

Integrated Science Assessment for Particulate Matter

Second External Review Draft

ISA: EPA/600/R-08/139B
ANNEXES: EPA/600/R-08/139BA

National Center for Environmental Assessment-RTP Division
Office of Research and Development
U.S. Environmental Protection Agency
Research Triangle Park, NC

Disclaimer

This document is the second external review draft for review purposes only and does not constitute U.S. Environmental Protection Agency policy. Mention of trade names or commercial products doesnot constitute endorsement or recommendation for use.

Table of Contents

LIST OF TABLES	XIII
LIST OF FIGURES	XXI
PM ISA PROJECT TEAM	XLI
AUTHORS, CONTRIBUTORS, REVIEWERS	XLIV
CLEAN AIR SCIENTIFIC ADVISORY COMMITTEE FOR PARTICULATE MATTER NAAQS	L
ACRONYMS AND ABBREVIATIONS	I
CHAPTER 1. INTRODUCTION	1-1
1.1. Legislative Requirements	1-4
1.2. History of Reviews of the NAAQS for PM	1-5
1.3. ISA Development	1-12
1.4. Document Organization	1-16
1.5. EPA Framework for Causal Determination	1-18
1.5.1. Scientific Evidence Used in Establishing Causality	1-19
1.5.2. Association and Causation	1-19
1.5.3. Evaluating Evidence for Inferring Causation	1-20
1.5.4. Application of Framework for Causal Determination	1-25
1.5.5. First Step—Determination of Causality	1-27
1.5.6. Second Step—Evaluation of Response	1-30
1.5.6.1. Effects on Human Populations	1-30
1.5.6.2. Effects on Public Welfare	1-31
1.5.7. Concepts in Evaluating Adversity of Health Effects	1-32
1.6. Summary	1-33
CHAPTER 2. INTEGRATIVE HEALTH AND WELFARE EFFECTS OVERVIEW	2-1
2.1. Concentrations and Sources of Atmospheric PM	2-2
2.1.1. Ambient PM Variability and Correlations	2-2
2.1.1.1. Spatial Variability across the U.S.	2-3
2.1.1.2. Spatial Variability on the Urban and Neighborhood Scales	2-4
2.1.2. Trends and Temporal Variability	2-4
2.1.3. Correlations between Copollutants	2-5
2.1.4. Measurement Techniques	2-5
2.1.5. PM Formation in the Atmosphere and Removal	2-6
2.1.6. Source Contributions to PM	2-7
2.1.7. Policy-Relevant Background	2-8
2.2. Human Exposure	2-8
2.2.1. Spatial Scales of PM Exposure Assessment	2-9
2.2.2. Exposure to PM Components and Copollutants	2-10
2.2.3. Implications for Epidemiologic Studies	2-11
2.3. Health Effects	2-12

2.3.1.	Exposure to PM _{2.5}	2-13
2.3.1.1.	Effects of Short-Term Exposure to PM _{2.5}	2-13
2.3.1.2.	Effects of Long-Term Exposure to PM _{2.5}	2-16
2.3.2.	Integration of PM _{2.5} Health Effects	2-19
2.3.3.	Exposure to PM _{10-2.5}	2-25
2.3.3.1.	Effects of Short-Term Exposure to PM _{10-2.5}	2-25
2.3.4.	Integration of PM _{10-2.5} Effects	2-27
2.3.5.	Exposure to Ultrafine PM	2-30
2.3.5.1.	Effects of Short-Term Exposure to UFPs	2-30
2.3.6.	Integration of UFP Effects	2-31
2.4.	Policy Relevant Considerations	2-32
2.4.1.	Potentially Susceptible Subpopulations	2-32
2.4.2.	Lag Structure of PM—Morbidity and PM—Mortality Associations	2-34
2.4.2.1.	PM—Cardiovascular Morbidity Associations	2-34
2.4.2.2.	PM—Respiratory Morbidity Associations	2-35
2.4.2.3.	PM—Mortality Associations	2-35
2.4.3.	PM Concentration—Response Relationship	2-36
2.5.	Ecological and Welfare Effects	2-37
2.5.1.	Summary of Effects on Visibility	2-37
2.5.2.	Summary of Effects on Climate	2-39
2.5.3.	Summary of Ecological Effects of PM	2-41
2.5.4.	Summary of Effects on Materials	2-43

CHAPTER 3. SOURCE TO HUMAN EXPOSURE **3-1**

3.1.	Introduction	3-1
3.2.	Overview of Basic Aerosol Properties	3-2
3.3.	Sources, Emissions and Deposition of Primary and Secondary PM	3-6
3.3.1.	Emissions of Primary PM and Precursors to Secondary PM	3-9
3.3.2.	Formation of Secondary PM	3-12
3.3.2.1.	Formation of Nitrate and Sulfate	3-12
3.3.2.2.	Formation of Secondary Organic Aerosol	3-12
3.3.2.3.	Formation of new particles	3-15
3.3.3.	Mobile Source Emissions	3-16
3.3.3.1.	Emissions from Gasoline Fueled Engines	3-16
3.3.3.2.	Emissions from Diesel Fueled Engines	3-17
3.3.4.	Deposition of PM	3-19
3.3.4.1.	Deposition Forms	3-21
3.3.4.2.	Methods for Estimating Dry Deposition	3-23
3.3.4.3.	Factors Affecting Dry Deposition Rates and Totals	3-24
3.4.	Monitoring of PM	3-27
3.4.1.	Ambient Measurement Techniques	3-27
3.4.1.1.	PM Mass	3-27
3.4.1.2.	PM Speciation	3-31
3.4.1.3.	Multiple-Component Measurements on Individual Particles	3-39
3.4.1.4.	Ultrafine PM: Mass, Surface Area, and Number	3-39
3.4.1.5.	PM Size Distribution	3-40
3.4.1.6.	Satellite Measurement	3-41
3.4.2.	Ambient Network Design	3-42
3.4.2.1.	Monitor Siting Requirements	3-42
3.4.2.2.	Spatial and Temporal Coverage	3-44
3.4.2.3.	Network Application for Exposure Assessment with Respect to Susceptible Sub-populations	3-48
3.5.	Ambient PM Concentrations	3-52
3.5.1.	Spatial Distribution	3-54

3.5.1.1.	Variability across the U.S.	3-54
3.5.1.2.	Urban-Scale Variability	3-74
3.5.1.3.	Neighborhood-Scale Variability	3-98
3.5.2.	Temporal Variability	3-106
3.5.2.1.	Regional Trends	3-106
3.5.2.2.	Seasonal Variations	3-111
3.5.2.3.	Hourly Variability	3-113
3.5.3.	Statistical Associations with Copollutants	3-117
3.5.4.	Summary	3-120
3.6.	Mathematical Modeling of PM	3-122
3.6.1.	Estimating Source Contributions to PM Using Receptor Models	3-122
3.6.1.1.	Receptor Models	3-123
3.6.2.	Chemistry Transport Models	3-130
3.6.2.1.	Global Scale	3-132
3.6.2.2.	Regional Scale	3-132
3.6.2.3.	Local or Neighborhood Scale	3-135
3.6.3.	Air Quality Model Evaluation for Air Concentrations	3-136
3.6.3.1.	Ground-based Comparisons of Photochemical Dynamics	3-142
3.6.3.2.	Predicted Chemistry for Nitrates and Related Compounds	3-142
3.6.4.	Evaluating Concentrations and Deposition of PM Components with CTMs	3-149
3.6.4.1.	Global CTM Performance	3-149
3.6.4.2.	Regional CTM Performance	3-151
3.7.	Background PM	3-162
3.7.1.	Contributors to PRB concentrations of PM	3-163
3.7.1.1.	Estimates of PRB Concentrations in Previous Assessments	3-164
3.7.1.2.	Chemistry Transport Models (CTMs) for Predicting PRB Concentrations	3-167
3.8.	Issues in Exposure Assessment for PM and its Components	3-178
3.8.1.	General Exposure Concepts	3-179
3.8.2.	Exposure Modeling	3-182
3.8.2.1.	Time-Weighted Microenvironmental Models	3-182
3.8.2.2.	Stochastic Population Exposure Models	3-184
3.8.2.3.	Dispersion Models	3-186
3.8.2.4.	Land Use Regression (LUR) and GIS-Based Models	3-187
3.8.3.	Personal and Microenvironmental Exposure Monitoring	3-190
3.8.3.1.	New Developments in Personal Exposure Monitoring Techniques	3-190
3.8.3.2.	New Developments in Microenvironmental Exposure Monitoring Techniques	3-191
3.8.4.	Exposure Assessment Studies at Different Spatial Scales	3-192
3.8.4.1.	Urban Scale Ambient PM Exposure	3-193
3.8.4.2.	Micro-to-Neighborhood Scale Ambient PM Exposure	3-197
3.8.4.3.	Indoor Exposure to Ambient: Infiltration and Differential Infiltration	3-201
3.8.5.	Multicomponent and Multipollutant PM Exposures	3-203
3.8.5.1.	Exposure Issues Related to PM Composition	3-203
3.8.5.2.	Exposure to PM and Copollutants	3-209
3.8.6.	Implications of Exposure Assessment Issues for Interpretation of Epidemiologic Studies	3-211
3.8.6.1.	Measurement Error	3-211
3.8.6.2.	Model-Related Errors	3-212
3.8.6.3.	Spatial Variability	3-215
3.8.6.4.	Temporal Variability	3-219
3.8.6.5.	Use of Surrogates for PM Exposure	3-220
3.8.6.6.	Compositional Differences	3-222
3.8.6.7.	Conclusions	3-223
3.9.	Summary and Conclusions	3-224
3.9.1.	Concentrations and Sources of Atmospheric PM	3-224
3.9.1.1.	Ambient PM Variability and Correlations	3-224
3.9.1.2.	Temporal Variability	3-227
3.9.1.3.	Correlations between Copollutants	3-228

3.9.1.4.	Measurement Techniques	3-228
3.9.1.5.	PM Source Characteristics	3-229
3.9.1.6.	Source Contributions to PM	3-229
3.9.1.7.	Policy-Relevant Background	3-230
3.9.2.	Human Exposure	3-231
3.9.2.1.	Characterizing Human Exposure	3-231
3.9.2.2.	Spatial Scales of PM Exposure Assessment	3-232
3.9.2.3.	Multicomponent and Multipollutant PM Exposures	3-233
3.9.2.4.	Implications for Epidemiologic Studies	3-234

CHAPTER 4. DOSIMETRY **4-1**

4.1.	Introduction	4-1
4.1.1.	Size Characterization of Inhaled Particles	4-2
4.1.2.	Structure of the Respiratory Tract	4-3
4.2.	Particle Deposition	4-6
4.2.1.	Mechanisms of Deposition	4-7
4.2.2.	Deposition Patterns	4-9
4.2.2.1.	Total Respiratory Tract Deposition	4-11
4.2.2.2.	Extrathoracic Region	4-11
4.2.2.3.	Tracheobronchial and Alveolar Region	4-12
4.2.2.4.	Localized Deposition Sites	4-13
4.2.3.	Interspecies Patterns of Deposition	4-14
4.2.4.	Biological Factors Modulating Deposition	4-15
4.2.4.1.	Physical Activity	4-15
4.2.4.2.	Age	4-17
4.2.4.3.	Gender	4-19
4.2.4.4.	Anatomical Variability	4-19
4.2.4.5.	Respiratory Tract Disease	4-20
4.2.4.6.	Hygroscopicity of Aerosols	4-22
4.2.5.	Summary	4-22
4.3.	Clearance of Poorly Soluble Particles	4-23
4.3.1.	Clearance Mechanisms and Kinetics	4-24
4.3.1.1.	Extrathoracic Region	4-24
4.3.1.2.	Tracheobronchial Region	4-24
4.3.1.3.	Alveolar Region	4-26
4.3.2.	Interspecies Patterns of Clearance and Retention	4-27
4.3.3.	Particle Translocation	4-29
4.3.3.1.	Alveolar Region	4-29
4.3.3.2.	Olfactory Region	4-31
4.3.4.	Factors Modulating Clearance	4-33
4.3.4.1.	Age	4-33
4.3.4.2.	Gender	4-34
4.3.4.3.	Respiratory Tract Disease	4-34
4.3.4.4.	Particle Overload	4-36
4.3.5.	Summary	4-36
4.4.	Clearance of Soluble Materials	4-37
4.4.1.	Clearance Mechanisms and Kinetics	4-38
4.4.2.	Factors Modulating Clearance	4-40
4.4.2.1.	Age	4-40
4.4.2.2.	Physical Activity	4-40
4.4.2.3.	Disease	4-41
4.4.2.4.	Concurrent Exposures	4-42
4.4.3.	Summary	4-43

CHAPTER 5. POSSIBLE PATHWAYS/ MODES OF ACTION **5-1**

5.1. Pulmonary Effects	5-2
5.1.1. Reactive Oxygen Species	5-2
5.1.2. Activation of Cell Signaling Pathways	5-4
5.1.3. Pulmonary Inflammation	5-6
5.1.4. Respiratory Tract Barrier Function	5-7
5.1.5. Antioxidant Defenses and Adaptive Responses	5-8
5.1.6. Pulmonary Function	5-10
5.1.7. Allergic Disorders	5-10
5.1.8. Impaired Lung Defense Mechanisms	5-11
5.1.9. Resolution of Inflammation/Progression or Exacerbation of Disease	5-11
5.1.9.1. Factors Affecting the Retention of PM	5-11
5.1.9.2. Factors Affecting the Balance of Pro/Anti-Inflammatory Mediators, Oxidants/Anti-Oxidants and Proteases/Anti-Proteases	5-12
5.1.9.3. Pre-Existing Disease	5-13
5.1.10. Pulmonary DNA Damage	5-14
5.1.11. Epigenetic Changes	5-14
5.1.12. Lung Development	5-16
5.2. Systemic Inflammation	5-16
5.2.1. Endothelial Dysfunction and Altered Vasoreactivity	5-18
5.2.2. Activation of Coagulation and Acute Phase Response	5-19
5.2.3. Atherosclerosis	5-20
5.2.4. Activation of the Autonomic Nervous System by Pulmonary Reflexes	5-22
5.3. Translocation of Ultrafine PM or Soluble PM Components	5-24
5.4. Disease of the Cardiovascular and Other Organ Systems	5-26
5.5. Acute and Chronic Responses	5-27
5.6. Results of New Inhalation Studies which Contribute to Modes of Action	5-28

CHAPTER 6. INTEGRATED HEALTH EFFECTS OF SHORT-TERM PM EXPOSURE **6-1**

6.1. Introduction	6-1
6.2. Cardiovascular and Systemic Effects	6-2
6.2.1. Heart Rate and Heart Rate Variability	6-2
6.2.1.1. Epidemiologic Studies	6-3
6.2.1.2. Controlled Human Exposure Studies	6-12
6.2.1.3. Toxicological Studies	6-14
6.2.2. Arrhythmia	6-18
6.2.2.1. Epidemiologic Studies	6-19
6.2.2.2. Toxicological Studies	6-26
6.2.3. Ischemia	6-29
6.2.3.1. Epidemiologic Studies	6-29
6.2.3.2. Controlled Human Exposure Studies	6-32
6.2.3.3. Toxicological Studies	6-32
6.2.4. Vasomotor Function	6-34
6.2.4.1. Epidemiologic Studies	6-35
6.2.4.2. Controlled Human Exposure Studies	6-37
6.2.4.3. Toxicological Studies	6-41
6.2.5. Blood Pressure	6-47
6.2.5.1. Epidemiologic Studies	6-48
6.2.5.2. Controlled Human Exposure Studies	6-51
6.2.5.3. Toxicological Studies	6-52
6.2.6. Cardiac Contractility	6-53
6.2.6.1. Toxicological Studies	6-54
6.2.7. Systemic Inflammation	6-55

6.2.7.1.	Epidemiologic Studies	6-55
6.2.7.2.	Controlled Human Exposure Studies	6-59
6.2.7.3.	Toxicological Studies	6-61
6.2.8.	Hemostasis, Thrombosis and Coagulation Factors	6-63
6.2.8.1.	Epidemiologic Studies	6-63
6.2.8.2.	Controlled Human Exposure Studies	6-65
6.2.8.3.	Toxicological Studies	6-67
6.2.9.	Systemic and Cardiovascular Oxidative Stress	6-70
6.2.9.1.	Epidemiologic Studies	6-70
6.2.9.2.	Controlled Human Exposure Studies	6-72
6.2.9.3.	Toxicological Studies	6-73
6.2.10.	Hospital Admissions and ED Visits	6-75
6.2.10.1.	All Cardiovascular Disease	6-81
6.2.10.2.	Cardiac Diseases	6-87
6.2.10.3.	Ischemic Heart Disease	6-88
6.2.10.4.	Acute MI	6-90
6.2.10.5.	Congestive Heart Failure	6-92
6.2.10.6.	Cardiac Arrhythmias	6-94
6.2.10.7.	Cerebrovascular Disease	6-96
6.2.10.8.	Peripheral Vascular Disease	6-98
6.2.10.9.	Copollutant Models	6-100
6.2.10.10.	Concentration Response	6-101
6.2.10.11.	Out of Hospital Cardiac Arrest	6-103
6.2.11.	Short-term Exposure to PM and Cardiovascular Mortality	6-105
6.2.12.	Summary and Causal Determinations	6-106
6.2.12.1.	PM _{2.5}	6-106
6.2.12.2.	PM _{10-2.5}	6-111
6.2.12.3.	Ultrafine PM	6-113
6.3.	Respiratory Effects	6-115
6.3.1.	Respiratory Symptoms and Medication Use	6-115
6.3.1.1.	Epidemiologic Studies	6-116
6.3.1.2.	Controlled Human Exposure Studies	6-127
6.3.2.	Pulmonary Function	6-128
6.3.2.1.	Epidemiologic Studies	6-129
6.3.2.2.	Controlled Human Exposure Studies	6-134
6.3.2.3.	Toxicological Studies	6-136
6.3.3.	Pulmonary Inflammation	6-138
6.3.3.1.	Epidemiologic Studies	6-138
6.3.3.2.	Controlled Human Exposure Studies	6-143
6.3.3.3.	Toxicological Studies	6-146
6.3.4.	Oxidative Responses	6-153
6.3.4.1.	Controlled Human Exposure Studies	6-153
6.3.4.2.	Toxicological Studies	6-154
6.3.5.	Pulmonary Injury	6-158
6.3.5.1.	Epidemiologic Studies	6-158
6.3.5.2.	Controlled Human Exposure Studies	6-158
6.3.5.3.	Toxicological Studies	6-159
6.3.6.	Allergic Responses	6-168
6.3.6.1.	Epidemiologic Studies	6-168
6.3.6.2.	Controlled Human Exposure Studies	6-168
6.3.6.3.	Toxicological Studies	6-169
6.3.7.	Host Defense	6-178
6.3.7.1.	Epidemiologic Studies	6-178
6.3.7.2.	Toxicological Studies	6-179
6.3.8.	Respiratory ED Visits, Hospital Admissions and Physician Visits	6-183
6.3.8.1.	All Respiratory Diseases	6-184
6.3.8.2.	Asthma	6-190
6.3.8.3.	COPD	6-197

6.3.8.4.	Pneumonia and Respiratory Infections	6-198
6.3.8.5.	Copollutant Models	6-204
6.3.9.	Short-term Exposure to PM and Respiratory Mortality	6-205
6.3.10.	Summary and Causal Determinations	6-206
6.3.10.1.	PM _{2.5}	6-206
6.3.10.2.	PM _{10-2.5}	6-210
6.3.10.3.	Ultrafine PM	6-212
6.4.	Central Nervous System Effects	6-214
6.4.1.	Epidemiologic Studies	6-214
6.4.2.	Controlled Human Exposure Studies	6-215
6.4.3.	Toxicological Studies	6-215
6.4.3.1.	Urban Air	6-215
6.4.3.2.	CAPS	6-216
6.4.3.3.	Diesel Exhaust	6-217
6.4.4.	Summary and Causal Determination	6-219
6.5.	Mortality Associated with Short-Term Exposure	6-219
6.5.1.	Summary of Findings from 2004 PM AQCD	6-220
6.5.2.	Associations of Mortality and Short-Term Exposure to PM	6-221
6.5.2.1.	PM ₁₀	6-223
6.5.2.2.	PM _{2.5}	6-241
6.5.2.3.	Thoracic Coarse Particles (PM _{10-2.5})	6-252
6.5.2.4.	Ultrafine PM	6-259
6.5.2.5.	Chemical Components of PM	6-261
6.5.2.6.	Source-Appportioned PM Analyses	6-267
6.5.2.7.	Investigation of Concentration-Response Relationship	6-268
6.5.3.	Summary and Causal Determinations	6-271
6.5.3.1.	PM _{2.5}	6-271
6.5.3.2.	PM _{10-2.5}	6-272
6.5.3.3.	Ultrafine PM	6-273
6.6.	Attribution of Ambient PM Health Effects to Specific Constituents or Sources	6-274
6.6.1.	Evaluation Approach	6-275
6.6.2.	Findings	6-276
6.6.2.1.	Epidemiologic Studies	6-276
6.6.2.2.	Controlled Human Exposure Studies	6-280
6.6.2.3.	Toxicological Studies	6-281
6.6.3.	Summary by Health Effects	6-285

CHAPTER 7. INTEGRATED HEALTH EFFECTS OF LONG-TERM PM EXPOSURE **7-1**

7.1.	Introduction	7-1
7.2.	Cardiovascular and Systemic Effects	7-1
7.2.1.	Atherosclerosis	7-2
7.2.1.1.	Epidemiologic Studies	7-2
7.2.1.2.	Toxicological Studies	7-6
7.2.2.	Venous Thromboembolism	7-9
7.2.2.1.	Epidemiologic Studies	7-9
7.2.3.	Diabetes	7-10
7.2.3.1.	Toxicological Studies	7-10
7.2.4.	Systemic Inflammation, Immune Function, and Blood Coagulation	7-10
7.2.4.1.	Epidemiologic Studies	7-10
7.2.4.2.	Toxicological Studies	7-12
7.2.5.	Renal and Vascular Function	7-13
7.2.5.1.	Epidemiologic Studies	7-14
7.2.5.2.	Toxicological Studies	7-15
7.2.6.	Autonomic Function	7-16
7.2.6.1.	Toxicological Studies	7-16

7.2.7.	Cardiac changes	7-17
7.2.7.1.	Toxicological studies	7-17
7.2.8.	Left Ventricular Mass and Function	7-18
7.2.9.	Clinical Outcomes in Epidemiologic Studies	7-18
7.2.10.	Cardiovascular Mortality	7-23
7.2.11.	Summary and Causal Determinations	7-25
7.2.11.1.	PM _{2.5}	7-25
7.2.11.2.	PM _{10-2.5}	7-27
7.2.11.3.	Ultrafine PM	7-27
7.3.	Respiratory Effects	7-28
7.3.1.	Respiratory Symptoms and Disease Incidence	7-29
7.3.1.1.	Epidemiologic Studies	7-29
7.3.2.	Pulmonary Function	7-37
7.3.2.1.	Epidemiologic Studies	7-37
7.3.2.2.	Toxicological Studies	7-43
7.3.3.	Pulmonary Inflammation	7-45
7.3.3.1.	Epidemiologic Studies	7-45
7.3.3.2.	Toxicological Studies	7-45
7.3.4.	Pulmonary Oxidative Response	7-49
7.3.4.1.	Toxicological Studies	7-49
7.3.5.	Pulmonary Injury	7-49
7.3.5.1.	Toxicological Studies	7-49
7.3.6.	Allergic Responses	7-55
7.3.6.1.	Epidemiologic Studies	7-55
7.3.6.2.	Toxicological Studies	7-56
7.3.7.	Host Defense	7-57
7.3.7.1.	Epidemiologic Studies	7-57
7.3.7.2.	Toxicological Studies	7-58
7.3.8.	Respiratory Mortality	7-59
7.3.9.	Summary and Causal Determinations	7-59
7.3.9.1.	PM _{2.5}	7-59
7.3.9.2.	PM _{10-2.5}	7-62
7.3.9.3.	Ultrafine PM	7-63
7.4.	Reproductive, Developmental, Prenatal and Neonatal Outcomes	7-63
7.4.1.	Epidemiologic Studies	7-63
7.4.2.	Toxicological Studies	7-84
7.4.2.1.	Female Reproductive Effects	7-85
7.4.2.2.	Male Reproductive Effects	7-86
7.4.2.3.	Multiple Generation Effects	7-90
7.4.2.4.	Receptor Mediated Effects	7-91
7.4.2.5.	Developmental Effects	7-92
7.4.3.	Summary and Causal Determinations	7-97
7.4.3.1.	PM _{2.5}	7-97
7.4.3.2.	PM _{10-2.5}	7-98
7.5.	Cancer, Mutagenicity, and Genotoxicity	7-99
7.5.1.	Epidemiologic Studies	7-101
7.5.1.1.	Lung Cancer Mortality and Incidence	7-101
7.5.1.2.	Other Cancers	7-105
7.5.1.3.	Markers of Exposure or Susceptibility	7-105
7.5.2.	Toxicological Studies	7-108
7.5.2.1.	Mutagenesis and Genotoxicity	7-109
7.5.2.2.	Carcinogenesis	7-114
7.5.3.	Epigenetic Studies and Other Heritable DNA mutations	7-115
7.5.4.	Summary and Causal Determinations	7-117
7.6.	Mortality Associated with Long-term Exposure	7-118
7.6.1.	Recent Studies of Long-Term Exposure to PM and Mortality	7-120

7.6.2.	Composition and Source-Oriented Analyses of PM	7-129
7.6.3.	Within-City Effects of PM Exposure	7-130
7.6.4.	Effects of Different Long-term Exposure Windows	7-132
7.6.5.	Summary and Causal Determinations	7-135
7.6.5.1.	PM _{2.5}	7-135
7.6.5.2.	PM _{10-2.5}	7-138

CHAPTER 8. SUSCEPTIBLE SUBPOPULATIONS **8-1**

8.1.	Potentially Susceptible Subpopulations	8-1
8.1.1.	Age	8-3
8.1.1.1.	Older Adults	8-3
8.1.1.2.	Children	8-6
8.1.2.	Pregnancy and Developmental Effects	8-7
8.1.3.	Gender	8-7
8.1.4.	Race/Ethnicity	8-8
8.1.5.	Gene-Environment Interaction	8-9
8.1.6.	Pre-Existing Disease	8-12
8.1.6.1.	Cardiovascular Diseases	8-12
8.1.6.2.	Respiratory Illnesses	8-16
8.1.6.3.	Respiratory Contributions to Cardiovascular Effects	8-18
8.1.6.4.	Diabetes and Obesity	8-19
8.1.7.	Socioeconomic Status	8-21
8.1.8.	Summary	8-22

CHAPTER 9. WELFARE EFFECTS **9-1**

9.1.	Introduction	9-1
9.2.	Effects on Visibility	9-1
9.2.1.	Introduction	9-1
9.2.2.	Background	9-3
9.2.2.1.	Non-PM Visibility Effects	9-6
9.2.2.2.	PM Visibility Effects	9-7
9.2.2.3.	Direct Optical Measurements	9-11
9.2.2.4.	Value of Good Visual Air Quality	9-13
9.2.3.	Monitoring and Assessment	9-14
9.2.3.1.	Aerosol Properties	9-15
9.2.3.2.	Spatial Patterns	9-22
9.2.3.3.	Urban and Regional Patterns	9-29
9.2.3.4.	Temporal Trends	9-37
9.2.3.5.	Causes of Haze	9-44
9.2.4.	Urban Visibility Valuation and Preference	9-74
9.2.4.1.	Urban Visibility Preference Studies	9-75
9.2.4.2.	Denver, Colorado Urban Visibility Preference Study	9-77
9.2.4.3.	Phoenix, Arizona Urban Visibility Preference Study	9-78
9.2.4.4.	British Columbia, Canada Urban Visibility Preference Study	9-79
9.2.4.5.	Washington, DC Urban Visibility Pilot Preference Study	9-79
9.2.4.6.	Urban Visibility Valuation Studies	9-81
9.2.5.	Summary of Effects on Visibility	9-83
9.3.	Effects on Climate	9-86
9.3.1.	The Climate Effects of Aerosols	9-87
9.3.2.	Overview of Aerosol Measurement Capabilities	9-94
9.3.2.1.	Satellite Remote Sensing	9-94
9.3.2.2.	Focused Field Campaigns	9-100
9.3.2.3.	Ground-Based In Situ Measurement Networks	9-101
9.3.2.4.	In Situ Aerosol Profiling Programs	9-103
9.3.2.5.	Ground-Based Remote Sensing Measurement Networks	9-107
9.3.2.6.	Synergy of Measurements and Model Simulations	9-108

9.3.3.	Assessments of Aerosol Characterization and Climate Forcing	9-111
9.3.3.1.	The Use of Measured Aerosol Properties to Improve Models	9-111
9.3.3.2.	Intercomparisons of Satellite Measurements and Model Simulation of Aerosol Optical Depth	9-114
9.3.3.3.	Satellite-Based Estimates of Aerosol Direct Radiative Forcing	9-116
9.3.3.4.	Satellite-Based Estimates of Anthropogenic Component of Aerosol Direct Radiative Forcing	9-123
9.3.3.5.	Aerosol-Cloud Interactions and Indirect Forcing	9-124
9.3.3.6.	Remote Sensing of Aerosol-Cloud Interactions and Indirect Forcing	9-125
9.3.3.7.	In Situ Studies of Aerosol-Cloud Interactions	9-128
9.3.4.	Outstanding Issues	9-129
9.3.5.	Concluding Remarks	9-132
9.3.6.	Modeling the Effect of Aerosols on Climate	9-134
9.3.6.1.	Introduction	9-134
9.3.6.2.	Modeling of Atmospheric Aerosols	9-136
9.3.6.3.	Calculating Aerosol Direct Radiative Forcing	9-141
9.3.6.4.	Calculating Aerosol Indirect Forcing	9-150
9.3.6.5.	Aerosol in the Climate Models	9-157
9.3.6.6.	Impacts of Aerosols on Climate Model Simulations	9-165
9.3.6.7.	Outstanding Issues	9-169
9.3.6.8.	Conclusions	9-170
9.3.7.	Fire as a Special Source of PM Welfare Effects	9-171
9.3.8.	Radiative Effects of Volcanic Aerosols	9-173
9.3.8.1.	Explosive Volcanic Activity	9-173
9.3.9.	Other Special Sources and Effects	9-178
9.3.9.1.	Glaciers and Snowpack	9-181
9.3.9.2.	Radiative Forcing by Anthropogenic Surface Albedo Change: BC in Snow and Ice	9-184
9.3.9.3.	Effects on Local and Regional Climate	9-185
9.3.10.	Summary of Effects on Climate	9-187
9.4.	Ecological Effects of PM	9-188
9.4.1.	Introduction	9-188
9.4.1.1.	Ecosystem Scale, Function, and Structure	9-191
9.4.1.2.	Ecosystem Services	9-192
9.4.2.	Deposition of PM	9-192
9.4.2.1.	Forms of Deposition	9-192
9.4.2.2.	Components of PM Deposition	9-194
9.4.2.3.	Magnitude of Dry Deposition	9-198
9.4.3.	Direct Effects of PM on Vegetation	9-203
9.4.3.1.	Effects of Coarse-mode Particles	9-204
9.4.4.	PM and Diffuse Light Effects	9-205
9.4.5.	Effects of Trace Metals on Ecosystems	9-206
9.4.5.1.	Direct Effects of Metals	9-207
9.4.5.2.	Effects on Soil Chemistry	9-209
9.4.5.3.	Effects on Soil Microbes and Plant Uptake via Soil	9-210
9.4.5.4.	Plant Response to Metals	9-215
9.4.5.5.	Effects on Aquatic Ecosystems	9-218
9.4.5.6.	Effects on Animals	9-219
9.4.5.7.	Biomagnification across trophic levels	9-221
9.4.5.8.	Effects near Smelters and Roadsides	9-223
9.4.6.	Organic Compounds	9-225
9.4.7.	Summary of Ecological Effects of PM	9-230
9.5.	Effects on Materials	9-232
9.5.1.	Effects on Paint	9-234
9.5.2.	Effects on Metal Surfaces	9-234
9.5.3.	Effects on Stone	9-235
9.5.4.	Summary of Effects on Materials	9-236

ANNEX A. ATMOSPHERIC SCIENCE	A-1
A.1. Ambient Air Particle Monitoring	A-1
A.1.1. Measurements and Analytical Specifications	A-1
A.1.2. Networks	A-49
A.1.3. Monitor Distribution with Respect to Population Density	A-54
A.2. Ambient PM Concentration	A-82
A.2.1. Speciation Trends Network Site Data	A-82
A.2.2. Intraurban Variability	A-88
A.2.3. Speciation	A-170
A.2.4. Diel Trends	A-192
A.2.5. Copollutant Measurements	A-201
A.3. Source Apportionment	A-215
A.3.1. Type of Receptor Models	A-215
A.3.2. Source Profiles	A-228
A.3.3. Receptor Model Results	A-231
A.4. Exposure Assessment	A-232
A.4.1. Exposure Assessment Study Findings	A-232
 ANNEX B. DOSIMETRY	 B-1
B.1. Ultrafine Disposition	B-1
B.2. Olfactory Translocation	B-3
B.3. Clearance and Age	B-4
 ANNEX C. CONTROLLED HUMAN EXPOSURE STUDIES	 C-1
 ANNEX D. TOXICOLOGICAL STUDIES	 D-1
D.1. Carcinogenesis, Mutagenesis, Genotoxicity	D-172
 ANNEX E. EPIDEMIOLOGIC STUDIES	 E-1
E.1. Short-Term Exposure and Cardiovascular Outcomes	E-1
E.1.1. Cardiovascular Morbidity Studies	E-1
E.1.2. Cardiovascular Emergency Department Visits and Hospital Admissions	E-84
E.2. Short-Term Exposure and Respiratory Outcomes	E-146
E.2.1. Respiratory Morbidity Studies	E-146
E.2.2. Respiratory Emergency Department Visits and Hospital Admissions	E-276
E.3. Short-Term Exposure and Mortality	E-351
E.4. Long-Term Exposure and Cardiovascular Outcomes	E-468
E.5. Long-Term Exposure and Respiratory Outcomes	E-490
E.6. Long-Term Exposure and Cancer	E-555
E.7. Long-Term Exposure and Reproductive Effects	E-563
E.8. Long-Term Exposure and Mortality	E-630
E.9. Long-Term Exposure and Mortality	E-639
 ANNEX F. SOURCE APPORTIONMENT STUDIES	 F-1

List of Tables

Table 1-1.	Summary of NAAQS promulgated for PM, 1971-2006. _____	1-6
Table 1-2	Aspects to aid in judging causality. _____	1-26
Table 1-3.	Weight of evidence for causal determination. _____	1-29
Table 2-1	Summary of causal determinations for short-term exposure to PM _{2.5} . _____	2-13
Table 2-2.	Summary of causal determinations for long-term exposure to PM _{2.5} . _____	2-16
Table 2-3.	Summary of causal determinations for short-term exposure to PM _{10-2.5} . _____	2-25
Table 2-4.	Summary of causal determinations for short-term exposure to UFPs. _____	2-30
Table 2-5.	Summary of causality determination for welfare effects. _____	2-37
Table 3-1.	Characteristics of ambient fine (ultrafine plus accumulation-mode) and coarse particles. _____	3-4
Table 3-2.	Constituents of atmospheric particles and their major sources. _____	3-7
Table 3-3.	Proximity to PM ₁₀ and PM _{2.5} monitors for total population ^a by city. _____	3-47
Table 3-4.	Proximity to PM ₁₀ and PM _{2.5} monitors for children 0-4 y, children 5-17 y, and adults 65 y and older. ^a The figures presented here are cumulative for the 15 CSAs/CBSAs examined in Chapter 3. _____	3-49
Table 3-5.	Proximity to PM ₁₀ and PM _{2.5} monitors for adults aged 65 and older ^a by city. _____	3-50
Table 3-6.	Proximity to PM ₁₀ and PM _{2.5} monitors based on the population identified as white, black, Hispanic, or non-Hispanic _____	3-51
Table 3-7.	Proximity to PM ₁₀ and PM _{2.5} monitors based on the population below or above the poverty line _____	3-52
Table 3-8.	PM _{2.5} distributions derived from AQS data (concentration in $\mu\text{g}/\text{m}^3$). _____	3-56
Table 3-9.	PM _{10-2.5} distributions derived from AQS data (concentration in $\mu\text{g}/\text{m}^3$). _____	3-59
Table 3-10.	PM ₁₀ distributions derived from AQS data (concentration in $\mu\text{g}/\text{m}^3$). _____	3-60
Table 3-11.	Inter-sampler comparison statistics for each pair of 24-h PM _{2.5} monitors reporting to AQS for Boston, MA. _____	3-78
Table 3-12.	Inter-sampler comparison statistics for each pair of 24-h PM _{2.5} monitors reporting to AQS for Pittsburgh, PA. _____	3-81
Table 3-13.	Inter-sampler comparison statistics for each pair of 24-h PM _{2.5} monitors reporting to AQS for Los Angeles, CA. _____	3-83
Table 3-14.	Inter-sampler comparison statistics for each pair of 24-h PM ₁₀ monitors reporting to AQS for Boston, MA. _____	3-88
Table 3-15.	Inter-sampler comparison statistics for each pair of 24-h PM ₁₀ monitors reporting to AQS for Pittsburgh, PA. _____	3-90
Table 3-16.	Inter-sampler comparison statistics for each pair of 24-h PM ₁₀ monitors reporting to AQS for Los Angeles, CA. _____	3-93
Table 3-17.	Example of emissions factors (ng/kg) for trace elements under variable speed and steady speed driving conditions for PM emitted by diesel and gasoline engines. _____	3-125

Table 3-18.	Estimates of annual average natural background concentrations of PM _{2.5} and PM ₁₀ _____	3-165
Table 3-19.	Annual and quarterly mean PM _{2.5} concentrations (µg/m ³) measured at IMPROVE sites in 2004. _____	3-166
Table 3-20.	Annual and quarterly mean PM _{2.5} concentrations (µg/m ³) for the CMAQ “base case” at IMPROVE sites in 2004. _____	3-176
Table 3-21.	Annual and quarterly mean PM _{2.5} concentrations (µg/m ³) for the CMAQ PRB simulations at IMPROVE sites in 2004. _____	3-177
Table 3-22.	Annual and quarterly mean of the CMAQ-predicted base case PM _{2.5} concentrations (µg/m ³) in the U.S. EPA CONUS regions in 2004. _____	3-177
Table 3-23.	Annual and quarterly mean of the CMAQ-predicted PRB PM _{2.5} concentrations (µg/m ³) in the U.S. EPA CONUS regions in 2004. _____	3-177
Table 3-24.	Examples of studies comparing near-road personal exposures with fixed site ambient concentrations. _____	3-199
Table 4-1.	Breathing patterns with activity level in adult human male. _____	4-16
Table 6-1.	Characteristics of epidemiologic/panel studies investigating associations between PM and changes in HRV. _____	6-9
Table 6-2.	Studies of ventricular arrhythmia and ambient PM concentration, in patients with implantable cardioverter defibrillators. _____	6-22
Table 6-3.	Median particle concentrations. _____	6-48
Table 6-4.	Ambient concentrations in six European cities. _____	6-56
Table 6-5.	Description of ICD-9 and ICD-10 codes for diseases of the circulatory system. _____	6-77
Table 6-6.	Characterization of ambient PM concentrations in studies of hospital admission and ED visits for cardiovascular diseases. _____	6-86
Table 6-7.	Characterization of ambient PM concentrations from studies of respiratory morbidity and short-term exposures in asthmatic children and adults. All concentrations are for the 24-h avg unless otherwise noted. _____	6-119
Table 6-8.	PAMCHAR PM _{10-2.5} inflammation results with ambient PM. _____	6-164
Table 6-9.	Other ambient PM – in vivo PM _{10-2.5} studies – BALF results, 18-24 h post-IT exposure _____	6-164
Table 6-10.	Description of ICD-9 and ICD-10 codes for diseases of the respiratory system. _____	6-183
Table 6-11.	PM concentrations in studies of respiratory diseases published since 2002. _____	6-204
Table 6-12.	Overview of U.S. and Canadian multicity PM studies of mortality analyzed in the 2004 PM AQCD and the PM ISA ^b _____	6-222
Table 6-13.	NMMAPS national and regional percentage increase in all-cause, cardio-respiratory, and other-cause mortality associated with a 10 µg/m ³ increase in PM ₁₀ at lag 1 day for the periods 1987-1994, 1995-2000, and 1987-2000. _____	6-226
Table 6-14.	Key to Figure 6-24 _____	6-246
Table 6-15.	Key for Figure 6-29 _____	6-256
Table 6-16.	Effect modification of composition on the estimated percent increase in mortality with a 10 µg/m ³ increase in PM _{2.5} . _____	6-264
Table 6-17.	Study-specific PM _{2.5} factor/source categories associated with health effects. _____	6-282

Table 7-1.	Characterization of ambient PM concentrations from studies of subclinical measures of cardiovascular diseases. _____	7-15
Table 7-2.	Characterization of ambient PM concentrations from studies of clinical cardiovascular diseases. _____	7-18
Table 7-3.	Characterization of ambient PM concentrations from studies of respiratory symptoms/disease and long-term exposures. _____	7-31
Table 7-4.	Characterization of ambient PM concentrations from studies of FEV ₁ and long-term exposures. _____	7-37
Table 7-5.	Characterization of ambient PM concentrations from studies of reproductive, developmental, prenatal and neonatal outcomes and long-term exposure. _____	7-65
Table 7-6.	Characterization of ambient PM concentrations from recent studies of cancer and long-term exposures to PM. _____	7-102
Table 7-7.	Associations* between ambient PM concentrations from select studies of lung cancer mortality and incidence. _____	7-103
Table 7-8.	Characterization of ambient PM concentrations from studies of mortality and long-term exposures to PM. _____	7-119
Table 7-9:	Comparison of results from ACS intra-urban analysis of Los Angeles and new york city using kriging or land use regression to estimate exposure _____	7-131
Table 7-10.	Distribution of the effect of a hypothetical reduction of 10 $\mu\text{g}/\text{m}^3$ PM ₁₀ in 2000 on all-cause mortality 2000-2009 in Switzerland. _____	7-134
Table 8-1.	Definitions of susceptible and vulnerable in the PM literature. _____	8-1
Table 8-2.	Susceptibility Factors. _____	8-3
Table 8-3.	Percent of the U.S. population with respiratory diseases, cardiovascular diseases, and diabetes. _____	8-16
Table 9-1.	Regional Planning Organization websites with visibility characterization and source attribution assessment information. _____	9-23
Table 9-2.	Summary of urban visibility preference studies. _____	9-76
Table 9-3.	Top-of-atmosphere, cloud-free, instantaneous direct aerosol radiative forcing dependence on aerosol and surface properties. _____	9-93
Table 9-4.	Summary of major satellite measurements currently available for the tropospheric aerosol characterization and radiative forcing research. _____	9-95
Table 9-5.	List of major intensive field experiments that are relevant to aerosol research in a variety of aerosol regimes around the globe conducted in the past two decades. _____	9-105
Table 9-6.	Summary of major U.S. surface in situ and remote sensing networks for the tropospheric aerosol characterization and radiative forcing research. _____	9-106
Table 9-7.	Summary of approaches to estimating the aerosol direct radiative forcing in three categories: (A) satellite retrievals; (B) satellite-model integrations; and (C) model simulations. _____	9-117
Table 9-8.	Summary of seasonal and annual average clear-sky DRF (W/m^2) at the TOA and the surface (SFC) over global OCEAN derived with different methods and data. _____	9-121
Table 9-9.	Summary of seasonal and annual average clear-sky DRF (W/m^2) at the TOA and the surface (SFC) over global LAND derived with different methods and data. _____	9-122

Table 9-10.	Estimates of anthropogenic components of aerosol optical depth (T_{ant}) and clear-sky DRF at the TOA from model simulations _____	9-124
Table 9-11.	Anthropogenic emissions of aerosols and precursors for 2000 and 1750. _____	9-138
Table 9-12.	Summary of statistics of AeroCom Experiment A results from 16 global models. _____	9-139
Table 9-13.	SO_4^{2-} mass loading, MEE and AOD at 550 nm, shortwave radiative forcing at the top of the atmosphere, and normalized forcing with respect to AOD and mass. _____	9-143
Table 9-14.	Particulate organic matter (POM) and BC mass loading, AOD at 550 nm, shortwave radiative forcing at the top of the atmosphere, and normalized forcing with respect to AOD and mass. _____	9-144
Table 9-15.	Differences in present day and pre-industrial outgoing solar radiation (W/m^2) in the different experiments. _____	9-153
Table 9-16.	Forcings used in IPCC AR4 simulations of 20th century climate change. _____	9-157
Table 9-17.	Climate forcings (1880-2003) used to drive GISS climate simulations, along with the surface air temperature changes obtained for several periods. _____	9-166
Table 9-18.	Overview of the different aerosol indirect effects and their sign of the net radiative flux change at the top of the atmosphere (TOA). _____	9-180
Table 9-19.	Overview of the different aerosol indirect effects and their implications for the global mean net shortwave radiation of the surface F_{sc} (columns 2-4) and for precipitation (columns 5-7). _____	9-180
Table 9-20.	Recent studies highlighting POP occurrence and fate in the major arctic compartments. _____	9-182
Table 9-21.	Factors potentially important in estimating mercury exposure. _____	9-195

Annex Tables

Table A-1.	Summary of integrated and continuous samplers included in the field comparison. _____	A-1
Table A-2.	Summary of $PM_{2.5}$ and PM_{10} FRM and FEM samplers. _____	A-4
Table A-3.	Measurement and analytical specifications for filter analysis of mass, elements, ions, and carbon. _____	A-6
Table A-4.	Measurement and analytical specifications for filter analysis of organic species. _____	A-8
Table A-5.	Measurement and analytical specifications for continuous mass and mass surrogate instruments. _____	A-10
Table A-6.	Measurement and analytical specifications for continuous elements. _____	A-12
Table A-7.	Measurement and analytical specifications for continuous NO_3^- . _____	A-12
Table A-8.	Measurement and analytical specifications for continuous SO_4^{2-} . _____	A-14
Table A-9.	Measurement and analytical specifications for ions other than NO_3^- and SO_4^{2-} . _____	A-16
Table A-10.	Measurement and analytical specifications for continuous carbon. _____	A-17
Table A-11.	Summary of mass measurement comparisons. _____	A-19
Table A-12.	Summary of element and liquid water content measurement comparisons. _____	A-27
Table A-13.	Summary of $PM_{2.5}$ NO_3^- measurement comparisons. _____	A-28
Table A-14.	Summary of $PM_{2.5}$ SO_4^{2-} measurement comparisons _____	A-32

Table A-15.	Summary of PM _{2.5} carbon measurement comparisons. _____	A-35
Table A-16.	Summary of particle mass spectrometer measurement comparisons. _____	A-40
Table A-17.	Summary of particle mass spectrometer measurement comparisons. _____	A-44
Table A-18.	Summary of key parameters for TD-GC/MS and pyrolysis-GC/MS. _____	A-47
Table A-19.	Relevant Spatial Scales for PM ₁₀ , PM _{2.5} , and PM _{10-2.5} Measurement _____	A-49
Table A-20.	Major routine operating air monitoring networks ^d _____	A-51
Table A-21.	Inter-sampler correlation statistics for each pair of PM _{2.5} monitors reporting to AQS for Atlanta, GA. _____	A-90
Table A-22.	Inter-sampler correlation statistics for each pair of PM _{2.5} monitors reporting to AQS for Birmingham, AL. _____	A-94
Table A-23.	Inter-sampler correlation statistics for each pair of PM _{2.5} monitors reporting to AQS for Chicago, IL. _____	A-97
Table A-24.	Inter-sampler correlation statistics for each pair of PM _{2.5} monitors reporting to AQS for Denver, CO. _____	A-101
Table A-25.	Inter-sampler correlation statistics for each pair of PM _{2.5} monitors reporting to AQS for Detroit, MI. _____	A-105
Table A-26.	Inter-sampler correlation statistics for each pair of PM _{2.5} monitors reporting to AQS for Houston, TX. _____	A-109
Table A-27.	Inter-sampler correlation statistics for each pair of PM _{2.5} monitors reporting to AQS for New York City, NY. _____	A-113
Table A-28.	Inter-sampler correlation statistics for each pair of PM _{2.5} monitors reporting to AQS for Philadelphia, PA. _____	A-118
Table A-29.	Inter-sampler correlation statistics for each pair of PM _{2.5} monitors reporting to AQS for Phoenix, AZ. _____	A-121
Table A-30.	Inter-sampler correlation statistics for each pair of PM _{2.5} monitors reporting to AQS for Riverside, CA. _____	A-125
Table A-31.	Inter-sampler correlation statistics for each pair of PM _{2.5} monitors reporting to AQS for Seattle, WA. _____	A-127
Table A-32.	Inter-sampler correlation statistics for each pair of PM _{2.5} monitors reporting to AQS for St. Louis, MO. _____	A-131
Table A-33.	Inter-sampler correlation statistics for each pair of PM ₁₀ monitors reporting to AQS for Atlanta, GA. _____	A-133
Table A-34.	Inter-sampler correlation statistics for each pair of PM ₁₀ monitors reporting to AQS for Birmingham, AL. _____	A-136
Table A-35.	Inter-sampler correlation statistics for each pair of PM ₁₀ monitors reporting to AQS for Chicago, IL. _____	A-140
Table A-36.	Inter-sampler correlation statistics for each pair of PM ₁₀ monitors reporting to AQS for Denver, CO. _____	A-143
Table A-37.	Inter-sampler correlation statistics for each pair of PM ₁₀ monitors reporting to AQS for Detroit, MI. _____	A-146
Table A-38.	Inter-sampler correlation statistics for each pair of PM ₁₀ monitors reporting to AQS for Houston, TX. _____	A-149

Table A-39.	Inter-sampler correlation statistics for each pair of PM ₁₀ monitors reporting to AQS for New York City, NY. _____	A-150
Table A-40.	Inter-sampler correlation statistics for each pair of PM ₁₀ monitors reporting to AQS for Philadelphia, PA. _____	A-153
Table A-41.	Inter-sampler correlation statistics for each pair of PM ₁₀ monitors reporting to AQS for Phoenix, AZ. _____	A-157
Table A-42.	Inter-sampler correlation statistics for each pair of PM ₁₀ monitors reporting to AQS for Riverside, CA. _____	A-162
Table A-43.	Inter-sampler correlation statistics for each pair of PM ₁₀ monitors reporting to AQS for Seattle, WA. _____	A-165
Table A-44.	Inter-sampler correlation statistics for each pair of PM ₁₀ monitors reporting to AQS for St. Louis, MO. _____	A-168
Table A-45.	Correlation coefficients of hourly and daily average particle number, surface and volume concentrations in selected particle size ranges. _____	A-169
Table A-46.	Different receptor models used in the Supersite source apportionment studies: chemical mass balance. _____	A-215
Table A-47.	Different receptor models used in the Supersites source apportionment studies: factor analysis. _____	A-216
Table A-48.	Different receptor models used in the Supersites source apportionment studies: tracer-based methods. _____	A-220
Table A-49.	Different receptor models used in the Supersites source apportionment studies: meteorology-based methods. _____	A-222
Table A-50.	Source Profiles _____	A-228
Table A-51.	PM ₁₀ receptor model results _____	A-231
Table A-52.	PM _{2.5} receptor model results _____	A-232
Table A-53.	Exposure Assessment Study Summaries _____	A-232
Table A-53.	Examples of studies showing developments with UFP sampling methods since the 2004 PM AQCD. _____	A-279
Table A-54.	Summary of in-vehicle studies of exposure assessment. _____	A-280
Table A-55.	Summary of personal PM exposure studies with no indoor source during 2002-2008. _____	A-283
Table A-56.	Summary of PM species exposure studies. _____	A-287
Table A-57.	Summary of personal PM exposure source apportionment studies. _____	A-299
Table A-54.	Summary of PM infiltration studies. _____	A-301
Table A-55.	Summary of PM – copollutant exposure studies. _____	A-312
Table A-56.	Summary of studies relating PM, SES, and mortality and/or morbidity. _____	A-316
Table B-1.	Ultrafine disposition in humans. _____	B-1
Table B- 2.	Ultrafine disposition in animals. _____	B-2
Table B- 3.	In vitro studies of ultrafine disposition. _____	B-2
Table B-4.	Olfactory particle translocation. _____	B-3
Table B-5.	Studies of respiratory tract mucosal and macrophage clearance as a function. _____	B-4

Table C-1.	Cardiovascular Effects _____	C-1
Table C-2.	Respiratory effects _____	C-8
Table C- 3.	Central Nervous System Effects _____	C-13
Table D-1.	Cardiovascular effects. _____	D-1
Table D-2.	Respiratory effects: in vitro studies. _____	D-29
Table D-3.	Respiratory effects: in vivo studies. _____	D-78
Table D-4.	Effects related to immunity and allergy. _____	D-123
Table D-5.	Effects of the central nervous system. _____	D-165
Table D-6.	Reproductive and developmental effects. _____	D-167
Table D-7.	Mutagenic/genotoxic effects in bacterial cultures. _____	D-172
Table D-8.	Mutagenicity and genotoxicity data summary: in vitro studies. _____	D-175
Table D-9.	Mutagenicity and genotoxicity data summary: in vivo studies. _____	D-181
Table E-1	Short-term exposure - cardiovascular morbidity outcomes - PM ₁₀ _____	E-1
Table E-2.	Short-term exposure - cardiovascular morbidity studies: PM _{10-2.5} . _____	E-18
Table E-3.	Short-term exposure - cardiovascular morbidity studies: PM _{2.5} (including PM components/sources). _____	E-20
Table E-4.	Short-term exposure – cardiovascular morbidity studies - other size fractions. _____	E-77
Table E-5.	Short-term exposure–cardiovascular–ED/HA PM ₁₀ _____	E-84
Table E-6.	Short-term exposure–cardiovascular–ED/HA - PM _{10-2.5} . _____	E-109
Table E-7.	Short-term exposure - cardiovascular–ED/HA – PM _{2.5} (including PM components/sources) _____	E-112
Table E-8.	Short-term exposure-cardiovascular–ED/HA-other size fractions. _____	E-140
Table E-9.	Short-term exposure–respiratory morbidity outcomes -PM ₁₀ _____	E-146
Table E-10.	Short-term exposure - respiratory morbidity outcomes - PM _{10-2.5} . _____	E-194
Table E-11.	Short-term exposure - respiratory morbidity outcomes - PM _{2.5} (including components/sources). _____	E-198
Table E-12.	Short-term exposure–respiratory–ED/HA-PM ₁₀ _____	E-276
Table E-13.	Short-term exposure–respiratory–ED/HA-PM _{10-2.5} _____	E-308
Table E-14.	Short-term exposure–respiratory–ED/HA-PM _{2.5} (including PM components/sources). _____	E-316
Table E-15.	Short-term exposure–respiratory–ED/HA-Other Size Fractions _____	E-340
Table E-16.	Short-term exposure – mortality - PM ₁₀ . _____	E-351
Table E-17.	Short-term exposure – mortality - PM _{10-2.5} . _____	E-433
Table E-18.	Short-term exposure – mortality - PM _{2.5} (including PM components/sources). _____	E-439
Table E-19.	Short-term exposure – mortality - other PM size fractions. _____	E-464
Table E-20.	Long-term exposure - cardiovascular morbidity outcomes - PM ₁₀ _____	E-468
Table E-21.	Long-term effects–cardiovascular– PM _{2.5} (including PM components/sources) _____	E-476
Table E-22.	Long-term exposure - respiratory morbidity outcomes - PM ₁₀ . _____	E-490

Table E-23.	Long-term exposure - respiratory morbidity outcomes - PM _{10-2.5} . _____	E-521
Table E-24.	Long-term exposure - respiratory morbidity outcomes - PM _{2.5} (including PM components/sources). _____	E-528
Table E-25.	Long-term exposure - respiratory morbidity outcomes - other PM size fractions. _____	E-553
Table E-26.	Long-term exposure - cancer outcomes - PM ₁₀ . _____	E-555
Table E-27.	Long-term exposure - cancer outcomes - PM _{2.5} (including PM components/sources). _____	E-559
Table E-28.	Long-term exposure - cancer outcomes - other PM size fractions. _____	E-562
Table E-29.	Long-term exposure - reproductive outcomes - PM ₁₀ . _____	E-563
Table E-30.	Long-term exposure – mortality - PM ₁₀ . _____	E-630
Table E-31.	Long-term exposure – mortality - PM ₁₀ . _____	E-639
Table E-32.	Long-term exposure – mortality - PM _{10-2.5} . _____	E-640
Table E-33.	Long-term exposure – mortality - PM _{2.5} (including PM components/sources). _____	E-641
Table E-34.	Long-term exposure - central nervous system outcomes - PM. _____	E-672
Table F-1.	Epidemiologic studies of ambient PM sources, factors, or constituents. _____	F-1
Table F-2.	Human clinical studies of ambient PM sources, factors, or constituents. _____	F-4
Table F-3.	Toxicological studies of ambient PM sources, factors, or constituents _____	F-5

List of Figures

Figure 1-1	Identification of studies for inclusion in the ISA.	1-13
Figure 2-1.	Excess risk estimates from epidemiologic studies of PM _{2.5} ordered by mean 24-h avg concentration as reported by the investigator.	2-20
Figure 2-2.	Summary of U.S. studies examining the association between long-term exposure to PM _{2.5} and CVD morbidity/mortality, respiratory morbidity/mortality, and all-cause mortality conducted in locations where the mean annual PM _{2.5} concentration ranged from 10.7-29 $\mu\text{g}/\text{m}^3$. All effect estimates have been standardized to reflect a 10 $\mu\text{g}/\text{m}^3$ increase in mean annual PM _{2.5} concentration.	2-21
Figure 2-3.	Effect estimates from epidemiologic studies of PM _{10-2.5} ordered by mean 24-h avg concentration as reported by the investigator.	2-28
Figure 3-1.	Particle size distributions by number and volume.	3-3
Figure 3-2.	X-ray spectra and scanning electron microscopy images of individual particles	3-5
Figure 3-3.	Detailed source categorization of anthropogenic emissions of primary PM _{2.5} , PM ₁₀ and gaseous precursor species SO ₂ , NO _x , NH ₃ and VOCs for 2002 in units of million metric tons (MMT). (EGUs = Electricity Generating Units)	3-11
Figure 3-4.	Primary emissions and formation of SOA through gas, cloud and condensed phase reactions.	3-15
Figure 3-5.	Schematic of the resistance-in-series analogy for atmospheric deposition.	3-20
Figure 3-6.	The relationship between particle diameter and V_d for particles.	3-25
Figure 3-7.	PM ₁₀ monitor distribution in comparison with population density, Boston CSA.	3-45
Figure 3-8.	PM _{2.5} monitor distribution in comparison with population density, Boston CSA.	3-46
Figure 3-9.	Three-yr avg 24-h PM _{2.5} concentration by county derived from FRM or FRM-like data, 2005-2007.	3-55
Figure 3-10.	Three-yr avg 24-h PM _{10-2.5} concentration by county derived from co-located low volume FRM PM ₁₀ and PM _{2.5} monitors, 2005-2007.	3-58
Figure 3-11.	Three-yr avg 24-h PM ₁₀ concentration by county derived from FRM or FEM monitors, 2005-2007.	3-60
Figure 3-12.	Three-yr avg 24-h PM _{2.5} OC concentrations measured at CSN sites across the U.S., 2005-2007.	3-65
Figure 3-13.	Three-yr avg 24-h PM _{2.5} EC concentrations measured at CSN sites across the U.S., 2005-2007.	3-66
Figure 3-14.	Three-yr avg 24-h PM _{2.5} SO ₄ ²⁻ concentrations measured at CSN sites across the U.S., 2005-2007.	3-67
Figure 3-15.	Three-yr avg 24-h PM _{2.5} NO ₃ ⁻ concentrations measured at CSN sites across the U.S., 2005-2007.	3-68
Figure 3-16.	Three-yr avg 24-h PM _{2.5} NH ₄ ⁺ concentrations measured at CSN sites across the U.S., 2005-2007.	3-69
Figure 3-17.	Three-yr avg PM _{2.5} speciation estimates for 2005-2007 derived using the SANDWICH method	3-70

Figure 3-18.	Seasonally-stratified three-yr avg PM _{2.5} speciation estimates for 2005-2007 derived using the SANDWICH method _____	3-71
Figure 3-19.	Locations of PM _{2.5} monitors and major highways, Boston, MA. _____	3-76
Figure 3-20.	Seasonal distribution of 24-h avg PM _{2.5} concentrations by site for Boston, MA, 2005-2007. Box plots show the median and interquartile range with whiskers extending to the 5th and 95th percentiles at each site during (1) winter (December-February), (2) spring (March-May), (3) summer (June-August) and (4) fall (September-November). _____	3-77
Figure 3-21.	Locations of PM _{2.5} monitors and major highways, Pittsburgh, PA. _____	3-79
Figure 3-22.	Seasonal distribution of 24-h avg PM _{2.5} concentrations by site for Pittsburgh, PA, 2005-2007. _____	3-80
Figure 3-23.	Locations of PM _{2.5} monitors and major highways, Los Angeles, CA. _____	3-82
Figure 3-24.	Seasonal distribution of 24-h avg PM _{2.5} concentrations by site for Los Angeles, CA, 2005-2007. _____	3-83
Figure 3-25.	Inter-sampler correlations for 24-h PM _{2.5} as a function of distance between monitors in Boston, MA. _____	3-84
Figure 3-26.	Inter-sampler correlations for 24-h PM _{2.5} as a function of distance between monitors in Pittsburgh, PA. _____	3-84
Figure 3-27.	Inter-sampler correlations for 24-h PM _{2.5} as a function of distance between monitors in Los Angeles, CA. _____	3-85
Figure 3-28.	Seasonal distribution of 24-h avg PM _{10-2.5} concentrations by site _____	3-86
Figure 3-29.	Locations of PM ₁₀ monitors and major highways, Boston, MA. _____	3-87
Figure 3-30.	Seasonal distribution of 24-h avg PM ₁₀ concentrations by site for Boston, MA, 2005-2007. _____	3-88
Figure 3-31.	Locations of PM ₁₀ monitors and major highways, Pittsburgh, PA. _____	3-89
Figure 3-32.	Seasonal distribution of 24-h avg PM ₁₀ concentrations by site for Pittsburgh, PA, 2005-2007. _____	3-90
Figure 3-33.	Locations of PM ₁₀ monitors and major highways, Los Angeles, CA. _____	3-92
Figure 3-34.	Seasonal distribution of 24-h avg PM ₁₀ concentrations by site for Los Angeles, CA, 2005-2007. _____	3-93
Figure 3-35.	Inter-sampler correlations for 24-h PM ₁₀ as a function of distance between monitors in Boston, MA. _____	3-95
Figure 3-36.	Inter-sampler correlations for 24-h PM ₁₀ as a function of distance between monitors in Pittsburgh, PA. _____	3-95
Figure 3-37.	Inter-sampler correlations for 24-h PM ₁₀ as a function of distance between monitors in Los Angeles, CA. _____	3-96
Figure 3-38.	Bin-wise Spearman correlation coefficients in aerosol particle number concentrations _____	3-97
Figure 3-39.	Dimensionless concentration as a function of height at windward and leeward locations and street canyon aspect ratios _____	3-99
Figure 3-40.	Inter-sampler correlations for 24-h PM _{2.5} and PM ₁₀ as a function of distance between monitors for samplers located within 4 km (neighborhood scale). _____	3-100
Figure 3-41.	Particle size distributions measured at various distances from the 710 freeway _____	3-102
Figure 3-42.	Mass distributions for BaP _____	3-105

Figure 3-43.	Mass distributions for 16 PAHs at a high traffic city center in Seville, Spain. _____	3-105
Figure 3-44.	Ambient 24-h PM _{2.5} concentrations in the U.S., 1999-2007, _____	3-107
Figure 3-45.	Ambient annual PM _{2.5} concentrations in the U.S., 1999-2007, _____	3-108
Figure 3-46.	Ambient 24-h PM ₁₀ concentrations in the U.S., 1988-2007, _____	3-109
Figure 3-47.	Regional and seasonal trends in annual PM _{2.5} composition from 2002 to 2007 derived using the SANDWICH method. _____	3-110
Figure 3-48.	Ultrafine particle size distribution _____	3-112
Figure 3-49.	Diel plot generated from hourly FRM-like PM _{2.5} data _____	3-114
Figure 3-50.	Diel plots generated from hourly FEM PM ₁₀ data _____	3-115
Figure 3-51.	Average diel variation _____	3-116
Figure 3-52.	Distribution of correlations between 24-h avg PM _{2.5} and co-located 24-h avg PM ₁₀ , PM _{10-2.5} , SO ₂ , NO ₂ and CO _____	3-117
Figure 3-53.	Distribution of correlations between 24-h avg PM ₁₀ and co-located 24-h avg PM _{2.5} , PM _{10-2.5} , SO ₂ , NO ₂ and CO _____	3-118
Figure 3-54.	Schematic of organic composition of particulate emissions from gasoline-fueled vehicles. _____	3-124
Figure 3-55.	Source category contributions to PM _{2.5} at a number of sites in the East derived using PMF. _____	3-128
Figure 3-56.	Pearson correlation coefficients for source category contributions to PM _{2.5} between the ten Regional Air Pollution Study/Regional Air Monitoring System (RAPS/RAMS) monitoring sites in St. Louis. _____	3-129
Figure 3-57.	Pearson correlation coefficients for source contributions to PM _{10-2.5} between the ten Regional Air Pollution Study/Regional Air Monitoring System (RAPS/RAMS) monitoring sites in St. Louis. _____	3-129
Figure 3-58.	Eight km southeast U.S. CMAQ-UCD domain zoomed over Tampa Bay, FL. _____	3-137
Figure 3-59.	Two km southeast U.S. CMAQ-UCD domain zoomed over Tampa Bay, FL. _____	3-137
Figure 3-60.	Hourly average CMAQ-UCD predictions and measured observations of NO (top), NO ₂ (middle), and total NO _x (bottom) concentrations for May 1-31, 2002. _____	3-138
Figure 3-61.	CMAQ-UCD predictions and measured observations of ethene concentrations at Sydney, FL for May 1-31, 2002. _____	3-139
Figure 3-62.	CMAQ-UCD predictions and measured observations of isoprene concentrations at Sydney, FL for May 1-31, 2002. _____	3-140
Figure 3-63.	CMAQ-UCD predictions and measured observations of PM _{2.5} concentrations at St. Petersburg, FL for May 1-31, 2002. _____	3-141
Figure 3-64.	CMAQ-UCD predictions of HNO ₃ ⁻ concentrations and corresponding measured observations at Sydney, FL _____	3-144
Figure 3-65.	CMAQ-UCD predictions of NH ₃ concentrations and corresponding measured observations at Sydney, FL, for May 1-31, 2002. _____	3-145
Figure 3-66.	CMAQ-UCD predictions of pNO ₃ ⁻ concentrations and corresponding measured observations at Sydney, FL, for 1-31 May, 2002. _____	3-146
Figure 3-67.	CMAQ-UCD predictions of the ratio of HNO ₃ to total NO ₃ and corresponding measured observations at Sydney, FL, for May 1-31, 2002. _____	3-147

Figure 3-68.	CMAQ-UCD predicted size and chemical-form fractions of total NO_3^- for days in May 2002 with measured observations. Measured concentrations (top panel); 8 km solution (middle panel); 2 km solution (bottom panel).	3-148
Figure 3-69.	Scatter plot of total nitrate (HNO_3 plus pNO_3^-) wet deposition ($\text{mg N/m}^2/\text{yr}$) of the model mean versus measurements	3-150
Figure 3-70.	Scatter plot of total SO_4^{2-} wet deposition ($\text{mg S/m}^2/\text{yr}$) of the model mean versus measurements	3-150
Figure 3-71.	CMAQ modeling domains for the OAQPS risk and exposure assessments	3-151
Figure 3-72.	12-km EUS Summer sulfate PM.	3-152
Figure 3-73.	12-km EUS Winter nitrate PM.	3-153
Figure 3-74.	12-km EUS Winter total nitrate (HNO_3 + total pNO_3^-).	3-154
Figure 3-75.	12-km EUS annual sulfate wet deposition.	3-155
Figure 3-76.	12-km EUS annual nitrate wet deposition.	3-156
Figure 3-77.	CMAQ vs. measured air concentrations from east-coast sites in the IMPROVE, CSN (labeled STN), and CASTNet sites in the summer of 2002 for sulfate (left) and ammonium (right). Solid lines indicate a factor of 2 around the 1:1 line shown between them.	3-157
Figure 3-78.	Comparison of CMAQ-predicted and NADP-measured NH_4^+ wet deposition	3-157
Figure 3-79.	CMAQ-predicted (red symbols and lines) and 12-h measured (blue symbols and lines) NH_3 and SO_4^{2-} surface concentrations at high and low concentration grid cells	3-158
Figure 3-80.	Surface grid cell (layer 1) analysis of the sensitivity of NH_x deposition and transport to the change in $\text{NH}_3 V_d$ in CMAQ.	3-159
Figure 3-81.	Total column analysis for NH_3 (left) and NH_x (right) showing modeled NH_3 emissions, transformation, and transport throughout the mixed layer and up to the free troposphere.	3-160
Figure 3-82.	Range of influence (where 50% of emitted NH_3 deposits) from the high concentration Sampson County grid cell in the June 2002 CMAQ simulation of V_d sensitivities.	3-161
Figure 3-83.	Areal extent of the change in NH_x range of influence as predicted by CMAQ	3-162
Figure 3-84.	IMPROVE monitoring site locations.	3-165
Figure 3-85.	12-km EUS Summer SO_4^{2-} PM.	3-169
Figure 3-86.	12-km EUS Winter NO_3^- PM.	3-170
Figure 3-87.	12-km EUS Winter total nitrate (HNO_3 + total particulate NO_3^-).	3-170
Figure 3-88.	Monthly average of $\text{PM}_{2.5}$ concentrations measured at IMPROVE sites in the East and Midwest for 2004.	3-172
Figure 3-89.	Monthly average of $\text{PM}_{2.5}$ concentrations measured at IMPROVE sites in the West for 2004.	3-173
Figure 3-90.	Distribution of $\text{PM}_{2.5}$ concentrations measured at IMPROVE sites in the East and Midwest for 2004.	3-174
Figure 3-91.	Distribution of $\text{PM}_{2.5}$ concentrations measured at IMPROVE sites in the West for 2004.	3-175
Figure 3-92.	Model of total personal exposure to PM as a function of ambient and nonambient sources.	3-180

Figure 3-93.	Distribution of time sample population spends in various environments, from the National Human Activity Pattern Survey. _____	3-186
Figure 3-94.	Total exposure to SO_4^{2-} as a function of measured ambient SO_4^{2-} concentration _____	3-194
Figure 3-95.	Estimated ambient exposure to $\text{PM}_{2.5}$ as a function of measured ambient $\text{PM}_{2.5}$ concentration _____	3-195
Figure 3-96.	Total exposure to $\text{PM}_{2.5}$ as a function of measured ambient $\text{PM}_{2.5}$ concentration. _____	3-195
Figure 3-97.	F_{inf} as a function of particle size. _____	3-203
Figure 3-98.	Apportionment of aliphatic carbon, carbonyl and SO_4^{2-} components _____	3-206
Figure 3-99.	Apportionment of infiltrated mechanically-generated _____	3-207
Figure 3-100.	Results of the positive matrix factorization model _____	3-208
Figure 3-101.	Grid resolution of the CMAQ model in Philadelphia compared with distribution of census tracts in which exposure assessment is performed. _____	3-213
Figure 4-1.	Diagrammatic representation of respiratory tract regions in humans. _____	4-4
Figure 4-2.	Structure of lower airways with progression from the large airways to the alveolus. _____	4-5
Figure 4-3.	Comparison of total and regional deposition results from the ICRP and MPPD models for a resting breathing pattern ($V_T = 625 \text{ mL}$, $f = 12 \text{ min}^{-1}$) and corrected for particle inhalability. _____	4-10
Figure 4-4.	Comparison of total and regional deposition results from the ICRP and MPPD models for a light exercise breathing pattern ($V_T = 1250 \text{ mL}$, $f = 20 \text{ min}^{-1}$) and corrected for particle inhalability. _____	4-10
Figure 4-5.	Total lung deposition measured in healthy adults (ultrafine, 11 M, 11 F, 31 ± 4 years; fine and coarse, 11 M, 11 F, 25 ± 4 years) during controlled breathing on a mouthpiece. _____	4-11
Figure 4-6.	Total deposition of hygroscopic sodium chloride and hydrophobic aluminosilicate aerosols during oral breathing ($V_T = 1.0 \text{ L}$; $f = 15 \text{ min}^{-1}$). _____	4-22
Figure 4-7.	Retention of poorly soluble particles ($0.5\text{-}5 \mu\text{m}$) in the alveolar region of the lung over various mammalian species. _____	4-28
Figure 5-1.	PM oxidative potential. _____	5-2
Figure 5-2.	PM stimulates pulmonary cells to produce ROS/RNS. _____	5-4
Figure 5-3.	PM activates cell signaling pathways leading to pulmonary inflammation. _____	5-5
Figure 5-4.	Potential pathways for the effects of PM on the respiratory system. _____	5-9
Figure 5-5.	Potential pathways for the effects of PM on the cardiovascular system. _____	5-17
Figure 6-1.	Excess risk estimates per $10 \mu\text{g}/\text{m}^3$ increase in PM_{10} , $\text{PM}_{2.5}$ and $\text{PM}_{10-2.5}$ for studies of CVD ED visits* and hospitalizations. Studies represented in the figure include all multicity studies. Single-city studies conducted in the U.S. or Canada are also included. _____	6-85
Figure 6-2.	Excess risk estimates per $10 \mu\text{g}/\text{m}^3$ increase in PM_{10} , $\text{PM}_{2.5}$, $\text{PM}_{10-2.5}$ for studies of EDvisits * and hospitalizations for IHD and MI. _____	6-89
Figure 6-3.	Excess risk estimates per $10 \mu\text{g}/\text{m}^3$ increase in PM_{10} , $\text{PM}_{10-2.5}$ and $\text{PM}_{10-2.5}$ for studies of CHF ED visits* and hospitalizations. _____	6-94
	Studies represented in the figure include all multicity studies. Single-city studies conducted in the U.S. and Canada are also included. _____	6-94

Figure 6-4.	Excess risk estimates per 10 $\mu\text{g}/\text{m}^3$ increase in PM_{10} and $\text{PM}_{2.5}$ for studies of ED visits* and hospitalizations for CBVDs. _____	6-99
Figure 6-5.	Excess risk estimates per 10 $\mu\text{g}/\text{m}^3$ increase in $\text{PM}_{2.5}$, and $\text{PM}_{10-2.5}$ for studies of ED visits* and hospitalizations for CVDs. _____	6-101
Figure 6-6.	Combined random-effect estimate of the dose-response relationship between MI emergency hospital admissions and PM_{10} , computed by fitting a piecewise linear spline, with slope changes at 20 $\mu\text{g}/\text{m}^3$ and 50 $\mu\text{g}/\text{m}^3$. _____	6-103
Figure 6-7.	Respiratory symptoms and/or medication use among asthmatic children following acute exposure to $\text{PM}_{2.5}$. _____	6-117
Figure 6-8.	Respiratory symptoms and/or medication use among asthmatic adults following acute exposure to particles. _____	6-125
Figure 6-9.	Respiratory symptoms following acute exposure to particles and additional criteria pollutants. _____	6-127
Figure 6-10.	Excess risk estimates per 10 $\mu\text{g}/\text{m}^3$ 24-h avg PM concentration for studies of ED visits and hospitalizations for respiratory diseases in children. _____	6-189
Figure 6-11.	Excess risks estimates per 10 $\mu\text{g}/\text{m}^3$ increase in 24-h avg PM for studies of ED visits and hospitalizations for respiratory diseases among adults. _____	6-192
Figure 6-12.	Excess risk estimates per 10 $\mu\text{g}/\text{m}^3$ increase in 24-h avg PM_{10} , $\text{PM}_{2.5}$ and $\text{PM}_{10-2.5}$ for studies of asthma ED visits* and hospitalizations. _____	6-195
Figure 6-13.	Excess risks estimates per 10 $\mu\text{g}/\text{m}^3$ increase in 24-h avg PM_{10} , $\text{PM}_{2.5}$ and $\text{PM}_{10-2.5}$ for studies of COPD ED visits* and hospitalizations among older adults (65+ yr, unless other age group is noted). _____	6-199
Figure 6-14.	Excess risks estimates per 10 $\mu\text{g}/\text{m}^3$ increase in 24-h avg PM_{10} , $\text{PM}_{2.5}$ and $\text{PM}_{10-2.5}$ for studies of respiratory infection ED visits* and hospitalizations. Studies represented in the figure include all multicity studies. Single-city studies conducted in the U.S. are also included. _____	6-202
Figure 6-15.	Excess risk estimates per 10 $\mu\text{g}/\text{m}^3$ increase in $\text{PM}_{2.5}$, and $\text{PM}_{10-2.5}$ for studies of ED visits* and HAs for respiratory diseases. _____	6-203
Figure 6-16.	National and regional estimates of smooth seasonal effects for PM_{10} at a 1-day lag and their sensitivity to the degrees of freedom assigned to the smooth function of time in the updated NMMAPS data 1987-2000. _____	6-224
Figure 6-17.	Percent increase in the daily number of deaths, for all ages, associated with a 10- $\mu\text{g}/\text{m}^3$ increase in PM_{10} _____	6-231
Figure 6-18.	Effect modification by city characteristics in 20 U.S. cities. _____	6-234
Figure 6-19.	PM_{10} risk estimates (per 10 $\mu\text{g}/\text{m}^3$) by individual-level characteristics. _____	6-236
Figure 6-20.	PM_{10} risk estimates (per 10 $\mu\text{g}/\text{m}^3$) by location of death and by season. _____	6-237
Figure 6-21.	PM_{10} risk estimates (per 10 $\mu\text{g}/\text{m}^3$) by contributing causes of deaths. _____	6-238
Figure 6-22.	Summary of PM_{10} risk estimates (per 10 $\mu\text{g}/\text{m}^3$) for all-cause mortality from recent multicity studies. _____	6-240
Figure 6-23.	Percent increase in mortality for 10 $\mu\text{g}/\text{m}^3$ increase in the average of 0- and 1-day lagged $\text{PM}_{2.5}$, combined by climatic regions. _____	6-244
Figure 6-24.	Empirical Bayes-adjusted city-specific effect estimates for total, cardiovascular, and respiratory mortality for 10 $\mu\text{g}/\text{m}^3$ increase in the average of 0- and 1-day lagged $\text{PM}_{2.5}$ by decreasing mean 24-h avg $\text{PM}_{2.5}$ concentrations. _____	6-245

Figure 6-25.	Summary of all-cause mortality PM _{2.5} risk estimates per 10 µg/m ³ by various effect modifiers. _____	6-248
Figure 6-26.	Summary of PM _{2.5} risk estimates per 10 µg/m ³ for major underlying causes of death. _____	6-250
Figure 6-27.	Summary of PM _{2.5} risk estimates (per 10 µg/m ³) for cause-specific mortality for all U.S.- and Canadian-based studies. _____	6-251
Figure 6-28.	Percent increase in mortality for 10 µg/m ³ increase in the average of 0- and 1-day lagged PM _{10-2.5} , combined by climatic regions. _____	6-254
Figure 6-29.	Empirical Bayes-adjusted city-specific effect estimates for total, cardiovascular, and respiratory mortality for 10 µg/m ³ increase in the average of 0- and 1-day lagged PM _{10-2.5} by decreasing 98th percentile of mean 24-h avg PM _{2.5} concentrations. _____	6-255
Figure 6-30.	Summary of PM _{10-2.5} risk estimates (per 10 µg/m ³) for cause-specific mortality for all U.S., Canadian-, and international-based studies. _____	6-258
Figure 6-31.	Percent increase in PM ₁₀ risk estimates (point estimates and 95% confidence intervals) associated with a 5th-to-95th percentile: increase in PM _{2.5} and PM _{2.5} chemical components. _____	6-262
Figure 6-32.	Sensitivity of the percent increase in PM ₁₀ risk estimates (point estimates and 95% confidence intervals) associated with an interquartile increase in Ni. _____	6-262
Figure 6-33.	Excess risk (CI) of total mortality per IQR of concentrations. _____	6-266
Figure 6-34.	Relative risk and CI of cardiovascular mortality associated with estimated PM _{2.5} source contributions. _____	6-268
Figure 6-35.	Concentration-response curves (spline model) for all-cause, cardiovascularrespiratory and other cause mortality from the 20 NMMAPS cities. _____	6-269
Figure 6-36.	Percent increase in the risk death on days with PM ₁₀ concentrations in the ranges of 15-24, 25-34, 35-44, and 45 µg/m ³ and greater, compared to a reference of days when concentrations were below 15 µg/m ³ . _____	6-270
Figure 6-37.	Combined concentration-response curves (spline model) for all-cause, cardiovascular, and respiratory mortality from the 22 APHEA cities. _____	6-271
Figure 7-1.	Risk estimates for the associations of clinical outcomes with long-term exposure to ambient PM _{2.5} and PM ₁₀ . _____	7-21
Figure 7-2.	Adjusted ORs and 95% CIs of symptoms and respiratory diseases associated with a decline of 10 µg/m ³ PM ₁₀ levels in Swiss Surveillance Program of Childhood Allergy and Respiratory Symptoms _____	7-32
Figure 7-3.	Effect of PM _{2.5} on the association of lung function with asthma. _____	7-34
Figure 7-4.	Proportion of 18-year olds with a FEV ₁ below 80% of the predicted value plotted against the average levels of pollutants _____	7-40
Figure 7-5.	Percent increase in postneonatal mortality per 10 µg/m ³ in PM ₁₀ , comparing risk for total and respiratory mortality. _____	7-83
Figure 7-6.	Mortality risk estimates associated with long-term exposure to PM _{2.5} from the Harvard Six Cities Study (SCS) and the American Cancer Society Study (ACS). _____	7-123
Figure 7-7.	Mortality risk estimates associated with long-term exposure to PM _{2.5} in recent cohort stud _____	7-124
Figure 7-8.	Plots of the relative risk of death from cardiovascular disease from the Women's Health Initiative study _____	7-132

Figure 7-9.	The model-averaged estimated effect of a $10\text{-}\mu\text{g}/\text{m}^3$ increase in $\text{PM}_{2.5}$ on all-cause mortality _____	7-133
Figure 7-10.	Time course of relative risk of death after a sudden decrease in air pollution exposure during the year 2000, assuming a steady state model (solid line) and a dynamic model (bold dashed line). The thin dashed line refers to the reference scenario. _____	7-134
Figure 7-11.	Experts' mean effect estimates and uncertainty distributions for the $\text{PM}_{2.5}$ mortality _____	7-137
Figure 9-1.	Important factors involved in seeing a scenic vista are outlined. Image-forming information from an object is reduced (scattered and absorbed) as it passes through the atmosphere to the human observer. _____	9-4
Figure 9-2.	Schematic of remote-area (top) and urban (bottom) nighttime sky visibility showing the effects of PM and light pollution. _____	9-5
Figure 9-3.	Effect of relative humidity on light scattering by mixtures of ammonium nitrate and ammonium sulfate. _____	9-8
Figure 9-4.	Estimated fractions of total particulate nitrate during each field campaign comprised of ammonium nitrate, reacted sea salt nitrate (shown as NaNO_3), and reacted soil dust nitrate (shown as $\text{Ca}(\text{NO}_3)_2$). _____	9-17
Figure 9-5.	A scatter plot of the original IMPROVE algorithm estimated particle light scattering versus measured particle light scattering. _____	9-21
Figure 9-6.	Scatter plot of the revised algorithm estimates of light scattering versus measured light scattering. _____	9-21
Figure 9-7.	IMPROVE network PM species estimated light extinction for 2000 (left) and for 2004 (right). _____	9-24
Figure 9-8.	Mean estimated light extinction from PM speciation measurements for the first (top left), second (top right), third (bottom left), and fourth (bottom right) calendar quarters of 2004. _____	9-24
Figure 9-9.	Percent contributions of ammonium nitrate (left column) and ammonium sulfate (right column) to particulate light extinction for each calendar quarter of 2004 (first through fourth quarter arranged from top to bottom). _____	9-26
Figure 9-10.	Percent contributions of organic mass (left column) and EC (right column) to particulate light extinction for each calendar quarter of 2004 (first through fourth quarter arranged from top to bottom). _____	9-27
Figure 9-11.	Percent contributions of coarse mass (left column) and fine soil (right column) to particulate light extinction for each calendar quarter of 2004 (first through fourth quarter arranged from top to bottom). _____	9-28
Figure 9-12.	IMPROVE Mean $\text{PM}_{2.5}$ mass concentration determined by summing the major components for the 2000-2004. _____	9-30
Figure 9-13.	IMPROVE and CSN (STN) mean $\text{PM}_{2.5}$ mass concentration determined by summing the major components for 2000-2004 _____	9-30
Figure 9-14.	IMPROVE mean ammonium nitrate concentrations for 2000-2004. _____	9-31
Figure 9-15.	IMPROVE and CSN (STN) mean ammonium nitrate concentrations for 2000-2004. _____	9-31
Figure 9-16.	IMPROVE mean ammonium sulfate concentrations for 2000-2004. _____	9-32
Figure 9-17.	IMPROVE and CSN (STN) mean ammonium sulfate concentrations for 2000-2004. _____	9-32
Figure 9-18.	IMPROVE monitored mean organic mass concentrations for 2000-2004. _____	9-34

Figure 9-19.	IMPROVE and CSN (STN) mean organic mass concentrations for 2000-2004.	9-35
Figure 9-20.	IMPROVE mean EC concentrations for 2000-2004.	9-35
Figure 9-21.	IMPROVE and CSN (STN) mean EC concentrations for 2000-2004.	9-36
Figure 9-22.	IMPROVE mean fine soil concentrations for 2000-2004.	9-36
Figure 9-23.	IMPROVE and CSN (STN) fine soil concentrations, 2000-2004.	9-37
Figure 9-24.	Regional and local contributions to annual average PM _{2.5} by particulate SO ₄ ²⁻ , nitrate and total carbon (i.e., organic plus EC) for select urban areas based on paired IMPROVE and CSN monitoring sites.	9-38
Figure 9-25.	IMPROVE mean coarse mass concentrations for 2000-2004.	9-39
Figure 9-26.	Ten-yr (1995-2004) haze trends for the mean of the 20% best annual haze conditions.	9-40
Figure 9-27.	Ten-yr (1995-2004) haze trends for the mean of the 20% worst annual haze conditions.	9-40
Figure 9-28.	Ten-yr trends in the 80th percentile particulate SO ₄ ²⁻ concentration based on IMPROVE and CASTNet monitoring and net SO ₂ emissions from the National Emissions Trends (NET) data base by region of the U.S.	9-42
Figure 9-29.	Map of 10-yr trends (1994-2003) in haze by particulate nitrate contribution to haze for the worst 20% annual haze periods.	9-43
Figure 9-30.	Contributions of the Pacific Coast area to the ammonium sulfate (μg/m ³) at 84 remote-area monitoring sites in western U.S. based on trajectory regression for all sample periods from 2000-2002 (dots denote locations of the IMPROVE aerosol monitoring sites).	9-46
Figure 9-31.	Shows the IMPROVE monitoring sites in the WRAP region with at least three yr of valid data and identifies the six sites selected to demonstrate the apportionment tools.	9-48
Figure 9-32.	Particulate SO ₄ ²⁻ (a) and nitrate (b) source attribution by region using CAMx modeling for six western remote area monitoring sites	9-50
Figure 9-33.	Monthly averaged model predicted organic mass concentration apportioned into primary and anthropogenic and biogenic secondary PM categories for the Olympic NP (top) and San Geronio Wilderness (bottom) monitoring sites.	9-51
Figure 9-34.	Monthly averaged model predicted organic mass concentration apportioned into primary and anthropogenic and biogenic secondary PM categories for the Yellowstone NP (top) and Grand Canyon (Hopi Point) (bottom) monitoring sites.	9-52
Figure 9-35.	Monthly averaged model predicted organic mass concentration apportioned into primary and anthropogenic and biogenic secondary PM categories for the Badland NP (top) and Salt Creek Wilderness (bottom) monitoring sites.	9-53
Figure 9-36.	Comparison of carbon concentrations between Seattle (Puget Sound site) and Mt. Rainer (left) and between Phoenix and Tonto (right) showing the background site concentration (gray) and the urban excess concentration (black) for total, fossil and contemporary carbon during the summer and winter studies.	9-54
Figure 9-37.	Average contemporary fraction of PM _{2.5} carbon for the summer (top) and winter (bottom), estimated from IMPROVE monitoring data (6/04 to 2/06) based on EC/TC ratios.	9-55
Figure 9-38.	Results of the weighted emissions potential tool applied to primary OC emissions (top) and EC emissions (bottom) for the baseline and projected 2018 emissions inventories for Olympic NP	9-57

Figure 9-39.	Results of the weighted emissions potential tool applied to primary OC emissions (top) and EC emissions (bottom) for the baseline and projected 2018 emissions inventories for San Geronio W. _____	9-58
Figure 9-40.	Results of the weighted emissions potential tool applied to primary OC emissions (top) and EC emissions (bottom) for the baseline and projected 2018 emissions inventories for Yellowstone NP. _____	9-60
Figure 9-41.	Results of the weighted emissions potential tool applied to primary OC emissions (top) and EC emissions (bottom) for the baseline and projected 2018 emissions inventories for Grand Canyon NP. _____	9-61
Figure 9-42.	Results of the weighted emissions potential tool applied to primary OC emissions (top) and EC emissions (bottom) for the baseline and projected 2018 emissions inventories for Badlands NP. _____	9-62
Figure 9-43.	Results of the weighted emissions potential tool applied to primary OC emissions (top) and EC emissions (bottom) for the baseline and projected 2018 emissions inventories for Salt Creek W. _____	9-63
Figure 9-44.	BRAVO study haze contributions for Big Bend NP, TX during a 4-mo period in 1999. _____	9-65
Figure 9-45.	Maps of spatial patterns for average annual particulate nitrate measurements (top), and for ammonia emissions for April 2002 from the WRAP emissions inventory (bottom). _____	9-66
Figure 9-46.	Maps of spatial patterns of annual NO (left) and NO ₂ (right) emissions for 2002 from the WRAP emissions inventory. _____	9-67
Figure 9-47.	Midwest ammonia monitoring network. _____	9-69
Figure 9-48.	Upwind transport probability fields associated with high particulate nitrate concentrations _____	9-70
Figure 9-49.	Trajectory probability fields for periods with high particulate SO ₄ ²⁻ measured at Underhill, VT and Brigantine, NJ (shown as white stars) associated with oil-burning trace components (left) and with coal-burning trace components (right). _____	9-71
Figure 9-50.	Scatter plots of particulate SO ₄ ²⁻ (left) and particulate nitrate and organic mass (right) versus nephelometer measured particle light scattering for Acadia NP, ME. _____	9-72
Figure 9-51.	CMAQ air quality modeling projections of visibility responses on the 20% worst haze days at Great Smoky Mountains NP, NC (top) and Swanquarter Wilderness, NC (bottom) to 30% reductions from a projected 2009 emission inventory of visibility-reducing pollutants by source category and geographic areas. _____	9-73
Figure 9-52.	Aerosol radiative forcing. _____	9-88
Figure 9-53.	Global average radiative forcing (RF) estimates and uncertainty ranges in 2005, relative to the pre-industrial climate. _____	9-90
Figure 9-54.	Probability distribution functions (PDFs) for anthropogenic aerosol and GHG RFs. _____	9-91
Figure 9-55.	The clear-sky forcing efficiency E _T _____	9-92
Figure 9-56.	A composite of MODIS/Terra observed aerosol optical depth (at 550 nm, green light near the peak of human vision) and fine-mode fraction that shows spatial and seasonal variations of aerosol types. _____	9-99
Figure 9-57.	Oregon fire on September 4, 2003 as observed by MISR: _____	9-100
Figure 9-58.	Global maps at 18 km resolution showing monthly average _____	9-101

Figure 9-59.	A dust event that originated in the Sahara desert on 17 August 2007 and was transported to the Gulf of Mexico. _____	9-103
Figure 9-60.	A constellation of five spacecraft that overfly the Equator _____	9-104
Figure 9-61.	Geographical coverage of active AERONET sites in 2006. _____	9-107
Figure 9-62.	Comparison of the mean concentration ($\mu\text{g}/\text{m}^3$) and standard deviation of the modeled (STEM) aerosol chemical components _____	9-110
Figure 9-63.	Location of aerosol chemical composition measurements with aerosol mass spectrometers. _____	9-112
Figure 9-64.	Scatterplots of the submicrometer POM measured during NEAQS versus A) acetylene and B) iso-propyl nitrate. _____	9-113
Figure 9-65.	Comparison of annual mean aerosol optical depth (AOD) _____	9-116
Figure 9-66.	Percentage contributions of individual aerosol components _____	9-116
Figure 9-67.	Geographical patterns of seasonally (MAM) averaged aerosol optical depth _____	9-119
Figure 9-68.	Summary of observation- and model-based (denoted as OBS and MOD, respectively) estimates of clear-sky, annual average DRF at the TOA and at the surface. _____	9-120
Figure 9-69.	Scatter plots showing mean cloud drop effective radius (r_e) vs. aerosol extinction coefficient _____	9-127
Figure 9-70.	Sampling the Arctic Haze. Pollution and smoke aerosols can travel long distances, from mid-latitudes to the Arctic, causing "Arctic Haze." _____	9-135
Figure 9-71.	Global annual averaged AOD (upper panel) and aerosol mass loading (lower panel) _____	9-142
Figure 9-72.	Aerosol direct radiative forcing in various climate and aerosol models. Observed values are shown in the top section. _____	9-146
Figure 9-73.	Aerosol optical thickness and anthropogenic shortwave all-sky radiative forcing from the AeroCom study. _____	9-148
Figure 9-74.	Radiative forcing from the cloud albedo effect (1st aerosol indirect effect) in the global climate models used from _____	9-149
Figure 9-75.	Anthropogenic impact on cloud cover, planetary albedo, radiative flux at the surface (while holding sea surface temperatures and sea ice fixed) and surface air temperature change from the direct aerosol forcing (top row), the first indirect effect (second row) and the second indirect effect (third row). _____	9-151
Figure 9-76.	Global average present-day short wave cloud forcing at TOA (top) and change in whole sky net outgoing shortwave radiation (bottom) between the present-day and pre-industrial simulations for each model in each experiment. _____	9-152
Figure 9-77.	Direct radiative forcing by anthropogenic aerosols in the GISS model (including sulfates, BC, OC and nitrates). _____	9-161
Figure 9-78.	Percentage of aerosol optical depth in the GISS, left, based on Liu et al. (2006, 190422), provided by A. Lacis, GISS, and GFDL, right, from Ginoux et al. (2006, 190582). Models associated with the different components _____	9-163
Figure 9-79.	Most probable aerosol altitude (in pressure, hPa) from the GISS model in January (top) and July (bottom). _____	9-165
Figure 9-80.	Time dependence of aerosol optical thickness (left) and climate forcing (right). _____	9-167
Figure 9-81.	Change in global mean ocean temperature (left axis) and ocean heat content (right axis) for the top 3000 m due to different forcings in the GFDL model. _____	9-168

Figure 9-82.	Visible (wavelength 0.55 μm) optical depth estimates of stratospheric SO_4^{2-} aerosols formed in the aftermath of explosive volcanic eruptions that occurred between 1860 and 2000. _____	9-176
Figure 9-83.	The transfer of POPs between the major abiotic compartments of the Arctic. Shaded arrows represent inputs/outputs of POPs to the Arctic. _____	9-184
Figure 9-84.	Relationship of plant nutrients and trace metals with vegetation. _____	9-207

Annex Figures

Figure A-1.	PM _{2.5} monitor distribution in comparison with population density, Atlanta, GA. _____	A-54
Figure A-2.	PM ₁₀ monitor distribution in comparison with population density, Atlanta, GA. _____	A-55
Figure A-3.	PM _{2.5} monitor distribution in comparison with population density, Birmingham, AL. _____	A-56
Figure A-4.	PM ₁₀ monitor distribution in comparison with population density, Birmingham, AL. _____	A-57
Figure A-5.	PM _{2.5} monitor distribution in comparison with population density, Chicago, IL. _____	A-58
Figure A-6.	PM ₁₀ monitor distribution in comparison with population density, Chicago, IL. _____	A-59
Figure A-7.	PM _{2.5} monitor distribution in comparison with population density, Denver, CO. _____	A-60
Figure A-8.	PM ₁₀ monitor distribution in comparison with population density, Denver, CO. _____	A-61
Figure A-9.	PM _{2.5} monitor distribution in comparison with population density, Detroit, MI. _____	A-62
Figure A-10.	PM ₁₀ monitor distribution in comparison with population density, Detroit, MI. _____	A-63
Figure A-11.	PM ₁₀ monitor distribution in comparison with population density, Detroit, MI. _____	A-64
Figure A-12.	PM ₁₀ monitor distribution in comparison with population density, Houston, TX. _____	A-65
Figure A-13.	PM _{2.5} monitor distribution in comparison with population density, Los Angeles, CA. _____	A-66
Figure A-14.	PM ₁₀ monitor distribution in comparison with population density, Los Angeles, CA. _____	A-67
Figure A-15.	PM _{2.5} monitor distribution in comparison with population density, New York City, NY. _____	A-68
Figure A-16.	PM ₁₀ monitor distribution in comparison with population density, New York City, NY. _____	A-69
Figure A-17.	PM _{2.5} monitor distribution in comparison with population density, Philadelphia, PA. _____	A-70
Figure A-18.	PM ₁₀ monitor distribution in comparison with population density, Philadelphia, PA. _____	A-71
Figure A-19.	PM _{2.5} monitor distribution in comparison with population density, Phoenix, AZ. _____	A-72
Figure A-20.	PM ₁₀ monitor distribution in comparison with population density, Phoenix, AZ. _____	A-73
Figure A-21.	PM _{2.5} monitor distribution in comparison with population density, Pittsburgh, PA. _____	A-74
Figure A-22.	PM ₁₀ monitor distribution in comparison with population density, Pittsburgh, PA. _____	A-75
Figure A-23.	PM _{2.5} monitor distribution in comparison with population density, Riverside, CA. _____	A-76
Figure A-24.	PM ₁₀ monitor distribution in comparison with population density, Riverside, CA. _____	A-77
Figure A-25.	PM _{2.5} monitor distribution in comparison with population density, Seattle, WA. _____	A-78
Figure A-26.	PM _{2.5} monitor distribution in comparison with population density, Seattle, WA. _____	A-79
Figure A-27.	PM _{2.5} monitor distribution in comparison with population density, St. Louis, MO. _____	A-80
Figure A-28.	PM ₁₀ monitor distribution in comparison with population density, St. Louis, MO. _____	A-81
Figure A-29.	Three-yr avg of 24-h PM _{2.5} Cu concentrations measured at CSN sites across the U.S., 2005-2007. _____	A-82

Figure A-30.	Three-yr avg of 24-h PM _{2.5} iron concentrations measured at CSN sites across the U.S., 2005-2007 _____	A-83
Figure A-31.	Three-yr avg of 24-h PM _{2.5} nickel concentrations measured at CSN sites across the U.S., 2005-2007 _____	A-84
Figure A-32.	Three-yr avg of 24-h PM _{2.5} lead concentrations measured at CSN sites across the U.S., 2005-2007 _____	A-85
Figure A-33.	Three-yr avg of 24-h PM _{2.5} selenium concentrations measured at CSN sites across the U.S., 2005-2007 _____	A-86
Figure A-34.	Three-yr avg of 24-h PM _{2.5} vanadium concentrations measured at CSN sites across the U.S., 2005-2007 _____	A-87
Figure A-35.	PM _{2.5} monitor distribution and major highways, Atlanta, GA. _____	A-89
Figure A-36.	Box plots illustrating the seasonal distribution of 24-h avg PM _{2.5} concentrations for Atlanta, GA. _____	A-90
Figure A-37.	PM _{2.5} inter-sampler correlations as a function of distance between monitors for Atlanta, GA. _____	A-91
Figure A-38.	PM _{2.5} monitor distribution and major highways, Birmingham, AL. _____	A-92
Figure A-39.	Box plots illustrating the seasonal distribution of 24-h avg PM _{2.5} concentrations for Birmingham, AL. _____	A-93
Figure A-40.	PM _{2.5} inter-sampler correlations as a function of distance between monitors for Birmingham, AL. _____	A-94
Figure A-41.	PM _{2.5} monitor distribution and major highways, Chicago, IL. _____	A-95
Figure A-42.	Box plots illustrating the seasonal distribution of 24-h avg PM _{2.5} concentrations for Chicago, IL. _____	A-97
Figure A-43.	PM _{2.5} inter-sampler correlations as a function of distance between monitors for Chicago, IL. _____	A-99
Figure A-44.	PM _{2.5} monitor distribution and major highways, Denver, CO. _____	A-100
Figure A-45.	Box plots illustrating the seasonal distribution of 24-h avg PM _{2.5} concentrations for Denver, CO. _____	A-101
Figure A-46.	PM _{2.5} inter-sampler correlations as a function of distance between monitors for Denver, CO. _____	A-102
Figure A-47.	PM _{2.5} monitor distribution and major highways, Detroit, MI. _____	A-103
Figure A-48.	Box plots illustrating the seasonal distribution of 24-h avg PM _{2.5} concentrations for Detroit, MI. _____	A-104
Figure A-49.	PM _{2.5} inter-sampler correlations as a function of distance between monitors for Detroit, MI. _____	A-106
Figure A-50.	PM _{2.5} monitor distribution and major highways, Houston, TX. _____	A-107
Figure A-51.	Box plots illustrating the seasonal distribution of 24-h avg PM _{2.5} concentrations for Houston, TX. _____	A-108
Figure A-52.	PM _{2.5} inter-sampler correlations as a function of distance between monitors for Houston, TX. _____	A-109
Figure A-53.	PM _{2.5} monitor distribution and major highways, New York City, NY. _____	A-110

Figure A-54.	Box plots illustrating the seasonal distribution of 24-h avg PM _{2.5} concentrations for New York City, NY. _____	A-112
Figure A-55	PM _{2.5} inter-sampler correlations as a function of distance between monitors for New York City, NY. _____	A-115
Figure A-56.	PM _{2.5} monitor distribution and major highways, Philadelphia, PA. _____	A-116
Figure A-57.	Box plots illustrating the seasonal distribution of 24-h avg PM _{2.5} concentrations for Philadelphia, PA. _____	A-117
Figure A-58.	PM _{2.5} inter-sampler correlations as a function of distance between monitors for Philadelphia, PA. _____	A-119
Figure A-59.	PM _{2.5} monitor distribution and major highways, Phoenix, AZ. _____	A-120
Figure A-60.	Box plots illustrating the seasonal distribution of 24-h avg PM _{2.5} concentrations for Phoenix, AZ. _____	A-121
Figure A-61.	PM _{2.5} inter-sampler correlations as a function of distance between monitors for Phoenix, AZ. _____	A-122
Figure A-62.	PM _{2.5} monitor distribution and major highways, Riverside, CA. _____	A-123
Figure A-63.	Box plots illustrating the seasonal distribution of 24-h avg PM _{2.5} concentrations for Riverside, CA. _____	A-124
Figure A-64.	PM _{2.5} inter-sampler correlations as a function of distance between monitors for Riverside CA. _____	A-125
Figure A-65.	PM _{2.5} monitor figudistribution and major highways, Seattle, WA. _____	A-126
Figure A-66.	Box plots illustrating the seasonal distribution of 24-h avg PM _{2.5} concentrations for Seattle, WA. _____	A-127
Figure A-67.	PM _{2.5} inter-sampler correlations as a function of distance between monitors for Seattle, WA. _____	A-128
Figure A-68.	PM _{2.5} monitor distribution and major highways, St. Louis, MO. _____	A-129
Figure A-69.	Box plots illustrating the seasonal distribution of 24-h avg PM _{2.5} concentrations for St. Louis, MO. _____	A-130
Figure A-70	PM _{2.5} inter-sampler correlations as a function of distance between monitors for St. Louis, MO. _____	A-131
Figure A-71.	PM ₁₀ monitor distribution and major highways, Atlanta, GA. _____	A-132
Figure A-72.	Box plots illustrating the seasonal distribution of 24-h avg PM ₁₀ concentrations for Atlanta, GA. _____	A-133
Figure A-73.	PM ₁₀ inter-sampler correlations as a function of distance between monitors for Atlanta, GA. _____	A-134
Figure A-74.	PM ₁₀ monitor distribution and major highways, Birmingham, AL. _____	A-135
Figure A-75.	Box plots illustrating the seasonal distribution of 24-h avg PM ₁₀ concentrations for Birmingham, AL. _____	A-136
Figure A-76	PM ₁₀ inter-sampler correlations as a function of distance between monitors for Birmingham, AL. _____	A-137
Figure A-77.	PM ₁₀ monitor distribution and major highways, Chicago, IL. _____	A-138
Figure A-78.	Box plots illustrating the seasonal distribution of 24-h avg PM ₁₀ concentrations for Chicago, IL. _____	A-139

Figure A-79.	PM ₁₀ inter-sampler correlations as a function of distance between monitors for Chicago, IL. _____	A-141
Figure A-80.	PM ₁₀ monitor distribution and major highways, Denver, CO. _____	A-142
Figure A-81.	Box plots illustrating the seasonal distribution of 24-h avg PM ₁₀ concentrations for Denver, CO. _____	A-143
Figure A-82.	PM ₁₀ inter-sampler correlations as a function of distance between monitors for Denver, CO. _____	A-144
Figure A-83.	PM ₁₀ monitor distribution and major highways, Detroit, MI. _____	A-145
Figure A-84.	Box plots illustrating the seasonal distribution of 24-h avg PM ₁₀ concentrations for Detroit, MI. _____	A-146
Figure A-85.	PM ₁₀ inter-sampler correlations as a function of distance between monitors for Detroit, MI. _____	A-147
Figure A-86.	PM ₁₀ monitor distribution and major highways, Houston, TX. _____	A-148
Figure A-87.	Box plots illustrating the seasonal distribution of 24-h avg PM ₁₀ concentrations for Houston, TX. _____	A-149
Figure A-88.	Box plots illustrating the seasonal distribution of 24-h avg PM ₁₀ concentrations for New York City, NY. _____	A-150
Figure A-89.	PM ₁₀ inter-sampler correlations as a function of distance between monitors for New York City, NY. _____	A-151
Figure A-90.	PM ₁₀ monitor distribution and major highways, Philadelphia, PA. _____	A-152
Figure A-91.	Box plots illustrating the seasonal distribution of 24-h avg PM ₁₀ concentrations for Philadelphia, PA. _____	A-153
Figure A-92.	PM ₁₀ inter-sampler correlations as a function of distance between monitors for Philadelphia, PA. _____	A-154
Figure A-93.	PM ₁₀ monitor distribution and major highways, Phoenix, AZ. _____	A-155
Figure A-94.	Box plots illustrating the seasonal distribution of 24-h avg PM ₁₀ concentrations for Phoenix, AZ. _____	A-157
Figure A-95.	PM ₁₀ inter-sampler correlations as a function of distance between monitors for Phoenix, AZ. _____	A-159
Figure A-96.	PM ₁₀ monitor distribution and major highways, Riverside, CA. _____	A-160
Figure A-97.	Box plots illustrating the seasonal distribution of 24-h avg PM ₁₀ concentrations for Riverside, CA. _____	A-161
Figure A-98.	PM ₁₀ inter-sampler correlations as a function of distance between monitors for Riverside, CA. _____	A-163
Figure A-99.	PM ₁₀ monitor distribution and major highways, Seattle, WA. _____	A-164
Figure A-100.	Box plots illustrating the seasonal distribution of 24-h avg PM ₁₀ concentrations for Seattle, WA. _____	A-165
Figure A-101.	PM ₁₀ inter-sampler correlations as a function of distance between monitors for Seattle, WA. _____	A-166
Figure A-102.	PM ₁₀ monitor distribution and major highways, St. Louis, MO. _____	A-167
Figure A-103.	Box plots illustrating the seasonal distribution of 24-h avg PM ₁₀ concentrations for St. Louis, MO. _____	A-168

Figure A-104.	PM ₁₀ inter-sampler correlations as a function of distance between monitors for St. Louis, MO. _____	A-169
Figure A-105.	Seasonally averaged PM _{2.5} speciation data for 2005-2007 for a) annual, b) winter, c) spring, d) summer and e) fall derived using the SANDWICH method in Atlanta, GA. _____	A-170
Figure A-106.	Seasonally averaged PM _{2.5} speciation data for 2005-2007 for a) annual, b) winter, c) spring, d) summer and e) fall derived using the SANDWICH method in Birmingham, AL. _____	A-171
Figure A-107.	Seasonally averaged PM _{2.5} speciation data for 2005-2007 for a) annual, b) winter, c) spring, d) summer and e) fall derived using the SANDWICH method in Boston, MA. _____	A-172
Figure A-108.	Seasonally averaged PM _{2.5} speciation data for 2005-2007 for a) annual, b) winter, c) spring, d) summer and e) fall derived using the SANDWICH method in Chicago, IL. _____	A-173
Figure A-109.	Seasonally averaged PM _{2.5} speciation data for 2005-2007 for a) annual, b) winter, c) spring, d) summer and e) fall derived using the SANDWICH method in Denver, CO. _____	A-174
Figure A-110.	Seasonally averaged PM _{2.5} speciation data for 2005-2007 for a) annual, b) winter, c) spring, d) summer and e) fall derived using the SANDWICH method in Detroit, MI. _____	A-175
Figure A-111.	Seasonally averaged PM _{2.5} speciation data for 2005-2007 for a) annual, b) winter, c) spring, d) summer and e) fall derived using the SANDWICH method in Houston, TX. _____	A-176
Figure A-112.	Seasonally averaged PM _{2.5} speciation data for 2005-2007 for a) annual, b) winter, c) spring, d) summer and e) fall derived using the SANDWICH method in Los Angeles, CA. _____	A-177
Figure A-113.	Seasonally averaged PM _{2.5} speciation data for 2005-2007 for a) annual, b) winter, c) spring, d) summer and e) fall derived using the SANDWICH method in New York City, NY. _____	A-178
Figure A-114.	Seasonally averaged PM _{2.5} speciation data for 2005-2007 for a) annual, b) winter, c) spring, d) summer and e) fall derived using the SANDWICH method in Philadelphia. _____	A-179
Figure A-115.	Seasonally averaged PM _{2.5} speciation data for 2005-2007 for a) annual, b) winter, c) spring, d) summer and e) fall derived using the SANDWICH method in Phoenix, AZ. _____	A-180
Figure A-116.	Seasonally averaged PM _{2.5} speciation data for 2005-2007 for a) annual, b) winter, c) spring, d) summer and e) fall derived using the SANDWICH method in Pittsburgh, PA. _____	A-181
Figure A-117.	Seasonally averaged PM _{2.5} speciation data for 2005-2007 for a) annual, b) winter, c) spring, d) summer and e) fall derived using the SANDWICH method in Riverside, CA. _____	A-182
Figure A-118.	Seasonally averaged PM _{2.5} speciation data for 2005-2007 for a) annual, b) winter, c) spring, d) summer and e) fall derived using the SANDWICH method in Seattle, WA. _____	A-183
Figure A-119.	Seasonally averaged PM _{2.5} speciation data for 2005-2007 for a) annual, b) winter, c) spring, d) summer and e) fall derived using the SANDWICH method in St. Louis, MO. _____	A-184
Figure A-120.	Seasonal patterns in PM _{2.5} chemical composition from city-wide monthly average values for Atlanta, GA, 2005-2007. The gray line represents the difference in OCM calculated using material balance and blank corrected OC x 1.4. _____	A-185
Figure A-121.	Seasonal patterns in PM _{2.5} chemical composition from city-wide monthly average values for Birmingham, AL, 2005-2007. The gray line represents the difference in OCM calculated using material balance and blank corrected OC x 1.4. _____	A-185
Figure A-122.	Seasonal patterns in PM _{2.5} chemical composition from city-wide monthly average values for Boston, MA, 2005-2007. The gray line represents the difference in OCM calculated using material balance and blank corrected OC x 1.4. _____	A-186

Figure A-123.	Seasonal patterns in PM _{2.5} chemical composition from city-wide monthly average values for Chicago, IL, 2005-2007. The gray line represents the difference in OCM calculated using material balance and blank corrected OC x 1.4. _____	A-186
Figure A-124.	Seasonal patterns in PM _{2.5} chemical composition from city-wide monthly average values for Denver, CO, 2005-2007. The gray line represents the difference in OCM calculated using material balance and blank corrected OC x 1.4. _____	A-187
Figure A-125.	Seasonal patterns in PM _{2.5} chemical composition from city-wide monthly average values for Detroit, MI, 2005-2007. The gray line represents the difference in OCM calculated using material balance and blank corrected OC x 1.4. _____	A-187
Figure A-126.	Seasonal patterns in PM _{2.5} chemical composition from city-wide monthly average values for Houston, TX, 2005-2007. The gray line represents the difference in OCM calculated using material balance and blank corrected OC x 1.4. _____	A-188
Figure A-127.	Seasonal patterns in PM _{2.5} chemical composition from city-wide monthly average values for Los Angeles, CA, 2005-2007. The gray line represents the difference in OCM calculated using material balance and blank corrected OC x 1.4. _____	A-188
Figure A-128.	Seasonal patterns in PM _{2.5} chemical composition from city-wide monthly average values for New York City, NY, 2005-2007. The gray line represents the difference in OCM calculated using material balance and blank corrected OC x 1.4. _____	A-189
Figure A-129.	Seasonal patterns in PM _{2.5} chemical composition from city-wide monthly average values for Philadelphia, PA, 2005-2007. The gray line represents the difference in OCM calculated using material balance and blank corrected OC x 1.4. _____	A-189
Figure A-130.	Seasonal patterns in PM _{2.5} chemical composition from city-wide monthly average values for Phoenix, AZ, 2005-2007. The gray line represents the difference in OCM calculated using material balance and blank corrected OC x 1.4. _____	A-190
Figure A-131.	Seasonal patterns in PM _{2.5} chemical composition from city-wide monthly average values for Pittsburgh, PA, 2005-2007. The gray line represents the difference in OCM calculated using material balance and blank corrected OC x 1.4. _____	A-190
Figure A-132.	Seasonal patterns in PM _{2.5} chemical composition from city-wide monthly average values for Riverside, CA, 2005-2007. The gray line represents the difference in OCM calculated using material balance and blank corrected OC x 1.4. _____	A-191
Figure A-133.	Seasonal patterns in PM _{2.5} chemical composition from city-wide monthly average values for Seattle, WA, 2005-2007. The gray line represents the difference in OCM calculated using material balance and blank corrected OC x 1.4. _____	A-191
Figure A-134.	Seasonal patterns in PM _{2.5} chemical composition from city-wide monthly average values for St. Louis, MO, 2005-2007. The gray line represents the difference in OCM calculated using material balance and blank corrected OC x 1.4. _____	A-192
Figure A-135.	Diel plots generated from all available hourly FRM-like PM _{2.5} data, stratified by weekday (left) and weekend (right), in Atlanta, GA. Included are the number of monitor days (N) and the median, mean, 5th, 10th, 90th and 95th percentiles for each hour. _____	A-192
Figure A-136.	Diel plots generated from all available hourly FRM-like PM _{2.5} data, stratified by weekday (left) and weekend (right), in Chicago, IL. Included are the number of monitor days (N) and the median, mean, 5th, 10th, 90th and 95th percentiles for each hour. _____	A-193
Figure A-137.	Diel plots generated from all available hourly FRM-like PM _{2.5} data, stratified by weekday (left) and weekend (right), in Houston, TX. Included are the number of monitor days (N) and the median, mean, 5th, 10th, 90th and 95th percentiles for each hour. _____	A-193

Figure A-138.	Diel plots generated from all available hourly FRM-like PM _{2.5} data, stratified by weekday (left) and weekend (right), in New York City, NY. Included are the number of monitor days (N) and the median, mean, 5th, 10th, 90th and 95th percentiles for each hour. _____	A-194
Figure A-139.	Diel plots generated from all available hourly FRM-like PM _{2.5} data, stratified by weekday (left) and weekend (right), in Pittsburgh, PA. Included are the number of monitor days (N) and the median, mean, 5th, 10th, 90th and 95th percentiles for each hour. _____	A-194
Figure A-140.	Diel plots generated from all available hourly FRM-like PM _{2.5} data, stratified by weekday (left) and weekend (right), in Seattle, WA. Included are the number of monitor days (N) and the median, mean, 5th, 10th, 90th and 95th percentiles for each hour. _____	A-195
Figure A-141.	Diel plots generated from all available hourly FRM-like PM _{2.5} data, stratified by weekday (left) and weekend (right), in St. Louis, MO. Included are the number of monitor days (N) and the median, mean, 5th, 10th, 90th and 95th percentiles for each hour. _____	A-195
Figure A-142.	Diel plot generated from all available hourly FRM/FEM PM ₁₀ data, stratified by weekday (left) and weekend (right), in Atlanta, GA. Included are the number of monitor days (N) and the median, mean, 5th, 10th, 90th and 95th percentiles for each hour. _____	A-196
Figure A-143.	Diel plot generated from all available hourly FRM/FEM PM ₁₀ data, stratified by weekday (left) and weekend (right), in Chicago, IL. Included are the number of monitor days (N) and the median, mean, 5th, 10th, 90th and 95th percentiles for each hour. _____	A-196
Figure A-144.	Diel plot generated from all available hourly FRM/FEM PM ₁₀ data, stratified by weekday (left) and weekend (right), in Denver, CO. Included are the number of monitor days (N) and the median, mean, 5th, 10th, 90th and 95th percentiles for each hour. _____	A-197
Figure A-145.	Diel plot generated from all available hourly FRM/FEM PM ₁₀ data, stratified by weekday (left) and weekend (right), in Detroit, MI. Included are the number of monitor days (N) and the median, mean, 5th, 10th, 90th and 95th percentiles for each hour. _____	A-197
Figure A-146.	Diel plot generated from all available hourly FRM/FEM PM ₁₀ data, stratified by weekday (left) and weekend (right), in Los Angeles, CA. Included are the number of monitor days (N) and the median, mean, 5th, 10th, 90th and 95th percentiles for each hour. _____	A-198
Figure A-147.	Diel plot generated from all available hourly FRM/FEM PM ₁₀ data, stratified by weekday (left) and weekend (right), in Philadelphia, PA. Included are the number of monitor days (N) and the median, mean, 5th, 10th, 90th and 95th percentiles for each hour. _____	A-198
Figure A-148.	Diel plot generated from all available hourly FRM/FEM PM ₁₀ data, stratified by weekday (left) and weekend (right), in Phoenix, AZ. Included are the number of monitor days (N) and the median, mean, 5th, 10th, 90th and 95th percentiles for each hour. _____	A-199
Figure A-149.	Diel plot generated from all available hourly FRM/FEM PM ₁₀ data, stratified by weekday (left) and weekend (right), in Pittsburgh, PA. Included are the number of monitor days (N) and the median, mean, 5th, 10th, 90th and 95th percentiles for each hour. _____	A-199
Figure A-150.	Diel plot generated from all available hourly FRM/FEM PM ₁₀ data, stratified by weekday (left) and weekend (right), in Riverside, CA. Included are the number of monitor days (N) and the median, mean, 5th, 10th, 90th and 95th percentiles for each hour. _____	A-200

Figure A-151.	Diel plot generated from all available hourly FRM/FEM PM ₁₀ data, stratified by weekday (left) and weekend (right), in Seattle, WA. Included are the number of monitor days (N) and the median, mean, 5th, 10th, 90th and 95th percentiles for each hour. _____	A-200
Figure A-152.	Diel plot generated from all available hourly FRM/FEM PM ₁₀ data, stratified by weekday (left) and weekend (right), in St. Louis, MO. Included are the number of monitor days (N) and the median, mean, 5th, 10th, 90th and 95th percentiles for each hour. _____	A-201
Figure A-153.	Correlations between 24-h PM _{2.5} and co-located 24-h avg PM ₁₀ , PM _{10-2.5} , SO ₂ , NO ₂ and CO and daily maximum 8-h avg O ₃ for Atlanta, GA, stratified by season (2005-2007). One point is included for each available monitor pair. _____	A-201
Figure A-154.	Correlations between 24-h PM _{2.5} and co-located 24-h avg PM ₁₀ , PM _{10-2.5} , SO ₂ , NO ₂ and CO and daily maximum 8-h avg O ₃ for Birmingham, AL, stratified by season (2005-2007). One point is included for each available monitor pair. _____	A-202
Figure A-155.	Correlations between 24-h PM _{2.5} and co-located 24-h avg PM ₁₀ , PM _{10-2.5} , SO ₂ , NO ₂ and CO and daily maximum 8-h avg O ₃ for Boston, MA, stratified by season (2005-2007). One point is included for each available monitor pair. _____	A-202
Figure A-156.	Correlations between 24-h PM _{2.5} and co-located 24-h avg PM ₁₀ , PM _{10-2.5} , SO ₂ , NO ₂ and CO and daily maximum 8-h avg O ₃ for Chicago, IL, stratified by season (2005-2007). One point is included for each available monitor pair. _____	A-203
Figure A-157.	Correlations between 24-h PM _{2.5} and co-located 24-h avg PM ₁₀ , PM _{10-2.5} , SO ₂ , NO ₂ and CO and daily maximum 8-h avg O ₃ for Denver, CO, stratified by season (2005-2007). One point is included for each available monitor pair. _____	A-203
Figure A-158.	Correlations between 24-h PM _{2.5} and co-located 24-h avg PM ₁₀ , PM _{10-2.5} , SO ₂ , NO ₂ and CO and daily maximum 8-h avg O ₃ for Houston, TX, stratified by season (2005-2007). One point is included for each available monitor pair. _____	A-204
Figure A-159.	Correlations between 24-h PM _{2.5} and co-located 24-h avg PM ₁₀ , PM _{10-2.5} , SO ₂ , NO ₂ and CO and daily maximum 8-h avg O ₃ for Los Angeles, CA, stratified by season (2005-2007). One point is included for each available monitor pair. _____	A-204
Figure A-160.	Correlations between 24-h PM _{2.5} and co-located 24-h avg PM ₁₀ , PM _{10-2.5} , SO ₂ , NO ₂ and CO and daily maximum 8-h avg O ₃ for Philadelphia, PA, stratified by season (2005-2007). One point is included for each available monitor pair. _____	A-205
Figure A-161.	Correlations between 24-h PM _{2.5} and co-located 24-h avg PM ₁₀ , PM _{10-2.5} , SO ₂ , NO ₂ and CO and daily maximum 8-h avg O ₃ for Phoenix, AZ, stratified by season (2005-2007). One point is included for each available monitor pair. _____	A-205
Figure A-162.	Correlations between 24-h PM _{2.5} and co-located 24-h avg PM ₁₀ , PM _{10-2.5} , SO ₂ , NO ₂ and CO and daily maximum 8-h avg O ₃ for Pittsburgh, PA, stratified by season (2005-2007). One point is included for each available monitor pair. _____	A-206
Figure A-163.	Correlations between 24-h PM _{2.5} and co-located 24-h avg PM ₁₀ , PM _{10-2.5} , SO ₂ , NO ₂ and CO and daily maximum 8-h avg O ₃ for Riverside, CA, stratified by season (2005-2007). One point is included for each available monitor pair. _____	A-206
Figure A-164.	Correlations between 24-h PM _{2.5} and co-located 24-h avg PM ₁₀ , PM _{10-2.5} , SO ₂ , NO ₂ and CO and daily maximum 8-h avg O ₃ for St. Louis, MO, stratified by season (2005-2007). One point is included for each available monitor pair. _____	A-207
Figure A-165.	Correlations between 24-h PM ₁₀ and co-located 24-h avg PM _{2.5} , PM _{10-2.5} SO ₂ , NO ₂ and CO and daily maximum 8-h avg O ₃ for Atlanta, GA, stratified by season (2005-2007). One point is included for each available monitor pair. _____	A-207

Figure A-166.	Correlations between 24-h PM ₁₀ and co-located 24-h avg PM _{2.5} , PM _{10-2.5} SO ₂ , NO ₂ and CO and daily maximum 8-h avg O ₃ for Birmingham, AL, stratified by season (2005-2007). One point is included for each available monitor pair.	A-208
Figure A-167.	Correlations between 24-h PM ₁₀ and co-located 24-h avg PM _{2.5} , PM _{10-2.5} SO ₂ , NO ₂ and CO and daily maximum 8-h avg O ₃ for Boston, MA, stratified by season (2005-2007). One point is included for each available monitor pair.	A-208
Figure A-167.	Correlations between 24-h PM ₁₀ and co-located 24-h avg PM _{2.5} , PM _{10-2.5} SO ₂ , NO ₂ and CO and daily maximum 8-h avg O ₃ for Chicago, IL, stratified by season (2005-2007). One point is included for each available monitor pair.	A-209
Figure A-168.	Correlations between 24-h PM ₁₀ and co-located 24-h avg PM _{2.5} , PM _{10-2.5} SO ₂ , NO ₂ and CO and daily maximum 8-h avg O ₃ for Denver, CO, stratified by season (2005-2007). One point is included for each available monitor pair.	A-209
Figure A-169.	Correlations between 24-h PM ₁₀ and co-located 24-h avg PM _{2.5} , PM _{10-2.5} SO ₂ , NO ₂ and CO and daily maximum 8-h avg O ₃ for Detroit, MI, stratified by season (2005-2007). One point is included for each available monitor pair.	A-210
Figure A-170.	Correlations between 24-h PM ₁₀ and co-located 24-h avg PM _{2.5} , PM _{10-2.5} SO ₂ , NO ₂ and CO and daily maximum 8-h avg O ₃ for Houston, TX, stratified by season (2005-2007). One point is included for each available monitor pair.	A-210
Figure A-171.	Correlations between 24-h PM ₁₀ and co-located 24-h avg PM _{2.5} , PM _{10-2.5} SO ₂ , NO ₂ and CO and daily maximum 8-h avg O ₃ for Los Angeles, CA, stratified by season (2005-2007). One point is included for each available monitor pair.	A-211
Figure A-172.	Correlations between 24-h PM ₁₀ and co-located 24-h avg PM _{2.5} , PM _{10-2.5} SO ₂ , NO ₂ and CO and daily maximum 8-h avg O ₃ for New York City, NY, stratified by season (2005-2007). One point is included for each available monitor pair.	A-211
Figure A-173.	Correlations between 24-h PM ₁₀ and co-located 24-h avg PM _{2.5} , PM _{10-2.5} SO ₂ , NO ₂ and CO and daily maximum 8-h avg O ₃ for Philadelphia, PA, stratified by season (2005-2007). One point is included for each available monitor pair.	A-212
Figure A-174.	Correlations between 24-h PM ₁₀ and co-located 24-h avg PM _{2.5} , PM _{10-2.5} SO ₂ , NO ₂ and CO and daily maximum 8-h avg O ₃ for Phoenix, AZ, stratified by season (2005-2007). One point is included for each available monitor pair.	A-212
Figure A-175.	Correlations between 24-h PM ₁₀ and co-located 24-h avg PM _{2.5} , PM _{10-2.5} SO ₂ , NO ₂ and CO and daily maximum 8-h avg O ₃ for Pittsburgh, PA, stratified by season (2005-2007). One point is included for each available monitor pair.	A-213
Figure A-176.	Correlations between 24-h PM ₁₀ and co-located 24-h avg PM _{2.5} , PM _{10-2.5} SO ₂ , NO ₂ and CO and daily maximum 8-h avg O ₃ for Riverside, CA, stratified by season (2005-2007). One point is included for each available monitor pair.	A-213
Figure A-177.	Correlations between 24-h PM ₁₀ and co-located 24-h avg PM _{2.5} , PM _{10-2.5} SO ₂ , NO ₂ and CO and daily maximum 8-h avg O ₃ for St. Louis, MO, stratified by season (2005-2007). One point is included for each available monitor pair.	A-214

PM ISA Project Team

Executive Direction

Dr. John Vandenberg (Director)—National Center for Environmental Assessment-RTP Division, U.S. Environmental Protection Agency, Research Triangle Park, NC

Dr. Ila Cote (Acting Director)—National Center for Environmental Assessment-RTP Division, U.S. Environmental Protection Agency, Research Triangle Park, NC

Ms. Debra Walsh (Deputy Director)—National Center for Environmental Assessment-RTP Division, U.S. Environmental Protection Agency, Research Triangle Park, NC

Dr. Mary Ross (Branch Chief)—National Center for Environmental Assessment, U.S. Environmental Protection Agency, Research Triangle Park, NC

Scientific Staff

Dr. Lindsay Wichers Stanek (PM Team Leader)—National Center for Environmental Assessment, U.S. Environmental Protection Agency, Research Triangle Park, NC

Dr. Jeffrey Arnold—National Center for Environmental Assessment, U.S. Environmental Protection Agency, Research Triangle Park, NC

Dr. Christal Bowman—National Center for Environmental Assessment, U.S. Environmental Protection Agency, Research Triangle Park, NC

Dr. James S. Brown—National Center for Environmental Assessment, U.S. Environmental Protection Agency, Research Triangle Park, NC

Dr. Barbara Buckley—National Center for Environmental Assessment, U.S. Environmental Protection Agency, Research Triangle Park, NC

Mr. Allen Davis—National Center for Environmental Assessment, U.S. Environmental Protection Agency, Research Triangle Park, NC

Dr. Jean-Jacques Dubois— Oak Ridge Institute for Science and Education, Postdoctoral Research Fellow to National Center for Environmental Assessment, U.S. Environmental Protection Agency, Research Triangle Park, NC

Dr. Steven J. Dutton—National Center for Environmental Assessment, U.S. Environmental Protection Agency, Research Triangle Park, NC

Dr. Erin Hines—National Center for Environmental Assessment, U.S. Environmental Protection Agency, Research Triangle Park, NC

Dr. Douglas Johns—National Center for Environmental Assessment, U.S. Environmental Protection Agency, Research Triangle Park, NC

Dr. Ellen Kirrane—National Center for Environmental Assessment, U.S. Environmental Protection Agency, Research Triangle Park, NC

Dr. Dennis Kotchmar—National Center for Environmental Assessment, U.S. Environmental Protection Agency, Research Triangle Park, NC

Dr. Thomas Long—National Center for Environmental Assessment, U.S. Environmental Protection Agency, Research Triangle Park, NC

Dr. Thomas Luben—National Center for Environmental Assessment, U.S. Environmental Protection Agency, Research Triangle Park, NC

Dr. Qingyu Meng—Oak Ridge Institute for Science and Education, Postdoctoral Research Fellow to National Center for Environmental Assessment, U.S. Environmental Protection Agency, Research Triangle Park, NC

Dr. Kristopher Novak—National Center for Environmental Assessment, U.S. Environmental Protection Agency, Research Triangle Park, NC

Dr. Joseph Pinto—National Center for Environmental Assessment, U.S. Environmental Protection Agency, Research Triangle Park, NC

Dr. Jennifer Richmond-Bryant—National Center for Environmental Assessment, U.S. Environmental Protection Agency, Research Triangle Park, NC

Dr. Mary Ross—National Center for Environmental Assessment, U.S. Environmental Protection Agency, Research Triangle Park, NC

Mr. Jason Sacks—National Center for Environmental Assessment, U.S. Environmental Protection Agency, Research Triangle Park, NC

Dr. David Svendsgaard—National Center for Environmental Assessment, U.S. Environmental Protection Agency, Research Triangle Park, NC

Dr. Lisa Vinikoor—National Center for Environmental Assessment, U.S. Environmental Protection Agency, Research Triangle Park, NC

Dr. William Wilson—National Center for Environmental Assessment, U.S. Environmental Protection Agency, Research Triangle Park, NC

Dr. Lori White—National Institute for Environmental Health Sciences, Research Triangle Park, NC

Technical Support Staff

Mattie Arnold—Senior Environmental Employee Program, National Center for Environmental Assessment, U.S. Environmental Protection Agency, Research Triangle Park, NC

Laeda Baston—Senior Environmental Employee Program, National Center for Environmental Assessment, U.S. Environmental Protection Agency, Research Triangle Park, NC

Kimberly Branch—Student Services Contractor, National Center for Environmental Assessment, U.S. Environmental Protection Agency, Research Triangle Park, NC

Ken Breito—Senior Environmental Employee Program, National Center for Environmental Assessment, U.S. Environmental Protection Agency, Research Triangle Park, NC

Eleanor Jamison—Senior Environmental Employee Program, National Center for Environmental Assessment, U.S. Environmental Protection Agency, Research Triangle Park, NC

Ryan Jones—Oak Ridge Institute for Science and Education, at National Center for Environmental Assessment, U.S. Environmental Protection Agency, Research Triangle Park, NC

Erica Lee—Oak Ridge Institute for Science and Education, at National Center for Environmental Assessment, U.S. Environmental Protection Agency, Research Triangle Park, NC

Barbara Liljequist—Senior Environmental Employee Program, National Center for Environmental Assessment, U.S. Environmental Protection Agency, Research Triangle Park, NC

Ellen Lorang—National Center for Environmental Assessment, U.S. Environmental Protection Agency, Research Triangle Park, NC

Kelsey Matson—Student Services Contractor, National Center for Environmental Assessment, U.S. Environmental Protection Agency, Research Triangle Park, NC

Sandy Pham—Student Services Contractor, National Center for Environmental Assessment, U.S. Environmental Protection Agency, Research Triangle Park, NC

Olivia Phillpott—Senior Environmental Employee Program, National Center for Environmental Assessment, U.S. Environmental Protection Agency, Research Triangle Park, NC

Deborah Wales—National Center for Environmental Assessment, U.S. Environmental Protection Agency, Research Triangle Park, NC

Erica Wilson—Oak Ridge Institute for Science and Education, at National Center for Environmental Assessment, U.S. Environmental Protection Agency, Research Triangle Park, NC

Richard Wilson—National Center for Environmental Assessment, U.S. Environmental Protection Agency, Research Triangle Park, NC

Barbara Wright—Senior Environmental Employee Program, National Center for Environmental Assessment, U.S. Environmental Protection Agency, Research Triangle Park, NC

Authors, Contributors, Reviewers

AUTHORS

Dr. Lindsay Wichers Stanek (PM Team Leader)—National Center for Environmental Assessment, U.S. Environmental Protection Agency, Research Triangle Park, NC

Dr. Jeffrey Arnold—National Center for Environmental Assessment, U.S. Environmental Protection Agency, Research Triangle Park, NC

Dr. Christal Bowman—National Center for Environmental Assessment, U.S. Environmental Protection Agency, Research Triangle Park, NC

Dr. James S. Brown—National Center for Environmental Assessment, U.S. Environmental Protection Agency, Research Triangle Park, NC

Dr. Barbara Buckley—National Center for Environmental Assessment, U.S. Environmental Protection Agency, Research Triangle Park, NC

Mr. Allen Davis—National Center for Environmental Assessment, U.S. Environmental Protection Agency, Research Triangle Park, NC

Dr. Jean-Jacques Dubois—Oak Ridge Institute for Science and Education, Postdoctoral Research Fellow to National Center for Environmental Assessment, U.S. Environmental Protection Agency, Research Triangle Park, NC

Dr. Steven J. Dutton—National Center for Environmental Assessment, U.S. Environmental Protection Agency, Research Triangle Park, NC

Dr. Tara Greaver—National Center for Environmental Assessment, U.S. Environmental Protection Agency, Research Triangle Park, NC

Dr. Erin Hines—National Center for Environmental Assessment, U.S. Environmental Protection Agency, Research Triangle Park, NC

Dr. Douglas Johns—National Center for Environmental Assessment, U.S. Environmental Protection Agency, Research Triangle Park, NC

Dr. Ellen Kirrane—National Center for Environmental Assessment, U.S. Environmental Protection Agency, Research Triangle Park, NC

Dr. Dennis Kotchmar—National Center for Environmental Assessment, U.S. Environmental Protection Agency, Research Triangle Park, NC

Dr. Thomas Long—National Center for Environmental Assessment, U.S. Environmental Protection Agency, Research Triangle Park, NC

Dr. Thomas Luben—National Center for Environmental Assessment, U.S. Environmental Protection Agency, Research Triangle Park, NC

Dr. Qingyu Meng—Oak Ridge Institute for Science and Education, Postdoctoral Research Fellow to National Center for Environmental Assessment, U.S. Environmental Protection Agency, Research Triangle Park, NC

Dr. Kristopher Novak—National Center for Environmental Assessment, U.S. Environmental Protection Agency, Research Triangle Park, NC

Dr. Joseph Pinto—National Center for Environmental Assessment, U.S. Environmental Protection Agency, Research Triangle Park, NC

Dr. Jennifer Richmond-Bryant—National Center for Environmental Assessment, U.S. Environmental Protection Agency, Research Triangle Park, NC

Dr. Mary Ross—National Center for Environmental Assessment, U.S. Environmental Protection Agency, Research Triangle Park, NC

Mr. Jason Sacks—National Center for Environmental Assessment, U.S. Environmental Protection Agency, Research Triangle Park, NC

Dr. Timothy J. Sullivan—E&S Environmental Chemistry, Inc., Corvallis, OR

Dr. David Svendsgaard—National Center for Environmental Assessment, U.S. Environmental Protection Agency, Research Triangle Park, NC

Dr. Lisa Vinikoor—National Center for Environmental Assessment, U.S. Environmental Protection Agency, Research Triangle Park, NC

Dr. William Wilson—National Center for Environmental Assessment, U.S. Environmental Protection Agency, Research Triangle Park, NC

Dr. Lori White—National Institute for Environmental Health Sciences, Research Triangle Park, NC

Dr. Christy Avery—University of North Carolina, Chapel Hill, NC

Dr. Kathleen Belanger —Center for Perinatal, Pediatric and Environmental Epidemiology, Yale University, New Haven, CT

Dr. Michelle Bell—School of Forestry & Environmental Studies, Yale University, New Haven, CT

Dr. William D. Bennett—Center for Environmental Medicine, Asthma and Lung Biology, University of North Carolina, Chapel Hill, NC

Dr. Matthew J. Campen—Lovelace Respiratory Research Institute, Albuquerque, NM

Dr. Leland B. Deck— Stratus Consulting, Inc., Washington, DC

Dr. Janneane F. Gent—Center for Perinatal, Pediatric and Environmental Epidemiology, Yale University, New Haven, CT

Dr. Yuh-Chin Tony Huang—Department of Medicine, Division of Pulmonary Medicine, Duke University Medical Center, Durham, NC

Dr. Kazuhiko Ito—Nelson Institute of Environmental Medicine, NYU School of Medicine, Tuxedo, NY

Mr. Marc Jackson—Integrated Laboratory Systems, Inc., Research Triangle Park, NC

Dr. Michael Kleinman—Department of Community and Environmental Medicine, University of California, Irvine

Dr. Sergey Napelenok—National Exposure Research Laboratory, U.S. Environmental Protection Agency, Research Triangle Park, NC

Dr. Marc Pitchford—National Oceanic and Atmospheric Administration, Las Vegas, NV

Dr. Les Recio—Genetic Toxicology Division, Integrated Laboratory Systems, Inc., Research Triangle Park, NC

Dr. David Quincy Rich—Department of Epidemiology, University of Medicine and Dentistry of New Jersey, Piscataway, NJ

Dr. Timothy Sullivan— E&S Environmental Chemistry, Inc., Corvallis, OR

Dr. George Thurston—Department of Environmental Medicine, NYU, Tuxedo, NY

Dr. Gregory Wellenius—Cardiovascular Epidemiology Research Unit, Beth Israel Deaconess Medical Center, Boston, MA

Dr. Eric Whitsel—Departments of Epidemiology and Medicine, University of North Carolina, Chapel Hill, NC

CONTRIBUTORS

Dr. Philip Bromberg—Department of Medicine, University of North Carolina, Chapel Hill, NC

Mr. Michael Burr—National Center for Environmental Assessment, U.S. Environmental Protection Agency, Research Triangle Park, NC

Mr. Turhan Carroll—Student Services Contractor, National Center for Environmental Assessment, U.S. Environmental Protection Agency, Research Triangle Park, NC

Mr. Rosana Datti—Student Services Contractor, National Center for Environmental Assessment, U.S. Environmental Protection Agency, Research Triangle Park, NC

Mr. Neil Frank—Office of Air Quality Planning and Standards, U.S. Environmental Protection Agency, Research Triangle Park, NC

Mr. Jonathan Krug—Student Services Contractor, National Center for Environmental Assessment, U.S. Environmental Protection Agency, Research Triangle Park, NC

Ms. Katie Lane—Student Services Contractor, National Center for Environmental Assessment, U.S. Environmental Protection Agency, Research Triangle Park, NC

Mr. Phil Lorang—Office of Air Quality Planning and Standards, U.S. Environmental Protection Agency, Research Triangle Park, NC

Ms. Christina Miller—National Center for Environmental Assessment, U.S. Environmental Protection Agency, Research Triangle Park, NC

Ms. Irina Mordukhovich—Oak Ridge Institute for Science and Education, at National Center for Environmental Assessment, U.S. Environmental Protection Agency, Research Triangle Park, NC

Dr. Elizabeth Oesterling Owens—Oak Ridge Institute for Science and Education, Postdoctoral Research Fellow to National Center for Environmental Assessment, U.S. Environmental Protection Agency, Research Triangle Park, NC

Dr. Adam Reff—Office of Air Quality Planning and Standards, U.S. Environmental Protection Agency, Research Triangle Park, NC

Ms. Vicki Sandiford— Office of Air Quality Planning and Standards, U.S. Environmental Protection Agency, Research Triangle Park, NC

Dr. Mark Schmidt—Office of Air Quality Planning and Standards, U.S. Environmental Protection Agency, Research Triangle Park, NC

Ms. Angelina Schultz—Student Services Contractor, National Center for Environmental Assessment, U.S. Environmental Protection Agency, Research Triangle Park, NC

Ms. Kirsten Simmons—Student Services Contractor, National Center for Environmental Assessment, U.S. Environmental Protection Agency, Research Triangle Park, NC

Ms. Genee Smith—Oak Ridge Institute for Science and Education, at National Center for Environmental Assessment, U.S. Environmental Protection Agency, Research Triangle Park, NC

Mr. Kurt Susdorf—Student Services Contractor, National Center for Environmental Assessment, U.S. Environmental Protection Agency, Research Triangle Park, NC

Ms. Rebecca Yang—Student Services Contractor, National Center for Environmental Assessment, U.S. Environmental Protection Agency, Research Triangle Park, NC

PEER REVIEWERS

Dr. Sara Dubowsky Adar, Department of Epidemiology, University of Washington, Seattle, WA

Mr. Chad Bailey, Office of Transportation and Air Quality, Ann Arbor, MI

Mr. Richard Baldauf, Office of Transportation and Air Quality, Ann Arbor, MI

Dr. Prakash Bhave, National Exposure Research Laboratory, U.S. Environmental Protection Agency, Research Triangle Park, NC

Mr. George Bowker, Office of Atmospheric Programs, U.S. Environmental Protection Agency, Washington, D.C.

Dr. Judith Chow, Division of Atmospheric Sciences, Desert Research Institute, Reno, NV

Dr. Dan Costa, Office of Research and Development, U.S. Environmental Protection Agency, Research Triangle Park, NC

Dr. Ila Cote, National Center for Environmental Assessment, U.S. Environmental Protection Agency, Research Triangle Park, NC

Dr. Robert Devlin, National Health and Environmental Effects Research Laboratory, U.S. Environmental Protection Agency, Research Triangle Park, NC

Dr. David DeMarini, National Health and Environmental Effects Research Laboratory, U.S. Environmental Protection Agency, Research Triangle Park, NC

Dr. Neil Donahue, Department of Chemical Engineering, Carnegie Mellon University, Pittsburgh, PA

Dr. Aimen Farraj, National Health and Environmental Effects Research Laboratory, U.S. Environmental Protection Agency, Research Triangle Park, NC

Dr. Mark Frampton, Department of Environmental Medicine, University of Rochester Medical Center, Rochester, NY

Mr. Neil Frank, Office of Air Quality Planning and Standards, U.S. Environmental Protection Agency, Research Triangle Park, NC

Mr. Tyler Fox, Office of Air Quality Planning and Standards, U.S. Environmental Protection Agency, Research Triangle Park, NC

Dr. Jim Gauderman, Department of Environmental Medicine, Department of Preventive Medicine, University of Southern California, Los Angeles, CA

Dr. Barbara Glenn, National Center for Environmental Research, U.S. Environmental Protection Agency, Washington, D.C.

Dr. Terry Gordon, School of Medicine, New York University, Tuxedo, NY

Mr. Tim Hanley, Office of Air Quality Planning and Standards, U.S. Environmental Protection Agency, Research Triangle Park, NC

Dr. Jack Harkema, Department of Pathobiology and Diagnostic Investigation, Michigan State University, East Lansing, MI

Ms. Beth Hassett-Sipple, Office of Air Quality Planning and Standards, U.S. Environmental Protection Agency, Research Triangle Park, NC

Dr. Amy Herring, Department of Biostatistics, University of North Carolina, Chapel Hill, NC

Dr. Israel Jirak, Department of Meteorology, Embry-Riddle Aeronautical University, Prescott, AZ

Dr. Mike Kleeman, Department of Civil and Environmental Engineering, University of California, Davis, CA

Dr. Petros Koutrakis, Exposure, Epidemiology and Risk Program, Harvard School of Public Health, Boston, MA

Dr. Sagar Krupa, Department of Plant Pathology, University of Minnesota, St. Paul, MN

Mr. John Langstaff, Office of Air Quality Planning and Standards, U.S. Environmental Protection Agency, Research Triangle Park, NC

Dr. Meredith Lassiter, Office of Air Quality Planning and Standards, U.S. Environmental Protection Agency, Research Triangle Park, NC

Mr. Phil Lorang, Office of Air Quality Planning and Standards, U.S. Environmental Protection Agency, Research Triangle Park, NC

Dr. Karen Martin, Office of Air Quality Planning and Standards, U.S. Environmental Protection Agency, Research Triangle Park, NC

Ms. Connie Meacham—National Center for Environmental Assessment, U.S. Environmental Protection Agency, Research Triangle Park, NC

Mr. Tom Pace, Office of Air Quality Planning and Standards, U.S. Environmental Protection Agency, Research Triangle Park, NC

Dr. Jennifer Peel, Department of Environmental and Radiological Health Sciences, College of Veterinary Medicine and Biomedical Sciences, Colorado State University, Fort Collins, CO

Dr. Zackary Pekar, Office of Air Quality Planning and Standards, U.S. Environmental Protection Agency, Research Triangle Park, NC

Mr. Rob Pinder, National Exposure Research Laboratory, U.S. Environmental Protection Agency, Research Triangle Park, NC

Mr. Norm Possiel, Office of Air Quality Planning and Standards, U.S. Environmental Protection Agency, Research Triangle Park, NC

Dr. Sanjay Rajagopalan, Division of Cardiovascular Medicine, Ohio State University, Columbus, OH

Dr. Pradeep Rajan, Office of Air Quality Planning and Standards, U.S. Environmental Protection Agency, Research Triangle Park, NC

Mr. Venkatesh Rao, Office of Air Quality Planning and Standards, U.S. Environmental Protection Agency, Research Triangle Park, NC

Ms. Joann Rice, Office of Air Quality Planning and Standards, U.S. Environmental Protection Agency, Research Triangle Park, NC

Mr. Harvey Richmond, Office of Air Quality Planning and Standards, U.S. Environmental Protection Agency, Research Triangle Park, NC

Ms. Victoria Sandiford, Office of Air Quality Planning and Standards, U.S. Environmental Protection Agency, Research Triangle Park, NC

Dr. Stefanie Sarnat, Department of Environmental and Occupational Health, Emory University, Atlanta, GA

Dr. Frances Silverman, Gage Occupational and Environmental Health, University of Toronto, Toronto, ON

Mr. Steven Silverman, Office of General Council, U.S. Environmental Protection Agency, Washington, D.C.

Dr. Barbara Turpin, Department of Environmental Sciences, Rutgers University, New Brunswick, NJ

Dr. Robert Vanderpool, National Exposure Research Laboratory, U.S. Environmental Protection Agency, Research Triangle Park, NC

Dr. Alan Vette, National Exposure Research Laboratory, U.S. Environmental Protection Agency, Research Triangle Park, NC

Mr. Tim Watkins, National Exposure Research Laboratory, U.S. Environmental Protection Agency, Research Triangle Park, NC

Dr. Christopher Weaver, National Center for Environmental Assessment, U.S. Environmental Protection Agency, Research Triangle Park, NC

Mr. Lewis Weinstock, Office of Air Quality Planning and Standards, U.S. Environmental Protection Agency, Research Triangle Park, NC

Ms. Karen Wesson, Office of Air Quality Planning and Standards, U.S. Environmental Protection Agency, Research Triangle Park, NC

Dr. Jason West, Department of Environmental Sciences and Engineering, University of North Carolina, Chapel Hill, NC

Mr. Ronald Williams, National Exposure Research Laboratory, U.S. Environmental Protection Agency, Research Triangle Park, NC

Dr. George Woodall, National Center for Environmental Assessment, U.S. Environmental Protection Agency, Research Triangle Park, NC

Dr. Antonella Zanobetti, Department of Environmental Health, Harvard School of Public Health, Boston, MA

Clean Air Scientific Advisory Committee for Particulate Matter NAAQS

CHAIRPERSON

Dr. Jonathan Samet, Department of Preventive Medicine, Keck School of Medicine, University of Southern California, Los Angeles, CA

MEMBERS

Dr. Lowell Ashbaugh, Crocker Nuclear Lab, University of California, Davis, CA

Dr. Ed Avol, Department of Preventive Medicine, Keck School of Medicine, University of Southern California, Los Angeles, CA

Dr. Joseph Brain*, Department of Environmental Health, Harvard School of Public Health, Harvard University, Boston, MA

Dr. Wayne Cascio, Brody School of Medicine, East Carolina University, Greenville, NC

Dr. Ellis B. Cowling*, Colleges of Natural Resources and Agriculture and Life Sciences, North Carolina State University, Raleigh, NC

Dr. James Crapo*, Department of Medicine, National Jewish Medical and Research Center, Denver, CO

Dr. Douglas Crawford-Brown, Department of Environmental Sciences and Engineering, University of North Carolina at Chapel Hill, Chapel Hill, NC

Dr. H. Christopher Frey*, Department of Civil, Construction and Environmental Engineering, College of Engineering, North Carolina State University, Raleigh, NC

Dr. David Grantz, Botany and Plant Sciences and Air Pollution Research Center, Riverside Campus and Kearney Agricultural Center, University of California, Parlier, CA

Dr. Joseph Helble, Thayer School of Engineering, Dartmouth College, Hanover, NH

Dr. Rogene Henderson**, Lovelace Respiratory Research Institute, Albuquerque, NM

Dr. Philip Hopke, Department of Chemical Engineering, Clarkson University, Potsdam, NY

Dr. Donna Kenski*, Lake Michigan Air Directors Consortium, Rosemont, IL

Dr. Morton Lippmann, Nelson Institute of Environmental Medicine, New York University School of Medicine, Tuxedo, NY

Dr. Helen Suh MacIntosh, Environmental Health, School of Public Health, Harvard University, Boston, MA

Dr. William Malm, National Park Service Air Resources Division, Cooperative Institute for Research in the Atmosphere, Colorado State University, Fort Collins, CO

Mr. Charles Thomas (Tom) Moore, Jr., Western Regional Air Partnership, Western Governors' Association, Fort Collins, CO

Dr. Robert F. Phalen, Center for Occupation & Environment Health, College of Medicine, Department of Community and Environmental Medicine, Air Pollution Health Effects Laboratory, University of California Irvine, Irvine, CA

Dr. Kent Pinkerton, Center for Health and the Environment, University of California, Davis, CA

Mr. Richard L. Poirot, Air Pollution Control Division, Department of Environmental Conservation, Vermont Agency of Natural Resources, Waterbury, VT

Dr. Armistead (Ted) Russell*, Department of Civil and Environmental Engineering, Georgia Institute of Technology, Atlanta, GA

Dr. Frank Speizer, Channing Laboratory, Harvard Medical School, Boston, MA

Dr. Sverre Vedal, Department of Environmental and Occupational Health Sciences, School of Public Health and Community Medicine, University of Washington, Seattle, WA

*Members of the statutory Clean Air Scientific Advisory Committee (CASAC) appointed by the EPA Administrator.

**As immediate past CASAC Chair, Dr. Henderson is invited to participate in CASAC advisory activities for FY 2009.

SCIENCE ADVISORY BOARD STAFF

Dr. Holly Stallworth, Economist and Designated Federal Officer, Clean Air Scientific Advisory Committee, Environmental Economics Advisory Committee, Washington, D.C.

Acronyms and Abbreviations

α	alpha, ambient exposure factor (varies between 0 and 1)
α -HCH	alpha-hexachlorocyclohexane
\AA	Ångström exponent; determined by the contrast between the AOD at two or more different wavelengths and is related to aerosol particle size
A	surface albedo (varies between 0 and 1), the fraction of the total light striking a surface that gets reflected back off that surface. An object that has a high albedo (near 1) is very bright; an object that has a low albedo (near 0) is dark. The Earth's albedo is about 0.37. The Moon's is about 0.12.
A549	human epithelial cell line
AAC	abdominal aortic calcium
AAS	atomic absorption spectrophotometry
AB	Alcian Blue stain
ABC	Asian Brown Cloud: (ABC: Climate and Other Environmental Impacts; UNEP Report)
ABI	ankle-arm or resting blood pressure index
AC	air conditioning
Ace	acenaphthene
ACE-1	angiotensin converting enzyme
ACEAsia	(Asian Pacific Regional) Aerosol Characterization Experiment (study of radiative forcing due to anthropogenic aerosols over the Asian Pacific region)
ACGIH	American Conference of Governmental Industrial Hygienists
ACh	acetylcholine
Acl	acenaphthylene
ACP	accumulation mode particle
ACS	American Cancer Society
actinomycetes	bacteria, gram-positive, anaerobic, filamentous/branching growth pattern
Ad4BP	adrenal-4-binding protein (also known as steroidogenic factor-1 (SF-1), Ad4BP/SF-1, or NR5A1)
ADEOS-1	Advanced Earth Observing Satellite-1
A-DEP	automobile diesel exhaust particles
ADM	angular distribution model(s), angular dependence model
ADMA	asymmetric dimethylarginine
AD-Net	Asian Dust Network
Ae	AERONET

AeroCom	Aerosol Comparisons between Observations and Models
AERONET	NASA AERosol RObotic NETwork, aerosol observation system
Aerosols 99	1999 NOAA aerosol research cruise across the Atlantic
aethalometer	instrument that measures mass concentration of soot (BC or EC) particles in aerosols or in an air stream
AF	atrial fibrillation
AGA	appropriate for gestational age
AGE	advanced glycation end product
AHR	airway hyperresponsiveness, airway hyperreactivity
AhR	arylhydrocarbon receptor
AHSMOG	California Seventh Day Adventist study
AI	aerosol index
AIC	Akaike's information criterion
AIM	ambient ion monitor
AIOP	2003 Aerosol Intensive Operating Period, a DOE program
air light	light scattered or diffused in the air by dust, haze, etc., especially as it limits the visibility of distant, dark objects by causing them to blend with the background sky
AIRS	Aerometric Information Retrieval System
Al	aluminum
albedo	a measure of light reflectance, See "A" abbreviation
ALI	air liquid interface
AM	alveolar macrophage(s)
AM, AMF	arbuscular mycorrhizal (fungi)
AMAP	Arctic Monitoring and Assessment Programme
AMDP	annual maximum of daily precipitation
AMI	acute myocardial infarction
AMS	aerosol mass spectrometry
Ang II	angiotensin II
ANOVA	analysis of variance
ANP	atrial natriuretic peptide
ANS	autonomic nervous system
Ant	anthracene
AOD	aerosol optical depth
AP-1	activator protein 1
APC	antigen presenting cell(s)
APCS	Absolute Principal Components Scores

APEX	Air Pollutants Exposure Model
APHEA	Air pollution and Health: a European Approach (study)
APHEA2	extended analysis of APHEA
APO	apocynin
ApoE	apolipoprotein E
ApoE ^{-/-}	mouse strain devoid of ApoE protein
APS	aerodynamic particle sizer, aerosol polarimetry sensor
aPTT	activated partial thromboplastin time
AQCD	Air Quality Criteria Document
AQI	Air Quality Index
AQM	air quality model
AQS	U.S. EPA Air Quality System database
Aqua	NASA satellite to study Earth's water cycle, radiative energy fluxes, aerosols, vegetation cover on the land, phytoplankton and dissolved organic matter in the oceans, and temperatures
AR4	Fourth Assessment Report (AR4) from the IPCC
ARCTAS	Arctic Research of the Composition of the Troposphere from Aircraft and Satellites
ARD	Air Resources Division (U.S. Dept. of Interior, National Park Service)
ARDS	adult respiratory distress syndrome
ARI	acute respiratory infection
ARIC	Atherosclerosis Risk in Communities study
ARIES	Aerosol Research and Inhalation Epidemiology Study
ARM	DOE's Atmospheric Radiation Measurement program
ARQM	Air Quality Research Branch (Meteorological Service of Canada Toronto)
ARS	Air Resource Specialists
As	arsenic
ASDNN5	mean of the standard deviation in all 5-min segments of a EKG 24 h recording
ASOS	Automated Surface Observing System
ATOFMS	aerosol time-of-flight mass spectrometry
ATP	adenosine triphosphate
A-Train	a group of 5 afternoon overpass satellites (Aura, PARASOL, CALIPSO, CloudSat, Aqua) that overfly the Equator, carrying sensors to study aerosols
ATS	American Thoracic Society
AURA	(Latin for breeze) NASA satellite to study the Earth's ozone, air quality and climate

avg	average
AVHRR	Advanced Very High Resolution Radiometer
β	beta, beta coefficient, slope
β -HCH	beta-hexachlorocyclohexane(s)
3 β HSD	3 β -hydroxysteroid dehydrogenase
β TGF	β transforming growth factor
b_{ag}	absorption by gases coefficient
<i>BAP</i>	absorption by particles coefficient
<i>BEXT</i>	light extinction coefficient, in units of Mm ⁻¹
<i>BSG</i>	scattering by gases coefficient
<i>BSP</i>	sum of light scattering by (aerosol) particles coefficient, aerosol light scattering
Ba	barium
BaA	benz[a]anthracene
BAD	bronchial artery diameter
BAL	bronchoalveolar lavage
BALB/c	albino inbred mouse strain
BALF	bronchoalveolar lavage fluid
BALT	bronchus-associated lymphoid tissues
BAM	beta attenuation monitor
BaP	benzo[a]pyrene
BASIC	Brain Attack Surveillance in Corpus Christi (project)
BASE-A	(Biomass) Burning Airborne and Spaceborne Experiment - Amazon and Brazil
BbF	benzo[b]fluoranthene
BC	black carbon
BCC-CMI	Beijing Climate Center – Carbon Mitigation Initiative
BCCR	Bjerknes Centre for Climate Research, Univ. of Bergen, Norway
BCM2.0	BCCR's Bergen Climate Model, Version 2
BEAS-2B	human bronchial epithelial cell line
BeP	benz[e]pyrene
BghiP, BpPe	benzo[g,h,i]perylene
BGT	beta-gauge technique
BH ₄	tetrahydrobiopterin
bhp	brake horsepower
BkF	benzo[k]fluoranthene

BMI	body mass index
BMP	bone morphogenetic protein (e.g., BMP-6, BMP-15)
BN/BR	Brown Norway rat strain
BNP	brain natriuretic peptide, B-type natriuretic peptide
BOSS	BYU Organic Sampling System; multichannel diffusion denuder sampling system
BP	blood pressure
BPM	blowing PM _{2.5}
BpPe, BghiP	benzo[ghi]perylene
BPQ	benz(a)pyrene (BaP)-quinone
Br	bromine
BRAVO	Big Bend Regional Aerosol and Visibility Observational (Study)
BrdU	bromodeoxyuridine
BS	black smoke
BUC	bucillamine (N-[2-mercapto-2-methylpropionyl]-L-cysteine)
BVAIT	B-Vitamin Atherosclerosis Intervention Trial
BW, bw	body weight
BYU	Brigham Young University
C	carbon
C ⁴	Center of Clouds, Chemistry and Climate
¹² C	carbon-12
¹³ C	carbon-13
¹⁴ C	carbon-14
C ₆₀ (OH) ₂₄	water-soluble fullerene
C ₆₀ Cs C ₆₀	fullerenes
Ca	calcium
CAA	Clean Air Act
CAAA	1977 Clean Air Act Amendments
CAAM	continuous ambient mass monitor
CAC	coronary artery calcification
CaCO ₃	calcium carbonate
CAD	coronary artery disease
CALINE	California Line Source Dispersion Model
CALIOP	Cloud and Aerosol Lidar with Orthogonal Polarization
CALIPSO	Cloud-Aerosol Lidar and Infrared Pathfinder Satellite Observations

CAM	Community Atmosphere Model (replaced NCAR CCM3 atmospheric model)
CAMM	continuous ambient mass monitor
CAMP	Childhood Asthma Management Program
CAMx	comprehensive air quality model with extensions (modeling system)
Ca(NO ₃) ₂	calcium nitrate
CAP	concentrated ambient particle
CAPMoN	Canadian Air and Precipitation Monitoring Network
CASAC	Clean Air Scientific Advisory Committee
CaSO ₄	calcium sulfate
CASTNet	Clean Air Status and Trends Network
CATS	cumulative air toxics surface
CB	carbon black, chronic bronchitis
CB-Fe	carbon black particles artificially coated with Fe(II) salt.
CB(P)	carbon black (particles)
CBSA	Core-Based Statistical Area based on the 2000 U.S. Census
CB-V	carbon black particles artificially coated with a targeted concentration of Vanadium (IV) salt
CBVD	cerebrovascular disease
CC16	Clara cell protein, Clara cell 16 protein
CCCma	Canadian Centre for Climate Modeling and Analysis
CCM3	NCAR Community Climate Model
CCM-MATCH	general circulation model (NCAR CCM), in tandem with a related chemical transport model (MATCH), and observations
CCN	cloud condensation nuclei; cloud seed, small particles about which cloud droplets coalesce (A typical raindrop is about 2 mm in diameter, a typical cloud droplet is on the order of 0.02 mm, and a typical cloud condensation nucleus (aerosol) is on the order of 0.0001 mm or 0.1 micrometer or greater in diameter.)
CCPM	continuous coarse particle monitor
CCSM3	NCAR community climate system model, version 3
CCSP	U.S. Climate Change Science Program
Cd	cadmium
CD1	albino outbred mouse strain
CDC	Centers for Disease Control and Prevention
CDE	conjugated diene
CDNC	cloud droplet number concentration
CDPHE	Colorado Department of Public Health and Environment
Ce	cerium

CEN	European Committee for Standardization
CenRAP	Central Regional Air Planning Association
CERES	Clouds and the Earth's Radiant Energy System
CERFACS	European Centre for Research and Advanced Training in Scientific Computation
CF	coronary flow, cystic fibrosis
CFA	coal fly ash
CFD	cystic fibrosis disease
CFR	Code of Federal Regulations
CGCM3.1	Canada's CCCma third generation coupled global climate model, runs at 2 resolutions (T47 and T63)
cGMP	cyclic guanosine monophosphate
CH ₂ Cl ₂	methylene chloride
CH ₂ O	formaldehyde
CH ₄	methane
CHAD	Consolidated Human Activity Database
CHD	chronic heart disease
CHF	congestive heart failure
CHL	crown heel length
CHO	Chinese hamster ovary cells
Chr	chrysene
CHS	Children's Health Study
CI	confidence interval
CIF	carbon-impregnated charcoal filter
CIIT	The Chemical Industry Institute of Toxicology
CIMT	carotid intimal-medial thickness
Cl	chlorine
CL	chemiluminescence
CLAMS	ARM's Chesapeake Lighthouse and Aircraft Measurements for Satellites
CloudSat	satellite to provide observations necessary to advance understanding of cloud abundance, distribution, structure, and radiative properties
CM	conditioned medium, cell culture medium
CMAQ	Community Multi-scale Air Quality modeling system
CMAR	CSIRO Marine and Atmospheric Research; houses Australia's leading regional climate change modeling research
CMB	chemical mass balance
CMD	count median diameter

CNES	Centre National d'Etudes Spatiales, or National Space Study Center Toulouse, France
CNP	carbon nano particle
CNRM	Centre National de Recherches Meteorologiques, Meteo France, France
CNRM-CM3	Center National Weather Research - global coupled system, third version (of the ocean-atmosphere model initially developed at CERFACS (Toulouse, France))
CNS	central nervous system
Co	cobalt
CO	carbon monoxide
CO ₂	carbon dioxide
COD	coefficient of divergence
COH, CoH	coefficient of haze (a measurement of visibility interference in the atmosphere, as the quantity of dust and smoke in a theoretical 1,000 linear feet of air).
Cong	U.S. Congress
CONUS	continental United States
COO ⁻	carboxyl group
COPD	chronic obstructive pulmonary disease
CoPP	cobalt protoporphyrin a potent inhibitor of HO-1 (heme oxygenase)
COX-2	cyclooxygenase 2 enzyme
CPC	condensation particle counter
CPZ	capsazepine
Cr	chromium
C-R	concentration-response (relationship)
CRP	C-reactive protein
cryosphere	land or sea covered by snow or ice
Cs	cesium
¹³⁷ Cs	cesium-137
CS	cigarette smoke
CSA	Combined Statistical Area based on the 2000 U.S. Census
CSC	cigarette smoke condensates
CSE	cigarette smoke extract
cSHMT	cytosolic serine hydroxymethyltransferase gene
CSIRO	Commonwealth Scientific and Industrial Research Organization (Australia National Science Agency)
CSIRO-Mk3.x	CSIRO Mark 3.x coupled climate system model
CSN	Chemical Speciation Network

CTM	chemistry-transport model, chemical transport model
Cu	copper
CuSO ₄	copper sulfate
Cu/Zn SOD	Cu/Zn superoxide dismutase
CUP	Current Use Pesticide (excluding DDT)
CV	cardiovascular, coefficient of variation
CVD	cardiovascular disease(s)
CVM	contingent valuation method – used in urban visibility valuation studies
CYP	cytochrome P450
CYP 1A1	cytochrome P450 1A1
Δ	delta, change, difference
ΔFEV ₁	change in forced expiratory volume in one second
d ₅₀	50 percent cut point or 50 percent diameter
d _{ae}	aerodynamic diameter of a particle
D	diameter
D _a	Dalton (measure of molecular weight)
DAAC	Distributed Active Archive Center
DAASS	Dry Ambient Aerosol Size Spectrometer
DABEX	Dust and Biomass-burning Experiment (in West Africa)
DAR	denuded aortic ring
DAX-1	x-chromosome gene-1
DBA	dibenzo(a,h)thracene
DBP	diastolic blood pressure
DC	dendritic cell
DC	diesel exhaust particles + cigarette smoke condensates
D.C.	District of Columbia
DC8	Douglas aircraft, originally designed as an 80 passenger airliner
DCF	direct climate forcing, 2',7'-dichlorofluorescein
DDT	dichlorodiphenyltrichloroethane, an insecticide
DE	diesel exhaust

deciview haze index	See d_v log transformation of light extinction, similar in many ways to the decibel index for acoustic measurements. The name deciview is used because of the similarity of the decibel scale in acoustics. Both use 10 times the logarithm of a ratio of a measured physical quantity to a reference value to create scales that are approximately linear with respect to changes as perceived by human senses. Because the index increases from zero as haze increases, it is characterized as a haziness index. Expressed in terms of extinction coefficient (b_{ext}) and visual range (vr): haziness (d_v) = $10 \ln (b_{ext}/0.01 \text{ km}^{-1}) = 10 \ln (391 \text{ km/vr})$
DEE	diesel exhaust extract
DEP	diesel exhaust particle
DEPAL	diesel exhaust particles methylene chloride extracts aliphatic (hexane)
DEPAR	diesel exhaust particles methylene chloride extracts aromatic (hexane/methylene chloride)
DEPE	5 grams diesel exhaust particles in 5 mL PBS containing 0.05% Tween 80
DEPM	diesel exhaust particles methanol extract
DEPME	diesel exhaust particles methylene chloride extracts
DEPPO	diesel exhaust particles methylene chloride extracts polar (methylene chloride/methanol)
Dex	dexamethasone
d Fld	change fold, unit change in property
DFO	desferrioxamine (Desferral) an iron chelator
DFX	deferasirox (Exjade) an oral iron chelator
DHR	dihydrorhodamine 123
diel	a 24-hour period, usually involving a day and the adjoining night
DLCO	carbon monoxide diffusing capacity
DMEM	Dulbecco's modified Eagle's medium (culture medium)
DMSO	dimethyl sulfoxide
DMT1	divalent metal transporter-1 protein (transport and detoxification of metals)
DMTU	dimethylthiourea
DNA	deoxyribonucleic acid
DOE	U.S. Department of Energy
downwelling	when ocean winds cause the surface water to move toward a coastline, the nutritionally-depleted warmer surface water will move deeper downward, thereby creating a downwelling current
dpc	days post conception
DPC	dodecylphosphocholine
DPCC	1,2-dipalmitoyl-SN-glycero-3-phosphocholine
DPI	diphenyleneiodonium
DPM	diesel particulate matter

DPPC	dipalmitoylphosphatidylcholine, the major phospholipid constituent of pulmonary surfactant
DRE	direct radiative effects
DRF	direct radiative forcing
DRUM	Davis Rotating Uniform size-cut Monitor – UC Davis aerosol sampling technique
DS	diffusion screens
DSP	daily sperm production
DTMA	Dynamic mechanical thermal analysis
DTPA	diethylene triamine pentaacetic acid
DU	dust
<i>dv</i>	deciview(s) unit, convenient, numerical method for presentation of visibility values. The log scale of this visibility index, expressed in deciview(s) (<i>dv</i>), is linear with respect to humanly-perceived changes in visual air quality over its entire range, analogous to the decibel scale for sound. The <i>dv</i> scale is near zero for a pristine environment and increases as visibility degrades. One deciview is about a 10% change in light extinction. See deciview haze index.
DVT	deep vein thrombosis
EAD	electrical aerosol detector
EANET	Acid Deposition Monitoring Network in East Asia
EARLINET	European Aerosol Research Lidar Network
EarthCARE	Earth Clouds, Aerosols and Radiation Explorer (European Space Agency satellite)
EAST-AIRE	East Asian Study for Tropospheric Aerosols: An International Regional Experiment
EBCT	electron beam computed tomography
EC	elemental carbon
ECE-1	endothelin converting enzyme
ECG, EKG	electrocardiogram, electrical activity of the heart over time, measured by an electrocardiograph
ECHAM5	European Centre Hamburg with Hamburg Aerosol Module, 5th generation model of the ECHAM general atmosphere circulation model, studies the climate of the troposphere
ECHAMS5-HAM	European Centre Hamburg, with Hamburg Aerosol Module;
ECHO-G	(ECHAM4 + HOPE-G): Global climate model used at MPI, and Meteorological Institute of the University of Bonn (Germany) and Institute of KMA (Korea)
ECRHS	European Community Respiratory Health Survey
EC/TC	ratio of elemental carbon to total carbon
ED	emergency room, emergency department
EDGAR	Emissions Database for Global Atmospheric Research, version 2

EDTA	ethylenediaminetetraacetic acid
ED-XRF	energy dispersive X-ray fluorescence
EGM	electrogram
EGU	electricity-generating unit
EHC-93	Ottawa dust: urban air particulate matter PM ₁₀ , collected in 1993 in Ottawa, Canada
EKG, ECG	electrocardiogram
ELISA	enzyme-linked immunosorbent assay
EMECAS	Spanish Multi-centric Study on the Relation between Air Pollution and Health
EMEP	European Monitoring and Evaluation Programme
eNO	exhaled nitric oxide
eNOS	endothelial nitric oxide synthase
EOS	Earth Observing System
EPA	U.S. Environmental Protection Agency
ER	estrogen receptor
ERBS	Earth Radiation Budget Satellite
ERK1/2	ERK-1 (MAPK p42) and ERK-2 (MAPK p44) (extracellular signal-regulated kinases [in cell signaling pathway])
ESRL	NOAA Earth System Research Laboratory
ESTR	expanded simple tandem repeat
E_r	forcing efficiency
ET	extrathoracic region of respiratory tract
ET	endothelin
ET-1	endothelin-1
ET-2	endothelin-2
ET-3	endothelin-3
ET _A	endothelin A receptor subtype
ET _B	endothelin B receptor subtype
ETS	environmental tobacco smoke
EU	endotoxin units
EXPOLIS	EXPOLIS (exposure + polis [Greek for city]); six-city European air pollution study
F	breathing frequency
f	the ratio of ambient aerosol mass (wet) to dry aerosol mass M .
$F()$	function of variable inside parentheses
$f_{\text{osp}}(\text{RH})$	total light scattering coefficient at given relative humidity(RH) values

faf	anthropogenic fraction of fine-mode fraction
ff	fine mode fraction
$f(RH)$	the unitless water growth term that depends on relative humidity
F	fine particles, aerosol direct Radiative Forcing (RF) at the Top of the Atmosphere (TOA)
F344	Fisher 344 strain of rats
F_a	adjusted forcings
FA	filtered air
FAC	ferric ammonium citrate
FBI	Federal Bureau of Investigation
FBS	fetal bovine serum
FCS	fetal calf serum
FDMS	Filter Dynamics Measurement System, a self referencing airborne particulate monitor that provides a measurement of the mass of nonvolatile and semivolatile airborne particulate matter
FDMS-TEOM	Filter Dynamics Measurement System - Tapered Element Oscillating Microbalance
F_e	effective (F_e) forcings
Fe	iron
$Fe_2(SO_4)_3$	ferric sulfate
$FeCl_3$	ferric chloride
FEF	forced expiratory flow
FEF_{25-75}	mean forced expiratory flow over the middle half of the forced vital capacity
$FEF_{50\%}$	mid-expiratory flow
FEM	Federal Equivalent Method
$FeNO$	fractional exhaled nitric oxide
FERA	Fire and Environmental Research Applications Team (Pacific Northwest Research Station, U.S. Forest Service)
FEV_1	forced expiratory volume in one second
FGA	one fibrinogen alpha chain
FGB	one fibrinogen beta chain
FGOALS-g1.0	Flexible Global Ocean-Atmosphere-Land System Model, a global climate system model developed at the Laboratory of Numerical Modeling for Atmospheric Sciences and Geophysical Fluid Dynamics (LASG), Institute of Atmospheric Physics, Chinese Academy of Sciences, Beijing, China
F_I	instantaneous forcing, simplest measure of radiative climate forcing
FID	flame ionization detection
FIMS	fast integrated mobility scanners

<i>FINF</i>	infiltration factors
FKHR	Proapoptotic Factor FOXO1
Fle	fluorine
Flu	fluoranthene
FMD	flow-mediated dilation
forcing	changes in composition of the Earth's atmosphere, leading to changes in the global energy balance; "forcing" the climate to change
FPG	formamidopyrimidine-DNA glycosylase
f-PM, FPM	fine particulate matter
FR	Federal Register
FRM	Federal Reference Method
FROSTFIRE	The landscape-scale prescribed research burn in the boreal forest of interior Alaska, July 1999; conducted by FERA.
Fs	SST forcing(s), forcing driven by sea surface temperature (SST)
Fsfc	mean net solar flux at the (Earth) surface
FT	free troposphere
FTIR	Fourier transform infrared spectrometry
F/UFP	mix of fine and ultrafine particles, all < 2.5 μm
FVC	forced vital capacity
γGCS	gamma glutamylcysteine sythetase
Ga	gallium
GAM	generalized additive model
GATOR	Gas, Aerosol, Transport, and Radiation model
GATORG	Gas, Aerosol, Transport, Radiation, and General circulation model
GAW	Global Atmospheric Watch network
GBS	group B streptococcus
GC	gas chromatography
GCM(s)	general circulation model(s), global climate model
GCMOM	General Circulation, Mesoscale and Ocean Model
GC/MS	gas chromatography/mass spectrometry
GCS	gamma glutamylcysteine sythetase
GD	gestational day
GDF	growth differentiation factor (e.g., GDF-9)
GEE	generalized estimating equations, gasoline engine exhaust
GEIA	Global Emissions Inventory Activity
GEM	gaseous elemental mercury

GEOS-Chem	NASA Goddard Earth Observing System-CHEMistry (global 3-D chemical transport model (CTM) for atmospheric composition)
GFAAS	graphite furnace atomic absorption spectrometry
GFAP	glial fibrillary acidic protein
GFDL	NOAA's Geophysical Fluid Dynamics Laboratory
GFDL-CM2.x	GFDL Climate Models
GFED	Global Fire Emission Database (U.S. Oak Ridge National Laboratory)
GGT	gamma-glutamyltranspeptidase; a marker of epithelial injury
GHG	greenhouse gas
GIS	Geographic Information System
GISS	NASA Goddard Institute for Space Studies
GISS-AOM	GISS Atmosphere-Ocean Model climate prediction model
GISS-EH	GISS AOM for sea ice model
GISS-ER	GISS AOM for liquid sea model
GLAS	Geoscience Laser Altimeter System
GLM	generalized linear models
GM	geometric mean
GM-CSF	granulocyte macrophage colony-stimulating factor
GMD	NOAA Global Monitoring Division of the Earth System Research Laboratory
GMS	Greater Mekong Subregion (Cambodia, the People's Republic of China, Lao People's Democratic Republic, Myanmar, Thailand, and Viet Nam) Core Environment Program
GOCART	NASA Goddard Chemistry Aerosol Radiation and Transport; a model simulation of major tropospheric aerosol components
GOES	Geostationary Operational Environmental Satellite
GoMACCS	Texas Air Quality Study (TexAQS) - Gulf of Mexico Atmospheric Composition and Climate Study
GPS	Global Positioning System
GSD	geometric standard deviation
GSFC	NASA Goddard Space Flight Center
GSH	glutathione
GSH:GSSG	ratio of reduced glutathione to glutathione disulfide (oxidized glutathione)
GSO, GSNO	S-Nitrosoglutathione
GSSG	glutathione disulfide; oxidized glutathione
GST	glutathione-S-transferase
GSTM1	glutathione S-transferase polymorphism M1
GSTP1	glutathione-S-transferase polymorphism P1

GSTT1	glutathione-S-transferase polymorphism T1
GWP	global warming potential
h	hour
H	atomic hydrogen, hydrogen radical, height, heart rate, high dose, high exposure
H ⁺	hydrogen ion
HR	heart rate
H ₂	molecular hydrogen
H ₂ CO	formaldehyde
H ₂ O	water
H ₂ O ₂	hydrogen peroxide
H ₂ S	hydrogen sulfide
H ₂ SO ₄	sulfuric acid
H9c2	rat embryonic cardiomyocytes cell line
HA	hospital admission
HAEC	Human Aortic Endothelial Cell
HAPC	Harvard ambient particle concentrator
haze index	expressed in deciview (<i>dv</i>) units - log transformation of light extinction, similar in many ways to the decibel index for acoustic measurements (see <i>dv</i>)
HBE, HBEC	Human Bronchial Epithelial cells
HC	hydrocarbon(s); head circumference
HCB	hexachlorobenzene
HCH	hexachlorocyclohexane(s) (e.g. α -HCH, β -HCH)
HDL	high density lipoprotein
HEAPSS	Health Effects of Air Pollution among Susceptible Subpopulations study
HEI	Health Effects Institute
HEPA	high efficiency particle air (filter)
HERO	Health and Environmental Research Online, NCEA Database System
HF	heart failure, high frequency (HRV parameter), high (dose/exposure) filtered
HFCD	High-Fat Chow Diet
HFE	HFE gene, HFE protein
Hg	mercury
Hg(0)	gaseous elemental mercury
Hg(II)	gaseous divalent (oxidized) mercury
HH	hereditary hemochromatosis

HNRS	Hans Nixdorf Recall Study
HO-1	heme oxygenase-1
hOGG1	8-hydroxyguanine DNA-glycosylase
HOPE-G	Hamburg Atmosphere-Ocean Coupled Circulation Model
hPA	hectopascal (unit of pressure); 1 hPA = 1 millibar, = 100 Pascals
hPAEC	human pulmonary artery endothelial cells
hPBMC	human peripheral blood mononuclear cells
HPLC	high pressure liquid chromatography
HPMF	high particulate matter filtered
hPMVEC	human pulmonary microvascular endothelial cells
HR	heart rate, hazard ratio, high level DE, Hunter College, NY
HRV	heart rate variability
HSD	17 β -hydroxysteroid dehydrogenase
HSP-70	heat shock protein
HSPH	Harvard School of Public Health
HSRL	NASA's High Spectral Resolution Lidar
HUVEC	human umbilical vein endothelial cells
h ν	photon
H/W	height to width ratio
HWS	hardwood smoke
Hz	hertz
IC	ion chromatography
ICAM-1	intercellular adhesion molecule-1
ICARTT	International Consortium for Atmospheric Research on Transport and Transformation
ICAS	Inner-City Asthma Study
ICD	implantable/implanted cardioverter defibrillator
ICD-9	International Classification of Disease 9th revision
ICD-10	International Classification of Disease 10th revision
ICESat	NASA Ice, Cloud and land Elevation Satellite
ICP-AES	inductively coupled plasma-atomic emission spectroscopy
ICP-MS	inductively-coupled plasma-mass spectrometry
ICR	imprinting control region, mouse strain
ICRP	International Commission on Radiological Protection
ID	identification number
IDP	indeno[1,2,3-c,d]pyrene

IFN- γ	interferon-gamma
IFS	Integrated Forest Study
Ig	immunoglobulin (e.g., IgE)
IGS	International Genetic Standard
IHD	ischemic heart disease
IIASA	International Institute for Applied Systems Analysis, Luxemburg Austria
IL	interleukin (e.g., IL-4, IL-5, IL-6, IL-8)
IM	IMPACT (Michigan, USA)
iMDDC	immature monocyte-derived dendritic cells
IMPACT	NASA Langley Research Center's Interactive Modeling Project for Atmospheric Chemistry and Transport (model)
IMPROVE	Interagency Monitoring of Protected Visual Environment, operated by the National Park Service Air Resources Division
IN	ice nuclei
INAA	instrumental neutron activation analysis
INCA	Interactions between Chemistry and Aerosol, a LMDz model
index of refraction	refractive index - a measure of how much the speed of light is seemingly reduced by a medium (in a vacuum = 1.0; through air at STP = 1.000029, through ice = 1.31, etc.)
INDOEX	NOAA 1999 Indian Ocean Experiment
INGV-SXG	Istituto Nazionale di Geofisica e Vulcanologia, Italy; SINTEX-G model (A Coupled Atmosphere Ocean Sea-Ice General Circulation Climate Model evolving from the the SINTEX and SINTEX-F models)
INM-CM3.0	Institute of Numerical Mathematics climate model, Russian Academy of Science, Russia
iNOS	inducible nitric oxide synthase
INTEX-A	INTEX – Phase A (2004)
INTEX-B	INTEX – Phase B (2006)
INTEX-NA	NASA Intercontinental Chemical Transport Experiment – North America
I/O	indoor-outdoor ratio
IOM	Institute of Medicine
i.p.	intraperitoneal (injection)
IP	inhalable particle
IPCC	Intergovernmental Panel on Climate Change
IPSL-CM4	climate model developed at the Institut Pierre Simon Laplace (IPSL), a federation of five research laboratories in the Paris area studying terrestrial and planetary environments (Des Sciences de L'Environnement)
IQR	interquartile range

Ir	iridium
IR	incidence rate, infrared radiation
IRE	iron responsive element
IRMS	isotope ratio mass spectrometer
ISA	Integrated Science Assessment
ISO	International Standards Organization
ISO	isoprene, 2-methyl analog of 1,3-butadiene
IT	intratracheal, intratracheally (region or installation)
IUGG	International Union of Geodesy and Geophysics
IUGR	intrauterine growth restriction, intrauterine growth retardation
i.v.	intravenous
JNK	c-jun N-terminal kinase
κ B	kappa B transcription factor
K	potassium
KC	local neutrophil chemoattractant protein, the murine analog of interleukin-8
kHz	kilohertz
kJ	kilojoules
KLH	keyhole limpet hemocyanin
km	kilometer
km^{-1}	inverse kilometer
K_{ow}	octanol-water partition coefficient
L, dL, mL, μ L	Liter, deciLiter, milliLiter, microLiter
L	low (dose / exposure)
La	lanthanum
LAC	light-absorbing carbon
LACE98	Lindenberg Aerosol Characterization Experiment 1998 (The Lindenberg Meteorological Observatory, Berlin)
lag	time between one event and another
lag 0	same day as the death, test, hospital, ED, clinic, physician visit; that occurs on the same day as the exposure to the pollution
lag 0-3	all the deaths, tests, hospital, ED, clinic, physician visits; that occurred on the same day as the exposure to the pollution and the two days following the day of exposure
LBA-SMOCC	Brazil's Large-Scale Atmosphere-Biosphere Experiment in Amazon – European Commission's Smoke Aerosols, Clouds, Rainfall and Climate: Aerosols from Biomass Burning Perturb Global and Regional Climate
LBW	low birth weight
LC	lethal concentration

LC ₅₀	median lethal concentration
LDH	lactate dehydrogenase
LDL	low-density lipoprotein
LDLR	low-density lipoprotein receptor
LDVP	left developing ventricular pressure
LES	large eddy simulations model
LF	low frequency an HRV parameter
LF/HF	ratio of LF to HF an HRV parameter
LIBS	laser induced breakdown spectroscopy
lidar	(light detection and ranging) A lidar instrument uses short pulses of laser light to detect particles or gases in the atmosphere, like a radar bounces radio waves off rain drops in clouds. The resulting reflected laser radiation is measured and used to determine the location, distribution and nature of the atmospheric particles.
LIF	leukemia inhibitory factor
light extinction	fractional loss of intensity in a light beam per unit distance due to scattering and absorption by the gases and particles in the air
LITE	NASA Lidar In-space Technology Experiment (1994)
litterfall	leaves, branches, and other organic fuel deposition that fall to the ground and decompose allow nutrients and organic matter to transfer back to the soil
LMD	Laboratoire de Meteorologie Dynamique
LMDz	Laboratoire de Meteorologie Dynamique with Zoom
LMDZ-INCA	IPSL Laboratoire de Météorologie Dynamique's INTERactive Chemistry and Aerosols model
LMDZ-LOA	IPSL-LMDZ model with model from Laboratoire d'Optique Atmosphérique – Université des Sciences et Technologies de Lille, France
ln	natural logarithm
L-NAME	arginine analog; N(G)-nitro-L- arginine methyl ester
L-NMMA	N(G)-mono-methyl-L-arginine
LnRMSSD	natural log of RMSSD; measure of HRV
lnSDNN	natural log of the standard deviation of NN intervals in an EKG
LOA	Laboratoire d'Optique Atmosphérique, Université des Sciences et Technologies de Lille, France
LOESS	locally weighted scatterplot smoothing
log	logarithm of a number raised to a given base (e.g., log ₁₀)
longwave emissivity	a material's ability to emit or release the longwave (thermal) energy which it has absorbed
LOSU	level of scientific understanding
Lpm	liters per minute (L/min)

LPMF	low particulate matter filtered
LPO	plasma lipid peroxides
LPS	lipopolysaccharide
LRAT	long range atmospheric transport
LROT	long range oceanic transport
LSCE	Laboratoire des Sciences du Climat et de l'Environnement, Gif sur Yvette, France
LSDF	low-sulfur diesel fuel
LTB ₄	leukotriene B ₄
LTE ₄	leukotriene E ₄
LUA NRW	The North Rhine-Westphalia State Environment Agency
LUDEP	LUNG Dose Evaluation Program
LUR	land use regression (model)
LV	left ventricle
LVEDP	left-ventricular end-diastolic pressure,
LVSP	left-ventricular systolic pressure, left ventricular developed pressure
L/W	ratio of lumen to wall
LWC	liquid water content
LWDE	Low Whole Diesel Exhaust
LWP	liquid water path
µg	microgram
µg/m ³	micrograms per cubic meter (unit of chemical concentration in air)
µm	micrometer, micron
µM	microMolar (10 ⁻⁶ Molar)
m, cm, µm, nm	meter(s), centimeter(s), micrometer(s) = micron(s), nanometer(s)
M, mM, µM, nM, pM	Molar, milliMolar (10 ⁻³ Molar), microMolar (10 ⁻⁶ Molar), nanoMolar (10 ⁻⁹ Molar), picoMolar (10 ⁻¹² Molar)
M	dry aerosol mass, medium dose/exposure
ma	moving average
MAM	March-April-May
MAN	Maritime Aerosol Network
MANE-VU	Mid-Atlantic/Northeast Visibility Union
MAP	mitogen-activated protein, mean arterial pressure
MAPK	mitogen-activated protein kinase(s), MAP kinase
MARAMA	Mid Atlantic Regional Air Management Association
MATCH	NCAR Model of Atmospheric Transport and Chemistry

max	maximum
MBP	major basic protein
MCAPS	Medicare Air Pollution Study
Mch	methacholine
MCN	mixed carbon nanoparticle
MCP-1	monocyte chemoattractant protein 1
MCV	mean corpuscular volume
MD	mineral dust
MDA	malondialdehyde
MDCT	multidetector computed tomography
ME	Multilinear Engine
MEE	mass extinction efficiency, (in units of m^2/g), a parameter linking the particle mass concentration to light scattering
MEF	maximal expiratory flow
MEF ₅₀	maximum expiratory flow rate at 50% of vital capacity
MeHg	methyl mercury
MENTOR	Modeling Environment for Total Risk Studies
MEP	motorcycle exhaust particulate(s)
MEPE	motorcycle exhaust particulate extract (particle-free)
MESA	Multi-Ethnic Study of Atherosclerosis
MFFSR	multifilter rotating shadowband radiometer
mg/m ³	milligrams per cubic meter
Mg	magnesium
MI	myocardial infarction
MIROC3.x	Model for Interdisciplinary Research on Climate, Center for Climate System Research, University of Tokyo
Mie solution	solves Maxwell's equations for light scattering; valid for all possible ratios of diameter to wavelength, used by optical scattering measurements to accurately calculate light scattering and absorption of particles
MILAGRO	Megacity Initiative: Local and Global Research Observations, study of air pollution in Mexico City
min	minute(s), minimum
MINOS	MPI Mediterranean INTensive Oxidant Study
MIP-2	macrophage inflammatory protein-2
MIRAGE	Megacities Impact on Regional and Global Environment program
MIS	mullerian inhibiting substance
MISR	Multi-angle Imaging SpectroRadiometer

Mm	megameter [1 million meters]
Mm ⁻¹	inverse megameter
Mm ⁻¹ /(µg/m ³)	units used in light scattered per unit of mass concentration (mass scattering efficiency), reduces to m ² /g
MM	monocyte-derived macrophages
MM5	PSU/NCAR mesoscale model used to predict mesoscale atmospheric circulation. (Pennsylvania State University / National Center for Atmospheric Research, Mesoscale and Microscale Meteorology Division)
MMAD	mass median aerodynamic diameter
MMD	mass median diameter
MMEF	maximal mid-expiratory flow; synonymous with FEF ₂₅₋₇₅
mmHg	millimeters of mercury
MMP	mitochondria membrane potential
MMP(2,9)	matrix metalloproteinase (2, or 9)
MMT	million metric tons
Mn	manganese
MN	micronuclei
MnSO ₄	manganese sulfate
MnSOD	manganese superoxide dismutase
MnTBAP	manganese tetrakis (4-benzoic acid) porphyrin (membrane-permeable SOD mimetic)
mo	month
MO_GO	satellite-model integration, MODIS over ocean and GOCART simulated AOD
MO_MI_GO	satellite-model integration, MODIS over ocean and MISR over land and GOCART simulated AOD
MOA	mode(s) of action
MODIS	MODerate resolution Imaging Spectroradiometer, an aerosol sensor
MOUDI	Micro-Orifice Uniform Deposit Impactor (a University of Minnesota sampling technique)
MOZART	MOdel for Ozone and Related chemical Tracers; a chemical transport model
MP	mid polar, myelopeptide
MPC	mean platelet component
MPF	median power frequency
MPG	synthetic aminothiols, N-(2-mercaptopropionyl) glycine
MPI	Max Planck Institute for Meteorology in Hamburg, Germany
MPLNET	NASA Micro-Pulse Lidar Network
MPO	myeloperoxidase

MPPD	Multiple-Path Particle Dosimetry model
MPV	mean platelet volume
MRI	Meteorological Research Institute, Japan
MRI-CGCM	MRI coupled general circulation model
mRNA	messenger RNA
MRPO	Midwest Regional Planning Organization
ms	millisecond
MSA	metropolitan statistical area based on the 1990 U.S. Census
MSH	melanocyte stimulating hormone
MSHA	Mount St. Helen ash
MSU	monosodium urate crystals
MT	metric ton (1000 kg)
MTHFR	methylenetetrahydrofolate reductase
MTT	methyl thiazol tetrazolium
MV	motor vehicle
MWNT	multiplewall nanotube
<i>M/Z</i>	mass-to-charge ratio
N	nitrogen
N, n	number of observations
N ₂ O	nitrous oxide
Na	sodium
Na ₂ SO ₄	sodium sulfate
NAAQS	National Ambient Air Quality Standards
NAC	N-acetylcysteine, a thiol antioxidant
NaCl	sodium chloride
NADPH	reduced form of nicotinamide adenine dinucleotide phosphate
NAG	N-acetyl-β-D-glucosaminidase
Na,K-ATPase	sodium-potassium adenosine triphosphatase
NAMS	National Ambient Monitoring Stations
NaN ₃	sodium azide
NaNO ₃	sodium nitrate
nano-BAM	low pressure-drop ultrafine particle impactor coupled with a Beta Attenuation Monitor
NAPAP	National Acid Precipitation Assessment Program

NAPCA	National Air Pollution Control Administration, formerly in the Environmental Health Service (Environmental Control Administration), Public Health Service (PHS), U.S. Department of Health, Education, and Welfare (HEW)
NAS	National Academy of Sciences
NASA	U.S. National Aeronautics and Space Administration
NASDA	National Space Development Agency, Japan
NATA	U.S. EPA's National Air Toxics Assessment
2-NB	2-nitrobenzanthrone
NC	total (particle) number concentration
NC _{0.01-0.1}	10–100 nm number concentrations
NCAR	National Center for Atmospheric Research (Pennsylvania State University)
NCC-MPSP	negatively charged carboxylate-modified polystyrene particle(s)
NCD	Normal Chow Diet
NCEA	National Center for Environmental Assessment
NCHS	National Center for Health Statistics
NCICAS	National Cooperative Inner-City Asthma Study
NCore	National Core (a multi pollutant network of measurement systems for ambient particles, pollutant gases and meteorology)
Nd	drop number concentration (cloud droplets/cm ³)
Nd:YAG	neodymium-doped yttrium aluminum garnet laser
NDDN	National Dry Deposition Network
NEAQS	NOAA New England Air Quality Study
nephelometer	an instrument for measuring the concentration of a suspension by its scattering of a beam of light
NEI	National Emissions Inventory
NESCAUM	Northeast States for Coordinated Air Use Management
NET	National Emissions Trends database
net irradiance	the difference between incoming and outgoing radiation energy in a climate system, measured in watts per square meter (W/m ²)
NFκB	nuclear factor kappa-B; transcription factor, light-chain enhancer of B cells
NG	neutrophil granulocytes
NH	northern hemisphere
NH ₃	ammonia
NH ₄ ⁺	ammonium ion
NH ₄ NO ₃	ammonium nitrate

(NH ₄) ₂ SO ₄	ammonium sulfate
NHANES	National Health and Nutrition Examination Survey
NHBE(C)	normal human bronchial epithelial cells
NHPAE	normal human pulmonary artery endothelial cells
NHS	Nurses' Health Study
Ni	nickel
NIOSH	National Institute for Occupational Safety and Health
NIST	National Institute of Standards and Technology
nm	nanometers
NMHC	non-methane volatile hydrocarbon
NMMAPS	U.S. National Morbidity, Mortality, and Air Pollution Study
NN intervals	normal-to-normal (NN or RR, sinus) time interval between each QRS complex in the EKG
NO	nitric oxide
NO ₂ , NO ₂ [·]	nitrogen dioxide, nitrogen dioxide radical
NO ₃ ⁻	nitrate
NOAA	National Oceanic and Atmospheric Administration
NOAEL	no observed adverse effect level
NOS	nitric oxide synthase
NOS3	nitric oxide synthase 3
NO _x	nitrogen oxides, oxides of nitrogen (NO + NO ₂)
NP	National Park
NPM	non-blowing PM _{2.5}
NPOESS	National Polar-orbiting Operational Environment Satellite System
NPS	National Park Service, U.S. Department of the Interior
NR	not reported
NR5A1	nuclear receptor subfamily 5, group A, member 1 (previously known as AD4BP/SF-1 or SF-1)
NRC	National Research Council
NRPB	National Radiological Protection Board
NSA	North Slope Alaska
NT	neurotrophin, nitrotyrosine
NWS	National Weather Service
NYHA	New York Heart Association (NYHA) Classification Scale
NYHA I	Class I: No symptoms at any level of exertion
NYHA II	Class II: Mild symptoms and slight limitation during regular activity

NYHA III	Class III: Noticeable limitation due to symptoms, even during minimal activity
NYHA IV	Class IV: Severe limitations. Experience symptoms even while at rest
O	oxygen
O ₂	molecular oxygen
O ₃	ozone
OAQPS	Office of Air Quality Planning and Standards
OC	organic carbon
OCM	organic carbon mass
OE	organic extracts
OGG1	8 oxo-guanine repair enzyme
OH, OH·	hydroxyl group, hydroxyl radical
8-OHdG	8-hydroxydeoxyguanosine
OM	organic matter
OMI	Ozone Monitoring Instrument
OMM	organic molecular marker
OR	odds ratio(s)
Orographic fog	formed as the air rises up a slope and will often envelope the summit. When the humid rising air expands and cools, the cloud cannot hold moisture as well as a warm cloud, and some of the moisture will fall as rain on the windward slope and on the summit.
OSM	oncostatin M, a cytokine
OSPM	Operational Street Pollution Model
OVA	ovalbumin
oxLDL	oxidation of LDL, marker of oxidative stress
8-oxodG	8-oxo-7-hydrodeoxyguanosine
ox-PAPC	oxidized 1-palmitoyl-2-arachidonoyl-sn-glycero-3-phosphorylcholine (an atherogenic oxidized phospholipid)
P450	cytochrome P450
P450c17	cytochrome P450 17- α -hydroxylase
P450scc	cytochrome P450 cholesterol side chain cleavage enzyme
P90	90th percentile of the absolute difference in concentrations
P90	Printex 90, industrial (Degussa) carbon black ultrafine particles
p	probability value
P	phosphorus
PA	photoacoustic analyzer, physical activity, plasminogen activator, pulmonary arterial, alveolar pressure
PAF	platelet-activating factor

PAH	polycyclic aromatic hydrocarbon(s)
PAI	plasminogen activator inhibitor, (e.g. PAI-1)
PALMS	NOAA Particle Analysis by Laser Mass Spectrometry instrument
PAMCHAR	Chemical and Biological Characterisation of Ambient Air Coarse, Fine, and Ultrafine Particles for Human Health Risk Assessment in Europe
PAMS	Photochemical Assessment Monitoring Stations network
PAR	photosynthetically active radiation
PAR(s)	Pulmonary Artery Rings
PARASOL	Polarization and Directionality of the Earth's Reflectances, coupled with observations from a Lidar, a CNES satellite
PARP	poly(ADP-ribose) polymerase
PAS	Periodic Acid Schiff stain
Pb	lead
²⁰⁷ Pb	lead-207
PBDE	polybrominated diphenyl ether
PBL	planetary boundary layer
PBMC	peripheral blood mononuclear cell
PBMM	peripheral blood monocyte-derived macrophages
PBP	primary biological particle(s)
PBS	phosphate buffered saline
PC	synthetic carboxylate-modified particles
PCA	principal component analysis
PCA-MPSP	positively-charged amine modified polystyrene particle
PCB	polychlorinated biphenyl(s)
PCDD	polychlorinated dibenzo-p-dioxin
PCIS	Personal Cascade Impactor Sampler
PCM	NCAR Parallel Climate Model
PCPSP	positively charged polystyrene particle
PCR	polymerase chain reaction
PDF	probability distribution functions
pDR	personal DataRam
PE	post exposure, post exercise, phenylephrine
PEACE	Pollution Effects on Asthmatic Children in Europe study
PEC	particulate elemental carbon
PECAM-1	platelet endothelial cell adhesion molecule 1
pedogenesis	soil evolution or soil formation - the process in which soil is created

PEF	peak expiratory flow (L/min)
PEFR	peak expiratory flow rate
PEFT	time to peak flow
PEM	personal exposure monitor
PEM-West	NASA Pacific Exploratory Missions in the western Pacific
Penh	enhanced pause (altered ventilatory timing)
Per	perylene
PESA	particle elastic scattering analysis
PFDE	particle free diesel exhaust
PGE ₂	prostaglandin E ₂
PGI ₂	prostacyclin
pH	scale of acidity (log of hydrogen ion concentration); decreased breath pH is a biomarker for airway inflammation
Phe	phenanthrene
photoacoustic	based on the photoacoustic effect (thin discs emit sound when exposed to laser beams, with the sound proportional to the light intensity) photoacoustic spectroscopy is a sensitive technique to study concentrations of gases down to the ppb or ppt levels
photopic	photopic vision, the vision of the eye under well-lit conditions
Phytochelatin	oligomers of glutathione, produced by the enzyme phytochelatase. They are found in plants, fungi, nematodes, and all groups of algae, including all groups of algae, including cyanobacteria. Phytochelatin act as chelators and are important for heavy metal detoxification.
PI	post instillation, posterior interval, pulmonary inflammation
PICT	pollution-induced community tolerance
PILS	Particle Into Liquid Sampler
PILS-IC	Particle Into Liquid Sampler-Ion Chromatography
PIXE	Particle Induced X-ray Emission
PKA	protein kinase A/cAMP-dependent protein kinase
planet brightening	an increase in the amount of sunlight reaching the planet's land surface
planet dimming	a decrease in the amount of sunlight reaching the planet's land surface
PLS	partial least squares, projection to latent structures
PM	particulate matter
PM _x	particulate matter of a specific size range. X refers to the diameter at which the sampler collects 50% of the particles and rejects 50% of the particles. Collection efficiency increases for particles with smaller diameters and decreases for particles with larger diameters. The variation of collection efficiency with size is given by a collection efficiency curve. The definition of PM _x is frequently abbreviated as "particles with a nominal mean aerodynamic diameter less than or equal to x μm.

PM _{x-y}	particulate matter with a nominal mean diameter greater than x μm and less than y μm where x and y are the numeric mean aerodynamic or mobility diameters (μm).
PM _{0.1}	particulate matter with a nominal mean mobility diameter less than or equal to 0.1 μm (referred to as ultrafine PM)
PM _{2.5}	particulate matter with a nominal mean aerodynamic diameter less than or equal to 2.5 μm (referred to as fine PM)
PM ₁₀	particulate matter with a nominal mean aerodynamic diameter less than or equal to 10 μm
PM _{10-2.5}	particulate matter with a nominal mean aerodynamic diameter greater than 2.5 μm and less than or equal to 10 μm (referred to as thoracic coarse particulate matter or the coarse fraction of PM ₁₀) Concentration may be measured with a dichotomous sampler or calculated as the difference between measured PM ₁₀ and measured PM _{2.5} concentrations.
PMA	phorbol 12-myristate 13-acetate
PMF	particulate matter filtrate, positive matrix factorization
PM-HD	particulate matter at high concentration
PM-LD	particulate matter at low concentration
PMN	polymorphonuclear leukocytes
PN	particle number
PNC	particle number concentration, particle number count
PND, pnd	post-natal day
PNMD	particle number median diameter
PNN	proportion of interval differences of successive normal-beat intervals in EKG
pNN50	proportion of interval differences of successive normal-beat intervals greater than 50 ms in an EKG
PNNL	DOE Pacific Northwest National Laboratory
pNO ₃	particulate nitrate
POA	primary organic aerosol
POC	particulate organic carbon
polarimeter	a laboratory instrument used to determine the angle of optical rotation of plane-polarized light passing through a sample of material
POLDER	CNES satellite - POLarization and Directionality of the Earth's Reflectance
polymorphism	an inherited genetic variation occurring in a population
POM	particulate organic matter
POP	persistent organic pollutant
P _p	particle density
PP	pulse pressure
ppb	parts per billion

PPFL	percent predicted lung function
ppm	parts per million
ppt	parts per trillion
PRB	policy-relevant background
PRE	AeroCom Experiment
PRELC	Primary Rat Epithelial Lung Cells
PRIDE	NASA Puerto Rico Dust Experiment
PS	public school
PSAS	The French National Program on Air Pollution Health Effects
PSO	Public Service Company of Oklahoma (subsidiary of American Electric Power)]
pSO ₄	particulate sulfate
PSS	physiologic saline solution
PSU	Pennsylvania State University
PT	prothrombin time
PTT	partial thromboplastin time
PTV	programmable temperature vaporization
PVD	peripheral vascular disease
Pyr	pyrene
Q	cardiac output
Q	coronary flow of the heart
QAI	QA interval (simple systolic time interval)
QBQ	backup quartz-fiber filter behind a quartz-fiber filter
QEEG	quantitative electroencephalography
Q_{ext}	the extinction coefficient (a function of particle size distribution and refractive index)
r	correlation coefficient
R^2	coefficient of determination
radiative forcing	a way to compare different causes of perturbations in a climate system, radiative forcing measures change in net irradiance (W/m ²) at the tropopause; atmospheric aerosols and particles can scatter and bounce incoming solar radiation back into space, resulting in negative radiative forcing (or absorb solar and infrared radiation, resulting in positive radiative forcing) on the climate system.
RAIN	Regional Aerosol Intensive Network, established by MANE-VU
RAMS	real-time total ambient mass sampler
RANTES	regulated upon activation, normal T cell expressed and secreted (a chemotactic cytokine)
RAPS/RAMS	Regional Air Pollution Study/ Regional Air Monitoring Study

RAR	rapidly activating receptor(s)
RASMC	rat aortic smooth muscle cells
RAW 264.7	mouse macrophage cell line
Rayleigh scattering	describes the elastic scattering of light by particles much smaller than the wavelength of the light. Rayleigh scattering of sunlight in a clear atmosphere is the main reason why the sky appears to be blue.
RBC	red blood cell
RD	respiratory disease
r_e	cloud drop effective radius r_e
REALM	Regional East Atmospheric Lidar Mesonet (REALM) in North America
RF	radiative forcing(s) measured in Watts per square meter (W/m^2) - the change in net irradiance at the tropopause. A positive forcing (more incoming energy) tends to warm the system, while a negative forcing (more outgoing energy) tends to cool it. Affected by variations in the amount of radiatively active gases and aerosols present.
r_{eff}	particle effective radius
restinga	a distinct type of ecoregion - coastal tropical and subtropical moist broadleaf forest found in Brazil. Restingas form on sandy, acidic, and nutrient-poor soils, and are characterized by medium sized trees and shrubs adapted to the drier and nutrient-poor conditions.
RFL	Fetal Lung Fibroblasts
RH	relative humidity
RHMVE	rat heart micro-vessel endothelial cell
rho(0)	rho(0) cells (cell lacking mitochondrial DNA)
RHR	Regional Haze Rule
RLF	rat lung fibroblasts
RMC	rat cardiomyocyte(s)
RME r	rapeseed oil methyl ester
RMSSD	root mean squared differences of successive normal-beat to normal-beat (NN or RR) time intervals between each QRS complex in the EKG, also referred to as: r-MSSD and rMSSD
RMV	respiratory minute volume
RNA	ribonucleic acid
RNS	reactive nitrogen species
RO	residual oil
ROCK	rho associated kinase
ROFA	residual oil fly ash (particles)
ROFA-L	residual oil fly ash leachate
ROI	reactive oxygen intermediates
ROS	reactive oxygen species

RPO	Regional Planning Organizations
RR	risk ratio, relative risk, normal-to-normal (NN or RR) time interval between each QRS complex in the EKG, using the R-wave peak as the reference point.
RS	resuspended soil
RSV	respiratory syncytial virus
RTI	respiratory tract infection
RTM	Radiative Transfer Model
RTP	Research Triangle Park, North Carolina
RV	right ventricular
RVCFB	right ventricular cardio fibroblasts
RVCM	right ventricular cardiomyopathy, rat ventricular cardiomyocytes, reduced volume culture medium
σ	sigma, standard deviation
1σ	one sigma; one standard deviation
σ_g	sigma-g; geometric standard deviation
s	second
S	sulfur
SAB	(EPA) Science Advisory Board
SAFARI	South African Fire-Atmosphere Research Initiative
SAGE	Stratospheric Aerosol and Gas Experiment
SALIA	German study on the Influence of Air Pollution on Lung Function, Inflammation, and Aging
SAM	Stratospheric Aerosol Measurement
SAMUM	NASA Saharan Mineral Dust Experiment
SAP2.3	(CCSP Final Report) Synthesis and Assessment Product 2.3, <i>Atmospheric Aerosol Properties and Climate Impacts</i> (CCSP Final Report)
Sb	antimony
SB	strand breaks
SBL	stable boundary layer
SBP	systolic blood pressure
Sc	scandium
SC	summer curbside particles
SCAB	California South Coast Air Basin
SCAR-A	NASA Smoke/Sulfates, Clouds and Radiation - America experiment
SCAR-B	NASA Sulfates, Clouds and Radiation - Brazil
SCARPOL	Swiss Study on Childhood Allergy and Respiratory Symptoms with Respect to Air Pollution

sCD40L	soluble CD40 ligand
SCE	sister chromatid exchange
SCS	Harvard Six Cities Study
Sd	standard deviation
SD	Sprague-Dawley rat
SDANN5	standard deviation of the average of normal to normal (N:N) intervals in all 5-min intervals in a 24-h period
SDNN	standard deviation normal-to-normal (NN or RR) time interval between each QRS complex in the EKG
SDNN24HR	standard deviation of the average of all normal to normal intervals in a 24-h period
Se	selenium
se	standard error
SEARCH	Southeastern Aerosol Research and Characterization
sem	standard error of mean
SEM	scanning electron microscopy
SES	socioeconomic status, sample equilibration system
Sess	Session of U.S. Congress
SF-1	steroidogenic factor -1
SF-UFID	suspension, particle free ultrafine industrial exhaust
SGA	small for gestational age
sGC	soluble guanylate cyclase
SGP	Southern Great Plains
-SH	sulfhydryl group
SH	Mount Saint Helen's ash
SH, SHR	spontaneously hypertensive disease model rat
SHADE	Saharan Dust Experiment
SHEDS	Stochastic Human Exposure and Dose Simulation model
shortwave albedo	the fraction of shortwave (solar) radiation reflected from the earth back into space
shortwave emissivity	a material's ability to emit or release the shortwave (solar) energy which it has absorbed
Si	silicon
sICAM-1	soluble intercellular adhesion molecule
SIDS	sudden infant death syndrome
SiO ₂	silicone dioxide
SIPS	State Implementation Plan
SJV	San Joaquin Valley

Skyglow	A kind of light pollution, human-made electrical lighting contributes to sky glow, visible by the "glowing" effect seen in the skies over many cities and towns as a dome of light. Light can be emitted directly upward or reflected from the ground and is scattered by dust and gas molecules in the atmosphere, producing a luminous background. It has the effect of reducing one's ability to view the stars.
SLAMS	State and Local Air Monitoring Stations
SME	soybean oil methyl ester
SMOCC	European Commission's Smoke Aerosols, Clouds, Rainfall and Climate (Aerosols from Biomass Burning Perturb Global and Regional Climate)
SMOKE	Spare-Matrix Operator Kernel Emissions system
SMPS	scanning mobility particle sizer
SMPS-APS	scanning mobility particle sizer-- aerodynamic particle sizer (in tandem)
SMRA	small mesenteric rat arteries
SNP	single-nucleotide polymorphism, sodium nitroprusside
SNS	sympathetic nervous system
SO ₂	sulfur dioxide
SO ₃	sulfur trioxide
SO ₄ ²⁻	sulfate
SOA	secondary organic aerosol
SOC	semi-volatile organic compound
SOD	superoxide dismutase
SOPHIA	Study of Particulates and Health in Atlanta
SO _x	sulfur oxides, oxides of sulfur
SP	surfactant protein (e.g., SPA, SPD)
SPA	surfactant protein A (present in lung surfactant)
SPD	surfactant protein D (present in lung surfactant)
SPEW	Speciated Pollutant Emission Wizard
SPG	Southern Great Plains site established by DOE's ARM Program.
SPM	suspended particulate matter
SPRINTARS	Spectral Radiation-Transport Model for Aerosol Species
SRM-154b	NIST standard reference material 154b; (TiO ₂ Titanium dioxide)
SRM1648	NIST standard reference material 1648; (urban particulate matter)
SRM-1649	NIST standard reference material 1649 (Washington, D. C. urban air particulate matter, urban dust)
SRM-1650	NIST standard reference material 1650 (diesel exhaust particulate matter)
SRM-1879	NIST standard reference material 1859; (silicon dioxide, respirable cristobalite [respirable crystalline silica])

SRM-2975	NIST standard reference material 2975 (diesel exhaust particulate matter)
s-ROFA	soluble portion of residual oil fly ash
SS	secondary sulfate, sea salt
SSA	single-scattering albedo (the ratio of scattering efficiency to total light extinction, or a sum of scattering and absorption)
SSR	standardized sex ratio
SST	sea surface temperature
STEM	Sulfur / Sulfate Transport Eulerian Model
stemflow	during precipitation (rain, snow, etc.) when the plant, forest system, ecosystem can hold no more, the water will drip from the plant (throughfall) or run down the stem (stemflow) before reaching the ground
STN	EPA Speciation Trend Network
Stokes velocity	the terminal velocity at which a sphere of a given density will sink (or rise) in a medium of a given density.
STP	standard temperature and pressure
STZ	Streptozotocin
SUB	summer urban background particles
Sunglint	an area of a satellite image viewing the ocean surface, which appears smooth and silver, due to the sun reflecting off the surface of the ocean at the same angle as the satellite
SURFRAD	NOAA GMD Surface Radiation network
SVA	supraventricular arrhythmia
sVCAM-1	soluble vascular adhesion molecule 1
SVEB	supraventricular ectopic beats
SWNT	singlewalled nanotube
SXRF	Synchrotron X-ray fluorescence
SZA	solar zenith angle
τ	photochemical lifetime
T	body temperature
TAR	IPCC 3rd Assessment Report
TARC	thymus and activation-regulated chemokine
TARFOX	Tropospheric Aerosol Radiative Forcing Observational Experiment
TAT	thrombin-anti-thrombin complexes
TB	tracheobronchial region of the respiratory tract
TBA	thiobarbituric acid
TBAP	tetrakis(4-benzoic acid) porphyrin
TBARS	thiobarbituric acid reactive substances

TBQ	backup quartz-fiber filter behind a Teflon-membrane filter
^{99m} Tc	Technetium-99m
^{99m} Tc-DMTA	^{99m} Tc Dynamic mechanical thermal analysis
^{99m} Tc-DTPA	^{99m} Tc-diethylenetriaminepentaacetic acid
T _{co}	core temperature
TD	thermal desorption, tire debris extracted in methanol
TD-GC/MS	thermal desorption-gas chromatography/mass spectrometry
TEAC	Trolox Equivalent Antioxidant Capacity assay
TEOM	Tapered Element Oscillating Microbalance
Terra	multi-national, multi-disciplinary satellite mission involving partnerships between NASA and the aerospace agencies of Canada and Japan
TexAQs	Texas Air Quality Field Study
TF	tissue factor
TFPI	tissue factor pathway inhibitor
Tg	teragram (one trillion grams 1 x 10 ¹² grams; one billion kilograms 1 x 10 ⁹ kg; one million metric tons)
TG	terminal ganglion (neurons)
TGF	transforming growth factor
TGF β	β transforming growth factor
Th	thorium
Th1	T helper cell type 1
Th2	T helper cell type 2
tHcy	total homocysteine
throughfall	during precipitation (rain, snow, etc.) when the plant, forest system, ecosystem can hold no more, the water will drip from the plant (throughfall) or run down the stem (stemflow) before reaching the ground
Ti	titanium
TIA	transient ischemic attack
TiFe	iron-loaded fine titanium oxide
TIMP-2	tissue inhibitor of MMP
TiO ₂	titanium dioxide
TK	thymidine kinase
TM	transition metals
TM5	Thematic Mapper, a sensor on Landsat5 satellite, for mapping temporal-spatial dynamics
TMTU	tetramethylthiourea
TNF-α	tumor necrosis factor alpha

TOA	top of the atmosphere
TOF-SIMS	time-of-flight - secondary ion mass spectrometry
TOMS	Total Ozone Mapping Spectrometer
TOT/GC	thermal optical transmission analyzer coupled with gas chromatography
TOVS	TIROS-N Operational Vertical Sounder
toxaphene	an insecticide used before 1982, not used in U.S. after 1990
tPA, t-PA	tissue plasminogen activator
TRACE	Transition Region and Coronal Explorer (satellite)
TRACE-A	Transport and Chemical Evolution Over the Atlantic
TRACE-P	Transport and Chemical Evolution Over the Pacific mission model
Transmissometer	an instrument for approximating the visual range, by measuring the extinction coefficient of the atmosphere at the middle of the visible waveband (550 nm). Also called hazemeter, or transmittance meter.
TRP	transient receptor potential family of ion channels
TRPV1	transient receptor potential vanilloid-1 receptor
TR-XRF	total reflection X-ray fluorescence
TSA	trichostatin A
TSP	total suspended particulate
TSP-10	total suspended particulates up to 10 μm
TSS	WRAP Technical Support System website
TVOC	total VOC
Twomey effect	first "indirect" climate effect; an increase in cloud brightness (describes how aerosols and cloud condensation nuclei from anthropogenic pollution may increase the amount of solar radiation reflected by clouds, changing cloud brightness)
TWP	Tropical West Pacific island
TXB ₂	thromboxane B-2
U	uranium
UACR	urinary albumin / creatinine ratio
UAE ²	United Arab Emirates Unified Aerosol Experiment
UAP	urban ambient particle
UF	ultrafine, uncertainty factor
UFAA	ultrafine ambient air
UFC	ultrafine carbon
UfCB	ultrafine carbon black
UFDG	ultrafine diesel engine exhaust
UFID	ultrafine industrial exhaust

UFP	ultrafine particle
UFPM	ultrafine particulate matter
UFTiO ₂	ultrafine titanium dioxide
UIO	University of Oslo
U.K.	United Kingdom
UKMO	United Kingdom Meteorological Office
ULAQ	University of IL'Aquila.
ULTRA	Exposure and Risk Assessment for Fine and Ultrafine Particles in Ambient Air (study)
UMI	University of Michigan
UNEP	United Nations Environmental Programme
UP	urban particle
UPM	ultrafine particulate matter
UPSP	unmodified polystyrene particle(s)
upwelling	when ocean winds cause surface water to move away from a coastline the deeper, colder water will move upward to the surface, creating a upwelling current; which brings replenishing nutritional components to the surface
URI	upper respiratory infection
URS	upper respiratory symptoms
U.S.	United States of America
USC, U.S.C.	U.S. Code
UV	ultraviolet radiation
V	vanadium
V, mV, μ V	volt, millivolt, microvolt
VAQ	visual air quality, used here to refer to the visibility effects caused solely by air quality conditions, so for example it excludes the reduced visibility caused by fog
VCAM-1	vascular adhesion molecule 1
V _a	deposition velocity
VEAPS	Vitamin E Atherosclerosis Progression Study
VEGF	vascular endothelial growth factor
VEWS	Visibility Information Exchange Web Site, ambient monitoring data system,
VISTAS	Visibility Improvement State and Tribal Association of the Southeast
VOC	volatile organic compound
VOSO ₄	vanadyl sulfate
VPB	ventricular premature beat
VR	visual range

VR1	vanilloid receptor 1
VSCC	very sharp cut cyclone
VSMC	Vascular Smooth Muscle Cells
V_T	tidal volume
vWF	von Willebrand factor
W	Wilderness
WACAP	Western Airborne Contaminates Assessment Project
WBC	white blood cell(s)
WC	winter curbside particles
WHI	Women's Health Initiative
WHI OS	Women's Health Initiative Observational Study
WinHaze	imaging software from ARS, simulates visual air quality differences of various scenes
wk	week(s)
WKY	Wistar-Kyoto rat strain
W/m ² , W m ⁻²	watts per square meter
WMO	World Meteorological Organization
Wnt	wingless gene family, encoding oncogenesis signaling pathways (e.g., Wnt-4, Wnt-7a [MMTV integration site family, member 4 or 7a])
WRAP	Western Regional Air Partnership
WRF	Weather Research and Forecasting model
WS	wood smoke
WSOC	water soluble organic carbon
WUB	winter urban background particles
XAD	polystyrene-divinyl benzene
XPS	X-ray photoelectron spectroscopy
Y	yttrium
yr	year
Z	radar reflectivity (measured in dBZ [decibels of Z, where Z represents the energy reflected back to the radar.]
Zn	zinc
ZnO	zinc oxide
ZnS	zinc sulfide
ZnSO ₄	zinc sulfate
Zr	zirconium

Chapter 1. Introduction

1 The second external review draft Integrated Science Assessment (ISA) is a review,
2 synthesis, and evaluation of the most policy-relevant evidence, and communicates critical
3 science judgments relevant to the National Ambient Air Quality Standards (NAAQS)
4 review. As such, the ISA forms the scientific foundation for the review of the primary
5 (health-based) and secondary (welfare-based) NAAQS for particulate matter (PM). The ISA
6 accurately reflects “the latest scientific knowledge useful in indicating the kind and extent
7 of identifiable effects on public health which may be expected from the presence of [a]
8 pollutant in ambient air” (42 U.S.C. 7408). Key information and judgments formerly
9 contained in an Air Quality Criteria Document (AQCD) for PM are incorporated in this
10 assessment. Additional details of the pertinent literature published since the last review, as
11 well as selected older studies of particular interest, are included in a series of annexes. This
12 ISA thus serves to update and revise the evaluation of the scientific evidence available at
13 the time of the previous review of the NAAQS for PM that was concluded in 2006.

14 The *Integrated Review Plan for the National Ambient Air Quality Standards for*
15 *Particulate Matter* identifies a series of policy-relevant questions that provide a framework
16 for this assessment of the scientific evidence (U.S. EPA, 2008, [157072](#)). These questions
17 frame the entire review of the NAAQS for PM, and thus are informed by both science and
18 policy considerations. The ISA organizes and presents the scientific evidence such that,
19 when considered along with findings from risk analyses and policy considerations, will help
20 the EPA address these questions during the NAAQS review for PM. In evaluating the
21 health evidence, the focus of this assessment will be on scientific evidence that is most
22 relevant to the following questions that have been taken directly from the Integrated
23 Review Plan:

- 24 ▪ Has new information altered the body of scientific support for the occurrence of
25 health effects following short- and/or long-term exposure to levels of fine and
26 thoracic coarse particles found in the ambient air?

- 27 ▪ Has new information altered conclusions from previous reviews regarding the
28 plausibility of adverse health effects associated with exposures to PM_{2.5}, PM₁₀, PM_{10-2.5},
29 or alternative PM indicators that might be considered?

- 30 ▪ What evidence is available from recent studies focused on specific size fractions,
31 chemical components, sources, or environments (e.g., urban and non-urban areas) of

Note: Hyperlinks to the reference citations throughout this document will take you to the NCEA HERO database (Health and Environmental Research Online) at <http://epa.gov/hero>. HERO is a database of scientific literature used by U.S. EPA in the process of developing science assessments such as the Integrated Science Assessments (ISA) and the Integrated Risk Information System (IRIS).

1
2
3
4
5
6
7
8
9
10
11
12
13
14
15
16
17
18
19
20
21
22
23
24
25
26
27
28
29
30
31
32
33
34

- To what extent is key scientific evidence becoming available to improve our understanding of the health effects associated with various time periods of PM exposures, including not only short-term (daily or multi-day) and chronic (months to years) exposures, but also peak PM exposures (less than 24 hours)? To what extent is critical research becoming available that could improve our understanding of the relationship between various health endpoints and different lag periods (e.g., less than one day, single day, multi-day distributed lags)?
- What data are available to improve our understanding of spatial and/or temporal heterogeneity of PM exposures considering different size fractions and/or components?
- At what levels of PM exposure do health effects of concern occur? Is there evidence for the occurrence of adverse health effects at levels of PM lower than those observed previously? If so, at what levels and what are the important uncertainties associated with that evidence? What is the nature of the dose-response relationships of PM for the various health effects evaluated?
- What evidence is available linking particle number concentration with adverse health effects of ultrafine particles?
- Do risk/exposure estimates suggest that exposures of concern for PM-induced health effects will occur with current ambient levels of PM or with levels that just meet the current standards? If so, are these risks/exposures of sufficient magnitude such that the health effects might reasonably be judged to be important from a public health perspective? What are the important uncertainties associated with these risk/exposure estimates?
- To what extent is key evidence becoming available that could inform our understanding of subpopulations that are particularly sensitive or vulnerable to PM exposures? In the last review, sensitive or vulnerable subpopulations that appeared to be at greater risk for PM-related effects included individuals with pre-existing heart and lung diseases, older adults, and children. Has new evidence become available to suggest additional sensitive subpopulations should be given increased focus in this review (e.g., fetuses, neonates, genetically susceptible subpopulations)?
- To what extent is key evidence becoming available to inform our understanding of populations that are particularly vulnerable to PM exposures? Specifically, is there

1
2
3
4
5
6
7
8
9
10
11
12
13
14
15
16
17
18
19
20
21
22
23
24
25
26
27
28
29
30
31
32

- To what extent have important uncertainties identified in the last review been reduced and/or have new uncertainties emerged?
- To what extent is new information available to inform our understanding of non-PM-exposure factors that might influence the associations between PM levels and health effects being considered (e.g., weather-related factors; behavioral factors such as heating/air conditioning use; driving patterns; and time-activity patterns)?

In evaluating evidence on welfare effects of PM, the focus will be on evidence that can help inform these questions from the Integrated Review Plan:

- What new evidence is available on the relationship between PM mass/size fraction and/or specific PM components and visibility impairment and climate-related and other welfare effects?
- To what extent has key scientific evidence now become available to improve our understanding of the nature and magnitude of visibility, climate, and ecosystem responses to PM and the variability associated with those responses (including ecosystem type, climatic conditions, environmental effects and interactions with other environmental factors and pollutants)?
- Do the evidence, the air quality assessment, and the risk/exposure assessment provide support for considering alternative averaging times?
- At what levels of ambient PM do visibility impairment and/or environmental effects of concern occur? Is there evidence for the occurrence of adverse visibility and other welfare-related effects at levels of PM lower than those observed previously? If so, at what levels and what are the important uncertainties associated with the evidence?
- Do the analyses suggest that PM-induced visibility impairment and/or other welfare-effects will occur with current ambient levels of PM or with levels that just meet the current standards? If so, are these effects of sufficient magnitude and/or frequency such that these effects might reasonably be judged to be important from a public welfare perspective? What are the uncertainties associated with these estimates?
- What new evidence and/or techniques are available to quantify the benefits of improved visibility and/or other welfare-related effects?

- 1 ▪ To what extent have important uncertainties identified in the last review been
2 reduced and/or have new uncertainties emerged?

1.1. Legislative Requirements

3 Two sections of the Clean Air Act (CAA, the Act) govern the establishment and
4 revision of the NAAQS. Section 108 of the Act (42 U.S.C. 7408) directs the Administrator to
5 identify and list “air pollutants” that “in his judgment, may reasonably be anticipated to
6 endanger public health and welfare” and whose “presence... in the ambient air results from
7 numerous or diverse mobile or stationary sources” and to issue air quality criteria for those
8 that are listed (42 U.S.C. 7408). Air quality criteria are intended to “accurately reflect the
9 latest scientific knowledge useful in indicating the kind and extent of identifiable effects on
10 public health or welfare which may be expected from the presence of [a] pollutant in
11 ambient air...” 42 U.S.C. 7408(b).

12 Section 109 of the Act (42 U.S.C. 7409) directs the Administrator to propose and
13 promulgate “primary” and “secondary” NAAQS for pollutants listed under Section 108. 42
14 U.S.C. 7409(a). Section 109(b)(1) defines a primary standard as one “the attainment and
15 maintenance of which in the judgment of the Administrator, based on such criteria and
16 allowing an adequate margin of safety, are requisite to protect the public health.”¹ 42 U.S.C.
17 7409(b)(1). A secondary standard, as defined in Section 109(b)(2), must “specify a level of air
18 quality the attainment and maintenance of which, in the judgment of the Administrator,
19 based on such criteria, is required to protect the public welfare from any known or
20 anticipated adverse effects associated with the presence of [the] pollutant in the ambient
21 air.”² 42 U.S.C. 7409(b)(2).

22 The requirement that primary standards include an adequate margin of safety was
23 intended to address uncertainties associated with inconclusive scientific and technical
24 information available at the time of standard setting. It was also intended to provide a
25 reasonable degree of protection against hazards that research has not yet identified. See
26 *Lead Industries Association v. EPA*, 647 F.2d 1130, 1154 (D.C. Cir 1980), cert. denied, 449
27 U.S. 1042 (1980); *American Petroleum Institute v. Costle*, 665 F.2d 1176, 1186 (D.C. Cir.
28 1981), cert. denied, 455 U.S. 1034 (1982); *American Farm Bureau Federation v. EPA*, 559 F.
29 3d 512, 533 (D.C. Cir. 2009). Both kinds of uncertainties are components of the risk
30 associated with pollution at levels below those at which human health effects can be said to
31 occur with reasonable scientific certainty. Thus, in selecting primary standards that include

¹ The legislative history of section 109 indicates that a primary standard is to be set at “the maximum permissible ambient air level...which will protect the health of any [sensitive] group of the population,” and that for this purpose “reference should be made to a representative sample of persons comprising the sensitive group rather than to a single person in such a group” [S. Rep. No. 91-1196, 91st Cong., 2d Sess. 10 (1970)].

² Welfare effects as defined in Section 302(h) [42 U.S.C. 7602(h)] include, but are not limited to, “effects on soils, water, crops, vegetation, man-made materials, animals, wildlife, weather, visibility and climate, damage to and deterioration of property, and hazards to transportation, as well as effects on economic values and on personal comfort and well-being.”

1 an adequate margin of safety, the Administrator is seeking not only to prevent pollution
2 levels that have been demonstrated to be harmful but also to prevent lower pollutant levels
3 that may pose an unacceptable risk of harm, even if the risk is not precisely identified as to
4 nature or degree.

5 In selecting a margin of safety, the EPA considers such factors as the nature and
6 severity of the health effects involved, the size of the sensitive population(s) at risk, and the
7 kind and degree of the uncertainties that must be addressed. The selection of any particular
8 approach to providing an adequate margin of safety is a policy choice left specifically to the
9 Administrator’s judgment. See *Lead Industries Association v. EPA*, supra, 647 F.2d 1161-62.

10 In setting standards that are “requisite” to protect public health and welfare, as
11 provided in Section 109(b), the Administrator’s task is to establish standards that are
12 neither more nor less stringent than necessary. In so doing, EPA may not consider the costs
13 of implementing the standards. See generally *Whitman v. American Trucking Associations*,
14 531 U.S. 457, 465-472, 475-76 (2001).

15 Section 109(d)(1) requires that “not later than December 31, 1980, and at 5-yr
16 intervals thereafter, the Administrator shall complete a thorough review of the criteria
17 published under Section 108 and the national ambient air quality standards...and shall
18 make such revisions in such criteria and standards and promulgate such new standards as
19 may be appropriate...” 42 U.S.C. 7409(d)(1). Section 109(d)(2) requires that an independent
20 scientific review...committee “shall complete a review of the criteria and the national
21 primary and secondary ambient air quality standards...and shall recommend to the
22 Administrator any new standards and revisions of existing criteria and standards as may
23 be appropriate...” 42 U.S.C. 7409(d)(2). Since the early 1980s, this independent review
24 function has been performed by the Clean Air Scientific Advisory Committee (CASAC).

1.2. History of Reviews of the NAAQS for PM

25 PM is the generic term for a broad class of chemically and physically diverse
26 substances that exist as discrete particles (liquid droplets or solids) over a wide range of
27 sizes. Particles originate from a variety of anthropogenic stationary and mobile sources as
28 well as from natural sources. Particles may be emitted directly or formed in the atmosphere
29 by transformations of gaseous emissions such as sulfur oxides (SO_x), nitrogen oxides (NO_x),
30 and volatile organic compounds (VOC). The chemical and physical properties of PM vary
31 greatly with time, region, meteorology, and source category, thus complicating the
32 assessment of health and welfare effects. Table 1-1 summarizes the NAAQS that have been
33 promulgated for PM to date. These reviews are briefly described below, and further details
34 are provided in the Integrated Review Plan (U.S. EPA, 2008, [157072](#)).

Table 1-1. Summary of NAAQS promulgated for PM, 1971-2006.

Final Rule	Indicator	Avg Time	Level	Form
1971 (36 FR 8186)	TSP (Total Suspended Particulates)	24-h	260 $\mu\text{g}/\text{m}^3$ (primary) 150 $\mu\text{g}/\text{m}^3$ (secondary)	Not to be exceeded more than once per yr
		Annual	75 $\mu\text{g}/\text{m}^3$ (primary)	Annual geometric mean
1987 (52 FR 24634)	PM ₁₀	24-h	150 $\mu\text{g}/\text{m}^3$	Not to be exceeded more than once per yr on average over a 3-yr period
		Annual	50 $\mu\text{g}/\text{m}^3$	Annual arithmetic mean, averaged over 3 yrs
1997 (62 FR 38652)	PM _{2.5}	24-h	65 $\mu\text{g}/\text{m}^3$	98th percentile, averaged over 3 yrs
		Annual	15 $\mu\text{g}/\text{m}^3$	Annual arithmetic mean, averaged over 3 yrs ¹
	PM ₁₀	24-h	150 $\mu\text{g}/\text{m}^3$	Initially promulgated 99th percentile, averaged over 3 yrs; when 1997 standards were vacated in 1999, the form of 1987 standards remained in place (not to be exceeded more than once per yr on average over a 3-yr period)
		Annual	50 $\mu\text{g}/\text{m}^3$	Annual arithmetic mean, averaged over 3 yrs
2006 (71 FR 61144)	PM _{2.5}	24-h	35 $\mu\text{g}/\text{m}^3$	98th percentile, averaged over 3 yrs
		Annual	15 $\mu\text{g}/\text{m}^3$	Annual arithmetic mean, averaged over 3 yrs ²
	PM ₁₀	24-h	150 $\mu\text{g}/\text{m}^3$	Not to be exceeded more than once per yr on average over a 3-yr period

Note: When not specified, primary and secondary standards are identical.

1 EPA first established NAAQS for PM in 1971 (36 FR 8186, April 30, 1971), based on
 2 the original criteria document (NAPCA, 1969, [014684](#)). The reference method specified for
 3 determining attainment of the original standards was the high-volume sampler, which
 4 collects PM up to a nominal size of 25 to 45 micrometers (μm) (referred to as total
 5 suspended particulates or TSP). The primary standards (measured by the indicator TSP)
 6 were 260 $\mu\text{g}/\text{m}^3$ ($\mu\text{g}/\text{m}^3$), 24-h avg, not to be exceeded more than once per year, and 75 $\mu\text{g}/\text{m}^3$,
 7 annual geometric mean. The secondary standard was 150 $\mu\text{g}/\text{m}^3$, 24-h avg, not to be
 8 exceeded more than once per year. In October 1979 (44 FR 56730, October 2, 1979), EPA
 9 announced the first periodic review of the air quality criteria and NAAQS for PM, and
 10 significant revisions to the original standards were promulgated in 1987 (52 FR 24634, July
 11 1, 1987). In that decision, EPA changed the indicator for particles from TSP to PM₁₀, the
 12 latter including particles with a mean aerodynamic diameter³ less than or equal to 10 μm ,
 13 which delineated that subset of inhalable particles small enough to penetrate to the
 14 thoracic region (including the tracheobronchial and alveolar regions) of the respiratory tract

¹ The level of the 1997 annual PM_{2.5} standard was to be compared to measurements made at the community-oriented monitoring site recording the highest level, or, if specific constraints were met, measurements from multiple community-oriented monitoring sites could be averaged ("spatial averaging"). This approach was judged to be consistent with the short-term epidemiologic studies on which the annual PM_{2.5} standard was primarily based, in which air quality data were generally averaged across multiple monitors in an area or were taken from a single monitor that was selected to represent community-wide exposures, not localized "hot spots" (62 FR 38672). These criteria and constraints were intended to ensure that spatial averaging would not result in inequities in the level of protection afforded by the PM_{2.5} standards. Community-oriented monitoring sites were specified to be consistent with the intent that a spatially averaged annual standard provide protection for persons living in smaller communities, as well as those in larger population centers.

² In the revisions to the PM NAAQS finalized in 2006, EPA tightened the constraints on the spatial averaging criteria by further limiting the conditions under which some areas may average measurements from multiple community-oriented monitors to determine compliance (see 71 FR 61165-61167, October 17, 2006).

³ The more precise term is 50% cut point or 50% diameter (d_{50}). This is the aerodynamic particle diameter for which the efficiency of particle collection is 50%. Larger particles are not excluded altogether, but are collected with substantially decreasing efficiency and smaller particles are collected with increasing (up to 100%) efficiency.

1 (referred to as thoracic particles). EPA also revised the level and form of the primary
2 standards by (1) replacing the 24-h TSP standard with a 24-h PM₁₀ standard of 150 µg/m³
3 with no more than one expected exceedence per year; and (2) replacing the annual TSP
4 standard with a PM₁₀ standard of 50 µg/m³, annual arithmetic mean, averaged over three
5 years.

6 The secondary standard was revised by replacing it with 24-h and annual standards
7 identical in all respects to the primary standards. The revisions also included a new
8 reference method for the measurement of PM₁₀ in the ambient air and rules for determining
9 attainment of the new standards. On judicial review, the revised standards were upheld in
10 all respects. *Natural Resources Defense Council v. Administrator*, 902 F. 2d 962 (D.C. Cir.
11 1990), cert. denied, 498 U.S. 1082 (1991).

12 In April 1994, EPA announced its plans for the second periodic review of the air
13 quality criteria and NAAQS for PM, and promulgated significant revisions to the NAAQS in
14 1997 (62 FR 38652, July 18, 1997). In that decision, EPA revised the PM NAAQS in several
15 respects. Most significantly, EPA determined that the fine and coarse¹ fractions of PM₁₀
16 should be considered separately. The Administrator's decision to modify the standards was
17 based on evidence that serious health effects were associated with short- and long-term
18 exposure to fine particles in areas that met the existing PM₁₀ standards. EPA accordingly
19 added new standards, using PM_{2.5} as the indicator for fine particles (with PM_{2.5} referring to
20 particles with a nominal mean aerodynamic diameter less than or equal to 2.5 µm), and
21 PM₁₀ as the indicator for thoracic coarse particles or coarse-fraction particles (generally
22 including particles with a nominal mean aerodynamic diameter greater than 2.5 µm and
23 less than or equal to 10 µm, or PM_{10-2.5}). The EPA established two new PM_{2.5} standards: an
24 annual standard of 15 µg/m³, based on the 3-yr avg of annual arithmetic mean PM_{2.5}
25 concentrations from single or multiple community-oriented monitors; and a 24-h standard
26 of 65 µg/m³, based on the 3-yr avg of the 98th percentile of 24-h PM_{2.5} concentrations at
27 each population-oriented monitor within an area. Also, EPA established a new reference
28 method for measuring PM_{2.5} in the ambient air and adopted protocols for determining
29 attainment of the new standards. To continue to address thoracic coarse particles, EPA
30 retained the annual PM₁₀ standard, while revising the form, but not the level, of the 24-h
31 PM₁₀ standard to be based on the 99th percentile of 24-h PM₁₀ concentrations at each
32 monitor in an area. The EPA revised the secondary standards by making them identical in
33 all respects to the primary standards.

34 Following promulgation of the 1997 PM NAAQS, petitions for review were filed by a
35 large number of parties, addressing a broad range of issues. In May 1999, a three-judge
36 panel of the U.S. Court of Appeals for the District of Columbia Circuit issued an initial
37 decision that upheld EPA's decision to establish fine particle standards, holding that "the
38 growing empirical evidence demonstrating a relationship between fine particle pollution

¹ See definitions of "fine" and "coarse" particles in Section 3.2.

1 and adverse health effects amply justifies establishment of new fine particle standards.”
2 *American Trucking Associations v. EPA* (175 F. 3d 1027, 1055-56 (D.C. Cir. 1999); rehearing
3 granted in part and denied in part, 195 F. 3d 4 (D.C. Cir. 1999), affirmed in part and
4 reversed in part, *Whitman v. American Trucking Associations* 531 U.S. 457 (2001). The
5 panel also found “ample support” for EPA’s decision to regulate coarse particle pollution, but
6 vacated the 1997 PM₁₀ standards, concluding that EPA had not provided a reasonable
7 explanation justifying use of PM₁₀ as an indicator for coarse particles (175 F. 3d at 1054-55).
8 Pursuant to the court’s decision, EPA removed the vacated 1997 PM₁₀ standards from the
9 Code of Federal Regulations. The pre-existing 1987 PM₁₀ standards remained in place (65
10 FR 80776, December 22, 2000). The Court also upheld EPA’s determination not to establish
11 more stringent secondary standards for fine particles to address effects on visibility (175 F.
12 3d at 1027).

13 More generally, the panel held (over one judge’s dissent) that EPA’s approach to
14 establishing the level of the standards in 1997, both for the PM and ozone (O₃) NAAQS
15 promulgated on the same day, effected “an unconstitutional delegation of legislative
16 authority” (id. at 1034-40). Although the panel stated that “the factors EPA uses in
17 determining the degree of public health concern associated with different levels of ozone
18 and PM are reasonable,” it remanded the rule to EPA, stating that when EPA considers
19 these factors for potential non-threshold pollutants “what EPA lacks is any determinate
20 criterion for drawing lines” to determine where the standards should be set. Consistent
21 with EPA’s long-standing interpretation and D.C. Circuit precedent, the panel also
22 reaffirmed its prior holdings that in setting NAAQS EPA is “not permitted to consider the
23 cost of implementing those standards” (id. at 1040-41).

24 On EPA’s petition for rehearing, the panel adhered to its position on these points.
25 *American Trucking Associations v. EPA*, 195 F. 3d 4 (D.C. Cir. 1999). The full Court of
26 Appeals denied EPA’s suggestion for rehearing en banc, with five judges dissenting (id. at
27 13).

28 Both sides filed cross appeals on these issues to the U.S. Supreme Court, and the
29 Court granted *certiorari*. In February 2001, the Supreme Court issued a unanimous
30 decision upholding EPA’s position on both the constitutional and cost issues. *Whitman v.*
31 *American Trucking Associations*, 531 U.S. 457, 464, 475-76. On the constitutional issue, the
32 Court held that the statutory requirement that NAAQS be “requisite” to protect public
33 health with an adequate margin of safety sufficiently guided EPA’s discretion, affirming
34 EPA’s approach of setting standards that are neither more nor less stringent than
35 necessary. The Supreme Court remanded the case to the Court of Appeals for resolution of
36 any remaining issues that had not been addressed in that court’s earlier rulings. Id. at
37 475-76. In March 2002, the Court of Appeals rejected all remaining challenges to the
38 standards, holding under the traditional standard of judicial review that PM_{2.5} standards

1 were reasonably supported by the administrative record and were not “arbitrary and
2 capricious” *American Trucking Associations v. EPA*, 283 F. 3d 355, 369-72 (D.C. Cir. 2002).

3 In October 1997, EPA published its plans for the third periodic review of the air
4 quality criteria and NAAQS for PM (62 FR 55201). After CASAC and public review, EPA
5 finalized the 2004 PM AQCD (U.S. EPA, 2004, [056905](#)) and 2005 Staff Paper (U.S. EPA,
6 2005, [090209](#)). For the primary fine particle standards, most CASAC PM Panel members
7 favored the option of revising the level of the 24-h PM_{2.5} standard in the range of 35 to 30
8 µg/m³ with a 98th percentile form, in concert with revising the level of the annual PM_{2.5}
9 standard in the range of 14 to 13 µg/m³ (Henderson, 2005, [188316](#)). Most of the members of
10 the CASAC PM Panel also strongly supported establishing a new, secondary PM_{2.5} standard
11 to protect urban visibility and recommended establishing a sub-daily (4- to 8-h averaging
12 time) PM_{2.5} standard within the range of 20 to 30 µg/m³ with a form within the range of the
13 92nd to 98th percentile (Henderson, 2005, [188316](#)). For thoracic coarse particles, there was
14 general concurrence among CASAC PM Panel members to revise the PM₁₀ standards by
15 establishing a primary standard specifically targeted to address particles in the size range
16 of 2.5 to 10 µm. The CASAC PM Panel was also in general agreement “that coarse particles
17 in urban or industrial areas are likely to be enriched by anthropogenic pollutants that tend
18 to be inherently more toxic than the windblown crustal material which typically dominates
19 coarse particle mass in arid rural areas.” Based on its review of the Staff Paper, there was
20 general agreement among the CASAC PM Panel members that a 24-h PM_{10-2.5} standard
21 with a level in the range of 50 to 70 µg/m³, with a 98th percentile form, was reasonably
22 justified and that a PM_{10-2.5} standard with an annual averaging time was not warranted
23 (Henderson, 2005, [156537](#)). On January 17, 2006, EPA proposed to revise the NAAQS for
24 PM (71 FR 2620). For fine particles, EPA proposed to retain PM_{2.5} as the indicator, to retain
25 standards for 24-h and annual exposures, and to revise the form of the annual standard to
26 tighten conditions for demonstrating compliance using spatially averaged monitoring. EPA
27 also proposed to revise the level of the 24-h PM_{2.5} standard to 35 µg/m³ to provide increased
28 protection against health effects associated with short-term PM_{2.5} exposures, including
29 premature mortality and increased hospital admission and emergency room visits, but
30 proposed to retain the level of the annual PM_{2.5} standard at 15 µg/m³, continuing protection
31 against health effects associated with long-term exposure including premature mortality
32 and development of chronic respiratory disease. With regard to the primary standards for
33 thoracic coarse particles, EPA proposed to revise the 24-h PM₁₀ standard in part by
34 establishing a new indicator for thoracic coarse particles (particles generally between 2.5
35 and 10 µm in PM_{10-2.5} diameter), qualified so as to include any ambient mix of PM_{10-2.5} that
36 was dominated by resuspended dust from high density traffic on paved roads and PM
37 generated by industrial sources and construction sources, and proposed to exclude any
38 ambient mix of PM_{10-2.5} that was dominated by rural windblown dust and soils and PM_{10-2.5}
39 generated by agricultural and mining sources. EPA also proposed a detailed monitoring

1 regime in conjunction with this proposed indicator. 71 FR 2710, 2731-42. The EPA proposed
2 to set a 24-h standard (using the proposed indicator) at a level of 70 $\mu\text{g}/\text{m}^3$ to continue to
3 provide a level of protection against health effects associated with short-term exposure
4 (including hospital admissions for cardiopulmonary diseases, increased respiratory
5 symptoms and possibly premature mortality) in those areas where the proposed indicator
6 was found, generally equivalent to the level of protection provided by the existing 24-h PM_{10}
7 standard. Also, EPA proposed to revoke, upon finalization of a primary 24-h standard for
8 thoracic coarse particles, the 24-h PM_{10} standard as well as the annual PM_{10} standard.

9 EPA proposed to revise the secondary standards by making them identical to the suite
10 of proposed primary standards for fine and coarse particles, providing protection against
11 PM-related public welfare effects including visibility impairment, effects on vegetation and
12 ecosystems, and materials damage and soiling. EPA also solicited comment on adding a new
13 sub-daily $\text{PM}_{2.5}$ secondary standard to address visibility impairment in urban areas.

14 CASAC provided additional advice to EPA in a letter to the Administrator requesting
15 reconsideration of CASAC's recommendations for both the primary and secondary $\text{PM}_{2.5}$
16 standards as well as standards for thoracic coarse particles (Henderson, 2006, [156538](#)).

17 On September 21, 2006, EPA announced its final decisions to revise the primary and
18 secondary NAAQS for PM to provide increased protection of public health and welfare,
19 respectively (71 FR 61144). With regard to the primary and secondary standards for fine
20 particles, EPA revised the level of the 24-h $\text{PM}_{2.5}$ standard to 35 $\mu\text{g}/\text{m}^3$, retained the level of
21 the annual $\text{PM}_{2.5}$ standard at 15 $\mu\text{g}/\text{m}^3$, and revised the form of the annual $\text{PM}_{2.5}$ standard
22 by narrowing the constraints on the optional use of spatial averaging. EPA established the
23 secondary standard for fine particles identical to the primary standards. With regard to the
24 primary and secondary standards for thoracic coarse particles, EPA retained PM_{10} as the
25 indicator for coarse particles, retained the level and form of the 24-h PM_{10} standard (so the
26 standard remains 150 $\mu\text{g}/\text{m}^3$ with a one expected exceedence form) and revoked the annual
27 standard because available evidence generally did not support a link between long-term
28 exposure to current ambient levels of coarse particles and health or welfare effects.

29 Following promulgation of the revised PM NAAQS in 2006, several parties filed
30 petitions for review with respect to: (1) selecting the level of the annual primary $\text{PM}_{2.5}$
31 standard; (2) setting the secondary $\text{PM}_{2.5}$ standards identical to the primary standards; (3)
32 retaining PM_{10} as the indicator for coarse particles and retaining the level and form of the
33 PM_{10} 24-h standard, and (4) revoking the PM_{10} annual standard. On judicial review, the
34 D.C. Circuit remanded the annual standard for fine particles to EPA because EPA failed to
35 adequately explain why the annual $\text{PM}_{2.5}$ standard provided the requisite protection from
36 both short- and long-term exposures to fine particles including protection for vulnerable
37 subpopulations. With respect to protection from short-term exposures, in 1997 EPA
38 determined that the annual standard was the generally controlling standard for lowering
39 both short- and long-term $\text{PM}_{2.5}$ concentrations and the 24-h standard was set to "provide

1 an adequate margin of safety against infrequent or isolated peak concentrations that could
2 occur in areas that attain the annual standard” (62 FR 38676-77, July 18, 1997). In the
3 2006 decision, the Administrator considered it appropriate to use a somewhat different
4 evidence-based approach from that used in 1997 to set the level of the 24-h and annual
5 PM_{2.5} standards. In that decision, the Administrator relied upon evidence from the short-
6 term exposure PM_{2.5} studies as the principal basis for selecting the proposed level of the 24-
7 h standard and relied upon evidence from the long-term exposure PM_{2.5} studies as the
8 principal basis for selecting the level of the annual standard. The court found EPA failed to
9 adequately explain this change in approach in light of CASAC and staff’s recommendations
10 to do otherwise. The court also found that EPA had failed to adequately explain why a
11 short-term 24-h standard by itself would provide the protection needed from short-term
12 exposures. *American Farm Bureau Federation v. EPA*, 559 F. 3d 512, 520-24 (D.C. Cir.
13 2009). With respect to protection from long-term exposure, the court found that EPA failed
14 to adequately explain how the current standard provided ”an adequate margin of safety for
15 vulnerable subpopulations, such as children, the elderly, or those with conditions that
16 exposure them to greater risk from from fine particles”. Specifically, EPA did not provide a
17 reasonable explanation of why certain studies, including a study of children in Southern
18 California showing lung damage from long-term exposure, did not call for a more stringent
19 annual standard. *Id.* at 522-23.

20 The court also remanded the secondary standard for fine particles, based on EPA’s
21 failure to adequately explain why setting the secondary NAAQS equivalent to the primary
22 standards provided the required protection for public welfare including protection from
23 visibility impairment. The court found that EPA failed to identify a target level of visibility
24 impairment that would be requisite to protect public welfare. This was contrary to the
25 statute and resulted in a lack of a reasoned basis for the final decision. In addition, EPA’s
26 near exclusive reliance on a comparison of numbers of counties that would be in
27 nonattainment under various types of standards was an inadequate basis for making a
28 decision. It did not take into account the relative visibility protection of different standards,
29 as well as the failure of a 24-h standard to address regional differences in humidity and its
30 effect on visibility. *Id.* at 528-31.

31 The court upheld EPA’s decision to retain the 24-h PM₁₀ standard to provide protection
32 for coarse particle exposures and to revoke the annual PM₁₀ standard. The court found that
33 EPA reasonably included all coarse PM within the standard, both urban and non-urban, to
34 provide nationwide protection for exposure to coarse PM. It rejected arguments that the
35 evidence showed there are no risks from exposure to non-urban coarse PM. *Id.* at 531-33.
36 The court further found that EPA had a reasonable basis to not set separate standards for
37 urban and non-urban coarse PM, namely the inability to reasonably define what ambient
38 mixes would be included under either “urban” or “non-urban.” In addition, the court found
39 that record evidence supported EPA’s cautious decision to provide “some protection from

1 exposure to thoracic coarse particles... in all areas.” The court also upheld EPA’s decision to
2 use PM₁₀ as the indicator for coarse particles, and to retain the level of the standard at 150
3 µg/m³. EPA’s final rule acknowledged that evidence of harm from urban-type coarse PM is
4 stronger than for other types, and targeted protection at areas where urban-type coarse PM
5 is most likely present. The targeting is done by using the indicator PM₁₀ for coarse
6 particles. PM₁₀ includes both coarse PM and fine PM. Urban and industrial areas tend to
7 have higher levels of fine PM than rural areas, so that in those areas less coarse PM is
8 allowed – the desired targeting. Conversely, fine PM levels tend to be lower in rural areas,
9 so more coarse particles are allowed in those areas – again the desired targeting. Likewise,
10 the court concluded that the EPA’s choice of the level for the PM₁₀ standard was reasonable,
11 for many of the same reasons. *Id.* at 533-36. The court also upheld EPA’s decision to revoke
12 the annual PM₁₀ standard. *Id.* at 537-38.

1.3. ISA Development

13 EPA initiated the current formal review of the NAAQS for PM on June 28, 2007 with
14 a call for information from the public (72 FR 35462). In addition to the call for information,
15 publications were identified through an ongoing literature search process that includes
16 extensive computer database mining on specific topics. Literature searches were conducted
17 routinely to identify studies published since the last review, focusing on publications from
18 2002 to May 2009. Search strategies were iteratively modified in an effort to optimize the
19 identification of pertinent publications. Additional papers were identified for inclusion in
20 several ways: review of pre-publication tables of contents for journals in which relevant
21 papers may be published; independent identification of relevant literature by expert
22 authors; and identification by the public and CASAC during the external review process.
23 Generally, only information that had undergone scientific peer review and had been
24 published or accepted for publication was considered. All relevant epidemiologic, controlled
25 human exposure, and animal toxicological studies, including those related to
26 exposure-response relationships, mode(s) of action (MOA), or susceptible or vulnerable
27 subpopulations, and welfare effects studies published since the last review were considered.

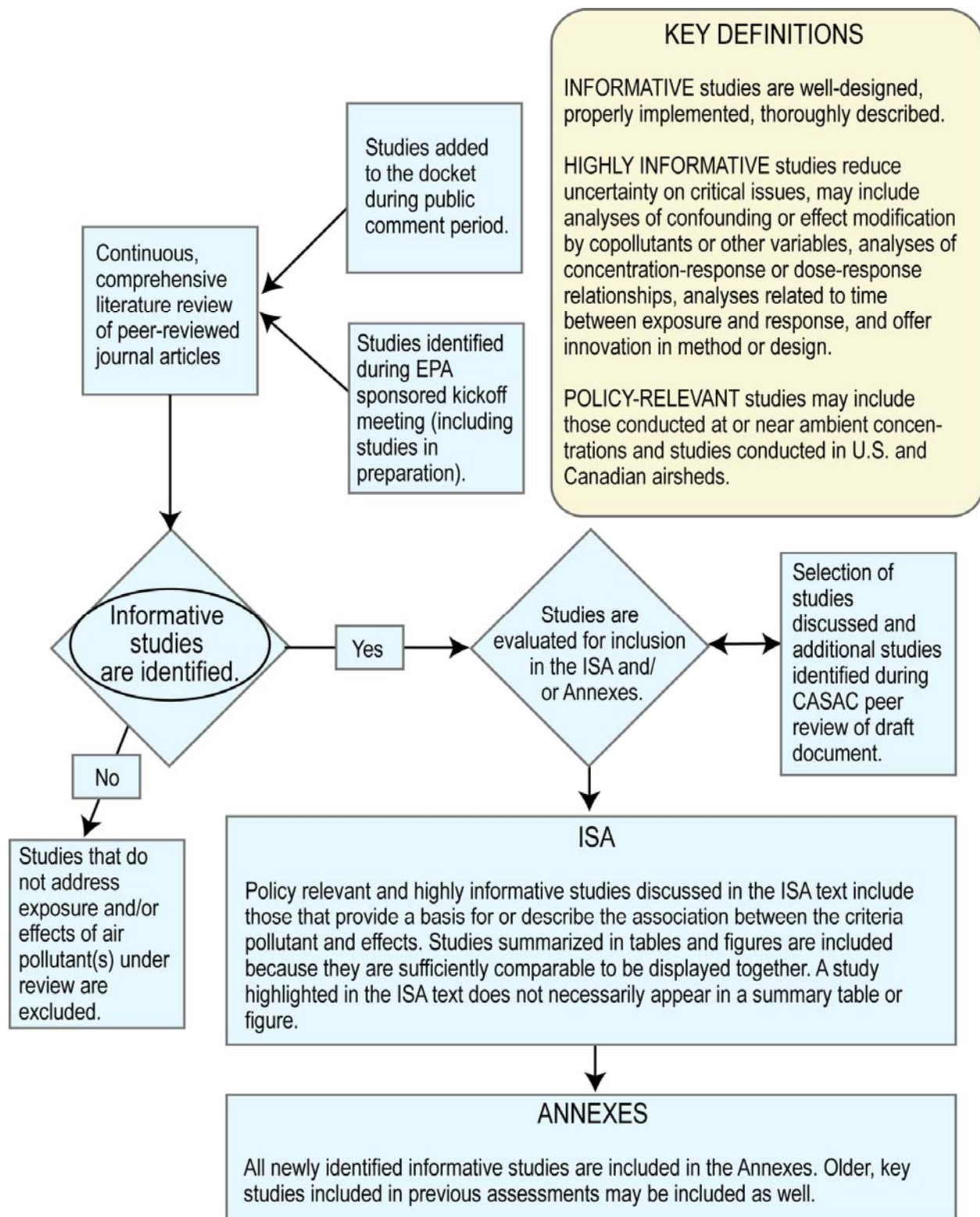


Figure 1-1 Identification of studies for inclusion in the ISA.

1 In general, in assessing the scientific quality and relevance of health and
2 environmental effects studies, the following considerations have been taken into account
3 when selecting studies for inclusion in the ISA or its annexes. The selection process for
4 studies included in this ISA is shown in Figure 1-1.

- 5 ▪ Are the study populations, subjects, or animal models adequately selected and are
6 they sufficiently well defined to allow for meaningful comparisons between study or
7 exposure groups?
- 8 ▪ Are the statistical analyses appropriate, properly performed, and properly
9 interpreted? Are likely covariates adequately controlled or taken into account in the
10 study design and statistical analysis?
- 11 ▪ Are the PM aerometric data, exposure, or dose metrics of adequate quality and
12 sufficiently representative of information regarding ambient PM?
- 13 ▪ Are the health or welfare effect measurements meaningful and reliable?

14 In selecting epidemiologic studies, EPA considered whether a given study contained
15 information on associations with short- or long-term PM exposures at or near ambient
16 levels of PM; evaluated health effects of PM size fractions, components or source-related
17 indicators; considered approaches to evaluate issues related to potential confounding and
18 modification of effects by other pollutants; and evaluated important methodologic issues
19 (e.g., lag or time period between exposure and effects, model specifications, thresholds,
20 mortality displacement) related to interpretation of the health evidence. Among the
21 epidemiologic studies selected, particular emphasis was placed on those studies most
22 relevant to the review of the NAAQS. Specifically, studies conducted in the United States
23 (U.S.) or Canada were discussed in more detail than those from other geographical regions.
24 Particular emphasis was placed on: (1) recent multicity studies that employ standardized
25 analysis methods for evaluating effects of PM and that provide overall estimates for effects
26 based on combined analyses of information pooled across multiple cities, (2) studies that
27 help understand quantitative relationships between exposure concentrations and effects,
28 (3) new studies that provide evidence on effects in susceptible or vulnerable populations,
29 and (4) studies that consider and report PM as a component of a complex mixture of air
30 pollutants.

31 Criteria for the selection of research evaluating controlled human exposure or animal
32 toxicological studies included a focus on studies conducted using relevant pollutant
33 exposures. For both types of studies, relevant pollutant exposures are considered to be
34 those generally within one or two orders of magnitude of ambient PM concentrations.
35 Studies in which higher doses were used may also be considered if they provide information
36 relevant to understanding MOAs or mechanisms, as noted below.

1 Evaluation of controlled human exposure studies focused on those that approximated
2 expected human exposure conditions in terms of concentration and duration. In the
3 selection of controlled human exposure studies, emphasis is placed on studies that (1)
4 investigate potentially susceptible populations such as people with cardiovascular diseases
5 or asthmatics, particularly studies that compare responses in susceptible individuals with
6 those in age-matched healthy controls; (2) address issues such as concentration-response or
7 time-course of responses; (3) investigate exposure to PM separately and in combination
8 with other pollutants such as O₃; (4) include control exposures to filtered air; and (5) have
9 sufficient statistical power to assess findings.

10 For selecting toxicological studies for highlighting in the text, emphasis is placed on
11 inhalation studies conducted at concentrations <2 mg/m³ and those studies that
12 approximate expected human dose conditions in terms of concentration, size distributions,
13 and duration, which will depend on the toxicokinetics and biological sensitivity of the
14 particular laboratory animals examined. Studies that elucidated mechanisms of action
15 and/or susceptibility, particularly if the studies were conducted under atmospherically
16 relevant conditions, were emphasized whenever possible. A limited number of toxicological
17 studies were included that employed intratracheal instillation (IT) techniques, mainly for
18 PM_{10-2.5} studies in rodents, that explored new emerging areas of investigation (e.g.,
19 vasomotor function), or that evaluated specific potential MOA or mechanisms of response.
20 The sources, transport, and fate of fibers and unique nano-materials (viz., dots, hollow
21 spheres, rods, fibers, tubes) are not reviewed herein because the in vivo disposition of these
22 unique nanomaterials is not necessarily relevant to the behavior of ultrafine aerosols in the
23 urban environment that are created by combustion sources and photochemical formation of
24 secondary organic aerosols. In considering the potential effects of different components of
25 PM, EPA has focused on studies that have assessed effects for a range of PM sources or
26 components, including those using source apportionment methods or comparing effects for
27 numerous PM components, and not on studies of individual constituents or species.

28 These criteria provide benchmarks for evaluating various studies and for focusing on
29 the policy relevant studies in assessing the body of health and welfare effects evidence.
30 Detailed critical analysis of all PM health and welfare effects studies, especially in relation
31 to the above considerations, is beyond the scope of this document. Of most relevance for
32 evaluation of studies is whether they provide useful qualitative or quantitative information
33 on exposure-effect or exposure-response relationships for effects associated with current
34 ambient air concentrations of PM that can inform decisions on whether to retain or revise
35 the standards.

36 In developing the PM ISA, EPA began by reviewing and summarizing the evidence on
37 (1) atmospheric sciences and exposure; (2) the welfare effects of PM, including visibility,
38 climate, and ecological effects; and (3) the health effects evidence from in vivo and in vitro
39 animal toxicology, controlled human exposure, and epidemiology studies. In June 2008, EPA

1 held a workshop to obtain review of the scientific content of initial draft materials or
2 sections for the draft ISA and its annexes, that primarily contain summary information.
3 The purpose of the initial peer review workshop was to ensure that the ISA is up-to-date
4 and focused on the most policy-relevant findings, and to assist EPA with integration of
5 evidence within and across disciplines. Following the peer review workshop, EPA addressed
6 comments from the peer review workshop and completed the initial integration and
7 synthesis of the evidence.

8 The integration of evidence on health or welfare effects involves collaboration between
9 scientists from various disciplines. As described in the section below, the ISA organization is
10 based on health or welfare effect categories. As an example, an evaluation of health effects
11 evidence would include summaries of findings from epidemiologic, controlled human
12 exposure, and toxicological studies, and integration of the results to draw conclusions based
13 on the causal framework described below. Using the causal framework described in
14 Section 1.5, EPA scientists consider aspects such as strength, consistency, coherence and
15 biological plausibility of the evidence, and develop draft judgments on the whether the
16 relationships are causal. The draft integrative synthesis sections and conclusions are
17 reviewed by EPA internal experts and, as appropriate, by outside expert authors. In
18 practice, causality determinations often entail an iterative process of review and evaluation
19 of the evidence. The draft ISA is released for review by the CASAC and the public.
20 Comments on the characterization of the science as well as the implementation of the
21 causal framework are carefully considered in revising and completing the ISA.

1.4. Document Organization

22 This ISA is composed of nine chapters. This introductory chapter presents background
23 information, and provides an overview of EPA's framework for making causal judgments.
24 Key findings and conclusions for consideration in the review of the NAAQS for PM from the
25 atmospheric sciences, ambient air data analyses, exposure assessment, dosimetry, health
26 and welfare effects, including judgments on causality for the health and welfare effects of
27 PM exposure, are presented in Chapter 2. More detailed summaries, evaluations and
28 integration of the evidence are included in Chapters 3 through 9.

29 Chapter 3 highlights key concepts or issues relevant to understanding the
30 atmospheric chemistry, sources, and exposure of and to PM following a "source-to-exposure"
31 paradigm. Chapter 4 summarizes key concepts and recent findings on the dosimetry of PM
32 and Chapter 5 discusses possible pathways and MOA for the effects of PM. Chapters 6 and
33 7 evaluate and integrate epidemiologic, controlled human exposure, and animal
34 toxicological information relevant to the review of the primary NAAQS for PM. Health
35 effects related to short-term exposures (hours to days) to PM are the focus of Chapter 6.
36 Chapter 7 evaluates health evidence related to long-term exposures (months to years) to

1 PM. Chapters 6 and 7 are organized by health outcome categories, such as cardiovascular
2 or respiratory effects, and each section includes effects of the various types of PM studied.
3 For each health outcome category, summary sections then integrate the findings to draw
4 conclusions on the evidence for the main size classes of PM (i.e., PM_{2.5}, PM_{10-2.5}, and
5 ultrafine particles). PM₁₀ studies are included in this assessment where they provide
6 insights into relationships between PM and effects, but the ISA draws no conclusions
7 regarding causality between exposure to PM₁₀ and effects; to the extent possible, the
8 findings of these studies are considered insofar as they provide information relevant to the
9 review of the standards for fine and thoracic coarse particles. Chapter 6 also includes a
10 summary and synthesis of the recent health evidence that uses apportionment methods to
11 assess health effects of sources and constituents of ambient PM; most such studies have
12 evaluated effects of short-term exposure. Chapter 8 evaluates evidence related to
13 populations potentially susceptible to PM-related effects.

14 Chapter 9 evaluates welfare effects evidence that is relevant to the review of the
15 secondary NAAQS for PM. This chapter includes consideration of effects of PM on visibility
16 impairment, materials damage, effects of PM on climate, and ecological effects of PM that
17 were not addressed in the *Integrated Science Assessment for Oxides of Nitrogen and*
18 *Sulfur—Ecological Criteria* (NO_xSO_x ISA) (U.S. EPA, 2008, [157074](#)). The chapter also
19 presents key conclusions and scientific judgments regarding causality for welfare effects of
20 PM. In 2008, EPA completed the NO_xSO_x ISA (U.S. EPA, 2008, [157074](#)), that focused on
21 ecological effects related to the deposition of nitrogen (N)- and sulfur (S)-containing
22 compounds. The 2008 NO_xSO_x ISA included ecological effects from particle-phase
23 compounds (e.g., nitrates and sulfates), primarily effects from acidification and N-nutrient
24 enrichment and eutrophication. In the PM ISA, EPA focuses on recent data for direct
25 welfare effects of particle-phase NO_x and SO_x in the ambient air — primarily visibility
26 impairment, damage to materials, and positive and negative climate interactions — not the
27 welfare effects related to deposition of particle-phase NO_x and SO_x.

28 A series of annexes supplement this ISA. The annexes provide additional details of
29 the pertinent literature published since the last review, as well as selected older studies of
30 particular interest. These annexes contain information on:

- 31 ▪ atmospheric chemistry of PM, sampling and analytic methods for measurement of
32 PM, concentrations, emissions, sources and human exposure to PM (Annex A)
- 33 ▪ studies on the dosimetry of PM (Annex B)
- 34 ▪ controlled human exposure studies of health effects related to exposure to PM
35 (Annex C)
- 36 ▪ toxicological studies of health effects in laboratory animals (Annex D); and

- 1 ▪ epidemiologic studies of health effects from short- and long-term exposure to PM
2 (Annex E);
- 3 ▪ studies that evaluate PM-induced health effects attributable to specific constituents
4 or sources.

5 Within the annexes, detailed information about methods and results of health studies
6 is summarized in tabular format, and generally includes information about: concentrations
7 of PM and averaging times; study methods employed; results; and quantitative results for
8 relationships between effects and exposure to PM. As noted in the section above, the most
9 pertinent results of this body of studies are brought into the ISA.

1.5. EPA Framework for Causal Determination

10 The EPA has developed a consistent and transparent basis to evaluate the causal
11 nature of air pollution-induced health or environmental effects. The framework described
12 below establishes uniform language concerning causality and brings more specificity to the
13 findings. It drew standardized language from across the federal government and wider
14 scientific community, especially from the recent National Academy of Sciences (NAS)
15 Institute of Medicine (IOM) document, *Improving the Presumptive Disability*
16 *Decision-Making Process for Veterans* (IOM, 2008, [156586](#)), the most recent comprehensive
17 work on evaluating causality.

18 This introductory section focuses on the evaluation of health effects evidence; while
19 focusing on human health outcomes, the concepts are also generally relevant to causality
20 determination for welfare effects. This section:

- 21 ▪ describes the kinds of scientific evidence used in establishing a general causal
22 relationship between exposure and health effects;
- 23 ▪ defines cause, in contrast to statistical association;
- 24 ▪ discusses the sources of evidence necessary to reach a conclusion about the existence
25 of a causal relationship;
- 26 ▪ highlights the issue of multifactorial causation;
- 27 ▪ identifies issues and approaches related to uncertainty; and
- 28 ▪ provides a framework for classifying and characterizing the weight of evidence in
29 support of a general causal relationship.

30 Approaches to assessing the separate and combined lines of evidence (e.g.,
31 epidemiologic, controlled human exposure, and animal toxicological studies) have been

1 formulated by a number of regulatory and science agencies, including the IOM of the NAS
2 (IOM, 2008, [156586](#)), International Agency for Research on Cancer (IARC, 2006, [093206](#)),
3 EPA Guidelines for Carcinogen Risk Assessment (U.S. EPA, 2005, [086237](#)), Centers for
4 Disease Control and Prevention (CDC, 2004, [056384](#)), and National Acid Precipitation
5 Assessment Program (NAPAP) (NAPAP, 1991, [095894](#)). These formalized approaches offer
6 guidance for assessing causality. The frameworks are similar in nature, although adapted
7 to different purposes, and have proven effective in providing a uniform structure and
8 language for causal determinations. Moreover, these frameworks have supported
9 decision-making under conditions of uncertainty.

1.5.1. Scientific Evidence Used in Establishing Causality

10 Causality determinations are based on the evaluation and synthesis of evidence from
11 across scientific disciplines; the type of evidence that is most important for such
12 determinations will vary by assessment. The most direct evidence of a causal relationship
13 between pollutant exposures and human health effects comes from controlled human
14 exposure studies. This type of study experimentally evaluates the health effects of
15 administered exposures in human volunteers under highly-controlled laboratory conditions.

16 In most epidemiologic or observational studies of humans, the investigator does not
17 control exposures or intervene with the study population. Broadly, observational studies
18 can describe associations between exposures and effects. These studies fall into several
19 categories: cross-sectional, prospective cohort, and time-series studies. “Natural
20 experiments” offer the opportunity to investigate changes in health with a change in
21 exposure; these include comparisons of health effects before and after a change in
22 population exposures, such as the closure of a pollution source.

23 Experimental animal data complement the controlled human exposure and
24 observational data; these studies can help characterize effects of concern,
25 exposure-response relationships, susceptible subpopulations, MOAs and enhance
26 understanding of biological plausibility of observed effects. In the absence of clinical or
27 epidemiologic data, animal data alone may be sufficient to support a likely causal
28 determination, assuming that similar responses are expected in humans.

1.5.2. Association and Causation

29 “Cause” is a significant, effectual relationship between an agent and an effect on
30 health or public welfare. “Association” is the statistical dependence among events,
31 characteristics, or other variables. An association is prima facie evidence for causation;
32 alone, however, it is insufficient proof of a causal relationship between exposure and disease
33 or health effect. Determining whether an observed association is causal rather than
34 spurious involves consideration of a number of factors, as described below. Much of the

1 newly available health information evaluated in this ISA comes from epidemiologic studies
2 that report a statistical association between ambient exposure and health outcomes.

3 Many of the health and environmental outcomes reported in these studies have
4 complex etiologies. Diseases such as asthma, coronary artery disease or cancer are typically
5 initiated by a web of multiple agents. Outcomes depend on a variety of factors, such as age,
6 genetic susceptibility, nutritional status, immune competence, and social factors (Gee and
7 Payne-Sturges, 2004, [093070](#); IOM, 2008, [156586](#)). Effects on ecosystems are also
8 multifactorial with a complex web of causation. Further, exposure to a combination of
9 agents could cause synergistic or antagonistic effects. Thus, the observed risk represents
10 the net effect of many actions and counteractions.

1.5.3. Evaluating Evidence for Inferring Causation

11 Moving from association to causation involves elimination of alternative explanations
12 for the association. In estimating the causal influence of an exposure on health or
13 environmental effects, it is recognized that scientific findings include uncertainty.
14 Uncertainty can be defined as a state of having limited knowledge where it is impossible to
15 exactly describe an existing state or future outcome; the lack of knowledge about the correct
16 value for a specific measure or estimate. Uncertainty characterization and uncertainty
17 assessment are two activities that lead to different degrees of sophistication in describing
18 uncertainty. Uncertainty characterization generally involves a qualitative discussion of the
19 thought processes that lead to the selection and rejection of specific data, estimates,
20 scenarios, etc. The uncertainty assessment is more quantitative. The process begins with
21 simpler measures (e.g., ranges) and simpler analytical techniques and progresses, to the
22 extent needed to support the decision for which the assessment is conducted, to more
23 complex measures and techniques. Data will not be available for all aspects of an
24 assessment and those data that are available may be of questionable or unknown quality.
25 In these situations, evaluation of uncertainty can include professional judgment or
26 inferences based on analogy with similar situations. The net result is that the assessments
27 will be based on a number of assumptions with varying degrees of uncertainty.
28 Uncertainties commonly encountered in evaluating health evidence for the criteria air
29 pollutants are outlined below for epidemiologic and experimental studies. Various
30 approaches to characterizing uncertainty include classical statistical methods, sensitivity
31 analysis, or probabilistic uncertainty analysis, in order of increasing complexity and data
32 requirements. The ISA generally evaluates uncertainties qualitatively in assessing the
33 evidence from across studies; in some situations quantitative analysis approaches, such as
34 meta-regression may be used.

35 It is important to note here that, although the following discussion refers primarily to
36 health effect studies, many parallels exist with welfare effects studies. Controlled exposure

1 studies have been conducted in which plant species have been directly exposed to air
2 pollutants, and the strengths and limitations of that body of studies mirror those of the
3 controlled human exposure studies discussed below. Ecological field or natural gradient
4 studies are similar to epidemiologic studies, for example, in the study of free-living
5 populations and in the challenges faced in distinguishing effects of pollutants within a
6 mixture.

7 Controlled human exposure studies evaluate the effects of exposures to a variety of
8 pollutants in a highly-controlled laboratory setting. Also referred to as human clinical
9 studies, these experiments allow investigators to expose subjects to fixed concentrations of
10 air pollutants under carefully regulated environmental conditions and activity levels.
11 Controlled human exposures to PM typically involve exposing subjects either at rest or
12 while engaged in intermittent exercise in a whole-body exposure chamber, although
13 mouthpiece and facemask systems can also be used. A variety of different types of particles
14 are used in these studies including ambient outdoor particles, concentrated ambient
15 particles (CAPs), diesel exhaust (DE) from a diesel engine, wood smoke (WS) generated in a
16 wood stove, laboratory generated model particles (e.g., elemental carbon [EC] or zinc oxide
17 [ZnO]), or particles collected on a filter, resuspended in saline, and administered either
18 through instillation or inhalation (aerosolized and delivered using a nebulizer). The
19 recovery of particles on filters is variable and some components, such as organics, may be
20 too volatile to be collected. Exposures to artificially generated particles may provide
21 important information on the health effects of PM, but are not truly representative of
22 ambient air pollution particles. The direct exposure of humans to ambient air pollution
23 particles may be complicated by factors that cannot be controlled such as coexposures to
24 other air pollutants (e.g., O₃, SO₂, and NO₂). In concentrating ambient particles, gaseous
25 copollutants are not proportionately concentrated and interactions between PM and the
26 copollutants cannot be investigated unless the latter are re-introduced. These limitations as
27 well as daily variability in concentration and composition can make it difficult to compare
28 the results from controlled human exposure studies employing particles from different
29 sources.

30 In some instances, controlled human exposure studies can also be used to characterize
31 concentration-response relationships at pollutant concentrations relevant to ambient
32 conditions. Controlled human exposures are typically conducted using a randomized
33 crossover design with subjects exposed both to PM and a clean air control. In this way,
34 subjects serve as their own controls, effectively controlling for many potential confounders.
35 However, controlled human exposure studies are limited by a number of factors including a
36 small sample size and short exposure time. These laboratory studies are often conducted at
37 PM concentrations much higher than those typically observed under ambient conditions,
38 which may result in an overestimate of the acute response to exposure in the general
39 population. Although the repetitive nature of ambient PM exposures may lead to

1 cumulative health effects, this type of exposure is not practical to replicate in a laboratory
2 setting. In addition, while subjects do serve as their own controls, personal exposure to
3 pollutants in the hours and days preceding the controlled exposures may vary significantly
4 between and within individuals. Finally, controlled human exposure studies require
5 investigators to adhere to stringent health criteria for a subject to be included in the study,
6 and therefore the results cannot necessarily be generalized to an entire population.
7 Although some controlled human exposure studies have included health comprised
8 individuals such as asthmatics or individuals with chronic obstructive pulmonary disease
9 (COPD) or coronary artery disease, these individuals must also be relatively healthy and do
10 not represent the most sensitive individuals in the population. Thus, a lack of observation
11 of effects from controlled human exposure studies does not necessarily mean that a causal
12 relationship does not exist. While controlled human exposure studies provide important
13 information on the biological plausibility of associations observed between air pollutant
14 exposure and health outcomes in epidemiologic studies, observed effects in these studies
15 may underestimate the response in certain subpopulations.

16 Epidemiologic studies provide important information on the associations between
17 health effects and exposure of human populations to ambient air pollution. In the
18 evaluation of epidemiologic evidence, one important consideration is potential confounding.
19 Confounding is “. . . a confusion of effects. Specifically, the apparent effect of the exposure
20 of interest is distorted because the effect of an extraneous factor is mistaken for or mixed
21 with the actual exposure effect (which may be null)” (Rothman and Greenland S, 1998,
22 [086599](#)). One approach to remove spurious associations from possible confounders is to
23 control for characteristics that may differ between exposed and unexposed persons; this is
24 frequently termed “adjustment.” Scientific judgment is needed regarding likely sources and
25 magnitude of confounding, together with consideration of how well the existing
26 constellation of study designs, results, and analyses address this potential threat to
27 inferential validity. One key consideration in this review is evaluation of the potential
28 contribution of PM to health effects when it is a component of a complex air pollutant
29 mixture. Reported PM effect estimates in epidemiologic studies may reflect independent
30 PM effects on respiratory and cardiovascular health. Ambient PM may also be serving as an
31 indicator of complex ambient air pollution mixtures that share the same source as PM
32 (i.e., combustion of S-containing fuels or motor vehicle emissions). Alternatively,
33 copollutants may mediate the effects of PM or PM may influence the toxicity of
34 copollutants.

35 Multivariable regression models constitute one tool for estimating the association
36 between exposure and outcome after adjusting for characteristics of participants that might
37 confound the results. The use of multipollutant regression models has been the prevailing
38 approach for controlling potential confounding by copollutants in air pollution health effects
39 studies. Finding the likely causal pollutant from multipollutant regression models is made

1 difficult by the possibility that one or more air pollutants may be acting as a surrogate for
2 an unmeasured or poorly-measured pollutant or for a particular mixture of pollutants. In
3 addition, more than one pollutant may exert similar health effects, resulting in
4 independently observed associations for multiple pollutants. Further, the correlation
5 between the air pollutant of interest and various copollutants may make it difficult to
6 discern associations between different pollutant exposures and health effects. Thus, results
7 of models that attempt to distinguish gaseous and particle effects must be interpreted with
8 caution. The number and degree of diversity of covariates, as well as their relevance to the
9 potential confounders, remain matters of scientific judgment. Despite these limitations, the
10 use of multipollutant models is still the prevailing approach employed in most air pollution
11 epidemiologic studies, and provides some insight into the potential for confounding or
12 interaction among pollutants.

13 Another way to adjust for potential confounding is through stratified analysis,
14 i.e., examining the association within homogeneous groups with respect to the confounding
15 variable. Stratified analysis can also be used to examine potential effect modification. The
16 use of stratified analyses has an additional benefit: it allows examination of effect
17 modification through comparison of the effect estimates across different groups. If
18 investigators successfully measured characteristics that distort the results, adjustment of
19 these factors help separate a spurious from a true causal association. Appropriate
20 statistical adjustment for confounders requires identifying and measuring all reasonably
21 expected confounders. Deciding which variables to control for in a statistical analysis of the
22 association between exposure and disease or health outcome depends on knowledge about
23 possible mechanisms and the distributions of these factors in the population under study.
24 Identifying these mechanisms makes it possible to control for potential sources that may
25 result in a spurious association.

26 Adjustment for potential confounders can be influenced by differential exposure
27 measurement error. There are several components that contribute to exposure
28 measurement error in epidemiologic studies, including the difference between true and
29 measured ambient concentrations, the difference between average personal exposure to
30 ambient pollutants and ambient concentrations at central monitoring sites, and the use of
31 average population exposure rather than individual exposure estimates. Previous AQCDs
32 have examined the role of measurement error in time-series epidemiologic studies using
33 simulated data and mathematical analyses and suggested that “transfer of effects” would
34 only occur under unusual circumstances (i.e., “true” predictors having high positive or
35 negative correlation; substantial measurement error; or extremely negatively correlated
36 measurement errors) (U.S. EPA, 2004, [056905](#)).

37 Confidence that unmeasured confounders are not producing the findings is increased
38 when multiple studies are conducted in various settings using different subjects or
39 exposures; each of which might eliminate another source of confounding from consideration.

1 Thus, multicity studies which use a consistent method to analyze data from across locations
2 with different levels of covariates can provide insight on potential confounding in
3 associations. Intervention studies, because of their quasi-experimental nature, can be
4 particularly useful in characterizing causation.

5 In addition to clinical and epidemiologic studies, the tools of experimental biology
6 have been valuable for developing insights into human physiology and pathology. Animal
7 toxicological studies explore the effects of pollutants on human health, especially through
8 the study of model systems in other species. These studies evaluate the effects of exposures
9 to a variety of pollutants in a highly-controlled laboratory setting, and allow exploration of
10 MOAs or mechanisms by which a pollutant may cause effects. Background knowledge of the
11 biological mechanisms by which an exposure might or might not cause disease can prove
12 crucial in establishing, or negating, a causal claim. There are, however, uncertainties
13 associated with quantitative extrapolations between laboratory animals and humans on the
14 pathophysiological effects of any pollutant. Animal species can differ from each other in
15 fundamental aspects of physiology and anatomy (e.g., metabolism, airway branching,
16 hormonal regulation) that may limit extrapolation. The differences between humans and
17 rodents with regard to pollutant absorption and distribution profiles based on breathing
18 pattern, exposure dose, and differences in lung structure and anatomy all have to be taken
19 into consideration.

20 A relatively new tool available for experimental studies of PM exposure is the particle
21 concentrator. Particle concentrators enable human subjects, animals, or cell culture
22 systems to be exposed to atmospheric PM at concentrations much greater than that
23 observed under ambient conditions. As ambient PM is just one component of a complex
24 mixture that interacts with gases and other aerosols, CAPs systems provide a method of
25 exposing subjects to the particle phase. Gases (such as O₃ and SO₂) are not concentrated
26 nor are thoracic coarse particles (except for the coarse particle concentrator) and only
27 certain systems are capable of concentrating ultrafine PM. In ultrafine CAPs systems,
28 increased number fraction of organic carbon and PAHs, along with decreased relative
29 percentage of EC particles have been reported in concentrated PM compared to ambient PM
30 (Su et al., 2006, [157021](#)). These data suggest that for ultrafine concentrators, the CAPs do
31 not accurately reflect atmospheric ultrafine composition. There are several instrument
32 systems used to concentrate ambient PM in controlled human or animal exposure studies
33 (Gordon et al., 1999, [001176](#); Maciejczyk and Chen, 2005, [087456](#); Sioutas et al., 1995,
34 [001629](#); Sioutas et al., 1999, [001633](#)).

35 The ability to extrapolate between species has not generally changed since the 2004
36 PM AQCD but some considerations related to coarse particles merit attention. The
37 inhalability of particles greater than 2.5 µm in diameter is considerably lower in rats than
38 in humans; however, once inhaled, deposition in the extrathoracic region is near 100%
39 percent for particles greater than 5 µm for most laboratory animal species (rat, mouse,

1 hamster, guinea pig, and dogs). By contrast, penetration of thoracic coarse particles into the
2 lower respiratory tract is greater in humans than rodents due to the moderately less
3 efficient nasal deposition of humans and oronasal breathing (especially during exercise).
4 The extent to which coarse particle deposition in the lower respiratory tract differs between
5 the species is highly dependent on the activity level of the human exposure scenario in
6 contrast with the resting exposure conditions common to rodent exposures. Endotracheal
7 exposures of rodents may be needed to achieve coarse particle tissue doses in the lower
8 respiratory tract of rodents similar to those experienced by humans. For particles less than
9 1 μm , including ultrafine particles, deposition is expected to be relatively similar between
10 the species.

11 There are also differences between species in both the rates of particle clearance from
12 and retention in the lung. The clearance rate of particles from the ciliated airways of rats is
13 considerably greater than humans. There is also evidence of prolonged particle retention in
14 the smaller bronchioles of humans that does not appear to exist or has not been observed in
15 rats. Under most circumstances, clearance from the alveolar region of rats is also more
16 rapid than observed in humans. Thus, these combined effects contribute to a greater
17 particle burden in the lower respiratory tract of humans relative to rats. An important
18 consideration in studies where rats are chronically exposed to high concentrations of
19 insoluble particles, is the potential for “overload conditions.” Rats, unlike other laboratory
20 animals or humans, may experience a reduction in their alveolar clearance rates and an
21 accumulation of interstitial particle burden and under these conditions, the relevance of
22 tissue burdens and responses to humans is questionable. Considering interspecies
23 differences in both deposition and clearance, greater exposure concentrations are required
24 to achieve coarse particle tissue doses in the lower respiratory tract of rodents similar to
25 those experienced by humans.

1.5.4. Application of Framework for Causal Determination

26 EPA uses a two-step approach to evaluate the scientific evidence on health or
27 environmental effects of criteria pollutants. The first step determines the weight of
28 evidence in support of causation and characterizes the strength of any resulting causal
29 classification. The second step includes further evaluation of the quantitative evidence
30 regarding the concentration-response relationships and the loads or levels, duration and
31 pattern of exposures at which effects are observed.

Table 1-2 Aspects to aid in judging causality.

Aspect	Description
Consistency of the observed association	An inference of causality is strengthened when a pattern of elevated risks is observed across several independent studies, conducted in multiple locations by multiple investigators. The reproducibility of findings constitutes one of the strongest arguments for causality. If there are discordant results among investigations, possible reasons such as differences in exposure, confounding factors, and the power of the study are considered.
Coherence	An inference of causality from epidemiologic associations may be strengthened by other lines of evidence (e.g., controlled human exposure and animal toxicological studies) that support a cause-and-effect interpretation of the association. Causality is also supported when epidemiologic associations are reported across study designs and across related health outcomes. Evidence on ecological or welfare effects may be drawn from a variety of experimental approaches (e.g., greenhouse, laboratory, and field) and subdisciplines of ecology (e.g., community ecology, biogeochemistry and paleological/ historical reconstructions). The coherence of evidence from various fields greatly adds to the strength of an inference of causality. The absence of other lines of evidence, however, is not a reason to reject causality
Biological plausibility	An inference of causality tends to be strengthened by consistency with data from experimental studies or other sources demonstrating plausible biological mechanisms. A proposed mechanistic linking between an effect, and exposure to the agent, is an important source of support for causality, especially when data establishing the existence and functioning of those mechanistic links are available. A lack of biological understanding, however, is not a reason to reject causality.
Biological gradient (exposure-response relationship)	A well characterized exposure-response relationship (e.g., increasing effects associated with greater exposure) strongly suggests cause and effect, especially when such relationships are also observed for duration of exposure (e.g., increasing effects observed following longer exposure times). There are, however, many possible reasons that a study may fail to detect an exposure-response relationship. Thus, although the presence of a biological gradient may support causality, the absence of an exposure-response relationship does not exclude a causal relationship.
Strength of the observed association	The finding of large, precise risks increases confidence that the association is not likely due to chance, bias, or other factors. However, given a truly causal agent, a small magnitude in the effect could follow from a lower level of exposure, a lower potency, or the prevalence of other agents causing similar effects. While large effects support causality, modest effects therefore do not preclude it.
Experimental evidence	The strongest evidence for causality can be provided when a change in exposure brings about a change in occurrence or frequency of health or welfare effects.
Temporal relationship of the observed association	Evidence of a temporal sequence between the introduction of an agent and appearance of the effect constitutes another argument in favor of causality.
Specificity of the observed association	As originally intended, this refers to increased inference of causality if one cause is associated with a single effect or disease (Hill, 1965, 071664). Based on the current understanding this is now considered one of the weaker guidelines for causality; for example, many agents cause respiratory disease and respiratory disease has multiple causes. At the scale of ecosystems, as in epidemiology, complexity is such that single agents causing single effects, and single effects following single causes, are extremely unlikely. The ability to demonstrate specificity under certain conditions remains, however, a powerful attribute of experimental studies. Thus, although the presence of specificity may support causality, its absence does not exclude it.
Analogy	Structure activity relationships and information on the agent's structural analogs can provide insight into whether an association is causal. Similarly, information on mode of action for a chemical, as one of many structural analogs, can inform decisions regarding likely causality.

1 To aid judgment, various “aspects”¹ of causality have been discussed by many
2 philosophers and scientists. The most widely cited aspects of causality in epidemiology, and
3 public health, in general, were articulated by Sir Austin Bradford Hill in 1965 and have
4 been widely used (CDC, 2004, [056384](#); Hill, 1965, [071664](#); IARC, 2006, [093206](#); IOM, 2008,
5 [156586](#); NRC, 2004, [156814](#); U.S. EPA, 2005, [086237](#)). Several adaptations of the Hill
6 aspects have been used in aiding causality judgments in the ecological sciences (Adams,
7 2003, [156192](#); Collier, 2003, [155736](#); Fox, 1991, [156444](#); Gerritsen et al., 1998, [156465](#)).
8 These aspects (Hill, 1965, [071664](#)) have been modified (Table 1-2) for use in causal
9 determinations specific to health and welfare effects or pollutant exposures.² Some aspects
10 are more likely than others to be relevant for evaluating evidence on the health or
11 environmental effects of criteria air pollutants. For example, the analogy aspect does not
12 always apply and specificity would not be expected for multi-etiological health outcomes such
13 as asthma or cardiovascular disease, or ecological effects related to acidification. Aspects
14 that usually play a larger role in determination of causality are consistency of results across
15 studies, coherence of effects observed in different study types or disciplines, biological
16 plausibility, exposure-response relationship, and evidence from “natural” experiments.

17 Although these aspects provide a framework for assessing the evidence, they do not
18 lend themselves to being considered in terms of simple formulas or fixed rules of evidence
19 leading to conclusions about causality (Hill, 1965, [071664](#)). For example, one cannot simply
20 count the number of studies reporting statistically significant results or statistically
21 nonsignificant results and reach credible conclusions about the relative weight of the
22 evidence and the likelihood of causality. In addition, it is important to note that the aspects
23 in Table 1-2 cannot be used as a strict checklist, but rather to determine the weight of the
24 evidence for inferring causality. While these aspects are particularly salient in this
25 assessment, it is also important to recognize that no one aspect is either necessary or
26 sufficient for drawing inferences of causality.

1.5.5. First Step—Determination of Causality

27 In the ISA, EPA assesses the results of recent relevant publications, building upon
28 evidence available during the previous NAAQS review, to draw conclusions on the causal
29 relationships between relevant pollutant exposures and health or environmental effects.
30 This ISA uses a five-level hierarchy that classifies the weight of evidence for causation, not

¹ The “aspects” described by Hill (1965, [071664](#)) have become, in the subsequent literature, more commonly described as “criteria.” The original term “aspects” is used here to avoid confusion with ‘criteria’ as it is used, with different meaning, in the Clean Air Act.

² The Hill aspects were developed for interpretation of epidemiologic results. They have been modified here for use with a broader array of data, i.e., epidemiologic, controlled human exposure, and animal toxicological studies, as well as in vitro data, and to be more consistent with EPA’s Guidelines for Carcinogen Risk Assessment.

1 just association¹. In developing this hierarchy, EPA has drawn on the work of previous
2 evaluations, most prominently the IOM's *Improving the Presumptive Disability*
3 *Decision-Making Process for Veterans* (IOM, 2008, [156586](#)), EPA's Guidelines for
4 Carcinogen Risk Assessment (U.S. EPA, 2005, [086237](#)) and the U.S. Surgeon General's
5 smoking reports (CDC, 2004, [056384](#)). This weight of evidence evaluation is based on
6 various lines of evidence from across the health and environmental effects disciplines.
7 These separate judgments are integrated into a qualitative statement about the overall
8 weight of the evidence and causality. The five descriptors for causal determination are
9 described in Table 1-3.

10 For PM, this determination of causality step involved a rather complex evaluation of
11 evidence for different PM indices, different types of health or environmental effects, and for
12 short- and long-term exposure periods. Determination of causality was made for both the
13 PM measure (PM_{2.5}, PM_{10-2.5}, and ultrafine particles, to the extent evidence was available for
14 each measure) and for the overall effect category. As noted above, to the extent possible,
15 results of PM₁₀ studies are considered in causality determinations for PM_{2.5} and PM_{10-2.5}. In
16 the evaluation of health effects findings in Chapter 6 (for short-term exposure) and Chapter
17 7 (for long-term exposure), evidence was evaluated for health outcome categories, such as
18 cardiovascular effects, and then conclusions were drawn based upon the integration of
19 evidence from across disciplines (e.g., epidemiology, controlled human exposure, and
20 toxicology) and also across the suite of related individual health outcomes. These chapters
21 initially summarize and evaluate findings for individual health outcomes, then integrate
22 the results in summary sections to draw conclusions on causality for each PM indicator. The
23 causality narratives present the weight of evidence that highlights the quality and breadth
24 of the data, including any limitations or uncertainties. In the integrative synthesis and
25 conclusions in Chapter 2, the ISA presents causality determinations and a summary of the
26 underlying basis for those determinations for the PM indicator (e.g., PM_{2.5}), for the
27 exposure time period (e.g., short- and long-term exposure) and for the major health effect
28 categories.

¹ It should be noted that the CDC and IOM frameworks use a four-category hierarchy for the strength of the evidence. A five-level hierarchy is used here to be consistent with the EPA Guidelines for Carcinogen Risk Assessment and to provide a more nuanced set of categories.

Table 1-3. Weight of evidence for causal determination.

Determination	Health Effects	Ecological and Welfare Effects
Causal relationship	Evidence is sufficient to conclude that there is a causal relationship with relevant pollutant exposures. That is, the pollutant has been shown to result in health effects in studies in which chance, bias, and confounding could be ruled out with reasonable confidence. For example: a) controlled human exposure studies that demonstrate consistent effects; or b) observational studies that cannot be explained by plausible alternatives or are supported by other lines of evidence (e.g., animal studies or mode of action information). Evidence includes replicated and consistent high-quality studies by multiple investigators.	Evidence is sufficient to conclude that there is a causal relationship with relevant pollutant exposures. That is, the pollutant has been shown to result in effects in studies in which chance, bias, and confounding could be ruled out with reasonable confidence. Controlled exposure studies (laboratory or small- to medium-scale field studies) provide the strongest evidence for causality, but the scope of inference may be limited. Generally, determination is based on multiple studies conducted by multiple research groups, and evidence that is considered sufficient to infer a causal relationship is usually obtained from the joint consideration of many lines of evidence that reinforce each other.
Likely to be a causal relationship	Evidence is sufficient to conclude that a causal relationship is likely to exist with relevant pollutant exposures, but important uncertainties remain. That is, the pollutant has been shown to result in health effects in studies in which chance and bias can be ruled out with reasonable confidence but potential issues remain. For example: a) observational studies show an association, but copollutant exposures are difficult to address and/or other lines of evidence (controlled human exposure, animal, or mode of action information) are limited or inconsistent; or b) animal toxicological evidence from multiple studies from different laboratories that demonstrate effects, but limited or no human data are available. Evidence generally includes replicated and high-quality studies by multiple investigators.	Evidence is sufficient to conclude that there is a likely causal association with relevant pollutant exposures. That is, an association has been observed between the pollutant and the outcome in studies in which chance, bias and confounding are minimized, but uncertainties remain. For example, field studies show a relationship, but suspected interacting factors cannot be controlled, and other lines of evidence are limited or inconsistent. Generally, determination is based on multiple studies in multiple research groups.
Suggestive of a causal relationship	Evidence is suggestive of a causal relationship with relevant pollutant exposures, but is limited because chance, bias and confounding cannot be ruled out. For example, at least one high-quality epidemiologic study shows an association with a given health outcome but the results of other studies are inconsistent.	Evidence is suggestive of a causal relationship with relevant pollutant exposures, but chance, bias and confounding cannot be ruled out. For example, at least one high-quality study shows an effect, but the results of other studies are inconsistent.
Inadequate to infer a causal relationship	Evidence is inadequate to determine that a causal relationship exists with relevant pollutant exposures. The available studies are of insufficient quantity, quality, consistency or statistical power to permit a conclusion regarding the presence or absence of an effect .	The available studies are of insufficient quality, consistency or statistical power to permit a conclusion regarding the presence or absence of an effect.
Not likely to be a causal relationship	Evidence is suggestive of no causal relationship with relevant pollutant exposures. Several adequate studies, covering the full range of levels of exposure that human beings are known to encounter and considering susceptible or vulnerable subpopulations, are mutually consistent in not showing an effect at any level of exposure.	Several adequate studies, examining relationships with relevant exposures, are consistent in failing to show an effect at any level of exposure.

1.5.6. Second Step—Evaluation of Response

1 Beyond judgments regarding causality are questions relevant to quantifying health or
2 environmental risks based on our understanding of the quantitative relationships between
3 pollutant exposures and health or welfare effects.

1.5.6.1. Effects on Human Populations

4 Once a determination is made regarding the causal relationship between the
5 pollutant and outcome category, important questions regarding quantitative relationships
6 include:

- 7 ▪ What is the concentration-response or dose-response relationship in the human
8 population?
- 9 ▪ What exposure conditions (dose or exposure, duration and pattern) are important?
- 10 ▪ What subpopulations appear to be differentially affected i.e., more
11 susceptible/vulnerable to effects?

12 To address these questions, in the second step of the EPA framework, the entirety of
13 quantitative evidence is evaluated to best quantify those concentration-response
14 relationships that exist. This requires evaluation of levels of pollutant and exposure
15 durations at which effects were observed for exposed populations including potentially
16 susceptible subpopulations. This integration of evidence results in identification of a study
17 or set of studies that best approximates the concentration-response relationships between
18 health outcomes and PM indicators for the U.S. population or subpopulations, given the
19 current state of knowledge and the uncertainties that surrounded these estimates.

20 To accomplish this, evidence from multiple and diverse types of studies is considered.
21 To the extent available, the ISA evaluates results from across epidemiologic studies that
22 use various methods to evaluate the form of relationships between PM and health
23 outcomes, and draws conclusions on the most well-supported shape of these relationships.
24 Animal data may also inform evaluation of concentration-response relationships,
25 particularly relative to MOAs, and characteristics of susceptible subpopulations. For some
26 health outcomes, the probability and severity of health effects and associated uncertainties
27 can be characterized. Chapter 2 presents the integrated findings informative for evaluation
28 of population risks.

29 An important consideration in characterizing the public health impacts associated
30 with exposure to a pollutant is whether the concentration-response relationship is linear
31 across the full concentration range encountered, or if nonlinear relationships exist along
32 any part of this range. Of particular interest is the shape of the concentration-response
33 curve at and below the level of the current standards. The shape of the

1 concentration-response curve varies, depending on the type of health outcome, underlying
2 biological mechanisms and dose. At the human population level, however, various sources of
3 variability and uncertainty tend to smooth and “linearize” the concentration-response
4 function (such as the low data density in the lower concentration range, possible influence
5 of measurement error, and individual differences in susceptibility to air pollution health
6 effects). In addition, many chemicals and agents may act by perturbing naturally occurring
7 background processes that lead to disease, which also linearizes population
8 concentration-response relationships (Clewell and Crump, 2005, [156359](#); Crump et al.,
9 1976, [003192](#); Hoel, 1980, [156555](#)). These attributes of population dose-response may
10 explain why the available human data at ambient concentrations for some environmental
11 pollutants (e.g., PM, O₃, lead [Pb], environmental tobacco smoke [ETS], radiation) do not
12 exhibit evident thresholds for health effects, even though likely mechanisms include
13 nonlinear processes for some key events. These attributes of human population
14 dose-response relationships have been extensively discussed in the broader epidemiologic
15 literature (Rothman and Greenland S, 1998, [086599](#)).

16 Publication bias is a source of uncertainty regarding the magnitude of health risk
17 estimates. It is well understood that studies reporting non-null findings are more likely to
18 be published than reports of null findings, and publication bias can also result in
19 overestimation of effect estimate sizes (Ioannidis, 2008, [188317](#)). For example, effect
20 estimates from single-city epidemiologic studies have been found to be generally larger than
21 those from multicity studies (Anderson et al., 2005, [087916](#)).

22 Finally, identification of the susceptible or vulnerable population groups contributes
23 to an understanding of the public health impact of pollutant exposures. Epidemiologic
24 studies can help identify susceptible or vulnerable subpopulations by evaluating health
25 responses in the study population. Examples include stratified analyses for subsets of the
26 population under study, or testing for interactions or effect modification by factors such as
27 gender, age group, or health status. Experimental studies using animal models of
28 susceptibility or disease can also inform the extent to which health risks are likely greater
29 in specific population subgroups. Further discussion of these groups is in Chapter 8.

1.5.6.2. Effects on Public Welfare

30 Key questions for understanding the quantitative relationships between exposure (or
31 concentration or deposition) to a pollutant and risk to the public welfare (e.g., ecosystems,
32 visibility, materials, climate):

- 33 ▪ What elements of the ecosystem (e.g., types, regions, taxonomic groups, populations,
34 functions, etc.) appear to be affected, or are more sensitive to effects?
- 35 ▪ Under what exposure conditions (amount deposited or concentration, duration and
36 pattern) are effects seen?

- 1 ▪ What is the shape of the concentration-response or exposure-response relationship?

2 Evaluations of causality typically consider the probability of welfare effects changing
3 in response to exposure. A challenge to the quantification of exposure-response relationships
4 for ecological effects is the variability across ecosystems. Ecological responses are evaluated
5 within the range of observations, so a quantitative relationship may be determined for a
6 given ecological system and scale. However, there is great regional and local variability in
7 ecosystems. Thus, exposure-response relationships are often available site by site, rather
8 than at the national or even regional scale. Quantitative relationships therefore are
9 available site by site. For example, an ecological response to deposition of a given pollutant
10 can differ greatly between ecosystems. Where results from greenhouse or natural ecological
11 studies are available, they may be used to aid in characterizing exposure-response
12 relations, particularly relative to mechanisms of action, and characteristics of sensitive
13 biota.

1.5.7. Concepts in Evaluating Adversity of Health Effects

14 In evaluating the health evidence, a number of factors can be considered in deter-
15 mining the extent to which health effects are “adverse” for health outcomes such as changes
16 in lung function. What constitutes an adverse health effect may vary between populations.
17 Some changes in healthy individuals may not be considered adverse while those of a similar
18 type and magnitude are potentially adverse in more susceptible individuals.

19 The American Thoracic Society (ATS) published an official statement titled *What*
20 *Constitutes an Adverse Health Effect of Air Pollution?* (ATS, 2000, [011738](#)). This statement
21 updated the guidance for defining adverse respiratory health effects that had been
22 published 15 years earlier (ATS, 1985, [006522](#)), taking into account new investigative
23 approaches used to identify the effects of air pollution and reflecting concern for impacts of
24 air pollution on specific susceptible groups. In the 2000 update, there was an increased
25 focus on quality of life measures as indicators of adversity and a more specific consideration
26 of population risk. Exposure to air pollution that increases the risk of an adverse effect to
27 the entire population is viewed as adverse, even though it may not increase the risk of any
28 identifiable individual to an unacceptable level; estimated mean population effects do not
29 reflect more severe effects in individuals. For example, a population of asthmatics could
30 have a distribution of lung function such that no identifiable individual has a level
31 associated with significant impairment. Exposure to air pollution could shift the
32 distribution such that no identifiable individual experiences clinically-relevant effects; this
33 shift toward decreased lung function, however, would be considered adverse because
34 individuals within the population would have diminished reserve function and, therefore,
35 would be at increased risk to further environmental insult.

1.6. Summary

1 This second external review draft ISA is a review, synthesis, and evaluation of the
2 most policy-relevant science, and communicates critical science judgments relevant to the
3 NAAQS review. It reviews the most policy-relevant evidence from environmental
4 effects studies and includes information on atmospheric chemistry, PM sources and
5 emissions, exposure, and dosimetry. This draft ISA incorporates clarification and revisions
6 based on advice and comments provided by EPA's CASAC (Samet, 2009, [190992](#)). Annexes
7 to the ISA provide additional details of the literature published since the last review. A
8 framework for making critical judgments concerning causality appears in this chapter. It
9 relies on a widely accepted set of principles and standardized language to express evaluation
10 of the evidence. This approach can bring rigor and clarity to the current and future
11 assessments. This ISA should assist EPA and others, now and in the future, to accurately
12 represent what is presently known—and what remains unknown—concerning the effects of
13 PM on human health and public welfare.

Chapter 1 References

- Adams SM. (2003). Establishing causality between environmental stressors and effects on aquatic ecosystems. *Human and Ecological Risk Assessment*, 9: 17-35. [156192](#)
- Anderson HR; Atkinson RW; Peacock JL; Sweeting MJ; Marston L. (2005). Ambient particulate matter and health effects: Publication bias in studies of short-term associations. *Epidemiology*, 16: 155-163. [087916](#)
- ATS. (1985). Guidelines as to what constitutes an adverse respiratory health effect, with special reference to epidemiologic studies of air pollution. American Thoracic Society . *Am Rev Respir Dis*, 131: 666-668. [006522](#)
- ATS. (2000). What constitutes an adverse health effect of air pollution? Official statement of the American Thoracic Society. *Am J Respir Crit Care Med*, 161: 665-673. [011738](#)
- CDC. (2004). The health consequences of smoking: A report of the Surgeon General. Centers for Disease Control and Prevention, U.S. Department of Health and Human Services. Washington, DC. [056384](#)
- Clewell HJ; Crump KS. (2005). Quantitative estimates of risk for noncancer endpoints. *Risk Anal*, 25: 285-289. [156359](#)
- Collier TK. (2003). Forensic ecotoxicology: Establishing causality between contaminants and biological effects in field studies. *Human and Ecological Risk Assessment*, 9: 259 - 266. [155736](#)
- Crump KS; Hoel DG; Langley CH; Peto R. (1976). Fundamental carcinogenic processes and their implications for low dose risk assessment. *Cancer Res*, 36: 2973-2979. [003192](#)
- Fox GA. (1991). Practical causal inference for ecotoxicologists. *J Toxicol Environ Health*, 33: 359-373. [156444](#)
- Gee GC; Payne-Sturges DC. (2004). Environmental health disparities: A framework integrating psychosocial and environmental concepts. *Environ Health Perspect*, 112: 1645-1653. [093070](#)
- Gerritsen J; Carlson RE; Dycus DL; Faulkner C; Gibson GR. (1998). Lake and reservoir bioassessment and biocriteria: Technical guidance document. US Environmental Protection Agency, Office of Water. Washington, DC. EPA 841-B-98-007. <http://www.epa.gov/owow/monitoring/tech/lakes.html> . [156465](#)
- Gordon T; Gerber H; Fang CP; Chen LC. (1999). A centrifugal particle concentrator for use in inhalation toxicology. *Inhal Toxicol*, 11: 71-87. [001176](#)
- Henderson R. (2005). Clean Air Scientific Advisory Committee (CASAC) review of the EPA staff recommendations concerning a Potential Thoracic Coarse PM standard in the Review of the National Ambient Air Quality Standards for Particulate Matter: Policy Assessment of Scientific and Technical Information. U.S. Environmental Protection Agency. RTP, NC. [156537](#)
- Henderson R. (2005). EPA's Review of the National Ambient Air Quality Standards for Particulate Matter (Second Draft PM Staff Paper, January 2005): A review by the Particulate Matter Review Panel of the EPA Clean Air Scientific Advisory Committee. U.S. Environmental Protection Agency. Washington D.C.. [188316](#)
- Henderson R. (2006). Clean Air Scientific Advisory Committee recommendations concerning the proposed National Ambient Air Quality Standards for particulate matter. U.S. Environmental Protection Agency. Washington, DC. [156538](#)
- Hill AB. (1965). The environment and disease: Association or causation. *J R Soc Med*, 58: 295-300. [071664](#)
- Hoel DG. (1980). Incorporation of background in dose-response models. *Fed Proc*, 39: 73-75. [156555](#)
- IARC. (2006). IARC monographs on the evaluation of carcinogenic risks to humans: Preamble. International Agency for Research on Cancer. Lyon, France . <http://monographs.iarc.fr/ENG/Preamble/CurrentPreamble.pdf> . [093206](#)
- Ioannidis JPA. (2008). Why most discovered true associations are inflated. *Epidemiology*, 19: 640-648. [188317](#)
- IOM. (2008). Improving the Presumptive Disability Decision-Making Process for Veterans: Committee on Evaluation of the Presumptive Disability Decision-Making Process for Veterans, Board on Military and Veterans Health. Washington, DC: Institute of Medicine of the National Academies, National Academies Press. [156586](#)
- Maciejczyk P; Chen LC. (2005). Effects of subchronic exposures to concentrated ambient particles (CAPs) in mice: VIII source-related daily variations in in vitro responses to CAPs. *Inhal Toxicol*, 17: 243-253. [087456](#)
- NAPAP. (1991). The experience and legacy of NAPAP report of the Oversight Review Board. National Acid Precipitation Assessment Program. Washington, DC. [095894](#)
- NAPCA. (1969). Air quality criteria for particulate matter. National Air Pollution Control Administration. Washington, DC. [014684](#)
- NRC. (2004). Research priorities for airborne particulate matter: IV Continuing research progress. National Academies Press . Washington, DC. [156814](#)

- Rothman KJ; Greenland S eds. (1998). Modern epidemiology. Philadelphia, PA: Lippincott-Raven Publishers. [086599](#)
- Samet JM. (2009). Review of EPA's Integrated Science Assessment for Particulate Matter (First External Review Draft, December 2008). Clean Air Scientific Advisory Committee (CASAC) and members of the CASAC Particulate Matter (PM) Review Panel, Science Advisory Board, U.S. Environmental Protection Agency. Washington, D.C.. EPA-CASAC-09-008. [190992](#)
- Sioutas C; Kim S; Chang M. (1999). Development and evaluation of a prototype ultrafine particle concentrator. J Aerosol Sci, 30: 1001-1017. [001633](#)
- Sioutas D; Koutrakis P; Ferguson ST; Burton RM. (1995). Development and evaluation of a prototype ambient particle concentrator for inhalation exposure studies. Inhal Toxicol, 7: 633-644. [001629](#)
- Su Y; Sipin MF; Spencer MT; Qin X; Moffet RC; Shields LG; Prather KA; Venkatachari P; Jeong C-H; Kim E; Hopke PK; Gelein RM; Utell MJ; Oberdörster G; Berntsen J; Devlin RB; Chen LC. (2006). Real-time characterization of the composition of individual particles emitted from ultrafine particle concentrators. Aerosol Sci Technol, 40: 437 - 455. [157021](#)
- U.S. EPA. (2004). Air quality criteria for particulate matter. U.S. Environmental Protection Agency. Research Triangle Park, NC. EPA/600/P-99/002aF-bF. [056905](#)
- U.S. EPA. (2005). Guidelines for carcinogen risk assessment, Risk Assessment Forum Report. U.S. Environmental Protection Agency. Washington, DC. EPA/630/P-03/001F. <http://cfpub.epa.gov/ncea/index.cfm> . [086237](#)
- U.S. EPA. (2005). Review of the national ambient air quality standards for particulate matter: Policy assessment of scientific and technical information OAQPS staff paper. Office of Air Quality Planning and Standards, U.S. EPA. Research Triangle Park, North Carolina. EPA/452/R-05-005a. http://www.epa.gov/ttn/naaqs/standards/pm/data/pmstaffpaper_20051221.pdf . [090209](#)
- U.S. EPA. (2008). Integrated review plan for the national ambient air quality standards for particulate matter. U.S. Environmental Protection Agency, Office of Research and Development, National Center for Environmental Assessment. Research Triangle Park, NC. [157072](#)
- U.S. EPA. (2008). Integrated science assessment for oxides of nitrogen and sulfur: Ecological criteria. EPA. Research Triangle Park, NC. EPA/600/R-08/082F. [157074](#)

Chapter 2. Integrative Health and Welfare Effects Overview

1 The subsequent chapters of this ISA will present the most policy-relevant information
2 related to this review of the NAAQS for PM. This chapter integrates the key findings from
3 the disciplines evaluated in this current assessment of the PM scientific literature, which
4 includes the atmospheric sciences, ambient air data analyses, exposure assessment,
5 dosimetry, health studies (e.g., toxicological, controlled human exposure, and
6 epidemiologic), and ecological and welfare effects. The EPA framework for causal
7 determinations described in Chapter 1 has been applied to the body of scientific evidence in
8 order to collectively examine the health effects, or ecological and welfare effects attributed
9 to PM exposure in a two-step process.

10 As described in Chapter 1, EPA assesses the results of recent relevant publications,
11 building upon evidence available during the previous NAAQS review, to draw conclusions
12 on the causal relationships between relevant pollutant exposures and health or
13 environmental effects. This ISA uses a five-level hierarchy that classifies the weight of
14 evidence for causation:

- 15 ▪ Causal relationship
- 16 ▪ Likely to be a causal relationship
- 17 ▪ Suggestive of a causal relationship
- 18 ▪ Inadequate to infer a causal relationship
- 19 ▪ Not likely to be a causal relationship

20 Beyond judgments regarding causality are questions relevant to quantifying health or
21 environmental risks based on our understanding of the quantitative relationships between
22 pollutant exposures and health or welfare effects. Once a determination is made regarding
23 the causal relationship between the pollutant and outcome category, important questions
24 regarding quantitative relationships include:

- 25 ▪ What is the concentration-response or dose-response relationship?
- 26 ▪ Under what exposure conditions (amount deposited, dose or concentration, duration
27 and pattern) are effects seen?

Note: Hyperlinks to the reference citations throughout this document will take you to the NCEA HERO database (Health and Environmental Research Online) at <http://epa.gov/hero>. HERO is a database of scientific literature used by U.S. EPA in the process of developing science assessments such as the Integrated Science Assessments (ISA) and the Integrated Risk Information System (IRIS).

- 1 ▪ What subpopulations appear to be differentially affected i.e., more susceptible to
2 effects? What elements of the ecosystem (e.g., types, regions, taxonomic groups,
3 populations, functions, etc.) appear to be affected, or are more sensitive to effects?

4 To address these questions, in the second step of the EPA framework, the entirety of
5 quantitative evidence is evaluated to identify and characterize potential
6 concentration-response relationships. This requires evaluation of levels of pollutant and
7 exposure durations at which effects were observed for exposed populations including
8 potentially susceptible subpopulations.

9 This chapter summarizes and integrates the newly available scientific evidence that
10 best informs consideration of the policy-relevant questions that frame this assessment,
11 presented in Chapter 1. Section 2.1 discusses the trends in ambient concentrations and
12 sources of PM and provides a brief summary of ambient air quality for short- and long-term
13 exposure durations. Section 2.2 presents the evidence regarding personal exposure to
14 ambient PM in outdoor and indoor microenvironments, and it discusses the relationship
15 between ambient PM concentrations and exposure to PM from ambient sources. Section 2.3
16 integrates the evidence for studies that examine the health effects associated with short-
17 and long-term exposure to PM and discusses important uncertainties identified in the
18 interpretation of the scientific evidence. In addition, this section presents the evidence for
19 potentially susceptible subpopulations to PM exposure. Section 2.4 provides discussion of
20 policy-relevant considerations, such as potentially susceptible subpopulations, lag
21 structure, and the PM concentration-response relationship. Finally, Section 2.5 summarizes
22 the evidence for ecological and welfare effects related to PM exposure.

2.1. Concentrations and Sources of Atmospheric PM

2.1.1. Ambient PM Variability and Correlations

23 Recently, advances in understanding the spatiotemporal distribution of PM mass and
24 its constituents have been made, particularly with regard to PM_{2.5} and its components as
25 well as ultrafine particles (UFP). Emphasis in this ISA is placed on the period from 2005-
26 2007 incorporating the most recent validated EPA Air Quality System (AQS) data. The AQS
27 is EPA's repository for ambient monitoring data reported by the national, and state and
28 local air monitoring networks. Measurements of PM_{2.5} and PM₁₀ are reported into AQS
29 while PM_{10-2.5} concentrations are obtained as the difference between PM₁₀ and PM_{2.5} (after
30 converting PM₁₀ concentrations from STP to local conditions; Section 3.5). Note, however,
31 that a majority of U.S. counties were not represented in AQS because their population fell
32 below the regulatory monitoring threshold. Moreover, monitors reporting to AQS were not
33 uniformly distributed across the U.S. or within counties, and conclusions drawn from AQS

1 data may not apply equally to all parts of a geographic region. Furthermore, biases can
2 exist for some PM constituents (and hence total mass) owing to volatilization losses of
3 nitrates and other semi-volatile compounds, and, conversely, to retention of particle-bound
4 water by hygroscopic species. The degree of spatial variability in PM was likely to be
5 region-specific and strongly influenced by local sources and meteorological and topographic
6 conditions.

2.1.1.1. Spatial Variability across the U.S.

7 AQS data for concentrations of PM_{2.5} for 2005-2007 showed considerable variability
8 across the U.S. (Section 3.5.1.1). Counties with the highest average concentrations of PM_{2.5}
9 (>18 µg/m³) were reported for several counties in the San Joaquin Valley and inland
10 southern California as well as Jefferson County, AL (containing Birmingham) and
11 Allegheny County, PA (containing Pittsburgh). Relatively few regulatory monitoring sites
12 have the appropriate co-located monitors for computing PM_{10-2.5}, resulting in poor
13 geographic coverage on a national scale (Figure 3-10). Although the general understanding
14 of PM differential settling leads to an expectation of greater spatial heterogeneity in the
15 PM_{10-2.5} fraction, deposition of particles as a function of size depends strongly on local
16 meteorological conditions. Better geographic coverage is available for PM₁₀, where the
17 highest reported annual average concentrations (>50 µg/m³) occurred in southern
18 California, southern Arizona and central New Mexico. The size distribution of PM varied
19 substantially by location, with a generally larger fraction of PM₁₀ mass in the PM_{10-2.5} size
20 range in western cities (e.g., Phoenix and Denver) and a larger fraction of PM₁₀ in the PM_{2.5}
21 size range in eastern U.S. cities (e.g., Pittsburgh and Philadelphia). UFPs are not measured
22 as part of AQS or any other routine regulatory network in the U.S. Therefore, limited
23 information is available regarding regional variability in the spatiotemporal distribution of
24 UFPs.

25 Spatial variability in PM_{2.5} components obtained from the Chemical Speciation
26 Network (CSN) varied considerably by species from 2005-2007 (Figures 3-12 through 3-18).
27 The highest annual average organic carbon (OC) concentrations were observed in the
28 western and southeastern U.S. OC concentrations in the western U.S. peaked in the fall
29 and winter, while OC concentrations in the Southeast peaked anytime between spring and
30 fall. Elemental carbon (EC) exhibited less seasonality than OC and showed lowest seasonal
31 variability in the eastern half of the U.S. The highest annual average EC concentrations
32 were present in Los Angeles, Pittsburgh, New York, and El Paso. Concentrations of sulfate
33 (SO₄²⁻) were higher in the eastern U.S. as a result of higher sulfur dioxide (SO₂) emissions
34 in the East compared with the West. There is also considerable seasonal variability with
35 higher SO₄²⁻ concentrations in the summer months when the oxidation of SO₂ proceeds at a
36 faster rate than during the winter. Nitrate (NO₃⁻) concentrations were highest in California
37 and during the winter in the Upper Midwest. In general, NO₃⁻ was higher in the winter

1 across the country, in part as a result of temperature-driven partitioning and volatilization.
2 Exceptions existed in Los Angeles and Riverside, CA, where high NO_3^- concentrations
3 appeared year-round. There is variation in both $\text{PM}_{2.5}$ mass and composition among cities,
4 some of which might be due to regional differences in meteorology, sources, and topography.

2.1.1.2. Spatial Variability on the Urban and Neighborhood Scales

5 In general, $\text{PM}_{2.5}$ has a longer atmospheric lifetime than $\text{PM}_{10-2.5}$. As a result, $\text{PM}_{2.5}$ is
6 more homogeneously distributed than $\text{PM}_{10-2.5}$, whose concentrations more closely reflect
7 proximity to local sources (Section 3.5.1.2). Since PM_{10} incorporates $\text{PM}_{10-2.5}$ in addition to
8 $\text{PM}_{2.5}$, it also exhibits more spatial heterogeneity than $\text{PM}_{2.5}$. Urban- and neighborhood-
9 scale variability in PM mass and composition was examined by focusing on fifteen
10 metropolitan areas, which were chosen based on their geographic distribution and coverage
11 in recent health effects studies. The urban areas selected were Atlanta, Birmingham,
12 Boston, Chicago, Denver, Detroit, Houston, Los Angeles, New York, Philadelphia, Phoenix,
13 Pittsburgh, Riverside, Seattle and St. Louis. Inter-monitor correlation remained higher
14 over long distances for $\text{PM}_{2.5}$ as compared with PM_{10} in these 15 urban areas. To a large
15 extent, greater variation in $\text{PM}_{2.5}$ and PM_{10} concentrations within cities was observed in
16 areas with lower ratios of $\text{PM}_{2.5}$ to PM_{10} . When the data was limited to only sampler pairs
17 with less than 4 km separation (i.e., on a neighborhood scale), inter-sampler correlations
18 remained higher for $\text{PM}_{2.5}$ than for PM_{10} . Average correlation was maintained at 0.93 for
19 $\text{PM}_{2.5}$, while it dropped to 0.70 for PM_{10} (Section 3.5.1.3). Insufficient data were available in
20 the 15 metropolitan areas to perform similar analyses for $\text{PM}_{10-2.5}$ using co-located, low
21 volume FRM monitors.

22 As previously mentioned, UFPs are not measured as part of AQS or any other routine
23 regulatory network in the U.S. Therefore, information about the spatial variability of UFPs
24 is sparse; however, their number concentrations are expected to be highly spatially and
25 temporally variable. This has been shown on the urban scale in studies in which UFP
26 number concentrations drop off quickly with distance from roads compared to accumulation
27 mode particle numbers.

2.1.2. Trends and Temporal Variability

28 Overall, $\text{PM}_{2.5}$ concentrations decreased from 1999 (the beginning of nationwide
29 monitoring for $\text{PM}_{2.5}$) to 2007 in all 10 EPA Regions, with the 3-yr avg of the 98th percentile
30 of 24-h $\text{PM}_{2.5}$ concentrations dropping 10% over this time period. However from 2002 to
31 2007, concentrations of $\text{PM}_{2.5}$ were nearly constant with decreases observed in only some
32 EPA Regions (Section 3.5.2.1). Concentrations of $\text{PM}_{2.5}$ components were only available for
33 2002-2007 using CSN data and showed little decline over this time period. This trend in
34 $\text{PM}_{2.5}$ components is consistent with trends in $\text{PM}_{2.5}$ mass concentration observed after 2002

1 (shown in Figures 3-44 through 3-47). Concentrations of PM₁₀ also declined from 1988 to
2 2007 in all 10 EPA Regions.

3 Using hourly PM observations in the 15 metropolitan areas, diel variation showed
4 average hourly peaks that differ by size fraction and region (Section 3.5.2.3). For both PM_{2.5}
5 and PM₁₀, a morning peak was typically observed starting at approximately 6:00 a.m.,
6 corresponding with the start of morning rush hour. There was also an evening
7 concentration peak that was broader than the morning peak and extended into the
8 overnight period, reflecting the concentration increase caused by the usual collapse of the
9 mixing layer after sundown. The magnitude and duration of these peaks varied
10 considerably by metropolitan area investigated.

11 UFPs were found to exhibit similar two-peaked diel patterns in Los Angeles and the
12 San Joaquin Valley of CA, Rochester, NY as well as in Kawasaki City, Japan and
13 Copenhagen, Denmark. The morning peak in UFPs likely represents primary source
14 emissions, such as rush-hour traffic, while the afternoon peak likely represents the
15 combination of primary source emissions and nucleation of new particles.

2.1.3. Correlations between Copollutants

16 Correlations between PM and gaseous copollutants including SO₂, nitrogen dioxide
17 (NO₂), carbon monoxide (CO) and ozone (O₃) varied both seasonally and spatially between
18 and within metropolitan areas (Section 3.5.3). On average, PM_{2.5} and PM₁₀ were correlated
19 with each other better than with the gaseous copollutants. There was relatively little
20 seasonal variability in the mean correlation between PM in both size fractions and SO₂ and
21 NO₂. CO, however, showed higher correlations with PM_{2.5} and PM₁₀ on average in the
22 winter compared with the other seasons. This seasonality results in part because a larger
23 fraction of PM is primary in origin during the winter. To the extent that this primary
24 component of PM is associated with common combustion sources of NO₂ and CO, then
25 higher correlations with these gaseous copollutants are to be expected. Increased
26 atmospheric stability in colder months also results in higher correlations between primary
27 pollutants (Section 3.5).

28 The correlation between daily maximum 8-h avg O₃ and PM_{2.5} showed the highest
29 degree of seasonal variability with positive correlations on average in the spring, summer
30 and fall, and negative correlations on average in the winter. This situation arises as the
31 result of seasonal differences in sources and photochemical production of secondary PM_{2.5}
32 and O₃. However, this relationship was not present in Birmingham, Boston and St. Louis.

2.1.4. Measurement Techniques

33 The federal reference methods (FRMs) for PM_{2.5} and PM₁₀ are based on criteria
34 outlined in the Code of Federal Regulations. They are, however, subject to several

1 limitations that should be kept in mind when using compliance monitoring data for health
2 studies. For example, FRM techniques are subject to the loss of semi-volatile species such
3 as organic compounds and ammonium nitrate (especially in the West). Since FRMs based
4 on gravimetry use 24-h integrated filter samples to collect PM mass, no information is
5 available for variations over shorter averaging times from these instruments. However,
6 reliable methods have been developed to measure real-time PM mass concentrations. Real-
7 time (or continuous and semi-continuous) measurement techniques are also available for
8 PM species, such as particle into liquid sampler (PILS) for multiple ions analysis and
9 aerosol mass spectrometer (AMS) for multiple components analysis (Section 3.4.1).
10 Advances have also been achieved in PM organic speciation. New 24-h FRMs and Federal
11 Equivalent Methods (FEMs) based on gravimetry and continuous FEMs for PM_{10-2.5} are
12 available. FRMs for PM_{10-2.5} rely on calculating the difference between co-located PM₁₀ and
13 PM_{2.5} measurements and a dichotomous sampler is designated as an FEM.

2.1.5. PM Formation in the Atmosphere and Removal

14 PM in the atmosphere contains both primary (i.e., emitted directly by sources) and
15 secondary components, which can be anthropogenic or natural in origin. Secondary PM
16 components can be produced by the oxidation of precursor gases such as SO₂ and NO_x to
17 acids followed by neutralization with ammonia (NH₃) and the partial oxidation of organic
18 compounds. In addition to being emitted as primary particles, UFPs are produced by the
19 nucleation of H₂SO₄ vapor and perhaps NH₃ and certain organic compounds. Over most of
20 the earth's surface, nucleation is probably the major mechanism forming new UFPs. New
21 UFP formation has been observed in environments ranging from relatively unpolluted
22 marine and continental environments to polluted urban areas as an ongoing background
23 process and during nucleation events. However, as noted above a large percentage of UFPs
24 come from combustion-related sources such as mobile sources.

25 Developments in the chemistry of formation of secondary organic aerosol (SOA)
26 indicate that oligomers are likely a major component of OC in aerosol samples. Recent
27 observations also suggest that small but significant quantities of SOA are formed from
28 isoprene oxidation of terpenes and organic hydrocarbons with six or more carbon atoms.
29 Gasoline engines have been found to emit a mix of nucleation-mode heavy and large
30 polycyclic aromatic hydrocarbons on which unspent fuel and trace metals can condense,
31 while diesel particles are composed of a soot nucleus on which sulfates and hydrocarbons
32 can condense. To the extent that the primary component of organic aerosol is overestimated
33 in emissions from combustion sources, the semi-volatile components are underestimated.
34 This situation results from the lack of capture of evaporated semi-volatile components upon
35 dilution in common emissions tests. As a result, near-traffic sources of precursors to
36 secondary organic aerosol would be underestimated. The oxidation of these precursors

1 results in more oxidized forms of SOA than previously considered, both in near source
2 urban environments and further downwind. Organic peroxides constitute a significant
3 fraction of SOA and represent an important class of reactive oxygen species (ROS) that
4 have high oxidizing potential. More information on sources, emissions and deposition of PM
5 are included in Section 3.3.

6 Wet and dry deposition are important processes for removing PM and other pollutants
7 from the atmosphere on urban, regional, and global scales. Wet deposition includes
8 incorporation of particles into cloud droplets that fall as rain (rainout) and collisions with
9 falling rain (washout). Other hydrometeors (snow, ice) can also serve the same purpose. Dry
10 deposition involves transfer of particles through gravitational settling and/or by impaction
11 on surfaces by turbulent motions. The effects of deposition of PM on ecosystems and
12 materials are discussed in Section 2.5 and in Chapter 9.

2.1.6. Source Contributions to PM

13 Results of receptor modeling calculations indicate that PM_{2.5} is produced mainly by
14 combustion of fossil fuel, either by stationary sources or by transportation. A relatively
15 small number of broadly defined source categories, compared to the total number of
16 chemical species that typically are measured in ambient monitoring source receptor
17 studies, account for the majority of the observed PM mass. Some ambiguity is inherent in
18 identifying source categories. For example, quite different mobile sources such as trucks
19 and locomotives rely on diesel engines and ancillary data is often required to resolve these
20 sources. A compilation of study results shows that secondary SO₄²⁻ (mainly from Electric
21 Generating Units [EGUs]), NO₃⁻ (from the oxidation of NO_x emitted mainly from
22 transportation sources and EGUs), and primary mobile source categories constitute most of
23 PM_{2.5} (and PM₁₀) in the East. PM_{10-2.5} is mainly a primary pollutant, having been emitted
24 from pollution sources as fully formed particles derived from abrasion and crushing
25 processes, soil disturbances, desiccation of marine aerosol emitted from bursting bubbles,
26 hygroscopic fine PM expanding with humidity to coarse mode, and/or gas condensation
27 directly onto preexisting coarse particles. Suspended primary coarse PM may contain iron,
28 silica, aluminum, and base cations from soil, plant and insect fragments, pollen, fungal
29 spores, bacteria, and viruses, as well as fly ash, brake lining particles, debris, and
30 automobile tire fragments. Quoted uncertainties in the source apportionment of
31 constituents in ambient aerosol samples typically range from 10 to 50%. An
32 intercomparison of source apportionment techniques indicated that the same major source
33 categories of PM_{2.5} were consistently identified by several independent groups working with
34 the same data sets. Soil-, sulfate-, residual oil-, and salt-associated mass were most clearly
35 identified by the groups. Other sources with more ambiguous signatures, such as vegetative
36 burning and traffic-related emissions were less consistently identified.

1 Spatial variability in source contributions across urban areas is an important
2 consideration in assessing the likelihood of exposure error in epidemiologic studies relating
3 health outcomes to sources. Concepts similar to those for using ambient concentrations as
4 surrogates for personal exposures apply here. Some source attribution studies for PM_{2.5}
5 indicate that intra-urban variability increases in the following order: regional sources (e.g.,
6 secondary SO₄²⁻ originating from EGUs) < area sources (e.g., on-road mobile sources)
7 < point sources (e.g., stacks). Although limited information was available for PM_{10-2.5}, it does
8 indicate a similar ordering, but without a regional component (resulting from the short
9 lifetime of PM_{10-2.5} compared to transport times on the regional scale). More discussion on
10 source contributions to PM is available in Section 3.6.

2.1.7. Policy-Relevant Background

11 The background concentrations of PM that are useful for risk and policy assessments,
12 which inform decisions about the NAAQS are referred to as policy-relevant background
13 (PRB) concentrations. PRB concentrations have historically been defined by EPA as those
14 concentrations that would occur in the U.S. in the absence of anthropogenic emissions in
15 continental North America defined here as the U.S., Canada, and Mexico. For this
16 document, PRB concentrations include contributions from natural sources everywhere in
17 the world and from anthropogenic sources outside continental North America. Background
18 concentrations so defined facilitated separation of pollution that can be controlled by U.S.
19 regulations or through international agreements with neighboring countries from those
20 that were judged to be generally uncontrollable by the U.S. Over time, consideration of
21 potential broader ranging international agreements may lead to alternative determinations
22 of which PM source contributions should be considered by EPA as part of PRB.
23 Contributions to PRB concentrations of PM include both primary and secondary natural
24 and anthropogenic components. For this document, PRB concentrations of PM_{2.5} for the
25 continental U.S. were estimated using EPA's Community Multi-scale Air Quality (CMAQ)
26 modeling system, a deterministic, chemical-transport model (CTM), using output from
27 GEOS-Chem a global-scale model for CMAQ boundary conditions. PRB concentrations of
28 PM_{2.5} were estimated to be less than 1 µg/m³ on an annual basis, with maximum daily
29 average values in a range from 3.1 to 20 µg/m³ and having a peak of 63 µg/m³ at the nine
30 national park sites across the U.S. used to evaluate model performance for this analysis. A
31 description of the models and evaluation of their performance is given in Section 3.6 and
32 further details about the calculations of PRB concentrations is given in Section 3.7.

2.2. Human Exposure

33 This section summarizes the findings from the recent exposure assessment literature,
34 which includes the assessment of exposure to ambient PM, infiltration of ambient PM to

1 indoor environments, and source apportionment of exposure. This summary is intended to
2 support the interpretation of the findings from epidemiologic studies (Section 3.8).

2.2.1. Spatial Scales of PM Exposure Assessment

3 Assessing population-level exposure at the urban scale is particularly relevant for
4 time-series epidemiologic studies, which provide information on the relationship between
5 health effects and community-average exposure, rather than an individual's exposure. PM
6 concentrations measured at a central-site ambient monitor are used as surrogates for
7 personal PM exposure. However, the correlation between the PM concentration measured
8 at central-site ambient monitor(s) and the unknown true community average concentration
9 depends on the spatial distribution of PM, the location of the monitoring site(s) chosen to
10 represent the community average, and division of the community by terrain features or
11 local sources into several sub-communities that differ in the temporal pattern of pollution.
12 Concentrations of SO_4^{2-} and some components of SOA measured at central-site monitors are
13 expected to be uniform in urban areas because of the regional nature of their sources.
14 However, this is not true for primary components like EC whose sources are strongly
15 spatially variable in urban areas.

16 At micro-to-neighborhood scales, heterogeneity of sources and topography are sources
17 of variability in exposure. This is particularly true for $\text{PM}_{10-2.5}$ and for UFPs, which have
18 spatially variable urban sources and loss processes (mainly gravitational settling for $\text{PM}_{10-2.5}$
19 and coagulation for UFPs) that also limit their transport from sources more readily than
20 for $\text{PM}_{2.5}$. Personal activity patterns also vary across urban areas and across regions. Some
21 studies, conducted mainly in Europe, have found personal $\text{PM}_{2.5}$ and PM_{10} exposures for
22 pedestrians in street canyons to be higher than ambient concentrations measured by urban
23 central site ambient monitors. Likewise, microenvironmental UFP concentrations were
24 observed to be substantially higher in near-road environments, street canyons, and tunnels
25 when compared with background concentrations. In-vehicle UFP and $\text{PM}_{2.5}$ exposures can
26 also be important. As a result, ambient monitors located at background, central urban, road
27 side, or near-residential sites might not reflect the contributions in UFP or $\text{PM}_{2.5}$ exposures
28 to individuals who commute.

29 There is significant variability within and across regions of the country with respect
30 to indoor exposures to ambient PM. Infiltrated ambient PM concentrations depend in part
31 on the ventilation properties of the building or vehicle in which the person is exposed. PM
32 infiltration factors depend on particle size, chemical composition, season, and region of the
33 country. Infiltration can best be modeled dynamically rather than being represented by a
34 single value. Season is important to PM infiltration because it affects the ventilation
35 practices (e.g., open windows) used. In addition, ambient temperature and humidity
36 conditions affect the transport, dispersion, and size distribution of PM. Residential air

1 exchange rates have been observed to be higher in the summer for regions with low air
2 conditioning usage. Regional differences in air exchange rates (Southwest < Southeast
3 < Northeast < Northwest) also reflect ventilation practices. Differential infiltration occurs
4 as a function of PM size and composition (the latter of which is described below). PM
5 infiltration is larger for accumulation mode particles than for UFPs and PM_{10-2.5}.
6 Differential infiltration by size fraction can affect exposure estimates if not accurately
7 characterized.

2.2.2. Exposure to PM Components and Copollutants

8 Emission inventories and source apportionment studies suggest that sources of PM
9 exposure vary by region. Comparison of studies performed in the eastern U.S. with studies
10 performed in the western U.S. suggest that the contribution of SO₄²⁻ to exposure is higher
11 for the East (16-46%) compared with the West (~4%) and that motor vehicle emissions and
12 secondary NO₃⁻ are larger sources of exposure for the West (~9%) as compared with the
13 East (~4%). Results of source apportionment studies of exposure to SO₄²⁻ indicate that SO₄²⁻
14 exposures are mainly attributable to ambient sources. Source apportionment for OC and
15 EC is difficult because they originate from both indoor and outdoor sources. Exposure to OC
16 of indoor and outdoor origin can be distinguished by the presence of aliphatic C-H groups
17 generated indoors, since outdoor concentrations of aliphatic C-H are low. Studies of
18 personal exposure to ambient trace metal have shown significant variation among cities
19 and over seasons. This is in response to geographic and seasonal variability in sources
20 including incinerator operation, fossil fuel combustion, biomass combustion (wildfires), and
21 the resuspension of crustal materials in the built environment. Differential infiltration is
22 also affected by variations in particle composition and volatility. For example, EC infiltrates
23 more readily than OC. This can lead to outdoor-indoor differentials in PM composition.

24 Some studies have explored the relationship between PM and copollutant gases and
25 suggested that certain gases can serve as surrogates for describing exposure to other air
26 pollutants. The findings indicate that ambient concentrations of gaseous copollutants can
27 act as surrogates for personal exposure to ambient PM. Several studies have concluded that
28 ambient concentrations of O₃, NO₂, and SO₂ are associated with the ambient component of
29 personal exposure to total PM_{2.5} as opposed to the ambient component of personal
30 exposures to the gases. However, in some of these studies this result may have arisen in
31 part because personal exposure to the gases was often beneath the detection limits of the
32 personal monitoring devices. If associations between ambient gases and personal exposure
33 to PM_{2.5} of ambient origin exist, such associations are complex and vary by season and
34 location.

2.2.3. Implications for Epidemiologic Studies

1 In epidemiologic studies, exposure may be estimated using various approaches most
2 of which rely on measurements obtained using central site monitors. The magnitude and
3 direction of the biases introduced through error in exposure measurement depend on the
4 extent to which the error is associated with the measured PM concentration. In general,
5 when exposure error is not strongly correlated with the measured PM concentration, bias is
6 toward the null and effect estimates are underestimated. Moreover, lack of information
7 regarding exposure measurement error can also add uncertainty to the health effects
8 estimate.

9 One important factor to be considered is spatial variation in PM concentrations. The
10 degree of urban-scale spatial variability in PM concentrations varies across the country and
11 with size fraction. PM_{2.5} concentrations are relatively well-correlated across monitors in the
12 urban areas examined for this assessment. The limited available evidence indicates that
13 there is greater spatial variability in PM_{10-2.5} concentrations than PM_{2.5} concentrations,
14 resulting in increased exposure error for the larger size fraction. Likewise, studies have
15 shown UFP to be more spatially variable across urban areas compared to PM_{2.5}. Even if
16 PM_{2.5}, PM_{10-2.5}, or UFP concentrations measured at sites within an urban area are generally
17 highly correlated, significant spatial variation in their concentrations can occur on any
18 given day. In addition, there can be differential exposure errors for PM components (e.g.,
19 sulfates, OC, EC). Current information suggests that UFP, PM_{10-2.5}, and some PM
20 components are more spatially variable than PM_{2.5}. For these PM indicators their spatial
21 variability adds uncertainty to exposure estimates.

22 Overall, recent studies generally confirm and build upon the key conclusions of the
23 2004 PM AQCD: separation of total PM exposures into ambient and nonambient
24 components reduces potential uncertainties in the analysis and interpretation of PM health
25 effects data; and ambient PM concentration can be used as a surrogate for ambient PM
26 exposure in community time-series epidemiologic studies because the change in ambient
27 PM concentration should be reflected in the change in the health risk coefficient. The use of
28 the community average ambient PM_{2.5} concentration as a surrogate for the community
29 average personal exposure to ambient PM_{2.5} is not expected to change the principal
30 conclusions from time-series and most panel epidemiologic studies that use community
31 average health and pollution data. Several recent studies support this by showing how the
32 ambient component of personal exposure to PM_{2.5} could be estimated using various tracer
33 and source apportionment techniques and by showing that the ambient component is highly
34 correlated with ambient concentrations of PM_{2.5}. These studies show that the non-ambient
35 component of personal exposure to PM_{2.5} is largely uncorrelated with ambient PM_{2.5}
36 concentrations. A few panel epidemiologic studies have included personal as well as
37 ambient monitoring data, and generally reported associations with all types of PM

1 measurements. Epidemiologic studies of long-term exposure typically exploit the differences
2 in PM concentration across space as well as time to estimate the effect of PM on the health
3 outcome of interest. Long-term exposure estimates are most accurate for pollutants that do
4 not vary substantially within the geographical area studied.

2.3. Health Effects

5 This section evaluates the evidence from toxicological, controlled human exposure,
6 and epidemiologic studies that examined the health effects associated with short- and
7 long-term exposure to PM (i.e., PM_{2.5}, PM_{10-2.5} and UFPs). The results from the health
8 studies evaluated in combination with the evidence from atmospheric chemistry and
9 exposure assessment studies contribute to the causal determinations made for the health
10 outcomes discussed in this assessment (Section 1.5.4). In the following sections a discussion
11 of the causal determinations will be presented by PM size fraction and exposure duration
12 (i.e., short- or long-term exposure) for the health effects for which sufficient evidence was
13 available to conclude a **causal, likely to be causal, or suggestive** relationship. To the extent
14 possible, results of PM₁₀ studies were considered in causality determinations for PM_{2.5} and
15 PM_{10-2.5}. Although an extensive amount of research has been conducted to examine
16 PM-related health effects, a limited body of evidence is currently available to examine the
17 presence or absence of associations between some health outcomes and PM size fractions.
18 The evaluation of the aforementioned factors together has resulted in evidence that is
19 **inadequate** to infer whether a causal relationship exists for the following exposure
20 durations, PM size fractions, and health categories:

- 21 ▪ Short-term exposure to UFPs and mortality
- 22 ▪ Short-term exposure to all PM size fractions and central nervous system (CNS)
23 effects
- 24 ▪ Long-term exposure to PM_{10-2.5} and all health effects and mortality
- 25 ▪ Long-term exposure to UFPs and all health effects and mortality

26 Although not presented in depth in this chapter, a detailed discussion of the
27 underlying evidence used to formulate each causal determination can be found in Chapters
28 6 and 7.

2.3.1. Exposure to PM_{2.5}

2.3.1.1. Effects of Short-Term Exposure to PM_{2.5}

Table 2-1 Summary of causal determinations for short-term exposure to PM_{2.5}.

Size Fraction	Outcome	Causality Determination
PM _{2.5}	Cardiovascular Effects	Causal
	Respiratory Effects	Likely to be causal
	Mortality	Likely to be causal

Cardiovascular Effects

1 Epidemiologic studies that examined the effect of PM_{2.5} on cardiovascular emergency
2 department (ED) visits and hospital admissions (HA) reported consistent positive
3 associations (predominantly for ischemic heart disease [IHD] and congestive heart failure
4 [CHF]), with the majority reporting increases ranging from 0.5 to 3.4% per 10 µg/m³
5 increase in PM_{2.5}. These effects were observed in study locations with mean¹ 24-h avg PM_{2.5}
6 concentrations ranging from 7-18 µg/m³ (Section 6.2.10), with effects becoming more precise
7 and consistently positive in locations with mean PM_{2.5} concentrations of 13 µg/m³ and above
8 (Figure 2-1). Toxicological studies have provided biologically plausible mechanisms (e.g.,
9 increased right ventricular pressure and diminished cardiac contractility) for the
10 associations observed between PM_{2.5} and CHF in epidemiologic studies. The largest U.S.-
11 based multicity study evaluated, Medicare Air Pollution Study (MCAPS), provided evidence
12 of regional heterogeneity (e.g., the largest excess risks occurred in the Northeast [1.08%])
13 and seasonal variation (e.g., the largest excess risks occurred during the winter season
14 [1.49%]) in PM_{2.5} CVD risk estimates, which is consistent with the null findings of several
15 single-city studies conducted in the Western U.S. These associations are supported by
16 multicity epidemiologic studies that observed consistent positive associations between
17 short-term exposure to PM_{2.5} and cardiovascular mortality as well as regional and seasonal
18 variability in risk estimates. The multicity studies evaluated reported consistent, precise
19 increases in cardiovascular mortality ranging from 0.47 to 0.85% in study locations with
20 mean 24-h avg PM_{2.5} concentrations above 13 µg/m³ (Table 6-12).

¹ In this context mean represents the arithmetic mean of 24-h average PM concentrations.

1 Controlled human exposure studies have demonstrated PM_{2.5}-induced changes in
2 various measures of cardiovascular function among healthy and health-compromised
3 adults. The most consistent evidence is for altered vasomotor function following exposure to
4 diesel exhaust (DE) or concentrated ambient particles (CAPs) with ozone (O₃) (Section
5 6.2.4.2). Although these findings provide biological plausibility for the observations from
6 epidemiologic studies, the fresh DE used in the controlled human exposure studies
7 evaluated contains gaseous components (e.g., CO, NO_x), and therefore, the possibility that
8 some of the changes in vasomotor function might be due to gaseous components cannot be
9 ruled out. Furthermore, the prevalence of UF particles in fresh DE limits the ability to
10 conclusively attribute the observed effects to either the UF fraction or PM_{2.5} as a whole. An
11 evaluation of toxicological studies found evidence for altered vessel tone and microvascular
12 reactivity, which provide coherence and biological plausibility for the vasomotor effects that
13 have been observed in both the controlled human exposure and epidemiologic studies
14 (Section 6.2.4.3). However, most of these toxicological studies exposed animals via
15 intratracheal instillation (IT) or using relatively high inhalation concentrations.

16 In addition to the effects observed on vasomotor function, myocardial ischemia has
17 been observed across disciplines through PM_{2.5} effects on ST-segment depression, with
18 toxicological studies providing biological plausibility by demonstrating reduced blood flow
19 during ischemia (Section 6.2.3). There is also a growing body of evidence from controlled
20 human exposure and toxicological studies demonstrating PM_{2.5}-induced changes on
21 markers of systemic oxidative stress and heart rate variability (HRV) (Section 6.2.1 and
22 Section 6.2.9). Additional, but inconsistent effects of PM_{2.5} on BP, blood coagulation
23 markers, and markers of systemic inflammation have also been reported across disciplines.

24 Together, the collective evidence from epidemiologic, controlled human exposure, and
25 toxicological studies is sufficient to conclude that **a causal relationship exists between short-**
26 **term exposures to PM_{2.5} and cardiovascular effects.**

Respiratory Effects

27 The recent epidemiologic studies evaluated report consistent positive associations
28 between short-term exposure to PM_{2.5} and respiratory ED visits and HAs for chronic
29 obstructive pulmonary disease (COPD) and respiratory infections (Section 6.3). Positive
30 associations were also observed for asthma ED visits and HAs for adults and children
31 combined, but effect estimates are imprecise and not consistently positive for children
32 alone. Most effects were in the range of ~1% to 4% and were observed in study locations
33 with mean 24-h avg PM_{2.5} concentrations ranging from 6.1 - 19.2 µg/m³, with effects
34 becoming more precise and consistently positive in locations with mean PM_{2.5}
35 concentrations of 13 µg/m³ and above (Figure 2-1). Additionally, multicity epidemiologic
36 studies observed consistent positive associations between short-term exposure to PM_{2.5} and
37 respiratory mortality as well as regional and seasonal variability in risk estimates. The

1 multicity studies evaluated reported consistent, precise increases in respiratory mortality
2 ranging from 1.67 to 2.20% in study locations with mean 24-h avg PM_{2.5} concentrations
3 above 13 µg/m³ (Table 6-12). Evidence for PM_{2.5}-related respiratory effects was also
4 observed in panel studies, which indicate associations with respiratory symptoms,
5 pulmonary function, and pulmonary inflammation among asthmatic children. Although not
6 consistently observed, some controlled human exposure studies have reported small
7 decrements in various measures of pulmonary function following controlled exposures to
8 PM_{2.5} (Section 6.3.2.2).

9 Controlled human exposure studies using adult volunteers have demonstrated
10 increased markers of pulmonary inflammation following exposure to a variety of different
11 particle types: oxidative responses to DE and WS; and exacerbations of allergic responses
12 and allergic sensitization following exposure to DE particles (Section 6.3). Toxicological
13 studies have provided additional support for PM_{2.5}-related respiratory effects through
14 inhalation exposures of animals to CAPs, DE, other traffic-related PM and WS. These
15 studies reported an array of respiratory effects including altered pulmonary function, mild
16 pulmonary inflammation and injury, oxidative responses, airway hyperresponsiveness
17 (AHR) in allergic and non-allergic animals, exacerbations of allergic responses, and
18 increased susceptibility to infections (Section 6.3). Overall, there is limited coherence across
19 disciplines for the PM_{2.5}-induced respiratory outcomes observed. Epidemiologic studies have
20 reported variable results among specific respiratory outcomes, specifically in asthmatics
21 (e.g., increased respiratory symptoms in asthmatic children, but not increased asthma HAs
22 and ED visits) (Section 6.3.8). Additionally, respiratory effects have not been consistently
23 demonstrated following controlled exposures to PM_{2.5} among asthmatics or individuals with
24 COPD. Collectively, the studies evaluated demonstrate a wide range of respiratory
25 responses, and although results are not fully consistent and coherent across studies the
26 evidence is sufficient to conclude that **a causal relationship is likely to exist between short-**
27 **term exposures to PM_{2.5} and respiratory effects.**

Mortality

28 An evaluation of the epidemiologic literature indicates consistent positive associations
29 between short-term exposure to PM_{2.5} and all-cause, cardiovascular-, and respiratory-
30 related mortality (Section 6.5.2.2.). The evaluation of multicity studies found that risk
31 estimates for all-cause (non-accidental) mortality ranged from 0.29% to 1.21% per 10 µg/m³
32 increase in PM_{2.5} at lags of 1 and 0-1 days. These consistent, precise effects were observed
33 in study locations with mean 24-h avg PM_{2.5} concentrations of 13 µg/m³ and above (Table 6-
34 12). Cardiovascular-related mortality risk estimates were found to be similar to those for
35 all-cause mortality whereas, the risk estimates for respiratory-related mortality were
36 consistently larger: 1.01-2.2% using the same lag periods and averaging indices. Regional
37 and seasonal patterns in PM_{2.5} risk estimates were observed with the greatest effect

1 estimates occurring in the eastern U.S. and during the spring. Of the studies evaluated, no
 2 U.S.-based multicity studies conducted a detailed analysis of the potential confounding of
 3 PM_{2.5} risk estimates by gaseous pollutants but Burnett et al. (2004, [086247](#)) found mixed
 4 results, with possible confounding by NO₂ when analyzing gaseous pollutants in a multicity
 5 Canadian-based study (Section 6.5.2.1). However, it should be noted that U.S.-based
 6 multicity studies that focused on the association between PM₁₀ and mortality found that
 7 gaseous pollutants are not likely to confound the PM-mortality relationship. An
 8 examination of effect modifiers (e.g., demographic and socioeconomic factors), specifically
 9 air conditioning use as an indicator for decreased pollutant penetration indoors, has
 10 suggested that PM_{2.5} risk estimates increase as the percent of the population with access to
 11 air conditioning decreases. Collectively, the epidemiologic literature provides evidence that
 12 **a causal relationship is likely to exist between short-term exposures to PM_{2.5} and mortality.**

2.3.1.2. Effects of Long-Term Exposure to PM_{2.5}

Table 2-2. Summary of causal determinations for long-term exposure to PM_{2.5}.

Size Fraction	Outcome	Causality Determination
PM _{2.5}	Cardiovascular Effects	Causal
	Respiratory Effects	Likely to be causal
	Mortality	Likely to be causal
	Reproductive and Developmental	Suggestive
	Cancer, Mutagenicity, and Genotoxicity	Suggestive

Cardiovascular Effects

13 The strongest evidence for CVD health effects related to long-term exposure to PM_{2.5}
 14 comes from large, multicity U.S.-based studies, which provide consistent evidence of an
 15 association between long-term exposure to PM_{2.5} and cardiovascular mortality (Section
 16 7.2.10). These associations are supported by a large U.S.-based epidemiologic study (i.e.,
 17 Women’s Health Initiative [WHI] study) that reports associations between PM_{2.5} and CVDs
 18 among post-menopausal women using a 1-yr avg PM_{2.5} concentration (mean = 13.5 µg/m³)
 19 (Section 7.2). Epidemiologic studies that examined subclinical markers of CVD report
 20 inconsistent findings. In addition, epidemiologic studies have provided some evidence for
 21 potential modification of the PM_{2.5}-CVD association when examining individual-level data,
 22 specifically smoking status and the use of anti-hyperlipidemics. Although epidemiologic

1 studies have not consistently detected effects on markers of atherosclerosis due to long-
2 term exposure to PM_{2.5}, toxicological studies have provided strong evidence for accelerated
3 development of atherosclerosis in ApoE^{-/-} mice exposed to CAPs and have shown effects on
4 coagulation, experimentally-induced hypertension, and vascular reactivity (Section 7.2.1.2).
5 Evidence from toxicological studies provides biological plausibility and coherence with
6 studies of short-term exposure and CVD morbidity and mortality, as well as with studies
7 that examined long-term exposure to PM_{2.5} and CVD mortality. Taken together, the
8 evidence from epidemiologic and toxicological studies is sufficient to conclude that **a causal**
9 **relationship exists between long-term exposures to PM_{2.5} and cardiovascular effects.**

Respiratory Effects

10 Recent epidemiologic studies conducted in the U.S. and abroad provide evidence of
11 associations between long-term exposure to PM_{2.5} and decrements in lung function growth,
12 increased respiratory symptoms, and asthma development in study locations with mean
13 PM_{2.5} concentrations ranging from 13.8 to 30 µg/m³ during the study periods (Section 7.3.1.1
14 and 7.3.2.1), with effects becoming more precise and consistently positive in locations with
15 mean PM_{2.5} concentrations of 14 µg/m³ and above (Figure 2-2). These results are supported
16 by studies that observed associations between long-term exposure to PM₁₀ and an increase
17 in respiratory symptoms and reductions in lung function growth in areas where PM₁₀ is
18 dominated by PM_{2.5}. However, the evidence to support an association with long-term
19 exposure to PM_{2.5} and respiratory mortality is limited (Figure 7-8). Subchronic and chronic
20 toxicological studies of CAPs, DE, roadway air and woodsmoke provide coherence and
21 biological plausibility for the effects observed in the epidemiologic studies. These
22 toxicological studies have presented some evidence for altered pulmonary function, mild
23 inflammation, oxidative responses, immune suppression, and histopathological changes
24 including mucus cell hyperplasia (Section 7.3). Exacerbated allergic responses have been
25 demonstrated in animals exposed to DE and WS. In addition, pre- and postnatal exposure
26 to ambient levels of urban particles was found to affect lung development in an animal
27 model. This finding is important because impaired lung development is one mechanism by
28 which PM exposure may decrease lung function growth in children. Collectively, the
29 evidence from epidemiologic and toxicological studies is sufficient to conclude that **a causal**
30 **relationship is likely to exist between long-term exposures to PM_{2.5} and respiratory effects.**

Mortality

31 The recent epidemiologic literature reports associations between long-term PM_{2.5}
32 exposure and increased risk of mortality in areas with mean PM_{2.5} concentrations during
33 the study period ranging from 13.2 to 29 µg/m³ (Section 7.6), with effects becoming more
34 precise and consistently positive in locations with mean PM_{2.5} concentrations of 13.5 µg/m³
35 and above (Figure 2-2). When evaluating cause-specific mortality, the strongest evidence

1 can be found when examining associations between PM_{2.5} and cardiovascular mortality, and
2 positive associations were also reported between PM_{2.5} and lung cancer mortality
3 (Figure 7-8). The cardiovascular mortality association has been confirmed further by the
4 extended Harvard Six Cities and ACS studies, which both report strong associations
5 between long-term exposure to PM_{2.5} and cardiopulmonary and IHD mortality (Figure 7-7).
6 The most recent evidence for the association between long-term exposure to PM_{2.5} and
7 CVD-mortality is particularly strong for women. Fewer studies evaluate the respiratory
8 component of cardiopulmonary mortality, and the evidence to support an association with
9 long-term exposure to PM_{2.5} and respiratory mortality is limited (Figure 7-8). The evidence
10 for cardiovascular and respiratory morbidity due to short- and long-term exposure to PM_{2.5}
11 discussed above provides biological plausibility for cardiovascular- and respiratory-related
12 mortality. Collectively, the evidence is sufficient to conclude that **a causal relationship is**
13 **likely to exist between long-term exposures to PM_{2.5} and mortality.**

Reproductive and Developmental

14 Evidence is accumulating for PM_{2.5} effects on low birth weight and infant mortality,
15 especially due to respiratory causes during the post-neonatal period. The mean PM_{2.5}
16 concentrations during the study periods ranged from 5.3-27.4 µg/m³ (Section 7.4), with
17 effects becoming more precise and consistently positive in locations with mean PM_{2.5}
18 concentrations of 15 µg/m³ and above (Section 7.4). Exposure to PM_{2.5} was usually
19 associated with greater reductions in birth weight than exposure to PM₁₀. The evidence
20 from a few U.S. studies that investigated PM₁₀ effects on fetal growth, which reported
21 similar decrements in birth weight, provide consistency for the PM_{2.5} associations observed
22 and strengthen the interpretation that particle exposure may be causally related to
23 reductions in birth weight. The epidemiologic literature does not consistently report
24 associations between long-term exposure to PM and preterm birth, growth restriction, birth
25 defects or decreased sperm quality. Toxicological evidence supports an association between
26 PM_{2.5} and PM₁₀ exposure and adverse reproductive and developmental outcomes, but
27 provided little mechanistic information or biological plausibility for an association between
28 long-term PM exposure and adverse birth outcomes (e.g., low birth weight or infant
29 mortality). New evidence from animal toxicological studies on heritable mutations is of
30 great interest, and warrants further investigation. Overall, the epidemiologic and
31 toxicological evidence is **suggestive of a causal relationship between long-term exposures to**
32 **PM_{2.5} and reproductive and developmental outcomes.**

Cancer, Mutagenicity, and Genotoxicity

33 Multiple epidemiologic studies have shown a consistent positive association between
34 PM_{2.5} and lung cancer mortality, but studies have generally not reported associations
35 between PM_{2.5} and lung cancer incidence (Section 7.5). Animal toxicological studies have

1 examined the potential relationship between PM and cancer, but have not focused on
2 specific size fractions of PM. Instead they have examined ambient PM, WS, and DEP. A
3 number of recent studies indicate that ambient urban PM, emissions from wood/biomass
4 burning, emissions from coal combustion, and gasoline and DE are mutagenic, and that
5 PAHs are genotoxic. These findings are consistent with earlier studies that concluded that
6 ambient PM and PM from specific combustion sources are mutagenic and genotoxic and
7 provide biological plausibility for the results observed in the epidemiologic studies. A
8 limited number of epidemiologic and toxicological studies examined epigenetic effects, and
9 demonstrate that PM induces some changes in methylation. However, it has yet to be
10 determined how these alterations in the genome could influence the initiation and
11 promotion of cancer. Collectively, the evidence from epidemiologic studies, primarily those
12 of lung cancer mortality, along with the toxicological studies that show some evidence of the
13 mutagenic and genotoxic effects of PM is **suggestive of a causal relationship between long-**
14 **term exposures to PM_{2.5} and cancer.**

2.3.2. Integration of PM_{2.5} Health Effects

15 In epidemiologic studies, short-term exposure to PM_{2.5} is associated with a broad
16 range of respiratory and cardiovascular effects, as well as mortality. For effects on the
17 cardiovascular system, the evidence supports the existence of a causal relationship with
18 short-term PM_{2.5} exposure; the evidence indicates that a causal relationship is likely to exist
19 between short-term PM_{2.5} exposure and effects on the respiratory system. The effect
20 estimates from U.S. and Canadian-based epidemiologic studies (Figure 2.1) have found
21 consistent positive associations in study areas with mean PM_{2.5} concentrations ranging
22 from 6.1 to 22 µg/m³.

23 Long-term exposure to PM_{2.5} has been associated with health outcomes similar to
24 those found in the short-term exposure studies, specifically for respiratory and
25 cardiovascular morbidity and mortality. As found for short-term PM_{2.5} exposure, the
26 evidence indicates that a causal relationship exists between long-term PM_{2.5} exposure and
27 cardiovascular effects and that a causal relationship is likely to exist between long-term
28 PM_{2.5} exposure and effects on the respiratory system. Figure 2.2 highlights these findings,
29 which show a range of health effects and outcomes occurring in studies with long-term
30 mean PM_{2.5} concentrations ranging from 10.7 to 29 µg/m³ during the study periods.
31 Additional studies not included in this figure that focus on subclinical outcomes, such as
32 changes in lung function or atherosclerotic markers also report effects in areas with similar
33 concentrations (Sections 7.2 and 7.3). The long-term exposure studies provide additional
34 evidence for reproductive and developmental effects (i.e., LBW) and cancer (i.e., lung cancer
35 mortality) in response to PM_{2.5}.

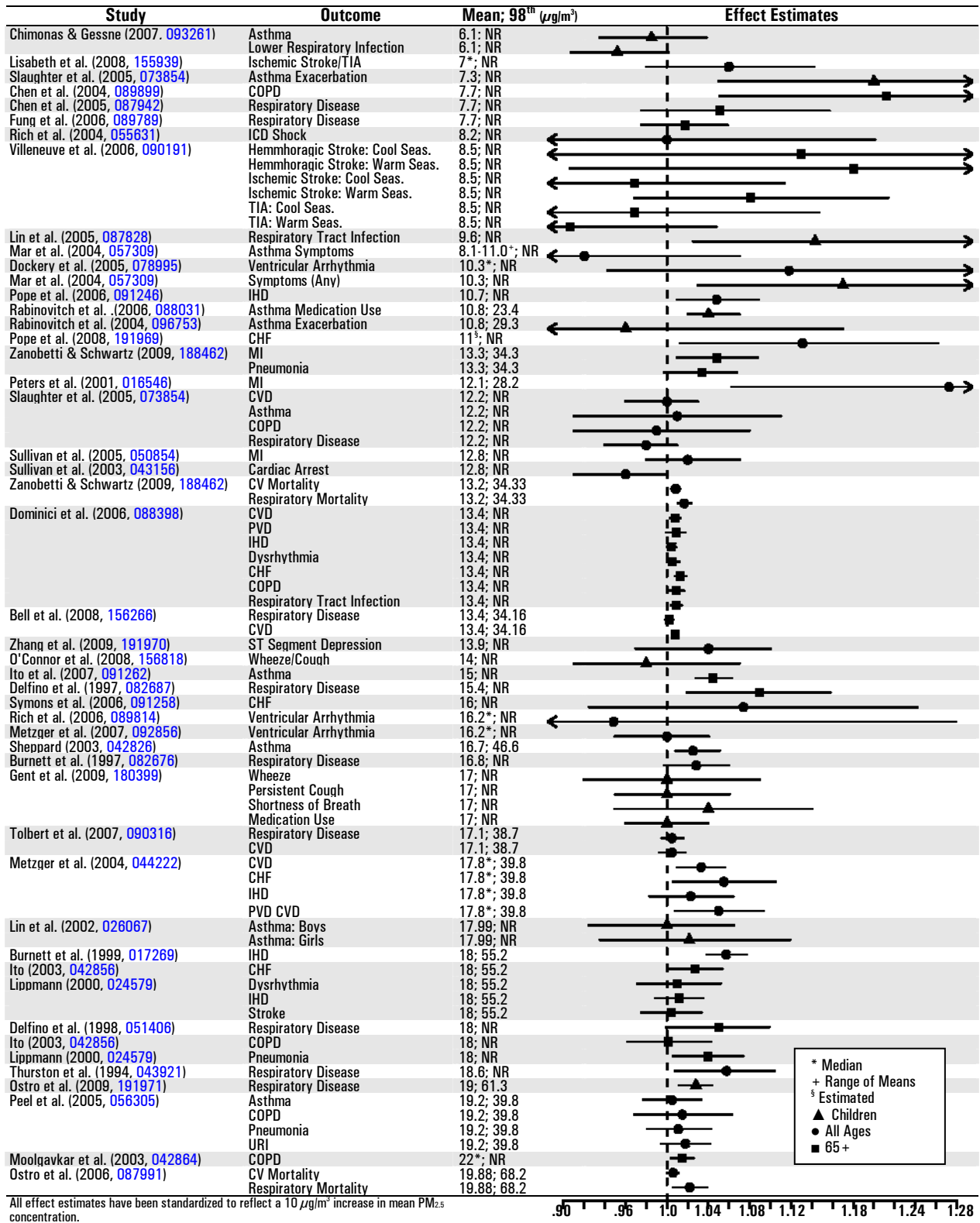


Figure 2-1. Excess risk estimates from epidemiologic studies of PM_{2.5} ordered by mean 24-h avg concentration as reported by the investigator.

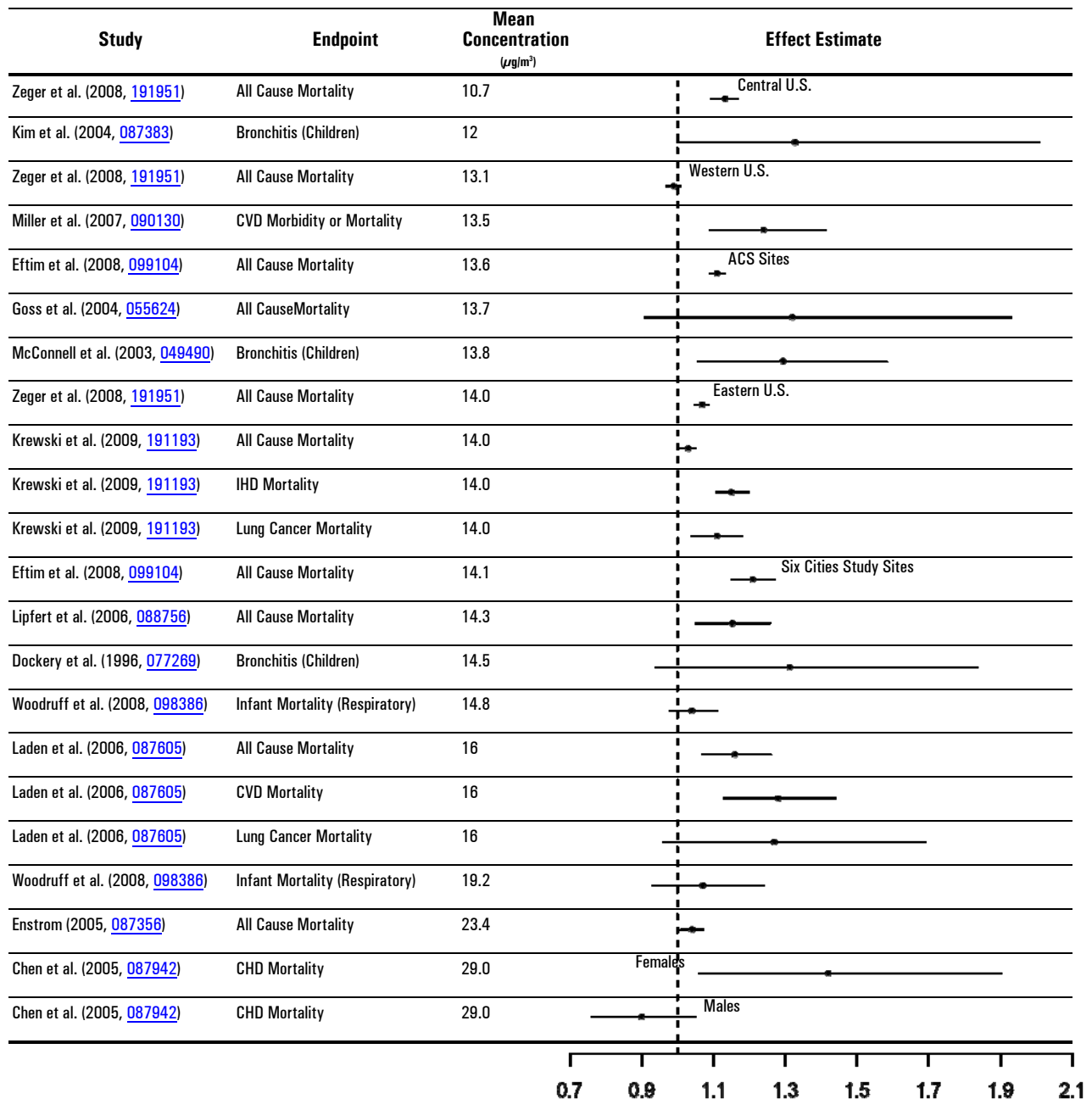


Figure 2-2. Summary of U.S. studies examining the association between long-term exposure to $\text{PM}_{2.5}$ and CVD morbidity/mortality, respiratory morbidity/mortality, and all-cause mortality conducted in locations where the mean annual $\text{PM}_{2.5}$ concentration ranged from 10.7-29 $\mu\text{g}/\text{m}^3$. All effect estimates have been standardized to reflect a 10 $\mu\text{g}/\text{m}^3$ increase in mean annual $\text{PM}_{2.5}$ concentration.

1 The observations from both the short- and long-term exposure studies are supported
 2 by experimental findings of $\text{PM}_{2.5}$ -induced subclinical and clinical cardiovascular effects.
 3 Epidemiologic studies have shown an increase in ED visits and HAs for IHD upon exposure
 4 to $\text{PM}_{2.5}$. These effects are coherent with the changes in vasomotor function and ST-segment
 5 depression observed in both toxicological and controlled human exposure studies. It has

1 been postulated that exposure to PM_{2.5} can lead to myocardial ischemia through an effect on
2 the autonomic nervous system or by altering vasomotor function. PM-induced systemic
3 inflammation, oxidative stress and/or endothelial dysfunction may contribute to altered
4 vasomotor function. These effects have been demonstrated in recent animal toxicological
5 studies, along with altered microvascular reactivity, altered vessel tone, and reduced blood
6 flow during ischemia. Toxicological studies demonstrating increased right ventricular
7 pressure and diminished cardiac contractility also provide biological plausibility for the
8 associations observed between PM_{2.5} and CHF in epidemiologic studies.

9 Thus, the overall evidence from the short-term epidemiologic, controlled human
10 exposure, and toxicological studies evaluated provide coherence and biological plausibility
11 for cardiovascular effects related to myocardial ischemia and congestive heart failure.
12 Coherence in the cardiovascular effects observed can be found in long-term exposure
13 studies, especially for CVDs among post-menopausal women. Additional studies provide
14 limited evidence for subclinical measures of atherosclerosis in epidemiologic studies with
15 stronger evidence from toxicological studies that have demonstrated accelerated
16 development of atherosclerosis in ApoE^{-/-} mice exposed to PM_{2.5} CAPs along with effects on
17 coagulation, experimentally-induced hypertension, and vascular reactivity. Repeated acute
18 responses to PM may lead to cumulative effects that manifest as chronic disease, such as
19 atherosclerosis. Contributing factors to atherosclerosis development include systemic
20 inflammation, endothelial dysfunction, and oxidative stress all of which are associated with
21 PM_{2.5} exposure. However, it has not yet been determined whether PM initiates or promotes
22 atherosclerosis. Collectively the evidence from both short- and long-term exposure studies
23 on cardiovascular morbidity is consistent with the cardiovascular mortality effects observed
24 when examining both exposure durations. In addition, CVD HA and mortality studies that
25 examined the PM₁₀ concentration-response relationship found evidence of a log-linear no-
26 threshold relationship between PM exposure and CVD-related morbidity (Section 6.2) and
27 mortality (Section 6.5).

28 Epidemiologic studies have also reported respiratory effects related to short-term
29 exposure to PM_{2.5}, which include increased ED visits and HAs, as well as alterations in lung
30 function and respiratory symptoms in asthmatic children. These respiratory effects were
31 found to be generally robust to the inclusion of gaseous pollutants in copollutant models
32 with the strongest evidence from the higher powered studies (Figures 6-9 and 6-15). The
33 respiratory effects observed in epidemiologic studies are consistent with those from studies
34 that examined the association between short-term exposure to PM_{2.5} and respiratory
35 mortality. However, the effect of gaseous pollutants on PM_{2.5} respiratory mortality risk
36 estimates has not been extensively examined in PM_{2.5} mortality studies. Important new
37 findings, which support the PM_{2.5}-induced respiratory effects mentioned above, include
38 associations with post-neonatal (between 1 month and 1 year of age) mortality. Controlled
39 human exposure studies provide some support for the respiratory findings from

1 epidemiologic studies, with demonstrated increases in pulmonary inflammation following
2 short-term exposure. However, there is limited and inconsistent evidence of effects in
3 response to controlled exposures to PM_{2.5} on respiratory symptoms or pulmonary function
4 among healthy adults or adults with respiratory disease. Long-term exposure epidemiologic
5 studies provide additional evidence for PM_{2.5}-induced respiratory morbidity, but little
6 evidence for an association with respiratory mortality. These epidemiologic morbidity
7 studies have found decrements in lung function growth, as well as increased respiratory
8 symptoms, and asthma. Toxicological studies provide coherence and biological plausibility
9 for the respiratory effects observed in response to short and long-term exposures to PM by
10 demonstrating a wide array of biological responses including: altered pulmonary function,
11 mild pulmonary inflammation and injury, oxidative responses, and histopathological
12 changes in animals exposed by inhalation to PM_{2.5} derived from a wide variety of sources.
13 In some cases, prolonged exposures led to adaptive responses. Important evidence was also
14 found in an animal model for altered lung development following perinatal exposure to
15 urban air, which may provide a mechanism to explain the reduction in lung function growth
16 observed in children in response to long-term exposure to PM.

17 Additional respiratory-related effects have been tied to allergic responses.
18 Epidemiologic studies have provided evidence for increased HAs for allergic symptoms (e.g.,
19 allergic rhinitis) in response to short- and long-term exposure to PM_{2.5}. Panel studies also
20 positively associate long-term exposure to PM_{2.5} and PM₁₀ with indicators of allergic
21 sensitization. Controlled human exposure and toxicological studies provide coherence for
22 the exacerbation of allergic symptoms, by showing that PM_{2.5} can promote allergic
23 responses and intensify existing allergies. Allergic responses require repeated exposures to
24 antigen over time and co-exposure to an adjuvant (possibly DEP or ultrafine CAPs) can
25 enhance this response. Allergic sensitization often underlies allergic asthma, characterized
26 by inflammation and AHR. In this way, repeated or chronic exposures involving
27 multifactorial responses (immune system activation, oxidative stress, inflammation) can
28 lead to irreversible outcomes. Epidemiologic studies have also reported evidence for
29 increased HAs for respiratory infections in response to both short- and long-term exposures
30 to PM_{2.5}. Toxicological studies suggest that PM impairs innate immunity, which is the first
31 line of defense against infection, providing coherence for the respiratory infection effects
32 observed in epidemiologic studies.

33 The difference in effects observed across studies and between cities may be attributed,
34 at least in part, to the differences in PM composition across the U.S.; however, the available
35 evidence and the limited amount of city-specific speciated PM_{2.5} data does not allow
36 conclusions to be drawn that specifically differentiate effects of PM in different locations.
37 Regional differences in PM_{2.5} composition are outlined briefly in Section 2.1 above and in
38 Section 3.5 in more detail. Although PM_{2.5} is produced mainly by the combustion of fossil
39 fuels, either by stationary sources or by transportation, there is a large degree of regional

1 variability in PM mass concentration, composition, and sources. It remains a challenge to
2 determine relationships between specific constituents, combination of constituents, or
3 sources of PM_{2.5} and the various health effects observed. Source apportionment studies of
4 PM_{2.5} have attempted to decipher some of these relationships and in the process have
5 identified associations between multiple sources and various respiratory and cardiovascular
6 health effects, as well as mortality. Although different source apportionment methods have
7 been used across these studies, the methods used have been validated and found to
8 generally identify the same sources and associations between sources and health effects
9 (Section 6.6). While uncertainty remains, it has been recognized that many components of
10 PM_{2.5} may contribute to health effects. Overall, the results displayed in Table 6-17 indicate
11 that many constituents of PM_{2.5} can be linked with multiple health effects and the evidence
12 is not yet sufficient to allow differentiation of those constituents or sources that are more
13 closely related to specific health outcomes.

14 Variability in the associations observed, specifically across epidemiologic studies may
15 be due in part to exposure error related to the use of air quality data at the county level.
16 Because western U.S. counties tend to be much larger than eastern U.S. counties and more
17 diverse in topography and population characteristics, the day-to-day variations in
18 concentration at one site, or even for the average of several sites, may not correlate well
19 with the day-to-day variations in all parts of the county. For example, site-to-site
20 correlations as a function of distance between sites (Section 3.5.1.2) fall off rapidly with
21 distance in Los Angeles, but high correlations extend to larger distances in cities such as
22 Boston and Pittsburgh. These differences cannot be attributed solely to topographic
23 differences between East and West because some eastern cities (e.g., Pittsburgh) are located
24 in complex topography. Regional differences in climate which can lead to more time
25 outdoors or indoors along with more or less air conditioning, and housing stock (e.g., new
26 homes tend to be tighter with lower infiltration ratios than older homes) may also cause
27 regional differences in effect estimates. Overall, the various differences between eastern
28 and western U.S. counties can result in exposure misclassification and an underestimation
29 of effects in western counties.

30 The new evidence reviewed in this ISA greatly expands upon the evidence available in
31 the 2004 PM AQCD particularly in providing greater understanding of the underlying
32 mechanisms for PM_{2.5} induced cardiovascular and respiratory effects for both short- and
33 long-term exposures. Recent studies have provided new evidence linking long-term
34 exposure to PM_{2.5} with cardiovascular outcomes that has expanded upon the continuum of
35 effects ranging from the more subtle subclinical measures to cardiopulmonary mortality.

2.3.3. Exposure to PM_{10-2.5}

2.3.3.1. Effects of Short-Term Exposure to PM_{10-2.5}

Table 2-3. Summary of causal determinations for short-term exposure to PM_{10-2.5}.

Size Fraction	Outcome	Causality Determination
PM _{10-2.5}	Cardiovascular Effects	Suggestive
	Respiratory Effects	Suggestive
	Mortality	Suggestive

Cardiovascular Effects

1 Of the epidemiologic studies evaluated, generally positive associations were reported
2 between short-term exposure to PM_{10-2.5} and HAs or ED visits for CVDs. These results are
3 supported by a large U.S. multicity study of older adults that reported PM_{10-2.5} associations
4 with CVD HAs, and only a slight reduction in the PM_{10-2.5} risk estimate when included in a
5 copollutant model with PM_{2.5} (Section 6.2.10). The PM_{10-2.5} associations with cardiovascular
6 HAs and ED visits were observed in study locations with mean 24-h avg PM_{10-2.5}
7 concentrations ranging from 7.4 to 13 µg/m³, with effects becoming more precise and
8 consistently positive in locations with mean PM_{10-2.5} concentrations of 10 µg/m³ and above
9 (Figure 2-3). These results are supported by the associations observed between PM_{10-2.5} and
10 cardiovascular mortality in areas with similar 24-h avg PM_{10-2.5} concentrations ranging
11 from 6.1-16.4 µg/m³ (Section 6.2.11), with effects becoming more precise and consistently
12 positive in locations with mean PM_{10-2.5} concentrations of 12 µg/m³ and above (Figure 2-3).
13 The results of the epidemiologic studies were further confirmed by studies that examined
14 dust storm events, which contain high concentrations of crustal material, and found an
15 increase in CVD ED visits and HAs. Other epidemiologic studies have reported PM_{10-2.5}
16 associations with other cardiovascular health effects including supraventricular ectopy and
17 changes in HRV (6.2.1.1). Although limited in number, studies of controlled human
18 exposures provide some evidence to support the alterations in HRV observed in the
19 epidemiologic studies (Section 6.2.1.2). The few toxicological studies that examined the
20 effect of PM_{10-2.5} on cardiovascular health effects used IT instillation due to the technical
21 challenges in exposing rodents via inhalation to PM_{10-2.5}, and, as a result, provide only
22 limited evidence on the biological plausibility of PM_{10-2.5} induced cardiovascular effects. The
23 potential for coarse particles to elicit an effect is supported by dosimetric studies, which

1 show that a large proportion of inhaled coarse particles in the 3-6 micron (d_{ae}) range can
2 reach and deposit in the lower respiratory tract, particularly the tracheobronchial (TB)
3 airways (Figures 4-3 and 4-4). Collectively, the evidence from epidemiologic studies, along
4 with the more limited evidence from controlled human exposure and toxicological studies **is**
5 **suggestive of a causal relationship between short-term exposures to $PM_{10-2.5}$ and cardiovascular**
6 **effects.**

Respiratory Effects

7 A number of recent epidemiologic studies conducted in Canada and France found
8 consistent, positive associations between respiratory ED visits and hospital admissions and
9 short-term exposure to $PM_{10-2.5}$ in studies with mean 24-h avg concentrations ranging from
10 5.6-13.5 $\mu\text{g}/\text{m}^3$ (Section 6.3.8), with effects becoming more precise and consistently positive
11 in locations with mean $PM_{10-2.5}$ concentrations of 10 $\mu\text{g}/\text{m}^3$ and above (Figure 2-3). In these
12 studies, the strongest relationships were observed among children, with less consistent
13 evidence for adults and older adults (i.e., ≥ 65). In a large multicity study of older adults,
14 $PM_{10-2.5}$ was positively associated with respiratory HAs in both single and copollutant
15 models with $PM_{2.5}$. In addition, a U.S.-based multicity study found evidence for an increase
16 in respiratory mortality upon short-term exposure to $PM_{10-2.5}$, but these associations have
17 not been consistently observed in single-city studies (Section 6.3.9). A limited number of
18 epidemiologic studies have focused on specific respiratory morbidity outcomes, and found no
19 evidence of an association with lower respiratory symptoms, wheeze, and medication use
20 (Section 6.3.1.1). While controlled human exposure studies have not observed an effect on
21 lung function or respiratory symptoms in healthy or asthmatic adults in response to
22 exposure to $PM_{10-2.5}$, healthy volunteers have exhibited an increase in markers of
23 pulmonary inflammation. Toxicological studies using inhalation exposures are still lacking,
24 but pulmonary injury has been observed in animals after IT exposure (Section 6.3.5.3). In
25 some cases, $PM_{10-2.5}$ was found to be more potent than $PM_{2.5}$ and effects were not
26 attributable to endotoxin. Both rural and urban $PM_{10-2.5}$ have induced inflammation and
27 injury responses in rats or mice exposed via IT instillation, making it difficult to distinguish
28 effects of $PM_{10-2.5}$ from different environments. Overall, epidemiologic studies, along with
29 the limited number of controlled human exposure and toxicological studies that examined
30 $PM_{10-2.5}$ respiratory effects provide evidence that **is suggestive of a causal relationship**
31 **between short-term exposures to $PM_{10-2.5}$ and respiratory effects.**

Mortality

32 The majority of studies evaluated in this review provide some evidence for mortality
33 associations with $PM_{10-2.5}$. A new U.S.-based multicity study, which estimated $PM_{10-2.5}$ by
34 calculating the difference between the county-average PM_{10} and $PM_{2.5}$, found associations

1 between PM_{10-2.5} and mortality across the U.S., including evidence for regional variability in
2 PM_{10-2.5} risk estimates (Section 6.5.2.3). Additionally, the U.S.-based multicity study
3 provides preliminary evidence for greater effects during the warmer months (i.e., spring
4 and summer). A multicity Canadian study provides additional evidence for an association
5 between short-term exposure to PM_{10-2.5} and mortality (Section 6.5.2.3). Uncertainty
6 surrounds the PM_{10-2.5} associations reported in the studies evaluated due to the limited
7 number of PM_{10-2.5} studies that have investigated confounding by gaseous copollutants or
8 the influence of model specification on PM_{10-2.5} risk estimates. Overall, the consistent
9 positive association between short-term exposure to PM_{10-2.5} and mortality observed in the
10 U.S. and Canadian-based multicity studies, along with the positive associations from
11 single-city studies conducted in these locations, provides evidence that **is suggestive of a**
12 **causal relationship between short-term exposures to PM_{10-2.5} and mortality.**

2.3.4. Integration of PM_{10-2.5} Effects

13 Epidemiologic, controlled human exposure, and toxicological studies have provided
14 evidence that is suggestive for relationships between short-term exposure to PM_{10-2.5} and
15 cardiovascular effects, respiratory effects, and mortality. Conclusions regarding causation
16 for the various health effects and outcomes were made for PM_{10-2.5} as a whole regardless of
17 origin, since PM_{10-2.5}-related effects have been demonstrated for a number of different
18 environments. These effects have been observed in locations with mean PM_{10-2.5}
19 concentrations ranging from 5.6 to 13 µg/m³ (Figure 2-3). To date, a sufficient amount of
20 evidence does not exist in order to draw conclusions regarding the health effects and
21 outcomes associated with long-term exposure to PM_{10-2.5}.

22 In epidemiologic studies, associations between short-term exposure to PM_{10-2.5} and
23 cardiovascular outcomes (i.e., IHD HAs, supraventricular ectopy, and changes in HRV) have
24 been found that are similar in magnitude to those observed in PM_{2.5} studies. Controlled
25 human exposure studies have also observed alterations in HRV, providing consistency and
26 coherence for the effects observed in the epidemiologic studies. To date, only a limited
27 number of toxicological studies have been conducted to examine the effects of PM_{10-2.5} on
28 cardiovascular outcomes. All of these studies involved IT instillation due to the technical
29 challenges of using PM_{10-2.5} for rodent inhalation studies. As a result, the toxicological
30 studies evaluated provide limited biological plausibility for the PM_{10-2.5} effects observed in
31 the epidemiologic and controlled human exposure studies.

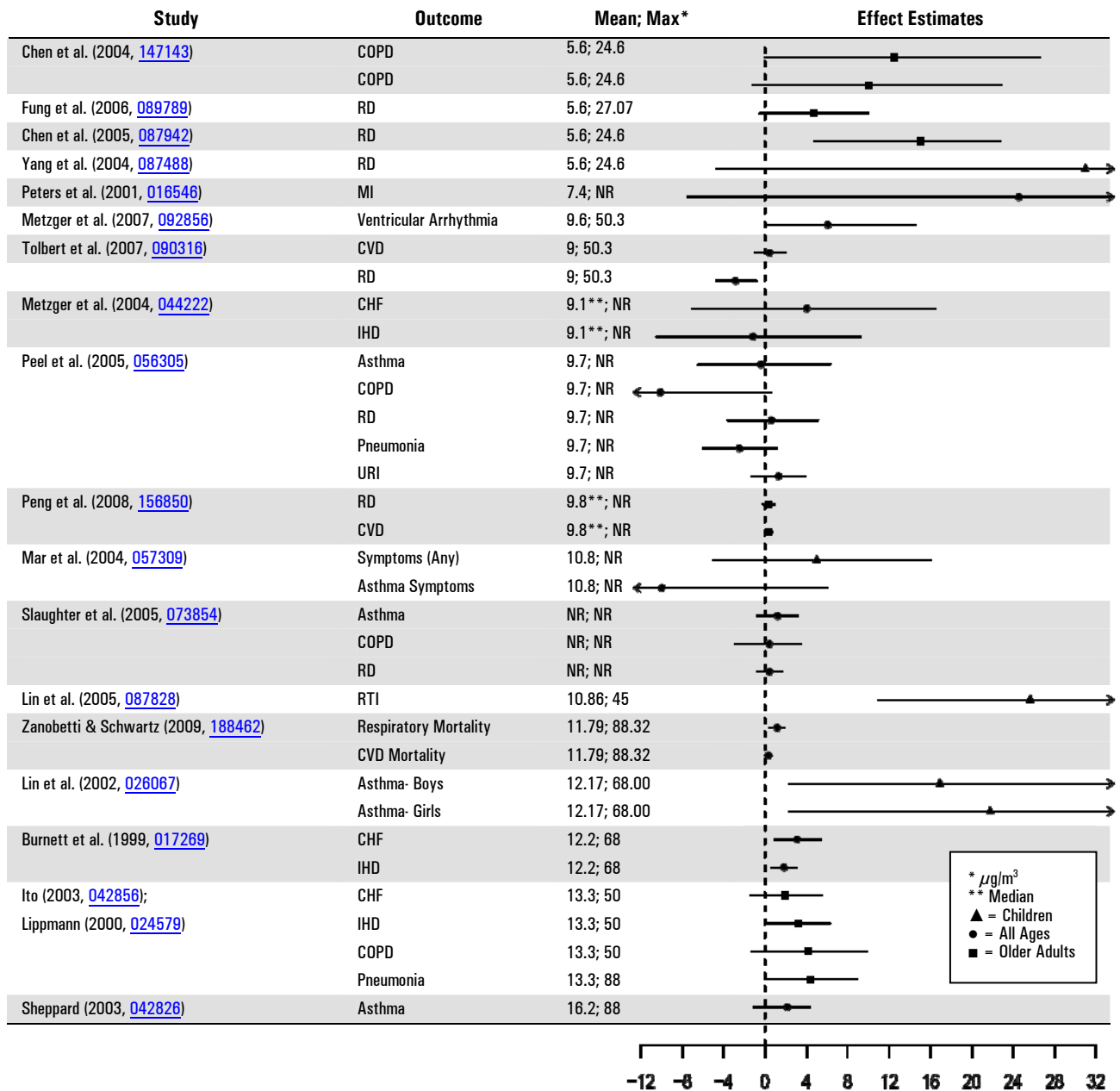


Figure 2-3. Effect estimates from epidemiologic studies of PM_{10-2.5} ordered by mean 24-h avg concentration as reported by the investigator.

1 Limited evidence is available from epidemiologic studies for respiratory health effects
2 and outcomes in response to short-term exposure to PM_{10-2.5}. An increase in respiratory HA
3 and ED visits has been observed, but primarily in studies conducted in Canada and Europe.
4 In addition, associations are not reported for lower respiratory symptoms, wheeze, or
5 medication use. Controlled human exposure studies have not observed an effect on lung
6 function or respiratory symptoms in healthy or asthmatic adults, but healthy volunteers
7 have exhibited pulmonary inflammation. The toxicological studies (all IT) provide evidence

1 of pulmonary injury and inflammation. In some cases, PM_{10-2.5} was found to be more potent
2 than PM_{2.5} and effects were not solely attributable to endotoxin.

3 Currently, a national network is not in place to monitor PM_{10-2.5} concentrations. As a
4 result, uncertainties surround the concentration at which the observed associations occur.
5 Ambient concentrations of PM_{10-2.5} are generally determined by the subtraction of PM₁₀ and
6 PM_{2.5} measurements, using various methods. For example, some epidemiologic studies
7 estimate PM_{10-2.5} by taking the difference between collocated PM₁₀ and PM_{2.5} monitors while
8 other studies have taken the difference between county average PM₁₀ and PM_{2.5}
9 concentrations. Therefore, there is greater error in ambient exposure to PM_{10-2.5} compared to
10 PM_{2.5}. This would tend to increase uncertainty and make it more difficult to detect effects of
11 PM_{10-2.5} in epidemiologic studies. In addition, the various differences between eastern and
12 western U.S. counties can lead to exposure misclassification, and the potential
13 underestimation of effects in western counties (as discussed for PM_{2.5} in Section 2.3.2).

14 It is also important to note that the chemical composition of PM_{10-2.5} can vary
15 considerably by location, but city-specific speciated PM_{10-2.5} data are limited. However, PM₁₀₋
16 _{2.5} may contain iron, silica, aluminum, and base cations from soil, plant and insect
17 fragments, pollen, fungal spores, bacteria, and viruses, as well as fly ash, brake lining
18 particles, debris, and automobile tire fragments.

19 The 2004 PM AQCD presented the limited amount of evidence available that
20 examined the potential association between exposure to PM_{10-2.5} and health effects and
21 outcomes. The current evidence, primarily from epidemiologic studies, builds upon the
22 results from the 2004 PM AQCD and indicates that short-term exposure to PM_{10-2.5} is
23 associated with effects on both the cardiovascular and respiratory systems. However,
24 variability in the chemical and biological composition of PM_{10-2.5}, limited evidence regarding
25 effects of the various components of PM_{10-2.5}, and lack of clearly defined biological
26 mechanisms for PM_{10-2.5}-related effects are important sources of uncertainty.

2.3.5. Exposure to Ultrafine PM

2.3.5.1. Effects of Short-Term Exposure to UFPs

Table 2-4. Summary of causal determinations for short-term exposure to UFPs.

Size Fraction	Outcome	Causality Determination
Ultrafine Particles	Cardiovascular Effects	Suggestive
	Respiratory Effects	Suggestive

Cardiovascular Effects

1 Controlled human exposure studies provide the majority of the evidence for
2 cardiovascular health effects in response to short-term exposure to UFP. While there are a
3 limited number of studies that have examined the association between UFP and
4 cardiovascular morbidity, there is a larger body of evidence from studies that exposed
5 subjects to fresh DE, which is typically dominated by UFPs. These studies have
6 consistently demonstrated effects on vasomotor function (Section 6.2.4.2). Markers of
7 systemic oxidative stress have also been observed to increase after exposure to various
8 particle types that are predominantly in the UFP size range. In addition controlled human
9 exposure studies have observed alterations in HRV parameters in response to exposure to
10 ultrafine CAPs, with inconsistent evidence for changes in markers of blood coagulation
11 following exposure to ultrafine CAPs and DE (Sections 6.2.1.2 and 6.2.8.2). A few
12 toxicological studies have also observed consistent changes in vasomotor function, which
13 provides coherence with the effects demonstrated in the controlled human exposure studies
14 (Section 6.2.4.3). Additional UFP-induced effects observed in toxicological studies include
15 alterations in HRV, with less consistent effects observed for systemic inflammation and
16 blood coagulation. Only a few epidemiologic studies have examined the effect of UFP on
17 cardiovascular morbidity and collectively they found inconsistent evidence for an
18 association between UFP and CVD hospital admissions, but some positive associations for
19 subclinical measures of CVD (i.e., arrhythmias and supraventricular beats) (Section
20 6.2.2.1). These studies were conducted in the U.S. and Europe at mean particle number
21 concentration ranges of ~8,500-36,000 particles/cm³. However, UFP number concentrations
22 are highly dependent on monitor location (i.e., concentrations drop off quickly from the road
23 compared to accumulation mode particles), and therefore, more subject to exposure error
24 than accumulation mode particles. In conclusion, the evidence from the studies evaluated **is**

1 **suggestive of a causal relationship between short-term exposures to UFP and cardiovascular**
2 **effects.**

Respiratory Effects

3 A limited number of epidemiologic studies have examined the potential association
4 between short-term exposure to UFP and respiratory morbidity. Of the studies evaluated,
5 there is limited, and predominately inconsistent evidence for an association between short-
6 term exposure to UFPs and respiratory symptoms, as well as asthma hospital admissions
7 at a median particle number concentration of ~6,200 to a mean of 38,000 particles/cm³
8 (Section 6.3.8). The spatial and temporal variability of UFPs also affects these associations.
9 Although controlled human exposure studies have not extensively examined the effect of
10 UFP on respiratory outcomes, a few studies have observed small UFP-induced decreases in
11 pulmonary function. However, these studies have not reported an increase in respiratory
12 symptoms and the observed effects on pulmonary inflammation are not consistent.
13 Toxicological studies have also reported mixed results when examining the effect of UFP on
14 respiratory effects, but several studies demonstrate oxidative, inflammatory, and allergic
15 responses (Section 6.3). Some effects, such as inflammation or pulmonary histopathology,
16 are only observed when using particular animal models (e.g., immature or compromised).
17 Additionally, although a number of controlled human exposure and toxicological studies
18 that used controlled exposures to fresh DE report respiratory effects, the relative
19 contributions of gaseous copollutants to the health effects observed remain unresolved.
20 Thus, the current collective evidence **is suggestive of a causal relationship between short-term**
21 **exposures to UFP and respiratory effects.**

2.3.6. Integration of UFP Effects

22 The controlled human exposure studies evaluated have consistently demonstrated
23 effects on vasomotor function and systemic oxidative stress with additional evidence for
24 alterations in HRV parameters in response to exposure to ultrafine CAPs. The toxicological
25 studies provide coherence for the changes in vasomotor function observed in the controlled
26 human exposure studies. Epidemiologic studies are limited because a national network is
27 not in place to measure UFP in the U.S. UFP concentrations are spatially variable, which
28 would increase uncertainty and make it difficult to detect associations between health
29 effects and UFPs in epidemiologic studies. In addition, data on the composition of UFPs and
30 potential effects of UFP constituents are sparse.

31 More limited evidence is available regarding the effect of UFP on respiratory effects.
32 Controlled human exposure studies have not extensively examined the effect of UFPs on
33 respiratory measurements, but a few studies have observed small decrements in pulmonary
34 function. Additional effects including oxidative, inflammatory, and pro-allergic outcomes

1 have been demonstrated in toxicological studies, but the lack of coherence with the
2 controlled human exposure studies limits the interpretation of these findings.

3 Overall, a limited number of studies have examined the association between exposure
4 to UFP and morbidity and mortality. Of the studies evaluated, controlled human exposure
5 studies provide the most evidence for UFP-induced cardiovascular and respiratory effects;
6 however, these studies focus on exposure to DE. As a result, it is unclear if the effects
7 observed are due to UFP, larger particles (i.e., PM_{2.5}), or the gaseous components of DE.
8 Additionally, ultrafine CAPs systems are limited as the atmospheric ultrafine PM
9 composition is modified when concentrated, which adds uncertainty to the health effects
10 observed in controlled human exposure studies (Chapter 1).

2.4. Policy Relevant Considerations

2.4.1. Potentially Susceptible Subpopulations

11 Upon evaluating the association between short- and long-term exposure to PM and
12 various health outcomes, studies also attempted to identify subpopulations that are more
13 susceptible to PM (i.e., populations that have a greater likelihood of experiencing health
14 effects related to PM exposure). These studies did so by: conducting stratified analyses;
15 examining individuals with an underlying health condition; or developing animal models
16 that mimic the physiological conditions associated with an adverse health effect. These
17 studies identified a multitude of factors that could potentially contribute to whether an
18 individual is susceptible to PM (Table 8-2). Although studies have primarily used exposures
19 to PM_{2.5} or PM₁₀, the available evidence suggests that the identified factors may also
20 enhance susceptibility to PM_{10-2.5}. The examination of susceptible subpopulations to PM
21 exposure allows for the NAAQS to provide an adequate margin of safety for both the
22 general population and for sensitive subpopulations.

23 During specific periods of life (i.e., childhood and advanced age), individuals may be
24 more susceptible to environmental exposures, which in turn can render them more
25 susceptible to PM-related health effects. An evaluation of age-related health effects
26 suggests that older adults have heightened responses for cardiovascular morbidity with PM
27 exposure. In addition, epidemiologic and toxicological studies provide evidence that
28 indicates children are at an increased risk of PM-related respiratory effects. It should be
29 noted that the health effects observed in children could be initiated by exposures to PM that
30 occurred during key windows of development, such as in utero. Epidemiologic studies that
31 focus on exposures during development have reported inconsistent findings (Section 7.4),
32 but a recent toxicological study suggests that inflammatory responses during pregnancy
33 due to exposure to PM could result in health effects in the developing fetus.

1 Epidemiologic studies have also examined whether additional factors, such as gender,
2 race, or ethnicity modify the association between PM and morbidity and mortality
3 outcomes. Although gender and race do not seem to modify PM risk estimates, limited
4 evidence from two studies conducted in California suggest that Hispanic ethnicity may
5 modify the association between PM and mortality.

6 Recent epidemiologic and toxicological studies provided evidence that individuals with
7 null alleles or polymorphisms in genes that mediate the antioxidant response to oxidative
8 stress (i.e., GSTM1), regulate enzyme activity (i.e., MTHFR and cSHMT), or regulate
9 physiological levels of inflammatory markers (i.e., fibrinogen) are more susceptible to PM
10 exposure. However, some studies have shown that polymorphisms in genes (e.g., HFE) can
11 have a protective effect against effects of PM exposure. Additionally, preliminary evidence
12 suggests that PM exposure can impart epigenetic effects (i.e., DNA methylation); however,
13 this requires further investigation.

14 Collectively, the evidence from epidemiologic and toxicological, and to a lesser extent,
15 controlled human exposure studies indicate increased susceptibility of individuals with
16 underlying CVDs and respiratory illnesses, particularly asthma, to PM exposure.
17 Controlled human exposure and toxicological studies provide additional evidence for
18 increased PM-related cardiovascular effects in individuals with underlying respiratory
19 health conditions.

20 Recently studies have begun to examine the influence of preexisting chronic
21 inflammatory conditions, such as diabetes and obesity, on PM-related health effects. These
22 studies have found some evidence for increased associations for cardiovascular outcomes
23 along with physiological alterations in markers of inflammation, oxidative stress, and acute
24 phase response. However, more research is needed to thoroughly examine the affect of PM
25 exposure on obese individuals and to identify the biological pathway(s) that could increase
26 the susceptibility of diabetic and obese individuals to PM.

27 There is also evidence that socioeconomic status (SES), measured using surrogates
28 such as educational attainment or residential location, modifies the association between
29 PM and morbidity and mortality outcomes. In addition, nutritional status, another
30 surrogate measure of SES, has been shown to have protective effects against PM exposure
31 in individuals that have a higher intake of some vitamins and nutrients.

32 Overall, the epidemiologic, controlled human exposure, and toxicological studies
33 evaluated in this review provide evidence for increased susceptibility for various
34 subpopulations, including children and older adults, people with pre-existing
35 cardiopulmonary diseases, and people with lower SES.

2.4.2. Lag Structure of PM—Morbidity and PM—Mortality Associations

1 Epidemiologic studies have attempted to identify the time-frame in which exposure to
2 PM can impart a health effect. Although PM exposure-response relationships have
3 traditionally been examined using air quality data for a defined lag period (e.g, 1 day or
4 average of 0-1 days), the relationship can potentially be influenced by a multitude of
5 factors, such as the underlying susceptibility of an individual (e.g., age, pre-existing
6 diseases), which could increase or decrease the lag times observed.

7 An attempt has been made to identify whether certain lag periods are more strongly
8 associated with specific health outcomes. The epidemiologic evidence evaluated in the 2004
9 PM AQCD supported the use of lags of 0-1 days for cardiovascular effects and longer
10 moving averages or distributed lags for respiratory diseases (U.S. EPA, 2004, [056905](#)).
11 However, currently, little consensus exists as to the most appropriate a priori lag times to
12 use when examining morbidity and mortality outcomes. As a result, many investigators
13 have chosen to examine the lag structure of associations between PM concentration and
14 health outcome instead of focusing on a priori lag times. This approach is informative
15 because if effects are cumulative, higher overall risks may exist than would be observed for
16 any given single day lag. An examination of lag times used in the epidemiologic studies
17 evaluated in this assessment can provide further insight on the relationship between PM
18 exposure and morbidity and mortality outcomes.

2.4.2.1. PM—Cardiovascular Morbidity Associations

19 Most of the studies evaluated that examined the association between cardiovascular
20 HAs and ED visits report strong associations with short-term PM exposure at lags 0- to 2-
21 days, with more limited evidence for shorter durations (i.e., hours) between exposure and
22 response for some health effects (e.g., onset of MI) (Section 6.2.10). However, these studies
23 have rarely examined alternative lag structures. Controlled human exposure and
24 toxicological studies provide biological plausibility for the health effects observed in the
25 epidemiologic studies at immediate or concurrent day lags. Although the majority of the
26 evidence supports shorter lag times for cardiovascular health effects, a recent study has
27 provided preliminary evidence suggesting that longer lag times (i.e., 14-day distributed lag
28 model) may be plausible for non-ischemic cardiovascular conditions (Section 6.2.10). Panel
29 studies of short-term exposure to PM and cardiovascular endpoints have also examined lag
30 times using a wide range of lag times. Studies of ECG changes, indicating ischemia, show
31 effects at lags from several hours to 2 days, while lag times ranging from hours to several
32 week moving averages have been observed in studies of arrhythmias, ECG measures of
33 arrhythmia, vasomotor function and blood markers of inflammation, coagulation and
34 oxidative stress (Section 6.2). The longer lags observed in these panel studies may be

1 explained if the effects of PM are cumulative. Although few studies of cumulative effects
2 have been conducted, toxicological studies have demonstrated PM-dependent progression of
3 atherosclerosis. It should be noted that PM exposure could also lead to an acute event (e.g.,
4 infarction or stroke) in individuals with atherosclerosis that may have progressed in
5 response to cumulative PM exposure. Therefore, effects have been observed at a range of
6 lag periods from a few hours to several days with no clear evidence for any lag period
7 having stronger associations than another.

2.4.2.2. PM–Respiratory Morbidity Associations

8 Generally, recent studies of respiratory HAs that evaluate multiple lags, have found
9 effect sizes to be larger when using longer moving averages or distributed lag models. For
10 example, when examining HAs for all respiratory diseases among older adults, the
11 strongest associations were observed when using PM concentrations 2 days prior to the HA
12 (Section 6.3.8). Longer lag periods were also found to be most strongly associated with
13 asthma HAs and ED visits children (3-5 days) with some evidence for more immediate
14 effects in older adults (lags of 0 and 1 day), but these observations were not consistent
15 across studies (Section 6.3.8). These variable results could be due to the biological
16 complexity of asthma, which inhibits the identification of a specific lag period. The longer
17 lag times identified in the epidemiologic studies evaluated are biologically plausible
18 considering that PM effects on allergic sensitization and lung immune defenses have been
19 observed in controlled human exposure and toxicological studies. These effects could lead to
20 respiratory illnesses over a longer time course (e.g., within several days respiratory
21 infection may become evident, resulting in respiratory symptoms or hospital visits).
22 However, inflammatory responses, which contribute to some forms of asthma, may results
23 in symptoms requiring medical care within a shorter time frame (e.g., 0-1 days).

2.4.2.3. PM–Mortality Associations

24 Epidemiologic studies that focused on the association between short-term PM
25 exposure and mortality (i.e., all-cause, cardiovascular, and respiratory) mostly examined a
26 priori lag structures of either 1 or 0-1 days. Although mortality studies do not often
27 examine alternative lag structures, the selection of the aforementioned a priori lag days has
28 been confirmed in additional studies, with the strongest PM-mortality associations
29 consistently being observed at lag 1 and 0-1-days (Section 6.5). However, of note is recent
30 evidence for larger effect estimates when using a distributed lag model.

31 Epidemiologic studies that examined the association between long-term exposure to
32 PM and mortality have also attempted to identify the latency period from PM exposure to
33 death (Section 7.6.4). Results of the lag comparisons from several cohort studies indicate
34 that the effects of changes in exposure on mortality are seen within five years, with the

1 strongest evidence for effects observed within the first two years. Additionally, there is
2 evidence, albeit from one study, that the mortality effect had larger cumulative effects
3 spread over the follow-up year and 3 preceding years.

2.4.3. PM Concentration—Response Relationship

4 An important consideration in characterizing the PM-morbidity and mortality
5 association is whether the C-R relationship is linear across the full concentration range
6 that is encountered or if there are concentration ranges where there are departures from
7 linearity (i.e., nonlinearity). In this ISA studies have been identified that attempt to
8 characterize the shape of the PM C-R curve along with possible PM “thresholds” (i.e., levels
9 which PM concentrations must exceed in order to elicit a health response). The
10 epidemiologic studies evaluated that examined the shape of the C-R curve and the potential
11 presence of a threshold have focused on cardiovascular HAs and ED visits and mortality
12 associated with short-term exposure to PM₁₀ and mortality associated with long-term
13 exposure to PM_{2.5}.

14 A limited number of studies have been identified that examined the shape of the PM-
15 cardiovascular HA and ED visits C-R relationship. Of these studies, some conducted an
16 exploratory analysis during model selection to determine if a linear curve most adequately
17 represented the C-R relationship; whereas, only one study conducted an extensive analysis
18 to examine the shape of the C-R curve at different concentrations (Section 6.2.10.10).
19 Overall, the limited evidence from the studies evaluated supports the use of a no-threshold,
20 log-linear model, which is consistent with the observations made in studies that examined
21 the PM-mortality relationship.

22 Although multiple studies have previously examined the PM-mortality C-R
23 relationship and whether a threshold exists, more complex statistical analyses continue to
24 be developed to analyze this association. Using a variety of methods and models, most of
25 the studies evaluated support the use of a no-threshold, log-linear model; however, one
26 study did observe heterogeneity in the shape of the C-R curve across cities (Section 6.5).
27 Overall, the studies evaluated further support the use of a no-threshold log-linear model,
28 but additional issues such as the influence of heterogeneity in estimates between cities, and
29 the effect of seasonal and regional differences in PM on the C-R relationship still require
30 further investigation.

31 In addition to examining the C-R relationship between short-term exposure to PM
32 and mortality, Schwartz et al. (2008, [156963](#)) conducted an analysis of the shape of the C-R
33 relationship associated with long-term exposure to PM. Using a variety of statistical
34 methods, the C-R curve was found to be indistinguishable from linear, and, therefore, little
35 evidence was observed to suggest that a threshold exists in the association between
36 long-term exposure to PM_{2.5} and the risk of death (Section 7.6).

2.5. Ecological and Welfare Effects

1 This section presents key conclusions and scientific judgments regarding causality for
2 welfare and ecological effects of PM as discussed in Chapter 9. The effects of particulate
3 NO_x and SO_x have recently been evaluated in the *ISA for Oxides of Nitrogen and Sulfur –*
4 *Ecological Criteria* (U.S. EPA, 2008, [157074](#)). That ISA focused on the effects from
5 deposition of gas- and particle-phase pollutants related to ambient NO_x and SO_x
6 concentrations that can lead to acidification and nutrient enrichment. Thus, emphasis in
7 Chapter 9 is placed on the effects of airborne PM on visibility and climate, and on the
8 effects of deposition of PM constituents other than NO_x and SO_x, primarily metals and
9 carbonaceous compounds. EPA's framework for causality, described in Chapter 1, was
10 applied and the causal determinations are highlighted.

Table 2-5. Summary of causality determination for welfare effects.

Welfare Effects	Causality Determination
Effects on Visibility	Causal
Effects on Climate	Causal
Ecological Effects	Likely to be causal
Effects on Materials	Causal

2.5.1. Summary of Effects on Visibility

11 Visibility impairment is caused by light scattering and absorption by suspended
12 particles and gases. There is strong and consistent evidence that PM is the overwhelming
13 source of visibility impairment in both urban and remote areas. EC and some crustal
14 minerals are the only commonly occurring airborne particle components that absorb light.
15 All particles scatter light, and generally light scattering by particles is the largest of the
16 four light extinction components (i.e., absorption and scattering by gases and particles).
17 Although a larger particle scatters more light than a similarly shaped smaller particle of
18 the same composition, the light scattered per unit of mass is greatest for particles with
19 diameters from ~0.3-1.0 μm.

20 For studies where detailed data on particle composition by size are available, accurate
21 calculations of light extinction can be made. However, routinely available PM speciation
22 data can be used to make reasonable estimates of light extinction using relatively simple
23 algorithms that multiply the concentrations of each of the major PM species by its dry

1 extinction efficiency and by a water growth term that accounts for particle size change as a
2 function of relative humidity for hygroscopic species (e.g., sulfate, nitrate, and sea salt).
3 This permits the visibility impairment associated with each of the major PM components to
4 be separately approximated from PM speciation monitoring data.

5 Direct optical measurement of light extinction measured by transmissometer, or by
6 combining the PM light scattering measured by integrating nephelometers with the PM
7 light absorption measured by an aethalometer, offer a number of advantages compared to
8 algorithm estimates of light extinction based on PM composition and relative humidity
9 data. The direct measurements are not subject to the uncertainties associated with
10 assumed scattering and absorption efficiencies used in the PM algorithm approach. The
11 direct measurements have higher time resolution (i.e., minutes to hours), which is more
12 commensurate with visibility effects compared with calculated light extinction using
13 routinely available PM speciation data (i.e., 24-h duration).

14 Particulate sulfate and nitrate have comparable light extinction efficiencies (haze
15 impacts per unit mass concentration) at any relative humidity value. Their light scattering
16 per unit mass concentration increases with increasing relative humidity, and at sufficiently
17 high humidity values (RH>85%) they are the most efficient particulate species contributing
18 to haze. Particulate sulfate is the dominant source of regional haze in the eastern U.S.
19 (>50% of the particulate light extinction) and an important contributor to haze elsewhere in
20 the country (>20% of particulate light extinction). Particulate nitrate is a minor component
21 of remote-area regional haze in the non-California western and eastern U.S., but an
22 important contributor in much of California and in the upper Midwestern U.S., especially
23 during winter when it is the dominant contributor to particulate light extinction.

24 EC and OC have the highest dry extinction efficiencies of the major PM species and
25 are responsible for a large fraction of the haze, especially in the northwestern U.S., though
26 absolute concentrations are as high in the eastern U.S. Smoke plume impacts from large
27 wildfires dominate many of the worst haze periods in the western U.S. Carbonaceous PM is
28 generally the largest component of urban excess PM_{2.5} (i.e., the difference between urban
29 and regional background concentration). Western urban areas have more than twice the
30 average concentrations of carbonaceous PM than remote areas sites in the same region. In
31 eastern urban areas PM_{2.5} is dominated by about equal concentrations of carbonaceous and
32 sulfate components, though the usually high relative humidity in the East causes the
33 hydrated sulfate particles to be responsible for about twice as much of the urban haze as
34 that caused by the carbonaceous PM.

35 PM_{2.5} crustal material (referred to as fine soil) and PM_{10-2.5} are significant contributors
36 to haze for remote areas sites in the arid southwestern U.S. where they contribute a
37 quarter to a third of the haze, with PM_{10-2.5} usually contributing twice that of fine soil.
38 Coarse mass concentrations are as high in the Central Great Plains as in the deserts
39 though there are no corresponding high concentrations of fine soil as in the Southwest. Also

1 the relative contribution to haze by the high coarse mass in the Great Plains is much
2 smaller because of the generally higher haze values caused by the high concentrations of
3 sulfate and nitrate PM in that region.

4 Visibility has direct significance to people's enjoyment of daily activities and their
5 overall sense of wellbeing. A number of social science disciplines have attempted to link
6 perceived urban visibility to an array of effects reflecting the overall desire for good visual
7 air quality (VAQ), and the benefits of improving currently degraded VAQ. For example,
8 psychological research has demonstrated that people are emotionally affected by poor VAQ
9 such that their overall sense of wellbeing is diminished. Urban visibility has been examined
10 in two types of studies directly relevant to the NAAQS review process: urban visibility
11 preference studies and urban visibility valuation studies. Both types of studies are designed
12 to evaluate individuals' desire for good VAQ where they live, using different metrics. Urban
13 visibility preference studies examine individuals' preferences by investigating the amount
14 of visibility degradation considered unacceptable, while economic studies examine the value
15 an individual places on improving VAQ by eliciting how much the individual would be
16 willing to pay for different amounts of VAQ improvement.

17 There are three urban visibility preference studies and one additional pilot study
18 (designed as a survey instrument development project) that have been conducted to date
19 that provide useful information on individuals' preferences for good VAQ in the urban
20 setting. The completed studies were conducted in Denver, Colorado, two cities in British
21 Columbia, Canada, and Phoenix, Arizona. The pilot study was conducted in Washington,
22 DC. One notable finding of the three visibility preference studies and the one pilot study is
23 the general degree of consistency in the median preferences for an acceptable amount of
24 visibility degradation. The range of median acceptable visibility preference values from the
25 four studies is 19-25 deciviews (dv). Measured in terms of visual range (VR), these median
26 acceptable values are between 59 km and 32 km.

27 The economic importance of urban visibility has been examined by a number of
28 studies designed to quantify the benefits (or willingness to pay) associated with potential
29 improvements in urban visibility. Urban visibility valuation research was described in the
30 2004 PM AQCD and the 2005 OAQPS PM NAAQS Staff Paper. Since the mid-1990s, little
31 new information has become available regarding urban visibility valuation (Section 9.2.4).

32 Collectively, the evidence is sufficient to conclude that **a causal relationship exists**
33 **between PM and visibility impairment.**

2.5.2. Summary of Effects on Climate

34 Aerosols affect climate through direct and indirect effects. The direct effect is
35 primarily realized as planet brightening when seen from space because most aerosols
36 scatter most of the visible spectrum light that reaches them. The IPCC AR4 reported that

1 the radiative forcing from this direct effect was $-0.5 (\pm 0.4)$ W/m² and identified the level of
2 scientific understanding of this effect as “medium-low.” The global mean direct radiative
3 forcing from individual aerosol components varies from strongly negative for sulfate to
4 positive for black carbon with weaker positive or negative effects for other components, all
5 of which can vary strongly over space and time and with aerosol size. The indirect effects
6 are primarily realized as an increase in cloud brightness (termed the “first indirect” or
7 “Twomey” effect), changes in precipitation, and possible changes in cloud lifetime. The IPCC
8 AR4 reported that the radiative forcing from the Twomey effect was -0.7 (range: -1.1 to $+4$)
9 and identified the level of scientific understanding of this effect as “low.” The other indirect
10 effects from aerosols were not considered to be radiative-forcing.

11 Taken together, direct and indirect effects from aerosols increase Earth's shortwave
12 albedo or reflectance, thereby reducing the radiative flux reaching Earth's surface from the
13 Sun. This produces net climate cooling from aerosols. The current scientific consensus
14 reported by IPCC AR4 is that the direct and indirect radiative forcing from anthropogenic
15 aerosols computed at the top of the atmosphere, on a global average, is about -1.3 (range: $-$
16 2.2 to -0.5) W/m². Although the magnitude of this negative radiative forcing appears large
17 in comparison to the analogous IPCC AR4 estimate of positive radiative forcing from
18 anthropogenic GHG of about $2.9 (\pm 0.3)$ W/m², the spatial and temporal distributions of
19 these two very different radiative forcing agents are dissimilar; therefore, they do not
20 simply cancel and regional differences can be large. These differences result from the much
21 shorter atmospheric lifetime of aerosols than for the radiatively important trace gases,
22 implying that the radiative effects of aerosols respond much more quickly to changes in
23 emissions than do the effects from the gas-phase forcing agents. Moreover, the effect of
24 present-day aerosols is to cool Earth's surface but, on average, to heat the atmosphere
25 itself: within the atmospheric column, the radiative forcing effect from aerosols is estimated
26 to range from $+0.8$ to $+2$ W/m².

27 Considerable progress has been made with in situ and remotely-sensed aerosols
28 concentrations including the MODIS, MISR, POLDER, and OMI satellite instruments
29 (Section 3.4.1.6). The accuracy for aerosol optical depth (AOD) measured with these global-
30 coverage remote sensing instruments is on the order of 0.05 or 20% of the AOD, but is still
31 much lower than for the limited-area surface-based sun photometers which have accuracy
32 in the range of 0.01-0.02. The differences remaining between surface and remotely sensed
33 AOD and between estimates computed from measurements and from numerical model
34 predictions are important because AOD is a significant element in determining radiative
35 forcing. Hence, uncertainty and error in AOD measurements and modeling propagate into
36 the range of estimates for total radiative forcing reported here.

37 Numerical modeling of aerosol effects on climate has also sustained remarkable
38 progress since the 2004 PM AQCD, though model solutions still display large heterogeneity
39 in their estimation of the direct radiative forcing effect from anthropogenic aerosols.

1 Differences among models are due in large measure to differences in: emissions of PM and
2 precursors to secondary PM formation; the representation of aerosol microphysical and
3 optical processes; and regional- and global-scale transport and transformation; as well as in
4 the effects of aerosol radiative forcing. The clear-sky direct radiative forcing over ocean due
5 to anthropogenic aerosols is estimated from satellite instruments to be on the order of -1.1
6 (± 0.37) W/m^2 while model estimates are $-0.6 W/m^2$. The models' low bias over ocean is
7 carried through for the global average: global average direct radiative forcing from
8 anthropogenic aerosols is estimated from measurements to range from -0.9 to $-1.9 W/m^2$,
9 larger than the estimate of $-0.8 W/m^2$ from the models. Spatial heterogeneity in radiative
10 forcing is expected to exert significant effects on regional climate, but because the effects of
11 climate warming and cooling are not strictly co-located spatially or temporally with
12 radiative forcing or with emissions in particular for precursors for secondary PM formation,
13 assessments of effects for sub-global domains are even more uncertain than the global
14 averages reported here.

15 Overall, the evidence is sufficient to conclude that **a causal relationship exists between**
16 **PM and effects on climate, including both direct effects on radiative forcing and indirect effects**
17 **that involve cloud feedbacks that influence precipitation formation and cloud lifetimes.**

2.5.3. Summary of Ecological Effects of PM

18 Ecological effects of PM include direct effects to metabolic processes of plant foliage;
19 contribution to total metal loading resulting in alteration of soil biogeochemistry, plant
20 growth and animal growth and reproduction; and contribution to total organics loading
21 resulting in bioaccumulation and biomagnification across trophic levels. These effects were
22 well-characterized in the 2004 PM AQCD. Thus, the summary below builds upon the
23 conclusions provided in that review.

24 PM deposition comprises a heterogeneous mixture of particles differing in origin, size,
25 and chemical composition. Exposure to a given concentration of PM may, depending on the
26 mix of deposited particles, lead to a variety of phytotoxic responses and ecosystem effects.
27 Moreover, many of the ecological effects of PM are due to the chemical constituents (e.g.,
28 metals and organics) and their contribution to total loading within an ecosystem.

29 Investigations of the direct effects of PM deposition on foliage have suggested little or
30 no effects on foliar processes, unless deposition levels were higher than is typically found in
31 the ambient environment. However, consistent and coherent evidence of direct effects of PM
32 has been found in heavily polluted areas adjacent to industrial point sources such as
33 limestone quarries, cement kilns, and metal smelters (Sections 9.4.3. and 9.4.5.8.). Where
34 toxic responses have been documented, they generally have been associated with the
35 acidity, trace metal content, surfactant properties, or salinity of the deposited materials.

1 An important characteristic of fine particles is their ability to affect the flux of solar
2 radiation passing through the atmosphere directly, by scattering and absorbing solar
3 radiation, and, indirectly, by acting as cloud condensation nuclei (CCN) that, in turn,
4 influence the optical properties of clouds. Regional haze has been estimated to diminish
5 surface solar visible radiation. Crop yields can be sensitive to the amount of sunlight
6 received, and crop losses have been attributed to increased airborne particle concentrations
7 in some areas of the world. PM has been observed to cause a decrease in photosynthetically
8 active radiation (PAR) via thick haze occurring in China that decreases plant growth in the
9 diffuse light portion of PAR. However, a global model showed that PM can increase the
10 diffuse light fraction of PAR. On a global scale, the diffuse light fraction of PAR has been
11 shown to increase growth. Consequently, it was shown that when PM is decreased, plant
12 growth and C storage are also decreased. Further research is needed to determine net
13 effects of PM alteration of light conditions on the growth of vegetation in the U.S.

14 The deposition of PM onto vegetation and soil, depending on its chemical composition,
15 can produce responses within an ecosystem. The ecosystem response to pollutant deposition
16 is a direct function of the level of sensitivity of the ecosystem and its ability to ameliorate
17 resulting change. Many of the most important ecosystem effects of PM deposition occur in
18 the soil. Upon entering the soil environment, PM pollutants can alter ecological processes of
19 energy flow and nutrient cycling, inhibit nutrient uptake, change ecosystem structure, and
20 affect ecosystem biodiversity. The soil environment is one of the most dynamic sites of
21 biological interaction in nature. It is inhabited by microbial communities of bacteria, fungi,
22 and actinomycetes, in addition to plant roots and soil macro-fauna. These organisms are
23 essential participants in the nutrient cycles that make elements available for plant uptake.
24 Changes in the soil environment can be important in determining plant and ultimately
25 ecosystem response to PM inputs.

26 There is strong and consistent evidence from field and laboratory experiments that
27 metal components of PM alter numerous aspects of ecosystem structure and function.
28 Changes in the soil chemistry, microbial communities and nutrient cycling, can result from
29 the deposition of trace metals. Exposures to trace metals are highly variable, depending on
30 whether deposition is by wet or dry processes. Although metals can cause phytotoxicity at
31 high concentrations, few heavy metals (e.g., Cu, Ni, Zn) have been documented to cause
32 direct phytotoxicity under field conditions. Exposure to coarse particles and elements such
33 as Fe and Mg are more likely to occur via dry deposition, while fine particles are more likely
34 to contain elements such as Ca, Cr, Pb, Ni, and V. Ecosystems immediately downwind of
35 major emissions sources can receive locally heavy deposition inputs. Phytochelatins
36 produced by plants as a response to sublethal concentrations of heavy metals are indicators
37 of metal stress to plants. Increased concentrations of phytochelatins across regions and at
38 greater elevation have been associated with increased amounts of forest injury in the
39 northeastern U.S.

1 Overall, the ecological evidence is sufficient to conclude that **a causal relationship is**
2 **likely to exist between deposition of PM and a variety of effects on individual organisms and**
3 **ecosystems, based on information from the previous review and limited new findings in this**
4 **review.** However, in many cases, it is difficult to characterize the nature and magnitude of
5 effects and to quantify relationships between ambient concentrations of PM and ecosystem
6 response due to significant data gaps and uncertainties as well as considerable variability
7 that exists in the components of PM and their various ecological effects.

2.5.4. Summary of Effects on Materials

8 Building materials (metals, stones, cements, and paints) undergo natural weathering
9 processes from exposure to environmental elements (wind, moisture, temperature
10 fluctuations, sunlight, etc.). Metals form a protective film of oxidized metal (e.g., rust) that
11 slows environmentally induced corrosion. However, the natural process of metal corrosion is
12 enhanced by exposure to anthropogenic pollutants. For example, formation of hygroscopic
13 salts increases the duration of surface wetness and enhances corrosion.

14 A significant detrimental effect of particle pollution is the soiling of painted surfaces
15 and other building materials. Soiling changes the reflectance of opaque materials and
16 reduces the transmission of light through transparent materials. Soiling is a degradation
17 process that requires remediation by cleaning or washing, and, depending on the soiled
18 surface, repainting. Particulate deposition can result in increased cleaning frequency of the
19 exposed surface and may reduce the usefulness of the soiled material.

20 Attempts have been made to quantify the pollutant exposure levels at which
21 materials damage and soiling have been perceived. However, to date, insufficient data are
22 available to advance the knowledge regarding perception thresholds with respect to
23 pollutant concentration, particle size, and chemical composition. Nevertheless, the evidence
24 is sufficient to conclude that **a causal relationship exists between PM and effects on materials.**

Chapter 2 References

- Bell ML; Ebisu K; Peng RD; Walker J; Samet JM; Zeger SL; Dominic F. (2008). Seasonal and regional short-term effects of fine particles on hospital admissions in 202 U.S. counties, 1999-2005. *Am J Epidemiol*, 168: 1301-1310. [156266](#)
- Burnett RT; Brook JR; Yung WT; Dales RE; Krewski D. (1997). Association between ozone and hospitalization for respiratory diseases in 16 Canadian cities. *Environ Res*, 72: 24-31. [082676](#)
- Burnett RT; Smith-Doiron M; Stieb D; Cakmak S; Brook JR. (1999). Effects of particulate and gaseous air pollution on cardiorespiratory hospitalizations. *Arch Environ Occup Health*, 54: 130-139. [017269](#)
- Burnett RT; Stieb D; Brook JR; Cakmak S; Dales R; Raizenne M; Vincent R; Dann T. (2004). Associations between short-term changes in nitrogen dioxide and mortality in Canadian cities. *Arch Environ Occup Health*, 59: 228-236. [086247](#)
- Chen B; Hong C; Kan H. (2004). Exposures and health outcomes from outdoor air pollutants in China. *Toxicology*, 198: 291-300. [089899](#)
- Chen LH; Knutsen SF; Shavlik D; Beeson WL; Petersen F; Ghamsary M; Abbey D. (2005). The association between fatal coronary heart disease and ambient particulate air pollution: Are females at greater risk?. *Environ Health Perspect*, 113: 1723-1729. [087942](#)
- Chen SJ; Hsieh LT; Kao MJ; Lin WY; Huang KL; Lin CC. (2004). Characteristics of particles sampled in southern Taiwan during the Asian dust storm periods in 2000 and 2001. *Atmos Environ*, 38: 5925-5934. [147143](#)
- Chimonas MA; Gessner BD. (2007). Airborne particulate matter from primarily geologic, non-industrial sources at levels below National Ambient Air Quality Standards is associated with outpatient visits for asthma and quick-relief medication prescriptions among children less than 20 years old enrolled in Medicaid in Anchorage, Alaska. *Environ Res*, 70: 2021-2026. [093261](#)
- Delfino RJ; Murphy-Moulton AM; Burnett RT; Brook JR; Becklake MR. (1997). Effects of air pollution on emergency room visits for respiratory illnesses in Montreal, Quebec. *Am J Respir Crit Care Med*, 155: 568-576. [082687](#)
- Delfino RJ; Zeiger RS; Seltzer JM; Street DH. (1998). Symptoms in pediatric asthmatics and air pollution: differences in effects by symptom severity, anti-inflammatory medication use and particulate averaging time. *Environ Health Perspect*, 106: 751-761. [051406](#)
- Dockery DW; Cunningham J; Damokosh AI; Neas LM; Spengler JD; Koutrakis P; Ware JH; Raizenne M; Speizer FE. (1996). Health effects of acid aerosols on North American children: respiratory symptoms. *Environ Health Perspect*, 104: 500-505. [077269](#)
- Dockery DW; Luttmann-Gibson H; Rich DQ; Link MS; Mittleman MA; Gold DR; Koutrakis P; Schwartz JD; Verrier RL. (2005). Association of air pollution with increased incidence of ventricular tachyarrhythmias recorded by implanted cardioverter defibrillators. *Environ Health Perspect*, 113: 670-674. [078995](#)
- Dominici F; Peng RD; Bell ML; Pham L; McDermott A; Zeger SL; Samet JL. (2006). Fine particulate air pollution and hospital admission for cardiovascular and respiratory diseases. *JAMA*, 295: 1127-1134. [088398](#)
- Eftim SE; Samet JM; Janes H; McDermott A; Dominici F. (2008). Fine particulate matter and mortality: a comparison of the six cities and American Cancer Society cohorts with a medicare cohort. *Epidemiology*, 19: 209-216. [099104](#)
- Enstrom JE. (2005). Fine particulate air pollution and total mortality among elderly Californians, 1973-2002. *Inhal Toxicol*, 17: 803-816. [087356](#)
- Fung KY; Khan S; Krewski D; Chen Y. (2006). Association between air pollution and multiple respiratory hospitalizations among the elderly in Vancouver, Canada. *Inhal Toxicol*, 18: 1005-1011. [089789](#)
- Gent JF; Koutrakis P; Belanger K; Triche E; Holford TR; Bracken MB; Leaderer BP. (2009). Symptoms and medication use in children with asthma and traffic-related sources of fine particle pollution. *Environ Health Perspect*, In Press: 1-41. [180399](#)
- Goss CH; Newsom SA; Schildcrout JS; Sheppard L; Kaufman JD. (2004). Effect of ambient air pollution on pulmonary exacerbations and lung function in cystic fibrosis. *Am J Respir Crit Care Med*, 169: 816-821. [055624](#)

Note: Hyperlinks to the reference citations throughout this document will take you to the NCEA HERO database (Health and Environmental Research Online) at <http://epa.gov/hero>. HERO is a database of scientific literature used by U.S. EPA in the process of developing science assessments such as the Integrated Science Assessments (ISA) and the Integrated Risk Information System (IRIS).

- Ito K. (2003). Associations of particulate matter components with daily mortality and morbidity in Detroit, Michigan. [042856](#)
- Ito K; Thurston GD; Silverman RA. (2007). Association between coarse particles and asthma emergency department (ED) visits in New York City. [091262](#)
- Kim JJ; Smorodinsky S; Lipsett M; Singer BC; Hodgson AT; Ostro B. (2004). Traffic-related air pollution near busy roads: the East Bay children's Respiratory Health Study. *Am J Respir Crit Care Med*, 170: 520-526. [087383](#)
- Krewski D; Jerrett M; Burnett RT; Ma R; Hughes E; Shi Y; Turner MC; Pope AC III; Thurston G; Calle EE; Thun MJ. (2009). Extended follow-up and spatial analysis of the American Cancer Society study linking particulate air pollution and mortality. Health Effects Institute. Cambridge, MA. 140. [191193](#)
- Laden F; Schwartz J; Speizer FE; Dockery DW. (2006). Reduction in fine particulate air pollution and mortality: extended follow-up of the Harvard Six Cities study. *Am J Respir Crit Care Med*, 173: 667-672. [087605](#)
- Lin M; Chen Y; Burnett RT; Villeneuve PJ; Krewski D. (2002). The influence of ambient coarse particulate matter on asthma hospitalization in children: case-crossover and time-series analyses. *Environ Health Perspect*, 110: 575-581. [026067](#)
- Lin M; Stieb DM; Chen Y. (2005). Coarse particulate matter and hospitalization for respiratory infections in children younger than 15 years in Toronto: a case-crossover analysis. , 116: 235-240. [087828](#)
- Lipfert FW; Baty JD; Miller JP; Wyzga RE. (2006). PM2.5 constituents and related air quality variables as predictors of survival in a cohort of U.S. military veterans. *Inhal Toxicol*, 18: 645-657. [088756](#)
- Lippmann M. (2000). Environmental toxicants: human exposures and their health effects. [024579](#)
- Lisabeth LD; Escobar JD; Dvonch JT; Sanchez BN; Majersik JJ; Brown DL; Smith MA; Morgenstern LB. (2008). Ambient air pollution and risk for ischemic stroke and transient ischemic attack. , 64: 53-59. [155939](#)
- Mar TF; Larson TV; Stier RA; Claiborn C; Koenig JQ. (2004). An analysis of the association between respiratory symptoms in subjects with asthma and daily air pollution in Spokane, Washington. *Inhal Toxicol*, 16: 809-815. [057309](#)
- McConnell R; Berhane K; Gilliland F; Molitor J; Thomas D; Lurmann F; Avol E; Gauderman WJ; Peters JM. (2003). Prospective study of air pollution and bronchitic symptoms in children with asthma. *Am J Respir Crit Care Med*, 168: 790-797. [049490](#)
- Metzger KB; Klein M; Flanders WD; Peel JL; Mulholland JA; Langberg JJ; Tolbert PE. (2007). Ambient air pollution and cardiac arrhythmias in patients with implantable defibrillators. *Epidemiology*, 18: 585-592. [092856](#)
- Metzger KB; Tolbert PE; Klein M; Peel JL; Flanders WD; Todd KH; Mulholland JA; Ryan PB; Frumkin H. (2004). Ambient air pollution and cardiovascular emergency department visits. , 15: 46-56. [044222](#)
- Miller KA; Siscovick DS; Sheppard L; Shepherd K; Sullivan JH; Anderson GL; Kaufman JD. (2007). Long-term exposure to air pollution and incidence of cardiovascular events in women. , 356: 447-458. [090130](#)
- Moolgavkar SH. (2003). Air pollution and daily deaths and hospital admissions in Los Angeles and Cook counties. [042864](#)
- O'Connor GT; Neas L; Vaughn B; Kattan M; Mitchell H; Crain EF; Evans R, 3rd; Gruchalla R; Morgan W; Stout J; Adams GK; Lippmann M. (2008). Acute respiratory health effects of air pollution on children with asthma in US inner cities. *J Allergy Clin Immunol*, 121: 1133-1139 e1131. [156818](#)
- Ostro B; Broadwin R; Green S; Feng W-Y; Lipsett M. (2006). Fine particulate air pollution and mortality in nine California counties: results from CALFINE. *Environ Health Perspect*, 114: 29-33. [087991](#)
- Ostro B; Roth L; Malig B; Marty M. (2009). The effects of fine particle components on respiratory hospital admissions in children. *Environ Health Perspect*, 117: 475. [191971](#)
- Peel JL; Tolbert PE; Klein M; Metzger KB; Flanders WD; Knox T; Mulholland JA; Ryan PB; Frumkin H. (2005). Ambient air pollution and respiratory emergency department visits. , 16: 164-174. [056305](#)
- Peng RD; Chang HH; Bell ML; McDermott A; Zeger SL; Samet JM; Dominici F. (2008). Coarse particulate matter air pollution and hospital admissions for cardiovascular and respiratory diseases among Medicare patients. *JAMA*, 299: 2172-2179. [156850](#)
- Peters A; Dockery DW; Muller JE; Mittleman MA. (2001). Increased particulate air pollution and the triggering of myocardial infarction. , 103: 2810-2815. [016546](#)
- Pope C; Renlund D; Kfoury A; May H; Horne B. (2008). Relation of heart failure hospitalization to exposure to fine particulate air pollution. , 102: 1230-1234. [191969](#)
- Pope CA III; Muhlestein JB; May HT; Renlund DG; Anderson JL; Horne BD. (2006). Ischemic heart disease events triggered by short-term exposure to fine particulate air pollution. *Circulation*, 114: 2443-2448. [091246](#)
- Rabinovitch N; Strand M; Gelfand EW. (2006). Particulate levels are associated with early asthma worsening in children with persistent disease. *Am J Respir Crit Care Med*, 173: 1098-1105. [088031](#)

- Rabinovitch N; Zhang LN; Murphy JR; Vedal S; Dutton SJ; Gelfand EW. (2004). Effects of wintertime ambient air pollutants on asthma exacerbations in urban minority children with moderate to severe disease. *J Allergy Clin Immunol*, 114: 1131-1137. [096753](#)
- Rich DQ; Kim MH; Turner JR; Mittleman MA; Schwartz J; Catalano PJ; Dockery DW. (2006). Association of ventricular arrhythmias detected by implantable cardioverter defibrillator and ambient air pollutants in the St Louis, Missouri metropolitan area. *Occup Environ Med*, 63: 591-596. [089814](#)
- Rich KE; Petkau J; Vedal S; Brauer M. (2004). A case-crossover analysis of particulate air pollution and cardiac arrhythmia in patients with implantable cardioverter defibrillators. *Inhal Toxicol*, 16: 363-372. [055631](#)
- Schwartz J; Coull B; Laden F; Ryan L. (2008). The effect of dose and timing of dose on the association between airborne particles and survival. *Environ Health Perspect*, 116: 64-69. [156963](#)
- Sheppard L. (2003). Ambient air pollution and nonelderly asthma hospital admissions in Seattle, Washington, 1987-1994. [042826](#)
- Slaughter JC; Kim E; Sheppard L; Sullivan JH; Larson TV; Claiborn C. (2005). Association between particulate matter and emergency room visits, hospital admissions and mortality in Spokane, Washington. *J Expo Sci Environ Epidemiol*, 15: 153-159. [073854](#)
- Sullivan J; Ishikawa N; Sheppard L; Siscovick D; Checkoway H; Kaufman J. (2003). Exposure to ambient fine particulate matter and primary cardiac arrest among persons with and without clinically recognized heart disease. *Am J Epidemiol*, 157: 501-509. [043156](#)
- Sullivan J; Sheppard L; Schreuder A; Ishikawa N; Siscovick D; Kaufman J. (2005). Relation between short-term fine-particulate matter exposure and onset of myocardial infarction. *Am J Epidemiol*, 161: 41-48. [050854](#)
- Symons JM; Wang L; Guallar E; Howell E; Dominici F; Schwab M; Ange BA; Samet J; Ondov J; Harrison D; Geyh A. (2006). A case-crossover study of fine particulate matter air pollution and onset of congestive heart failure symptom exacerbation leading to hospitalization. *Am J Epidemiol*, 164: 421-33. [091258](#)
- Thurston GD; Ito K; Hayes CG; Bates DV; Lippmann M. (1994). Respiratory hospital admissions and summertime haze air pollution in Toronto, Ontario: consideration of the role of acid aerosols. *Environ Res*, 65: 271-290. [043921](#)
- Tolbert PE; Kleina M; Peelb JL; Sarnata SE; Sarnata JA. (2007). Multipollutant modeling issues in a study of ambient air quality and emergency department visits in Atlanta. *J Expo Sci Environ Epidemiol*, 24: 938-945. [090316](#)
- U.S. EPA. (2004). Air quality criteria for particulate matter. U.S. Environmental Protection Agency. Research Triangle Park, NC. EPA/600/P-99/002aF-bF. [056905](#)
- U.S. EPA. (2008). Integrated science assessment for oxides of nitrogen and sulfur: Ecological criteria. EPA. EPA. EPA/600/R-08/082F. [157074](#)
- Villeneuve PJ; Chen L; Stieb D; Rowe BH. (2006). Associations between outdoor air pollution and emergency department visits for stroke in Edmonton, Canada. *Eur J Epidemiol*, 21: 689-700. [090191](#)
- Woodruff TJ; Darrow LA; Parker JD. (2008). Air pollution and postneonatal infant mortality in the United States, 1999-2002. *Environ Health Perspect*, 116: 110-5. [098386](#)
- Yang Q; Chen Y; Krewski D; Shi Y; Burnett RT; McGrail KM. (2004). Association between particulate air pollution and first hospital admission for childhood respiratory illness in Vancouver, Canada. *Arch Environ Occup Health*, 59: 14-21. [087488](#)
- Zanobetti A; Schwartz J. (2009). The effect of fine and coarse particulate air pollution on mortality: A national analysis. *Environ Health Perspect*, 117: 1-40. [188462](#)
- Zeger S; Dominici F; McDermott A; Samet J. (2008). Mortality in the Medicare population and chronic exposure to fine particulate air pollution in urban centers (2000-2005). *Environ Health Perspect*, 116: 1614. [191951](#)
- Zhang Z; Whitsel E; Quibrera P; Smith R; Liao D; Anderson G; Prineas R. (2009). Ambient Fine Particulate Matter Exposure and Myocardial Ischemia in the Environmental Epidemiology of Arrhythmogenesis in the Women's Health Initiative (EEAWHI) Study. *Environ Health Perspect*, 117: 751. [191970](#)

Chapter 3. Source to Human Exposure

3.1. Introduction

1 This chapter describes basic concepts and new and established findings in
2 atmospheric sciences and human exposure assessment relevant to PM to establish a
3 foundation for the health and ecological effects discussed in subsequent chapters.
4 Information in this chapter builds on previous AQCDs for PM using new data and re-
5 interpretations of extant studies as well. This includes new knowledge of PM chemistry, the
6 latest developments in monitoring methodologies, recent national and local measurements
7 and trends in PM concentrations as a function of size range and composition, advances in
8 receptor and chemistry-transport modeling, revised estimates of policy-relevant background
9 PM, and recent work on exposure assessment.

10 The chapter and its associated annex material are organized as follows: Section 3.2
11 presents an overview of basic information related to the size distribution and composition of
12 airborne particles. Section 3.3 provides a brief description of the sources, emissions, and
13 deposition of PM, including discussions of possible mechanisms of secondary PM formation
14 from gaseous precursors and of the atmospheric processes that deposit PM to the earth's
15 surface. Issues related to the measurement of PM and its chemical components and to
16 monitors and networks in the U.S. are covered in Section 3.4; supplementary material on
17 these topics is contained in Annex A, Section A.1. Analyses of data for ambient
18 concentrations of PM and its components are characterized in Section 3.5, and
19 supplementary information can be found in Annex A, Section A.2. Section 3.6 describes
20 methods for determining source contributions to ambient samples by receptor models and
21 presents results from recent receptor modeling studies. In addition, the construction of
22 chemistry-transport models (CTMs) to determine pollutant concentrations is described in
23 Section 3.6. Supplementary information about receptor model methods and results is given
24 in Annex A, Section A.3. Policy relevant background concentrations of PM, i.e., those
25 concentrations defined to result from natural sources everywhere in the world together

Note: Hyperlinks to the reference citations throughout this document will take you to the NCEA HERO database (Health and Environmental Research Online) at <http://epa.gov/hero>. HERO is a database of scientific literature used by U.S. EPA in the process of developing science assessments such as the Integrated Science Assessments (ISA) and the Integrated Risk Information System (IRIS).

1 with anthropogenic sources outside of Canada, the United States, and Mexico, are
2 presented in Section 3.7. Issues related to human exposure assessment including sources of
3 exposure and implications for epidemiologic studies are discussed in Section 3.8.
4 Supplementary information on exposure studies is included in Annex A, Section A.4.
5 Finally, the summary and conclusions from Chapter 3 are presented in Section 3.9.

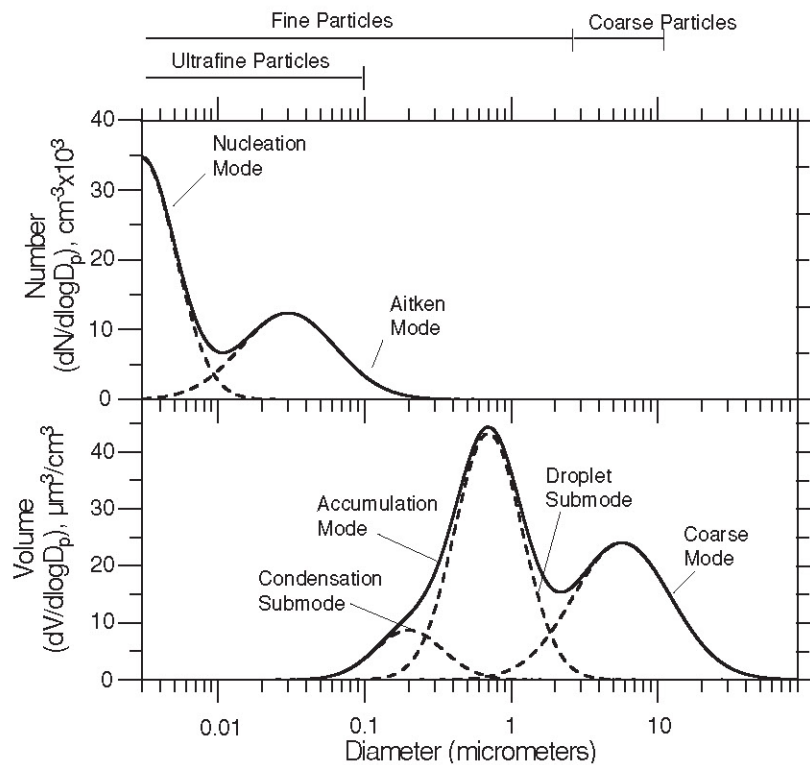
3.2. Overview of Basic Aerosol Properties

6 Unlike gas-phase pollutants such as SO₂, CO, H₂CO and O₃, which are well-defined
7 chemical entities, atmospheric PM varies in size, shape, and chemical composition.
8 Atmospheric chemical and microphysical processing of direct emissions of PM and its
9 precursors together with mechanical generation of particles tend to produce distinct
10 lognormal modes (Whitby, 1978, [071181](#)) as shown in Figure 3-1. To the extent that
11 information is available, discussions in this and subsequent chapters will focus on particles
12 in specific size ranges (i.e., PM_{2.5}, PM_{10-2.5} and PM₁₀). The subscripts after PM refer to the
13 aerodynamic diameter¹ (d_{ae}) in micrometers (μm) of 50% cut points of sampling devices. For
14 example, EPA defines PM₁₀ as particles collected by a sampler with an upper 50% cut point
15 of 10 μm d_{ae} and a specific, fairly sharp, penetration curve, as defined in the Code of Federal
16 Regulations (40 CFR Part 58). PM_{2.5} is defined in an analogous way. Ultrafine particles,
17 defined here as particles with a diameter ≤ 0.1 μm (typically based on physical size, thermal
18 diffusivity, or electrical mobility), will also be discussed.

19 The terms “fine particles” and “coarse particles” have lost the precise meaning as
20 defined in Whitby (1978, [071181](#)), where “fine particles” refers to all particles in the
21 nucleation, Aitken, and accumulation modes; and “coarse particles” characterizes all
22 particles larger than these. Ultrafine particles correspond loosely to the nucleation plus
23 Aitken modes (in earlier literature, these modes were not separated and the combination,
24 unresolved by older instruments, was called the Aitken mode). Now, the term “fine
25 particles” is most often associated with the PM_{2.5} fraction, which includes the nucleation,

¹ Aerodynamic diameter is the diameter of a unit density (1 g/cm³) sphere that has the same gravitational settling velocity as the particle of interest and is a useful metric for characterizing particles >~ 1 μm. For sub-micron particles, forces other than gravity increase in importance in determining a particle’s motion and air can no longer be considered a continuum. Regardless, aerodynamic diameter is frequently reported down to ~ 0.1 μm where the assumptions used in its derivation no longer hold. A useful metric for characterizing particles <~ 0.5 μm is the mobility diameter defined as the diameter of a particle having the same diffusivity or electrical mobility in air as the particle of interest. In the region between ~ 0.5–1.0 μm, aerodynamic and mobility diameters are not necessarily the same. The question of how best to merge these diameters is unresolved and depends on the particle properties of interest.

1 Aitken and accumulation modes and some particles from the lower-size tail of the coarse
 2 particle mode between about 1 and 2.5 μm aerodynamic diameter. “Thoracic coarse” is
 3 frequently used in reference to $\text{PM}_{10-2.5}$, which does not include the low-end tail of the coarse
 4 particle mode. With high relative humidity, larger particles in the accumulation mode could
 5 also extend into the 1 to 3 μm size range. These relationships can be seen in Figure 3-1,
 6 which shows the number distribution for ultrafine particles and the volume distribution (or
 7 mass distribution if particle density is constant across the size range) for fine and (thoracic)
 8 coarse particles. The figure is arranged this way because particle number is most highly
 9 concentrated in the ultrafine size range but volume (or mass) is most concentrated in the
 10 larger size ranges.



Source: Pandis (2004, [156838](#)).

Figure 3-1. Particle size distributions by number and volume. Dashed lines refer to values in individual modes and solid lines to their sum. Note that ultrafine particles are a subset of fine particles.

11 Characterizing particle size is important because different size particles penetrate to
 12 different regions of the human respiratory tract. Thoracic particles refer to particles that

1 travel past the larynx to reach the lung airways and the gas-exchange region of the lung,
 2 and respirable particles are those that reach the gas-exchange region. The selection of PM₁₀
 3 as an indicator of thoracic particles was based in large part on dosimetry (U.S. EPA, 1996,
 4 [079380](#)). However, the selection of PM_{2.5} to characterize respirable particles was driven
 5 mainly by considerations related to measurement techniques available at the time rather
 6 than dosimetry. Currently, cut points other than 2.5 μm are attainable and frequently put
 7 into use. For example, the American Conference of Governmental Industrial Hygienists
 8 (ACGIH, 2005, [156188](#)), the International Standards Organization, and the European
 9 Standardization Committee have adopted a 50% cut point of 4 μm as an indicator of
 10 respirable particles. Most commonly, however, PM_{2.5} is used as an indicator of respirable
 11 particles, PM_{10-2.5} is used as an indicator of the thoracic component of coarse particles that
 12 is sometimes referred to as thoracic coarse (noting that it excludes some coarse particles
 13 below 2.5 μm and above 10 μm), and PM₁₀ is used as an indicator of thoracic particles.

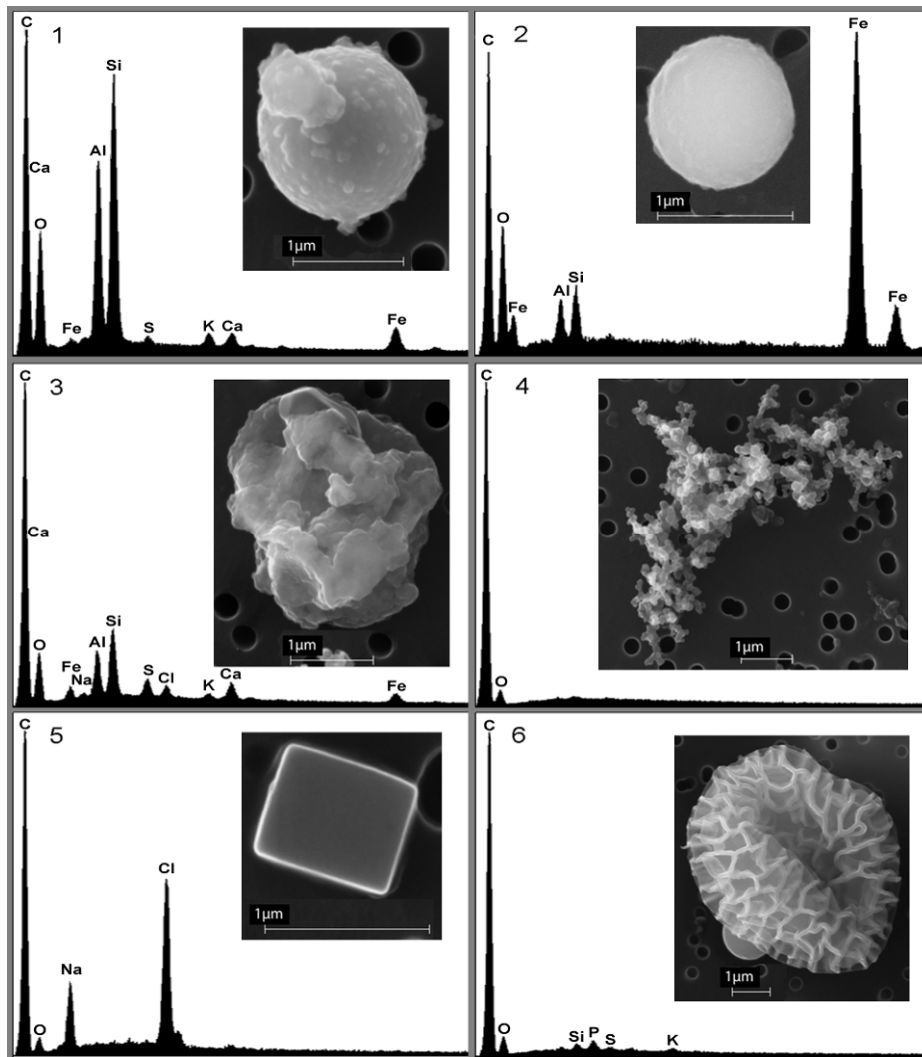
14 As can be seen from Table 3-1, particles in individual size modes are characterized by
 15 rather distinct sources, composition, chemical properties, lifetimes in the atmosphere (τ)
 16 and distances over which they can travel. Whereas particles in the smaller size modes are
 17 formed mainly by combustion processes and by nucleation and condensation of gases,
 18 coarse particles are generated mainly by mechanical activity, such as by the action of wind
 19 on either the ground or the sea surface or by construction or by resuspension by traffic.
 20 Particles in the ultrafine size range are either emitted directly to the atmosphere or are
 21 formed by nucleation of gaseous constituents in the atmosphere as shown in Table 3-1. The
 22 properties of fibers and engineered nano-objects and nanometer scale products (e.g., dots,
 23 hollow spheres, rods, fibers, and tubes) are not reviewed in this chapter because these
 24 classes of objects are found mainly in certain occupational settings and not in ambient air.

Table 3-1. Characteristics of ambient fine (ultrafine plus accumulation-mode) and coarse particles.

	Fine		Coarse
	Ultrafine	Accumulation	
Formation Processes	Combustion, high-temperature processes, and atmospheric reactions		Break-up of large solids/droplets
Formed by	Nucleation of atmospheric gases including H ₂ SO ₄ , NH ₃ and some organic compounds Condensation of gases	Condensation of gases Coagulation of smaller particles Reactions of gases in or on particles Evaporation of fog and cloud droplets in which gases have dissolved and reacted	Mechanical disruption (crushing, grinding, abrasion of surfaces) Evaporation of sprays Suspension of dusts Reactions of gases in or on particles

Fine			
Composed of	Sulfate EC Metal compounds Organic compounds with very low saturation vapor pressure at ambient temperature	Sulfate, nitrate, ammonium, and hydrogen ions EC Large variety of organic compounds Metals: compounds of Pb, Cd, V, Ni, Cu, Zn, Mn, Fe, etc. Particle-bound water Bacteria, viruses	Nitrates/chlorides/sulfates from HNO ₃ /HCl/SO ₂ reactions with coarse particles Oxides of crustal elements (Si, Al, Ti, Fe) CaCO ₃ , CaSO ₄ , NaCl, sea salt Bacteria, pollen, mold, fungal spores, plant and animal debris
Solubility	Not well characterized	Largely soluble, hygroscopic, and deliquescent	Largely insoluble and nonhygroscopic
Sources	High temperature combustion Atmospheric reactions of primary, gaseous compounds.	Combustion of fossil and biomass fuels, and high temperature industrial processes, smelters, refineries, steel mills etc. Atmospheric oxidation of NO ₂ , SO ₂ , and organic compounds, including biogenic organic species (e.g., terpenes)	Resuspension of particles deposited onto roads Tire, brake pad, and road wear debris Suspension from disturbed soil (e.g., farming, mining, unpaved roads) Construction and demolition Fly ash from uncontrolled combustion of coal, oil, and wood Ocean spray
Atmospheric half-life	Minutes to hours	Days to weeks	Minutes to hours
Removal Processes	Grows into accumulation mode Diffuses to raindrops	Forms cloud droplets and rains out Dry deposition	Dry deposition by fallout Scavenging by falling rain drops
Travel distance	< 1 to 10s of km	100s to 1000s of km	< 1 to 10s of km (100s to 1,000s of km in dust storms for the small size tail)

Source: Wilson and Suh (1997, [077408](#)) (adapted).



Source: National Exposure Research Laboratory.

Figure 3-2. X-ray spectra and scanning electron microscopy images of individual particles including:(1) an aluminum-silicate fly ash sphere emitted from a coal-fired power plant, (2) an iron oxide sphere emitted from a steel manufacturing facility, (3) An aluminum-silicate particle, probably of crustal origin, (4) a carbon soot aggregate from a diesel engine consisting of many sub-micron size carbon particles, (5) a sodium chloride crystal, potentially of marine origin, and (6) a partially collapsed pollen particle. The polycarbonate filter substrate used to collect the particles contributes to the carbon peak in each spectrum.

- 1 Particles appear in a wide variety of shapes such as spheres, ellipsoids, cubes, and
- 2 irregular or fractal geometries. This is one reason why a standard metric such as
- 3 aerodynamic diameter is useful for describing the mechanical properties of the particles.
- 4 The shape of particles is important for determining the optical properties of the particles.
- 5 The directionality of sunlight scattered by certain shapes of particles, such as plates, also

1 depends strongly on their physical orientation while suspended. The shape of particles also
2 affects the surface area of the particles in contact with the surface it is deposited on,
3 including cell membranes.

4 Images of six types of individual particles obtained using scanning electron
5 microscope (SEM) and their corresponding x-ray spectra showing their major elemental
6 composition are shown in Figure 3-2. The images show particles sitting on a thin
7 polycarbonate film with pores and a 1 μm scale bar for size reference. Air is pulled through
8 the filter pores with a vacuum pump and the particles are left behind on the surface. The
9 metal dominated spherical particles (image 2) were formed at high temperatures and were
10 quickly cooled. Particles which are liquid such as sulfate are also spherical. Sodium chloride
11 (NaCl) crystals are cubic (image 5); this particular particle could be marine sea salt due to
12 the proximity to the ocean where the sample was collected. Other particles, such as the
13 carbon chain agglomerates from diesel engines have much more irregular and complex
14 shapes (image 4). Note that these particles were placed under vacuum resulting in
15 volatilization of water and other volatile components and partial collapse of the pollen grain
16 (image 6). Changes in composition and possibly morphology could occur during the
17 sampling, collection and analysis of aerosol samples. For example, particles may be coated
18 with semi-volatile material that evolves off the particles under vacuum and under the
19 electron beam. Similarly, particles in ambient air are generally mixtures or agglomerates of
20 particles coming from multiple sources and have a diverse chemical make-up.

3.3. Sources, Emissions and Deposition of Primary and Secondary PM

21 PM is composed of both primary (derived directly from emissions) or secondary
22 (derived from atmospheric reactions involving gaseous precursors) components. Table 3-2
23 summarizes anthropogenic and natural sources for the major primary and secondary
24 aerosol constituents of fine and coarse particles. Anthropogenic sources can be further
25 divided into stationary and mobile sources. Stationary sources include fuel combustion for
26 electrical utilities, residential space heating and cooking; industrial processes; construction
27 and demolition; metal, mineral, and petrochemical processing; wood products processing;
28 mills and elevators used in agriculture; erosion from tilled lands; waste disposal and
29 recycling; and biomass combustion. Biomass combustion encompasses many emission

1 activities including burning of wood for fuel, burning of vegetation to clear land for
2 agriculture and construction, to dispose of agricultural and domestic waste, to control the
3 growth of animal or plant pests, and to manage forest resources (prescribed burning).
4 Wildlands also burn due to lightning strikes and arson. Mobile or transportation-related
5 sources include direct emissions of primary PM and secondary PM precursors from highway
6 vehicles and non-road sources as well as fugitive dust from paved and unpaved roads. Also
7 shown in Table 3-2 are sources for several precursor gases, the oxidation of which can form
8 secondary PM. An overview of estimates of emissions of primary PM and precursors to
9 secondary PM from major sources is given in Section 3.3.1. The transformations from
10 gaseous precursors shown in Table 3-2 to secondary PM are described in Section 3.3.2.

11 In general, the sources of fine PM are very different from those of coarse PM. Some of
12 the mass in the fine size fraction forms during combustion from material that has
13 volatilized in combustion chambers and then recondensed before emission to the
14 atmosphere. Some ambient $PM_{2.5}$ forms in the atmosphere from photochemical reactions
15 involving precursor gases. Included in this category is the formation of new ultrafine
16 particles by homogeneous nucleation of precursor gases in addition to the condensation of
17 gases on pre-existing particles. PM formed by the first mechanism is referred to as primary,
18 and PM formed by the second mechanism is referred to as secondary. Biological material
19 also exists in the fine fraction including many types of microorganisms, especially viruses
20 and bacteria and fragments of pollens and fungal spores. $PM_{10-2.5}$ is mainly primary in
21 origin, as it is produced by surface abrasion or by suspension of biological material and
22 fragments of living things (e.g., plant and insect debris). In addition, atmospheric reaction
23 products condense on coarse particles. Because precursor gases undergo mixing during
24 transport from their sources and reactions in the atmosphere can produce the same
25 products, it is difficult to identify individual sources of secondary PM. Transport and
26 transformation of precursors can occur over distances of hundreds of kilometers. $PM_{10-2.5}$
27 has a shorter lifetime in the atmosphere, so its effects tend to be more localized. However,
28 intercontinental transport of dust from African and Asian deserts occurs and some of this
29 material is in the $PM_{10-2.5}$ size range. Major events are highly episodic but much smaller
30 contributions can be made at other times (see Section 3.7).

Table 3-2. Constituents of atmospheric particles and their major sources.

Aerosol species	Primary (PM < 2.5 μm)		Primary (PM > 2.5 μm)		Secondary PM Precursors (PM < 2.5 μm)	
	Natural	Anthropogenic	Natural	Anthropogenic	Natural	Anthropogenic
Sulfate (SO ₄ ²⁻)	Sea spray	Fossil fuel combustion	Sea spray	—	Oxidation of reduced sulfur gases emitted by the oceans and wetlands and SO ₂ and H ₂ S emitted by volcanism and forest fires	Oxidation of SO ₂ emitted from fossil fuel combustion
Nitrate (NO ₃ ⁻)	—	Mobile source exhaust	—	—	Oxidation of NO _x produced by soils, forest fires, and lighting	Oxidation of NO _x emitted from fossil fuel combustion and in motor vehicle exhaust
Minerals	Erosion and re-entrainment	Fugitive dust from paved and unpaved roads, agriculture, forestry, construction, and demolition	Erosion and re-entrainment	Fugitive dust, paved and unpaved road dust, agriculture, forestry, construction, and demolition	—	—
Ammonium (NH ₄ ⁺)	—	Mobile source exhaust	—	—	Emissions of NH ₃ from wild animals, and undisturbed soil	Emissions of NH ₃ from motor vehicles, animal husbandry, sewage, and fertilized land
Organic carbon (OC)	Wildfires	Prescribed burning, wood burning, motor vehicle exhaust, cooking, tire wear and industrial processes	Soil humic matter	Tire and asphalt wear, paved and unpaved road dust	Oxidation of hydrocarbons emitted by vegetation (terpenes, waxes) and wild fires	Oxidation of hydrocarbons emitted by motor vehicles, prescribed burning, wood burning, solvent use and industrial processes
EC	Wildfires	Mobile source exhaust (mainly diesel), wood biomass burning, and cooking	—	Tire and asphalt wear, paved and unpaved road dust	—	—
Metals	Volcanic activity	Fossil fuel combustion, smelting and other metallurgical processes, and brake wear	Erosion, re-entrainment, and organic debris	—	—	—
Bioaerosols	Viruses and bacteria	—	Plant and insect fragments, pollen, fungal spores, and bacterial agglomerates	—	—	—

Dash (—) indicates either very minor source or no known source of component.
 Source: U.S. EPA (2004, [056905](#)).

1 Only major sources for each constituent within each broad category shown at the top
 2 of Table 3-2 are listed. Not all sources are equal in magnitude. Chemical characterizations
 3 of primary particulate emissions for a wide variety of natural and anthropogenic sources (as
 4 shown in Table 3-2) were given in Chapter 5 of the 1996 PM AQCD (U.S. EPA, 1996,
 5 [079380](#)). Summary tables of the composition of source emissions presented in the 1996 PM
 6 AQCD (U.S. EPA, 1996, [079380](#)) and updates to that information are provided in Appendix
 7 3D to the 2004 PM AQCD (U.S. EPA, 2004, [056905](#)). Source composition profiles are

1 archived by the EPA at <http://www.epa.gov/ttn/chief/software/speciate/>. The profiles of
2 source composition were based in large measure on the results of studies that collected
3 source signatures for use in source apportionment studies.

4 Natural sources of primary PM include windblown dust from undisturbed land, sea
5 spray, and biological material. The oxidation of a fraction of terpenes emitted by vegetation
6 and reduced sulfur species from anaerobic environments leads to secondary PM formation.
7 Ammonium (NH_4^+) ions, which play a major role in regulating the pH of particles, are
8 derived from emissions of NH_3 gas. Source categories for NH_3 have been divided into
9 emissions from undisturbed soils (natural) and emissions that are related to human
10 activities (e.g., fertilized lands, domestic and farm animal waste). There is ongoing debate
11 about characterizing emissions from wildfires (i.e., unwanted fire) as either natural or
12 anthropogenic. Wildfires have been listed in Table 3-2 as natural in origin, but land
13 management practices and other human actions affect the occurrence and scope of
14 wildfires. For example, fire suppression practices allow the buildup of combustible fuels and
15 increase the susceptibility of forests to more severe and infrequent fires from whatever
16 cause, including lightning strikes. Similarly, prescribed burning is listed as anthropogenic,
17 but can be viewed as a substitute for wildfires that would otherwise occur eventually on the
18 same land.

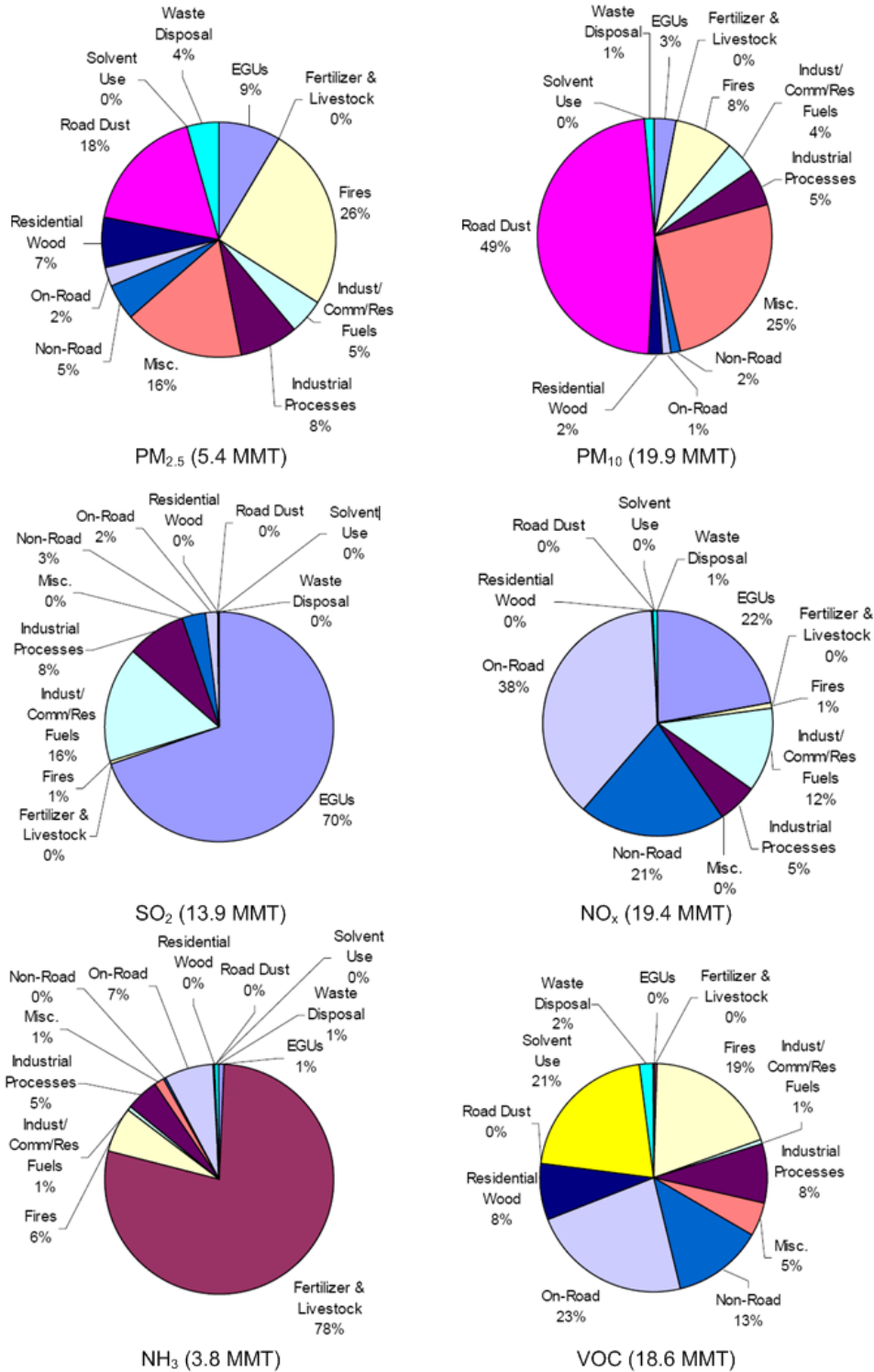
3.3.1. Emissions of Primary PM and Precursors to Secondary PM

19 U.S. national average emissions of primary $\text{PM}_{2.5}$, PM_{10} and gaseous precursor species
20 (SO_2 , NO_x , NH_3 and VOCs) from different source categories are shown in Figure 3-3. Note
21 that the entries refer mainly to anthropogenic sources, with little information about natural
22 sources. However, for categories such as VOCs, the contribution from biogenic emissions of
23 isoprene and terpenes can be quite large. The entries are continually undergoing revision
24 and are subject to varying degrees of uncertainty. For example, almost all of the sulfur in
25 fuel is released as volatile components (SO_2 or SO_3) during combustion. Hence, sulfur
26 emissions can be calculated on the basis of sulfur content in fuels to a greater accuracy than
27 can be done for other pollutants like nitrogen oxides or primary PM. There have been
28 notable downward revisions to the inventories since 2002 in the emissions of dust from
29 roads. These have resulted in large measure from incorporation of emissions test data that

1 relies on updated measurement methods. Also, the spatial and temporal characterization of
2 wildfire emissions has improved since 2002 by integrating satellite-derived fire detection
3 and state-of-the-art fuels characterization and consumption models (Pouliot et al., 2008,
4 [156883](#)). Emission measurements from high-temperature combustion sources are sensitive
5 to the dilution, temperature, and pre-treatment of dilution air (England et al., 2007,
6 [156420](#); England et al., 2007, [156421](#); Sheya et al., 2008, [156977](#)).

7 To a large extent, especially with regard to the contribution of road dust to PM,
8 refinements in emission estimates have been guided by the use of receptor modeling. See
9 Section 3.6.1 in this chapter for a description of receptor modeling techniques and the last
10 PM AQCD (U.S. EPA, 2004, [056905](#)) for the role of receptor models in refining emissions
11 estimates. Note that since the estimates given in Figure 3-3 are U.S. national averages,
12 they may not accurately reflect the contribution of specific local sources determining a
13 person's exposures to PM at any given time and location.

14 As can be seen from a comparison of the total U.S. emissions (in million metric tons)
15 shown in Figure 3-3, estimates of total emissions of potential precursors to secondary PM
16 formation including SO₂, NO_x, NH₃ and VOCs are considerably larger than those for
17 primary PM sources. The emissions of SO₂, NO_x, and NH₃ that are converted to PM should
18 be multiplied by factors of 1.5, 1.35, and 1.07, respectively, to account for their chemical
19 form in the aerosol phase. Estimating a factor for VOCs is somewhat less straightforward.
20 In addition, OC mass, whether primary or secondary, must be adjusted to account for aging
21 in the atmosphere. Turpin and Lim (2001, [017093](#)) recommend factors ranging from 1.4 to
22 2.0 to account for the conversion of OC to oxygen- and nitrogen-containing compounds in
23 the aerosol phase. In general, however, the emissions of precursors cannot be translated
24 directly into rates of PM formation. Dry deposition and precipitation scavenging of some of
25 these gaseous precursors and their intermediate oxidation products occur before they are
26 converted to PM in the atmosphere, and most of the VOCs are oxidized to carbon dioxide
27 (CO₂) rather than PM. In addition, some fraction of these gases is transported outside the
28 domain of the continental United States before being oxidized. Likewise, emissions of these
29 gases from areas outside the United States can result in the transport of their oxidation
30 products into the United States.



Source: U.S. EPA (2006, [157070](#))

Figure 3-3. Detailed source categorization of anthropogenic emissions of primary PM_{2.5}, PM₁₀ and gaseous precursor species SO₂, NO_x, NH₃ and VOCs for 2002 in units of million metric tons (MMT). (EGUs = Electricity Generating Units)

3.3.2. Formation of Secondary PM

1 Precursors to secondary PM have natural and anthropogenic sources, just as primary
2 PM has natural and anthropogenic sources. A substantial fraction of the fine particle mass,
3 especially during the warmer months of the year, is secondary in nature, formed as the
4 result of atmospheric reactions involving both inorganic and organic gaseous precursors.
5 The major atmospheric chemical transformations leading to the formation of particulate
6 nitrate (pNO_3) and sulfate (pSO_4) are relatively well understood; whereas those involving
7 the formation of secondary organic aerosol (SOA) are less well understood and are subject
8 to much current investigation. A large number of organic precursors are involved and many
9 of the kinetic details still need to be determined. Also, many of the products of the oxidation
10 of hydrocarbons have yet to be identified. However, there has been substantial progress
11 made in understanding the chemistry of SOA formation in the past few years.

3.3.2.1. Formation of Nitrate and Sulfate

12 The basic mechanism of the gas and aqueous phase oxidation of NO_2 and SO_2 has long
13 been studied and can be found in numerous texts on atmospheric chemistry, e.g., Seinfeld
14 and Pandis (1998, [018352](#)), Finlayson-Pitts and Pitts (2000, [055565](#)), Jacob (1999, [091122](#)),
15 and Jacobson (2002, [090667](#)). The reader is referred to the 2004 PM AQCD (U.S. EPA, 2004,
16 [056905](#)) where these processes are described in great detail, as well as the 2008 NO_x ISA
17 (U.S. EPA, 2008, [157073](#)) and the 2008 SO_x ISA (U.S. EPA, 2008, [157074](#)).

3.3.2.2. Formation of Secondary Organic Aerosol

18 Some key new findings have altered perceptions of SOA formation since the 2004 PM
19 AQCD (see especially the reviews by Kroll and Seinfeld (2008, [155910](#)) and Rudich et al.
20 (2007, [156059](#)). New measurement techniques for estimating the speciation and water
21 solubility of organic aerosols have noted the dominant contribution of oxygenated species in
22 atmospheric particles. Recent measurements show that the abundance of oxidized SOA
23 exceeds that of more reduced hydrocarbon like organic aerosol in Pittsburgh (Zhang et al.,
24 2005, [157185](#)) and in about 30 other cities across the Northern Hemisphere (Zhang et al.,
25 2007, [101119](#)). Based on aircraft and ship-based sampling of organic aerosols in coastal

1 waters downwind of northeastern U.S. cities, de Gouw et al. (2008, [191757](#)) reported that
2 40-70% of measured organic mass was water soluble and estimated that approximately 37%
3 of SOA is attributable to aromatic precursors using PM mass yields estimated for NO_x-
4 limited conditions, while 63% of mass was unexplained, possibly due to oxidation of
5 semivolatile precursors not measured by standard gas chromatography. Aerosol yields from
6 the oxidation of aromatic compounds have been reported to be higher when reactions with
7 NO_x are not dominant, suggesting that transport of less reactive compounds (e.g., benzene)
8 out of source regions with high NO_x levels could result in greater overall SOA yields than
9 previously estimated (Ng et al., 2007, [090983](#)). Furthermore, Zhang et al. (2007, [157186](#))
10 noted that the most common mass spectrum of oxygenated OA measured in ambient air
11 resembles mass spectra measured in irradiated diesel exhaust reported by Robinson et al.
12 (2007, [156053](#)) and Sage et al. (2008, [191758](#)).

13 Typical dilution sampling of combustion sources employ dilution rate, temperature,
14 pressure, and background aerosol concentrations that can differ substantially from ambient
15 conditions. Lipsky and Robinson (2006, [189891](#)) and Robinson et al. (2007, [156053](#)) showed
16 that under higher dilution conditions, the fraction of diesel engine organic emissions that
17 volatilizes is higher than that measured using common test methods.

18 Murphy and Pandis (2009, [190095](#)) pointed out the importance of characterizing the
19 volatility distribution of emissions of organic species from combustion sources for more
20 accurately predicting the abundance and oxidation state of SOA in both urban and
21 surrounding regional background environments. They note that in urban areas, volatile
22 emissions can be photochemically oxidized to more non-volatile compounds which then
23 condense, forming oxidized SOA. Braun (2009, [189997](#)) suggested that the weathering of
24 diesel exhaust particles involves the desorption of semi-volatile organic compounds followed
25 by the decomposition and reaction of the amorphous non-volatile carbon. These reactions
26 would result in the formation of a number of functional groups on the surface of the carbon
27 core including quinones, carbohydroxide and carboxyl groups as well as sulfate. In general,
28 all the above studies underscore the importance of accurately describing the phase
29 distribution of semivolatile organic compounds emitted by combustion sources under
30 atmospheric conditions, and of atmospheric photochemical reactions in modifying the
31 composition of emissions.

32 Until a few years ago, the oxidation of terpenes and aromatic compounds were
33 considered as sources of SOA, and the oxidation of isoprene was not considered a source of

1 SOA. However, observations of 2-methyl tetrols in ambient samples from a number of
2 different environments suggest that small but not insignificant quantities of SOA are
3 formed (Claeys et al., 2004, [058608](#)). Laboratory studies also indicate the formation of
4 2-methyl tetrols from isoprene oxidation (Edney et al., 2005, [155760](#); Kleindienst et al.,
5 2006, [156650](#)). Xia and Hopke (2006, [179947](#)) observed the seasonal variations for the two
6 major diastereoisomers produced during the oxidation of isoprene with highest
7 concentrations occurring during summer and lowest concentrations occurring during
8 winter. During summer, their maximum contribution to OC was 2.8%.

9 Kroll and Seinfeld (2008, [155910](#)) and Rudich et al. (2007, [156059](#)) noted that the
10 composition of SOA evolves from repeated cycles of volatilization and condensation of
11 chemical reaction products in both the particle and gas phases. Rudich et al. (2007, [156059](#))
12 focused on the oxidation of particle phase species by reaction with gas phase oxidants. Kroll
13 and Seinfeld (2008, [155910](#)) identified three factors that determine the SOA forming
14 potential of organic compounds in the atmosphere:

- 15 1. Oxidation reactions of gas-phase organic species. These species include alkanes, alkenes,
16 aromatics, cyclic olefins, isoprene and terpenes. Note that oxidation reactions can either lower
17 volatility by addition of functional groups or increase volatility by cleavage of carbon-carbon
18 bonds;
- 19 2. Reactions in the particle, or condensed, phase that can change volatility either by oxidation or
20 formation of high-molecular-weight species. These reactions can lead to the formation of
21 oligomers, thereby decreasing volatility or to the formation of more volatile products; and
- 22 3. Ongoing reactions that result from the varied volatility of oxidation products.

23 Other detailed work has focused on the formation of higher molecular weight
24 particle-phase oligomers (Gao et al., 2004, [156460](#); Kalberer et al., 2004, [156619](#); Tolocka et
25 al., 2004, [087578](#)) the importance of cloud processing in the evolution of SOA (Blando and
26 Turpin, 2000, [155692](#); Gelencser and Varga, 2005, [156463](#)) and the role of acid seeds in
27 oligomer formation (Tolocka et al., 2004, [087578](#)). These results imply that ambient samples
28 could contain mixtures of SOA from different sources at different stages of processing, some
29 with common reaction products making source identification of SOA problematic.
30 Figure 3-4 shows a schematic of processes involved in the formation of SOA.

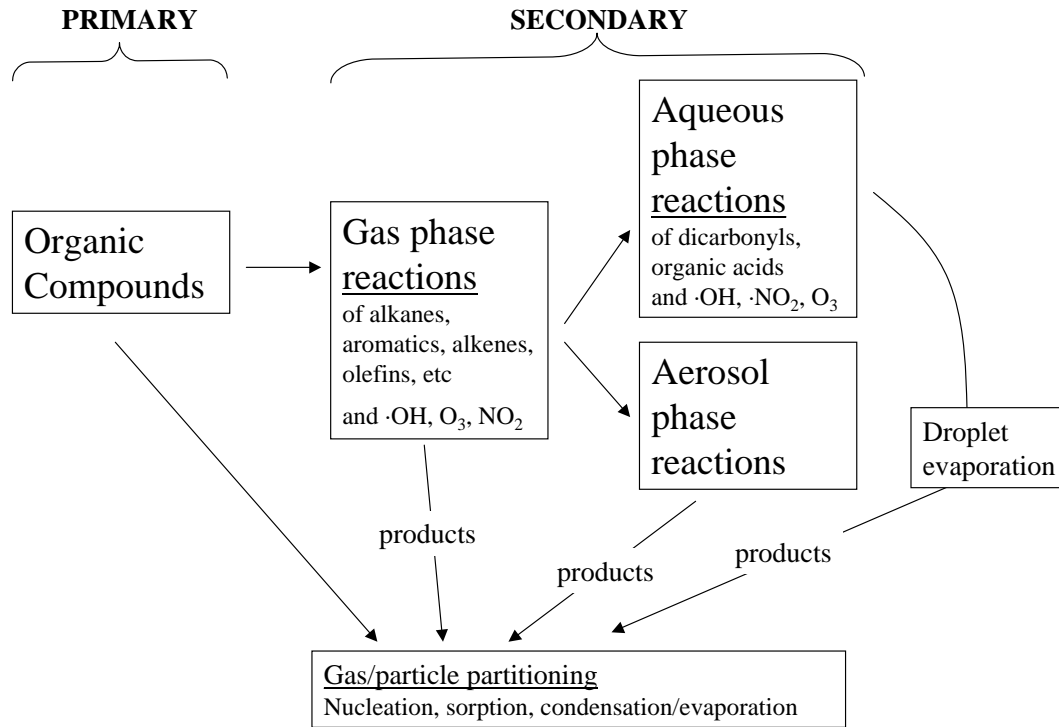


Figure 3-4. Primary emissions and formation of SOA through gas, cloud and condensed phase reactions.

1 It should be noted that many of the products of terpene oxidation are oxidative in
 2 nature, and are not merely nonreactive oxidation products. Organic peroxides represent an
 3 important class of reactive oxygen species (ROS) that have high oxidizing potential and
 4 could cause oxidative stress in cells on which these species deposit. For example, Docherty
 5 (2005, [087613](#)) found that 47 to 85% of SOA is composed of peroxides. Biogenic terpenoids
 6 can be oxidized outdoors by ozone to form SOA. Various terpenoid compounds are used in a
 7 number of household products and can be oxidized by ozone that has infiltrated from
 8 outdoors. The oxidation of terpenoid compounds indoors produces ultrafine particles as
 9 described in the 2006 Ozone AQCD (U.S. EPA, 2006, [088089](#)).

3.3.2.3. Formation of new particles

10 In addition to emission by high temperature combustion sources, atmospheric gases
 11 nucleate to form new particles. New particle formation has been observed in environments
 12 ranging from relatively unpolluted marine and continental environments to polluted urban
 13 areas (Kulmala et al., 2004, [089159](#)). These new, nucleation mode particles are formed from
 14 molecular clusters. Competition between condensation of gases and clusters onto existing

1 particles and coagulation of clusters determines which process will dominate (McMurry et
2 al., 2005, [191759](#)). Because of this competition, it is expected that particle number
3 concentrations are dominated by primary anthropogenic emissions in highly polluted
4 settings and by nucleation in remote continental sites. However, nucleation still occurs in
5 urban environments and can still be the major source under certain conditions. The
6 composition of ultrafine particles will differ depending on the nature of their sources.
7 Nucleation is observed in the morning and extending into the afternoon, and occurs at
8 higher rates during summer than during winter, consistent with a photochemical process.
9 New particle formation events have been observed to occur over distances of several
10 hundred kilometers in what have been called regional nucleation events (Shi et al., 2007,
11 [191760](#)).

12 The major gas phase nucleating species involved are sulfuric acid vapor and water
13 vapor. Kuang et al. (2008, [191196](#)) suggested that the rate of nucleation is 2nd order with
14 respect to H₂SO₄ vapor depending on mechanism. However, other studies (e.g., Kulmala et
15 al., 2007, [191761](#)) have suggested that the nucleation rate is first order with respect to
16 H₂SO₄ vapor. These differences imply that a number of mechanistic details still remain to
17 be determined, including the interactions with other species. However, this disparity is
18 small compared to classical thermodynamic binary nucleation theory involving H₂SO₄ and
19 water vapor, in which the nucleation rate is given by H₂SO₄ vapor to at least the 10th power
20 (Kulmala et al., 1998, [129411](#)). H₂SO₄ vapor is produced by the gas phase oxidation of SO₂
21 by OH radicals (U.S. EPA, 2008, [157075](#)). Ammonia (Gaydos et al., 2005, [191762](#)) and
22 organic acids and bases (amines) are also involved to some extent (Smith et al., 2008,
23 [190037](#)). The formation of ultrafine particles indoors from the oxidation of terpenoids by O₃
24 as mentioned above also indicates that nucleation occurs indoors as well (U.S. EPA, 2006,
25 [088089](#)).

3.3.3. Mobile Source Emissions

3.3.3.1. Emissions from Gasoline Fueled Engines

26 PM emitted from gasoline fueled engines is a mix of OC, EC and small quantities of
27 trace metals and sulfates, with OC constituting anywhere from 26-88% of PM (Cadle et al.,
28 1999, [007636](#); Geller et al., 2006, [139644](#); Schauer et al., 2002, [035332](#)). Most of the
29 compounds in OC have yet to be characterized, though constituents of unburned or

1 partially oxidized fuel and lube oil are the dominant components of OC emitted by diesel
2 engines. High molecular weight and large PAHs have been identified in gasoline fueled
3 vehicle emissions (Phuleria et al., 2006, [156867](#); Riddle et al., 2007, [115272](#)). EPA exhaust
4 emission standards do not control PM from gasoline vehicles as stringently as diesel
5 vehicles. PM emissions from gasoline fueled vehicles decreased greatly as other exhaust
6 emissions (primarily hydrocarbons and carbon monoxide) were controlled by improvements
7 in the catalytic converter and better control of air-to-fuel mixture ratios for the engine
8 intake. When leaded gasoline was used in pre-1975 model year vehicles, gasoline engine
9 PM emissions were relatively large (about 300 mg/mile) and consisted largely of lead salts
10 from combustion of the lead additive. A current gasoline fueled vehicle emits far lower PM,
11 about 1-10 mg/mile. Emissions of gasoline PM increase at colder ambient temperatures and
12 recent rulemaking for air toxics will result in significant reduction of gasoline PM at colder
13 temperatures. Further details about the composition of motor vehicle emissions in the
14 context of source apportionment modeling can be found in Section 3.6.1.

3.3.3.2. Emissions from Diesel Fueled Engines

15 Matti Maricq (2007, [155973](#)) presents a conceptual model of diesel PM as a mix of
16 nucleation-mode SO_4^{2-} and hydrocarbons from unspent fuel and soot embedded with trace
17 metals on which SO_4^{2-} and hydrocarbons condense. PM emissions from pre 2007 diesels
18 consist largely of EC (about 70% by mass) and OC (high molecular weight compounds
19 derived from both diesel fuel and lubricating oil) which is responsible for about 25% of the
20 PM (Matti Maricq, 2007, [155973](#)). The elemental carbon is non-volatile, while the organic
21 material present exhibits temperature-dependent evaporation in similar fashion to a
22 mixture of C₂₄-C₃₂ alkanes (Sakurai et al., 2003, [113924](#)). Sulfates constitute about 5% of
23 the PM. A small fraction of the diesel fuel sulfur (typically about 1-2%) is oxidized to
24 sulfate. Trace elements (such as zinc and halogens, mainly from lubricating oil; and others)
25 are also present. Mass spectra of organic diesel particles from pre-2007 engines appear to
26 be largely similar to engine lube oil with minor contributions from unburned diesel fuel.

27 Effective with the 2007 model year for on-road diesel heavy-duty highway truck
28 engines, the new EPA PM standard (0.01 g per brake horsepower-hour, g/bhp-hr) reduced
29 PM emission limits by 90% from the prior standard (0.10 g/bhp-hr). By comparison,
30 uncontrolled heavy-duty diesels (pre-1988 model years) emitted about 1-2 g/bhp-hour of

1 PM. The 2007 standard resulted in the introduction of new emission control technology,
2 mainly the diesel particulate filter (DPF). Other elements of the new control technology also
3 include water-cooled exhaust gas recirculation (mostly for control of NO_x), a diesel oxidation
4 catalyst (DOC) used in some vehicles and improved fuel injection systems.

5 Besides the large reduction in diesel PM on a mass basis, the composition of diesel
6 PM changed greatly. EPA regulations required that diesel fuel for on-road vehicles contain
7 no more than 15 ppm sulfur as of January 2007 (Lim et al., 2007, [155931](#)). Prior to that, the
8 limit on diesel fuel sulfur established in 1995 for on-road vehicles was 500 ppm. The HEI-
9 ACES study characterizes emissions from four engines and shows that PM emissions are
10 about 0.001 g/BHP-hr or 90% below the level of the current (2007) emission standard
11 (Shimpi et al., 2009, [189888](#)). This study also characterizes the composition of the much
12 lower mass of PM emitted with this new technology. PM samples collected over a composite
13 type test consisted of 53% sulfate, 30% OC, 13% EC and 4% other components, including
14 metals. A substantial fraction of sulfur is converted to sulfate over the diesel particulate
15 filter resulting in the higher fractional content of sulfate emissions. However, due to the
16 much lower mass of PM being emitted (over a 90% reduction compared to earlier diesels) as
17 well as the low sulfur content of the fuel, the total mass of sulfate emitted is somewhat less
18 than that from earlier diesels. This work also shows that ultrafine particle number
19 emissions are lower (about 90% lower) and that a number of other emissions are also
20 controlled, including PAHs, nitro-PAHs, carbonyls (such as aldehydes), and metals and that
21 their emissions are lower than those from earlier diesels.

22 Pre-2007 engines can be retrofitted with exhaust after treatment devices, including
23 DPFs, DOCs, and selective catalytic reduction (SCR) systems to reduce emissions
24 (U.S. EPA, 2009, [189885](#)). Hu et al. (2009, [189886](#)) examined emissions of various metals
25 (vanadium, platinum) from various diesel retrofit systems including those using vanadium-
26 SCR and a zeolite-based SCR with a DPF. Pakbin et al. (2009, [189893](#)) shows significant
27 reductions in emissions of various PAHs for diesels with SCR retrofit systems for NO_x
28 control. Biswas et al. (2008, [189969](#)) examined PM size distribution and composition
29 (including semi-volatiles and non-volatiles) from several advanced technology diesels
30 including those with SCR. They showed major reductions in PM number in most driving
31 conditions but did not show a reduction in PM number under cruise conditions. Biswas et
32 al. (2009, [189880](#)) examined four heavy-duty diesel vehicles with various retrofits showing,

1 in general, large reductions in PM but, in some cases, somewhat higher emissions (or
2 smaller decreases than expected) for EC and OC.

3 In general, under light load conditions such as idle, diesel PM has a higher percentage
4 of OC emissions than at high load conditions. Under lighter loads, organic compounds are
5 not oxidized as effectively as under high loads. Under higher loads, PM contains more EC
6 than under light loads. Also, newer model year diesels through the 2006 model year tend to
7 have a higher fraction of PM that is EC than older models.

8 Emissions have been measured with the new technology engines under a number of
9 driving cycles besides the Federal Test Procedure. The HEI ACES study examined
10 emissions during a range of test procedures. In general, the low-load test cycle resulted in
11 lower exhaust temperatures and higher emission than did the high-load cycles.
12 Regeneration events also produced short-term increases in particle emissions. However,
13 particle emission measurements on the ACES engines were consistently lower than those
14 on a typical 2004 engine (Shimpi et al., 2009, [189888](#)).

15 EPA standards will result in non-road diesels also having technology like catalyzed
16 diesel particulate filters starting in 2012. Similar standards have also been promulgated for
17 locomotives powered by diesel engines. Some work has been done with prototype SCR
18 systems for diesel NO_x control such as would be used for the 2010 diesel NO_x standard.
19 This standard will also result in reductions for NO_x similar to those seen for PM in the
20 2007 standard.

21 There is no information on emissions from diesel engines with this new technology, at
22 temperatures of $\leq 10^{\circ}$ C. In general, the ratio of emissions under cold start conditions at low
23 temperatures to emissions at 24 $^{\circ}$ C is significantly higher for diesel engines with new
24 technology compared to emissions from non-catalyst systems. Note that the engines with
25 the newer technology require time to allow the catalyst to reach normal operating
26 temperatures for full emission reductions. During the period of catalyst heating, particles
27 will be trapped in the DPF, but volatile components can pass through. As a result of this
28 particle-trapping, post-2007 model year engines still emit less than the older engines, even
29 under cold start conditions.

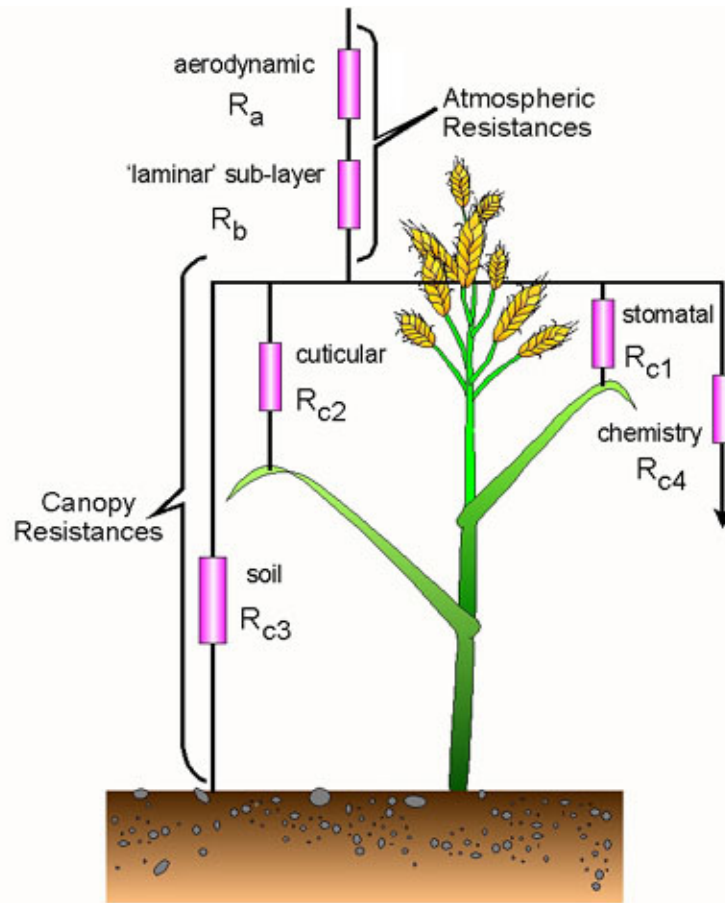
3.3.4. Deposition of PM

1 Wet and dry deposition are important processes for removing PM and other pollutants
2 from the atmosphere on urban, regional, and global scales. The conceptual model for dry
3 deposition is to view the flux deposited on a surface as the product of a concentration (mass
4 or moles of a pollutant/m³) times a deposition velocity (V_d) (m/s). Therefore, deposition has
5 the units of mass per unit time per unit area, or flux. The general approach used to
6 estimate V_d is the resistance-in-series method represented by Equation 3.1:

$$V_d = 1 / (R_a + R_b + R_c)$$

Equation 3-1

7 where R_a , R_b , and R_c represent the resistance due to atmospheric turbulence, transport in
8 the fluid sublayer very near the elements of surface such as leaves or soil, and the
9 resistance to uptake of the surface itself, respectively. These processes are shown
10 schematically in Figure 3-5. This approach works for a range of substances, although it is
11 inappropriate for species with substantial re-emissions from the surface or for species
12 where deposition to the surface depends on concentrations at the surface itself. The
13 approach is also modified somewhat for aerosols in that the terms R_b and R_c are replaced
14 with a surface V_d to account for gravitational settling.



Resistance analogy for the deposition of atmospheric pollutants

Source: Courtesy of T. Pierce, USEPA / ORD / NERL / Atmospheric Modeling Division.

Figure 3-5. Schematic of the resistance-in-series analogy for atmospheric deposition. Function of wind speed, solar radiation, plant characteristics, precipitation/moisture, and soil/air temperature.

1 Wesley and Hicks (2000, [025018](#)) listed several shortcomings of the then-current
 2 knowledge of dry deposition. Among those shortcomings were difficulties in representing
 3 dry deposition over varying terrain where horizontal advection plays a significant role in
 4 determining the magnitude of R_a and difficulties in adequately determining V_d for
 5 extremely stable conditions such as those occurring at night; see the discussion by Mahrt
 6 (1998, [048210](#)). Under optimal conditions, when a model is exercised over a relatively small
 7 area where dry deposition measurements have been made, models still generally showed
 8 uncertainties on the order of $\pm 30\%$ (see, e.g., Brook et al., 1996, [024023](#); Massman et al.,
 9 1994, [043681](#); Padro, 1996, [052446](#); Wesely and Hicks, 2000, [025018](#)).

10 Wesley and Hicks (2000, [025018](#)) concluded that an important result of those
 11 comparisons was that the level of sophistication of most dry deposition models was

1 relatively low, and that deposition estimates, therefore, must rely heavily on empirical data.
2 Still larger uncertainties exist when the surface features in the built environment are not
3 well known or when the surface comprises a patchwork of different surface types, as is
4 common in the eastern U.S.

3.3.4.1. Deposition Forms

Wet Deposition

5 Wet deposition results from the incorporation of atmospheric particles and gases into
6 cloud droplets and their subsequent precipitation as rain or snow, or from the scavenging of
7 particles and gases by raindrops or snowflakes as they fall (Lovett, 1994, [024049](#)). Wet
8 deposition depends on precipitation amount and ambient pollutant concentrations.
9 Receptor (i.e., vegetation) surface properties have little effect on wet deposition, although
10 leaves can retain liquid and solubilized PM. In terrain containing extensive vegetative
11 canopies, any material deposited via precipitation to the upper stratum of foliage is likely to
12 be intercepted by several foliar surfaces before reaching the soil. This allows such processes
13 as foliar uptake, chemical transformation, and re-suspension into the atmosphere to occur.

14 Landscape characteristics can affect wet deposition via orographic effects and by the
15 closer aerodynamic coupling to the atmosphere of tall forest canopies as compared to the
16 shorter shrub and herbaceous canopies. Following wet deposition, humidity and
17 temperature conditions further affect the extent of drying versus concentrating of solutions
18 on foliar surfaces, which influence the rate of metabolic uptake of surface solutes (Swietlik
19 and Faust, 1984, [046678](#)). The net consequence of these factors on direct physical effects of
20 wet deposited PM on leaves is not known (U.S. EPA, 2004, [056905](#)).

21 Rainfall introduces new wet deposition and also redistributes throughout the canopy
22 previously dry-deposited particles (Peters and Eiden, 1992, [045277](#)). The concentrations of
23 suspended and dissolved materials are typically highest at the onset of precipitation and
24 decline with duration of individual precipitation events (Hansen et al., 1994, [046634](#)).
25 Sustained rainfall removes much of the accumulation of dry-deposited particles from foliar
26 surfaces, reducing direct foliar effects and combining the associated chemical burden with
27 the wet-deposited material (Lovett, 1994, [024049](#)) for transfer to the soil. Intense rainfall
28 may contribute substantial total particulate inputs to the soil, but it also removes
29 bioavailable or injurious pollutants from foliar surfaces. This washing effect, combined with

1 differential foliar uptake and foliar leaching of different chemical constituents from
2 particles, alters the composition of the rainwater that reaches the soil and the pollutant
3 burden that is taken-up by plants. Once in the soil, these particle constituents may affect
4 biogeochemical cycles of major, minor, and trace elements. Low intensity precipitation
5 events, in contrast, may deposit significantly more particulate pollutants to foliar-surfaces
6 than high intensity precipitation events. Additionally, low-intensity events may enhance
7 foliar uptake through the hydrating of some previously dry-deposited particles (U.S. EPA,
8 2004, [056905](#))

Dry Deposition

9 Dry particulate deposition, especially of heavy metals, base cations, and organic
10 contaminants, is a complex and poorly characterized process. It appears to be controlled
11 primarily by such variables as atmospheric stability, macro- and micro-surface roughness,
12 particle diameter, and surface characteristics (Hosker RP and Lindberg, 1982, [019118](#)). The
13 range of particle sizes, the diversity of canopy surfaces, and the variety of chemical
14 constituents in airborne particles have made it difficult to predict and to estimate dry
15 particulate deposition (U.S. EPA, 2004, [056905](#)).

16 Dry deposition of atmospheric particles to plant and soil surfaces affects all exposed
17 surfaces. Larger particles >5 µm diameter are dry-deposited mainly by gravitational
18 sedimentation and inertial impaction. Smaller particles, especially those with diameters
19 between 0.2 and 2.0 µm, are not readily dry-deposited and may travel long distances in the
20 atmosphere until their eventual deposition, most often via precipitation. Plant parts of all
21 types, along with exposed soil and water surfaces, receive steady deposits of dry dusts, EC,
22 and heterogeneous secondary particles formed from gaseous precursors (U.S. EPA, 1982,
23 [017610](#)).

24 Estimates of regional particulate dry deposition infer fluxes from the product of
25 variable and uncertain measured or modeled particulate concentrations in the atmosphere
26 and even more variable and uncertain estimates of V_d parameterized for a variety of
27 specific surfaces (e.g., Brook et al., 1996, [024023](#)). Even for specific sites and well-defined
28 particles, uncertainties are large. Modeling the dry deposition of particles to vegetation is at
29 a relatively early stage of development, and it is not currently possible to identify a best or
30 most generally applicable modeling approach (U.S. EPA, 2004, [056905](#)).

Deposition from Clouds and Fog

1 The occurrence of cloud and fog deposition tends to be geographically restricted to
2 coastal and high mountain areas. Several factors make it particularly effective for the
3 delivery of dissolved and suspended particles to vegetation. Concentrations of particulate-
4 derived materials are often many-fold higher in cloud or fog water than in precipitation or
5 ambient air due to orographic effects and gas-liquid partitioning. In addition, fog and cloud
6 water deliver particulate chemical species in a bioavailable-hydrated form to foliar surfaces.
7 This enhances deposition by sedimentation and impaction of submicron aerosol particles
8 that exhibit low V_d before fog droplet formation (Fowler et al., 1989, [002515](#)). Deposition to
9 vegetation in fog droplets is proportional to wind speed, droplet size, concentration, and fog
10 density. In some areas, typically along foggy coastlines or at high elevations, this deposition
11 represents a substantial fraction of total deposition to foliar surfaces (Fowler et al., 1991,
12 [046630](#)).

3.3.4.2. Methods for Estimating Dry Deposition

13 Methods for estimating dry deposition of particles are more restricted than for
14 gaseous species and fall into two major categories: surface analysis methods, which include
15 all types of estimates of contaminant accumulation on surfaces of interest; and atmospheric
16 deposition rate methods, which use measurements of contaminant concentrations in the
17 atmosphere and descriptions of surrounding surface elements to estimate deposition rates
18 (Davidson and Wu, 1990, [036799](#)). Surface extraction or washing methods characterize the
19 accumulation of particles on natural receptor surfaces of interest or on experimental
20 surrogate surfaces. These techniques rely on methods designed specifically to remove only
21 surface-deposited material. Total surface rinsate may be equated to accumulated deposition
22 or to the difference in concentrations in rinsate between exposed and control (sheltered)
23 surfaces and may be used to refine estimates of deposition. Foliar extraction techniques
24 may underestimate deposition to leaves because of uptake and translocation processes that
25 remove pollutants from the leaf surface (Garten CT and Hanson, 1990, [036803](#); Taylor GE
26 et al., 1988, [019289](#)). Foliar extraction methods also cannot distinguish gas from particle-
27 phase sources (Bytnerowicz et al., 1987, [036493](#); Dasch, 1987, [036496](#); Kelly, 1988, [037379](#);
28 Lindberg and Lovett, 1985, [036530](#); Van Aalst, 1982, [036481](#)).

1 The National Dry Deposition Network was established in 1986 to document the
2 magnitude, spatial variability, and trends in dry deposition across the United States.
3 Currently, the network operates as a component of the CASTNet (Clarke et al., 1997,
4 [025022](#)). A significant limitation on current capacity to estimate regional effects of NO_x and
5 SO_x deposition is inadequate knowledge of the mechanisms and factors governing particle
6 dry deposition to diverse surfaces (U.S. EPA, 2004, [056905](#)).

7 Dry deposition cannot be directly measured. Deposition rates and totals are often
8 calculated as the product of measured ambient concentration and a modeled V_d. This
9 method is widely used because atmospheric concentrations are easier to measure than are
10 dry deposition rates, and models have been developed to estimate V_d. Ambient pollutant
11 concentrations and meteorological conditions required for application of inferential models
12 are routinely collected at CASTNet dry deposition sites. Monitored chemical species are
13 limited to O₃, SO₄²⁻, NO₃⁻, NH₄⁺, SO₂, and HNO₃. The temporal resolution for the ambient
14 concentration measurements and dry deposition flux calculations is hourly for O₃ and
15 weekly for all the other species (Clarke et al., 1997, [025022](#)).

16 Collection and analysis of stem flow and throughfall can also provide useful estimates
17 of particulate deposition when compared to directly sampled precipitation. The method is
18 most precise for particle deposition when gaseous deposition is a small component of the
19 total dry deposition and when leaching or uptake of compounds of interest out of or into the
20 foliage is not a significant fraction of the deposition because these lead to positive and
21 negative artifacts in the calculated totals.

22 Foliar washing, whether using precipitation or experimental lavage, is one of the best
23 available methods to determine dry deposition to vegetated ecosystems. Major limitations
24 include the site specificity of the measurements and the restriction to elements that are
25 largely conserved within the vegetative system. Surrogate surfaces have not been found
26 that can adequately replicate essential features of natural surfaces; and therefore do not
27 produce reliable estimates of particle deposition to the landscape.

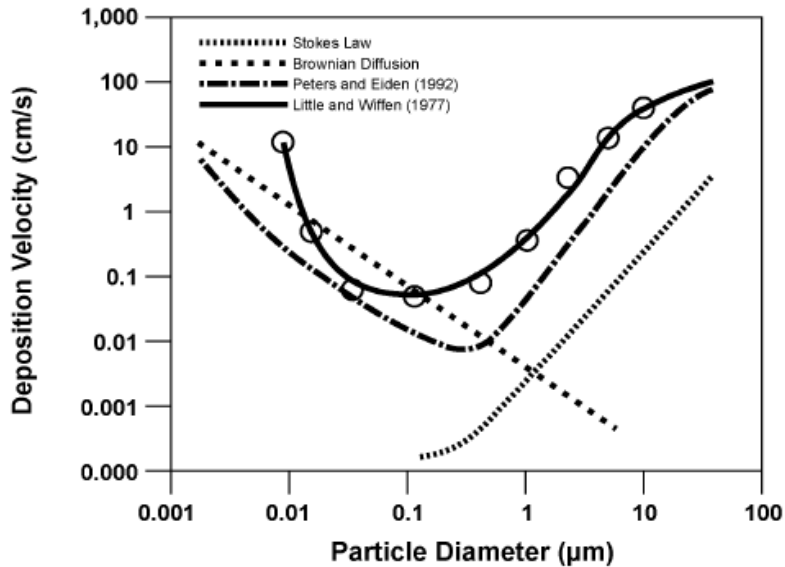
28 Micrometeorological methods employ eddy covariance, eddy accumulation, or flux
29 gradient protocols for quantifying dry deposition. These techniques require measurements
30 of particulate concentrations and of atmospheric transport processes. They are currently
31 well developed for ideal conditions of flat, homogeneous, and extensive landscapes and for
32 chemical species for which accurate and rapid sensors are available. Additional studies are
33 needed to extend these techniques to more complex terrain and more chemical species.

1 The eddy covariance technique measures vertical fluxes of gases and fine particles
2 from calculations of the mean covariance between the vertical component of wind velocity
3 and pollutant concentration (Wesely et al., 1982, [036564](#)) using sensors acquiring
4 concentration data at 5 to 20 Hz. For the flux gradient or profile techniques, vertical fluxes
5 are calculated from a concentration difference and an eddy exchange coefficient determined
6 at discrete heights (Erisman et al., 1988, [036510](#); Huebert et al., 1988, [036569](#)). Most
7 measurements of eddy transport of PM have used chemical sensors (rather than mass or
8 particle counting) to focus on specific PM components. These techniques have not been well
9 developed for generalized particles and may be less suitable for coarse particles that are
10 transported efficiently in high frequency eddies (Gallagher et al., 1988, [046631](#)).

3.3.4.3. Factors Affecting Dry Deposition Rates and Totals

11 In the size range of ~ 0.1 - $1.0 \mu\text{m}$ where V_d is relatively independent of particle
12 diameter as shown in Figure 3-6, particulate deposition is controlled by roughness of the
13 surface and by the stability and turbulence of the atmospheric surface layer. Impaction and
14 interception dominate over diffusion as dry deposition processes, and the V_d is considerably
15 lower than for particles that are either smaller than $\sim 0.1 \mu\text{m}$ or larger than $\sim 1.0 \mu\text{m}$ (Shinn,
16 1978, [071426](#)).

17 Deposition of particles between 1 and $10 \mu\text{m}$ diameter is strongly dependent on
18 particle size (Shinn, 1978, [071426](#)). Larger particles within this size range are collected
19 more efficiently at typical wind speeds than are smaller particles (Clough, 1975, [070850](#)),
20 suggesting the importance of impaction. Impaction is related to wind speed, the square of
21 particle diameter, and the inverse of receptor diameter as a depositing particle fails to
22 follow the streamlines of the air in which it is suspended around the receptor. When
23 particle trajectory favors a collision, increasing either wind speed or the ratio of particle
24 size to receptor cross-section increases the probability of collision.



Source: U.S. EPA (2004, [056905](#)).

Figure 3-6. The relationship between particle diameter and V_d for particles. Values measured in wind tunnels by Little and Wiffen (1977, [070869](#)) over short grass with wind speed of 2.5 mi/s closely approximate the theoretical distribution determined by Peters and Eiden (1992, [045277](#)) for a tall spruce forest. These distributions reflect the interaction of Brownian diffusivity (descending dashed line), which decreases with particle size and sedimentation velocity (ascending dotted line derived from Stokes Law), which increases with particle size. Intermediate-sized particles (0.1-1.0 μm) are influenced strongly by both particle size and sedimentation velocity, and deposition is relatively independent of size.

1 Empirical estimates of V_d for fine particles under wind tunnel and field conditions are
 2 often several-fold greater than predicted by theory (Unsworth and Wilshaw, 1989, [046682](#)).
 3 A large number of transport phenomena, including streamlining of foliar obstacles,
 4 turbulence structure near surfaces, and various phoretic transport mechanisms are not well
 5 characterized (U.S. EPA, 2004, [056905](#)). The discrepancy between estimated and predicted
 6 values of V_d may reflect model limitations or experimental limitations in the specification of
 7 the effective size and number of receptor obstacles. Previous reviews (e.g., U.S. EPA, 1996,
 8 [079380](#); U.S. EPA, 2004, [056905](#)) suggest the following generalizations: (1) particles $>10 \mu\text{m}$
 9 exhibit variable V_d between 0.5 and 1.1 cm/s depending on friction velocities, whereas a
 10 minimum particle V_d of 0.03 cm/s exists for particles in the size range 0.1 to 1.0 μm , (2) the
 11 V_d of particles is approximately a linear function of friction velocity, and (3) deposition of
 12 particles from the atmosphere to a forest canopy is from 2 to 16 times greater than
 13 deposition in adjacent open terrain like grasslands or other low vegetation.

Leaf Surface Effects on V_d

1 The chemical composition of a particle is not usually considered to be a primary
2 determinant of its V_d . Rather, the plant leaf surface has an important influence on the V_d of
3 particles, and therefore on the flux of dry deposition to the terrestrial environment.
4 Relevant leaf surface properties include stickiness, microscale roughness, and cross-
5 sectional area. These properties affect the probability of impaction and particle bounce. The
6 efficiency of deposition to vegetation also varies with leaf shape. Particles impact more
7 frequently on the adaxial (upper) surface than on the abaxial (lower) surface. Most particles
8 accumulate in the midvein, central portion of leaves. The greatest particle loading on
9 dicotyledonous leaves is frequently on the adaxial surface at the base of the blade, just
10 above the petiole junction. Precipitation washing probably plays an important role in this
11 distribution pattern (U.S. EPA, 2004, [056905](#)).

12 Lead particles have been shown to accumulate to a greater extent on older as
13 compared with younger needles and twigs of white pine, suggesting that wind and rain may
14 be insufficient to fully wash the foliage. Fungal mycelia (derived from windborne spores)
15 were frequently observed in intimate contact with other particles on leaves, which may
16 reflect minimal re-entrainment of the spore due to shelter by the particles, mycelia
17 development near sources of soluble nutrients provided by the particles, or simply co-
18 deposition (Smith and Staskawicz, 1977, [046675](#)).

19 Leaves with complex shapes tend to collect more particles than do those with shapes
20 that are more regular. For example, conifer needles are more efficient than broad leaves in
21 collecting particles by impaction as a result of the small cross-section of the needles relative
22 to the larger leaf laminae of broadleaves allowing for greater penetration of wind into
23 conifer canopies than broadleaf ones (U.S. EPA, 2004, [056905](#)).

Canopy Surface Effects on V_d

24 Surface roughness increases particulate deposition, and V_d is usually greater for a
25 forest than for a nonforested area and greater for a field than for a water surface. Different
26 size particles have different transport properties and V_d . The upwind leading edges of
27 forests, hedgerows, and individual plants are primary sites of coarse particle deposition.
28 Impaction at high wind speed and the sedimentation that follows the reduction in wind
29 speed and carrying capacity of the air in these areas lead to preferential deposition of larger
30 particles (U.S. EPA, 2004, [056905](#)).

1 Air movement is slowed in proximity to vegetated surfaces. Canopies of uneven age or
2 with a diversity of species are typically aerodynamically rougher and receive larger inputs
3 of dry-deposited pollutants than do smooth, low, or monoculture vegetation (Garner et al.,
4 1989, [042085](#); U.S. EPA, 2004, [056905](#)). Canopies on slopes facing the prevailing winds
5 receive larger inputs of pollutants than more sheltered, interior canopy regions.

6 All foliar surfaces within a forest canopy are not equally exposed to particle
7 deposition. Upper canopy foliage tends to receive maximum exposure to coarse and fine
8 particles, but foliage within the canopy tends to receive primarily fine aerosol exposures.
9 The dry deposition of fine-mode particles and unreactive gases tends to be more evenly
10 distributed throughout the canopy.

11 Both uptake and release of PM constituents can occur within the canopy. The leaf
12 surface is a region of leaching and uptake. Exchange also occurs with epiphytic organisms
13 and bark and through solubilization of previously dry-deposited PM. Vegetation emits a
14 variety of particles and particulate precursor materials.

3.4. Monitoring of PM

3.4.1. Ambient Measurement Techniques

3.4.1.1. PM Mass

15 Federal Reference Methods (FRMs) and Federal Equivalent Methods (FEMs) for PM
16 were discussed in detail in the 2004 PM AQCD (U.S. EPA, 2004, [056905](#)). Issues discussed
17 there include the definition or description of FRMs and FEMs for PM₁₀, PM_{2.5}, and
18 measurement methods for PM_{10-2.5} with detailed descriptions of the WINS impactor, virtual
19 and cascade multistage impactors for PM_{10-2.5} measurement, high-volume and low-volume
20 PM₁₀ samplers, and real-time or continuous methods for PM₁₀ and PM_{2.5} including:

- 21 ▪ Tapered Element Oscillating Microbalance (TEOM) operated at various
22 temperatures;
- 23 ▪ Sample Equilibration System (SES)-TEOM;
- 24 ▪ Differential TEOM;
- 25 ▪ β -Gauge Techniques (BGT);

- 1 ▪ Piezoelectric Microbalance;
- 2 ▪ Real-Time Total Ambient Mass Sampler (RAMS);
- 3 ▪ Continuous Ambient Mass Monitor (CAMM);
- 4 ▪ Continuous Coarse Particle Monitor (CCPM);
- 5 ▪ Micro-orifice Uniform Deposit Impactor (MOUDI);
- 6 ▪ Multichannel diffusion denuder sampling system (BOSS); and
- 7 ▪ Light scattering photometric instruments.

8 In this section, FRMs and FEMs for PM₁₀, PM_{2.5}, and PM_{10-2.5} will be revisited and
9 evaluated based on the cumulative understanding of these methods with a focus on
10 evaluations performed following the 2004 PM AQCD, followed by the discussion of new
11 techniques under development or evaluation.

Federal Reference Method and Federal Equivalent Method

12 The FRM and FEM are designed to measure the mass concentrations of ambient
13 particles. The FRMs for measuring PM₁₀, PM_{2.5}, and PM_{10-2.5} are specified in CFR 40 Part
14 50, Appendices J, L, and O, respectively. The PM₁₀ FRM is a performance-based method in
15 which particles are inertially separated with a penetration efficiency of 50% at 10 ± 0.5 μm
16 aerodynamic diameter. The collection efficiency specified in the CFR approaches 100% as
17 particle size decreases and approaches 0% as particle size increases. Particles are collected
18 on filters for which mass concentrations are determined gravimetrically. In contrast, the
19 FRM for PM_{2.5} is a design-based method that specifies certain details of the sampler design,
20 as well as of sample handling and analysis, whereas other aspects (e.g., flow control) have
21 performance specifications (U.S. EPA, 2004, [056905](#)) PM_{10-2.5} concentration is computed as
22 the difference between concurrent and co-located PM₁₀ and PM_{2.5} concentrations obtained
23 from co-located FRM samplers of the same make and model. It should be noted that the
24 FRM for PM₁₀ operates and reports data corrected to standard temperature (298K) and
25 pressure (101.3 kPa) (STP), while the FRM for PM_{2.5} and PM_{10-2.5} operates and reports data
26 under local conditions.

27 A very sharp cut cyclone (VSCC) was approved in 2004 as a Class II PM_{2.5} FEM
28 method (Kenny et al., 2004, [155895](#)). The VSCC provides superior performance over long
29 sampling periods under heavy loading and was also incorporated as an optional second-

1 stage separator for the PM_{2.5} FRM (71 FR 61214, October 17, 2006). In 2006, EPA finalized
2 new performance criteria (40 CFR Part 53) for the approval of FEMs as Class II equivalent
3 methods when based on integrated filter sampling and as Class III equivalent methods
4 when based on continuous technologies that can provide at least hourly data reporting. The
5 performance criteria include evaluating additive bias (intercept) and multiplicative bias
6 (slope) as well as correlation from co-located candidate and FRM methods at field studies
7 covering multiple seasons and locations. As a result of these new performance criteria, EPA
8 has recently approved two PM_{2.5} and two PM_{10-2.5} Class II FEMs based on the virtual
9 impactor techniques (dichotomous sampler), and five PM_{2.5} and one PM_{10-2.5} Class III FEMs
10 based on BGT or TEOM techniques. The most recent list of FRMs and FEMs can be found
11 in Annex A, Table A-2 and on the following EPA web site:

12 <http://www.epa.gov/ttn/amtic/files/ambient/criteria/reference-equivalent-methods-list.pdf>.

13 Evaluations of FRMs and FEMs were conducted both in supersite studies and in other
14 research studies (Ayers, 2004, [097440](#); Brown et al., 2006, [097665](#); Butler et al., 2003,
15 [156313](#); Cabada et al., 2004, [148859](#); Chang and Tsai, 2003, [155718](#); Charron et al., 2004,
16 [053849](#); Cowburn et al., 2008, [191142](#); Grover et al., 2005, [156500](#); Hains et al., 2007,
17 [091039](#); Hering et al., 2004, [155837](#); Jaques et al., 2004, [155878](#); Krieger et al., 2007,
18 [129657](#); Lee et al., 2005, [156679](#); Lee et al., 2005, [155924](#); Price et al., 2003, [098082](#); Rees et
19 al., 2004, [097164](#); Russell et al., 2004, [156061](#); Salminen and Karlsson, 2003, [156070](#);
20 Schwab et al., 2004, [098450](#); Schwab et al., 2006, [098449](#); Solomon et al., 2003, [156994](#); Tsai
21 et al., 2006, [098312](#); Vega et al., 2003, [105974](#); Wilson et al., 2006, [091142](#); Yi et al., 2004,
22 [156169](#); Zhu et al., 2007, [098367](#)) (see Annex A, Tables A-3, A-5 and A-11). In general, the
23 co-located FRMs showed very good precision with coefficient of variation (CV) <5%. For
24 different co-located FRMs, the regression slope of one sampler on another is commonly close
25 to unity and with R² >0.95. The PM_{2.5} and PM₁₀ concentrations measured by dichotomous
26 samplers were within 10% of the FRM methods, and the differences can be attributed to the
27 sampling artifacts of semi-volatile components; see Section 3.4.1.2 for details. The precision
28 of various TEOMs ranges from 10-30%. The concentration measured by the TEOM operated
29 at 50°C was consistently lower than those measured by the TEOM operated at 30°C. The
30 differences between these monitors were also found to be a function of season and location.
31 BGTs were highly correlated with FRMs but BGT mass could be higher than the FRM mass
32 (30% higher at the Fresno supersite) (Chow et al., 2008, [156355](#)). CAMMs did not show a
33 consistent pattern when compared with FRMs. These differences could be largely attributed

1 to the sampler operating principles and design, ambient conditions (copollutants and
2 meteorological parameters), and the built-in default calibration factors for non-FRM/FEM
3 instruments. Additionally, a number of techniques have been developed to reduce positive
4 and negative sampling artifacts. These are described in the ISA for NO_x and SO_x –
5 Environmental Criteria (U.S. EPA, 2008, [157074](#)).

6 For PM_{2.5} and PM₁₀, it has long been known that FRMs are subject to sampling
7 artifacts, i.e., the loss of semi-volatile components of PM (e.g., NH₄NO₃, and some organics).
8 Therefore, the FRMs cannot provide the “true” PM mass concentrations. The accuracy of
9 the method cannot be directly evaluated due to the lack of standard reference materials.
10 However, in comparison with other sampling techniques that can measure both semi-
11 volatile and nonvolatile PM, FRMs reported PM_{2.5} or PM₁₀ mass concentrations biased low
12 by 10-30%. The bias of the FRMs depends on the components of ambient PM and the
13 sampling conditions (e.g., ambient temperature and relative humidity), which vary from
14 day to day and from season to season. Another limitation of the current FRM sampling
15 frequency is that filter samples are often collected every three or six days (approximately
16 150 of the 900 plus PM_{2.5} FRMs operating in 2007 were scheduled to sample each day).
17 Under this operating condition, the concentration-response relationship in air pollution
18 health studies (especially in time-series studies) cannot be fully evaluated in terms of lag
19 structures and distributed lags between ambient concentration and health outcome
20 (Lippmann, 2009, [190083](#); Solomon and Hopke, 2008, [156997](#)). Despite these issues, the
21 precision of the FRMs are usually quite high (CV <5%), thereby providing consistent and
22 reliable PM measurements.

Development and Evaluation of New Techniques

23 Several new innovations have recently emerged to measure both fine and coarse PM
24 fractions in the ambient air. These techniques include the Filter Dynamics Measurement
25 System-TEOM (FDMS-TEOM) (Grover et al., 2006, [138080](#)) for real-time measurement of
26 PM_{2.5} or PM₁₀ and several new methods for measurement of PM_{10-2.5}. In addition, several
27 new techniques exist for measuring ultrafine particles (discussed later in Section 3.4.1.4)
28 and for estimating PM mass concentration indirectly using particle size (discussed later in
29 Section 3.4.1.5).

Real-time Measurement of PM_{2.5} or PM₁₀ using the FDMS-TEOM

1 The FDMS-TEOM incorporates self-referencing capability to the traditional TEOM by
2 alternating measurement of ambient air and chilled clean air (particles and semivolatile
3 gases are removed by filtration at 4°C after which the clean air is reheated to 30°C) in
4 6-min intervals. As clean air flows over the sample filter, the semivolatile PM on the sample
5 filter is evaporated. Thus, the instrument provides direct measurements of the monvolatile
6 particle mass and incorporates an adjustment for the semivolatile NH₄NO₃ and organic
7 material. In a comparison between the TEOM, FDMS-TEOM, and FRM mass, the PM_{2.5}
8 concentration measured by the TEOM operated at 50°C was consistently lower than those
9 measured by the TEOM operated at 30°C. The TEOM operated at 30°C provided
10 concentrations 50% lower than the FDMS-TEOM, and the FDMS-TEOM provided
11 concentrations 10-30% higher than the FRM mass (Chow et al., 2008, [156355](#); Schwab et
12 al., 2006, [098449](#)).

Techniques for Measurement of PM_{10-2.5}

13 Methods developed to measure PM_{10-2.5} are based on three measurement techniques:
14 1) virtual impactors using low-volume, high-volume, and real-time techniques; 2) cascade
15 impactors; and 3) passive samplers.

16 A low-volume dichotomous sampler (operated at 16.7 L/min), based on virtual
17 impaction, was described in the 2004 AQCD (U.S. EPA, 2004, [056905](#)). Since then, a high-
18 volume dichotomous sampler was developed to operate at 1,000 L/min (Sardar et al., 2006,
19 [156071](#)). The sampler was evaluated in the field by comparison with a MOUDI sampler,
20 and the measured PM_{10-2.5} mass concentrations were within 10%. The high-volume
21 dichotomous sampler provides sufficient mass collection for comprehensive standard
22 chemical analyses over short sampling intervals. Using the virtual impactor technique in
23 conjunction with a TEOM or BGT as the detector, continuous PM_{10-2.5} measurement
24 techniques were developed (Miller GT, 1975, [018988](#); Misra et al., 2003, [180217](#); Solomon
25 and Sioutas, 2008, [190139](#)). The TEOM method was highly correlated with the PM_{10-2.5}
26 FRM, but mass concentrations measured by the TEOM were 20-30% lower (Solomon and
27 Sioutas, 2008, [190139](#)). The BGT method also agreed well with the PM_{10-2.5} FRM (slopes =
28 0.88-1.17, and R² >0.95) (Solomon and Sioutas, 2008, [190139](#)).

29 Case et al. (2008, [155149](#)) evaluated a cascade PM sampler designed to collect PM_{10-2.5}
30 on a foam impactor. Particle bouncing on impactors has long been a concern for PM

1 collection. Porous foam was used to serve as the impactor substrate to reduce particle
2 bounce and to collect relatively large amounts of particles (Demokritou et al., 2004, [186901](#);
3 Demokritou et al., 2004, [190115](#); Huang et al., 2005, [186991](#); Kuo et al., 2005, [186997](#)). The
4 sampler was operated at 5 L/min, and it agreed with a low-volume dichotomous sampler
5 within $\pm 20\%$. The precision of the sampler was 20% as determined by the CV.

6 An inexpensive passive sampler for $PM_{10-2.5}$ was also developed (Leith et al., 2007,
7 [098241](#); Ott et al., 2008, [191765](#); Wagner and Leith, 2001, [190153](#); Wagner and Leith, 2001,
8 [190154](#)). The passive sampler collects particles by gravity, diffusion, and convective
9 diffusion onto a glass coverslip, and then an image analysis is conducted on the collected
10 particles to estimate mass flux as a function of aerodynamic diameter. Leith et al. (2007,
11 [098241](#)) conducted a field evaluation of the passive sampler, and the difference between an
12 FRM and the co-located passive sampler was within 1σ of concentrations measured with
13 $PM_{10-2.5}$ FRM samplers. Ott et al. (2008, [191765](#)) reported the precision of the sampler was
14 11.6% (CV), and the detection limit was $2.3 \mu\text{g}/\text{m}^3$ for a 5-day sample.

3.4.1.2. PM Speciation

15 The following sections describe recent developments regarding measurement
16 techniques to ascertain quantities of particle-bound water, cations and anions, elemental
17 composition, carbon, and organic species.

Particle-Bound Water

18 Particle-bound water is an important component of ambient PM (U.S. EPA, 2006,
19 [157071](#)). Recently, a differential method was developed to measure particle-bound water
20 (Santarpia et al., 2004, [156944](#); Stanier et al., 2004, [095955](#)). The dry ambient aerosol size
21 spectrometer (DAASS) can measure particle-bound water in the particle size range from 3
22 nm-10 μm (Stanier et al., 2004, [095955](#)), by alternatively measuring ambient PM size
23 distribution at low relative humidity (RH) and ambient RH. A comparison of the two size
24 distributions provides information on the water absorption and change in particle size due
25 to RH. Khlystov et al. (2005, [156635](#)) reported that the particle-bound water, measured by
26 DAASS, was underestimated for particles < 200 nm and overestimated for particles > 200
27 nm compared with thermodynamic models. The loss of semi-volatile components during
28 measurement may bias the particle-bound water measurement results. Methods and
29 analytical specifications for particle-bound water are listed in Annex A, Table A-12.

Cations and Anions

1 The measurement of cations and anions including SO_4^{2-} , NO_3^- , NH_4^+ , Cl^- , Na^+ , and K^+
2 still relies primarily on filter-based collection, water based extraction and ion
3 chromatography (IC) based chemical speciation and quantification. In addition, denuders
4 are frequently used in the sampling system to adjust for sampling artifacts. These methods
5 have been reviewed in the 2004 PM AQCD (U.S. EPA, 2004, [056905](#)). Filter-denuder based
6 integrated sampling methods for SO_4^{2-} , NO_3^- , and NH_4^+ have been detailed in the 2008 SO_x
7 ISA and 2008 NO_xSO_x ISA (U.S. EPA, 2008, [157075](#); U.S. EPA, 2008, [157074](#)).

8 Recent developments in multiple ion measurements have focused on the coupling of
9 IC and a sample dissolution system, represented by the Particle into Liquid Sampler-Ion
10 Chromatography (PILS-IC) and the Ambient Ion Monitor (AIM) (Dasgupta et al., 2007,
11 [156383](#); Orsini et al., 2003, [156008](#); Weber et al., 2001, [024640](#)). When ambient PM passes
12 through the PILS-IC system, water droplets are generated by mixing ambient PM with
13 saturated water vapor and collected by impaction. The resulting liquid stream is then
14 introduced into the IC system for ion speciation and quantification. Hourly concentrations
15 of multiple ions can be obtained with the system, with a CV of 10%. For the AIM system, a
16 parallel plate denuder is used to remove the interfering gases, and then particles enter a
17 super-saturation chamber to form droplets. The collected droplets are then introduced into
18 the IC for analysis. The AIM system can provide hourly concentrations for multiple ions.
19 The particle mass spectrometer is another advance in multiple PM component
20 measurements, but most of these types of measurements are semi-quantitative and will be
21 detailed later in Section 3.4.1.3. Note that measurement and analytical specifications for
22 ions other than SO_4^{2-} and NO_3^- are listed in Annex A, Table A-9.

Sulfate

23 Methods used for continuous (sampling interval of minutes) measurements of SO_4^{2-}
24 include Aerosol Mass Spectrometry (AMS) (Drewnick et al., 2003, [099160](#); Hogrefe et al.,
25 2004, [156560](#)), PILS-IC (Weber et al., 2001, [024640](#)), flash volatilization techniques (Bae,
26 2007, [155669](#); Stolzenburg and Hering, 2000, [013289](#)) and the Harvard School of Public
27 Health (HSPH) tube furnace to convert SO_4^{2-} to SO_2 for detection by a SO_2 analyzer (Allen
28 et al., 2001, [156205](#)). These methods are described in detail by Drewnick et al. (2003,
29 [099160](#)), along with an inter-sampler comparison that found overall agreement within 2.9%
30 for all continuous instruments with R^2 of 0.87 or better. When compared with filter

1 samples, Drewnick et al. (2003, [099160](#)) showed differences were less than 25% for the
2 AMS, PILS, flash vaporization, and HSPH continuous SO_4^{2-} monitors. The Thermo 5020
3 particulate sulfate analyzer (based on the HSPH technique) compared within 80% of 24-h
4 filter-based measurement at a rural site in New York (Schwab et al., 2006, [098449](#)). Annex
5 A, Tables A-8 and A-14, list detailed methods and analytical specifications for sampling
6 SO_4^{2-} .

Nitrate

7 In addition to the nylon filter-based method and the new developments mentioned for
8 SO_4^{2-} , methods based on flash volatilization-chemiluminescence analysis and catalytic
9 conversion-chemiluminescence analysis have also been developed for continuous NO_3^-
10 measurement (averaging time 30 seconds to 10 minutes). For the flash volatilization system
11 (Fine et al., 2003, [155775](#); Stolzenburg and Hering, 2000, [013289](#); Stolzenburg et al., 2003,
12 [156102](#)), particles are collected by a humidified impaction process and analyzed in place by
13 flash vaporization and chemiluminescent detection of the evolved NO_x . For the catalytic
14 conversion-chemiluminescence analysis system (Weber et al., 2003, [157129](#)), NO_3^- was
15 measured by conversion of particle NO_3^- into NO , and then detected with the
16 chemiluminescence method. Field and lab comparisons were conducted to compare the
17 different instruments mentioned above. Although the R&P 8400N ambient particulate NO_3^-
18 monitor, which is based on the Stolzenburg flash vaporization technique, could provide
19 10-min resolution data and showed excellent precision (with a CV <10%) (Harrison et al.,
20 2004, [136787](#); Hogrefe et al., 2004, [156560](#); Long and McClenny, 2006, [098214](#); Rattigan et
21 al., 2006, [115897](#)), it consistently reported NO_3^- concentrations ~30% lower than the
22 denuder-filter systems in both the Baltimore supersite and the multiyear field study in New
23 York (Harrison et al., 2004, [136787](#); Hogrefe et al., 2004, [156560](#); Rattigan et al., 2006,
24 [115897](#)). In the New York measurement campaign, an AMS was also co-located with other
25 instruments to obtain the real-time NO_3^- information. AMS did not always agree well with
26 the denuder-filter system for reasons not entirely apparent. However, Bae et al. (2007,
27 [156244](#)) reported that some organic compounds can also produce signals at mass-to-charge
28 ratio $m/z = 30$, which is one of the characteristic m/z for NO_3^- . Therefore, the disagreement
29 between the AMS and the filter-based method could be a result of the interference of
30 organic compounds using the AMS. Annex A, Tables A-7 and A-13, list methods and
31 analytical specifications for sampling NO_3^- .

Ammonium

1 Several continuous and semi-continuous instruments can be used to monitor ambient
2 ammonium concentrations (Al-Horr et al., 2003, [153951](#); Bae, 2007, [155669](#)) including
3 many listed above for SO_4^{2-} and NO_3^- . Bae et al. (2007, [155669](#)) conducted an
4 inter-comparison of three semi-continuous instruments during the New York multiyear air
5 sampling campaign: a PILS-IC, an AMS, and a wet scrubbing-long path absorption
6 photometer. Bae et al. (2007, [155669](#)) reported the inter-sampler coefficients of
7 determination (R^2) between these instruments were above 0.75, and the slopes (with zero
8 intercept) were between 0.71 and 1.04. Annex A, Table A-9 describes measurement of ions
9 other than NO_3^- and SO_4^{2-} , including NH_4^+ .

Elemental Composition

10 Techniques for measuring the elemental composition of PM samples were reviewed in
11 the 2004 PM AQCD (U.S. EPA, 2004, [056905](#)). These methods include:

- 12 ▪ Energy dispersive X-ray fluorescence (ED-XRF);
- 13 ▪ Synchrotron X-ray fluorescence (SXRF);
- 14 ▪ Particle-induced X-ray emission (PIXE);
- 15 ▪ Particle elastic scattering analysis (PESA);
- 16 ▪ Total reflection X-ray fluorescence (TR-XRF);
- 17 ▪ Instrumental neutron activation analysis (INAA);
- 18 ▪ Atomic absorption spectrophotometry (AAS);
- 19 ▪ Inductively-coupled plasma-atomic emission spectroscopy (ICP-AES);
- 20 ▪ Inductively-coupled plasma-mass spectrometry (ICP-MS); and
- 21 ▪ Scanning electron microscopy (SEM).

22 Recent development in this area focused on the semi-continuous measurement
23 methods, in which elements were analyzed in the lab using the methods mentioned above
24 on time-resolved and/or size resolved samples (Kidwell and Ondov, 2004, [155898](#)). The
25 concentrated slurry/graphite furnace atomic absorption spectrometry (GFAAS) method
26 collects ambient PM as a slurry using impactors, and then the collected PM is analyzed by
27 AAS in the lab. Laser induced breakdown spectroscopy (LIBS) was used to measure seven

1 metals at the Pittsburgh supersite. LIBS concentrates ambient PM using a virtual impactor
2 into a sample cell, and then a Nd:YAG laser-spectrometer is used to identify and quantify
3 different elements. A full listing of measurement techniques and analytical specifications
4 for trace elements is provided in Annex A, Table A-6.

Elemental and Organic Carbon

5 The large variety of aspects of carbon analyses were reviewed in the 2004 PM AQCD
6 (U.S. EPA, 2004, [056905](#)). Measurement and analytical specifications for carbon
7 measurements are listed in Annex A, Tables A-10 and A-15. Aspects of the measurements
8 include sampling artifacts associated with the integrated filter-based OC and EC sampling
9 methods, the IMPROVE vs. CSN thermal optical protocols (i.e., different thermal optical
10 methods) and optical techniques to measure light-absorption or BC. One significant change
11 taking place in the CSN is that the method for carbon measurements is being changed from
12 the CSN method to a method designed to be consistent with the IMPROVE carbon analysis
13 protocol. This is a phased process that began in May of 2007 with the conversion of 56
14 stations. Phase 2 of the carbon sampler conversion occurred in April of 2009 with another
15 62 stations. The balance of the CSN is scheduled to be converted to IMPROVE-like
16 sampling and IMPROVE analysis in late 2009 (Henderson, 2005, [156537](#)). The CSN
17 network was implemented to support the PM_{2.5} NAAQS and provides data for PM_{2.5} mass,
18 SO₄²⁻, NO₃⁻, NH₄⁺, Na, K, EC, OC, and select trace elements (Al through Pb) at many sites
19 across the U.S. This conversion will increase consistency between these two networks. Also,
20 since the release of the 2004 PM AQCD, more studies have been conducted to extend the
21 understanding of sampling artifact issues (Chow et al., 2008, [156355](#); Watson et al., 2005,
22 [157125](#)), evaluate different thermal and optical procedures (Chen et al., 2004, [147143](#);
23 Chow et al., 2004, [156347](#); Chow et al., 2005, [155728](#); Chow et al., 2007, [156354](#); Conny et
24 al., 2003, [145948](#); Han et al., 2007, [155823](#); Subramanian et al., 2004, [081203](#); Watson et
25 al., 2005, [157125](#)), develop reference materials (Klouda et al., 2005, [130382](#); Lee, 2007,
26 [155926](#)), create water soluble organic carbon (WSOC) measurement techniques (Andracchio
27 et al., 2002, [155657](#); Yang et al., 2003, [156167](#)), develop
28 semi-continuous/continuous/real-time carbon measurement techniques (Chow et al., 2008,
29 [156355](#); Watson et al., 2005, [157125](#)), and introduce isotope identification into the OC/EC
30 measurement (Huang et al., 2006, [097654](#)).

1 OC sampling artifact issues were further addressed in various studies (Arhami et al.,
2 2006, [156224](#); Bae et al., 2004, [156243](#); Chow et al., 2005, [155728](#); Fan et al., 2003, [058628](#);
3 Fan et al., 2004, [155770](#); Grover et al., 2008, [156502](#); Lim et al., 2003, [156697](#); Mader et al.,
4 2003, [155955](#); Matsumoto et al., 2003, [124293](#); Muller et al., 2004, [097109](#); Offenberg et al.,
5 2007, [156822](#); Olson and Norris, 2005, [156005](#); Park et al., 2006, [098104](#); Rice, 2004,
6 [156049](#); Subramanian et al., 2004, [081203](#); ten Brink et al., 2004, [097110](#); ten Brink et al.,
7 2005, [156115](#); Viana et al., 2006, [096384](#)), and were well summarized by Watson et al.
8 (2005, [157125](#)) and Chow et al. (2008, [156355](#)). There are two commonly used methods to
9 correct OC sampling artifacts: the filter with backup filter system (TBQ: placing a backup
10 quartz-fiber filter behind the front Teflon-membrane filter; QBQ: placing a backup
11 quartz-fiber filter behind the front quartz-fiber filter); and the denuder-filter-adsorbent
12 system. Subramanian et al. (2004, [081203](#)) and Chow et al. (2006, [099031](#)) reported that
13 during the Pittsburgh and Fresno supersite studies the positive artifact (organic gases
14 condensed on filters) from TBQ (24-34%, up to 4 $\mu\text{g}/\text{m}^3$ OC) was nearly twice that from QBQ
15 (13-17%). With the denuder-filter-adsorbent system, the negative artifact (OC evaporating
16 from the filter) was 5-10%. Watson and Chow (2002, [037873](#)) reported that the XAD-coated
17 denuder could function as efficiently as a parallel plate denuder using carbon-impregnated
18 charcoal filters (CIF) with frequent denuder changes. Huebert and Charlson (2000, [156577](#))
19 reported that using tandem filter packs may hinder a quantitative analysis of the artifacts.

20 Different temperature protocols and optical correction methods in thermal-optical
21 analyses were further evaluated by Watson et al. (2005, [157125](#)), Chow et al. (2004, [156347](#);
22 2005, [155728](#); 2007, [156354](#)), Subramanian et al. (2006, [156107](#)), Conny et al. (2005,
23 [155728](#); 2003, [145948](#)), Han et al. (2007, [155823](#)), Chen et al. (2004, [147143](#)), and (Conny et
24 al., 2009, [191999](#)). Solomon et al. (2003, [156994](#)) reported a 20-50% difference for OC and a
25 20-200% difference for EC using 11 filter samples and 4 different analytical protocols. In an
26 assessment of the different thermal-optical analysis protocols used around the world,
27 Watson et al. (2005, [157125](#)) reported that differences of a factor of 2 to 7 in EC between
28 different methods could be observed, and a factor of 2 was common, while the relative
29 differences in OC between different methods were relatively small. As Watson et al. (2007,
30 [157127](#)) stated, there are 12 major differences among the thermal methods: (1) analysis
31 atmosphere; (2) temperature ramping rates; (3) temperature plateaus; (4) residence time at
32 each plateau; (5) optical pyrolysis monitoring configuration and wavelength; (6)
33 standardization; (7) oxidation and reduction catalysts; (8) sample aliquot and size; (9)

1 evolved carbon detection method; (10) carrier gas flow through or across the sample; (11)
2 location of the temperature monitor relative to the sample; and (12) oven flushing
3 conditions. Chow et al. (2004, [156347](#)) and Chen et al. (2004, [147143](#)) addressed the
4 difference between optical transmission and optical reflectance methods for charring
5 correction, and they reported that the charring OC on the surface of or inside a filter
6 dominated the differences between these two correction methods. The differences between
7 different sampling and measurement methods are also applied to the
8 in-situ/semi-continuous methods, since most of these methods are also based on
9 thermal-optical analysis of collected filters. Most of these methods agree with integrated
10 filter methods within 30%.

11 The differences observed between methods for OC and EC come largely from how OC
12 and EC are defined. They are defined on an operational basis, as there are no standard
13 reference materials. Initial efforts have been made to produce OC/EC reference materials at
14 the National Institute of Science and Technology (NIST) (Klouda et al., 2005, [130382](#); Lee,
15 2007, [155926](#)). Klouda et al. (2005, [130382](#)) described the development of Reference
16 Material 8785: Air Particulate Matter on Filter Media. Each reference filter is uniquely
17 identified by its air PM number and its gravimetrically determined mass of fine Standard
18 Reference Material (SRM) 1649a, and each filter has values assigned for total carbon, EC,
19 and organic carbon mass fractions measured according to both IMPROVE and NIOSH
20 protocols. Lee et al. (2007, [155926](#)) reported a method to create a reference filter with a
21 known amount of OC (as potassium hydrogen phthalate), and EC (as carbon black
22 hydrosol).

23 Measurement methods for WSOC have been developed recently (Greenwald et al.,
24 2007, [155809](#); Miyazaki et al., 2006, [156767](#); Sullivan and Weber, 2006, [157031](#); Sullivan et
25 al., 2004, [157029](#); Sullivan et al., 2006, [157030](#); Sullivan et al., 2007, [100083](#); Yu et al.,
26 2004, [156172](#)). WSOC can be measured on integrated filter samples, or in-situ
27 measurement can be conducted by coupling with the PILS-IC (Sullivan et al., 2004,
28 [157029](#)). For integrated filter samples, filters are extracted with deionized water and
29 followed by oxidation of total WSOC to CO₂. CO₂ can then be detected by either infrared
30 spectroscopy (IR) (Decesari et al., 2000, [155748](#); Kiss et al., 2002, [156646](#); Yang et al., 2003,
31 [156167](#)), FID (Yang et al., 2003, [156167](#)), or pyrolysis gas chromatography/mass
32 spectrometry (GC/MS) (Gelencsér et al., 2000, [155785](#)). A correlation coefficient of 0.84 was

1 reported by Sullivan et al. (Sullivan et al., 2004, [157029](#)) between in-situ and filter based
2 measurement of WSOC.

3 Further development and evaluation has been conducted on the measurement of BC
4 with light absorption instruments (Andreae and Gelencsér, 2006, [156215](#); Arnott et al.,
5 2003, [037711](#); Bae et al., 2004, [156243](#); Borak et al., 2003, [156284](#); Cyrus et al., 2003,
6 [049634](#); Kurniawan and Schmidt-Ott, 2006, [098823](#); Park et al., 2006, [098104](#); Saathoff et
7 al., 2003, [156066](#); Sadezky et al., 2005, [097499](#); Slowik et al., 2007, [096177](#); Taha et al.,
8 2007, [096277](#); Virkkula et al., 2007, [157098](#); Wallace, 2000, [000803](#); Weingartner et al.,
9 2003, [156149](#); Williams et al., 2006, [157148](#); Wu et al., 2005, [157155](#)). These instruments
10 include the aethalometer, particle absorption photometer, and photoacoustic analyzer.
11 However, these instruments are subject to interferences by particle scattering, interactions
12 with the filter substrate, particle loading on filters, and other pollutants (e.g., NO₂).
13 Uncertainties of up to 50% were observed in the studies mentioned above by comparing
14 these methods with integrated filter methods and thermal analysis methods.

15 Huang et al. (2006, [097654](#)) reported the measurement of a stable isotope, ¹³C, in OC
16 and EC with a thermal optical transmission analyzer coupled with gas
17 chromatography-isotope ratio mass spectrometer (TOT-GC-IRMS). The ratio of ¹³C/¹²C in
18 OC and EC can provide useful information on OC/EC source categories and origin. The
19 method was applied to Pacific2001 aerosol samples from the Greater Vancouver area in
20 Canada and produced a precision of ~0.03%. Gustafsson et al. (2009, [192000](#)) applied the
21 radiocarbon measurement technique and quantified the source contributions of
22 carbonaceous aerosols to the Indian Ocean “brown cloud,” with particular relevance for
23 understanding and mitigating the climate effects of EC/BC.

Organic Speciation

24 Organic matter makes up a substantial fraction of PM in all regions of the U.S.
25 (U.S. EPA, 2004, [056905](#)), and 10 to 40% of the total organic matter is currently
26 quantifiable at the individual compound level (Pöschl, 2005, [156882](#)). Recent advancements
27 in traditional solvent extraction gas chromatography/mass spectrometry (GC/MS) and high
28 pressure liquid chromatography (HPLC) as well as application of thermal desorption (TD)
29 techniques are helping to expand the understanding of the composition of organic matter as
30 well as improving detection limits for quantification of organic molecular marker (OMM)
31 compounds (Robinson et al., 2006, [156918](#); Schnelle-Kreis et al., 2005, [112944](#); Sheesley et

1 al., 2007, [112017](#); Shrivastava et al., 2007, [111594](#)). In addition, information about organic
2 functional groups can be obtained with Fourier transform infrared spectrometry (FTIR)
3 (Tsai and Kuo, 2006, [156127](#)).

4 Recent advancements in GC/MS technology including inert electron ionization sources
5 and improved instrument sensitivity and scan rates for better OMM quantification, have
6 increased its application in organic aerosol characterization studies (Cass, 1998, [155716](#);
7 Fraser et al., 2003, [042231](#); Graham et al., 2003, [156489](#); Hays et al., 2002, [026104](#);
8 Robinson et al., 2006, [156918](#); Schauer et al., 1996, [051162](#); Sheesley et al., 2007, [112017](#);
9 Subramanian et al., 2006, [156107](#); Watson et al., 1998, [012257](#); Zheng et al., 2002, [026100](#);
10 Zheng et al., 2006, [157189](#)). Incorporation of high volume injection using programmable
11 temperature vaporization (PTV) (Engewald et al., 1999, [155765](#)) has further lowered
12 detection limits for trace level OMM compounds. High volume injection has the added
13 benefit of preventing the loss of semivolatile compounds (Swartz et al., 2003, [157035](#)), and
14 has been applied for analysis of PAHs using low volume samplers (down to 5 Lpm), allowing
15 for smaller required mass loadings (Bruno et al., 2007, [155706](#); Crimmins and Baker, 2006,
16 [097008](#)). Since last review, HPLC analysis with fluorescence detection has also been used
17 frequently for quantification of semivolatile organic compounds in both the particle and gas
18 phase (Albinet et al., 2007, [154426](#); Barreto et al., 2007, [155676](#); Chow, 2007, [157209](#);
19 Eiguren-Fernandez et al., 2003, [142609](#); Goriaux et al., 2006, [156484](#); Murahashi, 2003,
20 [096539](#); Rynö et al., 2006, [156065](#); Stracquadanio et al., 2005, [156104](#); Temime-Roussel et
21 al., 2004, [098530](#); Temime-Roussel et al., 2004, [098521](#)). Lengthy extraction and analysis
22 times remain a limiting factor for these methods.

23 TD techniques bypass one of the time consuming steps in traditional solvent
24 extraction analysis for nonpolar organic compounds (n-alkanes, branched alkanes,
25 cyclohexanes, hopanes, steranes, alkenes, phthalates and PAHs). This is achieved by
26 vaporizing and analyzing organic constituents directly from the collection substrate,
27 thereby bypassing the extraction step (Chow et al., 2007, [156354](#)). Methods exist for both
28 off-line TD analysis of previously collected filter samples and semi-continuous TD analysis.
29 Annex A, Table A-17 is adapted from Chow et al. (2007, [157209](#)) and summarizes recent
30 TD-GC/MS studies. The most common off-line method is thermal desorption-gas
31 chromatography/mass spectrometry (TD-GC/MS) (Hays and Lavrich, 2007, [155831](#)).
32 Continuous or semi-continuous methods have been developed for direct analysis of
33 individual organic constituents by coupling TD with various forms of mass spectrometry

1 (Smith et al., 2004, [156090](#); Tobias and Ziemann, 1999, [157053](#); Tobias et al., 2000, [156121](#);
2 Voisin et al., 2003, [156141](#); Williams et al., 2006, [156157](#)). A comparison of measurement
3 and analytical specifications for filter analysis using solvent extraction and TD methods for
4 organic speciation are summarized in Annex A, Table A-17.

3.4.1.3. Multiple-Component Measurements on Individual Particles

5 The 2004 PM AQCD discussed the aerosol time-of-flight mass spectrometry
6 (ATOFMS). Recently, the ATOFMS and several other aerosol mass spectrometry methods
7 have been further developed. Both lab and field comparisons have been conducted to
8 evaluate the reliability of these types of instruments.

9 There are four types of commonly used aerosol mass spectrometry: (1) particle
10 analysis by laser MS (PALMS; National Oceanic and Atmospheric Administration [NOAA]);
11 (2) rapid single particle mass spectrometer (RSMS; University of Delaware); (3) aerosol
12 time-of-flight MS (ATOFMS; TSI, Inc.); and (4) AMS (Aerodyne) (Chow et al., 2008, [156355](#);
13 Nash et al., 2006, [156795](#)). The differences between these instruments primarily come from
14 the particle sizing methods of mass spectrometers, as shown in Annex A, Table A-16.
15 Although the technique varies, the underlying principle is to fragment each particle into
16 ions, using either a high-power laser or a heated surface, and then a mass spectrometer to
17 measure the mass to charge ratio of each ion fragment in a vacuum.

18 These instruments were evaluated at the Atlanta, Houston, Fresno, Pittsburgh, New
19 York, and Baltimore supersites (Bein et al., 2005, [156265](#); Drewnick et al., 2004, [155755](#);
20 Drewnick et al., 2004, [155754](#); Hogrefe et al., 2004, [156560](#); Jimenez et al., 2003, [156611](#);
21 Lake et al., 2003, [156669](#); Lake et al., 2004, [088411](#); Middlebrook et al., 2003, [042932](#);
22 Phares et al., 2003, [156866](#); Qin and Prather, 2006, [156895](#); Wenzel et al., 2003, [157139](#);
23 Zhang et al., 2008, [155144](#)). Measurements of the gross composition and abundance of
24 particles by these instruments were generally semi-quantitative, with the exception of
25 AMS. Particles of similar composition (e.g., OC/SO₄²⁻, Na/K/SO₄²⁻, soot/hydrocarbon, and
26 mineral particle types) were characterized by these instruments during the studies
27 mentioned above. NO₃⁻ and SO₄²⁻ concentrations measured with AMS were comparable
28 with other continuous and filter-based methods, as mentioned in Section 3.4.1.2. In
29 addition, concentrations of different particle types can be obtained by the co-location of

1 these aerosol mass spectrometers and other particle sizing instruments, such as particle
2 counters or the MOUDI.

3.4.1.4. Ultrafine PM: Mass, Surface Area, and Number

3 Instruments for measuring ultrafine PM developed during the past decade permit
4 measurement of size distributions of particles down to 3 nm in diameter with mobility
5 particle sizers. Concentrations down to this size range can be obtained by a Micro-Orifice
6 Uniform Deposit Impactor (MOUDI). The recently developed low pressure-drop ultrafine
7 particle impactor coupled with a β Attenuation Monitor (nano-BAM) can also provide
8 ultrafine PM (<150 nm) mass concentrations (Chakrabarti et al., 2004, [147867](#)). A high
9 correlation coefficient was observed between MOUDIs and nano-BAMs, with a correlation
10 of 0.96. A 50% cutpoint (d_{50}) of 13-200 nm can be achieved by a high-volume slot-type
11 ultrafine PM virtual impactor (Middha and Wexler, 2006, [155982](#)).

12 Methods are also being developed to measure the surface area of ultrafine particles.
13 Particle surface area is usually measured by attaching labeled (radioactive or electrical
14 labeling) molecules to particles and detect the radioactive or electrical properties of the
15 attached molecules. Wilson et al. (2007, [157149](#)) suggested that the electrical aerosol
16 detector (EAD, based on diffusion charging) measurement might be a useful indicator of the
17 particle surface area deposited in the lung. This method can be potentially useful for
18 examining the association between health effects and particle surface areas.

19 Developments involving the condensation particle counter include use of de-ionized
20 water as a condensation media in lieu of butanol or n-propanol in condensation particle
21 counters (Hering et al., 2005, [155838](#); Hermann et al., 2007, [155840](#); Petäjä, 2006, [156021](#)).
22 This development makes the condensation particle counter (CPC) easier to use in field
23 studies because water does not have some of the same chemical properties (with respect to
24 hazard and odor) as butanol or n-propanol. The performance of this CPC was reported to be
25 similar to the conventional butanol based CPC (Hering et al., 2005, [155838](#)). Use of a
26 battery of water and butanol-based CPCs was demonstrated to detect a range of solubilities
27 in nucleation-mode particles (Kulmala et al., 2007, [155911](#)). Additionally, CPCs have been
28 used to measure particles in the smaller end of the ultrafine scale through adjustment of
29 CPC cut-off diameters through tuning the temperature difference between the CPC
30 saturator and condenser (Kulmala et al., 2007, [155911](#)) and improved charge reduction

1 techniques (Winkler et al., 2008, [156160](#)). The latter method was effective in reducing the
2 size of particles detected by a CPC to less than 2 nm. These studies include assessment of
3 errors related to these developments with the CPC and generally show that counting
4 efficiencies with these devices is upwards of 95% (Hermann et al., 2007, [155840](#)).
5 Additionally, recent advancements have been made in development of fast scanning
6 methods for ultrafine particle size distributions, including diffusion screens (DS)
7 (Feldpausch et al., 2006, [155773](#)) and fast integrated mobility scanners (FIMS) (Olfert et
8 al., 2008, [156004](#)).

3.4.1.5. PM Size Distribution

9 Along with particle density and shape (U.S. EPA, 2004, [056905](#)), the particle size
10 distribution can be used to estimate PM mass concentrations. For particles $>0.1 \mu\text{m}$, several
11 instruments, including DRUM, MOUDI_s, and aerodynamic particle sizer (APS), are
12 available to measure mass-based or count-based particle size distribution. An APS
13 incorporating very sharp cut points between 0.1 and 10 μm is now available (Peters, 2006,
14 [156860](#); Zeng, 2006, [098375](#)). For particles in this range, inertial forces are used to separate
15 particles based on impaction. For particles $<0.1 \mu\text{m}$, particles can be separated by their
16 electrical mobility, and as a result, electrical mobility diameter is often used to describe
17 ultrafine PM size distribution in lieu of aerodynamic diameter. It has been necessary to
18 develop techniques to convert mobility diameters, measured by the scanning mobility
19 particle sizer (SMPS) or the Engine Exhaust Particle Sizer (EEPS), to aerodynamic
20 diameters, measured by the APS, or vice versa, in order to merge the distributions
21 spanning the ultrafine, accumulation, and coarse modes. A variety of techniques for
22 combining SMPS and APS diameters have been reported in the literature (Hand and
23 Kreidenweis, 2002, [155824](#); Khlystov et al., 2004, [155897](#); Morawska et al., 1999, [007609](#);
24 Morawska et al., 2007, [155990](#); Shen et al., 2002, [156086](#); TSI, 2005, [157196](#)). However,
25 each of these techniques incurs some uncertainty of which the user must be aware.

3.4.1.6. Satellite Measurement

26 Instruments sensing back scattered solar radiation on satellites have made it possible
27 to derive information about tropospheric aerosol properties on the global scale. The satellite
28 borne instruments vary in their complexity and in the aerosol properties they can measure.

1 Satellite instruments measure radiance (or brightness temperature) that can then be used
2 to provide information on the aerosol column amount, or the aerosol optical depth (AOD).
3 Depending on the wavelengths sampled and the spectral resolution of the instruments,
4 information about the composition of particles of diameter $<2 \mu\text{m}$ and particles of diameter
5 $>2\mu\text{m}$ can be obtained. Data from two main instruments, the moderate resolution imaging
6 spectroradiometer (MODIS) and the multiangle imaging spectroradiometer (MISR) have
7 been used to estimate surface PM in the U.S. MODIS measures the intensity of back
8 scattered sunlight at seven wavelengths through the visible to the near infrared at one
9 viewing direction; and MISR measures the intensity at four wavelengths (from the visible
10 to the near IR) and the same ground pixel at nine viewing angles. The spatial resolution of
11 reported AOD is $17.6 \times 17.6 \text{ km}$ for MISR and either 10×10 or $1 \times 1 \text{ km}$ for MODIS,
12 depending on retrieval algorithm. Since both instruments are located on the same satellite,
13 their times of overpass are the same, about 1330 local time. Due to precession of the
14 satellite's orbit, the satellite does not pass over the same path every day, and instruments
15 cannot sense aerosol properties beneath cloud tops.

16 The problem of using satellite data to retrieve properties of the atmospheric aerosol is
17 complex because the surface contribution to satellite measured reflectance must be
18 separated from the aerosol signal. Difficulties can arise when attempting to derive aerosol
19 information over land surfaces because of uncertainties in surface reflectivity, similarities
20 between aerosol and surface composition, and high signal-to-noise ratio when viewing AOD
21 over reflective surfaces such as desert and snow. To overcome this difficulty, data from
22 MODIS have been applied over dark land surfaces and ongoing improvements in retrieval
23 algorithms are being developed. Instruments such as the multiangle imaging
24 spectroradiometer (MISR) that sense at multiple viewing angles can better cope with the
25 problems over land surfaces because they can use the information on the angular
26 dependence of reflection from the surface and the atmosphere to distinguish between their
27 signals. Not only can total AODs be derived, but fractional AODs that reflect external
28 mixtures characterized by particle shape, effective radius, and single scattering albedo can
29 also be derived. These properties can then be used to infer particle composition. Retrievals
30 over the oceans have had less difficulty because the optical properties of sunlight reflected
31 from the sea surface are much better known, and reflectivities are low over most zenith
32 angles at less than grazing incidence.

1 Kokhanovsky et al. (2007, [190009](#)) examined the errors associated with MODIS,
2 MISR, and a number of other satellite instruments with respect to associated retrieval
3 algorithms for retrievals over Central Europe. They found a correlation coefficient between
4 MODIS and MISR AOD of 0.62. Both MODIS and MISR AOD tended to underestimate
5 ground-based AOD measurements from AERONET (NASA's AErosol RObotic NETwork)
6 slightly with MODIS generally retrieving higher AODs than MISR. Chu et al. (2003,
7 [190049](#)) found correlations between MODIS and AERONET AODs ranging from 0.82-0.91;
8 and Kahn et al. (2005, [189961](#)) found correlations of 0.7-0.9 between MISR and AERONET
9 AODs.

10 Further complexity is added when attempting to relate surface PM_{2.5} to aerosol optical
11 depths. The detailed comparisons of surface measurement and satellite measurements are
12 given in Chapter 9.

3.4.2. Ambient Network Design

3.4.2.1. Monitor Siting Requirements

13 The AQS contains measurements of air pollutant concentrations in the 50 states, plus
14 the District of Columbia, Puerto Rico, and the Virgin Islands, for the 6 criteria air
15 pollutants as well as a more limited dataset of hazardous air pollutants. In 2007, there
16 were 4,693 PM₁₀ monitors and 2,194 PM_{2.5} monitors reporting values to the EPA Air Quality
17 System database (AQS). Where SLAMS PM₁₀ and PM_{2.5} monitoring is required, at least one
18 of the sites must be a maximum concentration site for that specific area. The appropriate
19 spatial scales for PM₁₀, PM_{2.5}, and PM_{10-2.5} monitoring differ given the contrasting spatial
20 gradients of coarse PM relative to fine. The relevant scales for each size classification are
21 provided in Annex A, Table A-18.

22 Criteria for siting ambient monitors for PM at national monitoring networks are
23 summarized below by PM size, and details are given in the CFR 40 Part 58 Appendix D,
24 and SLAMS/NAMS/PAMS Network Review Guidance (U.S. EPA, 1998, [083151](#)). Table A-19
25 in Annex A provides a summary of the number of sites and operating specifications of these
26 networks. Probing and monitoring path siting criteria for any specific monitoring site are
27 given in CFR 40 Part 58 Appendix E, including horizontal and vertical placement, spacing
28 from minor source, spacing from obstructions, spacing from trees, and spacing from
29 roadways.

PM₁₀

1 Metropolitan Statistical Areas (MSAs) with populations in excess of one million are
2 required to have between 2 and 10 monitors (depending on concentration), while MSAs with
3 populations less than one million are required to have between 0 and 8 monitors (40 CFA
4 Part 58, Appendix D). Except from some circumstances where microscale (<100 m, for
5 maximum PM₁₀ exposure) monitoring may be appropriate, the most important scales to
6 characterize the emissions of PM₁₀ effectively from both mobile and stationary sources are
7 the middle (for short-term public exposure) and neighborhood scales (for trends and
8 compliance with standards). PM₁₀ measurements are obtained at standard temperature
9 and pressure across the NAMS/SLAMS networks (40 CFR Part 58).

PM_{2.5}

10 Monitor requirements for PM_{2.5} based on MSA population are similar to those for
11 PM₁₀ above, but also include pollutant concentration as a factor in determining the number
12 of required stations. Continuous PM_{2.5} monitors must be operated in no fewer than one-half
13 of the minimum required sites in each area. Most PM_{2.5} monitoring in urban areas should
14 be representative of a neighborhood scale (for trends and compliance with standards).
15 Urban or regional scale sites are located to characterize regional transport of PM_{2.5}. In
16 certain instances where population-oriented micro- or middle-scale PM_{2.5} monitoring are
17 determined by the Regional Administrator to represent many such locations throughout a
18 metropolitan area, these smaller scales can be considered to represent community-wide air
19 quality. PM_{2.5} measurements are obtained at local temperature and pressure across the
20 NAMS/SLAMS networks (40 CFR Part 58).

21 PM species are monitored at both mostly urban (CSN) and mostly rural (IMPROVE)
22 locations. PM_{2.5} chemical speciation monitoring is currently conducted at 197 CSN sites
23 (<http://www.epa.gov/ttn/amtic/specgen.html>). Within the CSN network, 53 locations are
24 recognized as the Speciation Trends Network (STN) operating on a sample schedule of one
25 in every three days, while the rest of the CSN typically operates every sixth day.

PM_{10-2.5}

26 PM_{10-2.5} has not been required to be monitored at SLAMS sites, but will be required at
27 NCore¹ Stations (which is a sub-set of the SLAMS) by January 1, 2011. Middle and
28 neighborhood scale measurements are the most important station classifications for PM_{10-2.5}

¹ For more information on NCore, see the NCore web site at: <http://www.epa.gov/ttn/amtic/ncore/index.html>

1 to assess the variation in coarse particle concentrations that would be expected across
2 populated areas that are in proximity to large emissions sources. PM_{10-2.5} chemical
3 speciation monitoring and analyses is required at NCore sites, also by January 1, 2011. EPA
4 has already approved FRMs and FEMs for PM_{10-2.5} mass; however, methods for PM_{10-2.5}
5 speciation are still being developed (Henderson, 2009, [192001](#)). PM_{10-2.5} measurements are
6 obtained at local temperature and pressure by recalculating the co-located PM₁₀ for local
7 conditions.

3.4.2.2. Spatial and Temporal Coverage

Locations of PM_{2.5} and PM₁₀ Monitors in Selected Metropolitan Areas in the U.S.

8 Fifteen metropolitan regions were chosen for closer investigation of monitor siting
9 based on their distribution across the nation and relevance to health studies analyzed in
10 subsequent chapters of this ISA. These regions were: Atlanta, Birmingham, Boston,
11 Chicago, Denver, Detroit, Houston, Los Angeles, New York City, Philadelphia, Phoenix,
12 Pittsburgh, Riverside, Seattle, and St. Louis. Core-Based Statistical Areas (CBSAs) and
13 Combined Statistical Areas (CSAs), as defined by the U.S. Census Bureau
14 (<http://www.census.gov/>), were used to determine which counties, and hence which
15 monitors, to include for each metropolitan region.¹ Figures 3-7 and 3-8 display PM₁₀ and
16 PM_{2.5} monitor density with respect to population density for Boston. Annex A includes
17 similar information for the remaining fourteen metropolitan regions (Figures A-1-A-28).

¹ A CBSA represents a county-based region surrounding an urban center of at least 10,000 people determined using 2000 census data and replaces the older Metropolitan Statistical Area (MSA) definition from 1990. The CSA represents an aggregate of adjacent CBSAs tied by specific commuting behaviors. The broader CSA definition was used when selecting monitors for the cities listed above with the exception of Los Angeles, Riverside and Phoenix. Los Angeles and Riverside are contained within the same CSA, so the smaller CBSA definition was used to delineate these two cities. Phoenix is not contained within a CSA, so the smaller CBSA definition was used for this city as well.

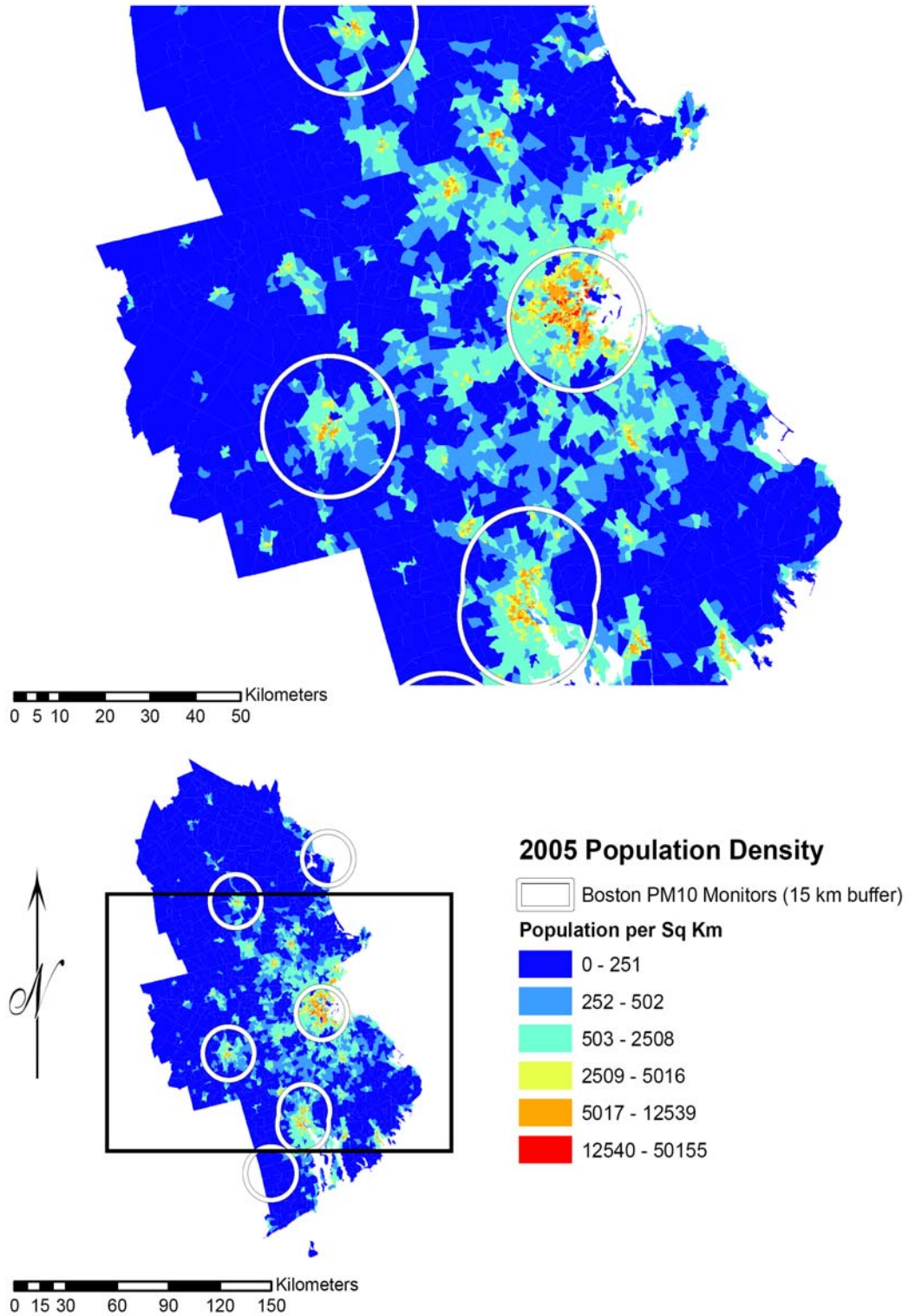


Figure 3-7. PM₁₀ monitor distribution in comparison with population density, Boston CSA.

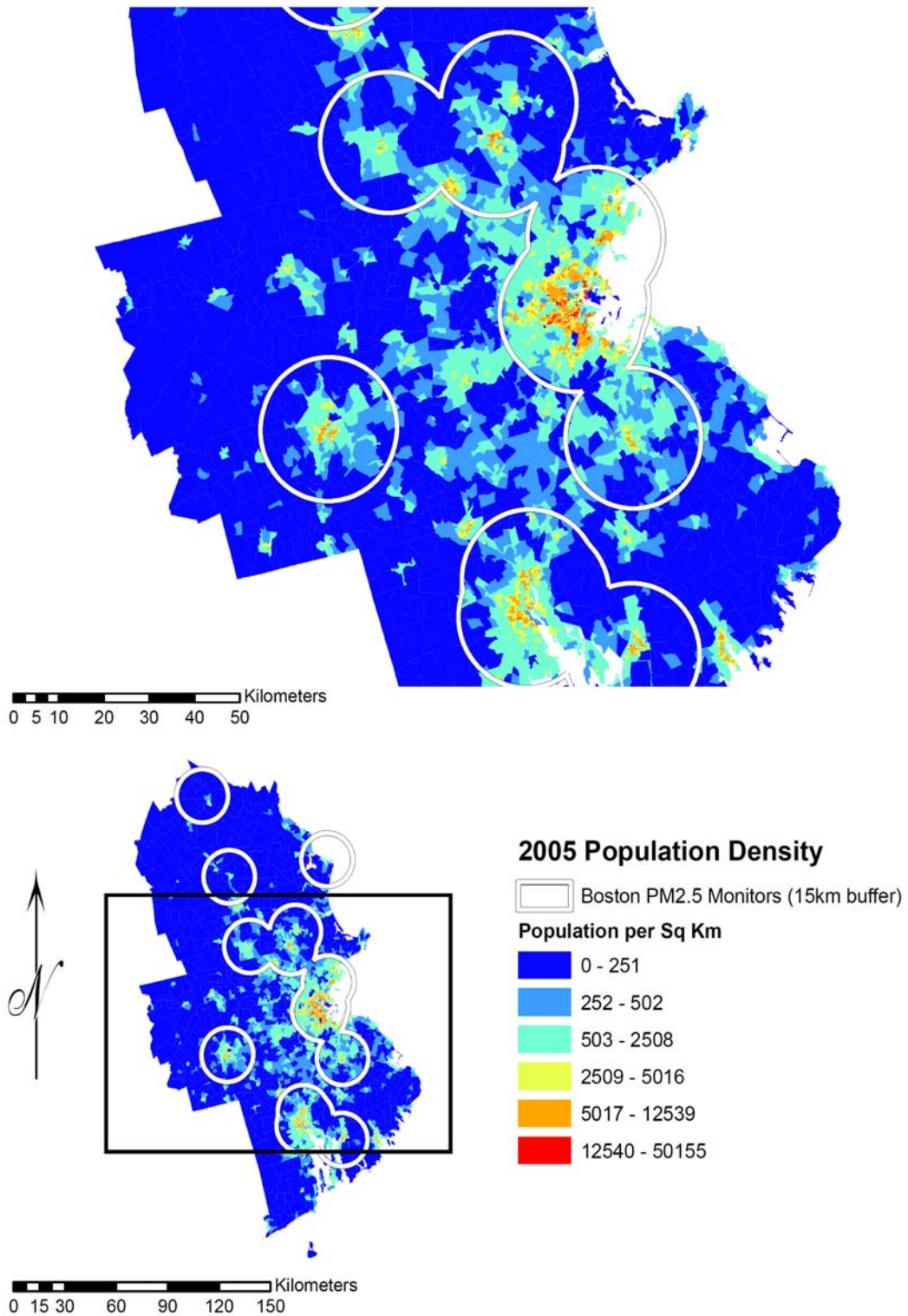


Figure 3-8. PM_{2.5} monitor distribution in comparison with population density, Boston CSA.

Table 3-3. Proximity to PM₁₀ and PM_{2.5} monitors for total population^a by city.

Region	Proximity to PM Monitors ^b									
	Total CSA/CBSA		≤ 1 km		≤ 5 km		≤ 10 km		≤ 15 km	
	N		N	%	N	%	N	%	N	%
PROXIMITY TO PM₁₀ MONITORS										
Atlanta	5316742	30973	0.58	416440	7.83	1090497	20.51	1837983	34.57	
Birmingham	1166100	23943	2.05	251310	21.55	473054	40.57	638472	54.75	
Boston	7502707	63614	0.85	1090172	14.53	2087770	27.83	2939870	39.18	
Chicago	9754262	55642	0.57	844714	8.66	2374972	24.35	3844297	39.41	
Denver	2952039	38449	1.30	521201	17.66	1146286	38.83	1799187	60.95	
Detroit	5553465	14050	0.25	309623	5.58	748971	13.49	1300995	23.43	
Houston	5503320	36795	0.67	832767	15.13	2227314	40.47	3141150	57.08	
Los Angeles	13061361	52052	0.40	1404389	10.75	4899254	37.51	9075863	69.49	
New York	22050940	19842	0.09	292105	1.32	592631	2.69	773962	3.51	
Philadelphia	6388913	23988	0.38	376966	5.90	1091532	17.08	2238309	35.03	
Phoenix	3818147	99520	2.61	1255430	32.88	2615738	68.51	3416682	89.49	
Pittsburgh	2515383	65906	2.62	706413	28.08	1291700	51.35	1705451	67.80	
Riverside	3781063	61356	1.62	895615	23.69	2360272	62.42	2922799	77.30	
Seattle	3962434	4851	0.12	220539	5.57	709887	17.92	1211430	30.57	
St. Louis	2869955	27872	0.97	380411	13.25	891695	31.07	1212543	42.25	
PROXIMITY TO PM_{2.5} MONITORS										
Atlanta	5316742	23461	0.44	581461	10.94	1990477	37.44	3179844	59.81	
Birmingham	1166100	12925	1.11	240383	20.61	666926	57.19	848447	72.76	
Boston	7502707	185457	2.47	1877180	25.02	3356019	44.73	4641175	61.86	
Chicago	9754262	177076	1.82	3091573	31.69	6473463	66.37	8185010	83.91	
Denver	2952039	40601	1.38	649953	22.02	1548976	52.47	2252657	76.31	
Detroit	5553465	54997	0.99	1174733	21.15	2791555	50.27	3845190	69.24	
Houston	5503320	11586	0.21	213708	3.88	905007	16.44	1599079	29.06	
Los Angeles	13061361	115477	0.88	2579809	19.75	7544466	57.76	10792727	82.63	
New York	22050940	717094	3.25	8107764	36.77	13493867	61.19	16571764	75.15	
Philadelphia	6388913	117389	1.84	1878373	29.40	3517321	55.05	4393136	68.76	
Phoenix	3818147	37133	0.97	490072	12.84	1099069	28.79	1739542	45.56	
Pittsburgh	2515383	40574	1.61	587148	23.34	1331230	52.92	1883301	74.87	
Riverside	3781063	43739	1.16	723829	19.14	1855296	49.07	2344394	62.00	
Seattle	3962434	13723	0.35	287373	7.25	931630	23.51	1561792	39.41	
St. Louis	2869955	37329	1.30	563176	19.62	1338349	46.63	1760985	61.36	

^aBased on 2005 population totals.

^bPercentages are given with respect to the total population per city provided.

1 Table 3-3 shows the population density around PM_{2.5} and PM₁₀ monitors for the total
 2 population for each CSA/CBSA individually. Population totals within various distances of

1 PM monitors were calculated assuming equal internal population distribution for
2 individual census blocks. Between-city disparities in population density were large and
3 were dependent primarily on the location and number of PM monitoring sites per
4 CSA/CBSA. For PM_{2.5}, Los Angeles (83%) and Denver (76%) had the largest proportion of
5 the total population within 15 km of a monitor. Houston (29%) had the least population
6 coverage with their PM_{2.5} monitors. For PM₁₀, Phoenix (89%) had the largest proportion of
7 the total population within 15 km of a monitor. Detroit (23%), Boston (39%), Seattle (31%),
8 and Philadelphia (35%) had the smallest proportions of the population within 15 km of a
9 PM₁₀ monitor. Proximity to monitoring stations is considered further in Sections 3.5 and 3.7
10 regarding spatial variability within cities. Figure 3-8 shows that the PM_{2.5} network more
11 closely samples near population centers in the Boston CSA compared with the PM₁₀
12 network shown in Figure 3-7, although both PM₁₀ and PM_{2.5} networks place at least one
13 monitor in the city center.

3.4.2.3. Network Application for Exposure Assessment with Respect to Susceptible Sub-populations

Subject Age

14 Table 3-4 breaks down the population density around PM_{2.5} and PM₁₀ monitors for
15 sub-populations of children aged 0-4, children aged 5-17, and elderly adults aged 65 and
16 over cumulatively for the fifteen CSAs/CBSAs examined, and Table 3-5 shows the
17 distribution for adults aged 65 and over for each CSA/CBSA individually. This detail of
18 information is not provided for the 0-4 y and 5-17 y age groups because variation in
19 percentage within a certain radius of the monitor was generally fairly low for each city
20 across the child age groups when compared to total population. In the cases of Denver,
21 Detroit, Phoenix, Riverside, and St. Louis for PM_{2.5} and Birmingham, Denver, Riverside,
22 and St. Louis for PM₁₀, the elderly population's distribution around the samplers varied
23 more from the total population compared to other age groups. When all CSAs/CBSAs were
24 considered cumulatively, the percentage of the population within 15 km of a monitor was
25 similar for all age groups for both PM_{2.5} and PM₁₀. Between-city disparities in elderly
26 population density within a sampler radius were larger. For PM_{2.5}, Chicago (86%) and
27 Denver (84%) had the largest proportion of the total population within 15 km of a monitor.
28 Houston (31%) had the least population coverage with their PM_{2.5} monitors. For PM₁₀,
29 Phoenix (90%) had the largest proportion of the total population within 15 km of a monitor.

1 New York (4%), Detroit (27%), Seattle (32%), and Philadelphia (38%) had the smallest
 2 proportions of the population within 15 km of a PM₁₀ monitor. These differences may reflect
 3 overall density of the samplers within a given city, with PM_{2.5} monitors more numerous
 4 than PM₁₀ monitors in most of the CSAs/CBSAs, and retirement and settlement trends
 5 among elderly adults.

Table 3-4. Proximity to PM₁₀ and PM_{2.5} monitors for children 0-4 y, children 5-17 y, and adults 65 y and older.^aThe figures presented here are cumulative for the 15 CSAs/CBSAs examined in Chapter 3.

Age Grouping	Proximity to PM Monitors ^b									
	Total CSA/CBSA	≤ 1 km		≤ 5 km		≤ 10 km		≤ 15 km		
	N	N	%	N	%	N	%	N	%	
PROXIMITY TO PM₁₀ MONITORS										
0-4	6400785	44384	0.69	695120	10.86	1725419	26.96	2636782	41.19	
5-17	17212825	110882	0.64	1756246	10.20	4441239	25.80	6942001	40.33	
> 64	10391023	68367	0.66	1056375	10.17	2631243	25.32	4041802	38.90	
PROXIMITY EAR GLASS-IN WOONPDSALTO PM_{2.5} MONITORS										
0-4	6400785	109466	1.71	1603000	25.04	3361922	52.52	4462403	69.72	
5-17	17212825	275427	1.60	4164132	24.19	8814179	51.21	11813997	68.63	
> 64	10391023	175113	1.69	2570909	24.74	5483776	52.77	7288049	70.14	

^aBased on 2000 population totals.

^bPercentages are given with respect to the total population per city provided.

Race and Hispanic Origin

6 Table 3-6 shows the percent of the population self-identified as white or black and
 7 having a Hispanic or non-Hispanic origin within 1, 5, 10, or 15 kilometer distances of PM_{2.5}
 8 and PM₁₀ monitors cumulatively across the fifteen CSAs/CBSAs. For PM₁₀, Hispanics (54%)
 9 represented the subpopulation with the largest percentage of total population within 15 km
 10 of a monitor across the fifteen CSAs/CBSAs studied. The percentage of blacks within that
 11 same distance was marginally lower (48%), whereas the percentage of whites and non-
 12 Hispanics within 15 km of a monitor was approximately two-thirds that of Hispanics (35%
 13 and 37%, respectively). For PM_{2.5}, blacks and Hispanics had similar percentages of the
 14 population within 15 km of a monitor (86% and 82%, respectively), while a smaller
 15 proportion of whites and non-Hispanics were within that same distance (63% and 67%,
 16 respectively), across the fifteen CSAs/CBSAs studied. Higher percentages of individual
 17 ethnic subpopulations within 15 km of a PM_{2.5} monitor most likely represents the fact that

1 more PM_{2.5} monitors are currently deployed compared with PM₁₀ monitors. While no ethnic
 2 subpopulation appears to be well represented at the neighborhood scale, greater
 3 percentages of the black and Hispanic populations (1% each) are within 1 km of a PM₁₀
 4 monitor than the corresponding white and non-Hispanic populations (0.5% each). Likewise,
 5 2.5% of the black population and 2.8% of the Hispanic population reside within 1 km of a
 6 PM_{2.5} monitor compared to 1.4% of the white population and 1.5% of the non-Hispanic
 7 population. Furthermore, it is notable that at any scale shown in Table 3-6, for both PM₁₀
 8 and PM_{2.5} monitors, those self-identified as black or Hispanic actually have greater
 9 representation by the monitors than those identified as white or non-Hispanic.

Table 3-5. Proximity to PM₁₀ and PM_{2.5} monitors for adults aged 65 and older^a by city.

Region	Proximity to PM Monitors ^b								
	Total CSA/CBSA	≤ 1 km		≤ 5 km		≤ 10 km		≤ 15 km	
	N	N	%	N	%	N	%	N	%
PROXIMITY TO PM₁₀ MONITORS									
Atlanta	362201	2115	0.58	35448	9.79	93903	25.93	139240	38.44
Birmingham	145905	3663	2.51	35628	24.42	66839	45.81	86299	59.15
Boston	945790	6852	0.72	124911	13.21	262854	27.79	385046	40.71
Chicago	1018983	7619	0.75	107540	10.55	291705	28.63	441771	43.35
Denver	232974	3675	1.58	43658	18.74	107548	46.16	168447	72.30
Detroit	626216	1555	0.25	41833	6.68	99680	15.92	167760	26.79
Houston	377586	2085	0.55	57413	15.21	166715	44.15	219615	58.16
Los Angeles	1207436	4693	0.39	126696	10.49	422725	35.01	810078	67.09
New York	2710675	2463	0.09	37580	1.39	80222	2.96	104951	3.87
Philadelphia	834110	2740	0.33	49413	5.92	154535	18.53	322700	38.69
Phoenix	388150	8605	2.22	119306	30.74	267456	68.91	348464	89.78
Pittsburgh	449544	13302	2.96	133285	29.65	243723	54.22	314941	70.06
Riverside	342334	4181	1.22	65499	19.13	182615	53.34	236900	69.20
Seattle	390372	503	0.13	22333	5.72	72979	18.69	123054	31.52
St. Louis	358747	4316	1.20	55833	15.56	117743	32.82	172535	48.09
PROXIMITY TO PM_{2.5} MONITORS									
Atlanta	362201	1757	0.49	36772	10.15	136179	37.60	207122	57.18
Birmingham	145905	1619	1.11	29952	20.53	84223	57.72	106488	72.98
Boston	945790	18821	1.99	224628	23.75	438920	46.41	606231	64.10
Chicago	1018983	18539	1.82	348656	34.22	713194	69.99	883112	86.67
Denver	232974	3891	1.67	59625	25.59	140523	60.32	196361	84.28
Detroit	626216	5765	0.92	138672	22.14	345808	55.22	469462	74.97
Houston	377586	1010	0.27	14911	3.95	66741	17.68	117661	31.16
Los Angeles	1207436	9653	0.80	229893	19.04	688844	57.05	984889	81.57

Proximity to PM Monitors ^b									
New York	2710675	78918	2.91	921599	34.00	1619177	59.73	2048842	75.58
Philadelphia	834110	13323	1.60	251459	30.15	487003	58.39	605663	72.61
Phoenix	388150	2738	0.71	39833	10.26	90304	23.27	142084	36.61
Pittsburgh	449544	8933	1.99	111050	24.70	249269	55.45	347711	77.35
Riverside	342334	3024	0.88	50901	14.87	129836	37.93	170933	49.93
Seattle	390372	1721	0.44	29429	7.54	101223	25.93	156562	40.11
St. Louis	358747	5401	1.51	83528	23.28	192532	53.67	244929	68.27

^aBased on 2000 population totals.

^bPercentages are given with respect to the total population per city provided.

Table 3-6. Proximity to PM₁₀ and PM_{2.5} monitors based on the population identified as white, black, Hispanic, or non-Hispanic^a. The figures presented here are cumulative for the 15 CSAs/CBSAs examined in Chapter 3.

Proximity to PM Monitors ^b									
Race or Hispanic Origin	Total CSA/CBSA	≤ 1 km		≤ 5 km		≤ 10 km		≤ 15 km	
	N	N	%	N	%	N	%	N	%
PROXIMITY TO PM₁₀ MONITORS									
White	61936855	325771	0.53	5554906	8.97	14041215	22.67	21913907	35.38
Black	12668004	134174	1.06	1611263	12.72	3867436	30.53	6020348	47.52
Hispanic	15916208	169305	1.06	2496959	15.69	5905322	37.10	8589819	53.97
Non-Hispanic	74611962	421917	0.57	6767187	9.07	17261734	23.14	27254421	36.53
PROXIMITY TO PM_{2.5} MONITORS									
White	61936855	863823	1.39	12257978	19.79	27553900	44.49	39030037	63.02
Black	12668004	320447	2.53	4780620	37.74	9241172	72.95	10906346	86.09
Hispanic	15916208	445126	2.80	5782482	36.33	10661947	66.99	13094618	82.27
Non-Hispanic	74611962	1135999	1.52	16553574	22.19	36318474	48.68	49629054	66.52

^aBased on 2000 population totals

^bPercentages are given with respect to the total population per city provided.

Socioeconomic Status

1 Table 3-7 shows the percent of the population below and above the poverty level and
2 the percent of the population over age 25 with less than high school, high school or more,
3 and college graduate education levels that reside within 1 km, 5 km, 10 km, and 15 km of a
4 PM₁₀ and PM_{2.5} monitor cumulatively across the fifteen CSAs/CBSAs for which PM
5 concentration data were examined. For PM₁₀, 47% of the population below the poverty level
6 and 45% of the population with less than a high school education are within 15 km of a
7 monitor, whereas the percentage of those above the poverty line (39%), those with a high

1 school or more education (38%), and those with a college education (35%) were slightly less.
 2 For PM_{2.5}, 80% of the population below poverty level and 77% of the population with less
 3 than high school education are within 15 km of a monitor for the fifteen CSAs/CBSAs
 4 studied. Again, populations of those above the poverty line, those with a high school or more
 5 education, and those with a college education within 15 km of a monitor were less than the
 6 low SES groups (67% for each). Higher percentages of individual SES subpopulations
 7 within PM_{2.5} monitors likely reflect the fact that more PM_{2.5} monitors are currently
 8 deployed within 15 CSAs/CBSAs studied compared with PM₁₀ monitors. Lower SES groups
 9 are not shown to be well-represented at the neighborhood scale, with 1.2% of the population
 10 below the poverty level and 1.0% of the population with less than a high school education
 11 residing within 1 km of a PM₁₀ monitor. Likewise, 3.1% of the population below the poverty
 12 level and 2.4% of the population with less than high school education reside within 1 km of
 13 a PM_{2.5} monitor. However, the populations of low SES groups are more represented at the
 14 neighborhood scale than those for higher SES groups. For example, only about 1.5-1.7% of
 15 those above the poverty line, those with a high school or more education, or those with a
 16 college education are within 1 km of a PM_{2.5} monitor. Moreover, it is notable that at any
 17 scale shown in Table 3-7 and for both PM₁₀ and PM_{2.5}, those living under the poverty line
 18 and those with less than high school education have greater representation by the monitors
 19 than those above the poverty line or those age 25 and older with high school or college
 20 education.

Table 3-7. Proximity to PM₁₀ and PM_{2.5} monitors based on the population below or above the poverty line, population over age 25 with less than high school education, population over 25 with high school education, and population over 25 with college education or more^a. The figures presented here are cumulative for the 15 CSAs/CBSAs examined in Chapter 3.

SES	Total CSA/CBSA	Proximity to PM Monitors ^b							
		≤ 1 km		≤ 5 km		≤ 10 km		≤ 15 km	
		N	%	N	%	N	%	N	%
PROXIMITY TO PM₁₀ MONITORS									
Below poverty line	10645411	132979	1.25	1626694	15.28	3504957	32.92	5024714	47.20
Above poverty line	85551420	485874	0.57	8171398	9.55	21096615	24.66	33034279	38.61
Less than HS education	11606042	112901	0.97	1544594	13.31	3537414	30.48	5186441	44.69

Proximity to PM Monitors^b									
HS education	30583598	185439	0.61	2975200	9.73	7580000	24.78	11747653	38.41
College education	16433811	59892	0.36	1229885	7.48	3447148	20.98	5722347	34.82
<i>PROXIMITY TO PM_{2.5} MONITORS</i>									
Below poverty line	10645411	330970	3.11	3951549	37.12	7107192	66.76	8528731	80.12
Above poverty line	85551420	1297591	1.52	19094985	22.32	41736460	48.79	57070312	66.71
Less than HS education	11606042	276942	2.39	3806208	32.80	7225291	62.25	8930174	76.94
HS education	30583598	444262	1.45	6940261	22.69	15152047	49.54	20489904	67.00
College education	16433811	280810	1.71	3451717	21.00	7776218	47.32	11000917	66.94

^aBased on 2000 population totals

^bPercentages are given with respect to the total population per city provided.

3.5. Ambient PM Concentrations

1 This section describes measurements of ambient PM mass concentration and
 2 composition made since the 2004 PM AQCD (U.S. EPA, 2004, [056905](#)) including analyses
 3 using EPA Air Quality System (AQS) data as well as published findings. Emphasis is placed
 4 on the period from 2005-2007 which incorporates the most recent validated AQS data
 5 available at the time this document was prepared.

6 When the 2004 PM AQCD was written, the full nationwide PM_{2.5} compliance
 7 monitoring network had only recently been deployed, providing three years (1999 to 2001)
 8 of completed measurements. Based on observations from these first three years, the 2004
 9 PM AQCD found that PM_{2.5} in eastern cities was generally more highly correlated across
 10 monitoring sites than in western cities. The higher spatial correlations in the eastern cities
 11 resulted from the more regionally dispersed sources of PM_{2.5} in the East. Although PM_{2.5}
 12 concentrations at sites within an urban area can be highly correlated, significant
 13 differences in concentrations can occur on any given day. The ratio of PM_{2.5} to PM₁₀ was
 14 found to be higher in the East than in the West in general, and values for this ratio are
 15 consistent with those found in numerous earlier studies presented in the 1996 PM AQCD
 16 (U.S. EPA, 1996, [079380](#)). Differences in the composition of PM_{2.5} between eastern and
 17 western cities were also found to be consistent with differences found in the 1996 PM
 18 AQCD. Much more limited data were available for describing the spatial variability of
 19 coarse particulate mass measured as PM_{10-2.5}, ultrafine PM, and PM composition. The 2004
 20 AQCD noted that components produced by area (e.g., traffic) and point sources are more

1 spatially variable than regionally dispersed components (e.g., secondary SO_4^{2-}). Spatial
2 variability will affect estimates of community-scale human exposure and caution should be
3 exercised in extrapolating conclusions from one area to another, particularly on a regional
4 scale.

5 For this PM ISA, the $\text{PM}_{2.5}$ monitoring network has been active for eight or nine years
6 depending on location. Observations and analyses based on $\text{PM}_{2.5}$ measurements reported
7 to AQS are included in this chapter. Furthermore, by selecting locations where PM_{10} and
8 $\text{PM}_{2.5}$ measurements are co-located, information about the spatiotemporal distribution of the
9 $\text{PM}_{10-2.5}$ size fraction is investigated. Given the form of the current standard and the relative
10 abundance of PM_{10} monitors in the AQS network, PM_{10} mass concentrations are also
11 included in this section with the understanding that PM_{10} includes mass contributions from
12 the smaller size fractions and therefore overlaps with $\text{PM}_{2.5}$, $\text{PM}_{10-2.5}$ and ultrafine particle
13 mass concentrations. Although compliance monitoring does not apply for ultrafine particles
14 because there is no ambient standard for them, new observational information is available
15 from detailed studies in several cities. Similarly, advancements have been made in
16 understanding PM composition from the CSN and IMPROVE networks. Descriptions of
17 ultrafine particles and speciated PM are covered where information is available.

18 Unless otherwise specified, the $\text{PM}_{2.5}$, $\text{PM}_{10-2.5}$ and PM_{10} data utilized in this
19 section comes from the AQS. Based on the population and exposure requirements for
20 monitor siting of 40 CFR Part 58 described in Section 3.4.2, monitors reporting to the AQS
21 are not uniformly distributed across the U.S. Monitors are far more abundant in urban
22 areas than rural ones, so actual rural spatiotemporal distributions may differ considerably
23 from those reported here. Furthermore, biases exist for some PM constituents (and hence,
24 total mass) owing to volatilization losses of NO_3^- and other semi-volatile compounds and,
25 conversely, retention of particle-bound water with hygroscopic species. The magnitude of
26 these effects is likely to be region-specific.

27 Spatial distributions of PM across a range of geographic scales are covered in
28 Section 3.5.1. Temporal behavior including trends, seasonality and hourly variability are
29 covered in Section 3.5.2. The section ends with statistical associations between different
30 size fractions of PM and copollutants including CO , NO_2 , O_3 and SO_2 in Section 3.5.3.

3.5.1. Spatial Distribution

1 Spatial scales of interest for PM range from global and continental scales (>1000 km)
2 down to micro scale (~5-100m). Variation in PM concentration depends on the spatial scale
3 and magnitude of PM sources, formation and removal mechanisms, and transport and
4 dispersion of PM. These different sources and processes can cause substantial variation in
5 particle size distribution and chemistry. This section addresses the spatial variability of PM
6 by focusing primarily on AQS data across three different scales: variability across the U.S.,
7 urban-scale variability and neighborhood-scale variability. These sections are further
8 subdivided to the extent possible into PM size fractions and composition.

3.5.1.1. Variability across the U.S.

PM_{2.5}

9 Figure 3-9 shows the three-yr mean of the 24-h PM_{2.5} concentrations by county across
10 the U.S. for 2005-2007. The data used in generating this map are from the AQS database
11 after applying a completeness criterion of 75% per quarter (or 11 out of 15 quarterly
12 measurements for a one-in-six-day sampling schedule). Counties shown in white did not
13 contain sufficient PM_{2.5} data meeting the completeness criterion for inclusion. Of the 3,225
14 U.S. counties, 540 (17%) had PM_{2.5} data meeting the completeness criterion in all three
15 years (2005-2007) and have been included in Figure 3-9. These 540 counties represent
16 roughly 63% of the U.S. population. The fraction of the population residing within each
17 county-average concentration range is shown on the left-hand margin of the figure. Given
18 the number of counties with no data, the varying size of counties, and the non-uniform
19 spacing of the monitors and population within each reporting county, this should only be
20 taken as a rough estimate of the relationship between population and average ambient
21 concentrations. Kern County, CA reported the highest 3-yr avg 24-h PM_{2.5} concentration in
22 excess of 20 µg/m³. Average concentrations between 18 and 20 µg/m³ were reported for
23 several counties in the San Joaquin Valley and inland southern California as well as
24 Jefferson County, AL containing Birmingham and Allegheny County, PA containing
25 Pittsburgh.

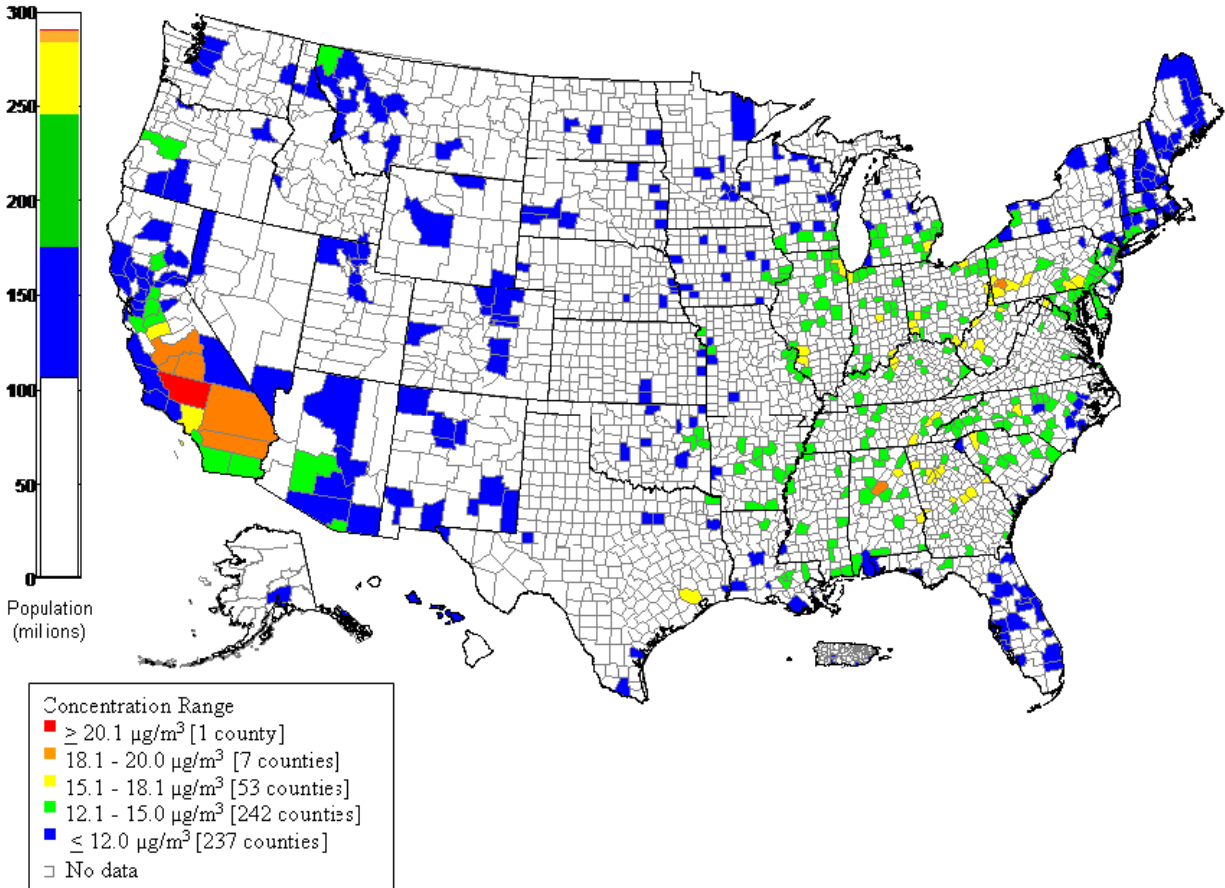


Figure 3-9. Three-yr avg 24-h $\text{PM}_{2.5}$ concentration by county derived from FRM or FRM-like data, 2005-2007. The population bar shows the number of people residing within counties that reported county-wide average concentrations within the specified ranges.

1 Table 3-8 contains summary statistics for $\text{PM}_{2.5}$ reported to AQS for the period 2005-
 2 2007. All 24-h FRM and 1-h FRM-like¹ data reported to AQS and meeting the completeness
 3 criterion outlined above are included in the table. The table provides a distributional
 4 comparison between annual, 24-h and 1-h averaging times, calendar years (2005, 2006 and

¹ FRM-like refers to $\text{PM}_{2.5}$ concentration data associated with the parameter code “88502 - Acceptable $\text{PM}_{2.5}$ AQI and Speciation Mass” in the EPA Air Quality System. These data were collected by continuous instruments which are not approved as FRM or FEM, and consequently EPA does not use these data for regulatory purposes. These data are denoted as “FRM-like” because state and local monitoring agencies have individually decided that the continuous instruments reporting these data have a degree of agreement with FRM/FEM methods that is sufficient in their opinion for the data to be used in public advisories regarding current air quality. In some cases, these data include statistical adjustments by the state/local monitoring agency based on one-time or ongoing correlation analysis with co-located FRM/FEM monitors, intended to improve the “FRM-likeness” of the continuous concentration data (see, for example, Bortnick et al. (2002, 156285) State/local monitoring agency decisions about whether to adjust continuous $\text{PM}_{2.5}$ data and whether their raw or adjusted continuous $\text{PM}_{2.5}$ data should be associated with parameter code 88502 were informed by non-binding EPA guidance issued in 2006 (Technical Note on Reporting $\text{PM}_{2.5}$ Continuous Monitoring and Speciation Data to AQS <http://www.epa.gov/ttn/amtic/files/ambient/pm25/datamang/contrept.pdf>).

1 2007) and seasons: winter (December-February), spring (March-May), summer
2 (June-August), and fall (September-November). In addition, fifteen CSAs/CBSAs were
3 chosen for their importance in recent PM health studies, as described in Section 3.4, and
4 have been included individually in the table.

5 The distribution of PM_{2.5} annual averages—calculated without seasonal weighting
6 and presented in Table 3-8—was generated from 2382 individual annual means reported by
7 794 24-h FRM monitors reporting to AQS between 2005 and 2007. The mean of the annual
8 averages was 12 µg/m³, equivalent to the mean of the individual 24-h avg. The maximum
9 annual average PM_{2.5} concentration calculated from 24-h FRM data over these three years
10 was 23 µg/m³ in Bakersfield, CA (AQS monitor ID: 060290010) during 2007. This site is
11 located in the heavily populated portion of the San Joaquin Valley where air pollution
12 frequently becomes trapped at ground level due to local topography. The distribution of the
13 24-h and 1-h avg, both generated from the same 1-h FRM-like data, are comparable up to
14 the 90th percentile. The 1-h avg is 3 µg/m³ higher than the 24-h avg at the 95th percentile
15 and 7 µg/m³ higher at the 99th percentile. This deviation between 1-h and 24-h averaging
16 times is a result of short duration spikes in PM_{2.5} mass lasting long enough to influence the
17 upper percentiles of the 1-h distribution but not the 24-h avg distribution. Exceptional
18 events were not removed from this data set and are responsible for at least some of the
19 higher concentrations observed. For example, the maximum 1-h reading of 828 µg/m³ was
20 reported by a monitor in Boise, ID (AQS monitor ID: 160010011) on July 4, 2007. Nine of
21 the top 12 1-h PM_{2.5} concentrations reported across the country also occurred on July 4th,
22 implicating fireworks as the common source for these high values.

23 The distribution of the 24-h FRM PM_{2.5} data was similar across the three years (2005-
24 2007) investigated. Summer (June-August) had the highest mean and median relative to
25 other seasons, but only by a small margin. At the 99th percentile, winter (December-
26 February) was slightly higher than the other seasons. This is consistent with wintertime
27 stagnation events resulting in short-term elevated PM_{2.5} concentrations. Of the 15
28 CSAs/CBSAs investigated, the highest mean of 24-h PM_{2.5} concentrations was reported for
29 Riverside (17 µg/m³), Birmingham (16 µg/m³) and Pittsburgh (16 µg/m³); the lowest was
30 reported for Denver (9 µg/m³) and Seattle (9 µg/m³).

Table 3-8. PM_{2.5} distributions derived from AQS data (concentration in µg/m³).

	n	Mean	Percentiles									Max
			1	5	10	25	50	75	90	95	99	
2005-2007 PM_{2.5} FOR DIFFERENT AVERAGING PERIODS												
Annual avg ^a (24-h FRM)	2382	12	5	7	8	10	12	14	16	17	19	23
24-h avg (24-h FRM)	349,028	12	2	4	4	7	10	16	23	28	39	193
24-h avg (1-h FRM-like)	183,057	10	1	2	3	5	8	13	19	24	35	126
1-h avg (1-h FRM-like)	4,403,817	10	0	1	2	4	8	13	21	27	42	828
PM_{2.5} ANNUAL AND SEASONAL STRATIFICATION USING 24-H AVG FRM DATA												
2005	114,346	13	2	4	5	7	11	17	24	30	42	133
2006	113,197	12	2	4	4	7	10	15	21	26	36	193
2007	121,485	12	2	4	4	7	10	16	22	27	40	145
Winter (December-February)	86,286	12	2	4	5	7	10	15	22	27	44	193
Spring (March-May)	88,489	11	2	3	4	6	9	14	20	24	33	145
Summer (June-August)	86,830	14	2	4	5	8	12	19	26	31	40	133
Fall (September-November)	87,423	12	2	3	4	6	10	15	22	26	39	126
2005-2007 PM_{2.5} IN INDIVIDUAL CSAS/CBSAS USING 24-H AVG FRM DATA												
Atlanta	4,939	15	4	6	7	10	14	19	25	29	37	145
Birmingham	4,869	16	4	6	7	10	15	21	29	34	47	64
Boston	8,464	10	2	3	4	5	9	13	20	24	32	50
Chicago	10,308	14	3	4	6	8	13	18	25	31	42	65
Denver	4,192	9	2	3	4	6	8	10	14	18	31	61
Detroit	5,223	14	2	3	5	7	12	19	26	31	45	82
Houston	1,342	15	4	6	8	10	14	18	23	26	34	44
Los Angeles	6,600	15	3	5	6	9	13	18	25	32	50	133
New York	15,826	13	2	4	4	6	10	17	24	29	39	58
Philadelphia	7,541	14	3	4	5	8	12	18	25	30	38	63
Phoenix	1,634	10	2	3	4	6	9	12	17	21	32	77
Pittsburgh	5,783	16	3	5	6	9	13	20	29	36	52	101
Riverside	2,751	17	3	5	6	10	14	21	31	40	58	106
Seattle	1,297	9	2	3	3	4	7	10	20	29	43	68
St. Louis	6,887	14	3	5	6	9	13	18	24	29	40	50
All 15 CSAs/CBSAs	87,656	14	2	4	5	7	12	17	25	30	42	145
Not in the 15 CSAs/CBSAs	261,372	12	2	3	4	6	10	15	22	27	38	193

^aStraight annual average without quarterly weighting.

PM_{10-2.5}

- 1 Since PM_{10-2.5} is not routinely measured and reported to AQS, co-located PM₁₀ and
- 2 PM_{2.5} measurements from the AQS network were used to investigate the spatial
- 3 distribution in PM_{10-2.5}. Only low-volume FRM or FRM-like samplers were considered in

1 calculating $PM_{10-2.5}$ to avoid complications with vastly different sampling protocols (e.g.,
2 flow rates) between the independent PM_{10} and $PM_{2.5}$ measurements. The same 11+ days per
3 quarter completeness criterion discussed above was applied to the PM_{10} and $PM_{2.5}$
4 measurements. The $PM_{2.5}$ concentrations are reported to AQS at local conditions whereas
5 the PM_{10} concentrations are reported at standard conditions. Therefore, prior to calculating
6 $PM_{10-2.5}$ by subtraction, the PM_{10} AQS data were adjusted to local conditions on a daily basis
7 using temperature and pressure measurements from the nearest National Weather Service
8 station. Figure 3-10 shows the three-yr mean of the 24-h $PM_{10-2.5}$ concentration by county
9 across the U.S. for 2005-2007. There is considerably less coverage than for $PM_{2.5}$ or PM_{10}
10 alone since only a small subset of PM monitors are co-located and low-volume. The 40
11 counties included in Figure 3-10 incorporate less than 5% of the U.S. population. Of the
12 3,225 U.S. counties, only 40 (1%) met the completeness and co-location criteria in all three
13 years (2005-2007), and therefore the available measurements do not provide sufficient
14 information to adequately characterize regional-scale coarse PM spatial concentration
15 distributions.

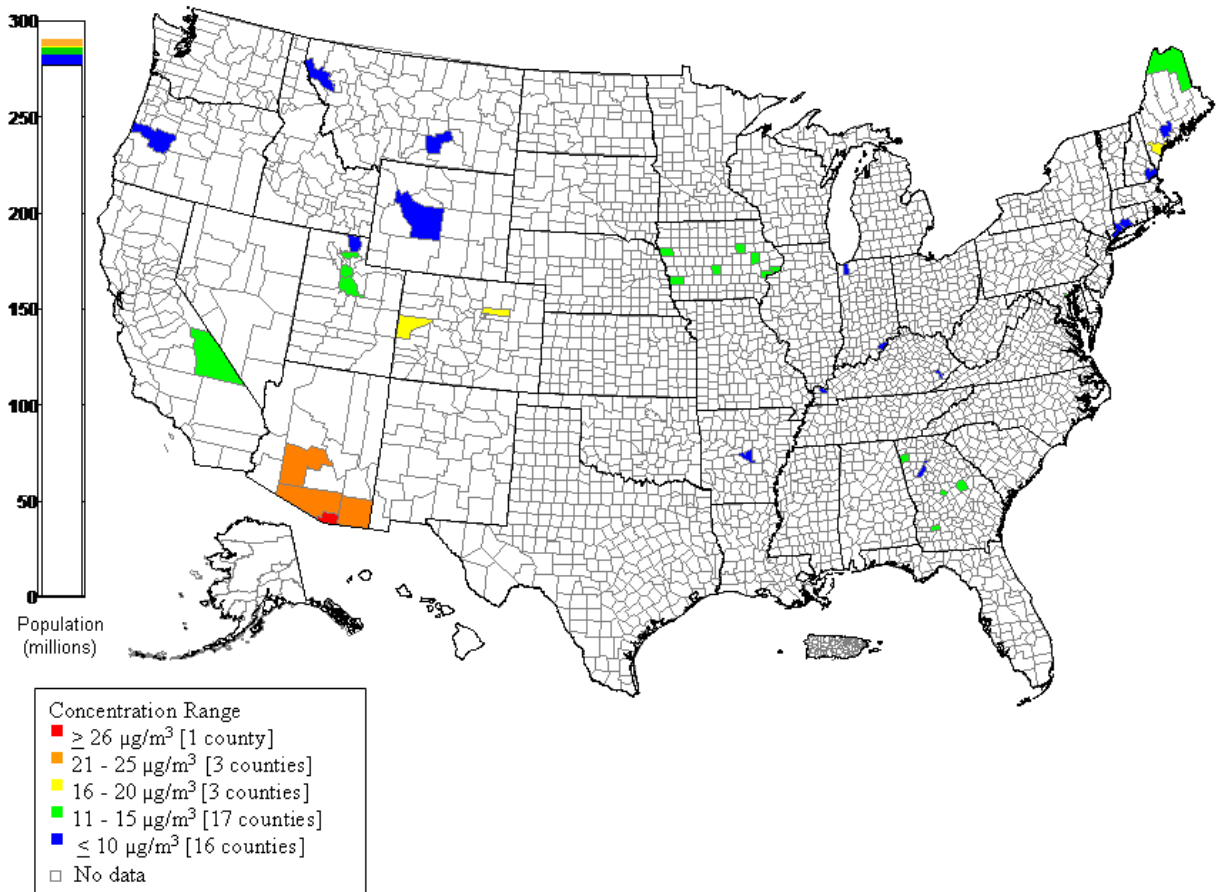


Figure 3-10. Three-yr avg 24-h $\text{PM}_{10-2.5}$ concentration by county derived from co-located low volume FRM PM_{10} and $\text{PM}_{2.5}$ monitors, 2005-2007. The population bar shows the number of people residing within counties that reported county-wide average concentrations within the specified ranges.

1 Table 3-9 contains summary statistics for $\text{PM}_{10-2.5}$ for the period 2005-2007 similar to
 2 those reported in Table 3-8 for $\text{PM}_{2.5}$. Only six of the 15 CSAs/CBSAs had sufficient data for
 3 inclusion in Table 3-9. Although fewer monitoring sites within these CSAs/CBSAs were
 4 used for $\text{PM}_{10-2.5}$ than for $\text{PM}_{2.5}$, Table 3-8 and 3-9 provide a rough comparison of the PM
 5 present in the fine and thoracic coarse modes for these six cities. The eastern cities
 6 including Atlanta, Boston, Chicago and New York all had a higher fraction in the fine mode
 7 with the greatest ratio of fine to thoracic coarse in Chicago ($14 \mu\text{g}/\text{m}^3 \text{PM}_{2.5}$, $5 \mu\text{g}/\text{m}^3 \text{PM}_{10-2.5}$,
 8 ratio = 2.8). In contrast, Denver ($9 \mu\text{g}/\text{m}^3 \text{PM}_{2.5}$, $20 \mu\text{g}/\text{m}^3 \text{PM}_{10-2.5}$, ratio = 0.45) and Phoenix
 9 ($10 \mu\text{g}/\text{m}^3 \text{PM}_{2.5}$, $22 \mu\text{g}/\text{m}^3 \text{PM}_{10-2.5}$, ratio = 0.45) had a higher fraction in the thoracic coarse
 10 mode. Given the limited information available from AQS for $\text{PM}_{10-2.5}$ and the current
 11 National Ambient Air Quality Standard for PM_{10} , the next section characterizes the more

1 prevalent PM₁₀ data, acknowledging that PM₁₀ incorporates both thoracic coarse and fine
 2 particles.

Table 3-9. PM_{10-2.5} distributions derived from AQS data (concentration in µg/m³).

	n	Mean	Percentiles									Max
			1	5	10	25	50	75	90	95	99	
2005-2007 PM_{10-2.5} FOR DIFFERENT AVERAGING PERIODS												
Annual avg ^a (low volume FRM)	130	12	3	5	6	9	11	14	19	23	39	43
24-h avg (low volume FRM)	12,027	13	-3	1	2	6	10	17	26	33	54	246
PM_{10-2.5} ANNUAL AND SEASONAL STRATIFICATION USING 24-H AVG LOW VOLUME FRM DATA												
2005	3,990	12	-5	0	2	5	10	16	26	33	52	246
2006	4,037	13	-2	1	2	6	10	17	27	34	56	182
2007	4,000	13	-2	1	3	6	11	18	26	33	56	148
Winter (December-February)	2,942	11	-5	-1	1	4	8	15	27	34	56	246
Spring (March-May)	3,088	13	-2	1	2	5	10	17	26	33	62	151
Summer (June-August)	2,968	14	-2	3	5	8	12	18	25	31	44	93
Fall (September-November)	3,029	14	-2	1	3	6	11	18	28	34	60	148
2005-2007 PM_{10-2.5} IN INDIVIDUAL CSAS/CBSAS USING 24-H AVG LOW VOLUME FRM DATA^b												
Atlanta	167	10	-4	1	2	5	9	13	18	21	30	46
Boston	340	7	-2	1	2	4	6	9	12	16	25	27
Chicago	161	5	-8	-4	-3	1	4	8	14	19	37	37
Denver	353	20	0	4	6	11	19	28	36	42	59	78
New York	338	9	-16	-2	1	5	8	12	17	23	34	56
Phoenix	163	22	-3	8	11	16	20	29	35	46	67	70
All 6 CSAs/CBSAs	1,522	12	-6	0	2	5	10	17	27	34	51	78
Not in the 6 CSAs/CBSAs	10,505	13	-2	1	2	6	10	17	26	33	56	246

^aStraight annual average without quarterly weighting.

^bNo co-located FRM PM₁₀ and FRM-like PM_{2.5} monitors present in Birmingham, Detroit, Houston, Los Angeles, Philadelphia, Pittsburgh, Riverside, Seattle or St. Louis.

PM₁₀

3 Figure 3-11 shows the 3-yr mean of the 24-h PM₁₀ concentrations by county across the
 4 U.S. for 2005-2007. Both FRM and FEM PM₁₀ data reported to AQS were included and the
 5 same 11+ days per quarter completeness criterion described above for PM_{2.5} was applied.
 6 The highest 3-yr avg for PM₁₀ (>50 µg/m³) occurred in inland southern California and the
 7 populous counties of southern Arizona and central New Mexico. Of the 3,225 U.S. counties,
 8 676 (12%) contained PM₁₀ data meeting the completeness criterion in all three years; these
 9 676 counties incorporate approximately 43% of the U.S. population.

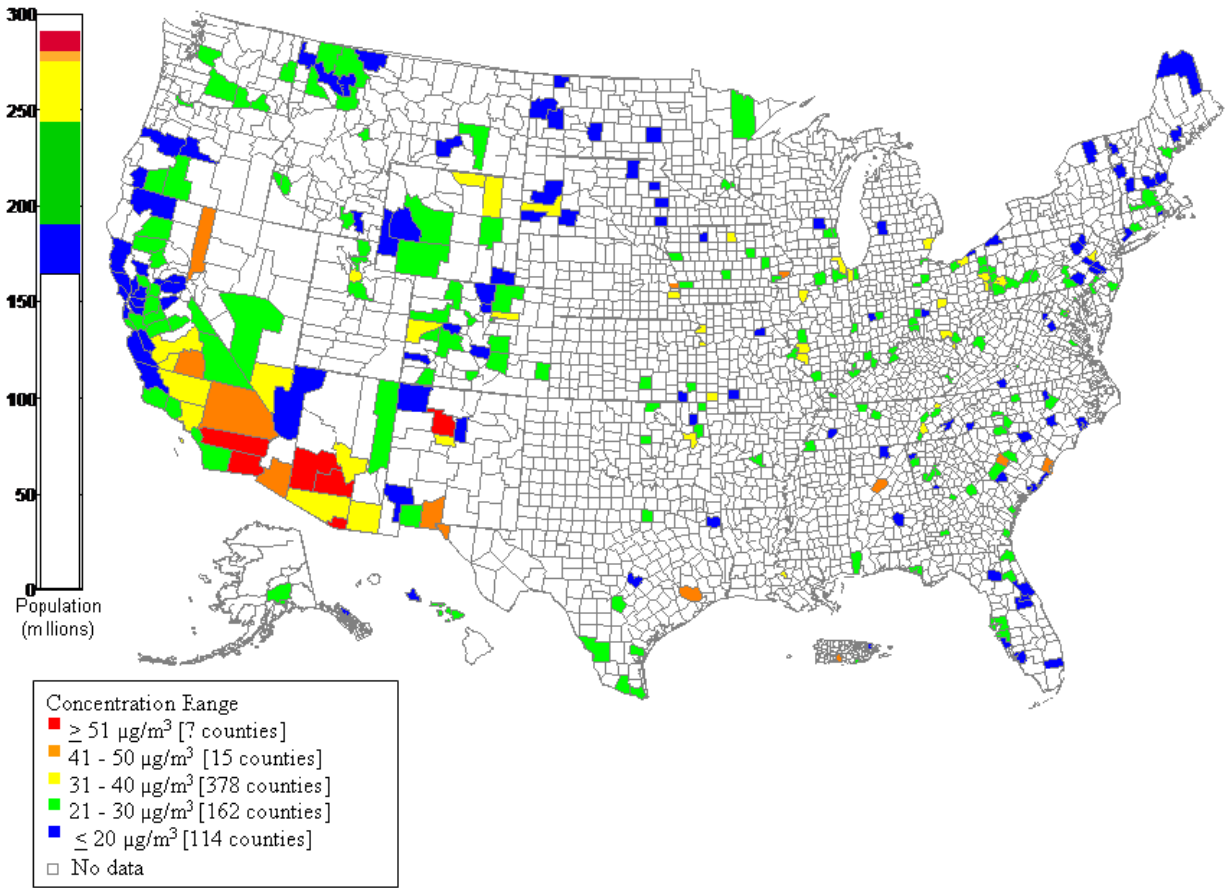


Figure 3-11. Three-yr avg 24-h PM₁₀ concentration by county derived from FRM or FEM monitors, 2005-2007. The population bar shows the number of people residing within counties that reported county-wide average concentrations within the specified ranges.

1 Table 3-10 contains summary statistics for PM₁₀ reported to AQS for the period 2005-
 2 2007. Both 24-h FRM and 1-h FEM data are included in the table. To facilitate a
 3 distributional comparison between averaging times, annual, 24-h and 1-h averaging times
 4 using the FRM and FEM data have been included separately in Table 3-10. As in the earlier
 5 tables, the data is also stratified by year and season and includes the 15 CSAs/CBSAs
 6 individually.

Table 3-10. PM₁₀ distributions derived from AQS data (concentration in µg/m³).

	n	Mean	Percentiles										Max
			1	5	10	25	50	75	90	95	99		
2005-2007 PM₁₀ FOR DIFFERENT AVERAGING PERIODS													
Annual avg ^a (24-h FRM and 1-h FEM)	2022	25	10	14	16	19	23	28	35	44	60	85	
24-h avg (24-h FRM and 1-h FEM)	326,675	26	3	6	9	14	21	32	46	59	97	8299	
24-h avg (24-h FRM)	167,310	25	2	6	9	14	21	31	45	57	91	8299	
24-h avg (1-h FEM)	156,931	26	4	7	9	14	21	32	48	62	105	979	
1-h avg (1-h FEM)	3,767,533	27	1	4	6	11	19	32	51	69	145	8540	
PM₁₀ ANNUAL AND SEASONAL STRATIFICATION USING 24-H AVG FRM AND FEM DATA													
2005	107,524	25	2	6	9	13	21	31	46	58	93	1441	
2006	109,505	26	3	6	9	13	21	32	46	59	101	8299	
2007	109,646	26	4	7	9	14	21	32	47	60	99	2253	
Winter (December-February)	80,959	23	2	5	7	11	17	27	42	57	99	8299	
Spring (March-May)	82,772	25	2	6	8	13	20	31	45	58	96	2253	
Summer (June-August)	81,351	29	6	10	12	18	25	35	49	60	92	1839	
Fall (September-November)	81,593	26	3	7	9	14	21	32	48	62	102	1212	
2005-2007 PM₁₀ IN INDIVIDUAL CSAS/CBSAS USING 24-H AVG FRM AND FEM DATA													
Atlanta	1,868	24	6	9	11	16	23	31	39	44	57	108	
Birmingham	5,478	34	6	9	12	19	28	43	64	82	120	241	
Boston	1,412	17	2	5	7	10	15	22	30	36	50	58	
Chicago	6,165	26	6	9	11	16	23	32	45	55	78	214	
Denver	4,706	28	5	10	12	18	25	35	47	54	75	118	
Detroit	1,407	30	7	10	12	18	26	38	53	64	81	182	
Houston	1,397	31	7	10	12	17	23	34	56	80	137	248	
Los Angeles	2,020	27	4	8	11	18	25	33	42	51	74	489	
New York	514	19	2	6	7	11	17	25	35	40	51	83	
Philadelphia	4,207	19	4	7	9	12	17	24	34	40	52	84	
Phoenix	12,005	52	7	14	19	29	44	65	91	112	166	2253	
Pittsburgh	12,677	24	4	7	9	13	19	31	45	57	83	157	
Riverside	4,327	35	4	8	11	19	30	45	64	75	111	1212	
Seattle	2,136	19	5	7	9	12	17	23	31	37	52	79	
St. Louis	2,464	33	6	10	12	18	28	42	59	74	114	315	
All 15 CSAs/CBSAs	62,783	32	5	8	10	16	25	39	60	77	120	2253	
Not in the 15 CSAs/CBSAs	263,892	24	2	6	8	13	20	30	43	54	88	8299	

^aStraight annual average without quarterly weighting

1 The maximum annual average PM₁₀ concentration calculated from 24-h FRM data
 2 over these three years was 85 µg/m³ in Stanfield, AZ (AQS monitor ID: 040213008) during
 3 2007. Stanfield is a small agricultural town (2007 population = 1074) approximately 64 km
 4 south of Phoenix and is in a region heavily influenced by windblown dust. Many of the

1 maximum 24-h and 1-h avg PM₁₀ concentrations in Table 3-10 exceed 1,000 µg/m³, but
2 these represent rare events given the much lower 99th percentiles. Exceptional events were
3 not removed from this data set and are responsible for at least some of the higher
4 concentrations observed.

5 The distribution of the 24-h FRM and FEM PM₁₀ data was similar across the three
6 years (2005-2007) investigated. Summer (June-August) had the highest mean and median
7 relative to other seasons, consistent with PM_{2.5} observations. Of the 15 CSAs/CBSAs
8 investigated, the highest mean of 24-h PM₁₀ concentrations was reported for Phoenix (52
9 µg/m³), considerably higher than the means for the other CSAs/CBSAs investigated. The
10 lowest was reported for Boston (17 µg/m³) with New York, Philadelphia and Seattle only
11 slightly higher (19 µg/m³).

12 On average using the 2005-2007 data for PM_{2.5} in Table 3-8 and PM₁₀ in Table 3-10,
13 the distribution between fine and coarse PM varies substantially by location. A larger
14 fraction of PM mass is present in the thoracic coarse mode in Phoenix and Denver (3-yr
15 mean PM_{2.5}/PM₁₀ ratios of 0.19 and 0.32, respectively). In contrast, a larger fraction is
16 present in the fine mode in Philadelphia (0.74), New York (0.68) and Pittsburgh (0.67).
17 Comparisons of PM_{2.5} to PM₁₀ as reported to AQS should be used with caution, however,
18 since PM_{2.5} concentrations are reported for local conditions while PM₁₀ concentrations are
19 converted to STP before reporting. Nevertheless, these findings are consistent with those in
20 Table 3-9 for PM_{10-2.5} in the subset of 6 cities with available co-located low-volume PM data
21 that have been properly adjusted for temperature and pressure. These findings are also
22 consistent with those reported in the previous PM AQCD (U.S. EPA, 2004, [056905](#)) where
23 ratios of PM_{2.5} to PM₁₀ were observed to be highest in the northeast (0.70), southeast (0.70),
24 and industrial Midwest (0.70) and lower in the upper Midwest (0.53), northwest (0.50),
25 southern California (0.47) and southwest (0.38).

Ultrafine Particles

26 Little is known about the spatiotemporal distribution or composition of ultrafine
27 particles on a regional scale. New particle formation has been observed in environments
28 ranging from relatively unpolluted marine and continental environments to polluted urban
29 areas as an ongoing background process and during nucleation events (Kulmala et al.,
30 2004, [089159](#)). During nucleation events, which may last for several hours, ultrafine
31 particle number concentrations can exceed 10⁴ cm³ over distances of several hundred

1 kilometers (Kulmala et al., 2004, [089159](#); Qian et al., 2007, [116435](#)). These events occur
2 throughout the year on 5-40% of days, depending on location (Qian et al., 2007, [116435](#)).
3 Cloud condensation nuclei, with diameters between 10 and ~100 nm have been monitored
4 for several years at a number of nonurban sites in the U.S.
5 (<http://cmdl.noaa.gov/aero/data/>). Average particle number counts at these sites in the U.S.
6 range from several hundred to several thousand per cm³. The particles are formed by
7 nucleation of atmospheric gases with a secondary contribution from primary emissions in
8 these environments (Pierce and Adams, 2009, [191189](#)).

9 In an urban setting, a large percentage of ultrafine particles come from combustion-
10 related emissions from mobile sources (Sioutas et al., 2005, [088428](#)). Ultrafine particle
11 number concentrations drop off quickly with distance from the roadway (Reponen et al.,
12 2003, [088425](#); Zhu et al., 2005, [157191](#); Levy et al., 2003, [052661](#)), and therefore
13 concentrations can be highly heterogeneous in the near-road environment depending on
14 traffic, meteorological and topographic conditions (Baldauf et al., 2008, [190239](#)). Studies
15 characterizing spatial variability in ultrafine particles are currently limited to a handful of
16 close proximity locations and therefore are discussed in Sections 3.5.1.2 and 3.5.1.3 in the
17 context of urban- and neighborhood-scale variability. Further elaboration on the
18 composition of ultrafine particles is included below.

PM Constituents

19 Only PM_{2.5} is collected routinely at CSN network sites so the majority of this
20 section on PM constituents is devoted to PM_{2.5}. PM_{10-2.5} and ultrafine PM composition is
21 discussed to the extent possible below. Figures 3-12 through 3-16 contain U.S.
22 concentration maps for OC, EC, SO₄²⁻, NO₃⁻, and NH₄⁺ mass from PM_{2.5} measurements
23 taken as part of the CSN network for the period 2005-2007. Data used in these figures are
24 as reported to AQS: no correction was applied to OC for non-carbon mass and NO₃⁻
25 represents total particulate NO₃⁻. Figure 3-12 shows regions of high PM_{2.5} OC mass
26 concentration with annual average concentrations greater than 5 µg/m³ in the western and
27 the southeastern U.S. Concentrations at the western monitors peak in the fall and winter
28 while those in the Southeast peak anywhere from spring through fall. The central and
29 northeastern portions of the U.S. generally contain lower measured OC. Bell et al. (2007,
30 [155683](#)) present a similar map for estimated organic carbon mass (OCM) from 2000-2005
31 calculated by multiplying the blank corrected OC measurement by 1.4 to account for

1 non-carbon mass. This differs from the raw OC values shown in Figure 3-12. There are a
2 range of estimates in the literature for suggested scaling factors (Turpin and Lim, 2001,
3 [017093](#)), depending predominantly on how highly oxygenated the aerosol is (Pang et al.,
4 2006, [156012](#)). Turpin and Lim (2001, [017093](#)) recommended ratios of 1.6 ± 0.2 for urban
5 and 2.1 ± 0.2 for non-rurban aerosols. Fresh PM, more common in urban regions, has
6 undergone limited chemical transformation. As the aerosol is transported to rural regions,
7 it becomes more oxygenated. As a result, the necessary correction factor to account for non-
8 carbon mass (e.g., oxygen) is higher in rural locations compared to urban locations, with an
9 average of 1.9 and estimates ranging from 1.6 to 2.6 for rural IMPROVE monitors (El-
10 Zanan et al., 2005, [155764](#)). Therefore, applying one correction factor of 1.4 across the
11 entire U.S. will lead to an underestimate of the OCM in rural regions. Therefore, the data
12 presented in Figure 3-12 represent OC as measured and with a national blank correction,
13 but no adjustment to OCM.

14 Figure 3-13 contains a similar map for $PM_{2.5}$ EC mass concentration that exhibits
15 smaller seasonal variability than OC, particularly in the eastern half of the U.S. There are
16 isolated monitors spread throughout the country that measure high annual average EC
17 concentrations. These EC 'hot spots' are primarily associated with larger metropolitan
18 areas such as Los Angeles, Pittsburgh, and New York, but El Paso, TX, also reported high
19 annual average EC concentrations (driven by a wintertime average concentration greater
20 than $2 \mu\text{g}/\text{m}^3$). In a similar analysis for EC by Bell et al. (2007, [155683](#)) for 2000-2005 data,
21 there were also high wintertime EC concentrations in eastern Kentucky and western
22 Montana. These particular locations do not stand out in the 2005-2007 data in Figure 3-13.

23 Figure 3-14 contains a map for $PM_{2.5}$ SO_4^{2-} mass concentration which shows that
24 SO_4^{2-} is more prevalent in the eastern U.S. owing to the strong west-to-east gradient in SO_2
25 emissions. This gradient is magnified in the summer months when more sunlight is
26 available for photochemical formation of SO_4^{2-} . In contrast, $PM_{2.5}$ NO_3^- mass concentration
27 in Figure 3-15 is highest in the west, particularly in California. There are also elevated
28 concentrations of NO_3^- in the upper midwest. The seasonal plots show generally higher
29 NO_3^- in the wintertime as a result of temperature driven partitioning. Exceptions exist in
30 Los Angeles and Riverside where high NO_3^- readings appear year-round. The $PM_{2.5}$ NH_4^+
31 mass concentration concentration maps in Figure 3-16 shows spatial patterns related to
32 both SO_4^{2-} and NO_3^- resulting from its presence in both $(\text{NH}_4)_2\text{SO}_4$ and NH_4NO_3 . Figures A-
33 29 through A-34 in Annex A show similar U.S. concentration maps for $PM_{2.5}$ Cu, Fe, Ni, Pb,

1 Se and V mass concentrations as measured by XRF. There is considerably less seasonal
2 variation in the concentration profile for these metals than OC or the ions.

3 For the fifteen metropolitan areas identified earlier, the contribution of the major
4 component classes to total PM_{2.5} mass was derived using the measured sulfate, adjusted
5 NO₃⁻, derived water, inferred carbonaceous mass approach (SANDWICH) (Frank, 2006,
6 [098909](#)). This approach uses the measured FRM PM_{2.5} mass and co-located CSN chemical
7 constituents to perform a mass balance-based estimation of the PM_{2.5} mass fraction
8 attributed to SO₄²⁻, NO₃⁻, EC, OCM, and crustal material. SO₄²⁻ and NO₃⁻ include
9 associated NH₄⁺ mass and estimated particle-bound water. Furthermore, NO₃⁻ is assumed
10 to be fully neutralized as NH₄NO₃ and has been adjusted to represent the amount retained
11 by the FRM monitor. EC is taken as measured, and the crustal component is derived from
12 common oxides contained in the Earth's crust (Pettijohn, 1957, [156862](#)), but can also
13 include significant anthropogenic contributions, such as coal fly ash that are unrelated to
14 soil resuspension. Finally, OCM is estimated using mass balance by subtracting the sum of
15 all other constituents from the FRM PM_{2.5} mass. The SANDWICH method takes into
16 account passive collection of semi-volatile or handling-related mass on the FRM filters in
17 the mass balance calculation. The magnitude of this artifact is assigned a nominal value of
18 0.5 µg/m³, which is derived from limited analysis of FRM field blanks. Other constituents
19 such as salt and other metallic oxides, however, are not included in these calculations and
20 therefore the OCM fraction estimated by mass balance represents an upper bound on the
21 FRM retained OCM. The calculations and assumptions that go into the SANDWICH
22 method are discussed in detail in Frank (2006, [098909](#)) with further information available
23 on EPA's AirExplorer web site
24 (http://www.epa.gov/cgi-bin/htmSQL/mxplorer/query_spe.hsql).

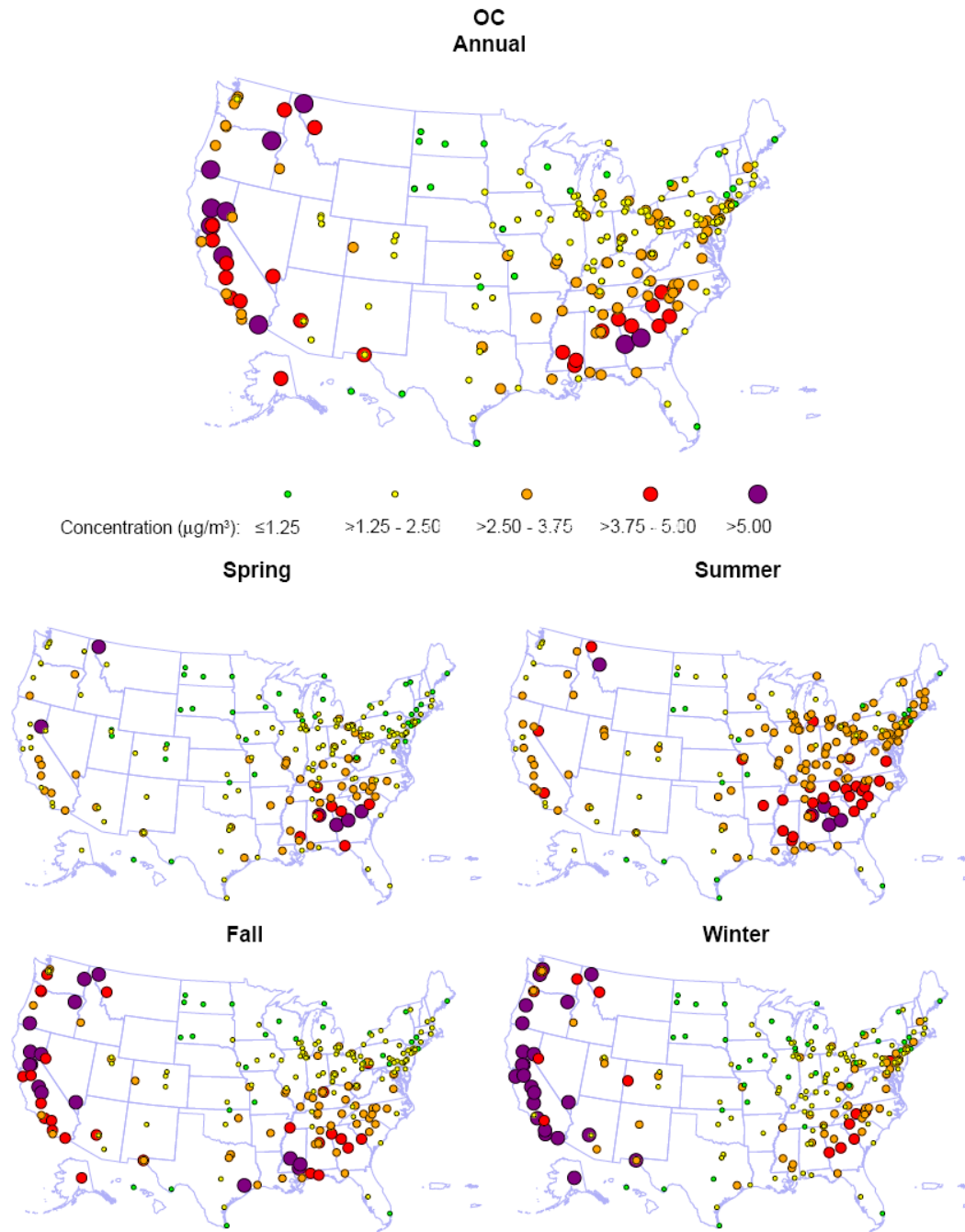


Figure 3-12. Three-yr avg 24-h $\text{PM}_{2.5}$ OC concentrations measured at CSN sites across the U.S., 2005-2007.

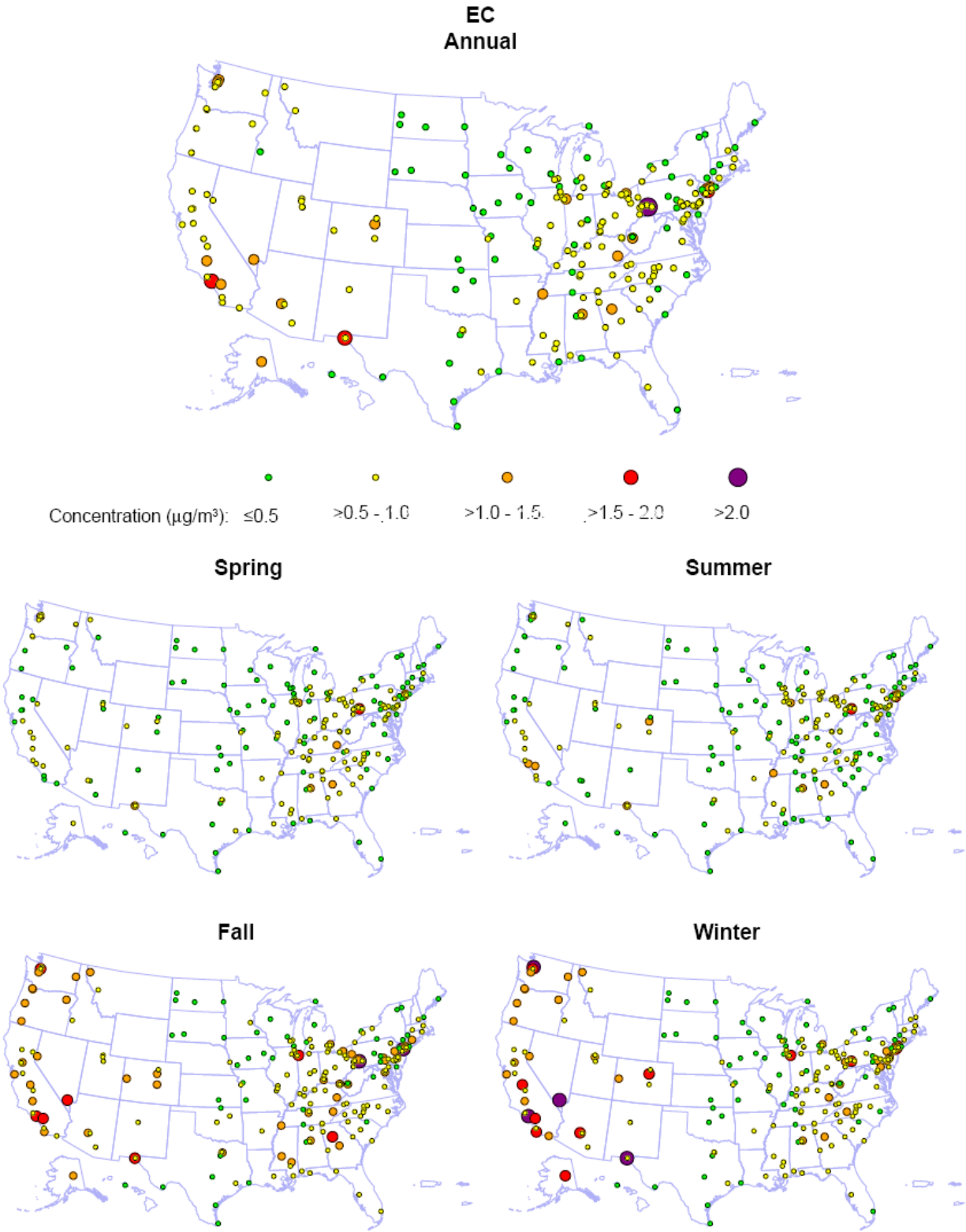


Figure 3-13. Three-yr avg 24-h $\text{PM}_{2.5}$ EC concentrations measured at CSN sites across the U.S., 2005-2007.

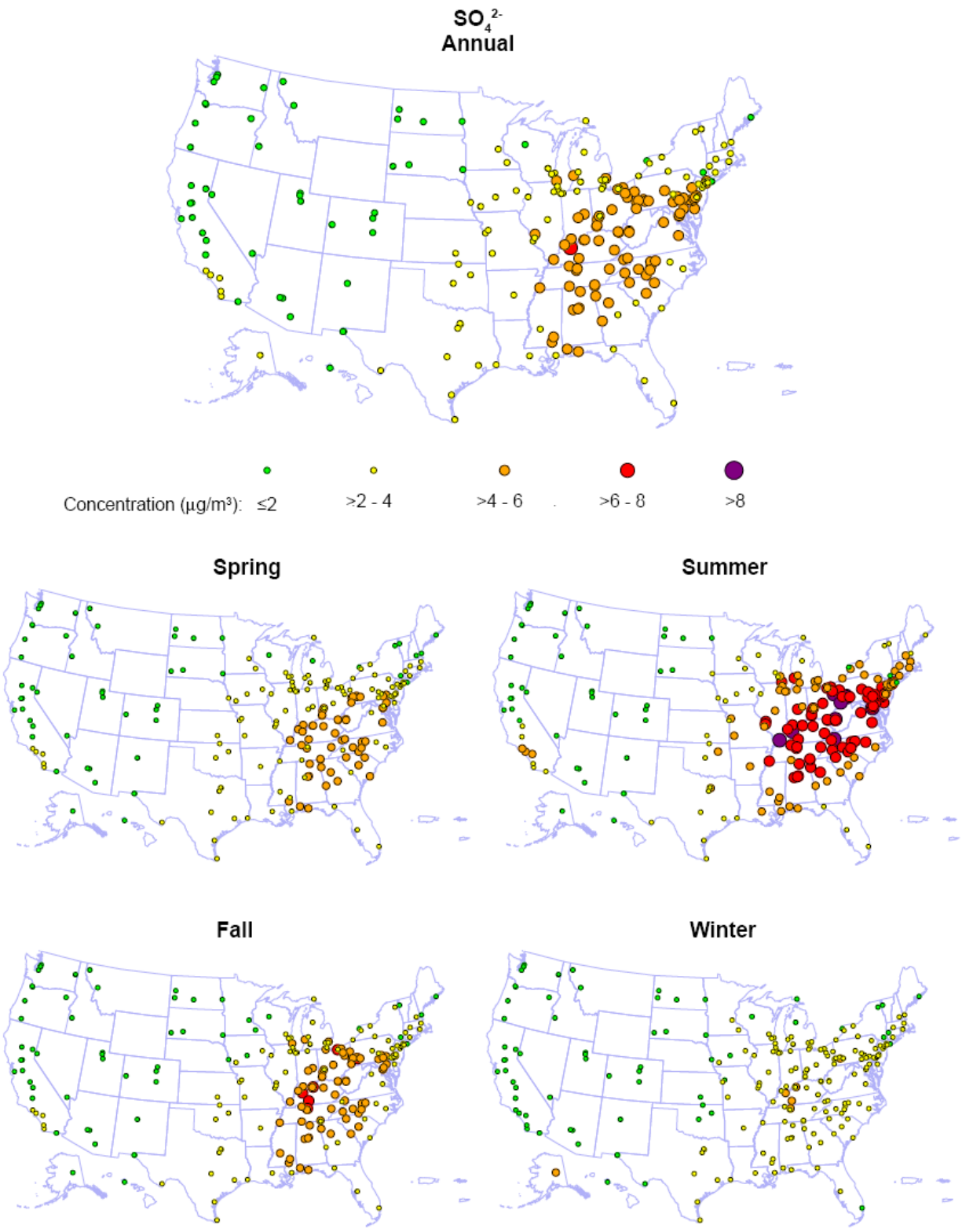


Figure 3-14. Three-yr avg 24-h PM_{2.5} SO₄²⁻ concentrations measured at CSN sites across the U.S., 2005-2007.

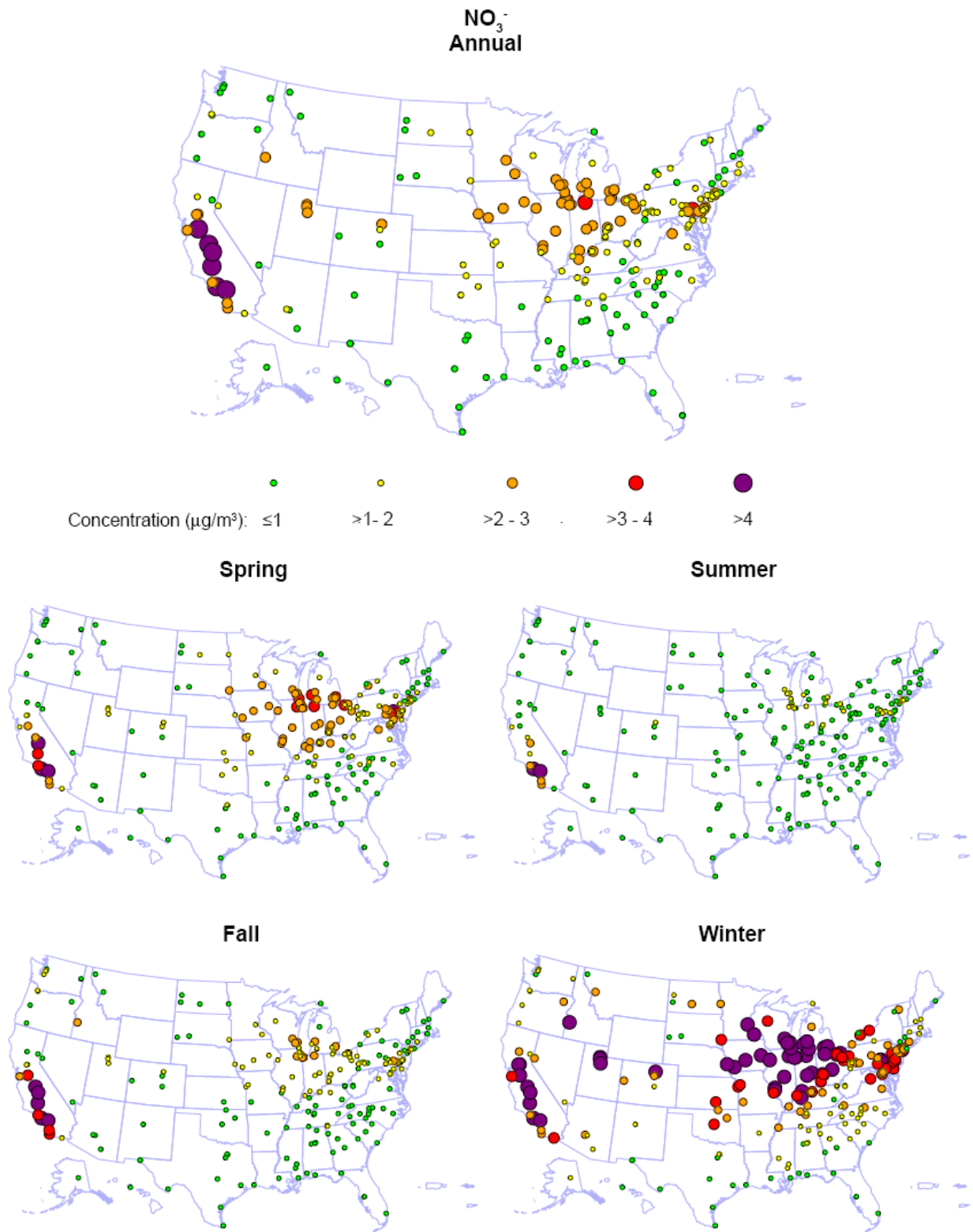


Figure 3-15. Three-yr avg 24-h PM_{2.5} NO₃⁻ concentrations measured at CSN sites across the U.S., 2005-2007.

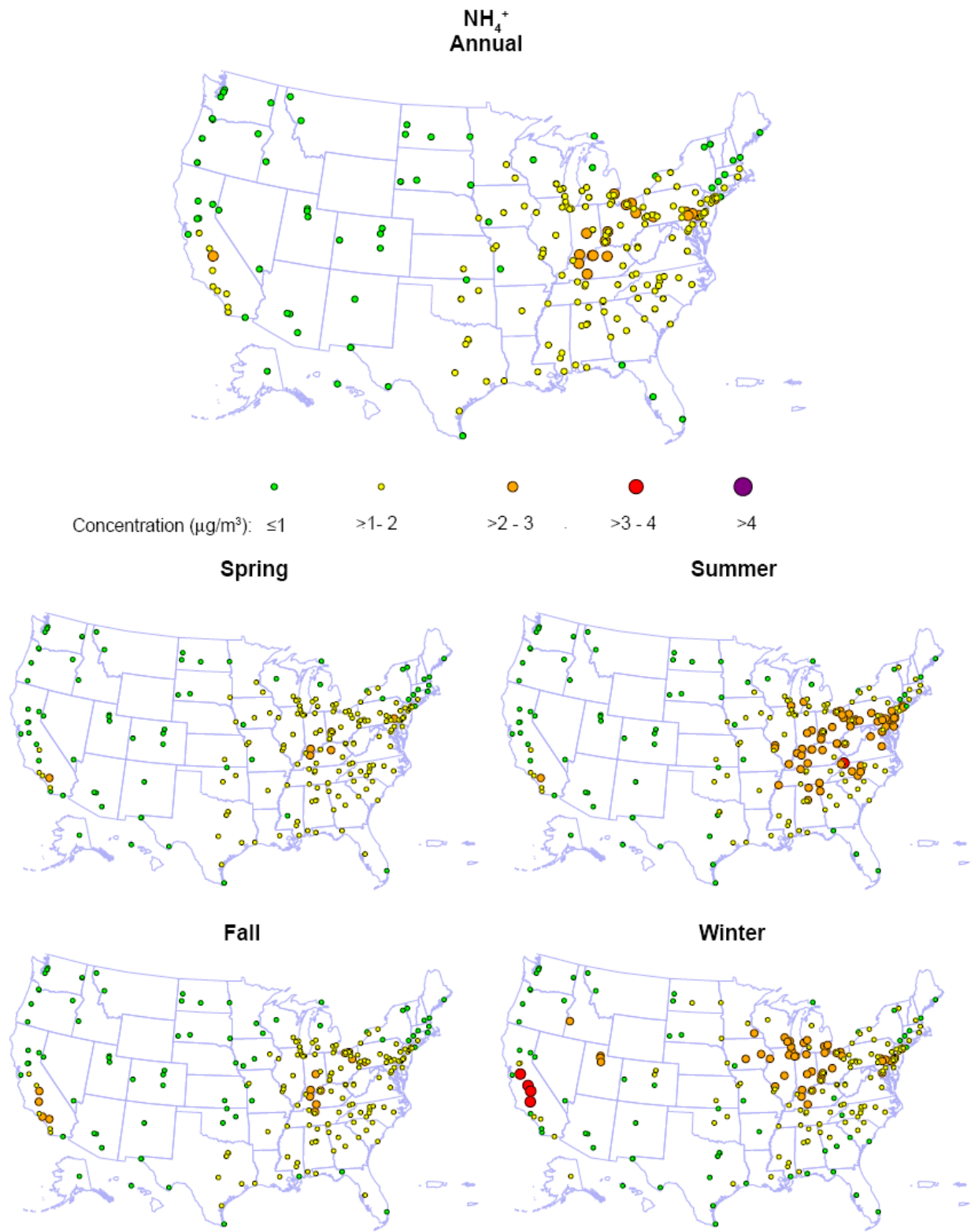


Figure 3-16. Three-yr avg 24-h PM_{2.5} NH₄⁺ concentrations measured at CSN sites across the U.S., 2005-2007.

1 Figure 3-17 shows the PM_{2.5} compositional breakdown for the fifteen CSAs/CBSAs. All
2 available monitoring sites with co-located FRM PM_{2.5} and CSN speciation data reporting in
3 all four seasons for at least one calendar year from 2005-2007 were included. Furthermore,
4 each season was required to contain five reported values for mass and the major PM_{2.5}
5 constituents. This resulted in a varying number of sites (ranging from one to seven, as
6 indicated in the caption to Figure 3-17) used to create the averages shown in the figure.
7 Variability in PM_{2.5} composition within each CSA/CBSA where multiple monitors were
8 available and trends in composition over time are discussed in subsequent sections.

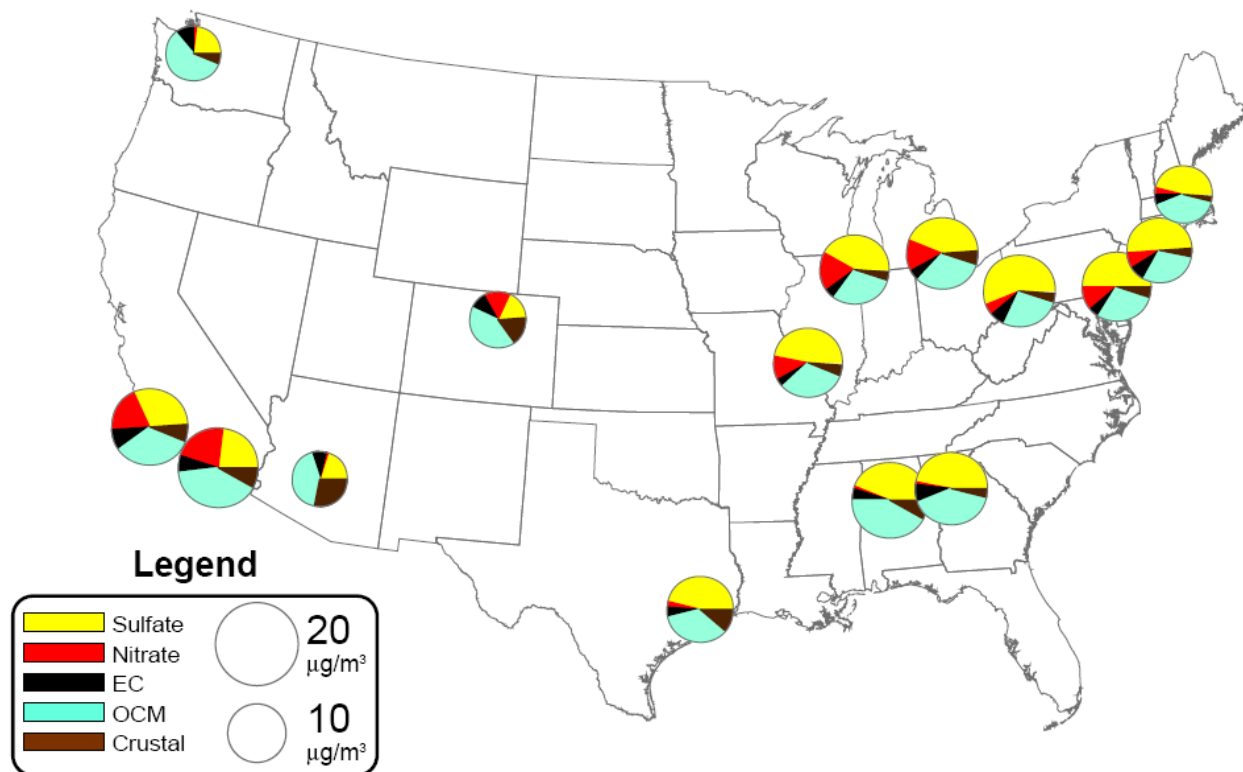


Figure 3-17. Three-yr avg PM_{2.5} speciation estimates for 2005-2007 derived using the SANDWICH method for the following fifteen CSAs/CBSAs (with the number of sites per CSA/CBSA listed in parenthesis): Atlanta, GA (1); Birmingham, AL (3); Boston, MA (4); Chicago, IL (7); Denver, CO (2); Detroit, MI (4); Houston, TX (1); Los Angeles, CA (1); New York City, NY (7); Philadelphia, PA (6); Phoenix, AZ (2); Pittsburgh, PA (4); Riverside, CA (1); Seattle, WA (4); and St. Louis, MO (3). SO₄²⁻ and NO₃⁻ estimates include NH₄⁺ and particle bound water and the circles are scaled in proportion to FRM PM_{2.5} mass as indicated in the legend.

1 On an annual average basis, SO₄²⁻ is a dominant PM component in the eastern U.S.
 2 cities. For the presented cities, this includes everything east of Houston where the SO₄²⁻
 3 fraction of PM_{2.5} ranges from 42% in Chicago to 56% in Pittsburgh on an annual average
 4 basis. OCM is the next largest component in the east ranging from 27% in Pittsburgh to
 5 42% in Birmingham. In the west, OCM is the largest constituent on an annual basis,
 6 ranging from 34% in Los Angeles to 58% in Seattle. SO₄²⁻, NO₃⁻ and crustal material are
 7 also important in many of the included western cities. In the west, fractional SO₄²⁻ ranges
 8 from 18% in Denver to 32% in Los Angeles while fractional NO₃⁻ is relatively large in
 9 Riverside (22%), Los Angeles (19%) and Denver (15%) and less important on an annual

1 basis in Phoenix (1%) and Seattle (2%). Crustal material is particularly prevalent in
 2 Phoenix (28%). EC makes up a smaller fraction of the PM_{2.5} (4 to 11%), but it is consistently
 3 present in all included cities regardless of region.

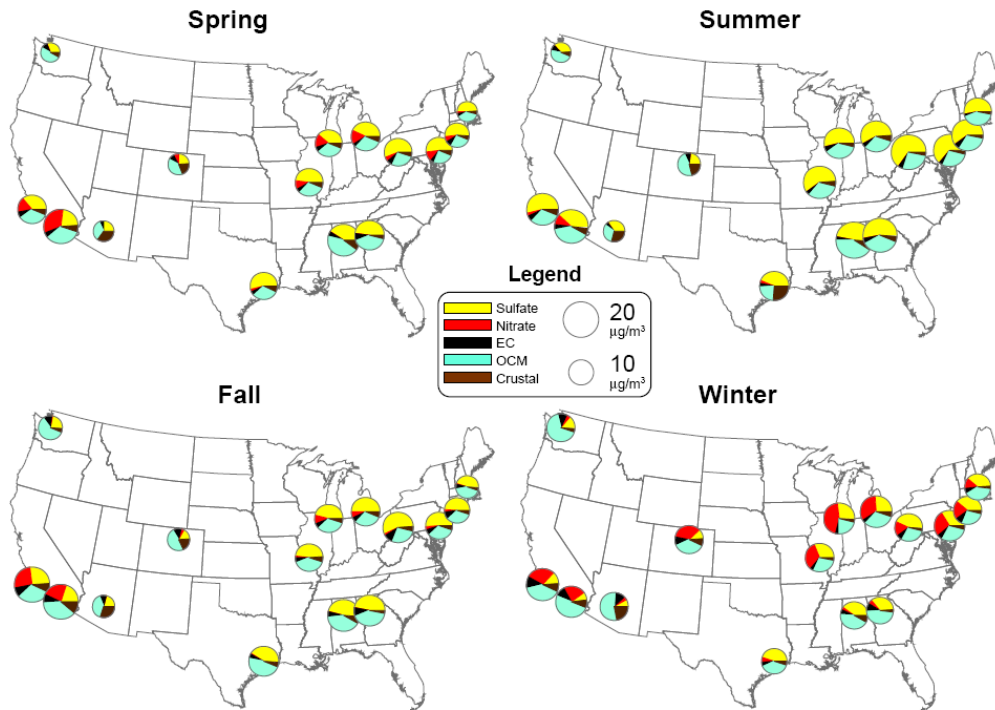


Figure 3-18. Seasonally-stratified three-yr avg PM_{2.5} speciation estimates for 2005-2007 derived using the SANDWICH method for the following fifteen CSAs/CBSAs: Atlanta, GA; Birmingham, AL; Boston, MA; Chicago, IL; Denver, CO; Detroit, MI; Houston, TX; Los Angeles, CA; New York City, NY; Philadelphia, PA; Phoenix, AZ; Pittsburgh, PA; Riverside, CA; Seattle, WA; and St. Louis, MO. SO₄²⁻ and NO₃⁻ estimates include NH₄⁺ and particle bound water and the circles are scaled in proportion to FRM PM_{2.5} mass as indicated in the legend.

4 The seasonal variation in PM_{2.5} composition across the fifteen CSAs/CBSAs is shown
 5 in Figure 3-18 where the seasons are defined as before. SO₄²⁻ dominates in most metropoli-
 6 tan areas in the summertime, while NO₃⁻ becomes important in the colder wintertime
 7 months. Notable summertime exceptions include Denver, Phoenix, and Seattle, where SO₄²⁻-
 8 makes up a smaller fraction of the PM_{2.5} mass. Likewise, NO₃⁻ is less pronounced in the
 9 wintertime in Atlanta, Birmingham, Houston, Phoenix, and Seattle. Los Angeles and
 10 Riverside exhibit elevated NO₃⁻ from fall through spring. Crustal material is a substantial

1 summertime component in Houston (26%), and is generally low elsewhere in the East in all
2 seasons. In the West, crustal material represents a substantial component year-round in
3 Phoenix and Denver.

4 Only speciated $PM_{2.5}$ is collected routinely at CSN network sites, resulting in far less
5 information on speciated $PM_{10-2.5}$. Edgerton et al. (2005, [088686](#); 2009, [180385](#)) published
6 speciated measurements for $PM_{2.5}$ and $PM_{10-2.5}$ obtained using dichotomous samplers from
7 four locations included in the Southeastern Aerosol Research and Characterization
8 (SEARCH) study: Yorkville, GA, Centreville, AL, Birmingham, AL and Atlanta, GA.
9 Samples were collected between 1999 and 2003 on a 1-in-3 day or 1-in-6 day schedule,
10 depending on site. Speciated measurements for both $PM_{2.5}$ and $PM_{10-2.5}$ included SO_4^{2-} , NO_3^-
11 , NH_4^+ , and major metal oxides (MMO). In addition, OC and either black carbon (BC) or EC
12 were reported for $PM_{2.5}$ over the entire study period and for $PM_{10-2.5}$ for a subset of samples
13 extending from April 2003 to April 2004.

14 For the Atlanta and Birmingham SEARCH sites, the annual average NO_3^- mass
15 fraction was approximately equal for $PM_{2.5}$ (5.6% and 5.0%, respectively, for Atlanta and
16 Birmingham) and $PM_{10-2.5}$ (4.9% and 3.3%). Likewise, the OC mass fraction was
17 approximately equal for $PM_{2.5}$ (26% and 26%) and $PM_{10-2.5}$ (24% and 27%). MMO
18 contributed an order of magnitude smaller mass fraction to $PM_{2.5}$ (2.6% and 4.7%) than
19 $PM_{10-2.5}$ (38% and 35%). In contrast, SO_4^{2-} contributed an order of magnitude greater mass
20 fraction to $PM_{2.5}$ (25.1% and 24.1%) than $PM_{10-2.5}$ (2.8 and 2.1%). BC also represented a
21 slightly larger mass fraction of $PM_{2.5}$ (8.6% and 10.5%) than EC did for $PM_{10-2.5}$ (2.9% &
22 2.4%). Based on these findings, MMO are present primarily in the thoracic coarse mode
23 while SO_4^{2-} and EC/BC are present primarily in the fine mode. NO_3^- and OC are present in
24 both modes in approximately equal mass fractions. These results are specific to Atlanta and
25 Birmingham and may not represent other geographic regions. However, they are consistent
26 with the current understanding of sources and formation of these constituents and
27 therefore likely resemble the general compositional split between fine and thoracic coarse
28 mode particles.

29 Information about the composition of ambient ultrafine particles directly emitted by
30 sources is still sparse compared to that for the larger size modes. However, their
31 composition is expected to reflect that of their sources. As noted in Section 3.3 (and
32 references therein), particle number emissions from motor vehicles are dominantly in the
33 ultrafine size range. The composition of gasoline vehicle emissions consists mainly of a mix

1 of OC, EC and small quantities of trace metals and sulfates, with OC constituting
2 anywhere from 26-88% of PM. Diesel PM is generally comprised of an EC and trace metal
3 ash core onto which organic material condenses, and nucleation-mode SO_4^{2-} . With the
4 introduction of new diesel emissions standards in 2007, total emissions have decreased
5 dramatically, particularly for carbon. In areas where nucleation is the dominant source of
6 ultrafine particles, sulfate along with ammonium, and secondary organic compounds are
7 the likely major components of ultrafine particles.

8 In a study conducted at several urban sites in Southern California, Cass et al. (2000,
9 [020680](#)) found that the composition of ultrafine particles ranged from 32-67% organic
10 compounds, 3.5-17.5% elemental carbon, 1-18% sulfate, 0-19% NO_3^- , 0-9% ammonium,
11 1-26% metal oxides, 0-2% sodium, and 0-2% chloride. Thus carbon, in various forms, was
12 found to be the major contributor to the mass of ultrafine particles. However, ammonium
13 was found to contribute 33% of the mass of ultrafine particles at one site in Riverside. Iron
14 was the most abundant metal found in the ultrafine particles. Chung et al. (2001, [017105](#))
15 found that carbon was the major component of the mass of ultrafine particles in a study
16 conducted during January of 1999 in Bakersfield, CA. However, in the study of Chung et
17 al., the contribution of carbonaceous species (OC and EC; typically 20-30%) was much lower
18 than that found in the cities in Southern California. They found that calcium was the
19 dominant cation, accounting for about 20% of the mass of ultrafine particles in their
20 samples. Sizable contributions from silicon (0-4%) and aluminum (6-14%) were also found.
21 MOUDIs are used to collect size-segregated filter samples in the ultrafine particle
22 compositional analyses described above. Coarse particle bounce is a concern when using
23 MOUDIs and further studies, including scanning electron microscopy, may be needed to
24 quantify the effect of this sampling artifact on ultrafine particle compositional analyses.

25 Herner et al. (2005, [135983](#)) reported a gradual increase in OC mass fraction as
26 particle size decreases from 1 μm (20% OC) to 100 nm (80% OC) in the San Joaquin Valley
27 of California. Sardar et al. (2005, [180086](#)) found OC to be the major component of ultrafine
28 particles at four locations in California, with higher OC mass fraction in the wintertime
29 relative to summertime. EC and SO_4^{2-} were also present in the ultrafine samples but at
30 much smaller mass fractions; EC was present year-round whereas SO_4^{2-} had a summertime
31 preference. More detailed chemical characterization of the OC fraction of ambient ultrafine
32 particles is extremely limited, but recent studies have identified specific organic molecular
33 markers affiliated with motor vehicle emissions including hopanes and polycyclic aromatic

1 hydrocarbons (Fine et al., 2004, [141283](#); Ning et al., 2007, [156809](#); Phuleria et al., 2007,
2 [117816](#)).

3 As noted in the 2004 PM AQCD (U.S. EPA, 2004, [056905](#)), primary biological aerosol
4 particles (PBAP), which include microorganisms, fragments of living things, and organic
5 compounds of miscellaneous origin in surface deposits on filters, are not distinguishable in
6 analyses of total OC. A clear distinction should be made between PBAP and primary OC
7 produced by organisms (e.g., waxes coating the surfaces of organisms) and precursors to
8 secondary OC such as isoprene and terpenes. Indeed, the fields of view of many
9 photomicrographs of PM samples obtained by scanning electron microscopy are often
10 dominated by large numbers of pollen spores, plant and insect fragments, and
11 microorganisms. Bioaerosols such as pollen, fungal spores, and most bacteria are expected
12 to be found mainly in the coarse size fraction (see Figure 3-2 for an illustrative example of a
13 pollen particle). However, allergens from pollens can also be found in respirable particles
14 (Edgerton et al., 2009, [180385](#); Taylor, 2002, [025693](#)). Matthias-Maser et al. (2000, [155972](#))
15 summarized information about the size distribution of PBAP in and around Mainz,
16 Germany in what is perhaps the most complete study of this sort. Matthias-Maser found
17 that PBAP constituted up to 30% of total particle number and volume in the approximate
18 size range from 0.35-50 μm on an annual basis. Additionally, whereas the contribution of
19 PBAP to the total aerosol volume did not change appreciably with season, the contribution
20 of PBAP to total particle number ranged from about 10% in December and March to about
21 25% in June and October. Bauer et al. (2008, [189986](#)) measured contributions of fungal
22 spores to OC at an urban and a suburban site in Vienna, Austria in spring and summer.
23 Fungal spores at the suburban site contributed on average 10% to OC in PM_{10} and 5% at
24 the urban site. At the suburban site, in summer, fungal spores accounted on average for
25 60% of the OC ($0.56 \mu\text{g}/\text{m}^3$) in $\text{PM}_{10-2.1}$ ($2.6 \mu\text{g}/\text{m}^3$). The contribution to $\text{PM}_{2.1}$ was estimated
26 to be about 10% that in $\text{PM}_{10-2.1}$. Womiloju et al. (2003, [179954](#)) estimated that fungal
27 spores contribute 14-22% of OC in $\text{PM}_{2.5}$ in and around Toronto.

28 Edgerton et al. (2009, [180385](#)) found that PBAP contributed 60-70% of OC (average \sim
29 $1.7 \mu\text{g}/\text{m}^3$) in $\text{PM}_{10-2.5}$ at an urban and a rural site in Alabama in fall of 2000 and spring of
30 2001. The percentage contributions were similar at both sites and higher concentrations
31 were found in spring than in fall. Although results for the U.S. are more limited, they are
32 broadly consistent with the results of the other studies in illustrating the importance of
33 PBAP, at least for fungal spores in OC.

3.5.1.2. Urban-Scale Variability

PM_{2.5}

1 Data from the fifteen CSAs/CBSAs were used to investigate urban-scale variability in
2 PM reported to AQS. PM_{2.5} has a longer residence time in the atmosphere compared to
3 PM_{10-2.5} resulting from a slower V_d. As a result, PM_{2.5} exhibits increased spatial
4 homogeneity with less localized influence from point sources. Maps of PM_{2.5} monitor
5 locations and box plots of seasonal PM_{2.5} mass concentration data are provided for Boston
6 (Figure 3-19 and 3-23), Pittsburgh (Figure 3-21 and 3-25), and Los Angeles (Figure 3-23 and
7 3-27). Figures A-35 through A-70 in Annex A contain similar information for the remainder
8 of the 15 CSAs/CBSAs under investigation. With very few exceptions, the PM_{2.5}
9 concentration is quite uniformly distributed across the monitors. Los Angeles has one
10 monitor (Site I) that reported noticeably less PM_{2.5} in all four seasons than the rest of the
11 monitors in the region. This monitor is located at Lancaster CA, separated from the rest of
12 the Los Angeles region by the San Gabriel Mountains. In general, however, PM_{2.5} varies
13 approximately the same magnitude between monitors as it does between seasons for the 15
14 selected cities.

15 Tables 3-11 through 3-13 contain pair-wise statistics for PM_{2.5} in Boston, Pittsburgh,
16 and Los Angeles, respectively. Tables A-20 through A-31 in Annex A contain pair-wise
17 statistics for PM_{2.5} measured within the remaining CSAs/CBSAs. Comparison statistics
18 shown include the Pearson correlation coefficient (R), the 90th percentile of the absolute
19 difference in concentrations (P90), the coefficient of divergence (COD) and the number of
20 paired observations (N). The COD provides an indication of the variability across the
21 monitoring sites in each CSA/CBSA and is defined as follows:

$$COD_{jk} = \sqrt{\frac{1}{P} \sum_{i=1}^p \left(\frac{X_{ij} - X_{ik}}{X_{ij} + X_{ik}} \right)^2}$$

Equation 3-2

22 where X_{ij} and X_{ik} represent observed concentrations averaged over some measurement
23 averaging period i (hourly, daily, etc.) at sites j and k , and p is the number of paired
24 observations. A COD of 0 indicates there are no differences between concentrations at
25 paired sites (spatial homogeneity), while a COD approaching 1 indicates extreme spatial
26 heterogeneity.

1 Temporal correlations between 24-h $PM_{2.5}$ concentrations in Boston range from 0.61 to
2 0.97 in Table 3-11. The lowest correlation in this CSA was between Site A located in Fall
3 River, MA 1 km from the Narragansett Bay and Site L located in Nashua, NH on the bank
4 of the Merrimack River, 120 km north. The highest correlation was between Sites P and R,
5 located less than a kilometer apart in Providence, RI.

6 In Pittsburgh, 24-h $PM_{2.5}$ correlations range from 0.65 to 0.97. The lowest correlation
7 in this CSA was between Sites B and D, located diametrically opposite downtown
8 Pittsburgh and 33 km apart. The highest correlation was for Sites K and D, located 21 km
9 apart and both west of downtown. The prevailing wind in Pittsburgh is from the west,
10 which explains the higher correlation between the two upwind sites.

11 In Los Angeles, 24-h $PM_{2.5}$ correlations range from 0.21 to 0.96. The lowest correlation
12 was between Sites I and J located 123 km apart and separated by the San Gabriel
13 Mountains as discussed earlier. The highest correlation was for sites G and H, located 3.7
14 km apart and both in Long Beach, CA. Therefore, while distance between monitors plays an
15 important role in how well any two monitors correlate, other factors such as meteorology
16 and topography can be important.

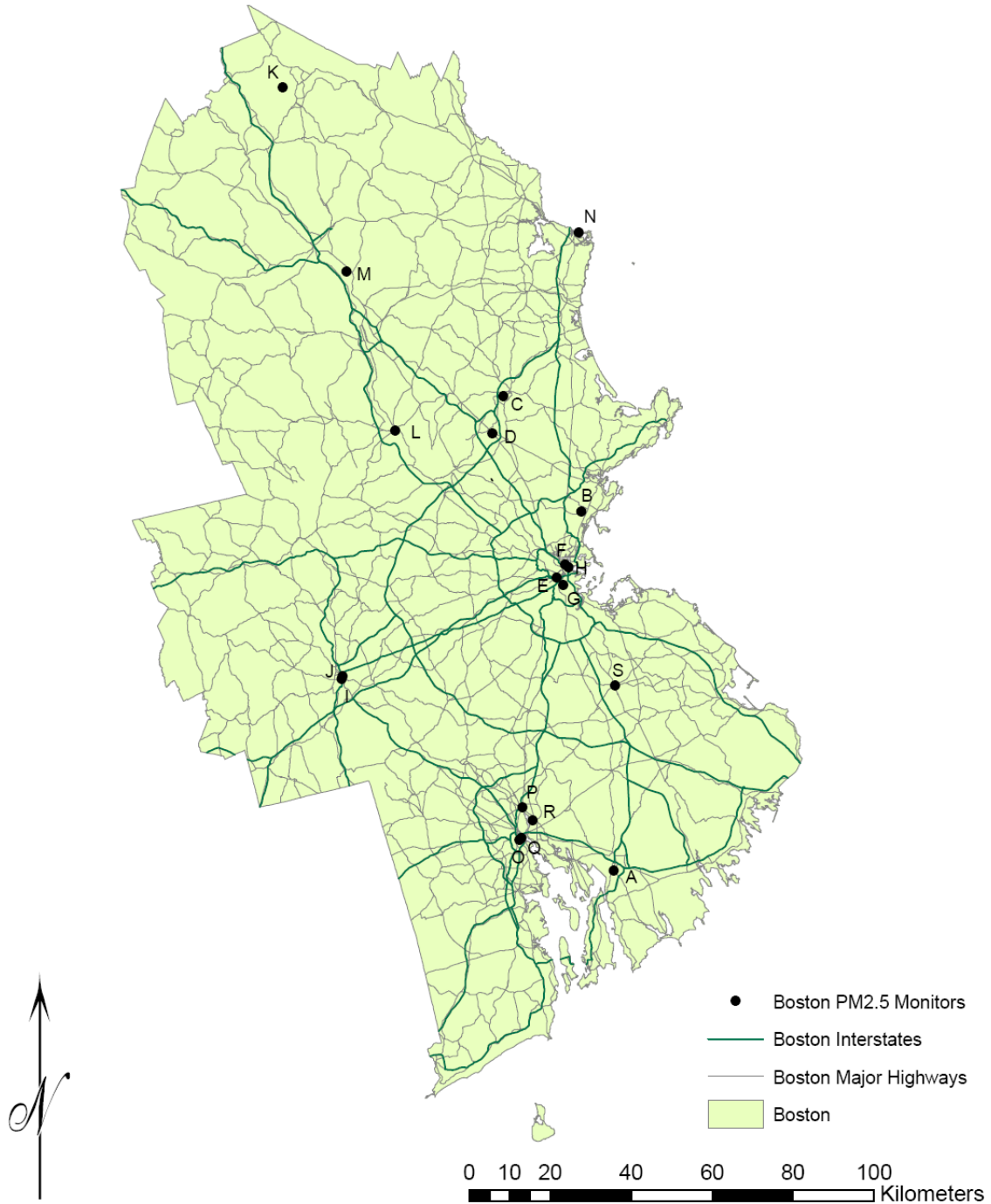


Figure 3-19. Locations of PM_{2.5} monitors and major highways, Boston, MA.

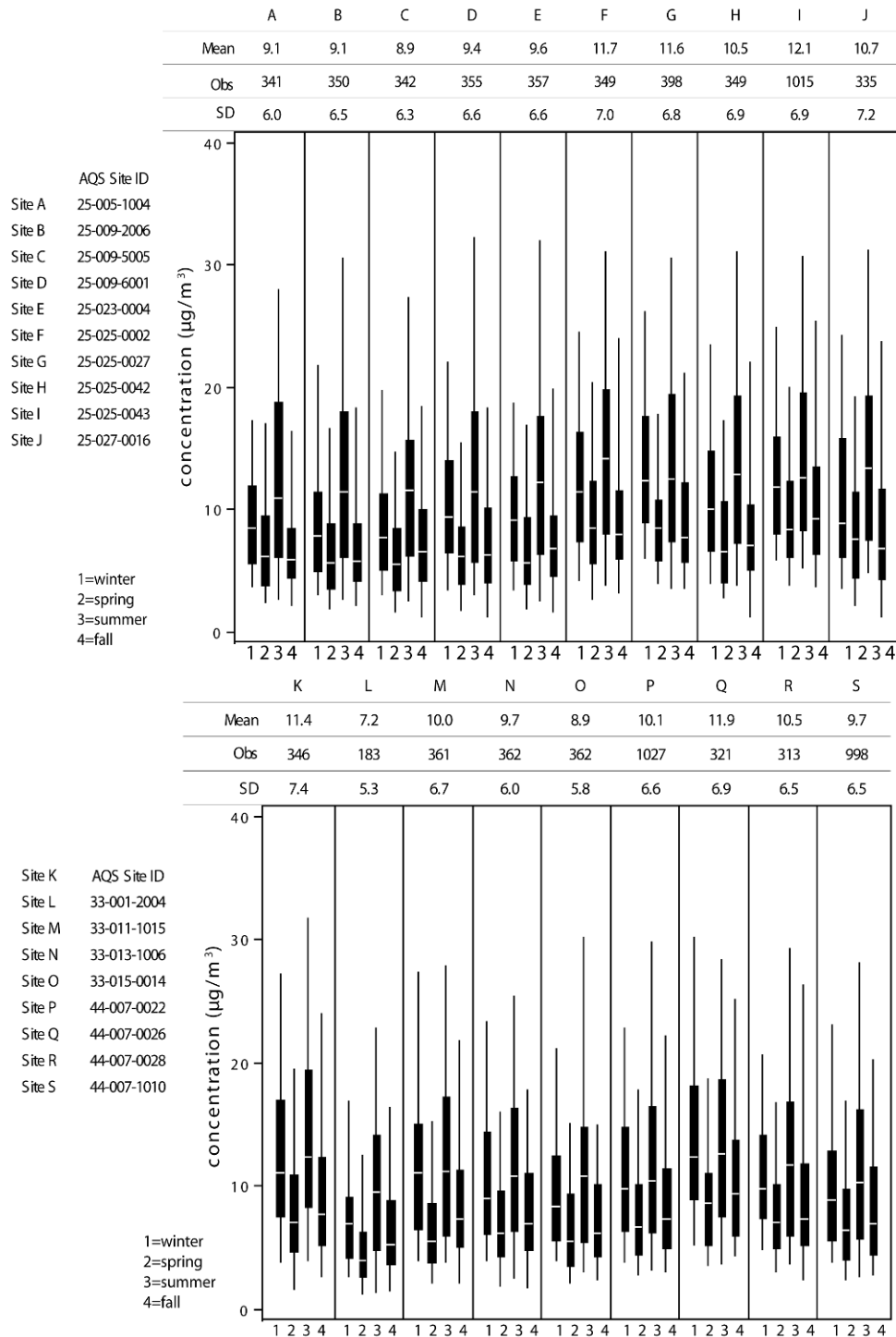


Figure 3-20. Seasonal distribution of 24-h avg PM_{2.5} concentrations by site for Boston, MA, 2005-2007. Box plots show the median and interquartile range with whiskers extending to the 5th and 95th percentiles at each site during (1) winter (December-February), (2) spring (March-May), (3) summer (June-August) and (4) fall (September-November).

Table 3-11. Inter-sampler comparison statistics for each pair of 24-h PM_{2.5} monitors reporting to AQS for Boston, MA.

Site	A	B	C	D	E	F	G	H	I	J
A	1.00 (0.0, 0.00)	0.80 (6.6, 0.21)	0.77 (6.2, 0.22)	0.71 (6.9, 0.23)	0.84 (4.8, 0.19)	0.79 (8.1, 0.23)	0.78 (7.7, 0.24)	0.79 (6.8, 0.22)	0.79 (7.9, 0.25)	0.77 (7.5, 0.24)
	341	326	318	323	329	318	319	325	338	310
B		1.00 (0.0, 0.00)	0.92 (4.1, 0.17)	0.87 (4.1, 0.18)	0.87 (4.7, 0.19)	0.90 (6.3, 0.21)	0.90 (6.2, 0.23)	0.90 (4.9, 0.19)	0.90 (7.1, 0.26)	0.85 (5.5, 0.21)
		350	328	331	339	326	323	333	343	317
C			1.00 (0.0, 0.00)	0.90 (3.5, 0.17)	0.85 (5.3, 0.21)	0.90 (6.3, 0.23)	0.89 (6.3, 0.24)	0.90 (5.0, 0.20)	0.88 (6.8, 0.26)	0.86 (6.2, 0.21)
			342	321	331	316	318	326	336	311
D				1.00 (0.0, 0.00)	0.80 (5.6, 0.20)	0.88 (5.8, 0.21)	0.88 (5.8, 0.22)	0.86 (4.6, 0.19)	0.86 (7.0, 0.26)	0.87 (5.8, 0.19)
				355	336	324	329	332	345	313
E					1.00 (0.0, 0.00)	0.90 (5.9, 0.19)	0.90 (5.8, 0.21)	0.89 (5.0, 0.19)	0.87 (6.9, 0.24)	0.87 (5.4, 0.20)
					357	330	333	340	350	322
F						1.00 (0.0, 0.00)	0.94 (3.8, 0.14)	0.94 (3.5, 0.15)	0.92 (4.5, 0.17)	0.92 (5.4, 0.18)
						349	324	324	339	310
G							1.00 (0.0, 0.00)	0.94 (4.0, 0.16)	0.94 (4.3, 0.15)	0.89 (5.7, 0.20)
							398	325	338	308
H								1.00 (0.0, 0.00)	0.93 (4.7, 0.19)	0.89 (5.0, 0.17)
								349	342	318
I									1.00 (0.0, 0.00)	0.86 (6.9, 0.23)
									1015	330
J										1.00 (0.0, 0.00)
										335

Site	K	L	M	N	O	P	Q	R	S
A	0.77 (8.1, 0.23)	0.61 (8.3, 0.29)	0.71 (8.0, 0.23)	0.68 (7.9, 0.23)	0.73 (7.0, 0.22)	0.87 (5.3, 0.18)	0.81 (7.2, 0.23)	0.85 (5.6, 0.20)	0.86 (5.2, 0.18)
	320	173	324	334	331	326	292	285	306
B	0.86 (6.6, 0.21)	0.80 (6.2, 0.23)	0.87 (5.3, 0.19)	0.83 (6.0, 0.21)	0.88 (4.7, 0.18)	0.86 (5.8, 0.19)	0.80 (7.9, 0.26)	0.85 (5.7, 0.21)	0.85 (6.0, 0.19)
	329	175	331	341	336	335	300	288	314
C	0.86 (6.9, 0.21)	0.89 (4.8, 0.23)	0.93 (4.4, 0.17)	0.90 (4.6, 0.19)	0.93 (3.8, 0.18)	0.83 (5.9, 0.21)	0.79 (7.8, 0.26)	0.81 (6.2, 0.23)	0.82 (6.0, 0.21)
	321	173	323	335	328	329	290	281	309
D	0.88 (6.4, 0.19)	0.79 (5.7, 0.25)	0.91 (3.5, 0.16)	0.85 (4.7, 0.19)	0.86 (4.2, 0.18)	0.80 (6.2, 0.20)	0.75 (7.8, 0.25)	0.79 (6.2, 0.21)	0.80 (5.8, 0.20)
	325	174	329	339	334	342	300	287	321
E	0.87 (6.3, 0.20)	0.72 (8.3, 0.27)	0.83 (5.8, 0.17)	0.79 (6.3, 0.20)	0.84 (4.8, 0.18)	0.91 (4.5, 0.17)	0.86 (6.3, 0.22)	0.88 (4.9, 0.18)	0.91 (3.9, 0.17)
	333	179	338	347	343	343	306	295	324
F	0.91 (4.7, 0.17)	0.78 (9.6, 0.33)	0.90 (5.3, 0.18)	0.85 (6.4, 0.20)	0.85 (7.5, 0.22)	0.89 (5.2, 0.16)	0.86 (6.0, 0.16)	0.88 (4.9, 0.16)	0.89 (5.5, 0.17)
	323	168	323	334	330	336	295	281	316
G	0.90 (5.0, 0.19)	0.77 (9.0, 0.33)	0.90 (5.3, 0.19)	0.85 (6.3, 0.20)	0.87 (7.0, 0.22)	0.88 (5.5, 0.17)	0.86 (5.3, 0.17)	0.87 (5.2, 0.17)	0.88 (5.7, 0.19)
	320	172	326	335	329	383	296	282	356
H	0.90 (4.4, 0.17)	0.75 (9.4, 0.30)	0.88 (4.9, 0.18)	0.83 (5.6, 0.21)	0.84 (6.8, 0.21)	0.89 (4.5, 0.16)	0.86 (6.0, 0.19)	0.87 (4.5, 0.16)	0.88 (5.1, 0.17)
	327	175	332	341	336	335	299	289	314
I	0.87 (6.1, 0.20)	0.75 (10.0, 0.36)	0.86 (6.7, 0.22)	0.82 (7.2, 0.23)	0.83 (8.2, 0.25)	0.88 (6.1, 0.20)	0.84 (6.0, 0.16)	0.85 (6.0, 0.18)	0.87 (6.3, 0.21)
	341	181	352	356	357	957	314	306	936
J	0.95 (3.0, 0.14)	0.73 (9.2, 0.28)	0.87 (5.2, 0.18)	0.84 (5.9, 0.20)	0.80 (7.5, 0.22)	0.90 (5.0, 0.17)	0.86 (5.9, 0.20)	0.87 (5.3, 0.17)	0.88 (5.2, 0.18)
	316	167	314	326	323	321	283	272	302
K	1.00 (0.0, 0.00)	0.71 (10.3, 0.31)	0.88 (6.0, 0.16)	0.85 (6.5, 0.19)	0.81 (8.2, 0.22)	0.89 (5.2, 0.16)	0.86 (5.8, 0.18)	0.87 (5.5, 0.16)	0.88 (5.5, 0.18)
	346	170	326	337	332	331	296	286	313
L		1.00 (0.0, 0.00)	0.89 (6.7, 0.24)	0.91 (5.9, 0.23)	0.90 (4.8, 0.21)	0.88 (10.0, 0.29)	0.63 (12.1, 0.35)	0.72 (9.1, 0.30)	0.69 (9.8, 0.29)
		183	176	181	177	181	153	149	164
M			1.00 (0.0, 0.00)	0.94 (3.8, 0.13)	0.80 (4.6, 0.16)	0.83 (5.5, 0.16)	0.81 (7.4, 0.20)	0.82 (5.8, 0.17)	0.84 (5.1, 0.16)
			361	341	336	345	300	288	326
N				1.00 (0.0, 0.00)	0.90 (4.4, 0.17)	0.77 (6.7, 0.19)	0.75 (8.1, 0.22)	0.78 (6.4, 0.20)	0.78 (6.2, 0.19)
				362	347	347	309	327	327
O					1.00 (0.0, 0.00)	0.80 (5.8, 0.19)	0.75 (8.8, 0.25)	0.79 (6.8, 0.21)	0.80 (6.0, 0.19)
					362	348	304	292	330
P						1.00 (0.0, 0.00)	0.95 (3.6, 0.14)	0.97 (2.0, 0.09)	0.97 (2.1, 0.08)
						1027	307	299	943

Site	K	L	M	N	O	P	Q	R	S
Q							1.00	0.92	0.94
							(0.0, 0.00)	(3.1, 0.13)	(4.0, 0.16)
							321	268	290
R								1.00	0.94
								(0.0, 0.00)	(2.7, 0.12)
								313	280
S									1.00
									(0.0, 0.00)
									988

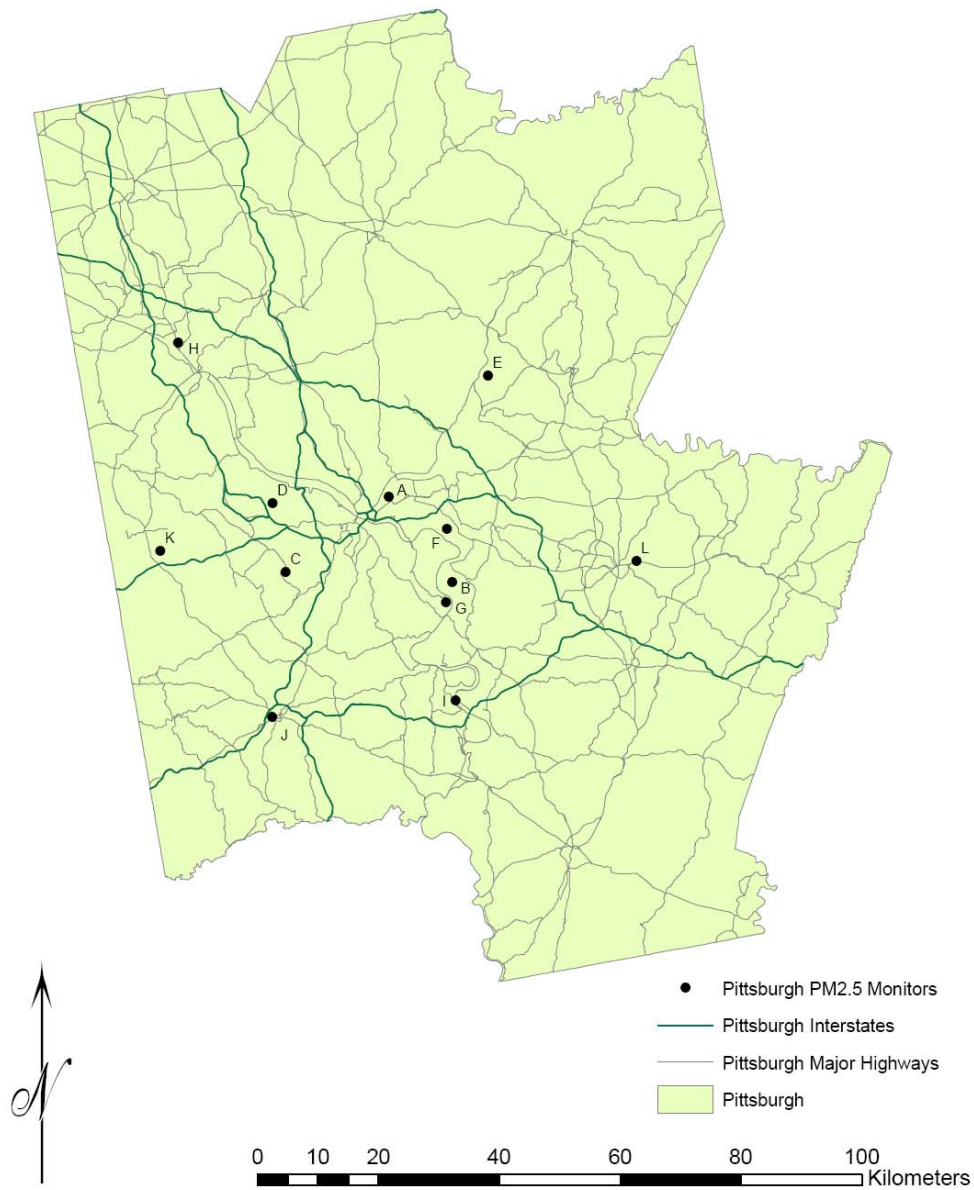


Figure 3-21. Locations of PM_{2.5} monitors and major highways, Pittsburgh, PA.

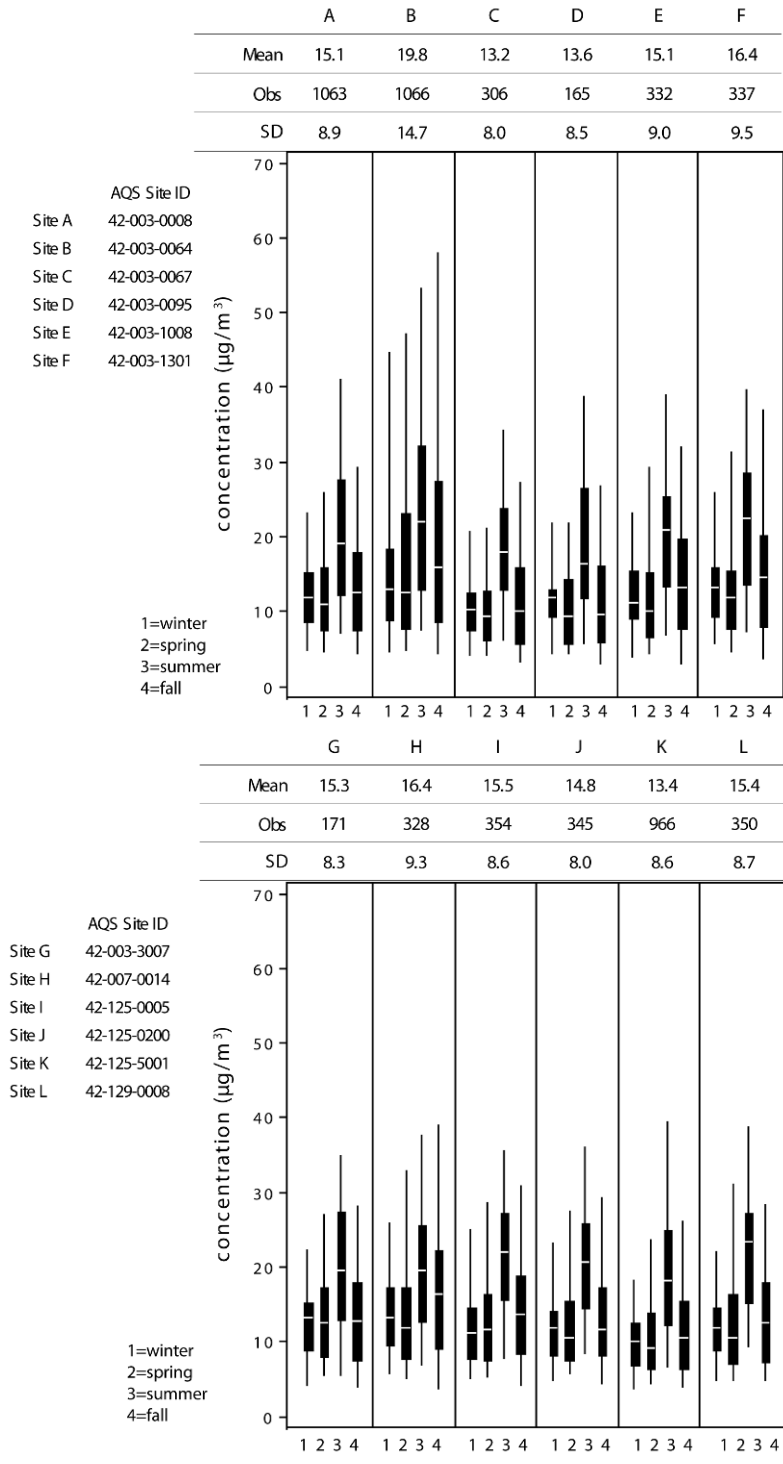


Figure 3-22. Seasonal distribution of 24-h avg PM_{2.5} concentrations by site for Pittsburgh, PA, 2005-2007. Box plots show the median and interquartile range with whiskers extending to the 5th and 95th percentiles at each site during (1) winter (December-February), (2) spring (March-May), (3) summer (June-August) and (4) fall (September-November).

Table 3-12. Inter-sampler comparison statistics for each pair of 24-h PM_{2.5} monitors reporting to AQS for Pittsburgh, PA.

	A	B	C	D	E	F	G	H	I	J	K	L
A	1.00 (0.0, 0.00) 1063	0.79 (15.9, 0.19) 1035	0.95 (5.6, 0.13) 298	0.92 (4.7, 0.11) 164	0.93 (4.7, 0.11) 323	0.95 (4.9, 0.10) 329	0.95 (3.8, 0.10) 170	0.85 (6.4, 0.13) 319	0.90 (6.4, 0.13) 344	0.93 (5.0, 0.12) 337	0.91 (6.0, 0.13) 934	0.88 (5.6, 0.12) 340
B		1.00 (0.0, 0.00) 1066	0.71 (16.9, 0.24) 303	0.65 (17.4, 0.25) 165	0.80 (14.4, 0.19) 329	0.85 (12.5, 0.14) 335	0.76 (15.7, 0.20) 171	0.69 (17.0, 0.19) 324	0.71 (15.7, 0.21) 350	0.68 (17.8, 0.23) 341	0.68 (19.3, 0.25) 938	0.67 (15.9, 0.21) 346
C			1.00 (0.0, 0.00) 306	0.93 (2.8, 0.09) 144	0.90 (6.6, 0.16) 282	0.91 (6.7, 0.17) 282	0.94 (6.0, 0.14) 148	0.80 (9.4, 0.19) 268	0.93 (6.7, 0.15) 290	0.96 (4.6, 0.12) 286	0.95 (4.5, 0.10) 270	0.91 (6.5, 0.15) 286
D				1.00 (0.0, 0.00) 165	0.84 (6.4, 0.15) 153	0.87 (8.5, 0.16) 161	0.91 (5.8, 0.13) 158	0.79 (9.2, 0.17) 156	0.89 (5.9, 0.13) 158	0.91 (4.6, 0.11) 155	0.97 (3.1, 0.08) 146	0.85 (6.5, 0.15) 157
E					1.00 (0.0, 0.00) 332	0.90 (6.4, 0.13) 313	0.90 (6.5, 0.13) 157	0.84 (6.8, 0.14) 295	0.85 (8.3, 0.16) 320	0.86 (7.7, 0.16) 315	0.88 (7.6, 0.15) 290	0.83 (7.3, 0.15) 318
F						1.00 (0.0, 0.00) 337	0.91 (6.7, 0.13) 167	0.82 (7.4, 0.14) 302	0.88 (7.1, 0.15) 327	0.88 (7.9, 0.15) 319	0.89 (8.8, 0.17) 296	0.86 (7.0, 0.14) 322
G							1.00 (0.0, 0.00) 171	0.78 (7.3, 0.16) 159	0.94 (4.0, 0.10) 163	0.93 (5.0, 0.11) 159	0.90 (6.6, 0.15) 149	0.91 (5.0, 0.13) 161
H								1.00 (0.0, 0.00) 328	0.80 (8.4, 0.15) 317	0.78 (8.2, 0.17) 309	0.82 (9.0, 0.18) 288	0.70 (9.2, 0.18) 314
I									1.00 (0.0, 0.00) 354	0.93 (5.0, 0.11) 334	0.89 (7.2, 0.16) 310	0.88 (6.0, 0.13) 339
J										1.00 (0.0, 0.00) 345	0.93 (5.5, 0.12) 302	0.88 (5.9, 0.13) 331
K											1.00 (0.0, 0.00) 966	0.86 (6.9, 0.15) 306
L												1.00 (0.0, 0.00) 350

1 To further investigate the relationship between correlation and distance, Figures 3-28
2 through 3-30 plot inter-sampler correlation as a function of distance between monitors for
3 PM_{2.5} in Boston, Pittsburgh, and Los Angeles. These three cities were selected to illustrate
4 how this relationship varies across urban areas with different topography and climatology
5 as well as different PM_{2.5} sources, compositions and monitor densities. Plots are provided in
6 Annex A for the remainder of the 15 CSAs/CBSAs under investigation beginning with
7 Figure A-1. The Boston data exhibit the strongest relationship between inter-sampler
8 correlation and distance, with average inter-sampler correlation remaining higher than
9 80% when samplers are 95 km apart ($R^2 = 0.55$). This small amount of variability is
10 expected given the consistency between distributions shown in the corresponding box plots
11 (Figure 3-20). The Pittsburgh data show some reductions in inter-sampler correlations at
12 short distances, with the samplers at Sites B and G having only 76% correlation with a
13 distance of less than 4 km. Site B is located in Liberty, PA, a mountainous suburb of
14 Pittsburgh where emissions from steel manufacturing and frequent stable conditions in the
15 planetary boundary layer cause localized events of elevated concentration. In contrast, Site

1 G is in the neighboring town of Clairton, PA, located at a lower elevation on the bank of the
2 opposite side of the Monongahela River from Liberty. On average, inter-sampler correlation
3 remained higher than 80% when samplers were separated by 61 km, but in this case with
4 much greater scatter ($R^2 = 0.22$) than observed in the Boston data. This scatter is driven by
5 the measurements at Site B; Figure 3-22 shows an elevated mean and variability for this
6 site compared with other monitors situated around the Pittsburgh CSA. When data from
7 Site B are removed, the inter-sampler correlation vs. distance plot for Pittsburgh $PM_{2.5}$
8 resembles the one from Boston (with R^2 increasing to 0.68). The Los Angeles data exhibit a
9 much steeper slope, with average inter-sampler correlation remaining higher than 80%
10 when samplers are 29 km apart ($R^2 = 0.74$). This suggests that other factors, such as
11 mountainous topography separating monitors, the distribution of traffic and suspension of
12 crustal components, and occurrence of stable boundary layers, may cause more spatial
13 variation in the $PM_{2.5}$ concentration profile within the Los Angeles region when compared
14 with other parts of the country. The Site I monitor, separated from the rest of the Los
15 Angeles region by the San Gabriel Mountains as mentioned above, provides the low
16 correlations grouped in the lower right portion of Figure 3-27. It should also be noted in
17 examining Figures 3-19 through 3-23 that some monitors are often located close to major
18 interstate highways while others in the same urban area are not. These differences in
19 proximity of monitors to nearby major roads will also result in lower inter-monitor
20 correlations.



Figure 3-23. Locations of PM_{2.5} monitors and major highways, Los Angeles, CA.

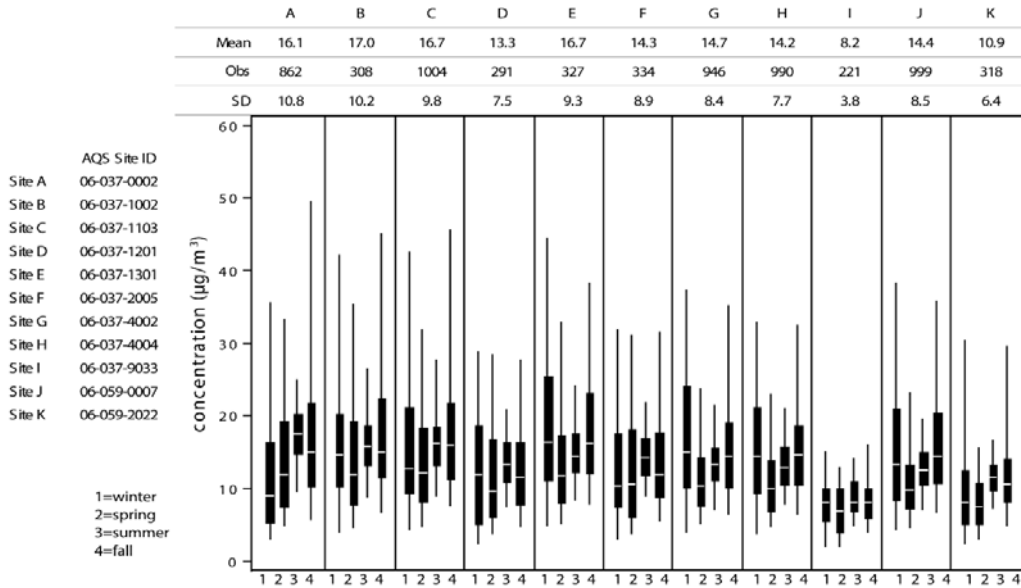


Figure 3-24. Seasonal distribution of 24-h avg PM_{2.5} concentrations by site for Los Angeles, CA, 2005-2007. Box plots show the median and interquartile range with whiskers extending to the 5th and 95th percentiles at each site during (1) winter (December-February), (2) spring (March-May), (3) summer (June-August) and (4) fall (September-November).

Table 3-13. Inter-sampler comparison statistics for each pair of 24-h PM_{2.5} monitors reporting to AQ5 for Los Angeles, CA.

	A	B	C	D	E	F	G	H	I	J	K
A	1.00 (0.0, 0.00)	0.86 (9.0, 0.18)	0.87 (7.7, 0.16)	0.81 (9.0, 0.19)	0.80 (9.7, 0.21)	0.88 (5.8, 0.14)	0.68 (11.5, 0.22)	0.64 (12.4, 0.23)	0.30 (18.0, 0.36)	0.70 (10.5, 0.21)	0.82 (11.4, 0.23)
	862	252	803	238	262	269	761	793	179	804	259
B		1.00 (0.0, 0.00)	0.92 (5.5, 0.11)	0.87 (9.1, 0.19)	0.83 (9.0, 0.15)	0.88 (7.6, 0.15)	0.77 (9.8, 0.17)	0.73 (11.6, 0.18)	0.31 (24.1, 0.38)	0.74 (11.9, 0.19)	0.71 (15.0, 0.27)
		308	293	250	278	279	268	282	177	292	277
C			1.00 (0.0, 0.00)	0.80 (9.6, 0.20)	0.89 (5.8, 0.11)	0.92 (6.4, 0.13)	0.84 (9.0, 0.15)	0.79 (10.0, 0.17)	0.29 (18.6, 0.38)	0.82 (9.4, 0.16)	0.78 (13.2, 0.25)
			1004	274	315	319	880	913	213	920	305
D				1.00 (0.0, 0.00)	0.69 (10.9, 0.23)	0.77 (7.4, 0.18)	0.63 (11.3, 0.22)	0.60 (11.1, 0.22)	0.41 (14.8, 0.31)	0.64 (9.6, 0.21)	0.60 (11.6, 0.23)
				291	263	263	256	268	164	274	261
E					1.00 (0.0, 0.00)	0.79 (9.1, 0.19)	0.95 (5.9, 0.11)	0.92 (7.6, 0.13)	0.34 (19.7, 0.39)	0.88 (8.2, 0.15)	0.76 (13.7, 0.27)
					327	301	289	301	192	307	291
F						1.00 (0.0, 0.00)	0.70 (10.5, 0.18)	0.70 (9.2, 0.19)	0.33 (14.8, 0.34)	0.69 (9.8, 0.19)	0.72 (9.9, 0.21)
						KEY					
						Pearson R					
						(P90, COD)					
G							1.00 (0.0, 0.00)	0.96 (4.0, 0.09)	0.23 (17.0, 0.35)	0.92 (5.4, 0.12)	0.78 (11.0, 0.21)
							n				
							946	859	194	882	277
H								1.00 (0.0, 0.00)	0.26 (15.3, 0.34)	0.91 (5.9, 0.12)	0.78 (9.5, 0.21)
								990	208	914	294
I									1.00 (0.0, 0.00)	0.21 (18.3, 0.35)	0.31 (9.7, 0.28)
									221	205	180
J										1.00 (0.0, 0.00)	0.84 (9.8, 0.19)
										999	298
K											1.00 (0.0, 0.00)
											318

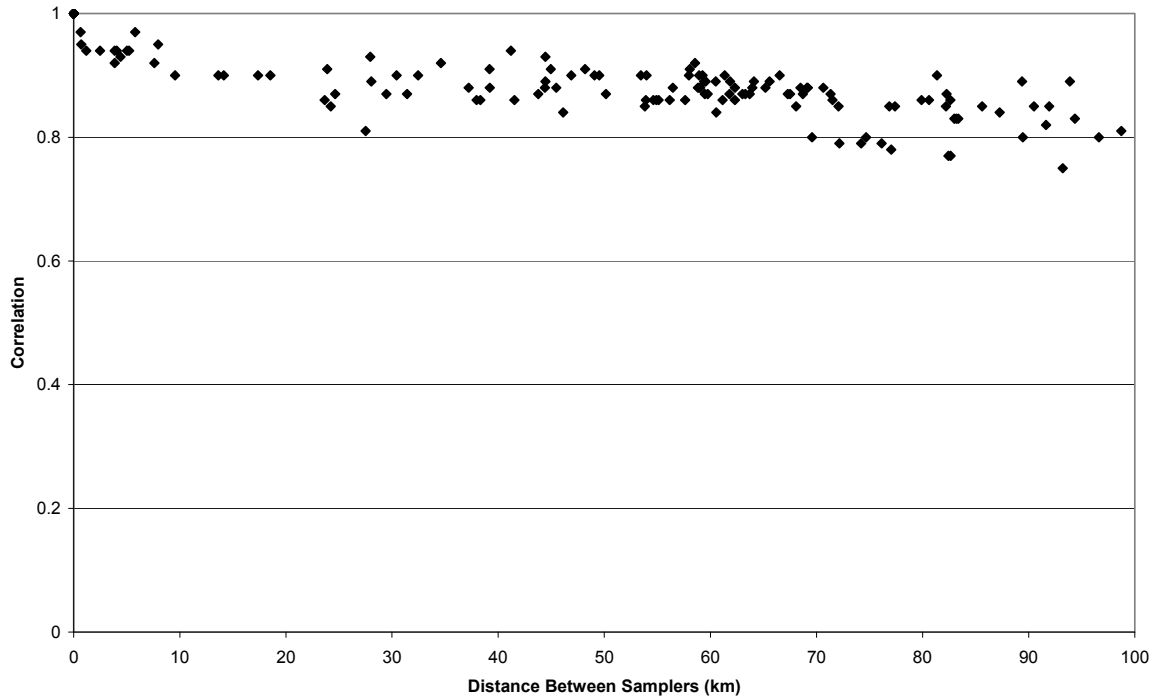


Figure 3-25. Inter-sampler correlations for 24-h PM_{2.5} as a function of distance between monitors in Boston, MA.

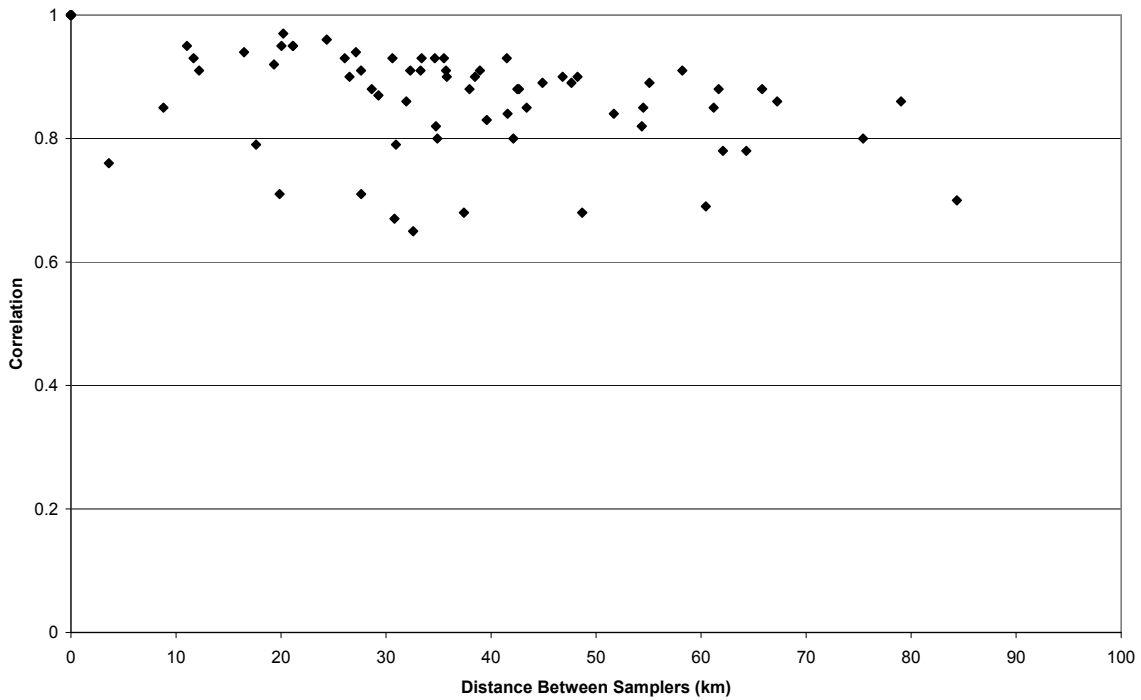


Figure 3-26. Inter-sampler correlations for 24-h PM_{2.5} as a function of distance between monitors in Pittsburgh, PA.

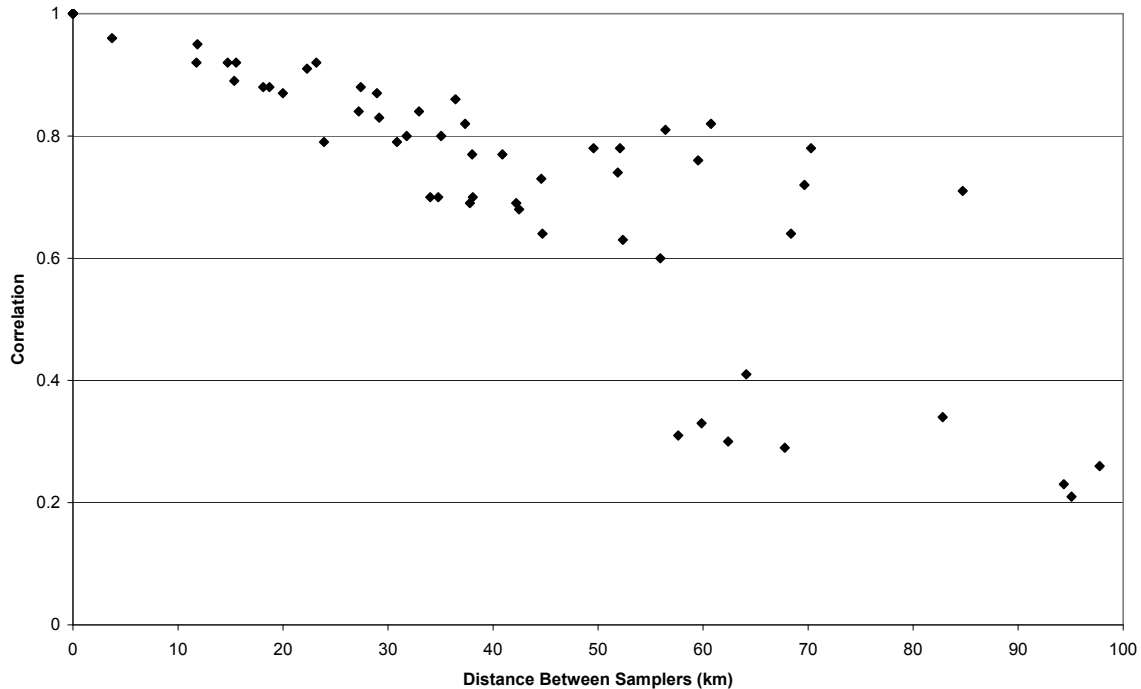


Figure 3-27. Inter-sampler correlations for 24-h PM_{2.5} as a function of distance between monitors in Los Angeles, CA.

PM_{10-2.5}

1 Given the limited number of co-located low-volume FRM PM₁₀ and FRM PM_{2.5}
 2 monitors, only a very limited investigation into the intra-urban spatial variability of PM₁₀₋
 3 _{2.5} was possible using AQS data. Of the 15 cities under investigation, only six (Atlanta,
 4 Boston, Chicago, Denver, New York and Phoenix) contained data sufficient for calculating
 5 PM_{10-2.5} according to the data completeness and monitor specification requirements
 6 discussed earlier. Figure 3-28 contains box plots of PM_{10-2.5} for one or two available sites per
 7 CSA/CBSA providing adequate PM_{10-2.5} concentration data. For Boston, the correlation
 8 between the two sites for PM_{10-2.5} was 0.45 compared with 0.73 for PM_{2.5} alone and 0.84 for
 9 PM₁₀ alone (using the same two monitoring sites). For New York, the correlation was
 10 slightly higher for the two sites: 0.74 for PM_{10-2.5} compared with 0.93 for PM_{2.5} alone and
 11 0.82 for PM₁₀ alone. The COD for PM_{10-2.5} also increases in both cities compared with PM_{2.5}
 12 and PM₁₀ alone, suggesting less spatial homogeneity for thoracic coarse particles compared
 13 with fine particles. Wilson and Suh (1997, [077408](#)) reported PM_{10-2.5} correlations between
 14 eight sites in Philadelphia ranging from 0.14 to 0.63 with an average of 0.38. This was
 15 considerably less than the corresponding average correlation for PM_{2.5} (r = 0.90) and PM₁₀
 16 (r = 0.87) from the same study. Thornburg et al. (2009, [190999](#)) also reported a high degree

1 of spatial variability in $PM_{10-2.5}$ in Detroit with between-monitor correlations ranging from
 2 0.03 to 0.76. These results suggest that local sources can have a substantial impact on
 3 $PM_{10-2.5}$ concentrations, resulting in a higher degree of spatial variability in $PM_{10-2.5}$ relative
 4 to $PM_{2.5}$ or PM_{10} .

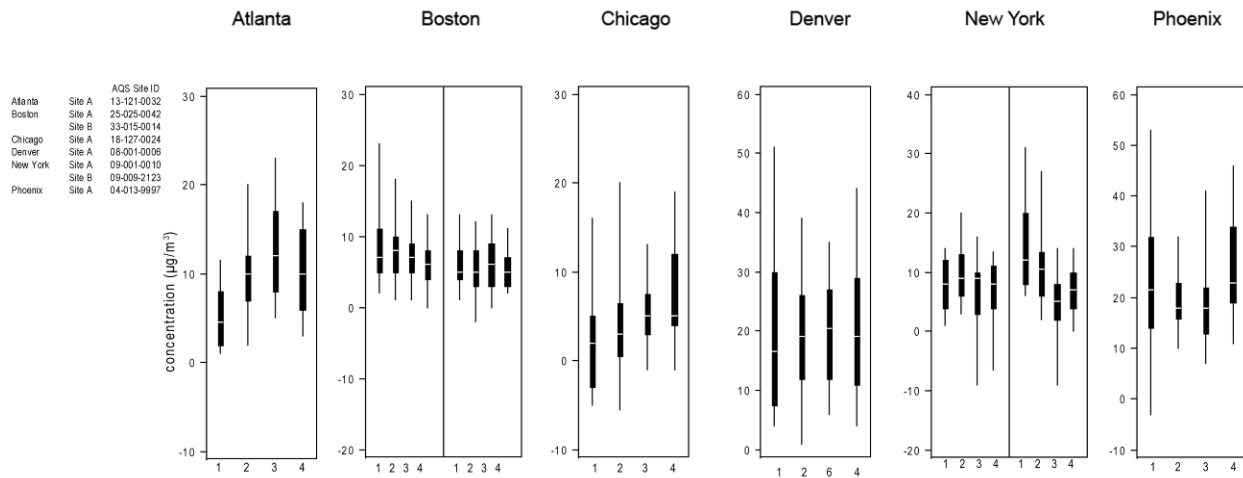


Figure 3-28. Seasonal distribution of 24-h avg $PM_{10-2.5}$ concentrations by site for Atlanta, GA; Boston, MA; Chicago, IL; Denver, CO; New York City, NY; and Phoenix, AZ; 2005-2007. Box plots show the median and interquartile range with whiskers extending to the 5th and 95th percentiles at each site during (1) winter (December-February), (2) spring (March-May), (3) summer (June-August) and (4) fall (September-November). Note the different concentration scales on the y-axes.

PM_{10}

5 PM_{10} mass concentration has been shown to vary as much as a factor of five over
 6 urban-scale distances of 100 km or less, and by a factor of 2 or more on scales as small as 30
 7 km in an analysis of California air quality (Alexis et al., 2001, [079886](#)). This can be
 8 attributed to the rapid V_d and resulting short atmospheric lifetime of the coarse-mode
 9 particles making up much of PM_{10} mass. As a result, local emission sources often dominate
 10 PM_{10} annual average mass at certain monitors. Data from the fifteen CSAs/CBSAs were
 11 used to investigate urban variability in PM_{10} reported to the AQS database.

12 Maps of PM_{10} monitor locations and box plots of seasonal PM_{10} mass concentration
 13 data are provided for Boston (Figures 3-32 and 3-33), Pittsburgh (Figures 3-34 and 3-35),
 14 and Los Angeles (Figures 3-36 and 3-37) similar to the $PM_{2.5}$ maps and box plots shown
 15 earlier in Figures 3-38 through 3-40 Annex A, Figures A-71 through A-106 incorporate

1 similar information for the remainder of the 15 CSAs/CBSAs. Tables 3-14 through 3-16
2 contain pair wise, within-city comparison statistics (R, P90, COD and N, as defined above)
3 for PM₁₀ measured at the available monitors in Boston (Table 3-14), Pittsburgh (Table 3-15)
4 and Los Angeles (Table 3-16); the remainder of the 15 CSAs/CBSAs are included in Annex
5 A, Tables A-32 through A-43.

6 Boston is an example of a city with a wide range in concentrations measured at
7 different sites. Inter-monitor variation in PM₁₀ is frequently larger than the seasonal
8 variation measured at any given site. Pairwise correlations between monitors in Boston
9 range from 0.45 to 0.95 in Table 3-14. Pittsburgh is an example of a city with a large
10 number of PM₁₀ monitors providing consistent values with a select few reporting higher
11 concentrations (sites D, H, I and K in Figure 3-32). This illustrates the potential influence
12 of localized point or area sources or topography. Correlations between monitors in
13 Pittsburgh range from 0.47 to 0.97 in Table 3-15. Los Angeles shows a high degree of
14 between-season and within-season variability, which is on the order of the between-monitor
15 variation. Correlations between monitors in Los Angeles range from 0.29 to 0.93 in
16 Table 3-16. Once again, the lowest correlations are with the monitor separated from the
17 other monitors by the San Gabriel Mountains (Site E in Figure 3-33).

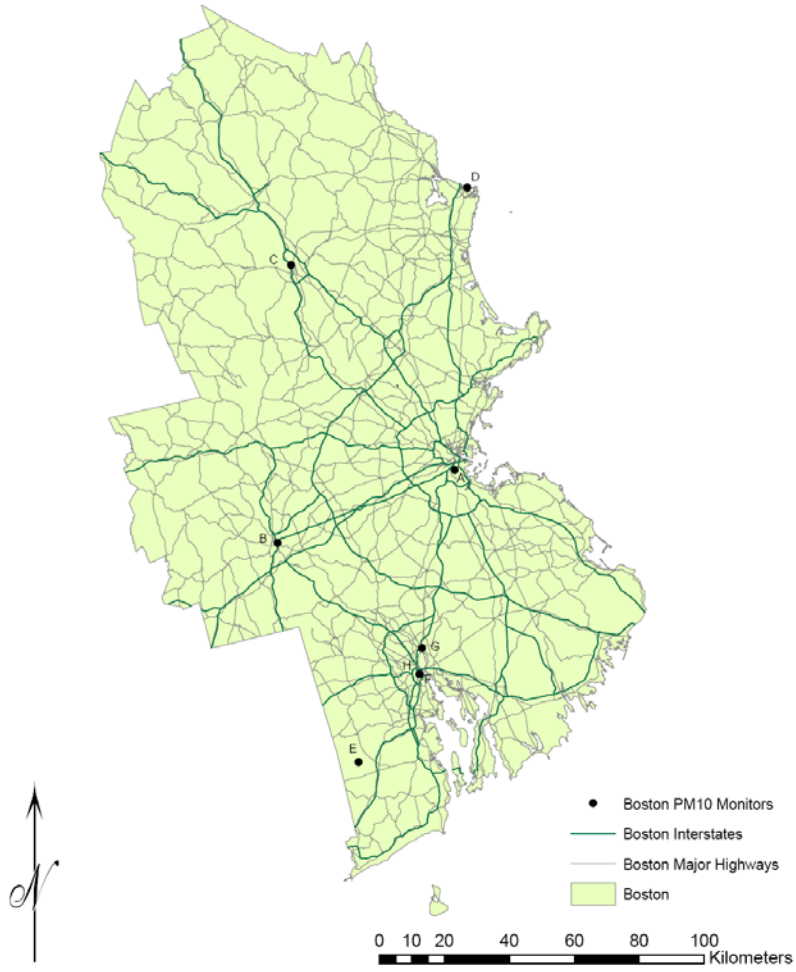


Figure 3-29. Locations of PM₁₀ monitors and major highways, Boston, MA.

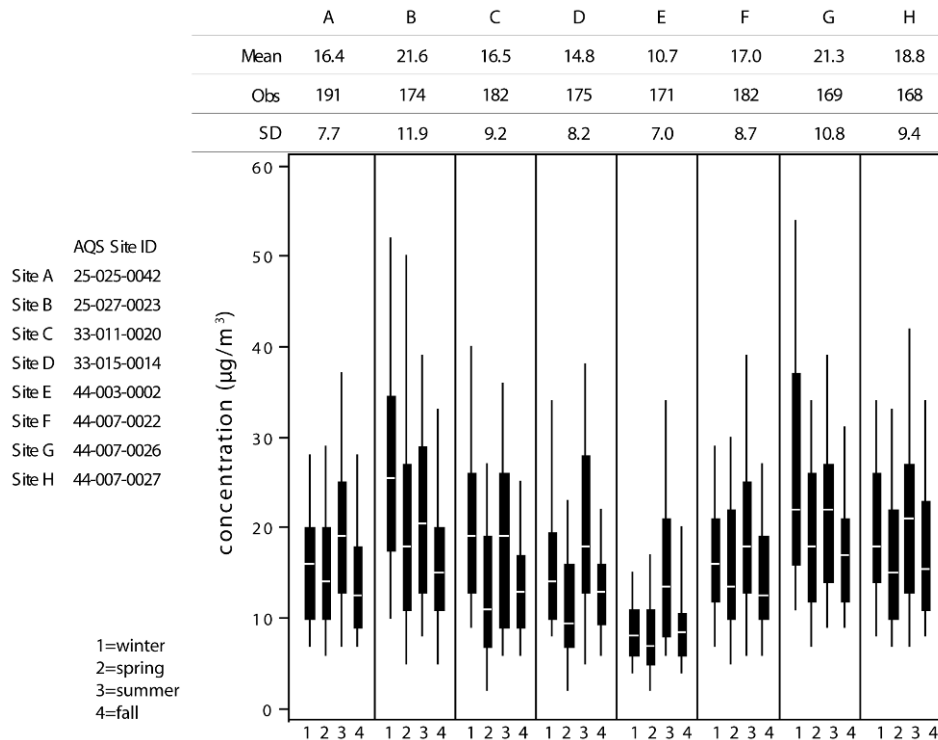


Figure 3-30. Seasonal distribution of 24-h avg PM₁₀ concentrations by site for Boston, MA, 2005-2007. Box plots show the median and interquartile range with whiskers extending to the 5th and 95th percentiles at each site during (1) winter (December-February), (2) spring (March-May), (3) summer (June-August) and (4) fall (September-November).

Table 3-14. Inter-sampler comparison statistics for each pair of 24-h PM₁₀ monitors reporting to AQS for Boston, MA.

Site	A	B	C	D	E	F	G	H
A	1.00 (0.0, 0.00) 191	0.69 (15.0, 0.22) 169	0.69 (12.0, 0.20) 179	0.73 (10.0, 0.22) 173	0.71 (13.0, 0.30) 171	0.84 (8.0, 0.14) 182	0.70 (15.0, 0.20) 169	0.79 (10.0, 0.17) 167
B		1.00 (0.0, 0.00) 174	0.66 (17.0, 0.24) 167	0.56 (19.0, 0.28) 161	0.45 (24.0, 0.39) 158	0.69 (15.0, 0.21) 169	0.77 (12.0, 0.17) 156	0.65 (16.0, 0.20) 154
C			1.00 (0.0, 0.00) 182	0.72 (10.0, 0.22) 170	0.47 (17.0, 0.33) 168	0.62 (12.0, 0.21) 179	0.64 (16.0, 0.26) 166	0.59 (16.0, 0.24) 164
D				1.00 (0.0, 0.00) 175	0.63 (11.0, 0.29) 163	0.68 (10.0, 0.23) 173	0.59 (19.0, 0.30) 161	0.69 (13.0, 0.26) 158
E					1.00 (0.0, 0.00) 171	0.84 (13.0, 0.29) 171	0.58 (22.0, 0.38) 161	0.80 (15.0, 0.33) 157
F						1.00 (0.0, 0.00) 182	0.81 (11.0, 0.16) 169	0.95 (5.0, 0.11) 167
G							1.00 (0.0, 0.00) 169	0.79 (10.0, 0.13) 154
H								1.00 (0.0, 0.00) 168

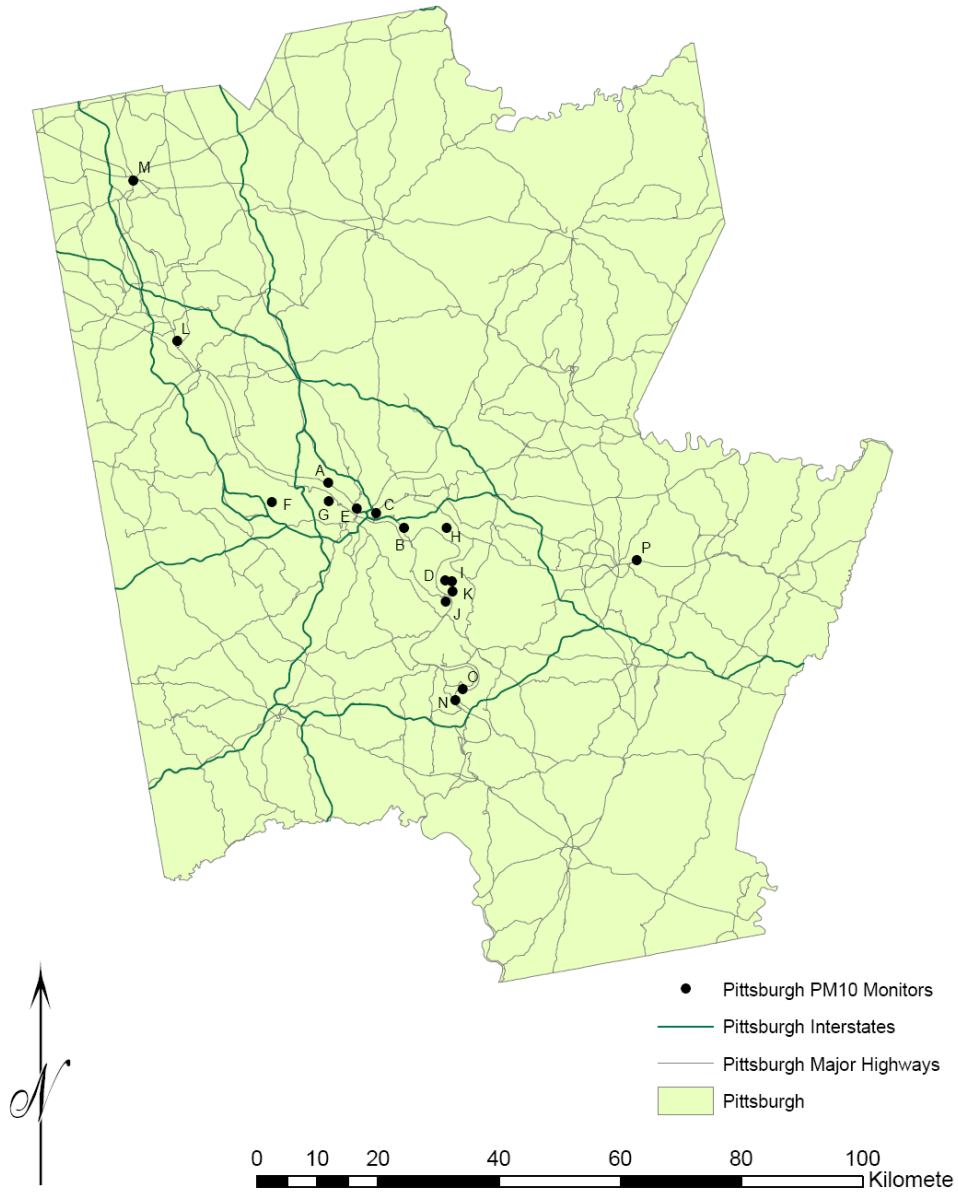


Figure 3-31. Locations of PM₁₀ monitors and major highways, Pittsburgh, PA.

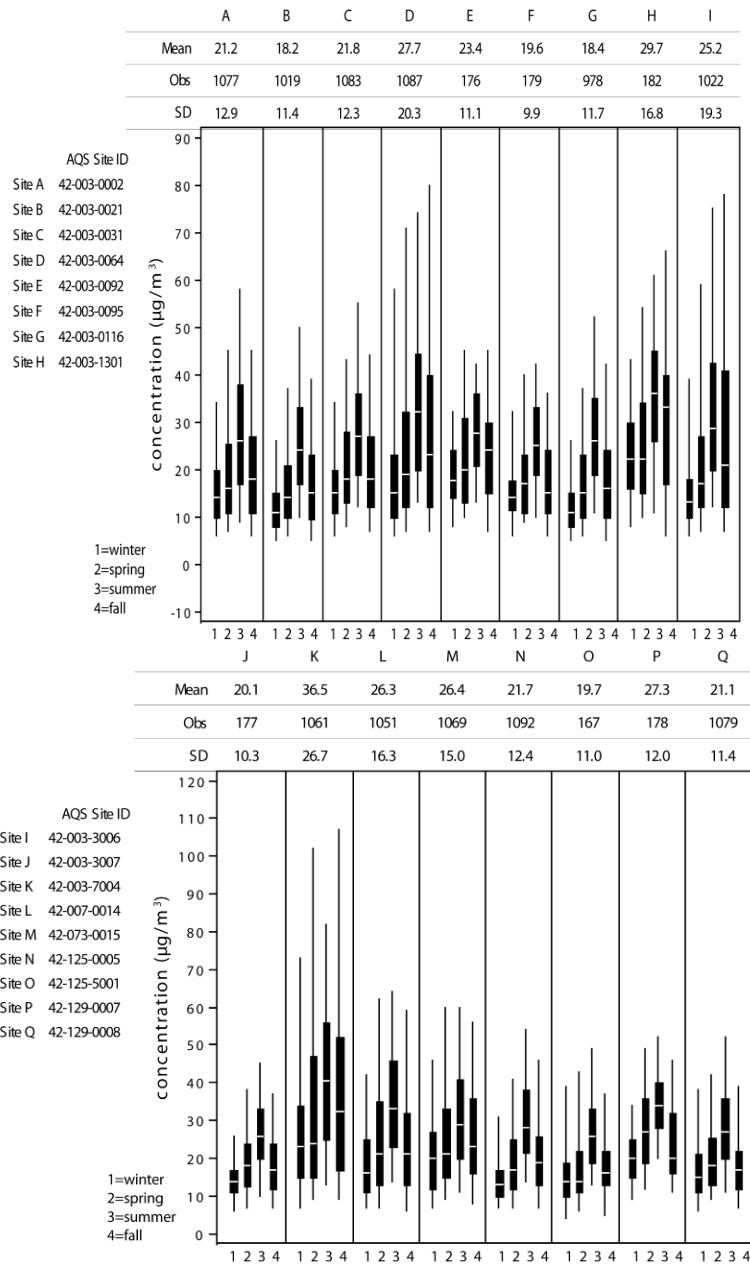


Figure 3-32. Seasonal distribution of 24-h avg PM₁₀ concentrations by site for Pittsburgh, PA, 2005-2007. Box plots show the median and interquartile range with whiskers extending to the 5th and 95th percentiles at each site during (1) winter (December-February), (2) spring (March-May), (3) summer (June-August) and (4) fall (September-November).

Table 3-15. Inter-sampler comparison statistics for each pair of 24-h PM₁₀ monitors reporting to AQS for Pittsburgh, PA.

Site	A	B	C	D	E	F	G	H	I
------	---	---	---	---	---	---	---	---	---

Site	A	B	C	D	E	F	G	H	I
A	1.00 (0.0, 0.00)	0.93 (9.0, 0.15)	0.93 (8.0, 0.14)	0.90 (23.0, 0.21)	0.92 (8.0, 0.12)	0.89 (14.0, 0.18)	0.93 (8.0, 0.14)	0.79 (16.0, 0.17)	0.86 (18.0, 0.18)
T	1077	1002	1065	1070	175	178	960	181	1005
B		1.00 (0.0, 0.00)	0.96 (8.0, 0.15)	0.80 (29.0, 0.24)	0.91 (11.0, 0.20)	0.92 (6.0, 0.16)	0.87 (5.0, 0.10)	0.81 (25.0, 0.29)	0.89 (22.0, 0.20)
		1019	1007	1012	163	166	911	169	954
C			1.00 (0.0, 0.00)	0.81 (23.0, 0.20)	0.94 (6.0, 0.11)	0.93 (7.0, 0.12)	0.94 (8.0, 0.13)	0.77 (21.0, 0.22)	0.87 (19.0, 0.17)
			1083	1075	173	176	966	179	1010
D				1.00 (0.0, 0.00)	0.72 (21.0, 0.20)	0.66 (26.0, 0.24)	0.76 (27.0, 0.24)	0.83 (14.0, 0.18)	0.88 (16.0, 0.14)
				1087	176	179	970	182	1014
E					1.00 (0.0, 0.00)	0.90 (10.0, 0.14)	0.90 (10.0, 0.17)	0.78 (20.0, 0.20)	0.77 (20.0, 0.19)
					176	173	154	175	166
F						1.00 (0.0, 0.00)	0.94 (7.0, 0.12)	0.70 (25.0, 0.27)	0.74 (25.0, 0.22)
						179	157	178	168
G							1.00 (0.0, 0.00)	0.70 (22.0, 0.28)	0.87 (20.0, 0.19)
							978	160	910
H								1.00 (0.0, 0.00)	0.76 (17.0, 0.20)
								182	171
I									1.00 (0.0, 0.00)
									1022

KEY
Pearson R
(P90, COD)
n

	J	K	L	M	N	O	P	Q
A	0.84 (14.0, 0.20)	0.76 (40.0, 0.30)	0.88 (15.0, 0.18)	0.85 (16.0, 0.19)	0.86 (11.0, 0.16)	0.77 (16.0, 0.22)	0.78 (15.0, 0.19)	0.86 (11.0, 0.15)
	176	1044	1033	1052	1074	166	177	1061
B	0.93 (7.0, 0.16)	0.76 (43.0, 0.36)	0.88 (19.0, 0.23)	0.81 (20.0, 0.26)	0.91 (10.0, 0.16)	0.76 (12.0, 0.19)	0.83 (18.0, 0.28)	0.88 (10.0, 0.18)
	164	986	982	994	1016	157	165	1003
C	0.90 (8.0, 0.13)	0.75 (39.0, 0.30)	0.88 (14.0, 0.17)	0.83 (15.0, 0.19)	0.89 (9.0, 0.12)	0.78 (12.0, 0.18)	0.88 (13.0, 0.19)	0.90 (9.0, 0.12)
	174	1049	1039	1057	1080	164	175	1067
D	0.73 (24.0, 0.22)	0.84 (24.0, 0.22)	0.80 (20.0, 0.18)	0.78 (20.0, 0.20)	0.76 (25.0, 0.20)	0.57 (28.0, 0.26)	0.64 (20.0, 0.25)	0.74 (26.0, 0.21)
	177	1055	1043	1061	1084	167	178	1071
E	0.86 (10.0, 0.16)	0.65 (36.0, 0.29)	0.83 (16.0, 0.16)	0.80 (14.0, 0.17)	0.84 (12.0, 0.14)	0.77 (14.0, 0.19)	0.84 (13.0, 0.16)	0.85 (11.0, 0.15)
	171	169	169	172	176	161	172	174
F	0.90 (7.0, 0.12)	0.57 (41.0, 0.34)	0.82 (20.0, 0.20)	0.75 (19.0, 0.22)	0.86 (11.0, 0.14)	0.83 (9.0, 0.15)	0.84 (16.0, 0.22)	0.86 (9.0, 0.14)
	174	172	172	175	179	164	175	177
G	0.92 (7.0, 0.13)	0.73 (45.0, 0.35)	0.87 (18.0, 0.21)	0.78 (19.0, 0.24)	0.89 (9.0, 0.15)	0.81 (11.0, 0.17)	0.84 (17.0, 0.26)	0.86 (10.0, 0.16)
	156	955	938	952	975	146	157	967
H	0.74 (23.0, 0.26)	0.68 (26.0, 0.22)	0.77 (15.0, 0.18)	0.78 (17.0, 0.18)	0.74 (21.0, 0.22)	0.60 (27.0, 0.29)	0.65 (19.0, 0.22)	0.76 (21.5, 0.24)
	176	175	175	178	182	167	177	180
I	0.79 (22.0, 0.20)	0.83 (30.0, 0.25)	0.82 (16.0, 0.17)	0.78 (18.0, 0.20)	0.81 (20.0, 0.17)	0.66 (26.0, 0.24)	0.69 (21.0, 0.25)	0.78 (22.0, 0.19)
	166	992	978	998	1019	158	167	1009
J	1.00 (0.0, 0.00)	0.66 (44.5, 0.33)	0.79 (18.0, 0.20)	0.72 (18.0, 0.22)	0.88 (8.0, 0.13)	0.78 (11.0, 0.17)	0.86 (16.0, 0.21)	0.86 (8.0, 0.15)
	177	170	170	173	177	163	173	175
K		1.00 (0.0, 0.00)	0.74 (31.0, 0.26)	0.75 (33.0, 0.24)	0.70 (40.0, 0.30)	0.47 (44.0, 0.36)	0.58 (34.0, 0.30)	0.68 (43.0, 0.30)
		1061	1017	1035	1058	160	171	1048
L			1.00 (0.0, 0.00)	0.87 (13.0, 0.16)	0.85 (16.0, 0.17)	0.70 (22.0, 0.24)	0.74 (17.0, 0.21)	0.80 (18.0, 0.19)
			1051	1025	1048	160	171	1035
M				1.00 (0.0, 0.00)	0.74 (18.0, 0.21)	0.64 (19.0, 0.26)	0.67 (17.0, 0.22)	0.77 (18.0, 0.19)
				1069	1067	163	174	1053
N					1.00 (0.0, 0.00)	0.72 (13.0, 0.18)	0.86 (14.0, 0.20)	0.86 (10.0, 0.14)
					1092	167	178	1076
O						1.00 (0.0, 0.00)	0.75 (18.0, 0.25)	0.69 (14.0, 0.19)
						167	163	165
P							1.00 (0.0, 0.00)	0.84 (15.0, 0.21)
							178	176
Q								1.00 (0.0, 0.00)
								1079

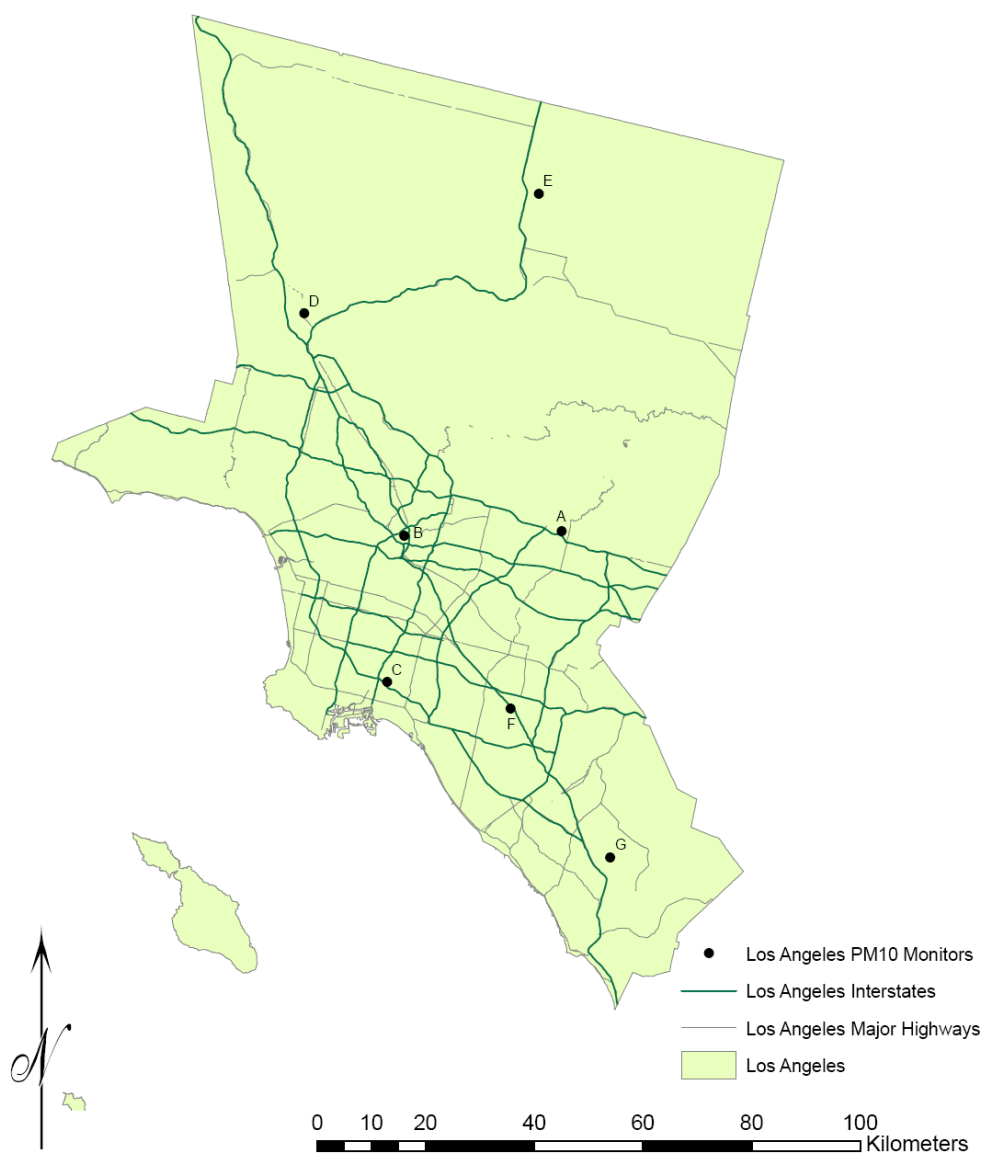


Figure 3-33. Locations of PM₁₀ monitors and major highways, Los Angeles, CA.

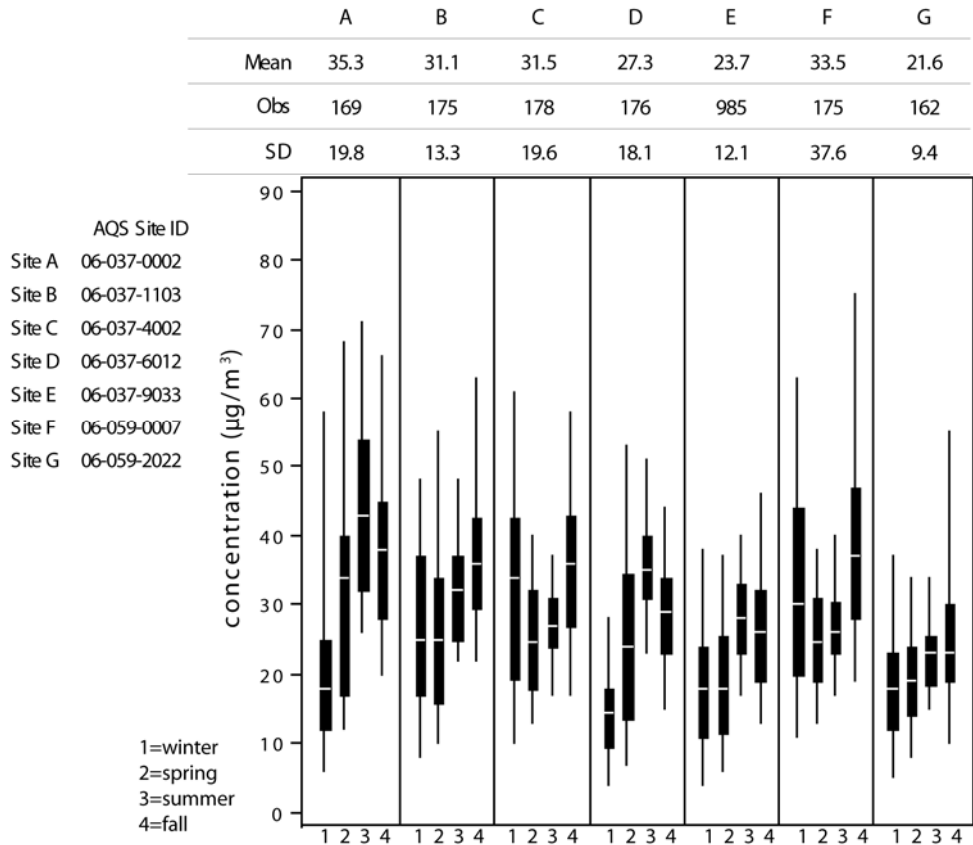


Figure 3-34. Seasonal distribution of 24-h avg PM₁₀ concentrations by site for Los Angeles, CA, 2005-2007. Box plots show the median and interquartile range with whiskers extending to the 5th and 95th percentiles at each site during (1) winter (December-February), (2) spring (March-May), (3) summer (June-August) and (4) fall (September-November).

Table 3-16. Inter-sampler comparison statistics for each pair of 24-h PM₁₀ monitors reporting to AQS for Los Angeles, CA.

Site	A	B	C	D	E	F	G
A	1.00 (0.0, 0.00)	0.73 (17.0, 0.17)	0.44 (27.0, 0.24)	0.73 (24.0, 0.22)	0.47 (28.0, 0.26)	0.41 (29.0, 0.24)	0.65 (30.0, 0.28)
	169	153	154	157	169	155	143
B		1.00 (0.0, 0.00)	0.61 (14.0, 0.14)	0.57 (21.0, 0.24)	0.52 (23.0, 0.23)	0.42 (15.0, 0.16)	0.73 (20.0, 0.23)
		175	159	159	173	162	149
C			1.00 (0.0, 0.00)	0.65 (27.0, 0.28)	0.43 (22.0, 0.24)	0.93 (11.0, 0.11)	0.73 (21.0, 0.22)
			178	158	176	159	148
D				1.00 (0.0, 0.00)	0.70 (16.0, 0.20)	0.65 (26.0, 0.28)	0.57 (19.5, 0.24)
				176	175	161	150
E					1.00 (0.0, 0.00)	0.29 (26.0, 0.25)	0.38 (20.0, 0.24)
					985	173	159
F						1.00 (0.0, 0.00)	0.65 (21.5, 0.22)
						175	150
G							1.00 (0.0, 0.00)
							162

1 Figures 3-38 through 3-42 illustrate the relationship between inter-sampler
2 correlation and distance between sites for PM₁₀ measurements obtained in Boston,
3 Pittsburgh and Los Angeles. Annex A contain similar plots for the remainder of the fifteen
4 CSAs/CBSAs under investigation beginning with Figure A-2. In each plot, substantially
5 more scatter is observed when compared to those for PM_{2.5} (Figure 3-25 through 3-30). This
6 is consistent with the variability observed in the seasonal box plots of concentration shown
7 in Figures 3-33, 3-35, and 3-37. The Boston data exhibit the strongest relationship between
8 inter-sampler correlation and distance, with average inter-sampler correlation remaining
9 higher than 80% when samplers are 44 km apart ($R^2 = 0.61$). The lowest correlations on
10 this plot originate from comparisons between Site B (rural Worcester, MA) and samplers
11 located at Sites E (West Greenwich, RI) and G (Providence, RI). Boston is subject to long
12 range transport of SO₄²⁻, which is a regional pollutant and is a major component of PM_{2.5}
13 and PM₁₀ in the eastern U.S. The Pittsburgh data shows some lower inter-sampler
14 correlations, with one sampler pair having only 66% correlation within a distance of 2 km.
15 On average, inter-sampler correlation remained higher than 80% when samplers were also
16 separated by 44 km, but in this case with much greater scatter ($R^2 = 0.28$) than observed in
17 the Boston data. As seen for the Pittsburgh PM₁₀ box plots in Figure 3-32, sites D, H, I, and
18 K have elevated means and high variability that is driving the observed scatter. These four
19 sites are all located in mountainous suburbs of Pittsburgh (North Braddock, PA, Liberty,
20 PA, Lincoln Boro, PA, and Beaver Falls, PA, respectively), where emissions from steel
21 manufacturing and frequent stable conditions in the planetary boundary layer cause
22 localized events of elevated concentration. When those four sites are removed, scatter
23 decreases greatly ($R^2 = 0.56$). The Los Angeles data exhibit a much steeper slope, with
24 average inter-sampler correlation remaining higher than 80% when samplers are only 30
25 km apart ($R^2 = 0.56$). The lower inter-sampler correlations in part reflect the fact that some
26 of these monitoring sites are separated from each other by hills or, in the case of one sited
27 at Lancaster, CA (Site D), by the San Gabriel Mountains. The Los Angeles data exhibit
28 greater scatter than the Pittsburgh data. However, the smallest inter-sampler separation
29 distance is 23 km, and there are relatively fewer PM₁₀ samplers. It is not possible to judge
30 how data would correlate on smaller spatial scales.

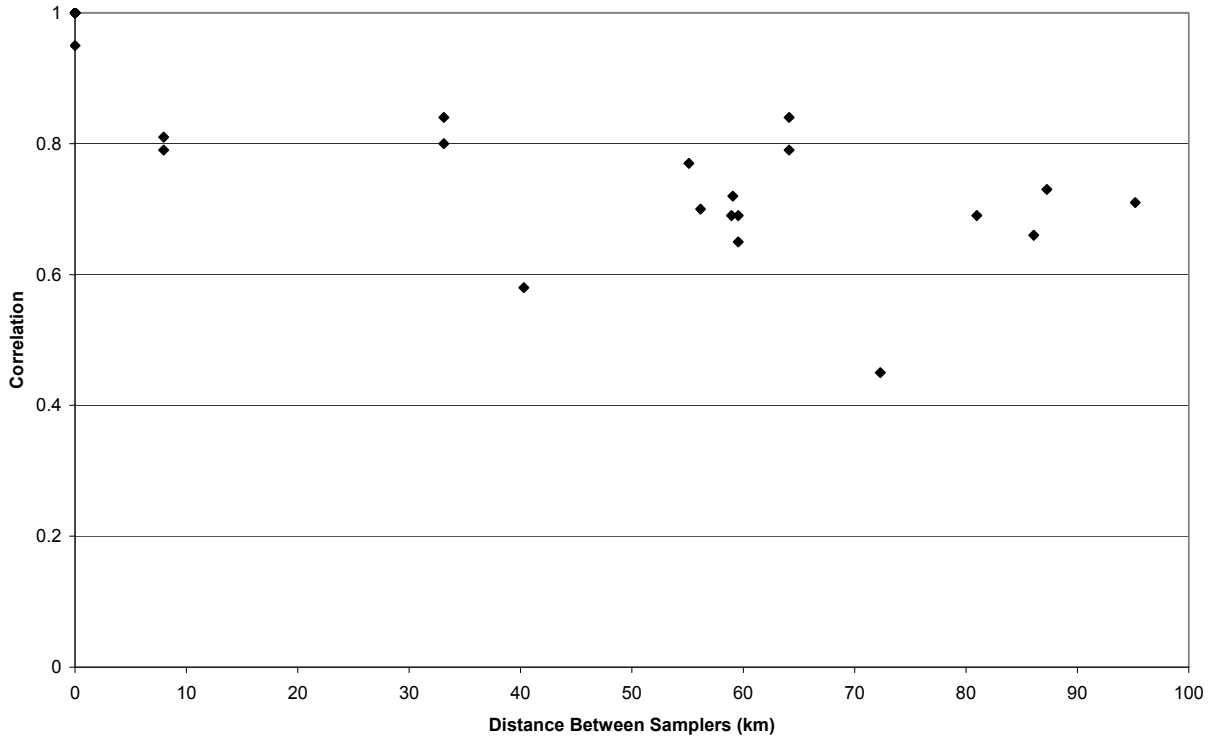


Figure 3-35. Inter-sampler correlations for 24-h PM₁₀ as a function of distance between monitors in Boston, MA.

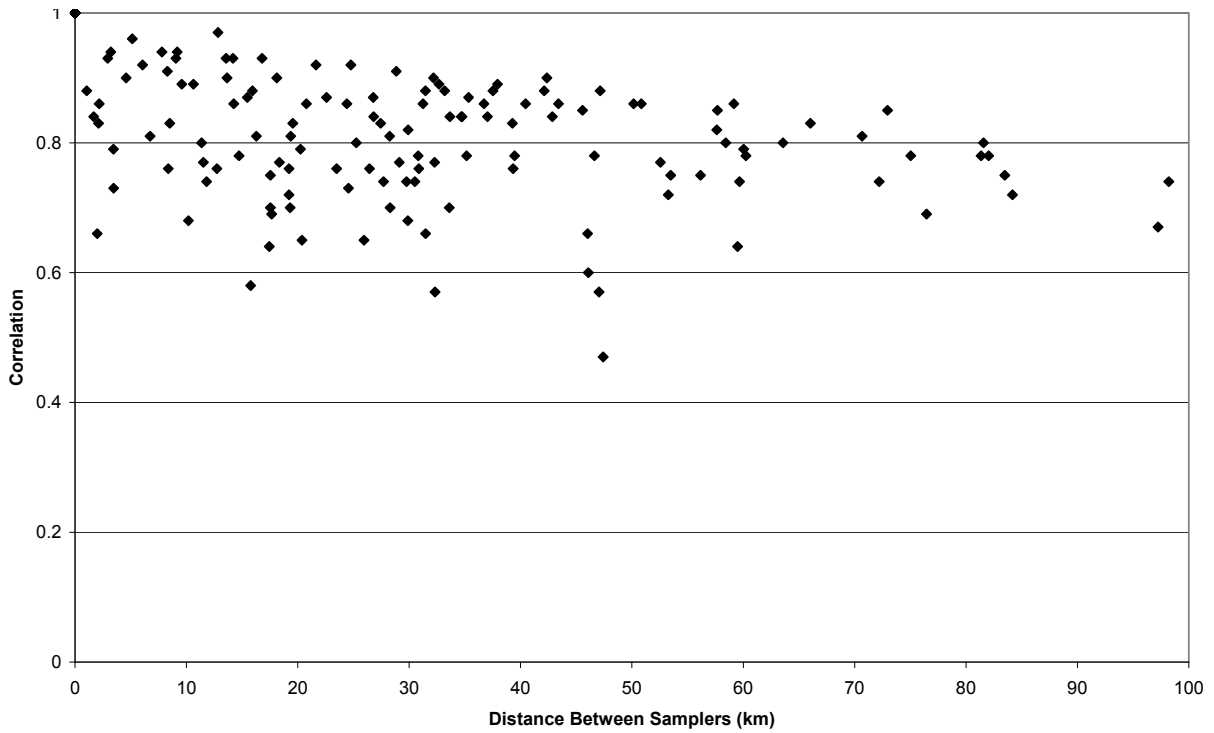


Figure 3-36. Inter-sampler correlations for 24-h PM₁₀ as a function of distance between monitors in Pittsburgh, PA.

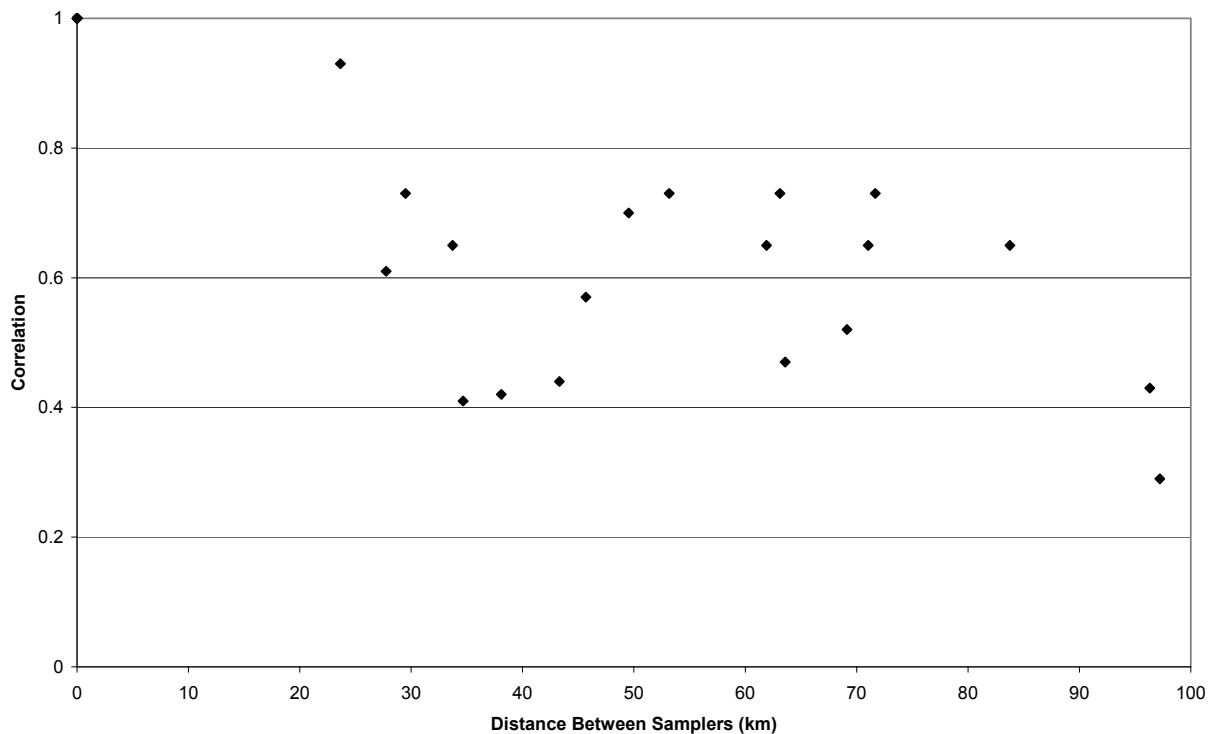


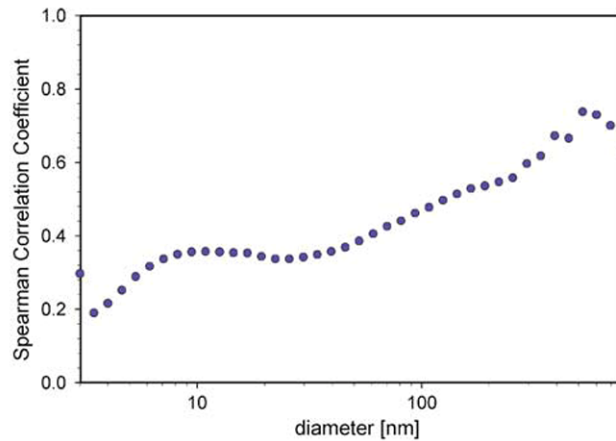
Figure 3-37. Inter-sampler correlations for 24-h PM₁₀ as a function of distance between monitors in Los Angeles, CA.

Ultrafine Particles

1 Relatively few studies compare ultrafine measurements at multiple locations within
 2 an urban center. An early study by Buzorius et al. (1999, [081205](#)) suggested spatial
 3 homogeneity in total particle number concentrations between multiple locations in
 4 Helsinki, Finland. They found correlations in 10-min avg at three sites within the city as
 5 high as 0.84. The sites, however, were relatively close together (2 km) and all near the same
 6 roadway. There was a high degree of correlation between traffic intensity and total aerosol
 7 number concentrations, suggesting that traffic was the primary source of the measured
 8 particles and the driving force behind the high correlations. Weekend correlations
 9 (0.28-0.47) and correlations with a fourth monitor located 22 km outside the city (0.05-0.64)
 10 were much lower.

11 Tuch et al. (2006, [157060](#)) found more spatial heterogeneity in ultrafine particle
 12 concentrations measured for an entire year at two locations 1.5 km apart in Leipzig,
 13 Germany. Figure 3-38 shows the correlation as a function of particle size (mobility
 14 diameter) dropping off as the particle size decreases from 0.5 at 100 nm down to 0.2 at 3
 15 nm. Table A-44 in Annex A contains correlation coefficients of hourly and daily average

1 particle number, surface area and volume concentrations as a function of particle diameter
2 adapted from the Tuch et al. (2006, [157060](#)) study. For all days (N = 5481 hourly
3 observations), the correlation between ultrafine particles (10-100 nm) measured at the two
4 sites was 0.31.



Source: Tuch et al. (2006, [157060](#))

Figure 3-38. Bin-wise Spearman correlation coefficients in aerosol particle number concentrations between the Ift (urban background) and the Eisenbahn-strasse (city/urban center) sites in Leipzig, Germany.

5 The two sites represented in Figure 3-38 and Table A-44 were relatively close to each
6 other, but one was located in a mixed semi-industrial region while the other was in a street
7 canyon in a residential neighborhood near busy roadways. This suggests a high degree of
8 spatial heterogeneity in ultrafine particles driven primarily by differences in nearby source
9 characteristics. Sioutas et al. (2005, [088428](#)) reviewed studies of the distribution of
10 ultrafine particles and came to the similar conclusion that mobile sources make a large
11 contribution to ultrafine particles and therefore ultrafine concentrations can exhibit
12 substantial variability in space and time. This is to be expected since ultrafine particle
13 concentrations drop off much quicker with distance from roadways than larger particle
14 sizes (Levy et al., 2003, [156688](#); Levy et al., 2003, [052661](#); Reponen et al., 2003, [088425](#);
15 Zhu et al., 2005, [157191](#)). Hagler et al. (2009, [191185](#)) showed similar exponential decreases
16 in ultrafine particle number concentrations with distance from the road for multiple
17 locations in the U.S. Neighborhood-scale variability and near-roadway concentration
18 gradients for ultrafine particles are discussed further in Section 3.1.1.3.

PM Constituents

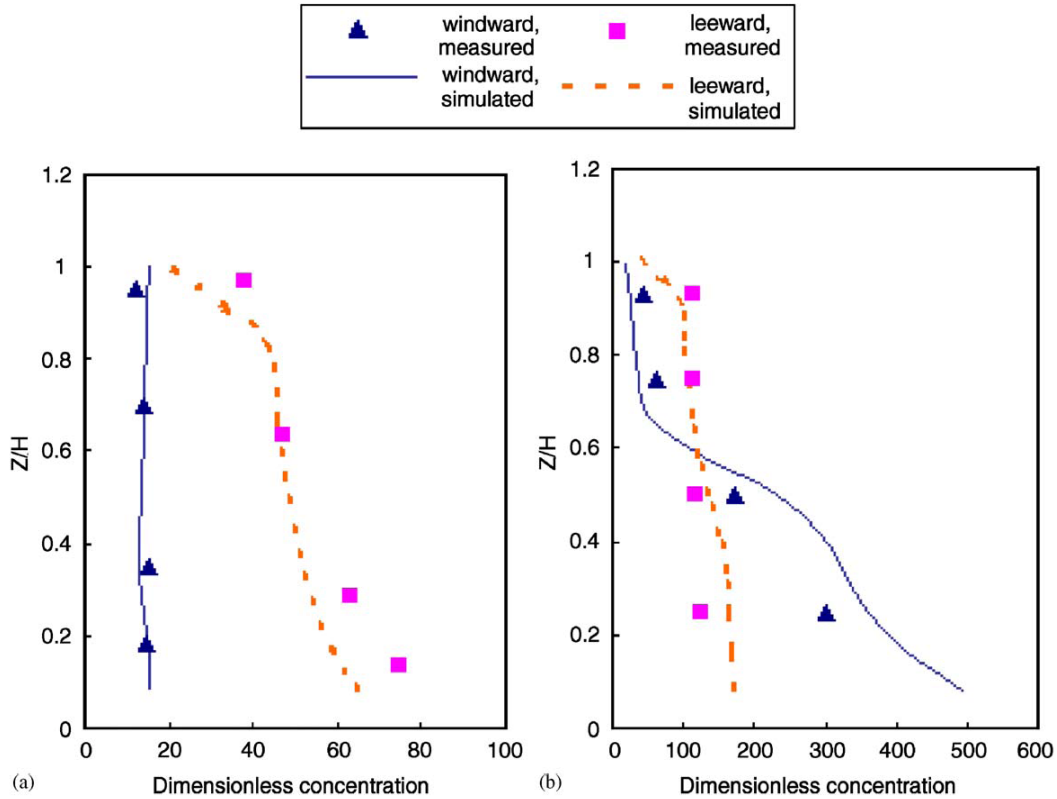
1 The pie charts showing PM_{2.5} composition that were generated using the SANDWICH
2 method for the fifteen CSAs/CBSAs presented earlier in Figures 3-17 and 3-18 represent
3 the average of all available monitors within each region. Individual pie charts for each
4 monitor are included in Figures A-107 through A-121 in Annex A and provide an indication
5 of the urban-scale spatial variability in PM_{2.5} composition. In the instances where multiple
6 monitors were available, there was a fair degree of spatial homogeneity in PM_{2.5} bulk
7 chemistry within each metropolitan area. Some notable exceptions exist, however.
8 Birmingham and Detroit show variation in the amount of crustal material, both spatially
9 and seasonally. Denver exhibits some spatial variation in NO₃⁻ during the winter, the
10 season with the highest measured PM_{2.5} mass. Several sites in New York and one in
11 Pittsburgh have elevated fractions of EC relative to the other sites within the respective
12 cities. In Phoenix, high winter PM_{2.5} mass is site specific and appears to be associated with
13 high organic carbon; the crustal component also varies and is inversely proportional to total
14 measured mass.

3.5.1.3. Neighborhood-Scale Variability

15 Neighborhood scale spatial variability in the particle concentration profile is affected
16 by land and building topography, meteorology, particle size distribution, particle
17 composition, and particle volatility. Population density at the neighborhood scale is also an
18 important determinant of the spatial distribution of PM concentration because density
19 impacts source prevalence, source magnitude, topographical-driven ventilation, and heat
20 island effects (Crist et al., 2008, [156372](#); Makar et al., 2006, [155959](#); Mfula et al., 2005,
21 [123359](#); Rigby and Toumi, 2008, [156050](#)). These considerations are crucial to understanding
22 variability in community monitoring data and for monitor deployment planning.

23 A number of computational and wind tunnel modeling street canyon studies have
24 demonstrated the potential variability in pollutant concentrations within a street canyon
25 (Borrego et al., 2006, [155697](#); Chang and Meroney, 2003, [090298](#); Chang and Tsai, 2003,
26 [155718](#); Kastner-Klein and Plate, 1999, [001961](#); So et al., 2005, [110746](#); Xiaomin et al.,
27 2006, [156165](#)). Influential parameters include street canyon height to width ratio (H/W),
28 source positioning, wind speed and direction, building shape and upstream configuration of
29 buildings. Figure 3-39 shows pollutant concentrations obtained from wind tunnel and

1 computational fluid dynamics simulations of transport and dispersion in an infinitely long
2 street canyon with a line source centered at the bottom of the canyon (Xiaomin et al., 2006,
3 [156165](#)). When the canyon height was equal to the street width (typical of moderate density
4 suburban or urban fringe residential neighborhoods) and lower background wind speed
5 existed, concentrations on the leeward canyon wall were four times those of the windward
6 wall near ground level. When the canyon height was twice the street width (typical of
7 higher-density urban planning) and background winds were somewhat higher, near ground
8 level concentrations on the windward canyon wall were roughly three times higher than
9 those measured at the leeward wall. Baldauf et al. (2008, [191017](#); 2009, [191766](#)) noted that
10 the presence of noise barriers, vegetation, or changes in topography adjacent to the road
11 can also alter particle dispersion characteristics. Specifically, depressed road sections,
12 where the road bed is below the surrounding terrain, leads to increased air turbulence and
13 pollutant dispersion. These results suggest that micro- and neighborhood-scale variation
14 related to urban topography may have a significant impact on pollutant concentrations at
15 this scale.



Source: Xiaomin et al. (2006, [156165](#)).

Figure 3-39. Dimensionless concentration as a function of height at windward and leeward locations and street canyon aspect ratios (H/W). (a) Dimensionless concentration on the windward and leeward sides of the canyon when $H/W = 1$ and wind speed = 3 m/s. (b) Dimensionless concentration on the windward and leeward sides of the canyon when $H/W = 2$ and wind speed = 5 m/s. Computational fluid dynamics modeling was performed, and measurements were obtained in wind tunnel simulations.

PM_{2.5} and PM₁₀

1 Knowledge of neighborhood-scale variability is important for interpreting data from
 2 PM_{2.5} and PM₁₀ community monitors. Figure 3-40 shows data derived from the fifteen
 3 CSAs/CBSAs for PM_{2.5} and PM₁₀ discussed in Section 3.5.1.2. This figure is limited to the
 4 inter-sampler correlations obtained for sampler pairs located within a distance of 4 km (i.e.,
 5 neighborhood scale). PM_{2.5} data exhibit a flatter slope, with average correlation maintained
 6 at 93% within 4 km ($R^2 = 0.22$). There is more scatter and variability among the PM₁₀ data,
 7 with an average correlation of 70% within 4 km ($R^2 = 0.03$). The degree of variability in
 8 PM₁₀ compared with PM_{2.5} relates to transport and dispersion of the PM_{10-2.5} component of

1 PM₁₀ compared with PM_{2.5}. However, differences in composition, source location,
 2 topography, and monitor height—all of which could affect concentrations—could drive the
 3 relatively high degree of scatter for both size classes, considering the low computed R²
 4 values for each of these curves.

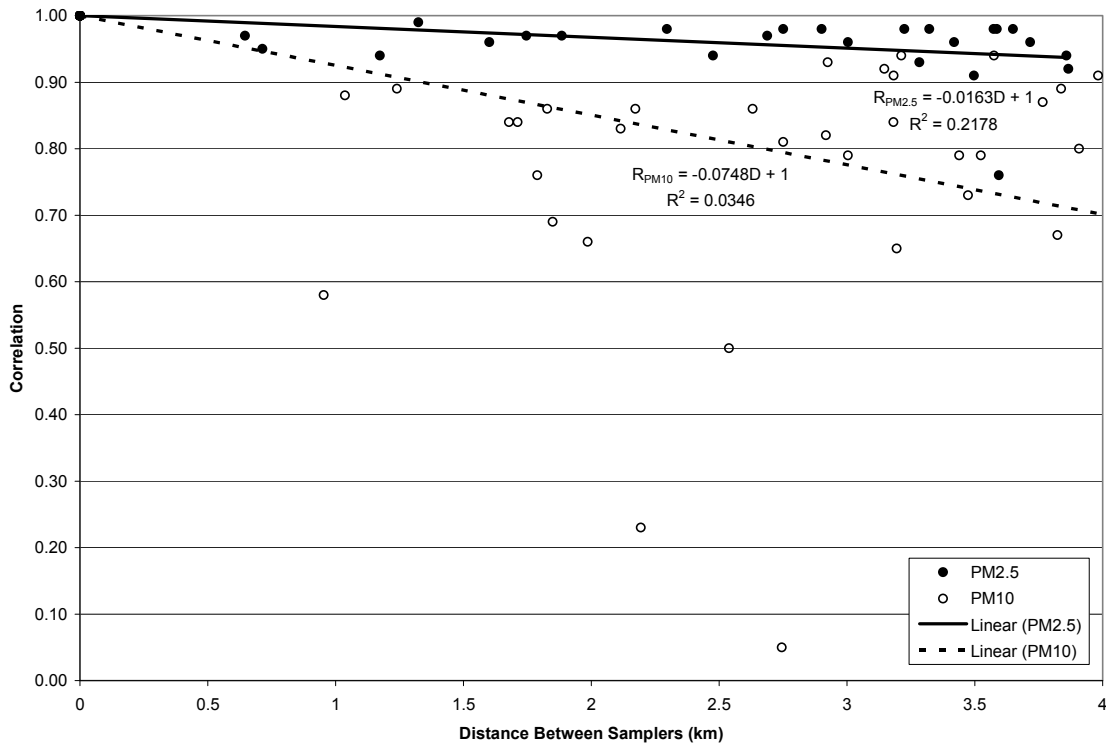


Figure 3-40. Inter-sampler correlations for 24-h PM_{2.5} and PM₁₀ as a function of distance between monitors for samplers located within 4 km (neighborhood scale).

5 Isakov et al. (2007, [156588](#)) compared PM_{2.5} concentrations from a central monitoring
 6 site in Wilmington, DE with PM_{0.3} measurements taken on a mobile platform driven
 7 through mostly quite residential streets within a 4 km x 4 km grid containing the central
 8 monitor. Correlations were generally high (average r = 0.87) over all time periods and
 9 locations monitored, consistent with the range of correlations for PM_{2.5} shown in
 10 Figure 3-40.

PM_{10-2.5}

11 Neighborhood-scale variability in PM_{10-2.5} was investigated by Chen et al. (2007,
 12 [147318](#)) in the Raleigh/Durham area of NC. The average correlation between 26 residential

1 monitors located throughout the region and a centrally located monitor representing a
2 maximum inter-sampler range of 60 km was found to be 0.75 for PM_{10-2.5} compared with
3 0.92 and 0.94 for PM_{2.5} and PM₁₀, respectively. Based on this study, neighborhood-scale
4 variability is greater for PM_{10-2.5} than for PM_{2.5} or PM₁₀, matching the conclusion drawn
5 above on the broader urban-scale.

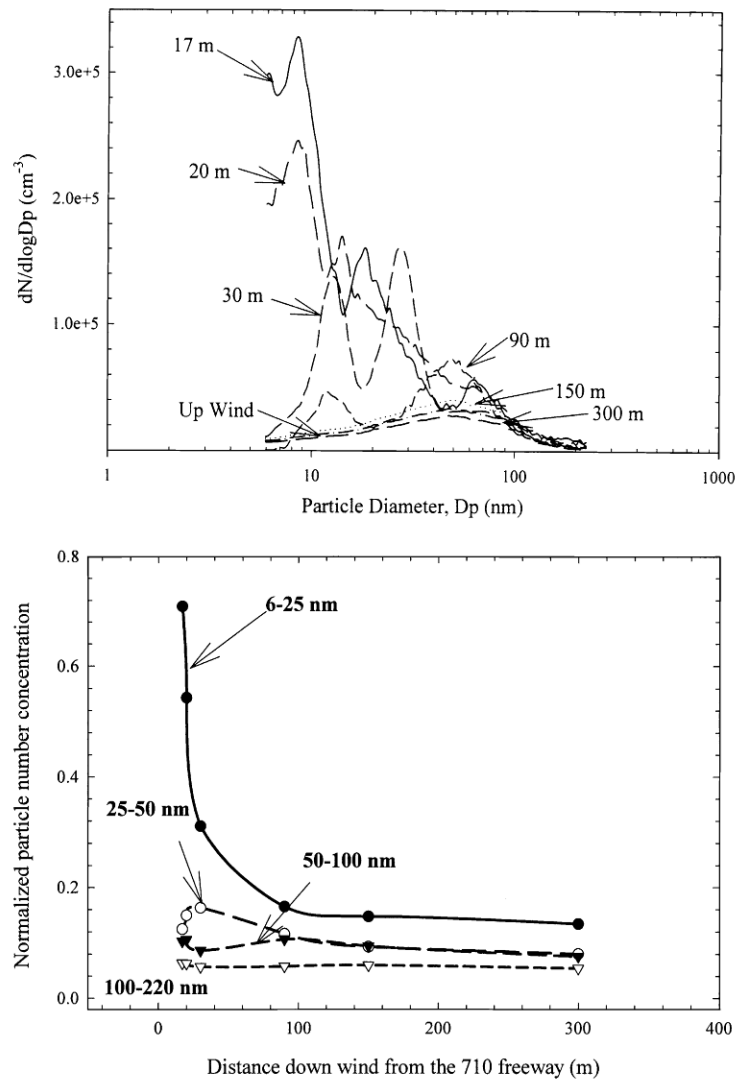
Ultrafine Particles

6 Moore et al. (2009, [191002](#)) monitored ultrafine PM concentrations throughout the
7 Ports of Los Angeles and Long Beach, through which an interstate highway runs and found
8 that concentrations varied by a factor of 5-7 across sites with substantial differences in the
9 daily concentration time series at each site. Such variability reflects diversity of the sources
10 (some near the Interstate, some near the Port), and the influence of changing meteorology
11 over an urban area. In a mobile platform sampling study, Westerdahl et al. (2005, [086502](#))
12 and Fruin et al. (2008, [097183](#)) also reported substantial peaks in ultrafine PM
13 concentration when sampling at highways in comparison with a background site (the
14 University of Southern California) using the same data set.

15 Near roadway environments can exhibit high concentration gradients, particularly for
16 ultrafine particles. Ntziachristos et al. (2007, [089164](#)) observed that the near-road particle
17 size distribution was substantially higher in the ultrafine mobility diameter range and that
18 these results were very sensitive to meteorology (rain) and time of day. Baldauf et al. (2008,
19 [190239](#)) reported elevated ultrafine particle number concentrations downwind of a highway
20 in Raleigh, North Carolina when compared to measurements approximately 100 m upwind
21 of the road. Hagler et al. (2009, [191185](#)) noted a 5-12% decrease in number concentrations
22 per 10 m distance from the road for a number of studies in the U.S. with unobstructed air
23 flow.

24 After initial emission from a motor vehicle, the evolution of the PM distribution
25 within the plume is a function of (1) the turbulence that dilutes the plume and (2)
26 evaporation or condensation of the volatile portion of the aerosol that results from rapid
27 cooling of the exhaust. Figure 3-41 shows the size distribution measured by Zhu and Hinds
28 (2002, [041552](#)) at distances of 17-300 m away from the roadway (in this case, highway 710
29 in Los Angeles) and at an upwind site. It can be seen that a mode originally measured
30 around 9 nm increases in diameter and decreases in magnitude as distance from the
31 highway increases. Smaller secondary modes appear around 30 m from the roadway with

1 multiple modes at some particle sizes. By 150 m away from the highway, the size
 2 distribution flattens with a small mode around 50 nm. It is clear from the bottom
 3 figure that the larger particles are better represented by one sampler than ultrafine
 4 particles because the 100-220 nm number concentration is fairly constant with distance up
 5 to at least 300 m whereas the <100 nm particle sizes measured show more variation with
 6 distance, in both an absolute and relative sense.



Source: Zhu and Hinds (2002, [041552](#)).

Figure 3-41. Particle size distributions measured at various distances from the 710 freeway in Los Angeles, CA (top), and particle number concentration as a function of distance from the 710 freeway (bottom).

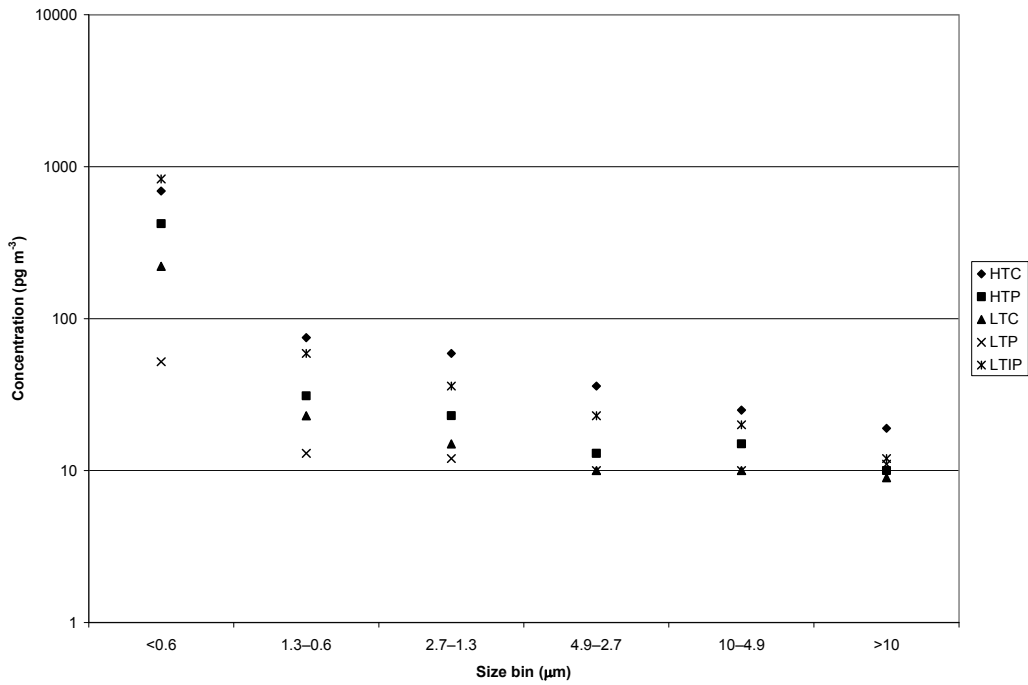
1 Zhou and Levy (2007, [098633](#)) performed a meta-analysis of traffic-related air
2 pollution literature and found that background pollution and meteorology can have
3 important impacts on the size of the elevated concentration region around the highway. Zhu
4 and Hinds (2002, [041552](#)) and Zhang et al. (2005, [157185](#)) noted in field measurements of
5 ultrafine PM that small particles can be lost due to evaporation or to coagulation during
6 Brownian diffusion to form bigger particles, resulting in an upward shift in mode diameter
7 with distance from the roadway. Studies of particle sizes on roads (Kittelson et al., 2006,
8 [156649](#); Kittelson et al., 2006, [156648](#)), in tunnels (Venkataraman et al., 1994, [002475](#)), and
9 upwind and downwind of roads (Wilson and Suh, 1997, [077408](#); Zhu and Hinds, 2002,
10 [041552](#)) suggest that for well-maintained spark-ignition vehicles, a large fraction of the
11 mass of particles emitted from the vehicles are in the nuclei mode (i.e., smaller than
12 accumulation mode). High-speed highway driving may be associated with a larger fraction
13 of particle mass being emitted in the ultrafine size range, while lower speed operation
14 results in a higher mass fraction in the accumulation mode (Cadle et al., 2001, [017192](#)).
15 Traffic may also generate some coarse mode particles (Wilson and Suh, 1997, [077408](#))
16 (Wilson and Suh, 1997, 077408) from material resuspended from the road and brake and
17 tire wear. In situations in which the dilution rates are lower than in a short tunnel or
18 downwind of a road way, condensation of vapors can give rise to particles in the
19 accumulation mode (Kittelson, 1998, [051098](#); Wilson and Suh, 1997, [077408](#)). Diesel
20 engines, in particular, emit elemental (black) carbon in the lower end of the accumulation
21 mode, with number emissions dominated by semi-volatile material in the nuclei mode
22 (Kittelson, 1998, [051098](#); Kittelson et al., 2006, [156649](#); Kittelson et al., 2006, [156648](#)).
23 Sharp gradients in black carbon mass have been observed along roadways with high diesel
24 traffic (Zhu and Hinds, 2002, [041552](#)). As the traffic pollution moves downwind, the
25 ultrafine particles may grow into the accumulation mode by coagulation or condensation. In
26 addition to Gaussian dispersion and wind eddies caused by the presence of natural and
27 anthropogenic barriers, Sahlodin et al. (2007, [114058](#)) demonstrated that turbulence
28 produced by vehicles can result in modification of the plume emanating from the highway.
29 Hence, on-road turbulence could potentially alter the aerosol size distribution. This added
30 turbulence could cause some evaporation of tiny nucleation particles that have not absorbed
31 or adsorbed onto soot nuclei, which may affect the rate of coagulation (Jacobson et al., 2005,
32 [191187](#)). The roadway configuration may also affect particle transport and dispersion.
33 Depressed road sections, where the road bed is below the surrounding terrain, leads to

1 increased air turbulence and mixing as air flows up and out of the road depression. This
2 configuration can result in lower particulate concentrations and flatter concentration decay
3 curves away from the road. On the other hand, configurations with the road bed at-grade
4 with surrounding terrain, or elevated above the surrounding terrain with solid fill material
5 resulted in the highest pollutant concentrations and sharpest concentration gradients
6 downwind from the road.

PM Constituents

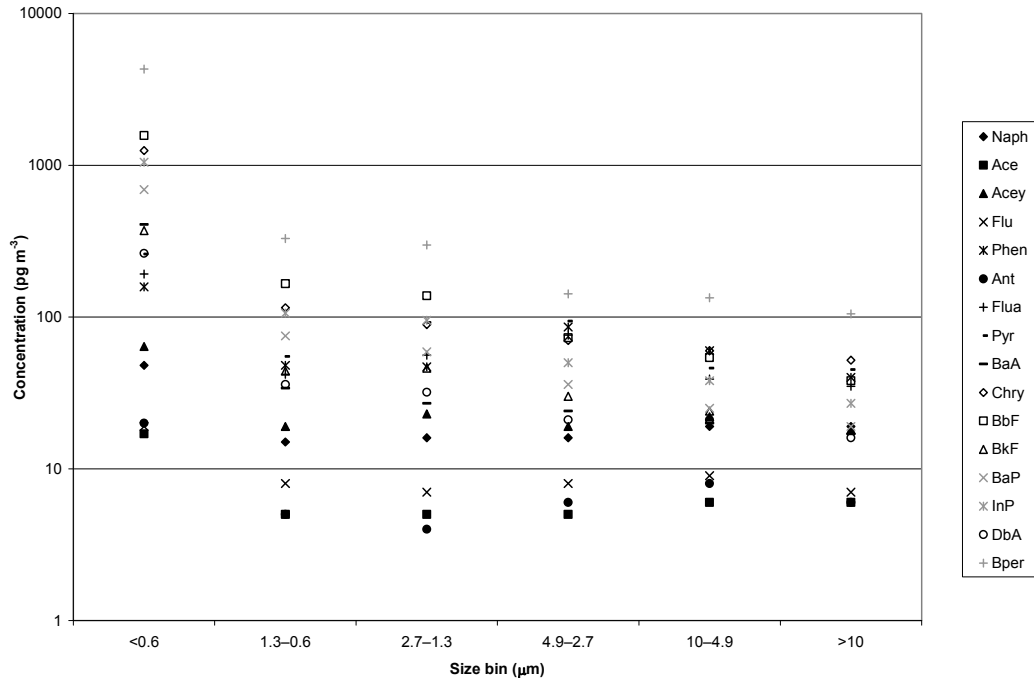
7 The composition of PM will also vary on the neighborhood-scale in response to local
8 sources and differential dispersion, resulting in variable spatial distribution of individual
9 components. Krudysz et al. (2008, [190064](#)) investigated spatial variation in size-
10 fractionated (<0.25 μm , 0.25-2.5 μm , >2.5 μm) PM composition data at four sites located
11 within 3-6 km of each other in the Long Beach, CA area. Inter-site R^2 values in the 0.25-2.5
12 μm size range were higher for mass (ranging from 0.56-0.91) than for EC (0.02-0.71) for pair
13 wise site comparisons. Spatial heterogeneity in all size ranges investigated was also found
14 for several elements associated with motor vehicle emissions and resuspended road dust
15 including Cu, Mg, Ba, Ca and Al. Viana et al. (2008, [156135](#)) observed higher
16 concentrations of crustal elements in $\text{PM}_{2.5}$ and PM_{10} samples in rural neighborhoods and
17 higher concentrations of combustion-derived $\text{PM}_{2.5}$ and PM_{10} , such as EC and NO_3^- , in
18 higher density urban areas. Gutiérrez-Dabán et al. (2005, [155818](#)) examined the mass
19 distribution of various PAHs under different traffic and urban density conditions.
20 Figure 3-42 displays the distributions for benz[a]pyrene (BaP) at high and low traffic sites
21 at the urban center, periphery, and industrial areas found in Gutiérrez-Dabán et al. (2005,
22 [155818](#)). It can be seen that concentrations were nearly an order of magnitude lower for the
23 low traffic urban periphery location when compared with the high traffic or industrial
24 locations. Particles smaller than ~ 600 nm had roughly an order of magnitude higher
25 concentration than those at larger sizes and tended to have a larger spread in
26 concentrations among sampling sites. Figure 3-43 shows the distributions for sixteen PAHs
27 at a high traffic location at the city center from Gutiérrez-Dabán et al. (2005, [155818](#)). PAH
28 species varied in concentration by up to two orders of magnitude for each particle size bin,
29 and the highest concentrations of individual PAHs were generally found for particles
30 smaller than approximately 600 nm. Olson and McDow (2009, [191188](#)) reported decreases
31 by a factor of 1.04 to 2.37 in select PAH and organic source marker concentrations when

1 comparing measurements 10 m and 275 m from a highway in Raleigh, North Carolina.
 2 Phuleria et al. (2006, [156867](#)) sampled ultrafine PM and PM_{2.5} concentrations and PAH
 3 species at the mouth of the Caldecott Tunnel in Orinda, CA and found that the two size
 4 classes were highly correlated ($R^2 = 0.97$). Given the size differentials of each size bin
 5 presented in the Gutiérrez-Dabán et al. (2005, [155818](#)) study, it is possible that the PM_{2.5}
 6 sampled at the tunnel mouth represented secondary PM_{2.5} that grew from ultrafine PM
 7 emissions trapped within the tunnel.



Source: Gutiérrez-Dabán et al. (2005, [155818](#)).

Figure 3-42. Mass distributions for BaP at a high traffic urban center (HTC), high traffic urban periphery (HTP), low traffic urban center (LTC), low traffic urban periphery (LTP), and low traffic industrial urban periphery (LTIP) in Seville, Spain.



Source: Gutiérrez-Dabán et al. (2005, [155818](#)).

Figure 3-43. Mass distributions for 16 PAHs at a high traffic city center in Seville, Spain.

3.5.2. Temporal Variability

1 Temporal variability is another important factor in characterizing PM. This
 2 section addresses trends as well as seasonal and hourly variability. Trends in PM₁₀ and
 3 PM_{2.5} are addressed in Section 3.5.2.1 based on AQS data. Seasonality is coupled with
 4 spatial variability and has been discussed in the regional context above. Section 3.5.2.2
 5 below briefly investigates the seasonality on a finer time scale, thereby addressing issues
 6 relating to the seasonal definitions used earlier. Section 3.5.2.3 addresses hourly patterns,
 7 an issue particularly important to understanding the behavior of PM concentrations in
 8 reference to sources, human activity patterns and exposure. Hourly patterns are
 9 investigated using AQS data on a national basis for PM_{2.5} and PM₁₀. Data for ultrafine
 10 particles and PM constituents are presented where available.

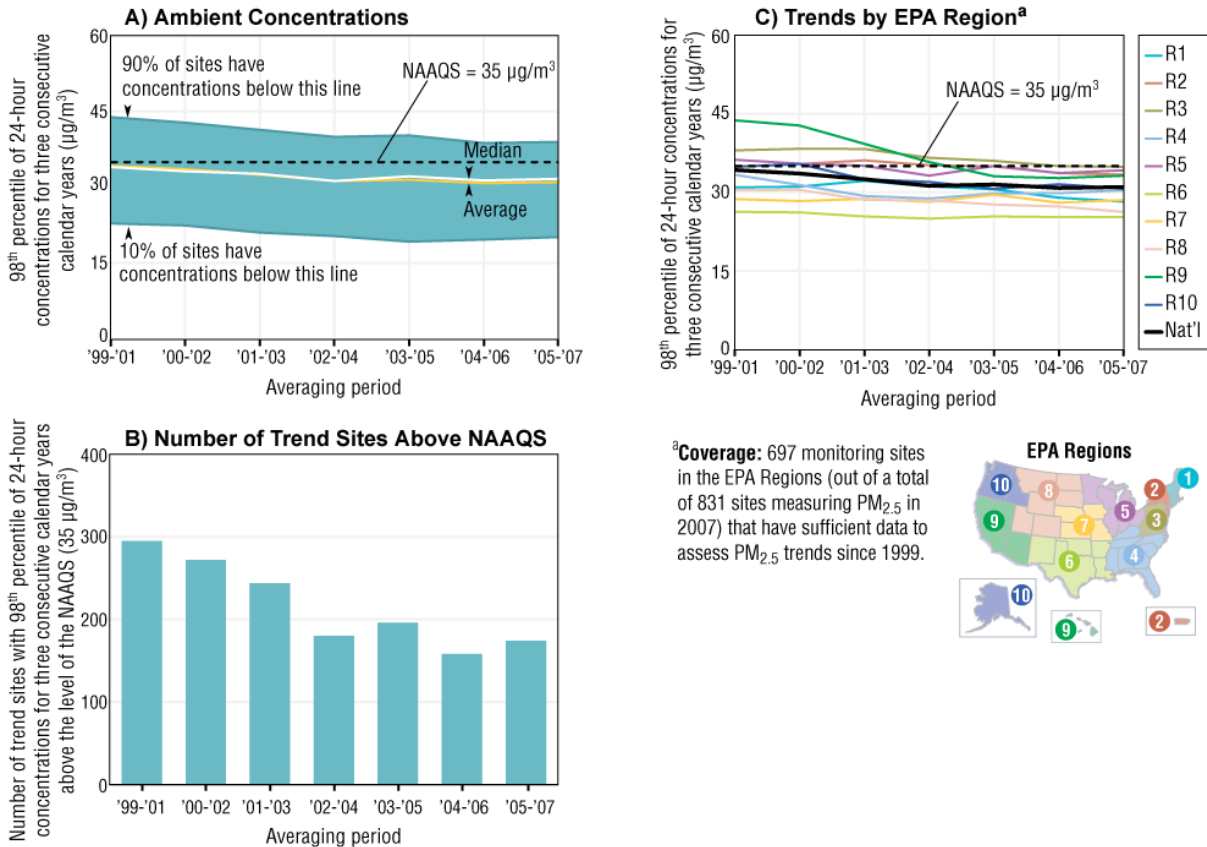
3.5.2.1. Regional Trends

11 This section summarizes available information on trends in PM mass and
 12 composition. Mass concentration trends are based on AQS data and incorporate nine years
 13 (1999-2007) of PM_{2.5} data and 20 years (1988-2007) of PM₁₀ data. Composition trends are

1 based on six years of available CSN data (2002-2007). Several monitoring sites were
2 excluded from the following trend analyses to provide a consistent basis for comparison over
3 the desired years of monitoring. This included exclusion of sites when there was no
4 corresponding site in later or earlier years. Region-average trends were calculated to
5 facilitate presentation and extrapolation of the results. These region-averages, however,
6 may not necessarily represent the trends that are being observed at any individual monitor
7 or geographical location within the specified region.

PM_{2.5}

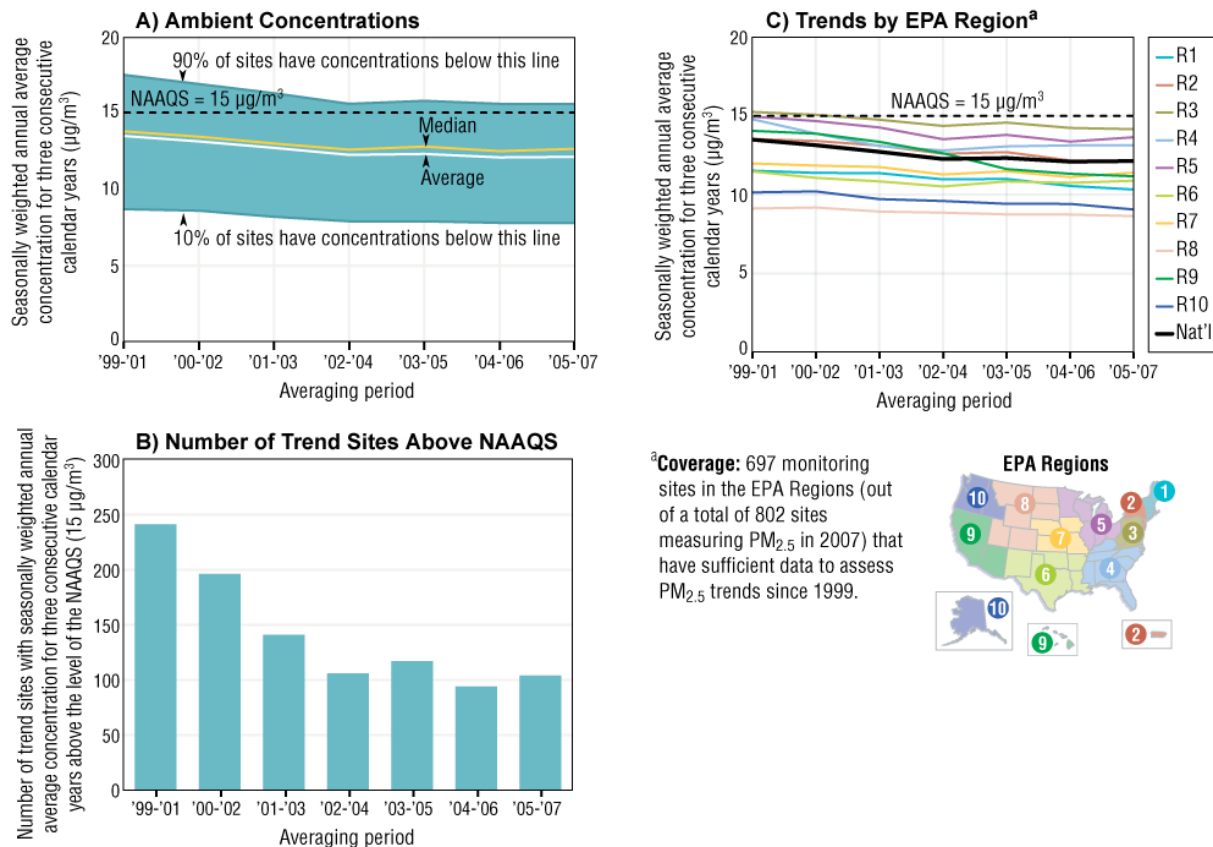
8 Figure 3-44 shows trends in U.S. ambient 24-h PM_{2.5} concentrations from 1999 to
9 2007. In the period 2005-2007, the three-yr avg of the 98th percentile of 24-h PM_{2.5}
10 concentrations fell 10% relative to the 1999-2001 period (see Figure 3-44a). The number of
11 sites reporting values greater than the 24-h NAAQS was shown to decline 40% in
12 Figure 3-44b. Figure 3-44c illustrates the downward trend in the 98th percentile of 24-h
13 PM_{2.5} concentrations for three consecutive calendar years in all U.S. EPA regions. This
14 trend is most pronounced in Region 9 incorporating Arizona, California and Nevada where
15 this value dropped 25% from the 1999-2001 period to the 2005-2007 period.



Source: U.S. EPA (2008, [157076](#))

Figure 3-44. Ambient 24-h $\text{PM}_{2.5}$ concentrations in the U.S., 1999-2007, showing A) ambient concentrations, B) number of trends sites above the 24-h NAAQS and C) trends by U.S. EPA Region.

1 Figure 3-45 contains similar trend information for the annual $\text{PM}_{2.5}$ NAAQS. The
 2 seasonally weighted 3-yr avg $\text{PM}_{2.5}$ concentrations for the years 2005 to 2007 were at the
 3 lowest since national monitoring began in 1999 (see Figure 3-45a). The seasonally weighted
 4 3-yr avg fell 10% between the 1999-2001 averaging period and the 2005-2007 averaging
 5 period. The number of sites reporting concentrations above the annual average $\text{PM}_{2.5}$
 6 NAAQS fell 56% over these same periods in Figure 3-45b. Figure 3-45c illustrates the
 7 annual trends in $\text{PM}_{2.5}$ by U.S. EPA region. Declines were the greatest in Region 9 again
 8 where $\text{PM}_{2.5}$ concentrations fell 20% from the 1999-2001 averaging period to the 2005-2007
 9 averaging period.

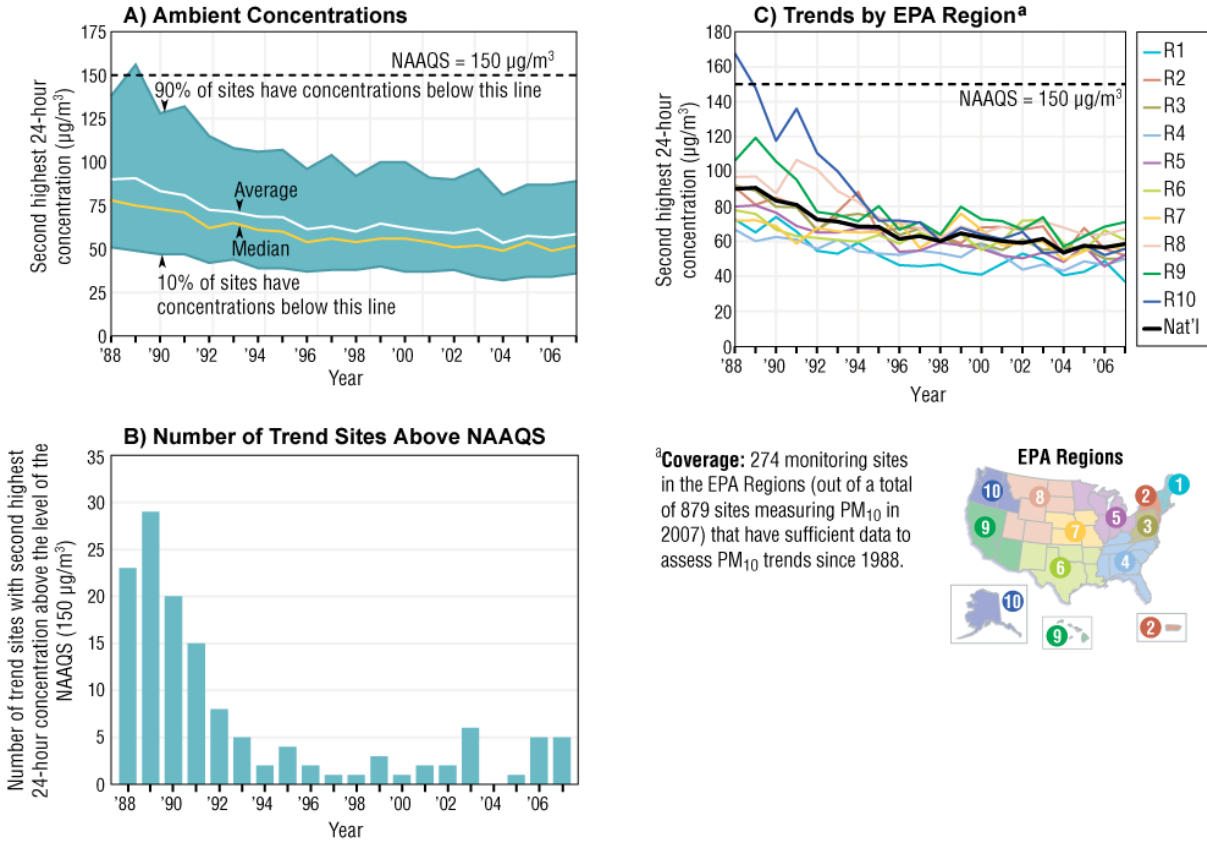


Source: U.S. EPA (2008, [157076](#)).

Figure 3-45. Ambient annual $\text{PM}_{2.5}$ concentrations in the U.S., 1999-2007, showing A) ambient concentrations, B) number of trends sites above the annual NAAQS and C) trends by U.S. EPA Region.

PM_{10}

1 Figure 3-46 shows trends in U.S. ambient 24-h PM_{10} concentrations from 1988 to
 2 2007. In 2007, the U.S. national average second highest PM_{10} concentration was 37% lower
 3 than in 1988 (see Figure 3-46a). Of 281 sites used in this trend analysis, the number
 4 reporting concentrations above the 24-h PM_{10} NAAQS ($150 \mu\text{g}/\text{m}^3$) fell from 23 in 1988 to 5
 5 in 2007 with a max of 29 in 1989 (see Figure 3-46b). Figure 3-46c shows trends in the
 6 second highest 24-h PM_{10} concentrations broken down by U.S. EPA region. All regions
 7 exhibit an overall decrease from 1988 to 2007. Largest decreases occurred in EPA Region
 8 10, which incorporates Washington, Oregon, Idaho and Alaska. Most of the decrease
 9 occurred between 1988 and 1995.



Source: U.S. EPA (2008, 157078).

Figure 3-46. Ambient 24-h PM_{10} concentrations in the U.S., 1988-2007, showing A) ambient concentrations, B) number of trends sites above the 24-h NAAQS and C) trends by U.S. EPA Region.

PM Constituents

1 The SANDWICH method discussed in Section 3.5.1.1 for estimating $\text{PM}_{2.5}$ composition

2 from FRM mass measurements and CSN bulk composition measurements was used to

3 evaluate trends in $\text{PM}_{2.5}$ constituents. Figure 3-47 includes stacked bar charts of $\text{PM}_{2.5}$

4 composition from 2002 to 2007 stratified by region and season. The regions used in

5 Figure 3-47 were selected based on common aerosol characteristics including trends,

6 seasonality, size distributions and/or composition as described in chapter 6 of the 1996

7 AQCD and differ from the EPA regions used in the preceding figures. Figure 3-47 is based

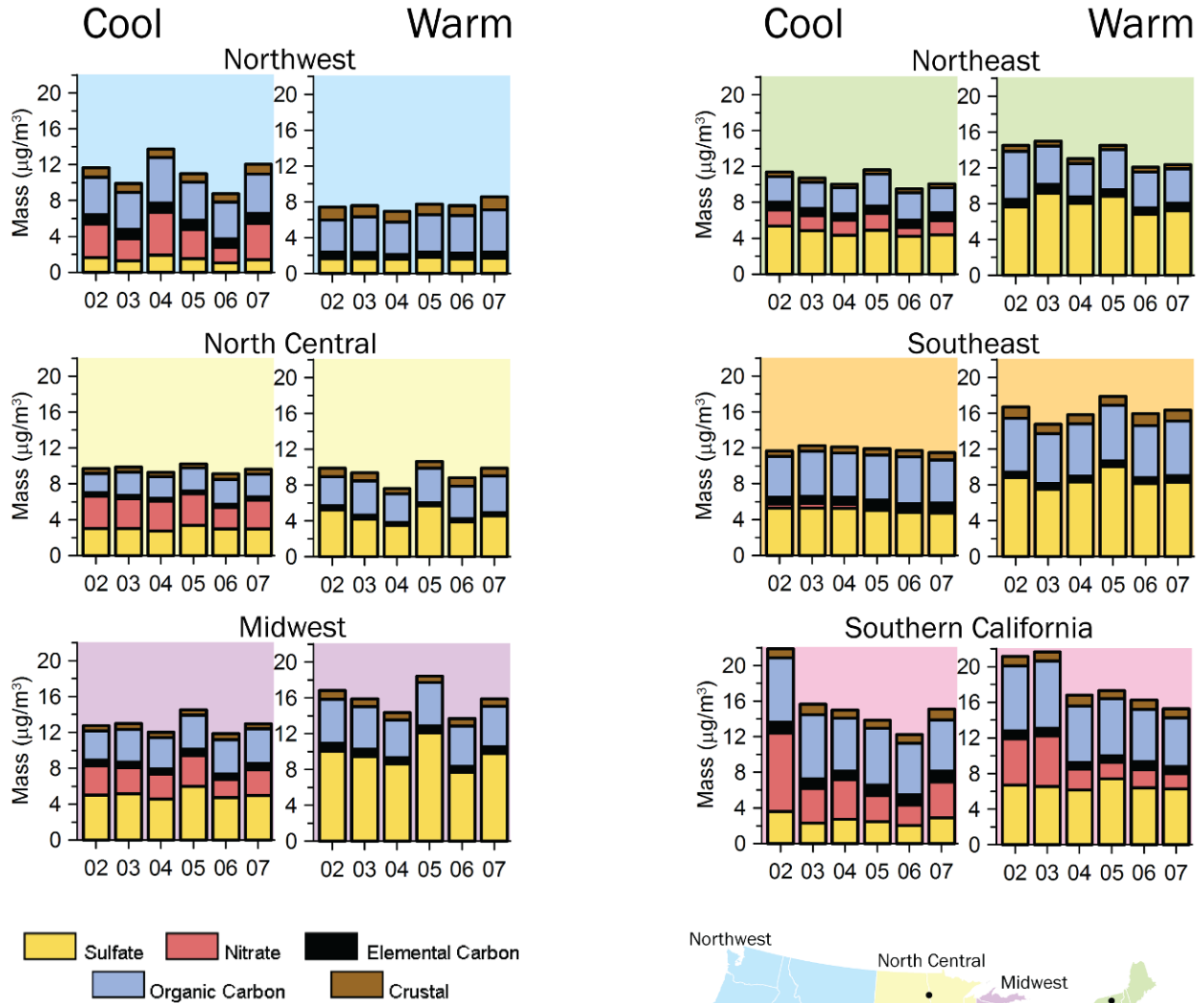
8 on 42 monitoring locations reporting complete CSN data with 2002 being the first year with

9 sufficient speciation data. The Southwest region incorporating Arizona, New Mexico and

10 parts of Texas and Oklahoma did not contain any complete data and therefore is not

11 represented in this analysis. Two seasons representing different temperature ranges—cool

- 1 (October-April) and warm (May-September)—were considered in the figure since many
- 2 PM_{2.5} components exhibit strong temperature dependence.



Source: U.S. EPA (2008, [191190](#)).

Figure 3-47. Regional and seasonal trends in annual PM_{2.5} composition from 2002 to 2007 derived using the SANDWICH method. Data from the 42 monitoring locations shown on the map were stratified by region and season including cool months (October-April) and warm months (May-September). SO₄²⁻ and NO₃⁻ estimates include NH₄⁺ and particle bound water.

1 Most of the components showed little discernable trend over the 6-yr period. SO_4^{2-}
2 showed a peak during the warm months of 2005 in the Southeast, Northeast and Midwest,
3 partly due to atypical weather conditions (U.S. EPA, 2008, [191190](#)). However, no trend over
4 the 6-yr time period is present for SO_4^{2-} in any of the regions or seasons. The same is true
5 for EC and crustal material. A slight decline in OC was observed for the Northeast during
6 warm months and in Southern California year-round. The largest decline was for NO_3^- in
7 Southern California during both cool and warm months. A smaller decline in NO_3^- is also
8 observed in the other regions with the exception of the Northwest where no discernible
9 trend is present. This analysis is limited in time and space by the availability of CSN data
10 so a high degree of uncertainty remains regarding $\text{PM}_{2.5}$ compositional trends. However,
11 with the exception of NO_3^- concentrations in Southern California, no major changes in $\text{PM}_{2.5}$
12 composition are evident based on available CSN data from 2002-2007. This is consistent
13 with Figures 3-44 through 3-47 where the downward trend in $\text{PM}_{2.5}$ mass begins to level off
14 after 2002.

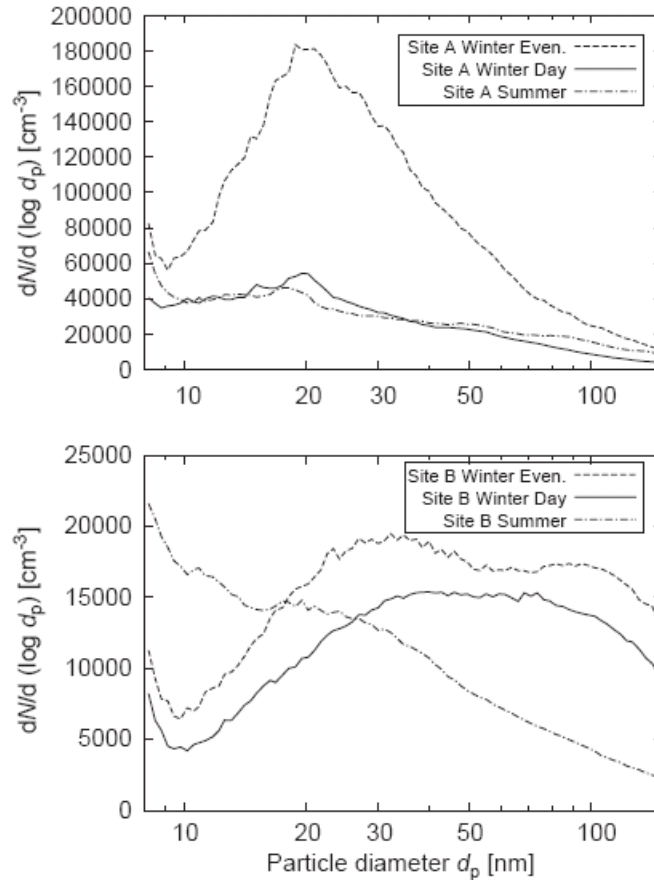
3.5.2.2. Seasonal Variations

15 Many of the figures and tables presented in the preceding sections have included a
16 seasonal break-down based on the following climatological seasons: winter
17 (December-February), spring (March-May), summer (June-August) and fall
18 (September-November). Figures A-122 through A-136 in Annex A show bar charts of $\text{PM}_{2.5}$
19 composition by individual month, illustrating intra-annual variability on a finer time scale.
20 The same 15 CSAs/CBSAs are investigated and included in these plots; they are generated
21 from the same data used in the seasonal and annual pie charts based on the SANDWICH
22 method discussed in Section 3.5.1.1 and illustrated in Figures 3-17 and 3-18.

23 Monthly plots for most of the areas reveal heterogeneity in PM composition within the
24 3-month long seasonal bins defined earlier. This is especially true in the spring and fall
25 when daily average weather conditions (e.g., temperature) are changing most rapidly,
26 driving fluctuation in $\text{PM}_{2.5}$ composition on relatively short timescales in many cities. For
27 example, the NO_3^- mass in Los Angeles (Figure A-129) and Riverside (Figure A-134) can
28 vary from a small fraction to the most prevalent fraction of $\text{PM}_{2.5}$ mass in a month's time
29 based on the 3-yr aggregate data. Therefore, selecting a different delineation point for the

1 seasons can have an influence on the seasonal composition analysis, specifically for
2 constituents that fluctuate rapidly (e.g., NO₃⁻).

3 Relatively little is known about the seasonal variability in ultrafine particles. Kuhn et
4 al. (2005, [129448](#)) and Zhu et al. (2004, [156184](#)) found that the concentrations in the
5 ultrafine mode in Los Angeles, CA can be much higher during winter, particularly during
6 evenings, because atmospheric dilution is reduced in response to lower mixing heights. This
7 can be seen in Figure 3-48. Jeong et al. (2004, [180350](#)) made similar observations in
8 Rochester, NY, suggesting an inverse relationship between temperature and ultrafine
9 particle formation in the 11-470 nm size range. Singh et al. (2006, [190136](#)) reported higher
10 particle number concentrations during winter months, relative to summer and spring, at
11 urban sites in Southern California, and that afternoon particle number concentrations in
12 warm months either occurred during a peak in ozone concentrations or followed shortly
13 thereafter, suggesting a role for photochemistry in addition to meteorological changes in the
14 formation of aerosols. The study also reported increased concentrations of 60-200 nm
15 particles during a labor strike at the Port of Long Beach, suggesting contributions from
16 idling ships. Moore et al. (2009, [191004](#)) also report higher particle number concentrations
17 during cooler months at 14 sites in Long Beach, San Pedro, and Wilmington, CA, a location
18 with diverse industrial and transportation sources. However, they noted substantial
19 heterogeneity in seasonal trends between sites with seasonal numerical size distributions
20 not generalizable across the study area with a maximum monitor separation of under 10
21 km.



Source: Kuhn et al. (2005, [129448](#)).

Figure 3-48. Ultrafine particle size distribution at highway (site A) and background (site B) sites in Los Angeles, CA, during summer and winter seasons, with winter broken into day and evening distributions.

1 Studies reporting higher cold-season particle number concentrations are consistent
 2 with vehicle emission studies that found particle emission rates elevated during lower
 3 ambient temperatures (Baldauf et al., 2005, [191184](#); Mathis et al., 2005; [155970](#); U.S. EPA,
 4 2008, [191767](#)). Mathis et al. (2005, [155970](#)) found that cold-start conditions produce roughly
 5 an order of magnitude greater PM number emissions in gasoline engines and more than
 6 two orders of magnitude higher PM number emissions in diesel engines when compared
 7 with warm start conditions.

3.5.2.3. Hourly Variability

8 Hourly PM₁₀ and PM_{2.5} measurements are conducted at many sites using beta gauge
 9 or TEOM monitors. Many of the hourly measurements for PM₁₀ have FRM or FEM status.

1 All available hourly data from FRM, FEM and FRM-like monitors in the fifteen
2 CSAs/CBSAs discussed earlier were used to investigate diel variation in PM. Of the fifteen
3 CSAs/CBSAs, Atlanta, Chicago, Pittsburgh, Seattle and St. Louis had qualifying hourly
4 PM_{2.5} and PM₁₀ data available. Houston and New York had only qualifying PM_{2.5} data.
5 Denver, Detroit, Los Angeles, Philadelphia, Phoenix, and Riverside had only qualifying
6 hourly PM₁₀ data. Birmingham and Boston had no qualifying hourly PM_{2.5} or PM₁₀ data.

7 Diel plots for PM_{2.5} stratified by weekdays and weekends for seven of the fifteen
8 CSAs/CBSAs with available data between 2005 and 2007 are included in Annex A, Figures
9 A-137 through A-143. In most cities investigated, a morning PM_{2.5} peak is present starting
10 at approximately 6:00 a.m., corresponding with the start of the morning rush hour just
11 before the break-up of overnight stagnation. In Pittsburgh, dispersion behavior during the
12 night results in elevated PM_{2.5} concentrations throughout the night that blend in with any
13 morning peak. With the exception of Pittsburgh, all seven metropolitan areas show two
14 distinct daily peaks on both the weekdays and weekends. The evening PM_{2.5} concentration
15 peak is broader than the morning peak and extends to overnight hours, reflecting the
16 concentration increase caused by a drop in boundary layer height at night. Figure 3-49
17 compares the two-peak diel distribution in PM_{2.5} for Seattle with the one-peak distribution
18 in PM_{2.5} for Pittsburgh. Since these figures represent the distribution of hourly observations
19 over a 3-yr period, any fluctuations or changes in the timing of the daily peaks would result
20 in a broadening of the curves shown in the diel plot.

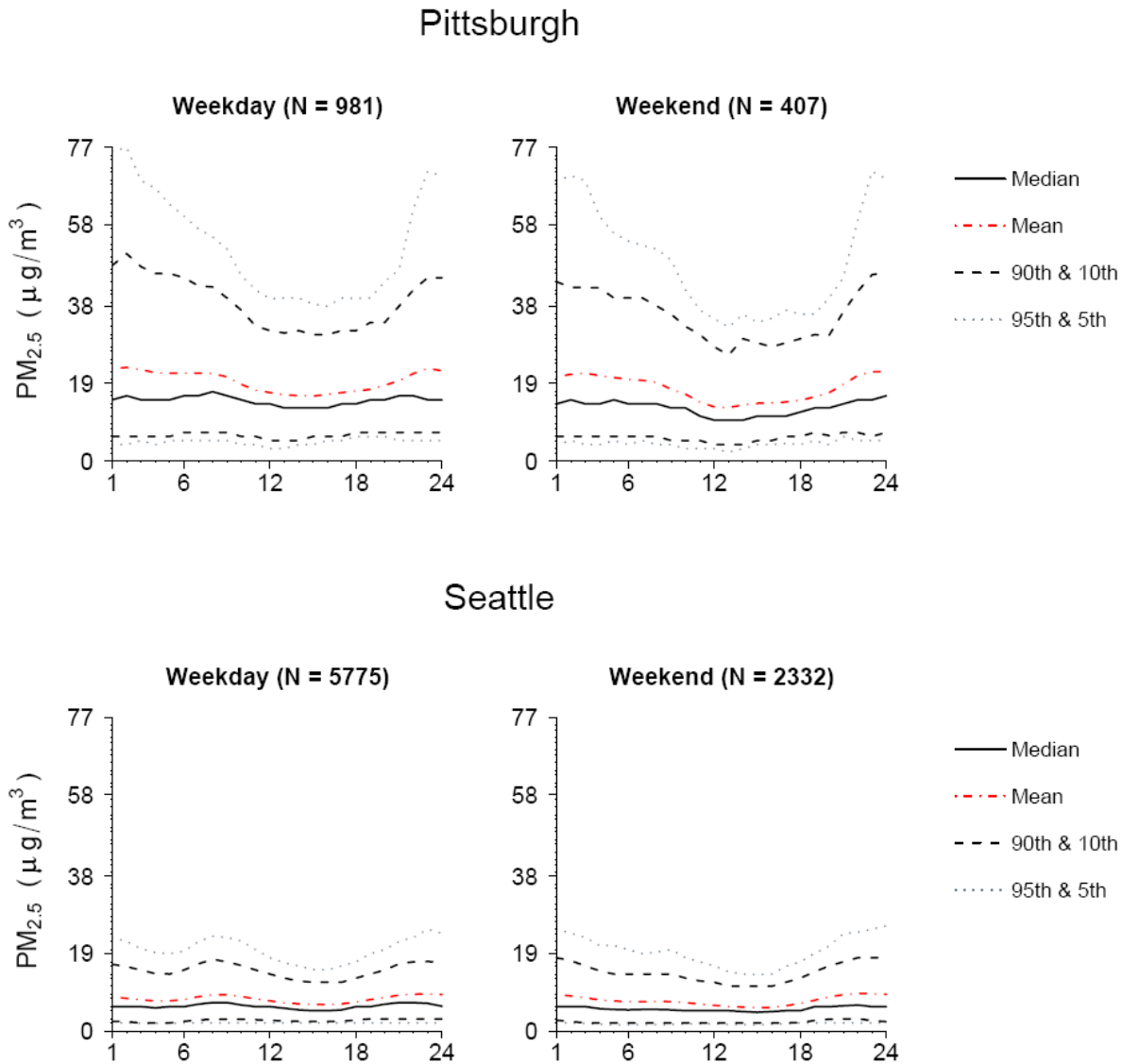
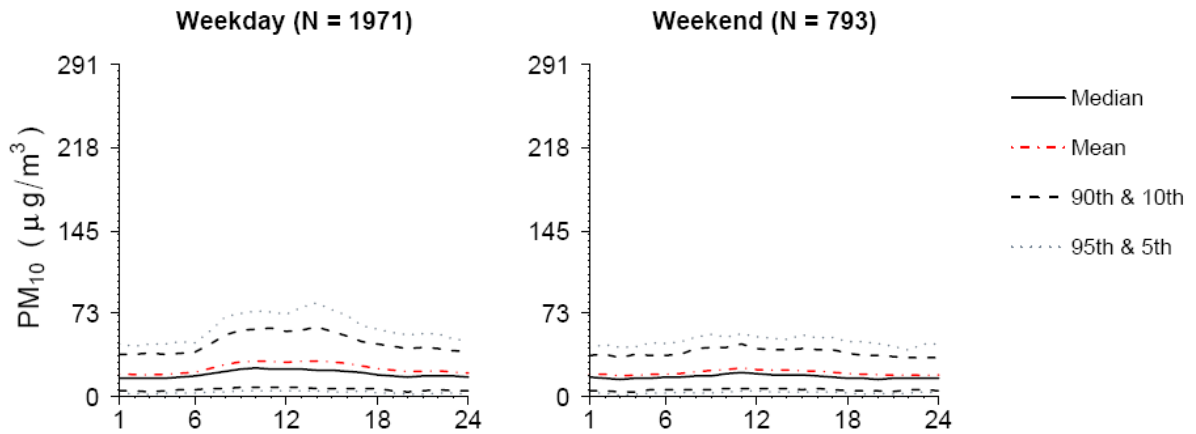


Figure 3-49. Diel plot generated from hourly FRM-like PM_{2.5} data (µg/m³) stratified by weekday (left) and weekend (right) for Pittsburgh, PA, and Seattle, WA, from 2005 to 2007. Included are the number of monitor days (N) and the median, mean, 5th, 10th, 90th and 95th percentiles for each hour of the day shown on the horizontal axis.

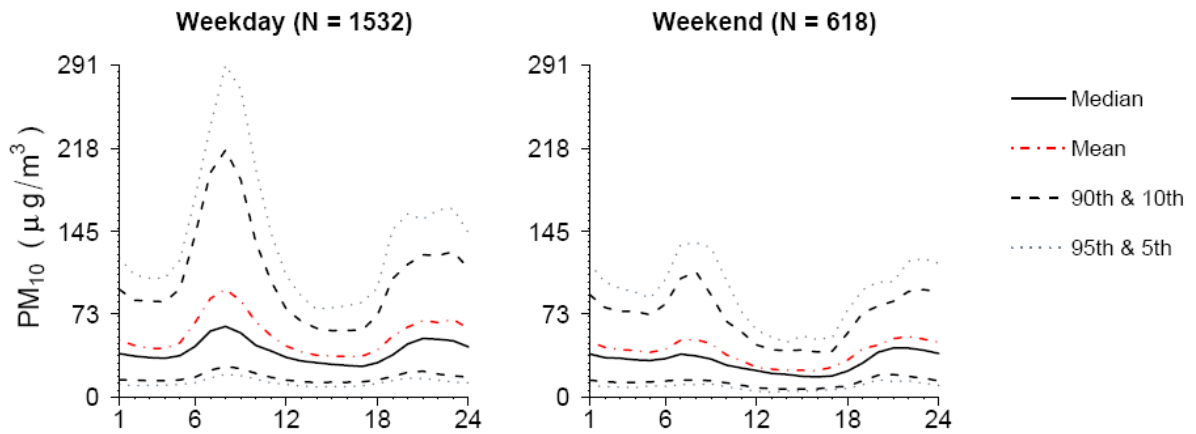
1 Annex A, Figures A-144 through A-154 show diel patterns for PM₁₀ stratified by
 2 weekdays and weekends for eleven of the fifteen CSAs/CBSAs with available data between
 3 2005 and 2007. All cities show a gradual morning increase in mean PM₁₀ starting at
 4 approximately 6:00 a.m. on weekdays, corresponding with the start of the morning rush
 5 hour before the break-up of overnight stagnation. The magnitude and duration of this peak,
 6 however, varies considerably by area. Phoenix shows the most pronounced morning PM₁₀

1 peak concentration, which drops off during the day and reappears in the evening. In
 2 contrast, Chicago shows a less pronounced peak with the PM₁₀ concentration remaining
 3 elevated throughout the day. Figure 3-50 shows the diel plots of PM₁₀ for Chicago and
 4 Phoenix. In both instances, the weekend diel pattern is similar in shape to the weekday
 5 pattern with less pronounced peaks. Once again, any fluctuations in the timing of the daily
 6 peaks could result in a broadening of the peaks in the 3-yr composite diel figures.

Chicago



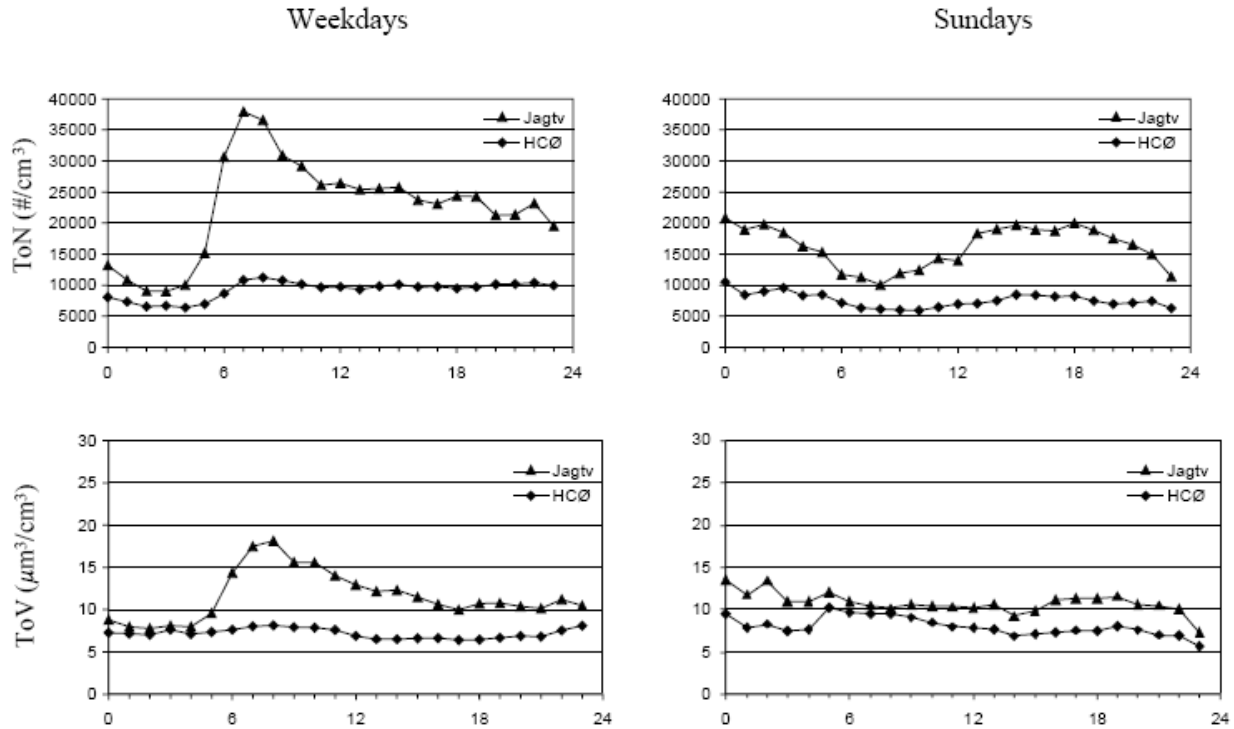
Phoenix



7

Figure 3-50. Diel plots generated from hourly FEM PM₁₀ data (µg/m³) stratified by weekday (left) and weekend (right) for Chicago, IL, and Phoenix, AZ, from 2005 to 2007. Included are the number of monitor days (N) and the median, mean, 5th, 10th, 90th and 95th percentiles for each hour of the day shown on the horizontal axis.

1 Ultrafine particles in urban environments have been shown to exhibit a similar
2 two-peaked diel pattern in Los Angeles (Moore et al., 2007, [122445](#); Sardar et al., 2005,
3 [180086](#)) and the San Joaquin Valley (Herner et al., 2005, [135983](#)) in CA, Rochester, NY
4 (Jeong et al., 2004, [180350](#)), Raleigh, NC (Baldauf et al., 2008, [190239](#)) as well as in
5 Kawasaki City, Japan (Hasegawa et al., 2005, [157355](#)) and Copenhagen, Denmark (Ketzel
6 et al., 2003, [131251](#)). Figure 3-51 from the Denmark study shows a large peak in total
7 particle number (dominated by ultrafine particles) corresponding with the morning rush
8 hour. The morning peak is absent on Sundays, however. Many studies also show a broad
9 afternoon ultrafine concentration peak, which likely originates from a combination of
10 evening rush-hour traffic, decreased atmospheric dilution and formation of ultrafine
11 particles through nucleation involving products of active photochemistry. Nucleation likely
12 plays an important role since the afternoon peak is present on weekends whereas the
13 morning traffic related peak is absent. This is consistent with observations of particle
14 counts in Atlanta peaking during the mid-afternoon for particles less than 10 nm (Woo et
15 al., 2001, [011702](#)) resulting from nucleation.



Source: Ketzel et al. (2003, [131251](#))

Figure 3-51. Average diel variation in total particle number (ToN) and total particle volume (ToV) on weekdays (left column) and Sundays (right column) from two sites in Denmark: one in a busy street canyon (Jagtv) and one measuring urban background (HCØ).

1 Hourly variability in particle-phase OC and EC were investigated by Bae et al. (2004,
 2 [156243](#)) in the urban St. Louis atmosphere. OC diel patterns were similar during weekdays
 3 and weekends with a broad morning and evening concentration peak most likely reflecting
 4 daily fluctuations in atmospheric mixing height. Weekend EC diel patterns were similar to
 5 those for OC, but the weekday patterns showed more abrupt EC concentration peaks in the
 6 morning and afternoon, coinciding with rush-hour traffic. The divergent weekday patterns
 7 between OC and EC suggests motor vehicles or other EC sources with temporal profiles
 8 tracking traffic patterns are primarily responsible for the daily fluctuations in EC
 9 concentrations in St. Louis.

3.5.3. Statistical Associations with Copollutants

10 Associations between PM and other copollutants including SO₂, NO₂, CO and O₃ are
 11 investigated in this section. AQS data were obtained from all available co-located monitors
 12 across the U.S. after application of an 11 or more observations per quarter completeness

1 criterion. Pearson correlation coefficients (R) were calculated using 2005-2007 data. The
 2 results are displayed graphically in Figure 3-52 for correlations with PM_{2.5} and Figure 3-53
 3 for correlations with PM₁₀.

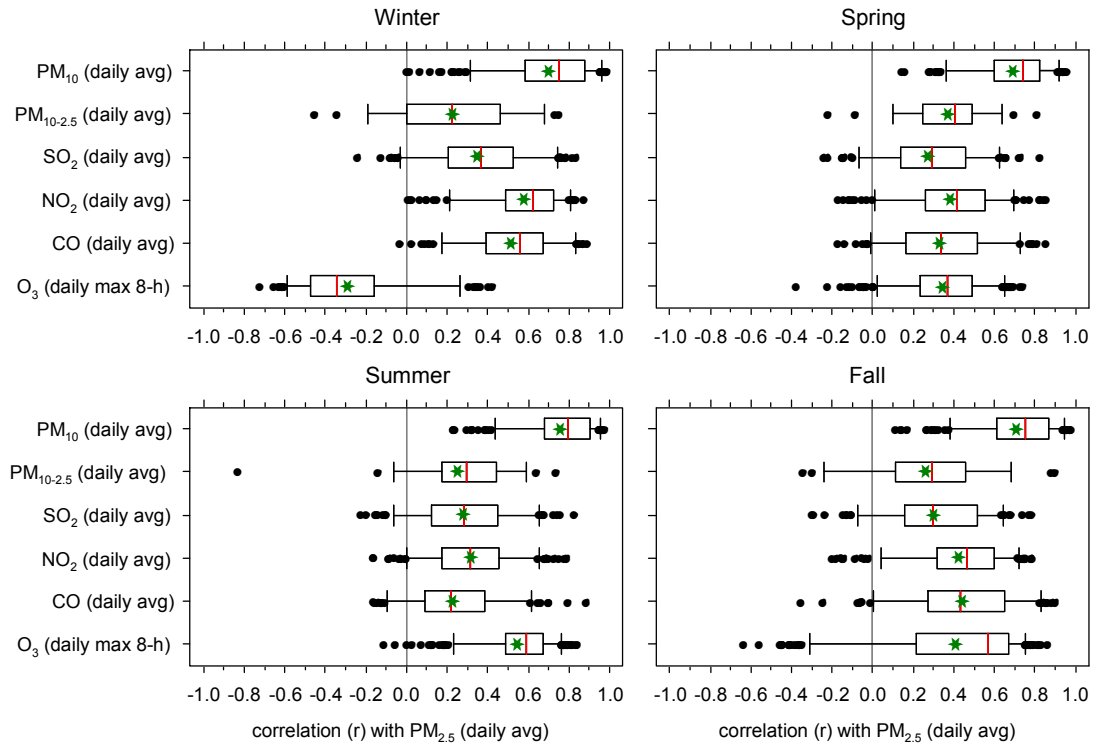


Figure 3-52. Distribution of correlations between 24-h avg PM_{2.5} and co-located 24-h avg PM₁₀, PM_{10-2.5}, SO₂, NO₂ and CO and daily max 8-h avg O₃ for the U.S. stratified by season (2005-2007). Statistics shown include the mean (green star), median (red line), inner quartile range (box), 5th/95th percentiles (whiskers) and outliers (black circles).

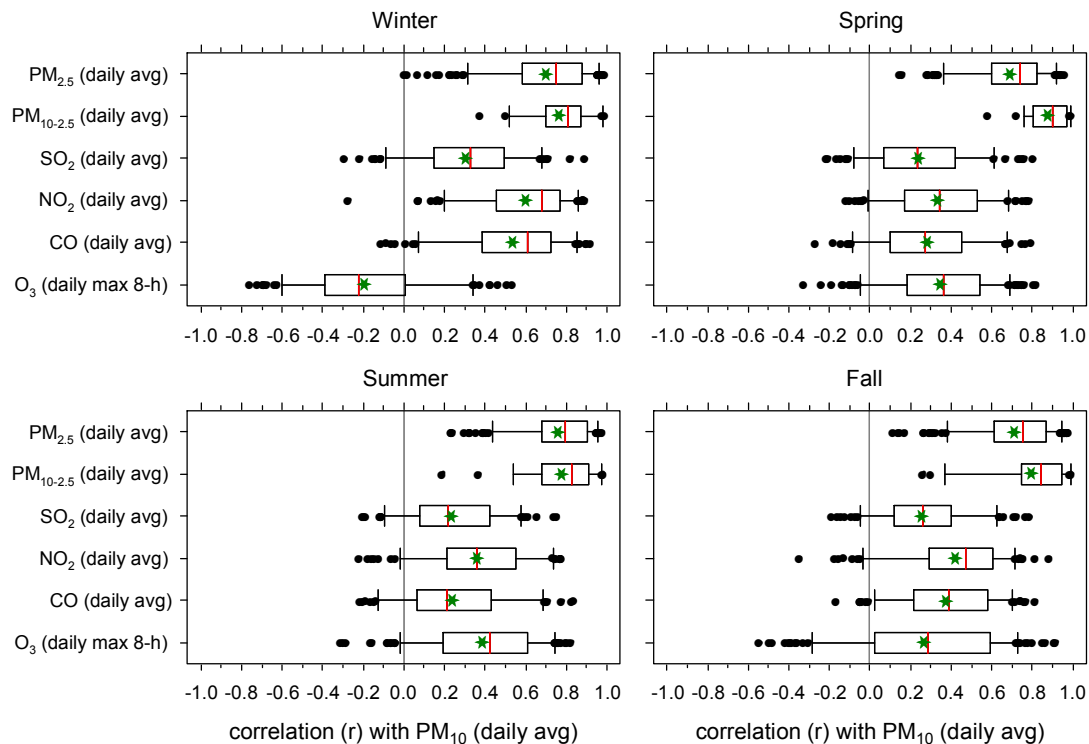


Figure 3-53. Distribution of correlations between 24-h avg PM₁₀ and co-located 24-h avg PM_{2.5}, PM_{10-2.5}, SO₂, NO₂ and CO and daily max 8-h avg O₃ for the U.S. stratified by season (2005-2007). Statistics shown include the mean (green star), median (red line), inner quartile range (box), 5th/95th percentiles (whiskers) and outliers (black circles).

1 For both PM_{2.5} and PM₁₀ national composite copollutant correlations, there is
 2 considerable spread in the observed correlations in all four seasons. On average, PM_{2.5} and
 3 PM₁₀ correlate with each other more than with the gaseous copollutants. The correlations
 4 between PM_{2.5} and PM₁₀ are all positive but span the range from just above zero to near
 5 one. This illustrates the wide variability in correlation between these two PM metrics.
 6 Fewer points are available for correlation with PM_{10-2.5} because only data from low-volume
 7 FRM/FRM-like samplers were used to calculate PM_{10-2.5}. The available data suggest a
 8 stronger correlation between PM₁₀ and PM_{10-2.5} than between PM_{2.5} and PM_{10-2.5} on a
 9 national basis.

10 The correlation between PM and the gaseous pollutants included in Figures 3.5-47
 11 and 3.5-48 also have a large range in values based on the national composite data. There is
 12 little seasonal variability in the mean correlation between PM and SO₂, NO₂ and CO,
 13 however, show higher correlations with PM on average in the wintertime than in the other
 14 seasons. This is possibly driven by meteorology with increased frequency of stagnation

1 events in colder months as well as potential concurrent increases in emissions of these
2 compounds from motor vehicles with colder temperatures. The correlation between daily
3 max 8-h avg O₃ and PM shows high seasonal variability with positive correlations on
4 average in the spring, summer and fall and negative correlations on average in the winter.
5 The highest positive correlations are in the summer, likely driven by favorable
6 photochemical formation conditions for both O₃ and secondary aerosols (Joseph, 2008,
7 [155219](#); Meng et al., 1997, [083324](#)). The mean correlation drops below zero (-0.3 for PM_{2.5}
8 and -0.2 for PM₁₀) in the wintertime. As discussed in Chapter 3 of the last AQCD for Ozone
9 and other Photochemical Oxidants (U.S. EPA, 2006, [088089](#)), this situation arises because
10 photochemical production of ozone in the planetary boundary layer is much smaller during
11 the winter than summer, while primary PM concentrations are elevated in many areas as a
12 product of heating emissions and lower mixing heights. Ozone in the boundary layer is
13 mainly associated with the subsidence from above the boundary layer following the passage
14 of cold fronts. This subsiding air has much lower PM concentrations than were present in
15 the boundary layer. Therefore, a negative association between O₃ and PM_{2.5} is frequently
16 observed in the wintertime. Bell et al. (2007, [155683](#)) also observed a wintertime minima in
17 same-day correlations between 24-h avg PM₁₀ and O₃ using data from 98 U.S. urban
18 communities over a 14-yr period (1987-2000). The average correlations were not negative in
19 wintertime, however, as seen in Figure 3-53. Furthermore, the highest national average
20 correlations were in spring and fall in the Bell et al. (2007, [155683](#)) analysis rather than
21 summer as observed in Figure 3-53. This discrepancy could be a result of the different
22 averaging times used for O₃ or the selection of different monitoring networks and/or time
23 periods.

24 Correlations among copollutants for individual CSAs/CBSAs are included in Annex A,
25 Figures A-155 through A-166 for PM_{2.5} and Figures A-167 through A-180 for PM₁₀. The 15
26 CSAs/ CBSAs were chosen for further investigation, but several had an insufficient amount
27 of co-located data to be included. As can be seen from the individual CSAs/CBSAs in these
28 figures with multiple pairs of co-located monitors per pollutant, there can be considerable
29 variation in the correlations even within an individual urban area. Birmingham, Boston,
30 and St. Louis all show positive wintertime correlations between PM₁₀ and daily maximum
31 8-h avg O₃; Denver, Detroit, Houston, Los Angeles and Phoenix show negative wintertime
32 correlations. The remaining seven CSAs/CBSAs have insufficient data. For PM_{2.5}, all
33 selected cities with sufficient data show negative correlations in the wintertime with daily

1 max 8-h avg O₃ (including Birmingham, Boston, Chicago, Denver, Houston, Los Angeles,
2 Philadelphia, Phoenix, Pittsburgh, Riverside and St. Louis). The remaining four
3 CSAs/CBSAs have insufficient data. In Baltimore (not one of the fifteen CSAs/CBSAs
4 included in this investigation), Sarnat et al. (2001, [019401](#)) found a significant (at the
5 p <0.05 level) positive (0.67) and negative (-0.72) correlation between daily PM_{2.5} and O₃ in
6 the summer (June 19-August 23, 1998) and winter (February 2-March 13, 1999),
7 respectively. These copollutant correlations illustrate the importance of considering
8 seasonality when assessing temporal relationships between air pollutants, particularly PM
9 and O₃.

3.5.4. Summary

10 Many analyses in this section were based on 2005-2007 AQS data, which has varying
11 degrees of availability depending on the PM size fraction or component of interest. Overall,
12 PM_{2.5} mass has the broadest geographic coverage with PM₁₀ having slightly less coverage.
13 PM_{10-2.5} mass is not routinely measured and reported to AQS and therefore was calculated
14 by difference using data from co-located PM₁₀ and PM_{2.5} monitors. After applying data
15 completeness criterion and limiting the calculation to low-volume FRM and FRM-like
16 monitors for measurement consistency, only 1% of U.S. counties, incorporating less than 5%
17 of the U.S. population, had qualifying PM_{10-2.5} data. Therefore, insufficient information was
18 available using AQS data to adequately characterize regional-scale PM_{10-2.5} concentrations
19 for this review. In all cases, monitors reporting to AQS were not uniformly distributed
20 across the U.S. or within counties, and conclusions drawn from AQS data may not apply
21 equally to all parts of a geographic region.

22 In general, for the eastern metropolitan areas investigated including Atlanta, Boston,
23 Chicago and New York, most of the mass of PM₁₀ was in the PM_{2.5} size fraction, with the
24 highest ratio of PM_{2.5} to PM_{10-2.5} in Chicago. In contrast, Denver and Phoenix contained
25 most of PM₁₀ mass as PM_{10-2.5}. This is consistent with the conclusion drawn in the 1996 PM
26 AQCD (U.S. EPA, 1996, [079380](#)) where ratios of PM_{2.5} to PM₁₀ were generally found to be
27 higher in the east than the west. However, expanded monitoring specifically designed for
28 PM_{10-2.5} is needed before a more conclusive regional characterization of PM_{10-2.5} can be
29 made.

1 Chemical Speciation Network (CSN) data was used to characterize PM_{2.5} composition
2 by region and CSA/CBSA. The highest annual average OC concentrations (>5 µg/m³) were
3 observed in the western and southeastern U.S. EC exhibited less seasonal variability than
4 OC with annual average EC concentrations greater than 1.5 µg/m³ in Los Angeles,
5 Pittsburgh, New York and El Paso. Concentrations of SO₄²⁻ were higher in the eastern U.S.
6 resulting from higher SO₂ emissions in the East, compared with the West. There was also
7 considerable seasonal variability with higher SO₄²⁻ concentrations in the summer months
8 when the oxidation of SO₂ proceeds at a faster rate than during the winter. NO₃⁻
9 concentrations were highest in California, with annual averages >4 µg/m³ at many
10 monitoring locations. There were also elevated concentrations of NO₃⁻ in the Midwest
11 (>2 µg/m³), with wintertime concentrations exceeding 4 µg/m³. In general, NO₃⁻ was higher
12 in the winter across the country, resulting from a number of factors including (1) lower
13 temperatures favoring partitioning into particles, (2) higher relative humidity, particularly
14 in arid and semi-arid regions, (3) lower sulfate concentrations allowing higher uptake of
15 NO₃⁻ and (4) increased residential wood burning in specific areas of the U.S., especially in
16 the Northwest. Exceptions existed in Los Angeles and Riverside, where high NO₃⁻ readings
17 appeared year-round. Crustal material constituted a substantial fraction of PM_{2.5} year-
18 round in Phoenix (28%) and Denver (16%), and during the summer in Houston (26%).

19 In general, PM_{2.5} has a longer atmospheric lifetime than PM_{10-2.5} because larger
20 particles have a higher gravitational settling velocity. For PM_{2.5}, most metropolitan areas
21 investigated exhibited high inter-monitor correlations (generally >0.75) out to a distance of
22 100 km. PM₁₀ data from the same metropolitan areas, however, showed sharper declines in
23 inter-monitor correlations as a function of distance. Insufficient data were available in the
24 15 metropolitan areas to perform similar analyses for PM_{10-2.5} using co-located, low volume
25 FRM or FRM-like monitors. Although the general understanding of PM differential settling
26 leads to an expectation of greater spatial heterogeneity in the PM_{10-2.5} fraction relative to
27 the PM_{2.5} fraction in urban areas, deposition of particles as a function of size depends
28 strongly on local meteorological conditions, in particular on the degree of turbulence in the
29 mixing layer. Therefore, the findings from the 15 CSAs/CBSAs investigated may not apply
30 to all locations or at all times. Population density and associated building density are also
31 important determinants of the spatial distribution of PM concentrations.

32 Few studies performed direct comparisons of ultrafine particle measurements at
33 multiple locations within an urban area. A decrease in the number of ultrafine particles was

1 demonstrated with shifts from a dominant mode at around 10 nm within 20 m of a freeway
2 to a flattened dominant mode at around 50 nm fat a distance of roughly 100-150 m. At the
3 same time, accumulation mode particle number concentration remained relatively constant
4 to within ~300 m from the freeway. These findings suggest a high degree of spatial
5 heterogeneity in ultrafine particles compared with accumulation mode particles on the
6 urban scale.

7 Using hourly PM_{2.5} and PM₁₀ observations in the 15 metropolitan areas, diel variation
8 showed a morning peak starting at approximately 6:00 a.m., corresponding with the start of
9 morning rush hour. There was also an evening concentration peak that was broader than
10 the morning peak and extended into the overnight period, likely reflecting a combination of
11 evening rush hour and the concentration increase caused by the usual collapse of the mixed
12 layer after sundown. The magnitude and duration of these peaks varied considerably by
13 size fraction and metropolitan area. Studies indicate that ultrafine particles in urban
14 environments exhibit similar two-peaked diel patterns. Comparison between weekdays and
15 weekends as well as between urban street canyon and urban background sites suggest
16 traffic is a major source of ultrafine particles during the morning rush hour. The afternoon
17 peak in ultrafine particles likely represents the combination of primary source emissions
18 such as evening rush-hour traffic and photochemical formation of secondary organic and
19 sulfate aerosols.

20 Correlations between PM and gaseous copollutants varied both seasonally and
21 spatially between and within metropolitan areas. On average, PM₁₀ and PM_{2.5} were
22 correlated with each other better than with the gaseous copollutants. There was relatively
23 little seasonal variability in the mean correlation between PM in both size fractions and
24 SO₂ and NO₂. CO, however, showed higher correlations with PM₁₀ and PM_{2.5} on average in
25 the winter compared with the other seasons. This seasonality results in part because a
26 larger fraction of PM is primary in origin during the winter. To the extent that this primary
27 component of PM is associated with common sources of NO₂ and CO, then higher
28 correlations with these gaseous copollutants are to be expected. Increased atmospheric
29 stability in colder months would also reinforce these associations. The correlation between
30 daily maximum 8-h avg O₃ and PM_{2.5} showed the highest degree of seasonal variability with
31 positive correlations on average in the spring, summer and fall, and negative correlations
32 on average in the winter. This situation arises as the result of seasonal differences in PM
33 primary emissions and photochemical production of secondary PM_{2.5} and O₃.

3.6. Mathematical Modeling of PM

1 There are two main classes of models used to study atmospheric PM, receptor models
2 and chemistry-transport models (CTMs). Receptor models are statistical models whereas
3 CTMs are numerical models, i.e., they approximate derivatives by finite difference
4 approximations. Finite element models are also numerical models but have not been used
5 as extensively for applications described here, and so are not discussed further. Receptor
6 models are diagnostic in their approach, in that they try to derive source contributions at
7 monitoring locations using either ambient data alone or in combination with data for the
8 chemical composition of sources or in combination with meteorological data. Three-
9 dimensional chemistry and transport models are formulated in a prognostic, or predictive
10 manner, that is, they attempt to predict species concentrations by solving a set of coupled,
11 non-linear partial differential equations (continuity equations) for chemical species that
12 include terms based on emissions inventories, atmospheric transport, chemical
13 transformations, and deposition. Monitoring data is used to evaluate the performance of
14 CTMs. Each of these approaches has its own advantages and disadvantages.

3.6.1. Estimating Source Contributions to PM Using Receptor Models

15 Methods for analyzing the composition of ambient PM samples in terms of
16 contributions from different sources are reviewed in this section. Associations between
17 exposures to ambient PM, as represented by ambient monitors, and health outcomes have
18 been extensively studied. Some health studies, described in Section 6.6, have used source
19 apportionment modeling to evaluate relationships between health outcomes and PM
20 (mainly PM_{2.5}) from different sources. This section is intended to provide background
21 concerning the uses of source apportionment techniques in such studies. Understanding the
22 contribution of different emissions sources to ambient PM has also been used extensively in
23 evaluating air quality data for use in developing control strategies.

3.6.1.1. Receptor Models

24 Receptor models have been used mainly as part of the development of air quality
25 management plans. However, there have been several publications relating apportioned

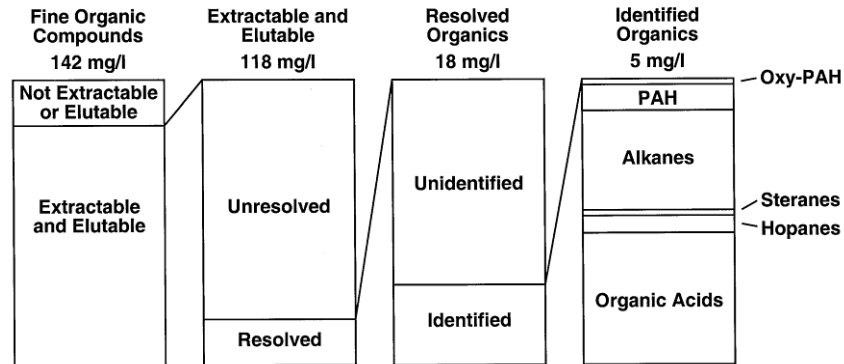
1 source types based on receptor models to human health effects. Discussions in this
2 section will focus mainly on those methods that have been used to relate health outcomes to
3 sources. More complete descriptions of a large number of types of receptor models currently
4 in use are given in Watson et al. (2008, [157128](#)), who summarize the properties of these
5 methods, including the strengths and weaknesses. This compilation of receptor models,
6 broken down into different approaches (i.e., chemical mass balance, factor analysis,
7 tracer-based, meteorology based) is included in Tables A-45 through A-48 in Annex A.

8 Receptor models such as the chemical mass balance (CMB) model (Watson et al.,
9 1990, [004848](#)) relate source category contributions to ambient PM concentrations based on
10 analyses of the compositional profiles of ambient and source emissions samples. It uses as
11 its basis a mass balance equation that represents all chemical species in an aerosol sample
12 as linear combinations of contributions from a fixed number of independent sources plus an
13 error term representing the portion of the measurement that cannot be fit by the model.

14 The compositional profiles used in receptor models can be extensive (see for example
15 the SPECIATE data base, (<http://www.epa.gov/ttnchie1/software/speciate/index.html>) for a
16 comprehensive collection of results from a large number of studies. As an example, several
17 studies have identified EC and over 100 organic carbon compounds in gasoline PM
18 emissions, including alkanes, PAHs, oxy-PAHs, steranes, hopanes, and organic acids (Matti
19 Maricq, 2007, [155973](#); Schauer et al., 1999, [010582](#); Schauer et al., 2002, [035332](#)). This
20 breakdown in identifiable groups of organic compounds is illustrated in Figure 3-54 and
21 Table 3-17 shows emissions factors for trace elements. Data for the compositional profiles
22 for several other important sources of PM that could be used for CMB modeling are shown
23 in Table A-49 in Annex A.

24 Source categories are amenable to refinement and to analysis as information on
25 tracers becomes available. For example, primary biological aerosol particles (PBAP) have
26 long been known to be significant constituents of the atmospheric aerosol, but not many
27 studies have evaluated their contributions, largely because of the lack of suitable tracers
28 and the additional equipment needs for sampling and analysis of bioaerosols. Bauer et al.
29 (2008, [189986](#)) reviewed studies estimating the contribution of fungal spores to PM_{2.5} and
30 PM_{10-2.5} as fungal spores were expected to be major contributors to PBAP. They proposed the
31 use of arabitol and mannitol as unique tracers with an estimated accuracy of $\pm 50\%$ to
32 apportion the contribution of fungal spores to OC in both PM_{2.5} and PM_{10-2.5}. They estimated

1 24-h avg contributions of ~ 40% to OC in PM_{10-2.5} during spring and summer in Vienna, with
2 a smaller contribution to PM_{2.5}.



Source: Fraser et al. (1999, [010819](#))

Figure 3-54. Schematic of organic composition of particulate emissions from gasoline-fueled vehicles.

3 One recently-identified concern in the application of CMB-based receptor models with
4 detailed organic marker compounds is the photochemical stability of those species.
5 Robinson et al. (2006, [156918](#)) reported evidence of significant summertime photooxidation
6 of hopanes and long-chain alkenoic acids, low-volatility compounds often used as mobile
7 source and cooking emissions, respectively. Seasonal differences in hopanes/EC ratios
8 differed in a manner consistent with oxidation. Photochemical loss of particle-phase marker
9 species mass complicates the interpretation of model results, as long-range transport and
10 photochemistry may result in the loss of markers for distant sources. Furthermore,
11 photochemical breakdown of organic marker species may cause losses in CMB model
12 performance criteria and possible bias in source contribution estimates. The photooxidation
13 of condensed-phase organic compounds also may affect the polarity and volatility of these
14 compounds

15 In other methods, various forms of factor analysis are used that rely on the varying
16 mix of species present in ambient observations of compositional data to derive the source
17 contributions. Standard factor analytic approaches such as Principal Component Analysis
18 (PCA) have been used but PCA alone can apportion only the variance, not the mass, in an
19 aerosol composition data set. Additional steps such as those applied in Absolute Principal
20 Components Scores (APCS) are required to apportion mass from PCA (Miller et al., 2002,

1 [030661](#); Thurston and Spengler, 1985, [056074](#)). In Positive Matrix Factorization (PMF)
 2 (Paatero and Tapper, 1994, [086998](#)), the ambient compositional data matrix is decomposed
 3 into the product of a matrix representing the source contributions and one representing the
 4 source profiles. Solutions are obtained by minimizing an object function with respect to
 5 these two matrices, and solutions are subject to non-negativity constraints. PMF also allows
 6 for the treatment of missing data and data near or below detection limits by weighting
 7 elements inversely according to their uncertainties. The PMF approach requires a large
 8 number of samples (n typically >50) and are most often applied to time series data, whereas
 9 CMB can be applied to a single sample. Both the CMB and the PMF approaches find
 10 solutions based on least squares fitting and minimization of an object function. Both
 11 methods provide error estimates for the solutions based on estimates of the errors in the
 12 input parameters. It should be noted, though, that the error estimates for both methods
 13 often contain subjective judgments about the magnitude of the analytical and monitoring
 14 errors.

Table 3-17. Example of emissions factors (ng/kg) for trace elements under variable speed and steady speed driving conditions for PM emitted by diesel and gasoline engines. Note that emissions are highly variable.

Element	Diesel		Gasoline	
	Transient	Steady State	Transient	Steady State
Al	9108 (5224)	2706	2273 (545)	252
Ca	69,443 (23,640)	16,128	18,247 (3044)	2324
Fe	22,910 (21,448)	2036	10,266 (9928)	138
K	4672 (752)	1191	1935 (558)	117
Mg	3087 (461)	997	5183 (1706)	183
Na	7736 (1751)	1945	2237 (1125)	321
Ba	583 (349)	73	331 (55)	4.8
Be	26 (12)	23	6.7 (1.1)	1.5
Cr	634 (354)	93	138 (6.7)	8.6
Cu	1944 (679)	627	1745 (1803)	16
Li	13 (0.2)	7.9	3.0 (1.4)	0.9
Mn	368 (183)	76	152 (85)	3.4
Ni	2310 (656)	644	107 (0.7)	21
Pb	793 (593)	79	237 (2.3)	11
S	23,750 (5295)	6713	8705 (3375)	349
Ti	2036 (320)	345	118 (9.3)	24

		Diesel		Gasoline
V	28 (9.4)	11	15 (11)	1.8
Zn	21,118 (4422)	5620	4650 (1225)	198

Source: Geller and Solomon (2006, [139645](#)).

1 The nature of the solutions in terms of source categories is different in the CMB and
2 PMF approaches. In the CMB approach, the composition of the source emissions is assumed
3 to be known based on measurements. These assumptions may or may not reflect the
4 composition of emissions affecting a particular site at any given time or place. However,
5 there may be variations in the composition of individual source categories (e.g., soils, motor
6 vehicle emissions) across a given airshed and even in the composition of the same source
7 with time. Source profiles can also be altered between emission and receptor locations
8 resulting from atmospheric reactions, depending on the source type and species under
9 analysis. The CMB technique was developed for apportioning source categories of primary
10 PM and was not formulated to include sources of secondary PM. CMB might not explain
11 all the mass or produce a valid result unless there is information for the composition of all
12 major sources affecting a given site, and there is confidence that the existing source profiles
13 are specific to those sources. For example, Volckens et al. (2008, [105465](#)) describe PAH
14 emission profiles from hand-held gasoline lawn and garden equipment as found in some
15 CMB source profiles for motor vehicles.

16 In PMF, the source solutions are more general in that they contain information about
17 the entrainment of emissions from additional sources during transport, the time
18 dependence of the composition of emissions from particular sources, the formation of
19 secondary species and local differences in source compositions. PMF differs from CMB
20 because it derives the mix of factors from measured data. However, the procedure used to
21 find a solution results in some rotational ambiguity (Paatero and Tapper, 1994, [086998](#)).
22 The assignment of sources to PMF factors depends largely on past experience and
23 judgments. Judgments are based to large extent on comparison with data for source profiles
24 and also on the factors that could modify the assignments. These issues are alleviated to
25 some degree by incorporating information about local wind fields and other physical
26 parameters.

27 The UNMIX model takes a geometric approach that exploits the covariance of the
28 ambient data to determine the number of independent sources, the composition and
29 contributions of the sources, and corresponding uncertainties (Henry, 1997, [020941](#)).

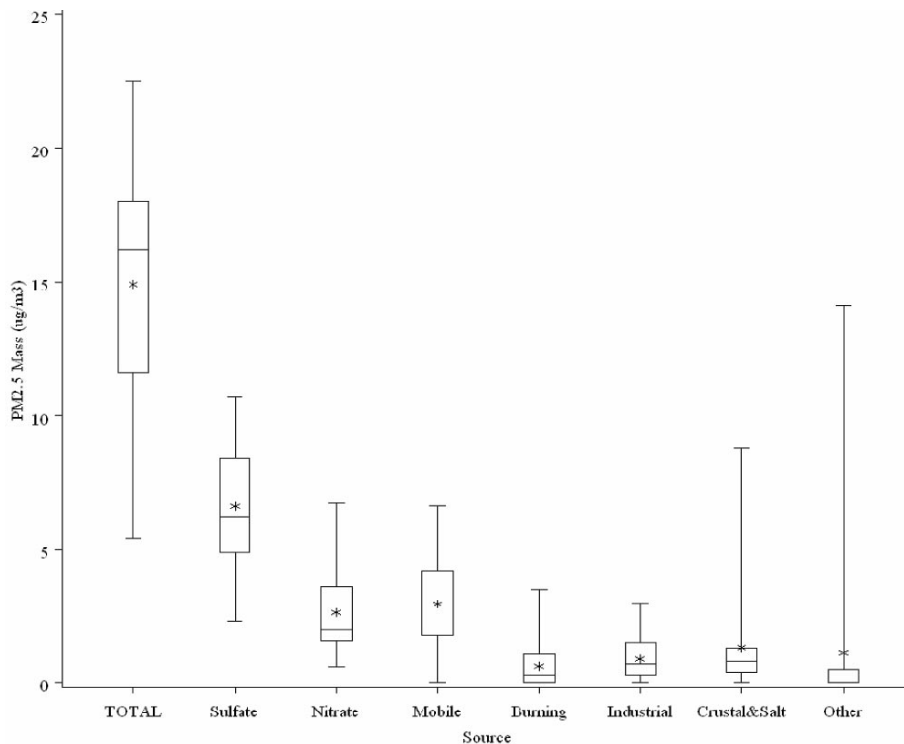
1 UNMIX uses PCA to find edges in m-dimensional space, where m is the number of ambient
2 species. Success of the UNMIX model hinges on the ability to find these “edges” in the
3 ambient data from which the number of source types and the source compositions are
4 extracted. In simplest terms, the approach can be seen to be similar to that for deriving
5 ternary mixing diagrams, except there is extension to higher dimensionality. Measurement
6 errors in the ambient data “fuzz” the edges, making them difficult to find. UNMIX employs
7 an “edge-finding” algorithm to find the best edges in the presence of error. UNMIX does not
8 make explicit use of errors or uncertainties in the ambient concentrations, unlike the
9 methods outlined above. Rather they are implicitly incorporated into the analyses. PMF
10 and UNMIX have also used data for particle size distributions to obtain further information
11 about sources.

12 Partial least squares (PLS) is another mathematical model related to PCA which has
13 been used in a limited number of PM toxicology studies to establish a relationship between
14 PM constituents and health outcomes (McDonald et al., 2004, [087458](#); Seagrave et al., 2006,
15 [091291](#); Veranth et al., 2006, [087479](#)). Unlike PCA and other receptor models discussed in
16 this section, PLS incorporates both predictor variables (e.g., PM component concentrations)
17 and outcome variables (e.g., toxicological responses) into one coupled regression model. Like
18 PCA, PLS groups the observable variables into a reduced number of latent variables,
19 thereby reducing the dimensionality of the model. Typically, PM toxicology studies have
20 been limited to two-component models (two latent variables on the predictor side compared
21 with two on the outcome side), thereby producing a 2x2 loading plot revealing relationships
22 between predictors and outcomes. PLS is particularly useful when there are more predictor
23 variables than observations, which is a situation that other multivariate factor analysis
24 approaches do not handle well. However, since PLS is a variance based approach, it shares
25 the same shortcomings discussed earlier for PCA. PLS has also traditionally been limited to
26 two-component applications even though this is not a strict mathematical limitation.

Results from Receptor Models

27 Results from receptor modeling calculations indicate that PM_{2.5} is most often
28 produced mainly by fossil fuel combustion. Fugitive dust, found mainly in the PM_{10-2.5} size
29 range, represents the largest source of measured ambient PM₁₀ in many locations in the
30 western U.S. Quoted uncertainties in the source apportionment of constituents in ambient
31 aerosol samples typically range from 10 to 50%. It is apparent that a relatively small

1 number of broadly defined source categories, compared to the total number of chemical
 2 species that typically are measured in ambient monitoring-source receptor model studies,
 3 are needed to account for the majority of the observed mass of PM in these studies. Trying
 4 to be more specific about contributions from source categories could result in ambiguity. For
 5 example, some stationary sources (e.g., agriculture use engines) and quite different mobile
 6 sources (e.g., trucks and locomotives) rely on diesel power and ancillary data is required to
 7 resolve contributions from these sources. Compilations of source attribution studies using
 8 CMB for PM₁₀ have appeared in the PM AQCD (U.S. EPA, 2004, [056905](#)) and using PMF
 9 for PM_{2.5} in Engel-Cox and Weber (2007, [156419](#)). Results of the compilation by Engel-Cox
 10 and Weber (2007, [156419](#)) for the eastern U.S. are shown in Figure 3-53. There are only
 11 three main source categories in the figure constituting most of the PM_{2.5} mass. Two of these
 12 are predominantly secondary and not identified by sources of precursors. Tables A-50 and
 13 A-51 in Annex A list results of other receptor modeling studies for PM₁₀ and PM_{2.5}, many of
 14 which are in the western U.S.

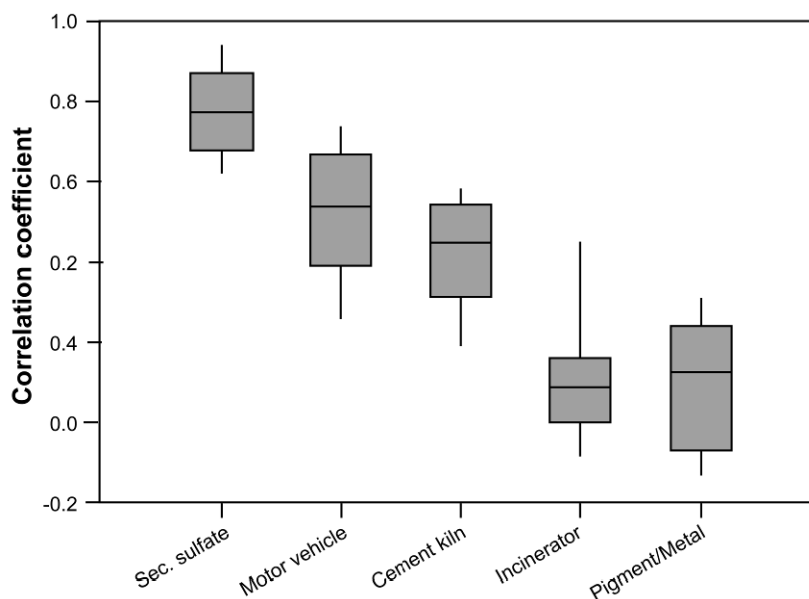


Source: Engel-Cox and Weber (2007, [156419](#)).

Figure 3-55. Source category contributions to PM_{2.5} at a number of sites in the East derived using PMF.

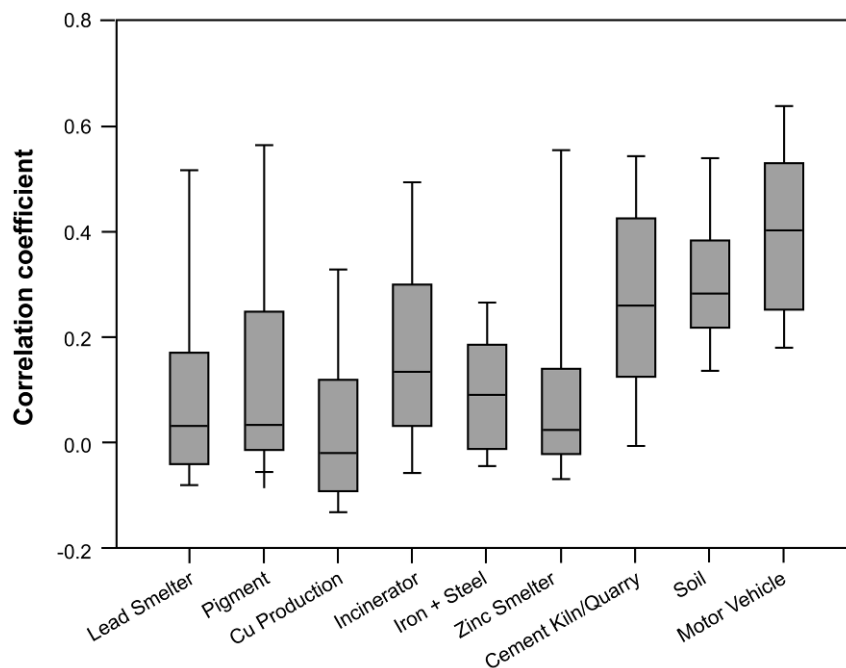
Spatial Variability in Source Contributions to PM Based on Receptor Models

1 Spatial variability in source contributions across urban areas is an important
2 consideration in assessing the likelihood of exposure measurement error in epidemiologic
3 studies relating health endpoints to sources. Arguments similar to those for using ambient
4 concentrations as surrogates for personal exposures apply here. Studies for $PM_{2.5}$ (Kim et
5 al., 2005, [083181](#); Wongphatarakul et al., 1998, [049281](#)) indicate that intra-urban
6 variability increases in the following order: regional sources (e.g., secondary SO_4^{2-}
7 originating from EGUs) < area sources (e.g., on-road mobile sources) < point sources (e.g.,
8 stacks). This point is illustrated in Figure 3-56. The only study available for $PM_{10-2.5}$
9 (Hwang et al., 2008, [134420](#)) indicates a similar ordering, but without a regional component
10 (resulting from the short lifetime of coarse PM compared to transport times on the regional
11 scale) as shown in Figure 3-57.



Source: Kim et al. (2005, [083181](#))

Figure 3-56. Pearson correlation coefficients for source category contributions to $PM_{2.5}$ between the ten Regional Air Pollution Study/Regional Air Monitoring System (RAPS/RAMS) monitoring sites in St. Louis.



Source: Hwange et al. (2008, [134420](#))

Figure 3-57. Pearson correlation coefficients for source contributions to PM_{10-2.5} between the ten Regional Air Pollution Study/Regional Air Monitoring System (RAPS/RAMS) monitoring sites in St. Louis.

3.6.2. Chemistry Transport Models

1 Chemistry Transport Models (CTMs) are the prime tools used to compute the
 2 interactions among atmospheric pollutants and their transformation products, the
 3 production of secondary aerosols, the evolution of particle size distribution, and transport
 4 and deposition of pollutants. CTMs are driven by emissions inventories for primary species
 5 such as NO_x, SO_x, NH₃, VOCs, and primary PM, and by meteorological fields produced by
 6 other numerical prediction models. Values for meteorological state variables such as winds
 7 and temperatures are taken from operational analyses, reanalyses, or weather circulation
 8 models. In most cases, these are off-line meteorological analyses, meaning that they are not
 9 modified by radiatively active species generated by the air quality model (AQM). Work to
 10 integrate meteorology and chemistry was done in the mid 1990s by Lu et al. (1997, [048202](#)
 11 and references therein; 1997, [191768](#)) although limits to computing power prevented their
 12 wide-spread application. More recently, new, integrated models of meteorology and
 13 chemistry are now available as well; see, for example, (Binkowski et al., 2007, [090563](#)) and

1 the Weather Research and Forecast model with chemistry (WRF-Chem)
2 (<http://ruc.fsl.noaa.gov/wrf/WG11>).

3 CTMs have been developed for application over a wide range of spatial scales ranging
4 up from neighborhood to global. CTMs are used to: (1) obtain better understanding of the
5 processes controlling the formation, transport, and destruction of gas- and particle-phase
6 criteria and hazardous air pollutants; (2) understand the relations between concentrations
7 of secondary pollutant products and concentrations of their precursors; (3) understand
8 relations among the concentration patterns of various pollutants that may exert adverse
9 effects; and (4) evaluate how changes in emissions propagate through the atmospheric
10 system to secondary products and deposition.

11 Emissions of precursor compounds can be divided into anthropogenic and natural
12 source categories. Natural sources can be further divided into biogenic from vegetation,
13 microbes, and animals, and abiotic from biomass burning, lightning, and geogenic sources.
14 However, the distinction between natural sources and anthropogenic sources is often
15 difficult to make in practice, as human activities affect directly or indirectly emissions from
16 what would have been considered natural sources during the preindustrial era. Thus,
17 emissions from plants and animals used in agriculture have been referred to as
18 anthropogenic or biogenic in different applications. Wildfire emissions may be considered
19 natural, except that forest management practices can lead to buildup of fuels on the forest
20 floor, thereby altering the frequency and severity of forest fires.

21 The initial conditions, or starting concentration fields of all species computed by a
22 model, and the boundary conditions, or concentrations of species along the horizontal and
23 upper boundaries of the model domain throughout the simulation, must be specified at the
24 beginning of the simulation. Both initial and boundary conditions can be estimated from
25 models or data or, more generally, model + data hybrids. Because data for vertical profiles
26 of most species of interest are very sparse, results of model simulations over larger, usually
27 global, domains are often used. As might be expected, the influence of boundary conditions
28 depends on the lifetime of the species under consideration and the time scales for transport
29 from the boundaries to the interior of the model.

30 Each of the model components described above has associated uncertainties and the
31 relative importance of these uncertainties varies with the modeling application. The largest
32 errors in photochemical modeling are still thought to arise from the meteorological and
33 emissions inputs to the model (Russell and Dennis, 2000, [035563](#)). While the effects of

1 poorly specified boundary conditions propagate through the model's domain, the effects of
2 these errors remain undetermined. Because many meteorological processes occur on spatial
3 scales smaller than the model's vertical or horizontal grid spacing and thus are not
4 calculated explicitly, parameterizations of these processes must be used. These
5 parameterizations introduce additional uncertainty. Because the chemical production and
6 loss terms in the continuity equations for individual species are numerically coupled, the
7 chemical calculations must be performed iteratively until calculated concentrations
8 converge to within some preset criterion. The number of iterations and the convergence
9 criteria chosen also can introduce error.

10 CTMs in current use mostly have one of two forms. The first, grid-based or Eulerian
11 air quality models subdivide the region to be modeled, the modeling domain, into a three-
12 dimensional array of grid cells. Spatial derivatives in the species continuity equations are
13 cast in finite-difference form over this grid and a system of equations for the concentrations
14 of all the chemical species in the model are solved numerically at each grid point. Finite
15 element Eulerian models also exist and have been exercised, but less frequently. Time-
16 dependent continuity or mass conservation equations are solved for each species including
17 terms for transport, chemical production and destruction, and emissions and deposition (if
18 relevant), in each grid cell. Chemical processes are simulated with ordinary differential
19 equations, and transport processes are simulated with partial differential equations.
20 Because of a number of factors such as the different time scales inherent in different
21 processes, the coupled, nonlinear nature of the chemical process terms, and computer
22 storage limitations, not all of the terms in the equations are solved simultaneously in three
23 dimensions. Instead, operator splitting, in which terms in the continuity equation involving
24 individual processes are solved sequentially, is used.

25 In the second common CTM formulation, trajectory or Lagrangian models, a number
26 of hypothetical air parcels are specified as though following wind trajectories. In these
27 models, the original system of partial differential equations is transformed into a system of
28 ordinary differential equations.

29 A less common approach is to use a hybrid Lagrangian-Eulerian model, in which
30 certain aspects of atmospheric chemistry and transport are treated with a Lagrangian
31 approach and others are treated in an Eulerian manner (see, e.g., Stein et al., 2000,
32 [048341](#)).

1 Each approach has advantages and disadvantages. The Eulerian approach is more
2 general in that it includes processes that mix air parcels and allows integrations to be
3 carried out for long periods during which individual air parcels lose their identity. There
4 are, however, techniques for including the effects of mixing in Lagrangian models such as
5 FLEXPART (Zanis et al., 2003, [053423](#)), ATTILA (Reithmeier and Sausen, 2002, [053447](#)),
6 and CLaMS (McKenna et al., 2002, [053445](#)). Because both the accuracy and the
7 computational intensity of Eulerian models depend strongly on the size of the horizontal
8 and vertical grid spacing, speed and fidelity to actual atmospheric conditions much
9 sometimes be traded-off; that is to say, while finer grid spacing will often capture effects
10 missed at larger grid intervals, models set up in this way require longer to solve. In a
11 similar manner, the accuracy of Lagrangian models depends on the number of air parcels
12 deployed; thus they, too, become computationally intensive when higher-order accuracy is
13 desired. More detailed discussion of CTM applications appears in the 2008 ISA for NO_x and
14 SO_x - Ecological Criteria (U.S. EPA, 2008, [157074](#)).

3.6.2.1. Global Scale

15 Global-scale CTMs are used to address issues associated with climate change and
16 stratospheric O₃ depletion to characterize long-range air pollution transport, and to provide
17 boundary conditions for the regional-scale models. The CTMs include parameterizations of
18 atmospheric transport; the transfer of solar radiation through the atmosphere; chemical
19 reactions; and removal to the surface by turbulent motions and precipitation for emitted
20 pollutants. The upper boundaries of the CTMs extend anywhere from the tropopause (~8
21 km at the poles to ~16 km in the tropics) to the mesopause at ~80 km in order to obtain
22 more realistic boundary conditions for problems involving stratospheric dynamics and
23 chemistry.

24 Global simulations are typically conducted with a horizontal grid spacing of 200 km or
25 more, although some models such as GEOS-Chem have been run at grid spacings of about
26 100 km (see e.g., Wu et al., 2008, [190039](#)) and efforts are being made to go to even higher
27 spatial resolution. Simulations of the effects of long-range transport at particular locations
28 link multiple horizontal resolutions from the global to the local scale. Finer resolution can
29 only improve scientific understanding to the extent that the governing processes are more

1 accurately described at that scale. Consequently, there is a crucial need for observations at
2 the appropriate scales to evaluate the scientific understanding represented by the models.

3.6.2.2. Regional Scale

3 Most major regional-scale air-related modeling efforts at EPA use the Community
4 Multi-scale Air Quality modeling system (CMAQ) (Byun and Ching, 1999, [156314](#); Byun
5 and Schere, 2006, [090560](#)). A number of other modeling platforms using Lagrangian and
6 Eulerian frameworks were reviewed in the 2006 AQCD for O₃ (U.S. EPA, 2006, [088089](#)) and
7 in Russell and Dennis (Russell and Dennis, 2000, [035563](#)). The capabilities of a number of
8 CTMs designed to study local- and regional-scale air pollution problems were summarized
9 by Russell and Dennis (2000, [035563](#)). Evaluations of the performance of CMAQ are given
10 in Arnold et al. (2003, [087579](#)) Eder and Yu (2005, [089229](#)) Appel et al. (2005, [089227](#)), and
11 Fuentes and Raftery (2005, [087580](#)). CMAQ's horizontal domain can extend from a few
12 hundred kilometers on a side to the entire hemisphere. CMAQ is most often driven by the
13 MM5 mesoscale meteorological model (Seaman, 2000, [035562](#)), though it may be driven by
14 other meteorological models including WRF and the Regional Atmospheric Modeling
15 System (RAMS); see <http://atmet.com>. Simulations of pollution episodes over regional
16 domains have been performed with a horizontal resolution as low as 1 km; see the
17 application and general survey results reported in Ching et al. (2006, [090300](#)). However,
18 simulations at such high resolutions require better parameterizations of meteorological
19 processes such as boundary layer fluxes, deep convection and clouds (Seaman, 2000,
20 [035562](#)). Finer spatial resolution is necessary to resolve features such as urban heat island
21 circulation; sea, bay, and land breezes; mountain and valley breezes; and the nocturnal low-
22 level jet, all of which can affect pollutant concentrations.

23 The most common approach to setting up the horizontal domain is to nest a finer grid
24 within a larger domain of coarser resolution. However, there are other strategies such as
25 the stretched grid (see, e.g., Fox-Rabinovitz et al., 2002, [047806](#)) and the adaptive grid (see,
26 e.g., Hansen et al., 1994, [046634](#)). In a stretched grid, the grid's resolution continuously
27 varies throughout the domain, thereby eliminating any potential problems with the sudden
28 change from one resolution to another at the boundary. Caution should be exercised in
29 using such a formulation because certain parameterizations like those for convection might
30 be valid on a relatively coarse grid scale but may not be valid on finer scales. Adaptive grids

1 are not fixed at the start of the simulation, but instead adapt to the needs of the simulation
2 as it evolves. They have the advantage that they can resolve processes at relevant spatial
3 scales. However, they can be very slow if the situation to be modeled is complex.
4 Additionally, if adaptive grids are used for separate meteorological, emissions, and
5 photochemical models, there is no reason a priori why the resolution of each grid should
6 match, and the gains realized from increased resolution in one model will be wasted in the
7 transition to another model. The use of finer horizontal resolution in CTMs will necessitate
8 finer-scale inventories of land use and better knowledge of the exact paths of roads,
9 locations of factories, and, in general, better methods for locating sources and estimating
10 their emissions.

11 The vertical resolution of these CTMs is variable and usually configured to have more
12 layers in the PBL and fewer higher up. Because the height of the boundary layer is of
13 critical importance in simulations of air quality, improved resolution of the boundary layer
14 height would likely improve air quality simulations. Additionally, current CTMs do not
15 adequately resolve fine-scale features such as the nocturnal low-level jet in part because
16 little is known about the nighttime boundary layer.

17 CTMs require time-dependent, three-dimensional wind fields for the period of
18 simulation. The winds may be generated either by a model using initial fields alone or with
19 four-dimensional data assimilation to improve the model's performance; i.e., model
20 equations can be updated periodically to bring results into agreement with observations.
21 Modeling series durations can range from simulations of several days duration, the typical
22 time scale for individual O₃ episodes, to several months or multiple seasons of the year. The
23 current trend in modeling applications is towards annual simulations. This trend is driven
24 in part by the need to improve understanding of observations of periods of high wintertime
25 PM (Blanchard et al., 2002, [047598](#)) and the need to simulate O₃ episodes occurring in
26 spring, fall, and winter.

27 Chemical kinetics mechanisms representing the important reactions occurring in the
28 atmosphere are used in CTMs to estimate the rates of chemical formation and destruction
29 of each pollutant simulated as a function of time. Mechanisms that treat the reactions of all
30 individual reactive species explicitly are computationally too demanding to be incorporated
31 into CTMs for regulatory use. Similarly, very extensive "master mechanisms" (Derwent et
32 al., 2001, [047912](#)) that include approximately 10,500 reactions involving 3603 chemical
33 species (Derwent et al., 2001, [047912](#)) can be combined into mechanisms that group

1 together compounds with similar chemistry. Because of different approaches to the lumping
2 of organic compounds into surrogate groups for computational efficiency, chemical
3 mechanisms can produce different results under similar conditions. The Carbon Bond
4 chemical mechanisms starting with CB-IV (Gery et al., 1989, [043039](#)), the RADM II
5 mechanism (Stockwell et al., 1990, [043095](#)), the SAPRC (see, e.g., Carter, 1990, [042893](#);
6 Wang et al., 2000, [048357](#); Wang et al., 2000, [048365](#)), and the RACM mechanisms can be
7 used in CMAQ. Jimenez et al. (Jimenez et al., 2003, [156611](#)) provided brief descriptions of
8 the features of the main mechanisms in use and compared concentrations of several key
9 species predicted by seven chemical mechanisms in a box-model simulation over 24 h.

10 CMAQ and other state-of-the-science CTMs incorporate processes and interactions of
11 aerosol-phase chemistry (Binkowski and Roselle, 2003, [191769](#); Gaydos et al., 2007, [139738](#))
12 Zhang and Wexler (2008, [191770](#)). There have also been several attempts to study the
13 feedbacks of chemistry on atmospheric dynamics using meteorological models like MM5
14 and WRF (Grell et al., 2000, [048047](#); Liu et al., 2001, [048201](#); Lu et al., 1997, [048202](#); Park
15 et al., 2001, [156841](#)). This coupling is necessary to accurately simulate feedbacks which
16 may be caused by the heavy aerosol loading found in forest fire plumes (Lu et al., 1997,
17 [048202](#); Park et al., 2001, [156841](#)) or in heavily polluted areas. Photolysis rates in CMAQ
18 can now be calculated interactively with model produced O₃, NO₂, and aerosol fields
19 (Goldstein et al., 1973, [015674](#)).

20 Spatial and temporal characterizations of anthropogenic and biogenic precursor
21 emissions must be specified as inputs to a CTM. Emissions inventories have been compiled
22 on grids of varying resolution for many HCs, aldehydes, ketones, CO, NH₃, and NO_x.
23 Emissions inventories for many species require the application of algorithms for calculating
24 the dependence of emissions on physical variables such as temperature and to convert the
25 inventories into formatted emission files which can be used by a CTM. For example,
26 preprocessing of emissions data for CMAQ often is done by the Sparse-Matrix Operator
27 Kernel Emissions (SMOKE) system (<http://smoke-model.org>). For many species,
28 information concerning the temporal variability of emissions is lacking, so long-term
29 annual averages are used in short-term, episodic simulations. Annual emissions estimates
30 are often modified by the emissions model to produce emissions more characteristic of the
31 time of day and season. Significant errors in emissions can occur if inappropriate time
32 dependence is used. Additional complexity arises in model calculations because different

1 chemical mechanisms can include different species, and inventories constructed for use
2 with one mechanism must be adjusted to reflect these differences in another.

3.6.2.3. Local or Neighborhood Scale

3 The grid spacing in regional CTMs, usually between 1 and 12 km², is usually too
4 coarse to resolve spatial variations on the neighborhood scale. The interface between
5 regional scale models and models of smaller exposure scales is provided by smaller scale
6 dispersion models. Several models could be used to simulate concentration fields near
7 roads, each with its own set of strengths and weaknesses. The California Department of
8 Transportation's most recent line dispersion model is CALINE4; see
9 <http://www.dot.ca.gov/hq/env/air/pages/calinesw.htm>. The CALINE family of models is not
10 supported by the California Department of Transportation for modeling of highway-source
11 PM, however, but only for roadway CO, although PM work with CALINE has performed for
12 more than ten years; see Wu et al. (2009, [191773](#)) and references therein.

13 In addition, AERMOD (http://www.epa.gov/scram001/dispersion_prefrec.htm) is a
14 steady-state plume model formulated as a replacement to the ISC3 dispersion model. In the
15 stable boundary layer (SBL), it assumes the concentration distribution to be Gaussian in
16 both the vertical and horizontal dimensions. In the convective boundary layer, the
17 horizontal distribution is also assumed to be Gaussian, but the vertical distribution is
18 described with a bi-Gaussian probability density function (pdf). AERMOD has provisions to
19 be applied to flat and complex terrain and multiple source types (including, point, area and
20 volume sources) in both urban and rural areas. It incorporates air dispersion based on PBL
21 turbulence structure and scaling concepts and is meant to treat both surface and elevated
22 sources and simple and complex terrain in rural and urban areas. The dispersion of
23 emissions from line sources like highways in AERMOD is handled as a source with
24 dimensions set using an area or volume source algorithm in the model; however, actual
25 emissions are usually not in steady state and there are different functional relationships
26 between buoyant plume rise in point and line sources. Moreover, most simple dispersion
27 models including AERMOD are designed without chemical mechanisms and so cannot
28 produce secondary pollutants from their primary emissions .

29 There are also non-steady state models that incorporate plume rise explicitly from
30 different types of sources. For example, CALPUFF

1 (<http://www.src.com/calpuff/calpuff1.htm>), which is EPA's recommended dispersion model
2 for transport in ranges >50 km, is a non-steady-state puff dispersion model that simulates
3 the effects of time- and space-varying meteorological conditions on pollution transport,
4 transformation, and removal and has provisions for calculating dispersion from surface
5 sources. However, CALPUFF was not designed to treat the dispersion of emissions from
6 roads, and like AERMOD does not include production of secondary pollutants. The
7 distinction between a steady-state and time varying model could be unimportant for long
8 time scales; however, at short time scales, the temporal variability in traffic emissions could
9 result in underestimation of peak concentration and exposures.

3.6.3. Air Quality Model Evaluation for Air Concentrations

10 Urban and regional air quality is determined by a complex system of coupled chemical
11 and physical processes including emissions of pollutants and pollutant precursors, complex
12 chemical reactions, physical transport and diffusion, and wet and dry deposition. NO_x in
13 these systems has long been known to act nonlinearly in the production of O₃ and other
14 secondary pollutants (Dodge, 1977, [038646](#)) to extend over multiple spatial and temporal
15 scales; and to involve complicated cross-media environmental issues such as acidic or
16 nutrient deposition to sensitive biota and degradation of visibility.

17 NO_y species emitted and transformed from emissions control the production and fate
18 of both O₃ and aerosols by sustaining or suppressing OH cycling. Correctly characterizing
19 the interrelated NO_y and OH dynamics for O₃ formation and fate in the polluted
20 troposphere depends on new techniques using combinations of several NO_y species for
21 diagnostically probing the complex atmospheric dynamics in typical urban and regional
22 airsheds.

23 Evaluation results from a recent EPA exercise of CMAQ in the Tampa Bay, FL,
24 airshed are presented here as an example of the present level of skill of state-of-the-science
25 AQMs for predicting atmospheric concentrations of some of the relevant species for this PM
26 NAAQS assessment. This modeling series exercised CMAQ version 4.4 and with the
27 University of California at Davis (UCD) sectional aerosol module in place of the standard
28 CMAQ modal aerosol module and was driven by meteorology from MM5 v3.6 and with NEI
29 emissions as augmented by continuous emissions monitoring data where available. The
30 UCD size-segregated module was preferred for this application because of the importance of

1 sea salt particles in the bay airshed. Testing of this new engineering extension to CMAQ
2 (termed CMAQ-UCD below) revealed that its performance was very similar to that of
3 CMAQ's standard modal module; hence, model behavior and performance reported here can
4 stand as a general indication of CMAQ's skill.

5 The CTM was run with 21 vertical layers for the month of May 2002. For this
6 evaluation, CMAQ-UCD was run in a one-way nested series of three domains with 32 km, 8
7 km, and 2 km horizontal grid spacings from the CONUS (32 km) to central Florida and the
8 eastern Gulf of Mexico (2 km). Depictions of the 8 km and 2 km domains used here zoomed
9 over the central Tampa area are shown in Figure 3-58 and Figure 3-59.



Figure 3-58. Eight km southeast U.S. CMAQ-UCD domain zoomed over Tampa Bay, FL.

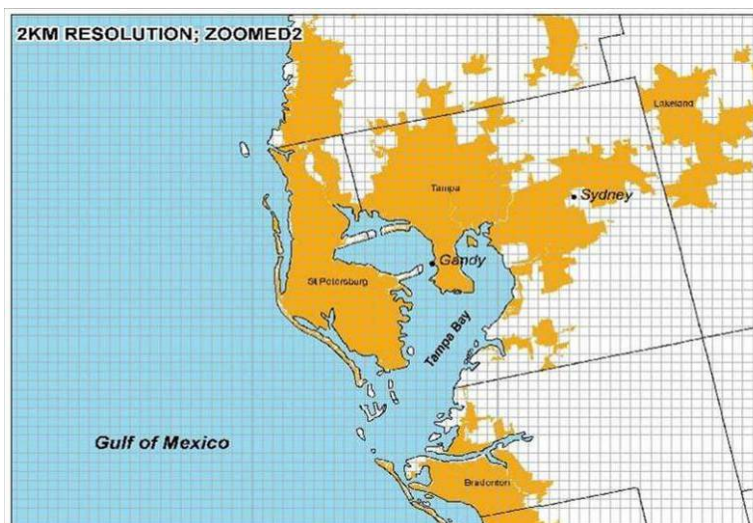


Figure 3-59. Two km southeast U.S. CMAQ-UCD domain zoomed over Tampa Bay, FL.

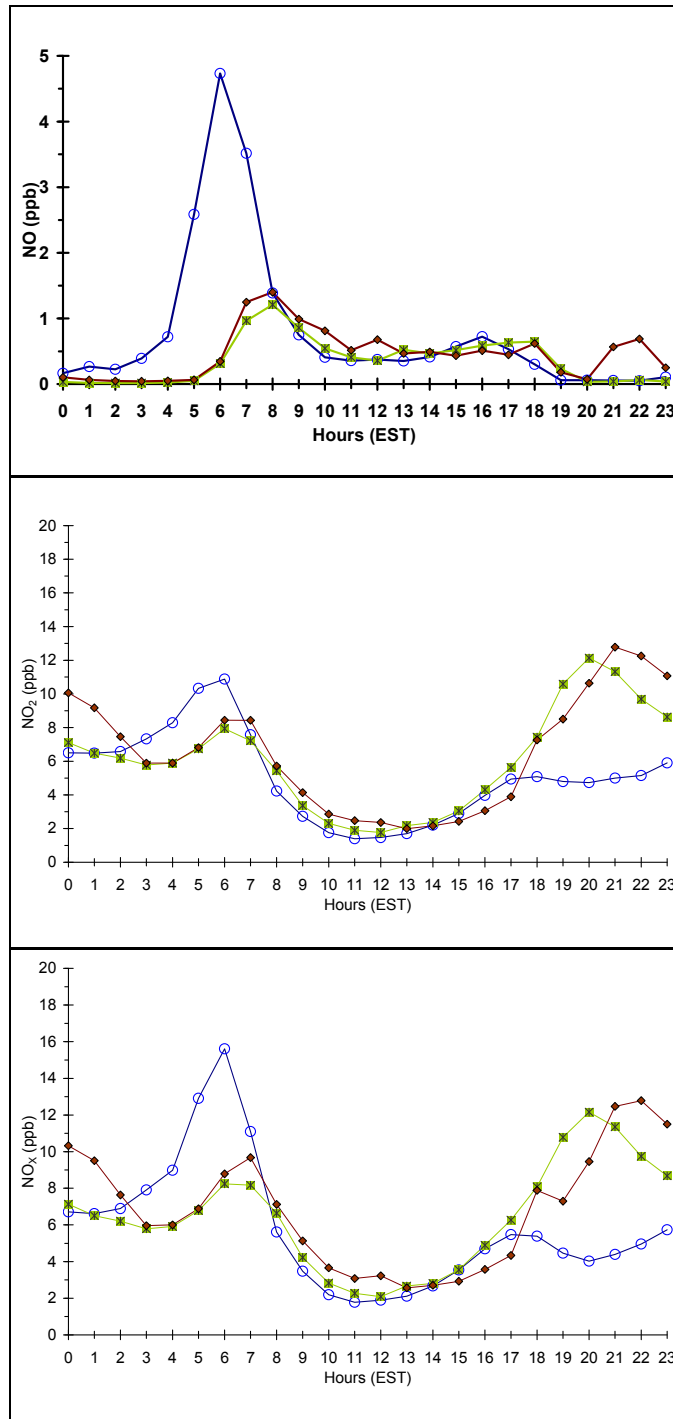


Figure 3-60. Hourly average CMAQ-UCD predictions and measured observations of NO (top), NO₂ (middle), and total NO_x (bottom) concentrations for May 1-31, 2002. Green squares = 8 km solution, red diamonds = 2 km solution, blue circles = observations.

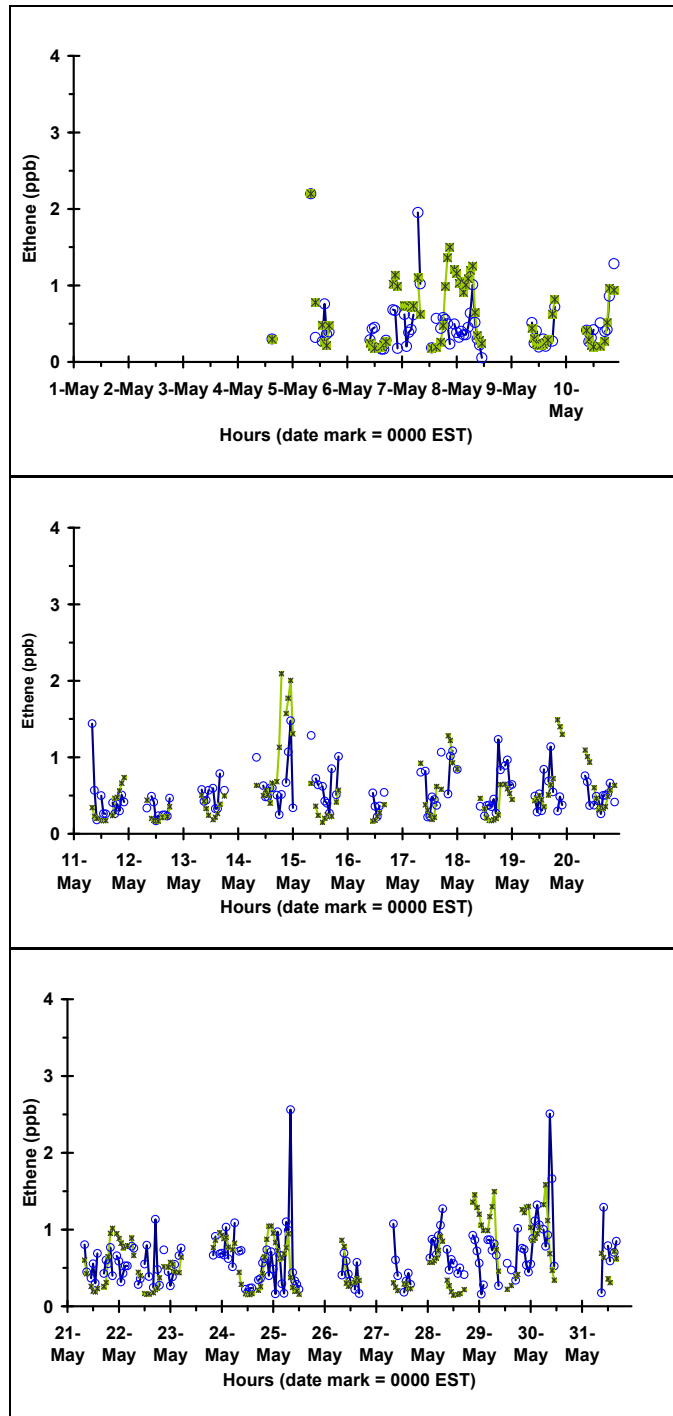


Figure 3-61. CMAQ-UCD predictions and measured observations of ethene concentrations at Sydney, FL for May 1-31, 2002. Green squares = 8 km solution, blue circles = observations .

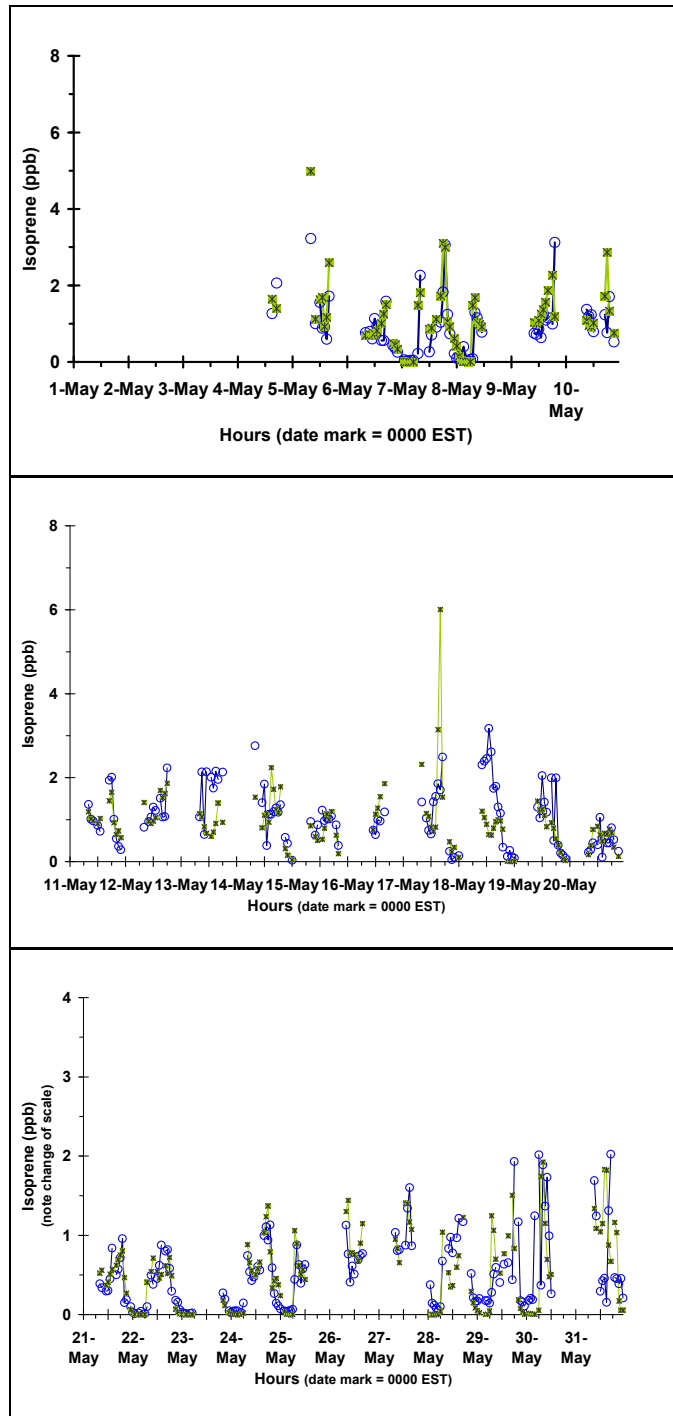


Figure 3-62. CMAQ-UCD predictions and measured observations of isoprene concentrations at Sydney, FL for May 1-31, 2002. Green squares = 8 km solution, blue circles = observations .

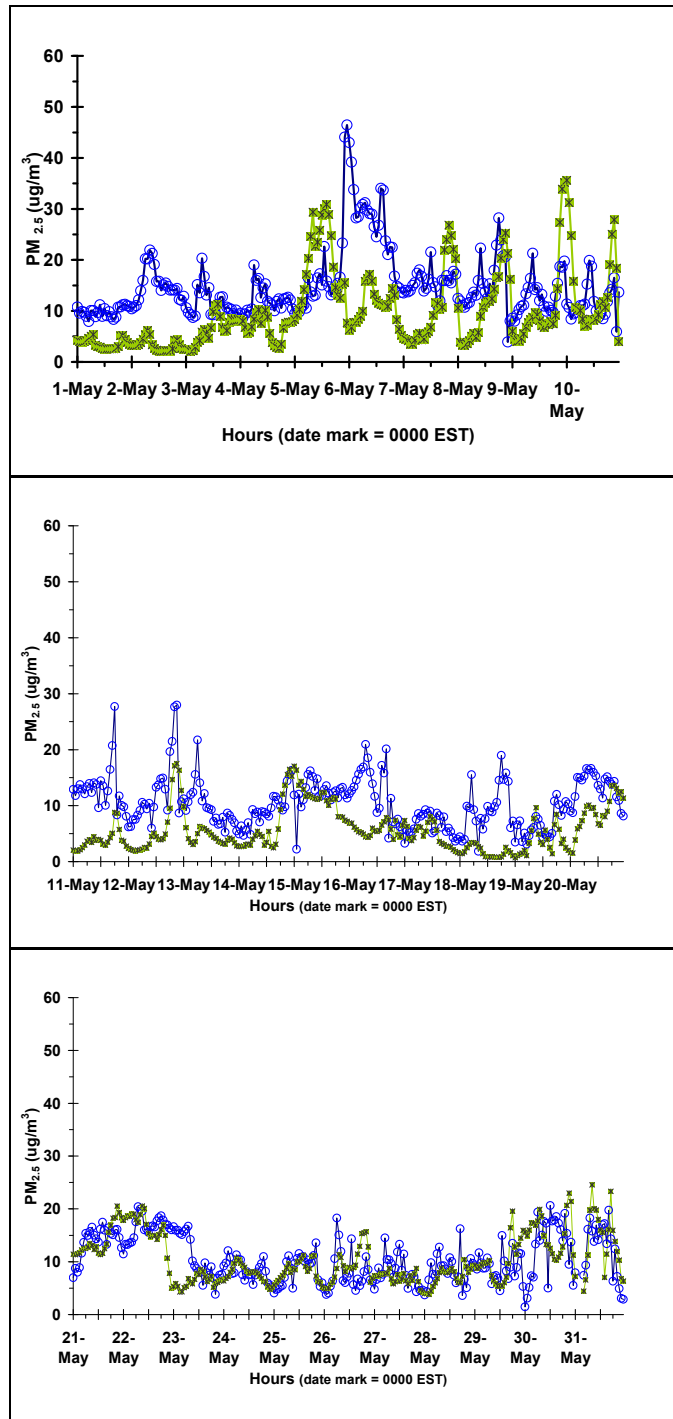


Figure 3-63. CMAQ-UCD predictions and measured observations of PM_{2.5} concentrations at St. Petersburg, FL for May 1-31, 2002. Green squares = 8 km solution, blue circles = observations .

3.6.3.1. Ground-based Comparisons of Photochemical Dynamics

1 Errors in the NO_x concentrations in the model, most likely from on-road emissions,
2 affected NO_x predictions shown in Figure 3-60, but CMAQ-UCD's general responses were
3 reasonable. The model also replicated anthropogenic and biogenic VOC emissions well; see
4 Figure 3-61 and Figure 3-62, respectively. After initial errors leading to underprediction in
5 the first 21 days, CMAQ-UCD's predictions of hourly PM_{2.5} concentrations and trends over
6 the whole month also replicated the observed concentrations well; see Figure 3-63.

3.6.3.2. Predicted Chemistry for Nitrates and Related Compounds

7 Particulate NO₃⁻ (pNO₃⁻) plays a crucial and complex role in the health of aquatic and
8 estuarine ecosystems and human drinking water systems. Gas-phase NO₃⁻ replacement of
9 Cl⁻ on sea salt particles is often favored thermodynamically and the V_d of the coarse pNO₃⁻
10 formed through this replacement is more than an order of magnitude greater than for fine
11 pNO₃⁻. Over open bodies of salt water such as the Gulf of Mexico and Tampa Bay, FL,
12 pNO₃⁻ from this reaction dominates dry deposition and is estimated to be of the same order
13 as pNO₃⁻ wet deposition.

14 However, total NO₃⁻ concentrations are driven, buffered, and altered by a wide range
15 of photochemical gas-phase reactions, heterogeneous reactions, and aerosol dynamics, mak-
16 ing them especially difficult to model. Because pNO₃⁻ is derived mostly from gas-phase
17 HNO₃ and will interact with Na⁺, NH₄⁺, Cl⁻, and SO₄²⁻, all these species and the physical
18 parameters governing their creation, transport, transformation, and fate must be accu-
19 rately replicated to predict pNO₃⁻ with high fidelity. This has historically been a difficult
20 problem for numerical process models, owing not least to the pervasive dearth of reliable
21 ambient measurements of NO₃⁻ in its various forms. Normalized mean error (NME) for the
22 large-scale Eulerian CTM-predicted pNO₃⁻ has typically been on the order of a factor of 3
23 greater than the NME for particulate SO₄²⁻ (pSO₄²⁻) (Odman et al., 2002, [092474](#); Pun et al.,
24 2003, [047775](#)).

25 SO₄²⁻, NH₄⁺, Na⁺, and Cl⁻ were all predicted to within a factor of 2 and with no signifi-
26 cant bias during the photochemical day in the 8 km CMAQ-UCD solution, although a
27 significant bias in Na⁺ and Cl⁻ was evident in the 2 km solution for two near-water sites.
28 This grid-size dependent bias is still being explored. Size segregation maxima were correct
29 to within two size bins every day for which there were observations for both SO₄²⁻ and NH₄⁺

1 (0.2 to 1.0 μm), and Na^+ and Cl^- (2.0 to 10.0 μm). Cl^- concentrations were greatly overpre-
2 dicted during dark hours, but were nearer to observed values during the photochemical day.
3 CMAQ-UCD performance for HNO_3 and NH_3 are shown in Figure 3-64 and Figure 3-65, re-
4 spectively.

5 Figure 3-66 shows that CMAQ-UCD systematically underpredicted the hourly time
6 series of measured pNO_3^- concentrations at the Sydney supersite, the only location with
7 discrete pNO_3^- data. These time series data establish that CMAQ-UCD's largest errors
8 were on four days in the first two weeks of the month, but that the total peak pNO_3^- concen-
9 trations were nearly all underpredicted.

10 Since pNO_3^- is derived in large part from gas-phase HNO_3 , its underprediction may be
11 due to an underprediction of HNO_3 concentrations or an underrepresentation of the gas- to
12 aerosol-phase change. At Sydney, FL, in fact, both these conditions held. Figure 3-64 depicts
13 the model's bias for HNO_3 underprediction in both the 8 km and 2 km solutions, excepting
14 four days of very large peak overpredictions. This trend was especially true overnight; on
15 eight other days the model overpredicted the one hour peak concentration as well, though
16 not so substantially, but the chief effect was still one of an artificial and inappropriate N
17 limitation in the model.

18 A time series molar equivalent ratio of HNO_3 to total NO_3^- depicts which phase stores
19 the NO_3^- and how that storage ratio changes over time. Figure 3-67 shows that at Sydney,
20 FL, CMAQ-UCD stored too much NO_3^- in the gas phase as HNO_3 (and recall that the day-
21 time HNO_3 concentrations were sometimes overpredicted by the model) and too little in the
22 gas phase overnight, when the model was regularly low against the measurements; com-
23 pare Figures 3-64 and 3-65. Note again here the self-similarity of the 8 km and 2 km solu-
24 tions in this comparison.

25 Interestingly, the 23-h integrated data did not reveal this important difference in NO_3^-
26 form between the model and measurements as Figure 3-68 shows in the stacked bar
27 percentage plots of fine and coarse pNO_3^- together with gas-phase HNO_3 . Both the 8 km
28 (Figure 3-68, middle panel) and the 2 km (Figure 3-68, bottom panel) solutions predicted
29 distributions between the two general ranges of aerosol size, and between gas and aerosol
30 phases, with good fidelity to the daily observations (Figure 3-68, top panel) at Sydney, FL.
31 This result illustrates that while discrete time series data are crucial for diagnosing model
32 behavior, on the integrated total daily and longer basis used for computing total annual N

- 1 loads, CMAQ-UCD predicted approximately the correct distributions for $p\text{NO}_3^-$, even
- 2 though the total NO_3^- concentration prediction was biased low.

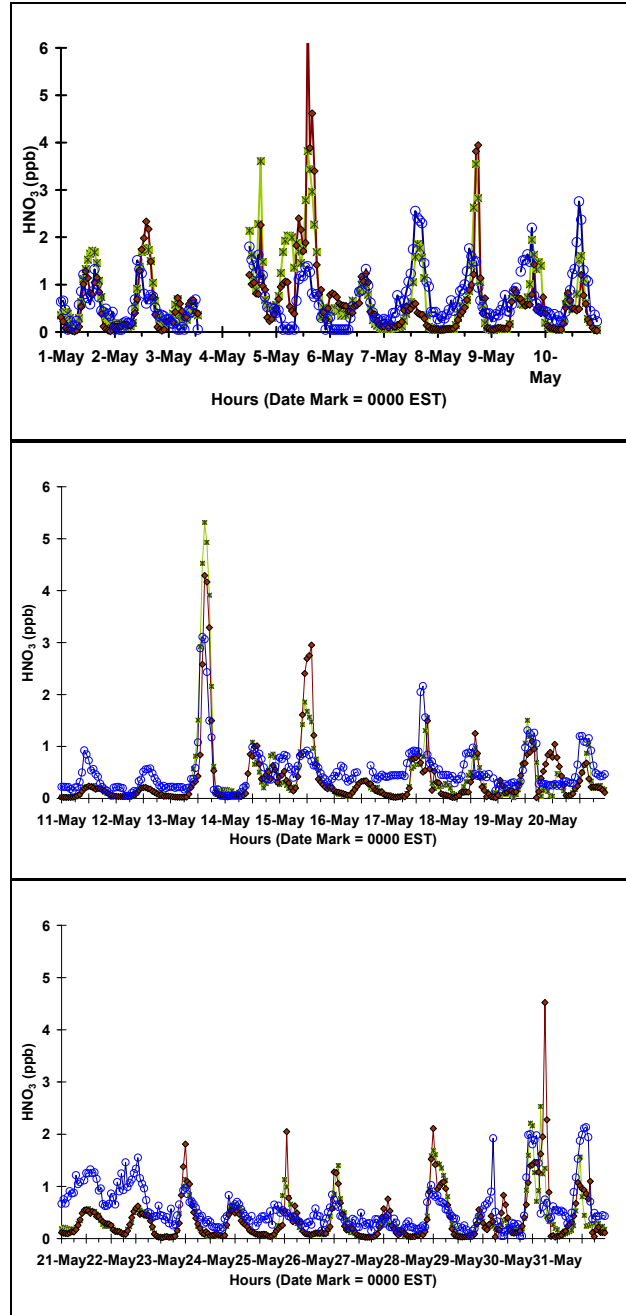


Figure 3-64. CMAQ-UCD predictions of HNO_3^- concentrations and corresponding measured observations at Sydney, FL, for May 1-31, 2002. Green x = 8 km solution, red diamonds = 2 km solution, blue circles = observations.

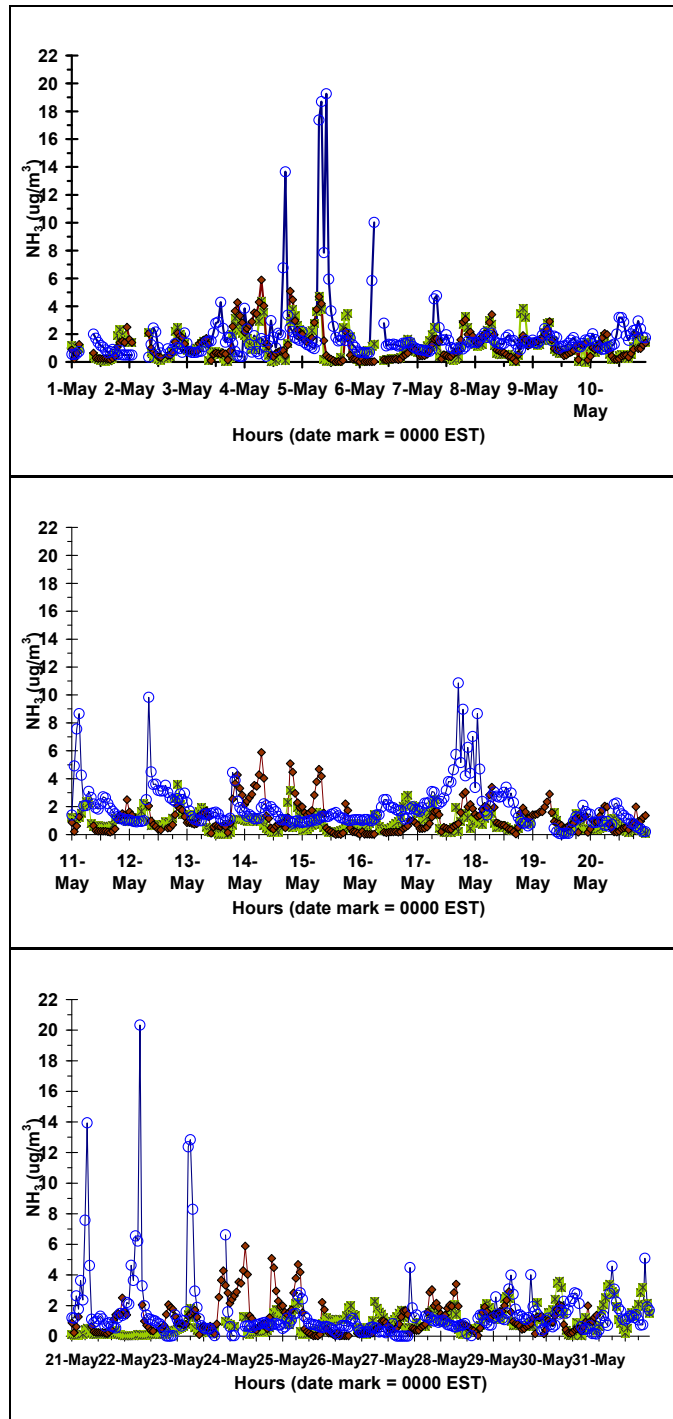


Figure 3-65. CMAQ-UCD predictions of NH_3 concentrations and corresponding measured observations at Sydney, FL, for May 1-31, 2002. Green squares = 8 km solution, red

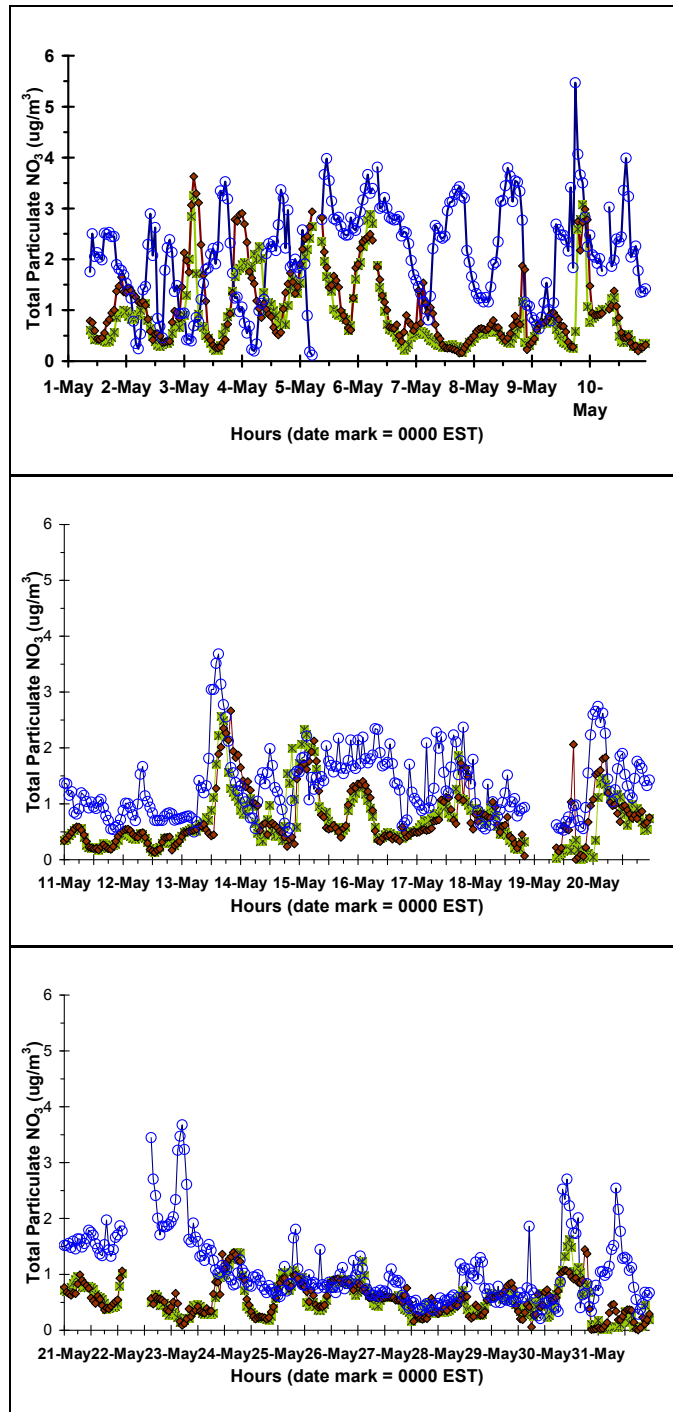


Figure 3-66. CMAQ-UCD predictions of pNO_3^- concentrations and corresponding measured observations at Sydney, FL, for 1-31 May, 2002. Green x = 8 km solution, red diamonds = 2 km solution, blue circles = observations.

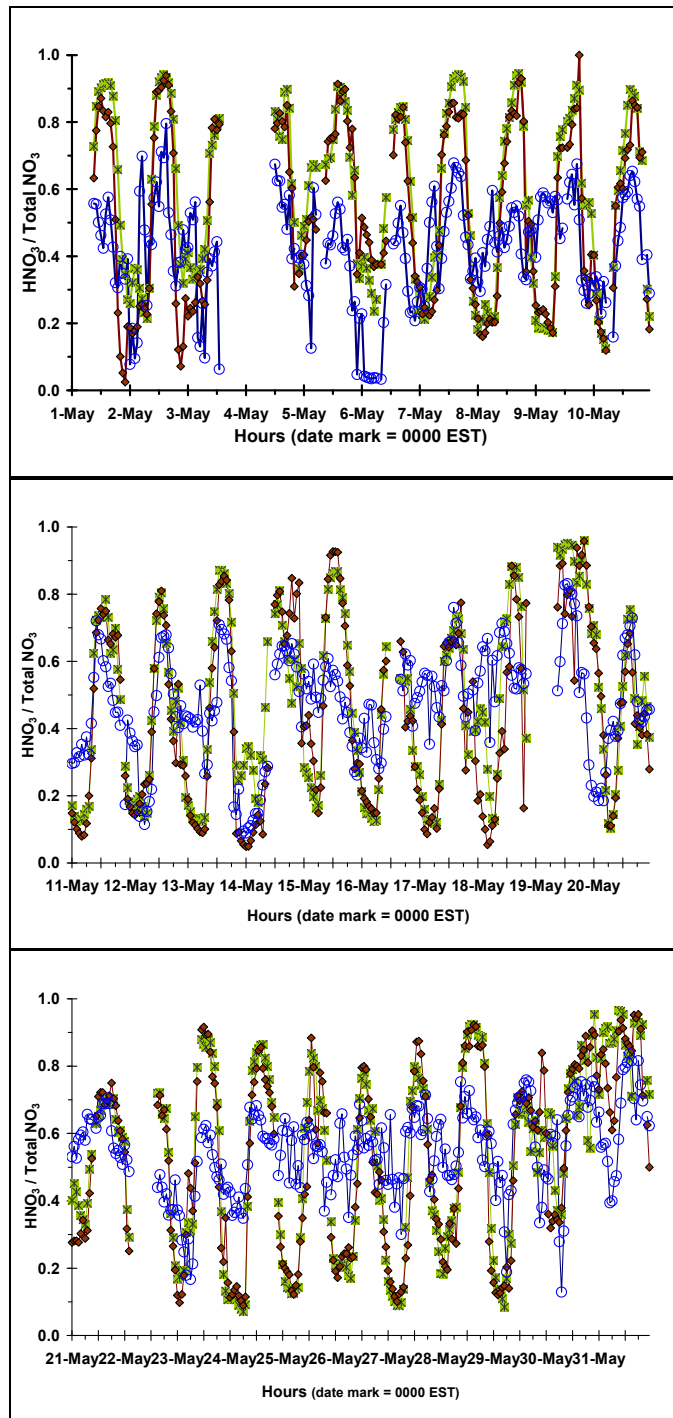


Figure 3-67. CMAQ-UCD predictions of the ratio of HNO_3 to total NO_3 and corresponding measured observations at Sydney, FL, for May 1-31, 2002. Green x = 8 km solution, red diamonds = 2 km solution, blue circles = observations.

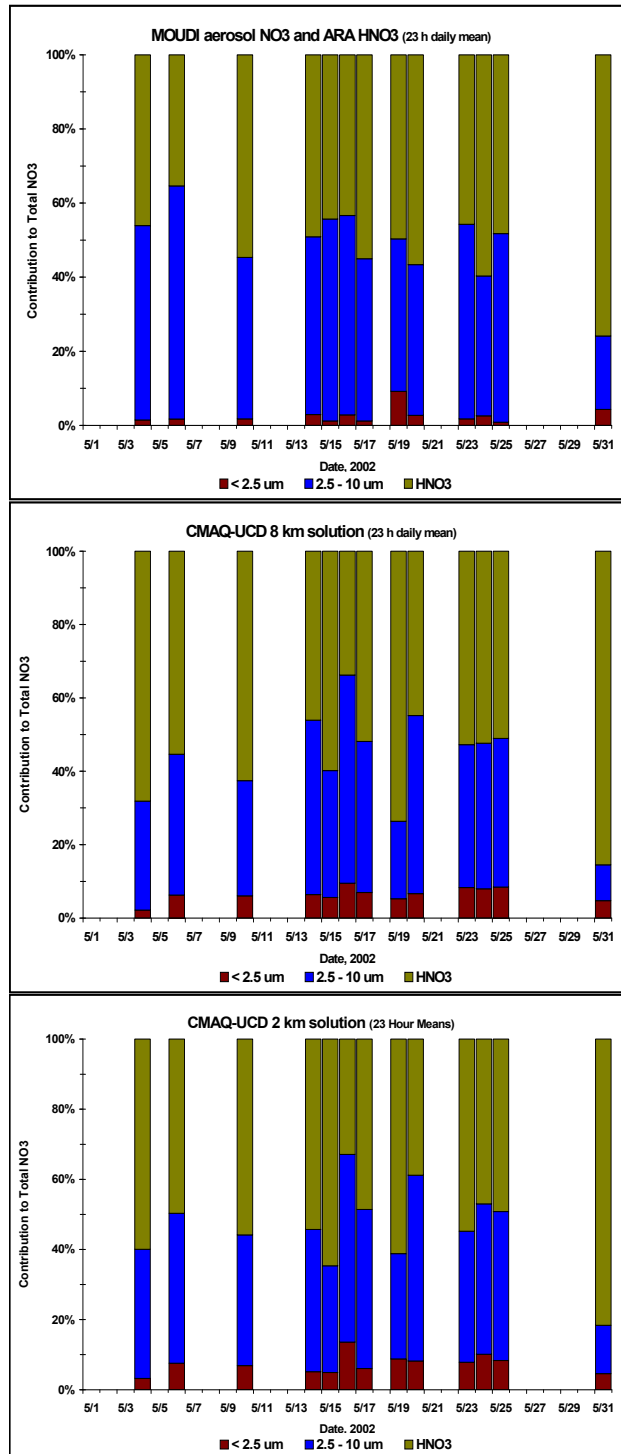


Figure 3-68. CMAQ-UCD predicted size and chemical-form fractions of total NO₃⁻ for days in May 2002 with measured observations. Measured concentrations (top panel); 8 km solution (middle panel); 2 km solution (bottom panel). Red bars = pNO₃⁻ < 2.5 μm; blue bars = pNO₃⁻ 2.5-10 μm; green bars = HNO₃.

1 While inorganic aerosol anion totals were dominated by NO_3^- in the coarse fraction
2 and by SO_4^{2-} in the fine fraction, there was sufficient NH_x ($\text{NH}_x = \text{NH}_3 + \text{NH}_4^+$) at Sydney,
3 FL, to form fine aerosol NH_4NO_3 in some circumstances. Figure 3-65 depicts the hourly
4 mass concentration of NH_3 at Sydney, FL, showing again the strong self-similarity of the 8
5 km and 2 km solutions. Each solution, however, underpredicted the measured NH_3
6 concentrations consistently, and especially for the nine very large excursions of 10 to 20
7 $\mu\text{g}/\text{m}^3$ during the month.

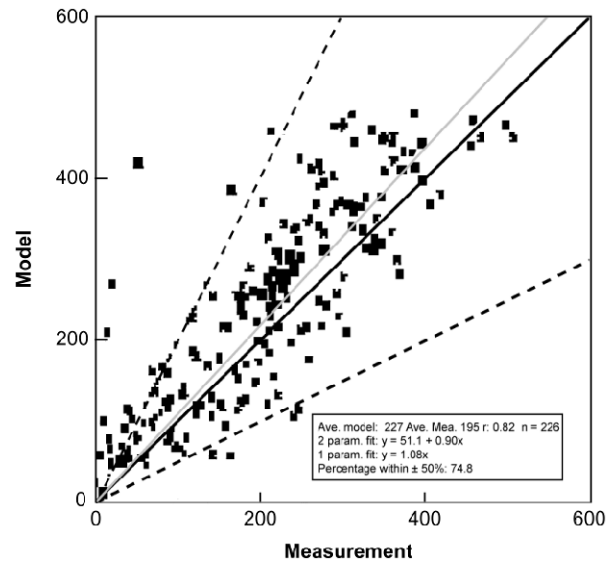
8 Overall, CMAQ-UCD was found to be operationally sound in this evaluation of its 8
9 km and 2 km solutions for the Tampa Bay airshed using the ground-based and aloft data
10 (not shown here) from the May 2002 field intensive. Moreover, results from diagnostic tests
11 of the model's photochemical dynamics were generally in excellent agreement with results
12 from the ambient atmosphere. However, CMAQ-UCD was biased low in this application for
13 total NO_3 and for NO_3 present as gas-phase HNO_3 . In addition, the model was biased low
14 for the HO_x radical reservoir species CH_2O and H_2O_2 (not shown here), though this bias
15 appeared to have been limited to these species. Performance of the new UCD aerosol
16 module was judged to be entirely adequate, allocating aerosols by chemical makeup to the
17 appropriate size fractions. Model performance for fine-mode aerosols was also judged to be
18 fully adequate.

3.6.4. Evaluating Concentrations and Deposition of PM Components with CTMs

3.6.4.1. Global CTM Performance

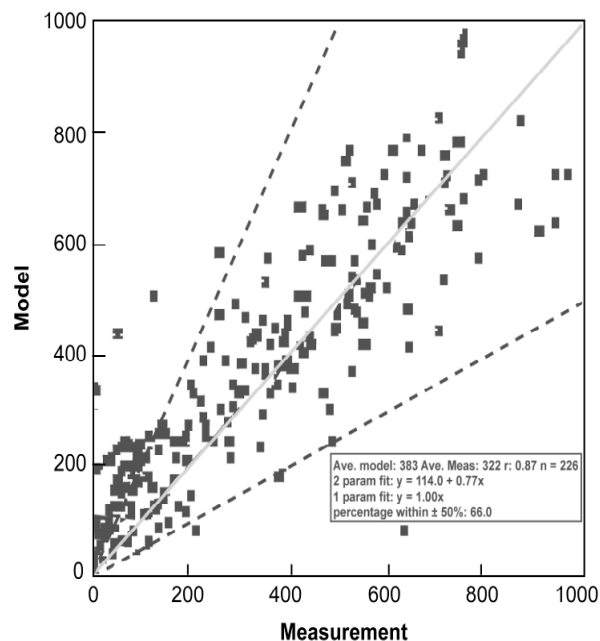
19 The wet and dry deposition processes described in Section 3.3 are of necessity highly
20 parameterized in all CTMs. While all current models implement resistance schemes for dry
21 deposition, the V_d generated from different models can vary highly across terrain types
22 (Stevenson et al., 2006, [089222](#)). The accuracy of wet deposition in global CTMs is tied to
23 spatial and temporal distribution of model precipitation and the treatment of chemical
24 scavenging. Dentener et al. (2006, [088434](#)) compared wet deposition across 23 models with
25 available measurements around the globe. Figures 3-69 and 3-70 extract results of a
26 comparison of the 23-model mean versus observations over the eastern U.S. for pNO_3^- and
27 pSO_4^{2-} deposition, respectively. The mean model results were strongly correlated with the

1 observations ($r > 0.8$), and usually captured the magnitude of wet deposition to within a
2 factor of two over the eastern U.S. Dentener et al. (2006, [088434](#)) concluded that 60 to 70%
3 of the participating models captured the measurements to within 50% in regions with
4 quality controlled observations.



Source: Dentener et al. (2006, [088434](#)). Reprinted with permission.

Figure 3-69. Scatter plot of total nitrate (HNO_3 plus pNO_3^-) wet deposition ($\text{mg N/m}^2/\text{yr}$) of the model mean versus measurements for the North American Deposition Program (NADP) network. Dashed lines indicate a factor of two. The gray line is a linear regression through zero.



Source: Dentener et al. (2006, [088434](#)). Reprinted with permission.

Figure 3-70. Scatter plot of total SO_4^{2-} wet deposition ($\text{mg S/m}^2/\text{yr}$) of the model mean versus measurements for the National Atmospheric Deposition Program (NADP) network. Dashed lines indicate a factor of two. The gray line is a linear regression through zero.

3.6.4.2. Regional CTM Performance

1 Regional CTM performance for concentration and deposition of some of the most
 2 relevant PM species is illustrated here with examples from CMAQ version 4.6.1 as
 3 configured and run for exposure and risk assessments reported in the Draft Risk and
 4 Exposure Assessment for the Review of the Secondary National Ambient Air Quality
 5 Standards for Oxides of Nitrogen and Oxides of Sulfur (U.S. EPA, 2009, [191774](#)); additional
 6 details on the model configuration and application are found there. A map of the 36 km
 7 parent domain and two 12 km (east and west) progeny domains appears in Figure 3-71.

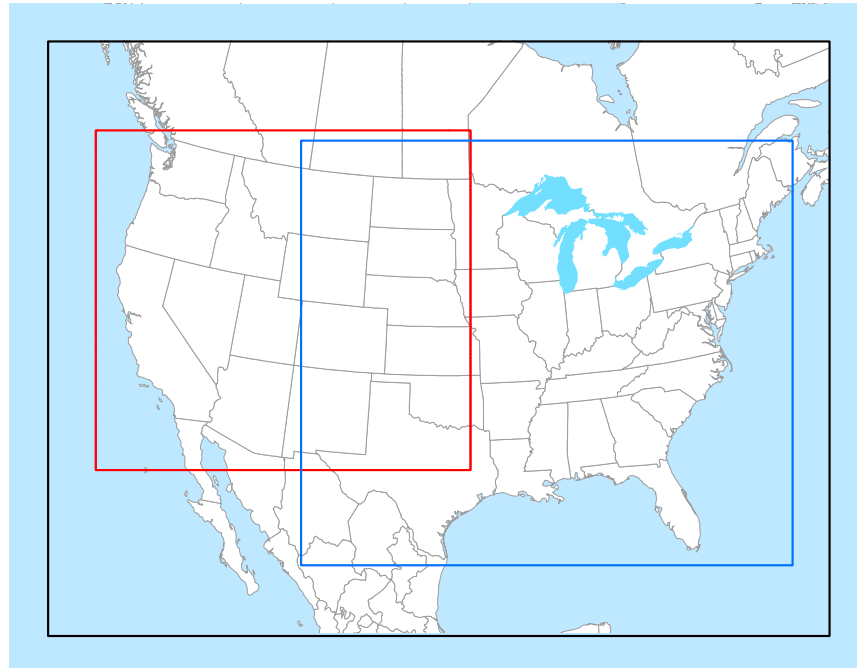


Figure 3-71. CMAQ modeling domains for the OAQPS risk and exposure assessments: 36 km outer parent domain in black; 12 km western U.S. (WUS) domain in red; 12 km eastern U.S. (EUS) domain in blue.

1 Comparisons from the 2002 annual run of CMAQ for the exposure assessment are
 2 shown here against measured concentrations and deposition totals from nodes in three
 3 networks: IMPROVE, CSN (labeled STN in the plots) and CASTNet. Comparisons were
 4 made as model-observation pairs at all sites having sufficient data for the seasonal or the
 5 2002 annual time period in the two 12 km east and west domains and were evaluated with
 6 the following descriptive statistics: correlation, root mean square error, normalized mean
 7 bias, and normalized mean error.

8 Summertime pSO_4^{2-} concentrations are well predicted by CMAQ, to within a factor of
 9 2 at nearly every point, and with $R^2 > 0.8$ across all three networks; see Figure 3-72. This
 10 result tracks the generally well-predicted SO_4^{2-} concentrations found in earlier CMAQ
 11 evaluations: see Eder and Yu (2005, [089229](#); Mebust et al., 2003, [156749](#)), Mebust et al.
 12 (2003, [156749](#)) and Tesche et al. (2006, [157050](#)). Since pSO_4^{2-} concentrations are strongly a
 13 function of precipitation, care must be taken to ensure that the meteorological solution
 14 driving individual CMAQ chemical applications produces precipitation fields with low bias
 15 as discussed by Appel et al. (2008, [155660](#)).

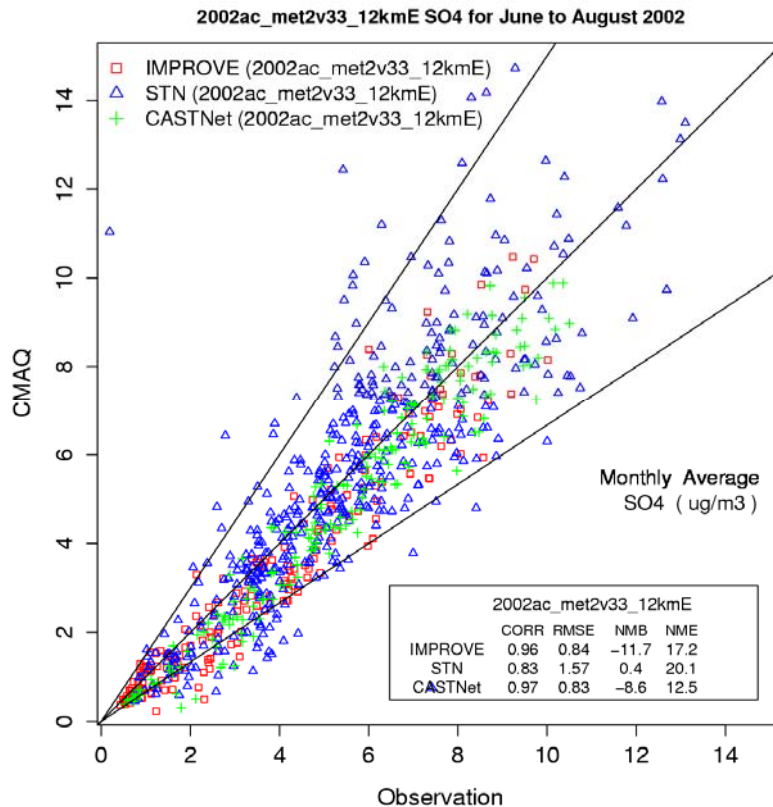


Figure 3-72. 12-km EUS Summer sulfate PM. Each data point represents a paired monthly averaged (June/July/August) observation and CMAQ prediction at a particular IMPROVE, STN, and CASTNet site. Solid lines indicate a factor of two around the 1:1 line shown between them.

1 Wintertime pNO_3^- (Figure 3-73) and total NO_3 ($HNO_3+pNO_3^-$) (Figure 3-74)
 2 concentrations are predicted less well by CMAQ; but NO_3 is a pervasively difficult species
 3 to measure and model. Still, at the CASTNet nodes where the total NO_3 concentrations are
 4 higher than they are at all but a few of the remote IMPROVE sites, CMAQ predicts
 5 concentrations for nearly every node to within a factor of 2 and with an $R^2 > 0.8$. These
 6 CMAQ-predicted concentrations, coupled with modeled cloud and precipitation fields
 7 produce wet deposition fields for SO_4^{2-} and NO_3^- in the east domain as shown in Figures
 8 3-75 and 3-76, respectively.

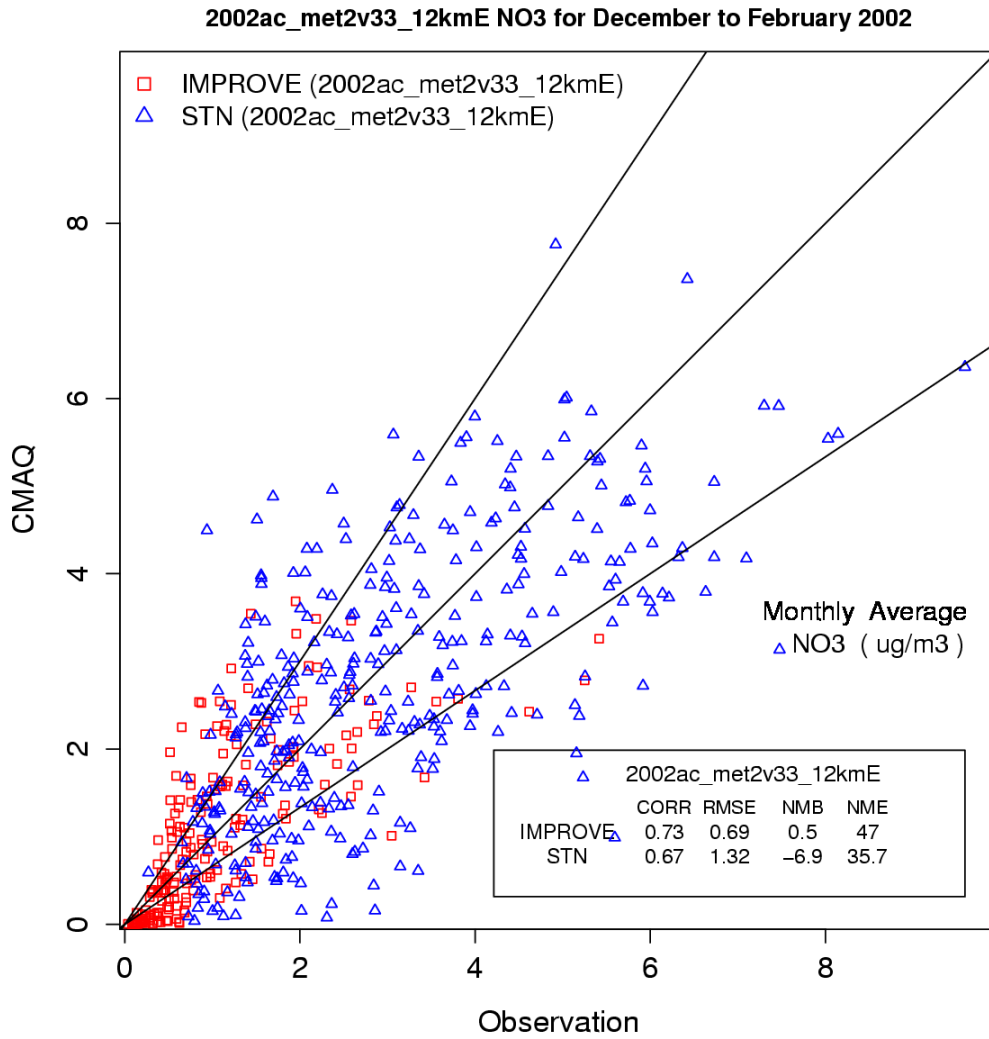


Figure 3-73. 12-km EUS Winter nitrate PM. Each data point represents a paired monthly averaged (December/January/February) observation and CMAQ prediction at a particular IMPROVE and STN site. Solid lines indicate a factor of two around the 1:1 line shown between them.

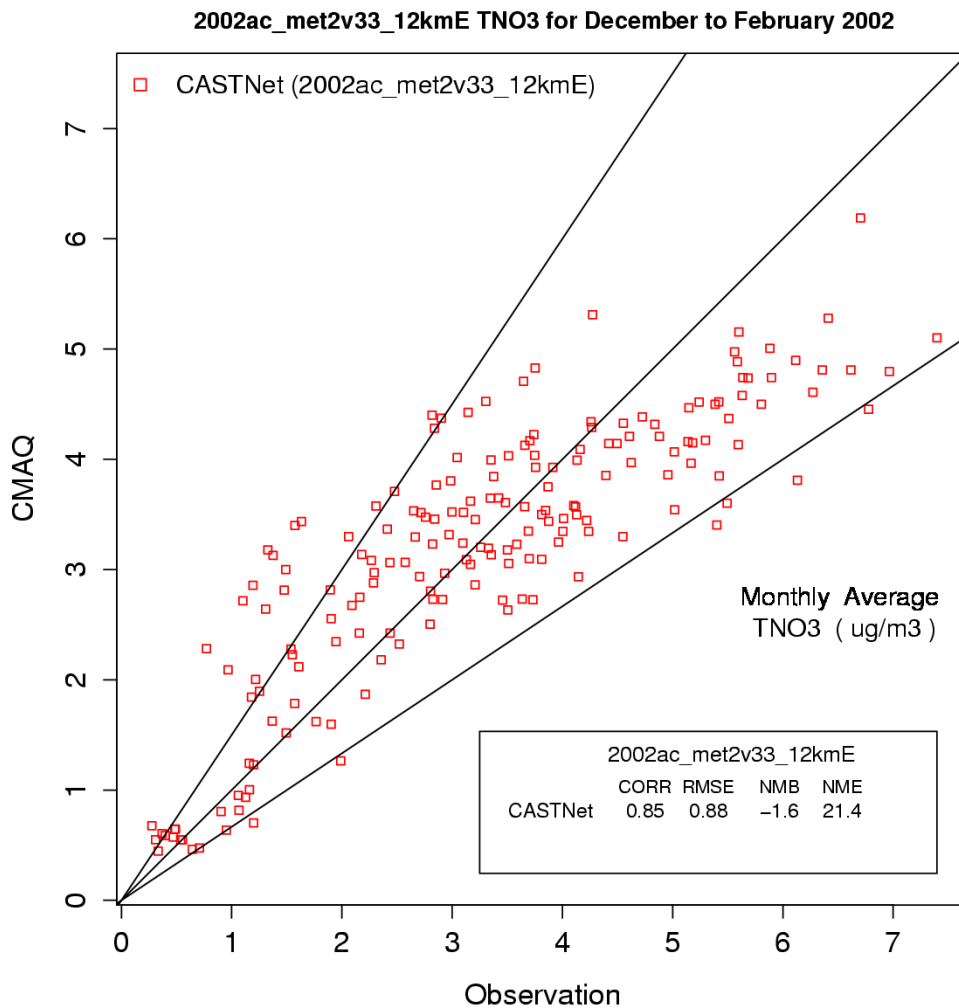


Figure 3-74. 12-km EUS Winter total nitrate ($\text{HNO}_3 + \text{total pNO}_3^-$). Each data point represents a paired monthly averaged (December/January/February) observation and CMAQ prediction at a particular CASTNet site. Solid lines indicate a factor of two around the 1:1 line shown between them.

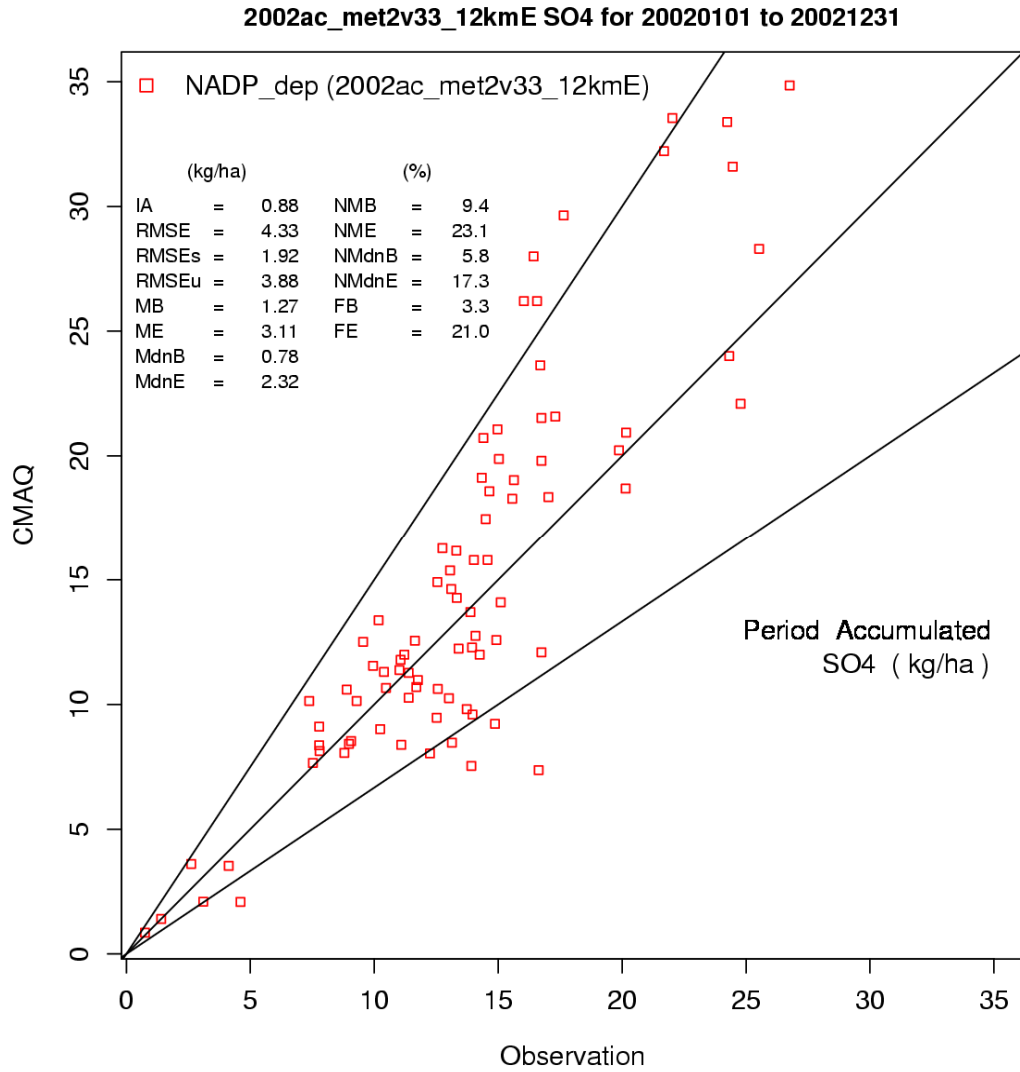


Figure 3-75. 12-km EUS annual sulfate wet deposition. Each data point represents an annual average paired observation and CMAQ prediction at a particular NADP site. Solid lines indicate the factor of 2 around the 1:1 line shown between them.

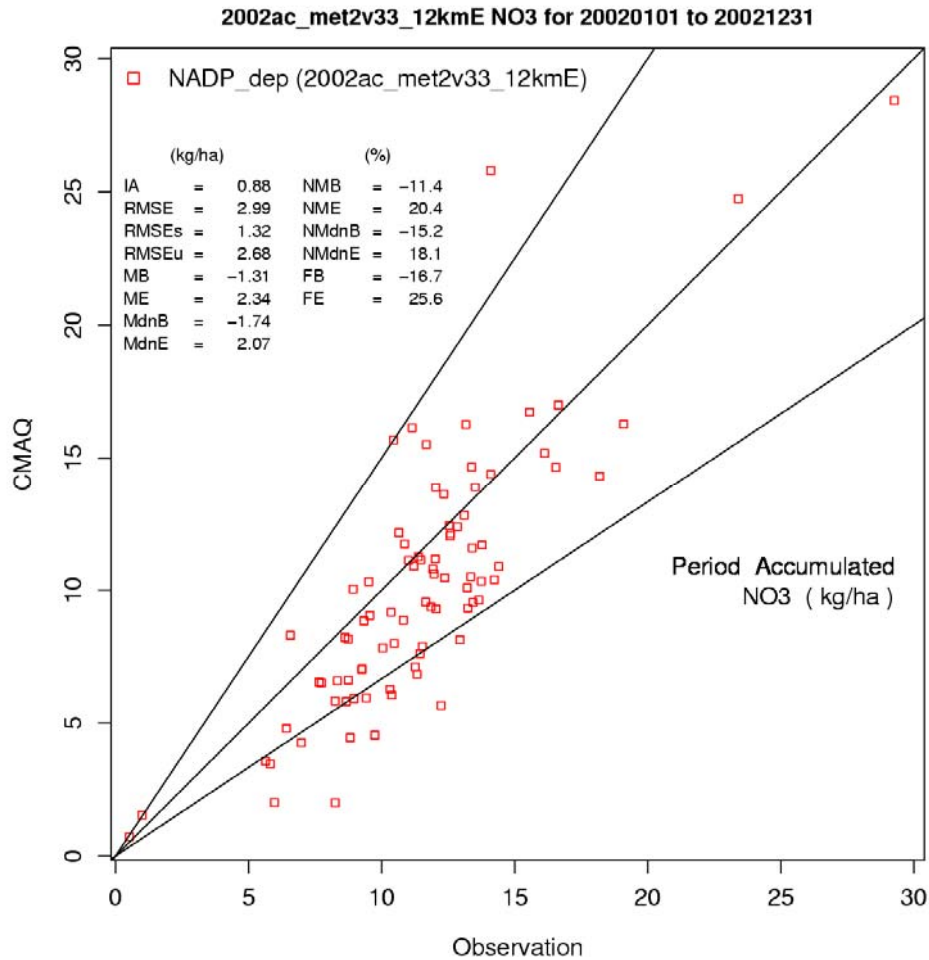


Figure 3-76. 12-km EUS annual nitrate wet deposition. Each data point represents an annual average paired observation and CMAQ prediction at a particular NADP site. Solid lines indicate a factor of two around the 1:1 line shown between them.

1 Importantly, CMAQ captured the chief spatial patterns and magnitudes of air
 2 concentrations and wet deposition relevant to computing concentration and deposition
 3 budgets, as shown in Figures 3-77 for concentrations and 3-78 for deposition. More
 4 specifically, CMAQ's predictions of NH_3 and SO_4^{2-} for both high and low concentration sites
 5 are well within the range of measurements there; see Figure 3-79.

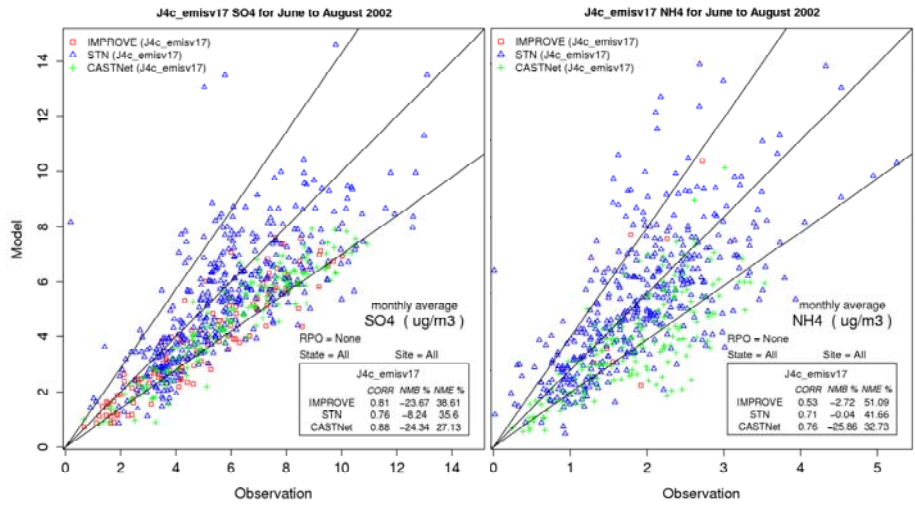


Figure 3-77. CMAQ vs. measured air concentrations from east-coast sites in the IMPROVE, CSN (labeled STN), and CASTNet sites in the summer of 2002 for sulfate (left) and ammonium (right). Solid lines indicate a factor of 2 around the 1:1 line shown between them.

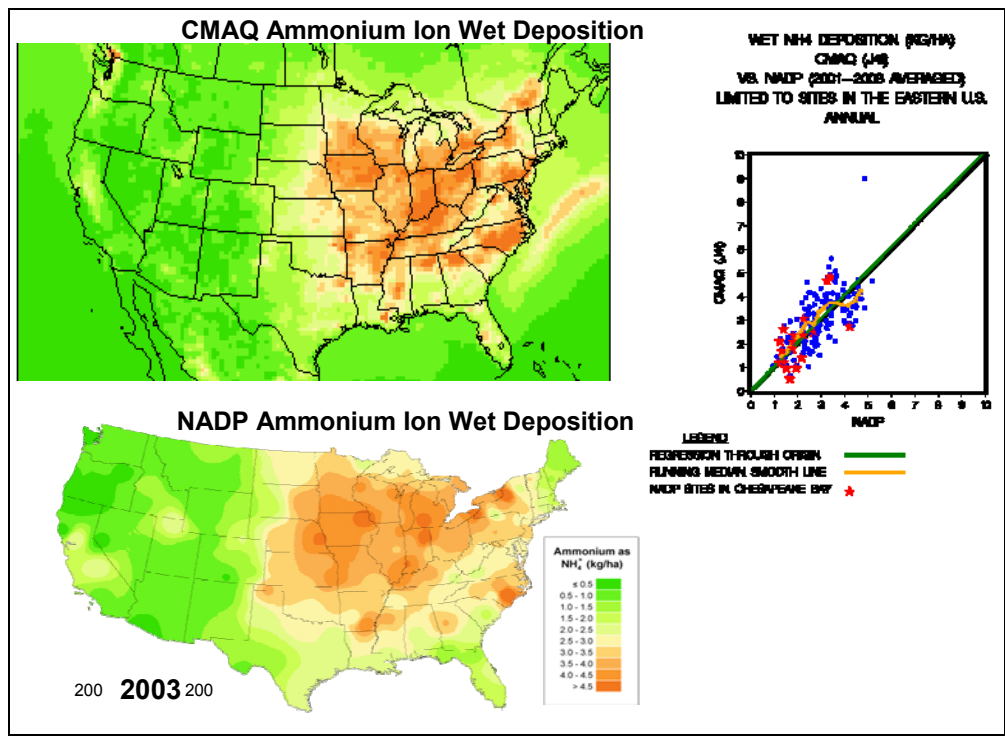


Figure 3-78. Comparison of CMAQ-predicted and NADP-measured NH₄⁺ wet deposition: (top left) CMAQ prediction; (bottom left) NADP-measurements; (right) regression and smoothed median line through CMAQ predictions and NADP measurements with sites in the Chesapeake Bay watershed highlighted.

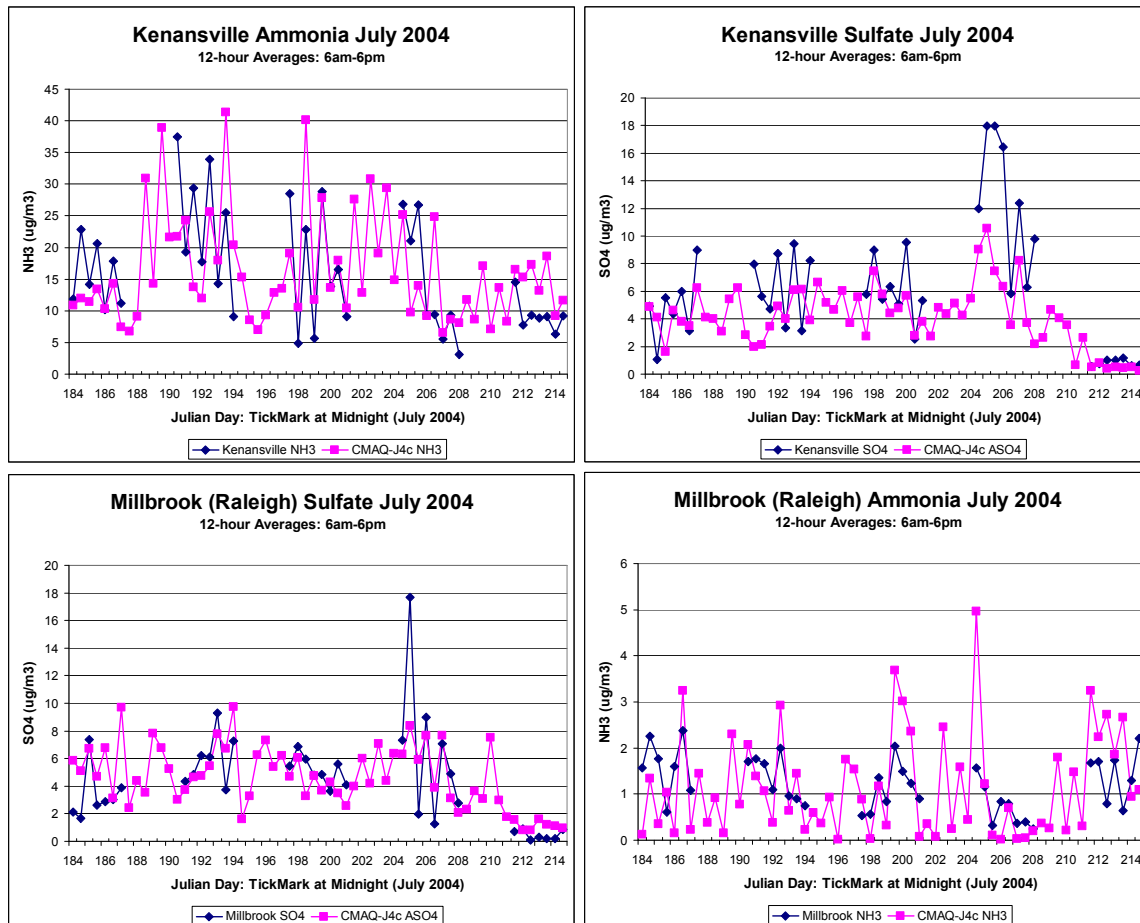


Figure 3-79. CMAQ-predicted (red symbols and lines) and 12-h measured (blue symbols and lines) NH₃ and SO₄²⁻ surface concentrations at high and low concentration grid cells in North Carolina in July 2004. (top left) High concentration NH₃ in Kenansville; (top right) high concentration SO₄²⁻ in Kenansville; (bottom left) low concentration NH₃ in Raleigh; (bottom right) low concentration SO₄²⁻ in Raleigh.

1 Deposition velocities are difficult to estimate for reasons described in Section 3.3.3.
 2 Recent work in EPA's Atmospheric Modeling and Analysis Division with CMAQ showed
 3 that the original V_d for NH₃ was very likely too high and should be nearer to the values for
 4 SO₂ deposition, or even lower over some land use surface types. A sensitivity study with the
 5 model was performed to test the effects of changing V_d for NH₃ on the fraction of NH₃
 6 available for transport away from grid cells with high emissions concentrations.
 7 Comparisons were made for the surface grid cells and total column NH₃ concentrations.
 8 In the highest emissions grid cells during June 2002, the surface NH_x budget was
 9 dominated by turbulent transport or vertical mixing moving a majority of the surface NH₃
 10 emissions up and away from the surface into the mixed layer. Figure 3-80 depicts the NH_x

1 budget under the base case (Base V_d) and the sensitivity case (SO₂ V_d) for which the NH₃ V_d
 2 was set equal to the SO₂ V_d. Lower NH₃ V_d decreased NH_x deposition to the surface from 15
 3 to 8 %, leaving more NH_x for transport horizontally, 22% up from 20% in the base case, and
 4 vertically, 69% up from 64% in the base case. Typically, ~67% of surface emissions were
 5 moved aloft where most was advected away from the high emissions grid cell, with a small
 6 fraction converted to pNH₄⁺ and an even smaller fraction wet-deposited to the surface. The
 7 total column analyses for NH₃ and NH_x are shown in Figure 3-81.

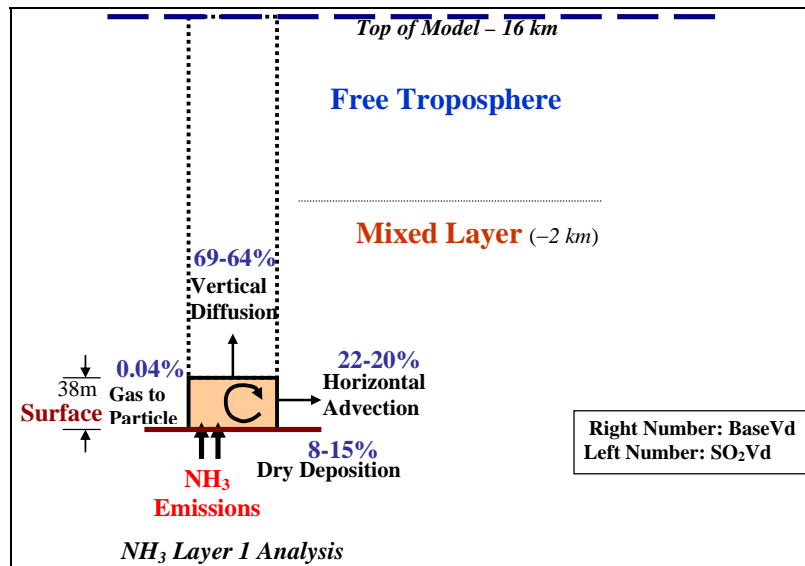


Figure 3-80. Surface grid cell (layer 1) analysis of the sensitivity of NH_x deposition and transport to the change in NH₃ V_d in CMAQ.

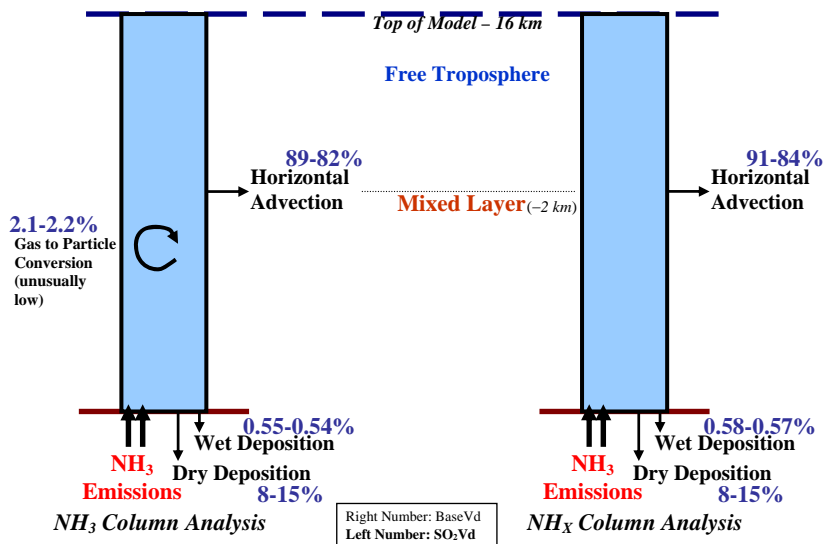


Figure 3-81. Total column analysis for NH_3 (left) and NH_x (right) showing modeled NH_3 emissions, transformation, and transport throughout the mixed layer and up to the free troposphere.

1 Local total deposition (wet + dry) is a significant but not dominant loss pathway for
 2 surface NH_3 emissions. In these simulations, CMAQ deposited ~25% of the NH_3 emissions
 3 from the single high concentration grid cell in Sampson County, NC, back into that grid cell.
 4 By far, the largest contribution to the local deposition total was dry deposition; dry-to-wet
 5 deposition ratios for the Sampson County high emissions grid cell and surrounding surface
 6 grid cells ranged from 2 to 10.

7 Deposition to grid cells farther away from the high concentration, immediately
 8 surrounding grid cells was significantly affected by the change in NH_3 V_d tested in this
 9 case. Figure 3-82 depicts the range of influence of the high concentration grid cell, where
 10 that range is defined to be the distance by which 50% of the emissions attributable to that
 11 grid cell have deposited. The range of influence of the high concentration Sampson County
 12 grid cell was extended in the V_d sensitivity tested here from ~180 km in the base case to
 13 ~400 km in the case using the lower, more realistic V_d for NH_3 . The areal extent of this
 14 difference in range of influence is mapped in Figure 3-83.

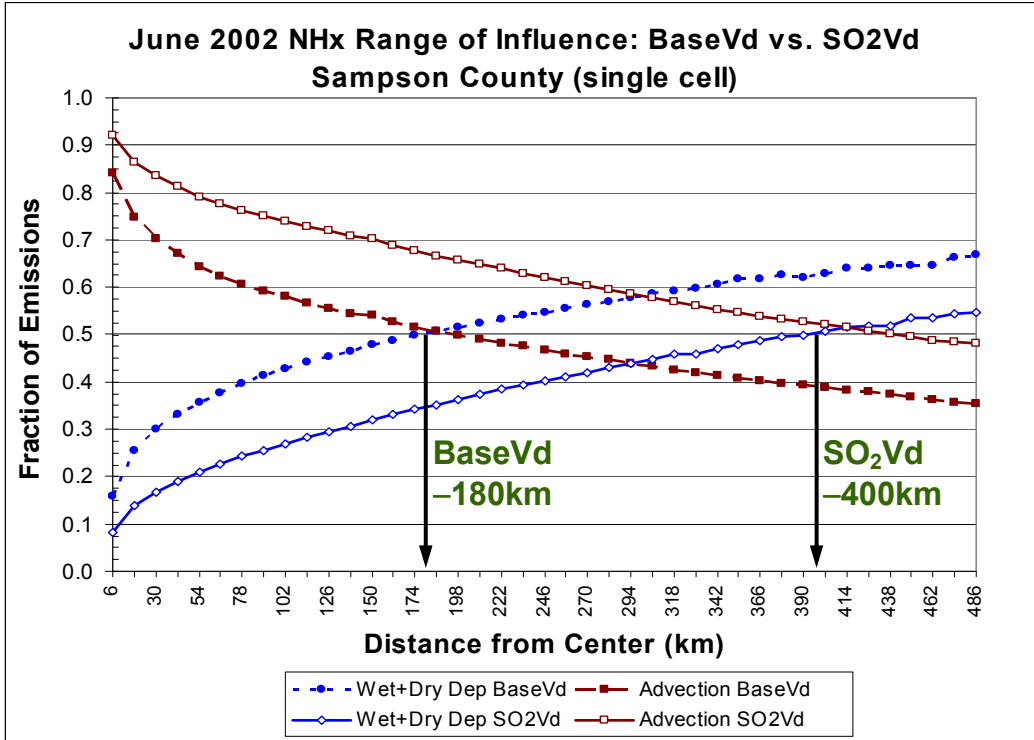


Figure 3-82. Range of influence (where 50% of emitted NH₃ deposits) from the high concentration Sampson County grid cell in the June 2002 CMAQ simulation of V_d sensitivities. Base case and sensitivity case total deposition (blue symbols and lines); base case and sensitivity case advection totals (red symbols and lines).

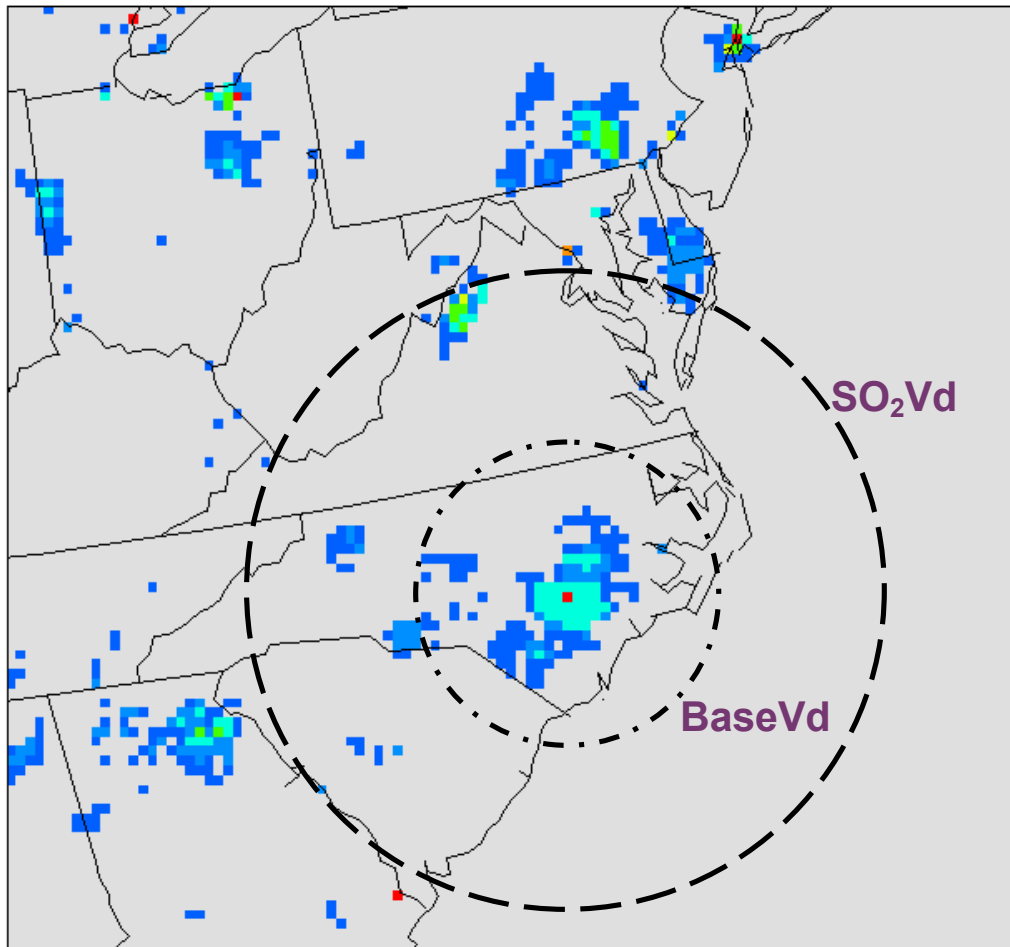


Figure 3-83. Areal extent of the change in NH_x range of influence as predicted by CMAQ for the Sampson County high concentration grid cell (center of range circles) in June 2002 using the base case and sensitivity case V_d .

3.7. Background PM

1 The background concentrations of PM that are useful for risk and policy assessments
 2 informing decisions about the NAAQS are referred to as policy-relevant background (PRB)
 3 concentrations. PRB concentrations have historically been defined by EPA as those
 4 concentrations that would occur in the U.S. in the absence of anthropogenic emissions in
 5 continental North America defined here as the U.S., Canada, and Mexico. For this
 6 document, PRB concentrations include contributions from natural sources everywhere in
 7 the world and from anthropogenic sources outside continental North America. Background
 8 concentrations so defined facilitated separation of pollution that can be controlled by U.S.
 9 regulations or through international agreements with neighboring countries from those

1 that were judged to be generally uncontrollable by the U.S. Over time, consideration of
2 potential broader ranging international agreements may lead to alternative determinations
3 of which PM source contributions should be considered by EPA as part of PRB.

3.7.1. Contributors to PRB concentrations of PM

4 Contributions to PRB concentrations of PM include both primary and secondary
5 natural and anthropogenic components. Natural sources include wind erosion of natural
6 surfaces (Gillette and Hanson, 1989, [030212](#)); volcanic production of SO_4^{2-} , primary
7 biological aerosol particles (PBAP); wildfires producing EC, OC, and inorganic and organic
8 PM precursors; and SOA produced by oxidation of biogenic hydrocarbons such as isoprene
9 and terpenes. However, human intervention can be involved in the formation of SOA, as
10 production of natural SOA depends to a large extent on the presence of anthropogenic NO_x .
11 As described earlier in Section 3.3, prescribed fires are considered part of PRB. In addition
12 to emissions from forest fires in the U.S., emissions from forest fires in other countries can
13 be transported to the U.S. For example, Boreal forest fires in Canada (Mathur, 2008,
14 [156742](#)) and Siberia (Generoso et al., 2007, [155786](#)) and tropical forest fires in the Yucatan
15 Peninsula and Central America (Wang et al., 2006, [157109](#)) have affected PM
16 concentrations in the U.S. PRB PM varies across the contiguous United States (CONUS) by
17 region and season as a function of complex mechanism of transport, dispersion, deposition,
18 and reentrainment.

19 Dust from the Sahara desert and the Sahel in North Africa (Chiapello et al., 2005,
20 [156339](#)) affects mainly the eastern U.S.; dust from the Gobi and Taklimikan deserts in Asia
21 (VanCuren and Cahill, 2002, [157087](#); Yu et al., 2008, [157168](#)) have the largest effects in the
22 western U.S. but also affect air quality in the eastern U.S. Husar et al. (2001, [024947](#))
23 report that the average PM_{10} concentration at 25 reporting stations throughout the
24 northwestern U.S. reached $65 \mu\text{g}/\text{m}^3$ during an episode in the last week in April 1998,
25 compared to an average of $10\text{-}25 \mu\text{g}/\text{m}^3$ during the rest of April and May. This was
26 accompanied by visual reports of milky-white discoloration of the normally blue sky in non-
27 urban areas along the west coast.

28 PRB contributions to $\text{PM}_{2.5}$, $\text{PM}_{10-2.5}$, and PM_{10} can also be viewed as coming from two
29 conceptually separate components: a reasonably consistent “baseline” component and an
30 episodic component. The baseline component consists of contributions that are generally

1 well characterized by a reasonably consistent distribution of daily values each year,
2 although there is variability by region and season. The episodic component consists of
3 infrequent, sporadic contributions from natural high-concentration events occurring over
4 shorter periods of time (e.g., hours to several days) both within North America (e.g.,
5 volcanic eruptions, large forest fires, dust storms) and outside North America (e.g.,
6 transport related to dust storms from deserts in North Africa and China and storms at sea).
7 These episodic natural events, as well as events like the uncontrolled biomass burning in
8 Central America, are essentially uncontrollable and do not necessarily occur in all years.

9 In-situ measurements provide evidence for the transport of anthropogenic PM from
10 Asia on Mt. Batchelor, OR by Jaffe et al. (2003, [041957](#)). These data show sporadic but well
11 correlated increases in CO, O₃, total Hg, and aerosol backscatter associated with air coming
12 from Asia. The ITCT-2K2 campaign also found evidence for the oxidation of SO₂ to H₂SO₄
13 during trans-Pacific transport of Asian emissions. If particulate SO₄²⁻ were to be formed in
14 the polluted boundary layer where it originated, it would likely be deposited prior to
15 transport across the Pacific Ocean (Brock et al., 2004, [156295](#)). Thus primary species
16 emitted directly and secondary species formed during transport contribute to PRB
17 concentrations. Satellite data have provided images to track clouds of dust and pollution
18 across the oceans and have been used for some quantitative estimation of the flux of
19 material leaving continents. Yu et al. (2008, [157168](#)) used optical thickness data to estimate
20 column loadings from the Moderate Resolution Imaging Spectroradiometer (MODIS) along
21 with satellite assimilated wind fields to estimate the transport of PM from Asia.
22 Three-dimensional, global-scale chemistry-transport models have also been used to
23 estimate intercontinental transport of PM pollution (UNCEC, 2007, [157078](#)) and
24 trans-Pacific transport of mineral dust from Asian deserts (Fairlie et al., 2007, [141923](#)) and
25 the Sahara Desert (McKendry et al., 2007, [156748](#)).

26 Estimates for the contribution of PBAP are highly problematic. Heald and Spracklen
27 (2009, [190014](#)) estimated the contribution of fungal spores to PM_{2.5} based on GEOS-Chem
28 simulations of mannitol, considered to be a unique tracer for fungal spores (Bauer et al.,
29 2008, [189986](#)). They estimated an annual mean contribution of fungal spores to OC ranging
30 from <0.1 µg/m³ in the desert Southwest to ~ 0.5 µg/m³ in the more humid Southeast. It
31 should be noted that these are model derived estimates that still require evaluation against
32 measurements in the U.S. They do, however, provide the only quantitative estimates of
33 PBAP concentrations across the continental U.S.

3.7.1.1. Estimates of PRB Concentrations in Previous Assessments

1 Estimates of PRB concentrations reported in the 1996 AQCD for PM (U.S. EPA, 1996,
2 [079380](#)) and earlier AQCDs were based in large measure on estimates by Trijonis et al.
3 (1990, [157058](#)) for the national Acid precipitation Assessment Program as shown in
4 Table 3-18. Different approaches for estimating PRB concentrations in the western and
5 eastern U.S. were taken in the 2004 PM AQCD (U.S. EPA, 2004, [056905](#)). Data obtained at
6 IMPROVE monitoring sites in the western U.S. shown in Figure 3-84 were chosen as
7 estimates of the distribution of daily average PRB concentrations in the West because they
8 were thought to be among the least likely influenced by regional pollution sources
9 especially at the upper end of the concentration distribution. This conclusion was drawn
10 from back trajectory analyses and examination of the trace elemental composition at
11 IMPROVE sites. Because of likely unresolved contamination from pollution sources at other
12 IMPROVE sites, it was recommended to use averaged data from these sites throughout the
13 West. Concentrations distributions from 1988 through 2001 can be found in Appendix 3E of
14 the 2004 PM AQCD. Median concentrations were around 3 $\mu\text{g}/\text{m}^3$. Little interannual
15 variability was observed below the 90th percentile values. However, at the upper end of the
16 concentration distribution substantial interannual variability was observed due mainly to
17 forest fires and dust transport from Asian deserts. It was also recognized that this method
18 would likely overestimate PRB concentrations.

Table 3-18. Estimates of annual average natural background concentrations of PM_{2.5} and PM₁₀ ($\mu\text{g}/\text{m}^3$) from Trijonis et al. (1990, [157058](#)). Estimates of PM_{10-2.5} were obtained by subtraction.

	PM _{2.5}	PM ₁₀	PM _{10-2.5}
East	2-5	5-11	□ 1-9
West	1-4	4-8	□ 1-7

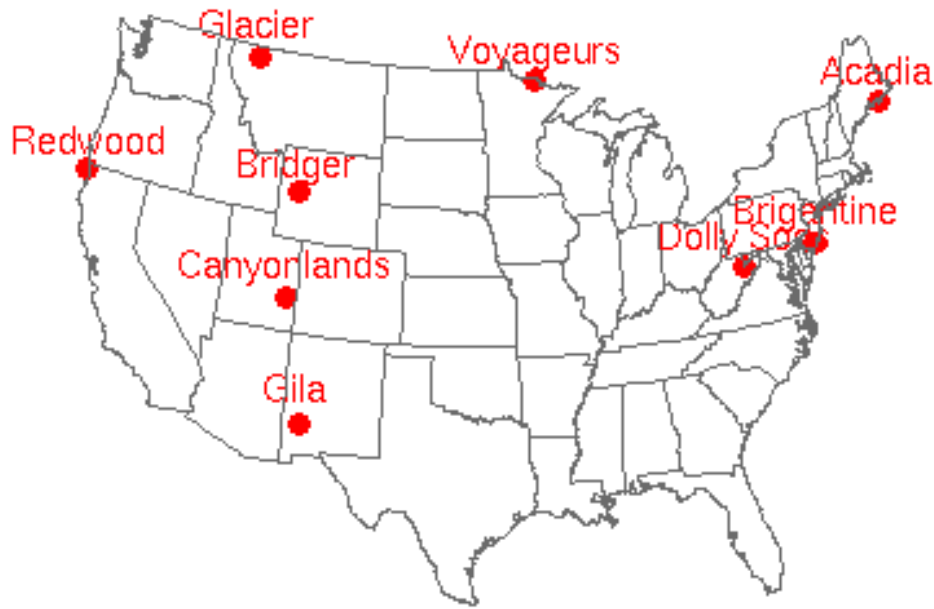


Figure 3-84. IMPROVE monitoring site locations.

1 Table 3-19 shows annual and quarterly average PM_{2.5} concentrations measured at the
 2 IMPROVE sites shown in Figure 3-82 for 2004. Annual average concentrations tend to be
 3 slightly higher in the East, particularly in Brigantine and Dolly Sods. When the data are
 4 broken down by season, a more complex picture emerges. Highest values in the East and
 5 Midwest are found during the 3rd calendar quarter, whereas in the West highest quarterly
 6 averages can occur during other quarters. As can also be seen from a comparison with
 7 values shown in Table 3-18, PM_{2.5} values measured in the East are much higher than the
 8 PRB concentration estimates by Trijonis et al. (1990, [157058](#)) for the NAPAP.

Table 3-19. Annual and quarterly mean PM_{2.5} concentrations (µg/m³) measured at IMPROVE sites in 2004.

	Mean	January-March	April-June	July-September	October-December
<i>EAST</i>					
Acadia	4.5	3.9	4.6	6.0	3.5
Brigantine	9.5	8.1	11.3	11.6	7.3
Dolly Sods	9.5	6.7	9.8	15.5	5.7
<i>MIDWEST</i>					
Voyageurs	3.8	4.1	3.1	4.2	3.6
<i>WEST</i>					
Bridger	2.1	1.2	3.1	2.8	1.3

	Mean	January-March	April-June	July-September	October-December
Canyonlands	2.6	2.2	3.2	2.9	2.1
Gila	2.9	2.0	4.0	3.8	1.8
Glacier	4.8	4.6	4.2	5.3	5.0
Redwood	3.5	2.7	3.6	3.7	3.9

1 Thus, estimating daily average PRB concentrations in the eastern U.S. using
2 observations is highly problematic because of the widespread mixing of precursors and
3 anthropogenic PM generated in the East. Therefore, results from receptor modeling studies
4 using PMF by Song et al. (2001, [036064](#)) were used in the 2004 PM AQCD for the East to
5 separate contributions from likely regional pollution sources from natural and imported
6 pollution. The “background” sources contribute about 7% to annual average PM_{2.5}
7 concentrations at Underhill, VT and about 12% at Brigantine, NJ, i.e., values between 1
8 and 2 µg/m³. These sites were chosen because they were outside of urban areas making it
9 easier to separate pollution from background components. However, some contribution of
10 regional anthropogenic pollution was still present.

11 The PM Staff Paper (U.S. EPA, 2006, [157071](#)) adopted a different approach for
12 estimating PRB concentrations. This approach separated out components mainly thought to
13 be emitted by regional pollution sources such as SO₄²⁻, which are obtained directly from
14 observations at many more IMPROVE sites than are shown in Figure 3-84, and to use the
15 remaining PM components in both the East and the West to estimate PRB. Removing
16 regional pollution from data obtained at IMPROVE sites is problematic as it involves
17 assumptions about the relative contributions of regional pollution and background sources.
18 Although sulfate in the East is mainly produced by regional pollution sources, it is not the
19 only component with a regional pollution source. By comparison, sulfate is a very minor
20 component of PM_{2.5} in the West, leading to substantial overestimates in populated states
21 like California. Annual mean estimates in the continental U.S. ranged from 2.5 µg/m³ in the
22 Central West (ID, MT, WY, ND, SD, CO, UT, NZ, AZ) to 5.2 µg/m³ for the Southwest Coast
23 (most of CA), the latter value likely reflecting contributions from local, non-sulfate
24 pollution.

25 In general, the methods outlined in both these documents are of limited utility for two
26 reasons: (1) they lack detailed spatial coverage across the whole U.S., since both methods
27 rely on monitoring data that are limited both spatially and temporally; and (2) PM
28 measurements from even the limited, remote sites used in the previous estimates of PRB

1 can not be completely devoid of contributions from anthropogenic PM. Because of these
2 limitations, numerical modeling can provide superior PM background estimates, as
3 described just below.

3.7.1.2. Chemistry Transport Models (CTMs) for Predicting PRB Concentrations

4 CTMs can be used to estimate the PRB concentrations of atmospheric components
5 including PM using a “zero-out” approach in which anthropogenic emissions inside
6 continental North America are set to zero while global biogenic emissions and
7 anthropogenic emissions outside continental North America remain. Numerical modeling
8 can provide more precision in the estimate of PRB PM than measurements since even the
9 most remote measurement sites like some of those in the IMPROVE network (see the
10 discussion in Section 6.1.1. above) will necessarily be affected by non-local non-biogenic
11 pollution, thereby confusing the contributions from these sources. Numerical models are
12 also capable of supplying estimates of PRB concentrations at much higher spatial and
13 temporal resolution than can be obtained by relying on measurements obtained at even the
14 most remote monitoring sites. In this approach, the monitoring data are used to evaluate
15 the CTM’s performance.

16 For this assessment, the global-scale circulation model GEOS-Chem was coupled with
17 the regional scale air quality model CMAQ (see the discussion of CMAQ in Section 3.6.2) to
18 simulate 1-yr of air quality data over the CONUS in two series of runs, the first annual
19 series with all anthropogenic and biogenic emissions included and the second annual series
20 with the zero-out approach employed.

21 The global-scale scale circulation model was set up as follows. GEOS-Chem version 7
22 was used, with modifications to include aromatic and biogenic SOA formation; emissions
23 were computed from a variety of sources including the Global Emissions Inventory Activity
24 (GEIA) (Benkovitz et al., 1996, [156267](#)), and Emissions Database for Global Atmospheric
25 Research, version 2 (EDGAR) (Olivier et al., 1996, [156828](#); Olivier et al., 1999, [156829](#)).

26 Particularized emissions in specific areas used the European Monitoring and
27 Evaluation Program (EMEP) for Europe (Auvray and Bey, 2005, [156237](#)), BRAVO (Kuhns
28 and Knipping, 2005, [156663](#)) for Mexico, Streets et al. (2006, [157019](#)) for Asia, Martin et al.
29 (2002, [089380](#)) for additional NO_x emissions from biofuels, lightning, and ship traffic, Bond
30 et al. (2004, [056389](#)) for global primary organic aerosols, and Cooke et al. (1999, [156365](#))

1 and Park et al. (2003, [156842](#)) for U.S. primary organic aerosols. Biomass burning
2 emissions are not climatological but were computed with GFEDv2 (Giglio et al., 2006,
3 [156469](#); van der Werf et al., 2006, [157084](#)) monthly values using active fire observations
4 from MODIS; global dust fields were computed off-line using GOCART (see emissions from
5 DEAD: <http://dust.ess.uci.edu/dead/>) to make annual adjustments to photolysis rates and
6 heterogeneous-phase chemistry.

7 The regional CTM was set up as follows. CMAQ version 4.7 (excluding the dynamic
8 coarse mode updates) was used with the SAPRC_99 chemical mechanism and AERO5
9 aerosol module; emissions were processed through SMOKE (<http://smoke-model.org>)
10 version 2.4 based on the 2004 projections from the NEI with specific CEM, biogenics, and
11 fire updates; MM5 version 3.7.4 was used with the Asymmetric Convective Mixing, version
12 2.2, PBL scheme; and data nudging was used to analyze fields for winds and temperature.

Model Evaluation

13 Details from evaluations of the performance of a number of CMAQ applications are
14 given in Arnold et al. (2003, [087579](#)), Eder and Yu (2006, [142721](#)), Appel et al. (2005,
15 [089227](#)), and Fuentes and Raftery (2005, [087580](#)).

16 In an annual simulation series for 2002 using CMAQ v4.6.1 in two 12 km domains for
17 the CONUS (see Figure 3-85), predicted concentrations of summertime particulate SO₄,
18 often a major determinant of surface-layer PM concentrations, were well-predicted by
19 CMAQ at a 12 km grid spacing, to within a factor of 2 at nearly every point of comparison
20 and with R² >0.8 across all three national networks (CASTNet, IMPROVE and CSN); a
21 more detailed description is included in the 2008 NO_xSO_x ISA (U.S. EPA, 2008, [157074](#)).
22 This result for CMAQ v4.6.1 for 2002 tracks the generally well-predicted SO₄²⁻
23 concentrations found in most earlier CMAQ evaluations: see Mebust et al. (2003, [156749](#)),
24 Eder and Yu (2006, [142721](#)), and Tesche et al. (2006, [157050](#)). Since particulate SO₄²⁻
25 concentrations are strongly a function of precipitation, care must be taken to ensure that
26 the meteorological solution driving individual CMAQ chemical applications produces
27 precipitation fields with low bias as discussed by Appel et al. (2008, [155660](#)).

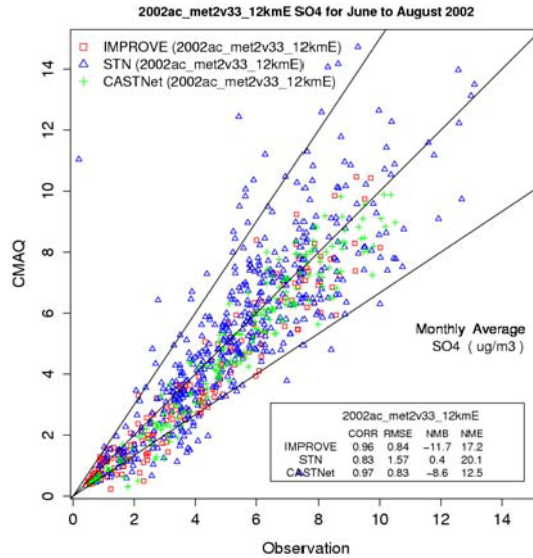


Figure 3-85. 12-km EUS Summer SO₄²⁻ PM. Each data point represents a paired monthly averaged (June/July/August) observation and CMAQ prediction at a particular IMPROVE, STN, and CASTNet site. Solid lines indicate the factor of 2 around the 1:1 line shown between them.

1 Wintertime particulate NO₃⁻ (Figure.3-86) and total NO₃ (HNO₃ + particulate NO₃⁻)
 2 (Figure 3-87) concentrations are predicted as well by CMAQ; but NO₃⁻ is a pervasively
 3 difficult species to measure and model. Still, at the CASTNet nodes where the total NO₃⁻
 4 concentrations are higher than they are at all but a few of the remote IMPROVE sites,
 5 CMAQ predicts concentrations for nearly every node to within a factor of 2 and with an R²
 6 >0.8.

7 A “base case” in which conditions for 2004 including all the anthropogenic and natural
 8 sources both within and outside of continental North America was run for comparison with
 9 measurements. A PRB simulation was also run by shutting off the anthropogenic sources of
 10 primary PM and precursors to secondary PM inside continental North America.

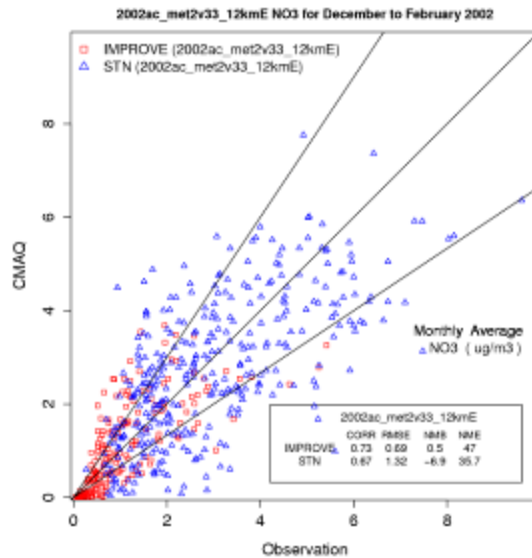


Figure 3-86 12-km EUS Winter NO_3 PM. Each data point represents a paired monthly averaged (December/January/February) observation and CMAQ prediction at a particular IMPROVE and STN site. Solid lines indicate the factor of 2 around the 1:1 line shown between them.

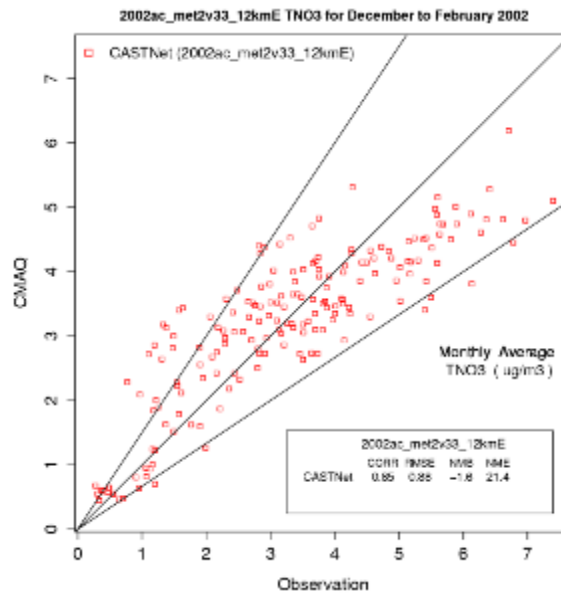


Figure 3-87. 12-km EUS Winter total nitrate (HNO_3 + total particulate NO_3^-). Each data point represents a paired monthly averaged (December/January/February) observation and CMAQ prediction at a particular CASTNet site. Solid lines indicate the factor of 2 around the 1:1 line shown between them.

1 Figures 3-88 through 3-90 show monthly average concentrations, and Figures 3-91
 2 through 3.7-10 show 24-h avg concentration distributions for 2004 predicted by CMAQ for

1 the base case and for PRB. Measurements are also included for the five Western and four
2 Eastern/Midwestern IMPROVE sites shown in Figure 3-84. Wildfires could have affected
3 the grid cell containing the Midwestern Voyageurs site resulting in the high PRB values
4 found for the July average compared to the PRB values for the rest of the year. The “base
5 case” simulations tend to underestimate concentrations throughout most western sites as
6 shown in Figures 3-89 and 3-90. These underestimates are still within the range of a
7 few $\mu\text{g}/\text{m}^3$. However, the base case simulation also greatly over-predicts $\text{PM}_{2.5}$
8 concentrations at the upper end of the distribution at the Redwoods site (Figure 3-90). This
9 over-prediction results from emissions from wildfires in northern California that are
10 included in the grid cell containing the Redwoods site, but may not have affected the site.
11 However, wildfires indicated by MODIS would have affected other areas either close to
12 these sites or could have affected other locations in between the IMPROVE sites. The
13 simulated monthly average PRB concentrations in the East/Midwest range from a
14 minimum of $0.6 \mu\text{g}/\text{m}^3$ at Acadia NP in July to $3.7 \mu\text{g}/\text{m}^3$ at Voyageurs NP in July. However,
15 most values are $<1 \mu\text{g}/\text{m}^3$. The monthly average PRB concentrations calculated for the West
16 tend to be lower than for the East and range from $0.2 \mu\text{g}/\text{m}^3$ at Bridger and Glacier NPs in
17 January and February, respectively, to $8.7 \mu\text{g}/\text{m}^3$ at Redwoods NP in November. Excluding
18 values at Redwoods NP which greatly exceed measurements, the highest monthly average
19 concentration was $3.7 \mu\text{g}/\text{m}^3$ at Voyageurs NP in the East/Midwest and $2.4 \mu\text{g}/\text{m}^3$ at Gila NP
20 in the West.

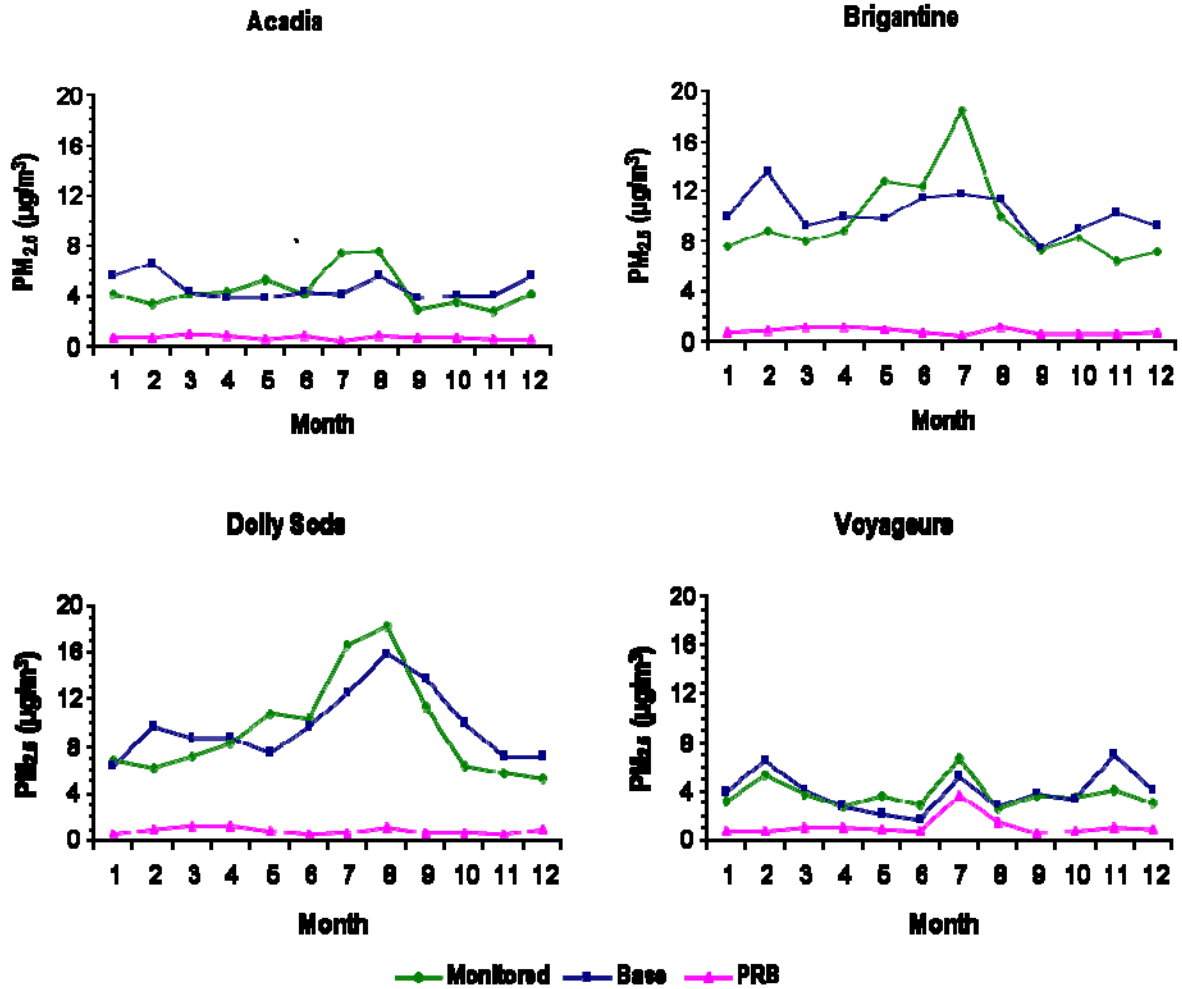


Figure 3-88. Monthly average of PM_{2.5} concentrations measured at IMPROVE sites in the East and Midwest for 2004. Also shown are distributions of PM_{2.5} concentrations calculated by CMAQ for the base case and for PRB.

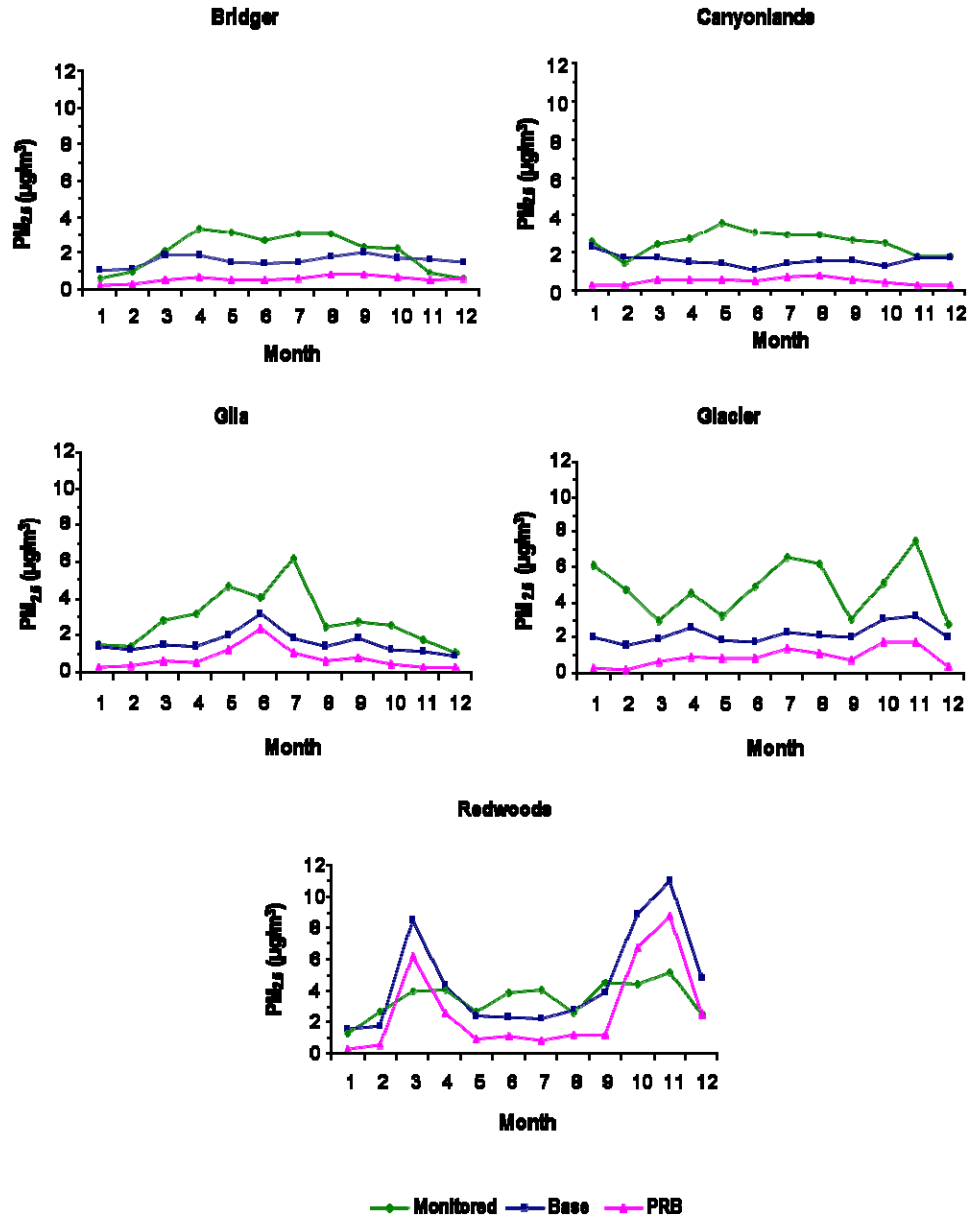


Figure 3-89. Monthly average of PM_{2.5} concentrations measured at IMPROVE sites in the West for 2004. Also shown are distributions of PM_{2.5} concentrations calculated by CMAQ for the base case and for PRB.

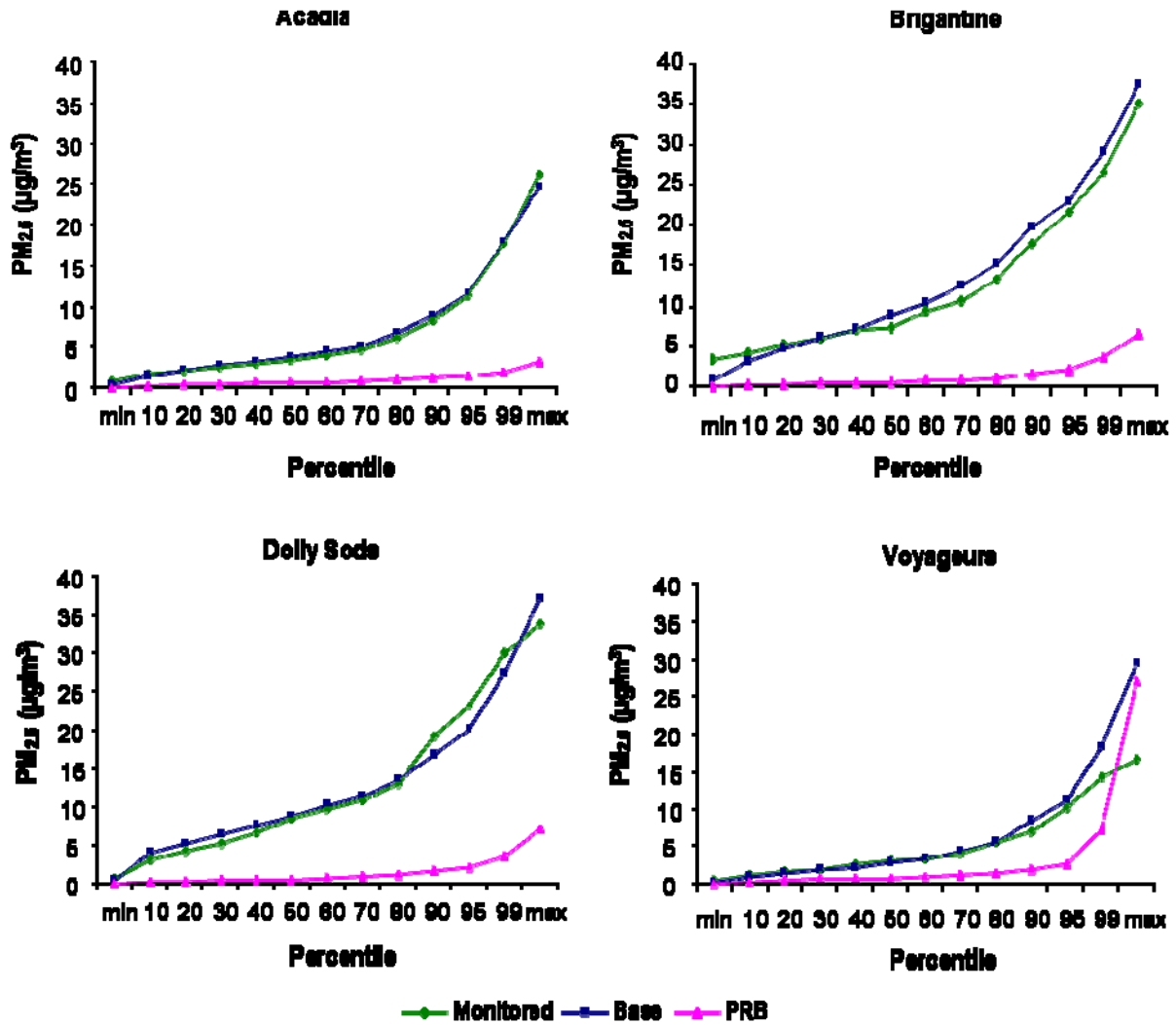


Figure 3-90. Distribution of PM_{2.5} concentrations measured at IMPROVE sites in the East and Midwest for 2004. Also shown are distributions of PM_{2.5} concentrations calculated by CMAQ for the base case and for PRB.

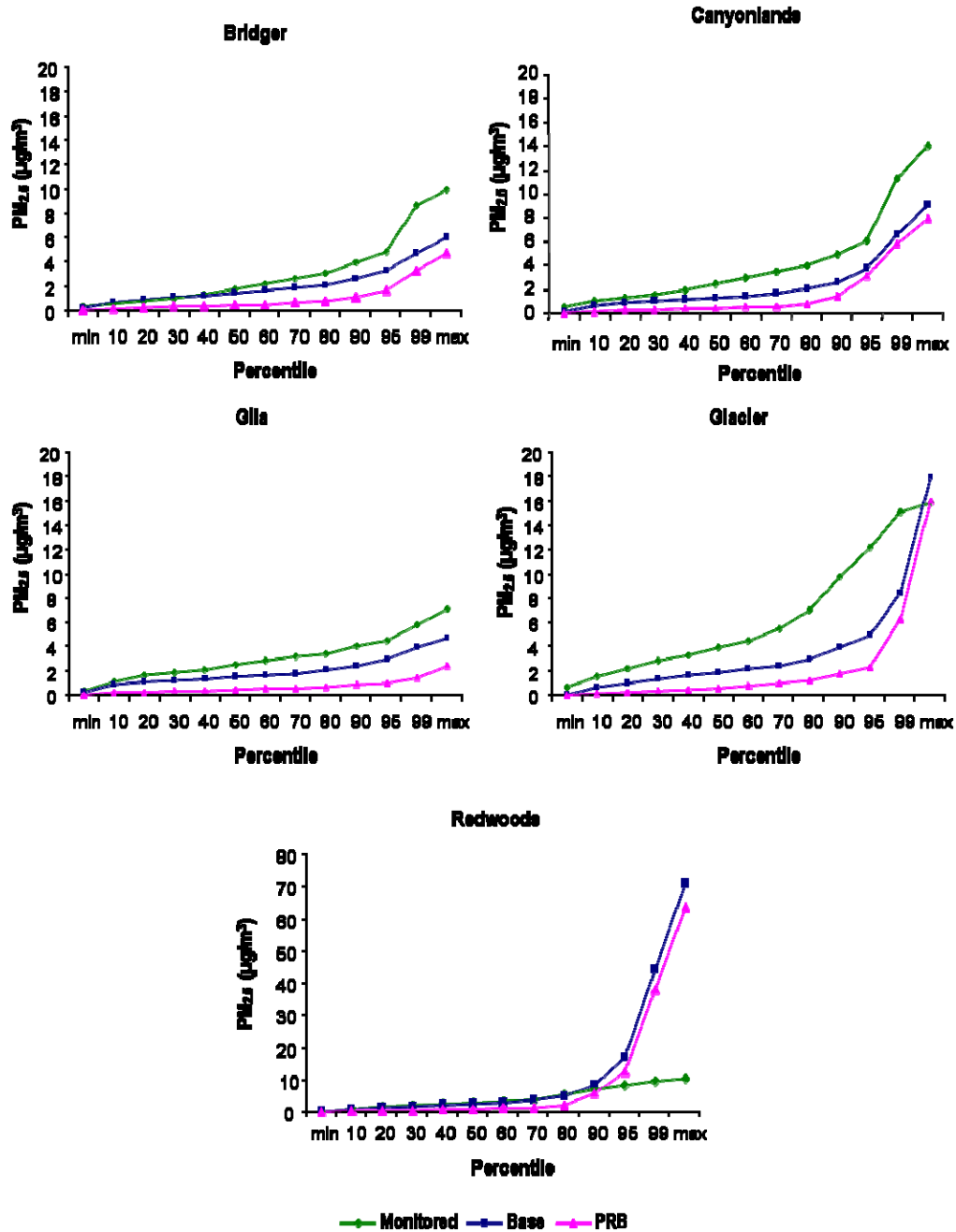


Figure 3-91. Distribution of PM_{2.5} concentrations measured at IMPROVE sites in the West for 2004. Also shown are distributions of PM_{2.5} concentrations calculated by CMAQ for the base case and for PRB. Note the scale change on the y-axis for Redwoods NP.

1 Table 3-20 gives the annual and quarterly average CMAQ predictions at IMPROVE
 2 sites for the “base case” and the ratio of CMAQ predictions to the measured concentrations
 3 at those sites in 2004. CMAQ performance for the annual average concentrations and most
 4 of the seasonal averages is very good in the East and Midwest, generally falling within 35%.

1 In the West, CMAQ’s prediction of PM_{2.5} mass averages at these remote sites is generally
 2 too low in all seasons, often by 50%. Air quality model predictions in the mountainous West
 3 are often not as good as those over the flatter terrain in the East and Midwest because the
 4 model’s grid spacing (36 km in this case) smoothes over significant variation at the surface
 5 which results in differences at such remote sites. However, the model’s trend relative to the
 6 geospatial difference is correct: the predicted PM_{2.5} concentrations are lower at the western
 7 sites than they are at the eastern sites, just as the measurements are. Table 3-21 shows
 8 corresponding annual and quarterly mean PRB PM_{2.5} concentrations at IMPROVE sites.

Table 3-20. Annual and quarterly mean PM_{2.5} concentrations (µg/m³) for the CMAQ “base case” at IMPROVE sites in 2004.

	Annual; mod/obs	Jan-March; mod/obs	Apr-Jun; mod/obs	Jul-Sep; mod/obs	Oct-Dec; mod/obs
<i>EAST</i>					
Acadia	4.7; 1.04	5.6; 1.44	4.0; 0.87	4.6; 0.77	4.6; 1.31
Brigantine	10.2; 1.07	10.9; 1.35	10.3; 0.91	10.2; 0.88	9.4; 1.29
Dolly Sods	9.8; 1.03	8.3; 1.24	8.6; 0.88	14.0; 0.90	8.0; 1.40
<i>MIDWEST</i>					
Voyageurs	4.0; 1.05	4.9; 1.19	2.2; 0.71	3.9; 0.93	4.9; 1.36
<i>WEST</i>					
Bridger	1.6; 0.76	1.3; 1.08	1.6; 0.52	1.8; 0.64	1.7; 1.30
Canyonlands	1.6; 0.62	1.9; 0.86	1.4; 0.44	1.5; 0.52	1.6; .76
Gila	1.6; 0.55	1.4; 0.70	2.2; 0.55	1.7; 0.45	1.1; 0.61
Glacier	2.2; 0.45	1.8; 0.39	2.1; 0.50	2.1; 0.40	2.8; 0.56
Redwood	4.6; 1.31	4.0; 1.48	3.0; 0.83	2.9; 0.78	8.4; 2.15

9 Table 3-22 illustrates CMAQ predictions of seasonal variation in the base case PM_{2.5}
 10 concentrations across regions of the CONUS, while Table 3-23 shows CMAQ predictions of
 11 the seasonal variation in regional PRB PM_{2.5} concentrations. Highest base case PM_{2.5}
 12 concentrations were observed for the Northeast, Southeast, and Industrial Midwest with
 13 highest concentrations during the fall and winter (and comparably high concentrations in
 14 the summer for the Industrial Midwest). PRB PM_{2.5} concentrations were highest on an
 15 annual basis in the Southeast, and peaking during the winter. In the summer, PRB PM_{2.5} is
 16 roughly comparable for the Northwest, and Southern California and elevated but slightly
 17 lower for the Southwest. These results also likely indicate the influence of sources that are
 18 more strongly related to hot and dry conditions such as wildfires and dust suspension.

Table 3-21. Annual and quarterly mean PM_{2.5} concentrations (µg/m³) for the CMAQ PRB simulations at IMPROVE sites in 2004.

	Annual	January-March	April-June	July-September	October-December
<i>EAST</i>					
Acadia	0.70	0.76	0.76	0.65	0.65
Brigantine	0.77	0.86	0.91	0.70	0.63
Dolly Sods	0.79	0.88	0.83	0.75	0.66
<i>MIDWEST</i>					
Voyageurs	1.2	0.83	0.91	2.0	0.93
<i>WEST</i>					
Bridger	0.57	0.33	0.57	0.76	0.61
Canyonlands	0.49	0.38	0.54	0.68	0.35
Gila	0.74	0.42	1.4	0.80	0.32
Glacier	0.91	0.36	0.87	1.1	1.3
Redwood	2.8	2.4	1.5	1.1	6.1

Table 3-22. Annual and quarterly mean of the CMAQ-predicted base case PM_{2.5} concentrations (µg/m³) in the U.S. EPA CONUS regions in 2004.

	Annual	January-March	April-June	July-September	October-December
Northeast	9.76	10.74	8.38	9.55	10.38
Southeast	10.05	12.28	7.72	9.78	10.42
Industrial Midwest	11.38	12.22	9.37	11.89	12.00
Upper Midwest	6.70	8.83	4.95	5.34	7.67
Southwest	3.30	4.08	2.77	3.31	3.03
Northwest	2.72	2.49	2.21	2.71	3.44
Southern California	4.43	4.64	3.93	4.34	4.82

Table 3-23. Annual and quarterly mean of the CMAQ-predicted PRB PM_{2.5} concentrations (µg/m³) in the U.S. EPA CONUS regions in 2004.

	Annual	January-March	April-June	July-September	October-December
Northeast	0.74	0.85	0.78	0.67	0.68
Southeast	1.72	2.43	1.41	1.41	1.64
Industrial Midwest	0.86	0.89	0.89	0.94	0.73
Upper Midwest	0.84	0.79	0.93	0.99	0.66

	Annual	January-March	April-June	July-September	October-December
Southwest	0.62	0.61	0.76	0.70	0.40
Northwest	1.01	0.48	0.81	1.42	1.32
Southern California	0.84	0.54	0.92	1.21	0.67

3.8. Issues in Exposure Assessment for PM and its Components

1 The purpose of this section is to present the latest exposure assessment studies to
2 characterize the exposure of individuals and populations to PM of ambient origin. Such
3 information will aid the interpretation of epidemiologic studies described in subsequent
4 chapters of this Integrated Science Assessment. This section includes descriptions of
5 modeling and monitoring techniques used to capture personal PM exposure, observations
6 reported in the literature at various relevant spatial scales, observations related to PM
7 composition and PM in a mix of copollutants, and the effect of exposure estimates on
8 epidemiologic results. Attention is given to use of community-based monitors at urban
9 spatial scales and use of personal and microenvironmental exposure data to present how
10 each metric can be used in exposure assessment and what errors and uncertainties exist for
11 each approach. Understanding of exposure errors is important because exposure error can
12 potentially bias an estimate of a health effect endpoint, or increase the size of confidence
13 intervals around a health effect estimate. Typically, exposure error biases analyses of
14 health effects towards the null (i.e., no relationship between exposure and health effect).

15 The information presented in this section builds upon the key findings of the 2004 PM
16 AQCD (U.S. EPA, 2004, [056905](#)). One key finding was that separation of total PM
17 exposures into ambient and nonambient components reduces potential uncertainties in the
18 analysis and interpretation of PM health effects data. At the time of the 2004 PM AQCD
19 (U.S. EPA, 2004, [056905](#)), one study had reported that individual daily values of the total
20 and nonambient personal PM exposure were both poorly correlated with the daily ambient
21 PM concentrations while individual daily values of ambient PM exposure and daily ambient
22 PM concentrations were highly correlated. In pooled studies (different subjects measured on
23 different days), individual, daily values of the total PM exposure were generally shown to
24 be poorly correlated with the daily ambient PM concentrations. In longitudinal studies

1 (each subject measured for multiple days), individual, daily values of the total PM personal
2 exposure and the daily ambient PM concentrations were found to be highly correlated for
3 some, but not all, subjects. Using the PTEAM study data, the 2004 PM AQCD (U.S. EPA,
4 2004, [056905](#)) also analyzed exposure measurement errors in the context of time-series
5 epidemiology to show that the error introduced by using ambient PM concentrations as a
6 surrogate for ambient PM exposure negatively biases the estimation of health risk
7 coefficients by the ratio of ambient PM exposure to ambient PM concentration (called α , the
8 ambient exposure factor). However, it was concluded that the health risk coefficient
9 determined using ambient PM concentrations provides the correct information on the
10 change in health risks that would be produced by a change in ambient concentrations.

11 The material in this section is designed to help interpret findings from epidemiologic
12 studies presented in Chapters 6 and 7 of this ISA. The chapter is structured as follows. A
13 conceptual model of PM exposure is presented in Section 3.8.1, followed by exposure
14 modeling techniques in Section 3.8.2. Next, new developments in techniques for measuring
15 personal and indoor PM are presented. In Section 3.8.4, exposure assessment field studies
16 in the literature are presented. This section is divided into urban and neighborhood-to-
17 micro spatial scales of ambient exposure with attention to near-road, in-vehicle, and indoor
18 environments. Section 3.8.5 presents issues related to PM composition and PM in
19 multipollutant mixtures. The section culminates with implications of exposure assessment
20 issues for epidemiologic studies in Section 3.8.6.

3.8.1. General Exposure Concepts

21 A theoretical model of personal exposure is presented to highlight what is measurable
22 and what uncertainties exist in this framework. An individual's time-integrated total
23 exposure to airborne PM can be described based on a compartmentalization of the person's
24 activities throughout a given time period:

$$E_T = \int C_j dt$$

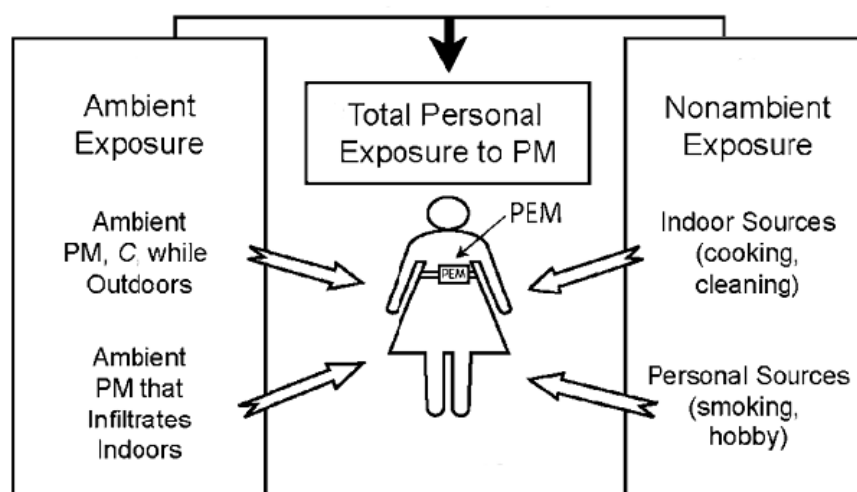
Equation 3-3

25 where E_T = total exposure over a time-period of interest, C_j = airborne PM concentration at
26 microenvironment j , and dt = portion of the time-period spent in microenvironment j .
27 Equation 3-3 can be decomposed into a microenvironmental model that accounts for
28 exposure to PM of ambient (E_a) and nonambient (E_{na}) origin of the form:

$$E_T = E_a + E_{na}$$

Equation 3-4

1 Figure 3-92 illustrates Equation 3-4. Examples of ambient PM sources include
2 industrial and mobile source emissions, resuspended dust, biomass combustion, and
3 secondary formation. Examples of nonambient sources include smoking, cooking, home
4 heating, cleaning, and indoor air chemistry. PM concentrations generated by ambient and
5 nonambient sources are subject to spatial and temporal variability that can affect estimates
6 of exposure and resulting health effects. Exposure factors affecting interpretation of
7 epidemiology are discussed in detail in Section 3.8.6.



Source: Wilson and Brauer (2008).

Figure 3-92. Model of total personal exposure to PM as a function of ambient and nonambient sources.

8 This assessment focuses on the ambient component of exposure because this is more
9 relevant to the NAAQS review. E_a can be expressed in terms of the fraction of time spent in
10 various outdoor and indoor microenvironments (Wallace et al., 2006, [089190](#); Wilson et al.,
11 2000, [010288](#)):

$$E_a = \sum f_o C_o + \sum f_i F_{inf,i} C_{o,i}$$

Equation 3-5

1 where f = fraction of the relevant time period (equivalent to dt in Equation 3-2),
 2 subscript o = index of outdoor microenvironments, subscript i = index of indoor
 3 microenvironments, subscript o,i = index of outdoor microenvironments adjacent to a given
 4 indoor microenvironment i , and $F_{inf,i}$ = infiltration factor for indoor microenvironment i .
 5 Equation 3-5 is subject to the constraint $\sum f_o + \sum f_i = 1$, and each term on the right hand side
 6 of the equation has a summation because it reflects various microenvironmental exposures.
 7 Here, “indoors” refers to being inside any aspect of the built environment, e.g., home, office
 8 buildings, enclosed vehicles (automobiles, trains, buses), and/or recreational facilities
 9 (movies, restaurants, bars). “Outdoor” exposure can occur in parks or yards, on sidewalks,
 10 and on bicycles or motorcycles.

11 F_{inf} represents the equilibrium fraction of the PM concentration outside the
 12 microenvironment that penetrates inside the microenvironment and remains suspended. It
 13 is a function of the microenvironmental air exchange characteristics and the particle
 14 properties. Assuming steady state ventilation conditions, the infiltration factor is a function
 15 of the penetration, P (P is the ratio of indoor to outdoor PM), of PM, the air exchange rate,
 16 a , of the indoor microenvironment, and the rate of PM loss, k , within the indoor
 17 microenvironment: $F_{inf} = Pa/(a+k)$. Determination of E_a can be complicated by PM loss
 18 through chemical and physical processes in microenvironments and the composition of PM
 19 can be modified during infiltration of outdoor air into microenvironments (Sarnat et al.,
 20 2006, [089166](#); Meng et al., 2007, [091197](#))

21 In the context of interpreting epidemiologic studies of the effects of ambient
 22 pollutants on human health, the association between E_a and concentrations from a central
 23 site monitor, C_a , is more relevant than the association between E_T (which includes both the
 24 ambient and nonambient component of PM exposure) and C_a because nonambient PM is
 25 uncorrelated with C_a , as shown in Section 3.8.4. In ecologic studies of large panels or
 26 cohorts, C_a is often used in lieu of outdoor microenvironmental data to represent these
 27 exposures based on the availability of data. Thus it is often assumed that $C_o = C_a$ and that
 28 the fraction of time spent outdoors can be expressed cumulatively as f_o ; the indoor terms
 29 still retain a summation because infiltration differs among different microenvironments.
 30 Under these assumptions, an individual’s exposure to ambient PM, first given in Equation

1 3-5, can be re-expressed as a function of C_a . The following approximation has been
2 employed in the literature to describe ambient exposure based on these assumptions
3 (Wallace et al., 2006, [089190](#); Wilson and Brauer, 2006, [088933](#); Wilson et al., 2000,
4 [010288](#)):

$$E_a = (f_o + \sum f_i F_{\text{inf},i}) C_a$$

Equation 3-6

5 Particle size, particle composition, meteorology, urban and natural topography, and
6 other factors determine whether or not Equation 3-6 is a reasonable approximation for
7 Equation 3-5. Errors and uncertainties inherent in use of Equation 3-6 in lieu of Equation
8 3-5 are described in Section 3.8.6 with respect to implications for epidemiology. If
9 concentration measured at a central site monitor is used to represent ambient
10 concentration, then α , the ratio between personal exposure to ambient PM and the ambient
11 concentration of PM, can be defined as:

$$\alpha = \frac{E_a}{C_a}$$

Equation 3-7

12 If the assumptions forming the basis for Equation 3-6 are valid, then α is the
13 proportionality factor in Equation 3-6:

$$\alpha = f_o + \sum f_i F_{\text{inf},i}$$

Equation 3-8

14 α varies between 0 and 1. If a person's exposure occurs in a single microenvironment, the
15 ambient component of a microenvironmental PM concentration can be represented as the
16 product of the ambient concentration and F_{inf} . Wallace et al. (2006, [089190](#)) note that time-
17 activity data and corresponding estimates of F_{inf} for each microenvironmental exposure are
18 needed to compute an individual's α with accuracy. If local sources and sinks exist and are
19 significant but not captured by central site monitors, then the ambient component of
20 outdoor air must be estimated using dispersion models, land use regression models,
21 receptor models, fine scale chemistry-transport models or some combination of these
22 techniques. These techniques are described in Section 3.8.2.

3.8.2. Exposure Modeling

1 This section describes a variety of techniques used to model PM exposure. Many of
2 these methods are used in combination to link ambient PM levels in the atmosphere or
3 source characteristics to human exposure among individuals or sample populations. Recent
4 developments in exposure modeling are described in this subsection, and errors and
5 uncertainties of these approaches are described in the Section 3.8.6.2.

3.8.2.1. Time-Weighted Microenvironmental Models

6 An individual's exposure is dictated by his or her activity patterns, as modeled by f_o
7 and f_i in Equation 3-5. A number of panel studies have tracked subject exposures using
8 questionnaires, time-activity diaries, or global positioning systems (e.g. Cohen et al., 2009,
9 [190639](#); Elgethun et al., 2003, [190640](#); Johnson et al., 2000, [001660](#); Olson and Burke,
10 2006, [189951](#); Wallace et al., 2006, [089190](#)). In many cases, the time-activity tracking is
11 performed in conjunction with personal exposure and/or indoor and outdoor PM
12 concentration monitoring to estimate overall PM exposure. Wu (2005, [086397](#)) described a
13 microenvironmental model of total personal exposure:

$$E_T = f_{oh}C_o + f_{oa}C_a + f_iC_i$$

Equation 3-9

14 where f_{oh} = fraction of time spent outdoors at home, f_{oa} = fraction of time spent
15 outdoors away from home, C_o = PM concentration outside the home, and C_i = indoor PM
16 concentration. In Equation 3-9, E_T can be calculated based on time-activity diary data and
17 time-resolved PM concentration measurements. E_T can be expressed as a time-resolved
18 value or cumulatively over a time period of interest using this formulation. In this model,
19 ambient and nonambient exposure cannot be separated because it incorporates indoor
20 concentrations that are a function of both ambient and nonambient sources. Additionally,
21 Equation 3-9 distinguishes ambient concentration measured at a monitor from that
22 measured immediately outside the home. Liu et al. (2003, [073841](#)) found that this model
23 predicted elderly exposures adequately but was a poor predictor of PM_{2.5} exposure for
24 asthmatic children. Wu et al. (2005, [086397](#)) point out that this may be due to lack of
25 availability of the children's time-activity data in school where children spend a substantial
26 portion of their day. In a study of school children's exposure patterns, DeCastro et al. (2007,

1 [190996](#)) computed odds ratios of a panel subject's location within a given microenvironment
 2 using multivariate logistic models of the indoor school, indoor home, and outdoor
 3 microenvironments and found that city of residence was a significant predictor of being
 4 indoors at school, having an afterschool job was a significant predictor of being indoors at
 5 home, and age and having an afterschool job were significant predictors of being outdoors.
 6 The results of the DeCastro et al. (2007, [190996](#)) study were designed to predict f_i and f_o in
 7 exposure modeling.

8 A second approach proposed by Wu et al. (2005, [086397](#)) is similar in formulation to
 9 Equation 3-5 because it computes ambient PM exposure by considering the amount of
 10 outdoor PM infiltrated indoors. This version also incorporates C_o and C_a :

$$E_a = f_{oh}C_o + f_{oa}C_a + f_iF_{inf}C_o$$

Equation 3-10

11 Equation 3-10 differs from 3-5 because it accounts for concentrations immediately
 12 outside the building rather than considering all outdoor exposures to be a function of that
 13 measured at a community monitor. Factors influencing the contribution of E_a to E_T may
 14 include sample population characteristics, location of a site for microenvironmental
 15 monitoring, seasonal trends in PM concentration, and regional differences affecting
 16 ambient concentration and infiltration.

17 Regression based approaches can also be incorporated into time-weighted
 18 microenvironmental modeling. Chang et al. (2003, [053789](#)) used data from the Scripted
 19 Activity Study and the Older Adults Study, both conducted in Baltimore in 1998 and 1999,
 20 to compute total personal exposure based on time-weighting microenvironmental exposures
 21 for each panel subject:

$$E_T = ME_i\beta_i \sum_k f_k C_k + ME_o\beta_o \sum_k f_k C_k$$

Equation 3-11

22 where ME = microenvironment (indoor or outdoor), β = regression coefficient
 23 reflecting the accuracy of the exposure estimate for a given microenvironment, f_k = fraction
 24 of time performing an activity k , and C_k = personal exposure while performing activity k . In
 25 this work, Chang et al. (2003, [053789](#)) tested the models with hourly personal exposure
 26 data, hourly ambient concentration data, and daily ambient concentration data. The study
 27 found that time-activity data improved estimates of 24-h $PM_{2.5}$ exposure in comparison with

1 using 24-h ambient PM_{2.5} data but use of hourly ambient data was comparable to personal
2 microenvironmental data in estimating exposure. When using ambient concentration data,
3 β reflected infiltration for the indoor microenvironmental estimates for a sample
4 population. Wallace et al. (2006, [089190](#)) also used a multivariate regression to assess the
5 impact of various factors on total and ambient PM_{2.5} personal exposure and found several
6 building- and activity-related variables were significant predictors of total and ambient
7 PM_{2.5} exposure. Using a similar activity-based exposure modeling approach for a panel
8 study in Seattle from 1999-2002, Allen et al. (2004, [190089](#)) found that subjects' PM
9 exposures were best represented by modeling ambient and nonambient exposures
10 separately because ambient PM exposure was well correlated with PM concentration at
11 central site monitors while nonambient PM exposure was not.

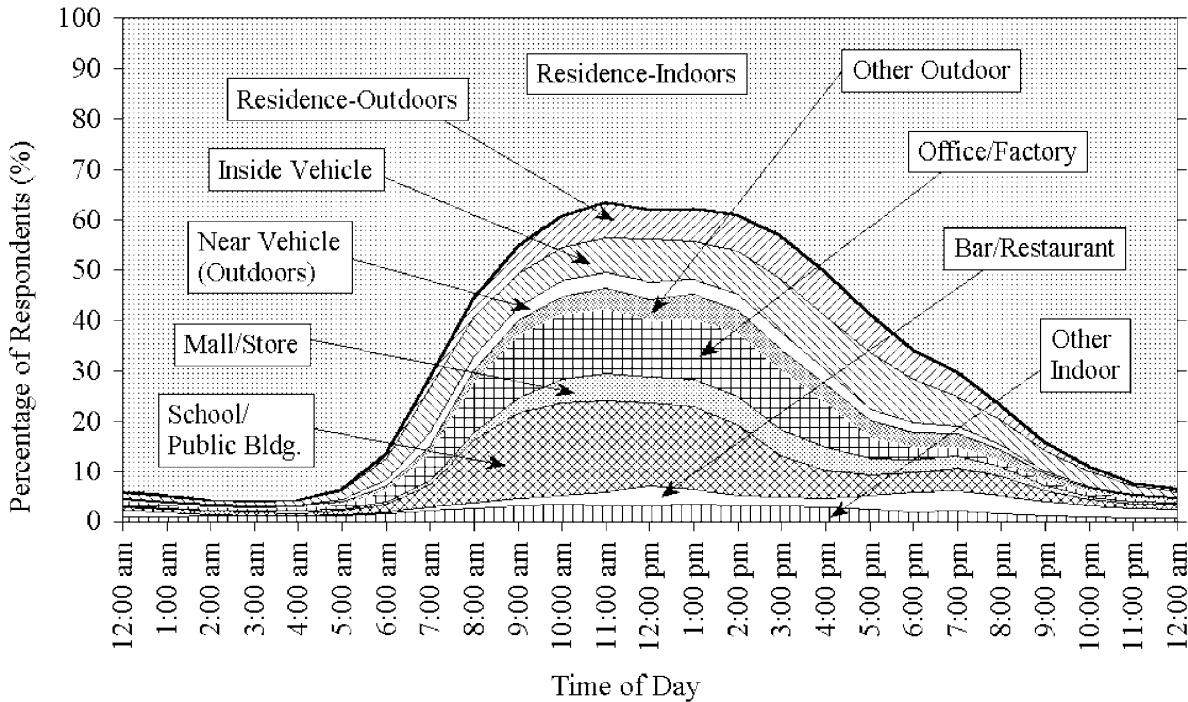
3.8.2.2. Stochastic Population Exposure Models

12 Population-based methods, such as the Air Pollution Exposure (APEX), Stochastic
13 Human Exposure and Dose Simulation (SHEDS), and EXPOLIS (exposure in polis, or
14 cities) models, involve stochastic treatment of the model input factors
15 (http://www.epa.gov/ttn/fera/human_apex.html) (Burke et al., 2001, [014050](#); Kruize et al.,
16 2003, [156661](#)). These are described in detail in Annex 3.7 of the 2008 NO_x ISA (U.S. EPA,
17 2008, [157073](#)). Stochastic models utilize distributions of pollutant-related and
18 individual-level variables, such as ambient and local PM concentration source contributions
19 and breathing rate respectively, to compute the distribution of individual exposures across
20 the modeled population. Using distributions of input parameters in the model framework
21 rather than point estimates allows the models to explicitly incorporate uncertainty and
22 variability into exposure estimates (Zidek et al., 2007, [190076](#)). These models estimate
23 time-weighted exposure for modeled individuals by summing exposure in each
24 microenvironment visited during the exposure period. The models also have the capability
25 to estimate received dose through a dosimetry model. The initial set of input data for
26 population exposure models is ambient air quality data, which may come from a monitoring
27 network or model estimates. Estimates of concentrations in a set of microenvironments are
28 generated either by mass balance methods or microenvironmental factors.
29 Microenvironments modeled include residential indoor microenvironments; other indoor
30 microenvironments, such as schools, offices, and public buildings; vehicles; and outdoor

1 microenvironments. The sequence of microenvironments and exertion levels during the
2 exposure period is determined from characteristics of each modeled individual. The APEX
3 model does this by generating a profile for each simulated individual by sampling from
4 distributions of demographic variables such as age, gender, and employment; physiological
5 variables such as height and weight; and situational variables such as living in a house
6 with a gas stove or air conditioning. Activity patterns from a database such as CHAD are
7 assigned to the simulated individual using age, gender, and biometric characteristics.
8 Breathing rates are calculated for each activity based on exertion level, and the
9 corresponding received dose is then computed. For APEX, the PM dosimetry algorithm is
10 based on the International Commission on Radiological Protection's Human Respiratory
11 Tract Model for Radiological Protection (ICRP, 1994, [006988](#)), and calculates the rate of
12 mass deposition of PM in the respiratory system (U.S. EPA, 2008, [191775](#)). Summaries of
13 individual- and population-level metrics are produced, such as maximum exposure or dose,
14 number of individuals exceeding a specified exposure/dose threshold, and number of person-
15 days at or above certain exposure levels. The models also consider the non-ambient
16 contribution to total exposure. Nonambient source terms are added to the infiltration of
17 ambient pollutants to calculate the total concentration in the microenvironment. Output
18 from model runs with and without nonambient sources can be compared to estimate the
19 ambient contribution to total exposure and dose.

20 Recent larger-scale human activity databases, such as those developed for the
21 Consolidated Human Activity Database (CHAD) or the National Human Activity Pattern
22 Survey (NHAPS), have been designed to characterize exposure patterns among much larger
23 population subsets than can be examined during individual panel studies (Klepeis et al.,
24 2001, [002437](#); McCurdy et al., 2000, [000782](#)). CHAD consists of a consolidation of human
25 activity data obtained during several panel studies in which diary or retrospective activity
26 data were obtained, while NHAPS acquired sample population time activity data through
27 surveys about human activity (Klepeis et al., 2001, [002437](#)). The complex human activity
28 patterns across the population (all ages) are illustrated in Figure 3-93 (Klepeis et al., 2001,
29 [002437](#)). This figure is presented to illustrate the diversity of daily activities among the
30 entire population as well as the proportion of time spent in each microenvironment.
31 Different patterns would be anticipated when breaking down activity patterns for
32 subgroups such as children or the elderly. With data for average PM concentrations in each

1 microenvironment, population exposures can be estimated from this break-down of time-
2 activity data.



Source: Klepeis et al. (2001, [002437](#)).

Figure 3-93. Distribution of time sample population spends in various environments, from the National Human Activity Pattern Survey.

3 Stochastic and deterministic methods are often combined, as described below.
4 Recently, SHEDS has been linked with the Modeling Environment for Total Risk Studies
5 (MENTOR) model to expand population exposure assessment to individual risk assessment
6 (Georgopoulos et al., 2005, [080269](#)). In this formulation, CMAQ was used to predict initial
7 concentrations at a coarse scale, and then a spatiotemporal random field method (Vyas and
8 Christakos, 1997, [156142](#)) or Bayesian max entropy method (Serre and Christakos, 1999,
9 [156968](#)) was applied to interpolate the concentration to census tract scale in which
10 exposure estimates are made. CHAD can also be incorporated into MENTOR so that
11 estimates of exposure are related to dose and metabolic distributions to estimate risk of
12 specific health impacts.

3.8.2.3. Dispersion Models

1 Dispersion models have been used both for direct estimation of exposure and as
2 inputs for stochastic modeling systems, as described above. Location-based exposures have
3 been predicted using a model such as California Line Source Dispersion Model (CALINE),
4 the American Meteorological Society/Environmental Protection Agency Regulatory Model
5 (AERMOD), CALPUFF (long-range plume transport model created by the California Air
6 Resources Board), or the Operational Street Pollution Model (OSPM) for estimation of
7 street-level PM pollution coupled with infiltration models to represent indoor exposure to
8 ambient levels (Gilliam et al., 2005, [056749](#); Hering, 2007, [155839](#); Mensink et al., 2008,
9 [155980](#); Wilson and Zawar-Reza, 2006, [088292](#)). For instance, CALPUFF was used to model
10 transport and dispersion in lower Manhattan following the September 11, 2001 World
11 Trade Center collapse (Gilliam et al., 2005, [056750](#)) to determine average location-based
12 exposures. Wilson and Zawar-Reza (2006, [088292](#)) used The Air Pollution Model (TAPM),
13 which integrated an emissions model with a mesoscale meteorological driver, to assess PM₁₀
14 dispersion and potential for exposure in Christchurch, New Zealand. Gulliver and Briggs
15 (2005, [191079](#)) used the Atmospheric Dispersion Modeling System (ADMS) to model
16 dispersion of “line-source” traffic emissions in an urban environment. In a method similar
17 to that employed by Georgopoulos et al. with SHEDS, Wu et al. (2005, [157155](#)) used
18 CALINE to predict street-level concentrations of pollutants and input the results of that
19 dispersion model into an individual exposure model that accounts for infiltration of specific
20 building characteristics. Wu et al. (2005, [086397](#)) employed CHAD to estimate the
21 time-basis of exposures from the CALINE predictions. With an individualized exposure
22 approach, the model is deterministic. However, population exposures can be estimated by
23 performing repeated simulations using various housing characteristics and then computing
24 a posterior probability distribution function for exposure. Isakov et al. (2009, [191192](#))
25 developed a methodology to link a chemical transport model, used to compute regional scale
26 spatiotemporally-varying concentration in an urban area, with stochastic population
27 exposure models to predict annual and seasonal variation in urban population exposure
28 within urban microenvironments.

3.8.2.4. Land Use Regression (LUR) and GIS-Based Models

1 Land use regression (LUR) models have also been developed to describe pollution
2 levels as a function of source characteristics (Briggs et al., 1997, [025950](#); Gilliland et al.,
3 2005, [098820](#); Ryan and LeMasters, 2007, [156063](#)). LUR develops a regression from
4 monitored concentration values as a function of data from a combination of factors such as
5 land use designation, traffic counts, home heating usage, point source strength, and
6 population density and then computes the regression at multiple locations based on the
7 independent variables at those particular locations without monitors. At the census tract
8 level, a LUR is a multivariate description of pollution as a function of traffic, land use, and
9 topographic variables (Briggs et al., 1997, [025950](#)). Originally, LUR was used for NO₂
10 dispersion, but it was adapted for PM_{2.5} exposure estimation by Brauer et al. (2003, [155702](#))
11 for Stockholm, Sweden, Munich, Germany, and throughout The Netherlands. This study
12 found a measure of traffic density to be the most significant variable predicting PM_{2.5}
13 exposure. Ryan et al. (2008, [156064](#)) reported on a LUR model for childhood exposure to
14 traffic-derived EC for the Cincinnati Allergy and Air Pollution Study and also found traffic
15 to be the most important determinant of diesel exhaust particle exposure. In this case, wind
16 direction was also factored into the model as a determinant of EC mixing. Like
17 deterministic dispersion models, LUR can be performed over wide areas to develop a
18 posterior probability distribution function of exposure at the urban scale. However, Hoek et
19 al. (2008, [156554](#)) warn of several limitations of LUR, including distinguishing real
20 associations between pollutants and covariates from those of correlated copollutants,
21 limitations in spatial resolution from monitor data, applicability of the LUR model under
22 changing temporal conditions, and introduction of confounding factors when LUR is used in
23 epidemiologic studies.

24 A GIS platform is typically used to organize the independent variable data and map
25 the results. The GIS software creates numerous lattice points for the regression of
26 concentration as a function of the covariates. For instance, Krewski et al. (2009, [191193](#))
27 computed PM_{2.5} concentrations for the New York City and Los Angeles metropolitan areas.
28 For the Los Angeles analysis, the LUR was applied at 18,000 points in the simulation
29 domain, and an inverse distance weighting kriging method was applied to interpolate the
30 predicted concentration. In New York City, the LUR was applied at 49 monitors for a 3-yr
31 model and 36 monitors for a model of winter 2000; kriging was employed only for the

1 purpose of visualizing the concentration between monitors. The models explained 69% and
2 66% of the variation in PM_{2.5} in Los Angeles and New York City, respectively.

3 GIS-based spatial smoothing models can be used to estimate PM concentration levels
4 where monitors are not located. Yanosky et al. (2008, [099467](#)) described an approach to
5 estimate concentrations using a combination of reported AQS data and GIS-based and
6 meteorological covariates. Temporally stationary covariates included distance to nearest
7 road for different PM size fractions, urban land use, population density, point source
8 emissions within 1 and 10 km buffers, and elevation above sea level. Time-varying
9 covariates included area source emissions, precipitation, and wind speed. In this analysis,
10 the GIS-based covariates were temporally stationary, while the meteorological and PM
11 monitored concentration inputs were time-varying. This approach was applied to estimate
12 PM₁₀, PM_{10-2.5}, and PM_{2.5} exposures for the Nurse's Health Study and provided estimates of
13 concentration at approximately 70,000 nodes with PM₁₀ and/or PM_{2.5} data input from more
14 than 900 AQS sites with good validation of the PM₁₀ and PM_{2.5} models (Paciorek et al.,
15 2008, [190090](#); Yanosky et al., 2008, [099467](#); Yanosky et al., 2009, [190114](#)).

16 GIS-based methods can also be applied to integrate exposures over different
17 microenvironments. For example, Gulliver and Briggs (2005, [191079](#)) described
18 development of the Space-Time Exposure Modeling System (STEMS) to model PM₁₀
19 concentration. STEMS is a multipronged model that links traffic emissions estimates,
20 dispersion, background PM estimates, and time-activity data within a GIS framework to
21 create exposure estimates. Traffic emissions estimates and meteorological parameters are
22 input into the ADMS dispersion model, which along with background PM measurements
23 are used to create hourly point estimates of PM concentration. Based on the time-activity
24 data, the concentration estimates were then used to calculate exposures to traffic-related
25 PM₁₀ along a commuting path while an individual is in transit. PM₁₀ was used by Gulliver
26 and Briggs (2005, [191079](#)) because ADMS had not yet been validated for smaller size
27 fractions. In an analysis of the sensitivity of included variables, Gulliver and Briggs (2005,
28 [191079](#)) showed the model to be most sensitive to fluctuations in local meteorology followed
29 by sudden speed reductions of 10 km/h. The STEMS model was primarily designed to model
30 exposures during transit, but the authors state that this technique can be applied to
31 modeling other microenvironmental exposures.

32 Source proximity is sometimes used as a covariate in GIS-based regression models.
33 For instance, Baxter et al. (2007, [092725](#)) predicted indoor exposure to PM_{2.5}, EC, and NO_x

1 based on distance to traffic sources, indoor source characteristics, window opening, and
2 ambient concentrations in the Boston metropolitan area. In this effort, Baxter et al.
3 examined a variety of factors estimated using GIS including roadway density, roadway
4 length, average daily traffic, and population density to determine which variables were
5 significant predictors. They found that point estimates of PM_{2.5} were largely influenced by
6 regional ambient PM_{2.5} while EC estimates were more influenced by local traffic sources.
7 However, Baxter et al. (2008, [191194](#)) found no association between distance to a bridge toll
8 booth station and indoor EC concentration in Detroit homes when studying the impact of
9 diesel emissions from traffic on the Ambassador Bridge as part of the Detroit Exposure and
10 Aerosol Research Study (DEARS). Being located downwind of the booth, however, was a
11 significant predictor of indoor EC concentration. Corburn (2007, [155738](#)) tested two distinct
12 modeling approaches, the cumulative air toxics surface (CATS) and the U.S. EPA's National
13 Air Toxics Assessment (NATA) to determine how these approaches can yield estimates of
14 human exposure to diesel exhaust and 33 air toxics for environmental impact assessment.
15 The CATS approach included an exposure term incorporating source density and distance
16 to source, and the sources could include traffic as well as bus depots and transfer stations,
17 airports, and industrial point sources. Corburn's paper demonstrated that robust land use
18 data can provide an approximation for urban exposures, although he cautioned that such
19 estimates should not supersede environmental monitoring. In using these approaches,
20 Huang and Batterman (2000, [156572](#)) warn that geographic divisions must be sufficiently
21 small to avoid inter-zone variability in source and exposure characteristics. Moreover, the
22 HEI Report on Traffic Related Health Effects (2009, [191009](#)) discourages use of source
23 proximity as a surrogate for traffic exposure in epidemiologic studies because it is not
24 specific to particular pollutants and can be subject to confounding factors such as
25 socioeconomic status.

3.8.3. Personal and Microenvironmental Exposure Monitoring

26 The purpose of this section is to present new discoveries related to measuring aerosol
27 concentration. A review of over 200 personal and microenvironmental PM exposure studies
28 published since 2002 (see Table A-52 of Annex A) reveals that the majority of the
29 monitoring techniques in use were previously reviewed in the 2004 PM AQCD (U.S. EPA,
30 2004, [056905](#)) for PM. Detailed descriptions of these methodologies are provided in the 2004

1 PM AQCD and therefore will not be repeated in this document. The following sections will
2 include only findings from 2002 or later regarding monitoring and modeling methodologies
3 in common use and significant advancements in understanding the capabilities and
4 limitations of these methods for assessment of PM exposure.

3.8.3.1. New Developments in Personal Exposure Monitoring Techniques

5 Current personal exposure sampling methodology consists largely of integrated filter
6 sampling using a cyclone or Personal Exposure Monitor (PEM) to achieve a cut-point at a
7 desired particle size (Hopke et al., 2003, [095544](#); Larson et al., 2004, [098145](#)). This method
8 of sampling facilitates speciation work because the filters can be archived for chemical and
9 gravimetric analysis. Additionally, light scattering aerosol detection instruments, such as
10 the personal DataRam (pDR) and SidePak personal aerosol monitor have seen some use in
11 personal PM₁₀, PM_{2.5}, and PM₁ monitoring (e.g. Lewne et al., 2006, [090556](#); Wallace et al.,
12 2006, [088211](#)). Several researchers have noted that relative humidity causes overestimation
13 of the estimated particle mass in light-scattering personal exposure monitors
14 (e.g. Lowenthal et al., 1995, [045134](#); Ramachandran et al., 2003, [191197](#)); a correction factor
15 has been applied to concentrations to address this issue. In the DEARS, Williams et al.
16 (2008, [191198](#)) attempted to reduce humidity of the sample stream by placing a drying
17 column upstream of the pDR's detector. Although this addressed the humidity issue,
18 Williams et al. (2008, [191198](#)) also found that the drying column occasionally released
19 particles and therefore caused artificial concentration peaks. For this reason, Williams et
20 al. (2008, [191198](#)) determined that the humidity correction approach is preferable.

21 One area of further development is in personal sampling of the thoracic and
22 respirable particle size distribution. Variations of the cascade impactor have been developed
23 for personal sampling and tested for use in field studies (Case et al., 2008, [155149](#); Lee et
24 al., 2006, [098249](#); Singh et al., 2003, [156088](#)). The model developed and tested by Lee et al.
25 (2006, [098249](#)) operates with a 1 µm cut point and therefore can characterize respirable
26 particles well. Case et al. (2008, [155149](#)) two-stage cascade impactor separated PM_{10-2.5} from
27 PM_{2.5} for personal monitoring and sampled within ± 20% of a reference method. Hsiao et al.
28 (2009, [191001](#)) developed a mini-cyclone with a 1 µm or 0.3 µm cutpoint for sampling
29 accumulation mode and ultrafine PM. The Personal Cascade Impactor Sampler (PCIS) has
30 the capability to sample down to a cutpoint of 250 nm (Singh et al., 2003, [156088](#)). For

1 PM_{2.5}, the difference between the PCIS and MOUDI cascade impactor was 11%, while
2 difference between the PCIS and SMPS-APS was only 2%. Difference in PM_{2.5} species
3 compared with the MOUDI was generally higher: 11% for SO₄²⁻, 22% for NO₃⁻, 19% for EC,
4 and 94% for OC. Mass was overestimated by 3%, 16%, and 31% for PM_{1-0.5}, PM_{0.5-0.25}, and
5 PM_{0.25}, respectively, when compared with the SMPS-APS. Similarly, Case et al. (2008,
6 [155149](#)) found a difference ranging from -11 to +10% for PM_{10-2.5} with the Personal
7 Respirable Particulate Sampler (PRPS), and Lee et al. (2006, [098249](#)) found a difference of
8 -6 to 0% for PM_{2.5} and -6 to -1% for PM₁₀ when comparing results from this device with
9 those from the PEM. Leith et al. (2007, [098241](#)) redesigned the Wagner-Leith passive
10 sampler for measuring PM_{10-2.5}. In this work,

11 Leith et al. (2007, [098241](#)) tested the passive PM_{10-2.5} sampler and found the
12 difference between a PM_{10-2.5} FRM and the co-located passive sampler was within 1
13 standard deviation of concentrations measured by the FRM samplers.

14 A number of personal PM monitors are under development as part of the National
15 Institutes of Health Genes, Environment, and Health Initiative
16 (<http://www.gei.nih.gov/exposurebiology/program/sensor.asp>). Funded projects for
17 miniature personal monitors include a platform that records real-time BC and PM
18 concentrations and archives PM for further analysis, a badge containing a sensor array that
19 detects several compounds found in diesel PM, a micro-nephelometer recording PM and
20 endotoxin exposure, a complimentary metal-oxide-semiconductor (CMOS) fitting in the nose
21 to measure allergen PM, and a micro-thermofluidic nanoparticle sensor. The mini-cyclone
22 cited above was designed to operate upwind of the micro-thermofluidic sensor (Hsiao et al.,
23 2009, [191001](#)). LeVine et al. (1999, [156687](#)) and Schwartz et al. (2008, [156963](#)) described
24 use of the CMOS technology for real-time DNA detection. Mulchandani et al. (2001, [191003](#))
25 reviewed amperometric biosensors used for organophosphate pesticide detection that are
26 the basis of the diesel detection badge; several articles have been published by that group
27 before and after Mulchandani et al's (2001, [191003](#)) review to describe applications of
28 amperometric sensors.

3.8.3.2. New Developments in Microenvironmental Exposure Monitoring Techniques

29 The majority of developments since the 2004 PM AQCD (U.S. EPA, 2004, [056905](#))
30 regarding microenvironmental PM characterization have involved real-time

1 instrumentation in the ultrafine PM size range. Because these methods are also used for
2 ambient sampling, they are described in Section 3.4.

3 New developments in microenvironmental sampling for exposure assessment have
4 also included construction, testing, and implementation of mobile environmental sampling
5 laboratories for PM mass, particle count, and composition, as well as other criteria
6 pollutants (CO, SO₂, NO₂, O₃). These mobile laboratories typically contain a suite of
7 real-time equipment with short sampling intervals (e.g., 1-10 minutes), such as an SMPS
8 with CPC, APS, laser photometers, and aethalometers for aerosols; monitors for the gaseous
9 criteria pollutants; weather station for meteorological variables, and a Global Positioning
10 System (GPS) for position. Videotape or journal observations are sometimes logged
11 simultaneously to track local on-road sources of pollution in this way. One key application
12 of mobile laboratory technology is assessment of the outdoor microscale environments and
13 in-vehicle microenvironments on roadways for determining exposure during on-road
14 transportation (Pirjola et al., 2004, [117564](#); Weijers et al., 2004, [104186](#); Westerdahl et al.,
15 2005, [086502](#); Sabin et al., 2005, [087728](#)). For instance, Sabin et al. (2005, [087728](#)) used
16 videotape records to determine whether BC detected on a school bus was the result of local
17 outdoor sources from other vehicles or “self-pollution” from the school bus’s own engine
18 exhaust. Westerdahl et al. (2005, [086502](#)) used the GPS time series to determine that
19 minima in the ultrafine PM time series corresponded to passage through residential areas
20 of Long Beach and Pasadena, in contrast to the pollution spikes observed along highways.
21 Studies have also shown that detection of PM from vehicle exhaust could be improved
22 through use of combined measurement results to improve statistical analysis (Ntziachristos
23 and Samaras, 2006, [116722](#)).

3.8.4. Exposure Assessment Studies at Different Spatial Scales

24 A number of exposure studies have been published since 2002. Table A-55 in Annex A
25 lists those studies performed in the U.S. by region of the country with personal,
26 microenvironmental, and ambient mass concentrations presented (note that chemical
27 speciation data where available are presented and discussed below). The majority of urban-
28 scale studies focus on PM_{2.5} because PM_{2.5} concentrations are more homogeneously
29 distributed. Studies of microscale to neighborhood scale dispersion more commonly include

1 data on ultrafine and thoracic coarse PM in addition to PM_{2.5} because they travel over
2 shorter distances from the site of generation, as described in Section 3.5. Some of these
3 studies present the outdoor concentration measured outside the test building, while others
4 use ambient concentration obtained from a community site monitor. As would be expected,
5 there is considerable variability within and across regions of the country with respect to
6 indoor exposures and ambient concentrations. Furthermore, some regions are represented
7 by only one or two studies, while other regions have many studies; in most regions, studies
8 have been conducted in only one or two metropolitan areas. Thus, the results presented
9 may not be broadly representative.

10 Results of these studies highlight the uncertainties surrounding various estimates of
11 the ambient contribution to personal exposure. This variation can be attributed to a
12 number of factors, including PM size distribution, scope and magnitude of
13 microenvironmental sources, proximity to microenvironmental sources, ambient
14 concentrations of PM, percentages of time spent in various microenvironments, the age and
15 condition of indoor microenvironments, natural and urban topography, and outdoor
16 meteorology. Errors in exposure estimation are linked to the spatial scale of concentration
17 measurements because pollutant transport and dispersion varies over different spatial
18 scales as a function of the many factors mentioned in the previous sentence. Findings
19 related to identifying the ambient components of personal exposure and modes of PM
20 infiltration indoors are discussed in the subsequent subsections with respect to urban,
21 neighborhood, and micro spatial scales.

3.8.4.1. Urban Scale Ambient PM Exposure

22 The following paragraphs describe assessment of personal exposure to ambient PM at
23 the urban scale. As shown in Figure 3-93, the large majority of an individual's time is spent
24 indoors. Although calculation of infiltration and indoor personal exposure is an important
25 part of this assessment, such exposures are described with respect to central site monitors.
26 Assessing population-level exposure at the urban scale is particularly relevant for
27 epidemiologic studies, which typically provide information on the relationship between
28 health effects and community-average exposure, rather than individual exposure.

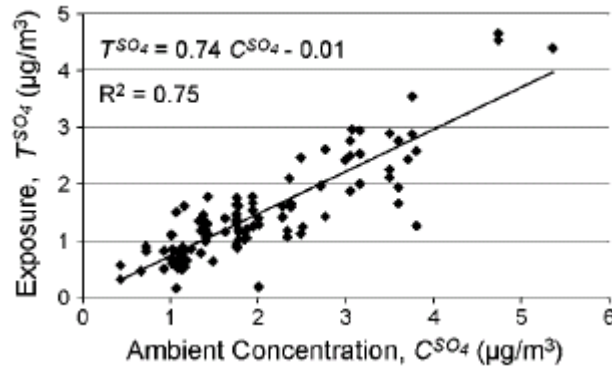
29 In the context of determining the effects of ambient pollutants on human health, the
30 association between E_a and C_a is more relevant than the association between E_T (which

1 includes both the ambient and nonambient component of PM exposure) and C_a . If there are
2 no indoor or other nonambient sources of a pollutant, the total personal exposure is equal to
3 the ambient personal exposure. However, indoor or other nonambient sources could
4 significantly affect a person's total exposure to many pollutants. Wilson and Brauer (2006,
5 [088933](#)) noted that exposure to nonambient PM will not affect the relationship between C_a
6 and E_a , but "the difference between ambient concentration and ambient exposure will bias
7 the relative risk derived from epidemiologic studies."

8 Some studies have used PM components to estimate the infiltration of ambient PM to
9 indoor environments. Wilson et al. (2000, [010288](#)) first proposed that SO_4^{2-} could be used as
10 a tracer of the ambient $\text{PM}_{2.5}$ infiltration rate. Sarnat et al. (2002, [037056](#)) also noted that it
11 is reasonable to assume that the size distribution of ambient SO_4^{2-} particles is sufficiently
12 similar to the size distribution of ambient $\text{PM}_{2.5}$, and therefore that the ambient SO_4^{2-} to
13 personal SO_4^{2-} ratio is an acceptable surrogate for the ratio of the ambient $\text{PM}_{2.5}$ exposure
14 to the ambient $\text{PM}_{2.5}$ concentration. Sulfate has been used this way in several studies,
15 including Ebel et al. (2005, [056907](#)), Wallace and Williams (2005, [057485](#); 2006, [089190](#))
16 and Wilson and Brauer (2006, [088933](#)). For this method to be successful, indoor or other
17 nonambient sources of the tracer must be small compared to ambient sources over the
18 period of sampling. Wilson and Brauer (2006, [088933](#)) noted that environmental tobacco
19 smoke and tap water used in showers or humidifiers are indoor sources of SO_4^{2-} . Other
20 concerns in using SO_4^{2-} as a tracer for $\text{PM}_{2.5}$ arise because SO_4^{2-} tends to be concentrated in
21 smaller particles and thus it might be a better tracer for fine mode particles than for total
22 $\text{PM}_{2.5}$, which can include larger particles in the tail end of the coarse mode (Wallace and
23 Williams, 2005, [057485](#)). Strand et al. (2006, [157017](#)) suggested that Fe be used as an
24 additional tracer to correct for the infiltration of larger $\text{PM}_{2.5}$ particles. Their study took
25 place in Denver, where indoor sources of Fe were small. However, there could be more
26 substantial contributions from tracking iron in soil indoors in other locations. The spatial
27 variability of Fe is also larger than that of $\text{PM}_{2.5}$ across urban areas. Volatilization of nitrate
28 or organic compounds after infiltration of $\text{PM}_{2.5}$ indoors could lead to bias in exposure
29 estimates (Lunden et al., 2003, [081201](#)). This could be a large problem in areas in which
30 PM contains a large semi-volatile component.

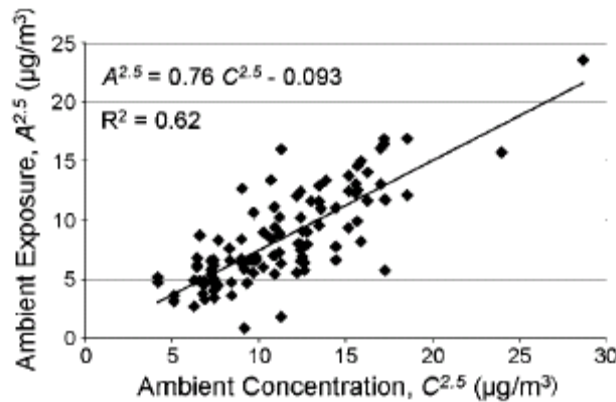
31 Figure 3-94 shows total exposure to SO_4^{2-} as a function of measured ambient SO_4^{2-}
32 concentration. Figure 3-95 shows estimated ambient exposure to $\text{PM}_{2.5}$ as a function of
33 measured ambient $\text{PM}_{2.5}$ concentration, where ambient personal exposure is calculated

1 from the ambient exposure factor for SO_4^{2-} . Close agreement between these figures can be
 2 observed. Figure 3-96 shows total exposure to $\text{PM}_{2.5}$ as a function of measured ambient
 3 $\text{PM}_{2.5}$ concentration. However, the total exposure to $\text{PM}_{2.5}$ shows virtually no association
 4 with ambient $\text{PM}_{2.5}$ because it contains nonambient contributions to $\text{PM}_{2.5}$.



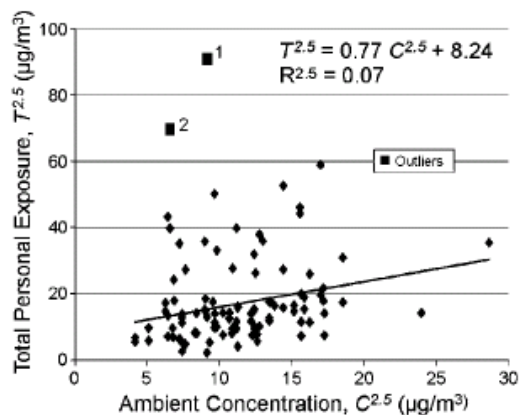
Source: Wilson and Brauer (2006, [088933](#))

Figure 3-94. Total exposure to SO_4^{2-} as a function of measured ambient SO_4^{2-} concentration, from the Vancouver study (Vancouver British Columbia, April-September 1998, with 16 non-smoking subjects aged 54-86).



Source: Wilson and Brauer (2006, [088933](#))

Figure 3-95. Estimated ambient exposure to $\text{PM}_{2.5}$ as a function of measured ambient $\text{PM}_{2.5}$ concentration, from the Vancouver study (Vancouver British Columbia, April-September 1998, with 16 non-smoking subjects aged 54-86).



Source: Wilson and Brauer (2006, [088933](#))

Figure 3-96. Total exposure to PM_{2.5} as a function of measured ambient PM_{2.5} concentration.

1 The estimated ambient exposure to PM_{2.5} is well correlated with measured ambient
 2 PM_{2.5} concentration with zero intercept implying that nonambient sources were minor. This
 3 technique works well in areas where sulfate is a regional pollutant insuring that its spatial
 4 variations are small (Kim et al., 2005, [156640](#); U.S. EPA, 2004, [056905](#)). Wilson and Brauer
 5 (2006, [088933](#)) reported that the pooled Pearson correlation coefficient was 0.79 for
 6 personal ambient exposures (estimated by tracer element method) versus ambient
 7 concentrations, and was 0.001 for personal nonambient exposure vs. ambient
 8 concentrations. Strand et al. (2007, [157018](#)) conducted an exposure study in Denver (from
 9 2002 to 2004) for 6-12-year-old school children. Up to 10 personal exposure samples were
 10 collected on each day, and ambient concentrations were measured simultaneously at a fixed
 11 site located at the school. The daily average personal sulfate exposure was strongly
 12 associated with ambient sulfate concentration ($r = 0.96$, $120 > N > 100$). Koutrakis et al.
 13 (2005, [095800](#)) reported the median Spearman correlation coefficients between personal
 14 sulfate exposure and ambient sulfate concentration were above 0.60 during both winter and
 15 summer in Boston and Baltimore (15 subjects with 12 consecutive measurements during
 16 each season in both Boston and Baltimore). For another Baltimore cohort (15 senior
 17 subjects with up to 23 consecutive measurements for each person), Hopke et al. (2003,
 18 [095544](#)) reported that the median Pearson correlation coefficient between personal
 19 exposure to sulfate factor and ambient sulfate factor was 0.91 (ranging from 0.56 to 0.95 for
 20 different subjects), while the median Pearson correlation coefficients were 0.34 for the
 21 crustal factor (ranging from -0.05 to 0.62), and 0.31 for a factor whose origin was not

1 identified (ranging from -0.01 to 0.88), respectively. The inferences drawn from using the
2 SO_4^{2-} component of $\text{PM}_{2.5}$ as an indicator for personal exposure to ambient $\text{PM}_{2.5}$ may apply
3 in areas where SO_4^{2-} is a minor component of $\text{PM}_{2.5}$ or in the absence of significant
4 nonambient sources of SO_4^{2-} (Sarnat et al., 2001, [019401](#)).

5 Source apportionment techniques could also be used, in principle, to derive ambient
6 personal $\text{PM}_{2.5}$ concentrations. They would be especially useful in areas where the
7 application of a tracer method might be problematic. Strand et al. (2007, [157018](#)) noted that
8 the four outdoor factors (nitrate-sulfate, sulfate, OC, motor vehicle exhaust) would
9 constitute an estimate of the personal ambient $\text{PM}_{2.5}$ concentration. However, the data used
10 in this portion of the analysis were obtained only with fixed monitors and did not include
11 measurements made by PEMs. They also used the Multilinear Engine (ME) to derive
12 factors that were required to contribute jointly to central indoor and outdoor, individual
13 apartment and individual PEM samples of a panel of residents. Hopke et al. (2003, [095544](#))
14 used PMF to derive source contributions to community, outdoor, and indoor PM exposures
15 at a retirement facility in Towson, MD. Hopke et al. (2003, [095544](#)) found three sources:
16 sulfate, unknown (perhaps combustion related, according to the authors) and soil, jointly
17 contributing 46%, 13% and 4% of $\text{PM}_{2.5}$ to the PEM samples. Further source resolution was
18 not possible because of a lack of data for a number of components in the PEM samples. The
19 largest and most clearly identified contribution to personal exposure was from the sulfate
20 factor. This study also determined that a few minor indoor and personal activity sources
21 contributed <10% of the ambient sulfate source to personal exposures.

22 Wilson and Brauer (2006, [088933](#)) presented an adaptation of the SO_4^{2-} method for
23 estimating exposure to $\text{PM}_{10-2.5}$. α is computed based on the SO_4^{2-} method as the ratio of
24 exposure to ambient SO_4^{2-} , as measured by a personal monitor, to ambient SO_4^{2-}
25 concentration. Then, knowing an individual subjects' time diary and the penetration and
26 loss properties of SO_4^{2-} , the air exchange rate for an individual location can be calculated
27 from Equations 3-5 and 3-7. Finally, the penetration and loss rates of $\text{PM}_{10-2.5}$ from the
28 PTEAM database (Ozkaynak et al., 1996, [073986](#)) can be input into the individual exposure
29 model along with the individual activity pattern and residential air exchange rate to
30 compute the ambient $\text{PM}_{10-2.5}$ exposure factor and ambient $\text{PM}_{10-2.5}$ exposure knowing PM_{10-}
31 $_{2.5}$ concentration. Given that $\text{PM}_{10-2.5}$ deposits more readily and therefore disperses over a
32 shorter distance than $\text{PM}_{2.5}$, it is possible that use of ambient $\text{PM}_{10-2.5}$ concentration may
33 incur more error than in using this method for $\text{PM}_{2.5}$. Ebel et al. (2005, [056907](#)) observed in

1 a Vancouver, Canada panel study that ambient PM_{10-2.5} exposure was less correlated with
2 ambient PM₁₀ exposure ($r = 0.72$) than was ambient PM_{2.5} ($r = 0.92$) exposure. In this study,
3 PM_{10-2.5} mass concentration was calculated from the difference between ambient PM₁₀ and
4 PM_{2.5} mass concentration. This is attributed to both a smaller F_{inf} for PM_{10-2.5} and PM_{2.5}
5 comprising a greater fraction of the PM₁₀ for the Vancouver study.

6 Wilson and Brauer (2006, [088933](#)) state that their methodology for computing the
7 ambient exposure factor based on the PM_{2.5} sulfate method can be applied to PM in the
8 0.1-0.5 μm size range. Little SO₄²⁻ mass is found below 0.1 μm , so the sulfate tracer method
9 would not be applicable for ultrafine PM. Given the short atmospheric lifetime of ultrafine
10 PM resulting from particle growth and evaporation processes, primary ultrafine PM is most
11 prevalent at microscale rather than urban scale (Sioutas et al., 2005, [088428](#)). Moore et al.
12 (2009, [191004](#)) found substantial spatial, hourly, and daily variability in ultrafine PM
13 concentration in a saturation study of Los Angeles. Moore et al. (2009, [191004](#)) and
14 Harrison and Jones (2005, [191005](#)) also found that ultrafine PM and PM_{2.5} measurements
15 were poorly correlated at the monitoring sites.

3.8.4.2. Micro-to-Neighborhood Scale Ambient PM Exposure

Near-Road Exposures

16 Sections 3.3 and 3.5 describe the physical and chemical composition of traffic
17 emissions as well as evolution of the plume away from roads. Table 3-24 contains data from
18 recent studies comparing outdoor personal exposure to fixed site monitors. Only studies
19 where samples were obtained outdoors and compared with a community-based ambient
20 monitoring site were included because indoor microenvironments have penetration losses
21 that impact the comparability of the results. Note that some of these studies included
22 enclosed transportation microenvironments (e.g., cars, buses, subways), but all studies
23 examined personal exposure in the outdoor microscale environment. Also note that studies
24 must be reviewed cautiously because most used different instrumentation for personal,
25 microenvironmental, and ambient measurements so that measurement artifacts related to
26 each instrument may differ. The Violante et al. (2006, [156140](#)) study showed that outdoor
27 personal exposure to PM₁₀ was significantly higher than fixed community-based ambient
28 monitoring site measurements in downtown Bologna, Italy. Likewise, the Kaur et al. (2005,
29 [088175](#)), Kaur et al. (2005, [086504](#)), and Adams et al. (2001, [019350](#)) studies showed PM_{2.5}

1 measurements to be significantly higher than fixed community-based ambient monitoring
2 site measurements in central London, U.K. However, Kinney et al. (2000, [001774](#)) showed
3 that on-street PM_{2.5} concentrations were not significantly different from ambient PM_{2.5}
4 measurements in a study of PM_{2.5} exposure in New York City; this is more consistent with
5 the urban-scale homogeneity in concentration of PM_{2.5}.

6 Morwaska et al. (2008, [191006](#)) stated that ultrafine PM number concentrations in
7 the near-road environment were roughly 18 times higher than in a non-urban background
8 environment, while measured concentrations in street canyons and tunnels were 27 and 64
9 times higher, respectively than background. This suggests that trapping of sources in a
10 semi-enclosed environment can lead to higher ultrafine PM exposures. Additionally, fresh
11 emission of short-lived ultrafine PM would explain substantially higher concentrations near
12 the site of emission. By sampling ultrafine PM count at multiple sites in Los Angeles,
13 Moore et al. (2009, [191004](#)) demonstrated five-to-seven-fold difference between
14 concentrations measured directly next to a freeway and an oceanside site during morning
15 rush hour with substantial variability among sites throughout the day. When comparing
16 sampling campaign data on clear weather and rainy days next to the I-710 freeway in Los
17 Angeles, Ntziachristos et al. (2007, [089164](#)) found that particle number concentration
18 obtained with an CPC was 2.4 times higher on clear weather than when raining; particle
19 surface area was 3.7 times higher in clear weather; and, black carbon concentration was 1.7
20 times higher in clear weather. However, SMPS data reported for rainy day particle number
21 concentrations were almost 29 times higher in this study. Likewise, Zhou and Levy (2007,
22 [098633](#)) noted in a meta-analysis of near-road studies that the zone of influence of the near-
23 road environment was generally within 300-400 m for EC and ultrafine PM counts. Kinney
24 et al. (2000, [001774](#)) showed EC to increase linearly with increasing traffic counts with
25 large spatial variations where two sites had concentrations significantly higher than
26 ambient measurements. These observations suggest caution should be taken regarding the
27 representativeness of community averaged monitoring data for assessing exposures.

28 Particle chemistry is also an important consideration, because exposure may differ for
29 PM components. Farmer et al. (2003, [156431](#)) found that exposure to particle-bound PAHs
30 including benzo[a]pyrene can be 2-3 times higher among those routinely exposed to outdoor
31 traffic emissions (e.g., police, bus drivers) compared with control subjects. Kinsey et al.
32 (2007, [190073](#)) estimated from continuous idling and restart school bus operating
33 conditions (without retrofitting) that over a 10-min period of waiting at a bus stop,

1 continuous idling resulted in exposure to 33% more particle-bound PAH than in the case
 2 where the bus was restarted 2 min into the simulation and idled for 8 min. Continuous
 3 idling produced 3380% more particle-bound PAH than the case where the bus was off for 10
 4 min then restarted and left at the end of the simulation.

Table 3-24. Examples of studies comparing near-road personal exposures with fixed site ambient concentrations.

Reference	Ambient monitors	Personal monitors	Microenvironment, other variables	Ambient v. Personal Association	Primary Findings																					
Violante et al. (2006, 156140) Bologna, Italy	Fixed PM ₁₀ and benzene monitoring station (method not specified).	Active pump with PM ₁₀ PEM, passive sample for benzene desorbed and analyzed by GC-MS.	Localized traffic density (vehicles/h); Meteorology (wind speed, wind direction, visibility, relative humidity).	Personal: 185.10 ± 38.52 μg/m ³ Fixed: 43.56 ± 24.10 μg/m ³ (p < 0.0001); small but significant correlation observed (R ² = 0.19, p = 0.035) but disappeared after outlier removal (R ² = 0.09, p = 0.165).	Fixed PM ₁₀ correlated with multivariate model of traffic and meteorology but not personal PM ₁₀ ; relationship between benzene and PM ₁₀ not explored.																					
Kaur et al. (2005, 086504) London, U.K.	Fixed TEOM for PM _{2.5} and fixed CO monitor at ambient and curbside sites.	High flow personal samplers for PM _{2.5} , P-Trak monitors for UFP, Langan T15 and T15v for CO.	Exposures stratified by mode of transport (walk, cycle, bus, car, taxi).	Average PM _{2.5} at TEOMS was 3 times lower than average personal PM _{2.5} sample, and 8 times lower than max personal PM _{2.5} sample.	PM _{2.5} exposures during walking significantly lower than during car and taxi rides, UFP exposures during walking significantly lower than bus and car rides, cycling exposures to PM _{2.5} and UFP not significantly different from those on bus, car, or taxi.																					
Kaur et al. (2005, 088175) London, U.K.	Fixed TEOM for PM _{2.5} and fixed CO monitor at ambient and curbside sites.	High flow personal samplers for PM _{2.5} analyzed post-sample for reflectance for EC, P-Trak monitors for UFP, Langan T15 and T15v for CO.	Volunteers walking at set times and directions along Marylborne Rd in London.	Fixed vs. personal PM _{2.5} : slope = 0.29, R = 0.6; personal PM _{2.5} measurements were > 2 times background levels and more than 15 μg/m ³ greater than curbside measurements.	Pedestrian exposures were significantly higher than fixed site curbside (or ambient) measurements. Results indicate that exposure decline up to 10% from curb-side to building edge within a street canyon.																					
Adams et al. (2001, 019350) London, U.K.	Fixed TEOM for PM _{2.5} and fixed CO monitor at ambient and curbside sites.	High flow personal samplers for PM _{2.5} .	Exposures stratified by mode of transport (cycle, bus, car, subway).	Median values: (μg/m ³) <table border="1" style="margin-left: auto; margin-right: auto;"> <tr> <td></td> <td>Summer</td> <td>Winter</td> </tr> <tr> <td>Cycle</td> <td>34.5</td> <td>23.5</td> </tr> <tr> <td>Bus</td> <td>39.0</td> <td>38.9</td> </tr> <tr> <td>Car</td> <td>37.7</td> <td>33.7</td> </tr> <tr> <td>Subway</td> <td>247.2</td> <td>157.3</td> </tr> <tr> <td>Fixed15</td> <td>13</td> <td></td> </tr> <tr> <td>Curb</td> <td>24</td> <td>37</td> </tr> </table>		Summer	Winter	Cycle	34.5	23.5	Bus	39.0	38.9	Car	37.7	33.7	Subway	247.2	157.3	Fixed15	13		Curb	24	37	Exposures were 2.3-16.5 times higher than ambient and 1.4-10.3 times higher than curbside during summer. During winter, only subway exposures were appreciably higher (4.3 times) than curbside.
	Summer	Winter																								
Cycle	34.5	23.5																								
Bus	39.0	38.9																								
Car	37.7	33.7																								
Subway	247.2	157.3																								
Fixed15	13																									
Curb	24	37																								
Kinney et al. (2000, 001774) New York City, NY (Harlem)	Ambient site filter in greased impactor with pump; absorbance testing on filter for EC.	Three high traffic sites filter in greased impactor with pump; absorbance testing on filter for EC.	Traffic counts per h.	Mean values: (μg/m ³) <table border="1" style="margin-left: auto; margin-right: auto;"> <tr> <td></td> <td>PM_{2.5}</td> <td>EC</td> </tr> <tr> <td>Site 1</td> <td>45.7 (10.1)</td> <td>6.2 (1.9)</td> </tr> <tr> <td>Site 2</td> <td>47.1 (16.4)</td> <td>3.7 (0.6)</td> </tr> <tr> <td>Site 3</td> <td>36.6 (10.8)</td> <td>2.3 (0.9)</td> </tr> <tr> <td>Ambient</td> <td>38.7 (10.9)</td> <td>1.5 (0.5)</td> </tr> </table>		PM _{2.5}	EC	Site 1	45.7 (10.1)	6.2 (1.9)	Site 2	47.1 (16.4)	3.7 (0.6)	Site 3	36.6 (10.8)	2.3 (0.9)	Ambient	38.7 (10.9)	1.5 (0.5)	PM _{2.5} at high traffic sites was not significantly higher than ambient; EC was significantly higher than ambient at 2 sites. EC increased linearly with traffic counts.						
	PM _{2.5}	EC																								
Site 1	45.7 (10.1)	6.2 (1.9)																								
Site 2	47.1 (16.4)	3.7 (0.6)																								
Site 3	36.6 (10.8)	2.3 (0.9)																								
Ambient	38.7 (10.9)	1.5 (0.5)																								

In-Vehicle and In-Transit Exposures

5 In-vehicle pollution has been identified in various studies as a source of exposure to
 6 PM₁₀, PM_{2.5}, and ultrafine PM (Briggs et al., 2008, [156294](#); Diapouli et al., 2007, [156397](#);
 7 Fruin et al., 2008, [097183](#); Gomez-Perales et al., 2004, [054418](#); Gomez-Perales et al., 2007,

1 [138816](#); Gulliver and Briggs, 2004, [053238](#); Gulliver and Briggs, 2007, [155814](#); Rossner et
2 al., 2008, [156927](#); Sabin et al., 2005, [088300](#)). Results from recent studies are provided in
3 Table A-54 of Annex A. In many of these studies, in-vehicle exposures are shown to be
4 comparable or less than that of walkers on the same route. Typically, in-vehicle exposures
5 were still higher than community-based ambient monitor concentrations for TSP and PM₁₀
6 (Diapouli et al., 2008, [190119](#)). Curbside measurements of ultrafine PM and PM_{2.5} obtained
7 at a fixed site in the Kaur et al. (2005, [088175](#); 2005, [086504](#)) studies were generally lower
8 than exposures during transit (including during walking and cycling), but in the Adams et
9 al. (1987, [019356](#)) study PM_{2.5} exposures were higher than curbside during the summer and
10 lower than curbside during the winter. As particle size decreased to the fine and ultrafine
11 range, less difference between in-vehicle and ambient concentrations was observed for PM
12 mass or count, with the exception of the Diapouli et al. (2008, [190119](#)) study where in-bus
13 ultrafine PM concentrations were several times higher than indoor or outdoor residential
14 and school concentrations.

15 Fruin et al. (2008, [097183](#)) and Westerdahl et al. (2005, [086502](#)) observed that
16 in-vehicle ultrafine PM concentrations increased for freeways in comparison with arterial
17 roads. They estimated that 36% of exposure to ultrafine PM occurred during a total daily
18 commuting time of 1.5 hours (6% of the day); 22% of total exposure occurred during 0.5
19 hours spent on freeways. Gong et al. (2009, [190124](#)) demonstrated that ultrafine PM
20 deposition rate increased with decreasing particle size (down to ~30 nm) and increasing
21 surface area inside the vehicle, where deposited PM on the seats and dashboard can be
22 resuspended and then inhaled or ingested. Ultrafine PM deposition also rose slightly with
23 increased number of passengers. Zhu et al. (2007, [179919](#)) found that in-vehicle ultrafine
24 PM counts were 85% lower than outdoors when the fan was operating and recirculation was
25 on. They estimated that a 1-h commute (4% of the day) accounts for 10-50% of daily
26 exposure to ultrafine PM generated by traffic. Based on the American Time Use Survey
27 estimation of 70.2 minutes spent in vehicles each day (U.S. Bureau of Labor Statistics
28 <http://www.bls.gov/tus/>), cumulative in-vehicle exposure can be found that PM_{2.5} on school
29 buses was two times higher than on-road levels and four times higher than central site
30 measurements. Sabin et al. (2005, [087728](#)) demonstrated for school buses that emissions
31 control technologies had a significant impact on in-bus concentrations of black carbon mass,
32 and Hammond et al. (2007, [190135](#)) demonstrated significant reductions of particle number
33 concentration measured for 0.02-1 µm particles when comparing buses using clean diesel or

1 retrofits compared with non-retrofitted buses. Although not tested here for other vehicle
2 types with respect to PM, these findings suggest that a portion of in-vehicle concentrations
3 are due to self-pollution, defined by Behrentz et al. (2004, [155682](#)) as the fraction of a
4 vehicle's own exhaust entering the vehicle microenvironment. Behrentz et al. (2004,
5 [155682](#)) tested self-pollution with school buses using SF₆ tracer gas and demonstrated that
6 0.3% of in-vehicle air comes from self-pollution, and that this number was roughly ten times
7 greater than in-vehicle concentrations related to self-pollution on newer buses. The
8 Behrentz et al. (2004, [155682](#)) study also measured EC and particle-bound PAH and found
9 that 25% of the variability in EC concentration was related to self-pollution. Adar et al.
10 (2008, [191200](#)) estimated that 7 µg/m³ of PM_{2.5} mass on school buses was from self-
11 pollution. These findings are important for exposure estimation when partitioning local and
12 ambient sources of pollution during transport in vehicles.

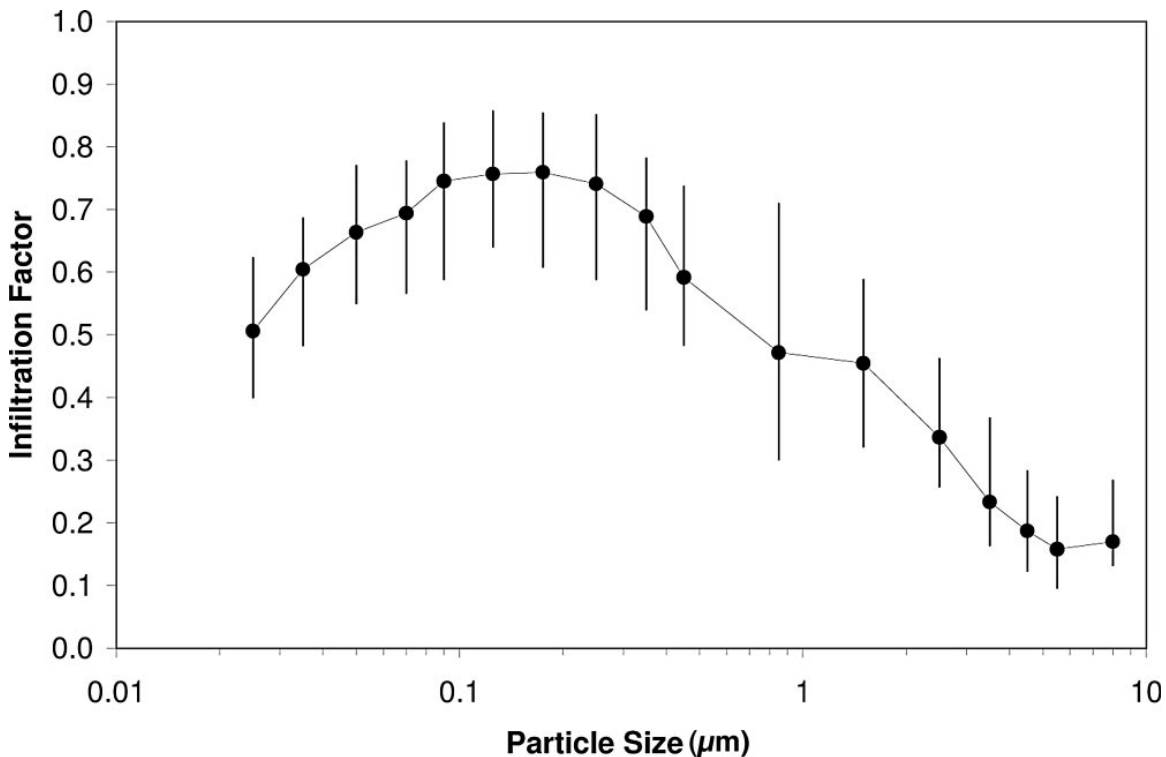
3.8.4.3. Indoor Exposure to Ambient: Infiltration and Differential Infiltration

13 F_{inf} varies substantially given a vast array of conditions, and it can best be modeled
14 dynamically based on a distribution of air exchange and deposition or other ultrafine,
15 accumulation mode, fine, and coarse PM loss rates rather than a single value (Bennett and
16 Koutrakis, 2006, [089184](#); Wallace et al., 2006, [089190](#)). Given that air exchange rates
17 within a building vary as a function of ambient temperature and pressure, F_{inf} is subject to
18 seasonal and regional changes (Meng et al., 2005, [058595](#); Sarnat et al., 2006, [089166](#);
19 Wallace and Williams, 2005, [057485](#)). These factors make F_{inf} a more accurate descriptor of
20 infiltration than a simple I/O ratio because the I/O ratio also includes contributions from
21 indoor sources in addition to PM that infiltrates from outdoors. Wallace et al. (2006,
22 [089190](#)) identified several significant factors affecting F_{inf} , including window opening, age of
23 an indoor microenvironment, number of occupants, location on a dirt road, dryer usage, and
24 air conditioning usage). This complex term becomes even more complicated when one
25 considers transformation of the size distribution and chemical composition of the PM
26 through chemical reactions on the particle surface, agglomeration, growth, and evaporation
27 given that F_{inf} depends on particle size (Keller and Siegmann, 2001, [025881](#)). F_{inf} for PM is
28 influenced by physical mechanisms, such as Brownian diffusion, thermophoresis, and
29 impaction, all of which are functions of particle size (Bennett and Koutrakis, 2006, [089184](#);
30 Tung et al., 1999, [049003](#)). These differential effects are summarized below. Recent studies

1 on infiltration are summarized in Table A-58 of Annex A. F_{inf} and I/O are listed where
2 available, although it is recognized that I/O is not as meaningful a descriptor but provides
3 an approximation of F_{inf} .

4 A number of studies have examined the impact of season on PM infiltration. Season is
5 important because it impacts the ventilation practices used (e.g., open windows, air
6 conditioning or heating use) and the ambient temperature and humidity conditions affect
7 the transport, dispersion, and size distribution of the PM. Pandian et al. (1998, [090552](#))
8 found that residential air exchange rates vary by season as: summer > spring > winter
9 > fall with summer air exchange roughly 1.5-2 times greater than average air exchange
10 rate for the entire year because the rates are driven by home air conditioning and heating
11 usage. Allen (2003, [053578](#)) gave information on the range and distribution of F_{inf} at 44
12 residences in Seattle. The mean F_{inf} (\pm SD) measured by light scattering for all sampling
13 days was 0.65 ± 0.21 . Differences in infiltration were observed for the heating season
14 (0.53 ± 0.16), when windows would be expected to be closed, versus non-heating season
15 (0.79 ± 0.18). Residences with open windows had a mean F_{inf} of 0.69 vs. 0.58 for residences
16 with closed windows. The authors combined the light scattering results with indoor and
17 outdoor sulfur measurements to estimate that $79 \pm 17\%$ of indoor $PM_{2.5}$ was generated
18 outdoors. This study provides important data on the distribution of residential F_{inf} values
19 and illustrates the magnitude of the effect of season and window position on infiltration
20 rates. Barn et al. (2008, [156252](#)) and Baxter et al. (2007, [092725](#)) both also noted that
21 window opening was an important variable. Barn et al. (2008, [156252](#)) found F_{inf} of
22 0.61 ± 0.27 for 13 homes during summer and 0.27 ± 0.18 for 19 homes during winter in
23 Canada. Likewise, location could impact residential ventilation practices and infiltration.
24 Cohen et al. (2009, [190639](#)) noted differences in median infiltration among eight areas
25 (among this eight were three comprising the Los Angeles region and two comprising the
26 New York City region). Indoor-outdoor SO_4^{2-} ratio was noted to be highest in New York City
27 (median: 0.85) and Los Angeles (median: 0.84) and lowest in St. Paul (median: 0.54).
28 Pandian et al. (1998, [090552](#)) observed that residential air exchange rates vary by region
29 as: southwest > southeast > northeast > northwest, which reflects regional use of air
30 conditioning. Sarnat et al. (2006, [089166](#)) noted differences in infiltration between coastal
31 and inland residences, although variability in these datasets made the differences not
32 statistically significant.

1 Differential infiltration as a function of particle size has been observed to occur.
2 Infiltration factors for particle diameters ranging from 20 nm to 10 μm were reported in
3 Boston by Long et al. (2001, [011526](#)) during summer and fall for nighttime periods, when
4 personal activity patterns would be less likely to generate indoor PM. The maximum
5 infiltration factor was reported for particles between 80 and 500 nm to range from 0.8-1.0.
6 Summer values were uniformly higher than fall values, consistent with higher observed air
7 exchange rates. The infiltration factor decreased with size above 500 nm, reaching 0.1-0.2
8 for 6-10 μm diameter particles. Particles smaller than 80 nm also were reported to have
9 lower infiltration factors. This demonstrates the size dependence of PM infiltration, which
10 has been further studied by recent investigators. Sarnat et al. (2006, [089166](#)) examined
11 infiltration as a function of particle size and found that F_{inf} varies by particle diameter, as
12 measured by a SMPS-APS system to estimate particle volume. Figure 3-97 presents F_{inf}
13 values for size fractions ranging from 0.02-10 μm . The maximum infiltration factors were
14 observed around the accumulation mode (0.1-0.5 μm), with $F_{\text{inf}} = 0.7-0.8$. Reduced
15 infiltration was observed for coarse-mode particles (0.1-0.2 for $D_p = 5-10 \mu\text{m}$) and, to a
16 lesser extent, ultrafine particles (0.5-0.7 for $D_p = 0.02-0.1 \mu\text{m}$). This is consistent with
17 increased removal mechanisms for those size fractions: deposition caused by settling for
18 coarse-mode particles and diffusion for ultrafine particles; for ultrafine PM, diffusion leads
19 to deposition by agglomeration into larger particles and settling as well as losses to walls.



Source: Sarnat et al. (2006, [089166](#)).

Figure 3-97. F_{int} as a function of particle size.

3.8.5. Multicomponent and Multipollutant PM Exposures

3.8.5.1. Exposure Issues Related to PM Composition

1 Annex A presents exposure studies that include chemical speciation data in Table A-
 2 56. Some of these studies focused on SO_4^{2-} , NO_3^- or carbonaceous aerosols (EC, OC,
 3 particle-bound PAHs), while others measured concentrations of trace elements from crustal
 4 (Ca, Fe, Mn, K, Al, S, Cl in salt), mobile (Al, Ca, Fe, K, Mg, Na, Ba, Cr, Cu, Mn, Ni, Pb, S,
 5 Ti, V, and Zn), or industrial (particle-bound Hg, Cl, V, Zn, Ti, Cu, Pb) sources. A number of
 6 source apportionment studies have been performed over the last five years to determine the
 7 contribution of outdoor sources to indoor and personal PM constituents.

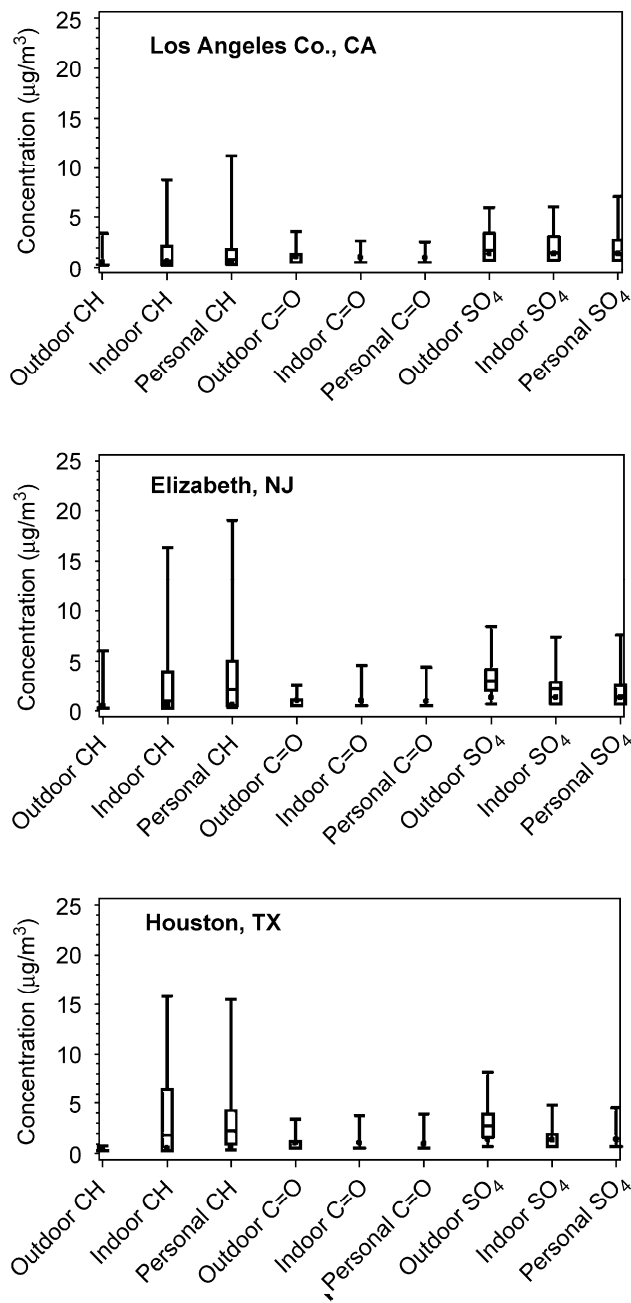
8 Several source apportionment studies by Kim et al. (2005, [156640](#)), Hopke et al.
 9 (2003, [095544](#)) and Zhao et al. (2006, [156181](#)) have shown that secondary SO_4^{2-} provides
 10 the largest ambient contribution to personal and indoor exposures. These studies took place
 11 on the east coast in Baltimore and Raleigh/Chapel Hill, NC. In Larson et al. (2004, [098145](#))
 12 source apportionment study in Seattle, vegetative burning was the most significant source

1 of outdoor origin. Zhao et al. (2007, [156182](#)) performed a source apportionment study of
2 personal exposure to PM_{2.5} among residents in Denver and also saw lower contributions
3 from secondary SO₄²⁻ in comparison with motor vehicle emissions and secondary NO₃⁻. This
4 suggests that personal exposure to SO₄²⁻ in parts of the West is lower than in the
5 Mid-Atlantic. These observations are consistent with the composition distribution shown in
6 Figures 3-17 and 3-18. Viana et al. (2008, [155269](#)) analyzed PM₁₀ and PM_{2.5} samples for
7 several species along urban-to-rural gradients centered in Valencia, Spain and found
8 gradients for both size fractions in anthropogenically-generated SO₄²⁻, OC, EC, NO₃⁻, Fe,
9 and NH₄⁺ but not in mineral species. Combined, these findings suggest urban- and regional-
10 scale variation in species composition can influence exposure estimates. Personal PM
11 exposure source apportionment studies are presented in Annex A, Table A-57.

12 Source apportionment for carbonaceous aerosols is complicated by the fact that they
13 can be derived from indoor and outdoor combustion sources. Carbonaceous aerosols are
14 difficult to trace to specific indoor and outdoor sources because combustion is widespread.
15 Sørensen et al. (2005, [089428](#)), Ho et al. (2004, [056804](#)), Larson et al. (2004, [098145](#)), and
16 Jansen et al. (2005, [082236](#)) all found that personal and microenvironmental exposure to
17 total carbon or BC was lower than that measured outdoors, while Sarnat et al. (2006,
18 [089166](#)) showed significant associations between personal and ambient measurements of
19 EC for measurements taken during the fall (slope = 0.66-0.73) and summer under high
20 ventilation conditions (slope = 0.41). Wu et al. (2006, [157156](#)), Delfino et al. (2006, [090745](#)),
21 Olson and Norris et al. (2005, [156005](#)) and Turpin et al. (2007, [157062](#)) all demonstrated
22 much higher levels of OC compared with EC in personal samples, possibly due to indoor
23 sources of OC from cooking and home heating. Reff et al. (2007, [156045](#)) and Meng et al.
24 (2007, [091197](#)) both reported findings from the Relationships between Indoor, Outdoor, and
25 Personal Air (RIOPA) study in Los Angeles, Houston, and Elizabeth, NJ. Results from Reff
26 et al. (2007, [156045](#)) are shown in Figure 3-98. These reveal significantly higher detection
27 of aliphatic C-H functional groups indoors and in personal samples compared with
28 outdoors. This information may help to distinguish carbonaceous compounds of indoor and
29 outdoor origin in future source apportionment studies of PM exposure. Little regional
30 variation in the aliphatic, carbonyl, or SO₄²⁻ groups tested were reported in this study. In
31 Meng et al. (2007, [091197](#)) indoor exposures were shown to decrease for secondary
32 formation aerosols including SO₄²⁻ but excluding NO₃⁻ (not tested) when compared with
33 outdoor concentrations, and indoor exposures to mechanically generated aerosols increased

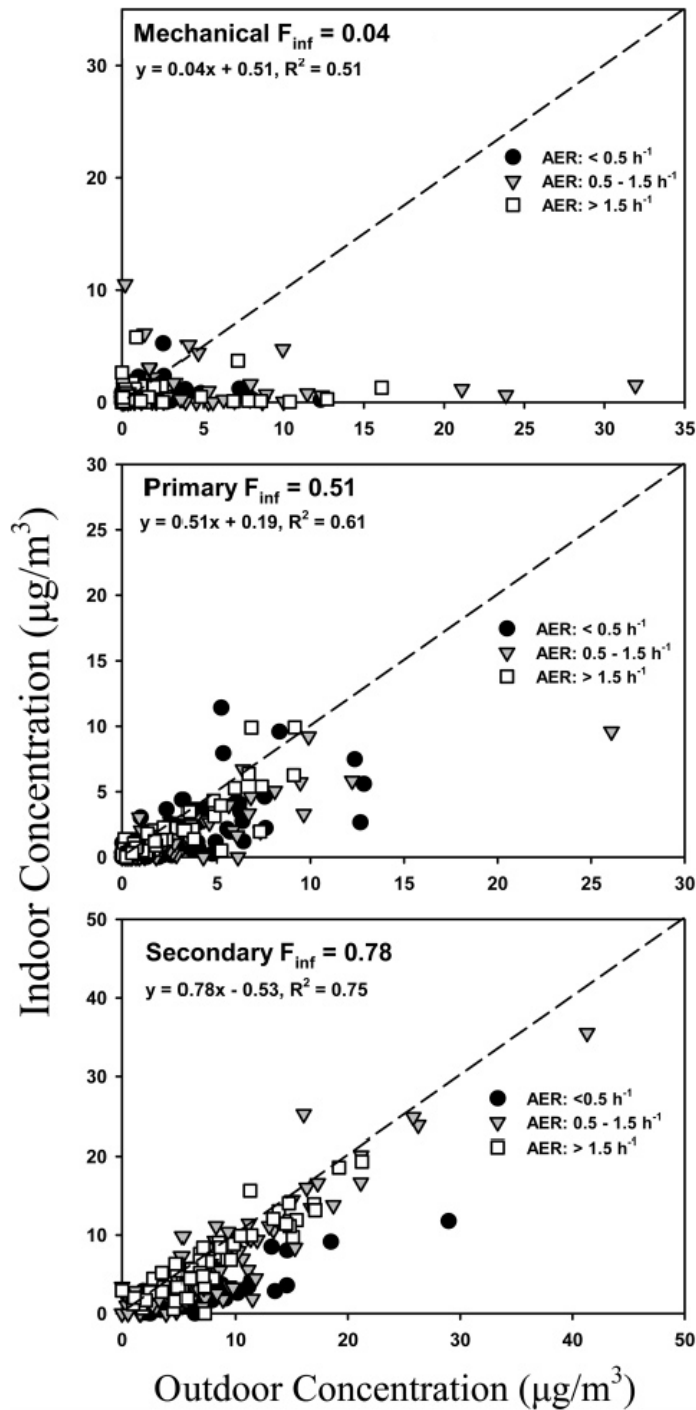
1 in comparison with outdoors. Differences in infiltration based on source category are shown
2 in Figure 3-99.

3 Trace metal studies have shown variable results regarding personal exposure to
4 ambient constituents. For instance, Molnár et al. (2006, [156773](#)) found that personal
5 exposure was higher than outdoor and ambient concentrations for mostly crustal Cl, K, Ca,
6 Ti, Fe, and Cu. However, Adgate et al. (2007, [156196](#)) found that personal exposures were
7 higher than ambient for Fe, Mg, K, Zn, Cu, Pb, and Mn but lower than ambient for Al, Na,
8 and Ti. Larson et al. (2004, [098145](#)) found that personal exposure to Ca and Cl were higher
9 than concentrations measured at ambient (central site) and residential outdoor monitors,
10 lower for Fe, K, Mn, and As and the same for Al, Br, Cr, Cu. Source apportionment for trace
11 metals can vary significantly among cities and over seasons. For instance, in a Baltimore
12 source apportionment study, exposure to Mn could be attributed nearly equally to the
13 Quebec wildfires, roadway wear, and soil, while Pb exposure was largely found to be due to
14 a local incinerator (Ogulei et al., 2006, [119973](#)). In this case, the Quebec wildfires were a
15 transient episodic source while roadway wear and incineration were continuous. However,
16 in Larson et al. (2004, [098145](#)), Mn and Pb exposures in Seattle were largely attributable to
17 mobile source and stationary source emissions. For this reason, source composition
18 behavior cannot be generalized for characterizing exposures and resulting health effects
19 across multiple locations or times.



Source: Reff et al. (2007, [156045](#))

Figure 3-98. Apportionment of aliphatic carbon, carbonyl and SO₄²⁻ components of outdoor, indoor, and personal PM_{2.5} samples, for Los Angeles (top), Elizabeth (center), and Houston (bottom).

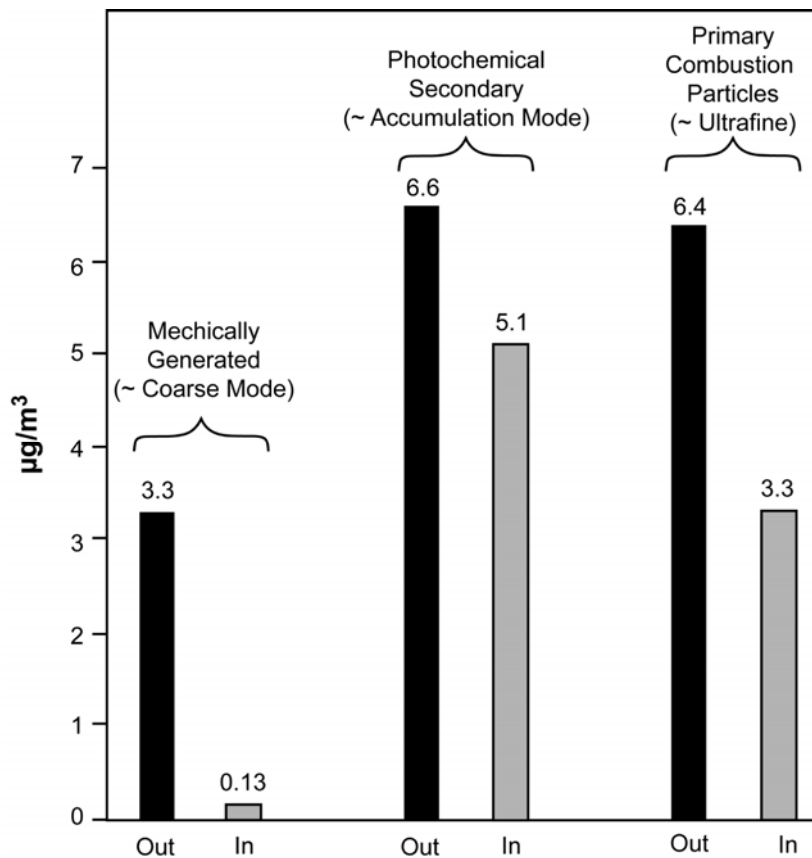


Source: Meng et al. (2007, [091197](#)).

Figure 3-99. Apportionment of infiltrated mechanically-generated (top), primary combustion (center), and secondary combustion (bottom).

- 1 A number of chemical factors influence the tendency for differential infiltration in PM.
- 2 Lunden et al. (2003, [156718](#)) studied infiltration of BC and OC aerosols and found that F_{inf}

1 can vary substantially as a function of gas transport properties within differing air
 2 exchange rates. This study and Sarnat et al. (2006, [090489](#)) also showed that BC aerosol
 3 infiltration is considerably higher than infiltration of OC, and that carbonaceous aerosol
 4 infiltration differed substantially from NO_3^- and SO_4^{2-} aerosols under the same building air
 5 exchange conditions. These differences are likely related to differences in the particle size
 6 distribution of PM components. As shown in Figure 3-100, the composition of indoor PM
 7 that has infiltrated from outdoors is different from that of outdoor PM. In this case, the
 8 particles containing photochemical products (primarily accumulation mode) have a higher
 9 infiltration rate than the larger (primarily coarse mode) mechanically generated particles
 10 or the smaller primary combustion particles (probably mostly ultrafine particles in the
 11 nucleation or Aitken nuclei mode).



Source: Meng et al. (2007, [091197](#)).

Figure 3-100. Results of the positive matrix factorization model showing differences in the mass of outdoor PM and PM that has infiltrated indoors based on source category.

12 PM species enriched in the accumulation mode, such as SO_4^{2-} , will infiltrate more
 13 efficiently than components with larger size distributions, such as iron (Strand et al., 2007,

1 [157018](#)). Lunden et al. (2008, [155949](#)) also compared I/O ratios for PM_{2.5}, total carbon in
2 PM, OC in PM, and BC in PM in an unoccupied house and found the lowest ratio for PM_{2.5}
3 (0.41 ± 0.2), the highest for BC (0.61 ± 0.2), and intermediate values for total carbon
4 (0.50 ± 0.2) and OC (0.47 ± 0.2). The authors attributed the lower PM_{2.5} I/O ratio to indoor
5 loss of NH₄NO₃ aerosol. The authors note that their BC I/O of 0.6 is somewhat lower than
6 BC ratios measured in occupied spaces (Polidori et al., 2007, [156877](#)). Conversely, indoor
7 sources in occupied residences contribute to observed OC I/O ratios greater than 1 in other
8 studies (Polidori et al., 2006, [156876](#); Sawant et al., 2008, [156949](#)). Analytical results for
9 PM_{2.5} components from the Baxter et al. (2007, [092726](#)) study found F_{inf} of 0.95 ± 0.07 for S
10 and 0.60 ± 0.04 for V, the two components identified as having no indoor sources and which
11 had I/O ratios significantly less than 1 (Baxter et al., 2007, [092726](#)). It is possible that
12 association of V with larger particles of lower penetration efficiency could contribute to a
13 lower infiltration rate. Meng et al. (2005, [058595](#)) also noted that the lack of indoor sources
14 of S and V result in much lower variability in penetration and loss rates.

15 Volatilization of PM during infiltration can cause differences between the composition
16 of indoor and outdoor PM. NO₃⁻, a prevalent PM component in the western U.S. year-round
17 and during winter throughout the mid-western and northeastern states, has a decreased
18 F_{inf} due to volatilization of NO₃⁻ indoors. Sarnat et al. (2006, [089166](#)) calculated F_{inf} values
19 for NO₃⁻, PM_{2.5}, and BC, and found the values to increase in that order. NO₃⁻ was low
20 (median = 0.18, IQR = 0.12-0.33), while BC was high (median = 0.84, IQR = 0.70-0.96); the
21 intermediate value of PM_{2.5} (median = 0.48, IQR = 0.39-0.57) reflected its composition as a
22 mixture of those two components (among others). Indoor volatilization of NO₃⁻ enriches
23 ambient PM in other components, creating differences in toxicity between indoor ambient
24 and outdoor ambient PM. The high infiltration of non-volatile BC creates additional
25 sorption sites for organics, including indoor-generated compounds. Meng et al. (2007,
26 [091197](#)) found that secondary formation accounts for 55% of indoor aerosols of outdoor
27 origin, while primary combustion accounts for 43% and mechanical generation for 2%.
28 Meng et al. (2007, [091197](#)) noted that secondary formation processes often result in more
29 accumulation mode particles so that diffusion losses are not as great as for primary
30 combustion particles, composed primarily of nucleation and condensation modes (see
31 Figure 3-97). Likewise, Polidori et al. (2007, [156877](#)) suggest that similarities in the EC and
32 OC size distributions and infiltration factors reflect low vapor pressure secondary organic
33 aerosols in the OC component. Sioutas et al. (2005, [088428](#)) suggest that volatilization of

1 ultrafine PM while crossing the building envelope may hamper infiltration in this size
2 range. Variations in the presence of outdoor PM indoors, and resulting changes in removal
3 behavior once indoors, relate to the species composition and makeup of PM.

3.8.5.2. Exposure to PM and Copollutants

4 Analysis of personal exposure to multipollutant mixtures is an area of growing
5 research. Several multipollutant studies involving ultrafine, fine, and coarse PM are
6 presented in Table A-59. Understanding the health impacts of complex multipollutant
7 mixtures, including multiple PM species, can have a substantial impact on the
8 interpretation of health effects data. Challenges are presented in accurately estimating the
9 components of a mixture, their concentrations, and personal exposure to those species.

10 One question that has been raised is whether copollutants act as confounders in PM
11 exposure assessments. Sarnat et al. (2001, [019401](#)) explored the relationship between PM
12 and copollutant gases and suggested that certain gases can serve as surrogates for
13 describing exposure to other air pollutants. Sarnat et al. (2001, [019401](#)) found significant
14 associations between personal exposure to PM_{2.5} and ambient concentrations of O₃, NO₂, CO
15 (significant only for winter), and SO₂ in a panel study conducted in Baltimore. Personal
16 exposures to PM_{2.5} and personal exposures to the gases were not correlated in this study.
17 This result may have arisen in part because personal exposures to the gases were often
18 beneath detection limits of the personal monitoring devices. Schwartz et al. (2007, [090220](#))
19 also used data from the Baltimore panel study to simulate distributions of personal
20 exposures and ambient concentrations of PM_{2.5}, PM₁₀, SO₄²⁻, NO₂, and O₃. They found that
21 personal exposure to ambient PM_{2.5} was significantly associated with ambient
22 concentrations of PM_{2.5}, NO₂, and O₃ (O₃ in an inverse relationship). They also reported that
23 personal exposure to SO₄²⁻ was significantly positively associated with ambient PM_{2.5} and
24 O₃ concentrations.

25 Seasonality of the associations could be a result of seasonal variability in
26 photochemistry, source generation, and building ventilation. Sarnat et al. (2005, [087531](#))
27 observed associations between personal PM_{2.5} and ambient O₃, NO₂, and SO₂ exposure for a
28 group of healthy senior citizens and school children in Boston for summer but not for
29 winter. In this study, significant associations between personal exposure to ambient PM_{2.5}
30 and personal O₃ exposures were observed in summer and between personal PM_{2.5} and

1 personal NO₂ in winter and summer, unlike the Baltimore study in which only summertime
2 personal PM_{2.5} and personal NO₂ were associated (Sarnat et al., 2001, [019401](#)). In their
3 study of personal exposure to ambient air pollutants in Steubenville, OH, Sarnat et al.
4 (2006, [090489](#)) found that, in the summer, low but significant associations existed for
5 ambient O₃ with personal PM_{2.5}, SO₄²⁻, and EC. In the summer, low but significant
6 associations between ambient SO₂ and personal PM_{2.5} and between ambient NO₂ and
7 personal EC were also observed. In the fall, ambient O₃ had a weak but significant
8 association with personal EC, and SO₂ had a weak but significant association with personal
9 SO₄²⁻. Ambient NO₂ was significantly associated with personal PM_{2.5}, SO₄²⁻, and EC with
10 somewhat higher coefficient of determination (R² = 0.25-0.49). There is evidence that
11 associations between ambient gases and personal exposure to PM_{2.5} of ambient origin exist
12 but are complex and vary by season and region.

3.8.6. Implications of Exposure Assessment Issues for Interpretation of Epidemiologic Studies

13 Environmental epidemiologic study designs vary by many factors, including study
14 sample size, measurement time interval, study duration, monitor type, and spatial
15 distribution of the study sample. A panel epidemiology study consists of a relatively small
16 sample (typically tens) of study participants followed over a period of days to months. Time-
17 activity diary studies are examples of panel studies (e.g. Cohen et al., 2009, [190639](#);
18 Elgethun et al., 2003, [190640](#); Johnson et al., 2000, [001660](#); Olson and Burke, 2006,
19 [189951](#)), and a microenvironmental model might be applied to represent exposure in this
20 case. Community time-series studies may involve millions of people whose exposure and
21 health status is estimated over the course of a few years using a short monitoring interval
22 (hours to days). Because so many people are involved, community-averaged concentration is
23 typically used as a surrogate for exposure in community time-series studies. Exposures and
24 health effects are spatially aggregated over the time intervals of interest because they are
25 designed to examine health effects and their potential causes at the community level
26 (e.g. Dominici et al., 2000, [005828](#); Peng et al., 2005, [087463](#)). A longitudinal cohort
27 epidemiology study typically involves hundreds or thousands of subjects followed over
28 several years or decades. Concentrations are generally aggregated over time and by
29 community to estimate exposures (e.g. Dockery et al., 1993, [044457](#); Krewski et al., 2000,

1 [012281](#)). The importance of exposure misclassification varies with study design based on
2 the spatial and temporal aspects of the design. Other factors that could influence exposure
3 estimates in PM epidemiologic studies include source characteristics, particle size
4 distribution, and particle composition. Potential issues that could influence estimates of PM
5 exposure include measurement, modeling, spatial variability, temporal variability, use of
6 surrogates for PM exposure, and compositional differences. These are described in detail in
7 the following sections.

3.8.6.1. Measurement Error

Measurement Error at Community-Based Ambient Monitors and Exposure Assessment

8 Community-based ambient monitors are employed for time-series and longitudinal
9 studies, although they can be used for panel studies as well. Section 3.4 discusses potential
10 errors in measuring ambient PM in detail. Because there will likely be some random
11 component to instrumental measurement error, the correlation of the measured PM mass
12 with the true PM mass will likely be less than 1. Sheppard et al. (2005, [079176](#)) indicate
13 that instrument error in the hourly or daily average concentrations has “the effect of
14 attenuating the estimate of α .” However, Zeger et al. (2000, [001949](#)) suggest that in order
15 for this error to cause substantial bias in later estimation of a health outcome, the
16 measurement error must be strongly correlated with the measured concentrations. Positive
17 and negative artifacts resulting from sampling volatile PM may therefore lead to lack of
18 association with health endpoints in time-series and longitudinal studies. In multicity
19 longitudinal studies, PM composition and associated artifacts may vary across cities.

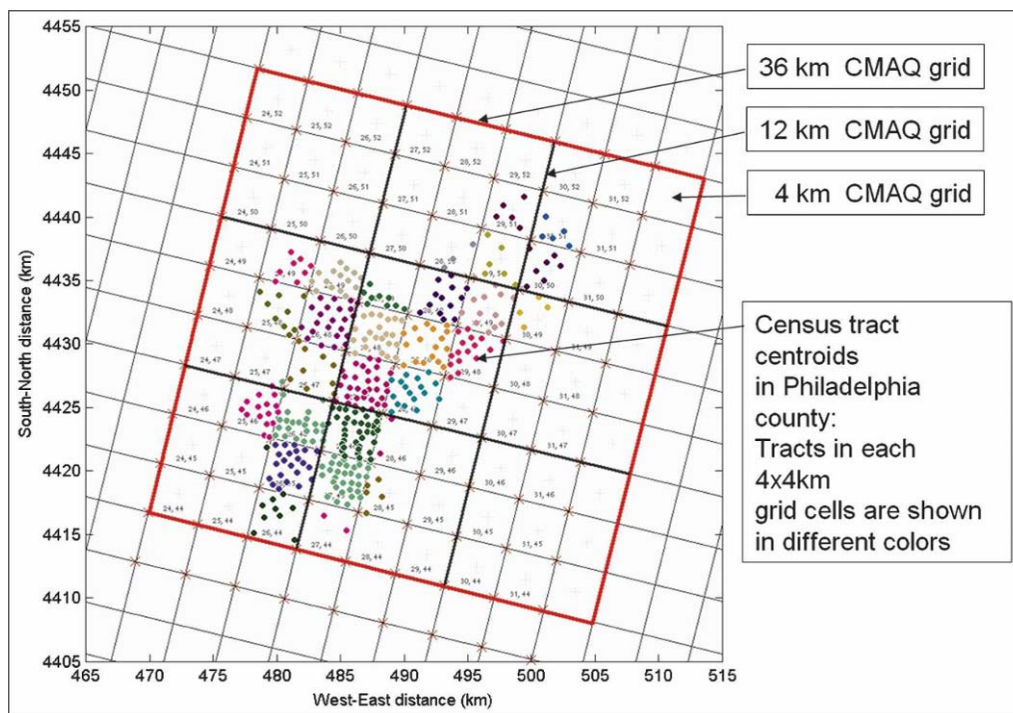
Measurement Error for Personal Exposure Monitors

20 Personal exposure monitors (PEM) are primarily used in panel exposure studies to
21 measure total exposure to PM (e.g. Cohen et al., 2009, [190639](#); Elgethun et al., 2003,
22 [190640](#); Johnson et al., 2000, [001660](#); Olson and Burke, 2006, [189951](#)). PEMs are
23 specialized monitors that, because people must carry them, have to be small, light, quiet,
24 and battery operated or passive. As a result, they may have lower face velocities across the
25 filter and pressure drops than ambient based filter measurements of PM, which typically
26 sample at much higher flow rates, and consequently at much higher face velocities. Light
27 scattering measurements are biased when relative humidity is high and are sensitive to
28 size distribution (Lowenthal et al., 1995, [045134](#); Sioutas et al., 2000, [025223](#)). Positive

1 artifacts resulting from adsorption of vapor-phase organic compounds and negative
2 artifacts from evaporation of semi-volatile PM also creates challenges for personal exposure
3 (e.g.Pang et al., 2002, [030353](#)). Olson and Norris et al. (2005, [156005](#)) attributed more OC
4 particle mass collection using PEMS than when using FRMs; this was attributed to face
5 velocity differences. Accuracy of PEMS is described in much greater detail in the 2004 PM
6 AQCD (U.S. EPA, 2004, [056905](#)). The artifacts listed here could result in either negative or
7 positive sampling bias.

3.8.6.2. Model-Related Errors

8 When models are used in lieu of or to supplement measurements of ambient PM
9 exposure or community-based ambient PM concentration, it is important to identify errors
10 and uncertainties that could affect estimates of PM-related health effects. Model-related
11 errors are determined by four factors: representativeness of the mathematical model,
12 accuracy of model inputs, scale of model resolution, and model sensitivity. If verification
13 errors related to these four factors are minimized, then the model can be evaluated against
14 physical data to determine how well the model truly captures a real situation (Roache,
15 1998, [156915](#)). Detail of the model design and inputs can have significant impact on
16 validation, as demonstrated in Meng et al.(2005, [058595](#)) and Hering (2007, [155839](#)). Meng
17 et al. (2005, [058595](#)) demonstrated how use of an increasingly more detailed mathematical
18 model decreases the variability of the results with respect to modeled indoor PM_{2.5}
19 concentration of outdoor origin and infiltration factor. Hering (2007, [155839](#)) compared
20 infiltration model results for PM-based EC, NO₃⁻, and SO₄²⁻. Model inputs were from a
21 central site monitor only, central site monitor with air exchange data, and detailed inputs
22 related to initial outdoor (outside test building) and indoor concentrations. Use of more
23 detailed inputs resulted in significant reductions in error for indoor EC concentration,
24 smaller improvements for indoor SO₄²⁻, and negligible improvement in model results for
25 indoor NO₃⁻.This illustrates the impact of differential infiltration discussed in
26 Sections 3.8.4 and 3.8.5.



Source: Isakov et al. (2007, [156588](#)).

Figure 3-101. Grid resolution of the CMAQ model in Philadelphia compared with distribution of census tracts in which exposure assessment is performed.

1 For any spatial interpolation models, grid resolution is another source of error
 2 addressed. Isakov et al. (2007, [156588](#)) linked CMAQ with the Hazardous Air Pollutant
 3 Exposure Model for exposure assessment in Philadelphia. Their simulation was
 4 implemented on a 4 km nested grid within 12 km and 36 km grids to bring the scale of their
 5 model from national to urban scale. However, the census tracts in which Isakov et al. (2007,
 6 [156588](#)) sought to describe exposure were distributed on a much finer scale (see
 7 Figure 3-101). They were required to supplement the CMAQ model with an Industrial
 8 Source Complex Short Term (ISCST) dispersion model to resolve the subgrid scale behavior.
 9 If concentrations were averaged across the cell in lieu of a more detailed subgrid
 10 representation, (Isakov et al., 2007, [156588](#)) found that exposures were overestimated by a
 11 factor of two. Appel et al. (2008, [155660](#)) noted that their 36 km simulations provided a
 12 closer estimate of SO_4^{2-} aerosol concentration than did their 12 km nested simulation,
 13 which overestimated concentrations. Hogrefe et al. (2007, [156561](#)) also noted
 14 overestimation of the CMAQ model at the 12 km scale, where multiple point interpolation
 15 was used to obtain subgrid estimates. Model convergence theory would suggest that the 36

1 km simulation is not actually more accurate but coincidentally closer to the physical values
2 (Roache, 1998, [156915](#)). It is possible that if secondary pollutants are more regionally
3 dispersed, lower spatial resolution would be required to attain a converged solution of the
4 spatial concentration distribution. However, higher spatial resolution in the simulation
5 should produce very similar results if the solution is convergent.

6 Use of geospatial statistical methods for grid interpolation, as performed in the
7 SHEDS/MENTOR simulation by Georgopoulos et al. (2005, [080269](#)), provides another
8 methodology for grid interpolation. Similar to Isakov et al. (2007, [156588](#)), Georgopoulos et
9 al. (Georgopoulos et al., 2005, [080269](#)) linked CMAQ with an exposure model for estimation
10 of neighborhood-scale exposures. The authors found that CMAQ underestimated PM_{2.5}
11 concentration at many times during the simulation. Kim et al. (2009, [188446](#)) compared
12 results from an exposure model using six different levels of spatial resolution. Kim et al.
13 (2009, [188446](#))'s model predicted PM_{2.5} at monitor locations as a function of the mean
14 concentration and spatial and random errors. The six levels of spatial resolution were
15 simulated through assignment of the spatial and random error terms and by defining the
16 distance over which spatial errors are correlated. Between monitors, Kim et al. (2009,
17 [188446](#)) compared results from assigning nearest monitor values and from kriging. They
18 found that model prediction error and bias in health effects estimates decreased with
19 increased spatial resolution of the error terms as well as with kriging over a nearest
20 monitor scheme.

21 For GIS-based models designed to improve spatial resolution of exposure estimates,
22 Yanosky et al. (2008, [099467](#)) described three sources from which they derived an estimate
23 of total model uncertainty: transient model components, stationary model components, and
24 residual spatial and temporal components of variance. When analyzing relative
25 contributions to uncertainty, they found that unexplained local spatial variability was the
26 largest contributor. With model inputs from PM₁₀ monitors for this study, Yanosky et al.
27 (2008, [099467](#)) observed poor model performance and high uncertainty where monitors
28 were sparsely located. High uncertainties were also calculated in a few select urban areas
29 (New York City, Detroit, Cleveland, and Pittsburgh) where concentrations tend to be higher,
30 although the latter may have been related to the Taylor series approximation Yanosky et al.
31 (2008, [099467](#)) used for the residual uncertainty term. Spatial and temporal uncertainties
32 were also reduced when temporal resolution was increased in the model implementation.

1 In his review of various exposure assessment modeling techniques, Jerrett et al.
2 (2005, [092864](#)) reviewed source proximity and LUR for application to exposure assessment.
3 The literature contains mixed evidence of the association between health effects and source
4 proximity (Langholz et al., 2002, [191771](#); Maheswaran and Elliott, 2003, [125271](#); e.g., Venn
5 et al., 2000, [007895](#); Venn et al., 2001, [023644](#)). Jerrett et al. (2005, [092864](#)) contend that
6 source proximity modeling is limited because other confounding covariates, such as
7 socioeconomic status, may be related to source proximity. Additionally, subjects' time-
8 activity patterns may vary from locations modeled through source proximity. Wind direction
9 and topography may bring PM plumes away from a site located even in very close proximity
10 to the source so that high concentrations would be found at distances far downwind of a
11 source. Jerrett et al. (2005, [092864](#)) state that LUR is an adaptable framework allowing
12 adaptation to localized conditions, but they caution that LUR is limited to fairly
13 homogeneous spatial regions. They point to Briggs' (2000, [191772](#)) simulation of Amsterdam
14 as an example of LUR surfaces produced with little spatial variability.

15 LUR and kriging were both used in the ACS data reanalysis by Krewski et al. (2009,
16 [191193](#)) to study mortality as a function of spatial variability in PM_{2.5} in New York and Los
17 Angeles. The LUR predicted 66% and 69% of the variability in PM_{2.5} concentration in New
18 York City and Los Angeles, respectively. The LUR solution produced some observed
19 overpredictions near freeways. Kriged results were compared with LUR for both cities. For
20 New York City, kriging produced slightly attenuated mortality risk estimates, while for Los
21 Angeles, kriging did not exhibit as much spatial variability as LUR. The latter may be due
22 to the fact that the monitoring network in Los Angeles was not situated to capture spatial
23 variability in PM_{2.5} concentration occurring near areas of high traffic. Despite similarities
24 in the LUR performance, health effects predictions were quite different for New York City
25 and Los Angeles, with increased hazard ratios of 1.56 and 1.39, respectively using the same
26 LUR covariates. Krewski et al. (2009, [191193](#)) noted that in New York City, the healthiest
27 (and wealthiest) segment of the population lived in the most polluted areas, while in Los
28 Angeles, there was a strong association between pollution and mortality. This finding
29 implies that, because geographic regions may differ by multiple factors such as building
30 and power plant fuel use, roadway design, traffic patterns, building design, traffic patterns,
31 and building design, significant variables in an LUR analysis may also differ by region.

3.8.6.3. Spatial Variability

1 For PM, spatial and temporal distribution as a function of particle size and
2 composition also plays a large role in the selection of an exposure model. For instance, use
3 of Equation 3-6 might be employed for a study of ambient $PM_{2.5}$ exposure because spatial
4 variability in $PM_{2.5}$ concentration can be low over urban to regional scales. $PM_{10-2.5}$ tends to
5 deposit and become resuspended over a neighborhood scale as a result of gravitational
6 forces. Ultrafine PM is generally limited to micro-to-neighborhood scale environments
7 because it tends to diffuse rapidly and then coagulate with other particles or serve as
8 condensation media. These phenomena cause rapid growth of ultrafine PM that limits their
9 lifetime and spatial extent. Spatial issues leading to exposure misclassification are
10 discussed below.

11 Spatial variability of ambient PM concentration can occur when there are local
12 sources, particularly for ultrafine PM and coarse PM with shorter spatial scales. In panel
13 studies, an exposure error will be introduced if the ambient PM concentration measured at
14 the central site monitor is used as an exposure surrogate and differs from the actual
15 ambient PM concentration outside a subject's residence and/or worksite. Filleul et al. (2006,
16 [089862](#)) computed exposure based on varying contributions of community-based ambient
17 monitors (deemed background) and proximal monitors (to represent a receptor) in Le
18 Havre, France for black smoke measurements. Filleul et al. (2006, [089862](#)) found that
19 increasing the weight of proximal monitors resulted in non-significant but increased mean
20 concentrations. Moore et al.'s (2009, [191002](#)) findings of high variability in ultrafine PM
21 across Los Angeles also suggest that exposure error would occur from using one or a few
22 ultrafine PM monitors. In an example using AQS data, PM_{10} monitors in the Chicago CSA
23 are south of the most populated areas within Chicago (see Figure A-6 in Annex A), and
24 intersampler correlations for urban scale PM_{10} data for several monitor pairs are below 0.4
25 (see Table A-22 in Annex A). In another example from AQS data, $PM_{2.5}$ and PM_{10} monitors
26 in the Riverside CBSA are shown to correspond more closely with higher population density
27 areas (see Figures A-23 and A-24 in Annex A), and urban scale intersampler correlations for
28 both $PM_{2.5}$ and PM_{10} are below 0.4 for several monitor pairs there. For most cities,
29 intersampler correlation is much higher for $PM_{2.5}$ than for PM_{10} . This is consistent with the
30 findings of Sarnat et al. (2009, [180084](#)) where, in a time-series study of the effect of spatial
31 variation in concentration on epidemiologic associations, spatially homogeneous $PM_{2.5}$ and

1 O₃ were found to be associated with emergency room visits while spatially heterogeneous
2 CO and NO₂ were not well associated. Considering results reported in the literature along
3 with inter-sampler correlations reported in Annex A, Section A.2 for PM₁₀ and PM_{2.5}, and
4 their corresponding monitor locations shown in Annex A, Section A.1, the magnitude of
5 spatial exposure error likely depends on particle size as well as monitor location, source
6 location, and characteristics such as urban and natural topography and meteorological
7 trends.

8 Spatial variability among various studies further suggests that use of a single or
9 small number of ambient monitors introduces uncertainty in exposure assessment panel
10 studies. Violante et al. (2006, [156140](#)) studied personal exposures to traffic of parking police
11 in Bologna, Italy to determine how personal exposure to outdoor PM₁₀ and benzene
12 compares with that measured at a community-based monitor. This study found that
13 personal exposures to PM₁₀ were significantly higher than at the community-based monitor,
14 although the authors were not able to demonstrate significant effects of meteorology or
15 traffic on those exposures. Spatial heterogeneity of personal exposures to metals in PM₁₀
16 and PM_{2.5}, with higher levels found near high-traffic and industrial areas, was observed by
17 Nerriere et al. (2007, [156801](#)). In a Bayesian hierarchical model analysis of personal
18 exposure and ambient data from the pilot Baltimore Epidemiology-Exposure Panel Study of
19 16 subjects, McBride et al. (2007, [124058](#)) showed that community monitors overestimated
20 personal exposures for the panel subjects, and that these results were not sensitive to
21 model selection.

22 For community time-series epidemiology, the community averaged concentration, not
23 the concentration at each fixed monitoring site, is the concentration variable of concern
24 (Zeger et al., 2000, [001949](#)). Because variation in trends is of interest, bias in the central
25 site monitor data will not affect health effects estimates unless the central site monitor is
26 not correlated with the community averaged concentration. The latter condition will cause
27 the health effect estimate to be biased towards the null (Sheppard et al., 2005, [079176](#)). The
28 correlation between the concentration at a central community ambient monitor and the
29 community averaged concentration depends on homogeneity of the spatial distribution and
30 representativeness of the central site monitor location. Regional pollutants such as SO₄²⁻
31 will be more spatially homogeneous than point source pollutants. Traffic emissions might
32 show spatial heterogeneity near sources but more homogeneous distribution farther
33 downwind from sources. Kim et al. (2005, [083181](#)) noted that spatial variability among PM

1 species can add uncertainty to exposure estimates in community time-series epidemiology
2 studies exploring source contributions to health effects. The monitoring site is selected to
3 represent the community average of the PM characteristic (mass and/or species) of interest.
4 If the selected site is far from PM sources, then the average measurement may be lower
5 than actual ambient PM concentrations. Likewise, if the site is selected to measure a “hot
6 spot” or pollution from a nearby source, exposure estimates across the community could be
7 skewed upwards.

8 Intra-urban spatial heterogeneity could affect health effects estimates derived from
9 community time-series studies if a community is divided by urban or natural topographic
10 features or by source locations into several sub-communities that differ in the temporal
11 pattern of pollution. Intra-urban spatial heterogeneity is discussed in detail in Section 3.5.
12 Community exposure may not be well-represented when monitors cover large areas with
13 several sub-communities having different sources and topographies. This point is
14 illustrated for Los Angeles in Figures 3-27 and 3-37. Using zip code classified mortality
15 data in a study of socioeconomic status and acute cardiovascular mortality in Phoenix, high
16 risk ratios were computed when a small area near the monitoring site was studied, (Mar et
17 al., 2003, [156731](#); Wilson et al., 2007, [157149](#)) while use of larger-area county-wide data
18 produced non-significant associations (Moolgavkar, 2000, [010305](#); Smith et al., 2000,
19 [010335](#)). At least part of the heterogeneity found between cities in multicity studies may be
20 due to the use of a large geographic area that is composed of several sub-communities that
21 differ in the spatiotemporal distribution of air pollutants. Note that when zip codes cover
22 large areas (e.g., in western mountain states) or when counties cover small areas (e.g., the
23 northeast), then assumptions change regarding use of zip code- or county-level data for
24 epidemiology studies. For all metropolitan areas investigated in this assessment, the PM₁₀
25 data have significantly more scatter. This suggests that the uncertainty of the community
26 average concentration would increase in the coarse PM range. Metrics have been developed
27 and used to compare the spatial variability of air pollutants (Wongphatarakul et al., 1998,
28 [049281](#)). These metrics are useful in assessing the potential for exposure error in the
29 epidemiologic studies, especially when different monitors are used on different days to
30 construct city-wide averages.

31 Epidemiologic studies of long-term exposure rely on differences among communities
32 in long-term average ambient concentrations. If exposure errors are different in the
33 different communities, the differences in long-term ambient concentrations among

1 communities may not represent the differences in long-term average exposures (Dockery et
2 al., 1993, [044457](#)). For example, there may be community to community differences in
3 measurement error if exposure to fresh pollutants generated by vehicular traffic or
4 pollutants from other localized sources differed among the spatial areas. Thus, in a
5 regression of health effects against average concentration as an indicator for average
6 exposure, there could be a different magnitude and direction of error in the exposure
7 indicator for each spatial area. This could bias the slope up or down. The following long-
8 term mortality studies, described in Section 7.6, are cited here to illustrate the effect of
9 spatial exposure error on health effects estimates; the reader is referred to Section 7.6 for a
10 more detailed description of these results. The Harvard Six-City Study dealt with this issue
11 by design, where the members of the cohort in each city were located in a relatively small
12 area near the monitor (Dockery et al., 1993, [044457](#)). In the ACS study, the spatial area was
13 the Metropolitan Statistical Area (MSA) (Krewski et al., 2000, [012281](#)); other studies have
14 used counties as the spatial area (Enstrom, 2005, [087356](#); Lipfert et al., 2000, [004087](#)). In a
15 comparison of several of the larger long-term cohort studies (Enstrom, 2005, [087356](#)), those
16 using county level spatial areas (Enstrom, 2005, [087356](#); Lipfert et al., 2000, [004087](#))
17 sometimes did not find significant associations whereas those using MSAs (Pope CA et al.,
18 1995, [045159](#); Pope CA et al., 2002, [024689](#)) or cities (Dockery et al., 1993, [044457](#)) did find
19 significant associations. Jerrett et al. (2005, [189405](#)) used smaller zip code areas within Los
20 Angeles County and found effects that were both significant and largest in magnitude
21 among those that have been reported for long-term cohort studies. Krewski et al. (2009,
22 [191193](#)) suggested that significant associations between cardiovascular health effects
23 estimates and PM_{2.5} observed in Low Angeles but not in New York City were related to
24 spatial homogeneity of PM_{2.5} concentration in New York City. The Nurses' Health Study
25 examined associations of mortality with PM₁₀ found higher and more significant
26 associations when using estimated concentrations at subjects' individual residences (Puett
27 et al., 2008, [156891](#)) in lieu of county-level concentrations (Fuentes et al., 2006, [097647](#)).
28 These considerations suggest that studies that include large U.S. counties as spatial areas
29 and find no significant associations of health effects with pollution cannot be considered
30 definitive, because the likelihood of exposure error increases in this situation. Reducing the
31 exposure error by using concentrations based on residence address or small zip code areas
32 is associated with larger relative risk than those obtained with county-wide averages of
33 concentrations.

3.8.6.4. Temporal Variability

Temporal Correlation

1 The time series analyzed together for community time-series epidemiology studies can
2 include those obtained from several central site monitors, a single central site monitor with
3 the true community average exposure, and the representative monitor and health effect
4 endpoint. Within a city, lack of correlation of relevant time series at various sites results in
5 smoothing the exposure/surrogate concentration function over time and resulting loss of
6 peak structure from the data series. Burnett and Goldberg (2003, [042798](#)) found that
7 community time-series epidemiology results reflect actual population dynamics only when
8 five conditions are met: environmental covariates are fixed spatially but vary temporally;
9 the probability of the health effect estimate is small at any given time; each member of the
10 population has the same probability of the health effect estimate at any given time after
11 adjusting for risk factors; each member of the population is equally affected by
12 environmental covariates; and, if risk factors are averaged across members of the
13 population, they will exhibit smooth temporal variation. Note that for this study, Burnett
14 and Goldberg (2003, [042798](#)) analyzed mortality, but the results are generalized here.
15 Dominici et al. (2000, [005828](#)) note that ensuring correlation between ambient and
16 community average exposure time series is made difficult by limitations in availability and
17 duration of detailed ambient concentration and exposure time series data and so this is
18 often a source of uncertainty. Sheppard et al. (2005, [079176](#)) also add that the health effect
19 estimate can be biased by time-dependent error in α in a time-series study, provided the
20 spatial variation in PM concentration is not significant and thus Equation 3-6 can be
21 assumed a valid exposure model. The direction of bias is related to seasonal correlation
22 between α and ambient concentration.

Seasonality

23 Community time-series studies can be designed to investigate seasonal effects by
24 incorporating seasonal interaction terms for the exposure surrogate and/or meteorology
25 (e.g. Dominici et al., 2000, [005828](#)). Studies from Section 6.5 are cited here to illustrate how
26 seasonal exposures can influence health effects estimates; the reader is referred to
27 Section 6.5 for a more detailed review of the results. Peng et al. (2005, [087463](#)) and Bell et
28 al. (2008, [156266](#)) observed higher health effects estimates and stronger seasonal

1 dependence in the northeast than the rest of the country for PM₁₀ and PM_{2.5} respectively.
2 Peng et al. (2005, [087463](#)) stated that these results generated three hypotheses. First, the
3 PM composition and resulting toxicity might vary with season. Bell et al. (2008, [156266](#))
4 results showed seasonal differences between respiratory and cardiovascular effects
5 estimates that the authors hypothesize relate to seasonal differences in dominance of a
6 given PM species. Second, Peng et al. (2005, [087463](#)) suggested that less seasonality in
7 regions other than the northeast may reflect regional tendencies for spending more or less
8 time outdoors. Exposure estimates for time spent outdoors may be less subject to exposure
9 error because uncertainties related to infiltration are not a factor during that time. At the
10 same time, air conditioning usage, which is more common in the summer and in warm
11 climates Pandian et al. (1998, [090552](#)), has been associated with decreased association
12 between PM_{2.5} and cardiovascular morbidity (Bell et al., 2009, [191007](#)). Third, infectious
13 diseases are more prevalent during winter and so may influence health outcomes. However,
14 it would be expected that regions other than the northeast would be affected by influenza in
15 winter. Uncertainty in sources of seasonal bias may also indicate other unknown factors.

Data Frequency

16 Most panel studies look at the associations of health outcomes only with exposure (or
17 exposure surrogates) on the day of exposure (lag 0). Zanobetti et al. (2000, [004133](#)) suggest
18 that health effects may not occur until subsequent days or be distributed over several days.
19 When PM measurements are obtained every three or every six days, it is difficult to refine
20 the study lag structure down to the day-level. In studies of the effects of short-term PM_{2.5}
21 exposure on cardiovascular and respiratory hospitalization in >200 urban U.S. counties,
22 Bell et al. (2008, [156266](#)) and Dominici et al. (2006, [088398](#)) worked with a combination of
23 measurements obtained daily and those obtained every three days, while their
24 hospitalization data were daily. Time lags of 0, 1, and 2 days were applied so that PM_{2.5}
25 data obtained only on day 0 would be applied as lag 0 for the corresponding day's
26 hospitalization record, as lag 1 for the next day's hospitalization, and as lag 2 for the
27 following day. No lag 0 data would be available for day 1, and no lag 0 or 1 data would be
28 available for day 2 in this example. This analysis could be performed with sufficient
29 statistical power despite the reduction in days of PM data because a large number of
30 counties were analyzed. Single city studies using data obtained every three or six days
31 could employ the same approach but would lose statistical significance compared with daily

1 data because fewer data points would exist for each lag. Likewise, Dominici et al. (2006,
2 [088398](#)) only applied distributed lag analysis to the daily hospitalization data where daily
3 PM_{2.5} concentration data were also available.

3.8.6.5. Use of Surrogates for PM Exposure

Surrogates for Infiltration Tracers

4 In panel studies, a tracer can be used for PM, such as sulfate as a surrogate for PM_{2.5},
5 as described in Section 3.8.4. For this method to be successful, indoor or other nonambient
6 sources of the tracer must be small compared to ambient sources over the period of
7 sampling. Wilson and Brauer (2006, [088933](#)) noted that environmental tobacco smoke and
8 tap water used in showers or humidifiers are indoor sources of SO₄²⁻. Wallace and Williams
9 (2005, [057485](#)) observed that, because SO₄²⁻ particles are typically smaller than other PM
10 contributing to measurable PM_{2.5} mass, F_{inf} may be biased by using this term to describe
11 PM_{2.5} infiltration. Other concerns in using SO₄²⁻ as a tracer for PM_{2.5} arise because SO₄²⁻
12 tends to be concentrated in smaller particles and thus it might be a better tracer for fine
13 mode particles than for all PM_{2.5} particles. Stand et al. (2006, [157017](#)) suggested that Fe be
14 used as an additional tracer to correct for the infiltration of larger PM_{2.5} particles. In their
15 study, they noted that indoor sources of Fe were small. However, in other environments
16 there could be more substantial contributions from tracking iron in soil indoors. The spatial
17 variability of Fe is also larger than that of PM_{2.5} across urban areas. Volatilization of nitrate
18 or organic compounds after infiltration of PM_{2.5} indoors results in these components being
19 poor surrogates for ambient PM in exposure estimates Lunden et al. (2003, [081201](#)).

Use of Ambient PM Concentration in Lieu of Ambient PM Exposure

20 Ambient PM concentration is often used as a surrogate for exposure to ambient PM in
21 epidemiologic studies. Based on the information presented in Section 3.8.4 related to urban-
22 scale PM distribution, there is less exposure error for accumulation mode PM because it has
23 a more homogeneous spatial distribution and higher filtration indoors, compared with for
24 coarse or ultrafine PM. The ambient concentration may be based on measurements made
25 just outside the primary microenvironment, at the nearest community monitor, at a single
26 community monitor, or as the average of several community monitors. If appropriate
27 measurements are made, it is also possible to estimate the ambient and nonambient
28 components of total personal exposure and use four exposure surrogates in panel

1 epidemiologic studies: C_a , E_T , E_a , and E_{na} (Ebelt et al., 2005, [056907](#); Koenig et al., 2005,
2 [087384](#); Strand et al., 2006, [157017](#); Wilson and Brauer, 2006, [088933](#)). Results from Wilson
3 and Brauer (Wilson and Brauer, 2006, [088933](#)) showed for their panel that exposure error is
4 introduced by 1) using C_a instead of E_a and 2) assuming E_a and E_{na} have the same effects on
5 health outcomes. There was essentially no association of the effect with E_T or E_{na} . Strand et
6 al. (2006, [157017](#)) also noted that inclusion of nonambient PM_{2.5} would not be expected to
7 change health effects estimates because ambient and nonambient PM_{2.5} calculations were
8 not correlated.

9 Zeger et al. (2000, [001949](#)) pointed out that for community time-series epidemiology,
10 which analyzes the association between health effects and potential causal factors at the
11 community level rather than the individual level, it is the correlation of the daily
12 community-averaged personal exposure to the ambient concentration with daily community
13 average concentration that is important, not the correlation of each individual's daily
14 exposure with the daily community average concentration. Thus, the low correlation of
15 individual daily exposure with the daily community average concentration, as frequently
16 found in pooled panel exposure studies, is not relevant to error in community time-series
17 epidemiologic analysis. Sheppard et al. (2005, [079176](#)) also notes that an insufficient
18 number of total personal exposure samples used in a time-series design would introduce
19 large classical measurement errors related to high variability in E_{na} . Sheppard et al. (2005,
20 [079176](#)) further maintain that these errors can be minimized by using the average of
21 concentration measured at community-based ambient monitors. However, overestimation of
22 the community-averaged exposure by substituting C_a for E_a leads to underestimation of the
23 effect estimate per unit mass of ambient PM. City-to-city variations in the indoor air
24 exchange rate, related to differences in climate or housing stock, will cause city-to-city
25 differences in the health effect endpoint estimate obtained from the study using C_a even if
26 the endpoint remained the same using the community-averaged exposure.

Relationship between PM and Copollutants

27 Section 3.8.5 describes studies exploring associations of PM_{2.5} and SO₄²⁻ with
28 copollutants O₃, NO₂, CO, and SO₂ observed in Sarnat et al. (2001, [019401](#)) and Schwartz et
29 al. (2007, [090220](#)). Strong associations between ambient O₃, NO₂, CO, and SO₂ with
30 personal PM_{2.5} and SO₄²⁻ were observed by Sarnat et al. (2001, [019401](#); 2005, [087531](#)). For
31 example, O₃ may be an indicator of photochemical oxidation products including organic

1 particulate matter. SO₂ may be an indicator of Ni emissions from smelters, V from oil fired
2 power plants, or As, Se or Hg from coal fired power plants. In another example, the HEI
3 Report on traffic-related health effects (2009, [191009](#)) lists CO, NO₂, PM₁₀ and PM_{2.5} mass,
4 ultrafine PM count, EC, benzene, and traffic metrics (e.g., count, fuel consumption) all as
5 potential surrogates for traffic or for the mix of PM and gaseous pollutants in traffic
6 because all of these pollutants are found in mobile source emissions. Furthermore, in a
7 multipollutant model, transfer of association can occur by an increase in the slope of a
8 confounding copollutant and a concurrent decrease in the slope of the truly causal
9 covariate. This can occur when copollutants are highly correlated with larger error for the
10 true copollutant, smaller error for the confounder, and correlation between the copollutant
11 measurement errors (U.S. EPA, 2004, [056905](#); Zeger et al., 2000, [001949](#); Zidek et al., 1996,
12 [051879](#)). For these reasons, this is an important area of uncertainty for interpretation of
13 the multipollutant models discussed in Chapter 6.

3.8.6.6. Compositional Differences

14 Differences between the composition of ambient PM and the ambient PM that has
15 infiltrated indoors may affect exposure estimates. Numerous differential infiltration studies
16 related to indoor-outdoor changes in size distribution and chemical composition are cited in
17 Sections 3.8.4 and 3.8.5, respectively. Differential infiltration can be caused by impaction of
18 coarse PM, diffusion of ultrafine PM, and evaporation of semi-volatile components during
19 infiltration for particles of different sources and sizes. Local meteorology and building air
20 exchange also influence differential infiltration rates for individual buildings. Differential
21 infiltration results in differences in PM size distribution and chemical composition between
22 indoor-ambient PM and outdoor-ambient PM. For instance, Adgate et al. (2007, [156196](#))
23 found that outdoor concentrations underestimate personal exposures to trace elements.
24 Baxter et al. (2007, [092726](#)) showed that V tends to have lower penetration efficiency,
25 perhaps because metals exist more in the coarse range, while S has penetration efficiency
26 close to unity. Epidemiologic studies cited in Section 6.6 indicate that significant
27 associations between health effects estimates and trace metal exposures exist and may be
28 modified by season. Trace metal penetration efficiency estimates are thus relevant to those
29 findings. Section 6.6 also discusses significant associations between health effects endpoints
30 and exposure to EC and OC. After initial emission, traffic-related PM is generally in the

1 accumulation mode with volatile components; accumulation mode PM tends to have the
2 highest infiltration factors but volatile components may be lost during infiltration (Sarnat
3 et al., 2006, [089166](#)). If outdoor residential or central-site measurements are used for an
4 exposure surrogate, differences in indoor and outdoor PM composition related to infiltration
5 could introduce uncertainty into effects estimates.

6 Ebel et al. (2005, [056907](#)) illustrated that exposure error occurs when the PM on one
7 or more days is not representative of the normal community PM. Section 6.3.2.1 cites Ebel
8 et al.'s (2005, [056907](#)) panel study of the association between chronic obstructive pulmonary
9 disease and PM_{2.5}, PM_{10-2.5}, and PM₁₀. In their analysis, one day of dust from the Gobi
10 Desert caused an increase in the concentration of fine and coarse PM. When this day was
11 deleted from the analysis, the relationships were changed and the associations of chronic
12 obstructive pulmonary disease with PM₁₀ and especially with PM_{10-2.5}, became larger and
13 more significant. Similar peaks in PM₁₀ concentration have been observed on the Iberian
14 Peninsula as a result of high transport events carrying dust from the Sahara Desert that
15 could affect epidemiologic associations on given days (Artinano et al., 2001, [190099](#)).

3.8.6.7. Conclusions

16 This section presents considerations for exposure assessment and the exposure
17 misclassification issues that can potentially affect health effects estimates. These issues can
18 be categorized into six areas: measurement, modeling, spatial variability, temporal
19 variability, use of surrogates for PM exposure, and compositional differences. Potential
20 influences of each of these sources on health effect estimates derived from panel, time-
21 series, and longitudinal epidemiologic studies are described above. Additionally, error
22 sources often interact with each other and are driven by particle size distribution. For
23 example, fresh diesel-generated PM is characterized by ultrafine PM that dynamically grow
24 and change in chemical composition over short time and spatial scales, and lack of spatial
25 and temporal resolution in measurements or models can result in misclassifying this
26 exposure (Moore et al., 2009, [191002](#)). For this reason, conclusions regarding ultrafine PM
27 exposure cannot be drawn from PM_{2.5} concentration data in part because PM_{2.5}
28 concentration is more spatially homogeneous across a city. In most circumstances, exposure
29 error tends to bias a health effect estimate downward (Sheppard et al., 2005, [079176](#); Zeger
30 et al., 2000, [001949](#)). Insufficient spatial or temporal resolution to capture true variability

1 and correlation of PM with copollutants are examples of sources of uncertainty that could
2 widen confidence intervals and so reduce the significance of health effects estimates.

3.9. Summary and Conclusions

3.9.1. Concentrations and Sources of Atmospheric PM

3 This section summarizes concentrations and sources of atmospheric PM. The
4 following summaries cover ambient variability and correlations, temporal variability and
5 copollutant correlations from Section 3.5, measurement techniques from Section 3.4, source
6 characteristics from Section 3.3, source contributions from Section 3.6 and policy relevant
7 background concentrations from Section 3.7.

3.9.1.1. Ambient PM Variability and Correlations

8 Advances in understanding the spatiotemporal distribution of PM mass and
9 constituents have recently been made, particularly with regard to PM_{2.5} mass and chemical
10 composition and ultrafine concentrations. Emphasis in this ISA was on the period from
11 2005-2007 so that the most recent validated EPA Air Quality System (AQS) data were used.
12 Note, however, that a majority of U.S. counties were not represented in AQS data, since
13 their population fell below the regulatory monitoring threshold for PM. Moreover, monitors
14 reporting to AQS were not uniformly distributed across the U.S. or within counties, and
15 conclusions drawn from AQS data may not apply equally to all parts of a geographic region.
16 Furthermore, biases can exist for some PM constituents (and hence total mass) owing to
17 volatilization losses of nitrates and other semi-volatile compounds, and, conversely, to
18 retention of particle-bound water by hygroscopic species. The degree of spatial variability in
19 PM is likely to be region-specific and strongly influenced by region-specific sources and
20 meteorological and topographic conditions.

Spatial Variability across the U.S.

21 County-scale, 24-h avg concentration data for PM_{2.5} between 2005-2007 showed
22 considerable variability across the U.S. (see Figure 3-9). The highest reported 3-yr avg
23 concentrations were reported for six counties within the San Joaquin Valley and inland
24 southern California, as well as Jefferson County, AL (containing Birmingham) and
25 Allegheny County, PA (containing Pittsburgh). The lowest reported annual average PM_{2.5}

1 concentrations were contained within 237 counties distributed throughout many western
2 and northern states as well as Florida and the Carolinas. Of the 15 individual CSAs/CBSAs
3 selected for detailed investigation based on their geographic distribution and importance in
4 recent health effect studies, the highest mean 24-h $PM_{2.5}$ concentrations were reported for
5 Riverside ($17 \mu\text{g}/\text{m}^3$), Birmingham ($16 \mu\text{g}/\text{m}^3$) and Pittsburgh ($16 \mu\text{g}/\text{m}^3$); the lowest were
6 reported for Denver ($9 \mu\text{g}/\text{m}^3$) and Seattle ($9 \mu\text{g}/\text{m}^3$).

7 Since $PM_{10-2.5}$ is not routinely measured and reported to AQS, co-located low-volume
8 PM_{10} and $PM_{2.5}$ measurements from the AQS network were used to investigate the spatial
9 distribution in $PM_{10-2.5}$. Current data coverage (see Figure 3-10) and measurement errors
10 limit the ability to draw any meaningful conclusions regarding the large-scale spatial
11 distribution of $PM_{10-2.5}$ in urban areas. Only six of the 15 CSAs/CBSAs chosen for closer
12 investigation had sufficient data for calculating $PM_{10-2.5}$. In general, in the eastern
13 metropolitan areas including Atlanta, Boston, Chicago and New York. Most of the mass of
14 PM_{10} was in the $PM_{2.5}$ size fraction, with the highest ratio of $PM_{2.5}$ to $PM_{10-2.5}$ in Chicago (14
15 $\mu\text{g}/\text{m}^3$ $PM_{2.5}$, $5 \mu\text{g}/\text{m}^3$ $PM_{10-2.5}$, ratio = 2.8). In contrast, in Denver ($9 \mu\text{g}/\text{m}^3$ $PM_{2.5}$, $20 \mu\text{g}/\text{m}^3$
16 $PM_{10-2.5}$, ratio = 0.45) and Phoenix ($10 \mu\text{g}/\text{m}^3$ $PM_{2.5}$, $22 \mu\text{g}/\text{m}^3$ $PM_{10-2.5}$, ratio = 0.45) most of
17 PM_{10} was in the thoracic coarse mode.

18 Given the limited information available from AQS for $PM_{10-2.5}$ and the current
19 National Ambient Air Quality Standard for PM_{10} , analyses were performed on the more
20 prevalent PM_{10} data (see Figure 3-11), acknowledging that PM_{10} incorporates both thoracic
21 coarse and fine particles. The highest reported 3-yr avg PM_{10} concentrations ($>51 \mu\text{g}/\text{m}^3$)
22 occurred in two counties in southern California and five counties in southern Arizona and
23 central New Mexico. The lowest reported annual average PM_{10} concentrations ($\leq 20 \mu\text{g}/\text{m}^3$)
24 were within 114 counties distributed fairly uniformly across the U.S. Of the 15
25 CSAs/CBSAs investigated, the highest mean 24-h PM_{10} concentrations was reported for
26 Phoenix ($52 \mu\text{g}/\text{m}^3$), considerably higher than the means for the other CSAs/CBSAs
27 investigated. The lowest was reported for Boston ($17 \mu\text{g}/\text{m}^3$) with New York, Philadelphia
28 and Seattle only slightly higher ($19 \mu\text{g}/\text{m}^3$).

29 Spatial variability in $PM_{2.5}$ components obtained from the Chemical Speciation
30 Network (CSN) varied considerably by species. The highest annual average OC
31 concentrations ($>5 \mu\text{g}/\text{m}^3$) were observed in the western and southeastern U.S. (see
32 Figure 3-12) Concentrations in the West peaked in the fall and winter, while concentrations
33 in the Southeast peaked anytime between spring and fall. Of the 15 CSAs/CBSAs

1 investigated, OC was the dominant PM_{2.5} component on an annual basis in the western
2 cities, ranging from 34% of PM_{2.5} mass in Los Angeles to 58% in Seattle (see Figure 3-17).
3 EC exhibited less seasonal variability than OC and was particularly stable in the eastern
4 half of the U.S. (see Figure 3-13). Annual average EC concentrations greater than 1.5 µg/m³
5 were present in Los Angeles, Pittsburgh, New York and El Paso. Concentrations of SO₄²⁻
6 were higher in the eastern U.S. (see Figure 3-14) resulting from higher SO₂ emissions in
7 the East, compared with the West. There is also considerable seasonal variability with
8 higher SO₄²⁻ concentrations in the summer months when the oxidation of SO₂ proceeds at a
9 faster rate than during the winter. Of the 15 CSAs/CBSAs selected, sulfate was the
10 dominant PM_{2.5} component on an annual basis in the eastern cities, ranging from 42% of
11 PM_{2.5} mass in Chicago to 56% in Pittsburgh (see Figure 3-17). NO₃⁻ concentrations were
12 highest in California, with annual averages >4 µg/m³ at many monitoring locations (see
13 Figure 3-15). There were also elevated concentrations of NO₃⁻ in the Midwest (>2 µg/m³),
14 with wintertime concentrations exceeding 4 µg/m³. In general, NO₃⁻ was higher in the
15 winter across the country, resulting from a number of factors including lower temperatures
16 which favor partitioning into particles; higher relative humidity, mainly in dry areas; lower
17 sulfate, allowing higher uptake of NO₃⁻; and residential wood burning in specific areas of
18 the U.S., especially in the Northwest. Exceptions existed in Los Angeles and Riverside,
19 where high NO₃⁻ readings appeared year-round. Crustal material constituted a substantial
20 fraction of PM_{2.5} year-round in Phoenix (28%) and Denver (16%), and during the summer in
21 Houston (26%) (see Figure 3-17).

22 Clearly there are variations in both PM_{2.5} mass and composition by city. Such
23 variability results from numerous controlling variables (e.g., meteorology, the nature of
24 sources, proximity to sources, topography) that are too poorly characterized on a broad scale
25 to allow conclusions to be drawn regarding PM_{2.5} mass and composition across all cities
26 within a given geographic region.

Spatial Variability on the Urban and Neighborhood Scales

27 In general, PM_{2.5} has a longer atmospheric lifetime than PM_{10-2.5} because larger
28 particles have a higher gravitational settling velocity. For PM_{2.5}, most metropolitan areas
29 exhibited high correlations (generally >0.75) out to a distance of 100 km (e.g., Figures 3-25
30 through 3-27). Notable exceptions were Denver, Los Angeles and Riverside where
31 correlations dropped below 0.75 somewhere between 20 and 50 km. Insufficient data were

1 available in the 15 metropolitan areas to perform similar analyses for PM_{10-2.5} using co-
2 located, low volume FRM monitors. More abundant PM₁₀ data, however, showed larger
3 declines in inter-monitor correlations as a function of distance (e.g., Figures 3-35 through
4 3-37) relative to PM_{2.5}. Atlanta, Boston, Denver, Los Angeles, New York City, Philadelphia,
5 Phoenix, Pittsburgh and Riverside all showed an average correlation of 0.75 at 40 km or
6 greater monitor separation while Birmingham, Chicago, Detroit, Houston and St. Louis had
7 correlations that dropped off much more quickly with distance (average correlation of 0.75
8 at 6 km or less monitor separation). Furthermore, correlations between PM₁₀
9 concentrations exhibited substantially more scatter relative to PM_{2.5}. Shorter atmospheric
10 lifetimes for PM₁₀ can result in local emission sources dominating PM₁₀ annual average
11 mass concentrations at particular monitors. Although the general understanding of PM
12 differential settling leads to an expectation of greater spatial heterogeneity in the PM_{10-2.5}
13 fraction relative to the PM_{2.5} fraction in urban areas, deposition of particles as a function of
14 size depends strongly on local meteorological conditions, in particular on the degree of
15 turbulence in the mixing layer. Therefore, the findings from these 15 CSAs/CBSAs may not
16 apply to all locations or at all times.

17 Population density and associated building density are also important determinants
18 of the spatial distribution of PM concentrations. Inter-sampler correlations as a function of
19 distance between monitors obtained for sampler pairs located less than 4 km apart (i.e., on
20 a neighborhood scale) showed a shallower slope for PM_{2.5} than for PM₁₀. The average
21 correlation was 0.93 for PM_{2.5}, but it dropped to 0.70 for PM₁₀ (see Figure 3-43).

22 Few studies performed direct comparisons of ultrafine particle measurements at
23 multiple locations within an urban area. A decrease in the number of ultrafine particles was
24 demonstrated with shifts from a dominant mode at around 10 nm within 20 m of a freeway
25 to a flattened dominant mode at around 50 nm at a distance of roughly 100-150 m. At the
26 same time, accumulation mode particle number concentration remained relatively constant
27 to within ~300 m from the freeway. These findings suggest a high degree of spatial
28 heterogeneity in ultrafine particles compared with accumulation mode particles on the
29 urban scale.

3.9.1.2. Temporal Variability

1 A steady decrease in PM_{2.5} concentrations from 1999 (the beginning of nationwide
2 monitoring for PM_{2.5}) to 2007 was observed in all 10 EPA Regions, with the three-yr avg of
3 the 98th percentile of 24-h PM_{2.5} concentrations dropping 10% over this time period.
4 Similar trends in PM₁₀ concentrations show a steady decline from 1988 to 2007 in all 10
5 EPA Regions.

6 Using hourly PM observations in the 15 metropolitan areas, diel variation showed
7 peaks that differ by PM size fraction and region. For PM_{2.5}, a morning peak was observed
8 starting at approximately 6:00 a.m., corresponding with the start of morning rush hour
9 (e.g., Figure 3-49b). There was also an evening PM_{2.5} concentration peak that was broader
10 than the morning peak and extended into the overnight period, likely reflecting a
11 combination of evening rush hour and the concentration increase caused by the usual
12 collapse of the mixed layer after sundown. PM_{2.5} concentrations in Pittsburgh remained
13 elevated throughout the night, obscuring the morning peak (see Figure 3-49a). For PM₁₀, all
14 areas showed a morning and afternoon peak in mean concentrations. The magnitude and
15 duration of this peak varied considerably by metropolitan area (e.g., Figure 3-50). Since
16 these figures represent the distribution of hourly observations over a 3-yr period, any
17 fluctuations or changes in the timing of the daily peaks would result in a broadening of the
18 curves shown in the diel plot.

19 Studies indicate that ultrafine particles in urban environments exhibit similar two-
20 peaked diel patterns in Los Angeles and the San Joaquin Valley as well as in Kawasaki
21 City, Japan and Copenhagen, Denmark. The afternoon peak in ultrafine particles likely
22 represents the combination of primary source emissions such as evening rush-hour traffic
23 and photochemical formation of secondary organic aerosol and sulfate. Several example diel
24 patterns are shown in Figure 3-51 for the study in Denmark. Comparison between
25 weekdays and Sundays as well as an urban street canyon site and an urban background
26 site in this figure suggest traffic is a major source of ultrafine particles within a street
27 canyon during the morning rush hour.

3.9.1.3. Correlations between Copollutants

28 Correlations between PM and gaseous copollutants including SO₂, NO₂, CO and O₃
29 varied both seasonally and spatially between and within metropolitan areas. On average,

1 PM₁₀ and PM_{2.5} were correlated with each other better than with the gaseous copollutants.
2 There was relatively little seasonal variability in the mean correlation between PM in both
3 size fractions and SO₂ and NO₂. CO, however, showed higher correlations with PM₁₀ and
4 PM_{2.5} on average in the winter compared with the other seasons. This seasonality results in
5 part because a larger fraction of PM is primary in origin during the winter. To the extent
6 that this primary component of PM is associated with common sources of NO₂ and CO, then
7 higher correlations with these gaseous copollutants are to be expected. Increased
8 atmospheric stability in colder months would also reinforce these associations.

9 The correlation between daily maximum 8-h avg O₃ and PM showed the highest
10 degree of seasonal variability with positive correlations on average in the spring, summer
11 and fall, and negative correlations on average in the winter. This situation arises as the
12 result of seasonal differences in PM primary emissions and photochemical production of
13 secondary PM_{2.5} and O₃. However, this relationship is not found in Birmingham, Boston and
14 St. Louis.

3.9.1.4. Measurement Techniques

15 The federal reference methods for PM_{2.5} and PM₁₀ are based on criteria outlined in the
16 Code of Federal Regulations. They are, however, subject to several limitations that should
17 be kept in mind when using compliance monitoring data for health outcome studies. FRM
18 methods are subject to the loss of semi-volatile species such as organic compounds and
19 ammonium nitrate (especially in the West). Since FRM gravimetric methods involve 24-h
20 integrated filter samples, no information is available for variations over shorter averaging
21 times. However, reliable methods have been developed to measure real-time PM_{2.5} or PM₁₀
22 mass concentrations (e.g., FDMS-TEOM). New FRMs and FEMs are available for PM_{10-2.5}
23 and various methods (dichotomous samplers, cascade impactors, and passive sampling
24 techniques) are under evaluation to improve PM_{10-2.5} measurements. Techniques are
25 available to characterize ultrafine PM mass, surface area, and number concentrations.
26 Continuous and semi-continuous measurement techniques are also available for PM
27 species, such as PILS for multiple ion analysis and AMS for multiple component analysis.
28 Advances have also been achieved in PM organic speciation (e.g., TD-GC-MS). For
29 additional information see Section 3.4.1.

3.9.1.5. PM Source Characteristics

1 PM in the atmosphere contains both primary (i.e., emitted directly by sources) and
2 secondary components, which can be anthropogenic or natural in origin. Secondary
3 components are produced by the oxidation of precursor gases such as SO₂, NO_x, and
4 reactions of acidic products with NH₃, and organic compounds.

5 Developments in the chemistry of formation of SOA indicate that oligomers are likely
6 a major component of OC in aerosol samples. Recent observations suggest that small, but
7 still significant quantities of SOA are formed from isoprene oxidation. Gasoline engines
8 have been found to emit a mix of OC, EC, and nucleation-mode heavy and large polycyclic
9 aromatic hydrocarbons on which unspent fuel and trace metals condense, while diesel
10 particles are composed of a soot nucleus on which SO₄²⁻ and hydrocarbons condense. Data
11 from standard emissions tests in which there is insufficient dilution of fresh exhaust from
12 combustion sources tend to overestimate the primary component of organic aerosol at the
13 expense of the semi-volatile components. These semi-volatile components are precursors to
14 secondary organic aerosol formation and their oxidation results in more oxidized forms of
15 SOA, both in near source urban environments and further downwind, than previously
16 considered, both in near source urban environments and further downwind.

3.9.1.6. Source Contributions to PM

17 Results of receptor modeling calculations indicate that PM_{2.5} is produced mainly by
18 combustion of fossil fuel, either by stationary sources or by transportation. It is apparent
19 that a relatively small number of source categories, compared to the total number of
20 chemical species that typically are measured in ambient monitoring source receptor model
21 studies, are needed to account for the majority of the observed mass of PM in these studies.
22 Trying to be more specific about contributions from source categories could result in
23 ambiguity. For example, quite different mobile sources (e.g., trucks and locomotives) rely on
24 diesel power and ancillary data is required to resolve contributions from these sources. A
25 compilation of study results shows that secondary sulfate (mainly from EGUs), nitrate
26 (from the oxidation of NO_x emitted mainly from transportation and EGUs), and primary
27 mobile source categories constitute most of PM_{2.5} (and PM₁₀) in the East. Fugitive dust,
28 found mainly in the PM_{10-2.5} size range, represents the largest source of ambient PM₁₀ in
29 many locations in the western U.S. Quoted uncertainties in the source apportionment of

1 constituents in ambient aerosol samples typically range from 10 to 50%. A comparison of
2 source apportionment techniques indicated that the same major source categories of PM_{2.5}
3 were consistently identified by several independent groups working with the same data
4 sets. Soil-, sulfate-, residual oil-, and salt-associated mass were most clearly identified by
5 the groups. Other sources with more ambiguous signatures, such as vegetative burning and
6 traffic-related emissions were less consistently identified.

7 Spatial variability in source contributions across urban areas is an important
8 consideration in assessing the likelihood of exposure error in epidemiologic studies relating
9 health endpoints to sources. Concepts similar to those for using ambient concentrations as
10 surrogates for personal exposures apply here. Studies for PM_{2.5} indicate that intra-urban
11 variability increases in the following order: regional (e.g., secondary SO₄²⁻ from EGUs)
12 < area (e.g., on-road mobile sources) < point (e.g., stacks) sources. Only one study was
13 available for PM_{10-2.5}, indicating a similar ordering, but without a regional component
14 (resulting from the short lifetime of PM_{10-2.5} compared to transport times on the regional
15 scale). Descriptions of receptor models and three dimensional chemistry transport models
16 are given in Section 3.6.

3.9.1.7. Policy-Relevant Background

17 The background concentrations of PM that are useful for risk and policy assessments
18 informing decisions about the NAAQS are referred to as policy-relevant background (PRB)
19 concentrations. PRB concentrations have historically been defined by EPA as those
20 concentrations that would occur in the U.S. in the absence of anthropogenic emissions in
21 continental North America defined here as the U.S., Canada, and Mexico. For this
22 document, PRB concentrations include contributions from natural sources everywhere in
23 the world and from anthropogenic sources outside continental North America. Background
24 concentrations so defined facilitated separation of pollution that can be controlled by U.S.
25 regulations or through international agreements with neighboring countries from those
26 that were judged to be generally uncontrollable by the U.S. Over time consideration of
27 potential broader ranging international agreements may lead to alternative determinations
28 of which PM source contributions should be considered by EPA as part of PRB.
29 Contributions to PRB concentrations of PM include both primary and secondary natural
30 and anthropogenic components. For this document, PRB concentrations for the continental

1 U.S. were estimated using EPA's Community Multi-scale Air Quality (CMAQ) modeling
2 system, a deterministic, chemical-transport model (CTM), and with GEOS-Chem, a global-
3 scale model for CMAQ boundary conditions. PRB concentrations of PM_{2.5} were estimated to
4 be less than 1 µg/m³ on an annual basis, with maximum daily average values in a range
5 from 3.1 to 20 µg/m³ and having a peak of 63 µg/m³ at the nine national park sites across
6 the U.S. used to evaluate model performance for this analysis. For further information on
7 methods used in modeling of PRB concentrations see Section 3.6, and for further
8 information on the results of calculation of PRB concentrations see Section 3.7.

3.9.2. Human Exposure

9 This section summarizes the findings from the recent exposure assessment literature,
10 which include the assessment of exposure to ambient PM, infiltration of ambient PM to
11 indoor environments, and source apportionment of PM exposure. This summary is intended
12 to support the interpretation of the findings from epidemiologic studies. For more detailed
13 explication see Section 3.8.

3.9.2.1. Characterizing Human Exposure

14 A number of techniques have been applied in the literature to model human exposure
15 to PM. Several studies have used time-weighted microenvironmental models to define total
16 or ambient PM exposure. Time-activity diaries or global positioning systems have been
17 employed to capture the time-basis for those models. Stochastic population exposure
18 models, such as APEX and SHEDS, are applied for PM exposure risk assessment among
19 the population. Concentrations from chemistry transport models have also been used to
20 provide input to the stochastic exposure models at particular locations. LUR models applied
21 for individual exposures at the intra-urban scale to examine exposure to pollution
22 surrogates, such as traffic counts, land use, or topographic variables. Source proximity and
23 kriging have also been applied. GIS-based models have been used to model exposure over
24 large regions (e.g., for the Nurse's Health Study) using spatial smoothing models of AQS
25 data and incorporating GIS-based and meteorological covariates. GIS approaches have also
26 been used for intra-urban scale exposure studies. These methods all have their own uses
27 and caveats. LUR is an adaptable framework allowing adaptation to localized conditions
28 but might best be applied in relatively spatially homogeneous areas. In a comparison of

1 LUR with kriging, kriging produced slightly attenuated mortality risk estimates for New
2 York City, while for Los Angeles, kriging did not exhibit as much spatial variability as LUR.
3 Source proximity modeling is relatively simple to apply but is limited because other
4 confounding covariates, such as socioeconomic status, may be related to source proximity.
5 Additionally, subjects' activities may take them away from residences located close to source
6 New advancements in personal and microenvironmental monitoring techniques have
7 been reported. Personal monitoring developments include new models of cascade impactors
8 and cyclones to sample in the ultrafine PM size range and miniature monitors for species
9 detection. Additionally, new work on microenvironmental modeling using mobile platforms
10 and GPS technology has been reported. The reader is referred to the 2004 AQCD for
11 descriptions of most real-time and filter-based personal and microenvironmental PM
12 monitors currently available (U.S. EPA, 2004, [056905](#)).

3.9.2.2. Spatial Scales of PM Exposure Assessment

13 Assessing population-level exposure at the urban scale is particularly relevant for
14 time-series epidemiologic studies, which provide information on the relationship between
15 health effects and community-average exposure, rather than variations in individual
16 exposure. The correlation between the PM concentration measured at a central-site
17 community ambient monitor and the true community average concentration depends on the
18 spatial distribution of the PM, location of the monitoring site chosen to represent the
19 community average, and division of the community by terrain features or source locations
20 into several sub-communities that differ in the temporal pattern of pollution.
21 Concentrations of SO_4^{2-} and some components of SOA measured at central-site monitors are
22 expected to be uniform in urban areas because of the regional nature of their sources.
23 However, this is not true for primary components like EC whose sources are strongly
24 spatially variable in urban areas. Given that roughly 90% of an individual's day is spent
25 indoors, assessment of exposure to infiltrated ambient SO_4^{2-} , whose formation and
26 dispersion also occurs over urban-to-regional scales and whose size distribution is in the
27 accumulation mode, is commonly used to assess ambient $\text{PM}_{2.5}$ exposure. This technique
28 has also been applied to assess $\text{PM}_{10-2.5}$ exposure but is likely to have more error than for
29 $\text{PM}_{2.5}$ because $\text{PM}_{10-2.5}$ is more highly spatially variable than $\text{PM}_{2.5}$. Source apportionment

1 techniques have also been applied to assess urban-scale PM_{2.5} exposures using community-
2 based ambient monitoring, outdoor, and indoor samples.

3 At micro-to-neighborhood scales, heterogeneity of sources and topography may cause
4 more variability in exposure. This is particularly true for PM_{10-2.5} and for ultrafine PM, both
5 of which are more highly spatially variable than PM_{2.5}. Particle chemistry and source
6 behavior also contribute to spatial heterogeneity of PM concentration. Some studies,
7 conducted mainly in Europe, have found personal PM_{2.5} and PM₁₀ exposures for pedestrians
8 in street canyons to be higher than ambient concentrations measured by urban background
9 ambient monitors. Likewise, microenvironmental ultrafine PM concentrations were
10 observed to be substantially higher in near-road environments, street canyons, and tunnels
11 when compared with other environments in urban areas. In-vehicle ultrafine PM exposures
12 can also be important. As a result, ambient monitors located at background, central urban,
13 road side, or near-residential sites might not reflect peak exposures to individuals who
14 commute.

15 PM infiltration factors, F_{inf} , depend on particle size, chemical composition, season, and
16 region of the country. Infiltration can best be modeled dynamically based on a distribution
17 of air exchange and deposition PM loss rates rather than being represented by a single
18 value. There is significant variability within and across regions of the country with respect
19 to indoor exposures to ambient PM. Infiltrated ambient PM concentrations depend in part
20 on the ventilation properties of the building or vehicle in which the person is exposed.
21 Season is important to PM infiltration because it affects the ventilation practices used, and
22 ambient temperature and humidity conditions affect the transport, dispersion, and size
23 distribution of PM. Residential air exchange rates have been observed to be higher in
24 summer for regions with low air conditioning usage, and regional differences in air
25 exchange rates (Southwest < Southeast < Northeast < Northwest) also reflect ventilation
26 practices. Differential infiltration occurs as a function of PM size and composition. PM
27 infiltration is largest for accumulation mode particles, and decreases for ultrafine PM lost
28 to diffusion and for coarse PM lost through inertial impaction mechanisms. Differential
29 infiltration by size fraction can affect exposure estimates if not properly characterized.

3.9.2.3. Multicomponent and Multipollutant PM Exposures

1 Emission inventories and source apportionment studies suggest that sources of PM
2 exposure vary by region. Comparison of studies performed in the eastern U.S. with studies
3 performed in the western U.S. suggest that the contribution of SO_4^{2-} to personal exposure is
4 higher for the East (16-46%) compared with the West (~4%) and that motor vehicle
5 emissions and secondary NO_3^- are larger sources of personal exposure for the West (~9%) as
6 compared with the East (~4%). Results of source apportionment studies of personal
7 exposure to SO_4^{2-} indicate that personal SO_4^{2-} exposures are mainly attributable to ambient
8 sources. Source apportionment for OC and EC is difficult because they originate from both
9 indoor and outdoor sources. Exposure to OC of indoor and outdoor origin can be
10 distinguished by the presence of aliphatic C-H groups generated indoors, since outdoor
11 concentrations of aliphatic C-H are low. Trace metal studies have shown variable results
12 regarding personal exposure to ambient constituents with significant variation among cities
13 and over seasons that can be related to incinerator operation, fossil fuel combustion,
14 biomass combustion (wildfires), and presence of crustal materials in the built environment,
15 among other sources. Differential infiltration is also affected by variations in particle
16 composition and volatility. For example EC infiltrates more readily than OC. This can lead
17 to outdoor-indoor differentials in PM toxicity.

18 A number of studies have examined whether gaseous copollutants could act as
19 surrogates for exposure to ambient PM. Several studies have concluded that ambient
20 concentrations of O_3 , NO_2 , and SO_2 are associated with the ambient component of personal
21 exposure to total $\text{PM}_{2.5}$ as opposed to the ambient component of personal exposures to the
22 gases. However, in some studies this result may have arisen in part because personal
23 exposure to the gases was often beneath the detection limits of the personal monitoring
24 devices. Thus, the evidence that ambient gases can be considered surrogates of $\text{PM}_{2.5}$
25 exposure is mixed. It is likely that associations between ambient gases and personal
26 exposure to $\text{PM}_{2.5}$ of ambient origin exist, but they are complex and vary by season and
27 location.

3.9.2.4. Implications for Epidemiologic Studies

28 The importance of exposure error varies with study design based on the spatial and
29 temporal aspects of the design. For PM epidemiology studies, source characteristics,

1 particle size distribution, and particle composition are also important factors in
2 interpreting exposure error for an epidemiology study. Potential sources of error that could
3 influence estimates of PM exposure include measurements, surrogacy, modeling, spatial
4 variability, temporal variability, and compositional differences.

5 PM exposure estimates are subject to monitoring and modeling errors. Ambient and
6 personal exposure monitoring errors can bias health effects estimates if the error is
7 strongly correlated with the measurements of concentration. This can be an issue for
8 sampling semi-volatile organic compounds in PM, especially where PM exposures in cities
9 with different PM composition are compared. Ambient monitor height also affects estimates
10 of exposure because PM concentration varies as a function of height. Within a street
11 canyon, changes in wind direction and speed cause significant variability over a small
12 distance, with findings showing up to a two order of magnitude change in benzo[a]pyrene
13 concentrations within the depth of a street canyon. Wind tunnel studies have shown street
14 canyon effects exist for suburban and not just for downtown, heavily urbanized settings.
15 Additionally, model-based exposure estimates are subject to errors related to the spatial
16 resolution of the modeling technique and the measurement-based inputs used.

17 Variations in PM and its components could lead to errors in using ambient PM
18 measures as surrogates for exposures to PM. PM_{2.5} concentrations are relatively well-
19 correlated across monitors in the urban areas examined. Correlation coefficients tend to be
20 lower, and concentration differences tend to be higher between PM₁₀ monitoring sites than
21 between PM_{2.5} monitoring sites. Likewise, studies have shown ultrafine PM to be more
22 spatially variable across urban areas. Even if PM_{2.5}, PM_{10-2.5}, and ultrafine PM
23 concentrations measured at sites within an urban area are highly correlated, significant
24 differences in their concentrations can occur on any given day. The degree of urban-scale
25 spatial variability in PM concentrations varies across the country and with size fraction.
26 Current information suggests that ultrafine PM, PM_{10-2.5}, and many PM components are
27 more spatially variable than PM_{2.5}. These factors should be considered in using data
28 obtained from monitoring networks to estimate community-scale human exposure to
29 ambient PM, and caution should be exercised in extrapolating conclusions obtained from
30 one urban area to another.

31 Community time-series epidemiologic studies use the average community PM
32 concentration as a surrogate for the average personal exposure to ambient PM. The
33 resulting health effect risk estimate, based on the average community ambient

1 concentration, differs from the risk that would be estimated if the average community
2 ambient exposure were used in the epidemiologic study. However, the risk estimate based
3 on the ambient concentration gives the change in health effects resulting from a change in
4 ambient PM concentration and is, therefore, an appropriate measure for risk assessment
5 and risk management. Variations in ambient concentrations across a community, variations
6 in individual ambient exposures around the community average, and seasonal or daily
7 variation in the ambient exposure estimate may increase standard errors of PM health
8 effects estimates, making it more difficult to detect a true underlying association between
9 the correct exposure metric and the health outcome studied. Likewise, sampling time
10 interval and lag time selection both determine whether an epidemiologic model captures
11 the phenomena of interest with sufficient resolution. The use of the community average
12 ambient PM_{2.5} concentration as a surrogate for the community average personal exposure
13 to ambient PM_{2.5} is not expected to change the principal conclusions from PM_{2.5}
14 epidemiologic studies that use community average health and pollution data. Several
15 recent studies support this by showing how the ambient component of personal exposure to
16 PM_{2.5} could be estimated using various tracer and source apportionment techniques and
17 that it is highly correlated with ambient concentrations of PM_{2.5}. These studies also show
18 that the non-ambient component of personal exposure to PM_{2.5} is basically uncorrelated
19 with ambient PM_{2.5} concentrations. For long-term studies that use differences in long-term
20 community average ambient PM concentrations as an exposure metric, the effect of possible
21 community-to-community differences in the average ambient exposure factor or in the
22 average non-ambient exposure are less understood. For panel epidemiologic studies, the
23 most appropriate exposure metric may depend on the health outcome measured. However,
24 sufficient information should be obtained to enable determining the association of the
25 health outcome with ambient concentration, ambient exposure, non-ambient exposure, and
26 total personal exposure.

27 Health effect estimates are often not clearly associated with a given PM constituent
28 because questions persist whether the measured surrogate or a different component are
29 actually responsible for the effect. Two studies have suggested that if PM composition data
30 are accurate, resulting health effects estimates are more significant than when the PM are
31 poorly characterized. Differences between composition of outdoor and indoor ambient PM
32 may also cause error in exposure assessment related either to differential losses of ultrafine
33 or coarse PM from diffusion, evaporation of semi-volatile PM, or impaction. The resulting

1 differences in PM size distribution and chemical composition between indoor-ambient PM
2 and outdoor-ambient PM are expected to cause differences in toxicity that could affect
3 health effects outcomes. Lack of information regarding these relationships adds uncertainty
4 to the health effects estimate.

Chapter 3 References

- ACGIH. (2005). TLVs and BEIs: Based on the documentation of the threshold limit values for chemical substances and physical agents and biological exposure indices. [156188](#)
- Adams HS; Nieuwenhuijsen MJ; Colvile RN; McMullen MAS; Khandelwal P. (2001). Fine particle (PM_{2.5}) personal exposure levels in transport microenvironments, London, UK. *Sci Total Environ*, 279: 29-44. [019350](#)
- Adar SD; Davey M; Sullivan JR; Compther M; Szpiro A; Liu L-J. (2008). Predicting airborne particle levels aboard Washington State school buses . *Atmos Environ*, 42: 7590-7599. [191200](#)
- Adgate JL; Mongin SJ; Pratt GC; Zhang J; Field MP; Ramachandran G; Sexton K. (2007). Relationships between personal, indoor, and outdoor exposures to trace elements in PM_{2.5}. *Sci Total Environ*, 386: 21-32. [156196](#)
- Al-Horr R; Samanta G; Dasgupta PK. (2003). A Continuous Analyzer for Soluble Anionic Constituents and Ammonium in Atmospheric Particulate Matter. *Environ Sci Technol*, 37: 5711-5720. [153951](#)
- Albinet A; Leoz-Garziandia E; Budzinski H; Villenave E. (2007). Sampling precautions for the measurement of nitrated polycyclic aromatic hydrocarbons in ambient air. *Atmos Environ*, 41: 4988-4994. [154426](#)
- Alexis A; Garcia A; Nystrom M; Rosenkranz K. (2001). The 2001 California almanac of emissions and air quality. Retrieved , from . [079886](#)
- Allen GA; Harrison D; Koutrakis P. (2001). A New Method for Continuous Measurement of Sulfate in the Ambient Atmosphere. Presented at American Association for Aerosol Research, 20th Annual Conference. [156205](#)
- Allen R; Larson T; Sheppard L; Wallace L; Liu L-J. (2003). Use of real-time light scattering data to estimate the contribution of infiltrated and indoor-generated particles to indoor air. *Environ Sci Technol*, 37: 3484-3492. [053578](#)
- Allen R; Wallace L; Larson T; Sheppard L; Liu L-J. (2004). Estimated hourly personal exposures to ambient and nonambient particulate matter among sensitive populations in Seattle, Washington. , 54: 1197-1211. [190089](#)
- Andracchio A; Cavicchi C; Tonelli D; Zappoli S. (2002). A new approach for the fractionation of water-soluble organic carbon in atmospheric aerosols and cloud drops. *Atmos Environ*, 36: 5097-5107. [155657](#)
- Andreae MO; Gelencsér A. (2006). Black carbon or brown carbon? The nature of light-absorbing carbonaceous aerosols. , 6: 3131-3148. [156215](#)
- Appel K; Bhawe PV; Gilliland AB; Sarwar G; Roselle SJ. (2008). Evaluation of the community multiscale air quality (CMAQ) model version 4.5: Sensitivities impacting model performance; Part II – particulate matter. *Atmos Environ*, 42: 6057-6066. [155660](#)
- Appel KW; Gilliland A; Eder B. (2005). An operational evaluation of the 2005 release of models-3 CMAQ version 4.5. National Oceanic and Atmospheric Administration–Air Resources. Washington DC. [089227](#)
- Arhami M; Kuhn T; Fine PM; Delfino RJ; Sioutas C. (2006). Effects of Sampling Artifacts and Operating Parameters on the Performance of a Semicontinuous Particulate Elemental Carbon/Organic Carbon Monitor. *Environ Sci Technol*, 40: 945-954. [156224](#)
- Arnold JR; Dennis RL; Tonnesen GS. (2003). Diagnostic evaluation of numerical air quality models with specialized ambient observations: testing the Community Multiscale Air Quality modeling system (CMAQ) at selected SOS 95 ground sites. *Atmos Environ*, 37: 1185-1198. [087579](#)
- Arnott WP; Moosmüller H; Sheridan PJ; Ogren JA; Raspert R; Slaton WV; Hand JL; Kreidenweis SM; Collett JL Jr. (2003). Photoacoustic and filter-based ambient aerosol light absorption measurements: Instrument comparisons and the role of relative humidity. *J Geophys Res*, 108: AAC 15-1. [037711](#)
- Artinano B; Querol X; Salvador P; Rodriguez S; Alonso DG; Alastuey A. (2001). Assessment of airborne particulate levels in Spain in relation to the new EU-directive . *Atmos Environ*, 35: S43-S53. [190099](#)
- Auvray M; Bey I. (2005). Long-range transport to Europe: Seasonal variations and implications for the European ozone budget. *J Geophys Res*, 110: D11303.1-D11303.22. [156237](#)
- Ayers GP. (2004). Potential for simultaneous measurement of PM₁₀, PM_{2.5} and PM₁ for air quality monitoring purposes using a single TEOM. *Atmos Environ*, 38: 3453-3458. [097440](#)

Note: Hyperlinks to the reference citations throughout this document will take you to the NCEA HERO database (Health and Environmental Research Online) at <http://epa.gov/hero>. HERO is a database of scientific literature used by U.S. EPA in the process of developing science assessments such as the Integrated Science Assessments (ISA) and the Integrated Risk Information System (IRIS).

- Bae MS. (2007). Intercomparison of Real Time Ammonium Measurements at Urban and Rural Locations in New York. *Aerosol Sci Technol*, 41: 329-341. [155669](#)
- Bae MS; Schauer JJ; Deminter JT; Turner JR. (2004). Hourly and daily patterns of particle-phase organic and elemental carbon concentrations in the urban atmosphere. *J Air Waste Manag Assoc*, 54: 823-833. [156243](#)
- Bae MS; Schwab JJ; Zhang Q; Hogrefe O; Demerjian KL; Weimer S; Rhoads K; Orsini D; Venkatachari P; Hopke PK. (2007). Interference of organic signals in highly time resolved nitrate measurements by low mass resolution aerosol mass spectrometry. *J Geophys Res*, 112: D22305-D22305 (1-16). [156244](#)
- Baldauf R; Thoma E; Hays M; Shores R; Kinsey J; Gullett B; Kimbrough S; Isakov V; Long T; Snow R; Khlystov A; Weinstein J; Chen FL; Seila R; Olson D; Gilmour I; Cho SH; Watkins N; Rowley P; Bang J. (2008). Traffic and meteorological impacts on near-road air quality: Summary of methods and trends from the raleigh near-road study. , 58: 865-878. [190239](#)
- Baldauf R; Thoma E; Khlystov A; Isakov V; Bowker G; Long T; Snow R. (2008). Impacts of noise barriers on near-road air quality. *Atmos Environ*, 42: 7502-7507. [191017](#)
- Baldauf R; Watkins N; Heist D; Bailey C; Rowley P; Shores R. (2009). Near-road air quality monitoring: Factors affecting network design and interpretation of data. , 2: 1-9. [191766](#)
- Baldauf RW; Gabele P; Crews W; Snow R; Cook JR. (2005). Criteria and air-toxic emissions from in-use automobiles in the national low-emission vehicle program. , 55: 1263-1268. [191184](#)
- Barn P; Larson T; Noullett M; Kennedy S; Copes R; Brauer M. (2008). Infiltration of forest fire and residential wood smoke: an evaluation of air cleaner effectiveness. *J Expo Sci Environ Epidemiol*, 18: 503-511. [156252](#)
- Barreto RP; Albuquerque FC; Netto ADP. (2007). Optimization of an improved analytical method for the determination of 1-nitropyrene in milligram diesel soot samples by high-performance liquid chromatography–mass spectrometry. *J Chromatogr*, 1163: 219-227. [155676](#)
- Bauer H; Schueller E; Weinke G; Berger A; Hitzenberger R; Marr I; Puxbaum H. (2008). Significant contributions of fungal spores to the organic carbon and to the aerosol mass balance of the urban atmospheric aerosol. *Atmos Environ*, 42: 5542-5549. [189986](#)
- Baxter LK; Barzyk TM; Vette VF; Croghan C; Williams RW. (2008). Contributions of diesel truck emissions to indoor elemental carbon concentrations in homes in proximity to Ambassador Bridge . *Atmos Environ*, 42: 9080-9086 . [191194](#)
- Baxter LK; Clougherty JE; Laden F; Levy JI. (2007). Predictors of concentrations of nitrogen dioxide, fine particulate matter, and particle constituents inside of lower socioeconomic status urban homes. *J Expo Sci Environ Epidemiol*, 17: 433-444. [092726](#)
- Baxter LK; Clougherty JE; Paciorek CJ; Wright RJ; Levy JI. (2007). Predicting residential indoor concentrations of nitrogen dioxide, fine particulate matter, and elemental carbon using questionnaire and geographic information system based data. *Atmos Environ*, 41: 6561-6571. [092725](#)
- Behrentz E; Fitz DR; Pankratz DV; Sabin LD; Colome SD; Fruin SA; Winer AM. (2004). Measuring self-pollution in school buses using a tracer gas technique. *Atmos Environ*, 38: 3735-3746. [155682](#)
- Bein KJ; Zhao Y; Wexler AS; Johnston MV. (2005). Speciation of size-resolved individual ultrafine particles in Pittsburgh, Pennsylvania. *J Geophys Res*, 110: D07S05. [156265](#)
- Bell ML; Dominici F; Ebisu K; Zeger SL; Samet JM. (2007). Spatial and Temporal Variation in PM_{2.5} Chemical Composition in the United States for Health Effects Studies. , 115: 989. [155683](#)
- Bell ML; Ebisu K; Peng RD; Dominici F. (2009). Adverse health effects of particulate air pollution: modification by air conditioning. *Epidemiology*, in press: in press. [191007](#)
- Bell ML; Ebisu K; Peng RD; Walker J; Samet JM; Zeger SL; Dominici F. (2008). Seasonal and regional short-term effects of fine particles on hospital admissions in 202 U.S. counties, 1999-2005. *Am J Epidemiol*, 168: 1301-1310. [156266](#)
- Benkovitz CM; Scholtz MT; Pacyna J; Tarrason L; Dignon J; Voldner EC; Spiro PA; Logan JA; Graedel TE. (1996). Global gridded inventories of anthropogenic emissions of sulfur and nitrogen: North Atlantic Regional Experiment(NARE). *J Geophys Res*, 101: 29239-29253. [156267](#)
- Bennett DH; Koutrakis P. (2006). Determining the infiltration of outdoor particles in the indoor environment using a dynamic model. *J Aerosol Sci*, 37: 766-785. [089184](#)
- Binkowski F; Roselle S. (2003). Models-3 Community Multiscale Air Quality(CMAQ) model aerosol component 1. Model description. , 108: np. [191769](#)
- Binkowski FS; Arunachalam S; Adelman Z; Pinto JP. (2007). Examining photolysis rates with a prototype online photolysis module in CMAQ. , 46: 1252-1256. [090563](#)

- Biswas S; Hu S; Verma V; Herner J; Robertson W; Ayala A; Sioutas C. (2008). Physical properties of particulate matter (PM) from late model heavy-duty diesel vehicles operating with advanced PM and NO_x emission control technologies. *Atmos Environ*, 42: 5622-5634. [189969](#)
- Biswas S; Verma V; Schauer JJ; Sioutas C. (2009). Chemical speciation of PM emissions from heavy-duty diesel vehicles equipped with diesel particulate filter (DPF) and. *Atmos Environ*, 43: 1917-1925. [189880](#)
- Blanchard P; Brook JR; Brazil P. (2002). Chemical characterization of the organic fraction of atmospheric aerosol at two sites in Ontario, Canada. *J Geophys Res*, 107: ICC10.1-ICC10.8 . [047598](#)
- Blando JD; Turpin BJ. (2000). Secondary organic aerosol formation in cloud and fog droplets: a literature evaluation of plausibility. *Atmos Environ*, 34: 1623-1632. [155692](#)
- Bond TC; Streets DG; Yarber KF; Nelson SM; Woo J-H; Klimont Z. (2004). A technology-based global inventory of black and organic carbon emissions from combustion. *J Geophys Res*, 109: D14203. [056389](#)
- Borak J; Sirianni G; Cohen HJ; Chemerynski S; Wheeler R. (2003). Comparison of NIOSH 5040 Method versus Aethalometer™ to Monitor Diesel Particulate in School Buses and at Work Sites. *AIHA J*, 64: 260-268. [156284](#)
- Borrego C; Tchepel O; Costa AM; Martins H; Ferreira J; Miranda AI. (2006). Traffic-related particulate air pollution exposure in urban areas. *Atmos Environ*, 40: 7205-7214. [155697](#)
- Bortnick SM; Coutant BW; Eberly SI. (2002). Using continuous PM_{2.5} monitoring data to report an air quality index. *J Air Waste Manag Assoc*, 52: 104-112. [156285](#)
- Brauer M; Hoek G; van Vliet P; Meliefste K; Fischer P; Gehring U; Heinrich J; Cyrus J; Bellander T; Lewne M; Brunekreef B. (2003). Estimating long-term average particulate air pollution concentrations: application of traffic indicators and geographic information systems. , 14: 228-239. [155702](#)
- Braun A. (2009). Two-process model for the atmospheric weathering, oxidation and ageing of diesel soot. *Geophys Res Lett*, 36: L07810. [189997](#)
- Briggs D. (2000). Exposure assessment. In *Spatial Epidemiology: Methods and Applications* (pp. 335-359). Oxford: Oxford University Press. [191772](#)
- Briggs DJ; Collins S; Elliott P; Fischer P; Kingham S; Lebret E; Pryn K; Van Reeuwijk H; Smallbone K; Van Der Veen A. (1997). Mapping urban air pollution using GIS: a regression-based approach. *Int J Geogr Inform Sci*, 11: 699-718. [025950](#)
- Briggs DJ; de Hoogh K; Morris C; Gulliver J. (2008). Effects of travel mode on exposures to particulate air pollution. *Environ Int*, 34: 12-22. [156294](#)
- Brock CA; Hudson PK; Lovejoy ER; Sullivan A; Nowak JB; Huey LG; Cooper OR; Cziczo DJ; de Gouw J; Fehsenfeld FC. (2004). Particle characteristics following cloud-modified transport from Asia to North America. *J Geophys Res*, 109: D23S26. [156295](#)
- Brook JR; Sirois A; Clarke JF. (1996). Comparison of dry deposition velocities for SO₂, HNO₃, and SO₄(2-) estimated with two inferential models. *Water Air Soil Pollut*, 87: 205-218. [024023](#)
- Brown AS; Yardley RE; Quincey PG; Butterfield DM. (2006). Studies of the effect of humidity and other factors on some different filter materials used for gravimetric measurements of ambient particulate matter. *Atmos Environ*, 40: 4670-4678. [097665](#)
- Bruno P; Caselli M; de Gennaro G; Tutino M. (2007). Determination of polycyclic aromatic hydrocarbons (PAHs) in particulate matter collected with low volume samplers. *Talanta*, 72: 1357-1361. [155706](#)
- Burke JM; Zufall MJ; Ozkaynak H. (2001). A population exposure model for particulate matter: case study results for PM_{2.5} in Philadelphia, PA. *J Expo Sci Environ Epidemiol*, 11: 470-489. [014050](#)
- Burnett RT; Goldberg MS. (2003). Size-fractionated particulate mass and daily mortality in eight Canadian cities. [042798](#)
- Butler AJ; Andrew MS; Russell AG. (2003). Daily sampling Of PM_{2.5} in Atlanta: Results of the first year of the Assessment of Spatial Aerosol Composition. *J Geophys Res*, 108: 8415. [156313](#)
- Buzorius G; Hameri K; Pekkanen J; Kulmala M. (1999). Spatial variation of aerosol number concentration in Helsinki city. *Atmos Environ*, 33: 553-565. [081205](#)
- Bytnerowicz A; Miller PR; Olszyk DM. (1987). Dry deposition of nitrate, ammonium and sulfate to a *Ceanothus crassifolius* canopy and surrogate surfaces. *Atmos Environ*, 21: 1749-1757. [036493](#)
- Byun D; Schere KL. (2006). Review of the governing equations, computational algorithms, and other components of the models-3 community multiscale air quality (CMAQ) modeling system. *Appl. Mech. Rev.*, 59: 51-77. [090560](#)
- Byun DW; Ching JKS. (1999). Science Algorithms of the EPA Models-3 Community Multiscale Air Quality (CMAQ) Modeling System. [156314](#)
- Cabada JC; Rees S; Takahama S; Khlystov A; Pandis SN; Davidson CI; Robinson AL. (2004). Mass size distributions and size resolved chemical composition of fine particulate matter at the Pittsburgh supersite. *Atmos Environ*, 38: 3127-3141. [148859](#)

- Cadle SH; Mulawa P; Groblicki P; Laroo C; Ragazzi RA; Nelson K; Gallagher G; Zielinska B. (2001). In-use light-duty gasoline vehicle particulate matter emissions on the FTP, REPO5, and UC cycles [final report]. [017192](#)
- Cadle SH; Mulawa PA; Hunsanger EC; Nelson K; Ragazzi RA; Barrett R; Gallagher GL; Lawson DR; Knapp KT; Snow R. (1999). Composition of light-duty motor vehicle exhaust particulate matter in the Denver, Colorado area. *Environ Sci Technol*, 33: 2328-2339. [007636](#)
- Carter WPL. (1990). A detailed mechanism for the gas-phase atmospheric reactions of organic compounds. *Atmos Environ*, 24: 481-518. [042893](#)
- Case MW; Williams R; Yeatts K; Chen F-L; Scott J; Svendsen E; Devlin RB. (2008). Evaluation of a direct personal coarse particulate matter monitor. *Atmos Environ*, 42(19): 4446-4452. [155149](#)
- Cass GR. (1998). Organic molecular tracers for particulate air pollution sources. *Trends Analyt Chem*, 17: 356-366. [155716](#)
- Cass GR; Hughes LA; Bhave P; Kleeman MJ; Allen JO; Salmon LG. (2000). The chemical composition of atmospheric ultrafine particles. *Proc Biol Sci*, 358: 2581-2592. [020680](#)
- Chakrabarti B; Fine PM; Delfino R; Sioutas C. (2004). Performance evaluation of the active-flow personal DataRAM PM25 mass monitor (Thermo Anderson pDR-1200) designed for continuous personal exposure measurements. *Atmos Environ*, 38: 3329-3340. [147867](#)
- Chang C-H; Meroney RN. (2003). Concentration and flow distributions in urban street canyons: wind tunnel and computational data. *J Wind Eng Ind Aerod*, 91: 1141-1154. [090298](#)
- Chang CT; Tsai CJ. (2003). A model for the relative humidity effect on the readings of the PM10 beta-gauge monitor. *J Aerosol Sci*, 34: 1685-1697. [155718](#)
- Chang L-T; Koutrakis P; Catalano PJ; Suh HH. (2003). Assessing the importance of different exposure metrics and time-activity data to predict 24-h personal PM25 exposures. *J Toxicol Environ Health A*, 66: 1825-1846. [053789](#)
- Charron A; Harrison RM; Moorcroft S; Booker J. (2004). Quantitative interpretation of divergence between PM10 and PM25 mass measurement by TEOM and gravimetric (Partisol) instruments. *Atmos Environ*, 38: 415-423. [053849](#)
- Chen FL; Williams R; Svendsen E; Yeatts K; Creason J; Scott J; Terrell D; Case M. (2007). Coarse particulate matter concentrations from residential outdoor sites associated with the North Carolina Asthma and Children's Environment Studies (NC-ACES). *Atmos Environ*, 41: 1200-1208. [147318](#)
- Chen SJ; Hsieh LT; Kao MJ; Lin WY; Huang KL; Lin CC. (2004). Characteristics of particles sampled in southern Taiwan during the Asian dust storm periods in 2000 and 2001. *Atmos Environ*, 38: 5925-5934. [147143](#)
- Chiapello I; Moulin C; Prospero JM. (2005). Understanding the long-term variability of African dust transport across the Atlantic as recorded in both Barbados surface concentrations and large-scale Total Ozone Mapping Spectrometer (TOMS) optical thickness. *J Geophys Res*, 110: D18S10. [156339](#)
- Ching J; Herwehe J; Swall J. (2006). On joint deterministic grid modeling and sub-grid variability conceptual framework for model evaluation. *Atmos Environ*, 40: 4935-4945. [090300](#)
- Chow JC. (2007). The application of thermal methods for determining chemical composition of carbonaceous aerosols: A review. , 42: 1521-1541. [157209](#)
- Chow JC; Doraiswamy P; Watson JG; Chen LW; Ho SS; Sodeman DA. (2008). Advances in integrated and continuous measurements for particle mass and chemical composition. *J Air Waste Manag Assoc*, 58: 141-163. [156355](#)
- Chow JC; Watson JG; Chen LW; Chang MC; Robinson NF; Trimble D; Kohl S. (2007). The IMPROVE_A temperature protocol for thermal/optical carbon analysis: maintaining consistency with a long-term database. *J Air Waste Manag Assoc*, 57: 1014-1023. [156354](#)
- Chow JC; Watson JG; Chen LWA; Arnott WP; Moosmuller H; Fung K. (2004). Equivalence of elemental carbon by thermal/optical reflectance and transmittance with different temperature protocols. *Environ Sci Technol*, 38: 4414-4422. [156347](#)
- Chow JC; Watson JG; Louie PKK; Chen LWA; Sin D. (2005). Comparison of PM2.5 carbon measurement methods in Hong Kong, China. , 137: 334-344. [155728](#)
- Chow JC; Watson JG; Park K; Lowenthal DH; Robinson NF; Magliano KA. (2006). Comparison of particle light scattering and fine particulate matter mass in central California. *J Air Waste Manag Assoc*, 56: 398-410. [099031](#)
- Chu D; Kaufman Y; Zibordi G; Chern J; Mao J; Li C; Holben B. (2003). Global monitoring of air pollution over land from the Earth Observing System-Terra Moderate Resolution Imaging Spectroradiometer (MODIS). , 108: ACH4.1-ACH4.18. [190049](#)

- Chung A; Herner JD; Kleeman MJ. (2001). Detection of alkaline ultrafine atmospheric particles at Bakersfield, California. *Environ Sci Technol*, 35: 2184-2190. [017105](#)
- Claeys M; Graham B; Vas G; Wang W; Vermeylen R; Pashynska V; Cafmeyer J; Guyon P; Andreae MO; Artaxo P; Maenhaut W. (2004). Formation of secondary organic aerosols through photooxidation of isoprene. , 303: 1173-1176. [058608](#)
- Clarke JF; Edgerton ES; Martin BE. (1997). Dry deposition calculations for the clean air status and trends network. *Atmos Environ*, 31: 3667-3678. [025022](#)
- Clough WS. (1975). The deposition of particles on moss and grass surfaces. *Atmos Environ*, 9: 1113-1119. [070850](#)
- Cohen M; Adar S; Allen R; Avol E; Curl C; Gould T; Hardie D; Ho A; Kinney P; Larson T. (2009). Approach to estimating participant pollutant exposures in the multi-ethnic study of atherosclerosis and air pollution (MESA Air). , x: 709-742. [190639](#)
- Conny JM; Klinedinst DB; Wight SA; Paulsen JL. (2003). Optimizing thermal-optical methods for measuring atmospheric elemental (black) carbon: A response surface study. *Aerosol Sci Technol*, 37: 703-723. [145948](#)
- Conny JM; Norris GA; Gould TR. (2009). Factorial-based response-surface modeling with confidence intervals for optimizing thermal-optical transmission analysis of atmospheric black carbon. *Anal Chim Acta*, 635: 144-156. [191999](#)
- Cooke WF; Lioussé C; Cachier H; Feichter J. (1999). Construction of a 1 ° x 1 ° fossil fuel emission data set for carbonaceous aerosol and implementation and radiative impact in the ECHAM 4 model. *J Geophys Res*, 104: 22137-22162. [156365](#)
- Corburn J. (2007). Urban land use, air toxics and public health: Assessing hazardous exposures at the neighborhood scale. *Environ Impact Assess Rev*, 27: 145-160. [155738](#)
- Cowburn AS; Condliffe AM; Farahi N; Summers C; Chilvers ER. (2008). Advances in neutrophil biology: clinical implications. , 134: 606-12. [191142](#)
- Crimmins BS; Baker JE. (2006). Improved GC/MS methods for measuring hourly PAH and nitro-PAH concentrations in urban particulate matter. *Atmos Environ*, 40: 6764-6779. [097008](#)
- Crist KC; Liu B; Kim M; Deshpande SR; John K. (2008). Characterization of fine particulate matter in Ohio: Indoor, outdoor, and personal exposures. *Environ Res*, 106: 62-71. [156372](#)
- Cyrus J; Heinrich J; Hoek G; Meliefste K; Lewne M; Gehring U; Bellander T; Fischer P; Van Vliet P; Brauer M; Wichmann H-E; Brunekreef B. (2003). Comparison between different traffic-related particle indicators: elemental carbon (EC), PM_{2.5} mass, and absorbance. *J Expo Sci Environ Epidemiol*, 13: 134-143. [049634](#)
- Dasch JM. (1987). Measurement of dry deposition to surfaces in deciduous and pine canopies. , 44: 261-277. [036496](#)
- Dasgupta PK; Idowu AD; Li J. (2007). Method and Apparatus for Analyzing Arsenic Concentrations Using Gas Phase Ozone Chemiluminescence. [156383](#)
- Davidson CI; Wu Y-L. (1990). Dry deposition of particles and vapors. In Lindberg, S. E.; Page, A. L.; Norton, S. A. (Ed.), *Acidic precipitation: v. 3, sources, deposition, and canopy interactions* New York, NY: Springer-Verlag. [036799](#)
- de Gouw JA; Brock CA; Atlas EL; Bates TS; Fehsenfeld FC; Goldan PD; Holloway JS; Kuster WC; Lerner BM; Matthew BM. (2008). Sources of particulate matter in the northeastern United States in summer: 1. Direct emissions and secondary formation of organic matter in urban plumes. , 113: np. [191757](#)
- deCastro BR; Sax AN; Chillrud SN; Kinney PL; Spengler JD. (2007). Modeling time-location patterns of inner-city high school students in New York and Los Angeles using a longitudinal approach with generalized estimating equations. *J Expo Sci Environ Epidemiol*, 17: 233-247. [190996](#)
- Decesari S; Facchini MC; Fuzzi S; Tagliavini E. (2000). Characterization of water-soluble organic compounds in atmospheric aerosol: A new approach. *J Geophys Res*, 105: 1481-1489. [155748](#)
- Delfino RJ; Staimer N; Gillen D; Tjoa T; Sioutas C; Fung K; George SC; Kleinman MT. (2006). Personal and ambient air pollution is associated with increased exhaled nitric oxide in children with asthma. *Environ Health Perspect*, 114: 1736-1743. [090745](#)
- Demokritou P; Lee S; Koutrakis P. (2004). Development and Evaluation of a High Loading PM_{2.5} Speciation Sampler. *Aerosol Sci Technol*, 38: 111-119. [186901](#)
- Demokritou P; Lee SJ; Ferguson ST; Koutrakis P. (2004). A compact multistage (cascade) impactor for the characterization of atmospheric aerosols. *J Aerosol Sci*, 35: 281-299. [190115](#)

- Dentener F; Stevenson D; Ellingsen K; Van Noije T; Schultz M; Amann M; Atherton C; Bell N; Bergmann D; Bey I; Bouwman L; Butler T; Cofala J; Collins B; Drevet J; Doherty R; Eickhout B; Eskes H; Fiore A; Gauss M; Hauglustaine D; Horowitz L; Isaksen ISA; Josse B; Lawrence M; Krol M; Lamarque JF; Montanaro V; Muller JF; Peuch VH; Pitari G; Pyle J; Rast S; Rodriguez J; Sanderson M; Savage NH; Shindell D; Strahan S; et al. (2006). The global atmospheric environment for the next generation. *Environ Sci Technol*, 40: 3586-3594. [088434](#)
- Derwent RG; Collins WJ; Johnson CE; Stevenson DS. (2001). Transient behaviour of tropospheric ozone precursors in a global 3-D CTM and their indirect greenhouse effects. *Clim Change*, 49: 463-487. [047912](#)
- Diapouli E; Chaloulakou A; Spyrellis N. (2007). Levels of ultrafine particles in different microenvironments- implications to children exposure. *Sci Total Environ*, 388: 128-136. [156397](#)
- Diapouli E; Grivas G; Chaloulakou A; Spyrellis N. (2008). PM10 and ultrafine particles counts in-vehicle and on-road in the Athens area . , 8: 89-97. [190119](#)
- Docherty KS; Wu W; Lim YB; Ziemann PJ. (2005). Contributions of organic peroxides to secondary aerosol formed from reactions of monoterpenes with O₃. *Environ Sci Technol*, 39: 4049-4059. [087613](#)
- Dockery DW; Pope CA III; Xu X; Spengler JD; Ware JH; Fay ME; Ferris BG Jr; Speizer FE. (1993). An association between air pollution and mortality in six US cities. , 329: 1753-1759. [044457](#)
- Dodge MC. (1977). Combined use of modeling techniques and smog chamber data to derive ozone-precursor relationships. [038646](#)
- Dominici F; Peng RD; Bell ML; Pham L; McDermott A; Zeger SL; Samet JL. (2006). Fine particulate air pollution and hospital admission for cardiovascular and respiratory diseases. *JAMA*, 295: 1127-1134. [088398](#)
- Dominici F; Zeger SL; Samet JM. (2000). A measurement error model for time-series studies of air pollution and mortality. , 1: 157-175. [005828](#)
- Drewnick F; Jayne JT; Canagaratna M; Worsnop DR; Demerjian KL. (2004). Measurement of Ambient Aerosol Composition During the PMTACS-NY 2001 Using an Aerosol Mass Spectrometer. Part II: Chemically Speciated Mass Distributions. *Aerosol Sci Technol*, 38: 104-117. [155755](#)
- Drewnick F; Schwab J; Jayne J; Canagaratna M; Worsnop D; Demerjian K. (2004). Measurement of Ambient Aerosol Composition During the PMTACS-NY 2001 Using an Aerosol Mass Spectrometer. Part I: Mass Concentrations. *Aerosol Sci Technol*, 38: 92-103. [155754](#)
- Drewnick F; Schwab JJ; Hogrefe O; Peters S; Husain L; Diamond D; Weber R; Demerjian KL. (2003). Intercomparison and evaluation of four semi-continuous PM_{2.5} sulfate instruments. *Atmos Environ*, 37: 3335-3350. [099160](#)
- Ebelt ST; Wilson WE; Brauer M. (2005). Exposure to ambient and nonambient components of particulate matter: a comparison of health effects. *Epidemiology*, 16: 396-405. [056907](#)
- Eder B; Kang D; Mathur R; Yu S; Schere K. (2006). An operational evaluation of the Eta-CMAQ air quality forecast model. *Atmos Environ*, 40: 4894-4905. [142721](#)
- Eder B; Yu S. (2005). A performance evaluation of the 2004 release of Models-3 CMAQ. *Atmos Environ*, 40: 4811-4824. [089229](#)
- Edgerton ES; Casuccio GS; Saylor RD; Lersch TL; Hartsell BE; Jansen JJ; Hansen DA. (2009). Measurements of OC and EC in coarse particulate matter in the southeastern United States. *J Air Waste Manag Assoc*, 59: 78-90. [180385](#)
- Edgerton ES; Hartsell BE; Saylor RD; Jansen JJ; Hansen DA; Hidy GM. (2005). The Southeastern Aerosol Research and Characterization Study: Part II Filter-based measurements of fine and coarse particulate matter mass and composition. *J Air Waste Manag Assoc*, 55: 1527-1542. [088686](#)
- Edney EO; Lewandowski M; Offenberg JH; Wang W; Claeys M; Kleindienst TE; Jaoui M. (2005). Formation of 2-methyl tetrols and 2-methylglyceric acid in secondary organic aerosol from laboratory irradiated isoprene/NOX/SO₂/air mixtures and their detection in ambient PM_{2.5} samples collected in the eastern United States. *Atmos Environ*, 39: 5281-5289. [155760](#)
- Eiguren-Fernandez A; Miguel AH; Jaques PA; Sioutas C. (2003). Evaluation of a denuder-MOUDI-PUF sampling system to measure the size distribution of semi-volatile polycyclic aromatic hydrocarbons in the atmosphere. *Aerosol Sci Technol*, 37: 201-209. [142609](#)
- El-Zanan HS; Lowenthal DH; Zielinska B; Chow JC; Kumar N. (2005). Determination of the organic aerosol mass to organic carbon ratio in IMPROVE samples. *Chemosphere*, 60: 485-496. [155764](#)
- Elgethun K; Fenske R; Yost M; Palcisko G. (2003). Time-location analysis for exposure assessment studies of children using a novel global positioning system instrument. *Environ Health Perspect*, 111: 115-122. [190640](#)

- Engel-Cox JA; Weber SA. (2007). Compilation and assessment of recent positive matrix factorization and UNMIX receptor model studies on fine particulate matter source apportionment for the eastern United States. *J Air Waste Manag Assoc*, 57: 1307-1316. [156419](#)
- Engewald W; Teske J; Efer J. (1999). Programmed temperature vaporisers-based large volume injection in capillary gas chromatography. *J Chromatogr*, 842: 143-161. [155765](#)
- England GC; Watson JG; Chow JC; Zielinska B; Chang M. (2007). Dilution-Based Emissions Sampling from Stationary Sources: Part 2- Gas-Fired Combustors Compared with Other Fuel-Fired Systems. *J Air Waste Manag Assoc*, 57: 79-93. [156421](#)
- England GC; Watson JG; Chow JC; Zielinska B; Oliver Chang MC; Loos KR; Hidv GM. (2007). Dilution-based emissions sampling from stationary sources: Part 1-Compact sampler methodology and performance. *J Air Waste Manag Assoc*, 57: 65-78. [156420](#)
- Enstrom JE. (2005). Fine particulate air pollution and total mortality among elderly Californians, 1973-2002. *Inhal Toxicol*, 17: 803-816. [087356](#)
- Erisman J-W; Vermetten AWM; Asman WAH; Waijers-IJpelaan A; Slanina J. (1988). Vertical distribution of gases and aerosols: the behaviour of ammonia and related components in the lower atmosphere. *Atmos Environ*, 22: 1153-1160. [036510](#)
- Fairlie TD; Jacob DJ; Park RJ. (2007). The impact of transpacific transport of mineral dust in the United States. *Atmos Environ*, 41: 1251-1266. [141923](#)
- Fan X; Brook JR; Mabury SA. (2003). Sampling atmospheric carbonaceous aerosols using an integrated organic gas and particle sampler. *Environ Sci Technol*, 37: 3145-3151. [058628](#)
- Fan X; Lee PKH; Brook JR; Mabury SA. (2004). Improved Measurement of Seasonal and Diurnal Differences in the Carbonaceous Components of Urban Particulate Matter Using a Denuder-Based Air Sampler. *Aerosol Sci Technol*, 38: 63-69. [155770](#)
- Farmer PB; Singh R; Kaur B; Sram RJ; Binkova B; Kalina I; Popov TA; Garte S; Taioli E; Gabelova A; Cebulska-Wasilewska A. (2003). Molecular epidemiology studies of carcinogenic environmental pollutants. Effects of polycyclic aromatic hydrocarbons (PAHs) in environmental pollution on exogenous and oxidative DNA damage. , 544: 397-402. [156431](#)
- Feldpausch P; Fiebig M; Fritzsche L; Petzold A. (2006). Measurement of ultrafine aerosol size distributions by a combination of diffusion screen separators and condensation particle counters. *J Aerosol Sci*, 37: 577-597. [155773](#)
- Filleul L; Zeghnoun A; Cassadou S; Declercq C; Eilstein D; Le Tertre A; Medina S; Pascal L; Prouvost H; Saviuc P; Quenel P. (2006). Influence of set-up conditions of exposure indicators on the estimate of short-term associations between urban pollution and mortality. *Sci Total Environ*, 355: 90-97. [089862](#)
- Fine PM; Chakrabarti B; Krudysz M; Schauer JJ; Sioutas C. (2004). Diurnal Variations of Individual Organic Compound Constituents of Ultrafine and Accumulation Mode Particulate Matter in the Los Angeles Basin. *Environ Sci Technol*, 38: 1296-1304. [141283](#)
- Fine PM; Jaques PA; Hering SV; Sioutas C. (2003). Performance Evaluation and Use of a Continuous Monitor for Measuring Size-Fractionated PM 2.5 Nitrate. *Aerosol Sci Technol*, 37: 342 - 354. [155775](#)
- Finlayson-Pitts BJ; Pitts JN Jr. (2000). Chemistry of the upper and lower atmosphere: theory, experiments and applications. [055565](#)
- Fowler D; Cape JN; Unsworth MH. (1989). Deposition of atmospheric pollutants on forests. *Proc Biol Sci*, 324: 247-265. [002515](#)
- Fowler D; Duyzer JH; Baldocchi DD. (1991). Inputs of trace gases, particles and cloud droplets to terrestrial surfaces. *Proc Roy Soc Edinb B Biol*, 97: 35-59. [046630](#)
- Fox-Rabinovitz MS; Takacs LL; Govindaraju RC. (2002). A variable-resolution stretched-grid general circulation model and data assimilation system with multiple areas of interest: studying the anomalous regional climate events of 1998. *J Geophys Res*, 107D24. [047806](#)
- Frank NH. (2006). Retained nitrate, hydrated sulfates, and carbonaceous mass in federal reference method fine particulate matter for six eastern U.S. cities. *J Air Waste Manag Assoc*, 56: 500-11. [098909](#)
- Fraser MP; Cass GR; Simoneit BRT. (1999). Particulate organic compounds emitted from motor vehicle exhaust and in the urban atmosphere. *Atmos Environ*, 33: 2715-2724. [010819](#)
- Fraser MP; Yue ZW; Buzcu B. (2003). Source apportionment of fine particulate matter in Houston, TX, using organic molecular markers. *Atmos Environ*, 37: 2117-2123. [042231](#)
- Fruin S; Westerdahl D; Sax T; Sioutas C; Fine PM. (2008). Measurements and predictors of on-road ultrafine particle concentrations and associated pollutants in Los Angeles. *Atmos Environ*, 42: 207-219. [097183](#)
- Fuentes M; Raftery AE. (2005). Model evaluation and spatial interpolation by Bayesian combination of observations with outputs from numerical models. *Biometrics*, 61: 36-45. [087580](#)

- Fuentes M; Song HR; Ghosh SK; Holland DM; Davis JM. (2006). Spatial association between speciated fine particles and mortality. *Biometrics*, 62: 855-63. [097647](#)
- Gallagher MW; Choulaton TW; Morse AP; Fowler D. (1988). Measurements of the size dependence of cloud droplet deposition at a hill site. , 114: 1291-1303. [046631](#)
- Gao S; Ng NL; Keywood M; Varutbangkul V; Bahreini R; Nenes A; He J; Yoo KY; Beauchamp JL; Hodyss RP; Flagan RC; Seinfeld JH. (2004). Particle phase acidity and oligomer formation in secondary organic aerosol. *Environ Sci Technol*, 38: 6582-6589. [156460](#)
- Garner JHB; Pagano T; Cowling EB. (1989). An evaluation of the role of ozone, acid deposition, and other airborne pollutants in the forests of eastern North America. [042085](#)
- Garten CT Jr; Hanson PJ. (1990). Foliar retention of ¹⁵N-nitrate and ¹⁵N-ammonium by red maple (*Acer rubrum*) and white oak (*Quercus alba*) leaves from simulated rain. *Environ Exp Bot*, 30: 333-342. [036803](#)
- Gaydos TM; Pinder R; Koo B; Fahey KM; Yarwood G; Pandis SN. (2007). Development and application of a three-dimensional aerosol chemical transport model, PMCAMx. *Atmos Environ*, 41: 2594-2611. [139738](#)
- Gaydos TM; Stanier CO; Pandis SN. (2005). Modeling of in situ ultrafine atmospheric particle formation in the eastern United States. , 110: D07S12. [191762](#)
- Gelencser A; Varga Z. (2005). Evaluation of the atmospheric significance of multiphase reactions in atmospheric secondary organic aerosol formation. , 5: 2823-2831. [156463](#)
- Gelencsér A; Mészáros T; Blazsó M; Kiss G; Krivácsy Z; Molnár A; Mészáros E. (2000). Structural Characterisation of Organic Matter in Fine Tropospheric Aerosol by Pyrolysis-Gas Chromatography-Mass Spectrometry. , 37: 173-183. [155785](#)
- Geller M; Solomon P. (2006). Special issue of Aerosol Science and Technology for particulate matter supersites program and related studies. *Aerosol Sci Technol*, 40: 735-736. [139645](#)
- Geller MD; Ntziachristos L; Mamakos A; Samaras Z; Schmitz DA; Froines JR; Sioutas C. (2006). Physicochemical and redox characteristics of particulate matter (PM) emitted from gasoline and diesel passenger cars. *Atmos Environ*, 40: 6988-7004. [139644](#)
- Generoso S; Bey I; Attié J-L; Bréon F-M. (2007). A satellite- and model-based assessment of the 2003 Russian fires: impact on the arctic region. *J Geophys Res*, 112: 5302. [155786](#)
- Georgopoulos PG; Wang S-W; Vyas VM; Sun Q; Burke J; Vedantham R; McCurdy T; Ozkaynak H. (2005). A source-to-dose assessment of population exposures to fine PM and ozone in Philadelphia, PA, during a summer 1999 episode. *J Expo Sci Environ Epidemiol*, 15: 439-457. [080269](#)
- Gery MW; Whitten GZ; Killus JP; Dodge MC. (1989). A photochemical kinetics mechanism for urban and regional scale computer modeling. *J Geophys Res*, 94: 12,925-12,956. [043039](#)
- Giglio L; van der Werf GR; Randerson JT; Collatz GJ; Kasibhatla P. (2006). Global estimation of burned area using MODIS active fire observations. , 6: 957-974. [156469](#)
- Gillette DA; Hanson KJ. (1989). Spatial and temporal variability of dust production caused by wind erosion in the United States. *J Geophys Res*, 94: 2197-2206. [030212](#)
- Gilliam RC; Childs PP; Huber AH; Raman S. (2005). Metropolitan-scale transport and dispersion from the New York World Trade Center following September 11, 2001 Part I: an evaluation of the CALMET meteorological model. , 162: 1981-2003. [056749](#)
- Gilliam RC; Huber AH; Raman S. (2005). Metropolitan-scale transport and dispersion from the New York World Trade Center following September 11, 2001 Part II: an application of the CALPUFF plume model. , 162: 2005-2028. [056750](#)
- Gilliland F; Avol E; Kinney P; Jerrett M; Dvonch T; Lurmann F; Buckley T; Breyse P; Keeler G; de Villiers T; McConnell R. (2005). Air pollution exposure assessment for epidemiologic studies of pregnant women and children: lessons learned from the Centers for Children's Environmental Health and Disease Prevention Research. *Environ Health Perspect*, 113: 1447-54. [098820](#)
- Goldstein E; Eagle MC; Hoerprich PD. (1973). Effect of nitrogen dioxide on pulmonary bacterial defense mechanisms. *Arch Environ Occup Health*, 26: 202-204. [015674](#)
- Gomez-Perales JE; Colville RN; Fernandez-Bremauntz AA; Gutierrez-Avedoy V; Paramo-Figueroa VH; Blanco-Jimenez S; Bueno-Lopez E; Bernabe-Cabanillas R; Mandujano F; Hidalgo-Navarro M; Nieuwenhuijsen MJ. (2007). Bus, minibus, metro inter-comparison of commuters' exposure to air pollution in Mexico City. *Atmos Environ*, 41: 890-901. [138816](#)
- Gomez-Perales JE; Colville RN; Nieuwenhuijsen MJ; Fernandez-Bremauntz A; Gutierrez-Avedoy VJ; Paramo-Figueroa VH; Blanco-Jimenez S; Bueno-Lopez E; Mandujano F; Bernabe-Cabanillas R; Ortiz-Segovia E. (2004). Commuters' exposure to PM_{2.5}, CO, and benzene in public transport in the metropolitan area of Mexico City. *Atmos Environ*, 38: 1219-1229. [054418](#)
- Gong L; Xu B; Zhu Y. (2009). Ultrafine particles deposition inside passenger vehicles . *Aerosol Sci Technol*, 43: 544-553. [190124](#)

- Goriaux M; Jourdain B; Temime B; Besombes JL; Marchand N; Albinet A; Leoz-Garziandia E; Wortham H. (2006). Field comparison of particulate PAH measurements using a low-flow denuder device and conventional sampling systems. *Environ Sci Technol*, 40: 6398-6404. [156484](#)
- Graham B; Guyon P; Taylor PE; Artaxo P; Maenhaut W; Glovsky MM; Flagan RC; Andreae MO. (2003). Organic compounds present in the natural Amazonian aerosol: Characterization by gas chromatography-mass spectrometry. *J Geophys Res*, 108: 4766. [156489](#)
- Greenwald R; Bergin MH; Weber R; Sullivan A. (2007). Size-resolved, real-time measurement of water-insoluble aerosols in metropolitan Atlanta during the summer of 2004. *Atmos Environ*, 41: 519-531. [155809](#)
- Grell GA; Emeis S; Stockwell WR; Schoenemeyer T; Forkel R; Michalakes J; Knoche R; Seidl W. (2000). Application of a multiscale, coupled MM5/chemistry model to the complex terrain of the VOTALP valley campaign. *Atmos Environ*, 34: 1435-1453. [048047](#)
- Grover BD; Eatough NL; Eatough DJ; Chow JC; Watson JG; Ambs JL; Meyer MB; Hopke PK; Al-Horr R; Later DW; Wilson WE. (2006). Measurement of Both Nonvolatile and Semi-Volatile Fractions of Fine Particulate Matter in Fresno, CA. *Aerosol Sci Technol*, 40: 811-826. [138080](#)
- Grover BD; Hopke PK; Long RW; Wilson WE; Meyer MB; Ambs JL; Kleinman M; Eatough NL; Eatough DJ. (2005). Measurement of total PM_{2.5} mass (nonvolatile plus semivolatile) with the Filter Dynamic Measurement System tapered element oscillating microbalance monitor. *J Geophys Res*, 110: 1-9. [156500](#)
- Grover BD; Kleinman M; Eatough NL; Eatough DJ; Cary RA; Hopke PK; Wilson WE. (2008). Measurement of fine particulate matter nonvolatile and semi-volatile organic material with the Sunset Laboratory Carbon Aerosol Monitor. *J Air Waste Manag Assoc*, 58: 72-77. [156502](#)
- Gulliver J; Briggs DJ. (2004). Personal exposure to particulate air pollution in transport microenvironments. *Atmos Environ*, 38: 1-8. [053238](#)
- Gulliver J; Briggs DJ. (2005). Time-space modeling of journey-time exposure to traffic-related air pollution using GIS. *Environ Res*, 97: 10-25. [191079](#)
- Gulliver J; Briggs DJ. (2007). Journey-time exposure to particulate air pollution. *Atmos Environ*, 41: 7195-7207. [155814](#)
- Gustafsson O; Kruså M; Zencak Z; Sheesley RJ; Granat L; Engström E; Praveen PS; Rao PS; Leck C; Rodhe H. (2009). Brown clouds over South Asia: biomass or fossil fuel combustion?. , 323: 495-498. [192000](#)
- Gutiérrez-Dabán A; Fernández-Espinosa AJ; Ternero-Rodríguez M; Fernández-Álvarez F. (2005). Particle-size distribution of polycyclic aromatic hydrocarbons in urban air in southern Spain. *Anal Bioanal Chem*, 381: 721-736. [155818](#)
- Hagler GSW; Baldauf RW; Thoma ED; Long TR; Snow RF; Kinsey JS; Oudejans L; Gullett BK. (2009). Ultrafine particles near a major roadway in Raleigh, North Carolina: Downwind attenuation and correlation with traffic-related pollutants. *Atmos Environ*, 43: 1229-1234. [191185](#)
- Hains JC; Chen L-WA; Taubman BF; Doddridge BG; Dickerson RR. (2007). A side-by-side comparison of filter-based PM₂₅ measurements at a suburban site: a closure study. *Atmos Environ*, 41: 6167-6184. [091039](#)
- Hammond DM; Lalor MM; Jones SL. (2007). In-vehicle measurement of particle number concentrations on school buses equipped with diesel retrofits . , 179: 217-225. [190135](#)
- Han Y; Cao J; Chow JC; Watson JG; An Z; Jin Z; Fung K; Liu S. (2007). Evaluation of the thermal/optical reflectance method for discrimination between char-and soot-EC. *Chemosphere*, 69: 569-574. [155823](#)
- Hand JL; Kreidenweis SM. (2002). A New Method for Retrieving Particle Refractive Index and Effective Density from Aerosol Size Distribution Data. *Aerosol Sci Technol*, 36: 1012-1026. [155824](#)
- Hansen K; Draaijers GPJ; Ivens WPMF; Gundersen P; van Leeuwen NFM. (1994). Concentration variations in rain and canopy throughfall collected sequentially during individual rain events. *Atmos Environ*, 28: 3195-3205. [046634](#)
- Harrison D; Shik Park S; Ondov J; Buckley T; Roul Kim S; Jayanty RKM. (2004). Highly time resolved fine particle nitrate measurements at the Baltimore Supersite. *Atmos Environ*, 38: 5321-5332. [136787](#)
- Harrison RM; Jones AM. (2005). Multisite study of particle number concentrations in urban air. , 39: 6063-6070. [191005](#)
- Hasegawa S; Hirabayashi M; Kobayashi S; Moriguchi Y; Kondo Y; Tanabe K; Wakamatsu. (2005). Size Distribution and Characterization of Ultrafine Particles in Roadside Atmosphere. , 39: 2671-2690. [157355](#)
- Hays MD; Geron CD; Linna KJ; Smith ND; Schauer JJ. (2002). Speciation of gas-phase and fine particle emissions from burning of foliar fuels. *Environ Sci Technol*, 36: 2281-2295. [026104](#)
- Hays MD; Lavrich RJ. (2007). Developments in direct thermal extraction gas chromatography-mass spectrometry of fine aerosols. *Trends Analyt Chem*, 26: 88-102. [155831](#)
- Heald C; Spracklen D. (2009). Atmospheric budget of primary biological aerosol particles from fungal sources. *J Geophys Res Lett*, 36: L09806. [190014](#)

- Health Effects Institute. (2009). Traffic-related air pollution: A critical Review of the literature on emissions, exposure, and health effects . Health Effects Institute. Boston. [191009](#)
- Henderson R. (2005). Clean Air Scientific Advisory Committee (CASAC) Review of the EPA Staff Recommendations Concerning a Potential Thoracic Coarse PM Standard in the Review of the National Ambient Air Quality Standards for Particulate Matter: Policy Assessment of Scientific and Technical Information. U.S. Environmental Protection Agency. RTP, NC. [156537](#)
- Henderson R. (2009). Clean Air Scientific Advisory Committee (CASAC) letter the the Administrator: Consultation on monitoring issues related to the NAAQS for particulate matter. U.S. Environmental Protection Agency . Washington, DC. EPA-CASAC-09-006. [192001](#)
- Henry RC. (1997). History and fundamentals of multivariate air quality receptor models. , 37: 37-42. [020941](#)
- Hering S; Fine PM; Sioutas C; Jaques PA; Ambs JL; Hogrefe O; Demerjian KL. (2004). Field assessment of the dynamics of particulate nitrate vaporization using differential TEOM® and automated nitrate monitors. Atmos Environ, 38: 5183-5192. [155837](#)
- Hering SV. (2007). Using Regional Data and Building Leakage to Assess Indoor Concentrations of Particles of Outdoor Origin. Aerosol Sci Technol, 41: 639-654. [155839](#)
- Hering SV; Stolzenburg MR; Quant FR; Oberreit DR; Keady PB. (2005). A Laminar-Flow, Water-Based Condensation Particle Counter (WCPC). Aerosol Sci Technol, 39: 659-672. [155838](#)
- Hermann M; Wehner B; Bischof O; Han HS; Krinke T; Liu W; Zerrath A; Wiedensohler A. (2007). Particle counting efficiencies of new TSI condensation particle counters. J Aerosol Sci, 38: 674-682. [155840](#)
- Herner JD; Aw J; Gao O; Chang DP; Kleeman MJ. (2005). Size and composition distribution of airborne particulate matter in Northern California: I - Particulate mass, carbon, and water-soluble ions. J Air Waste Manag Assoc, 55: 30-51. [135983](#)
- Ho KF; Cao JJ; Harrison RM; Lee SC. (2004). Indoor/outdoor relationships of organic carbon (OC) and elemental carbon (EC) in PM_{2.5} in roadside environment of Hong Kong. Atmos Environ, 38: 6327-6335. [056804](#)
- Hoek G; de Hartog J; Meliefste K; ten Brink H; Katsouyanni K; Karakatsani A; Lianou M; Kotronarou A; Kavouras I; Pekkanen J; Vallius M; Kulmala M; Puustinen A; Thomas S; Meddings C; Ayres J; van Wijnen J; Hameri K; Kos G; Harrison R. (2008). Indoor-outdoor relationships of particle number and mass in four European cities. Atmos Environ, 42: 156-169. [156554](#)
- Hogrefe C; Hao W; Civerolo K; Ku JY; Sistla G; Gaza RS; Sedefian L; Schere K; Gilliland A; Mathur R. (2007). Daily Simulation of Ozone and Fine Particulates over New York State: Findings and Challenges. , 46: 961-979. [156561](#)
- Hogrefe O; Schwab JJ; Drewnick F; Lala GG; Peters S; Demerjian KL; Rhoads K; Felton HD; Rattigan OV; Husain L. (2004). Semicontinuous PM_{2.5} sulfate and nitrate measurements at an urban and a rural location in New York: PMTACS-NY Summer 2001 and 2002 Campaigns. J Air Waste Manag Assoc, 54: 1040-1060. [156560](#)
- Hopke PK; Ramadan Z; Paatero P; Norris GA; Landis MS; Williams RW; Lewis CW. (2003). Receptor modeling of ambient and personal exposure samples: 1998 Baltimore Particulate Matter Epidemiology-Exposure Study. Atmos Environ, 37: 3289-3302. [095544](#)
- Hosker RP Jr; Lindberg SE. (1982). Review: atmospheric deposition and plant assimilation of gases and particles. Atmos Environ, 16: 889-910. [019118](#)
- Hsiao T-C; Chen D-R; Son SY. (2009). Development of mini-cyclones as the size-selective inlet of miniature particle detectors. J Aerosol Sci, 40: 481-491. [191001](#)
- Hu S; Herner JD; Shafer M; Robertson W; Schauer JJ; Dwyer H; Collins J; Huai T; Ayala A. (2009). Metals emitted from heavy-duty diesel vehicles equipped with advanced PM and NO_x emission controls. Atmos Environ, 43: 2950-2959. [189886](#)
- Huang C; Chang C; Chang S; Tsai C; Shih T; Tang D. (2005). Use of porous foam as the substrate of an impactor for respirable aerosol sampling. J Aerosol Sci, 36: 1373-1386. [186991](#)
- Huang L; Brook JR; Zhang W; Li SM; Graham L; Ernst D; Chivulescu A; Lu G. (2006). Stable isotope measurements of carbon fractions (OC/EC) in airborne particulate: A new dimension for source characterization and apportionment. Atmos Environ, 40: 2690-2705. [097654](#)
- Huang YL; Batterman S. (2000). Selection and evaluation of air pollution exposure indicators based on geographic areas. Sci Total Environ, 253: 127-144. [156572](#)
- Huebert BJ; Charlson RJ. (2000). Uncertainties in data on organic aerosols. Tellus B Chem Phys Meteorol, 52: 1249-1255. [156577](#)
- Huebert BJ; Luke WT; Delany AC; Brost RA. (1988). Measurements of concentrations and dry surface fluxes of atmospheric nitrates in the presence of ammonia. J Geophys Res, 93: 7127-7136. [036569](#)

- Husar RB; Tratt DM; Schichtel BA; Falke SR; Li F; Jaffe D; Gasso S; Gill T; Laulainen NS; Lu F; Reheis MC; Chun Y; Westphal D; Holben BN; Gueymard C; McKendry I; Kuring N; Feldman GC; McClain C; Frouin RJ; Merrill J; DuBois D; Vignola F; Murayama T; Nickovic S; Wilson WE; Sassen K; Sugimoto N; Malm WC. (2001). Asian dust events of April 1998. *J Geophys Res*, 106: 18,317-18,330. [024947](#)
- Hwang K-W; Lee J-H; Jeong D-Y; Lee C-H; Bhatnagar A; Park J-M; Kim S-H. (2008). Observation of difference in the size distribution of carbon and major inorganic compounds of atmospheric aerosols after the long-range transport between the selected days of winter and summer. *Atmos Environ*, 42: 1057-1063. [134420](#)
- ICRP. (1994). Human respiratory tract model for radiological protection: a report of a task group of the International Commission on Radiological Protection. *Ann ICRP*, 24: 1-482. [006988](#)
- Isakov V; Touma JS; Burke J; Lobdell DT; Palma T; Rosenbaum A; Ozkaynak H. (2009). Combining regional- and local-scale air quality models with exposure models for use in environmental health studies. , 59: 461-472. [191192](#)
- Isakov V; Touma JS; Khlystov A. (2007). A method of assessing air toxics concentrations in urban areas using mobile platform measurements. *J Air Waste Manag Assoc*, 57: 1286-1295. [156588](#)
- Jacob DJ. (1999). Introduction to atmospheric chemistry. [091122](#)
- Jacobson MZ. (2002). Atmospheric pollution: history, science, and regulation. [090667](#)
- Jacobson MZ; Kittelson DB; Watts WF. (2005). Enhanced coagulation due to evaporation and its effect on nanoparticle evolution. , 39: 9486-9492. [191187](#)
- Jaffe DH; Singer ME; Rimm AA. (2003). Air pollution and emergency department visits for asthma among Ohio Medicaid recipients, 1991-1996. *Environ Res*, 91: 21-28. [041957](#)
- Jansen KL; Larson TV; Koenig JQ; Mar TF; Fields C; Stewart J; Lippmann M. (2005). Associations between health effects and particulate matter and black carbon in subjects with respiratory disease. *Environ Health Perspect*, 113: 1741-1746. [082236](#)
- Jaques PA; Ambs JL; Grant WL; Sioutas C. (2004). Field evaluation of the differential TEOM monitor for continuous PM 2.5 mass concentrations. *Aerosol Sci Technol*, 38: 49-59. [155878](#)
- Jeong CH; Hopke PK; Chalupa D; Utell M. (2004). Characteristics of nucleation and growth events of ultrafine particles measured in Rochester, NY. *Environ Sci Technol*, 38: 1933-1940. [180350](#)
- Jerrett M; Arain A; Kanaroglou P; Beckerman B; Potoglou D; Sahuvaroglu T; Morrison J; Giovis C. (2005). A review and evaluation of intraurban air pollution exposure models. *J Expo Sci Environ Epidemiol*, 15: 185-204. [092864](#)
- Jerrett M; Burnett RT; Ma R; Pope 3rd CA; Krewski D; Newbold KB; Thurston G; Shi Y; Finkelstein N; Calle EE; Thun MJ. (2005). Spatial analysis of air pollution and mortality in Los Angeles. *Epidemiology*, 16: 727-36. [189405](#)
- Jimenez JL; Jayne JT; Shi Q; Kolb CE; Worsnop DR; Yourshaw I; Seinfeld JH; Flagan RC; Zhang X; Smith KA. (2003). Ambient aerosol sampling using the Aerodyne Aerosol Mass Spectrometer. *J Geophys Res*, 108: 8425. [156611](#)
- Johnson T; Long T; Ollison W. (2000). Prediction of hourly microenvironmental concentrations of fine particles based on measurements obtained from the Baltimore scripted activity study. *J Expo Sci Environ Epidemiol*, 10: 403-411. [001660](#)
- Johnston IDA; Bland JM; Anderson HR. (1987). Ethnic variation in respiratory morbidity and lung function in childhood. *Thorax*, 42: 542-548. [019356](#)
- Joseph PM. (2008). Can fine particulate matter explain the paradoxical ozone associations?. *Environ Int*, 34(8): 1185-1191. [155219](#)
- Kahn R; Gaitley B; Martonchik J; Diner D; Crean K; Holben B. (2005). Multiangle Imaging Spectroradiometer (MISR) global aerosol optical depth validation based on 2 years of coincident Aerosol Robotic Network (AERONET) observations. *J Geophys Res*, 110: D10S04. [189961](#)
- Kalberer M; Paulsen D; Sax M; Steinbacher M; Dommen J; Prevot ASH; Fisseha R; Weingartner E; Frankevich V; Zenobi R. (2004). Identification of Polymers as Major Components of Atmospheric Organic Aerosols. , 303: 1659-1662. [156619](#)
- Kastner-Klein P; Plate EJ. (1999). Wind-tunnel study of concentration fields in street canyons. *Atmos Environ*, 33: 3973-3979. [001961](#)
- Kaur S; Nieuwenhuijsen M; Colville R. (2005). Personal exposure of street canyon intersection users to PM_{2.5}, ultrafine particle counts and carbon monoxide in central London, UK. *Atmos Environ*, 39: 3629-3641. [086504](#)
- Kaur S; Nieuwenhuijsen MJ; Colville RN. (2005). Pedestrian exposure to air pollution along a major road in Central London, UK. *Atmos Environ*, 39: 7307-7320. [088175](#)
- Keller A; Siegmund HC. (2001). The role of condensation and coagulation in aerosol monitoring. *J Expo Sci Environ Epidemiol*, 11: 441-448. [025881](#)

- Kelly JM. (1988). Annual elemental input/output estimates for two forested watersheds in eastern Tennessee. *J Environ Qual*, 17: 463-468. [037379](#)
- Kenny LC; Merrifield T; Mark D; Gussman R; Thorpe A. (2004). The Development and Designation Testing of a New USEPA-Approved Fine Particle Inlet: A Study of the USEPA Designation Process. *Aerosol Sci Technol*, 38: 15-22. [155895](#)
- Ketzel M; Wahlin P; Berkowicz R; Palmgren F. (2003). Particle and trace gas emission factors under urban driving conditions in Copenhagen based on street and roof-level observations. *Atmos Environ*, 37: 2735-2749. [131251](#)
- Khlystov A; Stanier C; Pandis SN. (2004). An Algorithm for Combining Electrical Mobility and Aerodynamic Size Distributions Data when Measuring Ambient Aerosol. *Aerosol Sci Technol*, 38: 229-238. [155897](#)
- Khlystov A; Stanier CO; Takahama S; Pandis SN. (2005). Water content of ambient aerosol during the Pittsburgh Air Quality Study. *J Geophys Res*, 110: D07S10. [156635](#)
- Kidwell CB; Ondov JM. (2004). Elemental Analysis of Sub-Hourly Ambient Aerosol Collections. *Aerosol Sci Technol*, 38: 205-218. [155898](#)
- Kim D; Sass-Kortsak A; Purdham JT; Dales RE; Brook JR. (2005). Sources of personal exposure to fine particles in Toronto, Ontario, Canada. *J Air Waste Manag Assoc*, 55: 1134-1146. [156640](#)
- Kim E; Hopke PK; Pinto JP; Wilson WE. (2005). Spatial variability of fine particle mass, components, and source contributions during the regional air pollution study in St Louis. *Environ Sci Technol*, 39: 4172-4179. [083181](#)
- Kim SY; Sheppard L; Kim H. (2009). Health effects of long-term air pollution: influence of exposure prediction methods. *Epidemiology*, 20: 442-50. [188446](#)
- Kinney PL; Aggarwal M; Northridge ME; Janssen NAH; Shepard P. (2000). Airborne concentrations of PM_{2.5} and diesel exhaust particles on Harlem sidewalks: a community-based pilot study. *Environ Health Perspect*, 108: 213-218. [001774](#)
- Kinsey JS; Williams DC; Dong Y; Logan R. (2007). Characterization of fine particle and gaseous emissions during school bus idling. *J Environ Health Perspect*, 115: 4972-4979. [190073](#)
- Kiss G; Varga B; Galambos I; Ganszky I. (2002). Characterization of water-soluble organic matter isolated from atmospheric fine aerosol. *J Geophys Res*, 107: 8339. [156646](#)
- Kittelson DB. (1998). Engines and nanoparticles: a review. *J Aerosol Sci*, 29: 575-588. [051098](#)
- Kittelson DB; Schauer JJ; Lawson DR; Watts WF; Johnson JP. (2006). On-road and laboratory evaluation of combustion aerosols-Part 2: Summary of spark ignition engine results. *J Aerosol Sci*, 37: 931-949. [156648](#)
- Kittelson DB; Watts WF; Johnson JP. (2006). On-road and laboratory evaluation of combustion aerosols—Part 1: Summary of diesel engine results. *J Aerosol Sci*, 37: 913-930. [156649](#)
- Kleindienst TE; Edney EO; Lewandowski M; Offenberg JH; Jaoui M. (2006). Secondary Organic Carbon and Aerosol Yields from the Irradiations of Isoprene and Pinene in the Presence of NO_x and SO₂. *Environ Sci Technol*, 40: 3807-3812. [156650](#)
- Klepeis NE; Nelson WC; Ott WR; Robinson JPTsang AM; Switzer P; Behar JV; Hern SC; Engelmann WH. (2001). The National Human Activity Pattern Survey (NHAPS): a resource for assessing exposure to environmental pollutants. *J Expo Sci Environ Epidemiol*, 11: 231-252. [002437](#)
- Klouda GA; Filliben JJ; Parish HJ; Chow JC; Watson JG; Cary RA. (2005). Reference material 8785: Air particulate matter on filter media. *Aerosol Sci Technol*, 39: 173-183. [130382](#)
- Koenig JQ; Mar TF; Allen RW; Jansen K; Lumley T; Sullivan JH; Trenga CA; Larson T; Liu LJ. (2005). Pulmonary effects of indoor- and outdoor-generated particles in children with asthma. *Environ Health Perspect*, 113: 499-503. [087384](#)
- Kohsaka A; Watanobe H; Kakizaki Y; Suda T. (1999). A comparative study of the effects of nitric oxide and carbon monoxide on the in vivo release of gonadotropin-releasing hormone and neuropeptide Y from rat hypothalamus during the estradiol-induced luteinizing hormone surge: estimation by push-pull perfusion. *Neuroendocrinology*, 69: 245-253. [191000](#)
- Kokhanovsky A; Breon F; Cacciari A; Carboni E; Diner D; Di Nicolantonio W; Grainger R; Grey W; Höller R; Lee K. (2007). Aerosol remote sensing over land: a comparison of satellite retrievals using different algorithms and instruments. *J Geophys Res*, 112: 372-394. [190009](#)
- Koutrakis P; Suh HH; Sarnat JA; Brown KW; Coull BA; Schwartz J. (2005). Characterization of particulate and gas exposures of sensitive subpopulations living in Baltimore and Boston. *J Environ Health Perspect*, 113: 1-65. [095800](#)
- Krewski D; Burnett RT; Goldberg MS; Hoover K; Siemiatycki J; Jerrett M; Abrahamowicz M; White WH. (2000). Reanalysis of the Harvard Six Cities study and the American Cancer Society study of particulate air pollution and mortality: a special report of the Institute's Particle Epidemiology Reanalysis Project. Health Effects Institute. Cambridge, MA. [012281](#)

- Krewski D; Jerrett M; Burnett RT; Ma R; Hughes E; Shi Y; Turner MC; Pope AC III; Thurston G; Calle EE; Thun MJ. (2009). Extended follow-up and spatial analysis of the American Cancer Society study linking particulate air pollution and mortality. Health Effects Institute. Cambridge, MA. 140. [191193](#)
- Krieger UK; Rupp S; Hausammann E; Peter T. (2007). Simultaneous measurements of PM₁₀ and PM₁ using a single TEOM. *Aerosol Sci Technol*, 41: 975-980. [129657](#)
- Kroll JH; Seinfeld JH. (2008). Chemistry of secondary organic aerosol: Formation and evolution of low-volatility organics in the atmosphere. *Atmos Environ*, 42: 3593-3624. [155910](#)
- Krudysz M; Froines J; Fine P; Sioutas C. (2008). Intra-community spatial variation of size-fractionated PM mass, OC, EC, and trace elements in the Long Beach, CA area. *Atmos Environ*, 42: 5374-5389. [190064](#)
- Kruize H; Hanninen O; Breugelmans O; Lebet E; Jantunen M. (2003). Description and demonstration of the EXPOLIS simulation model: two examples of modeling population exposure to particulate matter. , 13: 87-99. [156661](#)
- Kuang C; McMurry PH; McCormick AV; Eisele FL. (2008). Dependence of nucleation rates on sulfuric acid vapor concentration in diverse atmospheric locations. *J Geophys Res*, 113: D10209. [191196](#)
- Kuhn T; Biswas S; Sioutas C. (2005). Diurnal and seasonal characteristics of particle volatility and chemical composition in the vicinity of a light-duty vehicle freeway. *Atmos Environ*, 39: 7154-7166. [129448](#)
- Kuhns H; Knipping EM. (2005). Development of a United States-Mexico emissions inventory for the Big Bend Regional Aerosol and Visibility Observational (BRAVO) Study. *J Air Waste Manag Assoc*, 55: 677-692. [156663](#)
- Kulmala M; Laaksonen A; Pirjola L. (1998). Parameterizations for sulfuric acid/water nucleation rates. *J Geophys Res*, 103: 8301-8307. [129411](#)
- Kulmala M; Mordas G; Petäjä T; Grönholm T; Aalto PP; Vehkamäki H; Hienola AI; Herrmann E; Sipilä M; Riipinen I. (2007). The condensation particle counter battery (CPCB): A new tool to investigate the activation properties of nanoparticles. *J Aerosol Sci*, 38: 289-304. [155911](#)
- Kulmala M; Riipinen I; Sipilä M; Manninen HE; Petäjä T; Junninen H; Maso MD; Mordas G; Mirme A; Vana M; Hirsikko A; Laakso L; Harrison RM; Hanson I; Leung C; Lehtinen KE; Kerminen VM. (2007). Toward direct measurement of atmospheric nucleation. , 318: 89-92. [191761](#)
- Kulmala M; Vehkamäki H; Petäjä T; Dal Maso M; Lauri A; Kerminen V-M; Birmili W; McMurry PH. (2004). Formation and growth rates of ultrafine atmospheric particles: a review of observations. *J Aerosol Sci*, 35: 143-176. [089159](#)
- Kuo Y; Huang S; Shih T; Chen C; Weng Y; Lin W. (2005). Development of a size-selective inlet-simulating ICRP lung deposition fraction. *Aerosol Sci Technol*, 39: 437-443. [186997](#)
- Kurniawan A; Schmidt-Ott A. (2006). Monitoring the soot emissions of passing cars. *Environ Sci Technol*, 40: 1911-5. [098823](#)
- Lake DA; Tolocka MP; Johnston MV; Wexler AS. (2003). Mass Spectrometry of Individual Particles between 50 and 750 nm in Diameter at the Baltimore Supersite. *Environ Sci Technol*, 37: 3268-3274. [156669](#)
- Lake DA; Tolocka MP; Johnston MV; Wexler AS. (2004). The character of single particle sulfate in Baltimore. *Atmos Environ*, 38: 5311-5320. [088411](#)
- Langholz B; Ebi K; Thomas D; Peters J; London S. (2002). Traffic density and the risk of childhood leukemia in a Los Angeles case-control study. *Ann Epidemiol*, 12: 482-487. [191771](#)
- Larson T; Gould T; Simpson C; Liu LJ; Claiborn C; Lewtas J. (2004). Source apportionment of indoor, outdoor, and personal PM_{2.5} in Seattle, Washington, using positive matrix factorization. *J Air Waste Manag Assoc*, 54: 1175-87. [098145](#)
- Lee HM. (2007). Fabrication of Reference Filter for Measurements of EC (Elemental Carbon) and OC (Organic Carbon) in Aerosol Particles. *Aerosol Sci Technol*, 41: 284-294. [155926](#)
- Lee HM; Kim CS; Shimada M; Okuyama K. (2005). Effects of Mobility Changes and Distribution of Bipolar Ions on Aerosol Nanoparticle Diffusion Charging. *J Chem Eng Jpn*, 38: 486-496. [156679](#)
- Lee HM; Soo Kim C; Shimada M; Okuyama K. (2005). Bipolar diffusion charging for aerosol nanoparticle measurement using a soft X-ray charger. *J Aerosol Sci*, 36: 813-829. [155924](#)
- Lee SJ; Demokritou P; Koutrakis P; Delgado-Saborit JM. (2006). Development and evaluation of personal respirable particulate sampler (PRPS). *Atmos Environ*, 40: 212-224. [098249](#)
- Leith D; Sommerlatt D; Boundy MG. (2007). Passive sampler for PM_{10-2.5} aerosol. *J Air Waste Manag Assoc*, 57: 332-6. [098241](#)
- LeVine AM; Gwozdz J; Stark J; Bruno M; Whitsett J; Korfhagen T. (1999). Surfactant protein-A enhances respiratory syncytial virus clearance in vivo. *J Clin Invest*, 103: 1015-1021. [156687](#)
- Levy JI; Bennett DH; Melly SJ; Spengler JD. (2003). Influence of traffic patterns on particulate matter and polycyclic aromatic hydrocarbon concentrations in Roxbury, Massachusetts. *J Expo Sci Environ Epidemiol*, 13: 364-371. [052661](#)

- Levy JI; Wilson AM; Evans JS; Spengler JD. (2003). Estimation of primary and secondary particulate matter intake fractions for power plants in Georgia. *Environ Sci Technol*, 37: 5528-5536. [156688](#)
- Lewne M; Nise G; Lind ML; Gustavsson P. (2006). Exposure to particles and nitrogen dioxide among taxi, bus and lorry drivers. *Int Arch Occup Environ Health*, 79: 220-226. [090556](#)
- Lim HJ; Allen G; Maring H; Solomon P; Turpin BJ; Edgerton E; Hering SV. (2003). Semicontinuous aerosol carbon measurements: Comparison of Atlanta supersite measurements. *J Geophys Res*, 108: SOS-SOS. [156697](#)
- Lim MCH; Ayoko GA; Morawska L; Ristovski ZD; Jayaratne ER. (2007). The effects of fuel characteristics and engine operating conditions on the elemental composition of emissions from heavy duty diesel buses. , 86: 1831-1839. [155931](#)
- Lindberg SE; Lovett GM. (1985). Field measurements of particle dry deposition rates to foliage and inert surfaces in a forest canopy. *Environ Sci Technol*, 19: 238-244. [036530](#)
- Lipfert FW; Perry HM Jr; Miller JP; Baty JD; Wyzga RE; Carmody SE. (2000). The Washington University-EPRI veterans' cohort mortality study: preliminary results. *Inhal Toxicol*, 4: 41-73. [004087](#)
- Lippmann M. (2009). Semi-continuous speciation analyses for ambient air particulate matter: an urgent need for health effects studies. *J Expo Sci Environ Epidemiol*, 19: 235-247. [190083](#)
- Lipsky E; Robinson A. (2006). Effects of dilution on fine particle mass and partitioning of semivolatile organics in diesel exhaust and wood smoke. , 40: 155-162. [189891](#)
- Little P; Wiffen RD. (1977). Emission and deposition of petrol engine exhaust Pb-I deposition of exhaust Pb to plant and soil surfaces. *Atmos Environ*, 11: 437-447. [070869](#)
- Liu L-J; Box M; Kalman D; Kaufman J; Koenig J; Larson T; Lumley T; Sheppard L; Wallace L. (2003). Exposure assessment of particulate matter for susceptible populations in Seattle. *Environ Health Perspect*, 11: 909-918. [073841](#)
- Liu XH; Hegg DA; Stoelinga MT. (2001). Numerical simulation of new particle formation over the northwest Atlantic using the MM5 mesoscale model coupled with sulfur chemistry. *J Geophys Res*, 106: 9697-9715. [048201](#)
- Long CM; Suh HH; Catalano PJ; Koutrakis P. (2001). Using time- and size-resolved particulate data to quantify indoor penetration and deposition behavior. *Environ Sci Technol*, 35: 2089-2099. [011526](#)
- Long RW; McClenny WA. (2006). Laboratory and field evaluation of instrumentation for the semicontinuous determination of particulate nitrate (and other water-soluble particulate components). *J Air Waste Manag Assoc*, 56: 294-305. [098214](#)
- Lovett GM. (1994). Atmospheric deposition of nutrients and pollutants in North America: an ecological perspective. *Ecol Appl*, 4: 629-650. [024049](#)
- Lowenthal DH; Rogers CF; Saxena P; Watson JG; Chow JC. (1995). Sensitivity of estimated light extinction coefficients to model assumptions and measurement errors. *Atmos Environ*, 29: 751-766. [045134](#)
- Lu R; Turco RP; Jacobson MZ. (1997). An integrated air pollution modeling system for urban and regional scales: 1 Structure and performance. *J Geophys Res*, 102: 6063-6079. [048202](#)
- Lu R; Turco RP; Jacobson MZ. (1997). An integrated air pollution modeling system for urban and regional scales: 2. Simulations for SCAQS 1987 . *J Geophys Res*, 102: 6081-6098. [191768](#)
- Lunden MM; Kirchstetter TW; Thatcher TL; Hering SV; Brown NJ. (2008). Factors affecting the indoor concentrations of carbonaceous aerosols of outdoor origin. *Atmos Environ*, 42: 5660-5671. [155949](#)
- Lunden MM; Revzan KL; Fischer ML; Thatcher TL; Littlejohn D; Hering SV; Brown NJ. (2003). The transformation of outdoor ammonium nitrate aerosols in the indoor environment. *Atmos Environ*, 37: 5633-5644. [081201](#)
- Lunden MM; Thatcher TL; Hering SV; Brown NJ. (2003). The use of time-and chemically resolved particulate data to characterize the infiltration of outdoor PM_{2.5} into a residence in the San Joaquin Valley. , 37: 4724-4732. [156718](#)
- Mader BT; Schauer JJ; Seinfeld JH; Flagan RC; Yu JZ; Yang H; Lim HJ; Turpin BJ; Deminter JT; Heidemann G. (2003). Sampling methods used for the collection of particle-phase organic and elemental carbon during ACE-Asia. *Atmos Environ*, 37: 1435-1449. [155955](#)
- Maheswaran R; Elliott P. (2003). Stroke mortality associated with living near main roads in England and wales: a geographical study. , 34: 2776-80. [125271](#)
- Mahrt L. (1998). Stratified atmospheric boundary layers and breakdown of models. , 11: 263-279. [048210](#)
- Makar PA; Gravel S; Chirkov V; Strawbridge KB; Froude F; Arnold J; Brook J. (2006). Heat flux, urban properties, and regional weather. *Atmos Environ*, 40: 2750-2766. [155959](#)
- Mar TF; Norris GA; Larson TV; Wilson WE; Koenig JQ. (2003). Air pollution and cardiovascular mortality in Phoenix, 1995-1997. [156731](#)

- Martin RV; Chance K; Jacob DJ; Kurosu TP; Spurr RJD; Bucsela E; Gleason JF; Palmer PI; Bey I; Fiore AM; Li Q; Yantosca RM; Koelemeijer RBA. (2002). An improved retrieval of tropospheric nitrogen dioxide from GOME. *J Geophys Res*, 107: 1-21. [089380](#)
- Massman WJ; Pederson J; Delany A; Grantz D; Denhartog G; Neumann HH; Oncley SP; Pearson R; Shaw RH. (1994). An evaluation of the regional acid deposition model surface module for ozone uptake at 3 sites in the San-Joaquin valley of California. *J Geophys Res*, 99: 8281-8294. [043681](#)
- Mathis U; Mohr M; Forss AM. (2005). Comprehensive particle characterization of modern gasoline and diesel passenger cars at low ambient temperatures. *Atmos Environ*, 39: 107-117. [155970](#)
- Mathur R. (2008). Estimating the impact of the 2004 Alaskan forest fires on episodic particulate matter pollution over the eastern United States through assimilation of satellite-derived aerosol optical depths in a regional air quality model. *J Geophys Res*, 113: D17302. [156742](#)
- Matsumoto K; Hayano T; Uematsu M. (2003). Positive artifact in the measurement of particulate carbonaceous substances using an ambient carbon particulate monitor. *Atmos Environ*, 37: 4713-4717. [124293](#)
- Matthias-Maser S; Bogs B; Jaenicke R. (2000). The size distribution of primary biological aerosol particles in cloud water on the mountain Kleiner Feldberg/Taunus (FRG). , 54: 1-13. [155972](#)
- Matti Mariq M. (2007). Chemical characterization of particulate emissions from diesel engines: A review. *J Aerosol Sci*, 38: 1079-1118. [155973](#)
- McBride SJ; Williams RW; Creason J. (2007). Bayesian hierarchical modeling of personal exposure to particulate matter. *Atmos Environ*, 41: 6143-6155. [124058](#)
- McCurdy T; Glen G; Smith L; Lakkadi Y. (2000). The National Exposure Research Laboratory's Consolidated Human Activity Database. *J Expo Sci Environ Epidemiol*, 10: 566-578. [000782](#)
- McDonald JD; Eide I; Seagrave J; Zielinska B; Whitney K; Lawson DR; Mauderly JL. (2004). Relationship between composition and toxicity of motor vehicle emission samples. *Environ Health Perspect*, 112: 1527-1538. [087458](#)
- McKendry IG; Strawbridge KB; O'Neill NT; Macdonald AM; Liu PSK; Leitch WR; Anlauf KG; Jaegle L; Fairlie TD; Westphal DL. (2007). Trans-Pacific transport of Saharan dust to western North America: A case study. *J Geophys Res*, 112: D01103. [156748](#)
- McKenna DS; Konopka P; Grooss J-U; Gunther G; Muller R; Spang R; Offermann D; Orsolini Y. (2002). A new chemical Lagrangian model of the stratosphere (CLaMS) 1 formulation of advection and mixing. *J Geophys Res*, 107. [053445](#)
- McMurry PH; Fink M; Sakurai H; Stolzenburg MR; Mauldin RL, III; Smith J; Eisele F; Moore K; Sjostedt S; Tanner D; Huey LG; Nowak JB; Edgerton E; Voisin D. (2005). A criterion for new particle formation in the sulfur-rich Atlanta atmosphere. *J Geophys Res*, 110: np. [191759](#)
- Mebust MR; Eder BK; Binkowski FS; Roselle SJ. (2003). Models-3 community multiscale air quality (CMAQ) model aerosol component 2. Model evaluation. *J Geophys Res*, 108: 4184. [156749](#)
- Meng QY; Turpin BJ; Korn L; Weisel CP; Morandi M; Colome S; Zhang J; Stock T; Spector D; Winer A; Zhang L; Lee JH; Giovanetti R; Cui W; Kwon J; Alimokhtari S; Shendell D; Jones J; Farrar C; Maberti S. (2005). Influence of ambient (outdoor) sources on residential indoor and personal PM_{2.5} concentrations: analyses of RIOPA data. *J Expo Sci Environ Epidemiol*, 15: 17-28. [058595](#)
- Meng QY; Turpin BJ; Lee JH; Polidori A; Weisel CP; Morandi M; Colome S; Zhang JF; Stock T; Winer A. (2007). How does infiltration behavior modify the composition of ambient PM_{2.5} in indoor spaces? An analysis of RIOPA data. *Environ Sci Technol*, 41: 7315-7321. [091197](#)
- Meng YY; Wilhelm M; Rull RP; English P; Ritz B. (2007). Traffic and outdoor air pollution levels near residences and poorly controlled asthma in adults. *Ann Allergy Asthma Immunol*, 98: 455-63. [093275](#)
- Meng Z; Dabdub D; Seinfeld JH. (1997). Chemical coupling between atmospheric ozone and particulate matter. , 277: 116-119. [083324](#)
- Mensink C; De Ridder K; Deutsch F; Lefebvre F; Van de Vel K. (2008). Examples of scale interactions in local, urban, and regional air quality modelling. , 89: 351-357. [155980](#)
- Mfula AM; Kukadia V; Griffiths RF; Hall DJ. (2005). Wind tunnel modelling of urban building exposure to outdoor pollution. *Atmos Environ*, 39: 2737-2745. [123359](#)
- Middha P; Wexler A. (2006). Design of a Slot Nanoparticle Virtual Impactor. *Aerosol Sci Technol*, 40: 737-743. [155982](#)
- Middlebrook AM; Murphy DM; Lee S-H; Thomson DS; Prather KA; Wenzel RJ; Liu D-Y; Phares DJ; Rhoads KP; Wexler AS; Johnston MV; Jimenez JL; Jayne JT; Worsnop DR; Yourshaw I; Seinfeld JH; Flagan RC. (2003). A comparison of particle mass spectrometers during the 1999 Atlanta Supersites project. *J Geophys Res*, 108D7. [042932](#)

- Miller GT Jr. (1975). Carbon and oxygen cycles showing chemicals cycling and energy flow. In *Living in the Environment Concepts, Problems, and Alternatives* Belmont, CA: Wadsworth Publishing Company, Inc. [018988](#)
- Miller SL; Anderson MJ; Daly EP; Milford JB. (2002). Source apportionment of exposures to volatile organic compounds I Evaluation of receptor models using simulated exposure data. *Atmos Environ*, 36: 3629-3641. [030661](#)
- Misra C; Geller MD; Sioutas C; Solomon PA. (2003). Development and evaluation of a PM10 impactor-inlet for a continuous coarse particle monitor. *Aerosol Sci Technol*, 37: 271-281. [180217](#)
- Miyazaki Y; Kondo Y; Takegawa N; Komazaki Y; Fukuda M; Kawamura K; Mochida M; Okuzawa K; Weber RJ. (2006). Time-resolved measurements of water-soluble organic carbon in Tokyo. *J Geophys Res*, 111: D23206. [156767](#)
- Molnár P; Johannesson S; Boman J; Barregard L; Sallsten G. (2006). Personal exposures and indoor, residential outdoor, and urban background levels of fine particle trace elements in the general population. *J Environ Monit*, 8: 543-551. [156773](#)
- Moolgavkar SH. (2000). Air pollution and hospital admissions for diseases of the circulatory system in three US metropolitan areas. *J Air Waste Manag Assoc*, 50: 1199-1206. [010305](#)
- Moore K; Krudysz M; Pakbin P; Hudda N; Sioutas C. (2009). Intra-community variability in total particle number concentrations in the San Pedro Harbor Area (Los Angeles, California). *Aerosol Sci Technol*, 43: 587-603. [191002](#)
- Moore K; Krudysz M; Pakbin P; Hudda N; Sioutas C. (2009). Intra-community variability in total particle number concentrations in the San Pedro Harbor Area (Los Angeles, California). *Aerosol Sci Technol*, 43: 587-603. [191004](#)
- Moore KF; Ning Z; Ntziachristos L; Schauer JJ; Sioutas C. (2007). Daily variation in the properties of urban ultrafine aerosol-Part I: Physical characterization and volatility. *Atmos Environ*, 41: 8633-8646. [122445](#)
- Morawska L; Keogh DU; Thomas SB; Mengersen K. (2007). Modality in ambient particle size distributions and its potential as a basis for developing air quality regulation. *Atmos Environ*. [155990](#)
- Morawska L; Ristovski Z; Jayaratne ER; Keogh DU; Ling X. (2008). Ambient nano and ultrafine particles from motor vehicle emissions: Characteristics, ambient processing and implications on human exposure . , 42: 8113-8138. [191006](#)
- Morawska L; Thomas S; Jamriska M; Johnson G. (1999). The modality of particle size distributions of environmental aerosols. *Atmos Environ*, 33: 4401-4411. [007609](#)
- Mulchandani A; Chen W; Mulchandani P; Rogers KR. (2001). Biosensors for direct determination of organophosphate pesticides . , 16: 225-230. [191003](#)
- Muller K; Spindler G; Maenhaut W; Hitznerberger R; Wierprecht W; Baltensperger U; ten Brink H. (2004). INTERCOMP2000, a campaign to assess the comparability of methods in use in Europe for measuring aerosol composition. *Atmos Environ*, 38: 6459-6466. [097109](#)
- Murahashi T. (2003). Determination of mutagenic 3-nitrobenzanthrone in diesel exhaust particulate matter by three-dimensional high-performance liquid chromatography. *Analyst*, 128: 42-5. [096539](#)
- Murphy BN; Pandis SN. (2009). Simulating the formation of semivolatile primary and secondary organic aerosol in a regional chemical transport model. , in press: in press. [190095](#)
- Nash DG; Tolocka MP; Baer T. (2006). The uptake of O₃ by myristic acid-oleic acid mixed particles: evidence for solid surface layers. *Phys Chem Chem Phys*, 8: 4468-4475. [156795](#)
- Nerriere E; Guegan H; Bordigoni B; Hautemaniere A; Momas I; Ladner J; Target A; Lameloise P; Delmas V; Personnaz MB; Koutrakis P; Zmirou-Navier D. (2007). Spatial heterogeneity of personal exposure to airborne metals in French urban areas. *Sci Total Environ*, 373: 49-56. [156801](#)
- Ng LJ; Stuhmiller LM; Stuhmiller JH. (2007). Incorporation of acute dynamic ventilation changes into a standardized physiologically based pharmacokinetic model. *Inhal Toxicol*, 19: 247-263. [090983](#)
- Ning Z; Geller MD; Moore KF; Sheesley R; Schauer JJ; Sioutas C. (2007). Daily Variation in Chemical Characteristics of Urban Ultrafine Aerosols and Inference of Their Sources. *Environ Sci Technol*, 41: 6000-6006. [156809](#)
- Ntziachristos L; Ning Z; Geller MD; Sioutas C. (2007). Particle concentration and characteristics near a major freeway with heavy-duty diesel traffic. *Environ Sci Technol*, 41: 2223-2230. [089164](#)
- Ntziachristos L; Samaras Z. (2006). Combination of aerosol instrument data into reduced variables to study the consistency of vehicle exhaust particle measurements. *Atmos Environ*, 40: 6032-6042. [116722](#)
- Odman MT; Boylan JW; Wilkinson JG; Russell AG; Mueller SF; Imhoff RE; Doty KG; Norris WB; McNider RT. (2002). SAMI air quality modeling: final report. [092474](#)

- Offenberg JH; Lewis CW; Lewandowski M; Jaoui M; Kleindienst TE; Edney EO. (2007). Contributions of toluene and alpha-pinene to SOA formed in an irradiated toluene/alpha-pinene/NO(x)/ air mixture: comparison of results using ¹⁴C content and SOA organic tracer methods. *Environ Sci Technol*, 41: 3972-3976. [156822](#)
- Ogulei D; Hopke PK; Zhou L; Patrick Pancras J; Nair N; Ondov JM. (2006). Source apportionment of Baltimore aerosol from combined size distribution and chemical composition data. *Atmos Environ*, 40: 396-410. [119973](#)
- Olfert JS; Kulkarni P; Wang J. (2008). Measuring aerosol size distributions with the fast integrated mobility spectrometer. *J Aerosol Sci*, 39: 940-956. [156004](#)
- Olivier JGJ; Bouwman AF; Berdowski JJM; Veldt C; Bloos JPJ; Visschedijk AJH; van der Maas CWM; Zandveld PYJ. (1999). Sectoral emission inventories of greenhouse gases for 1990 on a per country basis as well as on 1° x 1°. , 2: 241-263. [156829](#)
- Olivier JGJ; Bouwman AF; Berdowski JJM; Veldt C; Bloos JPJ; Visschedijk AJH; Zandveld PYJ; Haverlag JL. (1996). Description of EDGAR Version 2.0: A set of global emission inventories of greenhouse gases and ozone-depleting substances for all anthropogenic and most natural sources on a per country basis and on 1 degree x 1 degree grid. [156828](#)
- Olson DA; Burke JM. (2006). Distributions of PM_{2.5} source strengths for cooking from the Research Triangle Park particulate matter panel study. *Environ Sci Technol*, 40: 163-169. [189951](#)
- Olson DA; Mcdow SR. (2009). Near roadway concentrations of organic source markers. *Atmos Environ*, 43: 2862-2867. [191188](#)
- Olson DA; Norris GA. (2005). Sampling artifacts in measurement of elemental and organic carbon: Low-volume sampling in indoor and outdoor environments. *Atmos Environ*, 39: 5437-5445. [156005](#)
- Orsini DA; Ma Y; Sullivan A; Sierau B; Baumann K; Weber RJ. (2003). Refinements to the particle-into-liquid sampler (PILS) for ground and airborne measurements of water soluble aerosol composition. *Atmos Environ*, 37: 1243-1259. [156008](#)
- Ott DK; Kumar N; Peters TM. (2008). Passive sampling to capture spatial variability in PM_{10-2.5}. *Atmos Environ*, 42: 746-756. [191765](#)
- Ozkaynak H; Xue J; Zhou H; Raizenne M. (1996). Associations between daily mortality and motor vehicle pollution in Toronto, Canada. [073986](#)
- Paatero P; Tapper U. (1994). Positive matrix factorization: a non-negative factor model with optimal utilization of error estimates of data values. *Environmetrics*, 5: 111-126. [086998](#)
- Paciorek CJ; Yanosky JD; Suh HH. (2008). Practical Large-Scale Spatio-Temporal Modeling of Particulate Matter Concentrations. , unknown: unknown. [190090](#)
- Padro J. (1996). Summary of ozone dry deposition velocity measurements and model estimates over vineyard, cotton, grass and deciduous forest in summer. *Atmos Environ*, 30: 2363-2369. [052446](#)
- Pakbin P; Ning Z; Schauer J; Sioutas C. (2009). Characterization of Particle Bound Organic Carbon from Diesel Vehicles Equipped with Advanced Emission Control Technologies. , In Press: 5622-5634. [189893](#)
- Pandian MD; Behar JV; Ott WR; Wallace LA; Wilson AL; Colome S D. (1998). Correcting errors in the nationwide data base of residential air exchange rates. *J Expo Sci Environ Epidemiol*, 8: 577-586. [090552](#)
- Pandis SN. (2004). Atmospheric aerosol processes. In McMurphy PH; Shepard, M; Vickery JS (Ed.), *Particulate Matter Science for Policy Makers: A NARSTO Assessment* Cambridge, UK: Cambridge University Press. [156838](#)
- Pang Y; Eatough NL; Modey WK; Eatough DJ. (2002). Evaluation of the RAMS continuous monitor for determination of PM_{2.5} mass including semi-volatile material in Philadelphia, PA. *J Air Waste Manag Assoc*, 52: 563-572. [030353](#)
- Pang Y; Turpin BJ; Gundel LA. (2006). On the Importance of Organic Oxygen for Understanding Organic Aerosol Particles. *Aerosol Sci Technol*, 40: 128-133. [156012](#)
- Park J; Mitchell MJ; McHale PJ; Christopher SF; Myers TP. (2003). Interactive effects of changing climate and atmospheric deposition on N and S biogeochemistry in a forested watershed of the Adirondack Mountains, New York State. , 9: 1602-1619. [156842](#)
- Park K; Chow JC; Watson JG; Trimble DL; Doraiswamy P; Arnott WP; Stroud KR; Bowers K; Bode R; Petzold A; Hansen AD. (2006). Comparison of continuous and filter-based carbon measurements at the Fresno supersite. *J Air Waste Manag Assoc*, 56: 474-91. [098104](#)
- Park RJ; Stenichikov GL; Pickering KE; Dickerson RR; Allen DJ; Kondragunta S. (2001). Regional air pollution and its radiative forcing- Studies with a single-column chemical and radiation transport model. *J Geophys Res*, 106: 28. [156841](#)
- Peng RD; Dominici F; Pastor-Barriuso R; Zeger SL; Samet JM. (2005). Seasonal analyses of air pollution and mortality in 100 US cities. *Am J Epidemiol*, 161: 585-594. [087463](#)

- Peters K; Eiden R. (1992). Modelling the dry deposition velocity of aerosol particles to a spruce forest. *Atmos Environ*, 26: 2555-2564. [045277](#)
- Peters TM. (2006). Use of the Aerodynamic Particle Sizer to Measure Ambient PM 10-2. 5: The Coarse Fraction of PM 10. *J Air Waste Manag Assoc*, 56: 411-416. [156860](#)
- Pettijohn FJ. (1957). Sedimentary rocks. [156862](#)
- Petäjä T. (2006). Detection Efficiency of a Water-Based TSI Condensation Particle Counter 3785. *Aerosol Sci Technol*, 40: 1090-1097. [156021](#)
- Phares DJ; Rhoads KP; Johnston MV; Wexler AS. (2003). Size-resolved ultrafine particle composition analysis 2. Houston. *J Geophys Res*, 108: 8420. [156866](#)
- Phuleria HC; Geller MD; Fine PM; Sioutas C. (2006). Size-Resolved emissions of organic tracers from light-and heavy-duty vehicles measured in a California roadway tunnel. *Environ Sci Technol*, 40: 4109-4118. [156867](#)
- Phuleria HC; Sheesley RJ; Schauer JJ; Fine PM; Sioutas C. (2007). Roadside measurements of size-segregated particulate organic compounds near gasoline and diesel-dominated freeways in Los Angeles, CA. *Atmos Environ*, 41: 4653-4671. [117816](#)
- Pierce JR; Adams PJ. (2009). Uncertainty in global CCN concentrations from uncertain aerosol nucleation and primary emission rates. , 9: 1339-1356. [191189](#)
- Pirjola L; Parviainen H; Hussein T; Valli A; Haemeri K; Aalto P; Virtanen A; Keskinen J; Pakkanen TA; Maekelae T; Hillamo RE. (2004). 'Sniffer'; a novel tool for chasing vehicles and measuring traffic pollutants. *Atmos Environ*, 38: 3625-3635. [117564](#)
- Polidori A; Arhami M; Sioutas C; Delfino RJ; Allen R. (2007). Indoor/Outdoor relationships, trends, and carbonaceous content of fine particulate matter in retirement homes of the Los Angeles Basin. *J Air Waste Manag Assoc*, 57: 366-379. [156877](#)
- Polidori A; Turpin B; Meng QY; Lee JH; Weisel C; Morandi M; Colome S; Stock T; Winer A; Zhang J; Kwon J; Alimokhtari S; Shendell D; Jones J; Farrar C; Maberti S. (2006). Fine organic particulate matter dominates indoor-generated PM_{2.5} in RIOPA homes. *J Expo Sci Environ Epidemiol*, 16: 321-331. [156876](#)
- Pope CA III; Burnett RT; Thun MJ; Calle EE; Krewski D; Ito K; Thurston GD. (2002). Lung cancer, cardiopulmonary mortality, and long-term exposure to fine particulate air pollution. *JAMA*, 287: 1132-1141. [024689](#)
- Pope CA III; Thun MJ; Namboodiri MM; Dockery DW; Evans JS; Speizer FE; Heath CW Jr. (1995). Particulate air pollution as a predictor of mortality in a prospective study of US adults. *Am J Respir Crit Care Med*, 151: 669-674. [045159](#)
- Pouliot G; Pace TG; Roy B; Pierce T; Mobley D. (2008). Development of a biomass burning emissions inventory by combining satellite and ground-based information. , 2: 021501-021517. [156883](#)
- Price M; Bulpitt S; Meyer MB. (2003). A comparison of PM₁₀ monitors at a Kerbside site in the northeast of England. *Atmos Environ*, 37: 4425-4434. [098082](#)
- Puett RC; Schwartz J; Hart JE; Yanosky JD; Speizer FE; Suh H; Paciorek CJ; Neas LM; Laden F. (2008). Chronic particulate exposure, mortality, and coronary heart disease in the nurses' health study. *Am J Epidemiol*, 168: 1161-1168. [156891](#)
- Pun BK; Seigneur C; White W. (2003). Day-of-week behavior of atmospheric ozone in three US cities. *J Air Waste Manag Assoc*, 53: 789-801. [047775](#)
- Pöschl U. (2005). Atmospheric aerosols: composition, transformation, climate and health effects. *Angew Chem Weinheim Bergstr Ger*, 44: 7520-7540. [156882](#)
- Qian S; Sakurai H; McMurry PH. (2007). Characteristics of regional nucleation events in urban East St Louis. *Atmos Environ*, 41: 4119-4127. [116435](#)
- Qin X; Prather KA. (2006). Impact of biomass emissions on particle chemistry during the California Regional Particulate Air Quality Study. *Int J Mass Spectrom*, 258: 142-150. [156895](#)
- Ramachandran G; Adgate JL; Pratt GC; Sexton K. (2003). Characterizing indoor and outdoor 15 minute average PM_{2.5} concentrations in urban neighborhoods . *Aerosol Sci Technol*, 37: 33-45. [191197](#)
- Rattigan OV; Hogrefe O; Felton HD; Schwab JJ; Roychowdhury UK; Husain L; Dutkiewicz VA; Demerjian KL. (2006). Multi-year urban and rural semi-continuous PM₂₅ sulfate and nitrate measurements in New York state: Evaluation and comparison with filter based measurements. *Atmos Environ*, 40: 192-205. [115897](#)
- Rees SL; Robinson AL; Khlystov A; Stanier CO; Pandis SNSN. (2004). Mass balance closure and the Federal Reference Method for PM_{2.5} in Pittsburgh, Pennsylvania. *Atmos Environ*, 38: 3305-3318. [097164](#)
- Reff A; Weisel CP; Zhang J; Morandi M; Stock T; Colome S; Winer A; Turpin BJ; Offenberg JH. (2007). A functional group characterization of organic PM_{2.5} exposure: Results from the RIOPA study. *Atmos Environ*, 41: 4585-4598. [156045](#)

- Reithmeier C; Sausen R. (2002). ATTILA: atmospheric tracer transport in a Lagrangian model. , 54B: 278-299. [053447](#)
- Reponen T; Grinshpun SA; Trakumas S; Martuzevicius D; Wang Z-M; LeMasters G; Lockey JE; Biswas P. (2003). Concentration gradient patterns of aerosol particles near interstate highways in the Greater Cincinnati airshed. *J Environ Monit*, 5: 557-562. [088425](#)
- Rice J. (2004). Comparison of Integrated Filter and Automated Carbon Aerosol Measurements at Research Triangle Park, North Carolina. *Aerosol Sci Technol*, 38: 23-36. [156049](#)
- Riddle SG; Jakober CA; Robert MA; Cahill TM; Charles MJ; Kleeman MJ. (2007). Large PAHs detected in fine particulate matter emitted from light-duty gasoline vehicles. *Atmos Environ*, 41: 8658-8668. [115272](#)
- Rigby M; Toumi R. (2008). London air pollution climatology: Indirect evidence for urban boundary layer height and wind speed enhancement. *Atmos Environ*, 42: 4932-4947. [156050](#)
- Roache PJ. (1998). Verification and validation in computational science and engineering. [156915](#)
- Robinson AL; Donahue NM; Rogge WF. (2006). Photochemical oxidation and changes in molecular composition of organic aerosol in the regional context. *J Geophys Res*, 111: D03302. [156918](#)
- Robinson AL; Donahue NM; Shrivastava MK; Weitkamp EA; Sage AM; Grieshop AP; Lane TE; Pierce JR; Pandis SN. (2007). Rethinking organic aerosols: semivolatile emissions and photochemical aging. , 315: 1259-1262. [156053](#)
- Rossner P; Svecova V; Milcova A; Lnenickova Z; Solansky N; Sram RJ. (2008). Seasonal variability of oxidative stress markers in city bus drivers - Part I. Oxidative damage to DNA. , 642: 14-20. [156927](#)
- Rudich Y; Donahue NM; Mentel TF. (2007). Aging of Organic Aerosol: Bridging the Gap Between Laboratory and Field Studies. *Annu Rev Phys Chem*, 58: 321. [156059](#)
- Russell A; Dennis R. (2000). NARSTO critical review of photochemical models and modeling. *Atmos Environ*, 34: 2283-2324. [035563](#)
- Russell M; Allen D; Collins D; Fraser M. (2004). Daily, Seasonal, and Spatial Trends in PM_{2.5} Mass and Composition in Southeast Texas. *Aerosol Sci Technol*, 38: 14-26. [156061](#)
- Ryan PH; LeMasters GK. (2007). A Review of Land-use Regression Models for Characterizing Intraurban Air Pollution Exposure. *Inhal Toxicol*, 19: 127. [156063](#)
- Ryan PH; LeMasters GK; Levin L; Burkle J; Biswas P; Hu S; Grinshpun S; Reponen T. (2008). A land-use regression model for estimating microenvironmental diesel exposure given multiple addresses from birth through childhood. *Sci Total Environ*. [156064](#)
- Rynö M; Rantanen L; Papaioannou E; Konstandopoulos AG; Koskentalo T; Savela K. (2006). Comparison of pressurized fluid extraction, Soxhlet extraction and sonication for the determination of polycyclic aromatic hydrocarbons in urban air and diesel exhaust particulate matter. *J Environ Monit*, 8: 488-493. [156065](#)
- Saathoff H; Naumann KH; Schnaiter M; Schöck W; Weingartner E; Baltensperger U; Krämer L; Bozoki Z; Pöschl U; Niessner R. (2003). Carbon mass determinations during the AIDA soot aerosol campaign 1999. *J Aerosol Sci*, 34: 1399-1420. [156066](#)
- Sabin LD; Kozawa K; Behrentz E; Winer AM; Fitz DR; Pankratz DV; Colome SD; Fruin SA. (2005). Analysis of real-time variables affecting children's exposure to diesel-related pollutants during school bus commutes in Los Angeles. *Atmos Environ*, 39: 5243-5254. [087728](#)
- Sabin LD; Lim JH; Stolzenbach KD; Schiff KC. (2005). Contribution of trace metals from atmospheric deposition to stormwater runoff in a small impervious urban catchment. *Water Res*, 39: 3929-3937. [088300](#)
- Sadezky A; Muckenhuber H; Grothe H; Niessner R; Poschl U. (2005). Raman microspectroscopy of soot and related carbonaceous materials: Spectral analysis and structural information. *Carbon N Y*, 43: 1731-1742. [097499](#)
- Sage AM; Weitkamp EA; Robinson AL; Donahue NM. (2008). Evolving mass spectra of the oxidized component of organic aerosol: results from aerosol mass spectrometer analyses of aged diesel emissions. , 8: 1139-1152. [191758](#)
- Sahlodin AM; Sotudeh-Gharebagh R; Zhu Y. (2007). Modeling of dispersion near roadways based on the vehicle-induced turbulence concept. *Atmos Environ*, 41: 92-102. [114058](#)
- Sakurai H; Tobias HJ; Park K; Zarling D; Docherty KS; Kittelson DB; McMurry PH; Ziemann PJ. (2003). On-line measurements of diesel nanoparticle composition and volatility. *Atmos Environ*, 37: 1199-1210. [113924](#)
- Salminen K; Karlsson V. (2003). Comparability of low-volume PM₁₀ sampler with β -attenuation monitor in background air. *Atmos Environ*, 37: 3707-3712. [156070](#)
- Santarpia JL; Li RJ; Collins DR. (2004). Direct measurement of the hydration state of ambient aerosol populations. *J Geophys Res*, 109: D18209. [156944](#)

- Sardar SB; Fine PM; Mayo PR; Sioutas C. (2005). Size-fractionated measurements of ambient ultrafine particle chemical composition in Los Angeles using the NanoMOUDI. *Environ Sci Technol*, 39: 932-944. [180086](#)
- Sardar SB; Fine PM; Sioutas C. (2005). Seasonal and spatial variability of the size-resolved chemical composition of particulate matter (PM₁₀) in the Los Angeles Basin. *J Geophys Res*, 110D07S08. [089165](#)
- Sardar SB; Solomon PA; Geller MD; Sioutas C. (2006). Development and evaluation of a high-volume dichotomous sampler for chemical speciation of coarse and fine particles. *J Aerosol Sci*, 37: 1455-1466. [156071](#)
- Sarnat JA; Brown KW; Schwartz J; Coull BA; Koutrakis P. (2005). Ambient gas concentrations and personal particulate matter exposures: implications for studying the health effects of particles. , 16: 385-395. [087531](#)
- Sarnat JA; Long CM; Koutrakis P; Coull BA; Schwartz J; Suh HH. (2002). Using sulfur as a tracer of outdoor fine particulate matter. *Environ Sci Technol*, 36: 5305-5314. [037056](#)
- Sarnat JA; Schwartz J; Catalano PJ; Suh HH. (2001). Gaseous pollutants in particulate matter epidemiology: confounders or surrogates?. *Environ Health Perspect*, 109: 1053-1061. [019401](#)
- Sarnat SE; Coull BA; Ruiz PA; Koutrakis P; Suh HH. (2006). The influences of ambient particle composition and size on particle infiltration in Los Angeles, CA residences. *J Air Waste Manag Assoc*, 56: 186-196. [089166](#)
- Sarnat SE; Klein M; Sarnat JA; Flanders WD; Waller LA; Mulholland JA; Russell AG; Tolbert PE. (2009). An examination of exposure measurement error from air pollutant spatial variability in time-series studies. *J Expo Sci Environ Epidemiol*, In Press: 1-12. [180084](#)
- Sarnat SE; Suh HH; Coull BA; Schwartz J; Stone PH; Gold DR. (2006). Ambient particulate air pollution and cardiac arrhythmia in a panel of older adults in Steubenville, Ohio. *Occup Environ Med*, 63: 700-706. [090489](#)
- Sawant AA; Cocker DR, 3rd; Miller JW; Taliaferro T; Diaz-Sanchez D; Linn WS; Clark KW; Gong H, Jr. (2008). Generation and characterization of diesel exhaust in a facility for controlled human exposures. *J Air Waste Manag Assoc*, 58: 829-837. [156949](#)
- Schauer JJ; Kleeman MJ; Cass GR; Simoneit BRT. (1999). Measurement of emissions from air pollution sources 2 C1 through C30 organic compounds from medium duty diesel trucks. *Environ Sci Technol*, 33: 1578-1587. [010582](#)
- Schauer JJ; Kleeman MJ; Cass GR; Simoneit BRT. (2002). Measurement of emissions from air pollution sources 5 C1 - C32 organic compounds from gasoline-powered motor vehicles. *Environ Sci Technol*, 36: 1169-1180. [035332](#)
- Schauer JJ; Rogge WF; Hildemann LM; Mazurek MA; Cass GR. (1996). Source apportionment of airborne particulate matter using organic compounds as tracers. *Atmos Environ*, 30: 3837-3855. [051162](#)
- Schnelle-Kreis J; Sklorz M; Peters A; Cyrys J; Zimmermann R. (2005). Analysis of particle-associated semi-volatile aromatic and aliphatic hydrocarbons in urban particulate matter on a daily basis. *Atmos Environ*, 39: 7702-7714. [112944](#)
- Schwab JJ; Felton HD; Rattigan OV; Demerjian KL. (2006). New York State urban and rural measurements of continuous PM_{2.5} mass by FDMS, TEOM, and BAM: Evaluations and Comparisons with the FRM . *J Air Waste Manag Assoc*, 56: 372-83. [098449](#)
- Schwab JJ; Hogrefe O; Demerjian KL; Ambs JL. (2004). Laboratory characterization of modified tapered element oscillating microbalance samplers. *J Air Waste Manag Assoc*, 54: 1254-63. [098450](#)
- Schwartz J; Coull B; Laden F; Ryan L. (2008). The effect of dose and timing of dose on the association between airborne particles and survival. *Environ Health Perspect*, 116: 64-69. [156963](#)
- Schwartz J; Sarnat JA; Coull BA; Wilson WE. (2007). Effects of exposure measurement error on particle matter epidemiology: a simulation using data from a panel study in Baltimore, MD. *J Expo Sci Environ Epidemiol*, 17: S2-S10. [090220](#)
- Seagrave JC; McDonald JD; Bedrick E; Edgerton ES; Gigliotti AP; Jansen JJ; Ke L; Naeher LP; Seilkop SK; Zheng M; Mauderley JL. (2006). Lung toxicity of ambient particulate matter from southeastern US sites with different contributing sources: relationships between composition and effects. *Environ Health Perspect*, 114: 1387-93. [091291](#)
- Seaman NL. (2000). Meteorological modeling for air quality assessments. *Atmos Environ*, 34: 2231-2259. [035562](#)
- Seinfeld JH; Pandis SN. (1998). Atmospheric chemistry and physics: from air pollution to climate change. [018352](#)
- Serre ML; Christakos G. (1999). Modern geostatistics: computational BME analysis in the light of uncertain physical knowledge-the Equus Beds study. *Stoch Environ Res Risk Assess*, 13: 1-26. [156968](#)
- Sheesley RJ; Schauer JJ; Meiritz M; Deminter JT; Bae M-S; Turner JR. (2007). Daily Variation in Particle-Phase Source Tracers in an Urban Atmosphere. *Aerosol Sci Technol*, 41: 981-993. [112017](#)

- Shen S; Jaques PA; Zhu Y; Geller MD; Sioutas C. (2002). Evaluation of the SMPS-APS system as a continuous monitor for measuring PM_{2.5}, PM₁₀ and coarse (PM_{2.5-10}) concentrations. *Atmos Environ*, 36: 3939-3950. [156086](#)
- Sheppard L; Slaughter JC; Schildcrout J; Liu L-JS; Lumley T. (2005). Exposure and measurement contributions to estimates of acute air pollution effects. *J Expo Sci Environ Epidemiol*, 15: 366-376. [079176](#)
- Sheya SA; Glowacki C; Chang MC; Chow JC; Watson JG. (2008). Hot filter/impinger and dilution sampling for fine particulate matter characterization from ferrous metal casting processes. *J Air Waste Manag Assoc*, 58: 553-561. [156977](#)
- Shi Q; Sakurai H; McMurry PH. (2007). Climatology of Regional Nucleation Events in Urban East St. Louis. *Atmos Environ*, 41: 4119-4127. [191760](#)
- Shimpi S; Khalek I; Bougher T; Tennant C. (2009). Number count measurements of particulate trap-equipped diesel truck exhaust from engines that meet 2007 US on-highway emission regulations. Presented at A&WMA's 102nd Annual Conference and Exhibition, June 16-19, 2009, Pittsburgh, PA. [189888](#)
- Shinn JH. (1978). A critical survey of measurements of foliar deposition of airborne sulfates and nitrates. Presented at Presented at: 71st annual meeting of the Air Pollution Control Association; June; Houston, TX. Pittsburgh, PA: Air Pollution Control Association; paper no. 78-7.2. [071426](#)
- Shrivastava MK; Subramanian R; Rogge WF; Robinson AL. (2007). Sources of organic aerosol: Positive matrix factorization of molecular marker data and comparison of results from different source apportionment models. *Atmos Environ*, 41: 9353-9369. [111594](#)
- Singh M; Misra C; Sioutas C. (2003). Field evaluation of a personal cascade impactor sampler (PCIS). *Atmos Environ*, 37: 4781-4793. [156088](#)
- Singh M; Phuleria HC; Bowers K; Sioutas C. (2006). Seasonal and spatial trends in particle number concentrations and size distributions at the children's health study sites in Southern California. *J Expo Sci Environ Epidemiol*, 16: 3-18. [190136](#)
- Sioutas C; Delfino RJ; Singh M. (2005). Exposure assessment for atmospheric ultrafine particles (UFPs) and implications in epidemiologic research. *Environ Health Perspect*, 113: 947-955. [088428](#)
- Sioutas C; Kim S; Chang M; Terrell LL; Gong H Jr. (2000). Field evaluation of a modified DataRAM MIE scattering monitor for real-time PM₂₅ mass concentration measurements. *Atmos Environ*, 34: 4829-4838. [025223](#)
- Slowik JG; Cross ES; Han J-H; Davidovits P; Onasch TB; Jayne JT; Williams LR; Canagaratna MR; Worsnop DR; Chakrabarty RK; Moosm; uuml; ller H; Arnott WP; Schwarz JP; Gao R-S; Fahey DW; Kok GL; Petzold A. (2007). An Inter-Comparison of Instruments Measuring Black Carbon Content of Soot Particles. *Aerosol Sci Technol*, 41: 295 - 314. [096177](#)
- Smith JN; Moore KF; McMurry PH; Eisele FL. (2004). Atmospheric Measurements of Sub-20 nm Diameter Particle Chemical Composition by Thermal Desorption Chemical Ionization Mass Spectrometry. *Aerosol Sci Technol*, 38: 100-110. [156090](#)
- Smith JR; Bailey MR; Etherington G; Shutt AL; Youngman MJ. (2008). Effect of particle size on slow particle clearance from the bronchial tree. *Exp Lung Res*, 34: 287 - 312. [190037](#)
- Smith RL; Spitzner D; Kim Y; Fuentes M. (2000). Threshold dependence of mortality effects for fine and coarse particles in Phoenix, Arizona. *J Air Waste Manag Assoc*, 50: 1367-1379. [010335](#)
- Smith WH; Staskawicz BJ. (1977). Removal of atmospheric particles by leaves and twigs of urban trees: some preliminary observations and assessment of research needs. *J Environ Manage*, 1: 317-330. [046675](#)
- So ESP; Chan ATY; Wong AYT. (2005). Large-eddy simulations of wind flow and pollutant dispersion in a street canyon. *Atmos Environ*, 39: 3573-3582. [110746](#)
- Solomon P; Baumann K; Edgerton E; Tanner R; Eatough D; Modey W; Marin H; Savoie D; Natarajan S; Meyer MB. (2003). Comparison of integrated samplers for mass and composition during the 1999 Atlanta supersites project. *J Geophys Res*, 108: 8423. [156994](#)
- Solomon PA; Hopke PK. (2008). A Special Issue of JA&WMA Supporting Key Scientific and Policy-and Health-Relevant Findings from EPA's Particulate Matter Supersites Program and Related Studies: An Integration and Synthesis of Results. *J Air Waste Manag Assoc*, 58: 137. [156997](#)
- Solomon PA; Sioutas C. (2008). Continuous and semicontinuous monitoring techniques for particulate matter mass and chemical components: a synthesis of findings from EPA's Particulate Matter Supersites Program and related studies. , 58: 164-195. [190139](#)
- Song CH; Carmichael GR. (2001). A three-dimensional modeling investigation of the evolution processes of dust and sea-salt particles in east Asia. *J Geophys Res*, 106: 18,131-18,154. [036064](#)
- Sorensen M; Loft S; Andersen HV; Raaschou-Nielsen O; Skovgaard LT; Knudsen LE; Nielsen IV; Hertel O. (2005). Personal exposure to PM₂₅, black smoke and NO₂ in Copenhagen: relationship to bedroom and outdoor concentrations covering seasonal variation. *J Expo Sci Environ Epidemiol*, 15: 413-422. [089428](#)

- Stanier CO; Khlystov AY; Chan WR; Mandiro M; Pandis SN. (2004). A Method for the In Situ Measurement of Fine Aerosol Water Content of Ambient Aerosols: The Dry-Ambient Aerosol Size Spectrometer (DAASS). *Aerosol Sci Technol*, 38: 215 - 228. [095955](#)
- Stein AF; Lamb D; Draxler RR. (2000). Incorporation of detailed chemistry into a three-dimensional Lagrangian-Eulerian hybrid model: application to regional tropospheric ozone. *Atmos Environ*, 34: 4361-4372. [048341](#)
- Stevenson D; Dentener FJ; Schultz MG; Ellingsen K; Van Noije TPC; Wild O; Zeng G; Amann M; Atherton CS; Bell N; Bergmann DJ; Bey I; Butler T; Cofala J; Collins WJ; Derwent RG; Doherty RM; Drevet J; Eskes HJ; Fiore AM; Gauss M; Hauglustaine DA; Horowitz LW; Isaksen ISA; Krol MC; Lamarque J-F; Lawrence MG; Montanaro V; Muller J-F; Pitari G; Prather MJ; Pyle JA; Rast S; Rodriguez JM; Sanderson MG. (2006). Multimodel ensemble simulations of present-day and near-future tropospheric ozone. *J Geophys Res*, 111. [089222](#)
- Stockwell WR; Middleton P; Chang JS; Tang X. (1990). The second generation Regional Acid Deposition Model chemical mechanism for regional air quality modeling. *J Geophys Res*, 95: 16,343-16,367. [043095](#)
- Stolzenburg MR; Dutcher DD; Kirby BW; Hering SV. (2003). Automated Measurement of the Size and Concentration of Airborne Particulate Nitrate. *Aerosol Sci Technol*, 37: 537-546. [156102](#)
- Stolzenburg MR; Hering SV. (2000). Method for the automated measurement of fine particle nitrate in the atmosphere. *Environ Sci Technol*, 34: 907-914. [013289](#)
- Stracquadanio M; Bergamini D; Massaroli E; Trombini C. (2005). Field evaluation of a passive sampler of polycyclic aromatic hydrocarbons (PAHs) in an urban atmosphere (Bologna, Italy). *J Environ Monit*, 7: 910-915. [156104](#)
- Strand M; Hopke PK; Zhao W; Vedal S; Gelfand E; Rabinovitch N. (2007). A study of health effect estimates using competing methods to model personal exposures to ambient PM_{2.5}. *J Expo Sci Environ Epidemiol*, 17: 549-558. [157018](#)
- Strand M; Vedal S; Rodes C; Dutton SJ; Gelfand EW; Rabinovitch N. (2006). Estimating effects of ambient PM_{2.5} exposure on health using PM_{2.5} component measurements and regression calibration (vol 16, pg 30, 2006). *J Expo Sci Environ Epidemiol*, 16: 471-471. [157017](#)
- Streets DG; Zhang Q; Wang L; He K; Hao J; Wu Y; Tang Y; Carmichael GR. (2006). Revisiting China's CO emissions after the Transport and Chemical Evolution over the Pacific (TRACE-P) mission: Synthesis of inventories, atmospheric modeling, and observations. *J Geophys Res*, 111: D14306. [157019](#)
- Subramanian R; Khlystov A; Robinson A. (2006). Effect of Peak Inert-Mode Temperature on Elemental Carbon Measured Using Thermal-Optical Analysis. *Aerosol Sci Technol*, 40: 763-780. [156107](#)
- Subramanian R; Khlystov AY; Cabada JC; Robinson AL. (2004). Positive and negative artifacts in particulate organic carbon measurements with denuded and undenuded sampler configurations. *Aerosol Sci Technol*, 1: 27-48. [081203](#)
- Sullivan AP; Peltier RE; Brock CA; de Gouw JA; Holloway JS; Warneke C; Wollny AG; Weber RJ. (2006). Airborne measurements of carbonaceous aerosol soluble in water over northeastern United States: Method development and an investigation into water-soluble organic carbon sources. *J Geophys Res*, 111: 1-14. [157030](#)
- Sullivan AP; Weber RJ. (2006). Chemical characterization of the ambient organic aerosol soluble in water: 1. Isolation of hydrophobic and hydrophilic fractions with a XAD-8 resin. *J Geophys Res*, 111: D05314. [157031](#)
- Sullivan AP; Weber RJ; Clements AL; Turner JR; Bae MS; Schauer JJ. (2004). A method for on-line measurement of water-soluble organic carbon in ambient aerosol particles: Results from an urban site. *Geophys Res Lett*, 31: L13105. [157029](#)
- Sullivan JH; Hubbard R; Liu SL; Shepherd K; Trenga CA; Koenig JQ; Chandler WL; Kaufman JD. (2007). A community study of the effect of particulate matter on blood measures of inflammation and thrombosis in an elderly population. *Environ Health Perspect*, 6: 3. [100083](#)
- Swartz E; Stockburger L; Gundel LA. (2003). Recovery of Semivolatile Organic Compounds during Sample Preparation: Implications for Characterization of Airborne Particulate Matter. *Environ Sci Technol*, 37: 597-605. [157035](#)
- Swietlik D; Faust M. (1984). Foliar nutrition of fruit crops. , 6: 287-355. [046678](#)
- Taha G; Box GP; Cohen DD; Stelcer E. (2007). Black Carbon Measurement using Laser Integrating Plate Method. *Aerosol Sci Technol*, 41: 266 - 276. [096277](#)
- Taylor DA. (2002). Dust in the wind. *Environ Health Perspect*, 110: A80-A87. [025693](#)

- Taylor GE Jr; Hanson PJ; Baldocchi DD. (1988). Pollutant deposition to individual leaves and plant canopies: sites of regulation and relationship to injury. In Heck, W. W.; Taylor, O. C.; Tingey, D. T. (Ed.), Assessment of crop loss from air pollutants (pp. 227-257). New York, NY: Elsevier Applied Science. [019289](#)
- Temime-Roussel B; Monod A; Massiani C; Wortham H. (2004). Evaluation of an annular denuder for atmospheric PAH partitioning studies--2: evaluation of mass and number particle losses. Atmos Environ, 38: 1925-1932. [098530](#)
- Temime-Roussel B; Monod A; Massiani C; Wortham H. (2004). Evaluation of an annular denuder tubes for atmospheric PAH partitioning studies--1: evaluation of the trapping efficiency of gaseous PAHS. Atmos Environ, 38: 1913-1924. [098521](#)
- ten Brink H; Hoek G; Khlystov A. (2005). An approach to monitor the fraction of elemental carbon in the ultrafine aerosol. Atmos Environ, 39: 6255-6259. [156115](#)
- ten Brink H; Maenhaut W; Hitzemberger R; Gnauk T; Spindler G; Even A; Chi X; Bauer H; Puxbaum H; Putaud J-P; Tursic J; Berner A. (2004). INTERCOMP2000: the comparability of methods in use in Europe for measuring the carbon content of aerosol. Atmos Environ, 38: 6507-6519. [097110](#)
- Tesche TW; Morris R; Tonnesen G; McNally D; Boylan J; Brewer P. (2006). CMAQ/CAMx annual 2002 performance evaluation over the eastern US. Atmos Environ, 40: 4906-4919. [157050](#)
- Thornburg J; Rodesa CE; Lawless PA; Williams R. (2009). Spatial and Temporal Variability of Outdoor Coarse Particulate Matter Mass Concentrations Measured with a New Coarse Particle Sampler During the Detroit Exposure and Aerosol Research Study. Atmos Environ, 43: 1909-1919. [190999](#)
- Thurston GD; Spengler JD. (1985). A quantitative assessment of source contributions to inhalable particulate matter pollution in metropolitan Boston. Atmos Environ, 19: 9-25. [056074](#)
- Tobias HJ; Kooiman PM; Docherty KS; Ziemann PJ. (2000). Real-Time Chemical Analysis of Organic Aerosols Using a Thermal Desorption Particle Beam Mass Spectrometer. Aerosol Sci Technol, 33: 170-190. [156121](#)
- Tobias HJ; Ziemann PJ. (1999). Compound Identification in Organic Aerosols Using Temperature-Programmed Thermal Desorption Particle Beam Mass Spectrometry. Anal Chem, 71: 3428-3435. [157053](#)
- Tolocka M; Jang PM; Ginter JM; Cox FJ; Kamens RM; Johnston MV. (2004). Formation of oligomers in secondary organic aerosol. Environ Sci Technol, 38: 1428-1434. [087578](#)
- Trijonis JC; Malm WC; Pitchford M; White WH; Charlson R. (1990). Acidic deposition: State of science and technology. Report 24. Visibility: Existing and historical conditions-causes and effects. Final report. [157058](#)
- Tsai CJ; Chang CT; Huang CH. (2006). Direct field observation of the relative humidity effect on the beta-gauge readings. J Air Waste Manag Assoc, 56: 834-40. [098312](#)
- Tsai YI; Kuo SC. (2006). Development of diffuse reflectance infrared Fourier transform spectroscopy for the rapid characterization of aerosols. Atmos Environ, 40: 1781-1793. [156127](#)
- TSI. (2005). Data Merge Software Module for merging and fitting of SMPA and APS Data Files, P/N 1930074, User's Guide, Model 390069, Revision A. St. Paul, MN. [157196](#)
- Tuch TM; Herbarth O; Franck U; Peters A; Wehner B; Wiedensohler A; Heintzenberg J. (2006). Weak correlation of ultrafine aerosol particle concentrations < 800 nm between two sites within one city. J Expo Sci Environ Epidemiol, 16: 486-491. [157060](#)
- Tung TCW; Chao CYH; Burnett J. (1999). A methodology to investigate the particulate penetration coefficient through building shell. Atmos Environ, 33: 881-893. [049003](#)
- Turpin BJ; Lim H-J. (2001). Species contributions to PM_{2.5} mass concentrations: revisiting common assumptions for estimating organic mass. Aerosol Sci Technol, 35: 602-610. [017093](#)
- Turpin BJ; Weisel CP; Morandi M; Colome S; Stock T; Eisenreich S; Buckley B. (2007). Relationships of Indoor, Outdoor, and Personal Air (RIOPA): Part II. Analyses of concentrations of particulate matter species. [157062](#)
- U.S. EPA. (1982). Air quality criteria for particulate matter and sulfur oxides. U.S. Environmental Protection Agency. Washington, D.C.. [017610](#)
- U.S. EPA. (1996). Air quality criteria for particulate matter. U.S. Environmental Protection Agency. Research Triangle Park, NC. EPA/600/P-95/001aF-cF. [079380](#)
- U.S. EPA. (1998). Particulate matter research needs for human health risk assessment to support future reviews of the National Ambient Air Quality Standards for particulate matter. U.S. Environmental Protection Agency. Durham, North Carolina. [083151](#)
- U.S. EPA. (2004). Air quality criteria for particulate matter. U.S. Environmental Protection Agency. Research Triangle Park, NC. EPA/600/P-99/002aF-bF. [056905](#)
- U.S. EPA. (2006). 2002 National Emissions Inventory Data and Documentation. [157070](#)
- U.S. EPA. (2006). Air quality criteria for ozone and related photochemical oxidants. EPA. DC. [088089](#)

- U.S. EPA. (2006). Provisional Assessment of Recent Studies on Health Effects of Particulate Matter Exposure. U.S. Environmental Protection Agency. Research Triangle Park, NC. [157071](#)
- U.S. EPA. (2008). Analysis of particulate matter emissions from light-duty gasoline vehicles in Kansas City. U.S. Environmental Protection Agency. Washington, D.C.. EPA420-R-08-010. [191767](#)
- U.S. EPA. (2008). Integrated Science Assessment for Oxides of Nitrogen - Health Criteria. U.S. Environmental Protection Agency. Research Triangle Park, NC. [157073](#)
- U.S. EPA. (2008). Integrated science assessment for oxides of nitrogen and sulfur: Ecological criteria. EPA. Research Triangle Park, NC. EPA/600/R-08/082F. [157074](#)
- U.S. EPA. (2008). Integrated Science Assessment for Sulfur Oxides?Health Criteria. U.S. Environmental Protection Agency. Research Triangle Park, NC. [157075](#)
- U.S. EPA. (2008). National Air Quality Status and Trends Through 2007. US EPA. Research Triangle Park. EPA-454/R-08-006 . [191190](#)
- U.S. EPA. (2008). Total Risk Integrated Methodology (TRIM) Air Pollutants Exposure Model Documentation (TRIM.Expo/APEX, Version 4.3). Volume 1: User's Guide. U.S. Environmental Protection Agency, Office of Air Quality Planning and Standards. Research Triangle Park, NC. EPA-452/B-08-001b. [191775](#)
- U.S. EPA. (2008). U.S. EPA's 2008 Report on the Environment (Final Report). EPA. DC. [157076](#)
- U.S. EPA. (2009). Risk and Exposure Assessment for Review of the Secondary National Ambient Air Quality Standards for Oxides of Nitrogen and Oxides of Sulfur Second Draft. U.S. Environmental Protection Agency. Washington, D.C.. EPA-452/P-09-004a. http://www.epa.gov/ttnnaqs/standards/no2so2sec/cr_rea.html. [191774](#)
- U.S. EPA. (2009). Verified Retrofit Technologies. [Online at <http://www.epa.gov/otaq/retrofit/index.htm>. [189885](#)
- UNCEC. (2007). Hemispheric Transport of Air Pollution 2007. [157078](#)
- Unsworth MH; Wilshaw JC. (1989). Wet, occult and dry deposition of pollutants on forests. , 47: 221-238. [046682](#)
- Van Aalst RM. (1982). Dry deposition of NO_x. In Schneider, T.; Grant, L. (Ed.), Air pollution by nitrogen oxides Amsterdam, The Netherlands: Elsevier Scientific Publishing Company. [036481](#)
- van der Werf GR; Randerson JT; Giglio L; Collatz GJ; Kasibhatla PS; Arellano Jr AF. (2006). Interannual variability in global biomass burning emissions from 1997 to 2004. , 6: 3423-3441. [157084](#)
- VanCuren RA; Cahill TA. (2002). Asian aerosols in North America: Frequency and concentration of fine dust. J Geophys Res, 107 (2002) pArticle Number: 4804: Article. [157087](#)
- Vega E; Reyes E; Wellens A; Sanchez G; Chow JC; Watson JG. (2003). Comparison of continuous and filter based mass measurements in Mexico City. Atmos Environ, 37: 2783-2793. [105974](#)
- Venkataraman C; Lyons JM; Friedlander SK. (1994). Size distributions of polycyclic aromatic hydrocarbons and elemental carbon 1 Sampling, measurement methods, and source characterization. Environ Sci Technol, 28: 555-562. [002475](#)
- Venn A; Lewis S; Cooper M; Hubbard R; Hill I; Boddy R; Bell M; Britton J. (2000). Local road traffic activity and the prevalence, severity and persistence of wheeze in school children: combined cross sectional and longitudinal study. Occup Environ Med, 57: 152-158. [007895](#)
- Venn AJ; Lewis SA; Cooper M; Hubbard R; Britton J. (2001). Living near a main road and the risk of wheezing illness in children. Am J Respir Crit Care Med, 164: 2177-2180. [023644](#)
- Veranth JM; Moss TA; Chow JC; Labban R; Nichols WK; Walton JC; Walton JG; Yost GS. (2006). Correlation of in vitro cytokine responses with the chemical composition of soil-derived particulate matter. Environ Health Perspect, 114: 341-349. [087479](#)
- Viana M; Kuhlbusch TAJ; Querol X; Alastuey A; Harrison RM; Hopke PK; Winiwarter W; Vallius M; Szidat S; Prévôt ASH; Hueglin C; Bloemen H; Wählin P; Vecchi R; Miranda AI; Kasper-Giebl A; Maenhaut W; Hitzenberger R. (2008). Source apportionment of particulate matter in Europe: A review of methods and results. J Aerosol Sci, 39(10): 827-849. [155269](#)
- Viana M; Querol X; Alastuey A. (2006). Chemical characterisation of PM episodes in NE Spain. Chemosphere, 62: 947-56. [096384](#)
- Viana M; Querol X; Alastuey A; Ballester F; Llop S; Esplugues A; FernÁndez-Patier R; GarcÁ-a dos Santos S; Hecce MD. (2008). Characterising exposure to PM aerosols for an epidemiological study. Atmos Environ, 42: 1552-1568. [156135](#)
- Violante FS; Barbieri A; Curti S; Sanguinetti G; Graziosi F; Mattioli S. (2006). Urban atmospheric pollution: Personal exposure versus fixed monitoring station measurements. Chemosphere, 64: 1722-1729. [156140](#)
- Virkkula A; Makela T; Hillamo R; Yli-Tuomi T; Hirsikko A; Hameri K; Koponen IK. (2007). A simple procedure for correcting loading effects of aethalometer data. J Air Waste Manag Assoc, 57: 1214-1222. [157098](#)
- Voisin D; Smith JN; Sakurai H; McMurry PH; Eisele FL. (2003). Thermal Desorption Chemical Ionization Mass Spectrometer for Ultrafine Particle Chemical Composition. Aerosol Sci Technol, 37: 471-475. [156141](#)

- Volckens J; Olson DA; Hays MD. (2008). Carbonaceous species emitted from handheld two-stroke engines. *Atmos Environ*, 42: 1239-1248. [105465](#)
- Vyas VM; Christakos G. (1997). Spatiotemporal analysis and mapping of sulfate deposition data over Eastern USA. *Atmos Environ*, 31: 3623-3633. [156142](#)
- Wagner J; Leith D. (2001). Passive aerosol sampler. Part I: Principle of operation. *Aerosol Sci Technol*, 34: 186-192. [190153](#)
- Wagner J; Leith D. (2001). Passive aerosol sampler. Part II: Wind tunnel experiments. *Aerosol Sci Technol*, 34: 193-201. [190154](#)
- Wallace L. (2000). Real-time monitoring of particles, PAH, and CO in an occupied townhouse. *J Occup Environ Hyg*, 15: 39-47. [000803](#)
- Wallace L; Williams R. (2005). Use of personal-indoor-outdoor sulfur concentrations to estimate the infiltration factor and outdoor exposure factor for individual homes and persons. *Environ Sci Technol*, 39: 1707-1714. [057485](#)
- Wallace L; Williams R; Rea A; Croghan C. (2006). Continuous weeklong measurements of personal exposures and indoor concentrations of fine particles for 37 health-impaired North Carolina residents for up to four seasons. *Atmos Environ*, 40: 399-414. [088211](#)
- Wallace L; Williams R; Suggs J; Jones P. (2006). Estimating contributions of outdoor fine particles to indoor concentrations and personal exposures: effects of household characteristics and personal activities. [089190](#)
- Wang J; Christopher SA; Nair US; Reid JS; Prins EM; Szykman J; Hand JL. (2006). Mesoscale modeling of Central American smoke transport to the United States: 1.??Top-down??assessment of emission strength and diurnal variation impacts. *J Geophys Res*, 111: D05S17. [157109](#)
- Wang LH; Milford JB; Carter WPL. (2000). Reactivity estimates for aromatic compounds Part 2 uncertainty in incremental reactivities. *Atmos Environ* 4349-4360. [048365](#)
- Wang LH; Milford JB; Carter WPL. (2000). Reactivity estimates for aromatic compounds Part I: uncertainty in chamber-derived parameters. *Atmos Environ*, 34: 4337-4348. [048357](#)
- Watson JG; Chen LW; Chow JC; Doraiswamy P; Lowenthal DH. (2008). Source apportionment: findings from the U.S. Supersites Program. *J Air Waste Manag Assoc*, 58: 265-288. [157128](#)
- Watson JG; Chow JC. (2002). Comparison and evaluation of in situ and filter carbon measurements at the Fresno Supersite. *J Geophys Res*, 107. [037873](#)
- Watson JG; Chow JC. (2007). Receptor models for source apportionment of suspended particles. In *Introduction to Environmental Forensics* (pp. 273-298). San Diego, CA: Academic Press. [157127](#)
- Watson JG; Chow JC; Chen LWA. (2005). Summary of organic and elemental carbon/black carbon analysis methods and intercomparisons. *Aerosol Air Qual Res*, 5: 69-102. [157125](#)
- Watson JG; Fujita EM; Chow JC; Zielinska B; Richards LW; Neff W; Dietrich D. (1998). Northern front range air quality study Final report. [012257](#)
- Watson JG; Robinson NF; Chow JC; Henry RC; Kim BM; Pace TG; Meyer EL; Nguyen Q. (1990). The USEPA/DRI chemical mass balance receptor model, CMB 70. *Environ Software*, 5: 38-49. [004848](#)
- Weber RJ; Orsini D; Daun Y; Lee Y-N; Kotz PJ; Brechtel F. (2001). A particle-into-liquid collector for rapid measurement of aerosol bulk chemical composition. *Aerosol Sci Technol*, 35: 718-727. [024640](#)
- Weber RJ; Orsini D; Duan Y; Baumann K; Kiang CS; Chameides W; Lee YN; Brechtel F; Klotz P; Jongejan P. (2003). Intercomparison of near real time monitors of PM_{2.5} nitrate and sulfate at the US Environmental Protection Agency Atlanta Supersite. *J Geophys Res*, 108: 8421. [157129](#)
- Weijers EP; Khlystov AY; Kos GPA; Erisman JW. (2004). Variability of particulate matter concentrations along roads and motorways determined by a moving measurement unit. *Atmos Environ*, 38: 2993-3002. [104186](#)
- Weingartner E; Saathoff H; Schnaiter M; Streit N; Bitnar B; Baltensperger U. (2003). Absorption of light by soot particles: determination of the absorption coefficient by means of aethalometers. *J Aerosol Sci*, 34: 1445-1463. [156149](#)
- Wenzel RJ; Liu DY; Edgerton ES; Prather KA. (2003). Aerosol time-of-flight mass spectrometry during the Atlanta Supersite Experiment: 2. Scaling procedures. *J Geophys Res*, 108: 8426. [157139](#)
- Wesely ML; Eastman JA; Stedman DH; Yalvac ED. (1982). An eddy-correlation measurement of NO₂ flux to vegetation and comparison to O₃ flux. *Atmos Environ*, 16: 815-820. [036564](#)
- Wesely ML; Hicks BB. (2000). A review of the current status of knowledge on dry deposition. *Atmos Environ*, 34: 2261-2282. [025018](#)
- Westerdahl D; Fruin S; Sax T; Fine PM; Sioutas C. (2005). Mobile platform measurements of ultrafine particles and associated pollutant concentrations on freeways and residential streets in Los Angeles. *Atmos Environ*, 39: 3597-3610. [086502](#)
- Whitby KT. (1978). The physical characteristics of sulfur aerosols. *Atmos Environ*, 12: 135-159. [071181](#)

- Williams B; Goldstein A; Kreisberg N; Hering S. (2006). An In-Situ Instrument for Speciated Organic Composition of Atmospheric Aerosols: Thermal Desorption Aerosol GC/MS-FID (TAG). *Aerosol Sci Technol*, 40: 627-638. [156157](#)
- Williams R; Rea A; Vette A; Croghan C; Whitaker D; Stevens C; McDow S; Fortmann R; Sheldon L; Wilson H; Thornburg J; Phillips M; Lawless P; Rodes C; Daughtrey H. (2008). The design and field implementation of the Detroit Exposure and Aerosol Research Study. *J Expo Sci Environ Epidemiol*, in press: in press. [191198](#)
- Williams TC; Shaddix CR; Jensen KA; Suo-Anttila JM. (2006). Measurements of the Dimensionless Extinction Coefficient of Soot Within Laminar Diffusion Flames. [157148](#)
- Wilson JG; Zawar-Reza P. (2006). Intraurban-scale dispersion modelling of particulate matter concentrations: applications for exposure estimates in cohort studies. *Atmos Environ*, 40: 1053-1063. [088292](#)
- Wilson WE; Brauer M. (2006). Estimation of ambient and non-ambient components of particulate matter exposure from a personal monitoring panel study. *J Expo Sci Environ Epidemiol*, 16: 264-274. [088933](#)
- Wilson WE; Grover BD; Long RW; Eatough NL; Eatough DJ. (2006). The measurement of fine particulate semivolatile material in urban aerosols. *J Air Waste Manag Assoc*, 56: 384-387. [091142](#)
- Wilson WE; Mage DT; Grant LD. (2000). Estimating separately personal exposure to ambient and nonambient particulate matter for epidemiology and risk assessment: why and how. *J Air Waste Manag Assoc*, 50: 1167-1183. [010288](#)
- Wilson WE; Mar TF; Koenig JQ. (2007). Influence of exposure error and effect modification by socioeconomic status on the association of acute cardiovascular mortality with particulate matter in Phoenix. *J Expo Sci Environ Epidemiol*, 17: S11. [157149](#)
- Wilson WE; Suh HH. (1997). Fine particles and coarse particles: concentration relationships relevant to epidemiologic studies. *J Air Waste Manag Assoc*, 47: 1238-1249. [077408](#)
- Winkler PM; Steiner G; Vrtala A; Vehkamäki H; Noppel M; Lehtinen KEJ; Reischl GP; Wagner PE; Kulmala M. (2008). Heterogeneous Nucleation Experiments Bridging the Scale from Molecular Ion Clusters to Nanoparticles. , 319: 1374. [156160](#)
- Womilaju TO; Miller JD; Mayer PM; Brook JR. (2003). Methods to determine the biological composition of particulate matter collected from outdoor air. *Atmos Environ*, 37: 4335-4344. [179954](#)
- Wongphatarakul V; Friedlander SK; Pinto JP. (1998). A comparative study of PM_{2.5} ambient aerosol chemical databases. *Environ Sci Technol*, 32: 3926-3934. [049281](#)
- Woo K-S; Chen D-R; Pui DYH; McMurry PH. (2001). Measurement of Atlanta aerosol size distributions: observations of ultrafine particle events. *Aerosol Sci Technol*, 34: 75-87. [011702](#)
- Wu C-F; Delfino RJ; Floro JN; Quintana. (2005). Exposure assessment and modeling of particulate matter for asthmatic children using personal nephelometers. *Atmos Environ*, 39: 3457-3469. [086397](#)
- Wu CF; Delfino RJ; Floro JN; Samimi BS; Quintana PJ; Kleinman MT; Liu LJ. (2005). Evaluation and quality control of personal nephelometers in indoor, outdoor and personal environments. , 15: 99-110. [157155](#)
- Wu J; Houston D; Lurmann F; Ong P; Winer A. (2009). Exposure of PM_{2.5} and EC from diesel and gasoline vehicles in communities near the Ports of Los Angeles and Long Beach, California. *Atmos Environ*, 43: 1962-1971. [191773](#)
- Wu J; M Winer A; J Delfino R. (2006). Exposure assessment of particulate matter air pollution before, during, and after the 2003 Southern California wildfires. *Atmos Environ*, 40: 3333-3348. [157156](#)
- Wu S; Mickley L; Jacob D; Rind D; Streets D. (2008). Effects of 2000-2050 changes in climate and emissions on global tropospheric ozone and the policy-relevant background surface ozone in the United States. *J Geophys Res*, 113: D18312. [190039](#)
- Xia X; Hopke PK. (2006). Seasonal Variation of 2-Methyltetrols in Ambient Air Samples. *Environ Sci Technol*, 40: 6934-6937. [179947](#)
- Xiaomin X; Zhen H; Jiasong W. (2006). The impact of urban street layout on local atmospheric environment. , 41: 1352-1363. [156165](#)
- Yang H; Li Q; Yu JZ. (2003). Comparison of two methods for the determination of water-soluble organic carbon in atmospheric particles. *Atmos Environ*, 37: 865-870. [156167](#)
- Yanosky JD; Paciorek CJ; Schwartz J; Laden F; Puett R; Suh HH. (2008). Spatio-temporal modeling of chronic PM₁₀ exposure for the Nurses' Health Study. *Atmos Environ*, 42(18): 4047-4062. [099467](#)
- Yanosky JD; Paciorek CJ; Suh HH. (2009). Predicting chronic fine and coarse particulate exposures using spatiotemporal models for the northeastern and midwestern United States. *Environ Health Perspect*, 117: 522-529. [190114](#)
- Yi SM; Ambs JL; Patashnick H; Rupprecht G; Hopke PK. (2004). Particle Collection Characteristics of a Prototype Electrostatic Precipitator (ESP) for a Differential TEOM System. *Aerosol Sci Technol*, 38: 46-51. [156169](#)

- Yu H; Remer LA; Chin M; Bian H; Kleidman RG; Diehl T. (2008). A satellite-based assessment of transpacific transport of pollution aerosol. *J Geophys Res*, 113: 1-15. [157168](#)
- Yu JZ; Yang H; Zhang H; Lau AKH. (2004). Size distributions of water-soluble organic carbon in ambient aerosols and its size-resolved thermal characteristics. *Atmos Environ*, 38: 1061-1071. [156172](#)
- Zanis P; Trickl T; Stohl A; Wernli H; Cooper O; Zerefos C; Gaeggeler H; Schnabel C; Tobler L; Kubik PW; Priller A; Scheel HE; Kanter HJ; Cristofanelli P; Forster C; James P; Gerasopoulos E; Delcloo A; Papayannis A; Claude H. (2003). Forecast, observation and modelling of a deep stratospheric intrusion event over Europe. , 3: 763-777. [053423](#)
- Zanobetti A; Wand MP; Schwartz J; Ryan LM. (2000). Generalized additive distributed lag models: quantifying mortality displacement. , 1: 279-292. [004133](#)
- Zeger SL; Thomas D; Dominici F; Samet JM; Schwartz J; Dockery D; Cohen A. (2000). Exposure measurement error in time-series studies of air pollution: concepts and consequences. *Environ Health Perspect*, 108: 419-426. [001949](#)
- Zeng Y. (2006). A comprehensive particulate matter monitoring system and dosimetry-based ambient particulate matter standards. *J Air Waste Manag Assoc*, 56: 518-29. [098375](#)
- Zhang K; Wexler A. (2008). Modeling urban and regional aerosols—Development of the UCD Aerosol Module and implementation in CMAQ model. *Atmos Environ*, 42: 3166-3178 . [191770](#)
- Zhang Q; Jimenez JL; Canagaratna MR; Jayne JT; Worsnop DR. (2005). Time- and size-resolved chemical composition of submicron particles in Pittsburgh: Implications for aerosol sources and processes. *J Geophys Res*, 110: 1-19. [157185](#)
- Zhang X; Kondragunta S; Schmidt C; Kogan F. (2008). Near Real-time Monitoring of Biomass Burning Particulate Emissions (PM25) across Contiguous United States Using Multiple Satellite Instruments. *Atmos Environ*, 42(29): 6959-6972. [155144](#)
- Zhang X; Zhuang G; Guo J; Yin K; Zhang P. (2007). Characterization of aerosol over the Northern South China Sea during two cruises in 2003. *Atmos Environ*, 41: 7821-7836. [101119](#)
- Zhang Z; Che W; Liang Y; Wu M; Li N; Shu Y; Liu F; Wu D. (2007). Comparison of cytotoxicity and genotoxicity induced by the extracts of methanol and gasoline engine exhausts. *Toxicol In Vitro*, 21: 1058-1065. [157186](#)
- Zhao W; Hopke PK; Norris G; Williams R; Paatero P. (2006). Source apportionment and analysis on ambient and personal exposure samples with a combined receptor model and an adaptive blank estimation strategy. *Atmos Environ*. [156181](#)
- Zhao W; Rabinovitch N; Hopke PK; Gelfand EW. (2007). Use of an expanded receptor model for personal exposure analysis in schoolchildren with asthma. *Atmos Environ*, 41: 4084-4096. [156182](#)
- Zheng M; Cass GR; Schauer JJ; Edgerton ES. (2002). Source apportionment of PM2.5 in the southeastern United States using solvent-extractable organic compounds as tracers. *Environ Sci Technol*, 36: 2361-2371. [026100](#)
- Zheng M; Ke L; Edgerton ES; Schauer JJ; Dong M; Russell AG. (2006). Spatial distribution of carbonaceous aerosol in the southeastern United States using molecular markers and carbon isotope data. *J Geophys Res*, 111: D10S06. [157189](#)
- Zhou Y; Levy JI. (2007). Factors influencing the spatial extent of mobile source air pollution impacts: a meta-analysis. *BMC Public Health*, 7: 89. [098633](#)
- Zhu K; Zhang J; Liou PJ. (2007). Evaluation and comparison of continuous fine particulate matter monitors for measurement of ambient aerosols. *J Air Waste Manag Assoc*, 57: 1499-506. [098367](#)
- Zhu Y; Eiguren-Fernandez A; Hinds WC; Miguel AH. (2007). In-Cabin Commuter Exposure to Ultrafine Particles on Los Angeles Freeways. *Environ Sci Technol*, 41: 2138-2145. [179919](#)
- Zhu Y; Hinds WC. (2002). Concentration and size distribution of ultrafine particles near a major highway. *J Air Waste Manag Assoc*, 52: 1032-1042. [041552](#)
- Zhu Y; Hinds WC; Shen S; Sioutas C. (2004). Seasonal trends of concentration and size distribution of ultrafine particles near major highways in Los Angeles. *Aerosol Sci Technol*, 38: 5-13. [156184](#)
- Zhu Y; Kuhn T; Mayo P; Hinds WC. (2005). Comparison of Daytime and Nighttime Concentration Profiles and Size Distributions of Ultrafine Particles near a Major Highway. *Environ Sci Technol*, 39: 2531-2536. [157191](#)
- Zidek JV; Shaddick G; Meloche J; Chatfield C; White R. (2007). A framework for predicting personal exposures to environmental hazards. , 14: 411-431. [190076](#)
- Zidek JV; Wong H; Le ND; Burnett R. (1996). Causality, measurement error and multicollinearity in epidemiology. *Environmetrics*, 7: 441-451. [051879](#)

Chapter 4. Dosimetry

4.1. Introduction

1 Particle dosimetry refers to the characterization of deposition, translocation,
2 clearance, and retention of particles and their constituents within the respiratory tract and
3 extrapulmonary tissues. This chapter summarizes basic concepts presented in dosimetry
4 chapters of the 1996 and 2004 PM AQCDs (U.S. EPA, 1996, [079380](#); U.S. EPA, 2004,
5 [056905](#)), and updates the state of the science based upon new literature appearing since
6 publication of these PM AQCDs. Although the basic understanding of the mechanisms
7 governing deposition and clearance of inhaled particles has not changed, there has been
8 significant additional information on the role of certain biological determinants such as
9 gender, age and lung disease on deposition and clearance. Additionally, new studies have
10 further characterized the retention and translocation of ultrafine particles (also commonly
11 referred to as nanoparticles) following deposition in the respiratory tract.

12 The dose from inhaled particles deposited and retained in the respiratory tract is
13 governed by a number of factors. These include exposure concentration and duration,
14 activity and ventilatory parameters, and particle properties (e.g., particle size,
15 hygroscopicity, and solubility in airway fluids and cellular components). The basic
16 characteristics of particles as they relate to deposition and retention, as well as anatomical
17 and physiological factors influencing particle deposition and retention, were discussed in
18 depth in Chapter 10 of 1996 PM AQCD and updated in Chapter 6 of the 2004 PM AQCD.
19 Species differences between humans and rats in particle exposures, deposition patterns,
20 and pulmonary retention were also reviewed in Brown et al. (2005, [089308](#)). The current
21 review of PM dosimetry focuses mainly on issues that may affect the susceptibility of an
22 individual to adverse effects as well as issues that affect our ability to extrapolate findings
23 between studies (e.g., in vitro to in vivo) and between species. Other than a brief overview
24 in this introductory section, the disposition (i.e., deposition, absorption, distribution,
25 metabolism, and elimination) of fibers and unique nano-objects (viz., dots, hollow spheres,
26 rods, fibers, tubes) is not reviewed herein. Exposures to fibers and unique nano-objects
27 generally occur in the occupational settings rather than the ambient environment.

28 The deposition by interception of micro-sized fibers was briefly discussed in the 1996
29 and 2004 PM AQCD, but fiber retention in the respiratory tract was not addressed.
30 Airborne fibers (length/diameter ratio ≥ 3), frequently exceed 150 μm in length and appear

Note: Hyperlinks to the reference citations throughout this document will take you to the NCEA HERO database (Health and Environmental Research Online) at <http://epa.gov/hero>. HERO is a database of scientific literature used by U.S. EPA in the process of developing science assessments such as the Integrated Science Assessments (ISA) and the Integrated Risk Information System (IRIS).

1 to be relatively stable in air. This is because their aerodynamic size is determined
2 predominantly by their diameter, not their length. Fibers, therefore, deposit largely by
3 interception and when aligned with the direction of airflow may penetrate deep into the
4 respiratory tract. Once deposited, macrophage mediated clearance is the primary
5 mechanism of removing micro-sized particles from the pulmonary region. The length of
6 fibers can, however, prevent their phagocytosis and clearance. For example, fibers of
7 greater than 17 μm in length are too long to be fully engulfed by rat alveolar macrophages
8 and can protrude from macrophages (i.e., macrophage frustration) (Zeidler-Erdely et al.,
9 2006, [190967](#)). Further discussion of the fiber disposition in the respiratory tract is beyond
10 the scope of this chapter.

11 The term “ultrafine particle” has traditionally been used by the aerosol research and
12 occupational and environmental health communities to describe airborne particles or other
13 laboratory generated aerosols used in toxicological studies that are smaller than 100 nm in
14 size (based on physical size, diffusivity, or electrical mobility). Generally consistent with the
15 definition of an ultrafine particle, the International Organization for Standardization (ISO)
16 recently defined a nanoparticle as an object with all three external dimensions in the
17 nanoscale, i.e., from approximately 1 and 100 nm (ISO, 2008, [190066](#)). The ISO also defined
18 a nano-object as a material with one or more external dimensions in the nanoscale. The
19 terms, nanoparticle and ultrafine particle, have been used rather synonymously in the
20 recent literature. However, the terms nanoparticle and nano-object are more commonly
21 associated with engineered materials that are created for consumer products and industrial
22 applications. With the current interest in nanotechnologies, many nano-objects have been
23 created by manipulating materials at the atomic or molecular scale for the purpose of
24 forming new materials, structures, and devices that exploit the unique physical and
25 chemical properties associated with their nanoscale. Toxicological studies are becoming
26 available that evaluate in vivo translocation and health effects unique of nano-objects (viz.,
27 dots, hollow spheres, rods, tubes). The in vivo disposition of these unique nano-objects is
28 not, however, necessarily relevant to the behavior of ultrafine aerosols in the urban
29 environment that are created by combustion sources and photochemical formation of
30 secondary organic aerosols. Therefore, the disposition of unique nano-objects (viz., dots,
31 hollow spheres, rods, fibers, tubes) is not considered in this chapter.

4.1.1. Size Characterization of Inhaled Particles

32 Particle size is a major determinant of the fraction of inhaled particles depositing in
33 and cleared from various regions of the respiratory tract. The distribution of particle sizes
34 in an aerosol is typically described by the lognormal distribution (i.e., the situation in which
35 the logarithms of particle diameter are distributed normally). The geometric mean is the

1 median of the distribution, and the variability around the median is the geometric standard
2 deviation (GSD or σ_g) and is given by:

$$GSD = \sigma_g = \frac{d_{84\%}}{d_{50\%}} = \frac{d_{50\%}}{d_{16\%}}$$

Equation 4-1

3 where: $d_{16\%}$, $d_{50\%}$, $d_{84\%}$ are the particle diameters associated with the 16th, 50th (i.e., the
4 median), and the 84th percentiles from the cumulative frequency distribution of particle
5 sizes. By definition, GSD must be greater than one. The particle size associated with any
6 percentile of the distribution, d_i , is given by:

$$d_i = d_{50\%} \sigma_g^{z(P)}$$

Equation 4-2

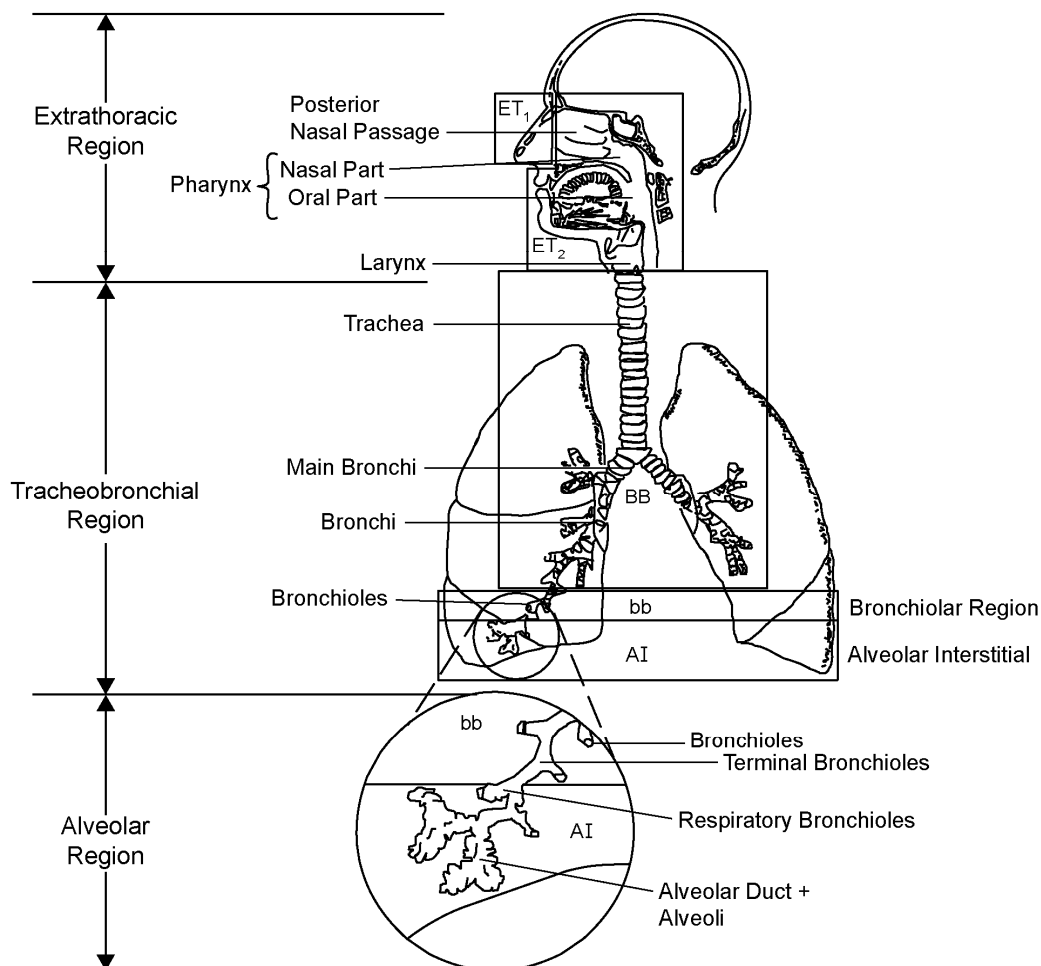
7 where: $z(P)$ is the normal standard deviate for a given probability. In most cases, the
8 aerosols to which people are naturally exposed are polydisperse. By contrast, most
9 experimental studies of particle deposition and clearance in the lung use monodisperse
10 particles (GSD <1.15). Ambient aerosols may also be composed of multiple size modes, each
11 mode should be described by its specific median diameter and GSD.

12 Aerosol size distributions may be measured and described in various ways. When a
13 distribution is described by counting particles, the median is called the count median
14 diameter (CMD). On the other hand, the median of a distribution based on particle mass in
15 an aerosol is the mass median diameter (MMD). Impaction and sedimentation of particles
16 in the respiratory tract depend on a particle's aerodynamic diameter (d_{ae}), which is the size
17 of a sphere of unit density that has the same terminal settling velocity as the particle of
18 interest. The size distribution is frequently described in terms of d_{ae} as the mass median
19 aerodynamic diameter (MMAD), which is the median of the distribution of mass with
20 respect to aerodynamic equivalent diameter. Alternative descriptions should be used for
21 particles with actual physical sizes below $\approx 0.5 \mu\text{m}$ because, for these sized particles,
22 aerodynamic properties become less important and diffusion becomes ever more important.
23 For these smaller particles, their physical diameter or CMD are typically used since
24 diffusivity is not a function of particle density. For aggregates, a thermodynamic-equivalent
25 size, i.e., the diameter of a spherical particle that has the same diffusion coefficient in air as
26 the aggregate, is appropriate.

4.1.2. Structure of the Respiratory Tract

27 The basic structure of the human respiratory tract is illustrated in Figure 4-1. In the
28 literature, the terms extrathoracic (ET) region and upper airways are used synonymously.
29 The term lower airways is used to refer to the intrathoracic airways, i.e., the combination of

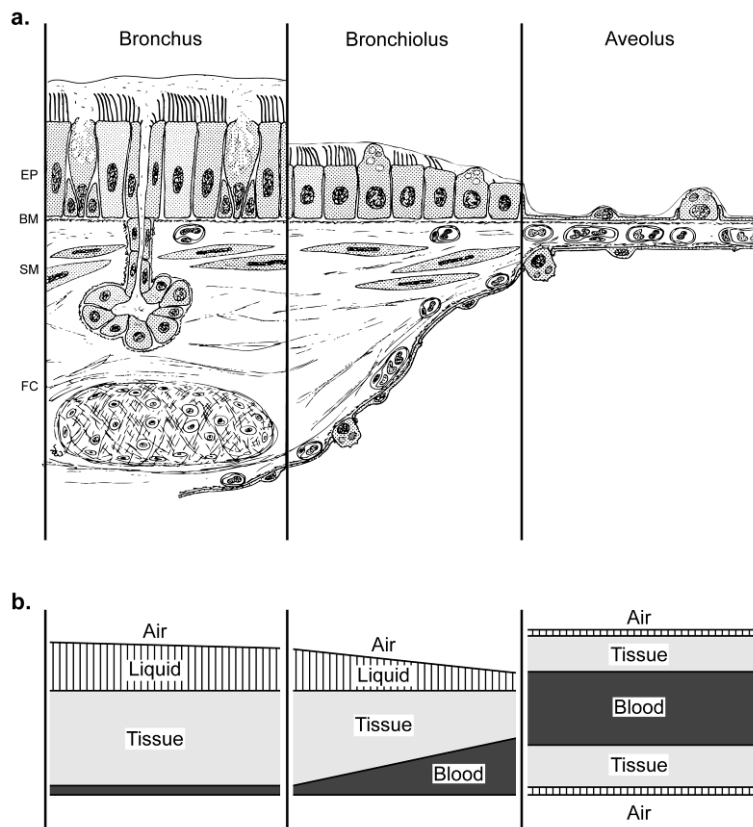
1 the tracheobronchial (TB) region which is the conducting airways and the alveolar region
 2 which is the functional part or parenchyma of the lung. A recent review of interspecies
 3 similarities and differences in the structure and function of the respiratory tract is provided
 4 by Phalen et al. (2008, [156865](#)). Although the structure varies, the illustrated anatomic
 5 regions are common to all mammalian species with the exception of the respiratory
 6 bronchioles. Respiratory bronchioles, the transition region between ciliated and fully
 7 alveolated airways, are found in humans, dogs, ferrets, cats, and monkeys. Respiratory
 8 bronchioles are absent in rats and mice and abbreviated in hamsters, guinea pigs, oxen,
 9 sheep, and pigs. The branching structure of the ciliated bronchi and bronchioles also differs
 10 between species from being a rather symmetric and dichotomous branching network of
 11 airways in humans to a more monopodial branching network in other mammals.



Source: Based on ICRP (1994, [006988](#)).

Figure 4-1. Diagrammatic representation of respiratory tract regions in humans. Structures are anterior nasal passages, ET₁; oral airway and posterior nasal passages, ET₂; bronchial airways, BB; bronchioles, bb; and alveolar interstitial, AI.

1 Another species difference relevant to particle dosimetry is the route of breathing. For
 2 instance, rats are obligate nose breathers, whereas most humans are oronasal breathers
 3 who breathe through the nose when at rest and increasingly through the mouth with
 4 increasing activity level. There is inter-individual variability in the route by which people
 5 breathe. Most people, 87% (26 of 30) in the Niinimaa et al. (1981, [071758](#)) study, breathed
 6 through their nose until an activity level was reached where they switched to oronasal
 7 breathing. Thirteen percent (4 of 30) of the subjects, however, were oronasal breathers even
 8 at rest. These two subject groups are commonly referred to in the literature (e.g. ICRP,
 9 1994, [006988](#)) as “normal augmenters” and “mouth breathers,” respectively. In contrast to
 10 healthy subjects, Chadha et al. (1987, [037365](#)) found that the majority (11 of 12) of patients
 11 with asthma or allergic rhinitis breathe oronasally even at rest.



Source: Panel (a) reproduced with permission (ER Weibel, Design and structure of the human lung, In: Pulmonary Diseases and Disorders, ed. AP Fishman, McGraw-Hill, New York, 1980, p. 231)(Fishman and Elias, 1980, [156436](#))

Figure 4-2. Structure of lower airways with progression from the large airways to the alveolus. Panel (a) illustrates basic airway anatomy. Structures are epithelial cells, EP; basement membrane, BM; smooth muscle cells, SM; and fibrocartilaginous coat, FC. Panel (b) illustrates the relative amounts of liquid, tissue, and blood with distal progression.

1 The site of particle deposition within the respiratory tract has implications related to
2 lung retention and surface dose of particles as well as potential systemic distribution of
3 particles or their constituents. Figure 4-2 illustrates the progressive change in airway
4 anatomy with distal progression into the lower respiratory tract. In the bronchi there is a
5 thick liquid lining and mucociliary clearance rapidly moves deposited particles toward the
6 mouth. In general, in the bronchi, only highly soluble materials moving from the air into
7 the liquid layer will have systemic access via the blood. With distal progression, the
8 protective liquid lining diminishes and clearance rates slow. Soluble compounds and some
9 poorly soluble ultrafine particles may cross the air-liquid interface to enter the tissues and
10 the blood especially in the alveolar region.

4.2. Particle Deposition

11 Inhaled particles may be either exhaled or deposited in the ET, TB, or alveolar region.
12 A particle becomes deposited when it moves from the airway lumen to the wall of an airway.
13 The deposition of particles in the respiratory tract depends primarily on inhaled particle
14 size, route of breathing (through the nasal or oronasal), tidal volume (V_T), breathing
15 frequency (f), and respiratory tract morphology. The distinction between air passing
16 through the nose versus the mouth is important since the nasal passages more effectively
17 remove inhaled particles than the oral passage. Respiratory tract morphology, which affects
18 particle transport and deposition, varies between species, the size of an animal or human,
19 and health status.

20 The fraction of inhaled aerosol becoming deposited in the human respiratory tract has
21 been measured experimentally. Studies, using light scattering or particle counting
22 techniques to quantify the amount of aerosol in inspired and expired breaths, have
23 characterized total particle deposition for varied breathing conditions and particle sizes.
24 The vast majority of in vivo data on the regional particle deposition has been obtained by
25 scintigraphic methods. These data have shown highly variable regional deposition with
26 sites of highly localized deposition or “hot spots” in the obstructed lung relative to the
27 healthy lung. Even in the healthy lung, “hot spots” occur in the region of airway
28 bifurcations. Mathematical models aid in predicting the mixed effects of particle size,
29 breathing conditions, and lung volume on total and regional deposition. Experimentally,
30 however, there is considerable inter-individual variability in total and regional deposition
31 even when inhaled particle size and breathing conditions are strictly controlled.
32 Section 4.2.4 on Biological Factors Modulating Deposition provides more detailed
33 information on factors affecting deposition among individuals.

34 In order to potentially become deposited in the respiratory tract, particles must first
35 be inhaled. The inspirable particulate mass fraction of an aerosol is that fraction of the
36 ambient airborne particles that can enter the uppermost respiratory tract compartment,

1 the head (Soderholm, 1985, [156992](#)). The American Conference of Governmental Industrial
2 Hygienists (ACGIH) and the International Commission on Radiological Protection (ICRP)
3 have established inhalability criteria for humans (ACGIH, 2005, [156188](#); ICRP, 1994,
4 [006988](#)). These criteria are indifferent to route of breathing and assume random orientation
5 with respect to wind direction. They are based on experimental inhalability data for $d_{ae} \leq$
6 $100 \mu\text{m}$ at wind speeds of between 1 and 8 m/s. For ACGIH criterion, inhalability is 97% for
7 an $d_{ae} = 1 \mu\text{m}$, 87% for an $d_{ae} = 5 \mu\text{m}$, 77% for an $d_{ae} = 10 \mu\text{m}$, and plateaus at 50% d_{ae} above
8 $\sim 40 \mu\text{m}$. The ICRP criterion, which also plateaus at 50% for very large d_{ae} , does not become
9 of real importance until an $d_{ae} = 5 \mu\text{m}$ where inhalability is 97%. Dai et al. (2006, [156377](#))
10 reported slightly lower nasal particle inhalability in humans during moderate exercise than
11 rest (e.g., 89.2 vs. 98.1% for $13 \mu\text{m}$ particles, respectively). Nasal particle inhalability is
12 similar between an adult and 7-year-old child (Hsu and Swift, 1999, [155855](#)). Inhalability
13 into the mouth from calm air in humans also becomes important for $d_{ae} > 10 \mu\text{m}$ (Anthony
14 and Flynn, 2006, [155659](#); Brown, 2005, [156299](#)). Unlike the inhalability from high wind
15 speeds which plateaus at 50% for d_{ae} greater than $\sim 40 \mu\text{m}$, particle inhalability from calm
16 air continues to decrease toward zero with increasing d_{ae} .

17 Inhalability data in laboratory animals, such as rats, are only available for breathing
18 from relatively calm air (velocity $\leq 0.3 \text{ m/s}$). For nasal breathing, inhalability becomes an
19 important consideration for d_{ae} of above $1 \mu\text{m}$ in rodents and $10 \mu\text{m}$ in humans (Ménache et
20 al., 1995, [006533](#)). The inhalability of particles having d_{ae} of 2.5, 5, and $10 \mu\text{m}$ is 80, 65, and
21 44% in rats, respectively, whereas it only decreases to 96% for a d_{ae} of $10 \mu\text{m}$ in humans
22 during nasal breathing (Ménache et al., 1995, [006533](#)). Asgharian et al. (2003, [153068](#))
23 suggested that an even more rapid decrease in inhalability with increasing d_{ae} may occur in
24 rats. Inhalability is a particularly important consideration for rodent exposures.
25 Section 4.2.3 provides additional discussion of interspecies patterns of particle deposition.

4.2.1. Mechanisms of Deposition

26 Particle deposition in the lung is predominantly governed by diffusion, impaction, and
27 sedimentation. Most discussion herein focuses on these three dominant mechanisms of
28 deposition. Simple interception, which is an important mechanism of fiber deposition, is not
29 discussed in this chapter. Electrostatic and thermophoretic forces as mechanisms of
30 deposition have not been thoroughly evaluated and receive limited discussion. Some
31 generalizations with regard to deposition by these mechanisms follows, but should not be
32 viewed as absolute rules. Both experimental studies and mathematical models have
33 demonstrated that breathing patterns can dramatically alter regional and total deposition
34 for all sized particles. The combined processes of aerodynamic and diffusive (or
35 thermodynamic) deposition are important for particles in the range of $0.1 \mu\text{m}$ to $1 \mu\text{m}$.

1 Aerodynamic processes predominate above and thermodynamic processes predominate
2 below this range.

3 Diffusive deposition, by the process of Brownian diffusion, is the primary mechanism
4 of deposition for particles having physical diameters of less than 0.1 μm . For particles
5 having physical diameters of roughly between 0.05 and 0.1 μm , diffusive deposition occurs
6 mainly in the small distal bronchioles and the pulmonary region of the lung. However, with
7 further decreases in particle diameter below $\sim 0.05 \mu\text{m}$, increases in particle diffusivity shift
8 more deposition proximally to the bronchi and ET regions.

9 Governed by inertial or aerodynamic properties, impaction and sedimentation
10 increase with d_{ae} . When a particle has sufficient inertia, it is unable to follow changes in
11 flow direction and strikes a surface thus depositing by the process of impaction. Impaction
12 occurs predominantly at bifurcations in the proximal airways, where linear velocities and
13 secondary eddies are at their highest. Sedimentation, caused by the gravitational settling of
14 a particle, is most important in the distal airways and pulmonary region of the lung. In
15 these regions, residence time is the greatest and the distances that a particle must travel to
16 reach the wall of an airway are minimal.

17 The electrical charge on some particles may result in an enhanced deposition over
18 what would be expected from size alone. With an estimated charge of 10-50 negative ions
19 per 0.5 μm particle, Scheuch et al. (1990, [006948](#)) found deposition in humans ($V_T = 500$
20 mL , $f = 15 \text{ min}^{-1}$) to increase from 13.4% (no charge) to 17.8% (charged). This increase in
21 deposition is thought to result from image charges induced on the surface of the airway by
22 charged particles. Yu (1985, [006963](#)) estimated a charge threshold level above which
23 deposition fractions would be increased of about 12, 30, and 54% for 0.3, 0.6, and 1.0 μm
24 diameter particles, respectively. Electrostatic deposition is generally considered negligible
25 for particles below 0.01 μm because so few of these particles carry a charge at Boltzmann
26 equilibrium. This mechanism is also thought to be a minor contributor to overall particle
27 deposition, but it may be important in some laboratory studies due to specific aerosol
28 generation techniques such as nebulization. Laboratory methods such as passage of the
29 aerosols through a Kr-85 charge neutralizer prior to inhalation are commonly used to
30 mitigate this effect.

31 The National Radiological Protection Board (NRPB) recently evaluated the potential
32 for corona discharges from high voltage power lines to charge particles and enhance
33 particulate doses (NRPB, 2004, [156815](#)). They concluded that electrostatic effects would be
34 the most important for particles in the size range from about 0.1-1 μm , where deposition
35 may theoretically increase by a factor of three to ten. However, given that the small fraction
36 of ambient particles would pass through the corona to become charged, the small range of
37 relevant particle sizes (0.1-1 μm), and the subsequent required transport of charged
38 particles to expose individuals; the NRPB concluded that effects, if any, of electric fields on
39 particle deposition in the human respiratory tract would likely be minimal.

1 Thermophoretic forces on particles occur due to temperature differences between
2 respired air and respiratory tract surfaces. Temperature gradients of around 20°C are
3 thought to produce sufficient thermophoretic force to oppose diffusive and electrostatic
4 deposition during inspiration and to perhaps augment deposition by these mechanisms
5 during expiration (Jeffers, 2005, [156608](#)). Thermophoresis is only relevant in the
6 extrathoracic and large bronchi airways and reduces to zero as the temperature gradient
7 decreases deeper in the lung. Theoretical analysis of thermophoresis has been done for
8 smooth walled tubes and is important over distances that are several orders of magnitude
9 smaller than the diameter of the trachea. The alteration of the flow patterns by airway
10 surface features such as cartilaginous rings may affect particle transport and deposition
11 over far greater distances than thermophoretic force.

4.2.2. Deposition Patterns

12 Knowledge of sites where particles of different sizes deposit in the respiratory tract
13 and the amount of deposition therein is necessary for understanding and interpreting the
14 health effects associated with exposure to particles. Particles deposited in the various
15 respiratory tract regions are subjected to large differences in clearance mechanisms and
16 pathways and, consequently, retention times. Deposition patterns in the human respiratory
17 tract were described in considerable detail in dosimetry chapters of prior PM AQCD
18 (U.S. EPA, 1996, [079380](#); U.S. EPA, 2004, [056905](#)); as such, they are only briefly described
19 here.

20 Predicted total and regional deposition for an adult male during rest and light
21 exercise are illustrated in Figures 4-3 and 4-4, respectively. Note that a large proportion of
22 inhaled coarse particles in the 3-6 micron (d_{ae}) range can reach and deposit in the lower
23 respiratory tract, particularly the TB airways. Although these figures were provided in
24 Chapter 6 of the 2004 PM AQCD, they are reproduced here to illustrate changes in
25 deposition as a function of particle size and breathing conditions. The predictions were
26 based on two publicly available particle deposition models, the ICRP (1994, [006988](#)) and the
27 Multi-Path Particle Dosimetry model (MPPD; Version 1.0, ©2002). The ICRP (1994,
28 [006988](#)) model was implemented by Lung Dose Evaluation Program (LUDEP; Version 2.07,
29 June 2000). The MPPD¹ model was developed by the CIIT Centers for Health Research
30 with support from the Dutch National Institute of Public Health and the Environment.

¹ For more information about this model, the reader is referred to: http://www.ara.com/products/mppd_capabilities.htm.

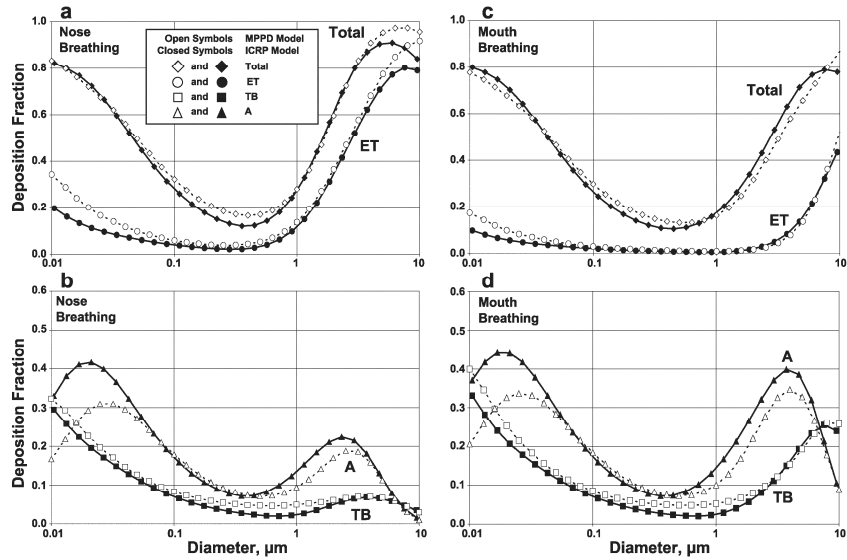


Figure 4-3. Comparison of total and regional deposition results from the ICRP and MPPD models for a resting breathing pattern ($V_T = 625 \text{ mL}$, $f = 12 \text{ min}^{-1}$) and corrected for particle inhalability. Regions are extrathoracic, ET; tracheobronchial, TB; and alveolar, A. Panels a-b are for nose breathing; panels c-d are for mouth breathing.

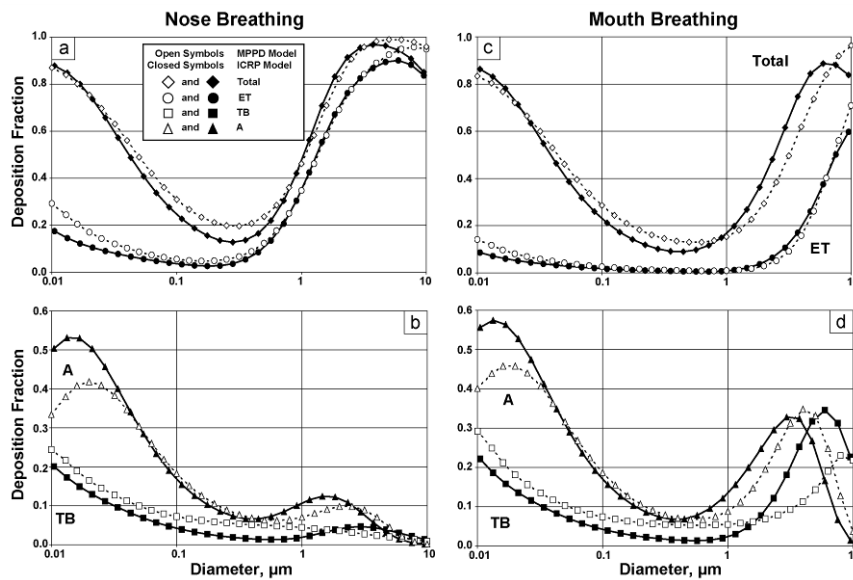
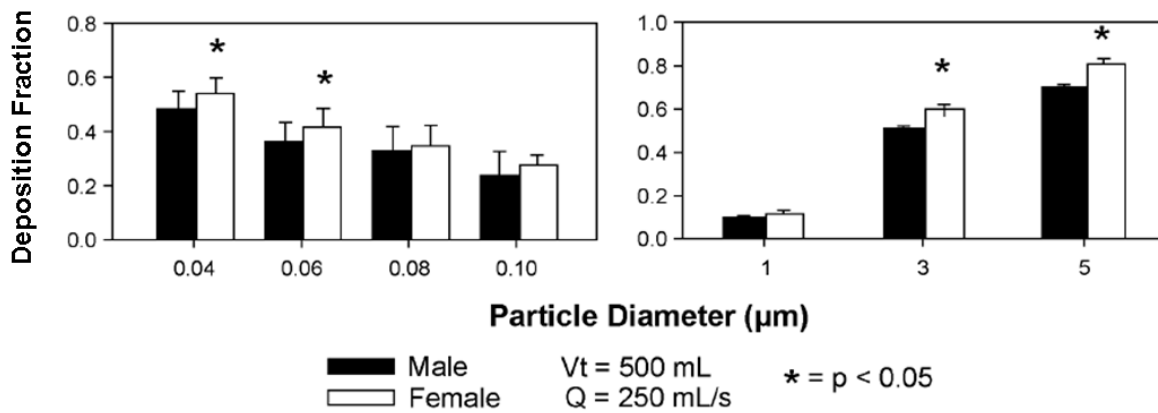


Figure 4-4. Comparison of total and regional deposition results from the ICRP and MPPD models for a light exercise breathing pattern ($V_T = 1250 \text{ mL}$, $f = 20 \text{ min}^{-1}$) and corrected for particle inhalability. Regions are extrathoracic, ET; tracheobronchial, TB; and alveolar, A. Panels a-b are for nose breathing; panels c-d are for mouth breathing.

4.2.2.1. Total Respiratory Tract Deposition

1 The efficiency of deposition in the respiratory tract may generally be described as a
2 “U-shaped” curve on a plot of deposition efficiency versus the of log particle diameter. Total
3 deposition shows a minimum for particle diameters in the range of 0.1 to 1.0 μm , where
4 particles are small enough to have minimal sedimentation or impaction and sufficiently
5 large so as to have minimal diffusive deposition. Total deposition does not decrease to zero
6 for any sized particle because of mixing between particle laden tidal air and residual lung
7 air. The particles mixed into residual air remain in the lung following a breath and are
8 removed on subsequent breaths or gradually deposited. Total deposition approaches 100%
9 for particles of roughly 0.01 μm (physical diameter) due to diffusive deposition and for
10 particles of around 10 μm (d_{ae}) due to the efficiency of sedimentation and impaction.

11 Total human lung deposition, as a function of particle size, is depicted in Figure 4-5.
12 These experimental data were obtained by using monodisperse spherical test particles in
13 healthy adults during controlled breathing on a mouthpiece. Despite the control of inhaled
14 particle size and breathing conditions, these figures illustrate variability in deposition
15 efficiencies due to inter-individual differences in lung size and anatomical variability in
16 airway dimensions and branching patterns.



Source: Data from Kim and Hu (1998, [086086](#)) and Kim and Jaques (2000, [012811](#)).

Figure 4-5. Total lung deposition measured in healthy adults (ultrafine, 11 M, 11 F, 31 ± 4 years; fine and coarse, 11 M, 11 F, 25 ± 4 years) during controlled breathing on a mouthpiece. Deposition calculated from aerosol bolus measurements between 50 and 500 mL into a breath with 50 mL increments. Illustrated data are means and standard errors.

4.2.2.2. Extrathoracic Region

17 The first line of defense for protecting the lower respiratory tract from inhaled
18 particles is the nose and mouth. Particle deposition the ET region, especially the nasal
19 passages, reduces the amount available for deposition in the TB and A regions. Newer data

1 have become available, but are largely derived from computational fluid dynamics (CFD)
2 modeling and experimental measurements in casts. As most of these studies do not
3 substantially improve our understanding of deposition in the ET region they are not
4 reviewed here.

5 For particles $>1 \mu\text{m } d_{ae}$, deposition efficiency in the oral and nasal passages has been
6 generally described as a function of an impaction parameter (Stokes number) with the
7 addition of a flow regime parameter (Reynolds number) for the oral passages (Finlay and
8 Martin, 2008, [155776](#); Grgic et al., 2004, [155810](#); Kelly et al., 2005, [155894](#); Schroeter et al.,
9 2006, [156076](#)). For an adult male, the CFD simulations of Schroeter et al. (2006, [156076](#))
10 predicted nasal deposition of $10 \mu\text{m } d_{ae}$ particles was 90%, and 100% for a V_e of 7.5 L/min
11 (rest) and 15 L/min (light activity), respectively. Thus, relatively few large coarse particles
12 will pass through the nasal passages into the lungs.

13 Since the nasal passages are more efficient at removing inhaled particles than the
14 oral passage, an individual's mode of breathing (i.e., oral vs. nasal) influences the quantity
15 of particles penetrating to the lung. In limited studies, it has been shown that children tend
16 to have more oral breathing both at rest and during exercise and also displayed more
17 variability than adults (Becquemin et al., 1999, [155679](#); Bennett et al., 2008, [156269](#);
18 James et al., 1997, [042422](#)). In contrast to adults, there is little data on the uptake of
19 particles for oral or nasal breathing in children. Theoretical calculations by Xu and Yu
20 (1986, [072697](#)) predict enhanced deposition of particles (greater than $2 \mu\text{m}$) in the head
21 region for children when compared to adults. Studies of fine particle deposition in physical
22 models of the nose, scaled to adult vs. children sizes, predict that deposition efficiency in
23 the nose is a function of pressure drop across the nose (Phalen et al., 1989, [156023](#)).
24 Consequently, these model analyses suggest that, when properly scaled physiological flows
25 are used in the calculation of nasal deposition, children, who have higher nasal resistance
26 than adults, should have higher nasal deposition compared to adults. Surprisingly, the few
27 studies reporting measures of nasal deposition in children, found lower nasal deposition
28 efficiencies for fine particles ($1\text{-}3 \mu\text{m } d_{ae}$) as compared to adults, despite their higher nasal
29 resistances (Becquemin et al., 1991, [009187](#); Bennett et al., 2008, [156269](#)). These findings of
30 lesser nasal vs oral breathing and less efficient nasal deposition suggest that children's
31 lower respiratory tract (i.e., the TB and alveolar regions) may receive a higher dose of
32 ambient PM compared to adults. Normalized to lung surface area, the dose rate to the lower
33 airways of children vs. adults is increased further because children breathe at higher
34 minute ventilations relative to their lung volumes (see Section 4.2.4.2 on Age as a factor
35 modulating deposition).

4.2.2.3. Tracheobronchial and Alveolar Region

36 Inhaled particles passing the ET region enter and may become deposited in the lungs.
37 For any given particle size, the pattern of particle deposition influences clearance by

1 partitioning deposited material between lung regions. Deposition in the tracheobronchial
2 airways and alveolar region cannot be directly measured in vivo. Much of the available
3 deposition data for the TB and A regions have been obtained from experiments with
4 radioactively labeled, poorly soluble particles (U.S. EPA, 1996, [079380](#)) or by use of aerosol
5 bolus techniques (U.S. EPA, 2004, [056905](#)). In general, the ability of these experimental
6 data to define specific sites of particle deposition is limited to anatomically large regions of
7 the respiratory tract such as the head, larynx, bronchi, bronchioles, and alveolar region.
8 Mathematical modeling can provide more refined predictions of deposition sites.
9 Comparisons of the modeling results obtained with two publicly available models were
10 provided in Figures 4-3 and 4-4. Highly localized sites of deposition within the bronchi are
11 described in Section 4.2.2.4. Both experimental and modeling techniques are based on many
12 assumptions that may be relatively good for the healthy lung but not for the diseased lung.
13 For discussion of these issues, the reader is referred to Sections 4.2.4.4 and 4.2.4.5.

4.2.2.4. Localized Deposition Sites

14 From a toxicological perspective, it is important to realize that not all epithelial cells
15 in an airway will receive the same dose of deposited particles. Localized deposition in the
16 vicinity of airway bifurcations has been analyzed using experimental and mathematical
17 modeling techniques. In the 1996 PM AQCD, experimental data were available illustrating
18 the peak deposition of coarse particles (3, 5, and 7 μm d_{ae}) in daughter airways during
19 inspiration and the parent airway during expiration, but always near the carinal ridge
20 (Kim and Iglesias, 1989, [078539](#); Kim et al., 1989, [078538](#)). In the 2004 PM AQCD,
21 mathematical models predicted distinct “hot spots” of deposition in the vicinity of the
22 carinal ridge for both coarse (10 μm) and ultrafine (0.01 μm) particles (Heistracher and
23 Hofmann, 1997, [047514](#); Hofmann et al., 1996, [047515](#)). In a model of lung generations 4-5
24 during inspiration, hot spots occurred at the carinal ridge for 10 μm d_{ae} particles due to
25 inertial impaction and for 0.01 μm particles due to secondary flow patterns formed at the
26 bifurcation. During expiration, preferential sites of deposition for both particle sizes
27 occurred 1) approaching the juncture of daughter airways on the walls forming and across
28 the lumen from the carinal ridge and 2) the top and bottom (visualizing the Y-shaped
29 geometry laying horizontal) of the parent airway downstream of the bifurcation.

30 Recent studies further support these findings (Balashazy et al., 2003, [155671](#); Farkas
31 et al., 2006, [155771](#); Farkas and Balásházy, 2008, [157358](#); Isaacs et al., 2006, [155861](#)). Most
32 of these studies quantified localized deposition in terms of an enhancement factor. Typically,
33 the enhancement factor is the ratio of the deposition in a pre-specified surface area (e.g.,
34 100 \times 100 μm which corresponds to $\sim 10 \times 10$ epithelial cells) to the average deposition
35 density for the whole airway geometry. These enhancement factors are very sensitive to the
36 size of the surface considered (Balashazy et al., 1999, [043201](#)). The studies by Farkas et al.
37 (2006, [155771](#)) and Farkas and Balásházy (2008, [157358](#)) investigated the phenomena of

1 localized deposition down to 0.001 μm particles. The deposition of 0.001 μm was rather
2 uniform, however, the deposition pattern became increasingly less uniform with increasing
3 particle size. These studies indicate that, for particles greater than $\sim 0.01 \mu\text{m}$, some cells
4 located near the carinal ridge of bronchial bifurcations may receive hundreds to thousands
5 times the average dose (particles per unit surface area) of the parent and daughter airways.
6 Furthermore, the inertial impaction of particles $\geq 1 \mu\text{m}$ d_{ae} at the carinal ridge of large
7 bronchi will increase with increasing inspiratory flows. In a comparison of constricted
8 versus healthy airways, Farkas et al. (2006, [155771](#)) also reported that the overall
9 deposition efficiency of 10 μm d_{ae} particles at bifurcations downstream of a constriction may
10 be increased by 18 times. Given these considerations, Phalen and Oldham (2006, [156024](#))
11 noted that substantial doses of particles ($\geq 1 \mu\text{m}$ d_{ae}) may be justified for in vitro studies
12 using tracheobronchial epithelial cell cultures.

4.2.3. Interspecies Patterns of Deposition

13 The primary purpose of this document is to assess the health effects of particles in
14 humans. As such, human dosimetry studies have been stressed in this chapter. Such
15 studies avoid the uncertainties associated with the extrapolation of dosimetric data from
16 laboratory animals to humans. However, animal models have been and continue to be used
17 in evaluating PM health effects because of ethical considerations regarding the types of
18 studies that can be performed with human subjects. Thus, there is a considerable need to
19 understand dosimetry in animals and dosimetric differences between animals and humans.
20 Limited new data are becoming available. Similar deposition efficiencies have been
21 reported in nasal casts of human and rhesus monkey for 1 to 10 μm d_{ae} for inspiratory flows
22 mimicking resting breathing patterns (Kelly et al., 2005, [155894](#)). Oldham and Robinson
23 (2007, [156003](#)) recently provided morphological data and predicted particle deposition in an
24 asthma mouse model.

25 Interspecies similarities and differences in deposition were described in detail in the
26 last two PM AQCDs (U.S. EPA, 1996, [079380](#); U.S. EPA, 2004, [056905](#)). It was concluded
27 that the general pattern of total particle deposition efficiency was similar between
28 laboratory animals and humans: deposition increases on both sides of a minimum that
29 occurs for particles of 0.2 to 1 μm . There are, however, marked interspecies differences in
30 uptake into the respiratory tract and regional deposition. For instance, the nasal
31 inhalability of 10 μm d_{ae} particles is predicted to be 96% in humans, whereas it is only 44%
32 in rats (Ménache et al., 1995, [006533](#)). In most laboratory animal species (rat, mouse,
33 hamster, guinea pig, and dogs), deposition in the ET region is near 100% for particles
34 greater than 5 μm d_{ae} (Raabe et al., 1988, [001439](#)), indicating greater efficiency than that
35 seen in humans. Detailed presentation of dosimetric difference between rats and humans
36 are available elsewhere (Brown et al., 2005, [089308](#); Jarabek et al., 2005, [056756](#)).

1 Brown et al. (2005, [089308](#)) conducted a thorough evaluation of extrapolations
2 between rats and humans in relation to PM exposures. One of many factors they considered
3 was the choice of a dose metric appropriate for comparison between species. For example,
4 deposited mass may be an appropriate PM indicator for health effects associated with
5 soluble PM constituents. For health effects associated with insoluble PM, the particle
6 number, surface area, or mass may be appropriate indicators. Given interspecies differences
7 in deposition patterns and clearance rates, the question of retained versus deposited dose
8 was also discussed. It was concluded that for acute effects, the maximum deposited
9 incremental dose may be the appropriate type of dose metric. For chronic effects, long-term
10 burden may be more appropriate. For various dose metrics, estimates of particle
11 concentration and exposure duration required for a rat to receive the same dose as received
12 by a human were obtained with consideration of activity levels and particle size
13 distributions. It was noted that high PM exposures over the period of months can lead to
14 particle overload in rats (see Section 4.3.4.4). Exposure regimes were derived as a function
15 of particle size and exposure duration that should avoid overwhelming macrophage
16 mediated clearance achieving particle overload in rats (see Table 12 in Brown et al., 2005,
17 [089308](#)). The dosimetric calculations indicated that to achieve nominally similar acute
18 doses per surface area in rats, relative to humans undergoing moderate to high exertion,
19 PM exposure concentrations for rats would need to be somewhat higher than for humans.
20 Since particle clearance from the lungs of rats is faster than humans, much higher exposure
21 concentrations are required for the rat to simulate retained burdens of humans. Illustrating
22 the complexity of such analyses, in some cases, rats were found to require lower exposures
23 than humans to have comparable doses (generally when considering a scenario of humans
24 at rest).

4.2.4. Biological Factors Modulating Deposition

25 Evaluation of factors affecting particle deposition is important to help understand
26 potentially susceptible subpopulations. Differences in biological response following
27 pollutant exposure may be caused by dosimetry differences as well as by differences in
28 innate sensitivity. The effects of different biological factors on deposition were discussed in
29 the 2004 PM AQCD (U.S. EPA, 2004, [056905](#)) and are summarized briefly here.

4.2.4.1. Physical Activity

30 The activity level of an individual is well recognized to affect their minute ventilation
31 and route of breathing. Changes in minute ventilation during exercise are accomplished by
32 increasing both V_T and f (Table 4-1). Humans are oronasal breathers tending to breathe
33 through the nose when at rest and increasingly through the mouth with increasing activity

1 level. There is considerable inter-individual variability in both the route by which people
2 breathe the way breathing pattern changes occur.

Table 4-1. Breathing patterns with activity level in adult human male.

Activity	Awake Rest ^a	Slow Walk ^a	Light Exertion ^a	Moderate Exertion ^a	Heavy Exertion ^b
Breaths/min	12	16	19	28	26
Tidal volume, mL	625	813	1000	1429	1923
Minute ventilation, L/min	7.5	13	19	40	50

Sources: ^aWinter-Sorkina and Cassee (2002, [043670](#)); ^bNCRP (1994, [006988](#))

3 Individuals typically breathe through their nose while at rest, switching to oronasal
4 breathing as ventilation increases (Bennett et al., 2003, [191977](#); Niinimaa et al., 1981,
5 [071758](#)). The role of the nose in filtering particles is diminished as airflow is diverted from
6 the nose to the mouth during exercise, bringing more particles to the lower respiratory
7 tract. A recent study in adults (Bennett et al., 2003, [191977](#)) found that nasal ventilation
8 during exercise varied as a function of both race and gender. African-Americans possessed a
9 greater nasal contribution to breathing during exercise than Caucasians. At similar
10 exercise efforts (i.e., normalized to a % maximum work capacity) the females also had a
11 greater nasal contribution to breathing during exercise than males.

12 In addition, when individuals increase their ventilation with activity the total number
13 of particles inhaled per unit time (i.e., exposure rate) increases, but the fractional
14 deposition of particles in each breath also changes with breathing pattern. Figures 4-3 and
15 4-4 illustrate predicted deposition fractions in the respiratory tract during rest vs. light
16 exercise, respectively. During exercise, both V_T and f increase. Fractional deposition for all
17 particles increases with increased V_T . Increasing the f , however, decreases the fractional
18 deposition of fine and ultrafine particles due to decreased time for gravitational and
19 diffusive deposition. For particles of larger than a d_{ae} of roughly 3 μm , increasing f can
20 increase the deposition fraction due to increased impaction in the extrathoracic and TB
21 airways. Thus, it should be expected that the change in deposition fraction with activity
22 will vary among individuals depending on the relative influences of these two variables (i.e.,
23 V_T and f) in a given subject and the particle size to which they are exposed. Experimentally,
24 the lung deposition fractions of fine particles during moderate exercise and mouth
25 breathing are unchanged between rest and exercise (Bennett et al., 1985, [190034](#); Morgan
26 et al., 1984, [190035](#)). Kim (2000, [013112](#)) evaluated differences in deposition of 1, 3, and 5
27 μm (MMAD) particles under varying breathing patterns (simulating breathing conditions of
28 sleep, resting, and mild exercise). Total lung deposition increased with increasing V_T at a
29 given flow rate and with increasing flow rate at a given breathing period. These
30 experimental studies suggest that the total deposited dose rate (i.e., deposition per unit

1 time) of particles will generally increase in direct proportion to the increase in minute
2 ventilation associated with exercise.

3 The changes in ventilation, i.e., breathing pattern and flow rate, may also alter the
4 regional deposition of particles. Coarse particle deposition increases in the TB and ET
5 regions during exercise due to the increased flow rates and associated impaction. A rapid-
6 shallow breathing pattern during exercise may result in more bronchial airway vs. alveolar
7 deposition, while a slow-deep pattern will shift deposition to deeper lung regions (Valberg et
8 al., 1982, [190019](#)). Bennett et al. (1985, [190034](#)) showed for 2.6 µm particles that moderate
9 exercise shifted deposition from the lung periphery towards ET and larger, bronchial
10 airways. Similarly, Morgan et al. (1984, [190035](#)) showed that even for fine particles (0.7 µm)
11 TB deposition was enhanced with exercise. This shift in deposition toward the bronchial
12 airways results in a much greater dose per unit surface area of tissue in those regions.
13 Morgan et al. (1984, [190035](#)) also found that the apical-to-basal distribution of fine particles
14 increased with exercise, i.e., a shift towards increased deposition in the lung apices. This
15 shift may be less likely for larger particles, however, whose deposition in large airway
16 bifurcations may preclude their transport to these more apical regions (Bennett et al., 1985,
17 [190034](#)).

4.2.4.2. Age

18 Airway structure and respiratory conditions vary with age, and these variations may
19 alter the amount and site of particle deposition in the respiratory tract. It was concluded in
20 the 2004 PM AQCD (U.S. EPA, 2004, [056905](#)) that significant differences between adults
21 and children had been predicted by mathematical models and observed in experimental
22 studies. Studies generally indicated that ET and TB deposition was greater in children and
23 that children received greater doses of particles per lung surface area than adults.
24 Deposition studies in the elderly are still quite limited.

25 A few studies have attempted to measure oronasal breathing in children as compared
26 to adults (Becquemin et al., 1999, [155679](#); Bennett et al., 2008, [156269](#); James et al., 1997,
27 [042422](#)). This is important since particles deposit with greater efficiency in the nose
28 relative to the mouth, thereby affecting exposure of the lower respiratory tract. James et al.
29 (1997, [042422](#)) found that children (age 7-16, n = 10) displayed more variability than adults
30 with respect to their oronasal pattern of breathing with exercise. However, it was not
31 possible to predict the pattern of the partitioning of ventilation during exercise based on
32 age, gender, or nasal airway resistance. Further, in a limited number of children (age 8-16,
33 n = 10), Becquemin et al. (1999, [155679](#)) found that the children tended to display more oral
34 breathing both at rest and during exercise than the adults. The highest oral fractions were
35 also found in the youngest children. None of these studies, however, was able to show a
36 relationship between nasal resistance and the relative contribution of nasal breathing in
37 their children. Bennett et al. (2008, [156269](#)) made preliminary measurements of the

1 relative contributions of oral versus nasal breathing at rest and during incrementally
2 graded submaximal exercise on the cycle ergometer for children (age 6-10, n = 12) adults
3 (age 18-27, n = 11). There was a trend for children to have a lesser nasal contribution to
4 breathing at rest and during exercise, but the differences from adults were not statistically
5 significant.

6 Breathing patterns are well recognized to change with increasing age, i.e., V_T increase
7 and respiratory rates decrease (Tabachnik et al., 1981, [157036](#); Tobin et al., 1983, [156122](#)).
8 Bennett and Zeman (Bennett and Zeman, 1998, [076182](#)) measured deposition fraction of
9 inhaled, fine particles ($2 \mu\text{m d}_{ae}$) in children as they breathed the aerosol with their natural,
10 resting breathing pattern. Among the children, variation in deposition fraction, measured
11 by photometry at the mouth, was highly dependent on intersubject variation in V_T . On the
12 other hand, they found no difference in deposition fraction for the children vs. adults for
13 these fine particles. This finding and the modeling predictions (Hofmann et al., 1989,
14 [006922](#)) are explained in part by the smaller V_T and faster breathing rate of children
15 relative to adults for natural breathing conditions. Bennett et al. (2008, [156269](#)) also
16 recently reported measures of fine particle (1 and $2 \mu\text{m d}_{ae}$) deposition fraction for
17 ventilation associated with light exercise in children and adults and showed that, like with
18 resting breathing, deposition fraction was predicted by breathing pattern and did not differ
19 or tended to be less in children compared to adults. On the other hand, because children
20 breathe at higher minute ventilations relative to their lung volumes, the rate of deposition
21 of fine particles normalized to lung surface area may be greater in children vs. adults
22 (Bennett and Zeman, 1998, [076182](#)).

23 Bennett and Zeman (2004, [155686](#)) expanded their measures of fine particle
24 deposition during resting breathing to a larger group of healthy children (6-13 yr; 20 boys,
25 16 girls) and found again that the variation in total deposition, was best predicted by V_T
26 ($r = 0.79$, $p < 0.001$). But both V_T and resting minute ventilation increased with both height
27 and body mass index (BMI) of the children. Interestingly, these data suggest that for a
28 given height and age, children with higher BMI have larger minute ventilations and V_T at
29 rest than those with lower BMI. These differences in breathing patterns as a function of
30 BMI translated into increased deposition of fine particles in the heaviest children. The rate
31 of deposition (i.e., particles depositing/time) in the overweight children was 2.8 times that of
32 the leanest children ($p < 0.02$). Among all children, the rate of deposition was significantly
33 correlated with BMI ($r = 0.46$, $p < 0.004$). Some of the increased deposition fraction in
34 heavier children may be due to their elevated V_T , which was well correlated with BMI
35 ($r = 0.72$, $p < 0.001$).

36 In 62 healthy adults with normal lung function aged 18-80, Bennett et al. (1996,
37 [083284](#)) showed there was no effect of age on the whole lung deposition fraction of $2\text{-}\mu\text{m}$
38 particles under natural breathing conditions. Across all subjects, the deposition fraction
39 was found to be independent of age, depending on breathing period ($r = 0.58$, $p < 0.001$) and

1 airway resistance ($r = 0.46$, $p < 0.001$). In the same adults breathing with a fixed pattern
2 (360 mL V_T , 3.4 sec breathing period), there was a mild decrease in deposition with
3 increasing age, which could be attributed to increased peripheral airspace dimensions in
4 the elderly.

4.2.4.3. Gender

5 Males and females differ in body size, conductive airway size, and ventilatory
6 parameters; therefore, gender differences in deposition might be expected. In some of the
7 controlled studies, however, the men and women were constrained to breathe at the same
8 V_T and f . Since women are generally smaller than men, the increased minute ventilation of
9 women compared to their normal ventilation could affect deposition patterns. This may
10 help explain why gender related effects on deposition have been observed in some studies.

11 Kim and Hu (1998, [086066](#)) assessed the regional deposition patterns of 1-, 3-, and 5-
12 μm MMAD particles in healthy adult males and females using controlled breathing. The
13 total fractional deposition in the lungs was similar for both genders with the 1- μm particle
14 size, but was greater in women for the 3- and 5- μm particles. Deposition also appeared to be
15 more localized in the lungs of females compared to those of males. Kim and Jaques (2000,
16 [012811](#)) measured deposition in healthy adults using sizes in the ultrafine mode
17 (0.04-0.1 μm). Total fractional lung deposition was greater in females than in males for
18 0.04- and 0.06- μm particles. The region of peak fractional deposition was shifted closer to
19 the mouth and peak height was slightly greater for women than for men for all exposure
20 conditions. The total and regional deposition data from these studies are illustrated in
21 Figure 4-5. These differences were generally attributed to the smaller size of the upper
22 airways, particularly of the laryngeal structure, in females.

23 In another study (Bennett et al., 1996, [083284](#)), the total respiratory tract deposition
24 of 2- μm particles was examined in adult males and females aged 18-80 years who breathed
25 with a normal resting pattern. There was a tendency for a greater deposition fraction in
26 females compared to males. However, since males had greater minute ventilation, the
27 deposition rate (i.e., deposition per unit time) was greater in males than in females. More
28 recently, Bennett and Zeman (2004, [155686](#)) found no difference in the deposition of 2- μm
29 particles in boys versus girls aged 6-13 yr ($n = 36$).

4.2.4.4. Anatomical Variability

30 Anatomical variability, even in the absence of respiratory disease, can affect
31 deposition throughout the respiratory tract. The ET region is the first exposed to inhaled
32 particles and, therefore, deposition within this region would reduce the amount of particles
33 available for deposition in the lungs. Variations in relative deposition within the ET region
34 will, therefore, propagate through the rest of the respiratory tract, creating differences in
35 calculated doses from individual to individual.

1 The influence of variations in nasal airway geometry on particle deposition has been
2 investigated. Cheng et al. (1996, [047520](#)) examined nasal airway deposition in healthy
3 adults using particles ranging in size from 0.004 to 0.15 μm and at two constant inspiratory
4 flow rates, 167 and 333 mL/s. Inter-individual variability in deposition was correlated with
5 the wide variation of nasal dimensions, in that greater surface area, smaller cross-sectional
6 area, and increasing complexity of airway shape were all associated with enhanced
7 deposition. Bennett and Zeman (2005, [155687](#)) have also shown that nasal anatomy
8 influences the efficiency of particle uptake in the noses of adults. For light exercise
9 breathing conditions in adults, their study demonstrated that nasal deposition efficiencies
10 for both 1- and 2- μm monodisperse particles were significantly less in African Americans
11 versus Caucasians. The lesser nasal efficiencies in African-Americans were associated with
12 both lower nasal resistance and less elliptical nostrils compared to Caucasians.

13 Within the lungs, the branching structure of the airways may also differ between
14 individuals. Zhao et al. (2009, [157187](#)) recently examined the bronchial anatomy of the left
15 lung in patients (132 M, 84 W; mean age 47 years) that under went conventional thoracic
16 computed tomography scans for various reasons. At the level of the segmental bronchus in
17 the upper and lower lobes, a bifurcation occurred in the majority of patients. A trifurcation,
18 however, was observed in 23% of the upper and 18% of the lower lobes. Other more unusual
19 findings were also reported such as four bronchi arising from the left upper lobe bronchus.
20 As described in Section 4.2.2.4, deposition can be highly localized near the carinal ridge of
21 bifurcations. The effect of a bifurcation versus other branching patterns on airflow patterns
22 and particle deposition has not been described in the literature. Martonen et al. (1994,
23 [000847](#)) showed that a wide blunt carinal ridge shape dramatically affected the flow stream
24 lines relative to a narrower and more rounded ridge shape. Specifically, there were high
25 flow velocities across the entire area of the blunt carinal ridge versus a smoother division of
26 the airstream in the case of the narrow rounded ridge shape. The implication may be that
27 localized particle deposition on the carinal ridge would increase with ridge width. A similar
28 situation might be expected for a trifurcation versus a bifurcation. These differences in
29 branching patterns provide a clear example of anatomical variability between individuals
30 that might affect both air flow patterns and sites of particle deposition.

4.2.4.5. Respiratory Tract Disease

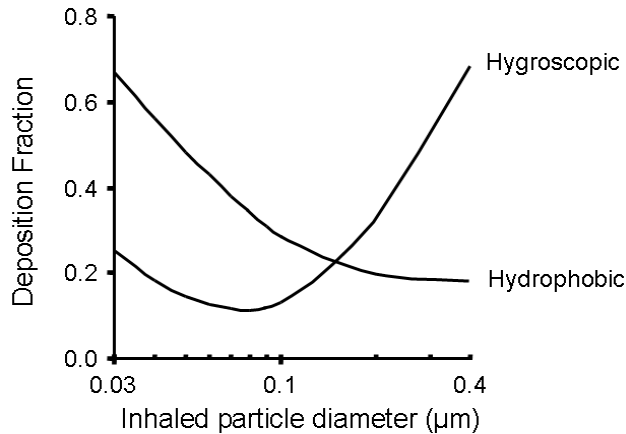
31 The presence of respiratory tract disease can affect airway structure and ventilatory
32 parameters, thus altering deposition compared to that occurring in healthy individuals. The
33 effect of airway diseases on deposition has been studied extensively, as described in the
34 1996 and 2004 PM AQCD (U.S. EPA, 2004, [056905](#); U.S. EPA, 1996, [079380](#)). Studies
35 described therein showed that people with chronic obstructive pulmonary disease (COPD)
36 had very heterogeneous deposition patterns and differences in regional deposition
37 compared to healthy individuals. People with obstructive pulmonary diseases tended to

1 have greater deposition in the TB region than did healthy people. Furthermore, there
2 tended to be an inverse relationship between bronchoconstriction and the extent of
3 deposition in the A region, whereas total respiratory tract deposition generally increased
4 with increasing degrees of airway obstruction.

5 The vast majority of deposition studies in individuals with respiratory disease have
6 been performed during controlled breathing, i.e., all subjects breathed with the same V_T
7 and f . However, although resting V_T is similar or elevated in people with COPD compared to
8 healthy individuals, the former tend to breathe at a faster rate, resulting in higher than
9 normal tidal peak flow and resting minute ventilation. Thus, given that breathing patterns
10 differ between healthy and obstructed individuals, particle deposition data for controlled
11 breathing may not be appropriate for estimating respiratory doses from ambient PM
12 exposures.

13 Bennett et al. (1997, [078839](#)) measured the fractional deposition of insoluble 2- μm
14 particles in moderate-to-severe COPD patients ($n = 13$; mean age 62 years) and healthy
15 older adults ($n = 11$; mean age 67 years) during natural resting breathing. COPD patients
16 had about a 50% greater deposition fraction and a 50% increase in resting minute
17 ventilation relative to the healthy adults. As a result, the patients had an average
18 deposition rate of about 2.5 times that of healthy adults. Similar to previously reviewed
19 studies (U.S. EPA, 1996, [079380](#); U.S. EPA, 2004, [056905](#)), these investigators observed an
20 increase in deposition with an increase in airway resistance, suggesting that deposition
21 increased with the severity of airway disease.

22 Brown et al. (2002, [043216](#)) measured the deposition of an ultrafine aerosol
23 (CMD = 0.033 μm) during natural resting breathing in 10 patients with moderate-to-severe
24 COPD (mean age 61 years) and 9 healthy adults (mean age 53 years). The COPD group
25 consisted of 7 patients with chronic bronchitis and 3 patients with emphysema. The total
26 deposition fraction in the bronchitic patients (0.67) was significantly ($p < 0.02$) greater than
27 in either the patients with emphysema (0.48) or the healthy subjects (0.54). Minute
28 ventilation increased with disease severity (healthy, 5.8 L/min; chronic bronchitic, 6.9
29 L/min; emphysema, 11 L/min). Relative to the healthy subjects, the average dose rate was
30 significantly ($p < 0.05$) increased by 1.5 times in the COPD patients, whereas the average
31 deposition fraction only tended to be increased by 1.1 times. These data further
32 demonstrate the need to consider dose rates (which depend on minute ventilation) rather
33 than just deposition fractions when evaluating the effect of respiratory disease on particle
34 deposition and dose.



Source: Adapted from Tu and Knutson (1984, [072870](#)).

Figure 4-6. Total deposition of hygroscopic sodium chloride and hydrophobic aluminosilicate aerosols during oral breathing ($V_T = 1.0$ L; $f = 15$ min⁻¹).

4.2.4.6. Hygroscopicity of Aerosols

1 Experimental and modeling studies of hygroscopic aerosol growth and deposition in
 2 the lung were extensively discussed in Section 10.4.3.1 of the 1996 PM AQCD (U.S. EPA,
 3 1996, [079380](#)). Hygroscopic ambient aerosols include sulfates, nitrates, some organics, and
 4 aerosols laden with sodium or potassium. The high relative humidity in the lungs
 5 contributes to rapid growth of hygroscopic particles and dramatically alters the deposition
 6 characteristics of ambient hygroscopic aerosols relative to nonhygroscopic aerosols.
 7 Nonhygroscopic particles in the range of 0.3 µm have minimal intrinsic mobility and low
 8 total deposition in the lungs. However, a 0.3 µm salt particle (dry) will grow in vivo to
 9 nearly 2 µm and deposit to a far greater extent (Anselm et al., 1990, [156217](#)). The
 10 hygroscopic growth of particles in the respiratory tract decreases diffusive deposition and
 11 increases aerodynamic deposition as illustrated in Figure 4-6.

4.2.5. Summary

12 Particle deposition in the respiratory tract occurs predominantly by diffusion,
 13 impaction, and sedimentation. Deposition is minimal for particle diameters in the range of
 14 0.1 to 1.0 µm, where particles are small enough to have minimal sedimentation or
 15 impaction and sufficiently large so as to have minimal diffusive deposition. In humans,
 16 total respiratory tract deposition approaches 100% for particles of roughly 0.01 µm
 17 (physical diameter) due to diffusive deposition and for particles of around 10 µm d_{ae} due to
 18 the efficiency of sedimentation and impaction.

19 The first line of defense for protecting the lower respiratory tract from inhaled
 20 particles is the nose and mouth. Nasal deposition approaches 100% in humans for 10 µm d_{ae}

1 particles. Experimental studies show lower nasal particle deposition in children than
2 adults. Relative to adults, children also tend to breathe more through their mouth which is
3 less efficient for removing inhaled particles than the nose. These findings suggest that the
4 lower respiratory tract of children may receive a higher dose of ambient PM compared to
5 adults. Since children breathe at higher minute ventilations relative to their lung volumes,
6 the rate of particle deposition normalized to lung surface area may be further increased
7 relative to adults.

8 People with COPD generally have greater total deposition and more heterogeneous
9 deposition patterns compared to healthy individuals. The observed increase in deposition
10 correlates with increases in airway resistance, suggesting that deposition increases with
11 the severity of airway disease. COPD patients also have an increased resting minute
12 ventilation relative to the healthy adults. This demonstrates the need to consider dose rates
13 (which depend on minute ventilation) rather than just deposition fractions when evaluating
14 the effect of respiratory disease on particle deposition and dose.

15 Modeling studies indicate that, for particles greater than $\sim 0.01 \mu\text{m}$, some cells located
16 near the carinal ridge of bronchial bifurcations may receive hundreds to thousands times
17 the average dose (particles per unit surface area) of the parent and daughter airways. The
18 inertial impaction of particles $\geq 1 \mu\text{m } d_{ae}$ at the carinal ridge of large bronchi increases with
19 increasing inspiratory flows. Airway constriction can further augment the overall
20 deposition efficiency of coarse particles at downstream bifurcations. These findings suggest
21 that substantial doses of particles ($\geq 1 \mu\text{m } d_{ae}$) may be justified for in vitro studies using
22 tracheobronchial epithelial cell cultures.

23 Our ability to extrapolate between species has not generally changed since the 2004
24 PM AQCD (U.S. EPA, 2004, [056905](#)). However, some considerations related to coarse
25 particles warrant comment. The inhalability of particles having d_{ae} of 2.5, 5, and 10 μm is
26 80, 65, and 44% in rats, respectively, whereas it remains near 100% for a d_{ae} of 10 μm in
27 humans. In most laboratory animal species (rat, mouse, hamster, guinea pig, and dogs),
28 deposition in the extrathoracic region is near 100% for particles greater than 5 $\mu\text{m } d_{ae}$. By
29 contrast, in humans nasal deposition approaches 100% for 10 $\mu\text{m } d_{ae}$. Oronasal breathing
30 versus obligate nasal breathing further contributes to greater penetration of coarse
31 particles into the lower respiratory tract of humans than rodents.

4.3. Clearance of Poorly Soluble Particles

32 This section discusses the clearance and translocation of poorly soluble particles that
33 have deposited in the respiratory tract. The term “clearance” is used here to refer to the
34 processes by which deposited particles are removed by mucociliary action or phagocytosis
35 from the respiratory tract. “Translocation” is used here mainly to refer to the movement of
36 free particles across cell membranes and to extrapulmonary sites. In the literature,

1 translocation may also refer to the extra- and intracellular dissolution of particles and the
2 subsequent transfer of dissociated material to the blood through extra- and intracellular
3 fluids and across the various cell membranes and lung tissues. The clearance and
4 distribution of soluble particles and soluble constituents of particles are discussed in
5 Section 4.4.

6 A basic overview of biological mechanisms and clearance pathways from various
7 regions of the respiratory tract are presented in the following sections. Then regional
8 kinetics of particle clearance are addressed. Subsequently, an update on interspecies
9 patterns and rates of particle clearance is provided. The translocation of ultrafine particles
10 is also discussed. Finally, information on biological factors that may modulate clearance is
11 presented.

4.3.1. Clearance Mechanisms and Kinetics

12 For any given particle size, the deposition pattern of poorly soluble particles
13 influences clearance by partitioning deposited material between lung regions.
14 Tracheobronchial clearance of poorly soluble particles in humans, with some exceptions, is
15 thought (in general) to be complete within 24 to 48 hours through the action of the
16 mucociliary escalator. Clearance of poorly soluble particles from the alveolar region is a
17 much slower process which may continue from months to years.

4.3.1.1. Extrathoracic Region

18 Particles deposited in either the nasal or oral passages are cleared by several
19 mechanisms. Particles depositing in the mouth may generally be assumed to be swallowed
20 or removed by expectoration. Particles deposited in the posterior portions of the nasal
21 passages are moved via mucociliary transport towards the nasopharynx and swallowed.
22 Mucus flow in the most anterior portion of the nasal passages is forward, toward the
23 vestibular region where removal occurs by sneezing, wiping, or nose blowing.

4.3.1.2. Tracheobronchial Region

24 Mucociliary clearance in the TB region has generally been considered to be a rapid
25 process that is relatively complete by 24-48 hours post-inhalation in humans. Mucociliary
26 clearance is frequently modeled as a series of “escalators” moving material proximally from
27 one generation to the next. As such, the removal rate of particles from an airway generation
28 increases with increasing tracheal mucus velocity. Assuming continuity in the amount of
29 mucus between airway generations, mucus velocities decrease and transit times within an
30 airway generation increase with distal progression. Although clearance from the TB region
31 is generally rapid, experimental evidence discussed in the 1996 and 2004 PM AQCD

1 (U.S. EPA, 1996, [079380](#); U.S. EPA, 2004, [056905](#)), showed that a fraction of material
2 deposited in the TB region is retained much longer.

3 The slow-cleared TB fraction (i.e., the fraction of particles deposited in the TB region
4 that are subject to slow clearance) was thought to increase with decreasing particle size.
5 For instance, Roth et al. (1993, [156928](#)) showed approximately 93% retention of ultrafine
6 particles (30 nm median diameter) thought to be deposited in the TB region at 24-h post
7 inhalation. The slow phase clearance of these ultrafine particles continued with an
8 estimated half-time ($t_{1/2}$) of around 40 days. Using a technique to target inhaled particles
9 (monodisperse 4.2 μm MMAD) to the conducting airways, Möller et al. (2004, [155987](#))
10 observed that $49 \pm 9\%$ of particles cleared rapidly ($t_{1/2}$ of 3.0 ± 1.6 h), whereas the remaining
11 fraction cleared considerably slower ($t_{1/2}$ of 109 ± 78 days). The ICRP (1994, [006988](#)) human
12 respiratory tract model assumes particles ≤ 2.5 μm (physical diameter) to have a slow-
13 cleared TB fraction of 50%. The slow-cleared fraction assumed by the ICRP (1994, [006988](#))
14 decreases with increasing particle size to $<1\%$ for 9 μm particles. Considering the ultrafine
15 data of Roth et al. (1993, [156928](#)) in addition to data considered by the ICRP (1994,
16 [006988](#)). Bailey et al. (1995, [190057](#)) estimated a slow-cleared TB fraction of 75% for
17 ultrafine particles. At that time, they (Bailey et al. 1995) also estimated the slow-cleared
18 fraction to decrease with increasing particle size to 0% for particles ≥ 6 μm . Recent
19 experimental evidence from the same group (Smith et al., 2008, [190037](#)) showed no
20 difference in TB clearance among humans for particles with geometric sizes of 1.2 vs. 5 μm ,
21 but the same d_{ae} (5 μm) so as to deposit similarly in the TB airways. For at least micron-
22 sized particles, these recent findings do not support the particle size dependence of a slow-
23 cleared TB fraction. As discussed further below, much of the apparent slow-cleared TB
24 fraction may be accounted for by differences in deposition patterns, i.e., greater deposition
25 in the alveolar region than expected.

26 A portion of the slow cleared fraction from the TB region appears to be associated with
27 small bronchioles. For large particles ($d_{ae} = 6.2$ μm) inhaled at very slow rate to
28 theoretically deposit mainly in small ciliated airways, 50% had cleared by 24-h post-
29 inhalation. Of the remaining particles, 20% cleared with a $t_{1/2}$ of 2.0 days and 80% with a
30 $t_{1/2}$ of 50 days (Falk et al., 1997, [086080](#)). Using the same techniques, Svartengren et al.
31 (2005, [157034](#)) also reported the existence of long-term clearance in humans from the small
32 airways. It should be noted that the clearance rates for the slow-cleared TB fraction still
33 exceeds the clearance rate of the alveolar region in humans. Kreyling et al. (1999, [039175](#))
34 targeted inhaled particle ($d_{ae} = 2.2$ and 2.5 μm) deposition to the TB airways of adult beagle
35 dogs and subsequently quantified particle retention using scintigraphic and morphometric
36 analyses. Despite the use of shallow aerosol bolus inhalation to a volumetric lung depth of
37 less than the anatomic dead space, 2.5 to 25% of inhaled particles deposited in alveoli. At 24
38 and 96 hours post inhalation, more than 50% of the retained particles were in alveoli.
39 However, 40% of particles present at 24 and 96 hours were localized to small TB airways of

1 between 0.3 and 1 mm in diameter. Collectively, these studies suggest that although
2 mucociliary clearance is fast and effective in healthy large airways, it is less effective and
3 sites of longer retention exist in the smaller TB airways.

4 The underlying sites and mechanisms of long-term TB retention in the smaller
5 airways remain largely unknown. Several factors may contribute to the existence or
6 experimental artifact of slow clearance from the smaller TB airways. Even when inhaled to
7 very shallow lung volumes, some particles reach the alveolar region (Kreyling et al., 1999,
8 [039175](#)). Therefore, experiments utilizing bolus techniques to target inhaled particle
9 deposition to the TB airways may have had some deposition in the alveolar region. This
10 may occur due to variability in path length and the number of generations to the alveoli
11 (Asgharian et al., 2001, [017025](#)) and/or differences in regional ventilation (Brown and
12 Bennett, 2004, [190032](#)). Nonetheless, the experimentally measured clearance rates
13 measured for the slow cleared TB fraction are faster than that of the alveolar region in both
14 humans and canines. Thus, although experimental artifacts likely occur, they do not
15 discount the existence of a slow cleared TB fraction. To some extent, it is possible that the
16 slow cleared TB fraction may be due to bronchioles that do not have a continuous ciliated
17 epithelium as in the larger bronchi. Neither path length, ventilation distribution, nor a
18 discontinuous ciliated epithelium explains an apparently slow cleared TB fraction with
19 decreasing particle size below 0.1 μm . As discussed in Section 4.3.3 on Particle
20 Translocation, ultrafine particles cross cell membranes by mechanisms different from larger
21 ($\sim 1 \mu\text{m}$) particles. Based on that body of literature, particles smaller than a micron may
22 enter epithelial cells resulting in their prolonged retention, particularly in the bronchioles
23 where the residence time is longer and distances necessary to reach the epithelium are
24 shorter compared to that in the bronchi.

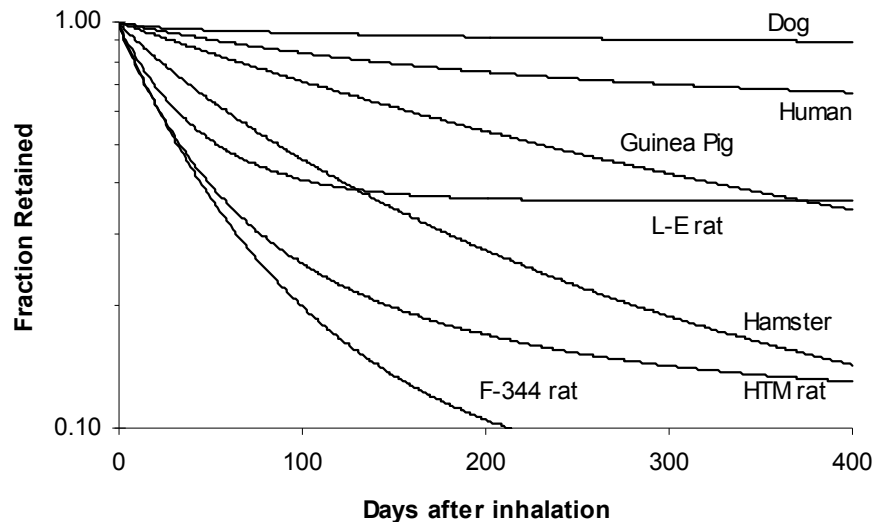
4.3.1.3. Alveolar Region

25 The primary alveolar clearance mechanism is macrophage phagocytosis and
26 migration to terminal bronchioles where the cells are cleared by the mucociliary escalator.
27 Alveolar macrophages originate from bone marrow, circulate briefly as monocytes in the
28 blood, and then become pulmonary interstitial macrophages before migrating to the
29 luminal surfaces. Under normal conditions, a small fraction of ingested particles may also
30 be cleared through the lymphatic system. This may occur by transepithelial migration of
31 alveolar macrophage following particle ingestion or free particle translocation with
32 subsequent uptake by interstitial macrophages. Snipes et al. (1997, [156092](#)) have also
33 demonstrated the importance of neutrophil phagocytosis in clearance of particles from the
34 alveolar region. Rates of alveolar clearance of poorly soluble particles vary between species
35 and are briefly discussed in Section 4.3.2. The translocation of particles from their site of
36 deposition is discussed in Section 4.3.3.

1 The efficiency of macrophage phagocytosis is thought to be greatest for particles
2 between 1.5 and 3 μm (Oberdörster, 1988, [006857](#)). The decreased efficiency of alveolar
3 macrophage for engulfing ultrafines increases the time available for these particles to be
4 taken up by epithelial cells and moved into the interstitium (Ferin et al., 1992, [044401](#)).
5 Consistent with this supposition (i.e., translocation increases with time), an increase in
6 titanium dioxide (TiO_2) particle transport to lymph nodes has been reported following
7 inhalation of a cytotoxin to macrophages (Greenspan et al., 1988, [045031](#)). Interestingly, the
8 long-term clearance kinetics of the poorly soluble ultrafine (15-20 nm CMD) iridium (Ir)
9 particles were found to be similar to the kinetics reported in the literature for micrometer-
10 sized particles (Semmler et al., 2004, [055641](#); Semmler-Behnke et al., 2007, [156080](#)).
11 Semmler-Behnke et al. (2007, [156080](#)) concluded that ultrafine Ir particles are less
12 phagocytized by alveolar macrophage than larger particles, but are effectively removed
13 from the airway surface into the interstitium. Particles are then engulfed by interstitial
14 macrophages which then migrate to the airway lumen and are removed by mucociliary
15 clearance to the larynx. The major role of macrophage-mediated clearance was supported
16 by lavage of relatively few free particles versus predominantly phagocytized particles at
17 time-points of up to 6-months. It is also possible that some free particles as well as particle-
18 laden macrophage were carried from interstitial sites via the lymph flow to bronchial and
19 bronchiolar sites, including bronchial-associated lymphatic tissue, where they were
20 excreted again into the airway lumen.

4.3.2. Interspecies Patterns of Clearance and Retention

21 There are differences between species in both the rates of particle clearance from the
22 lung and manner in which particles are retained in the lung. For instance, based on models
23 of mucociliary clearance from un-diseased airways, >95% of particles deposited in the
24 tracheobronchial airways of rats are predicted to be cleared by 5-h post deposition, whereas
25 it takes nearly 40 hours for comparable clearance in humans (Hofmann and Asgharian,
26 2003, [055579](#)). As noted in Section 4.3.1.2, however, there is considerable evidence that a
27 sizeable fraction of particles deposited at the bronchiolar level of the ciliated airways in
28 humans (as well as canines) are cleared at a far slower rate. The slowly cleared TB fraction
29 appears to increase with decreasing particle size. In contrast to humans and canines,
30 studies of mice and rats show negligible long-term retention of even ultrafine particles in
31 the ciliated airways .



Source: Adapted from Kreyling and Scheuch (2000, [056281](#)).

Figure 4-7. Retention of poorly soluble particles (0.5-5 μm) in the alveolar region of the lung over various mammalian species.

1 Figure 4-7 illustrates rates of alveolar clearance for 0.5-5 μm particles in various
 2 mammalian species. The alveolar clearance rate of particles smaller than 0.1 μm and larger
 3 than 5 μm is slower than that of particles in the 0.5 to 5 μm range. From interspecies
 4 comparisons of alveolar clearance, the path length from alveoli to ciliated terminal
 5 bronchioles may affect the particle transport rate (Kreyling and Scheuch, 2000, [056281](#)).
 6 The path length from alveoli to ciliated terminal bronchioli is longer in humans, monkeys,
 7 and dogs, than in sheep, rats, hamsters, and mice. Transport time and hence retention
 8 times may increase with path length. This hypothesis fits with all species in this
 9 comparison, except guinea pigs, which have a short path length yet particle retention that
 10 is nearly as long as in humans, monkeys, and dogs. However, sheep have a short path
 11 length and particle transport as fast as rodents. In general, alveolar clearance rates appear
 12 to increase with increasing path length from the alveoli to ciliated airways.

13 There are also distinct differences in the sites of particle retention between species.
 14 Large mammals retain particles in interstitial tissues under normal conditions, whereas
 15 rats retain particles in alveolar macrophages (Snipes, 1996, [076041](#)). In rats, with chronic
 16 high doses there is a shift in the pattern of dust accumulation and response from that
 17 observed at lower doses in the lungs (Snipes, 1996, [076041](#); Vincent and Donaldson, 1990,
 18 [002462](#)). Rats chronically exposed to high concentrations of insoluble particles experience a
 19 reduction in their alveolar clearance rates and an accumulation of interstitial particle
 20 burden (Bermudez et al., 2002, [055578](#); Bermudez et al., 2004, [056707](#); Ferin et al., 1992,
 21 [044401](#); Oberdörster et al., 1994, [046203](#); Oberdörster et al., 1994, [056285](#); Warheit et al.,
 22 1997, [086055](#)). The influence of exposure concentration on the pattern of particle retention
 23 in rats (exposed to diesel soot) and humans (exposed to coal dust) was examined by Nikula
 24 et al. (2001, [016641](#)). In rats, the DE particles were found to be primarily in the lumens of

1 the alveolar duct and alveoli; whereas in humans, retained dust was found primarily in the
2 interstitial tissue within the respiratory acini.

4.3.3. Particle Translocation

3 Mucociliary and macrophage mediated clearance of poorly soluble particles from the
4 respiratory tract was discussed in Section 4.3.1. There is evidence that particles may cross
5 cell membranes and move from their site of deposition by other mechanisms. The following
6 subsections discuss the movement of particles from the luminal surfaces of the alveolar
7 region and from the olfactory mucosa. The clearance and distribution of soluble particles
8 and soluble constituents of particles are discussed in Section 4.4.

4.3.3.1. Alveolar Region

9 Numerous studies have examined the translocation of ultrafine particles from their
10 site of deposition in the lung. Traditionally viewed as a relatively inert particle type,
11 ultrafine TiO₂ has received the most study. At the time the 2004 PM AQCD was released,
12 there were conflicting results regarding the rate and magnitude of ultrafine carbon
13 translocation from the human lung. Since that time, it has become well-established that the
14 transport of ultrafine carbon particles from the human lung is far slower than that of
15 soluble materials. However, it has also been shown in animal studies (primarily of rats)
16 that ultrafine particles cross cell membranes by mechanisms different from larger (~1 µm)
17 particles and that a small fraction of these particles enter capillaries and may distribute
18 systemically. Described in brief below, details of selected new studies investigating the
19 disposition of poorly soluble particles are provided in Annex B.

20 There has been some contention regarding ability of ultrafine carbon particles to
21 rapidly diffuse from the lungs into the systemic circulation. Based on their study of 5
22 healthy volunteers, Nemmar et al. (2002, [024914](#)) suggested that ultrafine carbon particles
23 (<100 nm) pass rapidly into the systemic circulation. However, Brown et al. (2002, [043216](#))
24 found that the majority of ultrafine carbon particles (CMD, 33 ± 2 nm) were still in the
25 lungs of healthy human adult volunteers (n = 9; aged 40 to 67 years) and COPD patients
26 (n = 10; 45 to 70 years) at 24-h post inhalation. Brown et al. (2002, [043216](#)) and Burch
27 (2002, [056754](#)) contended that the findings reported by Nemmar et al. (2002, [024914](#)) were
28 consistent with soluble pertechnetate clearance, but not insoluble ultrafine carbon
29 particles. Highly soluble in normal saline, pertechnetate clears rapidly from the lung with a
30 half-time of ~10 mins and accumulates most notably in the bladder, stomach, thyroid, and
31 salivary glands. Three recent studies have confirmed that the majority (>95%) of ultrafine
32 carbon particles deposited in the lungs of human volunteers are retained at 24-h post
33 inhalation (Mills et al., 2006, [088770](#); Wiebert et al., 2006, [157146](#); Wiebert et al., 2006,
34 [156154](#)). Wiebert et al. (2006, [157146](#)) modified their aerosol generation system to reduce

1 leaching of the ^{99m}Tc radiolabel from carbon particles. Except for a small amount of
2 radiotracer leaching from particles ($1.0 \pm 0.6\%$ of initially deposited activity in urine by 24
3 h), these investigators found negligible radiolabel and associated particle clearance from
4 the lungs by 70 h. The available data show that there is not a rapid or significant amount of
5 ultrafine carbon particle migration into circulation (Mills et al., 2006, [088770](#); Möller et al.,
6 2008, [156771](#); Wiebert et al., 2006, [157146](#); Wiebert et al., 2006, [156154](#); Brown et al., 2002,
7 [043216](#); Burch, 2002, [056754](#)).

8 Although human studies show that the vast majority of ultrafine carbon particles are
9 retained in the lungs until at least 24-h post inhalation, both in vitro and in vivo studies
10 support the rapid [≤ 1 h] translocation of free ultrafine TiO₂ particles across pulmonary cell
11 membranes (Churg et al., 1998, [085815](#); Ferin et al., 1992, [044401](#); Geiser et al., 2005,
12 [087362](#)). Peculiar to TiO₂ aerosols, there is evidence that particle aggregates may
13 disassociate once deposited in the lungs. This disassociation makes inhaled aggregate size
14 the determinant of deposition amount and site, but primary particle size the determinant of
15 subsequent clearance (Bermudez et al., 2002, [055578](#); Ferin et al., 1992, [044401](#); Takenaka
16 et al., 1986, [046210](#)). Following disaggregation, the ultrafine TiO₂ particles are cleared
17 more slowly and cause a greater inflammatory response (neutrophil influx) than fine TiO₂
18 particles (Bermudez et al., 2002, [055578](#); Ferin et al., 1992, [044401](#); Landry et al., 1983,
19 [003904](#); Oberdörster et al., 1994, [046203](#); Oberdörster et al., 1994, [056285](#); Putz-Anderson
20 et al., 1981, [003914](#)). The differences in inflammatory effects and possibly lymph burdens
21 between fine and ultrafine TiO₂ in many studies appear related to lung burden in terms of
22 particle surface area and not particle mass or number (Oberdorster, 1996, [039852](#);
23 Oberdorster et al., 1992, [045110](#); Oberdorster et al., 2000, [039014](#); Tran et al., 2000,
24 [013071](#)). More recently, others have noted that particle surface area is not an appropriate
25 metric across all particle types (Warheit et al., 2006, [088436](#)). Surface characteristics such
26 as roughness can also affect protein binding and potentially clearance kinetics, with
27 smoother TiO₂ surfaces being more hydrophobic (Sousa et al., 2004, [089866](#)).

28 Geiser et al. (2005, [087362](#)) conducted a detailed examination of the disposition of
29 inhaled ultrafine TiO₂ in 20 healthy adult rats. They found that distributions of particles
30 among lung tissue compartments appeared to follow the volume fraction of the tissues and
31 did not significantly differ between 1- and 24-h post-inhalation. Averaging 1- and 24-h data,
32 $79.3 \pm 7.6\%$ of particles were on the luminal side of the airway surfaces, $4.6 \pm 2.6\%$ were in
33 epithelial or endothelial cells, $4.8 \pm 4.5\%$ were in connective tissues, and $11.3 \pm 3.9\%$ were
34 within capillaries. Particles within cells were not membrane bound. It is not clear why the
35 fraction of particles identified in compartments such as the capillaries did not differ
36 between 1- and 24-h post-inhalation. These findings were consistent with the smaller study
37 of 5 rats by Kapp et al. (2004, [156624](#)) who reported identifying TiO₂ aggregates in a type II
38 pneumocyte; a capillary close to the endothelial cells; and within the surface-lining layer
39 close to the alveolar epithelium immediately following a 1-h exposure. These studies

1 effectively demonstrate that some inhaled ultrafine TiO₂ particles once deposited on the
2 pulmonary surfaces can rapidly [≤ 1 h] translocate beyond the epithelium and potentially
3 into the vasculature.

4 Extrapulmonary translocation has also been described for poorly soluble ultrafine
5 gold and Ir particles. In male Wistar-Kyoto rats exposed to ultrafine gold particles (5-8 nm),
6 Takenaka et al. (2006, [156110](#)) reported a low but significant fraction (0.03 to 0.06% of lung
7 concentration) of gold in the blood from 1 to 7 days post inhalation. Semmler et al. (2004,
8 [055641](#)) also found small but detectable amounts of poorly soluble Ir particle (15 and 20 nm
9 CMD) translocation from the lungs of male Wistar-Kyoto rats to secondary target organs
10 like the liver, spleen, brain, and kidneys. Each of these organs contained about 0.2% of
11 deposited Ir. The peak levels in these organs were found 7 days post inhalation. The
12 translocated particles were largely cleared from extrapulmonary organs by 20 days and Ir
13 levels were near background at 60 days post inhalation. Particles may have been
14 distributed systemically via the gastrointestinal tract. Immediately after the 6-h inhalation
15 exposure, $18 \pm 5\%$ of the deposited Ir particles had already cleared into the gastrointestinal
16 tract. After 3 weeks, $31 \pm 5\%$ of the deposited particles were retained in the lung. By 2 and
17 6 months post inhalation, lung retention was 17 ± 3 and $7 \pm 1\%$, respectively. The particles
18 appeared to be cleared predominantly from the peripheral lung via the mucociliary
19 escalator into the GI tract and were found in feces.

20 A few recent studies have characterized differences in the behavior of fine and
21 ultrafine particles in vitro. Geiser et al. (2005, [087362](#)) found that both ultrafine and fine
22 (0.025 μm gold, 0.078 μm TiO₂, and 0.2 μm TiO₂) particles cross cellular membranes by non-
23 endocytic (i.e., involving vesicle formation) mechanisms such as adhesive interactions and
24 diffusion, whereas the phagocytosis of larger 1 μm TiO₂ particles is ligand-receptor
25 mediated. Edetsberger et al. (2005, [155759](#)) found that ultrafine particles (0.020 μm
26 polystyrene) translocated into cells by first measurement (~ 1 min after particle
27 application). Intracellular agglomerates of 88-117 nm were seen by 15-20 mins and of 253-
28 675 nm by 50-60 mins after particle application. These intracellular aggregates were
29 thought to result from particle incorporation into endosomes or similar structures since
30 Genistein or Cytochalasin treatment generally blocked aggregate formation. Interestingly,
31 particles did not translocate into dead cells, rather they attached to the outside of the cell
32 membrane. Amine- or carboxyl-modified surfaces (46 nm polystyrene) did not affect
33 translocation across cultures of human bronchial epithelial cells with about 6% regardless
34 of the surface characteristics (Geys et al., 2006, [155789](#)).

4.3.3.2. Olfactory Region

35 Numerous studies have demonstrated the translocation of soluble and poorly soluble
36 particles from the olfactory mucosa via the axons to the olfactory bulb of the brain. The vast
37 majority of these studies were conducted in rodents. However, DeLorenzo (DeLorenzo, 1970,

1 [156391](#)) observed the rapid (within 30-60 mins) movement of 50 nm silver-coated colloidal
2 gold particles instilled on the olfactory mucosa into the olfactory bulb of squirrel monkeys.
3 The specifics of this and other key studies that have investigated the translocation of
4 particles to the olfactory bulb are provided in Annex B.

5 Two recent studies reported the movement of ultrafine particles deposited in the
6 olfactory region of the nose along the olfactory nerve and into the olfactory bulb of the brain
7 in rats. Oberdörster et al. (2004, [055639](#)) exposed rats to ultrafine carbon particles (36 nm
8 CMD, 1.7 σ_g) containing ^{13}C in a whole-body chamber for 6 h. The distribution of ^{13}C was
9 followed for 7 days postexposure. There was a significant increase in ^{13}C in the olfactory
10 bulb on Day 1 with persistent and continued increased through Day 7. Elder et al. (2006,
11 [089253](#)) exposed rats to manganese (Mn) oxide (~30 nm equivalent sphere with 3-8 nm
12 primary particles) via whole-body inhalation exposure for 12 days (6 h/day, 5 days/wk) with
13 both nares open or Mn oxide for 2 days (6 h/day) with right nostril blocked. After the 12
14 days exposure via both nostrils, Mn in the olfactory bulb increased 3.5-fold. After the 2-day
15 exposure with the right nostril blocked, Mn was found mainly in the left olfactory bulb (2.4-
16 fold increase). These studies suggest the neuronal uptake and translocation of ultrafine
17 particles without particle dissolution and in the absence of mucosal injury.

18 Elder et al. (2006, [089253](#)) also addressed the issue of whether solubilization of
19 particles was requisite for translocation along the olfactory nerve and into the brain.
20 Similar amounts of soluble manganese chloride (MnCl_2) and poorly soluble Mn oxide were
21 instilled onto the left naris of anesthetized rats. At 24-h post instillation, similar amounts of
22 Mn were found in the left olfactory bulb of rats instilled with MnCl_2 ($8.2 \pm 3.6\%$ of instilled)
23 and Mn oxide ($8.2 \pm 0.7\%$ of instilled). If solubilization were required for translocation, then
24 a lower amount of Mn oxide than MnCl_2 should have reached the olfactory bulb. Following
25 14 consecutive days of aerosol exposure, Dorman et al. (2001, [055433](#)) demonstrated that
26 more soluble Mn sulfate reaches the olfactory bulb and striatum of rat brains than the
27 poorly soluble form of Mn tetroxide. Nonetheless, the Mn levels were statistically increased
28 in both the olfactory bulb and striatum following exposure to Mn tetroxide relative to filter
29 air. In a subsequent 13-wk exposure study, Dorman et al. (2004, [155752](#)) also demonstrated
30 that more soluble manganese sulfate (MnSO_4) reached the olfactory bulb than was observed
31 for the less soluble Mn form (hureaulite). Both the soluble and less soluble forms of Mn
32 resulted in statistically increased levels of Mn in the olfactory bulb relative to air exposed
33 controls. The soluble MnSO_4 was also observed to reach the striatum and cerebellum. In
34 addition, Yu et al. (2003, [156171](#)) demonstrated increased Mn levels in the brains of rats
35 exposed to welding-fumes for 60 days, however, the role of transport via the blood is less
36 clear in this study.

37 The translocation of zinc (Zn) and TiO_2 to the olfactory bulb has also been reported in
38 the literature. Persson et al. (2003, [051846](#)) observed the translocation of Zn to the olfactory
39 bulbs following instillation in both rats and freshwater pike. Wang et al. (2007, [156146](#))

1 reported the translocation of both fine (155 nm) and ultrafine (21 and 71 nm) TiO₂ particles
2 in mice. Interestingly, a qualitative analysis of the data showed that more of the fine TiO₂
3 than ultrafine TiO₂ reached the olfactory bulb. Wang et al. (2007, [156146](#)) suggested that a
4 strong hydrophilic character and propensity for aggregation reduced the translocation of
5 the ultrafine TiO₂.

6 The importance of particle translocation to the brain is not yet understood.
7 Translocation via the axon to the olfactory bulb has been observed for numerous compounds
8 of varying composition, particle size, and solubility. Although the rate of translocation is
9 rapid, perhaps less than an hour, the magnitude of transport remains poorly characterized.
10 With regard to the magnitude of transport, Elder et al. (2006, [089253](#)) found that as much
11 as 8% of both soluble and insoluble forms of Mn were translocated to the olfactory bulb in
12 rats following intranasal instillation. It is also still unclear to what extent translocation to
13 the olfactory bulb and other brain regions may vary between species. The olfactory mucosa
14 covers approximately 50% of the nasal epithelium in rodents versus only about 5% in
15 primates (Aschner et al., 2005, [155663](#)). Additionally, a greater portion of inhaled air passes
16 through the olfactory region of rats relative to primates (Kimbell, 2006, [155902](#)). These
17 differences may predispose rats, more so than humans, to deposition of particles in the
18 olfactory region with subsequent particle translocation to the olfactory bulb.

4.3.4. Factors Modulating Clearance

4.3.4.1. Age

19 It was previously concluded that there appeared to be no clear evidence for any age-
20 related differences in clearance from the lung or total respiratory tract, either from child to
21 adult, or young adult to elderly (U.S. EPA, 2004, [056905](#); U.S. EPA, 1996, [079380](#)). Studies
22 showed either no change or some slowing in mucus clearance with age after maturity.
23 Although some differences in alveolar macrophage function were reported between mature
24 and senescent mice, no age-related decline in macrophage function had been observed in
25 humans. A comprehensive review of the recent and older literature supports a decrease in
26 mucociliary clearance with increasing age beyond adulthood in humans and animals.
27 Limited animal data also suggest macrophage-mediated alveolar clearance may also
28 decrease with age.

29 Studies addressing the effects of age on respiratory tract clearance are provided in
30 Annex B. Ho et al. (2001, [156549](#)) demonstrated that nasal mucociliary clearance rates
31 were about 40% lower in old (age >40-90) versus young (age 11-40) men and women.
32 Tracheal mucus velocities in elderly (or aged) humans and beagle dogs are about 50% that
33 of young adults (Goodman et al., 1978, [071130](#); Whaley et al., 1987, [156153](#)). Several
34 human studies have demonstrated decreasing rates of mucociliary particle clearance from

1 the large and small bronchial airways with increasing age (Puchelle et al., 1979, [006863](#);
2 Svartengren et al., 2005, [157034](#); Vastag et al., 1985, [157088](#)). Linear fits to the data show
3 that rapid clearance (within 1 h) from large bronchi and prolonged clearance (between 1-21
4 days) from the small bronchioles in an 80-year-old is only about 50% of that in 20-year-old
5 (Svartengren et al., 2005, [157034](#); Vastag et al., 1985, [157088](#)). One study reported that
6 alveolar particle clearance rates decreased by nearly 40% in old versus young rats (Muhle
7 et al., 1990, [006853](#)). Another study has reported that older rats have an increased
8 susceptibility to pulmonary infection due to altered alveolar macrophage function and
9 slowed bacterial clearance (Antonini et al., 2001, [156219](#)). Although data are somewhat
10 limited, they consistently show a depression of clearance throughout the respiratory tract
11 with increasing age from young adulthood in humans and laboratory animals.

4.3.4.2. Gender

12 Gender was not found to affect clearance rates in prior reviews (U.S. EPA, 1996,
13 [079380](#); U.S. EPA, 2004, [056905](#)). Studies not included in those reviews also show that
14 human males and females have similar nasal mucus clearance rates (Ho et al., 2001,
15 [156549](#)), tracheal mucus velocities (Yeates et al., 1981, [095391](#)), and large bronchial airway
16 clearance rates (Vastag et al., 1985, [157088](#)).

4.3.4.3. Respiratory Tract Disease

17 At the time of the last two reviews (U.S. EPA, 1996, [079380](#); U.S. EPA, 2004, [056905](#)),
18 it was well recognized that obstructive airways disease may influence both the site of initial
19 deposition and the rate of mucociliary clearance from the airways. When deposition
20 patterns are matched, mucociliary clearance rates are reduced in patients with COPD
21 relative to healthy controls. The effects of acute bacterial/viral infections and cough on
22 mucociliary clearance were briefly summarized in Section 10.4.2.5 (EPA, 1996, [079380](#)) and
23 Section 6.3.4.4 (EPA, 2004, [056905](#)) of past reviews. While cough is generally a reaction to
24 some inhaled stimulus, in some cases, especially respiratory disease, it can also serve to
25 clear the upper bronchial airways of deposited substances by dislodging mucus from the
26 airway surface. One of the difficulties in assessing effects on infection on mucociliary
27 clearance is that spontaneous coughing increases during acute infections. Cough has been
28 shown to supplement mucociliary clearance of secretions, especially in patients with
29 obstructive lung disease and primary ciliary dyskinesia.

30 Using a bolus technique to target specific lung regions, Möller et al. (2008, [156771](#))
31 examined particle clearance from the ciliated airways and alveolar region of healthy
32 subjects, smokers, and patients with COPD. Airway retention after 1.5 hours was
33 significantly lower in healthy subjects ($89 \pm 6\%$) than smokers ($97 \pm 3\%$) or COPD patients
34 ($96 \pm 6\%$). At 24 and 48 h, retention remained significantly higher in COPD patients
35 ($86 \pm 6\%$ and $82 \pm 6\%$, respectively) than healthy subjects ($75 \pm 10\%$ and $70 \pm 9\%$,

1 respectively). However, these findings are confounded by the more central pattern of
2 deposition in the healthy subjects than in the smokers and COPD patients. Alveolar
3 retention of particles was similar between the groups at 48-h post-inhalation.

4 The effect of asthma on lung clearance of particles may depend on disease status. Lay
5 et al. (2009, [190060](#)) found significantly ($p < 0.01$) more rapid particle ($0.22 \mu\text{m}$) mucociliary
6 clearance over a 2-h period post inhalation in mild asthmatics than in healthy volunteers.
7 Although the pattern of deposition tended to be more central in the asthmatics, there was
8 not a statistically significant difference from healthy controls. In vivo uptake by airway
9 macrophages in mild asthmatics was also enhanced relative to healthy volunteers ($p <$
10 0.01). In an ex vivo study, airway macrophages from individuals with more severe asthma
11 had impaired phagocytic capacity relative to less severely affect asthmatics and healthy
12 volunteers (Alexis et al., 2001, [190013](#)). Lay et al. (2009, [190060](#)) concluded that enhanced
13 uptake and processing of particulate antigens could contribute to the pathogenesis and
14 progression of allergic airways disease in asthmatics and may contribute to an increased
15 risk of exacerbations with particulate exposure.

16 Chen et al. (2006, [147267](#)) investigated the effect of endotoxin on the disposition of
17 particles. Healthy rats and those pretreated with endotoxin (12 hours before particle
18 instillation) were instilled with ultrafine (56.4 nm) or fine (202 nm) particles. In healthy
19 rats, there were no marked differences in lung retention or systemic distribution between
20 the ultrafine and fine particles. In healthy animals, ultrafine particles were primarily
21 retained in lungs ($72 \pm 10\%$ at 0.5-2 h; $65 \pm 1\%$ at 1 day; $62 \pm 5\%$ at 5 days). Particles were
22 also detected in the blood ($2 \pm 1\%$ at 0.5-2 h; $0.1 \pm 0.1\%$ at 5 days) and liver ($3 \pm 2\%$ at 0.5-2
23 h; $1 \pm 0.1\%$ at 5 days) of the healthy animals. At 1 day post-instillation, about 13% of the
24 particles were excreted in the urine or feces of the healthy animals. In rats pretreated with
25 endotoxin, by 2-h post-instillation, the ultrafine particles accessed the blood (5 vs. 2%) and
26 liver (11 vs. 4%) to a significantly greater extent than fine particles. The endotoxin-treated
27 rats also had significantly greater amounts of ultrafine particles in the blood (5% vs. 2%)
28 and liver (11% vs. 3%) relative to the healthy control rats. This study demonstrates that
29 acute pulmonary inflammation caused by endotoxin increases the migration of ultrafine
30 particles into systemic circulation.

31 Adamson and Preditis (1995, [189982](#)) investigated the possibility that particle
32 deposition into an already injured lung might affect particle retention and enhance the
33 toxicity of “inert” particles. Bleomycin was instilled into mice to induce epithelial necrosis
34 and subsequent pulmonary fibrosis. Instilled 3 days following bleomycin treatment, while
35 epithelial permeability was compromised, carbon black particles in treated mice were
36 translocated to the interstitium and showed increased pulmonary retention relative to
37 untreated mice. When instilled 4 weeks post bleomycin treatment, after epithelial integrity
38 was restored, carbon black particle retention was similar between treated and untreated
39 mice with minimal translocation to the interstitium. The instillation of carbon particles did

1 not appear to increase lung injury in the bleomycin treated mice at either time point. This
2 study shows that integrity of the epithelium affects particle retention and translocation into
3 interstitial tissues.

4.3.4.4. Particle Overload

4 Unlike other laboratory animals, rats appear susceptible to “particle overload” effects
5 due to impaired macrophage-mediated alveolar clearance. Numerous reviews have
6 discussed this phenomenon and the difficulties it poses for the extrapolation of chronic
7 effects in rats to humans (Miller, 2000, [011822](#); ILSI, 2000, [002892](#); Oberdorster, 1995,
8 [046596](#); Oberdorster, 2002, [021111](#); Morrow, 1994, [006850](#)). Large mammals have slow
9 pulmonary particle clearance and retain particles in interstitial tissues under normal
10 conditions, whereas rats have rapid pulmonary clearance and retain particles in alveolar
11 macrophages (Snipes, 1996, [076041](#)). With chronic high doses of PM there is a shift in the
12 pattern of dust accumulation and response from that observed at lower doses in rat lungs
13 (Snipes, 1996, [076041](#); Vincent and Donaldson, 1990, [002462](#)). Rats chronically exposed to
14 high concentrations of insoluble particles experience a reduction in their alveolar clearance
15 rates and an accumulation of interstitial particle burden (Bermudez et al., 2002, [055578](#);
16 Bermudez et al., 2004, [056707](#); Ferin et al., 1992, [044401](#); Oberdörster et al., 1994, [046203](#);
17 Oberdörster et al., 1994, [056285](#); Warheit et al., 1997, [086055](#)). With continued exposure,
18 some rats eventually develop pulmonary fibrosis and both benign and malignant tumors
19 (Lee et al., 1985, [003847](#); Lee et al., 1985, [067628](#); Lee et al., 1986, [067629](#); Warheit et al.,
20 1997, [086055](#)). Oberdörster (1996, [039852](#); 2002, [021111](#)) proposed that high-dose effects
21 observed in rats may be associated with two thresholds. The first threshold is the
22 pulmonary dose that results in a reduction in macrophage-mediated clearance. The second
23 threshold, occurring at a higher dose than the first, is the dose at which antioxidant
24 defenses are overwhelmed and pulmonary tumors develop. Intrapulmonary tumors
25 following TiO₂ exposures are exclusive to rats and are not found in mice or hamsters
26 (Mauderly, 1997, [084631](#)). Moreover, Lee et al. (1985, [003847](#)) noted that the squamous cell
27 carcinomas observed with prolonged high concentration TiO₂ exposures developed from the
28 alveolar lining cells adjacent to the alveolar ducts, whereas squamous cell carcinomas in
29 humans are generally linked with cigarette smoking are thought to arise from basal cells of
30 the bronchial epithelium. Quoting Lee et al. (1986, [067629](#)), “Since the lung tumors were a
31 unique type of experimentally induced tumor under exaggerated exposure conditions and
32 have not usually been seen in man or animals, their relevance to man in questionable.”

4.3.5. Summary

33 For any given particle size, the pattern of poorly soluble particle deposition influences
34 clearance by partitioning deposited material between regions of the respiratory tract.

1 Particles depositing in the mouth may generally be assumed to be swallowed or removed by
2 expectoration. Particles deposited in the posterior portions of the nasal passages or the TB
3 airways are moved via mucociliary transport towards the nasopharynx and swallowed.
4 Although clearance from the TB region is generally rapid, there appears to be fraction of
5 material deposited in the TB region of humans that is retained much longer. The
6 underlying sites and mechanisms of long-term TB retention are not known. In contrast to
7 humans, mice and rats appear to have negligible long-term retention of particles in TB
8 airways. The primary alveolar clearance mechanism is macrophage phagocytosis and
9 migration to terminal bronchioles where the cells are cleared by the mucociliary escalator.
10 Clearance from both the TB and alveolar region is more rapid in rodents than humans.
11 Mucociliary and macrophage-mediated clearance decreases with age beyond adulthood.

12 Human data show that there is not a rapid or significant amount of ultrafine carbon
13 particle migration into circulation. However, both in vitro and in vivo animal studies
14 support the rapid [≤ 1 h] translocation of free ultrafine TiO_2 particles across pulmonary cell
15 membranes. Extrapulmonary translocation has also been described in rats for poorly
16 soluble ultrafine gold and Ir particles. A low, but statistically significant, fraction (0.03 to
17 0.06% of lung concentration) of ultrafine gold particles has been observed in the blood of
18 rats from 1 to 7 days post inhalation. The translocation in detectable amounts ($<1\%$ of
19 deposited material) of poorly soluble Ir particles (15 and 20 nm CMD) from the lungs of rats
20 to secondary target organs like the liver, spleen, brain, and kidneys has also been reported.
21 However, the systemic distribution of particles may have occurred via normal clearance
22 from the lungs to the gastrointestinal tract.

23 Although the importance of particle translocation to the brain is not yet understood,
24 translocation from the olfactory mucosa via the axon to the olfactory bulb has been reported
25 in primates, rodents, and freshwater pike for numerous compounds of varying composition,
26 particle size, and solubility. The rate of translocation is rapid, perhaps less than an hour. In
27 rats, as much as 8% of material may become translocated to the olfactory bulb following
28 intranasal instillation. It is unclear to what extent translocation to the olfactory bulb and
29 other brain regions may vary between species. Interspecies differences may predispose rats,
30 more so than humans, to the deposition of particles in the olfactory region with subsequent
31 translocation to the olfactory bulb.

4.4. Clearance of Soluble Materials

32 Soluble particles and soluble constituents of particles may be absorbed through the
33 epithelium and distributed systemically or retained in the lung. The rate of dissolution
34 depends on a number of factors, including particle surface area and chemical structure.
35 Some dissolved materials bind to proteins or other components in the airway surface liquid
36 layer. In the ciliated airways, solutes are cleared by mucociliary transport and diffuse into

1 underlying tissues and the blood. In the alveolar regions, the thin barrier between the air
2 and blood allows for rapid transport of solutes into the blood. The movement of soluble
3 materials depends on the site of deposition in the lung, the rate of material dissolution from
4 particles, and the molecular weight of the solute. The rate of soluble material clearance
5 from the lungs depends on epithelial permeability which may be affected by age,
6 respiratory disease, and concurrent exposures. While enhanced clearance of insoluble
7 particles acts to reduce dose to airway tissue, increased transport of soluble matter into the
8 blood stream may enhance effects on extra-pulmonary organs.

4.4.1. Clearance Mechanisms and Kinetics

9 The rate of absorption across the epithelium for materials that dissolve in the airway
10 or alveolar lining fluid is fairly rapid (minutes to hours) and is a function of their molecular
11 size and their water or lipid solubility (Oberdörster, 1988, [006857](#); Enna and Schanker,
12 1972, [155767](#); Huchon et al., 1987, [024923](#); Schanker et al., 1986, [005100](#)). Huchon et al.
13 (1987, [024923](#)) studied the clearance of a variety of aerosolized solutes from the lungs of
14 dogs. Solute clearance was inversely related to molecular weight. Negligible clearance of
15 the largest molecular weight solute (transferrin; mol wt ~76,000 daltons) in their study was
16 found over a 30-min observation period. At the other extreme, free pertechnetate (mol wt
17 ~163 daltons) had a clearance rate of 6% per min. Clearance of hydrophilic solutes is
18 diffusion limited by pore sizes associated with intercellular tight junctions (estimated at
19 0.6-1.5 nm). Absorption of lipophilic compounds that pass easily through cell membranes is
20 perfusion limited and thus generally occurs very rapidly. However, if lipophilic materials
21 are adsorbed onto insoluble particles their retention in the lung may be prolonged (Creasia
22 et al., 1976, [059713](#)). In addition to diffusion through intercellular junctions, transcellular
23 transport of large solutes by pinocytosis in epithelial cells has also been observed (Chinard,
24 1980, [156341](#)).

25 A portion of poorly soluble particles may become dissolved with subsequent solute
26 clearance. More rapid dissolution of poorly soluble nano- or ultrafine particles relative to
27 micro-sized particles occurs due to an increasing surface-to-volume ratio with decreasing
28 particle size. Kreyling et al. (2002, [037332](#)) examined the dissolution of poorly soluble
29 ultrafine Ir particle agglomerates (15-80 nm CMD) composed of 5 nm primary particles.
30 After 7 days, less than 1% of the particles were dissolved in buffered saline, whereas 6%
31 dissolved in 1 N hydrochloric acid after 1 day. Thus, the high surface-to-volume ratio of
32 ultrafine particles should not be misconstrued to imply rapid dissolution of poorly soluble
33 particles following deposition in the respiratory tract. However, poorly soluble particles that
34 become phagocytosed may slowly dissolve in the acidic (pH of 4.3-5.3) environment of the
35 phagolysosome to be released in their solubilized form from the cell and potential move
36 across the epithelium into the bloodstream. The dissolution rate is inversely related to

1 particle size and directly related to specific surface area (Kreyling and Scheuch, 2000,
2 [056281](#)) and facilitated by the acidic environment of the macrophage (Kreyling, 1992,
3 [067243](#)).

4 There is considerable evidence as well that soluble particles depositing in the
5 bronchial airways are also cleared by mucociliary transport (Bennett and Ilowite, 1989,
6 [000835](#); Wagner and Foster, 2001, [156143](#); Matsui et al., 1998, [040405](#); Sakagami et al.,
7 2002, [156936](#); Lay et al., 2003, [155920](#)). The relative contribution of their removal by
8 transepithelial absorption vs. mucociliary clearance is likely a function of both the
9 molecular size and water or lipid solubility of the material (Oberdörster, 1988, [006857](#);
10 Enna and Schanker, 1972, [155767](#); Huchon et al., 1987, [024923](#); Sakagami et al., 2002,
11 [156936](#)). Furthermore, the rate of mucociliary transport for soluble particles may be less
12 than that of insoluble particles (Lay et al., 2003, [155920](#)). Consequently, non-permeating
13 hydrophilic solutes may remain in contact with the airway epithelium for a longer period
14 than insoluble particles. This may be due to diffusion of a greater portion of the solute into
15 the periciliary sol layer which may be transported less efficiently than the mucus layer
16 during mucociliary clearance. Bronchial blood flow has also been shown to modulate airway
17 retention of soluble particles (Wagner and Foster, 2001, [156143](#)), i.e., decreasing blood flow
18 increases airway retention of soluble particles.

19 As an example of how transport of soluble components of PM may clear the lung by
20 transepithelial absorption, Wallenborn et al. (2007, [156144](#)) measured elemental content of
21 lungs, plasma, heart, and liver of healthy male WKY rats (12-15 weeks old) 4 or 24 hours
22 following a single intratracheal (IT) instillation of saline or 8.33 mg/kg of oil combustion PM
23 containing a variety of transition metals with differing water and acid solubility. Metals
24 with high water solubility and relatively high concentration in oil combustion PM were
25 increased in extrapulmonary organs. Elements with low water or acid solubility, like silicon
26 and aluminum, were not detected in extrapulmonary tissues despite decreased levels in the
27 lung suggesting they cleared the lung primarily by mucociliary clearance. Thus, PM-
28 associated metals deposited in the lung may be released into systemic circulation at
29 different rates depending on their water/acid solubility.

30 The amount and type of water soluble or leachable metals associated with PM varies
31 with location and by source. Furthermore some metals such as Zn, copper, and iron are
32 essential to body function while others such as vanadium and nickel are nonessential
33 metals. Consequently the body and the lung have different ways of dealing with excesses in
34 inhaled soluble metals associated with PM. Bioavailability, and potentially the toxicity, of
35 leachable metals may be altered by protein binding within the lung and blood as well as the
36 affinities of these binding sites. For example Zn is tightly regulated by a variety of metal
37 binding proteins, including metallothionein and a family of Zn specific transporters. In the
38 plasma, Zn binds to many proteins, including α 2-macroglobulin and albumin. Zn is an
39 example of a common abundant water soluble metal in ambient air that may contribute to

1 increased respiratory and cardiovascular disease risk associated with PM exposure.
2 Wallenborn et al. (2009, [191172](#)) recently showed that soluble Zn sulfate (in the form of
3 ^{70}Zn , a rare isotope of Zn) introduced into the lungs by instillation not only reaches, but
4 accumulates in extrapulmonary organs, including the heart and liver, following pulmonary
5 exposure. However, the retention of greater than 50% of ^{70}Zn in the lung 4 hours post
6 instillation suggested that the transepithelial absorption of soluble Zn was indeed slowed
7 by binding to proteins in the lungs. While it could not be ascertained if ^{70}Zn measured in
8 the heart was replacing endogenous Zn pools, any accumulation in cardiac Zn levels could
9 lead to mitochondrial dysfunction and ion channel disruption, possibly explaining adverse
10 cardiac effects from inhalation of Zn-rich PM. Effects of Zn instillation on epithelial
11 integrity were not evaluated.

4.4.2. Factors Modulating Clearance

12 A number of studies have evaluated the epithelial permeability by measuring the
13 clearance of $^{99\text{m}}\text{Tc}$ -diethylenetriaminepentaacetic acid ($^{99\text{m}}\text{Tc}$ -DTPA), a small hydrophilic
14 solute (492 daltons, 0.57 nm). These studies are the basis for much of the discussion in this
15 section.

4.4.2.1. Age

16 In humans, the clearance of water-soluble particles ($^{99\text{m}}\text{Tc}$ -DTPA) from the alveolar
17 epithelium generally slows with increasing age (Pigorini et al., 1988, [156027](#); Braga et al.,
18 1996, [156289](#)). However, Tankersley et al. (2003, [096363](#)) recently showed enhanced
19 permeability of soluble particles ($^{99\text{m}}\text{Tc}$ -DTPA) in terminally senescent mice just before
20 death, suggesting that a disintegration of the epithelial barrier may be a feature of lung
21 homeostatic loss during this period of terminal senescence.

4.4.2.2. Physical Activity

22 The transepithelial transport rates of soluble particles, $^{99\text{m}}\text{Tc}$ -DTPA, have also been
23 found to increase during exercise (Hanel et al., 2003, [155826](#); Lorino et al., 1989, [155946](#);
24 Meignan et al., 1986, [156752](#)). This enhancement was linked to increases in V_T associated
25 with exercise (Lorino et al., 1989, [155946](#)). Regionally, this effect was dominated by
26 increased apical lung clearance and attributed to an increase in apical blood flow (Meignan
27 et al., 1986, [156752](#)). The increased permeability with exercise appears to resolve to
28 baseline after a short period post exercise, i.e., within a couple hours (Hanel et al., 2003,
29 [155826](#)).

4.4.2.3. Disease

1 Because the integrity of the epithelial surface lining of the lungs may be damaged
2 from lung disease, particles (either insoluble or soluble) may gain greater access to the
3 interstitium, lymph, and blood stream. Damage to the epithelial barrier is most likely to
4 acutely affect transepithelial transport rates of soluble particles. From bronchial biopsies,
5 Laitinen et al. (1985, [037521](#)) found various degrees of epithelial damage, from loosening of
6 tight junctions to complete denudation of the airway epithelium, in asthmatics. Consistent
7 with these findings, Ilowite et al. (1989, [156584](#)) found that asthmatics had increased
8 permeability of the bronchial mucosa to the hydrophilic solute ^{99m}Tc -DTPA. On the other
9 hand, a more recent study in a sheep model showed that the presence of bronchial edema
10 could slow the uptake of soluble DTPA into the blood and enhanced retention in the
11 airways, likely within the expanded interstitial barrier (Foster and Wagner, 2001, [155778](#)).
12 Both a leaky epithelial barrier and expanded interstitial barrier associated with asthma
13 may result in enhanced exposure of submucosal immune and smooth muscle cells to
14 xenobiotic substances.

15 Alveolar epithelial permeability was also shown to be affected by the presence of lung
16 inflammation. The most common finding has been a clear increase in alveolar permeability
17 induced by cigarette smoking (Jones et al., 1980, [155883](#)). This effect appears to be
18 dependent the recent cigarette smoke exposure as indexed by carboxyhaemoglobin (Jones et
19 al., 1983, [155884](#)) and is rapidly reversible within a week of smoking cessation (Mason et
20 al., 1983, [013169](#)). In fact, Huchon et al. (1984, [156576](#)) demonstrated that COPD patients
21 who have stopped smoking have normal clearance of ^{99m}Tc -DTPA.

22 In general, increased alveolar permeability to ^{99m}Tc -DTPA has been found to be
23 associated with any lung syndrome characterized by pulmonary edema. While the trans-
24 alveolar transport of a small solute like DTPA is very sensitive to even mild acute lung
25 injury (such as that associated with even mild cigarette smoking), increased transport rates
26 of larger molecules (>100K daltons) across the alveolar epithelium require more severe
27 damage like that seen in adult respiratory distress syndrome (ARDS) (Peterson et al., 1989,
28 [024922](#); Braude et al., 1986, [155701](#)). Interstitial lung disease and pulmonary fibrosis are
29 also characterized by increased alveolar permeability (Bodolay et al., 2005, [156280](#);
30 Antoniou et al., 2006, [156220](#); Watanabe et al., 2007, [157115](#)). Interestingly, these recent
31 studies have also shown that the increased permeability in these patients could be
32 corrected with immunosuppressive/steroid treatments (Bodolay et al., 2005, [156280](#);
33 Watanabe et al., 2007, [157115](#)). Furthermore, studies of DTPA clearance in bleomycin
34 injured dogs, a model of pulmonary fibrosis, suggest that the enhanced permeability is
35 associated with the initial acute phase of the lung damage, with clearance rates returning
36 to normal as chronic fibrosis developed over time (Suga et al., 2003, [157024](#)).

37 Finally, as evidence of lung complications associated with non-insulin dependent
38 diabetes (type 2) patients, Lin et al. (2002, [155932](#)) found impairment of alveolar integrity

1 as shown by increased transport rates of both hydrophilic and lipophilic solutes from the
2 lungs in these patients. By contrast, a number of other studies have found epithelial
3 permeability reduced, i.e., slower transport rates, in diabetes (Özsahin et al., 2006, [156833](#);
4 Caner, 1994, [156320](#); Mousa et al., 2000, [156786](#)) that may be related to disease duration
5 and metabolic control (Özsahin et al., 2006, [156833](#)). These findings are consistent with
6 thickening of alveolar basement membrane detected in autopsies of diabetes patients
7 (Weynand et al., 1999, [157140](#)).

4.4.2.4. Concurrent Exposures

8 The integrity of the alveolar epithelium may be disrupted by co-pollutants such that
9 soluble components of inhaled particles can more easily enter the interstitium and blood
10 stream. Like active cigarette smoking discussed previously, Beadsmoore et al. (2007,
11 [156259](#)) showed clearance half-times in healthy passive smokers to be shorter compared
12 with healthy non-smokers but still longer than in healthy smokers. These findings show a
13 progressive increase in epithelial permeability with exposure to cigarette smoke. Similarly,
14 acute exposure of humans to 0.4 ppm ozone for 2 hours with intermittent exercise has been
15 shown to alter epithelial integrity and increase clearance of soluble hydrophilic particles
16 from the alveolar surfaces of the lung (Kehrl et al., 1987, [040824](#)). This effect persists to at
17 least 24 hours post-exposure to even low concentrations (0.24 ppm average for 130 minutes)
18 of ozone (Foster and Stetkiewicz, 1996, [079920](#)). Similarly, 0.8 ppm O₃ exposure for 2 hours
19 in rats shows increased permeability to macromolecules at all levels of the respiratory tract
20 (Bhalla et al., 1986, [040407](#)) that persisted in the alveolar region beyond 24 hours post-
21 exposure. Cohen et al. (1997, [009213](#)) may have best illustrated the competing effects of
22 mucociliary and transepithelial transport by showing that coexposure to ozone affected the
23 retention of inhaled chromium in rats differently depending on its solubility. In its soluble
24 potassium chromate form, ozone decreased the retention of chromium, but when chromium
25 was inhaled as insoluble barium chromate, its retention in the lung was increased by ozone
26 coexposure. Similarly, a study that showed decreased clearance of insoluble cesium oxide
27 particles following influenza infection also showed a virus-induced enhancement of
28 clearance for a soluble cesium chloride (Lundgren et al., 1978, [155950](#)). Chang et al. (2005,
29 [097776](#)) also recently showed that ultrafine carbon black acts through a reactive oxygen
30 species (ROS) dependent pathway to increase epithelial permeability in mice.

31 But chronic exposure to other particulate or gaseous pollutants has not always led to
32 increased epithelial permeability. Studying subjects with a variety of occupational
33 exposures, Kaya et al. (2006, [156632](#)) showed that nonsmoking welders actually have
34 decreased epithelial permeability relative to nonsmoking control subjects, and occupational
35 exposure of painters to isocyanates has no effect on bronchoalveolar epithelial permeability
36 (Kaya et al., 2003, [156631](#)).

4.4.3. Summary

1 The healthy airway and alveolar epithelium is generally impermeable to very large
2 insoluble macromolecules and particles. Water and acid soluble particles may more rapidly
3 move through the epithelium as they dissolve on the airway surface or within the
4 phagolysosomes of macrophages. The presence of airway inflammation in a variety of airway
5 diseases (e.g., asthma, fibrosis, ARDS, pulmonary edema, inflammation from smoking)
6 alters epithelial integrity to allow more rapid movement of these solutes into the
7 bloodstream. While diabetics are another group recently shown to have increased
8 susceptibility to particulate air pollution (Zanobetti and Schwartz, 2002, [034821](#)), it is
9 unclear whether transport of soluble particles across the epithelium is affected in these
10 patients. In general, it appears that coexposure to irritant pollutants results in a disruption
11 of epithelial integrity and macrophage function which, on the one hand, retards mucociliary
12 and alveolar clearance, but also allows for a more rapid movement of soluble constituents
13 across the epithelial surface into the interstitium and blood stream. Alterations in
14 epithelial permeability by disease, pollutant exposure, or infection may partially explain
15 increased susceptibility to PM associated with these co-conditions.

Chapter 4 References

- ACGIH. (2005). TLVs and BEIs: Based on the documentation of the threshold limit values for chemical substances and physical agents and biological exposure indices. [156188](#)
- Adamson I; Frieditis H. (1995). Response of mouse lung to carbon deposition during injury and repair. *Environ Health Perspect*, 103: 72-76. [189982](#)
- Alexis N; Soukup J; Nierkens S; Becker S. (2001). Association between airway hyperreactivity and bronchial macrophage dysfunction in individuals with mild asthma. , 280: L369-L375. [190013](#)
- Anselm A; Heibel T; Gebhart J; Ferron GA. (1990). In vivo studies of growth factors of sodium chloride particles in the human respiratory tract. *J Aerosol Sci*, 21: S427-430. [156217](#)
- Anthony TR; Flynn MR. (2006). Computational fluid dynamics investigation of particle inhalability. *J Aerosol Sci*, 37: 750-765. [155659](#)
- Antonini JM; Roberts JR; Clarke RW; Yang HM; Barger MW; Ma JYC; Weissman DN. (2001). Effect of age on respiratory defense mechanisms: pulmonary bacterial clearance in Fischer 344 rats after intratracheal instillation of *Listeria monocytogenes*. , 120: 240-249. [156219](#)
- Antoniou KM; Malagari K; Tzanakis N; Perisinakis K; Symvoulakis EK; Karkavitsas N; Siafakas NM; Bouros D. (2006). Clearance of technetium-99m-DTPA and HRCT findings in the evaluation of patients with Idiopathic Pulmonary Fibrosis. , 6: 4. [156220](#)
- Aschner M; Erikson KM; Dorman DC. (2005). Manganese Dosimetry: Species Differences and Implications for Neurotoxicity. *Crit Rev Toxicol*, 35: 1-32. [155663](#)
- Asgharain B; Kelly JT; Tewksbury EW. (2003). Respiratory deposition and inhalability of monodisperse aerosols in Long-Evans rats. *Toxicol Sci*, 71: 104-111. [153068](#)
- Asgharian B; Hofmann W; Miller FJ. (2001). Mucociliary clearance of insoluble particles from the tracheobronchial airways of the human lung. *J Aerosol Sci*, 32: 817-832. [017025](#)
- Bailey M; Dorrian M; Birchall A. (1995). Implications of airway retention for radiation doses from inhaled radionuclides. , 8: 373-390. [190057](#)
- Balashazy I; Hofmann W; Heistracher T. (1999). Computation of local enhancement factors for the quantification of particle deposition patterns in airway bifurcations. *J Aerosol Sci*, 30: 185-203. [043201](#)
- Balashazy I; Hofmann W; Heistracher T. (2003). Local particle deposition patterns may play a key role in the development of lung cancer. , 94: 1719-1725. [155671](#)
- Beadsmoore C; Cheow HK; Szczepura K; Ruparella P; Peters AM. (2007). Healthy passive cigarette smokers have increased pulmonary alveolar permeability. , 28: 75. [156259](#)
- Becquemin MH; Swift DL; Bouchikhi A; Roy M; Teillac A. (1991). Particle deposition and resistance in the noses of adults and children. *Eur Respir J*, 4: 694-702. [009187](#)
- Becquemin MM; Bertholon JF; Bouchikhi A; Malarbet JL; Roy M. (1999). Oronasal Ventilation Partitioning in Adults and Children: Effect on Aerosol Deposition in Airways. *Radiat Prot Dosimetry*, 81: 221-228. [155679](#)
- Bennett W; Messina M; Smaldone G. (1985). Effect of exercise on deposition and subsequent retention of inhaled particles. *J Appl Physiol*, 59: 1046-1054. [190034](#)
- Bennett W; Zeman K; Jarabek A. (2003). Nasal contribution to breathing with exercise: effect of race and gender. *J Appl Physiol*, 95: 497-503. [191977](#)
- Bennett WD; Ilowite JS. (1989). Dual pathway clearance of 99mTc-DTPA from the bronchial mucosa. *Am Rev Respir Dis*, 139: 1132-1138. [000835](#)
- Bennett WD; Zeman KL. (1998). Deposition of fine particles in children spontaneously breathing at rest. *Inhal Toxicol*, 10: 831-842. [076182](#)
- Bennett WD; Zeman KL. (2004). Effect of body size on breathing pattern and fine-particle deposition in children. *J Appl Physiol*, 97: 821-826. [155686](#)
- Bennett WD; Zeman KL. (2005). Effect of Race on Fine Particle Deposition for Oral and Nasal Breathing. *Inhal Toxicol*, 17: 641-648. [155687](#)
- Bennett WD; Zeman KL; Jarabek AM. (2008). Nasal contribution to breathing and fine particle deposition in children versus adults. *J Toxicol Environ Health A*, 71: 227-237. [156269](#)
- Bennett WD; Zeman KL; Kim C. (1996). Variability of fine particle deposition in healthy adults: effect of age and gender. *Am J Respir Crit Care Med*, 153: 1641-1647. [083284](#)

Note: Hyperlinks to the reference citations throughout this document will take you to the NCEA HERO database (Health and Environmental Research Online) at <http://epa.gov/hero>. HERO is a database of scientific literature used by U.S. EPA in the process of developing science assessments such as the Integrated Science Assessments (ISA) and the Integrated Risk Information System (IRIS).

- Bennett WD; Zeman KL; Kim C; Mascarella J. (1997). Enhanced deposition of fine particles in COPD patients spontaneously breathing at rest. *Inhal Toxicol*, 9: 1-14. [078839](#)
- Bermudez E; Mangum JB; Asgharian B; Wong BA; Reverdy EE; Janszen DB; Hext PM; Warheit DB; Everitt JI. (2002). Long-term pulmonary responses of three laboratory rodent species to subchronic inhalation of pigmentary titanium dioxide particles. *Toxicol Sci*, 70: 86-97. [055578](#)
- Bermudez E; Mangum JB; Wong BA; Asgharian B; Hext PM; Warheit DB; Everitt JI. (2004). Pulmonary responses of mice, rats, and hamsters to subchronic inhalation of ultrafine titanium dioxide particles. *Toxicol Sci*, 77: 347-357. [056707](#)
- Bhalla DK; Mannix RC; Kleinman MT; Crocker TT. (1986). Relative permeability of nasal, tracheal, and bronchoalveolar mucosa to macromolecules in rats exposed to ozone. *J Toxicol Environ Health*, 17: 269-283. [040407](#)
- Bodolay E; Szekanez Z; Devenyi K; Galuska L; Csipo I; Vegh J; Garai I; Szegedi G. (2005). Evaluation of interstitial lung disease in mixed connective tissue disease (MCTD). , 44: 656-661. [156280](#)
- Braga F; Mango JC; Souza JF; Ferrioli E; De Andrade J; Iazigi N. (1996). Age-related reduction in 99Tcm-DTPA alveolar-capillary clearance in normal humans. , 17: 971-974. [156289](#)
- Braude S; Nolop KB; Hughes JMB; Barnes PJ; Royston D. (1986). Comparison of lung vascular and epithelial permeability indices in the adult respiratory distress syndrome. , 133: 1002-1005. [155701](#)
- Brown J; Bennett W. (2004). Deposition of coarse particles in cystic fibrosis: model predictions versus experimental results. , 17: 239-248. [190032](#)
- Brown JS. (2005). Particle inhalability at low wind speeds. *Inhal Toxicol*, 17: 831-837. [156299](#)
- Brown JS; Wilson WE; Grant LD. (2005). Dosimetric comparisons of particle deposition and retention in rats and humans. *Inhal Toxicol*, 17: 355-385. [089308](#)
- Brown JS; Zeman KL; Bennett WD. (2002). Ultrafine particle deposition and clearance in the healthy and obstructed lung. *Am J Respir Crit Care Med*, 166: 1240-1247. [043216](#)
- Burch WM. (2002). Comment on "Passage of inhaled particles into the blood circulation in humans". *Circulation*, 106: e141-e142. [056754](#)
- Caner B. (1994). Impaired lung epithelial permeability in diabetics detected by technetium-99m-DTPA aerosol scintigraphy. *J Nucl Med*, 35: 204-206. [156320](#)
- Chadha TS; Birch S; Sackner MA. (1987). Oronasal distribution of ventilation during exercise in normal subjects and patients with asthma and rhinitis. , 92: 1037-1041. [037365](#)
- Chang C-C; Chiu H-F; Wu Y-S; Li Y-C; Tsai M-L; Shen C-K; Yang C-Y. (2005). The induction of vascular endothelial growth factor by ultrafine carbon black contributes to the increase of alveolar-capillary permeability. , 113: 454-460. [097776](#)
- Chen J; Tan M; Nemmar A; Song W; Dong M; Zhang G; Li Y. (2006). Quantification of extrapulmonary translocation of intratracheal-instilled particles in vivo in rats: effect of lipopolysaccharide. *Toxicology*, 222: 195-201. [147267](#)
- Cheng K-H; Cheng Y-S; Yeh H-C; Guilmette RA; Simpson SQ; Yang Y-H; Swift DL. (1996). In vivo measurements of nasal airway dimensions and ultrafine aerosol deposition in the human nasal and oral airways. *J Aerosol Sci*, 27: 785-801. [047520](#)
- Chinard FP. (1980). The alveolar-capillary barrier: some data and speculations. *Microvasc Res*, 19: 1-17. [156341](#)
- Churg A; Stevens B; Wright JL. (1998). Comparison of the uptake of fine and ultrafine TiO₂ in a tracheal explant system. *Am J Physiol*, 274: L81-L86. [085815](#)
- Cohen MD; Zelikoff JT; Chen L-C; Schlesinger RB. (1997). Pulmonary retention and distribution of inhaled chromium: effects of particle solubility and coexposure to ozone. *Inhal Toxicol*, 9: 843-865. [009213](#)
- Creasia DA; Poggenburg JK Jr; Nettesheim P. (1976). Elution of benzo[a]pyrene from carbon particles in the respiratory tract of mice. *J Toxicol Environ Health*, 1: 967-975. [059713](#)
- Dai YT; Juang YJ; Wu Y; Breyse PN; Hsu DJ. (2006). In vivo measurements of inhalability of ultralarge aerosol particles in calm air by humans. *J Aerosol Sci*, 37: 967-973. [156377](#)
- DeLorenzo AJD. (1970). The olfactory neuron and the blood-brain barrier. In *Taste and Smell in Vertebrates* (pp. 151-175). London: Churchill Livingstone. [156391](#)
- Dorman DC; McManus BE; Parkinson CU; Manuel CA; McElveen AM; Everitt JI. (2004). Nasal Toxicity of Manganese Sulfate and Manganese Phosphate in Young Male Rats Following Subchronic (13-Week) Inhalation Exposure. *Inhal Toxicol*, 16: 481-488. [155752](#)
- Dorman DC; Struve MF; James RA; Marshall MW; Parkinson CU; Wong BA. (2001). Influence of particle solubility on the delivery of inhaled manganese to the rat brain: manganese sulfate and manganese tetroxide pharmacokinetics following repeated (14-day) exposure. *Toxicol Appl Pharmacol*, 170: 79-87. [055433](#)

- Edetsberger M; Gaubitzer E; Valic E; Waigmann E; Köhler G. (2005). Detection of nanometer-sized particles in living cells using modern fluorescence fluctuation methods. *Biochem Biophys Res Commun*, 332: 109-116. [155759](#)
- Elder A; Gelein R; Silva V; Feikert T; Opanashuk L; Carter J; Potter R; Maynard A; Ito Y; Finkelstein J; Oberdorster G. (2006). Translocation of inhaled ultrafine manganese oxide particles to the central nervous system. *Environ Health Perspect*, 114: 1172-1178. [089253](#)
- Enna SJ; Schanker LS. (1972). Absorption of drugs from the rat lung. *Am J Physiol*, 223: 1227-1231. [155767](#)
- Falk R; Philipson K; Svartengren M; Jarvis N; Bailey M; Camner P. (1997). Clearance of particles from small ciliated airways. , 23: 495-515. [086080](#)
- Farkas A; Balashazy I; SzQcs K. (2006). Characterization of Regional and Local Deposition of Inhaled Aerosol Drugs in the Respiratory System by Computational Fluid and Particle Dynamics Methods. , 19: 329-343. [155771](#)
- Farkas A; Balásházy I. (2008). Quantification of particle deposition in asymmetrical tracheobronchial model geometry. , 38: 508-18. [157358](#)
- Ferin J; Oberdorster G; Penney DP. (1992). Pulmonary retention of ultrafine and fine particles in rats. *Am J Respir Cell Mol Biol*, 6: 535-542. [044401](#)
- Finlay WH; Martin AR. (2008). Recent advances in predictive understanding of respiratory tract deposition. , 21: 189-206. [155776](#)
- Fishman AP; Elias JA. (1980). Fishman's Pulmonary diseases and disorders. [156436](#)
- Foster WM; Stekiewicz PT. (1996). Regional clearance of solute from the respiratory epithelia: 18-20 h postexposure to ozone. *J Appl Physiol*, 81: 1143-1149. [079920](#)
- Foster WM; Wagner EM. (2001). Bronchial edema alters 99mTc-DTPA clearance from the airway surface in sheep. *J Appl Physiol*, 91: 2567-2573. [155778](#)
- Geiser M; Rothen-Rutishauser B; Kapp N; Schurch S; Kreyling W; Schulz H; Semmler M; Im Hof V; Heyder J; Gehr P. (2005). Ultrafine particles cross cellular membranes by nonphagocytic mechanisms in lungs and in cultured cells. *Environ Health Perspect*, 113: 1555-1560. [087362](#)
- Geys J; Coenegrachts L; Vercammen J; Engelborghs Y; Nemmar A; Nemery B; Hoet PHM. (2006). In vitro study of the pulmonary translocation of nanoparticles A preliminary study. *Toxicol Lett*, 160: 218-226. [155789](#)
- Goodman RM; Yergin BM; Landa JF; Golinvaux MH; Sackner MA. (1978). Relationship of smoking history and pulmonary function tests to tracheal mucous velocity in nonsmokers, young smokers, ex-smokers, and patients with chronic bronchitis. *Am Rev Respir Dis*, 117: 205-214. [071130](#)
- Greenspan BJ; Morrow PE; Ferin J. (1988). Effects of aerosol exposures to cadmium chloride on the clearance of titanium dioxide from the lungs of rats. *Exp Lung Res*, 14: 491-499. [045031](#)
- Grgic B; Finlay WH; Burnell PKP; Heenan AF. (2004). In vitro intersubject and intrasubject deposition measurements in realistic mouth-throat geometries. *J Aerosol Sci*, 35: 1025-1040. [155810](#)
- Hanel B; Law I; Mortensen J. (2003). Maximal rowing has an acute effect on the blood-gas barrier in elite athletes. , 95: 1076-1082. [155826](#)
- Heistracher T; Hofmann W. (1997). Flow and deposition patterns in successive airway bifurcations. Presented at In: Cherry, N.; Ogden, T., eds. *Inhaled Particles VIII: proceedings of an international symposium on inhaled particles organised by the British Occupational Hygiene Society; August 1996; Cambridge, UK. Ann. Occup. Hyg.* 41(suppl.): 537-542. [047514](#)
- Ho JC; Chan KN; Hu WH; Lam WK; Zheng L; Tipoe GL; Sun J; Leung R; Tsang KW. (2001). The effect of aging on nasal mucociliary clearance, beat frequency, and ultrastructure of respiratory cilia. *Am J Respir Crit Care Med*, 163: 983-988. [156549](#)
- Hofmann W; Asgharian B. (2003). The effect of lung structure on mucociliary clearance and particle retention in human and rat lungs. *Toxicol Sci*, 73: 448-456. [055579](#)
- Hofmann W; Balashazy I; Heistracher T; Koblinger L. (1996). The significance of particle deposition patterns in bronchial airway bifurcations for extrapolation modeling. *Aerosol Sci Technol*, 25: 305-327. [047515](#)
- Hofmann W; Martonen TB; Graham RC. (1989). Predicted deposition of nonhygroscopic aerosols in the human lung as a function of subject age. : *J. Aerosol Med.* 2. [006922](#)
- Hsu DJ; Swift DL. (1999). The measurements of human inhalability of ultralarge aerosols in calm air using mannikins. *J Aerosol Sci*, 30: 1331-1343. [155855](#)
- Huchon GJ; Montgomery AB; Lipavsky A; Hoefel JM; Murray JF. (1987). Respiratory clearance of aerosolized radioactive solutes of varying molecular weight. *J Nucl Med*, 28: 894-902. [024923](#)
- Huchon GJ; Russell JA; Barrिताult LG; Lipavsky A; Murray JF. (1984). Chronic air-flow limitation does not increase respiratory epithelial permeability assessed by aerosolized solute, but smoking does. *Am Rev Respir Dis*, 130: 457-460. [156576](#)
- ICRP. (1994). Human respiratory tract model for radiological protection: a report of a task group of the International Commission on Radiological Protection. *Ann ICRP*, 24: 1-482. [006988](#)

- Ilowite JS; Bennett WD; Sheetz MS; Groth ML; Nierman DM. (1989). Permeability of the bronchial mucosa to ^{99m}Tc-DTPA in asthma. *Am Rev Respir Dis*, 139: 1139-1143. [156584](#)
- ILSI. (2000). The relevance of the rat lung response to particle overload for human risk assessment: a workshop consensus report. *Inhal Toxicol*, 12: 1-17. [002892](#)
- Isaacs KK; Schlesinger RB; Martonen TB. (2006). Three-dimensional computational fluid dynamics simulations of particle deposition in the tracheobronchial tree. , 19: 344-352. [155861](#)
- ISO. (2008). Nanotechnologies -- Terminology and definitions for nano-objects -- Nanoparticle, nanofibre and nanoplate. International Organization for Standardization. Geneva. [190066](#)
- James DS; Stidley CA; Lambert WE; Chick TW; Mermier CM; Samet JM. (1997). Oronasal distribution of ventilation at different ages. *Arch Environ Occup Health*, 52: 118-123. [042422](#)
- Jarabek AM; Asgharian B; Miller FJ. (2005). Dosimetric adjustments for interspecies extrapolation of inhaled poorly soluble particles (PSP). *Inhal Toxicol*, 17: 317-334. [056756](#)
- Jeffers DE. (2005). Relative magnitudes of the effects of electrostatic image and thermophoretic forces on particles in the respiratory tract. *Radiat Prot Dosimetry*, 113: 189-194. [156608](#)
- Jones JG; Minty BD; Lawler P; Hulands G; Crawley JC; Veall N. (1980). Increased alveolar epithelial permeability in cigarette smokers. *Lancet*, 1: 66-68. [155883](#)
- Jones JG; Minty BD; Royston D; Royston JP. (1983). Carboxyhaemoglobin and pulmonary epithelial permeability in man. *Thorax*, 38: 129-133. [155884](#)
- Kapp N; Kreyling W; Schulz H; Im Hof V; Gehr P; Semmler M; Geiser M. (2004). Electron energy loss spectroscopy for analysis of inhaled ultrafine particles in rat lungs. *Microsc Res Tech*, 63: 298-305. [156624](#)
- Kaya E; Fidan F; Unlu M; Sezer M; Tetik L; Acar M. (2006). Evaluation of alveolar clearance by Tc-99m DTPA radioaerosol inhalation scintigraphy in welders. , 20: 503. [156632](#)
- Kaya M; Salan A; Tabakoglu E; Aydogdu N; Berkarda S. (2003). The bronchoalveolar epithelial permeability in house painters as determined by Tc-99m DTPA aerosol scintigraphy. , 17: 305-308. [156631](#)
- Kehrl HR; Vincent LM; Kowalsky RJ; Horstman DH; O'Neil JJ; McCartney WH; Bromberg PA. (1987). Ozone exposure increases respiratory epithelial permeability in humans. *Am J Respir Crit Care Med*, 135: 1124-1128. [040824](#)
- Kelly JT; Asgharian B; Wong BA. (2005). Inertial Particle Deposition in a Monkey Nasal Mold Compared with that in Human Nasal Replicas. *Inhal Toxicol*, 17: 823-830. [155894](#)
- Kim CS. (2000). Methods of calculating lung delivery and deposition of aerosol particles. *Respir Care*, 45: 695-711. [013112](#)
- Kim CS; Hu SC. (1998). Regional deposition of inhaled particles in human lungs: comparison between men and women. *J Appl Physiol*, 84: 1834-1844. [086066](#)
- Kim CS; Iglesias AJ. (1989). Deposition of inhaled particles in bifurcating airway models: I inspiratory deposition. , 2: 1-14. [078539](#)
- Kim CS; Iglesias AJ; Garcia L. (1989). Deposition of inhaled particles in bifurcating airway models: II expiratory deposition. , 2: 15-27. [078538](#)
- Kim CS; Jaques PA. (2000). Respiratory dose of inhaled ultrafine particles in healthy adults. , 358: 2693-2705. [012811](#)
- Kimbell JS. (2006). Nasal Dosimetry of Inhaled Gases and Particles: Where Do Inhaled Agents Go in the Nose?. *Toxicol Pathol*, 34: 270-273. [155902](#)
- Kreyling WG. (1992). Intracellular particle dissolution in alveolar macrophages. *Environ Health Perspect*, 97: 121-126. [067243](#)
- Kreyling WG; Blanchard JD; Godleski JJ; Haeussermann S; Heyder J; Hutzler P; Schulz H; Sweeney TD; Takenaka S; Ziesenis A. (1999). Anatomic localization of 24- and 96-h particle retention in canine airways. *J Appl Physiol*, 87: 269-284. [039175](#)
- Kreyling WG; Scheuch G. (2000). Clearance of particles deposited in the lungs. In Gehr, P.; Heyder, J. (Ed.), *Particle-lung interactions* New York, NY: Marcel Dekker, Inc. [056281](#)
- Kreyling WG; Semmler M; Erbe F; Mayer P; Takenaka S; Schulz H; Oberdorster G; Ziesenis A. (2002). Translocation of ultrafine insoluble iridium particles from lung epithelium to extrapulmonary organs is size dependent but very low. *J Toxicol Environ Health A*, 65: 1513-1530. [037332](#)
- Laitinen LA; Heino M; Laitinen A; Kava T; Haahtela T. (1985). Damage of the airway epithelium and bronchial reactivity in patients with asthma. *Am Rev Respir Dis*, 131: 599-606. [037521](#)
- Landry TD; Gushow TS; Langvardt PW; Wall JM; McKenna MJ. (1983). Pharmacokinetics and metabolism of inhaled methyl chloride in the rat and dog. *Toxicol Appl Pharmacol*, 68: 473-486. [003904](#)
- Lay J; Alexis N; Zeman K; Peden D; Bennett W. (2009). In vivo uptake of inhaled particles by airway phagocytes is enhanced in patients with mild asthma compared with normal volunteers. *Thorax*, 64: 313-320. [190060](#)

- Lay JC; Stang MR; Fisher PE; Yankaskas JR; Bennett WD. (2003). Airway Retention of Materials of Different Solubility following Local Intrabronchial Deposition in Dogs. , 16: 153-166. [155920](#)
- Lee KP; Henry NW III; Trochimowicz HJ; Reinhardt CF. (1986). Pulmonary response to impaired lung clearance in rats following excessive TiO₂ dust deposition. Environ Res, 41: 144-167. [067629](#)
- Lee KP; Trochimowicz HJ; Reinhardt CF. (1985). Pulmonary response of rats exposed to titanium dioxide (TiO₂) by inhalation for two years. Toxicol Appl Pharmacol, 79: 179-192. [003847](#)
- Lee KP; Trochimowicz HJ; Reinhardt CF. (1985). Transmigration of titanium dioxide (TiO₂) particles in rats after inhalation exposure. Exp Mol Pathol, 42: 331-343. [067628](#)
- Lin CC; Chang CT; Li TC; Kao A. (2002). Objective Evidence of Impairment of Alveolar Integrity in Patients with Non-Insulin-Dependent Diabetes Mellitus Using Radionuclide Inhalation Lung Scan. Lung, 180: 181-186. [155932](#)
- Lorino AM; Meignan M; Bouissou P; Atlan G. (1989). Effects of sustained exercise on pulmonary clearance of aerosolized 99mTc-DTPA. , 67: 2055-2059. [155946](#)
- Lundgren DL; Hahn FF; Crain CR; Sanchez A. (1978). Effect of Influenza Virus Infection on the Pulmonary Retention of Inhaled 144Ce and Subsequent Survival of Mice. , 34: 557. [155950](#)
- Martonen TB; Yang Y; Xue ZQ. (1994). Effects of carinal ridge shapes on lung airstreams. Aerosol Sci Technol, 21: 119-136. [000847](#)
- Mason GR; Uszler JM; Effros RM; Reid E. (1983). Rapid reversible alterations of pulmonary epithelial permeability induced by smoking. , 83: 6-11. [013169](#)
- Matsui H; Randell SH; Peretti SW; Davis CW; Boucher RC. (1998). Coordinated clearance of periciliary liquid and mucus from airway surfaces. J Clin Invest, 102: 1125-1131. [040405](#)
- Mauderly JL. (1997). Relevance of particle-induced rat lung tumors for assessing lung carcinogenic hazard and human lung cancer risk. Presented at In: Driscoll, K. E.; Oberdorster, G., eds. Proceedings of the sixth international meeting on the toxicology of natural and man-made fibrous and non-fibrous particles; September 1996; Lake Placid, NY. Environ. Health Perspect. Suppl. 105(5): 1337-1346. [084631](#)
- Meignan M; Rosso J; Leveau J; Katz A; Cinotti L; Madelaine G; Galle P. (1986). Exercise increases the lung clearance of inhaled technetium-99m DTPA. J Nucl Med, 27: 274-280. [156752](#)
- Miller FJ. (2000). Dosimetry of particles in laboratory animals and humans in relationship to issues surrounding lung overload and human health risk assessment: a critical review. Inhal Toxicol, 12: 19-57. [011822](#)
- Mills NL; Amin N; Robinson SD; Anand A; Davies J; Patel D; de la Fuente JM; Cassee FR; Boon NA; Macnee W; Millar AM; Donaldson K; Newby DE. (2006). Do inhaled carbon nanoparticles translocate directly into the circulation in humans?. Am J Respir Crit Care Med, 173: 426-431. [088770](#)
- Morgan W; Ahmad D; Chamberlain M; Clague H; Pearson M; Vinitzki S. (1984). The effect of exercise on the deposition of an inhaled aerosol. , 56: 327-338. [190035](#)
- Morrow PE. (1994). Mechanisms and significance of "particle overload". Presented at . [006850](#)
- Mousa K; Onadeko BO; Mustafa HT; Mohamed M; Nabilla A; Omar A; Al-Bunni A; Elgazzar A. (2000). Technetium 99mTc-DTPA clearance in the evaluation of pulmonary involvement in patients with diabetes mellitus. Respir Med, 94: 1053-1056. [156786](#)
- Muhle H; Creutzenberg O; Bellmann B; Heinrich U; Mermelstein R. (1990). Dust overloading of lungs: investigations of various materials, species differences, and irreversibility of effects. , 1: S111-S128. [006853](#)
- Ménache MG; Miller FJ; Raabe OG. (1995). Particle inhalability curves for humans and small laboratory animals. Ann Occup Hyg, 39: 317-328. [006533](#)
- Möller W; Felten K; Sommerer K; Scheuch G; Meyer G; Meyer P; Haussinger K; Kreyling WG. (2008). Deposition, retention, and translocation of ultrafine particles from the central airways and lung periphery. Am J Respir Crit Care Med, 177: 426-432. [156771](#)
- Möller W; Haussinger K; Winkler-Heil R; Stahlhofen W; Meyer T; Hofmann W; Heyder J. (2004). Mucociliary and long-term particle clearance in the airways of healthy nonsmoker subjects. , 97: 2200-2206. [155987](#)
- Nemmar A; Hoet PHM; Vanquickenborne B; Dinsdale D; Thomeer M; Hoylaerts MF; Vanbilloen H; Mortelmans L; Nemery B. (2002). Passage of inhaled particles into the blood circulation in humans. Circulation, 105: 411-414. [024914](#)
- Niinimaa V; Cole P; Mintz S; Shephard RJ. (1981). Oronasal distribution of respiratory airflow. Respir Physiol Neurobiol, 43: 69-75. [071758](#)
- Nikula KJ; Vallyathan V; Green FHY; Hahn FF. (2001). Influence of exposure concentration or dose on the distribution of particulate material in rat and human lungs. Environ Health Perspect, 109: 311-318. [016641](#)
- NRPB. (2004). Particle deposition in the vicinity of power lines and possible effects on health: report of an independent advisory group on non-ionising radiation and its ad hoc group on corona ions. [156815](#)

- Oberdorster G. (1995). Lung particle overload: implications for occupational exposures to particles. *Regul Toxicol Pharmacol*, 27: 123-135. [046596](#)
- Oberdorster G. (1996). Significance of particle parameters in the evaluation of exposure-dose-response relationships of inhaled particles. *Inhal Toxicol*, 8 Supplement: 73-89. [039852](#)
- Oberdorster G. (2002). Toxicokinetics and effects of fibrous and nonfibrous particles. *Inhal Toxicol*, 14: 29-56. [021111](#)
- Oberdorster G; Ferin J; Gelein R; Soderholm SC; Finkelstein J. (1992). Role of the alveolar macrophage in lung injury: studies with ultrafine particles. *Environ Health Perspect*, 97: 193-199. [045110](#)
- Oberdorster G; Finkelstein JN; Johnston C; Gelein R; Cox C; Baggs R; Elder ACP. (2000). Acute pulmonary effects of ultrafine particles in rats and mice. [039014](#)
- Oberdorster G; Sharp Z; Atudorei V; Elder A; Gelein R; Kreyling W; Cox C. (2004). Translocation of inhaled ultrafine particles to the brain. *Inhal Toxicol*, 16: 437-445. [055639](#)
- Oberdorster G. (1988). Lung clearance of inhaled insoluble and soluble particles. , 1: 289-330. [006857](#)
- Oberdorster G; Ferin J; Lehnert BE. (1994). Correlation between particle size, in vivo particle persistence, and lung injury. *Environ Health Perspect*, 102 : 173-179. [046203](#)
- Oberdorster G; Ferin J; Soderholm S; Gelein R; Cox C; Baggs R; Morrow PE. (1994). Increased pulmonary toxicity of inhaled ultrafine particles: due to lung overload alone?. *Ann Occup Hyg*, 38: 295-302. [056285](#)
- Oldham MJ; Robinson RJ. (2007). Predicted tracheobronchial and pulmonary deposition in a murine asthma model. , 290: 1309-1314. [156003](#)
- Persson E; Henriksson J; Tallkvist J; Rouleau C; Tjalve H. (2003). Transport and subcellular distribution of intranasally administered zinc in the olfactory system of rats and pikes. *Toxicology*, 191: 97-108. [051846](#)
- Peterson BT; Dickerson KD; James HL; Miller EJ; McLarty JW; Holiday DB. (1989). Comparison of three tracers for detecting lung epithelial injury in anesthetized sheep. *J Appl Physiol*, 66: 2374-2383. [024922](#)
- Phalen RF; Oldham MJ. (2006). Aerosol dosimetry considerations. *Clin Occup Environ Med*, 5: 773-784. [156024](#)
- Phalen RF; Oldham MJ; Mautz WJ. (1989). Aerosol Deposition in the Nose As a Function of Body Size. , 57: 299-305. [156023](#)
- Phalen RF; Oldham MJ; Wolff RK. (2008). The relevance of animal models for aerosol studies. , 21: 113-124. [156865](#)
- Pigorini F; Maini CL; Pau F; Giosue S. (1988). The influence of age on the pulmonary clearance of ⁹⁹Tcm-DTPA radioaerosol. , 9: 965-971. [156027](#)
- Puchelle E; Zahm J-M; Bertrand A. (1979). Influence of age on bronchial mucociliary transport. , 60: 307-313. [006863](#)
- Putz-Anderson V; Setzer JV; Croxton JS; Phipps FC. (1981). Methyl chloride and diazepam effects on performance. *Scand J Work Environ Health*, 7: 8-13. [003914](#)
- Raabe OG; Al-Bayati MA; Teague SV; Rasolt A. (1988). Regional deposition of inhaled monodisperse, coarse, and fine aerosol particles in small laboratory animals. Presented at In: Dodgson, J.; McCallum, R. I.; Bailey, M. R.; Fischer, D. R., eds. *Inhaled particles VI: proceedings of an international symposium and workshop on lung dosimetry*; September 1985; Cambridge, United Kingdom. *Ann. Occup. Hyg.* 32(suppl. 1): 53-63. [001439](#)
- Roth C; Scheuch G; Stahlhofen W. (1993). Clearance of the human lungs for ultrafine particles. *J Aerosol Sci*, 24: S95-S96 . [156928](#)
- Sakagami M; Byron PR; Venitz J; Rypacek F. (2002). Solute disposition in the rat lung in vivo and in vitro: determining regional absorption kinetics in the presence of mucociliary escalator. *J Pharmacol Sci*, 91: 594-604. [156936](#)
- Schanker LS; Mitchell EW; Brown RA Jr. (1986). Species comparison of drug absorption from the lung after aerosol inhalation or intratracheal injection. *Drug Metab Dispos*, 14: 79-88. [005100](#)
- Scheuch G; Gebhart J; Roth C. (1990). Uptake of electrical charges in the human respiratory tract during exposure to air loaded with negative ions. *J Aerosol Sci*, 21: S439-S442. [006948](#)
- Schroeter JD; Kimbell JS; Asgharian B. (2006). Analysis of Particle Deposition in the Turbinate and Olfactory Regions Using a Human Nasal Computational Fluid Dynamics Model. , 19: 301-313. [156076](#)
- Semmler M; Seitz J; Erbe F; Mayer P; Heyder J; Oberdorster G; Kreyling WG. (2004). Long-term clearance kinetics of inhaled ultrafine insoluble iridium particles from the rat lung, including transient translocation into secondary organs. *Inhal Toxicol*, 16: 453-459. [055641](#)
- Semmler-Behnke M; Takenaka S; Fertsch S; Wenk A; Seitz J; Mayer P; Oberdorster G; Kreyling WG. (2007). Efficient elimination of inhaled nanoparticles from the alveolar region: evidence for interstitial uptake and subsequent reentrainment onto airways epithelium. *Environ Health Perspect*, 115: 728. [156080](#)
- Smith JR; Bailey MR; Etherington G; Shutt AL; Youngman MJ. (2008). Effect of particle size on slow particle clearance from the bronchial tree. *Exp Lung Res*, 34: 287 - 312. [190037](#)

- Snipes MB. (1996). Current information on lung overload in nonrodent mammals: contrast with rats. *Inhal Toxicol*, 8: 91-109. [076041](#)
- Snipes MB; Harkema JR; Hotchkiss JA; Bice DE. (1997). Neutrophil Involvement in the Retention and Clearance of Dust Intratracheally Instilled into the LUNGS of F344/N Rats. , 23: 65-84. [156092](#)
- Soderholm SC. (1985). Size-selective sampling criteria for inspirable mass fraction. . [156992](#)
- Sousa SR; Moradas-Ferreira P; Saramango B; Viseu ML; Barbosa MA. (2004). Human serum albumin adsorption on TiO₂ from single protein solutions and from plasma. *Langmuir*, 20: 9745-9754. [089866](#)
- Suga K; Yuan Y; Ogasawara N; Tsukuda T; Matsunaga N. (2003). Altered Clearance of Gadolinium Diethylenetriaminepentaacetic Acid Aerosol from Bleomycin-injured Dog Lungs: Initial Observations. *Am J Respir Crit Care Med*, 167: 1704-1710. [157024](#)
- Svartengren M; Falk R; Philipson K. (2005). Long-term clearance from small airways decreases with age. *Eur Respir J*, 26: 609-615. [157034](#)
- Tabachnik E; Muller N; Toye B; Levison H. (1981). Measurement of ventilation in children using the respiratory inductive plethysmograph. *J Pediatr*, 99: 895-899. [157036](#)
- Takenaka S; Dornhofer-Takenaka H; Muhle H. (1986). Alveolar distribution of fly ash and of titanium dioxide after long-term inhalation by Wistar rats. *J Aerosol Sci*, 17: 361-364. [046210](#)
- Takenaka S; Karg E; Kreyling W; Lentner B; Möller W; Behnke-Semmler M; Jennen L; Walch A; Michalke B; Schramel P. (2006). Distribution Pattern of Inhaled Ultrafine Gold Particles in the Rat Lung. *Inhal Toxicol*, 18: 733-740. [156110](#)
- Tankersley CG; Shank JA; Flanders SE; Soutiere SE; Rabold R; Mitzner W; Wagner EM. (2003). Changes in lung permeability and lung mechanics accompany homeostatic instability in senescent mice. *J Appl Physiol*, 95: 1681-1687. [096363](#)
- Tobin MJ; Chadha TS; Jenouri G; Birch SJ; Gazeroglu HB; Sackner MA. (1983). Breathing patterns. 1. Normal subjects. , 84: 202-205. [156122](#)
- Tran CL; Buchanan D; Cullen RT; Searl A; Jones AD; Donaldson K. (2000). Inhalation of poorly soluble particles II Influence of particle surface area on inflammation and clearance. *Inhal Toxicol*, 12: 1113-1126. [013071](#)
- Tu KW; Knutson EO. (1984). Total deposition of ultrafine hydrophobic and hygroscopic aerosols in the human respiratory system. *Aerosol Sci Technol*, 3: 453-465. [072870](#)
- U.S. EPA. (1996). Air quality criteria for particulate matter. U.S. Environmental Protection Agency. Research Triangle Park, NC. EPA/600/P-95/001aF-cF. [079380](#)
- U.S. EPA. (2004). Air quality criteria for particulate matter. U.S. Environmental Protection Agency. Research Triangle Park, NC. EPA/600/P-99/002aF-bF. [056905](#)
- Valberg P; Brain J; Sneddon S; LeMott S. (1982). Breathing patterns influence aerosol deposition sites in excised dog lungs. *J Appl Physiol*, 53: 824-837. [190019](#)
- Vastag E; Matthys H; Kohler D; Gronbeck L; Daikeler G. (1985). Mucociliary clearance and airways obstruction in smokers, ex-smokers and normal subjects who never smoked. , 139: 93-100. [157088](#)
- Vincent JH; Donaldson K. (1990). A dosimetric approach for relating the biological response of the lung to the accumulation of inhaled mineral dust. *Br J Ind Med*, 47: 302-307. [002462](#)
- Wagner EM; Foster WM. (2001). Interdependence of bronchial circulation and clearance of 99mTc-DTPA from the airway surface. *J Appl Physiol*, 90: 1275-1281. [156143](#)
- Wallenborn JG; Kovalcik KD; McGee JK; Landis MS; Kodavanti UP. (2009). Systemic translocation of (70)zinc: kinetics following intratracheal instillation in rats. *Toxicol Appl Pharmacol*, 234: 25-32. [191172](#)
- Wallenborn JG; McGee John K; Schladweiler Mette C; Ledbetter Allen D; Kodavanti Urmila P. (2007). Systemic translocation of particulate matter-associated metals following a single intratracheal instillation in rats. *J Toxicol Sci*, 98: 231-239. [156144](#)
- Wang JX; Chen CY; Yu HW; Sun J; Li B; Li YF; Gao YX; He W; Huang YY; Chai ZF. (2007). Distribution of TiO₂ particles in the olfactory bulb of mice after nasal inhalation using microbeam SRXRF mapping techniques. , 272: 527-531. [156146](#)
- Warheit DB; Hansen JF; Yuen IS; Kelly DP; Snajdr SI; Hartsky MA. (1997). Inhalation of high concentrations of low toxicity dusts in rats results in impaired pulmonary clearance mechanisms and persistent inflammation. *Toxicol Appl Pharmacol*, 145: 10-22. [086055](#)
- Warheit DB; Webb TR; Sayes CM; Colvin VL; Reed KL. (2006). Pulmonary instillation studies with nanoscale TiO₂ rods and dots in rats: toxicity is not dependent upon particle size and surface area. *Toxicol Sci*, 91: 227-236. [088436](#)
- Watanabe N; Tanada S; Sasaki Y. (2007). Pulmonary clearance of aerosolized 99mTc-DTPA in sarcoidosis I patients. , 51: 82-90. [157115](#)
- Weynand B; Jonckheere A; Frans A; Rahier J; Saint-Luc CU. (1999). Diabetes mellitus Induces a Thickening of the Pulmonary Basal Lamina. *Respiration*, 66: . [157140](#)

- Whaley SL; Muggenburg BA; Seiler FA; Wolff RK. (1987). Effect of aging on tracheal mucociliary clearance in beagle dogs. *J Appl Physiol*, 62: 1331-1334. [156153](#)
- Wiebert P; Sanchez-Crespo A; Falk R; Philipson K; Lundin A; Larsson S; Möller W; Kreyling W; Svartengren M. (2006). No Significant Translocation of Inhaled 35-nm Carbon Particles to the Circulation in Humans. *Inhal Toxicol*, 18: 741-747. [156154](#)
- Wiebert P; Sanchez-Crespo A; Seitz J; Falk R; Philipson K; Kreyling WG; Moller W; Sommerer K; Larsson S; Svartengren M. (2006). Negligible clearance of ultrafine particles retained in healthy and affected human lungs. *Eur Respir J*, 28: 286-290. [157146](#)
- Winter-Sorkina Rde; Cassee FR. (2002). From concentration to dose: factors influencing airborne particulate matter deposition in humans and rats. [043670](#)
- Xu GB; Yu CP. (1986). Effects of age on deposition of inhaled aerosols in the human lung. *Aerosol Sci Technol*, 5: 349-357. [072697](#)
- Yeates DB; Gerrity TR; Garrard CS. (1981). Particle deposition and clearance in the bronchial tree. *Ann Biomed Eng*, 9: 577-592. [095391](#)
- Yu CP. (1985). Theories of electrostatic lung deposition of inhaled aerosols. *Ann Occup Hyg*, 29: 219-227. [006963](#)
- Yu IJ; Park JD; Park ES; Song KS; Han KT; Han JH; Chung YH; Choi BS; Chung KH; Cho MH. (2003). Manganese Distribution in Brains of Sprague–Dawley Rats After 60 Days of Stainless Steel Welding-Fume Exposure. , 24: 777-785. [156171](#)
- Zanobetti A; Schwartz J. (2002). Cardiovascular damage by airborne particles: are diabetics more susceptible?. , 13: 588-592. [034821](#)
- Zeidler-Erdely PC; Calhoun WJ; Ameredes BT; Clark MP; Deye GJ; Baron P; Jones W; Blake T; Castranova V. (2006). In vitro cytotoxicity of Manville Code 100 glass fibers: Effect of fiber length on human alveolar macrophages. *Part Fibre Toxicol*, 28: 3:5. [190967](#)
- Zhao X; Ju Y; Liu C; Li J; Huang M; Sun J; Wang T. (2009). Bronchial anatomy of left lung: a study of multi-detector row CT. , 31: 85-91. [157187](#)
- Özsahin K; Tugrul A; Mert S; Yüksel M; Tugrul G. (2006). Evaluation of pulmonary alveolo-capillary permeability in Type 2 diabetes mellitus Using technetium 99mTc-DTPA aerosol scintigraphy and carbon monoxide diffusion capacity. , 20: 205-209. [156833](#)

Chapter 5. Possible Pathways/ Modes of Action

1 The mechanisms underlying pulmonary effects of inhaled PM have been well-studied
2 in the laboratory and there is general agreement regarding the key roles played by cellular
3 injury and inflammation. These pathways are initiated following the deposition of inhaled
4 particles on respiratory tract surfaces. Since most of these studies were conducted at
5 concentrations of PM higher than ambient levels, there is some question regarding the
6 relevance of these responses and mechanisms to ambient exposures.

7 Interestingly, inhaled PM may also affect the cardiovascular, hematopoietic and other
8 systems. Mechanisms underlying these extra-pulmonary effects are incompletely
9 understood. However, pulmonary inflammation can lead to systemic inflammation and
10 pulmonary reflexes can activate the autonomic nervous system (ANS). These latter
11 responses may mediate cardiovascular and other systemic effects, as will be discussed
12 below. In addition, it has been proposed that PM or soluble components of PM reach the
13 circulation by translocating across the epithelial and endothelial barriers of the respiratory
14 tract. In this way PM or its components may interact directly with cells in the vasculature
15 and blood and be transported to the heart and other organs. At this time, evidence clearly
16 supports the translocation of small solutes following inhalation exposures and the
17 translocation of soluble components of PM following some high dose exposures involving
18 intratracheal instillation. However there is insufficient evidence to support translocation of
19 appreciable amounts of intact particles following inhalation exposures at lower
20 concentrations (see Section 4.3.3.1). Future studies will be required to resolve these issues.

21 The following sections discuss biological pathways which comprise proposed modes of
22 action for the pulmonary and extra-pulmonary effects of inhaled PM. Overall themes are
23 emphasized and supportive evidence from new in vitro and in vivo animal studies is cited.
24 The characterization of evidence here is for PM in general, since most of the potential
25 pathways or modes of action do not appear to be specific to a particular size class of PM.
26 However, characteristics of ultrafine PM may allow for unique modes of action or effects
27 disproportionate to their mass, as will be described below. Finally, a compilation of results
28 from new inhalation studies which are relevant to ambient PM exposures and which
29 confirm and extend these proposed mechanisms is found at the end of this chapter. Detailed
30 descriptions of these key new studies are found in Chapters 6 and 7.

Note: Hyperlinks to the reference citations throughout this document will take you to the NCEA HERO database (Health and Environmental Research Online) at <http://epa.gov/hero>. HERO is a database of scientific literature used by U.S. EPA in the process of developing science assessments such as the Integrated Science Assessments (ISA) and the Integrated Risk Information System (IRIS).

5.1. Pulmonary Effects

5.1.1. Reactive Oxygen Species

1 A great deal of research interest has focused on the role of reactive oxygen species
2 (ROS) in the initiation of pulmonary injury and inflammation following exposure to PM.
3 Numerous studies have demonstrated PM oxidative potential in in vitro assay systems
4 (Ayres et al., 2008, [155666](#); Cho et al., 2005, [087937](#); Shi et al., 2003, [088248](#); Tao et al.,
5 2003, [156111](#)). Both redox active surface components such as metals and organic species
6 and the surface characteristics of crystal structures have been shown to contribute to
7 oxidative potential (Jiang et al., 2008, [156609](#); Tao et al., 2003, [156111](#); Warheit et al., 2007,
8 [090482](#)). In this way, PM may be a direct source of ROS in the respiratory tract
9 (Figure 5-1).

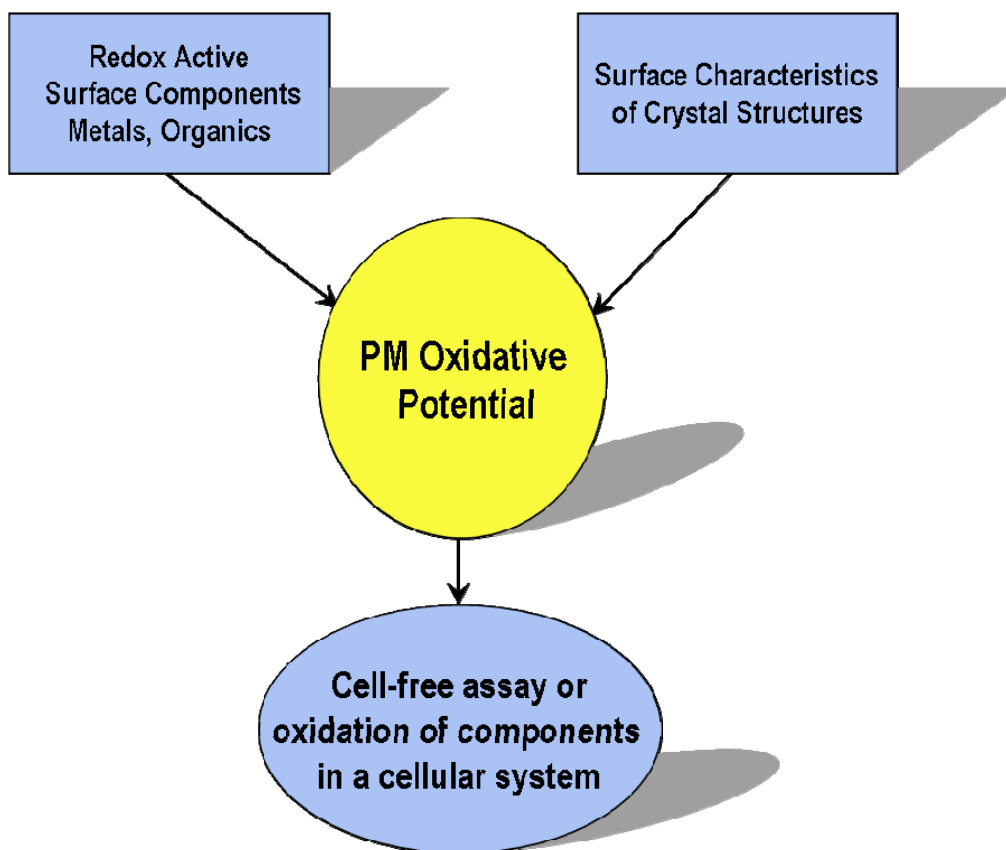


Figure 5-1. PM oxidative potential.

10 PM may also act as an indirect source of ROS in the respiratory tract by stimulating
11 cells to produce ROS (Ayres et al., 2008, [155666](#); Tao et al., 2003, [156111](#)) (Figure 5-2). This

1 may explain the observation that the oxidative potential of isolated PM does not always
2 correlate with cellular or tissue oxidative stress induced by PM exposure. Exposure to PM
3 increases intracellular production of ROS by a variety of mechanisms. For example, PM
4 interaction with cell surfaces results in stimulation of NADPH oxidase in macrophages (i.e.,
5 the respiratory burst) (Dostert et al., 2008, [155753](#)) and in epithelial cells (Amara et al.,
6 2007, [156212](#); Becher et al., 2007, [097125](#); Tamaoki et al., 2004, [157040](#)). Absorption of PM
7 soluble components (e.g., PAH, transition metals) by respiratory tract cells can occur (Penn
8 et al., 2005, [088257](#)) and be followed by microsomal transformation of PAHs to quinones or
9 by redox cycling of transition metals with production of intracellular ROS (Molinelli et al.,
10 2002, [035347](#); Xia et al., 2004, [087486](#)). Disruption of intracellular iron homeostasis with
11 the subsequent generation of ROS has also been demonstrated following PM exposure (Ghio
12 and Cohen, 2005, [088272](#)). In some cases, mitochondria serve as the source of ROS in
13 response to PM (Huang et al., 2003, [156573](#); Risom et al., 2005, [189016](#); Soberanes et al.,
14 2006, [156991](#); Soberanes et al., 2009, [190483](#)). Furthermore, PM interaction with cells can
15 lead to the induction of nitric oxide synthase (Becher et al., 2007, [097125](#); Lindbom et al.,
16 2007, [155934](#); Xiao et al., 2005, [156164](#); Zhao et al., 2006, [100996](#)) and the production of
17 nitric oxide and other reactive nitrogen species (RNS).

18 Although all size fractions of PM may contribute to oxidative and nitrosative stress,
19 ultrafine PM may contribute disproportionately to their mass due to their large
20 surface/volume ratio. The relative enrichment of redox active surface components such as
21 metals and organics per unit mass may translate to a relatively greater oxidative potential
22 of ultrafine PM compared with larger particles with similar surface components. In
23 addition, the greater surface per unit volume could potentially deliver relatively more
24 adsorbed soluble components to cells. These components may undergo intracellular redox
25 cycling following cellular uptake. Furthermore, per unit mass, ultrafine PM may have more
26 opportunity to interact with cell surfaces due to their greater surface area and their greater
27 particle number compared with larger PM. These interactions with cell surfaces can lead to
28 ROS generation, as described above. Recent studies have also demonstrated that ultrafine
29 PM have the capacity to cross cellular membranes by non-endocytotic mechanisms
30 involving adhesive interactions and diffusion (Geiser et al., 2005, [087362](#)), as described in
31 Chapter 4. This may allow ultrafine PM to interact with or penetrate intracellular
32 organelles.

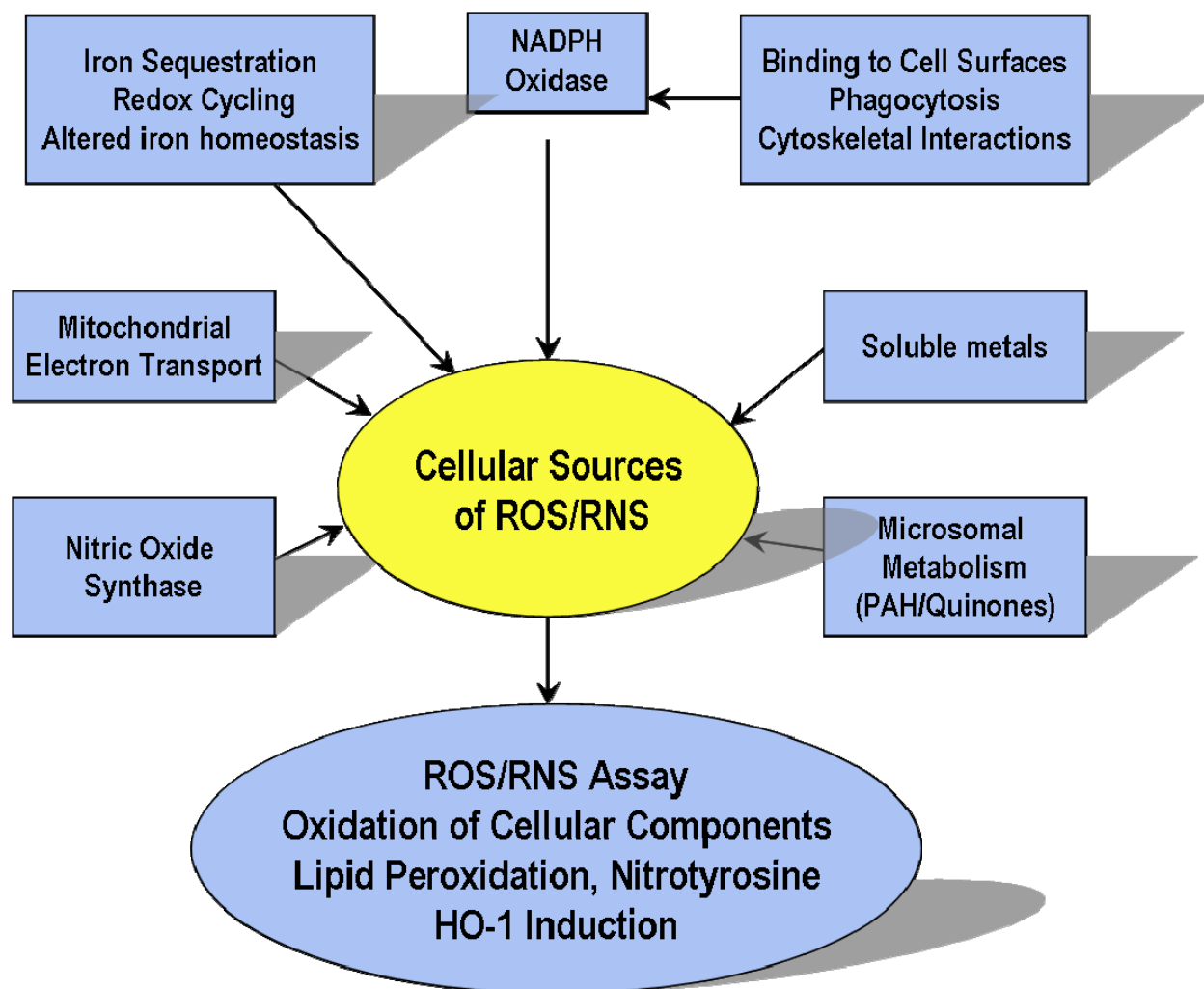


Figure 5-2. PM stimulates pulmonary cells to produce ROS/RNS.

1 In general, high levels of intracellular ROS/RNS can lead to irreversible protein
 2 modifications, loss of cellular membrane integrity, DNA damage and cellular toxicity. Lower
 3 levels of ROS/RNS may cause reversible protein modifications that trigger intracellular
 4 signaling pathways and/or adaptive responses. Thus PM-dependent generation of ROS may
 5 be responsible for a continuum of responses from cell signaling to cellular injury.

5.1.2. Activation of Cell Signaling Pathways

6 Activation of cell signaling pathways by ROS/RNS has received increasing attention
 7 in recent years. An early example was provided by Kaul and Forman (1996, [155892](#)) who
 8 demonstrated that respiratory burst-derived H_2O_2 activates the transcription factor nuclear
 9 factor kappa-light-chain-enhancer of activated B cells (NF κ B). Numerous studies since then
 10 have demonstrated that PM, which serves as both a direct and indirect source of ROS/RNS,
 11 activates cell signaling pathways by this mechanism.

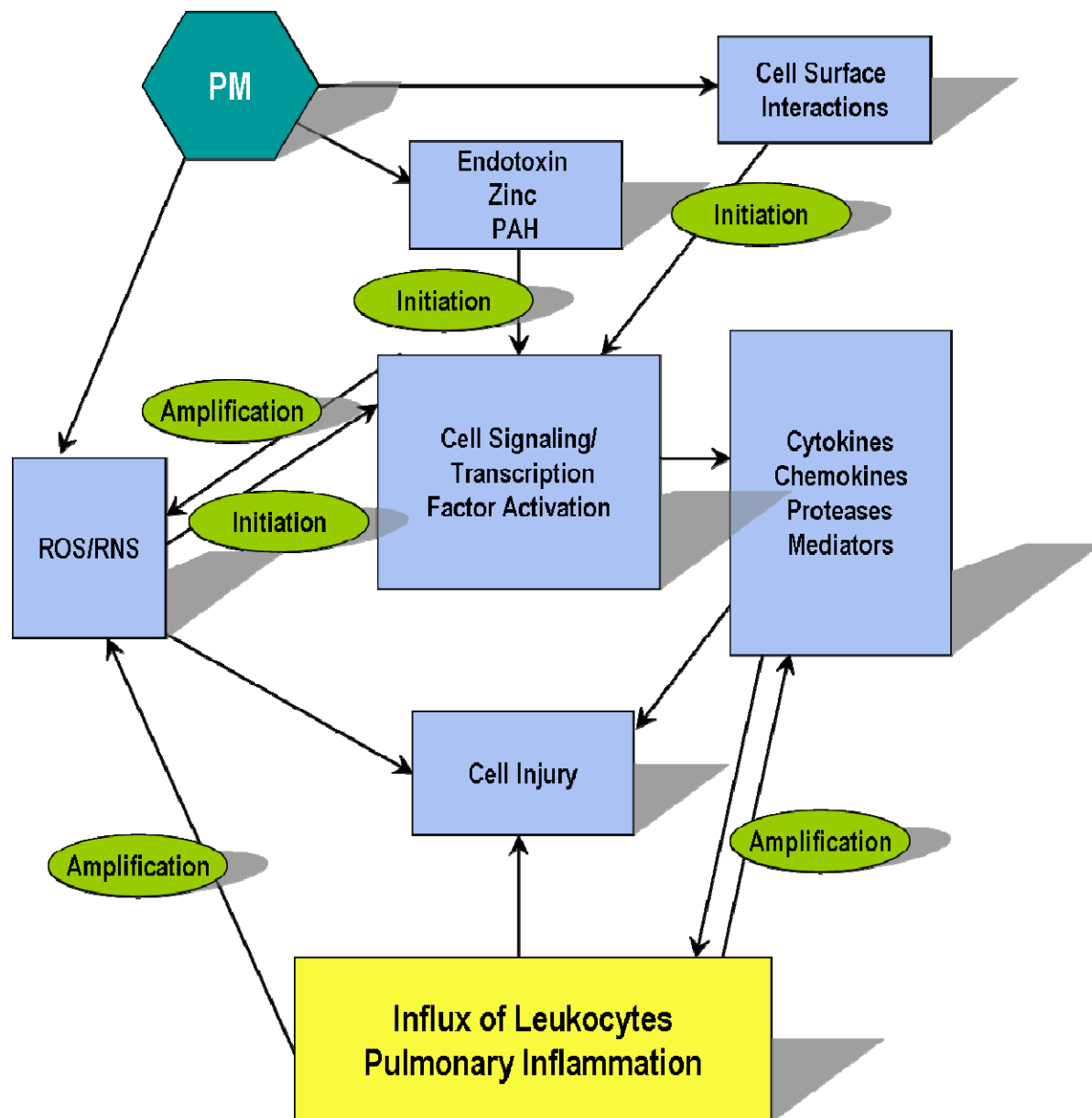


Figure 5-3. PM activates cell signaling pathways leading to pulmonary inflammation.

1 PM also has the potential to activate cell signaling by mechanisms that are
 2 independent of ROS/RNS. For example, PM delivers water-soluble components such as
 3 endotoxin and zinc to cell surfaces. Endotoxin binds to toll-like receptors on alveolar
 4 macrophages and other cells, resulting in the upregulation of cytokines (Becker et al., 2002,
 5 [052419](#)). Zinc, a transition metal which does not redox cycle, inhibits protein tyrosine
 6 phosphatases in airway epithelial cells resulting in a cascade of cell signaling events (Tal et
 7 al., 2006, [108588](#)). Similarly, PM-mediated delivery of lipid soluble components such as
 8 PAH results in binding and activation of the arylhydrocarbon receptor (AhR). AhR is a
 9 transcription factor responsible for the upregulation of CYP1A1, a cytochrome oxidase

1 involved in PAH biotransformation to metabolites capable of forming DNA adducts or
2 eliciting oxidative stress responses (Rouse et al., 2008, [156930](#)). In addition, interaction of
3 PM with cell surfaces may activate cell signaling by perturbation of the cytoskeleton,
4 adherence, internalization, or receptor-mediated pathways.

5 Ultrafine PM may activate cell signaling by ROS-dependent and -independent
6 mechanisms disproportionately to their mass compared with larger sized particles for
7 reasons described in Section 5.1.1.

8 Recent studies involving PM exposures have focused on intracellular pathways
9 involving protein kinases such as mitogen-activated protein kinase (MAPK) (Bayram et al.,
10 2006, [088439](#); Lee et al., 2005, [156682](#); Roberts et al., 2003, [156051](#); Soberanes et al., 2009,
11 [190483](#)), AKT (Ahsan et al., 2005, [156200](#)), src (Cao et al., 2007, [156322](#)) and epidermal
12 growth factor receptor (Blanchet et al., 2004, [087982](#); Cao et al., 2007, [156322](#); Tamaoki et
13 al., 2004, [157040](#)); as well as ras (Tamaoki et al., 2004, [157040](#)), toll-like receptors (Becker
14 et al., 2002, [052419](#); Becker et al., 2005, [088590](#); U.S. EPA, 2000, [052149](#)), protein tyrosine
15 phosphatases (Tal et al., 2006, [108588](#)) phospholipases A₂ (Lee et al., 2003, [156678](#)),
16 calcium (Agopyan et al., 2003, [155649](#); Brown et al., 2004, [155705](#); Brown et al., 2004,
17 [088663](#); Geng et al., 2005, [096689](#); 2006, [097026](#); Sakamoto et al., 2007, [096282](#)), caspases
18 (Soberanes et al., 2006, [156991](#); Zhang et al., 2007, [156179](#)), poly (ADP-ribose) polymerase
19 family member 1 (PARP-1) (Zhang et al., 2007, [156179](#)) and histone acetylation (Gilmour et
20 al., 2003, [096959](#)). The transcription factors regulated by these pathways, including NFκB
21 (Bayram et al., 2006, [088439](#); Lee et al., 2005, [156682](#); Takizawa et al., 2003, [157039](#)),
22 activator protein 1 (AP-1) (Donaldson et al., 2003, [156408](#)), signal transducers and
23 activators of transcription protein (STAT) (Cao et al., 2007, [156322](#)), antioxidant response
24 element (ARE) (Li and Nel, 2006, [156694](#)), and AhR (Rouse et al., 2008, [156930](#)) have also
25 been studied following PM exposures. Activation of these intracellular pathways and
26 transcription factors leads to the upregulation of genes responsible for inflammatory,
27 immune and acute phase responses as well as genes responsible for antioxidant defense and
28 xenobiotic metabolism.

5.1.3. Pulmonary Inflammation

29 Following PM exposure, transcription factor activation in macrophages and epithelial
30 cells stimulates the synthesis and release of proteins involved in inflammatory and immune
31 responses including cytokines, chemokines, proteases and eicosanoids (Figure 5-3). These
32 soluble mediators play a role in recruiting inflammatory cells such as neutrophils,
33 monocytes, mast cells and eosinophils to the lung. Interactions between macrophages and
34 epithelial cells enhance these responses (Tao and Kobzik, 2002, [157044](#)).

35 Inflammatory cells can serve as a source of extracellular ROS which, along with
36 soluble mediators derived from the inflammatory cells, amplify the inflammatory response.

1 Unchecked inflammation may cause cellular and tissue injury through the generation of
2 ROS and soluble mediators. In some cases the oxidative potential of PM is well-correlated
3 with the degree of inflammation (Dick et al., 2003, [036605](#)), suggesting that the
4 inflammation is a direct consequence of PM-generated ROS. However, in other cases the
5 oxidative potential of PM is not well-correlated with the degree of inflammation (Beck-
6 Speier et al., 2005, [156262](#)), suggesting that the inflammation is a consequence of the other
7 mechanisms by which PM activates intracellular signaling pathways.

8 Particle surface area has been identified as a key determinant of the extent of
9 inflammation in the case of low-toxicity, low-solubility particles (Donaldson et al., 2008,
10 [190217](#)). Given their large surface/volume ratio compared with other PM fractions,
11 ultrafine PM may cause inflammation disproportionately to their mass compared with PM
12 of larger sizes.

13 PM exposure often results in neutrophilic inflammation in laboratory studies (Tao et
14 al., 2003, [156111](#)). Neutrophilic inflammation is also associated with acute lung injury in
15 humans as well as chronic lung diseases such as COPD and certain forms of asthma
16 (Barnes, 2007, [191139](#); Cowburn et al., 2008, [191142](#)). Circulating neutrophils respond to
17 chemotactic factors in the lung such as leukotriene B₄ and IL-8 (Barnes, 2007, [191139](#)).
18 They migrate into the lung parenchyma across the pulmonary capillary network and into
19 the airways from the bronchial circulation (Cowburn et al., 2008, [191142](#)). As a consequence
20 of priming by inflammatory mediators or contact with extracellular matrix components,
21 neutrophils become hyperresponsive to activating signals and insensitive to chemotactic
22 signals (Cowburn et al., 2008, [191142](#)). Activation results in neutrophil degranulation,
23 respiratory burst responses and soluble mediator release (Cowburn et al., 2008, [191142](#)).
24 Neutrophils eventually undergo apoptosis and are phagocytized by inflammatory
25 macrophages (Cowburn et al., 2008, [191142](#)). This is accompanied by the release of anti-
26 inflammatory mediators such as IL-10 and transforming growth factor- β (TGF- β) (Cowburn
27 et al., 2008, [191142](#)). These steps are key to the resolution of inflammation and prevent
28 unregulated release of toxic neutrophil products such as neutrophil elastase (Cowburn et
29 al., 2008, [191142](#)). Thus, circumstances leading to the decreased ingestion of apoptotic
30 neutrophils by macrophages may lead to tissue injury. Impairment of macrophage function
31 may serve as an important mechanism by which PM contributes to disease.

5.1.4. Respiratory Tract Barrier Function

32 Epithelial injury can lead to an increase in permeability of the airway epithelial and
33 alveolar-capillary barriers (Braude et al., 1986, [155701](#)). Enhanced transport of soluble and
34 possibly of insoluble PM components into the circulation may occur under these conditions.
35 Increased epithelial permeability is also associated with enhanced immune responses to
36 proteins, including allergens, on the epithelial surface, presumably due to the greater

1 availability of antigens to underlying immune cells (Wan et al., 1999, [191903](#)).
2 Furthermore, endothelial injury can compromise the integrity of the the alveolar-capillary
3 barrier resulting in transvascular fluid and solute flux (Braude et al., 1986, [155701](#)).
4 Soluble mediators derived from inflammatory and lung cells (Chang et al., 2005, [097776](#))
5 and peptides released by some nerve cells (Widdicombe and Lee, 2001, [019049](#)) can increase
6 the permeability of the alveolar-capillary barrier and result in alveolar edema.
7 Compromised barrier function in the airways may lead to airway edema. Edema occurring
8 secondarily to nerve cell stimulation is one component of the process termed neurogenic
9 inflammation.

10 Given the small size of ultrafine PM, modest changes in epithelial permeability may
11 particularly affect the disposition of this fraction. Enhanced translocation to interstitial
12 compartments or to the circulation may be important sequelae. A recent study described in
13 Section 4.3.4.1 demonstrated greater translocation of ultrafine compared with PM_{2.5} into
14 the circulation of rodents treated with endotoxin to induce acute lung injury prior to
15 intratracheal instillation of PM (Chen et al., 2006, [147267](#)). Furthermore, epithelial injury
16 in another model resulted in greater translocation of ultrafine PM into the interstitial
17 compartment (Adamson and Prieditis, 1995, [189982](#)).

5.1.5. Antioxidant Defenses and Adaptive Responses

18 Antioxidant defenses and adaptive responses are important modulators of oxidative
19 stress and other cellular stresses resulting from PM exposure. Antioxidants are present in
20 the epithelial lining fluid in all regions of the respiratory tract. In addition, they are present
21 in cells of the lung parenchyma and inflammatory cells found in airways and alveoli. Some
22 antioxidants act directly against oxidant species (e.g., glutathione, ascorbate, superoxide
23 dismutase) while others act indirectly (e.g., gamma-glutamylcysteine synthetase [γ GCS],
24 glutathione reductase). Furthermore, some antioxidants (e.g., Phase 2 enzymes heme
25 oxygenase-1[HO-1], NADPH quinone oxidoreductase 1 [NQO1], glutathione-S-transferase
26 [GST]) are inducible via activation of the nuclear factor (erythroid-derived 2)- related factor
27 2 (Nrf2)-ARE pathway, which occurs as an adaptive response to stress (Cho et al., 2006,
28 [156345](#); Li and Nel, 2006, [156694](#)). Antioxidants play an important role in reducing the
29 oxidative potential of those PM species that directly generate ROS. They also inhibit
30 responses due to generation of intracellular ROS.

31 Recently a three-tier response to oxidative stress was proposed (Li and Nel, 2006,
32 [156694](#)). In this scheme, mild oxidative stress enhances antioxidant defenses by
33 upregulating Phase 2 and other antioxidant enzymes (Tier 1). Further increase in oxidative
34 stress induces inflammation (Tier 2) and cell death (Tier 3). Experimental evidence is
35 supportive of this scheme. Numerous studies have demonstrated that enhancement of lung
36 and cellular antioxidant defenses inhibits inflammation, cytotoxicity and other responses

1 following exposure to PM (Ahsan et al., 2005, [156200](#); Bachoual et al., 2007, [155667](#);
 2 Bayram et al., 2006, [088439](#); Chang et al., 2005, [097776](#); Imrich et al., 2007, [155859](#); Koike
 3 and Kobayashi, 2005, [088303](#); Koike et al., 2004, [058555](#); Li et al., 2007, [155929](#); Ramage
 4 and Guy, 2004, [055640](#); Rhoden et al., 2004, [087969](#); Steerenberg et al., 2004, [087981](#);
 5 Takizawa et al., 2003, [157039](#); Tao et al., 2003, [156111](#); Upadhyay et al., 2003, [097370](#); Wan
 6 and Diaz-Sanchez, 2006, [097399](#); Wan and Diaz-Sanchez, 2007, [156145](#); Yin et al., 2004,
 7 [087983](#)).

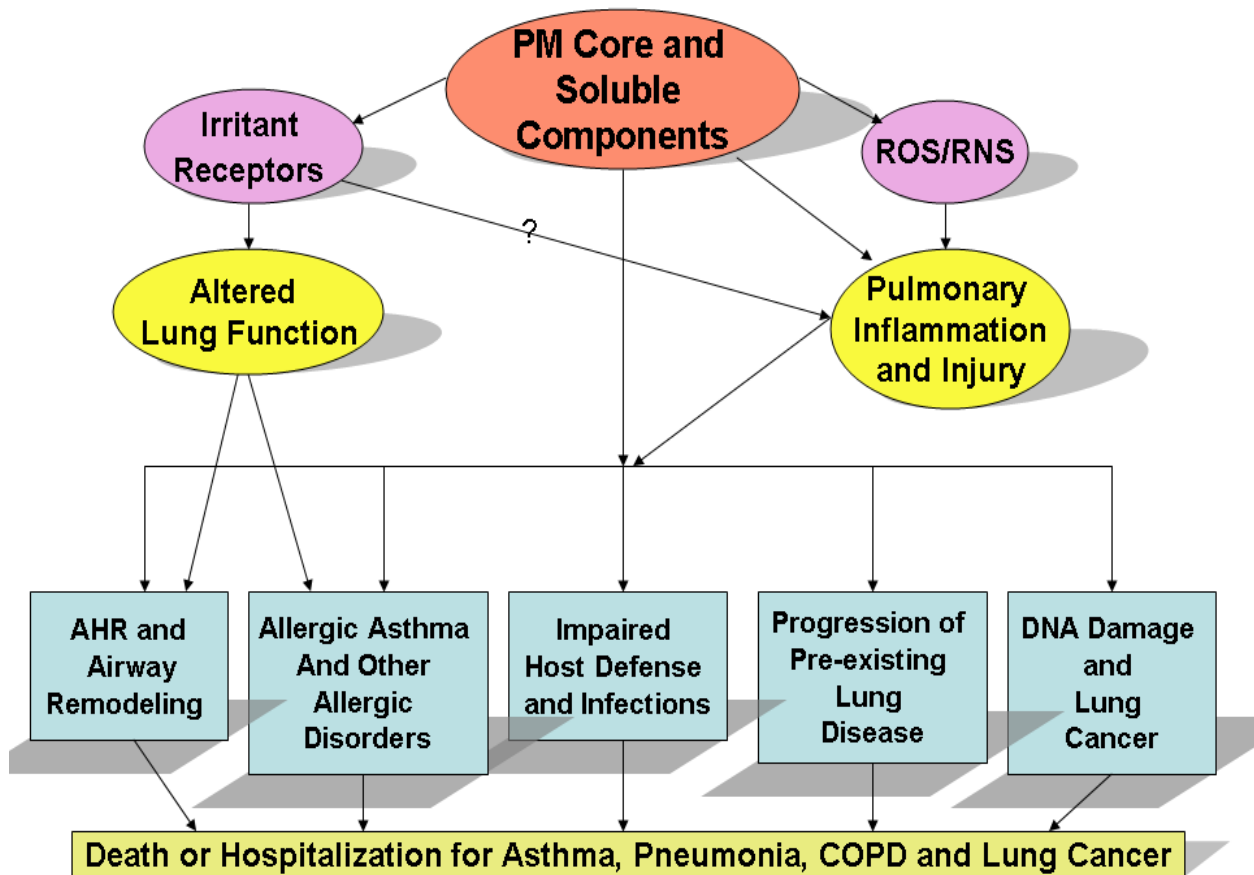


Figure 5-4. Potential pathways for the effects of PM on the respiratory system.

8 Cellular and tissue exposure to xenobiotics carried by PM can lead to induction of
 9 Phase 1 and Phase 2 detoxifying enzymes following the activation of cell signaling
 10 pathways and transcription factors AhR and ARE, respectively (Rengasamy et al., 2003,
 11 [156907](#); Rouse et al., 2008, [156930](#); Zhao et al., 2006, [100996](#)).

5.1.6. Pulmonary Function

1 PM exposure may alter pulmonary function by a variety of different mechanisms
2 (Figure 5-4). In the short term, airway hyperresponsiveness (AHR) may ensue due to the
3 influence of inflammatory mediators. In the long-term, morphological changes may occur, in
4 some cases leading to mucus hypersecretion and airway remodeling. Activation of irritant
5 receptors and stimulation of the ANS in the respiratory tract is another mechanism by
6 which PM exposure may alter pulmonary function (Section 5.3).

5.1.7. Allergic Disorders

7 PM exposure sometimes leads to the development of allergic immune responses
8 (Figure 5-4). These responses are predominately mediated by T helper 2 cells (Th2). Th1
9 responses, characterized by IFN- γ and classical macrophage activation, are inflammatory;
10 in excess they can lead to tissue damage. Alternatively, Th2 responses are associated with
11 allergy and asthma and are characterized by IL-4, IL-5, IL-13, influx of eosinophils, β -
12 lymphocyte production of IgE, and alternative macrophage activation. PM exposure can
13 also lead to the exacerbation of airway allergic responses, such as antigen-specific IgE
14 production and AHR.

15 Due to soluble mediators and immune cell trafficking, pulmonary exposure may result
16 in systemic immune alterations. Not only do macrophages ingest PM, but they are also
17 antigen presenting cells whose level of activation dictates costimulation and thus
18 subsequent T cell responses. These cells are highly mobile, and can transport PM to other
19 sites such as lymph nodes. Dendritic cells (DC) also play a key role as antigen presenting
20 cells and in modulating T and B cell activity. A cell culture model of the human epithelial
21 airway wall was used to demonstrate that DC extended processes between epithelial cells
22 through the tight junctions, collected particles in the luminal space and transported them
23 across the epithelium (Blank et al., 2007, [096521](#)). DC also transmigrated through the
24 epithelium to take up particles on the epithelial surface (Blank et al., 2007, [096521](#)).
25 Furthermore, DC interacted with particle-loaded macrophages on top of the epithelium and
26 with other DC within or beneath the epithelium to transfer particles (Blank et al., 2007,
27 [096521](#)). In vitro studies also demonstrated that the adjuvant activity of diesel exhaust
28 particles (DEPs) involved stimulation of immature monocyte-derived dendritic cells
29 (iMDDC) to undergo maturation in response to an altered airway epithelial cell-derived
30 microenvironment (Bleck et al., 2006, [096560](#)). Additionally, DEP directly influenced the
31 profile of cytokines secreted by DC and caused a predisposition toward Th2-mediated or
32 allergic responses (Chan et al., 2006, [097468](#)). Thus PM can negatively affect both innate
33 immunity through effects on macrophage pathogen handling (see Section 5.1.8) as well as
34 adaptive immunity by altering macrophage or DC antigen presenting activity and
35 subsequent T cell responses.

1 Given their larger surface area and particle number per unit mass as well as their
2 propensity for trans-epithelial movement, ultrafine PM may have a disproportionate ability
3 to enhance allergic sensitization compared with particles of larger size.

5.1.8. Impaired Lung Defense Mechanisms

4 PM exposure may impair lung defense mechanisms and result in frequent or
5 persistent infections (Figure 5-4). Potential targets include mucociliary transport,
6 surfactant function and pathogen clearance. Pathogen clearance is dependent on the
7 integrity of macrophages and their migration, phagocytosis and respiratory burst functions.
8 PM-mediated cytotoxicity of macrophages with the concomitant release of lysosomal
9 contents may affect pathogen clearance and cause damage to nearby cells and tissues.
10 Intratracheal instillation and cell culture experiments have demonstrated PM-dependent
11 impairment of lung defense mechanisms (Jaspers et al., 2005, [088115](#); Kaan and Hegele,
12 2003, [095753](#); Long et al., 2005, [087454](#); Moller et al., 2005, [156770](#); Monn et al., 2003,
13 [052418](#); Roberts et al., 2007, [097623](#); Yin et al., 2004, [087983](#)).

5.1.9. Resolution of Inflammation/Progression or Exacerbation of Disease

14 Resolution of pulmonary inflammation and injury has been demonstrated in many
15 experimental models using higher than ambient concentrations of PM. Factors contributing
16 to this complex process are likely to include the uptake and clearance of PM by
17 macrophages; the retention of PM in parenchymal cells and tissues; the balance of
18 pro/anti-inflammatory soluble mediators, oxidants/antioxidants and proteases/anti-
19 proteases; and the presence of pre-existing disease. These factors may also influence the
20 resolution of pulmonary responses to ambient PM exposures (Figure 5-4). The long-term
21 consequences of prolonged inflammation are not likely to be beneficial and may lead to
22 remodeling of the respiratory tract and to the progression or exacerbation of disease.

5.1.9.1. Factors Affecting the Retention of PM

23 Clearance of poorly soluble particles from ET, TB and alveolar regions is extensively
24 discussed in Section 4.3. While clearance from ET and TB regions generally occurs over
25 hours to days, clearance from the alveolar compartment is much slower, occurring over
26 months to years depending on the species. Phagocytosis by alveolar macrophages and
27 transport by the mucociliary escalator is the primary mechanism of clearance from the
28 alveolar compartment although neutrophil phagocytosis also plays a role (Snipes et al.,
29 1997, [156092](#)). Pre-existing disease can alter the extent and localization of PM deposition as
30 discussed in Section 4.2.4.5 and 4.2.5. In addition, mechanisms of clearance may be altered

1 in cases of pre-existing disease as discussed in Section 4.3.4.3. While mild asthma was
2 associated with enhanced mucociliary clearance, acute lung injury was associated with
3 enhanced translocation to the circulation and the interstitial compartment. Whether
4 retained particles are localized in alveolar macrophages or parenchymal tissue also differs
5 according to species (Snipes, 1996, [076041](#)).

6 Ultrafine PM may have a special propensity for retention given the decreased
7 efficiency of alveolar macrophages for phagocytosis of this size particle (Oberdörster, 1988,
8 [006857](#)) and the demonstration that ultrafine PM can readily cross cellular membranes
9 (Geiser et al., 2005, [087362](#)). Some studies suggest that ultrafine PM are taken up by
10 epithelial cells and move to the interstitium where they are cleared by other pathways
11 (Semmler-Behnke et al., 2007, [156080](#)); however clearance mechanisms are not entirely
12 understood.

13 Enhanced deposition of particles in “hot spots” may influence retention. For example,
14 deposition in the centriacinar region or proximal alveolar region, where clearance is slow,
15 may result in accumulated particle dose in this region and the potential for prolonged
16 inflammation at the site leading to the development of pulmonary fibrosis or emphysema
17 (Donaldson et al., 2008, [190217](#)). A recent study suggests an important role for retained
18 particles in the progression of disease. Complexation of endogenous iron by retained
19 particles resulted in retained particles growing larger over time. The authors suggested
20 that redox cycling of complexed iron may be responsible for disease progression (Ghio and
21 Cohen, 2005, [088272](#); Ghio et al., 2004, [155790](#)).

5.1.9.2. Factors Affecting the Balance of Pro/Anti-Inflammatory Mediators, Oxidants/Anti-Oxidants and Proteases/Anti-Proteases

22 Inflammation can be enhanced by pro-inflammatory mediators or dampened by anti-
23 inflammatory mediators. Production of anti-inflammatory mediators normally occurs at
24 several steps of the inflammation pathway, such as the release of IL-8 and TGF- β during
25 phagocytosis of apoptotic neutrophils by macrophages (Cowburn et al., 2008, [191142](#)).
26 Dysregulation of the inflammatory process may prevent the resolution of inflammation. PM
27 exposure may result in the production of pro-inflammatory mediators as well as decrease
28 the production of anti-inflammatory mediators by impairing macrophages function.

29 An unfavorable balance of oxidants to antioxidants in the lung is associated with
30 inflammatory lung diseases including asthma and COPD (Rahman et al., 2006, [191165](#)).
31 PM is likely to contribute to an unfavorable balance through its oxidative potential and
32 capacity to promote cellular production of ROS. Exacerbations of asthma and COPD
33 resulting from bacterial and viral infections are also associated with increased oxidative
34 stress (Barnes, 2007, [191139](#)). In addition, antioxidants may reduce neutrophilic
35 inflammation associated with oxidative stress (Barnes, 2007, [191139](#)).

1 Protease/anti-protease balance has long been tied to the pathogenesis of emphysema
2 and other forms of COPD (Owen, 2008, [191162](#)). Key steps include the release of
3 proteinases by inflammatory cells which degrade the extracellular matrix components of
4 alveolar walls. Destruction of alveolar walls and airspace enlargement ensues. Endogenous
5 anti-protease defenses in the lung modulate this response but may be insufficient to
6 prevent it during prolonged inflammation. Proteases also play a role in airways pathologies
7 which lead to small airway fibrosis (Owen, 2008, [191162](#)). Oxidative stress has been linked
8 to both activation of proteases and inactivation of anti-proteases (Owen, 2008, [191162](#)). PM
9 may contribute to an unfavorable protease/anti-protease balance through the generation of
10 ROS.

11 Although there are numerous inflammatory cell-derived proteases and lung anti-
12 proteases, many recent studies have focused on matrix metalloproteinases (MMPs). MMPs
13 are a family of zinc-containing enzymes normally found in an inactive pro-enzyme form.
14 Activation involves proteolytic cleavage or oxidation of the “cysteine switch” (Pardo and
15 Selman, 2005, [191163](#)). Inhibitors include tissue inhibitors of metalloproteinases (TIMPs)
16 (Pardo and Selman, 2005, [191163](#)). In particular, MMP-1 is well-studied and found to play
17 an important role in physiological processes such as development and wound repair as well
18 as in diseases such as pulmonary emphysema, fibrosis, asthma and bronchial carcinoma (Li
19 et al., 2009, [190424](#); Pardo and Selman, 2005, [191163](#)). In addition to its activity in
20 degrading collagenase, MMP-1 also acts on non-matrix substrates and cell surface
21 molecules suggesting that it may influence cell signaling (Pardo and Selman, 2005, [191163](#)).
22 MMP-2 and MMP-9 are thought to be involved in the pathogenesis of disease through their
23 gelatinase activity. Interestingly, recent in vitro studies have demonstrated upregulation of
24 MMP-1 by hydrogen peroxide, cigarette smoke and DEPs (Amara et al., 2007, [156212](#); Li et
25 al., 2009, [190424](#); Mercer et al., 2004, [191180](#)), and up-regulation of MMP-12 following
26 instillation of PM collected from the Paris subway (Bachoual et al., 2007, [155667](#)). These
27 considerations suggest that particulate air pollution may act via MMP-mediated
28 progression or exacerbation of lung disease.

5.1.9.3. Pre-Existing Disease

29 In addition to its effects on deposition, retention and clearance of PM described above,
30 pre-existing disease may also affect the balance of the afore-mentioned factors. For
31 example, acute exacerbations of COPD are characterized by a rapid influx of neutrophils
32 into the airways (Owen, 2008, [191162](#)). However, clearance of apoptotic neutrophils by
33 macrophages is impaired in COPD leading to greater release of neutrophil-derived
34 inflammatory mediators, oxidants and proteases (Owen, 2008, [191162](#)). Thus exacerbation
35 of disease may occur as a result of unchecked inflammation.

5.1.10. Pulmonary DNA Damage

1 Pulmonary DNA damage can occur primarily or secondarily to PM exposure. Primary
2 effects include oxidative DNA injury or DNA adduct formation due directly to PM while
3 secondary effects occur due to PM-mediated inflammation (Gallagher et al., 2003, [140171](#);
4 Gábelová et al., 2007, [156457](#); Schins and Knaapen, 2007, [156074](#); de Kok et al., 2005,
5 [189835](#)). These responses may lead to chromosomal aberrations or DNA strand breaks. PM
6 effects on cell cycle arrest, proliferation, apoptosis, and DNA repair mechanisms may also
7 influence the genotoxic, mutagenic or carcinogenic potential of DNA damage as reviewed by
8 Schins et al. (2007, [156074](#)).

5.1.11. Epigenetic Changes

9 Epigenetic mechanisms regulate the transcription of genes without altering the
10 nucleotide sequence of DNA. These mechanisms generally involve DNA methylation and
11 histone modifications, leading to alterations which may have long-term consequences or are
12 heritable (Jones et al., 2007, [156615](#); Keverne and Curley, 2008, [191154](#)). DNA methylation
13 and histone modifications, which include methylation, acetylation, phosphorylation,
14 ubiquitylation and sumoylation, are known to be linked (Hitchler and Domann, 2007,
15 [191151](#); Jones and Baylin, 2007, [191153](#)). Numerous studies have identified epigenetic
16 processes in the control of cancer (Foley et al., 2009, [191144](#); Gopalakrishnan et al., 2008,
17 [191147](#); Jones and Baylin, 2007, [191153](#); Valinluck et al., 2004, [191170](#)), embryonic
18 development (Foley et al., 2009, [191144](#); Gopalakrishnan et al., 2008, [191147](#); Keverne and
19 Curley, 2008, [191154](#)) and inflammation and other immune system functions (Adcock et al.,
20 2007, [191178](#)).

21 Epigenetic modifications resulting in decreased expression of tumor suppressor genes
22 and increased expression of transforming genes have been observed in human tumors
23 (Valinluck et al., 2004, [191170](#)). In general, transcription repression is associated with DNA
24 methylation in promoter regions of genes. Cytosine methylation in CpG dinucleotides has
25 emerged as an important, heritable epigenetic modification which can result in chromatin
26 remodeling and decreased gene expression (Valinluck et al., 2004, [191170](#)). Global changes
27 in DNA methylation are also seen in cancer and hypomethylation is associated with
28 genomic instability (Gopalakrishnan et al., 2008, [191147](#)).

29 Embryonic development is characterized by several phases of epigenetic
30 modifications. DNA methylation is very dynamic following fertilization, with demethylation
31 and re-methylation of egg and sperm genomes occurring immediately (Foley et al., 2009,
32 [191144](#)). Imprinted genes, however, retain the methylation profile of the parent of origin
33 (Foley et al., 2009, [191144](#)). Epigenetic changes accumulated through a life course may be
34 passed from parent to offspring in the germline (i.e germline transmission of epimutation) if
35 they survive the epigenetic remodeling that occurs during gametogenesis and early

1 embryogenesis (Foley et al., 2009, [191144](#)). Early development is characterized by the
2 process of cell differentiation, which produces different cell types and involves the selective
3 activation of some sets of genes and the silencing of others in a temporal pattern (Foley et
4 al., 2009, [191144](#); Gopalakrishnan et al., 2008, [191147](#)). DNA methylation is postulated to
5 provide a basis for cell differentiation (Gopalakrishnan et al., 2008, [191147](#)).

6 In the lung, histone acetylation and methylation have been linked to inflammatory
7 gene expression, T cell differentiation, and the regulation of macrophage function following
8 pathogen challenge (Adcock et al., 2007, [191178](#)). Furthermore, altered patterns of
9 methylation and acetylation have been reported in inflammatory diseases (Adcock et al.,
10 2007, [191178](#)). Histone deacetylase has been identified as a potential therapeutic target for
11 epigenetic therapy (Adcock et al., 2007, [191178](#); Jones and Baylin, 2007, [191153](#)). Reduced
12 expression and activity of histone deacetylase have been demonstrated in lung and
13 inflammatory cells in COPD and asthma (Adcock et al., 2007, [191178](#); Barnes, 2007,
14 [191139](#)).

15 Epigenetic mechanisms have been identified as potential targets for gene-
16 environment interactions and recent studies have demonstrated that diet, cigarette
17 smoking, endocrine disrupters, heavy metals and bacterial infection can alter the epigenetic
18 profile in animals and humans (Foley et al., 2009, [191144](#)). A role for PM in promoting
19 epigenetic changes has been proposed and new studies, discussed in later chapters, provide
20 some evidence for this pathway (Baccarelli et al., 2009, [188183](#); Liu et al., 2008, [156709](#);
21 Reed et al., 2008, [156903](#); Tarantini et al., 2009, [192010](#); Tarantini et al., 2009, [192153](#);
22 Yauk et al., 2008, [157164](#)). Early life exposures may be especially important in this regard
23 since periods of rapid cell division and epigenetic remodeling are likely to occur at this time
24 (Foley et al., 2009, [191144](#); Keverne and Curley, 2008, [191958](#); Wright and Baccarelli, 2007,
25 [191173](#)). This may provide a basis for fetal origins of adult disease.

26 It has been suggested that DNA methylation is regulated by oxygen gradients and
27 redox status (Hitchler and Domann, 2007, [191151](#)). While this is of particular importance
28 during development where oxygen gradients and redox status are linked to cellular
29 differentiation, these processes are also important for cell signaling during all stages of life.
30 A common metabolic precursor for both methylation reactions and glutathione availability
31 (involved in redox status) is methionine (Hitchler and Domann, 2007, [191151](#)). Methionine
32 availability regulates the cell's ability to generate S-adenosyl methionine which is directly
33 involved in DNA and histone methylation and the cell's ability to generate
34 homocysteine/cysteine which is involved in glutathione biosynthesis (Hitchler and Domann,
35 2007, [191151](#)). Furthermore the folate cycle is a key determinant of methionine
36 bioavailability (Hitchler and Domann, 2007, [191151](#)). In this way cellular intermediary
37 metabolism is linked to epigenetic processes, with oxidative stress necessitating a metabolic
38 shift resulting in decreased DNA methylation and increased glutathione production.

5.1.12. Lung Development

1 Lung development is a multi-step process which begins in embryogenesis and
2 continues to adult life (Pinkerton and Joad, 2006, [091237](#)). This allows for a long period of
3 potential vulnerability to environmental and other stressors. Furthermore, enzymatic
4 systems responsible for detoxification of xenobiotic compounds are not fully developed until
5 the postnatal period (Pinkerton and Joad, 2006, [091237](#)). Disruption of cell signaling during
6 development could affect cellular differentiation, branching morphogenesis and overall lung
7 growth, possibly leading to life-long consequences. Although very little is known about the
8 effects of maternal exposure to PM on the fetus or the effects of exposure during childhood,
9 recent animal studies demonstrate respiratory and immune system effects of perinatal
10 exposure to sidestream cigarette smoke (Pinkerton and Joad, 2006, [091237](#); Wang and
11 Pinkerton, 2007, [179975](#)).

5.2. Systemic Inflammation

12 Pulmonary inflammation resulting from PM exposure may trigger systemic
13 inflammation through the action of cytokines and other soluble mediators which leave the
14 lung and enter the circulation (Figure 5-5). Epithelial permeability may exert an important
15 influence on this process (see Section 5.1.4.) Cytokines released by alveolar macrophages
16 can stimulate bone marrow production of leukocytes resulting in an increased number of
17 total and immature leukocytes in the circulation (Van Eeden and Hogg, 2002, [088111](#); Van
18 Eeden et al., 2001, [019018](#)). They also activate neutrophils and promote their sequestration
19 in microvascular beds (Van Eeden et al., 2001, [019018](#)). The time course of these responses
20 varies according to the acute or chronic nature of the PM exposure (van Eeden et al., 2005,
21 [157086](#)).

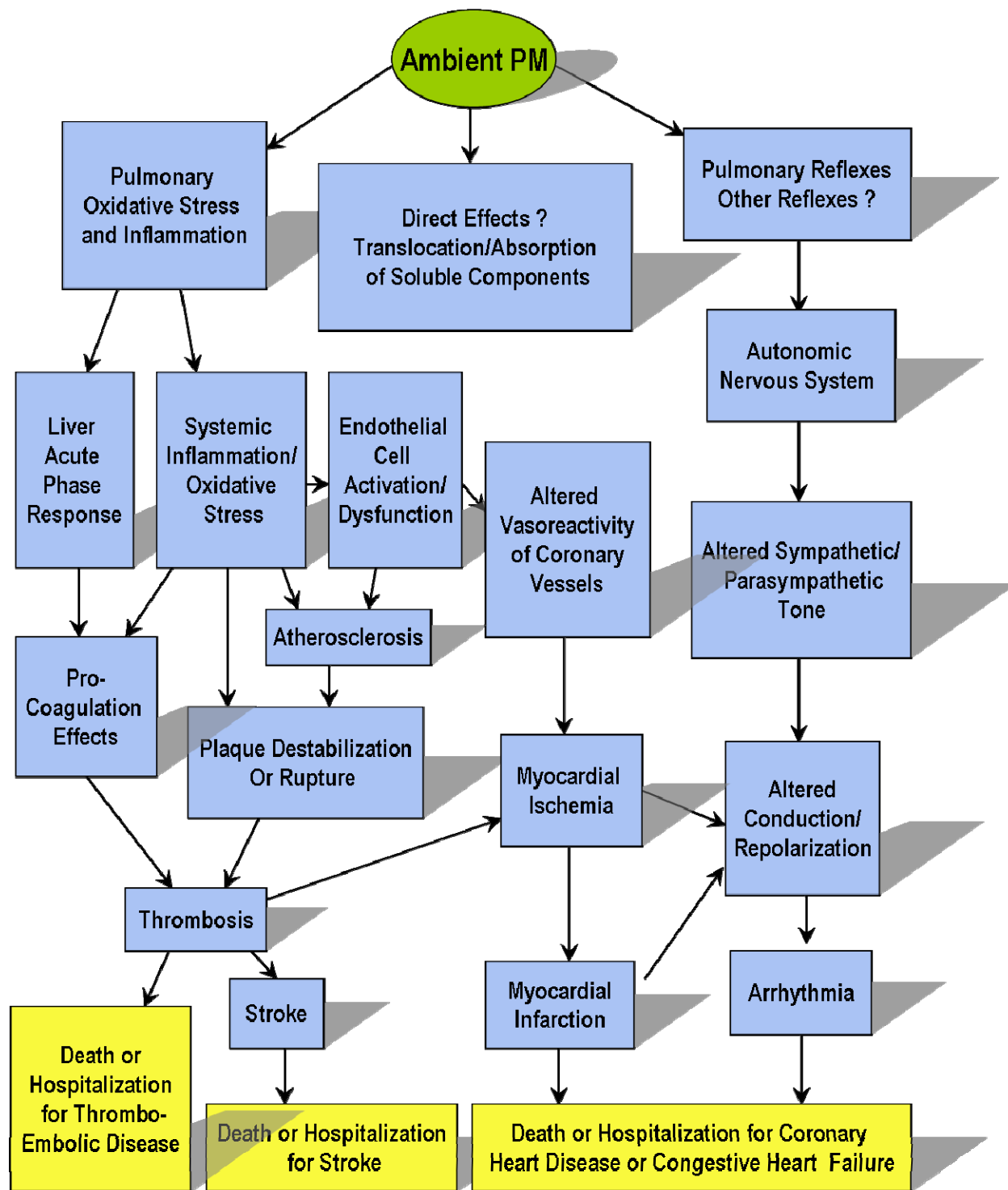


Figure 5-5. Potential pathways for the effects of PM on the cardiovascular system.

- 1 Systemic inflammation is seen under conditions of mild pulmonary inflammation –
- 2 and sometimes under conditions of no measurable pulmonary inflammation – following PM
- 3 exposure. The time-dependent nature of pulmonary and systemic inflammatory responses

1 may in part explain these findings since biomarkers of inflammation are frequently
2 measured only at one time point. Furthermore, chronic exposures may lead to adaptive
3 responses. In general, systemic inflammation is associated with changes in circulating
4 white blood cells, the acute phase response, pro-coagulation effects, endothelial dysfunction
5 and the development of atherosclerosis (Figure 5-5). Adverse effects on the cardiovascular
6 and cerebrovascular systems such as thrombosis, plaque rupture, MI and stroke may
7 result. Systemic inflammation may affect other organ systems such as the liver or the CNS.

8 One recent study demonstrated that alveolar macrophage-derived IL-6 mediated
9 pro-coagulation effects in mice exposed by intratracheal instillation to PM₁₀ (Mutlu et al.,
10 2007, [121441](#)). This study provides a clear link between lung cytokines and systemic
11 responses in one model system. Whether this mechanism or others account for the majority
12 of extra-pulmonary effects following PM exposure is not yet known.

5.2.1. Endothelial Dysfunction and Altered Vasoreactivity

13 The luminal surface of blood vessels is lined by endothelial cells which, in addition to
14 providing a barrier function, are key regulators of vascular homeostasis. Endothelial cells
15 synthesize and release vasodilators such as nitric oxide (NO) and prostacyclin and
16 vasoconstrictors such as endothelin (ET), which act on neighboring smooth muscle cells. ET
17 also stimulates endothelial NO synthesis through a feedback mechanism. Inhalation of
18 high concentrations of PM has been reported to increase ET levels in the circulation
19 (Thomson et al., 2005, [087554](#)). ET has also been proposed to play a role in hypoxia-induced
20 MI (Caligiuri et al., 1999, [156318](#)). However the role of ET in mediating cardiovascular
21 effects following ambient PM exposures is unclear.

22 Endothelial dysfunction can lead to or follow endothelial activation under conditions
23 of systemic inflammation and/or vascular oxidative stress. Both systemic inflammation and
24 vascular oxidative stress have been associated with PM exposure (Nurkiewicz et al., 2006,
25 [088611](#); Van Eeden et al., 2001, [019018](#)). Cytokines activate endothelial cells and
26 upregulate endothelial cell adhesion molecules. They also promote the sequestration of
27 neutrophils in microvascular beds. Neutrophil sequestration is sometimes associated with
28 the deposition of myeloperoxidase (MPO) on endothelial cell surfaces (Nurkiewicz et al.,
29 2006, [088611](#)). ROS-derived from neutrophils, MPO, other adhered inflammatory cells
30 and/or other sources can perturb the balance of vasodilator and vasoconstrictor species
31 produced by endothelial cells. Oxidative stress can result in decreased synthesis of NO due
32 to limitation of the redox-sensitive essential cofactor tetrahydrobiopterin and in decreased
33 bioavailability of NO due to reaction with superoxide. Prostacyclin synthesis is also
34 decreased by oxidative stress. Importantly, these processes can affect vasoreactivity such
35 that blood vessels may be unable to respond to vasoconstrictor stimuli with compensatory
36 vasodilation.

1 Loss of NO and prostacyclin synthesis due to PM-dependent vascular oxidative stress
2 may have other consequences since both exert negative influences on platelet and
3 neutrophil activation. While endothelial surfaces normally are antithrombotic, endothelial
4 dysfunction can contribute to thrombus formation. Furthermore inflammation and
5 oxidative stress associated with endothelial dysfunction can contribute to the development
6 or progression of atherosclerosis (van Eeden et al., 2005, [157086](#)).

5.2.2. Activation of Coagulation and Acute Phase Response

7 The primary function of the coagulation cascade is to stop the loss of blood after
8 vascular injury by forming a fibrin clot. However in some cases, activation of coagulation
9 can promote intravascular thrombosis (Karoly et al., 2007, [155890](#)). It has been proposed
10 that air pollution-associated PM can activate clotting pathways and enhance the likelihood
11 of an obstructive cardiac ischemic event (e.g., MI) or cerebral event (e.g., stroke) (Seaton et
12 al., 1995, [045721](#)).

13 Coagulation is regulated by intrinsic and extrinsic pathways. The intrinsic pathway
14 occurs following activation of Factor XII and does not require the addition of an exogenous
15 agent (Mackman, 2005, [156722](#)). On the other hand, the extrinsic pathway is an inducible
16 signaling cascade that can be activated by tissue factor (TF) produced in response to
17 inflammation or endothelial injury (Karoly et al., 2007, [155890](#)).

18 In general, platelets, red blood cells (RBCs) and endothelial cells are effector cells for
19 inducing a pro-coagulant state in the vasculature. Circulating factors may enhance
20 coagulation or promote activation of platelets. Cytokines formed during tissue damage and
21 inflammation lead to TF induction. TF is the initiating stimulus for coagulation following
22 vascular injury or plaque erosion. Complexes of TF:Factor VIIa form on endothelial cell
23 surfaces and play a key role in thrombin generation by initiating the extrinsic blood
24 coagulation pathway (Gilmour et al., 2005, [087410](#)). Thrombin generates fibrin from
25 fibrinogen and amplifies the intrinsic pathway (Karoly et al., 2007, [155890](#)). TF and
26 thrombin also have pro-inflammatory actions independent of coagulation functions (Chu,
27 2005, [155730](#)); thus activation of coagulation may lead to or potentiate inflammation. von
28 Willebrand factor, produced by endothelial cells, also plays an important role in
29 coagulation.

30 The fibrinolytic system opposes these processes by facilitating the removal of a clot.
31 The fibrinolytic pathway is regulated by the ratio of tissue plasminogen activator (tPA) and
32 plasminogen activator inhibitor (PAI). Furthermore, the endothelial cell surface has
33 antithrombotic properties due to the expression of tissue factor pathway inhibitor (TFPI)
34 and thrombomodulin (Mackman, 2005, [156722](#)).

35 Inhibition of the fibrinolytic pathway, along with increased plasma viscosity, plasma
36 fibrinogen and Factor VII concentrations, contributes to a pro-thrombotic state (Gilmour et

1 al., 2005, [087410](#)). In acute lung injury, vascular cells have enhanced procoagulant activity
2 and impaired fibrinolytic activity (Gilmour et al., 2005, [087410](#)). In arterial atherosclerosis,
3 TF expression is increased within plaques. As a result, spontaneous plaque rupture may
4 trigger intravascular clotting (Karoly et al., 2007, [155890](#)).

5 Acute phase responses also play a role in hemostasis by exerting procoagulant effects.
6 Cytokines such as IL-6 stimulate the liver to produce acute phase proteins including C-
7 reactive protein (CRP), fibrinogen and antiproteases (van Eeden et al., 2005, [157086](#)). To
8 date, there is limited evidence supporting a role for ambient PM in stimulating acute phase
9 responses (Ruckerl et al., 2007, [156931](#) and reviewed therein; see also Sections 6.2.7.3 and
10 6.2.8.3).

5.2.3. Atherosclerosis

11 Atherosclerosis is a chronic progressive disease which contributes greatly to
12 cardiovascular disease (Libby, 2002, [192009](#)). Mainly a disease of the large arteries, it is
13 characterized by the accumulation of lipid and fibrous tissue in atheromas, or swellings of
14 the vessel wall (Libby, 2002, [192009](#)). Although a strong link is known to exist between
15 hypercholesterolemia and atherogenesis, recent studies demonstrate a key role for
16 inflammation in the initiation and progression of atherosclerosis (Libby, 2002, [192009](#)).
17 Furthermore, inflammation has the potential to promote thrombosis which can complicate
18 this disorder and lead to MI and stroke (Libby, 2002, [192009](#)). As discussed above, PM
19 exposure is associated with systemic inflammation, suggesting a potential role in the
20 development of atherosclerosis.

21 Atheroma formation in experimental animals fed a high fat diet begins with the
22 accumulation of modified lipoprotein particles in the arterial intima, as reviewed by Libby
23 (2002, [192009](#)). The modification of lipoprotein particles often involves oxidation. As
24 discussed above, PM exposure is associated with oxidative stress, suggesting a potential
25 role for PM in the modification of lipoprotein particles. Endothelial dysfunction may also be
26 key to these early events (Halvorsen et al., 2008, [191149](#)). Recent studies, which are
27 discussed in later chapters, demonstrate PM-dependent endothelial dysfunction
28 (Nurkiewicz et al., 2009, [191961](#)). As described by Libby (2002, [191157](#)), oxidative stress
29 leads to enhance lipid modification and uptake by endothelial cells and initiates an
30 inflammatory response by activating NFκB. As a result, cell adhesion molecules such as
31 vascular cell adhesion molecule-1 (VCAM-1) are upregulated and expressed in endothelial
32 cells. Pro-inflammatory cytokines associated with systemic inflammation may also
33 contribute to adhesion molecule upregulation. Subsequently, monocytes and T cell
34 lymphocytes adhere to the activated endothelium, then migrate into the tunica intima
35 directed by chemokines such as monocyte chemoattractant protein-1 (MCP-1) and IL-8.
36 Monocytes undergo transformation to tissue macrophages and later to foam cells. As a part

1 of this transformation, monocyte/macrophages express scavenger receptors and bind to and
2 internalize the modified lipoprotein particles. These cells secrete growth factors and
3 cytokines, produce ROS, replicate within the lesion and contribute to further lesion
4 progression. Macrophage colony-stimulating factor (M-CSF) and granulocyte-macrophage
5 colony-stimulating factor (GM-CSF) are thought to be involved in these latter steps which
6 eventually lead to the formation of a fatty streak. T cell lymphocytes also become activated
7 in the atheroma and secrete pro- or anti-inflammatory cytokines. Degranulation of mast
8 cells found in the atheroma may also play an important role in the lesion.

9 Atheroma progression involves the proliferation of smooth muscle cells, which is
10 stimulated by macrophage-derived growth factors (Libby, 2002, [192009](#)). This results in
11 smooth muscle accumulation in the lesion, the elaboration of extracellular matrix material
12 and the formation of a more bulky lesion which can occlude the arterial lumen. Matrix
13 proteins contribute to the evolution of the lesion from a fatty streak to a fibrous plaque.
14 Mechanisms which trigger plaque disruption, including endothelial erosions and plaque
15 rupture, can result in thrombosis as well as in further expansion of the lesion. Resident T
16 cells, mast cells and circulating platelets may also play a role in destabilizing plaques
17 (Halvorsen et al., 2008, [191149](#)). It is thought that most atheromatous lesions progress in a
18 discontinuous manner due to cycles of disruption, expansion and repair.

19 A major factor regulating plaque disruption is the thickness of the fibrous cap, with
20 more stable plaques characterized by a thick fibrous cap (Libby, 2002, [192009](#)). Collagen in
21 the fibrous cap can be degraded by proteases, especially MMPs. Inflammation in the intima
22 reduces collagen production by smooth muscle cells and promotes the expression and
23 activation of MMPs. ROS may mediate effects on MMP upregulation (Lund et al., 2009,
24 [180257](#)). Both macrophages and smooth muscle produce MMPs in the lesion areas
25 (Halvorsen et al., 2008, [191149](#)); fully differentiated macrophages selectively upregulate
26 certain MMPs with more destructive potential (Newby, 2008, [191161](#)). Rupture of the
27 fibrous cap allows pro-thrombotic factors within the plaque (e.g., TF) to come into contact
28 with coagulation factors in the blood possibly resulting in the formation of an occlusive
29 blood clot. However in some cases, blood fibrinolytic mechanisms minimize clot formation
30 and repair processes ensue. The result is a more fibrous plaque and/or an expanded lesion.
31 The proposed role of PM in activating coagulation pathways, which was discussed above,
32 may influence the outcome of plaque disruption.

33 In this manner oxidative stress, inflammation and pro-coagulant activity in the blood
34 are involved in the initiation and progression of atheromatous lesions as well as plaque
35 disruption and occlusive blood clot formation. PM exposure may contribute to these
36 pathways and in fact, studies described in later chapters demonstrate PM-dependent effects
37 on atherosclerosis progression (Araujo et al., 2008, [156222](#); Chen and Nadziejko, 2005,
38 [087219](#); Sun et al., 2005, [186814](#); Ying et al., 2009, [190111](#)).

5.2.4. Activation of the Autonomic Nervous System by Pulmonary Reflexes

1 Chemosensitive receptors, including rapidly activating receptors (RARs) and sensory
2 C-fiber receptors, are found at all levels of the respiratory tract and are sensitive to irritant
3 particles as well as to irritant gases (Alarie, 1973, [070967](#); Coleridge and Coleridge, 1994,
4 [156362](#); Widdicombe, 2006, [155519](#)). Activation of trigeminal afferents in the nose causes
5 CNS reflexes resulting in decreases in respiratory rate through a lengthened expiratory
6 phase, closure of the glottis, closure of the nares with increased nasal airflow resistance and
7 effects on the cardiovascular system such as bradycardia, peripheral vasoconstriction and a
8 rise in systolic arterial blood pressure (Alarie, 1973, [070967](#)). Sneezing, rhinorrhea and
9 vasodilation with subsequent nasal vascular congestion are also nasal reflex responses
10 involving the trigeminal nerve (Sarin et al., 2006, [191166](#)). Activation of vagal afferents in
11 the tracheobronchial and alveolar regions of the respiratory tract causes CNS reflexes
12 resulting in bronchoconstriction, mucus secretion, mucosal vasodilation, cough, apnea
13 followed by rapid shallow breathing and effects on the cardiovascular system such as
14 bradycardia and hypotension or hypertension (Coleridge and Coleridge, 1994, [156362](#);
15 Widdicombe, 2003, [157145](#); 2006, [155519](#); Widdicombe and Lee, 2001, [019049](#)). Some
16 evidence suggests that cardiovascular responses may be mediated primarily by the C-fiber
17 receptors (Coleridge and Coleridge, 1994, [156362](#)) and that irritants in the lower
18 respiratory tract cause more pronounced cardiovascular responses than irritants in the
19 upper respiratory tract (Widdicombe and Lee, 2001, [019049](#)).

20 Early experiments demonstrated that sectioning of the trigeminal nerve abrogated
21 irritant effects on respiratory rate, heart rate and systolic arterial blood pressure (Alarie,
22 1973, [070967](#)). These nasal reflexes were attributed to the ophthalmic branch of the
23 trigeminal nerve since they were identical to reflex responses following diving or immersion
24 of the face in water (Alarie, 1973, [070967](#)). Early experiments also demonstrated that non-
25 nasal reflexes were mediated by cholinergic parasympathetic pathways involving the vagus
26 nerve and inhibited by atropine (Grunstein et al., 1977, [071445](#); Nadel et al., 1965, [014846](#)).
27 More recent experiments have shown that noncholinergic mechanisms may also be
28 involved. For example, stimulation of C-fiber receptors can activate local axon reflexes.
29 These local axon pathways are responsible for secretion of neuropeptides and the
30 development of neurogenic inflammation (Widdicombe and Lee, 2001, [019049](#)). It has been
31 proposed that, in some cases, neurogenic pulmonary responses can switch from their
32 normally protective function to one that perpetuates pulmonary inflammation (Wong et al.,
33 2003, [097707](#)). Differences in respiratory tract innervation between rodents and humans
34 suggest that C-fiber mediated neurogenic inflammation may be more important in rodents
35 than in humans (Groneberg et al., 2004, [138134](#); 2003, [157145](#); Widdicombe and Lee, 2001,

1 [019049](#)). However the role of neurogenic inflammation in mediating pulmonary responses
2 in humans is an active area of investigation.

3 VR1 receptors represent a subset of neuropeptide and acid-sensitive irritant receptors
4 which belong to the transient receptor potential (TRP) family. They are located on the
5 sensory C-fibers which lie underneath and between lung epithelial cells and on immune
6 and non-immune airway cells. Recent research interest has focused on the role played by
7 these receptors in mediating inflammation following exposure to PM (Veronesi and
8 Oortgiesen, 2001, [015977](#)). Exposure to PM has been shown to result in an immediate
9 increase in intracellular calcium followed by the release of neuropeptides and inflammatory
10 cytokines (Veronesi et al., 1999, [048764](#); Veronesi et al., 2000, [017062](#)). In one study this
11 response was found to be due to an intrinsic property of the particle core and was not
12 metal-dependent (Oortgiesen et al., 2000, [013998](#)), while in another study electrostatic
13 charge was found to activate VR1 receptors (Veronesi et al., 2003, [094384](#)). PM-mediated
14 activation of VR1 receptors which results in increases in intracellular calcium and
15 apoptosis in epithelial cells has also been demonstrated (Agopyan et al., 2003, [155649](#)).
16 Recent studies, discussed in later chapters, provide evidence for the involvement of TRPV1
17 irritant receptor involvement in PM-dependent responses (Ghelfi et al., 2008, [156468](#);
18 Rhoden et al., 2005, [087878](#)).

19 Recently it has been proposed that pulmonary reflex responses may be modulated by
20 CNS plasticity (Bonham et al., 2006, [191140](#); Sekizawa et al., 2008, [191167](#)). Plasticity is a
21 property of neurons or synapses which allows change in response to previous events. In the
22 case of the respiratory tract, visceral afferent inputs to the CNS are integrated primarily in
23 the nucleus tractus solitarius (NTS) region of the brain (Bonham et al., 2006, [191140](#)).
24 Inputs from local networks, higher brain regions and circulating mediators contribute to
25 the reflex output (Bonham et al., 2006, [191140](#)). This integration allows for plasticity in
26 that repeated or prolonged exposure to a particular stimuli may lead to altered reflex
27 responses to the same or subsequent stimuli. An exaggerated reflex response was recently
28 observed in guinea pigs exposed to ETS for an extended period of time (Sekizawa et al.,
29 2008, [191167](#)). It is not known whether CNS plasticity influences responses following acute
30 and chronic exposure to ambient PM, but it is a mechanism that may possibly explain
31 hyperresponsiveness and/or adaptation of reflex-related responses.

32 At this time, it is not clear how activation of the ANS by pulmonary reflexes
33 contributes to the kinds of altered conduction and/or repolarization properties of the heart
34 which may be linked to arrhythmias (Figure 5-5). Pulmonary reflexes, as they are currently
35 understood, initially lead to increases in parasympathetic tone. However decreased heart
36 rate variability appears to be reflective of decreased parasympathetic tone and/or increased
37 sympathetic tone. A PM-dependent sympathetic stress response mediated by cytokines has
38 been postulated (Godleski et al., 2000, [000738](#)) but there is little new information to
39 support this mechanism. Thus activation of the autonomic nervous system by mechanisms

1 other than pulmonary reflexes seems likely in response to PM. Very little is known about
2 putative alternative mechanisms leading to sympathoexcitatory responses although one
3 study demonstrated a role for the olfactory bulb-NTS pathway in regulating cardiovascular
4 functions following smoke exposure (Moffitt et al., 2002, [191160](#)). In addition,
5 sympathoexcitatory responses occur during myocardial ischemia, mediated by the release of
6 adenosine or the production of ROS by the myocardium (Longhurst et al., 2001, [191158](#)).
7 Hence, PM-dependent effects leading to myocardial ischemia may stimulate
8 sympathoexcitatory responses. Furthermore, the effects of pre-existing alterations in the
9 ANS due to disease processes (e.g., increased sympathetic tone observed in cardiac
10 diseases) on PM responses are not understood. Possibly, integration of neural signals
11 resulting from pulmonary and cardiac reflexes at the level of the NTS may have an
12 influence on ANS responses to PM. Further investigation will be required to clarify these
13 mechanisms.

5.3. Translocation of Ultrafine PM or Soluble PM Components

14 Ultrafine PM translocate into cells through non-endocytotic mechanisms involving
15 adhesive interactions and diffusion (Geiser et al., 2005, [087362](#)), as described in Chapter
16 4.3.3.1. In this study, inhaled ultrafine particles rapidly crossed cell membranes of alveolar
17 epithelial cells and capillary endothelial cells but there was no measurable loss of PM from
18 the lung over 24 h. In another study, ultrafine PM were localized in macrophage
19 mitochondria as demonstrated by electron microscopy (Li et al., 2003, [042082](#)). Other
20 studies demonstrated extrapulmonary translocation of poorly soluble ultrafine PM but the
21 process was slow and resulted in only a small amount leaving the lung. It is possible that in
22 these studies PM gained access to the circulation after initial transport to the lymph nodes
23 or the gastrointestinal system. To date, there is limited evidence that ultrafine or other PM
24 size fractions access the circulation by traversing the epithelial barrier of the respiratory
25 tract.

26 However, soluble components from all size fractions of PM have the potential to
27 translocate across the airway epithelium into the bronchial circulation or across the
28 alveolar epithelium into the systemic circulation as depicted in Figure 5-5. Absorption
29 across nasal epithelium may also occur (Illum, 2006, [191205](#)). Factors affecting this process
30 include the rate of dissolution of the solute from the particle and the molecular weight of
31 the solute (see Section 4.4.1). It should be noted that the high surface/volume ratio
32 characteristic of ultrafine PM may lead to more rapid dissolution of soluble components
33 associated with this size fraction compared with larger particles

34 Several interesting studies investigated the translocation of water-soluble metals
35 from the lung. Gilmour et al. (2006, [156472](#)) demonstrated the rapid appearance of zinc in

1 the plasma of rats intratracheally instilled with zinc sulfate. Similarly, Wallenborn et al.
2 (2007, [156144](#)) demonstrated the rapid appearance of water-soluble metals in the blood,
3 heart and liver following intratracheal instillation of oil combustion PM in rats. Using a
4 more sensitive technique, these same investigators demonstrated the accumulation of ^{70}Zn ,
5 a rare isotope of zinc, in blood, heart and liver following intratracheal instillation of zinc
6 sulfate (Wallenborn et al., 2009, [191172](#)). In three other studies, soluble zinc and copper
7 were associated with cardiac effects following intratracheal instillation of rats with
8 different forms of zinc and copper-containing PM (Gilmour et al., 2006, [088489](#); Gottipolu et
9 al., 2008, [191148](#); Kodavanti et al., 2008, [155907](#)). These results suggest the possibility that
10 PM-derived soluble zinc and copper translocated across the alveolar-capillary barrier into
11 the circulation and exerted effects on the heart. However, in the two studies in which
12 barrier function was measured it was found to be compromised (Gilmour et al., 2006,
13 [088489](#); Gottipolu et al., 2008, [191148](#)) suggesting an acute lung injury response to
14 instillation of high concentrations of metal. Acute lung injury is not likely to occur in
15 healthy individuals exposed to PM at concentrations relevant to ambient levels. Cardiac
16 effects were also observed following subchronic inhalation exposure to low concentrations of
17 aerosolized zinc sulfate (Wallenborn et al., 2008, [191171](#)). Since it was not possible to
18 measure extrapulmonary zinc in this study, it remains unclear whether cardiac effects were
19 a direct effect of translocated zinc or an indirect effect of exposure to zinc-containing PM.
20 Nonetheless, translocation of soluble components derived from inhaled PM remains a viable
21 hypothesis to explain some extra-pulmonary effects.

22 Epithelial permeability is a key determinant of translocation and is discussed in
23 detail in Section 4.4.2. In brief, a number of studies have measured clearance of $^{99\text{m}}\text{Tc}$ -DTPA
24 as an index of alveolar epithelial membrane integrity and permeability of alveolar-capillary
25 barrier (Braude et al., 1986, [155701](#)). Endothelial integrity also contributes to the alveolar-
26 capillary barrier and is measured by transvascular protein flux but is not discussed here
27 (Braude et al., 1986, [155701](#)). Interestingly, epithelial permeability was transiently
28 increased in human volunteers following 3 h of moderate exercise but not following 24-h
29 exposure to particle-rich urban air (Brauner et al., 2009, [190244](#)). A previous study found
30 that the exercise-induced increase in epithelial permeability was transient and suggested
31 that it was due to increased ventilation and elevated vascular pressure which altered the
32 properties of tight junctions (Hanel et al., 2003, [155826](#)). Smokers (Jones et al., 1983,
33 [155884](#)) and individuals with acute respiratory distress syndrome (Braude et al., 1986,
34 [155701](#)) or interstitial lung disease (Rinderknecht et al., 1980, [191965](#)) also exhibited
35 increased alveolar epithelial permeability. The changes in smokers were reversible upon
36 cessation of smoking. In laboratory animals, increased alveolar permeability was
37 demonstrated in terminally senescent mice (Tankersley et al., 2003, [096363](#)). Clearance of
38 $^{99\text{m}}\text{Tc}$ -DTPA was also used to measure permeability of the bronchial mucosa in a study by
39 Ilowite (Ilowite et al., 1989, [156584](#)) which found increased airway epithelial permeability

1 in asthmatics. These studies demonstrate that epithelial permeability is increased following
2 moderate exercise and in lung syndromes associated with inflammation and suggest that
3 compromised epithelial barrier functions in the lung may contribute to PM-mediated
4 effects.

5 Interaction of circulating PM or soluble PM components with vascular endothelial
6 cells, platelets, and other leukocytes is a potential mechanism underlying the
7 cardiovascular and systemic effects of inhaled PM. A role for PM-derived ROS and/or
8 cellular-derived ROS has been proposed. Furthermore, soluble metals that do not
9 redox-cycle may activate cell signaling pathways without the generation of ROS. In this
10 way PM may promote adverse cardiovascular effects such as endothelial dysfunction,
11 atherosclerosis and thrombosis. Circulating PM or soluble PM components also have the
12 potential to impact other organ systems. However convincing evidence that this occurs to
13 an appreciable extent in healthy individuals following inhalation of PM at concentrations
14 relevant to ambient exposures is lacking.

5.4. Disease of the Cardiovascular and Other Organ Systems

15 As discussed above, deposition of PM in the lung may lead not only to pulmonary
16 disease but also to diseases of other systems (Figure 5-5). In the cardiovascular system,
17 myocardial ischemia and MI may occur as a result of the above proposed effects of PM on
18 atherosclerosis, plaque instability, thrombosis, plaque rupture and/or altered vasoreactivity
19 of coronary vessels. Myocardial ischemia and MI may alter the conduction and
20 depolarization properties of the heart and lead to arrhythmic events. In addition,
21 thrombosis may lead to stroke and/or thromboembolic disease. Many of these processes may
22 be interlinked and responses to ambient PM exposures may involve multiple mechanisms
23 simultaneously with some variability depending on PM composition. Furthermore, it is not
24 clear at this time whether PM initiates cardiovascular disease or whether it perturbs
25 existing disease.

26 In addition, recent studies which are discussed in later chapters have demonstrated
27 PM-dependent effects on the CNS (Campbell et al., 2005, [087217](#); Kleinman et al., 2008,
28 [190074](#); Sirivelu et al., 2006, [111151](#); Veronesi et al., 2005, [087481](#); Win-Shwe et al., 2008,
29 [190146](#)). At this time, it is not known whether this is a direct or indirect consequence of PM
30 exposure. Translocation of soluble and poorly soluble particles from the olfactory mucosa
31 via the axons to the olfactory bulb of the brain has been proposed as a possible mechanism
32 by which PM or its components may directly access the CNS. Evidence for this pathway is
33 discussed in Section 4.3.2.2. Given their small size, ultrafine PM deposited onto nasal
34 epithelium may be more efficiently translocated by this mechanism compared with larger
35 size PM. Alternative mechanisms proposed for PM-mediated CNS effects involve systemic

1 inflammation and autonomic responses. These are new and intriguing possibilities which
2 warrant further investigation.

3 PM-dependent effects on the reproductive system, reproductive outcomes and
4 perinatal development have also been identified and are discussed in a later chapter.
5 Mechanisms involved in these responses have not been determined. However it seems
6 possible that systemic inflammation and/or oxidative stress may play a role. Developmental
7 windows of susceptibility may also be a key consideration. Furthermore it has been
8 hypothesized that oxygen gradients and redox status are key to cell differentiation and
9 epigenetic processes occurring during development (see Section 5.1.11) (Hitchler and
10 Domann, 2007, [191151](#)).

5.5. Acute and Chronic Responses

11 In general, repeated acute responses may lead to cumulative effects which manifest as
12 chronic disease. Several examples relevant to the modes of action discussed in this chapter
13 are that of allergic responses, atherosclerosis and lung development. Allergic responses
14 require repeated exposures to antigen over time. Co-exposure to an adjuvant, possibly DEP
15 or ultrafine concentrated ambient particles (CAPs), can enhance this response.
16 Furthermore, the presence of oxidative stress, as may occur in response to PM, can
17 contribute to allergic responses. Allergic sensitization often underlies allergic asthma,
18 characterized by inflammation and AHR. In this way, repeated or chronic exposures
19 involving multifactorial responses (immune system activation, oxidative stress,
20 inflammation) can lead to irreversible outcomes. Similarly, the development of
21 atherosclerosis involves inflammation and remodeling of the blood vessel wall. Factors
22 contributing to this process include systemic inflammation, endothelial dysfunction,
23 oxidative stress and high levels of circulating lipids. PM exposure is associated with three
24 out of four of these processes. The role of PM in initiating, promoting or complicating this
25 disease or its outcomes has yet to be determined. Critical windows of susceptibility during
26 development also provide an opportunity for repeated exposures to injurious agents to lead
27 to irreversible changes in organ structure and function. The extended period of postnatal
28 lung development in humans and other species heightens this vulnerability. PM may serve
29 as such an injurious agent as has been demonstrated previously for hyperoxia (Randell et
30 al., 1990, [191956](#)).

31 Furthermore, adverse outcomes may be precipitated by acute events imposed on
32 chronic disease states. In the case of allergic asthma, acute PM exposure may provoke
33 asthmatic responses through oxidative stress and inflammatory pathways. Additionally, PM
34 can act as a carrier of aeroallergens and other biological materials which can potentially
35 trigger asthma attacks. Similarly, PM exposure may provoke inflammatory or thrombotic
36 responses leading to rupture of an atherosclerotic plaque which subsequently leads to acute

1 myocardial infarction. In this way, the outcome of an acute exposure to PM may be
2 drastically worsened by the underlying chronic disease.

5.6. Results of New Inhalation Studies which Contribute to Modes of Action

3 Prior to this review, much of the evidence for the proposed modes of action was
4 obtained from animal studies involving intratracheal instillation or inhalation of high
5 concentrations of PM and from cell culture experiments. In many cases, the types of PM
6 used were of questionable relevance to ambient exposures (i.e., high concentrations of
7 ROFA, metals and ambient PM collected on filters). Since then, many inhalation studies
8 have been conducted using CAPs, combustion-derived PM, urban air and carbon black,
9 generally using concentrations of PM lower than 1 mg/m³. Much of this research has been
10 conducted in animal models of disease. These key new studies, described in detail in
11 Chapters 6 and 7, add to the understanding of modes of action which are relevant to
12 ambient PM exposure. A compilation of pertinent results is found below.

- 13 ▪ Altered lung function including changes in respiratory frequency and AHR following
14 short-term exposures to CAPs and combustion-derived PM (Section 6.3.2.3)
- 15 ▪ Mild pulmonary inflammation in response to short-term exposures to CAPs, urban
16 air, combustion-derived PM and carbon black (Section 6.3.3.3)
- 17 ▪ Mild pulmonary injury in response to short-term exposure to CAPs and combustion-
18 derived PM (Section 6.3.5.3)
- 19 ▪ Inhibition of cell proliferation in the proximal alveolar region of neonatal animals
20 following short-term exposure to iron-soot (Section 6.3.5.3)
- 21 ▪ Pulmonary oxidative stress in response to short-term exposure to CAPs, urban air,
22 combustion-derived PM, carbon black and iron-soot; pulmonary nitrosative stress in
23 response to titanium dioxide (TiO₂) (Section 6.3.4.2)
- 24 ▪ Antioxidant intervention which ameliorates PM effects on oxidative stress, allergic
25 responses, and AHR (Sections 6.3.4.2)
- 26 ▪ Allergic sensitization and exacerbation of allergic responses in response to CAPs and
27 combustion-derived PM (Section 6.3.6.3)
- 28 ▪ Altered methylation of promoter regions of IFN-γ and IL-4 genes suggestive of pro-
29 allergic Th2 gene activation following short-term exposure to combustion-derived
30 PM in an allergy model (Section 6.3.6.3)

- 1 ▪ Increased susceptibility to respiratory infection following exposure to combustion-
2 derived PM (Section 6.3.7.2)
- 3 ▪ Effects on nasal epithelial mucosubstances, airway morphology and airway
4 mucosubstances following chronic exposure to urban air-derived PM and woodsmoke
5 (Section 7.3.5.1)
- 6 ▪ Worsening of papain-induced emphysema following chronic exposure to urban air-
7 derived PM (Section 7.3.5.1)
- 8 ▪ Effects on lung development following chronic exposure to urban air-derived PM
9 (Section 7.3.2.2 and 7.3.5.1)
- 10 ▪ Prolonged exposure to CAPs and combustion-derived PM leading sometimes to mild
11 pulmonary inflammation, oxidative stress and injury and sometimes to loss of
12 inflammatory, oxidative stress and AHR responses which were observed after short-
13 term exposures (Sections 7.3.2.2, 7.3.3.2, 7.3.5.1 and 7.3.6.2)
- 14 ▪ Hypermethylation of lung DNA following chronic exposure to combustion-derived
15 PM (Section 7.3.5.1)
- 16 ▪ A role for TRPV1 irritant receptors in activating local axon and CNS reflexes
17 following short term exposure to CAPs and combustion-derived PM (see
18 Section 6.2.9.3)
- 19 ▪ A role for TRPV1 irritant receptors in mediating lung and heart oxidative stress
20 through increased parasympathetic and sympathetic activity in response to CAPs.
21 (see Section 6.2.9.3 and 6.3.2.3)
- 22 ▪ Altered heart rate variability in response to CAPs, combustion-derived PM and
23 carbon black (Section 6.2.1.3)
- 24 ▪ Arrhythmic events in response to CAPs and combustion-derived PM
25 (Section 6.2.2.2)
- 26 ▪ Decreased cardiac contractility following short-term exposure to CAPs and carbon
27 black (Section 6.2.6.1)
- 28 ▪ Enhanced myocardial ischemia following short-term exposure to CAPs
29 (Section 6.2.3.3).

- 1 ▪ Endothelial dysfunction and altered vascular reactivity following short-term
2 exposure to CAPs, combustion-derived PM and TiO₂ (Section 6.2.4.3)
- 3 ▪ Increases in blood pressure following short-term exposure to CAPs and carbon black
4 (Section 6.2.5.3)
- 5 ▪ Changes in blood leukocyte counts following short-term exposure to CAPs and
6 carbon black (Section 6.2.7.3)
- 7 ▪ Increased levels of blood coagulation factors following short-term exposure to CAPs
8 and on-road highway aerosols (Section 6.2.8.3)
- 9 ▪ Systemic and cardiovascular oxidative stress in response to short-term exposure to
10 CAPs, road dust and combustion-derived PM (Section 6.2.9.3)
- 11 ▪ Progression of atherosclerosis, induction of TF in aortic plaques, vascular oxidative
12 stress and altered vasomotor function following long-term exposure to CAPs in a
13 susceptible animal model (Section 7.2.1.2)
- 14 ▪ Vascular remodeling following chronic exposure to urban air-derived PM
15 (Section 7.2.1.2).
- 16 ▪ Enhanced angiotensin II-induced hypertension accompanied by vascular oxidative
17 stress and altered vasoreactivity in response to chronic exposure to CAPs
18 (Section 7.2.5.2)
- 19 ▪ Exaggerated insulin resistance, visceral adiposity and systemic inflammation in
20 response to chronic exposure to CAPs and a high-fat diet (Section 7.2.3.1)
- 21 ▪ CNS responses following short- and long-term exposures to CAPs and combustion-
22 derived PM (Section 6.4.3)
- 23 ▪ Effects on the reproductive system, reproductive outcomes and perinatal
24 development following chronic exposure to urban-air derived PM (Section 7.4.2)
- 25 ▪ DNA adducts in nose, lung and liver following chronic exposure to urban air
26 (Section 7. 5.2)
- 27 ▪ Germ line mutations, DNA strand breaks and global hypermethylation in sperm
28 following chronic exposure to urban air-derived PM (Section 7.5.3)

29 These new studies confirm and extend findings from older studies. However this
30 increasing body of evidence does not provide a complete picture of the biological pathways

1 involved in mediating PM effects. For example, a lack of information regarding the time-
2 dependence of many responses makes it difficult to understand the underlying biological
3 mechanisms. Existing gaps in knowledge include:

- 4 ▪ The spatial distribution of retained particles in the lung and its impact
- 5 ▪ The deposition, uptake and clearance of ultrafine particles in the lung
- 6 ▪ Effects of ambient PM exposures on epithelial barrier function in the lung
- 7 ▪ Time dependence of responses
- 8 ▪ The putative modulation of neural reflexes by pre-existing disease or other factors.
- 9 ▪ The putative role of neural reflexes besides those involving pulmonary irritant
10 receptors
- 11 ▪ The putative role of ET in altering vasomotor tone following PM exposure
- 12 ▪ The putative translocation of PM or soluble components across the epithelial barrier
13 of the lung into the circulation
- 14 ▪ The putative translocation of PM from olfactory epithelium to the olfactory bulb and
15 other brain regions.

16 Additional studies will be required to clarify the biological mechanisms underlying
17 the health effects of PM.

Chapter 5 References

- Adamson I; Frieditis H. (1995). Response of mouse lung to carbon deposition during injury and repair. *Environ Health Perspect*, 103: 72-76. [189982](#)
- Adcock IM; Tsaprouni L; Bhavsar P; Ito K. (2007). Epigenetic regulation of airway inflammation. *Curr Opin Allergy Clin Immunol*, 19: 694-700. [191178](#)
- Agopyan N; Bhatti T; Yu S; Simon SA. (2003). Vanilloid receptor activation by 2- and 10- μ m particles induces responses leading to apoptosis in human airway epithelial cells. *Toxicol Appl Pharmacol*, 192: 21-35. [155649](#)
- Ahsan MK; Nakamura H; Tanito M; Yamada K; Utsumi H; Yodoi J. (2005). Thioredoxin-1 suppresses lung injury and apoptosis induced by diesel exhaust particles (DEP) by scavenging reactive oxygen species and by inhibiting DEP-induced downregulation of Akt. *Free Radic Biol Med*, 39: 1549-1559. [156200](#)
- Alarie Y. (1973). Sensory irritation by airborne chemicals. *Crit Rev Toxicol*, 2: 299-363. [070967](#)
- Amara N; Bachoual R; Desmard M; Golda S; Guichard C; Lanone S; Aubier M; Ogier-Denis E; Boczkowski J. (2007). Diesel exhaust particles induce matrix metalloproteinase-1 in human lung epithelial cells via a NADPH oxidase/NOX4 redox-dependent mechanism. *Am J Physiol Lung Cell Mol Physiol*, 293: L170-181. [156212](#)
- Araujo JA; Barajas B; Kleinman M; Wang X; Bennett BJ; Gong KW; Navab M; Harkema J; Sioutas C; Lusis AJ; Nel AE. (2008). Ambient particulate pollutants in the ultrafine range promote early atherosclerosis and systemic oxidative stress. *Circ Res*, 102: 589-596. [156222](#)
- Ayres JG; Borm P; Cassee FR; Castranova V; Donaldson K; Ghio A; Harrison RM; Hider R; Kelly F; Kooter IM; Marano F; Maynard RL; Mudway I; Nel A; Sioutas C; Smith S; Baeza-Squiban A; Cho A; Duggan S; Froines J. (2008). Evaluating the Toxicity of Airborne Particulate Matter and Nanoparticles by Measuring Oxidative Stress Potential - A Workshop Report and Consensus Statement. *Inhal Toxicol*, 20: 75 - 99. [155666](#)
- Baccarelli A; Martinelli I; Pegoraro V; Melly S; Grillo P; Zanobetti A; Hou L; Bertazzi PA; Mannucci PM; Schwartz J. (2009). Living near Major Traffic Roads and Risk of Deep Vein Thrombosis. *Circulation*, x: x. [188183](#)
- Bachoual R; Boczkowski J; Goven D; Amara N; Tabet L; On D; Lecon-Malas V; Aubier M; Lanone S. (2007). Biological effects of particles from the paris subway system. , 20: 1426-1433. [155667](#)
- Barnes PJ. (2007). New molecular targets for the treatment of neutrophilic diseases. , 119: 1055-62; quiz 1063-4. [191139](#)
- Bayram H; Ito K; Issa R; Ito M; Sukkar M; Chung KF. (2006). Regulation of human lung epithelial cell numbers by diesel exhaust particles. *Eur Respir J*, 27: 705-713. [088439](#)
- Becher R; Bucht A; Ovrevik J; Hongslo Jan K; Dahlman Hans J; Samuelsen Jan T; Schwarze Per E. (2007). Involvement of NADPH Oxidase and iNOS in Rodent Pulmonary Cytokine Responses to Urban Air and Mineral Particles. , 19: 645-55. [097125](#)
- Beck-Speier I; Dayal N; Karg E; Maier KL; Schumann G; Schulz H; Semmler M; Takenaka S; Stettmaier K; Bors W; Ghio A; Samet JM; Heyder J. (2005). Oxidative stress and lipid mediators induced in alveolar macrophages by ultrafine particles. *Free Radic Biol Med*, 38: 1080-1092. [156262](#)
- Becker S; Fenton MJ; Soukup JM. (2002). Involvement of microbial components and toll-like receptors 2 and 4 in cytokine responses to air pollution particles. *Am J Respir Cell Mol Biol*, 27: 611-618. [052419](#)
- Becker S; Mundandhara S; Devlin RB; Madden M. (2005). Regulation of cytokine production in human alveolar macrophages and airway epithelial cells in response to ambient air pollution particles: further mechanistic studies. *Toxicol Appl Pharmacol*, 207: 269-275. [088590](#)
- Blanchet S; Ramgolam K; Baulig A; Marano F; Baeza-Squiban A. (2004). Fine particulate matter induces amphiregulin secretion by bronchial epithelial cells. *Am J Respir Cell Mol Biol*, 230: 421-427. [087982](#)
- Blank F; Rothen-Rutishauser B; Gehr P. (2007). Dendritic cells and macrophages form a transepithelial network against foreign particulate antigens. , 36: 669-77. [096521](#)
- Bleck B; Tse Doris B; Jaspers I; de Lafaille Maria AC; Reibman J. (2006). Diesel exhaust particle-exposed human bronchial epithelial cells induce dendritic cell maturation. , 176: 7431-7437. [096560](#)
- Bonham AC; Chen CY; Sekizawa S; Joad JP. (2006). Plasticity in the nucleus tractus solitarius and its influence on lung and airway reflexes. *J Appl Physiol*, 101: 322-7. [191140](#)
- Braude S; Nolop KB; Hughes JMB; Barnes PJ; Royston D. (1986). Comparison of lung vascular and epithelial permeability indices in the adult respiratory distress syndrome. , 133: 1002-1005. [155701](#)
- Brauner EV; Mortensen J; Moller P; Bernard A; Vinzents P; Wahlin P; Glasius M; Loft S. (2009). Effects of ambient air particulate exposure on blood-gas barrier permeability and lung function. , 21: 38-47. [190244](#)

- Brown DM; Donaldson K; Borm PJ; Schins RP; Dehnhardt M; Gilmour P; Jimenez LA; Stone V. (2004). Calcium and ROS-mediated activation of transcription factors and TNF-alpha cytokine gene expression in macrophages exposed to ultrafine particles. *Am J Physiol*, 286: L344-L353. [155705](#)
- Brown DM; Donaldson K; Stone V. (2004). Effects of PM10 in human peripheral blood monocytes and J774 macrophages. *Respir Res*, 5: 29. [088663](#)
- Caligiuri G; Levy B; Pernow J; Thoren P; Hansson GK. (1999). Myocardial infarction mediated by endothelin receptor signaling in hypercholesterolemic mice. Presented at . [156318](#)
- Campbell A; Oldham M; Becaria A; Bondy SC; Meacher D; Sioutas C; Misra C; Mendez LB; Kleinman M. (2005). Particulate matter in polluted air may increase biomarkers of inflammation in mouse brain. *Neurotoxicology*, 26: 133-140. [087217](#)
- Cao D; Tal TL; Graves LM; Gilmour I; Linak W; Reed W; Bromberg PA; Samet JM. (2007). Diesel exhaust particulate-induced activation of Stat3 requires activities of EGFR and Src in airway epithelial cells. *Am J Physiol Lung Cell Mol Physiol*, 292: L422-L429. [156322](#)
- Chan RC-F; Wang M; Li N; Yanagawa Y; Onoe K; Lee JJ; Nel AE. (2006). Pro-oxidative diesel exhaust particle chemicals inhibit LPS-induced dendritic cell responses involved in T-helper differentiation. *J Allergy Clin Immunol*, 118: 455-465. [097468](#)
- Chang C-C; Chiu H-F; Wu Y-S; Li Y-C; Tsai M-L; Shen C-K; Yang C-Y. (2005). The induction of vascular endothelial growth factor by ultrafine carbon black contributes to the increase of alveolar-capillary permeability. *Environ Health Perspect*, 113: 454-460. [097776](#)
- Chen J; Tan M; Nemmar A; Song W; Dong M; Zhang G; Li Y. (2006). Quantification of extrapulmonary translocation of intratracheal-instilled particles in vivo in rats: effect of lipopolysaccharide. *Toxicology*, 222: 195-201. [147267](#)
- Chen LC; Nadziejko C. (2005). Effects of subchronic exposures to concentrated ambient particles (CAPs) in mice V CAPs exacerbate aortic plaque development in hyperlipidemic mice. *Inhal Toxicol*, 17: 217-224. [087219](#)
- Cho AK; Sioutas C; Miguel AH; Kumagai Y; Schmitz DA; Singh M; Eiguren-Fernandez A; Froines JR. (2005). Redox activity of airborne particulate matter at different sites in the Los Angeles Basin. *Environ Res*, 99: 40-47. [087937](#)
- Cho H-Y; Reddy SP; Kleeberger SR. (2006). Nrf2 defends the lung from oxidative stress. *Antioxid Redox Signal*, 8: 76-87. [156345](#)
- Chu AJ. (2005). Tissue factor mediates inflammation. *Arch Biochem Biophys*, 440: 123-132. [155730](#)
- Coleridge HM; Coleridge JCG. (1994). Pulmonary Reflexes: Neural Mechanisms of Pulmonary Defense. *Annu Rev Physiol*, 56: 69-91. [156362](#)
- Cowburn AS; Condliffe AM; Farahi N; Summers C; Chilvers ER. (2008). Advances in neutrophil biology: clinical implications. , 134: 606-12. [191142](#)
- de Kok TM; Hogervorst JG; Briede JJ; van Herwijnen MH; Maas LM; Moonen EJ; Driee HA; Kleinjans JC. (2005). Genotoxicity and physicochemical characteristics of traffic-related ambient particulate matter. , 46: 71-80. [189835](#)
- Dick CAJ; Brown DM; Donaldson K; Stone V. (2003). The role of free radicals in the toxic and inflammatory effects of four different ultrafine particle types. *Inhal Toxicol*, 15: 39-52. [036605](#)
- Donaldson K; Borm PJ; Oberdorster G; Pinkerton KE; Stone V; Tran CL. (2008). Concordance between in vitro and in vivo dosimetry in the proinflammatory effects of low-toxicity, low-solubility particles: the key role of the proximal alveolar region. *Inhal Toxicol*, 20: 53-62. [190217](#)
- Donaldson K; Stone V; Borm PJ; Jimenez LA; Gilmour PS; Schins RP; Knaapen AM; Rahman I; Faux SP; Brown DM; MacNee W. (2003). Oxidative stress and calcium signaling in the adverse effects of environmental particles (PM10). *Free Radic Biol Med*, 34: 1369-1382. [156408](#)
- Dostert C; Petrilli V; Van Bruggen R; Steele C; Mossman BT; Tschopp J. (2008). Innate Immune Activation Through Nalp3 Inflammasome Sensing of Asbestos and Silica. , 320: 674. [155753](#)
- Foley DL; Craig JM; Morley R; Olsson CA; Dwyer T; Smith K; Saffery R. (2009). Prospects for epigenetic epidemiology. *Am J Epidemiol*, 169: 389-400. [191144](#)
- Gallagher J; Sams R; Inmon J; Gelein R; Elder A; Oberdorster G; Prahalad AK. (2003). Formation of 8-oxo-7,8-dihydro-2'-deoxyguanosine in rat lung DNA following subchronic inhalation of carbon black. *Toxicol Appl Pharmacol*, 190: 224-231. [140171](#)
- Geiser M; Rothen-Rutishauser B; Kapp N; Schurch S; Kreyling W; Schulz H; Semmler M; Im Hof V; Heyder J; Gehr P. (2005). Ultrafine particles cross cellular membranes by nonphagocytic mechanisms in lungs and in cultured cells. *Environ Health Perspect*, 113: 1555-1560. [087362](#)
- Geng H; Meng Z; Zhang Q. (2005). Effects of blowing sand fine particles on plasma membrane permeability and fluidity, and intracellular calcium levels of rat alveolar macrophages. , 157: 129-137. [096689](#)
- Geng H; Meng Z; Zhang Q. (2006). In vitro responses of rat alveolar macrophages to particle suspensions and water-soluble components of dust storm PM(2.5). *Toxicol In Vitro*, 20: 575-584. [097026](#)

- Ghelfi E; Rhoden CR; Wellenius GA; Lawrence J; Gonzalez-Flecha B. (2008). Cardiac oxidative stress and electrophysiological changes in rats exposed to concentrated air particles are mediated by TRP-dependent pulmonary reflexes. *Toxicol Sci*, 102: 328-336. [156468](#)
- Ghio AJ; Churg A; Roggli VL. (2004). Review: Ferruginous Bodies: Implications in the Mechanism of Fiber and Particle Toxicity. , 32: 643. [155790](#)
- Ghio AJ; Cohen MD. (2005). Disruption of iron homeostasis as a mechanism of biologic effect by ambient air pollution particles. *Inhal Toxicol*, 17: 709-716. [088272](#)
- Gilmour PS; Morrison ER; Vickers MA; Ford I; Ludlam CA; Greaves M; Donaldson K; MacNee W. (2005). The procoagulant potential of environmental particles (PM10). *Occup Environ Med*, 62: 164-171. [087410](#)
- Gilmour PS; Nyska A; Schladweiler MC; McGee JK; Wallenborn JG; Richards JH; Kodavanti UP. (2006). Cardiovascular and blood coagulative effects of pulmonary zinc exposure. *Toxicol Appl Pharmacol*, 211: 41-52. [088489](#)
- Gilmour PS; Rahman I; Donaldson K; MacNee W. (2003). Histone acetylation regulates epithelial IL-8 release mediated by oxidative stress from environmental particles. Retrieved , from . [096959](#)
- Gilmour PS; Schladweiler MC; Nyska A; McGee JK; Thomas R; Jaskot RH; Schmid J; Kodavanti UP. (2006). Systemic imbalance of essential metals and cardiac gene expression in rats following acute pulmonary zinc exposure. *J Toxicol Environ Health A*, 69: 2011-2032. [156472](#)
- Godleski JJ; Verrier RL; Koutrakis P; Catalano P; Coull B; Reinisch U; Lovett EG; Lawrence J; Murthy GG; Wolfson JM; Clarke RW; Nearing BD; Killingsworth C. (2000). Mechanisms of morbidity and mortality from exposure to ambient air particles. , 91: 5-88; discussion 89-103. [000738](#)
- Gopalakrishnan S; Van Emburgh BO; Robertson KD. (2008). DNA methylation in development and human disease. , 647: 30-8. [191147](#)
- Gottipolu RR; Landa ER; Schladweiler MC; McGee JK; Ledbetter AD; Richards JH; Wallenborn GJ; Kodavanti UP. (2008). Cardiopulmonary responses of intratracheally instilled tire particles and constituent metal components. *Inhal Toxicol*, 20: 473-84. [191148](#)
- Groneberg DA; Quarcoo D; Frossard N; Fischer A. (2004). Neurogenic mechanisms in bronchial inflammatory diseases. *Allergy*, 59: 1139-52. [138134](#)
- Grunstein MM; Hazucha M; Sorli J; Milic-Emili J. (1977). Effect of SO2 on control of breathing in anesthetized cats. *J Appl Physiol*, 43: 844-851. [071445](#)
- Gábelová A; Valovicova Z; Labaj J; Bacova G; Binkova B; Farmer Peter B. (2007). Assessment of oxidative DNA damage formation by organic complex mixtures from airborne particles PM(10). , 620: 135-144. [156457](#)
- Halvorsen B; Otterdal K; Dahl TB; Skjelland M; Gullestad L; Oie E; Aukrust P. (2008). Atherosclerotic plaque stability--what determines the fate of a plaque?. , 51: 183-94. [191149](#)
- Hanel B; Law I; Mortensen J. (2003). Maximal rowing has an acute effect on the blood-gas barrier in elite athletes. , 95: 1076-1082. [155826](#)
- Hitchler MJ; Domann FE. (2007). An epigenetic perspective on the free radical theory of development. *Free Radic Biol Med*, 43: 1023-36. [191151](#)
- Huang Y-CT; Soukup J; Harder S; Becker S. (2003). Mitochondrial oxidant production by a pollutant dust and NO-mediated apoptosis in human alveolar macrophage. *Am J Physiol Lung Cell Mol Physiol*, 284: C24-32. [156573](#)
- Illum L. (2006). Nasal clearance in health and disease. , 19: 92-99. [191205](#)
- Ilowite JS; Bennett WD; Sheetz MS; Groth ML; Nierman DM. (1989). Permeability of the bronchial mucosa to 99mTc-DTPA in asthma. , 139: 1139-1143. [156584](#)
- Imrich A; Ning Y; Lawrence J; Coull B; Gitin E; Knutson M; Kobzik L. (2007). Alveolar macrophage cytokine response to air pollution particles: oxidant mechanisms. *Toxicol Appl Pharmacol*, 218: 256-264. [155859](#)
- Jaspers I; Cienciewicki JM; Zhang W; Brighton LE; Carson JL; Beck MA; Madden MC. (2005). Diesel exhaust enhances influenza virus infections in respiratory epithelial cells. *Toxicol Sci*, 85: 990-1002. [088115](#)
- Jiang J; Oberdrster G; Elder A; Gelein R; Mercer P; Biswas P. (2008). Does nanoparticle activity depend upon size and crystal phase?. , 2: 33-42. [156609](#)
- Jones J; Stick S; Dingle P; Franklin P. (2007). Spatial variability of particulates in homes: implications for infant exposure. *Sci Total Environ*, 376: 317-323. [156615](#)
- Jones JG; Minty BD; Royston D; Royston JP. (1983). Carboxyhaemoglobin and pulmonary epithelial permeability in man. *Thorax*, 38: 129-133. [155884](#)
- Jones PA; Baylin SB. (2007). The epigenomics of cancer. *Cell*, 128: 683-92. [191153](#)
- Kaan PM; Hegele RG. (2003). Interaction between respiratory syncytial virus and particulate matter in guinea pig alveolar macrophages. *Am J Respir Cell Mol Biol*, 28: 697-704. [095753](#)
- Karoly ED; Li Z; Dailey LA; Hyseni X; Huang YCT. (2007). Up-regulation of Tissue Factor in Human Pulmonary Artery Endothelial Cells after Ultrafine Particle Exposure. , 115: 535. [155890](#)

- Kaul N; Forman HJ. (1996). Activation of NF κ B by the respiratory burst of macrophages. *Free Radic Biol Med*, 21: 401-405. [155892](#)
- Keverne EB; Curley JP. (2008). Epigenetics, brain evolution and behaviour. , 29: 398-412. [191154](#)
- Keverne EB; Curley JP. (2008). Epigenetics, brain evolution and behaviour. *Neuroendocrinology*, 29: 398-412. [191958](#)
- Kleinman MT; Araujo JA; Nel A; Sioutas C; Campbell A; Cong PQ; Li H; Bondy SC. (2008). Inhaled ultrafine particulate matter affects CNS inflammatory processes and may act via MAP kinase signaling pathways. *Toxicol Lett*, 178: 127-130. [190074](#)
- Kodavanti UP; Schladweiler MC; Gilmour PS; Wallenborn JG; Mandavilli BS; Ledbetter AD; Christiani DC; Runge MS; Karoly ED; Costa DL; Peddada S; Jaskot R; Richards JH; Thomas R; Madamanchi NR; Nyska A. (2008). The role of particulate matter-associated zinc in cardiac injury in rats. , 116: 13-20. [155907](#)
- Koike E; Hirano S; Furuyama A; Kobayashi T. (2004). cDNA microarray analysis of rat alveolar epithelial cells following exposure to organic extract of diesel exhaust particles. *Toxicol Appl Pharmacol*, 201: 178-185. [058555](#)
- Koike E; Kobayashi T. (2005). Organic extract of diesel exhaust particles stimulates expression of Ia and costimulatory molecules associated with antigen presentation in rat peripheral blood monocytes but not in alveolar macrophages. *Toxicol Appl Pharmacol*, 209: 277-285. [088303](#)
- Lee CC; Cheng YW; Kang JJ. (2005). Motorcycle exhaust particles induce IL-8 production through NF-kappaB activation in human airway epithelial cells. *J Toxicol Environ Health A*, 68: 1537-1555. [156682](#)
- Lee SS; Woo CH; Chang JD; Kim JH. (2003). Roles of Rac and cytosolic phospholipase A2 in the intracellular signalling in response to titanium particles. *Cell Signal*, 15: 339-345. [156678](#)
- Li J; Ghio AJ; Cho SH; Brinckerhoff CE; Simon SA; Liedtke W. (2009). Diesel exhaust particles activate the matrix-metalloproteinase-1 gene in human bronchial epithelia in a beta-arrestin-dependent manner via activation of RAS. *Environ Health Perspect*, 117: 400-409. [190424](#)
- Li N; Nel AE. (2006). Role of the Nrf2-mediated signaling pathway as a negative regulator of inflammation: Implications for the impact of particulate pollutants on asthma. *Antioxid Redox Signal*, 8: 88-98. [156694](#)
- Li N; Sioutas C; Froines JR; Cho A; Misr. (2003). Ultrafine particulate pollutants induce oxidative stress and mitochondrial damage. *Environ Health Perspect*, 111: 455-460. [042082](#)
- Li Y-J; Kawada T; Matsumoto A; Azuma A; Kudoh S; Takizawa H; Sugawara I. (2007). Airway inflammatory responses to oxidative stress induced by low-dose diesel exhaust particle exposure differ between mouse strains. , 33: 227-244. [155929](#)
- Libby P. (2002). Inflammation in atherosclerosis. *Nature*, 420: 868-874 . [192009](#)
- Libby P; Ridker PM; Maseri A. (2002). Inflammation and atherosclerosis. *Circulation*, 105: 1135-43. [191157](#)
- Lindbom J; Gustafsson M; Blomqvist G; Dahl A; Gudmundsson A; Swietlicki E; Ljungman AG. (2007). Wear particles generated from studded tires and pavement induces inflammatory reactions in mouse macrophage cells. , 20: 937-946. [155934](#)
- Liu J; Ballaney M; Al-Alem U; Quan C; Jin X; Perera F; Chen LC; Miller RL. (2008). Combined Inhaled Diesel Exhaust Particles and Allergen Exposure Alter Methylation of T Helper Genes and IgE Production In Vivo. *Toxicol Sci*, 102: 76-81. [156709](#)
- Liu X; Meng Z. (2005). Effects of airborne fine particulate matter on antioxidant capacity and lipid peroxidation in multiple organs of rats. *Inhal Toxicol*, 17: 467-473. [088650](#)
- Long JF; Waldman WJ; Kristovich R; Williams M; Knight D; Dutta PK. (2005). Comparison of ultrastructural cytotoxic effects of carbon and carbon/iron particulates on human monocyte-derived macrophages. *Environ Health Perspect*, 113: 170-174. [087454](#)
- Longhurst JC; Tjen ALSC; Fu LW. (2001). Cardiac sympathetic afferent activation provoked by myocardial ischemia and reperfusion. *Mechanisms and reflexes*. , 940: 74-95. [191158](#)
- Lund AK; Lucero A; Lucas S; Madden MC; McDonald JD; Seagrave JC; Knuckles TL; Campen MJ. (2009). Vehicular emissions induce vascular MMP-9 expression and activity associated with endothelin-1-mediated pathways. *Arterioscler Thromb Vasc Biol*, 29: 511-517. [180257](#)
- Mackman N. (2005). Tissue-Specific Hemostasis in Mice. *Arterioscler Thromb Vasc Biol*, 25: 2273-2281. [156722](#)
- Mercer BA; Kolesnikova N; Sonett J; D'Armiento J. (2004). Extracellular regulated kinase/mitogen activated protein kinase is up-regulated in pulmonary emphysema and mediates matrix metalloproteinase-1 induction by cigarette smoke. *J Biol Chem*, 279: 17690-17696. [191180](#)
- Moffitt JA; Grippo AJ; Holmes PV; Johnson AK. (2002). Olfactory bulbectomy attenuates cardiovascular sympathoexcitatory reflexes in rats. , 283: H2575-83. [191160](#)
- Molinelli AR; Madden MC; McGee JK; Stonebuerner JG; Ghio AJ. (2002). Effect of metal removal on the toxicity of airborne particulate matter from the Utah Valley. *Inhal Toxicol*, 14: 1069-1086. [035347](#)

- Moller W; Brown DM; Kreyling WG; Stone V. (2005). Ultrafine particles cause cytoskeletal dysfunctions in macrophages: role of intracellular calcium. *Part Fibre Toxicol*, 2: 7. [156770](#)
- Monn C; Naef R; Koller T. (2003). Reactions of macrophages exposed to particles <10 "micron"m. *Environ Res*, 91: 35-44. [052418](#)
- Mutlu GM; Green D; Bellmeyer A; Baker CM; Burgess Z; Rajamannan N; Christman JW; Foiles N; Kamp DW; Ghio AJ; Chandel NS; Dean DA; Sznajder JI; Budinger GR. (2007). Ambient particulate matter accelerates coagulation via an IL-6-dependent pathway. , 117: 2952-61. [121441](#)
- Nadel JA; Salem H; Tamplin B; Tokiwa Y. (1965). Mechanism of bronchoconstriction during inhalation of sulfur dioxide. *J Appl Physiol*, 20: 164-167. [014846](#)
- Newby AC. (2008). Metalloproteinase expression in monocytes and macrophages and its relationship to atherosclerotic plaque instability. , 28: 2108-14. [191161](#)
- Nurkiewicz TR; Porter DW; Barger M; Millecchia L; Rao KM; Marvar PJ; Hubbs AF; Castranova V; Boegehold MA. (2006). Systemic microvascular dysfunction and inflammation after pulmonary particulate matter exposure. *Environ Health Perspect*, 114: 412-419. [088611](#)
- Nurkiewicz TR; Porter DW; Hubbs AF; Stone S; Chen BT; Frazer DG; Boegehold MA; Castranova V. (2009). Pulmonary nanoparticle exposure disrupts systemic microvascular nitric oxide signaling. , 110: 191-203. [191961](#)
- Oberdörster G. (1988). Lung clearance of inhaled insoluble and soluble particles. , 1: 289-330. [006857](#)
- Oortgiesen M; Veronesi B; Eichenbaum G; Kiser PF; Simon SA. (2000). Residual oil fly ash and charged polymers activate epithelial cells and nociceptive sensory neurons. *Am J Physiol*, 278: L683-L695. [013998](#)
- Owen CA. (2008). Roles for proteinases in the pathogenesis of chronic obstructive pulmonary disease. , 3: 253-68. [191162](#)
- Pardo A; Selman M. (2005). MMP-1: the elder of the family. , 37: 283-8. [191163](#)
- Penn A; Murphy G; Barker S; Henk W; Penn L. (2005). Combustion-derived ultrafine particles transport organic toxicants to target respiratory cells. *Environ Health Perspect*, 113: 956-963. [088257](#)
- Pinkerton KE; Joad JP. (2006). Influence of air pollution on respiratory health during perinatal development. *Clin Exp Pharmacol Physiol*, 33: 269-272. [091237](#)
- Rahman I; Biswas SK; Kode A. (2006). Oxidant and antioxidant balance in the airways and airway diseases. , 533: 222-39. [191165](#)
- Ramage L; Guy K. (2004). Expression of C-reactive protein and heat-shock protein-70 in the lung epithelial cell line A549, in response to PM10 exposure. *Inhal Toxicol*, 16: 447-452. [055640](#)
- Randell S; Mercer R; Young S. (1990). Neonatal hyperoxia alters the pulmonary alveolar and capillary structure of 40-day-old rats. , 136: 1259. [191956](#)
- Reed MD; Barrett EG; Campen MJ; Divine KK; Gigliotti AP; McDonald JD; Seagrave JC; Mauderly JL; Seilkop SK; Swenberg JA. (2008). Health effects of subchronic inhalation exposure to gasoline engine exhaust. *Inhal Toxicol*, 20: 1125-1143. [156903](#)
- Rengasamy A; Barger MW; Kane E; Ma JKH; Castranova V; Ma JYC. (2003). Diesel exhaust particle-induced alterations of pulmonary phase I and phase II enzymes of rats. *J Toxicol Environ Health A*, 66: 153-167. [156907](#)
- Rhoden CR; Lawrence J; Godleski JJ; Gonzalez-Flecha B. (2004). N-acetylcysteine prevents lung inflammation after short-term inhalation exposure to concentrated ambient particles. *Toxicol Sci*, 79: 296-303. [087969](#)
- Rhoden CR; Wellenius GA; Ghelfi E; Lawrence J; Gonzalez-Flecha B. (2005). PM-induced cardiac oxidative stress and dysfunction are mediated by autonomic stimulation. *Biochim Biophys Acta*, 1725: 305-313. [087878](#)
- Rinderknecht J; Shapiro L; Krauthammer M; Taplin G; Wasserman K; Uszler JM; Effros RM. (1980). Accelerated clearance of small solutes from the lungs in interstitial lung disease. , 121: 105-117. [191965](#)
- Risom L; Moller P; Loft S. (2005). Oxidative stress-induced DNA damage by particulate air pollution. , 592: 119-137. [189016](#)
- Roberts ES; Richards JH; Jaskot R; Dreher KL. (2003). Oxidative stress mediates air pollution particle-induced acute lung injury and molecular pathology. *Inhal Toxicol*, 15: 1327-1346. [156051](#)
- Roberts JR; Young S-H; Castranova V; Antonini JM. (2007). Soluble metals in residual oil fly ash alter innate and adaptive pulmonary immune responses to bacterial infection in rats. *Toxicol Appl Pharmacol*, 221: 306-319. [097623](#)
- Rouse RL; Murphy G; Boudreaux MJ; Paulsen DB; Penn AL. (2008). Soot nanoparticles promote biotransformation, oxidative stress, and inflammation in murine lungs. *Am J Respir Cell Mol Biol*, 39: 198-207. [156930](#)

- Ruckerl R; Greven S; Ljungman P; Aalto P; Antoniadou C; Bellander T; Berglund N; Chrysohoou C; Forastiere F; Jacquemin B; von Klot S; Koenig W; Kuchenhoff H; Lanki T; Pekkanen J; Perucci CA; Schneider A; Sunyer J; Peters A. (2007). Air pollution and inflammation (interleukin-6, C-reactive protein, fibrinogen) in myocardial infarction survivors. *Environ Health Perspect*, 115: 1072-1080. [156931](#)
- Sakamoto N; Hayashi S; Gosselink J; Ishii H; Ishimatsu Y; Mukae H; Hogg JC; van Eeden SF. (2007). Calcium dependent and independent cytokine synthesis by air pollution particle-exposed human bronchial epithelial cells. *Toxicol Appl Pharmacol*, 225: 134-141. [096282](#)
- Sarin S; Udem B; Sanico A; Togias A. (2006). The role of the nervous system in rhinitis. , 118: 999-1016. [191166](#)
- Schins RPF; Knaapen AM. (2007). Genotoxicity of poorly soluble particles. *Inhal Toxicol*, 19 Suppl 1: 189-198. [156074](#)
- Seaton A; MacNee W; Donaldson K; Godden D. (1995). Particulate air pollution and acute health effects. *Lancet*, 346: 176-178. [045721](#)
- Sekizawa S; Chen CY; Bechtold AG; Tabor JM; Bric JM; Pinkerton KE; Joad JP; Bonham AC. (2008). Extended secondhand tobacco smoke exposure induces plasticity in nucleus tractus solitarius second-order lung afferent neurons in young guinea pigs. , 28: 771-81. [191167](#)
- Semmler-Behnke M; Takenaka S; Fertsch S; Wenk A; Seitz J; Mayer P; Oberdörster G; Kreyling WG. (2007). Efficient Elimination of Inhaled Nanoparticles from the Alveolar Region: Evidence for Interstitial Uptake and Subsequent Reentrainment onto Airways Epithelium. , 115: 728. [156080](#)
- Shi T; Knaapen AM; Begerow J; Birmili W; Borm PJ; Schins RP. (2003). Temporal variation of hydroxyl radical generation and 8-hydroxy-2'-deoxyguanosine formation by coarse and fine particulate matter. *Occup Environ Med*, 60: 315-321. [088248](#)
- Sirivelu MP; MohanKumar SMJ; Wagner JG; Harkema JR; MohanKumar PS. (2006). Activation of the stress axis and neurochemical alterations in specific brain areas by concentrated ambient particle exposure with concomitant allergic airway disease. *Environ Health Perspect*, 114: 870-874. [111151](#)
- Snipes MB. (1996). Current information on lung overload in nonrodent mammals: contrast with rats. *Inhal Toxicol*, 8: 91-109. [076041](#)
- Snipes MB; Harkema JR; Hotchkiss JA; Bice DE. (1997). Neutrophil Involvement in the Retention and Clearance of Dust Intratracheally Instilled into the LUNGS of F344/N Rats. , 23: 65-84. [156092](#)
- Soberanes S; Panduri V; Mutlu GM; Ghio A; Bundinger GRS; Kamp DW. (2006). p53 mediates particulate matter-induced alveolar epithelial cell mitochondria-regulated apoptosis. *Am J Respir Crit Care Med*, 174: 1229-1238. [156991](#)
- Soberanes S; Urich D; Baker CM; Burgess Z; Chiarella SE; Bell EL; Ghio AJ; De Vizcaya-Ruiz A; Liu J; Ridge KM; Kamp DW; Chandel NS; Schumacker PT; Mutlu GM; Budinger GRS. (2009). Mitochondrial complex III-generated oxidants activate ASK1 and JNK to induce alveolar epithelial cell death following exposure to particulate matter air pollution. *J Biol Chem*, 284: 2176-2186. [190483](#)
- Steerenberg P; Withagen C; Dalen W; Dormans J; Loveren H. (2004). Adjuvant Activity of Ambient Particulate Matter in Macrophage Activity-Suppressed, N-Acetylcysteine-Treated, iNOS- and IL-4-Deficient Mice. *Inhal Toxicol*, 16: 835-843. [087981](#)
- Sun Q; Wang A; Jin X; Natanzon A; Duquaine D; Brook RD; Aguinaldo J-GS; Fayad ZA; Fuster V; Lippmann M; Chen Lung C; Rajagopalan S. (2005). Long-term air pollution exposure and acceleration of atherosclerosis and vascular inflammation in an animal model. , 294: 3003-3010. [186814](#)
- Takizawa H; Abe S; Okazaki H; Kohyama T; Sugawara I; Saito Y; Ohtoshi T; Kawasaki S; Desaki M; Nakahara K; Yamamoto K; Matsushima K; Tanaka M; Sagai M; Kudoh S. (2003). Diesel exhaust particles upregulate eotaxin gene expression in human bronchial epithelial cells via nuclear factor-kappa B-dependent pathway. *Am J Physiol Lung Cell Mol Physiol*, 284: L1055-1062. [157039](#)
- Tal TL; Graves LM; Silbajoris R; Bromberg PA; Wu W; Samet JM. (2006). Inhibition of protein tyrosine phosphatase activity mediates epidermal growth factor receptor signaling in human airway epithelial cells exposed to Zn²⁺. *Toxicol Appl Pharmacol*, 214: 16-23. [108588](#)
- Tamaoki J; Isono K; Takeyama K; Tagaya E; Nakata J; Nagai A. (2004). Ultrafine carbon black particles stimulate proliferation of human airway epithelium via EGF receptor-mediated signaling pathway. *Am J Physiol Lung Cell Mol Physiol*, 287: L1127-1133. [157040](#)
- Tankersley CG; Shank JA; Flanders SE; Soutiere SE; Rabold R; Mitzner W; Wagner EM. (2003). Changes in lung permeability and lung mechanics accompany homeostatic instability in senescent mice. *J Appl Physiol*, 95: 1681-1687. [096363](#)
- Tao F; Gonzalez-Flecha B; Kobzik L. (2003). Reactive oxygen species in pulmonary inflammation by ambient particulates. *Free Radic Biol Med*, 35: 327-340. [156111](#)
- Tao F; Kobzik L. (2002). Lung macrophage-epithelial cell interactions amplify particle-mediated cytokine release. *Am J Respir Cell Mol Biol*, 26: 499-505. [157044](#)

- Tarantini L; Bonzini M; Apostoli P; Pegoraro V; Bollati V; Marinelli B; Cantone L; Rizzo G; Hou L; Schwartz J; Bertazzi PA; Baccarelli A. (2009). Effects of particulate matter on genomic DNA methylation content and iNOS promoter methylation. *Environ Health Perspect*, 117: 217-222. [192010](#)
- Tarantini L; Bonzini M; Apostoli P; Pegoraro V; Bollati V; Marinelli B; Cantone L; Rizzo G; Hou L; Schwartz J; Bertazzi PA; Baccarelli A. (2009). Errata to Effects of particulate matter on genomic DNA methylation content and iNOS promoter methylation. *Environ Health Perspect*, 117: A143. [192153](#)
- Thomson E; Kumarathasan P; Goegan P; Aubin RA; Vincent R. (2005). Differential regulation of the lung endothelin system by urban particulate matter and ozone. *Toxicol Sci*, 88: 103-113. [087554](#)
- U.S. EPA. (2000). Science Policy Council handbook: risk characterization. [052149](#)
- Upadhyay D; Panduri V; Ghio A; Kamp DW. (2003). Particulate matter induces alveolar epithelial cell DNA damage and apoptosis: role of free radicals and the mitochondria. *Toxicol Appl Pharmacol*, 29: 180-187. [097370](#)
- Valinluck V; Tsai HH; Rogstad DK; Burdzy A; Bird A; Sowers LC. (2004). Oxidative damage to methyl-CpG sequences inhibits the binding of the methyl-CpG binding domain (MBD) of methyl-CpG binding protein 2 (MeCP2). *J Biol Chem*, 279: 4100-8. [191170](#)
- Van Eeden SF; Hogg JC. (2002). Systemic inflammatory response induced by particulate matter air pollution: the importance of bone-marrow stimulation. *J Toxicol Environ Health A*, 65: 1597-1613. [088111](#)
- Van Eeden SF; Tan WC; Suwa T; Mukae H; Terashima T; Fujii T; Qui D; Vincent R; Hogg JC. (2001). Cytokines involved in the systemic inflammatory response induced by exposure to particulate matter air pollutants (PM10). *Am J Respir Crit Care Med*, 164: 826-830. [019018](#)
- van Eeden SF; Yeung A; Quinlan K; Hogg JC. (2005). Systemic response to ambient particulate matter: relevance to chronic obstructive pulmonary disease. Presented at . [157086](#)
- Veronesi B; Makwana O; Pooler M; Chen LC. (2005). Effects of subchronic exposures to concentrated ambient particles VII Degeneration of dopaminergic neurons in Apo E^{-/-} mice. *Inhal Toxicol*, 17: 235-241. [087481](#)
- Veronesi B; Oortgiesen M. (2001). Neurogenic inflammation and particulate matter (PM) air pollutants. *Neurotoxicology*, 22: 795-810. [015977](#)
- Veronesi B; Oortgiesen M; Carter JD; Devlin RB. (1999). Particulate matter initiates inflammatory cytokine release by activation of capsaicin and acid receptors in a human bronchial epithelial cell line. *Toxicol Appl Pharmacol*, 154: 106-115. [048764](#)
- Veronesi B; Oortgiesen M; Roy J; Carter JD; Simon SA; Gavett SH. (2000). Vanilloid (capsaicin) receptors influence inflammatory sensitivity in response to particulate matter. *Toxicol Appl Pharmacol*, 169: 66-76. [017062](#)
- Veronesi B; Wei G; Zeng JQ; Oortgiesen M. (2003). Electrostatic charge activates inflammatory vanilloid (VR1) receptors. *Neurotoxicology*, 24: 463-473. [094384](#)
- Wallenborn JG; Evansky P; Shannahan JH; Vallanat B; Ledbetter AD; Schladweiler MC; Richards JH; Gottipolu RR; Nyska A; Kodavanti UP. (2008). Subchronic inhalation of zinc sulfate induces cardiac changes in healthy rats. *Toxicol Appl Pharmacol*, 232: 69-77. [191171](#)
- Wallenborn JG; Kovalcik KD; McGee JK; Landis MS; Kodavanti UP. (2009). Systemic translocation of (70)zinc: kinetics following intratracheal instillation in rats. *Toxicol Appl Pharmacol*, 234: 25-32. [191172](#)
- Wallenborn JG; McGee John K; Schladweiler Mette C; Ledbetter Allen D; Kodavanti Urmila P. (2007). Systemic translocation of particulate matter-associated metals following a single intratracheal instillation in rats. *J Toxicol Sci*, 98: 231-239. [156144](#)
- Wan H; Winton HL; Soeller C; Tovey ER; Gruenert DC; Thompson PJ; Stewart GA; Taylor GW; Garrod DR; Cannell MB; Robinson C. (1999). Der p 1 facilitates transepithelial allergen delivery by disruption of tight junctions. *J Clin Invest*, 104: 123-133. [191903](#)
- Wan J; Diaz-Sanchez D. (2006). Phase II enzymes induction blocks the enhanced IgE production in B cells by diesel exhaust particles. *Toxicol Appl Pharmacol*, 177: 3477-3483. [097399](#)
- Wan J; Diaz-Sanchez D. (2007). Antioxidant enzyme induction: a new protective approach against the adverse effects of diesel exhaust particles. *Inhal Toxicol*, 19 Suppl 1: 177-182. [156145](#)
- Wang L; Pinkerton KE. (2007). Air Pollutant Effects on Fetal and Early Postnatal Development. *Toxicol Appl Pharmacol*, 81: 144-154. [179975](#)
- Warheit DB; Webb TR; Colvin VL; Reed KL; Sayes CM. (2007). Pulmonary bioassay studies with nanoscale and fine-quartz particles in rats: toxicity is not dependent upon particle size but on surface characteristics. *Toxicol Sci*, 95: 270-280. [090482](#)
- Widdicombe J. (2006). Reflexes from the lungs and airways: historical perspective. *J Appl Physiol*, 101: 628. [155519](#)
- Widdicombe J; Lee L-Y. (2001). Airway reflexes, autonomic function, and cardiovascular responses. *Environ Health Perspect*, 4: 579-584. [019049](#)
- Widdicombe JG. (2003). Overview of neural pathways in allergy and asthma. *Pulm Pharmacol Ther*, 16: 23-30. [157145](#)

- Win-Shwe TT; Yamamoto S; Fujitani Y; Hirano S; Fujimaki H. (2008). Spatial learning and memory function-related gene expression in the hippocampus of mouse exposed to nanoparticle-rich diesel exhaust. *Neurotoxicology*, 29: 940-947. [190146](#)
- Wong SS; Sun NN; Keith I; Kweon C-B; Foster DE; Schauer James J; Witten ML. (2003). Tachykinin substance P signaling involved in diesel exhaust-induced bronchopulmonary neurogenic inflammation in rats. , 77: 638-650. [097707](#)
- Wright RO; Baccarelli A. (2007). Metals and neurotoxicology. *J Nutr*, 137: 2809-13. [191173](#)
- Xia T; Korge P; Weiss JN; Li N; Venkatesen MI; Sioutas C; Nel A. (2004). Quinones and aromatic chemical compounds in particulate matter induce mitochondrial dysfunction: implications for ultrafine particle toxicity. *Environ Health Perspect*, 112: 1347-1358. [087486](#)
- Xiao GG; Nel AE; Loo JA. (2005). Nitrotyrosine-modified proteins and oxidative stress induced by diesel exhaust particles. *Electrophoresis*, 26: 280-292. [156164](#)
- Yauk C; Polyzos A; Rowan-Carroll A; Somers CM; Godschalk RW; Van Schooten FJ; Berndt ML; Pogribny IP; Koturbash I; Williams A; Douglas GR; Kovalchuk O. (2008). Germ-line mutations, DNA damage, and global hypermethylation in mice exposed to particulate air pollution in an urban/industrial location. , 105: 605-610. [157164](#)
- Yin XJ; Ma JYC; Antonini JM; Castranova V; Ma JKH. (2004). Roles of reactive oxygen species and heme oxygenase-1 in modulation of alveolar macrophage-mediated pulmonary immune responses to listeria monocytogenes by diesel exhaust particles. *Toxicol Sci*, 82: 143-153. [087983](#)
- Ying Z; Kampfrath T; Thurston G; Farrar B; Lippmann M; Wang A; Sun Q; Chen LC; Rajagopalan S. (2009). Ambient particulates alter vascular function through induction of reactive oxygen and nitrogen species. *Toxicol Sci*, 1: 1-36. [190111](#)
- Zhang J; Ghio AJ; Chang W; Kamdar O; Rosen GD; Upadhyay D. (2007). Bim mediates mitochondria-regulated particulate matter-induced apoptosis in alveolar epithelial cells. *FEBS Lett*, 581: 4148-4152. [156179](#)
- Zhao H; Barger MW; Ma JKH; Castranova V; Ma JYC. (2006). Cooperation of the inducible nitric oxide synthase and cytochrome P450 1A1 in mediating lung inflammation and mutagenicity induced by diesel exhaust particles. *Environ Health Perspect*, 114: 1253-1258. [100996](#)

Chapter 6. Integrated Health Effects of Short-Term PM Exposure

6.1. Introduction

This chapter summarizes, reviews, and integrates the evidence of relationships between short-term exposures to PM and a variety of health-related endpoints. Cardiovascular and respiratory health effects of short-term exposure to various size fractions and sources of PM have been examined in an expansive number of epidemiologic, controlled human exposure and toxicological studies. In addition, there is a large body of literature evaluating the relationship between mortality and short-term exposure to PM. The association between PM exposure and central nervous system function has also been assessed, although far fewer studies are available. The research approaches used to evaluate health effects of PM exposure are described in Section 1.5 along with advantages and limitations of the various study types. Chapter 5 provides an overview of the potential pathophysiological pathways and modes of action underlying the PM-induced health effects observed in animal and human studies. Evidence from the scientific literature of specific cardiovascular and systemic effects, respiratory effects, and central nervous system effects associated with exposure to PM are presented in Sections 6.2, 6.3, and 6.4, respectively. Evidence of associations between short-term exposure to PM and mortality are described in Section 6.5. The chapter concludes with a preliminary evaluation of PM-induced health effects attributable to specific constituents or sources (Section 6.6). More detailed descriptions of each study evaluated for this assessment are presented in Annexes C, D, and E.

Findings for cardiovascular and respiratory effects are presented by specific endpoint or measure of effect, leading from more subtle health outcome measures (e.g., heart rate variability [HRV]) to the more severe, such as hospitalization for cardiovascular disease. Conclusions from the 2004 PM AQCD (U.S. EPA, 2004, [056905](#)) are briefly summarized at the beginning of each section, and the evaluation of evidence from recent studies builds

Note: Hyperlinks to the reference citations throughout this document will take you to the NCEA HERO database (Health and Environmental Research Online) at <http://epa.gov/hero>. HERO is a database of scientific literature used by U.S. EPA in the process of developing science assessments such as the Integrated Science Assessments (ISA) and the Integrated Risk Information System (IRIS).

upon what was available during the previous review. For each health outcome, results are summarized for studies from the specific scientific discipline, i.e., epidemiologic, controlled human exposure, and toxicological studies. The sections conclude with summaries of the evidence on the various health outcomes and integration of the findings that leads to conclusions regarding causality based upon the framework described in Chapter 1. Determination of causality is made for the overall health effect category, such as cardiovascular effects, with coherence, consistency and plausibility being based upon the evidence from across disciplines and also across the suite of related health outcomes ranging from the more subtle health outcomes to cause-specific mortality. In the summary sections for cardiovascular and respiratory effects, the evidence is summarized and independent conclusions drawn for relationships with PM_{2.5}, PM_{10-2.5}, and UFPs (Sections 6.2.11 and 6.3.9, respectively). Evidence of central nervous system effects is also divided by scientific discipline (Section 6.4); however, the lack of data does not allow for informative summaries of effect by PM metric in discussing CNS effects.

6.2. Cardiovascular and Systemic Effects

6.2.1. Heart Rate and Heart Rate Variability

Heart rate (HR), HRV, and BP are all regulated, in part, by the sympathetic and parasympathetic nervous systems. Changes in one or more may increase the risk of cardiovascular events (e.g., arrhythmias, MI, etc.). Decreases in HRV have been associated with cardiovascular mortality/morbidity in older adults and those with significant heart disease (TFESC, 1996, [003061](#)).

HRV is measured using electrocardiograms (ECG) and can be analyzed in the time domain (e.g., standard deviation of all NN intervals [SDNN], square root of the mean squared successive NN interval differences [rMSSD]), and/or the frequency domain measured by power spectral analysis (e.g., high frequency [HF], low frequency [LF], ratio of LF to HF [LF/HF]). SDNN generally reflects the overall modulation of HR by the autonomic nervous system, whereas rMSSD generally reflects parasympathetic activity and high frequency variations in HR. Thus, rMSSD is generally well correlated with HF, which also reflects the parasympathetic modulation of HR. LF is predominately dictated by sympathetic tone and increased LF/HF indicates sympathoexcitation, which correlates

overall with decreased overall HRV (SDNN, rMSSD). Thus LF/HF is thought to estimate the ratio of sympathetic influences on HR to parasympathetic influences.

While HRV is commonly described as being a reflection of vagal and adrenergic input to the heart, there is clearly a more complex phenomenon reflected in HRV parameters. Rowan et al. (2007, [191911](#)) provide a review of HRV and its use and interpretation with respect to air pollution studies. To summarize, HRV indices are excellent measures of extrapulmonary effects from inhaled pollutants, but the characterization of the acute, reversible responses to air pollution as being either parasympathetic or sympathetic in origin, much less predictive of some adverse outcomes such as ventricular arrhythmia, is relatively unsupported by the clinical literature. This is consistent with the 2004 PM AQCD (U.S. EPA, 2004, [056905](#)) which stated that there is inherent variability in the minute-to-minute spectral measurements, but long-term HRV measures demonstrate excellent day-to-day reproducibility.

The 2004 PM AQCD (U.S. EPA, 2004, [056905](#)) presented limited evidence of PM-induced changes in HRV. However, findings from epidemiologic, controlled human exposure and toxicological studies were seemingly contradictory, with reports of both decreases and increases in HRV following PM exposure. Recent epidemiologic studies have demonstrated a more consistent decrease in HRV (SDNN and rMSSD), which is supported by several controlled human exposure studies published since 2003. In these studies, decreases in HRV were observed among healthy adults following short-term exposures to PM_{2.5} and PM_{10-2.5} CAPs. It is interesting to note that these effects were not observed in adults with asthma or COPD. The effect of PM on HRV observed in animal toxicological studies continues to vary greatly, which may be due in part to strain differences in baseline HRV.

6.2.1.1. Epidemiologic Studies

The 2004 PM AQCD (U.S. EPA, 2004, [056905](#)) reviewed several studies of PM exposure and HR or HRV and described discrepant findings across studies. Several studies have investigated the association between acute changes in multiple HRV parameters and ambient air pollutant concentrations in the U.S., Canada, Europe, Mexico, and Asia. Features and results of these studies are presented in Table 6-1, and are summarized below.

In a multicity study, Liao and colleagues (2004, [056590](#)) used data from the fourth cohort evaluation of the Atherosclerosis Risk in Communities (ARIC) Study (1996-1998).

The 6,784 subjects were 45-64 yr of age and lived in Washington County, MD, Forsyth County, NC, or the suburbs of Minneapolis, MN. At each HRV measurement session, each subject rested comfortably for 15 min in the supine position in a quiet, semi-dark room, with a constant temperature of 24°C. Then, resting, supine, 5-min beat-to-beat RR- interval data were collected. All measurements were made between 8:30 a.m. and 12:30 p.m. Linear regression models, adjusting for multiple covariates (i.e., age, ethnicity, gender, education, smoking, BMI, cardiovascular medications, presence of coronary heart disease, diabetes, hypertension, HR, humidity, temperature, and season), were used to examine the change in HRV associated with PM₁₀, O₃, SO₂, CO, and NO₂ concentrations in the 1-3 days prior to ECG measurement. Among all subjects, each 11.5 µg/m³ increase in mean daily PM₁₀ concentration 1 day before the ECG measurement was associated with a 0.06 ms² decrease in log-transformed HF (95% CI: -0.10 to -0.02) and a 1.03 m decrease in SDNN (95% CI: -1.64 to -0.42). A smaller non-significant decrease was also observed for log transformed LF. This reduction in cardiac autonomic control was larger among hypertensive subjects, suggesting that this group may be susceptible to the effects of PM.

In a study of 4,295 randomly selected participants in the Women's Health Initiative (WHI), a multicity U.S. study, Whitsel et al. (2009, [191980](#)) found decreases in rMMSD and SDNN in association with PM₁₀ concentration. The associations were stronger among participants with diabetes. For example, among those with impaired fasting glucose, the reduction in rMSSD was 8.3% (-13.9, 2.4) among those with high levels of insulin and 0.6% (-2.1, 1.6) among those with low levels of insulin. Similar results were observed comparing high and low levels of insulin resistance.

Timonen et al. (2006, [088747](#)) conducted a multicity panel study of n = 131 elderly subjects with stable coronary heart disease who lived in 3 European cities (Amsterdam, Netherlands; Erfurt, Germany; or Helsinki, Finland). They collected ECGs biweekly for six months in each subject. This analysis, done as part of the ULTRA Study, examined changes in HRV (resting, paced breathing, supine, and five min beat-to-beat NN intervals) associated with changes in fixed monitor particulate concentrations (PM_{2.5}, PM_{10-2.5}) with an emphasis on ultrafine particle counts (UFP; 0.01-0.1 µm particles) and counts of accumulation mode particles (ACP; 0.1-1.0 µm particles). Mixed models adjusting for time trend, weekday, humidity, barometric pressure, and temperature were first fit to estimate the change in HRV associated with PM (UFP, ACP, PM_{2.5}, and PM_{10-2.5}) concentrations on the same and previous four days in each city. Then, in pooled analyses, the most consistent

results were for LF/HF. During paced breathing, each 10,000 particles/cm³ increase in two day lagged UFP was associated with a 13.5% decrease in LF/HF (95% CI: -20.1 to -7.1). Each 1,000 particles/cm³ increase in 1 day lagged ACP was associated with a 7.8% decrease in LF/HF (95% CI: -13.0 to -0.2). Although not statistically significant, each 10 µg/m³ increase in 2 day lagged mean PM_{10-2.5} concentration was associated with a 3.3% decrease in LF/HF (95% CI: -12.7 to 6.1). For PM_{2.5}, however, results were not consistent across cities, and thus a pooled estimate was not appropriate. PM_{2.5} was associated with decreased HF power and increased LF/HF in Helsinki, increased HF power and decreased LF/HF in Erfurt, and not associated with any HRV metric in Amsterdam. The authors state that these contrasting city-specific PM_{2.5} findings do not clearly support a PM/HRV association, but suggest that effects may be dependent on PM sources and subject characteristics in each city. In a subsequent analysis, de Hartog et al. (2009, [191904](#)) investigated whether exposure misclassification, effect modification by medication use, or particle composition differences across the three cities could explain the result observed. They reported that 1 µg/m³ increases in traffic related and long range transported PM_{2.5} were associated with -0.28 ms (95% CI: -0.57 to 0.01) and -0.05 ms (95% CI: -0.17 to 0.07) changes in SDNN, respectively, with smaller sized reductions at lags 0, 1, and 3. Further, these source apportioned particles as well as outdoor PM_{2.5} were associated with reduced HRV only among those not taking beta-blockers. There were no consistent patterns for other medication classes. Thus, effect modification by medication use and particle composition differences across the three cities may, in part, explain the heterogeneous PM_{2.5} findings in the previous analysis (Timonen et al., 2006, [088747](#)).

The association between HRV and short-term increases in PM_{2.5}, PM_{10-2.5}, PM₁₀, other size fractions and components was also examined in single-city studies (Table 6-1). Among U.S. and Canadian cities, increases in PM_{2.5} were generally associated with decreased SDNN (Adar et al., 2007, [001458](#); Ebel et al., 2005, [056907](#); Fan et al., 2008, [191979](#); Luttmann-Gibson et al., 2006, [089794](#); Park et al., 2005, [057331](#); Pope et al., 2004, [055238](#); Schwartz et al., 2005, [074317](#)) and/or decreased HF power (Adar et al., 2007, [001458](#); Baccarelli et al., 2008, [157984](#); Ebel et al., 2005, [056907](#); Luttmann-Gibson et al., 2006, [089794](#); Park et al., 2005, [057331](#); Schwartz et al., 2005, [074317](#)), but not in all studies. Two studies reported increased SDNN associated with PM_{2.5} concentrations (Riediker et al., 2004, [056992](#); Wheeler et al., 2006, [088453](#)). Yeatts et al. (2007, [091266](#)) also reported increased rMSSD, SDANN5 (standard deviation of the average of normal to normal

intervals in all 5-min intervals in a 24-h period), and SDNN24HR (standard deviation of the average of all normal to normal intervals in a 24-h period), and HF power associated with increased PM_{2.5} concentrations. Lipsett et al. (2006, [088753](#)) reported significantly decreased SDNN associated with increases in 2- and 6-h mean PM₁₀ and PM_{10-2.5} concentrations. Similarly, Yeatts et al. (2007, [091266](#)) reported decreased rMSSD, SDNN24HR, SDANN5, ASDNN5 (mean of the standard deviation in all 5-min segments of a 24-h recording), proportion of NN intervals <50 ms apart (pNN50) (7-min and 24-h), and HF power associated with increased PM_{10-2.5} concentration. Of those studies examining HRV associations with particle counts (Adar et al., 2007, [001458](#); Park et al., 2005, [057331](#)), only Adar et al. (2007, [001458](#)) found clear evidence of such effects (e.g., decreased SDNN, LF, HF). Decreased HRV was also associated with increases in ambient mean SO₄²⁻ concentration (Luttmann-Gibson et al., 2006, [089794](#)), ambient mean BC concentration, (Park et al., 2005, [057331](#); Schwartz et al., 2005, [074317](#)), and traffic generated particles/pollution (Adar et al., 2007, [001458](#); Riediker et al., 2004, [056992](#)).

Studies in Asia, Europe, and Mexico have reported decreases in one or several HRV metrics (see Figure 6-1) associated with increases in PM_{2.5} concentration or other size fractions (Chan et al., 2004, [087398](#); Chuang et al., 2005, [087989](#); Chuang et al., 2007, [091063](#); Cárdenas et al., 2008, [191900](#); Folino et al., 2009, [191902](#); Holguin et al., 2003, [057326](#); Min et al., 2008, [191901](#); Riojas-Rodriguez et al., 2006, [156913](#); Romieu et al., 2005, [086297](#)). However, one study reported no PM-HRV associations (Barclay et al., 2009, [179935](#)). Langrish et al. (2009, [191908](#)) reported that study subjects, who were residents of Beijing, had decreased HRV when they wore a face mask while walking for 2 h on a predetermined route. HRV measures were higher when they did not wear the mask. In contrast, Riojas-Rodriguez et al. (2006, [156913](#)) reported significantly decreased LF and HF power associated with each 1 ppm increase in CO concentration, but only small non-significant decreases associated with PM_{2.5}.

HRV studies investigated lagged pollutant concentrations from 2 h to 5 days before ECG measurement, reporting effects associated with mean pollutant concentrations lagged as short as 1-2 h, and more consistently lagged 24-48 h. Taken together, these international and U.S./Canadian studies show decreases in HRV associated with PM_{2.5} in most studies that use SDNN, rMSSD or HF power. The effects of PM_{10-2.5}, UFP, and components were evaluated in fewer studies but associations with decreased HRV (e.g., both time and frequency measures) were observed. The proportion of studies reporting decreases in HRV

may be inflated by publication bias (i.e., studies showing little or no effects are not submitted for publication).

HRV Studies Investigating Specific Mechanisms

Panel studies investigating PM-HRV associations have also been useful in investigating potential mechanistic pathways by which PM may elicit a cardiovascular response. A series of analyses using data from the Normative Aging Study (NAS), a cohort of older men living in the Boston metropolitan area, has also provided mechanistic insights into the PM/HRV association (Baccarelli et al., 2008, [191959](#); Chahine et al., 2007, [156327](#); Park et al., 2005, [057331](#); Park et al., 2006, [091245](#); Park et al., 2008, [156845](#); Schwartz et al., 2005, [086296](#)).

Park et al. (2005, [057331](#)) studied the association between short-term increases in ambient air pollution and changes in HRV using $n = 497$ males enrolled in the NAS. Subjects had ECG measurements made during a 4-min rest period between 8:00 a.m. and 1:00 p.m. Using linear regression models, adjusted for age, BMI, fasting blood glucose, smoking, cardiac medications, room temperature, and season, the association between HRV metrics and $PM_{2.5}$, O_3 , NO_2 , SO_2 , CO, BC, and particle number count moving averages (ma) in the previous 4, 24, and 48 h was examined. The modifying effects of hypertension, diabetes, ischemic heart disease, and use of hypertensive medications were also estimated. Of the pollutants examined, only $PM_{2.5}$ and O_3 were associated with reductions in HRV, and each pollutant's effect appeared independent of the other. Each $8 \mu\text{g}/\text{m}^3$ increase in mean $PM_{2.5}$ concentration in the previous 48 h was associated with a 20.8% decrease in the component of HRV HF (95% CI: -34.2% to -4.6%), with larger effects among subjects with hypertension, ischemic heart disease (IHD), and diabetes. O_3 effects were strongest with the 4-h ma. The authors state that since BC concentrations were also associated with adverse changes in HRV, this suggests that traffic pollution may be particularly toxic.

Schwartz et al. (2005, [086296](#)) examined the hypothesis that adverse changes in HRV due to $PM_{2.5}$ are mediated by an oxidative stress response among participants in the NAS. They examined whether the change in the HF component of HRV associated with each $10 \mu\text{g}/\text{m}^3$ increase in 48-h mean $PM_{2.5}$ was modified by the presence or absence of the allele for glutathione S-transferase M1 (GSTM1), use of statins, obesity, high neutrophil counts, higher BP, and/or older age. In subjects without the GSTM1 allele and its protection against oxidative stress, each $10 \mu\text{g}/\text{m}^3$ increase in 48-h mean $PM_{2.5}$ concentration was associated

with a 34% decrease in HF (95% CI: -52% to -9%). There was no association among those with at least one copy of the allele. Obesity and high neutrophil counts also worsened the effect of PM on HRV regardless of allele.

Park et al. (2006, [091245](#)) investigated whether transition metals may be responsible for cardiorespiratory effects that are observed in association with PM_{2.5}. Again using the NAS cohort, they investigated whether subjects with two hemochromatosis (HFE) polymorphisms associated with increased iron uptake had a smaller decrease in HF HRV associated with PM than those subjects without either variant. Each 10 µg/m³ increase in 48-h mean PM_{2.5} was associated with a 31.7% decrease in HF (95% CI: -48.1 to -10.3%) among subjects without either polymorphism, but not among those with the two protective HFE alleles.

Chahine et al. (2007, [156327](#)) reported a 10.5% reduction in SDNN (95% CI: -18.2% to -2.2%) associated with each 10 µg/m³ increase in the mean 48-h PM_{2.5} concentration among NAS participants without the GSTM1 allele, but only a 2.0% SDNN decrease (95% CI: -11.3%, 8.3%) in those with the allele. This confirmed the PM/HF HRV findings of Schwartz et al. (2005, [074317](#)). Further, subjects with the long repeat polymorphism in the HO-1 promoter had a greater decline in SDNN associated with each 10 µg/m³ increase in the mean 48-h PM_{2.5} concentration (-8.5% [95% CI: -14.8% to -1.8%]) than those with the short repeat polymorphism in HO-1 (7.4 % increase [95% CI: -8.7% to 26.2%]). Again, this suggests that PM-HRV changes are mediated, in part, by oxidative stress.

Baccarelli et al. (2008, [191959](#)) investigated whether the HRV-PM_{2.5} association was modified by dietary intakes of methyl nutrients (folate, vitamins B6 and B12, and methionine) and related gene polymorphisms thought to either confer increased or decreased risk of CVD among men enrolled in the NAS. Each 10 µg/m³ increase in PM_{2.5} in the previous 48 h was associated with -8.8% (95% CI: -16.7 to -0.2) and -11.8% (95% CI: -20.8 to -1.8) decreases in SDNN, among those with CC/TT genotypes of the C677T methylenetetrahydrofolate reductase (MTHFR) polymorphism, and the CC genotype of the C1420T cytoplasmic serine hydroxymethyltransferase (cSHMT) polymorphism, respectively. There were no changes among those with CC MTHFR and CC/TT cSHMT. Further, there were similar HRV reductions in those subjects with lower intakes of B6, B12, and/or methionine, but no decreases in those with high intakes. Thus these genetic and nutritional variations in the methionine cycle may modify the PM/HRV association.

Finally, among those NAS subjects with high chronic lead exposure as measured using X-ray fluorescence of the tibia, each $7 \mu\text{g}/\text{m}^3$ increase in mean $\text{PM}_{2.5}$ concentration in the previous 48 h was associated with a 22% decrease in HF HRV (95% CI: -37.4% to -1.7%) (Park et al., 2008, [093027](#)). Decreases in HF HRV were also associated with each $2.5 \mu\text{g}/\text{m}^3$ increase in mean SO_4^{2-} concentration in the previous 48 h (22% decrease [95% CI: -40.4% to 1.6%]) and each 16 ppb increase in mean O_3 concentration in the previous 48 h (38% decrease [95% CI: -54.6% to -14.9%]). The authors suggest that these findings are consistent with an oxidative stress response. Although this series of studies suggest a role of oxidative stress and perhaps methyl nutrients and related polymorphisms in these short-term associations of $\text{PM}_{2.5}$ with HRV, replication by other investigators in other cities and in other populations will aid interpretations of these findings.

Using data from a randomized controlled trial in Mexico City, Romieu et al. (2005, [086297](#)) investigated whether omega-3 fatty acids in fish oil supplements would mitigate the adverse effects of acute PM exposure on HRV. Residents of a Mexico City nursing home (N=50, aged >60 yr), subjects were randomized to either 2 g/day of fish oil or 2 g/day of soy oil. They used random-effects regression models to estimate the change in HRV associated with mean $\text{PM}_{2.5}$ concentration in the pre-supplementation and supplementation phases. In the group receiving the fish oil supplement, each $8 \mu\text{g}/\text{m}^3$ increase in 24-h mean total $\text{PM}_{2.5}$ exposure (weighted average of indoor and outdoor $\text{PM}_{2.5}$ based on time activity diaries) was associated with a 54% reduction (95% CI: -72% to -24%) in log transformed HF in the pre-supplementation phase. However, in the supplementation phase of the trial, each $8 \mu\text{g}/\text{m}^3$ increase in 24-h mean total $\text{PM}_{2.5}$ concentration was associated with only a 7% reduction in log transformed HF (95% CI: -20% to 7%). Decreases in other HRV parameters associated with $\text{PM}_{2.5}$ were also muted in the supplementation phase. In the group receiving the soy oil supplement, the reduction in HF was also smaller in magnitude during the supplementation phase. However, among those receiving the soy oil supplement, the differences between the pre-supplementation $\text{PM}_{2.5}$ -HF change and the supplementation $\text{PM}_{2.5}$ -HF change were smaller compared to those receiving the fish oil, and were not statistically significant. Romieu et al. (2008, [156922](#)) also report that omega-3 polyunsaturated fatty acids appear to modulate the adverse effect of $\text{PM}_{2.5}$ based on measured biomarkers of oxidative response (see Section 6.2.9.1.).

In summary, several analyses of data from the Normative Aging Study have provided evidence that HRV is modulated by genetic polymorphisms related to oxidative stress

(Chahine et al., 2007, [156327](#); Park et al., 2006, [091245](#); Schwartz et al., 2005, [086296](#)) preexisting conditions such as diabetes, IHD, and hypertension (Park et al., 2005, [057331](#); Whitsel et al., 2009, [191980](#)), or dietary methyl nutrients or related genetic polymorphisms (Baccarelli et al., 2008, [191959](#)). Another analysis reported that the HRV-PM association was more pronounced among those with chronic lead exposure (Park et al., 2008, [093027](#)). In addition, omega-3 fatty acid was found to modulate the effect of PM_{2.5} on HRV in a randomized trial conducted in Mexico City (Romieu et al., 2005, [086297](#)) and beta-blocker use (Folino et al., 2009, [191902](#)) was found to modify the PM-HRV association in a study in Padua, Italy.

Table 6-1. Characteristics of epidemiologic/panel studies investigating associations between PM and changes in HRV.

	PM Type, Exposure Lag	Study Subjects	Ambient Concentration Mean (SD) **	Recording Length	SDNN	LF	HF, rMSSD	LF/HF
U.S. AND CANADIAN STUDIES								
Park et al. (2005, 057331)	PM _{2.5} , 48-h avg	497 men (mean age = 73[7] yr), Normative Aging Study Boston MA	24-h: 11.4 (8.0) $\mu\text{g}/\text{m}^3$ 98th: 30.58	4-min	↓	↓	↓	↑
	PN, 48-h avg		24-h: 28,942 (13,527) particles/cm ³		→	↓	↓	↓
	BC, 48-h avg		24-h: 0.92 (0.47) $\mu\text{g}/\text{m}^3$		↓	↓	↓	↑
Liao et al. (2004, 056590)	24-h PM ₁₀ , lag 1-day	6784 (mean age = 62[6] yr), ARIC study: MD, NC, MN	24.3 $\mu\text{g}/\text{m}^3$	5-min	↓	↓	↓	
Riediker et al. (2004, 056992)	In-vehicle PM _{2.5} (mass) 9-h avg	9 state troopers	9-h in-vehicle avg 23 $\mu\text{g}/\text{m}^3$	10-min	↑	→	↑	↓
Schwartz et al. (2005, 074317)	BC, 24-h	28 (61-89 yr), 12 wk follow-up, Boston, MA	24-h Median: 1.0 $\mu\text{g}/\text{m}^3$	23-min	↓		↓	↑
	PM _{2.5} , 24-h		24-h Median: 10 $\mu\text{g}/\text{m}^3$		↓		↓	↑
	Secondary PM (estimated), 24-h		1-h Median: 1.7 $\mu\text{g}/\text{m}^3$		↓		↓	↑
Yeatts et al. (2007, 091266)	24-h PM _{10-2.5}	12 adult asthmatics, Chapel Hill, NC	5.3 (2.8) $\mu\text{g}/\text{m}^3$	5-min	↓	↓	↓	
	24-h PM _{2.5}		12.5 (6.0) $\mu\text{g}/\text{m}^3$		↑	↓	↑	
Wheeler et al. (2006, 088453)	PM _{2.5} , 4-h avg	18 COPD, Atlanta, GA	17.8 $\mu\text{g}/\text{m}^3$	20-min	↑	↑	↑	↑
	PM _{2.5} , 4-h avg	12 MI, Atlanta, GA			↓	↑	↓	↓
	EC, 4-h avg	18 COPD, Atlanta, GA	2.3 $\mu\text{g}/\text{m}^3$		↑	Not presented	Not presented	Not presented
	EC, 4-h avg	12 MI, Atlanta, GA			↓	Not presented	Not presented	Not presented
Dales 2004 (2004, 099036)	PM _{2.5} 24-h avg (personal)	36 CAD patients, Toronto, Canada	19.9 (13.8) $\mu\text{g}/\text{m}^3$	Not described	→	→	→	→
Luttmann-Gibson et al. (2006, 089794)	PM _{2.5} , lag 1-day	32 (65+ yr), Steubenville OH	24-h: 19.7 $\mu\text{g}/\text{m}^3$	~ 30-min.	↓	↓	↓	
	Sulfate, lag 1-day		24-h: 6.9 $\mu\text{g}/\text{m}^3$		↓	↓	↓	
	Nonsulfate PM, lag 1-day		24-h: 10.0 $\mu\text{g}/\text{m}^3$		↓	↓	↓	

	PM Type, Exposure Lag	Study Subjects	Ambient Concentration Mean (SD) **	Recording Length	SDNN	LF	HF, rMSSD	LF/HF
	EC, lag 1-day		24-h: 1.1 $\mu\text{g}/\text{m}^3$		↑	↓	→	
Adar et al. (2007, 001458)	PM _{2.5} , 24-h avg	44 (60+ yr), diesel bus riders, St. Louis, MO	10.17 $\mu\text{g}/\text{m}^3$ 98th: 22.43	5-min.	↓	↓	↓	↑
	BC, 24-h avg		330 ng/m ³		↓	↓	↓	↑
	PC fine		42 particles/cm ³		↓	↓	↓	↑
	PC course		0.02 particles/cm ³		↑	↑	↑	↓
Pope et al. (2004, 055238)	24-h PM _{2.5} (FRM), lag 1-day	88 subjects (65+ yr; 250 p-days), Utah Valley	23.7 (20.2) $\mu\text{g}/\text{m}^3$	24-h	↓		↓	
Sullivan et al. (2005, 109418)	PM _{2.5} , 1, 2, 24-h avg	21 subjects (65+ yr) with CVD, Seattle WA 13 subjects (65+ yr) w/out CVD, Seattle WA	Median: 10.7 $\mu\text{g}/\text{m}^3$	20-min	→		→	
Lipsett et al. (2006, 088753)	PM ₁₀ , lag * PM _{10-2.5} , lag * PM _{2.5} , lag *	19 CAD patients (65+ yr), 12 wk fu, Coachella Valley, CA	31.0 and 46.1 $\mu\text{g}/\text{m}^3$ None given 14 & 23.2 $\mu\text{g}/\text{m}^3$	5-min F domain; 2-h, 24-h T domain	↓ ↓ ↓	↓ ↓ ↓	↓ → ↑	
Ebelt et al. (2005, 056907)	PM ₁₀ – 24 h PM _{10-2.5} (calculated from PM ₁₀ and PM _{2.5} values) PM _{2.5} – 24-h PM _{2.5} Sulfate – 24-h outdoor	16 subjects with COPD in Vancouver, Canada	17 (6) $\mu\text{g}/\text{m}^3$ 5.6 (3.0) $\mu\text{g}/\text{m}^3$ 11.4 (4.6) $\mu\text{g}/\text{m}^3$ 98th: 23 2.0 (1.1) $\mu\text{g}/\text{m}^3$	24-h	↓ ↑ ↓ ↓		↓ → ↓ →	
Baccarelli et al. (2008, 191959)	PM _{2.5} – 48 h	549 subjects in Normative Aging Study and residents of Boston metropolitan area	Geometric mean (95% confidence interval) 10.5 (10.0, 10.9) $\mu\text{g}/\text{m}^3$	7 min	↓			
Fan et al. (2008, 191979)	PM _{2.5} personal -1 h	11 crossing guards in New Jersey	Only change in 1-h PM _{2.5} reported Morning shift: 35.2 ± 25.9 $\mu\text{g}/\text{m}^3$ Afternoon shift: 24.1 ± 22.1 $\mu\text{g}/\text{m}^3$	24 h	↓			
Whitsel et al. (2009, 191980)	PM ₁₀ 24 h	4295 randomly selected participants in the WHI Trial	Mean ± se 28 ± 0.2 visit 1 27 ± 0.2 visit 2 27 ± 0.3 visit 3	10 second	↓		↓	
INTERNATIONAL STUDIES								
Timonen et al. (2006, 088747)	UF, lags 0-2 days AC, lags 0-2 days	Stable CHD patients (65+ yr) n = 37: Amsterdam n = 47: Erfurt n = 47: Helsinki	Amsterdam: 17,300 particles/cm ³ Erfurt: 21,100 particles/cm ³ Helsinki: 17,000 particles/cm ³ Amsterdam: 2100 particles/cm ³ Erfurt: 1800 particles/cm ³ Helsinki: 1400 particles/cm ³	5-min (Pooled estimates during paced breathing presented to the right)	↓ ↓		↑ ↑	↓ ↓

	PM Type, Exposure Lag	Study Subjects	Ambient Concentration Mean (SD) **	Recording Length	SDNN	LF	HF, rMSSD	LF/HF
	PM _{2.5} , lags 0-2 days		Amsterdam: 20.0 $\mu\text{g}/\text{m}^3$ Erfurt: 23.1 $\mu\text{g}/\text{m}^3$ Helsinki: 12.7 $\mu\text{g}/\text{m}^3$		↓		↑	↓
	PM _{10-2.5} , 2-day lag		Amsterdam: 15.3 $\mu\text{g}/\text{m}^3$ Erfurt: 3.7 $\mu\text{g}/\text{m}^3$ Helsinki: 6.7 $\mu\text{g}/\text{m}^3$		→		→	↓
Chan et al. (2003, 089398)	NC _{0.02-1} 1-4 h	9 adults (19-29 yr) with lung function impairment Taipei, Taiwan	23,407 (19,836) particles/cm ³	5 min	↓	↓	↓	↓
		10 adults (42-79 yr) with lung function impairment Taipei, Taiwan	25,529 (20,783) particles/cm ³		↓	↓	↓	↓
Chuang et al. (2005, 087989)	PM _{1.0-0.3} 1-4 h	16 CHD hypertensive patients, Taipei Taiwan	37.2 (25.8) $\mu\text{g}/\text{m}^3$	5-min	↓	↓	↓	↑
	PM _{2.5-1.0} 1-4 h		12.6 (7.8) $\mu\text{g}/\text{m}^3$		↓	↓	↓	↑
	PM _{10-2.5} 1-4 h		14.0 (11.1) $\mu\text{g}/\text{m}^3$		↓	↓	↓	↑
	PM _{1.0-0.3} 1-4 h	10 CHD patients, Taipei Taiwan	26.8 (25.9) $\mu\text{g}/\text{m}^3$		↓	↓	↓	→
	PM _{2.5-1.0} 1-4 h		10.9 (8.5) $\mu\text{g}/\text{m}^3$		↓	↓	↓	↓
	PM _{10-2.5} 1-4 h		16.4 (10.7) $\mu\text{g}/\text{m}^3$		↓	↓	↓	↑
Holguin et al. (2003, 057326)	24-h PM _{2.5}	21 without hypertension (60-96 yr), Mexico City	37.2 (13.5) $\mu\text{g}/\text{m}^3$	5-min		↓	↓	↑
		13 with hypertension (60-88 yr), Mexico City				↓	↓	↑
Romieu et al. (1995, 089297)	24-h PM _{2.5} (outdoor and indoor)	50 nursing home residents 65+ yr, Mexico City	Outdoor: 19.4 (5.7) $\mu\text{g}/\text{m}^3$ Indoor: 18.3 (5.8) $\mu\text{g}/\text{m}^3$	6-min (Indoor PM _{2.5} , pre-supplement phase presented)	↓	↓	↓	
Riojas-Rodriguez et al. (2006, 156913)	Personal PM _{2.5}	30 IHD patients, Mexico City	Geometric mean: 46.8 $\mu\text{g}/\text{m}^3$	5-min		↓	↓	
Barclay et al. (2009, 179935)	PM ₁₀ - daily Particle number count (PNC)-daily Estimated PM _{2.5} and PNC	132 subjects with stable coronary heart failure Aberdeen, Scotland	Range of daily means: 7.4 to 68 $\mu\text{g}/\text{m}^3$	24 hs	→			
Cárdenas et al. (2008, 191900)	PM _{2.5} -outdoor PM _{2.5} -indoor	52 subjects (31 women, 21 men; 20-40 yr), southeast of Mexico City	Median PM _{2.5} outdoor: 28.3 $\mu\text{g}/\text{m}^3$ Median PM _{2.5} indoor: 10.8 $\mu\text{g}/\text{m}^3$	15 min		↓	↓	↓
De Hartog et al. (2009, 191904)	PM _{2.5} outdoor – 24 h	Amsterdam, Netherlands (37 subject) Erfurt, Germany (47 subjects) Helsinki, Finland (47 subjects)	Median $\mu\text{g}/\text{m}^3$ Amsterdam: 16.7 Erfurt: 16.3 Helsinki: 10.6	5 min	↓		↓	

	PM Type, Exposure Lag	Study Subjects	Ambient Concentration Mean (SD) **	Recording Length	SDNN	LF	HF, rMSSD	LF/HF
Folino et al. (2009, 191902)	PM ₁₀ 24 h PM _{2.5} 24 h PM _{0.25} 24 h	39 subjects (36 male, 3 female; mean age = 60 yr) Padua Italy	PM ₁₀ Mean ± std μg/m ³ Summer 46.4 ± 16.1 Winter 73.0 ± 30.9 Spring 38.3 ± 15.4 PM _{2.5} Mean ± std μg/m ³ summer 33.9 ± 12.7 Winter 62.1 ± 27.9 Spring 30.8 ± 14.0 PM _{0.25} Mean ± std μg/m ³ Summer 17.6 ± 7.5 Winter 30.5 ± 17.4 Spring 18.8 ± 10.8	24 h	↓			
Langrish et al. (2009, 191908)	PM _{2.5} -personal 2 h PNC-personal 2 h	15 young healthy volunteers (median age = 28 yr) Beijing	PM _{2.5} with mask: Mean = 86 μg/m ³ Without mask: Mean = 140 μg/m ³ PNC with mask: Mean = 23,379 particles/cm ³ PNC without mask: Mean = 24,184 particles/cm ³	24 h	↓ withoutmask	↓ withoutmask		
Min et al. (2008, 191901)	PM ₁₀ 12 h	1349 subjects (596 males; mean age = 44 yr) Korea	Mean ± std: 1-h avg 33.244 ± 19.017	5 min	↓	↓	↓	

Notes: Increases (↑), decreases (↓) and no effects (→) in HRV associated with PM concentration are indicated. Statistical significance was not necessary to categorize an effect as an increase or decrease.

For time domain measures moving average lags up to 24-h were explored. For frequency domain measures lags of 2-h, 4-h and 24-h were explored.

** All concentrations are means, unless otherwise noted.

6.2.1.2. Controlled Human Exposure Studies

The 2004 PM AQCD (U.S. EPA, 2004, [056905](#)) cited one study in which HRV indicators of parasympathetic activity increased relative to filtered air control following a 2-h exposure with intermittent exercise to PM_{2.5} CAPs (average concentration 174 μg/m³) in both healthy and asthmatic volunteers (Gong et al., 2003, [042106](#)). This effect was observed immediately following exposure and at 1 day post-exposure, but not at 4 h post-exposure. Although not statistically significant, HRV (total power) increased following exposure to filtered air and decreased following exposure to CAPs. More recent controlled human exposure studies are described below.

CAPs

Two new studies have evaluated the effect of PM_{2.5} CAPs (2-h exposures to concentrations of 20-200 μg/m³) on HRV in elderly subjects (Devlin et al., 2003, [087348](#); Gong et al., 2004, [087964](#)). In both studies, subjects experienced significant decreases in HRV following exposure to CAPs relative to filtered air exposures. Interestingly, Gong et al. (2004, [087964](#)) found that decreases in HRV were more pronounced in healthy older adults

than in those with COPD. In another study, healthy and asthmatic adults were exposed to thoracic coarse CAPs (average concentration 157 $\mu\text{g}/\text{m}^3$) for 2 h with intermittent exercise (Gong et al., 2004, [055628](#)). HRV was not affected immediately following the exposure, but decreased in both groups at 4 and 22 h after the end of the exposure, with greater responses observed in non-asthmatics. In a recent study among healthy adults exposed for 2 h with intermittent exercise to thoracic coarse CAPs (average concentration 89 $\mu\text{g}/\text{m}^3$, MMAD 3.59 μm , Chapel Hill, NC), Graff et al. (2009, [191981](#)) observed a significant decrease in overall HRV (SDNN) at 20 h post-exposure, although no other measures of HRV were affected. Using a similar study design, the same laboratory also evaluated the effect of ultrafine CAPs (average concentration 49.8 $\mu\text{g}/\text{m}^3$, <0.16 μm in diameter) on various HRV parameters (Samet et al., 2009, [191913](#)) Relative to filtered air, HF and LF power were both observed to increase 18 h following exposure to UF CAPs (36-42% increase per 10^5 particles/ cm^3). Exposure to UF CAPs, expressed as mass concentration, was not associated with changes in HF power, and time domain parameters of HRV did not differ between CAPs and filtered air in the 24 h following exposure. Gong et al. (2008, [156483](#)) also recently evaluated changes in HRV following controlled human exposures to UF CAPs and reported a small and transient decrease in LF power ($p < 0.05$) among healthy ($n = 17$) and asthmatic ($n = 14$) adults 4 h after the completion of a 2-h exposure with intermittent exercise in Los Angeles (average concentration 100 $\mu\text{g}/\text{m}^3$, average particle count 145,000/ cm^3). No other measure of HRV was shown to be significantly affected by exposure to UF CAPs. In one of the largest studies of controlled human exposures to CAPs conducted to date, Fakhri et al. (2009, [191914](#)) evaluated changes in HRV among 50 adult volunteers during 2-h exposures to fine CAPs (127 $\mu\text{g}/\text{m}^3$) and O_3 (114 ppb), alone and in combination. Neither exposure to CAPs nor O_3 resulted in any significant changes in HRV relative to filtered air. However, trends were observed suggesting a negative concentration response relationship between CAPs concentration and SDNN, rMSSD, HF power and LF power when subjects were concomitantly exposed to O_3 .

Diesel Exhaust

In a double-blind, crossover, controlled-exposure study, Peretz et al. (2008, [156855](#)) exposed three healthy adult volunteers and 13 adults with metabolic syndrome while at rest to filtered air and two levels of diluted DE (reported $\text{PM}_{2.5}$ concentrations of 100 and 200 $\mu\text{g}/\text{m}^3$) in 2-h sessions. HRV parameters were assessed prior to exposure, as well as at

1, 3, 6 and 22 h following the start of exposure, and included both time domain (SDNN and rMSSD) and frequency domain parameters (HF power, LF power, and the LF/HF ratio). The authors observed an increase in HF power and a decrease in LF/HF 3 h after the start of exposure to 200 $\mu\text{g}/\text{m}^3$ relative to filtered air. Although these changes were statistically significant ($p < 0.05$) the effects were not consistent among the study subjects. No other significant effect of DE on HRV was observed at either concentration or time point. The authors attributed the lack of consistent effects to the small and non-homogeneous population and the timing of measurement. There was no difference in either baseline or diesel-induced changes in HRV parameters between normal individuals and patients with metabolic syndrome, although the number of normal individuals was quite small ($n = 3$). It is unclear if patients with metabolic syndrome were taking any medications.

Model Particles

Several additional recent controlled human exposure studies have evaluated the effect of laboratory generated particles on HRV in healthy and health-compromised individuals. In a random order crossover controlled human exposure study, Routledge et al. (2006, [088674](#)) examined the effects of ultrafine elemental carbon particles ($50 \mu\text{g}/\text{m}^3$) alone and in combination with 200 ppb SO_2 on HRV among 20 healthy older adults (age 56-75), as well as 20 older adults with coronary artery disease (age 52-74). Five minute recordings of HRV data were obtained prior to and immediately following the 1-h exposure, as well as 3 h post-exposure. In healthy subjects, exposure to carbon particles resulted in small increases in RR-interval, SDNN, rMSSD, and LF power immediately following exposure compared to filtered air control. At 3 h post-exposure, there were no significant differences in HRV measures between carbon particle and filtered air exposures. Conversely, SO_2 -induced decreases in HRV were observed at 3 h, but not immediately following exposure. Concomitant exposure to carbon particles and SO_2 followed a pattern similar to that observed with SO_2 alone, but did not reach statistical significance. Subjects with coronary artery disease did not experience any significant changes in HRV following exposure to either pollutant. The authors postulated that this lack of effect may be due to differences in medication between the two groups, as 70% of subjects with stable angina reported using β blockers, which are known to increase cardiac vagal control. The lack of any significant effects on HRV following exposure to carbon particles is an important finding, as it provides evidence to suggest that the health effects observed following exposure to PM may be due to

particle constituents other than carbon, or to reactive species found on the surface of the particle. These findings are in agreement with those of Zareba et al. (2009, [190101](#)) who reported small and variable changes in HRV among a group of healthy adults following exposure to UF elemental carbon. While exposure both at rest and during exercise to 10 $\mu\text{g}/\text{m}^3$ UF carbon resulted in an increase in time domain parameters (rMSSD and SNDD), no such effect was observed following exposure to a higher concentration of UF carbon (25 $\mu\text{g}/\text{m}^3$) in the same subjects. A recent pilot study reported no effect of exposure to elemental carbon and ammonium nitrate particles (250-300 $\mu\text{g}/\text{m}^3$) on HRV parameters in 5 adults with allergic asthma (Power et al., 2008, [191982](#)). However, when the exposure occurred concomitantly with O_3 (0.2 ppm), subjects were observed to experience significant changes in both time and frequency HRV parameters (decreases in SDNN and normalized HF and LF power). These observations should be considered very preliminary as the study was limited by a small sample size ($n = 5$) and did not evaluate the effect of exposure to O_3 without particles. However, these findings are in agreement with the previously described study of CAPs and O_3 conducted by Fakhri et al. (2009, [191914](#)). In addition to the studies of laboratory generated carbon described above, Beckett et al. (2005, [156261](#)) used ZnO as a model particle and exposed twelve resting, healthy adults for 2 h to filtered air and 500 $\mu\text{g}/\text{m}^3$ in the ultrafine (40.4 ± 2.7 nm) and fine (291.2 ± 20.2 nm) modes. Neither ultrafine nor fine ZnO produced a significant change in any time or frequency domain parameter of HRV.

Summary of Controlled Human Exposure Study Findings for Heart Rate Variability

The results of several new controlled human exposure studies provide limited evidence to suggest that acute exposure to near ambient levels of PM may be associated with small changes in HRV. Changes in HRV parameters, however, are variable with some showing increased parasympathetic activity relative to sympathetic activity and others showing the opposite. Although a direct comparison between younger and older adults has not been made, PM exposure appears to result in a decrease in HRV more consistently in healthy older adults (Devlin et al., 2003, [087348](#); Gong et al., 2004, [087964](#)).

6.2.1.3. Toxicological Studies

Toxicological studies that examined HR and HRV are presented in the 2004 PM AQCD (U.S. EPA, 2004, [056905](#)) and overall demonstrated differing responses, which were

collectively characterized as providing limited evidence for PM-related cardiovascular effects. The studies described that reported HR or HRV effects following PM exposure were conducted with a variety of particle types (CAPs, diesel, ROFA, metals), exposure methods (inhalation and IT instillation), and doses (100-3,000 $\mu\text{g}/\text{m}^3$ for inhalation; up to 8.3 mg/kg for IT instillation).

CAPs

Two groups of SH rats exposed to CAPs in Tuxedo, NY for 4 h (single-day mean $\text{PM}_{2.5}$ concentrations 80 and 66 $\mu\text{g}/\text{m}^3$; 2/2001 and 5/2001, respectively) demonstrated decreased HR when exposure groups were combined that returned to baseline values when exposure ceased (Nadziejko et al., 2002, [087460](#)). Fine or ultrafine H_2SO_4 exposure (mean concentration 225 and 468 $\mu\text{g}/\text{m}^3$) did not induce any HR effects. Another study demonstrated a trend toward increased HR in WKY rats following a 1- or 4-day $\text{PM}_{2.5}$ CAPs exposure in Yokohama City, Japan (4.5 h/day; 5/2004, 11/2004, 9/2005), but the correlation between change in HR and cumulative PM mass collected was not significant (Ito et al., 2008, [096823](#)). Increased HR was observed in SH rats exposed to $\text{PM}_{2.5}$ CAPs for two 5-h periods during the spring (mean mass concentration 202 $\mu\text{g}/\text{m}^3$) in a suburb of Taipei, Taiwan (Chang et al., 2004, [055637](#)). The response was less prominent in the summer (mean mass concentration 141 $\mu\text{g}/\text{m}^3$), despite the number concentrations being similar for the two seasons (2.30×10^5 and 2.78×10^5 particles/ cm^3 , respectively).

For HRV, decreased SDNN was observed in SH rats exposed to $\text{PM}_{2.5}$ CAPs (mean mass concentration 202 $\mu\text{g}/\text{m}^3$; mean number concentration 2.30×10^5 particles/ cm^3) for two 5-h periods separated by 24 h (Chang et al., 2005, [088662](#)). Each of the four animals served as their own control and the estimated mean PM effects for the SDNN decreases during exposure were 85-60% of baseline. CAPs effects on rMSSD were less remarkable. In a study of Tuxedo, NY, $\text{PM}_{2.5}$ CAPs, no acute changes in rMSSD or SDNN were observed in either ApoE^{-/-} or C57 mice when the 48-h time period postexposure was evaluated (6 h/day \times 5 day/wk; mean mass concentration over 5-month period 110 $\mu\text{g}/\text{m}^3$) (Chen and Hwang, 2005, [087218](#)).

Diesel Exhaust

Anselme et al. (2007, [097084](#)) used a MI model of CHF where the left anterior descending coronary artery of WKY rats was occluded to induce ischemia. After 3 months of recovery, rats were exposed to diesel emissions for 3 h (PM concentration 500 $\mu\text{g}/\text{m}^3$; mass

mobility diameter 85 nm; NO₂ 1.1 ppm; CO 4.3 ppm) and decreases in rMSSD were observed during the first 2 h of the exposure, which returned to baseline values for the last hour of exposure. Healthy rats also demonstrated decreased rMSSD when measured over the entire exposure period.

Model Particles

In WKY rats exposed to ultrafine carbon particles (mass concentration 180 µg/m³; mean number concentration 1.6 × 10⁷ particles/cm³) for 24 h, HR increased and SDNN decreased during particle inhalation (Harder et al., 2005, [087371](#)). These measures returned to baseline values during the recovery period. This study provides evidence that ultrafine carbon exerts its effects through changes in autonomic nervous system mediation, as the HR and HRV responses occurred quickly after exposure started and pulmonary inflammation was only observed at the 24-h time point (and not at 4 h). SH rats exposed to ultrafine carbon particles under the same conditions (mass concentration 172 µg/m³; mean number concentration 9.0 × 10⁶ particles/cm³) demonstrated similar responses, albeit not until recovery days 2 and 3 (Upadhyay et al., 2008, [159345](#)).

A model of premature senescence has been developed by Tankersley et al. (2003, [053919](#)), using aged AKR mice whose body weight abruptly declines ~5 wk prior to death and is accompanied by deficiencies in other vital physiological function including HR and temperature regulation. When exposed to CB (CB; mean concentration 160 µg/m³; 3 h/day × 3 day), terminal senescent mice responded with robust cardiovascular effects, including bradycardia and increased rMSSD and SDNN (Tankersley et al., 2004, [094378](#)). SDNN and LF/HF were also increased in healthy senescent mice exposed to CB. These studies indicate that HR regulatory mechanisms are altered in susceptible mice exposed to PM (sympathetic and parasympathetic changes in healthy senescent mice and increased parasympathetic influence in terminally senescent mice), which may translate into lowered homeostatic competence in these animals. Results from the near-terminal group should be interpreted with caution, as only 3 mice were in this group.

Subsequent research with a similar exposure protocol (mean CB concentration 159 µg/m³) used C57BL/6J and C3H/HeJ mice to determine whether an acute PM challenge can modify HR regulation in two mice strains with differing baseline HR (Tankersley et al., 2007, [097910](#)) There were no CB-specific effects on HR or HRV in C3H/HeJ compared to C57BL/6J mice (average HR ~80 bpm lower than C3H/HeJ at baseline). Administration of a

sympathetic antagonist (propranolol) to C57BL/6J mice prior to CB exposure resulted in elevated HR and decreased rMSSD compared to air during the last 2-h of exposure, indicating withdrawal of parasympathetic tone. There may be differences in regional particle deposition based on strain-specific breathing patterns that may affect HR and HRV responses. However, this study revealed that inherent autonomic tone, which is genetically varied between these mouse strains, may affect cardiovascular responses following PM exposure. In extrapolating these results to humans, individual variation in genetic factors likely plays some role in PM-induced adjustments in HR control via the ANS.

A recent study in mice (C3H/HeJ, C57BL/6J, and C3H/HeOuJ) examined the effects of a 2-h O₃ (mean concentration 0.584 ppm) pretreatment followed by a 3-h exposure to CB (mean concentration 536 µg/m³) on HR and HRV measures (Hamade et al., 2008, [156515](#)) HR decreased to the greatest extent during O₃ pre-exposure for all strains that were then exposed to CB. The percent change in SDNN and rMSSD were increased in C3H mice during O₃ pre-exposure and CB exposure compared to the filtered air group; however, these HRV parameters gradually decreased over the duration of the experiment and appeared to be O₃ dependent. Together, these findings indicate that increases in parasympathetic tone and/or decreases in sympathetic input may explain the observed bradycardia. In a subset of all mice pre-exposed to O₃, rMSSD remained significantly elevated during the CB exposure compared to filtered air. The results from this study confirm what was observed in Tankersly et al. (2007, [097910](#)) in that genetic determinants affect HR regulation in mice with exposure to air pollutants.

Summary of Toxicological Study Findings for Heart Rate and Heart Rate Variability

Both increases and decreases in HR have been observed in rats or mice following PM exposure. Fine or ultrafine H₂SO₄ did not result in HR changes in SH rats. Similarly, decreased SDNN was reported for ultrafine CAPs exposure and lowered rMSSD was observed with diesel exposure. In near-terminal senescent mice, HRV responses were robust following CB exposure and represented increased parasympathetic influence. Strain differences in baseline HR and HRV likely contribute to PM responses. HRV changes with preexposure to O₃ and CB appeared to be O₃ dependent, although rMSSD remained elevated during PM exposure.

Source Apportionment and PM Components

An additional analysis of CAPs data (Chen and Hwang, 2005, [087218](#); Hwang et al., 2005, [087957](#)) was conducted to link short-term HR and HRV effects to major PM source categories using source apportionment methodology (Lippmann et al., 2005, [087453](#)). The source categories were: (1) regional secondary SO_4^{2-} comprised of high S, Si, and OC (mean $63.41 \mu\text{g}/\text{m}^3$); (2) resuspended soil characterized by high concentrations of Ca, Fe, Al, and Si (mean concentration $5.88 \mu\text{g}/\text{m}^3$); (3) fly ash emissions from power plants burning residual oil in the eastern U.S. and containing high levels of V, Ni, and Se (mean concentration $1.53 \mu\text{g}/\text{m}^3$); and (4) motor vehicle traffic and other unknown sources ($34.92 \mu\text{g}/\text{m}^3$) (Lippmann et al., 2005, [087453](#)). Exposures occurred from 9:00 a.m. to 3:00 p.m., 5 days/wk for 5 months. $\text{PM}_{2.5}$ mass was associated with a daily interquartile change of -4.1 beat/min HR during exposure in $\text{ApoE}^{-/-}$ mice¹ and a similar magnitude of effect was observed with resuspended soil (-4.5 beat/min). Resuspended soil was also associated with a HR increase in the afternoon post-exposure (2.6 beat/min); the secondary SO_4^{2-} factor was linked to lowered HR in the same period (-2.5 beat/min). A 6.2% increase in rMSSD collected in the afternoon post-exposure was associated with the residual oil factor, compared to a 5.6% and 2.4% decrease in rMSSD at night for secondary SO_4^{2-} and $\text{PM}_{2.5}$ mass, respectively. Resuspended soil was associated with a 4.3% increase in rMSSD the night following CAPs exposure. The residual oil and secondary SO_4^{2-} categories showed similar statistically significant parameter estimates for SDNN as rMSSD.

Recent studies of ECG alterations in mice have indicated a role for PM-associated Ni in driving the cardiovascular effects. Lippman et al. (2006, [091165](#)) presented a posthoc analysis of daily variations in $\text{PM}_{2.5}$ CAPs (mean concentration: $85.6 \mu\text{g}/\text{m}^3$; 7/21/2004–1/12/2005; Tuxedo, NY) and changes in cardiac dynamics in $\text{ApoE}^{-/-}$ mice. On the 14 days that the exposed mice had unusually elevated HR, Ni, Cr, and Fe comprised 12.4% of the PM mass, compared to only 1.5% on the other 89 days. Back trajectory analyses indicated high-altitude winds from the northwest that did not traverse population centers and industrial areas except the Sudbury Ni smelter in Ontario, Canada. On the 14 days that

¹ Atherosclerosis and related pathways has been studied primarily in the Apolipoprotein E (ApoE) knockout mouse. Developed by Nobuyo Maeda's group in 1992 (Piedrahita et al., 1992, [156868](#); Zhang et al., 1992, [157180](#)), the $\text{ApoE}^{-/-}$ mouse and related models have become the workhorse of atherosclerosis research over the past 15 years. The ApoE molecule is involved in the clearance of fats and cholesterol. When ApoE (or the LDL receptor) is deleted from the genome, mice develop severely elevated lipid and cholesterol profiles; $\text{ApoE}^{-/-}$ mice on a high-fat ("Western") diet exhibit cholesterol levels exceeding 1000 mgdL (normal is ~150 mgdL) (Huber et al., 1999, [156575](#); Moore et al., 2005, [156780](#)). As a result, the lipid uptake into the vasculature is increased and the atherosclerotic process is dramatically hastened. Furthermore, the LDLs in $\text{ApoE}^{-/-}$ mice are highly susceptible to oxidation (Hayek et al., 1994, [156527](#)), which may be a crucial event in the air pollution-mediated vascular changes. However it should be noted that this model is primarily one of peripheral vascular disease rather than coronary artery disease.

high HR was observed, the HR elevation lasted for two days, but only the current day CAPs concentration was statistically significant. SDNN decreases were statistically significant for all 3 lags (0, 1, 2 days). The GAM regression analysis showed that only Ni produced a statistically significant effect for HR and SDNN.

6.2.2. Arrhythmia

Epidemiologic and toxicological studies presented in the 2004 PM AQCD (U.S. EPA, 2004, [056905](#)) provided some evidence of arrhythmia following exposure to PM. However, a positive association between PM and ventricular arrhythmias among patients with implantable cardioverter defibrillators was only observed in one study conducted in Boston, MA, while toxicological studies reported arrhythmogenesis in rodents following exposure to ROFA, DE (DE), or metals. Recent epidemiologic studies have confirmed the findings of PM-induced ventricular arrhythmias in Boston, MA, and have also reported increases in ectopic beats in studies conducted in the Midwest and Pacific Northwest regions of the U.S. In addition, two studies from Germany have demonstrated positive associations between traffic and combustion particles and changes in repolarization parameters among patients with ischemic heart disease. Findings of recent toxicological studies are mixed, with both demonstrated decreases and increases in frequency of arrhythmia following exposure to CAPs.

6.2.2.1. Epidemiologic Studies

Studies of Arrhythmias Using Implantable Cardioverter Defibrillators

One study reviewed in the 2004 PM AQCD assessed the effect of short-term fluctuations in PM_{2.5} on ventricular arrhythmias and several recent studies examining this relationship have been conducted. Ventricular ectopy and arrhythmia include ventricular premature beats (VPBs), ventricular tachycardia (VT), and ventricular fibrillation (VF). As their name implies, VPBs are early-occurring depolarizations of the right or left ventricle. VT refers to the succession of 3 or more VPBs at a rate of at least 100 beats/min while VF is characterized by the total absence of properly formed QRS complexes and P waves. Ventricular arrhythmia is commonly associated with myocardial infarction, heart failure, cardiomyopathy, and other forms of structural (e.g., valvular) heart disease. Pathophysiologic mechanisms underlying this established cause of sudden cardiac death

include dysfunction of the cardiac ion channels, gap junctions, and autonomic nervous system.

Previously, Peters et al. (2000, [011347](#)) conducted a pilot study in Boston, MA to examine the association between short-term changes in ambient air pollutant concentrations and increased risk of ventricular arrhythmias, among a cohort of patients with implantable cardioverter defibrillators (ICD). ICDs continuously monitor subject's HR and rhythm and upon detection of an abnormal rhythm (i.e., rapid HR), they can be programmed to deliver pacing and/or shock therapy to restore normal sinus rhythm. Those abnormal rhythms that are most severe or rapid are assumed to be due to ventricular tachycardia or ventricular fibrillation (i.e., life-threatening arrhythmias), and are thus treated with electric shock. These ICD devices also store information on each abnormal rhythm detected, including the date, time, and therapy given. Thus, using the date and time of those arrhythmias resulting in electric shock, Peters et al. (2000, [011347](#)) reported an increased risk of ICD shock associated with mean NO₂ concentration in the previous two days. Among subjects with frequent events (10 or more during 3 yr of follow-up) an increased risk of ICD shock was also associated with interquartile range increases in CO, NO₂, PM_{2.5}, and BC in the previous 2 days. Several studies were conducted to confirm these findings. The study characteristics, as well as the reported effect estimates and 95% CI associated with each PM metric, are shown in Table 6-2.

Dockery et al. (2005, [078995](#); 2005, [090743](#)) conducted a follow-up study of n = 203 ICD patients living in eastern Massachusetts and followed subjects for a longer period of time (up to 7 yr). They were the first to review the ECG, classify each ICD-detected arrhythmia (e.g., ventricular arrhythmia, ventricular fibrillation, atrial tachycardia, sinus tachycardia, etc.), and include only ventricular arrhythmias (ventricular fibrillation or ventricular tachycardia; excluding supraventricular arrhythmias). In single pollutant models using generalized estimating equations increased risks of confirmed ventricular arrhythmias were associated with IQR increases in every pollutant (PM_{2.5}, BC, SO₄²⁻, NO₂, SO₂, O₃, and particle number count). Among those with a prior ventricular arrhythmia in the past three days, interquartile range increases in 2 calendar day mean PM_{2.5}, NO₂, SO₂, CO, O₃, SO₄²⁻, and BC concentrations were all associated with significant and markedly higher risks of ventricular arrhythmia than among those without a prior arrhythmia. The pollutants associated with increased risk of ventricular arrhythmia implicate traffic pollution.

Rich et al. (2005, [079620](#)) conducted a case-crossover analysis of these same data to investigate moving average pollutant concentrations lagged <48 h. They reported an increased risk of ventricular arrhythmia associated with mean PM_{2.5} and O₃ concentrations in the 24 h before the arrhythmia. Each pollutant effect appeared independent in two pollutant models. In single pollutant models, NO₂ and SO₂ were associated with increased risk, but when included in two pollutant models with PM_{2.5}, only PM_{2.5} remained associated with increased risk. They did not, however, find evidence of a more acute arrhythmic response to pollution (i.e., larger risk estimates associated with moving averages <24-h before arrhythmia detection).

Rich et al. (2006, [089814](#)) conducted another case-crossover study in the St. Louis, MO metropolitan area. Using the same methods as in Boston, they reported increased risk of ventricular arrhythmia associated mean SO₂ concentration in the 24-h before the arrhythmia, but not PM_{2.5} (in single-pollutant models). Again, they found no evidence of an arrhythmic response with moving average pollutant concentrations <24-h before the arrhythmia.

In Vancouver, Canada, Vedal et al. (2004, [055630](#)) did not find increased risk of ICD shocks associated with increases in any pollutant concentration (PM₁₀, O₃, SO₂, NO₂, and CO), after adjusting for temporal trends, temperature, relative humidity, wind speed, barometric pressure, and proportion of hours with rain. Secondary analyses among those subjects with two or more discharges per year, and analyses stratified by season were also null for PM₁₀, although an association with SO₂ (lag 2 days) was observed. A case crossover analysis of these same data examining additional particle pollutant concentrations available for a shorter time frame (e.g., PM_{2.5}, SO₄²⁻, EC, and OC) also found no increased risk of ICD shock associated with any pollutant. Rich et al. (2004, [055631](#)) did not use the time-stratified control selection procedure. They used an ambi-directional approach, taking control periods 7 days before and after the case day when pollution data was available.

The largest ICD study to date examined the risk of ventricular arrhythmias associated with increases in the daily concentration of numerous particulate and gaseous pollutants in Atlanta, GA (Metzger et al., 2007, [092856](#)) (see Table 6-2 for specific pollutants evaluated). However, they also did not find significant or consistently increased risk of a ventricular arrhythmia associated with any IQR increase in mean daily particulate or gaseous pollutant concentration at any lag examined.

Ljungman et al. (2008, [180266](#)) conducted a similar study, using case-crossover methods, on 211 ICD patients in Gotheburg and Stockholm, Sweden from 2001-2006. They investigated the triggering of confirmed ventricular arrhythmias by ambient PM₁₀ and NO₂ concentrations, and reported increased relative odds of ventricular arrhythmia associated with each 10 µg/m³ increase in the 2-h ma PM₁₀ concentration (OR = 1.22 [95% CI: 1.00-1.51]), with a smaller non-significant risk associated with each 10.3 µg/m³ increase in the 24-h ma PM₁₀ concentration (OR = 1.23 [95% CI: 0.87-1.73]). The NO₂ and PM_{2.5} effect estimates were much smaller and not statistically significant. Effect estimates were larger for events occurring near the air pollution monitors, and larger in Gothenberg than Stockholm.

Albert et al. (2007, [156201](#)), although not investigating associations with ambient pollution, conducted a case-crossover study of the association between ventricular arrhythmia and traffic exposure in the hours before the arrhythmia. They reported an increased risk of ventricular arrhythmia associated with traffic exposure or driving in the previous hour. They hypothesized that this increased risk was due to either a stress response from being in a car in heavy traffic, or from traffic-generated air pollution, or a combination of both.

Although ICDs detect and treat potentially life-threatening ventricular arrhythmias, other arrhythmias including episodes of paroxysmal atrial fibrillation (AF) may also be detected. AF is the most common type of arrhythmia. In this condition, ectopic electrical impulses arising in the atria or pulmonary veins, i.e., outside their normal anatomic origin (the sinoatrial node), can result in atrioventricular dilatation, dysfunction, and/or thromboembolism. Despite being common, clinical and subclinical forms of AF are associated with reduced functional status and quality of life. Moreover, the arrhythmia accounts for a large proportion of ischemic stroke (Laupacis et al., 1994, [190901](#); Prystowsky et al., 1996, [156031](#)) and is a strong risk factor for congestive heart failure (Roy et al., 2009, [190902](#)), contributing to both cardiovascular disease (CVD) and all-cause mortality (Kannel et al., 1983, [156623](#)).

In an ancillary case-crossover analysis of data from the Boston ICD study described above, Rich et al. (2006, [088427](#)) identified 91 confirmed episodes of paroxysmal AF among 29 subjects. In single pollutant models, they reported a significantly increased risk of AF associated with mean O₃ and PM_{2.5} concentrations in the hour before the arrhythmia and BC concentration in the 24 h before the arrhythmia (Table 6-2).

Table 6-2. Studies of ventricular arrhythmia and ambient PM concentration, in patients with implantable cardioverter defibrillators.

Reference	Outcome and Sample Size	Study Design and Analytic Method	Copollutants	PM Metric	Ambient Concentration	Lag and its Increment Units	OR	95% Confidence Interval
Dockery et al. (2005, 078995 ; 2005, 090743) Eastern MA	N = 670 days with ≥ 1 confirmed ventricular arrhythmias among n = 84 subjects	Generalized estimating equations Lags Evaluated: 2 calendar day means	NO ₂ , CO, SO ₂ , O ₃	PM _{2.5}	Daily Median: 10.3 µg/m ³	2 day 6.9 µg/m ³	1.08	0.96, 1.22
				BC	Daily Median: 0.98 µg/m ³	2 day 0.74 µg/m ³	1.11	0.95, 1.28
				Sulfate	Daily Median: 2.55 µg/m ³	2 day 2.04 µg/m ³	1.05	0.92, 1.20
				Particle Number	Daily Median: 29,300 particles/cm ³	2 day 19,120 particles/cm ³	1.14	0.87, 1.50
Rich et al. (2005, 079620) Eastern MA	N = 798 confirmed ventricular arrhythmias among n = 84 subjects	Time-stratified case-crossover study. Conditional logistic regression. Lags evaluated: 3, 6, 24, 48-h ma	NO ₂ , CO, SO ₂ , O ₃	PM _{2.5}	Daily Median: 9.8 µg/m ³	24-h ma 7.8 µg/m ³	1.19	1.02, 1.38
				BC	Daily Median: 0.94 µg/m ³	24-h ma 0.83 µg/m ³	0.93	0.74, 1.18
Rich et al. (2006, 089814) St. Louis metro area	N = 139 confirmed ventricular arrhythmias among n = 56 subjects	Time-stratified case-crossover study. Conditional logistic regression. Lags Evaluated: 6, 12, 24, 48-h ma	NO ₂ , CO, SO ₂ , O ₃	PM _{2.5}	Daily Median: 16.2 µg/m ³	24-h ma 9.7 µg/m ³	0.95	0.72, 1.27
				EC	Daily Median: 0.6 µg/m ³	24-h ma 0.5 µg/m ³	1.18	0.93, 1.50
				Organic Carbon	Daily Median: 4.0 µg/m ³	24-h ma 2.3 µg/m ³	1.08	0.81, 1.43
Vedal et al. (2004, 055630) Vancouver, BC, Canada	N = 257 days with ≥ 1 ICD shock among n = 50 subjects	Generalized estimating equations Lags Evaluated: 0, 1, 2, 3 daily ma	NO ₂ , CO, SO ₂ , O ₃	PM ₁₀	Daily Median: 11.6 µg/m ³	Lag Day 0 5.6 µg/m ³	1.00*	0.82, 1.19*
Ljungman et al. (2008, 180266) Gothenberg and Stockholm, Sweden	N = 114 ventricular arrhythmias among 73 subjects. 211 total subjects were followed.	Conditional logistic regression Lags evaluated 2 h, 24 h	NO ₂	PM ₁₀	Median Gothenberg 2 h: 18.95 µg/m ³ 24 h: 19.92 µg/m ³ Stockholm 2 h: 14.62 µg/m ³ 24 h: 15.23 µg/m ³	2-h ma: 14.16 µg/m ³ 24-h ma: 11:49 µg/m ³	2 h: 1.31 24 h: 1.24	1.00, 1.72 0.87, 1.76
				PM _{2.5}	Median Stockholm µg/m ³ 2 h: 9.17 24 h: 9.49 µg/m ³	2-h ma: 6.69 µg/m ³ 24-h ma: 5.27 µg/m ³	2 h: 1.23 24 h: 1.28	0.84, 1.80 0.90, 1.84
				PM _{2.5}	Daily Mean: 8.2 µg/m ³	Lag Day 0 5.2 µg/m ³	1.0†	0.9, 1.1†
				PM ₁₀	Daily Mean: 13.3 µg/m ³	Lag Day 0 7.4 µg/m ³	0.9†	0.5, 1.5†
Rich et al. (2004, 055631) Vancouver, BC, Canada	N = 77 to 98 days with with ≥ 1 ICD shock among n = 34 subjects	Ambi-directional case-crossover study. Conditional logistic regression Lags Evaluated: 0, 1, 2, and 3 day ma	NO ₂ , CO, SO ₂ , O ₃	PM _{2.5}	Daily Mean: 8.2 µg/m ³	Lag Day 0 5.2 µg/m ³	1.0†	0.9, 1.1†
				PM ₁₀	Daily Mean: 13.3 µg/m ³	Lag Day 0 7.4 µg/m ³	0.9†	0.5, 1.5†
				EC	Daily Mean: 0.8 µg/m ³	Lag Day 0 0.4 µg/m ³	1.1†	0.9, 1.3†
				Organic Carbon	Daily Mean: 4.5 µg/m ³	Lag Day 0 2.2 µg/m ³	1.1†	0.9, 1.3†
Metzger et al. (2007, 092856) Atlanta, GA	N = 6287 confirmed ventricular arrhythmias among n = 518 subjects	Generalized estimating equations FLags Evaluated: 0, 1, and 2 day ma	NO ₂ , CO, SO ₂ , O ₃	PM _{2.5}	Daily Median: 16.2 µg/m ³	24-h ma 10 µg/m ³	1.00	0.95, 1.0
				PM ₁₀	Daily Median: 26.4 µg/m ³	24-h ma 10 µg/m ³	1.00	0.97, 1.03

Reference	Outcome and Sample Size	Study Design and Analytic Method	Copollutants	PM Metric	Ambient Concentration	Lag and its Increment Units	OR	95% Confidence Interval
				PM _{10-2.5}	Daily Median: 8.7 $\mu\text{g}/\text{m}^3$	24-h ma 5 $\mu\text{g}/\text{m}^3$	1.03	1.00, 1.07
				PM _{2.5} EC	Daily Median: 1.4 $\mu\text{g}/\text{m}^3$	24-h ma 1 $\mu\text{g}/\text{m}^3$	1.01	0.98, 1.05
				PM _{2.5} OC	Daily Median: 3.9 $\mu\text{g}/\text{m}^3$	24-h ma 2 $\mu\text{g}/\text{m}^3$	1.01	0.98, 1.03
				PM _{2.5} SO ₄ ²⁻	Daily Median: 4.1 $\mu\text{g}/\text{m}^3$	24-h ma 5 $\mu\text{g}/\text{m}^3$	0.99	0.93, 1.06
				PM _{2.5} water soluble elements	Daily Median: 0.022 $\mu\text{g}/\text{m}^3$	24-h ma 0.03 $\mu\text{g}/\text{m}^3$	0.95	0.90, 1.00

Estimated from Figure 3 Vedal et al. (2004, [055630](#)). † Estimated from Figure 3 Rich et al. (2004, [055631](#))

Since 2004, only two studies (in Boston and Sweden), reported adverse associations of PM_{2.5}, other size fractions and components with ICD detected ventricular arrhythmias (Dockery et al., 2005, [078995](#); Dockery et al., 2005, [090743](#); Ljungman et al., 2008, [180266](#); Rich et al., 2005, [079620](#)), while other studies done elsewhere did not (Metzger et al., 2007, [092856](#); Rich et al., 2004, [055631](#); Vedal et al., 2004, [055630](#); Dusek et al., 2006, [155756](#)). A range in exposure lags was evaluated in the Boston study (3 h to 3 days) (Dockery et al., 2005, [078995](#); Dockery et al., 2005, [090743](#); Rich et al., 2005, [079620](#)) and Sweden study (2 h and 24 h) (Ljungman et al., 2008, [180266](#)). Given the unique and homogenous nature of the study populations, it is not clear why there is not more consistency across these studies. Rich et al. (2005, [079620](#)) reported that use of the mean pollutant concentration from the specific 24 h before the arrhythmia rather than just the day of the arrhythmia, resulted in less exposure misclassification and less bias towards the null, possibly explaining the lack of association when using just the day of ICD discharge and daily PM concentrations. Other reasons for the inconsistent findings may include differing degrees of exposure misclassification within each study or city due to differences in PM composition and pollutant mixes (e.g., less transition metals and sulfates in the Pacific Northwest than the Northeast U.S.), and differences in the size of study areas (Boston: within 40 km of PM_{2.5} monitoring site; Vancouver: Lower Mainland of British Columbia 90 km east of Vancouver). Studies of ventricular arrhythmia and PM concentration in patients with ICDs are summarized in Table 6-2.

Ectopy Studies Using ECG Measurements

A few panel studies have used ECG recordings to evaluate associations between ectopic beats (ventricular or supraventricular) and mean PM concentrations in the previous hours and/or days (Berger et al., 2006, [098702](#); Ebel et al., 2005, [056907](#); Sarnat et al., 2006, [090489](#)). Ectopic beats are defined as heart beats that originate at a location in the heart outside of the sinus node. They are the most common disturbance in heart rhythm. Ectopic beats are usually benign, and may present with or without symptoms, such as palpitations or dizziness. Such beats can arise in the atria or ventricles. When the origin is in the atria the beat is called an atrial or supraventricular ectopic beat. When such a beat occurs earlier than expected it is referred to as a premature supraventricular or atrial premature beat. Likewise, when the origin is in the ventricle the beat is defined as a ventricular ectopic beat, or when early a premature ventricular beat. When three or more occur ectopic beats occur in succession, this is called a non-sustained run of either supraventricular (atrial) or ventricular origin. When the rate of the run is greater than 100 beats per minute it is defined as a tachycardia. Sustained ventricular tachycardias are the arrhythmias investigated in the ICD studies described above.

Sarnat et al. (2006, [090489](#)) conducted a panel study among 32 nonsmoking older adults residing in Steubenville, OH. In this study, the median daily PM_{2.5} concentration was 17.7 µg/m³. The median daily SO₄²⁻ concentration was 5.7 µg/m³, and the median daily EC concentration was 1.0 µg/m³. They used logistic regression models to examine lagged effects of 1-10-day mean concentrations of PM_{2.5}, SO₄²⁻, EC, O₃, NO₂, and SO₂. Supraventricular ectopy and ventricular ectopy were measured using Holter monitors during a 30-minute protocol of alternating rest in the supine position, standing, walking and paced breathing. In single pollutant models, each 10.0 µg/m³ increase in 5-day mean PM_{2.5} concentration was associated with increased risk of supraventricular ectopy (OR = 1.42 [95% CI: 0.99-2.04]), but not ventricular ectopy (OR = 1.02 [95% CI: 0.63-1.65]). Similarly, increased risk of supraventricular ectopy, but not ventricular ectopy, was associated with each interquartile range increase in 5-day mean SO₄²⁻ and O₃ concentration.

Ebel et al. (2005, [056907](#)) conducted a repeated measures panel study of 16 patients with COPD in the summer of 1998 in Vancouver, British Columbia. Their goal was to evaluate the relative impact of ambient and non-ambient exposures to PM_{2.5}, PM₁₀, and PM_{10-2.5} on several health measures. Subjects wore an ambulatory ECG monitor for 24 h to record heart rhythm data and ascertain supraventricular ectopic beats. The mean PM_{2.5}

concentration during this study was $11.4 \mu\text{g}/\text{m}^3$. Using mixed models with random subjects effects to investigate only same day PM concentrations, an increase in supraventricular ectopic beats was associated with same day ambient exposures to each PM size fraction.

Berger and colleagues (2006, [098702](#)) conducted a panel study of 57 men with coronary heart disease living in Erfurt, Germany. Using 24-h ECG measurements made once every 4 wk, they studied associations between runs of supraventricular and ventricular tachycardia and lagged concentrations of $\text{PM}_{2.5}$, UFP (0.01-0.1 μm), ACP (0.1-1.0 μm), SO_2 , NO_2 , CO, and NO. Using GAMs, as well as Poisson and linear regression models, they reported increases in supraventricular tachycardia and the number of runs of ventricular tachycardia associated with 5-day mean $\text{PM}_{2.5}$, UFP counts (0.01-0.1 μm), and ACP counts (0.1-1.0 μm). They found these associations at all lags evaluated (during ECG recording, 0-23 h before, 24-47 h before, 48-71-h before, 72-95 h before, and 5-day mean), but the largest effect estimates were generally associated with the 24-47-h mean and the 5-day mean.

Using data from the WHI done in 59 U.S. exam sites in 24 cities, Liao et al. (2009, [157456](#)) estimated mean $\text{PM}_{2.5}$ and PM_{10} concentrations at the address of 57,422 study subjects undergoing ECG monitoring. They then estimated the risks of ventricular and supraventricular ectopy during that 10 second ECG recording associated with increases in mean PM_{10} and $\text{PM}_{2.5}$ concentrations on the same day and previous 2 days, as well as over the previous 30 days. Mean $\text{PM}_{2.5}$ and PM_{10} concentrations during the study period were 13.8 and 27.5 $\mu\text{g}/\text{m}^3$, respectively. Using a 2-stage random effects model, they reported that among smoking subjects, each 10 $\mu\text{g}/\text{m}^3$ increase in $\text{PM}_{2.5}$ concentration on lag day 1 was associated with a significantly increased risk of ventricular ectopy (OR = 2.0 [95% CI: 1.32-3.3]). Similarly, each 10 $\mu\text{g}/\text{m}^3$ increase in lag 1 PM_{10} concentration was associated with an increased risk of ventricular ectopy (OR = 1.32 [95% CI: 1.07-1.65]). The lag day 2 $\text{PM}_{2.5}$ risk estimate was similar in size but not statistically significant. There were no associations between PM_{10} , $\text{PM}_{2.5}$ and supraventricular ectopy among smokers or non-smokers, and no association with any PM metric and ventricular ectopy among non-smokers.

Four studies of ectopic beats and runs of supraventricular and ventricular tachycardia, captured using ECG measurements, all report at least one positive association. Further, they report findings in regions other than Boston and Sweden (i.e., Midwest U.S., Pacific Northwest, 24 U.S. cities, and Erfurt, Germany). A range of lags and/or moving

averages were investigated (0-30 days) with the strongest effects observed for either the 5-day mean, same day, or 1-day lagged PM concentrations. Taken together, these ICD studies and ectopy studies provide evidence of an arrhythmic response to PM, although further study is needed to understand the variable ICD study findings.

ECG Abnormalities Indicating Arrhythmia

No reported investigations of the relationship of PM concentration and ECG abnormalities indicating arrhythmia were conducted prior to 2002 and thus were not included in the 2004 PM AQCD (U.S. EPA, 2004, [056905](#)). Abnormalities in the myocardial substrate, myocardial vulnerability, and resulting repolarization abnormalities are believed to be key factors contributing to the development of arrhythmogenic conditions such as those discussed above. These abnormalities include ECG measures of repolarization such as QT duration (time for depolarization and repolarization of the ventricles), T-wave complexity (a measure of repolarization morphology), and T-wave amplitude (height of the T-wave). Abnormalities in repolarization may also identify subjects potentially at risk of more serious events such as sudden cardiac death (Atiga et al., 1998, [156231](#); Berger et al., 1997, [155688](#); Chevalier et al., 2003, [156338](#); Okin et al., 2000, [156002](#); Zabel et al., 1998, [156176](#)). Recent studies of changes in these measures following acute increases in air pollution are described below.

Two studies conducted in Erfurt, Germany (Henneberger et al., 2005, [087960](#); Yue et al., 2007, [097968](#)) examined the association between measures of repolarization (QT duration, T-wave complexity, T-wave amplitude, T-wave amplitude variability) and particulate air pollution. Henneberger et al. (2005, [087960](#)) conducted a panel study of 56 males with ischemic heart disease. Each subject was measured every 2 wk for 6 months. During the study, the median daily PM_{2.5} concentration was 14.9 µg/m³. The median EC concentration was 1.8 µg/m³, while the median OC concentration was 1.4 µg/m³. The median count of UFP counts (0.01-0.1 µm) was 11,444 particles/cm³, while the median count of ACP (0.1-1.0 µm) was 1238 particles/cm³. They examined the change in these ECG parameters associated with the mean pollutant (UFP, ACP, PM_{2.5}, OC, and EC) concentrations 0-5, 6-11, 12-17, 18-23, and 0-23 h before, and 2-5 days before the ECG measurement. Significant decreases in T-wave amplitude were associated with PM_{2.5} mass, UFP, and ACP. Each 16.4 µg/m³ increase in the mean PM_{2.5} concentration in the previous 5 h was associated with a 6.46 µV decrease in T-wave amplitude (95% CI: -10.88 to -2.04).

Each 0.7 $\mu\text{g}/\text{m}^3$ increase in the mean OC concentration in the previous 5 h was associated with a 4.15 ms increase in QT interval (95% CI: 0.22-8.09). There was a similar sized effect for 24-h mean OC concentration. Significant increases in the variability of T-wave complexity were also associated with acute increases in EC and OC concentration.

Yue et al. (2007, [097968](#)) then used positive matrix factorization to identify 5 sources of ambient PM (airborne soil, local traffic-related UFP, combustion generated aerosols, diesel traffic-related particles, and secondary aerosols). Using similar statistical models, they examined the association between these same repolarization changes and incremental increases in the mean concentration of each particle source in the 24 h before the ECG measurement. They also examined associations with CRP and vWF concentrations in the blood. Both UFP from local traffic and diesel particles from traffic had the strongest associations with repolarization parameters.

These two analyses demonstrate associations between PM pollution and repolarization changes, at lags of 5 h to 2 days. Moreover, the findings from the Yue et al. (2007, [097968](#)) study demonstrate a potential role of traffic particles/pollution.

6.2.2.2. Toxicological Studies

The ECG of animal research models frequently exhibit different characteristics than that of humans. Mice and rats are notable in this regard, as they do not have an isoelectric ST-segment typical of larger species, likely owing to their rapid heart rates (~600 and ~350 bpm, respectively) and repolarizing currents. However, the ultimate function of the pumping heart is conserved and reflected by the ECG in a remarkably consistent manner across species. Thus, atrial depolarization causes an electrical inflection represented by the P-wave, ventricular depolarization elicits the QRS complex, and the T-wave represents repolarization of the ventricles.

The earliest indication that there may be cardiovascular system effects of PM came from ECG studies in susceptible animal models (rats with pulmonary hypertension and dogs with coronary occlusion), which were summarized in the 2004 PM AQCD (U.S. EPA, 2004, [056905](#)). However, a study of dogs exposed to ROFA did not demonstrate ECG changes, perhaps due to differences in disease state, as these were the oldest dogs in the colony with clinical signs of preexisting, naturally occurring heart disease (Muggenburg et al., 2000, [010279](#)). Much of the research conducted since the release of the last PM AQCD

has been focused on exploring susceptibility or varying exposure methodologies, with little new evidence into the mechanisms for ECG changes of inhaled PM.

CAPs

Wellenius et al. (2004, [087874](#)) used a susceptible model that was previously shown to produce significant results with exposures to ROFA (Wellenius et al., 2002, [025405](#)) to examine ECG-related PM_{2.5} effects. Using an anesthetized model of post-infarction myocardium sensitivity, Wellenius and colleagues tested the effects of Boston, MA CAPs on the induction of spontaneous arrhythmias in SD rats (1-h exposure; mean mass concentration 523.11 µg/m³; range of mass concentration 60.3-2202 µg/m³). Decreased (67.1%) ventricular premature beat (VPB) frequency was observed during the post-exposure period in rats with a high number of pre-exposure VPB. No interaction was observed with coexposure to CO (35 ppm). CAPs number concentration or the mass concentration of any single element did not predict VPB frequency. In a follow-up publication, decreased number of supraventricular ectopic beats (SVEB) was reported with CAPs (mean mass concentration 645.7 µg/m³) (Wellenius et al., 2006, [156152](#)). Furthermore, an increase in CAPs number concentration of 1,000 particles/cm³ was associated with a 3.3% decrease in SVEB frequency. The findings of decreased ventricular arrhythmia differ from those observed following ROFA exposure in the same animal model in that an increased frequency of premature ventricular complexes was observed with ROFA, albeit the ROFA exposure concentration was >3,000 µg/m³ (Wellenius et al., 2002, [025405](#)). It is difficult to directly compare the result of these studies due to differences in exposure concentrations and particle type, but collectively they may suggest an important role for the soluble components of PM, including transition metals, as only ROFA induced increases in ventricular arrhythmia occurrence.

In older rats (Fisher 344; ~18 months) exposed to PM_{2.5} CAPs in Tuxedo, NY (4 h; mean concentration 180 µg/m³; 8/2,000), the frequency of delayed beats was greater than in rats exposed to air (Nadziejko et al., 2004, [055632](#)). The majority of these beats were characterized as pauses (a delay of 2.5 times the adjacent interbeat intervals) rather than premature beats. When the same animals were exposed to generated ultrafine carbon particles (single-day concentrations 500 and 1280 µg/m³) or SO₂ (1.2 ppm), no significant differences were observed in arrhythmia frequency between air controls and exposed animals. The authors also report using the same protocol for young WKY rats

(concentration 215 $\mu\text{g}/\text{m}^3$) and very few arrhythmias were observed, thus precluding statistical analysis. The results of this study indicate 1) involvement of the sino-atrial node, as the observed arrhythmias were mostly of a delayed nature and 2) particle size and $\text{PM}_{2.5}$ constituents may play a role in these effects.

Diesel and Gasoline Exhaust

Anselme and colleagues (2007, [097084](#)) exposed rats with and without induced CHF to DE for 3 h (PM concentration 500 $\mu\text{g}/\text{m}^3$; mass mobility diameter 85 nm; NO_2 1.1 ppm; CO 4.3 ppm). While no dramatic change was noted in HR, prominent increases in the incidence of VPB were observed in CHF rats, which lasted at least 4-5 h after exposure ceased. The duration of VPB attributable to diesel exposure in CHF rats lasted much longer than the rMSSD change (>5 h post-exposure), indicating that the HRV response was not driving the increased arrhythmia incidence. It is interesting to contrast the work of Anselme with the studies by Wellenius et al. (2002, [025405](#); 2004, [087874](#); 2006, [156152](#)), as the arrhythmia incidence in the acute infarction model was greatest with ROFA, while the CHF model demonstrated sensitivity to diesel exposure. However, several differences in the research designs preclude strong comparisons.

Using ApoE^{-/-} mice on a high-fat diet as a model of pre-existing coronary insufficiency (Caligiuri et al., 1999, [156318](#)), Campen and colleagues studied the impact of inhaled diesel and gasoline exhaust and road dust (6 h/day \times 3 day) on ECG morphology (Campen et al., 2005, [083977](#); Campen et al., 2006, [096879](#)). Moreover, a high efficiency particle filter was used to compare the whole exhaust with an atmosphere containing only the gaseous components. For gasoline exhaust, the PM-containing atmosphere (PM mean concentration 61 $\mu\text{g}/\text{m}^3$; PNMD 15 nm; NO_x mean concentration 18.8 ppm; CO mean concentration 80 ppm) induced T-wave morphological alterations, while the PM-filtered atmosphere did not (Campen et al., 2006, [096879](#)). Resuspended road dust ($\text{PM}_{2.5}$), at up to 3500 $\mu\text{g}/\text{m}^3$ had no impact on ECG. For DE (PM mean concentration 512, 770, or 3634 $\mu\text{g}/\text{m}^3$; MMD 100 nm, CMD 80 nm; NO_x mean concentration 19, 105, 102 ppm for low whole exhaust, high PM filtered, and high whole exhaust, respectively), dramatic bradycardia, decreased T-wave area, and arrhythmia (atrioventricular-node block and VPB) were only observed in mice exposed to high filtered and high whole exhaust (Campen et al., 2005, [083977](#)). These effects remained after filtration of PM, suggesting that the gaseous components of the whole DE drove the cardiovascular findings. The diesel- and gasoline-induced ECG changes

contrast, in that the gasoline exhaust required particles to induce T-wave changes, whereas the DE did not require PM to cause an effect on ECG. However, the differing responses could be attributable to higher PM concentrations in the whole DE.

The above toxicological studies demonstrate mixed results for arrhythmias, which may be somewhat attributable to the different disease models used. Wellenius et al. (2004, [087874](#); 2006, [156152](#)) showed decreased frequency of VPB and SVEB following PM_{2.5} CAPs exposure in rats with induced MI (>12-h prior to exposure). One study reported increased frequency of premature beats in older rats exposed to CAPs, which were not observed with ultrafine carbon particles (Nadziejko et al., 2004, [055632](#)). Rats with a MI model of chronic heart failure (3-month recovery) had increased incidence of VPB with DE exposure (Anselme et al., 2007, [097084](#)). As for ECG morphology changes, T-wave alterations were reported for gasoline exhaust that were absent when the PM was filtered (Campen et al., 2006, [096879](#)). However, for DE, increased atrioventricular-node block, VPB, and decreased T-wave area were observed with whole exhaust and remained after filtration of PM, indicating that the gases were responsible for the effects (Campen et al., 2005, [083977](#)).

6.2.3. Ischemia

Although no evidence from epidemiologic or controlled human exposure studies of PM-induced myocardial ischemia was included in the 2004 PM AQCD (U.S. EPA, 2004, [056905](#)), one toxicological study was cited that observed ST-segment changes in dogs following a 3 day exposure to CAPs. In epidemiologic studies published since the 2004 PM AQCD (U.S. EPA, 2004, [056905](#)), associations have been demonstrated between PM and ST-segment depression, and one new controlled human exposure study reported significant increases in exercise-induced ST-segment depression among men with prior MI following a controlled exposure to DE. Results from recent toxicological studies confirm the findings presented in the 2004 PM AQCD (U.S. EPA, 2004, [056905](#)) and provide coherence and biological plausibility for the effects observed in epidemiologic and controlled human exposure studies.

6.2.3.1. Epidemiologic Studies

ECG Abnormalities Indicating Ischemia

The ST-segment duration is typically in the range of 0.08-0.12 s (80-120 ms). The direction of the ST change is influenced by the extent of the acute myocardial injury. If the ischemia or infarction is transmural, i.e., penetrates the entire thickness of the ventricular wall, it usually causes ST elevation, while ischemia confined primarily to the ventricular endocardium often causes ST-segment depression. Several short-term exposure studies of air pollution investigated the association of ST-segment depression with PM concentration.

Gold et al. (2005, [087558](#)) studied 24 elderly residents of Boston, MA (aged 61-88 yr) residing at or near an apartment complex that was ~ 0.5 km from an air pollution monitoring station. A protocol of continuous Holter monitoring including 5 min of rest, 5 min of standing, 5 min of outdoor exercise, 5 min of rest, and then 20 cycles of paced breathing was done up to 12 times for each subject (n = 269 ECG measurements for analysis). From these ECG measurements, they identified occurrences of ST-segment depression and examined whether mean BC, CO, and PM_{2.5} concentrations in the previous 5 and 12 h were associated with ST-segment depression. The median 5-h mean BC concentration was 1.28 µg/m³ and the median 12-h mean BC concentration was 1.14 µg/m³. The median 5-h mean PM_{2.5} concentration was 9.5 µg/m³, and the median 12-h mean PM_{2.5} concentration was 9.8 µg/m³. The mean BC concentrations in the 5 and 12 h before testing predicted ST-segment depression in most portions of the protocol. However, these effects were strongest in the post-exercise periods. For example, during the post-exercise rest period, each 10th-90th percentile increase (1.59 µg/m³) in the mean 5-h BC concentration was associated with a -0.11 mm ST-segment depression (95% CI: -0.18 to -0.05). In two pollutant models, CO did not appear to confound this association. PM_{2.5} was not associated with ST-segment depression in this study. These findings suggest traffic-generated particulate pollution may be associated with ST-segment depression.

Previously, Pekkanen et al. (2002, [035050](#)) conducted a panel study of 45 subjects with stable coronary heart disease living in Helsinki, Finland. Each subject had biweekly sub-maximal exercise testing for 6 months (n = 342 exercise tests with 72 exercise-induced ST-segment depressions). During this study, the median daily PM_{2.5} concentration was 10.6 µg/m³, and the median daily count of ACP (ACP: 0.1-1.0 µm) was 1,200 particles/cm³. They examined the risk of ST-segment depression associated with mean pollutant

concentrations (UFP, ACP, PM₁, PM_{2.5}, PM_{10-2.5}, NO₂, CO) in the previous 24 h, and the 3 previous lagged 24-h periods. Each 7.9 µg/m³ increase in mean PM_{2.5} concentration, lagged 2 days, was associated with significantly increased risk of ST-segment depression >0.1 mV (OR: 2.84 [95% CI: 1.42-5.66]). Each 760 particles/cm³ increase in the count of ACP, lagged 2 days, was also associated with significantly increased risk of ST-segment depression >0.1 mV (OR: 3.29 [95% CI: 1.57-6.92]). Similarly sized increased risks of ST-segment depression were also found for other particulate pollutants, including PM_{10-2.5}, PM₁, and the counts of UFP (0.01-0.1 µm).

This same research group, then conducted a principal components analysis to identify five PM_{2.5} sources (crustal, long range transport, oil combustion, salt, and local traffic) (Lanki et al., 2006, [088412](#)). Using similar statistical models, each 1 µg/m³ increase in “local traffic” particle concentration, lagged 2 days, was associated with increased risk of ST-segment depression (OR: 1.53 [95% CI: 1.19-1.97]). Similarly, each 1 µg/m³ increase in “long range transport” particle concentration was also associated with increased risk of ST-segment depression (OR: 1.11 [95% CI: 1.02-1.20]). No significant associations for other sources were reported for any lag time.

In Boston, Chuang et al. (2008, [155731](#)) studied 48 patients with a prior percutaneous intervention following MI, acute coronary syndrome (ACS) without MI, or stable coronary artery disease without ACS, no earlier than 1-yr previous. Each patient had a 24-h ECG measurement up to 4 times during study follow-up. Using logistic regression, they estimated the risk of ST-segment depression of ≥ 0.1 mm, during half hour segments, associated with increases in the mean PM_{2.5}, BC, CO, NO₂, O₃, and SO₂ concentration in the previous 24 h. Each 6.93 µg/m³ increase in mean PM_{2.5} concentration was associated with a significantly increased risk of ST-segment depression (OR = 1.50 [95% CI: 1.19-1.89]). Using linear additive models to estimate the change in ST level associated with the same PM_{2.5} change, they observed a significant -0.031 mm change (95% CI: -0.042 to -0.019). In single pollutant models, risk estimates were of similar magnitude and statistically significant for BC, NO₂, and SO₂. In two pollutant models, however, PM_{2.5} risk estimates were reduced to 1.0 in all models with BC, NO₂, and SO₂. In contrast, the risk estimates for BC, NO₂, and SO₂ remained elevated and statistically significant when modeled with PM_{2.5}.

In a panel study of 14 Helsinki resident, non-smoking, elderly subjects with coronary artery disease, Lanki et al. (2008, [191984](#)) used logistic regression to report that each 10 µg/m³ increase in personal PM_{2.5} concentration in the previous hour was associated with a

significantly increased risk of ST-segment depression (OR = 3.26 [95% CI: 1.07-9.98]). In addition, each 10 $\mu\text{g}/\text{m}^3$ increase in outdoor mean $\text{PM}_{2.5}$ concentration in the previous 4 h was also associated with an increased risk (OR = 2.47 [95% CI: 1.05-5.85]). Last, the risk estimates for all time lags examined (1, 4, 8, 12, and 22 or 24 h) for all PM size fractions were greater than 1.0, but none other than those described above were statistically significant.

In a study of 57,908 participants in the WHI Trial, Zhang et al. (2009, [191970](#)) examined the change and risk of ST-segment abnormalities, T wave abnormalities, and T wave amplitude associated with ambient $\text{PM}_{2.5}$ concentrations on the same and previous 6 days. Using logistic regression, each 10 $\mu\text{g}/\text{m}^3$ increase in the mean $\text{PM}_{2.5}$, on lag days 0 to 2, was associated with a 4% (95% CI: -3% to 10%) increase in the relative odds of a ST-segment abnormality, and a 5% (95% CI: 0-9%) increase in the relative odds of a T wave abnormality.

Summary of Epidemiologic Study Findings for Ischemia

These studies demonstrate associations between $\text{PM}_{2.5}$ pollution and ST-segment depression at lags of 1 h to 2 days. Moreover, these findings demonstrate a potential role for traffic (Chuang et al., 2008, [155731](#); Gold et al., 2005, [087558](#)) and long-range transported $\text{PM}_{2.5}$ (Lanki et al., 2006, [089788](#)).

6.2.3.2. Controlled Human Exposure Studies

Diesel Exhaust

Among a group of 20 men with prior MI, Mills et al. (2007, [091206](#)) found that DE (300 $\mu\text{g}/\text{m}^3$ particle concentration, median particle diameter 54 nm) significantly increased exercise-induced ischemic burden during exposure, calculated as the product of exercise duration and change in ST-segment amplitude. The mechanism by which DE induced the exacerbation of ischemic burden remains unclear, and appears to be unrelated to impaired vasodilation. However, the authors suggest that this discrepancy may be due to the timing of the vascular assessment, as measures of blood-flow were taken 5 h after the observed increase in ischemic burden. Although it is reasonable to assume that the observed increase in ST-segment depression during exercise represents an increased magnitude of ischemia, it is important to note that there are other potential explanations for the ST change. For example, it is possible that the ST-segment depression could be secondary to heterogeneity

of electrophysiological responses of particle exposure on the myocardium that is enhanced by the metabolic and ionic conditions associated with ischemia or increased heart rate. It is also important to note that the effects observed in this study cannot be conclusively attributed to the particles per se, as subjects were also exposed relatively high levels of NO (3.45 ppm), NO₂ (1.01 ppm), CO (2.9 ppm), and total hydrocarbons (2.8 ppm).

6.2.3.3. Toxicological Studies

There were no toxicological studies cited in the 2004 PM AQCD (U.S. EPA, 2004, [056905](#)) that directly examined myocardial ischemia. One study was reviewed in the 2004 PM AQCD that evaluated ST-segment changes in dogs during occlusion and following a 3-day exposure to Boston CAPs reported increased magnitude and decreased time to ST-segment elevation (Godleski et al., 2000, [000738](#)).

CAPs

A study that examined ECG changes in dogs (female; retired mongrel breeder dogs) following PM_{2.5} CAPs exposure in Boston, MA (mean mass concentration 345 µg/m³; 9/2000-3/2001) and left anterior descending coronary artery occlusion as an indicator of myocardial ischemia reported changes in ST-segment (Wellenius et al., 2003, [055691](#)). The experimental protocol was a 6-h exposure to CAPs via tracheostomy, followed by a preconditioning occlusion (5 min), rest interval (20 min), and the experimental occlusion (5 min). Increased ST-segment elevation was observed following PM_{2.5} during the experimental occlusion period compared to filtered air. Furthermore, peak ST-segment elevation attributable to CAPs was reported with the experimental occlusion, which remained elevated 24 h post-exposure. Ventricular arrhythmias were rarely observed during occlusion and when observed, were unrelated to CAPs exposure. The results from this study support those previously observed (Godleski et al., 2000, [000738](#)) and provides greater support that enhanced myocardial ischemia occurs relatively quickly (within h) following PM exposure.

A recent study in dogs (female mixed-breed canines) evaluated myocardial blood flow during myocardial ischemia following 5-h PM_{2.5} Boston CAPs exposures (daily mean mass concentration 94.1-1556.8 µg/m³; particle number concentration 3-69.3 × 10³ particles/cm³; BC concentration 1.3-32.0 µg/m³) (Bartoli et al., 2009, [179904](#)). Similar methods were used for the coronary occlusion and exposure method as Wellenius et al. (2003, [055691](#)).

Immediately following exposure, microspheres were injected (15 μm diameter) into the left atrium after 3 min of ischemia during the second occlusion. Post-mortem analysis of cardiac tissue and blood samples allowed for quantification of microspheres. CAPs-exposed dogs had decreased total myocardial blood flow and increased coronary vascular resistance during occlusion that was greatest in tissue within or near the ischemic zone. The rate-pressure product (product of HR and SBP) during occlusion was unchanged in animals exposed to CAPs, indicating that cardiac metabolic demand was not altered. The multilevel linear mixed models demonstrated that myocardial blood flow and coronary vascular resistance during occlusion were inversely and significantly associated with CAPs mass concentration, particle number concentration, and BC concentration, with the strongest effects observed with particle number concentration. The results of this study provide evidence that exacerbation of myocardial ischemia following PM exposure is due to reduced myocardial blood flow, perhaps via dysfunctional collateral vessels.

Intratracheal Instillation

Cozzi et al. (2006, [091380](#)) exposed ICR mice to ultrafine PM (100 μg IT instillation), and followed 24 h later by ischemia/reperfusion injury to the left anterior coronary artery. The area-at-risk (the region of tissue perfused by the left anterior descending coronary artery) and the infarct size were measured 2 h following reperfusion, and while the area-at-risk was not affected by PM exposure, the infarct size was nearly doubled in mice who received ultrafine PM. Increases in infarct size were associated with increased myocardial neutrophil density in the infarct zone and lipid peroxidation in the myocardium.

Summary of Toxicological Study Findings for Ischemia

The studies described above provide evidence that PM can induce greater myocardial responses following ischemic events, as demonstrated by, enhanced ischemia, decreased myocardial blood flow and increased coronary vascular resistance, and increased infarct size.

PM Components

The Wellenius et al. (2003, [055691](#)) study employing dogs also attempted to link ST-segment changes with four CAPs elements (Si, Ni, S, and BC) as tracers of PM_{2.5} sources in Boston. In the multivariate regression analyses, peak ST-segment elevation and integrated ST-segment change were significantly associated with only the mass

concentration of Si (Si mean concentration 8.17 $\mu\text{g}/\text{m}^3$; Si concentration 2.31-13.93 $\mu\text{g}/\text{m}^3$). In the univariate regression analyses, Pb also demonstrated a significant association for both ST-segment measures, although the p-value was greater than that observed with Si.

6.2.4. Vasomotor Function

The most noteworthy new health-related revelation in the past six yr with regards to PM exposure is that the systemic vasculature may be a target organ. The vasculature of all tissues is lined with endothelial cells that will naturally encounter any systemically absorbed toxin. The endothelium (1) maintains barrier integrity to ensure fluid compartmentalization, (2) communicates dilatory and constrictive stimuli to vascular smooth muscle cells, and (3) recruits inflammatory cells to injured regions. Smooth muscle cells lie within the layer of endothelium and are crucial to the regulation of blood flow and pressure. In states of injury and disease, both cell types can exhibit dysfunction and even pathological responses.

Endothelial dysfunction is a factor in many diseases and may contribute to the origin and/or exacerbation of perfusion-limited diseases, such as MI or IHD, as well as hypertension. Endothelial dysfunction is also a characteristic feature of early and advanced atherosclerosis. A primary outcome of endothelial dysfunction is impaired vasodilatation, frequently due to uncoupling of NOS. It is this uncoupling that appears central to impaired vasodilation and thus endothelial dysfunction.

One controlled human exposure study cited in the 2004 PM AQCD (U.S. EPA, 2004, [056905](#)) reported a decrease in bronchial artery diameter (BAD) among healthy adults following exposure to CAPs in combination with O₃. Conclusions based on this finding were limited due to the concomitant exposure to O₃ as well as a lack of published results from epidemiologic and toxicological studies. Recent controlled human exposure studies have provided support to the findings described in the 2004 PM AQCD (U.S. EPA, 2004, [056905](#)), with changes in vasomotor function observed following controlled exposures to DE and EC particles. In addition, epidemiologic studies have observed associations between PM and decreases in BAD and flow mediated dilatation in healthy adults and diabetics. These findings are further supported by a large body of new toxicological evidence of impaired vasodilation following exposure to PM.

6.2.4.1. Epidemiologic Studies

O'Neill et al. (2005, [088423](#)) examined the association between 2 measures of vascular reactivity (nitroglycerin mediated reactivity and flow-mediated reactivity) and ambient mean particulate pollutant concentration ($PM_{2.5}$, SO_4^{2-} , BC, particle number count [PNC]) on the same and previous few days. They studied a panel of 270 subjects with diabetes or at risk for diabetes, who lived in the greater Boston metropolitan area. The mean $PM_{2.5}$ concentration during this study (1998-2002) was $11.5 \mu\text{g}/\text{m}^3$. Using linear regression models adjusted individually for age, gender, BMI, and race, the change in vascular reactivity associated with moving average pollutant concentrations across the same and previous 5 days was estimated. Interquartile range (values not reported) increases in the mean $PM_{2.5}$ concentration, BC concentration, and PNC over the previous 6 days were associated with decreased vascular reactivity among diabetics, but not among subjects at risk for diabetes. For sulfates, the mean concentration on lag day 0, lag day 1, and the 3-day, 4-day, and 5-day ma all were associated with similarly sized reductions in both metrics of vascular reactivity. Among diabetics, each interquartile range increase in the mean SO_4^{2-} concentration over the previous 6 days was associated with a 5.4% decrease in nitroglycerin-mediated reactivity (95% CI: -10.5 to -0.1) and flow-mediated reactivity (-10.7% [95% CI: -17.3 to -3.5]). Also among diabetics, each interquartile range increase in the mean $PM_{2.5}$ concentration over the previous 6 days was associated with a significant 7.6% decrease in nitroglycerin-mediated reactivity (95% CI: -12.8 to -2.1) and a non-significant 7.6% decrease in flow-mediated reactivity (95% CI: -14.9 to 0.4). Each interquartile range increase in the mean BC concentration over the previous 6 days was associated with a 12.6% decrease in flow mediated reactivity (95% CI: -21.7 to -2.4), but not nitroglycerin-mediated reactivity. PNC was associated with non-significant decreases in both. Effect estimates were larger for type II diabetics than type 1 diabetics.

Dales et al. (2007, [155743](#)) conducted a panel study of 39 healthy volunteers who sat at 1 of 2 bus stops in Ottawa, Canada for 2 h. Flow-mediated vasodilation of the brachial artery was measured immediately after the bus stop exposure, but not before. The mean $PM_{2.5}$ concentrations, measured at the 2 bus stops, were 40 and $10 \mu\text{g}/\text{m}^3$. They examined the association between flow-mediated vasodilation and 2-h mean $PM_{2.5}$, PM_{10} , NO_2 , and traffic density at the bus stop (vehicles/h). The authors report that each $30 \mu\text{g}/\text{m}^3$ increase in 2-h mean $PM_{2.5}$ concentration was associated with a significant 0.48% reduction in flow-

mediated dilation (FMD) ($p = 0.05$). This represented a 5% relative change in the maximum ability to dilate.

This same research group conducted a panel study of 25 type I or II diabetic subjects living in Windsor, Ontario (aged 18-65) (Liu et al., 2007, [156705](#)). For each subject, personal PM_{10} concentrations were measured for 24 h before measurements of BAD, FMD, and other biomarkers. The mean 24-h mean PM_{10} concentration, measured with personal monitors, was $25.5 \mu\text{g}/\text{m}^3$. Each $10 \mu\text{g}/\text{m}^3$ increase in personal 24-h mean PM_{10} concentration was associated with a 0.20% increase in end-diastolic FMD (95% CI: 0.04 to 0.36) and a 0.38% increase in end-systolic FMD (95% CI: 0.03-0.73), but decreases in end-diastolic basal diameter ($-2.52 \mu\text{m}$ [95% CI: -8.93 to 3.89]) and end-systolic basal diameter ($-9.02 \mu\text{m}$ [95% CI: -16.04 to -2.00]).

Rundell et al. (2007, [156060](#)) examined the change in FMD associated with high and low PM_1 (0.02 - $1.0 \mu\text{m}$) pollution in a panel of 16 young intercollegiate athletes (mean age = 20.5 ± 2.4 yr) in Scranton, PA, who were non-smokers, non-asthmatics, and free of cardiovascular disease (Rundell et al., 2007, [156060](#)). Each subject had FMD of the brachial artery measured 10-20 min before and 20-30 min after each of two 30-min exercise tests (85-90% of maximal HR). The exercise tests were done outside either on an inner campus location free of automobile and truck traffic (low PM_1 ; mean = 5309 ± 1942 particles/ cm^3) or on a soccer field adjacent to a major highway (high PM_1 ; mean = $143,501 \pm 58,565$ particles/ cm^3). The order of the exercise test locations was chosen randomly. Using paired t-tests for analysis, they reported FMD was impaired after high PM_1 exposure (pre-exercise: $6.8\% \pm 3.58\%$; post-exercise: $0.30\% \pm 2.74\%$; $p = 0.0001$ for the change) but not low PM_1 exposure (pre-exercise: $6.6\% \pm 4.04\%$; post-exercise: $4.89\% \pm 4.42\%$; p-value for the change not given). Further, they found basal brachial artery vasoconstriction (4%; pre-exercise BAD: 4.66 ± 0.61 mm; post-exercise BAD: 4.47 ± 0.63 mm; $p = 0.0002$ for the change) after the 'high PM_1 ' exposure, but not the 'low PM_1 ' exposure (-0.3% pre-exercise BAD: 4.66 ± 0.63 mm; post-exercise BAD: 4.68 ± 0.61 mm; p-value for the change not given).

In a prospective panel study of $n = 22$ Type II diabetics (aged 61 ± 8 yr), Schneider et al. (2008, [191985](#)) examined the change in FMD, BAD, small artery elasticity index, larger artery elasticity index, and systemic vascular resistance associated with ambient $PM_{2.5}$ as measured in Chapel Hill, NC. The mean and standard deviation $PM_{2.5}$ concentrations during the study period (November 2004 to December 2005) were $13.6 \pm 7.0 \mu\text{g}/\text{m}^3$. Using additive mixed models with a random subject effect, each $10 \mu\text{g}/\text{m}^3$ increase in

PM_{2.5} in the previous 24 h was associated with a significant decrease in FMD (-17.3% [95% CI: -34.6 to 0.0]). Similarly, each 10 µg/m³ increases in PM_{2.5} was associated with a significant decrease in small artery elasticity index lagged 1 day (-15.1% [95% CI: -29.3 to -0.9]), and lagged 3 days (-25.4% [95% CI: -45.4 to -5.3]). Significant decreases in larger artery elasticity index and significant increases in systemic vascular resistance lagged 2 and 4 days were also observed. Further, effects were greatest among those with high BMI, high glycosylated hemoglobin A1c, low adiponectin, or the null GSTM1 polymorphism. However, high myeloperoxidase levels were associated with greater PM_{2.5} effects on these measures.

In a similar study done in Paris, France, Briet (2007, [093049](#)) similarly reported that each increase in PM_{2.5} was associated with a -0.32% (95% CI: -1.10 to 0.46) decrease in FMD, although this estimate was not statistically significant. Significant FMD reductions were associated with increased SO₂, NO₂, and CO concentrations. Each 1 standard deviation increase (units not given) in PM_{2.5} in the previous 2 wk was associated with a 15.68% (95% CI: 7.11-23.30) increase in small artery reactive hyperemia. Each 1 standard deviation increase (units not given) in PM₁₀ in the previous 2 wk was associated with a 15.91% (95% CI: 7.74-24.0) increase in small artery reactive hyperemia.

Summary of Epidemiologic Study Findings for Vasomotor Function

Vasomotor function has been evaluated using several metrics in the studies described above, including FMD, small artery elasticity index, larger artery index, systemic vascular resistance, BAD, end diastolic basal diameter, and nitroglycerin-mediated reactivity. The most common measures evaluated were BAD, a measure of the relatively static, anatomic/physiological baseline vasomotor function, and FMD, the dynamic measure of post- minus pre-occlusion BAD. Each study demonstrated an acute association between these measures of vascular function and ambient PM concentrations (Briet et al., 2007, [093049](#); Dales et al., 2007, [155743](#); Liu et al., 2007, [156705](#); O'Neill et al., 2005, [088423](#); Rundell et al., 2007, [156060](#); Schneider et al., 2008, [191985](#)). Three studied a panel of diabetics (Liu et al., 2007, [156705](#); O'Neill et al., 2005, [088423](#); Schneider et al., 2008, [191985](#)), and three a panel of young healthy subjects (Briet et al., 2007, [093049](#); Dales et al., 2007, [155743](#); Rundell et al., 2007, [156060](#)). Only two studies investigated multiple lags (lag days 0 to 6) (O'Neill et al., 2005, [088423](#); Schneider et al., 2008, [191985](#)), with one reporting the strongest association with the 6-day mean PM concentration (O'Neill et al.,

2005, [088423](#)), and the other with lag day 0. In other studies, responses were observed in as short as 30 min after the exposure (Rundell et al., 2007, [156060](#)). The Rundell et al. (2007, [156060](#)) findings are consistent with other studies showing an adverse response to ambient particulate pollution emitted from vehicular traffic (Adar et al., 2007, [098635](#); Adar et al., 2007, [001458](#); Riediker et al., 2004, [056992](#); Riediker et al., 2004, [091261](#)).

6.2.4.2. Controlled Human Exposure Studies

Some evidence of a PM-induced increase in brachial artery vasoconstriction is presented in the 2004 PM AQCD (U.S. EPA, 2004, [056905](#)). Brook et al. (2002, [024987](#)) exposed 24 healthy adults to PM_{2.5} CAPs (150 µg/m³) along with 120 ppb O₃ for a period of 2 h. A significant decrease in BAD was observed immediately following exposure compared with filtered air control. No significant changes were observed in either endothelial-dependent or endothelial-independent vasomotor function, as determined by FMD and nitroglycerin-mediated dilatation, respectively. As described below, many more recent studies have evaluated the effects of various types of particles on vasomotor function following controlled exposures among healthy and health-compromised individuals.

CAPs

A subsequent analysis of the CAPs constituents from the Brook et al. study revealed a significant negative association between the post-exposure change in BAD and both the OC and EC concentrations of CAPs (Urch et al., 2004, [055629](#)). However, the observed vasomotor effects cannot conclusively be attributed to PM_{2.5}, as subjects were exposed concurrently to PM_{2.5} and O₃. Mills et al. (2008, [156766](#)) evaluated the effect of fine and ultrafine CAPs on vasomotor function in a group of 12 males with stable coronary heart disease (average age 59 yr), as well as in 12 healthy males (average age 54 yr). Relative to filtered air exposure, exposure to PM (average concentration 190 µg/m³) did not significantly affect vascular function in either group. The authors attributed the lack of response in endothelial function to the composition of the CAPs used in the study, which were low in combustion-derived particles and consisted largely of sea salt.

Urban Traffic Particles

The effect of exposure to urban traffic particles on vasomotor function has recently been evaluated among a group of adult volunteers (Bräuner et al., 2008, [191966](#)). In this study, healthy young adults (average age 27 yr) exposed for 24 h to urban traffic particles

(average PM_{2.5} concentration 9.7 µg/m³) were not observed to experience any change in microvascular function after 6 or 24 h of exposure relative to filtered air.

Diesel Exhaust

Mills et al. (2005, [095757](#)) exposed 30 healthy men (20-38 years old) to both diluted DE (300 µg/m³) and filtered air control for 1 h with intermittent exercise. Half of the subjects underwent vascular assessments at 6 to 8 h following exposure to DE or filtered air, while in the other 15 subjects, vascular assessments were performed at 2-4 h post-exposure. DE attenuated forearm blood flow increase induced by bradykinin, acetylcholine, and sodium nitroprusside infusion measured 2 and 6 h after exposure. The authors postulated that the effect of diesel on vasomotor function may be the result of reduced NO bioavailability in the vasculature stemming from oxidative stress induced by the nanoparticulate fraction of DE. A diesel-induced decrease in the release of tPA was also observed at 6 h post-exposure, which may provide additional mechanistic evidence supporting the observed association between air pollution and MI. As presented in Tornqvist et al. (2007, [091279](#)), changes in vascular function were also evaluated 24 h following exposure in 15 of the 30 subjects. Compared with filtered air, exposure to DE significantly reduced endothelium-dependent (acetylcholine) vasodilation ($p = 0.01$) at 24 h post exposure. Bradykinin-induced vasodilation was marginally attenuated by DE ($p = 0.08$), while no effects of diesel on endothelium-independent vasodilation (sodium nitroprusside) were observed. Although the release of tPA was not affected by DE 24 h following exposure, the authors suggest that the persistent association between diesel exposure and vasomotor function observed in this study provides supporting mechanistic evidence of increases in cardiovascular events occurring 24 h after a peak in PM concentration.

To further investigate the effects of DE on vasomotor function, Mills et al. (2007, [091206](#)) exposed 20 men (average age 60 yr) with previous MI on two separate occasions to dilute DE (300 µg/m³; mean particle size 54 nm) or filtered air for 1 h with intermittent exercise. Contrary to previous findings in younger, healthy adults (Mills et al., 2005, [095757](#)), DE was found not to affect vasomotor function in peripheral resistance vessels at 6 h post-exposure as measured by endothelium-dependent (acetylcholine) and endothelium-independent (sodium nitroprusside) vasodilation (forearm blood flow). However, vascular assessments were not performed at 2 h post-exposure in this study. The

same laboratory evaluated the effect of exposure to DE with slightly higher particle concentrations ($330 \mu\text{g}/\text{m}^3$, particle number $1.26 \times 10^6/\text{cm}^3$) on arterial stiffness among healthy adults (Lundbäck et al., 2009, [191967](#)). Using radial artery pulse wave analysis, significant increases in augmentation pressure and augmentation index, as well as a significant reduction in the time to wave reflection were observed 10 and 20 min following exposure to DE relative to filtered air. This finding of a DE-induced reduction in arterial compliance provides additional evidence to suggest that exposure to particles may adversely affect vasomotor function.

Peretz et al. (2008, [156854](#)) exposed both healthy adults ($n = 10$) and adults with metabolic syndrome ($n = 17$) for 2 h to filtered air and two concentrations of diluted DE (fine PM concentrations of 100 and $200 \mu\text{g}/\text{m}^3$). Compared with filtered air, DE at $200 \mu\text{g}/\text{m}^3$ elicited a statistically significant decrease in BAD (0.11 mm [95% CI: 0.02-0.18 mm]) immediately following exposure. A smaller diesel-induced decrease in BAD (0.05 mm) was observed following exposure to $100 \mu\text{g}/\text{m}^3$. Although this decrease was not statistically significant, the average decrease was approximately one half the decrease at the higher particle concentration, which provides suggestive evidence of a linear concentration response in this range of concentrations. Exposure to DE was not shown to significantly affect endothelium-dependent flow-mediated dilatation. Plasma levels of endothelin-1 (ET-1) were observed to increase relative to filtered air exposure approximately 1-h after exposure to $200 \mu\text{g}/\text{m}^3$ DE ($p = 0.01$). The results of this study provide evidence of an acute endothelial response and arterial vasoconstriction resulting from short-term exposure to DE. Diesel-induced changes in vasoconstriction and ET-1 release were more pronounced in the healthy subjects than in the subjects with metabolic syndrome. The authors postulated that subjects with metabolic syndrome may have stiffer vessels that are not as responsive to vasoconstrictor stimuli. In a study utilizing a similar exposure protocol, Lund et al. (2009, [180257](#)) observed a significant increase in ET-1 in healthy adults following a 1-h exposure to DE with a particle concentration of $100 \mu\text{g}/\text{m}^3$, a concentration that was not shown to affect ET-1 levels in the Peretz et al. (2008, [156854](#)) study.

In the previously described studies by Mills et al. (2005, [095757](#); 2007, [091206](#)), Peretz et al. (2008, [156854](#)), Tornqvist et al. (2007, [091279](#)) and Lund et al. (2009, [180257](#)), subjects were exposed to DE, which, in addition to PM, includes DE gases such as NO_x , CO, and hydrocarbons. Therefore, it is possible that the observed effects may be due in part to exposure to non-particle components of DE. While the majority of these DE exposures have

contained relatively high levels of gaseous emissions including NO₂ concentrations >2 ppm, the concentrations of these gases were much lower in the Peretz et al. (2008, [156854](#)) study (NO₂ concentrations ≈ 20 ppb) which used a newer diesel engine (2002 Cummins B-series) operating under load at 75% of rated capacity. In this study, an apparent linear concentration response relationship was observed between increasing DE exposure and decreases in BAD at particle concentrations between 100 and 200 µg/m³.

Gasoline Emissions

Rundell and Caviston (2008, [191986](#)) exposed 15 college athletes to particles generated using a 2.5 hp gasoline engine, as well as a clean air control during 6 min periods of maximal exercise on a cycle ergometer. Subjects were exposed twice under each condition, with the two clean air exposures occurring first, separated by 3 days. The two exposures to gasoline emissions were also separated by 3 days, with the first exposure occurring 7 days after the second clean air exposure. During exposures to gasoline emissions, average particle counts of particulate matter <1.0 µm were reported as 336,730/cm³ and 396,200/cm³ during the first and second exposures, respectively, with an average CO concentration of 6.3 ppm. There were no differences observed in total work done (kJ) over the 6-minute exercise periods between the two clean air exposures or between the clean air exposures and the first exposure to gasoline exhaust. However, the second gasoline exhaust exposure was demonstrated to significantly decrease work accumulated over the 6-minute exercise period compared with either of the other exposure conditions (p < 0.01). The results of this study provide limited evidence to suggest that a very short term exposure to gasoline emissions may affect exercise performance in healthy adults. The authors speculated that the observed effect of exposure on work accumulated during maximal exercise could be due to vasoconstriction and decrease in blood flow in the skeletal muscle microcirculation. However, the effect of exposure on vasoreactivity was not explicitly assessed.

Model Particles

The results of a recent study by Shah et al. (2008, [156970](#)) provides evidence that exposure to ultrafine EC particles (50 µg/m³) without coexposure to organics, metals, or gaseous copollutants may alter vasomotor function in healthy adults. In this study, venous occlusion plethysmography was used to measure reactive hyperemia of the forearm prior to exposure, immediately following exposure, and 3.5 h, 21 h, and 45 h following a 2-h

exposure with intermittent exercise. Peak forearm blood flow was observed to increase after exposure to filtered air, but not following exposure to ultrafine EC at 3.5 h post-exposure ($p = 0.03$).

Summary of Controlled Human Exposure Study Findings for Vasomotor Function

Taken together, the two studies by Mills et al. (2005, [095757](#); 2007, [091206](#)) along with the studies by Peretz et al. (2008, [156854](#)), Lund et al. (2009, [180257](#)) and Tornqvist et al. (2007, [091279](#)) suggest that, in healthy subjects, DE exposure inhibits endothelium-dependent and endothelium-independent vasodilation acutely (within 2-6 h), and that the suppression of endothelium-dependent vasodilation may remain up to 24 h following exposure. In patients with coronary artery disease, vasodilator function does not appear to be affected 6-8 h following exposure; however, vascular assessments were not performed at earlier time points. In addition, the use of medications in these patients may have blunted the response to PM. The findings of Shah et al. (2008, [156970](#)) suggest that UFP carbon core may be sufficient to produce small changes in systemic vascular function, but the mechanisms remain obscure. The authors demonstrated a decrease in nitrate levels following exposure to EC UFP; however, venous nitrite level, which more closely reflects NO production, was unchanged. Exposure to urban traffic particles was not demonstrated to alter vasomotor function among healthy adults.

6.2.4.3. Toxicological Studies

Vascular dysfunction is a function of altered production of vasoconstrictors and vasodilators. In the 2004 PM AQCD (U.S. EPA, 2004, [056905](#)), studies examining ET as an activator of vasoconstriction were limited to those conducted by Bouthiller et al. (1998, [087110](#)) and Vincent et al. (2001, [021184](#)), in which increased plasma endothelin (ET) levels were observed in rats exposed to high concentrations (40 or 5 mg/m³) of resuspended Ottawa (EHC-93) or diesel PM, respectively. The authors postulated that PM altered vasoconstriction via elevated ET. No studies were cited in the 2004 PM AQCD (U.S. EPA, 2004, [056905](#)) that looked at direct measures of vasoreactivity.

As this area is newly emerging, numerous studies are included below that utilize IT exposure or high concentrations; the studies that exposed vessels directly to particles *ex vivo* are included in Annex D only, as their relevance is questionable. There is clearly a need for more toxicological research examining the relationship between vascular measurements

and PM exposures using ambient particles at lower concentrations. Furthermore, no new studies have advanced the knowledge in regards to ET as a biomarker of PM-induced vasoconstriction since the last PM review.

CAPs

SD rats were exposed to PM_{2.5} CAPs (5 h/day × 3 days; daily mean mass concentration 73.5-733 µg/m³; Boston, MA; 3/1997-6/1998) then the pulmonary arterial vasculature was evaluated (Batalha et al., 2002, [088109](#)). Some animals were repeatedly exposed to SO₂ (5 h/day × 5 days/wk × 6 wks) to induce chronic bronchitis. Morphometric measurements indicated that the pulmonary artery lumen-to-wall (L/W) ratio (an indicator of arterial narrowing) was decreased for the both CAPs groups compared to the normal/air group. Furthermore, decreased L/W ratio in CAPs-exposed animals (regardless of pre-treatment) was significantly associated with particle mass and composition when the mean concentrations from the second and third exposure days were used in a univariate linear regression. These results indicate a change in vascular tone following acute exposure to PM.

Diesel Exhaust

The venous circulation plays a prominent role in heart failure exacerbation (Gehlbach and Geppert, 2004, [155784](#)). In heart failure, patients are often volume overloaded and are subsequently placed on diuretics to alleviate symptoms of pulmonary congestion and chest pain. Knuckles et al. (2008, [191987](#)) hypothesized that if veins constrict in a manner similar to arteries, then patients with severe heart failure may have temporary shunting of fluid to the pulmonary circulation, which may elicit signs and symptoms of heart failure. Using mesenteric vessels from mice (C57BL/6) exposed to DE (350 µg/m³ × 4 h; MMD 100 nm, CMD 80 nm), the authors reported a significant enhancement of ET-1-induced vasoconstriction in veins with much weaker responses in arteries. In an ex vivo experiment, venous constriction was blocked by the arginine analog, L-NAME, which eliminates the feedback NOS activation via endothelial ET_B receptors; this is indicative of impaired or uncoupled eNOS. The authors hypothesized that volatile organic compounds might be responsible these effects, but no significant effects were observed for acetaldehyde, formaldehyde, acetone, hexadecane, or pristane.

Model Particles

A study by Nurkiewicz et al. (2008, [156816](#)) compared the arteriole dilation responses in the spinotrapezius muscle with inhalation exposure to fine or ultrafine TiO₂ (1 μm and 21 nm, respectively; mean mass concentration 3-16 and 1.5-12 mg/m³, respectively) for durations of 4-12 h in SD rats. Both size fractions of TiO₂ induced impaired dilation with a NO-dependent Ca²⁺ ionophore in a dose-dependent manner. When ultrafine and fine TiO₂ were compared at similar mass doses, the systemic microvascular dysfunction was greater with the UFPs. Furthermore, three exposures of differing durations and concentrations that produced equal calculated pulmonary deposition of ultrafine TiO₂ (30 μg) demonstrated similar dilation responses, indicating that impairment is dependent upon the time × concentration product. No effects on dilation were observed with a dose of 4 μg ultrafine TiO₂ (1.5 mg/m³ for 4 h) or 8 μg fine TiO₂ (3 mg/m³ for 4 h).

In a follow-up study, Nurkiewicz et al. (2009, [191961](#)) examined the effect of pulmonary fine and ultrafine TiO₂ exposure on endogenous microvasculature NO production in SD rats. The exposure concentrations and durations were selected to produce ~50% impairment of microvascular reactivity (67 and 10 μg for fine¹ and ultrafine² TiO₂, respectively). Similar to the study above (Nurkiewicz et al., 2008, [156816](#)), impaired endothelium-dependent arteriolar dilation was observed 24 h post-exposure with infusion of a Ca²⁺ ionophore. Earlier studies that used residual oil fly ash (ROFA) or TiO₂ IT instillation reported similar findings, regardless of particle type (Nurkiewicz et al., 2004, [087968](#); Nurkiewicz et al., 2006, [088611](#)). There was no difference in arteriolar dilation between sham and TiO₂ exposed groups with direct administration of the NO donor sodium nitroprusside (SNP) to the exterior arteriolar wall and this response was consistent with that observed following ROFA administered IT (Nurkiewicz et al., 2004, [087968](#)). The lack of response to SNP indicates that vascular smooth muscle sensitivity to NO is not altered after particle exposure. The amount of ROS in the microvascular wall was increased following exposure to either TiO₂ sizes. Local ROS may consume endothelial-derived NO and generate peroxynitrite radicals, as microvascular nitrotyrosine (NT) formation (the end product of peroxynitrite reactions) was demonstrated after TiO₂ exposure. NO production was compromised in a dose-dependent manner following particle exposure (8-90 μg for fine

¹ Produced by a 300-min exposure to 16 mg/m³ of fine TiO₂

² Produced by a 240-min exposure to 6 mg/m³ of ultrafine TiO₂

and 4-38 µg for ultrafine TiO₂), and was partially restored with agents for radical scavenging or enzyme inhibition for NADPH oxidase and myeloperoxidase (MPO).

Intratracheal Instillation

Nurkiewicz et al. (2004, [087968](#); 2006, [088611](#)) have shown impairment of endothelium-dependent dilation in the systemic microvasculature of SD rats following ROFA or TiO₂ exposure (0.1 or 0.25 mg/rat). NO-independent arteriolar dilation was also impaired by ROFA arteriole adrenergic sensitivity to phenylephrine (PHE) was not affected by 0.25 mg ROFA, indicating that contractile activity was unchanged. In addition, increased venular leukocyte rolling and adhesion in the spinotrapezius muscle was also observed following ROFA exposure (Nurkiewicz et al., 2004, [087968](#)).

Further characterization of the leukocyte adherence and “rolling” effects for both ROFA and TiO₂ were indicative of an activated endothelium (Nurkiewicz et al., 2006, [088611](#)). Vascular deposition of MPO was observed in the spinotrapezius muscle 24 h post-exposure and the authors suggested that the adherent leukocytes may have deposited the MPO to be taken up by endothelial cells (Nurkiewicz et al., 2006, [088611](#)). However, this is in contrast to another study (Cozzi et al., 2006, [091380](#)) that did not find changes in blood neutrophil MPO release in ICR mice exposed to ultrafine PM (100 µg from Chapel Hill, NC; assessed 24 h post-exposure), although this finding may be a reflection of differing protocols. Increased oxidative stress in the arteriolar wall was also reported with exposure to 0.25 mg ROFA. TiO₂ and ROFA induced varying degrees of pulmonary inflammation in these animals, but elicited very similar vascular effects, indicating that the vascular responses may be due to PM presence in the lung rather than its physiochemical properties or intrinsic pulmonary toxicity.

PM₁₀

Tamagawa et al. (2008, [191988](#)) reported reduced acetylcholine (ACh)-stimulated relaxation in carotid arteries from rabbits (New Zealand White) exposed to PM₁₀ (EHC-93) via intrapharyngeal instillation for 5 days or 4 wk (total doses 8 and 16 mg/kg, respectively). Endothelium-dependent NO-mediated vasorelaxation correlated with increased serum IL-6 levels in the acute study and during weeks 1 and 2 of the 4-wk exposure, which may indicate a role for systemic inflammation in the response. Maximal SNP-induced dilation was not affected by PM exposure, indicating that the dilatory response was not acting via endothelium-independent NO-mediated mechanisms. This

finding is consistent with that by Nurkiewicz et al. (2004, [087968](#)) and suggests that the arteriolar smooth muscle is not involved in the PM-impaired dilatation response.

Vasoreactivity of aortic rings was measured in SH rats following exposure to 10 mg/kg PM₁₀ (EHC-93), with an increase in ACh-induced vasorelaxation observed (Bagate et al., 2004, [087945](#)). This endothelium-dependent response was greatest at 4 h and was still present at 24 h. Similarly, vasorelaxation induced by SNP 4-h post-PM exposure was enhanced. The vasorelaxation response was attenuated after denudation of the aortic rings, suggesting that the effect was endothelium-dependent. The findings of enhanced dilation with PM exposure contrast with those reported by Nurkiewicz et al. (2004, [087968](#); 2006, [088611](#)), Tamagawa et al. (2008, [191988](#)), and Cozzi et al. (2006, [091380](#)) and may be attributable to differences in PM type, animal species, or disease models. The authors attribute their findings to the SH rat as a well-documented model of sympathetic hyperactivity (increased affinity of aortic smooth muscle α -adrenergic receptors) that demonstrates upregulation of NO formation and/or release (Safar et al., 2001, [156068](#)). No change in vasoconstriction was observed with PM with PHE or potassium chloride.

Consistent with the impaired vasodilatory responses observed in the microvasculature and aortic rings following PM exposure, Courtois et al. (2008, [156369](#)) demonstrated less relaxation to ACh in intrapulmonary arteries of Wistar rats exposed to a high dose (5 mg) of ambient PM (SRM1648). This response was only observed 12 h after PM exposure and not at shorter (6 h) or longer (24 or 72 h) time points. Fine TiO₂ did not alter ACh-induced relaxation.

Ultrafine PM

Cozzi et al. (2006, [091380](#)) used ICR mice to examine the effects of ultrafine PM exposure (100 μ g collected from Chapel Hill, NC) on vascular reactivity following PM exposure and ischemia/reperfusion injury. Aortic rings were evaluated for their contractile and dilatory responses 24 h post-exposure and following the ischemia/reperfusion protocol. Maximum ACh-induced relaxation was impaired in ultrafine PM-exposed vessels, as well as a rightward shift in sensitivity to ACh. There was no difference in constriction to PHE between aortic rings from control and PM-exposed mice. The reduced ACh-induced relaxation may be important for reperfusion of critical vascular beds following occlusion, potentially leading to a greater area of infarction (as in this study). A new study in dogs supports the results observed in the above study and provides evidence of reduced

myocardial blood flow following PM exposure (Bartoli et al., 2009, [179904](#)), and is discussed in more detail in Section 6.2.3.3.

Summary of Toxicological Study Findings for Vasoreactivity

The toxicological findings with respect to vascular reactivity are generally in agreement and demonstrate impaired dilation following PM exposure that is likely endothelium dependent. These effects have been demonstrated in varying vessels (right spinotrapezius muscle, carotid arteries, and aortic rings) and in response to different PM types (ROFA, TiO₂, EHC-93, ultrafine ambient PM). The work by Nurkiewicz et al. (2004, [087968](#); 2006, [088611](#); 2008, [156816](#); 2009, [191961](#)) supports a role for increased ROS and RNS production in the microvascular wall that leads to altered NO bioavailability and dysfunction following particle exposure. Only one study showed enhanced dilation with PM exposure, but the authors attributed the conflicting results to the SH rat. No constriction changes in response to PHE were observed following PM exposure. The responses observed in the pulmonary circulation after PM exposure include pulmonary vasoconstriction, decreased L/W ratio, and impaired vasodilation in intrapulmonary arteries. These results are consistent and indicate altered vascular tone. Enhancement of vasoconstriction in mesenteric veins following DE is the first study of its kind to report on venous circulatory effects.

Endothelin

In addition to studies that look at vascular reactivity, three recent studies have examined plasma ET levels following exposure to vehicle emissions and a few studies examined the mRNA expression of ET-1 and the ET receptors in the hearts of rodents following PM exposure.

CAPs

The upregulation of mRNA expressions of ET-1 and the ET_A receptor in WKY rats exposed to CAPs (1 or 4 days; 4.5 h/day; mean mass concentration range 1,000-1,900 µg/m³; 5/2004, 11/2004, 9/2005; Yokohama City, Japan) was correlated with increasing PM cumulative mass collected on chamber filters (Ito et al., 2008, [096823](#)). Furthermore, relative cardiac mRNA expressions of ET-1 and ET_A receptor were significantly correlated with CYP1B1 and HO-1 expression, indicating a possible relationship between ET-1 metabolism or oxidative stress.

Another plasma mediator of vasomotor tone is asymmetric dimethylarginine (ADMA), which is an endogenous inhibitor of NOS that is associated with impaired vascular function and increased cardiovascular events. Dvonch et al. (2004, [055741](#)) assessed levels of ADMA in Brown Norway rats 24-h following a 3-day PM_{2.5} CAPs exposure in southwest Detroit (8 h/day; 7/2002). CAPs (mean mass concentration 354 µg/m³) resulted in increased plasma ADMA compared to air controls, although the levels reported were well below the 2 µM/L range associated with increased CVD risk in humans in chronic studies. Therefore, the preliminary results identified a new potential biomarker of vascular tone that had not previously been used in air pollution toxicological studies.

Traffic-Related Particles

A study of old rats (21 month; Fischer 344) exposed to on-road highway aerosols (number concentration range 0.95-3.13 × 10⁵ particles/cm³; Interstate 90 between Rochester and Buffalo, NY) for 6 h demonstrated decreased plasma ET-2 (18 h post-exposure) and unchanged levels of ET-1 and ET-3 (Elder et al., 2004, [087354](#)).

Gasoline Exhaust

In contrast to the study above, circulating levels of ET-1 (measured 18 h post-exposure) were elevated in animals exposed to gasoline exhaust and filtration of particles did not reduce this effect (see study details in Section 6.2.2.2) (Campen et al., 2006, [096879](#)). The results of Campen et al. (2006, [096879](#)) are consistent with those observed by Bouthillier et al. (1998, [087110](#)) following a very high exposure to EHC-93, but it is difficult to attribute the effects to PM alone, as Campen et al. (2006, [096879](#)) showed that the gaseous components of the gasoline mixture were required for the ET-1 increase.

Aorta ET-1 mRNA expression was increased with a 7 day gasoline exhaust exposure (60 µg/m³) in ApoE^{-/-} mice, but was not changed following a single day exposure (Lund et al., 2009, [180257](#)). The expression and activity of MMP-2 and -9 and oxidative stress in aortas of exposed mice were also elevated. The ET-1 and MMP-9 mRNA expressions were attenuated with the addition of an ET_A receptor antagonist (but not a radical scavenger), indicating that ET-1 may mediate the expression of MMP-9 through the ET_A receptor.

Model Particles

Another study examined the effects of ultrafine carbon particles (mass concentration 172 µg/m³; mean number concentration 9.0 × 10⁶ particles/cm³) and there was no difference in ET-1, ET_A or ET_B receptor mRNA expression between air- and particle-exposed SH rats 1

or 3 days post-exposure (Upadhyay et al., 2008, [159345](#)). In lung homogenates, ET-1, ET_A and ET_B receptor mRNA expressions were elevated 3 days after exposure to ultrafine carbon particles (Upadhyay et al., 2008, [159345](#)).

Summary of Toxicological Study Findings for Endothelin

The ET responses were mixed, with one study demonstrating ET-1 increases after exposure to gasoline emissions that were particle independent and another reported decreased ET-2, but no change in ET-1 or ET-3 with on-road highway exposure. Elevated levels of ET-1 and ET_A receptor mRNA expression were noted in hearts of rats exposed to CAPs, but not in rats exposed to ultrafine carbon particles. However, ET-1, ET_A and ET_B receptor mRNA expressions were increased in lung homogenates of rats following ultrafine carbon exposure. The ET_A receptor was found to be involved in the ET-1 and MMP-9 responses in the aortas of mice exposed to gasoline exhaust. A relatively novel marker, ADMA, was used to evaluate vasomotor tone in rats and was found to be elevated following exposure to CAPs, although the results are preliminary and have not been confirmed.

PM Components

In the Batalha et al. (2002, [088109](#)) study described above, univariate analyses were conducted that regressed log L/W on differential exposure concentrations of tracer elements determined using principal components analysis. For CAPs exposure (regardless of pre-treatment), CAPs mass, Si, Pb, SO₄²⁻, EC, and OC were all negatively correlated with L/W ratio. Si and SO₄²⁻ were negatively correlated with L/W ratio in normal rats and Si and OC were negatively correlated with L/W ratio in bronchitic rats. When a multivariate analysis was conducted using normal and bronchitic animals, only the association with Si remained significant. V was not associated with L/W ratio in any analysis.

6.2.5. Blood Pressure

One of the potential outcomes of air pollution-mediated alterations in vascular tone is its impact on variable BP or hypertension. BP is tightly regulated by autonomic (central and local), cardiac, renal, and regional vascular homeostatic mechanisms with changes in arterial tone being countered by changes in cardiac contractility, HR, or fluid volume. The evidence of PM-induced changes in BP presented in the 2004 PM AQCD (U.S. EPA, 2004, [056905](#)) is limited and inconsistent. Recent epidemiologic, controlled human exposure, and

toxicological studies have similarly reported conflicting results regarding the effect of PM on BP. However, the majority of these studies have evaluated changes in BP at some point following exposure to PM. A significant increase in DBP was observed in the only controlled human exposure study that evaluated BP during exposure (concomitant exposure to CAPs and O₃). In addition, evidence from toxicological studies suggests that the effect of PM on BP may be modified by health status, as PM-induced increases in BP have been more consistently observed in SH rats.

6.2.5.1. Epidemiologic Studies

Increased BP was associated with PM concentration in two of three studies reviewed in the 2004 PM AQCD (U.S. EPA, 2004, [056905](#)). Increases in left ventricular BP (systolic and diastolic) are well established risk factors for cardiovascular mortality/morbidity (Welin et al., 1993, [156151](#)). Changes in HR and BP both reflect changes in autonomic tone, and have been examined following short-term increases in PM pollution in several recent studies.

Ibald-Mulli et al. (2004, [087415](#)) examined associations between BP (systolic [SBP], diastolic [DBP]) and ambient PM_{2.5} concentrations, UFP counts, and ACP counts in a multicity panel study (Amsterdam, Netherlands; Helsinki, Finland; Erfurt, Germany) of 131 adults with coronary heart disease. Although based on the same ULTRA Study (Timonen et al., 2006, [088747](#)) with study methods as described previously in Section 6.2.1.1, the study period was different. They investigated changes in BP (SBP and DBP) associated with mean PM_{2.5}, UFP, and ACP concentration/counts (lag days 0, 1, and 2, as well as the 5-day mean) in each city and then generated a pooled estimate across the cities. The median PM_{2.5} concentration, median UFP count, and median ACP count for each city are given below in Table 6-3. Pooled analyses across all 3 cities showed small, but statistically significant decreases in SBP and DBP associated with different lagged concentrations/counts of each particulate pollutant. Each 10 µg/m³ increase in the mean PM_{2.5} concentration over the previous 5 days was associated with a 0.36 mmHg decrease in SBP (95% CI: -0.99, 0.27) and a 0.39 mmHg decrease in DBP (95% CI: -0.75 to -0.03). Each 10,000 particles/cm³ increase in UFP was associated with a 0.72 mmHg decrease in SBP (95% CI: -1.92 to 0.49), and a 0.70 mmHg decrease in DBP (95% CI: -1.38 to -0.02). Each 1,000 particles/cm³ increase in 5 day avg ACP was associated with a 1.11 mmHg decrease in SBP (95% CI: -2.12 to -0.09) and a 0.95 mmHg decrease in DBP (95% CI: -1.53 to -0.37). The

authors concluded that these findings do not support previous findings of an increase in BP associated with increases in particulate pollutant concentrations.

Table 6-3. Median particle concentrations.

City	Median daily PM _{2.5} concentration (µg/m ³)	Median daily UFP concentration (0.01-0.1 µm; particles/cm ³)	Median daily ACP concentration (0.1-1.0 µm; particles/cm ³)
Amsterdam, Netherlands	16.9	17,147	1,874
Erfurt, Germany	16.3	19,198	1,492
Helsinki, Finland	10.6	14,886	1,200

Single-city studies examining the association between BP and particulate air pollution have been done in several U.S. and Canadian cities. Dales et al. (2007, [155743](#)) conducted a panel study of 39 healthy volunteers who sat outside at two different bus stops for 2-h in Ottawa, Canada. The median PM_{2.5} concentrations measured at the bus stops during each 2-h exposure session were 40 and 10 µg/m³. Post-exposure SBP and DBP were not associated with the mean PM_{2.5} concentration measured at the bus stops during the 2-h exposure session. The change in BP (post-exposure – pre-exposure) could not be evaluated, as health measurements were only made after the 2-h exposure session.

Jansen et al. (2005, [082236](#)) studied changes in BP among 16 older subjects (aged 60-86 yr) with asthma or COPD in Seattle, Washington, associated with indoor, outdoor, and personal PM₁₀, PM_{2.5}, and BC measurements (levels within the health measurement session) on 12 consecutive days. The mean daily outdoor PM₁₀ and PM_{2.5} concentrations were 13.47 and 10.47 µg/m³, respectively. The mean daily outdoor BC concentration was 2.01 µg/m³. The study authors reported that no associations were observed between BP and daily mean PM₁₀, PM_{2.5}, or BC concentrations, but did not present any of these results in the paper.

Zanobetti et al. (2004, [087489](#)) examined the association between BP (SBP, DBP, and mean arterial BP) and mean PM_{2.5} concentrations in the previous 24, 48, 72, 96, and 120 h in 62 elderly, cardiac rehabilitation patients in Boston, MA (Zanobetti et al., 2004, [087489](#)). The median PM_{2.5} concentration during the study was 8.8 µg/m³. Each 10.4 µg/m³ increase in mean PM_{2.5} concentration in the previous 120 h was associated with significant increases in resting DBP (2.82 mmHg [95% CI: 1.26-4.41]), SBP (2.68 mmHg [95% CI: 0.04-5.38]), and mean arterial BP (2.76 mmHg [95% CI: 1.07-4.48]).

Mar et al. (2005, [087566](#)) studied this same PM_{2.5}-BP association in 88 subjects aged >57 yr in Seattle, WA. Among healthy subjects taking medications (bronchodilators, inhaled corticosteroids, anti-hypertensives, β-blockers, calcium channel blockers, and/or cardiac glycosides), each 10 µg/m³ increase in mean outdoor PM_{2.5} concentration on the same day as the BP measurement was made was associated with small increases in SBP and DBP (the results for these analyses were presented in figures only). However, among all subjects, each 10 µg/m³ increase in same day mean PM_{2.5} concentration was associated with non-significant decreases in SBP (-0.81 mmHg [95% CI: -2.34 to 0.73]) and DBP (-0.46 mmHg [95% CI: -1.49 to 0.57]).

As described earlier, Ebel et al. (2005, [056907](#)) conducted a repeated measures panel study of 16 patients with COPD in the summer of 1998 in Vancouver, British Columbia to evaluate the relative impact of ambient and non-ambient exposures to PM_{2.5}, PM₁₀, and PM_{10-2.5} on multiple health outcomes including ectopy and BP. Using the same analytic methods, pollutant concentrations, and lags, they reported decreased SBP associated with same day ambient exposures to each PM size fraction (results were presented in figures only).

Two similar studies were done in Incheon, South Korea (Choi et al., 2007, [093196](#)) and Taipei, Taiwan (Chuang et al., 2005, [156356](#)). Both reported significant increases in BP associated with acute increases in ambient PM. Choi et al. (2007, [093196](#)) reported significantly increased SBP and DBP associated with the mean PM₁₀ concentration over the same and previous 2 days in the warm season only (July to September). Chuang et al. (2005, [156356](#)) reported significant increases in SBP and DBP associated with the mean UFP count (0.01 to 0.1 µm particles) 1-3 h before the BP measurement.

These studies (Choi et al., 2007, [093196](#); Chuang et al., 2005, [156356](#); Dales et al., 2007, [155743](#); Ibalid-Mulli et al., 2004, [087415](#); Mar et al., 2005, [087566](#); Zanobetti et al., 2004, [087489](#)) are not entirely consistent with regard to their BP-PM associations. Most have reported increases in SBP and DBP associated with increases in either PM_{2.5}, PM₁₀, or UFP (Choi et al., 2007, [093196](#); Chuang et al., 2005, [156356](#); Mar et al., 2005, [087566](#); Zanobetti et al., 2004, [087489](#)). However, two studies reported small decreases in BP associated with multiple particulate pollutants (Ibalid-Mulli et al., 2004, [087415](#); Mar et al., 2005, [087566](#)). Dales et al. (2007, [155743](#)) reported no change in BP associated with a 2-h exposure to bus stop PM_{2.5} and Jansen et al. (2005, [082236](#)) reported null findings among older adults in Seattle, WA. Exposure lags ranging from 1-3 h (Chuang et al., 2005,

[156356](#)), to the same day (Ebelt et al., 2005, [056907](#); Mar et al., 2005, [087566](#); Rich et al., 2008, [156910](#)), to the mean across the previous 5 days (Zanobetti et al., 2004, [087489](#)) were reported as having the strongest associations with BP.

Right Ventricular Pressure

Several recent studies, summarized in the section on hospital admissions and ED visits for CVD causes, have reported increased risk of hospital admissions for congestive heart failure associated with increased PM concentration on the same day (Wellenius et al., 2005, [087483](#); Wellenius et al., 2006, [088748](#)). As a possible mechanism for these reported associations, Rich et al. (2008, [156910](#)) hypothesized that these hospital admissions for decompensation of heart failure would be preceded by more subtle increases in pulmonary arterial (PA) and right ventricular (RV) diastolic pressures. They used passively monitored PA and RV pressures on 5807 person-days, among 11 subjects implanted with the Chronicle Implantable Hemodynamic Monitor [Medtronic, Inc. Medtronic, MN]). Using a two-stage modeling process (generalized additive model and mixed effects model adjusted for time trend, weekday, calendar month, apparent temperature, and barometric pressure), they examined the change in daily mean right heart pressures associated with mean PM_{2.5} concentration on the same and previous 6 days. Each 11.62 µg/m³ increase in same day mean PM_{2.5} concentration was associated with small but statistically significant increases in estimated PA diastolic pressure (0.19 mmHg [95% CI: 0.05-0.33]) and RV diastolic pressure (0.23 mmHg [95% CI: 0.11-0.34]). These effects were not attenuated when controlling for all lags simultaneously. Thus, PM induced right heart pressure increases may mark another potential pathway between PM exposure and incidence of cardiovascular events, but further studies on this same hypothesis are needed for confirmation.

Wellenius et al. (2007, [092830](#)) conducted a panel study of 28 subjects living in the greater Boston metropolitan area, each with chronic stable heart failure and impaired systolic function. They hypothesized that circulating levels of B-type natriuretic peptide (BNP), measured in whole blood at 0, 6, and 12 wk, were associated with acute changes in ambient air pollution, as a possible mechanistic explanation for the observed association between hospital admissions for heart failure and ambient PM concentration (Wellenius et al., 2005, [087483](#); Wellenius et al., 2006, [088748](#)). During the study, the mean PM_{2.5} concentration was 10.9 µg/m³, while the mean BC concentration was 0.73 µg/m³. Using linear mixed models, they reported no association between any pollutant (PM_{2.5}, CO, SO₂,

NO₂, O₃, and BC) and BNP at any lag (e.g., each 10 µg/m³ increase in mean daily PM_{2.5} concentration [0.8% increase in BNP (95% CI: -16.4 to 21.5)]) (Wellenius et al., 2007, [092830](#)). Yet, BNP the active peptide has a very short half-life and might not be the best biomarker for such a study. Thus the absence of a correlation between PM and BNP may not suggest that PM does not have an impact on RV or LV function in individuals with impaired cardiac mechanics.

6.2.5.2. Controlled Human Exposure Studies

Only one controlled human exposure study cited in the 2004 PM AQCD (U.S. EPA, 2004, [056905](#)) reported any PM-induced changes in BP. Gong et al. (2003, [042106](#)) found that exposure to PM_{2.5} (174 µg/m³) decreased SBP in asthmatics, but increased SBP in healthy subjects. Among healthy adults, BP was not affected following 2-h exposures to 200 µg/m³ diesel PM (Nightingale et al., 2000, [011659](#)), 150 µg/m³ PM_{2.5} CAPs with 120 ppb O₃ (Brook et al., 2002, [024987](#)), or 10 µg/m³ ultrafine carbon particles (Frampton, 2001, [019051](#)). The effect of PM on BP has been further investigated in several recent controlled human exposure studies, which are described below.

CAPs

One recent study demonstrated a significant increase (9.3%) in DBP among healthy adults immediately prior to the end of a 2-h exposure to 150 µg/m³ PM_{2.5} CAPs in combination with 120 ppb O₃ (Urch et al., 2005, [081080](#)). The authors also found that the magnitude of change in BP was significantly associated with PM_{2.5} carbon content, but not total PM_{2.5} mass. It was postulated that the disparity between these findings and those of a similar study by the same group (Brook et al., 2002, [024987](#)) could be due to differences in experimental methods. The Brook et al. (2002, [024987](#)) study measured post-exposure BP approximately 10 min following exposure, while the study by Urch et al. (2005, [081080](#)) measured BP during exposure. In a follow up study that evaluated changes in blood pressure during a 2-h exposure to PM_{2.5} CAPs, Fakhri et al. (2009, [191914](#)) reported a significant increase in DBP with exposure to CAPs with, but not without, coexposure to O₃.

Diesel Exhaust

Several recent studies have assessed BP changes following a 1-h exposure to DE with a particle concentration of 300 µg/m³. Mills et al. (2005, [095757](#)) evaluated changes in BP 2 h following exposure to DE and found a 6 mmHg increase in DBP of marginal statistical

significance ($p = 0.08$) compared to filtered air control. In this same group of subjects, Tornqvist et al. (2007, [091279](#)) did not observe any such changes in BP 24 h following DE exposure. At lower particle concentrations in diluted DE (100-200 $\mu\text{g}/\text{m}^3$ fine PM), Peretz et al. (2008, [156854](#)) did not observe any changes in systolic or DBP in either healthy adults or adults with metabolic syndrome immediately following a 2-h exposure. Further, although Lundback et al. (2009, [191967](#)) reported an increase in arterial stiffness following exposure to DE with a particle concentration of 330 $\mu\text{g}/\text{m}^3$ among healthy young adults, no changes in systolic or diastolic BP were observed during or following exposure relative to filtered air.

Model Particles

Routledge et al. (2006, [088674](#)) did not observe any changes in BP among healthy older adults and older adults with stable angina following a 1-h exposure to UF EC (50 $\mu\text{g}/\text{m}^3$), with or without coexposure to 200 ppb SO_2 . Similarly, neither Shah et al. (2008, [156970](#)), nor Beckett et al. (2005, [156261](#)) reported any changes in BP among healthy adults following exposure to UF EC (50 $\mu\text{g}/\text{m}^3$) or ZnO (500 $\mu\text{g}/\text{m}^3$ fine and ultrafine), respectively.

Summary of Controlled Human Exposure Study Findings for Blood Pressure

The findings of these new studies do not provide convincing evidence of an association between PM exposure and an increase in BP; however, they do suggest that there is a need for additional investigations of PM-induced changes in BP at various time points following exposure.

6.2.5.3. Toxicological Studies

In healthy animal models, little evidence exists for significant BP changes following inhalation exposure to environmentally-relevant concentrations of PM. Only one animal toxicological study is mentioned in the 2004 PM AQCD (U.S. EPA, 2004, [056905](#)) that examined BP with PM exposure and no effect was observed (Vincent et al., 2001, [021184](#)).

CAPs

In a recent study of dogs, exposure to $\text{PM}_{2.5}$ CAPs from Boston (mean mass concentration 358.1 $\mu\text{g}/\text{m}^3$; mass concentration 94.1-1557 $\mu\text{g}/\text{m}^3$) for 5 h resulted in increased SBP (2.7 mmHg), DBP (4.1 mmHg), mean arterial pressure (3.7 mmHg), and lowered pulse pressure (1.7 mmHg) when measured upstream of the femoral artery (Bartoli et al., 2009, [156256](#)). Administration of an α -adrenergic antagonist (prazosin) prior to CAPs

attenuated the BP responses. These findings indicate that CAPs exposure may have activated α -adrenergic receptors and increased peripheral vascular resistance. Baroreflex sensitivity was measured immediately before and after exposure during a transient elevation of arterial pressure that was induced by PHE; increased baroreflex sensitivity was observed in subgroup of dogs exposed to CAPs, which is consistent with an upregulation of vagal reflexes.

Chang et al. (2004, [055637](#)) noted slight increases in SH rat BP (5-10 mmHg) when exposed to PM_{2.5} CAPs (mean mass concentration 202 $\mu\text{g}/\text{m}^3$) during spring months. However, during summer months, when the CAPs exposure level was less (140 $\mu\text{g}/\text{m}^3$), this effect was not observed. It was unclear, therefore, whether the effects were seasonal or dose-related. In a preliminary study of SH rats exposed to CAPs during a dust storm event, mean BP was elevated the third and fourth hour of a 6-h exposure, although interpretation of this finding is difficult due to few animals in the exposure group ($n = 2$; details provided above) (Chang et al., 2007, [155719](#)). In another study, the increased change in mean BP measured using the tail cuff method following CAPs exposure weakly correlated with PM mass accumulated on chamber filters over the entire exposure duration (see Section 6.2.4.3 for details) (Ito et al., 2008, [096823](#)). Furthermore, ET_A receptor mRNA expression in cardiac tissue was positively correlated with the change in mean BP.

Model Particles

In WKY rats, 24-h exposure to ultrafine carbon particles (mass concentration 180 $\mu\text{g}/\text{m}^3$; mean number concentration 1.6×10^7 particles/ cm^3) did not alter mean BP during exposure or the recovery periods (Harder et al., 2005, [087371](#)). SH rats exposed to ultrafine carbon particles for 24 h (mass concentration 172 $\mu\text{g}/\text{m}^3$; mean number concentration $(9.0 \times 10^6$ particles/ cm^3) resulted in elevated mean BP (by 6 mmHg) on the first and second days of recovery following exposure that was attributable to increases in both SBP and DBP (Upadhyay et al., 2008, [159345](#)). Increased plasma renin concentrations were observed in CB-exposed rats on the first and second days of recovery, although renin activity and angiotensin (Ang) I and II concentrations were not affected by particle exposure.

Summary of Toxicological Study Findings for Blood Pressure

Limited toxicological evidence provides support for elevated BP in dogs or compromised rats with CAPs, ultrafine CAPs, CAPs during a dust storm event, or ultrafine

carbon particle exposure. However, most of the CAPs studies were conducted outside of the U.S.

6.2.6. Cardiac Contractility

The 2004 PM AQCD (U.S. EPA, 2004, [056905](#)) did not include any toxicological studies that evaluated cardiac contractility either directly or indirectly following exposure to PM. Two recent animal toxicological studies have demonstrated reductions in cardiac fractional shortening, diminished ejection shortening, or changes in the QA interval following PM exposure. The results of these studies provide some evidence of PM-induced changes in cardiac contractility in animal models.

6.2.6.1. Toxicological Studies

The strength of the contracting heart is reflected by its contractility. In heart failure, contractility wanes significantly and the heart cannot compensate during periods of increased physical activity. Measuring true contractility in a whole animal is difficult, requiring extensive surgical instrumentation and monitoring. There were no toxicological studies that examined cardiac contractility in the last PM AQCD.

CAPs

Using radiotelemetry to indirectly measure cardiac contractility through the QA interval, SH rats were repeatedly and alternately exposed to ultrafine CAPs in Taiwan on separate days in spring or summer (details provided in Section 6.2.5.3) (Chang et al., 2004, [055637](#)). The QA interval was calculated as the time duration between the Q wave in the ECG and point A (upstroke in aortic pressure) in the pressure trace and is not as reliable as other measures, such as echocardiography. During the spring exposure, QA interval decreased by 1.6 ms as demonstrated by fixed effects in linear mixed-effects modeling, which indicates an increase in cardiac contractility. There were no changes in QA interval observed for the summer months, which may be attributable to lower ultrafine PM concentrations (mean mass concentration 140 $\mu\text{g}/\text{m}^3$) or differing PM compositions.

Model Particles

A recent study using old (18 to 28-months-old) mice (C57BL/6, C3H/HeJ, and B6C3F1) demonstrated significant reductions in cardiac fractional shortening (due to increased left

ventricular end-diastolic and end-systolic diameters) following a 4-day (3 h/day) exposure to CB (PM_{2.5} mean concentration 401 µg/m³; PM₁₀ mean concentration 553 µg/m³) using echocardiography (Tankersley et al., 2008, [157043](#)). Hemodynamic measurements of diminished ejection fraction and maximum change in pressure over time further supported lowered myocardial contractility. Furthermore, increased right ventricular pressure associated with elevated right atrial and pulmonary vascular pressures and resistance, was indicative of pulmonary vasoconstriction in CB exposed mice. Heart tissue and isolated cardiomyocytes from exposed animals demonstrated enhanced ROS that was partially attributable to NOS3-uncoupling and elevated MMP2 and MMP9 levels, which may implicate myocardial remodeling. The combined results from this study suggest that cellular mechanisms involving NOS-uncoupled ROS generation likely mediate PM-induced cardiac effects. Furthermore, mRNA expression for atrial and brain natriuretic peptides (ANP and BNP, respectively) was increased in hearts from exposed mice compared to control, which is consistent with pulmonary congestion. There were no reported strain-related differences in any response.

Intratracheal Instillation

Similar to the responses observed by Tankersley et al. (2008, [157043](#)), decreases in fractional shortening and increases in left ventricular end diastolic diameter measured by echocardiography were also reported for SD rats at 24 h post-IT exposure to DEP (250 µg) (Yan et al., 2008, [098625](#)). A subset of rats received isoproterenol to induce myocardial injury prior to IT instillation of DEP and these animals demonstrated lowered fractional shortening at baseline, which was decreased to an even greater extent with DEP exposure; left ventricular end diastolic diameter was not affected by DEP in these rats.

Summary of Toxicological Study Findings for Cardiac Contractility

The studies above provide some evidence that cardiac contractility may be altered immediately following PM exposure in animal models. Results from the Tankersley (2008, [157043](#)) and Yan (2008, [098625](#)) studies provide the strongest support for PM-induced contractility changes, as echocardiography and hemodynamic measurements are well-established for examining cardiac function.

6.2.7. Systemic Inflammation

The evidence presented in the 2004 PM AQCD (U.S. EPA, 2004, [056905](#)) of increases in markers of systemic inflammation associated with PM was limited and not sufficient to formulate a definitive conclusion. Recent controlled human exposure and toxicological studies continue to provide mixed results for an effect of PM on markers of systemic inflammation including cytokine levels, C-reactive protein (CRP), and white blood cell count. While results from recent epidemiologic studies have also been inconsistent across studies, there is some evidence to suggest that PM levels may have a greater effect on inflammatory markers among populations with preexisting diseases.

6.2.7.1. Epidemiologic Studies

Several studies reviewed in the 2004 PM AQCD (U.S. EPA, 2004, [056905](#)) investigated the association of short-term fluctuations in PM concentration with markers of inflammation. These studies were found to offer limited support for mechanistic explanations of the associations between PM concentration and heart disease outcomes. Recent studies, published since 2002, are reviewed below. CRP was measured in multiple studies, allowing the consistency of findings across epidemiologic studies to be evaluated. Several other markers were examined in only a few studies, in relation to a wide range PM size fractions and components. These markers included IL-6, TNF- α , vascular cell adhesion molecule-1 (VCAM-1), intercellular adhesion molecule-1 (ICAM-1), soluble CD40 ligand (sCD40L), white blood cells (WBC) and soluble adhesion molecules (sP-selectin and e-selectin).

Diez-Roux et al. (2006, [156400](#)) examined whether CRP increased in response to changes in the mean ambient PM_{2.5} concentrations in the prior day, prior 2 days, prior week, prior 30 days, and prior 60 days among participants in the Multi-Ethnic Study of Atherosclerosis (MESA) cohort. Subjects (n = 5,634) lived in either Baltimore City or County, MD, Chicago, IL, Forsyth County, NC, Los Angeles County, CA, Northern Manhattan and the Bronx, NY, or St. Paul, MN. The authors report finding no evidence of a short-term effect of PM_{2.5} on CRP in their population based sample. Of the five exposure measures examined, only the 30-day and 60-day mean exposures showed positive associations with PM_{2.5} (3% [95% CI: -2% to 10%] and 4% [95% CI: -3% to 11%] per 10 $\mu\text{g}/\text{m}^3$, respectively).

Ruckerl et al. (2007, [156931](#)) conducted a multicity longitudinal study to examine whether changes in markers of inflammation were associated with short-term increases in particulate concentrations (PM₁₀, PM_{2.5}, particle number concentration [PNC]) and gaseous pollutant (NO₂, SO₂, CO, O₃). Study subjects were MI survivors (n= 1003) living in either Athens, Greece; Augsburg, Germany; Barcelona, Spain; Helsinki, Finland; Rome, Italy; or Stockholm, Sweden. Repeated measurements of IL-6 and CRP were made during the study. Fibrinogen was also measured in this study and results are discussed in Section 6.2.8.1. The mean city-specific pollutant concentrations during the study are shown below in Table 6-4.

Table 6-4. Ambient concentrations in six European cities.

Pollutant	Helsinki	Stockholm	Augsburg	Rome	Barcelona	Athens
PNC (particles/cm ³)	8,534	9,748	11,876	34,450	18,133	20,589
PM _{2.5} (μg/m ³)	8.2	8.8	17.4	24.5	24.2	23.0
PM ₁₀ (μg/m ³)	17.1	17.8	33.1	42.1	40.7	38.5

Source: Ruckerl et al. (2007, [156931](#))

In pooled analyses, each interquartile range (not provided) increase in PNC in the 12 to 17 h before the health measurement was associated with a 2.7% increase in the geometric mean IL-6 (95% CI: 1.0-4.6). None of the pollutants, at any lag, were associated with CRP levels in these subjects. There did not appear to be effect modification of these results by smoking, diabetes, or heart failure. Ljungman et al. (2009, [191983](#)) studied the modification of the IL-6 association with several PM size fractions (PM₁₀, PM_{2.5}, PNC) by three IL-6 SNPs, one fibrinogen alpha chain (FGA) SNP and one fibrinogen beta chain (FGB) SNP. The associations of PM_{2.5} and PM₁₀ with plasma level of IL-6 were stronger among those with the homozygous minor allele genotype of FGB rs1800790 and among those homozygous for the major allele genotype of IL-6 rs2069832. Gene-environment interactions were most pronounced for CO, modification the PNC-IL-6 association by genotype was not apparent in these data nor was modification of the PM-IL-6 associations by FBA.

Single-city studies of systemic inflammation have been conducted in the U.S. and Canada since 2002. Delfino et al. (2008, [156390](#)) measured CRP, IL-6, TNF-α, sP-selectin, sVCAM-1 and sICAM-1 in blood during a period of 12 wk. Associations of these markers with average PM concentration (PM_{0.25}, PM_{0.25-2.5}, PM_{10-2.5}, particle number concentration

(PNC), EC, OC, BC, primary OC, secondary OC) 24-h to 9 days prior to the blood draw were examined. Subjects included residents of two downtown Los Angeles nursing homes who were 65+ years old with a history of coronary artery disease. Both 24-h avg and multiday average concentrations of PM_{0.25}, EC, primary OC, BC, PNC and gaseous pollutants were associated with CRP, IL-6 and sP-selectin in this study.

Pope et al. (2004, [055238](#)) conducted a panel study of 88 non-smoking, elderly subjects residing in the Salt Lake City, Ogden, and Provo metropolitan area of Utah. The mean PM_{2.5} concentration during the study was 18.9 µg/m³. Each 100 µg/m³ increase in same day mean PM_{2.5} concentration was associated with a 0.81 mg/dL increase in CRP (95% CI: 0.48-1.14), but not WBCs. However, when excluding 1 influential subject, each 100 µg/m³ increase in same day mean PM_{2.5} concentration was associated with only a 0.19 mg/dL increase in CRP (95% CI: -0.01 to 0.39). Several markers of coagulation were examined in this study and are discussed in Section 6.2.8.1.

Zeka et al. (2006, [157177](#)) studied 710 elderly members of the VA Normative Aging Study to examine changes in CRP, sediment rate and WBC with acute changes in PM concentrations in the previous 48 h, 1 wk, and 2 wk. Results for fibrinogen will be discussed in Section 6.2.8.1. The median 48-h PNC was 24,200 particles/cm³, while the median 48-h PM_{2.5} concentration was 9.39 µg/m³. The median 48-h BC concentration was 0.61 µg/m³, while the median 48-h SO₄²⁻ concentration was 1.84 µg/m³. They did not find consistent or significant associations with any pollutant and CRP. The authors state that the largest effects were observed for the mean PNC and BC concentration in the previous 4 wk and their data suggests that effect PM may be modified by obesity, GSTM1 genotype and statin use may be present.

O'Neill et al. (2007, [091362](#)) conducted a cross-sectional study of 92 Boston residents with type 2 diabetes, to examine the association between plasma levels of ICAM-1, VCAM-1 and PM concentrations. Results for markers of coagulation measured in this study are discussed in Section 6.2.8.1. PM_{2.5}, BC, and SO₄²⁻ concentrations were measured 0.5 km from the patient exam site. The mean PM_{2.5} concentration during the study was 11.4 µg/m³. The mean BC concentration was 1.1 µg/m³, and the mean SO₄²⁻ concentration was 3.0 µg/m³. For all moving averages examined (1-6 days), increases in mean PM_{2.5} and BC concentration were associated with increased ICAM-1 and VCAM-1 concentrations. Each 7.6 µg/m³ increase in the mean PM_{2.5} concentration over the previous 6 days was associated with a 11.76 ng/mL increase in VCAM-1 (95% CI: 3.48-20.70), and each 0.6 µg/m³ increase

in the mean BC concentration over the previous 6 days was associated with a 27.51 ng/mL increase in VCAM-1 (95% CI: 11.96-45.21). However, there were no consistent associations between the mean SO₄²⁻ concentration at any lag and any marker.

Sullivan et al. (2007, [100083](#)) conducted a panel study of n = 47 subjects (aged >55 yr) either with COPD (n = 23) or without COPD (n = 24) in Seattle, WA. They examined the association between levels of CRP and mean daily PM_{2.5} concentration. Most values for IL-6 and TNF-α were below the limit of detection so these markers were not included in the analyses. Results for fibrinogen and d-Dimer are discussed in Section 6.2.8.1. The median PM_{2.5} concentration during the study was 7.7 µg/m³. They did not find any associations between 24-h mean PM_{2.5} concentrations and levels of CRP in individuals with or without COPD. In the study by Liu et al. (2006, [192002](#)), conducted in Toronto, Ontario, neither CRP (0.11 µg/mL [95% CI: -0.03 to 0.25]) nor TNF-α (0.03 pg/mL [95% CI: -0.07 to 0.13]) was associated with 24-h mean PM₁₀ concentration. However, significant positive associations with markers of oxidative stress, FMD and BP were found and are discussed in Sections 6.2.9.1, 6.2.4.1, and 6.2.5.1, respectively.

In the St. Louis Bus Study, each 5.4 µg/m³ increase in the mean PM_{2.5} concentration over the previous week was associated with 5.5% increase in WBC (95% CI: 0.10-11) (Dubowsky et al., 2006, [088750](#)). Each 6.1 µg/m³ increase in the mean PM_{2.5} concentration over the previous 5 days was associated with a 14% increase in CRP among all subjects (95% CI: -5.4 to 37), but an 81% increase in CRP (95% CI: 21-172) among subjects with diabetes, obesity, and/or hypertension. Associations between PM_{2.5} and IL-6 were only observed among those with diabetes, obesity, and/or or hypertension. In another study of in-vehicle PM_{2.5}, each 10 µg/m³ increase during a work-shift was associated with decreased lymphocytes, increased mean corpuscular volume, neutrophils, and CRP over the next 10-14 h among 9 healthy North Carolina state troopers (Riediker et al., 2004, [056992](#)). Associations of roadside and ambient PM_{2.5} were weaker and non-significant in this population. Personal exposure to PM₁₀ (24-h averaging time) was not associated with CRP, IL-6, ET-1 or TNF-α in as study 25 diabetic patients in Windsor, Ontario (Liu et al., 2006, [192002](#)).

International studies of the effect of air pollution on markers of inflammation have been conducted with mixed results. Two studies conducted among 57 male patients with coronary heart disease in Erfurt, Germany found associations of UFP, ACP and PM₁₀ with CRP (Ruckerl et al., 2006, [088754](#)) and UFP and ACP with sCD40L, a marker for platelet

activation (Ruckerl et al., 2007, [156931](#)). In a large cross-sectional study of healthy subjects in Tel Aviv, Steinvil et al. (2008, [188893](#)) examined biological markers of inflammation (CRP and WBC) collected as part of routine health examinations for 3,659 individuals. Associations with air pollutants (including PM₁₀) measured at local monitoring sites for the day of the examination and up to 7 days prior were examined. No significant associations were found between pollutant levels and indications of enhanced inflammation. By contrast, both PM₁₀ and PM_{2.5} SO₄²⁻ and nitrate (3-day avg concentrations) were associated with increases in hs-CRP in healthy students in Taiwan (Chuang et al., 2007, [091063](#)). PM₁₀, PM_{2.5} and PM_{0.25} were not associated with CRP in a study of MI patients in Italy, although associations with autonomic dysregulation and more severe arrhythmias were observed (Folino et al., 2009, [191902](#)). Kelishadi et al. (2009, [191960](#)) reports that CRP, as well as markers of insulin resistance and oxidative stress (discussed in Section 6.2.9.1), were associated in a cross sectional study, with PM₁₀ among a population based sample of children 10-18 years old in Iran (mean PM₁₀ concentration was 122.08 µg/m³).

Summary of Epidemiologic Study Findings for Systemic Inflammation

The most commonly measured marker of inflammation in the studies reviewed was CRP. CRP was not consistently associated with short-term PM concentrations (PM_{2.5}, PM₁₀, SO₄²⁻, EC, OC, PNC). A multicity study of MI survivors in Europe (Ruckerl et al., 2007, [156931](#)) failed to provide evidence of an effect of PM (e.g., PM₁₀, PM_{2.5}, PNC) on CRP and no effect was observed by Diez-Roux et al. (2006, [156400](#)) in a population based study when concentrations were averaged over periods less than 30 days. Several other markers of inflammation have been examined in relation to several PM size fractions and components but the number of studies examining the same marker/PM metric combination is too few to allow results to be compared across epidemiologic studies.

6.2.7.2. Controlled Human Exposure Studies

Several controlled human exposure studies were included in the 2004 PM AQCD (U.S. EPA, 2004, [056905](#)) which evaluated markers of systemic inflammation following exposure to PM. Salvi et al. (1999, [058637](#)) exposed 15 healthy volunteers (21-28 years old) for 1 h to DE (300 µg/m³ particle concentration) and observed a significant increase in neutrophils in peripheral blood 6 h post-exposure compared with filtered air control. However, Ghio et al. (2003, [087363](#)) reported no changes in plasma cytokine levels (e.g.,

IL-6 and TNF- α), WBC count, or CRP 0 or 24 h following a 2-h exposure to PM_{2.5} CAPs (120 $\mu\text{g}/\text{m}^3$). Gong et al. (2003, [042106](#)) did not observe any effect of PM_{2.5} CAPs (174 $\mu\text{g}/\text{m}^3$) on serum amyloid A, while Frampton (2001, [019051](#)) reported no change in leukocyte activation following exposure to a low concentration (10 $\mu\text{g}/\text{m}^3$) of UF carbon. The results of studies published since the completion of the 2004 PM AQCD (U.S. EPA, 2004, [056905](#)) are discussed below.

CAPs

In a study of exposures to PM_{2.5} CAPs (200 $\mu\text{g}/\text{m}^3$), Gong et al. (2004, [087964](#)) observed increased peripheral basophils 4 h following a 2-h exposure in a group of healthy older adults. While this provides some evidence of a CAPs-induced systemic inflammatory response, several other studies have reported no change in plasma CRP levels 0-24 h after exposure to ultrafine (average concentration 50–100 $\mu\text{g}/\text{m}^3$), fine (average concentration 190 - 200 $\mu\text{g}/\text{m}^3$), or coarse (average concentration 89 $\mu\text{g}/\text{m}^3$) CAPs (Gong et al., 2004, [055628](#); Gong et al., 2008, [156483](#); Graff et al., 2009, [191981](#); Mills et al., 2008, [156766](#); Samet et al., 2009, [191913](#)).

Urban Traffic Particles

In a recent investigation of controlled exposures (24 h) to urban traffic particles, Bräuner et al. (2008, [191966](#)) observed no effect of particulate matter concentration (PM_{2.5} concentration 9-10 $\mu\text{g}/\text{m}^3$)

on markers of inflammation including CRP, IL-6 and TNF- α in peripheral venous blood.

Diesel Exhaust

Recent controlled human exposure studies have observed no effect of DE on plasma CRP concentrations or peripheral blood cell counts (Blomberg et al., 2005, [191991](#); Carlsten et al., 2007, [155714](#); Mills et al., 2005, [095757](#); Mills et al., 2007, [091206](#); Tornqvist et al., 2007, [091279](#)). Mills et al. (2005, [095757](#)) found no effect of DE (300 $\mu\text{g}/\text{m}^3$) on serum IL-6 or TNF- α among healthy adult volunteers 6 h after exposure. However, as reported by Tornqvist et al. (2007, [091279](#)), a significant increase in these cytokines was observed 24 h after exposure. Although the physiological significance of this finding is unclear, this study does provide evidence of a mild systemic inflammatory response induced by exposure to DE. In an effort to better understand the inflammatory response of exposure to PM, Peretz et al.

(2007, [156853](#)) conducted a pilot study in which gene expression in peripheral blood mononuclear cells (PBMCs) of healthy human volunteers was evaluated following a 2-h controlled exposure to DE (200 $\mu\text{g}/\text{m}^3$ $\text{PM}_{2.5}$). Adequate RNA samples for microarray analysis (Affymetrix U133 Plus 2.0) from both pre- and 4 h post-exposure to filtered air and DE were available in 4 of the 11 subjects enrolled. The authors found differential expression of 10 genes involved in the inflammatory response when comparing DE exposure (8 upregulated, 2 downregulated) and exposure to filtered air. Two participants had paired samples from 20 h post-exposure which were adequate for analysis. At this time point, DE was associated with 4 differentially expressed genes (1 upregulated, 3 downregulated). However, this study is limited by a small sample size with limited statistical power.

Wood Smoke

Barregard et al. (2006, [091381](#)) recently reported an increase in serum amyloid A at 0, 3, and 20 h following a 4-h exposure to WS ($\text{PM}_{2.5}$ concentrations of 240-280 $\mu\text{g}/\text{m}^3$) among a group of 13 healthy adults (20-56 years old).

Model Particles

Frampton et al. (2006, [088665](#)) evaluated the effect of varying concentrations (10-50 $\mu\text{g}/\text{m}^3$) of UF elemental carbon on blood leukocyte expression of adhesion molecules in healthy and asthmatic adults. Healthy subjects (n = 40) were exposed for 2 h to filtered air and UF carbon under three separate protocols: 10 $\mu\text{g}/\text{m}^3$ at rest (n = 12), 10 and 25 $\mu\text{g}/\text{m}^3$ with intermittent exercise (n = 12), and 50 $\mu\text{g}/\text{m}^3$ with intermittent exercise (n = 16). Asthmatics (n = 16) were exposed at a single concentration (10 $\mu\text{g}/\text{m}^3$) for 2 h with intermittent exercise. Leukocyte expression of surface markers were quantified using flow cytometry on peripheral venous blood samples collected prior to and immediately following exposure, as well as at 3.5 and 21 h post-exposure. Among healthy resting adults, UFP exposure at a concentration of 10 $\mu\text{g}/\text{m}^3$ had no effect on blood leukocytes. The expression of adhesion molecules CD54 and CD18 on monocytes, and CD18 on PMNs was shown to decrease with UFP exposure in healthy exercising adults. In exercising asthmatics, expression of CD11b on monocytes and eosinophils, as well as CD54 on PMNs were reduced following exposure to UFP. In both asthmatics and healthy adults, a UFP-induced decrease in eosinophils and basophils was observed 0-21 h following exposure. Although the clinical significance of these findings is unclear, the authors concluded that their findings of UFP-induced changes in leukocyte distribution and expression were consistent with

increased retention of leukocytes in the pulmonary vasculature, which may be due to an increase in pulmonary vasoconstriction. Other studies have reported no changes in plasma cytokine levels, peripheral blood counts, or CRP following exposure to ZnO or ultrafine EC (Beckett et al., 2005, [156261](#); Routledge et al., 2006, [088674](#)).

Summary of Controlled Human Exposure Study Findings for Systemic Inflammation

New studies involving controlled exposures to various particle types have provided limited and inconsistent evidence of a PM-induced increase in markers of systemic inflammation.

6.2.7.3. Toxicological Studies

There has been limited evidence that enhanced hematopoiesis may occur in animals exposed to PM. Two studies in the 2004 PM AQCD (U.S. EPA, 2004, [056905](#)) provided support for this effect, with one study measured stimulated release of PMNs from bone marrow and another examined peripheral blood PMN and blood cell counts; however, one study did not find associations between CAPs and peripheral blood counts. Thus, it was concluded that consistent evidence of PM-induced hematopoiesis remained to be demonstrated. However, in a study of humans exposed to biomass burning during the 1997 Southeast Asian smoke-haze episodes, PM₁₀ demonstrated the best relationship with blood PMN band cell counts expressed as a percentage of total PMN at lag 0 and 1, indicating a relatively quick response (Tan et al., 2000, [002304](#)).

CAPs

A 2-day CAPs study employing SH rats did not report increased WBC 18-20 h post-exposure (Kodavanti et al., 2005, [087946](#)). A study utilizing fine and/or ultrafine CAPs demonstrated decreased WBC in SH rats 18 h after a 2-day (6 h/day) exposure (Kooter et al., 2006, [097547](#)). The decrease was largely attributable to lowered neutrophils in the fine CAPs-exposed rats and reduced lymphocytes in the ultrafine+fine CAPs animals.

Model Particles

In a study of fine and ultrafine CB particles (WKY rats; 7 h; mean mass concentration 1400 and 1660 µg/m³ for fine and ultrafine CB, respectively; mean number concentration 3.8 × 10³ and 5.2 × 10⁴ particles/cm³, respectively), only ultrafine CB induced elevated blood leukocytes at 0 and 48 h post-exposure compared to the control rats and no effect was

observed at 16 h (Gilmour et al., 2004, [054175](#)). In another study of SH rats exposed to ultrafine carbon particles for 24 h (mass concentration 172 $\mu\text{g}/\text{m}^3$; mean number concentration 9.0×10^6 particles/ cm^3), the percent neutrophils and lymphocytes were increased on the first recovery day, but not the third day (Upadhyay et al., 2008, [159345](#)); CRP was unchanged. In another study, blood neutrophils were decreased in SH rats exposed to ultrafine CB for 6 h and no effects were observed in old Fischer 344 rats (Elder et al., 2004, [055642](#)). Plasma IL-6 levels were unchanged (Elder et al., 2004, [055642](#)).

Coal Fly Ash

Smith et al. (2006, [110864](#)) examined the hematology parameters in SD rats following a 3-day inhalation exposure (4 h/day) to coal fly ash (mean mass concentration 1400 $\mu\text{g}/\text{m}^3$) and reported increased blood neutrophils and reduced blood lymphocytes at 36 h but not 18 h post-exposure.

Intratracheal Instillation

Elevated systemic IL-6 and TNF- α cytokine levels were observed following PM₁₀ instillation in mice (details provided in Section 6.2.8.3) (Mutlu et al., 2007, [121441](#)). IL-6 was decreased with PM exposure in macrophage-depleted mice, indicating that some of the IL-6 release originated in macrophages. For mice (male C57Bl/6J) exposed to PM_{10-2.5} derived from coal fly ash (200 μg), increased plasma IL-6 levels were only observed in animals that also received 100 μg of LPS (Finnerty et al., 2007, [156434](#)) and this response was not observed with LPS alone, indicating a role for PM_{10-2.5}.

Overall, these studies provide evidence of time-dependent responses of systemic inflammation induced by PM exposure. Alterations in WBC have been reported generally as elevations immediately (0 h) or <36 h post-exposure and no change or reductions are noted from 18-24 h.

6.2.8. Hemostasis, Thrombosis and Coagulation Factors

The 2004 PM AQCD (U.S. EPA, 2004, [056905](#)) presented limited and inconsistent evidence from epidemiologic, controlled human exposure, and toxicological studies of PM-induced changes in blood coagulation markers. The body of scientific literature investigating hemostatic effects of PM has grown significantly since the publication of the 2004 PM AQCD (U.S. EPA, 2004, [056905](#)), with a limited number of epidemiologic studies

demonstrating consistent increases in von Willebrand factor (vWf) associated with PM and less consistent associations with fibrinogen. Recent controlled human exposure and toxicological studies have also observed changes in blood coagulation markers (e.g., fibrinogen, vWf, factor VII, t-PA) following exposure to PM. However, the findings of these studies are somewhat inconsistent, which may be due in part to differences in the post-exposure timing of the assessment.

6.2.8.1. Epidemiologic Studies

Several studies investigating the association of short-term fluctuations in PM concentration with markers of coagulation (e.g., blood viscosity and fibrinogen) were included in the 2004 PM AQCD (U.S. EPA, 2004, [056905](#)). These preliminary studies offered limited support for mechanistic explanations of the associations of PM concentration with heart disease outcomes. New studies, published since 2002, are reviewed in this section. Only vWF and fibrinogen were measured in enough comparable studies to allow the consistency of findings to be evaluated across epidemiologic studies. Other markers of coagulation studied included D-dimer, prothombin time, Factor VII/VIII and tPA.

Liao et al. (2005, [088677](#)) used a cross-sectional study to examine the association between short-term increases in air pollutant concentrations (mean PM₁₀, NO₂, CO, SO₂, and O₃ over the previous 3 days) and several plasma hemostatic markers (fibrinogen, factor VIII-C, vWF, albumin). Study subjects were middle aged participants in the ARIC (Atherosclerosis Risk in Communities) study (n = 10,208), and were residents of Washington County, MD, Forsyth County, NC, selected suburbs of Minneapolis, MN, or Jackson, MS. The mean PM₁₀ concentration during the study was 29.9 µg/m³. Each 12.8 µg/m³ increase in the mean PM₁₀ concentration 1 day before the health measurements were made was associated with a 3.93% increase in vWF (95% CI: 0.40-7.46) among diabetics, but not among non-diabetics (-0.54% [95% CI: -1.68 to 0.60]). Each 12.8 µg/m³ increase in the mean PM₁₀ concentration 1 day before the health measurements were made was also associated with a 0.006 g/dL decrease in serum albumin (95% CI: -0.012 to 0.000) among those with CVD, but not among those without CVD (0.029 g/dL increase [95% CI: -0.004 to 0.062]). The mean CO concentration on the previous day was also associated with a significant decrease in serum albumin. The authors reported significant curvilinear associations between PM₁₀ and factor VIII-C, which may indicate a threshold effect. Similar curvilinear associations were observed between O₃ with fibrinogen, and vWF, and SO₂ with

factor VIII-C, WBC, and serum albumin (Liao et al., 2005, [088677](#)). A significant association with fibrinogen was not observed.

In the European multicity study described in Section 6.2.7.1, Ruckerl et al. (2007, [156931](#)) found that each 13.5 $\mu\text{g}/\text{m}^3$ increase in the mean PM_{10} concentration over the previous 5 days was associated with a 0.6% increase in the arithmetic mean fibrinogen level (95% CI: 0.1-1.1). Further these investigators found that promoter polymorphisms within FGA and FGB modified the association of 5-day avg PM_{10} concentration with plasma fibrinogen levels (Peters et al., 2009, [191992](#)). This association was 8-fold higher among those homozygous for the minor allele genotype of FGB rs1800790 compared with those homozygous for the major allele.

Several smaller studies have been conducted in the U.S. and Canada. Delfino et al. (2008, [156390](#)) measured fibrinogen and D-dimer in blood of subjects who resided at two downtown Los Angeles nursing homes. As described in Section 6.2.7.1, measurements were made over a period of 12 wk and subjects were 65+ years old with a history of coronary artery disease. These markers were not associated with the broad array PM metrics studied (e.g., $\text{PM}_{0.25}$, $\text{PM}_{0.25-2.5}$, $\text{PM}_{10-2.5}$, EC, OC, primary OC, BC). In the study of 92 Boston residents with type 2 diabetes described previously, O'Neill et al. (2007, [091362](#)) found that increases in mean $\text{PM}_{2.5}$ and BC concentration were associated with vWF concentrations for all moving averages examined (1-6 days). Reidiker et al. (2004, [056992](#)) reported that in-vehicle $\text{PM}_{2.5}$ was associated with increased vWF over the next 10-14 h among 9 police troopers. Sullivan et al. (2007, [100083](#)) did not observe associations with fibrinogen, or D-dimer in individuals with or without COPD. Neither RBC, platelets nor blood viscosity were associated with $\text{PM}_{2.5}$ concentration in a panel study of 88 non-smoking elderly subjects residing in the Salt Lake City, Ogden and Provo metropolitan area of Utah (Pope et al., 2004, [055238](#)). Although Zeka et al. (2006, [157177](#)) did not observe an association with CRP in the analysis of the NAS population in Boston (Section 6.3.7.1), increased fibrinogen level was associated with increases in the the number of particles/ cm^3 over the previous 48 h and 1 wk, and an incremental increase in BC concentration over the previous 4 wk. There were no consistent findings for lagged $\text{PM}_{2.5}$ or sulfates (Zeka et al., 2006, [157177](#)).

Several studies of coagulation markers were conducted outside the U.S. and Canada. In a study of healthy individuals in Taiwan, adverse associations were observed for $\text{PM}_{2.5}$, PM_{10} , nitrate, and SO_4^{2-} concentrations with fibrinogen and plasminogen activator fibrinogen inhibitor-1 (PAI-1) (Chuang et al., 2007, [091063](#)). In a large cross-sectional study

of healthy subjects in Tel-Aviv, Steinvil et al. (2008, [188893](#)) examined fibrinogen collected as part of routine health examinations for 3,659 individuals. No significant associations were found between pollutant levels (lagged 1-7 days) and fibrinogen. Finally, Baccarelli and colleagues reported adverse associations between PM₁₀ and prothrombin time among normal subjects (Baccarelli et al., 2007, [090733](#)).

Summary of Epidemiologic Study Findings for Hemostasis, Thrombosis and Coagulation

The most commonly measured markers of coagulation in the studies reviewed were fibrinogen and vWF. Associations of PM₁₀ (Liao et al., 2005, [088677](#)) and PM_{2.5} (O'Neill et al., 2007, [091362](#); Riediker et al., 2004, [056992](#)) with increased vWF were observed across the limited number of studies examining this association among both diabetics and healthy state troopers (Liao et al., 2005, [088677](#); Liao et al., 2007, [180272](#); Riediker et al., 2004, [056992](#)). Results for fibrinogen were not consistent across epidemiologic studies. Positive associations with fibrinogen were reported in older adults residing in Boston (Zeka et al., 2006, [157177](#)) and in the multicity European study of MI survivors. Liao et al. (2005, [088677](#)) in a population based multicity study and Sullivan et al. (2007, [100083](#)) did not observe associations of PM₁₀ or PM_{2.5} with fibrinogen. Several other markers have been examined (e.g., D-dimer, prothrombin time) but not in adequate numbers of studies to allow comparisons across epidemiologic studies.

6.2.8.2. Controlled Human Exposure Studies

In two separate studies conducted by Ghio and colleagues, controlled exposures (2 h) to fine CAPs (Chapel Hill, NC) at concentrations between 15 and 350 µg/m³ were shown to increase blood fibrinogen 18-24 h following exposure among healthy adults (Ghio et al., 2000, [012140](#); Ghio et al., 2003, [087363](#)). Increases in blood fibrinogen or factor VII would suggest an increase in blood coagulability, which could result in an increased risk of coronary thrombosis. However, a similar study conducted in Los Angeles observed a PM_{2.5} CAPs-induced decrease in factor VII blood levels in healthy subjects and found no association between PM_{2.5} CAPs and blood fibrinogen among healthy and asthmatic volunteers (Gong et al., 2003, [042106](#)). Since the publication of the 2004 PM AQCD (U.S. EPA, 2004, [056905](#)), several new controlled human exposure studies have evaluated the effects of PM on blood coagulation markers.

CAPs

Two studies of controlled human exposures to Los Angeles CAPs among older adults with COPD (fine CAPs) and adults with and without asthma (ultrafine CAPs) reported no significant association between exposure and blood coagulation markers at 0, 4, or 22 h post-exposure (Gong et al., 2004, [087964](#); Gong et al., 2008, [156483](#)). Graff et al. (2009, [191981](#)) observed a decrease in the concentration of D-dimer of marginal statistical significance in healthy adults (11.3% decrease per 10 $\mu\text{g}/\text{m}^3$, $p = 0.07$) following exposure to thoracic coarse CAPs (89 $\mu\text{g}/\text{m}^3$). At 20 h post-exposure, levels of tPA in plasma were shown to decrease by 32.9% from baseline per 10 $\mu\text{g}/\text{m}^3$ increase in CAPs concentration. No other markers of hemostasis or thrombosis were affected by exposure to thoracic coarse CAPs. However, in a similar study from the same laboratory, Samet et al. (2009, [191913](#)) reported a statistically significant increase in D-dimer immediately following, as well as 18 h after a 2-h exposure to UF CAPs (49.8 $\mu\text{g}/\text{m}^3$; 120,662 particles/ cm^3) in a group of healthy adults (18-35 years old). Plasma concentrations of PAI-1 were also reported to increase 18 h after exposure to UF CAPs, although this increase was not statistically significant ($p = 0.1$). No changes in fibrinogen, tPA, vWF, plasminogen, or factor VII were observed. The finding of an increase in D-dimer following exposure to UF CAPs provides potentially important information in elucidating the relationship between elevated concentrations of PM and cardiovascular morbidity and mortality observed in epidemiologic studies. Whereas many coagulation markers provide evidence of an increased potential to form clots (e.g., an increase in fibrinogen or a decrease in tPA), D-dimer is a degradation product of a clot that has formed.

Urban Traffic Particles

In a study of controlled 24-h exposures to urban traffic particles (average $\text{PM}_{2.5}$ concentration 9.7 $\mu\text{g}/\text{m}^3$) among 29 healthy adults, Bräuner et al. (2008, [191966](#)) did not observe any particle-induced change in plasma fibrinogen, factor VII, or platelet count after 6 or 24 h of exposure. Similarly, Larsson et al. (2007, [091375](#)) observed no change in PAI-1 or fibrinogen in peripheral blood of healthy adult volunteers 14 h after a 2-h exposure to road tunnel traffic with a fine particle concentration of 46-81 $\mu\text{g}/\text{m}^3$.

Diesel Exhaust

Mills and colleagues have recently demonstrated a significant effect of DE (particle concentration 300 $\mu\text{g}/\text{m}^3$) on fibrinolytic function both in healthy men ($n = 30$) and in men

with coronary heart disease (n = 20) (Mills et al., 2005, [095757](#); Mills et al., 2007, [091206](#)). In both groups of volunteers, bradykinin-induced release of tPA was observed to decrease 6 h following exposure to DE compared to filtered air exposure. The same laboratory did not observe an attenuation of tPA release 24 h after a 1-h exposure to DE (300 µg/m³) in a group of health adults (Tornqvist et al., 2007, [091279](#)), or observe any change in markers of hemostasis or thrombosis 6 or 24 h following DE exposure at the same particle concentration among a group of older adults with COPD (Blomberg et al., 2005, [191991](#)). Carlsten et al. (2007, [155714](#)) conducted a similar study involving exposure of healthy adults to DE with a fine particle concentration of 200 µg/m³. Although the authors observed an increase in D-dimer, vWF, and platelet count 6 h following exposure to DE, these increases did not reach statistical significance. In a subsequent study with a similar study design, the same laboratory found no effect of a 2-h exposure to DE (100 and 200 µg/m³ PM_{2.5}) on prothrombotic markers in a group (n = 16) of adults with metabolic syndrome (Carlsten et al., 2008, [156323](#)). The authors postulated that the lack of significant findings could be due to a relatively small sample size. In addition, Carlsten et al. (2007, [155714](#); 2008, [156323](#)) exposed subjects at rest while Mills et al. (2005, [095757](#)) exposed subjects to a higher concentration (300 µg/m³) with intermittent exercise. A more recent study of DE which exposed healthy adults to a slightly higher particle concentration (330 µg/m³) evaluated the effect of DE on thrombus formation using an ex vivo perfusion chamber (Lucking et al., 2008, 191993). Thrombus formation, as well as in vivo platelet activation, was observed to significantly increase 2 h following exposure to DE relative to filtered air, thus providing some evidence of a potential physiological mechanism which may explain in part the associations between PM and cardiovascular events observed in epidemiologic studies.

Wood Smoke

Barregard et al. (2006, [091381](#)) recently evaluated the effect of WS on markers of coagulation, inflammation, and lipid peroxidation. Subjects (n = 13) were healthy males and females (20-56 years old) and were exposed for 4 h to PM_{2.5} concentrations of 240-280 µg/m³. The authors reported an increase in the ratio of factor VIII/von Willebrand factor, which is an indicator of an increased risk of venous thromboembolism, at 0, 3, and 20 h following exposure to WS.

Model Particles

Routledge et al. (2006, [088674](#)) did not observe any changes in fibrinogen or D-dimer following a 1-h exposure to ultrafine carbon among a group of resting healthy older adults and older adults with stable angina. Similarly, Beckett et al. (2005, [156261](#)) found no changes in hemostatic markers (e.g., factor VII, fibrinogen, and vWF) following exposure to ultrafine and fine ZnO (500 $\mu\text{g}/\text{m}^3$).

Summary of Controlled Human Exposure Study Findings for Hemostasis, Thrombosis and Coagulation

Taken together, these new studies have provided some additional evidence that short-term exposure to PM at near ambient levels may have small, yet statistically significant effects on hemostatic markers in healthy subjects or patients with coronary artery disease.

6.2.8.3. Toxicological Studies

In general, the limited toxicological studies reviewed in the 2004 PM AQCD (U.S. EPA, 2004, [056905](#)) reported positive and negative findings for plasma fibrinogen levels or other factors involved in the coagulation cascade. Rats exposed to New York City CAPs did not have any exposure-related effects on any measured coagulation markers (Nadziejko et al., 2002, [050587](#)), whereas rats exposed to a high concentration of ROFA demonstrated increased plasma fibrinogen (Kodavanti et al., 2002, [025236](#)).

CAPs

A PM_{2.5} CAPs exposure conducted for 2 days (4 h/day; mean mass concentration 144-2758 $\mu\text{g}/\text{m}^3$; 8-10/2001; RTP, NC) in SH rats induced plasma fibrinogen increases (measured 18-20 h post-exposure) in 5 of 7 separate studies (Kodavanti et al., 2005, [087946](#)). Fibrinogen was not different from the air control group on the two days with the highest CAPs concentrations (1129 and 2758 $\mu\text{g}/\text{m}^3$), indicating that the response was likely not attributable to mass.

In SH rats exposed to PM_{2.5} CAPs for 6 h in one of three locations in the Netherlands (mean mass concentration range 270-2400, 335-3720, and 655-3660 $\mu\text{g}/\text{m}^3$), plasma fibrinogen was increased 48-h post-exposure when all CAP-exposed animals were combined in the analysis (Cassee et al., 2005, [087962](#)) (Cassee et al., 2005, [087962](#)). In WKY rats pre-exposed to O₃ (8 h; 1600 $\mu\text{g}/\text{m}^3$) and CAPs for 6 h, increases in RBC, hemoglobin, and

hematocrit were observed 2 days after CAPs exposure. For SH rats exposed to CAPs only, decreased mean corpuscular hemoglobin concentration were reported.

A similar study conducted by the same group (Kooter et al., 2006, [097547](#)) reported no changes in plasma fibrinogen measured 18 h after a 2-day exposure (6 h/day) to fine or fine+ultrafine CAPs (mean mass concentration range 399.0-1067.5 and 269.0-555.8 $\mu\text{g}/\text{m}^3$, respectively; 1/2003-4/2004). However, elevated vWF was observed in SH rats exposed to the highest concentration of fine CAPs. Decreases in mean corpuscular volume (MCV), and elevations in mean platelet volume (MPV) and mean platelet component (MPC) were reported in SH rats 18 h following a 2-day exposure to ultrafine+fine CAPs in a freeway tunnel.

Traffic-Related Particles

Plasma fibrinogen levels were elevated 18 h following a single 6-h exposure to on-road highway aerosols when groups of rats pretreated with saline or influenza virus were combined (i.e., there was a significant effect of particles) (Elder et al., 2004, [087354](#)).

Model Particles

The coagulation effects of inhaled ultrafine CB at a concentration of 150 $\mu\text{g}/\text{m}^3$ (number count not provided) for 6 h were evaluated 24-h post-exposure in two aged rat models (11-14 months SH and 23 months Fischer 344), some of which received LPS via intraperitoneal injection prior to particle exposure (Elder et al., 2004, [055642](#)). LPS has been shown to induce the expression of molecules involved in coagulation, inflammation, oxidative stress, and the acute-phase response. In those animals only exposed to CB, SH rats demonstrated increased thrombin-anti-thrombin complexes (TAT) and decreased fibrinogen. For F344 rats, TAT complexes and fibrinogen were elevated only in those that received LPS and CB. Whole-blood viscosity was not altered in either rat strain with particle exposure.

In another study of SH rats exposed to ultrafine carbon particles for 24 h (mass concentration 172 $\mu\text{g}/\text{m}^3$; mean number concentration 9.0×10^6 particles/ cm^3), the number of RBC and platelets and hematocrit percent, were unchanged 1 and 3 days following exposure (Upadhyay et al., 2008, [159345](#)). Fibrinogen levels were similar in both air and ultrafine carbon-exposed groups. However, mRNA expression of PAI-1 and TF in lung homogenates (but not in heart) was increased on recovery day 3 after exposure. A study of similar design that employed SH rats did not report any effect on plasma fibrinogen 4 or

24 h following ultrafine carbon exposure (mass concentration 180 $\mu\text{g}/\text{m}^3$; mean number concentration 1.6×10^7 particles/ cm^3) (Harder et al., 2005, [087371](#)). Similarly, clotting factor VIIa and thrombomodulin, PAI-1, and tPA mRNA expression were not affected by ultrafine carbon exposure at 24-h post-exposure.

Coal Fly Ash

One study that employed coal fly ash (mean mass concentration 1,400 $\mu\text{g}/\text{m}^3$; 4 h/day \times 3 days) demonstrated increases in hematocrit and MCV in SD rats at 36 h but not 16 h post-exposure (Smith et al., 2006, [110864](#)).

Intratracheal Instillation

Mutlu et al. (2007, [121441](#)) used a PM₁₀ sample collected from Dusseldorf, Germany in mice (C57BL/6) with and without the gene coding for IL-6. The authors report using a moderate IT dose (10 $\mu\text{g}/\text{mouse}$; roughly equivalent to 400-500 $\mu\text{g}/\text{kg}$); the PM sample had previously been characterized as having significant Fe, Ni, and V content (Upadhyay et al., 2003, [097370](#)). In C57BL/6 mice, the Dusseldorf PM shortened bleeding (32%), prothrombin (13%), and activated partial thromboplastin (16%) times and increased platelet count, fibrinogen, and Factors II, VIII, and X activities 24 h following exposure. The authors further demonstrated accelerated coagulation by a reduction in the left carotid artery occlusion time (experimentally-derived by direct application of FeCl₃). Additional experiments demonstrated that IL-6^{-/-} or macrophage-depleted mice showed dramatically attenuated effects of PM₁₀ on hemostatic indices, thrombin generation, and occlusion time. In IL-6^{-/-} mice, there was no change in total cell counts or differentials in BALF compared to the wild-type mice, despite the lack of IL-6. In contrast, the model of macrophage depletion had reduced levels of macrophages and IL-6 in BALF, following PM exposure. These studies suggest that instillation of Dusseldorf PM₁₀ activates clotting through an alveolar macrophage-dependent release of IL-6; however, other factors may also be involved in the prothrombotic response (i.e., activation of neutrophils, other inflammatory cells, or alterations in the levels of other cytokines).

In a study employing PM_{10-2.5} collected from six European locations with contrasting traffic profiles, fibrinogen increases were observed in SH rats exposed to 10 mg/kg IT at 24-h post-exposure and similar responses were observed with PM_{2.5} (Gerlofs-Nijland et al., 2007, [097840](#)). PM_{10-2.5} and PM_{2.5} samples from Prague or Barcelona administered IT to SH rats (7 mg/kg) resulted in elevated plasma fibrinogen levels 24-h post-exposure compared to

rats instilled with water (Gerlofs-Nijland et al., 2009, [190353](#)). No changes were observed in vWF for whole particle suspensions, but Barcelona PM_{10-2.5} organic extract induced greater levels of vWF than Barcelona PM_{10-2.5}.

Summary of Toxicological Study Findings for Hemostasis, Thrombosis and Coagulation

Increases in coagulation and thrombotic markers were observed in some studies of rats or mice exposed to PM. Plasma TAT complexes were increased in CB-exposed SH rats and shortened bleeding, prothrombin, and activated partial thromboplastin times were observed in mice exposed IT to PM₁₀. Furthermore, the latter study also reported increased levels of Factors II, VIII, and X activities in mice. Another study demonstrated increased vWF in response to PM_{2.5} CAPs. As for plasma fibrinogen, these studies provide some evidence that increased levels are observed 18 h to 48 h post-exposure to PM, although one study reported no change and another reported a decrease in this biomarker. Alterations in platelet measurements have also been observed with PM exposure, including increased platelet number, mean platelet volume, and mean platelet component. The toxicological results of RBC-related measurements are limited and inconsistent following PM exposure, which may be attributable to different exposure protocols, time of analysis, or rat strain.

6.2.9. Systemic and Cardiovascular Oxidative Stress

Very little information on systemic oxidative stress associated with PM was available for inclusion in the 2004 PM AQCD (U.S. EPA, 2004, [056905](#)). However, recent epidemiologic studies have provided consistent evidence of PM-induced increases in markers of systemic oxidative stress including plasma TBARS, CuZn-SOD, 8-oxodG, and total homocysteine. This is supported by a limited number of controlled human exposure studies that observed PM-induced increases in free-radical mediated lipid peroxidation as well as upregulation of the DNA repair gene hOGG1. In addition, recent toxicological studies have demonstrated an increase in cardiovascular oxidative stress following PM exposure in rats.

6.2.9.1. Epidemiologic Studies

No studies of markers of oxidative stress were reviewed in the 2004 PM AQCD (U.S. EPA, 2004, [056905](#)). Since 2002, numerous studies have examined whether short-

term increases in mean PM concentrations are associated with adverse changes in systemic markers of oxidative stress.

In an analysis of the randomized trial of omega-3 fatty acid supplementation in Mexico City nursing home residents described previously (Section 6.6.1.1), Romieu et al. (2008, [156922](#)) investigated the effect of this intervention on markers of systemic oxidative stress (Cu/Zn SOD activity, LPO in plasma and GSH in plasma). A significant decrease of Cu/Zn SOD was associated with a 10 $\mu\text{g}/\text{m}^3$ increase of $\text{PM}_{2.5}$ in both groups (Fish oil: $\beta = -0.17$ [SE = 0.05], $p = 0.002$; Soy oil: $\beta = -0.06$ [SE = 0.02] $p = < 0.001$). A decrease in GSH was associated with a 10 $\mu\text{g}/\text{m}^3$ increase in $\text{PM}_{2.5}$ in the fish oil group ($\beta = -0.09$ (SE = 0.04, $p = 0.017$).

Two studies evaluated plasma homocysteine levels in relation to PM. Baccarelli et al. (2007, [091310](#)) investigated fasting and postmethionine-load total homocysteine (tHcy) among 1,213 normal subjects in Lombardia, Italy. Plasma homocysteine is a risk factor for CVD and a marker for oxidative stress. Among smokers, average PM_{10} level during the 24-h preceding the measurement was associated with 6.3% (95% CI: 1.3-11.6) and 4.9% (95% CI: 0.5-9.6) increases in fasting and postmethionine-load tHcy, respectively. No associations were observed among non-smokers. Park et al. (2008, [156845](#)) investigated the association of BC, OC, SO_4^{2-} and $\text{PM}_{2.5}$ with tHcy among 960 male participants of the NAS. Effect modification by folate and vitamins B6 and B12 was also examined. BC and OC were associated with increases in tHcy and associations were more pronounced in those with lower plasma folate and vitamin B12.

In smaller studies with 25 to 50 healthy or diseased participants, several markers of oxidative stress have been associated with PM size fractions or components. These associations include thiobarbituric acid reactive substances (TBARS) with 24-h PM_{10} (Liu et al., 2006, [192002](#)); Cu/Zn-SOD with several PM metrics (e.g., ultrafine, coarse, EC, OC, BC and PN) (Delfino et al., 2008, [156390](#)); $\text{PM}_{2.5}$, BC, vanadium and chromium with plasma proteins (Sørensen et al., 2003, [157000](#)); DNA damage assessed by 7-hydro-8-oxo-2-deoxyguanosine (8-oxodG) in lymphocytes (Sørensen et al., 2003, [157000](#)) and, 8-OHdG with sulfates (Chuang et al., 2007, [091063](#)). In addition, a cross-sectional study of children (10-18 yr) in Iran showed an association of PM_{10} with oxidized LDL (oxLDL), malondialdehyde (MDA) and conjugated diene (CDE) (Kelishadi et al., 2009, [191960](#)).

Summary of Epidemiologic Study Findings for Systemic and Cardiovascular Oxidative Stress

Oxidative stress responses measured by plasma tHcy, CuZn-SOD, TBARS, 8-oxodG, oxLDL and MDA have been consistently observed (Baccarelli et al., 2007, [091310](#); Chuang et al., 2007, [091063](#); Delfino et al., 2008, [156390](#); Kelishadi et al., 2009, [191960](#); Liu et al., 2007, [156705](#); Romieu et al., 2008, [156922](#); Sørensen et al., 2003, [157000](#)). In addition, a series of analyses examining the modification the PM-HRV association by genetic polymorphisms related to oxidative stress has provided insight into the possible mechanisms of cardiovascular diseases observed in association with PM concentrations (see Section 6.2.1.1).

6.2.9.2. Controlled Human Exposure Studies

Urban Traffic Particles

Bräuner et al. (2007, [188507](#)) recently investigated the effect of urban traffic particles on oxidative stress-induced damage to DNA. Healthy adults (20-40 years old) were exposed to low concentrations of urban traffic particles as well as filtered air for periods of 24 h, with and without two 90-min periods of exercise. Exposures took place in an exposure chamber above a busy road with high traffic density in Copenhagen. Non-filtered air was pumped into the chamber from above the street, with average PM_{2.5} and PM_{10-2.5} mass concentrations of 9.7 µg/m³ and 12.6 µg/m³, respectively. The ultrafine/fine (6-700 nm) particle number concentration was continuously monitored throughout the exposure (average particle count 10,067/cm³). The PM_{2.5} fraction was rich in sulfur, vanadium, chromium, iron, and copper. PBMCs were isolated from blood samples collected at 6 and 24-h. DNA damage, as measured by strand breaks (SB) and formamidopyrimidine-DNA glycosylase (FPG) sites, was evaluated using the Comet assay. The activity and mRNA levels of the DNA repair enzyme 7,8-dihydro-8-oxoguanine-DNA glycosylase (OGG1) were also measured. The authors observed increased levels of DNA strand breaks and FPG sites following 6 and 24 h of exposure to PM. Using a mixed-effects regression model, the particle concentration at the 57 nm mode was found to be the major contributor of these measures of DNA damage. The results of this study suggest that short-term (6-24 h) exposure to ambient levels of UFPs cause systemic oxidative stress resulting in damage to DNA.

Diesel Exhaust

Tornqvist et al. (2007, [091279](#)) reported an increase in plasma antioxidant capacity in a group of healthy volunteers 24 h after a 1-h exposure to DE with a particle concentration of 300 $\mu\text{g}/\text{m}^3$. The investigators suggested that systemic oxidative stress occurring following exposure may have caused this up-regulation in antioxidant defense. Peretz et al. (2007, [156853](#)) observed some significant differences in expression of genes involved in oxidative stress pathways between exposure to DE (200 $\mu\text{g}/\text{m}^3$ $\text{PM}_{2.5}$) and filtered air. However, the conclusions of this investigation are limited by a small number of subjects ($n = 4$).

Wood Smoke

In a controlled human exposure study of controlled exposure to WS, Barregard et al. (2006, [091381](#)) found an increase in urinary excretion of free 8-iso-prostaglandin 2α among healthy adults ($n = 9$) approximately 20 h following a 4-h exposure to $\text{PM}_{2.5}$ (mass concentration of 240-280 $\mu\text{g}/\text{m}^3$). This finding provides evidence of a PM-induced increase in free-radical mediated lipid peroxidation. From the same study, Danielsen et al. (2008, [156382](#)) reported an increase in the mRNA levels of the DNA repair gene hOGG1 in peripheral mononuclear cells 20 h after exposure to WS relative to filtered air.

Summary of Controlled Human Exposure Study Findings for Systemic and Cardiovascular Oxidative Stress

Based on the results of these studies, it appears that exposure to PM at or near ambient levels may increase systemic oxidative stress in human subjects.

6.2.9.3. Toxicological Studies

Very little information was available for inclusion in the 2004 PM AQCD (U.S. EPA, 2004, [056905](#)) on oxidative stress in the cardiovascular system. A few new studies have evaluated ROS in blood or the heart following PM exposure. Some studies have used chemiluminescence (CL), which is measured using the decay of excited states of molecular oxygen, and may also be prone to artifact.

CAPs

Gurgueira et al. (2002, [036535](#)) measured oxidative stress in SD rats immediately following a 5-h CAPs exposure ($\text{PM}_{2.5}$ mean mass concentration 99.6-957.5 $\mu\text{g}/\text{m}^3$; Boston, MA; 7/2000 to 2/2001) and reported increased in situ CL in hearts of CAPs-exposed

animals. CL evaluated after 1- and 3-h CAPs exposure did not demonstrate changes from the filtered air group, although a 5-h exposure resulted in increased CL in hearts. When animals were allowed to recover for 24 h, oxidative stress returned to control values. To compare potential particle-induced differences in CL, rats were exposed to ROFA (1.7 mg/m³ for 30 min) or CB (170 µg/m³ for 5 h) and only the ROFA-treated animals exhibited increased CL in cardiac tissue. Additionally, levels of antioxidant enzymes in the heart (Cu/Zn-SOD and MnSOD) were increased in CAPs-exposed rats.

Recently, Rhoden et al. (2005, [087878](#)) tested the role of the ANS in driving CAPs-induced cardiac oxidative stress in heart tissues of SD rats. At PM_{2.5} mass concentrations of 700 µg/m³ (Boston, MA), pretreatment with an antioxidant, a β₁-receptor antagonist, or a muscarinic receptor antagonist attenuated the CL and TBARS effects observed in the heart following a 5-h PM_{2.5} exposure. The wet/dry ratio (edema) of cardiac tissue also returned to control values in animals treated with the antioxidant prior to CAPs. These combined results indicate involvement of both the sympathetic and parasympathetic pathways in the cardiac oxidative stress response observed following PM exposure.

More recently, a type of irritant receptor, the transient receptor potential vanilloid receptor 1 (TRPV1), was identified as central to the inhaled CAPS-mediated induction of cardiac tissue CL and TBARS in SD rats (Ghelfi et al., 2008, [156468](#)). In these studies (PM_{2.5} mean mass concentration 218 µg/m³; Boston, MA), capsazapine (a TRPV1 inhibitor) abrogated cardiac CL, TBARS, edema, and QT-interval shortening when measured at the end of the 5-h exposure. These studies provide some evidence that the ANS may be involved in producing cardiac oxidative stress following exposure to CAPs. Furthermore, this response could be acting, at least in part, via TRPV receptors.

In WKY rats exposed to PM_{2.5} CAPs in Japan, relative mRNA expression of HO-1 was increased in cardiac tissue and was also significantly correlated with the cumulative mass of PM collected on chamber filters throughout the exposure (Ito et al., 2008, [096823](#)).

Road Dust

A composite of PM_{2.5} road dust samples obtained from New York City, Los Angeles, and Atlanta induced cardiac ROS as measured by CL in the low exposure group (306 µg/m³) and TBARS in the high exposure group (954 µg/m³); thus, the CL and TBARS methods provided different results for the various source types (Seagrave et al., 2008, [191990](#)).

Gasoline and Diesel Exhaust

Gasoline exhaust exposure also resulted in increased ROS (measured by TBARS) in aortas of ApoE^{-/-} mice, as discussed in Section 6.2.4.3 (Lund et al., 2009, [180257](#)). Similarly, a 6-h exposure to gasoline exhaust (PM mass concentration 60 µg/m³, CMD 15-20 nm; MMD 150 nm; CO concentration 104 ppm, NO concentration 16.7 ppm, NO₂ concentration 1.1 ppm, SO₂ concentration 1.0 ppm) in SD rats demonstrated increased CL in the heart, but no change in TBARS and the CL response was not duplicated when the particles were filtered (Seagrave et al., 2008, [191990](#)). Increased lipid peroxides in the serum of male SH rats exposed to gasoline exhaust (PM mass concentration 59.1 µg/m³; NO concentration 18.4 ppm; NO₂ concentration 0.9 ppm; CO concentration 107.3 ppm; SO₂ concentration 0.62 ppm) was observed following a 1-wk exposure to gasoline exhaust and this effect was attenuated with particle filtration (Reed et al., 2008, [156903](#)). An IT instillation study of diesel particles in mice demonstrated increased myocardial MPO activity 12 and 24 h post-exposure to the residual particle component that remained after extraction with dichloromethane (Yokota et al., 2008, [190109](#)).

Model Particles

Other studies presented in earlier sections also demonstrated ROS (via CL) and NT expression (via ELISA) in the left ventricle with CB exposure (Tankersley et al., 2008, [157043](#)) and oxidative stress in the systemic microvasculature following TiO₂ inhalation exposure (Nurkiewicz et al., 2009, [191961](#)) or ROFA IT exposure (Nurkiewicz et al., 2006, [088611](#)). Decreased HO-1 mRNA expression in hearts of SH rats exposed to ultrafine carbon particles was observed 3 days following exposure (Upadhyay et al., 2008, [159345](#)) and there was a trend toward increased HO-1 mRNA expression 1 day post-exposure.

Summary of Toxicological Study Findings for Systemic and Cardiovascular Oxidative Stress

When considered together, the above studies provide evidence that PM exposure results in oxidative stress as measured in cardiac tissue by CL, TBARS, HO-1 mRNA expression, and NT expression. However, the PM concentration/dose and method of ROS measurement could also affect the response. Cardiac oxidative stress may have resulted from PM stimulation of the ANS, although these studies have only been conducted in one laboratory. Multiple studies from two different laboratories provide support for vascular

oxidative stress as demonstrated in aortas following gasoline exhaust exposure and in the microvasculature after TiO₂ inhalation or ROFA IT exposure.

PM Components

Individual PM component concentrations were linked to CL levels in rat heart tissue using separate univariate linear regression models, with total PM mass, Al, Si, Ti, and Fe having p-values ≤ 0.007 (Gurgueira et al., 2002, [036535](#)). The highest R² value in the regression analyses was for Al (0.67) and its concentration ranged from 0.000 to 8.938 $\mu\text{g}/\text{m}^3$.

6.2.10. Hospital Admissions and ED Visits

The 1996 PM AQCD (U.S. EPA, 1996, [079380](#)) considered just two time-series studies regarding the association between daily variations in PM levels and the risk of cardiovascular disease (CVD) morbidity as measured by the number of daily hospitalizations with primary discharge diagnoses related to CVD (Burnett et al., 1995, [077226](#); Schwartz and Morris, 1995, [046186](#)). In contrast, the 2004 PM AQCD (U.S. EPA, 2004, [056905](#)) reviewed more than 25 publications relating PM and risk of CVD hospitalizations. Results from a handful of larger multicity studies were emphasized, with the greatest emphasis placed on findings from the U.S. National Morbidity, Mortality, and Air Pollution Study (NMMAPS) (Samet et al., 2000, [010269](#)) and a subsequent reanalysis (Zanobetti and Schwartz, 2003, [157174](#)). The NMMAPS study evaluated the effect of daily changes in ambient PM levels on total CVD hospitalizations among elderly Medicare beneficiaries in 14 U.S. cities and found a ~1% excess risk per 10 $\mu\text{g}/\text{m}^3$ increase in PM₁₀. The 2004 PM AQCD concluded that these results, along with those of the other single- and multicity studies reviewed “generally appear to confirm likely excess risk of CVD-related hospital admissions for U.S. cities in the range of [0.6 to 1.7% per 10 $\mu\text{g}/\text{m}^3$] PM₁₀, especially among the elderly” (U.S. EPA, 2004, [056905](#)). The 2004 PM AQCD (U.S. EPA, 2004, [056905](#)) also concluded that there was some evidence from single-city studies suggesting an excess risk specifically for hospitalizations related to ischemic heart disease and heart failure. Furthermore, the 2004 PM AQCD (U.S. EPA, 2004, [056905](#)) found that “insufficient data exist from the time-series CVD admissions studies [...] to provide clear guidance as to which ambient PM components, defined on the basis of size or composition, determine ambient PM CVD effect potency” (U.S. EPA, 2004, [056905](#)). The key studies reviewed in the

2004 PM AQCD (U.S. EPA, 2004, [056905](#)) on this topic included those by Burnett and colleagues (1997, [084194](#); 1999, [017269](#)), Lippman and colleagues (2000, [024579](#)), Ito (2003, [042856](#)), and Peters et al. (2001, [016546](#)).

Recent large studies conducted in the U.S., Europe, and Australia and New Zealand have confirmed these findings for PM₁₀, and have also observed consistent associations between PM_{2.5} and cardiovascular hospitalizations. However, findings from single-city studies have demonstrated regional heterogeneity in effect estimates. It is apparent from these recent studies that the observed increases in cardiovascular hospitalizations are largely due to admissions for ischemic heart disease and congestive heart failure rather than CBVDs (such as stroke). The new literature on hospitalizations and ED visits for cardiovascular causes published since 2002 is reviewed in the following sections. First, the specific CVD outcomes captured using ICD codes from hospital admissions databases are discussed. Second, the methods used in the large and multicity studies are described. For each outcome considered, evidence from large/multicity studies is emphasized and results from U.S. and Canadian single-city studies are also discussed. Although the single-city studies may lack statistical power needed to evaluate interactions and detect some of the subtle effects of air pollution, they inform the interpretation of the heterogeneous effect estimates that have been observed across North America.

Cardiovascular Disease ICD Codes

When the 2004 PM AQCD (U.S. EPA, 2004, [056905](#)) was written, few studies had evaluated the link between ambient PM and specific CVD outcomes such as congestive heart failure, ischemic heart disease or ischemic stroke. In contrast, the majority of recent studies have focused on specific CVD outcomes. This trend is justified by the fact that the short-term exposure effects of PM may be very different for different cardiovascular outcomes. For example, given the current putative biological pathways involved in the acute response to PM exposure, there is no a priori reason why short-term fluctuations in PM levels would have similar effects on the risk of acute MI, chronic atherosclerosis of the coronary arteries, and hemorrhagic stroke.

Almost all of the published time-series studies of cardiovascular hospitalizations and ED visits identified cases based on administrative discharge diagnosis codes as defined by the International Classification of Disease 9th revision (ICD-9) or 10th revision (ICD-10) (NCHS, 2007, [157194](#)). A complicating factor in interpreting the results of these studies is

the lack of consistency in both defining specific health outcomes and in the nomenclature used.

Table 6-5. Description of ICD-9 and ICD-10 codes for diseases of the circulatory system.

Description	ICD-9 Codes	ICD-10 Codes
All Cardiovascular Disease	390-459	I00-I99
Ischemic Heart Disease	410-414	I20-I25
Acute MI	410	I21
Diseases Of Pulmonary Circulation	415-417	I26-I28
Heart Failure	428	I50
Arrhythmia	427	I47, I48, I49
CBVD	430-438	I60-I69
Ischemic Stroke And Transient Ischemic Attack (TIA)	430-432	I63
Hemorrhagic Stroke	433-435	I60-I62
Peripheral Vascular Disease (PVD)	440-448	I70-I79

Table 6-5 shows major groups of diagnostic codes used in air pollution studies for diseases of the circulatory system. The codes ICD-9: 390-459 are frequently used to identify all CVD morbidity. Note that this definition of CVD includes diseases of the heart and coronary circulation, CBVD, and peripheral vascular disease. In contrast, the term cardiac disease specifically excludes diseases not involving the heart or coronary circulation. While this distinction is conceptually straightforward, the implementation of the definition of cardiac disease in terms of ICD-9 or ICD-10 codes varies among authors. Even greater heterogeneity can be found among studies in the implementation of definitions related to CBVD.

Design and Methods of Large and Multicity Hospital Admission and ED Visit Studies

Recently, multiple research groups in the U.S., Europe, and Australia have created large datasets to evaluate specific CVD and respiratory endpoints using more detailed and relevant measures of PM concentration. In the U.S., the MCAPS analyses of Dominici et al. (2006, [088398](#)), Bell et al. (2008, [156266](#)) and Peng et al. (2008, [156850](#)) are large, comprehensive and informative studies based on Medicare hospitalization data. Likewise, the Atlanta-based SOPHIA study (Metzger et al., 2004, [044222](#); Peel et al., 2005, [056305](#); Tolbert et al., 2007, [090316](#)) is the largest and most comprehensive study of U.S. cardiovascular and respiratory ED visits. In Europe, the APHEA initiative (Le Tertre et al.,

2002, [023746](#); Le Tertre et al., 2003, [042820](#)) the more recent HEAPSS study (Von Klot et al., 2005, [088070](#)), and the French PSAS program (Host et al., 2008, [155852](#); Larrieu et al., 2007, [093031](#)) are similarly noteworthy for their large sample size, geographic diversity, and consideration of specific CVD and/or respiratory endpoints. These studies contain adequate data to examine interactions by season and region; the effects of different size fractions, components and sources of PM; or the effect of PM on susceptible subpopulations. The following section provides a detailed review of the study design and methods used by each of the large studies. A discussion of the results of each study can be found in later sections of the ISA.

MCAPS: Medicare Air Pollution Study

Dominici et al. (2006, [088398](#)) created a database of daily time-series of hospital admission rates (1999-2002) for a range of cardiovascular and respiratory outcomes among Medicare beneficiaries aged ≥ 65 yr, ambient PM_{2.5} levels, and meteorological variables for 204 U.S. urban counties. The specific CVD outcomes considered were: CBVD (ICD-9: 430-438), peripheral vascular disease (440-448), ischemic heart diseases (410-414, 429), heart rhythm disturbances (426, 427), and heart failure (428). Injuries (800-849) were evaluated as a control outcome. Gaseous and other particulate pollutant size fractions were not considered.

Data on PM_{2.5} were obtained from the AQS database of the U.S. EPA. Within each county, associations between cause-specific hospitalization rates and same-day PM_{2.5} levels were evaluated using Poisson regression models controlling for long-term temporal trends and meteorologic conditions with natural cubic splines. County-specific results were subsequently averaged using Bayesian hierarchical models. In addition to evaluating single day lags, 3-day distributed lag models (lags 0, 1, and 2 days) were also considered in a subset of 90 U.S. counties with daily PM_{2.5} data available during the study time period.

Subsequently, Peng et al. (2008, [156850](#)) and Bell et al. (2008, [156266](#)) extended the database of daily time-series of hospital admissions, PM_{2.5}, and other covariates for 202 U.S. counties through 2005. Importantly, Peng et al. (2008, [156850](#)) added data on PM_{10-2.5} to this database for 108 U.S. counties with one or more co-located PM_{2.5} and PM₁₀ monitors. Analyses with PM_{10-2.5} were carried out using similar methods to those of Dominici et al. (2006, [088398](#)). Peng et al. (2008, [156850](#)) evaluated the robustness of PM_{2.5} associations to adjustment for thoracic coarse PM (Peng et al., 2008, [156850](#)). Gaseous pollutants were not considered in these analyses.

SOPHIA: Study of Particulates and Health in Atlanta

SOPHIA investigators (Metzger et al., 2004, [044222](#); Peel et al., 2005, [056305](#); Tolbert et al., 2000, [010320](#)) compiled data on 4,407,535 ED visits between 1993 and 2000 to 31 hospitals in the Atlanta metropolitan statistical area (20 counties). Specific cardiovascular outcomes considered were: ischemic heart disease (ICD-9: 410-414), acute MI (410), cardiac dysrhythmias (427), cardiac arrest (427.5), congestive heart failure (428), peripheral vascular and CBVD (433-437, 440, 443-444, 451-453), atherosclerosis (440), and stroke (436). Finger wounds (883.0) were evaluated as a control outcome.

The air quality data included measurements of criteria pollutants (PM and gaseous pollutants) for the entire study period, as well as detailed measurements of mass concentrations for the fine (PM_{2.5}) and thoracic coarse fractions (PM_{10-2.5}) of PM and several physical and chemical characteristics of PM_{2.5} for the final 25 months of the study using data from the ARIES monitoring station. Rates of ED visits for specific causes were assessed in relation to the 3-day ma (lags 0-2 days) of daily measures of air pollutants using Poisson generalized linear models controlling for long-term temporal trends and meteorologic conditions with cubic splines. Tolbert et al. (2007, [090316](#)) published interim results of this study in relation to both cardiovascular and respiratory disease visits, Metzger et al. (2004, [044222](#)) published the main results for CVD visits, and Peel et al. (2005, [056305](#)) published the main results for respiratory conditions. An analysis of comorbid conditions that may make individuals more susceptible to PM-related cardiovascular risk was carried out by Peel et al. (2007, [090442](#)). Tolbert et al. (2007, [090316](#)) extended the available data through 2002 and compared results from single and multipollutant models while Sarnat et al. (2008, [097972](#)) evaluated the risk of ED visits for cardiovascular and respiratory diseases in relation to specific sources of ambient PM using the extended dataset.

APHEA and APHEA-2: Air pollution and Health: a European Approach

APHEA-2 investigators compiled daily data on cardiovascular (Le Tertre et al., 2002, [023746](#); Le Tertre et al., 2003, [042820](#)) and respiratory (Atkinson et al., 2001, [021959](#); Atkinson et al., 2003, [042797](#)) disease hospital admissions in the following 8 European cities: Barcelona, Birmingham, London, Milan, the Netherlands, Paris, Rome, and Stockholm. (The publications on respiratory diseases were reviewed in the 2004 PM AQCD). The specific CVD outcomes considered in each city were: cardiac diseases (ICD-9: 390-429), ischemic heart disease (410-413) and CBVDs (430-438). Routine registers in all cities

provided daily data on hospitalizations. Only emergency hospitalizations were considered, except in Milan, Paris, and Rome where only general admissions data were available.

Ambient PM₁₀ levels were available in all cities except Paris (PM₁₃ used), and Milan and Rome (TSP used). Data on gaseous pollutants (NO₂, SO₂, CO, and O₃) were also available in most cities. Five of the eight cities provided data on black smoke (BS). The length of the available time-series varied by city but generally spanned from the early to mid 1990s.

Within each city, associations between cause-specific hospitalization rates and same-day PM_{2.5} levels were evaluated using Poisson GAMs controlling for long-term temporal trends and meteorologic conditions. City-specific results were subsequently averaged using standard meta-analytic methods. The original analyses (Atkinson et al., 2001, [021959](#); Le Tertre et al., 2002, [023746](#)) were carried out using GAMs and LOESS smoothers. Following reports of problems associated with using the default convergence criteria in the standard S-plus GAM procedure (Dominici et al., 2002, [030458](#)), study authors reanalyzed the data on cardiac admissions using GAMs and stricter convergence criteria, and generalized linear models (GLMs) with natural splines and penalized splines (Atkinson et al., 2003, [042797](#); Le Tertre et al., 2003, [042820](#)). The authors found that the results of the original analyses were insensitive to the choice of convergence criteria and that the use of GLMs with penalized splines yielded very similar results.

HEAPSS: Health Effects of Air Pollution among Susceptible Subpopulations

HEAPSS investigators collected data on patients hospitalized for a first MI in five European cities between 1992 and 2000. Patients were identified from MI registers in Augsburg and Barcelona, and from hospital discharge registers in Helsinki, Rome and Stockholm. Data on daily levels of PM₁₀, were measured at central monitoring sites in each city. Particle number concentration, a proxy for UFPs, was measured for a year in each city and then modeled retrospectively for the whole study period. Associations of outcomes with gaseous criteria pollutants were also evaluated.

Von Klot et al. (2005, [088070](#)) identified 22,006 survivors of a first MI in the five participating European cities and collected data on subsequent first cardiac re-hospitalizations between 1992 and 2001. Readmissions of interest were those with primary diagnoses of acute MI, angina pectoris, or cardiac disease (which additionally includes dysrhythmias and heart failure). Within each city, associations between cause-specific hospitalization rates and same-day levels of PM₁₀ were evaluated using

Poisson GAMs controlling for long-term temporal trends and meteorologic conditions using penalized splines. City-specific results were combined using standard meta-analytic methods. Subsequently, Lanki et al. (2006, [089788](#)) used HEAPSS data from 26,854 patients to evaluate the association between daily PM₁₀ and particle number concentrations and the risk of hospitalization for first MI.

PSAS: The French National Program on Air Pollution Health Effects

Larrieu et al. (2007, [093031](#)) evaluated the association between PM₁₀ and the risk of hospitalization in 8 French cities between 1998 and 2003. The cities examined were: Bordeaux, Le Havre, Lille, Lyon, Marseille, Paris, Rouen and Toulouse. The specific CVD outcomes considered in each city included: total CVD (ICD-10: I00-I99), cardiac disease (I00-I52), ischemic heart diseases (I20-I25) and stroke (I60-I64, G45-G46). The available data did not differentiate between emergency and non-emergency hospitalizations. Daily mean PM₁₀ and NO₂ levels as well as 8-h max O₃ levels were obtained from a network of monitors in each city.

Within each city, associations between cause-specific hospitalization rates and 2-day ma (lag 0-1 days) levels of PM₁₀ were evaluated using Poisson GAMs controlling for long-term temporal trends and meteorologic conditions using penalized splines. City-specific results were combined using standard meta-analytic methods. Host et al. (2008, [155852](#)) used a subset of these data (6 cities, 2000-2003) to compare the effects of the fine (PM_{2.5}) and coarse fractions (PM_{10-2.5}) of ambient particles on the risk of cardiovascular and respiratory admissions. CVD outcomes assessed in this analysis were all CVD (ICD-10 I00-I99), cardiac (I00-I52) and IHD (I20-I25). PM_{2.5} levels were obtained from the same network of background monitors described above. PM_{10-2.5} was calculated by subtracting PM_{2.5} levels from PM₁₀ levels. Gaseous pollutants and hospital admissions for stroke were not considered in this analysis.

Multicity Studies in Australia and New Zealand

Barnett et al. (2006, [089770](#)) collected data on daily CVD emergency hospital admissions and pollution data between 1998 and 2001 in five Australian cities (Brisbane, Canberra, Melbourne, Perth, Sydney) and two cities in New Zealand (Auckland, Christchurch). In 2001, these cities covered 53% of the Australian population and 44% of the New Zealand population. The specific outcomes considered in each city were: all circulatory diseases (ICD-9 390-429, ICD-10 I00-I99 with exclusions); heart failure (ICD-9 428, ICD-10 I50); arrhythmia (ICD-9 427 ICD-10 I46-49); cardiac disease (ICD-9 390-429,

ICD-10 I00-I52, I97.0, I97.1, I98.1); ischemic heart disease (ICD-9 410-413, ICD-10 I20-24, I25.2); acute MI (ICD-9 410, ICD-10 I21-22); and stroke (ICD-9 430-438, ICD-10 I60-66, I67, I68, I69, G45-46 with exclusions).

Air pollutants considered were 24-h avg PM₁₀, 24-h avg PM_{2.5}, BSP and gaseous pollutants. Within each city, associations between cause-specific hospitalization rates and 2-day ma (lags 0-1 days) of PM₁₀ were evaluated using the time-stratified case-crossover approach which controls for long-term and seasonal time trends by design rather than analytically. City-specific results were combined using random effects meta-analytic methods.

EMECAS: Spanish Multicentric Study on the Relation between Air Pollution and Health

Ballester et al. (2006, [088746](#)) collected data on daily cardiovascular emergency hospital admission and air pollution data between approximately 1995 and 1999 in 14 cities in Spain. The specific outcomes considered in each city were: total CVD (ICD-9: 390-459) and heart diseases (410-414, 427, 428). Air pollutants considered were PM₁₀, TSP, BS, SO₂, NO₂ (24-h avg), CO and O₃ (8-h max).

Within each city, associations between cause-specific hospitalization rates and daily levels of each pollutant metric were evaluated using Poisson GAMs with strict convergence criteria. In all models, pollutants were entered as linear continuous variables and included control for confounding by meteorological variables, influenza rates, long-term time trends, and unusual events. The authors considered both distributed lag models (lags 0-3 days) and the 2-day ma of pollution (lags 0-1 days). City-specific results were combined using standard meta-analytic methods.

6.2.10.1. All Cardiovascular Disease

The 2004 PM AQCD (U.S. EPA, 2004, [056905](#)) incorporated the results of a large number of time-series studies in the U.S. and elsewhere relating ambient PM levels and risk of hospitalization for CVD. The 2004 PM AQCD (U.S. EPA, 2004, [056905](#)) noted that the strongest evidence for this association came from the NMMAPS study (Samet et al., 2000, [010269](#)) and the subsequent reanalysis by Zanobetti and Schwartz (2003, [042812](#)).

Since then, the U.S. MCAPS study evaluated the association between PM_{2.5} and risk of CVD hospitalization in 202 U.S. counties between 1999 and 2005 and found a 0.7% (95% posterior interval (PI): 0.5, 1.0) increase in risk per 10 µg/m³ increase in PM_{2.5} on the same day (Peng et al., 2008, [156850](#)). In 108 U.S. counties with co-located PM₁₀ and PM_{10-2.5}

monitors, the authors found a 0.4% (95% PI, 0.1 to 0.7, lag 0) increase in risk per 10 $\mu\text{g}/\text{m}^3$ $\text{PM}_{10-2.5}$ and no associations at lags of 1 and 2 days (Peng et al., 2008, [156850](#)). In a 2-pollutant model adjusted for $\text{PM}_{2.5}$, the association between $\text{PM}_{10-2.5}$ and CVD hospitalization lost precision (0.3% [95% PI: -0.1 to 0.6, lag 0]). Bell et al. (2008, [156266](#)) found evidence of substantial and statistically significant variability in the effects of $\text{PM}_{2.5}$ on cardiovascular hospitalizations by season and region, with the highest national average estimates occurring in the winter and the highest regional estimates in the northeastern U.S. (1.08% [95% PI: 0.79-1.37, lag 0, per 10 $\mu\text{g}/\text{m}^3$ increase in $\text{PM}_{2.5}$]). Estimates for the nation (1.49% [95% PI: 1.09-1.89, lag 0]) and northeast (2.01% [95% PI: 1.39-2.63, lag 0]) were highest in the winter.

Bell et al. (2009, [191997](#)) and Peng et al. (2009, [191998](#)) used data from the MCAPS study and the EPA's Speciation Trends Network (STN) to identify the components of $\text{PM}_{2.5}$ that are most strongly associated with hospitalizations for cardiovascular disease. Peng et al. (2009, [191998](#)) focused on the components that make up the majority of $\text{PM}_{2.5}$ mass (SO_4^{2-} , NO_3^- , Si, EC, OC, NA^+ and NH_4^+) and found that in multipollutant models only EC and OC were significantly associated with risk of hospitalization for cardiovascular disease. Bell et al. (2009, [191997](#)) used data from 20 $\text{PM}_{2.5}$ components and found that EC, Ni, and V were most positively and significantly associated with the risk of cardiovascular hospitalizations. These results suggest that the observed associations between $\text{PM}_{2.5}$ and cardiovascular disease hospitalizations may be primarily due to particles from oil combustion and traffic.

Additional evidence is provided by several large multicity studies conducted outside of the U.S. The European APHEA2 study (Le Tertre et al., 2002, [023746](#)) looked at admissions for CVD (defined as ICD-9 390-429) among those aged ≥ 65 and found a 0.7% (95% CI: 0.4-1.0, lag 0-1 day avg) increase in risk per 10 $\mu\text{g}/\text{m}^3$ PM_{10} . The Spanish EMECAS study (Ballester et al., 2006, [088746](#)) looked at admissions for CVD (defined as ICD-9 390-459) and found a 0.9% (95% CI: 0.4-1.5, lag 0-1 day avg) increase in risk per 10 $\mu\text{g}/\text{m}^3$ PM_{10} . The French PSAS program looked at CVD hospitalizations (defined as ICD-10 I00-I99) among the elderly and found a 1.1% (0.5, 1.7%) increase in risk with PM_{10} and a 1.9% (95% CI: 0.9-3.0, lag 0-1 day avg) increase in risk with a 10 $\mu\text{g}/\text{m}^3$ increase in $\text{PM}_{2.5}$ (Host et al., 2008, [155852](#); Larrieu et al., 2007, [093031](#)). Non-significant increases in association with $\text{PM}_{10-2.5}$ were reported (1.0% [95% CI: -1.0 to 3.0]) (Host et al., 2008, [155852](#)). In multiple cities across New Zealand and Australia, Barnett et al. (2006, [089770](#)) looked among the elderly

(CVD defined as ICD-9 390-459 and found a 1.3% (95% CI: 0.6-2.0, lag 0-1 day avg) increase in risk per 10 $\mu\text{g}/\text{m}^3$ increase in $\text{PM}_{2.5}$.

The Atlanta-based SOPHIA study found a 0.9% (95% CI: -0.2 to 1.9, lag 0-2 day avg) and a 3.3% (95% CI: 1.0-5.6, lag 0-2 day avg) increase in risk with a 10 $\mu\text{g}/\text{m}^3$ increase in PM_{10} and $\text{PM}_{2.5}$, respectively (Metzger et al., 2004, [044222](#)). In a more recent analysis from this study with an additional 4 yr of data, ED visits for CVD were not significantly associated with PM_{10} or $\text{PM}_{2.5}$, but were significantly associated with total carbon (1.6% [95% CI: 0.5-2.6, per IQR increase]), EC (1.5% [95% CI: 0.5-2.5, per IQR increase]) and organic carbon (1.5% [95% CI: 0.5-2.6, per IQR increase]) components of $\text{PM}_{2.5}$ (2007, [090316](#)). A weak non-significant association $\text{PM}_{10-2.5}$ was observed in these data (Tolbert et al., 2007, [090316](#)) More recently, Sarnat et al. (2008, [097972](#)) used multiple source-apportionment methods to evaluate the association between all CVD ED visits and specific $\text{PM}_{2.5}$ sources and found consistent positive associations with sources related to motor vehicles and biomass combustion. These results were insensitive to the source-apportionment technique used. It is noteworthy that other traffic-related gaseous pollutants were associated with CVD ED visits in the SOPHIA study (Metzger et al., 2004, [044222](#)).

Using meta-regression techniques and the reported association between PM_{10} and CVD hospitalizations from the 14 cities included in the NMMAPS analysis, Janssen et al. (2002, [016743](#)) examined whether the between-city variability in relative risk estimates were related to the local contribution of a number of PM sources. The authors found that in multivariate analyses PM_{10} coefficients increased significantly with increasing percentage of PM_{10} emissions from highway vehicles/diesels and oil combustion.

A small number of additional single-city studies have been published showing positive associations between hospital admissions and ambient PM in Copenhagen, Denmark (Andersen et al., 2007, [093201](#)), and weak nonsignificant associations in Spokane, WA (Schreuder et al., 2006, [097959](#); Slaughter et al., 2005, [073854](#)) and two small counties in Idaho (Ulirsch et al., 2007, [091332](#)). Schreuder et al. (2006, [097959](#)) performed a source apportionment analysis using seven yr of daily speciation data from the same residential monitor in Spokane, WA used by Slaughter et al. (2005, [073854](#)). These authors related daily levels of four sources (woodsmoke, an As-rich source, motor vehicle emissions, and airborne soil) to the excess risk of cardiovascular ED visits. During the heating season the only notable association for CVD-related ED visits was with WS, while in the non-heating

season the only notable association was with airborne soil. While neither of these associations reached statistical significance, the study likely lacked the statistical power to find effects of the expected magnitude. In fact, it is doubtful that studies conducted outside of large metropolitan areas have sufficient statistical power to detect associations of the expected magnitude. Delfino et al. (2009, [191994](#)) evaluated the effects of the 2003 California wildfires and observed a slightly larger excess risk of total cardiovascular disease admissions during the wildfire period compared to the period prior to the wildfire although excess risk estimates were generally weak and non-significant.

Studies in several cities in Australia have investigated the association of cardiovascular disease admissions with PM concentration and sources. A study from Sydney, Australia found a 0.3% (95% CI: -0.8 to 1.4) and 1.8% (95% CI: 0.4-3.2) excess risk per 10 $\mu\text{g}/\text{m}^3$ increase in the 2-day ma (lags 0-1 days) in PM_{10} and $\text{PM}_{2.5}$, respectively (Jalaludin et al., 2006, [189416](#)). Johnston et al. (2007, [155882](#)) and Hanigan et al. (2008, [156518](#)) studied the association between PM_{10} and cardiovascular and respiratory hospitalizations in Darwin, Australia, where the predominant source of PM is from biomass combustion. The authors found little or no evidence of an association between PM_{10} and cardiovascular disease hospital admissions in the general population.

Crustal material has also been investigated in an effort to explain associations of PM concentration with cardiovascular disease admissions. Studies of a dust storm in the Gobi desert that transported PM across the Pacific Ocean reaching the western U.S. in the spring of 1998 have been conducted. An analysis of the health impacts of this event on the population of British Columbia's (Canada) Lower Fraser Valley found no excess risk of cardiac or respiratory hospital admissions despite hourly PM_{10} levels $>100 \mu\text{g}/\text{m}^3$ (Bennett et al., 2006, [088061](#)). On the other hand, a number of studies in Asia and eastern Europe have identified some adverse health effects associated with dust storm events. Middleton et al. (Middleton et al., 2008, [156760](#)) found that dust storms in Cyprus were associated with a 4.7% (95% CI: 0.7-9.0) and 10.4% (95% CI: -4.7 to 27.9) increase in risk of hospitalization for all causes and cardiovascular diseases, respectively. Chan et al. (2008, [093297](#)) studied the effects of Asian dust storms on cardiovascular hospital admissions in Taipei, Taiwan and also found significant adverse effects during 39 Asian dust events with high PM_{10} levels (daily $\text{PM}_{10} >90 \mu\text{g}/\text{m}^3$). Bell et al. (2008, [091268](#)) analyzed these data independently and concluded that Asian dust storms were positively associated with risk of hospitalization for ischemic heart disease.

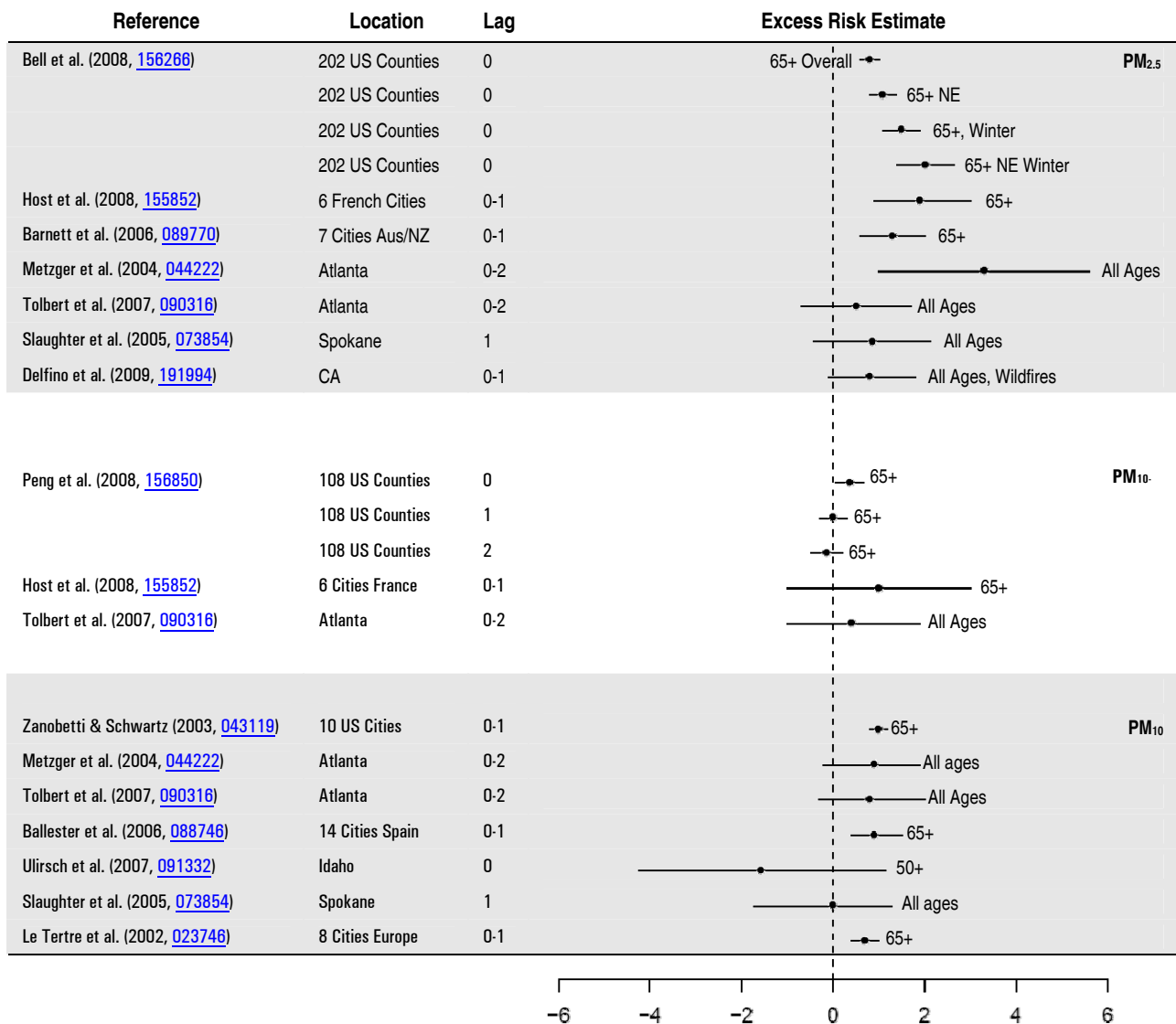


Figure 6-1. Excess risk estimates per 10 $\mu\text{g}/\text{m}^3$ increase in PM_{10} , $\text{PM}_{2.5}$ and $\text{PM}_{10-2.5}$ for studies of CVD ED visits* and hospitalizations. Studies represented in the figure include all multicity studies. Single-city studies conducted in the U.S. or Canada are also included.

Table 6-6. Characterization of ambient PM concentrations in studies of hospital admission and ED visits for cardiovascular diseases.

Pollutant	Author	Location	Mean Concentration ($\mu\text{g}/\text{m}^3$)	Upper Percentile Concentration ($\mu\text{g}/\text{m}^3$)
PM₁₀				
	Balelster et al. (2006, 088746)	14 cities in Spain	NR	NR
	Barnett et al. (2006, 089770)	5 cities in Australia and New Zealand	NR	NR
	Burnett et al. (1999, 017269)	Toronto, Canada	30.2	
	Ito et al. (2003, 042856); Lippman (2000, 024579)	Detroit, MI	31	
	Jalaludin et al. (2006, 189416)	Sydney, Australia	16.8	75th: 19.9 Max: 103.9
	Larrieu et al. (Larrieu et al., 2007, 093031)	8 cities in France		
	Le Tertre et al. (2002, 023746)	8 cities in Europe	Range: 15.5-55.7	Range 75th: 19.9-66
	Linn et al. (2000, 002839)	Los Angeles, California	45	78 (summer) - 132 (fall)
	Metzger et al. (2004, 044222)	Atlanta, GA	26.3	90th: 44.7
	Morris et al. (1998, 024924)	Chicago, Illinois	41	75th: 51 Max: 117
	Peters et al. (2001, 016546)	Boston, MA		
	Schwartz et al. (1995, 046186)	Detroit, MI	48	90th: 82
	Slaughter et al. (2005, 073854)	Spokane, WA	NR	90th: 41.9
	Tolbert et al. (2007, 090316)	Atlanta, GA		
	Ulirsch et al. (2007, 091332)*	2 cities in southeast Idaho	24.2/23.2	90th: 40.7/37.4
	Wellenius et al. (2005, 087483)	Pittsburgh, PA	31.1	95th: 70.5
	Wellenius et al. (2005, 087483)	9 cities in the U.S.	28.4 (median)	90th: 57.9
	Wellenius et al. (2005, 087483)	7 cities in the U.S.	28.3 (median)	90th: 57
	Zanobetti and Schwartz (2005, 088069)	Boston, MA	28.4 (median)	90th: 53.6
PM_{2.5}				
	Barnett et al. (2006, 089770)	7 cities in Australia		
	Bell et al. (2008, 156266)	202 counties in the U.S.	12.92	34.16
	Burnett et al. (1999, 017269)	Toronto Canada	18	
	Dominici et al. (2006, 088398)	204 counties in the U.S.	NR	NR
	Delfino et al. (2009, 191994)	6 counties CA	18.4-32.7	45.3-76.1 (wildfire period)
	Host et al. (2008, 155852)	6 cities in France	13.8-18.8	NR
	Ito et al. (2003, 042856); Lippman (2000, 024579)	Detroit, MI	18	98th: 55.2
	Lisabeth et al. (2008, 155939)		7	75th: 10
	Metzger et al. (2004, 044222)	Atlanta, GA	17.8	90th: 32.3 98th: 39.8
	Pope et al. (2006, 091246)	Wasatch Front, Utah		
	Slaughter et al. (2005, 073854)	Spokane, WA	NR	90th: 20.2
	Sullivan et al. (2005, 050854)	King County, WA	12.8	90th 27.3, Max: 147
	Symons et al. (2006, 091258)	Baltimore, MD	16	Max: 69.2
	Tolbert et al. (2007, 090316)	Atlanta, GA	17.1	98th: 38.7
	Villeneuve et al. (2006, 090191)	Edmonton, Canada	8.5	75th: 11
	Zanobetti and Schwartz (2005, 088069)	Boston, MA	11.1 (median)	95th: 26.31 98th: 55.2
PM_{10-2.5}				
	Burnett et al. (1999, 017269)	Toronto, Canada	12.2	Max: 68
	Host et al. (2008, 155852)	6 cities in France	7-11	NR
	Ito et al. (2003, 042856); Lippman (2000, 024579)	Detroit, MI	13	Max: 50
	Le Tertre et al. (2002, 023746)	8 cities in Europe	NR	NR
	Metzger et al. (2004, 044222)	Atlanta, GA	9.1	90th: 16.2
	Peng et al. (2008, 156850)	204 cities in the U.S.	9.8 (Median)	NR
	Peters et al. (2001, 016546)	Boston, MA	7.4	
	Slaughter et al. (2005, 073854)	Spokane, WA	NR	NR
	Tolbert et al. (2007, 090316)	Atlanta, GA	9	

*Results presented separately for 2 separate time series

The effect estimates from multicity studies and single-city studies conducted in the U.S. and Canada are included in Figure 6-1. Information on PM concentrations during the relevant study period is presented in Table 6-6. In summary, large studies from the U.S., Europe, and Australia/New Zealand published since the 2004 PM AQCD (U.S. EPA, 2004, [056905](#)) provide support for an association between short-term increases in ambient levels

of PM₁₀ and PM_{2.5} and increased risk of hospitalization for total CVD. The evidence for an association of CVD hospitalization with PM_{10-2.5} is relatively limited. Peng et al. (2008, [156850](#)) reported that their PM_{10-2.5} estimate was not robust to adjustment for PM_{2.5} and estimates from the other studies are imprecise. The average excess risk among the U.S. elderly is likely in the range of 0.5 to 1.0% per 10 µg/m³ increase in PM_{2.5}, although substantial variability by region of the country and season has been demonstrated. An excess risk of ED visits for CVD of a similar magnitude appears likely. The excess risk of CVD hospitalization may be somewhat greater in Europe and Australia/New Zealand than in the U.S. Sources including wood burning, oil burning, traffic and crustal material have been associated with increases in cardiovascular hospitalization or ED visits, but the best evidence suggests that in the U.S., oil combustion, wood burning, and traffic are likely the sources of PM_{2.5} most strongly associated with cardiovascular hospitalizations or ED visits.

6.2.10.2. Cardiac Diseases

Cardiac disease represents a subset of CVD which specifically excludes hospitalizations for CBVD, peripheral vascular disease, and other circulatory diseases not involving the heart or coronary circulation. Only a small number of studies published since the 2004 PM AQCD (U.S. EPA, 2004, [056905](#)) have evaluated the association between ambient PM and hospitalizations for cardiac diseases, as most investigators have focused instead on more narrowly defined outcomes.

The French PSAS program found a 1.5% (95% CI: 0.5-2.2, lag 0-1) and 2.4% (95% CI: 1.2-3.7, lag 0-1) excess risk among the elderly per 10 µg/m³ increase in PM₁₀ and PM_{2.5}, respectively (Host et al., 2007, [155851](#); Larrieu et al., 2007, [093031](#)). Host et al. (2008, [155852](#)) also found a positive less precise association with PM_{10-2.5}, (excess relative risk per 10 µg/m³: 1.6% [95% CI: -0.8 to 4.1%]). The European HEAPSS study looked at cardiac readmissions among survivors of a first MI and found a 2.1% (95% CI: 0.4-3.9, lag 0) excess risk per 10 µg/m³ increase in PM₁₀ (Von Klot et al., 2005, [088070](#)). A 1.9% (95% CI: 1.0-2.7, lag 0-1) excess risk per 10 µg/m³ increase in PM_{2.5} was observed in several cities in Australia and New Zealand (Barnett et al., 2006, [089770](#)). Single-city studies of hospital admissions from Kaohsiung and Taipei, Taiwan, and an ED visit study from Sydney, Australia also reported statistically significant positive associations (Chang et al., 2005, [088662](#); Jalaludin et al., 2006, [189416](#); Yang et al., 2004, [055603](#)). On the other hand,

Slaughter et al. (2005, [073854](#)) found no association between either PM₁₀ or PM_{2.5} and risk of cardiac hospitalization in Spokane, Washington.

In summary, although relatively few studies have focused on all cardiac diseases, large studies from Europe and Australia/New Zealand published since the 2004 PM AQCD (U.S. EPA, 2004, [056905](#)) report positive associations between short-term increases in ambient levels of PM₁₀, PM_{2.5} and PM_{10-2.5} and increased risk of hospitalization for cardiac disease. The results from small single-city studies are less consistent. The excess risk for cardiac hospitalizations may be somewhat larger than for total CVD hospitalizations.

6.2.10.3. Ischemic Heart Disease

IHD represents a subset of all cardiac disease hospitalizations and typically includes acute MI (ICD 9: 410), other acute and subacute forms of IHD (411), old MI (412), angina pectoris (413), and other forms of chronic ischemic heart disease (414). Some authors term this category coronary heart disease. Published studies evaluating IHD as a single outcome are considered first, followed by consideration of studies looking at acute MI, a specific form of IHD.

In 1995 Schwartz and Morris (1995, [046186](#)) reported a 0.6% (95% CI: 0.2-1.0%) excess risk of hospitalization for IHD per 10 µg/m³ increase in mean PM₁₀ levels over the previous two days among elderly Medicare beneficiaries living in Detroit between 1986 and 1989. As reviewed in the 2004 PM AQCD (U.S. EPA, 2004, [056905](#)), similar associations were subsequently observed in many single-city studies including: London, England (Atkinson et al., 1999, [007882](#)), Toronto, Canada (Burnett et al., 1999, [017269](#)), and Seoul, Korea (Lee et al., 2003, [095552](#)). Studies in Hong Kong (Wong et al., 1999, [009172](#); Wong et al., 2002, [023232](#)), Birmingham, England (Anderson et al., 2001, [017033](#)), and London, England (Wong et al., 2002, [025436](#)) yielded positive point estimates of a similar magnitude, but did not reach statistical significance.

The positive associations between short-term changes in PM and IHD hospitalizations observed in the early single-city studies have been confirmed in several large multicity studies. The U.S. MCAPS study (Dominici et al., 2006, [088398](#)) found a 0.4% (95% CI: 0.0-0.8) excess risk of hospitalization for IHD per 10 µg/m³ increase in PM_{2.5} two days earlier. The European APHEA-2 study (Le Tertre et al., 2002, [023746](#)) considered PM₁₀ and found a 0.8% (95% CI: 0.3-1.2, lag 0-1) excess risk among those aged ≥ 65 yr. Among the elderly in 5 cities in Australia and New Zealand (Barnett et al., 2006, [089770](#)) there was a

4.3% (95% CI: 1.9-6.4, lag 0-1) excess risk per 10 $\mu\text{g}/\text{m}^3$ increase in $\text{PM}_{2.5}$. Among the elderly in several French cities there was a 4.5% (95% CI: 2.3-6.8, lag 0-1), 6.4% (95% CI: 1.6-11.4%, lag 0-1) and 2.9% (95% CI: 1.5-4.3, lag 0-1) excess risk per 10 $\mu\text{g}/\text{m}^3$ increase in $\text{PM}_{2.5}$, $\text{PM}_{10-2.5}$, (Host et al., 2008, [155852](#)) and PM_{10} , respectively (Larrieu et al., 2007, [093031](#)).

With regard to ED visits, the Atlanta-based SOPHIA study (Metzger et al., 2004, [044222](#)) found positive associations with PM_{10} and $\text{PM}_{2.5}$ (ranging from 1.1 to 2.3%), but the effect estimates did not reach statistical significance. Similarly, associations of EC and OC with IHD were increased but not significant. In 6 cities across Canada, Szyszkowicz (2009, [191996](#)) observed a 1.4% (95% CI: 0.7-2.0%) and 2.4% (95% CI: 1.2-3.6%) excess risk of ED visits for angina per 10 $\mu\text{g}/\text{m}^3$ increase in same-day PM_{10} and $\text{PM}_{2.5}$, respectively. Although excess risks were generally weak and non-significant, Delfino et al. (2009, [191994](#)) observed a slightly larger excess risk of IHD during wildfires compared to the pre-wildfire period. In Sydney, Australia, Jalaludin et al. (2006, [189416](#)) found a 0.8% (95% CI: -1.2 to 2.8%) and 2.6% (95% CI: 0.1-5.2) excess risk of ED visits for IHD per 10 $\mu\text{g}/\text{m}^3$ increase in 2-day ma of PM_{10} and $\text{PM}_{2.5}$, respectively. A recent study in Helsinki, Finland found no evidence of an association with UFP, ACP, $\text{PM}_{2.5}$, $\text{PM}_{10-2.5}$, or source-specific $\text{PM}_{2.5}$ (Halonen et al., 2009, [180379](#)).

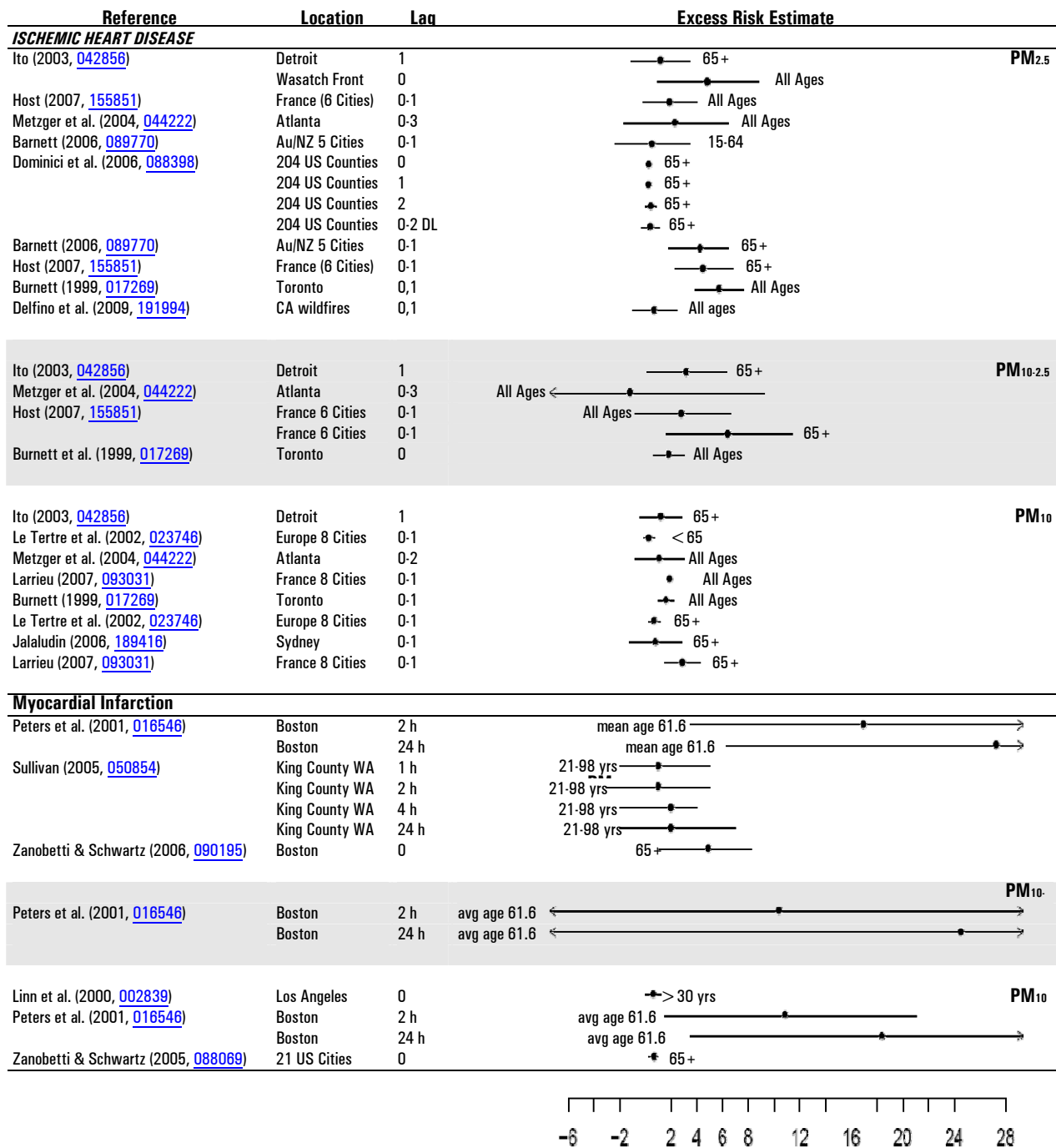


Figure 6-2. Excess risk estimates per 10 $\mu\text{g}/\text{m}^3$ increase in PM₁₀, PM_{2.5}, PM_{10-2.5} for studies of EDvisits * and hospitalizations for IHD and MI. Studies represented in the figure include all multicity studies. Single-city studies conducted in the U.S. and Canada are also included.

To explore this link further, Pope et al. (2006, [091246](#)) used data from an ongoing registry of patients undergoing coronary angiography at a single referral center in Salt

Lake City, UT, between 1994 and 2004. The authors found a 4.8% (95% CI: 1.0-8.8, lag 0) excess risk of acute MI or unstable angina per 10 $\mu\text{g}/\text{m}^3$ increase in $\text{PM}_{2.5}$ among 4,818 patients. These results were robust to changes in the definition of the outcome. The results of this study are particularly noteworthy given the high specificity of the outcome definition.

In summary, large studies from the U.S., Europe, and Australia/New Zealand published since the 2004 PM AQCD (U.S. EPA, 2004, [056905](#)) provide support for an association between short-term increases in ambient levels of PM_{10} and $\text{PM}_{2.5}$ and increased risk of hospitalization or ED visits for ischemic heart diseases. Although estimates are less precise for $\text{PM}_{10-2.5}$, most results from single pollutant models provide evidence of a positive association between $\text{PM}_{10-2.5}$ and IHD. Moreover, Host et al. (2008, [155852](#)) found that the effect estimates for the association of $\text{PM}_{2.5}$ and $\text{PM}_{10-2.5}$ with IHD were very similar when scaled to the IQR of each metric. Estimates of the excess risk vary considerably between studies, but as was the case for total CVD hospitalizations, the excess risk appears to somewhat greater in Europe and Australia/New Zealand. Results from multicity studies and U.S. and Canadian single-city studies are presented in Figure 6-2.

6.2.10.4. Acute MI

Because even IHD refers to a heterogeneous collection of diseases and syndromes, several authors have evaluated the association between short-term fluctuations in ambient PM and acute MI, a specific form of ischemic heart disease.

In 2001, Peters et al. (2001, [016546](#)) published their study evaluating the effects of PM on the risk of MI among 772 Boston-area participants in the Determinants of MI Onset Study. The authors found that a 10 $\mu\text{g}/\text{m}^3$ increase in the 2-h or 24-h avg levels of $\text{PM}_{2.5}$ was associated with a 17% (95% CI: 4-32) and 27% (95% CI: 6-53) excess risk of MI, respectively. An imprecise, non-significant association between $\text{PM}_{10-2.5}$ and onset of MI was observed in Boston. In contrast, a study among 5793 patients in King County, WA that used similar methods, found no association with $\text{PM}_{2.5}$ with lag times of 1, 2, 4, or 24 h (Sullivan et al., 2005, [050854](#)). Among 852 hospitalized patients in Augsburg, Germany, Peters et al. (2005, [087759](#)) also found no association between $\text{PM}_{2.5}$ and MI risk within this time frame, although they did find a positive and statistically significant association with time spent in traffic (Peters et al., 2004, [087464](#)).

These three studies are particularly important because in each one: (1) cases were prospectively identified based on clinical criteria rather than retrospectively based on discharge diagnoses; and (2) time of MI symptom onset was used for exposure assessment rather than date of hospital admission. Whether the discrepant results among these studies are due to regional differences in population characteristics and/or air pollution sources remains unclear. The King County study suggests that differences in statistical approaches are unlikely to account for the discrepant results (Sullivan et al., 2005, [050854](#)). Analyses from the U.S. MCAPS study suggest that substantial heterogeneity of effects are to be expected across regions of the country (Bell et al., 2008, [156266](#))

Several studies have assessed the association between acute exposure to ambient PM and MI using administrative databases. In the U.S., MI was not one of the specific endpoints evaluated in the MCAPS study (Dominici et al., 2006, [088398](#)) or in the Atlanta-based SOPHIA study of ED visits (Metzger et al., 2004, [044222](#)). However, Zanobetti and Schwartz (2005, [088069](#)) found a 0.7% (95% CI: 0.3-1.0) excess risk of MI per 10 $\mu\text{g}/\text{m}^3$ increase in same-day PM₁₀ among elderly Medicare beneficiaries in 21 cities. Subsequently, the same authors found that among elderly Medicare beneficiaries living in the Boston metropolitan region a 10 $\mu\text{g}/\text{m}^3$ increase in PM_{2.5} was associated with a 4.9% (95% CI: 1.1-8.2) excess risk on the same day (Zanobetti and Schwartz, 2006, [090195](#)).

This body of evidence may implicate traffic-related pollution generally as a risk factor for MI. In the study described above, Peters et al. (2001, [016546](#)) found positive associations between risk of hospitalization for MI and potential markers of traffic-related pollution measured at a central monitor including BC, CO and NO₂. However, none of these associations were statistically significant in models adjusting for season, meteorological variables, and day of week. Zanobetti and Schwartz (2006, [090195](#))

examined the association between traffic-related pollution and risk of hospitalization for MI among Medicare beneficiaries in the Boston area and found that MI risk was positively and significantly associated with measures of PM_{2.5}, BC, NO₂, and CO, but not with levels of non-traffic-related PM_{2.5}. Peters et al. (2004, [087464](#)) interviewed 691 subjects with MI who survived at least 24-h after the event and found a strong positive association between self-reported exposure to traffic and the onset of MI within 1 h (OR: 2.9 [95% CI: 2.2-3.8] $p < 0.001$). The association was somewhat stronger among subjects traveling by bicycle or public transportation in the hour prior to the event. Of note, however, this study did not directly measure traffic-related pollution.

Similar studies with administrative databases have been conducted in Europe, Australia, and New Zealand. In Rome, D'Ippoliti et al. (2003, [074311](#)) carried out a case-crossover study and found a statistically significant positive association between TSP and the risk of hospitalization for MI. Barnett et al. (2006, [089770](#)) observed that in 5 cities in Australia and New Zealand, a 10 $\mu\text{g}/\text{m}^3$ increase in $\text{PM}_{2.5}$ was associated with a 7.3% (95% CI: 3.5-11.4, lag 0-1 day) excess risk. In contrast, the HEAPSS study found no evidence of an association between PM_{10} and risk of hospitalization for a first MI in 5 European cities (Lanki et al., 2006, [089788](#)), although there is some indication that among survivors of a first MI, risk of re-hospitalization for MI may be related to transient elevations in PM_{10} (Von Klot et al., 2005, [088070](#)).

In summary, large studies from the U.S., Europe, and Australia/New Zealand published since the 2004 PM AQCD (U.S. EPA, 2004, [056905](#)) provide support for an association between short-term increases in ambient levels of PM_{10} and $\text{PM}_{2.5}$ and increased risk of hospitalization for MI, but not all studies have found statistically significant associations. Some of the heterogeneity of results is likely explained by regional differences in pollution sources, components, and measurement error. One study of the effect of 2- and 24-h avg $\text{PM}_{10-2.5}$ concentration on admissions for MI produced effect estimates that were positive but imprecise (Peters et al., 2001, [016546](#)). These results need to be interpreted together with those studies evaluating hospitalization for IHD since MIs make up the majority of hospitalizations for ischemic heart diseases. U.S. studies of MI are included in Figure 6-2.

6.2.10.5. Congestive Heart Failure

Perhaps the first suggestion of an association between ambient PM and hospitalization for congestive heart failure (CHF) was provided by the study of Schwartz and Morris (1990, [073222](#)). These authors reported that among elderly Medicare beneficiaries living in Detroit between 1986 and 1989, a 10 $\mu\text{g}/\text{m}^3$ increase in mean PM_{10} levels over the previous two days was associated with a 1.0% (95% CI: 0.4-1.6%) increase in risk of hospitalization for CHF. As reviewed in the 2004 PM AQCD (U.S. EPA, 2004, [056905](#)), using similar approaches, statistically significant positive associations with PM_{10} or $\text{PM}_{2.5}$ were subsequently reported in single-city studies looking at hospitalizations for CHF in Toronto (Burnett et al., 1999, [017269](#)), Hong Kong (Wong et al., 1999, [009172](#)), and Detroit (Lippmann, 2000, [024579](#)), but not Los Angeles (Linn et al., 2000, [002839](#)) or

Denver (Koken et al., 2003, [049466](#)). Burnett et al. (1999, [017269](#)) reports a significantly increased risk of CHF hospitalization with PM_{10-2.5} while Metzger et al. (2004, [044222](#)) and (Ito, 2003, [042856](#)) less precise associations.

Subsequent multicity studies support the presence of a positive association. In the U.S., Wellenius et al. (2006, [088748](#)) reported a 0.7% (95% CI: 0.4-1.1) excess risk of hospitalization for CHF per 10 µg/m³ increase in same-day PM₁₀ among elderly Medicare beneficiaries in 7 cities. The larger MCAPS study found a 1.3% (95% CI: 0.8-1.8) excess risk per 10 µg/m³ increase in same-day PM_{2.5} (Dominici et al., 2006, [088398](#)). In Australia and New Zealand, Barnett et al. (2006, [089770](#)) found a 9.8% (95% CI: 4.8-14.8, lag 0-1 day) and 4.6% (95% CI: 2.8-6.3, lag 0-1 days) excess risk of hospitalization for CHF associated with a 10 µg/m³ increase in PM_{2.5} and PM₁₀, respectively. Results from more recent single-city studies in Pittsburgh (Wellenius et al., 2005, [087483](#)), Utah's Wasatch Front (Pope et al., 2008, [191969](#)), Kaohsiung, Taiwan (Lee et al., 2007, [093042](#)) and Taipei, Taiwan (Yang, 2008, [157160](#)) have also reported positive associations. In addition, Yang et al. (2009, [190341](#)) found that hospitalizations for heart failure were elevated during or immediately following 54 Asian dust storm events (while single day lags 0 to 3 were evaluated, maximum excess risk occurred at lag 1: 11.4% [95% CI: -0.7% to 25.0%]). Delfino et al. (2009, [191994](#)) observed a slightly larger excess risk of total CHF during the wildfire occurring in California compared to the period before the wildfires (risks for CVD reported were generally weak and non-significant).

While most studies suggest an association at very short lags (0-1 days), the study by Pope et al. (2008, [191969](#)) failed to find such short term associations and instead suggested that PM_{2.5} levels averaged over the past 2-3 wk may be more important. Pope et al. (2008, [191969](#)) observed a 13.1% (1.3%, 26.2%) increase in CHF hospitalization per 10 µg/m³ increase in PM_{2.5} (imputed values used in analysis). Whether findings at longer lags in this population represent true cumulative effects of PM or are due to misclassification of symptom onset times remains to be determined.

Findings from the Atlanta-based SOPHIA study (Metzger et al., 2004, [044222](#)) also support the presence of a positive association. Specifically, the SOPHIA study found a 5.5% (95% CI: 0.6-10.5, lag 0-2 days) excess risk of ED visits for CHF per 10 µg/m³ increase in the 3-day ma of PM_{2.5}. Positive associations were also observed for CHF and EC and organic carbon components of PM_{2.5}. No associations were observed with PM₁₀ and a weak imprecise increase was observed in association with PM_{10-2.5}.

Only one published study has attempted to evaluate the effects of ambient particles on CHF symptom exacerbation using data which was not derived from administrative databases. Symons et al. (2006, [091258](#)) interviewed 135 patients with prevalent CHF hospitalized for symptom exacerbation in Baltimore, MD. The authors found a 7.4% (95% CI: -7.5 to 24.2) excess risk of hospitalization per 10 $\mu\text{g}/\text{m}^3$ increase in $\text{PM}_{2.5}$ two days prior to symptom onset. Although the authors' findings did not reach statistical significance, the study lacked the statistical power needed to find an effect of the expected magnitude.

In summary, large studies from the U.S., Europe, and Australia/New Zealand published since the 2004 PM AQCD (U.S. EPA, 2004, [056905](#)) provide support for an association between short-term increases in ambient levels of PM_{10} and $\text{PM}_{2.5}$ and increased risk of hospitalization and ED visits for heart failure. Although the number of studies is fewer (and only Metzger et al., 2004, [044222](#) is new since the 2005 AQCD), elevated risks of hospitalization or ED visits for CHF in association with $\text{PM}_{10-2.5}$ have been observed. The excess risk associate with heart failure hospitalizations and ED visits are consistently greater than those observed for other CVD endpoints. The results of multicity studies and U.S. and Canadian single-city studies are summarized in Figure 6-3.

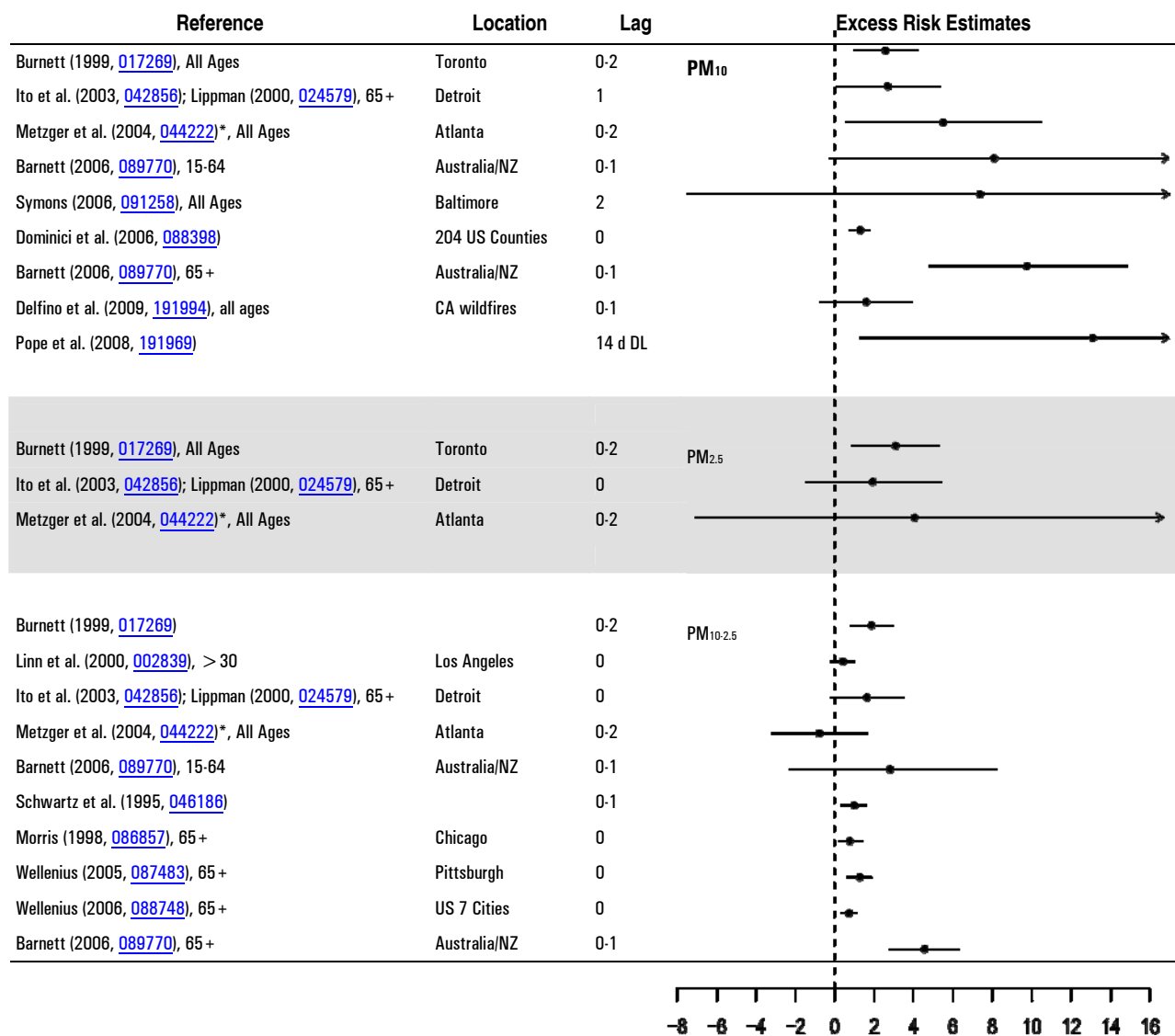


Figure 6-3. Excess risk estimates per 10 $\mu\text{g}/\text{m}^3$ increase in PM₁₀, PM_{10-2.5} and PM_{10-2.5} for studies of CHF ED visits* and hospitalizations. Studies represented in the figure include all multicounty studies. Single-city studies conducted in the U.S. and Canada are also included.

6.2.10.6. Cardiac Arrhythmias

A number of studies based on administrative databases have sought to evaluate the association between short-term fluctuations in ambient PM levels and the risk of hospitalization for cardiac arrhythmias (also known as dysrhythmias). Typically in these studies a primary discharge diagnosis of ICD-9 427 has been used to identify hospitalized patients. However, ICD-9 427 includes a heterogeneous group of arrhythmias including paroxysmal ventricular or supraventricular tachycardia, atrial fibrillation and flutter,

ventricular fibrillation and flutter, cardiac arrest, premature beats, and sinoarterial node dysfunction. One study in the Netherlands found that the positive predictive value of ICD-9 codes related to ventricular arrhythmias and sudden cardiac death was 82% (De Bruin et al., 2005, [155746](#)). The positive predictive value of other codes related to cardiac arrhythmias is unknown but likely to be lower.

The results from early studies of arrhythmia-related hospitalizations have been inconsistent with positive findings in Toronto (Burnett et al., 1999, [017269](#)) and null findings in Detroit (Schwartz and Morris, 1995, [046186](#)), Los Angeles (Linn et al., 2000, [002839](#)), and Denver (Koken et al., 2003, [049466](#)). The U.S. MCAPS study found a statistically significant 0.6% (95% CI: 0.0-1.2%) excess risk of hospitalization for the combined end point of cardiac arrhythmias and conduction disorders (ICD-9: 426, 427) per 10 $\mu\text{g}/\text{m}^3$ increase in same-day $\text{PM}_{2.5}$ (Dominici et al., 2006, [088398](#)). A multicity study in Australia and New Zealand found no evidence of an association between arrhythmia hospitalizations and either PM_{10} or $\text{PM}_{2.5}$ (Barnett et al., 2006, [089770](#)). A study in Helsinki, Finland found no evidence of an association between either $\text{PM}_{2.5}$ or $\text{PM}_{10-2.5}$ and risk of hospitalization for arrhythmias (Halonen et al., 2009, [180379](#)), although there was an association with smaller particles (0.03-0.1 μm).

With regard to ED visits, the Atlanta-based SOPHIA study found no evidence of an association between any measure of ambient PM and the rate of ED visits for cardiac arrhythmias (Metzger et al., 2004, [044222](#)). However, In Sao Paulo, Brazil, Santos et al. (2008, [192004](#)) found a 3.0% (95% CI: 0.5-5.4%) excess risk of ED visits for arrhythmias per 10 $\mu\text{g}/\text{m}^3$ increase in PM_{10} on the same day.

A number of studies in patients with ICD have been able to evaluate in more detail the potential link between ambient air pollution and the risk of atrial and ventricular arrhythmias (as opposed to hospital admissions or ED visits for these events) (Berger et al., 2006, [098702](#); Dockery et al., 2005, [078995](#); Dockery et al., 2005, [090743](#); Ljungman et al., 2009, [191983](#); Metzger et al., 2007, [092856](#); Peters et al., 2000, [011347](#); Rich et al., 2004, [055631](#); Vedal et al., 2004, [055630](#)). An important strength of these studies is the ability to examine recordings of arrhythmic episodes, thereby reducing misclassification of the outcome. These studies are reviewed in detail in Section 6.1.2.1.

In summary, the current evidence does not support the presence of a consistent association between short-term increases in ambient levels of PM_{10} , $\text{PM}_{2.5}$ or $\text{PM}_{10-2.5}$ and increased risk of hospitalization for cardiac arrhythmias. However, it should be noted that

studies of hospital admissions or ED visits are ill-suited to the study of cardiac arrhythmias since most arrhythmias do not lead to hospitalization. Studies in patients with implanted defibrillators, human panel studies with ambulatory ECG recordings, and animal toxicological studies provide a more appropriate setting for evaluating this endpoint. Results of these studies are described in Section 6.1.2.

6.2.10.7. Cerebrovascular Disease

Time-series studies evaluating the hypothesis that short-term increases in ambient PM₁₀ or PM_{2.5} levels are associated with increased risk of hospitalization for CBVD have been inconsistent with a minority of studies reporting statistically significant positive associations (Chan et al., 2006, [090193](#); Dominici et al., 2006, [088398](#); Metzger et al., 2004, [044222](#); Wordley et al., 1997, [082745](#)), and several studies reporting null or negative associations (Anderson et al., 2001, [017033](#); Barnett et al., 2006, [089770](#); Burnett et al., 1999, [017269](#); Halonen et al., 2009, [180379](#); Jalaludin et al., 2006, [189416](#); Larrieu et al., 2007, [093031](#); Le Tertre et al., 2002, [023746](#); Peel et al., 2007, [090442](#); Villeneuve et al., 2006, [090191](#); Wong et al., 1999, [009172](#)).

The U.S. MCAPS study found a 0.8% (95% CI: 0.3-1.4) excess risk of hospitalization for CBVD per 10 µg/m³ increase in same-day PM_{2.5} (Dominici et al., 2006, [088398](#)). The association showed regional variability with the strongest associations observed in the eastern U.S. The Atlanta-based SOPHIA study found a 2.0% (95% CI: -0.1 to 4.3, lag 0-2 days) excess risk of ED visits for a combined endpoint of cerebrovascular and peripheral vascular disease excluding hemorrhagic strokes per 10 µg/m³ increase in PM₁₀ and a 5.0% (95% CI: 0.8-9.3, lag 0-2 days) excess risk for PM_{2.5} (Metzger et al., 2004, [044222](#)). Delfino et al. (2009, [191994](#)) observed a similar weak excess risks of CBVD admissions before and during the wildfire occurring in California and slightly higher risks after the wildfire period (risks for CVD reported were generally weak and non-significant).

In contrast, large multicity studies outside of North America have failed to observe an association. The APHEA study, found no excess risk (0.0% [95% CI: -0.3 to 0.3]) of hospitalization for CBVD per 10 µg/m³ increase in the 2-day ma of PM₁₀ in 8 European cities (Le Tertre et al., 2002, [023746](#)). Investigators from the French PSAS program reported a 0.8% (95% CI: -0.9 to 2.5, lag 0-1 days) excess risk per 10 µg/m³ increase in PM₁₀ among patients aged ≥ 65 yr and a 0.2% (95% CI: -1.6 to 1.9, lag 0-1 days) excess risk among all patients (Larrieu et al., 2007, [093031](#)). Although neither estimate was

statistically significant, the estimated excess risk among the elderly is very similar to that observed in the U.S. MCAPS study. Barnett et al. (2006, [089770](#)) examined this hypothesis in New Zealand and Australia and found no association, but the authors did not report point estimates or confidence intervals.

All of the above studies have identified cases of CBVD based on ICD-9 or ICD-10 codes (most commonly ICD-9 430-438). However, the range of ICD codes commonly used in these studies includes ischemic strokes, hemorrhagic strokes, transient ischemic attacks (TIAs) and several poorly defined forms of acute neurological events (e.g., seizures from a vascular cause) (see Table 6-5). It is plausible that ambient PM has different effects on each of these disparate outcomes.

Ischemic Strokes and Transient Ischemic Attacks

An increasing number of studies have specifically evaluated the association between PM₁₀ and PM_{2.5} and the risk of ischemic stroke (Chan et al., 2006, [090193](#); Henrotin et al., 2007, [093270](#); Linn et al., 2000, [002839](#); Lisabeth et al., 2008, [155939](#); Tsai et al., 2003, [080133](#); Villeneuve et al., 2006, [090191](#); Wellenius et al., 2005, [087483](#); Low et al., 2006, [090441](#); Szyszkowicz, 2008, [192128](#)). Linn et al. (2000, [002839](#)) found a 1.3% (95% CI: 1.0-1.6 per 10 µg/m³, lag 0) excess risk of hospitalization for ischemic stroke in the Los Angeles metropolitan area. Wellenius et al. (2005, [087483](#)) reported a statistically significant 0.4% (95% CI: 0.0-0.9) excess risk per 10 µg/m³ increase in same-day PM₁₀ among elderly Medicare beneficiaries in 9 U.S. cities. Low et al. (2006, [090441](#)) reported an absolute increase of 0.08 (95% CI: 0.002-0.16) ischemic stroke hospitalizations per 10 µg/m³ increase in PM₁₀ in New York City. In Kaohsiung, Taiwan, Tsai et al. (2003, [080133](#)) found a 5.9% (95% CI: 4.3-7.4, lag 0-2 days) excess risk of hospitalization for ischemic stroke per 10 µg/m³ increase in PM₁₀ after excluding days with mean daily temperature <20°C. Meanwhile, in Taipei, Taiwan, Chan et al. (2006, [090193](#)) found a 1.6% (95% CI: -0.8 to 3.9, lag 3) and 3.0% (95% CI: -0.8 to 6.6, lag 3) excess risk per 10 µg/m³ increase in PM₁₀ and PM_{2.5}, respectively. Villeneuve et al. (2006, [090191](#)) and Szyszkowicz et al. (2008, [192128](#)) found no association between either PM_{2.5} or PM₁₀ and ED visits for acute ischemic stroke in Edmonton, Canada.

Two recent studies are particularly noteworthy given the high specificity of the outcome definition. Henrotin et al. (2007, [093270](#)) used data on 1432 confirmed cases of ischemic stroke from the French Dijon Stroke Register and found 0.9% (-7.0, 9.4%) excess

risk of ischemic stroke per 10 $\mu\text{g}/\text{m}^3$ increase in PM_{10} on the same day and a 1.1% (-0.2, 9.4%) excess risk on the previous day (lag 1 day). Lisabeth et al. (2008, [155939](#)) used data on 2,350 confirmed cases of ischemic stroke and 1,158 cases of TIA from the Brain Attack Surveillance in Corpus Christi Project (BASIC), a population-based stroke surveillance project designed to capture all strokes in Nueces County, Texas. The authors found a 6.0% (95% CI: -0.8 to 13.2) and 6.0% (95% CI: -1.8 to 14.4) excess risk of ischemic stroke/TIA per 10 $\mu\text{g}/\text{m}^3$ increase in $\text{PM}_{2.5}$ on the previous day and the same day, respectively.

Only the study by Villeneuve et al. (2006, [090191](#)) specifically evaluated the association between ambient PM and the risk of TIAs. This study failed to find any evidence of an association with either $\text{PM}_{2.5}$ or PM_{10} .

A limitation of all of these studies is that they have assessed exposure based on the date of hospital admission or ED presentation rather than the date and time of stroke symptom onset. It has been shown that this can bias health effect estimates towards the null by up to 60% (Lokken et al., 2009, [186774](#)). Therefore, if there is a causal link between PM and the risk of stroke, it is likely that the existing studies underestimate the true effects. Moreover, most of these studies have evaluated only very short-term effects (lags of 0-2 days) and none have considered lags longer than 5 days. It is possible that the lag structure of the association between PM and stroke differs from that of other cardiovascular diseases and it might even differ by stroke type.

Hemorrhagic Strokes

Most of the studies in the preceding section also evaluated the association between ambient PM and the risk of hemorrhagic stroke (Chan et al., 2006, [090193](#); Henrotin et al., 2007, [093270](#); Tsai et al., 2003, [080133](#); Villeneuve et al., 2006, [090191](#); Wellenius et al., 2005, [087483](#)). In Kaohsiung, Taiwan, Tsai et al. (2003, [080133](#)) noted a 6.7% (95% CI: 4.2-9.4, lag 0-2 days) excess risk of hospitalization for hemorrhagic stroke per 10 $\mu\text{g}/\text{m}^3$ increase in PM_{10} , after excluding days where the mean temperature was $<20^\circ\text{C}$. However, in the U.S., Wellenius et al. (2005, [087483](#)) failed to find any association between ambient PM_{10} levels and risk of hemorrhagic stroke among Medicare beneficiaries in 9 U.S. cities. Similarly, Villeneuve et al. (2006, [090191](#)) found no evidence of an association between ED visits for hemorrhagic stroke and either PM_{10} or $\text{PM}_{2.5}$ levels in Edmonton, Canada. Henrotin et al. (2007, [093270](#)) found no evidence of an association between risk of hospitalization and PM_{10} levels in Dijon, France, and Chan et al. (2006, [090193](#)) found no

evidence of an association between risk of hospitalization and either PM₁₀ or PM_{2.5} levels in Taipei, Taiwan.

In summary, large studies from the U.S., Europe, and Australia/New Zealand published since the 2004 PM AQCD (U.S. EPA, 2004, [056905](#)) provide inconsistent support for an association between short-term increases in ambient levels of PM₁₀ and PM_{2.5} and risk of hospitalization and ED visits for CBVD (Figure 6-4). Studies of PM_{10-2.5} and CBVD or stroke have not been conducted. The heterogeneity in results is likely partly attributed to: 1) differences in the sensitivity and specificity of the various outcome definitions used in the relevant studies; 2) lag structures between PM exposure and stroke onset which may vary by stroke type and patient characteristics; and 3) exposure misclassification due to the use of hospital admission date rather than stroke onset time, which may vary by region, population characteristics, and stroke type. Effect estimates from multicity studies and single-city U.S. and Canadian studies are included in Figure 6-4.

6.2.10.8. Peripheral Vascular Disease

In the U.S., the large MCAPS study Dominici et al. (2006, [088398](#)) evaluated the association between mean daily PM_{2.5} levels and the risk of hospitalization among elderly Medicare beneficiaries in 204 urban counties and found that a 10 µg/m³ increase in PM_{2.5} was not significantly associated with risk of hospitalization for peripheral vascular disease 0-2 days later. An earlier study in Toronto (Burnett et al., 1999, [017269](#)) found a negative association with PM_{2.5} (point estimate and confidence intervals not reported), a positive non-significant association with PM₁₀ (0.5% [95% CI: -0.5 to 1.6%]), and a positive statistically significant association with PM_{10-2.5} (2.2% [95% CI: 0.1-4.3%]). The Atlanta-based SOPHIA study (Metzger et al., 2004, [044222](#)) of ED visits grouped visits for PVD with those for CBVD, making interpretation of these results challenging.

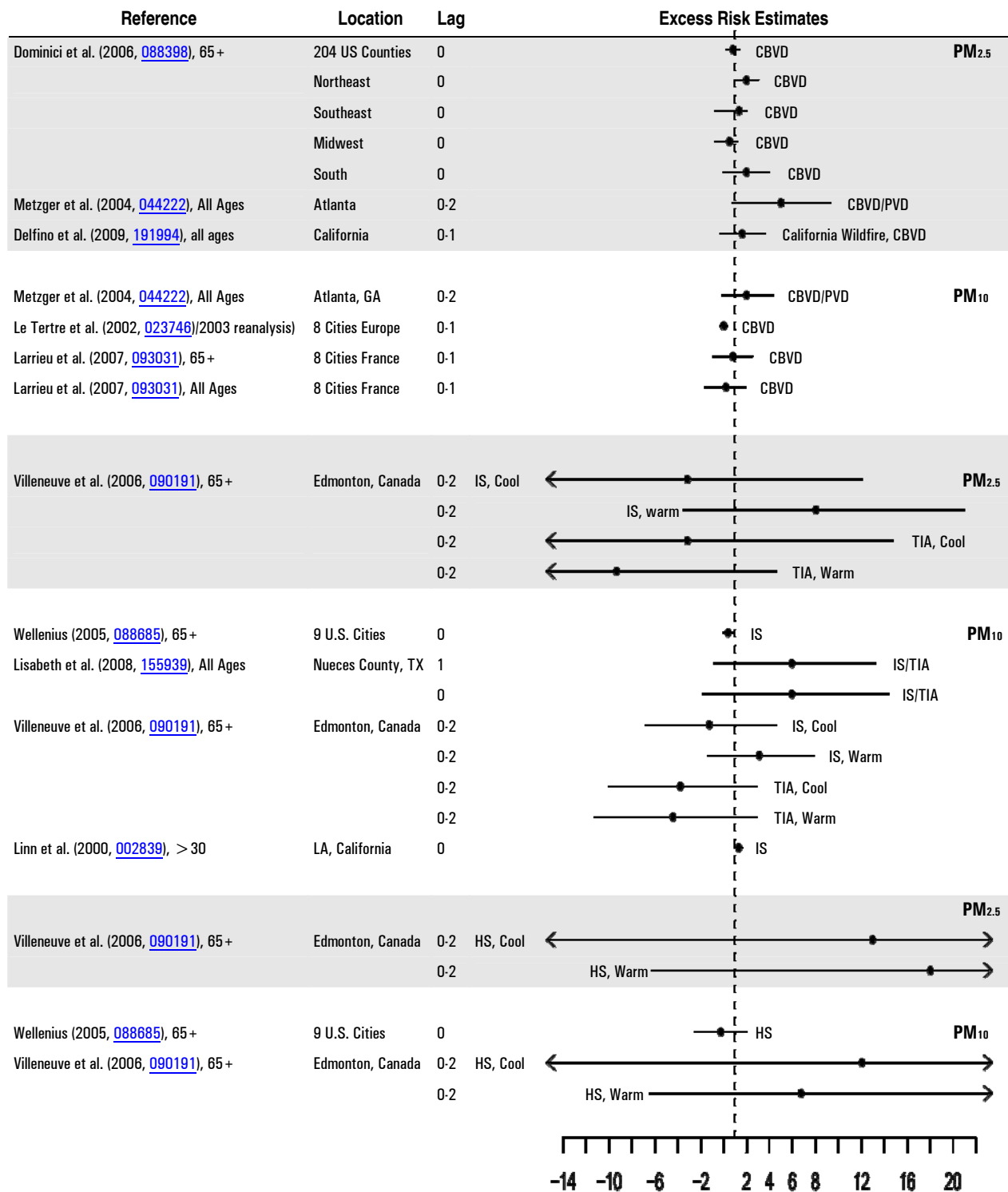


Figure 6-4. Excess risk estimates per 10 $\mu\text{g}/\text{m}^3$ increase in PM_{10} and $\text{PM}_{2.5}$ for studies of ED visits* and hospitalizations for CBVDs. Studies represented in the figure included all multicity studies. Single-city studies conducted in the U.S. and Canada are also included.

In summary, there is insufficient published data to determine whether or not there may be an association between short-term increases in ambient levels of PM₁₀, PM_{2.5}, or PM_{10-2.5} and increased risk of hospitalization and ED visits for PVD.

6.2.10.9. Copollutant Models

Relatively few studies have evaluated the effects of PM_{2.5} and PM_{10-2.5} on the risk of hospital admissions and ED visits in the context of 2 pollutant models. Generally, results for health effects of both size fractions are similar even after controlling for SO₂ or O₃ levels (Figure 6-5). However, controlling for NO₂ or CO has yielded conflicting results. Among the large multicity studies, the Atlanta-based SOPHIA study found that the association between PM_{2.5} (total carbon) and risk of cardiovascular ED visits was somewhat attenuated in 2-pollutant models additionally controlling for either CO or NO₂ (Tolbert et al., 2007, [090316](#)). Barnett et al. (2006, [089770](#)) found that the associations they observed between PM_{2.5} and cardiac hospitalizations in Australia and New Zealand were attenuated after control for 24-h NO₂, but not after control for CO.

Only a few studies have attempted to evaluate the effects of one PM size fraction while controlling for another PM size fraction. The large U.S. MCAPS study evaluating the effects of PM_{10-2.5} on cardiovascular hospital admissions lost precision after controlling for PM_{2.5}, but did not consider gaseous pollutants (Peng et al., 2008, [156850](#)). Andersen et al. (2008, [189651](#)) found that associations between both PM₁₀ and PM_{2.5} and cardiovascular hospitalizations in Copenhagen were not attenuated by control for particle number concentration, a measure of UFPs.

A number of studies have also evaluated PM₁₀ effects in the context of 2-pollutant models with inconsistent results. The multicity Spanish EMECAS study (Ballester et al., 2006, [088746](#)) found that the statistically significant positive associations observed between PM₁₀ and cardiac hospitalizations were robust to control for other pollutants in 2-pollutant models. Jalaludin et al. (2006, [189416](#)) found that the effects of PM₁₀ as well as PM_{2.5} on cardiovascular ED visits in Sydney Australia were attenuated by additional control for either NO₂ or CO. Wellenius et al. (2005, [087483](#)) found that the PM₁₀-related risk of hospitalization for CHF in Allegheny County, PA, was attenuated in 2-pollutant models controlling for either CO or NO₂. In contrast, Chang et al. (2004, [055637](#)) examined CHF hospitalizations in Taipei and found attenuation of PM₁₀ effects by control for NO₂ or CO, but only during warm days. In Kaohsiung, Taiwan, Tsai et al. (2003, [080133](#)) found that the

association between PM₁₀ and ischemic stroke hospitalizations was not materially attenuated in 2-pollutant models controlling for either NO₂ or CO.

The inconsistent findings after controlling for gaseous pollutants or other size fractions are likely due to differences in the correlation structure among pollutants as well as differing degrees of exposure measurement error.

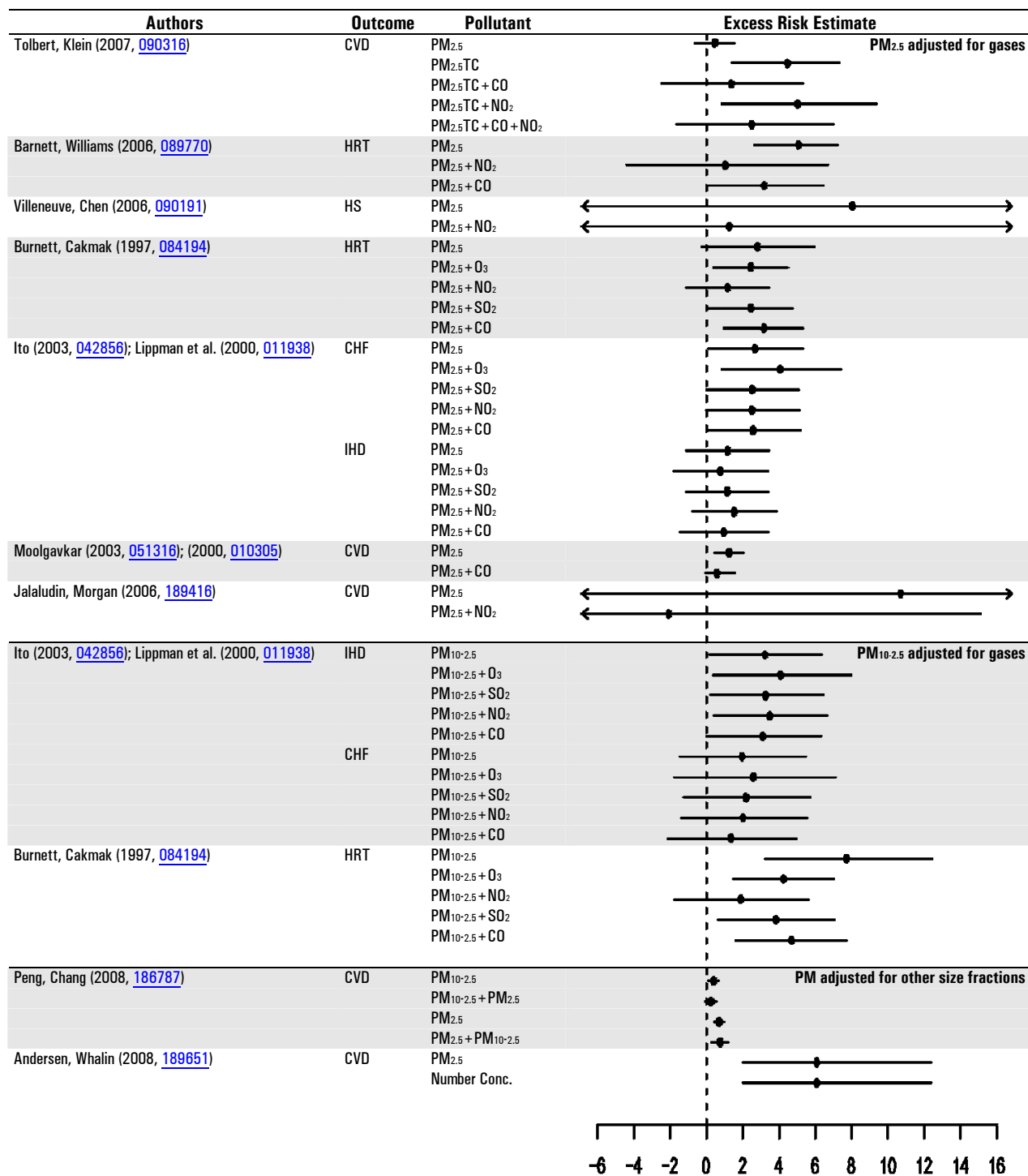


Figure 6-5. Excess risk estimates per 10 µg/m³ increase in PM_{2.5}, and PM_{10-2.5} for studies of ED visits* and hospitalizations for CVDs. Results presented for multipollutant models.

6.2.10.10. Concentration Response

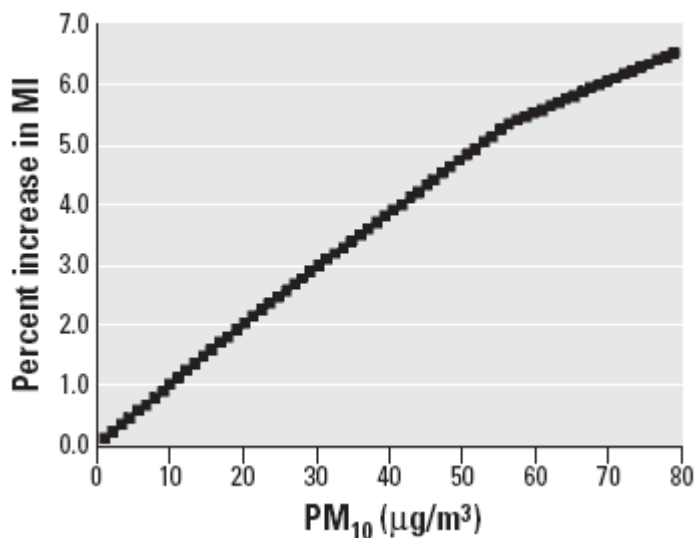
The concentration-response relationship has been extensively analyzed primarily through studies that examined the relationship between PM and mortality. These studies, which have focused on both short- and long-term exposures to PM have consistently found no evidence for deviations from linearity or a safe threshold (Daniels et al. 2004; Schwartz et al. 2004; Samoli et al. 2005; Schwartz et al. 2008) (see Section 6.5.2.7 and 7.1.4). Although on a more limited basis, studies that have examined PM effects on cardiovascular hospital admissions and ED visits have also analyzed the PM concentration-response relationship, and contributed to the overall body of evidence which suggests a log-linear, no-threshold PM concentration-response relationship.

The evaluation of cardiovascular hospital admission and ED visit studies in 2004 PM AQCD (U.S. EPA, 2004, [056905](#)) found no evidence for a threshold in the dose-response relationship between short-term exposure to PM₁₀ and IHD hospital admissions (Schwartz and Morris, 1995, [046186](#)). An evaluation of both recent single and multicity studies of hospital admission and ED visits for cardiovascular diseases further supports this finding.

Ballester et al. (2006, [088746](#)) examined the linearity of the relationship between air pollutants (including PM₁₀) and cardiovascular hospital admissions in 14 Spanish cities within the EMECAM project. In this exploratory analysis, the authors examined the models used when pollutants were added in either a linear or non-linear way (i.e., with a spline smoothing function) to the model. Although the study does not present the results for each of the pollutants evaluated individually, overall Ballester et al. (2006, [088746](#)) found that the shape of the pollutant-cardiovascular hospital admission relationship was most compatible with a linear curve. Wellenius et al. (2005, [087483](#)) conducted a similar analysis when examining the relationship between PM₁₀ and CHF hospital admissions among Medicare beneficiaries. The authors examined the assumption of linearity using fractional polynomials and linear splines. The results of both approaches contributed to Wellenius et al. (2005, [087483](#)) concluding that the assumption of linearity between the log relative risk of cardiovascular hospital admissions and PM concentration was reasonable.

Unlike the aforementioned studies that examined the linearity in the concentration-response curve as part of the model selection process (i.e., to determine the most appropriate model to use to examine the relationship between PM and cardiovascular hospital admissions and ED visits), Zanobetti and Schwartz (2005, [088069](#)) conducted an extensive analysis of the shape of the concentration-response curve and the potential

presence of a threshold when examining the association between PM₁₀ and MI hospital admissions among older adults in 21 U.S. cities. The authors examined the concentration-response curve by fitting a piecewise linear spline with slope changes at 20 µg/m³ and 50 µg/m³. This approach resulted in an almost linear concentration-response relationship between PM₁₀ and MI hospital admissions with a steeper slope occurring below 50 µg/m³ (see Figure 6-6). Additionally, Zanobetti and Schwartz (2005, [088069](#)) found no evidence for a threshold.



Source: Zanobetti and Schwartz (2005, 088069).

Figure 6-6. Combined random-effect estimate of the dose-response relationship between MI emergency hospital admissions and PM₁₀, computed by fitting a piecewise linear spline, with slope changes at 20 µg/m³ and 50 µg/m³.

Overall, the limited evidence from the studies that examined the concentration-response relationship between PM and cardiovascular hospital admissions and ED visits supports a no-threshold, log-linear model, which is consistent with the observations made in studies that examined the PM-mortality relationship (see Section 6.5.2.7).

6.2.10.11. Out of Hospital Cardiac Arrest

One study of out of hospital cardiac death conducted in Seattle, WA (Checkoway et al., 2000, [015527](#)), which reported no association with PM was included in the 2004 PM AQCD (U.S. EPA, 2004, [056905](#)). In the U.S., the survival rate of sudden cardiac arrest is less than

5%. In addition, as discussed above, Zeka et al. (2006, [088749](#)) found that the estimated mortality risk due to short-term exposure to PM₁₀ was much higher for out-of-hospital cardiovascular deaths than for in-hospital cardiovascular deaths. The analysis of studies that examine the association between PM and cardiac arrest could provide evidence for an important link between the morbidity and mortality effects attributed to PM.

Sullivan et al. (2003, [043156](#)) examined the association between the incidence of primary cardiac arrest and daily measures of PM_{2.5} (measured by nephelometry) using a case-crossover analysis of 1,206 Washington State out-of-hospital cardiac arrests (1985-1994) among persons with (n = 774) and without (n = 432) clinically recognized heart disease. The authors examined PM associations at 0- through 2-day lags using the time-stratified referent sampling scheme (i.e., the same day of the week and month of the same year). The estimated relative risk for a 13.8- $\mu\text{g}/\text{m}^3$ increase in 1-day lag PM_{2.5} (nephelometry: IQR = 0.54 km^{-1} *bsp*) was 0.94 (95% CI: 0.88-1.02), or 0.96 (95% CI: 0.91-1.0) per 10 $\mu\text{g}/\text{m}^3$ increase. Similar estimates were reported for 0- or 2-day lags. The presence or absence of clinically recognized heart disease did not alter the result. This finding is consistent with the previous study of cardiac arrest in Seattle (Levy et al., 2001, [017171](#)) that reported no PM association. It is also consistent with the Sullivan et al. (2005, [050854](#)) analysis of PM and onset of MI, and the Sullivan et al. (2007, [100083](#)) analysis of PM and blood markers of inflammation in the elderly population, both of which were conducted in Seattle. Note also that the analysis of the NMMAPS data for the year 1987-1994 also found no PM₁₀ association for all-cause mortality in Seattle. Overall, the results of studies conducted in Seattle consistently found no association between PM and cardiovascular outcomes or all-cause mortality.

Rosenthal et al. (2008, [156925](#)) examined associations between PM_{2.5} and out-of-hospital cardiac arrests in Indianapolis, Indiana for the years 2002-2006 using a case-crossover design with time-stratified referent sampling. Using all the cases (n = 1,374), they found no associations between PM_{2.5} and cardiac arrest in any of the 0 through 3-day lags or multiday averages thereof (e.g., for 0-day lag, OR = 1.02 [CI: 0.94-1.11] per 10 $\mu\text{g}/\text{m}^3$ increase in PM_{2.5}). However, for cardiac arrests witnessed by bystanders (n = 511), they found a significant association with PM_{2.5} exposure (by TEOM, corrected with FRM measurements) during the hour of the arrest (OR = 1.12 [CI: 1.01-1.25] per 10 $\mu\text{g}/\text{m}^3$ increase in PM_{2.5}), and even larger risk estimates for older adults (age 60-75) or those that

presented with asystole. There have been very few PM studies that used hourly PM measurements, and further studies are needed to confirm associations at such time scales.

In Rome, Forastiere et al. (2005, [086323](#)) examined associations between air pollution (particle number concentration, or PNC, PM₁₀, CO, NO₂, and O₃) and out-of-hospital coronary deaths (n = 5,144) for the study period of 1998-2000. A case-crossover design with the time-stratified referent sampling was used to examine the pollution indices at lag 0 through 3 days and the average of 0-1 lags. They found associations between deaths and PNC (lag 0 and 0-1), PM₁₀ (lag 0, 1, and 0-1), and CO (lag 0 and 0-1) but not with NO₂ or O₃. The risk estimate for 0-day lag PM₁₀ was 1.59% (CI: 0.03-3.18) per 10 µg/m³ increase. The older adults (65-74 and 75+ age groups) showed higher risk estimates than the younger (35-64) age group. Because PNC is considered to be associated with UFPs, and CO was also associated with out-of-hospital cardiac arrests, combustion sources were implicated.

In summary, only a few studies have examined out-of-hospital cardiac arrest or deaths. The two studies from Seattle, WA consistently found no association (also consistent with other cardiac effects and mortality studies conducted in that locale); a study in Indianapolis, IN found an association with hourly PM_{2.5} but not daily PM_{2.5}; and a study in Rome found an association with PM₁₀ but also with particle numbers and CO. Because multicity mortality studies examining this association found heterogeneity in PM risk estimates across regions, future studies of out-of-hospital cardiac arrest will need to consider location and the air pollution mixture during their design.

6.2.11. Short-term Exposure to PM and Cardiovascular Mortality

An evaluation of studies that examined the association between short-term exposure to PM_{2.5} and PM_{10-2.5} and mortality provides additional evidence for PM-related cardiovascular health effects. Although the primary analysis in the majority of mortality studies evaluated consists of an examination of the relationship between PM_{2.5} or PM_{10-2.5} and all-cause (non-accidental) mortality, some studies have examined associations with cause-specific mortality including cardiovascular-related mortality.

Multicity mortality studies that examined the PM_{2.5}-cardiovascular mortality relationship on a national scale: Franklin et al. (2007, [091257](#)) – 27 U.S. cities; Franklin et al. (2008, [155779](#)) – 25 U.S. cities; and Zanobetti and Schwartz (2009, [188462](#)) – 112 U.S. cities) have found consistent positive associations between short-term exposure to PM_{2.5} and

cardiovascular mortality ranging from 0.47 to 0.85% per 10 $\mu\text{g}/\text{m}^3$ at lag 0-1 (see Section 6.5). The associations observed on a national scale are consistent with those presented by Ostro et al. (2006, [087991](#)) in a study that examined the PM_{2.5}-mortality relationship in 9 California counties (0.6% [95% CI: 0-1.1] per 10 $\mu\text{g}/\text{m}^3$). Of the multicity studies evaluated, one examined single day lags and found evidence for slightly larger effects at lag 1 compared to the average of lag days 0 and 1 for cardiovascular mortality (94% [95% CI: -0.14 to 2.02] per 10 $\mu\text{g}/\text{m}^3$) (Franklin et al., 2007, [091257](#)). Although the overall effect estimates reported in the multicity studies evaluated are consistently positive, it should be noted that a large degree of variability exists between cities when examining city-specific effect estimates potentially due to differences between cities and regional differences in PM_{2.5} composition (see Figure 6-24). A limited number of studies that examined the PM_{2.5}-cardiovascular mortality association have not conducted extensive analyses of potential confounders, as a result, PM₁₀-mortality studies provide evidence which suggests that PM_{2.5} risk estimates are fairly robust to the inclusion of gaseous copollutants in models. Overall, the cardiovascular PM_{2.5} effects observed were similar to those reported for all-cause (non-accidental) mortality (see Section 6.5), and are consistent with the effect estimates observed in the single- and multicity studies evaluated in the 2004 PM AQCD.

Zanobetti and Schwartz (2009, [188462](#)) also examined PM_{10-2.5} mortality associations in 47 U.S. cities and found evidence for cardiovascular mortality effects (0.32% [95% CI: 0.00-0.64] per 10 $\mu\text{g}/\text{m}$ at lag 0-1) similar to those reported for all-cause (non-accidental) mortality (0.46% [95% CI: 0.21-0.67] per 10 $\mu\text{g}/\text{m}$). In addition, Zanobetti and Schwartz (2009, [188462](#)) reported seasonal (i.e., larger in spring and summer) and regional differences in PM_{10-2.5} cardiovascular mortality risk estimates. A few single-city studies evaluated also reported associations, albeit somewhat larger than the multicity study, between PM_{10-2.5} and cardiovascular mortality in Phoenix, AZ (Wilson et al., 2007, [157149](#)) (3.4-6.6% at lag 1) and Vancouver, CAN (Villeneuve et al., 2003, [055051](#)) (5.4% at lag 0). The difference in the PM_{10-2.5} risk estimates observed between the multi- and single-city studies could be due to a variety of factors including differences between cities and compositional differences in PM_{10-2.5} across regions (see Figure 6-29). Only a small number of studies have examined potential confounding by gaseous copollutants or the influence of model specification on PM_{10-2.5} mortality risk estimates, but the effects are relatively consistent with those studies evaluated in the 2004 PM AQCD.

6.2.12. Summary and Causal Determinations

6.2.12.1. PM_{2.5}

Several studies cited in the 2004 AQCD reported positive associations between short-term PM_{2.5} concentrations and hospital admissions or ED visits for cardiovascular diseases, although few were statistically significant. In addition, U.S. and Canadian-based studies (both multi- and single-city) that examined the PM_{2.5}-mortality relationship reported associations for cardiovascular mortality consistent with those observed for all-cause (nonaccidental) mortality and relatively stronger than those for respiratory mortality. Significant associations were also observed between MI and short-term PM_{2.5} concentration (averaged over 2 or 24 h) as well as decreased HRV in association with PM_{2.5}. Several controlled human exposure and animal toxicological studies demonstrated HRV effects from exposure to PM_{2.5} CAPs, as well as changes in blood coagulation markers. However, the effects in these studies were variable. Arrhythmogenesis was reported for toxicological studies and generally these results were observed in animal models of disease (SH rat, MI, pulmonary hypertension) exposed to combustion-derived PM_{2.5} (i.e., ROFA, DE, metals). One study demonstrated significant vasoconstriction in healthy adults following controlled exposures to CAPs, although this response could not be conclusively attributed to the particles as subjects were concomitantly exposed to relatively high levels of O₃. The results reported for systemic inflammation in toxicological studies were mixed.

A large body of evidence from studies of the effect of PM_{2.5} on hospital admissions and ED visits for cardiovascular diseases has been published since the 2004 PM AQCD. Associations with PM_{2.5} are consistently positive with the majority of studies reporting increases in hospital admissions or ED visits ranging from a 0.5 to 3.4% per 10 µg/m³ increase in PM_{2.5} (Section 6.2.10). The largest U.S.-based multicity study, MCAPs, reported excess risks in the range of approximately 0.7% with the largest excess risks in the North East (1.08%) and in the winter (1.49%), providing evidence of regional and seasonal heterogeneity (Bell et al., 2008, [156266](#); Dominici et al., 2006, [088398](#)). Weak or null findings for PM_{2.5} have been observed in two single-city studies both conducted in Washington state (Slaughter et al., 2003, [086294](#); Sullivan et al., 2007, [100083](#)) and may be explained by this heterogeneity. Weak associations were also reported in Atlanta for PM_{2.5} and CVD ED visits, with PM_{2.5} traffic components being more strongly associated with CVD

ED visits (Tolbert et al., 2007, [090316](#)). Multicity studies conducted outside the U.S. and Canada have shown positive associations with PM_{2.5}. Studies of specific CVD outcomes indicate that IHD and CHF may be driving the observed associations (Sections 6.2.10.3 and 6.2.10.5, respectively). Although estimates from studies of cerebrovascular diseases are less precise and consistent, ischemic diseases appear to be more strongly associated with PM_{2.5} compared to hemorrhagic stroke (Section 6.2.10.7). The available evidence suggests that these effects occur at very short lags (0-1 days), although effects at longer lags have rarely been evaluated. Overall, the results of these studies provide support for associations between short-term PM_{2.5} exposure and increased risk of cardiovascular hospital admissions in areas with mean concentrations ranging from 7 to 18 µg/m³.

Epidemiologic studies that examined the association between PM_{2.5} and mortality provide additional evidence for PM_{2.5}-related cardiovascular effects (Section 6.2.11). The multicity studies evaluated found consistent, precise positive associations between short-term exposure to PM_{2.5} and cardiovascular mortality ranging from 0.47 to 0.85% at mean 24-h avg PM_{2.5} concentrations above 13 µg/m³. These associations were reported at short lags (0-1 days), which is consistent with the associations observed in the HA and ED visit studies discussed above. Although examinations of potential confounders of the PM_{2.5}-cardiovascular mortality relationship are limited, the observed associations are supported by PM₁₀-mortality studies, which found that PM risk estimates remained robust to the inclusion of copollutants in models.

Recent studies that apportion ambient PM_{2.5} into sources and components suggest that cardiovascular hospital admissions associated with PM_{2.5} may be attributable to traffic-related pollution, and in some cases biomass burning (Section 6.2.10). Further supporting evidence is provided by studies that have used PM₁₀ collection filters (median diameter generally <2.5 µm) to identify combustion- or traffic-related sources associated with cardiovascular HA. Metals have also been implicated in these effects (Bell et al., 2009, [191997](#)). A limited number of older publications have reported that particle acidity of PM_{2.5} is not more strongly associated with CVD hospitalizations or ED visits than other PM metrics.

Changes in various measures of cardiovascular function have been demonstrated by multiple independent laboratories following controlled human exposures to different types of PM_{2.5}. The most consistent effect is changes in vasomotor function, which has been demonstrated following exposure to CAPs and DE. The majority of the new evidence of

particle-induced changes in vasomotor function comes from studies of exposures to DE (Section 6.2.4.2). None of these studies have evaluated the effects of DE with and without a particle trap. Therefore, the changes in vasomotor function cannot be conclusively attributed to the particles in DE as subjects are also concomitantly exposed to relatively high levels of NO₂, NO, CO, and hydrocarbons. However, it is important to note that a study by Peretz et al. (2008, [156854](#)) used a newer diesel engine with lower gaseous emissions and reported significant DE-induced decreases in BAD. In addition, increasing the particle exposure concentration from 100 to 200 µg/m³, without proportional increases in NO, NO₂, or CO, resulted in an approximate 100% increase in response. An additional consideration is that while fresh DE used in these studies contains relatively high concentrations of fine particles, the MMAD is typically ≤ 100 nm, which makes it difficult to determine whether the observed effects are due to the fine particles, or more specifically due to the ultrafine fraction. Further evidence of a particle effect on vasomotor function is provided by significant changes in BAD demonstrated in healthy adults following controlled exposure to CAPs with O₃ (Brook et al., 2002, [024987](#)). These findings are consistent with epidemiologic studies of various measures of vasomotor function (e.g., FMD and BAD were the most common), which have demonstrated an association with short-term PM_{2.5} concentration in healthy and diabetic populations (Section 6.2.4.1). A limited number of epidemiologic studies examined multiple lags and the strongest associations were with either the 6 day mean concentration (O'Neill et al., 2005, [098094](#)) or the concurrent day (Schneider et al., 2008, [191985](#)) either the 6 day mean concentration (O'Neill et al., 2005, [098094](#)) or the concurrent day (Schneider et al., 2008, [191985](#)).

The toxicological findings with respect to vascular reactivity are generally in agreement and demonstrate impaired dilation following PM_{2.5} exposure that is likely endothelium dependent (Section 6.2.4.3). These effects have been demonstrated in varying vessels and in response to different PM_{2.5} types, albeit using IT exposure in most studies. Further support is provided by IT studies of ambient PM₁₀ that also demonstrate impaired vasodilation and a PM_{2.5} CAPs study that reported decreased L/W ratio of the pulmonary artery. An inhalation study of Boston PM_{2.5} CAPs reported increases in coronary vascular resistance during ischemia, which indicated a possible role for PM-induced coronary vasoconstriction. The mechanism behind impaired dilation following PM exposure may include increased ROS and RNS production in the microvascular wall that leads to altered NO bioavailability and endothelial dysfunction. Despite the limited number of inhalation

studies conducted with concentrations near ambient levels, the toxicological studies collectively provide coherence and biological plausibility for the myocardial ischemia observed in controlled human exposure and epidemiologic studies.

Consistent with the observed effects on vasomotor function, one recent controlled human exposure study reported an increase in exercise-induced ST-segment depression (a potential indicator of ischemia) during exposure to DE in a group of subjects with prior MI (Mills et al., 2007, [091206](#)). In addition, toxicological studies from Boston that employed CAPs provide further evidence for PM_{2.5} effects on ischemia, with changes in ST-segment and decreases in total myocardial blood flow reported (Section 6.2.3.3). These findings from toxicological and controlled human exposure studies provide coherence and biological plausibility for the associations observed in epidemiologic studies, particularly those of increases in ED visits and hospital admissions for IHD. Several epidemiology studies have reported associations between short-term PM_{2.5} concentration (including traffic sources or components such as BC) and ST-segment depression or abnormality (Section 6.2.3.1).

Toxicological studies provide biological plausibility for the PM_{2.5} associations with CHF hospital admissions by demonstrating increased right ventricular pressure and diminished cardiac contractility in rodents exposed to CB and DE (Section 6.2.6.1). Similarly, increased coronary vascular resistance was observed following PM_{2.5} CAPs exposure in dogs with experimentally-induced ischemia. Further, a recent epidemiology study reported small but statistically significant decreases in passively monitored diastolic pressure and right ventricular diastolic pressure (Rich et al., 2008, [156910](#)).

In addition to the effects of PM on vasomotor response, there is a growing body of evidence that demonstrates changes in markers of systemic oxidative stress following controlled human exposures to DE, WS, and urban traffic particles. However, these effects may be driven in part by the ultrafine fraction of PM_{2.5}. Toxicological studies provide evidence of increased cardiovascular ROS following PM_{2.5} exposure to CAPs, road dust, CB, and TiO₂, as well as increased systemic ROS in rats exposed to gasoline exhaust (Section 6.2.9.3). Epidemiologic studies of markers of oxidative stress (e.g., tHcy, CuZn-SOD, TBARS, 8-oxodG, oxLDL and MDA) are consistent with these toxicological findings (Section 6.2.9.1).

A few epidemiologic studies of ventricular arrhythmias recorded on ICDs that were conducted in Boston and Sweden (Table 6-2) found associations with short-term PM_{2.5} concentration (also BC and sulfate). While Canadian and U.S. studies conducted outside of

Boston did not find positive associations between PM_{2.5} and ICD recorded ventricular arrhythmias, several such studies observed associations with ectopic beats and runs of supraventricular or ventricular tachycardias (Section 6.2.2.1). Toxicological studies also provide limited evidence of arrhythmia, mainly in susceptible animal models (i.e., older rats, rats with chronic heart failure) (Section 6.2.2.2).

Most epidemiologic studies of HRV have reported decreases in SDNN, LF, HF, and rMSSD (Section 6.2.1.1). While there are also a significant number of controlled human exposure studies reporting PM-induced changes in HRV, these changes are often variable and difficult to interpret (Section 6.2.1.2). Similarly, HRV increases and decreases have been observed in animal toxicological studies that employed CAPs or CB (Section 6.2.1.3). In a study in mice, resuspended soil, secondary sulfate, residual oil, and motor vehicle/other sources, as well as Ni were implicated in HRV effects (Lippmann et al., 2006, [091165](#)). Further, cardiac oxidative stress has been implicated as a consequence of ANS stimulation in response to CAPs. Modification of the PM-HRV association by genetic polymorphisms related to oxidative stress has been observed in a series of analyses of the population enrolled in the NAS. Changes in HRV measures (whether increased or decreased) are likely to be more useful as indicators of PM exposure rather than predictive of some adverse outcome. Furthermore, the HRV result may be reflecting a fundamental response of an individual that is determined in part by a number of factors including age and pre-existing conditions.

Although not consistently observed across studies, some investigators have reported PM_{2.5}-induced changes in BP, blood coagulation markers, and markers of systemic inflammation in controlled human exposure studies (Sections 6.2.5.2, 6.2.8.2, and 6.2.9.2, respectively). Findings from epidemiologic studies, which are largely cross-sectional and measure a wide array markers of inflammation and coagulation, are not consistent; however, a limited number of recent studies of gene environment interactions offer insight into potential individual susceptibility to these effects (Ljungman et al., 2009, [191983](#); Peters et al., 2009, [191992](#)). Similarly, toxicological studies demonstrate mixed results for systemic inflammatory markers and generally indicate relatively little change at 16-20 h post-exposure (Section 6.2.7.3). Increases in BP have been observed in toxicological studies (Section 6.2.5.3), with the strongest evidence coming from dogs exposed to PM_{2.5} CAPs. For blood coagulation parameters, the most commonly reported change in animal toxicological

studies is elevated plasma fibrinogen levels following PM_{2.5} exposure, but this response is not consistently observed (Section 6.2.8.3).

In summary, associations of hospital admissions or ED visits with PM_{2.5} for cardiovascular diseases (predominantly IHD and CHF) are consistently positive with the majority of studies reporting increases ranging from a 0.5 to 3.4% per 10 µg/m³ increase in PM_{2.5}. Seasonal and regional variation observed in the large multicity study of Medicare recipients is consistent with null findings reported in several single city studies conducted in the Western U.S. The results from the HA and ED visit studies are supported by the associations observed between PM_{2.5} and cardiovascular mortality, which also provide additional evidence for regional and seasonal variability in PM_{2.5} risk estimates. Changes in various measures of cardiovascular function that may explain these epidemiologic findings have been demonstrated by multiple independent laboratories following controlled human exposures to different types of PM_{2.5}. The most consistent PM_{2.5} effect is on vasomotor function, which has been demonstrated following exposure to CAPs and DE. Toxicological studies finding reduced myocardial blood flow during ischemia and altered vascular reactivity provide coherence and biological plausibility for the myocardial ischemia that has been observed in both controlled human exposure and epidemiologic studies. Further, PM_{2.5} effects on ST-segment depression have been observed across disciplines. In addition to ischemia, PM_{2.5} may act through several other pathways. Plausible biological mechanisms (e.g., increased right ventricular pressure and diminished cardiac contractility) for the associations of PM_{2.5} with CHF have also been proposed based on toxicological findings. There is a growing body of evidence from controlled human exposure, toxicological and epidemiologic studies demonstrating changes in markers of systemic oxidative stress with PM_{2.5} exposure. Inconsistent effects of PM on BP, blood coagulation markers and markers of systemic inflammation have been reported across the disciplines. Together, the collective **evidence is sufficient to conclude that a causal relationship exists between short-term PM_{2.5} exposures and cardiovascular effects.**

6.2.12.2. PM_{10-2.5}

There was little evidence in the 2004 AQCD regarding PM_{10-2.5} cardiovascular health effects. Two single-city epidemiologic studies found positive associations of PM_{10-2.5} with cardiovascular HA in Toronto (Burnett et al., 1999, [017269](#)) and Detroit, MI (Ito, 2003, [042856](#); Lippmann, 2000, [024579](#)) and the effect estimates were of the same general magnitude as for PM₁₀

and PM_{2.5}. Both studies reported positive associations and estimates appeared robust to adjustment for gaseous copollutants in 2-pollutant models. An imprecise, non-significant association between PM_{10-2.5} and onset of MI was observed in Boston (Peters et al., 2001, [016546](#)). No controlled human exposure or toxicological studies of PM_{10-2.5} were presented in the 2004 AQCD.

Several recent epidemiologic studies of the effect of ambient PM_{10-2.5} concentration on hospital admissions or ED visits for cardiovascular diseases were conducted (Section 6.2.10). In a study of Medicare patients in 108 U.S. counties, Peng et al. (2008, [156850](#)) reported a significant association between PM_{10-2.5} and cardiovascular disease hospitalizations in their single pollutant model. In a study of six French cities, Host et al. (2008, [155852](#)) reported a significant increase in IHD hospital admissions in association with PM_{10-2.5}. In contrast, associations of cardiovascular outcomes with PM_{10-2.5} were weak for CHF and null for IHD in the Atlanta-based SOPHIA study (Metzger et al., 2004, [044222](#)). Results from single city studies are generally positive but effect sizes are heterogeneous and estimates are imprecise (Section 6.2.10). Crustal material from a dust storm in the Gobi desert that was largely coarse PM (generally indicated using PM₁₀) was associated with hospitalizations for cardiovascular diseases including IHD and CHF in most studies (Section 6.2.10). Mean PM_{10-2.5} concentrations in the hospital admission and ED visit studies ranged from 7.4-13 µg/m³. A few epidemiologic studies that examined the association between short-term exposure to PM_{10-2.5} and cardiovascular mortality (Section 6.2.11) provide supporting evidence for the hospital admission and ED visit studies at similar 24-h avg PM_{10-2.5} concentrations (i.e., 6.1-16.4 µg/m³). A multicity study reported risk estimates for cardiovascular mortality of similar magnitude to those for all-cause (nonaccidental) mortality (Zanobetti and Schwartz, 2009, [188462](#)). However, the single-city studies evaluated (Wilson et al., 2007, [157149](#); Villeneuve et al., 2003, [055051](#)) reported substantially larger effect estimates, but this could be due to differences between cities and compositional differences in PM_{10-2.5} across regions. Of note is the lack of analyses within the studies evaluated that examined potential confounders of the PM_{10-2.5}-cardiovascular mortality relationship.

The U.S. study of Medicare patients (Peng et al., 2008, [156850](#)) and the multicity study that examined the association between PM_{10-2.5} and mortality (Zanobetti and Schwartz, 2009, [188462](#)) were the only studies to adjust PM_{10-2.5} for PM_{2.5}. Peng, et al. (2008, [156850](#)) found that the PM_{10-2.5} association with cardiovascular disease

hospitalizations remained, but diminished slightly after adjustment for PM_{2.5}. These results are consistent with those reported by Zanobetti and Schwartz (2009, [188462](#)), which found PM_{10-2.5}-cardiovascular mortality risk estimates remained relatively robust to the inclusion of PM_{2.5} in the model. Because of the greater spatial heterogeneity of PM_{10-2.5}, exposure measurement error is more likely to bias health effect estimates towards the null for epidemiologic studies of PM_{10-2.5} versus PM₁₀ or PM_{2.5}, making it more difficult to detect an effect of the coarse size fraction. In addition, models that include both PM_{10-2.5} and PM_{2.5} may suffer from instability due to collinearity. Further, the lag structure of PM_{10-2.5} effects on risk of cardiovascular hospital admissions and ED visits, as well as mortality, has not been examined in detail.

Several epidemiologic studies of cardiovascular endpoints including HRV, BP, ventricular arrhythmia, and ECG changes indicating ectopy or ischemia were conducted since publication of the 2004 PM AQCD. Supraventricular ectopy and ST-segment depression were associated with PM_{10-2.5} (Section 6.2.3.1) and the only study to examine the effect of PM_{10-2.5} on BP reported a decrease in SBP (Ebelt et al., 2005, [056907](#)) (Section 6.2.5.1). HRV findings were mixed across the epidemiologic studies (Section 6.2.1.1). A limited number of studies have evaluated the effect of controlled exposures to PM_{10-2.5} CAPs on cardiovascular endpoints in human subjects. These studies have provided some evidence of decreases in HRV (SDNN) and tPA concentration among healthy adults approximately 20 hours following exposure (Section 6.2.1.2). However, it is important to note that no other measures of HRV (e.g., LF, HF, or LF/HF), nor other hemostatic or thrombotic markers (e.g., fibrinogen) were significantly affected by particle exposure in these studies.

There are very few toxicological studies that examined the effect of exposure to PM_{10-2.5} on cardiovascular endpoints or biomarkers in animals. The only studies that evaluated cardiovascular responses were comparative studies of various size fractions and only blood or plasma parameters were measured (Sections 6.2.7.3 and 6.2.8.3). These studies used IT instillation methodologies, as there are challenges to exposing rodents via inhalation to PM_{10-2.5}, due to near 100% deposition in the ET region for particles >5 μm (Raabe et al., 1988, [001439](#)) and only 44% nasal inhalability of a 10 μm particle in the rat (Ménache et al., 1995, [006533](#)). These studies also employed relatively high doses of PM_{10-2.5}. Despite these shortcomings, increased plasma fibrinogen was observed and the response was similar to that observed with PM_{2.5}. At this time, evidence of biological plausibility for cardiovascular morbidity effects following PM_{10-2.5} exposure is sparse, due to

the small number of studies, few endpoints examined, and the limitations related to the interpretation of IT exposures.

In summary, several epidemiologic studies report associations with cardiovascular endpoints including IHD hospitalizations, supraventricular ectopy, and changes in HRV. In studies examining multiple size fractions, most of the effect estimates observed were of a similar magnitude (e.g., the PM_{2.5} effect was not larger in all studies). Further, dust storm events resulting in high concentrations of crustal material are linked to increases in cardiovascular disease hospital admissions or ED visits for cardiovascular diseases. A large proportion of inhaled coarse particles in the 3-6 μm (d_{ae}) range can reach and deposit in the lower respiratory tract, particularly the TB airways (see Figures 4-3 and 4-4). The few toxicological and controlled human exposure studies examining the effects of PM_{10-2.5} provide limited evidence of cardiovascular effects and biological plausibility to support the epidemiologic findings. Therefore the available evidence is **suggestive of a causal relationship between PM_{10-2.5} exposures and cardiovascular morbidity.**

6.2.12.3. Ultrafine PM

There was very little evidence available in the 2004 PM AQCD (U.S. EPA, 2004, [056905](#)) on the cardiovascular effects of ultrafine PM. Findings from one study presented in the 2004 PM AQCD (U.S. EPA, 2004, [056905](#)) of controlled exposures to ultrafine elemental carbon suggested no particle-related effects on various cardiovascular endpoints including blood coagulation, HRV, and systemic inflammation. No epidemiologic studies of short-term ultrafine particle concentration and cardiovascular endpoints were included in the 2004 AQCD and there were no relevant toxicological studies reviewed in the 2004 PM AQCD (U.S. EPA, 2004, [056905](#)) that exposed animals to ultrafine PM. A small number of new epidemiologic studies, as well as several controlled human exposure and toxicological studies have been conducted in recent years, but substantial uncertainties remain as to the cardiovascular effects of ultrafine PM. For a given mass, the enormous number and large surface area of UFPs highlight the importance of considering the size of the particle in assessing response. For example, UFPs with a diameter of 20 nm, when inhaled at the same mass concentration, have a number concentration that is approximately 6 orders of magnitude higher than for a 2.5-μm diameter particle. Particle surface area is also greatly increased with ultrafine PM. Many studies suggest that the surface of particles or substances released from the surface (e.g., transition metals, organics) interact with

biological substrates, and that surface-associated free radicals or free radical-generating systems may be responsible for toxicity, resulting in greater toxicity of ultrafine PM per particle surface area than larger particles. Additionally, smaller particles may have greater potential to cross cell membranes and epithelial barriers.

Controlled human exposure studies are increasingly being utilized to evaluate the effect of ultrafine PM on cardiovascular function. While the number of studies of exposure to UFPs per se is still limited, there is a large body of evidence from exposure to fresh DE, which is typically dominated by UFPs. As described under the summary for PM_{2.5}, studies of controlled exposures to DE (100-300 µg/m³) have consistently demonstrated effects on vasomotor function among adult volunteers (Section 6.2.4.2). In addition, exposure to ultrafine EC (50 µg/m³, particle count 10.8 × 10⁶/cm³) was recently shown to attenuate FMD (Shah et al., 2008, [156970](#)). Changes in vasomotor function have been observed in animal toxicological studies of ultrafine PM, although very few studies have been conducted (Section 6.2.4.3). Inhaled ultrafine TiO₂ impaired arteriolar dilation when compared to fine TiO₂ at similar mass doses (Nurkiewicz et al., 2008, [156816](#)). This response may have been due to ROS in the microvascular wall, which may have led to consumption of endothelial-derived NO and generation of peroxynitrite radicals. Support for an ultrafine PM effect on altered vascular reactivity is also provided by studies of DE and IT exposure to ambient PM. The response to DE did not appear to be due to VOCs. One epidemiologic study showed that particle number count was associated with a nonsignificant decrease in flow- and nitroglycerine-mediated reactivity as measures of vasomotor function in diabetics living in Boston (O'Neill et al., 2005, [088423](#)).

New studies have reported increases in markers of systemic oxidative stress in humans following controlled exposures to different types of PM consisting of relatively high concentrations of UFPs from sources including WS, urban traffic particles, and DE (Section 6.2.9.2). Increased cardiac oxidative stress has been observed in mice and rats following gasoline exhaust exposure and it appeared the effect was particle-dependent (Section 6.2.9.3).

The associations between ultrafine PM and HRV measures in epidemiologic studies include increases and decreases (Section 6.2.1.1), providing some evidence for an effect. Exposure to ultrafine CAPs has been observed to alter parameters of HRV in controlled human exposure studies, although this effect has been variable between studies (Section 6.2.1.2). Alterations in HR, HRV, and BP were reported in rats exposed to <200 µg/m³

ultrafine CB ($<1.6 \times 10^7$ particles/cm³) (Sections 6.2.1.3 and 6.2.5.3). The effects of ultrafine PM on BP have been mixed in epidemiologic studies (Section 6.2.5.1).

There is some evidence of changes in markers of blood coagulation in humans following controlled exposure to ultrafine CAPs, as well as WS and DE; however, these effects have not been consistently observed across studies (Section 6.2.8.2). Toxicological studies demonstrate mixed results for systemic inflammation and blood coagulation as well (Sections 6.2.7.3 and 6.2.8.3).

Few time-series studies of cardiovascular hospital admissions have evaluated ultrafine PM. The SOPHIA study found no association between any outcome studied (all CVD, dysrhythmia, CHF, IHD, peripheral vascular and cerebrovascular disease) and 24-h mean levels of UFP (Metzger et al. 2004). The median UF particle count in Atlanta during the study period was 25,900 particles/cm³. UFP were not associated with CVD hospitalizations in the elderly in Copenhagen, Denmark, but were associated with cardiac readmission or fatal MI in the European HEAPSS study (Section 6.2.10). In the Copenhagen study, the mean count of particles with a 100 nm mean diameter was 0.68×10^4 particles/cm³, whereas the PNC range was approximately $1.2\text{-}7.6 \times 10^4$ particles/cm³ in HEAPSS study. Spatial variation in UFP concentration, which diminishes within a short distance from the roadway, may introduce exposure measurement error, making it more difficult to observe an association if one exists.

A limited number of epidemiologic studies have evaluated subclinical cardiovascular measures and a number of these were conducted in Boston. Ultrafine PM has been linked to ICD-recorded arrhythmias in Boston and supraventricular ectopic beats in Erfurt, Germany (Section 6.2.2.1). One study reported no UFP association with ectopy (Barclay et al., 2009, [179935](#)). ST-segment depression in subjects with stable coronary heart disease was associated with ultrafine PM in Helsinki (Section 6.2.3.1). The limited number of studies that examine this size fraction makes it difficult to draw conclusions about these cardiovascular measures.

In summary, there is a large body of evidence from controlled human exposure studies of fresh DE, which is typically dominated by UFPs, demonstrating effects of UFP on the cardiovascular system. In addition, cardiovascular effects have been demonstrated by a limited number of laboratories in response to ultrafine CB, urban traffic particles and CAPs. Responses include altered vasomotor function, increased systemic oxidative stress and altered HRV parameters. Studies using ultrafine CAPs, as well as WS and DE, provide

some evidence of changes in markers of blood coagulation, but findings are not consistent. Toxicological studies conducted with ultrafine TiO₂, CB, and DE demonstrate changes in vasomotor function as well as in HRV. Effects on systemic inflammation and blood coagulation are less consistent. PM-dependent cardiac oxidative stress was noted following exposure to gasoline exhaust. The few epidemiologic studies of ultrafine conducted do not provide strong support for an association of UFPs with effects on the cardiovascular system. Based on the above findings, the **evidence is suggestive of a causal relationship between ultrafine PM exposure and cardiovascular effects.**

6.3. Respiratory Effects

6.3.1. Respiratory Symptoms and Medication Use

The 2004 PM AQCD (U.S. EPA, 2004, [056905](#)) presented evidence from epidemiologic studies of increases in respiratory symptoms associated with PM, although this was not supported by the findings of a limited number of controlled human exposure studies. Recent epidemiologic studies have provided evidence of an increase in respiratory symptoms and medication use associated with PM among asthmatic children, with less evidence of an effect in asthmatic adults. The lack of an observed effect of PM exposure on respiratory symptoms in controlled human exposure studies does not necessarily contradict these findings, as very few studies of controlled exposures to PM have been conducted among groups of asthmatic or healthy children.

6.3.1.1. Epidemiologic Studies

The 2004 PM AQCD (U.S. EPA, 2004, [056905](#)) concluded that the effects of PM₁₀ on respiratory symptoms in asthmatics tended to be positive, although they were somewhat less consistent than PM₁₀ effects on lung function. Most studies showed increases in cough, phlegm, difficulty breathing, and bronchodilator use, although these increases were generally not statistically significant for PM₁₀. The results from one study of respiratory symptoms and thoracic coarse particles (Schwartz and Neas, 2000, [007625](#)) found a statistically significant association with cough with PM_{10-2.5}. The results of two studies examining respiratory symptoms and PM_{2.5} revealed slightly larger effects for PM_{2.5} than for PM₁₀.

Asthmatic Children

Two large, longitudinal studies in urban areas of the U.S. investigated the effects of ambient PM on respiratory symptoms and/or asthma medication use with similar analytic techniques (i.e., multistaged modeling and generalized estimating equations [GEE]): the Childhood Asthma Management Program (CAMP) (Schildcrout et al., 2006, [089812](#)) and the National Cooperative Inner-City Asthma Study (NCICAS) (Mortimer et al., 2002, [030281](#)). A number of smaller panel studies conducted in the U.S. evaluated the effects of ambient PM concentrations on respiratory symptoms and medication use among asthmatic children (Delfino et al., 2002, [093740](#); Delfino et al., 2003, [090941](#); Delfino et al., 2003, [050460](#); Gent et al., 2003, [052885](#); Gent et al., 2009, [180399](#); 2006, [088031](#); Slaughter et al., 2003, [086294](#)).

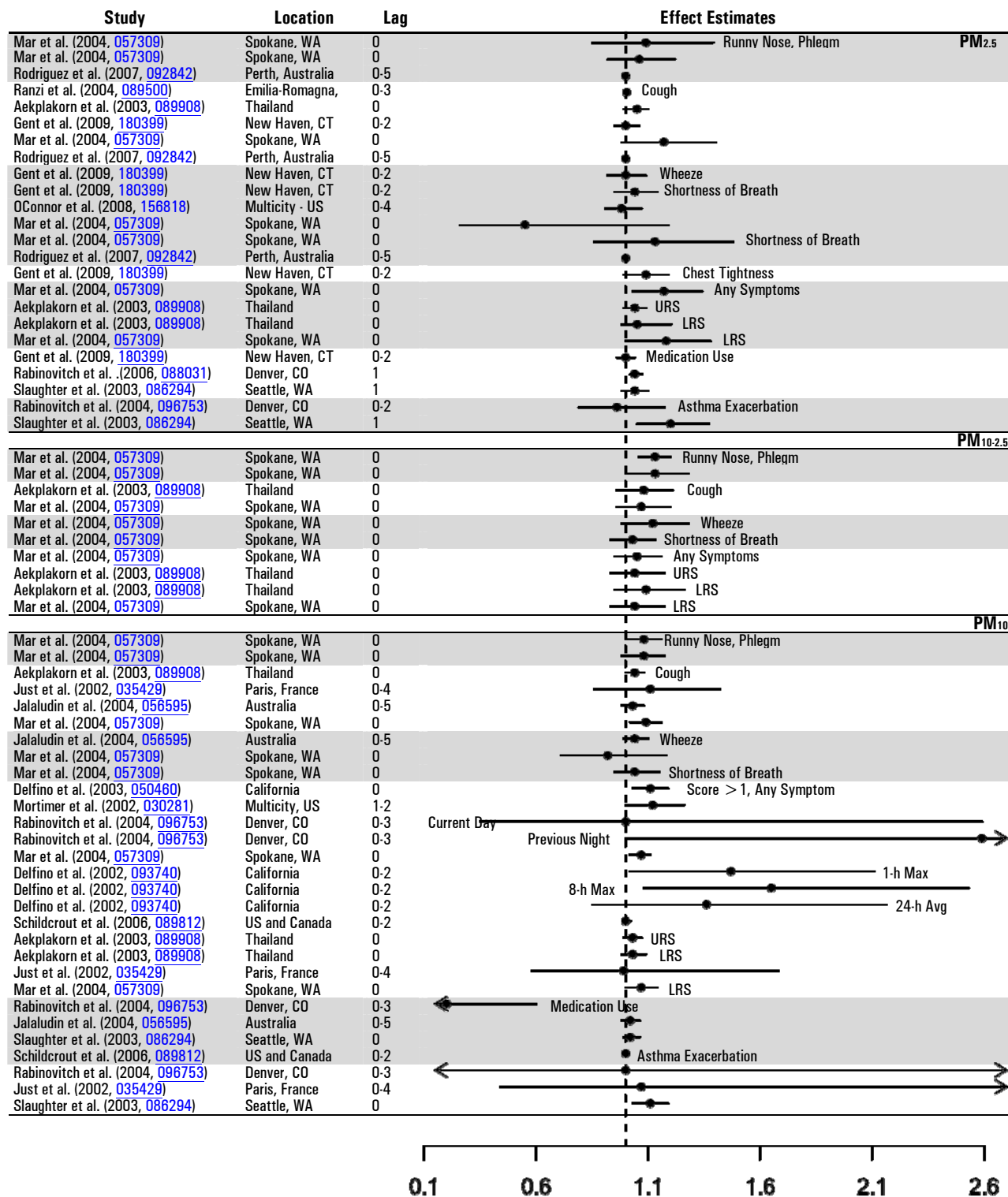


Figure 6-7. Respiratory symptoms and/or medication use among asthmatic children following acute exposure to PM_{2.5}. ORs and 95% CIs standardized to increments of 10 µg/m³.

In the CAMP study, the association between ambient air pollution and asthma exacerbations in children (n = 990) from eight North American cities was investigated (Schildcrout et al., 2006, [089812](#)). In contrast to several past studies (Delfino et al., 1996, [080788](#); 1998, [051406](#)), no associations were observed between PM₁₀ and asthma exacerbations or medication use. PM₁₀ concentrations were measured on less than 50% of study days in all cities except Seattle and Albuquerque. While PM₁₀ effects were not observed for the entire panel of children, they were observed in recent reports on the children participating at the Seattle center (Slaughter et al., 2003, [086294](#); Yu et al., 2000, [013254](#)). In a smaller panel study of asthmatic children (n = 133) enrolled in the CAMP study, daily particle concentrations averaged over 3 central sites in Seattle was used as the exposure metric (Slaughter et al., 2003, [086294](#)). Children were followed for 2 months, on average. Daily health outcomes included both a 3-category measure of asthma severity based on symptom duration and frequency, and inhaled albuterol use. In single-pollutant models, an increased risk of asthma severity was associated with a 10 µg/m³ increase in lag 1 PM_{2.5} (OR 1.20 [95% CI: 1.05-1.37]) and with a 10 µg/m³ increase in lag 0 PM₁₀ (OR 1.12 [95% CI: 1.05-1.22]). In copollutant models with CO, the associations remained (OR for PM_{2.5} 1.16 [95% CI: 1.03-1.30]; OR for PM₁₀ 1.11 [95% CI: 1.03-1.19]). Associations between inhaler use and PM were positive in single-pollutant models (RR lag 1 PM_{2.5} 1.08 [95% CI: 1.01-1.15]; RR lag 0 PM₁₀ 1.05 [95% CI: 1.00-1.09]), but attenuated and no longer statistically significant in copollutant models.

The eight cities included in the NCICAS (Mortimer et al., 2002, [030281](#)) were all in the East or Midwest: New York City (Bronx, E. Harlem), Baltimore, Washington DC, Cleveland, Detroit, St. Louis, and Chicago. In this study, 864 asthmatic children, aged 4-9 yr, were followed daily for four 2-wk periods over the course of nine months. Morning and evening asthma symptoms (analyzed as none vs. any) and peak flow were recorded. For the three urban areas with data, each 10 µg/m³ increase in the mean of the previous 2 days (lag 1-2) PM₁₀, increased the risk for morning asthma symptoms (OR 1.12 [95% CI: 1.00-1.26]). This effect was robust to the inclusion of O₃ (OR 1.12 [95% CI: 0.98-1.27]), though attenuated in models including O₃, SO₂, and NO₂ (OR 1.07 [95% CI: 0.89-1.22]). In a related study, O'Connor et al. (2008, [156818](#)) examined the relationship between short-term fluctuations in outdoor air pollutant concentrations and changes in pulmonary function and respiratory symptoms among children with asthma in 7 U.S. inner-city communities. PM_{2.5} concentration was not significantly associated with respiratory symptoms in this study.

Table 6-7. Characterization of ambient PM concentrations from studies of respiratory morbidity and short-term exposures in asthmatic children and adults. All concentrations are for the 24-h avg unless otherwise noted.

Reference	Location	Mean Concentration ($\mu\text{g}/\text{m}^3$)	Upper Percentile Concentrations ($\mu\text{g}/\text{m}^3$)
<i>PM_{2.5}</i>			
Adamkiewicz et al. (2004, 087925)	Steubenville, OH	20.43	75th: 23 98th: 51.79 Max: 51.79
Adar et al. (2007, 001458)	St. Louis, MO	10.13	98th: 22.43 Max: 23.24
Aekplakorn et al. (2003, 089908)	North Thailand		Max: 24.8-26.3
Allen et al. (2008, 156208)	Seattle, WA	11.2	
Barraza-Villarreal et al. (2008, 156254)	Mexico City	8-h max: 28.9	Max: 102.8
Bourotte et al. (2007, 150040)	Sao Paulo, Brazil	11.9	Max: 26.6
de Hartog et al. (2003, 001061)	Multicity, Europe	12.8-23.4	Max: 39.8-118.1
Delfino et al. (2006, 090745)	Southern CA	3.9-6.9	Max: 8.8-11.6
DeMeo et al. (2004, 087346)	Boston, MA	10.8	
Ebelt et al. (2005, 056907)	Vancouver, Canada	11.4	98th: 23 Max: 28.7
Ferdinands et al. (2008, 156433)	Atlanta, GA	27.2	Max: 34.7
Fischer et al. (2007, 156435)	The Netherlands	56	75th: 187
Gent et al. (2003, 052885)	CT & MA	13.1	60th: 12.1 80th: 19.0
Gent et al. (2009, 180399)	New Haven, CT	17.0	
Girardot et al. (2006, 088271)	Smoky Mountains	13.9	Max: 38.4
Hogervorst et al. (2006, 189460)	The Netherlands	19.0	
Hong et al. (2007, 091347)	Incheon City, Korea	20.27	Max: 36.28
Jansen et al. (2005, 082236)	Seattle, WA	14.0	Max: 44
Johnston et al. (2006, 091386)	Darwin, Australia	11.1	Max: 36.5
Koenig et al. (2003, 156653)	Seattle, WA	13.3	Max: 40.4
Lagorio et al. (2006, 089800)	Rome, Italy	27.2	Max: 100
Lee et al. (2007, 093042)	Seoul, South Korea	51.15	75th: 87.54 Max: 92.71
Lewis et al. (2004, 097498)	Detroit, MI	15.7-17.5	Max: 56.1
Liu et al. (2009, 192003)	Windsor, Ontario	7.1	95th: 19.0 98th: 19.0.
Mar et al. (2004, 057309)	Spokane, WA	8.1-11.0	
Mar et al. (2005, 088759)	Seattle, WA	5-26	
McCreanor et al. (2007, 092841)	London, England	1-h avg: 11.9-28.3	1-h max: 55.9-76.1
Moshammer et al. (2006, 090771)	Linz, Austria	8-h avg: 15.70	Max 24-h avg: 76.39
Murata et al. (2007, 156787)	Tokyo, Japan	39.0	Max 1-h avg: 120

Reference	Location	Mean Concentration ($\mu\text{g}/\text{m}^3$)	Upper Percentile Concentrations ($\mu\text{g}/\text{m}^3$)
O'Connor et al. (2008, 156818)	Multicity, U.S.	14	Max: 35
Peled et al. (2005, 156015)	Multicity, Israel	23.9-29.2	
Penttinen et al. (2006, 087988)	Helsinki, Finland	8.37	75th: 11.15 Max: 33.53
Rabinovitch et al. (2004, 096753)	Denver, CO	10.8	98th: 29.3 Max: 53.5
Rabinovitch et al. (2006, 088031)	Denver, CO	10.8	98th: 23.4
Ranzi et al. (2004, 089500)	Emilia-Romagna, Italy	Urban: 53.07 Rural: 29.11	
Rodriguez et al. (2007, 092842)	Perth, Australia	1-h avg: 20.8 24-h avg: 8.5	Max 1-h avg: 93.4 Max 24-h avg: 39.4
Slaughter et al. (2003, 086294)	Seattle, WA	7.3 ^a	75th: 11.3
Strand et al. (2006, 157017)	Denver, CO	12.7	
Timonen et al. (2004, 087915)	Multicity, Europe	12.7-23.1	Max: 39.8-118.1
Trenga et al. (2006, 155209)	Seattle, WA	8.6-9.6 ^a	75th: 13.1-14.8 Max: 40.4-41.5
von Klot et al. (2002, 034706)	Erfurt, Germany	30.3 ^b	75th: 41.3 ^b Max: 133.8 ^b
Ward et al. (2002, 025839)	Birmingham and Sandwell, U.K.	12.3-12.7	Max: 28-37
PM_{10-2.5}			
Aekplakorn et al. (2003, 089908)	North Thailand	NR	NR
Bourotte et al. (2007, 150040)	Sao Paulo, Brazil	21.7	Max: 62.0
Ebelt et al. (2005, 056907)	Vancouver, Canada	5.6	Max: 11.9
Lagorio et al. (2006, 089800)	Rome, Italy	15.6	Max: 39.6
Mar et al. (2004, 057309)	Spokane, WA	8.7-13.5	
von Klot et al. (2002, 034706)	Erfurt, Germany	10.3	75th: 14.6 Max: 64.3
PM₁₀			
Aekplakorn et al. (2003, 089908)	North Thailand	31.9-37.5	Max: 113.3-153.3
Boezen et al. (2005, 087396)	The Netherlands	26.6-44.1	Max: 89.9-242.2
de Hartog et al. (2003, 001061)	Multicity, Europe	19.6-36.5	Max: 67.4-112.0
Delfino et al. (2002, 093740)	Alpine, CA	20	90th: 32 Max: 42
Delfino et al. (2003, 050460)	Los Angeles, CA	59.9	90th: 86/0/Max: 126
Delfino et al. (2004, 056897)	Alpine, CA	29.7	90th: 40.9 Max: 50.7
Delfino et al. (2006, 090745)	Southern CA	35.7-70.8	Max: 105.5-154.1
Desqueyroux et al. (2002, 026052)	Paris, France	23-28	Max: 63-84
Ebelt et al. (2005, 056907)	Vancouver, Canada	17	Max: 36
Hong et al. (2007, 091347)	Incheon City, Korea	35.3	Max: 124.87
Jalaludin et al. (2004, 056595)	Sydney, Australia	22.8	75th: 122.8
Jansen et al. (2005, 082236)	Seattle, WA	18.0	Max: 51
Johnston et al. (2006, 091386)	Darwin, Australia	20	Max: 43.3

Reference	Location	Mean Concentration ($\mu\text{g}/\text{m}^3$)	Upper Percentile Concentrations ($\mu\text{g}/\text{m}^3$)
Just et al. (2002, 035429)	Paris, France	23.5	Max: 44.0
Lagorio et al. (2006, 089800)	Rome, Italy	42.8	Max: 123
Laurent et al. (2008, 156672)	Strasbourg, France	20.8	Max: 106.3
Lee et al. (2007, 093042)	Seoul, South Korea	71.40	75th: 87.54 Max: 148.34
Mar et al. (2004, 057309)	Spokane, WA	16.8-24.5	
Mortimer et al. (2002, 030281)	Multicity, UC	53	
Moshammer et al. (2006, 090771)	Linz, Austria	8-h avg: 24.85	Max 24-h: 76.39
Odajima et al. (2008, 192005)	Fukuoka, Japan	3-h avg: 32.6-41.5	Max 3-h avg: 126.0-191.3
Peacock et al. (2003, 042026)	Southern England	21.2	Max: 87.9
Peled et al. (2005, 156015)	Multicity, Israel	31.0-67.1	
Preutthipan et al. (2004, 055598)	Bangkok, Thailand	111.0	Max: 201
Rabinovitch et al. (2004, 096753)	Denver, CO	28.1	Max: 102.0
Ségala et al. (2004, 090449)	Paris, France	24.2	Max: 97.4
Schildcrout et al. (2006, 089812)	Multicity, U.S.	17.7-32.4 ^a	75th: 26.2-42.7 90th: 32.5-53.9
Slaughter et al. (2003, 086294)	Seattle, WA	21.0 ^b	75th: 29.3
Steinvil et al. (2008, 188893)	Tel Aviv, Israel	64.5	75th: 60.7
von Klot et al. (2002, 034706)	Erfurt, Germany	45.4	75th: 59.7 Max: 172.4

^aMedian

^bIncludes UFP, for complete information on number concentration from this study, please see corresponding table in Annex E.

Mar et al. (2004, [057309](#)) studied asthmatic children ($n = 9$) in Spokane, WA. Increases in 0, 1 or 2 day lags of each of the PM size classes studied were associated with cough. When all lower respiratory tract symptoms (wheeze, cough, shortness of breath, sputum production) were grouped together, positive associations were reported for each $10 \mu\text{g}/\text{m}^3$ increase in same-day PM_{10} (OR 1.07 [95% CI: 1.00-1.14]), or lag 0 or lag 1 $\text{PM}_{2.5}$ (OR 1.18 [95% CI: 1.00-1.38]; OR 1.21 [95% CI: 1.00-1.46], respectively), and $10 \mu\text{g}/\text{m}^3$ increase in lag 0 and lag 1 $\text{PM}_{1.0}$ (OR 1.21 [95% CI: 1.01-1.44]; OR 1.25 [95% CI: 1.01-1.55], respectively). No associations were reported for $\text{PM}_{10-2.5}$ and grouped lower respiratory tract symptoms (Mar et al., 2004, [057309](#)).

Gent et al. (2003, [052885](#)) reported on daily symptom and medication use during one summer for 271 asthmatic children living in southern New England. In single-pollutant models for users of maintenance medication ($n = 130$), $\text{PM}_{2.5} \geq 19 \mu\text{g}/\text{m}^3$ lagged by 1 day was associated with a 10 to 25% increase in risk of symptoms compared to $\text{PM}_{2.5} < 6.9 \mu\text{g}/\text{m}^3$: OR for persistent cough 1.12 (95% CI: 1.02-1.24); OR for chest tightness 1.21 (95% CI: 1.00-1.46); OR for shortness of breath 1.26 (95% CI: 1.02-1.54). Effects were attenuated in

models including O₃ (OR for persistent cough 1.00 95% CI: 0.88-1.15]; OR for chest tightness 0.91 [95% CI: 0.71-1.17]; OR for shortness of breath 1.20 [95% CI: 0.94-1.52]). No statistical associations between ambient particle exposure and respiratory health were found for asthmatic children not on maintenance medication.

Annual PM_{2.5} levels at monitoring sites in New Haven, CT exceed the annual standard of 15 µg/m³. Gent et al. (2009, [180399](#)) conducted a study here to examine the associations between daily exposure to PM_{2.5} components and sources identified through source apportionment, and daily symptoms and medication use in asthmatic children. Asthmatic children (n = 149) aged 4-12 yr were enrolled in the study between 2000 and 2003. Factor analysis was used to identify six sources of PM_{2.5} (motor vehicle, road dust, sulfur, biomass burning, oil, and sea salt). Total PM_{2.5} was not associated with any symptoms or medication use, however trace elements originating from motor vehicle, road dust, biomass burning and oil sources were associated with symptoms and/or medication use. For example, an increased risk of wheeze, shortness of breath, chest tightness or short-acting inhaler use was associated with increasing EC mass concentration. Risks remain in models that include all six PM_{2.5} sources as well as NO₂, which may be considered a marker for traffic. NO₂ was found to be an independent risk factor for increased wheeze.

Two panel studies were conducted over the course of three winters at a school in Denver (Rabinovitch et al., 2004, [096753](#); Rabinovitch et al., 2006, [088031](#)). In the first report, approximately 86 different children contributed data on asthma symptoms and medication use over three consecutive winters (Rabinovitch et al., 2004, [096753](#)). The exposure metric was a 3-day ma of PM_{2.5} measured at a site located next to the school for the first 2 winters and from a central site located 4.8 km (3 miles) away for the third. A strong correlation was observed during the first two winters between PM_{2.5} values measured locally and at a downtown monitoring station (Pearson product-moment correlation = 0.93) and between PM₁₀ values measured locally and at a downtown monitoring station (correlation = 0.84). Therefore, in year 3, all ambient data were collected from nearby community monitoring stations. No statistical associations were found between asthma symptoms or medication use and PM. Rabinovitch et al. (2006, [088031](#)) enrolled a panel of 73 children and evaluated associations with morning maximum PM_{2.5} measured at the central site. PM measurements were available hourly from 2 co-located monitors, an FRM and a TEOM monitor. Each 10 µg/m³ increase in morning maximum 1-h PM_{2.5} concentration was associated with an increased likelihood of rescue medication use

(OR for FRM exposure data 1.02 [95% CI: 1.01-1.03]; OR for TEOM 1.03 [95% CI: 1.00-1.6]). Interestingly, the association between inhaler use and particle exposure was not evident when the 24-h avg PM_{2.5} was used in the model.

Two smaller panel studies enrolling asthmatic children conducted by Delfino et al. (2002, [093740](#); 2003, [050460](#)) in southern California examined the health effects of different averaging times for PM₁₀ (1-h, 8-h, 24-h) (Delfino et al., 2002, [093740](#)), and 24-h avg of two PM₁₀ components (EC and OC) (Delfino et al., 2003, [050460](#)). In the first study, 22 children living in a “lower” pollution area were followed daily for two months in spring. In contrast with Gent et al. (2003, [052885](#)), positive statistical associations with asthma symptoms (measured on a 6-point severity scale) were found only for the children not taking anti-inflammatory medication. For these 12 children, in single-pollutant models each 10 µg/m³ increase in lag 0 1-h max PM₁₀ nearly doubled the risk of clinically meaningful symptoms (i.e., an asthma symptom score ≥ 3) (OR 1.14 [95% CI: 1.04-1.24]) and each 10 µg/m³ increase in 3-day avg 24-h PM₁₀ increased the risk by 1.25 (95% CI: 1.06-1.48). No statistical associations were found between exposure to ambient particles and symptoms in the 10 children who were taking anti-inflammatory medication. No multipollutant models were reported. The second study enrolled 22 asthmatic children living in an area of higher pollution. For children living in this community, each 10 µg/m³ increase in lag 0, 24-h PM₁₀ was associated with an increased risk of asthma symptom score >1: OR 1.10, (95% CI: 1.03-1.19) (Delfino et al., 2003, [050460](#)). The correlation among PM₁₀, EC and OC was substantial: 0.80 between PM₁₀ and either EC or OC, and 0.94 between EC and OC. Associations between EC or OC and asthma symptoms were very similar to those for PM₁₀: each 3 µg/m³ increase in lag 0, 24-h EC or 5 µg/m³ increase in lag 0, 24-h OC was associated with an increased risk of asthma symptoms (OR 1.85 [95% CI: 1.11-3.08] or OR 1.88 [95% CI: 1.12-3.17], respectively) (Delfino et al., 2003, [050460](#)).

Studies from Australia (Rodriguez et al., 2007, [092842](#)), Europe (Laurent et al., 2008, [156672](#); Ranzi et al., 2004, [089500](#); Laurent et al., 2009, [192129](#)), and Asia (Aekplakorn et al., 2003, [089908](#)) provide additional evidence of an association between ambient PM and respiratory symptoms and/or medication use among asthmatic children. Two studies (Jalaludin et al., 2004, [056595](#); Just et al., 2002, [035429](#)) found no association between ambient PM levels and these health endpoints.

Asthmatic Adults

Since the 2004 PM AQCD (U.S. EPA, 2004, [056905](#)), one U.S. and several European studies have investigated the effects of ambient PM levels on respiratory symptoms and medication use among asthmatic adults. The respiratory symptom and medication use results from these studies are summarized by particle size and displayed in Table 6.7 and Figure 6.8. Relatively few studies examined these effects in healthy adults, and they did not identify a relationship between ambient PM levels and respiratory symptoms or medication use. These studies of healthy adults are summarized in Annex E, but will not be described in detail in this section.

Mar et al. (2004, [057309](#)) studied asthmatic adults (N = 16) in Spokane, WA over a 3-yr time period. No associations were found between PM and respiratory symptoms among the adults.

Several panel studies conducted in Europe have examined effects of daily exposures to air pollution on adults with asthma, including studies in the Pollution Effects on Asthmatic Children in Europe (PEACE) study (Boezen et al., 2005, [087396](#)), Exposure and Risk Assessment for Fine and UFPs in Ambient Air (ULTRA) study (De Hartog et al., 2003, [001061](#)), in Germany (Von Klot et al., 2002, [034706](#)), and in Paris (Desqueyroux et al., 2002, [026052](#); 2004, [090449](#)). Boezen et al. (2005, [087396](#)) enrolled 327 elderly adults in the Netherlands to examine the role of AHR and IgE levels in susceptibility to air pollution. For subjects with both AHR (defined as $\geq 20\%$ FEV₁ decline at ≤ 2 mg cumulative methacholine) and high total IgE (>20 kU/L), each 10 $\mu\text{g}/\text{m}^3$ increase in lag 2 PM₁₀ concentration was associated with an increased risk of upper respiratory symptoms (URS) among males (OR 1.06 [95% CI: 1.02-1.10]), and at lag 0 with increased cough among females (OR 1.04 [95% CI: 1.00-1.08]). Each 10 $\mu\text{g}/\text{m}^3$ increase in BS at lag 0, lag 1, and the 5-day mean was associated with URS and cough among males. The strongest association in both cases was for the 5-day mean (OR for URS 1.43 [95% CI: 1.20-1.69]; OR for cough 1.16 [95% CI: 1.05-1.29]). The authors suggest that the sex differences observed may be explained by differential daily exposure to traffic exhaust experienced by men compared to women (Boezen et al., 2005, [087396](#)).

As part of the multicenter ULTRA study, de Hartog et al. (2003, [001061](#)) enrolled 131 older adults with coronary artery disease in three cities (Amsterdam, Erfurt [Germany], and Helsinki). Pooling data from all three cities, associations were observed between PM_{2.5} and shortness of breath and phlegm: each 10 $\mu\text{g}/\text{m}^3$ increase in the 5-day avg PM_{2.5} was

associated with an increased risk of symptoms (OR for shortness of breath 1.12 [95% CI: 1.02-1.24]; OR for phlegm 1.16 [95% CI: 1.03-1.32]). Unlike fine particles, UFPs were not consistently associated with symptoms.

In a study that took place in Erfurt, Germany, von Klot et al. (2002, [034706](#)) examined daily, winter time exposure to ambient PM_{10-2.5}, PM_{2.5-0.01} and PM_{0.1-0.01} particles and respiratory health effects in 53 β_2 -agonists or inhaled corticosteroids and exposure to particles in single and multipollutant models. Particle exposure metrics examined included same-day, 5-day and 14-day avg. No effects were observed for wheeze and exposure to PM_{10-2.5} for any averaging time. The strongest association between wheeze and exposure to UFPs was for a 14-day avg: each 7,700 increase in the NC_{0.01-0.1} increased the risk of wheeze by 27% (OR 1.27 [95% CI: 1.13-1.43]). The effect was attenuated in copollutant models that also included PM_{2.5-0.01} (OR 1.12 [95% CI: 1.01-1.24]), NO₂ (OR 1.12 [95% CI: 0.99-1.26]), CO (OR 1.05 [95% CI: 0.92-1.19]) or SO₂ (OR 1.14 [95% CI: 1.04-1.26]). The correlations between UFPs and two gaseous pollutants, NO₂ and CO, were high: 0.66 for each.

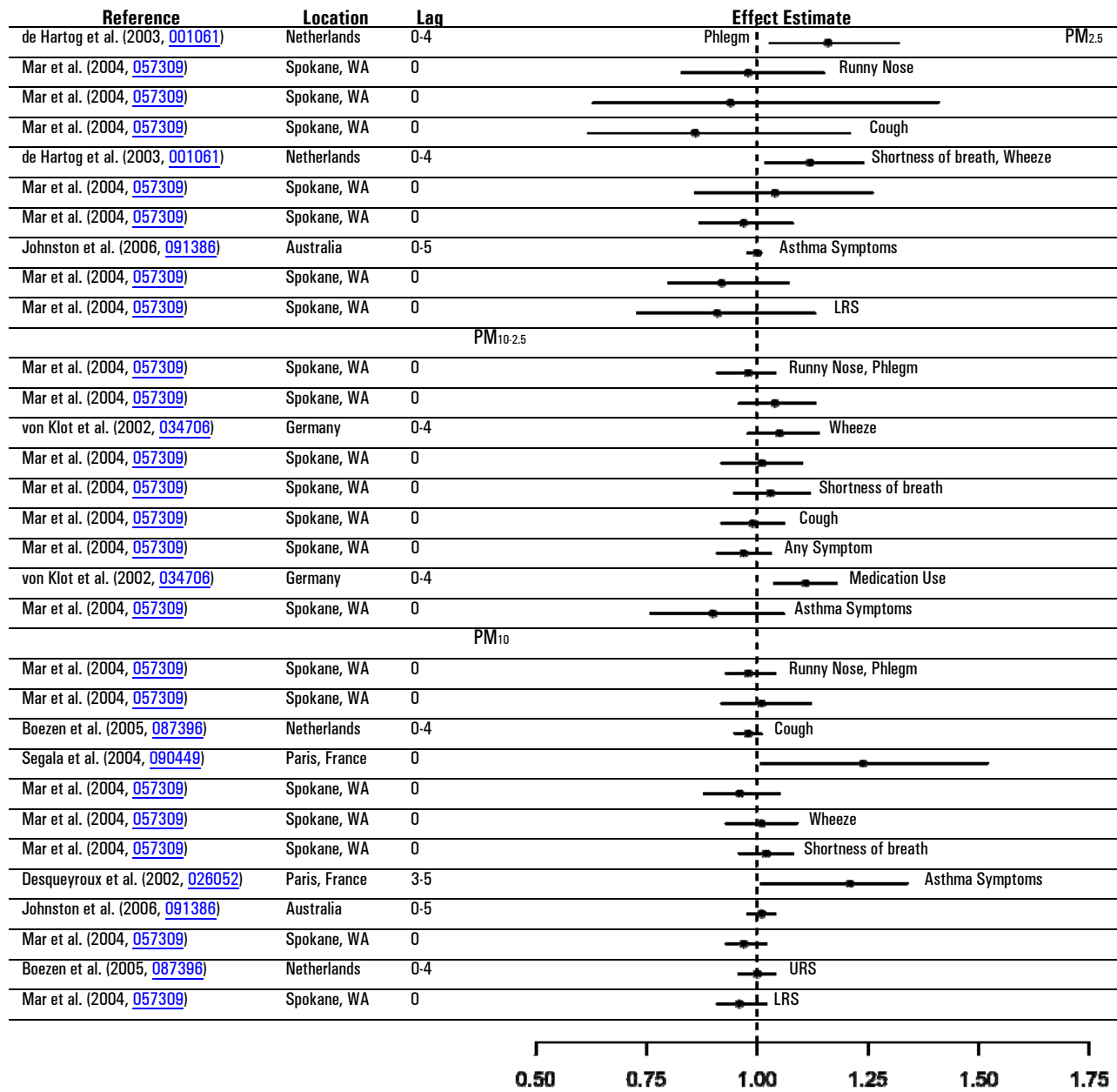


Figure 6-8. Respiratory symptoms and/or medication use among asthmatic adults following acute exposure to particles. Summary of studies using 24-h avg of PM₁₀, PM_{2.5}, PM_{10-2.5}. ORs and 95% CIs were standardized to increments of 10 µg/m³.

In the same study, no association was found between exposure to thoracic coarse, fine or UFPs and use of short-acting inhalers, though there was an association with maintenance medication. Increased likelihood of maintenance medication was significantly associated with PM of all sizes and all averaging times (same day, 5- and 14-day avg) and gaseous copollutants in single or multipollutant models. The strongest effects were seen for 14-day avg of PM_{10-2.5} (for each 10 µg/m³ increase OR 1.43 [95% CI: 1.28-1.60]), PM_{2.5-0.01} (for

each 20 $\mu\text{g}/\text{m}^3$ increase OR 1.54 [95% CI: 1.43-1.66]), $\text{NC}_{0.01-0.1}$ (for each 7,700 increase OR 1.45 [95% CI: 1.29-1.63]). For $\text{PM}_{2.5-0.01}$, effects were unchanged in copollutant models, including a model with UFPs. The authors conclude that this is evidence for independent effects of fine and UFPs (Von Klot et al., 2002, [034706](#)).

In Paris, Segala et al. (2004, [090449](#)) recruited 78 adults from an otolaryngology clinic and followed them for three months. Both PM_{10} and BS (which were very highly correlated [$r = .88$]) were associated with cough: OR 1.24 (95% CI: 1.01-1.52) for a 10 $\mu\text{g}/\text{m}^3$ increase in mean 0-4 day PM_{10} and OR 1.18 (95% CI: 1.02-1.39) for a 10 $\mu\text{g}/\text{m}^3$ increase in BS.

Also in Paris, 60 severe asthmatics were followed for 13 months and the relationship between daily air quality (including 24-h PM_{10} as measured at the site nearest to the subject's home) and asthma attack (defined as the need to increase rescue medication use and one or more positive signs on clinical exam of wheezing, expiratory brake, thoracic distention, hypertension with tachycardia, polypnea) were examined with GEE models (Desqueyroux et al., 2002, [026052](#)). Each 10 $\mu\text{g}/\text{m}^3$ increase in PM_{10} increased the risk of asthma attack, but only after lags of 3 to 5 days. The strongest effect was seen for the mean lag of days 3 to 5 (OR 1.21 [95% CI: 1.04-1.40]). Effect sizes were larger among patients not on regular oral steroid therapy: for PM_{10} lag 3-5 (OR 1.41 [95% CI: 1.15-1.73]). This effect persisted in multipollutant models for winter time levels of PM_{10} and SO_2 (OR 1.51 [95% CI: 1.20-1.90]) or NO_2 (OR 1.43 [95% CI: 1.16-1.76]), but not in summer time models with O_3 (OR 1.09 [95% CI: 0.71-1.67]).

Copollutant Models

A limited number of respiratory symptoms studies reported results of copollutant models. Generally, the associations between respiratory symptoms and PM were robust to the inclusion of copollutants (Figure 6-9), though Desqueyroux et al. (2002, [026052](#)) indicate the effects of PM may be potentiated by NO_2 and SO_2 during the winter months. Gent et al. (2003, [052885](#)) also reported the results of copollutant models, though the categorical exposure groups used in the analysis did not allow these results to be included in Figure 6-9. As reported above, the investigators found that effects were attenuated in models including O_3 .

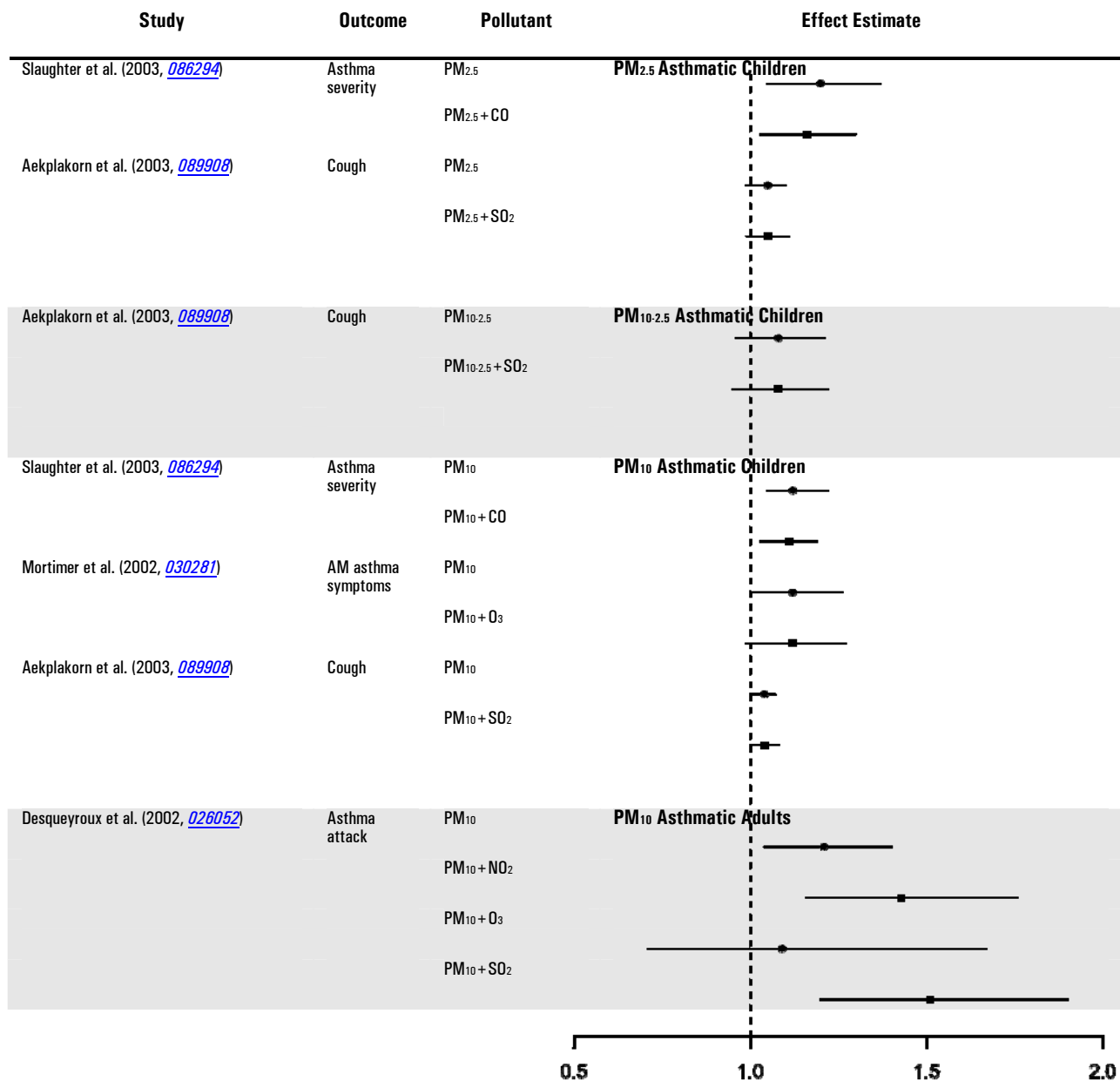


Figure 6-9. Respiratory symptoms following acute exposure to particles and additional criteria pollutants. Circles represent single pollutant effect estimates and squares represent copollutant effect estimates.

6.3.1.2. Controlled Human Exposure Studies

CAPs

Neither new controlled human exposure studies, nor studies cited in the 2004 PM AQCD (U.S. EPA, 2004, [056905](#)) have found significant effects of CAPs on respiratory symptoms among healthy or asthmatic adults, or among older adults with COPD (Gong et

al., 2000, [155799](#); Gong et al., 2003, [042106](#); Gong et al., 2004, [087964](#); Gong et al., 2004, [055628](#); Gong et al., 2005, [087921](#); Gong et al., 2008, [156483](#); Petrovic et al., 2000, [004638](#)).

Urban Traffic Particles

One new study reported an increase in respiratory symptoms (upper and lower airways) among healthy volunteers (19-59 years old) during a 2-h exposure to road tunnel traffic (PM_{2.5} concentration 46-81 µg/m³) (Larsson et al., 2007, [091375](#)). However, information on specific respiratory symptoms (e.g., throat irritation, wheeze or chest tightness) was not provided. In addition, this study only evaluated respiratory symptoms pre- versus post-exposure, and did not compare response with a filtered air control exposure.

Diesel Exhaust

Respiratory symptoms including mild nose and throat irritation have been reported following controlled exposure to DE; however, other symptoms such as cough, wheeze and chest tightness have not been observed (Mudway et al., 2004, [180208](#)).

Model Particles

Pietropaoli et al. (2004, [156025](#)) found no association between exposure to ultrafine carbon particles and respiratory symptoms in healthy adults at concentrations between 10 and 50 µg/m³, or asthmatics at a concentration of 10 µg/m³. Beckett et al. (2005, [156261](#)) exposed healthy subjects to ultrafine and fine ZnO (500 µg/m³) and observed no difference in respiratory symptoms compared to filtered air control 24 h following exposure. In a study evaluating respiratory effects of exposure to ammonium bisulfate or aerosolized H₂SO₄ (200 and 2,000 µg/m³) among healthy and asthmatic adults, Tunnicliffe et al. (2003, [088744](#)) observed no change in respiratory symptoms with either particle type or concentration relative to filtered air. This finding is in agreement with many similar older studies which have generally reported no increase in respiratory symptoms following exposure to acid aerosols at concentrations <1,000 µg/m³ (U.S. EPA, 1996, [079380](#); U.S. EPA, 2004, [056905](#)).

Summary of Controlled Human Exposure Study Findings for Respiratory Symptoms

These new studies confirm previous reports that have found no association between PM exposure and respiratory symptoms.

6.3.2. Pulmonary Function

Epidemiologic studies cited in the 2004 PM AQCD (U.S. EPA, 2004, [056905](#)) observed small decrements in pulmonary function associated with both PM₁₀ and PM_{2.5} (U.S. EPA, 2004, [056905](#)). The majority of controlled human exposure studies reported no effect of PM on pulmonary function, while the results from toxicological studies were mixed, with some evidence of changes in tidal volume and respiratory rate following exposure to CAPs. Epidemiologic studies published since the 2004 PM AQCD (U.S. EPA, 2004, [056905](#)) have reported an association between PM_{2.5} concentration and decrements in FEV₁, particularly among asthmatic children. These findings are coherent with results from a number of recent toxicological studies which have observed increases in airway hyperresponsiveness (AHR) following CAPs exposure. Results from recent controlled human exposure studies have been inconsistent, with some studies demonstrating small decreases in arterial oxygen saturation or maximal mid-expiratory flow following exposure to CAPs or EC. It is interesting to note that these effects appear to be more pronounced among healthy adults than adults with asthma or COPD.

6.3.2.1. Epidemiologic Studies

The 2004 PM AQCD (U.S. EPA, 2004, [056905](#)) concluded that both PM₁₀ and PM_{2.5} appeared to affect lung function in asthmatics. UFPs did not appear to have any notably stronger effect than other larger-diameter fine particles (U.S. EPA, 2004, [056905](#)). Few analyses were able to clearly distinguish the effects of PM₁₀ and PM_{2.5} from other pollutants. Results for PM₁₀ peak flow analyses in non-asthmatic studies were inconsistent, with fewer studies reporting strong associations.

Asthmatic Children

Seven recent panel studies have been conducted in the U.S. examining the association of exposure to ambient PM and lung function in asthmatic children (Allen et al., 2008, [156208](#) in Seattle; Lewis et al., 2003, [088413](#) in Southern California; 2004, [097498](#); Lewis et al., 2005, [081079](#) in Detroit; O'Connor et al., 2008, [156818](#); Rabinovitch et al., 2004, [096753](#) in Denver). Mean concentration data from these studies are summarized in Table 6-7.

In the Inner-City Asthma Study (ICAS), FEV₁ and PEFT were significantly related to the 5-day avg of PM_{2.5}, but not to the 1-day avg concentration (O'Connor et al., 2008, [156818](#)). The risk of experiencing a percent-predicted FEV₁ more than 10% below personal

best was significantly related to the 5-day avg concentration of PM_{2.5} (1.14 [95% CI: 1.01-1.29]). The risk of experiencing a percent-predicted PEFR more than 10% below personal best was significantly related to PM_{2.5} (1.18 [95% CI: 1.03-1.35]). This effect remained robust in multipollutant models with O₃ and NO₂ for the FEV₁ effect, but not the PEFR effect.

The Denver study (Rabinovitch et al., 2004, [096753](#)), described in Section 6.3.1.1, also examined daily forced expiratory volume in 1 sec (FEV₁) and peak expiratory flow (PEF) in 86 asthmatic children over the course of 3 winters (some subjects participated in more than one winter). Lung function measurements were performed under supervision daily at the elementary school where all subjects attended, and without supervision every evening and on nonschool days. As described above, the authors chose to use a 3-day ma of 24-h PM_{2.5} or PM₁₀ as the exposure metric. No statistical associations were observed between morning or afternoon FEV₁ or PEF and particle exposure. The same group of researchers (Strand et al., 2006, [157017](#)) used regression calibration to estimate personal exposures to ambient PM_{2.5} and found that a 10 µg/m³ increase in PM_{2.5} was associated with a 2.2% (95% CI: 0.0-4.3) decrease in FEV₁ at a 1-day lag as compared with the estimate of a 1.0% decrease in FEV₁ using ambient PM_{2.5} concentrations from fixed monitors. These results underscore the effects of exposure error on epidemiologic study results; the effect estimate using an estimate of personal exposure to ambient PM_{2.5} was twice that for central site PM_{2.5}.

From winter 2001 to the spring of 2002, the same number (n = 86) of primary school-age asthmatic children participated in six, 2-wk seasonal assessments of lung function in Detroit (Lewis et al., 2005, [081079](#)). Using a protocol similar to that used in Rabinovitch et al. (2004, [096753](#)), morning lung function measurements (FEV₁, PEF) were self-administered at school under supervision by research staff. Evening and weekend measurements were made without supervision by research staff at home. Community-level exposure was assessed using monitors placed on a school roof top of both of the two communities. Most of the subjects (82 of 86) lived within 5 km of their respective community monitors. In single-pollutant models using GEE and only among children reporting the use of maintenance medication (corticosteroids), each 10 µg/m³ increase in lag 2 PM₁₀ was associated with a decrease in the lowest daily percent predicted FEV₁ (a reduction of 1.15%, [95% CI: -2.1 to -0.25]). Among children reporting presence of URI on the day of lung function measurement, increases in the average of lag 3-5 of either PM_{2.5} or PM₁₀ resulted in a decrease in the lowest daily FEV₁ (for a 10 µg/m³ increase in PM_{2.5} the

reduction was 2.24% [95% CI: -4.4 to -0.25]; and for a 10 $\mu\text{g}/\text{m}^3$ increase in PM_{10} the reduction was 2.4% [95% CI: -4.5 to -0.3]). In copollutant models that included one particle pollutant and O_3 , and among children using maintenance medication, lag 3-5 $\text{PM}_{2.5}$ continued to be associated with lowest daily FEV_1 as well as diurnal FEV_1 variability: each 10 $\mu\text{g}/\text{m}^3$ increase was associated with a 2.23% decrease in FEV_1 (95% CI: -3.92 to -0.57) and a 2.22% increase in FEV_1 variability (95% CI: 1.0 to 3.50). Increases in lag 1 or lag 2 of PM_{10} were associated with FEV_1 and FEV_1 diurnal variability in copollutant models. The strongest association was with lag 2 for diurnal variability (for each 10 $\mu\text{g}/\text{m}^3$ increase variability increased by 7.0% [95% CI: 4.2 to 9.6]). It is unclear what role the lack of supervision during the evening and weekend measures may have had on these diurnal results.

Two panel studies in southern California examined the association of PM exposure on lung function in asthmatic children (Delfino et al., 2003, [050460](#); Delfino et al., 2004, [056897](#)). In Delfino et al. (2003, [050460](#)), described above, no association between exposure to particles and PEF was found for 22 Hispanic, asthmatic children living in an area of relatively high pollution. In Delfino et al. (2004, [056897](#)) 19 asthmatic children aged 9-17 yr were followed for 2 wk and daily, self-administered FEV_1 measurements were taken. Particle exposures studied included central-site PM_{10} in addition to personal PM (in the range of 0.1-10 μm range, with the highest response in the fine PM range), and home stationary measurements of both PM_{10} and $\text{PM}_{2.5}$. The authors report inverse associations between percent expected FEV_1 and PM indicators. The strongest association for exposure to personal PM was for a 5-day ma of 12-h daytime PM: for each 10 $\mu\text{g}/\text{m}^3$ increase, FEV_1 decreased by 7.1% (95% CI: -9.9 to -2.9). Effects for all stationary sites (inside and outside of residence, central site) for $\text{PM}_{2.5}$ were on the order of 1 to 2% reductions in FEV_1 , with the strongest associations for the 5-day ma (given in figures only). Likewise for PM_{10} measured at stationary sites, the strongest effects were for 5-day ma and ranged from approximately 3.8% reduction associated with indoor monitors to about 1.5% for both the outdoor and central site monitors (given in figures only). A helpful comparison among all 24-h measures is given for 10 $\mu\text{g}/\text{m}^3$ increases in personal PM and $\text{PM}_{2.5}$ associated with decreases in percent predicted FEV_1 : an increase of 10 $\mu\text{g}/\text{m}^3$ personal PM is associated with a decrease in FEV_1 of 3.0% (95% CI: -5.6 to -0.5); 10 $\mu\text{g}/\text{m}^3$ increase in indoor PM with 2.4% decrease (95% CI: -4.2 to -0.6); 10 $\mu\text{g}/\text{m}^3$ increase in outdoor PM with 1.5% decrease (95% CI: -3.4 to 0.1); 10 $\mu\text{g}/\text{m}^3$ increase in central site PM with 0.9% decrease (95% CI: -2.6 to 0.5).

Trenga et al. (2006, [155209](#)) reported associations among personal, residential, and central site PM_{2.5} and lung function in 17 asthmatic children in Seattle. The only statistical association with decline in FEV₁ was with indoor measurements of PM_{2.5}: each 10 µg/m³ increase in lag 1 indoor PM_{2.5} was associated with a decline in FEV₁ of 64.8 mL (95% CI: -111.3 to 18.3) (a 3.4% decline from the mean of 1.9 L). Indoor PM_{2.5} (lag 1) was also associated with declines in PEF (by 9.2 L/min [95% CI: -17.5 to -0.9], a 3.6% decline from the 254 L/min avg) and in MMEF for the 6 subjects not taking anti-inflammatory medication (by 12.6 L/min [95% CI: -20.7 to -4.6], a 13.7% decline from the 92 L/min avg). Personal PM_{2.5} (lag 1) was only statistically associated with PEF for the 6 subjects not on anti-inflammatory medication: each 10 µg/m³ increase resulted in a 10.5 L/min ([95% CI: -18.7 to -2.3], a 4.5% decline from the 233 L/min avg) reduction in PEF. Anti-inflammatory medication use significantly attenuated associations with PM_{2.5}.

Also in Seattle, Allen et al. (2008, [156208](#)) evaluated the effect of different PM_{2.5} exposure metrics in relation to lung function among children in WS-impacted areas. The authors found that the ambient-generated component of PM_{2.5} exposure was associated with decrements in lung function only among children not using inhaled corticosteroids, whereas no association was reported with the nonambient exposure component. All of the ambient concentrations were associated with decrements in both PEF and MEF. There were no associations between any exposure metrics and FVC. The authors suggest that lung function may be especially sensitive to the combustion-generated component of ambient PM_{2.5}, whereas airway inflammation may be more closely related to some other constituent.

In a longitudinal study, Liu et al. (2009, [192003](#)) examined the association between acute increases in ambient air pollutants and pulmonary function among children (ages 9-14 yr) with asthma. FEV₁ and FEF_{25-75%} exhibited a consistent trend of negative associations with PM_{2.5} across lag days 0, 1, 0-1, and 0-2, with the strongest effects for FEF_{25-75%} on lag day 0 (-1.12% [95% CI: -2.06 to -0.18]) and lag days 0-1 (-1.18% [95% CI: -2.24 to -0.12]). Two pollutant models including O₃, SO₂ or NO₂ did not result in marked changes in the PM_{2.5} risk estimates for FEV₁ or FEF_{25-75%}.

Moshhammer and Neuberger (2003, [041956](#)) used a novel technique for assessing exposure to PM in a study they conducted in Austria. They employed a diffusion charging particle sensor (model LQ 1-DC, Matter Engineering AG, Wohlen, Switzerland) and a photoelectric aerosol sensor (model PAS 2000 CE, EcoChem Analytics, League City, TX) to relate the spirometry scores of Upper Austrian children aged 7-10 to particle surface area

and particle-bound PAH concentration, respectively. Details on these methods for measuring surface area and PAH can be found in Shi et al. (2001, [078292](#)) and Burtscher (2005, [155710](#)), respectively. By measuring the surface area distribution, it was possible to understand potential for contact area with the respiratory tract cells. The authors found that acute decrements of pulmonary function (FVC, FEV₁, MEF₅₀) were related to the active surface of particles after adjustment for PM₁₀. For short-term lung impairments, this indicates that active particle surface is a better index of exposure than PM mass.

A number of additional panel studies conducted outside of the U.S. and Canada also examined lung function using more traditional exposure metrics. Several European and Asian studies reported associations with decrements in pulmonary function (FEV₁, FVC, FEF, MEF, PEFR) (Hogervorst et al., 2006, [189460](#); Hong et al., 2007, [091347](#); Moshhammer et al., 2006, [090771](#); Odajima et al., 2008, [192005](#); Peacock et al., 2003, [042026](#); Peled et al., 2005, [156015](#)). Others found little evidence for a relationship between PM and daily changes in PEF after correction for the confounding effects of weather, trends in the data, and autocorrelation (Fischer et al., 2002, [025731](#); Holguin et al., 2007, [099000](#); Just et al., 2002, [035429](#); Preutthipan et al., 2004, [055598](#); Ranzi et al., 2004, [089500](#); Ward, 2003, [157111](#)).

Adults

Trenga et al. (2006, [155209](#)) examined personal, residential, and central site monitoring of particles and the relationship with lung function in Seattle. In models controlling for gaseous copollutants (CO, NO₂), adults, regardless of COPD status, experienced a significant decline in FEV₁ associated only with measurements of PM_{2.5} at the central site: each 10 µg/m³ increase in lag 0 PM_{2.5} was associated with a 35.3 mL (95% CI: -70 to -1.0) decrease in FEV₁. This represents a 2.2% decline in mean FEV₁ (mean 1.6 L during the study). Results for personal, indoor and outdoor measures of PM_{2.5} were inconsistent. No significant associations were reported with outdoor PM_{10-2.5}.

Girardot et al. (2006, [088271](#)) assessed the effects of PM_{2.5} on the pulmonary function of adult day hikers in the Great Smoky Mountains National Park. Hikers performed spirometry both before their hike and when they returned from their hike. The authors reported no statistically significant responses in pulmonary function with an average of 5 h of outdoor exercise at ambient PM_{2.5} levels that were below the current NAAQS.

Specifically, posthike percentage changes in FVC, FEV₁, FEV₁/FVC, FEF₂₅₋₇₅, and PEF were not associated with PM_{2.5} exposure.

Ebelt et al. (2005, [056907](#)) developed an approach to separately estimate exposures to PM of ambient and nonambient origin based on a mass balance model. These exposures were linked with respiratory and cardiovascular health endpoints for 16 patients with COPD in Vancouver, Canada (mean age 74 yr). Effect estimates for estimated ambient exposure were generally equal to or larger than those for the respective ambient concentration levels for post-FEV and Δ FEV₁, and were statistically significant for all Δ FEV₁ comparisons (estimated from figure).

Several studies outside of the U.S. and Canada examined the relationship between PM concentrations and lung function and all reported a decrease in lung function in adults (FEV₁, FVC, PEF) associated with PM exposure (Boezen et al., 2005, [087396](#); Bourotte et al., 2007, [150040](#); Lagorio et al., 2006, [089800](#); Lee et al., 2007, [093042](#); McCreanor et al., 2007, [092841](#); Penttinen et al., 2006, [087988](#)).

Measures of Oxygen Saturation

Oxygen saturation measures the percentage of hemoglobin binding sites in the bloodstream occupied by oxygen. DeMeo et al. (2004, [087346](#)) estimated the change in oxygen saturation and mean PM_{2.5} concentration in the previous 24 h in a panel of elderly subjects. They used the same panel of elderly Boston residents (n = 28) and study protocol and analytic methods (12 wk of repeated oxygen saturation measurements) as Gold et al. (2005, [087558](#)) and Schwartz et al. (2005, [074317](#)) in studies of ST-segment depression and HRV, respectively. At each clinic visit, subjects had 5 min each of rest, standing, post-exercise rest, and 20 cycles of paced breathing. The median PM_{2.5} concentration during the study period was 10.0 $\mu\text{g}/\text{m}^3$ (Schwartz et al., 2005, [074317](#)). Each 13.4 $\mu\text{g}/\text{m}^3$ increase in the mean PM_{2.5} concentration in the previous 6 h was associated with a 0.2% decrease in oxygen saturation (95% CI: -0.3 to 0.0) during the baseline rest period. Each 13.4 $\mu\text{g}/\text{m}^3$ increase in mean 6-h PM_{2.5} concentration was also associated with a decline in oxygen saturation during the post-exercise period (-0.2% [95% CI: -0.3 to 0.0]), and post-exercise paced breathing period (-0.1% [95% CI: -0.3 to 0.0]), but not during the exercise period. The authors suggest that these oxygen saturation reductions may result from pulmonary vascular and inflammatory changes.

In a similar study, Goldberg et al. (2008, [180380](#)) examined the association between oxygen saturation, pulse rate, and ambient PM_{2.5}, NO₂, and SO₂ concentrations in a panel

of 31 subjects in Montreal, with NYHA Class II or III heart failure who were aged 50-85 yr. Although each 7.3 $\mu\text{g}/\text{m}^3$ increase in $\text{PM}_{2.5}$ on lag day 0 was associated with a -0.087 (95% CI = -0.143 to -0.031) change in oxygen saturation in unadjusted models, once adjusted for temperature and barometric pressure, the estimated change was smaller and no longer significant (-0.056 [95% CI = -0.117 to 0.005]). Only SO_2 was significantly associated with reduced oxygen saturation in multivariate adjusted models. None of the pollutants examined, including $\text{PM}_{2.5}$, were associated with a change in pulse rate.

6.3.2.2. Controlled Human Exposure Studies

As with respiratory symptoms, there is little evidence from controlled human exposure studies of PM -induced changes in pulmonary function. One study cited in the 2004 PM AQCD (U.S. EPA, 2004, [056905](#)) noted a significant decrement in thoracic gas volume in healthy adults following a 2-h exposure to $\text{PM}_{2.5}$ CAPs (92 $\mu\text{g}/\text{m}^3$); however, no significant changes were observed in spirometric measurements, diffusing capacity (DLCO), total lung capacity, or airways resistance (Petrovic et al., 2000, [004638](#)). Other studies found no significant changes in pulmonary function in healthy adults following exposure to inhaled iron oxide particles (Lay et al., 2001, [020613](#)), or in healthy and asthmatic adults following exposure to CAPs (Ghio et al., 2000, [012140](#); 2003, [087365](#); Gong et al., 2000, [155799](#)). Rudell et al. (1996, [056577](#)) reported a significant increase in specific airways resistance following exposure to DE, an effect that was not attenuated by reducing the particle number by 46% ($2.6 \times 10^6/\text{cm}^3$ compared with $1.4 \times 10^6/\text{cm}^3$) using a particle trap. The particle trap did not affect the concentrations of other measured diesel emissions including NO_2 , NO , CO , or total hydrocarbons. As described below, more recent controlled human exposure studies provide limited and inconsistent evidence of changes in lung function following exposure to particles from various sources.

CAPs

Among a group of healthy and asthmatic adults exposed to UFPs (Los Angeles, mean concentration 100 $\mu\text{g}/\text{m}^3$), Gong et al. (2008, [156483](#)) observed small, yet statistically significant decrements in arterial oxygen saturation immediately following exposure, 4 h post-exposure, and 22 h post-exposure (0.5% mean decrease relative to filtered air across all time points, $p < 0.05$). A statistically significant decrease in FEV_1 was also observed, but only at 22 h post-exposure (2% decrease relative to filtered air, $p < 0.05$). The responses

demonstrated in this study were not significantly affected by health status. No such effects were observed in a similar study conducted in Chapel Hill, NC which exposed healthy adults to a lower concentration of ultrafine CAPs ($49.8 \mu\text{g}/\text{m}^3$) (Samet et al., 2009, [191913](#)). In addition, two studies evaluating effects of exposure to thoracic coarse CAPs (average concentration $89\text{-}157 \mu\text{g}/\text{m}^3$) on lung function observed no changes in spirometric measurements, diffusing capacity or arterial oxygen saturation 0-22 h post-exposure in asthmatic or healthy adults (Gong et al., 2004, [055628](#); Graff et al., 2009, [191981](#)). While Gong et al. (2004, [087964](#)) did not observe a significant association between exposure to $\text{PM}_{2.5}$ CAPs and spirometry in older subjects (60-80 yr), the investigators did report a decrease in oxygen saturation immediately following CAPs exposure. This effect was observed more consistently in healthy older adults than in older adults with COPD. These findings were confirmed by a subsequent study conducted by the same laboratory (Gong et al., 2005, [087921](#)). The authors also observed a small decrease in maximal mid-expiratory flow (MMEF) following a 2-h exposure to $\text{PM}_{2.5}$ CAPs ($200 \mu\text{g}/\text{m}^3$) which was more pronounced in healthy subjects.

Urban Traffic Particles

Neither short term exposure to relatively high levels of urban traffic particle nor longer exposures to lower concentrations of urban particles have been observed to alter pulmonary function in controlled exposures among healthy adults. Larsson et al. (2007, [091375](#)) exposed 16 adults for 2 h to fine particle concentrations of $46\text{-}81 \mu\text{g}/\text{m}^3$ in a room adjacent to a busy road tunnel, with concomitant exposure to NO_2 (0.12 ppm), NO (0.71 ppm), and CO (5 ppm). Although respiratory effects in this study were not compared to filtered air control, no difference in lung function was observed 14 h after exposure to traffic particles relative to lung function measured on a day following typical activities that did not include transit through a road tunnel. In a study of 24-h exposures to urban traffic particles ($\text{PM}_{2.5}$ $9.7 \mu\text{g}/\text{m}^3$), no change in lung function was reported at 2.5 h after the start of exposure relative to filtered air (Bräuner et al., 2009, [191179](#)).

Diesel Exhaust

Mudway et al. (2004, [180208](#)) exposed 25 healthy adults to DE with an average particle concentration of $100 \mu\text{g}/\text{m}^3$ and observed mild bronchoconstriction (airways resistance) immediately following exposure relative to filtered air. No changes were observed in FEV1 or FVC following DE exposure in these subjects, or in a group of 15

asthmatics exposed using the same protocol (Mudway et al., 2004, [180208](#); Stenfors et al., 2004, [157009](#)).

Model Particles

Pietropaoli et al. (2004, [156025](#)) observed a reduction in MMEF and DLCO in healthy adults 21 h after a 2-h exposure to ultrafine carbon particles ($50 \mu\text{g}/\text{m}^3$). This reduction in DLCO may reflect a PM-induced vasoconstrictive effect on the pulmonary vasculature. Tunncliffe et al. (2003, [088744](#)) did not observe any significant change in lung function following exposure to ammonium bisulfate or aerosolized H_2SO_4 (200 and 2,000 $\mu\text{g}/\text{m}^3$) in healthy or asthmatic adults, which is consistent with findings of the majority of studies of controlled exposures to acid aerosols presented in the last two PM AQCDs (U.S. EPA, 1996, [079380](#); 2004, [056905](#)).

Summary of Controlled Human Exposure Study Findings for Pulmonary Function

Taken together, the majority of controlled human exposure studies do not provide evidence of PM-induced changes in pulmonary function; however, some investigators have observed slight decreases in DLCO, MMEF, FEV_1 , oxygen saturation, or increases in airways resistance following exposure to CAPs, DE, or ultrafine EC.

6.3.2.3. Toxicological Studies

The 2004 PM AQCD (U.S. EPA, 2004, [056905](#)) included three animal toxicological studies which measured pulmonary function following multiday short-term inhalation exposure to CAPs. A decreased respiratory rate was noted in one study involving dogs. Increased tidal volume was observed in one study involving rats while no changes were observed in the other rat study. AHR was found in 4 studies of mice, healthy rats or SH rats exposed to ROFA by IT instillation or inhalation. Studies conducted since the last review are discussed below.

CAPs

SH rats exposed to Tuxedo, NY CAPs via nose-only inhalation for 4 h (mean concentration $73 \mu\text{g}/\text{m}^3$; single-day concentrations 80 and $66 \mu\text{g}/\text{m}^3$; 2/2001 and 5/2001 respectively) had a statistically significant decreased respiratory rate compared with air-exposed controls (Nadziejko et al., 2002, [087460](#)). This measure was obtained from BP fluctuations using radiotelemetry. The decrease in respiratory rate of 25-30 breaths/min

was an immediate response to CAPs, beginning shortly after the exposure began and ceasing with the end of exposure. It was accompanied by a decrease in HR (see Section 6.2.1.3). Rats were also exposed to fine (MMAD 160 nm; 49-299 $\mu\text{g}/\text{m}^3$) and ultrafine H_2SO_4 (MMAD 50-75 nm; 140-750 $\mu\text{g}/\text{m}^3$) (Nadziejko et al., 2002, [087460](#)) because H_2SO_4 aerosols have the potential to activate irritant receptors. Irritant receptors, found at all levels of the respiratory tract, include rapidly-adapting receptors and sensory C-fiber receptors (Alarie, 1973, [191136](#); Coleridge and Coleridge, 1994, [156362](#); 2003, [157145](#); 2006, [155519](#); Widdicombe and Lee, 2001, [019049](#)) Activation of trigeminal afferents in the nose causes CNS reflexes resulting in decreases in respiratory rate through a lengthened expiratory phase, closure of the glottis, closure of the nares with increased nasal airflow resistance and effects on the cardiovascular system such as bradycardia, peripheral vasoconstriction and a rise in systolic arterial blood pressure. Sneezing, rhinorrhea and vasodilation with subsequent nasal vascular congestion are also nasal reflex responses involving the trigeminal nerve (Sarin et al., 2006, [191166](#)). Activation of vagal afferents in the tracheobronchial and alveolar regions of the respiratory tract causes CNS reflexes resulting in bronchoconstriction, mucus secretion, mucosal vasodilation, cough, and apnea followed by rapid shallow breathing. Besides effects on the respiratory system, effects on the cardiovascular system can also occur including bradycardia and hypotension or hypertension. Fine H_2SO_4 induced an overall decrease in respiratory rate, with ultrafine H_2SO_4 resulting in elevated respiratory rate compared to control (Nadziejko et al., 2002, [087460](#)). The authors suggested that both CAPs and fine H_2SO_4 aerosols activated sensory irritant receptors in the upper airways, resulting in a decreased respiratory rate. The response to ultrafine H_2SO_4 aerosols differed from the other responses and was thought to be due to deposition of UFPs deeper into the lung with the subsequent activation of pulmonary irritant receptors which trigger an increase in respiratory rate. Since irritant receptors in nasal, tracheobronchial and alveolar regions act via trigeminal- and vagal-mediated pathways, this study indicates a role for neural reflexes in respiratory responses to CAPs.

Kodavanti et al. (2005, [087946](#)) measured respiratory frequency 1 day after a 2-day exposure of SH and WKY rats to CAPs from RTP, NC (mean mass concentration range 144-2,758 $\mu\text{g}/\text{m}^3$; less than 2.5 μm in size; 8/27-10/24/2001) for 4 h/day. Increases in inspiratory and expiratory times were seen in SH, but not WKY rats, exposed to CAPs compared with filtered air controls.

Effects of CAPs on pulmonary function were also investigated in a rat model of pulmonary hypertension using SD rats pre-treated with monocrotaline (Lei et al., 2004, [087999](#)). In this study, rats were exposed to CAPs from an urban high traffic area in Taiwan (mean mass concentration 371 $\mu\text{g}/\text{m}^3$) for 6 h/day on 3 consecutive days and pulmonary function was evaluated 5 h post-exposure using whole-body plethysmography. A statistically significant decrease in respiratory frequency and an increase in tidal volume were observed following CAPs exposure, along with an increase in airway responsiveness (measured as Penh) following methacholine challenge.

In many animal studies changes in ventilatory patterns are assessed using whole body plethysmography, for which measurements are reported as enhanced pause (Penh). Some investigators report increased Penh as an indicator of AHR, but these are inconsistently correlated and many investigators consider Penh solely an indicator of altered ventilatory timing in the absence of other measurements to confirm AHR. Therefore use of the terms AHR or airway responsiveness has been limited to instances in which the terminology has been similarly applied by the study investigators.

Diesel Exhaust

Li et al. (2007, [155929](#)) exposed BALB/c and C57BL/6 mice to clean air or to low dose DE (containing 100 $\mu\text{g}/\text{m}^3$ DEP) for 7 h/day and 5 days/wk for 1, 4 and 8 wk. average gas concentrations were reported to be 3.5 ppm CO, 2.2 ppm NO₂, and less than 0.01 ppm SO₂. AHR was evaluated by whole body plethysmography at day 0 and after 1, 4 and 8 wk of exposure. Exposure to DE for 1 wk resulted in an increased sensitivity of airways to methacholine, measured as Penh, in C57BL/6, but not BALB/c, mice. Other short-term responses of this study are discussed in Sections 6.3.3.3 and 6.3.4.2.

McQueen et al. (2007, [096266](#)) investigated the role of vagally-mediated pathways in respiratory responses to PM. Respiratory minute volume (RMV) was increased in anesthetized Wistar rats 6 h after treatment with 500 μg DEP (SRM2975) by IT instillation. This response was blocked by severing the vagus nerve or pretreatment with atropine. The absence of a respiratory response with vagotomy or atropine indicated that the increase in RMV following DEP exposure involved a neural reflex acting via vagal afferents. No statistically significant changes in mean BP, HR or HRV were observed in response to DEP in this study. Vagally-mediated inflammatory responses to DEP were also observed in this study and are discussed in Section 6.3.3.3.

Model Particles

In a study by Last et al. (2004, [097334](#)), BALB/c mice were exposed to 250 µg/m³ laboratory-generated iron-soot (size range 80-110 nm; about 200 µg/m³ as soot) for 4 h/day and 3 days/wk for 2 wk. Pulmonary function was measured by whole-body plethysmography after challenge with methacholine. No increase in AHR, as measured by Penh, was observed following 2-wk exposure to iron-soot. Other findings of this study are reported in Sections 6.3.3.3, 6.3.5.2 and 7.3.2.2.

Summary of Toxicological Study Findings for Pulmonary Function

Several recent studies demonstrated alterations in respiratory frequency and AHR following short-term exposure to CAPs and DE. Two studies provide evidence for the involvement of irritant receptors and vagally-mediated neural reflexes in mediating changes in respiratory functions.

6.3.3. Pulmonary Inflammation

The discussion of the effects of PM on pulmonary inflammation in the 2004 PM AQCD (U.S. EPA, 2004, [056905](#)) was limited by a relative lack of information from controlled human exposure and toxicological studies. Although no epidemiologic studies of pulmonary inflammation were described in the 2004 PM AQCD (U.S. EPA, 2004, [056905](#)), several recent studies have observed a positive association between PM concentration and exhaled NO. New controlled human exposure and toxicological studies have also generally observed an increase in markers of inflammation in the airways following exposure to PM.

6.3.3.1. Epidemiologic Studies

No epidemiologic studies of pulmonary inflammation were described in the 2004 PM AQCD (U.S. EPA, 2004, [056905](#)).

Exhaled Nitrogen Oxide – Asthmatic Children

Exhaled NO, a biomarker for airway inflammation, was the outcome studied in panels of asthmatic children in southern California (Wu et al., 2006, [157156](#)) and Seattle (Allen et al., 2008, [156208](#); Koenig et al., 2003, [156653](#); 2005, [087384](#); Mar et al., 2005, [088759](#)). Mean concentration data from these studies are summarized in Table 6-7. Delfino et al. (2006, [157156](#)) followed 45 asthmatic children for 10 days with offline fractional eNO and

examined the associations with exposures to personal PM_{2.5} and 24-h PM_{2.5}, EC and OC as well as ambient PM_{2.5}, EC and OC. The strongest associations were between eNO and 2-day avg pollutant concentrations: for a 10 µg/m³ increase in personal PM_{2.5}, eNO increased by 0.46 ppb (95% CI: 0.04-0.79); for 0.6 µg/m³ personal EC, eNO increased by 0.7 ppb (95% CI: 0.3-1.1). An association with exposure to ambient PM_{2.5} was only statistically significant in 19 subjects taking inhaled corticosteroids: for each 10 µg/m³ increase in PM_{2.5}, eNO increased by 0.77 ppb (95% CI: 0.07-1.47).

In a panel of 19 asthmatic children in Seattle, effects were observed only among the 10 non-users of inhaled corticosteroids. For each 10 µg/m³ increase in personal, outdoor, indoor, or central site PM_{2.5}, eNO increased from 3.82 ppb (associated with central site, 95% CI: 1.22-6.43) to 4.48 ppb (with personal PM_{2.5}, 95% CI: 1.02-7.93) (Koenig et al., 2003, [156653](#)). Further analysis examining the association between eNO and outdoor and indoor-generated particles suggested that eNO was associated more strongly with ambient particles, but only for non-users of medication: each 10 µg/m³ increase in estimated ambient PM_{2.5} results in an increase in eNO of 4.98 ppb (95% CI: 0.28-9.69) (Koenig et al., 2005, [087384](#)).

Also in Seattle, WA, Mar et al. (2005, [088759](#)) examined the association between eNO and ambient PM_{2.5} concentration among children (aged 6-13 yr) recruited from an asthma/allergy clinic. Fractional exhaled nitric oxide (FeNO) was associated with hourly averages of PM_{2.5} up to 10-12 h after exposure. Each 10 µg/m³ increase in 1-h mean PM_{2.5} concentration was associated with a 6.99 ppb increase in eNO (95% CI: 3.43-10.55) among children not taking inhaled corticosteroids, but associated with only a 0.77 ppb decrease in eNO (95% CI: -4.58 to 3.04) among those taking inhaled corticosteroids.

Allen et al. (2008, [156208](#)), in a reanalysis of data from Koenig et al. (2005, [087384](#)), evaluated the effect of different PM_{2.5} exposure metrics in relation to airway inflammation among children in WS-impacted areas of Seattle. The authors found that for the 9 non-users of inhaled corticosteroids, the ambient-generated component of PM_{2.5} exposure was associated with respiratory responses, both airway inflammation and decrements in lung function, whereas the nonambient PM_{2.5} exposure component was not. They did note, however, different relationships for airway inflammation and decrements in lung function, with the former significantly associated with total personal PM_{2.5}, personal light-absorbing carbon (LAC), and ambient generated personal PM_{2.5} and the latter related to ambient PM_{2.5} and its combustion markers. The different results between FeNO and lung function

were not unexpected; epidemiologic data show that airway inflammation indicated by FeNO does not correlate strongly with either respiratory symptoms or lung function (Smith and Taylor, 2005, [192176](#)). The authors conclude that lung function decrements may be associated with the combustion-generated component of ambient PM_{2.5}, whereas airway inflammation may be related to some other constituent of the ambient PM_{2.5} mixture.

In a longitudinal study, Liu et al. (2009, [192003](#)) examined the association between acute increases in ambient air pollutants and FeNO among children (ages 9-14 yr) with asthma. Median PM_{2.5} = 6.5, 95th percentile = 19.0. FeNO had a trend of positive associations with PM_{2.5}, with the strongest association on lag day 0 (3.12% [95% CI: -2.12 to 8.82]). Two pollutant models including O₃, SO₂ or NO₂ did not result in marked changes in the PM_{2.5} risk estimates for FeNO.

Several studies outside of the U.S. examined eNO in relation to PM exposure among children. Fischer et al. (2002, [025731](#)) and Murata et al. (2007, [156787](#)) found a significant association between increases in PM and increases in the percent of eNO. Holguin et al. (2007, [099000](#)) found no association between exposure to PM and eNO. However, they did see significant associations between increases in eNO for the 95 asthmatic subjects and measures of road density of roads 50- and 75-m from the home.

Exhaled Nitrogen Oxide – Adults

Three recent panel studies examined the effects of particle exposure on eNO measured in older adults (Adamkiewicz et al., 2004, [087925](#) in Steubenville, OH; Adar et al., 2007, [001458](#); Jansen et al., 2005, [082236](#) in Seattle). Mean concentration data from these studies are characterized in Table 6-7. Breath samples were collected weekly for 12 wk from a group of 29 elderly adults in Steubenville, OH (Adamkiewicz et al., 2004, [087925](#)). In single-pollutant models, each 10 µg/m³ increase in 24-h ambient PM_{2.5} increased eNO by 0.82 ppb (95% CI: 0.19-1.45), a change of 15% compared to mean eNO (9.9 ppb). Effects were essentially unchanged in multipollutant models that included ambient and/or indoor NO. The effect estimates for the 7 COPD subjects were significantly higher than for normal subjects (2.20 vs. 0.45 ppb, p = 0.03) (Adamkiewicz et al., 2004, [087925](#)).

In the Seattle panel of older adults (aged 60-86 yr), 7 subjects were asthmatic and 9 had a diagnosis of COPD (5 with asthma and 4 without) (Jansen et al., 2005, [082236](#)). Exhaled NO was measured daily for 12 days, along with personal, indoor, outdoor and central site PM₁₀, PM_{2.5} and BC. Significant associations between 24-h avg PM and eNO

were found only for the asthmatic subjects: 10 $\mu\text{g}/\text{m}^3$ increases in outdoor levels (measured outside the subjects' homes) of $\text{PM}_{2.5}$ or PM_{10} were associated with increases in eNO of 4.23 ppb (95% CI: 1.33-7.13), an increase of 22% above the group mean of 19.2 ppb, and 5.87 ppb (95% CI: 2.87-8.88), an increase of 31%, respectively. BC measured indoors, outdoors or personally was also associated with significant increases in eNO (of 3.97, 2.32, and 1.20 ppb, respectively) (Jansen et al., 2005, [082236](#)).

Adar et al. (2007, [001458](#)) conducted a panel study of 44 non-smoking seniors residing in St. Louis, MO (60 yr). As part of the study, subjects were taken on group trips to a theater performance, Omni movie, outdoor band concert, and a Mississippi River boat cruise. Subjects were driven to and from each event aboard a diesel bus. Before and after each bus trip, eNO was measured on each subject. Two carts containing continuous air pollution monitors were used to measure group-level micro-environmental exposures to $\text{PM}_{2.5}$, BC, and size-specific particle counts (0.3-2.5 μm and 2.5-10 μm) on the day of each trip. Each 10 $\mu\text{g}/\text{m}^3$ increase in 24-h mean $\text{PM}_{2.5}$ concentration was associated with a 36% increase in eNO pre-trip (95% CI: 5-71). Each 10 $\mu\text{g}/\text{m}^3$ increase in micro-environmental $\text{PM}_{2.5}$ concentration (i.e., during the bus ride) was associated with a 27% increase in eNO post-trip (95% CI: 17-38).

These studies all demonstrated an association between increased levels of eNO and increases in PM in the previous 4-24 h. Further, three studies demonstrated effects in elderly populations (Adamkiewicz et al., 2004, [087925](#); Adar et al., 2007, [001458](#); Jansen et al., 2005, [082236](#)) while four others reported a similar acute increase in eNO among children (Delfino et al., 2006, [090745](#); Koenig et al., 2003, [156653](#); 2005, [087384](#); 2005, [088999](#)).

Outside of the U.S., one study examined eNO in a panel of 60 adult asthmatic subjects in London. McCreanor et al. (2007, [092841](#)) reported that 1 $\mu\text{g}/\text{m}^3$ increase in personal exposure to EC was associated with significant increases of approximately 1.75-2.25% in eNO (results were presented graphically only) for up to 22 h post-exposure.

Other Biomarkers of Pulmonary Inflammation and Oxidative Stress

Other biomarkers of respiratory distress that have been examined in recent panel studies include urinary leukotriene E4 (LTE_4) in asthmatic children (Rabinovitch et al., 2006, [088031](#)); two oxidative stress markers: thiobarbituric acid reactive substances (TBARS) and 8-isoprostane in asthmatic children (Liu et al., 2009, [192003](#)) and breath

acidification in adolescent athletes (Ferdinands et al., 2008, [156433](#)). Mean concentration data from these studies are characterized in Table 6-7.

In Rabinovitch et al. (2006, [088031](#)), LTE_4 , an asthma-related biological mediator, was used to study the response to short-term particle exposure. In the second winter of their 2-yr study of asthmatic children (described above in Section 6.3.1.1, under respiratory symptom and medication use outcomes), urine samples were collected at approximately the same time of day from 57 subjects for 8 consecutive days. Controlling for days with URI symptoms, each $10 \mu\text{g}/\text{m}^3$ increase in morning maximum $\text{PM}_{2.5}$ (measured by TEOM), was associated with an increase in LTE_4 levels by 5.1% (95% CI: 1.6-8.7). No significant effects were observed on the same day or up to 3 days later based on 24-h averaged concentrations from the TEOM monitor or from the FRM central site monitor.

In a longitudinal study conducted in Windsor, Ontario, Liu et al. (2009, [192003](#)) examined the association between acute increases in ambient air pollutants and TBARS and 8-isoprostane among children (ages 9-14 yr) with asthma. TBARS, but not 8-isoprostane, was positively associated with $\text{PM}_{2.5}$ (percent change in TBARS 40.6% [95% CI: 11.8-81.3], lag 0-2 days). The association with TBARS persisted for at least 3 days. Adverse changes in pulmonary function (see above) were consistent with those of TBARS in response to $\text{PM}_{2.5}$ with a similar lag structure, suggesting a coherent outcome for small airway function and oxidative stress.

The effects of vigorous outdoor exercise during peak smog season in Atlanta, GA on breath pH, a biomarker of airway inflammation, in adolescent athletes ($n = 16$, mean age = 14.9 yr) were examined by Ferdinands et al. (2008, [156433](#)). Median pre-exercise breath pH was 7.58 (range 4.39-8.09) and median post-exercise breath pH was 7.68 (range 3.78-8.17). The authors observed no significant association between ambient PM and post-exercise breath pH. However both pre- and post-exercise breath pH were strikingly low in these athletes when compared to 14 relatively sedentary healthy adults and to published values of breath pH in healthy subjects. The authors speculate that repetitive vigorous exercise may induce airway acidification.

Effect of Measurement Location on Studies of Pulmonary Function and Inflammation

A number of studies examining exposure to $\text{PM}_{2.5}$ and pulmonary function and inflammation have compared the results of exposure assessment based on concentrations recorded from personal, indoor, outdoor, and/or ambient monitors (Allen et al., 2008,

[156208](#); Delfino et al., 2004, [056897](#); Delfino et al., 2006, [090745](#); Koenig et al., 2005, [087384](#); Trenga et al., 2006, [155209](#)). Two investigations evaluated PM_{2.5} concentrations from indoor, outdoor, personal and central site monitors and the relationship with FEV₁. Delfino et al. (2004, [056897](#)) reported that personal exposure estimates showed a stronger association with FEV₁ than any of the stationary exposures, and that indoor exposure estimates were associated with a stronger effect than either outdoor or central site exposure estimates. However, Trenga et al. (2006, [155209](#)) reported the largest declines in FEV₁ associated with central site exposure estimates, though the most consistent association with declines in FEV₁ came from the exposure estimates measured by indoor monitors. Delfino et al. (2006, [090745](#)) used personal and ambient exposure estimates in a study of FeNO among asthmatic children and found that the personal exposure estimates were more robust than the ambient exposure estimates. Two studies conducted in Seattle, WA partitioned personal exposure to PM_{2.5} into its ambient-generated and indoor-generated components. Koenig et al. (2005, [087384](#)) reported that ambient-generated PM_{2.5} was consistently associated with an increase in FeNO, while the indoor-generated component of PM_{2.5} was less strongly associated with FeNO. This could reflect the difference in composition of indoor-generated PM_{2.5} as compared to ambient-generated PM_{2.5}. Similarly, Allen et al. (2008, [156208](#)) found that FeNO was associated with the ambient-generated component of personal PM_{2.5} exposure, but not with ambient PM_{2.5} concentrations measured by central site monitors. Overall, these studies provide a unique perspective on how measurement location influences the findings of epidemiologic studies. This small group of studies indicates that effects are associated with all types of PM measurement, suggesting health effects of both ambient-generated and indoor-generated particles. It is likely that variability in season, meteorology, topography, geography, behavior and exposure patterns contribute to the observed differences.

6.3.3.2. Controlled Human Exposure Studies

Studies of controlled human exposures presented in the 2004 PM AQCD (U.S. EPA, 2004, [056905](#)) provided evidence of pulmonary inflammation induced by exposure to PM. Lay et al. (1998, [007683](#)) found that instillation of iron oxide particles (2.6 µm) produced an increase in alveolar macrophages and neutrophils in BALF collected 24 h post-instillation. Ghio and Devlin (2001, [017122](#)) evaluated the inflammatory response following instillation of particles extracted from filters collected in the Utah Valley both prior to and after the

closure of an area steel mill. Subjects who underwent pulmonary instillation of particles (500 µg) collected while the steel mill was operating (n = 16) had significantly higher levels of neutrophils 24 h post-instillation compared with either saline instillation or with subjects (n = 8) who were instilled with the same mass of PM collected during the mill's closure. This finding indicates that metals may be an important PM component for this health outcome. In an inhalation study of exposure to fine CAPs (23-311 µg/m³) from Chapel Hill, NC, Ghio et al. (2000, [012140](#)) observed an increase in airway and alveolar neutrophils 18 h after the 2-h exposure. A similar finding was reported by Rudell et al. (1999, [001964](#)) following exposure to DE among healthy adults. In this study, reducing the particle number from 2.6 x 10⁶/cm³ to 1.3 x 10⁶/cm³ while maintaining the concentration of gaseous diesel emissions, was not observed to attenuate the response. As summarized below, several recent studies of controlled exposures have provided some additional evidence of pulmonary inflammation associated with PM.

CAPS

A series of exposures to ultrafine, fine, and thoracic coarse CAPs from Los Angeles with average particle concentrations between 100 and 200 µg/m³ have not been shown to have a significant effect on markers of airway inflammation in healthy or health-compromised adults (Gong et al., 2004, [087964](#); 2004, [055628](#); 2005, [087921](#); 2008, [156483](#)). However, two recent studies conducted in Chapel Hill, NC reported significant increases in percent PMNs and concentration of IL-8 in BALF among healthy adults 18-20 h following controlled exposures to coarse (89 µg/m³) and ultrafine (49.8 µg/m³) CAPs, respectively (Graff et al., 2009, [191981](#); Samet et al., 2009, [191913](#)). As discussed above, the same laboratory previously reported a mild inflammatory response in the lower respiratory tract following exposure to fine CAPs (Ghio et al., 2000, [012140](#)). In a follow-up analysis, Huang et al. (2003, [087377](#)) found the increase in BAL neutrophils demonstrated by Ghio et al. (2000, [012140](#)) to be positively associated with the Fe, Se, and SO₄²⁻ content of the particles.

Alexis et al. (2006, [154323](#)) recently evaluated the effect of PM_{10-2.5} on markers of airway inflammation, specifically focusing on the impact of biological components of PM_{10-2.5}. Healthy men and women (n = 9) between the ages of 18 and 35 inhaled nebulized saline (0.9%) as well as aerosolized PM_{10-2.5} collected from ambient air. Subjects were exposed to PM_{10-2.5} on two separate occasions, once using PM_{10-2.5} that had been heated to inactivate biological material and once using non-heated PM_{10-2.5}. Approximately 0.65 mg

PM_{10-2.5} was deposited in the respiratory tract of subjects during the exposures. Markers of inflammation and immune function were analyzed in induced sputum collected 2-3 h after inhalation of saline or PM_{10-2.5}. Both heated and non-heated PM_{10-2.5} were observed to increase the neutrophil response compared with saline. Exposure to non-heated PM_{10-2.5} was found to increase levels of monocytes, eotaxin, macrophage TNF- α mRNA, and was also associated with an upregulation of macrophage cell surface markers. No such effects were observed following exposure to biologically inactive PM_{10-2.5}. These results suggest that while thoracic coarse fraction PM-induction of neutrophil response is not dependent on biological components, heat sensitive components of coarse PM (e.g., endotoxin) may be responsible for PM-induced alveolar macrophage activation.

Traffic Particles

Larsson et al. (2007, [091375](#)) exposed 16 healthy adults to air pollution in a road tunnel for 2 h during the afternoon rush hour in Stockholm, Sweden. The median PM_{2.5} and PM₁₀ concentrations during the road tunnel exposures were 64 $\mu\text{g}/\text{m}^3$ and 176 $\mu\text{g}/\text{m}^3$, respectively. Bronchial biopsies were obtained and bronchoscopy and bronchoalveolar lavage were performed 14 h after the exposure. The results were compared with a control exposure which consisted of exposure to urban air during normal activity. The authors reported significant BALF increases in percentage of lymphocytes, total cell number, and alveolar macrophages following exposure to road tunnel exposure versus control. These results provide evidence of a significant association between exposure to road tunnel air pollution and airway inflammation. However, unlike other controlled exposure studies, the control exposure was not a true clean air control, but only a lower dose exposure group with no characterization of personal exposure. In addition, it is not possible to separate out the contributions of each air pollutant, including PM, on the observed inflammatory response.

Diesel Exhaust

In a recent study evaluating the effect of DE exposure on markers of airway inflammation, Behndig et al. (2006, [088286](#)) exposed healthy adults ($n = 15$) for 2 h with intermittent exercise to filtered air or DE with a reported PM₁₀ concentration of 100 $\mu\text{g}/\text{m}^3$. Eighteen hours after exposure to DE, the authors found significant increases in neutrophil and mast cell numbers in bronchial tissue, as well as significant increases in neutrophil numbers and IL-8 in bronchial lavage fluid compared with filtered air control. Similarly, Stenfors et al. (2004, [157009](#)) observed an increase in pulmonary inflammation (e.g.,

airways neutrophilia and an increase in IL-8 in BALF) among healthy adults 6 h following exposure to DE (PM₁₀ average concentration 108 µg/m³). It is interesting to note, however, that no such inflammatory effects were observed in a group of mild asthmatic subjects in the same study. The DE-induced neutrophil response in the airways of healthy subjects observed in these two studies (Behndig et al., 2006, [088286](#); Stenfors et al., 2004, [157009](#)) is qualitatively consistent with the findings of Ghio et al. (2000, [012140](#)) who exposed healthy subjects to Chapel Hill fine CAPs. In a group of healthy volunteers, Bosson et al. (2007, [156286](#)) demonstrated that exposure to O₃ (2 h at 0.2 ppm) may enhance the airway inflammatory response of DE relative to clean air (1-h exposure to 300 µg/m³). Exposure to O₃ was conducted 5 h after exposure to DE, and resulted in an increase in the percentage of neutrophils in induced sputum collected 18 h after exposure to O₃. In a subsequent study using a similar protocol at the same concentrations, prior exposure to DE was shown to increase the inflammatory effects of O₃ exposure, demonstrated as an increase in neutrophil and macrophage numbers in bronchial wash (Bosson et al., 2008, [156287](#)).

Wood Smoke

Barregard et al. (2008, [155675](#)) examined the effect of a short-term exposure (4 h) to WS (240-280 µg/m³) on markers of pulmonary inflammation in a group of healthy adults. Exposure to WS increased alveolar NO compared to filtered air (2.0 ppb versus 1.3 ppb) 3 h after exposure. Although these results provide some evidence of a PM-induced increase in pulmonary inflammation, the physiological significance of the relatively small increase in alveolar NO is unclear.

Model Particles

Pietropaoli et al. (2004, [156025](#)) observed a lack of airway inflammatory response 21 h after exposure to ultrafine EC particles (10-50 µg/m³) among healthy and asthmatic adults. The same laboratory reported no effect of exposure to ultrafine or fine ZnO (500 µg/m³) on total or differential sputum cell counts 24 h after exposure in a group of healthy adults (Beckett et al., 2005, [156261](#)). Tunnicliffe et al. (2003, [088744](#)) measured levels of eNO as a marker of airway inflammation following 1-h controlled exposures to ammonium bisulfate or aerosolized H₂SO₄ (200 and 2,000 µg/m³) in a group of healthy and asthmatic adults. While exposure to ammonium bisulfate increased the concentration of eNO immediately following exposure in asthmatics, no such effect was observed in healthy adults, or in either healthy or asthmatic adults following exposure to aerosolized H₂SO₄.

Instillation

Schaumann et al. (2004, [087966](#)) investigated the inflammatory response of human subjects instilled with PM_{2.5} (100 µg) collected from two different cities in Germany, Hettstedt and Zerbst. Although instillation of PM from both cities were shown to induce airway inflammation, instillation of PM from the more industrial area (Hettstedt) resulted in greater influxes of BALF monocytes compared to PM collected from Zerbst. The authors postulated that the difference in response between PM from the two cities may be due to the higher concentration of transition metals observed in the samples collected from Hettstedt. Another study reported no change in inflammatory markers in nasal lavage fluid 4 and 96 h following intranasal instillation of DEP (300 µg/nostril) in asthmatics and healthy adults (Kongerud et al., 2006, [156656](#)). Pre-exposure of DEP to O₃ was not shown to have any effect on the response. Although not a cross-over design, these findings suggest that exposure to DEP without the gaseous component of DE may have little effect on inflammatory responses in human subjects.

Summary of Controlled Human Exposure Study Findings for Pulmonary Inflammation

These new studies strengthen the evidence of PM-induced pulmonary inflammation, with the majority of the evidence associated with fine and thoracic coarse fractions. The response appears to vary significantly depending on the source and composition of the particles.

6.3.3.3. Toxicological Studies

The 2004 PM AQCD (U.S. EPA, 2004, [056905](#)) discussed numerous studies investigating pulmonary inflammation in response to CAPs, ROFA, DEPs, metals and acid aerosols. A wide variety of responses was reported depending on the type of PM and route of administration. In general, IT exposure to fly ash and metal PM resulted in notable pulmonary inflammation. In contrast, inhalation of sulfates and acid aerosols had minimal if any effect on pulmonary inflammation. More recent animal toxicological studies using CAPs, DE and other relevant PM types are summarized below.

CAPs

The 2004 PM AQCD (U.S. EPA, 2004, [056905](#)) found that exposure to fine CAPs at concentrations of 100-1,000 µg/m³ for 1-6 h/day and 1-3 days generally resulted in minimal to mild inflammation in rats and dogs. Somewhat enhanced inflammation was observed in

a model of chronic bronchitis. Since the last review, numerous studies have investigated inflammatory responses to fine and ultrafine CAPs in both healthy and compromised animal models.

In one study of healthy animals, SD rats were exposed to CAPs for 4 h/day on 3 consecutive days in Fresno, CA, in fall 2000 and winter 2001 (PM_{2.5}; mean mass concentration 190-847 µg/m³) (Smith et al., 2003, [042107](#)). The particle concentrator used in these studies was capable of enhancing the concentration of ultrafine as well as fine particles. Immediately after exposure on the third day, BALF was collected and analyzed for total cells and neutrophils. Statistically significant increases were observed in numbers of neutrophils during the first week of the fall exposure period and in numbers of total cells, neutrophils and macrophages during the first week of the winter exposure period. CAPs concentrations were >800 µg/m³ during both of those weeks.

Two studies were conducted using CAPs in Boston. In a study by Godleski et al. (2002, [156478](#)), healthy SD rats were exposed for 5 h/day for 3 consecutive days to CAPs ranging in concentration from 73.5-733.0 µg/m³. BALF and lung tissue were collected for analysis 1 day later. Neutrophilic inflammation was indicated by a statistically significant increase in percent neutrophils in BALF. Microarray analysis of RNA from lung tissue and BALF cells demonstrated increased gene expression of pro-inflammatory mediators, markers of vascular activation and enzymes involved in organic chemical detoxification. This study overlapped in part with previously described studies by Saldiva et al. (2002, [025988](#)) and Batalha et al. (2002, [088109](#)) (see Section 6.2.4.3). In another study, healthy SD rats were exposed for 5 h to CAPs (mean mass concentration 1228 µg/m³; 6/20-8/16/2002; (Rhoden et al., 2004, [087969](#)). A statistically significant increase in BALF neutrophils was observed 24-h following CAPs exposure. Histological analysis confirmed the influx of inflammatory cells (Section 6.3.5.3). Inflammation was accompanied by injury which is discussed in Section 6.3.5.3.

Kodavanti et al. (2005, [087946](#)) reported two sets of studies involving fine CAPs exposure during fall months in RTP, NC. In the first study, SH rats were exposed to filtered air or CAPs (mean mass concentration range 1,138-1,765 µg/m³; less than 2.5 µm in size) for 4 h and analyzed 1-3 h later. No increase in BALF inflammatory cells or other measured parameter was observed. In the second study, SH and WKY rats were exposed to filtered air or CAPs (mean mass concentration range 144-2,758 µg/m³; less than 2.5 µm in size) for 4 h/day on 2 consecutive days and analyzed 1 day afterward. Differences in baseline

parameters were noted for the two rat strains since SH rats had greater numbers of BALF neutrophils than WKY rats. Following the 2-day CAPs exposure, increased BALF neutrophils were observed in the WKY rats but not in the SH rats compared with filtered air controls. Inflammation was not accompanied by increases in BALF markers of injury (see Section 6.3.5.3).

Two CAPs studies involving SH rats were conducted in the Netherlands. In the first, SH rats were exposed by nose-only inhalation to CAPs (ranging in concentration from 270-3,660 $\mu\text{g}/\text{m}^3$ and in size from 0.15-2.5 μm) from 3 different sites in the Netherlands (suburban, industrial and near-freeway) for 6 h (Cassee et al., 2005, [087962](#)). Increased numbers of neutrophils were observed in BALF 2 days post-exposure compared to air controls. When CAPs exposure was used as a binary term, the relationship between CAPs concentration and number of PMN in BALF was statistically significant. In contrast, Kooter et al. (2006, [097547](#)) reported no changes in markers of pulmonary inflammation measured 18 h after a 2-day exposure (6 h/day) of SH rats to fine or fine+ultrafine CAPs from sites in the Netherlands (mean mass concentration range 399-3613 and 269-556 $\mu\text{g}/\text{m}^3$, respectively; fine CAPs site in Bilthoven and fine+ultrafine CAPs site in freeway tunnel in Hendrik Ido Ambacht).

Pulmonary inflammation was investigated in 2 studies using a rat model of pulmonary hypertension (i.e., SD rats pre-treated with monocrotaline). In the first study, rats were exposed to fine CAPs from an urban high traffic area in Taiwan (mean mass concentration of 371 $\mu\text{g}/\text{m}^3$) (Lei et al., 2004, [087999](#)) for 6 h/day on 3 consecutive days and BALF was collected 2 days later. A statistically significant increase in total cells and neutrophils was observed in BALF. Levels of TNF α and IL-6 in the BALF were not altered by CAPs exposure. In the second study, rats were exposed to fine CAPs (mean mass concentration 315.6 and 684.5 $\mu\text{g}/\text{m}^3$ for 6 and 4.5 h, respectively; Chung-Li area, Taiwan) during a dust storm event occurring 3/18-3/19/2002 (Lei et al., 2004, [087884](#)). Only one animal served as control during the 6-h exposure (from 2100-300 on the first exposure day) so results were combined with that of 3 control animals from the 4.5-h exposure (from 300-730) on the second exposure day. A statistically significant increase in total cells and neutrophils in BALF occurred in both CAPs-exposed groups. In addition, increases in BALF IL-6 and markers of injury (see Section 6.3.5.3) were observed as a function of CAPs exposure.

In summary, pulmonary inflammation was noted in all 3 studies involving multiday exposure of healthy rats to CAPs from different locations. No pulmonary inflammation was seen in one study of SH rats exposed to CAPs for 4 h and analyzed 1-3 h later. In studies involving multiday exposure of SH rats, one demonstrated pulmonary inflammation while two did not. In the rat monocrotaline model of pulmonary hypertension, both single-day and multiday exposures to CAPs resulted in mild pulmonary inflammation.

On-Road Exposures

In a study by Elder et al. (2004, [087354](#)) (21 months) were exposed to on-road highway aerosols (particle concentration range $0.95\text{-}3.13 \times 10^5$ particles/cm³; mass concentration estimated to be 37-106 µg/m³; Interstate 90 between Rochester and Buffalo, NY) for 6 h on 1 or 3 consecutive days. No increase in BALF inflammatory cells was observed 18 h post-exposure in any of the treatment groups.

Urban Air

To evaluate inflammatory responses to ambient particles from vehicles, Wistar rats were exposed to ambient urban air from a high traffic site (concentration range 22-225 µg/m³ PM₁₀; Porto Alegre, Brazil) or to the same air which was filtered to remove the PM (Pereira et al., 2007, [156019](#)). Concentrations of gases were not reported. Compared with filtered air controls, a significant increase in total number of BALF cells was observed 24 h following the 20 h continuous exposure but not following the 6 h of exposure to unfiltered urban air.

Diesel Exhaust

The 2004 PM AQCD (U.S. EPA, 2004, [056905](#)) summarized findings of the 2002 EPA Diesel Document regarding the health effects of DE. Short-term inhalation exposure to low levels of DE results in the accumulation of DPM in lung tissue, pulmonary inflammation and alveolar macrophage aggregation and accumulation near the terminal bronchioles. More recent studies are summarized below.

Pulmonary inflammatory responses were investigated in C57BL/6 mice exposed to diesel engine emissions 7 h/day for 6 consecutive days (Harrod et al., 2003, [097046](#)). Compared with controls, inflammatory cell counts in BALF were increased in mice exposed to the higher concentration of DE (1,000 µg/m³ DEP) but not in mice exposed to the lower

concentration of DE (30 $\mu\text{g}/\text{m}^3$ DEP). Concentrations of gases present in the higher dose DE were reported to be 43 ppm NO_x, 20 ppm CO and 364 ppb SO₂.

In a second study evaluating DE effects on BALF inflammatory cells, no increases in numbers of neutrophils, lymphocytes or eosinophils were observed in BALB/c mice exposed by inhalation to 500 or 2000 $\mu\text{g}/\text{m}^3$ DEP for 4 h/day on 5 consecutive days (Stevens et al., 2008, [157010](#)). Concentrations of gases reported in this study were 4.2 ppm CO, 9.2 ppm NO, 1.1 ppm NO₂, and 0.2 ppm SO₂ for the higher concentration of DE. Transcriptional microarray analysis demonstrated upregulation of chemokine and inflammatory cytokine genes, as well as genes involved in growth and differentiation pathways, in response to the higher concentration of DE. No gene expression results were reported for the lower concentration of DE. Sensitization and challenge with ovalbumin significantly altered these findings (see Section 6.3.6.2). These results demonstrate that changes in gene expression can occur in the absence of measurable pulmonary inflammation or injury markers (see Section 6.3.5.3).

Li et al. (2007, [155929](#)) exposed mice to clean air or to low dose DE (DEP 100 $\mu\text{g}/\text{m}^3$) for 7 h/day and 5 days/wk for 1, 4 and 8 wk as described in Section 6.3.2.3. Analysis of BALF and histology of lung tissues was carried out at day 0 and after 1, 4 and 8 wk of exposure. Total numbers of cells and macrophages in BALF were significantly increased in C57BL/6 mice but not in BALB/c mice after 1-wk exposure to DE compared with 0 day controls. Neutrophils and lymphocytes were increased after 1-wk exposure to DE in both strains compared with 0 day controls. Differences in BALF cytokines were also noted between the 2 strains after 1-wk exposure to DE. No changes were observed by histological analysis. Pulmonary function and oxidative responses were also evaluated (Sections 6.3.2.3 and 6.3.4.2) Long-term exposure responses are discussed in Sections 7.3.2.2, 7.3.3.2 and 7.3.4.1.

Healthy Fisher 344 rats and A/J mice were exposed to DE containing 30, 100, 300 and 1000 $\mu\text{g}/\text{m}^3$ PM by whole body inhalation for 6 h/day, 7 days/wk for either 1 wk or 6 months in a study by Reed et al. (2004, [055625](#)). Concentrations of gases were reported to be from 2.0-45.3 ppm NO, 0.2-4.0 ppm NO₂, 1.5-29.8 ppm CO and 8-365 ppb for SO₂ in these exposures. One week of exposure resulted in no measurable effects on pulmonary inflammation. Long-term exposure responses are discussed in Section 7.3.3.2.

In a study by Wong et al. (2003, [097707](#)) and Witten et al. (2005, [087485](#)), Fisher 344/NH rats were exposed nose-only to filtered room air or to DE at concentrations of

35.3 $\mu\text{g}/\text{m}^3$ and 669.3 $\mu\text{g}/\text{m}^3$ DEP (particle size range 7.2-294.3 nm) for 4 h/day and 5 days/wk for 3 wk. Gases associated with the high dose exposure were reported to be 3.59 ppm NO, 3.69 ppm NO_x, 0.1 ppm NO₂, 2.95 ppm CO, 518.96 ppm CO₂ and 0.031 ppm total hydrocarbon. The focus of this study was on the possible role of neurogenic inflammation in mediating responses to DE. Neurogenic inflammation is characterized by both the influx of inflammatory cells and plasma extravasation into the lungs following the release of neuropeptides from bronchopulmonary C-fibers. Pulmonary inflammation was evaluated by histological analysis of lung tissue at the end of the 3-wk exposure period. Following high, but not low, dose-exposure to DE, a large number of alveolar macrophages was found in the lungs. Small black particles, presumably DEP, were found in the cytoplasm of these alveolar macrophages. Perivascular cuffing consisting of mononuclear cells was also observed in high dose-exposed animals. Influx of neutrophils or eosinophils was not seen although mast cell number was increased in high-dose exposed animals. Pulmonary plasma extravasation was measured by the ^{99m}Tc-Technecium-albumin technique and found to be dose-dependently increased in the bronchi and lung parenchyma. Alveolar edema was also observed by histopathology in high dose-exposed animals. A significant decrease in substance P content in lung tissue was reported in DE-exposed rats. These responses initially suggested that DE resulted in stimulation of C-fibers and activation of a local neuron reflex resulting in the repeated release of the stored neuropeptide substance P. Subsequent experiments were conducted using capsaicin pretreatment, which inhibits neurogenic inflammation by activating C-fibers and causing the depletion of neuropeptide stores. Pretreatment with capsaicin was found to reduce the influx of inflammatory cells but not plasma extravasation in response to DE. Hence, DE is unlikely to act through bronchopulmonary C-fibers to cause neurogenic inflammation in this model, although there may be a different role for bronchopulmonary C-fibers in mediating the inflammatory cell influx.

Stimulation of bronchopulmonary C-fibers can result in activation of both local and CNS reflexes through vagal parasympathetic pathways. McQueen et al. (2007, [096266](#)) investigated the role of vagally-mediated pathways in acute inflammatory responses to DEP. A statistically significant increase in BAL neutrophils was observed 6 h after IT treatment of anesthetized Wistar rats with 500 μg DEP (SRM2975). This response was blocked by severing the vagus nerve or pretreatment with atropine (McQueen et al., 2007, [096266](#)). Similarly, atropine treatment blocked the increase in BAL neutrophils seen 6 h

after DEP exposure in conscious Wistar rats. These results provide evidence for the involvement of a pulmonary vagal reflex in the inflammatory response to DEP.

In summary, several studies demonstrate that short-term inhalation exposure to DE (100-1,000 $\mu\text{g}/\text{m}^3$ DEP) causes pulmonary inflammation in rodents. No attempt was made in these studies to determine whether the responses were due to PM components or to gaseous components. However, PM from DE was found to be capable of inducing an inflammatory response, as demonstrated by the one IT instillation study described above. Evidence was presented suggesting that DEP may act through bronchopulmonary C-fibers to stimulate pulmonary inflammation.

Gasoline Emissions and Road Dust

Healthy male Swiss mice were exposed to gasoline exhaust (635 $\mu\text{g}/\text{m}^3$ PM and associated gases) or filtered air for 15 min/day for 7, 14, and 21 days (Sureshkumar et al., 2005, [088306](#)). BALF was collected for analysis 1-h after the last exposure. Histological analysis was also carried out at 7, 14, and 21 days. The number of leukocytes in BALF was increased after exposure to gasoline exhaust but this increase did not achieve statistical significance. However, levels of the pro-inflammatory cytokines TNF α and IL-6 were significantly increased in BALF following 14 and 21 days of exposure. Furthermore, inflammatory cell infiltrate in the peribronchiolar and alveolar regions were observed by histology. Evidence of lung injury was also found (see Section 6.3.5.3). In this study, BALF analysis of inflammatory cells was a less sensitive indicator of pulmonary inflammation than BALF analysis of cytokines and histological analysis of lung tissue. Unfortunately results of this study cannot entirely be attributed to the presence of PM in the gasoline exhaust since 0.11 mg/m^3 SO $_x$, 0.49 mg/m^3 of NO $_x$ and 18.7 ppm of CO were also present during exposure.

Using ApoE $^{-/-}$ mice on a high-fat diet, Campen et al. (2006, [096879](#)) studied the impact of inhaled gasoline emissions and road dust (6 h/day \times 3 day) on pulmonary inflammation. Moreover, the investigators used a high efficiency particle filter to compare the whole exhaust with an atmosphere containing only the gaseous components. For gasoline emissions, the PM-containing atmosphere (PM mean concentration 61 $\mu\text{g}/\text{m}^3$; NO $_x$ mean concentration 18.8 ppm; CO mean concentration 80 ppm) failed to increase numbers of inflammatory cells in BALF collected 18 h after the last exposure. However, a statistically

significant increase in total cells and macrophages was observed in response to resuspended road dust (PM_{2.5}) at 3500 µg/m³, but not at 500 µg/m³.

Model Particles

In a study by Elder et al. (2004, [055642](#)), pulmonary inflammation was investigated in two compromised, aged animal models (11-14 mo old SH and 23 mo old Fischer 344) exposed by inhalation to ultrafine CB (count median diameter = 36 nm) at a relevant concentration (150 µg/m³). No changes in BALF cells were seen 24 h post-exposure in either model.

An increase in BALF neutrophils was observed at 24 h but not at 4 h in WKY rats exposed to ultrafine carbon particles (median particle size 38 nm; mass concentration 180 µg/m³; mean number concentration 1.6×10^7 particles/cm³) for up to 24 h (Harder et al., 2005, [087371](#)). Changes in HR and HRV demonstrated in this study (see Section 6.2.1.3) occurred much more rapidly than the inflammatory response.

No evidence of pulmonary inflammation was found by analysis of BALF or pulmonary histopathology 1 or 3 days following 24-h exposure of SH rats to ultrafine carbon particles under similar conditions (median particle size 31 nm; mass concentration 172 µg/m³; mean number concentration 9.0×10^6 particles/cm³) (Upadhyay et al., 2008, [159345](#)). However increased expression of HO-1, ET-1, ET_A and ET_B, tPA and, plasminogen activator-1 was found in lung tissue 3 days following exposure.

In a study by Gilmour et al. (2004, [054175](#)), adult Wistar rats were exposed for 7 h to fine and ultrafine CB particles (mean mass concentration 1400 and 1660 µg/m³ for fine and ultrafine CB, respectively; mean number concentration 3.8×10^3 and 5.2×10^4 particles/cm³, respectively; count median aerodynamic diameter 114 nm and 268 nm, respectively). Both treatments resulted in increased BALF neutrophils 16 h post-exposure, with the UFPs having the greater response. UFPs also increased total BALF leukocytes and macrophage inflammatory protein-2 mRNA in BALF cells. Although these exposures may not be relevant to ambient exposures, this study demonstrated the greater propensity of ultrafine CB particles to cause a pro-inflammatory response compared with fine CB particles.

In a study by Last et al. (2004, [097334](#)), mice were exposed to 250 µg/m³ laboratory-generated iron-soot over a 2-wk period as described in Section 6.3.2.3. BALF was collected 1-h after the last exposure and analyzed for total cells. No increase in total cell

number was observed following iron-soot exposure. Other findings of this study are described in Sections 6.3.2.3 and 6.3.5.3.

Pinkerton et al. (2008, [190471](#)) exposed young adult male SD rats to filtered air, iron, soot or iron-soot. Increased levels of the pro-inflammatory cytokine IL-1 β were observed in lung tissue of rats exposed for 6 h/day for 3 days to 90 $\mu\text{g}/\text{m}^3$, but not 57 $\mu\text{g}/\text{m}^3$, iron. No change in BALF inflammatory cells was observed after exposure to 57 $\mu\text{g}/\text{m}^3$ or 90 $\mu\text{g}/\text{m}^3$ iron. Exposures to 250 $\mu\text{g}/\text{m}^3$ soot in combination with 45 $\mu\text{g}/\text{m}^3$ iron also resulted in increased levels of lung IL-1 β and activation of the transcription factor NF κ B. Levels of lung IL-1 β were increased in neonatal rats exposed to 250 $\mu\text{g}/\text{m}^3$ soot in combination with 100, but not 30, $\mu\text{g}/\text{m}^3$ iron. This study is described in greater detail in Sections 6.1.4.2.

6.3.4. Oxidative Responses

The results of a small number of controlled human exposure and toxicological studies presented in the 2004 PM AQCD (U.S. EPA, 2004, [056905](#)) provided some initial evidence of an association between exposure to PM and pulmonary oxidative stress. Recent controlled human exposure studies have provided support to previous findings of an increase in markers of pulmonary oxidative stress following exposure to DE, and one new study has observed a similar effect following controlled exposure to WS. New findings from toxicological studies provide further evidence that oxidative species are involved in PM-mediated effects. No epidemiologic studies have evaluated the association between PM concentration and pulmonary oxidative response.

6.3.4.1. Controlled Human Exposure Studies

Two studies cited in the 2004 PM AQCD (U.S. EPA, 2004, [056905](#)) observed effects on markers of airway oxidative response in healthy adults following controlled exposures to fresh DE or resuspended DEP (Blomberg et al., 1998, [051246](#); Nightingale et al., 2000, [011659](#)). Several recent studies are described below which have further evaluated the oxidative response following exposure to particles in human volunteers.

Diesel Exhaust

Pourazar et al. (Pourazar et al., 2005, [088305](#)) exposed 15 adults (11 males and 4 females) for 1 h to air or DE (PM₁₀ concentration 300 $\mu\text{g}/\text{m}^3$) in a controlled cross-over study. Bronchoscopy with airway biopsy was performed 6 h after exposure. The expression of

NF- κ B, AP-1 (c-jun and c-fos), p38, and JNK in bronchial epithelium was quantified using immunohistochemical staining. DE was observed to significantly increase nuclear translocation of NF- κ B, AP-1, phosphorylated p38, and phosphorylated JNK; however, the findings of this study require confirmation with more quantitative methods such as Western blot analysis. The observed activation of redox-sensitive transcription factors by DE may result in the induction of pro-inflammatory cytokines. There is some evidence to suggest that this bronchial response to DE is mediated through the epidermal growth factor receptor signaling pathway (Pourazar et al., 2008, [156884](#)). Behndig et al. (Behndig et al., 2006, [088286](#)) evaluated the upregulation of endogenous antioxidant defenses following exposure to DE (100 $\mu\text{g}/\text{m}^3$ PM₁₀) in a group of 15 healthy adults. Increases in urate and reduced GSH were observed in alveolar lavage, but not bronchial wash, 18 h after exposure. In a study utilizing the same exposure protocol, Mudway et al. (2004, [180208](#)) observed an increase in GSH and ascorbate in nasal lavage fluid 6 h following exposure to DE in a group of 25 healthy adults.

Wood Smoke

Barregard et al. (2008, [155675](#)) observed a significant increase in malondialdehyde levels in breath condensate of healthy volunteers (n = 13) immediately following and 20 h after a 4-h exposure to WS (240-280 $\mu\text{g}/\text{m}^3$).

Instillation

Schaumann et al. (2004, [087966](#)) demonstrated an increased oxidant radical generation of BAL cells following instillation of urban particles compared with instillation of particles collected in a rural area. The authors suggested that this difference was likely due to the greater concentration of transition metals found in the urban particles.

Summary of Controlled Human Exposure Study Findings for Blood Pulmonary Oxidative Responses

Taken together, these studies suggest that short-term exposure to PM at near ambient levels may produce mild oxidative stress in the lung. Limited data suggest that proximal and distal lung regions may be subject to different degrees of oxidative stress during exposures to different pollutant particles.

6.3.4.2. Toxicological Studies

The 2004 PM AQCD (U.S. EPA, 2004, [056905](#)) reported one study which provided evidence that ROS were involved in PM-mediated responses. This particular study used pre-treatment with the antioxidant DMTU to block the neutrophilic response to ROFA. More recently, several studies evaluated the effects of PM exposure on pulmonary oxidative stress. Oxidative stress can be directly determined by measuring ROS or oxidation products of lipids and proteins. An indirect assay involves measurement of the enzyme HO-1 or of the antioxidant enzymes SOD or catalase, all of which can be induced by oxidative stress. Antioxidant interventions which inhibit or prevent responses are a further indirect measure of oxidative stress playing a role in the pathway of interest.

CAPs

Gurgueira et al. (2002, [036535](#)) measured oxidative stress as in situ chemiluminescence (CL). Immediately following a 5-h CAPs exposure (PM_{2.5}; mean mass concentration range 99.6-957.5 µg/m³; Boston, MA) increased CL was observed in lungs of CAPs-exposed SD rats. CL evaluated after CAPs exposure durations of 3 h was also increased but did not achieve statistical significance compared to the filtered air group. When animals were allowed to recover for 24 h following the 5-h CAPs exposure, CL levels returned to control values. Interestingly, a decrease in lung CL was observed in rats breathing filtered air for 3 days compared with rats breathing room air for the same duration. Exposure to CAPs for 3 and 5 h also increased lung wet/dry ratios, indicating the presence of mild edema. To compare potential particle-induced differences in in situ CL, rats were exposed to ROFA (1.7 mg/m³ for 30 min) or CB (170 µg/m³ for 5 h). Only the ROFA-treated animals exhibited increased CL in lung tissue. Additionally, levels of antioxidant enzymes in the lung (MnSOD and catalase) were increased in CAPs-exposed rats. A CAPs-associated increase in CL was also seen in the heart (see Section 6.2.9.3) but not the liver.

In a similar study, Rhoden et al. (2004, [087969](#)) exposed SD rats for 5 h to CAPs from Boston (mean mass concentration 1228 µg/m³) or to filtered air. Significant increases in TBARS (a measure of lipid peroxidation) and protein carbonyl content (a measure of protein oxidation) were observed 24 h post-exposure to CAPs. Pretreatment with the thiol antioxidant NAC (50 mg/kg i.p.) 1-h prior to exposure prevented not only the lipid and protein oxidation observed in response to CAPs, but also the increase in BALF neutrophils

and pulmonary edema in this model (see Sections 6.3.3.3 and 6.3.5.3). Results of this study demonstrate the key role played by oxidative stress in these CAPs-mediated effects.

A later study by Rhoden et al. (2008, [190475](#)) investigated the role of superoxide in mediating pulmonary inflammation following exposure to ambient air particles. In this study, adult SD rats were IT exposed to 1 mg of SRM1649. Two h prior to exposure, half of the rats were pretreated with the membrane-permeable SOD mimetic MnTBAP (10 mg/kg, i.p.). MnTBAP abrogated the inflammatory response, measured by increased BALF inflammatory cells, and the increase in lung superoxide, measured by CL observed 4 h following exposure to urban air particles.

Kooter et al. (2006, [097547](#)) reported an increase in HO-1 in BALF and lung tissue measured 18 h after a 2-day exposure (6 h/day) of SH rats to fine or fine+ultrafine CAPs (mean mass concentration range 399-3613 and 269-556 $\mu\text{g}/\text{m}^3$, respectively; fine CAPs site in Bilthoven and ultrafine+fine site in freeway tunnel in Hendrik Ido Ambacht, the Netherlands). This occurred in the absence of any measurable pulmonary inflammation (see Section 6.3.3.3).

Urban Air

To evaluate oxidative stress responses to ambient particles from vehicles, Wistar rats were exposed to ambient urban air from a high traffic site (concentration range 22-225 $\mu\text{g}/\text{m}^3$ PM₁₀; Porto Alegre, Brazil) or to the same air which was filtered to remove the PM (Pereira et al., 2007, [156019](#)). Several exposures regimens were carried out: 6 and 20-h continuous exposures or to intermittent exposures of 5 h/day for 4 consecutive days. A significant increase in lipid peroxidation (measured as malondialdehyde) was seen in lung tissue immediately following the 20-h continuous exposure but not following the 6-h exposure or the intermittent exposures.

Diesel Exhaust

Li et al. (2007, [155929](#)) exposed mice to clean air or to low dose DE (DEP 100 $\mu\text{g}/\text{m}^3$) for 7 h/day and 5 days/wk for 1, 4 and 8 wk as described in Section 6.3.2.3. HO-1 mRNA and protein were increased in lung tissues of both mouse strains after 1 wk of DE exposure. In addition, AHR and changes in BAL cells and cytokines were observed (see Sections 6.3.2.3 and 6.3.3.3). Pretreatment with the thiol antioxidant NAC (320 mg/kg, i.p.) on days 1-5 of DE exposure greatly attenuated the AHR and inflammatory response seen after 1 wk of DE exposure. Long-term responses are discussed in Sections 7.3.2.2, 7.3.3.2 and 7.3.4.1.

A study by Whitekus et al. (2002, [157142](#)) investigated the adjuvant effects of DEP in an allergic animal model and is discussed in detail below (see Section 6.3.6.3). Intervention with the thiol antioxidants bucillamine and NAC inhibited the increases in allergen-specific IgE and IgG₁ as well as the increases in protein carbonyl and lipid hydroperoxides in the lung following DE exposure.

Gasoline Exhaust

Pulmonary oxidative stress was evaluated by measurement of CL and TBARS following exposure of SD rats to gasoline engine exhaust (Seagrave et al., 2008, [191990](#)). Animals were exposed for 6 h in a nose-only inhalation exposure system. PM mass concentration was reported to be 60 µg/m³; count median diameter 20 nm; mass median diameter 150 nm; while the concentrations of gaseous copollutants were 104 ppm CO, 16.7 ppm NO, 1.1 ppm NO₂ and 1.0 ppm SO₂. A statistically significant increase in lung CL was observed without a concomitant increase in lung TBARS. Discordant results were also observed for road dust exposures in the heart (see Section 6.2.9.3). The discrepancy between oxidative stress indicators suggests that the responses may follow different time courses. Furthermore, no CL was seen when the gasoline exhaust was filtered to remove the particulate fraction.

Model Particles

Increased expression of HO-1 was observed in lung tissue 3 days following 24-h exposure of SH rats to ultrafine carbon particles (median particle size 31 nm; mass concentration 172 µg/m³; mean number concentration 9.0×10^6 particles/cm³) despite no evidence of pulmonary inflammation (see Section 6.3.3.3) (Upadhyay et al., 2008, [159345](#))

In a study conducted by Pinkerton et al. (2008, [190471](#)) young adult male SD rats were exposed to filtered air, soot, iron or iron-soot for 6 h/day for 3 days. The iron particulates were mainly less than 100 nm aerodynamic diameter, while the soot particulates were initially 20-40 nm in diameter but formed clusters of 100-200 nm in diameter. The size-distribution of iron-soot particulates was bimodal over 10-250 nm and averaged 70-80 nm in diameter. Rats were exposed 6 h/day for 3 days to 45, 57 and 90 µg/m³ iron or to 250 µg/m³ soot alone or in combination with 45 µg/m³ iron. A statistically significant decrease in total antioxidant power and a statistically significant increase in glutathione-S-transferase activity were observed in lung tissue from rats exposed to 90 µg/m³ iron. This high concentration iron exposure also resulted in increased levels of

ferritin protein in lung tissue, indicating the presence of free iron which has the potential to redox cycle and cause oxidative stress. Lung tissue total antioxidant power was decreased and glutathione redox ratio was increased by the combined exposure to 250 $\mu\text{g}/\text{m}^3$ soot and 45 $\mu\text{g}/\text{m}^3$ iron. The iron-soot exposure also increased oxidized glutathione in BALF and lung tissue. These results demonstrate that co-exposure to soot enhanced iron-mediated oxidative stress. Furthermore, co-exposure to soot and iron resulted in increased expression of cytochrome P450 isozymes CYP1A1 and CYP2E1 in lung tissue, an effect not observed in response to either agent alone. Other endpoints of this study are described in Sections 6.1.3.3.

In a parallel study, Pinkerton et al. (2008, [190471](#)) exposed neonatal male SD rats to iron-soot or filtered air 6 h/day for 3 days during the second and fourth week of life. Both 30 $\mu\text{g}/\text{m}^3$ and 100 $\mu\text{g}/\text{m}^3$ iron in combination with 250 $\mu\text{g}/\text{m}^3$ soot resulted in increased BALF oxidized glutathione, glutathione redox ratio and glutathione-S-transferase activity and decreased total antioxidant power. The higher concentration exposure resulted in increased ferritin expression in lung tissue. Effects on cellular proliferation in specific regions of the lung were also noted as described in Section 6.1.5.3.

Nurkiewicz et al. (2009, [191961](#)) exposed SD rats to fine (count median diameter 710 nm) and ultrafine (count median diameter 100 nm) TiO_2 particles via aerosol inhalation at concentrations of 1.5-16 mg/m^3 for 240-720 min. These exposures were chosen in order to produce deposition of 4-90 $\mu\text{g}/\text{rat}$, which was demonstrated in a previous study to result in different degrees of impaired microvascular function (Nurkiewicz et al., 2008, [156816](#)). Histopathological analysis of lung tissue did not find any significant inflammation although particle accumulation in alveolar macrophages and a frequent association of alveolar macrophage with the alveolar wall was observed 24 h following exposure (Nurkiewicz et al., 2008, [156816](#)). Although the main focus of the more recent study was on effects of TiO_2 on NO production and microvascular reactivity in the spinotrapezius muscle (see Section 6.2.4.3), the presence of nitrotyrosine was determined in both lung tissue and spinotrapezius muscle as a measure of peroxynitrite formation. Peroxynitrite formation occurs mainly as a result of the rapid reaction of NO with superoxide and suggests an increase in local superoxide production. The area of lung tissue containing nitrotyrosine immunoreactivity increased 3-fold 24 h following exposure to 10 μg ultrafine TiO_2 . Nitrotyrosine immunoreactivity was localized in inflammatory cells found in the alveolar region of the lung.

6.3.5. Pulmonary Injury

The 2004 PM AQCD (U.S. EPA, 2004, [056905](#)) presented evidence from several toxicological studies of small PM-induced increases in markers of pulmonary injury including thickening of alveolar walls and increases in BALF protein. These findings are consistent with the results of recent toxicological studies demonstrating mild pulmonary injury accompanying inflammatory responses to CAPs. One recent epidemiologic study has also observed a positive association between PM and urinary concentrations of lung Clara cell protein.

6.3.5.1. Epidemiologic Studies

One epidemiologic study examined biomarkers of pulmonary injury. The mean concentration data from this study are characterized in Table 6-7. Timonen et al. (2004, [087915](#)) enrolled subjects with coronary heart disease in Amsterdam (n = 37), Erfurt, Germany (n = 47) and Helsinki (n = 47) to study daily variation in PM and urinary concentrations of lung Clara cell protein (CC16). No associations were seen between the particle number concentration of the smallest particles (NC_{0.01-0.1}) and CC16. Significant associations with NC_{0.1-1} and PM_{2.5} (which were strongly correlated with each other [r = 0.8]) were seen only for Helsinki subjects: same day, lag 3 and 5-day mean NC_{0.1-1} increases of 1000/cm³ were associated with increases in ln (CC16/creatinine) of 15.5% (95% CI: 0.001-30.9), 17.4% (95% CI: 3.4-31.4), and 43.2% (95% CI: 17.4-69.0), respectively. Similar associations were seen for 10 µg/m³ increases in PM_{2.5}: lag 0 and 5-day mean PM_{2.5} were associated with increases in ln (CC16/creatinine) of 23.3% (95% CI: 6.3-40.3) and 38.8% (95% CI: 15.8-61.8), respectively.

6.3.5.2. Controlled Human Exposure Studies

No studies of controlled human exposures presented in the 2004 PM AQCD (U.S. EPA, 2004, [056905](#)) specifically examined the effect of PM on pulmonary injury. However, several recent studies have evaluated changes in markers of injury and increased alveolar permeability following exposures to various types of particles.

Urban Traffic Particles

Bräuner et al. (2009, [191179](#)) evaluated the effect of exposure to urban traffic particles (24-h exposure, PM_{2.5} 9.7 µg/m³) on the integrity of the alveolar epithelial

membrane in a group of 29 healthy adults, with and without exercise. Following 2.5 h of exposure, alveolar epithelial permeability was assessed by measuring the pulmonary clearance of ^{99m}Tc-DTPA, which was administered as an aerosol during 3 min of tidal breathing. While pulmonary clearance of ^{99m}Tc-DTPA was observed to increase following exercise, there was no significant difference in clearance between exposure to urban traffic particles and filtered air. In addition, PM exposure was not observed to affect the level of CC16 in plasma or urine at 6 or 24 h after the start of exposure.

Diesel Exhaust

Relative to filtered air, exposure for 1 h to DE (300 µg/m³ particle concentration) was not observed to affect the plasma CC16 concentration at 6 or 24 h post exposure in a group of 15 former smokers with COPD (Blomberg et al., 2005, [191991](#)).

Wood Smoke

In a study examining the respiratory effects of WS, Barregard et al. (2008, [155675](#)) exposed two groups of healthy adults in separate 4-h sessions to WS with median particle concentrations of 243 and 279 µg/m³. At 20 h post-exposure, the mean serum CC16 concentration was significantly higher after exposure to WS when compared with filtered air. However, when the analysis was stratified by exposure session, a statistically significant effect of WS on serum CC16 was observed in the subjects in session 1, but not those in session 2. It is interesting to note that while the mean particle concentration was only slightly higher in session 1, the mean particle number in session 1 was almost 90% higher than the particle number in session 2, with geometric mean particle diameters of 42 and 112 nm, respectively.

Summary of Controlled Human Exposure Study Findings for Pulmonary Injury

The findings from these studies provide limited evidence to suggest that exposures to particles may increase markers of pulmonary injury in healthy adults.

6.3.5.3. Toxicological Studies

The 2004 PM AQCD (U.S. EPA, 2004, [056905](#)) reported mild increases in BALF protein, a marker of pulmonary injury, in several studies involving inhalation exposure to CAPs. In addition, histopathological analysis demonstrated that the bronchoalveolar junction was the site of the greatest inflammation following CAPs exposure. Low level

exposure to DE was associated with Type 2 cell proliferation and thickening of alveolar walls near alveolar macrophages according to the 2002 EPA Diesel Document (U.S. EPA, 2002, [042866](#)). In addition, IT instillation of fly ash and metal-containing PM generally caused pulmonary injury as measured by increases in BALF protein, LDH and albumin. Proliferation of bronchiolar epithelium was also noted. More recent studies of BALF markers of pulmonary injury and histopathological analysis of lung tissue are summarized below.

BALF Markers of Pulmonary Injury and Increased Permeability

CAPs

Kodavanti et al. (2005, [087946](#)) exposed SH and WKY rats to filtered air or CAPs from RTP, NC as described in Section 6.3.3.3. Differences in baseline parameters were noted for the two rat strains since SH rats had greater levels of protein and lower levels of levels of LDH, NAG, ascorbate and uric acid in the BALF than WKY rats. One day after the 2-day CAPs exposure, increased levels of GGT were observed in BALF (a marker of epithelial injury) of SH rats but not WKY rats compared with filtered air controls. Injury was not accompanied by inflammation (see Section 6.3.3.3).

In a study by Cassee et al. (2005, [087962](#)), SH rats were exposed for 6 h by nose-only inhalation to CAPs from 3 different sites in the Netherlands as described in Section 6.3.3.3. The pulmonary injury marker CC16 was increased in BALF 2 days following CAPs exposure. Inflammation was also observed (see Section 6.3.3.3).

Gurgueira et al. (2002, [036535](#)) exposed to Boston, MA, CAPs as described in Section 6.3.4.2 and reported a small but statistically significant increase in lung wet/dry ratios after 3 and 5 h of exposure, indicating the presence of mild edema. This response was accompanied by increased oxidative stress as measured by in situ chemiluminescence (CL) (see Section 6.3.4.2). In a similar study, Rhoden et al. (2004, [087969](#)) reported an increase in lung wet/dry ratio 24 h following a 5-h exposure to Boston CAPs which was diminished by pre-treatment of the antioxidant NAC (see Section 6.3.4.2).

Pulmonary injury was investigated in 2 studies using a rat model of pulmonary hypertension (SD rats pre-treated with monocrotaline which is described in greater detail in Section 6.3.3.3 (Lei et al., 2004, [087999](#)). Significant increases in BALF LDH and protein were observed in response to CAPs. Pulmonary inflammation was observed in both of these studies (see Section 6.3.3.3).

Diesel Exhaust

In a study evaluating the effects of DE, no changes were observed in BALF protein and LDH in mice exposed by inhalation to concentrations of 50 and 2000 $\mu\text{g}/\text{m}^3$ DEP for 4 h/day on 5 consecutive days as described in Section 6.3.3.3 (Stevens et al., 2008, [157010](#)). Changes in gene expression were observed in the higher exposure group. This study demonstrates that changes in gene expression can occur in the absence of measurable markers of injury or pulmonary inflammation.

In a study by Wong et al. (2003, [097707](#)) and Witten et al. (Witten et al., 2005, [087485](#)), rats were exposed nose-only to filtered room air or to DE over a 3-wk period. This study, focusing on neurogenic inflammation, is described in greater detail in Section 6.3.3.3. Pulmonary plasma extravasation was measured by the $^{99\text{m}}$ Technecium-albumin technique and found to be dose-dependently increased in the bronchi and lung. Pretreatment with capsaicin, which inhibits neurogenic inflammation by activating C-fibers and causing the depletion of neuropeptide stores, did not reduce plasma extravasation following DE exposure. Hence, DE is unlikely to act through bronchopulmonary C-fibers to cause neurogenic inflammation in this model. Inflammatory responses measured in this study are discussed in Section 6.3.3.3.

Gasoline Exhaust

Healthy male Swiss mice were exposed to gasoline exhaust (635 $\mu\text{g}/\text{m}^3$ PM and associated gases) or filtered air for 15 min/day for 7, 14, and 21 days as described in Section 6.3.3.3 (Sureshkumar et al., 2005, [088306](#)). BALF was collected for analysis 1-h after the last exposure. Statistically significant increases in BALF markers of lung injury, alkaline phosphatase, gamma-glutamyl transferase and LDH, were observed at all time points studied. Alveolar edema was noted following 14 and 21 days of exposure. Other findings of this study including inflammation and histopathology are discussed in Section 6.3.3.3.

Histopathology

CAPs

Histopathological changes were demonstrated in rats exposed for 5 h to Boston CAPs as described in Section 6.3.3.3 (Rhoden et al., 2004, [087969](#)). Slight bronchiolar inflammation and thickened vessels at the bronchiole were observed 24 h post-exposure,

consistent with the influx of polymorphonuclear leukocytes observed in BALF (see Section 6.3.3.3).

Diesel Exhaust

In a study by Wong et al. (2003, [097707](#)) and Witten et al. (2005, [087485](#)), rats were exposed nose-only to filtered room air or to DE over a 3-wk period. This study, focusing on neurogenic inflammation, is described in greater detail in Section 6.3.3.3. Pulmonary inflammation was evaluated by histopathological analysis of lung tissue. Following high, but not low, dose-exposure to DE, a large number of alveolar macrophages was found in the lungs. Small black particles, presumably DEP, were found in the cytoplasm of these alveolar macrophages. Perivascular cuffing consisting of mononuclear cells was also observed in high dose-exposed animals. Influx of neutrophils or eosinophils was not seen although mast cell number was increased. Other indices of injury demonstrated in this study are described above.

Gasoline Exhaust

Another study, which is described in greater detail in Section 6.3.3.3, demonstrated histopathological responses to gasoline exhaust in mice exposed to gasoline exhaust or filtered air for 15 min/day for 7, 14, and 21 days (Sureshkumar et al., 2005, [088306](#)). Histological observations showed inflammatory cell infiltrate in the peribronchiolar and alveolar region, alveolar edema and thickened alveolar septa at 14 and 21 days post-exposure. Levels of pro-inflammatory cytokines and marker enzymes of lung damage were also increased in BALF. The numbers of inflammatory cells in BALF was increased but not significantly, demonstrating that BALF analysis of inflammatory cells was a less sensitive indicator of pulmonary inflammation in this study than histopathological analysis. Other indices of injury found in this study are described above.

Model Particles

In a study investigating the effects of iron-soot, mice were exposed to 250 $\mu\text{g}/\text{m}^3$ laboratory-generated iron-soot as described in Sections 6.3.2.3 and 6.3.3.3 (Last et al., 2004, [097334](#)). Analysis of airway collagen content was conducted by histology and by biochemical analysis of microdissected airways. No increases in airway collagen content were found by either method in mice exposed to iron-soot for 2 wk. Furthermore, no goblet cells were observed in airways of air or iron-soot exposed animals. Other findings of this study are described in Sections 6.3.2.3 and 6.3.3.3.

An interesting study demonstrating histopathological responses to PM in neonatal rats was reported by Pinkerton et al. (2004, [087465](#)). Rat pups (10 days old) were exposed to soot and iron particles (mean mass concentration of 243 $\mu\text{g}/\text{m}^3$; iron concentration 96 $\mu\text{g}/\text{m}^3$; size range 10-50 nm) for 6 h/day on 3 consecutive days. Cell proliferation in different lung regions was evaluated following bromodeoxyuridine injection 2-h prior to necropsy. The rate of cell proliferation in the proximal alveolar region (immediately beyond the terminal bronchioles) was significantly reduced in iron-soot exposed animals compared to controls. This was a region-specific response since the rate of cell proliferation was not altered in the terminal bronchioles or the general lung parenchyma. However alveolar septation, the process by which alveoli are formed during development, and alveolar growth were not altered by iron-soot exposure. Decreased cell viability and increased LDH was also noted in BALF of neonatal rats (Pinkerton et al., 2008, [190471](#)). The authors suggest the possibility of greater susceptibility to air pollution during the critical postnatal lung development period which occurs in animals and humans and that neonatal exposure to PM may contribute to impaired lung growth seen in children.

Relative Toxicity of PM Size Fractions

Ambient PM Studies

A recently undertaken multinational project entitled “Chemical and biological characterization of ambient thoracic coarse ($\text{PM}_{10-2.5}$), fine ($\text{PM}_{2.5-0.2}$), and UFPs ($\text{PM}_{0.2}$) for human health risk assessment in Europe” (PAMCHAR) takes a systematic approach to expanding the present knowledge about the physiochemical and toxicological effects of these three PM size fractions. Six European cities were selected that represented contrasting ambient PM profiles: Helsinki, Duisburg, Prague, Amsterdam, Barcelona, and Athens. For PM collected at all sites, $\text{PM}_{10-2.5}$ induced the greatest pulmonary effects in C57Bl/6J mice intratracheally instilled with 1, 3, or 10 mg/kg of particles (Happo et al., 2007, [096630](#)). Dose-response relationships in BALF parameters measured 24-h post-IT exposure, including BALF cell number and protein, were observed for all sites following $\text{PM}_{10-2.5}$ and neutrophils were the predominant cell type (Happo et al., 2007, [096630](#)). Prague $\text{PM}_{10-2.5}$ exposure resulted in decreased macrophages in BALF at 12 h and Amsterdam, Barcelona, and Athens $\text{PM}_{10-2.5}$ induced lymphoplasmacytic cells in BALF (Happo et al., 2007, [096630](#)). No inflammatory responses were observed for ultrafine PM measured 12-h after exposure. Protein was elevated for $\text{PM}_{10-2.5}$ for all locations with the 10

mg/kg dose; Athens ultrafine PM induced protein release only at the two lowest doses 12 h post-exposure. For TNF- α and IL-6, the greatest response was observed with PM_{10-2.5} 4 h following exposure (Happo et al., 2007, [096630](#)). Ultrafine Duisburg PM exposure resulted in elevated TNF- α for the 1 and 3 mg/kg doses. Only the Helsinki sample appeared to induce the same level of IL-6 release for PM_{10-2.5} and PM_{0.2} at 10 mg/kg, albeit the collection times differed. In vitro TNF- α and IL-6 responses did not always reflect in vivo effects (Table 6-8), as the Duisburg PM_{10-2.5} sample was the most potent in vivo compared to the other sites and elicited much lower cytokine release compared to other cities (except Helsinki) in vitro (Happo et al., 2007, [096630](#); Jalava et al., 2008, [098968](#)).

Helsinki PM was collected in the spring and generally had the lowest in vivo and in vitro activity for PM_{10-2.5} compared to the other cities (Happo et al., 2007, [096630](#); Jalava et al., 2008, [098968](#)). Spring-time samples were collected because episodes of resuspended road dust occur frequently during this season (Pennanen et al., 2007, [155357](#)). There was a high correlation between EC content in PM_{2.5} and PM_{10-2.5}, indicating that traffic impacted both size fractions (Sillanpaa et al., 2005, [156980](#)). Duisburg PM collected in fall had the greatest amounts of Mn and Zn compared to PM samples from other locations (Pennanen et al., 2007, [155357](#)). Metals industries in Duisburg are likely contributors to the observed PM metals concentrations. For the Prague winter PM samples, the As content was higher than any other location (Pennanen et al., 2007, [155357](#)). Prague also had the highest PAH levels in all three size fractions, possibly attributable to stable atmosphere conditions and incomplete combustion of coal and biomass in residential heating (Pennanen et al., 2007, [155357](#)). High levels of ammonium and nitrate in PM samples from Amsterdam suggest traffic as a large source of air pollution (Pennanen et al., 2007, [155357](#)). Approximately one-third of PM_{10-2.5} mass from Amsterdam was comprised of sea salt (Sillanpaa et al., 2005, [156980](#)), double that of any other city. In Barcelona and Athens, high calcium or Ca²⁺ contents in spring and summer PM_{2.5} and PM_{10-2.5} are indicative of resuspended soil-derived particles (Pennanen et al., 2007, [155357](#)).

Table 6-8. PAMCHAR PM_{10-2.5} inflammation results with ambient PM.

City and Season	In vivo ^a (mg/kg)					In vitro ^b (µg/mL)			
	BALF protein	BALF TNF-α	BALF IL-6	BALF KC	BALF PMN	BALF AM	TNF-α	IL-6	MIP-2
Helsinki spring	+10	+10	+10	[+3 10]	+10	--	+150,300	+150,300	+150,300
Duisburg fall	+10	+10	+10	+10	+10	--	+150,300	+150,300	+300
Prague winter	+10	[+3 10]	+10	[+3 10]	+10	+10	+150,300	+150,300	+150,300
Amsterdam winter	+10	+10	+10	+10	+10	--	+150	+150,300	+150,300
Barcelona spring	+10	+10	[+3 10]	+10	+10	--	+150,300	+150,300	+150,300
Athens summer	+10	[+3 10]	[+3 10]	[+3 10]	+10	--	+150,300	+150,300	+150,300

^aSource: Happonen et al. (2007, [096630](#)); 2 cell lines used for in vitro study were RAW264.7

^bSource: Jalava et al. (2006, [155872](#)); + indicates increased response and numbers that follow indicate at which dose the response was observed

Schins et al. (2004, [054173](#)) employed PM from two cities in Germany, Duisburg and Borken, in another study. In contrast to the PAMCHAR study where animals were administered PM suspended in pathogen-free water (Happonen et al., 2007, [096630](#)), animals received PM via IT instillation suspended in saline at a dose of 320 µg (Schins et al., 2004, [054173](#)). In female Wistar rats, neutrophils in BALF were significantly elevated for PM_{10-2.5} from Duisburg and Borken (Table 6-9), albeit the percent of neutrophils with the PM_{10-2.5} from Borken was nearly double that of Duisburg. The responses with PM_{2.5} were much smaller. When these PM_{10-2.5} particles were introduced into whole blood to determine overall inflammogenic capacity, IL-8 and TNF-α were released in greater quantities than in response to fine PM. Furthermore, PM_{10-2.5} from Borken induced higher cytokine responses than Duisburg PM_{10-2.5}.

An in vivo study involving SH rats was conducted using PM_{10-2.5} and PM_{2.5} from six different European locations with varying traffic densities (3 or 10 mg/kg IT; ultrafine PM was not collected) (Gerlofs-Nijland et al., 2007, [097840](#)). It was reported that PM_{10-2.5} generally induced greater responses than PM_{2.5}. IT instillation of PM_{10-2.5} from a location with high traffic influence in Munich, Germany demonstrated the greatest response in terms of LDH activity, BALF protein, total cells, neutrophils, and lymphocytes 24-h post-exposure. PM_{10-2.5} collected from a low traffic site in Munich induced the greatest cytokine response for TNF-α and MIP-2. Some correlations were observed between PM_{10-2.5} components (Ba and Cu) and BALF parameters, but were largely driven by one location (Gerlofs-Nijland et al., 2007, [097840](#)).

Table 6-9. Other ambient PM – in vivo PM_{10-2.5} studies – BALF results, 18-24 h post-IT exposure

Location	Endotoxin (~ Values)	Dose (mg/kg)	Cell Differentials	Cytokines	Injury Biomarkers	Reference
Germany, Borken; rural Feb-May 2000	6.6 EU/mg	0.58-0.91	↑* % PMN	↑ TNF-α		Schins et al. (2004, 054173)
Germany, Duisburg; heavy industry Feb-May 2000	5.0 EU/mg	0.58-0.91	↑ % PMN	↑ MIP-2		Schins et al. (2004, 054173)
USA, Seattle, WA Feb-March 2004	6.0 EU/mg	1.25, 5.0				Gilmour, et al. (2007, 096433)
USA, Salt Lake City, UT Apr-May 2004	6.3 EU/mg	1.25, 5.0			↑ protein	Gilmour, et al. (2007, 096433)
USA, South Bronx, NY Dec 2003-Jan 2004	2.8 EU/mg	1.25, 5.0	↑ PMN	↑ MIP-2		Gilmour, et al. (2007, 096433)
USA, Sterling Forest, NY Dec 2003-Jan 2004	2.9 EU/mg	1.25, 5.0				Gilmour, et al. (2007, 096433)
USA, RTP, NC Oct-Nov 1996	0.96 EU/mg	0.5, 2.5, 5.0	↑↑ PMN	↑ IL-6		Dick (2003, 088776)
Germany, Munich Ost Bahnhof; high traffic A Aug 2002	2.9 EU/mg	3, 10	↑↑* total cells ↑↑ AM ↑↑*PMN ↑↑* Lymph	↑↑ MIP-2 ↑↑ TNF-α	↑↑* LDH ↑* protein	Gerlofs-Nijland, et al. (2007, 097840)
Netherlands, Hendrik-Ido-Ambacht; high traffic Sept 2002	6.5 EU/mg	3, 10	↑↑ total cells ↑↑*AM ↑↑ PMN ↑↑ Lymph	↑ MIP-2 ↑↑ TNF-α	↑↑ LDH ↑ protein	Gerlofs-Nijland, et al. (2007, 097840)
Italy, Rome; high traffic Apr 2002	1.5 EU/mg	3, 10	↑ total cells ↑↑ AM ↑↑ PMN ↑↑ Lymph	↑↑ MIP-2 ↑↑ TNF-α	↑↑ LDH	Gerlofs-Nijland, et al. (2007, 097840)
Netherlands, Dordrecht; moderate traffic Apr 2002	0.6 EU/mg	3, 10	↑↑ total cells ↑ AM ↑↑ PMN ↑ Lymph		↑↑ LDH ↑ protein	Gerlofs-Nijland, et al. (2007, 097840)
Germany, Munich Grosshadern Hospital; low traffic Jun-Jul 2002	2.9 EU/mg	3, 10	↑ total cells ↑↑ AM ↑↑ PMN ↑↑ Lymph	↑↑* MIP-2 ↑↑* TNF-α	↑↑* LDH ↑ protein	Gerlofs-Nijland, et al. (2007, 097840)
Sweden, Lycksele; low traffic Feb-March 2002	0.9 EU/mg	3, 10	↑↑ total cells ↑ AM ↑↑ PMN ↑ Lymph		↑↑ LDH ↑ protein	Gerlofs-Nijland, et al. (2007, 097840)

For Gerlofs-Nijland study, composition data were averaged across seasons. ↑ significant only at highest dose. ↑↑ Significant at lowest and highest dose. * Greatest potency for that endpoint and study. Gilmour et al. (2007, [096433](#)) exposure was via aspiration.

A more recent study by these investigators (Gerlofs-Nijland et al., 2009, [190353](#)) compared responses to PM from 3 different European cities based on size fraction and content of metals and PAH. SH rats were intratracheally instilled with 7 mg/kg PM, and markers of toxicity and inflammation were measured in BALF 24 h later. Blood markers of systemic inflammation and coagulation were also measured and are described in Section 6.2.7.3 and 6.2.8.3. In the first part of the study, both fine and coarse fractions of PM from Duisburg were found to have dramatic effects on inflammatory cell influx and activation as well as on the injury markers LDH, protein and albumin in the BALF. The antioxidant species uric acid was increased in BALF from rats exposed to both size fractions and was interpreted as an adaptive response to oxidative stress. Statistical analysis demonstrated that coarse PM was more potent in eliciting these responses than fine PM. In the second part of the study, responses to metal-rich PM from Duisburg and metal-poor PM from Prague were determined. A statistically significant greater enhancement of BALF markers of inflammation and injury was observed for the Duisburg PM compared with the Prague PM. Furthermore, responses to PAH-rich coarse PM from Prague and PAH-poor coarse PM from Barcelona were determined. PM_{10-2.5} from Prague was found to have statistically significant greater effects compared with PM_{10-2.5} from Barcelona. However, organic extracts of these PM_{10-2.5} fractions had very little capacity to produce inflammation or toxicity in this model. These findings suggest an important role for specific components associated with the coarse fraction in mediating the pro-inflammatory effects.

In another study investigating specific components of PM_{10-2.5}, BALB/c mice were intratracheally-instilled with 25 and 50 µg PM_{10-2.5} from a rural area of the San Joaquin Valley, California (Wegesser and Last, 2008, [190506](#)). Inflammatory cell influx into BALF began at 6 h and peaked at 24 h following IT instillation with 50 µg PM, with the increase in neutrophils preceding the increase in macrophages. Pro-inflammatory effects were found to be mainly due to insoluble components of PM. Furthermore, heat-treatment, which was capable of inactivating endotoxin, had no effect on inflammation. Numbers of neutrophils in the BALF were found to correlate with the content of macrophage inflammatory protein-2, a known neutrophil chemoattractant released from macrophages and epithelial cells. Taken together, these results demonstrate that the pro-inflammatory effect of this PM_{10-2.5} was associated with insoluble components and not with endotoxin.

In an in vivo study that employed ambient PM collected in fall 1996 from Research Triangle Park (RTP), NC, neutrophilic influx was observed in BALF of female CD1 mice 18-

h post-IT exposure (10, 50 or 100 μg) of coarse PM (3.5-20 μm), although a dose-response relationship was not evident (Dick et al., 2003, [088776](#)). Only the two highest doses of PM for the smaller size fractions induced elevated neutrophils. Significant responses in albumin and TNF- α were only observed for the fine PM (1.7-3.5 μm) exposure group. Total protein, LDH and NAG responses were absent for all PM size fractions. Levels of IL-6 were elevated in mice exposed to 100 μg for coarse, fine, and fine/ultrafine (<1.7 μm) PM. When dimethylthiourea (DMTU) was administered intravenously prior to exposure, the neutrophil response was attenuated in all groups to levels below control.

Another study compared thoracic coarse, fine, and ultrafine PM collected in Seattle, WA, Salt Lake City, UT, South Bronx, NY, and Sterling Forest, NY (Gilmour et al., 2007, [096433](#)). In female BALB/c mice, the 100 μg dose of PM_{10-2.5} (approximately 5 mg/kg) from Salt Lake City induced a significant increase in protein in BALF and the level released was almost as high as that observed after LPS exposure. PM_{10-2.5} from the South Bronx resulted in dose-related increases in neutrophil number and MIP-2 levels in BALF. In contrast, no effects were observed with PM_{10-2.5} from Sterling Forest. The greatest amount of LPS was observed in the Salt Lake City and Seattle PM_{10-2.5} samples. There was a less discernable pattern of response with fine and ultrafine PM.

Coal Fly Ash

Coal fly ash of differing size fractions and composition was administered to female CD1 mice via oropharyngeal aspiration (25 or 100 μg) to assess lung inflammation and injury 18 h following exposure (Gilmour et al., 2004, [057420](#)). Montana (low-sulfur subbituminous; 0.83% sulfur, 11.72% ash content) or western Kentucky (high-sulfur bituminous; 3.11% sulfur, 8.07% ash content) coal was combusted using a laboratory-scale down-fired furnace. Interestingly, no significant PM_{10-2.5} effects for either coal fly ash were observed for BALF neutrophils, TNF- α , MIP-2, albumin, total protein, LDH activity, or NAG activity 18 h post-exposure. However, the ultrafine fraction (PM_{0.2}) of combusted Montana coal induced greater numbers of neutrophils than PM_{10-2.5} or PM_{2.5} at both doses. TNF- α was only elevated in animals exposed to 100 μg of the Montana ultrafine PM; MIP-2 was also increased at both doses. The PM_{2.5} western Kentucky coal fly ash caused increased BALF neutrophils, MIP-2, albumin, and protein (Gilmour et al., 2004, [057420](#)).

In a similar study employing Montana subbituminous coal fly ash particles >2.5 μm , C57Bl/6J mice were intratracheally instilled with PM alone or PM+LPS and BALF was obtained 18 h post-exposure (Finnerty et al., 2007, [156434](#)). TNF- α and IL-6 in lung

homogenates were only elevated in the animals exposed to PM+100 µg LPS, although it appeared that there was a greater-than additive effect. Total cells and cell differentials were not measured.

Summary of Toxicological Study Findings for Relative Toxicity of PM Size Fractions

Biomarkers of injury and inflammation were measured in in vivo and in vitro studies comparing the toxicity of different size fractions of ambient PM from various locations. Responses were measured in BALF of rodents following IT instillation or aspiration of PM. In general, the PM_{10-2.5} size fraction was more potent than fine or ultrafine PM and endotoxin levels did not appear responsible. In one study, rural PM_{10-2.5} from Germany induced a greater inflammatory and cytokine response than PM_{10-2.5} from an industrial location. In contrast, PM_{10-2.5} from Sterling Forest, NY did not lead to any change in BALF inflammation or injury markers. A study that employed coal fly ash indicated that the ultrafine PM fraction was the most inflammogenic. All of these studies were conducted using high doses of PM (0.58-10 mg/kg) and it is unclear if similar effects would be observed at lower doses.

6.3.6. Allergic Responses

A large number of toxicological and controlled human exposure studies cited in the 2004 PM AQCD (U.S. EPA, 2004, [056905](#)) reported an exacerbation of existing allergic airway disease following exposure to laboratory-generated and ambient particles. In addition, numerous studies have demonstrated that PM can alter the immune response to challenge with specific antigens and suggest that PM may act as an adjuvant to promote allergic sensitization. Recent toxicological studies have provided evidence of enhanced allergic responses and allergic sensitization following exposure to CAPs and diesel that is consistent with the findings presented in the 2004 PM AQCD. PM can enhance allergic responses by facilitating delivery of allergenic material and promoting subsequent immune reactivity. The initiation or exacerbation of allergic responses has important implications for allergic asthma, the most common form of asthma. Additionally, PM has been shown to alter ventilatory measures in non-allergic animal models, suggesting a possible role in other forms of asthma.

6.3.6.1. Epidemiologic Studies

Allergy contributes to a number of respiratory morbidity outcomes, including asthma. However, relatively few epidemiologic studies of PM have specifically examined indicators of allergy. The 2004 PM AQCD (U.S. EPA, 2004, [056905](#)) presented one study (Hajat et al., 2001, [016693](#)) showing an association between doctor visits for allergic rhinitis and PM₁₀ among children in London. This association was strongest at a lag of 3 or 4 days. Similar results were obtained in a new study by Tecer et al. (2008, [180030](#)), which found significant associations between PM_{2.5}, PM₁₀, and PM_{10-2.5} with hospital admissions for allergic rhinitis in Turkish children, particularly at lag day 4. While exacerbation of allergic symptoms may occur relatively rapidly, repeated or longer exposures may be required for allergic sensitization to develop; a number of studies associating long-term exposure to PM with specific indicators of allergic sensitization are described in Chapter 7.

6.3.6.2. Controlled Human Exposure Studies

Exacerbation of Allergic Responses

Diesel Exhaust and Diesel Exhaust Particles

Exposure to DEP was shown to increase the allergic response among atopic individuals in several controlled human exposure studies cited in the 2004 PM AQCD (U.S. EPA, 2004, [056905](#)). Nordenhall et al. (2001, [025185](#)) found that exposure to DE significantly decreased the concentration of methacholine required to induce a 20% decrease in FEV₁ in a group of atopic asthmatics 24 h post-exposure. In addition, Diaz-Sanchez et al. (1997, [051247](#)) demonstrated an increase in allergen-specific IgE following exposure via intranasal spray to ragweed plus DEP (0.3 mg) relative to ragweed allergen alone. Decreases in IFN- γ and IL-2, as well as increases in IL-4, IL-5, IL-6, IL-10, and IL-13 were also observed when ragweed allergen was administered with DEP. It should be noted that the DEP used in this study were collected during a cold start of a light-duty Isuzu diesel engine, and thus contained relatively high levels of incomplete combustion materials and semi-volatiles organics (e.g., PAHs). One new study using the same source of DEP (Bastain et al., 2003, [098690](#)) also observed an increase in IL-4 and allergen specific IgE, as well as a decrease in IFN- γ following intranasal administration of ragweed allergen with DEP (0.3 mg) in atopic adults. The protocol was repeated in this study for all subjects, and the enhancement of allergic response by coexposure to DEP was observed to be highly

reproducible within individuals. In addition, Gilliland et al. (2004, [156471](#)) demonstrated that GST polymorphisms may alter the adjuvant effects of DEP on allergic response, with individuals with GSTM1 null or GSTP1 I105 wild type genotypes showing the largest effects.

Allergic Sensitization

Diesel Exhaust and Diesel Exhaust Particles

One controlled human exposure study has demonstrated that de novo sensitization to a neoantigen can be induced by exposure to DEP. In this study, Diaz-Sanchez et al. (1999, [011346](#)) dosed 25 atopic adults intranasally with 1 mg keyhole limpet hemocyanin (KLH), followed by 2 biweekly challenges with 100 µg KLH. In 15 of the 25 subjects, cold-start DEP (0.3 mg) were administered intranasally 24-h prior to each KLH exposure, while in the other 10 subjects, no diesel particles were administered. No KLH-specific IgE was observed in the nasal lavage fluid of any of the subjects exposed to KLH without exposure to diesel particles. However, KLH-specific IgE was present in the nasal lavage fluid of 9 out of 15 subjects 28-32 days after the initial KLH immunization when exposures were preceded by administration of DEP.

6.3.6.3. Toxicological Studies

Exacerbation of Allergic Responses

Increased use of actual ambient air particle mixes in toxicological studies since the 2004 CD has greatly expanded evidence relevant to assessing these and other immunotoxic effects. A number of studies have also included ambient level doses, although many still include relatively high doses of questionable relevance compared to the doses inhaled by humans. Recent dosimetric models reveal that a small fraction of epithelial cells located at the carinal ridges of airway bifurcations can receive massive doses that may be even a few hundred times higher than the average dose for the whole airway (see Chapter 4). These areas, coincidentally, are locations of bronchus associated lymphoid tissues (BALT) which are sites at which interaction of T and B lymphocytes with antigen presenting cells (APC) occurs. Hence the deposited particles are in near-ideal proximity to immunologically active tissues. Doses used for assessing PM immunotoxicity should be viewed with this perspective. In many animal studies changes in ventilatory patterns are assessed using

whole body plethysmography, for which measurements are reported as enhanced pause (Penh). Some investigators report increased Penh as an indicator of airway hyperresponsiveness (AHR), but these are inconsistently correlated and many investigators consider Penh solely an indicator of altered ventilatory timing in the absence of other measurements to confirm AHR. Therefore use of the terms AHR or airway responsiveness has been limited to instances in which the terminology has been similarly applied by the study investigators.

CAPs

Existing allergic sensitization confers susceptibility to the effects of PM in rodent models. For example, studies in allergic rats (Harkema et al., 2004, [056842](#); Morishita et al., 2004, [087979](#)) suggest that allergic sensitization enhances the retention of PM in the airways. Recovery of anthropogenic trace elements (La, V, Mn, S) from lung tissue was greater for Detroit CAPs PM_{2.5} exposed ovalbumin (OVA) sensitized/challenged BN rats than for air exposed or non-allergic CAPs exposed controls (24-h post-exposure for 4 or 5 consecutive 10-h days during July or September; time weighted average mass concentration of 676 ± 288 or 313 ± 119 $\mu\text{g}/\text{m}^3$, respectively) (Harkema et al., 2004, [056842](#)). Interestingly, despite lower average mass concentration, increases in these elements were observed in September, when the average number concentration of UFPs was nearly double that of July ($10,879 \pm 5126$ vs. 5753 ± 2566 particles/cm³). September CAPs was associated with eosinophil influx and BALF protein content, as well as significantly increased airway mucosubstances, and the authors speculated that the high concentration of UFPs facilitated particle penetration into the alveolar region of the lungs. IT instillation of fractionated insoluble PM_{2.5} collected from this period resulted in a mild pulmonary neutrophilic inflammation in healthy BN rats, but no differential effects were obtained after IT instillation of total, soluble, or insoluble PM_{2.5} in allergic rats.

Research has also been conducted to determine the effect of proximity to the roadway on exacerbation of existing allergic disease. OVA-allergic BALB/c mice were exposed to CAPs (fine, F, ≤ 2.5 or ultrafine, UF, ≤ 0.15 , avg total concentration 400 $\mu\text{g}/\text{m}^3$) for five 4-h days a week over 2 wk at 50 or 150 m downwind of a heavily trafficked road (Kleinman et al., 2005, [189364](#)). Markers of allergy (serum OVA-specific IgE and IgG1, lung IL-5 and eosinophils) were significantly higher in mice exposed to CAPs (UF or F) than in air-exposed mice after OVA challenge. IL-5, IgG1, and eosinophils were higher in mice closer to the roadway (50 m) than in mice 150 m downwind. The authors suggest that the

enhanced responses closer to the roadway may reflect a greater proportion of UF particles in this vicinity, given that the concentrations of sub-25-nm particles decrease rapidly with distance from the roadway and the F CAPs nearer the roadway contained a greater number of particles for a similar mass, a portion of which are UF. Animal-to-animal variability among the biomarkers tested made it necessary to combine values from two exposures spanning two years for statistical power (determined prior to the start of the experiment). A subsequent publication (Kleinman et al., 2007, [097082](#)) included a third exposure regimen as well as compositional analysis. Fine CAPs mass concentration was intentionally adjusted to an average concentration of approximately 400 $\mu\text{g}/\text{m}^3$, ranging from 163 to 500 $\mu\text{g}/\text{m}^3$, with an estimated particle number of 2.1×10^5 particles/ cm^3 at 50 m and 1.6×10^5 particles/ cm^3 at 150 m. UF ranged from 146 to 430 $\mu\text{g}/\text{m}^3$, with particle counts of $4.9 \pm 1.4 \times 10^5$ particles/ cm^3 at 50 m, and $4.4 \pm 2.1 \times 10^5$ particles/ cm^3 at 150 m. Analysis of results from the three exposures indicated that OVA-sensitized mice exposed 50 m downwind of the roadway exhibited increased levels of IL-5 and IgG₁ compared to mice exposed 150 m downwind or exposed to air. No markers of allergy-related responses were observed in the 150 m exposure groups, and very little difference was seen between fine and ultrafine CAPs responses, perhaps because fine material contained 20-32% ultrafine components. The strongest associations between component concentrations and biological markers of allergy (IL-5 and IgG₁) were with EC and OC. These studies demonstrate that CAPs can enhance allergic responses, and that proximity to a source may be an important factor.

In a BN rat model for allergic asthma (Heidenfelder et al., 2009, [190026](#)), thirteen 8-h days of exposure to Grand Rapids, MI CAPs (PM_{2.5}) alone did not result in differential gene expression or indicators of asthmatic pathology in the lung, but the combination of CAPs and OVA resulted in differential expression of genes predominantly related to inflammation and airway remodeling, along with significant increases in IgE, mucin, and total protein in BALF. Consistent with these changes in gene expression and BALF markers, OVA with CAPs also induced a more severe allergic bronchopneumonia (distribution and severity of bronchiolitis and alveolitis), and increased mucus cell metaplasia/hyperplasia and mucosubstances, indicating exacerbation of allergic or asthmatic disease. CAPs was collected in July and characterized as having an average mass of 493 ± 391 , OC 244 ± 144 , EC 10 ± 4 , SO₄²⁻ 79 ± 131 (13 day avg was only about 10% of the CAPs, but a spike occurred during the first week), nitrate 39 ± 67 , ammonium 39 ± 59 , and urban dust (estimated from Fe, Al, Ca, and Si) 18 ± 6 (mean \pm SD in $\mu\text{g}/\text{m}^3$).

Diesel Exhaust Particles

Resuspended DEP influences airway responses in mice with existing allergic sensitization. A single 5-h nose-only exposure to 870 $\mu\text{g}/\text{m}^3$ aerosolized filter-collected DEP ($\text{PM}_{2.5}$) increased Mch-induced increases in ventilatory timing (Penh, a parameter that has been correlated with airways resistance in some studies) in OVA sensitized/challenged C57BL/6J mice (Farraj et al., 2006, [088469](#)). Intranasal pretreatment with an antibody against the pan neurotrophin receptor p75 attenuated the DEP-induced increase in airflow obstruction, indicating a role for neurotrophins. Neurotrophins are expressed by various structural, nerve and immune cells within the respiratory tract and are linked to the etiology of asthma in both humans and animal models. DEP alone in unsensitized mice caused a significant increase in lung macrophages; this response was also inhibited by anti-p75, which may suggest mediation of macrophage influx by neurotrophin or alternatively may reflect anti-p75 dependent depletion of macrophages due to expression of the p75 receptor. Aside from increased macrophages, the single exposure to DEP had little effect on other markers of airway inflammation. In a similar subsequent study, these authors demonstrate neurotrophin-mediated DEP-induced airflow obstruction in OVA sensitized and challenged BALB/c mice (Farraj et al., 2006, [141730](#)), in this case using a higher 2000 $\mu\text{g}/\text{m}^3$ single 5-h exposure to aerosolized filter-collected $\text{PM}_{2.5}$. Differences between whole body plethysmography and tracheal ventilation measurements indicated that airflow obstruction may have originated in the nasal passages. Again, very few indices of inflammation were increased; however, similar neurotrophin-dependent increases in lung macrophages were observed after DEP exposure alone, and BALF IL-4 protein levels were increased 5-fold in sensitized, challenged, DEP-exposed mice. This neurotrophin-dependent IL-4 response was not evident in the first study, and may be related to the higher dose used in the second study or the characteristic allergic/Th2 bias of the BALB/c strain. Airflow obstruction in the absence of airway inflammation in OVA-sensitized animals seen in both studies by Farraj et al. (2006, [088469](#); 2006, [141730](#)) may reflect DEP-induced acute enhancement of neurogenic as opposed to immunologic inflammation.

Diesel Exhaust

Exposure to relatively low doses of DE has been shown to exacerbate asthmatic responses in OVA sensitized/challenged BALB/c mice (Matsumoto et al., 2006, [098017](#)). Mice were intranasally challenged one day prior to chamber exposure to DE (DEP 100 $\mu\text{g}/\text{m}^3$; CO, 3.5 ppm; NO₂, 2.2 ppm; SO₂ <0.01 ppm) for 1 day or 1, 4, or 8 wk (7h/day, 5

days/wk, endpoints 12-h post-DE exposure). Results from the 8 wk study are described in Section 7.3.6.2. It should be noted that control mice were left in a clean room as opposed to undergoing chamber exposure to filtered air. Significant AHR upon Mch challenge was observed after 1 and 4 wk of exposure, and airway sensitivity (provocative concentration of Mch causing a 200% increase in Penh) was significantly increased after 1 wk of exposure but not 4 wk. DE had no effect on total cells in BALF, but transiently increased expression of IL-4, IL-5, and IL-13 after 1 day of exposure, MDC after 1 wk, and RANTES after 2 and 3 wk. Eotaxin, TARC, and MCP-1 were elevated without statistical significance after short-term (1 day or wk) exposure. Statistical power may have been lacking due to an n of 3. Protein levels of IL-4 and RANTES were significantly elevated after 1 day of DE exposure, respectively. DE had no effect on OVA challenge-induced peribronchial inflammatory or mucin positive cells. Therefore DE-induced airway hyperresponsiveness was observed in the absence of cellular inflammation, similar to the responses described for aerosolized or nebulized DEP by Farraj et al. (2006, [088469](#); 2006, [141730](#)) and Hao et al. (2003, [096565](#)).

Gasoline Exhaust

Acute exposure to fresh gasoline engine exhaust (GEE) PM does not appear to exacerbate allergic responses (Day et al., 2008, [190204](#)). BALB/c mice were exposed to whole exhaust diluted 1:10 (H), 1:15 (M), or 1:90 (L), filtered exhaust at the 1:10 (HF), or clean air for 6 h/day over three days. Analytes for the high (H) and high filtered (HF) concentrations were: PM mass ($\mu\text{g}/\text{m}^3$) 59.1 ± 28.3 (H) and 2.3 ± 2.6 (HF); PM number ($\#/\text{cm}^3$) 5.0×10^5 and 1.1×10^4 ; CO (mg/m^3) 102.8 ± 33.0 and 99.5 ± 1.6 ; NO (mg/m^3) 18.4 ± 2.8 and 17.2 ± 1.9 ; NO₂ (mg/m^3) 1.4 ± 0.3 and 1.7 ± 0.2 ; SO₂ ($\mu\text{g}/\text{m}^3$) 1366.8 ± 56.0 and 1051.1 ± 43.0 ; NH₃ ($\mu\text{g}/\text{m}^3$) 1957.7 ± 8.1 and 1241.5 ± 6.1 ; NMHC (mg/m^3) 15.9 and 25.9. Particles represented only 0.04% of the total exposure mass and particle size in the H exposure ranged from 5.5 - 150 nm with the majority between 5-20 nm (MMD 150 nm) (McDonald et al., 2008, [191978](#)). Although particles were filtered out, it should be noted that NMHC (non-methane volatile organics) increased by 62%. Mice were exposed with or without prior sensitization to OVA, after one aerosol challenge and with or without secondary challenge. Acute GEE exposure had variable effects on inflammatory and allergic markers depending on the exposure protocol, but there were no statistically significant differences between the H and HF exposure results, suggesting that the PM fraction of GEE does not appear to contribute significantly to observed health effects.

Hardwood Smoke

One study indicated that hardwood smoke (HWS) exposure only minimally exacerbated indices of allergic airway inflammation in an OVA-sensitized BALB/c mouse model and did not alter Th1/Th2 cytokine levels (Barrett et al., 2006, [155677](#)). Trend analysis indicated increasing BALF eosinophils with increasing dose of HWS, becoming significantly elevated at 300 $\mu\text{g}/\text{m}^3$ (CO, 1.6 ± 0.3 ppm; total vapor hydrocarbon, 0.6 ± 0.2 ppm; NO_x, below limit of quantitation, PM MMAD 0.35 ± 2.0 μm), and increasing but not statistically significant OVA-specific IgE levels with HWS up to 1000 $\mu\text{g}/\text{m}^3$.

Model Particles

Exposures to an aerosol of soot and iron oxide generated from ethylene (PM_{2.5}, 0.235 mg/m³) were conducted to test whether the sequence of exposure to OVA aerosol challenge and PM affected the observed response of OVA sensitized BALB/c mice (Last et al., 2004, [097334](#)). Though called PM_{2.5}, the authors characterized the PM material as ultrafine, 80-110 nm, with the iron oxide crystals often spatially segregated from the soot (200 $\mu\text{g}/\text{m}^3$ soot, remainder iron oxide, CO <0.8 ppm, NO_x <0.4 ppm, PAH below detection). Mice were exposed to PM via chamber inhalation for 2 wk (4h/day, 3 days/wk) before or after 4 wk of OVA inhalation, or simultaneously to PM and OVA for 6 wk. Among endpoints (BALF cells, Penh, airway collagen, and goblet cells) only goblet cell counts were significantly increased with PM exposure in any combination with OVA. There was a trend toward increased Penh responses with exposure to PM alone or with OVA, particularly when PM exposure immediately preceded Mch challenge (after or during OVA challenge). Results from this study are difficult to interpret due to the varied elapsed times between cessation of PM or OVA treatment and endpoint determination. The mild responses to PM may be related to the intraperitoneal sensitization protocol used, reputed to generate a highly allergic mouse in which any additive effects of PM may be obscured by maximal responses to antigen challenge (Deurloo et al., 2001, [156396](#); Hao et al., 2003, [096565](#)).

Residual Oil Fly Ash

Arantes-Costa and colleagues (2008, [187137](#)) estimated that 60 μg of ROFA would be inhaled by a mouse during one day of exposure to Sao Paulo air. This dose, given intranasally every other day for four days, increased AHR in both nonsensitized and OVA sensitized/challenged BALB/c mice upon Mch challenge two days after the last exposure. ROFA had no significant impact on eosinophil or macrophage numbers in the lung, nor did it increase the chronic lung inflammation or thickening induced by OVA. In many studies

particular effects such as airway obstruction are only evident when allergic sensitization precedes exposure, but this study and a few others demonstrate allergen-independent AHR after exposure to PM including CAPs (Lei et al., 2004, [087999](#)) and DEP or DE (Hao et al., 2003, [096565](#); Li et al., 2007, [155929](#)).

Allergy in pregnancy or early life

Pregnancy or in utero exposure may confer susceptibility to PM-induced asthmatic responses. Exposure of pregnant BALB/c mice to aerosolized ROFA leachate by inhalation or to DEP intranasally increased asthma susceptibility in their offspring (Fedulov et al., 2008, [097482](#); Hamada et al., 2007, [091235](#)). The offspring from dams exposed for 30 min to 50 mg/mL ROFA 1, 3, or 5 days prior to delivery responded to OVA immunization and aerosol challenge with AHR and increased antigen-specific IgE and IgG1 antibodies. AHR was also observed in the offspring of dams intranasally instilled with 50 µg of DEP or TiO₂, or 250 µg CB, indicating that the same effect could be demonstrated using relatively “inert” particles. Pregnant mice were particularly sensitive to exposure to DEP or TiO₂ particles, and genetic analysis indicated differential expression of 80 genes in response to TiO₂ on the pregnant background. Thus pregnancy may enhance responses to PM, and exposure to even relatively inert particles may result in offspring predisposed to asthma.

Allergic Sensitization

A large number of in vivo animal studies and in vitro studies have demonstrated that particles can alter the immune response to challenge with specific antigens and suggest that PM acts as an adjuvant to promote allergic sensitization. This phenomenon was introduced in the 2002 Diesel Document, and has been noted in multiple animal and human studies by the 2004 PM AQCD. Adjuvants enhance the immune response to antigens through various means, including chemoattraction, cytokines, or enhanced antigen presentation and costimulation, and may originate via effects on a number of cell types. Importantly, adjuvants may be major contributors to the development of inappropriate immune responses. These immune responses, mediated by T helper cells, fall along a continuum from T helper type 1 (Th1) to T helper type 2 (Th2). Th1 responses, characterized by IFN-γ, are inflammatory and in excess can lead to tissue damage. Alternatively, Th2 responses are characterized by IL-4, IL-5, IL-13, eosinophils, and IgE, and are associated with allergy and asthma. Autoimmune diseases may be driven by Th1,

Th2, or mixed responses, but allergic diseases are predominantly Th2 mediated, and many of the immunologic effects observed for PM fall into the Th2 category.

It has been suggested that the capacity of particles to enhance allergic sensitization is associated more strongly with particle number and surface area than particle mass, and several studies comparing size fractions of the same material show greater adjuvant activity for an equivalent mass dose of smaller particles (Inoue et al., 2005, [088625](#); Nygaard et al., 2004, [058558](#); de Haar et al., 2006, [144746](#)). This is particularly true of inert or homogeneous materials, such as carbon, polystyrene, and TiO₂, which vary little in composition with size fraction. Studies using CAPs have also observed that adjuvancy and allergic exacerbation are more strongly associated with the ultrafine fraction, possibly due to greater oxidative potential (Kleinman et al., 2005, [189364](#); 2007, [097082](#); Li et al., 2009, [190457](#)). In some studies of ambient PM, however, coarse particles have demonstrated equal or greater adjuvancy compared to fine particles (Nygaard et al., 2004, [058558](#); Steerenberg et al., 2004, [096024](#); Steerenberg et al., 2005, [088649](#)). More inhalation studies to compare size fractions are needed in order to elucidate the role of particle size in mediating adjuvancy, but this may prove difficult given the influence of composition, e.g., combustion related materials (Steerenberg et al., 2006, [088249](#)) and metal content (Gavett et al., 2003, [053153](#)), which differs among various size fractions and sources.

CAPs

As little as 0.1 µg of ultrafine Los Angeles CAPs administered intranasally with OVA was able to significantly boost allergic antibody responses in BALB/c mice (Li et al., 2009, [190457](#)). A comparison of UFPs (UFP, aerodynamic diameter <0.15 µm) with a mix of sub-2.5 µm particles (F/UFP) collected 200 m from a major freeway delivered intranasally five times over the course of nine days showed that UFP but not F/UFP were associated with significant adjuvant effects. 0.5 µg of UFP with OVA (but not alone) led to an increase in BALF eosinophils, allergic cytokines, inflammatory mediators, and serum OVA-specific IgE/IgG1, as well as allergic tissue inflammation in the upper and lower airways. Adjuvant effects of UFP were observed with two independently collected samples (Jan 07 and Sep 06) and could not be replicated by administering the same amount of endotoxin measured in the particles, indicating that the effects were not unique to the sampling period nor mediated by contaminating endotoxin. UFP had a greater OC and PAH content than F/UFP, and induced greater oxidative stress in vitro. Partial blocking of the adjuvant effects by antioxidant administration implicates redox potential as a key factor in mediating these

effects. The authors suggest that the lack of adjuvancy for ultrafine carbon particles (being mostly EC) is due to a lack of redox cycling compounds, but this was not tested. In contrast, ultrafine (30-50 nm) CB particles have demonstrated intranasal adjuvant activity in other studies (de Haar et al., 2005, [097872](#)) when administered with OVA over three consecutive days. A 200 µg dose increased serum OVA-specific IgE, local lymph node dendritic cells and OVA-specific Th2 lymphocytes in the lung draining lymph nodes and lung, as well as post-challenge airway eosinophilia. Doses as low as 20 µg were able to activate adoptively transferred OVA-specific T cells.

Diesel Exhaust Particles

Resuspended DEP have been shown to enhance OVA-specific IgG1 and IgE in BALB/c mice exposed via inhalation to doses as low as 200 and 600 µg/m³, respectively (Whitekus et al., 2002, [157142](#)). Mice were exposed to DEP (200, 600 and 2000 µg/m³) for 1-h daily for 10 days prior to aerosol OVA challenge. Compared with responses to OVA alone, antibody levels were increased by all OVA+DEP exposures. Statistical significance was reached for IgG1 at all DEP exposure levels, whereas OVA specific IgE was significantly increased at the 600 and 2000 µg/m³ doses and total IgE was significantly elevated at 2000 µg/m³. Although strong adjuvant effects were observed, no general markers of inflammation such as eosinophils, IL-5, GM-CSF, mucin, morphological changes, or eosinophilic major basic protein (MBP) deposition in the airways were observed in exposed mice. In vitro experiments using the RAW 264.7 macrophage-like cell line indicated a DEP-induced lipid peroxidation and protein oxidation, which could be inhibited by a variety of antioxidants. Also observed was a decrease in the GSH: GSSG ratio and an increase in HO-1 expression, both of which were inhibited only by the thiol antioxidants NAC and BUC. These same thiol antioxidants were able to completely block DEP-related increases in IgE and IgG1, as well as lipid peroxides and oxidized proteins recovered from lung lavage fluids at the 2000 µg/m³ dose. Thus solid correlations between in vivo and in vitro antioxidant activities were found, and the reversal of adjuvant effects by antioxidants in vivo clearly indicates a link between oxidative stress and DEP adjuvancy. However, the intranasal adjuvant activity of Ottawa, Canada, dust (EHC-93) in the same strain of mice was not inhibited by NAC pretreatment (Steerenberg et al., 2004, [087981](#)), suggesting that disparate pathways may be utilized by different materials to exert immune stimulation.

Diesel Exhaust

DEP inhalation during allergen exposure has been shown to augment IgE production and alter methylation of T helper genes in BALB/c mice (Liu et al., 2008, [156709](#)) Animals were exposed to 1280 $\mu\text{g}/\text{m}^3$ DEP over a 3-wk period, 5h per day, concurrent with periodic intranasal sensitization to the common fungus *Aspergillus fumigatus*. Gas concentrations were not reported. Total IgE and BALF eosinophils were elevated with *A. fumigatus* sensitization and further increased by concomitant DEP exposure. Greater methylation of the IFN- γ promoter was observed following DEP and *A. fumigatus* exposure (but not DEP alone) compared to *A. fumigatus* alone, indicating that combined DEP and allergen exposure might induce methylation and thus suppress expression of Th1 genes. Furthermore, hypomethylation of the IL-4 promoter was detected after exposure to *A. fumigatus* and DEP compared with exposure to *A. fumigatus* or DEP alone, suggesting pro-allergic Th2 gene activation upon combined exposure to allergen and DEP. The changes in methylation status of these genes were associated with alterations in IgE levels in individual animals, indicating that modifications at the genetic level could result in predicted downstream effects. This study shows for the first time that DEP exposure can exert pro-allergic in vivo effects on the mouse immune system at the epigenetic level.

A toxicogenomic approach to investigate early response mechanisms of DEP adjuvancy was taken by Stevens et al. (2008, [157010](#)). BALB/c mice were chamber exposed to filtered air, 500 or 2000 $\mu\text{g}/\text{m}^3$ PM in DE for 4 h/day over 5 consecutive days and intranasally exposed to OVA on each of the first 3 days. In the low vs. high PM exposures, CO, NO, NO₂, and SO₂ were <0.1 vs. 4.3, <2.5 vs. 9.2, <0.25 vs. 1.1 and <0.06 vs. 0.2 ppm; particle number median diameters were 80 and 86 nm, and volume median diameters were 184 and 195 nm, respectively. Lung tissues were assessed for alterations in global gene expression (n = 4) 4 h after the last DE exposure on day 4. Mice were intranasally challenged with OVA or saline on day 18 and then with OVA on day 28. Post-challenge results demonstrated mild adjuvancy with antigen and DE exposure as evidenced by significant increases in eosinophils, neutrophils, lymphocytes, and IL-6 in the BALF. Antibody responses were not significantly affected by DE exposure, although a slight increase in IgE after high dose exposure was observed. DE alone only increased neutrophils, indicating the need for combined exposure to DE and antigen in the development of allergic outcomes. Comparison of low DE (500 $\mu\text{g}/\text{m}^3$)/OVA versus air/OVA resulted in no significant changes in gene sets associated with this treatment. Comparison

of the high (2000 $\mu\text{g}/\text{m}^3$) DE/OVA versus air/OVA, however, showed significant changes in 23 gene sets, including neutrophil homing and other chemokines, inflammatory cytokines, numerous interleukins and TNF subtypes, and growth/differentiation pathways.

Summary of Findings for Allergic Responses

Studies conducted since the last review confirm and extend the 2004 PM AQCD's (U.S. EPA, 2004, [056905](#)) finding that PM can modulate immune reactivity in both humans and animals to promote allergic sensitization and exacerbate allergic responses. Numerous forms of PM, including inert materials, have been shown to function as adjuvants, and although toxicological studies of relatively homogeneous materials demonstrate greater adjuvancy for smaller particles, some analyses of ambient PM do not. Recent toxicological studies comparing size fractions of well-characterized ambient PM for adjuvant activity in a direct, controlled fashion via inhalation exposure suggest a role for oxidative potential, but thus far the relative contributions of size and composition are not entirely clear. Although epidemiologic studies examining specific allergic outcomes and short-term exposure PM are relatively rare, the available studies, conducted primarily in Europe, positively associate various PM size fractions with allergic rhinitis or hay fever and skin prick reactivity to allergens. Similar findings from a number of long term studies are described in Chapter 7.

6.3.7. Host Defense

The normal, and very important, role of respiratory immune defense is the detection and/or destruction of pathogens that enter the lung via inhalation and removal of damaged, transformed (cancerous), or infected cells. Innate immune defenses of the respiratory tract include mucociliary clearance, release of toxic antimicrobial proteins into airway surface liquid, and activation of alveolar macrophages. The innate immune system is the earliest responder to irritation or infection, initiating the normal inflammatory response including the majority of detrimental inflammatory processes discussed. Activated macrophages and epithelial cells release cytokines and chemokines that can bring into play the adaptive immune system, which in turn can produce long-lasting pathogen-specific immune responses critical for resolving and preventing infections.

6.3.7.1. Epidemiologic Studies

Collectively, results from multicity studies of hospital admissions and ED visits for respiratory infection as well as single-city studies conducted in the U.S. and Canada (summarized in Figure 6-14) show a positive association between PM and respiratory infections. Lag structure was not investigated in most studies and effects have been observed in association with current day concentration (Zanobetti and Schwartz, 2006, [090195](#)) as well as with concentrations modeled using a 14 day distributed lag function (Peel et al., 2005, [056305](#)). Of studies examining multiple lag times, associations with increasing lag times were observed (Dominici et al., 2006, [088398](#); Peel et al., 2005, [056305](#); Peng et al., 2008, [156850](#)). Although no significantly positive associations were reported, Slaughter et al. (2005, [073854](#)) observed a trend of increasing association with increasing lag for acute respiratory infection ED visits with PM₁, PM_{2.5}, PM₁₀ and PM_{10-2.5}. This delay in the onset of disease may reflect the time necessary for an infection to become established and symptomatic. The majority of toxicological evidence, described below and in the 2004 PM AQCD (U.S. EPA, 2004, [056905](#)), suggests that PM impairs innate immunity, the first line of defense in preventing infection.

6.3.7.2. Toxicological Studies

Several toxicological studies were cited in the 2004 PM AQCD (U.S. EPA, 2004, [056905](#)) that demonstrated increased susceptibility to infectious agents following exposure to PM. A limited number of new studies have evaluated the effect of PM on host defense in rodents. Two recent studies have observed an increase in susceptibility to influenza infection and respiratory syncytial virus in mice. However, one new study found that woodsmoke had no effect on bacterial clearance in rodents.

Bacterial Infection

Several studies included in the 2004 PM AQCD demonstrated increased susceptibility to infectious agents following exposure to various forms of PM. CAPs exposed aged rats demonstrated increased *S. pneumoniae* burdens when a 24-h exposure (65 µg/m³) followed infection (Zelikoff et al., 2003, [039009](#)). In another study, IT exposure to ROFA was found to affect bacterial clearance (Antonini et al., 2002, [035342](#)). Examinations of mechanisms related to PM interference with host defenses have demonstrated impaired mucociliary clearance and modified macrophage phagocytosis and chemotaxis. Prolonged exposure to

inhaled particles at sufficiently high concentrations can lead to diminished clearance of PM from the alveolar region of the lung, resulting in the accumulation of retained particles and an accompanying chronic alveolar inflammation. Diminished clearance of PM may also increase susceptibility to pulmonary infection by impeding clearance of pathogens. Impaired phagocytosis by alveolar macrophages may contribute to a decrease in the lung's capacity to deal with increased particle loads (as occurs during high-pollution episodes) or infections and affect the local and systemic responses through the release of biologically active compounds (cytokines, ROS, NO, isoprostanes).

Diesel Exhaust

Since the last review, several additional studies have reported impairment of pathogen clearance following exposure to various sources of PM. All levels of DE (30, 100, 300 or 1,000 $\mu\text{g}/\text{m}^3$) decreased lung bacterial clearance in C57BL/6 mice exposed for 1 wk (7 days/wk, 6 h/day) prior to infection with *Pseudomonas aeruginosa* (Harrod et al., 2005, [088144](#)). This effect appeared dose dependent up to 100 $\mu\text{g}/\text{m}^3$ and was not enhanced at higher doses. Lung inflammation was not induced by DE in the absence of infection, but infection-induced inflammation was exacerbated by DE at all concentrations without apparent dose dependency. Measures of histopathology in infected animals were dose dependently increased by DE exposure, peaking at 100 $\mu\text{g}/\text{m}^3$ and leveling off or decreasing with higher doses. Particle deposition was readily apparent in the lungs after exposure to the lowest concentration of 30 $\mu\text{g}/\text{m}^3$. A loss of ciliated cells was observed at 30 $\mu\text{g}/\text{m}^3$ and 100 $\mu\text{g}/\text{m}^3$ in large airways and in small airways at the higher dose. Alterations in Clara cell morphology and function were observed at both doses as well. Concentrations of gases were reported to be from 2.0-45.3 ppm NO, 0.2-4.0 ppm NO₂, 1.5-29.8 ppm CO and 8-365 ppb for SO₂ (McDonald et al., 2004, [055644](#)). PM mass median diameter was ~100-150 nm at all exposure levels (>90% below 1 μm in aerodynamic diameter), with lower exposure concentrations having a slightly smaller size distribution (Reed et al., 2004, [055625](#)).

Gasoline Exhaust

In a study by Reed et al. (2008, [156903](#)), short or long-term exposure to fresh gasoline exhaust (6h/day, 7day/wk for 1 wk or 6 months) did not affect clearance of *P. aeruginosa* from the lungs of C57BL/6 mice. [Atmospheric characterizations are described above for the Day et al. (2008, [190204](#)) and McDonald et al. (2008, [191978](#)) studies in Section 6.3.6.3, Exacerbation of Allergic Responses/Gasoline Exhaust.]

Hardwood Smoke

Similar to gasoline exhaust, HWS does not appear to have significant impact on pathogen clearance. C57BL/6 mice were exposed to 30-1000 $\mu\text{g}/\text{m}^3$ HWS by whole body inhalation for 1 wk and 6 months (Reed et al., 2006, [156043](#)). Long-term responses are discussed in Sections 7.3.3.2 and 7.3.7.2. Concentrations of gases ranged from 229.0-14887.6 mg/m^3 for CO, 54.9-139.3 $\mu\text{g}/\text{m}^3$ for ammonia, and 177.6-3455.0 $\mu\text{g}/\text{m}^3$ nonmethane volatile organic carbon in these exposures. Bacterial clearance of instilled *Pseudomonas aeruginosa* was unaffected by HWS.

Residual Oil Fly Ash

Antonini et al. (2004, [097199](#)) compared sources of ROFA in SD rats. Precipitator ROFA induced an inflammatory response and diminished pulmonary clearance of *L. monocytogenes* while air heater ROFA had no effect on lung bacterial clearance at the same dose of 1 mg/100g body weight. Precipitator ROFA generated a metal-dependent hydroxyl radical suggesting that differences in metal composition were a determinant of the immunotoxicity of ROFA. ROFA has also been shown to result in ciliated cell loss in BALB/c mice after intranasal administration of 60 μg every other day for four days (Arantes-Costa et al., 2008, [187137](#)).

Viral Infection

Diesel Exhaust

Viral respiratory infections in early life are associated with increased incidence of childhood asthma and other pulmonary diseases. DE exposure can enhance the progression of influenza infection. BALB/c mice that were chamber exposed to DE 4 h/day for 5 days and subsequently instilled with influenza A/Bangkok/1/79 virus had increased susceptibility to influenza infection (Ciencewicky et al., 2007, [096557](#)). Exposures to two doses of DEP were conducted: 500 $\mu\text{g}/\text{m}^3$ (0.9 ppm CO, <0.25 ppm NO₂, <2.5 ppm NO, and 0.06 ppm SO₂) and 2000 $\mu\text{g}/\text{m}^3$ (5.4 ppm CO, 1.13 ppm NO₂, 10.8 ppm NO, and 0.32 ppm SO₂). Responses were greater for animals exposed to 500 $\mu\text{g}/\text{m}^3$ DEP than to 2000 $\mu\text{g}/\text{m}^3$, and were associated with a significant increase in IL-6 protein and mRNA expression and IFN- β expression. The authors present the possibility that damage to the epithelium at the higher dose prevented viral infection and replication. After exposure to 500 $\mu\text{g}/\text{m}^3$ DEP alone or prior to infection, decreased expression of surfactant proteins (SP) A and D was observed. These proteins are part of the IFN-independent defense against influenza.

Similarly, Harrod et al. (2003, [097046](#)) demonstrated decreased SP-A expression in the lungs following DE exposure and linked it to increased susceptibility to respiratory syncytial virus (RSV), the most common cause of respiratory infection in young children. C57BL/6 mice, a relatively RSV-resistant strain, were exposed via inhalation to DE at a concentration of 30 or 1000 $\mu\text{g}/\text{m}^3$ DPM 6h/day for 7 consecutive days prior to intratracheal viral inoculation. Gaseous copollutants ranged from 2.0-43.3 ppm for NO_x (~ 90% NO), 0.94-29.0 ppm CO, and 8.3-364.9 ppb SO_2 . Exposure to 30 $\mu\text{g}/\text{m}^3$ DEP did not induce a statistically significant increase in BALF cell numbers compared to air-treated, infected animals. However, distinct consolidated inflammatory infiltrates were observed in the peribronchial regions of RSV-infected animals exposed to this dose, along with alterations in Clara cell morphology, decreased CCSP production by these cells, and occasional regional myofibril layer thickening. These changes were more pronounced in RSV-infected animals exposed to 1000 $\mu\text{g}/\text{m}^3$, and the higher dose also resulted in significant increases in inflammatory cells, predominantly macrophages, in both uninfected and infected mice compared to air-exposed controls. Both doses elicited significant levels of TNF- α and IFN- γ in the lungs of infected animals, but decreased levels of SP-A. Consistent with this study's finding of decreased SP-A and increased viral gene and inflammatory cytokine expression after DE exposure, SP-A^{-/-} mice demonstrate decreased clearance of RSV concordant with increased lung inflammation (LeVine et al., 1999, [156687](#)). Thus, DEP may enhance susceptibility to respiratory viral infections by reducing the expression and production of SP (Ciencewicz et al., 2007, [096557](#); Harrod et al., 2003, [097046](#)), although the contribution of gaseous copollutants, in some instances concentrated 1000x, should be considered for both studies. SP are also essential for clearance of other pathogens, including group B Streptococcus (GBS), *Haemophilus influenzae*, and *P. aeruginosa* (LeVine and Whitsett, 2001, [155928](#)).

A reduction in host defense molecules and an increase in viral entry sites was observed by Gowdy et al. (Gowdy et al., 2008, [097226](#)) after BALB/c mice were exposed to HEPA filtered room air or DE at 0.5 or 2.0 mg/m^3 for 4hr/day for one or five consecutive days [O_2 (%) 21.0 ± 0.10 or 20.7 ± 0.09 , CO (ppm) 1.7 ± 0.15 or 5.4 ± 0.07 , NO_x (ppm) 2.0 ± 0.36 or 7.4 ± 0.61 , SO_2 (ppm) 0.0 ± 0.0 or 0.4 ± 0.3 , number median (nm) 96.2 ± 2 or 97 ± 2 , volume median (nm) 238 ± 2 or 249 ± 2 , OC/EC (wt ratio) 0.4 ± 0.04 or 0.4 ± 0.07 for the 0.5 or 2.0 mg/m^3 exposures, respectively]. One of the more notable features of this study was the observation that effects of extended exposure to the lower dose (0.5 mg/m^3 for 5 days)

tended to persist beyond 18 h post-exposure. Exposure to DE significantly increased BAL neutrophils in the higher dose group, and this response persisted beyond 18 h only after the five day exposure. An increase in ICAM-1 expression (a viral entry site) was observed in both dose groups, and was persistent in the lower dose group after a 5 day exposure. Persistently elevated expression of pro-inflammatory cytokines IL-6 and TNF- α and pro-allergic cytokine IL-13 was observed after 5 days of low dose exposure. Non-statistically significant effects of either dose or dosing regimen included increased IFN- γ and MIP-2. Host defense molecules CCSP, SP-A and SP-D were decreased after either exposure regimen, persisting beyond 18 h in the low dose group.

Taken together, these data suggest that exposure to DE can weaken host defenses, in some cases persistently. A role for the PM component is supported by studies demonstrating changes in host defense molecules and viral entry sites in vitro consistent with those observed in vivo. In lung epithelial cells, DEP increased the mRNA expression of intercellular adhesion molecule-1 (ICAM-1), low-density lipoprotein (LDL) and platelet-activating factor (PAF) receptors, which can act as receptors for viruses or bacteria (Ito et al., 2006, [096648](#)). DEP may therefore enhance the susceptibility to infection by the upregulation of bacterial and viral invasion sites in the lungs. Expression of the β -defensin-2 gene, which is one antimicrobial mechanism of host defense in the airway, was significantly inhibited by V and not Ni or Fe in airway epithelial cells incubated with aqueous leachate of ROFA (Klein-Patel et al., 2006, [097092](#)).

Immunosuppressive Effects of PM

Diesel Exhaust

DEP may affect systemic immunity. Decreased thymus weight was observed in female F344 rats exposed to 300 $\mu\text{g}/\text{m}^3$ DEP for 1 wk by Reed et al. (2004, [055625](#)). Concentrations of gases for this dose were reported to be approximately 16.1 ppm for NO, 0.8 ppm for NO₂, 9.8 ppm for CO, and 115 ppb for SO₂. Long-term responses are discussed in Section 7.3.8.

Summary of Findings for Host Defense

Toxicological studies demonstrate that short-term inhalation exposures to CAPs and DE, but not gasoline exhaust or woodsmoke, can increase susceptibility to infection by bacterial and viral pathogens. While gaseous copollutants may be contributing factors, a role for particulate components is demonstrated by studies utilizing IT exposure and in

vitro studies of particles where biomarkers parallel those observed in vivo. Although ethical considerations limit controlled exposure studies in humans, epidemiologic evidence reflects an association between most PM size fractions and hospital admissions for respiratory infections. Importantly, toxicological studies demonstrate impaired host defense against the etiological agents of influenza, pneumonia (*S. pneumoniae*), and bronchiolitis (RSV), which are commonly reported respiratory morbidities associated with PM.

6.3.8. Respiratory ED Visits, Hospital Admissions and Physician Visits

The epidemiologic evidence presented in the 2004 PM AQCD (U.S. EPA, 2004, [056905](#)) linking short-term increases in PM concentration with respiratory hospitalizations and ED visits was consistent across studies. Recent investigations provide further support for this relationship, with larger effect estimates observed among children and older adults. However, effect estimates are clearly heterogeneous, with evidence of both regional and seasonal differences at play.

Excess risk estimates for hospitalizations or ED visits for all respiratory diseases combined, reported in studies reviewed in the 2004 PM AQCD (U.S. EPA, 2004, [056905](#)) fell within the range of approximately 1 to 4% per 10 $\mu\text{g}/\text{m}^3$ increase in PM_{10} . On average, excess risks for asthma were higher than excess risks for COPD and pneumonia. Associations with ambient fine particles ($\text{PM}_{2.5}$, PM_{1}) and coarse thoracic particles ($\text{PM}_{10-2.5}$) were also reported in the limited body of evidence reviewed in the 2004 AQCD. Excess risk estimates fell within the range of approximately 2.0 to 6.0% per 10 $\mu\text{g}/\text{m}^3$ increases in $\text{PM}_{2.5}$ or $\text{PM}_{10-2.5}$ for all respiratory diseases combined as well as COPD admissions. Larger estimates were reported for asthma admissions. Many of the associations of respiratory admissions and ED visits with short-term $\text{PM}_{2.5}$ concentration were statistically significant. The associations with $\text{PM}_{10-2.5}$ were less precise with fewer reaching statistical significance (U.S. EPA, 2004, [056905](#)). Finally, several studies reviewed in the 2004 AQCD reported associations of PM with outpatient physician visits suggesting that the population impacted by short-term increases in PM is not be restricted to those admitted to the hospital or seeking medical attention through an ED.

Table 6-10. Description of ICD-9 and ICD-10 codes for diseases of the respiratory system.

Description	ICD 9 Codes	ICD 10 Codes
Diseases of the Respiratory System	460-519	J00-J99
Asthma	493	J45
COPD and allied conditions	490-496 (asthma, chronic bronchitis, emphysema, bronchiectasis, extrinsic allergic alveolitis)	
Chronic lower respiratory diseases		J40-J47 (bronchitis, emphysema, other COPD, asthma, status asthmaticus, bronchiactasis)
Acute Respiratory Infections	460-466 (common cold, sinusitis, pharyngitis, tonsillitis, laryngitis & tracheitis, bronchitis & bronchiolitis)	
Acute Upper Respiratory Infections		J00-J06 (common cold, sinusitis, pharyngitis, tonsillitis, laryngitis & tracheitis, croup & epiglottitis)
Acute bronchitis and bronchiolitis	466	J20-J22
Allergic Rhinitis	477	J30.1
Pneumonia	480-486	J13-J18
Wheezing	786.09	

Hospital admissions or ED visits for respiratory diseases and ambient concentrations of PM have been the subject of more than 90 peer-reviewed research publications since 2002 (see Annex E). Included among these new publications are several large single-city and multicity studies. These new studies complement those reviewed in the 2004 AQCD by examining the effect of several PM size fractions and components on increasingly specific disease endpoints as well as evaluating the presence of effect modification by factors such as season and region.

Specific design and methodological considerations of the large and multicity studies included in this review were discussed previously (Section 4.4.10.2). Like the CVD endpoints discussed, the respiratory endpoints examined in these studies were heterogeneous and approaches to selecting cases for inclusion in the studies were varied. ICD codes commonly used in hospital admission and ED visits studies are found in Table 6-10.

6.3.8.1. All Respiratory Diseases

Findings from new studies of PM and respiratory hospitalization and ED visits among children are summarized in Figure 6-10. Results from new studies of adults are summarized in Figure 6-11. Information on the PM concentrations during the relevant study periods is found in Table 6-11.

Children

Barnett et al. (2005, [087394](#)) used a case-crossover design to study respiratory hospital admissions (ICD-9 460-519) of children (age groups 0, 1 to 4, 5 to 14 yr) in seven cities in Australia and New Zealand from 1998 to 2001. All respiratory diseases (ICD10 J00-J99) except Mendelson's Syndrome, post-procedural disorders, asphyxia and certain other symptoms (ICD10 codes J95.4-J95.9, R09.1, R09.8) were included in the study. In addition, scheduled admissions and transfers from other hospitals were excluded. Using an a priori lag (0-1 day avg), increases in respiratory hospital admissions of 2.0% (95% CI: -0.13 to 4.3) among infants less than 1 year old, 2.3% (95% CI: 1.9-7.3) among children 1-4 years old and 2.5% (95% CI: 0.1-5.1) among children 5-14 years old and, per 10 $\mu\text{g}/\text{m}^3$ increase in 24-h avg PM_{10} were observed. Increases of 6.4% (95% CI: 2.7-10.3) among infants less than 1 year and 4.5% (95% CI: 1.9-7.3) among children 1-4 yr per 10 $\mu\text{g}/\text{m}^3$ increase in $\text{PM}_{2.5}$ were observed.

Ostro et al. (2009, [191971](#)) studied the effect of $\text{PM}_{2.5}$ and components on respiratory disease (ICD9 460-519) hospitalizations among children less than 19 yr from 2000 to 2003 in six counties in California. The full-year and cool season mean $\text{PM}_{2.5}$ levels were 19.4 $\mu\text{g}/\text{m}^3$ and 24.8 $\mu\text{g}/\text{m}^3$, respectively. The nine components examined (EC, OC, nitrates, sulfates, Cu, Fe, K, Si and Zn), were chosen because they made up relatively large proportion of $\text{PM}_{2.5}$, had a signal to noise ratio greater than 2, or the majority of their values were greater than the LOD. Single day lags of 0-3 days were evaluated. The largest risks were observed at lag 3 days for $\text{PM}_{2.5}$ (2.8% 95%CI: 1.2-4.3 per 10 $\mu\text{g}/\text{m}^3$), EC (5.4 95% CI: 0.8-10.3 per IQR) and Fe (4.7% (95% CI: 2.2-7.2 per IQR increase). Although not as great, positive associations were also observed for OC, SO_4^{2-} , nitrate, Cu and Zn.

In a study of $\text{PM}_{2.5}$ from wildfires in California during 2003, Delfino et al. (2009, [191994](#)) evaluated conducted stratified analyses comparing $\text{PM}_{2.5}$ associations pre-, post- and during the wildfires. Four age groups (0-4, 5-19, 20-64 and 65+) were considered in these analyses. Authors found increased respiratory disease admissions in the periods before (2.6% 95%CI: -5.4 to 11.3) and during (2.7% 95%CI: -1.6 to 7.6) the wildfires among children 5-19 years old, but not after the wildfire period. Among younger children (0-4 yr), hospital admission were increased during fire periods (4.5% 95% CI: 1-8.2) but not before or after the wildfire period. Estimated zip code level $\text{PM}_{2.5}$ concentrations were 90 $\mu\text{g}/\text{m}^3$ and 75 $\mu\text{g}/\text{m}^3$ during heavy and light smoke conditions, respectively, compared to 20 $\mu\text{g}/\text{m}^3$ during non-fire periods.

In the study of six cities in France described previously (PSAS), investigators report a change of 0.4% (95%CI: -1.2 to 2) per 10 $\mu\text{g}/\text{m}^3$ increases in $\text{PM}_{2.5}$ for all respiratory diseases combined (ICD-10: J00-J99) among children from 0-14 years old (Host et al., 2008, [155852](#)). The same study reported a larger increase associated with $\text{PM}_{10-2.5}$ of 6.2% (95% CI: 0.4-12.3, 0-1 day avg) per 10 $\mu\text{g}/\text{m}^3$ increase among children. A relatively large effect for $\text{PM}_{10-2.5}$ (31% 95% CI: -4.7 to 80) was also observed in a single-city study of children less than 3 years old in Vancouver (Yang et al., 2004, [087488](#)). The non-significant $\text{PM}_{2.5}$ effect estimates were not presented in the publication. Luginaah et al. (2005, [057327](#)) did not observe significant increases in respiratory hospitalizations with increasing PM_{10} concentrations among male or female children in Ontario Canada, while Ulirsch et al. (2007, [091332](#)) reported increased admissions for respiratory hospitalizations, ED and urgent care visits combined among children <17 years old in association with PM_{10} .

Adults and All Ages Combined

In the study of 4 million ED visits from 31 hospitals in Atlanta described previously, SOPHIA investigators reported an excess risk of 1.3% (95% CI: 0.4-2.1, lag 0-2) per 10 $\mu\text{g}/\text{m}^3$ increase in 24-h avg PM_{10} for ED visits for respiratory causes combined (ICD-9: 460-466, 477, 480-486, 491-493, 496, 786.09) among all ages in Atlanta during the period January, 1993 to August, 2000 (Peel et al., 2005, [056305](#)). $\text{PM}_{2.5}$, $\text{PM}_{10-2.5}$, ultrafine number count and $\text{PM}_{2.5}$ components (SO_4^{2-} , acidity, EC, OC, and an index of water-soluble transition metals) were available for inclusion in analyses beginning August 1, 1998. Larger increases in ED visits for respiratory diseases were associated with $\text{PM}_{2.5}$ compared to $\text{PM}_{10-2.5}$. Excess risks of 1.6% (95% CI: -0.003 to 3.5) per 10 $\mu\text{g}/\text{m}^3$ increase in 24-h avg $\text{PM}_{2.5}$ and 0.6% (95% CI: -3.6 to 5.1) per 10 $\mu\text{g}/\text{m}^3$ increase in $\text{PM}_{10-2.5}$ were reported. Weaker, less precise associations with components were reported and no increase with ultrafine particle count was observed.

Analyses with four additional years of data were conducted and more recently reported by SOPHIA investigators (Tolbert et al., 2007, [090316](#)). Single pollutant results are included in Figure 6-11. As shown, effect of PM_{10} remains with the additional years of data, while the effect of $\text{PM}_{2.5}$ is diminished and a decrease in ED visits with $\text{PM}_{10-2.5}$ was observed. The association of PM_{10} with respiratory disease ED visits was robust to adjustment for O_3 , CO and NO_2 . In another recent analysis using SOPHIA data from 1998 through 2002 to compare source apportionment methods, Sarnat et al. (2008, [097972](#)) reported that $\text{PM}_{2.5}$ from mobile sources, $\text{PM}_{2.5}$ from biomass burning and SO_4^{2-} -rich

secondary PM_{2.5} were associated with respiratory ED visits and associations were robust to the choice of the method. Excess risks were statistically significant, ranging from approximately 2%-4%, depending on the method.

In the French multicity study, larger increases were observed in association with 24-h avg PM_{10-2.5} concentration compared to PM_{2.5} concentration among adults as well as children. Among adults 15-64 yr, investigators reported increases in respiratory hospitalizations of 0.8% (95%CI: -0.7, 2.3) and 2.6% (95%CI: -0.5 to 5.8) per 10 µg/m³ for PM_{2.5} and PM_{10-2.5}, respectively (lag 0-1 days) (Host et al., 2008, [155852](#)).

In a study of respiratory hospital admission and ED visits (ICD-9 Codes 460-519) among all ages conducted in Spokane, Washington, no associations were observed with any size fraction of PM considered (e.g., PM₁, PM_{2.5}, PM_{10-2.5}, PM₁₀) (Slaughter et al., 2005, [073854](#)). However, authors observe that there was a suggestion of greater effect estimates with PM_{2.5} compared to PM_{10-2.5}. Furthermore, several of the same investigators conducted a source apportionment analysis using daily fine PM filter samples from the same residential monitor in Spokane (Schreuder et al., 2006, [097959](#)). In this investigation, PM_{2.5} from vegetative burning in the previous day (lag 1) was associated with respiratory hospital admissions (2.3% [95% CI: 0.9-3.8] per interquartile range increase in the source marker). In a study of PM_{2.5} from wildfires in California during 2003, associations with respiratory hospitalizations were generally stronger relative to associations in the periods before and after the fires (Delfino et al., 2009, [191994](#)). Among adults 20-64 years, an increase of 2.4% (95% CI: 0.5-4.4 per 10 µg/m³) during the wildfire period compared to 0.9% (95%CI: -0.1 to 1.8 per 10 µg/m³) for all periods combined (pre-, post- and during wildfires).

Luginaah et al. (2005, [057327](#)) examined respiratory hospital admissions in relation to PM₁₀ concentration across strata for age and gender and compared time series to case crossover approaches. The results for all ages combined, which were relatively precise, stratified by gender and all lags are presented in the figure; the largest estimates for PM₁₀ were for adult males (15-64 years old), however. Fung et al. (2005, [093262](#)) did not report evidence of an association between respiratory admissions and 24-h PM₁₀ concentration among adults less than 65 yr, in a study in Vancouver, while Ulirsch et al. (2007, [091332](#)) reported a significant positive association among all ages and adults (18-64 yr) in two Southeast Idaho cities for hospitalizations, ED and urgent care visits combined. This estimate was robust to adjustment for gaseous pollutants.

Older Adults

Among older adults, MCAPS investigators observed largely null findings for PM_{2.5} and respiratory hospitalizations (ICD-9: 490-492, 464-466, 480-487) for the U.S. as a whole but reported heterogeneity in effect estimates across the country that were explained by regional and seasonal factors (Bell et al., 2008, [156266](#)). The nationwide excess risk of respiratory admissions with PM_{2.5} was 0.22% (95% posterior interval (PI): -0.12 to 0.56, lag 0) (Bell et al., 2008, [156266](#)). The largest increase was observed during the winter in the Northeast (1.76% [95% PI: 0.60-2.93], lag 0). Significant increases in respiratory admissions were also observed at lag 2. In an analysis of PM_{10-2.5}, MCAPS investigators observed small imprecise increases in respiratory admissions with 24-h PM_{10-2.5} concentration (0.33% [95% PI: -0.21 to 0.86, per 10 µg/m³, lag 0]) (Peng et al., 2008, [156850](#)), which decreased after adjustment for PM_{2.5} (0.26% [95% PI: -0.32 to 0.84 per 10 µg/m³ lag 0]). Associations with PM_{2.5} increased (0.7% [95% PI: 0-1.5, lag 0]) or persisted (0.6% [95% PI: -0.2 to 1.25, lag 2]), after adjustment for PM_{10-2.5}.

Two recent MCAPS analyses evaluate the effect of PM_{2.5} components on respiratory hospital admissions. Bell et al. (2009, [191997](#)) analyzed a subset of MCAPS data restricted to 106 counties with data available for both long-term average concentrations of PM_{2.5} components (Bell et al., 2007, [155683](#)) and PM_{2.5} total mass (1999-2005). The components evaluated included 20 chemicals with demonstrated toxicity or that contribute a large proportion of PM_{2.5} mass (Al, NH₄⁺, As, Ca, Cl, Cu, EC, OCM, Fe, Pb, Mg, Ni, NO₃⁻, K, Si, Na⁺, Ti, V, Zn). Increases in effect estimates of 511% (95% PI: 80.7-941) for EC, 223% (95% PI: 36.9-410) for nickel and 392% (95% CI: 46.3-738) for vanadium per IQR increases in county-specific component fraction were observed. Associations were somewhat reduced and non-significant in two pollutant models. When Queens or New York County were excluded the association of vanadium with hospital admissions lost significance. Associations were also diminished when alternative lag structures were considered.

Peng et al. (2009, [191998](#)) linked data on hospital admissions for respiratory causes among older adults from 2000-2006 to daily air levels from the STN in 119 counties in which both sets of data were available. Chemical components evaluated were SO₄²⁻, nitrate, silicon, EC, OCM, sodium and ammonium ions. Single day lags of 0-2 days were considered. These investigators found a 0.82% increase (95% PI: 0.22-1.44) per IQR increase in same day OCM. After adjustment for the other components, a 1.01% (95% PI: 0.04-1.98, lag 0)

increase in respiratory admissions was observed. A similar effect estimate was observed at lag 2.

French PSAS investigators reported a non-significant increase in hospitalizations for respiratory diseases (ICD-10 J00-J99) with 24-h avg $PM_{10-2.5}$ among older adults. $PM_{2.5}$ estimates were also not significant and were closer to the null than estimates for $PM_{10-2.5}$ (Host et al., 2008, [155852](#)). Adjusted estimates from 2-pollutant models were not presented. Positive associations of first hospitalization, overall hospitalizations and readmission for respiratory diseases and $PM_{10-2.5}$ were also reported among older adults in Vancouver (Chen et al., 2005, [087555](#)). $PM_{10-2.5}$ was associated with an increase of 15% (95% CI: 4.8-22.8) in overall admissions per $10 \mu\text{g}/\text{m}^3$. Increases associated with $PM_{10-2.5}$ were larger for readmissions compared to overall admissions. The association for $PM_{2.5}$ with overall admissions was 5.1% (95% CI: -4.9 to 13) and the association with readmissions was not larger. In this study, effect estimates for PM_{10} and $PM_{10-2.5}$ lost precision but were robust to adjustment for gaseous pollutants while the estimate for $PM_{2.5}$ was null after adjustment for gaseous pollutants. In Vancouver, Fung et al. (2006, [089789](#)) also report larger effect estimates for $PM_{10-2.5}$ than $PM_{2.5}$ among adults 65 yr and older. These authors report increased admissions of 1.8% (95% CI: -2.5 to 5.8) per $10 \mu\text{g}/\text{m}^3$ increase in $PM_{2.5}$ and 3.8% (95% CI: 0-7.6) per $10 \mu\text{g}/\text{m}^3$ increase in $PM_{10-2.5}$ (lag 0-1 day avg).

In a multicity Australian study, Simpson et al. (2005, [087438](#)) examined the association between fine particles measured by nephelometry and respiratory hospital admissions (ICD-9 460-519) among older adults (65+ yr) and reported significant associations (1.055 [95% CI: 1.008-1.1045], lag 0-1 day avg) from a meta-analysis combining effect estimates from all cities. Results from three statistical models were considered, including standard GAM, which produced similar results.

Delfino et al. (2009, [191994](#)) reported that $PM_{2.5}$ from wildfire in California was associated with respiratory hospital admissions among older adults (3% 95% CI: 1.1-4.9 per $10 \mu\text{g}/\text{m}^3$). In two analyses of data collected in Copenhagen Denmark between 1999 and 2004, several size fractions including ultrafine and accumulation mode (Andersen et al., 2008, [189651](#)) and PM_{10} sources (Andersen et al., 2007, [093201](#)) were investigated in relation to respiratory hospitalizations (J41-42, J43, J44-46) among adults greater than 65 yr of age. Of the size fractions examined (NC total, NC median diameter of 12 nm [NC_{a12}], NC_{a23} , NC_{a57} , NC_{a100} , NC_{a212} , PM_{10} , $PM_{2.5}$) NC_{a212} , typically aged secondary long-range transported, NC_{57} and PM_{10} were significantly associated with respiratory

hospitalizations (Andersen et al., 2008, [189651](#)). PM₁₀ sources including biomass combustion, secondary inorganic compounds, oil combustion and crustal were associated with respiratory hospitalizations (Excess risks ranged from 3.5% to 5.4% per interquartile range respectively) (Andersen et al., 2007, [093201](#)). PM₁₀ associations were diminished somewhat in 2 pollutant models (2007, [093201](#); Andersen et al., 2008, [189651](#)); the authors note that it was difficult to separate the effects of PM₁₀ and NC_{a212}, which were highly correlated in these data. PM_{2.5} was not associated with respiratory hospitalizations in these data.

Results from other single-city studies offer somewhat consistent evidence for the effect of PM₁₀ on respiratory admissions among older age groups. Ulirsch et al. (2007, [091332](#)) found increases in hospitalizations, ED and urgent care visits combined among this age group in 2 cities of Southeast Idaho. Two studies in Vancouver report increased admissions for respiratory causes with the largest effects observed for a 3 day ma (0-2 days) (Chen et al., 2005, [087555](#); Fung et al., 2006, [089789](#)). Fung et al. (2006, [089789](#)) observed non-significant increases in admissions with PM₁₀ among older adults in Ontario, Canada while the study by Luginaah et al. (2005, [057327](#)), which was also conducted in Ontario, did not provide compelling evidence for an effect that was robust to method selection, although some increases among males were observed. Finally, a study of hospital admissions for cardiopulmonary conditions combined among older adults (65+ yr) in Allegheny County, PA found a positive association with PM₁₀ at lag 0 (Arena et al., 2006, [088631](#)).

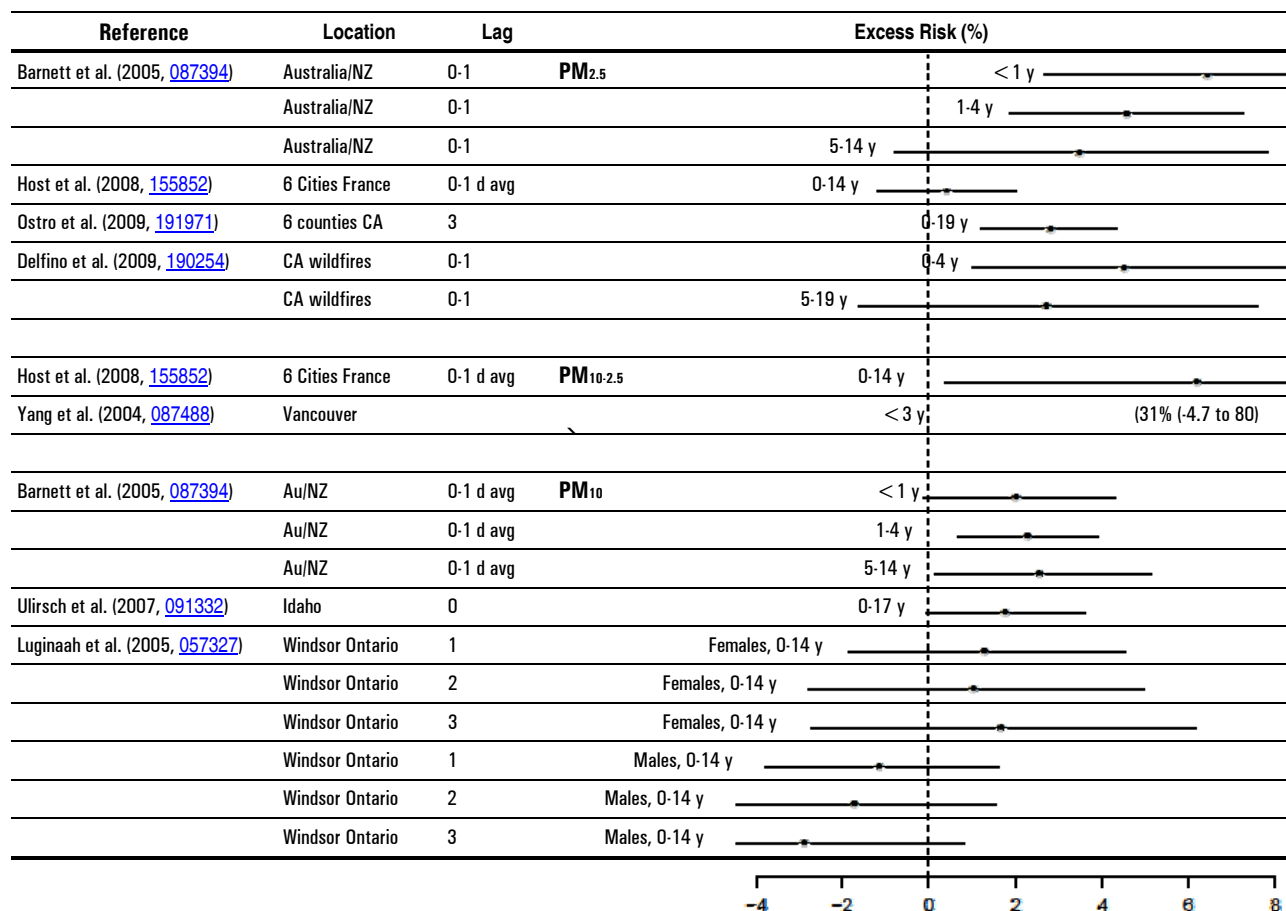


Figure 6-10. Excess risk estimates per 10 µg/m³ 24-h avg PM concentration for studies of ED visits and hospitalizations for respiratory diseases in children. Studies represented in the figure include all multicity studies. Single-city studies conducted in the U.S. or Canada are also included.

As shown in Figure 6-10, studies of respiratory hospitalizations or ED visits reported increased risks to children in association with all size fractions. However, increased risk among boys was not observed in Ontario (Luginaah et al., 2005, [057327](#)). Estimates are imprecise and it is not clear if associations with fine, coarse, or both are driving associations observed with PM₁₀. Effect estimates for adults (and combined age groups) as well as older adults are found in Figure 6-11. Effects observed in single-city studies are generally imprecise but most studies report positive associations. Regional and seasonal variation was observed with the largest effect estimate reported by Bell et al. (2008, [156266](#)) in the Northeast during the winter. Although the number of studies examining components or sources was limited, EC, OC, nickel, vanadium, and PM_{2.5} from mobile sources were associated with increased respiratory admissions. Several additional studies conducted outside the U.S. and Canada reported positive associations of respiratory

hospitalizations with PM₁₀ for different age groups and lags (Bedeschi et al., 2007, [090712](#); Chen et al., 2006, [087947](#); Hanigan et al., 2008, [156518](#); Middleton et al., 2008, [156760](#); Oftedal et al., 2003, [055623](#); Lai and Cheng, 2008, [180301](#); Larrieu et al., 2009, [180294](#)), PM_{2.5} (Hinwood et al., 2006, [088976](#); Neuberger et al., 2004, [093249](#); Vigotti et al., 2007, [090711](#)), BS (Bartzokas et al., 2004, [093252](#); Tecer et al., 2008, [180030](#)) and with PM_{10-2.5} (Tecer et al., 2008, [180030](#)). Other studies reported no associations with PM₁₀ (Vegni and Ros, 2004, [087448](#)) or TSP (Llorca et al., 2005, [087825](#)).

6.3.8.2. Asthma

Results from multicity studies of hospital admissions and ED visits for asthma as well as single-city studies conducted in the U.S. and Canada are summarized in Figure 6-12. Studies reviewed in the 2004 AQCD are included for continuity. Concentrations of PM for the relevant study period are found in Table 6-11.

Children

SOPHIA investigators (Peel et al., 2005, [056305](#)) reported that, of the PM mass indicators examined, the largest effect estimate observed using the a priori lag (0-2 day avg) was the association of PM₁₀ with pediatric (2-18 yr) asthma ED visits (1.6% [95% CI: -0.2 to 3.4]). ED visits for both asthma (ICD-9: 493) and wheezing (ICD-9: 786.09) were included in their study. Asthma hospital admissions (ICD-10 J45, J46, J44.8) in children less than 14 years old were examined in the Australia / New Zealand multicity study (Barnett et al., 2005, [087394](#)). In this study, associations for asthma hospital admissions with PM₁₀ and PM_{2.5} were increased but imprecise.

Lin et al. (2002, [026067](#)) used both time series and case crossover approaches to investigate the influence of PM on asthma hospitalization in children, 6-12 years old, in Toronto from 1981 to 1993. These authors report relatively small differences in results obtained through bi-directional case crossover and time series approaches but indicate that unidirectional case-crossover methods may overestimate the relative risks. Single to 7-day avg lags were investigated and estimates appeared to increase and then level off at the longer lags (0-2 day and 0-5 day lags are shown in figure). Effect estimates for PM_{2.5} are not easily distinguished from the null but PM_{10-2.5} is significantly associated with asthma admissions among boys and among girls. These associations were imprecise but robust to adjustment for gaseous pollutants among all children combined.

Although Ostro et al. (2009, [191971](#)) presented estimates for all respiratory diseases combined, these authors note that PM_{2.5} and its components were associated with asthma hospitalizations among the children in 6 counties of Los Angeles studied. Delfino et al. (2009, [191994](#)) examined the association of PM_{2.5} before, during, and after wildfires in California with asthma hospitalizations among age and gender subgroups. Significant associations were observed for children 0-4 yr among children during the wildfire period (8.3% 95% CI: 2.1-14.9, per 10 µg/m³) but not before or after the wildfire period. For older children, 5-19 yr, non-significant increases in asthma hospitalizations were found before the wildfire period but not during or after the fires.

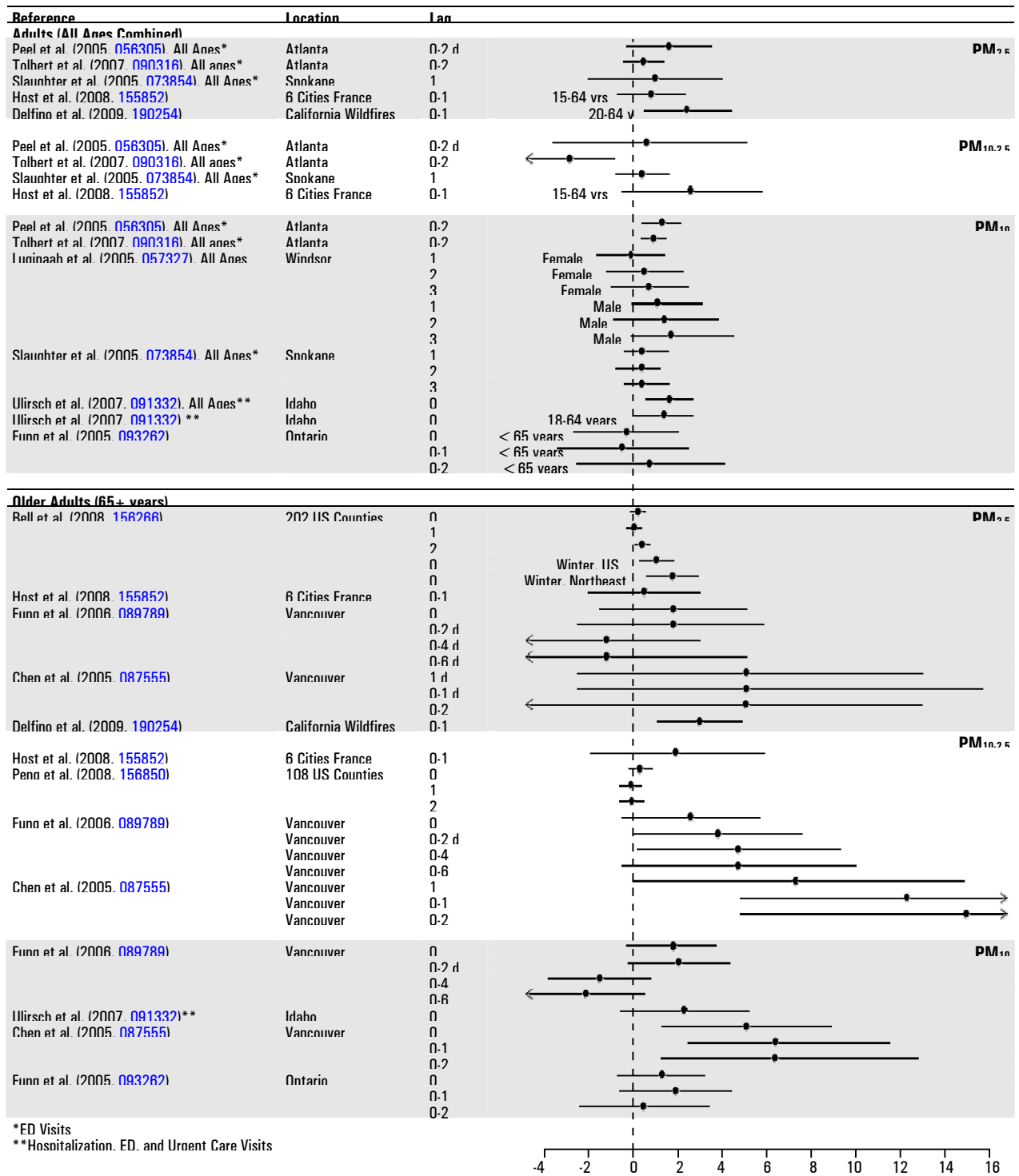


Figure 6-11. Excess risks estimates per 10 µg/m³ increase in 24-h avg PM for studies of ED visits and hospitalizations for respiratory diseases among adults. Studies represented in the figure include all multicity studies. Single-city studies conducted in the U.S. or Canada are also included.

Hirshon et al. (2008, [180375](#)) studied hospital admissions and ED visits by children 0-17 years old in Baltimore, MD from June 2002-November 2002 in relation to zinc as a component in PM_{2.5}. Single day lags from 0 to 2 days were tested with the highest estimates observed for the previous day. A 23% (95% CI: 7-41%) increase in admissions was observed comparing medium (8.63-20.76 ng/m³) concentrations on the previous day to low concentrations (<8.63 ng/m³) on the previous day. Previous day high concentration (>20.76 ng/m³) was associated with an increase in admissions of 16% (95% CI: -3 to 39) compared to previous day low concentration. Zinc associations were robust to adjustment for EC, CO, NO₂, nickel, and chromium. However, evidence of effect modification by EC and NO₂ at lags 1 and 2 was observed.

Mohr et al. (2008, [180215](#)) used measurements of EC, O₃, SO₂, and total NO_x from the EPA supersite in St. Louis for June 2001 through May 2003 to examine the association of EC, temperature and season with asthma ED visits among children 2-17 years old. The association of EC with asthma ED visits varied by age, season and weekday versus weekend. The largest associations were observed for 2-5 year olds during the fall weekends (3% 95% CI: 1-5 per 0.1 µg/m³) and 11-17 year olds during winter weekdays (3% 95% CI: 0-5, per 0.1 µg/m³) and summer weekends (9% 95% CI: 2-17, per 0.1 µg/m³). Investigators also report that temperature modified the effect of EC after adjusting for gaseous copollutants such that the association of ED visits with EC increased with increasing temperature during the summer and increased with decreasing temperature during the winter. Authors attribute the pattern of associations to time activity patterns among this age group.

In Copenhagen, Anderson et al. (2007, [093201](#)) found an association between PM₁₀ attributed to vehicle emissions and asthma hospitalizations among children 5-18 yr (5.4% 95% CI: 0.57, 22.9 per 10 µg/m³, 0-5 day avg) in Copenhagen, Denmark. In an analysis of size distribution and number concentration, accumulation mode particles were most strongly associated with asthma admissions (8% [95% CI: 0-17] per 495 particles per cm³, lag 0-5). (Andersen et al., 2008, [189651](#)). In Helsinki, Halonen et al. (2008, [189507](#)) examined the association of various size fractions of PM (e.g., Aitken, accumulation mode, PM_{2.5}, PM_{10-2.5}) with ED visits for asthma among children <15 yr. These authors evaluated lags 0 to 5 and noted a different lag structure depending on age with children experiencing greater effects at lags 3 to 5 days compared to adults at lag 0. Aitken, accumulation mode particles and traffic-related PM were significantly and most strongly associated with

asthma visits among children, while no association with PM_{10-2.5} was observed in this age group.

Sinclair and Tolsma (2004, [088696](#)) investigated respiratory ambulatory care visits using ARIES data in Atlanta, GA (also used by SOPHIA investigators) and health insurance records. These authors evaluated three 3-day ma lags (0-2, 2-5 and 6-8 days) and reported relative risks, with no confidence intervals, for significant results only (not included in Figure 6-12). For childhood asthma outpatient visits, OHC, PM_{10-2.5}, PM₁₀, EC and OC were significantly associated with ambulatory care visits at lags 0-2 or 2-5 days.

A study in Anchorage used medical records to examine effects of particle exposure on pediatric asthma outpatient visits, inpatient visits and prescriptions for short-acting inhalers (Chimonas and Gessner, 2007, [093261](#)). Authors examined Medicaid claims for asthma-related and lower respiratory infection visits among children less than 20 yr of age for five years (approximately 25,000 children were enrolled in Medicaid each year between 1999 and 2003). Citing work done in the mid-1980's, the authors describe their city's particles as arising primarily from natural, geologic sources (PM₁₀), and to a lesser extent from local automotive emissions (PM_{2.5}) (Pritchett and Cooper, 1985, [156886](#)). Using GEE in a time-series analysis of daily and weekly effects of particle exposure on health outcomes, the authors found that each 10 µg/m³ increase in 24-h avg PM₁₀ was associated with a 0.6% increase (95% CI: 0.1-1.3) in outpatient visits for asthma. The same increase in weekly PM₁₀ concentration resulted in a 2.1% increase (95% CI: 0.4-3.8) in asthma visits, after adjustment for gaseous pollutants. No meaningful associations were observed for PM_{2.5}.

Adults and All Ages Combined

Results from the Atlanta SOPHIA study based on the a priori models examining a 3-day ma (lag 0-2 days) revealed no statistically significant associations with asthma (ICD-9 493, 786.09) among all ages for any of the PM metrics studied (e.g., PM₁₀, PM_{2.5}, PM_{10-2.5}, ultrafine Particle Count, PM components) (Peel et al., 2005, [056305](#)). However, the 14-day unconstrained distributed lag model produced an excess risk of 9.9% (95% CI: 6.5-13.5). The authors note that associations of PM_{2.5} and OC with asthma tended to be stronger during the warmer months. Sinclair and Tolsma (2004, [088696](#)) report a significant association between adult outpatient visits for asthma and UFPs, but not other PM size fractions (not included in Figure 6-12 because only significant results were presented).

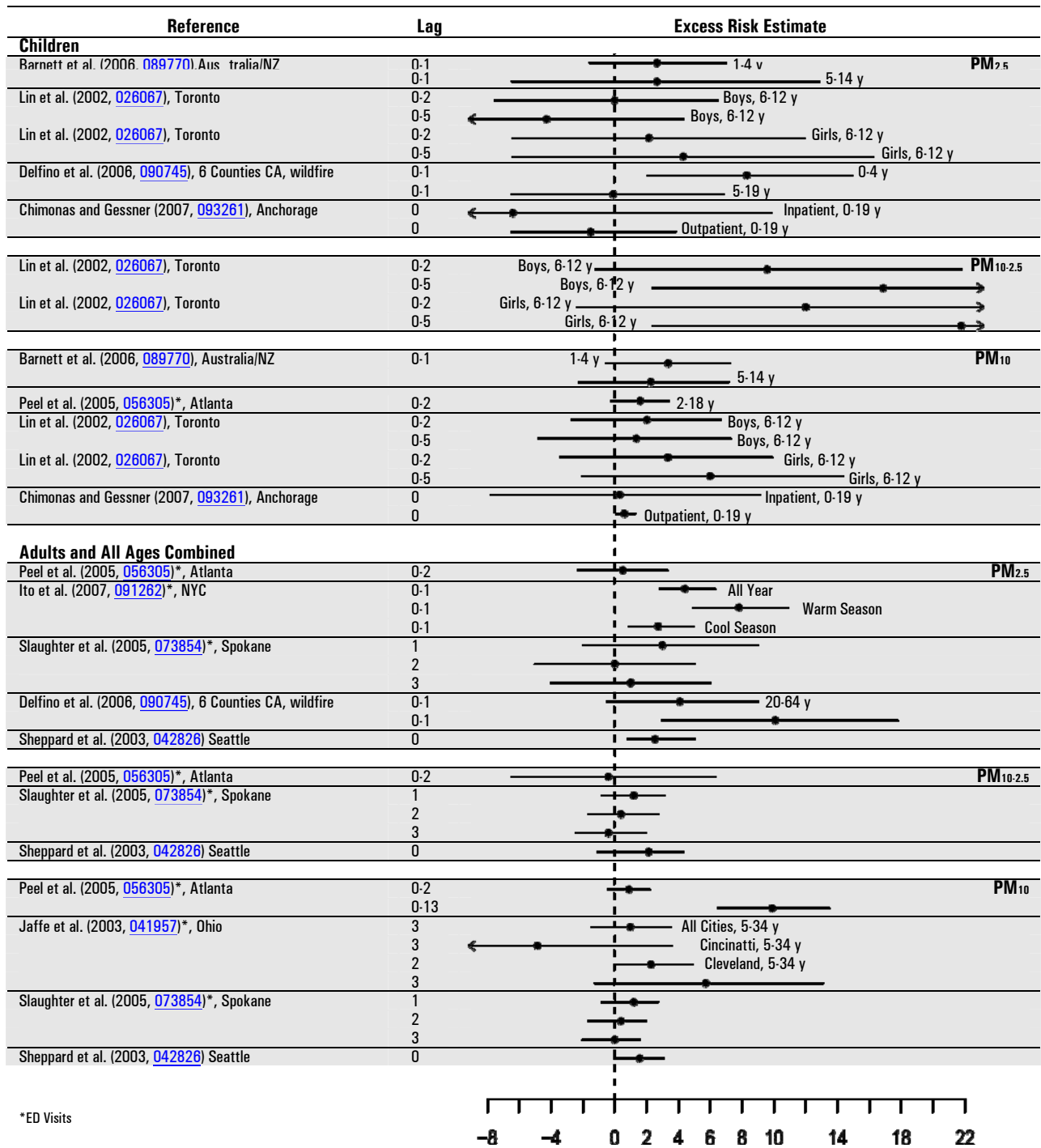


Figure 6-12. Excess risk estimates per 10 µg/m³ increase in 24-h avg PM₁₀, PM_{2.5} and PM_{10-2.5} for studies of asthma ED visits* and hospitalizations. Studies represented in the figure include all multicity studies. Single-city studies conducted in the U.S. or Canada are also included.

Jaffe et al. (2003, [041957](#)) examined the effects of ambient pollutants (PM₁₀, O₃, NO₂ and SO₂) during the summer months (June through August) on the daily number of ED

visits for asthma among Medicaid recipients aged 5 to 34 yr from 1991 to 1996 in Cincinnati, Columbus and Cleveland. Lags 1 to 3 were tested and only statistically significant lags were presented. For all cities combined, the overall effect estimate for 24-h avg PM₁₀ was 1.0% (95% CI: -1.44 to 3.54 per 10 µg/m³ increase). The effect estimate for Cleveland was the only significantly elevated estimate (2.3 95% CI: 0.0-4.9 per 10 µg/m³ increase) when the cities were examined independently. The authors report results from analyses indicating a possible concentration response for O₃ but no consistent effects for PM₁₀.

In New York City, Ito et al. (2007, [091262](#)) examined numbers of ED visits for asthma among all ages (ICD-9 493) in relation to pollution levels from 1999 to 2002; several weather models were evaluated. Although the association with NO₂ was the strongest, PM_{2.5} was significantly associated with asthma ED visits in each weather model (strongest during the warm months) and remained significant after adjustment for O₃, NO₂, CO and SO₂. Slaughter et al. (2005, [073854](#)) reported no associations with ED visits or hospitalizations for asthma, among all ages, in Spokane Washington for the PM size fractions studied (PM₁, PM_{2.5}, PM₁₀, PM_{10-2.5}). An association with CO, which the authors attribute to combustion related pollution in general, was observed. The effect of 24-h avg and 1-h maximum PM_{2.5}, PM_{10-2.5}, EC and OC on ED visits for asthma comparing two communities in New York City was investigated (New York State Department of, 2006, [090132](#)). In the Bronx, an increase in visits of 3.1% (95% CI: 0.6-6.2, per 10 µg/m³) was observed in relation to 24-h avg PM_{2.5} with similar findings for 1-h maximum PM_{2.5}. For PM_{10-2.5}, an increase of 2.7% (95% CI: 0.0-5.4) was observed in the Bronx. Smaller, less precise estimates were observed for Manhattan. Increased asthma visits were observed with OC, EC and total metals. The association of 1-h maximum PM_{2.5} with ED visits was robust to adjustment for copollutants.

Delfino et al. (2009, [191994](#)) examined the association of PM_{2.5} before, during and after wildfires in California with asthma hospitalizations among age and gender subgroups. The increase among older adults greater than 65 yr of 10% (95% CI: 3-17.8, per 10 µg/m³) was larger than the increase among adults 20-64 yr of 4.1% (95% CI: -0.5 to 9, per 10 µg/m³). For older adults, the association was stronger during the wildfire period compared to the pre-wildfire period and did not diminish during the post-wildfire period.

Effect estimates from studies of hospital admissions and ED visits for asthma are summarized in Figure 6-12. Associations with PM_{2.5} concentration among children are

imprecise and not consistently positive across different age groups and lags. Findings from two studies of PM_{10-2.5} (Sinclair and Tolsma, 2004, [088696](#)) as well as PM₁₀ studies both show positive associations, although estimates lack precision. Among adults and adults and children combined, associations of asthma hospital admissions and ED visits with PM_{2.5} concentration were observed in most studies. Positive, non-significant associations of PM_{10-2.5} concentration with asthma admissions and ED visits were observed in some studies of adults. Again, PM₁₀ estimates are more consistently positive and precise compared to other size fractions. Associations were observed with several PM_{2.5} components (e.g., EC, OC and zinc) and sources (e.g., traffic, wildfires). Many factors (e.g., the underlying distribution of individual sensitivity and severity, medication use and other personal behaviors) can influence the lag time observed in observational studies (Forastiere et al., 2008, [186937](#)). Excess risk estimates for asthma were generally sensitive to choice of lag and increase with longer or cumulative lags times. Most additional single-city studies conducted in Europe, South America and Asia, have investigated the associations of asthma hospitalizations, ED visits or doctor visits and most have reported evidence of an association with TSP (Arbex et al., 2007, [091637](#); Migliaretti and Cavallo, 2004, [087425](#); 2005, [088689](#)), PM₁₀ (Bell et al., 2008, [156266](#); Chardon et al., 2007, [091308](#); Chen et al., 2006, [087947](#); Erbas et al., 2005, [073849](#); Galan et al., 2003, [087408](#); Jalaludin et al., 2004, [056595](#); Kuo et al., 2002, [036310](#); Lee et al., 2002, [034826](#); Lee et al., 2006, [090176](#); Ko et al., 2007, [091639](#); Kim et al., 2007, [092837](#)) and PM_{2.5} (Chardon et al., 2007, [091308](#); Ko et al., 2007, [091639](#)), while a few have not shown an association with PM₁₀ (Larrieu et al., 2009, [180294](#); Masjedi et al., 2003, [052100](#); Tsai et al., 2006, [089768](#); Yang and Chen, 2007, [092847](#)).

6.3.8.3. COPD

Results from multicity studies of hospital admissions and ED visits for COPD as well as single-city studies conducted in the U.S. and Canada are summarized in Figure 6-13. Studies reviewed in the AQCD are included in the figure for continuity. Concentrations of PM for the relevant study period are found in Table 6-11.

In a study of Medicare recipients in 204 U.S. counties, Dominici et al. (2006, [088398](#)) reported an overall increase of about 1% in COPD hospitalizations (ICD-9 490-492) associated with 24-h avg PM_{2.5}, with the largest effects at lags 0 and 1. In this study effect

estimates were heterogeneous across the U.S. with a significant increase of about 4% observed in the Southeast at lag 0. In another study using Medicare data in 36 U.S. cities (1986-1999) short-term exposure to PM₁₀ was associated with an increase in COPD hospital admissions (ICD-9 490-496, excluding 493) of 1.47% (95% CI: 0.93-2.01, lag 1) during the warm season (Medina-Ramon et al., 2006, [087721](#)). A smaller effect was observed during the cold season.

In Atlanta, SOPHIA investigators reported a comparably sized effect estimate for COPD (ICD-9 491, 492, 496) and 24-h avg PM_{2.5} (1.5% [95% CI: -3.1 to 6.3, 0-2 day avg]). The association of PM₁₀ with COPD reported by Peel et al. (2005, [056305](#)) was 1.8% (95% CI: -0.6 to 4.3). No associations were observed for PM_{10-2.5}, ultrafine or PM_{2.5} components. Slaughter et al. (2005, [073854](#)) reported no associations between any size fraction of PM in Spokane, Washington (PM₁₀, PM_{2.5}, PM_{10-2.5}) and COPD (ICD-9 491, 492, 494, 496). In contrast, Chen et al. (2004, [087262](#)) reported increases in COPD admissions (ICD-9 490-492, 494, 496) for PM₁₀ (16.5% [95% CI: 6.88-27.02, 0-3 day avg]), PM_{2.5} (17.1% [95% CI: 4.6-31.0) and PM_{10-2.5} (10.0% [95% CI: -1.2 to 22.8, 0-3 day avg]). However, the estimates for PM metrics were diminished after adjustment for NO₂, however.

Delfino et al. (2009, [190254](#)) examined the association of PM_{2.5} from the wildfires of 2003 in California with COPD hospitalizations among age and gender subgroups. Among older adults (65+ years), associations were similar across pre-, post- and wildfire periods with none reaching significance. The increase for all periods combined in this age group was 1.9% (95% CI: -0.6 to 4.4, per 10 µg/m³). Michaud et al. (2004, [089900](#)) reported an association for asthma and COPD ED visits combined with PM₁ (lag 1) in Hilo, Hawaii in a study designed to investigate the effect of volcanic fog.

Halonen et al. (2008, [189507](#)) conducted a study of ED visits for COPD and asthma combined (J41, J44-J46) among adults 15-64 yr and older adults greater than 65 yr. These authors examined the effects of aitken mode particles, accumulation mode particles, PM_{2.5} and PM_{10-2.5} as well as several sources of PM_{2.5} (traffic, long range transported particles, road dust and coal/oil combustion). Concentrations, lagged from 0-5 days, were examined and the largest effects among older adults were observed in association with concurrent day PM_{2.5}, PM_{10-2.5} and accumulation mode particles, NO₂ and CO concentrations. The PM_{2.5} association was diminished with adjustment for UFPs, NO₂ and CO. A similar diminishment was observed when PM_{10-2.5} was adjusted for PM_{2.5}, NO₂ and CO. However, traffic related particles and long range transported particles (e.g., accumulation mode

particles such as carbon compounds, sulfates and nitrates from central Europe and Russia) were associated with COPD and asthma among older adults.

This same research group conducted additional analyses of hospital admissions using the same PM metrics focusing on older adults (65+ yr) (Halonen et al., 2009, [180379](#)). The PM_{2.5} results and lag structure were similar to the earlier ED visit study. The strongest effect was for accumulation mode particles with COPD/asthma admissions. Traffic related PM_{2.5} was associated with COPD/asthma admissions at lag 1 while no effect was observed with concurrent day concentration. Long range transported particles and road dust were also associated with admissions for asthma and COPD. With the exception of one study conducted in Spokane Washington (Slaughter et al., 2005, [073854](#)), associations have been consistently observed for PM_{2.5} and PM₁₀ with COPD in multicity and single-city studies conducted in the U.S. and Canada. Associations with PM_{10-2.5} are fewer and less consistent. A study that examined 7 single day lags in association with pooled COPD and asthma ED visits in Finland reports that PM_{2.5}, PM_{10-2.5}, traffic sources as well as gaseous pollutants had a more immediate effect in older adults (lags 0 and 1) compared to the children experiencing asthma (3-5 day lags) (Halonen et al., 2008, [189507](#)). Larger estimates at shorter lags were not observed consistently across other studies. Most single-city studies conducted outside of the U.S. or Canada focused on PM₁₀ (Chiu et al., 2008, [191989](#); Hapcioglu et al., 2006, [093263](#); Ko et al., 2007, [091639](#); Ko et al., 2007, [092844](#); Martins et al., 2002, [035059](#); Masjedi et al., 2003, [052100](#); Sauerzapf et al., 2009, [180082](#); Yang and Chen, 2007, [092847](#)).

6.3.8.4. Pneumonia and Respiratory Infections

Results from multicity studies of hospital admissions and ED visits for respiratory infection as well as single-city studies conducted in the U.S. and Canada are summarized in Figure 6-14. The figure includes studies of respiratory infection reviewed in the 2004 AQCD. Concentrations of PM for the relevant study period are found in Table 6-11.

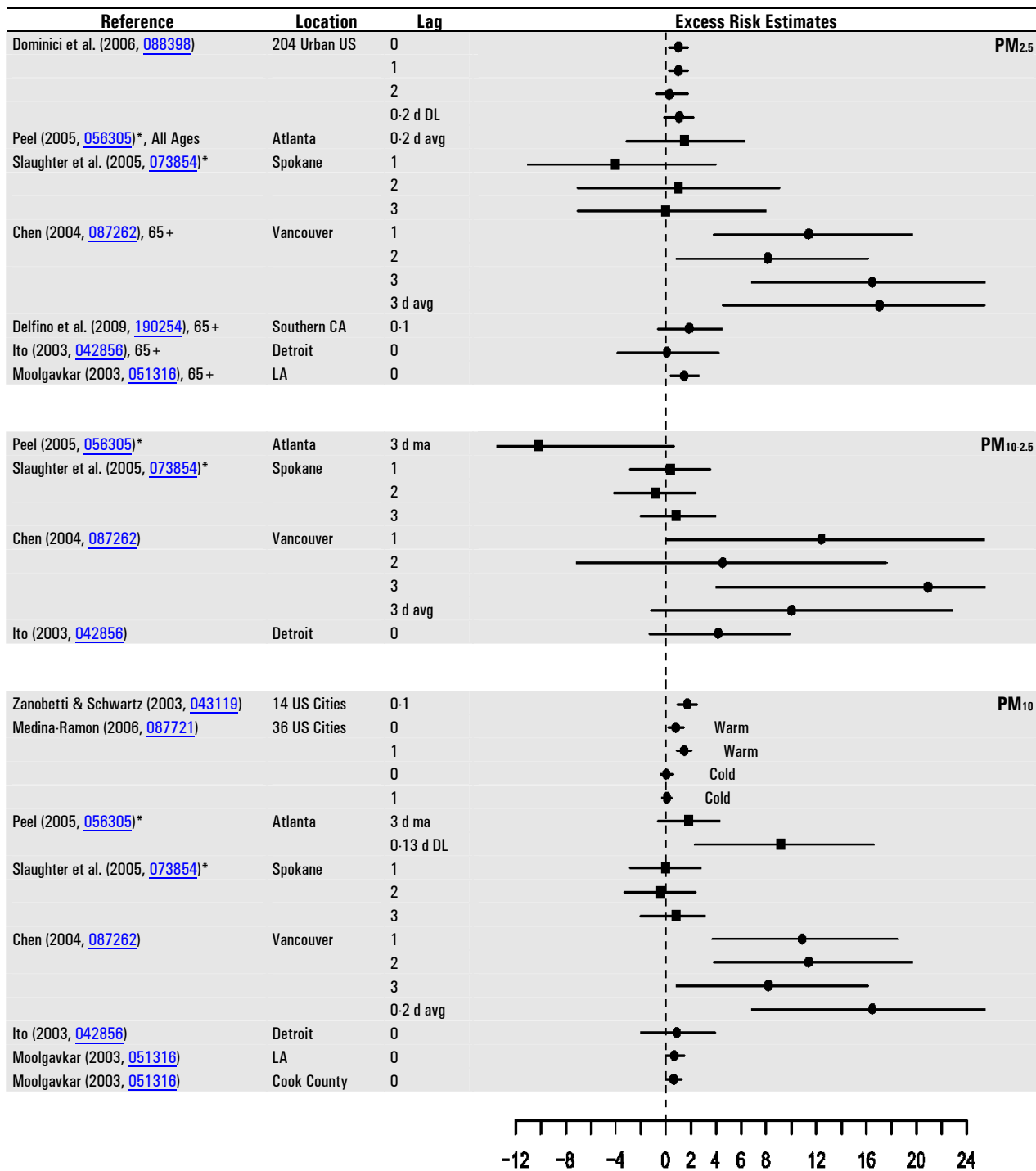


Figure 6-13. Excess risks estimates per 10 µg/m³ increase in 24-h avg PM₁₀, PM_{2.5} and PM_{10-2.5} for studies of COPD ED visits* and hospitalizations among older adults (65+ yr, unless other age group is noted). Studies represented in the figure include all multicity studies. Single-city studies conducted in the U.S. or Canada are also included.

Children

In the study of 7 cities in Australia and New Zealand, associations of PM_{2.5} with pneumonia and acute bronchitis (ICD-10 J12-J17, J18.0, J18.1, J18.8, J18.9, J20, J21) were observed among infants less than 1-years old (4.54% [95% CI: 0.00-9.20]) and children 1-4 years old (6.44% [95% CI: 0.26-12.85]) (Barnett et al., 2005, [087394](#)). Although quantitative results are only presented for all respiratory diseases combined, Ostro et al. (2009, [191971](#)) examined several specific respiratory diseases including acute bronchitis and pneumonia. They reported that PM_{2.5} and its components were more strongly associated with these endpoints compared to other respiratory diseases. Delfino et al. (2009, [190254](#)) reports imprecise increases in admissions among children during wildfire periods for acute bronchitis and bronchiolitis as well as pneumonia.

Inpatient and outpatient visits for lower respiratory tract infections among children in Anchorage, Alaska, were not associated with PM_{2.5} or PM₁₀ (Chimonas and Gessner, 2007, [093261](#)). Lin et al. (2005, [087828](#)) observed associations of respiratory infections (ICD-9 464, 466, 480-487) with PM_{10-2.5} and PM₁₀ that persisted after adjustment for gaseous pollutants among subjects less than 15 years old. Analyses were stratified by gender and both single and multiple day lags were examined (4 and 6 day avg were presented). The largest significant effect estimates were for PM_{10-2.5}. The size of the PM_{2.5} estimate varied by gender and was sensitive to the choice of lag. PM_{2.5} results were not generally robust to adjustment for gases.

All Ages and Older Adults

SOPHIA investigators examined ED visits for upper respiratory tract infections (URI) (ICD-9 460-466, 477) and pneumonia (ICD-9 480-486) among all ages. An excess risk of 1.4% (95% CI: 0.4-2.5 per 10 µg/m³, lag 0-2 day avg) for PM₁₀ was associated with URI visits. With the exception of a small increase in risk for OC of 2.8% (95% CI: 0.4-5.3, per 2 µg/m³, 0-2 day avg) with pneumonia visits, Peel et al. (2005, [056305](#)) reported no association with other PM size fractions or components evaluated. However, Sinclair and Tolsma (2004, [088696](#)), who also used ARIES data in their analysis, reported significant associations with outpatient visits for LRI. These associations were generally observed for 3-5-day ma lags, in association with PM_{10-2.5}, PM₁₀, EC, OC, and PM_{2.5} water soluble metals (not pictured in figure because only significant lags were reported). No associations with pneumonia for any size fractions were observed among all ages in a study conducted in

Spokane, Washington (not pictured because effect estimates were not reported) (Slaughter et al., 2005, [073854](#)).

French PSAS investigators examined the effect of fine and coarse PM on hospital admissions for respiratory infection (ICD-10: J10-22) among all ages. Increases of 2.5% (95% CI: 0.1-4.8) and 4.4% (95%CI: 0.9-8.0) per 10 $\mu\text{g}/\text{m}^3$ were observed in association with $\text{PM}_{2.5}$ and $\text{PM}_{10-2.5}$, respectively (Host et al., 2008, [155852](#)). In a multicity study of older adults (65+ yr) Medina-Ramon et al. (2006, [087721](#)) examined hospital admissions for pneumonia (ICD-9 480-487) in 36 U.S. cities in relation to 24-h avg PM_{10} concentration. An increase in pneumonia admissions of 0.84% (95% CI: 0.50-1.19, per 10 $\mu\text{g}/\text{m}^3$, lag 0) was reported by these investigators during the warm season. Cold season associations were weaker (0.30% 95% CI: 0.07-0.53, per 10 $\mu\text{g}/\text{m}^3$, lag 0) as were lag 1 associations. Dominici et al. (2006, [088398](#)) investigated hospital admissions for all respiratory infections including pneumonia (ICD-9 464-466, 480-487) among older adults in 204 urban U.S. counties in relation to $\text{PM}_{2.5}$ and reported a significant increased risk only at lag 2. Heterogeneity in effect estimates was observed across the U.S. with the largest associations reported for the South and Southeast.

In Boston, excess risks of pneumonia hospitalization in association with $\text{PM}_{2.5}$, BC, and CO were observed among older adults (Zanobetti and Schwartz, 2006, [090195](#)). A measure of non-traffic PM, e.g., the residuals from the regression of $\text{PM}_{2.5}$ on BC, was not associated with pneumonia hospitalization in these data. In a California study (Delfino et al., 2009, [190254](#)) effect estimates of similar magnitude for pneumonia admissions associated with $\text{PM}_{2.5}$ from wildfires among all ages combined and older adults (2.8% 95% CI: 0.7-5.0, per 10 $\mu\text{g}/\text{m}^3$, all ages combined). The $\text{PM}_{2.5}$ association with acute bronchitis and bronchiolitis admissions during the wildfire period for all age groups showed an approximately 10% increase (9.6% 95% CI: 1.8-17.9, per 10 $\mu\text{g}/\text{m}^3$). The increase was not larger during the wildfire period compared to the pre-fire period for either endpoint.

In a study of 4 cities in Australia, statistically significant associations of pneumonia and acute bronchitis with NO_2 and particles measured by nephelometry (but not $\text{PM}_{2.5}$ mass) were observed among older adults (Simpson et al., 2005, [087438](#)). Halonen et al. (2009, [180379](#)) examined pneumonia among older adults (ICD10 J12-J15) in their most recent analysis. Associations of $\text{PM}_{2.5}$ (5.0% 95% CI: 1.0-9.3, per 10 $\mu\text{g}/\text{m}^3$, lag 5-day mean) as well as accumulation mode particles with pneumonia admissions were observed.

Although the body of literature is small, several studies of children reported associations of PM_{2.5}, PM_{10-2.5} and PM₁₀ with respiratory infections but endpoints studied are heterogeneous and effect estimates are imprecise. Studies of adults show a similar pattern of increased risk for each of these size fractions. Several other single-city studies conducted outside the U.S. and Canada reported associations for PM₁₀ (Cheng et al., 2007, [093034](#); Hwang and Chan, 2002, [023222](#); Nascimento et al., 2006, [093247](#)) and PM_{2.5} (Hinwood et al., 2006, [088976](#)) with hospitalization or ED visits for respiratory infections.

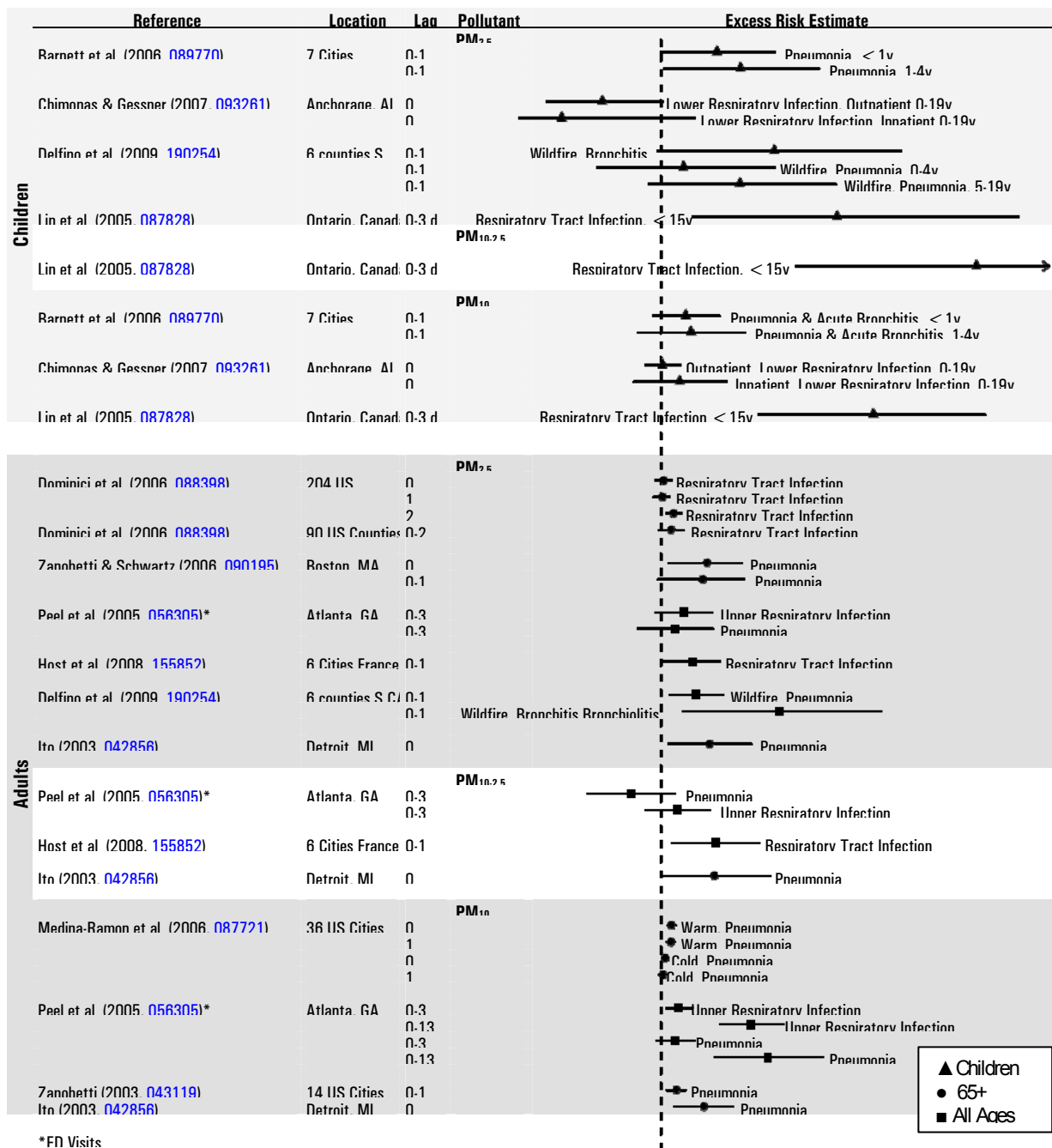


Figure 6-14. Excess risks estimates per 10 µg/m³ increase in 24-h avg PM₁₀, PM_{2.5} and PM_{2.5-10} for studies of respiratory infection ED visits* and hospitalizations. Studies represented in the figure include all multicounty studies. Single-city studies conducted in the U.S. are also included.

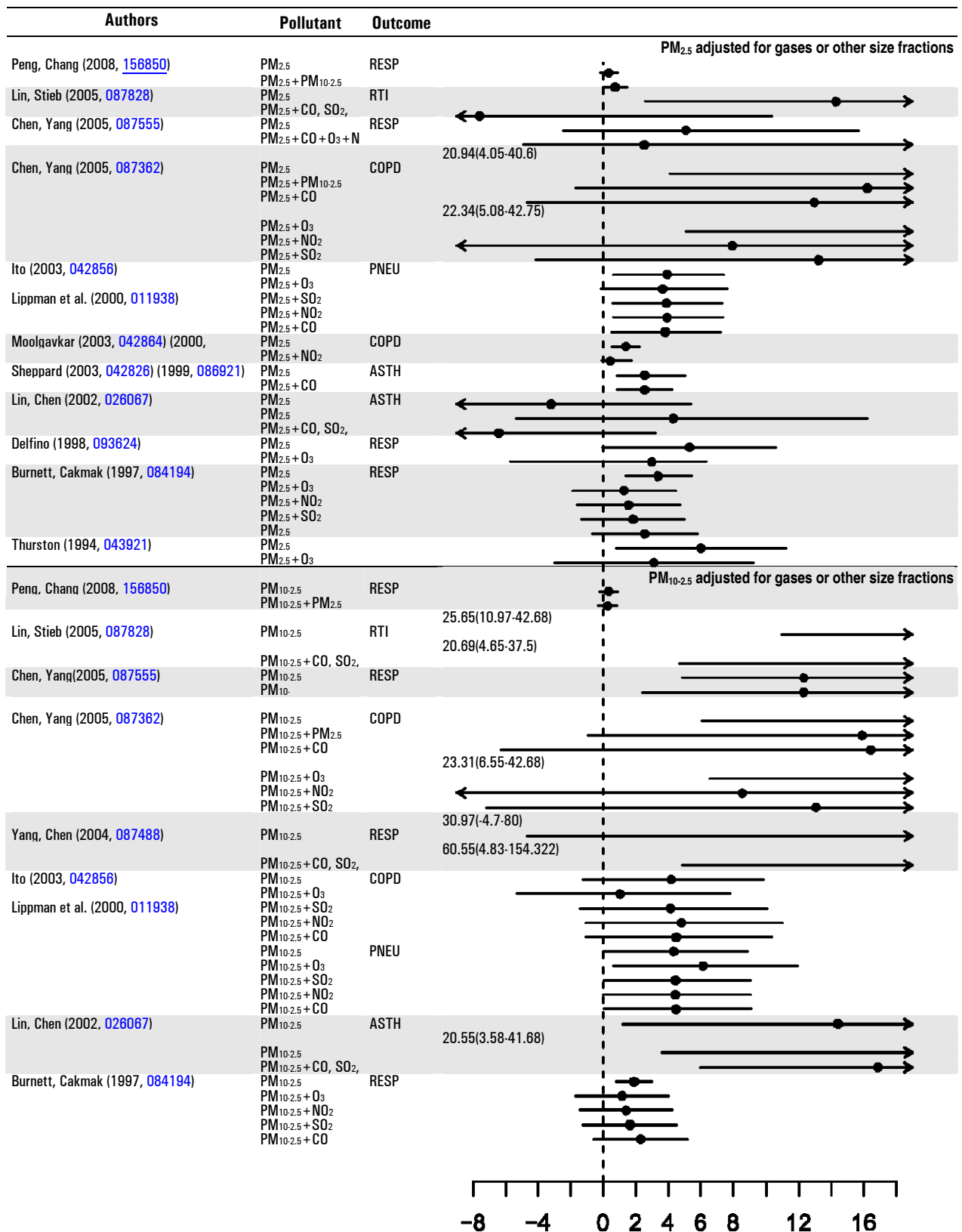


Figure 6-15. Excess risk estimates per 10 $\mu\text{g}/\text{m}^3$ increase in PM_{2.5}, and PM_{10-2.5} for studies of ED visits* and HAs for respiratory diseases. Results for multipollutant models.

Table 6-11. PM concentrations in studies of respiratory diseases published since 2002.

Pollutant	Author	Location	Mean Concentration ($\mu\text{g}/\text{m}^3$)	Upper Percentile concentrations ($\mu\text{g}/\text{m}^3$)
PM₁₀				
	Andersen et al. (2007, 093201)	Copenhagen, Denmark	25/24	75th: 30 / 99th: 72
	Barnett et al. (2005, 087394)	7 Cities, Australia, NZ	16.5-20.6	Max: 50.2-156.3
	Chardon et al. (2007, 091308)	Paris	23	Max: 97.3
	Chen et al. (2004, 087262 ; 2005, 087555)	Vancouver, Canada	13.3	Max: 52.2
	Chimonas and Gessner (2007, 093261)	Anchorage, Alaska	27.6	Max: 421
	Fung et al. (2005, 093262)	Ontario, Canada	38	Max: 248
	Fung et al. (2006, 089789)	Vancouver, Canada	13.3	Max: 52.17
	Gordian and Choudhury (2003, 054842)	Anchorage, AK	36.11	Max: 210.0
	Jaffe et al. (2003, 041957)	Cincinnati	43	Max: 90
	Jalaludin et al. (2004, 056695)	Sydney, Australia	22.8	Max: 44.9
	Lin et al. (2002, 026067)	Toronto, Canada	30.16	Max: 116.20
	Lin et al. (2005, 087828)	Ontario, Canada	20.41	Max: 73
	Luginaah et al. (2005, 057327)	Ontario, Canada	50.6	Max: 349
	Medina-Ramon et al. (2006, 087721)	36 U.S. Cities	15.9-44.0	NR
	Moolgavkar (2003, 051316)	Los Angeles, CA	22 (median)	Max: 86
	Moolgavkar (2003, 051316)	Cook County, IL	35 (median)	Max: 365
	Peel et al. (2005, 056305)	Atlanta, GA	27.9	Max: 44.7
	Sinclair and Tolsma (2004, 088696)	Atlanta, GA	29.03	NR
	Slaughter et al. (2005, 073854)	Spokane, WA	NR	Max: 41.9 (using 90% of concentrations)
	Tolbert et al. (2007, 090316)	Atlanta, GA	26.6	90th: 42.8
	Ulirsch et al. (2007, 091332)	Idaho	23.2	Max: 183.0
	Yang et al. (2004, 087488)	Vancouver, Canada	13.3	Max: 52.2
	Zanobetti (2003, 042812); Samet et al. (2000, 010269)	14 U.S. Cities	24.4-45.3	Max 94.8-605.8
PM_{2.5}				
	Andersen et al. (2007, 093201)	Copenhagen, Denmark	10	99 th : 28
	Barnett et al. (2005, 087394)	7 Cities Australia, NZ	8.1-11	Max: 29.3-122.8
	Bell et al. (2008, 156266)	202 U.S. counties	12.92	98th: 34.16
	Chardon et al. (2007, 091308)	Paris, France	14.7	75th: 18.2
	Chen et al. (2004, 087262 ; 2005, 087555)	Vancouver, Canada	7.7	Max: 32
	Chimonas and Gessner (2007, 093261)	Anchorage, AK	6.1	Max: 69.8
	Delfino et al. (2009, 190254)	6 counties, CA	18.4-32.7	45.3-76.1 (mean during wildfire period)
	Dominici et al. (2006, 088398)	204 U.S. counties	13.4	75th: 15.2
	Fung et al. (2006, 089789)	Vancouver, Canada	7.72	Max: 32
	Halonen et al. (2008, 189507)	Helsinki, Finland	NR; Median = 9.5	Max: 69.5
	Host et al. (2008, 155852)	6 Cities France	13.8-18.8	95th: 25.0-33.0
	Ito et al. (2007, 091262)	New York, NY	All yr: 15.1	All yr: 95th: 32
	Lin et al. (2002, 026067)	Toronto Canada	17.99	Max: 89.59
	Lin et al. (2005, 087828)	Ontario, Canada	9.59	Max: 73
	Moolgavkar (2003, 051316)	Los Angeles, CA	22 (median)	Max: 86
	Peel et al. (2005, 056305)	Atlanta, GA	19.2	90th: 32.3; 98th: 39.8
	Sinclair and Tolsma (2004, 088696)	Atlanta, GA	17.62	NR
	Sheppard et al. (2003, 042826)	Seattle, WA	16.7	98th: 46.6
	Slaughter et al. (2005, 073854)	Spokane, WA	NR	Max: 20.2 (using 90% of concentrations)
	Tolbert et al. (2007, 090316)	Atlanta, GA	17.1	90th: 28.8; 98th: 38.7
	Yang et al. (2004, 087488)	Vancouver, Canada	7.7	Max: 32.0
	Zanobetti and Schwartz (2009, 188462)	112 U.S. cities		
PM_{10-2.5}				
	Chen et al. (2004, 087262 ; 2005, 087555)	Vancouver, Canada	5.6	Max: 24.6
	Fung et al. (2006, 089789)	Vancouver, Canada	5.6	Max: 27.07
	Halonen et al. (2008, 189507)	Helsinki, Finland	NR; Median: 9.9	Max: 101.4
	Host et al. (2008, 155852)	6 Cities France	7.0-11.0	95th: 12.5-21.0
	Lin et al. (2002, 026067)	Toronto, Canada	12.17	Max: 68.00
	Lin et al. (2005, 087828)	Ontario, Canada	10.86	Max: 45
	Peel et al. (2005, 056305)	Atlanta, GA	9.7	90th: 16.2
	Peng et al. (2008, 156850)	108 U.S. counties	NR; Median: 9.8	75th: 15.0
	Sinclair and Tolsma (2004, 088696)	Atlanta, GA	9.67	NR
	Sheppard et al. (2003, 042826)	Seattle, WA	16.2	Max: 88
	Slaughter et al. (2005, 073854)	Spokane, WA	NR	NR
	Tolbert et al. (2007, 090316)	Atlanta, GA	9	90th: 15.1; Max: 50.3
	Yang et al. (2004, 087488)	Vancouver, Canada	7.7	Max: 24.6
ULTRAFINE				
	Andersen et al. (2008, 189651)	Copenhagen, Denmark	Mean particles/cm ³ : 6847	99th: 19,895 particles/cm ³
	Halonen et al. (2008, 189507)		NR: Median particles/cm ³ : 8,203	Max: 50,990 particles/cm ³

6.3.8.5. Copollutant Models

Some studies have investigated potential confounding by copollutants through the application of multipollutant models. Several Canadian studies of respiratory hospital admissions reported larger effects for $PM_{10-2.5}$ compared to $PM_{2.5}$ that were robust to adjustment for gaseous pollutants (Chen et al., 2005, [087555](#); Lin et al., 2002, [026067](#); Yang et al., 2004, [087488](#)). The COPD associations between $PM_{2.5}$ and $PM_{10-2.5}$ reported by Chen et al. 2004 remained positive but were diminished slightly after adjustment for NO_2 . The associations reported by Ito et al. 2003 of $PM_{2.5}$ and $PM_{10-2.5}$ with pneumonia hospital admissions remained after adjustment for gases while the association of $PM_{10-2.5}$ with COPD admissions was not robust to adjustment for O_3 . Associations reported by Burnett et al. (1986, [084184](#)), Moolgavkar et al. (2003, [042864](#)) and Delfino et al. (1998, [093624](#)) were not consistently robust to adjustment for gaseous copollutants. In the MCAPS study the effect of $PM_{2.5}$ was robust to adjustment for $PM_{10-2.5}$ while the $PM_{10-2.5}$ effect on respiratory admissions was diminished after adjustment for $PM_{2.5}$ (Peng et al., 2008, [156850](#)).

Multiple pollutant analyses for other size fractions and components have been conducted in a some additional studies. Effect estimates for PM_{10} were robust to adjustment for gases in several recent studies (Tolbert, 2007, [090316](#); Ulirsch et al., 2007, [091332](#); Anderson and Bogdan, 2007, [156214](#)). PM_{10} associations with respiratory disease did not change in models also containing total number concentration, nor did the association of ACP diminish after adjustment for UFP concentration (Anderson and Bogdan, 2007, [156214](#)). Finally, Peng et al. (2009, [191998](#)) reports an OCM effect that was robust to adjustment for other components while the associations with nickel, vanadium and EC were somewhat diminished in models containing multiple components.

Inconsistency across these study findings is likely due to differences in the correlation structure among pollutants as well as differing degrees of exposure measurement error.

6.3.9. Short-term Exposure to PM and Respiratory Mortality

An evaluation of studies that examined the association between short-term exposure to $PM_{2.5}$ and $PM_{10-2.5}$ and mortality provides additional evidence for PM-related respiratory health effects. Although the primary analysis in the majority of mortality studies evaluated consists of an examination of the relationship between $PM_{2.5}$ or $PM_{10-2.5}$ and all-cause (non-

accidental) mortality, some studies have examined associations with cause-specific mortality including respiratory-related mortality.

Multicity mortality studies that examine the PM-respiratory mortality relationship on a national scale – Franklin et al. (2007, [091257](#)): 27 U.S. cities and Zanobetti and Schwartz (2009, [188462](#)): 112 U.S. cities – have found consistent positive associations between short-term exposure to PM_{2.5} and respiratory mortality of approximately 1.68% per 10 µg/m³ at lag 0-1 (see Section 6.5). The associations observed on a national scale are consistent with those presented by Ostro et al. (2006, [087991](#)) in a study that examined the PM_{2.5}-mortality relationship in 9 California counties (2.2% [95% CI: 0.6-3.9] per 10 µg/m³). An evaluation of studies that examined additional lag structures of associations found smaller respiratory mortality effect estimates when using the average of lag days 1 and 2 (1.01% [95% CI: -0.03 to 2.05] per 10 µg/m³) (Franklin et al., 2008, [155779](#)), and associations consistent with those observed at lag 0-1 when examining single day lags, specifically lag 1 (1.78% [95% CI: 0.2-3.36]). Although the overall effect estimates reported in the multicity studies evaluated are consistently positive, it should be noted that a large degree of variability exists between cities when examining city-specific effect estimates potentially due to differences between cities and regional differences in PM_{2.5} composition (see Figure 6-25). A limited number of studies that examined the PM_{2.5}-respiratory mortality association have conducted extensive analyses of potential confounders, as a result, PM₁₀-mortality studies provide evidence which suggests that PM_{2.5} risk estimates are fairly robust to the inclusion of gaseous copollutants in models. Overall, the respiratory PM_{2.5} effects observed were larger, but less precise than those reported for all-cause (nonaccidental) mortality (see Section 6.5), and are consistent with the effect estimates observed in the single- and multicity studies evaluated in the 2004 PM AQCD.

Zanobetti and Schwartz (2009, [188462](#)) also examined PM_{10-2.5} mortality associations in 47 U.S. cities and found evidence for respiratory mortality effects (1.16% [95% CI: 0.43, 1.89] per 10 µg/m at lag 0-1), which are somewhat larger than those reported for all-cause (non-accidental) mortality (0.46% [95% CI: 0.21, 0.671] per 10 µg/m). In addition, Zanobetti and Schwartz (2009, [188462](#)) reported seasonal (i.e., larger in spring) and regional differences in PM_{10-2.5} respiratory mortality risk estimates. However, single-city studies conducted in Atlanta, GA (Klemm et al., 2004, [056585](#)) and Vancouver, CAN ((Villeneuve et al., 2003, [055051](#)) reported no associations between short-term exposure to PM_{10-2.5} and respiratory mortality. The difference in the results observed between the multi- and single-

city studies could be due to a variety of factors including differences between cities and compositional differences in PM_{10-2.5} across regions (see Figure 6-30). Only a small number of studies have examined potential confounding by gaseous copollutants or the influence of model specification on PM_{10-2.5} mortality risk estimates, but the effects are relatively consistent with those studies evaluated in the 2004 PM AQCD.

6.3.10. Summary and Causal Determinations

6.3.10.1. PM_{2.5}

Several studies of the effect of PM_{2.5} on hospital admissions for respiratory diseases reviewed in the 2004 AQCD reported positive associations for several diseases. The 2004 AQCD presented limited epidemiologic evidence of PM_{2.5} being associated with respiratory symptoms (including cough, phlegm, difficulty breathing, and bronchodilator use); observations for PM_{2.5} were positive, with slightly larger effects for PM_{2.5} than for PM₁₀. In addition, mortality studies reported relatively higher PM_{2.5} risk estimates for respiratory-related mortality compared to all-cause (non-accidental) mortality. Controlled human exposure studies did not provide support for effects of CAPs on respiratory symptoms. Small decrements in peak flow for both PM_{2.5} and PM₁₀ in asthmatics and nonasthmatics were reported in epidemiologic studies included in the 2004 PM AQCD, whereas controlled human exposure and animal toxicological studies reported few or no effects on pulmonary function with inhalation to CAPs. In addition, the 2004 PM AQCD presented a number of controlled human exposure and toxicological studies that reported mild pulmonary inflammation following exposure to PM_{2.5} CAPs and DE or DEP, as well as ROFA or other metal-containing PM in animals. The 2004 PM AQCD described controlled human exposure studies showing increases in allergic responses among previously sensitized atopic subjects after short term exposure to DEP. These observations were supported by many toxicological studies that added to existing evidence demonstrating that various forms of PM could promote allergic disease and exacerbate allergic asthma in animal models. Toxicological studies also indicated that PM_{2.5} increased susceptibility to respiratory infection.

Overall, in recent studies PM_{2.5} effects on respiratory hospitalizations and ED visits have been consistently observed. Most effect estimates were in the range of ~1-4% and were observed in areas with mean 24-h PM_{2.5} concentrations between 6.1 and 22 µg/m³. Further, recent studies have focused on increasingly specific disease endpoints such as asthma,

COPD and respiratory infection. The strongest evidence of an association comes from large multicity studies of COPD, respiratory tract infection and all respiratory diseases among Medicare recipients (65+ years old) published since 2004 (Dominici et al., 2006, [088398](#); Bell et al., 2008, [156266](#)). Studies of children have also found evidence of an effect of PM_{2.5} on hospitalization for all respiratory diseases, including asthma and respiratory infection. However, many of these effect estimates are imprecise, their magnitude and statistical significance are sensitive to choice of lag, and some null associations were observed. Although the association of PM_{2.5} with pediatric asthma was not examined specifically, it is noteworthy that one of the strongest associations observed in the Atlanta-based SOPHIA study was between PM₁₀ and pediatric asthma visits; PM_{2.5} makes up a large proportion of PM₁₀ in Atlanta (Peel et al., 2005, [056305](#)); Positive associations between PM_{2.5} (or PM₁₀) and hospital admissions for respiratory infection (Figure 6-14) are supported by animal toxicological studies which add to previous findings of increased susceptibility to infection following exposure to PM_{2.5}. These include studies demonstrating reduced clearance of bacteria (*Pseudomonas*, *Listeria*) or enhanced pathogenesis of viruses (influenza, RSV) after exposure to DE or ROFA.

Epidemiologic studies that examined the association between PM_{2.5} and mortality provide additional evidence for PM_{2.5}-related respiratory effects (Section 6.3.9). The multicity studies evaluated found consistent, precise positive associations between short-term exposure to PM_{2.5} and respiratory mortality ranging from 1.67 to 2.20% at mean 24-h PM_{2.5} avg concentrations above 13 µg/m³. Although examinations of potential confounders of the PM_{2.5}-respiratory mortality relationship are limited, the observed associations are supported by PM₁₀-mortality studies, which found that PM risk estimates remained robust to the inclusion of copollutants in models.

Epidemiologic studies of asthmatic children have observed increases in respiratory symptoms and asthma medication use associated with higher PM_{2.5} or PM₁₀ concentrations. Associations with respiratory symptoms and medication use are less consistent among asthmatic adults, and there is no evidence to suggest an association between respiratory symptoms with PM_{2.5} among healthy individuals. In addition, respiratory symptoms have not been reported following controlled exposures to PM_{2.5} among healthy or health-compromised adults (Section 6.3.1.2).

Although more recent epidemiologic studies of pulmonary function and PM_{2.5} have yielded somewhat inconsistent results, the majority of studies have found an association

between PM_{2.5} concentration and FEV₁, PEF, and/or MMEF. In asthmatic children, a 10 µg/m³ increase in PM_{2.5} is associated with a decrease in FEV₁ ranging from 1-3.4% (Section 6.3.2.1). A limited number of controlled human exposure studies have reported small decreases in arterial oxygen saturation and MMEF following exposure to PM_{2.5} CAPs with more pronounced effects observed in healthy adults than in asthmatics or older adults with COPD (Section 6.3.2.2). In toxicological studies, changes in pulmonary function have been observed in healthy and compromised rodents after inhalation exposures to CAPs from a variety of locations or DE. A role for the PM component of DE is supported by altered pulmonary function in healthy rats after IT instillation of DEP (Section 6.3.2.3).

Several lines of evidence suggest that fine PM promotes and exacerbates allergic disease, which often underlies asthma (Section 6.3.6). Although epidemiologic studies examining specific allergic outcomes and short-term exposure to PM are relatively rare, the available studies, conducted primarily in Europe, positively associate PM_{2.5} and PM₁₀ with allergic rhinitis or hay fever and skin prick reactivity to allergens. Short term exposure to DEP in controlled human exposure studies has been shown to increase the allergic response among previously sensitized atopic subjects, as well as induce de novo sensitization to an antigen. Toxicological studies continue to provide evidence that PM_{2.5}, in the form of CAPs, resuspended DEP, or DE, but not woodsmoke, spurs and intensifies allergic responses in rodents. Proposed mechanisms for these effects include mediation by neurotrophins and oxidative stress, and one study demonstrated that effects were mediated at the epigenetic level (Liu et al., 2008, [156709](#)).

A large body of evidence, primarily from toxicological studies, indicates that various forms of PM induce oxidative stress, pulmonary injury, and inflammation. Notably, CAPs from a variety of locations induce inflammatory responses in rodent models, although this generally requires multiday exposures. The toxicology findings are consistent with several recent epidemiologic studies of PM_{2.5} and the inflammatory marker eNO, which reported statistically significant, positive effect estimates with some inconsistency in the lag times and use of medication. In asthmatic children, a 10 µg/m³ increase in PM_{2.5} is associated with an increase in eNO ranging from 0.46 to 6.99 ppb. Several new controlled human exposure studies report traffic or diesel-induced increases in markers of inflammation (e.g., neutrophils and IL-8) in airway lavage fluid from healthy adults. Recent studies have provided additional evidence in support of a pulmonary oxidative response to DE in humans, including induction of redox-sensitive transcription factors and increased urate

and GSH concentrations in nasal lavage. In addition, exposure to WS has recently been demonstrated to increase the levels of eNO and malondialdehyde in breath condensate of healthy adults (Barregard et al., 2008, [155675](#)). Preliminary findings indicate little to no pulmonary injury in humans following controlled exposures to fine urban traffic particles or DE, in contrast to a number of toxicological studies demonstrating injury with CAPs or DE (Sections 6.3.5.2 and 6.3.5.3, respectively).

Recent studies have reported associations of hospital admissions, ED or urgent care visits for several respiratory diseases with PM_{2.5} components and sources including Ni, V, OC and EC, woodsmoke and traffic emissions, in studies of both children and adults. Delfino et al. (2003, [090941](#); 2006, [090745](#)) found positive associations between EC and OC components of PM and asthma symptoms and between EC and eNO. Particle composition and/or source also appears to heavily influence the increase in markers of pulmonary inflammation demonstrated in studies of controlled human exposures to PM_{2.5}. For example, whereas exposures to fine CAPs from Chapel Hill, NC have been shown to increase BAL neutrophils in healthy adults, no such effects have been observed in similar studies conducted in Los Angeles. In addition, differential inflammatory responses have been observed following bronchial instillation of particles collected at different times or from different areas (Section 6.3.3.2). One new study found that the increased airway neutrophils previously observed by Ghio et al. (2000, [012140](#)) in human volunteers after Chapel Hill CAPs exposure could be largely attributed to the content of sulfate, Fe, and Se in the soluble fraction (Huang et al., 2003, [087377](#)).

In summary, new evidence of ED visits and hospital admissions builds upon the positive and statistically significant evidence presented in the 2004 PM AQCD to support a consistent association with ambient concentrations of PM_{2.5}. Most effect estimates with respiratory hospitalizations and ED visits were in the range of ~1% to 4% and were observed in areas with mean 24-h PM_{2.5} concentrations between 6.1 and 22 µg/m³. The evidence for PM_{2.5} induced respiratory effects is strengthened by similar HA and ED visit associations for PM₁₀, along with the consistent positive associations observed between PM_{2.5} and respiratory mortality in multicity studies. Panel studies also indicate associations with PM_{2.5} and respiratory symptoms, pulmonary function, and pulmonary inflammation among asthmatic children. Further support for these observations is provided by recent controlled human exposure studies in adults demonstrating increased markers of pulmonary inflammation following DE and other traffic-related exposures, oxidative

responses to DE and woodsmoke, and exacerbations of allergic responses and allergic sensitization following exposure to DEP. Although not consistent across studies, some controlled human exposure studies have reported small decrements in various measures of pulmonary function following controlled exposures to PM_{2.5}. Numerous toxicological studies demonstrating a wide range of responses provide biological plausibility for the associations between PM_{2.5} and respiratory morbidity observed in epidemiologic studies. Altered pulmonary function, mild pulmonary inflammation and injury, oxidative responses, AHR in allergic and non-allergic animals, exacerbations of allergic responses and increased susceptibility to infections were observed in a large number of studies involving exposure to CAPs, DE, other traffic-related PM and woodsmoke. The evidence for an effect of PM_{2.5} on respiratory outcomes is somewhat restricted by limited coherence between some of the findings from epidemiologic and controlled human exposure studies for the specific health outcomes reported and the sub-populations in which those health outcomes occur. Although there is evidence for respiratory symptoms among asthmatic children in epidemiologic panel studies, the studies of hospital admissions and ED visits provide more evidence for effects from COPD and respiratory infections than for asthma. Additionally, controlled human exposure studies report greater effects in healthy adults when compared to asthmatics or those suffering from COPD. Finally, there is limited information which could explain the relationship between the clinical and subclinical respiratory outcomes observed and the magnitude of the PM_{2.5}-respiratory mortality associations reported. Therefore, the evidence is sufficient to conclude that a **causal relationship is likely to exist between short-term PM_{2.5} exposures and respiratory effects.**

6.3.10.2. PM_{10-2.5}

The 2004 PM AQCD presented the results from several epidemiologic studies of respiratory symptoms and thoracic coarse particles, which provided limited evidence for cough and effects on morning PEF. Toxicology data for PM_{10-2.5} were extremely limited, and there were no controlled human exposure studies presented in the 2004 PM AQCD that evaluated the effect of PM_{10-2.5} on respiratory symptoms, pulmonary function, or inflammation. Epidemiologic studies of the effect of PM_{10-2.5} on hospitalizations or ED visits for respiratory diseases (i.e., pneumonia, COPD and respiratory diseases combined) reviewed in the 2004 AQCD reported positive associations. Additionally, the few mortality

studies that examined cause-specific mortality suggested somewhat larger risk estimates for respiratory mortality compared to all-cause (non-accidental) mortality.

Several new studies report associations between $PM_{10-2.5}$ and respiratory hospitalizations with the most consistent evidence among children (Figures 6-10 through 6-14), however, effect estimates are imprecise. Although a number of studies provide evidence of respiratory effects in older adults, a recent analysis of MCAPS data reports that weak associations of $PM_{10-2.5}$ with respiratory hospitalizations are further diminished after adjustment for $PM_{2.5}$. It is not clear that $PM_{10-2.5}$ estimates across all populations and regions are confounded by $PM_{2.5}$. An examination of $PM_{10-2.5}$ mortality associations on a national scale found a strong association between $PM_{10-2.5}$ and respiratory mortality, but this association varied when examining city-specific risk estimates (Zanobetti and Schwartz, 2009, [188462](#)). Additionally, copollutant analyses were not conducted in this study, and the associations observed are inconsistent with those reported in single-city studies. There is greater spatial heterogeneity in $PM_{10-2.5}$ compared to $PM_{2.5}$ and consequently greater potential for exposure measurement error in epidemiologic studies relying on central site monitors. This exposure measurement error may bias effect estimates toward the null.

Mar et al. (2004, [057309](#)) provide evidence for an association with increased respiratory symptoms in asthmatic children but not asthmatic adults. Consistent with this, controlled human exposures to $PM_{10-2.5}$ have not been observed to affect lung function or respiratory symptoms in healthy or asthmatic adults. However, increases in markers of pulmonary inflammation have been demonstrated in healthy volunteers. In these studies, an increase in neutrophils in BAL fluid or induced sputum was observed, with additional evidence of alveolar macrophage activation associated with biological components of $PM_{10-2.5}$ (i.e., endotoxin). Toxicological studies using inhalation exposures are still lacking, but pulmonary injury and inflammation have been observed in animals after IT exposure and both rural and urban $PM_{10-2.5}$ have induced these responses. In some cases, $PM_{10-2.5}$ from urban air was more potent than $PM_{2.5}$ (Section 6.3.3.3). $PM_{10-2.5}$ respiratory effects may be due to components other than endotoxin (Wegesser and Last, 2008, [190506](#)).

Overall, the most compelling new evidence comes from a number of recent epidemiology studies conducted in Canada and France showing significant associations between respiratory ED visits or hospitalization and short-term exposure to $PM_{10-2.5}$. Effects have been observed in areas where the mean 24-h avg $PM_{10-2.5}$ concentrations ranged from

7.4 to 13.0 $\mu\text{g}/\text{m}^3$. The strongest relationships were observed among children, whereas studies of adults and older adults show less consistent evidence of an association. While controlled human exposure studies have not observed an effect on lung function or respiratory symptoms in healthy or asthmatic adults in response to exposure to $\text{PM}_{10-2.5}$, healthy volunteers have exhibited increases in markers of pulmonary inflammation. Toxicological studies using inhalation exposures are still lacking, but pulmonary injury has been observed in animals after IT exposure to both rural and urban $\text{PM}_{10-2.5}$, which may not be entirely attributed to endotoxin. Overall, epidemiologic studies, along with the limited number of controlled human exposure and toxicological studies that examined $\text{PM}_{10-2.5}$ and respiratory outcomes, provide evidence that is **suggestive of a causal relationship between short-term $\text{PM}_{10-2.5}$ exposures and respiratory effects.**

6.3.10.3. Ultrafine PM

The 2004 PM AQCD included a few epidemiologic or controlled human exposure studies which provided limited evidence of an association between ultrafine PM and respiratory symptoms, medication use, or decreased pulmonary function; none assessed inflammation and no studies of controlled human exposure to ultrafine PM were available. Evidence from toxicological studies presented in the 2004 AQCD, although limited, suggested that exposure via inhalation to high concentrations of ultrafine TiO_2 may increase pulmonary inflammation in healthy rodents. Since the publication of the 2004 AQCD there has been an increased focus among the scientific community on gaining a better understanding of the potential health effects associated with exposure to ultrafine particles (UFPs). A number of recent controlled human exposure and toxicological studies have evaluated respiratory responses following exposures to fresh DE. While these atmospheres contain both fine and UFPs, the MMAD is typically ≤ 100 nm, and therefore the results of these studies may be used to support findings from studies utilizing other sources of UFP.

Recent epidemiologic studies conducted in Copenhagen, Denmark and Helsinki, Finland reported associations between UFPs and HA or ED visits for respiratory diseases including childhood asthma and pneumonia in adults (Halonen et al., 2008, [189507](#); Andersen et al., 2008, [189651](#)). The median UFP number concentrations in Copenhagen and Helsinki were 6,243 particles/ cm^3 and 8,203 particles/ cm^3 , respectively. Associations

between UFP and ED visits for respiratory diseases were not observed in the Atlanta-based SOPHIA study, where the mean UFP number concentration was 38,000 particles/cm³.

A single recent epidemiologic study has examined associations between UFP and pulmonary function, and observed that asthmatic adults exhibited decreased lung function after exposure to diesel traffic pollution in London (McCreanor et al., 2007, [092841](#)). Two new controlled human exposure studies have reported small decreases in pulmonary function among healthy adults approximately 20 hours following exposure to Los Angeles UF CAPs (100 µg/m³, particle count 145,000/cm³) or UF EC (50 µg/m³, particle count 10.8 x 10⁶/cm³) (Pietropaoli et al., 2004, [156025](#); Gong, 2008, [156483](#)). Exposures to lower concentrations of UF CAPs (~50 µg/m³, particle count 120,662/cm³) from Chapel Hill, NC did not result in any changes in pulmonary function between 0 and 18 hours after exposure (Samet et al., 2009, [191913](#)). However, while Gong et al. (2008, [156483](#)) did not observe any effect of exposure to UF CAPs on markers of pulmonary inflammation, Samet et al. (2009, [191913](#)) reported an UF CAPs-induced increase in IL-8 in BAL fluid at 18 hours post-exposure. A limited number of studies have also demonstrated increases in the pulmonary inflammatory response following exposure to ultrafine and fine particles from DE, which may be enhanced by exposure to O₃ (Section 6.3.3.2).

Altered pulmonary function and inflammation have also been observed in toxicological studies of DE and ultrafine model particles (see Sections 6.3.2.3 and 6.3.3.3). Although the contributions of gaseous components of DE to changes in respiratory function are unknown, IT instillation of DEP can result in similar effects. In one rat model, pulmonary inflammation is observed after exposure to ultrafine carbon black at concentrations as low as 180 µg/m³ (Harder et al., 2005, [087371](#)). However, inflammatory responses vary considerably depending on the animal model, dose, test material, and exposure duration. In cases where pulmonary inflammation is not observed, oxidative stress is often evident (Section 6.3.4.2). For example, although gasoline exhaust does not appear to induce inflammation, the exhaust particles have been shown to increase ROS. Oxidative stress is a major mechanism by which PM may exert effects (see Chapter 5), and some toxicological studies suggest that UFPs are more potent than fine particles, possibly due to a higher proportion of pro-oxidative OC and PAH content and greater surface area with which to deliver these components.

The relationship between exposure to UFP and pulmonary injury has not been widely examined. No association with pulmonary injury biomarkers was found for UFP in a

European multicity epidemiologic study (Timonen et al., 2004, [087915](#)). In controlled human exposure studies, UFP from woodsmoke resulted in significantly increased markers of injury in healthy adults, but this effect was not evident in COPD sufferers exposed to DE (Section 6.3.5.2). Exposure of neonatal rats to ultrafine iron-soot particles resulted in a significantly reduced rate of cell proliferation in the proximal alveolar region, which suggests that postnatal lung development may be susceptible to air pollution, consistent with impaired lung function growth observed in children (Pinkerton et al., 2004, [087465](#)). In contrast, no histopathological responses were evident in adult mice exposed to ultrafine iron-soot particles (Last et al., 2004, [097334](#)). Some toxicological studies have observed pulmonary injury after inhalation of DE or gasoline exhaust (Section 6.3.5.3). In studies that evaluated ambient PM size fractions from a variety of European and U.S. cities for relative toxicity in rodents following IT exposure, ultrafine PM was generally less injurious than the larger size fractions. However, the ultrafine fraction of Montana coal fly ash induced greater injury and inflammation than the PM_{10-2.5} fraction (Gilmour et al., 2004, [057420](#)).

In rodent studies, ultrafine CAPs appeared to be more potent than fine CAPs in inducing and exacerbating allergic responses (Section 6.3.6.3). In addition to CAPs, ultrafine carbon black or iron-soot particles, but not particles from fresh gasoline exhaust, have been shown to induce or exacerbate allergic responses in mice. Bacterial clearance appears unaffected by HWS or gasoline engine exhaust. Diesel exhaust, however, has been shown to reduce bacterial clearance, impair defenses against viral infection, and reduce thymus weight, which may indicate systemic immunosuppression.

Taken together, a limited number of epidemiologic studies have provided some evidence of an association between short-term exposure to UFPs and respiratory symptoms as well as asthma hospitalizations. However, these findings have been inconsistent across studies. The ultrafine number concentrations reported in the hospital admissions studies ranged from a median of 6243 particles/cm³ to a mean of 38,000 particles/cm³. Although the effect of controlled exposures to UFPs has not been extensively examined in humans, two controlled human exposure studies have observed small ultrafine particle-induced decreases in pulmonary function. However, no increases in respiratory symptoms have been reported and effects on pulmonary inflammation are not consistent. The results from animal toxicological studies examining the respiratory effects of UFPs are mixed, but several studies demonstrate oxidative, inflammatory, and allergic responses. Some effects,

such as inflammation or pulmonary histopathology, may be observed only in particular animal models (e.g., immature or compromised). Additionally, although a number of controlled human exposure and toxicological studies using controlled exposures to fresh DE report respiratory effects, the relative contributions of gaseous copollutants remain unresolved. Thus, the current collective evidence is **suggestive of a causal relationship between short-term UFP exposure and respiratory effects.**

6.4. Central Nervous System Effects

While evidence of an effect of PM on the central nervous system was not presented in the 2004 PM AQCD (U.S. EPA, 2004, [056905](#)), a limited number of recent epidemiologic, controlled human exposure and toxicological studies provide some evidence that exposure to PM may be associated with changes in neurological function. The majority of studies included in this section are of short-term exposure, however, there are also a few studies of long-term exposure. As CNS effects of PM are a newly emerging area, and since there are so few studies, all studies that evaluate CNS responses are included in this section.

6.4.1. Epidemiologic Studies

Chen and Schwartz (2009, [179945](#)) used extant data on CNS function from the Third National Health and Nutrition Examination Survey (NHANES III) to characterize the association between cognitive function in adults (ages 20-59) and exposure to ambient air pollution. Three computerized neurobehavioral tests were used: a simple reaction time test (SRTT), a basic measure of visuomotor speed; a symbol digit substitution test (SDST) on coding ability; and a serial digit learning test (SDLT) on attention and short-term memory. The authors used annual PM₁₀ concentrations to approximate the long-term exposure to ambient air pollution prior to the NHANES-III examination. Increased PM₁₀ levels were associated with reduced performance in all three neurobehavioral tests, and were particularly strong for SDST and SDLT scores in models adjusted for age and sex. However, after additional adjustment for race/ethnicity or SES, the magnitudes of these associations were greatly diminished and largely null. It is possible that the observed associations disappeared after adjustment for race/ethnicity and SES due to the potential confounding by residential segregation of ethnic minorities and poorer people in areas with high levels of ambient PM₁₀ concentrations.

Two additional epidemiologic studies evaluated the effect of ambient PM on the CNS (Calderon-Garciduenas et al., 2008, [156317](#); Suglia et al., 2008, [157027](#)). These studies examined long-term exposure to non-specific PM indicators and are detailed in Annex E.

6.4.2. Controlled Human Exposure Studies

In a recent controlled human exposure study, Cruts et al. (2008, [156374](#)) exposed 10 healthy males (18-39 years old) to filtered air and dilute DE (300 µg/m³ particulate concentration) for 1-h using a randomized crossover study design. Changes in brain activity were measured during and following exposure using quantitative electroencephalography (QEEG). Exposure to DE was observed to significantly increase the median power frequency (MPF) in the frontal cortex during exposure, as well as in the hour following the completion of the exposure. While this study does provide some evidence of an acute cortical stress response to DE, it is important to note that the QEEG findings are very nonspecific, and could have been caused by factors other than diesel PM such DE gases (e.g., CO, NO and NO₂) or the odor of the DE.

6.4.3. Toxicological Studies

Evidence is mounting that the CNS may be a critical target of PM and that adverse health effects may result from PM exposure. Whether these health effects are a direct or indirect effect of PM has not yet been established. One hypothesis suggests that ultrafine PM which deposits onto nasal olfactory epithelium enters the CNS by axonal olfactory transport to the olfactory bulb and leads to a cascade of effects involving inflammatory cytokines and ROS. An increased potential for neurodegenerative processes may ensue. Evidence for translocation of ultrafine PM to the olfactory bulb via olfactory neurons is discussed in Chapter 4, but its relevance to CNS health effects is unknown. Another hypothesis suggests that brain inflammation occurs secondarily to PM-mediated systemic inflammation. Finally, it has been suggested that PM-stimulation of the autonomic nervous system via respiratory tract receptors results in inflammatory or other effects in the CNS. This is an emerging field with many unknowns.

6.4.3.1. Urban Air

Calderon-Garciduenas et al. (2003, [156316](#)) conducted a long-term observational study in mongrel dogs from Mexico City and Tlaxcala. DNA damage and inflammation in the brain and respiratory tract were evaluated in dogs living in Mexico City (exposed group) and dogs living in Tlaxcala (control group). These cities are similar in altitude but differ in air pollutant levels. Measurements of air pollutant levels were presented only for Mexico City, the more polluted city. Statistically significant greater levels of apurinic/apyrimidinic sites (an indicator of DNA damage) were observed in the olfactory bulbs and hippocampus of Mexico City dogs compared with controls. These differences were not seen in other brain regions examined or in nasal respiratory epithelium. In addition, Mexico City dogs demonstrated greater histopathological changes in the respiratory and olfactory epithelium of the nasal cavity compared with controls. Immunohistochemical staining of brain tissue from the Mexico City dogs demonstrated greater immunoreactivity for NFκB, iNOS, cyclooxygenase-2, glial fibrillary acidic protein (GFAP), ApoE, amyloid precursor product and β-amyloid compared with controls. These results are indicative of inflammation and stress protein responses. This study has several limitations given that the dogs were of mixed breeds and of variable ages and that there was no standardization of exposures or diets. However results suggest a possible relationship between air pollution and brain inflammation.

6.4.3.2. CAPS

Several new inhalation studies have provided evidence of CNS effects due to ambient PM exposures. In one study, Campbell et al. (2005, [087217](#)) exposed ovalbumin-sensitized BALB/c mice to filtered air or near-highway Los Angeles CAPs (a 20-fold concentration of fine+ultrafine or ultrafine only; mean exposure concentration ultrafine 282.5 μg/m³ and fine 441.7 μg/m³) for 4 h/day and 5 days/wk over a 2-wk period. The animals were subsequently challenged with ovalbumin to elicit an allergic response in the lungs; brain tissue was obtained 1 day later. Exposure to CAPs, but not filtered air, resulted in activation of the immune-related transcription factor NF-κB and upregulation of the cytokines TNFα, and IL-1α in the brain, demonstrating pro-inflammatory responses that could contribute to neurodegenerative disease. While this study demonstrates CAPs effects in an allergic animal model, it is not known whether these responses also occur in non-allergic animals.

In a second study, control or ovalbumin-sensitized and challenged Brown Norway rats were exposed for 8-h to filtered air or fine CAPs (Grand Rapids, MI; 500 $\mu\text{g}/\text{m}^3$ fine PM) (Sirivelu et al., 2006, [111151](#)). Brain tissue was obtained 1 day later. CAPs exposure resulted in brain region-specific modulation of neurotransmitters. In animals which were not pretreated with ovalbumin, statistically significant increases in norepinephrine were observed in the paraventricular nucleus and olfactory bulb of CAPs-exposed rats compared with filtered air controls. In animals which were pretreated with ovalbumin, a statistically significant increase in dopamine was observed in the medial preoptic area in CAPs-exposed rats compared with controls. Furthermore, exposure to CAPs resulted in a statistically significant increase in serum corticosterone. These data suggest that the hypothalamo-pituitary-adrenal axis (i.e., stress axis) may be activated by PM exposure, causing aggravation of allergic airway disease. The authors discuss the possible role of the olfactory bulb in mediating neuroendocrine control of autonomic activities involved in respiratory and cardiovascular functions; however these relationships require clarification.

Pro-inflammatory responses were examined in a subchronic CAPs study involving normal (C57BL/6J) and ApoE^{-/-} (Kleinman et al., 2008, [190074](#)). Mice were exposed to filtered air or to two concentrations of ultrafine CAPs from a near-highway area of central Los Angeles (average of 30.4 and 114.2 $\mu\text{g}/\text{m}^3$) for 5 h/day and 3 days/wk over a 6-wk period. Brain tissue was harvested one day after the last exposure and cortical samples prepared. CAPs exposure resulted in activation of transcription factors, with a dose-dependent increase observed for AP-1 and an increase in NF κ B observed at the higher concentration. Increased levels of GFAP (representing activation of astrocytes) and phosphorylated JNK (representing MAP kinase activation) were observed at the lower but not higher concentration of CAPs. No changes were observed in levels of or activation of the other MAP kinases p38 and ERK or of I κ B. These findings provide evidence that inhalation of CAPs can lead to activation of cell signaling pathways involved in upregulation of pro-inflammatory cytokine genes in the cortical region of the mouse brain.

In another study utilizing normal (C57BL/6) and ApoE^{-/-} mice, brain histopathology was examined following a 4-mo chronic exposure to fine CAPs from Tuxedo, NY (March, April or May through September 2003) (Veronesi et al., 2005, [087481](#)). The average PM_{2.5} exposure concentration was 110 $\mu\text{g}/\text{m}^3$. CAPs exposure resulted in a statistically significant decrease in dopaminergic neurons, measured by tyrosine hydroxylase immunoreactivity, in the substantia nigra of ApoE^{-/-} mice but not in control mice. This population of neurons is

targeted in neurodegenerative diseases such as Parkinson's. Furthermore, a statistically significant increase in GFAP immunoreactivity, a marker for astrocytes, was observed in the nucleus compacta of CAPs-exposed ApoE^{-/-} mice compared to air-exposed ApoE^{-/-} mice. These results suggest that the ApoE^{-/-} mice, a genetic model involving increased oxidative stress, are susceptible to PM-induced neurodegeneration. Evidence for brain oxidative stress has also been found in normal animals following IT instillation of high concentrations of PM_{2.5} from Taiyuan, China (Liu and Meng, 2005, [088650](#)) and of gasoline exhaust (Che et al., 2007, [096460](#)) and following chronic exposure to ROFA by intranasal instillation (Zanchi et al., 2008, [157173](#)).

6.4.3.3. Diesel Exhaust

A recent study tested the effects of DE inhalation on spatial learning and memory function-related gene expression in the hippocampus (Win-Shwe et al., 2008, [190516](#)). Male BALB/c mice were exposed to DE (148.86 µg/m³ particulate concentration) for 5 h/day and 5 day/wk over a 4-wk period. Particle size was 26.21 ± 1.50 nm and particle number count was 1.92 x 10⁶ ± 6.18 x 10⁴. Concentrations of gases were 3.27 ppm CO, 0.01 ppm SO₂, 0.53 ppm NO₂, 0.98 ppm NO and 0.07 ppm CO₂. Half of the animals were injected i.p. once per week with lipoteichoic acid (LTA), a bacterial cell wall component used to induce systemic inflammation. The ability of the mice to perform spatial learning tasks was examined the day after the final exposure to DE and on two subsequent days. Impaired acquisition of spatial learning was observed in DE-exposed mice on the first day and on all three days in DE-exposed mice which had also been treated with LTA. LTA by itself had no effect. Since the NMDA (a type of neurotransmitter) receptors in the hippocampus play an important role in spatial learning ability, mice were sacrificed and total RNA from hippocampus was extracted and analyzed for expression of NMDA receptor subunits. DE exposure resulted in a statistically significant increase in the expression of one subunit while the combined exposure to DE and LTA resulted in statistically significant increases in the expression of three subunits compared with controls. The expression of pro-inflammatory cytokines was also examined in the hippocampus. DE exposure resulted in a statistically significant increase in TNFα mRNA while LTA exposure resulted in a statistically significant increase IL-1β mRNA compared with controls. Neither exposure altered the expression of HO-1. These results demonstrated that subchronic exposure to ultrafine-rich DE resulted in impaired spatial learning and altered expression of

hippocampal genes involved in memory function and inflammation. These responses were modulated by systemic inflammation.

In summary, PM may produce adverse effects in the CNS by direct or indirect mechanisms which are at present incompletely understood. Two recent short-term fine CAPs inhalation studies demonstrated pro-inflammatory responses in the brain and brain region-specific modulation of neurotransmitters and suggest the involvement of neuroimmunological pathways. One recent chronic fine CAPs inhalation study demonstrated loss of dopaminergic neurons in the substantia nigra and suggested that oxidative stress contributes to neurodegeneration. Veronesi et al. (2005, [087481](#)) have noted that the brain is very vulnerable to the oxidative stress induced by PM due to the brain's high energy demands, low levels of endogenous free radical scavengers, and high content of lipids and proteins. PM-mediated upregulation of inflammatory cytokines and mediators may also contribute to neurodegeneration. In fact, a recent subchronic study involving ultrafine CAPs demonstrated the activation of cell signaling pathways associated with upregulation of pro-inflammatory cytokines in brain cortical regions. Furthermore, a subchronic study involving ultrafine-rich DE demonstrated impaired spatial learning and altered expression of pro-inflammatory and neurotransmitter receptor genes in the hippocampus. Further investigations are required to delineate mechanisms involved in these responses.

6.4.4. Summary and Causal Determination

Recent animal toxicological studies involving acute or chronic CAPs exposure have demonstrated pro-inflammatory responses in the brain, brain region-specific modulation of neurotransmitters and loss of dopaminergic neurons in the substantia nigra (Campbell et al., 2005, [087217](#); Kleinman et al., 2008, [190074](#); Sirivelu et al., 2006, [111151](#); Veronesi et al., 2005, [087481](#)). However, the mechanisms underlying these effects need to be delineated. A single controlled human exposure study provides some evidence of an acute cortical stress response to DE, though these findings are nonspecific and could have been caused by DE gases rather than diesel PM (Cruts et al., 2008, [156374](#)). Similar consideration is warranted for the single animal toxicological study involving DE which demonstrated impaired spatial learning and altered expression of pro-inflammatory and neurotransmitter genes in the hippocampus following subchronic exposure (Win-Shwe et al., 2008, [190516](#)). The single epidemiology study that examined CNS outcomes did not find associations

between long-term exposure to PM₁₀ and cognitive function in adults after adjustment for race/ethnicity or SES (Chen and Schwartz, 2009, [179945](#)). Though the effect of ambient air pollution on CNS outcomes has recently begun to draw more attention, the evidence for a PM-induced CNS effect is limited. While most available studies have evaluated the effects of fine particle exposures, there is insufficient evidence to draw conclusions regarding effects of specific PM size fractions. Overall, the **evidence is inadequate to determine if a causal relationship exists between short-term exposures to PM_{2.5}, PM_{10-2.5}, UFPs, or specific PM components and CNS effects.**

6.5. Mortality Associated with Short-Term Exposure

The relationship between short-term exposure to PM and mortality has been extensively addressed in previous PM assessments (Burnett et al., 2004, [086247](#); U.S. EPA, 1982, [017610](#); U.S. EPA, 1996, [079380](#); 2004, [056905](#)). A positive association between PM concentration and mortality was consistently demonstrated across studies cited in the 2004 PM AQCD (U.S. EPA, 2004, [056905](#)); these results are summarized below in Section 6.5.1. Numerous studies have been published since the previous review, including a number of multicity analyses and many single-city studies. The current body of evidence examines the association between short-term exposure to PM of various size fractions (i.e., PM₁₀, PM_{10-2.5}, PM_{2.5}, and UFPs [0.01-0.1 µm]) and mortality through the use of time-series and/or case-crossover studies. Both study designs aim to disentangle the PM-mortality effect through either complex modeling (i.e., time-series) or matching strategies (i.e., case crossover). Overall, the results of the more recent studies build upon the conclusions from the previous review, showing consistent positive associations between mortality and short-term exposure to PM_{2.5} and PM_{10-2.5}.

Section 6.5.2 reviews and summarizes the results of recent studies that examined mortality associations with the four PM size classes listed above. Each section integrates the results of recent studies with those available in previous PM reviews. This assessment first focuses on multicity studies that examined mortality associations with PM₁₀ because this is a large body of literature that provides important information on potential effect modifiers, potential confounding by copollutants, evaluation of concentration-response relationships, and the influence of different modeling approaches on the PM-mortality relationship (Section 6.5.2.1). The PM₁₀ studies have provided the most data among the PM

indices thus far; therefore this evaluation begins with the consideration of those findings as they relate to the general association between PM and mortality. It is difficult to interpret the extent to which these studies inform an evaluation of the effects of PM_{2.5} or PM_{10-2.5}, since data are combined from multiple cities with different PM composition. Interpretations of the PM size fraction that contributes the most to the PM₁₀ effects observed are provided when appropriate in the following review. The multicity studies that examine the association between PM₁₀ and mortality also offer new evidence on regional and seasonal differences in effect estimates, building upon observations made in the 2004 PM AQCD (U.S. EPA, 2004, [056905](#)).

Recent study findings on associations with PM_{2.5}, PM_{10-2.5}, and UFPs are evaluated in Sections 6.5.2.2, 6.5.2.3, and 6.5.2.4, respectively. For PM_{2.5}, the focus of the assessment remains on multicity study findings; however, for PM_{10-2.5} and UFPs, some additional emphasis is placed on single-city studies, due to the relative sparseness of the evidence base for these size fractions. Some studies have also evaluated relationships between mortality and specific components and sources of PM, and the results are summarized in Sections 6.5.2.4 and 6.5.2.5. Finally, Section 6.5.2.6 assesses evidence on the concentration-response relationship between short-term PM exposure and mortality.

6.5.1. Summary of Findings from 2004 PM AQCD

The 2004 PM AQCD (U.S. EPA, 2004, [056905](#)) found strong evidence that PM₁₀ and PM_{2.5}, or one or more PM_{2.5} components, acting alone and/or in combination with gaseous copollutants, are associated with total (non-accidental) mortality and various cause-specific mortality outcomes. For PM₁₀, several multicity studies in the U.S., Canada, and Europe provided strong support for this conclusion, reporting associations with total mortality highlighted by effect estimates ranging from ~0.2 to 0.7% (per 10 µg/m³ increase in PM₁₀) (U.S. EPA, 2004, [056905](#)). Numerous studies also reported PM₁₀ associations with cause-specific mortality, specifically cardiovascular- and respiratory-related mortality. For PM_{2.5}, the strength of the evidence varied across endpoints, with relatively stronger evidence for associations with cardiovascular compared to respiratory endpoints. The resulting effect estimates reported from the U.S.- and Canadian-based studies (both multi- and single-city) analyzed for these two endpoints ranged from 1.2 to 2.7% for cardiovascular-related mortality and 0.8 to 2.7% for respiratory-related mortality, per 10 µg/m³ increase in PM_{2.5} (U.S. EPA, 2004, [056905](#)). In regards to thoracic coarse particles

(PM_{10-2.5}), the PM AQCD found a limited body of evidence that was suggestive of associations between short-term exposure to ambient PM_{10-2.5} and various mortality outcomes (e.g., 0.08-2.4% increase in total [non-accidental] mortality per 10 µg/m³ increase in PM_{10-2.5}). The positive effect estimates obtained from studies that analyzed the association between PM_{10-2.5} and mortality resulted in the conclusion that PM_{10-2.5}, or some constituent component(s) (including those on the surface) of PM_{10-2.5}, may contribute, in certain circumstances, to increased human health risks.

Some additional studies examined the association between specific PM_{2.5} chemical components and mortality. These studies observed associations for SO₄²⁻, nitrate, and CoH, but not crustal particles. The strength of the association for each component varied from city to city (U.S. EPA, 2004, [056905](#)). Source-oriented analyses were also conducted to identify specific source-types associated with mortality. These studies implicate fine particles from anthropogenic origin, such as motor vehicle emissions, coal combustion, oil burning, and vegetative burning, as being important in contributing to increased mortality (U.S. EPA, 2004, [056905](#)).

6.5.2. Associations of Mortality and Short-Term Exposure to PM

The recent literature examines the association between short-term exposure to various PM size fractions (i.e., PM₁₀, PM_{10-2.5}, PM_{2.5}, UFPs [UFP], or species [e.g., OC, EC, transition metals, etc.]) and mortality. This ISA, similar to previous AQCDs, focuses more heavily on multicity studies, and especially those conducted in the U.S. and Canada (see Table 6-12). By using this approach it is possible to: (1) obtain a more representative sample of or insight into the PM-mortality relationship observed across the U.S.; (2) analyze the association between mortality and short-term exposure to PM at or near ambient conditions observed in the U.S.; (3) examine the potential heterogeneity in effect estimates between cities and regions; and (4) analyze the confounders and/or effect modifiers that may explain the PM-mortality relationship in the U.S. Although this section focuses on mortality outcomes in response to short-term exposure to PM, it does not evaluate studies that examine the association between PM and infant mortality. These studies are evaluated in Section 7.5, Reproductive, Developmental, Prenatal and Neonatal Outcomes, although it is possible that short- and long-term in utero exposures may contribute to infant mortality. In addition, the exposure windows of interest for this unique

health outcome can be difficult to characterize and may span both short- and long-term periods.

Table 6-12. Overview of U.S. and Canadian multicity PM studies of mortality analyzed in the 2004 PM AQCD and the PM ISA^b

Reference	Location	Mean Concentration ($\mu\text{g}/\text{m}^3$)	98 th ; 99 th Percentiles ($\mu\text{g}/\text{m}^3$)	Upper Percentile: Concentrations ($\mu\text{g}/\text{m}^3$)
<i>PM₁₀</i>				
Dominici et al. (2003, 156407) ^a	90 U.S. cities	15.3-53.2	---	NR
Burnett and Goldberg (2003, 042798) ^a	8 Canadian cities	25.9	---	95th: 54 Maximum: 121
Peng et al. (2005, 087463)	100 U.S. cities	13-49	---	50th: 27.1; 75th: 32.0 Maximum: 48.7
Dominici et al. (2006, 088398) ^f	100 U.S. cities	13-49	---	50th: 27.1; 75th: 32.0 Maximum: 48.7
Welty and Zeger (2005, 087484) ^f	100 U.S. cities	13-49	---	50th: 27.1 75th: 32.0 Maximum: 48.7
Bell et al. (2009, 191997)	84 U.S. urban communities	NR	---	NR
Burnett et al. (2004, 086247)	12 Canadian cities	NR	---	NR
Samoli et al. (2008, 188455)	12 Canadian cities 90 U.S. cities ^e 22 European cities	NR	---	NR
Schwartz (2004, 078998)	14 U.S. cities	23-36 ^d	---	75th: 31-57
Schwartz (2004, 053506)	14 U.S. cities	23-36 ^d	---	75th: 31-57
Zeka et al. (2005, 088068)	20 U.S. cities	15-37.5	---	NR
Zeka et al. (2006, 088749)	20 U.S. cities	15.9-37.5	---	NR
<i>PM_{2.5}</i>				
Burnett and Goldberg (2003, 042798) ^a	8 Canadian cities	13.3	---	95th: 32 Maximum: 86
Dominici et al. (2007, 099135)	100 U.S. cities	NR	---	NR
Zanobetti and Schwartz (2009, 188462)	112 U.S. cities	13.2	34.3; 38.6	Maximum: 57.4
Franklin et al. (2007, 091257)	27 U.S. cities	15.6	45.8; 54.7	Maximum: 239
Franklin et al. (2008, 097426) ^g	25 U.S. cities	Winter: 9.6-34.4 Spring: 6.7-27.6 Summer: 7.6-26.0 Fall: 9.5-32.1	---	NR
Ostro et al. (2006, 087991)	9 California counties	19.9	68.2; 82.0	95th: 61.3 Maximum: 160.0
Ostro et al. (2007, 091354)	6 California counties	18.4	61.2; 70.1	Maximum: 116.1
Burnett et al. (2004, 086247)	12 Canadian cities	12.8	---	NR

Reference	Location	Mean Concentration ($\mu\text{g}/\text{m}^3$)	98 th ; 99 th Percentiles ($\mu\text{g}/\text{m}^3$)	Upper Percentile: Concentrations ($\mu\text{g}/\text{m}^3$) ³
PM_{10-2.5}				
Burnett and Goldberg (2003, 042798) ^a	8 Canadian cities	12.6	---	95th: 30 Maximum: 99
Zanobetti and Schwartz (2009, 188462)	47 U.S. cities	11.8	40.2; 47.2	Maximum: 88.3
Burnett et al. (2004, 086247)	12 Canadian cities	11.4	---	NR
Villeneuve et al. (2003, 055051)	Vancouver, Canada	6.1	---	90th: 13.0 Maximum: 72.0
Klemm et al. (2004, 056585)	Atlanta, Georgia	9.7	---	50th: 9.34; 75th: 11.94 Maximum: 25.17
Slaughter et al. (2005, 073854)	Spokane, Washington	NR	---	NR
Wilson et al. (2007, 157149)	Phoenix, Arizona	NR	---	NR
Kettunen et al. (2007, 091242)	Helsinki, Finland	Cold season: 6.7 ^d Warm season: 8.4 ^d	---	Cold season 50th: 6.7; 75th: 12.5 Maximum: 101.4 Warm season 50th: 8.4; 75th: 11.8 Maximum: 42.0
Perez et al. (2008, 156020)	Barcelona, Spain	Saharan Dust Days: 16.4 Non-Saharan Dust Days: 14.9	---	Saharan Dust Days 50th: 14.8; 75th: 21.8 Maximum: 36.7 Non-Saharan Dust Days 50th: 12.6; 75th: 18.9 Maximum: 93.1

^a Multicity studies examined in the 2004 PM AQCD (U.S. EPA, 2004, [056905](#))

^b Because only two multicity study was identified that examined PM_{10-2.5}, single-city and international studies that examined PM_{10-2.5} were analyzed in this ISA and are included in this table.

^c The majority of multicity studies examined in the PM ISA provide the mean PM concentration of each individual city, not an overall PM concentration across all cities. As a result, the range of PM concentrations for a particular study are presented, which represents the lowest and highest mean PM concentrations reported across cities, if an overall mean is not provided within the study.

^d Median PM concentration.

^e The study included 90 U.S. cities in the 1-day lag analysis, but only 15 U.S. cities in the analysis of the average of lag days 0-1.

^f The concentrations reported for these studies were estimated from Peng et al. (2005, [087463](#)) because they used the same number of cities and years of data from NMMAPS.

^g This study did not present an overall mean 24-h ave PM_{2.5} concentration across all cities for each season. The range of mean 24-h avg concentrations reported in this table for each season represents the lowest mean 24-h avg PM_{2.5} concentration and the highest 24-h avg PM_{2.5} concentration reported across all cities included in the study.

6.5.2.1. PM₁₀

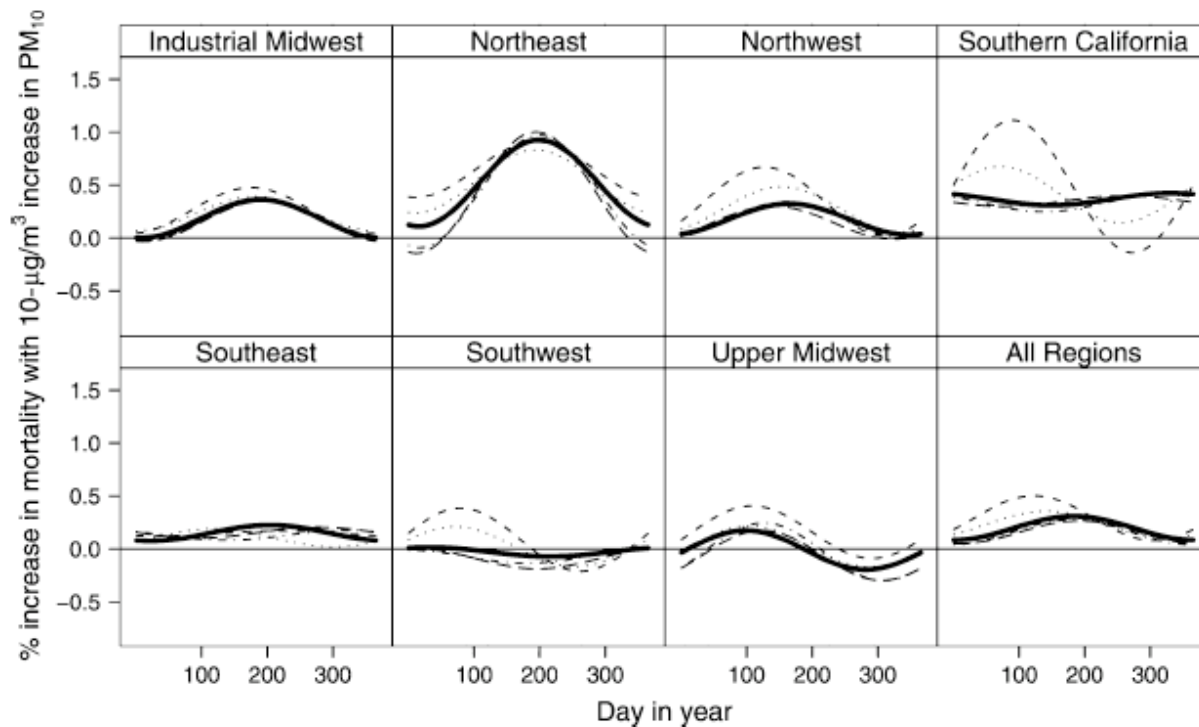
The majority of studies that examined the association between short-term exposure to PM and mortality focused on effects attributed to PM₁₀. Although these studies do not characterize the compositional differences in PM₁₀ across the cities examined in each of the studies evaluated, they can provide an underlying basis for the overall pattern of associations observed when examining the relationship between PM_{10-2.5} and PM_{2.5} and

mortality. The studies evaluated in this review analyzed the PM₁₀-mortality relationship through either a time-series or case-crossover design.¹

Time-Series Analyses

Mortality associations with short-term exposure to PM₁₀ in the U.S. have been examined in several updated time-series analyses of the National Morbidity and Mortality Air Pollution Study (NMMAPS). In the previous NMMAPS analysis (Dominici et al., 2003, [156407](#); Samet et al., 2000, [005809](#); Samet et al., 2000, [010269](#)) of the 1987-1994 data, which was reviewed in the 2004 PM AQCD (U.S. EPA, 2004, [056905](#)), the strongest association was found for non-accidental mortality for 1-day lag, with a combined estimate across 90 cities of 0.21% (95% posterior interval [PI]: 0.09, 0.33) per 10 µg/m³ increase in PM₁₀. The association was found to be robust to the inclusion of other gaseous copollutants in the regression models, but the investigators found heterogeneity across regions, with the strongest associations in northeastern cities. In the new updated analyses, the investigators examined additional issues surrounding the association between PM and mortality including: seasonal effect modification; change in risk estimates over time; sensitivity of results to alternative weather models; and effect modification by air conditioning use. The NMMAPS data has also been used to examine the PM concentration-response relationship using PM₁₀ data from 20 cities (see Section 6.5.2.7). A few multicity studies conducted in Canada and Europe provide additional information, which further clarifies and supports the association between PM and mortality presented in the NMMAPS analyses.

¹ Schwartz (2004, [188945](#)) used a case-crossover study design, but also conducted a time-series analysis to validate the results obtained using the case-crossover approach.



Source: Peng et al. (2005, [087463](#))

Figure 6-16. National and regional estimates of smooth seasonal effects for PM₁₀ at a 1-day lag and their sensitivity to the degrees of freedom assigned to the smooth function of time in the updated NMMAPS data 1987-2000. Note: The degrees of freedom chosen were 3 df (short-dashed line), 5 df (dotted line), 7 df (solid line), 9 df (dotted-and-dashed line), and 11 df (long-dashed line) per year of data.

Seasonal Analyses of PM₁₀-Mortality Associations

Using the updated NMMAPS data, which consisted of 100 U.S. cities for the period 1987-2000, Peng et al. (2005, [087463](#)) examined the effect of season on PM₁₀-mortality associations. In their first stage regression model, for each city, the PM₁₀ effect was modeled to have a sinusoidal shape that completes a cycle in a year, but was constrained to be periodic across years using sine/cosine terms. The authors also considered a model that consisted of PM₁₀-season interactions using season indicators. Both of these models also included covariates that were used in their earlier NMMAPS analyses. In the second stage model, the seasonal patterns of PM₁₀ mortality coefficients were estimated for seven geographic regions and on average for the entire U.S. Peng et al. (2005, [087463](#)) found for 1-day lag, at the national level, season specific increases in non-accidental mortality per 10 µg/m³ increase in PM₁₀ of: 0.15% (PI: -0.08 to 0.39), 0.14% (PI: -0.14 to 0.42), 0.36% (PI: 0.11-0.61), and 0.14% (PI: -0.06 to 0.34) for winter, spring, summer, and fall, respectively.

The corresponding all-season estimate was 0.19% (PI: 0.10-0.28). After the inclusion of SO₂, O₃, or NO₂ in the model with PM₁₀ in a subset of cities (i.e., 45 cities) for which data existed for all pollutants resulted in fairly robust PM₁₀ risk estimates. An analysis by geographic region found a strong seasonal pattern in the Northeast. Figure 6-16 presents the estimated seasonal pattern of PM₁₀ risk estimates by region from Peng et al. (2005, [087463](#)), which includes a sensitivity analysis aimed to determine the appropriate number of degrees of freedom for temporal adjustment. It is clear from Figure 6-16 that the Northeast has the strongest association, which peaks in the summer and is robust to the extent of temporal adjustment. The industrial Midwest also shows the summer peak, but with smaller risk estimates. Other regions have either no seasonal pattern (Southeast) or a suggestion of a spring peak that appears to be sensitive to the extent of temporal adjustment. On a nationwide basis, the PM₁₀ risk estimates appear to peak between spring and summer. Overall, this study identified an effect modifier that may be useful in identifying the specific chemical component(s) of PM that are related to specific regions and times of the year.

Change in PM₁₀-Mortality Associations over Time

Dominici et al. (2007, [099135](#)) conducted an analysis of the extended NMMAPS data set (i.e., 1987-2000) to examine if short-term PM₁₀-mortality risk estimates changed during the course of the study period. The investigators estimated the average PM₁₀ mortality risk coefficient for 1-day lag, using essentially the same model specification as in their 2003 analysis, separately for three time periods: 1987-1994, 1995-2000, and 1987-2000, for the “eastern U.S.” (62 counties), the “western U.S.” (38 counties), and all 100 U.S. counties. To produce national and regional estimates, two-stage hierarchical models were used as in the previous NMMAPS studies. As shown in Table 6-13, the authors found a continuation of the PM₁₀-mortality association in the nationwide data for the entire study period. A comparison of the relative risk estimates for 1987-1994 vs. 1995-2000 suggests weak evidence (not a significant difference) that short-term effects declined. Most of the decline in the national estimate appears to be attributable to the eastern U.S. counties. However, the decline in the risk estimate for all-cause mortality in the eastern U.S. appears to be disproportionately influenced by the reduction in the risk estimate for the “other” mortality category (i.e., all-cause minus cardio-respiratory category, which may be 40 to 50% of all-cause deaths in U.S. cities). Likewise, the apparent increase in the risk estimate for all-cause mortality in the western U.S. appears to be affected by the increase in the risk estimate for

the “other” mortality category. Because the study does not clearly identify the specific cause(s) in the “other” mortality category that are affected by PM, interpreting the reduction in risk estimates for all-cause mortality requires caution. In contrast, the apparent reductions (~23%) in PM₁₀ risk estimates for cardio-respiratory deaths were more comparable between the two regions.

In addition, the investigators estimated time-varying PM₁₀ mortality risk as a linear function of calendar time for the period 1987-2000, producing the percentage rate change in the PM₁₀ risk estimate with a change in time of 1 year. The estimated rate of decline in slope for all-cause mortality and the combination of cardiovascular and respiratory mortality were -0.012 (PI: -0.037, 0.014) and -0.016 (PI: -0.058, 0.027), respectively. The authors also estimated a PM_{2.5} mortality risk for the period 1999-2000 (discussed in Section 6.5.2.2.).

Table 6-13. NMMAPS national and regional percentage increase in all-cause, cardio-respiratory, and other-cause mortality associated with a 10 µg/m³ increase in PM₁₀ at lag 1 day for the periods 1987-1994, 1995-2000, and 1987-2000.

	1987-1994	95% PI	1996-2000	95% PI	1987-2000	95% PI
ALL CAUSE						
East	0.29	0.12, 0.46	0.13	-0.19, 0.44	0.25	0.11, 0.39
West	0.12	-0.07, 0.30	0.18	-0.07, 0.44	0.12	-0.02, 0.26
National	0.21	0.10, 0.32	0.18	0.00, 0.35	0.19	0.10, 0.28
CARDIORESPIRATORY						
East	0.39	0.16, 0.63	0.30	-0.13, 0.73	0.34	0.15, 0.54
West	0.17	-0.07, 0.40	0.13	-0.23, 0.50	0.14	-0.05, 0.33
National	0.28	0.14, 0.43	0.21	-0.03, 0.44	0.24	0.13, 0.36
OTHER						
East	0.21	-0.03, 0.44	0.00	-0.49, 0.50	0.15	-0.09, 0.39
West	0.09	-0.21, 0.38	0.23	-0.15, 0.62	0.11	-0.10, 0.33
National	0.15	-0.02, 0.32	0.17	-0.07, 0.41	0.15	0.00, 0.29

Source: Dominici et al. (2007, [099135](#))

The objective of the Dominici et al. (2007, [099135](#)) study described above was motivated by accountability research, the idea of measuring the impact of policy interventions. However, unlike the intervention studies conducted in Hong Kong (Hedley et al., 2002, [040284](#)) and Dublin, Ireland (Clancy et al., 2002, [035270](#)) that were reviewed in the 2004 PM AQCD (U.S. EPA, 2004, [056905](#)), this study was not designed to estimate a reduction in mortality in response to a sudden change in air pollution. In fact, the figure of

observed trend in PM₁₀ levels presented in the Dominici et al. (2007, [099135](#)) study indicates that the decline in PM₁₀ levels during the study period was very gradual, with much of the decline appearing in the first few years (median values of ~33 µg/m³ in 1987 to ~25 µg/m³ in 1992, then down to ~23 µg/m³ in 2000). A flaw in the use of the time-series study design for this type of analysis is that it adjusts for long-term trends, and, therefore, does not estimate the change in mortality in response to the gradual change in PM₁₀. The apparent change, though weak, in the PM₁₀ risk estimates may also reflect a potential change in the composition of PM₁₀ (i.e., PM_{10-2.5} or PM_{2.5}). The study listed a number of PM₁₀-related air pollution control programs that were implemented between 1987 and 2000. Some of these programs, such as the Acid Rain Control Program, did result in major reductions in emissions, and, therefore, could have contributed to the results observed, but the analytic approach used in the study does not allow for a systematic analysis of the effect of air pollution policies on the risk of mortality.

Sensitivity of PM-Mortality Associations to Alternative Weather Models

To examine the sensitivity of PM₁₀ mortality risk estimates to alternative weather models that consider longer lags, Welty and Zeger (2005, [087484](#)) analyzed the updated NMMAPS 100 U.S. cities data. All of the previous NMMAPS analyses only considered temperature and dew point up to 3-day lags. In this analysis, the authors considered various forms of a constrained distributed lag model: (1) containing a step function of temperature with steps at lag 0, 2, 7 and extended to 14 days; (2) similar to (1) but with time-varying coefficients to change over season and study period; and, (3) containing a smooth function to account for non-linearity in the temperature-mortality relationship. With the combination of degrees of freedom for temporal trends and the number of distributed lags, more than 20 models were applied to each of the three lag days (0, 1, and 2) of PM₁₀. These city-specific risk estimates were then combined across the 100 cities in the second stage Bayesian model. The combined PM₁₀ risk estimates were generally consistent within the lag. In particular, the risk estimates for non-accidental mortality for lag 1-day ranged between 0.15% and 0.25% per 10 µg/m³ increase in PM₁₀, and were always statistically significant regardless of the model used. In addition, the range of these point estimates across the models was found to be much narrower than the regression posterior intervals. Thus, the PM₁₀ risk estimates at lag 1 day were robust to alternative temperature models that considered temperature effects lasting up to a 2-wk period.

In summary, the above three analyses of the updated NMMAPS data provided useful information on PM mortality risks, resulting in the following conclusions: (1) estimated PM₁₀ risk is particularly high in the northeast and in the summer; (2) there remains an overall PM₁₀-mortality association in the 1987-2000 time period as well as the 1995-2000 time period; (3) there is a weak indication that PM₁₀ mortality risk estimates are declining; and (4) PM₁₀ risk estimates were not sensitive to alternative temperature models.

Effect Modification of PM₁₀-Mortality Associations by Air Conditioning Use

It has been hypothesized that air conditioning use reduces an individual's exposure to PM and subsequently modifies the PM-mortality association. Bell et al. (2009, [191997](#)) investigated the role of air conditioning (AC) use on the relationship between PM₁₀ and all-cause mortality using the NMMAPS PM₁₀ risk estimates from 84 U.S. urban communities from 1987-2000.¹ Bayesian hierarchical modeling was used to examine if AC prevalence (i.e., fraction of households with central or any AC) explained city-to-city variation in PM₁₀ risk estimates. The authors calculated yearly, summer-only, and winter-only effect estimates stratified by housing stock that had either central AC or any AC, which includes window units. Risk estimates for lag 1 (previous day) were used in the analysis because this lag has been found to show the strongest association with mortality in the original NMMAPS analyses. Community-specific AC prevalence was calculated from national survey U.S. Census American Housing Survey (AHS) data, which is available every two years. The investigators computed percent change in PM₁₀ effect estimates per an additional 20% of the population acquiring AC.

The AC variables were not strongly correlated with socio-economic variables (poverty rate, unemployment, and education) from the U.S. Census (correlation ranged from -0.27 to 0.29). Bell et al. (2009, [191997](#)) found that communities with higher AC prevalence had lower PM₁₀ mortality risk estimates for all-cause mortality (-30.4% [95% P.I.: -80.4 to 19.6] per an additional 20% of the population acquiring any AC; -39.0% [95% P.I.: -81.4 to 3.3] for central AC), but results were not statistically significant. When restricting the analysis to the summer months and focusing on the 45 cities with summer-peaking PM₁₀ concentrations, the authors reported positive (i.e., lower PM₁₀ risks in cities with lower AC use) non-significant risk estimates. A similar analysis was conducted for winter months

¹ This study also examined risk estimates for cardiovascular and respiratory hospital admissions in older adults (≥ 65).

using data from 6 cities with winter peaking PM₁₀ concentrations, but the confidence bands were too wide (due to small sample size) for meaningful interpretation.

Although the estimated reductions in PM₁₀ all-cause mortality risks from AC use reported in the Bell et al. (2009, [191997](#)) study were not statistically significant, their large magnitude suggests that AC use may reduce an individual's exposure to PM. Given the expected additional increase in AC use in the future, and the results from recent multicity studies, which have reported stronger PM-mortality associations during the warm season, AC use may play a larger role in determining an individual's exposure to PM. Studies that have examined the effect of AC use on the PM_{2.5}-mortality association have reported similar results. For example, Franklin et al. (2007, [091257](#)) (discussed in detail in Section 6.1.2.2) found that AC use non-significantly modified PM_{2.5} mortality risk estimates, but the result was suggestive of higher PM_{2.5} effects in cities with lower AC use, especially in cities with summer-peaking PM_{2.5} concentrations. Overall, further investigation is needed to fully understand the relationship between AC use and mortality attributed to short-term exposure to PM.

PM₁₀-Mortality Associations in Canada and Europe

Burnett et al. (2004, [086247](#)) examined the association between mortality and various air pollutants in 12 Canadian cities, and reported that the most consistent association was found for NO₂. For this analysis, PM was measured every 6th -day for the majority of the study period, and the PM₁₀ concentrations used in the study represent the sum of the PM_{2.5} and PM_{10-2.5}, which were directly measured by dichotomous samplers. The authors found that the simultaneous inclusion of NO₂ and PM₁₀ in a model, on those days with PM data, greatly reduced the PM₁₀ association with non-accidental mortality, from 0.47% (95% CI: 0.04-0.89) to 0.07% (95% CI: -0.44 to 0.58) per 10 µg/m³ increase. The previous Canadian multicity analysis (Burnett and Goldberg, 2003, [042798](#)), a re-analysis of Burnett et al. (2000, [010273](#)) reviewed in the 2004 PM AQCD (U.S. EPA, 2004, [056905](#)), did not consider gaseous pollutants. Thus, PM₁₀ risk estimates in the Canadian data appear to be more sensitive to NO₂ than those estimates reported in U.S. studies.

The association between PM₁₀ and mortality in Europe was also reviewed in the 2004 PM AQCD (U.S. EPA, 2004, [056905](#)) through Katsouyanni et al. (2003, [042807](#)), which presented results from the Air Pollution and Health: a European Approach (APHEA2) study, a multicity study that examined PM₁₀ effects on total mortality in 29 European cities. Analitis et al. (2006, [088177](#)) published a brief report on effect estimates for cardiovascular

and respiratory deaths also based on the 29 European cities, within the APHEA2 study. They reported for the average of 0- and 1-day lags, PM₁₀ risk estimates per 10 µg/m³ of 0.76% (95% CI: 0.47-1.05) for cardiovascular deaths and 0.71% (95% CI: 0.22-1.20) for respiratory deaths in random effects models.

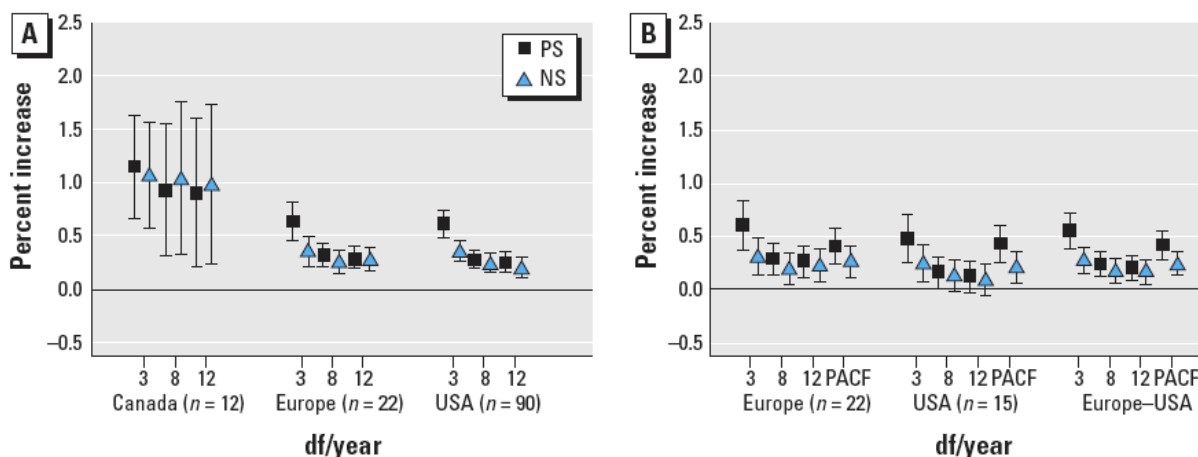
Comparison of PM-Mortality Associations in Europe, Canada, and the U.S.

The APHENA study (Samoli et al., 2008, [188455](#)) was a collaborative effort by the APHEA, NMMAPS, and the Canadian multicity study investigators to evaluate the coherence of PM₁₀ mortality risk estimates across locations and possible effect modifiers of the PM-mortality relationship using a common protocol. In this study, to adjust for temporal trends Samoli et al. (2008, [188455](#)) used 3, 8, and 12 df with natural splines and penalized splines, as well as the minimization of the sum of the absolute values of the partial auto-correlation function (PACF). The investigators also included a smooth function of temperature on the same day of death and the day before death. The study reported risk estimates for a 1-day lag (from all three data sets), the average of lag day 0 and 1 (all but for the Canadian data because PM data was collected every 6th day), and an unconstrained distributed lag model using lags of 0, 1, and 2 days (all but for the Canadian data). The second-stage regression included: (a) the average pollution level and mix in each city; (b) air pollution exposure characterization (e.g., number of monitors, density of monitors); (c) the health status of the population (e.g., cardio-respiratory deaths as a percentage of total mortality, crude mortality rate, etc.); and (d) climatic conditions (e.g., mean and variance of temperature). In addition, unemployment rate was examined for 14 European cities and all U.S. cities. Effect modification patterns were examined only for cities with complete time-series data and using the average of lags 0 and 1 day, resulting in the exclusion of the Canadian data.

Generally, the risk estimates from Europe and the U.S. were similar, but those from Canada were substantially higher.¹ For example, the percent excess risks per 10 µg/m³ increase in PM₁₀ for all ages using 8 df/yr and penalized splines were 0.84% (0.30, 1.40), 0.33% (0.22, 0.44), and 0.29% (0.18, 0.40) for the Canadian, European, and U.S. data, respectively. Note that the risk estimate for the 90 U.S. cities is slightly larger than that reported in the original NMMAPS study (0.21%, using natural splines, and more

¹ The risk estimate reported for the 12 Canadian cities examined in the APHENA study is higher than that reported by Burnett et al. (2004, [086247](#)). This is because the APHENA study did not use the 12 cities data from Burnett et al. (2004, [086247](#)), but instead used a composite of the data from three previous studies conducted by the same group (Burnett et al., 2000, [010273](#); Burnett et al., 1998, [029505](#); Burnett and Goldberg, 2003, [042798](#))

temperature variables). In the all ages model, the average of lag days 0 and 1, and the distributed lag model with lags 0, 1, and 2 did not result in larger risk estimates compared to those for a 1 day lag. In copollutant models, PM₁₀ risk estimates did not change when controlling for O₃. Figure 6-17 shows the risk estimates from the three data sets for alternative extent of temporal smoothing and smoothing methods. The Canadian data appear less sensitive to the extent of temporal smoothing or smoothing methods (see Panel A of Figure 6-17). When stratifying by age the risk estimates for the older age group (age ≥ 75) were consistently larger than those for the younger age group (age <75) (e.g., 0.47% vs. 0.12% for the U.S. data) for all the three data sets. Although the study did not quantitatively present the results from the effect modification analyses, some evidence of effect modification across the study regions was observed. The investigators reported that, in the European data, higher levels of NO₂ and a larger NO₂/PM₁₀ ratio were associated with greater PM₁₀ risk estimates, and that while this pattern was also present in the U.S. data, it was less pronounced. Additionally, in the U.S. data, smaller PM₁₀ risk estimates were observed among older adults in cities with higher O₃ levels. Effect modification by temperature was also observed, but only in the European data.



Source: Samoli et al. (2008, [188455](#))

Figure 6-17. Percent increase in the daily number of deaths, for all ages, associated with a 10-µg/m³ increase in PM₁₀: lag 1 (A) and lags 0 and 1 (B) for all three centers. PACF indicates df based on minimization of PACF.

In this study, the underlying basis for the larger PM₁₀ risk estimates (by 2-fold) in the Canadian data compared to the European and U.S. data could not be identified, even when

consistent statistical methods were applied across each of the data sets. Because the effect modification of PM₁₀ risk estimates were not examined in the Canadian data, the potential influence of air pollution type or mixture could not be ruled out as a potential source of heterogeneity across the three data sets. It should be noted that both the original U.S. and European studies reported regional heterogeneity in PM risk estimates while the U.S. data also reported seasonal heterogeneity. In both of these cases the specific characteristics associated with the regions that contributed to the heterogeneity observed were not identified. Thus, further investigation is needed to identify factors that influence the heterogeneity in PM risk estimates observed between different countries and across regions.

Case-Crossover Analyses

Since the 2004 PM AQCD (U.S. EPA, 2004, [056905](#)) investigators have used the case-crossover study design more frequently as an alternative to time-series analyses to examine the association between short-term exposure to PM and mortality. This study design allows for the control of seasonal variation, time trends, and slow time varying confounders without the use of complex models. However, similar to any study design, biases can be introduced into the study depending on the control (i.e., referent) period selected (Janes et al., 2005, [087535](#)). The multicity case-crossover analyses discussed below match cases (i.e., days in which a death occurred) to controls (i.e., days in which a death did not occur), to control for (1) seasonal patterns and gaseous pollutants, or (2) temperature. In addition, the studies attempted to examine the heterogeneity of effect estimates through the analysis of individual-level and city-specific effect modification.

Controlling for Temperature

Schwartz (2004, [078998](#)) investigated the PM₁₀-mortality association in 14 U.S. cities for the years 1986-1993 (some cities started in later years because of PM₁₀ data availability) using a case-crossover study design. Note that in this analysis, four more cities (Boulder, CO; Cincinnati, OH; Columbus, OH; and Provo-Orem, UT) were added to the cities Schwartz (2003, [042800](#)) previously analyzed using a time-series study design. These cities were chosen for this analysis because they collected daily PM₁₀ data, unlike most U.S. cities, which only monitor PM₁₀ every six days. Lag 1-day PM₁₀ risk estimates were computed using several methods. Models (1) (i.e., the main model) and (2) were constructed from a case-crossover analysis with bidirectional control days (7-15 days before and after

the case). Model (1) obtained city-specific estimates in the first stage analysis, followed by a second stage random-effects model to obtain a combined estimate. Model (2) is the same as model (1), but consisted of a single stage model, which included data from all 14 cities. Models (3) and (4) were also constructed from a case-crossover analysis, but used time-stratified control days (i.e., matched on season and temperature within the same degree in Celsius). Model (3) obtained single-city estimates in the first stage analysis, followed by a second stage random-effects model to obtain combined estimates. Model (4) used the same approach as model (3), but consisted of a single stage model including data from all 14 cities. The final model, (5), consisted of a two-stage Poisson time-series model, which produced city-specific estimates in the first stage, and combined estimates across cities in the second stage. In the main model, (1) above, the estimated excess risk for non-accidental mortality was 0.36% (CI: 0.22, 0.50) per 10 $\mu\text{g}/\text{m}^3$ increase in PM_{10} . The other models yielded a similar magnitude of effect estimates, ranging from 0.32% (model 2) to 0.53% (model 4). Thus, the methods used to select control days and adjust for weather in the case-crossover design did not result in major differences in effect estimates, and in addition, were comparable to the estimates obtained from the time-series analysis, 0.40% (model 5).

Controlling for Gaseous Pollutants

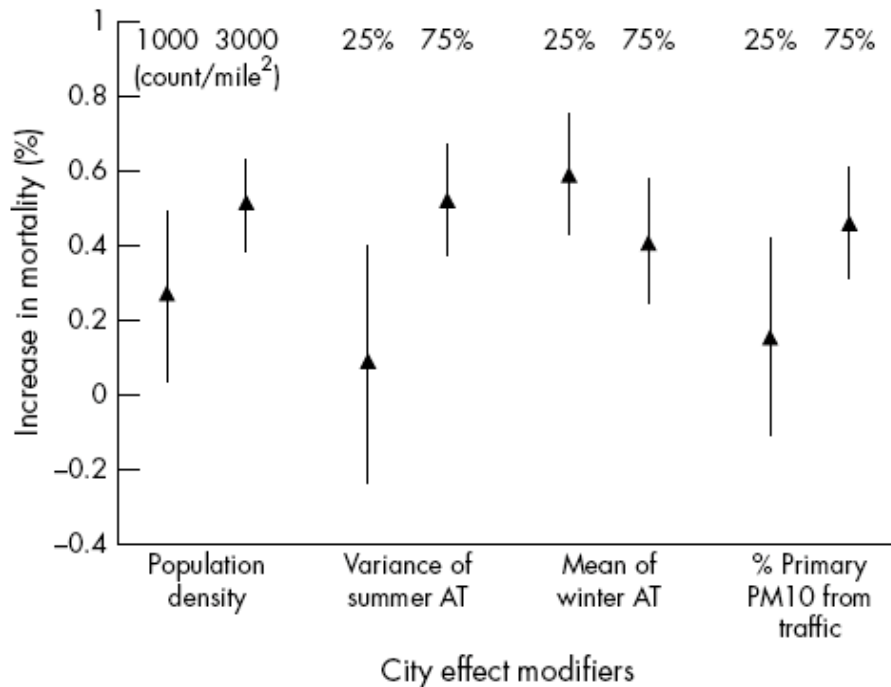
In a subsequent analysis, Schwartz (2004, [053506](#)) analyzed the same 14 cities data described above, using a case-crossover design, to investigate the potential confounding effects of gaseous pollutants. For each case day, control days were selected from all other days of the same month of the same year. In addition, case days were matched to control days that had gaseous pollutant levels that were within a defined concentration: 1 ppb, 1 ppb, 2 ppb, and 0.03 ppm for SO_2 , NO_2 , 1-h max O_3 , and CO, respectively. Unlike the study described above (Schwartz, 2004, [078998](#)) in this analysis, the excess risk was estimated for the average of 0- and 1-day lag PM_{10} (rather than 1-day lag). In addition, apparent temperature (a composite index of temperature and humidity) was used rather than temperature and humidity individually. The case-crossover analysis was conducted in each city, and a combined estimate was computed in a second-stage random effects model. The number of cities analyzed varied across pollutants depending on the availability of monitors. The study reported PM_{10} risk estimates for non-accidental mortality of 0.81% (CI: 0.47-1.15), 0.78% (CI: 0.42-1.15), 0.45% (CI: 0.12-0.78), and 0.53% (CI: 0.04-1.02) per

10 $\mu\text{g}/\text{m}^3$ increase, for the analysis matched by SO_2 (10 cities), NO_2 (8 cities), O_3 (13 cities), and CO (13 cities), respectively.

Schwartz (2004, [053506](#)) only presented PM_{10} risk estimates matched by gaseous pollutants, therefore, it is unclear in this analysis how matching by gaseous pollutants affected (i.e., reduced or increased) unmatched PM_{10} risk estimates. The estimates reported were computed using the average of 0- and 1-day lagged PM_{10} and, therefore, cannot be directly compared to the 1-day lag PM_{10} risk estimates obtained in the Schwartz (2004, [078998](#)) 14-city study described above. The estimates reported in Schwartz (2004, [053506](#)) are generally larger than those obtained in the Schwartz (2004, [078998](#)) analysis, which was expected since the Schwartz (2004, [053506](#)) analysis used two-day avg PM_{10} . However, the estimates reported in Schwartz (2004, [053506](#)) are comparable to the average of 0- and 1-day lagged PM_{10} risk estimate for non-accidental mortality (0.55% [CI: 0.39-0.70]) per 10 $\mu\text{g}/\text{m}^3$ increase from the 10-city study (Schwartz, 2003, [042800](#)), which was reviewed in the 2004 PM AQCD (U.S. EPA, 2004, [056905](#)). Overall, Schwartz (2004, [053506](#)) provided an alternative method to assess the influence of gaseous copollutants. The results suggest that PM_{10} is significantly associated with all-cause mortality after controlling for each of the gaseous copollutants.

City-Level Effect Modification

Zeka et al. (2006, [088749](#)) expanded the 14 cities analyses conducted by Schwartz (2004, [078998](#); 2004, [053506](#)) to 20 cities, added more years of data (1989-2000), and investigated PM_{10} effects on total and cause-specific mortality using a case-crossover design. Individual 0-, 1-, and 2-day lags as well as an unconstrained distributed lag model with 0, 1, and 2 lag days were examined. For each case day, control days were defined as every third day in the same month of the same year, to eliminate serial correlation. The authors also investigated potential effect modifiers in the second stage regression using city-specific variables including percent using air conditioning, population density, standardized mortality rates, the proportion of elderly in each city, daily minimum apparent temperature in summer, daily maximum apparent temperature in winter, and the estimated percentage of primary PM_{10} from traffic sources.



Source: Zeka et al. (2005, [088068](#))

Figure 6-18. Effect modification by city characteristics in 20 U.S. cities. Note: The two estimates and their CI for each of the modifying factors represent the percentage increase in mortality for a $10 \mu\text{g}/\text{m}^3$ increase in PM_{10} , for the 25th percentile, and 75th percentile of the modifier distribution across the 20 cities.

The investigators found that, for all-cause (non-accidental) mortality, lag 1-day showed the largest risk estimate (0.35% [CI: 0.21-0.49] per $10 \mu\text{g}/\text{m}^3$) among the individual lags. Respiratory mortality exhibited associations at lag 0, 1, and 2 days (0.34-0.52, and 0.51%, respectively), whereas cardiovascular mortality was most strongly associated with PM_{10} at lag day 2 (0.37%). The sum of the distributed lag risk estimates (e.g., 0.45% [CI: 0.25-0.65] for all-cause mortality) was generally larger than those for single-day lag estimates. The excess risk estimates for single-day lags for specific respiratory and cardiovascular causes had generally wider confidence intervals due to their smaller daily mortality counts, but some of the categories showed markedly larger estimates when included in the combined distributed lag model (e.g., pneumonia 1.24% [CI: 0.46-2.02]). As shown in Figure 6-18, Zeka et al. (2005, [088068](#)) also found evidence indicative of several PM_{10} effect modifiers including higher population density and the estimated percentage of primary PM_{10} from traffic. When 25th vs. 75th percentiles of these city-specific variables were evaluated, the estimated percent increase in mortality attributed to PM_{10} appears to

contrast substantially (e.g., 0.09 vs. 0.52% for variance of summer time apparent temperature).

The effect modifiers investigated by Zeka et al. (2005, [088068](#)) consisted of city-specific variables. Some of these variables are ecological in nature, and therefore, interpreting the meaning of “effect modification” requires some caution. As the investigators pointed out, the population density and the estimated percentage of primary PM₁₀ from traffic were correlated in this data set ($r = 0.65$)¹. These variables may also be a surrogate for another or composite aspects of “urban” characteristics. Thus, the apparent effect modification by traffic associated PM₁₀ needs further investigation. Interestingly, the percent of homes with central air conditioning was not a significant effect modifier of PM₁₀ risk estimates, which questions the impact of reduced ventilation rates on PM exposure. Overall, this study presented PM₁₀ risk estimates that are consistent with those found in other analyses, but also provided new information on the risk estimated for broad and specific respiratory and cardiovascular mortality, along with possible effect modifying city-specific characteristics.

¹ The correlation coefficient was calculated based on the numbers provided in Table 1 of Zeka et al. (2005, [088068](#)).

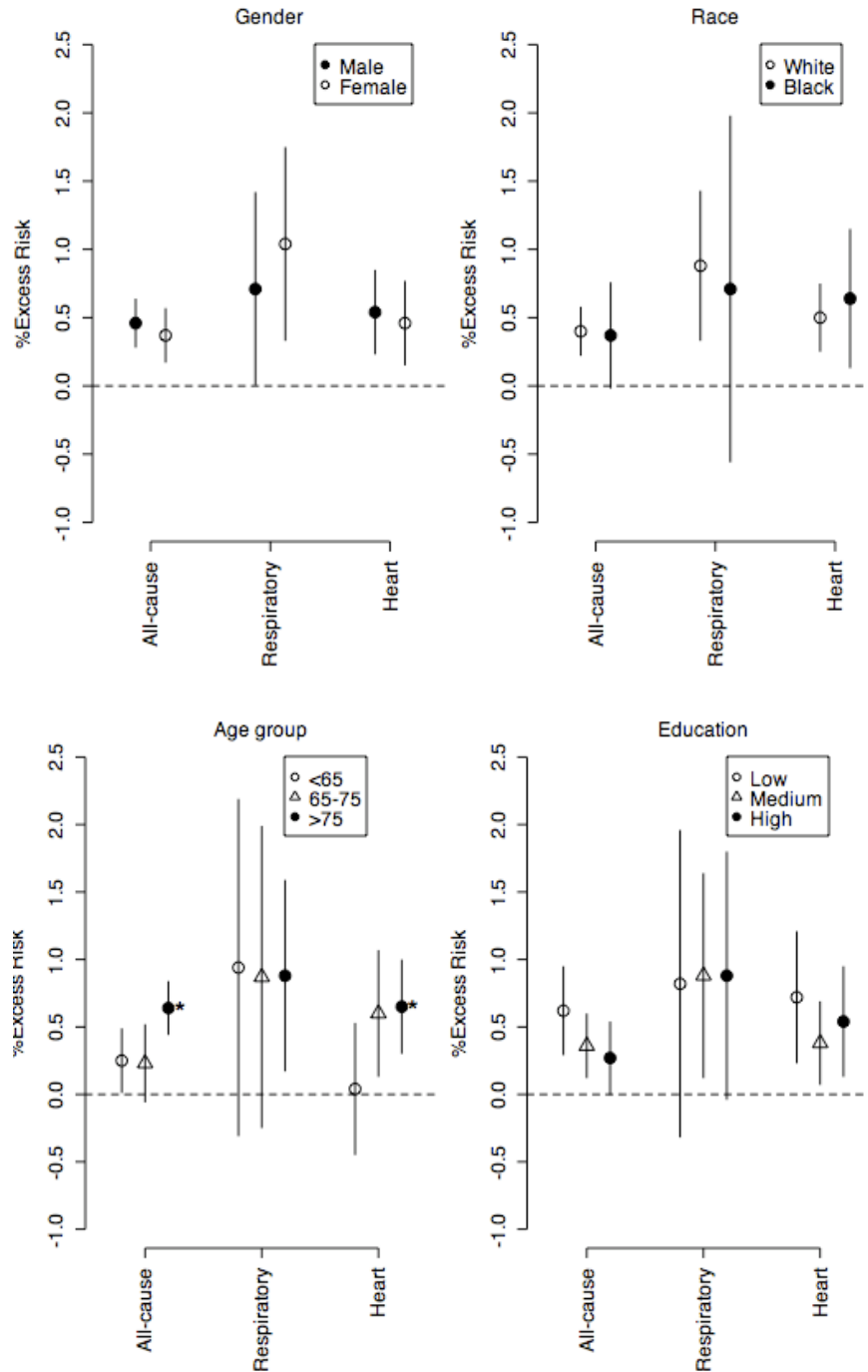


Figure 6-19. PM₁₀ risk estimates (per 10 $\mu\text{g}/\text{m}^3$) by individual-level characteristics. The risk estimates and 95% confidence intervals were plotted using numerical results from tables in Zeka et al. (2006, [088749](#)). The estimates with '*' next to them are significantly higher than the lowest estimate in the group.

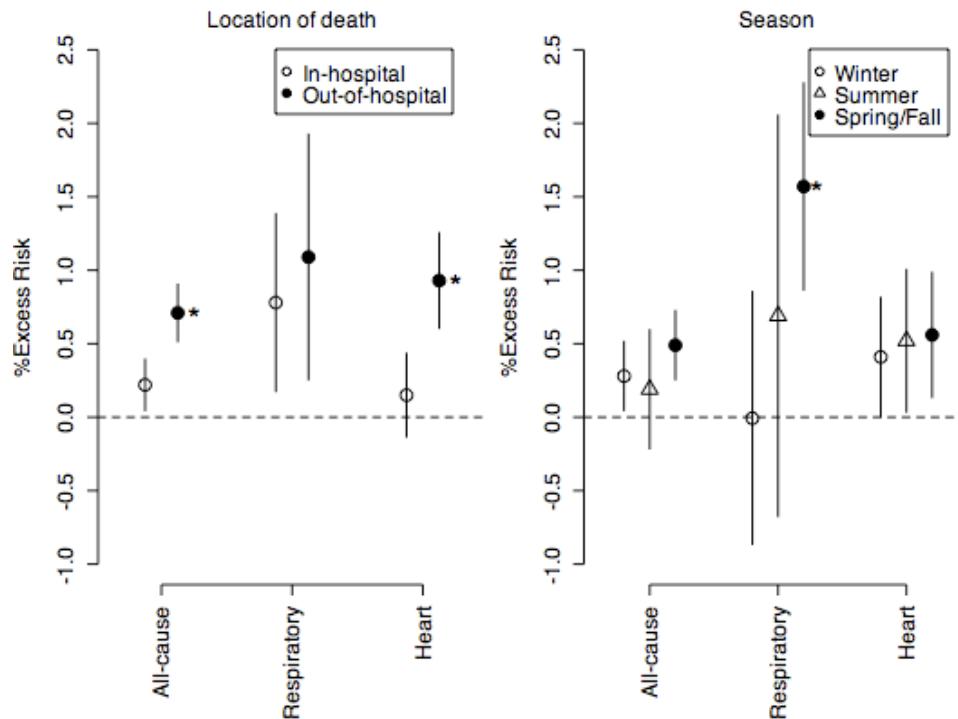


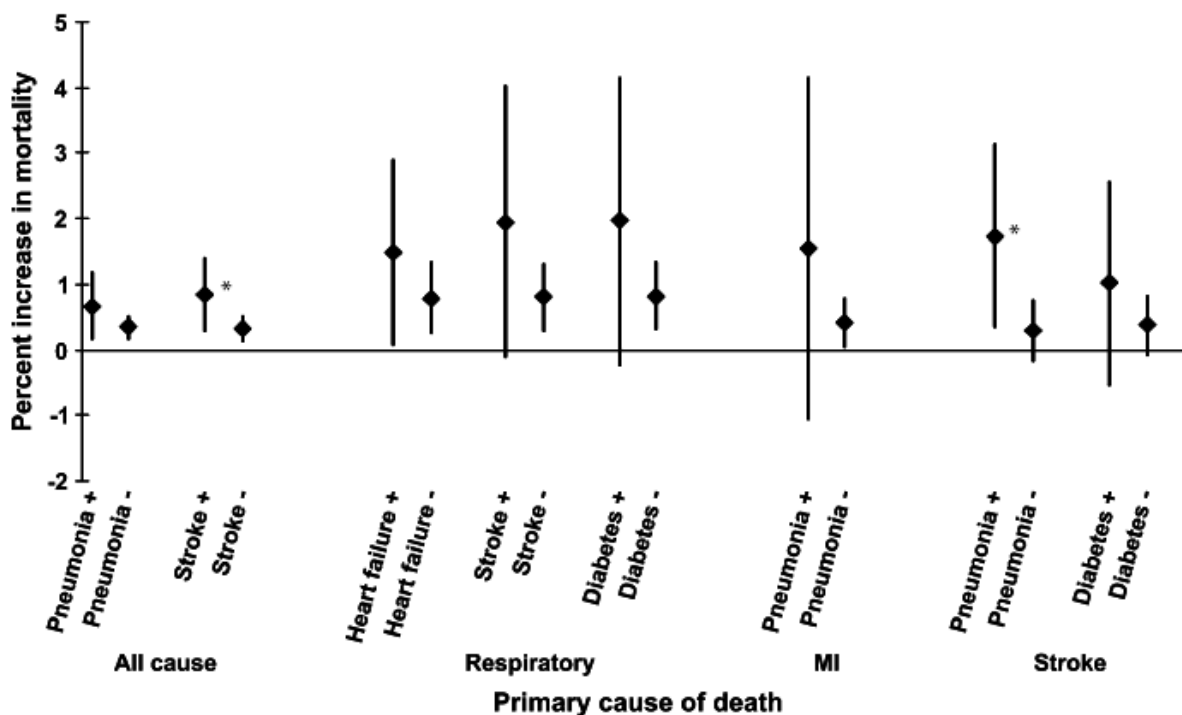
Figure 6-20. PM₁₀ risk estimates (per 10 $\mu\text{g}/\text{m}^3$) by location of death and by season. The risk estimates and 95% confidence intervals were plotted using numerical results from tables in Zeka et al. (2006, [088749](#)). The estimates with '' next to them are significantly higher than the lowest estimate in the group.**

Individual-level Effect Modification

In an additional analysis, Zeka et al. (2006, [088749](#)) examined individual-level, instead of city-specific, effect modification of PM₁₀-mortality associations in the 20 U.S. cities described above using the same case-crossover design. City-specific estimates were obtained in the first stage model, followed by a second stage model which estimated the overall effects across all cities. Figure 6-19 shows PM₁₀ excess risks by four of the individual characteristics examined in the study (i.e., gender, race, age group, and education). It should be noted that the lag and averaging of days for the associations reported varied across the outcomes: all-cause and heart disease deaths used the average of lag 1 and 2 days; respiratory deaths used the average of lag 0 through 2 days; MI deaths used lag 0 day; and stroke deaths used lag 1 day. PM₁₀ risk estimates do not appear to differ by gender or by race. However, significant differences were found for the youngest vs. oldest age groups for all-cause and heart disease mortality. For all-cause mortality, the level of education appeared to be inversely related to the PM₁₀ risk estimates, but this observation

was not statistically significant. The study also examined effect modification by location of death (“out-of-hospital” vs. “in-hospital”) and season (see Figure 6-20). The “out-of-hospital” deaths showed larger PM₁₀ risk estimates than were found for “in-hospital deaths” with a significant contrast per 10 µg/m³ for all-cause (0.71% vs. 0.22%) and heart disease (0.93% vs. 0.15%) deaths. Stroke deaths also showed a significant contrast (0.87% vs. 0.06%, not shown in Figure 6-20).

Overall, Zeka et al. (2006, [088749](#)) showed a consistent pattern of effect modification by contributing causes of death (i.e., pneumonia, stroke, heart failure, and diabetes) on PM₁₀ risk estimates for primary causes of death (Figure 6-21; not all results for contributing cause are shown). However, because the contributing causes of death counts were relatively small, as reflected by the wide confidence intervals in Figure 6-21, most of the contrasts observed did not achieve statistical significance.



Source: Zeka et al. (2006, [088749](#))

Figure 6-21. PM₁₀ risk estimates (per 10 µg/m³) by contributing causes of deaths. The estimates with ‘*’ (added to the original figure) indicates a significant difference.

In addition, when examining the other effect modifiers, the results that show no gender or race differences in PM₁₀ risk estimates for all-cause and cardiovascular deaths

are important, given the relatively narrow confidence bands of these estimates. The effect modification by the location of death has been reported previously in smaller studies, but the large contrast found for all-cause and cardiovascular mortality in this large multicity analysis is noteworthy. The elevated PM₁₀ risks reported by Zeka et al. (2006, [088749](#)) for all-cause, heart disease (and stroke) “out-of-hospital” deaths are also consistent with the hypothesis of acute PM₁₀ effects on “sudden deaths” brought on by systemic inflammation or dysregulation of the autonomic nervous system. The finding regarding the seasonal effect modification, though significant only for respiratory deaths, is somewhat in contrast with the Peng et al. (2005, [087463](#)) analysis of the extended NMMAPS data, which observed the greatest effects during the summer season. The apparent inconsistency may be due to the difference in geographic coverage (i.e., 20 vs. 100 cities) or methodology (i.e., case-crossover with referent days in the same month of the same year vs. time-series analysis with adjustment for temporal trend in the regression model).

Summary of PM₁₀ Risk Estimates

Overall, the recent studies continue to show an association between short-term exposure to PM and mortality. Although these studies do not examine mortality effects attributed to PM size fractions that compose PM₁₀, the regional, seasonal, and effect modification analyses conducted contribute to the evidence for the PM_{2.5} and PM_{10-2.5} associations presented in Sections 6.5.2.2 and 6.5.2.3, respectively. Of the PM₁₀ studies evaluated, depending on the lag/averaging time and the number of cities included, the estimates for all-cause (non-accidental) mortality for all ages ranged from 0.12% (Dominici et al., 2007, [099135](#)) to 0.84% (Samoli et al., 2008, [188455](#)) per 10 µg/m³ increase in PM₁₀, regardless of the study design used (i.e., time-series vs. case crossover) (see Figure 6-22). Although this range of PM mortality risk estimates is smaller than those reported for PM_{10-2.5} and PM_{2.5} they do support the association between PM and mortality. The majority of studies examined present estimates for either a lag of 1 day or a 2-day avg (lag 0-1), both of which have been found to be strongly associated with the risk of death (Schwartz, 2004, [078998](#); 2004, [053506](#)) The use of a distributed lag model (using lag 0, 1, and 2 days) was found to result in slightly larger (by ~30%) estimates compared to those for single-day lags in the 20 cities study (Zeka et al., 2005, [088068](#)), but when using the 15 cities data from NMMAPS analyzed in the APHENA study (Samoli et al., 2008, [188455](#)), the 1-day lag combined risk estimate was larger than the distributed lag (lag, 0, 1, and 2 days) estimate.

Overall, an examination of the PM₁₀ risk estimates stratified by cause-specific mortality and age, for all U.S.- and Canadian-based studies, further supports the findings of the multicity studies discussed in the 2004 PM AQCD (U.S. EPA, 2004, [056905](#)) and this ISA, however, it must be noted that a large degree of variability exists between cities when examining city-specific risk estimates.

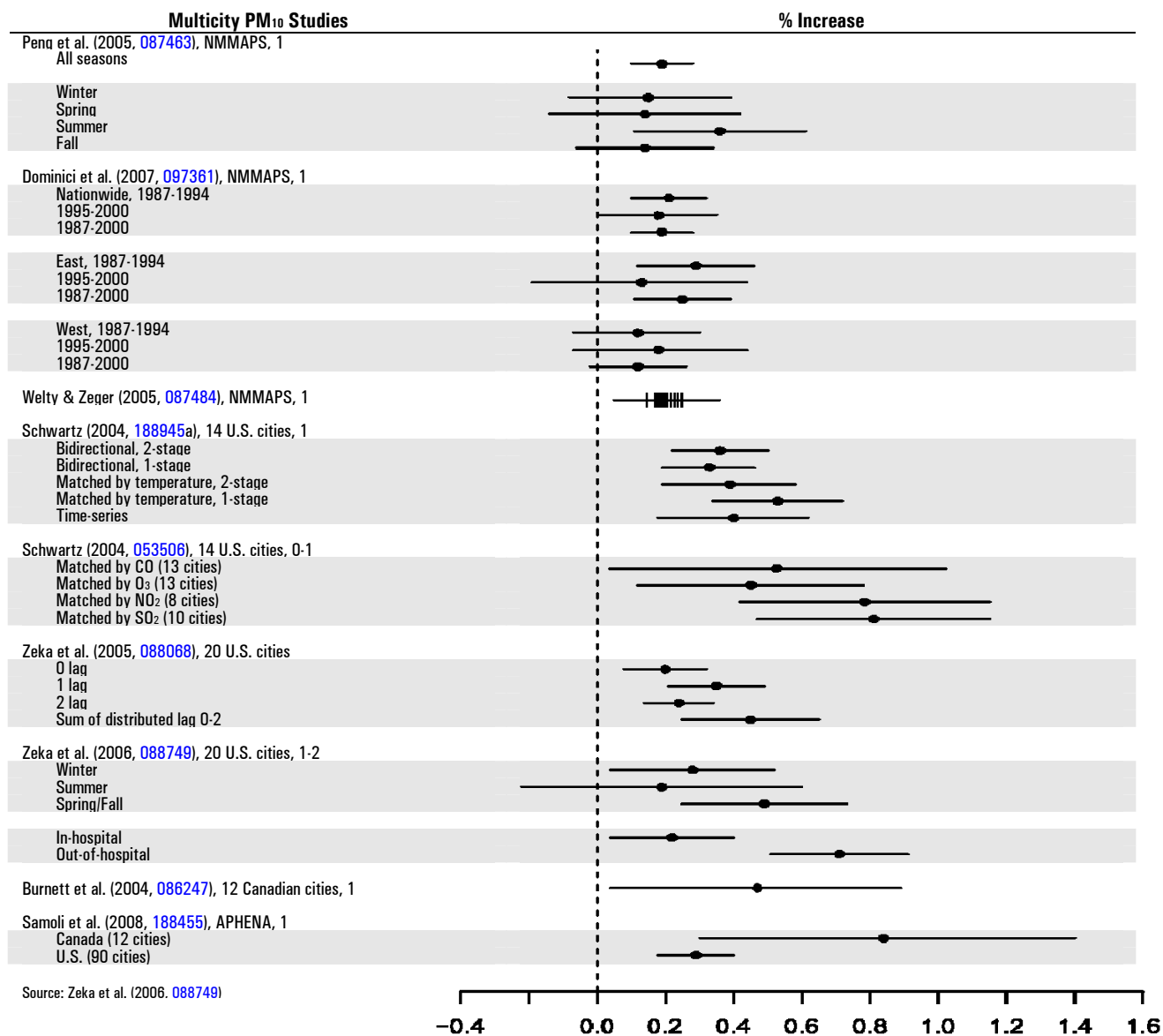


Figure 6-22. Summary of PM₁₀ risk estimates (per 10 $\mu\text{g}/\text{m}^3$) for all-cause mortality from recent multicity studies. The number after the study location indicates lag/average used for PM₁₀ (e.g., "01" indicates the average of lag 0 and 1 days). For Welty and Zeger (2005, [087484](#)), the vertical lines represent point estimates for 23 different weather models, and the horizontal band spans the 95% posterior intervals of these point estimates.

The variability in PM₁₀ mortality risk estimates reported within and between multicity studies may be due to the difference in the cities analyzed and the potential regional differences in PM composition. The NMMAPS studies have found that geographic regions and seasons are the two most important factors that determine the variability in risk estimates, with estimates being larger in the eastern U.S. and during the summer, respectively. These findings were fairly consistent across studies, but Zeka et al. (2006, [088749](#)) did observe the strongest association during the transition period (spring and fall); however, this may be due to the difference in geographic coverage or the difference in the model specification used compared to Peng et al. (2005, [087463](#)).

Finally, examination of potential confounders showed that the size of PM₁₀ risk estimates are fairly robust to the inclusion of gaseous copollutants in models (Peng et al., 2005, [087463](#)) or by matching days with similar gaseous pollutant concentrations (Schwartz, 2004, [078998](#)). These findings further confirmed that PM₁₀ risk estimates are not, at least in a straightforward manner, confounded by gaseous copollutants.

6.5.2.2. PM_{2.5}

A nationwide monitoring system for PM_{2.5} was not established until 1999. This in conjunction with the unavailability of nationwide mortality data from the National Center of Health Statistics (NCHS) starting in 2001¹, has contributed to the relatively small literature base that has examined the association between short-term exposure to PM_{2.5} and mortality. To date, the studies that have been conducted examined national (i.e., in multiple cities across the country) or regional (i.e., in one location of the country) PM_{2.5} associations with mortality.

PM_{2.5} – Mortality Associations on a National Scale

The NMMAPS study conducted by Dominici et al. (2007, [099135](#)) (described in Section 6.5.2.1.), also conducted a national analysis of PM_{2.5}-mortality associations using the same methodology and data for 1999-2000. The PM_{2.5} risk estimates at lag 1-day were 0.29% (PI: 0.01-0.57) and 0.38% (PI: -0.07 to 0.82) per 10 µg/m³ increase for all-cause and cardio-respiratory mortality, respectively. The authors also conducted a sensitivity analysis of the risk estimates based on the extent of adjustment for temporal trends in the model,

¹ In 2008 the EPA facilitated the availability of the mortality data for EPA-funded researchers, which should eventually increase the literature base of studies that examine the association between short-term exposure to PM_{2.5} and mortality.

changing the degrees of freedom (df) of temporal adjustment from 1 to 20/yr (the main result used 7 df/yr). In comparison to the PM₁₀ results, the PM_{2.5} risk estimates appeared more sensitive to the extent of temporal adjustment between 5 and 10 df/yr, but this may be in part due to the much smaller sample size used for the PM_{2.5} analysis compared to the PM₁₀ analysis.

Franklin et al. (2007, [091257](#)) analyzed 27 cities across the U.S. that had PM_{2.5} monitoring and daily mortality data for at least 2 yr of a 6-yr period 1997 to 2002. The mortality data up to year 2000 were obtained from the NCHS, while the 2001-2002 data were obtained from six states (CA, MI, MN, PA, TX, and WA), resulting in 12 out of the 27 cities having data up to 2002. The start year for each city included in the study was set at 1999, except for Milwaukee, WI (1997) and Boston, MA (1998), which is due to PM_{2.5} data availability in these two cities. In the case-crossover analysis in each city, control days for each death were chosen to be every third day within the same month and year that death occurred in order to reduce auto-correlation. The first stage regression examined the interaction of effects with age and gender, while the second stage random effects model combined city-specific PM_{2.5} risk estimates and examined possible effect modifiers using city-specific characteristics (e.g., prevalence of central air conditioning and geographic region). For all of the mortality categories, the estimates for lag 1-day showed the largest estimates. The combined estimates at lag 1 day were: 1.2% (CI: 0.29-2.1), 0.94% (CI: -0.14 to 2.0), 1.8% (CI: 0.20-3.4), and 1.0% (CI: 0.02-2.0) for all-cause, cardiovascular, respiratory, and stroke deaths, respectively, per 10 µg/m³. When examining the city-specific risk estimates most of the cities with negative estimates are also those with a high prevalence of central air conditioning (Dallas, 89%; Houston, 84%; Las Vegas, 93%; Birmingham, 77%). It is unclear why these cities exhibit negative (and significant) risk estimates rather than null effects.

In the analysis of effect modifiers, Franklin et al. (2007, [091257](#)) found that individuals ≥ 75 showed significantly higher PM_{2.5} risk estimates. The estimated effects were also found to vary by geographic location with larger estimates in the East than in the West, which are consistent with the regional pattern found in the NMMAPS PM₁₀ risk estimates. In addition, a higher prevalence of central air conditioning was associated with decreased PM_{2.5} risk estimates when comparing the lower (25th percentile) vs. the higher (75th percentile) air conditioning use rates, especially in the cities where PM_{2.5} concentrations peak in the summer. Finally, the risk estimates were not found to be

different between communities with PM_{2.5} levels less than or equal to vs. higher than 15 µg/m³. The risk estimates for each effect modifier are presented in Figure 6-25. Note the wide confidence intervals associated with each of the risk estimates, specifically for Franklin et al. (2007, [091257](#)) and Ostro et al. (2006, [087991](#)), which suggests low statistical power for testing the differences between effect modifiers.

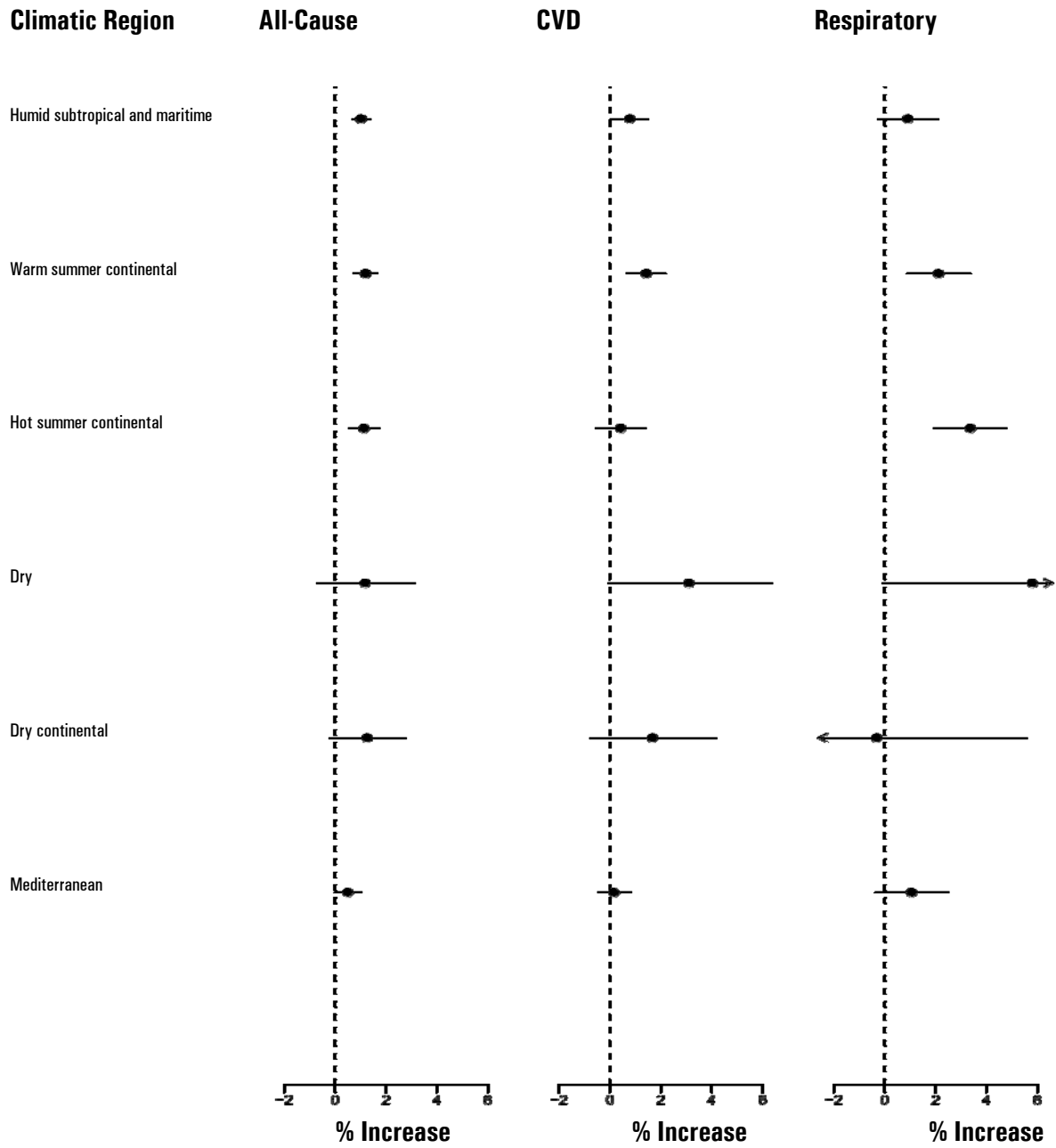
Franklin et al. (2008, [097426](#)) analyzed 25 cities that had PM_{2.5} monitoring and daily mortality data between the years 2000 to 2005 (with the study period varying from city to city). The choice of the 25 communities was based on the availability of PM_{2.5} mass concentrations and daily mortality records for at least 4 yr, along with PM_{2.5} speciation data for at least 2 yr between 2000 and 2005. Similar to Franklin et al. (2007, [091257](#)), all-cause, cardiovascular, respiratory, and stroke deaths were examined; however, of the 25 cities included in the study, only 15 overlap with the 27 cities analyzed in Franklin et al. (2007, [091257](#)). The authors obtained mortality data from the NCHS and various state health departments (California, Massachusetts, Michigan, Minnesota, Missouri, Ohio, Pennsylvania, Texas, and Washington). Although the main objective of the study was to examine the role of PM_{2.5} chemical species in the second stage analysis, the first stage analysis conducted a time-series regression of mortality on PM_{2.5}. In addition, the first stage regression performed a seasonal analysis in order to take advantage of seasonal variation in PM_{2.5} chemical species across cities and to possibly explain the city-to-city variation in PM_{2.5} mortality risk estimates. From this analysis a strong seasonal pattern was observed with the greatest effects occurring in the spring and summer seasons (see Figure 6-25).

Overall, the risk estimates for all-cause, cardiovascular, and respiratory deaths reported by Franklin et al. (Franklin et al., 2008, [097426](#)) are comparable to those presented in the 27 cities study (2007, [091257](#)), as shown in Figure 6-26. When comparing the 2007 and 2008 studies conducted by Franklin et al. (2007, [091257](#); 2008, [097426](#)), although only 15 cities overlap between the two studies and each study was designed differently (i.e., time-series vs. case-crossover), the magnitude of the PM_{2.5} risk estimates reported were similar for the same averaging time, and both studies reported a regional pattern (East > West) similar to that found in the NMMAPS studies previously discussed.

Zanobetti and Schwartz (2009, [188462](#)) conducted a multicity time-series study to examine associations between PM_{2.5} and mortality in 112 U.S. cities. The cities included in this analysis encompass the majority of cities included in the Franklin et al. (2007, [091257](#))

and (2008, [097426](#)) analyses. In this analysis a city represents a single county; however, 14 of the cities represent a composite of multiple counties. In addition to examining PM_{2.5}, the investigators also analyzed PM_{10-2.5}; these results are discussed in Section 6.5.2.3. Zanobetti and Schwartz (2009, [188462](#)) analyzed PM_{2.5} associations with all-cause, cardiovascular disease (CVD), MI, stroke, and respiratory mortality for the years 1999-2005. To be included in the analysis, each of the cities selected had to have at least 265 days of PM_{2.5} data per year and at least 300 days of mortality data per year. The authors conducted a city- and season-specific Poisson regression to estimate excess risk for PM_{2.5} lagged 0- and 1-days, adjusting for smooth functions (natural cubic splines) of days (1.5 df per season), the same-day and previous day temperature (3 df each), and day-of-week. The city specific estimates were then combined using a random effects model. Based on the assumption that climate affects PM exposures (e.g., ventilation and particle characteristics), the investigators combined city-specific estimates into six regions classified based on the Köppen climate classification scheme (e.g., “Mediterranean climates” for CA, OR, WA, etc.).

The overall combined excess risk estimates were: 0.98 % (0.75, 1.22) for all-cause; 0.85 % (0.46, 1.24) for CVD, 1.18 % (0.48, 1.89) for MI; 1.78 % (0.96, 2.62) for stroke, and 1.68 % (1.04, 2.33) for respiratory mortality for a 10 µg/m³ increase in PM_{2.5} at lag 0-1. When the risk estimates were combined by season, the spring estimates were the largest for all-cause and for all of the cause-specific mortality outcomes examined. For example, the risk estimate for all-cause mortality for the spring was 2.57% (1.96-3.19) with the estimates for the other seasons ranging from 0.25% to 0.95%. When examining cities that had both PM_{2.5} and PM_{10-2.5} data (i.e., 47 cities), the addition of PM_{10-2.5} in the model did not alter the PM_{2.5} estimates substantially, only decreasing slightly from 0.94% in a single pollutant model to 0.77% in a copollutant model with PM_{10-2.5}. When the risk estimates were combined by climatic regions, the estimated PM_{2.5} risk for all-cause mortality were similar (all above 1% per 10 µg/m³ increase) for all the regions except for the “Mediterranean” region (0.5%) which include cities in CA, OR and WA, though the estimates in that region were significantly heterogeneous (Figure 6-24).



Source: Zanobetti and Schwartz (2009, [188462](#)).

Figure 6-23. Percent increase in mortality for 10 µg/m³ increase in the average of 0- and 1-day lagged PM_{2.5}, combined by climatic regions.

The PM_{2.5} risk estimate for all-cause mortality reported by Zanobetti and Schwartz (2009, [188462](#)) for 112 cities (0.98% per 10 µg/m³ increase in the average of 0- and 1-day

lags) is generally consistent with that reported by Franklin et al. (2007, [091257](#)) for 27 cities (0.82% [0.02-1.63]) and Franklin et al. (2008, [097426](#)) for 25 cities (0.74% [0.41-1.07]) using the same 0- and 1-day avg exposure time. The seasonal pattern (i.e., higher risk estimates in the spring) found in this study is also consistent with the result from Franklin et al. (2008, [097426](#)). Figure 6-23 highlights the risk estimates for all-cause, CVD, and respiratory mortality combined by region. The regional division based on climatic types used in this study makes it difficult to directly compare the regional pattern of results from previous studies. However, an examination of empirical Bayes-adjusted effect estimates for each of the cities included in the analysis further confirms the heterogeneity observed between some cities and regions of the country (see Figure 6-24). It is noteworthy that, unlike NMMAPS, which focused on PM₁₀ and indicated larger risk estimates in the northeast, Zanobetti and Schwartz (2009, [188462](#)) found that the all-cause mortality risk estimates were fairly uniform across the climatic regions, except for the “Mediterranean” region.

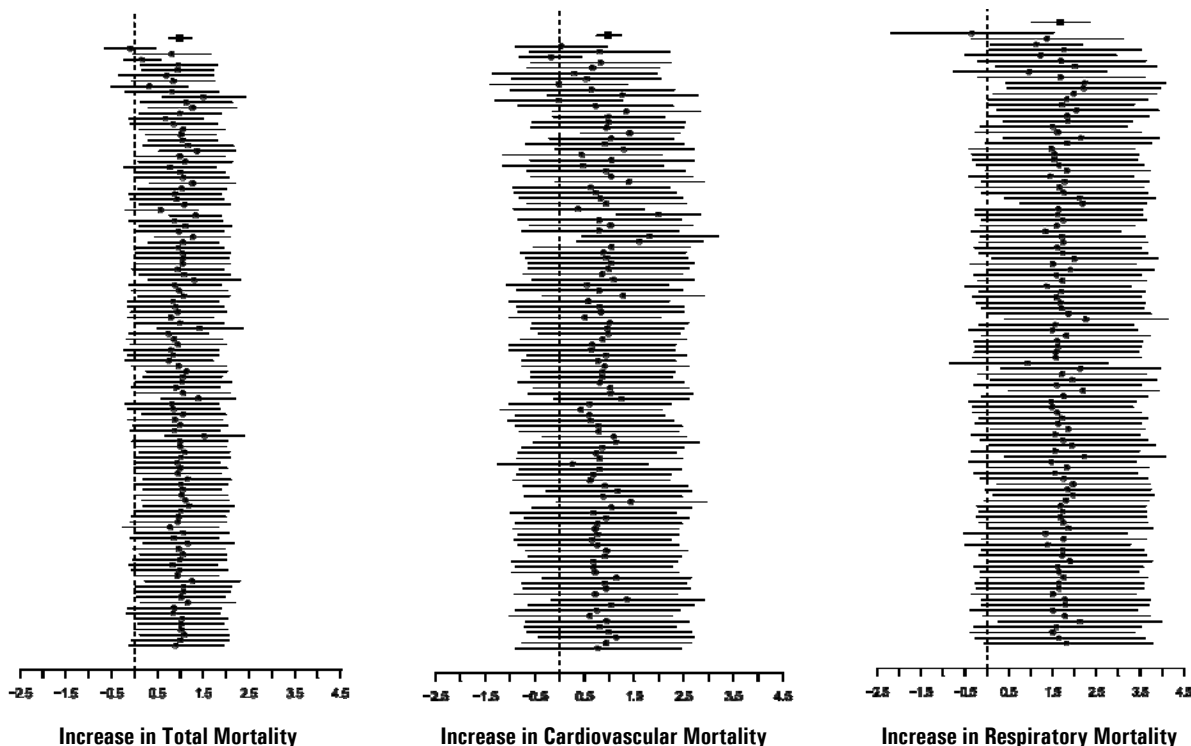


Figure 6-24. Empirical Bayes-adjusted city-specific effect estimates for total, cardiovascular, and respiratory mortality for 10 $\mu\text{g}/\text{m}^3$ increase in the average of 0- and 1-day lagged $\text{PM}_{2.5}$ by decreasing mean 24-h avg $\text{PM}_{2.5}$ concentrations. Based on estimates calculated from Zanobetti and Schwartz (2009, [188462](#)) using the approach specified in Le Tertre et al. (2005, [087560](#)).

Table 6-14. Key to Figure 6-24

City	Mean	98 th	City	Mean	98 th	City	Mean	98 th	City	Mean	98 th
Rubidoux, CA	24.7	68.0	Taylors, SC	15.0	32.2	Waukesha, WI	13.4	35.3	Phoenix, AZ	11.4	30.7
Bakersfield, CA	21.7	80.3	Toledo, OH	14.9	36.6	BatonRouge, LA	13.4	30.1	Tacoma, WA	11.4	38.1
Los Angeles, CA	19.7	51.1	Anaheim, CA	14.9	44.1	Memphis, TN	13.3	32.4	Port Arthur, TX	11.1	25.7
Fresno, CA	18.7	64.9	NewYork, NY	14.7	38.1	Erie, PA	12.9	36.1	Cedar Rapids, IA	11.0	31.0
Atlanta, GA	17.6	38.2	Washington, PA	14.7	37.0	Dallas, TX	12.8	28.7	Dodge, WI	10.9	32.9
Steubenville, OH	17.1	41.4	Winston, NC	14.7	34.1	Houston, TX	12.8	27.5	Oklahoma, OK	10.8	26.1
Cincinnati, OH	17.1	39.9	Elizabeth, NJ	14.6	38.2	Chesapeake, VA	12.8	29.8	Des Moines, IA	10.5	27.9
Birmingham, AL	16.5	38.8	Philadelphia, PA	14.6	36.6	Wilkesbarre, PA	12.8	32.5	Jacksonville, FL	10.5	25.3
Middletown, OH	16.5	38.4	St. Louis, MO	14.5	33.7	Norfolk, VA	12.7	29.6	Omaha, NE	10.5	28.0
Indianapolis, IN	16.4	38.2	Allentown, PA	14.4	38.9	Sacramento, CA	12.6	45.0	Denver, CO	10.5	26.4
Cleveland, OH	16.3	40.5	Richmond, VA	14.3	33.0	Springfield, MA	12.5	35.1	Pinellas, FL	10.4	23.1
Dayton, OH	16.3	38.3	Spartanburg, SC	14.2	31.4	NewOrleans, LA	12.5	29.0	Austin, TX	10.4	24.5

City	Mean	98 th	City	Mean	98 th	City	Mean	98 th	City	Mean	98 th
Columbus, OH	16.2	38.3	Durham, NC	14.2	32.9	Ft. Worth, TX	12.4	27.7	Orlando, FL	10.3	24.3
Detroit, MI	16.2	41.0	LittleRock, AR	14.2	31.8	Pensacola, FL	12.3	31.2	Klamath, OR	10.2	40.7
Akron, OH	16.0	39.0	Easton, PA	14.2	39.7	Davenport, IA	12.3	32.1	Seattle, WA	10.1	27.9
Louisville, KY	15.9	38.0	Raleigh, NC	14.1	31.8	Avondale, LA	12.3	28.6	Medford, OR	10.0	37.3
Chicago, IL	15.8	39.1	Greensboro, NC	14.1	31.0	Boston, MA	12.3	30.2	Bath, NY	9.6	29.3
Pittsburgh, PA	15.7	43.1	Mercer, PA	14.1	36.4	Holland, MI	12.1	35.0	Provo, UT	9.5	38.5
Harrisburg, PA	15.6	40.2	Annandale, VA	14.0	34.6	Charleston, SC	12.1	27.9	Miami, FL	9.4	20.5
Baltimore, MD	15.6	38.8	Nashville, TN	13.9	31.0	Tampa, FL	12.1	25.8	El Paso, TX	9.0	24.4
Youngstown, OH	15.6	38.1	Dumbarton, VA	13.8	31.9	Tulsa, OK	12.1	32.3	Spokane, WA	8.9	30.6
Knoxville, TN	15.5	32.9	Columbia, SC	13.7	30.7	Kansas, MO	12.0	28.6	SanAntonio, TX	8.9	21.9
Gary, IN	15.5	37.5	Milwaukee, WI	13.7	36.3	Scranton, PA	11.9	33.0	Portland, OR	8.9	25.4
Charlotte, NC	15.3	32.7	NewHaven, CT	13.6	36.8	Hartford, CT	11.8	33.5	Davie, FL	8.4	19.1
Warren, OH	15.2	37.4	Grand Rapids, MI	13.6	36.4	Minneapolis, MN	11.6	31.6	Eugene, OR	8.1	29.9
Washington, DC	15.2	37.2	El Cajon, CA	13.5	34.9	Worcester, MA	11.5	30.2	Palm Beach, FL	7.8	18.4
Wilmington, DE	15.1	37.6	Gettysburg, PA	13.4	36.5	Salt Lake, UT	11.5	52.4	Bend, OR	7.7	23.5
Carlisle, PA	15.1	40.0	State College, PA	13.4	38.5	Providence, RI	11.5	30.5	Albuquerque, NM	6.6	17.9

Note: The top effect estimate in the figures represents the overall effect estimate for that mortality outcome across all cities. The remaining effect estimates are ordered by the highest (i.e., Rubidoux, CA) to lowest (i.e., Albuquerque, NM) mean 24-h PM_{2.5} concentrations across the cities examined. In the key the cities are reported in this order, which represents the policy relevant concentrations for the annual standard, but the policy relevant PM_{2.5} concentrations for the daily standard (i.e., 98th percentile of the 24-h average) are also listed for each city (from Zanobetti and Schwartz (2009))

PM_{2.5} - Mortality Associations on a Regional Scale: California

Ostro et al. (2006, [087991](#)) examined associations between PM_{2.5} and daily mortality in nine heavily populated California counties (Contra Costa, Fresno, Kern, Los Angeles, Orange, Riverside, Sacramento, San Diego, and Santa Clara) using data from 1999 through 2002. The authors used a two-stage model to examine all-cause, respiratory, cardiovascular, ischemic heart disease, and diabetes mortality individually and by potential effect modifier (i.e., age, gender, race, ethnicity, and education level). The a priori exposure periods examined included the average of 0- and 1-day lags (lag 0-1) and the 2-day lag (lag 2). The authors selected these non-overlapping lags (i.e., rather than selecting lag 1 as the single-day lag) because previous studies have reported stronger associations at lags of 1 or 2 days or with cumulative exposure over three days. It is unclear why the investigators chose these non-overlapping lags (i.e., single-day lag of 2 instead of 1) even though they state they based the selection of their lag days on results presented in previous studies, which found the strongest association for PM lagged 1 or 2 days. Using the average of 0- and 1-day lags Ostro et al. (2006, [087991](#)) reported combined estimates of: 0.6%(CI: 0.2-1.0), 0.6% (CI: 0.0-1.1), 0.3% (CI: -0.5 to 1.0), 2.2% (CI: 0.6-3.9), and 2.4% (CI: 0.6-4.2) for all-cause, cardiovascular, ischemic heart disease, respiratory, and diabetes deaths, respectively, per 10 µg/m³. The authors also conducted a sensitivity analysis of risk

estimates based on the extent of temporal adjustment, which showed monotonic reductions for all of the death categories examined when 4, 8, and 12 degrees of freedom per year were used.

Five of the nine counties examined in the Ostro et al. (2006, [087991](#)) analysis contain cities that are among the 27 cities examined in the Franklin et al. (2007, [091257](#)) analysis for the same period, 1999-2002. While the lags used were different between these two studies, both presented PM_{2.5} risk estimates in individual cities or counties (graphically in the Franklin et al. study (2007, [091257](#)); in a table in the Ostro et al. study (2006, [087991](#)), which allowed for a cursory evaluation of consistency between the two analyses. In Franklin et al. (2007, [091257](#)), PM_{2.5} risk estimates at lag 1 day for the cities Los Angeles and Riverside were slightly negative, whereas Fresno, Sacramento, and San Diego showed positive values above 1% per 10 µg/m³ increase in PM_{2.5}. The 2-day lag result presented in Ostro et al. (2006, [087991](#)) is qualitatively consistent, with Los Angeles and Riverside, both of which show slightly negative estimates, while the other 3 locations all show positive, but somewhat smaller estimates, than those reported by Franklin et al. (2007, [091257](#)). The estimates for the average of 0- and 1-day lags for these five counties in Ostro et al. (2006, [087991](#)), which contain cities examined in Franklin et al. (2007, [091257](#)), were all positive. Thus, these two PM_{2.5} studies showed some consistencies in risk estimates even though they used different lag periods and a different definition for the study areas of interest (i.e., counties vs. cities). The risk estimates for Franklin et al. (2007, [091257](#)) and Ostro et al. (2006, [087991](#)), stratified by various effect modifiers (gender, race, etc.), are summarized in Figure 6-25. Of note is the contrast in the results presented for the effect modification analysis for “in-hospital” vs. “out-of-hospital” deaths for Ostro et al. (2006, [087991](#)), which differs from the results presented in the PM₁₀ study conducted by Zeka et al. (2006, [088749](#)). Ostro et al. (2006, [087991](#)) observed comparable risk estimates for “in-hospital” vs. “out-of-hospital” deaths, whereas Zeka et al. (2006, [088749](#)) observed a large difference between the two in the 20 cities study discussed earlier. This difference in effects observed between the two studies is more than likely due to the compositional differences in PM₁₀ in the cities examined in Zeka et al. (2006, [088749](#)) (i.e., PM₁₀ more or less dominated by PM_{2.5} and the subsequent composition of PM_{2.5}).

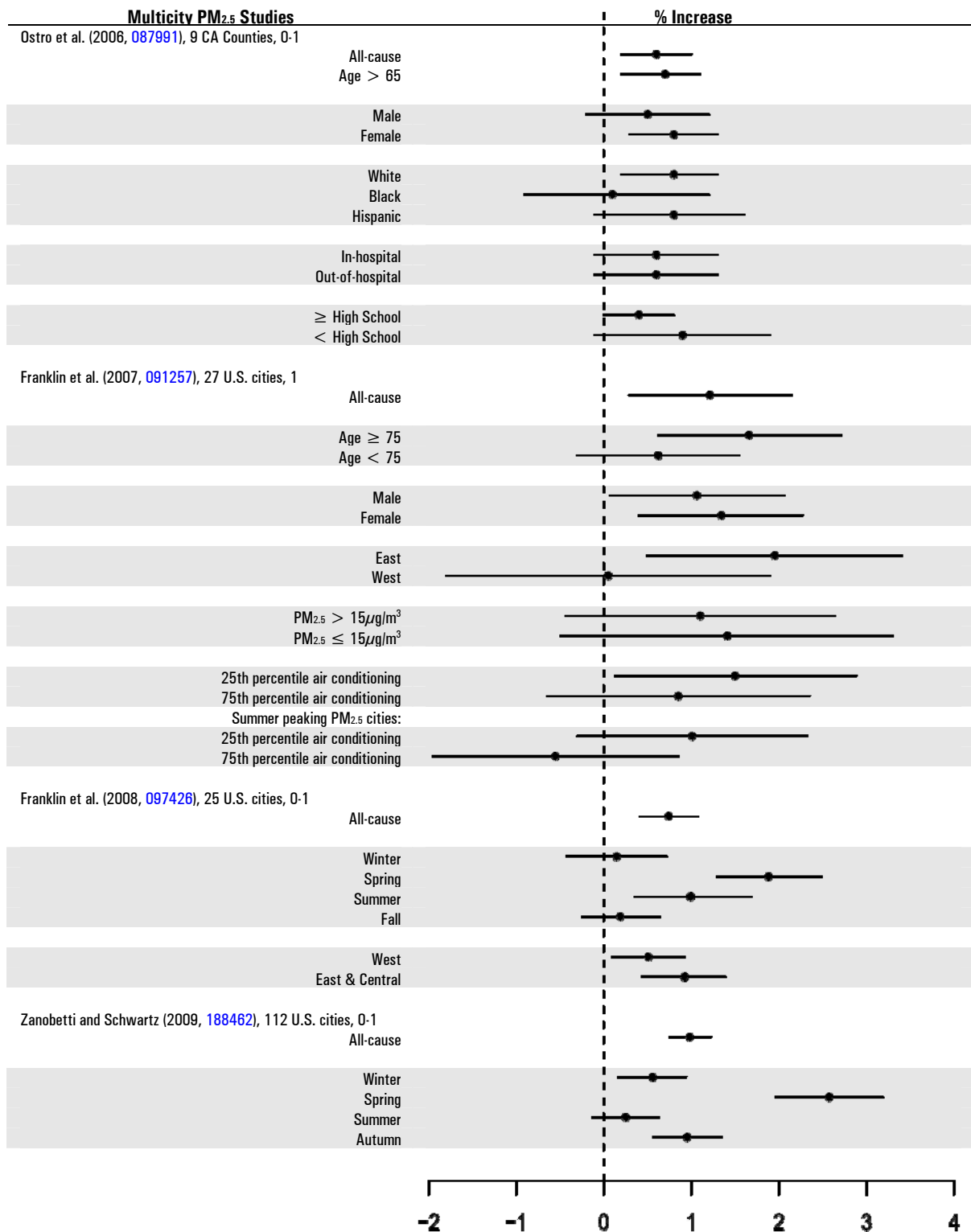


Figure 6-25. Summary of all-cause mortality PM_{2.5} risk estimates per 10 µg/m³ by various effect modifiers.

PM_{2.5}-Mortality Associations in Canada

An analysis of multiple pollutants, including PM_{2.5}, in 12 Canadian cities found the most consistent associations for NO₂ (Burnett et al., 2004, [086247](#)). In this analysis, PM_{2.5} was only measured every 6th-day in much of the study period, and the simultaneous inclusion of NO₂ and PM_{2.5} in a model on the days when PM_{2.5} data were available eliminated the PM_{2.5} association (from 0.60% to -0.10% per 10 µg/m³ increase in PM_{2.5}). However, the investigators noted that during the later study period of 1998-2000 when daily TEOM PM_{2.5} data were available for 11 of the 12 cities, a simultaneous inclusion of NO₂ and PM_{2.5} resulted in considerable reduction of the NO₂ risk estimate, while the PM_{2.5} risk estimate was only slightly reduced from 1.1% to 0.98% (CI: -0.16 to 2.14). Thus, the relative importance of NO₂ and PM_{2.5} on mortality effect estimates has not been resolved when using the Canadian data sets.

Summary of PM_{2.5} Risk Estimates

The risk estimates for all-cause mortality for all ages ranged from 0.29% Dominici et al. (2007, [099135](#)) to 1.21% Franklin et al. (2007, [091257](#)) per 10 µg/m³ increase in PM_{2.5} (see Figure 6-26). An examination of cause-specific risk estimates found that PM_{2.5} risk estimates for cardiovascular deaths are similar to those for all-cause deaths (0.30-1.03%), while the effect estimates for respiratory deaths were consistently larger (1.01-2.2%), albeit with larger confidence intervals, than those for all-cause or cardiovascular deaths using the same lag/averaging indices. Figure 6-27 summarizes the PM_{2.5} risk estimates for all U.S.- and Canadian-based studies by cause-specific mortality.

An examination of lag structure observed results similar to those reported for PM₁₀ with most studies reporting either single day lags or two-day avg lags with the strongest effects observed on lag 1 or lag 0-1. In addition, seasonal patterns of PM_{2.5} risk estimates were found to be similar to those reported for PM₁₀, with the warmer season showing the strongest association. An evaluation of regional associations found that in most cases the eastern U.S. had the highest PM_{2.5} mortality risk estimates, but this was dependent on the geographic designations made in the study. When grouping cities by climatic regions, similar PM_{2.5} mortality risk estimates were observed across the country except in the Mediterranean region, which included CA, OR, and WA. Unlike the examination of PM₁₀ risk estimates, the recently evaluated U.S.-based multicity studies did not analyze potential confounding of PM_{2.5} risk estimates by gaseous pollutants. Burnett et al. (2004,

[086247](#)) in a Canadian multicity study did analyze gaseous pollutants and found mixed results, with possible confounding by NO₂. Therefore, it is unclear if gaseous pollutants confound the PM_{2.5} mortality association.

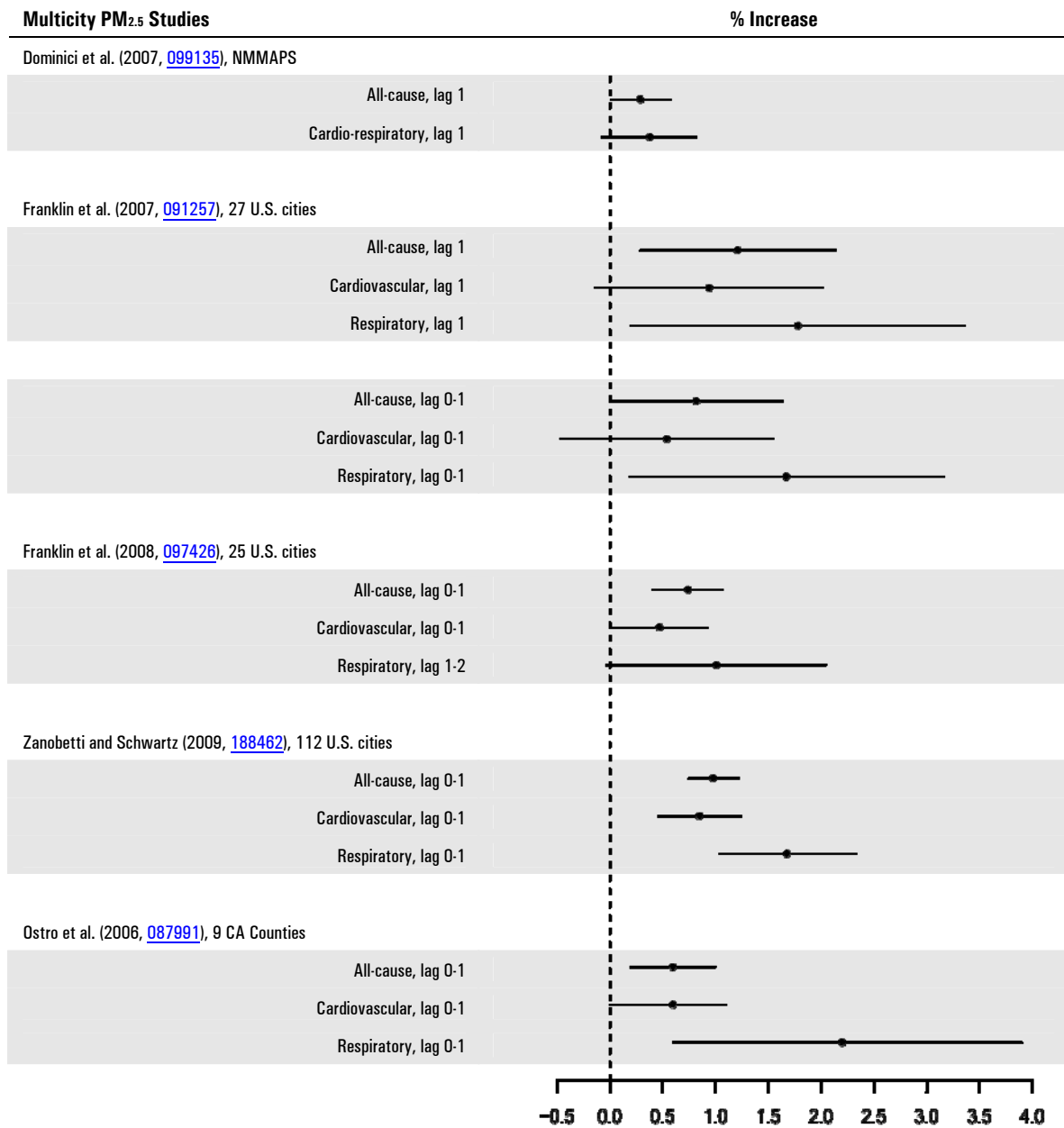


Figure 6-26. Summary of PM_{2.5} risk estimates per 10 µg/m³ for major underlying causes of death.

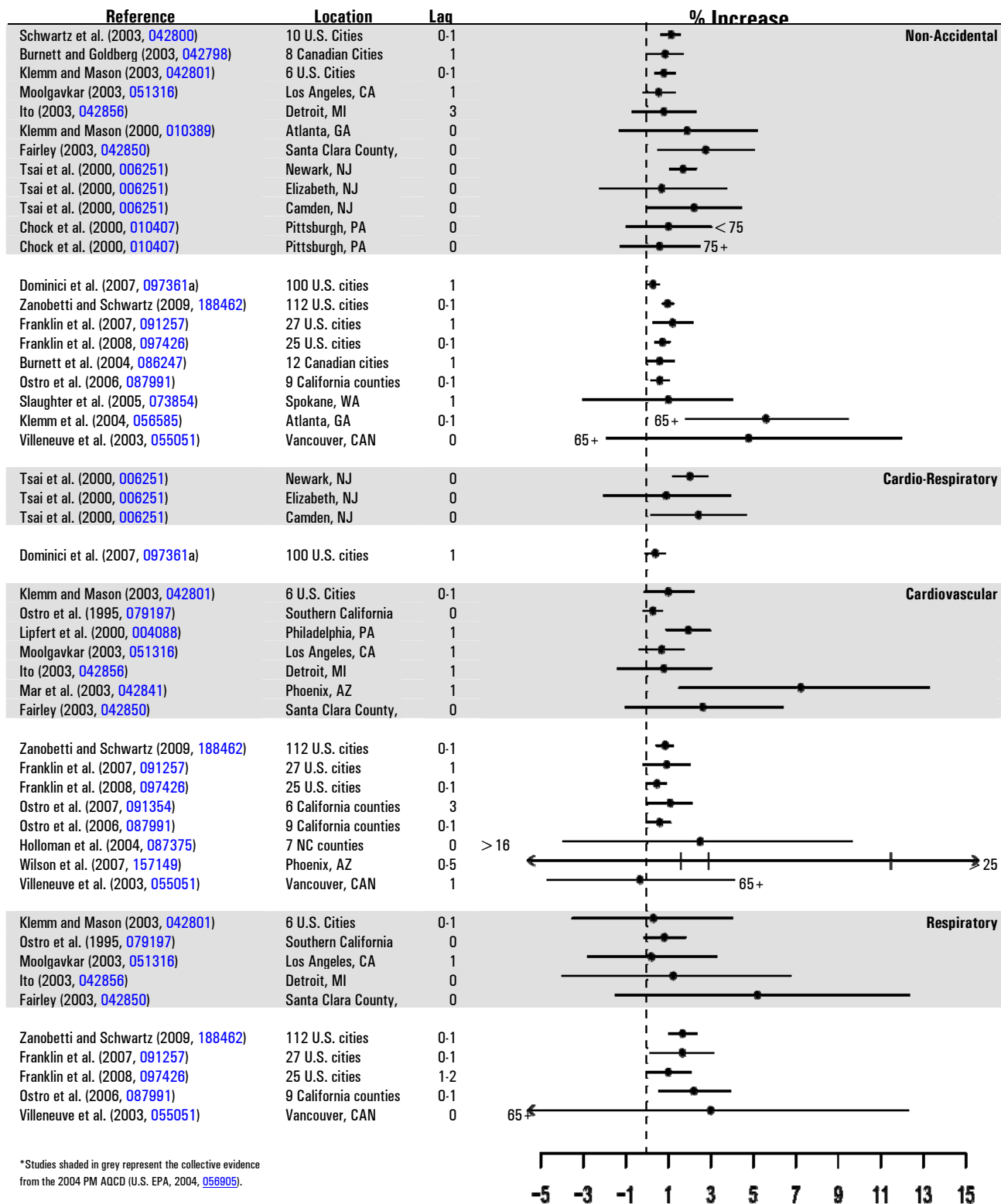


Figure 6-27. Summary of PM_{2.5} risk estimates (per 10 $\mu\text{g}/\text{m}^3$) for cause-specific mortality for all U.S.- and Canadian-based studies. The three vertical lines for the Wilson et al. (2007, [157149](#)) estimate represent the central, middle, and outer Phoenix estimates.

6.5.2.3. Thoracic Coarse Particles (PM_{10-2.5})

In the 2004 PM AQCD (U.S. EPA, 2004, [056905](#)), a limited number of studies, mostly single-city analyses, were evaluated that examined thoracic coarse (PM_{10-2.5}) PM for its association with mortality. Of these studies a small number examined both PM_{2.5} and PM_{10-2.5} effects, and found some evidence for PM_{10-2.5} effects of the same magnitude as PM_{2.5}. However, multiple limitations in these studies were identified including measurement and exposure issues for PM_{10-2.5} and the correlation between PM_{2.5} and PM_{10-2.5}. These limitations increased the uncertainty surrounding the concentrations at which PM_{10-2.5} mortality associations are observed.

A thorough analysis of PM_{10-2.5} mortality associations requires information on the speciation of PM_{10-2.5}. This is because, while a large percent of the composition of coarse particles may consist of crustal materials by mass, depending on available sources, the surface chemical characteristics of PM_{10-2.5} may also vary from city to city. Thus, without information on the chemical speciation of PM_{10-2.5}, the apparent variability in observed associations between PM_{10-2.5} and mortality across cities is difficult to characterize. Although this type of information is not available in the current literature, the relative importance of the associations observed between PM_{10-2.5} and mortality in the following studies is of interest.

PM_{10-2.5} Concentrations Estimated Using the Difference Method

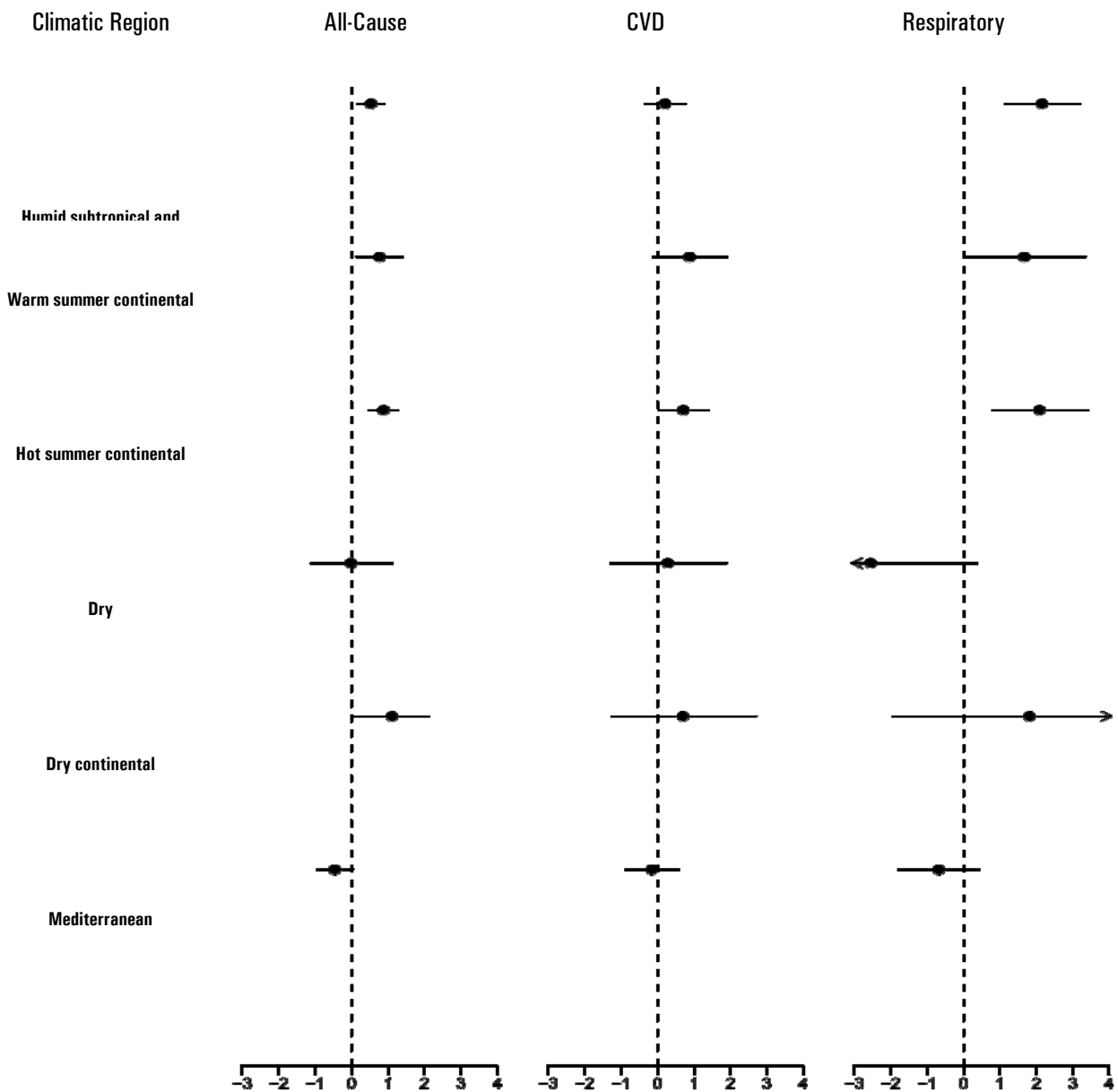
The Zanobetti and Schwartz (2009, [188462](#)) multicity analysis, described for PM_{2.5} section (Section 6.5.2.2), also examined the association between computed PM_{10-2.5} and all-causes, cardiovascular disease (CVD), MI, stroke, and respiratory mortality for the years 1999-2005. Of the 112 cities included in the PM_{2.5} analysis only 47 cities had both PM_{2.5} and PM₁₀ data available. PM_{10-2.5} was estimated in these cities by differencing the countywide averages of PM₁₀ and PM_{2.5}. In addition to examining the association between PM_{10-2.5} and mortality for the average of lags 0- and 1-day, the investigators also considered a distributed lag of 0-3 days. The risk estimates for PM_{10-2.5} were presented for both a single pollutant model and a copollutant model with PM_{2.5}, and were also combined by season and climatic regions as was done in the PM_{2.5} analysis.

The study found a significant association between the computed PM_{10-2.5} and all-cause, CVD, stroke, and respiratory mortality. The combined estimate for the 47 cities using the average of 0- and 1-day lag PM_{10-2.5} for all-cause mortality was 0.46% (95% CI:

0.21-0.71) per 10 $\mu\text{g}/\text{m}^3$ increase with the estimate obtained using the distributed lag model being smaller (0.31% [95% CI: 0.00-0.63]). The seasonal analysis showed larger risk estimates in the spring for all-cause (1.01%) and respiratory mortality (2.56%) (i.e., the same pattern observed in the $\text{PM}_{2.5}$ analysis); however, for CVD mortality, the estimates for spring (0.95%) and summer (1.00%) were comparable. When the risk estimates were combined by climatic region (Figure 6-28), for all-cause mortality, the “dry, continental” region (which included Salt Lake City, Provo, and Denver, all of which had relatively high estimated $\text{PM}_{10-2.5}$ concentrations) showed the largest risk estimate (1.11% [95% CI: 0.11-2.11]), but the “dry” region (which included Phoenix and Albuquerque, the two cities with high $\text{PM}_{10-2.5}$ concentrations) and the “Mediterranean” region (which included cities in CA, OR, and WA) did not show positive associations. The other three regions (i.e., “hot summer, continental,” “warm summer, continental,” and “humid, subtropical and maritime”), which included cities that correspond to the mid-west, southeast, and northeast geographic regions as defined in previous NMMAPS analyses, all showed significantly positive associations. Similar regional patterns of associations were found for CVD and respiratory mortality, which are further confirmed when examining the empirical Bayes-adjusted city-specific estimates in Figure 6-29. The regional pattern of associations for MI and stroke are less clear, because of the wider confidence intervals due to the smaller number of deaths in these specific categories. The lack of a $\text{PM}_{10-2.5}$ -mortality association in the “dry” region reported in this study is in contrast to the result from three studies that analyzed Phoenix data and found associations, as reviewed in the 2004 PM AQCD (U.S. EPA, 2004, [056905](#)), and Wilson et al. (2007, [157149](#)) (discussed below).

Although the results from this analysis are informative because it is the first multicity U.S.-based study that examined the association between short-term exposure to $\text{PM}_{10-2.5}$ and mortality on a large scale, some limitations do exist. Specifically, it is not clear how the computed $\text{PM}_{10-2.5}$ measurements used by Zanobetti and Schwartz (2009, [188462](#)) compare with the $\text{PM}_{10-2.5}$ concentrations obtained by directly measuring $\text{PM}_{10-2.5}$ using a dichotomous sampler, or the $\text{PM}_{10-2.5}$ concentrations computed using the difference of PM_{10} and $\text{PM}_{2.5}$ measured at co-located samplers.

Additional studies evaluated the association between short-term exposure to $\text{PM}_{10-2.5}$ and mortality using $\text{PM}_{10-2.5}$ concentrations estimated by subtracting PM_{10} from $\text{PM}_{2.5}$ concentrations at co-located monitors. Although $\text{PM}_{10-2.5}$ concentrations estimated using this approach are not ideal, the results from these studies are informative in evaluating the $\text{PM}_{10-2.5}$ mortality association.



Source: Zanobetti and Schwartz (2009, [188462](#)).

Figure 6-28. Percent increase in mortality for $10 \mu\text{g}/\text{m}^3$ increase in the average of 0- and 1-day lagged $\text{PM}_{10-2.5}$, combined by climatic regions.

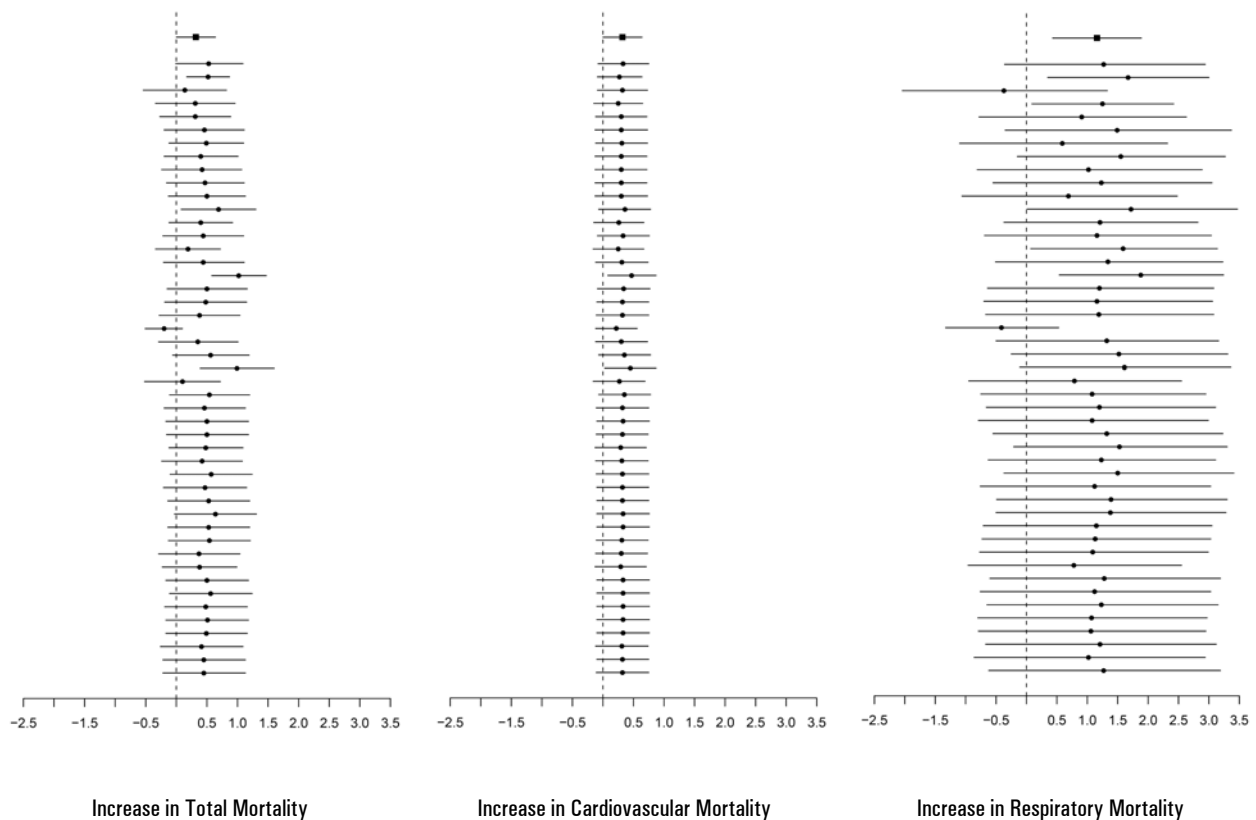


Figure 6-29. Empirical Bayes-adjusted city-specific effect estimates for total, cardiovascular, and respiratory mortality for $10 \mu\text{g}/\text{m}^3$ increase in the average of 0- and 1-day lagged $\text{PM}_{10-2.5}$ by decreasing 98th percentile of mean 24-h avg $\text{PM}_{2.5}$ concentrations. Based on estimates calculated from Zanobetti and Schwartz (2009, [188462](#)) using the approach specified in Le Tertre et al. (2005, [087560](#)).

Slaughter et al. (2005, [073854](#)) examined the association of various PM size fractions (PM_1 , $\text{PM}_{2.5}$, PM_{10} , $\text{PM}_{10-2.5}$) and CO with ED visits, HAs, and mortality in Spokane, WA for the period 1995-2001. Although the authors did not report mortality risk estimates for $\text{PM}_{10-2.5}$, they did not find an association between any PM size fraction (or CO) and mortality or cardiac HAs at lags of 0- to 3-days.

Wilson et al. (2007, [157149](#)) examined the association between size-fractionated PM ($\text{PM}_{2.5}$ and $\text{PM}_{10-2.5}$) and cardiovascular mortality in Phoenix for the study period 1995-1997, using mortality data aggregated for three geographic regions: “Central Phoenix,” “Middle Ring,” and “Outer Phoenix,” which were constructed as a composite of ZIP codes of residence in order to compare population size among the three areas. The authors reported apparently different patterns of associations between $\text{PM}_{2.5}$ and $\text{PM}_{10-2.5}$ in terms of the size

of the risk estimate across the three areas and temporal patterns of associations. In the “Middle Ring” where PM_{10-2.5} showed the strongest association, the estimated risk per 10 µg/m³ increase for a 1 day lag was 3.4% (95% CI: 1.0-5.8). The estimated risk for PM_{2.5} found for “Central Phoenix” was 6.6% (95% CI: 1.1-12.5) for lag 1. The authors speculated that the apparent difference in estimated risks across the areas might be due to the lower SES in “Central Phoenix” or the lower exposure error, but the relatively wide confidence bands of these estimates make it difficult to establish such relationships (see Section 8.1.7 for a detailed discussion on SES and susceptibility to PM exposure).

Table 6-15. Key for Figure 6-29

City	98th	Mean	City	98th	Mean	City	98th	Mean	City	98th	Mean
El Paso, TX	105.1	25.4	Cleveland, OH	51.2	15.2	Sacramento, CA	31.5	10.2	Louisville, KY	23.3	8.3
St. Louis, MO	81.9	15.2	Davenport, IA	49.9	15.3	Tampa, FL	29.1	12.9	Wilkesbarre, PA	22.2	6.2
Phoenix, AZ	80.1	33.3	Birmingham, AL	49.6	14.2	Toledo, OH	28.8	7.6	New York, NY	22.0	6.4
Detroit, MI	77.5	17.3	Provo, UT	49.3	18.2	Washington, PA	27.8	6.5	Wilmington, DE	21.8	7.0
Gary, IN	71.3	6.9	Chicago, IL	46.1	12.4	Allentown, PA	27.8	4.5	Raleigh, NC	20.9	6.9
Omaha, NE	65.6	24.7	Easton, PA	43.9	12.0	Atlanta, GA	27.4	8.6	Scranton, PA	19.2	6.1
Albuquerque, NM	64.3	22.9	Steubenville, OH	43.5	12.1	Davie, FL	25.5	9.4	Harrisburg, PA	18.6	5.4
New Haven, CT	58.4	11.9	Columbia, SC	42.9	8.4	Taylors, SC	25.4	8.0	Akron, OH	17.7	5.3
Bakersfield, CA	55.9	16.1	Los Angeles, CA	42.5	13.5	Memphis, TN	24.3	9.3	Charleston, SC	17.6	6.6
Des Moines, IA	55.0	16.2	Spokane, WA	41.8	13.8	Seattle, WA	23.7	9.0	Winston, NC	16.5	7.4
Denver, CO	53.8	18.1	Columbus, OH	40.0	11.2	Baltimore, MD	23.5	8.9	Erie, PA	14.9	3.1
Salt Lake, UT	52.6	19.2	Pittsburgh, PA	32.0	9.4	Cincinnati, OH	23.3	7.8			

Note: The top effect estimate in the figures represents the overall effect estimate for that mortality outcome across all cities. The remaining effect estimates are ordered by the highest (i.e., Rubidoux, CA) to lowest (i.e., Albuquerque, NM) 98th percentile of the mean 24-h PM_{10-2.5} concentrations across the cities examined, which is the policy relevant concentration for the daily standard (from Zanobetti and Schwartz (2009)).

Kettunen et al. (2007, [091242](#)) analyzed UFPs, PM_{2.5}, PM₁₀, PM_{10-2.5}, and gaseous pollutants for their associations with stroke mortality in Helsinki during the study period of 1998-2004. The authors did not observe an association between air pollution and mortality for the whole year or cold season, but they did find associations for PM_{2.5} (13.3% [95% CI: 2.3-25.5] per 10 µg/m³), PM₁₀, and CO during the warm season, most strongly at lag 1 day. An association was also observed for PM_{10-2.5} during the warm season (7.8% [95% CI: -7.4 to 25.5] per 10 µg/m³ at lag 1 day); however, it was weaker than PM_{2.5}.

The Perez et al. (2008, [156020](#)) analysis tested the hypothesis that outbreaks of Saharan dust exacerbate the effects of PM_{2.5} and PM_{10-2.5} on daily mortality. Changes of effects between Saharan and non-Saharan dust days were assessed using a time-stratified case-crossover design involving 24,850 deaths between March 2003 and December 2004 in

Barcelona, Spain. Saharan dust days were identified from back-trajectory and satellite images. Chemical speciation, but not an analysis for microbes or fungi, was conducted approximately once a week during the study period. On Saharan dust days, mean concentrations were 1.2 times higher for PM_{2.5} (29.9 µg/m³) and 1.1 times higher for PM_{10-2.5} (16.4 µg/m³) than on non-Saharan dust days. During Saharan dust days (90 days out of 602), the PM_{10-2.5} risk estimate was 8.4% (95% [CI: 1.5-15.8]) per 10 µg/m³ increase at lag 1 day, compared with 1.4% (95% CI: -0.8% to 3.4%) during non-Saharan dust days. In contrast, there was not an additional increased risk of daily mortality for PM_{2.5} during Saharan dust days (5.0% [95% CI: 0.5-9.7]) compared with non-Saharan dust days (3.5% [95% CI: 1.6-5.5]). However, differences in chemical composition (i.e., PM_{2.5} was primarily composed of nonmineral carbon and secondary aerosols; whereas PM_{10-2.5} was dominated by crustal elements) did not explain these observations. Note also when examining all days combined, both size fractions were associated with mortality, but the PM_{2.5} association was found to be stronger.

PM_{10-2.5} Concentrations Directly Measured

In Burnett et al. (2004, [086247](#)), which analyzed the association of multiple pollutants with mortality in 12 Canadian cities, described previously; the authors also examined PM_{10-2.5}. In this study the authors collected PM_{10-2.5} using dichotomous samplers with an every-6th-day schedule. When both NO₂ and PM_{10-2.5} were included in the regression model, the PM_{10-2.5} effect estimate was reduced from 0.65% (CI: -0.10 to 1.4) to 0.31% (95% CI: -0.49 to 1.1) per 10 µg/m³ increase in 1-day lag PM_{10-2.5}. These risk estimates are similar to those reported for PM_{2.5}, which were also reduced upon the inclusion of NO₂ in the two-pollutant model, but to a greater extent, from 0.60% (95% [CI: -0.03 to 1.2]) to -0.1% (95% [CI: -0.86 to 0.67]).

Villeneuve et al. (2003, [055051](#)) analyzed the association between PM_{2.5}, PM_{10-2.5}, TSP, PM₁₀, SO₄²⁻, and gaseous copollutants in Vancouver, Canada, using a cohort of approximately 550,000 whose vital status was ascertained between 1986 and 1999. In this study PM_{2.5} and PM_{10-2.5} were directly measured using dichotomous samplers. The authors examined the association of each air pollutant with all-cause, cardiovascular, and respiratory mortality, but only observed significant results for cardiovascular mortality at lag 0 for both PM_{10-2.5} and PM_{2.5}. They found that PM_{10-2.5} (5.4% [95% CI: 1.1-9.8] per

10 $\mu\text{g}/\text{m}^3$), was more strongly associated with cardiovascular mortality than $\text{PM}_{2.5}$ (4.8% [95% CI: -1.9 to 12.0] per 10 $\mu\text{g}/\text{m}^3$).

Klemm et al. (2004, [056585](#)) analyzed various components of PM and gaseous pollutants for their associations with mortality in Fulton and DeKalb Counties, Georgia for the two-yr period, 1998-2000. $\text{PM}_{10-2.5}$ concentrations were obtained from the ARIES database, which directly measured $\text{PM}_{10-2.5}$ using dichotomous samplers. In this analysis the authors adjusted for temporal trend using quarterly, monthly, and biweekly knots, and reported estimates for all-cause, circulatory, respiratory, cancer, and other causes mortality for each scenario. Overall, $\text{PM}_{2.5}$ was, generally, more strongly associated with mortality than $\text{PM}_{10-2.5}$. For example, using the average of 0- and 1-day lags, the risk estimates for $\text{PM}_{2.5}$ and $\text{PM}_{10-2.5}$ in the monthly knots model for all-cause mortality, ages ≥ 65 were 5.6% (95% [CI: 1.9-9.5]) and 6.4% (95% [CI: -0.5 to 14.1]) per 10 $\mu\text{g}/\text{m}^3$ increase, respectively.¹

¹ The monthly knot model was selected for comparison because, overall, $\text{PM}_{2.5}$ showed the strongest association with all-cause mortality among the 15 air pollution indices examined when using this model.

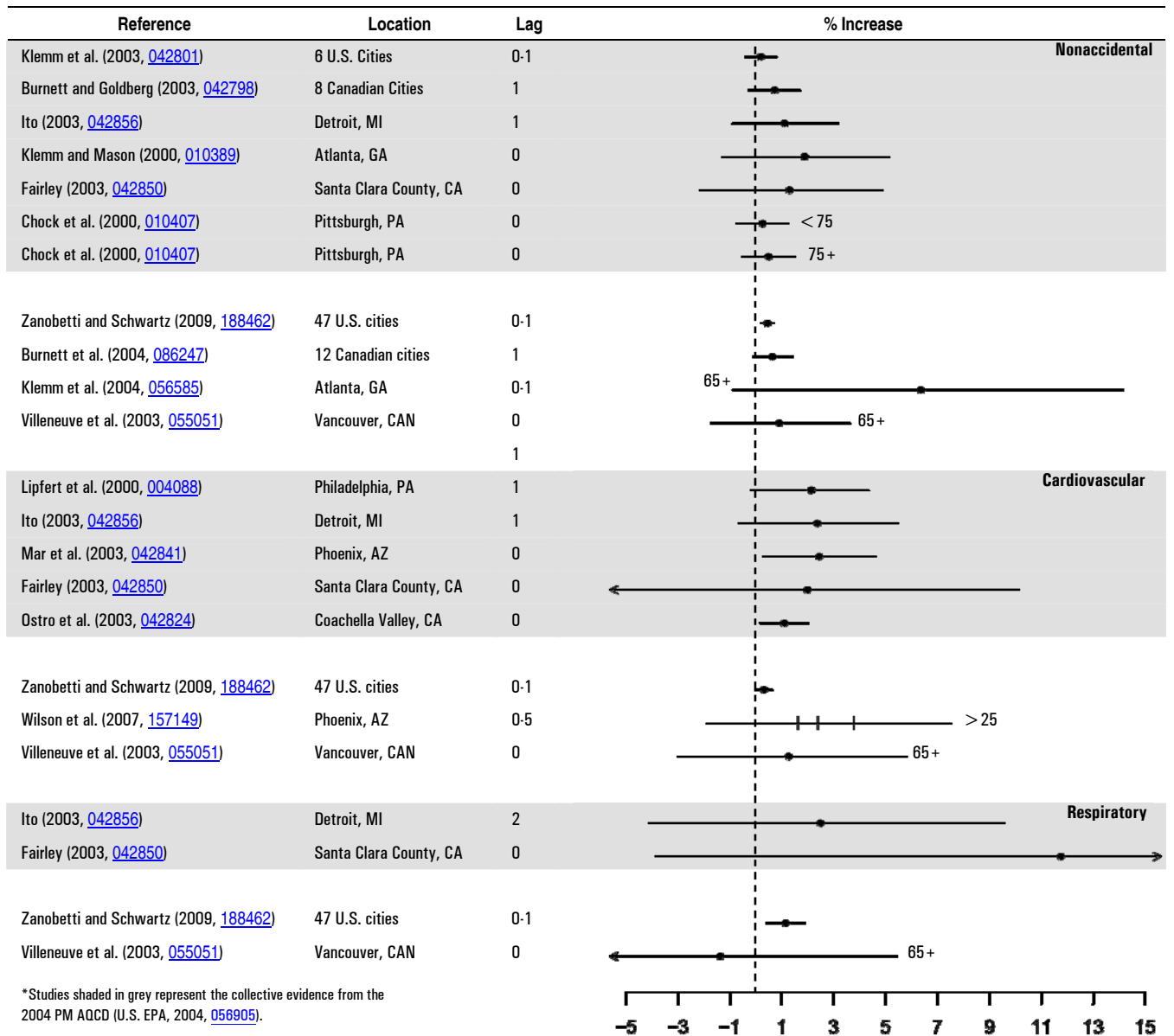


Figure 6-30. Summary of PM_{10-2.5} risk estimates (per 10 $\mu\text{g}/\text{m}^3$) for cause-specific mortality for all U.S., Canadian-, and international-based studies. The three vertical lines for the Wilson et al. (2007, [157149](#)) estimate represent the central, middle, and outer Phoenix estimates.

Summary of PM_{10-2.5} Risk Estimates

The results from newly available studies that examined the association between short-term exposure to PM_{10-2.5} primarily consisted of single-city studies. Collectively these studies found inconsistent associations, which varied depending on the study location. The evidence from those single-city studies conducted in the U.S. and Canada in combination

with the multicity studies evaluated (i.e., in the U.S. and Canada), provide evidence for $PM_{10-2.5}$ effects. Although there are limitations in the method used in the new U.S. multicity study (Zanobetti and Schwartz, 2009, [188462](#)) to estimate $PM_{10-2.5}$ (i.e., $PM_{10-2.5}$ was estimated by the difference between the county-average PM_{10} and $PM_{2.5}$), associations between $PM_{10-2.5}$ and mortality were observed throughout regions of the country. However, some of the findings of this new multicity study (e.g., no associations in “dry” region where $PM_{10-2.5}$ levels are high) are not consistent with the findings of the $PM_{10-2.5}$ studies evaluated in the 2004 PM AQCD (U.S. EPA, 2004, [056905](#)), and suggest that the coarse fraction is associated with mortality in areas of the U.S. where $PM_{10-2.5}$ levels are not high. Limitations also exist in the $PM_{10-2.5}$ associations reported due to the small number of $PM_{10-2.5}$ studies that have investigated confounding by gaseous copollutants or the influence of model specification on $PM_{10-2.5}$ risk estimates. Additionally, more data is needed to characterize the chemical and biological components that may modify the potential toxicity of $PM_{10-2.5}$. Figure 6-30 summarizes the $PM_{10-2.5}$ risk estimates for all U.S.-, Canadian-, and international-based studies by cause-specific mortality.

6.5.2.4. Ultrafine PM

The 2004 PM AQCD (U.S. EPA, 2004, [056905](#)) reviewed Wichmann et al.’s (2000, [013912](#); reanalyzed by Stolzel et al., 2003, [042842](#)) study of fine and ultrafine particles (UFP) (diameter: 0.01-0.1 μm) in Erfurt, Germany for the study period 1995-1998. Stölzel et al. (2007, [091374](#)) extended the study period to include the years 1995-2001 and updated the analysis. Number concentrations (NC) for four size ranges of UFP (0.01-0.1, 0.01-0.03, 0.03-0.05, and 0.05-0.1 μm) as well as mass concentration (MC) for three size ranges (0.01-2.5, 0.1-0.5, and 10 μm) were analyzed. The authors found associations with UFP NC and all-cause as well as cardio-respiratory mortality, each for a 4 day lag. The risk estimates associated with a 9,748/cm³ increase in UFP NC was 2.9% (95% CI: 0.3-5.5) for all-cause mortality and 3.1% (95% CI: 0.3-6.0) for cardio-respiratory mortality. The UFP-mortality association, and the lag structure of association, is consistent with the results from their earlier analysis, but the $PM_{2.5}$ association found in the previous study was not observed in the updated analysis. Both UFP and $PM_{2.5}$ concentrations were higher during the cold season in this locale.

Breitner et al. (2009) analyzed UFP data from Erfurt, Germany over a 10.5-yr period (October 1991 through March 2002) after the German unification, when air quality

improved. In this analysis associations between all-cause mortality and UFP and PM_{2.5} were analyzed from September 1995 to March 2002, while PM₁₀, NO₂ and CO was analyzed for the whole study duration. The exposure time window / averages used in this study were different from those used by Stölzel (2003, [042842](#)) and Stölzel et al. (2007, [091374](#)). Breitner et al. investigated the cumulative effect of air pollution on mortality at lags 0-5 and, 0-14 using (a) a semiparametric Poisson regression model and (b) a third degree polynomial distributed lag (PDL) model. The authors estimated the mortality risk for the entire study period as well as specific time periods to examine the effect of declining air pollution levels on the air pollution-mortality association. Of the air pollutants examined, UFP were found to be most consistently associated with mortality. NO₂ and CO were also found to be significantly associated with mortality using the 15-day PDL and 15-day avg models, respectively. PM_{2.5} and PM₁₀ also showed positive, but much weaker associations with mortality. In this data set, UFP were only moderately correlated with PM_{2.5} ($r = 0.48$) and PM₁₀ ($r = 0.57$). Of the pollutants examined, NO₂ showed the strongest (but overall a moderate) correlation with UFP ($r = 0.62$). When the risk estimates were compared between the two latter time periods of the study (September 1995 to February 1998; and March 1998 to March 2002), the estimates obtained using the 6-day avg for these pollutants generally declined. For example, the all-cause mortality risk estimates associated with a 8,439/cm³ increase in UFP NC was 5.5% (95% CI: 1.1-10.5) for the earlier period and -1.1% (95% CI: -6.8 to 4.9) for the later period. However, such patterns were less clear when using 15-day avg pollutants concentrations. In summary, UFP appear to be the pollutant most consistently associated with mortality in Erfurt, Germany, but combined with the results for NO₂ and CO, these associations may implicate the role of local combustion sources on the mortality association observed.

Kettunen et al.'s (2007, [091242](#)) study in Helsinki also examined the relationship between UFP and stroke mortality. As described earlier, PM_{2.5}, PM₁₀, and CO was associated with stroke mortality only during the warm season. The association with UFP was borderline non-significant (8.5% [95% CI: -1.2 to 19.1] per 4,979/cm³ increase in UFP at lag 1 day), but its lag structure of association and the magnitude of the effect estimate per interquartile-range are similar to those for PM_{2.5}. Note that the UFP NC levels in Helsinki (median equals 8,986/cm³ during the cold season and 7,587/cm³ during the warm season) are lower than those in Erfurt (mean = 13,549/cm³), but clearly higher in the cold season.

Summary of Ultra-Fine Particle (UFP) Risk Estimates

Only a few new studies, all of them from Europe, examined and reported associations between UFP and mortality. In Erfurt, UFP showed the strongest associations with mortality among all of the PM indices, but its lag structure of association is either unique (strongest association at lag 4 days in Stölzel et al., 2007, [091374](#)), and not consistent with the lag structure of associations found in other mortality studies, or the time-windows examined are longer (0-5 and 0-14 days in Breitner et al., 2009), making it difficult to compare whether the associations observed are consistent with those reported in other studies. In Helsinki, the association between UFP and stroke mortality was weaker than that for PM_{2.5}, but its lag structure of association was similar to that for PM_{2.5} (strongest at lag 1 day). However, Kettunen et al. (2007, [091242](#)) only examined lags 0 through 3 days. Overall, the results of these studies should be viewed with caution because UFP were consistently found to be correlated with gaseous pollutants derived from local combustion sources, and one or more of the gaseous pollutants were also found to be associated with mortality. Clearly, more research is needed to further investigate the role of UFP on PM-mortality associations.

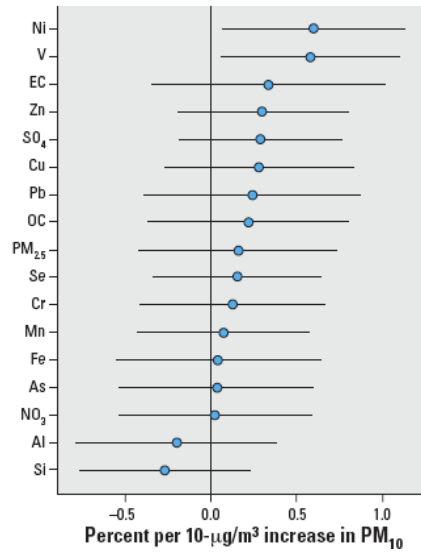
6.5.2.5. Chemical Components of PM

A few recent studies have examined the association between mortality and components of PM_{2.5}. This endeavor has been undertaken by some investigators through the use of the newly available PM_{2.5} chemical speciation network data. The PM_{2.5} chemical speciation network consists of more than 250 monitors that have been collecting over 40 chemical species since 2000; however, most sites started collecting data in 2001. One caveat to the new network is that because the sampling frequencies of the monitors are either every third day or every sixth day, there have not been, generally, a sufficient number of days to examine associations with mortality in single cities. To circumvent this issue, some investigators (Bell et al., 2009, [191997](#); Dominici et al., 2007, [099135](#); Franklin et al., 2008, [097426](#); Lippmann et al., 2006, [091165](#)) have used the PM_{2.5} chemical species data in a second stage regression to explain the heterogeneity in PM₁₀ or PM_{2.5} mortality risk estimates across cities. However, it should be noted these studies assume that the relative contributions of PM_{2.5} have remained the same over time. There have also been some studies that directly analyzed speciated PM_{2.5} data (e.g., Klemm et al., 2004, [056585](#); Ostro et al., 2007, [091354](#)).

Explaining the Heterogeneity of PM₁₀ Risk Estimates Using PM_{2.5} Chemical Speciation Data

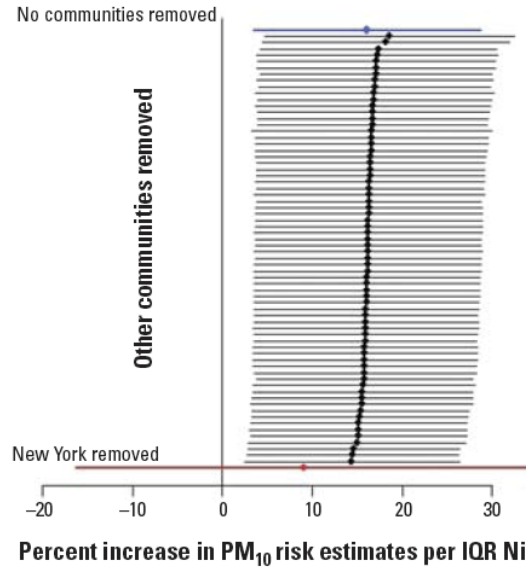
Lippmann et al. (2006, [091165](#)), in addition to their primary analysis¹, investigated the consistency of the associations between specific elements and health outcomes by examining the heterogeneity of published 1-day lagged NMMAPS PM₁₀ mortality risk estimates for 1987-1994 across cities as a function of the average PM_{2.5} chemical components across cities. They matched PM_{2.5} chemical species in 60 out of 90 cities. Lippmann et al. (2006, [091165](#)) noted that the concentrations of the 16 chemical species examined averaged over the years 2000-2003 were highly skewed across cities. They therefore regressed PM₁₀ risk estimates on each of the PM_{2.5} components, raw and log-transformed, with weights based on the standard error of the PM₁₀ risk estimates. The log-transformed values yielded better predictive power, and the authors subsequently presented the results with log-transformed values. As shown in Figure 6-31, the 16 PM_{2.5} species showed varying extent of predictive power in explaining the PM₁₀ risk estimates across 60 cities, with Ni and V being the best predictors.

¹ The main focus of the study was to examine the role of PM_{2.5} chemical components in a mouse model of atherosclerosis (ApoE^{-/-}) exposed to concentrated fine PM (CAPs) in Tuxedo, NY.



Source: Lippmann et al. (2006, [091165](#))

Figure 6-31. Percent increase in PM₁₀ risk estimates (point estimates and 95% confidence intervals) associated with a 5th-to-95th percentile: increase in PM_{2.5} and PM_{2.5} chemical components. The PM_{2.5} chemical components were log-transformed in the regression. The PM₁₀ risk estimates were for 60 NMMAP cities for 1987-1994.



Source: Dominici et al. (2007, [099135](#))

Figure 6-32. Sensitivity of the percent increase in PM₁₀ risk estimates (point estimates and 95% confidence intervals) associated with an interquartile increase in Ni. The Ni concentration was not log-transformed in this regression model. The PM₁₀ risk estimates were for 72 NMMAP cities for 1987-2000. The top estimate is achieved by including data for all the 69 communities. The other estimates are calculated by excluding one of the 69 communities at a time.

Dominici et al. (2007, [099135](#)) analyzed Ni and V on the updated NMMAPS PM₁₀ mortality risk estimates for 1987-2000, using 72 counties in which Ni and V data were collected. A Bayesian hierarchical model was used to estimate the role of Ni and V on the heterogeneity of PM₁₀ risk estimates. While they found both Ni and V to be significant predictors of variation in PM₁₀ mortality risk estimates across cities, they also noted that this result was sensitive to the inclusion of the New York City data. Lippmann et al. (2006, [091165](#)) and Dominici et al. (2007, [099135](#)) both reported that the Ni levels in New York City are particularly high (~10 times the national average). Figure 6-32 shows the result of the sensitivity analysis for Ni. Note that the Ni in this result was not log-transformed, as clearly reflected in the change in the width of confidence bands when the New York data were removed (i.e., a skewed distribution produces narrow bands). Dominici et al. (2007, [099135](#)) further noted that they reached “the same conclusion” when log-transformed data were used in the analysis, but the results were not presented.

Bell et al. (2009, [191997](#)) presented a supplemental analysis similar to both Lippmann et al. (2006, [091165](#)) and Dominici et al. (2007, [099135](#)) in their examination of whether the variation in PM_{2.5} risks for cardiovascular and respiratory hospital admissions

is due to differences in PM_{2.5} chemical composition. The authors used the 100 U.S. cities included in the Peng et al. (2005, [087463](#)) analysis and PM₁₀ data for the years 1987-2000 along with PM_{2.5} chemical component data for 2000-2005. Using a Bayesian hierarchical model, Bell et al. (2009, [191997](#)) found that PM₁₀ relative risks for total mortality were greater in counties and during seasons with higher PM_{2.5} Ni concentrations. However, in a sensitivity analysis when selectively removing cities from the overall estimate, the significant association between the PM₁₀ mortality risk estimate and the PM_{2.5} Ni fraction was diminished upon removing New York city from the analysis, which is consistent with the results presented by Dominici et al. (2007, [099135](#)).

Explaining the Heterogeneity of PM_{2.5} Risk Estimates Using PM_{2.5} Chemical Speciation Data

The first stage of the Franklin et al. (2008, [097426](#)) 25 cities study, described previously, focused on a time-series regression of mortality on PM_{2.5} by season. In the second stage random effects meta regression, the PM_{2.5} mortality risk estimates (25 cities x 4 seasons = 100 estimates) were regressed on the ratio of mean seasonal PM_{2.5} species to the total PM_{2.5} mass. The authors included those species that had at least 25% of the reported concentrations above the minimum detection limit, which resulted in 18 species being included in the analysis. Their rationale for using species proportions as effect modifiers, according to the investigators, was that “in the first stage of the analysis the mortality risk was estimated per unit of the total PM_{2.5} mass, which encompassed all measured species, and therefore it would not be meaningful to use the species concentrations directly as the effect modifier” (Franklin et al., 2008, [097426](#)). In the second stage regression model, Franklin et al. (2008, [097426](#)) also included a quadratic function of seasonally averaged temperature to capture the inverted U-shape relationship between PM_{2.5} penetration and temperature. They found that the fitted relationship between PM_{2.5} risk estimates across cities and seasonally averaged temperature substantiates the use of temperature as a surrogate for ventilation (Franklin et al., 2008, [097426](#)). Table 6-16 shows the resulting effect modification by PM_{2.5} species. Al, As, Ni, Si, and SO₄²⁻ were found to be significant effect modifiers of PM_{2.5} risk estimates, and simultaneously including Al, Ni, and SO₄²⁻ together, or Al, Ni, and As together further increased explanatory power. Of all the species examined, Al and Ni explained the most residual heterogeneity. Franklin et al. (2008, [097426](#)) also examined the effect of demographic variables on PM_{2.5} risk estimates and found that only median household income was significantly associated with mortality.

Table 6-16. Effect modification of composition on the estimated percent increase in mortality with a 10 µg/m³ increase in PM_{2.5}.

Cause	Species	p-value for effect modification by species to PM _{2.5} mass proportion	% increase in non-accidental mortality per 10 µg/m ³ increase in PM _{2.5} for an interquartile increase in species to PM _{2.5} mass proportion*	Heterogeneity explained (%)†
Non-accidental Univariate	Al	<0.001	0.58	45
	As			
	Br	0.02	0.55	35
	Cr			
	EC	0.11	0.38	5
	Fe			
	K	0.12	0.33	16
	Mn			
	Na ⁺	0.79	0.06	0
	Ni			
	NO ₃	0.43	0.12	3
	NH ₄			
	OC	0.10	0.41	28
	Pb			
	Si	0.42	0.14	10
	SO ₄ ²⁻	0.22	0.20	14
	V			
	Zn	0.01	0.37	41
		0.07	-0.49	28
		0.84	0.04	3
		0.59	-0.02	4
		0.31	0.17	11
		0.03	0.41	25
		0.01	0.51	33
		0.28	0.30	3
		0.19	0.23	15
Non-accidental Multivariate (1)	Al	<0.001	0.79	
	Ni			
	SO ₄ ²⁻	0.01	0.34	100
		<0.001	0.75	
Non-accidental Multivariate (2)	Al	<0.001	0.61	
	Ni			
	As	0.01	0.35	100
		<0.001	0.58	

Adjusted for temperature

†Includes heterogeneity explained by temperature

Source: Franklin et al. (2008, [097426](#))

Although Lippmann et al. (2006, [091165](#)) used NMMAPS PM₁₀ risk estimates and Franklin et al. (2008, [097426](#)) used PM_{2.5} risk estimates to examine effect modification due to various PM species, 14 out of the 18 species analyzed in these two studies overlap (see Figure 6-31 and Table 6-16). Both studies found that Ni explained the heterogeneity in PM risk estimates. Note that New York City was not included in the 25 cities examined in Franklin et al. (2008, [097426](#)) and, thus, could not influence the result. Sulfate positively, but not significantly, explained the PM₁₀ risk estimates in the Lippmann et al. (2006, [091165](#)) analysis. However, SO₄²⁻ was a significant predictor of PM_{2.5} risk estimates in the

Franklin et al. (2008, [097426](#)) analysis. Al and Si were negative (i.e., less than the average PM₁₀ risk estimates across cities), though not significant, predictors in the Lippmann et al. (2006, [091165](#)) analysis. Unlike the Franklin et al. (2008, [097426](#)) analysis, arsenic (As) showed no association with mortality in the Lippmann et al. (2006, [091165](#)) analysis. The source of these differences may be due to the difference in geographic coverage, PM size (PM_{2.5} may represent more secondary aerosols than PM₁₀), or the difference in the analytical methods used in each study. Specifically, the analytical approach used by Franklin et al. (2008, [097426](#)) does have an advantage of delineating seasonal variations in PM components and the associated potential seasonal mortality effects.

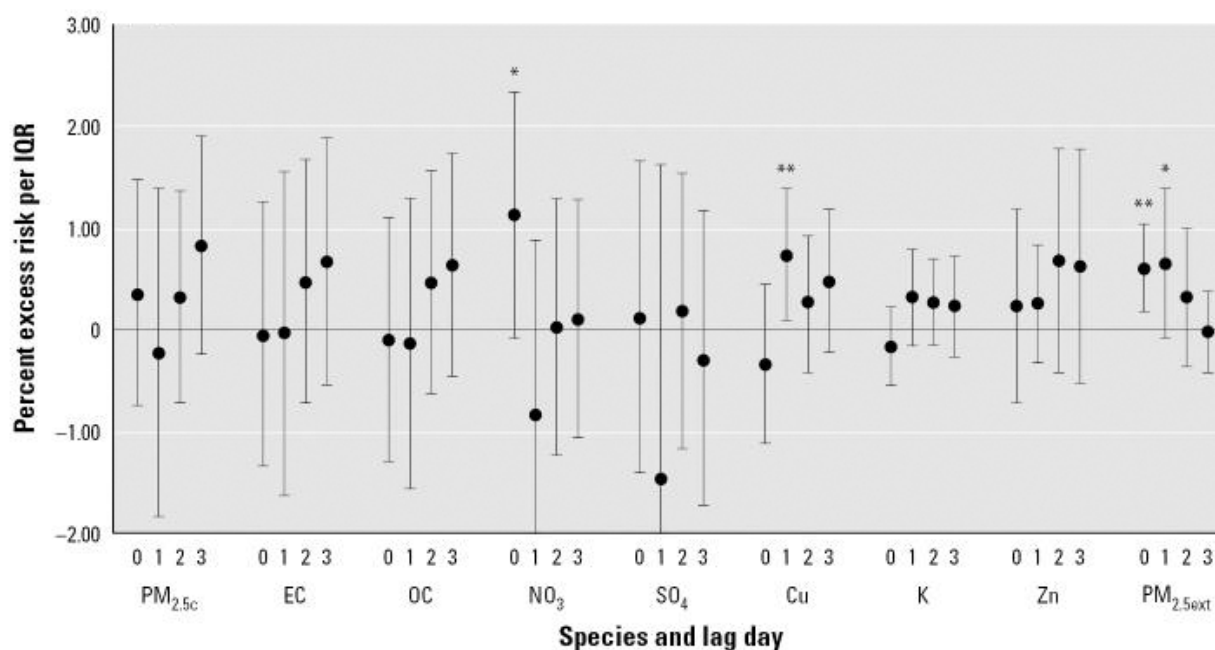
In light of the results presented in speciation studies it must be noted that second stage analyses that use PM chemical species as effect modifiers have some limitations. Unlike analyses that directly examine the associations between chemical species and mortality, if an effect modification is observed it may be confounded if the variations of the mean levels of the chemical species examined are correlated with other demographic factors that vary across cities. Thus, more concrete conclusions could be formulated if direct associations are found between mortality and PM chemical components in time-series analyses.

Association between PM_{2.5} Chemical Components and Mortality

Ostro et al. (2007, [091354](#)) examined associations between PM_{2.5} chemical components and mortality in six California counties (Fresno, Kern, Riverside, Sacramento, San Diego, and Santa Clara), which had at least 180 days of speciation data for the years 2000 to 2003. The study examined all-cause, cardiovascular, and respiratory mortality for individual lags of 19 specific PM_{2.5} chemical components. The second stage random-effects model combined risk estimates at each lag across cities. The number of available days for chemical species data ranged from 243 (San Diego County) to 395 (Sacramento County). The authors found an association between mortality, especially cardiovascular mortality, and several chemical components. For example, cardiovascular mortality was associated with EC, OC, nitrate, Fe, K, and Ti at various lags.

Even though this was a multicity study, the relatively small number of available days and the every-third-day (or every-sixth-day) sampling frequency for PM_{2.5} chemical species made it difficult to interpret the results of the lag structure of associations observed for the chemical species. To evaluate the impact of non-daily sampling frequency, Ostro et al. (2007,

[091354](#)) examined both the PM_{2.5} series that coincides with the speciation sampling days (for the initial six counties [i.e., PM_{2.5c}]) and PM_{2.5} data that was available on all days for an extended set of counties (the initial six counties plus Contra Costa, Los Angeles, and Orange Counties [i.e., PM_{2.5ext}]). Figure 6-33 shows the association between all-cause mortality and selected PM_{2.5} chemical species as well as for PM_{2.5c} and PM_{2.5ext}. Note the wide confidence bands for the risk estimates for each PM_{2.5} chemical species and PM_{2.5c}, apparently reflecting the low statistical power of the data. The lag structure of associations is more clearly defined for PM_{2.5ext}, and appears to be different from that for PM_{2.5}.



Source: Ostro et al. (2007, [091354](#))

Figure 6-33. Excess risk (CI) of total mortality per IQR of concentrations. Note: PM_{2.5} has the same sampling days as chemical species. PM_{2.5} has all available PM_{2.5ext} data for nine counties. * p < 0.10; ** p < 0.05

Ostro et al. (2008, [097971](#)) used the speciation data from the six counties analyzed in their 2007 analysis, described above, in an additional analysis to examine effect modification of cardiovascular mortality effects, which showed the strongest association in the 2007 analysis, attributed to PM_{2.5} and 13 chemical components by socio-economic and demographic factors. The results of the analysis were combined using random effects meta-analysis. The investigators tested statistical differences in risk estimates between

strata using a t-test, and reported that, for many of the PM_{2.5} chemical species; there were significantly higher effect estimates among those with lower educational attainment and Hispanics. While these patterns were apparent in their results table, interpretation of the results is not straightforward because the table only presented the most significant (and positive) lags, and they were often different between the strata (e.g., the most frequent significant lag for the Hispanic group was 1 day, while it was 2 or 3 days for the White group). As the investigators pointed out, the every-third-day sampling frequency of the speciation data also complicates the interpretation of the results for different lags.

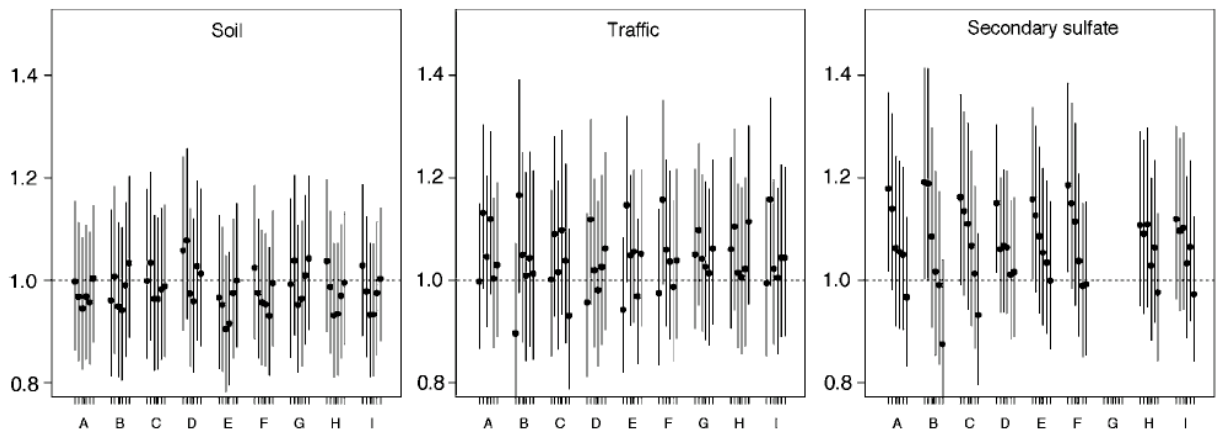
Overall, the two studies by Ostro et al. (2007, [091354](#)) were the first attempt to directly analyze associations between the newly available chemical speciation data and mortality. While suggestive associations between several chemical species and mortality were reported, a longer length of observations is needed to more clearly determine the associations.

6.5.2.6. Source-Apportioned PM Analyses

Chemically speciated PM data allow for the source apportionment of PM. The idea of using source-apportioned PM for health effects analyses is appealing because, if such source-apportionment could be reliably conducted, it will allow for an evaluation of PM_{2.5} mass concentrations by source types. However, the uncertainties associated with source-apportionment methods have not been well characterized.

To address this issue, in 2003, several groups of EPA-funded researchers organized a workshop and independently conducted source apportionment on two sets of data: Phoenix, AZ, and Washington, DC, compared the results (Hopke et al., 2006, [088390](#)), and then conducted time-series mortality regression analyses using each group's source-apportioned data (Thurston et al., 2005, [097949](#)) Ito, 2006 #5669 (Mar et al., 2006, [086143](#)). The various research groups generally identified the same major source types, each with similar elemental compositions. Inter-group correlation analyses indicated that soil-, SO₄²⁻-, residual oil-, and salt-associated mass concentrations were most unambiguously identified by various methods, whereas vegetative burning and traffic were less consistent. Aggregate source-specific mortality relative risk (RR) estimate confidence intervals overlapped each other, but the SO₄²⁻-related PM_{2.5} component was most consistently significant across analyses in these cities.

The results from the source-apportionment workshop quantitatively characterized the uncertainties associated with the factor analysis-based methods, but they also raised new issues. The mortality analyses conducted in Phoenix, AZ, and Washington, DC, both found that different source-types showed varying lag structure of associations with mortality. For example, Figure 6-34 shows cardiovascular mortality risk estimates for three of the PM_{2.5} sources from the Phoenix, AZ, analysis (Mar et al., 2006, [086143](#)). The strongest associations for “traffic” PM_{2.5} was found for lag 1-day, while for “secondary SO₄²⁻” PM_{2.5}, it was lag 0, with a monotonic decline towards longer lags. These results are consistent with those in the 2004 PM AQCD (U.S. EPA, 2004, [056905](#)), in which associations were reported with combustion-related PM_{2.5}, but not crustal source PM_{2.5}. It is conceivable that PM from different source types produces different lagged effects, but it is also likely that different PM species have varying lagged correlations with the covariates in the health effects regression models (e.g., temperature, day-of-week) resulting in apparent differences in lagged associations with mortality. Thus, interpretation of these source-apportioned PM health effect estimates remains challenging.



Source: Mar et al. (2006, [086143](#))

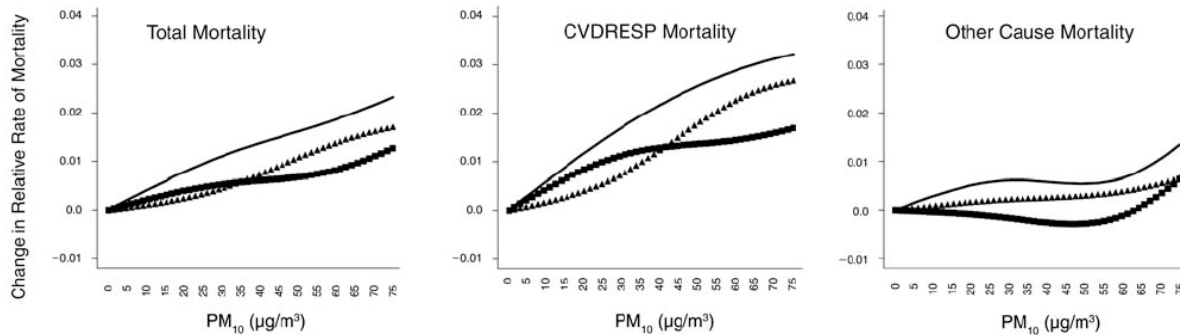
Figure 6-34. Relative risk and CI of cardiovascular mortality associated with estimated PM_{2.5} source contributions. Y-axis: relative risk per 5th-to-95th percentile increment of estimated PM_{2.5} source contribution. X-axis: the β bet denotes investigator/ method; lagged PM_{2.5} source contribution for lag 0 through 5 days, left to right, are shown for each investigator/method.

6.5.2.7. Investigation of Concentration-Response Relationship

The results from large multicity studies reviewed in the 2004 PM AQCD (U.S. EPA, 2004, [056905](#)) suggested that strong evidence did not exist for a clear threshold for PM mortality effects. However, as discussed in the 2004 PM AQCD (U.S. EPA, 2004, [056905](#)), there are several challenges in determining and interpreting the shape of PM-mortality concentration-response functions and the presence of a threshold, including: (1) limited range of available concentration levels (i.e., sparse data at the low and high end); (2) heterogeneity of susceptibility in at-risk populations; and (3) the influence of measurement error. Regardless of these limitations, studies have continued to investigate the PM-mortality concentration-response relationship.

Daniels et al. (2004, [087343](#)) evaluated three concentration-response models: (1) log-linear models (i.e., the most commonly used approach, from which the majority of risk estimates are derived); (2) spline models that allow data to fit possibly non-linear relationship; and (3) threshold models, using PM₁₀ data in 20 cities from the 1987-1994 NMMAPS data. They reported that the spline model, combined across the cities, showed a linear relation without indicating a threshold for the relative risks of death for all-causes and for cardiovascular-respiratory causes in relation to PM₁₀, but “the other cause” deaths (i.e., all cause minus cardiovascular-respiratory) showed an apparent threshold at around 50 µg/m³ PM₁₀, as shown in Figure 6-35. For all-cause and cardio-respiratory deaths, based on the Akaike’s Information Criterion (AIC), a log-linear model without threshold was preferred to the threshold model and to the spline model.

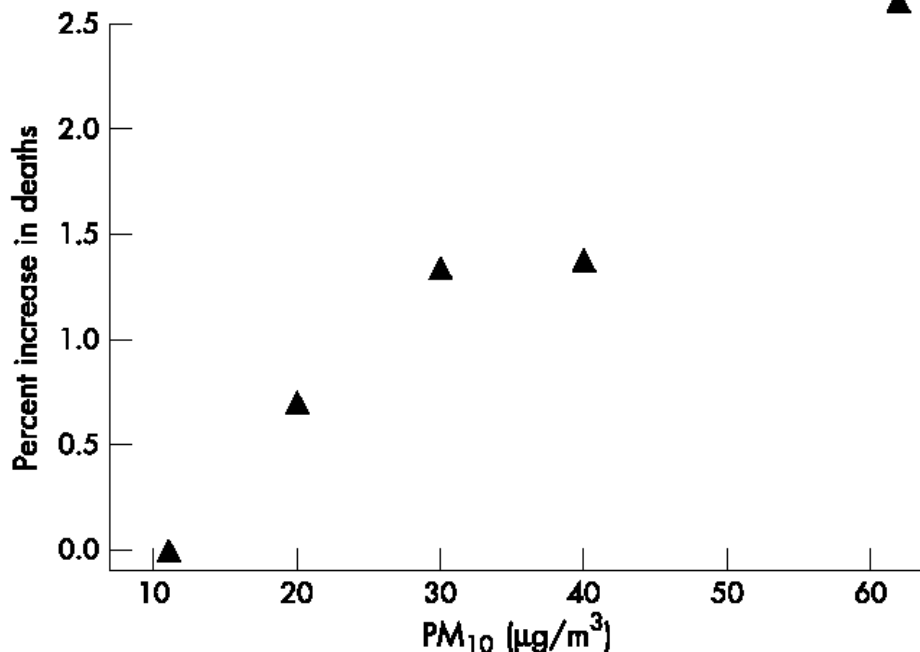
The HEI review committee commented that interpretation of these results required caution, because (1) the measurement error could obscure any threshold; (2) the city-specific concentration-response curves exhibited a variety of shapes; and (3) the use of AIC to choose among the models might not be appropriate due to the fact it was not designed to assess scientific theories of etiology. Note, however, that there has been no etiologically credible reason suggested thus far to choose one model over others for aggregate outcomes. Thus, at least statistically, the result of Daniels et al. (2004, [087343](#)) suggests that the log-linear model is appropriate in describing the relationship between PM₁₀ and mortality.



Source: Daniels et al. (2004, [087343](#))

Figure 6-35. Concentration-response curves (spline model) for all-cause, cardiovascularrespiratory and other cause mortality from the 20 NMMAPS cities. Estimates are posterior means under Bayesian random effects model. Solid line is mean lag, triangles are lag 0 (current day), and squares are lag 1 (previous day).

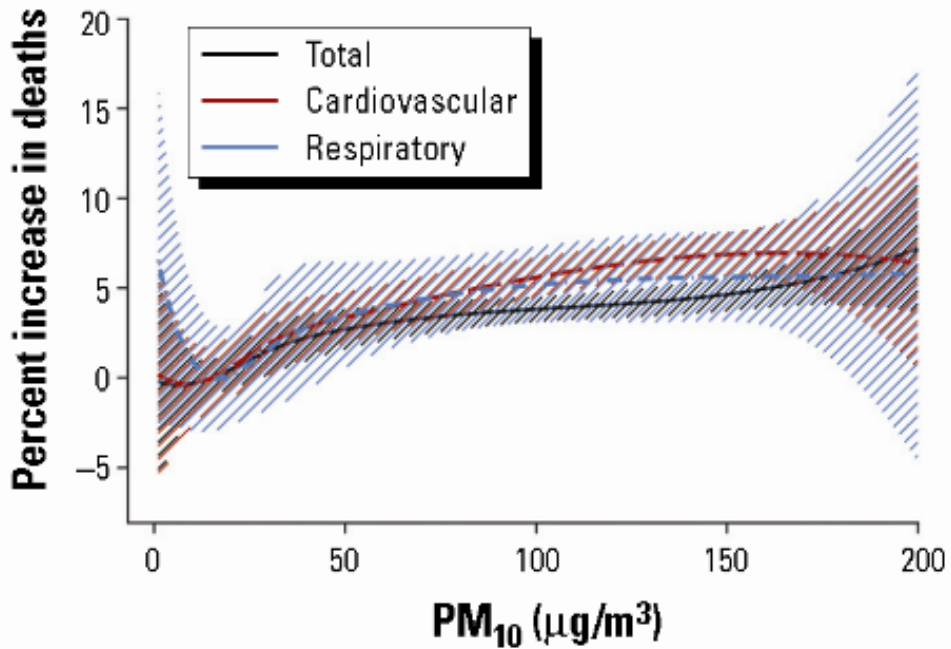
The Schwartz (2004, [078998](#)) analysis of PM₁₀ and mortality in 14 U.S. cities, described in Section 6.5.2.1., also examined the shape of the concentration-response relationship by including indicator variables for days when concentrations were between 15 and 25 µg/m³, between 25 and 34 µg/m³, between 35 and 44 µg/m³, and 45 µg/m³ and above. In the model, days with concentrations below 15 µg/m³ served as the reference level. This model was fit using the single stage method, combining strata across all cities in the case-crossover design. Figure 6-36 shows the resulting relationship, which does not provide sufficient evidence to suggest that a threshold exists. The authors did not examine city-to-city variation in the concentration-response relationship in this study.



Source: Schwartz (2004, [078998](#))

Figure 6-36. Percent increase in the risk death on days with PM₁₀ concentrations in the ranges of 15-24, 25-34, 35-44, and 45 µg/m³ and greater, compared to a reference of days when concentrations were below 15 µg/m³. Risk is plotted against the mean PM₁₀ concentration within each category.

Samoli et al. (2005, [087436](#)) investigated the concentration-response relationship between PM₁₀ and mortality in 22 European cities (and BS in 15 of the cities) participating in the APHEA project. In nine of the 22 cities, PM₁₀ levels were estimated using a regression model relating co-located PM₁₀ to BS or TSP. They used regression spline models with two knots (30 and 50 µg/m³) and then combined the individual city estimates of the splines across cities. The investigators concluded that the association between PM and mortality in these cities could be adequately estimated using the log-linear model. However, in an ancillary analysis of the concentration-response curves for the largest cities in each of the three distinct geographic areas (western, southern, and eastern European cities): London, England; Athens, Greece; and Cracow, Poland, Samoli et al. (2005, [087436](#)) observed a difference in the shape of the concentration-response curve across cities. Thus, while the combined curves (Figure 6-37) appear to support no-threshold relationships between PM₁₀ and mortality, the heterogeneity of the shapes across cities makes it difficult to interpret the biological relevance of the shape of the combined curves.



Source: Samoli et al. (2005, [087436](#))

Figure 6-37. Combined concentration-response curves (spline model) for all-cause, cardiovascular, and respiratory mortality from the 22 APHEA cities.

The results from the three multicity studies discussed above support no-threshold log-linear models, but issues such as possible influence of exposure error and heterogeneity of shapes across cities remains to be resolved. Also, given the pattern of seasonal and regional differences in PM risk estimates depicted in recent multicity study results (e.g. Peng et al., 2005, [087463](#)), the very concept of a concentration-response relationship estimated across cities and for all-year data may not be very informative.

6.5.3. Summary and Causal Determinations

6.5.3.1. PM_{2.5}

The 2004 PM AQCD (U.S. EPA, 2004, [056905](#)) found that the strength of evidence from U.S.- and Canadian-based studies (both multi- and single-city) for PM_{2.5} mortality associations varied across outcomes, with relatively stronger evidence for associations with cardiovascular compared to respiratory causes. The resulting effect estimates reported for these two endpoints ranged from 1.2 to 2.7% for cardiovascular-related mortality and 0.8 to

2.7% for respiratory-related mortality, per 10 $\mu\text{g}/\text{m}^3$ increase in $\text{PM}_{2.5}$ (U.S. EPA, 2004, [056905](#)).

In the current review, $\text{PM}_{2.5}$ risk estimates were found to be consistently positive, and slightly larger than those reported for PM_{10} for all-cause, and respiratory- and cardiovascular-related mortality. The risk estimates for all-cause (non-accidental) mortality ranged from 0.29% (Dominici et al., 2007, [099135](#)) to 1.21% (Franklin et al., 2007, [091257](#)) per 10 $\mu\text{g}/\text{m}^3$ increase in $\text{PM}_{2.5}$. These associations were consistently observed at lag 1 and lag 0-1, which have been confirmed through extensive analyses in PM_{10} -mortality studies. Cardiovascular-related mortality risk estimates were found to be similar to those for all-cause mortality; whereas, the risk estimates for respiratory-related mortality were consistently larger: 1.01% (Franklin et al., 2007, [091257](#)) to 2.2% (Ostro et al., 2006, [087991](#)) using the same lag (i.e., lag 1 and lag 0-1) and averaging indices. Regional and seasonal patterns in $\text{PM}_{2.5}$ risk estimates were observed with results similar to those presented for PM_{10} (Dominici et al., 2007, [099135](#); Peng et al., 2005, [087463](#); Zeka et al., 2006, [088749](#)), with the greatest effects occurring in the eastern U.S. (Franklin et al., 2007, [091257](#); Franklin et al., 2008, [097426](#)) and during the spring (Franklin et al., 2007, [091257](#); Zanobetti and Schwartz, 2009, [188462](#)). Of the studies evaluated, no U.S.-based multi-city studies conducted a detailed analysis of the potential confounding of $\text{PM}_{2.5}$ risk estimates by gaseous pollutants, but Burnett et al. (2004, [086247](#)) found mixed results, with possible confounding by NO_2 when analyzing gaseous pollutants in a multi-city Canadian-based study. However, it should be noted that U.S.-based multi-city studies that focused on the association between PM_{10} and mortality found that gaseous pollutants are not likely to confound the PM-mortality relationship. An examination of effect modifiers (e.g., demographic and socioeconomic factors), specifically air conditioning use which is sometimes used as a surrogate for decreased pollutant penetration indoors, has suggested that $\text{PM}_{2.5}$ risk estimates increase as the percent of the population with access to air conditioning decreases (Franklin et al., 2007, [091257](#); Franklin et al., 2008, [097426](#)). Collectively, the epidemiologic evidence on **the effect of short-term exposure to $\text{PM}_{2.5}$ on mortality is sufficient to conclude that a causal relationship is likely to exist at ambient concentrations.**

6.5.3.2. PM_{10-2.5}

The 2004 PM AQCD (U.S. EPA, 2004, [056905](#)) found a limited body of evidence that was suggestive of associations between short-term exposure to ambient PM_{10-2.5} and various mortality outcomes (e.g., 0.08 to 2.4% increase in total [non-accidental] mortality per 10 µg/m³ increase in PM_{10-2.5}). As a result, the AQCD concluded that PM_{10-2.5}, or some constituent component(s) (including those on the surface) of PM_{10-2.5}, may contribute, in certain circumstances, to increased human health risks.

The majority of studies evaluated in this review that examined mortality associations with PM_{10-2.5} reported mixed results in terms of the relative impact of PM_{10-2.5} on mortality. These studies were conducted in areas with mean 24-h avg concentrations ranging from 6.1-16.4 µg/m³. This can primarily be attributed to the majority of studies being conducted in individual cities and the city-to-city variation in the chemical composition of PM_{10-2.5}. A new study of 47 U.S. cities (Zanobetti and Schwartz, 2009, [188462](#)), which estimated PM_{10-2.5} by calculating the difference between the county-average PM₁₀ and PM_{2.5}, found associations between PM_{10-2.5} and mortality across the U.S., including regions where PM_{10-2.5} levels are not high. One well conducted multicity Canadian study (Burnett et al., 2004, [086247](#)) also provides evidence for an association between short-term exposure to PM_{10-2.5} and mortality. However, unlike PM_{2.5} not many of the PM_{10-2.5} studies have investigated confounding by gaseous copollutants or the influence of model specification on PM_{10-2.5} risk estimates. Zanobetti and Schwartz (2009, [188462](#)) did provide preliminary evidence for greater effects during the warmer months (i.e., spring and summer), which is consistent with the PM₁₀-mortality studies (Peng et al., 2005, [087463](#); Zeka et al., 2006, [088749](#)). Overall, although more data is needed to adequately characterize the chemical and biological components that may modify the potential toxicity of PM_{10-2.5}, consistent positive associations between short-term exposure to PM_{10-2.5} and mortality were observed in the U.S. and Canadian-based multicity studies, as well as in single-city studies conducted in these locations. Therefore, the epidemiologic evidence on **the effect of short-term exposure to PM_{10-2.5} on mortality is suggestive of a causal relationship at ambient concentrations.**

6.5.3.3. Ultrafine PM

Limited evidence was available during the review of the 2004 PM AQCD (U.S. EPA, 2004, [056905](#)) regarding the potential association between UFP and mortality. The lone study evaluated was conducted in Germany and provided some evidence for an association, but this association was reduced upon the inclusion of gaseous copollutants in a two-pollutant model.

Only a few new studies, all of them from Europe, were identified during this review, which examined the association between short-term exposure to UFP and mortality. Inconsistencies were observed in the lag structure of association reported by each study in terms of both the lag day with the greatest association and the number of lag days considered in the study. Overall the studies consistently found that UFP were correlated with gaseous pollutants derived from local combustion sources and that one or more of the gaseous pollutants were also associated with mortality. The limited number of studies available and the discrepancy in results between studies further confirms the need for additional data to examine the UFP-mortality relationship. In conclusion, the epidemiologic evidence on **the effect of short-term exposure to UFP on mortality is inadequate to infer a causal association at ambient concentrations.**

6.6. Attribution of Ambient PM Health Effects to Specific Constituents or Sources

From a mechanistic perspective, it is highly plausible that the chemical composition of PM would be a better predictor of health effects than particle size. This would be consistent with observed regional heterogeneity in PM-related health effects in some epidemiologic studies. Also, data from the CSN demonstrate gradients in a number of PM_{2.5} components, including EC, OC, nitrate, and SO₄²⁻ (Section 3.5.1.1). Recent studies in epidemiology, controlled human exposure, and toxicology have begun using apportionment of ambient PM into chemical constituents and sources, in an attempt to link them to health outcomes and endpoints, and thus examine their possible role in health effects.

This section focuses on studies that have assessed effects for a range of PM sources or components. Some of the studies reviewed earlier in this chapter evaluated the relationship between specific chemical constituents derived from ambient PM and health effects, including mortality and cardiovascular and respiratory morbidity. However, many of these

studies, as well as others only included in the Annexes, only considered one or a small number of PM constituents. Controlled human exposure and toxicological studies that use a single compound found in PM rather than ambient PM are also included in this category. Additionally, studies that presented ambient PM composition and health data without systematically and explicitly investigating relationships are also excluded from this section. In contrast, other epidemiologic, controlled human exposure, and toxicological studies took into consideration a large set of PM constituents (typically minerals, metals, EC, OC, and ions such as SO_4^{2-}), aiming to segregate which constituents or groups of constituents may be responsible for the PM-related health effects observed. This section compiles these latter studies and provides a review of their findings. The focus of this section is limited to those studies that use ambient measurements of chemically speciated PM to examine associations with health outcomes and endpoints. One of the most salient characteristics of ambient PM speciation data is the large number of constituents that compose PM and the strength of the correlation between each constituents.

Prior to the 2004 PM AQCD (U.S. EPA, 2004, [056905](#)), only a handful of epidemiologic studies had attempted to relate specific constituents or sources of ambient PM to health outcomes without selecting constituents a priori. In this review, approximately 40 new epidemiologic, controlled human exposure, and toxicological studies explore the health effects attributed to chemical constituents and sources of ambient PM. The following summary (Section 6.6.3) provides a synthesis of the findings, including discussions on the robustness, coherence, and consistency of the results.

6.6.1. Evaluation Approach

Relating a large number of ambient PM constituents with a large number of health outcomes presents difficulties that are related to both the nature of PM, and the methods of quantitative analysis. First, the number of constituents that comprise PM is not only large, but the correlations between them are inherently high. Reducing the correlation between constituents has been accomplished in most of the recent studies through various forms of factor analysis, which limits the correlations between constituents by grouping the most highly correlated ambient PM constituents into less correlated groups or factors. Some studies identify the resulting groups or factors with named sources of ambient PM, but many do not draw explicit links between factors and actual sources. The methods for estimating source contributions to ambient PM are reviewed in Section 3.5.4.

Most studies, regardless of discipline, were based on data for between 7 and 20 ambient PM constituents, with EC, OC, SO₄, and NO₃ most commonly measured. Most, but not all of the studies, reduced the number of ambient PM constituents by grouping them with various factorization or source apportionment techniques before using a separate analysis to examine the relationship between the grouped PM constituents and various health effects. However, not all studies labeled the constituent groupings according to their presumed source. A few performed these steps simultaneously using Partial Least Squares (PLS) procedures or Structural Equation Modeling (SEM). A small number of controlled human exposure and toxicological studies did not apply any kind of grouping to the ambient PM speciation data.

There are some differences in the type of PM constituent data used in epidemiologic, controlled human exposure and toxicological studies. In epidemiologic studies, ambient PM speciation data is obtained from atmospheric monitors; for controlled human exposure and toxicological studies, the experimental exposure technique used determines the type of PM data. Thus, all epidemiologic studies relied on monitor data, while all of the controlled human exposure and the majority of the toxicological studies used CAPs. The remaining toxicological studies used ambient PM samples collected on filters at various U.S. sites. Further details on the studies included can be found in Appendix F.

Some important limitations in interpreting these studies together is that few, if any of the results are easily comparable, due to: differences in the sets of ambient PM constituents that make up each of the factors; the subjectivity involved in labeling factors as sources; the numerous potential health effects examined in these studies, including definitive outcomes (e.g., HAs) as well as physiological alterations (e.g., increased inflammatory response); and the various statistical methods and analytical approaches used in the studies. There are no well-established, objective methods for conducting the various forms of factor analysis and source apportionment, leaving much of the model operation and factor assignment open to judgment by the individual investigator. For example, the Al/Si factor identified in one study may differ from the Al/Ca/Fe/Si factor from another study, and the “Resuspended Soil” factor from a third study.

After factorization or apportionment of the ambient PM data, various methods were used for analyzing the potential association between ambient PM constituents or sources and health effects. Except for the studies that used PLS or SEM, controlled human exposure and toxicological studies all used univariate mixed model regression for every

identified PM factor or source. A number of toxicological studies followed the univariate step with multivariate regression for all factors. Epidemiologic studies generally related short-term exposure to sources with health outcomes through various forms of Poisson regression; whereas, one long-term exposure study used time-to-event data analysis (survival analysis) methodology.

6.6.2. Findings

The results that follow are organized by discipline, with epidemiologic studies followed by controlled human exposure and toxicological studies. This section ends with a summary table, Table 6-17. Table 6-17 is broken out by PM_{2.5} sources, and includes those epidemiologic, controlled human exposure, and in vivo toxicological studies that either grouped ambient PM_{2.5} constituents or used tracers for each source. The table does not include all factors or sources examined in the studies listed: those factors or sources for which *no* association with effects was found are excluded.

6.6.2.1. Epidemiologic Studies

Results from the 2004 PM AQCD

Three epidemiologic studies were evaluated in the 2004 PM AQCD (U.S. EPA, 2004, [056905](#)) that examined the association between PM constituents or sources and specific health effects. Of these studies, one study associated daily mortality with a mobile sources PM factor in Knoxville, TN and St. Louis, MO and coal in Boston, MA; while the crustal factor was not found to be significant for any of the six cities studied (Laden et al., 2000, [012102](#)). Another study demonstrated an association between a regional SO₄²⁻ factor and total mortality at lag 0 in Phoenix and factors for regional SO₄²⁻, motor vehicles, and vegetative burning with cardiovascular mortality at lags of 0, 1, and 3, respectively (Mar et al., 2000, [001760](#); 2003, [042841](#)). Negative associations were observed between total mortality and regional SO₄²⁻ at lag 3, along with local SO₂ and soil factors (Mar et al., 2000, [001760](#); 2003, [042841](#)). Finally, Tsai et al. (2000, [006251](#)) identified significant associations between PM₁₅-derived industrial sources and total daily deaths in Newark and Camden, NJ; SO₄²⁻ was also linked to cardiopulmonary deaths in both locations. Total mortality and cardiopulmonary deaths were also significantly associated with PM from oil burning in Camden (2000, [006251](#)).

Comparative Analyses of Source Apportionment Methods

Hopke et al. (2006, [088390](#)) conducted a comparative analysis of source apportionment techniques used by investigators at multiple institutions, and subsequently used in epidemiologic analyses (Ito et al., 2006, [088391](#); Mar et al., 2006, [086143](#)). An overarching conclusion of this set of analyses, reported in Thurston et al. (2005, [097949](#)), is that variation in the source apportionment methods was not a major source of uncertainty in the epidemiologic effect estimates. In the primary analyses, mortality was associated with secondary SO_4^{2-} in both Phoenix and Washington D.C., although lag times differed (0 and 3, respectively). The SO_4^{2-} effect was stronger for total mortality in Washington D.C. and for cardiovascular mortality in Phoenix (Ito et al., 2006, [088391](#); Mar et al., 2006, [086143](#)). In addition, Ito et al. (2006, [088391](#)) found some evidence for associations with primary coal and traffic with total mortality in Washington D.C. (Ito et al., 2006, [088391](#)) while copper smelter, traffic, and sea salt were associated with cardiovascular mortality in Phoenix at various lag times (Mar et al., 2006, [086143](#)). In contrast to Phoenix, sea salt and traffic were not associated with mortality in Washington D.C. (Ito et al., 2006, [088391](#)), but in both locations no associations were observed between biomass/wood combustion and mortality (Ito et al., 2006, [088391](#); Mar et al., 2006, [086143](#)). In an additional study that compared three source apportionment methods in Atlanta - PMF, modified CMB, and a single-species tracer approach - found that the epidemiologic results were robust to the analytic method used (Sarnat et al., 2008, [097972](#)). There were consistent associations between ED visits for cardiovascular diseases with $\text{PM}_{2.5}$ from mobile sources (gasoline and diesel) and biomass combustion (primarily prescribed forest burning and residential wood combustion), whereas $\text{PM}_{2.5}$ from secondary SO_4^{2-} was associated with respiratory disease ED visits (Sarnat et al., 2008, [097972](#)). Sarnat et al. (2008, [097972](#)) also found that the primary power plant $\text{PM}_{2.5}$ source identified by the CMB approach was negatively associated with respiratory ED visits while no association was found for $\text{PM}_{2.5}$ from soil and secondary nitrates/ammonium nitrate. In these studies, effect estimates based on the different source apportionment methods were generally in close agreement.

Source Apportionment Studies

A study that examined associations with mortality in Santiago, Chile identified a motor vehicle source of $\text{PM}_{2.5}$ as having the greatest association with total and cardiac mortality at lag 1 (Cakmak et al., 2009, [191995](#)). There was effect modification by age, with

the total mortality relative risks associated with PM_{2.5} from motor vehicles being greatest for those >85 yr. Soil and combustion sources were also associated with cardiac mortality. Risk estimates for respiratory mortality were the greatest for the motor vehicle source, with combustion and soil source factors also demonstrating positive associations for lag 1 (Cakmak et al., 2009, [191995](#)).

An epidemiologic study that evaluated respiratory ED visits was conducted in Spokane, WA and used tracers as indicators of ambient PM_{2.5} sources (Schreuder et al., 2006, [097959](#)). In this study, only PM_{2.5} from vegetative burning (total carbon) was associated with increased respiratory ED visits for lag 1, while PM_{2.5} indicators for motor vehicles (Zn) and soil (Si) were not associated with cardiac hospital or respiratory ED visits. Andersen et al. (2007, [093201](#)) conducted a source apportionment analysis to identify the sources of ambient PM₁₀ associated with cardiovascular and respiratory hospital admissions in older adults and children (ages 5-18) in Copenhagen, including two-pollutant models with various sources of PM₁₀. Andersen et al. (2007, [093201](#)) found that secondary and crustal sources of PM₁₀ were associated with cardiovascular hospital admissions; biomass sources were associated with respiratory hospital admissions; and vehicle sources were associated with asthma hospital admissions.

Several panel epidemiologic studies have examined the association between PM sources and physiological alterations in cardiovascular function. Lanki et al. (2006, [089788](#)) reported associations between PM_{2.5} from local traffic and ST-segment depression in elderly adults in a study conducted in Helsinki, Finland. In an additional study, Yue et al. (2007, [097968](#)) found that adult males with coronary artery disease in Erfurt, Germany demonstrated changes in repolarization parameters associated with traffic-related PM_{2.5}, with increased vWF linked to traffic and combustion-generated particles, although the source apportionment analysis was based solely on particle size distribution. In addition, elevated CRP levels were associated with all sources of PM_{2.5} (soil, local traffic, secondary aerosols from local fuel combustion, diesel, and secondary aerosols from multiple sources) (Yue et al., 2007, [097968](#)). Reidiker et al. (2004, [056992](#)), in a study of young highway patrol officers, found that the most significant effects (HRV, supraventricular ectopic beats, hematological markers, vWF) were associated with a “speed-change” factor for PM_{2.5} (2004, [056992](#)). In addition, the authors observed an association between crustal factor and cardiovascular effects, but no health-related associations with steel wear or gasoline PM_{2.5} source factors.

Two recent studies have examined the associations between ambient PM_{2.5} sources and respiratory symptoms and lung function. Positive associations with PM_{2.5} motor vehicle and road dust sources were reported for respiratory symptoms and inhaler use in asthmatic children in New Haven, CT, and negative associations with wheeze or inhaler use for biomass burning at lag 0-2 (Gent et al., 2009, [180399](#)). These positive effects for motor vehicle and road dust sources were robust to the inclusion of a gaseous copollutant (NO₂, CO, SO₂, or O₃) in the regression model. Penttinen et al. (2006, [087988](#)) in a study consisting of asthmatic adults living in Helsinki, Finland, found that decrements in PEF were associated with ambient PM_{2.5} soil, long-range transport, and local combustion sources at lags from 0-5 days. In addition, negative associations with asthma symptoms and medication use were reported for PM_{2.5} from sea salt and long-range transport sources (Penttinen et al., 2006, [087988](#)).

PM Constituent Studies

Some studies considered large sets of ambient PM constituents and attempted to identify which were associated with various health effects, but without grouping them into factors, or identifying sources. The majority of these studies focused on health effects associated with short-term exposure to PM_{2.5}. Peng et al. (2009, [191998](#)) examined the association between PM_{2.5} constituents (i.e., EC, OC, SO₄²⁻, NO₃⁻, Si, Na, NH₄⁺) and cardiovascular and respiratory hospital admissions in 119 U.S. cities. When including each constituent in a multipollutant model, Peng et al. (2009, [191998](#)) found that EC and OC were robust to the inclusion of the other constituents at lag 0 for cardiovascular and respiratory hospital admissions, respectively. Although this study did not conduct analyses to identify sources of the constituents examined, EC and OC are often attributed to motor vehicle emissions, particularly diesel engines, and wood burning (Peng et al., 2009, [191998](#)). Ostro et al. (2007, [091354](#); 2008, [097971](#)) conducted two studies in six California counties to examine the association between ambient PM constituents and mortality. In the 2007 analysis, Ostro et al. (2006, [087991](#)) found associations for Cu and all-cause mortality; EC, K, and Zn and CVD mortality; and Cu and Ti and respiratory mortality at lags ranging from 0 to 3 days. Associations during the summer were only observed for K for both CVD and respiratory mortality; and Al, Cl, Cu, Pb, Ti, and Zn for respiratory mortality. Overall, the most consistent associations were observed during the cool season. In a subsequent analysis, Ostro et al. (2008, [097971](#)) examined the association between ambient PM

constituents and cardiovascular mortality in potentially susceptible subpopulations. The authors found positive associations between EC, OC, NO₃⁻, SO₄²⁻, K, Cu, Fe, and Zn and cardiovascular mortality. These associations were higher in individuals with lower educational attainment and of Hispanic ethnicity. In addition, similar to the 2007 analysis, associations were observed at lags ranging from 0 to 3 days.

One study long-term exposure to PM_{2.5} has included evaluation of multiple PM_{2.5} components and an indicator of traffic density (Lipfert et al., 2006, [088756](#)). Using health data from a cohort of U.S. military veterans and PM_{2.5} data from EPA's CSN, Lipfert et al. (2006, [088756](#)) reported a positive association for mortality with sulfates. Positive associations were found between mortality and long-term exposures to nitrates, EC, Ni and V, as well as traffic density and peak O₃ concentrations. In multipollutant models, associations with traffic density remained significant, as did nitrates, Ni and V in some models.

Evaluation of Effect Modification by PM Constituents

Several studies have conducted secondary analyses to examine the whether variation in associations between PM_{2.5} and morbidity or PM₁₀ and mortality reflects differences in PM_{2.5} constituents. An assumption in these types of analyses, especially when examining the effects on PM₁₀-mortality risk estimates, is that the relative contributions of PM_{2.5} have remained the same over time, since these studies used PM₁₀ data for years prior to 2000, while PM_{2.5} speciation data has only been routinely collected since about 2000. Bell et al. (2009, [191997](#)) found statistically significant associations between the county average concentrations of V, Ni, and EC (106 counties) and effect estimates for both cardiovascular and respiratory hospital admissions with short-term exposure to PM_{2.5}. In this analysis the authors only focused on those ambient PM_{2.5} constituents (i.e., NH₄⁺, EC, OC, NO₃⁻, and SO₄²⁻) that comprised the majority of PM_{2.5} total mass in the study locations. Bell et al. (2009, [191997](#)) also conducted a similar analysis for PM₁₀-mortality risk estimates and found that only Ni increased the risk estimate. However, in a sensitivity analysis, when selectively dropping out the communities examined one-by-one, the Ni association was diminished when removing New York City. Both Lippmann et al. (2006, [091165](#)) and Dominici et al. (2007, [099135](#)) conducted similar analyses, albeit using a smaller subset of cities and/or different years of PM₁₀ data. In both studies, Ni and V were found to modify the PM₁₀-mortality risk estimates. In addition, Dominici et al. (2007, [099135](#)) also found in

a sensitivity analysis that the association with Ni and V was diminished when excluding New York City from the analysis.

6.6.2.2. Controlled Human Exposure Studies

A few controlled human exposure studies employed PCA, although not all linked groupings of PM constituents to the measured physiological parameters. Huang et al. (2003, [087377](#)) demonstrated associations between increased fibrinogen and Cu/Zn/V and increased BALF neutrophils and Fe/Se/SO₄ in young, healthy adults exposed to RTP, NC CAPs; however, only water-soluble constituents were analyzed. In the other study that examined physiological cardiovascular effects, Fe and EC were associated with changes in ST-segment, while SO₄²⁻ was associated with decreased SBP in asthmatic and healthy human volunteers exposed to Los Angeles CAPs (2003, [087377](#)). In Gong et al. (2003, [087365](#)) the majority of the PM was in the thoracic coarse fraction. In the other study that used Los Angeles CAPs, the only observed association was between SO₄²⁻ content and decreased lung function (FEV₁ and FVC) in elderly volunteers with and without COPD (Gong et al., 2005, [087921](#)). Two additional controlled human exposure studies that did not perform grouping and employed Toronto CAPs plus O₃ demonstrated increased DBP and increased brachial artery vasoconstriction associated with carbon content (2004, [055629](#); Urch et al., 2005, [081080](#)).

6.6.2.3. Toxicological Studies

The only toxicological in vivo study that characterized PM sources corresponding to identified sources was conducted in Tuxedo, NY, over a 5-month period. This study reported that all sources (regional SO₄²⁻, resuspended soil, residual oil, traffic and other unknown sources) were linked to HR or HRV changes in mice at one time or another during or after daily exposure (Lippmann et al., 2005, [087453](#)). In a similar in vitro study using CAPs from the same location, NF-κB in BEAS-2B cells were correlated with the oil combustion factor ($r = 0.289$ and 0.302 for V and Ni, respectively) (Maciejczyk and Chen, 2005, [087456](#)). The other in vitro toxicological study (Duvall et al., 2008, [097969](#)) that named sources employed samples from five U.S. cities and found a good fit for the regression model with increased IL-8 release in primary human airway epithelium cells and coal combustion ($R^2 = 0.79$), secondary nitrate ($R^2 = 0.63$), and mobile sources ($R^2 = 0.39$). In addition, soil ($R^2 = 0.48$), residual oil combustion ($R^2 = 0.38$), and wood combustion ($R^2 = 0.33$) were associated with

COX-2 effects; whereas, secondary SO_4^{2-} ($R^2 = 0.51$) was correlated with HO-1. Wood combustion and soil were negatively associated with HO-1.

Several toxicological studies employed Boston CAPs and identified at least four groupings of ambient $\text{PM}_{2.5}$ constituents (V/Ni, S, Al/Si, and Br/Pb), but they named sources only partially and tentatively (Batalha et al., 2002, [088109](#); Clarke et al., 2000, [011806](#); Godleski et al., 2002, [156478](#); Nikolov et al., 2008, [156808](#); Saldiva et al., 2002, [025988](#); Wellenius et al., 2003, [055691](#)). When examining cardiovascular effects these studies reported that Si was associated with changes in the ST-segment of dogs (Wellenius et al., 2003, [055691](#)) and decreased L/W ratio in rat pulmonary arteries (Batalha et al., 2002, [088109](#)) in multivariate analyses. In addition, blood hematological results were associated with V/Ni, Al/Si, Na/Cl, and S in dogs (Clarke et al., 2000, [011806](#)). An examination of respiratory effects in the latter study found that V/Ni and Br/Pb were associated with increased inflammation in BALF for only the 3rd day of exposure (Clarke et al., 2000, [011806](#)). Decreased respiratory rate and increased airway irritation (Penh) in dogs were associated with road dust (Al) and motor vehicles (OC), respectively (Nikolov et al., 2008, [156808](#)). Individual $\text{PM}_{2.5}$ constituents associated with elevated neutrophils in BALF were Br, EC, OC, Pb, and SO_4^{2-} (Godleski et al., 2002, [156478](#)), which is consistent with the findings (Br, EC, OC, Pb, V, and Cl) of Saldiva et al. (2002, [025988](#)).

The toxicological studies that used PLS methodologies identified $\text{PM}_{2.5}$ constituents linked to respiratory parameters. Seagrave et al. (2006, [091291](#)) demonstrated associations between cytotoxic responses and a gasoline plus nitrates source factor (OC, Pb, hopanes/steranes, nitrate, and As) along with inflammatory responses and a gasoline plus diesel source factor (including major metal oxides) in rats exposed IT. In the other study, Veranth et al. (2006, [087479](#)) collected loose surface soil from 28 sites in the Western U.S. and exposed BEAS-2B cells to $\text{PM}_{2.5}$. In the multivariate redundancy analysis, OC₁, OC₃, OC₂, EC₂, Br, EC₁, and Ni correlated with IL-8 release, decreased IL-6 release, and decreased viability at low and high doses (10 and 80 $\mu\text{g}/\text{cm}^2$, respectively).

Table 6-17. Study-specific PM_{2.5} factor/source categories associated with health effects.

Source Category	Location	Health Effects	Time	Type of Study ¹	Species	Reference
CRUSTAL/SOIL/ROAD DUST						
Al, Si, Fe	Phoenix, AZ	negative association with total mortality	Lag 2	E	Human	Mar et al. (2000, 001760)
Not provided	Washington, D.C.	↑ CV mortality	Lag 4	E	Human	Ito et al. (2006, 088391)
Al, Ca, Fe, Si	Santiago, Chile	↑ CV mortality ↑ respiratory mortality	Lag 1	E	Human	Cakmak et al. (2009, 191995)
Al, Si, Ca, K, Fe	Helsinki, Finland	ST-segment depression	Lag 3	E	Human	Lanki et al. (2006, 089788)
Al, Si, Ca, K, Fe	Los Angeles, CA	↓ ST-segment voltage	2 days post-exposure	H	Human	Gong et al. (2003, 042106)
Al, Si	Boston, MA	ST-segment change	Following exposure	T	Dog	Wellenius et al. (2003, 055691)
Al, Si, Ca	Boston, MA	↓ lumen/wall ratio	24 h post-exposure	T	Rat	Batalha et al. (2002, 088109)
Al, Si, Ti, Fe	Wake County, NC	↑ uric acid ↑ mean cycle length	Lag 15 h	E	Human	Riediker et al. (2004, 056892)
Al, Si, Ca, Fe	Tuxedo, NY	↓ HR ↑ HR ↑ SDNN, ↑ RMSSD	During exposure Afternoon post-exposure e. Night post-exposure	T	Mouse	Lippmann et al. (2005, 087453)
Al, Si	Boston, MA	↑ blood PMN % ↓ blood lymphocytes % ↑ WBC	Following exposure	T	Dog	Clarke et al. (2000, 011806)
Si, Fe, Al, Ca, Ba, Ti	New Haven, CT	↑ respiratory symptoms and inhaler use	Lag 0-2	E	Human	Gent et al. (2009, 180399)
Si, Al, Ca, Fe, Mn	Helsinki, Finland	↓ mean PEF	Lag 3	E	Human	Penttinen et al. (2006, 087988)
Al	Boston, MA	↓ airway irritation (penh)	During exposure	T	Dog	Nikolov et al. (2008, 156808)
SALT						
Not provided	Phoenix, AZ	↑ CV mortality ↑ total mortality negative association with total mortality	Lag 5 Lag 0	E	Human	Mar et al. (2006, 086143)
Na, Cl	Helsinki, Finland	ST-segment depression	Lag 3	E	Human	Lanki et al. (2006, 089788)
Na, Cl	Boston, MA	↑ blood lymphocyte %	Following exposure	T	Dog	Clarke et al. (2000, 011806)
Na, Cl	Helsinki, Finland	Negatively associated with bronchodilator use and corticosteroid use	Lag 0-5 avg	E	Human	Penttinen et al. (2006, 087988)
Na, Cl	Boston, MA	↑ lung PMN density	24 h post-exposure	T	Rat	Saldiva et al. (2002, 025988)
SECONDARY SO₂ / LONG-RANGE TRANSPORT						
S	Phoenix, AZ	↑ total mortality negative association with total mortality	Lag 0 Lag 5	E	Human	Mar et al. (2000, 001760)
Not provided	Washington, D.C.	↑ total mortality	Lag 3	E	Human	Ito et al. (2006, 088391)
Not provided	Phoenix, AZ	↑ CV mortality	Lag 0	E	Human	Mar et al. (2006, 086143)
S, K, Zn, Pb	Helsinki, Finland	ST-segment depression	Lag 2	E	Human	Lanki et al. (2006, 089788)

Source Category	Location	Health Effects	Time	Type of Study ¹	Species	Reference
SO ₄ ²⁻	Los Angeles, CA	↓ SBP	4 h post-exposure	H	Human	Gong et al. (2003, 042106)
S, Si, OC	Tuxedo, NY	↓ HR ↓ SDNN, ↓ RMSSD	Afternoon post-exposure Night post-exposure	T	Mouse	Lippmann et al. (2005, 087453)
S	Boston, MA	↓ RBC ↑ hemoglobin	Following exposure	T	Dog	Clarke et al. (2000, 011806)
SO ₄ ²⁻ , NH ₄ ⁺ , OC	Atlanta, GA	↑ respiratory ED visits	Lag 0	E	Human	Sarnat et al. (2008, 097972)
S, K, Zn, PM mass	Helsinki, Finland	↓ mean PEF. Negative association with asthma symptom prevalence	Lag 1 Lag 3	E	Human	Penttinen et al. (2006, 087988)
SO ₄ ²⁻ (+NO ₂)	Los Angeles, CA	↓ FEV ₁ ↓ FVC	Following exposure	H	Human	Gong et al. (2005, 087921)
TRAFFIC						
Pb, Br, Cu	Harvard Six Cities	↑ total mortality	Lag 0-1	E	Human	Laden et al. (2000, 012102)
Not provided	Phoenix, AZ	↑ CV mortality	Lag 1	E	Human	Mar et al. (2006, 086143)
Mn, Fe, Zn, Pb, OC, EC, CO, NO ₂	Phoenix, AZ	↑ CV mortality	Lag 1	E	Human	Mar et al. (2000, 001760)
CO, NO ₂ , EC, OC	Santiago, Chile	↑ CV mortality ↑ respiratory mortality	Lag 1	E	Human	Cakmak et al. (2009, 191995)
Gasoline (OC, NO _s , NH ₄ ⁺)	Atlanta, GA	↑ CVD ED visits	Lag 0	E	Human	Sarnat et al. (2008, 097972)
Diesel (EC, OC, NO _s)	Atlanta, GA	↑ CVD ED visits	Lag 0	E	Human	Sarnat et al. (2008, 097972)
NO _x , EC, ultrafine count	Helsinki, Finland	ST-segment depression	Lag 2	E	Human	Lanki et al. (2006, 089788)
Speed-change factor (Cu, S, aldehydes)	Wake County, NC	↑ blood urea nitrogen ↑ mean red cell volume ↑ blood PMN % ↓ blood lymphocytes % ↑ von Willebrand factor (vWF) ↓ protein C ↑ mean cycle length ↑ SDNN ↑ PNN50 ↑ supraventricular ectopic beats	Lag 15 h	E	Human	Riediker et al. (2004, 056992)
Motor vehicle/other (Br, Pb, Se, Zn, NO ₃ -)	Tuxedo, NY	↓ RMSSD	Afternoon post-exposure	T	Mouse	Lippmann et al. (2005, 087453)
EC, Zn, Pb, Cu, Se	New Haven, CT	↑ respiratory symptoms	Lag 0-2	E	Human	Gent et al. (2009, 180399)
Local combustion (NO _x , ultrafine PM, Cu, Zn, Mn, Fe)	Helsinki, Finland	↓ mean PEF	Lag 0-5 avg	E	Human	Penttinen et al. (2006, 087988)
Gasoline + secondary nitrate*	Birmingham, AL; Atlanta, GA; Pensacola, FL; Centreville, AL	cytotoxic responses (potency)	24 h post-exposure	T	Rat	Seagrave et al. (2006, 091291)
Gasoline + diesel*	Birmingham, AL; Atlanta, GA; Pensacola, FL; Centreville, AL	inflammatory responses (potency)	24 h post-exposure	T	Rat	Seagrave et al. (2006, 091291)

Source Category	Location	Health Effects	Time	Type of Study ¹	Species	Reference
OIL COMBUSTION						
V, Ni	Boston, MA	↑ blood PMN % ↓ blood lymphocytes % ↑ BALF AM %	Following exposure Following exposure 24 h post-exposure	T	Dog	Clarke et al. (2000, 011806)
V, Ni, Se	Tuxedo, NY	↓ SDNN ↓ RMSSD	Afternoon post-exposure	T	Mouse	Lippmann et al. (2005, 087453)
Ni	Boston, MA	↓ respiratory rate	During exposure	T	Dog	Nikolov et al. (2008, 156808)
V, Ni	Boston, MA	↑ lung PMN density	24 h post-exposure	T	Rat	Saldiva et al. (2002, 025988)
COAL COMBUSTION						
Se, SO ₄ ²⁻	Harvard Six Cities	↑ total mortality	Lag 0-1	E	Human	Laden et al. (2000, 012102)
Not provided	Washington, D.C.	↑ total mortality	Lag 3	E	Human	Ito et al. (2006, 088391)
OTHER METALS						
Cu smelter (not provided)	Phoenix, AZ	↑ CV mortality ↑ total mortality	Lag 0	E	Human	Mar et al. (2006, 086143)
Incinerator	Washington, D.C.	Negative association with total and CV mortality	Lag 0	E	Human	Ito et al. (2006, 088391)
Metal processing (SO ₄ ²⁻ , Fe, NH ₄ ⁺ , EC, OC)	Atlanta, GA	↑ CVD ED visits	Lag 0	E	Human	Sarnat et al. (2008, 097972)
Combustion (Cr, Cu, Fe, Mn, Zn)	Santiago, Chile	↑ CV mortality ↑ respiratory mortality	Lag 1	E	Human	Cakmak et al. (2009, 191995)
WOODSMOKE / VEGETATIVE BURNING						
OC, K	Phoenix, AZ	↑ CV mortality	Lag 3	E	Human	Mar et al. (2000, 001760)
OC, EC, K, NH ₄ ⁺	Atlanta, GA	↑ CVD ED visits	Lag 0	E	Human	Sarnat et al. (2008, 097972)
Total C	Spokane, WA	↑ respiratory ED visits	Lag 1	E	Human	Schreuder et al. (2006, 097959)
UNNAMED FACTORS						
Zn-Cu-V	Chapel Hill, NC	↑ blood fibrinogen	18 h post-exposure	H	Human	Huang et al. (2003, 087377)
Fe-Se-SO ₄ ²⁻	Chapel Hill, NC	↑ BALF PMN	18 h post-exposure	H	Human	Huang et al. (2003, 087377)
Br, Cl, Pb	Santiago, Chile	↑ CV mortality ↑ respiratory mortality	Lag 1	E	Human	Cakmak et al. (2009, 191995)
Br, Pb	Boston, MA	↑ BALF PMN %	24 h post-exposure	T	Dog	Clarke et al. (2000, 011806)
Br, Pb	Boston, MA	↑ lung PMN density	24 h post-exposure	T	Rat	Saldiva et al. (2002, 025988)

*Constituents not provided.

¹ E = Epidemiologic study; h = Controlled human exposure study; T = Toxicological study

An in vitro toxicological study that employed Chapel Hill PM₁₀ used PCA but did not name specific PM sources (Becker et al., 2005, [088590](#)). In this study, the release of IL-6 from human alveolar macrophages and IL-8 from normal human bronchial epithelial cells was associated with a PM₁₀ factor comprised of Cr, Al, Si, Ti, Fe, and Cu. No statistically significant effects were observed for a second PM₁₀ factor (Zn, As, V, Ni, Pb, and Se).

Those toxicological studies that did not apply groupings to the ambient PM_{2.5} speciation data demonstrated a variety of results. Two Boston CAPs studies demonstrated lung oxidative stress correlated with a number of individual PM_{2.5} constituents including, Mn, Zn, Fe, Cu, and Ca (Gurgueira et al., 2002, [036535](#)) (Gurgueira et al., 2002, [036535](#)) and Al, Si, Fe, K, Pb, and Cu (Rhoden et al., 2004, [087969](#)) in rats using univariate regression. The remaining toxicological study that did not use ambient PM constituent groupings reported a correlation between Zn and plasma fibrinogen in SH rats when constituents were normalized per unit mass of CAPs (Kodavanti et al., 2002, [035344](#)).

6.6.3. Summary by Health Effects

Recent epidemiologic, toxicological, and controlled human exposure studies have evaluated the health effects associated with ambient PM constituents and sources, using a variety of quantitative methods applied to a broad set of PM constituents, rather than selecting a few constituents a priori. As shown in Table 6-17, numerous ambient PM_{2.5} source categories have been associated with health effects, including factors for PM from crustal and soil, traffic, secondary SO₄²⁻, power plants, and oil combustion sources. There is some evidence for trends and patterns that link particular ambient PM constituents or sources with specific health outcomes, but there is insufficient evidence to determine whether these patterns are consistent or robust.

For cardiovascular effects, multiple outcomes have been linked to a PM crustal/soil/road dust source, including cardiovascular mortality in Washington D.C. (Ito et al., 2006, [088391](#)) and Santiago, Chile (Cakmak et al., 2009, [191995](#)) and ST-segment changes in Helsinki (Lanki et al., 2006, [089788](#)), Los Angeles (Gong et al., 2003, [042106](#)), and Boston (Wellenius et al., 2003, [055691](#)). Interestingly, the ST-segment changes have been observed in an epidemiologic panel study, a controlled human exposure study, and a toxicological study, although the majority of the CAPs in the controlled human exposure study was PM_{10-2.5}. Further support for a crustal/soil/road dust source associated with cardiovascular health effects comes from a PM₁₀ source apportionment study in Copenhagen that reported increased cardiovascular hospital admissions (Andersen et al., 2007, [093201](#)).

PM_{2.5} traffic and WS/vegetative burning sources have also been linked to cardiovascular effects. Cardiovascular mortality in Phoenix (Mar et al., 2000, [001760](#); Mar et al., 2006, [086143](#)) and Santiago, Chile (Cakmak et al., 2009, [191995](#)) was associated with

traffic at lag 1. Gasoline and diesel sources were associated with ED visits in Atlanta for cardiovascular disease at lag 0 (Sarnat et al., 2008, [097972](#)). Cardiovascular mortality in Phoenix (Mar et al., 2000, [001760](#)) and ED visits in Atlanta (Sarnat et al., 2008, [097972](#)) were associated with WS/vegetative burning.

Studies that only examined the effects of individual PM_{2.5} constituents linked EC to cardiovascular hospital admissions in a multicity analysis (Peng et al., 2009, [191998](#)) and cardiovascular mortality in California (Ostro et al., 2007, [091354](#); 2008, [097971](#)).

These studies suggest that cardiovascular effects may be associated with PM_{2.5} from motor vehicle emissions, wood or biomass burning, and PM (both PM_{2.5} and PM_{10-2.5}) from crustal or road dust sources. In addition, there are many studies that observed associations between other sources (i.e., salt, secondary SO₄²⁻/long-range transport, other metals) and cardiovascular effects, but at this time, there does not appear to be a consistent trend or pattern of effects for those factors.

There is less consistency in observed associations between PM sources and respiratory health effects, which may be partially due to the fact that fewer studies have been conducted that evaluated respiratory-related outcomes and measures. However, there is some evidence for associations with secondary SO₄²⁻ PM_{2.5}. Sarnat et al. (2008, [097972](#)) found an increase in respiratory ED visits in Atlanta that was associated with a PM_{2.5} secondary SO₄²⁻ factor. Decrements in lung function in Helsinki (Lanki et al., 2006, [089788](#)) and Los Angeles (Gong et al., 2005, [087921](#)) in asthmatic and healthy adults, respectively, were also linked to this factor. Health effects relating to the crustal/soil/road dust and traffic sources of PM included increased respiratory symptoms in asthmatic children (Gent et al., 2009, [180399](#)) and decreased PEF in asthmatic adults (Penttinen et al., 2006, [087988](#)). Inconsistent results were also observed in those PM_{2.5} studies that use individual constituents to examine associations with respiratory morbidity and mortality, although Cu, Pb, OC, and Zn were related to respiratory health effects in two or more studies.

A few studies have identified PM_{2.5} sources associated with total mortality. These studies found an association between mortality and a PM_{2.5} coal combustion factor (Laden et al., 2000, [012102](#)), while others linked mortality to a secondary SO₄²⁻/long-range transport PM_{2.5} source (Ito et al., 2006, [088391](#); Mar et al., 2006, [086143](#)). One long-term exposure study reported an association between EC in PM_{2.5} and total mortality, and some evidence for associations with Ni and V, in a cohort of U.S. veterans (Lipfert et al., 2006, [088756](#)).

Recent studies have evaluated whether epidemiologic effect estimates from multicity studies were related to the specific PM_{2.5} constituents in the cities (Bell et al., 2009, [191997](#); Dominici et al., 2007, [099135](#); Lippmann et al., 2006, [091165](#)). In all three studies, PM₁₀-mortality effect estimates were greater in areas with higher proportion of Ni in PM_{2.5}, but when New York City was excluded in a sensitivity analysis in two of the studies, the association was diminished. A relationship was also found between V concentration in PM_{2.5} for PM₁₀-mortality effect estimates as well as those for PM_{2.5} with respiratory and cardiovascular hospital admissions (Bell et al., 2009, [191997](#)).

Recent studies show that source apportionment methods have the potential to add useful insights into which sources and/or PM constituents may contribute to different health effects. Of particular interest are several epidemiologic studies that compared source apportionment methods and the associated results. One set of studies compared epidemiologic associations with PM_{2.5} source factors using several methods - PCA, PMF, and UNMIX - independently analyzed by separate research groups (Hopke et al., 2006, [088390](#); Ito et al., 2006, [088391](#); Mar et al., 2006, [086143](#); Thurston et al., 2005, [097949](#)). Schreuder et al. (2006, [097959](#)) compared UPM and two versions of UNMIX to derive tracers and Sarnat et al. (2008, [097972](#)) compared PMF, modified CMB, and a single-species tracer approach. In all analyses, epidemiologic results based on the different methods were generally in close agreement. The variation in risk estimates for daily mortality between source categories was significantly larger than the variation between research groups (Ito et al., 2006, [088391](#); Mar et al., 2006, [086143](#); Thurston et al., 2005, [097949](#)). Additionally, the variation in risk estimates based on the source apportionment model used had a much smaller effect than the variation caused by the different source constituents. Further, the most strongly associated source types were consistent across all groups. This supports the general validity of such approaches, though integration of results would be simpler if the methods employed for grouping PM constituents were more consistent across studies and disciplines. Further research would aid understanding of the contribution of different factors, sources, or source tracers of PM to health effects by increasing the number of locations where similar health endpoints or outcomes are examined.

In summary, these findings are consistent with the conclusions of the 2004 PM AQCD (U.S. EPA, 2004, [056905](#)), that a number of source types, including motor vehicle emissions, coal combustion, oil burning, and vegetative burning, are associated with health effects (U.S. EPA, 2004, [056905](#)). Although the crustal factor of fine particles was not associated

with mortality in the 2004 PM AQCD (U.S. EPA, 2004, [056905](#)), recent studies have suggested that PM (both PM_{2.5} and PM_{10-2.5}) from crustal, soil or road dust sources or PM tracers linked to these sources are associated with cardiovascular effects. In addition, secondary SO₄²⁻ PM_{2.5} has been associated with both cardiovascular and respiratory effects. Overall, the results displayed in Table 6-17 indicate that many constituents of PM can be linked with differing health effects and the evidence is not yet sufficient to allow differentiation of those constituents or sources that are more closely related to specific health outcomes.

Chapter 6 References

- Adamkiewicz G; Ebelt S; Syring M; Slater J; Speizer FE; Schwartz J; Suh H; Gold DR. (2004). Association between air pollution exposure and exhaled nitric oxide in an elderly population. *Thorax*, 59: 204-209. [087925](#)
- Adar SD; Adamkiewicz G; Gold DR; Schwartz J; Coull BA; Suh H. (2007). Ambient and microenvironmental particles and exhaled nitric oxide before and after a group bus trip. *Environ Health Perspect*, 115: 507-12. [098635](#)
- Adar SD; Gold DR; Coull BA; Schwartz J; Stone PH; Suh H. (2007). Focused exposures to airborne traffic particles and heart rate variability in the elderly. *Epidemiology*, 18: 95-103. [001458](#)
- Aekplakorn W; Loomis D; Vichit-Vadakan N; Shy C; Plungchuchon S. (2003). Acute effects of SO₂ and particles from a power plant on respiratory symptoms of children, Thailand. , 34: 906-914. [089908](#)
- Alarie Y. (1973). Sensory irritation by airborne chemicals. , 2: 299-363. [191136](#)
- Albert CM; Rosenthal L; Calkins H; Steinberg JS; Ruskin JN; Wang P; Muller JE; Mittleman MA. (2007). Driving and Implantable Cardioverter-Defibrillator Shocks for Ventricular Arrhythmias: Results From the TOVA Study. *J Am Coll Cardiol*, 50: 2233-2240. [156201](#)
- Alexis NE; Lay JC; Zeman K; Bennett WE; Peden DB; Soukup JM; Devlin RB; Becker S. (2006). Biological material on inhaled coarse fraction particulate matter activates airway phagocytes in vivo in healthy volunteers. *J Allergy Clin Immunol*, 117: 1396-1403. [154323](#)
- Allen RW; Mar T; Koenig J; Liu LJ; Gould T; Simpson C; Larson T. (2008). Changes in lung function and airway inflammation among asthmatic children residing in a woodsmoke-impacted urban area. *Inhal Toxicol*, 20: 423-433. [156208](#)
- Analitis A; Katsouyanni K; Dimakopoulou K; Samoli E; Nikoloulopoulos AK; Petasakis Y; Touloumi G; Schwartz J; Anderson HR; Cambra K; Forastiere F; Zmirou D; Vonk JM; Clancy L; Kriz B; Bobvos J; Pekkanen J. (2006). Short-term effects of ambient particles on cardiovascular and respiratory mortality. , 17: 230-233. [088177](#)
- Andersen ZJ; Wahlin P; Raaschou-Nielsen O; Ketzler M; Scheike T; Loft S. (2008). Size distribution and total number concentration of ultrafine and accumulation mode particles and hospital admissions in children and the elderly in Copenhagen, Denmark. , 65: 458-66. [189651](#)
- Andersen ZJ; Wahlin P; Raaschou-Nielsen O; Scheike T; Loft S. (2007). Ambient particle source apportionment and daily hospital admissions among children and elderly in Copenhagen. 625-636. [093201](#)
- Anderson HR; Bremner SA; Atkinson RW; Harrison RM; Walters S. (2001). Particulate matter and daily mortality and hospital admissions in the west midlands conurbation of the United Kingdom: associations with fine and coarse particles, black smoke and sulphate. *Occup Environ Med*, 58: 504-510. [017033](#)
- Anderson ME; Bogdan GM. (2007). Environments, indoor air quality, and children. *Pediatr Clin North Am*, 54: 295-307, viii. [156214](#)
- Anselme F; Lorient S; Henry J-P; Dionnet F; Napoleoni J-G; Thnillez C; Morin J-P. (2007). Inhalation of diluted diesel engine emission impacts heart rate variability and arrhythmia occurrence in a rat model of chronic ischemic heart failure. *Arch Toxicol*, 81: 299-307. [097084](#)
- Antonini JM; Roberts JR; Jernigan MR; Yang H-M; Ma JYC; Clarke RW. (2002). Residual oil fly ash increases the susceptibility to infection and severely damages the lungs after pulmonary challenge with a bacterial pathogen. *Toxicol Sci*, 70: 110-119. [035342](#)
- Antonini JM; Taylor MD; Leonard SS; Lawryk NJ; Shi X; Clarke RW; Roberts JR. (2004). Metal composition and solubility determine lung toxicity induced by residual oil fly ash collected from different sites within a power plant. *Mol Cell Biochem*, 255: 257-265. [097199](#)
- Arantes-Costa F; Lopes F; Toledo A; Magliarelli-Filho P; Moriya H; Carvalho-Oliveira R; Mauad T; Saldiva P; Martins M. (2008). Effects of residual oil fly ash (ROFA) in mice with chronic allergic pulmonary inflammation. *Toxicol Pathol*, 36: 680. [187137](#)
- Arbex MA; Martins LC; De Oliveira RC; Pereira LA; Arbex FF; Cancado JE; Saldiva PH; Braga AL. (2007). Air pollution from biomass burning and asthma hospital admissions in a sugar cane plantation area in Brazil. *J Epidemiol Community Health*, 61: 395-400. [091637](#)

Note: Hyperlinks to the reference citations throughout this document will take you to the NCEA HERO database (Health and Environmental Research Online) at <http://epa.gov/hero>. HERO is a database of scientific literature used by U.S. EPA in the process of developing science assessments such as the Integrated Science Assessments (ISA) and the Integrated Risk Information System (IRIS).

- Arena VC; Mazumdar S; Zborowski JV; Talbott EO; He S; Chuang YH; Schwerha JJ. (2006). A retrospective investigation of PM10 in ambient air and cardiopulmonary hospital admissions in Allegheny County, Pennsylvania: 1995-2000. *J Occup Environ Med*, 48: 38-47. [088631](#)
- Atiga WL; Calkins H; Lawrence JH; Tomaselli GF; Smith JM; Berger RD. (1998). Beat-to-beat repolarization lability identifies patients at risk for sudden cardiac death. *Circulation*, 99: 899-908. [156231](#)
- Atkinson RW; Anderson HR; Sunyer J; Ayres J; Baccini M; Vonk JM; Boumghar A; Forastiere F; Forsberg B; Touloumi G; Schwartz J; Katsouyanni K. (2001). Acute effects of particulate air pollution on respiratory admissions: results from APHEA 2 project. *Am J Respir Crit Care Med*, 164: 1860-1866. [021959](#)
- Atkinson RW; Anderson HR; Sunyer J; Ayres J; Baccini M; Vonk JM; Boumghar A; Forastiere F; Forsberg B; Touloumi G; Schwartz J; Katsouyanni K. (2003). Acute effects of particulate air pollution on respiratory admissions. *Respiratory*, 10: 042797
- Atkinson RW; Bremner SA; Anderson HR; Strachan DP; Bland JM; Ponce de Leon A. (1999). Short-term associations between emergency hospital admissions for respiratory and cardiovascular disease and outdoor air pollution in London. *Arch Environ Occup Health*, 54: 398-411. [007882](#)
- Baccarelli A; Cassano P; Litonjua A; Park S; Suh H; Sparrow D; Vokonas P; Schwartz J. (2008). Cardiac autonomic dysfunction: effects from particulate air pollution and protection by dietary methyl nutrients and metabolic polymorphisms. *Am J Respir Crit Care Med*, 177: 1802. [191959](#)
- Baccarelli A; Martinelli I; Zanobetti A; Grillo P; Hou LF; Bertazzi PA; Mannucci PM; Schwartz J. (2008). Exposure to Particulate Air Pollution and Risk of Deep Vein Thrombosis. *Arch Intern Med*, 168: 920-927. [157984](#)
- Baccarelli A; Zanobetti A; Martinelli I; Grillo P; Hou L; Giacomini S; Bonzini M; Lanzani G; Mannucci PM; Bertazzi PA; Schwartz J. (2007). Effects of exposure to air pollution on blood coagulation. *J Thromb Haemost*, 5: 252-260. [090733](#)
- Baccarelli A; Zanobetti A; Martinelli I; Grillo P; Hou L; Lanzani G; Mannucci PM; Bertazzi PA; Schwartz J. (2007). Air pollution, smoking, and plasma homocysteine. *Environ Health Perspect*, 115: 176-181. [091310](#)
- Bagate K; Meiring JJ; Gerlofs-Nijland ME; Vincent R; Cassee FR; Borm PJA. (2004). Vascular effects of ambient particulate matter instillation in spontaneous hypertensive rats. *Toxicol Appl Pharmacol*, 197: 29-39. [087945](#)
- Ballester F; Rodriguez P; Iniguez C; Saez M; Daponte A; Galan I; Taracido M; Arribas F; Bellido J; Cirarda FB; Canada A; Guillen JJ; Guillen-Grima F; Lopez E; Perez-Hoyos S; Lertxundi A; Toro S. (2006). Air pollution and cardiovascular admissions association in Spain: results within the EMECAS project. *J Epidemiol Community Health*, 60: 328-336. [088746](#)
- Barclay JL; Miller BG; Dick S; Dennekamp M; Ford I; Hillis GS; Ayres JG; Seaton A. (2009). A panel study of air pollution in subjects with heart failure: negative results in treated patients. *Occup Environ Med*, 66: 325-334. [179935](#)
- Barnett AG; Williams GM; Schwartz J; Best TL; Neller AH; Petroeschevsky AL; Simpson RW. (2006). The effects of air pollution on hospitalizations for cardiovascular disease in elderly people in Australian and New Zealand cities. *Environ Health Perspect*, 114: 1018-1023. [089770](#)
- Barnett AG; Williams GM; Schwartz J; Neller AH; Best TL; Petroeschevsky AL; Simpson RW. (2005). Air pollution and child respiratory health: a case-crossover study in Australia and New Zealand. *Am J Respir Crit Care Med*, 171: 1272-1278. [087394](#)
- Barraza-Villarreal A; Sunyer J; Hernandez-Cadena L; Escamilla-Nunez MC; Sienra-Monge JJ; Ramirez-Aguilar M; Cortez-Lugo M; Holguin F; Diaz-Sanchez D; Olin AC; Romieu I. (2008). Air pollution, airway inflammation, and lung function in a cohort study of Mexico City schoolchildren. *Environ Health Perspect*, 116: 832-838. [156254](#)
- Barregard L; Sallsten G; Andersson L; Almstrand AC; Gustafson P; Andersson M; Olin AC. (2008). Experimental exposure to wood smoke: effects on airway inflammation and oxidative stress. *Occup Environ Med*, 65: 319-324. [155675](#)
- Barregard L; Sallsten G; Gustafson P; Andersson L; Johansson L; Basu S; Stigendal L. (2006). Experimental exposure to wood-smoke particles in health humans: effects on markers of inflammation, coagulation, and lipid peroxidation. *Inhal Toxicol*, 18: 845-853. [091381](#)
- Barrett EG; Henson RD; Seilkop SK; McDonald JD; Reed MD. (2006). Effects of hardwood smoke exposure on allergic airway inflammation in mice. *Inhal Toxicol*, 18: 33-43. [155677](#)
- Bartoli CR; Wellenius GA; Coull BA; Akiyama I; Diaz EA; Lawrence J; Okabe K; Verrier RL; Godleski JJ. (2009). Concentrated ambient particles alter myocardial blood flow during acute ischemia in conscious canines. *Environ Health Perspect*, 117: 333-337. [179904](#)
- Bartoli CR; Wellenius GA; Diaz EA; Lawrence J; Coull BA; Akiyama I; Lee LM; Okabe K; Verrier RL; Godleski JJ. (2009). Mechanisms of Inhaled Fine Particulate Air Pollution-Induced Arterial Blood Pressure Changes. *Environ Health Perspect*, 117: 361-366. [156256](#)

- Bartzokas A; Kassomenos P; Petrakis M; Celessides C. (2004). The effect of meteorological and pollution parameters on the frequency of hospital admissions for cardiovascular and respiratory problems in Athens. *Indoor Built Environ*, 13: 271-275. [093252](#)
- Bastain TM; Gilliland FD; Li Y-F; Saxon A; Diaz-Sanchez D. (2003). Intraindividual reproducibility of nasal allergic responses to diesel exhaust particles indicates a susceptible phenotype. , 109: 130-136. [098690](#)
- Batalha JR; Saldiva P H; Clarke RW; Coull BA; Stearns RC; Lawrence J; Murthy GG; Koutrakis P; Godleski JJ. (2002). Concentrated ambient air particles induce vasoconstriction of small pulmonary arteries in rats. *Environ Health Perspect*, 110: 1191-1197. [088109](#)
- Becker S; Mundandhara S; Devlin RB; Madden M. (2005). Regulation of cytokine production in human alveolar macrophages and airway epithelial cells in response to ambient air pollution particles: further mechanistic studies. *Toxicol Appl Pharmacol*, 207: 269-275. [088590](#)
- Beckett WS; Chalupa DF; Pauly-Brown A; Speers DM; Stewart JC; Frampton MW; Utell MJ; Huang LS; Cox C; Zareba W; Oberdorster G. (2005). Comparing inhaled ultrafine versus fine zinc oxide particles in healthy adults - A human inhalation study. *Am J Respir Crit Care Med*, 171: 1129-1135. [156261](#)
- Bedeschi E; Campari C; Candela S; Collini G; Caranci N; Frasca G; Galassi C; Francesca G; Vigotti MA. (2007). Urban air pollution and respiratory emergency visits at pediatric unit, Reggio Emilia, Italy. *J Toxicol Environ Health A*, 70: 261-265. [090712](#)
- Behndig AF; Mudway IS; Brown JL; Stenfors N Helleday R Duggan ST; Wilson SJ; Boman C Cassee FR; Frew AJ; Kelly FJ; Sandstrom T Blomberg A. (2006). Airway antioxidant and inflammatory responses to diesel exhaust exposure in healthy humans. *Eur Respir J*, 27: 359-365. [088286](#)
- Bell M; Ebisu K; Peng R; Samet J; Dominici F. (2009). Hospital Admissions and Chemical Composition of Fine Particle Air Pollution. *Am J Respir Crit Care Med*, 179: 1115-1120. [191997](#)
- Bell ML; Dominici F; Ebisu K; Zeger SL; Samet JM. (2007). Spatial and Temporal Variation in PM_{2.5} Chemical Composition in the United States for Health Effects Studies. , 115: 989. [155683](#)
- Bell ML; Ebisu K; Peng RD; Walker J; Samet JM; Zeger SL; Dominic F. (2008). Seasonal and regional short-term effects of fine particles on hospital admissions in 202 U.S. counties, 1999-2005. *Am J Epidemiol*, 168: 1301-1310. [156266](#)
- Bell ML; Levy JK; Lin Z. (2008). The effect of sandstorms and air pollution on cause-specific hospital admissions in Taipei, Taiwan. *Occup Environ Med*, 65: 104-111. [091268](#)
- Bennett CM; McKendry IG; Kelly S; Denike K; Koch T. (2006). Impact of the 1998 Gobi dust event on hospital admissions in the Lower Fraser Valley, British Columbia. *Sci Total Environ*, 366: 918-925. [088061](#)
- Berger A; Zareba W; Schneider A; Ruckerl R; Ibal-Mulli A; Cyrys J; Wichmann HE; Peters A. (2006). Runs of ventricular and supraventricular tachycardia triggered by air pollution in patients with coronary heart disease. *J Occup Environ Med*, 48: 1149-58. [098702](#)
- Berger RD; Kasper EK; Baughman KL; Marban E; Calkins H; Tomaselli GF. (1997). Beat-to-Beat QT Interval Variability : Novel Evidence for Repolarization Lability in Ischemic and Nonischemic Dilated Cardiomyopathy. , 96: 1557-1565. [155688](#)
- Blomberg A; Sainsbury C; Rudell B; Frew AJ; Holgate ST; Sandstrom T; Kelly FJ. (1998). Nasal cavity lining fluid ascorbic acid concentration increases in healthy human volunteers following short term exposure to diesel exhaust. *Free Radic Res*, 28: 59-67. [051246](#)
- Blomberg A; Tornqvist H; Desmyter L; Deneyts V; Hermans C. (2005). Exposure to diesel exhaust nanoparticles does not induce blood hypercoagulability in an at-risk population. *J Thromb Haemost*, 3: 2103-2105. [191991](#)
- Boezen HM; Vonk JM; Van Der Zee SC; Gerritsen J; Hoek G; Brunekreef B; Schouten JP; Postma DS. (2005). Susceptibility to air pollution in elderly males and females. *Eur Respir J*, 25: 1018-1024. [087396](#)
- Bosson J; Barath S; Pourazar J; Behndig AF; Sandstrom T; Blomberg A; Adelroth E. (2008). Diesel exhaust exposure enhances the ozone-induced airway inflammation in healthy humans. *Eur Respir J*, 31: 1234-1240. [156287](#)
- Bosson J; Pourazar J; Forsberg B; Adelroth E; Sandstrom T; Blomberg A. (2007). Ozone enhances the airway inflammation initiated by diesel exhaust. *Respir Med*, 101: 1140-1146. [156286](#)
- Bourotte C; Curi-Amarante A-P; Forti M-C; APereira LA; Braga AL; Lotufo PA. (2007). Association between ionic composition of fine and coarse aerosol soluble fraction and peak expiratory flow of asthmatic patients in Sao Paulo city (Brazil). *Atmos Environ*, 41: 2036-2048. [150040](#)
- Bouthillier L; Vincent R; Goegan P; Adamson IYR; Bjarnason S; Stewart M; Guenette J; Potvin M; Kumarathasan P. (1998). Acute effects of inhaled urban particles and ozone: lung morphology, macrophage activity, and plasma endothelin-1. *Am J Pathol*, 153: 1873-1884. [087110](#)
- Brauner EV; Forchhammer L; Moller P; Simonsen J; Glasius M; Wahlin P; Raaschou-Nielsen O; Loft S. (2007). Exposure to ultrafine particles from ambient air and oxidative stress-induced DNA damage. , 115: 1177-82. [188507](#)

- Briet M; Collin C; Laurent S; Tan A; Azizi M; Agharazii M; Jeunemaitre X; Alhenc-Gelas F; Boutouyrie P. (2007). Endothelial function and chronic exposure to air pollution in normal male subjects. *Hypertension*, 50: 970-976. [093049](#)
- Brook RD; Brook JR; Urch B; Vincent R; Rajagopalan S; Silverman F. (2002). Inhalation of fine particulate air pollution and ozone causes acute arterial vasoconstriction in healthy adults. , 105: 1534-1536. [024987](#)
- Bräuner EV; Mortensen J; Møller P; Bernard A; Vinzents P; Wählin P; Glasius M; Loft S. (2009). Effects of ambient air particulate exposure on blood-gas barrier permeability and lung function. *Inhal Toxicol*, 21: 38-47. [191179](#)
- Bräuner EV; Møller P; Barregard L; Dragsted LO; Glasius M; Wählin P; Vinzents P; Raaschou-Nielsen O; Loft S. (2008). Exposure to ambient concentrations of particulate air pollution does not influence vascular function or inflammatory pathways in young healthy individuals. *Part Fibre Toxicol*, 5: 13. [191966](#)
- Burnett RT; Brook J; Dann T; Delocla C; Philips O; Cakmak S; Vincent R; Goldberg MS; Krewski D. (2000). Association between particulate- and gas-phase components of urban air pollution and daily mortality in eight Canadian cities. *Inhal Toxicol*, 12: 15-39. [010273](#)
- Burnett RT; Cakmak S; Brook JR. (1998). The effect of the urban ambient air pollution mix on daily mortality rates in 11 Canadian cities. *Can J Public Health*, 89: 152-156. [029505](#)
- Burnett RT; Cakmak S; Brook JR; Krewski D. (1997). The role of particulate size and chemistry in the association between summertime ambient air pollution and hospitalization for cardiorespiratory diseases. *Environ Health Perspect*, 105: 614-620. [084194](#)
- Burnett RT; Dales R; Krewski D; Vincent R; Dann T; Brook JR. (1995). Associations between ambient particulate sulfate and admissions to Ontario hospitals for cardiac and respiratory diseases. *Am J Epidemiol*, 142: 15-22. [077226](#)
- Burnett RT; Goldberg MS. (2003). Size-fractionated particulate mass and daily mortality in eight Canadian cities. [042798](#)
- Burnett RT; Smith-Doiron M; Stieb D; Cakmak S; Brook JR. (1999). Effects of particulate and gaseous air pollution on cardiorespiratory hospitalizations. *Arch Environ Occup Health*, 54: 130-139. [017269](#)
- Burnett RT; Stieb D; Brook JR; Cakmak S; Dales R; Raizenne M; Vincent R; Dann T. (2004). Associations between short-term changes in nitrogen dioxide and mortality in Canadian cities. *Arch Environ Occup Health*, 59: 228-236. [086247](#)
- Burtscher H. (2005). Physical characterization of particulate emissions from diesel engines: a review. *J Aerosol Sci*, 36: 896-932. [155710](#)
- Cakmak S; Dales R; Vida C. (2009). Components of particulate air pollution and mortality in Chile. *Int J Occup Environ Health*, 15: 152. [191995](#)
- Calderon-Garciduenas L; Maronpot RR; Torres-Jardon R; Henriquez-Roldan C; Schoonhoven R; Acuna-Ayala H; Villarreal-Calderon A; Nakamura J; Fernando R; Reed W; Azzarelli B; Swenberg JA. (2003). DNA damage in nasal and brain tissues of canines exposed to air pollutants is associated with evidence of chronic brain inflammation and neurodegeneration. *Toxicol Pathol*, 31: 524-538. [156316](#)
- Calderon-Garciduenas L; Mora-Tiscareno A; Ontiveros E; Gomez-Garza G; Barragan-Mejia G; Broadway J; Chapman S; Valencia-Salazar G; Jewells V; Maronpot RR; Henriquez-Roldan C; Perez-Guille B; Torres-Jardon R; Herrit L; Brooks D; Osnaya-Brizuela N; Monroy M. (2008). Air pollution, cognitive deficits and brain abnormalities: A pilot study with children and dogs. *Brain Cognit*, 68: 117-127. [156317](#)
- Caligiuri G; Levy B; Pernow J; Thoren P; Hansson GK. (1999). Myocardial infarction mediated by endothelin receptor signaling in hypercholesterolemic mice. Presented at . [156318](#)
- Campbell A; Oldham M; Becaria A; Bondy SC; Meacher D; Sioutas C; Misra C; Mendez LB; Kleinman M. (2005). Particulate matter in polluted air may increase biomarkers of inflammation in mouse brain. *Neurotoxicology*, 26: 133-140. [087217](#)
- Campen MJ; Babu NS; Helms GA; Pett S; Wernly J; Mehran R; McDonald JD. (2005). Nonparticulate components of diesel exhaust promote constriction in coronary arteries from ApoE^{-/-} mice. *Toxicol Sci*, 88: 95-102. [083977](#)
- Campen MJ; McDonald JD; Reed MD; Seagrave J. (2006). Fresh gasoline emissions, not paved road dust, alter cardiac repolarization in ApoE^{-/-} mice. *Cardiovasc Toxicol*, 6: 199-210. [096879](#)
- Carlsten C; Kaufman JD; Trenga CA; Allen J; Peretz A; Sullivan JH. (2008). Thrombotic markers in metabolic syndrome subjects exposed to diesel exhaust. *Inhal Toxicol*, 20: 917-921. [156323](#)
- Carlsten C; Kaufman Joel D; Peretz A; Trenga Carol A; Sheppard L; Sullivan Jeffrey H. (2007). Coagulation markers in healthy human subjects exposed to diesel exhaust. , 120: 849-855. [155714](#)
- Cassee FR; Boere AJF; Fokkens PHB; Leseman DLAC; Sioutas C; Kooter IM; Dormans JAMA. (2005). Inhalation of concentrated particulate matter produces pulmonary inflammation and systemic biological effects in compromised rats. *J Toxicol Environ Health A*, 68: 773-796. [087962](#)

- Chahine T; Baccarelli A; Litonjua A; Wright RO; Suh H; Gold DR; Sparrow D; Vokonas P; Schwartz J. (2007). Particulate air pollution, oxidative stress genes, and heart rate variability in an elderly cohort. *Environ Health Perspect*, 115: 1617-1622. [156327](#)
- Chan C-C; Chuang K-J; Chien L-C; Chen W-J; Chang W-T. (2006). Urban air pollution and emergency admissions for cerebrovascular diseases in Taipei, Taiwan. *Eur Heart J*, 27: 1238-1244. [090193](#)
- Chan CC; Chuang KJ; Chen WJ; Chang WT; Lee CT; Peng CM. (2008). Increasing cardiopulmonary emergency visits by long-range transported Asian dust storms in Taiwan. *Environ Res*, 106: 393-400. [093297](#)
- Chan CC; Chuang KJ; Shiao GM; Lin LY. (2004). Personal exposure to submicrometer particles and heart rate variability in human subjects. *Environ Health Perspect*, 112: 1063-1067. [087398](#)
- Chang C-C; Hwang J-S; Chan C-C; Wang P-Y; Cheng T-J. (2007). Effects of concentrated ambient particles on heart rate, blood pressure, and cardiac contractility in spontaneously hypertensive rats during a dust storm event. *Inhal Toxicol*, 19: 973-978. [155719](#)
- Chang C-C; Hwang J-S; Chan C-C; Wang P-Y; Hu T-H; Cheng T-J. (2004). Effects of concentrated ambient particles on heart rate, blood pressure, and cardiac contractility in spontaneously hypertensive rats. *Inhal Toxicol*, 16: 421-429. [055637](#)
- Chang CC; Hwang JS; Chan CC; Wang PY; Hu TH; Cheng TJ. (2005). Effects of concentrated ambient particles on heart rate variability in spontaneously hypertensive rats. *J Occup Health*, 47: 471-480. [088662](#)
- Chardon B; Lefranc A; Granados D; Gremy I. (2007). Air pollution and doctors' house calls for respiratory diseases in the greater Paris area (2000-3). *Occup Environ Med*, 64: 320-4. [091308](#)
- Che W; Zhang Z; Zhang H; Wu M; Liang Y; Liu F; Shu Y; Li N. (2007). Compositions and oxidative damage of condensate, particulate and semivolatile organic compounds from gasoline exhausts. *Environ Toxicol Pharmacol*, 24: 11-18. [096460](#)
- Checkoway H; Levy D; Sheppard L; Kaufman J; Koenig J; Siscovick D. (2000). A case-crossover analysis of fine particulate matter air pollution and out-of-hospital sudden cardiac arrest. [015527](#)
- Chen C-H; Xirasagar S; Lin H-C. (2006). Seasonality in adult asthma admissions, air pollutant levels, and climate: a population-based study. *J Asthma*, 43: 287-292. [087947](#)
- Chen J; Schwartz J. (2009). Neurobehavioral effects of ambient air pollution on cognitive performance in US adults. *Neurotoxicology*, 30: 231-239. [179945](#)
- Chen LC; Hwang JS. (2005). Effects of subchronic exposures to concentrated ambient particles (CAPs) in mice IV Characterization of acute and chronic effects of ambient air fine particulate matter exposures on heart-rate variability. *Inhal Toxicol*, 17: 209-216. [087218](#)
- Chen Y; Yang Q; Krewski D; Burnett RT; Shi Y; McGrail KM. (2005). The effect of coarse ambient particulate matter on first, second, and overall hospital admissions for respiratory disease among the elderly. *Inhal Toxicol*, 17: 649-655. [087555](#)
- Chen Y; Yang Q; Krewski D; Shi Y; Burnett RT; McGrail K. (2004). Influence of relatively low level of particulate air pollution on hospitalization for COPD in elderly people. *Inhal Toxicol*, 16: 21-25. [087262](#)
- Cheng M-F; Tsai S-S; Wu T-N; Chen P-S; Yang C-Y. (2007). Air pollution and hospital admissions for pneumonia in a tropical city: Kaohsiung, Taiwan. *J Toxicol Environ Health A*, 70: 2021-6. [093034](#)
- Chevalier P; Burri H; Adeleine P; Kirkorian G; Lopez M; Leizorovicz A; Andre-Fouet X; Chapon P; Rubel P; Touboul P. (2003). QT dynamicity and sudden death after myocardial infarction: results of a long-term follow-up study. *J Am Coll Cardiol*, 41: 227-233. [156338](#)
- Chimonas MA; Gessner BD. (2007). Airborne particulate matter from primarily geologic, non-industrial sources at levels below National Ambient Air Quality Standards is associated with outpatient visits for asthma and quick-relief medication prescriptions among children less than 20 years old enrolled in Medicaid in Anchorage, Alaska. *Environ Res*, 70: 2021-2026. [093261](#)
- Chiu H; Tiao M; Ho S; Kuo H; Wu T; Yang C. (2008). Effects of Asian Dust Storm events on hospital admissions for chronic obstructive pulmonary disease in Taipei, Taiwan. *Inhal Toxicol*, 20: 777-781. [191989](#)
- Chock DP; Winkler SL; Chen C. (2000). A study of the association between daily mortality and ambient air pollutant concentrations in Pittsburgh, Pennsylvania. *J Air Waste Manag Assoc*, 50: 1481-1500. [010407](#)
- Choi JH; Xu QS; Park SY; Kim JH; Hwang SS; Lee KH; Lee HJ; Hong YC. (2007). Seasonal variation of effect of air pollution on blood pressure. *J Epidemiol Community Health*, 61: 314-318. [093196](#)
- Chuang K-J; Chan C-C; Chen N-T; Su T-C; Lin L-Y. (2005). Effects of particle size fractions on reducing heart rate variability in cardiac and hypertensive patients. *Environ Health Perspect*, 113: 1693-1697. [087989](#)
- Chuang K-J; Chan C-C; Su T-C; Lee C-T; Tang C-S. (2007). The effect of urban air pollution on inflammation, oxidative stress, coagulation, and autonomic dysfunction in young adults. *Am J Respir Crit Care Med*, 176: 370-6. [091063](#)
- Chuang KJ; Chan CC; Shiao GM; Su TC. (2005). Associations between submicrometer particles exposures and blood pressure and heart rate in patients with lung function impairments. *J Occup Environ Med*, 47: 1093-1098. [156356](#)

- Chuang KJ; Coull BA; Zanobetti A; Suh H; Schwartz J; Stone PH; Litonjua A; Speizer FE; Gold DR. (2008). Particulate Air Pollution as a Risk Factor for ST-Segment Depression in Patients With Coronary Artery Disease. [155731](#)
- Ciencewicki J; Gowdy K; Krantz QT; Linak WP; Brighton L; Gilmour MI; Jaspers I. (2007). Diesel exhaust enhanced susceptibility to influenza infection is associated with decreased surfactant protein expression. , 19: 1121-33. [096557](#)
- Clancy L; Goodman P; Sinclair H; Dockery DW. (2002). Effect of air pollution control on death rates in Dublin, Ireland: an intervention study. *Lancet*, 360: 1210-1214. [035270](#)
- Clarke RW; Catalano P; Coull B; Koutrakis P; Krishna Murthy GG; Rice T; Godleski JJ. (2000). Age-related responses in rats to concentrated urban air particles (CAPs). Presented at In: Phalen, R. F., ed. *Inhalation toxicology: proceedings of the third colloquium on particulate air pollution and human health (first special issue)*; June, 1999; Durham, NC. *Inhalation Toxicol.* 12(suppl. 1): 73-84. [011806](#)
- Coleridge HM; Coleridge JCG. (1994). Pulmonary Reflexes: Neural Mechanisms of Pulmonary Defense. *Annu Rev Physiol*, 56: 69-91. [156362](#)
- Courtois A; Andujar P; Ladeiro Y; Baudrimont I; Delannoy E; Leblais V; Begueret H; Galland MAB; Brochard P; Marano F. (2008). Impairment of NO-Dependent Relaxation in Intralobar Pulmonary Arteries: Comparison of Urban Particulate Matter and Manufactured Nanoparticles. *Environ Health Perspect*, 116: 1294. [156369](#)
- Cozzi E; Hazarika S; Stallings HW; Cascio WE; Devlin RB; Lust RM; Wingard CJ; Van Scott MR. (2006). Ultrafine particulate matter exposure augments ischemia-reperfusion injury in mice. *Am J Physiol*, 291: H894-H903. [091380](#)
- Cruts B; van Etten L; Tornqvist H; Blomberg A; Sandstrom T; Mills NL; Borm PJ. (2008). Exposure to diesel exhaust induces changes in EEG in human volunteers. *Part Fibre Toxicol*, 5: 4. [156374](#)
- Cárdenas M; Vallejo M; Romano-Riquer P; Ruiz-Velasco S; Ferreira-Vidal AD; Hermosillo AG. (2008). Personal exposure to PM_{2.5} air pollution and heart rate variability in subjects with positive or negative head-up tilt test. *Environ Res*, 108: 1-6. [191900](#)
- D'Ippoliti D; Forastiere F; Ancona C; Agabiti N; Fusco D; Michelozzi P; Perucci CA. (2003). Air pollution and myocardial infarction in Rome: a case-crossover analysis. , 14: 528-535. [074311](#)
- Dales R. (2004). Ambient carbon monoxide may influence heart rate variability in subjects with coronary artery disease. *J Occup Environ Med*, 46: 1217-21. [099036](#)
- Dales R; Liu L; Szyszkowicz M; Dalipaj M; Willey J; Kulka R; Ruddy TD. (2007). Particulate air pollution and vascular reactivity: the bus stop study. *Int Arch Environ Health*, 81: 159-164. [155743](#)
- Daniels MJ; Dominici F; Zeger SL; Samet JM. (2004). The national morbidity, mortality, and air pollution study Part III: PM₁₀ concentration-response curves and thresholds for the 20 largest US cities. [087343](#)
- Danielsen PH; Brauner EV; Barregard L; Sallsten G; Wallin M; Olinski R; Rozalski R; Moller P; Loft S. (2008). Oxidatively damaged DNA and its repair after experimental exposure to wood smoke in healthy humans. , 642: 37-42. [156382](#)
- Day KC; Reed MD; McDonald JD; Keilkop SK; Barrett EG. (2008). Effects of Gasoline Engine Emissions on Preexisting Allergic Airway Responses in Mice. *Inhal Toxicol*, 20: 1145-1155. [190204](#)
- De Bruin ML; van Hemel NM; Leufkens HG; Hoes AW. (2005). Hospital discharge diagnoses of ventricular arrhythmias and cardiac arrest were useful for epidemiologic research. , 58: 1325-1329. [155746](#)
- de Haar C; Hassing I; Bol M; Bleumink R; Pieters R. (2005). Ultrafine carbon black particles cause early airway inflammation and have adjuvant activity in a mouse allergic airway disease model. , 87: 409-418. [097872](#)
- de Haar C; Hassing I; Bol M; Bleumink R; Pieters R. (2006). Ultrafine but not fine particulate matter causes airway inflammation and allergic airway sensitization to co-administered antigen in mice. *Clin Exp Allergy*, 36: 1469-1479. [144746](#)
- De Hartog JJ; Hoek G; Peters A; Timonen KL; Ibaldo-Mulli A; Brunekreef B; Heinrich J; Tiittanen P; Van Wijnen JH; Kreyling W; Kulmala M; Pekkanen J. (2003). Effects of fine and ultrafine particles on cardiorespiratory symptoms in elderly subjects with coronary heart disease: the ULTRA study. *Am J Epidemiol*, 157: 613-623. [001061](#)
- Delfino R; Brummel S; Wu J; Stern H; Ostro B; Lipsett M; Winer A; Street D; Zhang L; Tjoa T. (2009). The relationship of respiratory and cardiovascular hospital admissions to the southern California wildfires of 2003. *Occup Environ Med*, 66: 189. [191994](#)
- Delfino RJ; Chang J; Wu J; Ren C; Tjoa T; Nickerson B; Cooper D; Gillen DL. (2009). Repeated hospital encounters for asthma in children and exposure to traffic-related air pollution near the home. *Ann Allergy Asthma Immunol*, 102: 138-44. [190254](#)
- Delfino RJ; Coate BD; Zeiger RS; Seltzer JM; Street DH; Koutrakis P. (1996). Daily asthma severity in relation to personal ozone exposure and outdoor fungal spores. *Am J Respir Crit Care Med*, 154: 633-641. [080788](#)

- Delfino RJ; Gone H; Linn WS; Pellizzari ED; Hu Y. (2003). Asthma symptoms in Hispanic children and daily ambient exposures to toxic and criteria air pollutants. *Environ Health Perspect*, 111: 647-656. [050460](#)
- Delfino RJ; Gong H; Linn WS; Hu Y; Pellizzari ED. (2003). Respiratory symptoms and peak expiratory flow in children with asthma in relation to volatile organic compounds in exhaled breath and ambient air. *J Expo Sci Environ Epidemiol*, 13: 348-363. [090941](#)
- Delfino RJ; Murphy-Moulton AM; Becklake MR. (1998). Emergency room visits for respiratory illnesses among the elderly in Montreal: association with low level ozone exposure. *Environ Res*, 76: 67-77. [093624](#)
- Delfino RJ; Quintana PJE; Floro J; Gastanaga VM; Samimi BS; Kleinman MT; Liu L-JS; Bufalino C; Wu C-F; McLaren CE. (2004). Association of FEV1 in asthmatic children with personal and microenvironmental exposure to airborne particulate matter. *Environ Health Perspect*, 112: 932-941. [056897](#)
- Delfino RJ; Staimer N; Gillen D; Tjoa T; Sioutas C; Fung K; George SC; Kleinman MT. (2006). Personal and ambient air pollution is associated with increased exhaled nitric oxide in children with asthma. *Environ Health Perspect*, 114: 1736-1743. [090745](#)
- Delfino RJ; Staimer N; Tjoa T; Polidori A; Arhami M; Gillen DL; Kleinman MT; Vaziri ND; Longhurst J; Zaldivar F; Sioutas C. (2008). Circulating biomarkers of inflammation, antioxidant activity, and platelet activation are associated with primary combustion aerosols in subjects with coronary artery disease. *Environ Health Perspect*, 116: 898-906. [156390](#)
- Delfino RJ; Zeiger RS; Seltzer JM; Street DH. (1998). Symptoms in pediatric asthmatics and air pollution: differences in effects by symptom severity, anti-inflammatory medication use and particulate averaging time. *Environ Health Perspect*, 106: 751-761. [051406](#)
- Delfino RJ; Zeiger RS; Seltzer JM; Street DH; McLaren CE. (2002). Association of asthma symptoms with peak particulate air pollution and effect modification by anti-inflammatory medication use. *Environ Health Perspect*, 110: A607-A617. [093740](#)
- DeMeo DL; Zanobetti A; Litonjua AA; Coull BA; Schwartz J; Gold DR. (2004). Ambient air pollution and oxygen saturation. *Am J Respir Crit Care Med*, 170: 383-387. [087346](#)
- Desqueyroux H; Pujet J-C; Prosper M; Squinazi F; Momas I. (2002). Short-term effects of low-level air pollution on respiratory health of adults suffering from moderate to severe asthma. *Environ Res*, 89: 29-37. [026052](#)
- Deurloo DT; van Esch BC; Hofstra CL; Nijkamp FP; van Oosterhout AJ. (2001). CTLA4-IgG reverses asthma manifestations in a mild but not in a more "severe" ongoing murine model. *Am J Respir Cell Mol Biol*, 25: 751-760. [156396](#)
- Devlin RB; Ghio AJ; Kehrl H; Sanders G; Cascio W. (2003). Elderly humans exposed to concentrated air pollution particles have decreased heart rate variability. *Eur Respir J*, 40: 76S-80S. [087348](#)
- de Hartog JJ; Lanki T; Timonen KL; Hoek G; Janssen NA; Ibaldo-Mulli A; Peters A; Heinrich J; Tarkiainen TH; van Grieken R; van Wijnen JH; Brunekreef B; Pekkanen J. (2009). Associations between PM2.5 and heart rate variability are modified by particle composition and beta-blocker use in patients with coronary heart disease. *Environ Health Perspect*, 117: 105-111. [191904](#)
- Diaz-Sanchez D; Garcia MP; Wang M; Jyrala M; Saxon A. (1999). Nasal challenge with diesel exhaust particles can induce sensitization to a neoallergen in the human mucosa. *J Allergy Clin Immunol*, 104: 1183-1188. [011346](#)
- Diaz-Sanchez D; Tsien A; Fleming J; Saxon A. (1997). Combined diesel exhaust particulate and ragweed allergen challenge markedly enhances human in vivo nasal ragweed-specific IgE and skews cytokine production to a T helper cell 2-type pattern. *J Immunol*, 158: 2406-2413. [051247](#)
- Dick CA; Singh P; Daniels M; Evansky P; Becker S; Gilmour MI. (2003). Murine pulmonary inflammatory responses following instillation of size-fractionated ambient particulate matter. *J Toxicol Environ Health A*, 66: 2193-2207. [088776](#)
- Diez-Roux AV; Auchincloss AH; Astor B; Barr RG; Cushman M; Dvorchak T; Jacobs DR Jr; Kaufman J; Lin X; Samson P. (2006). Recent exposure to particulate matter and C-reactive protein concentration in the multi-ethnic study of atherosclerosis. *Am J Epidemiol*, 164: 437-448. [156400](#)
- Dockery DW; Luttmann-Gibson H; Rich DQ; Link MS; Mittleman MA; Gold DR; Koutrakis P; Schwartz JD; Verrier RL. (2005). Association of air pollution with increased incidence of ventricular tachyarrhythmias recorded by implanted cardioverter defibrillators. *Environ Health Perspect*, 113: 670-674. [078995](#)
- Dockery DW; Luttmann-Gibson H; Rich DQ; Link MS; Schwartz JD; Gold DR; Koutrakis P; Verrier RL; Mittleman MA. (2005). Particulate air pollution and nonfatal cardiac events Part II Association of air pollution with confirmed arrhythmias recorded by implanted defibrillators. [090743](#)
- Dominici F; McDermott A; Daniels M; Zeger SL; Samet J. (2003). Revised Analyses of Time-Series Studies of Air Pollution and Health: Mortality Among Residents of 90 Cities. [156407](#)
- Dominici F; McDermott A; Zeger SL; Samet JM. (2002). On the use of generalized additive models in time-series studies of air pollution and health. *Am J Epidemiol*, 156: 193-203. [030458](#)

- Dominici F; Peng RD; Bell ML; Pham L; McDermott A; Zeger SL; Samet JL. (2006). Fine particulate air pollution and hospital admission for cardiovascular and respiratory diseases. *JAMA*, 295: 1127-1134. [088398](#)
- Dominici F; Peng RD; Ebisu K; Zeger SL; Samet JM; Bell ML. (2007). Does the effect of PM10 on mortality depend on PM nickel and vanadium content? A reanalysis of the NMMAPS data. *Environ Health Perspect*, 115: 1701-3. [099135](#)
- Dominici F; Peng RD; Zeger SL; White RH; Samet JM. (2007). Particulate air pollution and mortality in the United States: did the risks change from 1987 to 2000?. *Am J Epidemiol*, 166: 880-8. [097361](#)
- Dubowsky SD; Suh H; Schwartz J; Coull BA; Gold DR. (2006). Diabetes, obesity, and hypertension may enhance associations between air pollution and markers of systemic inflammation. *Environ Health Perspect*, 114: 992-998. [088750](#)
- Dusek R; Frank GP; Hildebrandt L; Curtius J; Schneider J; Walter S; Chand D; Drewnick F; Hings S; Jung D; Borrmann S; Andreae MO. (2006). Size matters more than chemistry for cloud-nucleating ability of aerosol particles. 1375-1378. [155756](#)
- Duvall RM; Norris GA; Dailey LA; Burke JM; McGee JK; Gilmour MI; Gordon T; Devlin RB. (2008). Source apportionment of particulate matter in the US and associations with lung inflammatory markers. *Inhal Toxicol*, 20: 671-83. [097969](#)
- Dvonch JT; Brook RD; Keeler GJ; Rajagopalan S; D'Alecy LG; Marsik FJ; Morishita M; Yip FY; Brook JR; Timm EJ; Wagner JG; Harkema JR. (2004). Effects of concentrated fine ambient particles on rat plasma levels of asymmetric dimethylarginine. *Inhal Toxicol*, 16: 473-480. [055741](#)
- Ebelt ST; Wilson WE; Brauer M. (2005). Exposure to ambient and nonambient components of particulate matter: a comparison of health effects. *Epidemiology*, 16: 396-405. [056907](#)
- Elder A; Gelein R; Finkelstein J; Phipps R; Frampton M; Utell M; Kittelson DB; Watts WF; Hopke P; Jeong CH; Kim E; Liu W; Zhao W; Zhuo L; Vincent R; Kumarathasan P; Oberdorster G. (2004). On-road exposure to highway aerosols 2 Exposures of aged, compromised rats. *Inhal Toxicol*, 16 Suppl 1: 41-53. [087354](#)
- Elder ACP; Gelein R; Azadniv M; Frampton M; Finkelstein J; Oberdorster G. (2004). Systemic effects of inhaled ultrafine particles in two compromised, aged rat strains. *Inhal Toxicol*, 16: 461-471. [055642](#)
- Erbas B; Kelly A-M; Physick B; Code C; Edwards M. (2005). Air pollution and childhood asthma emergency hospital admissions: estimating intra-city regional variations. *Int J Environ Health Res*, 15: 11-20. [073849](#)
- Fairley D. (2003). Mortality and air pollution for Santa Clara County, California, 1989-1996. [042850](#)
- Fakhri AA; Ilic LM; Wellenius GA; Urch B; Silverman F; Gold DR; Mittleman MA. (2009). Autonomic effects of controlled fine particulate exposure in young healthy adults: Effect modification by ozone. *Environ Health Perspect*, In Press: In Press. [191914](#)
- Fan Z; Meng Q; Weisel C; Laumbach R; Ohman-Strickland P; Shalat S; Hernandez M; Black K. (2008). Acute exposure to elevated PM (2.5) generated by traffic and cardiopulmonary health effects in healthy older adults. *J Expo Sci Environ Epidemiol*, 19: 525-533. [191979](#)
- Farraj AK; Haykal-Coates N; Ledbetter AD; Evansky PA; Gavett SH. (2006). Inhibition of pan neurotrophin receptor p75 attenuates diesel particulate-induced enhancement of allergic airway responses in C57/B16J mice. *Inhal Toxicol*, 18: 483-491. [088469](#)
- Farraj AK; Haykal-Coates N; Ledbetter AD; Evansky PA; Gavett SH. (2006). Neurotrophin mediation of allergic airways responses to inhaled diesel particles in mice. , 94: 183-92. [141730](#)
- Fedulov AV; Leme A; Yang Z; Dahl M; Lim R; Mariani TJ; Kobzik L. (2008). Pulmonary exposure to particles during pregnancy causes increased neonatal asthma susceptibility. , 38: 57-67. [097482](#)
- Ferdinands JM; Crawford CA; Greenwald R; Van Sickle D; Hunter E; Teague WG. (2008). Breath acidification in adolescent runners exposed to atmospheric pollution: a prospective, repeated measures observational study. *Environ Health*, 7: 10. [156433](#)
- Finnerty K; Choi J-E; Lau A; Davis-Gorman G; Diven C; Seaver N; Linak William P; Witten M; McDonagh Paul F. (2007). Instillation of coarse ash particulate matter and lipopolysaccharide produces a systemic inflammatory response in mice. *J Toxicol Environ Health A*, 70: 1957-1966. [156434](#)
- Fischer PH; Steerenberg PA; Snelder JD; Van Loveren H; Van Amsterdam JGC. (2002). Association between exhaled nitric oxide, ambient air pollution and respiratory health in school children. *Int Arch Occup Environ Health*, 75: 348-353. [025731](#)
- Fischer SL; Koshland CP. (2007). Daily and peak 1 h indoor air pollution and driving factors in a rural Chinese village. *Environ Sci Technol*, 41: 3121-3126. [156435](#)
- Folino AF; Scapellato ML; Canova C; Maestrelli P; Bertorelli G; Simonato L; Iliceto S; Lotti M. (2009). Individual exposure to particulate matter and the short-term arrhythmic and autonomic profiles in patients with myocardial infarction. *Eur Heart J*, 30: 1614-1620. [191902](#)

- Forastiere F; Stafoggia M; Berti G; Bisanti L; Cernigliaro A; Chiusolo M; Mallone S; Miglio R; Pandolfi P; Rognoni M; Serinelli M; Tessari R; Vigotti M; Perucci C. (2008). Particulate Matter and Daily Mortality: A Case-Crossover Analysis of Individual Effect Modifiers. *Epidemiology*, 19: 571-580. [186937](#)
- Forastiere F; Stafoggia M; Picciotto S; Bellander T; D'Ippoliti D; Lanki T; Von Klot S; Nyberg F; Paatero P; Peters A; Pekkanen J; Sunyer J; Perucci CA. (2005). A case-crossover analysis of out-of-hospital coronary deaths and air pollution in Rome, Italy. *Am J Respir Crit Care Med*, 172: 1549-1555. [086323](#)
- Frampton MW. (2001). Systemic and cardiovascular effects of airway injury and inflammation: ultrafine particle exposure in humans. *Environ Health Perspect*, 109: 529-532. [019051](#)
- Frampton MW; Stewart JC; Oberdorster G; Morrow PE; Chalupa D; Pietropaoli AP; Frasier LM; Speers DM; Cox C; Huang LS; Utell MJ. (2006). Inhalation of ultrafine particles alters blood leukocyte expression of adhesion molecules in humans. *Environ Health Perspect*, 114: 51-58. [088665](#)
- Franklin M; Koutrakis P; Schwartz J. (2008). PM25 composition & daily mortality in 25 US communities. [097426](#)
- Franklin M; Koutrakis P; Schwartz J. (2008). The role of particle composition on the association between PM2.5 and mortality. *Epidemiology*, 19: 680-689. [155779](#)
- Franklin M; Zeka A; Schwartz J. (2007). Association between PM2.5 and all-cause and specific-cause mortality in 27 US communities. *J Expo Sci Environ Epidemiol*, 17: 279-287. [091257](#)
- Fung KY; Khan S; Krewski D; Chen Y. (2006). Association between air pollution and multiple respiratory hospitalizations among the elderly in Vancouver, Canada. *Inhal Toxicol*, 18: 1005-1011. [089789](#)
- Fung KY; Luginaah IKMG; Webster G. (2005). Air pollution and daily hospitalization rates for cardiovascular and respiratory diseases in London, Ontario. *Int J Environ Stud*, 62: 677-685. [093262](#)
- Galan I; Tobias A; Banegas JR; Aranguiz E. (2003). Short-term effects of air pollution on daily asthma emergency room admissions. *Eur Respir J*, 22: 802-808. [087408](#)
- Gavett SH; Haykal-Coates N; Copeland L B; Heinrich J; Gilmour MI. (2003). Metal composition of ambient PM2.5 influences severity of allergic airways disease in mice. *Environ Health Perspect*, 111: 1471-1477. [053153](#)
- Gehlbach BK; Geppert E. (2004). The pulmonary manifestations of left heart failure. , 125: 669-682. [155784](#)
- Geiser M; Rothen-Rutishauser B; Kapp N; Schurch S; Kreyling W; Schulz H; Semmler M; Im Hof V; Heyder J; Gehr P. (2005). Ultrafine particles cross cellular membranes by nonphagocytic mechanisms in lungs and in cultured cells. *Environ Health Perspect*, 113: 1555-1560. [087362](#)
- Gent JF; Koutrakis P; Belanger K; Triche E; Holford TR; Bracken MB; Leaderer BP. (2009). Symptoms and medication use in children with asthma and traffic-related sources of fine particle pollution. *Environ Health Perspect*, In Press: 1-41. [180399](#)
- Gent JF; Triche EW; Holford TR; Belanger K; Bracken MB; Beckett WS; Leaderer BP. (2003). Association of low-level ozone and fine particles with respiratory symptoms in children with asthma. *JAMA*, 290: 1859-1867. [052885](#)
- Gerlofs-Nijland ME; Rummelhard M; Boere AJF; Leseman DLAC; Duffin R; Schins RPF; Borm PJA; Sillanpaa M; Salonen RO; Cassee FR. (2009). Particle induced toxicity in relation to transition metal and polycyclic aromatic hydrocarbon contents. *Environ Sci Technol*, In Press: 1-8. [190353](#)
- Gerlofs-Nijland ME; Dormans JA; Bloemen HJ; Leseman DL; John A; Boere F; Kelly FJ; Mudway IS; Jimenez AA; Donaldson K; Guastadisegni C; Janssen NA; Brunekreef B; Sandstrom T; van Bree L; Cassee FR. (2007). Toxicity of coarse and fine particulate matter from sites with contrasting traffic profiles. , 19: 1055-69. [097840](#)
- Ghelfi E; Rhoden CR; Wellenius GA; Lawrence J; Gonzalez-Flecha B. (2008). Cardiac oxidative stress and electrophysiological changes in rats exposed to concentrated air particles are mediated by TRP-dependent pulmonary reflexes. *Toxicol Sci*, 102: 328-336. [156468](#)
- Ghio AJ; Devlin RB. (2001). Inflammatory lung injury after bronchial instillation of air pollution particles. *Am J Respir Crit Care Med*, 164: 704-708. [017122](#)
- Ghio AJ; Hall A; Bassett MA; Cascio WE; Devlin RB. (2003). Exposure to concentrated ambient air particles alters hematologic indices in humans. *Inhal Toxicol*, 15: 1465-1478. [087363](#)
- Ghio AJ; Kim C; Devlin RB. (2000). Concentrated ambient air particles induce mild pulmonary inflammation in healthy human volunteers. *Am J Respir Crit Care Med*, 162: 981-988. [012140](#)
- Gilliland FD; Li YF; Saxon A; Diaz-Sanchez D. (2004). Effect of glutathione-S-transferase M1 and P1 genotypes on xenobiotic enhancement of allergic responses: randomised, placebo-controlled crossover study. *Lancet*, 363: 119-125. [156471](#)
- Gilmour MI; McGee J; Duvall Rachele M; Dailey L; Daniels M; Boykin E; Cho S-H; Doerfler D; Gordon T; Devlin Robert B. (2007). Comparative toxicity of size-fractionated airborne particulate matter obtained from different cities in the United States. , 19 Suppl 1: 7-16. [096433](#)

- Gilmour MI; O'Connor S; Dick CAJ; Miller CA; Linak WP. (2004). Differential pulmonary inflammation and in vitro cytotoxicity of size-fractionated fly ash particles from pulverized coal combustion. *J Air Waste Manag Assoc*, 54: 286-295. [057420](#)
- Gilmour PS; Ziesenis A; Morrison ER; Vickers MA; Drost EM; Ford I; Karg E; Mossa C; Schroepel A; Ferron GA; Heyder J; Greaves M; MacNee W; Donaldson K. (2004). Pulmonary and systemic effects of short-term inhalation exposure to ultrafine carbon black particles. *Toxicol Appl Pharmacol*, 195: 35-44. [054175](#)
- Girardot SP; Ryan PB; Smith SM; Davis WT; Hamilton CB; Obenour RA; Renfro JR; Tromatore KA; Reed GD. (2006). Ozone and PM25 exposure and acute pulmonary health effects: a study of hikers in the Great Smoky Mountains National Park. *Environ Health Perspect*, 113: 612-617. [088271](#)
- Godleski JJ; Clarke RW; Coull BA; Saldiva PHN; Jiang NF; Lawrence J; Koutrakis P. (2002). Composition of inhaled urban air particles determines acute pulmonary responses. *Ann Occup Hyg*, 46: 419-424. [156478](#)
- Godleski JJ; Verrier RL; Koutrakis P; Catalano P; Coull B; Reinisch U; Lovett EG; Lawrence J; Murthy GG; Wolfson JM; Clarke RW; Nearing BD; Killingsworth C. (2000). Mechanisms of morbidity and mortality from exposure to ambient air particles. , 91: 5-88; discussion 89-103. [000738](#)
- Gold DR; Litonjua AA; Zanobetti A; Coull BA; Schwartz J; MacCallum G; Verrier RL; Nearing BD; Canner MJ; Suh H; Stone PH. (2005). Air pollution and ST-segment depression in elderly subjects. *Environ Health Perspect*, 113: 883-887. [087558](#)
- Goldberg MS; Giannetti N; Burnett RT; Mayo NE; Valois MF; Brophy JM. (2008). A panel study in congestive heart failure to estimate the short-term effects from personal factors and environmental conditions on oxygen saturation and pulse rate. *Occup Environ Med*, 65: 659-666. [180380](#)
- Gong H Jr; Sioutas C; Linn WS. (2003). Controlled exposures of healthy and asthmatic volunteers to concentrated ambient particles in metropolitan Los Angeles. [087365](#)
- Gong H; Sioutas C; Linn WS; Clark KW; Terrell SL; Terrell LL; Anderson KR; Kim S; Chang MC. (2000). Controlled human exposures to concentrated ambient fine particles in metropolitan Los Angeles: Methodology and preliminary health-effect findings. *Inhal Toxicol*, 12: 107-119. [155799](#)
- Gong H Jr; Linn WS; Clark KW; Anderson KR; Geller MD; Sioutas C. (2005). Respiratory responses to exposures with fine particulates and nitrogen dioxide in the elderly with and without COPD. *Inhal Toxicol*, 17: 123-132. [087921](#)
- Gong H Jr; Linn WS; Clark KW; Anderson KR; Sioutas C; Alexis NE; Cascio WE; Devlin RB. (2008). Exposures of healthy and asthmatic volunteers to concentrated ambient ultrafine particles in Los Angeles. *Inhal Toxicol*, 20: 533-545. [156483](#)
- Gong H Jr; Linn WS; Sioutas C; Terrell SL; Clark KW; Anderson KR; Terrell LL. (2003). Controlled exposures of healthy and asthmatic volunteers to concentrated ambient fine particles in Los Angeles. *Inhal Toxicol*, 15: 305-325. [042106](#)
- Gong H Jr; Linn WS; Terrell SL; Anderson KR; Clark KW; Sioutas C; Cascio WE; Alexis N; Devlin RB. (2004). Exposures of elderly volunteers with and without chronic obstructive pulmonary disease (COPD) to concentrated ambient fine particulate pollution. *Inhal Toxicol*, 16: 731-744. [087964](#)
- Gong H Jr; Linn WS; Terrell SL; Clark KW; Geller MD; Anderson KR; Cascio WE; Sioutas C. (2004). Altered heart-rate variability in asthmatic and healthy volunteers exposed to concentrated ambient coarse particles. *Inhal Toxicol*, 16: 335-343. [055628](#)
- Gordian ME; Choudhury AH. (2003). PM10 and asthma medication in schoolchildren. *Arch Environ Occup Health*, 58: 42-47. [054842](#)
- Gowdy K; Krantz QT; Daniels M; Linak WP; Jaspers I; Gilmour MI. (2008). Modulation of pulmonary inflammatory responses and antimicrobial defenses in mice exposed to diesel exhaust. *Toxicol Appl Pharmacol*, 229(3): 310-319. [097226](#)
- Graff D; Cascio W; Rappold A; Zhou H; Huang Y; Devlin R. (2009). Exposure to concentrated coarse air pollution particles causes mild cardiopulmonary effects in healthy young adults . *Environ Health Perspect*, 117: 1089-1094. [191981](#)
- Gurgueira SA; Lawrence J; Coull B; Murthy GGK; Gonzalez-Flecha B. (2002). Rapid increases in the steady-state concentration of reactive oxygen species in the lungs and heart after particulate air pollution inhalation. *Environ Health Perspect*, 110: 749-755. [036535](#)
- Hajat S; Haines A; Atkinson RW; Bremner SA; Anderson HR; Emberlin J. (2001). Association between air pollution and daily consultations with general practitioners for allergic rhinitis in London, United Kingdom. *Am J Epidemiol*, 153: 704-714. [016693](#)
- Halonen JI; Lanki T; Yli-Tuomi T; Kulmala M; Tiittanen P; Pekkanen J. (2008). Urban air pollution, and asthma and COPD hospital emergency room visits. *Thorax*, 63: 635-41. [189507](#)
- Halonen JI; Lanki T; Yli-Tuomi T; Tiittanen P; Kulmala M; Pekkanen. (2009). Particulate air pollution and acute cardiorespiratory hospital admissions and mortality among the elderly. *Epidemiology*, 20: 143-153. [180379](#)

- Hamada K; Suzuki Y; Leme A; Ito T; Miyamoto K; Kobzik L; Kimura H. (2007). Exposure of pregnant mice to an air pollutant aerosol increases asthma susceptibility in offspring. *J Toxicol Environ Health A*, 70: 688-695. [091235](#)
- Hamade AK; Rabold R; Tankersley CG. (2008). Adverse cardiovascular effects with acute particulate matter and ozone exposures: interstrain variation in mice. *Environ Health Perspect*, 116: 1033-1039. [156515](#)
- Hanigan IC; Johnston FH; Morgan GG. (2008). Vegetation fire smoke, indigenous status and cardio respiratory hospital admissions in Darwin, Australia, 1996-2005: a time-series study. , 7: 42. [156518](#)
- Hao M; Comier S; Wang M; Lee James J; Nel A. (2003). Diesel exhaust particles exert acute effects on airway inflammation and function in murine allergen provocation models. *J Allergy Clin Immunol*, 112: 905-914. [096565](#)
- Hapcioglu B; Issever H; Kocyigit E; Disci R; Vatansever S; Ozdilli K. (2006). The effect of air pollution and meteorological parameters on chronic obstructive pulmonary disease at an Istanbul hospital. *Indoor Built Environ*, 15: 147-153. [093263](#)
- Happo MS; Salonen RO; Halinen AI; Jalava PI; Pennanen AS; Kosma VM; Sillanpaa M; Hillamo R; Brunekreef B; Katsouyanni K; Sunyer J; Hirvonen MR. (2007). Dose and time dependency of inflammatory responses in the mouse lung to urban air coarse, fine, and ultrafine particles from six European cities. , 19: 227-246. [096630](#)
- Harder V; Gilmour P; Lentner B; Karg E; Takenaka S; Ziesenis A; Stampfl A; Kodavanti U; Heyder J; Schulz H. (2005). Cardiovascular responses in unrestrained WKY rats to inhaled ultrafine carbon particles. *Inhal Toxicol*, 17: 29-42. [087371](#)
- Harkema JR; Keeler G; Wagner J; Morishita M; Timm E; Hotchkiss J; Marsik F; Dvonch T; Kaminski N; Barr E. (2004). Effects of concentrated ambient particles on normal and hypersecretory airways in rats. [056842](#)
- Harrod KS; Jaramillo RJ; Berger JA; Gigliotti AP; Seilkop SK; Reed MD. (2005). Inhaled diesel engine emissions reduce bacterial clearance and exacerbate lung disease to *Pseudomonas aeruginosa* infection in vivo. *Toxicol Sci*, 83: 155-165. [088144](#)
- Harrod KS; Jaramillo RJ; Rosenberger CL; Wang S-Z; Berger JA; McDonald JD; Reed MD. (2003). Increased susceptibility to RSV infection by exposure to inhaled diesel engine emissions. , 28: 451-463. [097046](#)
- Hayek T; Oiknine J; Brook JG; Aviram M. (1994). Increased plasma and lipoprotein lipid peroxidation in apo E-deficient mice. *Biochem Biophys Res Commun*, 201: 1567-1574. [156527](#)
- Hedley AJ; Wong C-M; Thach TQ; Ma S; Lam T-H; Anderson HR. (2002). Cardiorespiratory and all-cause mortality after restrictions on sulphur content of fuel in Hong Kong: an intervention study. *Lancet*, 360: 1646-1652. [040284](#)
- Heidenfelder BL; Reif DM; Harkema JR; Cohen Hubal EA; Hudgens EE; Bramble LA; Wagner JG; Morishita M; Keeler GJ; Edwards SW; Gallagher JE. (2009). Comparative microarray analysis and pulmonary changes in brown norway rats exposed to ovalbumin and concentrated air particulates. *Toxicol Sci*, 108: 207-221. [190026](#)
- Henneberger A; Zareba W; Ibald-Mulli A; Ruckerl R; Cyrys J; Couderc J-P; Mykins B; Woelke G; Wichmann H-E; Peters A. (2005). Repolarization changes induced by air pollution in ischemic heart disease patients. *Environ Health Perspect*, 113: 440-446. [087960](#)
- Henrotin JB; Besancenot JP; Bejot Y; Giroud M. (2007). Short-term effects of ozone air pollution on ischaemic stroke occurrence: a case-crossover analysis from a 10-year population-based study in Dijon, France. *Occup Environ Med*, 64: 439-445. [093270](#)
- Hinwood AL; De Klerk N; Rodriguez C; Jacoby P; Runnion T; Rye P; Landau L; Murray F; Feldwick M; Spickett J. (2006). The relationship between changes in daily air pollution and hospitalizations in Perth, Australia 1992-1998: a case-crossover study. *Int J Environ Health Res*, 16: 27-46. [088976](#)
- Hirshon JM; Shardell M; Alles S; Powell JL; Squibb K; Ondov J; Blaisdell CJ. (2008). Elevated ambient air zinc increases pediatric asthma morbidity. *Environ Health Perspect*, 116: 826-831. [180375](#)
- Hogervorst JG; de Kok TM; Briede JJ; Wesseling G; Kleinjans JC; van Schayck CP. (2006). Relationship between radical generation by urban ambient particulate matter and pulmonary function of school children. , 69: 245-62. [189460](#)
- Holguin F; Flores S; Ross Z; Cortez M; Molina M; Molina L; Rincon C; Jerrett M; Berhane K; Granados A; Romieu I. (2007). Traffic-related exposures, airway function, inflammation, and respiratory symptoms in children. *Am J Respir Crit Care Med*, 176: 1236-42. [099000](#)
- Holguin F; Tellez-Rojo MM; Hernandez M; Cortez M; Chow JC; Watson JG; Mannino D; Romieu I. (2003). Air pollution and heart rate variability among the elderly in Mexico City. , 14: 521-527. [057326](#)
- Holloman CH; Bortnick SM; Morara M; Strauss WJ; Calder CA. (2004). A Bayesian hierarchical approach for relating PM_{2.5} exposure to cardiovascular mortality in North Carolina. *Environ Health Perspect*, 112: 1282-1288. [087375](#)

- Hong Y-C; Hwang S-S; Kim JH; Lee K-H; Lee H-J; Lee K-H; Yu S-D; Kim D-S. (2007). Metals in particulate pollutants affect peak expiratory flow of schoolchildren. *Environ Health Perspect*, 115: 430-434. [091347](#)
- Hopke PK; Ito K; Mar T; Christensen WF; Eatough DJ; Henry RC; Kim E; Laden F; Lall R; Larson TV; Liu H; Neas L; Pinto J; Stolzel M; Suh H; Paatero P; Thurston GD. (2006). PM source apportionment and health effects: 1 Intercomparison of source apportionment results. *J Expo Sci Environ Epidemiol*, 16: 275-286. [088390](#)
- Host S; Larrieu S; Pascal L; Blanchard M; Declercq C; Fabre P; Jusot JF; Chardon B; Le Tertre A; Wagner V; Prouvost H; Lefranc A. (2007). Short-term Associations between Fine and Coarse Particles and Cardiorespiratory Hospitalizations in Six French Cities. *Occup Environ Med*. [155851](#)
- Host S; Larrieu S; Pascal L; Blanchard M; Declercq C; Fabre P; Jusot JF; Chardon B; Le Tertre A; Wagner V; Prouvost H; Lefranc A. (2008). Short-term associations between fine and coarse particles and hospital admissions for cardiorespiratory diseases in six French cities. *Occup Environ Med*, 65: 544-551. [155852](#)
- Huang Y-CT; Ghio AJ; Stonehuerner J; McGee J; Carter JD; Grambow SC; Devlin RB. (2003). The role of soluble components in ambient fine particles-induced changes in human lungs and blood. *Inhal Toxicol*, 15: 327-342. [087377](#)
- Huber SA; Sakkinen P; Conze D; Hardin N; Tracy R. (1999). Interleukin-6 exacerbates early atherosclerosis in mice. *Arterioscler Thromb Vasc Biol*, 19: 2364-2367. [156575](#)
- Hwang J-S; Chan C-C. (2002). Effects of air pollution on daily clinic visits for lower respiratory tract illness. *Am J Epidemiol*, 155: 1-10. [023222](#)
- Hwang J-S; Nadziejko C; Chen LC. (2005). Effects of subchronic exposures to concentrated ambient particles (CAPs) in mice: III Acute and chronic effects of CAPs on heart rate, heart-rate fluctuation, and body temperature. *Inhal Toxicol*, 17: 199-207. [087957](#)
- Ibald-Mulli A; Timonen KL; Peters A; Heinrich J; Wolke G; Lanki T; Buzorius G; Kreyling WG; De Hartog J; Hoek G; Ten Brink HM; Pekkanen J. (2004). Effects of particulate air pollution on blood pressure and heart rate in subjects with cardiovascular disease: a multicenter approach. *Environ Health Perspect*, 112: 369-377. [087415](#)
- Inoue K; Takano H; Yanagisawa R; Sakurai M; Ichinose T; Sadakane K; Yoshikawa T. (2005). Effects of nano particles on antigen-related airway inflammation in mice. *Respir Res*, 16. [088625](#)
- Ito K. (2003). Associations of particulate matter components with daily mortality and morbidity in Detroit, Michigan. [042856](#)
- Ito K; Christensen WF; Eatough DJ; Henry RC; Kim E; Laden F; Lall R; Larson TV; Neas L; Hopke PK; Thurston GD. (2006). PM source apportionment and health effects: 2 An investigation of intermethod variability in associations between source-apportioned fine particle mass and daily mortality in Washington, DC. *J Expo Sci Environ Epidemiol*, 16: 300-310. [088391](#)
- Ito K; Thurston GD; Silverman RA. (2007). Association between coarse particles and asthma emergency department (ED) visits in New York City. [091262](#)
- Ito T; Okumura H; Tsukue N; Kobayashi T; Honda K; Sekizawa K. (2006). Effect of diesel exhaust particles on mRNA expression of viral and bacterial receptors in rat lung epithelial L2 cells. , 165: 66-70. [096648](#)
- Ito T; Suzuki T; Tamura K; Nezu T; Honda K; Kobayashi T. (2008). Examination of mRNA expression in rat hearts and lungs for analysis of effects of exposure to concentrated ambient particles on cardiovascular function. *Toxicol Sci*, 243: 271-283. [096823](#)
- Jaffe DH; Singer ME; Rimm AA. (2003). Air pollution and emergency department visits for asthma among Ohio Medicaid recipients, 1991-1996. *Environ Res*, 91: 21-28. [041957](#)
- Jalaludin B; Morgan G; Lincoln D; Sheppard V; Simpson R; Corbett S. (2006). Associations between ambient air pollution and daily emergency department attendances for cardiovascular disease in the elderly (65+ years), Sydney, Australia. , 16: 225-37. [189416](#)
- Jalaludin BB; O'Toole BI; Leeder SR. (2004). Acute effects of urban ambient air pollution on respiratory symptoms, asthma medication use, and doctor visits for asthma in a cohort of Australian children. *Environ Res*, 95: 32-42. [056595](#)
- Jalava PI; Salonen RO; Halinen AI; Penttinen P; Pennanen AS; Sillanpaa M; Sandell E; Hillamo R; Hirvonen M-R. (2006). In vitro inflammatory and cytotoxic effects of size-segregated particulate samples collected during long-range transport of wildfire smoke to Helsinki. *Toxicol Appl Pharmacol*, 215: 341-353. [155872](#)
- Jalava PI; Salonen RO; Pennanen AS; Happonen MS; Penttinen P; Halinen AI; Sillanpaa M; Hillamo R; Hirvonen MR. (2008). Effects of solubility of urban air fine and coarse particles on cytotoxic and inflammatory responses in RAW 264.7 macrophage cell line. *Toxicol Appl Pharmacol*, 229: 146-60. [098968](#)
- Janes H; Sheppard L; Lumley T. (2005). Case-crossover analyses of air pollution exposure data: referent selection strategies and their implications for bias. , 16: 717-726. [087535](#)

- Jansen KL; Larson TV; Koenig JQ; Mar TF; Fields C; Stewart J; Lippmann M. (2005). Associations between health effects and particulate matter and black carbon in subjects with respiratory disease. *Environ Health Perspect*, 113: 1741-1746. [082236](#)
- Janssen NAH; Schwartz J; Zanobetti A; Suh HH. (2002). Air conditioning and source-specific particles as modifiers of the effect of PM10 on hospital admissions for heart and lung disease. *Environ Health Perspect*, 110: 43-49. [016743](#)
- Johnston FH; Bailie RS; Pilotto LS; Hanigan IC. (2007). Ambient biomass smoke and cardio-respiratory hospital admissions in Darwin, Australia. , 7: 240. [155882](#)
- Johnston FH; Webby RJ; Pilotto LS; Bailie RS; Parry DL; Halpin SJ. (2006). Vegetation fires, particulate air pollution and asthma: a panel study in the Australian monsoon tropics. *Int J Environ Health Res*, 16: 391-404. [091386](#)
- Just J; Segala C; Sahraoui F; Priol G; Grimfeld A; Neukirch F. (2002). Short-term health effects of particulate and photochemical air pollution in asthmatic children. *Eur Respir J*, 20: 899-906. [035429](#)
- Kannel WB; Abbott RD; Savage DD; McNamara PM. (1983). Coronary heart disease and atrial fibrillation: the Framingham Study. *Am Heart J*, 106: 389-396. [156623](#)
- Katsouyanni K; Touloumi G; Samoli E; Petasakis Y; Analitis A; Le Tertre A; Rossi G; Zmirou D; Ballester F; Boumghar A; Anderson HR; Wojtyniak B; Paldy A; Braunstein R; Pekkanen J; Schindler C; Schwartz J. (2003). Sensitivity analysis of various models of short-term effects of ambient particles on total mortality in 29 cities in APHEA2. [042807](#)
- Kelishadi R; Mirghaffari N; Poursafa P; Gidding S. (2009). Lifestyle and environmental factors associated with inflammation, oxidative stress and insulin resistance in children. *Atherosclerosis*, 203: 311-319. [191960](#)
- Kettunen J; Lanki T; Tiittanen P; Aalto PP; Koskentalo T; Kulmala M; Salomaa V; Pekkanen J. (2007). Associations of fine and ultrafine particulate air pollution with stroke mortality in an area of low air pollution levels. *Stroke*, 38: 918-922. [091242](#)
- Kim SY; O'Neill MS; Lee JT; Cho Y; Kim J; Kim H. (2007). Air pollution, socioeconomic position, and emergency hospital visits for asthma in Seoul, Korea. *Int Arch Occup Environ Health*, 80: 701-710. [092837](#)
- Klein-Patel ME; Diamond G; Boniotto M; Saad S; Ryan LK. (2006). Inhibition of beta-defensin gene expression in airway epithelial cells by low doses of residual oil fly ash is mediated by vanadium. , 92: 115-125. [097092](#)
- Kleinman MT; Araujo JA; Nel A; Sioutas C; Campbell A; Cong PQ; Li H; Bondy SC. (2008). Inhaled ultrafine particulate matter affects CNS inflammatory processes and may act via MAP kinase signaling pathways. *Toxicol Lett*, 178: 127-130. [190074](#)
- Kleinman MT; Hamade A; Meacher D; Oldham M; Sioutas C; Chakrabarti B; Stram D; Froines JR; Cho AK. (2005). Inhalation of concentrated ambient particulate matter near a heavily trafficked road stimulates antigen-induced airway responses in mice. , 55: 1277-88. [189364](#)
- Kleinman MT; Sioutas C; Froines JR; Fanning E; Hamade A; Mendez L; Meacher D; Oldham M. (2007). Inhalation of concentrated ambient particulate matter near a heavily trafficked road stimulates antigen-induced airway responses in mice. , 19 Suppl 1: 117-26. [097082](#)
- Klemm RJ; Lipfert FW; Wyzga RE; Gust C. (2004). Daily mortality and air pollution in Atlanta: two years of data from ARIES. *Inhal Toxicol*, 16 Suppl 1: 131-141. [056585](#)
- Klemm RJ; Mason R. (2003). Replication of reanalysis of Harvard Six-City mortality study. [042801](#)
- Klemm RJ; Mason RM Jr. (2000). Aerosol Research and Inhalation Epidemiological Study (ARIES): air quality and daily mortality statistical modeling--interim results. *J Air Waste Manag Assoc*, 50: 1433-1439. [010389](#)
- Knuckles T; Lund A; Lucas S; Campen M. (2008). Diesel exhaust exposure enhances vasoconstriction via uncoupling of eNOS. *Toxicol Appl Pharmacol*, 230: 346. [191987](#)
- Ko FWS; Tam W; Wong TW; Chan DPS. (2007). Temporal relationship between air pollutants and hospital admissions for chronic obstructive pulmonary disease in Hong Kong. *Thorax*, 62: 780-785. [091639](#)
- Ko FWS; Tam W; Wong TW; Lai CKW;. (2007). Effects of air pollution on asthma hospitalization rates in different age groups in Hong Kong. *Clin Exp Allergy*, 37: 1312-1319. [092844](#)
- Kodavanti UP; Schladweiler MC; Ledbetter AD; Hauser R; Christiani DC; McGee J; Richards JR; Costa DL. (2002). Temporal association between pulmonary and systemic effects of particulate matter in healthy and cardiovascular compromised rats. *J Toxicol Environ Health A*, 65: 1545-1569. [025236](#)
- Kodavanti UP; Schladweiler MC; Ledbetter AD; McGee JK; Walsh L; Gilmour PS; Highfill JW; Davies D; Pinkerton KE; Richards JH; Crissman K; Andrews D; Costa DL. (2005). Consistent pulmonary and systemic responses from inhalation of fine concentrated ambient particles: roles of rat strains used and physicochemical properties. *Environ Health Perspect*, 113: 1561-1568. [087946](#)

- Kodavanti UP; Schladweiler MCJ; Ledbetter AD; Hauser R; Christiani DC; Samet JM; McGee J; Richards JH; Costa DL. (2002). Pulmonary and systemic effects of zinc-containing emission particles in three rat strains: multiple exposure scenarios. *Toxicol Sci*, 70: 73-85. [035344](#)
- Koenig J; Allen R; Larson T; Liu S. (2005). Response to "Indoor- and Outdoor-Generated Particles and Children with asthma" [letter]. *Environ Health Perspect*, 113: A581. [088999](#)
- Koenig JQ; Jansen K; Mar TF; Lumley T; Kaufman J; Trenga CA; Sullivan J; Liu LJ; Shapiro GG; Larson TV. (2003). Measurement of offline exhaled nitric oxide in a study of community exposure to air pollution. *Environ Health Perspect*, 111: 1625-1629. [156653](#)
- Koenig JQ; Mar TF; Allen RW; Jansen K; Lumley T; Sullivan JH; Trenga CA; Larson T; Liu LJ. (2005). Pulmonary effects of indoor- and outdoor-generated particles in children with asthma. *Environ Health Perspect*, 113: 499-503. [087384](#)
- Koken PJM; Piver WT; Ye F; Elixhauser A; Olsen LM; Portier CJ. (2003). Temperature, air pollution, and hospitalization for cardiovascular diseases among elderly people in Denver. *Environ Health Perspect*, 111: 1312-1317. [049466](#)
- Kongerud J; Madden MC; Hazucha M; Peden D. (2006). Nasal responses in asthmatic and nonasthmatic subjects following exposure to diesel exhaust particles. *Inhal Toxicol*, 18: 589-594. [156656](#)
- Kooter IM; Boere AJ; Fokkens PH; Leseman DL; Dormans JA; Cassee FR. (2006). Response of spontaneously hypertensive rats to inhalation of fine and ultrafine particles from traffic: experimental controlled study. *Part Fibre Toxicol*, 15: 3-7. [097547](#)
- Kuo HW; Lai JS; Lee MC; Tai RC; Lee MC. (2002). Respiratory effects of air pollutants among asthmatics in central Taiwan. *Arch Environ Occup Health*, 57: 194-200. [036310](#)
- Laden F; Neas LM; Dockery DW; Schwartz J. (2000). Association of fine particulate matter from different sources with daily mortality in six US cities. *Environ Health Perspect*, 108: 941-947. [012102](#)
- Lagorio S; Forastiere F; Pistelli R; Iavarone I; Michelozzi P; Fano V; Marconi A; Ziemacki G; Ostro BD. (2006). Air pollution and lung function among susceptible adult subjects: a panel study. , 5: 11. [089800](#)
- Lai LW; Cheng WL. (2008). The impact of air quality on respiratory admissions during Asian dust storm periods. *Int J Environ Health Res*, 18: 429-450. [180301](#)
- Langrish JP; Mills NL; Chan JK; Leseman DL; Aitken RJ; Fokkens PH; Cassee FR; Li J; Donaldson K; Newby DE; Jiang L. (2009). Beneficial cardiovascular effects of reducing exposure to particulate air pollution with a simple facemask. *Part Fibre Toxicol*, 6: 8. [191908](#)
- Lanki T; De Hartog JJ; Heinrich J; Hoek G; Janssen NAH; Peters A; Stolzel M; Timonen KL; Vallius M; Vanninen E; Pekkanen J. (2006). Can we identify sources of fine particles responsible for exercise-induced ischemia on days with elevated air pollution? The ULTRA study. *Environ Health Perspect*, 114: 655-660. [088412](#)
- Lanki T; Hoek G; Timonen K; Peters A; Tiittanen P; Vanninen E; Pekkanen J. (2008). Hourly variation in fine particle exposure is associated with transiently increased risk of ST segment depression. *Br Med J*, 65: 782. [191984](#)
- Lanki T; Pekkanen J; Aalto P; Elosua R; Berglund N; D'Ippoliti D; Kulmala M; Nyberg F; Peters A; Picciotto S; Salomaa V; Sunyer J; Tiittanen P; Von Klot S; Forastiere F; for the HEAPSS Study Group. (2006). Associations of traffic-related air pollutants with hospitalisation for first acute myocardial infarction: the HEAPSS study. *Occup Environ Med*, 63: 844-851. [089788](#)
- Larrieu S; Jusot J-F; Blanchard M; Prouvost H; Declercq C; Fabre P; Pascal L; Le Tertre A; Wagner V; Riviere S; Chardon B; Borelli D; Cassadou S; Eilstein D; Lefranc A. (2007). Short term effects of air pollution on hospitalizations for cardiovascular diseases in eight French cities: The PSAS program. *Sci Total Environ*, 387: 105-112. [093031](#)
- Larrieu S; Lefranc A; Gault G; Chatignoux E; Couvy F; Jouves B; Filleul L. (2009). Are the Short-term Effects of Air Pollution Restricted to Cardiorespiratory Diseases?. *Am J Epidemiol*, 169: 1-8. [180294](#)
- Larsson B-M; Sehistedt M; Grunewald J; Skold CM; Lundin A; Blomberg A; Sandstrom T; Eklund A; Svartengren M. (2007). Road tunnel air pollution induces bronchoalveolar inflammation in healthy subjects. *Eur Respir J*, 29: 699-705. [091375](#)
- Last JA; Ward R; Temple L; Pinkerton KE; Kenyon NJ. (2004). Ovalbumin-induced airway inflammation and fibrosis in mice also exposed to ultrafine particles. , 16: 93-102. [097334](#)
- Laupacis A; Boysen G; Connolly S. (1994). Risk factors for stroke and efficacy of antithrombotic therapy in atrial fibrillation: Analysis of pooled data from five randomized controlled trials. , 154: 1449-1457. [190901](#)
- Laurent O; Pedrono G; Filleul L; Segala C; Lefranc A; Schillinger C; Riviere E; Bard D. (2009). Influence of socioeconomic deprivation on the relation between air pollution and beta-agonist sales for asthma. *Chest*, 135: 717-723. [192129](#)

- Laurent O; Pedrono G; Segala C; Filleul L; Havard S; Deguen S; Schillinger C; Riviere E; Bard D. (2008). Air pollution, asthma attacks, and socioeconomic deprivation: a small-area case-crossover study. *Am J Epidemiol*, 168: 58-65. [156672](#)
- Lay JC; Bennett WD; Kim CS; Devlin RB; Bromberg PA. (1998). Retention and intracellular distribution of instilled iron oxide particles in human alveolar macrophages. *Am J Respir Cell Mol Biol*, 18: 687-695. [007683](#)
- Lay JC; Zeman KL; Ghio AJ; Bennett WD. (2001). Effects of inhaled iron oxide particles on alveolar epithelial permeability in normal subjects. *Inhal Toxicol*, 13: 1065-1078. [020613](#)
- Le Tertre A; Medina S; Samoli E; Forsberg B; Michelozzi P; Boumghar A; Vonk JM; Bellini A; Atkinson R; Ayres JG; Sunyer J; Schwartz J; Katsouyanni K. (2002). Short term effects of particulate air pollution on cardiovascular diseases in eight European cities. *J Epidemiol Community Health*, 56: 773-779. [023746](#)
- Le Tertre A; Medina S; Samoli E; Forsberg B; Michelozzi P; Boumghar A; Vonk JM; Bellini A; Atkinson R; Ayres JG; Sunyer J; Schwartz J; Katsouyanni K. (2003). Short-term effects of particulate air pollution on cardiovascular diseases in eight European cities. [042820](#)
- Le Tertre A; Schwartz J; Touloumi G. (2005). Empirical Bayes and adjusted estimates approach to estimating the relation of mortality to exposure of PM10. *Risk Anal*, 25: 711-718. [087560](#)
- Lee J-T; Kim H; Song H; Hong Y-C; Cho Y-S; Shin S-Y; Hyun Y-J; Kim Y-S. (2002). Air pollution and asthma among children in Seoul, Korea. , 13: 481-484. [034826](#)
- Lee J-T; Son J-Y; Cho Y-S. (2007). A comparison of mortality related to urban air particles between periods with Asian dust days and without Asian dust days in Seoul, Korea, 2000-2004. *Environ Res*, 105: 409-13. [093042](#)
- Lee JT; Kim H; Cho YS; Hong YC; Ha EH; Park H. (2003). Air pollution and hospital admissions for ischemic heart diseases among individuals 64+ years of age residing in Seoul, Korea. , 58: 617-623. [095552](#)
- Lee SL; Wong WHS; Lau YL. (2006). Association between air pollution and asthma admission among children in Hong Kong. *Clin Exp Allergy*, 36: 1138-1146. [090176](#)
- Lei Y-C; Chan C-C; Wang P-Y; Lee C-T; Cheng T-J. (2004). Effects of Asian dust event particles on inflammation markers in peripheral blood and bronchoalveolar lavage in pulmonary hypertensive rats. *Environ Res*, 95: 71-76. [087884](#)
- Lei YC; Chen MC; Chan CC; Wang PY; Lee CT; Cheng TJ. (2004). Effects of concentrated ambient particles on airway responsiveness and pulmonary inflammation in pulmonary hypertensive rats. *Inhal Toxicol*, 16: 785-792. [087999](#)
- LeVine AM; Gwozdz J; Stark J; Bruno M; Whitsett J; Korfhagen T. (1999). Surfactant protein-A enhances respiratory syncytial virus clearance in vivo. *J Clin Invest*, 103: 1015-1021. [156687](#)
- LeVine AM; Whitsett JA. (2001). Pulmonary collectins and innate host defense of the lung. , 3: 161-166. [155928](#)
- Levy D; Sheppard L; Checkoway H; Kaufman J; Lumley T; Koenig J; Siscovick D. (2001). A case-crossover analysis of particulate matter air pollution and out-of-hospital primary cardiac arrest. , 12: 193-199. [017171](#)
- Lewis CW; Klouda GA; Ellenson WD. (2004). Radiocarbon measurement of the biogenic contribution to summertime PM-2.5 ambient aerosol in Nashville, TN. *Atmos Environ*, 38: 6053-6061. [097498](#)
- Lewis CW; Norris GA; Conner TL; Henry RC. (2003). Source apportionment of Phoenix PM2.5 aerosol with the Unmix Receptor model. *J Air Waste Manag Assoc*, 53: 325-338. [088413](#)
- Lewis TC; Robins TG; Dvonch JT; Keeler GJ; Yip FY; Mentz GB; Lin X; Parker EA; Israel BA; Gonzalez L; Hill Y. (2005). Air pollution-associated changes in lung function among asthmatic children in Detroit. *Environ Health Perspect*, 113: 1068-1075. [081079](#)
- Li N; Wang M; Bramble LA; Schmitz DA; Schauer JJ; Sioutas C; Harkema JR; Nel AE. (2009). The adjuvant effect of ambient particulate matter is closely reflected by the particulate oxidant potential. *Environ Health Perspect*, 117: 1116-1123. [190457](#)
- Li Y-J; Kawada T; Matsumoto A; Azuma A; Kudoh S; Takizawa H; Sugawara I. (2007). Airway inflammatory responses to oxidative stress induced by low-dose diesel exhaust particle exposure differ between mouse strains. , 33: 227-244. [155929](#)
- Liao C-M; Chiang Y-H; Chio C-P. (2009). Assessing the airborne titanium dioxide nanoparticle-related exposure hazard at workplace. *J Hazard Mater*, 162: 57-65. [157456](#)
- Liao D; Duan Y; Whitsel EA; Zheng Z-J; Heiss G; Chinchilli VM; Lin H-M. (2004). Association of higher levels of ambient criteria pollutants with impaired cardiac autonomic control: a population-based study. *Am J Epidemiol*, 159: 768-777. [056590](#)
- Liao D; Heiss G; Chinchilli VM; Duan Y; Folsom AR; Lin HM; Salomaa V. (2005). Association of criteria pollutants with plasma hemostatic/inflammatory markers: a population-based study. *J Expo Sci Environ Epidemiol*, 15: 319-328. [088677](#)

- Liao KJ; Tagaris E; Manomaiphiboon K; Napelenok SL; Woo JH; He S; Amar P; Russell AG. (2007). Sensitivities of Ozone and Fine Particulate Matter Formation to Emissions under the Impact of Potential Future Climate Change. *Environ Sci Technol*, 41: 8355-8361. [180272](#)
- Lin M; Chen Y; Burnett RT; Villeneuve PJ; Krewski D. (2002). The influence of ambient coarse particulate matter on asthma hospitalization in children: case-crossover and time-series analyses. *Environ Health Perspect*, 110: 575-581. [026067](#)
- Lin M; Stieb DM; Chen Y. (2005). Coarse particulate matter and hospitalization for respiratory infections in children younger than 15 years in Toronto: a case-crossover analysis. , 116: 235-240. [087828](#)
- Linn WS; Szlachcic Y; Gong H Jr; Kinney PL; Berhane KT. (2000). Air pollution and daily hospital admissions in metropolitan Los Angeles. *Environ Health Perspect*, 108: 427-434. [002839](#)
- Lipfert FW; Baty JD; Miller JP; Wyzga RE. (2006). PM_{2.5} constituents and related air quality variables as predictors of survival in a cohort of U.S. military veterans. *Inhal Toxicol*, 18: 645-657. [088756](#)
- Lipfert FW; Morris SC; Wyzga RE. (2000). Daily mortality in the Philadelphia metropolitan area and size-classified particulate matter. *J Air Waste Manag Assoc*, 50: 1501-1513. [004088](#)
- Lippmann M. (2000). Environmental toxicants: human exposures and their health effects. [024579](#)
- Lippmann M; Hwang J; Maciejczyk P; Chen L. (2005). PM source apportionment for short-term cardiac function changes in ApoE^{-/-} mice. *Environ Health Perspect*, 113: 1575-1579. [087453](#)
- Lippmann M; Ito K; Hwang JS; Maciejczyk P; Chen LC. (2006). Cardiovascular effects of nickel in ambient air. *Environ Health Perspect*, 114: 1662-9. [091165](#)
- Lippmann M; Ito K; Nadas A; Burnett RT. (2000). Association of particulate matter components with daily mortality and morbidity in urban populations. [011938](#)
- Lipsett MJ; Tsai FC; Roger L; Woo M; Ostro BD. (2006). Coarse particles and heart rate variability among older adults with coronary artery disease in the Coachella Valley, California. *Environ Health Perspect*, 114: 1215-1220. [088753](#)
- Lisabeth LD; Escobar JD; Dvonch JT; Sanchez BN; Majersik JJ; Brown DL; Smith MA; Morgenstern LB. (2008). Ambient air pollution and risk for ischemic stroke and transient ischemic attack. , 64: 53-59. [155939](#)
- Liu J; Ballaney M; Al-Alem U; Quan C; Jin X; Perera F; Chen LC; Miller RL. (2008). Combined Inhaled Diesel Exhaust Particles and Allergen Exposure Alter Methylation of T Helper Genes and IgE Production In Vivo. *Toxicol Sci*, 102: 76-81. [156709](#)
- Liu L; Poon R; Chen L; Frescura AM; Montuschi P; Ciabattini G; Wheeler A; Dales R. (2009). Acute effects of air pollution on pulmonary function, airway inflammation, and oxidative stress in asthmatic children. *Environ Health Perspect*, 117: 668-674. [192003](#)
- Liu L; Ruddy TD; Dalipaj M; Szyszkowicz M; You H; Poon R; Wheeler A; Dales R. (2007). Influence of personal exposure to particulate air pollution on cardiovascular physiology and biomarkers of inflammation and oxidative stress in subjects with diabetes. *J Occup Environ Med*, 49: 258-265. [156705](#)
- Liu SX; Hou FF; Guo ZJ; Nagai R; Zhang WR; Liu ZQ; Zhou ZM; Zhou M; Xie D; Wang GB; Zhang X. (2006). Advanced oxidation protein products accelerate atherosclerosis through promoting oxidative stress and inflammation. , 26: 1156-1162. [192002](#)
- Liu X; Meng Z. (2005). Effects of airborne fine particulate matter on antioxidant capacity and lipid peroxidation in multiple organs of rats. *Inhal Toxicol*, 17: 467-473. [088650](#)
- Ljungman P; Bellander T; Schneider A; Breitner S; Forastiere F; Hampel R; Illig T; Jacquemin B; Katsouyanni K; von Klot S. (2009). Modification of the interleukin-6 response to air pollution by interleukin-6 and fibrinogen polymorphisms. *Environ Health Perspect*, x: x. [191983](#)
- Ljungman PLS; Berglind N; Holmgren C; Gadler F; Edvardsson N; Pershagen G; Rosenqvist M; Sjögren B; Bellander T. (2008). Rapid effects of air pollution on ventricular arrhythmias. *Eur Heart J*, 29: 2894-2901. [180266](#)
- Llorca J; Salas A; Prieto-Salceda D; Chinchon-Bengoechea V; Delgado-Rodriguez M. (2005). Nitrogen dioxide increases cardiorespiratory admissions in Torrelavega (Spain). *J Environ Health*, 68: 30-35. [087825](#)
- Lokken PR; Wellenius GA; Coull BA; Burger MR; Schlaug G; Suh HH; Mittleman MA. (2009). Air Pollution and Risk of Stroke: Underestimation of Effect Due to Misclassification of Time of Event Onset. *Epidemiology*, 20: 137. [186774](#)
- Low RB; Bielory L; Qureshi AI; Dunn V; Stuhlmiller DF; Dickey DA. (2006). The relation of stroke admissions to recent weather, airborne allergens, air pollution, seasons, upper respiratory infections, and asthma incidence, September 11, 2001, and day of the week. , 37: 951-957. [090441](#)
- Lucking A; Lundback M; Mills N; Faratian D; Barath S; Pourazar J; Cassee F; Donaldson K; Boon N; Badimon J. (2008). Diesel exhaust inhalation increases thrombus formation in man. *Eur Heart J*, 29: 3043. [191993](#)

- Luginaah IN; Fung KY; Gorey KM; Webster G; Wills C. (2005). Association of ambient air pollution with respiratory hospitalization in a government designated "area of concern": the case of Windsor, Ontario. *Environ Health Perspect*, 113: 290-296. [057327](#)
- Lund AK; Lucero A; Lucas S; Madden MC; McDonald JD; Seagrave JC; Knuckles TL; Campen MJ. (2009). Vehicular emissions induce vascular MMP-9 expression and activity associated with endothelin-1-mediated pathways. *Arterioscler Thromb Vasc Biol*, 29: 511-517. [180257](#)
- Lundbäck M; Mills NL; Lucking A; Barath S; Donaldson K; Newby DE; Sandström T; Blomberg A. (2009). Experimental exposure to diesel exhaust increases arterial stiffness in man. *Part Fibre Toxicol*, 6: 7. [191967](#)
- Luttmann-Gibson H; Suh HH; Coull BA; Dockery DW; Sarnet SE; Schwartz J; Stone PH; Gold DR. (2006). Short-term effects of air pollution on heart rate variability in senior adults in Steubenville, Ohio. *J Occup Environ Med*, 48: 780-788. [089794](#)
- Maciejczyk P; Chen LC. (2005). Effects of subchronic exposures to concentrated ambient particles (CAPs) in mice: VIII source-related daily variations in in vitro responses to CAPs. *Inhal Toxicol*, 17: 243-253. [087456](#)
- Mar TF; Ito K; Koenig JQ; Larson TV; Eatough DJ; Henry RC; Kim E; Laden F; Lall R; Neas L; Stolzel M; Paatero P; Hopke PK; Thurston GD. (2006). PM source apportionment and health effects: 3 Investigation of inter-method variations in associations between estimated source contributions of PM_{2.5} and daily mortality in Phoenix, AZ. *J Expo Sci Environ Epidemiol*, 16: 311-320. [086143](#)
- Mar TF; Jansen K; Shepherd K; Lumley T; Larson TV; Koenig JQ. (2005). Exhaled nitric oxide in children with asthma and short-term PM_{2.5} exposure in Seattle. *Environ Health Perspect*, 113: 1791-1794. [088759](#)
- Mar TF; Koenig JQ; Jansen K; Sullivan J; Kaufman J; Trenga CA; Siahpush SH; Liu L-JS; Neas L. (2005). Fine particulate air pollution and cardiorespiratory effects in the elderly. *Environ Health Perspect*, 113: 681-687. [087566](#)
- Mar TF; Larson TV; Stier RA; Claiborn C; Koenig JQ. (2004). An analysis of the association between respiratory symptoms in subjects with asthma and daily air pollution in Spokane, Washington. *Inhal Toxicol*, 16: 809-815. [057309](#)
- Mar TF; Norris GA; Koenig JQ; Larson TV. (2000). Associations between air pollution and mortality in Phoenix, 1995-1997. *Environ Health Perspect*, 108: 347-353. [001760](#)
- Mar TF; Norris GA; Larson TV; Wilson WE; Koenig JQ. (2003). Air pollution and cardiovascular mortality in Phoenix, 1995-1997. [042841](#)
- Martins LC; Latorre MRDO; Saldiva PHN; Braga ALF. (2002). Air pollution and emergency room visits due to chronic lower respiratory diseases in the elderly: an ecological time-series study in Sao Paulo, Brazil. *J Occup Environ Med*, 44: 622-627. [035059](#)
- Masjedi MR; Jamaati HR; Dokouhaki P; Ahmadzadeh Z; Taheri SA; Bigdeli M; Izadi S; Rostamian A; Aagin K; Ghavam SM. (2003). The effects of air pollution on acute respiratory conditions. *Respirology*, 8: 213-230. [052100](#)
- Matsumoto A; Hiramatsu K; Li Y; Azuma A; Kudoh S; Takizawa H; Sugawara I. (2006). Repeated exposure to low-dose diesel exhaust after allergen challenge exaggerates asthmatic responses in mice. *Environ Health Perspect*, 114: 227-235. [098017](#)
- McCreanor J; Cullinan P; Nieuwenhuijsen MJ; Stewart-Evans J; Malliarou E; Jarup L; Harrington R; Svartengren M; Han I-K; Ohman-Strickland P; Chung KF; Zhang J. (2007). Respiratory effects of exposure to diesel traffic in persons with asthma. *Environ Health Perspect*, 115: 2348-2358. [092841](#)
- McDonald J; Barr E; White R; Kracko D; Chow J; Zielinska B; Grosjean E. (2008). Generation and characterization of gasoline engine exhaust inhalation exposure atmospheres. *Inhal Toxicol*, 20: 1157-1168. [191978](#)
- McDonald JD; Barr EB; White RK; Chow JC; Schauer JJ; Zielinska B; Grosjean E. (2004). Generation and characterization of four dilutions of diesel engine exhaust for a subchronic inhalation study. *Environ Sci Technol*, 38: 2513-2522. [055644](#)
- McQueen DS; Donaldson K; Bond SM; McNeilly JD; Newman S; Barton NJ; Duffin R. (2007). Bilateral vagotomy or atropine pre-treatment reduces experimental diesel-soot induced lung inflammation. *Toxicol Appl Pharmacol*, 219: 62-71. [096266](#)
- Medina-Ramon M; Zanobetti A; Schwartz J. (2006). The effect of ozone and PM₁₀ on hospital admissions for pneumonia and chronic obstructive pulmonary disease: a national multicity study. *Am J Epidemiol*, 163: 579-588. [087721](#)
- Metzger KB; Klein M; Flanders WD; Peel JL; Mulholland JA; Langberg JJ; Tolbert PE. (2007). Ambient air pollution and cardiac arrhythmias in patients with implantable defibrillators. *Epidemiology*, 18: 585-592. [092856](#)
- Metzger KB; Tolbert PE; Klein M; Peel JL; Flanders WD; Todd KH; Mulholland JA; Ryan PB; Frumkin H. (2004). Ambient air pollution and cardiovascular emergency department visits. *Environ Health Perspect*, 112: 46-56. [044222](#)

- Michaud J-P; Grove JS; Krupitsky D. (2004). Emergency department visits and "vog"-related air quality in Hilo, Hawai'i. *Environ Res*, 95: 11-19. [089900](#)
- Middleton N; Yiallourous P; Kleanthous S; Kolokotroni O; Schwartz J; Dockery DW; Demokritou P; Koutrakis P. (2008). A 10-year time-series analysis of respiratory and cardiovascular morbidity in Nicosia, Cyprus: the effect of short-term changes in air pollution and dust storms. , 7: 39. [156760](#)
- Migliaretti G; Cadum E; Migliore E; Cavallo F. (2005). Traffic air pollution and hospital admission for asthma: a case-control approach in a Turin (Italy) population. *Int Arch Occup Environ Health*, 78: 164-169. [088689](#)
- Migliaretti G; Cavallo F. (2004). Urban air pollution and asthma in children. *Pediatr Pulmonol*, 38: 198-203. [087425](#)
- Mills NL; Robinson SD; Fokkens PH; Leseman DL; Miller MR; Anderson D; Freney EJ; Heal MR; Donovan RJ; Blomberg A; Sandstrom T; MacNee W; Boon NA; Donaldson K; Newby DE; Cassee FR. (2008). Exposure to concentrated ambient particles does not affect vascular function in patients with coronary heart disease. *Environ Health Perspect*, 116: 709-715. [156766](#)
- Mills NL; Tornqvist H; Robinson SD; Gonzalez M; Darnley K; MacNee W; Boon NA; Donaldson K; Blomberg A; Sandstrom T; Newby DE. (2005). Diesel exhaust inhalation causes vascular dysfunction and impaired endogenous fibrinolysis. , 112: 3930-3936. [095757](#)
- Mills NL; Törnqvist H; Gonzalez MC; Vink E; Robinson SD; Soderberg S; Boon NA; Donaldson K; Sandstrom T; Blomberg A; Newby DE. (2007). Ischemic and thrombotic effects of dilute diesel-exhaust inhalation in men with coronary heart disease. , 357: 1075-1082. [091206](#)
- Min KB; Min JY; Cho SI; Paek D. (2008). The relationship between air pollutants and heart-rate variability among community residents in Korea. *Inhal Toxicol*, 4: 435-444. [191901](#)
- Mohr LB; Luo S; Mathias E; Tobing R; Homan S; Sterling D. (2008). Influence of season and temperature on the relationship of elemental carbon air pollution to pediatric asthma emergency room visits. *J Asthma*, 45: 936-943. [180215](#)
- Moolgavkar SH. (2000). Air pollution and daily mortality in three US counties. *Environ Health Perspect*, 108: 777-784. [012054](#)
- Moolgavkar SH. (2000). Air pollution and hospital admissions for diseases of the circulatory system in three US metropolitan areas. *J Air Waste Manag Assoc*, 50: 1199-1206. [010305](#)
- Moolgavkar SH. (2003). Air pollution and daily deaths and hospital admissions in Los Angeles and Cook counties. [042864](#)
- Moolgavkar SH. (2003). Air pollution and daily mortality in two US counties: season-specific analyses and exposure-response relationships. *Inhal Toxicol*, 15: 877-907. [051316](#)
- Moore KJ; Kunjathoor VV; Koehn SL; Manning JJ; Tseng AA; Silver JM; McKee M; Freeman MW. (2005). Loss of receptor-mediated lipid uptake via scavenger receptor A or CD36 pathways does not ameliorate atherosclerosis in hyperlipidemic mice. *J Clin Invest*, 115: 2192-2201. [156780](#)
- Morishita M; Keeler G; Wagner J; Marsik F; Timm E; Dvonch J; Harkema J. (2004). Pulmonary retention of particulate matter is associated with airway inflammation in allergic rats exposed to air pollution in urban Detroit. *Inhal Toxicol*, 16: 663-674. [087979](#)
- Morris RD; Naumova EN. (1998). Carbon monoxide and hospital admissions for congestive heart failure: evidence of an increased effect at low temperatures. *Environ Health Perspect*, 106: 649-653. [086857](#)
- Morrison D; Skwarski D; Millar AM; Adams W; MacNee W. (1998). A comparison of three methods of measuring ^{99m}Tc-DTPA lung clearance and their repeatability. *Eur Respir J*, 11: 1141-1146. [024924](#)
- Mortimer KM; Neas LM; Dockery DW; Redline S; Tager IB. (2002). The effect of air pollution on inner-city children with asthma. *Eur Respir J*, 19: 699-705. [030281](#)
- Moshhammer H; Hutter H-P; Hauck H; Neuberger M. (2006). Low levels of air pollution induce changes of lung function in a panel of schoolchildren. *Eur Respir J*, 27: 1138-1143. [090771](#)
- Moshhammer H; Neuberger M. (2003). The active surface of suspended particles as a predictor of lung function and pulmonary symptoms in Austrian school children. *Atmos Environ*, 37: 1737-1744. [041956](#)
- Mudway IS; Stenfors N; Duggan ST; Roxborough H; Zielinski H; Marklund SL; Blomberg A; Frew AJ; Sandstrom T; Kelly FJ. (2004). An in vitro and in vivo investigation of the effects of diesel exhaust on human airway lining fluid antioxidants. *Arch Biochem Biophys*, 423: 200-212. [180208](#)
- Mudzinski SP; Rudofsky UH; Mitchell DG; Lawrence DA. (1986). Analysis of lead effects on in vivo antibody-mediated immunity in several mouse strains. *Toxicol Appl Pharmacol*, 83: 321-330. [084184](#)
- Muggenburg BA; Barr EB; Cheng YS; Seagrave JC; Tilley LP; Mauderly JL. (2000). Effect of inhaled residual oil fly ash on the electrocardiogram of dogs. Presented at In: Grant, L. D., ed. PM2000: particulate matter and health. *Inhalation Toxicol*. 12(suppl. 4): 189-208. [010279](#)
- Murata A; Kida K; Hasunuma H; Kanegae H; Ishimaru Y; Motegi T; Yamada K; Yoshioka H; Yamamoto K; Kudoh S. (2007). Environmental influence on the measurement of exhaled nitric oxide concentration in school children: special reference to methodology. , 74: 30-36. [156787](#)

- Mutlu GM; Green D; Bellmeyer A; Baker CM; Burgess Z; Rajamannan N; Christman JW; Foiles N; Kamp DW; Ghio AJ; Chandel NS; Dean DA; Sznajder JI; Budinger GR. (2007). Ambient particulate matter accelerates coagulation via an IL-6-dependent pathway. , 117: 2952-61. [121441](#)
- Ménache MG; Miller FJ; Raabe OG. (1995). Particle inhalability curves for humans and small laboratory animals. *Ann Occup Hyg*, 39: 317-328. [006533](#)
- Nadziejko C; Fang K; Chen LC; Cohen B; Karpatkin M; Nadas A. (2002). Effect of concentrated ambient particulate matter on blood coagulation parameters in rats. [050587](#)
- Nadziejko C; Fang K; Nadziejko E; Narciso SP; Zhong M; Chen LC. (2002). Immediate effects of particulate air pollutants on heart rate and respiratory rate in hypertensive rats. , 2: 245-252. [087460](#)
- Nadziejko C; Fang K; Narciso S; Zhong M; Su WC; Gordon T; Nadas A; Chen LC. (2004). Effect of particulate and gaseous pollutants on spontaneous arrhythmias in aged rats. *Inhal Toxicol*, 16: 373-380. [055632](#)
- Nascimento LF; Pereira LA; Braga AL; Modolo MC; Carvalho JA Jr. (2006). Effects of air pollution on children's health in a city in southeastern Brazil. *Rev Saude Publica*, 40: 77-82. [093247](#)
- NCHS. (2007). Classification of Diseases, Functioning, and Disability...Monitoring the Nation's Health. Retrieved , from #http://www.cdc.gov/nchs/icd9.htm#RTF#. [157194](#)
- Neuberger M; Schimek MG; Horak F Jr; Moshhammer H; Kundi M; Frischer T; Gomiscek B; Puxbaum H; Hauck H; AUPHEP-Team. (2004). Acute effects of particulate matter on respiratory diseases, symptoms and functions: epidemiological results of the Austrian Projects on Health Effects of Particulate Matter (AUPHEP). *Atmos Environ*, 38: 3971-3981. [093249](#)
- New York State Department of Health. (2006). Study of ambient air contaminants and asthma in New York City, parts A and B. [090132](#)
- Nightingale JA; Maggs R; Cullinan P; Donnelly LE; Rogers DF; Kinnersley R; Chung KF; Barnes PJ; Ashmore M; Newman-Taylor A. (2000). Airway inflammation after controlled exposure to diesel exhaust particulates. *Am J Respir Crit Care Med*, 162: 161-166. [011659](#)
- Nikolov MC; Coull BA; Catalano PJ; Diaz E; Godleski JJ. (2008). Statistical methods to evaluate health effects associated with major sources of air pollution: a case-study of breathing patterns during exposure to concentrated Boston air particles. *J Roy Stat Soc C Appl Stat*, 57: 357-378. [156808](#)
- Nordenhall C; Pourazar J; Ledin M-C; Levin J-O; Sandstrom T; Adelroth E. (2001). Diesel exhaust enhances airway responsiveness in asthmatic subjects. *Eur Respir J*, 17: 909-915. [025185](#)
- Nurkiewicz TR; Porter DW; Barger M; Castranova V; Boegehold MA. (2004). Particulate matter exposure impairs systemic microvascular endothelium-dependent dilation. *Environ Health Perspect*, 112: 1299-1306. [087968](#)
- Nurkiewicz TR; Porter DW; Barger M; Millecchia L; Rao KM; Marvar PJ; Hubbs AF; Castranova V; Boegehold MA. (2006). Systemic microvascular dysfunction and inflammation after pulmonary particulate matter exposure. *Environ Health Perspect*, 114: 412-419. [088611](#)
- Nurkiewicz TR; Porter DW; Hubbs AF; Cumpston JL; Chen BT; Frazer DG; Castranova V. (2008). Nanoparticle inhalation augments particle-dependent systemic microvascular dysfunction. *Part Fibre Toxicol*, 5: 1. [156816](#)
- Nurkiewicz TR; Porter DW; Hubbs AF; Stone S; Chen BT; Frazer DG; Boegehold MA; Castranova V. (2009). Pulmonary nanoparticle exposure disrupts systemic microvascular nitric oxide signaling. , 110: 191-203. [191961](#)
- Nygaard UC; Samuelsen M; Aase A; Lovik M. (2004). The capacity of particles to increase allergic sensitization is predicted by particle number and surface area, not by particle mass. *Toxicol Sci*, 82: 515-524. [058558](#)
- O'Connor GT; Neas L; Vaughn B; Kattan M; Mitchell H; Crain EF; Evans R, 3rd; Gruchalla R; Morgan W; Stout J; Adams GK; Lippmann M. (2008). Acute respiratory health effects of air pollution on children with asthma in US inner cities. *J Allergy Clin Immunol*, 121: 1133-1139 e1131. [156818](#)
- O'Neill MS; Hajat S; Zanobetti A; Ramirez-Aguilar M; Schwartz J. (2005). Impact of control for air pollution and respiratory epidemics on the estimated associations of temperature and daily mortality. *Int J Biometeorol*, 50: 121-9. [098094](#)
- O'Neill MS; Veves A; Sarnat JA; Zanobetti A; Gold DR; Economides PA; Horton ES; Schwartz J. (2007). Air pollution and inflammation in type 2 diabetes: a mechanism for susceptibility. *Occup Environ Med*, 64: 373-379. [091362](#)
- O'Neill MS; Veves A; Zanobetti A; Sarnat JA; Gold DR; Economides PA; Horton ES; Schwartz J. (2005). Diabetes enhances vulnerability to particulate air pollution-associated impairment in vascular reactivity and endothelial function. , 111: 2913-2920. [088423](#)
- Odajima H; Yamazaki S; Nitta H. (2008). Decline in peak expiratory flow according to hourly short-term concentration of particulate matter in asthmatic children. *Inhal Toxicol*, 20: 1263. [192005](#)

- Oftedal B; Nafstad P; Magnus P; Bjorkly S; Skrondal A. (2003). Traffic related air pollution and acute hospital admission for respiratory diseases in Drammen, Norway 1995-2000. *Eur J Epidemiol*, 18: 671-675. [055623](#)
- Okin PM; Devereux RB; Howard BV; Fabsitz RR; Lee ET; Welty TK. (2000). Assessment of QT interval and QT dispersion for prediction of all-cause and cardiovascular mortality in American Indians: The Strong Heart Study. , 101: 61-66. [156002](#)
- Ostro B. (1995). Fine particulate air pollution and mortality in two Southern California counties. *Environ Res*, 70: 98-104. [079197](#)
- Ostro B; Broadwin R; Green S; Feng W-Y; Lipsett M. (2006). Fine particulate air pollution and mortality in nine California counties: results from CALFINE. *Environ Health Perspect*, 114: 29-33. [087991](#)
- Ostro B; Feng W-Y; Broadwin R; Green S; Lipsett M. (2007). The effects of components of fine particulate air pollution on mortality in California: results from CALFINE. *Environ Health Perspect*, 115: 13-9. [091354](#)
- Ostro B; Roth L; Malig B; Marty M. (2009). The effects of fine particle components on respiratory hospital admissions in children. *Environ Health Perspect*, 117: 475. [191971](#)
- Ostro BD; Broadwin R; Lipsett MJ. (2003). Coarse particles and daily mortality in Coachella Valley, California. [042824](#)
- Ostro BD; Feng WY; Broadwin R; Malig BJ; Green RS; Lipsett MJ. (2008). The impact of components of fine particulate matter on cardiovascular mortality in susceptible subpopulations. *Occup Environ Med*, 65: 750-756. [097971](#)
- Park SK; O'Neill MS; Vokonas PS; Sparrow D; Schwartz J. (2005). Effects of air pollution on heart rate variability: the VA normative aging study. *Environ Health Perspect*, 113: 304-309. [057331](#)
- Park SK; O'Neill MS; Vokonas PS; Sparrow D; Spiro A, 3rd; Tucker KL; Suh H; Hu H; Schwartz J. (2008). Traffic-related particles are associated with elevated homocysteine: the VA normative aging study. *Am J Respir Crit Care Med*, 178: 283-289. [156845](#)
- Park SK; O'Neill MS; Vokonas PS; Sparrow D; Wright RO; Coull B; Nie H; Hu H; Schwartz J. (2008). Air pollution and heart rate variability: effect modification by chronic lead exposure. , 19: 111-120. [093027](#)
- Park SK; O'Neill MS; Wright RO; Hu H; Vokonas PS; Sparrow D; Suh H; Schwartz J. (2006). HFE genotype, particulate air pollution, and heart rate variability A gene-environmental interaction. , 114: 2798-2805. [091245](#)
- Peacock JL; Symonds P; Jackson P; Bremner SA; Scarlett JF; Strachan DP; Anderson HR. (2003). Acute effects of winter air pollution on respiratory function in schoolchildren in southern England. *Occup Environ Med*, 60: 82-89. [042026](#)
- Peel JL; Metzger KB; Klein M; Flanders WD; Mulholland JA; Tolbert PE. (2007). Ambient air pollution and cardiovascular emergency department visits in potentially sensitive groups. *Am J Epidemiol*, 165: 625-633. [090442](#)
- Peel JL; Tolbert PE; Klein M; Metzger KB; Flanders WD; Knox T; Mulholland JA; Ryan PB; Frumkin H. (2005). Ambient air pollution and respiratory emergency department visits. , 16: 164-174. [056305](#)
- Pekkanen J; Peters A; Hoek G; Tiittanen P; Brunekreef B; de Hartog J; Heinrich J; Ibaldo-Mulli A; Kreyling WG; Lanki T; Timonen KL; Vanninen E. (2002). Particulate air pollution and risk of ST-segment depression during repeated submaximal exercise tests among subjects with coronary heart disease: the exposure and risk assessment for fine and ultrafine particles in ambient air (ULTRA) study. , 106: 933-938. [035050](#)
- Peled R; Friger M; Bolotin A; Bibi H; Epstein L; Pilpel D; Scharf S. (2005). Fine particles and meteorological conditions are associated with lung function in children with asthma living near two power plants. *Public Health*, 119: 418-425. [156015](#)
- Peng R; Bell M; Geyh A; McDermott A; Zeger S; Samet J; Dominici F. (2009). Emergency admissions for cardiovascular and respiratory diseases and the chemical composition of fine particle air pollution. *Environ Health Perspect*, 117: 957-963. [191998](#)
- Peng RD; Chang HH; Bell ML; McDermott A; Zeger SL; Samet JM; Dominici F. (2008). Coarse particulate matter air pollution and hospital admissions for cardiovascular and respiratory diseases among Medicare patients. *JAMA*, 299: 2172-2179. [156850](#)
- Peng RD; Dominici F; Pastor-Barriuso R; Zeger SL; Samet JM. (2005). Seasonal analyses of air pollution and mortality in 100 US cities. *Am J Epidemiol*, 161: 585-594. [087463](#)
- Peng RD; Chang HH; Bell ML; McDermott A; Zeger SL; Samet JM; Dominici F. (2008). Coarse particulate matter air pollution and hospital admissions for cardiovascular and respiratory diseases among Medicare patients. , 299: 2172-9. [186787](#)
- Pennanen AS; Sillanpaa M; Hillamo R; Quass U; John AC; Branis M; Hunova I; Meliefste K; Janssen NA; Koskentalo T; Castano-Vinyals G; Bouso L; Chalbot MC; Kavouras IG; Salonen RO. (2007). Performance of a high-volume cascade impactor in six European urban environments: mass measurement and chemical characterization of size-segregated particulate samples. , 374: 297-310. [155357](#)

- Penttinen P; Vallius M; Tiittanen P; Ruuskanen J; Pekkanen J. (2006). Source-specific fine particles in urban air and respiratory function among adult asthmatics. *Inhal Toxicol*, 18: 191-198. [087988](#)
- Pereira CEL; Heck TG; Saldiva PHN; Rhoden CR. (2007). Ambient particulate air pollution from vehicles promotes lipid peroxidation and inflammatory responses in rat lung. , 40: 1353-1359. [156019](#)
- Peretz A; Kaufman JD; Trenga CA; Allen J; Carlsten C; Aulet MR; Adar SD; Sullivan JH. (2008). Effects of diesel exhaust inhalation on heart rate variability in human volunteers. *Environ Res*, 107: 178-184. [156855](#)
- Peretz A; Peck EC; Bammler TK; Beyer RP; Sullivan JH; Trenga CA; Srinouanprachnah S; Farin FM; Kaufman JD. (2007). Diesel exhaust inhalation and assessment of peripheral blood mononuclear cell gene transcription effects: an exploratory study of healthy human volunteers. *Inhal Toxicol*, 19: 1107-1119. [156853](#)
- Peretz A; Sullivan JH; Leotta DF; Trenga CA; Sands FN; Allen J; Carlsten C; Wilkinson CW; Gill EA; Kaufman JD. (2008). Diesel exhaust inhalation elicits acute vasoconstriction in vivo. *Environ Health Perspect*, 116: 937-942. [156854](#)
- Perez L; Tobias A; Querol X; Kunzli N; Pey J; Alastuey A; Viana M; Valero N; Gonzalez-Cabre M; Sunyer J. (2008). Coarse particles from Saharan dust and daily mortality. , 19: 800-807. [156020](#)
- Peters A. (2005). Particulate matter and heart disease: evidence from epidemiological studies. *Toxicol Appl Pharmacol*, 207: S477-S482. [087759](#)
- Peters A; Dockery DW; Muller JE; Mittleman MA. (2001). Increased particulate air pollution and the triggering of myocardial infarction. , 103: 2810-2815. [016546](#)
- Peters A; Greven S; Heid I; Baldari F; Breitner S; Bellander T; Chrysohoou C; Illig T; Jacquemin B; Koenig W. (2009). Fibrinogen Genes Modify the Fibrinogen Response to Ambient Particulate Matter. *Am J Respir Crit Care Med*, 179: 484-491. [191992](#)
- Peters A; Liu E; Verrier RL; Schwartz J; Gold DR; Mittleman M; Baliff J; Oh JA; Allen G; Monahan K; Dockery DW. (2000). Air pollution and incidence of cardiac arrhythmia. , 11: 11-17. [011347](#)
- Peters A; Von Klot S; Heier M; Trentinaglia I; Hormann A; Wichmann HE; Lowel H. (2004). Exposure to traffic and the onset of myocardial infarction. , 351: 1721-1730. [087464](#)
- Petrovic S; Urech B; Brook J; Datema J; Purdham J; Liu L; Lukic Z; Zimmerman B; Tofler G; Downar E; Corey P; Tarlo S; Broder I; Dales R; Silverman F. (2000). Cardiorespiratory effects of concentrated ambient PM_{2.5}: a pilot study using controlled human exposures. *Inhal Toxicol*, 1: 173-188. [004638](#)
- Piedrahita JA; Zhang SH; Hagaman JR; Oliver PM; Maeda N. (1992). Generation of mice carrying a mutant apolipoprotein E gene inactivated by gene targeting in embryonic stem cells. Presented at Proceedings of the National Academy of Science, 5/15/1992. [156868](#)
- Pietropaoli AP; Frampton MW; Hyde RW; Morrow PE; Oberdorster G; Cox C; Speers DM; Frasier LM; Chalupa DC; Huang LS; Utell MJ. (2004). Pulmonary function, diffusing capacity, and inflammation in healthy and asthmatic subjects exposed to ultrafine particles. *Inhal Toxicol*, 16: 59-72. [156025](#)
- Pinkerton KE; Zhou Y; Teague SV; Peake JL; Walther RC; Kennedy IM; Leppert VJ; Aust AE. (2004). Reduced lung cell proliferation following short-term exposure to ultrafine soot and iron particles in neonatal rats: key to impaired lung growth?. *Inhal Toxicol*, 1: 73-81. [087465](#)
- Pinkerton KE; Zhou Y; Zhong C; Smith KR; Teague SV; Kennedy IM; Ménache MG. (2008). Mechanisms of particulate matter toxicity in neonatal and young adult rat lungs. Health Effects Institute. Boston, MA. 135. [190471](#)
- Pirrone N; Keeler GJ; Warner PO. (1995). Trends of ambient concentrations and deposition fluxes of particulate trace metals in Detroit from 1982 to 1992. *Sci Total Environ*, 162: 43-61. [089297](#)
- Pope C; Renlund D; Kfoury A; May H; Horne B. (2008). Relation of heart failure hospitalization to exposure to fine particulate air pollution. , 102: 1230-1234. [191969](#)
- Pope CA; Hansen ML; Long RW; Nielsen KR; Eatough NL; Wilson WE; Eatough DJ. (2004). Ambient particulate air pollution, heart rate variability, and blood markers of inflammation in a panel of elderly subjects. *Environ Health Perspect*, 112: 339-345. [055238](#)
- Pope CA III; Muhlestein JB; May HT; Renlund DG; Anderson JL; Horne BD. (2006). Ischemic heart disease events triggered by short-term exposure to fine particulate air pollution. *Circulation*, 114: 2443-2448. [091246](#)
- Pourazar J; Blomberg A; Kelly FJ; Davies DE; Wilson SJ; Holgate ST; Sandstrom T. (2008). Diesel exhaust increases EGFR and phosphorylated C-terminal Tyr 1173 in the bronchial epithelium. *Part Fibre Toxicol*, 5: 8. [156884](#)
- Pourazar J; Mudway IS; Samet JM; Helleday R; Blomberg A; Wilson SJ; Frew AJ; Kelly FJ; Sandstrom T. (2005). Diesel exhaust activates redox-sensitive transcription factors and kinases in human airways. *Am J Physiol*, 289: L724-L730. [088305](#)

- Power K; Balmes J; Solomon C. (2008). Controlled exposure to combined particles and ozone decreases heart rate variability. *J Occup Environ Med*, 50: 1253. [191982](#)
- Preuththipan A; Udomsubpayakul U; Chaisupamongkollarp T; Pentamwa P. (2004). Effect of PM10 pollution in Bangkok on children with and without asthma. *Pediatr Pulmonol*, 37: 187-192. [055598](#)
- Pritchett LC; Cooper JA. (1985). *Aerosol Characterization Study of Anchorage, Alaska: Chemical Analysis and Source Apportionment*. [156886](#)
- Prystowsky EN; Benson DW Jr; Fuster V; Hart RG; Kay GN; Myerburg RJ; Naccarelli GV; Wyse DG. (1996). Management of patients with atrial fibrillation. A Statement for Healthcare Professionals. From the Subcommittee on Electrocardiography and Electrophysiology, American Heart Association. , 93: 1262-1277. [156031](#)
- Raabe OG; Al-Bayati MA; Teague SV; Rasolt A. (1988). Regional deposition of inhaled monodisperse, coarse, and fine aerosol particles in small laboratory animals. In *Inhaled particles VI: Proceedings of an international symposium and workshop on lung dosimetry* (pp. 53-63). Cambridge, United Kingdom: Pergamon Press. [001439](#)
- Rabinovitch N; Strand M; Gelfand EW. (2006). Particulate levels are associated with early asthma worsening in children with persistent disease. *Am J Respir Crit Care Med*, 173: 1098-1105. [088031](#)
- Rabinovitch N; Zhang LN; Murphy JR; Vedal S; Dutton SJ; Gelfand EW. (2004). Effects of wintertime ambient air pollutants on asthma exacerbations in urban minority children with moderate to severe disease. *J Allergy Clin Immunol*, 114: 1131-1137. [096753](#)
- Ranzi A; Gambini M; Spattini A; Galassi C; Sesti D; Bedeschi M; Messori A; Baroni A; Cavagni G; Lauriola P. (2004). Air pollution and respiratory status in asthmatic children: hints for a locally based preventive strategy AIRE study. *Eur J Epidemiol*, 19: 567-576. [089500](#)
- Reed MD; Barrett EG; Campen MJ; Divine KK; Gigliotti AP; McDonald JD; Seagrave JC; Mauderly JL; Seilkop SK; Swenberg JA. (2008). Health effects of subchronic inhalation exposure to gasoline engine exhaust. *Inhal Toxicol*, 20: 1125-1143. [156903](#)
- Reed MD; Campen MJ; Gigliotti AP; Harrod KS; McDonald JD; Seagrave JC; Mauderly JL; Seilkop SK. (2006). Health effects of subchronic exposure to environmental levels of hardwood smoke. *Inhal Toxicol*, 18: 523-539. [156043](#)
- Reed MD; Gigliotti AP; McDonald JD; Seagrave JC; Seilkop SK; Mauderly JL. (2004). Health effects of subchronic exposure to environmental levels of diesel exhaust. *Inhal Toxicol*, 16: 177-193. [055625](#)
- Rhoden CR; Ghelfi E; González-Flecha B. (2008). Pulmonary inflammation by ambient air particles is mediated by superoxide anion. *Inhal Toxicol*, 20: 11-15. [190475](#)
- Rhoden CR; Lawrence J; Godleski JJ; Gonzalez-Flecha B. (2004). N-acetylcysteine prevents lung inflammation after short-term inhalation exposure to concentrated ambient particles. *Toxicol Sci*, 79: 296-303. [087969](#)
- Rhoden CR; Wellenius GA; Ghelfi E; Lawrence J; Gonzalez-Flecha B. (2005). PM-induced cardiac oxidative stress and dysfunction are mediated by autonomic stimulation. *Biochim Biophys Acta*, 1725: 305-313. [087878](#)
- Rich DQ; Freudenberger RS; Ohman-Strickland P; Cho Y; Kipen HM. (2008). Right heart pressure increases after acute increases in ambient particulate concentration. *Environ Health Perspect*, 116: 1167-1171. [156910](#)
- Rich DQ; Kim MH; Turner JR; Mittleman MA; Schwartz J; Catalano PJ; Dockery DW. (2006). Association of ventricular arrhythmias detected by implantable cardioverter defibrillator and ambient air pollutants in the St Louis, Missouri metropolitan area. *Occup Environ Med*, 63: 591-596. [089814](#)
- Rich DQ; Mittleman MA; Link MS; Schwartz J; Luttmann-Gibson H; Catalano PJ; Speizer FE; Gold DR; Dockery DW. (2006). Increased risk of paroxysmal atrial fibrillation episodes associated with acute increases in ambient air pollution. *Environ Health Perspect*, 114: 120-123. [088427](#)
- Rich DQ; Schwartz J; Mittleman MA; Link M; Luttmann-Gibson H; Catalano PJ; Speizer FE; Dockery DW. (2005). Association of short-term ambient air pollution concentrations and ventricular arrhythmias. *Am J Epidemiol*, 161: 1123-1132. [079620](#)
- Rich KE; Petkau J; Vedal S; Brauer M. (2004). A case-crossover analysis of particulate air pollution and cardiac arrhythmia in patients with implantable cardioverter defibrillators. *Inhal Toxicol*, 16: 363-372. [055631](#)
- Riediker M; Cascio WE; Griggs TR; Herbst MC; Bromberg PA; Neas L; Williams RW; Devlin RB. (2004). Particulate matter exposure in cars is associated with cardiovascular effects in healthy young men. *Am J Respir Crit Care Med*, 169: 934-940. [056992](#)
- Riediker M; Devlin RB; Griggs TR; Herbst MC; Bromberg PA; Williams RW; Cascio WE. (2004). Cardiovascular effects in patrol officers are associated with fine particulate matter from brake wear and engine emissions. *Part Fibre Toxicol*, 1: 2. [091261](#)

- Riojas-Rodriguez H; Escamilla-Cejudo JA; Gonzalez-Hermosillo JA; Tellez-Rojo MM; Vallejo M; Santos-Burgoa C; Rojas-Bracho L. (2006). Personal PM_{2.5} and CO exposures and heart rate variability in subjects with known ischemic heart disease in Mexico City. *J Expo Sci Environ Epidemiol*, 16: 131-137. [156913](#)
- Rodriguez C; Tonkin R; Heyworth J; Kusel M; De Klerk N; Sly PD; Franklin P; Runnion T; Blockley A; Landau L; Hinwood AL. (2007). The relationship between outdoor air quality and respiratory symptoms in young children. *Int J Environ Health Res*. [092842](#)
- Romieu I; Garcia-Esteban R; Sunyer J; Rios C; Alcaraz-Zubeldia M; Velasco SR; Holguin F. (2008). The effect of supplementation with omega-3 polyunsaturated fatty acids on markers of oxidative stress in elderly exposed to PM_{2.5}. *Environ Health Perspect*, 116: 1237-1242. [156922](#)
- Romieu I; Tellez-Rojo MM; Lazo M; Manzano-Patino Cortez-Lugo M; Julien P; Belanger MC; Hernandez-Avila MHolguin F. (2005). Omega-3 fatty acid prevents heart rate variability reductions associated with particulate matter. *Am J Respir Crit Care Med*, 172: 1534-1540. [086297](#)
- Rosenthal FS; Carney JP; Olinger ML. (2008). Out-of-hospital cardiac arrest and airborne fine particulate matter: a case-crossover analysis of emergency medical services data in Indianapolis, Indiana. *Environ Health Perspect*, 116: 631-636. [156925](#)
- Routledge HC; Manney S; Harrison RM; Ayres JG; Townend JN. (2006). Effect of inhaled sulphur dioxide and carbon particles on heart rate variability and markers of inflammation and coagulation in human subjects. *Heart*, 92: 220-227. [088674](#)
- Rowan 3rd WH; Campion MJ; Wichers LB; Watkinson WP. (2007). Heart rate variability in rodents: uses and caveats in toxicological studies. *Cardiovasc Toxicol*, 7: 28-51. [191911](#)
- Roy D; Talajic M; Dubuc M; Thibault B; Guerra P; Macle L; Khairy P. (2009). Atrial fibrillation and congestive heart failure. *Curr Opin Cardiol*, 24: 29. [190902](#)
- Ruckerl R; Greven S; Ljungman P; Aalto P; Antoniadou C; Bellander T; Berglind N; Chrysohoou C; Forastiere F; Jacquemin B; von Klot S; Koenig W; Kuchenhoff H; Lanki T; Pekkanen J; Perucci CA; Schneider A; Sunyer J; Peters A. (2007). Air pollution and inflammation (interleukin-6, C-reactive protein, fibrinogen) in myocardial infarction survivors. *Environ Health Perspect*, 115: 1072-1080. [156931](#)
- Ruckerl R; Ibald-Mulli A; Koenig W; Schneider A; Woelke G; Cyrus J; Heinrich J; Marder V; Frampton M; Wichmann HE; Peters A. (2006). Air pollution and markers of inflammation and coagulation in patients with coronary heart disease. *Environ Health Perspect*, 114: 432-441. [088754](#)
- Rudell B; Blomberg A; Helleday R; Ledin M-C; Lundback B; Stjernberg N; Horstedt P; Sandstrom T. (1999). Bronchoalveolar inflammation after exposure to diesel exhaust: comparison between unfiltered and particle trap filtered exhaust. *Occup Environ Med*, 56: 527-534. [001964](#)
- Rudell B; Ledin M-C; Hammarstrom U; Stjernberg N; Lundback B; Sandstrom T. (1996). Effects on symptoms and lung function in humans experimentally exposed to diesel exhaust. *Occup Environ Med*, 53: 658-662. [056577](#)
- Rundell KW; Caviston R. (2008). Ultrafine and fine particulate matter inhalation decreases exercise performance in healthy subjects. *Environ Health Perspect*, 116: 2-5. [191986](#)
- Rundell KW; Hoffman JR; Caviston R; Bulbulian R; Hollenbach AM. (2007). Inhalation of ultrafine and fine particulate matter disrupts systemic vascular function. *Inhal Toxicol*, 19: 133-140. [156060](#)
- Safar M; Chamiot-Clerc P; Dagher G; Renaud JF. (2001). Pulse pressure, endothelium function, and arterial stiffness in spontaneously hypertensive rats. *Hypertension*, 38: 1416-1421. [156068](#)
- Saldiva PHN; Clarke RW; Coull BA; Stearns RC; Lawrence J; Krishna-Murthy GG; Diaz E; Koutrakis P; Suh H; Tsuda A; Godleski JJ. (2002). Lung inflammation induced by concentrated ambient air particles is related to particle composition. *Am J Respir Crit Care Med*, 165: 1610-1617. [025988](#)
- Salvi S; Blomberg A; Rudell B; Kelly F; Sandstrom T; Holgate ST; Frew A. (1999). Acute inflammatory responses in the airways and peripheral blood after short-term exposure to diesel exhaust in healthy human volunteers. *Am J Respir Crit Care Med*, 159: 702-709. [058637](#)
- Samet JM; Dominici F; Zeger SL; Schwartz J; Dockery DW. (2000). National morbidity, mortality, and air pollution study Part I: methods and methodologic issues. [005809](#)
- Samet JM; Rappold A; Graff D; Cascio WE; Berntsen JH; Huang YC; Herbst M; Bassett M; Montilla T; Hazucha MJ; Bromberg PA; Devlin RB. (2009). Concentrated ambient ultrafine particle exposure induces cardiac changes in young healthy volunteers. *Am J Respir Crit Care Med*, 179: 1034-1042. [191913](#)
- Samet JM; Zeger SL; Dominici F; Curriero F; Coursac I; Dockery DW; Schwartz J; Zanobetti A. (2000). The national morbidity, mortality, and air pollution study Part II: morbidity, mortality, and air pollution in the United States. [010269](#)
- Samoli E; Analitis A; Touloumi G; Schwartz J; Anderson HR; Sunyer J; Bisanti L; Zmirou D; Vonk JM; Pekkanen J; Goodman P; Paldy A; Schindler C; Katsouyanni K. (2005). Estimating the exposure-response relationships between particulate matter and mortality within the APHEA multicity project. *Environ Health Perspect*, 113: 88-95. [087436](#)

- Samoli E; Peng R; Ramsay T; Pipikou M; Touloumi G; Dominici F; Burnett R; Cohen A; Krewski D; Samet J. (2008). Acute effects of ambient particulate matter on mortality in Europe and North America: results from the APHENA study. *Environ Health Perspect*, 116: 1480. [188455](#)
- Santos U; Terra-Filho M; Lin C; Pereira L; Vieira T; Saldiva P; Braga A. (2008). Cardiac arrhythmia emergency room visits and environmental air pollution in Sao Paulo, Brazil. *J Epidemiol Community Health*, 62: 267. [192004](#)
- Sarin S; Udem B; Sanico A; Togias A. (2006). The role of the nervous system in rhinitis. , 118: 999-1016. [191166](#)
- Sarnat JA; Marmur A; Klein M; Kim E; Russell AG; Sarnat SE; Mulholland JA; Hopke PK; Tolbert PE. (2008). Fine particle sources and cardiorespiratory morbidity: an application of chemical mass balance and factor analytical source-apportionment methods. *Environ Health Perspect*, 116: 459-66. [097972](#)
- Sarnat SE; Suh HH; Coull BA; Schwartz J; Stone PH; Gold DR. (2006). Ambient particulate air pollution and cardiac arrhythmia in a panel of older adults in Steubenville, Ohio. *Occup Environ Med*, 63: 700-706. [090489](#)
- Sauerzapf V; Jones AP; Cross J. (2009). Environmental factors and hospitalisation for chronic obstructive pulmonary disease in a rural county of England. *J Epidemiol Community Health*, 63: 324-328. [180082](#)
- Schaumann F; Borm PJA; Herbrich A; Knoch J; Pitz M; Schins RPF; Luettig B; Hohlfeld JM; Heinrich J; Krug N. (2004). Metal-rich ambient particles (particulate matter 25) cause airway inflammation in healthy subjects. *Am J Respir Crit Care Med*, 170: 898-903. [087966](#)
- Schildcrout JS; Sheppard L; Lumley T; Slaughter JC; Koenig JQ; Shapiro GG. (2006). Ambient air pollution and asthma exacerbations in children: an eight-city analysis. *Am J Epidemiol*, 164: 505-517. [089812](#)
- Schins RPF; Lightbody JH; Borm PJA; Shi T; Donaldson K; Stone V. (2004). Inflammatory effects of coarse and fine particulate matter in relation to chemical and biological constituents. *Toxicol Appl Pharmacol*, 195: 1-11. [054173](#)
- Schmitz H; Hilgers U; Weidner M. (2000). Assimilation and metabolism of formaldehyde by leaves appear unlikely to be of value for indoor air purification. *New Phytol*, 147: 307-315. [015623](#)
- Schneider A; Neas L; Herbst M; Case M; Williams R; Cascio W; Hinderliter A; Holguin F; Buse J; Dungan K. (2008). Endothelial dysfunction: associations with exposure to ambient fine particles in diabetic individuals. *Environ Health Perspect*, 116: 1666. [191985](#)
- Schreuder AB; Larson TV; Sheppard L; Claiborn CS. (2006). Ambient woodsmoke and associated respiratory emergency department visits in Spokane, Washington. *Int J Occup Environ Health*, 12: 147-53. [097959](#)
- Schwartz J. (2003). Airborne particles and daily deaths in 10 US cities. [042800](#)
- Schwartz J. (2004). Is the association of airborne particles with daily deaths confounded by gaseous air pollutants? An approach to control by matching. *Environ Health Perspect*, 112: 557-561. [053506](#)
- Schwartz J. (2004). The effects of particulate air pollution on daily deaths: a multi-city case crossover analysis. , 61: 956-961. [188945](#)
- Schwartz J. (2004). The effects of particulate air pollution on daily deaths: a multi-city case crossover analysis. *Occup Environ Med*, 61: 956-961. [078998](#)
- Schwartz J; Litonjua A; Suh H; Verrier M; Zanobetti A; Syring M; Nearing B; Verrier R; Stone P; MacCallum G; Speizer FE; Gold DR. (2005). Traffic related pollution and heart rate variability in a panel of elderly subjects. *Thorax*, 60: 455-461. [074317](#)
- Schwartz J; Marcus A. (1990). Mortality and air pollution in London: a time series analysis. *Am J Epidemiol*, 131: 185-194. [073222](#)
- Schwartz J; Morris R. (1995). Air pollution and hospital admissions for cardiovascular disease in Detroit, Michigan. *Am J Epidemiol*, 142: 23-35. [046186](#)
- Schwartz J; Neas LM. (2000). Fine particles are more strongly associated than coarse particles with acute respiratory health effects in schoolchildren. , 11: 6-10. [007625](#)
- Schwartz J; Park SK; O'Neill MS; Vokonas PS; Sparrow D; Weiss S; Kelsey K. (2005). Glutathione-S-transferase M1, obesity, statins, and autonomic effects of particles: gene-by-drug-by-environment interaction. *Am J Respir Crit Care Med*, 172: 1529-1533. [086296](#)
- Seagrave J; Campen M; McDonald J; Mauderly J; Rohr A. (2008). Oxidative stress, inflammation, and pulmonary function assessment in rats exposed to laboratory-generated pollutant mixtures. , 71: 1352. [191990](#)
- Seagrave JC; McDonald JD; Bedrick E; Edgerton ES; Gigliotti AP; Jansen JJ; Ke L; Naeher LP; Seilkop SK; Zheng M; Mauderly JL. (2006). Lung toxicity of ambient particulate matter from southeastern US sites with different contributing sources: relationships between composition and effects. *Environ Health Perspect*, 114: 1387-93. [091291](#)
- Segala C; Poizeau D; Neukirch F; Aubier M; Samson J; Gehanno P. (2004). Air pollution, passive smoking, and respiratory symptoms in adults. *Arch Environ Occup Health*, 59: 669-676. [090449](#)

- Shah AP; Pietropaoli AP; Frasier LM; Speers DM; Chalupa DC; Delehanty JM; Huang LS; Utell MJ; Frampton MW. (2008). Effect of inhaled carbon ultrafine particles on reactive hyperemia in healthy human subjects. *Environ Health Perspect*, 116: 375-380. [156970](#)
- Sheppard L. (2003). Ambient air pollution and nonelderly asthma hospital admissions in Seattle, Washington, 1987-1994. [042826](#)
- Sheppard L; Levy D; Norris G; Larson TV; Koenig JQ. (1999). Effects of ambient air pollution on nonelderly asthma hospital admissions in Seattle, Washington, 1987-1994. , 10: 23-30. [086921](#)
- Shi JP; Harrison RM; Evans D. (2001). Comparison of ambient particle surface area measurement by epiphaniometer and SMPS/APS. *Atmos Environ*, 35: 6193-6200. [078292](#)
- Sillanpaa M; Frey A; Hillamo R; Pennanen AS; Salonen RO. (2005). Organic, elemental and inorganic carbon in particulate matter of six urban environments in Europe. , 5: 2869-2879. [156980](#)
- Simpson R; Williams G; Petroschevsky A; Best T; Morgan G; Denison L; Hinwood A; Neville G. (2005). The short-term effects of air pollution on hospital admissions in four Australian cities. *Aust N Z J Public Health*, 29: 213-221. [087438](#)
- Sinclair AH; Tolsma D. (2004). Associations and lags between air pollution and acute respiratory visits in an ambulatory care setting: 25-month results from the aerosol research and inhalation epidemiological study. *J Air Waste Manag Assoc*, 54: 1212-1218. [088696](#)
- Sirivelu MP; MohanKumar SMJ; Wagner JG; Harkema JR; MohanKumar PS. (2006). Activation of the stress axis and neurochemical alterations in specific brain areas by concentrated ambient particle exposure with concomitant allergic airway disease. *Environ Health Perspect*, 114: 870-874. [111151](#)
- Slaughter JC; Kim E; Sheppard L; Sullivan JH; Larson TV; Claiborn C. (2005). Association between particulate matter and emergency room visits, hospital admissions and mortality in Spokane, Washington. *J Expo Sci Environ Epidemiol*, 15: 153-159. [073854](#)
- Slaughter JC; Lumley T; Sheppard L; Koenig JQ; Shapiro GG. (2003). Effects of ambient air pollution on symptom severity and medication use in children with asthma. *Ann Allergy Asthma Immunol*, 91: 346-353. [086294](#)
- Smith AD; Taylor DR. (2005). Is exhaled nitric oxide measurement a useful clinical test in asthma?. *Curr Opin Allergy Clin Immunol*, 5: 49-56. [192176](#)
- Smith KR; Kim S; Recendez JJ; Teague SV; Menache MG; Grubbs DE; Sioutas C; Pinkerton KE. (2003). Airborne particles of the California Central Valley alter the lungs of healthy adult rats. *Environ Health Perspect*, 111: 902-908. [042107](#)
- Smith KR; Veranth JM; Kodavanti UP; Aust AE; Pinkerton KE. (2006). Acute pulmonary and systemic effects of inhaled coal fly ash in rats: comparison to ambient environmental particles. , 93: 390-9. [110864](#)
- Steenenbergh P; Withagen C; Dalen W; Dormans J; Loveren H. (2004). Adjuvant Activity of Ambient Particulate Matter in Macrophage Activity-Suppressed, N-Acetylcysteine-Treated, iNOS- and IL-4-Deficient Mice. *Inhal Toxicol*, 16: 835-843. [087981](#)
- Steenenbergh PA; Van Amelsvoort L; Lovik M; Hetland RB; Alberg T; Halatek T; Bloemen HJT; Rydzynski K; Swaen G; Schwarze P; Dybing E; Cassee FR. (2006). Relation between sources of particulate air pollution and biological effect parameters in samples from four European cities: an exploratory study. *Inhal Toxicol*, 18: 333-346. [088249](#)
- Steenenbergh PA; Withagen CE; van Dalen WJ; Dormans JA; Heisterkamp SH; van Loveren H; Cassee FR. (2005). Dose dependency of adjuvant activity of particulate matter from five European sites in three seasons in an ovalbumin-mouse model. *Inhal Toxicol*, 17: 133-145. [088649](#)
- Steenenbergh PA; Withagen CET; van Dalen WJ; Dormans JAMA; Cassee FR; Heisterkamp SH; van Loveren H. (2004). Adjuvant activity of ambient particulate matter of different sites, sizes, and seasons in a respiratory allergy mouse model. *Toxicol Appl Pharmacol*, 200: 186-200. [096024](#)
- Steinvil A; Kordova-Biezuner L; Shapira I; Berliner S; Rogowski O. (2008). Short-term exposure to air pollution and inflammation-sensitive biomarkers. , 106: 51-61. [188893](#)
- Stenfors N; Nordenhall C; Salvi SS; Mudway I; Soderberg M; Blomberg A; Helleday R; Levin JO; Holgate ST; Kelly FJ; Frew AJ; Sandstrom T. (2004). Different airway inflammatory responses in asthmatic and healthy humans exposed to diesel. *Eur Respir J*, 23: 82-86. [157009](#)
- Stevens T; Krantz QT; Linak WP; Hester S; Gilmour MI. (2008). Increased transcription of immune and metabolic pathways in naive and allergic mice exposed to diesel exhaust. *Toxicol Sci*, 102: 359-370. [157010](#)
- Stolzel M; Peters A; Wichmann H-E. (2003). Daily mortality and fine and ultrafine particles in Erfurt, Germany. [042842](#)
- Strand M; Vedal S; Rodes C; Dutton SJ; Gelfand EW; Rabinovitch N. (2006). Estimating effects of ambient PM2.5 exposure on health using PM2.5 component measurements and regression calibration (vol 16, pg 30, 2006). *J Expo Sci Environ Epidemiol*, 16: 471-471. [157017](#)

- Stölzel M; Breitner S; Cyrus J; Pitz M; Wolke G; Kreyling W; Heinrich J; Wichmann H-E; Peters A. (2007). Daily mortality and particulate matter in different size classes in Erfurt, Germany. *J Expo Sci Environ Epidemiol*, 17: 458-467. [091374](#)
- Suglia SF; Gryparis A; Wright RO; Schwartz J; Wright RJ. (2008). Association of black carbon with cognition among children in a prospective birth cohort study. *Am J Epidemiol*, 167: 280-286. [157027](#)
- Sullivan J; Ishikawa N; Sheppard L; Siscovick D; Checkoway H; Kaufman J. (2003). Exposure to ambient fine particulate matter and primary cardiac arrest among persons with and without clinically recognized heart disease. *Am J Epidemiol*, 157: 501-509. [043156](#)
- Sullivan J; Sheppard L; Schreuder A; Ishikawa N; Siscovick D; Kaufman J. (2005). Relation between short-term fine-particulate matter exposure and onset of myocardial infarction. *Am J Epidemiol*, 161: 41-48. [050854](#)
- Sullivan JH; Hubbard R; Liu SL; Shepherd K; Trenga CA; Koenig JQ; Chandler WL; Kaufman JD. (2007). A community study of the effect of particulate matter on blood measures of inflammation and thrombosis in an elderly population. *Environ Health Perspect*, 115: 3. [100083](#)
- Sullivan JH; Schreuder AB; Trenga CA; Liu SL; Larson TV; Koenig JQ; Kaufman JD. (2005). Association between short term exposure to fine particulate matter and heart rate variability in older subjects with and without heart disease. *Thorax*, 60: 462-6. [109418](#)
- Sureshkumar V; Paul B; Uthirappan M; Pandey R; Sahu AP; Lal K; Prasad AK; Srivastava S; Saxena A; Mathur N; Gupta YK. (2005). Proinflammatory and anti-inflammatory cytokine balance in gasoline exhaust induced pulmonary injury in mice. *Inhal Toxicol*, 17: 161-168. [088306](#)
- Symons JM; Wang L; Guallar E; Howell E; Dominici F; Schwab M; Ange BA; Samet J; Ondov J; Harrison D; Geyh A. (2006). A case-crossover study of fine particulate matter air pollution and onset of congestive heart failure symptom exacerbation leading to hospitalization. *Am J Epidemiol*, 164: 421-33. [091258](#)
- Szyszkowicz M. (2008). Ambient air pollution and daily emergency department visits for ischemic stroke in Edmonton, Canada. *Int J Occup Med Environ Health*, 21: 295-300. [192128](#)
- Szyszkowicz M. (2009). Air pollution and ED visits for chest pain. *Am J Emerg Med*, 27: 165-168. [191996](#)
- Sørensen M; Daneshvar B; Hansen M; Dragsted LO; Hertel O; Knudsen L; Loft S. (2003). Personal PM_{2.5} exposure and markers of oxidative stress in blood. *Environ Health Perspect*, 111: 161-166. [157000](#)
- Tamagawa E; Bai N; Morimoto K; Gray C; Mui T; Yatera K; Zhang X; Xing L; Li Y; Laher I. (2008). Particulate matter exposure induces persistent lung inflammation and endothelial dysfunction. *Am J Respir Crit Care Med*, 178: L79. [191988](#)
- Tan WC; Qiu D; Liam BL; Ng TP; Lee SH; Van Eeden SF; D'Yachkova Y; Hogg JC. (2000). The human bone marrow response to acute air pollution caused by forest fires. *Am J Respir Crit Care Med*, 161: 1213-1217. [002304](#)
- Tankersley CG; Bierman A; Rabold R. (2007). Variation in heart rate regulation and the effects of particle exposure in inbred mice. *Am J Physiol*, 293: 621-9. [097910](#)
- Tankersley CG; Campen M; Bierman A; Flanders SE; Broman KW; Rabold R. (2004). Particle effects on heart-rate regulation in senescent mice. *Inhal Toxicol*, 16: 381-390. [094378](#)
- Tankersley CG; Champion HC; Takimoto E; Gabrielson K; Bedja D; Misra V; El-Haddad H; Rabold R; Mitzner W. (2008). Exposure to inhaled particulate matter impairs cardiac function in senescent mice. *Am J Physiol Regul Integr Comp Physiol*, 295: R252-263. [157043](#)
- Tankersley CG; Irizarry R; Flanders SE; Rabold R; Frank R. (2003). Unstable heart rate and temperature regulation predict mortality in AKR/J mice. *Am J Physiol*, 284: R742-R750. [053919](#)
- Tecer LH; Alagha O; Karaca F; Tuncel G; Eldes N. (2008). Particulate Matter (PM_{2.5}, PM_{10-2.5}, and PM₁₀) and Children's Hospital Admissions for Asthma and Respiratory Diseases: A Bidirectional Case-Crossover Study. *J Toxicol Environ Health A*, 71: 512-520. [180030](#)
- TFESC. (1996). Heart rate variability: standards of measurement, physiological interpretation, and clinical use. Task Force of the European Society of Cardiology. North American Society of Pacing and Electrophysiology. *Eur Heart J*, 17: 354-381. [003061](#)
- Thurston G; Ito K; Mar T; Christensen WF; Eatough DJ; Henry RC; Kim E; Laden F; Lall R; Larson TV; Liu H; Neas L; Pinto J; Stolzel M; Suh H; Hopke PK. (2005). Results and implications of the workshop on the source apportionment of PM health effects. *Environ Health Perspect*, 113: S134-S135. [097949](#)
- Thurston GD; Ito K; Hayes CG; Bates DV; Lippmann M. (1994). Respiratory hospital admissions and summertime haze air pollution in Toronto, Ontario: consideration of the role of acid aerosols. *Environ Res*, 65: 271-290. [043921](#)
- Timonen KL; Hoek G; Heinrich J; Bernard A; Brunekreef B; De Hartog J; Hameri K; Ibaldo-Mulli A; Mirme A; Peters A; Tiittanen P; Kreyling WG; Pekkanen J. (2004). Daily variation in fine and ultrafine particulate air pollution and urinary concentrations of lung Clara cell protein CC16. *Occup Environ Med*, 61: 908-914. [087915](#)

- Timonen KL; Vanninen E; De Hartog J; Ibaldo-Mulli A; Brunekreef B; Gold DR; Henrich J; Hoek G; Lanki T; Peters A; Tarkiainen T; Tiittanen P; Kreyling W; Pekkanen J. (2006). Effects of ultrafine and fine particulate and gaseous air pollution on cardiac autonomic control in subjects with coronary artery disease: the ULTRA study. *J Expo Sci Environ Epidemiol*, 16: 332-341. [088747](#)
- Tolbert PE; Klein M; Metzger KB; Peel J; Flanders WD; Todd K; Mulholland JA; Ryan PB; Frumkin H. (2000). Interim results of the study of particulates and health in Atlanta (SOPHIA). *J Expo Sci Environ Epidemiol*, 10: 446-460. [010320](#)
- Tolbert PE; Kleina M; Peelb JL; Sarnata SE; Sarnata JA. (2007). Multipollutant modeling issues in a study of ambient air quality and emergency department visits in Atlanta. *J Expo Sci Environ Epidemiol*, 24: 938-945. [090316](#)
- Tornqvist H; Mills NL; Gonzalez M; Miller MR; Robinson SD; Megson IL; MacNee W; Donaldson K; Soderberg S; Newby DE; Sandstrom T; Blomberg A. (2007). Persistent endothelial dysfunction in humans after diesel exhaust inhalation. *Am J Respir Crit Care Med*, 176: 395-400. [091279](#)
- Trenga CA; Sullivan JH; Schildcrout JS; Shepherd KP; Shapiro GG; Liu LJ; Kaufman JD; Koenig JQ. (2006). Effect of particulate air pollution on lung function in adult and pediatric subjects in a Seattle panel study. , 129: 1614-22. [155209](#)
- Tsai FC; Apte MG; Daisey JM. (2000). An exploratory analysis of the relationship between mortality and the chemical composition of airborne particulate matter. *Inhal Toxicol*, 12: 121-135. [006251](#)
- Tsai S-S; Cheng M-H; Chiu H-F; Wu T-N; Yang C-Y. (2006). Air pollution and hospital admissions for asthma in a tropical city: Kaohsiung, Taiwan. *Inhal Toxicol*, 18: 549-554. [089768](#)
- Tsai S-S; Goggins WB; Chiu H-F; Yang C-Y. (2003). Evidence for an association between air pollution and daily stroke admissions in Kaohsiung, Taiwan. , 34: 2612-2616. [080133](#)
- Tunnicliffe WS; Harrison RM; Kelly FJ; Dunster C; Ayres JG. (2003). The effect of sulphurous air pollutant exposures on symptoms, lung function, exhaled nitric oxide, and nasal epithelial lining fluid antioxidant concentrations in normal and asthmatic adults. *Occup Environ Med*, 60. [088744](#)
- U.S. EPA. (1982). Air quality criteria for particulate matter and sulfur oxides. U.S. Environmental Protection Agency. Washington, D.C.. [017610](#)
- U.S. EPA. (1996). Air quality criteria for particulate matter. U.S. Environmental Protection Agency. Research Triangle Park, NC. EPA/600/P-95/001aF-cF. [079380](#)
- U.S. EPA. (2002). Health assessment document for diesel engine exhaust. [042866](#)
- U.S. EPA. (2004). Air quality criteria for particulate matter. U.S. Environmental Protection Agency. Research Triangle Park, NC. EPA/600/P-99/002aF-bF. [056905](#)
- Ulirsch GV; Ball LM; Kaye W; Shy CM; Lee CV; Crawford-Brown D; Symons M; Holloway T. (2007). Effect of particulate matter air pollution on hospital admissions and medical visits for lung and heart disease in two southeast Idaho cities. *J Expo Sci Environ Epidemiol*, 17: 478-487. [091332](#)
- Upadhyay D; Panduri V; Ghio A; Kamp DW. (2003). Particulate matter induces alveolar epithelial cell DNA damage and apoptosis: role of free radicals and the mitochondria. , 29: 180-187. [097370](#)
- Upadhyay S; Stoeger T; Harder V; Thomas RF; Schladweiler MC; Semmler-Behnke M; Takenaka S; Karg E; Reitmeir P; Bader M; Stampfl A; Kodovanti U; Schulz H. (2008). Exposure to ultrafine carbon particles at levels below detectable pulmonary inflammation affects cardiovascular performance in spontaneously hypertensive rats. *Part Fibre Toxicol*, 5: 19. [159345](#)
- Urch B; Brook JR; Wasserstein D; Brook RD; Rajagopalan S; Corey P; Silverman F. (2004). Relative contributions of PM_{2.5} chemical constituents to acute arterial vasoconstriction in humans. *Inhal Toxicol*, 16: 345-352. [055629](#)
- Urch B; Silverman F; Corey P; Brook JR; Lukic KZ; Rajagopalan S; Brook RD. (2005). Acute blood pressure responses in healthy adults during controlled air pollution exposures. *Environ Health Perspect*, 113: 1052-1055. [081080](#)
- Van der Werf GR; Randerson JT; Collatz J; Giglio L. (2003). Carbon emissions from fires in tropical and subtropical ecosystems. , 9: 547-562. [089398](#)
- Vedal S; Rich K; Brauer M; White R; Petkau J. (2004). Air pollution and cardiac arrhythmias in patients with implantable cardiovascular defibrillators. *Inhal Toxicol*, 16: 353-362. [055630](#)
- Vegni FE; Ros O. (2004). Hospital accident and emergency burden is unaffected by today's air pollution levels. *Eur J Emerg Med*, 11: 86-88. [087448](#)
- Veranth JM; Moss TA; Chow JC; Labban R; Nichols WK; Walton JC; Walton JG; Yost GS. (2006). Correlation of in vitro cytokine responses with the chemical composition of soil-derived particulate matter. *Environ Health Perspect*, 114: 341-349. [087479](#)
- Veronesi B; Makwana O; Pooler M; Chen LC. (2005). Effects of subchronic exposures to concentrated ambient particles VII Degeneration of dopaminergic neurons in Apo E^{-/-} mice. *Inhal Toxicol*, 17: 235-241. [087481](#)

- Vigotti MA; Chiaverini F; Biagiola P; Rossi G. (2007). Urban air pollution and emergency visits for respiratory complaints in Pisa, Italy. *J Toxicol Environ Health A*, 70: 266-269. [090711](#)
- Villeneuve PJ; Burnett RT; Shi Y; Krewski D; Goldberg MS; Hertzman C; Chen Y; Brook J. (2003). A time-series study of air pollution, socioeconomic status, and mortality in Vancouver, Canada. *J Expo Sci Environ Epidemiol*, 13: 427-435. [055051](#)
- Villeneuve PJ; Chen L; Stieb D; Rowe BH. (2006). Associations between outdoor air pollution and emergency department visits for stroke in Edmonton, Canada. *Eur J Epidemiol*, 21: 689-700. [090191](#)
- Vincent R; Kumarathasan P; Goegan P; Bjarnason SG; Guenette J; Berube D; Adamson IY; Desjardins S; Burnett RT; Miller FJ; Battistini B. (2001). Inhalation toxicology of urban ambient particulate matter: acute cardiovascular effect in rats. [021184](#)
- Von Klot S; Peters A; Aalto P; Bellander T; Berglind N; D'Ippoliti D; Elosua R; Hormann A; Kulmala M; Lanki T; Lowel H; Pekkanen J; Picciotto S; Sunyer J; Forastiere F; Health Effects of Particles on Susceptible Subpopulations (HEAPSS) Study Group. (2005). Ambient air pollution is associated with increased risk of hospital cardiac readmissions of myocardial infarction survivors in five European cities. *Circulation*, 112: 3073-3079. [088070](#)
- Von Klot S; Wolke G; Tuch T; Heinrich J; Dockery DW; Schwartz J; Kreyling WG; Wichmann HE; Peters A. (2002). Increased asthma medication use in association with ambient fine and ultrafine particles. *Eur Respir J*, 20: 691-702. [034706](#)
- Ward DJ; Roberts KT; Jones N; Harrison RM; Ayres JG; Hussain S; Walters S. (2002). Effects of daily variation in outdoor particulates and ambient acid species in normal and asthmatic children. *Thorax*, 57: 489-502. [025839](#)
- Ward PA. (2003). Acute lung injury: how the lung inflammatory response works. *Eur Respir J*, 44: 22s-23s. [157111](#)
- Wegesser TC; Last JA. (2008). Lung response to coarse PM: bioassay in mice. *Toxicol Appl Pharmacol*, 230: 159-166. [190506](#)
- Welin L; Eriksson H; Larsson B; Svärdsudd K; Wilhelmsen L; Tibblin G. (1993). Risk Factors for Coronary Heart Disease during 25 Years of Follow-Up. *Cardiology*, 82: 223-228. [156151](#)
- Wellenius GA; Batalha JRF; Diaz EA; Lawrence J; Coull BA; Katz T; Verrier RL; Godleski JJ. (2004). Cardiac effects of carbon monoxide and ambient particles in a rat model of myocardial infarction. *Toxicol Sci*, 80: 367-376. [087874](#)
- Wellenius GA; Bateson TF; Mittleman MA; Schwartz J. (2005). Particulate air pollution and the rate of hospitalization for congestive heart failure among medicare beneficiaries in Pittsburgh, Pennsylvania. *Am J Epidemiol*, 161: 1030-1036. [087483](#)
- Wellenius GA; Coull BA; Batalha JRF; Diaz EA; Lawrence J; Godleski JJ. (2006). Effects of ambient particles and carbon monoxide on supraventricular arrhythmias in a rat model of myocardial infarction. *Inhal Toxicol*, 18: 1077-1082. [156152](#)
- Wellenius GA; Coull BA; Godleski JJ; Koutrakis P; Okabe K; Savage ST. (2003). Inhalation of concentrated ambient air particles exacerbates myocardial ischemia in conscious dogs. *Environ Health Perspect*, 111: 402-408. [055691](#)
- Wellenius GA; Saldiva PHN; Batalha JRF; Murthy GKG; Coull BA; Verrier RL; Godleski JJ. (2002). Electrocardiographic changes during exposure to residual oil fly ash (ROFA) particles in a rat model of myocardial infarction. *Toxicol Sci*, 66: 327-335. [025405](#)
- Wellenius GA; Schwartz J; Mittleman MA. (2005). Air pollution and hospital admissions for ischemic and hemorrhagic stroke among medicare beneficiaries. *Am J Epidemiol*, 162: 2549-2553. [088685](#)
- Wellenius GA; Schwartz J; Mittleman MA. (2006). Particulate air pollution and hospital admissions for congestive heart failure in seven United States cities. *Am J Cardiol*, 97: 404-408. [088748](#)
- Wellenius GA; Yeh GY; Coull BA; Suh HH; Phillips RS; Mittleman MA. (2007). Effects of ambient air pollution on functional status in patients with chronic congestive heart failure: a repeated-measures study. *Am J Epidemiol*, 165: 6: 26. [092830](#)
- Welty LJ; Zeger SL. (2005). Are the acute effects of particulate matter on mortality in the National Morbidity, Mortality, and Air Pollution study the result of inadequate control for weather and season? A sensitivity analysis using flexible distributed lag models. *Am J Epidemiol*, 162: 80-88. [087484](#)
- Wheeler A; Zanobetti A; Gold DR; Schwartz J; Stone P; Suh HH. (2006). The relationship between ambient air pollution and heart rate variability differs for individuals with heart and pulmonary disease. *Environ Health Perspect*, 114: 560-566. [088453](#)
- Whitekus MJ; Li N; Zhang M; Wang M; Horwitz MA; Nelson SK; Horwitz LD; Brechun N; Diaz-Sanchez D; Nel AE. (2002). Thiol antioxidants inhibit the adjuvant effects of aerosolized diesel exhaust particles in a murine model for ovalbumin sensitization. *J Immunol*, 168: 2560-2567. [157142](#)

- Whitsel E; Quibrera P; Christ S; Liao D; Prineas R; Anderson G; Heiss G. (2009). Heart rate variability, ambient particulate matter air pollution, and glucose homeostasis: the environmental epidemiology of arrhythmogenesis in the Women's Health Initiative. *Am J Epidemiol*, x: x. [191980](#)
- Wichmann H-E; Spix C; Tuch T; Wolke G; Peters A; Heinrich J; Kreyling WG; Heyder J. (2000). Daily mortality and fine and ultrafine particles in Erfurt, Germany Part I: role of particle number and particle mass. [013912](#)
- Widdicombe J. (2006). Reflexes from the lungs and airways: historical perspective. *J Appl Physiol*, 101: 628. [155519](#)
- Widdicombe J; Lee L-Y. (2001). Airway reflexes, autonomic function, and cardiovascular responses. *Environ Health Perspect*, 4: 579-584. [019049](#)
- Widdicombe JG. (2003). Overview of neural pathways in allergy and asthma. *Pulm Pharmacol Ther*, 16: 23-30. [157145](#)
- Wilson WE; Mar TF; Koenig JQ. (2007). Influence of exposure error and effect modification by socioeconomic status on the association of acute cardiovascular mortality with particulate matter in Phoenix. *J Expo Sci Environ Epidemiol*, 17: S11. [157149](#)
- Win-Shwe TT; Yamamoto S; Fujitani Y; Hirano S; Fujimaki H. (2008). Spatial learning and memory function-related gene expression in the hippocampus of mouse exposed to nanoparticle-rich diesel exhaust. *Neurotoxicology*, 29: 940-947. [190516](#)
- Witten ML; Wong SS; Sun NN; Keith I; Kweon C; Foster DE; Schauer JJ; Sherrill DL. (2005). Neurogenic responses in rat lungs after nose-only exposure to diesel exhaust. [087485](#)
- Wong C-M; Atkinson RW; Anderson HR; Hedley AJ; Ma S; Chau PY-K; Lam T-H. (2002). A tale of two cities: effects of air pollution on hospital admissions in Hong Kong and London compared. *Environ Health Perspect*, 110: 67-77. [023232](#)
- Wong SS; Sun NN; Keith I; Kweon C-B; Foster DE; Schauer James J; Witten ML. (2003). Tachykinin substance P signaling involved in diesel exhaust-induced bronchopulmonary neurogenic inflammation in rats. , 77: 638-650. [097707](#)
- Wong TW; Lau TS; Yu TS; Neller A; Wong SL; Tam W; Pang SW. (1999). Air pollution and hospital admissions for respiratory and cardiovascular diseases in Hong Kong. *Occup Environ Med*, 56: 679-683. [009172](#)
- Wong TW; Tam WS; Yu TS; Wong AHS. (2002). Associations between daily mortalities from respiratory and cardiovascular diseases and air pollution in Hong Kong, China. *Occup Environ Med*, 59: 30-35. [025436](#)
- Wordley J; Walters S; Ayres JG. (1997). Short term variations in hospital admissions and mortality and particulate air pollution. *Occup Environ Med*, 54: 108-116. [082745](#)
- Wu J; M Winer A; J Delfino R. (2006). Exposure assessment of particulate matter air pollution before, during, and after the 2003 Southern California wildfires. *Atmos Environ*, 40: 3333-3348. [157156](#)
- Yan YH; Huang CH; Chen WJ; Wu MF; Cheng TJ. (2008). Effects of diesel exhaust particles on left ventricular function in isoproterenol-induced myocardial injury and healthy rats. *Inhal Toxicol*, 20: 199-203. [098625](#)
- Yang C-Y; Chang C-C; Chuang H-Y; Tsai S-S; Wu T-N; Ho C-K. (2004). Relationship between air pollution and daily mortality in a subtropical city: Taipei, Taiwan. *Environ Int*, 30: 519-523. [055603](#)
- Yang CY. (2008). Air pollution and hospital admissions for congestive heart failure in a subtropical city: Taipei, Taiwan. *J Toxicol Environ Health A*, 71: 1085-1090. [157160](#)
- Yang CY; Chen CJ. (2007). Air pollution and hospital admissions for chronic obstructive pulmonary disease in a subtropical city: Taipei, Taiwan. *J Toxicol Environ Health A*, 70: 1214-9. [092847](#)
- Yang CY; Cheng MH; Chen CC. (2009). Effects of Asian Dust Storm Events on Hospital Admissions for Congestive Heart Failure in Taipei, Taiwan. , 72: 324-328. [190341](#)
- Yang Q; Chen Y; Krewski D; Shi Y; Burnett RT; McGrail KM. (2004). Association between particulate air pollution and first hospital admission for childhood respiratory illness in Vancouver, Canada. *Arch Environ Occup Health*, 59: 14-21. [087488](#)
- Yeatts K; Svendsen E; Creason J; Alexis N; Herbst M; Scott J; Kupper L; Williams R; Neas L; Cascio W; Devlin RB; Peden DB. (2007). Coarse particulate matter (PM_{2.5-10}) affects heart rate variability, blood lipids, and circulating eosinophils in adults with asthma. *Environ Health Perspect*, 115: 709-714. [091266](#)
- Yokota S; Seki T; Naito Y; Tachibana S; Hirabayashi N; Nakasaka T; Ohara N; Kobayashi H. (2008). Tracheal instillation of diesel exhaust particles component causes blood and pulmonary neutrophilia and enhances myocardial oxidative stress in mice. *J Toxicol Sci*, 33: 609-620. [190109](#)
- Yu O; Sheppard L; Lumley T; Koenig JQ; S. (2000). Effects of ambient air pollution on symptoms of asthma in Seattle-area children enrolled in the CAMP study. *Environ Health Perspect*, 108: 1209-1214. [013254](#)
- Yue W; Schneider A; Stolz M; Ruckerl R; Cyrys J; Pan X; Zareba W; Koenig W; Wichmann HE; Peters A. (2007). Ambient source-specific particles are associated with prolonged repolarization and increased levels of inflammation in male coronary artery disease patients. , 621: 50-60. [097968](#)

- Zabel M; Klingenheben T; Franz MR; Hohnloser SH. (1998). Assessment of QT Dispersion for Prediction of Mortality or Arrhythmic Events After Myocardial Infarction : Results of a Prospective, Long-term Follow-up Study. , 97: 2543-2550. [156176](#)
- Zanchi AC; Venturini CD; Saiki M; Nascimento Saldiva PH; Tannhauser Barros HM; Rhoden CR. (2008). Chronic nasal instillation of residual-oil fly ash (ROFA) induces brain lipid peroxidation and behavioral changes in rats. *Inhal Toxicol*, 20: 795-800. [157173](#)
- Zanobetti A; Canner MJ; Stone PH; Schwartz J; Sher D; Eagan-Bengston E; Gates KA; Hartley LH; Suh H; Gold DR. (2004). Ambient pollution and blood pressure in cardiac rehabilitation patients. , 110: 2184-2189. [087489](#)
- Zanobetti A; Schwartz J. (2003). Airborne particles and hospital admissions for heart and lung disease. [043119](#)
- Zanobetti A; Schwartz J. (2003). Airborne particles and hospital admissions for heart and lung disease. In: Revised analyses of time-series studies of air pollution and health. Special Report. [157174](#)
- Zanobetti A; Schwartz J. (2003). Multicity assessment of mortality displacement within the APHEA2 project. [042812](#)
- Zanobetti A; Schwartz J. (2005). The effect of particulate air pollution on emergency admissions for myocardial infarction: a multicity case-crossover analysis. *Environ Health Perspect*, 113: 978-982. [088069](#)
- Zanobetti A; Schwartz J. (2006). Air pollution and emergency admissions in Boston, MA. *J Epidemiol Community Health*, 60: 890-895. [090195](#)
- Zanobetti A; Schwartz J. (2009). The effect of fine and coarse particulate air pollution on mortality: A national analysis. *Environ Health Perspect*, 117: 1-40. [188462](#)
- Zareba W; Couderc JP; Oberdörster G; Chalupa D; Cox C; Huang LS; Peters A; Utell MJ; Frampton MW. (2009). ECG parameters and exposure to carbon ultrafine particles in young healthy subjects. *Inhal Toxicol*, 21: 223-233. [190101](#)
- Zeka A; Sullivan JR; Vokonas PS; Sparrow D; Schwartz J. (2006). Inflammatory markers and particulate air pollution: characterizing the pathway to disease. *Int J Epidemiol*, 35: 1347-1354. [157177](#)
- Zeka A; Zanobetti A; Schwartz J. (2005). Short term effects of particulate matter on cause specific mortality: effects of lags and modification by city characteristics. *Occup Environ Med*, 62: 718-725. [088068](#)
- Zeka A; Zanobetti A; Schwartz J. (2006). Individual-level modifiers of the effects of particulate matter on daily mortality. *Am J Epidemiol*, 163: 849-859. [088749](#)
- Zelikoff JT; Chen LC; Cohen MD; Fang K; Gordon T; Li Y; Nadziejko C; Schlesinger RB. (2003). Effects of inhaled ambient particulate matter on pulmonary antimicrobial immune defense. *Inhal Toxicol*, 15: 131-150. [039009](#)
- Zhang SH; Reddick RL; Piedrahita JA; Maeda N. (1992). Spontaneous hypercholesterolemia and arterial lesions in mice lacking apolipoprotein E. , 258: 468-471. [157180](#)
- Zhang Z; Whitsel E; Quibrera P; Smith R; Liao D; Anderson G; Prineas R. (2009). Ambient Fine Particulate Matter Exposure and Myocardial Ischemia in the Environmental Epidemiology of Arrhythmogenesis in the Women's Health Initiative (EEAWHI) Study. *Environ Health Perspect*, 117: 751. [191970](#)

Chapter 7. Integrated Health Effects of Long-Term PM Exposure

7.1. Introduction

1 This chapter summarizes reviews and integrates the evidence on relationships
2 between health effects and long-term exposures to various size fractions and sources of PM.
3 Cardiopulmonary health effects of long-term exposure to PM have been examined in an
4 extensive body of epidemiologic, human clinical, and toxicological studies. Both
5 epidemiologic and toxicological studies provide a basis for examining reproductive and
6 developmental and cancer health outcomes with regard to long-term exposure to PM. In
7 addition, there is a large body of epidemiologic literature evaluating the relationship
8 between mortality and long-term exposure to PM.

9 Conclusions from the 2004 PM AQCD are summarized briefly at the beginning of each
10 section, and the evaluation of evidence from recent studies builds upon what was available
11 during the previous review. For each health outcome (e.g., respiratory infections, lung
12 function), results are summarized for studies from the specific scientific discipline,
13 i.e., epidemiologic and toxicological studies. The sections conclude with summaries of the
14 evidence on the various health outcomes and integration of the findings that leads to
15 conclusions regarding causality based upon the framework described in Chapter 1.
16 Determination of causality is made for the overall health effect category, such as
17 cardiovascular effects, with coherence and plausibility being based upon the evidence from
18 across disciplines and also across the suite of related health outcomes. In these summary
19 sections, the evidence is summarized and independent conclusions drawn for relationships
20 with PM_{2.5}, PM_{10-2.5}, and ultrafine particles.

7.2. Cardiovascular and Systemic Effects

21 Studies examining associations between long-term exposure to ambient PM (over
22 months to years) and CVD morbidity had not been conducted and thus were not included in
23 the 1996 or 2004 PM Air Quality Criteria Documents (U.S. EPA, 1996, [079380](#); U.S. EPA,
24 2004, [056905](#)). A number of studies were included in the 2004 PM AQCD that evaluated the
25 effect of long-term PM_{2.5} exposure on cardiovascular mortality and found consistent
26 associations. No toxicological studies examined chronic atherosclerotic effects of PM

Note: Hyperlinks to the reference citations throughout this document will take you to the NCEA HERO database (Health and Environmental Research Online) at <http://epa.gov/hero>. HERO is a database of scientific literature used by U.S. EPA in the process of developing science assessments such as the Integrated Science Assessments (ISA) and the Integrated Risk Information System (IRIS).

1 exposure in animal models. However, a subchronic study that evaluated atherosclerosis
2 progression in hyperlipidemic rabbits was discussed and this study provided the foundation
3 for the subsequent work that has been conducted in this area (Suwa et al., 2002, [028588](#)).
4 No previous toxicological studies evaluated effects of subchronic or chronic PM exposure on
5 diabetes measures, or HR or HRV changes, nor were there animal toxicological studies
6 included in the 2004 PM AQCD that evaluated systemic inflammatory or blood coagulation
7 markers following subchronic or chronic PM exposure.

8 Several new epidemiologic studies have examined the long-term PM-CVD association
9 among U.S. and European populations. The studies investigate the association of both
10 PM_{2.5} and PM₁₀ exposures with a variety of clinical and subclinical CVD outcomes.
11 Epidemiologic and toxicological studies have provided evidence of the adverse effects of
12 long-term exposure to PM_{2.5} on cardiovascular outcomes, including atherosclerosis, clinical
13 and subclinical markers of cardiovascular morbidity, and cardiovascular mortality. The
14 evidence of these effects from long-term exposure to PM_{10-2.5} is weaker.

7.2.1. Atherosclerosis

15 Atherosclerosis is a progressive disease that contributes to several adverse outcomes,
16 including myocardial infarction and aortic aneurysm. It is multifaceted, beginning with an
17 early injury or inflammation that promotes the extravasation of inflammatory cells. Under
18 conditions of oxidative or nitrosative stress and high lipid or cholesterol concentrations, the
19 vessel wall undergoes a chronic remodeling that is characterized by the presence of foam
20 cells, migrated and differentiated smooth muscle cells, and ultimately a fibrous cap. The
21 advanced lesion that develops from this process can occlude perfusion to distal tissue,
22 causing ischemia, and erode, degrade, or even rupture, revealing coagulant initiators
23 (tissue factor) that promote thrombosis, stenosis, and infarction or stroke. Several detailed
24 reviews of atherosclerosis pathology have been published elsewhere (Ross, 1999, [156926](#);
25 Stocker and Keaney JF, 2004, [157013](#)).

7.2.1.1. Epidemiologic Studies

Measures of Atherosclerosis

26 Although no study has examined the association between long-term PM exposure and
27 longitudinal change in subclinical markers of atherosclerosis, several cross sectional studies
28 have been conducted. Markers of atherosclerosis used in these studies include coronary
29 artery calcium (CAC), carotid intima-media thickness (CIMT), ankle-brachial index (ABI),
30 and abdominal aortic calcium (AAC). These measures are described briefly below.

31 CAC is a measure of atherosclerosis assessed by non-contrast, cardiac-gated electron
32 beam computed tomography (EBCT) or multidetector computed tomography (MDCT) of the

1 coronary arteries in the heart (Greenland and Kizilbash, 2005, [156496](#); Hoffmann et al.,
2 2005, [156556](#); Mollet et al., 2005, [155988](#)). The prevalence of CAC is strongly related to age.
3 Few people have detectable CAC in their second decade of life but the prevalence of CAC
4 rises to approximately 100% by age 80 (Ardehali et al., 2007, [155662](#)). Previous studies
5 suggest that while the absence of CAC does not rule out atherosclerosis, it does imply a
6 very low likelihood of significant arterial obstruction (Achenbach and Daniel, 2001, [156189](#);
7 Arad et al., 1996, [155661](#); Shaw et al., 2003, [156083](#); Shemesh et al., 1996, [156085](#)).
8 Conversely, the presence of CAC confirms the existence of atherosclerotic plaque and the
9 amount of calcification varies directly with the likelihood of obstructive disease (Ardehali et
10 al., 2007, [155662](#)). CAC is a quantified using the Agatston method (Agatston et al., 1990,
11 [156197](#)). Its repeatability depends on the laboratory and the method of calculation
12 (O'Rourke et al. 2000). Agatston scores are frequently used to classify individuals into one
13 of five groups (zero; mild; moderate; severe; extensive) or according to age- and sex-specific
14 percentiles of the CAC distribution (Erbel et al., 2007, [155768](#)).

15 CIMT is a measure of atherosclerosis assessed by high-resolution, B-mode
16 ultrasonography of the carotid arteries in the neck, the walls of which have inner (intimal),
17 middle (medial) and outer (adventitial) layers (Craven et al., 1990, [155740](#); O'Leary et al.,
18 1999, [156826](#); Wendelhag et al., 1993, [157136](#)). CIMT estimates the distance in mm or μm
19 between the innermost (blood-intima) and outermost (media-adventitia) interfaces, often by
20 averaging over three arterial segments in the common carotid, carotid bulb, and internal
21 carotid artery (Amato et al., 2007, [155656](#)). CIMT has been associated with atherosclerosis
22 risk factors (Heiss et al., 1991, [156535](#); O'Leary et al., 1992, [156825](#); Salonen and Salonen,
23 1991, [156938](#)), prevalent coronary heart disease (Chambless et al., 1997, [156329](#);
24 Geroulakos et al., 1994, [155788](#)), and incident coronary and cerebral events (O'Leary et al.,
25 1999, [156826](#); van der Meer et al., 2004, [156129](#)). Several studies have indicated that CIMT
26 measurements are accurate (Girerd et al., 1994, [156474](#); Pignoli et al., 1986, [156026](#);
27 Wendelhag et al., 1991, [157135](#)) and reproducible (Montauban van Swijndregt et al., 1999,
28 [156777](#); Smilde et al., 1997, [156988](#); Willekes et al., 1999, [157147](#)), especially for the
29 common carotid artery (Montauban van Swijndregt et al., 1999, [156777](#)).

30 ABI, which is also known as the ankle-arm or resting (blood) pressure index, is a
31 measure of lower extremity arterial occlusive disease commonly caused by advanced
32 atherosclerosis (Weitz et al., 1996, [156150](#)). It is assessed by continuous wave Doppler and
33 manual or automated oscillometric sphygmomanometry, the latter having been shown to
34 have higher repeatability and validity (Weitz et al., 1996, [156150](#)). ABI is defined as the
35 unitless ratio of ankle to brachial systolic blood pressures measured in mmHg. As ankle
36 pressure is normally equal to or slightly higher than arm pressure (resulting in an $\text{ABI} \geq$
37 1.0), epidemiologic studies typically define the normal ABI range as 0.90 to 1.50 (Resnick et
38 al., 2004, [156048](#)). Low ABI has been associated with all-cause and CVD mortality

1 (Newman et al., 1993, [156805](#); Vogt et al., 1993, [157100](#)), as well as myocardial infarction
2 and stroke (Karthikeyan and Lip, 2007, [156626](#)).

3 AAC is a measure of atherosclerosis assessed by non-contrast, EBCT or MDCT of the
4 abdominal aorta. It is scored much like CAC (Agatston et al., 1990, [156197](#)), but the age-
5 specific prevalence and extent of AAC is greater, particularly among women and at ages
6 >50 years. Although AAC has not been studied as extensively as CAC, it is associated with
7 carotid and coronary atherosclerosis as well as cardiovascular morbidity and mortality
8 (Allison et al., 2004, [156210](#); Allison et al., 2006, [155653](#); Hollander et al., 2003, [156562](#);
9 Khoury et al., 1997, [156636](#); Oei et al., 2002, [156820](#); Walsh et al., 2002, [157103](#); Wilson et
10 al., 2001, [156159](#); Witteman et al., 1986, [156161](#)) and measurements are sufficiently
11 reproducible to allow serial investigations over time (Budoff et al., 2005, [192105](#)).

Study Findings

12 Diez et al. (2008, [156401](#)) conducted cross-sectional analyses of the association of
13 three of these subclinical markers of atherosclerosis (CAC, CIMT and ABI), collected from
14 2000 to 2003 during baseline examinations of participants enrolled in the Multi-Ethnic
15 Study of Atherosclerosis (MESA), with long-term exposure to PM_{2.5} and PM₁₀. The study
16 population included 5,172 ethnically diverse people (53% female) residing in Baltimore,
17 MD; Chicago, IL; Forsyth County, NC; Los Angeles, CA; New York, NY; and St. Paul, MN
18 ranging in age from 45 to 84 years old. Authors used spatio-temporal modeling of pollutant
19 concentrations, weather and demographic data to impute 20-yr avg exposures to PM_{2.5} and
20 PM₁₀. They reported small increases in CIMT of 1% (95% CI: 0%-1.4%) and 0.5% (95%
21 CI: 0%-1%), which correspond to absolute changes of 8 (95% CI: 0-12) and 7 (95%
22 CI: 0-14) μm , per 10 $\mu\text{g}/\text{m}^3$ increase in 20-yr avg PM₁₀ and PM_{2.5} concentration, respectively.
23 Evidence of age-, gender-, lipid- and smoking-related susceptibility was lacking. They also
24 reported weak, non-significant increases in the relative prevalence of CAC of 1% (95%
25 CI: -2% to 4%) and 0.5% (95% CI: -2% to 3%) per 10 $\mu\text{g}/\text{m}^3$ increase in PM₁₀ and PM_{2.5},
26 respectively. Among the subset of 2,586 participants with EBCT-identified calcification,
27 similarly weak associations were observed. There was little evidence of modification of the
28 CAC associations by demographic, socioeconomic or clinical characteristics. Finally, the
29 authors report no differences in mean ABI with PM₁₀ or PM_{2.5} concentrations. The null
30 findings for ABI exhibited little heterogeneity among participant subgroups and were
31 similarly null when ABI was modeled as a dichotomous outcome using a cutpoint of 0.9
32 units.

33 MESA investigators also examined the chronic PM_{2.5}-AAC association in a
34 residentially stable subset of 1,147 participants (mean age = 66 yr; 50% female) randomly
35 selected from all MESA centers, except Baltimore, MD for enrollment in its Aortic Calcium
36 Ancillary Study (Allen et al., 2009, [189644](#)). The authors used kriging and inverse
37 residence-to-monitor distance-weighted averaging of EPA AQS data to estimate 2-yr mean
38 exposures to PM_{2.5}. In cross-sectional analyses, the authors found a 6% (95% CI: -4% to

1 16%) excess risk of a non-zero Agatston score and an 8% (95% CI: -30% to 46%) increase in
2 AAC, i.e., approximately 50 (95% CI: -251 to 385) Agatston units, per 10 $\mu\text{g}/\text{m}^3$ increase in
3 $\text{PM}_{2.5}$ concentration. These associations were stronger among users than non-users of anti-
4 hyperlipidemics.

5 Kunzli et al. (2005, [087387](#)) used baseline data collected between 1998-2003 from two
6 randomized placebo-controlled clinical trials, the Vitamin E Atherosclerosis Progression
7 Study (VEAPS) and the B-Vitamin Atherosclerosis Intervention Trial (BVAIT), for their
8 ancillary cross-sectional analyses of the effect of long-term $\text{PM}_{2.5}$ exposure on CIMT. The
9 study population included 798 residents of the greater Los Angeles, CA area who were more
10 than 40 years old at baseline and 44% were female. The authors used universal kriging of
11 $\text{PM}_{2.5}$ data from 23 state and local monitors operating in 2000 to estimate 1-yr avg exposure
12 to $\text{PM}_{2.5}$ at each participant's geocoded U.S. Postal Service ZIP code. They found a 4.2%
13 (95% CI: -0.2% to 8.9%) or approximately 32 (95% CI: -2 to 68) μm increase in CIMT per
14 10 $\mu\text{g}/\text{m}^3$ increase in $\text{PM}_{2.5}$ concentration. In contrast to findings from the relatively large,
15 ethnically diverse, yet geographically overlapping MESA ancillary study described above,
16 PM-related increases in CIMT were two- to three-fold larger among older and female
17 participants taking anti-hyperlipidemics in this study. PM-related increases in CIMT were
18 also higher in never smokers when compared with current or former smokers.

19 Hoffmann et al. (2007, [091163](#)) conducted a cross-sectional analysis of data collected
20 at baseline (2000 to 2003) for 4,494 residents of Essen, Mülheim and Bochum, Germany
21 enrolled in the Heinz Nixdorf Recall Study from 2000 to 2003. The age of participants
22 ranged from 45-74 years and 51% were female. In this cross-sectional study the authors
23 used dispersion and chemistry transport modeling of emissions, climate and topography
24 data to estimate one-yr avg exposure to $\text{PM}_{2.5}$ in 2002 (the midpoint of the baseline exam.) They reported
25 an imprecise 43% (95% CI: -15% to 115%) or 102 (95% CI: -77 to 273) Agatston unit increase
26 in CAC per 10 $\mu\text{g}/\text{m}^3$ increase in $\text{PM}_{2.5}$. Differences in strength of association between
27 subgroups defined by demographic and clinical characteristics were small. The authors
28 reported a more consistent association of CAC with traffic exposure (distance from a major
29 roadway) than with $\text{PM}_{2.5}$ in this study.

30 In a subsequent analysis of these data, Hoffmann et al. (2009, [190376](#)) examined the
31 PM-ABI association in this population. In this cross-sectional study, no changes in ABI were
32 observed in association with $\text{PM}_{2.5}$ concentration nor was evidence of effect modification by
33 demographic and clinical characteristics apparent. As in the previous study, residing near a
34 major roadway was a stronger predictor of atherosclerotic changes. Absolute changes in ABI
35 of -0.024 (95% CI: -0.047 to -0.001) were associated with living within 50 m of a major
36 roadway compared to living more than 200 m away.

37 Each of the studies described above relied on cross-sectional analyses examining
38 differences in long-term average $\text{PM}_{2.5}$ concentrations across space (as well as time to the
39 extent baseline examinations were conducted over time). Such associations may reflect the

1 effect of compositional differences in PM_{2.5} as well as the effect of higher PM_{2.5}
2 concentrations. Most associations of PM_{2.5} with CAC (Diez Roux et al., 2008, [156401](#);
3 Hoffmann et al., 2007, [091163](#)), CIMT (Diez Roux et al., 2008, [156401](#); Kunzli et al., 2005,
4 [087387](#)), ABI (Diez Roux et al., 2008, [156401](#); Hoffmann et al., 2009, [190376](#)) and AAC
5 (Allen et al., 2009, [189644](#)) reviewed in this section were weak and/or imprecise. However,
6 several factors including exposure measurement error, variation in baseline measures
7 atherosclerosis, as well as limited power may contribute to the insensitivity of these cross-
8 sectional studies to detect small differences in CAC, CIMT, ABI and AAC. The study by
9 Hoffmann et al. (2007, [091163](#)), which reported large, imprecise and non-significant
10 increases in CAC in association with PM_{2.5}, is not distinguished from the other studies
11 reviewed by a superior study design or larger sample size. The several fold difference in the
12 magnitude of CIMT associations reported by Kunzli et al. (2005, [087387](#)) and Diez Roux et
13 al. (2008, [156401](#)) may be related to differences between the study populations. The
14 ambient PM concentrations from these studies are characterized in Table 7-1.

7.2.1.2. Toxicological Studies

15 In the only study of this kind described in the 2004 PM AQCD, Suwa et al. (2002,
16 [028588](#)) demonstrated more advanced atherosclerotic lesions based on phenotype and
17 volume fraction in the left main and right coronary arteries of rabbits exposed to PM₁₀ (5
18 mg/kg, 2 times/wk × 4 wks). Although this study was conducted using IT exposure
19 methodology at a relatively high dose, it provided the first experimental evidence that PM
20 exposure may result in progression of atherosclerosis. Recent toxicological studies
21 conducted using inhalation exposures have replicated these findings at relevant
22 concentrations and are discussed below.

CAPs

23 New studies have demonstrated increased atherosclerotic plaque area in aortas of
24 ApoE^{-/-} mice exposed to PM_{2.5} CAPs for 4-6 months (6 h/day × 5 days/wk). Average CAPs
25 concentrations ranged from 85 to 138 µg/m³ and all were conducted in Tuxedo or
26 Manhattan, NY. Chen and Nadziejko (2005, [087219](#)) reported that the percentage of aortic
27 intimal surface covered by atherosclerotic lesions in ApoE^{-/-} mice was increased. In male
28 ApoE^{-/-}/LDLR^{-/-} mice, both lesion area and cellularity in the aortic root were enhanced by
29 Tuxedo, NY CAPs exposure, although there was no change in lipid content. Genetic profiles
30 within plaques recovered from ApoE^{-/-} mice included many of the molecular pathways
31 known to contribute to atherosclerosis, including inflammation (Floyd et al., 2009, [190350](#)).
32 Sun (2005, [186814](#)) similarly demonstrated an enhancement of atherosclerosis in ApoE^{-/-}
33 mice exposed Tuxedo, NY CAPs. Plaque area in the aortic arch and abdominal aorta was
34 significantly increased in the PM-exposed, high fat-chow group compared to air-exposed,
35 high fat-chow group. Macrophage infiltration in the abdominal aorta was also observed in

1 the groups exposed to CAPs. A study conducted in Manhattan for 4-months (5-9/2007)
2 showed that PM_{2.5} CAPs exposure increased atherosclerotic plaque area and led to higher
3 levels of macrophage infiltration, collagen deposition, and lipid composition in thoracic
4 aortas of ApoE^{-/-} mice (Ying et al., 2009, [190111](#)), which is consistent with the previous two
5 studies described that were conducted in Tuxedo, NY.

6 Alteration of vasomotor function has been observed in aortic rings of ApoE^{-/-} mice on a
7 high fat diet with long-term exposure to CAPs (Sun et al., 2005, [186814](#); Ying et al., 2009,
8 [190111](#)). Sun (2005, [186814](#)) reported that PM_{2.5}-exposed animals exhibited increased
9 vasoconstrictor responsiveness to serotonin and PE. Increased ROS and elevated iNOS
10 protein expression in aortic sections of CAPs-exposed mice may have resulted alterations in
11 the NO pathway and generation of peroxynitrite that could have affected vascular
12 reactivity. In contrast, Ying, et al. (2009, [190111](#)) demonstrated decreased maximum
13 constriction induced by PE following Manhattan CAPs exposure. Pretreatment with the
14 soluble guanylate cyclase (sGC) inhibitor ODQ attenuated the response, indicating that
15 CAPs exposure resulted in abnormal NO/sGC signaling. iNOS mRNA and protein
16 expression was increased in aortas of CAPs-exposed mice, further supporting a role for NO
17 production. In conjunction with increased NO, aortic superoxide production was
18 demonstrated that appeared to be partially driven by increased NADPH oxidase activity.
19 The difference in vasoconstrictor responses between these two studies may be attributable
20 to varying durations (6 vs. 4 months, respectively) or CAPs compositions.

21 Sun (2005, [186814](#)) and Ying et al. (2001, [019011](#)) reported similar relaxation
22 responses to ACh for air- and CAPs-exposed mice. However, Manhattan CAPs-exposed mice
23 had a markedly decreased response to A23187, indicating that NO release occurred via
24 Ca²⁺-dependent mechanisms (Ying et al., 2009, [190111](#)). Abnormal eNOS function is likely
25 responsible for the decreased relaxation response, as activation of eNOS (but not iNOS) is
26 Ca²⁺-dependent.

27 A recent study (Sun et al., 2008, [157033](#)) that was part of the research described
28 above (Sun et al., 2005, [186814](#)) investigated tissue factor (TF) expression in aortas, which
29 is a major regulator of hemostasis and thrombosis following vascular injury or plaque
30 erosion. In PM_{2.5}-exposed ApoE^{-/-} mice on a high-fat diet, TF was significantly elevated in
31 the plaques of aortic sections compared to air-exposed mice on the high-fat diet. TF
32 expression was generally detected in (1) the extracellular matrix surrounding macrophages
33 and foam cell-rich areas and (2) around smooth muscle cells.

34 One new study of CAPs PM_{2.5} or ultrafine PM derived from traffic was conducted.
35 Araujo et al. (2008, [156222](#)) compared the relative impact of ultrafine (0.01-0.18 μm) and
36 fine (0.01-2.5 μm) PM inhalation on aortic lesion development in ApoE^{-/-} mice following a
37 40-day exposure (5 h/day × 3 days/wk for 75 total hours). Animals were on a normal chow
38 diet and exposed to CAPs in a mobile inhalation laboratory parked 300 m from a freeway in
39 downtown Los Angeles. Exposure concentrations were ~440 μg/m³ for PM_{2.5} and ~110 μg/m³

1 for ultrafine PM, and the number concentrations were roughly equivalent (4.56×10^5 and
2 5.59×10^5 particles/cm³ for PM_{2.5} and ultrafine PM, respectively). Significant increases in
3 plaque size (estimated by lesions at the aortic root) were reported for mice exposed to
4 ultrafine PM only. The lesions were largely comprised of macrophages with intracellular
5 lipid accumulation. Increased total cholesterol measured at the end of the exposure protocol
6 was observed only in the PM_{2.5} group. HDL isolated from the ultrafine PM-exposed mice
7 demonstrated decreased anti-inflammatory protective capacity against LDL-induced
8 monocyte chemotactic activity in an in vitro assay. The livers from the ultrafine
9 PM-exposed mice demonstrated significant increases in lipid peroxidation and several
10 stress-related gene products (catalase, glutathione S-transferase Y_a, NADPH-quinone
11 oxidoreductase1, superoxide dismutase 2). Thus, ultrafine PM in these exposures had a
12 substantially greater impact on the systemic response than did PM_{2.5}.

PM₁₀

13 A study employing young BALB/c mice examined the effects of a 4-month exposure (24
14 h/day \times 7 days/wk) to ambient air on arterial histopathology (Lemos et al., 2006, [088594](#)).
15 Outdoor exposure chambers were located in downtown Sao Paulo, Brazil next to streets of
16 high traffic density. In the control chamber, PM₁₀ and NO₂ were filtered with 50% and 75%
17 efficiency, respectively. The average pollutant concentrations were 2.06 ppm for CO (8-h
18 mean), 104.75 $\mu\text{g}/\text{m}^3$ for NO₂ (24-h mean), 11.07 $\mu\text{g}/\text{m}^3$ for SO₂ (24-h mean), and 35.52 $\mu\text{g}/\text{m}^3$
19 for PM₁₀ (24-h mean) at a monitoring site within 100 m of the inhalation chambers. The
20 pulmonary and coronary arteries demonstrated significant decreases in L/W ratio for
21 animals exposed to the entire ambient mixture compared to controls, indicating thicker
22 walls in these vessels. There was no difference reported for the L/W ratio in renal arteries.
23 Morphologic examination suggested that the increases in L/W ratio were due to muscular
24 hypertrophy rather than fibrosis. The results of this study indicate vascular remodeling of
25 the pulmonary and coronary arteries, as opposed to changes in tone.

26 To examine the role of systemic inflammation and recruitment of monocytes into
27 plaque tissue as a possible pathway for accelerated atherosclerosis, Yatera et al. (2008,
28 [157162](#)) exposed female Watanabe heritable hyperlipidemic rabbits (42 weeks old) to
29 Ottawa PM₁₀ (EHC-93) via intratracheal instillation (5 mg/rabbit; approximately 1.56
30 mg/kg) twice a week for 4 wk. Transfusion of whole blood harvested to from exposed and
31 non-exposed animals to donor rabbits supplied labeled monocytes for assessment of
32 monocyte recruitment from the blood to the aortic wall. The fraction of aortic surface and
33 volume of aortic wall taken up by atherosclerotic plaque was increased and the number of
34 labeled monocytes in the atherosclerotic plaques was elevated in rabbits exposed to PM₁₀.
35 In addition, labeled monocytes were attached onto the endothelium overlying
36 atherosclerotic plaques and the number that migrated into the smooth muscle underneath
37 plaques in aortic vessel walls was greater with PM₁₀ exposure compared to control. These

1 responses were not observed in normal vessel walls. ICAM-1 and VCAM-1 expression was
2 elevated in atherosclerotic lesions, likely indicating enhanced monocyte adhesion to
3 endothelium and migration into plaques. Monocytes in plaque tissue stained with
4 immunogold demonstrated foam cell characteristics, which were more numerous in the
5 rabbits exposed to PM₁₀.

Gasoline Exhaust

6 Lund and colleagues (2007, [125741](#)) used whole emissions from gasoline exhaust to
7 investigate changes in the transcriptional regulation of several gene products with known
8 roles in both the chronic promotion and acute degradation/destabilization of atheromatous
9 plaques. These 50-day exposures (6 h/day × 7 days/wk) employed ApoE^{-/-} mice on high-fat
10 chow and the concentrations of the high exposure group were 61 µg/m³ for PM, 19 ppm for
11 NO_x, 80 ppm for CO, and 12.0 ppm for total hydrocarbons. The average particle number
12 median diameter was approximately 15 nm (McDonald et al., 2007, [156746](#)). Dilutions of
13 gasoline engine emissions induced a concentration-dependent increase in transcription of
14 matrix metalloproteinase (MMP) isoform 9, ET-1, and HO-1 in aortas; MMP-3 and -9 mRNA
15 levels were only increased in animals in the highest exposure group. Strong increases in
16 oxidative stress markers (nitrotyrosine and TBARS) in the aortas were also observed.
17 However, using a high-efficiency particle trap, they established that most of the effects were
18 caused by the gaseous portion of the emissions and not the particles. This study did not
19 directly address lesion area.

7.2.2. Venous Thromboembolism

20 One epidemiologic study examined the relationship between long term PM₁₀
21 concentration, venous thromboembolism, and laboratory measures of hemostasis
22 (prothrombin and activated partial thromboplastin times [PT; PTT]). PT and PTT measure
23 the extrinsic and intrinsic blood coagulation pathways, the former activated in response to
24 blood vessel injury, the latter, key to subsequent amplification of the coagulation cascade
25 and propagation of thrombus (Mackman et al., 2007, [156723](#)). Decreases in PT and PTT are
26 consistent with a hypercoagulable, prothrombotic state.

7.2.2.1. Epidemiologic Studies

27 Baccarelli et al. (2007, [090733](#)) studied 2,081 residents (56% female) of the Lombardy
28 region of Italy whose ages ranged from 18 to 84 years old. In this case-control study of 871
29 patients with ultrasonographically or venographically diagnosed lower extremity deep vein
30 thrombosis (DVT) and 1,210 of their healthy friends or relatives (1995-2005), the authors
31 used arithmetic averaging of PM₁₀ data available at 53 monitors in nine geographic areas to
32 estimate one-yr avg residence-specific exposures. They found -0.09 (95% CI: -0.16 to 0) and

1 -0.18 (95% CI: -0.35 to 0) decreases in standardized correlation coefficients for PT as well as
2 0.02 (95% CI: -0.05 to 0.06) and -0.11 (95% CI: -0.29 to 0.12) decreases in standardized
3 correlation coefficients for PTT among cases and controls, respectively, per 10 $\mu\text{g}/\text{m}^3$
4 increase in PM_{10} . Patients with DVT who were taking heparin or coumarin anticoagulants
5 were not asked to stop taking them before measurement of PT and aPTT. Of additional
6 note, PT was neither adjusted for differences in reagents used to determine it nor
7 conventionally reported as the International Normalized Ratio (INR). The ambient PM
8 concentrations from this study are characterized in Table 7-1.

7.2.3. Diabetes

7.2.3.1. Toxicological Studies

9 Diabetics as a potentially susceptible subpopulation have only recently been
10 evaluated. A toxicological study of a diet-induced obesity mouse model (C57BL/6 fed high-
11 fat chow for 10 wk) examined the effects of a 128-day $\text{PM}_{2.5}$ CAPs exposure (mean mass
12 concentration 72.7 $\mu\text{g}/\text{m}^3$; Tuxedo, NY) on insulin resistance, adipose inflammation, and
13 visceral adiposity (Sun et al., 2009, [190487](#)). Elevated fasting glucose and insulin levels
14 were observed in CAPs-exposed mice compared to air-exposed during the glucose tolerance
15 test. Aortic rings of mice exposed to CAPs demonstrated decreased peak relaxation to ACh
16 or insulin, which was associated with reduced NO bioavailability. Additionally, insulin
17 signaling was impaired in aortic tissue via lowered endothelial Akt phosphorylation.
18 Increases in adipokines and systemic inflammatory markers (i.e., TNF- α , IL-6, E-selectin,
19 ICAM-1, PAI-1, resistin, leptin) were reported for CAPs-exposed mice. CAPs resulted in
20 increased visceral and mesenteric fat mass, as well as greater adipose tissue macrophages
21 in epididymal fat pads and larger adipocyte size compared to mice in the filtered air group.
22 The results of this study demonstrate that $\text{PM}_{2.5}$ exposure can exaggerate insulin
23 resistance, visceral adiposity, and inflammation in mice fed high-fat chow.

7.2.4. Systemic Inflammation, Immune Function, and Blood Coagulation

7.2.4.1. Epidemiologic Studies

24 Chen and Schwartz (2008, [190106](#)) studied 2,978 residentially stable participants in
25 33 U.S. communities (age range = 20-89 years; 49% female) who were examined during
26 phase 1 of the National Health and Nutrition Examination Survey III (1989-1991). In this
27 cross-sectional study, the authors used inverse-distance weighted averaging of U.S. EPA
28 AQS monitored data from participant and adjacent counties of residence to estimate one-

1 yr avg exposures to PM₁₀ (median concentration within quartiles = 23.1, 31.2, 38.8 and 53.7
2 µg/m³). They found that after adjustment, residents of communities in quartile 1 had 138
3 (95% CI: 2-273) fewer white blood cells (x 10⁶/L) than residents of communities in quartiles
4 2-4. This difference increased with increasing number of metabolic abnormalities (insulin
5 resistance; hypertension; hypertriglyceridemia; low high-density lipoprotein cholesterol;
6 abdominal obesity) reported by the participant.

7 Forbes et al. (2009, [190351](#)) studied approximately 25,000 adults (age ≥ 16 yr; 53%
8 female) who were representatively sampled from 720 English postcode sectors and
9 participated in the Health Survey for England (1994, 1998 and 2003). In this fixed-effects
10 meta-analysis of year-specific cross-sectional findings, the authors used dispersion
11 modeling of emissions and weather data to estimate two-yr avg exposures to PM₁₀ at
12 participant postcode sector centroids (median in 1994, 1998 and 2003 = 19.5, 17.9 and 16.2
13 µg/m³). They found little evidence of a PM₁₀-inflammatory marker association, i.e., only a
14 0.08% (95% CI: -0.25% to 0.10%) decrease in fibrinogen concentration and a 0.14% (95%
15 CI: -1.00% to 1.30%) increase in CRP concentration per 1 µg/m³ increase in PM₁₀.

16 Calderon-Garciduenas et al. (2007, [091252](#)) compared residentially stable, non-
17 smoking healthy children (age range: 6-13 yr) living and attending school between 2003-
18 2004 in Mexico City (historically high PM; altitude 2,250 m) and Polotitlán (historically low
19 PM; altitude 2,380 m). In this ecologic study, residents of Mexico City (n = 59; 93% female)
20 had fewer white blood cells and neutrophils (x 10⁹/L) than residents of Polotitlán (n = 22;
21 69% female): unadjusted mean 6.2 (95% CI: 5.7-6.6) versus 6.9 (95% CI: 6.3-7.5) and 2.9
22 (95% CI: 2.3-3.5) versus 3.8 (95% CI: 3.2-4.4), respectively.

23 Calderon-Garciduenas et al. (2009) subsequently compared 37 unadjusted mean
24 measures of immune function and inflammation among an expanded number of these
25 participants. They found that under a two-sided type I error rate (α) = 0.05, sixteen (43%) of
26 the measures were significantly different in residents of southwest Mexico City (n = 66;
27 48% female) than those in Polotitlán (n = 93; 57% female). However, only eight measures
28 were significantly different after Bon Ferroni-correction (α = 0.05 / 37 = 0.001) and even
29 fewer would be after adjustment for reported correlation between the measures of immune
30 function and inflammation, e.g., CRP and lipopolysaccharide binding protein (Pearson's r =
31 0.71).

32 Only two cross-sectional analyses of PM₁₀ concentration and markers of immune
33 function or inflammation have been conducted with significant changes observed in the
34 NHANES population (stronger effects among those with metabolic disorders) but not in a
35 relative large survey of adults, which was conducted in England. Ecological analyses
36 comparing children in high versus low pollution regions in Mexico show differences in
37 unadjusted blood markers that may be related to PM concentration or other unmeasured
38 risk factors that differs across the communities studied.

7.2.4.2. Toxicological Studies

1 In addition to the PM_{2.5} study mentioned previously that showed increased TF
2 expression (an important initiator of thrombosis) in aortas of ApoE^{-/-} mice following
3 subchronic CAPs exposure (Sun et al., 2008, [157033](#)), three recent studies examined
4 hematology and clotting parameters in rats and mice exposed to DE, gasoline exhaust, or
5 HWS for 1 week or 6 months (Reed et al., 2004, [055625](#); Reed et al., 2006, [156043](#); Reed et
6 al., 2008, [156903](#)). In all studies, male and female F344 rats were exposed to the mixtures
7 by whole-body inhalation for 6 h/day, 7 day/wk. Respiratory effects for these studies are
8 presented in Section 7.3.3.

Diesel Exhaust

9 The target PM concentrations in the diesel exhaust study was 30, 100, 300, and
10 1000 µg/m³ and the MMAD was 0.10-0.15 µm (Reed et al., 2004, [055625](#)). Male and female
11 rats exposed to DE at the highest concentration (NO concentration 45.3 ppm; NO₂
12 concentration 4.0 ppm; CO concentration 29.8 ppm; SO₂ concentration 365 ppb) for 6
13 months demonstrated decreased serum Factor VII, but no change in plasma fibrinogen or
14 TAT (Reed et al., 2004, [055625](#)). White blood cells were decreased only in female rats in the
15 highest exposure group. Another DE study of shorter duration (4 wk, 4 h/day, 5day/wk; PM
16 mass concentration 507 or 2201 µg/m³, CO 1.3 and 4.8 ppm, NO <2.5 and 5.9 ppm, NO₂
17 <0.25 and 1.2 ppm, SO₂ 0.2 and 0.3 ppm for low and high PM exposures, respectively) did
18 not demonstrate changes in hematologic parameters or those related to coagulation (i.e.,
19 plasma prothrombin time, activated partial thromboplastin time, plasma fibrinogen, D-
20 dimer) or inflammation (i.e., CRP) in SH or WKY rats (Gottipolu et al., 2009, [190360](#)).
21 Together, these findings do not support a DE-related stimulation of blood coagulation
22 following 1 or 6 months of exposure.

Hardwood Smoke

23 The target PM concentrations in the HWS study was 30, 100, 300, and 1000 µg/m³
24 and the MMAD was 0.25-0.36 µm (Reed et al., 2006, [156043](#)). In male rats exposed to HWS,
25 the mid-low group (PM concentration 113 µg/m³; NO, NO₂, SO₂ concentrations 0 ppm; CO
26 concentration 1832.3 ppm) had the greatest responses in hematology parameters, including
27 increased hematocrit, hemoglobin, lymphocytes, and decreased segmented neutrophils
28 (Reed et al., 2006, [156043](#)). Platelets were elevated in male and female rats after 1 week of
29 exposure, but this response returned to control values following the 6 month exposure. No
30 changes were observed for any coagulation markers at 6 months.

Gasoline Exhaust

31 PM mass in the gasoline exhaust study ranged from 6.6 to 59.1 µg/m³, with the
32 corresponding number concentration between 2.6×10^4 and 5.0×10^5 particles/cm³; the

1 dilutions for the gasoline exhaust were 1:10, 1:15 or 1:90 and filtered PM at the 1:10
2 dilution (Reed et al., 2008, [156903](#)). Similar to the responses observed with HWS, male and
3 female rats in the mid and high gasoline exhaust exposure groups (NO concentrations 11.9
4 and 18.4 ppm; NO₂ concentrations 0.5 and 0.9 ppm; CO concentration 73.2 and 107.3 ppm;
5 SO₂ concentration 0.38 and 0.62 ppm, respectively) demonstrated elevated hematocrit and
6 hemoglobin; RBC count was also elevated in these groups (Reed et al., 2008, [156903](#)). The
7 only response that appeared somewhat dependent on the presence of particles was
8 increased RBC in female rats at 6 months, although the authors attributed the observed
9 increases to the high concentration of CO.

10 Collectively, these studies do not indicate robust systemic inflammation or coagulation
11 responses in F344 rats following 6-month exposures to diesel, HWS, or gasoline exhaust.
12 The limited effects that were observed could possibly be due to the varying gas
13 concentrations in the exposure mixtures.

7.2.5. Renal and Vascular Function

14 Two recent epidemiologic studies have tested associations between PM exposure and
15 indicators of renal and vascular function (urinary albumin to creatinine ratio [UACR] and
16 blood pressure). UACR is a measure of urinary albumin excretion (National Kidney, 2008,
17 [156796](#)). When calculated as the ratio of albumin to creatinine concentrations in untimed
18 (“spot”) urine samples, UACR approximates 24-h urinary albumin excretion and can be
19 used to identify albuminuria, a marker of generalized vascular endothelial damage (Xu et
20 al., 2008, [157157](#)). Values ≥ 30 mg/g (3.5 mg/mmol) and ≥ 300 mg/g (34 mg/mmol) usually
21 define micro- and macroalbuminuria, both of which are associated with increases in CVD
22 incidence and mortality (Bigazzi et al., 1998, [156272](#); Deckert et al., 1996, [156389](#); Dinneen
23 and Gerstein, 1997, [156403](#); Gerstein et al., 2001, [156466](#); Mogensen, 1984, [156769](#)).
24 Several researchers have called the dichotomization of albuminuria into question, observing
25 that there is no threshold below which risk of cardiovascular and end-stage kidney disease
26 disappears (Forman and Brenner, 2006, [156439](#); Knight and Curhan, 2003, [179900](#);
27 Ruggenti and Remuzzi, 2006, [156933](#)).

28 Systolic, diastolic, pulse, and mean arterial blood pressures (SBP; DBP; PP; MAP) in
29 mmHg have also been used as measures of cardiovascular disease. Franklin et al. (1997,
30 [156446](#)) suggested that SBP and PP were the only two measures predictive of carotid
31 stenosis in a multivariable analysis considering all four measures, whereas Khattar et al.
32 (2001, [155896](#)) suggested that their prognostic significance in hypertensive populations
33 may differ by age, with SBP and PP being most predictive among those ≥ 60 and DBP
34 among those <60 years old (Khattar et al., 2001, [155896](#)).

7.2.5.1. Epidemiologic Studies

1 O'Neill et al. (2007, [156006](#)) examined the association of UACR with PM_{2.5} and PM₁₀
2 among members of the MESA population described previously (Diez Roux et al., 2008,
3 [156401](#)). For this study of UACR, which included cross-sectional and longitudinal analyses,
4 the study population was restricted to a subset of 3,901 participants (mean age = 63 yr; 52%
5 female) with complete covariate, outcome and exposure data at their first through third
6 exams (2000-2004). In cross-sectional analyses, the authors found that after adjustment for
7 demographic and clinical characteristics, 10 µg/m³ increases in 20-year imputed exposures
8 to PM_{2.5} and PM₁₀ were associated with negligible 0.002 (95% CI: -0.048 to 0.052) and -0.002
9 (95% CI: -0.038 to 0.035) mean differences in baseline log UACR, respectively. Similarly,
10 small non-statistically significant decreases in the prevalence of microalbuminuria (defined
11 in this setting as ≥ 25 mg/g) provided little evidence of an effect on renal function. These
12 largely null cross-sectional findings mirrored those based on the study's shorter-term (30-
13 and 60-day) PM_{2.5} and PM₁₀ exposures. Moreover, longitudinal analyses revealed only a
14 weak association between three-year change in log UACR and 20-yr PM₁₀ exposure.
15 Evidence of effect modification by demographic and geographic characteristics was not
16 apparent in either the cross-sectional or longitudinal analyses.

17 Auchincloss et al. (2008, [156234](#)) focused on automated, oscillometric,
18 sphygmomanometric measures of blood pressures in mmHg (SBP; DBP; PP; MAP). Like
19 O'Neill (2007, [156006](#)), Diez et al. (2008, [156401](#)) and Allen et al. (2007, [156006](#)),
20 Auchincloss et al. (2008, [156234](#)) based their examination on the previously described
21 MESA population. The authors included 5,112 study participants (age range = 45-84 years;
22 52% female) who were free of clinically manifested CVD at their baseline exam in one of six
23 primarily urban U.S. locations (2000-2002). In this cross-sectional study, they used
24 arithmetic averaging of EPA AQS PM_{2.5} data available at the monitor nearest to each
25 participant's geocoded U.S. Postal Service ZIP code centroid to estimate 30- and 60-day avg
26 exposures to PM_{2.5}. They found small nonsignificant increases of 1.5 (95% CI: -0.2 to 3.2),
27 0.2 (95% CI: -0.7 to 1.0), 1.3 (95% CI: 0.1 to 2.6), and 0.6 (95% CI: -0.4 to 1.7) mmHg
28 increases in SBP, DBP, PP and MAP, respectively, per 10 µg/m³ increase in 30-day avg PM_{2.5}
29 exposure. Associations were slightly weaker for 60-day avg PM_{2.5} exposure and among
30 participants without hypertension, during cooler weather, in the presence of low NO₂,
31 residing >300 m from a highway, or surrounded by lower road density.

32 Finally, the Calderon-Garciduenas et al. (2007, [091252](#)) ecologic study introduced in
33 Section 7.2.3.1 also found that children residing in Mexico City had higher mean pulmonary
34 artery pressure as assessed by Doppler echocardiography and fasting plasma endothelin-1
35 (ET-1) than residents in Polotitlán: unadjusted mean 17.5 (95% CI: 15.7-19.4) versus 14.6
36 (95% CI: 13.8-15.4) mmHg and 2.23 (95% CI: 1.93-2.53) versus 1.23 (95% CI: 1.11-1.35)
37 pg/mL, respectively. Within Mexico City, ET-1 was higher in residents of the Northeast
38 (historically higher PM_{2.5}) than those of the Southwest (historically lower PM_{2.5}).

1 The MESA analyses of UACR (O'Neill et al., 2007, [156006](#)) and the ecologic study of
 2 children living in a highly polluted area of Mexico (Calderon-Garciduenas et al., 2007,
 3 [091252](#)) provide little evidence that long-term exposure to PM_{2.5} had an effect on renal and
 4 vascular function. Auchincloss et al. (2008, [156234](#)) reports small nonsignificant
 5 associations of blood pressure with 30 and 60 day avg PM_{2.5} concentrations. PM
 6 concentrations from the analyses are characterized in Table 7-1.

Table 7-1. Characterization of ambient PM concentrations from studies of subclinical measures of cardiovascular diseases.

Reference	Location	Mean Concentration (µg/m ³)	Upper Percentile Concentrations (µg/m ³)
<i>PM₁₀</i>			
Diez et al. (2008, 156401)	MESA: 6 Cities U.S.	20 yr imputed mean: 34	NR
O'Neill et al. (2007, 156006)	MESA: 6 Cities U.S.	Long-Term Exposure: 1982-2002: 34.7 1982-1987: 40.5 1988-1992: 38 1993-1997: 30.6 1998-2002: 29.7 Previous Month: 27.5	NR
Baccarelli et al. (2008, 157984)	Lombardy Italy	Annual avg: 41	NR
Rosenlund et al. (2006, 089796)	Stockholm, Sweden	30-y avg PM ₁₀ (traffic) Cases: 2.6 Controls: 2.4	5th-95th %: 0.5-6 0.6-5.9
<i>PM_{2.5}</i>			
Hoffmann et al. (2007, 091163)	HNRS, 3 Cities Germany	Annual avg: 22.8	NR
Allen et al. (2007, 156006)	MESA: 5 Cities	Annual avg: 15.8	Min-Max: 10.6-24.7
Kunzli et al. (2005, 087387)	VEAPS BVAIT	Annual avg: 20.3	Min-Max: 5.2-26.9
Auchincloss et al. (2008, 156234)	MESA: 6 Cities	Prior 30 days: 16.8 Prior 60 days: 16.7	NR
O'Neill (2007, 156006)	MESA: 6 Cities U.S.	Previous Month: 16.5	NR
Diez et al. (2008, 156401)	MESA: 6 Cities U.S.	20-y imputed mean: 21.7	NR
Hoffmann et al. (2009, 190376)	HNRS: 3 Cities Germany	Annual avg: 22.8	Min-max: 19.8-26.8

MESA: Multi-Ethnic Study of Atherosclerosis
 HNRS: Heinz Nixdorf Recall Study
 VEAPS: Vitamin E Atherosclerosis Progression Study
 BVAIT: B-Vitamin Atherosclerosis Intervention Trial

7.2.5.2. Toxicological Studies

7 In a PM_{2.5} CAPs study of 10 wk (6 h/day × 5 days/wk) in Tuxedo, NY (mean mass
 8 concentration 79.1 µg/m³), there was no difference in mean arterial pressure (MAP) in SD
 9 rats between groups (Sun et al., 2008, [157032](#)). When angiotensin II (Ang II) was infused
 10 during the last week of exposure to induce systemic hypertension, the MAP slope was
 11 consistently greater in the CAPs-exposed rats compared to the filtered air group.
 12 Furthermore, thoracic aortic rings were more responsive to phenylephrine-induced
 13 constriction and less responsive to ACh-induced relaxation in the PM+Ang II vessels. In

1 contrast to the latter findings, the relaxation response was exaggerated in the PM+Ang II
2 aortic segments with a Rho-kinase (ROCK) inhibitor. Superoxide production in aortic rings
3 increased in the PM+Ang II group compared to the filtered air group and the addition of
4 NAD(P) oxidase inhibitor (apocymine) or a NOS inhibitor (L-NAME) attenuated the
5 superoxide generation. The levels of tetrahydrobiopterin (BH₄) were decreased in
6 mesenteric vasculature and the heart by 46% and 41% in the PM+Ang II group compared to
7 controls, respectively; furthermore, levels of BH₄ in the liver were similarly reduced, which
8 is consistent with a systemic effect of CAPs. Together, these findings indicate that CAPs
9 potentiate Ang II-induced hypertension and alter vascular reactivity, perhaps through
10 activated NADPH oxidase and eNOS uncoupling that result in oxidative stress generation
11 and triggering of the Rho/ROCK signaling pathway.

7.2.6. Autonomic Function

7.2.6.1. Toxicological Studies

12 Hwang et al. (2005, [087957](#)) and Chen and Hwang (2005, [087218](#)) used
13 radiotelemetry to examine the chronic changes in HR and HRV resulting from the same
14 CAPs exposures described previously (Chen and Nadziejko, 2005, [087219](#)). The overall
15 average CAPs exposure concentration was 133 µg/m³ and results indicate differing
16 responses to CAPs between ApoE^{-/-} mice and their genetic background strain, C57BL/6J
17 mice (Hwang et al., 2005, [087957](#)). Using the time period of 1:30 to 4:30 a.m., C57BL/6J
18 mice showed a HR increase only over the last month of exposure. In contrast, ApoE^{-/-} mice
19 had chronic decreases of 33.8 beat/min for HR. Changes in HRV (SDNN and rMSSD) were
20 somewhat more complicated, with biphasic responses in ApoE^{-/-} mice over the 5 month
21 period (initial increase over first 6 wk, decrease over next 12 wk, and slight upward turn for
22 remainder of the study)(Chen and Hwang, 2005, [087218](#)). Increasing linear trends were
23 observed in C57BL/6J mice for SDNN and rMSSD. The average CAPs concentration for the
24 HRV study was 110 µg/m³. However, only 3 C57BL/6J mice in the exposure group were
25 included in the analysis compared to 10 ApoE^{-/-} animals, thus making it difficult to
26 interpret the C57BL/6J mice responses (Chen and Hwang, 2005, [087218](#); Hwang et al.,
27 2005, [087957](#)).

7.2.7. Cardiac changes

7.2.7.1. Toxicological studies

1 Two recent toxicological studies have evaluated the effects of PM on cardiac effects
2 including pathology and gene expression. Cardiac mitochondrial function has also been
3 evaluated following PM exposure in rats.

Diesel Exhaust

4 A recent study of DE exposure (PM mass concentration 507 or 2201 $\mu\text{g}/\text{m}^3$, CO 1.3 or
5 4.8 ppm, NO <2.5 or 5.9 ppm, NO₂ <0.25 or 1.2 ppm, SO₂ 0.2 or 0.3 ppm for low and high
6 PM exposures, respectively; geometric median number diameter 85 nm) indicated a
7 hypertensive-like cardiac gene expression in WKY rats that mimicked baseline patterns in
8 air-exposed SH rats (Gottipolu et al., 2009, [190360](#)). Exposure to the high concentration of
9 DE for 4 wk (4 h/day, 5 day/wk) led to downregulation of genes involved in stress,
10 antioxidant compensatory response, growth and extracellular matrix regulation, membrane
11 transport of molecules, mitochondrial function, thrombosis regulation, and immune
12 function. No genes were affected by DE in SH rats. A dose-dependent inhibition of
13 mitochondrial aconitase activity in both rat strains was observed, indicating a DE effect on
14 oxidative stress. It should be noted that while DE-related cardiovascular effects were found
15 in WKY rats only, pulmonary inflammation and injury were observed in both strains (see
16 Sections 7.3.3.2. and 7.3.5.1.).

Model Particles

17 Wallenborn et al. (2008, [191171](#)) examined the subchronic (5 h/day, 3 day/wk, 16 wk)
18 pulmonary, cardiac, and systemic effects of nose-only exposure to particulate ZnSO₄ (9, 35,
19 or 120 $\mu\text{g}/\text{m}^3$) in WKY rats. Particle size was reported to be 31-44 nm measured as number
20 median diameter. Although changes in pulmonary inflammation or injury and cardiac
21 pathology were not observed, effects on cardiac mitochondrial protein and enzyme levels
22 were noted (i.e., increased ferritin levels, decrease in succinate dehydrogenase activity),
23 possibly indicating a small degree of mitochondrial dysfunction. Glutathione peroxidase, an
24 antioxidant enzyme, was also decreased in the cardiac cytosol. Gene expression analysis
25 identified alterations in cardiac genes involved in cell signaling events, ion channels
26 regulation, and coagulation in animals exposed to the highest ZnSO₄ concentration only.
27 This study demonstrates a possible direct effect of ZnSO₄ on extrapulmonary systems, as
28 suggested by the lack of pulmonary effects (see Section 7.3.3.2).

7.2.8. Left Ventricular Mass and Function

1 Van Hee et al. (2009) studied 3,827 participants (age range = 45-84 yr; 53% female)
 2 who underwent magnetic resonance imaging (MRI) of the heart at the baseline examination
 3 of the MESA cohort (2000-2002). This cross-sectional study focused on two MRI-based
 4 outcome measures: left ventricular mass index (LVMI, g/m²) and ejection fraction (EF, %),
 5 the former estimated using the DuBois formula for body surface area, the latter as the ratio
 6 of stroke volume to end diastolic volume. The study also estimated annual mean exposures
 7 to PM_{2.5} at participants' geocoded residential addresses in 2000 using ordinary kriging of
 8 U.S. EPA AQS concentration data. In fully adjusted models, it found 3.8 (95% CI: -6.1 to
 9 13.7) g/m² and -3.0% (-8.0% to 2.0%) differences in LVMI and EF per 10 µg/m³ increment in
 10 PM_{2.5}. The findings were small and imprecise, albeit suggestive of a slight, PM-associated
 11 increase in the mass and decrease in the function of the left ventricle. The effect of living
 12 within 50 m of a major roadway on LVMI was greater than the effect of PM_{2.5} (i.e., 1.4 g/m²
 13 [95% CI: 0.3-2.5] per 10 µg/m³.)

Table 7-2. Characterization of ambient PM concentrations from studies of clinical cardiovascular diseases.

Reference	Location	Mean Annual Concentration (µg/m ³)	Upper Percentile Concentrations (µg/m ³)
PM₁₀			
Puett et al. (2008, 156891)	13 U.S. States	21.6	
Zanobetti and Schwartz (2007, 091247)	21 U.S. Cities	28.8	Overall range NR
Rosenlund et al. (2006, 089796)	Stockholm, Sweden	30 y avg PM ₁₀ (traffic) Cases: 2.6 Controls: 2.4	5th-95th Percentile 0.5-6.0 0.6-5.9
Maheswaran et al. (2005, 090769)	Sheffield, U.K.	Range of means in each quintile: 16-23.3	NR
Baccarelli et al. (2007, 090733)	Lombardy, Italy	Sep-Nov: 51.2 Dec-Feb: 68.5 Mar-May: 64.1 Jun-Aug: 44.3	148.9 238.3 158.5 94.7
PM_{2.5}			
Miller et al. (2007, 090130)	WHI: 36 Metropolitan areas	Citywide avg (yr 2000): 13.5	Min-max: 4-19.3
Hoffmann et al. (2006, 091162)	HNRS: 2 Cities Germany	23.3	NR

WHI: Womens Health Initiative
 HNRS: Hans Nixdorf Recall Study

7.2.9. Clinical Outcomes in Epidemiologic Studies

14 Several epidemiologic studies of U.S. and European populations have examined
 15 associations between long-term PM exposures and clinical CVD events (Baccarelli et al.,

1 2008, [157984](#); Hoffmann et al., 2006, [091162](#); Hoffmann et al., 2009, [190376](#); Maheswaran
2 et al., 2005, [088683](#); Maheswaran et al., 2005, [090769](#); Miller et al., 2007, [090130](#);
3 Rosenlund et al., 2006, [089796](#); Solomon et al., 2003, [156994](#); Zanobetti and Schwartz,
4 2007, [091247](#)). Results from these studies are summarized in Figure 7-1. The ambient PM
5 concentrations from these studies are characterized in Table 7-2.

Coronary Heart Disease

6 Epidemiologic studies examining the association of coronary heart disease (CHD) with
7 long-term PM exposure are discussed below (Hoffmann et al., 2006, [091162](#); Maheswaran et
8 al., 2005, [090769](#); Miller et al., 2007, [090130](#); Rosenlund et al., 2006, [089796](#); Rosenlund et
9 al., 2009, [190309](#); Zanobetti and Schwartz, 2007, [091247](#)). Cases of CHD were variably
10 defined in these studies to include history of angina pectoris, MI, coronary artery
11 revascularization (bypass graft; angioplasty; stent; atherectomy), and congestive heart
12 failure (CHF). Results pertaining to death from CHD are described in Section 7.6.

13 Miller et al. (2007, [090130](#)) studied incident, validated MI, revascularization, and
14 CHD death, both separately and collectively, among 58,610 post-menopausal female
15 residents of 36 U.S. metropolitan areas (age range = 50-79 yr) enrolled in the Women's
16 Health Initiative Observational Study (WHI OS, 1994-1998). In this prospective cohort
17 study of participants free of CVD at baseline (median duration of follow-up = 6 yr), the
18 authors used arithmetic averaging of year 2000 EPA AQS PM_{2.5} data available at the
19 monitor nearest to each participant's geocoded U.S. Postal Service five-digit ZIP code
20 centroid to estimate one-yr avg exposures. They found 6% (95% CI: -15% to 34%), 20% (95%
21 CI: 0-43%) and 21% (95% CI: 4-42%) increases in the overall risk of MI, revascularization,
22 and their combination with CHD death per 10 µg/m³ increase in PM_{2.5}, respectively. Hazards
23 were higher within than between cities and in the obese. For the combined CVD outcome
24 (MI, revascularization, stroke, CHD death, cerebrovascular disease), authors reported a
25 24% (95% CI: 9-41%) increase in risk that was higher among participants at higher than
26 lower quintiles of body mass index, waist-to-hip ratio, and waist circumference. The
27 PM_{2.5}-CVD association was stronger among non-diabetic than diabetic participants.

28 Puett et al. (2008, [156891](#)) studied incident, validated CHD, CHD death, and non-
29 fatal MI among 66,250 female residents (mean age = 62 years) of metropolitan statistical
30 areas in thirteen northeastern U.S. states who were enrolled in the Nurses' Health Study
31 (NHS, 1992-2002). In this prospective cohort study of women without a history of non-fatal
32 MI at baseline (maximum duration of follow-up = 4 years), the authors used two-stage,
33 spatially smoothed, land use regression to estimate residence-specific, 1-yr ma PM₁₀
34 exposures from U.S. EPA AQS and emissions, IMPROVE, and Harvard University monitor
35 data. They found a 10% (95% CI: -6 to 29) increase in risk of first CHD event per 10 µ/m³
36 increase in 1-yr avg PM₁₀ exposure, while the association with MI was close to the null
37 value. The association with fatal CHD event of 30% (95% CI: 0-71%) was stronger.

1 Furthermore, associations with CHD death were higher in the obese and in the never
2 smokers.

3 Rosenlund et al. (2006, [089796](#)) studied 2,938 residents of Stockholm County, Sweden
4 (age range = 45-70 years; 34% female). In this case-control study of 1,085 patients with
5 their first, validated non-fatal MI and an age-, gender- and catchment-stratified random
6 sample of 1,853 controls without MI (1992-1994), the authors used street canyon-adjusted
7 dispersion modeling of emissions data to estimate 30-yr avg exposure to PM₁₀
8 (median = 2.4 µg/m³). They found that the OR for prevalent MI per 10 µg/m³ increase in
9 PM₁₀ was 0.85 (95% CI: 0.50-1.42). The OR for fatal MI was non-significantly elevated.

10 In a more recent study, Rosenlund et al. (2009, [190309](#)) evaluated 554,340 residents
11 (age range = 15-79 years; 49% female) of Stockholm County, Sweden (1984-1996). In this
12 population-based, case-control study of 43,275 cases of incident, validated MI, the authors
13 used dispersion modeling of traffic emissions and land use data to estimate 5-yr avg
14 exposure to PM₁₀. They found that after adjustment for demographic, temporal, and
15 socioeconomic characteristics, the OR for MI per 5 µg/m³ increase in PM₁₀ was 1.04 (95% CI:
16 1.00-1.09). ORs were higher after restriction to fatal cases, in- or out-of-hospital deaths, and
17 participants who did not move between population censuses. Authors state that control for
18 confounding was superior in their previous study (Rosenlund et al., 2006, [089796](#)) although
19 the size of the population was larger in this recent study (Rosenlund et al., 2009, [190309](#)).

20 Zanobetti and Schwartz (2007, [091247](#)) studied ICD-coded recurrent MI (ICD-9 410)
21 and post-infarction CHF (ICD-9 428) among 196,131 Medicare recipients (age ≥ 65 years;
22 50% female) discharged alive following MI hospitalization in 21 cities from 12 U.S. states
23 (1985-1999). In this ecologic, open cohort study of re-hospitalization among MI survivors
24 (mean duration of follow-up = 3.6 and 3.7 years for MI and CHF, respectively), the authors
25 used arithmetic averaging of EPA AQS PM₁₀ data available in the county of hospitalization
26 to estimate one-yr avg exposures. They found 17% (95% CI: 5-31%) and 11% (95% CI: 3-
27 21%) increases in the risk of recurrent MI and post-infarction CHF, respectively, per
28 10 µg/m³ increase in PM₁₀ exposure. Hazards were somewhat higher among persons aged
29 >75 years.

30 Hoffmann et al. (2006, [091162](#)) studied self-reported CHD (MI or revascularization)
31 among 3,399 residents of Essen and Mülheim, Germany (age range = 45-75 years; 51%
32 female) at the baseline exam of the Heinz Nixdorf Recall Study (2000-2003) introduced
33 previously. In this cross-sectional ancillary study, the authors used dispersion modeling of
34 emissions, climate and topography data to estimate 1-yr avg exposure to PM_{2.5}
35 (mean = 23.3 µg/m³). They found little evidence of an association between PM_{2.5} and CHD in
36 these data. After adjustment for geographic, demographic and clinical characteristics, the
37 OR for prevalent CHD per 10 µg/m³ increase in exposure was 0.55 (95% CI: 0.14-2.11).

38

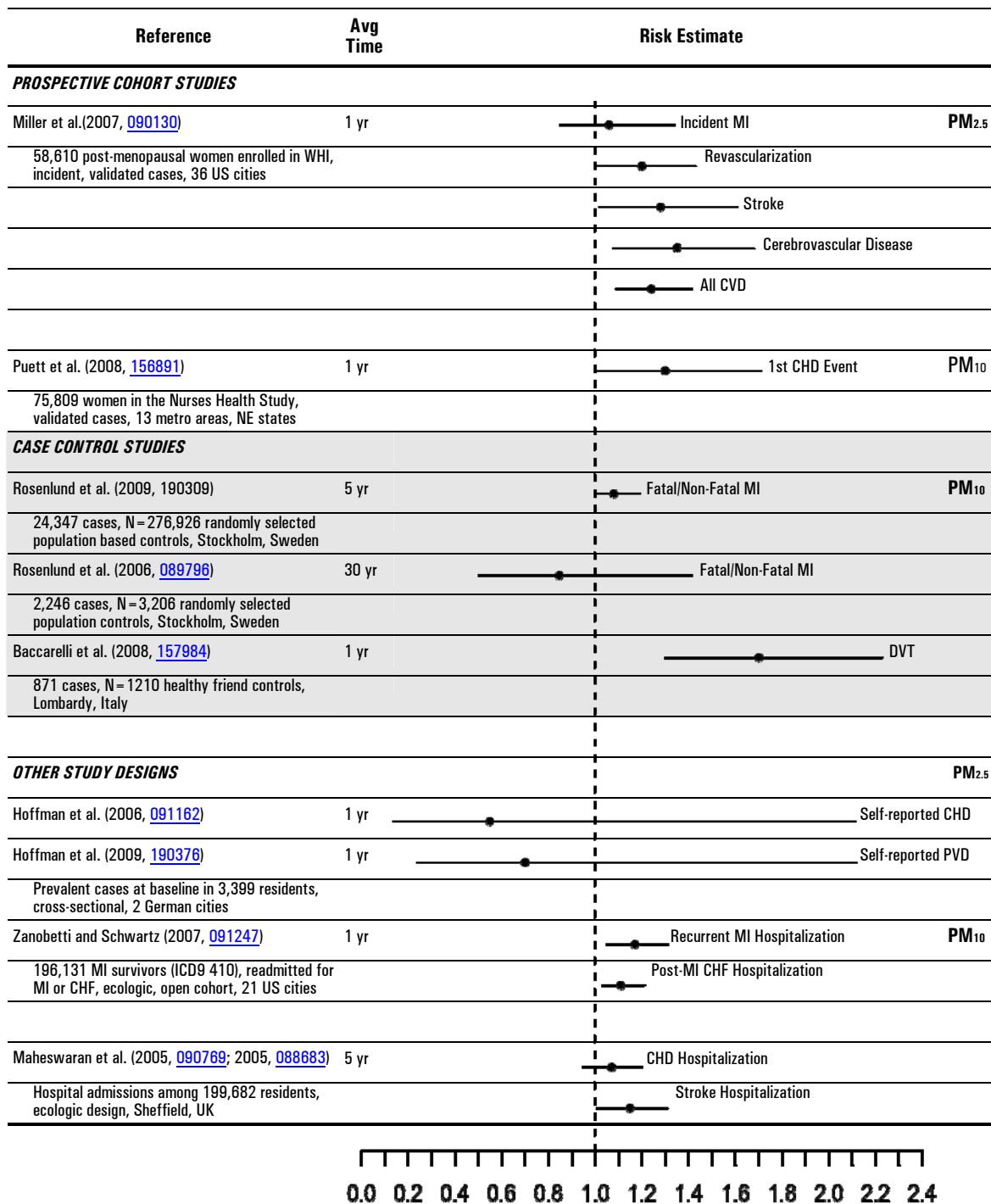


Figure 7-1. Risk estimates for the associations of clinical outcomes with long-term exposure to ambient PM_{2.5} and PM₁₀.

1 In the study of 1030 census enumeration districts in Sheffield, U.K. described
2 previously, Maheswaran et al. (2005, [090769](#)) studied 11,407 ICD-10-coded emergency
3 hospitalizations for CHD (ICD10 I20-25) among 199,682 residents (age ≥ 45 years; 45%
4 female). In this ecologic study, the authors used dispersion modeling of emissions and
5 climate data to estimate 5-yr avg exposure to PM₁₀. They found that after adjusting for

1 smoking prevalence, controlling for socioeconomic factors, and smoothing, the age- and
2 gender-standardized rate ratios for CHD admission were 1.01 (95% CI: 0.92-1.11), 1.04
3 (95% CI: 0.93-1.15), 0.97 (95% CI: 0.87-1.08), and 1.07 (95% CI: 0.95-1.20) across PM₁₀
4 quintiles. The linear trend was somewhat stronger for CHD mortality (see Section 7.3).

5 The study of post-menopausal women enrolled in the WHI OS by Miller et al. (2007,
6 [090130](#)) was the only U.S. study to examine the effect of PM_{2.5} rather than PM₁₀. This
7 study, which provides strong evidence of an association, was distinguished by its
8 prospective cohort design, validation of incident cases and large population. Puett et al.
9 (2008, [156891](#)), the other U.S. study with comparable design features, provides evidence of
10 an association of incident CHD with long-term PM₁₀ exposure. Findings from Swedish case
11 control studies of incident validated cases of MI were not consistent. A cross-sectional study
12 of self-reported CHD did not provide evidence of an association with PM_{2.5}, while findings
13 from two ecologic studies of PM₁₀ indicated positive associations of CHD hospitalizations
14 with PM₁₀ (Maheswaran et al., 2005, [088683](#); Zanobetti and Schwartz, 2007, [091247](#)).

Stroke

15 Miller et al. (2007, [090130](#)) found 28% (95% CI: 2-61%) and 35% (95% CI: 8-68%)
16 increases in the overall risk of validated stroke and cerebrovascular disease, respectively,
17 per 10 µg/m³ increase in one-yr avg PM_{2.5} exposure. Risks were higher within than between
18 cities. In the study of 1030 Census of enumeration districts in Sheffield, U.K. described
19 previously, Maheswaran et al. (2005, [088683](#)) studied 5,122 ICD-10-coded emergency
20 hospital admissions for stroke (I60-69) among 199,682 residents (age ≥ 45 yr; 45% female)
21 of 1,030 census enumeration districts in Sheffield, U.K. (1994-1999). In this ecologic study,
22 the authors used dispersion modeling of emissions and climate data to estimate five-yr avg
23 exposure to PM₁₀. They found that the age- and gender-standardized rate ratios for stroke
24 admission were 1.05 (95% CI: 0.94-1.17), 1.07 (95% CI: 0.95-1.20), 1.06 (95% CI: 0.94-1.20),
25 and 1.15 (95% CI: 1.01-1.31) across PM₁₀ quintiles. Linear trend was somewhat stronger for
26 stroke mortality (see Section 7.6).

27 These studies examining the long-term PM-stroke relationship provide evidence of
28 association. Maheswaran et al. (2005, [088683](#)) examined emergency room HAs in Sheffield,
29 U.K. using an ecologic design while results reported by Miller et al. (2007, [090130](#)) are
30 based on the prospective cohort study of the WHI OS population (both introduced
31 previously).

Peripheral Arterial Disease

32 The German Heinz Nixdorf Recall cross-sectional study described in Section 7.2.1.1
33 (Hoffmann et al., 2009, [190376](#)) also evaluated the association between one-yr avg exposure
34 to PM_{2.5} and peripheral arterial disease (self-reported history of a surgical or procedural
35 intervention or an ABI <0.9 in one or both legs). The authors found no evidence of an

1 increase in risk. The OR for peripheral arterial disease was 0.87 (95% CI: 0.57-1.34) per 3.9
2 $\mu\text{g}/\text{m}^3$ increase in $\text{PM}_{2.5}$. However, evidence of an association with traffic exposure was
3 present in these data. ORs of 1.77 (95% CI: 1.01-3.10), 1.02 (95% CI: 0.58-1.80), and 1.07
4 (95% CI: 0.68-1.68) for residing ≤ 50 , 50-100, and 100-200 m of a major road (reference
5 category: >200 m), respectively were observed. ORs were higher among participants with
6 CAC scores ≤ 75 th percentile, women, and smokers.

Deep Vein Thrombosis

7 The Italian case-control study (introduced in Section 7.2.1.2) also examined the
8 chronic PM_{10} -DVT association (Baccarelli et al., 2008, [157984](#)). The authors found a 70%
9 (95% CI: 30-223%) increase in the odds of deep vein thrombosis (DVT) per 10 $\mu\text{g}/\text{m}^3$ increase
10 in one-yr avg PM_{10} exposure. This finding was consistent with the decreases in PT and PTT
11 also observed among controls in this context as well as the 47% (95% CI: 11-96%) increase
12 in the odds of DVT per inter-decile range (242 m) increase in the residence-to-major-
13 roadway distance observed among a subset of cases and controls (Baccarelli et al., 2009,
14 [188183](#)). The PM_{10} -DVT and distance-DVT associations were both weaker among women
15 and among users of oral contraceptives or hormone therapy.

7.2.10. Cardiovascular Mortality

16 New epidemiologic evidence reports a consistent association between long-term
17 exposure to $\text{PM}_{2.5}$ and increased risk of cardiovascular mortality. There is little evidence for
18 the long-term effects of $\text{PM}_{10-2.5}$ on cardiovascular mortality. This section focuses on
19 cardiovascular mortality outcomes in response to long-term exposure to PM. The studies
20 that investigate long-term exposure and mortality due to any specific or all (non-accidental)
21 causes are evaluated in Section 7.6. A summary of the mean PM concentrations reported for
22 the studies characterized in this section is presented in Table 7-8, and the effect estimates
23 are presented in Figures 7-7 and 7-8.

24 A number of large, U.S. cohort studies have found consistent associations between
25 long-term exposure to $\text{PM}_{2.5}$ and cardiovascular mortality. The American Cancer Society
26 (ACS) (Pope et al. 2004, [055880](#)) reported positive associations with deaths from specific
27 cardiovascular diseases, particularly ischemic heart disease, and a group of cardiac
28 conditions including dysrhythmia, heart failure and cardiac arrest (RR for cardiovascular
29 mortality = 1.12 [95% CI: 1.08-1.15] per 10 $\mu\text{g}/\text{m}^3$ $\text{PM}_{2.5}$). In an additional reanalysis that
30 extended the follow-up period for the ACS cohort to 18 years (1982-2000) (Krewski et al.,
31 2009, [191193](#)), investigators found effect estimates that were similar, though generally
32 higher, than those reported in previous ACS analyses.

33 A follow-up to the Harvard Six Cities study (Laden et al., 2006, [087605](#)) used updated
34 air pollution and mortality data and found positive associations between long-term

1 exposure to PM_{2.5} and mortality. Of special note is a statistically significant **reduction** in
2 mortality risk reported with **reduced** long-term fine particle concentrations. This reduced
3 mortality risk was observed for deaths due to cardiovascular and respiratory causes, but
4 not for lung cancer deaths.

5 The WHI cohort study (Miller et al., 2007, [090130](#)) (described previously) found that
6 each 10 µg/m³ increase of PM_{2.5} was associated with a 76% increase in the risk of death
7 from cardiovascular disease (hazard ratio, 1.76 [95% CI: 1.25-2.47]). The WHI study not
8 only confirms the ACS and Six City Study associations with cardiovascular mortality in yet
9 another well characterized cohort with detailed individual-level information, it also has
10 been able to consider the individual medical records of the thousands of WHI subjects over
11 the period of the study. This has allowed the researchers to examine not only mortality, but
12 also related morbidity in the form of heart problems (cardiovascular events) experienced by
13 the subjects during the study. These morbidity co-associations with PM_{2.5} in the same
14 population lend even greater support to the biological plausibility of the air pollution-
15 mortality associations found in this study.

16 In an analysis for the Seventh-Day Adventist cohort in California (AHSMOG), a
17 positive, association with coronary heart disease mortality was reported among females (92
18 deaths; RR = 1.42 [95% CI: 1.06-1.90] per 10 µg/m³ PM_{2.5}), but not among males (53 deaths;
19 RR = 0.90 [95% CI: 0.76-1.05] per 10 µg/m³ PM_{2.5}) (Chen et al., 2005, [087942](#)). Associations
20 were strongest in the subset of postmenopausal women (80 deaths; RR = 1.49 [95% CI: 1.17-
21 1.89] per 10 µg/m³ PM_{2.5}). The authors speculated that females may be more sensitive to air
22 pollution-related effects, based on differences between males and females in dosimetry and
23 exposure. As was found with fine particles, a positive association with coronary heart
24 disease mortality was reported for PM_{10-2.5} and PM₁₀ among females (RR = 1.38 [95% CI:
25 0.97-1.95] per 10 µg/m³ PM_{10-2.5}; RR = 1.22 [95% CI: 1.01-1.47] per 10 µg/m³ PM₁₀), but not
26 for males (RR = 0.92 [95% CI: 0.66-1.29] per 10 µg/m³ PM_{10-2.5}; RR = 0.94 [95% CI: 0.82-1.08]
27 per 10 µg/m³ PM₁₀); associations were strongest in the subset of postmenopausal women
28 (80 deaths) (Chen et al., 2005, [087942](#)).

29 Two additional studies explored the effects of PM₁₀ on cardiovascular mortality. The
30 Nurses' Health Study (Puett et al., 2008, [156891](#)) is an ongoing prospective cohort study
31 examining the relation of chronic PM₁₀ exposures with all-cause mortality and incident and
32 fatal coronary heart disease consisting of 66,250 female nurses in MSAs in the northeastern
33 region of the U.S. The association with fatal CHD occurred with the greatest magnitude
34 when compared with other specified causes of death (hazard ratio 1.42 [95% CI: 1.11-1.81]).
35 The North Rhine-Westphalia State Environment Agency (LUA NRW) initiated a cohort of
36 approximately 4,800 women, and assessed whether long-term exposure to air pollution
37 originating from motorized traffic and industrial sources was associated with total and
38 cause-specific mortality (Gehring et al., 2006, [089797](#)). They found that cardiopulmonary
39 mortality was associated with PM₁₀ (RR = 1.52 [95% CI: 1.09-2.15] per 10 µg/m³ PM₁₀).

1 In summary, the 2004 PM AQCD concluded that there was strong evidence that long-
2 term exposure to PM_{2.5} was associated with increased cardiopulmonary mortality. Recent
3 studies investigating cardiovascular mortality provide some of the strongest evidence for a
4 cardiovascular effect of PM. A number of large cohort studies have been conducted
5 throughout the U.S. and reported consistent increases in cardiovascular mortality related
6 to PM_{2.5} concentrations. The results of two of these studies have been replicated in
7 independent reanalyses. These effects are biologically plausible and coherent with
8 epidemiologic and toxicological studies of short-term exposure and CVD morbidity and
9 mortality, and long-term exposure to PM_{2.5} and CVD morbidity.

7.2.11. Summary and Causal Determinations

7.2.11.1. PM_{2.5}

10 Epidemiologic studies examining associations between long-term exposure to ambient
11 PM (over months to years) and CVD morbidity had not been conducted and thus were not
12 included in the 1996 or 2004 PM AQCDs (U.S. EPA, 1996, [079380](#); U.S. EPA, 2006, [157071](#)).
13 A number of studies were included in the 2004 AQCD that evaluated the effect of long-term
14 PM_{2.5} exposure on cardiovascular mortality and found strong and consistent associations.
15 No toxicological studies had evaluated the effects of subchronic or chronic PM exposure on
16 CVD outcomes in the 2004 PM AQCD. Recently, epidemiologic and toxicological studies
17 have provided evidence of the adverse effects of long-term exposure to PM_{2.5} on
18 cardiovascular outcomes, including atherosclerosis and clinical and subclinical markers of
19 cardiovascular morbidity.

20 The strongest evidence for a CVD health effect related to long-term PM_{2.5} exposure
21 comes from epidemiologic studies of cardiovascular mortality. A number of large, multicity
22 U.S. studies (the ACS, Six Cities Study, WHI, and AHSMOG) provide consistent evidence of
23 an effect between long-term exposure to PM_{2.5} and cardiovascular mortality (Section 7.2.10).
24 These studies were conducted in urban areas across the U.S. where mean concentrations
25 ranged from 10.2–29.0 µg/m³ (Table 7-8). An epidemiologic study investigating the
26 relationship between PM_{2.5} and clinical CVD morbidity among post-menopausal women
27 (Miller et al., 2007, [090130](#)) provides evidence of an effect that is coherent with the
28 cardiovascular mortality studies. This large, prospective cohort study of incident, validated
29 cases found large increases in the adjusted risk of MI, revascularization, and stroke using a
30 1-yr avg PM_{2.5} concentration (mean = 13.5 µg/m³). A cross-sectional analyses of self-reported
31 prevalence of CHD and peripheral arterial disease found no such increase in the odds of
32 CVD morbidity (Hoffmann et al., 2006. [091162](#)); the inconsistency of these findings with
33 Miller et al. (2007, [090130](#)) may be explained by differences in study design or location.

1 The effect of long-term PM_{2.5} exposure on pre-clinical measures of atherosclerosis
2 (CIMT, CAC, AAC or ABI) has been studied in several populations using a cross-sectional
3 study design. The magnitude of the PM_{2.5} effects and their consistency across different
4 measures of atherosclerosis in these studies varies widely, and they may be limited in their
5 ability to discern small changes in these measures. Kunzli et al. (2005, [087387](#)) observed a
6 non-significant 4.2% increase in CIMT associated with long-term PM_{2.5} exposure among
7 participants of a clinical trial in greater Los Angeles, which was several fold higher than
8 the 0.5% increase observed by Diez-Roux et al. (2008, [156401](#)) in their analyses of MESA
9 baseline data. The associations in MESA of CAC and ABI with long-term PM_{2.5} exposure
10 were largely null (Diez Roux et al., 2008, [156401](#)), while an increase in AAC with long-term
11 PM_{2.5} exposure was reported (Chang et al., 2008, [180393](#)). By contrast, a 43% increase in
12 CAC was associated with long-term PM_{2.5} exposure in a German study but no similar
13 association with ABI was observed (Hoffmann et al., 2009, [190376](#)). Although the number of
14 studies examining these relationships is limited, effect modification by use of
15 hyperlipidemics and smoking status was reported in more than one study of long-term PM
16 exposure.

17 Evidence of enhanced atherosclerosis development was demonstrated in new
18 toxicological studies that demonstrate increased plaque and lesion areas, lipid deposition,
19 and TF in aortas of ApoE^{-/-} mice exposed to CAPs (Section 7.2.1.2). In addition, alterations
20 in vasoreactivity were observed, suggesting an impaired NO pathway. Additional
21 toxicological studies of PM₁₀ are consistent with these results. Further support is provided
22 by a study that reported decreased L/W ratio in the pulmonary and coronary arteries of
23 mice exposed to ambient air. However, PM_{2.5} CAPs derived from traffic in Los Angeles did
24 not affect plaque size (Araujo et al., 2008, [156222](#)). Collectively, these toxicological studies
25 provide biological plausibility for the small effects observed in epidemiologic studies.

26 There is limited evidence for the effects of PM_{2.5} on renal or vascular function. Cross-
27 sectional and longitudinal epidemiologic analyses of PM_{2.5} and UACR revealed no evidence
28 of an effect (O'Neill et al., 2007, [156006](#)) while small non-statistically significant increases
29 in BP with 30- and 60-day avg PM_{2.5} concentrations were reported (Auchincloss et al., 2008,
30 [156234](#)). A toxicological study did not show changes in MAP with CAPs, but indicated a
31 CAPs-related potentiation of experimentally-induced hypertension (Sun et al., 2008,
32 [157032](#)). In addition, CAPs has induced changes in insulin resistance, visceral adiposity,
33 and inflammation in a diet-induced obesity mouse model (Sun et al., 2009, [190487](#)),
34 indicating that diabetics may be a potentially susceptible population to PM exposure.

35 In summary, a number of large U.S. cohort studies report associations of long-term
36 PM_{2.5} concentration with cardiovascular mortality. These studies provide the strongest
37 evidence for an effect of long-term PM_{2.5} exposure on CVD effects. Additional evidence
38 comes from a methodologically rigorous epidemiology study that demonstrates coherent
39 associations between long-term PM_{2.5} exposure and CVD morbidity among post-menopausal

1 women. Toxicological studies demonstrate that this effect is biologically plausible and the
2 effect is coherent with studies of short-term PM_{2.5} exposure and CVD morbidity and
3 mortality, and with long-term exposure to PM_{2.5} and CVD mortality. Associations between
4 PM_{2.5} and subclinical measures of atherosclerosis are inconsistent, but cross-sectional
5 studies may be limited in their ability to discern small changes in these measures. In
6 addition, potential modification of the PM_{2.5}-CVD association by smoking status and the use
7 of anti-hyperlipidemics has been demonstrated in epidemiologic studies that used
8 individual-level data. Toxicological studies provide evidence for accelerated development of
9 atherosclerosis in ApoE^{-/-} mice exposed to CAPs and show effects on coagulation factors,
10 experimentally-induced hypertension, and vascular reactivity. Available studies of clinical
11 cardiovascular disease outcomes report inconsistent results. Based on the above findings,
12 the epidemiologic and toxicological evidence is **sufficient to infer a causal relationship**
13 **between long-term PM_{2.5} exposures and cardiovascular effects.**

7.2.11.2. PM_{10-2.5}

14 One epidemiologic study evaluated the relationship between long-term exposure to
15 PM_{10-2.5} and cardiovascular mortality and found a positive association with coronary heart
16 disease mortality among females, but not for males; associations were strongest in the
17 subset of postmenopausal women (Chen et al., 2005, [087942](#)). No toxicological studies of
18 long-term exposure to ambient PM_{10-2.5} and cardiovascular effects have been conducted to
19 date. Evidence is **inadequate to infer the presence or absence of a causal relationship.**

7.2.11.3. Ultrafine PM

20 A few toxicological studies of long-term exposure to ultrafine PM have been
21 conducted. Increased plaque size was reported in mice exposed to ultrafine CAPs derived
22 from traffic (Araujo et al., 2008, [156222](#)). Studies of diesel and gasoline exhaust reported
23 relatively few changes in hematologic or coagulation parameters (Section 7.2.4.2) and one
24 DE study demonstrated altered cardiac gene expression in normotensive rats that reflected
25 the development of hypertension (Gottipolu et al., 2009, [190360](#)). Whole and filtered
26 gasoline exhaust induced increases in gene products involved in atheromatous plaque
27 formation and/or degradation, but these effects were largely due to the gaseous emissions
28 (Lund et al., 2007, [125741](#)). Evidence from these studies alone is **inadequate to infer the**
29 **presence or absence of a causal relationship** due to a few studies being conducted without
30 gaseous co-pollutants.

7.3. Respiratory Effects

1 Several cohort studies reviewed in the 2004 PM AQCD provided evidence for
2 relationships between long-term PM exposure and effects on the respiratory system, though
3 it did not rule out the possibility that the observed respiratory effects may have been
4 confounded by other pollutants. In 12 southern California communities in the Children's
5 Health Study (CHS), Gauderman et al. (2000, [012531](#); 2002, [026013](#)) found that decreases
6 in lung function growth among schoolchildren were associated with long-term exposure to
7 PM. Declines in pulmonary function were reported with all three major PM size classes –
8 PM₁₀, PM_{10-2.5} and PM_{2.5} – though the three PM measures were highly correlated. In
9 another analysis of data from the CHS cohort, McConnell et al. (1999, [007028](#)), reported an
10 increased risk of bronchitis symptoms in children living in communities with higher PM₁₀
11 and PM_{2.5} concentrations. These results were found to be consistent with results of cross-
12 sectional analyses of the 24-cities study by Dockery et al. (1996, [077269](#)) and Raizenne et
13 al. (1996, [077268](#)), that were assessed in the 1996 PM AQCD. These studies reported
14 associations between increased bronchitis rates and decreased peak flow with fine particle
15 sulfate and fine particle acidity. However, the high correlation of PM₁₀, acid vapor and NO₂
16 precluded clear attribution of the bronchitis effects reported by McConnell et al. (1999,
17 [007028](#)) to PM alone. In a prospective cohort study among a subset of children in the CHS
18 (n = 110) who moved to other locations during the study period, Avol et al. (2001, [020552](#))
19 reported that those subjects who moved to areas of lower PM₁₀ showed increased growth in
20 lung function compared with subjects who moved to communities with higher PM₁₀
21 concentrations. Finally, the 2004 PM AQCD concluded that there was strong epidemiologic
22 evidence for associations between long-term exposures to PM_{2.5} and cardiopulmonary
23 mortality, though the respiratory effects were not separated from the cardiovascular effects
24 in this conclusion.

25 The 2004 PM AQCD (U.S. EPA, 2004, [056905](#)) concluded that the evidence for an
26 association between long-term exposure to PM and respiratory effects may be confounded
27 by other pollutants. Gauderman et al. (2002, [026013](#)) reported declines for FEV₁ and
28 McConnell et al. (1999, [007028](#)) reported increased ORs for bronchitic symptoms in
29 asthmatics for PM₁₀ and PM_{2.5}. Recent epidemiologic literature includes results from
30 several prospective cohort studies, which found consistent, positive associations between
31 long-term exposure to PM and respiratory morbidity. Associations were reported with PM_{2.5}
32 and PM₁₀, and the studies showing associations only with PM₁₀ were conducted in locations
33 where the PM was predominantly fine particles, providing support for associations with
34 long-term exposure to fine particles. These results are summarized below; further details
35 of these studies are summarized in Annex E.

36 Very few subchronic and chronic toxicological studies investigating respiratory effects
37 were available in the 2004 PM AQCD. However, the 2002 EPA Health Assessment

1 Document for DE reported that chronic exposure to DE was associated with histopathology
2 including alveolar histiocytosis, aggregation of alveolar macrophages, tissue inflammation,
3 increased polymorphonuclear leukocytes, hyperplasia of bronchiolar and Type 2 epithelial
4 cells, thickened alveolar septa, edema, fibrosis, emphysema and lesions of the trachea and
5 bronchi. Since then a number of animal toxicological studies have been conducted involving
6 inhalation exposure to CAPs, urban air, DE, gasoline exhaust, and woodsmoke. These
7 subchronic and chronic studies provide evidence of altered pulmonary function,
8 inflammation, histopathological changes and oxidative and allergic responses following
9 PM_{2.5} exposures. These results are summarized below; further details of these studies are
10 summarized in Annex D.

7.3.1. Respiratory Symptoms and Disease Incidence

7.3.1.1. Epidemiologic Studies

11 New longitudinal cohort studies provide the best evidence to evaluate the relationship
12 between long-term exposure to ambient PM and increased incidence of respiratory
13 symptoms or disease. A summary of the mean PM concentrations reported for the long-term
14 exposure studies characterized in this section is presented in Table 7-3.

15 Bayer-Oglesby et al. (2005, [086245](#)) examined the decline of ambient pollution levels
16 and improved respiratory health demonstrated by a reduction in respiratory symptoms and
17 diseases in school children (n = 9,591) in Switzerland. Reduced air pollution exposure
18 resulted in improved respiratory health of children. Further, the average reduction of
19 symptom prevalence was more pronounced in areas with stronger reduction of air pollution
20 levels. The average decline of PM₁₀ between 1993 and 2000 across the nine study regions
21 was 9.8 µg/m³ (29%). Declining levels of PM₁₀ were associated with declining prevalence of
22 chronic cough, bronchitis, common cold, nocturnal dry cough, and conjunctivitis symptoms,
23 but no significant associations were reported for wheezing, sneezing, asthma, and hay fever,
24 as shown in Figure 7-2. In Figure 7-2, Panel (B) illustrates that on an aggregate level
25 across region, the mean change in adjusted prevalence of chronic cough is associated with
26 the mean change in PM₁₀ levels (r = 0.78; p = 0.02). Similar associations were seen for
27 nocturnal dry cough and conjunctivitis symptoms and PM₁₀ levels. Rössli et al. (2000,
28 [010296](#); 2001, [108738](#); 2005, [156923](#)) have demonstrated that PM₁₀ levels are
29 homogeneously distributed within regions of Basel, Switzerland and are not significantly
30 affected by local traffic, justifying the single-monitor approach for assignment of PM₁₀
31 exposures. Based on parallel measurements of PM_{2.5} and PM₁₀ at seven sites in
32 Switzerland, PM_{2.5} and PM₁₀ at all sites are generally highly correlated (r² ranging from
33 0.85 to 0.98 for the seven cities) (Gehrig and Buchmann, 2003, [139678](#)), indicating that
34 PM₁₀ is predominantly fine particles in these locations.

1 Schindler et al. (2009, [191950](#)) reported that sustained reduction in ambient PM₁₀
2 concentrations can lead to decreases in respiratory symptoms among Swiss adults in the
3 SAPALDLIA study. They compared baseline data in 1991 to a follow-up interview in 2002
4 after a substantial decline in PM₁₀ concentrations served as a natural experiment. Each
5 subject was assigned model-based estimates of PM₁₀ concentrations averaged over the 12
6 months preceding each health assessment with mean decline in PM₁₀ levels of 6.2 µg/m³
7 (SD = 3.9 µg/m³). When the authors tested the joint hypothesis of no association between
8 the PM₁₀ difference and symptom incidence or persistence, positive results were obtained
9 for regular cough, chronic cough or phlegm and wheezing but not regular phlegm or
10 wheezing without a cold.

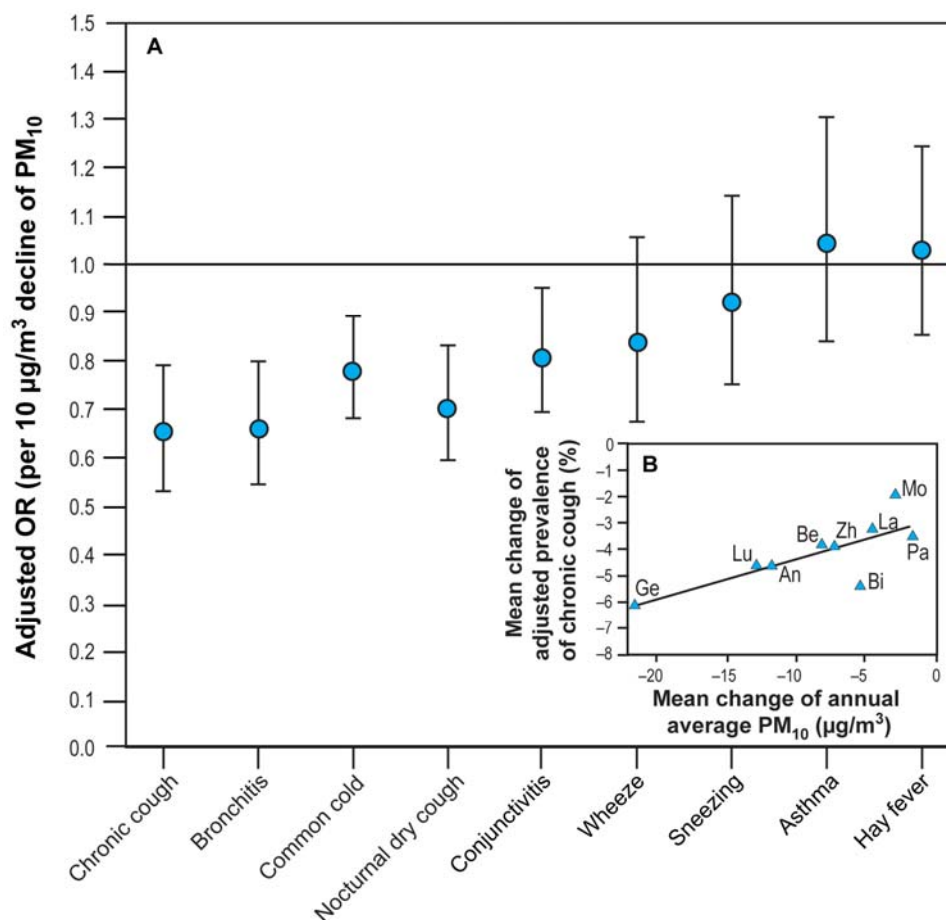
11 Pierse et al. (2006, [088757](#)) studied the association between primary PM₁₀ (particles
12 directly emitted from local sources/traffic) and the prevalence and incidence of respiratory
13 symptoms in a randomly sampled cohort of 4,400 children (aged 1-5 years) in
14 Leicestershire, England surveyed in 1998 and again in 2001. Annual exposure to primary
15 PM₁₀ was calculated for the home address using the Airviro statistical dispersion model.
16 After adjusting for confounders, mean annual exposure to locally generated PM₁₀ was
17 associated with an increased prevalence of cough without a cold in both the 1998 (OR 1.21
18 [95% CI: 1.07-1.38], n = 2164) and 2001 surveys (OR 1.56 [95% CI: 1.32-1.84], n = 1756).

19 Nordling et al. (2008, [097998](#)) examined the relationship between estimated PM
20 exposure levels and respiratory health effects in a Swedish birth cohort (n = 4089) of
21 preschool children. The spatial distributions of PM from traffic in the study area were
22 estimated with emission databases and statistical dispersion modeling. Children were
23 examined at 2 months and 1, 2, and 4 years of age. Using GIS methods, the average
24 contribution of traffic-generated PM₁₀ above regional background to the children's
25 residential outdoor air pollution levels was determined. To evaluate the exposure
26 assessment, the authors compared the estimated levels of traffic-generated PM₁₀ with PM_{2.5}
27 measurements from 42 locations (Hoek et al., 2002, [042364](#)) and reported modeled traffic-
28 generated PM₁₀ correlated reasonably well with measured PM_{2.5} (r = 0.61). Persistent
29 wheezing (cumulative incidence up to age 4) was associated with exposure to traffic-
30 generated PM₁₀ (OR 2.28 [95% CI: 0.84-6.24] per 10 µg/m³ increase) while transient and
31 late onset wheezing was not associated. This study demonstrates that respiratory effects
32 may be present in preschool children.

Table 7-3. Characterization of ambient PM concentrations from studies of respiratory symptoms/disease and long-term exposures.

Reference	Location	Mean Annual Concentration ($\mu\text{g}/\text{m}^3$)	Upper Percentile Concentrations ($\mu\text{g}/\text{m}^3$)
<i>PM_{2.5}</i>			
Annesi-Maesano et al. (2007, 093180)	6 French Cities	Range of means across sites: 8.7-23.0 Avg of means across sites: 15.5	
Brauer et al. (2007, 090691)	The Netherlands	16.9	75th: 18.1 90th: 19.0 Max: 25.2
Goss et al. (2004, 055624)	U.S.	13.7	75th: 15.9
Islam et al. (2007, 090697)	12 CHS/CA communities		Max: 29.5
Janssen et al. (2003, 133555)	The Netherlands	20.5	75th: 22.1 Max: 24.4
Kim et al. (2004, 087383)	San Francisco, CA	Range of means across sites: 11-15 Avg of means across sites: 12	
McConnell et al. (2003, 049490)	12 CHS/CA communities	13.8	Max: 28.5
Morgenstern et al. (2008, 156782)	Munich, Germany	11.1	
<i>PM₁₀</i>			
Bayer-Oglesby et al. (2005, 086245)	Nine study regions in Switzerland		Max: 46
Kunz li et al. (2009, 191949)	Switzerland	21.5	
Nord ling et al. (2008, 097998)	Sweden	4*	
Schin dler et al. (2009, 191950)	Switzerland		
McConnell et al. (2003, 049490)	12 CHS/CA communities	30.8	Max: 63.5
Pierse et al. (2006, 088757)	Leicestershire, U.K.	1.33	75th: 1.84

*Source specific; PM₁₀ from traffics



Source: Bayer-Oglesby et al. (2005, [086245](#))

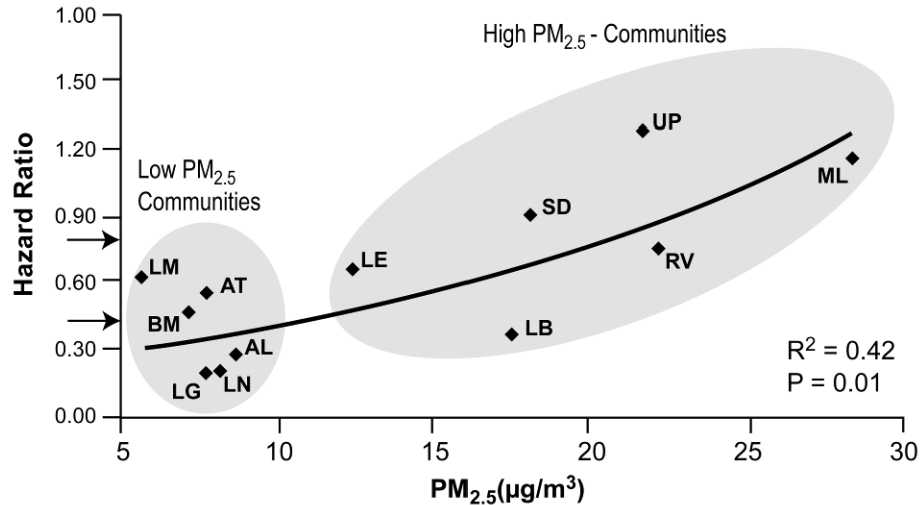
Figure 7-2. Adjusted ORs and 95% CIs of symptoms and respiratory diseases associated with a decline of 10 µg/m³ PM₁₀ levels in Swiss Surveillance Program of Childhood Allergy and Respiratory Symptoms¹. Inset: Mean change in adjusted prevalence (1998-2001 to 1992-1993) versus mean change in regional annual averages of PM₁₀ (1997-2000 to 1993) for chronic cough, across nine SCARPOL regions (An: Anières. Be: Bern. Bi: Biel. Ge: Geneva. La: Langnau. Lu: Lugano. Mo: Montana. Pa: Payerne. Zh: Zürich).

1 McConnell et al. (2003, [049490](#)) conducted a prospective study examining the
 2 association between air pollution and bronchitic symptoms in 475 school children with
 3 asthma in 12 Southern California communities as part of the CHS from 1996 to 1999. They
 4 investigated both the differences between- communities with 4-yr avg and within-
 5 communities yearly variation in PM (i.e., PM₁₀, PM_{2.5}, PM_{10-2.5}, EC, and OC). Based on a
 6 10 µg/m³ change in PM_{2.5}, within-communities effects were larger (OR 1.90 [95% CI: 1.10-
 7 2.70]) than those for between-communities (OR 1.30 [95% CI: 1.10-1.50]). The OR for the
 8 10 µg/m³ range in 4-yr avg PM_{2.5} concentrations across the 12 communities was 1.29 (95%

¹ Adjusted for age, sex, nationality, parental education, number of siblings; farming status, low birth weight, breastfeeding, child who smokes, family history of asthma, bronchitis, and/or atopy, mother who smokes, indoor humidity, mode of heating and cooking, carpeting, pets allowed in bedroom, removal of carpet and/or pets for health reasons, person who completed questionnaire, month when questionnaire was completed, number of days with the maximum temperature <0°C, and belief of mother that there is an association between environmental exposures and children's respiratory health

1 CI: 1.06-1.58). Similar results were reported for PM₁₀ and PM_{10-2.5} but the effect estimates
2 were smaller in magnitude and generally not statistically significant. Within-community
3 associations were not confounded by any time-fixed personal covariates. In two-pollutant
4 models, the within-community effect estimates for PM_{2.5} and OC were significant in the
5 presence of several other pollutants. While the within-community single-pollutant effect of
6 PM_{2.5} ($\beta = 0.085/\mu\text{g}/\text{m}^3$) was only modestly attenuated after adjusting for some pollutants, it
7 was markedly reduced after adjusting for NO₂ or OC. The between-community effect
8 estimates generally were not significant in the presence of other pollutants in two-pollutant
9 models.

10 In the CHS already discussed, Islam et al. (2007, [090697](#)) examined the hypothesis
11 that ambient air pollution attenuates the reduced risk for childhood asthma that is
12 associated with higher lung function (n = 2057). At each age a distribution of pulmonary
13 functions exists. Haland et al. (2006, [156511](#)) found evidence that children with high lung
14 function have a reduced risk for asthma. Islam et al. (2007, [090697](#)) used the CHS data to
15 study how the association of asthma incidence with lung function is modified by long-term
16 PM exposure. The incidence rate (IR) of newly diagnosed asthma increased from 9.5/1000
17 person-years for children with percent-predicted FEF₂₅₋₇₅ values $\geq 120\%$ to 20.4/1000
18 person-years for children with FEF₂₅₋₇₅ value $\leq 100\%$. Over the 10th-90th percentile range
19 for FEF₂₅₋₇₅ (57.1%), the hazard ratio of new onset asthma was 0.50 (95% CI: 0.35-0.71). The
20 IR of asthma for FEF₂₅₋₇₅ $\geq 120\%$ in the “high” PM_{2.5} (13.7-29.5 $\mu\text{g}/\text{m}^3$) communities was
21 15.9/1000 person-years compared to 6.4/1000 person-years in “low” PM_{2.5} (5.7-8.5 $\mu\text{g}/\text{m}^3$)
22 communities. Loss of protection by high lung function against new onset asthma in the
23 “high” PM_{2.5} communities was observed for all the lung function measures. Figure 7.3
24 shows the effect of PM_{2.5} on the association of lung function with asthma. Of all the
25 pollutants examined (NO₂, PM₁₀, PM_{2.5}, acid vapor, O₃, EC, and OC), PM_{2.5} appeared to
26 have the strongest modifying effect on the association between lung function with asthma
27 as it had the highest R² value (0.42). Over the 10th-90th percentile range of FEF₂₅₋₇₅, the
28 hazard ratio of new onset asthma was 0.34 (95% CI: 0.21-0.56) in a community with low
29 PM_{2.5} ($<13.7 \mu\text{g}/\text{m}^3$) and 0.76 (95% CI: 0.45-1.26) in a community with high PM_{2.5}
30 ($\geq 13.7 \mu\text{g}/\text{m}^3$). The data do not indicate that PM exposure increased rates of incident
31 asthma among children with poor lung function at study entry because rates among those
32 with poor lung function were similar in both low and high pollution communities.



Source: Islam et al. (2007, [090697](#))

Figure 7-3. Effect of PM_{2.5} on the association of lung function with asthma. Community-specific hazard ratio of newly diagnosed asthma over 10-90th percentile range (57.1%) of FEF_{25-75%} by level of ambient PM_{2.5} (µg/m³). The 12 CHS communities are shown.

1 In a prospective birth cohort study (n = 4,000) in The Netherlands, Brauer et al.
 2 (2007, [090691](#)) assessed the development of asthma, allergic symptoms, and respiratory
 3 infection during the first four years of life in relation to long-term PM_{2.5} concentration at
 4 the home address with a validated model using GIS. PM_{2.5} was associated with doctor-
 5 diagnosed asthma (OR = 1.32 [95% CI: 1.04-1.69]) for a cumulative lifetime indicator. These
 6 findings extend observations made at 2 years of age in the same cohort (Brauer et al., 2002,
 7 [035192](#)) providing greater confidence in the association. No associations were observed for
 8 bronchitis.

9 Kunzli et al. (2009, [191949](#)) used the SAPALDIA cohort study discussed previously in
 10 this section to evaluate the relationship between the 11-year change (1991-2002) in traffic-
 11 related PM₁₀ and asthma incidence-adult onset asthma. In a cohort of 2,725 never-smokers
 12 without asthma at baseline (ages: 18-60 years in 1991), subjects reporting doctor-diagnosed
 13 asthma at follow-up were considered incident cases. Modeled traffic-related PM₁₀ levels
 14 were used. Cox proportional hazard models for time to asthma onset were used with
 15 adjustments for cofounders. The study findings suggest that PM contributes to asthma
 16 development and that reductions in PM decrease asthma risk. A strong feature of
 17 SAPALDIA is the ability to assign space, time, and source-specific pollution to each subject.
 18 Further, Kunzli et al. (2008, [129258](#)) discusses the impact of attributable health risk models
 19 for exposures that are assumed to cause both chronic disease and its exacerbations. The
 20 added impact of causing disease increases the risk compared to only exacerbations.

21 A matched case-control study of infant bronchiolitis (ICD 9 code 466.1) hospitalization
 22 and two measures of long-term exposure – the month prior to hospitalization (subchronic)
 23 and the lifetime average (chronic) – to PM_{2.5} and gaseous air pollutants in the South Coast

1 Air Basin of southern California was conducted by Karr et al. (2007, [090719](#)) among 18,595
2 infants born between 1995-2000. For each case, 10 controls matched on date were randomly
3 selected from birth records. Exposure was based on PM_{2.5} measurements collected every
4 third day. The mean distance between the subjects' residential ZIP code and the assigned
5 monitor was generally 4-6 miles with a maximum distance of 30 miles. For 10 µg/m³
6 increases in both sub-chronic and chronic PM_{2.5} exposure, an adjusted OR of 1.09 (95% CI:
7 1.04-1.14) was observed. In multipollutant model analyses, the association with PM_{2.5} was
8 robust to the inclusion of gaseous pollutants. Also, in a cohort of children in Germany,
9 Morgenstern et al. (2008, [156782](#)) modeled PM_{2.5} data at birth addresses found statistically
10 significant effects for asthmatic bronchitis, hay fever, and allergic sensitization to pollen.

11 Goss et al. (2004, [055624](#)) conducted a national study examining the relationship
12 between air pollutants and health effects in a cohort of cystic fibrosis (CF) patients (n =
13 11,484) over the age of 6 years (mean age = 18.4, SD = 10) enrolled in the Cystic Fibrosis
14 Foundation National Patient Registry in 1999 and 2000. Exposure was assessed by linking
15 air pollution values from the closest population monitor from the Air Quality System (AQS)
16 with the centroid of the patient's home ZIP code that was within 30 miles. The mean
17 distance from the patient's ZIP code to monitors for PM_{2.5} and PM₁₀ was 10.8 miles (SD 7.8)
18 and 11.5 miles (SD 7.9), respectively. PM_{2.5} and PM₁₀ 24-h avg were collected every 1 to 12
19 days. CF diagnosis involves genetic screening panels and a common severe mutation used is
20 the loss of phenylalanine at the 508th position. Genotyping was available in 74% of the
21 population and of those genotyped, 66% carried one or more delta F508 deletions. After
22 adjusting for confounders, a 10 µg/m³ increase in PM_{2.5} or PM₁₀ was associated with a 21%
23 (95% CI: 7-33) or 8% (95% CI: 2-15), respectively, increase in the odds of two or more
24 exacerbations defined as a CF-related pulmonary condition requiring admission to the
25 hospital or use of home intravenous antibiotics. The estimate for the associations between
26 pulmonary exacerbations and PM_{2.5} and PM₁₀ were attenuated when the models were
27 adjusted for lung function. Brown et al. (2001, [012307](#)) found that particle deposition was
28 increased in CF and that particle distribution in the lungs was enhanced in poorly
29 ventilated tracheobronchial regions in CF patients. Such focal deposition may partially
30 explain the association of PM and CF exacerbation.

31 Annesi-Maesano (2007, [093180](#)) from 5,338 school children (10.4 ± 0.7 years)
32 attending 108 randomly chosen schools in 6 French cities to the concentration of PM_{2.5}
33 monitored in school yards. Atopic asthma was related to PM_{2.5} (OR 1.43 [95% CI: 1.07-1.91])
34 when high PM_{2.5} concentrations (20.7 µg/m³) were compared to low PM_{2.5} concentrations
35 (8.7 µg/m³). The report is consistent with the results in an earlier paper (Penard-Morand et
36 al., 2005, [087951](#)) in the same sample of children that related the findings to PM₁₀.

37 Kim et al. (2004, [087383](#)) conducted a school-based cross-sectional study in the San
38 Francisco metropolitan area in 2001 comprised of 10 neighborhoods to examine the
39 relationship between traffic-related pollutants and current bronchitic symptoms and

1 asthma obtained by parental questionnaire (n = 1109). They related traffic-related
2 pollutants (PM) and bronchitic and asthma symptoms in the past 12 months. No
3 multipollutant models were evaluated because of the high interpollutant correlations. PM_{2.5}
4 levels ranged across the school sites from 11 to 15 µg/m³.

5 Schikowski et al. (2005, [088637](#)) examined the relationship between both long-term
6 air pollution exposure and living close to busy roads and COPD in the Rhine-Ruhr Basin of
7 Germany from 1985 to 1994 using consecutive cross-sectional studies. Seven monitoring
8 stations that were <8 km to a woman's home address provided TSP data that PM₁₀ was
9 estimated from using a conversion factor (obtained from parallel measurement of TSP and
10 PM₁₀ conducted at 7 sites in the Ruhr area). Distance to a major road was determined using
11 GIS. The results of the study suggest that long-term exposure to air pollution from PM₁₀
12 and living near a major road might increase the risk of developing COPD and can have a
13 detrimental effect on lung function. All ORs for 5-yr exposures were stronger than those for
14 1-yr exposures.

15 In summary, the 2004 PM AQCD evaluated the available studies which primarily
16 related effects to bronchitic symptoms in school-age children. The new evidence is more
17 informative, as it includes longitudinal cohort studies that have been conducted in different
18 countries by different researchers that use different study designs. Some new studies are
19 using several different methods to include individual estimates of exposure to ambient PM
20 that may reduce the impact of exposure error. The strength and consistency of the outcomes
21 is enhanced by results being reported by several different researchers in different countries
22 using different designs. Most recent studies have focused on children, but a few studies
23 have also reported associations in adults.

24 The CHS (McConnell et al., 2003, [049490](#)) provides evidence in a prospective
25 longitudinal cohort study that relates PM_{2.5} and bronchitic symptoms and reports larger
26 associations for within-community effects that are less subject to confounding than
27 between-community effects. Several new studies report similar findings with long-term
28 exposure to PM₁₀ in areas where fine particles predominate PM₁₀. In England, in a cohort of
29 4,400 children (aged 1-5), an association is seen with an increased prevalence of cough
30 without a cold. Further evidence includes a reduction of respiratory symptoms
31 corresponding to decreasing PM levels in "natural experiments" in both a cohort of Swiss
32 school children (Bayer-Oglesby et al., 2005, [086245](#)) and adults (Schindler et al., 2009,
33 [191950](#)).

34 In a separate analysis of the CHS, Islam et al. (2007, [090697](#)) showed that PM_{2.5} had
35 the strongest modifying effect on the association between lung function with asthma such
36 that loss of protection by high lung function against new onset asthma in high PM_{2.5}
37 communities was observed for all the lung function measures from 10 to 18 years of age.
38 This relates new onset asthma to long-term PM exposure. In the Netherlands, Brauer et al.
39 (2007, [090691](#)) augments the literature with data examining the first 4 years of life in a

1 birth cohort showing an association with doctor-diagnosed asthma. Further, in an adult
 2 cohort in the SALPALDIA study, Kunzli et al. (2009, [191949](#)) relate PM to asthma
 3 incidence.

7.3.2. Pulmonary Function

4 Several cohort studies reviewed in the 2004 PM AQCD provided evidence for
 5 relationships between long-term PM exposure and effects on the respiratory system. In 12
 6 southern California communities in the Children’s Health Study (CHS), Gauderman et al.
 7 (2000, [012531](#); 2002, [026013](#)) found that decreases in lung function growth among school
 8 children were associated with long-term exposure to PM. Declines in pulmonary function
 9 were reported with all three major PM size classes – PM₁₀, PM_{10-2.5} and PM_{2.5} – though the
 10 three PM measures were highly correlated. These results were found to be consistent with
 11 results of cross-sectional analyses of Raizenne et al. (1996, [077268](#)), that was assessed in
 12 the 1996 PM AQCD. That study reported associations between decreased peak flow with
 13 fine particle sulfate and fine particle acidity. Finally, in a prospective cohort study among a
 14 subset of children in the CHS (n = 110) who moved to other locations during the study
 15 period, Avol et al. (2001, [020552](#)) reported that those subjects who moved to areas of lower
 16 PM₁₀ showed increased growth in lung function compared with subjects who moved to
 17 communities with higher PM₁₀ concentrations who showed decrease growth in lung
 18 function.

7.3.2.1. Epidemiologic Studies

19 New longitudinal cohort studies have evaluated the relationship between long-term
 20 exposure to PM and changes in measures of pulmonary function (FVC, FEV₁, and measures
 21 of expiratory flow). Cross-sectional studies also offer supportive information (see Annex E)
 22 and may provide insights derived from within community analysis. Lung function increases
 23 continue through early adulthood with growth and development, then declines with aging
 24 (Stanojevic et al., 2008, [157007](#); Thurlbeck, 1982, [093260](#); Zeman and Bennett, 2006,
 25 [157178](#)). A summary of the mean PM concentrations reported for the long-term exposure
 26 studies characterized in this section is presented in Table 7-4.

Table 7-4. Characterization of ambient PM concentrations from studies of FEV₁ and long-term exposures.

Reference	Location	Mean Annual Concentration (µg/m ³)	Upper Percentile Concentrations (µg/m ³)
<i>PM_{2.5}</i>			
Gauderman et al. (2002, 026013)	12 CHS/CA communities	5-30	
Gauderman et al. (2004, 056569)	12 CHS/CA communities	6-27	
Goss et al. (2004, 055624)	U.S.	13.7	75th: 15.9

Reference	Location	Mean Annual Concentration ($\mu\text{g}/\text{m}^3$)	Upper Percentile Concentrations ($\mu\text{g}/\text{m}^3$)
Gotschi et al. (2008, 180364)	21 European cities	Range of means across sites: 3.7-44.7 Avg of mean across sites: 16.8	
<i>PM₁₀</i>			
Downs et al. (2007, 092853)	8 cities in Switzerland	Range of means across sites: 9-46 Avg of mean across sites: 21.6	
Gauderman et al. (2002, 026013)	12 CHS/CA communities	Range of means across sites: 13-78 Avg of mean across sites: NR	
Gauderman et al. (2004, 056569)	12 CHS/CA communities	Range of means across sites: 18-68 Avg of mean across sites: NR	
Nordling et al. (2008, 097998)	Sweden		
Avol et al. (2001, 020552)	Southern CA/CHS		
Rojas-Martinez (2007, 188508)	Mexico City, Mexico	75.6	75th: 92.2 90th: 112.7

1 The CHS prospectively examined the relationship between air pollutants and lung
2 function (FVC, FEV₁, MMEF) in a cohort (n = 1,759) of children between the ages of 10 and
3 18 years, a period of rapid lung development (Gauderman et al., 2004, [056569](#)). Air
4 pollution monitoring stations provided data in each of the 12 study communities from 1994-
5 2000. The results for O₃, PM₁₀, NO₂, PM_{2.5}, acid vapor, and EC are depicted in Figure 7-4. In
6 general, two-pollutant models for any pair of pollutants did not provide a substantially
7 better fit to the data than the corresponding single-pollutant models due to the strong
8 correlation between most pollutants. The pollution-related deficits in the average growth in
9 lung function over the eight-yr period resulted in clinically important deficits in attained
10 lung function at the age of 18 years.

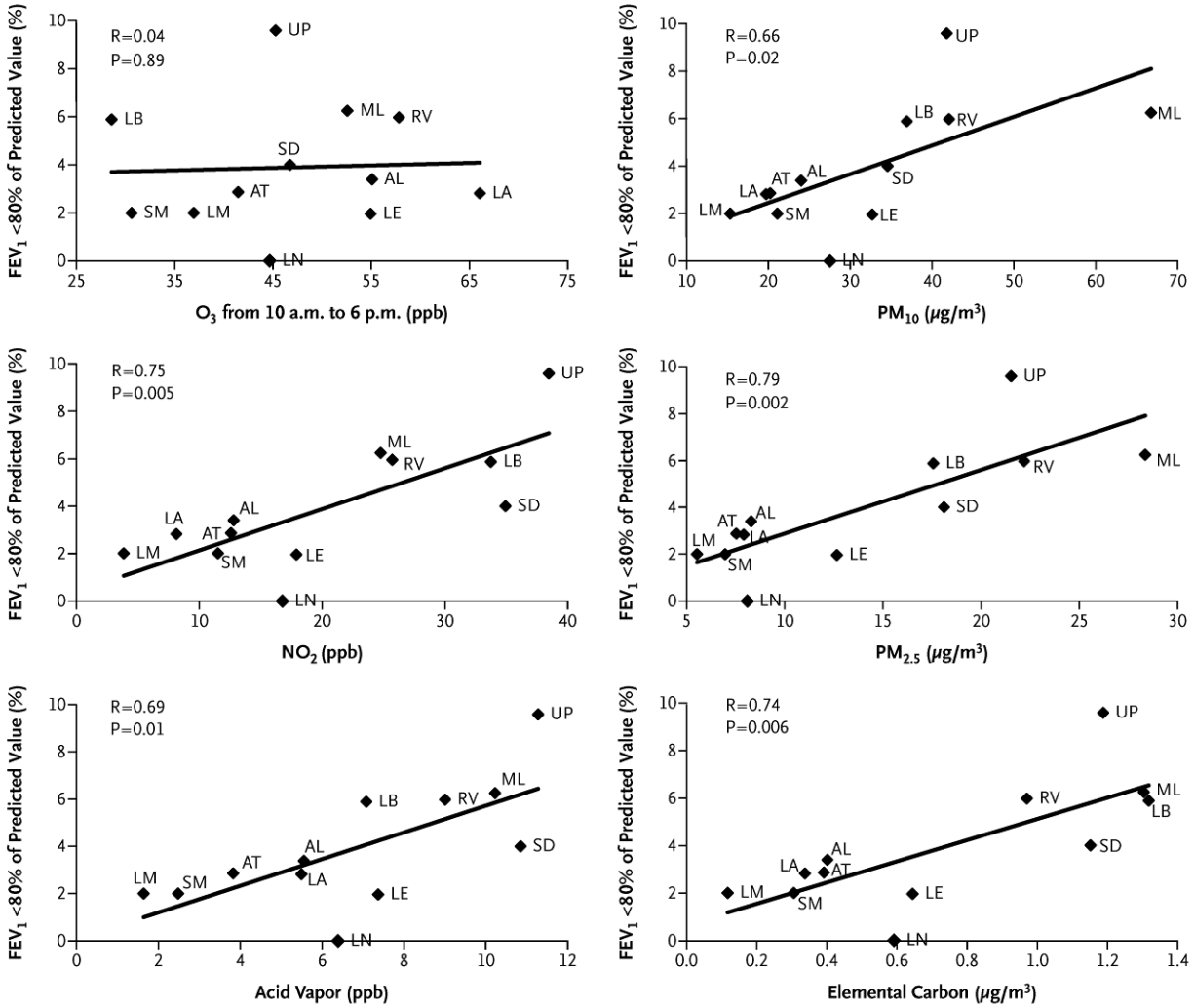
11 Downs et al. (2007, [092853](#)) prospectively examined 9,651 randomly selected adults
12 (18-60 years of age) in 8 cities in Switzerland (see also Ackermann-Liebrich et al., 1997,
13 [077537](#)) to ascertain the relationship between reduced exposure to PM₁₀ and age-related
14 decline in lung function (FVC, FEV₁, and FEF₂₅₋₅₀). An evaluated statistical dispersion
15 model (Liu et al., 2007, [093093](#)) provided spatially resolved concentrations of PM₁₀ that
16 enabled assignment to residential addresses for the participant examinations in 1991 and
17 2002 that yielded a median decline of 5.3 $\mu\text{g}/\text{m}^3$ (IQR 4.1-7.5). Decreasing PM₁₀
18 concentrations attenuated the decline in lung function. Effects were greater in tests
19 reflecting small airway function. No other pollutant relationships were evaluated, though a
20 related study indicated that levels of NO₂ also declined over the same period (Ackermann-
21 Liebrich et al., 2005, [087826](#)). Generalized cross-validation essentially chose a linear fit for
22 the the concentration-response curve for age-related decline in lung function.

23 These data show that improvement in air quality may slow the annual rate of decline
24 in lung function in adulthood indicating positive consequences for public health. Further
25 evidence on improvement in respiratory health with reduction in air pollution levels is
26 provided from studies conducted in East Germany related to dramatic emissions reductions
27 after the reunification in 1990 (Fryer and Collins, 2003, [156454](#); Heinrich et al., 2002,

1 [034825](#); Sugiri et al., 2006, [088760](#)). This type of “natural experiment” provides additional
2 support for epidemiologic findings that relatively low levels of airborne particles have
3 respiratory effects.

4 In a prospective cohort study consisting of school-age children (n = 3,170) who were 8
5 years of age at the beginning of the study, had not been diagnosed with asthma, and were
6 located in Mexico City (Rojas-Martinez et al., 2007, [188508](#)), evaluated the association
7 between long-term exposure to PM₁₀, O₃ and NO₂ and lung function growth every 6 months
8 from April 1996 through May 1999. Exposure data were provided by 10 air quality monitor
9 stations located within 2 km of each child’s school. The multipollutant model effect of PM₁₀
10 over the age of 8 to 10 years of life in this cohort on FVC, FEV₁, and FEF₂₅₋₇₅ showed an
11 association. Single pollutant models showed an association between ambient pollutants (O₃,
12 PM₁₀ and NO₂) and deficits in lung function growth. The association between PM₁₀ and
13 FEF₂₅₋₇₅ was not statistically significant. While the estimates from two-pollutant models
14 were not substantially different than single pollutant models, independent effects for
15 pollutants could not be estimated accurately because the traffic-related pollutants were
16 correlated. Although no PM_{2.5} data were presented in this study, Chow et al. (2002) in a
17 separate study report that for Mexico City during the winter of 1997 that approximately
18 50% of PM₁₀ was in the PM_{2.5} fraction.

19 Gotschi et al. (2008, [156485](#)) examined the relationship between air pollution and
20 lung function in adults in the European Community Respiratory Health Survey (ECRHS).
21 FEV₁ and FVC were assessed at baseline and after 9 years of follow-up from 21 European
22 centers (followed-up sample n = 5,610). No significant associations were found between city-
23 specific annual mean PM_{2.5} and average lung function levels which is in contrast to the
24 results seen by Ackermann-Lieblich (1997, [077537](#)) (SAPALDIA) and Schikowski et al.
25 (2005, [088637](#)) (SALIA) which compared across far more homogenous populations than for
26 the population assessed in the ECRHS. Misclassification and confounding may partially
27 explain the discrepancy in findings.



Source: Adapted from Gauderman et al. (2004, [056569](#))

Figure 7-4. Proportion of 18-year olds with a FEV₁ below 80% of the predicted value plotted against the average levels of pollutants from 1994 through 2000 in the 12 southern California communities of the Children’s Health Study (AL = Alpine; AT = Atascadero; LA = Lake Arrowhead; LB = Long Beach; LE = Lake Elsinore; LM = Lompoc; LN = Lancaster; ML = Mira Loma; RV = Riverside; SD = San Dimas; SM = Santa Maria; UP = Upland.)

1 In a birth cohort (n = 2,170) in Oslo, Norway, Oftedal et al. (2008, [093202](#)) examined
 2 effects of exposure to PM_{2.5} and PM₁₀ on lung function (FVC, FEV₁, FEF_{50%}). Spirometry was
 3 performed in 2,307 children aged 9-10 years old in 2001-2002. Residential air pollution
 4 levels over the time period 1992-2002 were calculated using EPISODE dispersion models to
 5 provide three time scales of exposure: 1) first year of life, 2) lifetime exposure, and 3) just
 6 before the lung function test. Only single pollutant models were evaluated because air
 7 pollutants were highly correlated (r = 0.83-0.95). PM exposure was associated with changes
 8 in adjusted peak respiratory flow, especially in girls. No effect was found for forced volumes.

1 Adjusting for contextual socioeconomic factors diminished associations. Results for PM₁₀
2 were similar to those for PM_{2.5}.

3 In an exploratory study, Mortimer et al. (2008, [187280](#)) examined the association of
4 prenatal and lifetime exposure to air pollutants using geocoded monthly average PM₁₀
5 levels with pulmonary function in a San Joaquin Valley, California cohort of 232 children
6 (aged 6-11) with asthma. First and second trimester PM₁₀ exposures (based on monthly
7 average concentrations) had a negative effect on pulmonary function and may relate to
8 prenatal exposures affecting the lungs as they begin to develop at 6 wk gestation.

9 Dales et al. (2008, [156378](#)) in a cross-sectional prevalence study examined the
10 relationship of pulmonary function and PM measures, other pollutants, and indicators of
11 motor vehicle emissions in Windsor, Ontario, in a cohort of 2,402 school children. PM_{2.5} and
12 PM₁₀ concentrations were estimated for each child's residence at the postal code level. Each
13 10 µg/m³ increase in PM_{2.5} was associated with a 7.0% decrease in FVC expressed in a
14 percentage of predicted.

15 In Leicester, England, investigators examined the carbon content of airway
16 macrophages in induced sputum in 64 of 114 healthy children 8 to 15 years of age (Grigg et
17 al., 2008, [156499](#); Kulkarni et al., 2006, [089257](#)). The carbon content of airway
18 macrophages (Finch et al., 2002, [054603](#); Strom et al., 1990, [157020](#)) was used as a marker
19 of individual exposure to PM₁₀. Near each child's home, exposure to PM₁₀ was estimated
20 using a statistical dispersion model (Pierse et al., 2006, [088757](#)). The authors reported a
21 dose-dependent inverse association between the carbon content of airway macrophages and
22 lung function in children and found no evidence that reduced lung function itself causes an
23 increase in carbon content. Consistent results were obtained for both FVC and FEF₂₅₋₇₅.
24 Caution should be used when interpreting these results as the accuracy of the estimates on
25 individual PM₁₀ exposures were not validated; there is potential for confounding by ethnic
26 origin; and there is concern that the magnitude of the changes in pulmonary function
27 associated with increased particle area appear large (Boushey et al. 2008).

28 Nordling et al. (2008, [097998](#)) discussed above in the respiratory symptoms section,
29 also reported that lower PEF at age 4 was associated with exposure to traffic-related PM₁₀
30 (-8.93 L/min [95% CI: -17.78 to -0.088]). Goss et al. (2004, [055624](#)), discussed in the
31 respiratory symptoms section, found strong inverse relationships between FEV₁ and PM_{2.5}
32 concentrations in both cross-sectional and longitudinal analyses.

33 In summary, recent studies have greatly expanded the evidence available for the 2004
34 PM. The earlier CHS studies followed young children for 2-4 years. New analyses have been
35 conducted that include longer follow-up periods of this cohort through 18 years of age
36 (considered early adulthood for lung development (Stanojevic et al., 2008, [157007](#)) and
37 provide evidence that effects from exposure to PM_{2.5} persist into early adulthood.
38 Longitudinal studies follow effects over time and are considered to provide the best
39 evidence as opposed to studies across communities as in cross-sectional studies. The

1 longitudinal cohort studies in the 2004 PM AQCD provided data for children in one location
2 in one study and new longitudinal studies have been conducted in other locations.

3 Gauderman et al. (2004, [056569](#)) reported that PM_{2.5} exposure was associated with
4 clinically and statistically significant deficits in FEV₁ attained at the age of 18 years.
5 Clinical significance was defined as a FEV₁ below 80% of the predicted value, a criterion
6 commonly used in clinical settings to identify persons at increased risk for adverse
7 respiratory conditions. This clinical aspect is an important enhancement over the earlier
8 results reported in the 2004 PM AQCD. Further, the association reported in this study that
9 evaluated the 8-yr time period into early adulthood not only provided evidence for the
10 persistence of the effect, but in addition the strength and robustness of the outcomes were
11 more positive, larger, and more certain than previous CHS studies of shorter follow-up.

12 Supporting this result are new longitudinal cohort studies conducted by other
13 researchers in other locations with different methods. Though these studies report results
14 for PM₁₀, available data discussed above indicate that the majority of PM₁₀ is composed of
15 PM_{2.5} in these areas. New studies provide positive results from Mexico City, Sweden, and a
16 national cystic fibrosis cohort in the U.S. One study reported null results in a European
17 cohort described as having potential misclassification and confounding concerns as well as
18 lacking a homogenous population potentially rendering the outcome as non-informative. A
19 natural experiment in Switzerland, where PM levels had decreased, reported that
20 improvement in air quality may slow the annual rate of decline in lung function in
21 adulthood, indicating positive consequences for public health. These natural experiments
22 are considered especially supportive.

23 The relationship between long-term PM exposure and decreased lung function is thus
24 seen during lung growth and lung development in school-age children into adulthood. At
25 adult ages studies continue to show a relationship between decreased lung function and
26 long-term PM exposure. Some newer studies attempting to study the relationship of long-
27 term PM exposure from birth through preschool are reporting a relationship. Thus, the
28 impact of long-term PM exposure is seen over the time period of lung function growth and
29 development and the decline of lung function with aging.

30 Overall, effect estimates from these studies are negative (i.e., indicating decreasing
31 lung function) and the pattern of effects are similar between the studies for FVC and FEV₁.
32 Thus, the data are consistent and coherent across several designs, locations, and
33 researchers. With cautions noted, the results relating carbon content of airway
34 macrophages to decreased measures of pulmonary function add plausibility to the
35 epidemiologic findings. Some new studies are using individual estimates of exposure to
36 ambient PM to reduce the impact of exposure error (Downs et al., 2007, [092853](#); Jerrett et
37 al., 2005, [087381](#)).

38 As was found in the 2004 PM AQCD, the studies report associations with PM_{2.5} and
39 PM₁₀, while most did not evaluate PM_{10-2.5}. Associations have been reported with fine

1 particle components, particularly EC and OC. Source apportionment methods generally
2 have not been used in these long-term exposure studies. However, numerous studies have
3 evaluated exposures to PM related to traffic or motor vehicle sources. For example, Meng et
4 al. (2007, [093275](#)) investigated the associations between traffic and outdoor pollution levels
5 and poorly controlled asthma among adults who were respondents to the California Health
6 Interview Survey and found associations for traffic density and PM₁₀, but not PM_{2.5}.

7.3.2.2. Toxicological Studies

Urban Air

7 An important new study evaluated the effects of chronic exposure to ambient levels of
8 urban particles on lung development in the mouse (Mauad et al., 2008, [156743](#)). Both
9 functional and anatomical indices of lung development were measured. Male and female
10 BALB/c mice were continuously exposed to ambient or filtered Sao Paulo air for 8 months.
11 Concentrations in the “polluted chamber” vs. “clean chamber” were 16.8 vs. 2.9 µg/m³ PM_{2.5}.
12 Thus PM levels were reduced by filtration but not entirely eliminated. Ambient
13 concentrations of CO, NO₂ and SO₂ were 1.7 ppm, 89.4 µg/m³ and 8.1 µg/m³, respectively.
14 Concentrations of gaseous pollutants were assumed to be similar to ambient levels in both
15 chambers. After 4 months, the animals were mated and the offspring were divided into 4
16 groups to provide for a prenatal exposure group, a postnatal exposure group, a pre and
17 postnatal exposure group and a control group. Animals were sacrificed at 15 and 90 days of
18 age for histological analysis of lungs. Pulmonary pressure-volume measurements were also
19 conducted in the 90 day old offspring. Statistically significant reductions in inspiratory and
20 expiratory volumes were found in the pre and postnatal exposure group, but not in the
21 prenatal or postnatal exposure group, compared with controls. These changes in pulmonary
22 function correlated with anatomical changes which are discussed in Section 7.3.5.1.

Diesel Exhaust

23 Li et al. (2007, [155929](#)) exposed BALB/c and C56BL/6 mice to clean air or to low dose
24 DE (at a PM concentration of 100 µg/m³) for 7 hs/day and 5 days/week for 1, 4 and 8 wk.
25 Average gas concentrations were reported to be 3.5 ppm CO, 2.2 ppm NO₂, and less than
26 0.01 ppm SO₂. AHR was evaluated by whole body plethysmography at Day 0 and after 1, 4
27 and 8 wk of exposure. Short-term responses are discussed in Section 6.3.2.3, 6.3.3.3 and
28 6.3.4.2. The increased sensitivity of airways to methacholine (measured as Penh) seen in
29 C57BL/6 but not BALB/c mice at 1 week was also seen at 4 wk but not at 8 wk. This study
30 suggests that adaptation occurs during prolonged DE exposure. Influx of inflammatory
31 cells, histopathology, markers of oxidative stress and effects of antioxidant intervention
32 were also evaluated (see Sections 7.3.3.2 and 7.3.4.1). Although no attempt was made in
33 this study to determine the effects of gaseous components of DE on the measured responses,

1 concentrations of gases were very low suggesting that PM may have been responsible for
2 the observed effects.

3 In many animal studies changes in ventilatory patterns are assessed using whole
4 body plethysmography, for which measurements are reported as enhanced pause (Penh).
5 Some investigators report increased Penh as an indicator of AHR, but these are
6 inconsistently correlated and many investigators consider Penh solely an indicator of
7 altered ventilatory timing in the absence of other measurements to confirm AHR. Therefore
8 use of the terms AHR or airway responsiveness has been limited to instances in which the
9 terminology has been similarly applied by the study investigators.

10 Gottipolu et al. (2009, [190360](#)) exposed WKY and SH rats to filtered air or DE
11 (particulate concentration 500 and 2000 $\mu\text{g}/\text{m}^3$) for 4 h/day and 5 days/week over a 4-week
12 period. Concentrations of gases were 1.3 and 4.8 ppm CO, NO <2.5 and 5.9 ppm NO, <0.25
13 and 1.2 ppm NO₂, 0.2 and 0.3 ppm SO₂ for low and high PM exposures, respectively. Particle
14 size, measured as geometric median number and volume diameters, was 85 and 220 nm,
15 respectively. No DE-related effects were found for breathing parameters measured by
16 whole-body plethysmography. Other pulmonary effects are described in Sections 7.3.3.2 and
17 7.3.5.1.

Woodsmoke

18 One study evaluated the effects of subchronic woodsmoke exposure on pulmonary
19 function in Brown Norway rats. Rats were exposed 3 h/day and 5 days/week for 4 and 12 wk
20 to air or to 1000-10,000 $\mu\text{g}/\text{m}^3$ concentrated wood smoke from the pinon pine which is native
21 to the U.S. Southwest (Tesfaigzi et al., 2002, [025575](#)). PM concentrations in the woodsmoke
22 were 1,000 and 10,000 $\mu\text{g}/\text{m}^3$ PM. The particles in this woodsmoke had a bimodal size
23 distribution with the smaller size fraction (74%) characterized by a MMAD of 0.405 μm and
24 the larger size fraction (26%) characterized by a MMAD of 6.7-11.7 μm . Many of these
25 larger particles would not be inhalable by the rat since 8 μm MMAD particles are about
26 50% inhalable (Menache et al., 1995, [006533](#)). Concentrations of gases were reported to be
27 15-106.4 ppm CO, 2.2-18.9 ppm NO, 2.4-19.7 ppm NO_x and 3.5-13.8 ppm total hydrocarbon
28 in these exposures. Respiratory function measured by whole-body plethysmography
29 demonstrated a statistically significant increase in total pulmonary resistance in rats
30 exposed to 1000 $\mu\text{g}/\text{m}^3$ woodsmoke. Additional effects were found at 10,000 $\mu\text{g}/\text{m}^3$.
31 Inflammatory and histopathological responses were also evaluated (see Sections 7.3.3.2 and
32 7.3.5.1).

7.3.3. Pulmonary Inflammation

7.3.3.1. Epidemiologic Studies

1 One epidemiologic study examined the relationship of airway inflammation (eNO) and
2 PM measures, other pollutants, and indicators of motor vehicle emissions in Windsor,
3 Ontario (Dales et al., 2008, [156378](#)). This cohort of 2,402 school children estimated PM_{2.5}
4 and PM_{10-2.5} for each child's residence at the postal code level with an evaluated statistical
5 model (Wheeler et al., 2006, [103905](#)). Each 10 µg/m³ increase in 1-yr PM_{2.5} was associated
6 with a 39% increase in eNO (p = 0.058). Associations between eNO and PM_{10-2.5} were
7 positive but not statistically significant.

7.3.3.2. Toxicological Studies

CAPs Studies

8 An important set of subchronic studies involved exposure of normal (C57BL1/6) mice,
9 ApoE^{-/-} and the double-knockout ApoE^{-/-}/LDLR^{-/-} mice to Tuxedo, NY CAPs for 5-6 month
10 (March, April or May through September 2003 (Lippmann et al., 2005, [087452](#)). The
11 average PM_{2.5} exposure concentration was 110 µg/m³. Animals were fed a normal chow diet
12 during the CAPs exposure period. No pulmonary inflammation was observed in response to
13 CAPs exposure as measured by BALF cell counts and histology. The lack of a persistent
14 pulmonary response may have been due to adaptation of the lung following repeated
15 exposures. In fact, a parallel study examined CAPs-related gene expression in the double-
16 knockout animals and found upregulation of numerous genes in lung tissue (Gunnison and
17 Chen, 2005, [087956](#)). An in vitro study conducted simultaneously found daily variations in
18 CAPs-mediated NFκB activation in cultured human bronchial epithelial cells, suggesting
19 that transcription factor-mediated gene upregulation could occur in response to CAPs
20 (Maciejczyk and Chen, 2005, [087456](#)). It should be noted that significant cardiovascular
21 effects were observed in these subchronic studies which are discussed in Section 7.2.1.2.

22 Araujo et al. (2008, [156222](#)) compared the relative impact of ultrafine (0.01-0.18 µm)
23 versus fine (0.01-2.5 µm) PM inhalation in ApoE^{-/-} mice following a 40 day exposure (5
24 hs/day × 3 days/week for 75 total hours). Animals were fed a normal chow diet and exposed
25 to PM from November 3-December 12, 2005 in a mobile inhalation laboratory that was
26 parked 300 m from the 110 Freeway in downtown Los Angeles. Particles were concentrated
27 to ~440 µg/m³ for the fine exposures and ~110 µg/m³ for the ultrafine exposures,
28 representing a roughly 15-fold increase in concentration from ambient levels; the number
29 concentration of PM in the fine and ultrafine chambers were roughly equivalent (4.56×10^5
30 and 5.59×10^5 particles/cm³, respectively). Over 50% of the ultrafine PM was comprised of
31 organic carbon compared to only 25% for PM_{2.5}. No major increase in BALF inflammatory

1 cells was found in response to PM. However ultrafine PM exposure resulted in significant
2 cardiovascular and systemic effects (see Section 7.3.5.2).

Diesel Exhaust

3 Gottipolu et al. (2009, [190360](#)) exposed WKY and SH rats to filtered air or DE for
4 4 wk as described in Section 7.3.2.2. Previous studies from this laboratory have shown
5 enhanced effects of PM in SH compared with WKY rats. Although the main focus of this
6 recent study was on DE-induced mitochondrial oxidative stress and hypertensive gene
7 expression in the heart (see Section 7.2.7.1), some pulmonary effects were also found.
8 Subchronic exposure to DE resulted in a dose-dependent increase in BALF neutrophils in
9 both rat strains although levels of measured cytokines were not altered. Histopathological
10 analysis of lung tissue rats exposed to the higher concentration of DE demonstrated
11 accumulation of particle-laden macrophages as well as focal alveolar hyperplasia and
12 inflammation. Effect on indices of injury are discussed in Section 7.3.5.1.

13 Ishihara and Kagawa (2003, [096404](#)) exposed Wistar rats to filtered air and DE
14 containing 200, 1,000 and 3,000 $\mu\text{g}/\text{m}^3$ PM for 16 h/day and 6 days/week for 6, 12, 18 or 24
15 months. The mass median particle diameter was reported to be between 0.3 and 0.5 μm .
16 Concentrations of gases ranged from 2.93-35.67 ppm NO_x, 0.23-4.57 ppm SO₂, 1.8-21.9 ppm
17 CO in the DE exposures. Statistically significant increases in total numbers of
18 inflammatory cells and neutrophils in BALF were observed beginning at 6-12 months of
19 exposure to DE containing 1,000 and 3,000 $\mu\text{g}/\text{m}^3$ PM. When rats were exposed to DE
20 containing 1,000 $\mu\text{g}/\text{m}^3$ PM, which was filtered to remove PM, the inflammatory cell
21 response was significantly diminished. These results implicate the PM fraction of DE as a
22 key determinant of the inflammation. The PM fraction was also found to mediate the
23 increase in protein levels, the decrease in PGE₂ levels and alterations in mucus and
24 surfactant components observed in BALF (see Section 7.3.5.1).

25 Li et al. (2007, [155929](#)) exposed BALB/c and C56BL/6 mice to low dose DE as
26 described in Section 7.3.2.2. for 1, 4 and 8 wk. Increases in numbers of BALF macrophages
27 and total inflammatory cells were observed in BALB/c mice at 8 wk but not 4 wk of DE
28 exposure. Persistent increases in numbers of BALF neutrophils and lymphocytes were
29 observed in both strains at 4 and 8 wk of DE exposure. Corresponding increases in BALF
30 cytokines differed between the two strains. These results should be interpreted with
31 caution since comparisons were made with Day 0 controls rather than age-matched
32 controls. No histopathological changes in the lungs were seen at any time point after DE
33 exposure. This study demonstrated differences in pulmonary responses to low dose DE
34 between 2 mouse strains. Altered AHR, pulmonary inflammation, markers of oxidative
35 stress and effects of antioxidant intervention were also evaluated (see Sections 7.3.2.2 and
36 7.3.4.1). Although no attempt was made in this study to determine the effects of gaseous

1 components of DE on the measured responses, concentrations of gases were very low
2 suggesting that PM may have been responsible for the observed effects.

3 In a study by Hiramatsu et al. (2003, [155846](#)), BALB/c and C57BL/6 mice were
4 exposed to DE (PM concentrations 100 and 3000 $\mu\text{g}/\text{m}^3$) for 1 or 3 months. Concentrations of
5 gases were reported to be 3.5-9.5 ppm CO, 2.2-14.8 ppm NO_x, and less than 0.01 ppm SO₂.
6 Modest increases in BALF neutrophils and lymphocytes were observed in response to DE in
7 both mouse strains at 1 and 3 months. Histological analysis demonstrated DEP-laden
8 alveolar macrophages in alveoli and peribronchial tissues at both time points. Bronchus-
9 associated lymphoid tissue developed after 3 months exposure to the higher concentration
10 of DE in both mouse strains. Mac-1 positive cells (a marker of phagocytic activation of
11 alveolar macrophages) were also increased in BALF of BALB/c mice exposed to the higher
12 concentration of DE for 1 and 3 months. Increased expression of several cytokines and
13 decreased expression of iNOS mRNA was observed in DE-exposed mice at 1 and 3 months.
14 NF κ B activation was also noted following 1 month exposure to the lower concentration of
15 DE. No attempt was made in this study to determine the responses to gaseous components
16 of the DE.

17 In a study by Reed et al. (2006, [156043](#)), healthy Fisher 344 rats and A/J mice were
18 exposed to DE (PM concentration = 30, 100, 300 and 1000 $\mu\text{g}/\text{m}^3$) by whole body inhalation
19 for 6 h/day, 7 days/week for either 1 week or 6 months. Concentrations of gases were
20 reported to be 2.0-45.3 ppm NO, 0.2-4.0 ppm NO₂, 1.5-29.8 ppm CO and 8-365 ppb SO₂.
21 Short-term responses are discussed in Section 6.3.3.3 and 6.3.7.1, and sub-chronic systemic
22 effects are presented in Section 7.2.4.1. Six months of exposure resulted in no measurable
23 effects on pulmonary inflammation. However numerous black particles were observed
24 within alveolar macrophages after 6 months of exposure.

25 Seagrave et al. (2005, [088000](#)) evaluated pulmonary responses in male and female
26 CDF (F-344)/CrIBR rats exposed 6 h/day for 6 months to filtered air or DE at concentrations
27 ranging from 30-1000 $\mu\text{g}/\text{m}^3$ PM. Concentrations of gases were reported for the highest
28 exposure as 45.3 ppm NO, 4.0 ppm NO₂, 29.8 ppm CO and 2.2 ppm total vapor
29 hydrocarbon. No changes in BALF cells were noted. A small decrease in TNF α was seen in
30 BALF of female rats exposed to the highest concentration of DE for 6 months. Pulmonary
31 injury also was evaluated (Section 7.3.5.1). Thus changes in BALF markers are modest and
32 gender specific.

Woodsmoke

33 Seagrave et al. (2005, [088000](#)) also evaluated pulmonary responses in male and
34 female CDF (F344)/CrIBR rats exposed 6 h/day for 6 months to filtered air or HWS
35 concentrations ranging from 30-1000 $\mu\text{g}/\text{m}^3$ PM. Concentrations of gases were reported for
36 the highest exposure as 3.0 ppm CO and 3.1 ppm total vapor hydrocarbon. A small increase
37 in BALF neutrophils was observed in male rats exposed to the lowest concentration of

1 HWS. Female rats exhibited a decrease in BALF MIP-2 at the highest concentration of
2 HWS. Pulmonary injury also was evaluated (Section 7.3.5.1). In general, responses to HWS
3 were more remarkable than responses to DE seen in a parallel study. However these
4 gender-specific responses are modest and difficult to interpret.

5 In a study by Reed et al. (2006, [156043](#)), Fisher 344 rats, SHR rats, A/J mice and
6 C57BL/6 mice were exposed to clean air or HWS (PM concentrations 30, 100, 300 and
7 1000 $\mu\text{g}/\text{m}^3$) by whole body inhalation for 6 h/day, 7 days/week for either 1 week or 6
8 months. Concentrations of gases ranged from 229.0-14887.6 mg/m^3 for CO, 54.9-139.3 $\mu\text{g}/\text{m}^3$
9 for ammonia, and 177.6- 3455.0 $\mu\text{g}/\text{m}^3$ nonmethane VOC in these exposures. Short-term
10 responses are discussed in Section 6.3.7.2 and sub-chronic effects are presented in
11 Section 7.2.4.1. Histological analysis of lung tissue showed minimal increases in alveolar
12 macrophages. The effects of HWS on bacterial clearance are discussed below
13 (Section 7.3.7.2).

14 Another study evaluated the effects of subchronic woodsmoke exposure in Brown
15 Norway rats and is described in detail in Section 7.3.2.2 (Tesfaigzi et al., 2002, [025575](#)).
16 Numbers of alveolar macrophages in BALF were significantly increased in rats exposed to
17 1000 $\mu\text{g}/\text{m}^3$ woodsmoke for 12 wk, but no changes were seen in numbers of other
18 inflammatory cells. A large percent of BALF macrophages contained carbonaceous material.
19 Histological analysis of lung tissue showed minimal to mild inflammation in the epiglottis
20 of the larynx in rats exposed to both concentrations of woodsmoke.

21 Ramos et al. (2009, [190116](#)) examined the effects of subchronic woodsmoke exposure
22 on the development of emphysema in guinea pigs. Inflammation is thought to be involved in
23 the pathogenesis of this form of COPD. Statistically significant increases in total numbers
24 of BALF cells were observed in guinea pigs exposed to smoke for 1-7 months, with numbers
25 of macrophages increased at 1-4 months and numbers of neutrophils increased at 4-7
26 months. At 4 months, alveolar mononuclear phagocytic and lymphocytic peribronchiolar
27 inflammation were observed by histopathological analysis of lung tissue. This study is
28 discussed in depth in Section 7.3.5.1.

Model Particles

29 Wallenborn et al. (2008, [191171](#)) examined the pulmonary, cardiac and systemic
30 effects of subchronic exposure to particulate ZnSO_4 . WKY rats were exposed nose-only to
31 10, 30, or 100 $\mu\text{g}/\text{m}^3$ ultrafine particulate ZnSO_4 for 5 h/day and 3 day/wk over a 16-week
32 period. Particle size was reported to be 31-44 nm measured as number median diameter. No
33 changes in pulmonary inflammation or injury were observed although cardiac effects were
34 noted (see Section 7.2.7.1.). This study possibly demonstrates a direct effect of ZnSO_4 on
35 extrapulmonary systems, as suggested by the lack of pulmonary effects.

7.3.4. Pulmonary Oxidative Response

7.3.4.1. Toxicological Studies

Urban Air

1 An interesting new study evaluated the effects of subchronic exposure to ambient
2 levels of urban particles on the development of emphysema in papain-treated mice (Lopes
3 et al., 2009, [190430](#)). Since oxidative stress is thought to contribute to the development of
4 emphysema, 8-isoprostane levels were measured in lung tissue from the 4 groups of mice
5 used in this study. A statistically significant increase in 8-isoprostane, a marker of oxidative
6 stress, was observed in lungs from mice treated with papain and exposed to ambient air
7 compared with the other groups of mice. This study is described in greater depth in
8 Section 7.3.5.1.

Diesel Exhaust

9 Li et al. (2007, [155929](#)) exposed mice to low dose DE for 1, 4 and 8 wk as described in
10 Section 7.3.2.2. Markers of oxidative stress and effects of antioxidant intervention were
11 evaluated in this model. While HO-1 mRNA and protein were increased in lung tissues of
12 both mouse strains after 1 week of DE exposure (see Section 6.3.4.2), at 8 wk of DE
13 exposure, HO-1 protein levels remained high in C57BL/6 mice but returned to control
14 values in BALB/c mice. This study demonstrates differences in pulmonary responses to low
15 dose DE between two mouse strains. Furthermore, this study suggests that adaptation
16 occurs in BALB/c mice during prolonged DE exposure since the increase in HO-1 protein
17 seen in both strains at 1 week of exposure was only seen in C57BL/6 mice at 8 wk. Altered
18 AHR (Section 7.3.2.2) and pulmonary inflammation (Section 7.3.3.2) were also evaluated.
19 Although no attempt was made in this study to determine the effects of gaseous
20 components of DE on the measured responses, concentrations of gases were very low. This
21 suggests that PM may have been responsible for the observed effects.

7.3.5. Pulmonary Injury

7.3.5.1. Toxicological Studies

Urban Air

22 An important new study evaluated the effects of chronic exposure to ambient levels of
23 urban particles on lung development in the mouse (Mauad et al., 2008, [156743](#)). Both
24 functional and anatomical indices of lung development were measured in mice exposed

1 prenatally and/or postnatally as described in Section 7.3.2.2. Animals were sacrificed at 15
2 and 90 days of age for histological analysis of lungs. Histological analysis demonstrated the
3 presence of mild foci of macrophages containing black dots of carbon pigment in the
4 prenatal and postnatal exposure group at 90 days. In addition, the alveolar spaces of 15-day
5 old mice in the prenatal and postnatal exposure group were enlarged compared with
6 controls. Morphometric analysis demonstrated statistically significant decreases in surface
7 to volume ratio at 15 and 90 days in the pre and postnatal group compared with controls.
8 Since alveolarization is normally complete by 15 days of age, these results suggest
9 incomplete alveolarization in the 15-day old group and an enlargement of air spaces in the
10 90-day old group. These anatomical changes correlated with decrements in pulmonary
11 function which are discussed in Section 7.3.2.2.

12 Prolonged exposure to low levels of ambient air pollution beginning in early life has
13 been linked to secretory changes in the nasal cavity of mice, specifically increased
14 production of acidic mucosubstances (Pires-Neto et al., 2006, [096734](#)). Six day-old Swiss
15 mice were continuously chamber exposed to ambient or filtered São Paulo air for 5 months.
16 Concentrations in the “polluted chamber” vs. “clean chamber” were (in $\mu\text{g}/\text{m}^3$) 59.52 vs.
17 37.08 for NO_2 , 12.52 vs. 0 for BC, and 46.49 vs. 18.62 for $\text{PM}_{2.5}$. Thus, pollutant levels were
18 reduced by filtration but not entirely eliminated. Compared to filtered air, exposure to
19 ambient air resulted in increased total mucus and acidic mucus in the epithelium lining the
20 nasal septum, but no statistically significant differences in other parameters (amount of
21 neutral mucus, volume proportions of neutral mucus, total mucus, or nonsecretory
22 epithelium, epithelial thickness, or ratio between neutral and acidic mucus). The
23 physicochemical properties of mucus glycoproteins are critical to the protective function of
24 the airway mucus layer. Acidified mucus is more viscous, and is associated with a decrease
25 in mucociliary transport. Thus acidic mucosubstances may represent impaired defense
26 mechanisms in the respiratory tract.

27 An interesting new study evaluated the effects of subchronic exposure to ambient
28 levels of urban particles on the development of emphysema in papain-treated mice (Lopes
29 et al., 2009, [190430](#)). Emphysema is a form of COPD caused by the destruction of
30 extracellular matrix in the alveolar region of the lung which results in airspace
31 enlargement, airflow limitation and a reduction of the gas-exchange area of the lung.
32 Inflammation, oxidative stress, protease imbalance and apoptosis are thought to contribute
33 to the development of emphysema. In this study, male BALB/c mice were continuously
34 exposed to ambient or filtered Sao Paulo air for 2 months. Concentrations of $\text{PM}_{2.5}$ in the
35 “polluted chamber” vs. “clean chamber” were 33.86 ± 2.09 vs. 2.68 ± 0.38 $\mu\text{g}/\text{m}^3$. Thus
36 filtration reduced PM levels considerably. Ambient concentrations of CO and SO_2 were 1.7
37 ppm and 16.2 $\mu\text{g}/\text{m}^3$ respectively. No significant difference was observed in the
38 concentrations of NO_2 in the “polluted chamber” vs “clean chamber” ($60\text{-}80$ $\mu\text{g}/\text{m}^3$). Half of
39 the mice were pre-treated with papain by intranasal instillation in order to induce

1 emphysema. Morphometric analysis of lung tissue demonstrated a statistically significant
2 increase in mean linear intercept, a measure of airspace enlargement, in papain-treated
3 mice compared with saline-treated controls exposed to filtered air. While exposure to
4 ambient air failed to increase mean linear intercept values in saline-treated mice, mean
5 linear intercept values were significantly increased in papain-treated mice exposed to
6 ambient air compared with papain-treated mice exposed to filtered air. A similar pattern of
7 responses was observed for the volume proportion of collagen and elastin fibers in alveolar
8 tissue, which are markers of alveolar wall remodeling. Lung immunohistochemical analysis
9 demonstrated an effect of papain, but not ambient air, on macrophage cell density and
10 matrix metalloproteinase 12-positive cell density. No differences in caspase-3 positive cells,
11 a marker of apoptosis, were observed between the 4 groups of mice. Oxidative stress was
12 evaluated in this model as described in see Section 7.3.4.1. Taken together, results of this
13 study demonstrate that urban levels of PM, mainly from traffic sources, worsen protease-
14 induced emphysema in an animal model.

15 Pulmonary vascular remodeling, measured by a decrease in the lumen to wall ratio,
16 was observed in mice exposed to ambient Sao Paulo air for 4 months (Lemos et al., 2006,
17 [088594](#)). This study is described in greater detail in Section 7.2.1.2.

18 Kato and Kagawa (2003, [089563](#)) exposed Wistar rats to roadside air contaminated
19 mainly with automobile emissions (55.7 to 65.2 ppb NO₂ and 63 to 65 µg/m³ suspended PM
20 [SPM]) and examined the effects on respiratory tissue after 24, 48, or 60 wk of exposure.
21 The surface of the lungs was light gray in color after all durations of exposure, and BC
22 particle deposits accumulated with prolonged exposure. These characteristics were not
23 evident in filtered air-exposed control animals, although filtered air contained low levels of
24 air pollutants (≤ 6.2 ppb NO₂ and 15 µg/m³ SPM). The most common change observed using
25 transmission electron microscopy was the presence of particle laden (anthracotic) alveolar
26 macrophages, or anthracosis, in a wide range of pulmonary tissues, including the
27 submucosa, tracheal- and bronchiole-associated lymph nodes, alveolar wall and space,
28 pleura, and perivascular connective tissue. These changes were evident after 24 wk and
29 increased with duration of exposure. Other changes included increases in the number of
30 mucus granules in goblet cells, mast cell infiltration (but no degranulation) after 24 wk,
31 increased lysosomes in ciliated cells, some altered morphology of Clara cells, and
32 hypertrophy of the alveolar walls after 48 wk. No goblet cell proliferation was observed, but
33 slight, variable acidification of mucus granules appeared after 24 and 48 wk and
34 disappeared after 60 wk. Anthracotic macrophages were seen in contact with plasma cells
35 and lymphocytes in the lymphoid tissue, suggesting immune cell interaction in the
36 immediate vicinity of particles. Even after 60 wk, no lymph node anthracosis was observed
37 in the filtered air group.

38 In a post-mortem study of lung tissues from 20 female lifelong residents of Mexico
39 City, a high PM locale, histology demonstrated significantly greater amounts of fibrous

1 tissue and muscle in the airway walls compared to subjects from Vancouver (Churg et al.,
2 2003, [087899](#)), a city with relatively low PM levels. Electron microscopy showed
3 carbonaceous aggregates of ultrafine particles, which the authors conclude penetrate into
4 and are retained in the walls of small airways. The study shows an association between
5 retained particles and airway remodeling in the form of excess muscle and fibrotic walls.
6 The subjects were deemed suitable for examination based on never-smoker status, no use of
7 biomass fuels for cooking, no known occupational particle/dust exposure, death by cause
8 other than respiratory disease, and extended residence in each locale (lifelong for Mexico
9 City and >20 years for Vancouver). However, subjects from the two locales were not
10 matched with respect to ethnicity, sex (20 females from Mexico City vs. 13 females and 7
11 males from Vancouver), or mean age at death (66 ± 9 vs. 76 ± 11), and other possibly
12 influential factors such as exercise or diet were not considered.

Diesel Exhaust

13 Gottipolu et al. (2009, [190360](#)) exposed WKY and SH rats to filtered air or DE as
14 described in Section 7.3.2.2. (Previous studies from this laboratory have shown enhanced
15 effects of PM in SH compared with WKY rats. Although the main focus of this recent study
16 was on DE-induced mitochondrial oxidative stress and hypertensive gene expression in the
17 heart (see Section 7.2.7.1), some pulmonary effects were found. Inflammatory effects are
18 described in Section 7.3.3.2. GGT activity in BALF was increased in both strains in
19 response to the higher concentration of DE. No DE-related changes were observed in BALF
20 protein or albumin. Histopathological analysis of lung tissue rats exposed to the higher
21 concentration of DE demonstrated accumulation of particle-laden macrophages as well as
22 focal alveolar hyperplasia and inflammation. No effects on indices of pulmonary function
23 were observed (see Section 7.3.2.2.)

24 Ishihara and Kagawa (2003, [096404](#)) exposed rats to DE for up to 24 months as
25 described in Section 7.3.3.2. A statistically significant increase in BALF protein was
26 observed at 12 months of exposure to DE containing $1000 \mu\text{g}/\text{m}^3$ PM. This response was
27 attenuated when the DE was filtered to remove PM. Pulmonary inflammation was noted
28 and is described in Section 7.3.3.2.

29 Seagrave et al. (2005, [088000](#)) evaluated pulmonary responses in rats exposed to DE
30 for up to 6 months as described in Section 7.3.3.2. A small increase in LDH was seen in
31 BALF of female rats exposed to the highest concentration of DE for 6 months. Pulmonary
32 inflammation was also evaluated (Section 7.3.3.2). The changes in BALF markers in this
33 study were modest and gender specific.

Gasoline Exhaust

34 Reed et al. (2008, [156903](#)) examined a variety of health effects following subchronic
35 inhalation exposure to gasoline engine exhaust. Male and female CDF (F344)/Cr1BR rats,

1 SHR rats and male C57BL/6 mice were exposed for 6 h/day and 7 days/week for a period of
2 3 days to 6 months. The dilutions for the gasoline exhaust were 1:10, 1:15 and 1:90; filtered
3 PM was at the 1:10 dilution. PM mass ranged from 6.6 to 59.1 $\mu\text{g}/\text{m}^3$, with the
4 corresponding number concentration between 2.6×10^4 and 5.0×10^5 particles/ cm^3 .
5 Concentrations of gases ranged from 12.8-107.3 ppm CO, 2.0-17.9 ppm NO, 0.1-0.9 ppm
6 NO₂, 0.09-0.62 ppm SO₂ and 0.38-3.37 ppm NH₃. Other effects for these studies are
7 presented in Sections 7.2.4.1. and 7.3.6.1. No pulmonary inflammation or histopathological
8 changes were noted in the F344 rats and A/J mice, except for a time-dependent increase in
9 the number of macrophages containing PM. However statistically significant increases of
10 47% and 29% in BALF LDH were observed in female and male F344 rats, respectively, after
11 6 months of exposure to the highest concentration of engine exhaust. This response was
12 absent when gasoline exhaust was filtered, implicating PM as a key determinant of this
13 response. In addition, exposure to the highest concentration of gasoline exhaust resulted in
14 statistically significant decreases in hydrogen peroxide and superoxide production in
15 unstimulated and stimulated BALF macrophages. Interestingly, hypermethylation of lung
16 DNA was observed in male F344 rats following 6 months of exposure to gasoline exhaust
17 containing 30 $\mu\text{g}/\text{m}^3$ particulates. This response was PM-dependent since it was absent in
18 mice exposed to filtered gasoline exhaust. The significance of this epigenetic change in
19 terms of respiratory health effects is not known. However, altered patterns of DNA
20 methylation can affect gene expression and are sometimes associated with altered immune
21 responses and/or the development of cancer.

Woodsmoke

22 Seagrave et al. (2005, [088000](#)) also evaluated pulmonary responses in rats to HWS for
23 6 months as described in Section 7.3.3.2. Increases in BALF LDH and protein were seen in
24 male but not female rats. Female rats exhibited a decrease in BALF glutathione at the
25 highest concentration of HWS. Decreases in BALF alkaline phosphatase were found in both
26 males and females exposed to 1000 $\mu\text{g}/\text{m}^3$ HWS. Male rats exposed to 100 and 300 $\mu\text{g}/\text{m}^3$
27 HWS exhibited a decrease in BALF β -glucuronidase activity. Pulmonary inflammation was
28 also evaluated (Section 7.3.3.2). These changes in BALF markers in this study were modest
29 and gender specific.

30 Another study evaluated the effects of subchronic woodsmoke exposure in Brown
31 Norway rats as described in Section 7.3.2.2. (Tesfaigzi et al., 2002, [025575](#)). Exposure to
32 1,000 $\mu\text{g}/\text{m}^3$ woodsmoke for 12 wk resulted in a statistically significant increase in Alcian
33 Blue- (AB) and Periodic Acid Schiff- (PAS) positive airway epithelial cells compared to
34 controls, indicating an increase in mucous secretory cells containing neutral and acid
35 mucus, respectively. More significant histopathological responses were found following
36 exposure to 10,000 $\mu\text{g}/\text{m}^3$ of DE. Pulmonary function and inflammation were evaluated also

1 but are not discussed here due to the extremely high exposure level (Sections 7.3.2.2 and
2 7.3.3.2).

3 Ramos et al. (2009, [190116](#)) examined the effects of subchronic woodsmoke exposure
4 on the development of emphysema in guinea pigs. In particular, the involvement of
5 macrophages and macrophage-derived matrix metalloproteinases (MMP) in woodsmoke-
6 related responses was investigated. Guinea pigs were exposed to ambient air or to whole
7 smoke from pine wood for 3 h/day and 5 days/week over a 7-month period. PM₁₀ and PM_{2.5}
8 concentrations in the exposure chambers were reported to be 502 ± 34 and 363 ± 23 µg/m³,
9 respectively, while the concentration of CO was less than 80 ppm. COHb levels were
10 reported to be 6% in controls and 15-20% in smoke-exposed guinea pigs. Statistically
11 significant decreases in body weight were observed in guinea pigs exposed to smoke for 4 or
12 more months compared with controls. Statistically significant increases in total numbers of
13 BALF cells were observed in guinea pigs exposed to smoke for 1-7 months, with numbers of
14 macrophages increased at 1-4 months and numbers of neutrophils increased at 4-7 months.
15 At 4 months, alveolar mononuclear phagocytic and lymphocytic peribronchiolar
16 inflammation, as well as bronchiolar epithelial and smooth muscle hyperplasia, were
17 observed by histopathological analysis of lung tissue. Emphysematous lesions, smooth
18 muscle hyperplasia and pulmonary arterial hypertension were noted at 7 months.
19 Morphometric analysis of lung tissue demonstrated statistically significant increases in
20 mean linear intercept values, a measure of airspace enlargement, in guinea pigs at 6 and 7
21 months of exposure. Statistically significant increases in elastolytic activity was observed in
22 BAL macrophages and lung tissue homogenates at 1-7 months of exposure. Lung
23 collagenolytic activity was also increased at 4-7 months of exposure and corresponded in
24 time with the presence of active forms of MMP-2 and MMP-9 in lung tissue homogenates
25 and BALF. Furthermore, MMP-1 and MMP-9 immunoreactivity was detected in
26 macrophages, epithelial and interstitial cells in smoke-exposed animals at 7 months.
27 Increased levels of MMP-2 and MMP-9 mRNA were also found in smoke-exposed guinea
28 pigs after 3-7 months. Apoptosis was found in BAL macrophages (TUNEL assay) from
29 guinea pigs exposed to smoke for 3-7 months and in alveolar epithelial cells (caspase-3
30 immunoreactivity) after 7 months. Taken together, these results provide evidence that
31 subchronic exposure to woodsmoke leads to the development of emphysematous lesions
32 accompanied by the accumulation of alveolar macrophages, increased levels and activation
33 of MMP's, connective tissue remodeling and apoptosis. Unfortunately, the high levels of CO
34 and COHb reported in this study make it difficult to conclude that woodsmoke PM alone is
35 responsible for these dramatic effects.

7.3.6. Allergic Responses

7.3.6.1. Epidemiologic Studies

1 A number of epidemiologic studies have found associations between PM and allergic
2 (or atopic) indicators. Allergy is a major driver of asthma, which has been associated with
3 PM in studies discussed in previous sections. In a study by Annesi-Maesano (2007, [093180](#))
4 (described in Section 7.3.1.1) atopic asthma was related to PM_{2.5} (OR 1.43 [95% CI:
5 1.07-1.91]) and positive skin prick test to common allergens was also increased with higher
6 PM levels. This report is consistent with the results from an earlier study (Penard-Morand
7 et al., 2005, [087951](#)) in the same sample of children that associated allergic rhinitis and
8 atopic dermatitis with PM₁₀. Also, Morgenstern et al. (2008, [156782](#)) found statistically
9 significant effects for asthmatic bronchitis, hay fever, and allergic sensitization to pollen in
10 a cohort of children in Germany examining modeled PM_{2.5} data at birth addresses. Distance
11 to a main road had a dose-response relationship with sensitization to outdoor allergens.
12 Nordling et al. (2008, [097998](#)) (discussed above in Section 7.3.2.1) reported a positive
13 association of PM₁₀ exposure during the first year of life with allergenic sensitization (IgE
14 antibodies) to inhaled allergens, especially pollen. In a study by Brauer et al. (2007,
15 [090691](#)) (discussed above in Section 7.3.1.1) an interquartile range increase in PM_{2.5} was
16 associated with an increased risk of sensitization to food allergens (OR 1.75 [95% CI
17 1.23-2.47]). A significant association was found for sensitization to any allergen, but none
18 was found for sensitization to specific indoor or outdoor aeroallergens or atopic dermatitis
19 (eczema). In a study by Janssen et al. (2003, [133555](#)), PM_{2.5} was associated with allergic
20 indicators such as hay fever (ever), skin prick test reactivity to outdoor allergens, current
21 itchy rash, and conjunctivitis in Dutch children. These same outcomes were also associated
22 with proximity of the school to truck traffic but not car traffic, suggesting a role for diesel-
23 related pollution. Consistent with the aforementioned Dutch study by Brauer et al. (2007,
24 [090691](#)), PM_{2.5} was not associated with eczema.

25 Mortimer et al. (2008, [187280](#)) examined the association between prenatal and early-
26 life exposures to air pollutants with allergic sensitization in a cohort of 170 children with
27 asthma, age 6-11, living in central California. Sensitization to at least one allergen was
28 associated with higher levels of PM₁₀ and CO during the entire pregnancy and 2nd
29 trimester and higher PM₁₀ during the first two years of life. Sensitization to at least one
30 indoor allergen was associated with higher exposures to PM₁₀ and CO in during the entire
31 pregnancy and during the 2nd trimester. However, no significant associations remained for
32 PM₁₀ after adjustment for co-pollutants, effect modifiers, or potential cofounders in addition
33 to year of birth. The authors advise that the large number of comparisons may be of concern
34 and this study should be viewed as an exploratory, hypothesis-generating undertaking. In
35 examining the National Health Interview Survey for the years 1997-2006, Bhattacharyya

1 et al. (2009, [180154](#)) found relationships between air quality and the prevalence of hay
2 fever and sinusitis. However, the air quality data were not clearly defined and as such
3 caution is required in interpretation of these results. In contrast, Bayer-Oglesby et al.
4 (2005, [086245](#)) found no significant association between declining levels of PM₁₀ and hay
5 fever in Switzerland. In a study by Oftedal et al. conducted in Oslo, Norway (2007, [191948](#)),
6 early-life exposure to PM₁₀ or PM_{2.5} was generally not associated with sensitization to
7 allergens in 9-10-year-old children; lifetime exposures to PM₁₀ and PM_{2.5} were associated
8 with dust mite allergy, but the association was diminished by adjustment for socioeconomic
9 factors . In Norway, wood burning in the wintertime is thought to account for about half of
10 the PM_{2.5} levels. Although associations between PM and reactivity to specific allergens have
11 been reported in long-term studies, there is a consistent lack of correlation between PM and
12 total IgE levels, indicating a selective enhancement of allergic responses.

7.3.6.2. Toxicological Studies

Diesel Exhaust

13 Exposure to relatively low doses of DE has been shown to exacerbate asthmatic
14 responses in OVA sensitized and challenged BALB/c mice (Matsumoto et al., 2006, [098017](#)).
15 Mice were intraperitoneally sensitized and intranasally challenged 1day prior to inhalation
16 exposure to DE (PM concentration 100 µg/m³; CO, 3.5 ppm; NO₂, 2.2 ppm; SO₂ <0.01 ppm)
17 for 1 day or 1, 4, or 8 wk (7h/day, 5 days/week, endpoints 12-h post DE exposure). Results
18 from the 1- and 4-week exposures are described in Section 6.3.6.3. It should be noted that
19 control mice were left in a clean room as opposed to undergoing chamber exposure to
20 filtered air. The significant increases in AHR and airway sensitivity observed following
21 shorter exposure periods did not persist at 8 wk. BALF cytokines were altered by DE
22 exposure with only RANTES significantly elevated after 8 wk. DE had no effect on OVA
23 challenge-induced peribronchial inflammatory or mucin positive cells. These results suggest
24 that adaptive processes may have occurred during prolonged exposure to DE.

Gasoline Exhaust

25 In a study by Reed et al. (2008, [156903](#)), BALB/c mice were exposed to whole gasoline
26 exhaust diluted 1:10 (H), 1:15 (M), or 1:90 (L), filtered exhaust at the 1:10 (HF), or clean air
27 for 6 h/day (atmospheric characterization described in Section 6.3.6.3). GEE exposure from
28 conception through four weeks of age induced slight but non-significant increases in ova-
29 specific IgG1 in offspring but had no significant effect on airway reactivity, BAL cytokine or
30 cell concentrations, although there were non-significant increases in lung neutrophils and
31 eosinophils. Significant increases in total serum IgE were observed, but this effect persisted
32 after filtration of particles and was thus attributed to gas phase components.

Woodsmoke

1 In a study by Tesfaigzi et al. (2005, [156116](#)), Brown Norway rats were sensitized and
2 challenged with ovalbumin. Rats were exposed for 70 days to filtered air or to 1000 $\mu\text{g}/\text{m}^3$
3 HWS. Particles were characterized by a MMAD of 0.36 μm . Concentrations of gases were
4 reported to be 13.0 ppm CO and 3.1 ppm total vapor hydrocarbon with negligible NO_x.
5 Respiratory function was measured in anesthetized animals by whole-body
6 plethysmography and demonstrated a significant increase in functional residual capacity as
7 well as a significant increase in dynamic lung compliance in HWS-exposed animals
8 compared to controls. No change in total pulmonary resistance or airway responsiveness to
9 methacholine was observed. BALF inflammatory cells were not increased, although
10 histological analysis demonstrated focal inflammation including granulomatous lesion and
11 eosinophilic infiltrations in HWS-exposed rats. Alterations of several cytokines in BALF
12 and plasma were noted. Changes in airway epithelial mucus cells and intraepithelial stored
13 mucosubstances were modest and did not achieve statistical significance. Results of this
14 study demonstrate that subchronic exposure to HWS had minimal effects on pulmonary
15 responses in a rat model of allergen sensitization and challenge.

7.3.7. Host Defense

7.3.7.1. Epidemiologic Studies

16 Epidemiologic studies of respiratory infections indicate an association with PM. This
17 is more evident when considering short-term exposures (Chapter 6), but studies of long-
18 term exposures have observed associations with general respiratory symptoms often caused
19 by infection, such as bronchitis. In a birth cohort study of approximately 4,000 Dutch
20 children, Brauer et al. (2007, [090691](#))(described in Section 7.3.1.1) found significant positive
21 associations for PM_{2.5} with ear/nose/throat infections and doctor-diagnosed flu/serious cold
22 in the first four years of life. These results are consistent with an earlier study by Brauer et
23 al. (2006, [090757](#)), which found that an increase of 3 $\mu\text{g}/\text{m}^3$ PM_{2.5} was associated with
24 modestly increased risk for ear infections in the Netherlands [OR 1.13 (95% CI, 1.00-1.27)].
25 A Swiss study by Bayer-Oglesby et al. (2005, [086245](#)), discussed in Section 7.3.1.1 above,
26 demonstrated that declining levels of PM₁₀ were associated with declining prevalence of
27 common cold and conjunctivitis. Because traffic-related pollutants such as ultrafine
28 particles are high near major roadways and then decay exponentially over a short distance,
29 Williams, et al. (2009, [191945](#)) assessed exposure according to residential proximity to
30 major roads in a Seattle area study of postmenopausal women. Proximity to major roads
31 was associated with a 21% decrease in natural killer cell function, which is an important
32 defense against viral infection and tumors. This finding was limited to women who reported
33 exercising near traffic; other markers of inflammation and lymphocyte proliferation did not

1 consistently differ according to proximity to major roads. In the Puget Sound region of
2 Washington, Karr et al. (2009, [191946](#)) reported that there may be a modest increased risk
3 of bronchiolitis related to PM_{2.5} exposure for infants born just before the peak respiratory
4 syncytial virus (RSV) season. Risk estimates were stronger when restricted to cases
5 specifically attributed to RSV and for infants residing closer to highways. Emerging
6 evidence suggests that respiratory infections, particularly infection by viruses such as RSV,
7 can cause asthma or trigger asthma attacks.

7.3.7.2. Toxicological Studies

Diesel Exhaust

8 DE may affect systemic immunity. The proliferative response of A/J mouse spleen
9 cells following stimulation with T cell mitogens was suppressed by 6 months of daily
10 exposure to DE at concentrations at or above 300 µg/m³ PM (Burchiel et al., 2004, [055557](#)).
11 B cell proliferation was increased at 300 µg/m³ but unaffected at higher concentrations (up
12 to 1000 µg/m³). Concentrations of gases and were reported in the parallel study by Reed et
13 al. (2004, [055625](#)), described in Section 7.3.3.2 Pulmonary Inflammation/Diesel exhaust.
14 The Reed study reported a decrease in spleen weight in male mice (27% reduction in the
15 300 µg/m³ exposure group). The immunosuppressive effects of DE were not due to PAHs or
16 benzo(a)pyrene (BaP)-quinones (BPQs) since there were little, if any, of these compounds
17 present in the chamber atmosphere. It should be noted that sentinel animals were negative
18 for mouse parvovirus at the start of the study, but seroconverted by the end of the study,
19 indicating possible infection. Parvovirus can interfere with the modulation of lymphocyte
20 mitogenic responses (Baker, 1998, [156245](#)). A six month exposure (6h/day, 7d/week) to 30,
21 100, 300 or 1000 µg/m³ of PM in DE did not significantly affect bacterial clearance in
22 C57BL/6 mice infected with *Pseudomonas aeruginosa*, although all levels reduced bacterial
23 clearance when the exposure only lasted a week (Harrod et al., 2005, [088144](#)).
24 Characterization of the exposure atmosphere was given by Reed et al. (2004, [055625](#))
25 (Section 7.3.3.2 Pulmonary Inflammation/Diesel exhaust).

Gasoline Exhaust

26 In a study by Reed et al. (2008, [156903](#)) (described in Section 6.3.6.3) long-term
27 exposure to fresh gasoline exhaust (6h/day, 7d/week for 6 months) did not affect clearance of
28 *P. aeruginosa* from the lungs of C57BL/6 mice.

Hardwood Smoke

29 One study demonstrated immunosuppressive effects of HWS (Burchiel et al., 2005,
30 [088090](#)). Exposure to HWS increased proliferation of T cells from A/J mice exposed daily to
31 100 µg/m³ PM for 6 months, but produced a concentration-dependent suppression of

1 proliferation at PM concentrations >300 µg/m³. No effects on B cell proliferation were
2 observed. Concentrations of NO and NO₂ were not detectable or <40 ppb for all exposure
3 levels. CO was reported to be 2, 4, and 13 ppm for the 100, 300 and 1000 µg/m³ PM
4 concentrations, respectively. Exposure atmospheres contained significant levels of
5 naphthalene and methylated naphthalenes, fluorene, phenanthrene, and anthracene, as well
6 as low concentrations of several metals (K, Ca, and Fe) (Burchiel et al., 2005, [088090](#)). It
7 should be noted that serologic analysis of study sentinel animals indicated infection with
8 parvovirus, which can interfere with the modulation of lymphocyte mitogenic responses
9 (Baker, 1998, [156245](#)). In another study by Reed et al. (2006, [156043](#)) C57BL/6 mice were
10 exposed to 30-1000 µg/m³ HWS by whole body inhalation for 6 months prior to instillation
11 of *P. aeruginosa*. Exposure characterizations are described in Section 7.3.3.2. Although
12 there was a trend toward increased clearance with increasing exposure concentrations,
13 there was no statistically significant effect of HWS exposure on bacterial clearance.

7.3.8. Respiratory Mortality

14 Two large U.S. cohort studies examined the effect of long-term exposure to PM_{2.5} on
15 respiratory mortality with mixed results. In the ACS, Pope et al. (2004, [055880](#)) reported
16 positive associations with deaths from specific cardiovascular diseases, but no PM_{2.5}
17 associations were found with respiratory mortality. A follow-up to the Harvard Six Cities
18 study (Laden et al., 2006, [087605](#)) used updated air pollution and mortality data and found
19 positive associations between long-term exposure to PM_{2.5} and mortality. Of special note is a
20 statistically significant **reduction** in mortality risk reported with **reduced** long-term fine
21 particle concentrations observed for deaths due to cardiovascular and respiratory causes,
22 but not for lung cancer deaths. There is some evidence for an association between PM_{2.5} and
23 respiratory mortality among post-neonatal infants (ages 1 mo to 1 yr) (see Section 7.4.1). In
24 summary, when deaths due to respiratory causes are separated from all-cause (non-
25 accidental) and cardiopulmonary deaths, there is limited and inconsistent evidence for an
26 effect of PM_{2.5} on respiratory mortality, with one large cohort study finding a reduction in
27 deaths due to respiratory causes associated with reduced PM_{2.5} concentrations, and another
28 large cohort study finding no PM_{2.5} associations with respiratory mortality.

7.3.9. Summary and Causal Determinations

7.3.9.1. PM_{2.5}

29 The epidemiologic studies reviewed in the 2004 PM AQCD suggested relationships
30 between long-term PM₁₀ and PM_{2.5} (or PM_{2.1}) exposures and increased incidence of
31 respiratory symptoms and disease. One of these studies indicated associations with

1 bronchitis in the 24-city cohort (Dockery et al., 1996, [077269](#)). They also suggested
2 relationships between long-term exposure to PM_{2.5} and pulmonary function decrements in
3 the CHS (Gauderman et al., 2000, [012531](#); Gauderman et al., 2002, [026013](#)). These findings
4 added to the database of the earlier 22-city study of PM_{2.1} (Raizenne et al., 1996, [077268](#))
5 that found an association between exposure to ambient particle strong acidity and
6 impairment of lung function in children. No long-term exposure toxicological studies were
7 reported in the 2004 PM AQCD.

8 Recent studies have greatly expanded the evidence available since the 2004 PM
9 AQCD. New analyses have been conducted that include longer follow-up periods of the CHS
10 cohort through 18 years of age and provide evidence that effects from exposure to PM_{2.5}
11 persist into early adulthood. Gauderman et al. (2004, [056569](#)) reported that PM_{2.5} exposure
12 was associated with clinically and statistically significant deficits in FEV₁ attained at the
13 age of 18 years. In addition the strength and robustness of the outcomes were larger in
14 magnitude, and more precise than previous CHS studies with shorter follow-up periods.
15 Supporting this result are new longitudinal cohort studies conducted by other researchers
16 in other locations with different methods. These studies report results for PM₁₀ that is
17 dominated by PM_{2.5}. New studies provide positive associations from Mexico City, Sweden,
18 and a national cystic fibrosis cohort in the U.S. A natural experiment in Switzerland, where
19 PM levels had decreased, reported that improvement in air quality may slow the annual
20 rate of decline in lung function in adulthood, indicating positive consequences for public
21 health. Thus, the data are consistent and coherent across several study designs, locations
22 and researchers. As was found in the 2004 PM AQCD, the studies report associations with
23 PM_{2.5} and PM₁₀, while most did not evaluate PM_{10-2.5}. Associations have been reported with
24 fine particle components, particularly EC and OC. Source apportionment methods generally
25 have not been used in these long-term exposure studies.

26 Coherence and biological plausibility for the observed associations with lung function
27 decrements is provided by recent toxicological studies (Section 7.3.2.2). A recent study
28 demonstrated that pre- and postnatal exposure to ambient levels of urban particles affected
29 mouse lung development, as measured by anatomical and functional indices (Mauad et al.,
30 2008, [156743](#)). Another study suggested that the developing lung may be susceptible to PM
31 since acute exposure to ultrafine iron-soot decreased cell proliferation in the proximal
32 alveolar region of neonatal rats (Pinkerton et al., 2004, [087465](#)) (Section 6.3.5.3). Impaired
33 lung development is a viable mechanism by which PM may reduce lung function growth in
34 children. Other animal toxicological studies have demonstrated alterations in pulmonary
35 function following exposure to DE and WS (Section 7.3.2.2).

36 An expanded body of epidemiologic evidence for the effect of PM_{2.5} on respiratory
37 symptoms and asthma incidence now includes prospective cohort studies conducted by
38 different researchers in different locations, both within and outside the U.S. with different
39 methods. The CHS provides evidence in a prospective longitudinal cohort study that relates

1 PM_{2.5} and bronchitic symptoms and reports larger associations for within-community
2 effects that are less subject to confounding than between-community effects (McConnell et
3 al., 2003, [049490](#)). Several new studies report similar findings with long-term exposure to
4 PM₁₀ in areas where fine particles predominate. In England, an association was seen with
5 an increased prevalence of cough without a cold. Further evidence includes a reduction of
6 respiratory symptoms corresponding to decreasing PM levels in natural experiments in
7 cohorts of Swiss school children (Bayer-Oglesby et al., 2005, [086245](#)) and adults (Schindler
8 et al., 2009, [191950](#)).

9 New studies examine the relationship between long-term PM_{2.5} exposure and asthma
10 incidence. PM_{2.5} had the strongest modifying effect on the association between lung function
11 with asthma in an analysis of the CHS (Islam et al., 2007, [090697](#)). The loss of protection
12 by high lung function against new onset asthma in high PM_{2.5} communities was observed
13 for all the lung function measures. In the Netherlands, an association with doctor-
14 diagnosed asthma was found in a birth cohort examining the first 4 years of life (Brauer et
15 al., 2007, [090691](#)) Further, findings from an adult cohort suggest that traffic-related PM₁₀
16 contributes to asthma development and that reductions in PM decrease asthma risk
17 (Kunzli et al., 2009, [191949](#)).

18 A large proportion of asthma is driven by allergy, and the majority of recent
19 epidemiologic studies examining allergic (or atopic) indicators found positive associations
20 with PM_{2.5} or PM₁₀ (Section 7.3.6.1). Limited evidence for PM-mediated allergic responses is
21 provided by toxicological studies of DE and woodsmoke, while effects of gasoline exhaust
22 were attributed to gaseous components (Section 7.3.6.2).

23 Long-term PM_{2.5} exposure is associated with pulmonary inflammation and oxidative
24 responses. An epidemiologic study found a relationship between PM_{2.5} and increased
25 inflammatory marker eNO among school children (Dales et al., 2008, [156378](#)). Toxicological
26 studies of pulmonary inflammation have demonstrated mixed results, with subchronic DE
27 exposures generating increases and CAPs and WS inducing little or no response (Section
28 7.3.3.2). The pulmonary inflammation observed with DE was attributable to the particle
29 fraction. Toxicological studies also reported evidence of oxidative responses (Section 7.3.4.1).
30 Adaptation to prolonged DE was observed for some oxidative responses in addition to some
31 allergic and pulmonary function responses (Section 7.3.2.2 and 7.3.6.2).

32 Additional support for the relationship between long-term PM_{2.5} exposures and
33 respiratory outcomes is provided by pulmonary injury responses observed in toxicological
34 studies (Section 7.3.5.1). Markers of pulmonary injury were increased in rats exposed to DE
35 and gasoline exhaust; and these changes were attributable to PM. Further, lung DNA
36 methylation was observed in the gasoline exhaust study. Histopathological changes have
37 also been reported following exposure to heavily-trafficked urban air and to woodsmoke.
38 Findings include nasal and airway mucous cell hyperplasia accompanied by alterations in
39 mucus production which can lead to a loss of mucus-mediated protective functions;

1 exacerbation of protease-induced emphysema; and mast cell infiltration and hypertrophy of
2 alveolar walls. These results provide biological plausibility for adverse respiratory outcomes
3 following long-term PM exposure.

4 Limited information is available on host defense responses (Section 7.3.7) and
5 respiratory mortality (Section 7.3.8) resulting from PM_{2.5} exposure. Several recent
6 epidemiologic studies suggest a relationship between long-term exposure to PM_{2.5} or PM₁₀
7 and infection in children and infants (Section 7.3.7.1). A few toxicological studies suggest
8 that DE exposure affects systemic immunity, and although impaired bacterial clearance is
9 associated with short-term exposures to DE, neither DE or gasoline exhaust seems to have
10 this effect after longer exposures (Section 7.3.7.2).

11 In summary, the strongest evidence for a relationship between long-term exposure to
12 PM_{2.5} and respiratory morbidity is provided by epidemiologic studies demonstrating
13 associations with decrements in lung function growth in children and with respiratory
14 symptoms and disease incidence in adults. Mean PM_{2.5} concentrations in these study
15 locations ranged from 13.8 to 30 µg/m³ during the study periods. These studies provide
16 evidence for associations in areas where PM is predominantly fine particles. A major
17 challenge to interpreting the results of these studies is that the PM size fractions and
18 concentrations of other air pollutants are often correlated; however, the consistency of
19 findings across different locations supports an independent effect of PM_{2.5}. Recent
20 toxicological studies provide support for the associations with PM_{2.5} and decreases in lung
21 function growth in children. Pre- and postnatal exposure to ambient levels of urban
22 particles was found to affect mouse lung development, which provides biological plausibility
23 for the epidemiologic findings. Recent subchronic and chronic toxicological studies also
24 demonstrate altered pulmonary function, mild inflammation, oxidative responses,
25 histopathological changes including mucus cell hyperplasia and enhanced allergic
26 responses in response to CAPs, DE, urban air and woodsmoke and provide further
27 coherence and biological plausibility. Exacerbation of emphysematous lesions was noted in
28 one study involving exposure to urban air in a heavily-trafficked area. **Collectively, the
29 evidence is sufficient to conclude that the relationship between long-term PM_{2.5} exposure and
30 respiratory effects is likely to be causal.**

7.3.9.2. PM_{10-2.5}

31 The 2004 PM AQCD did not report long-term exposure studies for PM_{10-2.5}. The only
32 recent study to evaluate long-term exposure to PM_{10-2.5} found positive, but not statistically
33 significant associations with eNO (Dales et al., 2008, [156378](#)). The evidence is **inadequate to
34 determine if a causal relationship exists between long-term PM_{10-2.5} exposures and respiratory
35 effects.**

7.3.9.3. Ultrafine PM

1 The 2004 PM AQCD did not report long-term exposure studies for ultrafine PM. The
2 current evidence for long-term ultrafine PM effects is limited to toxicological studies.
3 Generally, subchronic exposure to DE induced pulmonary inflammation, which was in
4 contrast to ultrafine CAPs exposure (Section 7.3.3.2) It appeared that the PM fraction was
5 responsible for the inflammatory response with DE exposure. Long-term exposure to DE
6 also resulted in oxidative and allergic responses, although lung injury was not remarkable
7 (Sections 7.3.4.1 and 7.3.6.2). The evidence is **inadequate to determine if a causal relationship**
8 **exists between long-term UFP exposures and respiratory effects.**

7.4. Reproductive, Developmental, Prenatal and Neonatal Outcomes

7.4.1. Epidemiologic Studies

9 This section evaluates and summarizes the scientific evidence on PM and
10 developmental and pregnancy outcomes and infant mortality. Infants and fetal development
11 processes may be particularly vulnerable to PM exposure, and although the physical
12 mechanisms are not fully understood, several hypotheses have been proposed involving
13 direct effects on fetal health, altered placenta function, or indirect effects on the mother's
14 health (Bracken et al., 2003, [156288](#); Clifton et al., 2001, [156360](#); Maisonet et al., 2004,
15 [156725](#); Schatz et al., 1990, [156073](#); Sram et al., 2005, [087442](#)). Study of these outcomes
16 can be difficult given the need for detailed data and potential residential movement of
17 mothers during pregnancy. Two recent articles have reviewed methodological issues
18 relating to the study of outdoor air pollution and adverse birth outcomes (Ritz and Wilhelm,
19 2008, [156914](#); Slama et al., 2008, [156985](#)). Some of the key challenges to interpretation of
20 these study results include the difficulty in assessing exposure as most studies use existing
21 monitoring networks to estimate individual exposure to ambient PM; the inability to
22 control for potential confounders such as other risk factors that affect birth outcomes (e.g.,
23 smoking); evaluating the exposure window (e.g., trimester) of importance; and limited
24 evidence on the physiological mechanism of these effects (Ritz and Wilhelm, 2008, [156914](#);
25 Slama et al., 2008, [156985](#)). Another uncertainty is whether PM effects differ by the child's
26 sex. A review of pre-term birth and low birth weight studies found limited indication that
27 effects may differ by gender, however sample size was limited (Ghosh et al., 2007, [091233](#)).

28 Previous summaries of the association between PM concentrations and pregnancy
29 outcomes and infant mortality were presented in previous PM AQCDs. The 1996 PM AQCD
30 concluded that although few studies had been conducted on the link between PM and infant
31 mortality, the research “suggested an association,” particularly for post-neonates (U.S. EPA,

1 1996, [079380](#)). In the 2004 PM AQCD, additional evidence was available on PM's effect on
2 fetal and early postnatal development and mortality (U.S. EPA, 2004, [056905](#)) and although
3 some studies indicated a relationship between PM and pregnancy outcomes, others did not.
4 Studies identifying associations found that exposure to PM₁₀ early during pregnancy (first
5 month of pregnancy) or late in the pregnancy (six weeks prior to birth) were linked with
6 higher risk of preterm birth, including models adjusted for other pollutants, and that PM_{2.5}
7 during the first month of pregnancy was associated with interuterine growth restriction.
8 However, other work did not identify relationships between PM₁₀ exposure and low birth
9 weight. The state of the science at that time, as indicated in the 2004 PM AQCD, was that
10 the research provided mixed results based on studies from multiple countries, and that
11 additional research was required to better understand the impact of PM on pregnancy
12 outcomes and infant mortality. Considering evidence from recent studies discussed below,
13 along with previous AQCD conclusions, epidemiologic studies consistently report
14 associations between PM₁₀ and PM_{2.5} exposure and low birth weight and infant mortality,
15 especially during the post-neonatal period. Animal toxicological evidence supports these
16 associations with PM_{2.5}, but provides little mechanistic information or biological
17 plausibility. Information on the ambient concentrations of PM₁₀ and PM_{2.5} in these study
18 sites can be found in Table 7-5.

Low Birth Weight

19 A large number of studies have investigated exposure to ambient PM and low birth
20 weight at term, including a U.S. national study, as well as two studies in the northeast
21 U.S., and four in California have been conducted. Parker and Woodruff (2008, [156846](#))
22 linked U.S. birth records for singletons delivered at 40 wk gestation in 2001-2003 during
23 the months of March, June, September and December to quarterly estimates of PM
24 exposure by county of residence and month of birth. They found an association between
25 PM_{10-2.5} and birthweight (-13 g [95% CI: -18.3 to -7.6]) per 10 µg/m³ increase), but no such
26 association for PM_{2.5}.

27 Maisonet et al. (2001, [016624](#)) analyzed 89,557 births (1994-96) in six northeastern
28 cities (Boston and Springfield MA, Hartford CT, Philadelphia and Pittsburgh PA,
29 Washington DC). Each city had three PM₁₀ monitors measuring every sixth day. Results
30 from multiple monitors were averaged in each city. Exposure was determined for each
31 trimester of pregnancy and categorized by quartiles (<25, 25-30, 31-35, 36-43 µg/m³) and
32 95th percentile (>43µg/m³). There was no increased risk for low birth weight at term
33 associated with PM₁₀ exposure during any trimester of pregnancy. When birth weight was
34 considered as a continuous outcome, exposure to PM₁₀ was not associated with a reduction
35 in mean birth weight.

Table 7-5. Characterization of ambient PM concentrations from studies of reproductive, developmental, prenatal and neonatal outcomes and long-term exposure.

Reference	Location	Mean Annual Concentration ($\mu\text{g}/\text{m}^3$)	Upper Percentile Concentrations ($\mu\text{g}/\text{m}^3$)
<i>PM_{2.5}</i>			
Basu et al. (2004, 087896)	CA	Range of means across sites: 14.5-18.2 Avg of means across sites: 16.2	Max: 26.3-34.1
Bell et al. (2007, 091059)	CT & MA	22.3	
Brauer et al. (2008, 156292)	Vancouver, Canada	5.3	Max: 37.0
Huynh et al. (2006, 091240)	CA	Range of means across trimesters: 17.5-18.8 Avg of means across trimesters: 18.2	
Jalaludin et al. (2007, 156601)	Sydney, Australia	9.0	
Liu (2007, 090429)	Multicity, Canada	12.2	75th: 15
Loomis et al. (1999, 087288)	Mexico City	27.4	Max: 85
Mannes et al. (2005, 087895)	Sydney, Australia	9.4	75th: 11.2; Max: 82.1
Parker et al. (2005, 087462)	CA	15.4	
Ritz et al. (2007, 096146)	Los Angeles, CA	20.0	
Wilhelm and Ritz (2005, 088668)	Los Angeles, CA	21.0	Max: 38.9-48.5
Woodruff et al. (2006, 088758)	CA	19.2 ^a	75th: 22.7
Woodruff et al. (2008, 098386)	U.S.	Range of means across effects: 14.5-14.9 ^a Avg of means across effects: 14.8 ^a	75th: 18.5-18.7
<i>PM_{10.2.5}</i>			
Parker et al. (2008, 156013)	U.S.	13.2	75th: 17.5
<i>PM₁₀</i>			
Bell et al. (2007, 093256)	CT & MA	22.3	
Brauer et al. (2008, 156292)	Vancouver, Canada	12.7	Max: 35.4
Chen et al. (2002, 024945)	Washoe County, NV	31.53	75th: 39.35; Max: 157.32
Gilboa et al. (2005, 087892)	TX	23.8 ^a	75th: 29
Ha et al. (2003, 042552)	Seoul, South Korea	69.2	75th: 87.7; Max: 245.4
Hansen et al. (2006, 089818)	Brisbane, Australia	19.6	Max: 171.7
Hansen et al. (2007, 090703)	Brisbane, Australia	19.6	75th: 22.7; Max: 171.7
Jalaludin et al. (2007, 156601)	Sydney, Australia	16.3	
Kim et al. (2007, 156642)	Seoul, Korea	Range of means across time: 88.7-89.7 Avg of means across time: 89.2	
Lee et al. (2003, 043202)	Seoul, Korea	71.1	75th: 89.3; Max: 236.9
Leem et al. (2006, 089828)	Incheon, Korea	53.8 ^a	75th: 64.6; Max: 106.39
Lipfert et al. (2000, 004103)	U.S.	33.1	Max: 59
Maisonet et al. (2001, 016624)	NE U.S.	31.0 ^a	75th: 36.1; Max: 46.5
Mannes et al. (2005, 087895)	Sydney, Australia	16.8	75th: 19.9; Max: 104.0
Pereira et al. (1998, 007264)	Sao Paulo, Brazil	65.04	Max: 192.8
Ritz et al. (2000, 012068)	CA	49.3	Max: 178.8
Ritz et al. (2006, 089819)	CA	46.3	Max: 83.5
Rogers and Dunlop (2006, 091232)	GA	3.75	75th: 15.07
Romieu et al. (2004, 093074)	Ciudad Juarez, Mexico	33.0-45.9	

Reference	Location	Mean Annual Concentration ($\mu\text{g}/\text{m}^3$)	Upper Percentile Concentrations ($\mu\text{g}/\text{m}^3$)
Sagiv et al. (2005, 087468)	PA	Range of means across time: 25.3-27.1 Avg of means across time: 26.2	Max: 68.9-156.3
Salam et al. (2005, 087885)	CA	Range of means across trimesters: 45.4-46.6 Avg of means across trimesters: 45.8	
Suh et al. (2008, 192077)	Seoul, Korea	Range of means across trimesters: 54.6-61.1 Avg of means across trimesters: 58.27	75th: 62.8-67.8 Max: 85.1-107.36
Tsai et al. (2006, 090709)	Kaohsiung, Taiwan	81.5	75th: 111.5; Max: 232.0
Wilhelm and Ritz (2005, 088668)	Los Angeles, CA	38.1	Max: 74.6-103.7
Woodruff et al. (2008, 098386)	U.S.	Range of means across effects: 28.6-29.8 ^a Avg of means across effects: 29.1 ^a	75th: 33.8-36.5
Yang et al. (2006, 090760)	Taipei, Taiwan	53.2	75th: 64.9; Max: 234.9

^aMedian concentration

1 In contrast, Bell et al. (2007, [093256](#)) reported positive associations for both PM_{2.5} and
2 PM₁₀ with birth weight in a study of births (n = 358,504) in Connecticut and Massachusetts
3 (1999-2002). Birth data indicated county, not street address or ZIP code, so women were
4 assigned exposure based on county residence at delivery. The difference in birth weight per
5 10 $\mu\text{g}/\text{m}^3$ associated with PM_{2.5} was -66.8 (95% CI: 77.7 to -55.9) gm. For PM₁₀ it was -11.1
6 (95% CI: -15.0 to -7.2) gm. The increased risk for low birth weight was OR = 1.054 (95% CI:
7 1.022-1.087) for PM_{2.5} and OR = 1.027 (95% CI: 0.991-1.064) for PM₁₀, based on average
8 exposure during pregnancy. Reductions in birth weight were also associated with third
9 trimester exposure to PM₁₀ and second and third trimester exposure to PM_{2.5}. Comparing
10 this study to Maisonet et al. (2001, [016624](#)), a larger sample size was able to detect a small
11 increase in risk. In addition, birth weight was reduced more by exposure to PM_{2.5} than by
12 exposure to PM₁₀. Measured PM_{2.5} concentrations were not available in the earlier study.

13 The Children's Health Study is a population based cohort of children living in 12
14 southern California communities, selected on the basis of differing levels of air pollution
15 (Salam et al., 2005, [087885](#)), as previously discussed in Section 7.3. The children in grades
16 4, 7 and 10 were recruited through schools. A subset of this cohort (n = 6,259) were born in
17 California from 1975-1987. Of these, birth certificates were located for 4,842, including
18 3,901 infants born at term and 72 cases of low birth weight at term. Using the mother's ZIP
19 code at the time of birth, exposure was determined by inverse distance weighting of up to 3
20 PM₁₀ monitors within 50 km of the ZIP code centroid. If there was a PM₁₀ monitor within 5
21 km of the ZIP code centroid (40% of data), exposure from that monitor was used. Exposure
22 was calculated for the entire pregnancy, and for each trimester of pregnancy. A 10 $\mu\text{g}/\text{m}^3$
23 increase in PM₁₀ during the third trimester reduced mean birth weight -10.9 g (95% CI:
24 -21.1 to -0.6) in single pollutant models, but became non-significant in multipollutant
25 models controlling for the effects of O₃. Increased risks of low birth weight (<2500 gm) were
26 not statistically significant (OR = 1.3 [95% CI: 0.9-1.9]). A strength of this study was the
27 cohort data available included information on SES and smoking during pregnancy. A

1 limitation is the assignment of exposure based on monitoring stations up to 50 km distant;
2 this may have introduced significant exposure misclassification obscuring some
3 associations.

4 Parker et al. examined births in California within 5 miles of a monitoring station
5 (n = 18,247) (Parker et al., 2005, [087462](#)). Only infants born at 40 wk gestation were
6 included. Thus all infants were the same gestational age, and had been exposed in the same
7 year. Exposure to PM_{2.5} in quartiles (<11.9, 11.9-13.9, 14.0-18.4, >18.4) was associated with
8 decrements in birth weight. Infants exposed to >13.9 µg/m³ experienced reductions in birth
9 weight (third quartile -13.7 g (95% CI: -34.2 to 6.9), fourth quartile -36.1 g (95% CI: -55.8 to
10 -16.5). These are larger reductions than have been seen in some other studies. However,
11 this study reduced misclassification by including only women living within 5 miles of a
12 monitoring station, and only included births at 40 wk gestation. Reducing misclassification
13 should lead to a stronger association, if the association is causal.

14 The effects of spatial variation in exposure were also investigated by Wilhelm and
15 Ritz (2005, [088668](#)). Their study included all women living in ZIP codes where 60% of the
16 ZIP code was within two miles of a monitoring station in the Southern California Basin,
17 and women with known addresses in Los Angeles County within 4 miles of a monitoring
18 station. Exposure to average PM₁₀ in the third trimester was analyzed for increased risk of
19 low birth weight at term (≥ 37-wk gestation). Analysis at the ZIP code level did not detect
20 increased risk (per 10 µg/m³ PM₁₀, OR = 1.03 [95% CI: 0.97-1.09]). However the analysis
21 based on geocoded addresses indicated that increasing exposure to PM₁₀ was associated
22 with increased risk of low birth weight for women living within 1 mile of the station where
23 PM₁₀ was measured. For these women (n = 247 cases, 10,981 non-cases), each 10 µg/m³
24 increase in PM₁₀ was associated with a 22% increase in risk of term low birth weight
25 (OR = 1.22 [95% CI: 1.05-1.41]). In the categorical analysis, exposure to PM₁₀ >44.4 µg/m³
26 was associated with a 48% increase in risk (OR = 1.48 [95% CI: 1.00-2.19]). Increased risk
27 of low birth weight also was associated with exposure to CO in single pollutant models.
28 However, when multipollutant models were considered, the effects of CO were attenuated
29 but the effects of PM₁₀ increased. Controlling for CO, NO₂, and O₃, each 10 µg/m³ increase
30 in exposure to PM₁₀ increased risk of low birth weight 36% (OR = 1.36 [95% CI: 1.12-1.65]).

31 Spatial variation in PM_{2.5} exposure was investigated by Basu et al. (2004, [087896](#)).
32 They included only mothers who lived within 5 miles of a PM_{2.5} monitor and within a
33 California county with at least one monitor. To minimize potential confounding, they
34 included only white (n = 8597) or Hispanic (n = 8114) women, who were married, between
35 20-30 years of age, completed at least high school and were having their first child.
36 Consistently, PM_{2.5} exposure measured by the county monitor was more strongly associated
37 with reductions in birth weight than exposure measured by the neighborhood monitor. The
38 results were replicated in both the white and the Hispanic samples. Reductions in birth
39 weight ranged from 15.2 g to 43.5 g per 10 µg/m³ increase in PM_{2.5}.

1 In the remaining U.S. study, Chen et al. (2002, [024945](#)) analyzed 33,859 birth
2 certificates of residents of Washoe County in northern Nevada (1991-1999). There were four
3 sites monitoring PM₁₀ during the study period, it appears (not stated) that exposure was
4 averaged over the county. A 10 µg/m³ increase in exposure to PM₁₀ during the third
5 trimester of pregnancy was associated with an 11 gm reduction in birth weight (95% CI:
6 -2.3 to -19.8). Effects on risk of low birth weight were not significant. For exposure in the
7 third trimester of 19.77 to 44.74 µg/m³ compared to <19.74 µg/m³ the odds ratio for low
8 birth weight was 1.05 (95% CI: 0.81-1.36). Comparing exposure >44.74 to the same
9 reference category, the odds ratio was 1.10 (95% CI: 0.71-1.71). Misclassification of exposure
10 may have occurred when exposure was averaged over a large geographic area (16,968 km²).

11 Recent international studies investigating effects of particles on low birth weight
12 include one in Munich (Slama et al., 2007, [093216](#)), two in Canada (Brauer et al., 2008,
13 [156292](#); Dugandzic RDodds et al., 2006, [088681](#)), two in Australia (Hansen et al., 2007,
14 [090703](#); Mannes et al., 2005, [087895](#)), two in Taiwan (Lin et al., 2004, [089827](#); Yang et al.,
15 2003, [087886](#)) one in Korea (Ha et al., 2003, [042552](#)) and two in Sao Paulo, Brazil (Gouveia
16 et al., 2004, [055613](#); Medeiros and Gouveia, 2005, [089824](#)). The majority of these studies
17 found that PM concentrations were associated with low birth weight, though two studies
18 (Hansen et al., 2007, [090703](#); Lin et al., 2004, [089827](#)) found no associations. The effect
19 estimates were similar in magnitude to those reported in the U.S. studies.

Issues in Interpreting Results of Low Birth Weight Studies

20 Studies included subjects at distances from monitoring stations varying from as close
21 as 1 mile or 2 km, to as far as 50 km or the size of the county. However, studies that only
22 included subjects living within a short distance (1 mile, 2 km) of the monitoring station
23 (thus likely reducing exposure measurement error) were more likely to find that PM
24 exposure was associated with increased risk of low birth weight. However, Basu et al.
25 (2004, [087896](#)) reported a stronger association between PM_{2.5} exposure and birth weight
26 when exposure was estimated based on the county monitor, rather than the monitor within
27 5 miles of the residence. They suggest that county level exposure may be more
28 representative of where women spend their time, including not only home, but also other
29 time spent away from home. Other pollutants also appeared to influence the risk associated
30 with particle exposure. In one study, exposure to PM₁₀ in a single pollutant model reduced
31 birth weight by 11 g, but became non-significant in multipollutant models with O₃ (Salam et
32 al., 2005, [087885](#)). In another study the risk associated with PM₁₀ exposure increased from
33 22% to 36% when other pollutants were included in the model (Wilhelm and Ritz, 2005,
34 [088668](#)). All but one study in the U.S. found some association between particle exposure
35 and reduced birth weight (Maisonet et al., 2001, [016624](#)). The results of international
36 studies were inconsistent. This might be related to the chemical composition of particles in
37 the U.S., or to differences in the pollutant mixture. Studies with null results must be

1 interpreted with caution when the comparison groups have significant exposure. This was
2 certainly the situation in studies in Taiwan and Korea (Lee et al., 2003, [043202](#); Lin et al.,
3 2004, [089827](#); Yang et al., 2003, [087886](#)). Differences in geographical locations, study
4 samples and linkage decisions may contribute to the diverse findings in the literature on
5 the association between PM and birthweight, even within the U.S. (Parker and Woodruff,
6 2008, [156846](#)).

Preterm Birth

7 A potential association of exposure to airborne particles and preterm birth has been
8 investigated in numerous epidemiologic studies, including some conducted in the U.S. and
9 others in foreign countries. Three U.S. studies have been carried out by the same group of
10 investigators in California.

11 A natural experiment occurred when an open-hearth steel mill in Utah Valley was
12 closed from August 1986 through September 1987. Parker et al. (2008, [156013](#)) compared
13 birth outcomes for Utah mothers within and outside of the Utah Valley, before, during, and
14 after the mill closure. They report that mothers who were pregnant around the time of the
15 closure of the mill were less likely to deliver prematurely than mothers who were pregnant
16 before or after. The strongest effect estimates were observed for exposure during the second
17 trimester (14% decrease in risk of preterm birth during mill closure). Preterm birth outside
18 of the Utah Valley did not change during the time of the mill closure.

19 In 2000, Ritz et al. (2000, [012068](#)) published the first study investigating the
20 association of preterm birth with PM in the U.S. The study population was women living in
21 the southern California Basin. There were 8 monitoring stations measuring PM₁₀ every
22 sixth day during the study period. Birth certificates (1989-1993) were analyzed for women
23 living in zip codes within 2 miles of a monitoring station. Women with multiple gestations,
24 chronic disease prior to pregnancy and women who delivered by cesarean section were
25 excluded resulting in a study population of 48,904 women. The risk of preterm birth
26 increased by 4% (RR = 1.04 [95% CI: 1.02-1.6]) per 10 µg/m³ increase in PM₁₀ averaged in
27 the 6 wk before birth. Exposure to PM₁₀ in the first month of pregnancy resulted in a 3%
28 increase in risk (RR = 1.03 [95% CI: 1.01-1.05]). These results were robust in multipollutant
29 models.

30 Wilhelm and Ritz (2005, [088668](#)) reinvestigated this association among women in the
31 same area in 2005, when air pollution had declined from a mean level near 50 µg/m³ to a
32 mean level near 40 µg/m³. Birth certificate data from 1994-2000 was analyzed for women
33 living in ZIP codes within 2 miles of a monitoring station, or with addresses within 5 miles
34 of the monitoring station. No significant effects of exposure to PM₁₀ were reported.
35 Exposure to PM_{2.5} 6 wk before birth resulted in an increase in preterm birth (RR = 1.19
36 [95% CI: 1.02-1.40]) for the highest quartile of exposure (PM_{2.5} >24.3 µg/m³). Using a

1 continuous measure of PM_{2.5}, there was a 10% increase in risk for each 10 µg/m³ increase in
2 PM_{2.5} (RR = 1.10 [95% CI: 1.00-1.21]).

3 There have been two major criticisms of air pollution studies using birth certificate
4 data. First, that birth certificates only indicate the address at birth and the exposure of
5 women who moved during pregnancy may be misclassified; second, that information about
6 some important confounders may not be available (e.g., smoking). To obtain more precise
7 information about these variables, Ritz et al. (2007, [096146](#)) conducted a case control study
8 nested within a cohort of birth certificates (Jan 2003-Dec 2003) in Los Angeles County.
9 Births to women residing in ZIP codes (n = 24) close to monitoring stations or major
10 population centers or roadways (n = 87) were eligible (n = 58,316 births). All cases of low
11 birth weight or preterm birth and an equal number of randomly sampled controls in the 24
12 zip codes close to monitors were selected. In the other 87 ZIP codes, 30% of cases and an
13 equal number of controls were randomly sampled. Of 6,374 women selected for the case
14 control study, 2,543 (40%) were interviewed. The association of preterm birth with exposure
15 to PM_{2.5} differed between women responding to the survey and women who did not respond.
16 Among responders, exposure to each 10 µg/m³ increase in PM_{2.5} concentration in the first
17 trimester increased risk to preterm birth by 23% (RR = 1.23 [95% CI: 1.02-1.48]). There was
18 no increase in risk among non-responders (RR = 0.95 [95% CI: 0.82-1.10]), or in the entire
19 birth cohort (RR = 1.00 [95% CI: 0.94-1.07]).

20 An additional case control study of preterm birth and PM_{2.5} exposure Huynh et al.
21 (2006, [091240](#)) used California birth certificate data. Singleton preterm infants (24-36-wk
22 gestation) born in California (1999-2000) whose mothers lived within 5 miles of a PM_{2.5}
23 monitor were eligible. Each of these 10,673 preterm infants were matched to three term
24 (39-44-wk gestation) controls (having a last menstrual period within 2 wk of the case
25 infant), resulting in a study population of 42,692. Controlling for maternal race/ethnicity,
26 education, marital status, parity and CO exposure, exposure to PM_{2.5} >17.7 µg/m³ increased
27 the risk of preterm birth by 14% (OR = 1.14 [95% CI: 1.07-1.23]). Averaging PM_{2.5} exposure
28 over the first month of pregnancy, the last 2 wk before birth, or the entire pregnancy did not
29 substantially change the risk estimate.

30 Two additional studies of preterm birth and exposure to particulate air pollution have
31 been conducted in the U.S. Each has used a unique methodology. Sagiv et al. (2005, [087468](#))
32 used time series to analyze births in four Pennsylvania counties between January 1997 and
33 December 2001. In this analysis, exposure to PM₁₀ is compared to the rate of preterm births
34 each day. Both acute exposure (on the day of birth) and longer term exposure (average
35 exposure for the preceding six weeks) were considered in the analysis. An advantage of this
36 analysis is that days, rather than individuals are compared, so confounding by individual
37 risk factors is minimized. For exposure averaged over the 6 wk prior to birth, there was a
38 non-significant increase in risk (RR = 1.07 [95% CI: 0.98-1.18]); for acute exposure with a 2

1 day lag (RR = 1.10 [95% CI: 1.00-1.21]) and 5 day lag (RR = 1.07 95% CI: 0.98-1.18]) results were marginal.

3 Rogers and Dunlop (2006, [091232](#)) examined exposure to particles and risk of delivery of an infant weighing less than 1500 g (all of which were preterm) from 24 counties in Georgia. The study included 69 preterm small for gestational age (SGA) infants, 59 preterm appropriate for gestational age (AGA) infants and 197 term AGA controls. Exposure was estimated using an environmental transport model that considered PM₁₀ emissions from 32 geographically located industrial point sources, meteorological factors, and geographic location of the birth home. Exposure was categorized by quartiles. Comparing women who delivered a preterm AGA infant to those who delivered a term AGA infant, exposure to PM₁₀>15.07 µg/m³ tripled the risk (OR = 3.68 [95% CI: 1.44-9.44]).

12 Brauer et al. (2008, [156292](#)) evaluated the impacts of PM_{2.5} on preterm birth using spatiotemporal exposure metrics in Vancouver, Canada. The authors found similar results when they used a land-use regression model or inverse distance weighting as the exposure metric. For preterm births <37 wk, they reported an OR of 1.06 (95% CI: 1.01-1.11), and for preterm births <35 wk the OR increased to 1.12 (95% CI: 1.02-1.24). There were no consistent trends for early or late gestational period to be more strongly associated with preterm births.

19 Suh et al. (2008, [192077](#)) conducted a study to determine if the effects of exposure to PM₁₀ during pregnancy on preterm delivery are modified by maternal polymorphisms in metabolic genes. They analyzed the effects of the gene-environment interaction between the GSTM1, GSTT1, CYP1a1-T6235C and -1462V polymorphisms and exposure to PM₁₀ during pregnancy on preterm birth in a case-control study in Seoul, Korea. PM₁₀ concentration ≥ 75th percentile alone was significant in the third trimester of pregnancy (OR = 2.33 [95% CI: 1.33-4.80]), but not in the first or second trimester. The risk of preterm delivery conferred by the GSTM1 null genotype was increased, and the highest risk was found during the third trimester of pregnancy (OR = 2.58 [95% CI: 1.34-4.97]). There were no statistical associations with the GSTT1 or CYP1A1 genotypes. When the gene-environment interaction was analyzed, the risk for preterm birth was significantly higher for women who carried the GSTM1 null genotype and were exposed to high levels of PM₁₀ (≥ 75th percentile) than for those who carried the GSTM1 positive genotype but were only exposed to low levels of PM₁₀ (<75th percentile) during the third trimester of pregnancy (OR = 6.22, 95% CI: 2.14-18.08).

34 In Incheon, Korea, Leem et al. (2006, [089828](#)) estimated PM₁₀ exposure spatially as well as temporally. Exposure was based on 26 monitors and kriging was used to determine exposure for 120 dong (administrative districts, mean area 7.82 km², median area 1.42 km³). The sample included 52,113 births, from 2001-2002. PM₁₀ was very weakly correlated with other pollutants. Exposure was compared in quartiles for the first and third trimester of pregnancy. In the first trimester, relative risks for the second, third and fourth quartiles

1 were RR = 1.14 (95% CI: 0.97-1.34), RR = 1.07 (95% CI: 0.94-1.37), and RR = 1.24 (95% CI:
2 1.09-1.41), respectively. Exposure to PM₁₀ in quartile one (reference group) was 26.9 -
3 45.9 µg/m³; fourth quartile exposure equaled 64.6-106.4 µg/m³. The p-value for trend was
4 0.02. Exposure in the third trimester was not related to preterm birth, however no
5 information was provided to determine how exposure in the third trimester was adjusted
6 for women who delivered preterm.

7 Two studies investigating risks of preterm birth related to particle exposure have
8 been reported from Australia. In Brisbane, Hansen et al. (2006, [089818](#)) studied 28,200
9 births (2000-2003) in an area of low PM₁₀ concentrations. Exposure to an interquartile
10 range increase in PM₁₀ exposure in the first trimester resulted in a 15% increased risk of
11 preterm birth (OR = 1.15 [95% CI: 1.06-1.25]). This result was strongly influenced by the
12 effect of PM₁₀ exposure in the first month of pregnancy (OR = 1.19 [95% CI: 1.13-1.26]).
13 PM₁₀ was correlated with ozone r = (0.77) in this study and ozone also increased risk in the
14 first trimester. No effects were associated with exposure to PM₁₀ in the third trimester.

15 In Sydney, associations between exposure to particles and preterm birth varied by
16 season. Jalaludin et al. (2007, [156601](#)) obtained information on all births in metropolitan
17 Sydney (1998-2000). Exposure to PM_{2.5} in the three months preceding birth was associated
18 with an increased risk of preterm birth (OR = 1.11 [95% CI: 1.04-1.19]). Additional effects
19 were dependent on season of conception. Both PM₁₀ (OR = 1.3 95% CI: 1.2-1.5) and PM_{2.5}
20 (OR = 1.4 [95% CI: 1.3-1.6]) were associated with increased risk for conceptions in the
21 winter. Conceptions in summer were associated with reductions in risk (PM₁₀ OR = 0.91
22 [95% CI: 0.88-0.93]) (PM_{2.5} OR = 0.87 [95% CI: 0.84-0.92]). Due to both positive and
23 negative findings, the authors recommend caution in interpreting their results.

Issues in Analyzing Environmental Exposures and Preterm Birth

24 A major issue in studying environmental exposures and preterm birth is selecting the
25 relevant exposure period, since the biological mechanisms leading to preterm birth and the
26 critical periods of vulnerability are poorly understood (Bobak, 2000, [011448](#)). Exposures
27 proximate to the birth may be most relevant if exposure causes an acute effect. However,
28 exposure occurring in early gestation might affect placentation, with results observable
29 later in pregnancy, or cumulative exposure during pregnancy may be the most important
30 determinate. The studies reviewed have dealt with this issue in different ways. Many have
31 considered several exposure metrics based on different periods of exposure.

32 Often the time periods used are the first month (or first trimester) of pregnancy and
33 the last month (or six weeks) prior to delivery. Using a time interval prior to delivery
34 introduces an additional problem since cases and controls are not in the same stage of
35 development when they are compared. For example, a preterm infant delivered at 36 wk, is
36 a 32 wk fetus 4 wk prior to birth, while an infant born at term (40 wk) is a 36 wk fetus 4 wk
37 prior to birth. Only one study (Huynh et al., 2006, [091240](#)) adjusted for this in the design.

1 Many of these studies compare exposure in quartiles, using the lowest quartile as the
2 reference (or control) group. No studies use a truly unexposed control group. If exposure in
3 the lowest quartile confers risk, than it may be difficult to demonstrate additional risk
4 associated with a higher quartile. Thus negative studies must be interpreted with caution.

5 Preterm birth occurs both naturally (idiopathic preterm), and as a result of medical
6 intervention (iatrogenic preterm). Ritz et al. (2000, [012068](#); 2007, [096146](#)) excluded all
7 births by Cesarean section, to limit their studies to idiopathic preterm. No other studies
8 attempted to distinguish the type of preterm birth, although PM exposure maybe associated
9 with only one type. This is a source of potential effect misclassification.

Growth Restriction

10 Low birth weight has often been used as an outcome measure because it is easily
11 available and accurately recorded on birth certificates. However, low birth weight may
12 result from either short gestation, or inadequate growth in utero. Most of the studies
13 investigating air pollution exposure and low birth weight, limited their analysis to term
14 infants to focus on inadequate growth. A number of studies were identified that specifically
15 addressed growth restriction in utero by identifying infants who failed to meet specific
16 growth standards. Usually these infants had birth weights less than the 10th percentile for
17 gestational age, using an external standard. Many of these studies have been previously
18 discussed, since they also examined other reproductive outcomes (low birth weight or
19 preterm delivery).

20 Three studies in the U.S. examined intrauterine growth. A recent study (Rich et al.,
21 2009, [180122](#)) investigated very small for gestational age (defined as a fetal growth ratio
22 <0.75), small for gestational age (defined as ≥ 75 and <85) and “reference” births (≥ 85) to
23 women residing in New Jersey and mean air pollutant concentrations during the first,
24 second and third trimesters. They reported an increased risk of SGA associated with first
25 and third trimester PM_{2.5} concentrations (1.116 [95% CI: 1.012, 1.232], and 1.106 [1.008-
26 1.212], per 10 $\mu\text{g}/\text{m}^3$ PM_{2.5}, respectively). Parker et al. (2005, [087462](#)) reported a positive
27 association between exposure to PM_{2.5}. Since this study only included singleton live births
28 at 40-wk gestation, birth weights less than 2872 g for girls and 2986 g for boys were
29 designated SGA, based on births in California. Infants exposed to the highest quartile PM_{2.5}
30 ($>18.4 \mu\text{g}/\text{m}^3$) compared to the lowest quartile PM_{2.5} ($<11.9 \mu\text{g}/\text{m}^3$) were 23% more likely to
31 be small for gestational age (OR = 1.23 [95% CI: 1.03-1.50]). Very similar results were found
32 for exposure in each of the three trimesters respectively (OR = 1.26 [95% CI: 1.04-1.51],
33 OR = 1.24 [95% CI: 1.04-1.49], OR = 1.21 [95% CI: 1.02-1.43]). These results controlled for
34 exposure to CO, which did not increase risk for SGA.

35 In contrast, Salam et al. (2005, [087885](#)) found no association between exposure to
36 PM₁₀ and intrauterine growth retardation (IUGR) in the California Children’s Health
37 Study. IUGR was defined as less than the 15th percentile of predicted birth weight based on

1 gestational age and sex in term infants. Apparently no external standard was used since
2 15% of infants in the study were designated as IUGR. An IQR increase in PM₁₀ exposure
3 was not significantly associated with IUGR for the whole pregnancy (OR = 1.1 [95% CI: 0.9-
4 1.3]) or for any specific trimester. Differences between this study and the study by Parker et
5 al. (2005, [087462](#)) include measurement of PM₁₀ vs. PM_{2.5}, a less stringent definition of
6 IUGR, and exposures determined by monitors located much farther away from the subjects'
7 residences (up to 50 km vs. within 5 miles). All of these factors could lead to
8 misclassification.

9 Two studies investigating particle exposure and SGA were conducted in Australia,
10 with differing results (Hansen et al., 2007, [090703](#); Mannes et al., 2005, [087895](#)). Mannes et
11 al. (2005, [087895](#)) defined SGA as birth weight less than two standard deviations below the
12 national mean birth weight for gestational age. In this study there was a statistically
13 significant effect of exposure to both PM₁₀ (OR = 1.10 [95% CI: 1.00-1.48], per 10 µg/m³
14 increase) and PM_{2.5} (OR = 1.34 [95% CI: 1.10-1.63], per 10 µg/m³ increase) for exposure
15 during the second trimester. When analysis was restricted to births within 5 km of the
16 monitoring station, the association for PM₁₀ became slightly stronger (OR = 1.22 [95% CI:
17 1.10-1.34]). Exposure during other trimesters of pregnancy was not associated with IUGR.

18 In Brisbane, Hansen et al. (2007, [090703](#)) examined head circumference (HC), crown
19 heel length (CHL) and risk of SGA, defined as less than the tenth percentile of weight for
20 gestational age and gender based on an Australian national standard. There was no
21 consistent relationship between PM₁₀ exposure and SGA, HC or CHL in any trimester of
22 pregnancy. PM₁₀ exposure was determined by averaging values from the five monitoring
23 stations. Due to the sample size and limited number of monitoring stations, it was not
24 possible to analyze the data for women living within 5 km of a monitoring station, as was
25 done in Sydney.

26 In Canada, Liu et al. (2007, [090429](#)) investigated the effect of PM_{2.5} exposure on fetal
27 growth in three cities, Calgary, Edmonton and Montreal. Intrauterine growth retardation
28 (IUGR) was defined as birth weight below the tenth percentile, by sex and gestational week
29 (37-42) for all singleton live births in Canada between 1986 and 2000. Models were
30 adjusted for maternal age, parity, infant sex, season of birth, city of residence, and year of
31 birth. A 10 µg/m³ increase in PM_{2.5} was associated with an increased risk for IUGR
32 (OR = 1.07 [95% CI: 1.03-1.10]) in the first trimester, and similar risks were associated with
33 exposure in the second or third trimesters. The effect of PM_{2.5} was reduced in
34 multipollutant models including CO and NO₂.

35 Brauer et al. (2008, [156292](#)) observed consistent increased risks of SGA for PM_{2.5},
36 PM₁₀, NO₂, NO and CO in Vancouver, Canada (20% increase in risk in PM_{2.5} and PM₁₀ per
37 10 µg/m³ increase). The effects were similar for exposure estimates based on nearest
38 monitor, inverse distance weighting, and land-use regression modeling. ORs for early or

1 late pregnancy exposure windows were remarkably similar to those for the full duration of
2 pregnancy.

Birth Defects

3 Four recent studies examined PM and birth defects. The Seoul, Korea study discussed
4 above also considered congenital anomalies, defined as a defect in the child's body structure
5 (Kim et al., 2007, [156642](#)). PM₁₀ levels were associated with higher risk of birth defects for
6 the second trimester, with a 16% (95% CI: 0-34) increase in risk per 10 µg/m³ in PM₁₀.

7 Two U.S. studies examined air pollution and risk of birth defects. Data were collected
8 from the California Birth Defects Monitoring Program for four counties in Southern
9 California (Los Angeles, Riverside, San Bernardino, and Orange) for the period 1987 to
10 1993, although each county included a subset of this period (Ritz et al., 2002, [023227](#)).
11 Cases (i.e., infants with birth defects) were identified as live birth infants and fetal deaths
12 from 20-wk gestation to 1 year post birth, with isolated, multiple, syndrome, or
13 chromosomal cardiac or orofacial cleft defects. Cases were restricted to those with registry
14 data for gestational age and residence zip code, and those with residences <10 miles from
15 an air pollution monitor. Six types of categories were included: aortic defects; atrium and
16 atrium septum defects; endocrinal and mitral valve defects; pulmonary artery and valve
17 defects; conotruncal defects; and ventricular septal defects not part of the conotruncal
18 category. PM₁₀ measurements were available every six days. While results indicated
19 increased risk of birth defects for higher levels of CO or O₃, the authors determined that
20 results for PM₁₀ were inconclusive, finding no consistent trend of effect after adjustment for
21 CO and O₃.

22 The other U.S. study examined birth defects through a case-control design in seven
23 Texas counties for the period 1997 to 2000 (Gilboa et al., 2005, [087892](#)). Births were
24 excluded for parents <18 years and several non-air pollution risk factors known to be
25 associated with birth defects (e.g., maternal diabetes, holoprosencephaly in addition to oral
26 cleft). Comparison of the highest (≥ 29.0 µg/m³) and lowest (<19.521 µg/m³) quartiles of PM₁₀
27 for exposure defined as the third to eighth weeks of pregnancy generated an OR of 2.27
28 (95% CI: 1.43-3.60) for risk of isolated atrial septal defects and 1.26 (95% CI: 1.03-1.55) for
29 individual atrial septal defects. Including other pollutants (CO, NO₂, O₃, SO₂) in the model
30 did not greatly alter results; numerical results for co-pollutant analysis were not provided.
31 Strong evidence was not observed for a relationship between PM₁₀ and the other birth
32 defect categories. Review articles have concluded that the scientific literature is not
33 sufficient to conclude a relationship between air pollution and birth defects (Sram et al.,
34 2005, [087442](#)).

35 A recent study of oral clefts conducted in Taiwan found no association between this
36 birth defect and concentrations of PM₁₀ during the first or second gestational month

1 (Hwang et al., 2006, [088971](#)). This population-based case-control study included 653 cases
2 and a random sample of 6,530 controls born in Taiwan between 2001 and 2003.

Infant Mortality

3 Many studies have identified strong associations between exposure to particles and
4 increased risk of mortality in adults or the general population, including for short- and
5 long-term exposure (see Section 7.6). Less evidence is available for the potential impact on
6 infant mortality, although studies have been conducted in several countries. The results of
7 these infant mortality studies are presented here with the other reproductive and
8 developmental outcomes because it is likely that in vitro exposures contribute to this
9 outcome. Both long-term and short-term exposure studies of infant mortality are included
10 in this section. Results on PM and infant mortality includes a range of findings, with some
11 studies finding associations and many non-statistically significant or null effects. Yet, more
12 consistency is observed when results are divided into the type of health outcome based on
13 the age of infant and cause of death.

14 An important question regarding the association between PM and infant mortality is
15 the critical window of exposure during development for which infants are susceptible.
16 Several age structures have been explored: infants (<1 year); neonatal (<1 month); and
17 postneonatal (1 month to 1 year). Within these various age categories, multiple causes of
18 deaths have been investigated, particularly total deaths and respiratory-related deaths.
19 The studies reflect a variety of study designs, particle size ranges, exposure periods,
20 regions, and adjustment for confounders.

Stillbirth

21 Only one study of stillbirths and PM was identified. A prospective cohort of pregnant
22 women in Seoul, Korea from 2001 to 2004 was examined with respect to exposure to PM₁₀
23 (Kim et al., 2007, [156642](#)). Gestational age was estimated by the last menstrual period or
24 by ultrasound. Whereas many of the previously discussed studies of PM and pregnancy
25 outcomes were based on national registries, this study examined medical records and
26 gathered individual information through interviews on socio-economic condition, medical
27 history, pregnancy complications, smoking, second-hand smoke exposure, and alcohol use.
28 Mother's exposure to PM₁₀ was based on residence for each month of pregnancy, each
29 trimester defined as a three month period, and the six weeks prior to death. Exposure was
30 assigned by the nearest monitor. A 10 µg/m³ increase in PM₁₀ in the third trimester was
31 associated with an 8% (95% CI: 2-14) increase in risk of stillbirth.

32 In São Paulo, Brazil, Poisson regression of stillbirth counts for the period 1991 and
33 1992 found that a 10 µg/m³ increase in PM₁₀ was associated with a 0.8% increase in
34 stillbirth rates (Pereira et al., 1998, [007264](#)). When other pollutants (NO₂, SO₂, CO, O₃)
35 were included simultaneously in the model, the association did not remain. Stillbirths were
36 defined as fetal loss at >28 wk of pregnancy age, weight >1000 g, or length of fetus >35 cm.

1 As discussed below, there exists some limited evidence for a link between PM and
2 stillbirth.

Infant Mortality and Infant Respiratory Mortality, < 1Year

3 A literature search did not reveal new studies on PM and infant mortality (<1 year)
4 since the previous PM AQCD. Previously conducted studies include a case-control study
5 that reported associations between infant mortality and TSP levels over the period between
6 birth and death for infants in the Czech Republic (Bobak and Leon, 1999, [007678](#)). An
7 ecological study evaluated U.S. PM₁₀ data for the year 1990 using long-term pollution levels
8 in 180 U.S. counties (Lipfert et al., 2000, [004103](#)). The authors found a 9.64% (95% CI: 4.60-
9 14.9) increase in risk of infant mortality for non-low birth weight infants per 10 µg/m³
10 increase in PM₁₀, a 13.4% (95% CI: -10.3 to 43.5%) increase in non-low birth weight
11 respiratory-disease related deaths (ICD-9 460-519) and a 19.5% (95% CI: 0.07-42.8)
12 increase in all non-low birth weight respiratory-related infant deaths (ICD 9 460-519, 769,
13 770).

Neonatal Mortality and Neonatal Respiratory Mortality, < 1 month

14 Studies on PM and neonatal mortality (<1 month) included a time-series analysis of
15 PM₁₀ for four years of data (1998-2000) for São Paulo, Brazil (Lin et al., 2004, [095787](#)). The
16 analysis used daily counts of deaths from government registries and adjusted for temporal
17 trend, day of the week, weather, and holidays. Findings indicated that a 10 µg/m³ increase
18 in PM₁₀ was associated with a 1.71% (95% CI: 0.31-3.32) increase in risk of neonatal death.

19 A case-crossover study of 11 years (1989-2000) in Southern California did not find an
20 association between PM₁₀ and neonatal deaths (Ritz et al., 2006, [089819](#)). Quantitative
21 results were not provided. The authors considered adjustment for season, county, parity,
22 gender, prenatal care, and maternal age, education, and race/ethnicity. The overall levels of
23 PM₁₀ in these studies were similar.

24 These results add to previous work on PM and neonatal death, including studies
25 identifying higher risk of neonatal mortality with higher TSP in the Czech Republic in an
26 ecological analysis (Bobak and Leon, 1992, [044415](#)) and case-crossover study (Bobak and
27 Leon, 1999, [007678](#)), and a Poisson model study in Kagoshima City, Japan (Shinkura et al.,
28 1999, [156978](#)). An ecological study evaluated U.S. PM₁₀ data for the year 1990 using long-
29 term pollution levels in 180 U.S. counties (Lipfert et al., 2000, [004103](#)). Analysis considered
30 birth weight, sex, month of birth, location by state and county, prenatal care, and mother's
31 race, age, educational level, marital status, and smoking status. County-level variables
32 were included for socio-economic status, altitude, and climate. Results indicate a 13.1%
33 increase in neonatal mortality (95% CI: 4.4-22.6) per 10 µg/m³ PM₁₀ for non-low birth
34 weight infants. Statistically significant associations were also observed considering all
35 infants or low birth weight infants. However, higher levels of SO₂ were associated with
36 lower risk of infant mortality. When sulfate and an estimate of non-sulfate particles were

1 included in the regression simultaneously, associations were observed with non-sulfate
2 particles and an inverse relationship with sulfate particles. Respiratory neonatal mortality
3 was not associated with higher TSP in the Czech Republic case-control study (Bobak and
4 Leon, 1999, [007678](#)).

Postneonatal Mortality and Post-neonatal Respiratory Mortality, 1 Month–1 Year

5 Several studies have been conducted on PM and postneonatal mortality since the
6 previous PM AQCD, including three from the U.S., one from Mexico, and three from Asia.
7 Two case-control studies examined the risk of PM to postneonatal death in California.
8 Research focused on Southern California for the period 1989 to 2000 linked birth and death
9 certificates and considered PM₁₀ two months prior to death with adjustment for prenatal
10 care, gender, parity, county, season, and mother's age, race/ethnicity, and education (Ritz et
11 al., 2006, [089819](#)). As previously noted, this study did not find an association between PM₁₀
12 and neonatal mortality (<1 month), however an association was observed for postneonatal
13 mortality, with a 10 µg/m³ increase in PM₁₀ associated with a 4% (95% CI: 1-6) increase in
14 risk. The exposure period of 2 wk before death was also considered, producing effect
15 estimates of 5% (95% CI: 1-10) for the same PM₁₀ increment. Even larger effect estimates
16 were observed for those who died at ages 4 to 12 months. When CO, NO₂, and O₃ were
17 simultaneously included with PM₁₀ in the model, the central estimate reduced to 2% for the
18 2-week exposure period and 4% for the 2-month exposure period, and both estimates lost
19 statistical significance. The other case-control study of California considered PM_{2.5} from
20 1999 to 2000 for infants born to mothers within five miles of a PM_{2.5} monitoring station
21 (Woodruff et al., 2006, [088758](#)). Infants who died during the postneonatal period were
22 matched to infants with date of birth within two weeks and birth weight category. Exposure
23 was estimated from the time of birth to death. Models considered parity and maternal race,
24 education, age, and marital status. A 10 µg/m³ increase in PM_{2.5} was associated with a 7%
25 (95% CI: -7 to 24) increase in postneonatal death

26 County-level PM₁₀ and PM_{2.5} for the first two months of life for births in urban U.S.
27 counties (≥ 250,000 residents) from 1999 to 2002 were evaluated in relation to postneonatal
28 mortality with GEE models (Woodruff et al., 2008, [098386](#)). Analyses were adjusted for
29 primiparity (first born), community-level poverty, region, month, year, and mother's race,
30 marital status, education, and age. Births were restricted to singleton births with
31 gestational age ≤ 44 wk, same county of residence at birth and death, and non-missing data
32 on birth order, birth weight, and maternal race, education, and marital status. Higher
33 levels of either PM metric were associated with higher risk of postneonatal mortality, with
34 4% (95% CI: -1 to 10) increase in mortality risk per 10 µg/m³ in PM₁₀ and 4% (95% CI: -2
35 to 11) increase in mortality risk for the same increment of PM_{2.5}. This work builds on a
36 previous study of 86 U.S. urban areas from 1989 to 1991, finding a 4% (95% CI: 2-7)
37 increase in postneonatal mortality per 10 µg/m³ county-level PM₁₀ over the first two months
38 of life (Woodruff et al., 1997, [084271](#)).

1 In Ciudad Juarez, Mexico, a case-crossover approach was applied to data from 1997 to
2 2001 based on death certificates and the cumulative PM₁₀ for the day of death and previous
3 two days (Romieu et al., 2004, [093074](#)). A case-crossover study of Kaohsiung, Taiwan from
4 1994-2000 compared the average of PM₁₀ on the day of death and two previous days to PM₁₀
5 in control periods a week before and week after death (Tsai et al., 2006, [090709](#)). A similar
6 approach was also applied to 1994 to 2000 data from Taipei, Taiwan, also using case-
7 crossover methods for the lag 0-2 PM₁₀ with referent periods the week before and after
8 death (Yang et al., 2006, [090760](#)). In these case-crossover studies, season was addressed
9 through matching in the study design. A 10 µg/m³ increase in PM₁₀ was associated with a
10 2.0% (95% CI: -2.8 to 7.0) increase in the Mexico study, a 0.59 (95% CI: -15.0 to 18.8)
11 increase in postneonatal death in the Kaohsiung study, and a 1.02% (95% CI: -13.2 to 17.6)
12 increase in the Taipei study. A study in Seoul, South Korea from 1995 to 1999 used time-
13 series approaches adjusted for temporal trend and weather, based on national death
14 registries excluding accidental deaths (Ha et al., 2003, [042552](#)). A 10 µg/m³ increase in PM₁₀
15 was associated with a 3.14% (95% CI: 2.16-4.14) increase in risk of death for postneonates.

16 A subset of the studies examining postneonatal mortality also considered the subset of
17 postneonatal deaths from respiratory causes. These include the time-series study in South
18 Korea, finding a 17.8% (95% CI: 14.4 to 21.2) increase in respiratory-mortality per 10 µg/m³
19 increase in PM₁₀ (Ha et al., 2003, [042552](#)) and the case-crossover study in Mexico, for which
20 the same increment in PM₁₀ was associated with a 1.5% (95% CI: -14.1 to 13.0) decrease in
21 risk (Romieu et al., 2004, [093074](#)). Both case-control California studies identified
22 associations, with a 5% (1, 10%) increase in risk in Southern California (Ritz et al., 2006,
23 [089819](#)) and 57.4% (95% CI: 7.0-132) increase in California per 10 µg/m³ PM₁₀ (Woodruff et
24 al., 2006, [088758](#)). The U.S. study found this increment in PM₁₀ to be linked with a 16%
25 (95% CI: 6.0-28.0) increase in respiratory postneonatal mortality, although effect estimates
26 for PM_{2.5} were not statistically significant (Woodruff et al., 2008, [098386](#)). Earlier studies on
27 respiratory-related postneonatal mortality include the study of 86 U.S. urban areas, finding
28 statistically significant effects (Woodruff et al., 1997, [084271](#)).

Sudden Infant Death Syndrome

29 Three studies examining the relationship between PM and sudden infant death
30 syndrome have been published from 2002 onward. These studies examined infant mortality
31 and were thereby discussed in this section previously. A case-control study over a 12-yr
32 period (1989 to 2000) matched 10 controls to deaths (cases) in Southern California (Ritz et
33 al., 2006, [089819](#)). A 10 µg/m³ increase in PM₁₀ the two months prior to death was
34 associated with a 3% (95% CI: -1 to 8) increased in SIDS. Adjusted for other pollutants (CO,
35 NO₂, and O₃), the effect estimate reduced to 1% (95% CI: -5 to 7).

36 A case-control study, also based in California, found an OR of 1.008 (95% CI: 1.006-
37 1.012) per 10 µg/m³ increase in PM_{2.5}, considering a SIDS definition of ICD 10 R95
38 (Woodruff et al., 2006, [088758](#)). Due to changes in SIDS diagnosis, another SIDS definition

1 was explored for ICD 10 R99 in addition to ICD 10 R95. Under this SIDS definition, the
2 effect estimate changed to 1.03 (95% CI: 0.79-1.35). The authors also examined whether the
3 relationship between PM_{2.5} and SIDS differed by season, finding no significant difference.
4 PM₁₀ and PM_{10-2.5} were not associated with risk of SIDS; numerical results were not
5 provided for these PM metrics. The third recent study of PM and SIDS examined U.S.
6 urban counties from 1999 to 2002 (Woodruff et al., 2008, [098386](#)). Non-statistically
7 significant relationships were observed between SIDS and PM₁₀ or PM_{2.5} in the first two
8 months of life.

9 These studies add to earlier work, such as a U.S. study that found higher risk of SIDS
10 with higher annual PM_{2.5} levels, including in a separate analysis of normal birth weight
11 infants (Lipfert et al., 2000, [004103](#)), and a U.S. study identifying a 12% (95% CI: 7-17)
12 increase in SIDS risk per 10 µg/m³ in PM₁₀ for the first two months of life for normal weight
13 births (Woodruff et al., 1997, [084271](#)). A study based on Taiwan found higher SIDS risk
14 with lower visibility (Knöbel et al., 1995, [155905](#)), whereas a 12 city Canadian time-series
15 study identified no significant associations (Dales et al., 2004, [087342](#)).

16 Deaths by SIDS were identified by different methods in the studies, partly due to
17 transition from ICD 9 to ICD 10, but also due to different choices within the research
18 design. Two studies examined multiple approaches (ICD 10 R95, ICD 10 R95 and R99)
19 (Woodruff et al., 2006, [088758](#); Woodruff et al., 2008, [098386](#)), and other studies
20 investigated ICD 9 798.0 and ICD 10 R95 (Ritz and Wilhelm, 2008, [156914](#)), ICD 9 798.0
21 (Woodruff et al., 1997, [084271](#)), ICD 9 798.0 and 799.0 (Knöbel et al., 1995, [155905](#)), as well
22 as a sudden unexplained death of infant <1 year for which an autopsy did not identify a
23 specific cause of death (Dales et al., 2004, [087342](#)). These variations in the definition of
24 health outcomes add to differences in populations and study designs.

25 Although some findings indicate a potential effect of PM on risk of SIDS, with the
26 strongest evidence perhaps from the case-control study in California (Woodruff et al., 2006,
27 [088758](#)), others do not find an effect or observe an uncertain association. For the
28 relationship between PM and SIDS, a 2004 review article concluded consistent evidence
29 exists compared to evidence for other infant mortality effects (Glinianaia et al., 2004,
30 [087898](#)), whereas other reviews found weaker or insufficient evidence (Heinrich and Slama,
31 2007, [156534](#)). Another review concluded that the scientific literature on air pollution and
32 SIDS suggests an effect, but that further research is needed to draw a conclusion (Tong and
33 Colditz, 2004, [087883](#)).

Comparisons across Studies and Key Issues

34 Comparison of results across studies can be challenging due to several issues,
35 including differences in methodologies, populations and study areas, pollution levels, and
36 the exposure timeframes used. Given the large variation in study designs, the methods to
37 address potential confounders vary. For example, weather and season were addressed in

1 the case-control studies by matching, in the time-series study through non-linear functions
2 of temperature and temporal trend, and in the ecological study through county-level
3 variables. All studies included consideration of seasonality and weather. Researchers used
4 different definitions of respiratory-related deaths, including ICD 9 460-519 (Bobak and
5 Leon, 1999, [007678](#); Lipfert et al., 2000, [004103](#)); ICD 9 460-519, 769-770 (Lipfert et al.,
6 2000, [004103](#)); ICD 9 codes 460-519, 769, 770.4, 770.7, 770.8, 770.9, and ICD 10 J00-J98,
7 P22.0, P22.9, P27.1, P27.9, P28.0, P28.4, P28.5, and P28.9 (Ritz et al., 2006, [089819](#)); and
8 ICD 9 460-519 and ICD 10 J00-J99 for any cause on death certificate (Romieu et al., 2004,
9 [093074](#)); ICD 10 J00-99 and P27.1 excluding J69.0 (Woodruff et al., 2006, [088758](#); Woodruff
10 et al., 2008, [098386](#)); and ICD 9 460-519 (Woodruff et al., 1997, [084271](#)).

11 Socioeconomic conditions were included at the individual level, typically maternal
12 education, in many studies (e.g., Bobak and Leon, 1999, [007678](#); Ritz and Wilhelm, 2008,
13 [156914](#); Ritz et al., 2006, [089819](#); Woodruff et al., 1997, [084271](#); Woodruff et al., 2006,
14 [088758](#)) and at the community-level in others (e.g., Bobak and Leon, 1992, [044415](#); Penna
15 and Duchade, 1991, [073325](#)) or for both individual and community-level data (e.g., Lipfert
16 et al., 2000, [004103](#)). The time-series approach is unlikely to be confounded by
17 socioeconomic and other variables that do not exhibit day-to-day variation. Similarly, case-
18 crossover methods use each case as his/her own control, thereby negating the need for
19 individual-level confounders such as socioeconomic status (e.g., Romieu et al., 2004, [093074](#);
20 Tsai et al., 2006, [090709](#); Yang et al., 2006, [090760](#)). All studies published after 2001
21 incorporated individual-level socioeconomic data or were of case-crossover or time-series
22 design. One study specifically examined whether socioeconomic status modified the PM and
23 mortality relationship, dividing subjects into three socioeconomic strata based on the zip
24 code of residence at death (Romieu et al., 2004, [093074](#)). This work, based in Mexico, found
25 that at lower socio-economic levels the association between PM₁₀ and postneonatal
26 mortality increased. Although the overall association showed higher risk of death with
27 higher PM₁₀ with statistical uncertainty, for the lowest socio-economic group, a 10 µg/m³
28 increment in cumulative PM₁₀ over the two days before death was associated with a 60%
29 (95% CI: 3-149) increase in postneonatal death. A trend of higher effect for lower socio-
30 economic condition is observed in all three lag structures.

31 Studies differ in terms of the timeframe of pregnancy that was used to estimate
32 exposure. Exposure to PM for infant mortality (<1 year) was estimated as the levels
33 between birth and death (Bobak and Leon, 1999, [007678](#)), annual community levels (Lipfert
34 et al., 2000, [004103](#); Penna and Duchade, 1991, [073325](#)) and the 3 to 5 days prior to death
35 (Loomis et al., 1999, [087288](#)). For neonatal deaths, exposure timeframes considered were
36 the time between birth and death (Bobak and Leon, 1992, [044415](#); Bobak and Leon, 1999,
37 [007678](#)), annual levels (Bobak and Leon, 1999, [007678](#); Lipfert et al., 2000, [004103](#)),
38 monthly levels (Shinkura et al., 1999, [156978](#)), the same day concentrations (Lin et al.,
39 2004, [095787](#)), and the two months or two weeks prior to death (Ritz et al., 2006, [089819](#)).

1 Postneonatal mortality was associated with PM concentrations based on annual levels
2 (Bobak and Leon, 1992, [044415](#); Lipfert et al., 2000, [004103](#)), between birth and death
3 (Bobak and Leon, 1999, [007678](#); Woodruff et al., 2006, [088758](#)), two months before death
4 (Ritz et al., 2006, [089819](#)), the first two months of life (Woodruff et al., 1997, [084271](#);
5 Woodruff et al., 2006, [088758](#)), the day of death (Ha et al., 2003, [042552](#)), and the average of
6 the same day as death and previous two days (Romieu et al., 2004, [093074](#); Tsai et al., 2006,
7 [090709](#); Yang et al., 2006, [090760](#)). Thus, no consistent window of exposure was identified
8 across the studies.

9 PM₁₀ concentrations were highest in South Korea (69.2 µg/m³) (Ha et al., 2003,
10 [042552](#)) and Taiwan (81.45 µg/m³) (Tsai et al., 2006, [090709](#)), and lowest in the U.S.
11 (29.1 µg/m³) (Woodruff et al., 2008, [098386](#)) and Japan (21.6 µg/m³) (Shinkura et al., 1999,
12 [156978](#)). All studies used community-level exposure information based on ambient
13 monitors, as opposed to exposure measured at the individual level (e.g., subject's home) or
14 personal monitoring.

15 Given similar sources for multiple pollutants (e.g., traffic), disentangling the health
16 responses of co-pollutants is a challenge in the study of ambient air pollution. Several
17 studies examined multiple pollutants, most by estimating the effect of different pollutants
18 through several univariate models. Some studies noted the difficulty of separating particle
19 impacts from those of other pollutants, but noted stronger evidence for particles than other
20 pollutants (Bobak and Leon, 1999, [007678](#)). A few studies applied co-pollutant models by
21 including multiple pollutants simultaneously in the same model. Effect estimates for the
22 relationship between PM₁₀ and neonatal deaths in São Paulo were reduced to a null effect
23 when SO₂ was incorporated (Lin et al., 2004, [095787](#)). Associations between PM₁₀ and
24 postneonatal mortality or respiratory postneonatal mortality remained but lost statistical
25 significance in a multiple pollutant model with CO, NO₂, and O₃ (Ritz et al., 2006, [089819](#)).

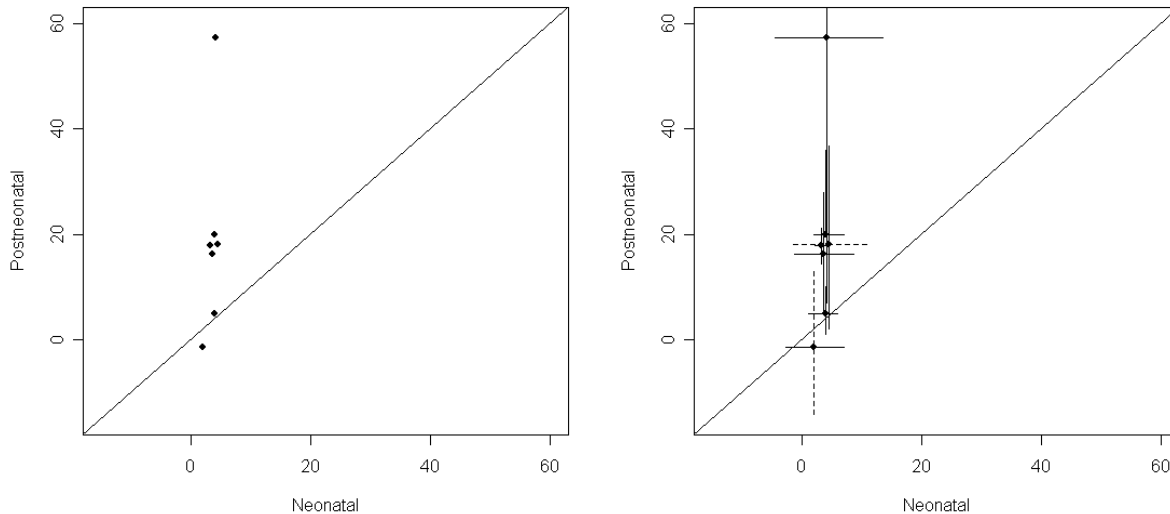


Figure 7-5. Percent increase in postneonatal mortality per $10 \mu\text{g}/\text{m}^3$ in PM_{10} , comparing risk for total and respiratory mortality.

Panel a (left) provides central estimates; panel b (right) also adds the 95% intervals. The points reflect central estimates and the lines the 95% intervals. Solid lines represent statistically significant effect estimates; dashed lines represent non-statistically significant estimates.¹

1 Several review articles in recent years have examined whether exposure to PM affects
 2 risk of infant mortality, generally concluding that more consistent evidence has been
 3 observed for postneonatal mortality, particularly from respiratory causes (Bobak and Leon,
 4 1999, [007678](#); Heinrich and Slama, 2007, [156534](#); Lacasaña et al., 2005, [155914](#); Sram et
 5 al., 2005, [087442](#)). In one review authors identified 14 studies on infant mortality and air
 6 pollution and determined that studies on PM and infant mortality do not provide consistent
 7 results, although more evidence was present for an association for some subsets of infant
 8 mortality such as postneonatal respiratory-related mortality (Bobak and Leon, 1999,
 9 [007678](#)). The relationship between PM and postneonatal respiratory mortality was
 10 concluded to be causal in one review (Sram et al., 2005, [087442](#)), and strong and consistent
 11 in another (Heinrich and Slama, 2007, [156534](#)). Meta-analysis using inverse-variance
 12 weighting of PM_{10} studies found that a $10 \mu\text{g}/\text{m}^3$ increase in acute PM_{10} exposure was
 13 associated with 3.3% (95% CI: 2.4-4.3) increase in risk of postneonatal mortality, whereas
 14 the same increment of chronic PM_{10} exposure was linked with a 4.8% (95% CI: 2.2-7.2)

¹ Studies included are Bobak and Leon (1999, [007678](#)), Ha et al. (2003, [042552](#)), Ritz et al. (2006, [089819](#)), Romieu et al. (2004, [093074](#)), Romieu et al. (2008, [156922](#)), Woodruff et al. (1997, [084271](#)), Woodruff et al. (2006, [088758](#)). Findings from Bobak and Leon (1999, [007678](#)) were based on TSP and were converted to PM_{10} estimates assuming $\text{PM}_{10}/\text{TSP} = 0.8$ as per summary data in the original article (Bobak and Leon, 1999, [007678](#)). Findings from Woodruff et al. (1997, [084271](#)) for respiratory-related mortality were based on non-low birth weight infants. Results for Woodruff et al. (2006, [088758](#)) were based on $\text{PM}_{2.5}$ and were converted to PM_{10} assuming $\text{PM}_{2.5}/\text{PM}_{10} = 0.6$.

1 increase in postneonatal mortality and a 21.6% (95% CI: 10.2-34.2) increase for respiratory
2 postneonatal mortality (Lacasaña et al., 2005, [155914](#)).

3 Studies that examined multiple outcomes and ages of death allow a direct comparison
4 based on the same study population and methodologies, thereby negating the concern that
5 inconsistent results are due to underlying variation in population, approaches, etc. In this
6 review, one study finds higher effect estimates for postneonatal mortality, for both total and
7 respiratory-related mortality, and the other study found higher effects for risk in the
8 neonatal period. Another study, based in Southern California identified no association for
9 neonatal effects (numerical results not provided) but statistically significant results for
10 postneonatal mortality (Ritz et al., 2006, [089819](#)). Figure 7.6 compares risk for the
11 postneonatal period for respiratory and total mortality. In six of the seven studies, higher
12 effect estimates were observed for respiratory-related mortality. Results from the neonatal
13 period found higher effects for total mortality compared to respiratory mortality (Bobak and
14 Leon, 1999, [007678](#)) and the reverse for a study examining infant mortality (Lipfert et al.,
15 2000, [004103](#)). Thus, there exists evidence for a stronger effect at the postneonatal period
16 and for respiratory-related mortality, although this trend is not consistent across all
17 studies.

Decrements in Sperm Quality

18 Limited research conducted in the Czech Republic on the effect of ambient air
19 pollution on sperm production has found associations between elevated air pollution and
20 decrements in proportionately fewer motile sperm, proportionately fewer sperm with
21 normal morphology or normal head shape, proportionately more sperm with abnormal
22 chromatin (Selevan et al., 2000, [012578](#)), and an increase in the percentage of sperm with
23 DNA fragmentation (Rubes et al., 2005, [078091](#)). These results were not specific to PM, but
24 for exposure to a high-, medium- or low-polluted air mixture. Similarly, in Salt Lake City,
25 Utah, fine particulate matter (PM_{2.5}) was associated with decreased sperm motility and
26 morphology (Hammoud et al. 2009). Research in Los Angeles, California examined 5134
27 semen samples from 48 donors in relation to ambient air pollution measured 0-9, 10-14, 70-
28 90 days before semen collection over a 2-yr period (1996-1998). Ambient ozone during all
29 exposure periods had a significant negative correlation with average sperm concentration,
30 and no other pollutant measures were significantly associated with sperm quality
31 parameters, or presented quantitatively (Sokol et al., 2006, [098539](#)).

7.4.2. Toxicological Studies

32 This section summarizes recent evidence on reproductive health effects reported with
33 exposure to ambient PM; no evidence was presented in this area in the 2004 PM AQCD.
34 Studies from different toxicological rodent models allow for investigation of specific
35 mechanisms and modes of action for reproductive changes. Emphasis is placed here on

1 results from different windows of development, i.e., if exposure in utero, neonatally or as an
2 adult can affect reproductive outcomes as an adult. In addition, studies evaluating whether
3 fertility is affected in female and/or male animals equally by a similar exposure, and how
4 exposures are transmitted to the fertility of the F1 offspring, are summarized. Hormonal
5 changes which can lead to decreased sperm count or changes in the estrous cycle are also of
6 interest. Pregnancy losses and placental sufficiency are also followed. Most recently, the
7 role of environmental chemicals in shifting sex ratios (also seen in epidemiologic studies)
8 and in affecting heritable DNA changes have become endpoints of interest.

7.4.2.1. Female Reproductive Effects

9 Significant work has been done in male rodent models to determine the effect of PM
10 exposure on reproductive success; fewer studies have been done on female rodents. Tsukue
11 et al. (2004, [096643](#)) exposed pregnant C57-BL mice to DE 0.1 mg DEP/m³ diluted in
12 charcoal and HEPA-filtered clean air or to for 8 h/day GD 2-13 and at GD 14 collected the
13 female fetuses for analysis of mRNA for Ad4BP-1/SF-1 and MIS, and found no significant
14 changes. The concentration of the gaseous materials including NO, NO_x, NO₂, CO and SO₂
15 are 2.2 + 0.34 ppm, 2.5 + 0.34 ppm, 0.0 ppm, 9.8 ± 0.69 ppm, and <0.1ppm (not detectable),
16 respectively. Work by Yoshida et al. (2006, [097015](#)) showed changes in these two transcripts
17 in male ICR fetuses exposed to similar doses of DEP, albeit with different daily durations of
18 exposure. Further work by Yoshida et al. showed that of three mouse strains tested, ICR
19 male fetuses were the most sensitive to DE-dependent changes in these two genes.
20 Nonetheless, strain sensitivity to DEP may also differ by sex. Thus, it appears that female
21 mice exposed in utero to DE show a lack of response at the mRNA level of MIS or Ad4bP-
22 1/SF-1, important genes in male sexual differentiation that showed DE-dependent changes
23 in male pups from dams exposed in utero. Female fetuses do however show a decrease in
24 BMP-15, which is related to oocyte development. Possible ingestion exposure by the
25 animals during grooming cannot be ruled out in this study.

26 Windows of exposure are important in determining reproductive success as an adult.
27 Exposure as a neonate may have a drastically more profound impact than does a similar
28 adult exposure in females. To test this, female BALB/C mice were exposed to ambient air in
29 Sao Paulo as neonates or as adults and then were bred to non-exposed males (Mohallem et
30 al., 2005, [088657](#)). Concentrations of pollutants in this ambient air including CO, NO₂,
31 PM₁₀, and SO₂ as measured locally were 2.2 ± 1.0, 107.8 ± 42.3, 35.5 ± 12.8, and 11.2 ± 5.3,
32 respectively. They reported decreased fertility in animals exposed as newborn but not in
33 adult-exposed female BALB/c mice. There were a significantly higher number of liveborn
34 pups from dams housed in filtered chambers (PM removed as well as chemical substances)
35 versus animals exposed to ambient air as newborns. There was also a higher incidence of
36 implantation failures in dams reared as newborns in polluted chambers. Sex ratio (unlike
37 in epidemiologic studies), number of pregnancies per group, resorptions, fetal deaths, and

1 fetal placental weights did not differ significantly by treatment group. Thus, in these
2 studies, exposure to ambient air pollution and its associated PM affected future
3 reproductive success of females if they were exposed as neonates and not if they are
4 exposed as adults.

5 Environmental chemicals have been shown to act as endocrine disruptors by acting on
6 the androgen pathway, including the phthalates, which have manifested their anti-
7 androgenic activity in numerous ways including decreased anogenital distance in male
8 rodents (Foster et al., 1980, [094701](#); Foster et al., 2001, [156442](#)). To assess the role of DE
9 exposure on reproductive success and anti-androgenic effects on offspring, Tsukue et al.
10 (2002, [030593](#)) exposed 6-weeks-old female C57-BL mice to 4 months of DE (0.3, 1.0, or 3.0
11 mg/m³) or filtered air (controls). Some animals were euthanized at the end of this exposure;
12 DE-exposed estrous females from this group were found to have significantly decreased
13 uterine weight (1.0 mg/m³). Some of these DE-exposed females were bred to unexposed
14 males. It was determined that DE-exposure led to increased but not significant rates of
15 pregnancy loss in mated females (up to 25%). The rate of good nest construction of the
16 pregnant exposed dams at the highest dose group was significantly lower than control (3.0
17 mg DEP/m³). Offspring were weighed after birth with significant decreases in body weight
18 seen at 6 and 8 wk (males and females 1.0 and 3.0 mg DEP/m³) and in female offspring
19 (9 wk of age, 1.0 and 3.0 mg/m³). Anogenital distance, a sensitive marker of anti-androgen
20 activity in males, was significantly decreased in 30-day old DEP exposed male offspring (0.3
21 mg DEP/m³) v. controls. Thymus weight was significantly decreased in 30-day old female
22 offspring (3.0 mg DEP/m³) and remained decreased at 70 days (0.3 and 1.0 mg DEP/m³).
23 Ovary weight of female offspring was significantly decreased (3.0 mg DEP/m³) at 30 days,
24 but no longer significantly different at 70 days. In males at 70 days of age, body weights
25 were significantly decreased and AGD was significantly shorter (3.0 mg DEP/m³). In
26 females at 70 days of age, the 1.0 mg DEP/m³ group showed significantly lower organ
27 weights (adrenals, liver, and thymus) and the 3.0 mg DEP/m³ group had decreased body
28 weight. Thymus weight of the 0.3 mg/m³ females was significantly lower at 70 days. Also,
29 crown to rump length in females from dams exposed to DEP (1.0 and 3.0 mg DEP/m³) was
30 also significantly lower. In conclusion, adult exposure to DEP led to maternal-dependent
31 reproductive changes that affected outcomes in offspring manifesting as decreased pup body
32 weight, anti-androgenic effects like decreased AGD and decreased organ weight (which may
33 be confounded by changes in body weight).

7.4.2.2. Male Reproductive Effects

34 Rodent strains differ in their sensitivity and response to various environmental
35 chemicals. Studies were performed to determine PM-dependent strain sensitivity using
36 male steroidogenic enzymes as the model pathway. In utero exposure of 3 strains of
37 pregnant mice (ICR, C57Bl/6J or ddY mice) via inhalation exposure of DE at 0.1 mg DE

1 particles (DEP)/m³ in HEPA-filtered clean air occurred or clean air as controls continuously
2 over gestational days 2-13 (Yoshida et al., 2006, [156170](#)). At gestational day 14, dams were
3 euthanized and fetuses were collected from the uteri. Male fetuses were collected from each
4 dam for mRNA analysis of genes related to male gonad development including mullerian
5 inhibiting substance (MIS), steroid transgenic factor (Ad4BP/SF-1), an enzyme in the
6 testosterone synthesis pathway, cytochrome P450 cholesterol side chain cleavage enzyme
7 (P450sc), and other steroidogenic enzymes [17 β -hydroxysteroid dehydrogenase (HSD),
8 cytochrome P450 17- α -hydroxylase (P450c17), and 3 β -hydroxysteroid dehydrogenase
9 (3 β HSD)]. There were significant decreases in MIS (ICR, and C57BL/6 mice) and
10 Ad4BP/SF-1 (ICR mice) versus control at gestational day (GD) 14. SF-1 transcriptionally
11 regulates T secretion. MIS is crucial in for sexual differentiation including mullerian duct
12 regression in males. The ddY strain showed no significant changes in Ad4BP/SF-1 or MIS
13 which the authors hypothesized may be due to changes in 3 β -hD, which had marked
14 changes in expression in the ddY strain when compared to non-DE exposed controls. From
15 these studies, it appears that mouse strains with in utero exposure to DE show differential
16 sensitivity in gonadal differentiation genes (mRNA) expression in male offspring; ICR are
17 the most sensitive, followed by C57BL/6 with ddY mice the least sensitive.

18 Yoshida et al. (2006, [097015](#)) also monitored changes in the male reproductive tract
19 after in utero exposure to DE. Timed-pregnant ICR dams were exposed during gestation
20 (2dpc to 16dpc) to continuous DE generated to concentrations of 0.3, 1.0 or 3.0 mg DEP/m³
21 in HEPA-filtered air or clean air as controls. PM deposition on the fur and ingestion of the
22 dams by grooming is another possible exposure route in this study. The reproductive tracts
23 of male offspring were monitored at 4 wk postnatally. These pups received possible
24 continued exposure through lactation as dams exposed to DE during gestation nursed pups.
25 There was a threshold effect; 0.3 mg/m³ had no effect on male reproductive organ weight or
26 serum testosterone (T). Exposure to the higher doses (1.0 and 3.0 mg/m³) of DEP led to
27 significant increases in reproductive gland weight [testis, prostate, seminal vesicle (3.0 mg
28 DEP/m³ only) and coagulating gland]. The intermediate dose of 1.0 mg DEP/m³ induced
29 significant increases in serum T. The organ weights are presented as absolute numbers and
30 not adjusted for body weight, which is sometimes problematic for complete representation
31 of hormonal changes as body weight may confound absolute organ weight changes.
32 Nonetheless, there were also significant decreases in mRNA for the steroidogenesis related
33 enzymes 3 β HSD (3.0 mg DEP/m³) and aromatase (3.0 mg DEP/m³). Transcripts relating to
34 male sexual differentiation [Mullerian inhibitory substance (mis) and steroid transgenic
35 factor (AD4BP/SF-1), 1.0 and 3.0 mg DEP/m³] were also significantly decreased. Sexual
36 differentiation is a tightly regulated process. For example, SF-1 missense mutations result
37 in XY individuals with external female genitalia. Thus the effect of environmental DE-
38 exposure should not be underscored.

1 This study demonstrated effects of DE exposure on male spermatogenesis. Exposure
2 of pregnant ICR mice to DE (2 dpc-16 dpc continuous inhalation exposure to 1.0 mg DEP/m³
3 in filtered air or to filtered clean air) led to impaired spermatogenesis in offspring (Ono et
4 al., 2007, [156007](#)). Male offspring were followed at PND 8, 16, 21 (3 wk), 35 (5 wk) and 84
5 (12 wk). After 16dpc but before termination of the study, all of the animals were transferred
6 to a regular animal care facility. No cross fostering was performed in this experiment, so
7 pups that were born to DE-exposed dams were also nursed on these dams and may have
8 received lactational exposure to DE from milk. The gaseous components of the diluted DE
9 included nitric oxide (NO), NO₂, sulfur dioxide (SO₂), and CO₂ at concentrations of 11.75 ±
10 1.18, 4.62 ± 0.36, 0.21 ± 0.01, and 4922 ± 244 ppm, respectively. The average proportion of
11 sulfur in the fuel during this study was 0.043%. Body weight was significantly depressed at
12 PNDs 8 and 35. Accessory gland relative weight was significantly increased at PND 8 and
13 16 only. Serum testosterone was significantly decreased at 3 wk and at 12 wk was
14 significantly increased. At 5 and 12 wk, daily sperm production (DSP) was significantly
15 decreased. FSH receptor and star mRNA levels were significantly increased at 5 and 12 wk,
16 respectively. Relative testis weight and relative epididymal weight were unchanged at all
17 time points. All endpoints were measured at each time point and if not mentioned above,
18 those data reported no significant changes. Histological changes showed sertoli cells with
19 partial vacuolization and a significant increase in testicular multinucleated giant cells in
20 the seminiferous tubules of DE exposed animals compared to control. This study indicates
21 that in utero exposure to DE had effects on spermatogenesis in offspring at the
22 histologically, hormonally and functionally.

23 In utero exposure to DE and its effect on adult body weight, sex ratio, and male
24 reproductive gland weight was measured by Yoshida et al. (2006, [097015](#)). Pregnant ICR
25 mice were exposed by inhalation to DE (0.3, 1.0 or 3.0 mg DEP/m³ or to clean air) from 2dpc
26 to 16dpc. Pups were allowed to nurse in clean air on exposed dams until weaning and at
27 PND 28, male pups were sacrificed. At this time, serum testosterone and pup reproductive
28 gland weight was determined. Significant increases in relative reproductive organ weights
29 were reported at 1.0 and 3.0 mg DEP/m³ for the seminal vesicle, testis, epididymis,
30 coagulating gland, prostate and liver. Male pup serum testosterone was significantly
31 increased at 1.0 mg DEP/m³. Mean testosterone positively correlated with testis weight,
32 daily sperm production, aromatase and steroidogenic enzyme message level (P450cc, c17
33 lyase, and P450 aromatase). Sex ratio did not differ in DE-exposed animals versus control.
34 Male pup body weight of DE-exposed animals was significantly increased at PND 28 (1.0
35 and 3.0 mg DEP/m³). These studies show that in utero DE-exposure led to increased serum
36 testosterone and increased reproductive gland weight in male offspring early in life.

37 The effects of DE on murine adult male reproductive function were studied by
38 exposing ICR male mice (6 wk of age) to DE (clean air control, 0.3, 1.0 or 3.0 mg DECP/m³)
39 for 12 h/day for 6 months with another group receiving a one month recovery of clean air

1 exposure post-exposure (Yoshida and Takedab, 2004, [097760](#)). After six months exposure,
2 there was a dose-dependent significant increase in degeneration of seminiferous tubules of
3 mice exposed to DEP. After six months, there was a significant decrease in daily sperm
4 production (DSP)/g of testis tissue in DEP exposed animals. After six months exposure to
5 DEP plus one month recovery with clean air exposure, significant decreases remained in
6 DSP at the higher doses; the effect was lost at 0.3 mg/m³. This adult exposure and other
7 work with in utero exposure to DE showed similar outcomes. The effect of ingestion of
8 deposited PM from the fur during grooming post-inhalation exposure cannot be ruled out as
9 a possible mechanism of exposure in this experiment.

10 Earlier studies showed an inverse correlation between environmental levels of PM
11 and sperm count in adult men (Mehta and Anad Kumar, 1997, [157197](#)). To expand on PM-
12 dependent changes in spermatogenesis, an eloquent DE-exposure model was designed to
13 determine if PM or the gaseous phase of DE was responsible for changes in sperm
14 production in rodents (Watanabe, 2005, [087985](#)). Pregnant dams (F344/DuCrj rats) exposed
15 to DE (6 hs/day exposure to 0.17 or 1.71 mg DEP/m³) or filtered air (removing PM only, high
16 dose filtered air and low dose filtered air) from GD7 to parturition produced adult offspring
17 with a decreased number of sertoli cells and decreased daily sperm production (PND 96)
18 when compared to control mice exposed to clean air (Watanabe, 2005, [087985](#)). The
19 concentrations of NO₂ for the high filtered and low filtered exposure groups were 0.8 and
20 0.1 ppm, respectively. Because both filtered and DE-exposure groups showed the same
21 outcomes, the effects are likely due to gaseous components of DE.

22 Another source of PM emissions that is common around the world is motorcycle
23 exhaust. Adult male (8 weeks old) Wistar rats were exposed to motorcycle exhaust (ME) for
24 one hour in the morning and one hour in the afternoon Monday through Friday at 1:50
25 dilution in filtered clean air for 4 wk (group A) or 1:10 for 2 (group B) or 4 wk (group C) or to
26 clean air (Huang et al., 2008, [156574](#)) via a head and nose inhalation chamber. After 4 wk of
27 exposure, both exposed groups had significantly decreased body weight v. control. All three
28 groups showed a decreased number of spermatids in the testis after ME exposure. Both
29 1:10 exposure groups also showed a decrease in caudal epididymal sperm counts. Group C
30 showed significant decreases in testicular weight. Group C had decreased mRNA for the
31 cytochrome P450 substrate 7-ethoxycoumarin O-de-ethylase, and increased IL-6, IL-1B,
32 and cox-2 mRNA control. Decreased protein levels of antioxidant superoxide dismutase and
33 increased IL-6 protein were reported for group C when compared to control. Serum
34 testosterone was significantly decreased in group C and co-treatment of group C with the
35 antioxidant vitamin E resulted in partial rescue of serum T levels and caudal epididymal
36 sperm counts (albeit still significantly decreased versus control), and returned IL-6, IL-1β,
37 and COX-2 ME-exposure-dependent message levels to baseline. The glutathione
38 antioxidant system and lipid peroxidation were unchanged after these ME exposures at the
39 time points measured. Male animals exposed to ME in this experiment showed significant

1 decrements in body weight, spermatid number, and serum testosterone with an increase in
2 inflammatory cytokines. Vitamin E co-treatment with ME-exposure led to an attenuation of
3 inflammation and a partial rescue of testosterone levels and sperm numbers. No filtration
4 was done in this experiment to determine if the effects were gas- or particle-dependent.

5 In summary, laboratory animals exposed to DE in utero or as adults manifest with
6 abnormal effects on the male reproductive system. In utero exposure to DE induced
7 increased reproductive gland weight and increased serum testosterone in early life
8 (PND28), which may lead to early puberty (albeit not measured in this study). With similar
9 in utero DE exposures, later life outcomes include decreased DSP, aberrant sperm
10 morphology, and hormonal changes (T and FSHr decrements). Chronic exposure of adult
11 mice to DE also induced decreased DSP and seminiferous tubule degeneration. DE-
12 dependent effects on male reproductive function have been reported in multiple animal
13 models with only one model separating exposure based on particulate versus gaseous
14 components. DE and filtered air (gaseous phase only) exposure in utero induced sertoli cell
15 and DSP decrements in both groups, indicating that the gaseous phase of DE was
16 causative. Adult male rats exposed to ME manifested with decreased spermatid number,
17 serum T, and an increase in inflammatory cytokines. Significant effects on the male
18 reproductive system have been demonstrated after exposure to ambient PM sources (DE,
19 ME, or PAHs). Nonetheless, these models often include a complex mixture of gaseous
20 component and PM exposure, which makes interpreting the contribution from PM alone
21 difficult.

7.4.2.3. Multiple Generation Effects

22 Multi-generational, chronic exposure to traffic-generated fine PM affects reproductive
23 and fetal outcomes in female mice including estrous cyclicity, follicle development, mating,
24 fertility, and pregnancy success. In this study, Veras et al. (2009, [190496](#)) investigated
25 pregnancy and female reproductive outcomes in BalbC female mice exposed to ambient air
26 (NF) or filtered air (F) at one of two different time periods (before conception and during
27 pregnancy) at the University of Sao Paulo School of Medicine near an area of high traffic
28 density. The exposure system is described by Mohallem et al., earlier in this ISA. Two
29 groups of 2nd generation (G2) nulliparous female mice were continuously exposed to
30 filtered air (F) or non-filtered ambient air (NF) since birth. Estrous cyclicity and ovarian
31 follicle classification were followed at PND60 (reproductive maturation) in one group. A
32 further group was subdivided into 4 groups by exposures during pregnancy following
33 reproductive capability and pregnancy outcomes of the G2 mice. Exposure were 27.5 and
34 6.5 ug/m³ PM_{2.5}, respectively for NF and F chambers with 101 ug/m³ NO₂, 1.81 ug/m³ CO,
35 and 7.66 ppm SO₂ in both chambers (Veras et al., 2009, [190496](#)).

36 The results of this study showed that animals exposed to NF air versus F air had an
37 extended time in estrous and thus a reduction in the number of cycles during the

1 experiment study period. The number of antral follicles was significantly decreased in the
2 NF versus the F animals. Other follicular quantification (number of small, growing or
3 preovulatory follicles) showed no significant differences between the two chambers. There
4 was a significant increase in the time necessary for mating, a significant decrease in the
5 fertility index, and a significant increase in the pregnancy index in the NF group versus the
6 F group. Specifically, in the NF1 and NF2 groups, there was a significant increase in rate of
7 the post-implantation loss. However, there was no statistically significant change in
8 number of pups in the litter. Fetal weight was significantly decreased in all treatment
9 groups (F2, NF1, and NF2) when compared to F1 or animals raised entirely in filtered air,
10 showing that fetal weight was affected by both pre-gestational and gestational PM exposure
11 (Veras et al., 2009, [190496](#)).

12 PM exposure prior to conception is associated with increased time in estrous, which in
13 other animal models can be related to ovarian hormone dysfunction and ovulatory
14 problems. These estrous issues can contribute to fecundity issues. There was no significant
15 difference in number of preovulatory follicles in this model, but there was a statistically
16 significant decrease in the number of antral follicles. Antral follicles are the last stage in
17 follicle development prior to ovulation, and a decrease in antral follicle number can be
18 related to premature reproductive senescence, premature ovarian failure, or early
19 menopause, which was not followed in this model (Veras et al., 2009, [190496](#)).

20 From the experimental design, one sees that the males that were used to generate the
21 G1 and G2 generations were also exposed to NF or F air, and thus the reproductive
22 contribution of these males to the overall fertility and mating changes in the females
23 mentioned above cannot be totally eliminated as a possible confounder as the literature has
24 characterized PM exposure as being associated with adverse male reproductive outcomes.
25 Thus these effects are hard to differentiate as male or female-dependent and can thus
26 indicate a general loss of reproductive fitness. Interestingly, both pre and gestational
27 exposure to NF induced a significant loss in post-implantation of fetuses and this may be
28 related to placental insufficiency as has been described in other work by this lab (Veras et
29 al., 2008, [190493](#)).

7.4.2.4. Receptor Mediated Effects

Arylhydrocarbon Receptor (AhR) and DEP

30 The AhR is often activated by chemicals classified as endocrine disrupting compounds
31 (EDCs), exogenous chemicals that behave as hormonally active agents, disrupting the
32 physiological function of endogenous hormones. DEPs are known to activate the AhR. A
33 recent study by Izawa et al. (2007, [190387](#)) showed that certain polyphenols (quercetin from
34 the onion) and food extracts (Ginkgo biloba extract (GBE)) are able to attenuate DEP-

1 dependent AhR activation when measured with the Ah-Immunoassay, thus possibly
2 attenuating the EDC activity of DEP.

7.4.2.5. Developmental Effects

Sex Ratio

3 A direct correlation between air pollution (PM₁₀) exposure and a decrease in
4 standardized sex ratios (SSRs) has been reported in humans exposed to air pollution
5 (Lichtenfels et al., 2007, [097041](#); Wilson et al., 2000, [010288](#)) pollution, with fewer numbers
6 of male births reported. To understand this shift, two groups (control and exposed) of male
7 Swiss mice were housed concurrently in Sao Paulo and received either ambient air
8 exposure or filtered air (chemical and particulate filtering) from PND10 for four months.
9 Filtration efficiency for PM_{2.5}, carbon black, and NO₂ inside the chamber was found to be
10 55%, 100%, and 35%, respectively. After this exposure, non-exposed females were placed in
11 either chamber to mate. After mating, the males were sacrificed and testes collected; males
12 exposed to ambient air showed decreased testicular and epididymal sperm counts,
13 decreased total number of germ cells, and decreased elongated spermatids, but no
14 significant change in litter size. Females were housed in the chambers and sacrificed on
15 GD19 when the number of pups born alive and the sex ratio were obtained. There was a
16 significant decrease in the SSR for pups born after living in the ambient air-exposed
17 chamber compared to the filtered chamber. In this study, a shift in SSR has been shown for
18 both humans and rodents exposed to air pollution, but other studies with DE exposure
19 (Yoshida et al., 2006, [156170](#)) or ambient air in Sao Paulo (Mohallem et al., 2005, [088657](#))
20 showed no changes in rodent sex ratio. Possible exposure to PM and other components of
21 ambient air via ingestion during grooming cannot be ruled out in this rodent model.

Immunological Effect-Placenta

22 Placental insufficiency can lead to the loss of a pregnancy or to adverse fetal
23 outcomes. DE-exposure has been shown to induce inflammation in various models.
24 Fujimoto et al. (2005, [096556](#)) assessed cytokine/immunological changes of DE-dependent
25 inhalation exposure on the placenta during pregnancy. Pregnant Slc: CR mice were exposed
26 to DE (0.3, 1.0, or 3.0 mg DEP/m³ in HEPA and charcoal-filtered clean air from 2dpc to 13
27 dpc) or clean air in inhalation chambers; dams, placenta, and pups were collected at 14dpc.
28 There was a significant increase in the number of absorbed placentas in DE exposed
29 animals (0.3 and 3.0 mg DEP/m³) with a significant decrease in the number of absorbed
30 placentas in DE exposed animals at the middle dose (1.0 mg DEP/m³). Absorbed placentas
31 from DE exposed mice had undetectable levels of CYP1A1 and two fold increases in TNF- α ;
32 CYP1A1 placental mRNA from healthy placentas of DE-exposed mice was unchanged
33 versus control. Interleukin (IL)-2, IL-5, IL-12 α , IL-12 β and granulocyte macrophage colony-

1 stimulating factor (GM-CSF) mRNA significantly increased in placentas of DE-exposed
2 animals (0.3 and 3 mg DEP/m³). Placental IL-6 mRNA was increased ten-fold in DE-
3 exposed mice (3.0 mg DEP/m³). Fujimoto et al. reported DE-induced significant increases in
4 multiple inflammatory markers in the placenta with significant increases in the number of
5 absorbed placentas.

Immunological Effects: Asthma

6 In utero exposure may confer susceptibility to PM-induced asthmatic responses in
7 offspring. Exposure of pregnant BALB/c mice to aerosolized ROFA leachate by inhalation or
8 to DEP intranasally increases asthma susceptibility to their offspring (Fedulov et al., 2008,
9 [097482](#); Hamada et al., 2007, [091235](#)). The offspring from dams exposed for 30 min to 50
10 mg/mL ROFA 1, 3, or 5 days prior to delivery responded to OVA immunization and aerosol
11 challenge with airway hyperreactivity and increased antigen-specific IgE and IgG1
12 antibodies. Airway hyperreactivity was also observed in the offspring of dams intra-nasally
13 instilled with 50 µg of DEP or TiO₂, or 250 µg CB, indicating that the same effect could be
14 demonstrated using relatively “inert” particles. Pregnant mice were particularly sensitive
15 to exposure to DEP or TiO₂ particles, and genetic analysis indicated differential expression
16 of 80 genes in response to TiO₂ in pregnant dams. Thus pregnancy and in utero exposure
17 may enhance responses to PM, and exposure to even relatively inert particles may result in
18 offspring predisposed to asthma.

Placental Morphology and Urban PM Exposure

19 Exposure to ambient air pollution during pregnancy is associated with reduced fetal
20 weight in both human and animal models. The effect of particular urban air pollution on
21 the functional morphology of the mouse placenta was explored by exposing second
22 generation mice in one of four groups to urban Sao Paulo air (PM was 67% PM_{2.5}, mainly of
23 vehicular origin) or filtered air (Veras et al., 2008, [190493](#)). Experimental design follows
24 with group F-F being comprised of mice that were raised in filtered air chambers and
25 completed pregnancy in filtered air chambers; group F-nF was raised in filtered air and
26 pregnant in ambient air; group nF-nF was raised and completed pregnancy in non-filtered
27 air chambers; group nF-F mice were raised in ambient air and received filtered air during
28 pregnancy. Exposure was from PND20-PND60. At this time, the animals were mated and
29 then maintained in their respective chambers during pregnancy; pregnancy was terminated
30 at GD18 (near term) with placentas and fetuses collected then for analysis.

31 Exposure to ambient PM pregestationally or gestationally led to significantly smaller
32 fetal weight (total litter weight). Pregestational exposure to ambient air induced significant
33 increases in fetal capillary surface area and in total mass-specific conductance. But
34 maternal/dam blood space and diameters were reduced. Gestational exposure to non-
35 filtered air was associated with reduced volume, diameter (caliber) and surface area of

1 maternal blood space with compensatory greater fetal capillary surface and oxygen
2 diffusion conduction rates. Intravascular barrier thickness, a quantitative relationship
3 between trophoblast volume and the combined surfaces of maternal blood spaces and fetal
4 capillaries, was not reduced with ambient air exposure. Fetal/placental circulatory
5 adaptation to maternal blood deficits after ambient PM exposure seems to be insufficient to
6 overcome PM-dependent birth weight deficits in mice exposed to ambient air with the
7 magnitude of this effect greater in the gestationally exposed groups.

Placental Weights and Birth Outcomes

8 Pregnant female Swiss mice were exposed to ambient air (Sao Paulo) or filtered air
9 over various portions of gestation to determine if there was an association between fetal or
10 placental weight or birth outcomes with exposure to air pollution. The concentration of
11 various components of the ambient air as measured by a State Environmental Sanitation
12 Agency 100 m away from the rodent exposure chambers reported PM₁₀ ($42 \pm 17 \mu\text{m}/\text{m}^3$),
13 NO₂ ($97 \pm 39 \mu\text{g}/\text{m}^3$), and SO₂ ($9 \pm 4 \mu\text{g}/\text{m}^3$) concentrations. By using six windows of
14 exposure that covered one to three weeks of gestation, which is all of gestation in a mouse,
15 these authors (Silva et al., 2008, [156981](#)) determined that a significant decrease in near-
16 term fetal weight(GD19) could be induced by ambient air-exposure at least during the first
17 week of gestation. Decreased placental weight could be induced by ambient air exposure
18 during any of the three weeks of gestation. These studies point to possible windows of
19 exposure that may be important in evaluating epidemiologic study results.

Neurodevelopmental Effects

20 The diagnosis of autism is on the rise in the Western world with its etiology mostly
21 unknown. Autism is associated cell loss in specific brain regions that is hypothesized to be
22 developmental in origin. Sugamata et al. (2006, [097166](#)) exposed pregnant ICR mice to DE
23 ($0.3 \text{ mg DEP}/\text{m}^3$) continuously from 2 days post-coitus (dPC) to 16 dPC. Pups with in utero
24 exposure to DE were nursed in clean air chambers but may have received gastro-intestinal
25 exposure via lactational transfer of various components of DE. At 11 wk of age, cerebellar
26 brain tissue was collected. Twenty animals were in each group (10 females, 10 males) with
27 one group receiving clean air exposure and one receiving DE; no filtration was used to
28 compare PM v. gaseous DE exposure. Earlier work has shown that DEP ($<0.1 \mu\text{m}$) have
29 been detected in the brains (cerebral cortex and hippocampus) of newborn pups who were
30 born to dams who were exposed to DE during pregnancy (Sugamata et al., 2006, [097166](#)).
31 Histological analysis of DE-exposed pup cerebella revealed significant increases in caspase-
32 3 (c-3) positive cells compared to control and significant decreases in cerebella Purkinje cell
33 numbers in DE-exposed animals versus control. The ratio of cells positive for apoptosis (c-3
34 positive) showed a nearly significant sex difference with males displaying increased
35 apoptosis versus females ($p = 0.09$). In humans with autism, the cerebellum has a decreased

1 number of Purkinje cells, which is thought to be fetal and developmental in origin; further,
2 these authors speculate that humans may be more sensitive to DE-dependent neuronal
3 brain changes as the human placenta is 2 layers thick whereas the mouse placenta is 4
4 layers thick.

Behavioral Effects

5 Body weight decrements at birth have recently been associated through the Barker
6 hypothesis with adverse adult outcomes. Thus, many publications have begun to focus on
7 decreased birth weight for gestational age and associated adult changes. Hougaard et al.
8 (2008, [156570](#)) exposed 40 timed-pregnant C57BL/6 dams to DEP reference materials (aged
9 DE particulate extract) via inhalation chamber over GD7-GD19 of pregnancy. They found
10 significantly decreased pup weight at weaning, albeit not at birth. PM-dependent liver
11 changes were monitored by following various inflammatory and genotoxicity-related mRNA
12 transcripts; there were no significant differences in pups at PND2. The comet assay from
13 PND2 pup livers showed no significant differences between DEP-exposed and control
14 animals. Thyroxine was unchanged in control and DEP-exposed dams and offspring at
15 weaning. At two months, female DEP-exposed pups required less time than controls to
16 locate the platform in its new location during the first trial of the spatial reversal learning
17 task in the Morris water maze ($p < 0.05$). DEP extract exposure during in utero
18 development led to decreased body weight at weaning and no changes in inflammatory
19 markers, or thyroid hormone levels.

20 The effect of in utero DE exposure on CNS motor function was evaluated in male pups
21 (ICR mice); dams received DE exposure 8hxd/5d/wk via total body inhalation GD2-GD17
22 (Yokota et al., 2009, [190518](#)). Spontaneous motor activity was significantly decreased in
23 pups (PND35) as was the dopamine metabolite homovanillic acid (HVA) as measured in the
24 striatum and nucleus accumbens indicating decreased dopamine (DA) turnover. DA levels
25 were unchanged in the same areas of the brain. The authors conclude that these data
26 demonstrate that maternal exposure to DE induced hypolocomotion, similar to earlier
27 studies with adult and neonatal DEP exposure (Peters et al., 2000, [001756](#)), with decreased
28 extracellular DA release. Concentrations of DE constituents in the Yokota study for DE
29 particle mass, CO, NO₂, and SO₂ are 1.0 mg/m³, 2.67 ppm, 0.23 ppm, and <0.01ppm,
30 respectively.

Lactation

31 Lactational exposure to various environmental compounds is an area of research that
32 is often overlooked. Breast milk is a complex matrix, which is essential for the survival of
33 many species. Compounds that are especially lipophilic are commonly found in breast milk
34 of exposed dams and this maternal load can be transferred to the developing neonate. PM
35 in DE adsorbs many chemicals, including polycyclic aromatic hydrocarbons (PAHs), which

1 have been shown to have to be mutagenic and to be estrogenic/antiestrogenic and
2 antiandrogenic (Hirose et al., 2001, [156548](#); Kizu et al., 2003, [096196](#)). Thus, Tozuka et al.
3 (2004, [090864](#)) monitored the transfer of aromatic hydrocarbons to fetuses and breast milk
4 of Fisher 344 rats exposed to DE for 2 wk from GD7-GD 20 (minus four days of the weekend
5 with no exposures) for 6h/day with PM₁₀ concentration of 1.73 mg/m³. Concentrations of
6 individual PAHs were monitored in the inhalation chambers including Ace, Fle, Phe, Ant,
7 Flu, Pyr, BaA, Chr, BbF, BkF, BaP, DBA, BghiP, and IDP at 150 ± 34, 3160 ± 401,
8 2280 ± 291, 70.3 ± 10.9, 148 ± 19, 133 ± 5, 17.2 ± 2.7, 39.9 ± 6.8, 9.9 ± 2.1, 4.9 ± 1.1, 3.7 ± 0.5,
9 <1.4, <6.0, and 4.2 ± 0.1 ng/m³, respectively. At PND 14, milk was collected from exposed
10 and control rats. Fifteen PAHs were monitored in DE-generated air. Seven of these were
11 quantified in dam blood with levels of phenanthrene (Phe), anthracene (Ant) and
12 benz[a]anthracene (BaA) in the DE group being significantly higher than control group. In
13 breast milk, acenaphthene (Ace), fluorene (Fle), Phe, Ant, fluoranthene (Flu), pyrene (Pyr),
14 BaA and chrysene (Chr) were quantified. Ant, Flu, Pyr and Chr showed significant
15 increases in the DE group compared to control milk. BaA tended to be about four fold
16 higher than the control group in breast milk, but the increase was not significant. PAHs in
17 dam livers of DE versus control were not significantly different. PAHs are transferred
18 across the placenta from the DE-exposed dam to the fetus. Lactational transfer through the
19 breast milk is also likely as PAHs are detected in dam breast milk, but this should be
20 confirmed in future studies that cross foster control and exposed dams and pups. The
21 lipophilicity of the PAH based on its structure affected its uptake to the dam from the air as
22 PAHs with 3 or 4 rings were found in maternal blood and PAHs with 5 or 6 rings were not
23 detected in dam blood.

Heritable DNA Changes and Heritable Epigenetic Changes

24 To address the role of ambient air exposure on heritable changes, Somers et al. (2004,
25 [078098](#)) exposed mice to ambient air in at a rural Canadian site or at an urban site near a
26 steel mill. They showed that offspring of mice exposed to ambient air in urban regions
27 inherited paternal-origin expanded simple tandem repeat (ESTR) mutations 1.9 to 2.1
28 times more frequently than offspring of mice exposed to HEPA filtered air or those exposed
29 to rural ambient air. Mouse expanded simple tandem repeat (ESTR) DNA is composed of
30 short base pair repeats which are unstable in the germline and tend to mutate by insertion
31 or deletion of repeat units. In vivo and in situ studies have shown that murine ESTR loci
32 are susceptible to ionizing radiation, and other environmental mutagen-dependent
33 germline mutations, and are thus good markers of exposure to environmental
34 contaminants.

35 Expanding upon the above work and to determine if PM or the gaseous phase of the
36 urban air was responsible for heritable mutations, Yauk et al. (2008, [157164](#)) exposed
37 mature male C57Blx/CBA F1 hybrid mice to either HEPA-filtered air or to ambient air in

1 Hamilton, Ontario, Canada for three, ten, or 10 wk plus 6 wk of clean air exposure (16 wk).
2 Sperm DNA was monitored for expanded simple tandem repeat (ESTR) mutations. In
3 addition, male-germ line (spermatogonial stem cell) DNA methylation was monitored post-
4 exposure. This area in Hamilton is near 2 steel mills and a major highway. Air composition
5 provided by the Ontario Ministry of the Environment showed TSP concentration of
6 $9.38 \pm 17 \mu\text{g}/\text{m}^3$, PAH concentration of $8.3 \pm 1.7 \text{ ng}/\text{m}^3$, and metal at $3.6 \pm 0.7 \text{ mg}/\text{m}^3$.
7 Mutation frequency at ESTR Ms6-hm locus in sperm DNA from mice exposed 3 or 10 wk
8 did not show elevated ESTR mutation frequencies, but there was a significant increase in
9 ESTR mutation frequency at 16 wk in ambient air exposed males versus HEPA-filter
10 exposed animals, pointing to a PM-dependent mechanism of action. When compared to
11 HEPA-filter air exposed males, ambient air exposed males manifested with
12 hypermethylation of germ-line DNA at 10 and 16 wk. These PM-dependent epigenetic
13 modifications (hypermethylation) were not seen in the haploid stage (3 wk) of
14 spermatogenesis, but were nonetheless seen in early stages of spermatogenesis (10 wk) and
15 remained significantly elevated in mature sperm even after removal of the mouse from the
16 environmental exposure (16 wk). Thus, these studies indicate that the ambient PM phase
17 and not the gaseous phase is responsible for the increased frequency of heritable DNA
18 mutations and epigenetic modifications.

7.4.3. Summary and Causal Determinations

7.4.3.1. PM_{2.5}

19 The 1996 PM AQCD concluded that while few studies had been conducted on the link
20 between PM and infant mortality, the research “suggested an association,” particularly for
21 post-neonates (U.S. EPA, 1996, [079380](#)). In the 2004 PM AQCD, additional evidence was
22 available on PM’s effect on fetal and early postnatal development and mortality and while
23 some studies indicated a relationship between PM and pregnancy outcomes, others did not
24 (U.S. EPA, 2004, [056905](#)). Studies identifying associations found that exposure to PM₁₀
25 early during pregnancy (first month of pregnancy) or late in the pregnancy (six weeks prior
26 to birth) were linked with higher risk of preterm birth, including models adjusted for other
27 pollutants, and that PM_{2.5} during the first month of pregnancy was associated with IUGR.
28 However, other work did not identify relationships between PM₁₀ exposure and LBW. The
29 state of the science at that time, as indicated in the 2004 PM AQCD, was that the research
30 provided mixed results based on studies from multiple countries.

31 Building on the evidence characterized in the previous AQCDs, recent epidemiologic
32 studies conducted in the U.S. and Europe were able to examine the effects of PM_{2.5}, and all
33 found an increased risk of LBW (Section 7.4.1). Exposure to PM_{2.5} was usually associated
34 with greater reductions in birth weight than exposure to PM₁₀. All of the studies that

1 examined the relationship between PM_{2.5} and preterm birth report positive associations,
2 and most were statistically significant. The studies evaluating the association between
3 PM_{2.5} and growth restriction all found positive associations, with the strongest evidence
4 coming when exposure was assessed during the first or second trimester (Section 7.4.1). For
5 infant mortality (<1 year), several studies examined PM_{2.5} and found positive associations
6 (Section 7.4.1).

7 Animal toxicological studies reported effects including decreased uterine weight,
8 limited evidence of male reproductive effects, and conflicting reports of reproductive
9 outcomes in male offspring, particularly in studies of DE (Section 7.4.2). Toxicological
10 studies also reported effects for several development outcomes, including immunological
11 effects in the placenta and related to asthma and neurodevelopmental and behavioral
12 effects (Section 7.4.2).

13 In summary evidence is accumulating from epidemiologic studies for effects on LBW
14 and infant mortality, especially due to respiratory causes during the post-neonatal period.
15 The mean PM_{2.5} concentrations during the study periods ranged from 5.3-27.4 µg/m³.
16 Exposure to PM_{2.5} was usually associated with greater reductions in birth weight than
17 exposure to PM₁₀. Several U.S. studies of PM₁₀ investigating fetal growth reported 11-g
18 decrements in birth weight associated with PM₁₀ exposure. The consistency of these results
19 strengthens the interpretation that particle exposure may be causally related to reductions
20 in birth weight. Similarly, animal evidence supported an association between PM_{2.5} and
21 PM₁₀ exposure and adverse reproductive and developmental outcomes, but provided little
22 mechanistic information or biological plausibility for an association between long-term PM
23 exposure and adverse birth outcomes, including LBW, or infant mortality. Epidemiologic
24 studies do not consistently report associations between PM exposure and preterm birth,
25 growth restriction, birth defects or decreased sperm quality. New evidence from animal
26 toxicological studies on heritable mutations is of great interest, and warrants further
27 investigation. Overall, the epidemiologic and toxicological evidence is **suggestive of a causal**
28 **relationship between long-term exposures to PM_{2.5} and reproductive and developmental**
29 **outcomes.**

7.4.3.2. PM_{10-2.5}

30 Evidence is **inadequate to determine if a causal relationship exists between long-term**
31 **exposure to PM_{10-2.5} or other PM components and developmental and reproductive outcomes**
32 because studies have not been conducted in sufficient quantity or quality to draw any
33 conclusion. A single study found an association between PM_{10-2.5} and birthweight (-13 g
34 [95% CI: -18.3 to -7.6] per 10 µg/m³ increase), but no such association for PM_{2.5} (Parker et
35 al., 2008, [156013](#)).

7.5. Cancer, Mutagenicity, and Genotoxicity

1 Evidence from epidemiologic and animal toxicological studies has been accumulating
2 for more than three decades regarding the mutagenicity and carcinogenicity of PM in the
3 ambient air. Diesel exhaust (DE) has been identified as one source of PM in ambient air,
4 and has been extensively studied for its carcinogenic potential. In 1989, the International
5 Agency for Research on Cancer (IARC) found that there was sufficient evidence that
6 extracts of DEP were carcinogenic in experimental animals and that there was limited
7 evidence for the carcinogenic effect of DE in humans (IARC, 1989, [002958](#)). This conclusion
8 was based on studies in which organic extracts of DEP were used to evaluate the effects of
9 concentrates of the organic compounds associated with carbonaceous soot particles. These
10 extracts were applied to the skin or administered by IT or intrapulmonary implantation to
11 mice, rats, or Syrian hamsters and an excess of tumors on the skin, lung or at the site of
12 injection were observed.

13 In 2002, the U.S. EPA reviewed over 30 epidemiologic studies that investigated the
14 potential carcinogenicity of DE. These studies, on average, found that long-term
15 occupational exposures to DE were associated with a 40% increase in the relative risk of
16 lung cancer (U.S. EPA, 2002, [042866](#)). In the same report the U.S. EPA concluded that
17 extensive studies with salmonella had unequivocally demonstrated mutagenic activity in
18 both particulate and gaseous fractions of DE. They further concluded that DE may present
19 a lung cancer hazard to humans (U.S. EPA, 2002, [042866](#)). The particulate phase appeared
20 to have the greatest contribution to the carcinogenic effect. Both the particle core and the
21 associated organic compounds demonstrated carcinogenic properties, although a role for the
22 gas-phase components of DE could not be ruled out. Almost the entire diesel particle mass
23 is $\leq 10 \mu\text{m}$ in diameter (PM_{10}), with approximately 94% of the mass of these particles
24 $< 2.5 \mu\text{m}$ in diameter ($\text{PM}_{2.5}$), including a subgroup with a large number of ultrafine
25 particles (U.S. EPA, 2002, [042866](#)). U.S. EPA considered the weight of evidence for potential
26 human carcinogenicity for DE to be strong, even though inferences were involved in the
27 overall assessment, and concluded that DE is “likely to be carcinogenic to humans by
28 inhalation” and that this hazard applies to environmental exposures (U.S. EPA, 2002,
29 [042866](#)).

30 Two recent reviews of the mutagenicity (Claxton et al., 2004, [089008](#)) and
31 carcinogenicity (Claxton and Woodall GM, 2007, [180391](#)) of ambient air have characterized
32 the animal toxicological literature on ambient air pollution and cancer. The majority of
33 these toxicological studies have been conducted using IT or dermal routes of exposure.
34 Generally, the toxicological evidence reviewed in this ISA has been limited to inhalation
35 studies conducted with lower concentrations of PM ($< 2 \text{ mg/m}^3$), relevant to current ambient
36 concentrations and the current regulatory standard (See Section 1.3). This ISA focuses on
37 toxicological studies which use the inhalation route of exposure, therefore it is possible that

1 important evidence for the role of PM in mutagenicity, tumorigenicity, and/or
2 carcinogenicity may be missed. In order to accurately characterize the relationship between
3 PM and cancer and be consistent with the EPA Guidelines for Carcinogen Risk Assessment
4 (U.S. EPA, 2005, [086237](#)), these reviews (that include studies that employ IT and dermal
5 routes of exposure) are summarized briefly.

6 Claxton et al. (2004, [089008](#)) reviewed the mutagenicity of air in the Salmonella
7 (Ames) assay, and showed that hundreds of compounds identified in ambient air from
8 varying chemical classes are mutagenic and that the commonly monitored PAHs could not
9 account for the majority of mutagenicity associated with most airborne particles. They
10 concluded that the smallest particles have the highest toxicity per particulate mass, with
11 the PM_{2.5} size fraction having greater mutagenic and cytotoxic potential than the PM₁₀ size
12 fraction, which had a higher mutagenic potential than the TSP size fraction. One study
13 reviewed by Claxton et al. (2004, [089008](#)) found that the cytotoxic potential of PM_{2.5} was
14 higher in wintertime samples than in summertime samples. A series of studies on source
15 apportionment for ambient particle mutagenic activity reviewed by Claxton et al. (2004,
16 [089008](#)) indicate that mobile sources (cars and diesel trucks) account for most of the
17 mutagenic activity.

18 Claxton and Woodall (2007, [180391](#)) reviewed many studies that examined the rodent
19 carcinogenicity of extracts of ambient PM samples; the PM was of various size classes, often
20 from TSP samples. Among a variety of mouse and rat strains, application methods, and
21 samples employed, the authors found no pattern that would suggest the routine use of a
22 particular strain or protocol would be more informative than another. The primary
23 conclusion that comes from the analysis of rodent carcinogenicity studies is that the most
24 polluted urban air samples tested to date are carcinogenic; the contribution of PM and
25 different size classes of PM to the carcinogenic effects of ambient air has not been
26 delineated. The differences in response by the various strains of inbred mice indicate that
27 the genetic background of an individual influences how likely a tumorigenic response is to
28 occur. Studies examining different components of ambient PM (e.g., PAHs) confirm that
29 ambient air contains multiple carcinogens, and that the carcinogenic potential of particles
30 from different airsheds can be quite different. Therefore, one would expect the incidence of
31 cancers related to ambient air exposure in different metropolitan areas to differ.

32 Numerous epidemiologic and animal toxicological studies of ambient PM and their
33 contributing sources have been conducted to assess the relative mutagenic or genotoxic
34 potential. Studies previously reviewed in the 2004 PM AQCD (U.S. EPA, 2004, [056905](#))
35 provide evidence that ambient PM as well as PM from specific combustion sources (e.g.,
36 fossil fuels) is mutagenic in vivo and in vitro. Building on these results, data from recent
37 epidemiologic and animal toxicological studies that evaluated the carcinogenic, mutagenic
38 and/or genotoxic effects of PM, PM-constituents, and combustion emission source particles
39 are reviewed in this section.

7.5.1. Epidemiologic Studies

1 The 2004 PM AQCD reported on original and follow-up analyses for three prospective
2 cohort studies that examined the relationship between PM and lung cancer incidence and
3 mortality. Based on these findings, as well as on the results from case-control and ecologic
4 studies, the 2004 PM AQCD concluded that long-term PM exposure may increase the risk of
5 lung cancer incidence and mortality. The largest of the three prospective cohort studies
6 included in the 2004 PM AQCD was the ACS study (Pope CA et al., 2002, [024689](#)). This
7 study was the follow-up to the original ACS study (Pope CA et al., 1995, [045159](#)), and
8 included a longer follow-up period and reported a statistically significant association
9 between PM_{2.5} exposure and lung cancer mortality.

10 A 14- to 16-yr prospective study conducted using the Six Cities Study cohort reported
11 a slightly elevated risk of lung cancer mortality for individuals living in the most polluted
12 city (mean PM₁₀: 46.5 µg/m³; mean PM_{2.5} 29.6 ug/m³) as compared to the least polluted city
13 (mean PM₁₀: 18.2 µg/m³; mean PM_{2.5} 11.0 µg/m³) but the association was not statistically
14 significant (Dockery et al., 1993, [044457](#)).

15 Re-analysis of the AHSMOG cohort, a study of non-smoking whites living in
16 California, concluded that elevated long-term exposure to PM₁₀ was associated with lung
17 cancer incidence among both men and women (Beeson et al., 1998, [048890](#)). The original
18 study had reported an excess of incident lung cancers only among women (Abbey et al.,
19 1991, [042668](#)). Further reanalysis of this cohort revealed an association between PM₁₀ and
20 lung cancer mortality among men but no association among women (Abbey et al., 1999,
21 [047559](#)). In addition, McDonnell et al. (2000, [010319](#)) reported increases in lung cancer
22 mortality with long-term exposure to PM_{2.5} in the AHSMOG cohort; no association was seen
23 for PM_{10-2.5}.

7.5.1.1. Lung Cancer Mortality and Incidence

24 The following sections will examine extensions of the above mentioned cohort studies
25 and new studies published since the 2004 PM AQCD. The section includes discussion of
26 both lung cancer incidence and mortality, as well as markers of exposure/susceptibility. A
27 summary of the mean PM concentrations reported for the new studies is presented in
28 Table 7.6. In addition, a summary of the associations for lung cancer mortality and
29 incidence are presented in Table 7.7 and Figure 7.8 (see Section 7.6) Further discussion of
30 all-cause and cause-specific mortality is presented in Section 7.6.

Table 7-6. Characterization of ambient PM concentrations from recent studies of cancer and long-term exposures to PM.

Reference	Location	Pollutant	Mean Annual Concentration ($\mu\text{g}/\text{m}^3$)	Upper Percentile Concentrations ($\mu\text{g}/\text{m}^3$)
Brunekreef et al. (2009, 191947)	The Netherlands	PM _{2.5}	28.3	Max: 36.8
Bonner et al. (2005, 088993)	Western NY State	TSP	44	
Jerret et al. (2005, 189405)	Los Angeles, California	PM _{2.5}		Max:27.1
Laden et al. (2006, 087605)	6 U.S. cities	PM _{2.5}	Range of means across sites: 10.2-29.0 Avg of means across sites: 16.4	
Naess et al. (2007, 090736)	Oslo, Norway	PM _{2.5}	15	Max: 22
		PM ₁₀	19	Max: 30
Palli et al. (2008, 156837)	Florence, Italy	PM ₁₀	NR	
Pedersen et al. (2006, 156848)	Czech Republic	PM _{2.5}		Max: 46-120
		PM ₁₀		Max: 120-238.6
Sorensen et al. (2005, 188901)	Copenhagen, Denmark	PM _{2.5}	Range of means across sites: 12.6-20.7 Avg of means across sites: 16.7	75th: 24.3-27.7
Sram et al. (2007, 188457)	Czech Republic	PM ₁₀		Max: 55
		PM _{2.5}		Max: 38
Sram et al. (2007, 192084)	Czech Republic	PM ₁₀	Range of means across sites: 36.4-55.6 Avg of means across sites: 46.0	
		PM _{2.5}	Range of means across sites: 24.8-44.4 Avg of means across sites: 34.6	
Vineis et al. (2006, 192089)	Multi-city, Europe	PM ₁₀	Range of means across sites: 19.9-73.4 Avg of means across sites: 35.4	
Vinzents et al. (2005, 087482)	Copenhagen, Denmark	PM ₁₀	Range of means across sites: 16.9-23.5 Avg of means across sites: 20.2	

1 A subset of the ACS cohort study from 1982-2000 that included only residents of Los
2 Angeles, California was used to examine the association between PM_{2.5} and lung cancer
3 mortality while adjusting for both individual and neighborhood covariates (Jerrett et al.,
4 2005, [189405](#)). There was a positive association between PM_{2.5} and lung cancer mortality
5 when adjusting for 44 individual covariates [RR 1.44 (95% CI: 0.98-2.11) per 10 $\mu\text{g}/\text{m}^3$
6 increase in PM_{2.5}]. However, including all potential individual and neighborhood covariates
7 associated with mortality reduced the association [RR 1.20 (95% CI: 0.79-1.82) per 10 $\mu\text{g}/\text{m}^3$
8 increase in PM_{2.5}]. A recent re-analysis of the full ACS cohort by the Health Effects Institute
9 also demonstrated a positive association between PM_{2.5} and lung cancer mortality [RR 1.11
10 (95% CI: 1.04-1.18)] (Krewski et al., 2009, [191193](#)). The authors observed modification of
11 this risk by educational attainment, with those completing a high school degree or less
12 having greater risk. In addition to utilizing the ACS cohort for a nationwide analysis, this
13 same study conducted two regional assessments, one in the New York City area and the
14 other in the Los Angeles area. No association was detected between PM_{2.5} and lung cancer

1 mortality in the analysis of the region included in the New York City analysis. A positive
 2 association was observed in the Los Angeles-area analysis using an unadjusted model, but
 3 this association did not persist after control for individual, ecologic, and co-pollutant
 4 covariates.

5 The Six Cities Study was extended to include data from 1990-1998, a period including
 6 1,368 deaths and 54,735 person-years (Laden et al., 2006, [087605](#)). An elevated risk ratio
 7 for lung cancer mortality was reported when the entire follow-up period (1974-1998) was
 8 included in the analysis [RR 1.27 (95% CI 0.96, 1.69) per 10 µg/m³ increase in average
 9 annual PM_{2.5}]. However, estimated decreases in PM_{2.5} were not associated with reduced
 10 lung cancer mortality [RR 1.06 (95% CI: 0.43-2.62) for every 10 µg/m³ reduction in PM_{2.5}].

11 Naess et al. (2007, [090736](#)) studied individuals aged 51-90 living in Oslo, Norway in
 12 1992. Death certificate data were obtained for 1992-1998 and information on PM was
 13 collected from 1992-1995. Women had a larger association of lung cancer mortality with
 14 PM_{2.5} compared to men. Similar results were reported for PM₁₀.

15 Most recently, Brunekreef et al. (2009, [191947](#)) used the Netherlands cohort study
 16 (NLCS) on diet and cancer to conduct a re-analysis of the research performed by Beelen et
 17 al. (2008, [156263](#)) examining the association between PM and both lung cancer mortality
 18 and incidence. After ten years of follow-up, there was no association between PM_{2.5} and lung
 19 cancer mortality for either the analysis of the full cohort (n = 105,296) [RR 1.06 (95% CI
 20 0.82-1.38) per 10 µg/m³ increase in PM_{2.5}] or the case-cohort (n = 4075) [RR 0.87 (95% CI:
 21 0.52-1.47)]. There was also no association with black smoke or traffic density variables,
 22 although living near a major roadway was associated with an elevated relative risk for lung
 23 cancer in the full cohort analysis [RR 1.20 (95% CI: 0.98-1.47)]. The association was not
 24 present in the case-cohort analysis [RR 1.07 (95% CI: 0.70-1.64)].

25 In addition to lung cancer mortality, Brunekreef et al. (2009, [191947](#)) also examined
 26 the association with lung cancer incidence using 11.3 years of follow-up data. In both the
 27 full cohort and the case-cohort analyses no association was reported between PM_{2.5} and lung
 28 cancer incidence [full cohort: RR 0.81 (95% CI: 0.63-1.04); case-cohort: RR 0.67 (95% CI:
 29 0.41-1.10) per 10 µg/m³ increase in PM_{2.5}]. The same was true for analyses of black smoke
 30 and traffic density variables.

Table 7-7. Associations* between ambient PM concentrations from select studies of lung cancer mortality and incidence.

Study	Cohort	Location	Yrs	Analysis subgroup	Effect Estimate (95% CI)
<i>MORTALITY - PM_{2.5}</i>					
Dockery et al. (1993, 044457) [†]	Six-Cities	Six cities across the U.S.	1974-1991		1.18 (0.89-1.57)
Krewski et al. (2000, 012281) [†]	Six-Cities-Re-analysis	Six cities across the U.S.	1974-1991		1.16 (0.86-1.23)
Laden et al. (2006, 087605)	Six-Cities	Six cities across the U.S.	1974-1998		1.27 (0.96-1.69)
Beelen et al. (2008, 156263)	NLCS	Netherlands	1987-1996	Full Cohort	1.06 (0.82-1.38)

Study	Cohort	Location	Yrs	Analysis subgroup	Effect Estimate (95% CI)
Beelen et al. (2008, 156263)	NLCS	Netherlands	1987-1996	Case Cohort	0.87 (0.52-1.47)
Brunekreef et al. (2009, 191947)	NLCS-Re-analysis	Netherlands	1987-1996	Full Cohort	1.06 (0.82-1.38)
Brunekreef et al. (2009, 191947)	NLCS-Re-analysis	Netherlands	1987-1996	Case Cohort	0.87 (0.52-1.47)
Pope et al. (1995, 045159) [‡]	ACS	U.S.	1982-1989		1.01 (0.91-1.12)
Pope et al. (2002, 024689) [‡]	ACS	U.S.	1982-2000		1.13 (1.04-1.22)
Jerret et al. (2005, 189405)	ACS-LA	Los Angeles	1982-2000	Intra-metro Los Angeles	1.44 (0.98-2.11)
Krewski et al. (2009, 191193)	ACS-Re-analysis	U.S.	1982-2000		1.11 (1.04-1.18)
Krewski et al. (2009, 191193)	ACS-Re-analysis	New York City	1982-2000	Intra-metro New York City	0.90 (0.29-2.78)
Krewski et al. (2009, 191193)	ACS-Re-analysis	Los Angeles	1982-2000	Intra-metro Los Angeles	1.31 (0.90-1.92)
McDonnell et al. (2000, 010319) [†]	AHSMOG	California	1973-1977	Men	1.39 (0.79-2.46)
Naess et al. (2007, 090736) [†]		Oslo, Norway	1992-1998	Men, 51-70 yrs	1.18 (0.93-1.52)
Naess et al. (2007, 090736) [†]		Oslo, Norway	1992-1998	Men, 71-90 yrs	1.18 (0.93-1.52)
Naess et al. (2007, 090736) [†]		Oslo, Norway	1992-1998	Women, 51-70 yrs	1.83 (1.36-2.47)
Naess et al. (2007, 090736) [†]		Oslo, Norway	1992-1998	Women, 71-90 yrs	1.45 (1.05-2.02)
MORTALITY - PM₁₀					
McDonnell et al. (2000, 010319) [†]	AHSMOG	California	1973-1977	Men	1.23 (0.84-1.80)
Naess et al. (2007, 090736) [†]		Oslo, Norway	1992-1998	Men, 51-70 yrs	1.12 (0.95-1.33)
Naess et al. (2007, 090736) [†]		Oslo, Norway	1992-1998	Men, 71-90 yrs	1.14 (0.97-1.36)
Naess et al. (2007, 090736) [†]		Oslo, Norway	1992-1998	Women, 51-70 yrs	1.50 (1.23-1.84)
Naess et al. (2007, 090736) [†]		Oslo, Norway	1992-1998	Women, 71-90 yrs	1.29 (1.03-1.60)
INCIDENCE - PM_{2.5}					
Beelen et al. (2008, 155681)	NLCS	Netherlands	1987-1996	Full Cohort	0.81 (0.63-1.04)
Beelen et al. (2008, 155681)	NLCS	Netherlands	1987-1996	Case Cohort	0.65 (0.41-1.04)
Brunekreef et al. (2009, 191947)	NLCS-Re-analysis	Netherlands	1987-1996	Full Cohort	0.81 (0.63-1.04)
Brunekreef et al. (2009, 191947)	NLCS-Re-analysis	Netherlands	1987-1996	Case Cohort	0.67 (0.41-1.10)
INCIDENCE - PM₁₀					
Beesn et al. (1998, 048890)	AHSMOG	California	1977-1992	Men	1.99 (1.32-3.00)
Vineis et al. (2006, 192089)	GenAir	Europe	1993-1999	Case-Control	0.91 (0.70-1.18)

*per 10 µg/m³ increase

†Results from the paper were standardized to 10 µg/m³ [For McDonnell et al. the non-standardized results were reported based on IQR increments (24.3 µg/m³ for PM_{2.5} and 29.5 µg/m³ for PM₁₀). For Naess et al. the original hazard ratios were calculated based on quartiles of PM exposure. The results were converted to 10 µg/m³ using the mean range of the four quartiles (3.95 µg/m³ for PM_{2.5} and 5.88 µg/m³ for PM₁₀)].

‡Study was included in the 2004 PM AQCD

1 The association between PM and incident lung cancers was examined in the European
2 Prospective Investigation into Cancer and Nutrition study (EPIC) (Vineis et al., 2006,
3 [192089](#)). Within this cohort, a nested case-control study, the GenAir study, included cases of
4 incident cancer and controls matched on age, gender, smoking status, country of
5 recruitment, and time between recruitment and diagnosis. Only non-smokers and former
6 smokers who had quit smoking at least ten years prior were included. The study included
7 113 cases and 312 controls. No association was seen between PM₁₀ and lung cancer [OR
8 0.91 (95% CI: 0.70-1.18) per 10 µg/m³]. The OR was elevated when cotinine, a marker for
9 cigarette exposure, was included in the model but the authors state that this is probably
10 due to small study size [OR 2.85 (95% CI: 0.97-8.33) comparing ≥ 11 µg/m³ to <11 µg/m³].

1 Control for other potential confounders, such as BMI, education level, and intake of fruit
2 and vegetables, did not have a large impact on the estimate.

7.5.1.2. Other Cancers

3 Bonner et al. (2005, [088993](#)) conducted a population-based, case-control study of the
4 association between ambient exposure to polycyclic aromatic hydrocarbons (PAHs) in early
5 life and breast cancer incidence among women living in Erie and Niagara counties in the
6 state of New York. Cases (n = 1166 of which 841 were post-menopausal) were women with
7 primary breast cancer, and controls (n = 2105 of which 1495 were post-menopausal) were
8 frequency matched to the cases by age, race, and county of residence. TSP was used as a
9 proxy for PAH exposure. Annual average TSP concentrations (1959-1997) were obtained
10 from the New York State Department of Environmental Conservation for Erie and Niagara
11 Counties. Among postmenopausal women, exposure to high concentrations of TSP
12 (>140 $\mu\text{g}/\text{m}^3$) at birth was associated with an OR of 2.42 for breast cancer (95% CI: 0.97-
13 6.09) relative to low concentrations of TSP (<84 $\mu\text{g}/\text{m}^3$). ORs were elevated for pollution
14 exposures at age of menarche (OR: 1.45 [95% CI: 0.74-2.87]) and age at first birth (OR: 1.33
15 [95% CI: 0.87-2.06]) among postmenopausal women. Among premenopausal women,
16 exposure to high concentrations of TSP at birth was associated with an OR for breast
17 cancer incidence of 1.79 (95% CI: 0.62-5.10) relative to low exposure levels, exposure at age
18 of menarche was associated with an OR of 0.66 (95% CI: 0.38-1.16), and exposure at age of
19 first birth was associated with an OR of 0.52 (95% CI: 0.22-1.20).

7.5.1.3. Markers of Exposure or Susceptibility

20 Several studies looked at markers of exposure or susceptibility as the outcome
21 associated with short-term exposure. These studies are included here because they may be
22 relevant to the mechanism that leads to cancer associated with long-term exposures.

23 A study performed in the Czech Republic compared 53 male policemen working at
24 least eight hours per day outdoors in urban air with age- and sex-matched controls who
25 spent at least 90% of their day indoors (n = 52) (Sram et al., 2007, [188457](#)). During the
26 sampling period, two monitors from downtown and suburban areas detected levels of air
27 pollutants in the following ranges: PM₁₀ 32-55 $\mu\text{g}/\text{m}^3$, P_{2.5} 27-38 $\mu\text{g}/\text{m}^3$, c-PAHs 18-22 ng/m^3 ,
28 and B[a]P 2.5-3.1 ng/m^3 using a VAPS monitor (measurements taken with a HiVol monitor,
29 which has a lower flow rate, had a mean for PM₁₀ of 62.6 $\mu\text{g}/\text{m}^3$). c-PAHs detected on
30 personal monitors during sampling days had a mean of 12.04 ng/m^3 among the policemen
31 and 6.17 ng/m^3 among the controls. No difference in percent of chromosomal aberrations
32 was observed between the policemen and control group using conventional cytogenetic
33 analysis. However, using fluorescent in situ hybridization (FISH), a difference in
34 chromosomal aberrations between the policemen and control group was reported. For
35 example, the percentage of aberrant cells, as well as the genomic frequency of

1 translocations per 100 cells, was about 1.4-fold greater in the policemen. This was largely
2 driven by a difference in chromosomal aberrations between nonsmoking policemen and
3 nonsmoking controls. A similar study that included only the policemen (n = 60), reported
4 that the mean exposure to c-PAHs and B[a]P for 40-50 days before sampling were
5 associated with chromosomal aberrations when analyzed with FISH (Sram et al., 2007,
6 [192084](#)). However, when included in a model with other covariates, the association with
7 these variables was null. No association was present with use of conventional cytogenetic
8 analysis.

9 Palli et al. (2008, [156837](#)) investigated the correlation between ambient PM₁₀
10 concentrations and individual levels of DNA bulky adducts. Study participants were 214
11 healthy adults aged 35-64 years at enrollment who resided in the city of Florence, Italy.
12 This study was conducted between 1993 and 1998. PM₁₀ exposure levels were based on
13 daily environmental measures provided by two types of urban monitoring stations (high-
14 traffic and low-traffic). The researchers assessed correlation between DNA bulky adducts
15 measured in blood samples and PM₁₀ concentrations prior to blood sample collection. Time
16 windows of PM₁₀ exposure evaluated in this study were 0-5 days, 0-10 days, 0-15 days, 0-30
17 days, 0-60 days, and 0-90 days prior to blood sample collection. Overall, average PM₁₀
18 concentrations decreased during the study period, with some fluctuations. Quantitative
19 values were not reported, but PM₁₀ appeared to range between approximately 30 and
20 100 µg/m³ for high-traffic stations, and between approximately 20 and 50 µg/m³ for low-
21 traffic stations. This study found that levels of DNA bulky adducts among non-smoking
22 workers with occupational traffic exposure were positively correlated with cumulative PM₁₀
23 levels from high-traffic stations during approximately 2 wk preceding blood sample
24 collection (0-5 days: r = 0.55, p = 0.03; 0-10 days: r = 0.58, p = 0.02; 0-15 days: r = 0.56,
25 p = 0.02). DNA bulky adducts were not associated with PM₁₀ levels among Florence
26 residents with no occupational exposure to vehicle emissions or among smokers. DNA bulky
27 adducts were not associated with PM₁₀ levels assessed by low-traffic urban monitoring
28 stations.

29 The association between personal exposure to water-soluble transition metals in PM_{2.5}
30 and oxidative stress-induced DNA damage was investigated among 49 students from
31 Central Copenhagen, Denmark (Sorensen et al., 2005, [188901](#)). Researchers assessed PM_{2.5}
32 exposure by personal sampling over two weekday periods twice in 1-yr (November, 1999
33 and August, 2000), and determined the concentration of water-soluble transition metals (V,
34 Cr, Fe, Ni, Cu and Pt) in these samples. In addition, lymphocyte and 24-h urine samples
35 were analyzed for DNA damage by measuring 7-hydro-8-oxo-2'-deoxyguanosine (8-oxodG).
36 Mean concentrations and corresponding IQR of these metals differed between months of
37 sample collection. This study found that 8-oxodG concentration in lymphocytes was
38 significantly associated with V and Cr concentrations, with a 1.9% increase in 8-oxodG per
39 1 µg/L increase in V concentration and a 2.2% increase in 8-oxodG per 1 µg/L increase in Cr

1 concentration; these associations were independent of the PM_{2.5} mass concentration. The
2 other transition metals were not significantly associated with the 8-oxodG concentration in
3 lymphocytes, and none of the six measured transition metals was associated with the 8-
4 oxodG concentration in urine.

5 Vinzents et al. (2005, [087482](#)) investigated the association between ultrafine particles
6 (UFP) and PM₁₀ concentrations with levels of purine oxidation and strand breaks in DNA
7 using a crossover design. Study participants were 15 healthy nonsmoking individuals with
8 a mean age of 25. UFP exposure was evaluated using number concentration obtained in the
9 breathing zone by portable instruments in six 18-h weekday periods from March to June
10 2003. Ambient concentrations for PM₁₀ and UFP were also measured on all exposure days
11 at curbside street stations and at one urban background station. Oxidative DNA damage
12 was assessed by evaluating strand breaks and oxidized purines in mononuclear cells
13 isolated from venous blood the morning after exposure measurement. Mean number
14 concentration of UFPs (street station) was 30.4×10^3 UFPs/mL (standard deviation [SD]:
15 1.38), mean mass concentration of PM₁₀ at a background monitoring station was $16.9 \mu\text{g}/\text{m}^3$
16 (SD: 1.53), and mean mass concentration of PM₁₀ at a street station was $23.5 \mu\text{g}/\text{m}^3$ (SD:
17 1.48). Mean personal exposure to UFPs was 32.4×10^3 UFPs/mL (SD: 1.49) while bicycling
18 (5 occasions), 19.6×10^3 UFPs/mL (SD: 1.78) during other outdoor activities (6 occasions),
19 and 13.4×10^3 UFPs/mL (SD: 1.96) while indoors (6 occasions). The regression coefficients of
20 the mixed-effects models looking at level of purine oxidation were estimated as 1.50×10^{-3}
21 (95% CI: 0.59×10^{-3} to 2.42×10^{-3} ; $p = 0.002$) for cumulative outdoor exposure and $1.07 \times$
22 10^{-3} (95% CI: 0.37×10^{-3} to 1.77×10^{-3} ; $p = 0.003$) for cumulative indoor exposure. Neither
23 cumulative outdoor nor cumulative indoor exposures to UFPs were associated with strand
24 breaks. Neither ambient air concentrations of PM₁₀ nor number concentrations of UFPs at
25 monitoring stations were significant predictors of DNA damage.

26 Additionally, a number of studies employed ecologic study designs, comparing the
27 prevalence of biomarkers in populations from more polluted locations to those in less
28 polluted locations. In a pilot study conducted in the Czech Republic (Pedersen et al., 2006,
29 [156848](#)), children age 5-11 provided 5 mL blood samples and the frequency of micronuclei in
30 peripheral blood lymphocytes was analyzed for cytogenetic effects. Significantly higher
31 frequencies of micronuclei were found in younger children living in Teplice (PM_{2.5}
32 concentration = $120 \mu\text{g}/\text{m}^3$) than in Prachatice (PM_{2.5} concentration = $46 \mu\text{g}/\text{m}^3$). The levels
33 of c-PAHs were also much higher in Teplice (nearly $30 \text{ ng}/\text{m}^3$ in Teplice and about $15 \text{ ng}/\text{m}^3$
34 in Prachatice). The difference in micronuclei frequencies observed in the children from the
35 two locations may be attributable to differences in exposure to air pollution, but could also
36 be due to differences in diet or other environmental exposures. This finding is noteworthy
37 considering micronuclei formation in peripheral blood lymphocytes is thought to be
38 biologically relevant for carcinogenesis.

1 Avogbe et al. (2005, [087811](#)) showed that there appeared to be a correlation between
2 the level of oxidative DNA damage in individuals and exposure to ambient ultrafine
3 particulate matter. Formamidopyrimidine DNA glycosylase sensitive sites and the presence
4 of DNA strand breaks were assessed from blood and urine samples obtained from healthy,
5 non-smoking male volunteers that lived and worked in different areas of Cotonou, Benin.
6 Exposure to benzene was assessed by urinary excretion of S-phenylmercapturic acid. There
7 was a high degree of correlation between exposure to benzene and ultrafine particles and
8 the presence of DNA strand breaks and formamidopyrimidine DNA glycosylase sensitive
9 sites (rural subjects < suburban subjects < residents living near high traffic roads < taxi
10 drivers). Genotyping studies showed that the magnitude of the effects of benzene and
11 ultrafine particulates may be modified by polymorphisms in GSTP1 and NQO1 genes.

12 Tovalin et al. (2006, [091322](#)) evaluated the association between exposure to air
13 pollutants and the level of DNA damage using the single cell gel electrophoresis (comet)
14 assay. Mononuclear lymphocytes from outdoor and indoor workers from two areas in
15 Mexico, Mexico City (large city) and Puebla (medium size city), were evaluated. The
16 outcomes showed that the outdoor workers in Mexico City exhibited greater DNA damage
17 than indoor workers in the same region. Similar levels of DNA damage were observed
18 between indoor and outdoor workers in Puebla. The level of observed DNA damage was
19 correlated with exposure to ozone and PM_{2.5}.

20 In summary, several recent studies have reported an association between lung cancer
21 mortality and long-term PM_{2.5} exposure. Although many of the estimates include the null in
22 the confidence interval, overall the results have shown a positive relationship. The two
23 recent studies that looked at lung cancer incidence did not report an association with PM_{2.5}
24 (Brunekreef et al., 2009, [191947](#)) or PM₁₀ (Vineis et al., 2006, [192089](#)). Studies of
25 exposure/susceptibility markers have reported inconsistent outcomes, with some markers
26 being associated with PM and others not.

7.5.2. Toxicological Studies

27 Over the past 30 years numerous mutagenicity and genotoxicity studies of ambient
28 PM and their contributing sources have been conducted to assess the relative mutagenic or
29 genotoxic potential. Studies previously reviewed in the 2004 PM AQCD (U.S. EPA, 2004,
30 [056905](#)) provide compelling evidence that ambient PM and PM from specific combustion
31 sources (e.g., fossil fuels) are mutagenic in vivo and in vitro. Research cited in the 2004
32 AQCD demonstrated mutagenic activity of ambient PM from urban centers in California,
33 Germany and the Netherlands. These studies suggested that ubiquitous emission sources,
34 particularly motor vehicle emissions, rather than isolated point sources were largely
35 responsible for the mutagenic effects. In addition, the mutagenicity was dependent upon
36 the chemical composition of the PM with unsubstituted polyaromatic compounds and semi-

1 polar compounds being highly mutagenic. Mutagenicity was also dependent on size, with
2 the fine fraction of urban PM having greater effects than the coarse fraction. Genotoxic
3 activity was demonstrated for ambient PM from two high traffic areas (one upwind and one
4 downwind) and a rural site. In addition, the 2004 AQCD reported that exhausts from
5 gasoline and diesel engines were mutagenic and that DE was more potent. More
6 mutagenicity was observed for exhaust from cold starts than starts at room temperature.
7 Both gaseous and particulate fractions of DE were found to be mutagenic. Sequential
8 fractionation of extracts from gasoline and diesel exhaust implicated the polar fractions,
9 especially nitrated polynuclear aromatic compounds, as contributing greatly to
10 mutagenicity. Among some of the other mutagenically active compounds found in the gas
11 phase of DE are ethylene, benzene, 1,3-butadiene, acrolein and several PAHs, all of which
12 are also present in gasoline exhaust. Also cited in the 2004 AQCD were studies
13 demonstrating mutagenic effects of emissions from wood/biomass burning, which were
14 primarily attributable to the organic fraction and not the condensate. It was noted that
15 wood smoke induced both frameshift mutations and base pair substitution but not DNA
16 adducts. Further, emissions from coal combustion in China were found to be mutagenic,
17 with both polar and aromatic fractions contributing to effects. Little data were available on
18 the mutagenicity of coal fly ash emissions from U.S. conventional combustion plants. In
19 conclusion, these studies provide evidence that ambient PM and combustion-derived PM
20 are mutagenic/genotoxic. The 2004 AQCD noted that there is not a simple relationship
21 between mutagenic potential and carcinogenic potential in animals or humans. No studies
22 evaluating carcinogenic effects of PM were reported in the 2004 AQCD.

23 Building on results of earlier studies in the 2004 PM AQCD, data from newly
24 published studies that evaluated the mutagenic, genotoxic and carcinogenic effects of PM,
25 PM-constituents, and combustion emission source particles are reviewed. Pertinent studies
26 are described briefly in the following paragraphs. A summary table is provided in Annex D
27 (Tables D7-D9).

7.5.2.1. Mutagenesis and Genotoxicity

In Vitro Studies

28 In general, studies have focused on PM and PM extracts for mutagenicity testing
29 using bacteria and mammalian cell lines. PM and/or PM extracts from ambient air samples,
30 wood smoke, and coal, diesel, or gasoline combustion have all been reported to induce
31 mutation in *S. typhimurium* and in cultured human cells (Abou Chakra et al., 2007,
32 [098819](#); Gábelová et al., 2007, [156457](#); Gábelová et al., 2007, [156458](#); Hannigan et al., 1997,
33 [083598](#); Hornberg et al., 1998, [155849](#)). In addition, effects associated with PM and PM-
34 associated constituents include induction of micronucleated reticulocytes (MN) formation,
35 DNA adduct formation, SCE, DNA strand breaks, frameshifts and inhibition of gap-

1 junctional intercellular communication (Alink et al., 1998, [087159](#); Arlt et al., 2007, [097257](#);
2 Avogbe et al., 2005, [087811](#); Gábelová et al., 2007, [156457](#); Gábelová et al., 2007, [156458](#);
3 Healey et al., 2006, [156532](#); Hornberg et al., 1996, [087164](#); Hornberg et al., 1998, [155849](#);
4 Sevastyanova et al., 2007, [156969](#))

5 Constituents adsorbed onto individual particles play a large role in the genotoxic
6 potential of PM. Poma et al. (2006, [096903](#)) showed that fine carbon black particles were
7 consistently less genotoxic than similar concentrations of PM_{2.5} extracts, suggesting that
8 the adsorbed components play a role in the genotoxic potential of PM. Total PAH and
9 carcinogenic PAH content is correlated with the genotoxic effects of PM (De Kok et al.,
10 2005, [088656](#); Sevastyanova et al., 2007, [156969](#)). Comparison of different extracts (water
11 vs. organic) by Gutierrez-Castillo et al. (2006, [089030](#)) indicated that water soluble extracts
12 were more genotoxic than the corresponding organic extracts. Sharma et al. (2007, [156975](#))
13 reported that mutagenic activity of extracted PM samples collected in and around a waste
14 incineration plant was attributed to the moderately polar and polar fractions. The polar and
15 crude fractions were mutagenic without metabolic activation, suggesting a direct mutagenic
16 effect. No mutagenic activity was observed from any of the nonpolar samples evaluated.
17 Arlt and colleagues (2007, [097257](#)) have shown that the PM constituents 2-
18 nitrobenzanthrone and 3-nitrobenzanthrone were genotoxic in a variety of bacterial and
19 mammalian cell systems.

20 Conflicting data have been reported for the role of metabolic enzymes on the
21 genotoxicity of PM and their adsorbed constituents. Arlt et al. (2007, [097257](#)) reported that
22 the PM constituent 2-nitrobenzanthrone (2-NB) was genotoxic in bacterial and mammalian
23 cells. However, metabolic activation with the human N-acetyltransferase 2 or
24 sulfotransferase (SULT1A1) enzyme was needed for the effect to be observed in human
25 cells. Erdinger et al. (2005, [156423](#)) demonstrated that mutagenic activity was not affected
26 when metabolism was induced. de Kok et al. (2005, [088656](#)) evaluated the relationship
27 between the physical, chemical, and genotoxic effects of ambient PM. TSP, PM₁₀, and PM_{2.5}
28 were sampled at different locations and the extracts were assessed for mutagenicity and
29 induction of DNA adducts in cells. Overall, induction of rat liver S9 metabolism generally
30 reduced the mutagenic potential via the Ames assay of the particle fractions and DNA
31 reactivity (induction of DNA adducts) was generally higher after metabolic activation.
32 Binková et al. (2003, [156274](#)) found that the addition of S9 increased PM₁₀-dependent DNA
33 adduct formation.

Ambient Air

34 A limited number of studies evaluated the impact of the season on the genotoxic
35 effects of ambient PM. A few studies however have indicated that greater genotoxic effects
36 were associated with samples collected during the winter months compared to those
37 collected in the summer (Abou Chakra et al., 2007, [098819](#); Gábelová et al., 2007, [156457](#);
38 Gábelová et al., 2007, [156458](#)). In contrast, Hannigan et al. (1997, [083598](#)) indicated that

1 no seasonal variation was observed. Studies have also shown that greater genotoxic effects
2 were associated with smaller particle size extracts (e.g., PM_{2.5}>PM₁₀) and from samples
3 collected in urban areas or closer to higher trafficked areas (Abou Chakra et al., 2007,
4 [098819](#); Hornberg et al., 1998, [155849](#)).

5 de Kok et al. (2005, [088656](#)) found the direct mutagenicity (Ames assay) and the
6 direct DNA reactivity (DNA adduct formation) of the PM_{2.5} size fraction was significantly
7 higher than that of the larger size fractions (TSP, PM₁₀) at most locations.

8 DNA damage was assessed by the Comet assay in A549 cells exposed to PM collected
9 from a high traffic area in Copenhagen, Denmark (TSP approximately 30 µg/m³) and
10 compared to the results from exposure of A549 cells to standard reference materials
11 (SRM1650 or SRM2975) at the same concentrations (2.5-250 µg/ml) (Danielsen et al., 2008,
12 [192092](#)). All three particles induced strand breaks and oxidized purines in a dose-dependent
13 manner and there were no obvious differences in potency. In contrast, only the ambient PM
14 formed 8-oxo-7,8-dihydro-2'-deoxyguanosine (8-oxodG) when incubated with calf thymus
15 DNA, which may be due to the levels of transition metals.

Diesel and Gasoline Exhaust

16 Automobile DEP (A-DEP) was tested in *S. typhimurium* strains TA98, TA100, and its
17 derivatives (e.g., TA98NR and YG1021) and found to be more mutagenic than forklift DEP
18 (i.e., SRM2975) particles, based on PM mass. A-DEP had 227 times more PAH-type
19 mutagenic activity and 8-45 times more nitroarene-type mutagenic activity due to the
20 different conditions for generating and collecting the two DEP samples (DeMarini et al.,
21 2004, [066329](#)). Using a diesel engine without an oxidation catalytic converter (OCC), the
22 diesel engine exhaust particle (DEP) extract produced the highest number of revertant
23 colonies in strains TA98 and TA100 with and without S9 at several tested loads when
24 compared to extracts from low-sulfur diesel fuel (LSDF), rapeseed oil methyl ester (RME),
25 and soybean oil methyl ester (SME). When an OCC was installed in the exhaust pipe of the
26 engine, all extracts reduced the number of revertant colonies in both strains with and
27 without S9 at partial loads but increased the number of revertant colonies without S9 at
28 rated power. At idling, DEP extracts increased the number of revertant colonies with and
29 without S9 (Bunger et al., 2006, [156303](#)). In a separate study, engine emissions (particle
30 extracts and condensates) from rapeseed (canola) oil were found to produce greater
31 mutagenic effects in *S. typhimurium* strains TA98 and TA100 than DEP (Bunger et al.,
32 2007, [156304](#)). Additionally, DE extract (DEE) from diesel fuel containing various
33 percentages of ethanol was also observed to induce mutational response in two *Salmonella*
34 strains. Base diesel fuel DEE and DEE from fuel with 20% ethanol caused more significant
35 DNA damage in rat fibrocytes L-929 cells than extracts containing 5, 10, or 15% ethanol
36 (Song et al., 2007, [188903](#)).

37 DE and gasoline engine exhaust particles, as well as their semi-volatile organic
38 compound (SVOC) extracts, induced mutations in the two *S. typhimurium* strains YG1024

1 and YG1029 in the absence and presence of S9; the PM extracts were more mutagenic than
2 the SVOC extracts. Additionally, all extracts except the DE extract induced DNA damage
3 and MN in Chinese hamster lung V79 cells (Liu et al., 2005, [192098](#)). Another study
4 demonstrated that gasoline engine exhaust significantly increased colony formation in
5 TA98 with and without S9 (Zhang et al., 2007, [157186](#)).

6 Jacobsen et al. (2008, [156597](#)) used the FE1-Muta™ Mouse lung epithelial cell line to
7 investigate putative mechanisms of DEP-induced mutagenicity. Mutation ion frequencies
8 and ROS were determined after cells were incubated with 37.5 or 75 µg/ml DEP (SRM1650)
9 for 72-h (n = 8). The mutation frequency at the 75 µg/ml dose was significantly increased
10 (1.55-fold; p<0.001) in contrast to cells treated with 37.5 µg/ml DEP. DEP induced ROS
11 generation 1.6-1.9-fold in the epithelial cell cultures after 3 hours of exposure compared
12 with the 3-10-fold increase in ROS production previously reported for carbon black. The
13 authors concluded that the mutagenic activity of DEP is likely attributable to activity from
14 the organic fraction that both contains reactive species and can generate ROS.

15 In human A549 and CHO-K1 cells, the organic fraction of DEP significantly increased
16 the amount of Comet and MN formation, respectively, in the presence and absence of SKF-
17 525A (a CYP450 inhibitor) and S9, respectively (Oh and Chung, 2006, [088296](#)). The organic
18 base and neutral fractions of DEP also significantly induced DNA damage but only without
19 SKF-525A, and all fractions but the moderately polar fraction (phthalates and PAH
20 oxyderivatives) induced MN formation with and without S9 (Bao et al., 2007, [097258](#)).
21 Gasoline engine exhaust significantly induced DNA damage as measured in the Comet
22 assay and increased the frequency of MN in human A549 cells (Zhang et al., 2007, [157186](#)).
23 In human-hamster hybrid (AL) cells, DEP (SRM 2975) dose-dependently increased the
24 mutation yield at the *CD59* locus; this was significantly reduced by simultaneous treatment
25 with phagocytosis inhibitors (Bao et al., 2007, [097258](#)).

Wood Smoke

26 The mutagenicity of wood smoke (WS) and cigarette smoke (CS) extracts was assayed
27 in *Salmonella typhimurium* strains TA98 and TA100 (Ames assay) using the pre-incubation
28 assay with exogenous metabolic activation (rat liver S-9). Extracts of both samples (62.5 or
29 125 µg TPM equivalent/ml) were equally mutagenic to strain TA98 but the WS extract was
30 less mutagenic than the CS extracts in strain TA100 (Iba et al., 2006, [156582](#)).

In vivo studies

Ambient Air

31 The contribution of ambient urban roadside air exposure (4, 12, 24, 48 or 60 wk) to
32 DNA damage was examined in the lungs, nasal mucosa, and livers of adult male Wistar
33 rats in Kawasaki, Japan (Sato et al., 2003, [096615](#)). Messenger RNA levels of CYP450
34 enzymes that catalyze the transformation of PAHs to reactive metabolites were also

1 evaluated. Concentrations of gases were reported to be 12-182 ppb NO and 0-9 ppb NO₂ in
2 the filtered air chamber and 33-280 ppb NO and 42-81 ppb NO₂ in the experimental group
3 chamber. Suspended PM concentrations were 11-19 µg/m³ in the filtered air chamber and
4 42-100 µg/m³ (average 63 µg/m³) in the experimental group chamber. Body weight
5 significantly decreased in exposed animals at 24, 48 and 60 wk. Exposure of 4 wk to urban
6 roadside air resulted in significant increases in multiple DNA adducts (lung, nasal, and
7 liver DNA adducts). With longer exposures, there were significant increases in lung (48 wk),
8 nasal (60 wk), and liver DNA adducts (60 wk). Changes were seen in CYP1A2 mRNA at
9 4 wk with a 2.3 fold increase in exposed animals compared to the control group with no
10 change observed at 60 wk; CYP1A1 mRNA was unchanged. These results indicate that
11 exposure to ambient air in this roadside area could induce DNA adduct formation, which
12 may be important for carcinogenicity. Earlier studies (Ichinose et al., 1997, [053264](#)) have
13 shown that 8-oxo-dG, a DNA adduct, is elevated along with tumor formation in a dose-
14 dependent manner in mice administered DEP. The finding of adducts in the liver indicated
15 that deposition of PM and its associated PAHs in the lung can have indirect effects on
16 extrapulmonary organs. It should be noted that PM deposition on the fur and ingestion
17 during grooming cannot be ruled out as a possible exposure route.

18 Another animal toxicological study employed “non-carcinogenic” particles obtained
19 from pooled non-cancerous lung tissue collected during surgical lung resection from three
20 non-smoking male patients diagnosed with lung adenocarcinomas (Tokiwa et al., 2005,
21 [191952](#)). Particles were partially purified to remove organic compounds. Morphologically
22 the particles were similar to DE or ambient air PM and the organic extracts from the
23 particles were directly mutagenic in *S. typhimurium* tester strains TA98, YG1021 and
24 YG1024. BALB/c and ICR mice were intratracheally instilled with particles at doses of 0.25,
25 0.5, 1.0, or 2.0 mg/mouse. After 24 hours, 8-oxo-dG was measured in lung DNA and found to
26 be increased in ICR mice in a dose-dependent manner, reaching a maximum of ~2.75 8-oxo-
27 dG/10⁵ dG at the 2.0 mg dose. The response was statistically significant at doses of 0.5, 1.0,
28 and 2.0 mg. The increased 8-oxo-dG levels observed in vivo was reported to be likely due to
29 hydroxyl radicals presumed to be involved in phagocytosis of non-mutagenic particles by
30 inflammatory cells that could induce hydroxylation of guanine residue on DNA.

Diesel Exhaust

31 An in vivo study employed *gtp* delta transgenic mice carrying the lambda EG10 on
32 each Chromosome 17 from a C57BL/6J background to investigate the effects of DEP on
33 mutation frequency (Hashimoto et al., 2007, [097261](#)). Mice were exposed via inhalation to
34 DEP or via IT instillation to DEP or DEP extract and lambda EG10 phages were rescued;
35 *E. coli* YG6020 was infected with the phage and screened for 6-thioguanine resistance. The
36 mutagenic potency (mutation frequency per mg) caused by DEP extract was twice that of
37 DEP, suggesting that the mutagenicity of DEP is attributed primarily to compounds in the
38 extract, since ~50% of the weight of DEP was provided by the extract. Interestingly, there

1 was no difference in mutation frequency between the 1 and 3 mg/m³ DEP groups after
2 12 wk of exposure.

Wood Smoke

3 One recent study measured the effect of freshly generated hard wood smoke (HWS) on
4 CYP1A1 activity based on ethoxyresorufin O-deethylase in pulmonary microsomes
5 recovered from male Sprague-Dawley rats exposed to HWS by nose-only inhalation
6 exposure (Iba et al., 2006, [156582](#)). CYP1A1 activity in rat lung explants treated with
7 extracts of the total PM (TPM) from HWS samples and from freshly generated cigarette
8 smoke (CS) was also evaluated. Unlike CS, HWS did not induce pulmonary CYP1A1
9 activity or mRNA (assessed by northern blot analysis) nor did extracts of HWS TPM induce
10 CYP1A1 protein (assessed by western blot analysis) in cultured rat lung explants. The
11 results suggest that unique constituents that are activated by CYP1A1 may be present in
12 CS but not HWS.

7.5.2.2. Carcinogenesis

13 Studies published prior to the 2004 AQCD that evaluated the carcinogenicity of
14 ambient air were reviewed by Claxton and Woodall (2007, [180391](#)). Five studies involved
15 chronic inhalation exposures in rodents. No statistically significant increase in
16 tumorigenesis was observed following chronic exposure to urban air pollution in Los
17 Angeles (Gardner, 1966, [015129](#); Gardner et al., 1969, [015130](#); Wayne and Chambers, 1968,
18 [038537](#)). However in a study conducted in Brazil, urban air pollution was found to enhance
19 the formation of urethane-induced lung tumors in mice (Cury et al., 2000, [192100](#); Reymao
20 et al., 1997, [084653](#)).

21 Two recent studies evaluated the carcinogenic potential of chronic inhalation
22 exposures to DE (Reed et al., 2004, [055625](#)) and hardwood smoke (HWS) (Reed et al., 2006,
23 [156043](#)). Two indicators of carcinogenic potential, formation of MN and tumorigenesis were
24 measured in strain A/J mice, which is a mouse model that spontaneously develops lung
25 tumors. Exposure to DE or HWS at concentrations of 1000 µg/m³ and below did not cause
26 increased formation of MN or an increased rate of lung tumors in this cancer-prone rodent
27 model. These studies are described below.

Diesel Exhaust

28 A/J mice were exposed to 30, 100, 300 and 1000 µg/m³ DE for 6 h/day and 7 days/wk
29 for 6 months (Reed et al., 2004, [055625](#)). The concentration of gases in this including NO_x,
30 NO₂, CO, SO₂, NH₃, methane, non-methane VOC, and FID total hydrocarbon ranged from
31 control to high dose group values of 0 to 50.4 ± 0.6 ppm, 0.2 ± 0.2 to 6.9 ± 3.3 ppm, 0.3 ± 0.1
32 to 30.9 ± 4.5 ppm, not detectable to 955.2 ± 58.4 ppb, 176.5 ± 8.8 to 9.1 ± 0.2 µg/m³, 1406.5 ±
33 253.2 to 2642.1 ± 455.9 µg/m³, 134.0 ± 52.1 to 1578.6 ± 256.2 µg/m³, 0.1 ± 0.1 to 2.2 ± 0.2
34 ppm, respectively. Particle sizes in the 4 exposure groups ranged from 0.10-0.15 µm mass

1 median aerodynamic diameter with geometric standard deviations of 1.4-1.8. Following the
2 6 month exposure and a 6 month recovery period, mice were collected and MN formation in
3 blood and tumor multiplicity and tumor incidence were measured in lungs. No increases in
4 formation of MN or numbers of lung adenomas were observed in DE-exposed mice
5 compared with controls.

Wood Smoke

6 A/J mice were exposed to 30, 100, 300 and 1000 $\mu\text{g}/\text{m}^3$ HWS for 30, 100, 300 and 1000
7 $\mu\text{g}/\text{m}^3$ DE for 6 h/day and 7 days/wk for 6 month (Reed et al., 2006, [156043](#)). Gaseous
8 components of the HWS included CO, NH₃, and non-methane VOC with concentrations
9 from control levels to high dose HWS exposure ranging from 229 ± 31 to 14887.6 ± 832.3
10 ppm, 139.3 ± 2.3 to 54.9 ± 1.2 $\mu\text{g}/\text{m}^3$ and 177.6 ± 10.4 to 3455.0 ± 557.2 $\mu\text{g}/\text{m}^3$, respectively.
11 Concentrations of NO_x, NO₂ and SO₂ were reported to be null. Particle sizes in the 4 exposure groups
12 ranged from 0.25-0.36 μm mass median aerodynamic diameter with geometric standard
13 deviations of 2.0-3.3. Following the 6 month exposure and a 6-month recovery period, mice
14 were collected and MN formation in blood and tumor multiplicity and tumor incidence were
15 measured in lungs. No increases in formation of MN or numbers of lung adenomas were
16 observed in HWS-exposed mice compared with controls. However, HWS from this study was
17 mutagenic in the Ames reverse mutation assay.

18 In summary, numerous new in vitro studies confirm and extend findings reported in
19 the 2004 AQCD that ambient PM from urban sites and combustion-derived PM are
20 mutagenic and genotoxic. A small number of new studies were conducted in vivo. One of
21 these studies demonstrated increased mutagenic potency in mice exposed to DEP and DEP
22 extract. Another study found increased formation of 8-oxo-dG, a DNA adduct, following
23 intratracheal instillation of PM in mice. A chronic inhalation study of rats exposed to urban
24 roadside air reported increased formation of DNA adducts in nose, lung, and liver and
25 induction of CYP1A2. Inhalation exposure of rats to HWS failed to induce CYP1A1 in
26 another study. Finally, two chronic inhalation studies found no evidence of carcinogenic
27 potential for DE and HWS in a cancer-prone mouse model. Collectively, these results
28 provide some evidence, mainly from in vitro studies, to support the biological plausibility of
29 ambient PM-lung cancer relationships observed in epidemiology studies.

7.5.3. Epigenetic Studies and Other Heritable DNA mutations

30 Two epidemiologic epigenetic studies examined the effect of PM on DNA methylation. Both
31 studies examined methylation of Alu and long interspersed nuclear element-1 (LINE-1) sequences, which
32 are located in repetitive elements. In previous studies, methylation of these sequences has been linked to
33 global genomic DNA methylation content (Weisenberger et al., 2005, [192101](#); Yang et al., 2004,
34 [192102](#)).

1 The first study included men age 55 and older who were part of the Normative Aging Study in the
2 Boston area. A stationary monitoring site located 1 km from the examination site was used to estimate
3 ambient PM_{2.5} exposure for the duration of the study (1999-2007). During the study period, the median
4 level of PM_{2.5}, averaged over 7 day periods, was 9.8 µg/m³ (interquartile range 8.0-12.0 µg/m³). There
5 was no association between PM_{2.5} and Alu methylation. LINE-1 methylation was associated with PM_{2.5}
6 measured over the 7 days before the examinations.

7 The second study included 63 healthy men aged 27 to 55 working at an electric furnace steel
8 plant (Tarantini et al., 2009, [192010](#)). Blood samples were taken twice, once in the morning after two
9 days of not working and once in the morning after three full days of work. PM₁₀ was measured in 11 work
10 areas and individuals completed daily logs about the amount of time spent in each area. On average,
11 individuals had an estimated exposure of 233.4 µg/m³ PM₁₀ (range 73.4-1220.2 µg/m³). Short-term
12 exposure did not alter the methylation of Alu and LINE-1. To examine effects of long-term exposure,
13 both blood samples were considered independent of time, and Alu and LINE-1 were examined with
14 respect to overall estimated PM₁₀ exposure using mixed effects models. There was a negative association
15 between increasing levels of PM₁₀ exposure and Alu and LINE-1 methylation, indicating that PM₁₀ causes
16 epigenetic changes to occur with long-term exposure. This study also looked at levels of inducible nitric
17 oxide synthase gene (*iNOS*), which is a gene suppressed by DNA methylation. *iNOS* expression was not
18 associated with long term exposure to PM₁₀ but was affected by methylation in the short term.

19 Animal toxicology studies evaluating the effect of PM exposure on changes in the
20 epigenome and other non-epigenetic heritable DNA changes have only recently been
21 conducted. After earlier work showed increased germline mutation rates in herring gulls
22 nesting near steel mills on Lake Ontario (Yauk and Quinn, 1996, [157163](#)) further work was
23 conducted to address air-dependent contribution to germline mutations by housing male
24 and female Swiss Webster mice in the same area and comparing mutation rates in those
25 animals with mutation rates of animals housed in a rural setting with less air pollution
26 (Somers et al., 2002, [078100](#)). To determine if PM or the gaseous phase of the urban air was
27 responsible for heritable mutations, Yauk et al. (2008, [157164](#)) exposed mature male
28 C57Bl×CBA F1 hybrid mice to either HEPA-filtered air or to ambient air in Hamilton,
29 Ontario, Canada for 3 or 10 wk, or 10 wk plus 6 wk of clean air exposure (16 wk). Sperm
30 DNA was monitored for expanded simple tandem repeat (ESTR) mutations, testicular
31 sample bulky DNA adducts, and DNA single or double strand breaks. In addition, male-
32 germ line (spermatogonial stem cell) DNA methylation was monitored post-exposure. This
33 area in Hamilton is near 2 steel mills and a major highway. Air composition showed mean
34 concentrations for TSP of 93.8 ± 17 µg/m³, PAH of 8.3 ± 1.7 ng/m³, and metal of 3.6 ± 0.7
35 µg/m³. Mutation frequency at ESTR Ms6-hm locus in sperm DNA from mice exposed 3 or
36 10 wk did not show elevated ESTR mutation frequencies, but there was a significant
37 increase in ESTR mutation frequency at 16 wk compared to HEPA-filter control animals,
38 pointing to a PM-dependent mechanism of action. No detectable DNA adducts were
39 observed in testes samples at any of the time points monitored. To verify inhalation

1 exposure to particles, DNA adducts were reported in the lungs of mice exposed for 3 wk to
2 ambient-air; no other time points showed detectable DNA adduct formation.

3 Hypermethylation of germ-line DNA was also observed in mice exposed to ambient air for
4 10 and 16 wk. These PM-dependent epigenetic modifications (hypermethylation) were not
5 seen in the haploid stage (3 wk) of spermatogenesis, but were nonetheless seen in early
6 stages of spermatogenesis (10 wk) and remained significantly elevated in mature sperm
7 even after removal of the mouse from the environmental exposure (16 wk). Thus, these
8 studies indicate that the ambient PM phase and not the gaseous phase is responsible for
9 the increased frequency of heritable DNA mutations and epigenetic modifications.

10 Based on the limited evidence from these epigenetics studies, long-term exposure to
11 PM₁₀ may result in epigenetic changes. PM_{2.5} also potentially affects some DNA methylation
12 content. As epigenetic research progresses, future studies examining the relationship
13 between PM and DNA methylation will be important in more thoroughly characterizing
14 these associations.

15 The effect of ambient PM on heritable DNA mutations and the epigenome has been
16 well characterized in a Canadian steel mill area. Mice exposed to ambient PM plus gases
17 developed paternally-derived heritable DNA mutations and epigenetic changes in sperm
18 DNA that were not observed in mice exposed to ambient air that was HEPA-filtered. This is
19 the first animal toxicology study showing heritable effects of PM exposure on DNA
20 mutation and the epigenome. Because the epigenetics field is so new, further work in this
21 emerging area will expand on these PM-dependent methylation changes to determine if the
22 results can be recapitulated at other urban sites.

7.5.4. Summary and Causal Determinations

23 The 2004 PM AQCD reported on original and follow-up analyses for three prospective
24 cohort studies that reported positive relationships between PM_{2.5} and lung cancer mortality.
25 Several recent, well-conducted epidemiologic studies have extended the evidence for a
26 positive association between PM_{2.5} and lung cancer mortality (Section 7.5.1.1). Generally,
27 studies have not reported associations between long-term exposure to PM_{2.5} or PM₁₀ and
28 lung cancer incidence (Section 7.5.1.1). Animal toxicological studies did not focus on specific
29 size fractions of PM, but rather examined ambient PM, woodsmoke, and DEP (Section
30 7.5.2). A number of recent studies indicate that ambient urban PM, emissions from
31 wood/biomass burning, emissions from coal combustion, and gasoline and DE are
32 mutagenic and that PAHs are genotoxic (Section 7.5.2). These findings are consistent with
33 earlier studies that concluded that ambient PM and PM from specific combustion sources
34 are mutagenic and genotoxic and provide biological plausibility for the results observed in
35 the epidemiologic studies. A limited number of epidemiologic and toxicological studies on
36 the epigenome demonstrate that PM induces changes in methylation (Section 7.5.3), a new

1 area of research that will likely be expanded in the future. However, it has yet to be
2 determined how these alterations in the genome could influence the initiation and
3 promotion of cancer. Overall, the evidence is **suggestive of a causal relationship between**
4 **relevant PM_{2.5} exposures and cancer, with the strongest evidence from the epidemiologic studies**
5 **of lung cancer mortality.** This evidence is limited by the non-specific measure of PM size
6 fraction in some of the epidemiologic studies and most of the animal toxicological studies,
7 and the inconsistency in evidence with recent epidemiologic studies for an effect on cancer
8 incidence. There is no epidemiologic evidence for cancer related to long-term exposure to
9 PM in organs or systems other than the lung. The evidence is **inadequate to assess the**
10 **association between PM_{10-2.5} and UFP exposures and cancer.**

7.6. Mortality Associated with Long-term Exposure

11 In the 1996 PM AQCD, results were presented for three prospective cohort studies of
12 adult populations: the Six Cities Study (Dockery et al., 1993, [044457](#)); the American Cancer
13 Society (ACS) Study (Pope CA et al., 1995, [045159](#)); and the California Seventh Day
14 Adventist (AHSMOG) Study (Abbey et al., 1995, [000669](#)). The 1996 AQCD concluded that
15 the chronic exposure studies, taken together, suggested associations between increases in
16 mortality and long-term exposure to fine PM, though there was no evidence to support an
17 association with PM_{10-2.5} (U.S. EPA, 1996, [079380](#)).

18 Discussions of mortality and long-term exposure to PM in the 2004 PM AQCD
19 emphasized the results of four U.S. prospective cohort studies, but the greatest weight was
20 placed on the findings of the ACS and the Harvard Six Cities studies, which had each
21 undergone extensive independent reanalysis, and which were based on cohorts that were
22 broadly representative of the U.S. population. The 2004 PM AQCD concluded that the
23 results from the Seventh-Day Adventist (AHSMOG) cohort provided some suggestive (but
24 less conclusive) evidence for associations, while results from the Veterans Cohort provided
25 inconsistent evidence for associations between long-term exposures to PM_{2.5} and mortality.
26 Collectively, the 2004 PM AQCD found that these studies provided strong evidence that
27 long-term exposure to PM_{2.5} was associated with increased risk of human mortality. Effect
28 estimates for all-cause mortality ranged from 6 to 13% increased risk per 10 µg/m³ PM_{2.5},
29 while effect estimates for cardiopulmonary mortality ranged from 6 to 19% per 10 µg/m³
30 PM_{2.5}. For lung cancer mortality, the effect estimate was a 13% increase per 10 µg/m³ PM_{2.5},
31 based upon the results of the extended analysis from the ACS cohort (Pope CA et al., 2002,
32 [024689](#)). With regard to thoracic coarse particles, the 2004 PM AQCD reported that no
33 association was observed between mortality and long-term exposure to PM_{10-2.5} in the ACS
34 study (Pope CA et al., 2002, [024689](#)), while a positive but statistically non-significant
35 association was reported in males in the AHSMOG cohort (McDonnell et al., 2000, [010319](#)).
36 Thus, the 2004 PM AQCD concluded that there was insufficient evidence for associations

1 between long-term exposure to thoracic coarse particles and mortality. Overall, the 2004
 2 PM AQCD concluded that there was strong epidemiologic evidence for associations between
 3 long-term exposures to PM_{2.5} and excess all-cause and cardiopulmonary mortality.

4 At the time of the 2004 PM AQCD, only a limited number of the chronic-exposure
 5 cohort studies had considered direct measurements of constituents of PM, other than
 6 sulfates. With regard to source-oriented evaluations of mortality associations with long-
 7 term exposure, the 2004 PM AQCD noted only the study by Hoek et al. (2002, [042364](#)), in
 8 which the authors concluded that long-term exposure to traffic-related air pollution may
 9 shorten life expectancy. However, Hoek et al. (2002, [042364](#)) also noted that living near a
 10 major road might include other factors that contribute to mortality associations. There was
 11 not sufficient evidence at the time of the 2004 PM AQCD to draw conclusions on effects
 12 associated with specific components or sources of PM.

13 New epidemiologic evidence reports a consistent association between long-term
 14 exposure to PM_{2.5} and increased risk of mortality. There is little evidence for the long-term
 15 effects of PM_{10-2.5} on mortality. Although this section focuses on mortality outcomes in
 16 response to long-term exposure to PM, it does not evaluate studies that examine the
 17 association between PM and infant mortality. These studies are evaluated in Section 7.5:
 18 “Reproductive, developmental, prenatal and neonatal outcomes associated with long-term
 19 exposure to PM” because it is possible that in utero exposures contribute to infant
 20 mortality. A summary of the mean PM concentrations reported for the studies characterized
 21 in this section is presented in Table 7-8.

Table 7-8. Characterization of ambient PM concentrations from studies of mortality and long-term exposures to PM.

Reference	Location	Mean Concentration (µg/m ³)	Upper Percentile Concentrations (µg/m ³)
<i>PM_{2.5}</i>			
Brunekreef et al. (2009, 191947)	The Netherlands	28	95th: 32 99th: 33 Max: 37
Chen et al. (2005, 087942)	Multicity, CA	29.0	
Eftim et al. (2008, 099104)	U.S.	13.6-14.1	Max: 19.1-25.1
Enstrom (2005, 087356)	CA	23.4	Max: 36.1
Goss et al. (2004, 055624)	U.S.	13.7	75th: 15.9
Janes et al. (2007, 090927)	U.S.	14.0	
Jerrett et al. (2005, 189405)	Los Angeles, CA		Max: 27.1
Krewski et al. (2009, 191193)	U.S.	14.02	75 th : 16.00 90th: 26.75 95th: 27.89 Max: 30.01
Laden et al. (2006, 087605)	Multicity, U.S.	10.2-29.0	

Reference	Location	Mean Concentration ($\mu\text{g}/\text{m}^3$)	Upper Percentile Concentrations ($\mu\text{g}/\text{m}^3$)
Lipfert et al. (2006, 088218)	U.S.	14.3	
Miller et al. (2007, 090130)	U.S.	13.5	75th: 18.3 Max: 28.3
Pope et al. (2004, 055880)	U.S.	17.1	
Schwartz et al. (2008, 156963)	Multicity, U.S.	17.5	Max: 40
Zeger et al. (2007, 157176)	U.S.		17.0
Zeger et al. (2008, 191951)	U.S.	13.2	75th: 14.9
<i>PM_{10-2.5}</i>			
Chen et al. (2005, 087942)	Multicity, CA	25.4	
Lipfert et al. (2006, 088218)	U.S.	16.0	
<i>PM₁₀</i>			
Chen et al. (2005, 087942)	Multicity, CA	52.6	
Gehring et al. (2006, 089797)	North Rhine, Germany	43.7-48.0	Max: 52.5-56.1
Goss et al. (2004, 055624)	U.S.	24.8	75th: 28.9
Puett et al. (2008, 156891)	NE U.S.	21.6	
Zanobetti et al. (2008, 156177)	U.S.	29.4	

7.6.1. Recent Studies of Long-Term Exposure to PM and Mortality

1 Studies since the last PM AQCD include results of new analyses and insights for the
2 ACS and Harvard Six Cities studies, further analyses from the AHSMOG and Veterans
3 study cohorts, as well as analyses of a Cystic Fibrosis cohort and subsets of the ACS from
4 Los Angeles and New York City. In the original analyses of the Six Cities and ACS cohort
5 studies, no associations were found between long-term exposure to PM_{10-2.5} and mortality,
6 and the extended and follow-up analyses did not evaluate associations with PM_{10-2.5}. The
7 historical and more recent results for PM_{2.5} of both the ACS and the Harvard Six Cities
8 studies are compiled in Figure 7-6. Moreover, since the last PM AQCD, there is a major new
9 cohort that investigates the effects of PM_{2.5} on cardiovascular mortality in the literature:
10 the Women's Health Initiative (WHI) study (Miller et al., 2007, [090130](#)). Most recently, an
11 ecological cohort study of the nation's Medicare population has been completed (Eftim et al.,
12 2008, [099104](#)). These new findings further strengthen the evidence linking long-term
13 exposure to PM_{2.5} and mortality, while providing indications that the magnitude of the
14 PM_{2.5} -mortality association is larger than previously estimated (Figure 7-7). Two recent
15 reports from the AHSMOG and Veterans study cohorts have provided some limited
16 evidence for associations between long-term exposure to PM_{10-2.5} and mortality. The original
17 analyses of the AHSMOG cohort study found positive associations between long-term

1 concentrations of PM₁₀ and 15-yr mortality due to natural causes and lung cancer (Abbey et
2 al., 1999, [047559](#)). McDonnell et al. (2000, [010319](#)) reanalyzed these data and concluded
3 that previously observed association of long-term ambient PM₁₀ concentrations with
4 mortality for males were best explained by a relationship of mortality with the fine fraction
5 of PM₁₀ rather than the coarse fraction of PM₁₀. Recent reports from the AHSMOG study
6 cohort, as well as the Nurses' Health Study and a cohort of women in Germany have
7 provided some evidence for associations between long-term exposure to PM₁₀ and mortality
8 among women.

9 **Harvard Six Cities:** A follow-up study has used updated air pollution and mortality
10 data; an additional 1,368 deaths occurred during the follow-up period (1990-1998) vs. 1,364
11 deaths in the original study period (1974-1989) (Laden et al., 2006, [087605](#)). Statistically
12 significant associations are reported between long-term exposure to PM_{2.5} and mortality for
13 data for the two periods (RR = 1.16 [95% CI: 1.07-1.26] per 10 µg/m³ PM_{2.5}). Of special note
14 is a statistically significant **reduction** in mortality risk reported with **reduced** long-term fine
15 particle concentrations (RR = 0.73 [95% CI: 0.57-0.95] per 10 µg/m³ PM_{2.5}). This is
16 equivalent to an RR of 1.27 for reduced mortality risks with reduced long-term PM_{2.5}
17 concentrations. This reduced mortality risk was observed for deaths due to cardiovascular
18 and respiratory causes, but not for lung cancer deaths. The PM_{2.5} concentrations for recent
19 years were estimated from visibility data, which introduces some uncertainty in the
20 interpretation of the results from this study. Coupled with the results of the original
21 analysis (Dockery et al., 1993, [044457](#)), this study strongly suggests that a reduction in fine
22 PM pollution yields positive health benefits.

23 **ACS Extended Analyses/Reanalysis II:** Two new analyses further evaluated the
24 associations of long-term PM_{2.5} exposures with risk of mortality in 50 U.S. cities reported by
25 Pope and colleagues (2002, [024689](#)), adding new details about deaths from specific
26 cardiovascular and respiratory causes (Krewski, 2009, [190075](#); Pope CA et al., 2004,
27 [055880](#)). Pope et al. (2004, [055880](#)) reported positive associations with deaths from specific
28 cardiovascular diseases, particularly ischemic heart disease, and a group of cardiac
29 conditions including dysrhythmia, heart failure and cardiac arrest (RR for cardiovascular
30 mortality = 1.12, 95% CI 1.08-1.15 per 10 µg/m³ PM_{2.5}), but no PM associations were found
31 with respiratory mortality.

32 In an additional reanalysis that extended the follow-up period for the ACS cohort to
33 18 years (1982-2000) (Krewski et al., 2009, [191193](#)), investigators found effect estimates
34 that were similar, though generally higher, than those reported in previous ACS analyses.
35 This reanalysis also included data for seven ecologic (neighborhood-level) contextual (i.e.,
36 not individual-level) covariates, each of which represents local factors known or suspected
37 to influence mortality, such as poverty level, educational attainment, and unemployment.
38 The effect estimate for all cause mortality, based on PM_{2.5} concentrations measured in 1999
39 and 2000 was 1.03 (95% CI: 1.01-1.05). The corresponding effect estimates for deaths due to

1 IHD and lung cancer were 1.15 (95% CI: 1.04-1.18) and 1.11 (95% CI: 1.04-1.18),
2 respectively. In earlier analyses of this cohort, investigators found that increasing education
3 levels appeared to reduce the effect of PM_{2.5} exposure on mortality. Results from this
4 reanalysis show a similar pattern, although with somewhat less certainty, for all causes of
5 death except IHD, for which the pattern was reversed. Overall, although the addition of
6 random effects modeling and contextual covariates to the ACS model made most effect
7 estimates higher (but some lower), they were not statistically different from the earlier ACS
8 effect CPD=Cardio-Pulmonary Disease; CVD=Cardiovascular Disease; IHD=Ischemic Heart
9 estimates. Thus, these new analyses, with their more extensive consideration of potentially
10 confounding factors, confirm the published ACS PM_{2.5}-mortality results to be robust.

11 **California Cancer Prevention Study:** In a cohort of elderly people in 11 California
12 counties (mean age 73 years in 1983), an association was reported for long-term PM_{2.5}
13 exposure with all-cause deaths from 1973-1982 (RR = 1.04 [95% CI: 1.01-1.07] per 10 µg/m³
14 PM_{2.5}) (Enstrom, 2005, [087356](#)). However, no significant associations were reported with
15 deaths in later time periods when PM_{2.5} levels had decreased in the most polluted counties
16 (1983-2002) (RR = 1.00 [95% CI: 0.98-1.02] per 10 µg/m³ PM_{2.5}). The PM_{2.5} data were
17 obtained from the EPA's Inhalation Particle Network (collected 1979-1983), and the
18 locations represented a subset of data used in the 50-city ACS study (Pope CA et al., 1995,
19 [045159](#)). However, the use of average values for California counties as exposure surrogates
20 likely leads to significant exposure error, as many California counties are large and quite
21 topographically variable.

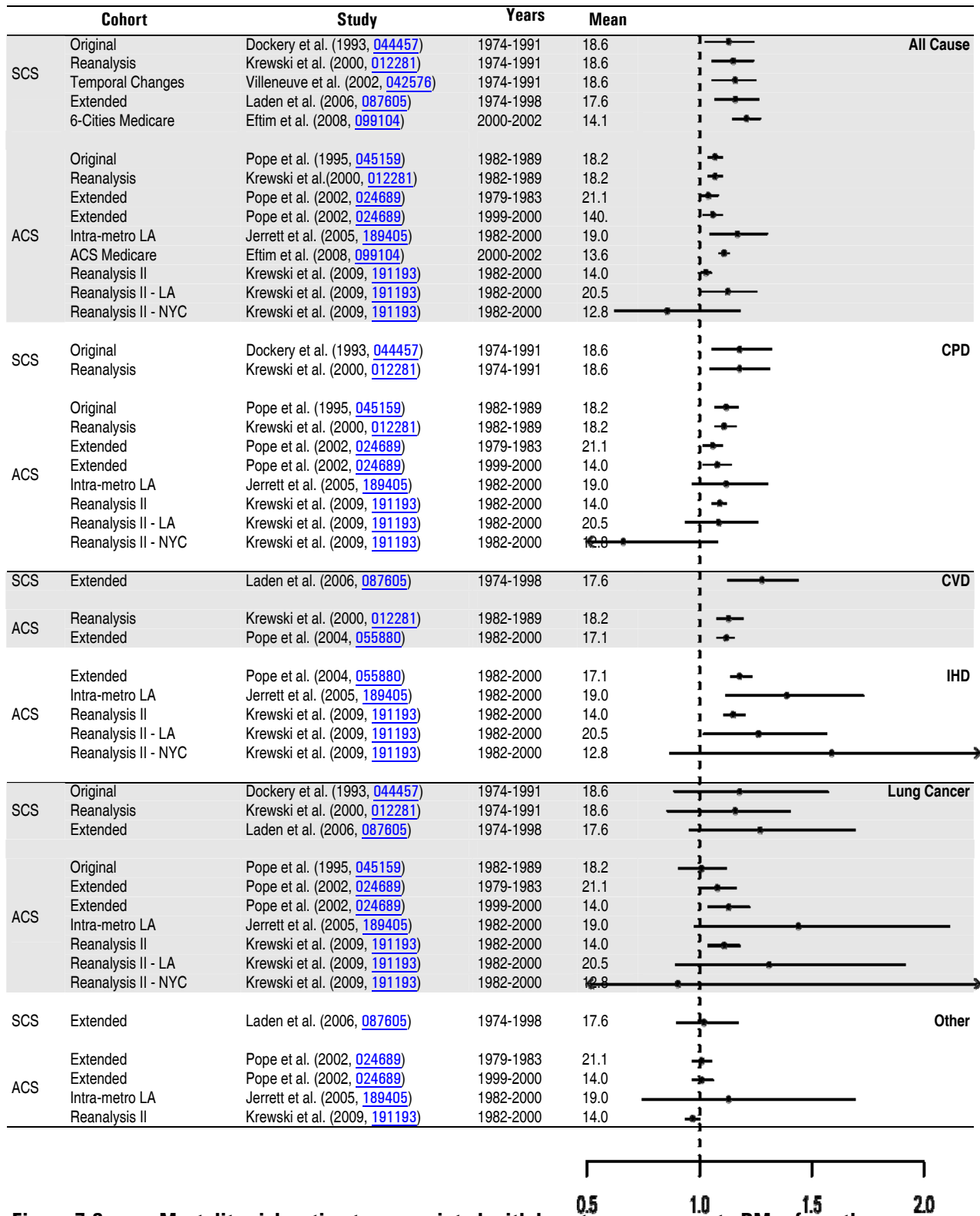


Figure 7-6. Mortality risk estimates associated with long-term exposure to PM_{2.5} from the Harvard Six Cities Study (SCS) and the American Cancer Society Study (ACS).

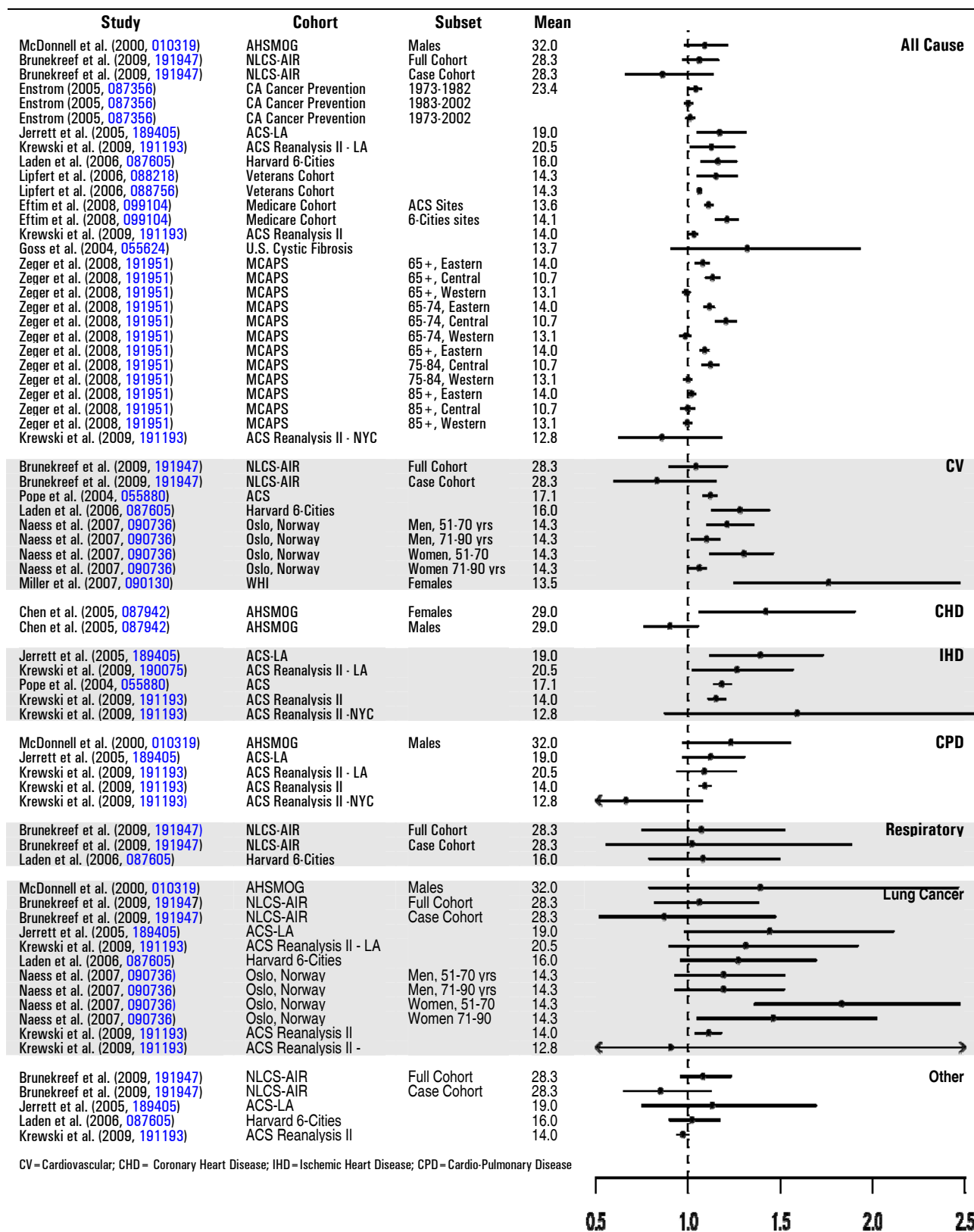


Figure 7-7. Mortality risk estimates associated with long-term exposure to PM_{2.5} in recent cohort studies.

1 **AHSMOG:** In this analysis for the Seventh-Day Adventist cohort in California, a
2 positive, statistically significant, association with coronary heart disease mortality was
3 reported among females (92 deaths; RR = 1.42 [95% CI: 1.06-1.90] per 10 $\mu\text{g}/\text{m}^3$ $\text{PM}_{2.5}$), but
4 not among males (53 deaths; RR = 0.90 [95% CI: 0.76-1.05] per 10 $\mu\text{g}/\text{m}^3$ $\text{PM}_{2.5}$) (Chen et al.,
5 2005, [087942](#)). Associations were strongest in the subset of postmenopausal women (80
6 deaths; RR = 1.49 [95% CI: 1.17-1.89] per 10 $\mu\text{g}/\text{m}^3$ $\text{PM}_{2.5}$). The authors speculated that
7 females may be more sensitive to air pollution-related effects, based on differences between
8 males and females in dosimetry and exposure. As was found with fine particles, a positive
9 association with coronary heart disease mortality was reported for PM_{10-25} and PM_{10} among
10 females (RR = 1.38 [95% CI: 0.97-1.95] per 10 $\mu\text{g}/\text{m}^3$ $\text{PM}_{10-2.5}$; RR = 1.22 [95% CI: 1.01-1.47]
11 per 10 $\mu\text{g}/\text{m}^3$ PM_{10}), but not for males (RR = 0.92 [95% CI: 0.66-1.29] per 10 $\mu\text{g}/\text{m}^3$ $\text{PM}_{10-2.5}$;
12 RR = 0.94 [95% CI: 0.82-1.08] per 10 $\mu\text{g}/\text{m}^3$ PM_{10}); associations were strongest in the subset
13 of postmenopausal women (80 deaths) (Chen et al., 2005, [087942](#)).

14 **U.S. Cystic Fibrosis cohort:** A positive, but not statistically significant, association was
15 reported for $\text{PM}_{2.5}$ in this cohort (RR = 1.32 [95% CI: 0.91-1.93] per 10 $\mu\text{g}/\text{m}^3$ $\text{PM}_{2.5}$) in a
16 study that primarily focused on evidence of exacerbation of respiratory symptoms (Goss et
17 al., 2004, [055624](#)). No clear association was reported for PM_{10} . However, only 200 deaths
18 had occurred in the cohort of over 11,000 people (average age in cohort was 18.4 years), so
19 the power of this study to detect associations was relatively low.

20 **Women's Health Initiative (WHI) Study:** This nationwide cohort study considered 65,893
21 postmenopausal women with no history of cardiovascular disease who lived in 36 U.S.
22 metropolitan areas from 1994 to 1998 (Miller et al., 2007, [090130](#)). The study had a median
23 subject follow-up time of six years. Miller and colleagues assessed each woman's exposure to
24 air pollutants using the monitor located nearest to their residence. Hazard ratios were
25 estimated for the first cardiovascular event, adjusting for age, race or ethnic group,
26 smoking status, educational level, household income, body-mass index, and presence or
27 absence of diabetes, hypertension, or hypercholesterolemia. Overall, this study concludes
28 that "long-term exposure to fine particulate air pollution is associated with the incidence of
29 cardiovascular disease and death among postmenopausal women." In terms of effect size,
30 the study found that each increase of 10 $\mu\text{g}/\text{m}^3$ of $\text{PM}_{2.5}$ was associated with a 24% increase
31 in the risk of a cardiovascular event (hazard ratio, 1.24 [95% CI: 1.09-1.41]) and a 76%
32 increase in the risk of death from cardiovascular disease (hazard ratio, 1.76 [95% CI: 1.25-
33 2.47]). While this study found results confirmatory to the ACS and Six Cities Study, it
34 reports much larger relative risk estimates per $\mu\text{g}/\text{m}^3$ $\text{PM}_{2.5}$. In addition, since the study
35 included only women without pre-existing cardiovascular disease, it could potentially be a
36 healthier cohort population than that considered by the ACS and Six Cities Study. Indeed,
37 the WHI Study reported only 216 cardiovascular deaths in 349,643 women-years of
38 followup, or a rate of 0.075% deaths per year (Miller et al., 2007, [090130](#)), while the ACS
39 Study reported that 10% of subjects died of cardiovascular disease over a 16 yr followup

1 period, yielding a rate of 0.625% per year, or approximately 8 times the cardiovascular
2 mortality rate of the WHI population (Pope CA et al., 2004, [055880](#)). Thus, PM_{2.5} impacts
3 may yield higher relative risk estimates in the WHI population because the PM_{2.5} risk is
4 being compared to a much lower prevailing risk of cardiovascular death in this select study
5 population.

6 The WHI study not only confirms the ACS and Six City Study associations with
7 mortality in yet another well characterized cohort with detailed individual-level
8 information, it also has been able to consider the individual medical records of the
9 thousands of WHI subjects over the period of the study. This has allowed the researchers to
10 examine not only mortality, but also related morbidity in the form of heart problems
11 (cardiovascular events) experienced by the subjects during the study. As reported in this
12 paper, this examination confirmed that there is an increased risk of cardiovascular
13 morbidity, as well (see Section 7.2.9). These morbidity co-associations with PM_{2.5} in the
14 same population lend even greater support to the biological plausibility of the air pollution-
15 mortality associations found in this study.

16 **Medicare Cohort Studies:** Using Medicare data, Eftim and co-authors (2008, [099104](#))
17 have assessed the association of PM_{2.5} with mortality for the same locations included in the
18 ACS and Six City Study. For these locations, they estimated the chronic effects of PM_{2.5} on
19 mortality for the period 2000-2002 using mortality data for cohorts of Medicare participants
20 and average PM_{2.5} levels from monitors in the same counties included in the two studies.
21 Using aggregate counts of mortality by county for three age groups, they estimated
22 mortality risk associated with air pollution adjusting for age and sex and area-level
23 covariates (education, income level, poverty, and employment), and controlled for potential
24 confounding by cigarette smoking by including standardized mortality ratios for lung
25 cancer and COPD. This study is, therefore, an ecological analysis, similar to past published
26 cross-sectional analyses, in that area-level covariates (education, income level, poverty, and
27 employment) are employed as controlling variables, since individual level information is not
28 available from the Medicare database (other than age and sex), which includes virtually all
29 Americans aged 65 or greater. Exposures are also ecological in nature, as central site data
30 are used as indices of exposure. These results indicated that a 10 µg/m³ increase in the
31 yearly average PM_{2.5} concentration is associated with 10.9% (95% CI: 9.0-12.8) and with
32 20.8% (95% CI: 14.8-27.1) increases in all-cause mortality for the ACS and Six Cities Study
33 counties, respectively. The estimates are somewhat higher than those reported by the
34 original investigators, and there may be several possible explanations for this apparent
35 increase, especially that this is an older population than the ACS cohort. Perhaps the most
36 likely explanation is that the lack of personal confounder information (e.g., past personal
37 smoking information) led to an insufficient control for the effects of these other variables'
38 effects on mortality, inflating the pollution effect estimates somewhat, similar to what has
39 been found in the ACS analyses when only ecological-level control variables were included.

1 The ability of the Eftim et al. (2008, [099104](#)) study results to qualitatively replicate the
2 original individual-level cohort study (e.g., ACS and Six Cities Study) results suggests that
3 past ecological cross-sectional mortality study results may also provide useful insights into
4 the nature of the association, especially when used for consideration of time trends, or for
5 comparisons of the relative (rather than absolute) sizes of risks between different pollutants
6 or PM components in health effects associations.

7 Janes et al. (2007, [090927](#)) use the same nationwide Medicare mortality data to
8 examine the association between monthly averages of fine particles (PM_{2.5}) over the
9 preceding 12 months and monthly mortality rates in 113 U.S. counties from 2000 to 2002.
10 They decompose the association between PM_{2.5} and mortality into 2 components: (1) the
11 association between “national trends” in PM_{2.5} and mortality; and (2) the association
12 between “local trends,” defined as county-specific deviations from national trends. This
13 second component is posited to provide evidence as to whether counties having steeper
14 declines in PM_{2.5} also have steeper declines in mortality relative to the national trend. They
15 report that the exposure effect estimates are different at these 2 spatiotemporal scales,
16 raising concerns about confounding bias in these analyses. The authors assert that the
17 association between trends in PM_{2.5} and mortality at the national scale is more likely to be
18 confounded than is the association between trends in PM_{2.5} and mortality at the local scale
19 and, if the association at the national scale is set aside, that there is little evidence of an
20 association between 12-month exposure to PM_{2.5} and mortality in this analysis. However, in
21 response, Pope and Burnett (2007, [090928](#)) point out that such use of long-term time trends
22 as the primary source of exposure variability has been avoided in most other air pollution
23 epidemiology studies because of such concerns about potential confounding of such time-
24 trend associations.

25 By linking monitoring data to the U.S. Medicare system by county of residence, Zeger
26 et al. (2007, [157176](#)) analyzed Medicare mortality records, comprising over 20 million
27 enrollees in the 250 largest counties during 2000-2002. The authors estimated log-linear
28 regression models having age-specific county level mortality rates as the outcome and, as
29 the main predictor, the average PM_{2.5} pollution level in each county during 2000. Area-level
30 covariates were used to adjust for socio-economic status and smoking. The authors reported
31 results under several degrees of adjustment for spatial confounding and with stratification
32 into eastern, central and western U.S. counties. A 10 µg/m³ increase in PM_{2.5} was associated
33 with a 7.6% increase in mortality (95% CI: 4.4-10.8). When adjusted for spatial
34 confounding, the estimated log-relative risks dropped by 50%. Zeger et al. (2007, [157176](#))
35 found a stronger association in the eastern counties than nationally, with no evidence of an
36 association in western counties.

37 In a subsequent report, Zeger et al. (2008, [191951](#)) created a new retrospective cohort,
38 the Medicare Cohort Air Pollution Study (MCAPS), consisting of 13.2 million persons
39 residing in 4,568 ZIP codes in urban areas having geographic centroids within 6 miles of a

1 PM_{2.5} monitor. Using this cohort, they investigated the relationship between 6-yr avg
2 exposure to PM_{2.5} and mortality risk over the period 2000-2005. When divided by region,
3 the associations between long-term exposure to PM_{2.5} and mortality for the eastern and
4 central ZIP codes were qualitatively similar to those reported in the ACS and Six Cities
5 Study, with 11.4% (95% CI: 8.8-14.1) and 20.4% (95% CI: 15.0-25.8) increases per 10 µg/m³
6 increase in PM_{2.5} in the eastern and central regions, respectively. The MCAPS results
7 included evidence of differing PM_{2.5} relative risks by age and geographic location, where
8 risk declines with increasing age category until there is no evidence of an association
9 among persons ≥ 85 years of age, and there is no evidence of a positive association for the
10 640 urban ZIP codes in the western region of the U.S.

11 Using hospital discharge data, Zanobetti et al. (2008, [156177](#)) constructed a cohort of
12 persons discharged with chronic obstructive pulmonary disease using Medicare data
13 between 1985 and 1999. Positive associations in the survival analyses were reported for
14 single year and multiple-year lag exposures, with a hazard ratio for total mortality of 1.22
15 (95% CI: 1.17-1.27) per 10 µg/m³ increase in PM₁₀ over the previous 4 years.

16 **Veterans cohort:** A recent reanalysis of the Veterans cohort data focused on exposure to
17 traffic-related air pollution (traffic density based on traffic flow rate data and road segment
18 length) reported a stronger relationship between mortality with long-term exposure to
19 traffic than with PM_{2.5} mass (Lipfert et al., 2006, [088218](#)). A significant association was
20 reported between total mortality and PM_{2.5} in single-pollutant models (RR = 1.12 [95% CI:
21 1.04-1.20] per 10 µg/m³ PM_{2.5}). This risk estimate is larger than results reported in a
22 previous study of this cohort. In multipollutant models including traffic density, the
23 association with PM_{2.5} was reduced and lost statistical significance. Traffic emissions
24 contribute to PM_{2.5} so it would be expected that the two would be highly correlated, and,
25 thus, these multipollutant model results should be interpreted with caution. In a
26 companion study, Lipfert et al. (2006, [088218](#)) used data from EPA's fine particle speciation
27 network, and reported findings for PM_{2.5} which were similar to those reported by Lipfert et
28 al. (2006, [088218](#)). In this study (Lipfert et al., 2006, [088218](#)), a significant association was
29 reported between long-term exposure to PM_{10-2.5} and total mortality in a single-pollutant
30 model (RR = 1.07, 95% CI 1.01-1.12 per 10 µg/m³ PM_{10-2.5}). However, the association became
31 negative and not statistically significant in a model that included traffic density. As it would
32 be expected that traffic would contribute to the thoracic coarse particle concentrations, it is
33 difficult to interpret the results of these multipollutant analyses.

34 **Nurses' Health Study Cohort:** The Nurses' Health Study (Puett et al., 2008, [156891](#)) is
35 an ongoing prospective cohort study examining the relation of chronic PM₁₀ exposures with
36 all-cause mortality and incident and fatal coronary heart disease consisting of 66,250
37 female nurses in MSAs in the northeastern region of the U.S. All cause mortality was
38 statistically significantly associated with average PM₁₀ exposures in the time period 3-48
39 months preceding death. The association was strongest with average PM₁₀ exposure in the

1 24 months prior to death (hazard ratio 1.16 [95% CI: 1.05-1.28]) and weakest with exposure
2 in the month prior to death (hazard ratio 1.04 [95% CI: 0.98-1.11]). The association with
3 fatal CHD occurred with the greatest magnitude with mean exposure in the 24 months
4 prior to death (hazard ratio 1.42 [95% CI: 1.11-1.81]).

5 **Netherlands Cohort Study (NLCS):** The Netherlands Cohort Study (Brunekreef et al.,
6 2009, [191947](#)) estimates the effects of traffic-related air pollution on cause specific mortality
7 in a cohort of approximately 120,000 subjects aged 55 to 69 year at enrollment. For a 10
8 $\mu\text{g}/\text{m}^3$ increase in $\text{PM}_{2.5}$ concentration, the relative risk for natural-cause mortality in the
9 full cohort was 1.06 (95% CI: 0.97-1.16), similar in magnitude to the results reported by the
10 ACS. In a case-cohort analysis adjusted for additional potential confounders, there were no
11 associations between air pollution and mortality.

12 **German Cohort:** The North Rhine-Westphalia State Environment Agency (LUA NRW)
13 initiated a cohort of approximately 4,800 women, and assessed whether long-term exposure
14 to air pollution originating from motorized traffic and industrial sources was associated
15 with total and cause-specific mortality (Gehring et al., 2006, [089797](#)). They found that
16 cardiopulmonary mortality was associated with PM_{10} (RR = 1.52 [95% CI: 1.09-2.15] per
17 $10 \mu\text{g}/\text{m}^3 \text{PM}_{10}$).

7.6.2. Composition and Source-Oriented Analyses of PM

18 As discussed in the 2004 PM AQCD, only a very limited number of the chronic
19 exposure cohort studies have included direct measurements of chemical-specific PM
20 constituents other than sulfates, or assessments of source-oriented effects, their analyses.
21 One exception is the Veterans Cohort Study, which looked at associations with some
22 constituents, and traffic.

23 **Veterans Cohort:** Using data from EPA's fine particle speciation network, Lipfert et al.
24 (2006, [088756](#)) reported a positive association for mortality with sulfates. Using 2002 data
25 from the fine particle speciation network, positive associations were found between
26 mortality and long-term exposures to nitrates, EC, Ni and V, as well as traffic density and
27 peak ozone concentrations. In multipollutant models, associations with traffic density
28 remained significant, as did nitrates, Ni and V in some models.

29 **Netherlands Cohort Study:** Beelen et al. (2008, [156263](#)) studied the association between
30 long-term exposure to traffic-related air pollution and mortality in a Dutch cohort. They
31 used data from an ongoing cohort study on diet and cancer with 120,852 subjects who were
32 followed from 1987 to 1996. Exposure to BS, NO_2 , SO_2 , and $\text{PM}_{2.5}$, as well as various
33 exposure variables related to traffic, were estimated at the home address. Cox analyses
34 were conducted in the full cohort, adjusting for age, sex, smoking, and area-level
35 socioeconomic status. Traffic intensity on the nearest road was independently associated
36 with mortality. Relative risks (95% confidence intervals) for a $10 \mu\text{g}/\text{m}^3$ increase in BS

1 concentrations (difference between 5th and 95th percentile) were 1.05 (95% CI: 1.00-1.11)
2 for natural cause, 1.04 (95% CI: 0.95-1.13) for cardiovascular, 1.22 (95% CI: 0.99-1.50) for
3 respiratory, 1.03 (95% CI: 0.88-1.20) for lung cancer, and 1.04 (95% CI: 0.97-1.12) for
4 mortality other than cardiovascular, respiratory, or lung cancer. Results were similar for
5 NO₂ and PM_{2.5}, but no associations were found for SO₂. Traffic-related air pollution and
6 several traffic exposure variables were associated with mortality in the full cohort, although
7 the relative risks were generally small. Associations between natural-cause and respiratory
8 mortality were statistically significant for NO₂ and BS. These results add to the evidence
9 that long-term exposure to traffic-related particulate air pollution is associated with
10 increased mortality.

11 Given the general dearth of published source-oriented studies of the mortality impacts
12 of long-term PM exposure components, and given that the recent Medicare Cohort study
13 now indicates that such ecological cross-sectional studies can be useful for evaluating time
14 trends and/or comparisons across pollution components, it may well be that examining past
15 cross-sectional studies comparing source-oriented components of PM may be informative. In
16 particular, Ozkaynak and Thurston (1987, [072960](#)), utilized the chemical speciation
17 conducted in the Inhalable Particle (IP) Network to conduct a chemical constituent and
18 source-oriented evaluation on long-term PM exposure and mortality in the U.S. They
19 analyzed the 1980 U.S. vital statistics and available ambient air pollution data bases for
20 sulfates and fine, inhalable, and TSP mass. Using multiple regression analyses, they
21 conducted a cross-sectional analysis of the association between various particle measures
22 and total mortality. Results from the various analyses indicated the importance of
23 considering particle size, composition, and source information in modeling of particle
24 pollution health effects. Of the independent mortality predictors considered, particle
25 exposure measures most related to the respirable fraction of the aerosols, such as fine
26 particles and sulfates, were most consistently and significantly associated with the reported
27 SMSA-specific total annual mortality rates. On the other hand, particle mass measures
28 that included thoracic coarse particles (e.g., total suspended particles and inhalable
29 particles) were often found to be non-significant predictors of total mortality. Furthermore,
30 based on the application of fine particle source apportionment, particles from industrial
31 sources and from coal combustion were indicated to be more significant contributors to
32 human mortality than fine soil-derived particles.

7.6.3. Within-City Effects of PM Exposure

33 Much of the exposure gradient in the national-scale cohort studies was due to city-to-
34 city differences in regional air pollution, raising the possibility that some or all of the
35 original PM-survival associations may have been driven instead by city-to-city differences

1 in some unknown (non-pollution) confounder variable. This has been evaluated by three
 2 recent studies.

3 **ACS, Los Angeles:** To investigate this issue, two new analyses using ACS data focused
 4 on neighborhood-to-neighborhood differences in urban air pollutants, using data from 23
 5 PM_{2.5} monitoring stations in the Los Angeles area, and applying interpolation methods
 6 Jerrett et al. (2005, [189405](#)) or land use regression methods (Krewski et al., 2009, [191193](#))
 7 to assign exposure levels to study individuals. This resulted in both improved exposure
 8 assessment and an increased focus on local sources of fine particle pollution. Significant
 9 associations between PM_{2.5} and mortality from all causes and cardiopulmonary diseases
 10 were reported with the magnitude of the relative risks being greater than those reported in
 11 previous assessments. In general, the associations for PM_{2.5} and mortality using these two
 12 methods for exposure assessment were similar, though the use of land use regression
 13 resulted in somewhat smaller hazard ratios and tighter confidence intervals (see Table 7-9)
 14 This indicates that city-to-city confounding was not the cause of the associations found in
 15 the earlier ACS Cohort studies. This provides evidence that reducing exposure error can
 16 result in stronger associations between PM_{2.5} and mortality than generally observed in
 17 broader studies having less exposure detail.

Table 7-9: Comparison of results from ACS intra-urban analysis of Los Angeles and new york city using kriging or land use regression to estimate exposure

Cause of Death	Los Angeles:	Los Angeles:	New York City:
	Hazard Ratio ¹ and 95% Confidence Interval Using Kriging ² (Jerrett et al., 2005, 189405)	Hazard Ratio ¹ and 95% Confidence Interval Using Land Use Regression ³ (Krewski et al., 2009, 191193)	Hazard Ratio ¹ and 95% Confidence Interval Using Land Use Regression ⁴ (Krewski et al., 2009, 191193)
All Cause	1.11 (0.99-1.25)	1.13 (1.01-1.25)	0.86 (0.63-1.18)
IHD	1.25 (0.99-1.59)	1.26 (1.02-1.56)	1.56 (0.87-2.88)
CPD	1.07 (0.91-1.26)	1.09 (0.94-1.26)	0.66 (0.41-1.08)
Lung Cancer	1.20 (0.79-1.82)	1.31 (0.90-1.92)	0.90 (0.29-2.78)

¹Hazard ratios presented per 10 µg/m³ increase in PM_{2.5}

²Model included parsimonious contextual covariates

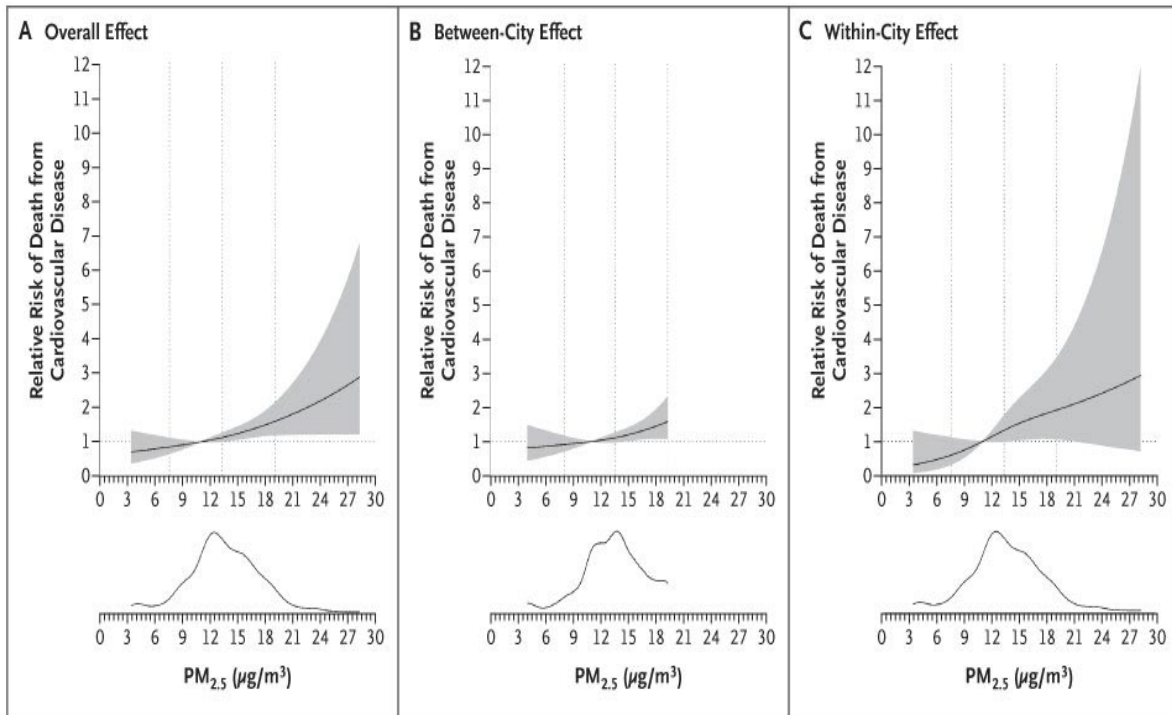
³Model included parsimonious individual level (23) and ecologic (4) covariates

⁴Model included all 44 individual level and 7 ecologic covariates.

18 **ACS, New York:** Krewski et al. (2009, [191193](#)) applied the same techniques used in the
 19 land use regression analysis of Los Angeles to an investigation conducted in New York City.
 20 Annual average concentrations were calculated for each of 62 monitors from 3 years of daily
 21 monitoring data for 1999 through 2001. Those data were combined with land-use data
 22 collected from traffic counting systems, roadway network maps, satellite photos of the study
 23 area, and local government planning and tax-assessment maps to assign estimated
 24 exposures to the ACS participants. The investigators did not observe elevated effect
 25 estimates for all cause, CPD or lung cancer deaths, but IHD did show a positive association
 26 with PM_{2.5} concentration. The difference between the 90th and 10th percentiles of the
 27 3-yr avg PM_{2.5} concentration was 1.5 µg/m³ and the difference between the minimum and

1 maximum values of the 3-yr avg $PM_{2.5}$ concentration was $7.8 \mu\text{g}/\text{m}^3$. This narrow range in
 2 $PM_{2.5}$ exposure contrasts across the New York City metropolitan area may well account for
 3 the inconclusive results in this city-specific analysis. Relatively uniform exposures would
 4 reduce the power of the statistical models to detect patterns of mortality relative to
 5 exposure and estimate the association with precision.

6 **WHI Study:** This study also investigated the within- vs. between-city effects in its
 7 cities. As shown in Figure 7-8, similar effects for both the within and between-city analyses
 8 demonstrate that this association is not due to some other (non-pollution) confounder
 9 differing between the various cities, strengthening confidence in the overall pollution-effect
 10 estimates.



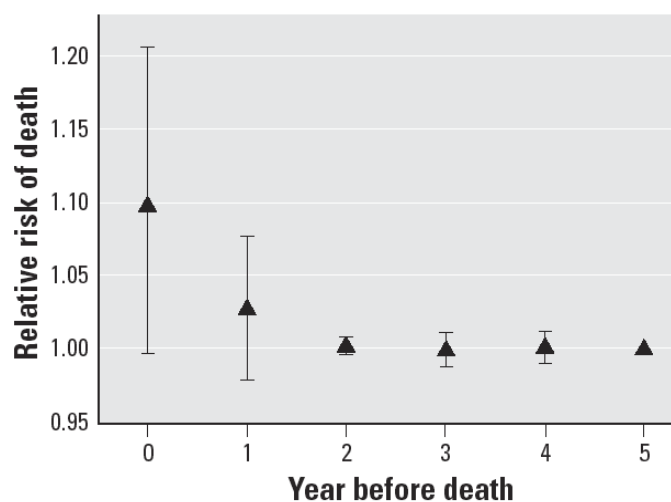
Source: Miller et al. (2007, [090130](#))

Figure 7-8. Plots of the relative risk of death from cardiovascular disease from the Women’s Health Initiative study displaying the between-city and within-city contributions to the overall association between $PM_{2.5}$ and cardiovascular mortality windows of exposure-effects.

7.6.4. Effects of Different Long-term Exposure Windows

11 The delay between changes in exposure and changes in health has important policy
 12 implications. Schwartz et al. (2008, [156963](#)) investigated this issue using an extended

1 follow-up of the Harvard Six Cities Study. Cox proportional hazards models were fit to
2 control for smoking, body mass index, and other covariates. Penalized splines were fit in a
3 flexible functional form to the concentration response to examine its shape, and the degrees
4 of freedom for the curve were selected based on Akaike's information criterion (AIC). The
5 researchers also used model averaging as an alternative approach, where multiple models
6 are fit explicitly and averaged, weighted by their probability of being correct given the data.
7 The lag relationship by model was averaged across a range of unconstrained distributed lag
8 models (i.e., same year, year prior, two years prior, etc.). Results of the lag comparison are
9 shown in Figure 7-9 indicating that the effects of changes in exposure on mortality are seen
10 within two years. The authors also noted that the concentration-response curve was linear,
11 clearly continuing below the level of the current U.S. air quality standard of $15 \mu\text{g}/\text{m}^3$.



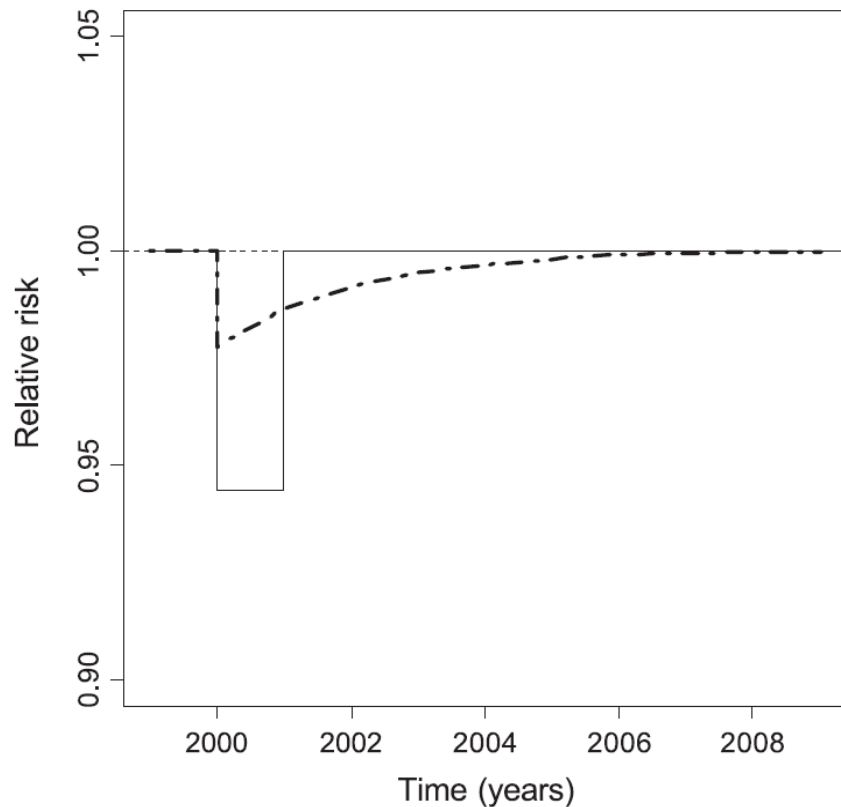
Source: Schwartz et al. (2008, [156963](#))

Figure 7-9. The model-averaged estimated effect of a $10\text{-}\mu\text{g}/\text{m}^3$ increase in $\text{PM}_{2.5}$ on all-cause mortality at different lags (in years) between exposure and death. Each lag is estimated independently of the others. Also shown are the pointwise 95% CIs for each lag, based on jackknife estimates.

12 Similarly, the effect of long-term exposure to PM_{10} on the risk of death in a large
13 multicity study of elderly subjects discharged alive following an admission for COPD found
14 the effect was not limited to the exposure in each year of follow-up, and had larger
15 cumulative effects spread over the follow-up year and 3 preceding years (Zanobetti et al.,
16 2008, [156177](#)).

17 Rösli et al. (2005, [156923](#)) took an alternative approach to determining the window
18 over which the mortality effects of long-term pollution exposures occurred. They fit the
19 model shown in Figure 7-10 using $k = 0.5$ based on the Utah Steel Strike (Pope CA, 1989,
20 [044461](#)) and the Ireland coal ban study (Clancy et al., 2002, [035270](#)). They found that

1 roughly 75% of health benefits are observed in the first 5 years, as shown in Table 7-10.
 2 These results are consistent with the findings of Schwartz et al. (2008, [156963](#)). Puett et al.
 3 (2008, [156891](#)) also compared different long-term lags, with exposure periods ranging from
 4 1 month to 48 months prior to death. They found statistically significant associations with
 5 average PM₁₀ exposures in the time period 3-48 months prior to death, with the strongest
 6 associations in the 24 months prior to death and the weakest with exposure in the 1 month
 7 prior to death.



Source: Rössli et al. (2005, [156923](#))

Figure 7-10. Time course of relative risk of death after a sudden decrease in air pollution exposure during the year 2000, assuming a steady state model (solid line) and a dynamic model (bold dashed line). The thin dashed line refers to the reference scenario. Table 7-10.

Distribution

of the effect of a hypothetical reduction of 10 µg/m³ PM₁₀ in 2000 on all-cause mortality 2000-2009 in Switzerland.

Yr	1999	2000	2001	2002	2003	2004	2005	2006	2007	2008	2009
Proportion of total effect (%)	-	39.3	23.9	14.5	8.8	5.3	3.2	2.0	1.2	0.7	0.4
Relative risk (per 10 µg/m ³ reduction in PM ₁₀)	1.0	0.9775	0.9863	0.9917	0.9950	0.9969	0.9981	0.9989	0.9993	0.9996	0.9997

Relative risk and proportion of total effect in each year are shown, assuming a time constant k of 0.5
 Source: Rössli et al. (2005, [156923](#))

1 In the reanalysis of the ACS cohort, the investigators calculated time windows of
2 exposure as average concentrations during successive five-yr periods preceding the date of
3 death (Krewski et al., 2009, [191193](#)). The investigators considered the time window with
4 the best-fitting model (judged by the AIC statistic) to be the period during which pollution
5 had the strongest influence on mortality. Overall, the differences between the time periods
6 were small and demonstrated no definitive patterns. High correlations between exposure
7 levels in the three periods may have reduced the ability of this analysis to detect any
8 differences in the relative importance of the time windows. The investigators did not
9 analyze any time periods smaller than five years, so the results are not directly comparable
10 to those reported by Schwartz et al. (2008, [156963](#)), Rösli et al. (2005, [156923](#)), and Puett
11 et al. (2008, [156891](#)).

12 Generally, these results indicate a developing coherence of the air pollution mortality
13 literature, suggesting that the health benefits from reducing air pollution do not require a
14 long latency period and would be expected within a few years of intervention.

7.6.5. Summary and Causal Determinations

7.6.5.1. PM_{2.5}

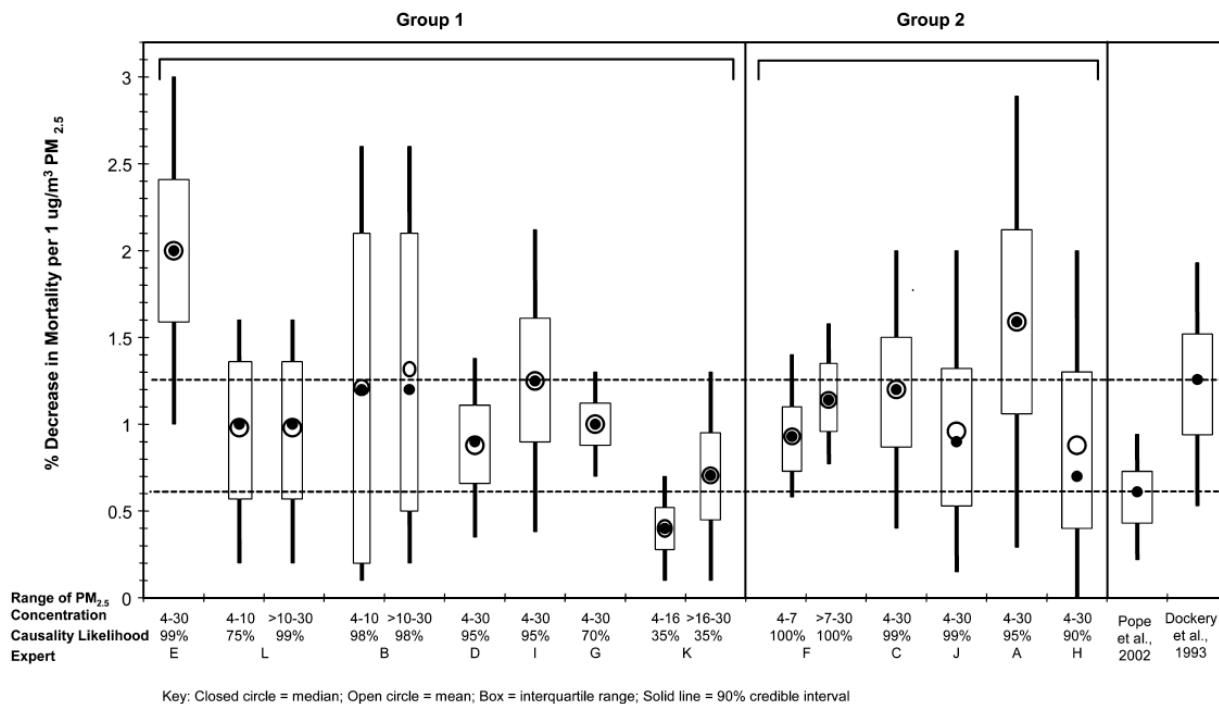
15 In the 1996 PM AQCD (U.S. EPA, 1996, [079380](#)), results were presented for three
16 prospective cohort studies of adult populations: the Six Cities Study (Dockery et al., 1993,
17 [044457](#)); the American Cancer Society (ACS) Study (Pope CA et al., 1995, [045159](#)); and the
18 California Seventh Day Adventist (AHSMOG) Study (Abbey et al., 1995, [000669](#)). The 1996
19 AQCD concluded that the chronic exposure studies, taken together, suggested associations
20 between increases in mortality and long-term exposure to fine PM, though there was no
21 evidence to support an association with PM_{10-2.5} (U.S. EPA, 1996, [079380](#)). Discussions of
22 mortality and long-term exposure to PM in the 2004 PM AQCD emphasized the results of
23 four U.S. prospective cohort studies, but the greatest weight was placed on the findings of
24 the ACS and the Harvard Six Cities studies, which had undergone extensive independent
25 reanalysis, and which were based on cohorts that were broadly representative of the U.S.
26 population. Collectively, the 2004 PM AQCD found that these studies provided strong
27 evidence that long-term exposure to PM_{2.5} was associated with increased risk of human
28 mortality.

29 The recent evidence is largely consistent with past studies, further supporting the
30 evidence of associations between long-term PM_{2.5} exposure and increased risk of human
31 mortality (Section 7.6) in areas with mean concentrations from 13.2 to 29 µg/m³
32 (Figure 7-7). New evidence from the Six Cities cohort study shows a relatively large risk
33 estimate for reduced mortality risk with decreases in PM_{2.5} (Laden et al., 2006, [087605](#)).
34 The results of new analyses from the Six Cities cohort and the ACS study in Los Angeles

1 suggest that previous and current studies may have underestimated the magnitude of the
2 association (Jerrett et al., 2005, [189405](#)). With regard to mortality by cause-of-death, recent
3 ACS analyses indicate that cardiovascular mortality primarily accounts for the total
4 mortality association with PM_{2.5} among adults, and not respiratory mortality. The recent
5 WHI cohort study shows even higher cardiovascular risks per µg/m³ than found in the ACS
6 study, but this is likely due to the fact that the study included only women without pre-
7 existing cardiovascular disease (Miller et al., 2007, [090130](#)). There is additional evidence for
8 an association between PM_{2.5} exposure and lung cancer mortality (Section 7.5.1.1). The WHI
9 study also considered within vs. between city mortality, as well as morbidity co-associations
10 with PM_{2.5} in the same population. The first showed that the results are not due to between
11 city confounding, and the morbidity analyses show the coherence of the mortality
12 association across health endpoints, supporting the biological plausibility of the air
13 pollution-mortality associations found in these studies.

14 Results from a new study examining the relationship between life expectancy and
15 PM_{2.5} and the findings from a multiyear expert judgment study that comprehensively
16 characterizes the size and uncertainty in estimates of mortality reductions associated with
17 decreases in PM_{2.5} in the U.S draw conclusions that are consistent with an association
18 between long-term exposure to PM_{2.5} and mortality (Pope et al., 2009, [190107](#); Roman et
19 al., 2008, [156921](#)). Pope et al. (2009, [190107](#)) report that a decrease of 10 µg/m³ in the
20 concentration of PM_{2.5} is associated with an estimated increase in mean (± SE) life
21 expectancy of 0.61 ± 0.20 year. For the approximate period of 1980-2000, the average
22 increase in life expectancy was 2.72 years among the 211 counties in the analysis. The
23 authors note that reduced air pollution was only one factor contributing to increased life
24 expectancies, with its effects overlapping with those of other factors.

25 Roman et al. (2008, [156921](#)) applied state-of-the-art expert judgment elicitation
26 techniques to develop probabilistic uncertainty distributions that reflect the broader array
27 of uncertainties in the concentration-response relationship. This study followed best
28 standard practices for expert elicitations based on the body of literature accumulated over
29 the past two decades. The resulting PM_{2.5} effect estimate distributions, elicited from 12 of
30 the world's leading experts on this issue, are shown in Figure 7-11. They indicate both
31 larger central estimates of mortality reductions for decreases in long-term PM_{2.5} exposure
32 in the U.S. (averaging almost 1% per µg/m³ PM_{2.5}) than reported (for example) by the ACS
33 Study (i.e., 0.6% per µg/m³ PM_{2.5} in Pope et al. (2002, [024689](#)), and a wider distribution of
34 uncertainty by each expert than provided by any one of the PM_{2.5} epidemiologic studies.
35 However, a composite uncertainty range of the overall mean effect estimate (i.e., based
36 upon all 12 experts' estimates, but not provided in Figure 7-11) would be much narrower,
37 and closer to that derived from the ACS study than indicated for any one expert shown in
38 Figure 7-11.



Source: Roman et al. (2008, [156921](#))

Figure 7-11. Experts' mean effect estimates and uncertainty distributions for the PM_{2.5} mortality concentration-response coefficient for a 1 $\mu\text{g}/\text{m}^3$ change in annual average PM_{2.5}

1 Overall, recent evidence supports the strong evidence reported in the 2004 PM AQCD
 2 (EPA, 2004, [056905](#)) that long-term exposure to PM_{2.5} is associated with an increased risk
 3 of human mortality. When looking at the cause of death, the strongest evidence comes from
 4 mortality due to cardiovascular disease, with additional evidence supporting an association
 5 between PM_{2.5} and lung cancer mortality (Figure 7-7). Fewer studies evaluate the
 6 respiratory component of cardiopulmonary mortality, and the evidence to support an
 7 association with long-term exposure to PM_{2.5} and respiratory mortality is weak (Figure 7-7).
 8 Together these findings are consistent and coherent with the evidence from epidemiologic,
 9 controlled human exposure, and animal toxicological studies for the effects of short- and
 10 long-term exposure to PM on cardiovascular effects presented in Sections 6.2 and 7.2,
 11 respectively. Evidence of short- and long-term exposure to PM_{2.5} and respiratory effects
 12 (Sections 6.3 and 7.3, respectively) and infant mortality (Section 7.4) are coherent with the
 13 weak respiratory mortality effects. Additionally, the evidence for short- and long-term
 14 cardiovascular and respiratory morbidity provides biological plausibility for mortality due
 15 to cardiovascular or respiratory disease. The most recent evidence for the association
 16 between long-term exposure to PM_{2.5} and mortality is particularly strong for women.
 17 Collectively, the evidence is **sufficient to conclude that the relationship between long-term**
 18 **PM_{2.5} exposures and mortality is likely to be causal.**

7.6.5.2. PM_{10-2.5}

1 In the 2004 PM AQCD, results from the ACS and Six Cities study analyses indicated
2 that thoracic coarse particles were not associated with mortality. Evidence is still limited to
3 adequately characterize the association between PM_{10-2.5} and PM sources and/or
4 components. The new findings from AHSMOG and Veterans cohort studies provide limited
5 evidence of associations between long-term exposure to PM_{10-2.5} and mortality in areas with
6 mean concentrations from 16 to 25 µg/m³. **The evidence for PM_{10-2.5} is inadequate to determine**
7 **if a causal relationship exists between long-term exposures and mortality.**

Chapter 7 References

- Abbey DE; Lebowitz MD; Mills PK; Petersen FF; Beeson WL; Burchette RJ. (1995). Long-term ambient concentrations of particulates and oxidants and development of chronic disease in a cohort of nonsmoking California residents. Presented at In: Phalen, R. F.; Bates, D. V., eds. Proceedings of the colloquium on particulate air pollution and human mortality and morbidity; January 1994; Irvine, CA. *Inhalation Toxicol.* 7: 19-34., Irvine, CA. [000669](#)
- Abbey DE; Mills PK; Petersen FF; Beeson WL. (1991). Long-term ambient concentrations of total suspended particulates and oxidants as related to incidence of chronic disease in California Seventh-Day Adventists. *Environ Health Perspect*, 94: 43-50. [042668](#)
- Abbey DE; Nishino N; McDonnell WF; Burchette RJ; Knutsen SF; Beeson WL; Yang JX. (1999). Long-term inhalable particles and other air pollutants related to mortality in nonsmokers. *Am J Respir Crit Care Med*, 159: 373-382. [047559](#)
- Abou Chakra OR; Joyeux M; Nerriere E; Strub MP; Zmirou-Navier D. (2007). Genotoxicity of organic extracts of urban airborne particulate matter: an assessment within a personal exposure study. *Chemosphere*, 66: 1375-81. [098819](#)
- Achenbach S; Daniel WG. (2001). Noninvasive coronary angiography--an acceptable alternative?. , 345: 1909-1910. [156189](#)
- Ackermann-Lieblich U; Kuna-Dibbert B; Probst-Hensch NM; Schindler C; Dietrich DF; Stutz EZ; Bayer-Oglesby L; Baum F; Brandli O; Brutsche M; Downs SH; Keidel D; Gerbase MW; Imboden M; Keller R; Knopfli B; Kunzli Nellweger J-P; Leuenberger P; SALPADIA Team. (2005). Follow-up of the Swiss Cohort study on air pollution and lung diseases in adults (SAPALDIA 2) 1991-2003: methods and characterization of participants. *Int J Public Health*, 50: 245-263. [087826](#)
- Ackermann-Lieblich U; Leuenberger P; Schwartz J; Schindler C; Monn C; Bolognini B; Bongard JP; Brandli O; Domenighetti G; Elsasser S; Grize L; Karrer W; Keller R; Keller-Wossidlo H; Kunzli N; Martin BW; Medici TC; Pliger B; Wuthrich B; Zellweger JP; Zemp E. (1997). Lung function and long term exposure to air pollutants in Switzerland. *Am J Respir Crit Care Med*, 155: 122-129. [077537](#)
- Agatston AS; Janowitz WR; Hildner FJ; Zusmer NR; Viamonte M Jr; Detrano R. (1990). Quantification of coronary artery calcium using ultrafast computed tomography. *J Am Coll Cardiol*, 15: 827-832. [156197](#)
- Alink GM; Sjogren M; Bos RP; Doekes G; Kromhout H; Scheepers PTJ. (1998). Effect of airborne particles from selected indoor and outdoor environments on gap-junctional intercellular communication. *Toxicol Lett*, 96/97: 209-213. [087159](#)
- Allen RW; Criqui MH; Diez Roux AV; Allison M; Shea S; Detrano R; Sheppard L; Wong N; Hinckley Stukovsky K; Kaufman JD. (2009). Fine particulate air pollution, proximity to traffic, and aortic atherosclerosis: The Multi-Ethnic Study of Atherosclerosis. *Epidemiology*, 20: 254-264. [189644](#)
- Allison MA; Cheung P; Criqui MH; Langer RD; Wright CM. (2006). Mitral and aortic annular calcification are highly associated with systemic calcified atherosclerosis. *Circulation*, 113: 861-866. [155653](#)
- Allison MA; Criqui MH; Wright CM. (2004). Patterns and risk factors for systemic calcified atherosclerosis. *Arterioscler Thromb Vasc Biol*, 24: 331-336. [156210](#)
- Amato M; Montorsi P; Ravani A; Oldani E; Galli S; Ravagnani PM; Tremoli E; Baldassarre D. (2007). Carotid intima-media thickness by B-mode ultrasound as surrogate of coronary atherosclerosis: correlation with quantitative coronary angiography and coronary intravascular ultrasound findings. *Eur Heart J*, 28: 2094-2101. [155656](#)
- Annesi-Maesano I; Moreau D; Caillaud D; Lavaud F; Le Moullec Y; Taytard A; Pauli G; Charpin D. (2007). Residential proximity fine particles related to allergic sensitisation and asthma in primary school children. *Respir Med*, 101: 1721-1729. [093180](#)
- Arad Y; Spadaro LA; Goodman K; Lledo-Perez A; Sherman S; Lerner G; Guerci AD. (1996). Predictive value of electron beam computed tomography of the coronary arteries. 19-month follow-up of 1173 asymptomatic subjects. *Circulation*, 93: 1951-1953. [155661](#)
- Araujo JA; Barajas B; Kleinman M; Wang X; Bennett BJ; Gong KW; Navab M; Harkema J; Sioutas C; Lusic AJ; Nel AE. (2008). Ambient particulate pollutants in the ultrafine range promote early atherosclerosis and systemic oxidative stress. *Circ Res*, 102: 589-596. [156222](#)

Note: Hyperlinks to the reference citations throughout this document will take you to the NCEA HERO database (Health and Environmental Research Online) at <http://epa.gov/hero>. HERO is a database of scientific literature used by U.S. EPA in the process of developing science assessments such as the Integrated Science Assessments (ISA) and the Integrated Risk Information System (IRIS).

- Ardehali R; Nasir K; Kolandaivelu A; Budoff MJ; Blumenthal RS. (2007). Screening patients for subclinical atherosclerosis with non-contrast cardiac CT. *Atherosclerosis*, 192: 235-242. [155662](#)
- Arlt VM; Glatt H; Gamboa da Costa G; Reynisson J; Takamura-Enya T; Phillips DH. (2007). Mutagenicity and DNA adduct formation by the urban air pollutant 2-nitrobenzanthrone. , 98: 445-57. [097257](#)
- Auchincloss AH; Roux AV; Dvornch JT; Brown PL; Barr RG; Daviglius ML; Goff DC; Kaufman JD; O'Neill MS. (2008). Associations between Recent Exposure to Ambient Fine Particulate Matter and Blood Pressure in the Multi-Ethnic Study of Atherosclerosis (MESA). *Environ Health Perspect*, 116: 486-491. [156234](#)
- Avogbe PH; Ayi-Fanou L; Autrup H; Loft S; Fayomi B; Sanni A; Vinzents P; Moller P. (2005). Ultrafine particulate matter and high-level benzene urban air pollution in relation to oxidative DNA damage. *Carcinogenesis*, 26: 613-620. [087811](#)
- Avol EL; Gauderman WJ; Tan SM; London SJ; Peters JM. (2001). Respiratory effects of relocating to areas of differing air pollution levels. *Am J Respir Crit Care Med*, 164: 2067-2072. [020552](#)
- Baccarelli A; Martinelli I; Pegoraro V; Melly S; Grillo P; Zanobetti A; Hou L; Bertazzi PA; Mannucci PM; Schwartz J. (2009). Living near Major Traffic Roads and Risk of Deep Vein Thrombosis. *Circulation*, x: x. [188183](#)
- Baccarelli A; Martinelli I; Zanobetti A; Grillo P; Hou LF; Bertazzi PA; Mannucci PM; Schwartz J. (2008). Exposure to Particulate Air Pollution and Risk of Deep Vein Thrombosis. *Arch Intern Med*, 168: 920-927. [157984](#)
- Baccarelli A; Zanobetti A; Martinelli I; Grillo P; Hou L; Giacomini S; Bonzini M; Lanzani G; Mannucci PM; Bertazzi PA; Schwartz J. (2007). Effects of exposure to air pollution on blood coagulation. *J Thromb Haemost*, 5: 252-260. [090733](#)
- Baker DG. (1998). Natural pathogens of laboratory mice, rats, and rabbits and their effects on research. *Clin Microbiol Rev*, 11: 231-266. [156245](#)
- Bao L; Chen S; Wu L; Hei Tom K; Wu Y; Yu Z; Xu A. (2007). Mutagenicity of diesel exhaust particles mediated by cell-particle interaction in mammalian cells. *Toxicol Sci*, 229: 91-100. [097258](#)
- Basu R; Woodruff TJ; Parker JD; Saulnier L; Schoendorf KC. (2004). Comparing exposure metrics in the relationship between PM_{2.5} and birth weight in California. *J Expo Sci Environ Epidemiol*, 14: 391-396. [087896](#)
- Bayer-Oglesby L; Grize L; Gassner M; Takken-Sahli K; Sennhauser FH; Neu U; Schindler C; Braun-Fahrlander C. (2005). Decline of ambient air pollution levels and improved respiratory health in Swiss children. *Environ Health Perspect*, 113: 1632-1637. [086245](#)
- Beelen R; Hoek G; van den Brandt PA; Goldbohm RA; Fischer P; Schouten LJ; Armstrong B; Brunekreef B. (2008). Long-term exposure to traffic-related air pollution and lung cancer risk. , 19: 702-710. [155681](#)
- Beelen R; Hoek G; van den Brandt PA; Goldbohm RA; Fischer P; Schouten LJ; Jerrett M; Hughes E; Armstrong B; Brunekreef B. (2008). Long-term effects of traffic-related air pollution on mortality in a Dutch cohort (NLCS-AIR study). *Environ Health Perspect*, 116: 196-202. [156263](#)
- Beeson WL; Abbey DE; Knutsen SF. (1998). Long-term concentrations of ambient air pollutants and incident lung cancer in California adults: results from the AHSMOG study. *Environ Health Perspect*, 106: 813-823. [048890](#)
- Bell ML; Ebisu K; Belanger K. (2007). Ambient air pollution and low birth weight in Connecticut and Massachusetts. *Environ Health Perspect*, 115: 1118-24. [091059](#)
- Bell ML; Kim JY; Dominici F. (2007). Potential confounding of particulate matter on the short-term association between ozone and mortality in multisite time-series studies. *Environ Health Perspect*, 115: 1591-1595. [093256](#)
- Bhattacharyya N. (2009). Air quality influences the prevalence of hay fever and sinusitis. *Laryngoscope*, 119: 429-433. [180154](#)
- Bigazzi R; Bianchi S; Baldari D; Campese VM. (1998). Microalbuminuria predicts cardiovascular events and renal insufficiency in patients with essential hypertension. *J Hypertens*, 16: 1325-1333. [156272](#)
- Binková B; Cerná M; Pastorková A; Jeli'nek R; Beneš I; Novák J; Šrám RJ. (2003). Biological activities of organic compounds adsorbed onto ambient air particles: comparison between the cities of Teplice and Prague during the summer and winter seasons 2000–2001. , 525: 43-59. [156274](#)
- Bobak M. (2000). Outdoor air pollution, low birth weight, and prematurity. *Environ Health Perspect*, 108: 173-176. [011448](#)
- Bobak M; Leon DA. (1992). Air pollution and infant mortality in the Czech Republic, 1986-1988. *Lancet*, 8826: 1010-1014. [044415](#)
- Bobak M; Leon DA. (1999). The effect of air pollution on infant mortality appears specific for respiratory causes in the postneonatal period. , 10: 666-670. [007678](#)

- Bonner MR; Han D; Nie J; Rogerson P; Vena JE; Muti P; Trevisan M; Edge SB; Freudenheim JL. (2005). Breast cancer risk and exposure in early life to polycyclic aromatic hydrocarbons using total suspended particulates as a proxy measure. *Cancer Epidemiol Biomarkers Prev*, 14: 53-60. [088993](#)
- Bracken MB; Triche EW; Belanger K; Saftlas A; Beckett WS; Leaderer BP. (2003). Asthma symptoms, severity, and drug therapy: a prospective study of effects on 2205 pregnancies. *Obstet Gynecol*, 102: 739-753. [156288](#)
- Brauer M; Gehring U; Brunekreef B; De Jongste J; Gerritsen J; Rovers M; Wichmann H-E; Wijga A; Heinrich J. (2006). Traffic-related air pollution and otitis media. *Environ Health Perspect*, 114: 1414-1418. [090757](#)
- Brauer M; Hoek G; Smit HA; De Jongste JC; Gerritsen J; Postma DS; Kerkhof M; Brunekreef B. (2007). Air pollution and development of asthma, allergy and infections in a birth cohort. *Eur Respir J*, 29: 879-888. [090691](#)
- Brauer M; Hoek G; Van Vliet P; Meliefste K; Fischer PH; Wijga A; Koopman LP; Neijens HJ; Gerritsen J; Kerkhof M; Heinrich J; Bellander T; Brunekreef B. (2002). Air pollution from traffic and the development of respiratory infections and asthmatic and allergic symptoms in children. *Am J Respir Crit Care Med*, 166: 1092-1098. [035192](#)
- Brauer M; Lencar C; Tamburic L; Koehoorn M; Demers P; Karr C. (2008). A cohort study of traffic-related air pollution impacts on birth outcomes. *Environ Health Perspect*, 116: 680-686. [156292](#)
- Brown JS; Zeman KL; Bennett WD. (2001). Regional deposition of coarse particles and ventilation distribution in healthy subjects and patients with cystic fibrosis. *Am J Respir Crit Care Med*, 14: 443-454. [012307](#)
- Brunekreef B; Beelen R; Hoek G; Schouten L; Bausch-Goldbohm S; Fischer P; Armstrong B; Hughes E; Jerrett M; van den Brandt P. (2009). Effects of long-term exposure to traffic-related air pollution on respiratory and cardiovascular mortality in the Netherlands: The NLCS-AIR Study. Health Effects Institute. Boston, MA. 139. [191947](#)
- Budoff MJ; Takasu J; Katz R; Mao S; Shavelle DM; O'Brien KD; Blumenthal RS; Carr JJ; Kronmal R. (2005). Reproducibility of CT measurements of aortic valve calcification, mitral annulus calcification, and aortic wall calcification in the multi-ethnic study of atherosclerosis. *Acad Radiol*, 13: 166-172. [192105](#)
- Bunger J; Krahl J; Weigel A; Schroder O; Bruning T; Muller M; Hallier E; Westphal G. (2006). Influence of fuel properties, nitrogen oxides, and exhaust treatment by an oxidation catalytic converter on the mutagenicity of diesel engine emissions. *Arch Toxicol*, 80: 540-546. [156303](#)
- Bunger J; Schappler-Scheele B; Hilgers R; Hallier E. (2007). A 5-year follow-up study on respiratory disorders and lung function in workers exposed to organic dust from composting plants. *Int Arch Occup Environ Health*, 80: 306-312. [156304](#)
- Burchiel SW; Lauer FT; Dunaway SL; Zawadzki J; McDonald JD; Reed MD. (2005). Hardwood smoke alters murine splenic T cell responses to mitogens following a 6-month whole body inhalation exposure. *Toxicol Appl Pharmacol*, 202: 229-236. [088090](#)
- Burchiel SW; Lauer FT; McDonald JD; Reed MD. (2004). Systemic immunotoxicity in AJ mice following 6-month whole body inhalation exposure to diesel exhaust. *Toxicol Appl Pharmacol*, 196: 337-345. [055557](#)
- Calderon-Garciduenas L; Vincent R; Mora-Tiscareno A; Franco-Lira M; Henriquez-Roldan C; Barragan-Mejia G; Garrido-Garcia L; Camacho-Reyes L; Valencia-Salazar G; Paredes R; Romero L; Osnaya H; Villarreal-Calderon R; Torres-Jardon. (2007). Elevated plasma endothelin-1 and pulmonary arterial pressure in children exposed to air pollution. *Environ Health Perspect*, 115: 1248-1253. [091252](#)
- Chambless LE; Heiss G; Folsom AR; Rosamond W; Szklo M; Sharrett AR; Clegg LX. (1997). Association of coronary heart disease incidence with carotid arterial wall thickness and major risk factors: the Atherosclerosis Risk in Communities (ARIC) Study, 1987-1993. *Am J Epidemiol*, 146: 483-494. [156329](#)
- Chang J; Delfino RJ; Gillen D; Tjoa T; Nickerson B; Cooper D. (2008). Repeated respiratory hospital encounters among children with asthma and residential proximity to traffic. *J Occup Environ Med*, 66: 90-98. [180393](#)
- Chen JC; Schwartz J. (2008). Metabolic syndrome and inflammatory responses to long-term particulate air pollutants. *Environ Health Perspect*, 116: 612-617. [190106](#)
- Chen L; Yang W; Jennison BL; Goodrich A; Omaye ST. (2002). Air pollution and birth weight in northern Nevada, 1991-1999. *Inhal Toxicol*, 14: 141-157. [024945](#)
- Chen LC; Hwang JS. (2005). Effects of subchronic exposures to concentrated ambient particles (CAPs) in mice IV Characterization of acute and chronic effects of ambient air fine particulate matter exposures on heart-rate variability. *Inhal Toxicol*, 17: 209-216. [087218](#)
- Chen LC; Nadziejko C. (2005). Effects of subchronic exposures to concentrated ambient particles (CAPs) in mice V CAPs exacerbate aortic plaque development in hyperlipidemic mice. *Inhal Toxicol*, 17: 217-224. [087219](#)
- Chen LH; Knutsen SF; Shavlik D; Beeson WL; Petersen F; Ghamsary M; Abbey D. (2005). The association between fatal coronary heart disease and ambient particulate air pollution: Are females at greater risk?. *Environ Health Perspect*, 113: 1723-1729. [087942](#)

- Churg A; Brauer M; del Carmen Avila-Casado M; Fortoul TI; Wright JL. (2003). Chronic exposure to high levels of particulate air pollution and small airway remodeling. *Environ Health Perspect*, 111: 714-718. [087899](#)
- Clancy L; Goodman P; Sinclair H; Dockery DW. (2002). Effect of air pollution control on death rates in Dublin, Ireland: an intervention study. *Lancet*, 360: 1210-1214. [035270](#)
- Claxton LD; Matthews PP; Warren SH. (2004). The genotoxicity of ambient outdoor air, a review: Salmonella mutagenicity. *DNA Repair (Amst)*, 567: 347-399. [089008](#)
- Claxton LD; Woodall GM Jr. (2007). A review of the mutagenicity and rodent carcinogenicity of ambient air. , 636: 36-94. [180391](#)
- Clifton VL; Giles WB; Smith R; Bisits AT; Hempenstall PA; Kessell CG; Gibson PG. (2001). Alterations of placental vascular function in asthmatic pregnancies. *Am J Respir Crit Care Med*, 164: 546-554. [156360](#)
- Craven TE; Ryu JE; Espeland MA; Kahl FR; McKinney WM; Toole JF; McMahan MR; Thompson CJ; Heiss G; Crouse JR, 3rd. (1990). Evaluation of the associations between carotid artery atherosclerosis and coronary artery stenosis. A case-control study. , 82: 1230-1242. [155740](#)
- Cury PM; Lichtenfels AJ; Reymão MS; Conceição GM; Capelozzi VL; Saldiva PH. (2000). Urban levels of air pollution modifies the progression of urethane-induced lung tumours in mice. *Pathol Res Pract*, 196: 627-633. [192100](#)
- Dales R; Burnett RT; Smith-Doiron M; Stieb DM; Brook JR. (2004). Air pollution and sudden infant death syndrome. , 113: 628-631. [087342](#)
- Dales R; Wheeler A; Mahmud M; Frescura AM; Smith-Doiron M; Nethery E; Liu L. (2008). The Influence of Living Near Roadways on Spirometry and Exhaled Nitric Oxide in Elementary Schoolchildren. *Environ Health Perspect*, 116: 1423. [156378](#)
- Danielsen PH; Loft S; Møller P. (2008). DNA damage and cytotoxicity in type II lung epithelial (A549) cell cultures after exposure to diesel exhaust and urban street particles. *Part Fibre Toxicol*, 5: 6. [192092](#)
- De Kok TM; Hogervorst JG; Briede JJ; Van Herwijnen MH; Maas LM; Moonen EJ; Driee HA; Kleinjans JC. (2005). Genotoxicity and physicochemical characteristics of traffic-related ambient particulate matter. *Environ Mol Mutagen*, 46: 71-80. [088656](#)
- Deckert T; Yokoyama H; Mathiesen E; Ronn B; Jensen T; Feldt-Rasmussen B; Borch-Johnsen K; Jensen JS. (1996). Cohort study of predictive value of urinary albumin excretion for atherosclerotic vascular disease in patients with insulin dependent diabetes. *Br Med J*, 312: 871-874. [156389](#)
- DeMarini DM; Brooks LR; Warren SH; Kobayashi T; Gilmour MI; Singh P. (2004). Bioassay-directed fractionation and Salmonella mutagenicity of automobile and forklift diesel exhaust particles. *Environ Health Perspect*, 112: 814-819. [066329](#)
- Diez Roux AV; Auchincloss AH; Franklin TG; Raghunathan T; Barr RG; Kaufman J; Astor B; Keeler J. (2008). Long-term exposure to ambient particulate matter and prevalence of subclinical atherosclerosis in the Multi-Ethnic Study of Atherosclerosis. *Am J Epidemiol*, 167: 667-675. [156401](#)
- Dinneen SF; Gerstein HC. (1997). The association of microalbuminuria and mortality in non-insulin-dependent diabetes mellitus. A systematic overview of the literature. , 157: 1413-1418. [156403](#)
- Dockery DW; Cunningham J; Damokosh AI; Neas LM; Spengler JD; Koutrakis P; Ware JH; Raizenne M; Speizer FE. (1996). Health effects of acid aerosols on North American children: respiratory symptoms. *Environ Health Perspect*, 104: 500-505. [077269](#)
- Dockery DW; Pope CA III; Xu X; Spengler JD; Ware JH; Fay ME; Ferris BG Jr; Speizer FE. (1993). An association between air pollution and mortality in six US cities. , 329: 1753-1759. [044457](#)
- Downs SH; Schindler C; Liu L-JS; Keidel D; Bayer-Oglesby L; Brutsche MH; Gerbase MW; Keller R; Kunzli N; Leuenberger P; Probst-Hensch NM; Tschopp J-M; Zellweger J-P; Rochat T; Schwartz J; Ackermann-Liebrich U. (2007). Reduced exposure to PM10 and attenuated age-related decline in lung function. , 15: 185-204. [092853](#)
- Dugandzic RDodds L; Stieb D; Smith-Doiron M. (2006). The association between low level exposures to ambient air pollution and term low birth weight: a retrospective cohort study. , 5: 3. [088681](#)
- Eftim SE; Samet JM; Janes H; McDermott A; Dominici F. (2008). Fine Particulate Matter and Mortality: A Comparison of the Six Cities and American Cancer Society Cohorts With a Medicare Cohort. , 19: 209-216. [099104](#)
- Enstrom JE. (2005). Fine particulate air pollution and total mortality among elderly Californians, 1973-2002. *Inhal Toxicol*, 17: 803-816. [087356](#)
- Erbel R; Mohlenkamp S; Kerkhoff G; Budde T; Schmermund A. (2007). Non-invasive screening for coronary artery disease: calcium scoring. *Heart*, 93: 1620-1629. [155768](#)
- Erdinger L; Durr M; Hopker KA. (2005). Correlations between mutagenic activity of organic extracts of airborne particulate matter, NOx and sulphur dioxide in southern Germany: results of a two-year study. *Environ Sci Pollut Res Int*, 12: 10-20. [156423](#)

- Fedulov AV; Leme A; Yang Z; Dahl M; Lim R; Mariani TJ; Kobzik L. (2008). Pulmonary exposure to particles during pregnancy causes increased neonatal asthma susceptibility. , 38: 57-67. [097482](#)
- Finch GL; Hobbs CH; Blair LF; Barr EB; Hahn FF; Jaramillo RJ; Kubatko JE; March TH; White RK; Krone JR; Menache MG; Nikula KJ; Mauderly JL; Van Gerpen J; Merceica MD; Zielinska B; Stankowski L; Burling K; Howell S; Mauderly JL. (2002). Effects of subchronic inhalation exposure of rats to emissions from a diesel engine burning soybean oil-derived biodiesel fuel. *Inhal Toxicol*, 14: 1017-1048. [054603](#)
- Floyd HS; Chen LC; Vallanat B; Dreher K. (2009). Fine ambient air particulate matter exposure induces molecular alterations associated with vascular disease progression within plaques of atherosclerotic susceptible mice. *Inhal Toxicol*, 21: 394-403. [190350](#)
- Forbes LJ; Patel MD; Rudnicka AR; Cook DG; Bush T; Stedman JR; Whincup PH; Strachan DP; Anderson RH. (2009). Chronic exposure to outdoor air pollution and markers of systemic inflammation. *Epidemiology*, 20: 245-253. [190351](#)
- Forman JP; Brenner BM. (2006). 'Hypertension' and 'microalbuminuria': the bell tolls for thee. *Kidney Int*, 69: 22-28. [156439](#)
- Foster PMD; Mylchreest E; Gaido KW; Sar M. (2001). Effects of phthalate esters on the developing reproductive tract of male rats. *Hum Reprod Update*, 7: 231-235. [156442](#)
- Foster PMD; Thomas LV; Cook MW; Gangolli SD. (1980). Study of the testicular effects and changes in zinc excretion produced by some n-alkyl phthalates in the rat. *Toxicol Appl Pharmacol*, 54: 392-398. [094701](#)
- Franklin SS; Sutton-Tyrrell K; Belle SH; Weber MA; Kuller LH. (1997). The importance of pulsatile components of hypertension in predicting carotid stenosis in older adults. *J Hypertens*, 15: 1143-1150. [156446](#)
- Fryer ME; Collins CD. (2003). Model intercomparison for the uptake of organic chemicals by plants. *Environ Sci Technol*, 37: 1617-1624. [156454](#)
- Fujimoto A; Tsukue N; Watanabe M; Sugawara I; Yanagisawa R; Takano H; Yoshida S; Takeda K. (2005). Diesel exhaust affects immunological action in the placentas of mice. , 20: 431-440. [096556](#)
- Gardner MB. (1966). Biological effects of urban air pollution III Lung tumors in mice. *Arch Environ Occup Health*, 12: 305-313. [015129](#)
- Gardner MB; Loosli CG; Hanes B; Blackmore W; Teebken D. (1969). Histopathologic findings in rats exposed to ambient and filtered air. *Arch Environ Occup Health*, 19: 637-647. [015130](#)
- Gauderman WJ; Avol E; Gilliland F; Vora H; Thomas D; Berhane K; McConnell R; Kuenzli N; Lurmann F; Rappaport E; Margolis H; Bates D; Peters J. (2004). The effect of air pollution on lung development from 10 to 18 years of age. , 351: 1057-1067. [056569](#)
- Gauderman WJ; Gilliland GF; Vora H; Avol E; Stram D; McConnell R; Thomas D; Lurmann F; Margolis HG; Rappaport EB; Berhane K; Peters JM. (2002). Association between air pollution and lung function growth in southern California children: results from a second cohort. *Am J Respir Crit Care Med*, 166: 76-84. [026013](#)
- Gauderman WJ; McConnell R; Gilliland F; London S; Thomas D; Avol E; Vora H; Berhane K; Rappaport EB; Lurmann F; Margolis HG; Peters J. (2000). Association between air pollution and lung function growth in southern California children. *Am J Respir Crit Care Med*, 162: 1383-1390. [012531](#)
- Gehrig R; Buchmann B. (2003). Characterising seasonal variations and spatial distribution of ambient PM10 and PM25 concentrations based on long-term Swiss monitoring data. *Atmos Environ*, 37: 2571-2580. [139678](#)
- Gehring U; Heinrich J; Kramer U; Grote V; Hochadel M; Sugiri D; Kraft M; Rauchfuss K; Eberwein HG; Wichmann H-E. (2006). Long-term exposure to ambient air pollution and cardiopulmonary mortality in women. , 17: 545-551. [089797](#)
- Geroulakos G; O'Gorman DJ; Kalodiki E; Sheridan DJ; Nicolaidis AN. (1994). The carotid intima-media thickness as a marker of the presence of severe symptomatic coronary artery disease. , 15: 781-785. [155788](#)
- Gerstein HC; Mann JF; Yi Q; Zinman B; Dinneen SF; Hoogwerf B; Halle JP; Young J; Rashkow A; Joyce C; Nawaz S; Yusuf S. (2001). Albuminuria and risk of cardiovascular events, death, and heart failure in diabetic and nondiabetic individuals. *JAMA*, 286: 421-426. [156466](#)
- Ghosh R; Rankin J; Pless-Mulloli T; Glinianaia S. (2007). Does the effect of air pollution on pregnancy outcomes differ by gender? A systematic review. *Environ Res*, 105: 400-408. [091233](#)
- Gilboa SM; Mendola P; Olshan AF; Langlois PH; Savitz DA; Loomis D; Herring AH; Fixler DE. (2005). Relation between ambient air quality and selected birth defects, seven county study, Texas, 1997-2000. *Am J Epidemiol*, 162: 238-252. [087892](#)
- Girerd X; Mourad JJ; Acar C; Heudes D; Chiche S; Bruneval P; Mignot JP; Billaud E; Safar M; Laurent S. (1994). Noninvasive measurement of medium-sized artery intima-media thickness in humans: in vitro validation. *J Vasc Res*, 31: 114-120. [156474](#)

- Glinianaia FV; Rankin J; Bell R; Pless-Mulloli T; Howel D. (2004). Does particulate air pollution contribute to infant death? A systematic review. *Environ Health Perspect*, 112: 1365-1371. [087898](#)
- Goss CH; Newsom SA; Schildcrout JS; Sheppard L; Kaufman JD. (2004). Effect of ambient air pollution on pulmonary exacerbations and lung function in cystic fibrosis. *Am J Respir Crit Care Med*, 169: 816-821. [055624](#)
- Gotschi T; Heinrich J; Sunyer J; Kunzli N. (2008). Long-term effects of ambient air pollution on lung function - A review. , 19: 690-701. [156485](#)
- Gotschi T; Sunyer J; Chinn S; de Marco R; Forsberg B; Gauderman JW; Garcia-Esteban R; Heinrich J; Jacquemin B; Jarvis D; Ponzio M; Villani S; Kunzli N. (2008). Air pollution and lung function in the European Community Respiratory Health Survey. *Int J Epidemiol*, 37: 1349-1358. [180364](#)
- Gottipolu RR; Wallenborn JG; Karoly ED; Schladweiler MC; Ledbetter AD; Krantz T; Linak WP; Nyska A; Johnson JA; Thomas R; Richards JE; Jaskot RH; Kodavanti UP. (2009). One-month diesel exhaust inhalation produces hypertensive gene expression pattern in healthy rats. *Environ Health Perspect*, 117: 38-46. [190360](#)
- Gouveia N; Bremner SA; Novaes HMD. (2004). Association between ambient air pollution and birth weight in Sao Paulo, Brazil. *J Epidemiol Community Health*, 58: 11-17. [055613](#)
- Greenland P; Kizilbash MA. (2005). Coronary computed tomography in coronary risk assessment. , 25: 3-10. [156496](#)
- Grigg J; Kulkarni N; Pierse N; Rushton L; O'Callaghan C; Rutman A. (2008). Black-pigmented material in airway macrophages from healthy children: association with lung function and modeled PM10. [156499](#)
- Gunnison A; Chen LC. (2005). Effects of subchronic exposures to concentrated ambient particles (CAPs) in mice VI Gene expression in heart and lung tissue. *Inhal Toxicol*, 17: 225-233. [087956](#)
- Gutierrez-Castillo ME; Roubicek DA; Cebrian-Garcia ME; De Vizcaya-Ruiz A; Sordo-Cedeno M; Ostrosky-Wegman P. (2006). Effect of chemical composition on the induction of DNA damage by urban airborne particulate matter. *Environ Mol Mutagen*, 47: 199-211. [089030](#)
- Gábelová A; Valovicova Z; Bacova G; Labaj J; Binkova B; Topinka J; Sevastyanova O; Sram RJ; Kalina I; Habalova V; Popov TA; Panev T; Farmer PB. (2007). Sensitivity of different endpoints for in vitro measurement of genotoxicity of extractable organic matter associated with ambient airborne particles (PM10). , 620: 103-113. [156458](#)
- Gábelová A; Valovicova Z; Labaj J; Bacova G; Binkova B; Farmer Peter B. (2007). Assessment of oxidative DNA damage formation by organic complex mixtures from airborne particles PM(10). , 620: 135-144. [156457](#)
- Ha E-H; Lee J-T; Kim H; Hong Y-C; Lee. (2003). Infant susceptibility of mortality to air pollution in Seoul, South Korea. , 111: 284-290. [042552](#)
- Haland G; Carlsen KC; Sandvik L; Devulapalli CS; Munthe-Kaas MC; Pettersen M; Carlsen KH. (2006). Reduced lung function at birth and the risk of asthma at 10 years of age. , 355: 1682-1689. [156511](#)
- Hamada K; Suzuki Y; Leme A; Ito T; Miyamoto K; Kobzik L; Kimura H. (2007). Exposure of pregnant mice to an air pollutant aerosol increases asthma susceptibility in offspring. *J Toxicol Environ Health A*, 70: 688-695. [091235](#)
- Hannigan MP; Cass GR; Penman BW; Crespi CL; Lafleur AL; Busby WF Jr; Thilly WG. (1997). Human cell mutagens in Los Angeles air. *Environ Sci Technol*, 31: 438-447. [083598](#)
- Hansen C; Neller A; Williams G; Simpson R. (2006). Maternal exposure to low levels of ambient air pollution and preterm birth in Brisbane, Australia. *BJOG*, 113: 935-941. [089818](#)
- Hansen C; Neller A; Williams G; Simpson R. (2007). Low levels of ambient air pollution during pregnancy and fetal growth among term neonates in Brisbane, Australia. *Environ Res*, 103: 383-389. [090703](#)
- Harrod KS; Jaramillo RJ; Berger JA; Gigliotti AP; Seilkop SK; Reed MD. (2005). Inhaled diesel engine emissions reduce bacterial clearance and exacerbate lung disease to *Pseudomonas aeruginosa* infection in vivo. *Toxicol Sci*, 83: 155-165. [088144](#)
- Hashimoto AH; Amanuma K; Hiyoshi K; Sugawara Y; Goto S; Yanagisawa R; Takano H; Masumura K-I; Nohmi T; Aoki Y. (2007). Mutations in the lungs of gpt delta transgenic mice following inhalation of diesel exhaust. , 48: 682-693. [097261](#)
- Healey K; Smith EC; Wild CP; Routledge MN. (2006). The mutagenicity of urban particulate matter in an enzyme free system is associated with the generation of reactive oxygen species. , 602: 1-6. [156532](#)
- Heinrich J; Hoelscher B; Frye C; Meyer I; Pitz M; Cyrys J; Wjst M; Neas L; Wichmann H-E. (2002). Improved air quality in reunified Germany and decreases in respiratory symptoms. , 13: 394-401. [034825](#)
- Heinrich J; Slama R. (2007). Fine particles, a major threat to children. *Int J Hyg Environ Health*, 210: 617-622. [156534](#)
- Heiss G; Sharrett AR; Barnes R; Chambless LE; Szklo M; Alzola C. (1991). Carotid atherosclerosis measured by B-mode ultrasound in populations: associations with cardiovascular risk factors in the ARIC study. *Am J Epidemiol*, 134: 250-256. [156535](#)

- Hiramatsu K; Azuma A; Kudoh S; Desaki M; Takizawa H; Sugawara I. (2003). Inhalation of diesel exhaust for three months affects major cytokine expression and induces bronchus-associated lymphoid tissue formation in murine lungs. , 29: 607-622. [155846](#)
- Hirose T; Morito K; Kizu R; Toriba A; Hayakawa K; Ogawa S; Inoue S; Muramatsu M; Masamune Y. (2001). Estrogenic/Antiestrogenic Activities of Benzo [a] pyrene Monohydroxy Derivatives. *Eisei Kagaku*, 47: 552-558. [156548](#)
- Hoek G; Brunekreef B; Goldbohm S; Fischer P; Van den Brandt PA. (2002). Association between mortality and indicators of traffic-related air pollution in the Netherlands: a cohort study. *Lancet*, 360: 1203-1209. [042364](#)
- Hoffmann B; Moebus S; Kroger K; Stang A; Mohlenkamp S; Dragano N; Schmermund A; Memmesheimer M; Erbel R; Jockel K-H. (2009). Residential exposure to urban pollution, ankle-brachial index, and peripheral arterial disease. *Epidemiology*, 20: 280-288. [190376](#)
- Hoffmann B; Moebus S; Mohlenkamp S; Stang A; Lehmann N; Dragano N; Schmermund A; Memmesheimer M; Mann K; Erbel R; Jockel K-H; Heinz Nixdorf Recall Study Investigative Group. (2007). Residential exposure to traffic is associated with coronary atherosclerosis. *Circulation*, 116: 489-496. [091163](#)
- Hoffmann B; Moebus S; Stang A; Beck E-M; Dragano N; Mohlenkamp S; Schmermund A; Memmesheimer M; Mann K; Erbel R; Jockel K-H; Heinz Nixdorf RECALL Study Investigative Group. (2006). Residence close to high traffic and prevalence of coronary heart disease. *Eur Heart J*, 27: 2696-2702. [091162](#)
- Hoffmann MH; Shi H; Schmitz BL; Schmid FT; Lieberknecht M; Schulze R; Ludwig B; Kroschel U; Jahnke N; Haerer W; Brambs HJ; Aschoff AJ. (2005). Noninvasive coronary angiography with multislice computed tomography. *JAMA*, 293: 2471-2478. [156556](#)
- Hollander M; Hak AE; Koudstaal PJ; Bots ML; Grobbee DE; Hofman A; Witteman JC; Breteler MM. (2003). Comparison between measures of atherosclerosis and risk of stroke: the Rotterdam Study. , 34: 2367-2372. [156562](#)
- Hornberg C; Maciuleviciute L; Seemayer NH. (1996). Sister chromatid exchanges in rodent tracheal epithelium exposed in vitro to environmental pollutants. *Toxicol Lett*, 88: 45-53. [087164](#)
- Hornberg C; Maciuleviciute L; Seemayer NH; Kainka E. (1998). Induction of sister chromatid exchanges (SCE) in human tracheal epithelial cells by the fractions PM-10 and PM-2.5 of airborne particulates. *Toxicol Lett*, 96: 215-220. [155849](#)
- Hougaard KS; Jensen KA; Nordly P; Taxvig C; Vogel U; Saber AT; Wallin H. (2008). Effects of prenatal exposure to diesel exhaust particles on postnatal development, behavior, genotoxicity and inflammation in mice. *Part Fibre Toxicol*, 5: 3. [156570](#)
- Huang JY; Liao JW; Liu YC; Lu SY; Chou CP; Chan WH; Chen SU; Ueng TH. (2008). Motorcycle exhaust induces reproductive toxicity and testicular interleukin-6 in male rats. *Toxicol Sci*, 103: 137-148. [156574](#)
- Huynh M; Woodruff TJ; Parker JD; Schoendorf KC. (2006). Relationships between air pollution and preterm birth in California. *Paediatr Perinat Epidemiol*, 20: 454-461. [091240](#)
- Hwang B-F; Jaakkola JJK; Lee Y-L; Lin Y-C; Guo Y-LL. (2006). Relation between air pollution and allergic rhinitis in Taiwanese schoolchildren. *Respir Res*, 7: 23. [088971](#)
- Hwang J-S; Nadziejko C; Chen LC. (2005). Effects of subchronic exposures to concentrated ambient particles (CAPs) in mice: III Acute and chronic effects of CAPs on heart rate, heart-rate fluctuation, and body temperature. *Inhal Toxicol*, 17: 199-207. [087957](#)
- IARC. (1989). Diesel and gasoline engine exhausts. Lyon, France: International Agency for Research on Cancer. [002958](#)
- Iba MM; Fung J; Chung L; Zhao J; Winnik B; Buckley BT; Chen LC; Zelikoff JT; Kou YR. (2006). Differential inducibility of rat pulmonary CYP1A1 by cigarette smoke and wood smoke. , 606: 1-11. [156582](#)
- Ichinose T; Yajima Y; Nagashima M; Takenoshita S; Nagamachi Y; Sagai M. (1997). Lung carcinogenesis and formation of 8-hydroxy-deoxyguanosine in mice by diesel exhaust particles. *Carcinogenesis*, 18: 185-192. [053264](#)
- Ishihara Y; Kagawa J. (2003). Chronic diesel exhaust exposures of rats demonstrate concentration and time-dependent effects on pulmonary inflammation. , 15: 473-492. [096404](#)
- Islam T; Gauderman WJ; Berhane K; McConnell R; Avol E; Peters JM; Gilliland FD. (2007). The relationship between air pollution, lung function and asthma in adolescents. *Thorax*, 62: 957-963. [090697](#)
- Izawa H; Watanabe G; Taya K; Sagai M. (2007). Inhibitory effects of foods and polyphenols on activation of aryl hydrocarbon receptor induced by diesel exhaust particles. , 14: 149-156. [190387](#)
- Jacobsen NR; Mrller P; Cohn CA; Loft S; Vogel U; Wallin H. (2008). Diesel exhaust particles are mutagenic in FE1-Muta™ Mouse lung epithelial cells. , 641: 54-57. [156597](#)
- Jalaludin B; Mannes T; Morgan G; Lincoln D; Sheppeard V; Corbett S. (2007). Impact of ambient air pollution on gestational age is modified by season in Sydney, Australia. , 6: 16. [156601](#)

- Janes H; Dominici F; Zeger SL. (2007). Trends in air pollution and mortality: an approach to the assessment of unmeasured confounding. , 18: 416-23. [090927](#)
- Janssen NAH; Brunekreef B; van Vliet P; Aarts F; Maliefste K; Harssema H; Fischer P. (2003). The relationship between air pollution from heavy traffic and allergic sensitization, bronchial hyperresponsiveness, and respiratory symptoms in Dutch schoolchildren. , 111: 1512-1518. [133555](#)
- Jerrett M; Burnett RT; Ma R; Pope 3rd CA; Krewski D; Newbold KB; Thurston G; Shi Y; Finkelstein N; Calle EE; Thun MJ. (2005). Spatial analysis of air pollution and mortality in Los Angeles. *Epidemiology*, 16: 727-36. [189405](#)
- Jerrett M; Buzzelli M; Burnett RT; DeLuca PF. (2005). Particulate air pollution, social confounders, and mortality in small areas of an industrial city. *Soc Sci Med*, 60: 2845-2863. [087381](#)
- Karr C; Lumley T; Schreuder A; Davis R; Larson T; Ritz B; Kaufman J. (2007). Effects of subchronic and chronic exposure to ambient air pollutants on infant bronchiolitis. *Am J Epidemiol*, 165: 553-560. [090719](#)
- Karr C; Rudra C; Miller K; Gould T; Larson T; Sathyanarayana S; Koenig J. (2009). Infant exposure to fine particulate matter and traffic and risk of hospitalization for RSV bronchiolitis in a region with lower ambient air pollution. *Environ Res*, 109: 321-327. [191946](#)
- Karthikeyan VJ; Lip GYH. (2007). Peripheral artery disease and hypertension: the relation between ankle-brachial index and mortality. *J Hum Hypertens*, 21: 762-765. [156626](#)
- Kato A; Kagawa J. (2003). Morphological effects in rat lungs exposed to urban roadside air. *Inhal Toxicol*, 15: 799-818. [089563](#)
- Khattar RS; Swales JD; Dore C; Senior R; Lahiri A. (2001). Effect of aging on the prognostic significance of ambulatory systolic, diastolic, and pulse pressure in essential hypertension. , 104: 783-789. [155896](#)
- Khoury Z; Schwartz R; Gottlieb S; Chenzbraun A; Stern S; Keren A. (1997). Relation of coronary artery disease to atherosclerotic disease in the aorta, carotid, and femoral arteries evaluated by ultrasound. *Am J Cardiol*, 80: 1429-1433. [156636](#)
- Kim JJ; Smorodinsky S; Lipsett M; Singer BC; Hodgson AT; Ostro B. (2004). Traffic-related air pollution near busy roads: the East Bay children's Respiratory Health Study. *Am J Respir Crit Care Med*, 170: 520-526. [087383](#)
- Kim OJ; Ha EH; Kim BM; Park HS; Jung WJ; Lee BE; Suh YJ; Kim YJ; Lee JT; Kim H; Hong YC. (2007). PM10 and pregnancy outcomes: a hospital-based cohort study of pregnant women in Seoul. *J Occup Environ Med*, 49: 1394-1402. [156642](#)
- Kizu R; Okamura K; Toriba A; Mizokami A; Burnstein KL; Klinge CM; Hayakawa K. (2003). Antiandrogenic activities of diesel exhaust particle extracts in PC3/AR human prostate carcinoma cells. , 76: 299-309. [096196](#)
- Knight EL; Curhan GC. (2003). Albuminuria: moving beyond traditional microalbuminuria cut-points. *Current Opinion Nephrol Hypertens*, 12: 283-284. [179900](#)
- Knöbel HH; Chen CJ; Liang KY. (1995). Sudden infant death syndrome in relation to weather and optometrically measured air pollution in Taiwan. , 96: 1106-1110. [155905](#)
- Krewski D. (2009). Evaluating the effects of ambient air pollution on life expectancy. *N Engl J Med*, 360: 413-415. [190075](#)
- Krewski D; Burnett RT; Goldberg MS; Hoover K; Siemiatycki J; Jerrett M; Abrahamowicz M; White WH. (2000). Reanalysis of the Harvard Six Cities study and the American Cancer Society study of particulate air pollution and mortality: a special report of the Institute's Particle Epidemiology Reanalysis Project. [012281](#)
- Krewski D; Jerrett M; Burnett RT; Ma R; Hughes E; Shi Y; Turner MC; Pope AC III; Thurston G; Calle EE; Thun MJ. (2009). Extended follow-up and spatial analysis of the American Cancer Society study linking particulate air pollution and mortality. Health Effects Institute. Cambridge, MA. 140. [191193](#)
- Kulkarni N; Pierse N; Rushton L; Grigg J. (2006). Carbon in airway macrophages and lung function in children. , 355: 21-30. [089257](#)
- Kunzli N; Bridevaux P-O; Liu S; Garcia-Esteban R; Schindler C; Gerbase M; Sunyer J; Keidel D; Rochat T. (2009). Traffic-related air pollution correlates with adult-onset asthma among never-smokers. *Thorax*, x: x. [191949](#)
- Kunzli N; Jerrett M; Mack WJ; Beckerman B; LaBree L; Gilliland F; Thomas D; Peters J; Hodis HN. (2005). Ambient air pollution and atherosclerosis in Los Angeles. *Environ Health Perspect*, 113: 201-206. [087387](#)
- Kunzli N; Perez L; Lurmann F; Hricko A; Penfold B; McConnell R. (2008). An Attributable Risk Model for Exposures Assumed to Cause Both Chronic Disease and its Exacerbations. , 19(2): 179-185. [129258](#)
- Lacasaña M; Esplugues A; Ballester F. (2005). Exposure to ambient air pollution and prenatal and early childhood health effects. , 20: 183-199. [155914](#)
- Laden F; Schwartz J; Speizer FE; Dockery DW. (2006). Reduction in fine particulate air pollution and mortality: extended follow-up of the Harvard Six Cities study. *Am J Respir Crit Care Med*, 173: 667-672. [087605](#)

- Lee BE; Ha EH; Park HS; Kim YJ; Hong YC; Kim H; Lee JT. (2003). Exposure to air pollution during different gestational phases contributes to risks of low birth weight. *Hum Reprod*, 18: 638-643. [043202](#)
- Leem J-H; Kaplan BM; Shim YK; Pohl HR; Gotway CA; Bullard SM; Rogers JF; Smith MM; Tylenda CA. (2006). Exposures to air pollutants during pregnancy and preterm delivery. *Environ Health Perspect*, 114: 905-910. [089828](#)
- Lemos M; Mohallen S; Macchione M; Dolhnikoff M; Assuncao J; Godleski J; Saldiva P. (2006). Chronic exposure to urban air Pollution induces structural alterations in murine pulmonary and coronary arteries. *Inhal Toxicol*, 18: 247-253. [088594](#)
- Li Y-J; Kawada T; Matsumoto A; Azuma A; Kudoh S; Takizawa H; Sugawara I. (2007). Airway inflammatory responses to oxidative stress induced by low-dose diesel exhaust particle exposure differ between mouse strains. , 33: 227-244. [155929](#)
- Lichtenfels AJFC; Gomes JB; Pieri PC; Miraglia SGEK; Hallak J; Saldiva PHN. (2007). Increased levels of air pollution and a decrease in the human and mouse male-to-female ration in Sao Paulo, Brazil. *Fertil Steril*, 87: 230-232. [097041](#)
- Lin C-M; Li C-Y; Mao I-F. (2004). Increased risks of term low-birth-weight infants in a petrochemical industrial city with high air pollution levels. *Arch Environ Occup Health*, 59: 663-668. [089827](#)
- Lin CA; Pereira LAA; Nishioka DC; Conceicao GMS; Graga ALF; Saldiva PHN. (2004). Air pollution and neonatal deaths in Sao Paulo, Brazil. *Braz J Med Biol Res*, 37: 765-770. [095787](#)
- Lipfert FW; Baty JD; Miller JP; Wyzga RE. (2006). PM2.5 constituents and related air quality variables as predictors of survival in a cohort of U.S. military veterans. *Inhal Toxicol*, 18: 645-657. [088756](#)
- Lipfert FW; Wyzga RE; Baty JD; Miller JP. (2006). Traffic density as a surrogate measure of environmental exposures in studies of air pollution health effects: long-term mortality in a cohort of US veterans. *Atmos Environ*, 40: 154-169. [088218](#)
- Lipfert FW; Zhang J; Wyzga RE. (2000). Infant mortality and air pollution: a comprehensive analysis of US data for 1990. *J Air Waste Manag Assoc*, 50: 1350-1366. [004103](#)
- Lippmann M; Gordon T; Chen LC. (2005). Effects of subchronic exposures to concentrated ambient particles in mice. IX. Integral assessment and human health implications of subchronic exposures of mice to CAPs. *Inhal Toxicol*, 17: 255-261. [087452](#)
- Liu L-JS; Curjuric I; Keidel D; Heldstab J; Kunzli N; Bayer-Oglesby L; Ackermann-Liebrich U; Schindler C; SAPALDIA team. (2007). Characterization of source-specific air pollution exposure for a large population-based Swiss cohort (SAPALDIA). *Environ Health Perspect*, 115: 1638-1645. [093093](#)
- Liu S; Krewski D; Shi Y; Chen Y; Burnett R. (2007). Association between maternal exposure to ambient air pollutants during pregnancy and fetal growth restriction. *J Expo Sci Environ Epidemiol*, 17: 426-432. [090429](#)
- Liu YQ; Keane M; Ensell M; Miller W; Kashon M; Ong TM; Mauderly J; Lawson D; Gautam M; Zielinska B; Whitney K; Eberhardt J; Wallace W. (2005). In vitro genotoxicity of exhaust emissions of diesel and gasoline engine vehicles operated on a unified driving cycle. *J Environ Monit*, 7: 60-66. [192098](#)
- Loomis D; Castillejos M; Gold DR; McDonnell W; Borja-Aburto VH. (1999). Air pollution and infant mortality in Mexico City. , 10: 118-123. [087288](#)
- Lopes FD; Pinto TS; Arantes-Costa FM; Moriya HT; Biselli PJ; Ferraz LF; Lichtenfels AJ; Saldiva PH; Mauad T; Martins MA. (2009). Exposure to ambient levels of particles emitted by traffic worsens emphysema in mice. *Environ Res*, 109: 544-551. [190430](#)
- Lund AK; Knuckles TL; Obot Akata C; Shoheit R; McDonald JD; Gigliotti A; Seagrave JC; Campen MJ. (2007). Gasoline exhaust emissions induce vascular remodeling pathways involved in atherosclerosis. , 95: 485-94. [125741](#)
- Maciejczyk P; Chen LC. (2005). Effects of subchronic exposures to concentrated ambient particles (CAPs) in mice: VIII source-related daily variations in in vitro responses to CAPs. *Inhal Toxicol*, 17: 243-253. [087456](#)
- Mackman N; Tilley RE; Key NS. (2007). Role of the extrinsic pathway of blood coagulation in hemostasis and thrombosis. *Arterioscler Thromb Vasc Biol*, 27: 1687-1693. [156723](#)
- Maheswaran R; Haining RP; Brindley P; Law J; Pearson T; Fryers PR; Wise S; Campbell MJ. (2005). Outdoor air pollution and stroke in Sheffield, United Kingdom: a small-area level geographical study. , 36: 239-243. [088683](#)
- Maheswaran R; Haining RP; Brindley P; Law J; Pearson T; Fryers PR; Wise S; Campbell MJ. (2005). Outdoor air pollution, mortality, and hospital admissions from coronary heart disease in Sheffield, UK: a small-area level ecological study. *Eur Heart J*, 26: 2543-2549. [090769](#)
- Maisonet M; Bush TJ; Correa A; Jaakkola JJK. (2001). Relation between ambient air pollution and low birth weight in the northeastern United States. *Environ Health Perspect*, 109: 351-356. [016624](#)

- Maisonet M; Correa A; Misra D; Jaakkola JJ. (2004). A review of the literature on the effects of ambient air pollution on fetal growth. *Environ Res*, 95: 106-115. [156725](#)
- Mannes T; Jalaludin B; Morgan G; Lincoln D; Sheppard V; Corbett S. (2005). Impact of ambient air pollution on birth weight in Sydney, Australia. *Occup Environ Med*, 62: 524-530. [087895](#)
- Matsumoto A; Hiramatsu K; Li Y; Azuma A; Kudoh S; Takizawa H; Sugawara I. (2006). Repeated exposure to low-dose diesel exhaust after allergen challenge exaggerates asthmatic responses in mice. , 121: 227-235. [098017](#)
- Mauad T; Rivero DH; de Oliveira RC; Lichtenfels AJ; Guimaraes ET; de Andre PA; Kasahara DI; Bueno HM; Saldiva PH. (2008). Chronic exposure to ambient levels of urban particles affects mouse lung development. *Am J Respir Crit Care Med*, 178: 721-728. [156743](#)
- McConnell R; Berhane K; Gilliland F; London SJ; Vora H; Avol E; Gauderman WJ; Margolis HG; Lurmann F; Thomas DC; Peters JM. (1999). Air pollution and bronchitic symptoms in southern California children with asthma. *Environ Health Perspect*, 107: 757-760. [007028](#)
- McConnell R; Berhane K; Gilliland F; Molitor J; Thomas D; Lurmann F; Avol E; Gauderman WJ; Peters JM. (2003). Prospective study of air pollution and bronchitic symptoms in children with asthma. *Am J Respir Crit Care Med*, 168: 790-797. [049490](#)
- McDonald JD; Reed MD; Campen MJ; Barrett EG; Seagrave J; Mauderly JL. (2007). Health effects of inhaled gasoline engine emissions. *Inhal Toxicol*, 19 Suppl 1: 107-116. [156746](#)
- McDonnell WF; Nishino-Ishikawa N; Petersen FF; Chen LH; Abbey DE. (2000). Relationships of mortality with the fine and coarse fractions of long-term ambient PM10 concentrations in nonsmokers. *J Expo Sci Environ Epidemiol*, 10: 427-436. [010319](#)
- Medeiros A; Gouveia N. (2005). Relacao entre baixo peso ao nascer e a poluicao do ar no Municipio de Sao Paulo [Relationship between low birthweight and air pollution in the city of Sao Paulo, Brazil]. *Rev Saude Publica*, 39: 65-72. [089824](#)
- Mehta RH; Anad Kumar TC. (1997). Declining semen quality in Bangaloreans: A preliminary report. *Curr Sci*, 72: 621-622. [157197](#)
- Menache MG; Miller FJ; Raabe OG. (1995). Particle inhalability curves for humans and small laboratory animals. *Ann Occup Hyg*, 39: 317-328. [006533](#)
- Meng YY; Wilhelm M; Rull RP; English P; Ritz B. (2007). Traffic and outdoor air pollution levels near residences and poorly controlled asthma in adults. *Ann Allergy Asthma Immunol*, 98: 455-63. [093275](#)
- Miller KA; Siscovick DS; Sheppard L; Shepherd K; Sullivan JH; Anderson GL; Kaufman JD. (2007). Long-term exposure to air pollution and incidence of cardiovascular events in women. , 356: 447-458. [090130](#)
- Mogensen CE. (1984). Microalbuminuria predicts clinical proteinuria and early mortality in maturity-onset diabetes. , 310: 356-360. [156769](#)
- Mohallem SV; de Araujo Lobo DJ; Pesquero CR; Assuncao JV; de Andre PA; Saldiva PH; Dolhnikoff M. (2005). Decreased fertility in mice exposed to environmental air pollution in the city of Sao Paulo. *Environ Res*, 98: 196-202. [088657](#)
- Mollet NR; Cademartiri F; de Feyter PJ. (2005). Non-invasive multislice CT coronary imaging. *Heart*, 91: 401-407. [155988](#)
- Montauban van Swijndregt AD; De Lange EE; De Groot E; Ackerstaff RG. (1999). An in vivo evaluation of the reproducibility of intima-media thickness measurements of the carotid artery segments using B-mode ultrasound. *Ultrasound Med Biol*, 25: 323-330. [156777](#)
- Morgenstern V; Zutavern A; Cyrys J; Brockow I; Koletzko S; Kramer U; Behrendt H; Herbarth O; von Berg A; Bauer CP; Wichmann HE; Heinrich J. (2008). Atopic diseases, allergic sensitization, and exposure to traffic-related air pollution in children. *Am J Respir Crit Care Med*, 177: 1331-1337. [156782](#)
- Mortimer K; Neugebauer R; Lurmann F; Alcorn S; Balmes J; Tager I. (2008). Early-Lifetime exposure to air pollution and allergic sensitization in children with asthma. *J Asthma*, 45: 874-881. [187280](#)
- Naess O; Nafstad P; Aamodt G; Claussen B; Rosland P. (2007). Relation between concentration of air pollution and cause-specific mortality: four-year exposures to nitrogen dioxide and particulate matter pollutants in 470 neighborhoods in Oslo, Norway. *Am J Epidemiol*, 165: 435-443. [090736](#)
- National Kidney Foundation. (2008). Chronic Kidney Disease: Evaluation, Classification, and Stratification. The National Kidney Foundation . Kidney Disease Outcomes Quality Initiative. [156796](#)
- Newman AB; Sutton-Tyrrell K; Vogt MT; Kuller LH. (1993). Morbidity and mortality in hypertensive adults with a low ankle/arm blood pressure index. *JAMA*, 270: 487-489. [156805](#)
- Nordling E; Berglind N; Melen E; Emenius G; Hallberg J; Nyberg F; Pershagen G; Svartengren M; Wickman M; Bellander T. (2008). Traffic-related air pollution and childhood respiratory symptoms, function and allergies. , 19: 401-8. [097998](#)

- O'Leary DH; Polak JF; Kronmal RA; Kittner SJ; Bond MG; Wolfson SK, Jr.; Bommer W; Price TR; Gardin JM; Savage PJ. (1992). Distribution and correlates of sonographically detected carotid artery disease in the Cardiovascular Health Study. The CHS Collaborative Research Group. , 23: 1752-1760. [156825](#)
- O'Leary DH; Polak JF; Kronmal RA; Manolio TA; Burke GL; Wolfson SK, Jr. (1999). Carotid-artery intima and media thickness as a risk factor for myocardial infarction and stroke in older adults. Cardiovascular Health Study Collaborative Research Group. , 340: 14-22. [156826](#)
- O'Neill MS; Diez-Roux AV; Auchincloss AH; Franklin TG; Jacobs Jnr DR; Astor BC; Dvorchak JT; Kaufman J. (2007). Airborne particulate matter exposure and urinary albumin excretion: The Multi-Ethnic Study of Atherosclerosis. *Occup Environ Med.* [156006](#)
- Oei HH; Vliegenthart R; Hak AE; Iglesias del Sol A; Hofman A; Oudkerk M; Witteman JC. (2002). The association between coronary calcification assessed by electron beam computed tomography and measures of extracoronary atherosclerosis: the Rotterdam Coronary Calcification Study. *J Am Coll Cardiol*, 39: 1745-1751. [156820](#)
- Oftedal B; Brunekreef B; Nystad W; Madsen C; Walker S-E; Nafstad P. (2008). Residential outdoor air pollution and lung function in schoolchildren. , 19: 129-137. [093202](#)
- Oftedal B; Brunekreef B; Nystad W; Nafstad P. (2007). Residential outdoor air pollution and allergen sensitization in schoolchildren in Oslo, Norway. , 37: 1632. [191948](#)
- Oh S-M; Chung K-H. (2006). Identification of mammalian cell genotoxins in respirable diesel exhaust particles by bioassay-directed chemical analysis. *Toxicol Lett*, 161: 226-235. [088296](#)
- Ono N; Oshio S; Niwata Y; Yoshida S; Tsukue N; Sugawara I; Takano H; Takeda K. (2007). Prenatal exposure to diesel exhaust impairs mouse spermatogenesis. *Inhal Toxicol*, 19: 275-281. [156007](#)
- Ozkaynak H; Thurston GD. (1987). Associations between 1980 US mortality rates and alternative measures of airborne particle concentration. *Risk Anal*, 7: 449-461. [072960](#)
- Palli D; Saieva C; Munnia A; Peluso M; Grechi D; Zanna I; Caini S; Decarli A; Sera F; Masala G. (2008). DNA adducts and PM10 exposure in traffic-exposed workers and urban residents from the EPIC-Florence City study. *Sci Total Environ*, 403: 105-112. [156837](#)
- Parker JD; Mendola P; Woodruff TJ. (2008). Preterm birth after the Utah valley steel mill closure: a natural experiment. , 19: 820-823. [156013](#)
- Parker JD; Woodruff TJ. (2008). Influences of study design and location on the relationship between particulate matter air pollution and birthweight. *Paediatr Perinat Epidemiol*, 22: 214-227. [156846](#)
- Parker JD; Woodruff TJ; Basu R; Schoendorf KC. (2005). Air pollution and birth weight among term infants in California. , 115: 121-128. [087462](#)
- Pedersen M; Vinzents P; Petersen JH; Kleinjans JC; Plas G; Kirsch-Volders M; Dostal M; Rossner P; Beskid O; Sram RJ; Merlo DF; Knudsen LE. (2006). Cytogenetic effects in children and mothers exposed to air pollution assessed by the frequency of micronuclei and fluorescence in situ hybridization (FISH): a family pilot study in the Czech Republic. , 608: 112-120. [156848](#)
- Penard-Morand C; Charpin D; Raheison C; Kopferschmitt C; Caillaud D; Lavaud F; Annesi-Maesano I. (2005). Long-term exposure to background air pollution related to respiratory and allergic health in schoolchildren. *Clin Exp Allergy*, 35: 1279-1287. [087951](#)
- Penna MLF; Duchade MP. (1991). Air pollution and infant mortality from pneumonia in the Rio de Janeiro metropolitan area. *Bull Pan Am Health Organ*, 25: 47-54. [073325](#)
- Pereira LAA; Loomis D; Conceicao GMS; Braga ALF; Arcas RM; Kishi HS; Singer JM; Bohm GM; Saldiva PHN. (1998). Association between air pollution and intrauterine mortality in Sao Paulo, Brazil. *Environ Health Perspect*, 106: 325-329. [007264](#)
- Peters A; Skorkovsky J; Kotesovec F; Brynda J; Spix C; Wichmann HE; Heinrich J. (2000). Associations between mortality and air pollution in central Europe. *Environ Health Perspect*, 108: 283-287. [001756](#)
- Pierse N; Rushton L; Harris RS; Kuehni CE; Silverman M; Grigg J. (2006). Locally-generated particulate pollution and respiratory symptoms in young children. *Thorax*, 61: 216-220. [088757](#)
- Pignoli P; Tremoli E; Poli A; Oreste P; Paoletti R. (1986). Intimal plus medial thickness of the arterial wall: a direct measurement with ultrasound imaging. , 74: 1399-1406. [156026](#)
- Pinkerton KE; Zhou Y; Teague SV; Peake JL; Walther RC; Kennedy IM; Leppert VJ; Aust AE. (2004). Reduced lung cell proliferation following short-term exposure to ultrafine soot and iron particles in neonatal rats: key to impaired lung growth?. *Inhal Toxicol*, 1: 73-81. [087465](#)
- Pires-Neto RC; Lichtenfels AJ; Soares SR; Macchione M; Saldiva PHN; Dolnikoff M. (2006). Effects of Sao Paulo air pollution on the upper airways of mice. , 101: 356-361. [096734](#)
- Poma A; Limongi T; Pisani C; Granato V; Picozzi P. (2006). Genotoxicity induced by fine urban air particulate matter in the macrophages cell line RAW 264.7. *Toxicol In Vitro*, 20: 1023-1029. [096903](#)
- Pope CA 3rd; Ezzati M; Dockery DW. (2009). Fine-particulate air pollution and life expectancy in the United States. *N Engl J Med*, 360: 376-386. [190107](#)

- Pope CA III. (1989). Respiratory disease associated with community air pollution and a steel mill, Utah Valley. *Am J Public Health*, 79: 623-628. [044461](#)
- Pope CA III; Burnett RT. (2007). Confounding in air pollution epidemiology: the broader context. , 18: 424-426. [090928](#)
- Pope CA III; Burnett RT; Thun MJ; Calle EE; Krewski D; Ito K; Thurston GD. (2002). Lung cancer, cardiopulmonary mortality, and long-term exposure to fine particulate air pollution. *JAMA*, 287: 1132-1141. [024689](#)
- Pope CA III; Burnett RT; Thurston GD; Thun MJ; Calle EE; Krewski D; Godleski JJ. (2004). Cardiovascular mortality and long-term exposure to particulate air pollution: epidemiological evidence of general pathophysiological pathways of disease. , 109: 71-77. [055880](#)
- Pope CA III; Thun MJ; Namboodiri MM; Dockery DW; Evans JS; Speizer FE; Heath CW Jr. (1995). Particulate air pollution as a predictor of mortality in a prospective study of US adults. *Am J Respir Crit Care Med*, 151: 669-674. [045159](#)
- Puett RC; Schwartz J; Hart JE; Yanosky JD; Speizer FE; Suh H; Paciorek CJ; Neas LM; Laden F. (2008). Chronic particulate exposure, mortality, and coronary heart disease in the nurses' health study. *Am J Epidemiol*, 168: 1161-1168. [156891](#)
- Raizenne M; Neas LM; Damokosh AI; Dockery DW; Spengler JD; Koutrakis P; Ware JH; Speizer FE. (1996). Health effects of acid aerosols on North American children: pulmonary function. *Environ Health Perspect*, 104: 506-514. [077268](#)
- Ramos C; Cisneros J; Gonzalez-Avila G; Becerril C; Ruiz V; Montaña M. (2009). Increase of matrix metalloproteinases in woodsmoke-induced lung emphysema in guinea pigs. *Inhal Toxicol*, 21: 119-132. [190116](#)
- Reed MD; Barrett EG; Campen MJ; Divine KK; Gigliotti AP; McDonald JD; Seagrave JC; Mauderly JL; Seilkop SK; Swenberg JA. (2008). Health effects of subchronic inhalation exposure to gasoline engine exhaust. *Inhal Toxicol*, 20: 1125-1143. [156903](#)
- Reed MD; Campen MJ; Gigliotti AP; Harrod KS; McDonald JD; Seagrave JC; Mauderly JL; Seilkop SK. (2006). Health effects of subchronic exposure to environmental levels of hardwood smoke. *Inhal Toxicol*, 18: 523-539. [156043](#)
- Reed MD; Gigliotti AP; McDonald JD; Seagrave JC; Seilkop SK; Mauderly JL. (2004). Health effects of subchronic exposure to environmental levels of diesel exhaust. *Inhal Toxicol*, 16: 177-193. [055625](#)
- Resnick HE; Lindsay RS; McDermott MM; Devereux RB; Jones KL; Fabsitz RR; Howard BV. (2004). Relationship of high and low ankle brachial index to all-cause and cardiovascular disease mortality: the Strong Heart Study. , 109: 733-739. [156048](#)
- Reymao MSF; Cury PM; Lichtenfels AJFC; Lemos M; Battlehner CN; Conceicao GMS; Capelozzi VL; Montes GS; Junior MF; Martins MA; Bohm GM; Saldiva PHN. (1997). Urban air pollution enhances the formation of urethane-induced lung tumors in mice. *Environ Res*, 74: 150-158. [084653](#)
- Rich DQ; Demissie K; Lu SE; Kamat L; Wartenberg D; Rhoads GG. (2009). Ambient air pollutant concentrations during pregnancy and the risk of fetal growth restriction. *J Epidemiol Community Health*, In Press: 1-9. [180122](#)
- Ritz B; Wilhelm M. (2008). Ambient air pollution and adverse birth outcomes: methodologic issues in an emerging field. , 102: 182-190. [156914](#)
- Ritz B; Wilhelm M; Hoggatt KJ; Ghosh JK. (2007). Ambient air pollution and preterm birth in the environment and pregnancy outcomes study at the University of California, Los Angeles. *Am J Epidemiol*, 166: 1045-52. [096146](#)
- Ritz B; Wilhelm M; Zhao Y. (2006). Air pollution and infant death in southern California, 1989-2000. , 118: 493-502. [089819](#)
- Ritz B; Yu F; Chapa G; Fruin S. (2000). Effect of air pollution on preterm birth among children born in Southern California between 1989 and 1993. , 11: 502-511. [012068](#)
- Ritz B; Yu F; Fruin S; Chapa G; Shaw GM; Harris JA. (2002). Ambient air pollution and risk of birth defects in Southern California. *Am J Epidemiol*, 155: 17-25. [023227](#)
- Rogers JF; Dunlop AL. (2006). Air pollution and very low birth weight infants: a target population?. , 118: 156-164. [091232](#)
- Rojas-Martinez R; Perez-Padilla R; Olaiz-Fernandez G; Mendoza-Alvarado L; Moreno-Macias H; Fortoul T; McDonnell W; Loomis D; Romieu I. (2007). Lung function growth in children with long-term exposure to air pollutants in Mexico City. , 176: 377-84. [188508](#)
- Roman HA; Walker KD; Walsh TL; Conner L; Richmond HM; Hubbell BJ; Kinney PL. (2008). Expert judgment assessment of the mortality impact of changes in ambient fine particulate matter in the U.S. *Environ Sci Technol*, 42: 2268-2274. [156921](#)

- Romieu I; Garcia-Esteban R; Sunyer J; Rios C; Alcaraz-Zubeldia M; Velasco SR; Holguin F. (2008). The effect of supplementation with omega-3 polyunsaturated fatty acids on markers of oxidative stress in elderly exposed to PM(2.5). *Environ Health Perspect*, 116: 1237-1242. [156922](#)
- Romieu I; Ramirez-Aguilar M; Moreno-Macias H; Barraza-Villarreal A; Miller P; Hernandez-Cadena L; Carbajal-Arroyo LA; Hernandez-Avila M. (2004). Infant mortality and air pollution: modifying effect by social class. *J Occup Environ Hyg*, 46: 1210-1216. [093074](#)
- Rosenlund M; Bellander T; Nordquist T; Alfredsson L. (2009). Traffic-generated air pollution and myocardial infarction. *Epidemiology*, 20: 265-71. [190309](#)
- Rosenlund M; Berglund N; Pershagen G; Hallqvist J; Jonson T; Bellander T. (2006). Long-term exposure to urban air pollution and myocardial infarction. , 17: 383-390. [089796](#)
- Ross R. (1999). Atherosclerosis--an inflammatory disease. , 340: 115-126. [156926](#)
- Rubes J; Selevan SG; Evenson DP; Zudova D; Vozdova M; Zudova Z; Robbins WA; Perreault SD. (2005). Episodic air pollution is associated with increased DNA fragmentation in human sperm without other changes in semen quality. *Hum Reprod*, 20: 2776-2783. [078091](#)
- Ruggenti P; Remuzzi G. (2006). Time to abandon microalbuminuria?. *Kidney Int*, 70: 1214-1222. [156933](#)
- Röösli M; Braun-Fahrlander C; Kunzli N; Oglesby L; Theis G; Camenzind M; Mathys P; Staehelin J. (2000). Spatial variability of different fractions of particulate matter within an urban environment and between urban and rural sites. *J Air Waste Manag Assoc*, 50: 1115-1124. [010296](#)
- Röösli M; Kunzli N; Braun-Fahrlander C; Egger M. (2005). Years of life lost attributable to air pollution in Switzerland: dynamic exposure-response model. *Int J Epidemiol*, 34: 1029-1035. [156923](#)
- Röösli M; Theis G; Kunzli N; Staehelin J; Mathys P; Oglesby L; Camenzind M; Braun-Fahrlander C. (2001). Temporal and spatial variation of the chemical composition of PM10 at urban and rural sites in the Basel area, Switzerland. *Atmos Environ*, 35: 3701-3713. [108738](#)
- Sagiv SK; Mendola P; Loomis D; Herring AH; Neas LM; Savitz DA; Poole C. (2005). A time-series analysis of air pollution and preterm birth in Pennsylvania, 1997-2001. *Environ Health Perspect*, 113: 602-606. [087468](#)
- Salam MT; Millstein J; Li Y-F; Lurmann FW; Margolis HG; Gilliland FD. (2005). Birth outcomes and prenatal exposure to ozone, carbon monoxide, and particulate matter: results from the Children's Health Study. *Environ Health Perspect*, 113: 1638-1644. [087885](#)
- Salonen JT; Salonen R. (1991). Ultrasonographically assessed carotid morphology and the risk of coronary heart disease. *Arterioscler Thromb Vasc Biol*, 11: 1245-1249. [156938](#)
- Sato H; Suzuki Kazuo T; Sone H; Yamano Y; Kagawa J; Aoki Y. (2003). DNA-adduct formation in lungs, nasal mucosa, and livers of rats exposed to urban roadside air in Kawasaki City, Japan. , 93: 36-44. [096615](#)
- Schatz M; Zeiger RS; Hoffman CP. (1990). Intrauterine growth is related to gestational pulmonary function in pregnant asthmatic women. *Kaiser-Permanente Asthma and Pregnancy Study Group*. , 98: 389-392. [156073](#)
- Schikowski T; Sugiri D; Ranft U; Gehring U; Heinrich J; Wichmann HE; Kramer U. (2005). Long-term air pollution exposure and living close to busy roads are associated with COPD in women. *Respir Res*, 22: 152-161. [088637](#)
- Schindler C; Keidel D; Gerbase MW; Zemp E; Bettschart R; Brandli O; Brutsche MH; Burdet L; Karrer W; Knopfli B; Pons M; Rapp R; Bayer-Oglesby L; Kunzli N; Schwartz J; Liu L-JS; Ackermann-Liebrich U; Rochat T; the SAPALDIA Team. (2009). Improvements in PM10 exposure and reduced rates of respiratory symptoms in a cohort of swiss adults (SAPALDIA). , 179: 579-587. [191950](#)
- Schwartz J; Coull B; Laden F; Ryan L. (2008). The effect of dose and timing of dose on the association between airborne particles and survival. *Environ Health Perspect*, 116: 64-69. [156963](#)
- Seagrave J; McDonald JD; Reed MD; Seilkop SK; Mauderly JL. (2005). Responses to subchronic inhalation of low concentrations of diesel exhaust and hardwood smoke measured in rat bronchoalveolar lavage fluid. *Inhal Toxicol*, 17: 657-670. [088000](#)
- Selevan SG; Borkovec L; Slott VL; Zudova Z; Rubes J; Evenson DP; Perreault SD. (2000). Semen quality and reproductive health of young Czech men exposed to seasonal air pollution. *Environ Health Perspect*, 108: 887-894. [012578](#)
- Sevastyanova O; Binkova B; Topinka J; Sram RJ; Kalina I; Popov T; Novakova Z; Farmer PB. (2007). In vitro genotoxicity of PAH mixtures and organic extract from urban air particles part II: human cell lines. , 620: 123-134. [156969](#)
- Sharma AK; Jensen KA; Rank J; White PA; Lundstedt S; Gagne R; Jacobsen NR; Kristiansen J; Vogel U; Wallin H. (2007). Genotoxicity, inflammation and physico-chemical properties of fine particle samples from an incineration energy plant and urban air. , 633: 95-111. [156975](#)
- Shaw LJ; Raggi P; Schisterman E; Berman DS; Callister TQ. (2003). Prognostic value of cardiac risk factors and coronary artery calcium screening for all-cause mortality. *Radiology*, 228: 826-833. [156083](#)

- Shemesh J; Tenenbaum A; Fisman EZ; Apter S; Rath S; Rozenman J; Itzhak Y; Motro M. (1996). Absence of coronary calcification on double-helical CT scans: predictor of angiographically normal coronary arteries in elderly women?. *Radiology*, 199: 665-668. [156085](#)
- Shinkura R; Fijuyama C; Akiba S. (1999). Relationship between ambient sulfur dioxide levels and neonatal mortality near the Mt. Sakurajima volcano in Japan. , 9: 344-349. [156978](#)
- Silva PJ; Erupe ME; Price D; Elias J; Malloy QG; Li Q; Warren B; Cocker DR, 3rd. (2008). Trimethylamine as precursor to secondary organic aerosol formation via nitrate radical reaction in the atmosphere. *Environ Sci Technol*, 42: 4689-4696. [156981](#)
- Slama R; Darrow L; Parker J; Woodruff TJ; Strickland M; Nieuwenhuijsen M; Glinianaia S; Hoggatt KJ; Kannan S; Hurley F; Kalinka J; Sram R; Brauer M; Wilhelm M; Heinrich J; Ritz B. (2008). Meeting report: atmospheric pollution and human reproduction. *Environ Health Perspect*, 116: 791-798. [156985](#)
- Slama R; Morgenstern V; Cyrus J; Zutavern A; Herbarth O; Wichmann HE; Heinrich J; LISA Study Group. (2007). Traffic-related atmospheric pollutants levels during pregnancy and offspring's term birth weight: a study relying on a land-use regression exposure model. *Environ Health Perspect*, 115: 1283-1292. [093216](#)
- Smilde TJ; Wollersheim H; Van Langen H; Stalenhoef AF. (1997). Reproducibility of ultrasonographic measurements of different carotid and femoral artery segments in healthy subjects and in patients with increased intima-media thickness. *Clin Sci (Lond)*, 93: 317-324. [156988](#)
- Sokol RZ; Kraft P; Fowle IM; Mamet R; Kim E; Berhane KT. (2006). Exposure to environmental ozone alters semen quality. *Environ Health Perspect*, 114: 360-5. [098539](#)
- Solomon P; Baumann K; Edgerton E; Tanner R; Eatough D; Modey W; Marin H; Savoie D; Natarajan S; Meyer MB. (2003). Comparison of integrated samplers for mass and composition during the 1999 Atlanta supersites project. *J Geophys Res*, 108: 8423. [156994](#)
- Somers CM; McCarry BE; Malek F; Quinn JS. (2004). Reduction of particulate air pollution lowers the risk of heritable mutations in mice. , 304: 1008-1010. [078098](#)
- Somers CM; Yauk CL; White PA; Parfett CLJ; Quinn JS. (2002). Air pollution induces heritable DNA mutations. *Proc Natl Acad Sci U S A*, 99: 15904-15907. [078100](#)
- Song CL; Zhou YC; Huang RJ; Wang YQ; Huang QF; Lu G; Liu KM. (2007). Influence of ethanol-diesel blended fuels on diesel exhaust emissions and mutagenic and genotoxic activities of particulate extracts. , 149: 355-63. [188903](#)
- Sorensen M; Schins RP; Hertel O; Loft S. (2005). Transition metals in personal samples of PM_{2.5} and oxidative stress in human volunteers. , 14: 1340-3. [188901](#)
- Sram R; Beskid O; Binkova B; Chvatalova I; Lnenickova Z; Milcova A; Solansky I; Tulupova E; Bavorova H; Ocadlikova D. (2007). Chromosomal aberrations in environmentally exposed population in relation to metabolic and DNA repair genes polymorphisms. , 620: 22-33. [188457](#)
- Sram RJ; Beskid O; Rössnerova A; Rössner P; Lnenickova Z; Milcova A; Solansky I; Binkova B. (2007). Environmental exposure to carcinogenic polycyclic aromatic hydrocarbons--the interpretation of cytogenetic analysis by FISH. *Toxicol Lett*, 172: 12-20. [192084](#)
- Sram RJ; Binkova B; Dejmek J; Bobak M. (2005). Ambient air pollution and pregnancy outcomes: a review of the literature. *Environ Health Perspect*, 113: 375-382. [087442](#)
- Stanojevic S; Wade A; Stocks J; Hankinson J; Coates AL; Pan H; Rosenthal M; Corey M; Lebecque P; Cole TJ. (2008). Reference ranges for spirometry across all ages: a new approach. *Am J Respir Crit Care Med*, 177: 253-260. [157007](#)
- Stocker R; Keaney JF Jr. (2004). Role of oxidative modifications in atherosclerosis. *Physiol Rev*, 84: 1381-1478. [157013](#)
- Strom KA; Garg BD; Johnson JT; D'Arcy JB; Smiler KL. (1990). Inhaled particle retention in rats receiving low exposures of diesel exhaust. *J Toxicol Environ Health*, 29: 377-398. [157020](#)
- Sugamata M; Ihara T; Takano H; Oshio S; Takeda K. (2006). Maternal diesel exhaust exposure damages newborn murine brains. *Eisei Kagaku*, 52: 82-84. [097166](#)
- Sugiri D; Ranft U; Schikowski T; Kramer U. (2006). The influence of large-scale airborne particle decline and traffic-related exposure on children's lung function. *Environ Health Perspect*, 114: 282-288. [088760](#)
- Suh YJ; Ha EH; Park H; Kim YJ; Kim H; Hong YC. (2008). GSTM1 polymorphism along with PM₁₀ exposure contributes to the risk of preterm delivery. , 656: 62-67. [192077](#)
- Sun Q; Wang A; Jin X; Natanzon A; Duquaine D; Brook RD; Aguinaldo J-GS; Fayad ZA; Fuster V; Lippmann M; Chen Lung C; Rajagopalan S. (2005). Long-term air pollution exposure and acceleration of atherosclerosis and vascular inflammation in an animal model. , 294: 3003-3010. [186814](#)

- Sun Q; Yue P; Deiuliis JA; Lumeng CN; Kampfrath T; Mikolaj MB; Cai Y; Ostrowski MC; Lu B; Parthasarathy S; Brook RD; Moffatt-Bruce SD; Chen LC; Rajagopalan S. (2009). Ambient air pollution exaggerates adipose inflammation and insulin resistance in a mouse model of diet-induced obesity. *Circulation*, 119: 538-546. [190487](#)
- Sun Q; Yue P; Kirk RI; Wang A; Moatti D; Jin X; Lu B; Schecter AD; Lippmann M; Gordon T; Chen LC; Rajagopalan S. (2008). Ambient air particulate matter exposure and tissue factor expression in atherosclerosis. *Inhal Toxicol*, 20: 127-137. [157033](#)
- Sun Q; Yue P; Ying Z; Cardounel AJ; Brook RD; Devlin R; Hwang JS; Zweier JL; Chen LC; Rajagopalan S. (2008). Air Pollution Exposure Potentiates Hypertension Through Reactive Oxygen Species-Mediated Activation of Rho/ROCK. *Arterioscler Thromb Vasc Biol*, 28: 1760-1766. [157032](#)
- Suwa T; Hogg JC; Quinlan KB; Ohgami A; Vincent R; Van Eeden SF. (2002). Particulate air pollution induces progression of atherosclerosis. *J Am Coll Cardiol*, 39: 935-942. [028588](#)
- Tarantini L; Bonzini M; Apostoli P; Pegoraro V; Bollati V; Marinelli B; Cantone L; Rizzo G; Hou L; Schwartz J; Bertazzi PA; Baccarelli A. (2009). Effects of particulate matter on genomic DNA methylation content and iNOS promoter methylation. *Environ Health Perspect*, 117: 217-222. [192010](#)
- Tesfaigzi Y; McDonald JD; Reed MD; Singh SP; De Sanctis GT; Eynott PR; Hahn FF; Campen MJ; Mauderly JL. (2005). Low-level subchronic exposure to wood smoke exacerbates inflammatory responses in allergic rats. *J Allergy Clin Immunol*, 115: 505-513. [156116](#)
- Tesfaigzi Y; Singh SP; Foster JE; Kubatko J; Barr EB; Fine PM; McDonald JD; Hahn FF; Mauderly JL. (2002). Health effects of subchronic exposure to low levels of wood smoke in rats. *Toxicol Sci*, 65: 115-125. [025575](#)
- Thurlbeck WM. (1982). Postnatal human lung growth. *Thorax*, 37: 564-571. [093260](#)
- Tokiwa H; Sera N; Nakanishi Y. (2005). Involvement of alveolar macrophages in the formation of 8-oxodeoxyguanosine associated with exogenous particles in human lungs. *Inhal Toxicol*, 17: 577. [191952](#)
- Tong S; Colditz P. (2004). Air pollution and sudden infant death syndrome: a literature review. *Paediatr Perinat Epidemiol*, 18: 327-335. [087883](#)
- Tovalin H; Valverde M; Morandi MT; Blanco S; Whitehead L; Rojas E. (2006). DNA damage in outdoor workers occupationally exposed to environmental air pollutants. *Occup Environ Med*, 63: 230-236. [091322](#)
- Tozuka Y; Watanabe N; Ohsawa M; Toriba A; Kizu R; Hayakawa K. (2004). Transfer of polycyclic aromatic hydrocarbons to fetuses and breast milk of rats exposed to diesel exhaust. *Eisei Kagaku*, 50: 497-502. [090864](#)
- Tsai S-S; Chen C-C; Hsieh H-J; Chang C-C; Yang C-Y. (2006). Air pollution and postneonatal mortality in a tropical city: Kaohsiung, Taiwan. *Inhal Toxicol*, 18: 185-189. [090709](#)
- Tsukue N; Tsubone H; Suzuki AK. (2002). Diesel exhaust affects the abnormal delivery in pregnant mice and the growth of their young. *Inhal Toxicol*, 14: 635-651. [030593](#)
- Tsukue N; Yoshida S; Sugawara I; Taked K. (2004). Effect of diesel exhaust on development of fetal reproductive function in ICR female mice. *Eisei Kagaku*, 50: 174-80. [096643](#)
- U.S. EPA. (1996). Air quality criteria for particulate matter. U.S. Environmental Protection Agency. Research Triangle Park, NC. EPA/600/P-95/001aF-cF. [079380](#)
- U.S. EPA. (2002). Health assessment document for diesel engine exhaust. [042866](#)
- U.S. EPA. (2004). Air quality criteria for particulate matter. U.S. Environmental Protection Agency. Research Triangle Park, NC. EPA/600/P-99/002aF-bF. [056905](#)
- U.S. EPA. (2005). Guidelines for carcinogen risk assessment. U.S. Environmental Protection Agency. Just. [086237](#)
- U.S. EPA. (2006). Provisional Assessment of Recent Studies on Health Effects of Particulate Matter Exposure. U.S. Environmental Protection Agency. Research Triangle Park, NC. [157071](#)
- Valentine R; Himmelstein MW. (2001). Overview of the acute, subchronic, reproductive, developmental and genetic toxicology of "beta"-chloroprene. *Chem Biol Interact*, 135: 81-100. [019011](#)
- van der Meer IM; Bots ML; Hofman A; del Sol AI; van der Kuip DA; Witteman JC. (2004). Predictive value of noninvasive measures of atherosclerosis for incident myocardial infarction: the Rotterdam Study. *Circulation*, 109: 1089-1094. [156129](#)
- Veras MM; Damaceno-Rodrigues NR; Caldini EG; Maciel Ribeiro AA; Mayhew TM; Saldiva PH; Dolhnikoff M. (2008). Particulate urban air pollution affects the functional morphology of mouse placenta. *Biol Reprod*, 79: 578-584. [190493](#)
- Veras MM; Damaceno-Rodrigues NR; Guimarães Silva RM; Scoriza JN; Saldiva PH; Caldini EG; Dolhnikoff M. (2009). Chronic exposure to fine particulate matter emitted by traffic affects reproductive and fetal outcomes in mice. *Environ Res*, 109: 536-543. [190496](#)
- Villeneuve PJ; Goldberg MS; Krewski D; Burnett RT; Chen Y. (2002). Fine particulate air pollution and all-cause mortality within the Harvard six-cities study: variations in risk by period of exposure. *Ann Epidemiol*, 12: 568-576. [042576](#)

- Vineis P; Hoek G; Krzyzanowski M; Vigna-Taglianti F; Veglia F; Airoidi L; Autrup H; Dunning A; Garte S; Hainaut P; Malaveille C; Matullo G; Overvad K; Raaschou-Nielsen O; Clavel-Chapelon F; Linseisen J; Boeing H; Trichopoulou A; Palli D; Peluso M; Krogh V; Tumino R; Panico S; Bueno-De-Mesquita HB; Peeters PH; Lund EE; Gonzalez CA; Martinez C; Dorronsoro M; Barricarte A; Cirera L; Quiros JR; Berglund G; Forsberg B; Day NE; Key TJ; Saracci R; Kaaks R; Riboli E. (2006). Air pollution and risk of lung cancer in a prospective study in Europe. *Int J Cancer*, 119: 169-174. [192089](#)
- Vinzents PS; Moller P; Sorensen M; Knudsen LE; Herte LQ; Jensen FP; Schibye B; Loft S. (2005). Personal exposure to ultrafine particles and oxidative DNA damage. *Environ Health Perspect*, 113: 1485-1490. [087482](#)
- Vogt MT; Cauley JA; Newman AB; Kuller LH; Hulley SB. (1993). Decreased ankle/arm blood pressure index and mortality in elderly women. *JAMA*, 270: 465-469. [157100](#)
- Wallenborn JG; Evansky P; Shannahan JH; Vallanat B; Ledbetter AD; Schladweiler MC; Richards JH; Gottipolu RR; Nyska A; Kodavanti UP. (2008). Subchronic inhalation of zinc sulfate induces cardiac changes in healthy rats. *Toxicol Appl Pharmacol*, 232: 69-77. [191171](#)
- Walsh CR; Cupples LA; Levy D; Kiel DP; Hannan M; Wilson PW; O'Donnell CJ. (2002). Abdominal aortic calcific deposits are associated with increased risk for congestive heart failure: the Framingham Heart Study. *Am Heart J*, 144: 733-739. [157103](#)
- Watanabe N. (2005). Decreased number of sperms and Sertoli cells in mature rats exposed to diesel exhaust as fetuses. *Toxicol Lett*, 155: 51-58. [087985](#)
- Wayne LG; Chambers LA. (1968). Biological effects of urban air pollution: V a study of effects of Los Angeles atmosphere on laboratory rodents. *Arch Environ Occup Health*, 16: 871-885. [038537](#)
- Weisenberger DJ; Campan M; Long TI; Kim M; Woods C; Fiala E; Ehrlich M; Laird PW. (2005). Analysis of repetitive element DNA methylation by MethyLight. *Nucleic Acids Res*, 33: 6823-36. [192101](#)
- Weitz JI; Byrne J; Clagett GP; Farkouh ME; Porter JM; Sackett DL; Strandness DE Jr; Taylor LM. (1996). Diagnosis and treatment of chronic arterial insufficiency of the lower extremities: a critical review. *Circulation*, 94: 3026-3049. [156150](#)
- Wendelhag I; Gustavsson T; Suurkula M; Berglund G; Wikstrand J. (1991). Ultrasound measurement of wall thickness in the carotid artery: fundamental principles and description of a computerized analysing system. *Clinical Physiol*, 11: 565-577. [157135](#)
- Wendelhag I; Wiklund O; Wikstrand J. (1993). Atherosclerotic changes in the femoral and carotid arteries in familial hypercholesterolemia. Ultrasonographic assessment of intima-media thickness and plaque occurrence. *Arterioscler Thromb Vasc Biol*, 13: 1404-1411. [157136](#)
- Wheeler AJ; Villeneuve P; Smith-Doiron M; Mahmud M; Dales R; Brook JR. (2006). Children's exposure to ambient air pollution: the application of different exposure assessment methodologies. *Epidemiology*, 17(6): S33-S34. [103905](#)
- Wilhelm M; Ritz B. (2005). Local variations in CO and particulate air pollution and adverse birth outcomes in Los Angeles County, California, USA. *Environ Health Perspect*, 113: 1212-1221. [088668](#)
- Willekes C; Brands PJ; Willigers JM; Hoeks AP; Reneman RS. (1999). Assessment of local differences in intima-media thickness in the human common carotid artery. *J Vasc Res*, 36: 222-228. [157147](#)
- Williams L; Ulrich C; Larson T; Wener M; Wood B; Campbell P; Potter J; McTiernan A; De Roos A. (2009). Proximity to Traffic, Inflammation, and Immune Function among Women in the Seattle, Washington, Area. *Environ Health Perspect*, 117: 373. [191945](#)
- Wilson PW; Kauppila LI; O'Donnell CJ; Kiel DP; Hannan M; Polak JM; Cupples LA. (2001). Abdominal aortic calcific deposits are an important predictor of vascular morbidity and mortality. *Circulation*, 103: 1529-1534. [156159](#)
- Wilson WE; Mage DT; Grant LD. (2000). Estimating separately personal exposure to ambient and nonambient particulate matter for epidemiology and risk assessment: why and how. *J Air Waste Manag Assoc*, 50: 1167-1183. [010288](#)
- Wittman JC; Kok FJ; van Saase JL; Valkenburg HA. (1986). Aortic calcification as a predictor of cardiovascular mortality. *Lancet*, 2: 1120-1122. [156161](#)
- Woodruff TJ; Darrow LA; Parker JD. (2008). Air pollution and postneonatal infant mortality in the United States, 1999-2002. *Environ Health Perspect*, 116: 110-5. [098386](#)
- Woodruff TJ; Grillo J; Schoendorf KC. (1997). The relationship between selected causes of postneonatal infant mortality and particulate air pollution in the United States. *Environ Health Perspect*, 105: 608-612. [084271](#)
- Woodruff TJ; Parker JD; Schoendorf KC. (2006). Fine particulate matter (PM_{2.5}) air pollution and selected causes of postneonatal infant mortality in California. *Environ Health Perspect*, 114: 785-790. [088758](#)

- Xu J; Lee ET; Devereux RB; Umans JG; Bella JN; Shara NM; Yeh J; Fabsitz RR; Howard BV. (2008). A longitudinal study of risk factors for incident albuminuria in diabetic American Indians: the Strong Heart Study. *Am J Kidney Dis*, 51: 415-424. [157157](#)
- Yang AS; Estéicio MR; Doshi K; Kondo Y; Tajara EH; Issa JP. (2004). A simple method for estimating global DNA methylation using bisulfite PCR of repetitive DNA elements. *Nucleic Acids Res*, 32: e38. [192102](#)
- Yang C-Y; Hsieh H-J; Tsai S-S; Wu T-N; Chiu H-F. (2006). Correlation between air pollution and postneonatal mortality in a subtropical city: Taipei, Taiwan. *J Toxicol Environ Health A*, 69: 2033-2040. [090760](#)
- Yang C-Y; Tseng Y-T; Chang C-C. (2003). Effects of air pollution on birthweight among children born between 1995 and 1997 in Kaohsiung, Taiwan. *J Toxicol Environ Health A*, 66: 807-816. [087886](#)
- Yatera K; Hsieh J; Hogg James C; Tranfield E; Suzuki H; Shih C-H; Behzad Ali R; Vincent R; van Eeden Stephan F. (2008). Particulate matter air pollution exposure promotes recruitment of monocytes into atherosclerotic plaques. *Am J Physiol Heart Circ Physiol*, 294: H944-H953. [157162](#)
- Yauk C; Polyzos A; Rowan-Carroll A; Somers CM; Godschalk RW; Van Schooten FJ; Berndt ML; Pogribny IP; Koturbash I; Williams A; Douglas GR; Kovalchuk O. (2008). Germ-line mutations, DNA damage, and global hypermethylation in mice exposed to pa. Presented at . [157164](#)
- Yauk CL; Quinn JS. (1996). Multilocus DNA fingerprinting reveals high rate of heritable genetic mutation in herring gulls nesting in an industrialized urban site. Presented at . [157163](#)
- Ying Z; Kampfrath T; Thurston G; Farrar B; Lippmann M; Wang A; Sun Q; Chen LC; Rajagopalan S. (2009). Ambient particulates alter vascular function through induction of reactive oxygen and nitrogen species. *Toxicol Sci*, 1: 1-36. [190111](#)
- Yokota S; Mizuo K; Moriya N; Oshio S; Sugawara I; Takeda K. (2009). Effect of prenatal exposure to diesel exhaust on dopaminergic system in mice. *Neurosci Lett*, 449: 38-41. [190518](#)
- Yoshida S; Ono N; Tsukue N; Oshio S; Umeda T; Takano H; Takeda K. (2006). In utero exposure to diesel exhaust increased accessory reproductive gland weight and serum testosterone concentration in male mice. , 13: 139-147. [097015](#)
- Yoshida S; Takeda K. (2004). The effects of diesel exhaust on murine male reproductive function. *Eisei Kagaku*, 50: 210-4. [097760](#)
- Yoshida S; Yoshida M; Sugawara I; Takeda K. (2006). Mice strain differences in effects of fetal exposure to diesel exhaust gas on male gonadal differentiation. , 13: 117-123. [156170](#)
- Zanobetti A; Bind MAC; Schwartz J. (2008). Particulate air pollution and survival in a COPD cohort. *Environ Health Perspect*, 7: 48. [156177](#)
- Zanobetti A; Schwartz J. (2007). Particulate air pollution, progression, and survival after myocardial infarction. *Environ Health Perspect*, 115: 769-775. [091247](#)
- Zeger S; Dominici F; McDermott A; Samet J. (2008). Mortality in the Medicare population and chronic exposure to fine particulate air pollution in urban centers (2000-2005). *Environ Health Perspect*, 116: 1614. [191951](#)
- Zeger S; McDermott A; Dominici F; Samet J. (2007). Mortality in the medicare population and chronic exposure to fine particulate air pollution. *Environ Health Perspect*, 116: 1614-1619. [157176](#)
- Zeman KL; Bennett WD. (2006). Growth of the small airways and alveoli from childhood to the adult lung measured by aerosol-derived airway morphometry. *J Appl Physiol*, 100: 965-971. [157178](#)
- Zhang Z; Che W; Liang Y; Wu M; Li N; Shu Y; Liu F; Wu D. (2007). Comparison of cytotoxicity and genotoxicity induced by the extracts of methanol and gasoline engine exhausts. *Toxicol In Vitro*, 21: 1058-1065. [157186](#)

Chapter 8. Susceptible Subpopulations

8.1. Potentially Susceptible Subpopulations

1 Interindividual variation in human responses to air pollutants indicates that some
2 subpopulations are at increased risk for the detrimental effects of ambient exposure to PM
3 (Kleeberger and Ohtsuka, 2005, [130489](#)). The NAAQS are intended to provide an adequate
4 margin of safety for both general populations and sensitive subpopulations, or those
5 subgroups potentially at increased risk for health effects in response to ambient air
6 pollution (see Section 1.1). To facilitate the identification of subpopulations at the greatest
7 risk for PM-related health effects, studies have evaluated factors that contribute to the
8 susceptibility and/or vulnerability of an individual to PM. These terms have sometimes
9 been used interchangeably in the literature, and in other cases have been defined to
10 represent two different categories that could contribute to a subpopulation experiencing
11 increased risk to PM-related health effects, resulting in the lack of a clear and consistent
12 definition (see Table 8-1). Additionally, in some cases, “at-risk” has been used as a term
13 encompassing these concepts more generally.

14 In this ISA, the term ‘susceptible’ will be used to represent populations that have a
15 greater likelihood of experiencing health effects related to PM exposure. This increased
16 likelihood of response to PM can result from a multitude of factors, including genetic or
17 developmental factors, race, gender, age, lifestyle (e.g., smoking status and nutrition) or
18 preexisting disease states. Population-level susceptibility factors (e.g., socioeconomic status
19 [SES], which includes reduced access to health care and low educational attainment) are
20 also discussed within this section due to the fact their non-random distribution appears to
21 play a dominant role in influencing the pattern of health effects observed in response to PM
22 exposure (American Lung Association, 2001, [016626](#)).

Table 8-1. Definitions of susceptible and vulnerable in the PM literature.

Definition	Reference
Susceptible: predisposed to develop a noninfectious disease	Merriam-Webster (2009, 192146)
Vulnerable: capable of being hurt: susceptible to injury or disease	
Susceptible: greater likelihood of an adverse outcome given a specific exposure, in comparison with the general population. Includes both host and environmental factors (e.g., genetics, diet, physiologic state, age, gender, social, economic, and geographic attributes).	American Lung Association (2001, 016626)
Vulnerable: periods during an individual’s life when they are more susceptible to environmental exposures.	

Note: Hyperlinks to the reference citations throughout this document will take you to the NCEA HERO database (Health and Environmental Research Online) at <http://epa.gov/hero>. HERO is a database of scientific literature used by U.S. EPA in the process of developing science assessments such as the Integrated Science Assessments (ISA) and the Integrated Risk Information System (IRIS).

Definition	Reference
Susceptible: innate (e.g., genetic or developmental) or acquired (e.g., age, disease or smoking or smoking) factors that make individuals more likely to experience effects with exposure to PM.	U.S. EPA. (2008, 157072)
Vulnerable: PM-related effects due to factors including socioeconomic status (e.g., reduced access to health care) or particularly elevated exposure levels.	
Susceptible: greater or lesser biological response to exposure.	U.S. EPA (2009, 192149)
Vulnerable: more or less exposed.	
Vulnerable: to be susceptible to harm or neglect, that is, acts of commission or omission on the part of others that can wound.	Aday, LA. (2001, 192150)
Susceptible: may be those who are significantly more liable than the general population to be affected by a stressor due to life stage (e.g., children, the elderly, or pregnant women), genetic polymorphisms (e.g., the small but significant percentage of the population who have genetic susceptibilities), prior immune reactions (e.g., individuals who have been "sensitized" to a particular chemical), disease state (e.g., asthmatics), or prior damage to cells or systems (e.g., individuals with damaged ear structures due to prior exposure to toluene, making them more sensitive to damage by high noise levels).	U.S. EPA (2003, 192145)
Vulnerable: differential exposure and differential preparedness (e.g., immunization).	
Susceptible: intrinsic (e.g., age, gender, pre-existing disease (e.g., asthma) and genetics) and extrinsic (previous exposure and nutritional status) factors.	Kleeberger and Ohtsuka (2005, 130489)
Susceptible: characteristics that contribute to increased risk of PM-related health effects (e.g., genetics, pre-existing disease, age, gender, race, socioeconomic status, healthcare availability, educational attainment, and housing characteristics).	Pope and Dockery (2006, 158881)

1 To examine whether PM differentially affects certain subpopulations, epidemiologic
2 studies conduct stratified analyses to identify the presence or absence of effect modification.
3 A thorough evaluation of potential effect modifiers may help identify subpopulations that
4 are more susceptible to PM. These analyses require the proper identification of confounders
5 and their subsequent adjustment in statistical models, which helps separate a spurious
6 association from a true causal association. Although the design of toxicological and
7 controlled human exposure studies do not allow for an extensive examination of effect
8 modifiers, the use of animal models of disease and the study of individuals with underlying
9 disease or genetic polymorphisms do allow for comparisons between subgroups. Therefore,
10 the results from these studies, combined with those results obtained through stratified
11 analyses in epidemiologic studies, contribute to the overall weight of evidence for the
12 increased susceptibility of specific subpopulations to PM.

13 This chapter discusses the epidemiologic, controlled human exposure, and
14 toxicological studies evaluated in Chapters 6 and 7 that provide information on potentially
15 susceptible subpopulations. The studies highlighted include only those studies that
16 presented stratified results (e.g., males vs. females or <65 vs. ≥ 65). This approach allowed
17 for a comparison between subpopulations exposed to similar PM concentrations and within
18 the same study design. Although this chapter does not provide a comprehensive evaluation
19 of all the studies that examined the effect of PM on potentially susceptible subpopulations
20 it does summarize the trends in the associations or health effects observed within the
21 identified subpopulations. Table 8-2 provides an overview of the factors identified in the
22 current toxicological, controlled human exposure, and epidemiologic literature that have
23 been shown to contribute to the susceptibility of a subpopulation to PM-related health
24 effects.

Table 8-2. Susceptibility Factors.

Factor	Exposure	PM Size Fraction Evaluated
Children (< 18) ¹⁵	Short-term	PM _{2.5} , PM _{10-2.5} , PM ₁₀
Older Adults (≥ 65)	Short-term	PM _{2.5} , PM _{10-2.5} , PM ₁₀
	Long-term	PM _{2.5}
Pregnancy and Developmental Effects	Long-term	PM _{2.5}
Gender	Short-term	PM _{2.5} , PM ₁₀
	Long-term	PM _{2.5} , PM _{10-2.5} , PM ₁₀
Race/Ethnicity	Short-term	PM _{2.5} , PM ₁₀
Genetic polymorphisms	Short-term	PM _{2.5}
	Long-term	PM ₁₀
Cardiovascular Diseases	Short-term	PM _{2.5} , PM ₁₀
	Long-term	PM _{2.5}
Respiratory Illnesses	Short-term	PM _{2.5} , PM ₁₀
	Long-term	PM ₁₀
Respiratory Contributions to Cardiovascular Effects	Short-term	PM _{2.5} , PM ₁₀
Diabetes	Short-term	PM ₁₀
Obesity	Short-term	PM _{2.5}
Health Status (e.g., Nutrition)	Short-term	PM _{2.5}
Socioeconomic Status (SES)	Short-term	PM _{2.5} , PM _{10-2.5} , PM ₁₀
Educational Attainment	Short-term	PM _{2.5} , PM ₁₀
	Long-term	PM _{2.5}
Residential Location	Short-term	PM ₁₀

8.1.1. Age

8.1.1.1. Older Adults

1 Evidence for PM-related health effects in older adults spans epidemiologic, controlled
2 human exposure, and toxicological studies. The 2004 PM AQCD found evidence for
3 increased risk of cardiovascular effects in older adults exposed to PM (U.S. EPA, 2004,
4 [056905](#)). Older adults represent a potentially susceptible subpopulation due to the higher
5 prevalence of pre-existing cardiovascular and respiratory diseases found in this age range
6 compared to younger age groups. The increased susceptibility in this subpopulation can
7 primarily be attributed to the gradual decline in physiological processes as part of the aging
8 process (U.S. EPA, 2006, [192082](#)). Therefore, some overlap exists between potentially
9 susceptible older adults and the subpopulation that encompasses individuals with pre-

¹⁵ The age range that defines a child varies from study to study. In some cases it is <21 years old while in others it is <18 years old (Firestone et al., 2007, [192071](#)). For the purposes of this exercise children are defined as those individuals <18 years old because the majority of epidemiologic studies consider individuals under the age of 18 children.

1 existing diseases (Kan et al., 2008, [156621](#)). Epidemiologic studies that conduct age
2 stratified analyses primarily focus on the association between short-term exposure to PM
3 and cardiovascular morbidity, but additional studies have examined the association
4 between PM and respiratory morbidity and mortality.

5 In recent publications, the epidemiologic evidence for cardiovascular effects in older
6 adults in response to short-term exposure to PM_{10-2.5} and PM_{2.5} is limited, but taken together
7 with evidence from studies of PM₁₀ (e.g., Larrieu et al., 2007, [093031](#); Le Tertre et al., 2002,
8 [023746](#)), supports the increased risk of cardiovascular morbidity in older adults. Host et al.
9 (2007, [155851](#)) found an increase in cardiovascular disease (CVD) hospital admissions
10 (HAs) in individuals >65 compared to all ages for short-term exposure to both PM_{10-2.5} and
11 PM_{2.5}. Barnett et al. (2006, [089770](#)) analyzed data from several cities across Australia and
12 New Zealand and found that the excess risk of hospitalizations for cardiac diseases,
13 congestive heart failure (CHF), ischemic heart disease (IHD), myocardial infarction (MI),
14 and all CVD was greater among patients aged ≥ 65 as compared to those individuals <65
15 years in response to short-term exposure to PM_{2.5}. U.S.-based studies that examined the
16 association between short-term exposure to PM and cardiovascular morbidity primarily
17 found no evidence for increased risk among older adults. Metzger et al. (2004, [044222](#))
18 found no evidence of effect modification by age for cardiovascular outcomes and short-term
19 exposure to PM_{2.5} in Atlanta, Georgia, which is supported by the results from other studies
20 that focused on short-term exposure to PM₁₀ (Fung et al., 2005, [074322](#); Zanobetti and
21 Schwartz, 2005, [088069](#)). However, Pope et al. (2008, [191969](#)) observed an increased risk of
22 HF hospital admissions in older adults (i.e., ≥ 65) in Utah, but the study used a 14-day
23 lagged cumulative moving average of PM_{2.5}, which is much longer than the lags examined
24 by the other U.S.-based studies. Although studies have not consistently found an
25 association between short-term exposure to PM and respiratory-related health effects in
26 older adults, some studies have reported an increase in respiratory hospital admissions in
27 individuals 65 years of age and older (e.g., Fung et al., 2005, [093262](#)).

28 Additional evidence for an increase in cardiovascular and respiratory effects among
29 older adults has been observed in controlled human exposure and dosimetric studies.
30 Devlin et al. (2003, [087348](#)) found that older subjects exposed to PM_{2.5} concentrated
31 ambient particles (CAPs) experienced significant decreases in heart rate variability (HRV)
32 (both in time and frequency) immediately following exposure, when compared to healthy
33 young subjects. In addition, Gong et al (2004, [055628](#)) reported that older subjects
34 demonstrated significant decreases in HRV when exposed to PM_{2.5} CAPs, but this study did
35 not compare the response in older subjects to those elicited by young, healthy individuals.
36 However, the study did find that healthy older adults were more susceptible to decreases in
37 HRV compared to those with an underlying health condition (i.e., chronic obstructive
38 pulmonary disease [COPD]) in response to PM exposure (Gong et al., 2004, [055628](#)).
39 Dosimetric studies have shown a depression of PM_{2.5} and PM_{10-2.5} clearance in all regions of

1 the respiratory tract with increasing age beyond young adulthood in humans and
2 laboratory animals. These results suggest that older adults are also susceptible to PM-
3 related respiratory health effects (Section 4.3.4.1).

4 Animal toxicological studies have attempted to characterize the relationship between
5 age and PM-related health effects through the development of models that mimic the
6 physiological conditions associated with older individuals. For example, Nadziejko et al.
7 (2004, [055632](#)) observed arrhythmias in older, but not younger, rats exposed to PM_{2.5} CAPs.
8 In addition, another study (Tankersley et al., 2004, [094378](#)) that used a mouse model of
9 terminal senescence observed various cardiovascular-related responses including altered
10 baseline autonomic tone in response to carbon black exposure that may subsequently affect
11 the quality and severity of cardiovascular responses (Tankersley, 2007, [188859](#)).
12 Reductions in cardiac fractional shortening and significant pulmonary vascular congestion
13 upon exposure to carbon black were also reported in older mice (Tankersley et al., 2008,
14 [157043](#)). Overall, these studies provide biological plausibility for the increase in
15 cardiovascular effects in older adults observed in the controlled human exposure and
16 epidemiologic studies.

17 Recent epidemiologic studies have also found that individuals >65 years old are more
18 susceptible to all-cause (non-accidental) mortality upon short-term exposure to both PM_{2.5}
19 (Franklin et al., 2007, [188502](#); Ostro et al., 2006, [087991](#)) and PM₁₀ (Samoli et al., 2008,
20 [188455](#); Zeka et al., 2006, [088749](#)), which is consistent with the findings of the 2004 PM
21 AQCD. Of note are the results from Ostro et al. (2006, [087991](#)) that reported a slight
22 increase in mortality for older adults compared to all ages in single-pollutant models, but a
23 robust effect estimate in co-pollutant models with gaseous pollutants (i.e., PM_{2.5}+CO and
24 PM_{2.5}+NO₂). These results differ from those in the all ages model (i.e., attenuation of the
25 effect estimate in co-pollutant models with CO and NO₂), which suggests that older adults
26 are more susceptible to PM exposures, even though the age-stratified effect estimates in
27 single-pollutant models did not significantly differ. Epidemiologic studies that examined the
28 association between mortality and long-term exposure to PM (i.e., PM_{2.5}) have found results
29 contradictory to those obtained in the short-term exposure studies. Villeneuve et al. (2002,
30 [042576](#)), Naess et al. (2007, [090736](#)) and Zeger et al. (2008, [191951](#)) report evidence of
31 differing PM_{2.5} relative risks by age, where risk declines with increasing age starting at age
32 60 until there is no evidence of an association among persons ≥ 85 years of age.

33 The evidence from epidemiologic, controlled human exposure, and toxicological
34 studies that focused on exposures to PM_{2.5}, PM_{10-2.5}, and PM₁₀, provide coherence and
35 biological plausibility for the association between PM and cardiovascular morbidity in older
36 adults. The clear pattern of positive associations only being observed in epidemiologic
37 studies conducted in non-U.S. locations brings into question the influence of PM
38 composition on health effects. However, the difference in effects observed between U.S. and
39 non-U.S. studies could also be due to possible differences in the identification of CVD-

1 related morbidity and mortality between the studies evaluated. The additional evidence
2 from epidemiologic studies that focus on mortality and respiratory morbidity in response to
3 short-term exposure to PM also indicate that older adults represent a susceptible
4 subpopulation. As the demographics of the U.S. population shift over the next 20 years with
5 a larger percentage of the population (i.e., 13% of the population in 2011 and a projected
6 20% in 2030) encompassing individuals ≥ 65 years (U.S. Census Bureau, 2000, [157064](#)), an
7 increase in the number of PM-related health effects (e.g., cardiovascular and respiratory
8 morbidity, and mortality) in individuals ≥ 65 years old could occur.

8.1.1.2. Children

9 Children have generally been considered more susceptible to PM exposure due to
10 multiple factors including more time spent outdoors, greater activity levels, exposures
11 resulting in higher doses per body weight and lung surface area, and the potential for
12 irreversible effects on the developing lung (U.S. EPA, 2004, [056905](#)). The 2004 PM AQCD
13 found that studies which stratify results by age typically report associations between PM
14 and respiratory-related health effects in children, specifically asthma (U.S. EPA, 2004,
15 [056905](#)). Of the recent epidemiologic studies evaluated, only a few have examined the
16 association between PM_{10-2.5} and PM_{2.5} and respiratory effects in children. Mar et al. (2004,
17 [057309](#)) found increased respiratory effects (e.g., wheeze, cough, lower respiratory
18 symptoms) in children 7-12 years of age compared to individuals 20-51 years of age in
19 response to exposure to both PM_{10-2.5} and PM_{2.5} in Spokane, Washington. In addition, Host et
20 al. (2007, [155851](#)) found an increase in respiratory-related hospital admissions with short-
21 term exposure to PM_{10-2.5} among children ages 0-14 years in 6 French cities. Further
22 support for these effects is provided by the results from studies that focused on PM₁₀ (Mar
23 et al., 2004, [057309](#); Peel et al., 2005, [056305](#)). A recent toxicological study provides
24 biological plausibility for the increase in PM-related respiratory effects in children observed
25 in the epidemiologic studies. Mauad et al. (2008, [156743](#)) using both prenatal and
26 postneonatal mice exposed to ambient PM_{2.5} in a “polluted chamber” found evidence for
27 changes in lung function and pulmonary injury (e.g., incomplete alveolarization).
28 Additionally, Pinkerton et al. (2004, [087465](#); 2008, [190471](#)) found evidence suggesting that
29 the developing lung is more susceptible to PM by demonstrating that neonatal rats exposed
30 to iron-soot PM had a reduction in cell proliferation in the lung. Overall, the evidence from
31 epidemiologic studies that have examined the health effects associated with all size
32 fractions of PM and toxicological studies that have examined individual PM components
33 provide additional support to the hypothesis that children are more susceptible to
34 respiratory effects from short-term exposure to PM.

8.1.2. Pregnancy and Developmental Effects

1 While the majority of the literature focuses on epidemiologic studies that examine the
2 potential health effects (e.g., low birth weight, growth restriction) attributed to in utero
3 exposure to PM (see Section 7.4), it is unclear if the health effects observed are due to
4 soluble fractions of PM that cross the placenta or physiological alterations in the pregnant
5 woman. In the case of exposure to PM, adverse health effects in the offspring could be
6 mediated by potentially greater susceptibility in the pregnant woman. For example, an
7 inflammatory response leads to differential activation of multiple genes involved in immune
8 response and regulation, cell metabolism, and proliferation all of which can lead to health
9 effects in the developing fetus (Fedulov et al., 2008, [097482](#)). Toxicological studies have
10 recently examined whether exposure to air pollutants during pregnancy leads to increased
11 allergic susceptibility in the offspring. Fedulov et al. (2008, [097482](#)) used an animal model
12 to examine the effect of diesel exhaust particles (DEPs) along with an immunologically
13 “inert” particle (TiO₂) on pregnant mice. The authors found that pregnant mice exhibited a
14 local and systemic inflammatory response when exposed to either DEP or TiO₂, which was
15 not observed in control, non-pregnant mice. In addition, the offspring of exposed pregnant
16 mice developed AHR and allergic inflammation. This study suggests that exposure to PM_{2.5},
17 and even relatively inert particles, during pregnancy can potentially lead to increased
18 allergic susceptibility in offspring and subsequently the development of asthma.

8.1.3. Gender

19 The 2004 PM AQCD did not find consistent evidence for a difference in health effects
20 by gender. However, there appeared to be gender differences in the localization of particles
21 when deposited in the respiratory tract and the deposition rate due to differences in body
22 size, conductive airway size, and ventilatory parameters (U.S. EPA, 2004, [056905](#)). For
23 example, females have proportionally smaller airways and slightly greater airway
24 reactivity than males (Yunginger et al., 1992, [192074](#)).

25 Few recent epidemiologic studies have conducted gender-stratified analyses when
26 examining the association between either short- or long-term exposure to PM_{10-2.5} or PM_{2.5}.
27 Similar to the studies evaluated in the 2004 PM AQCD, the current literature has not found
28 a consistent pattern of associations by gender for any health outcome. Pope et al. (2006,
29 [189048](#)) observed a slightly larger, non-significant, association between short-term
30 exposure to PM_{2.5} and daily HA for acute IHD events in males. An examination of gender-
31 specific effects by both Ostro et al. (2006, [087991](#)) and Franklin et al. (2007, [188502](#)) found
32 conflicting associations by gender for multiple cause-specific mortality outcomes. The
33 inconsistency in associations between males and females is further highlighted in studies
34 that examined the health effects associated with long-term exposure to PM_{10-2.5} and PM_{2.5}.

1 Chen et al. (2005, [087942](#)) found larger effects in females for congestive heart disease
2 (CHD) mortality upon long-term exposure to PM_{10-2.5} in 3 California cities. Naess et al.
3 (2006, [189048](#)), also observed slightly larger effect estimates in females for CVD and lung
4 cancer mortality upon long-term exposure to PM_{2.5}, but for COPD mortality the greatest
5 association was found in males.

6 The majority of the epidemiologic studies that examined the association between
7 exposure to PM and gender focused on exposure to PM₁₀. Although most of these studies do
8 not attribute the association to specific size fractions (i.e., PM_{10-2.5} or PM_{2.5}) or provide
9 insight as to whether one size fraction may be driving the observed effect, the studies of
10 PM₁₀ provide further support that gender does not appear to differentially affect PM-related
11 health outcomes. Neither Zanobetti and Schwartz (2005, [088069](#)) nor Wellenius et
12 al. (2006, [088748](#)) found gender to be a significant effect modifier of the risk estimates
13 associated with short-term exposure to PM₁₀ and cardiovascular hospital admissions. These
14 results are consistent with those found in other studies that examined the association
15 between short-term exposure to PM₁₀ and both cardiovascular and respiratory hospital
16 admissions (Luginaah et al., 2005, [057327](#); Middleton et al., 2008, [156760](#)). Additional
17 studies that examined the effects of short-term and long-term exposure to PM₁₀ on
18 respiratory morbidity and mortality (Boezen et al., 2005, [087396](#); Chen et al., 2005, [087942](#);
19 Zanobetti and Schwartz, 2005, [088069](#); Zeka et al., 2006, [088749](#)) found results that are
20 consistent with those reported in studies of PM_{10-2.5} and PM_{2.5} (i.e., gender is not likely to be
21 an effect modifier).

22 Although human clinical studies are not typically powered to detect differences in
23 response between males and females, one study did report significantly greater decreases in
24 blood monocytes, basophils, and eosinophils in females compared to males following
25 controlled exposures to UF EC (Frampton et al., 2006, [088665](#)). Overall, the evidence from
26 primarily epidemiologic studies that examined the association between short- and long-
27 term exposure to PM_{10-2.5} and PM_{2.5}, along with the supporting evidence from PM₁₀ studies,
28 further confirms that although differences in dosimetry exist between males and females,
29 neither gender consistently exhibits a higher disposition for PM-related health effects.

8.1.4. Race/Ethnicity

30 The 2004 PM AQCD did not evaluate the potential susceptibility of individuals of
31 different races and ethnicities to PM exposure. The results from epidemiologic studies
32 evaluated in this review that examined the potential effect modification of the PM-
33 morbidity and -mortality relationships by race and ethnicity varied depending on the study
34 location. In an analysis of the PM_{2.5}-mortality relationship, Ostro et al. (2006, [087991](#))
35 stratified the association by race and ethnicity, and observed a positive and marginally
36 significant effect for whites and Hispanics, but not for blacks, in response to short-term

1 exposure to PM_{2.5} in 9 California counties. An additional analysis performed by Ostro et al. (2008,
2 [097971](#)) in 6 California counties using PM_{2.5} and various PM_{2.5} components, also found a
3 significant association between mortality, specifically cardiovascular mortality, and
4 Hispanic ethnicity (Ostro et al., 2008, [097971](#)). It should be noted that neither study, Ostro
5 et al. (2006, [087991](#)) nor Ostro et al. (2008, [097971](#)), controlled for potential confounders
6 (e.g., SES factors and location of residence) of the association observed between PM_{2.5}
7 exposure and Hispanic ethnicity. As a result, Ostro et al (2008, [097971](#)) speculated that the
8 increased PM_{2.5}-mortality risks observed for Hispanics could be due to a variety of factors
9 including, higher rates of: non-high school graduates, obesity, no leisure-time activity, and
10 alcohol consumption within the Hispanic population in California. Additional evidence for
11 the potential susceptibility of individuals by race and ethnicity were derived from studies
12 on the health effects associated with short-term exposure to PM₁₀. Wellenius et al. (2006,
13 [088748](#)) observed that race (i.e., white vs. other) did not significantly modify the association
14 between short-term exposure to PM₁₀ and CHF hospital admissions. Additionally, Zeka et
15 al. (2006, [088749](#)) did not observe any difference in mortality effect estimates when
16 stratifying by race (i.e., black and white) upon short-term exposure to PM₁₀. To date,
17 dosimetric studies have not extensively examined differences in particle deposition between
18 races or ethnicities to confirm the epidemiologic findings. Although not extensively
19 analyzed, toxicological studies, have examined PM responses in different mouse and rat
20 strains have reported greater CV effects (Kodavanti et al., 2003, [051325](#); Tankersley et al.,
21 2007, [097910](#)) and compromised host defense (Ohtsuka et al., 2000, [004409](#)) for some
22 strains. These studies provide some support, in terms of biological plausibility, for
23 differences in PM-induced health effects by race or ethnicity. However, it is unclear how the
24 difference in the response to PM in different mouse or rat strains extrapolates to PM-
25 induced differences between races or ethnicities. Overall, the results from the studies that
26 examined the potential effect modification of PM associations by race and ethnicity provide
27 some evidence for increased risk of mortality in Hispanics upon short-term exposure to
28 PM_{2.5}. However, the evidence for this association is from two studies conducted in
29 California, it is unclear if the studies adequately controlled for potential confounders, and
30 additional studies in other locations that stratified results by race and ethnicity have not
31 yet been conducted.

8.1.5. Gene-Environment Interaction

32 A consensus now exists that gene-environment interactions merit serious
33 consideration when examining the relationship between ambient exposures to air
34 pollutants and the development of health effects (Gilliland et al., 1999, [155792](#); Kauffmann
35 and Post Genome Respiratory Epidemiology, 2004, [090968](#)). These potential interactions
36 were not evaluated in the 2004 PM AQCD. Inter-individual variation in human responses

1 to air pollutants suggests that some subpopulations are at increased risk of detrimental
2 effects due to pollutant exposure, and it has become clear that the genetic makeup of an
3 individual can increase their susceptibility (Kleeberger and Ohtsuka, 2005, [130489](#)).
4 Gene-environment interactions can result in health effects due to: genetic polymorphisms,
5 which result in the lack of a protein or a change that makes a functionally important
6 protein dysfunctional; or genetic damage in response to an exposure which potentially leads
7 to a health response (e.g., formation of benzo [a] pyrene DNA adducts in response to PM
8 exposure). In this review, the majority of studies examine gene-environment interactions
9 due to genetic polymorphisms. In order to establish useful links between polymorphisms in
10 candidate genes and adverse health effects, several criteria must be satisfied: the product of
11 the candidate gene must be significantly involved in the pathogenesis of the adverse effect
12 of interest; and polymorphisms in the gene must produce a functional change in either the
13 protein product or in the level of expression of the protein (U.S. EPA, 2008, [157075](#)).
14 Further, the issue of confounding by other environmental exposures must be carefully
15 considered.

16 It has been hypothesized that the cardiovascular and respiratory health effects that
17 occur in response to short-term PM exposure are mediated by oxidative stress (see
18 Section 5.1.1). Research has examined this hypothesis by primarily focusing on the
19 glutathione-S transferase (GST) genes because they have common, functionally important
20 polymorphic alleles that significantly affect antioxidant defense function in the lung (e.g.,
21 homozygosity for the null allele at the GSTM1 and GSTT1 loci, homozygosity for the A105G
22 allele at the GSTP1 locus), and approximately half of the white population has a
23 polymorphic null allele, resulting a large potential study population (Schwartz et al., 2005,
24 [086296](#)). Exposure to free radicals and oxidants in air pollution leads to a cascade of events,
25 which can result in a reduction in glutathione (GSH), and an increase in the transcription
26 of GSTs. Individuals with genotypes that result in reduced or absent enzymatic activity are
27 likely to have reduced antioxidant defenses and potentially increased susceptibility to
28 inhaled oxidants and free radicals.

29 Numerous studies have examined the role of genetic polymorphisms on PM-related
30 cardiovascular health effects using the Normative Aging Study cohort. Schwartz et al.
31 (2005, [086296](#)) and Chahine et al. (2007, [156327](#)) found that individuals with null GSTM1
32 alleles had a larger decrease in HRV upon short-term exposure to PM_{2.5} compared to
33 individuals with at least one allele. Polymorphisms in the HO-1 promoter resulted in
34 lowered HRV upon short-term exposure to PM_{2.5} in individuals with the long repeat
35 polymorphism compared to those individuals with the short repeat polymorphism (Chahine
36 et al., 2007, [156327](#)). In addition, Schneider et al. (2008, [191985](#)) found that diabetic
37 individuals with null GSTM1 alleles had larger decrements in FMD (i.e., flow-mediated
38 dialation of the brachial artery), suggesting alterations in endothelial function. A controlled
39 human exposure study examined whether genetic polymorphisms increase the

1 susceptibility of individuals to respiratory morbidity in response to PM exposure. Gilliland
2 et al. (2004, [156471](#)) examined the effect of allergens and DEPs on individuals with either
3 null genotypes for GSTM1 and GSTT1 or GSTP1 codon 105 variants. The authors found
4 that individuals with the GSTM1 null or the GSTP1 I105 wildtype genotypes were more
5 susceptible to allergic inflammation upon exposure to allergen and DEPs. Additional genes
6 within the GST pathway have also been examined (e.g., NQO1), but the sample sizes are
7 relatively small, which prohibits the analysis of the potential effect modification of PM-
8 related health effects by these genes (e.g., Schneider et al., 2008, [191985](#)).

9 The interaction between GST genes and PM exposure has recently been extended to
10 studies that examined the effect of PM exposure on birth outcomes. A recent study (Suh et
11 al., 2008, [192077](#)) that examined the effect of high PM10 exposures during the third
12 trimester of pregnancy on the risk of preterm delivery, found that women with the GSTM1
13 null genotype were at an increased risk of preterm birth. When examining the interaction
14 between high PM10 concentrations during the third trimester of pregnancy and the presence
15 of the GSTM1 null genotype on the risk of preterm delivery, there was evidence for a
16 synergistic gene-environment interaction in pregnant women. This effect could occur due to
17 oxidative stress induced by metals contained in PM10, which could be modified by
18 polymorphisms of the GSTM1 gene. This oxidative stress causes oxidative DNA damage in
19 fetal tissues, which may lead to preterm delivery by causing a reduction in placental blood
20 flow.

21 An examination of other genes outside the GST pathway have also been conducted to
22 determine if specific polymorphisms increase the susceptibility of individuals to PM.
23 Baccarelli et al. (2008, [157984](#)) in the Normative Aging Study observed that individuals
24 with polymorphisms in MTHFR (C677T methylenetetrahydrofolate reductase), an
25 alteration associated with reduced enzyme activity, and cSHMT (cytoplasmic serine
26 hydroxymethyltransferase) (i.e., [CT/TT] MTHFR and [CC] cSHMT genotypes), alterations
27 associated with higher homocysteine levels, have a reduction in SDNN, upon exposure to
28 PM_{2.5}. Peters et al. (2009, [191992](#)) examined single nucleotide polymorphisms (SNPs) in the
29 fibrinogen gene in myocardial infarction survivors to assess whether exposure to PM₁₀
30 altered physiologic levels of fibrinogen, which has been implicated in promoting
31 atherothrombosis. The authors found that individuals with single nucleotide
32 polymorphisms (SNPs) in the fibrinogen gene have higher steady state fibrinogen levels
33 which when combined with the inflammatory effects (i.e., increased fibrinogen levels)
34 associated with exposure to PM could increase their risk of PM-related cardiovascular
35 health effects. These results taken together suggest that individuals with null alleles or
36 specific polymorphisms in genes that mediate the antioxidant response to oxidative stress,
37 regulate enzyme activity, or regulate physiological levels of inflammatory markers are more
38 susceptible to PM. However, in some cases genetic polymorphisms may actually reduce an
39 individual's susceptibility to PM-related health effects. For example, Park et al. (2006,

1 [189099](#)) found that individuals with two hemochromatosis (HFE) polymorphisms (C282Y
2 and H63D), which result in an increase in iron uptake, had smaller reductions in HRV upon
3 exposure to PM_{2.5}. This effect could possibly be due to the reduction in free iron that enters
4 oxidation-reduction (redox) reactions and the subsequent reduction in reactive oxygen
5 species (ROS).

6 More recently, studies have begun to focus on epigenetic effects associated with PM
7 exposure (i.e., the effect of PM on DNA methylation) due to the fact that DNA methylation
8 can result in gene alterations. The limited number of epidemiologic studies that examined
9 epigenetic effects have found some evidence that long-term exposure to PM_{2.5} and PM₁₀ can
10 influence DNA methylation (Baccarelli et al., 2009, [188183](#); Tarantini et al., 2009, [192010](#)).
11 Additionally, a toxicological study found some evidence of hypermethylation of
12 spermatogonial stem cells in response to the PM component of ambient urban air (Yauk et
13 al., 2008, [157164](#)). Although epigenetic effects have been observed in response to PM
14 exposure in some studies additional research is needed to more accurately characterize
15 these associations.

16 Overall, the evidence suggests that specific genetic polymorphisms can potentially
17 increase the susceptibility of an individual to PM exposure, but protective polymorphisms
18 also exist, which may diminish the health effects attributed to PM exposure in some
19 individuals. In addition, the studies that examine genetic polymorphisms or epigenetics can
20 potentially provide additional information that can aid in identifying the specific pathways
21 and mechanisms by which PM initiates health effects.

8.1.6. Pre-Existing Disease

22 In 2004, the National Research Council (NRC) published a report that emphasized
23 the need to evaluate the effect of air pollution on susceptible and subpopulations, including
24 those with respiratory illnesses and cardiovascular diseases (NRC, 2004, [156814](#)). The 2004
25 PM AQCD included epidemiologic evidence suggesting that individuals with pre-existing
26 heart and lung diseases, as well as diabetes may be more susceptible to PM exposure. In
27 addition, toxicological studies that used animal models of cardiopulmonary diseases and
28 heightened allergic sensitivity found evidence of enhanced susceptibility. More recent
29 epidemiologic and human clinical studies have directly examined the effect of PM on
30 individuals with pre-existing diseases and toxicological studies have employed disease
31 models to identify whether exposure to PM disproportionately affects certain
32 subpopulations.

8.1.6.1. Cardiovascular Diseases

33 The potential effect of underlying cardiovascular diseases on PM-related health
34 responses has been examined using epidemiologic studies that stratify effect estimates by

1 underlying conditions or secondary diagnoses, and toxicological studies that use animal
2 models to mimic the physiological conditions associated with various cardiovascular
3 diseases (e.g., MI, ischemia, and atherosclerosis). A limited number of controlled human
4 exposure studies have also examined the potential relationship between cardiovascular
5 diseases and exposure to PM in individuals with underlying cardiovascular conditions, but
6 these studies have provided somewhat inconsistent evidence for these associations.

7 The majority of the epidemiologic literature that examined the association between
8 short-term exposure to PM and cardiovascular outcomes focuses on cardiovascular-related
9 hospital admissions and emergency department (ED) visits. Hypertension is the pre-
10 existing condition that has been considered to the greatest extent when examining the
11 association between short-term exposure to PM and cardiovascular-related HAs and ED
12 visits. Pope et al. (2006, [091246](#)) found no evidence of effect modification of the IHD ED
13 visit association with PM_{2.5} in individuals with secondary hypertension in Utah. This is
14 consistent with the results of both Wellenius et al. (2006, [088748](#)) in 7 U.S. cities and Lee et
15 al. (2008, [192076](#)) in Taipei, which found that hypertension did not modify the association
16 between PM₁₀ and cardiovascular-related health outcomes. These results differ from those
17 presented by Peel et al. (2007, [090442](#)), in Atlanta, which observed that exposure to PM₁₀
18 resulted in an increase in ED visits for arrhythmias and CHF in individuals with
19 underlying hypertension. An additional study conducted by Park et al. (2005, [057331](#)) in
20 Boston found that underlying hypertension increased associations between HRV,
21 specifically a reduction in the HF parameter, and short-term exposure to PM_{2.5}.

22 Park et al. (2005, [057331](#)), in the analysis mentioned above, examined other
23 underlying cardiovascular conditions and found associations between PM_{2.5} and HRV in
24 individuals with pre-existing IHD. In a toxicological study, Wellenius et al. (2003, [055691](#))
25 examined the effects of PM_{2.5} CAPs exposure on induced myocardial ischemia in dogs,
26 which mimics the effects associated with IHD. The authors found that exposure to PM_{2.5}
27 prior to the induced ischemia increased ST-segment elevation, indicating greater ischemia
28 than air-exposed animals. A follow-up study implicated impaired myocardial blood flow in
29 the response (Bartoli et al., 2009, [179904](#)).

30 Additional studies examined the effects of PM on cardiac function in individuals with
31 dysrhythmia. Peel et al. (2007, [090442](#)) observed some evidence for an increase in ED visits
32 for IHD for individuals with secondary dysrhythmia and PM₁₀ exposure. However, when
33 examining CHF hospital admissions in 7 U.S. cities, Wellenius et al. (2006, [088748](#)) found
34 no evidence for effect modification of PM₁₀ exposure in individuals with secondary
35 dysrhythmia.

36 Limited evidence is available from epidemiologic studies that examined other pre-
37 existing cardiovascular conditions, such as CHF and MI. Pope et al. (2006, [091246](#))
38 observed an increase in hospital admissions for acute IHD in individuals with underlying
39 CHF upon short-term exposure to PM_{2.5}. However, Peel et al. (2007, [090442](#)) did not find that

1 underlying CHF contributed to an increase in the association between IHD ED visits and
2 short-term exposure to PM₁₀. Zanobetti and Schwartz (2005, [088069](#)) also examined the
3 potential effect modification of the association between PM₁₀ and cardiovascular-related
4 health effects in individuals with CHF, but used MI hospital admissions as the outcome of
5 interest. Underlying CHF was not found to increase MI hospital admissions for exposure to
6 PM₁₀ in the cohort of more than 300,000 hospital admissions.

7 Wellenius et al. (2006, [088748](#)) examined the effect of previous diagnoses of acute MI
8 on the association between CHF hospital admissions and short-term exposure to PM₁₀ in 7
9 U.S. cities. In this study, Wellenius et al. (2006, [088748](#)) found no evidence of effect
10 modification of the relationship between PM₁₀ and CHF hospital admissions by previous
11 acute MI. Toxicological studies have provided additional evidence for the cardiovascular
12 health effects associated with exposure to PM in individuals with underlying MI. Anselme
13 et al. (2007, [097084](#)) and Wellenius et al. (2006, [156152](#)) examined the arrhythmic effects of
14 PM on rats that experienced an MI using two different models. Wellenius et al. (2006,
15 [156152](#)) used a post-myocardium sensitivity model (acute MI) and observed that exposure
16 to PM_{2.5} CAPs decreased ventricular premature beats and spontaneous supraventricular
17 ectopic beats. In contrast, the MI model of chronic heart failure (i.e., rats that experienced
18 an MI 3 months prior to exposure), demonstrated a prominent increase in the incidence of
19 premature ventricular contraction when exposed to DE (Anselme et al., 2007, [097084](#)). The
20 discrepancy in effects observed between studies could be due to differences in the MI model
21 or the PM exposure (i.e., CAPs vs. DE).

22 Additional toxicological studies examined the association between PM and
23 pre-existing cardiovascular diseases using a murine model of atherosclerosis (ApoE^{-/-}
24 mouse). For example, Campen et al. (2005, [083977](#); 2006, [096879](#)) examined the heart rate
25 and ECG effects of acute exposure to PM on ApoE^{-/-} mice. With DE, dramatic bradycardia
26 and T-wave depression were observed that were attributable to the gases (Campen et al.,
27 2005, [083977](#)), while whole gasoline emissions induced T-wave alterations that required
28 particles (Campen et al., 2006, [096879](#)). However, these studies along with others that used
29 this mouse model (see Section 6.2 and 7.2) did not compare the effects observed with the
30 ApoE^{-/-} mouse to other non-diseased mouse models, so it is unclear if the responses would
31 differ if other strains underwent the same experimental protocol.

32 Controlled human exposure studies that examined the effect of pre-existing diseases
33 on cardiovascular outcomes with exposure to PM are less consistent and difficult to
34 interpret in the context of the results from the epidemiologic and toxicological studies. Mills
35 et al. (2007, [091206](#); 2008, [156766](#)) investigated the effects of dilute DE, or fine and
36 ultrafine CAPs, respectively, on subjects with coronary artery disease and prior MI.
37 Exposure to dilute DE was found to promote exercise-induced ST-segment changes
38 indicating myocardial ischemia, as well as inhibit endogenous fibrinolytic capacity Mills et
39 al. (2007, [091206](#)). The physiological responses observed in Mills et al. provides a measure

1 of coherency with the cardiovascular effects observed in epidemiologic studies, including
2 increases in hospital admissions and ED visits for IHD and stroke associated with exposure
3 to PM. An examination of fine and ultrafine CAPs that were low in combustion derived
4 particles, were not found to exhibit any significant effects on vascular function (Mills et al.,
5 2008, [156766](#)). Routledge et al. (2006, [088674](#)) reported no change in HRV in a group of
6 adults with coronary artery disease following exposure to ultrafine carbon particles, which
7 may be explained in part by the use of medication (beta blockers) among the majority of the
8 subjects.

9 Although the epidemiologic studies did not examine potential effect modification of
10 pre-existing cardiovascular conditions on effects of long-term exposure to PM, a few
11 toxicological studies exposed animals with underlying cardiovascular conditions to PM for
12 months. In studies that focused on the cardiovascular effects following subchronic exposure
13 to PM in ApoE^{-/-} mice, relatively consistent physiological effects were observed across
14 studies. Araujo et al. (Araujo et al., 2008, [156222](#)) exposed mice to ultrafine CAPs and
15 observed enhanced size of early atherosclerotic lesions. Similarly, Chen and Nadziejko
16 (2005, [087219](#)) and Sun et al. (2005, [186814](#); Sun et al., 2008, [157033](#)) exposed mice to
17 PM_{2.5} CAPs with the same results. An additional long-term exposure study observed a
18 decreasing trend in heart rate, physical activity, and temperature along with biphasic
19 responses in HRV (SDNN and rMSSD) upon exposure to CAPs (Chen and Hwang, 2005,
20 [087218](#)).

21 While the majority of the literature examines the potential modification of the
22 association between PM and non-fatal cardiovascular health effects, a few new studies have
23 also examined effect modification in mortality associations. Zeka et al. (2006, [088749](#)) found
24 an increase in risk estimates for associations between PM₁₀ and mortality in individuals
25 with underlying stroke, while Bateson et al. (2004, [086244](#)) found evidence for effect
26 modification of the PM-mortality association in individuals with CHF.

27 Collectively, the evidence from epidemiologic and toxicological, and to a lesser extent,
28 controlled human exposure studies indicates increased susceptibility of individuals with
29 underlying cardiovascular diseases to PM exposure. Although the evidence for some
30 outcomes was inconsistent across epidemiologic and toxicological studies, this could be due
31 to a variety of issues including the PM size fraction used in the study along with the study
32 location. Even with these caveats, a large proportion of the U.S. population has been
33 diagnosed with cardiovascular diseases (i.e., approximately 51.6 million people with
34 hypertension, 24.1 million with heart disease, and 14.1 million with coronary heart disease
35 [see Table 8-3]), and therefore represents a large subpopulation that is potentially more
36 susceptible to PM exposure than the general population.

Table 8-3. Percent of the U.S. population with respiratory diseases, cardiovascular diseases, and diabetes.

Chronic Condition/ Disease	Adults (18+)*		Age				Regional			
	Number (x 10 ⁶)	%	18-44	45-64	65-74	75+	NE	MW	S	W
RESPIRATORY DISEASES										
Asthma*	24.2	11.0	11.5	10.5	11.7	9.3	11.7	11.5	10.5	10.8
Asthma (< 18 yrs)	6.8*	9.3*	---	---	---	---	---	---	---	---
COPD										
Chronic bronchitis	9.5	4.3	2.9	5.5	5.6	6.7	3.8	4.4	4.9	3.5
Emphysema	4.1	1.8	0.3	2.4	5.0	6.4	1.4	2.3	1.9	1.6
CARDIOVASCULAR DISEASES										
All heart disease	24.1	10.9	3.6	12.3	26.1	36.3	10.8	12.7	10.9	9.2
Coronary heart disease	14.1	6.4	0.9	7.2	18.4	25.5	6.4	7.6	6.6	4.7
Hypertension	51.6	23.4	7.7	32.4	52.7	53.5	22.2	23.7	25.3	20.6
Stroke	5.6	2.6	0.5	2.4	7.6	11.2	2.1	2.8	2.9	2.2
Diabetes	17.1	7.8	2.6	10.4	18.2	17.9	7.2	8.1	8.0	7.4

* All data for adults except asthma prevalence data for children under 18 years of age, from CDC (2008, [156324](#); 2008, [156325](#)). For adults prevalence data based off adults responding to "ever told had asthma."
Source: Pleis and Lethbridge-Çejku (2007, [156875](#)); CDC (2008, [156324](#); 2008, [156325](#)).

8.1.6.2. Respiratory Illnesses

1 Investigators have examined the effect of pre-existing respiratory illnesses on
2 multiple health outcomes (e.g., mortality, asthma symptoms, CHF) in response to exposure
3 to ambient levels of PM. Animal models have been developed and/or human clinical studies
4 conducted to examine the possible PM effects on pre-existing respiratory conditions in a
5 controlled setting.

6 Epidemiologic studies have examined the effect of short-term exposure to PM on the respiratory health of
7 asthmatic individuals measuring a variety of respiratory outcomes. Asthmatic individuals were found to
8 have an increase in medication use (Rabinovitch et al., 2006, [088031](#)), respiratory symptoms (i.e., asthma
9 symptoms, cough, shortness of breath, and chest tightness (Gent et al., 2003, [052885](#)), and asthma
10 symptoms (Delfino et al., 2002, [093740](#); 2003, [050460](#)) with short-term exposure to PM_{2.5}; and morning
11 symptoms (Mortimer et al., 2002, [030281](#)) and asthma attacks (Desqueyroux et al., 2002, [026052](#)) with
12 short-term exposure to PM₁₀.

13 Toxicological studies that have used ovalbumin-induced allergic airway disease models provide
14 evidence which supports the findings of the epidemiologic literature. Morishita et al. (2004, [087979](#)) used
15 this model to assess the health effects of PM_{2.5} components. In response to a short-term exposure to CAPs
16 from Detroit, an area with pediatric asthma rates three times the national average, rats with allergic airway
17 disease were found to preferentially retain PM derived from identified local combustion sources in
18 association with eosinophil influx and BALF protein content after an acute exposure (Morishita et al.,
19 2004, [087979](#)). These findings suggest that individuals with allergic airways conditions are more

1 susceptible to allergic airways responses upon exposure to PM_{2.5}, which may be partially attributed to
2 increased pulmonary deposition and localization of particles in the respiratory tract (Morishita et al.,
3 2004, [087979](#)). An additional study (Heidenfelder et al., 2009, [190026](#)) examined whether genes are
4 differentially expressed upon exposure to PM. They found that exposure to CAPs increased the
5 expression of genes associated with inflammation and airway remodeling in rats with allergic airway
6 disease. Although the evidence is much more limited, not all of the toxicological studies evaluated that
7 examined the effect of underlying respiratory conditions on PM-related respiratory morbidity focused on
8 allergic airways disease. Using an animal model of emphysema (i.e., papain-treated mice) Lopes et al.
9 (2009, [190430](#)) found that papain-treated mice exposed to urban ambient PM demonstrated a statistically
10 significant increase in mean linear intercept, a measure of airspace enlargement, compared to saline-
11 treated controls exposed to filtered air. These results provide preliminary evidence, which suggests that
12 non-allergic respiratory morbidities may also increase the susceptibility of an individual to PM-related
13 respiratory effects.

14 The results from the epidemiologic and toxicological studies that focused on underlying allergic
15 airways disease is supported by a series of controlled human exposure studies which have shown that
16 exposure to DEPs increases the allergic inflammatory response in atopic individuals (Bastain et al., 2003,
17 [098690](#); Diaz-Sanchez et al., 1997, [051247](#); Nordenhall et al., 2001, [025185](#)). However, not all controlled
18 human exposure studies have found evidence for differences between the respiratory effects exhibited by
19 healthy and asthmatic individuals. Studies by Gong et al. (2003, [042106](#); 2004, [055628](#); Gong et al.,
20 2008, [156483](#)) reported that healthy and asthmatic subjects exposed to coarse, fine and ultrafine CAPs,
21 exhibited similar respiratory responses. However, it should be noted that these studies excluded moderate
22 and severe asthmatics that would be expected to show increased susceptibility to PM exposure.

23 In addition to examining the association between exposure to PM and respiratory
24 effects in asthmatics, some studies examined whether individuals with COPD represent a
25 potentially susceptible subpopulation. Desqueyroux et al. (2002, [026052](#)) did not observe an
26 increase in the exacerbation¹⁶ of COPD in response to short-term exposure to PM_{2.5}.
27 However, studies that examined the effect of PM on lung function in individuals with COPD
28 (Lagorio et al., 2006, [089800](#); Trenga et al., 2006, [155209](#)) observed declines in FEV₁, and
29 FEV₁ and FVC, respectively in response to PM₁₀ and/or PM_{2.5}. Silkoff et al. (2005, [087471](#))
30 observed associations between PM₁₀ and a reduction in FEV₁ and PM_{2.5} and a reduction in
31 PEF, in those with COPD, but only during one winter of the analysis. Only one controlled
32 human exposure study examined the effects of PM on COPD subjects and found no
33 significant difference in respiratory effects between healthy and individuals with COPD
34 upon exposure to PM_{2.5} CAPs (Gong et al., 2004, [055628](#)). On the other hand the results
35 from dosimetric studies have shown that COPD patients have increased dose rates and
36 impaired mucociliary clearance relative to age matched healthy subjects, suggesting that

¹⁶ Desqueyroux et al. (2002, [026052](#)) defined a COPD exacerbation as (a) decrease in “vesicular” breath sound, (b) bronchial obstruction, (c) tachycardia or arrhythmia, or (d) cyanosis.

1 individuals with COPD are potentially at a greater risk of PM-related health effects
2 (Sections 4.2.4.5 and 4.3.4.3).

3 A few of the epidemiologic studies examined the effect of underlying respiratory
4 illnesses on the association between short- and long-term exposure to PM and mortality.
5 Using different pre-existing respiratory illnesses, Zeka et al. (2006, [088749](#)) and De Leon et
6 al. (2003, [055688](#)) found that short-term exposure to PM₁₀ increased the risk of
7 non-accidental mortality for pneumonia and circulatory mortality for all respiratory
8 illnesses, respectively. Additionally, Zanobetti et al. (2008, [156177](#)) observed an association
9 between long-term exposure to PM₁₀ and mortality in individuals that had previously been
10 hospitalized for COPD. Although these studies do not examine additional size fractions of
11 PM, together they highlight the potential effect of underlying respiratory illnesses on the
12 PM-mortality relationship.

13 Overall, the epidemiologic, controlled human exposure, and toxicological studies
14 evaluated provide biological plausibility for the increased health effects observed in
15 epidemiologic studies among asthmatic individuals in response to PM exposure. Although,
16 the evidence from studies that examined associations between PM and health effects in
17 individuals with COPD is inconsistent, taken together individuals with COPD and asthma
18 represent a large percent of the U.S. population, which may be more susceptible to PM-
19 related health effects (Table 8-3).

8.1.6.3. Respiratory Contributions to Cardiovascular Effects

20 Although the majority of health effects observed in individuals with pre-existing
21 respiratory illnesses were associated with respiratory illness exacerbations, studies also
22 examined whether underlying respiratory illnesses can lead to cardiovascular effects with
23 PM exposure. Controlled human exposure and toxicological studies have also observed some
24 cardiovascular effects in individuals with pre-existing respiratory illnesses. Gong et al.
25 (2003, [042106](#)) observed acute responses in the cardiovascular system and systemic
26 circulation among asthmatic individuals after exposure to PM_{2.5} CAPs. However,
27 respiratory disease has not consistently been observed to affect cardiovascular response in
28 controlled human exposure studies. In a toxicological study, Batalha et al. (2002, [088109](#)),
29 using a chronic bronchitis animal model, found that the pulmonary artery lumen-to-wall
30 ratio was decreased in rats exposed to PM_{2.5} CAPs, although the induced bronchitis didn't
31 seem to affect the response. The majority of epidemiologic studies that examined whether
32 underlying respiratory illnesses contributed to the manifestation of PM-related
33 cardiovascular hospital admission or ED visits, did not report increases in effects for a
34 variety of cardiovascular outcomes (e.g., IHD, arrhythmias, CHF, MI) for individuals with
35 underlying respiratory infection (Wellenius et al., 2006, [088748](#)), pneumonia (Zanobetti and
36 Schwartz, 2005, [088069](#)), or COPD (Peel et al., 2007, [090442](#); Wellenius et al., 2005,
37 [087483](#)). However, Yeatts et al. (2007, [091266](#)), in a panel study, found evidence for

1 cardiovascular effects, specifically reductions in HRV parameters, in asthmatic adults upon
2 short-term exposure to PM_{10-2.5}. It must be noted that most of the aforementioned
3 epidemiologic studies focused on exposure to PM₁₀, and, therefore, it is unclear how these
4 results compare to those found in the controlled human exposure and toxicological studies
5 that focused on exposure to PM_{2.5} (e.g., CAPs). Thus, it is unclear if individuals with
6 underlying respiratory illnesses represent a subpopulation that is potentially susceptible to
7 PM-related cardiovascular effects.

8.1.6.4. Diabetes and Obesity

8 It has been hypothesized that the systemic inflammatory cascade leads to an increase
9 in cardiovascular risk (Dubowsky et al., 2006, [088750](#)). As a result, individuals with
10 conditions linked to chronic inflammation (i.e., diabetes and obesity), have been examined
11 to determine whether diabetes or obesity facilitate the manifestation of PM-mediated
12 health effects, and, therefore, represent a potentially susceptible subpopulation.

13 Epidemiologic studies have examined whether diabetes modifies the association
14 between cardiovascular health effects and PM exposure, but these studies have primarily
15 focused on short-term exposure to PM₁₀. Time-series studies have provided evidence
16 through an examination of hospital admission and ED visits and mortality, which suggests
17 an increase in health effects in diabetic individuals in response to PM exposure. Multicity
18 studies have found upwards of 75% greater risk of hospitalization for cardiac diseases in
19 individuals with diabetes upon exposure to PM₁₀ (Zanobetti and Schwartz, 2002,
20 [034821](#)). Studies conducted in Atlanta, Georgia have also found increased risk for
21 cardiovascular-related ED visits in diabetics, specifically for IHD, arrhythmias, and CHF
22 (Peel et al., 2007, [090442](#)). Additional studies found some evidence that individuals with
23 diabetes are at increased risk of mortality upon exposure to PM₁₀ (Zeka et al., 2006,
24 [088749](#)) and PM_{2.5} (Goldberg et al., 2006, [088641](#)). However, some studies (both multicity
25 and single-city) have not observed a modification of the risk of cardiovascular ED visits and
26 hospital admissions in response to exposure to PM₁₀ in diabetics (Pope et al., 2006, [091246](#);
27 Wellenius et al., 2006, [088748](#); Zanobetti and Schwartz, 2005, [088069](#)).

28 Panel and cohort studies have been conducted to determine the physiological changes
29 that occur in individuals with diabetes in response to PM exposure. These studies examined
30 both changes in inflammatory markers along with specific physiological alterations in the
31 cardiovascular system. Schneider et al. (2008, [191985](#)) in a panel study of 22 individuals
32 with type 2 diabetes mellitus in Chapel Hill, NC found evidence that ambient exposure to
33 PM_{2.5} enhanced the reduction in various markers of endothelial function. Liu et al. (2007,
34 [156705](#)) observed an increase in end-diastolic FMD and end-systolic FMD, and decreases in
35 end-diastolic basal diameter and end-systolic basal diameter in diabetics upon exposure to
36 PM₁₀. The authors also observed positive associations with FMD and blood pressure in
37 diabetic individuals. A controlled human exposure study conducted by Carlsten et al. (2008,

1 [156323](#)) found that DE did not elicit any prothrombotic effects in subjects with metabolic
2 syndrome, which consists of physiological alterations similar to those observed in both
3 diabetic and obese individuals. An examination of biomarkers found mixed results, with
4 Liao et al. (2005, [088677](#)) observing an increase in vWF; Liu et al. (2007, [156705](#)) observing
5 an increase in TBARS, but not CRP or TNF- α ; and Dubowsky et al. (2006, [088750](#))
6 observing an increase in CRP and WBCs. Overall, it is unclear how differences in each of
7 the aforementioned biomarkers contribute to the potential overall cardiovascular effect
8 observed in diabetic individuals; however, an increase in inflammation, oxidative stress,
9 and acute phase response may contribute to cardiovascular effects. A recent toxicological
10 study, also demonstrated the potential for PM-related health effects in diabetics. Sun et al.
11 (2009, [190487](#)) found that PM_{2.5} CAPs exposure for 4 months can exaggerate insulin
12 resistance, visceral adiposity, and inflammation in a diet-induced obesity mouse model.

13 Overall, epidemiologic studies have reported evidence for increased effects in
14 diabetics in response to PM exposure, with preliminary evidence for physiological
15 alterations from toxicological studies. However, the limited evidence from toxicological and
16 controlled human exposure studies along with the lack of studies that examined additional
17 PM size fractions warrants additional research to confirm these associations and to identify
18 the biological pathway(s) that may result in a greater response to PM in diabetics. This
19 potentially susceptible subpopulation is large, with an estimated 17.1 million diabetic
20 individuals in the U.S. (Table 8-3).

21 In addition to diabetes, obesity has been examined as a health condition with the
22 potential to lead to an increase in PM-related health effects. Only a few recent studies have
23 examined the potential effect modification of PM risk estimates by obesity. Schwartz et al.
24 (2005, [086296](#)) reported a change in HRV in obese (i.e., BMI ≥ 30 kg/m²) compared to non-
25 obese subjects, while Dubowsky et al. (2006, [088750](#)) observed an increase in inflammatory
26 markers (i.e., CRP, IL-6, and WBC) in response to short-term exposure to PM_{2.5} among obese
27 individuals. Additionally, Schneider et al. (2008, [191985](#)) found some evidence for a larger
28 reduction in FMD in individuals with a BMI >30 kg/m³ in response to PM_{2.5} exposure.
29 These effects could be due, in part, to a higher PM dose rate in obese individuals, which has
30 been demonstrated in children by Bennett and Zeman (2004, [155686](#)). These investigators
31 also reported that tidal volume and resting minute ventilation increased with body mass
32 index. Although a limited amount of research has been conducted to examine PM-related
33 health effects in obese individuals there is an increasing trend of individuals within the
34 U.S. that have been defined as overweight or obese (BMI ≥ 25.0) (56-65% between NHANES
35 III and NHANES [1999-2002]).

8.1.7. Socioeconomic Status

1 Socioeconomic status (SES) is a composite measure that usually consists of economic
2 status, measured by income; social status measured by education; and work status
3 measured by occupation (Dutton and Levine, 1989, [192052](#)). Based on data from the U.S.
4 Census Bureau in 2006, from among commonly-used indicators of SES, about 12% of
5 individuals and 11% of families are below the poverty line (U.S., 2009, [192147](#)). Although
6 the measure of SES is composed of a multitude of determinants, each of these linked factors
7 can influence an individual's susceptibility to PM-related health effects. Additionally, low
8 SES individuals have been found to have a higher prevalence of pre-existing diseases;
9 inadequate medical treatment; and limited access to fresh foods leading to a reduced intake
10 of antioxidant polyunsaturated fatty acids and vitamins, which can increase this
11 subpopulations susceptibility to PM (Kan et al., 2008, [156621](#)).

12 SES and individual determinants of SES, such as educational attainment, are not
13 mutually exclusive and together can influence the susceptibility of a population. Within the
14 U.S. approximately 16% of the population does not have a high school degree and only 27%
15 have a bachelor's degree or higher level of education (U.S., 2009, [192148](#)). Educational
16 attainment generally coincides with an individual's income level, which is correlated to
17 other surrogates of SES, such as residential environment (Jerrett et al., 2004, [087379](#)). Low
18 SES, and surrogates of SES such as educational attainment, have been shown in some
19 studies to modify health outcomes of PM exposure for a population. Franklin et al. (2008,
20 [155779](#)) noted an increased risk in mortality associated with short-term exposure to PM_{2.5}
21 and its components for individuals with low SES while additional analyses stratified by
22 education level have also observed consistent trends of increased mortality for PM_{2.5} and
23 PM_{2.5} species for individuals with low educational attainment (Ostro et al., 2006, [087991](#);
24 Ostro et al., 2008, [097971](#); Zeka et al., 2006, [088749](#)) This is further supported by a
25 reanalysis of the ACS cohort (Krewski et al., 2009, [191193](#)), which found moderate evidence
26 for increased lung cancer mortality in individuals with a high school education or less
27 compared to individuals with more than a high school education in response to long-term
28 exposure to PM_{2.5}.

29 Epidemiologic studies have also examined additional surrogates of SES, such as
30 residential location and nutritional status to identify their influence on the susceptibility of
31 a subpopulation. Jerrett et al. (2004, [087379](#)) examined the modification of acute mortality
32 effects due to particulate air pollution exposure by residential location in Hamilton, Canada
33 using educational attainment as a surrogate for SES. The authors found that the area of
34 the city with the highest SES characteristics displayed no evidence of effect modification
35 while the area with the lowest SES characteristics had the largest health effects. Likewise,
36 Wilson et al. (2007, [157149](#)) examined the effect of SES on the association between
37 mortality and short-term exposure to PM in Phoenix, but used educational attainment and

1 income to represent SES. When stratifying Phoenix into central, middle, and outer rings of
2 varying urban density central Phoenix, the area with the lowest SES, was found to exhibit
3 the greatest association with PM_{2.5}. However, the association with urban density differed
4 when examining PM_{10-2.5}, with the greatest effect being observed for the middle ring.

5 Yanosky et al. (2008, [192081](#)) examined whether long-term exposure to traffic-related
6 pollutants, using NO₂ as a surrogate, varied by SES at the block group level. The authors
7 found higher levels of NO₂ associated with lower SES areas, which suggests that lower SES
8 individuals are disproportionately exposed to traffic-related pollutants, which includes PM.

9 Nutritional deficiencies have been associated with increased susceptibility to a variety
10 of infectious diseases and chronic health effects. Low SES may decrease access to fresh
11 foods, and thus be related to nutritional deficiencies that could increase susceptibility to
12 PM-related health effects. Baccarelli et al. (2008, [157984](#)) examined the association
13 between exposure to PM_{2.5} and HRV in individuals with polymorphisms in MTHFR and
14 cSHMT genes, which are associated with reduced enzyme activity and increased risk of
15 CVD. The authors found that when individuals with these genetic polymorphisms increased
16 their intake (above median levels) of B6, B12, or methionine no PM_{2.5} effect on HRV was
17 observed.

8.1.8. Summary

18 Upon evaluating the association between short- and long-term exposure to PM and various health
19 outcomes, studies also attempted to identify subpopulations that are more susceptible to PM. These
20 studies did so by: conducting stratified analyses; examining individuals with an underlying health
21 condition; or developing animal models that mimic the physiological conditions associated with an
22 adverse health effect. These studies identified a multitude of factors that could potentially contribute to
23 whether an individual is susceptible to PM (Table 8-2). Although studies have primarily used exposures
24 to PM₁₀ or PM_{2.5}, the available evidence suggests that the identified factors may also enhance
25 susceptibility to coarse fraction particles.

26 The majority of observations made during the evaluation of the literature reviewed in this ISA are
27 consistent with those reported in the 2004 PM AQCD. An evaluation of age-related health effects
28 suggests that older adults have heightened responses for cardiovascular morbidity with PM exposure. In
29 addition, epidemiologic and toxicological studies provide evidence, which indicates that children are at an
30 increased risk of PM-related respiratory effects. It should be noted that the health effects observed in
31 children could be initiated by exposures to PM that occurred during key windows of development, such as
32 in utero. Studies that focus on exposures during development have reported inconsistent findings (see
33 Section 7.4.), but a recent toxicological study suggests that inflammatory responses during pregnancy due
34 to exposure to PM could result in health effects in the developing fetus.

35 Epidemiologic studies have also examined whether additional factors, such as gender, race, or
36 ethnicity modify the association between PM and morbidity and mortality outcomes. Consistent with the

1 findings of the 2004 PM AQCD, gender and race do not seem to modify the association between PM and
2 morbidity and mortality outcomes. However, some evidence, albeit from two studies conducted in
3 California, suggest that Hispanic ethnicity may modify the association between PM and mortality.

4 Recent epidemiologic and toxicological studies provided evidence that individuals with null alleles
5 or polymorphisms in genes that mediate the antioxidant response to oxidative stress (i.e., GSTM1),
6 regulate enzyme activity (i.e., MTHFR and cSHMT), or regulate physiological levels of inflammatory
7 markers (i.e., fibrinogen) are more susceptible to PM exposure. However, some studies have shown that
8 polymorphisms in genes (e.g., HFE) can have a protective effect upon PM exposure. Additionally,
9 preliminary evidence suggests that PM exposure can impart epigenetic effects (i.e., DNA methylation),
10 however, these require further investigation.

11 Collectively, the evidence from epidemiologic and toxicological, and to a lesser extent, controlled
12 human exposure studies indicate increased susceptibility of individuals with underlying cardiovascular
13 diseases and respiratory illnesses, specifically asthma, to PM exposure. Additional controlled human
14 exposure and toxicological studies provide some evidence for increased PM-related cardiovascular effects
15 in individuals with underlying respiratory health conditions. However, the results are not consistent with
16 epidemiologic studies, resulting in the need for further investigation.

17 Recently studies have begun to examine the influence of preexisting chronic inflammatory
18 conditions, such as diabetes and obesity, on PM-related health effects. These studies have found some
19 evidence for increased associations for cardiovascular outcomes along with physiological alterations in
20 markers of inflammation, oxidative stress, and acute phase response. However more research is needed to
21 thoroughly examine the effect of PM exposure on obese individuals and to identify the biological
22 pathway(s) that could lead to increased susceptibility of diabetic and obese individuals to PM.

23 There is also evidence that socioeconomic status (SES), measured using surrogates such as
24 educational attainment or residential location, modifies the association between PM and morbidity and
25 mortality outcomes. In addition, nutritional status, another surrogate of SES, has been shown to have
26 protective effects against PM exposure in individuals that have a higher intake in some vitamins and
27 nutrients.

28 Overall, the epidemiologic, controlled human exposure, and toxicological studies evaluated in this
29 review provide evidence for increased susceptibility for various subpopulations. Although the level of
30 evidence varies depending on the factor being evaluated collectively, it can be concluded that some
31 subpopulations are more susceptible than the general population.

Chapter 8 References

- Aday LA. (2001). *At Risk in America: The Health and Health Care Needs of Vulnerable Populations in the United States*. San Francisco, CA: Jossey-Bass, Inc. [192150](#)
- American Lung Association. (2001). Urban air pollution and health inequities: A workshop report. *Environ Health Perspect*, 3: 357-374. [016626](#)
- Anselme F; Lorient S; Henry J-P; Dionnet F; Napoleoni J-G; Thnillez C; Morin J-P. (2007). Inhalation of diluted diesel engine emission impacts heart rate variability and arrhythmia occurrence in a rat model of chronic ischemic heart failure. *Arch Toxicol*, 81: 299-307. [097084](#)
- Araujo JA; Barajas B; Kleinman M; Wang X; Bennett BJ; Gong KW; Navab M; Harkema J; Sioutas C; Lusk AJ; Nel AE. (2008). Ambient particulate pollutants in the ultrafine range promote early atherosclerosis and systemic oxidative stress. *Circ Res*, 102: 589-596. [156222](#)
- Baccarelli A; Martinelli I; Pegoraro V; Melly S; Grillo P; Zanobetti A; Hou L; Bertazzi PA; Mannucci PM; Schwartz J. (2009). Living near Major Traffic Roads and Risk of Deep Vein Thrombosis. *Circulation*, x: x. [188183](#)
- Baccarelli A; Martinelli I; Zanobetti A; Grillo P; Hou LF; Bertazzi PA; Mannucci PM; Schwartz J. (2008). Exposure to Particulate Air Pollution and Risk of Deep Vein Thrombosis. *Arch Intern Med*, 168: 920-927. [157984](#)
- Barnett AG; Williams GM; Schwartz J; Best TL; Neller AH; Petroeschovsky AL; Simpson RW. (2006). The effects of air pollution on hospitalizations for cardiovascular disease in elderly people in Australian and New Zealand cities. *Environ Health Perspect*, 114: 1018-1023. [089770](#)
- Bartoli CR; Wellenius GA; Coull BA; Akiyama I; Diaz EA; Lawrence J; Okabe K; Verrier RL; Godleski JJ. (2009). Concentrated ambient particles alter myocardial blood flow during acute ischemia in conscious canines. *Environ Health Perspect*, 117: 333-337. [179904](#)
- Bastain TM; Gilliland FD; Li Y-F; Saxon A; Diaz-Sanchez D. (2003). Intraindividual reproducibility of nasal allergic responses to diesel exhaust particles indicates a susceptible phenotype. *Clin Immunol*, 109: 130-136. [098690](#)
- Batalha JR; Saldiva P H; Clarke RW; Coull BA; Stearns RC; Lawrence J; Murthy GG; Koutrakis P; Godleski JJ. (2002). Concentrated ambient air particles induce vasoconstriction of small pulmonary arteries in rats. *Environ Health Perspect*, 110: 1191-1197. [088109](#)
- Bateson TF; Schwartz J. (2004). Who is sensitive to the effects of particulate air pollution on mortality? A case-crossover analysis of effect modifiers. *Epidemiology*, 15: 143-149. [086244](#)
- Bennett WD; Zeman KL. (2004). Effect of body size on breathing pattern and fine-particle deposition in children. *J Appl Physiol*, 97: 821-826. [155686](#)
- Boezen HM; Vonk JM; Van Der Zee SC; Gerritsen J; Hoek G; Brunekreef B; Schouten JP; Postma DS. (2005). Susceptibility to air pollution in elderly males and females. *Eur Respir J*, 25: 1018-1024. [087396](#)
- Campen MJ; Babu NS; Helms GA; Pett S; Wernly J; Mehran R; McDonald JD. (2005). Nonparticulate components of diesel exhaust promote constriction in coronary arteries from ApoE^{-/-} mice. *Toxicol Sci*, 88: 95-102. [083977](#)
- Campen MJ; McDonald JD; Reed MD; Seagrave J. (2006). Fresh gasoline emissions, not paved road dust, alter cardiac repolarization in ApoE^{-/-} mice. *Cardiovasc Toxicol*, 6: 199-210. [096879](#)
- Carlsten C; Kaufman JD; Trenga CA; Allen J; Peretz A; Sullivan JH. (2008). Thrombotic markers in metabolic syndrome subjects exposed to diesel exhaust. *Inhal Toxicol*, 20: 917-921. [156323](#)
- CDC. (2008). Table 3-1: Current Asthma Population Estimates, in thousands by Age, United States: National Health Interview Survey, 2006. Retrieved , from . [156324](#)
- CDC. (2008). Table 4-1: Current Asthma Prevalence Percents by Age, United States: National Health Interview Survey, 2006. Retrieved , from . [156325](#)
- Chahine T; Baccarelli A; Litonjua A; Wright RO; Suh H; Gold DR; Sparrow D; Vokonas P; Schwartz J. (2007). Particulate air pollution, oxidative stress genes, and heart rate variability in an elderly cohort. *Environ Health Perspect*, 115: 1617-1622. [156327](#)

Note: Hyperlinks to the reference citations throughout this document will take you to the NCEA HERO database (Health and Environmental Research Online) at <http://epa.gov/hero>. HERO is a database of scientific literature used by U.S. EPA in the process of developing science assessments such as the Integrated Science Assessments (ISA) and the Integrated Risk Information System (IRIS).

- Chen LC; Hwang JS. (2005). Effects of subchronic exposures to concentrated ambient particles (CAPs) in mice
IV Characterization of acute and chronic effects of ambient air fine particulate matter exposures on
heart-rate variability. *Inhal Toxicol*, 17: 209-216. [087218](#)
- Chen LC; Nadziejko C. (2005). Effects of subchronic exposures to concentrated ambient particles (CAPs) in mice
V CAPs exacerbate aortic plaque development in hyperlipidemic mice. *Inhal Toxicol*, 17: 217-224. [087219](#)
- Chen LH; Knutsen SF; Shavlik D; Beeson WL; Petersen F; Ghamsary M; Abbey D. (2005). The association
between fatal coronary heart disease and ambient particulate air pollution: Are females at greater risk?.
Environ Health Perspect, 113: 1723-1729. [087942](#)
- De Leon SF; Thurston GD; Ito K. (2003). Contribution of respiratory disease to nonrespiratory mortality
associations with air pollution. *Am J Respir Crit Care Med*, 167: 1117-1123. [055688](#)
- Delfino RJ; Gone H; Linn WS; Pellizzari ED; Hu Y. (2003). Asthma symptoms in Hispanic children and daily
ambient exposures to toxic and criteria air pollutants. *Environ Health Perspect*, 111: 647-656. [050460](#)
- Delfino RJ; Zeiger RS; Seltzer JM; Street DH; McLaren CE. (2002). Association of asthma symptoms with peak
particulate air pollution and effect modification by anti-inflammatory medication use. *Environ Health
Perspect*, 110: A607-A617. [093740](#)
- Desqueyroux H; Pujet J-C; Prosper M; Squinazi F; Momas I. (2002). Short-term effects of low-level air pollution
on respiratory health of adults suffering from moderate to severe asthma. *Environ Res*, 89: 29-37. [026052](#)
- Devlin RB; Ghio AJ; Kehrl H; Sanders G; Cascio W. (2003). Elderly humans exposed to concentrated air
pollution particles have decreased heart rate variability. *Eur Respir J*, 40: 76S-80S.. [087348](#)
- Diaz-Sanchez D; Tsien A; Fleming J; Saxon A. (1997). Combined diesel exhaust particulate and ragweed
allergen challenge markedly enhances human in vivo nasal ragweed-specific IgE and skews cytokine
production to a T helper cell 2-type pattern. *J Immunol*, 158: 2406-2413. [051247](#)
- Dubowsky SD; Suh H; Schwartz J; Coull BA; Gold DR. (2006). Diabetes, obesity, and hypertension may enhance
associations between air pollution and markers of systemic inflammation. *Environ Health Perspect*, 114:
992-998. [088750](#)
- Dutton DB; Levine S. (1989). Overview, methodological critique, and reformulation. In JP Bunker; DS Gomby;
BH Kehrer (Ed.), *Pathways to health* (pp. 29-69). Menlo Park, CA: The Henry J. Kaiser Family
Foundation. [192052](#)
- Fedulov AV; Leme A; Yang Z; Dahl M; Lim R; Mariani TJ; Kobzik L. (2008). Pulmonary exposure to particles
during pregnancy causes increased neonatal asthma susceptibility. , 38: 57-67. [097482](#)
- Firestone M; Moya J; Cohen-Hubal E; Zartarian V; Xue J. (2007). Identifying childhood age groups for exposure
assessments and monitoring. *Risk Anal*, 27: 701-714. [192071](#)
- Frampton MW; Stewart JC; Oberdorster G; Morrow PE; Chalupa D; Pietropaoli AP; Frasier LM; Speers DM;
Cox C; Huang LS; Utell MJ. (2006). Inhalation of ultrafine particles alters blood leukocyte expression of
adhesion molecules in humans. *Environ Health Perspect*, 114: 51-58. [088665](#)
- Franklin M; Koutrakis P; Schwartz J. (2008). The role of particle composition on the association between PM2.5
and mortality. *Epidemiology*, 19: 680-689. [155779](#)
- Franklin M; Zeka A; Schwartz J. (2007). Association between PM2.5 and all-cause and specific-cause mortality
in 27 US communities. , 17: 279-87. [188502](#)
- Fung KY; Luginaah I; Gorey KM; Webster G. (2005). Air pollution and daily hospital admissions for
cardiovascular diseases in Windsor, Ontario. *Can J Public Health*, 96: 29-33. [074322](#)
- Fung KY; Luginaah IKMG; Webster G. (2005). Air pollution and daily hospitalization rates for cardiovascular
and respiratory diseases in London, Ontario. *Int J Environ Stud*, 62: 677-685. [093262](#)
- Gent JF; Triche EW; Holford TR; Belanger K; Bracken MB; Beckett WS; Leaderer BP. (2003). Association of
low-level ozone and fine particles with respiratory symptoms in children with asthma. *JAMA*, 290: 1859-
1867. [052885](#)
- Gilliland FD; Li YF; Saxon A; Diaz-Sanchez D. (2004). Effect of glutathione-S-transferase M1 and P1 genotypes
on xenobiotic enhancement of allergic responses: randomised, placebo-controlled crossover study. *Lancet*,
363: 119-125. [156471](#)
- Gilliland FD; McConnell R; Peters J; Gong Jr H. (1999). A Theoretical Basis for Investigating Ambient Air
Pollution and Children's Respiratory Health. *Environ Health Perspect*, 107: 403-407. [155792](#)
- Goldberg MS; Burnett RT; Yale JF; Valois MF; Brook JR. (2006). Associations between ambient air pollution
and daily mortality among persons with diabetes and cardiovascular disease. *Environ Res*, 100: 255-267.
[088641](#)
- Gong H Jr; Linn WS; Terrell SL; Clark KW; Geller MD; Anderson KR; Cascio WE; Sioutas C. (2004). Altered
heart-rate variability in asthmatic and healthy volunteers exposed to concentrated ambient coarse
particles. *Inhal Toxicol*, 16: 335-343. [055628](#)

- Gong H Jr; Linn WS; Clark KW; Anderson KR; Sioutas C; Alexis NE; Cascio WE; Devlin RB. (2008). Exposures of healthy and asthmatic volunteers to concentrated ambient ultrafine particles in Los Angeles. *Inhal Toxicol*, 20: 533-545. [156483](#)
- Gong H Jr; Linn WS; Sioutas C; Terrell SL; Clark KW; Anderson KR; Terrell LL. (2003). Controlled exposures of healthy and asthmatic volunteers to concentrated ambient fine particles in Los Angeles. *Inhal Toxicol*, 15: 305-325. [042106](#)
- Heidenfelder BL; Reif DM; Harkema JR; Cohen Hubal EA; Hudgens EE; Bramble LA; Wagner JG; Morishita M; Keeler GJ; Edwards SW; Gallagher JE. (2009). Comparative microarray analysis and pulmonary changes in brown norway rats exposed to ovalbumin and concentrated air particulates. *Toxicol Sci*, 108: 207-221. [190026](#)
- Host S; Larrieu S; Pascal L; Blanchard M; Declercq C; Fabre P; Jusot JF; Chardon B; Le Tertre A; Wagner V; Prouvost H; Lefranc A. (2007). Short-term Associations between Fine and Coarse Particles and Cardiorespiratory Hospitalizations in Six French Cities. *Occup Environ Med*. [155851](#)
- Jerrett M; Burnett RT; Brook J; Kanaroglou P; Giovis C; Finkelstein N; Hutchison B. (2004). Do socioeconomic characteristics modify the short term association between air pollution and mortality? Evidence from a zonal time series in Hamilton, Canada. *J Epidemiol Community Health*, 58: 31-40. [087379](#)
- Kan H; London SJ; Chen G; Zhang Y; Song G; Zhao N; Jiang L; Chen B. (2008). Season, sex, age, and education as modifiers of the effects of outdoor air pollution on daily mortality in Shanghai, China: The Public Health and Air Pollution in Asia (PAPA) Study. *Environ Health Perspect*. [156621](#)
- Kauffmann F; Post Genome Respiratory Epidemiology Group. (2004). Post-genome respiratory epidemiology: a multidisciplinary challenge. *Eur Respir J*, 24: 471-480. [090968](#)
- Kleeberger SR; Ohtsuka Y. (2005). Gene-particulate matter-health interactions. *Toxicol Appl Pharmacol*, 207: S276-S281. [130489](#)
- Kodavanti UP; Moyer CF; Ledbetter AD; Schladweiler MC; Costa DL; Hauser R; Christiani DC; Nyska A. (2003). Inhaled environmental combustion particles cause myocardial injury in the Wistar Kyoto rat. *Toxicol Sci*, 71: 237-245. [051325](#)
- Krewski D; Jerrett M; Burnett RT; Ma R; Hughes E; Shi Y; Turner MC; Pope AC III; Thurston G; Calle EE; Thun MJ. (2009). Extended follow-up and spatial analysis of the American Cancer Society study linking particulate air pollution and mortality. *Health Effects Institute*. Cambridge, MA. 140. [191193](#)
- Lagorio S; Forastiere F; Pistelli R; Iavarone I; Michelozzi P; Fano V; Marconi A; Ziemacki G; Ostro BD. (2006). Air pollution and lung function among susceptible adult subjects: a panel study. , 5: 11. [089800](#)
- Larrieu S; Jusot J-F; Blanchard M; Prouvost H; Declercq C; Fabre P; Pascal L; Le Tertre A; Wagner V; Riviere S; Chardon B; Borelli D; Cassadou S; Eilstein D; Lefranc A. (2007). Short term effects of air pollution on hospitalizations for cardiovascular diseases in eight French cities: The PSAS program. *Sci Total Environ*, 387: 105-112. [093031](#)
- Le Tertre A; Medina S; Samoli E; Forsberg B; Michelozzi P; Boumghar A; Vonk JM; Bellini A; Atkinson R; Ayres JG; Sunyer J; Schwartz J; Katsouyanni K. (2002). Short term effects of particulate air pollution on cardiovascular diseases in eight European cities. *J Epidemiol Community Health*, 56: 773-779. [023746](#)
- Lee IM; Tsai SS; Ho CK; Chiu HF; Wu TN; Yang CY. (2008). Air pollution and hospital admissions for congestive heart failure: are there potentially sensitive groups?. *Environ Res*, 108: 348-353. [192076](#)
- Liao D; Heiss G; Chinchilli VM; Duan Y; Folsom AR; Lin HM; Salomaa V. (2005). Association of criteria pollutants with plasma hemostatic/inflammatory markers: a population-based study. *J Expo Sci Environ Epidemiol*, 15: 319-328. [088677](#)
- Liu L; Ruddy TD; Dalipaj M; Szyszkowicz M; You H; Poon R; Wheeler A; Dales R. (2007). Influence of personal exposure to particulate air pollution on cardiovascular physiology and biomarkers of inflammation and oxidative stress in subjects with diabetes. *J Occup Environ Med*, 49: 258-265. [156705](#)
- Lopes FD; Pinto TS; Arantes-Costa FM; Moriya HT; Biselli PJ; Ferraz LF; Lichtenfels AJ; Saldiva PH; Mauad T; Martins MA. (2009). Exposure to ambient levels of particles emitted by traffic worsens emphysema in mice. *Environ Res*, 109: 544-551. [190430](#)
- Luginaah IN; Fung KY; Gorey KM; Webster G; Wills C. (2005). Association of ambient air pollution with respiratory hospitalization in a government designated "area of concern": the case of Windsor, Ontario. *Environ Health Perspect*, 113: 290-296. [057327](#)
- Mar TF; Larson TV; Stier RA; Claiborn C; Koenig JQ. (2004). An analysis of the association between respiratory symptoms in subjects with asthma and daily air pollution in Spokane, Washington. *Inhal Toxicol*, 16: 809-815. [057309](#)
- Mauad T; Rivero DH; de Oliveira RC; Lichtenfels AJ; Guimaraes ET; de Andre PA; Kasahara DI; Bueno HM; Saldiva PH. (2008). Chronic exposure to ambient levels of urban particles affects mouse lung development. *Am J Respir Crit Care Med*, 178: 721-728. [156743](#)

- Merriam-Webster. (2009). Merriam-Webster on-line: <http://www.merriam-webster.com/medical/susceptible>, <http://merriam-webster.com/medical/vulnerable>. Retrieved 15-JUN-09, from <http://www.merriam-webster.com/medical/>. [192146](#)
- Metzger KB; Tolbert PE; Klein M; Peel JL; Flanders WD; Todd KH; Mulholland JA; Ryan PB; Frumkin H. (2004). Ambient air pollution and cardiovascular emergency department visits. *Epidemiology*, 15: 46-56. [044222](#)
- Middleton N; Yiallourous P; Kleanthous S; Kolokotroni O; Schwartz J; Dockery DW; Demokritou P; Koutrakis P. (2008). A 10-year time-series analysis of respiratory and cardiovascular morbidity in Nicosia, Cyprus: the effect of short-term changes in air pollution and dust storms. , 7: 39. [156760](#)
- Mills NL; Robinson SD; Fokkens PH; Leseman DL; Miller MR; Anderson D; Freney EJ; Heal MR; Donovan RJ; Blomberg A; Sandstrom T; MacNee W; Boon NA; Donaldson K; Newby DE; Cassee FR. (2008). Exposure to concentrated ambient particles does not affect vascular function in patients with coronary heart disease. *Environ Health Perspect*, 116: 709-715. [156766](#)
- Mills NL; Törnqvist H; Gonzalez MC; Vink E; Robinson SD; Soderberg S; Boon NA; Donaldson K; Sandstrom T; Blomberg A; Newby DE. (2007). Ischemic and thrombotic effects of dilute diesel-exhaust inhalation in men with coronary heart disease. , 357: 1075-1082. [091206](#)
- Morishita M; Keeler G; Wagner J; Marsik F; Timm E; Dvonch J; Harkema J. (2004). Pulmonary retention of particulate matter is associated with airway inflammation in allergic rats exposed to air pollution in urban Detroit. *Inhal Toxicol*, 16: 663-674. [087979](#)
- Mortimer KM; Neas LM; Dockery DW; Redline S; Tager IB. (2002). The effect of air pollution on inner-city children with asthma. *Eur Respir J*, 19: 699-705. [030281](#)
- Nadziejko C; Fang K; Narciso S; Zhong M; Su WC; Gordon T; Nadas A; Chen LC. (2004). Effect of particulate and gaseous pollutants on spontaneous arrhythmias in aged rats. *Inhal Toxicol*, 16: 373-380. [055632](#)
- Naess O; Nafstad P; Aamodt G; Claussen B; Rosland P. (2007). Relation between concentration of air pollution and cause-specific mortality: four-year exposures to nitrogen dioxide and particulate matter pollutants in 470 neighborhoods in Oslo, Norway. *Am J Epidemiol*, 165: 435-443. [090736](#)
- Nordenhall C; Pourazar J; Ledin M-C; Levin J-O; Sandstrom T; Adelroth E. (2001). Diesel exhaust enhances airway responsiveness in asthmatic subjects. *Eur Respir J*, 17: 909-915. [025185](#)
- NRC. (2004). Research priorities for airborne particulate matter: IV Continuing research progress. National Academies Press . Washington, DC. [156814](#)
- Ohtsuka Y; Brunson KJ; Jedlicka AE; Mitzner W; Clarke RW; Zhang L-Y; Eleff SM; Kleeberger SR. (2000). Genetic linkage analysis of susceptibility to particle exposure in mice. *Am J Respir Cell Mol Biol*, 22: 574-581. [004409](#)
- Ostro B; Broadwin R; Green S; Feng W-Y; Lipsett M. (2006). Fine particulate air pollution and mortality in nine California counties: results from CALFINE. *Environ Health Perspect*, 114: 29-33. [087991](#)
- Ostro BD; Feng WY; Broadwin R; Malig BJ; Green RS; Lipsett MJ. (2008). The impact of components of fine particulate matter on cardiovascular mortality in susceptible subpopulations. *Occup Environ Med*, 65: 750-756. [097971](#)
- Park SK, O'Neill MS, Wright RO, Hu H, Vokonas PS, Sparrow D, Suh H, Schwartz J. (2006). HFE Genotype, Particulate Air Pollution, and Heart Rate Variability: A Gene-Environment Interaction. *Circulation*, 114: 2798-2805. [189099](#)
- Park SK; O'Neill MS; Vokonas PS; Sparrow D; Schwartz J. (2005). Effects of air pollution on heart rate variability: The VA normative aging study. *Environ Health Perspect*, 113: 304-309. [057331](#)
- Peel JL; Metzger KB; Klein M; Flanders WD; Mulholland JA; Tolbert PE. (2007). Ambient air pollution and cardiovascular emergency department visits in potentially sensitive groups. *Am J Epidemiol*, 165: 625-633. [090442](#)
- Peel JL; Tolbert PE; Klein M; Metzger KB; Flanders WD; Knox T; Mulholland JA; Ryan PB; Frumkin H. (2005). Ambient air pollution and respiratory emergency department visits. *Epidemiology*, 16: 164-174. [056305](#)
- Peters A; Greven S; Heid I; Baldari F; Breitner S; Bellander T; Chrysohoou C; Illig T; Jacquemin B; Koenig W. (2009). Fibrinogen Genes Modify the Fibrinogen Response to Ambient Particulate Matter. *Am J Respir Crit Care Med*, 179: 484-491. [191992](#)
- Pinkerton KE; Zhou Y; Teague SV; Peake JL; Walther RC; Kennedy IM; Leppert VJ; Aust AE. (2004). Reduced lung cell proliferation following short-term exposure to ultrafine soot and iron particles in neonatal rats: key to impaired lung growth?. *Inhal Toxicol*, 1: 73-81. [087465](#)
- Pinkerton KE; Zhou Y; Zhong C; Smith KR; Teague SV; Kennedy IM; Ménache MG. (2008). Mechanisms of particulate matter toxicity in neonatal and young adult rat lungs. Health Effects Institute. Boston, MA. 135. [190471](#)
- Pleis JR; Lethbridge-Cejku M. (2007). Summary health statistics for US adults: National Health Interview Survey, 2006. CDC. Maryland. [156875](#)

- Pope C; Renlund D; Kfoury A; May H; Horne B. (2008). Relation of heart failure hospitalization to exposure to fine particulate air pollution. , 102: 1230-1234. [191969](#)
- Pope CA, 3rd, Muhlestein JB, May HT, Renlund DG, Anderson JL, Horne BD. (2006). Ischemic heart disease events triggered by short-term exposure to fine particulate air pollution. , 114: 2443-8. [189048](#)
- Pope CA; Dockery DW. (2006). Health effects of fine particulate air pollution: Lines that connect. J Air Waste Manag Assoc, 56: 709-742. [156881](#)
- Pope CA III; Muhlestein JB; May HT; Renlund DG; Anderson JL; Horne BD. (2006). Ischemic heart disease events triggered by short-term exposure to fine particulate air pollution. Circulation, 114: 2443-2448. [091246](#)
- Rabinovitch N; Strand M; Gelfand EW. (2006). Particulate levels are associated with early asthma worsening in children with persistent disease. Am J Respir Crit Care Med, 173: 1098-1105. [088031](#)
- Routledge HC; Manney S; Harrison RM; Ayres JG; Townend JN. (2006). Effect of inhaled sulphur dioxide and carbon particles on heart rate variability and markers of inflammation and coagulation in human subjects. Heart, 92: 220-227. [088674](#)
- Samoli E; Peng R; Ramsay T; Pipikou M; Touloumi G; Dominici F; Burnett R; Cohen A; Krewski D; Samet J. (2008). Acute effects of ambient particulate matter on mortality in Europe and North America: results from the APHENA study. Environ Health Perspect, 116: 1480. [188455](#)
- Schneider A; Neas L; Herbst M; Case M; Williams R; Cascio W; Hinderliter A; Holguin F; Buse J; Dungan K. (2008). Endothelial dysfunction: associations with exposure to ambient fine particles in diabetic individuals. Environ Health Perspect, 116: 1666. [191985](#)
- Schwartz J; Park SK; O'Neill MS; Vokonas PS; Sparrow D; Weiss S; Kelsey K. (2005). Glutathione-S-transferase M1, obesity, statins, and autonomic effects of particles: gene-by-drug-by-environment interaction. Am J Respir Crit Care Med, 172: 1529-1533. [086296](#)
- Silkoff PE; Zhang L; Dutton S; Langmack EL; Vedal S; Murphy J; Make B. (2005). Winter air pollution and disease parameters in advanced chronic obstructive pulmonary disease panels residing in Denver, Colorado. J Allergy Clin Immunol, 115: 337-344. [087471](#)
- Suh YJ; Ha EH; Park H; Kim YJ; Kim H; Hong YC. (2008). GSTM1 polymorphism along with PM10 exposure contributes to the risk of preterm delivery. , 656: 62-67. [192077](#)
- Sun Q; Wang A; Jin X; Natanzon A; Duquaine D; Brook RD; Aguinaldo J-GS; Fayad ZA; Fuster V; Lippmann M; Chen Lung C; Rajagopalan S. (2005). Long-term air pollution exposure and acceleration of atherosclerosis and vascular inflammation in an animal model. , 294: 3003-3010. [186814](#)
- Sun Q; Yue P; Deiuliis JA; Lumeng CN; Kampfrath T; Mikolaj MB; Cai Y; Ostrowski MC; Lu B; Parthasarathy S; Brook RD; Moffatt-Bruce SD; Chen LC; Rajagopalan S. (2009). Ambient air pollution exaggerates adipose inflammation and insulin resistance in a mouse model of diet-induced obesity. Circulation, 119: 538-546. [190487](#)
- Sun Q; Yue P; Kirk RI; Wang A; Moatti D; Jin X; Lu B; Schechter AD; Lippmann M; Gordon T; Chen LC; Rajagopalan S. (2008). Ambient air particulate matter exposure and tissue factor expression in atherosclerosis. Inhal Toxicol, 20: 127-137. [157033](#)
- Tankersley CG, Bierman A, Rabold R. (2007). Variation in heart rate regulation and the effects of particle exposure in inbred mice. Inhal Toxicol, 19: 621-9. [188859](#)
- Tankersley CG; Bierman A; Rabold R. (2007). Variation in heart rate regulation and the effects of particle exposure in inbred mice. , 19: 621-9. [097910](#)
- Tankersley CG; Campen M; Bierman A; Flanders SE; Broman KW; Rabold R. (2004). Particle effects on heart-rate regulation in senescent mice. Inhal Toxicol, 16: 381-390. [094378](#)
- Tankersley CG; Champion HC; Takimoto E; Gabrielson K; Bedja D; Misra V; El-Haddad H; Rabold R; Mitzner W. (2008). Exposure to inhaled particulate matter impairs cardiac function in senescent mice. Am J Physiol Regul Integr Comp Physiol, 295: R252-263. [157043](#)
- Tarantini L; Bonzini M; Apostoli P; Pegoraro V; Bollati V; Marinelli B; Cantone L; Rizzo G; Hou L; Schwartz J; Bertazzi PA; Baccarelli A. (2009). Effects of particulate matter on genomic DNA methylation content and iNOS promoter methylation. Environ Health Perspect, 117: 217-222. [192010](#)
- Trenga CA; Sullivan JH; Schildcrout JS; Shepherd KP; Shapiro GG; Liu LJ; Kaufman JD; Koenig JQ. (2006). Effect of particulate air pollution on lung function in adult and pediatric subjects in a Seattle panel study. , 129: 1614-22. [155209](#)
- U.S. Census. (2009). Educational Attainment in the United States: 2007 (<http://www.census.gov/prod/2009pubs/p20-560.pdf>). U.S. Census Bureau, Economics and Statistics Administration, U.S. Department of Commerce, Washington, DC. P20-560. <http://www.census.gov/prod/2009pubs/p20-560.pdf>. [192148](#)
- U.S. Census. (2009). U.S. Census (2000) Poverty. Retrieved 01-JUL-09, from <http://www.census.gov/hhes/www/poverty/hispov/hstpov2.html>. [192147](#)

- U.S. EPA. (2003). Framework for cumulative risk assessment. National Center for Environmental Assessment, Office of Research and Development, U.S. Environmental Protection Agency. Washington, DC. EPA/630/P-02/001F. [192145](#)
- U.S. EPA. (2009). Susceptible subpopulations. Retrieved 15-MAY-09, from <http://www.epa.gov/nerl/goals/health/populations.html>. [192149](#)
- U.S. Census Bureau PIO. (2000). Census Bureau projects doubling of nation's population by 2100. Retrieved , from . [157064](#)
- U.S. EPA. (2004). Air quality criteria for particulate matter. U.S. Environmental Protection Agency. Research Triangle Park, NC. EPA/600/P-99/002aF-bF. [056905](#)
- U.S. EPA. (2006). Aging and Toxic Response: Issues Relevant to Risk Assessment (Final). U.S. Environmental Protection Agency. Washington, DC. <http://cfpub.epa.gov/ncea/cfm/recorddisplay.cfm?deid=156648>. [192082](#)
- U.S. EPA. (2008). Integrated review plan for the national ambient air quality standards for particulate matter. U.S. Environmental Protection Agency, Office of Research and Development, National Center for Environmental Assessment. Research Triangle Park, NC. [157072](#)
- U.S. EPA. (2008). Integrated Science Assessment for Sulfur Oxides?Health Criteria. U.S. Environmental Protection Agency. Research Triangle Park, NC. [157075](#)
- Villeneuve PJ; Goldberg MS; Krewski D; Burnett RT; Chen Y. (2002). Fine particulate air pollution and all-cause mortality within the Harvard six-cities study: variations in risk by period of exposure. *Ann Epidemiol*, 12: 568-576. [042576](#)
- Wellenius GA; Bateson TF; Mittleman MA; Schwartz J. (2005). Particulate air pollution and the rate of hospitalization for congestive heart failure among medicare beneficiaries in Pittsburgh, Pennsylvania. *Am J Epidemiol*, 161: 1030-1036. [087483](#)
- Wellenius GA; Coull BA; Batalha JRF; Diaz EA; Lawrence J; Godleski JJ. (2006). Effects of ambient particles and carbon monoxide on supraventricular arrhythmias in a rat model of myocardial infarction. *Inhal Toxicol*, 18: 1077-1082. [156152](#)
- Wellenius GA; Coull BA; Godleski JJ; Koutrakis P; Okabe K; Savage ST. (2003). Inhalation of concentrated ambient air particles exacerbates myocardial ischemia in conscious dogs. *Environ Health Perspect*, 111: 402-408. [055691](#)
- Wellenius GA; Schwartz J; Mittleman MA. (2006). Particulate air pollution and hospital admissions for congestive heart failure in seven United States cities. *Am J Cardiol*, 97: 404-408. [088748](#)
- Wilson WE; Mar TF; Koenig JQ. (2007). Influence of exposure error and effect modification by socioeconomic status on the association of acute cardiovascular mortality with particulate matter in Phoenix. *J Expo Sci Environ Epidemiol*, 17: S11-S19. [157149](#)
- Yanosky JD; Schwartz J; Suh HH. (2008). Associations between measures of socioeconomic position and chronic nitrogen dioxide exposure in Worcester, Massachusetts. , 71: 1593-1602. [192081](#)
- Yauk C; Polyzos A; Rowan-Carroll A; Somers CM; Godschalk RW; Van Schooten FJ; Berndt ML; Pogribny IP; Koturbash I; Williams A; Douglas GR; Kovalchuk O. (2008). Germ-line mutations, DNA damage, and global hypermethylation in mice exposed to particulate air pollution in an urban/industrial location. , 105: 605-610. [157164](#)
- Yeatts K; Svendsen E; Creason J; Alexis N; Herbst M; Scott J; Kupper L; Williams R; Neas L; Cascio W; Devlin RB; Peden DB. (2007). Coarse particulate matter (PM_{2.5-10}) affects heart rate variability, blood lipids, and circulating eosinophils in adults with asthma. *Environ Health Perspect*, 115: 709-714. [091266](#)
- Yunginger JW; Reed CE; O'Connell EJ; Melton LJ 3rd; O'Fallon WM; Silverstein MD. (1992). A community-based study of the epidemiology of asthma. Incidence rates, 1964-1983. , 146: 888-894. [192074](#)
- Zanobetti A; Bind MAC; Schwartz J. (2008). Particulate air pollution and survival in a COPD cohort. *Environ Health Perspect*, 7: 48. [156177](#)
- Zanobetti A; Schwartz J. (2002). Cardiovascular damage by airborne particles: are diabetics more susceptible?. *Epidemiology*, 13: 588-592. [034821](#)
- Zanobetti A; Schwartz J. (2005). The effect of particulate air pollution on emergency admissions for myocardial infarction: A multicity case-crossover analysis. *Environ Health Perspect*, 113: 978-982. [088069](#)
- Zeger S; Dominici F; McDermott A; Samet J. (2008). Mortality in the Medicare population and chronic exposure to fine particulate air pollution in urban centers (2000-2005). *Environ Health Perspect*, 116: 1614-1619. [191951](#)
- Zeka A; Zanobetti A; Schwartz J. (2006). Individual-level modifiers of the effects of particulate matter on daily mortality. *Am J Epidemiol*, 163: 849-859. [088749](#)

Chapter 9. Welfare Effects

9.1. Introduction

This chapter is a synthesis and evaluation of the most policy-relevant science used to help form the scientific foundation for review of the secondary (welfare-based) NAAQS aimed at protecting against welfare effects of ambient airborne PM. Specifically, Chapter 9 assesses the effects of atmospheric PM on the environment, including: (a) effects on visibility; (b) effects on climate; (c) ecological effects; and (d) effects on materials. These sections initially highlight the conclusions from the 2004 PM AQCD (U.S. EPA, 2004, [056905](#)), followed by an evaluation of recent publications and assessment of the expanded body of evidence. In some sections, few new publications are available, and the discussion is primarily a brief overview of the key conclusions from the previous review.

As discussed in Chapter 1, the effects of particulate NO_x and SO_x have recently been evaluated in the *ISA for Oxides of Nitrogen and Sulfur – Ecological Criteria* (U.S. EPA, 2008, [157074](#)). That ISA focused on the effects from deposition of gas- and particle-phase pollutants related to ambient NO_x and SO_x concentrations that can lead to acidification and nutrient enrichment, as well as on the potential for increased mercury methylation from SO₄²⁻ deposition. Thus, emphasis in this document is placed on the effects of airborne PM on visibility and climate, and on the deposition effects of PM constituents other than NO_x and SO_x, primarily metals and carbonaceous compounds.

Chapter 2 of this assessment provides an integrative overview of the major welfare effects evaluated. EPA's framework for causality, described in Chapter 1, is applied throughout the evaluation and the causal determinations are highlighted.

Note: Hyperlinks to the reference citations throughout this document will take you to the NCEA HERO database (Health and Environmental Research Online) at <http://epa.gov/hero>. HERO is a database of scientific literature used by U.S. EPA in the process of developing science assessments such as the Integrated Science Assessments (ISA) and the Integrated Risk Information System (IRIS).

9.2. Effects on Visibility

9.2.1. Introduction

In recent years, most visibility research involved characterizing visibility conditions and trends over broad regional scales, improving the understanding of the atmospheric processes and pollutants responsible for the regional impacts, and attribution of visibility-impairing pollutants to emission sources, source types, and regions. The motivation for much of this work has come from the visibility protection provisions of the 1977 Clean Air Act Amendments (CAAA) that called for the development of regulations to address reduction of regional haze in 156 national parks and wilderness areas to natural conditions, and from the subsequent RHR (RHR) promulgated in 1999 by EPA in response to the CAA mandate. Implementation of the RHR entails planned emissions reductions to reach natural haze conditions in these protected areas by 2064 in six ten-yr planning steps.

Haze conditions caused solely by PM from natural sources are generally much lower than contemporary conditions. The largest difference is between natural and current conditions for the inorganic salts ammonium sulfate and ammonium nitrate, with natural concentrations taken to be just a few tenths of a $\mu\text{g}/\text{m}^3$ each (Trijonis et al., 1990, [157058](#)), while current conditions of both over large regions of the country are an order of magnitude or more larger (DeBell, 2006, [156388](#)). However, natural source PM can be substantial on an episodic basis for crustal mineral PM components during high windblown dust conditions and for carbonaceous PM from biogenic combustion during wildfire and prescribed burning episodes. The need for information to generate RHR implementation plans has resulted in extensive use of continental-scale air quality simulation modeling and assessment of expanded ambient monitoring data sets.

Unlike the substantial remote-area visibility investigations that have been conducted in response to the RHR, relatively little work on urban visibility effects has been done in recent years. For example, there has been relatively little new research on the optical and human perceptual aspects of atmospheric visibility over the last decade or more. These topics have been the subjects of numerous earlier investigations that have been summarized in detail elsewhere (U.S. EPA, 1979, [157065](#); Latimer and Ireson, 1980, [035723](#); Middleton, 1952, [016324](#); Tombach and McDonald, 2004, [157054](#); Trijonis et al.,

1990, [157058](#); Watson et al., 2002, [035623](#)), including past criteria documents on PM, SO₂ and NO_x (U.S. EPA, 1982, [017610](#); U.S. EPA, 1993, [017649](#); U.S. EPA, 2004, [056905](#)).

In spite of this fact, the understanding of urban visibility conditions has continued to improve. By applying a well established algorithm that relates PM and haze conditions to data currently collected from routine filter-based PM chemical speciation monitors located in numerous urban areas (Jayanty, 2003, [156605](#)), and to data collected from the more recently deployed high time- and size-resolved PM speciation monitors located in several cities such as those in the PM Supersites program (Solomon and Hopke, 2008, [156997](#)) urban visibility conditions can be better characterized. Comparisons between urban and remote area data in the same region afford the opportunity to differentiate between regional and local visibility impacts. The availability of better size and time resolution PM composition data, compared to that available from the routine monitoring programs, reduces the number of simplifying assumptions required to estimate visibility conditions in these areas, thereby reducing the uncertainty of the estimates. Thus, the state of the science supporting urban visibility assessments continues to improve.

The background section below contains an overview of long-available information to help provide context to the more recently published literature summarized in subsequent sections.

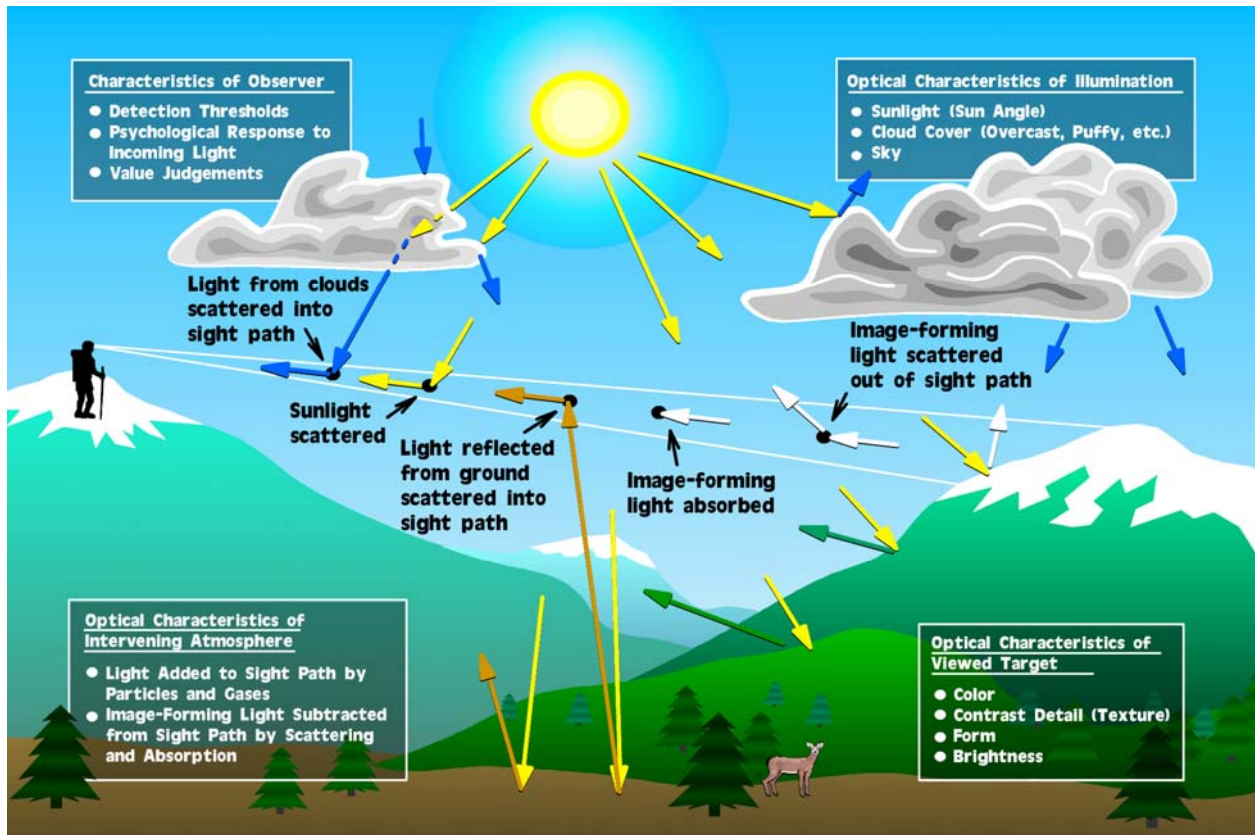
9.2.2. Background

Air pollution-induced visibility impairment is caused by the loss of image-forming light (i.e., signal) and the addition of non-image forming light (i.e., noise) between an observer and the object being viewed. These changes to the light reaching the observer are a result of light being scattered and absorbed by particles and gases in the sight path (see the schematic in Figure 9-1). Electromagnetic theory developed to characterize the interaction of light with matter (Mie, 1908, [155983](#)) permits the calculation of light scattering and absorption by particles and gas molecules where the index of refraction and shape of particles by size are known (Van de Hulst, 1981, [191972](#)).

The ability of human observers to visually detect distant objects or identify changes in their appearance depends on the apparent contrast of the object against its background. The apparent contrast is affected by changes in the transparency of the atmosphere caused by air pollution as well as factors not related to air quality such as length of the sight path, scenic lighting and the physical characteristics of the viewed object and other elements of

the scene. To rigorously determine the perceived visual effects of changes in the optical properties of the atmosphere requires the use of radiative transfer modeling to determine changes in light from the field of view experienced by the observer, followed by the use of psychophysical modeling to determine the response to the light by the eye-brain system. The complexity of such an approach discourages its common use.

Atmospheric light extinction is a fundamental atmospheric optics metric used to characterize air pollution impacts on visibility. It is the fractional loss of intensity in a light beam per unit distance due to scattering and absorption by the gases and particles in the air. Light extinction (b_{ext}) can be expressed as the sum of light scattering by particles ($b_{s,p}$), scattering by gases ($b_{s,g}$), absorption by particles ($b_{a,p}$) and absorption by gases ($b_{a,g}$). Light extinction and its components are expressed in units of inverse length, typically either inverse kilometers (km^{-1}) or, as will be the convention in this document, inverse megameters (Mm^{-1}). Traditionally, for visibility-protection applications, the most sensitive portion of the spectrum for human vision (550 nm) has been used to characterize light extinction and its components.



Source: Malm (1999, [025037](#)).

Figure 9-1. Important factors involved in seeing a scenic vista are outlined. Image-forming information from an object is reduced (scattered and absorbed) as it passes through the atmosphere to the human observer. Air light is also added to the sight path by scattering processes. Sunlight, light from clouds, and ground-reflected light all impinge on and scatter from particulates located in the sight path. Some of this scattered light remains in the sight path, and at times it can become so bright that the image essentially disappears. A final important factor in seeing and appreciating a scenic vista are the characteristics of the human observer.

A parametric analysis has shown that a constant fractional change in light extinction results in a similar perceptual change regardless of baseline conditions (Pitchford et al., 1990, [156871](#)). From this assessment, the deciview haze index, which is a log transformation of light extinction, similar in many ways to the decibel index for acoustic measurements, was developed (Pitchford and Malm, 1994, [044922](#)). A one deciview (1dv) change is about a 10% change in light extinction, which is a small change that is detectable for sensitive viewing situations. The haze index in deciview units is an appropriate metric for expressing the extent of haze changes where the perceptibility of the change is an issue. The RHR has adopted the deciview haze index as the metric for tracking long-term haze

trends of visibility-protected federal lands (EPA, 2001, [157068](#)). Light extinction and its components are more useful metrics for characterizing the apportionment of haze to its pollutant components due to the approximately linear relationship between pollutant species concentrations and their contributions to light extinction.

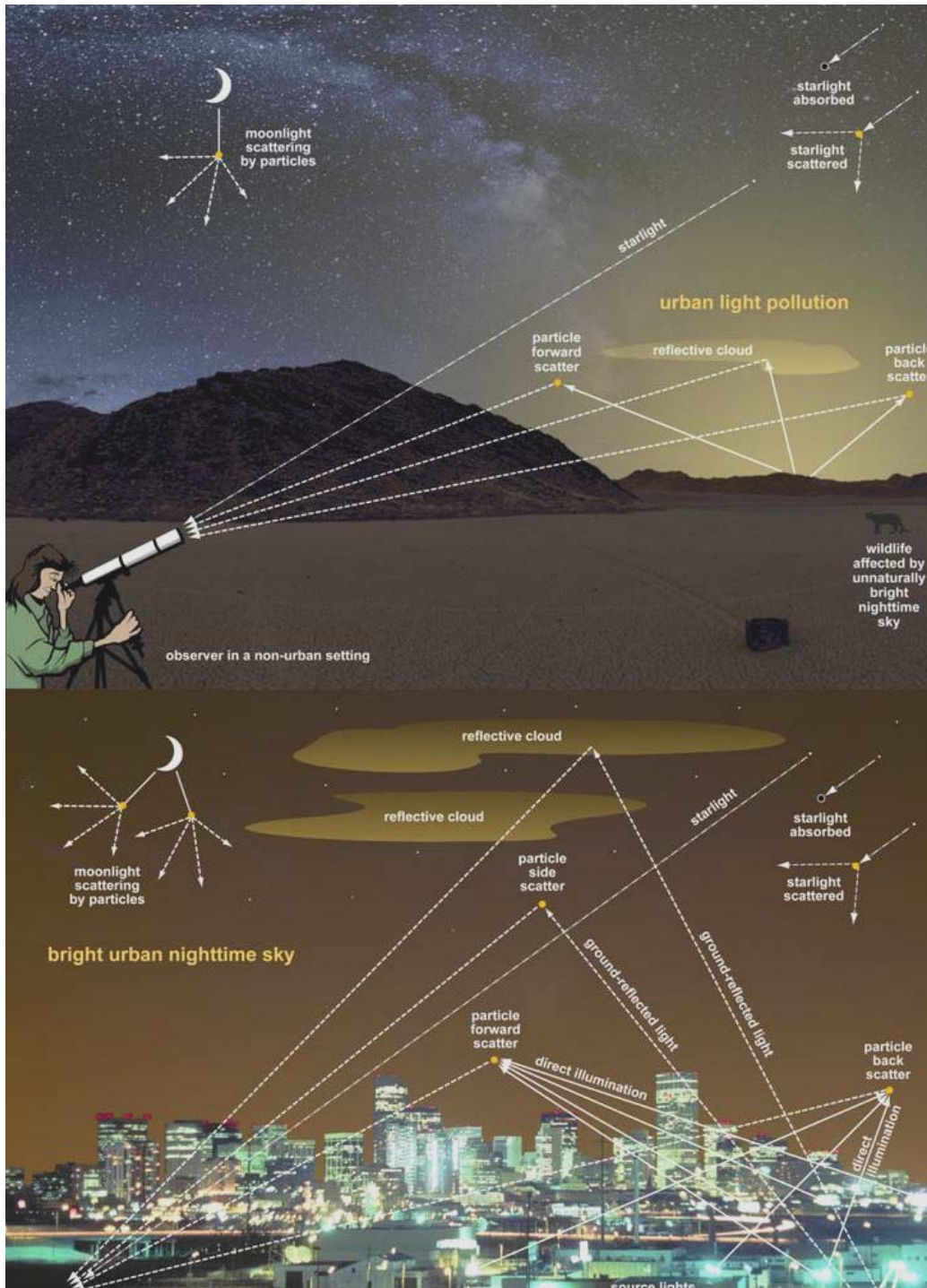


Figure 9-2. Schematic of remote-area (top) and urban (bottom) nighttime sky visibility showing the effects of PM and light pollution.

Daytime visibility has dominated the attention of those who have studied the visibility effects of air pollution, though nighttime visibility is also known to be affected by air pollution. Stargazing is a popular human activity in urban and remote settings. The

reduction in visibility of the night sky is primarily dependent on the addition of light into the sight path, the brightness of the night sky, and the reduction in contrast of stars against the background (see the schematic in Figure 9-2). These are controlled by the addition of PM, which enhances scattering, and the addition of anthropogenic sources of light. Scattering of anthropogenic light contributes to the “skyglow” within and over populated areas, adding to the total sky brightness. The visual result is a reduction of the number of visible stars and the disappearance of diffuse or subtle phenomena such as the Milky Way. The extinction of starlight is a secondary and minor effect also caused by increased scattering and absorption. Anthropogenic light sources include artificial outdoor lighting, which varies dramatically across space. Natural sources include the Moon, planets, and stars that have a predictable rhythm across time.

The nighttime visual environment has some important differences to note. Light sources and ambient conditions are typically five to seven orders of magnitude dimmer at night than in sunlight. Moonlight, like sunlight, introduces light throughout an observer’s sight path at a constant angle. On the other hand, dim starlight emanates from all over the celestial hemisphere while artificial lights are concentrated in cities and illuminate the atmosphere from below. Sight paths are often inclined upward at night as targets may be nearby terrain features or celestial phenomena. Extinction behaves the same at night as during the day, lowering the contrast of scenes through scattering and absorption; nevertheless the different light sources will yield variable changes in visibility as compared to what has been established for the daytime scenario. Little research has been conducted on nighttime visibility. Even if the air quality-visibility interactions are shown to be similar between day and night settings, the human psychophysical response at night is expected to differ. Though recent advances in the ability to instrument and quantify nighttime scenes (Duriscoe et al., 2007, [156411](#)) have been made and can be utilized to evaluate nocturnal visibility, the state of the science is not yet comparable to that associated with daytime visibility impairment. The remainder of this document focuses exclusively on daytime visibility.

9.2.2.1. Non-PM Visibility Effects

Light extinction due to the gaseous components of the atmosphere is relatively well understood and well estimated for any atmospheric conditions. Absorption of visible light by gases in the atmosphere is primarily by NO₂, and can be directly and accurately estimated

from NO₂ concentrations by multiplying by the absorption efficiency. Scattering by gases is described by the Rayleigh scattering theory. Rayleigh scattering occurs in a pollution-free atmosphere as a result of light scattering by the gas molecules that compose the atmosphere (i.e., N₂, O₂, CO₂, etc.) and depends only on the density of the atmosphere, with highest values at sea level (~12 Mm⁻¹) and diminishing with elevation (8 Mm⁻¹ at ~4 km), and varies somewhat at any elevation due to atmospheric temperature and pressure variations. Rayleigh scattering can be accurately determined for any elevation and meteorological conditions.

NO₂ absorbs more light in the short wavelength blue portion of the spectrum than at longer wavelengths. For this reason a plume or layer of NO₂ removes more of the blue light from the scene viewed through the layer giving a yellow or brown appearance to the layer or plume. This filtering of blue light by NO₂ can deepen the brown appearance of hazes over urban areas, although it is not the sole cause of such discoloration (EPA, 1993, [017649](#)). The photopic-weighted absorption efficiency at the 550 nm wavelength is incorporated into the revised version of the algorithm for estimating light extinction from aerosol data that is used for implementing the RHR (Pitchford et al., 2007, [098066](#)). However, NO₂ is not routinely measured at any of the monitoring sites representing visibility protected areas where its impacts are assumed to be inconsequential compared to those of PM. At background concentrations NO₂ absorption is generally less than five percent of the light scattering by clean air (Rayleigh scattering), making it unperceivable. Plume visibility models are available to assess both achromatic and discoloration associated with NO₂ light absorption, for point source emissions (Latimer and Ireson, 1980, [035723](#); Seigneur et al., 1984, [156965](#)).

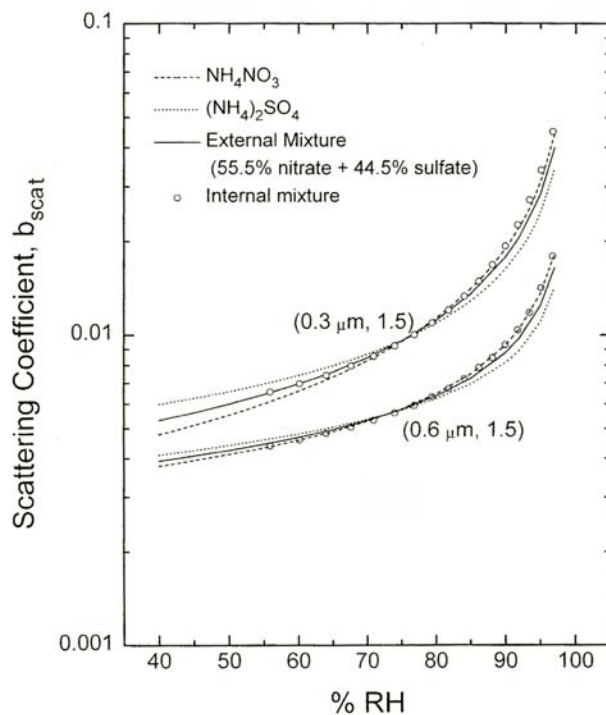
9.2.2.2. PM Visibility Effects

Particle light extinction is more complex than that caused by gaseous components. PM is responsible for most visibility impairment except under near-pristine conditions, where Rayleigh scattering is the largest contributor to light extinction or in plumes of combustion sources that are well-controlled for particulate emissions (e.g., coal-fired power plants with bag houses), where light absorption by NO₂ may dominate the light extinction.

Light-absorbing carbon (e.g., DE soot and smoke) and some crustal minerals are the only commonly occurring airborne particle components that absorb light. All particles scatter light, and generally particle light scattering is the largest of the four light extinction

components. While a larger particle scatters more light than a similar shaped smaller particle of the same composition, the light scattered per unit of mass concentration (i.e., mass scattering efficiency in units of $Mm^{-1}/[\mu\text{g}/\text{m}^3]$ which reduces to m^2/g) is greatest for particles with diameters from ~ 0.3 - $1.0 \mu\text{m}$. If the index of refraction, particle shape and concentration as a function of particle size are well characterized, Mie theory can be used to accurately calculate the light scattering and absorption by those particles. However, it is rare that these particle properties are known, so assumptions are used in place of missing information to develop a simplified calculation scheme that provides an estimate of the particle light extinction from available data sets.

Particles composed of water soluble inorganic salts (i.e., ammoniated sulfate, ammonium nitrate, sodium chloride, etc.) are hygroscopic in that they absorb water as a function of relative humidity to form a liquid solution droplet. Aside from the chemical consequences of this water growth, the droplets become larger when relative humidity increases, resulting in increased light scattering. Hence, the same PM dry concentration produces more haze. Figure 9-3 shows the effect of water growth as a function of relative humidity on light scattering for two size distributions of ammonium nitrate and ammonium sulfate particles as well as for internal and external mixtures (i.e., mixed within the same particle and in separate particles, respectively) of the two components. This figure illustrates a number of important points. The water growth effect is substantial with an increase in light scattering by about a factor of ten between 40% and 97% relative humidity for the same dry particle concentrations. The amount of scattering is significantly dependent on the dry particle size distribution. However the growth curves for ammonium sulfate, ammonium nitrate and mixtures of the two particle components are similar at any of the dry particle size distributions. Water growth curves are also available for sodium chloride, the major component in sea salt, which is an important PM component at coastal locations.



Source: Tang (1996, [157042](#)).

Figure 9-3. Effect of relative humidity on light scattering by mixtures of ammonium nitrate and ammonium sulfate.

Using Mie theory, the scattering and absorption of any wavelength of light by a particle of known size and index of refraction (a function of the wavelength of light) can be calculated (Van de Hulst, 1981, [191972](#)). Particle density is used to convert the particle light extinction to its mass extinction efficiency (i.e., the ratio of particle light extinction to its mass). To expand the calculations from one particle at a time to the multitude of particles in ambient aerosol, information about the aerosol size and composition distributions are needed. Aerosol mixture refers to how the major components that make up the particles are mixed. Methods have been developed to treat simple mixture models ranging from external mixtures where the various components are assumed to be in separate particles, to multi-component mixtures where individual particles contain several components (Ouimette and Flagan, 1982, [025047](#)). The latter includes internally mixed particles where two or more components are mixed within the particles, and layered aerosol with a core of one component covered by a shell of another component.

The Mie theory solution for an external mixture can be simplified to a linear relationship where the light extinction is the sum of the mass concentration of each species

multiplied by its specific mass extinction efficiency (Ouimette and Flagan, 1982, [025047](#)). This formulation promotes the concept of apportioning the light extinction among the various PM species. For internally mixed aerosol, the light extinction response to adding or removing mass of any component to the aerosol is dependent on how such changes would affect the particle size, density and index of refraction distribution of the aerosol. However, a number of investigators have shown that the differences among the calculated light extinction values using external and various internal mixture assumptions are generally less than about 10% (Lowenthal et al., 1995, [045134](#); Ramsey, 1966, [013946](#); Sloane, 1983, [025039](#); Sloane, 1984, [025040](#); Sloane, 1986, [045954](#); Sloane and Wolff, 1985, [045953](#); Wolff, 1985, [044680](#)). This provides a basis to accept the apportionment of light extinction to the PM components calculated using an external mixture assumption as a meaningful surrogate for their contributions.

Ambient aerosols are usually a complex and unknown combination of both internal and external mixtures of the particle components. Despite these complexities, PM light scattering can be accurately calculated for any relative humidity if the chemical composition as a function of dry particle size is known (Hand et al., 2002, [190367](#); Malm and Pitchford, 1997, [002519](#)). However, most routinely available ambient monitoring programs do not include data with sufficient detail to make such calculations. The IMPROVE network with its greater than 150 remote area monitoring sites (DeBell, 2006, [156388](#)) and the CSN (Jayanty, 2003, [156605](#)) with its greater than 150 urban area monitoring sites collect 24-h duration fine particle samples ($PM_{2.5}$) that are analyzed for the major PM components including SO_4^{2-} , nitrate, and carbonaceous particulate. CSN also analyzes for ammonium ion, but does not monitor coarse mass ($PM_{10-2.5}$), while IMPROVE measures coarse mass but does not analyze for ammonium ion. Neither data set has sufficient size resolution to make Mie theory calculations of light extinction, nor does either program routinely monitor NO_2 concentrations, which would be required to calculate its contribution to light extinction by absorption.

A simple algorithm similar in form to the linear equation that results from Mie theory applied with an external mixture assumption is frequently used to estimate light extinction from the concentrations of the major components. The concentration of each of the major aerosol components is multiplied by a dry extinction efficiency value and for the hygroscopic components (e.g., ammoniated sulfate and ammonium nitrate) an additional multiplicative term to account for the water growth to estimate that components contribution to light

extinction. Both the dry extinction efficiency and water growth terms are developed by some combination of empirical assessment and theoretical calculation using typical particle size distributions associated with each of the major aerosol components, and they are evaluated by comparing the algorithm estimates of light extinction with coincident optical measurements. Summing the contribution of each component gives the estimate of total light extinction. The most commonly used of these is referred to as the IMPROVE algorithm because it was developed specifically to use the IMPROVE aerosol monitoring data and was evaluated using IMPROVE optical measurements at the subset of sites that make those measurements (Malm et al., 1994, [044920](#)). The formula for the traditional IMPROVE algorithm is shown below.

$$\begin{aligned}
 b_{ext} \approx & 3 \times f(RH) \times [Sulfate] \\
 & + 3 \times f(RH) \times [Nitrate] \\
 & + 4 \times [Organic\ Mass] \\
 & + 10 \times [Elemental\ Carbon] \\
 & + 1 \times [Fine\ Soil] \\
 & + 0.6 \times [Coarse\ Mass] \\
 & + 10
 \end{aligned}$$

Equation 9-1

Light extinction (b_{ext}) is in units of Mm^{-1} , the mass concentrations of the components indicated in brackets are in $\mu g/m^3$, and $f(RH)$ is the unitless water growth term that depends on relative humidity. The dry extinction efficiency for particulate organic mass is larger than those for particulate SO_4^{2-} and nitrate principally because the density of the dry inorganic compounds are higher than that assumed for the PM organic mass components. Since IMPROVE does not include ammonium ion monitoring, the assumption is made that all SO_4^{2-} is fully neutralized ammonium sulfate and all nitrate is assumed to be ammonium nitrate. Though often reasonable, neither assumption is always true (see Section 9.2.3.1). In the eastern U.S. during the summer there is insufficient ammonia in the atmosphere to neutralize the SO_4^{2-} fully. Fine particle nitrates can include sodium or calcium nitrate, which are the fine particle fraction of generally much coarser particles due to nitric acid interactions with sea salt at near-coastal areas (sodium nitrate) or nitric acid interactions with calcium carbonate in crustal aerosol (calcium nitrate). Despite the simplicity of the algorithm, it performs reasonably well and permits the contributions to light extinction

from each of the major components (including the water associated with the SO_4^{2-} and nitrate compounds) to be separately approximated.

The $f(RH)$ terms inflate the particulate SO_4^{2-} and nitrate light scattering for high relative humidity conditions. For relative humidity below 40% the $f(RH)$ value is 1, but it increases to 2 at ~66%, 3 at ~83%, 4 at ~90%, 5 at ~93% and 6 at ~95% relative humidity. The result is that both particulate SO_4^{2-} and nitrate are more efficient per unit mass than any other aerosol component for relative humidity above ~85% where its total light extinction efficiency exceeds the $10\text{m}^2/\text{g}$ associated with EC. Based on this algorithm, particulate SO_4^{2-} and nitrate are estimated to have comparable light extinction efficiencies (i.e., the same dry extinction efficiency and $f(RH)$ water growth terms), so on a per unit mass concentration basis at any specific relative humidity they are treated as equally effective contributors to visibility effects. The strong relationship demonstrated between dry light scattering and fine PM mass concentration or ambient light extinction and fine PM mass concentration under low relative humidity conditions noted by a number of investigators (Charlson et al., 1968, [095355](#); Chow et al., 2002, [037784](#); Chow et al., 2002, [036166](#); McMurry, 2000, [081517](#); Samuels et al., 1973, [070601](#); Waggoner and Weiss, 1980, [070152](#); Waggoner et al., 1981, [095453](#)) is reasonable based on this algorithm when the PM fractional composition is either relatively constant or varies most among PM components with similar dry extinction efficiency values (e.g., SO_4^{2-} , nitrate and organic mass efficiencies).

9.2.2.3. Direct Optical Measurements

Light extinction and its components (i.e., scattering and absorption by particles and gases) can be determined directly by optical measurements using commercially available instruments (Trijonis et al., 1990, [157058](#)). Though these measurements are all wavelength dependent, the convention for visibility monitoring purposes is to make measurement at or near 550nm , which is the wavelength of maximum eye response. Direct PM light extinction, scattering and absorption measurements offer a number of advantages compared to estimates using an algorithm applied to PM speciation data. The direct optical measurements are considered more accurate because they do not depend on the assumed particle characteristics (e.g., size, shape, density, component mixture, etc.) thought to be associated with the major PM species. Also the optical measurements are made with high time resolution (e.g., minutes to hourly) compared with the filter composition based

estimates that are typically 24-h duration, allowing the former to better characterize sub-daily temporal patterns which can help in identifying influential source categories and characterize atmospheric phenomenon. The higher time resolution attainable with direct light extinction measurements are also more commensurate than the 24-h light extinction estimates from PM samples with the short exposure time associated with perceived visibility effects.

Path-averaged light extinction can be determined by long-path transmissometers that monitors the intensity of light that has traversed a known distance from a known initial intensity light source. Transmission (i.e., the ratio of the final to the initial light intensity) is the natural logarithm of the product of the path-averaged light extinction and the distance the light has traversed. Transmissometer path-length establishes the useful range of light extinction over which the measurements can be accurately measured, with path-lengths of 10km or more required for pristine conditions and less than 1km more appropriate for hazier situations or to measure the visibility impacts associated with fogs or precipitation events. The NP Service operated long-path transmissometers at up to 25 locations from 1986 through 2004 (DeBell, 2006, [156388](#)), but have more recently discontinued their use at all but one remote area location due to the cost of maintenance and the difficulties of performing calibration. Transmissometers are currently in routine service at five urban areas.

A number of instruments measure the light scattered by particles and gases from a source of known intensity. These include forward scattering, back scattering, polar, and integrating nephelometers. Of these the integrating nephelometers with its high sensitivity and sample control options has been more widely used for air quality-related visibility and PM monitoring purposes, while the robust design of the open air forward scattering instruments have seen extensive use by the National Weather Service (NWS) Automated Surface Observing System (ASOS) for characterizing visibility principally for transportation safety purposes (NOAA, 1998). The potential utility of the ASOS visibility network at about 900 locations for air quality monitoring has been established, but the lack of resolution in the reported data is a serious impediment to this use of the data (Richards et al., 1996, [190476](#)).

Integrating nephelometers draw air into a sample chamber, making it possible to modify the sample either by changing its humidity or controlling the particle size range that is measured. This feature makes it possible to use sample-controlled nephelometers to

investigate the effects of ambient PM size and water growth characteristic on light scattering (Covert et al., 1972, [072055](#); Rood et al., 1987, [046397](#); Malm and Day, 2001, [190431](#)). For instance the coarse particle contribution to light scattering can be estimated using a nephelometer that alternately samples through a 2.5 μm size selective inlet and a 10 μm size selective inlet. For routine monitoring, integrating nephelometers are typically either used to measure the PM component of light scattering when operated at ambient relative humidity or to measure dry PM light scattering as a high-time resolution surrogate for PM mass concentration when operated with a heater or other sample air drier. Integrating nephelometers operated at ambient conditions by the IMPROVE program have replaced the long-path transmissometer as the principal optical measurement at about 30 locations (DeBell, 2006, [156388](#)).

PM light absorption can also be inferred from measured changes in the light transmitted through a filter used to sample the PM compared to an identical clean filter (Bond et al., 1999, [156281](#)). Such measurements can be made subsequent to sampling (Campbell et al., 1995, [190171](#)) or continuously during sampling by using specifically designed sampler (Hansen et al., 1982, [190368](#); Hansen et al., 1984, [002396](#)). All of the filter-based methods require adjustments to the optical measurements to account for filter and sampled particle light scattering effects associated with particles concentrated on and within the matrix of the filters (Bond et al., 1999, [156281](#)). Often PM light absorption measurements are used to infer BC concentration by assuming it is the dominant PM contributor to light absorption with a near constant absorption efficiency (Allen et al., 1999, [048923](#); Babich et al., 2000, [156239](#)). In fact commercially available aethalometers incorporate an absorption efficiency value so they can directly report BC concentrations. Like nephelometers, commercially available aethalometers can be obtained with either single or multiple-wavelength measurement capabilities, where the multi-wavelength data can be used to better characterize the PM. More recently these have been used to distinguish BC that absorbs light strongly over the full visible light spectrum (e.g., DE) from brown carbon that absorbs appreciably more at shorter wavelengths than at long wavelengths (e.g., WS) (Andreae and Gelencsér, 2006, [156215](#)).

Other approaches to measure light absorption include a photoacoustic instrument that measures the heating associated with absorbed light by suspended PM (Arnott et al., 1999, [020650](#); Moosmüller et al., 1998, [192073](#)), as well as by the difference between light extinction and light scattering measurements (Bond et al., 1999, [156281](#)).

9.2.2.4. Value of Good Visual Air Quality

The term visual air quality (VAQ) is used here to refer to the visibility effects caused solely by air quality conditions. For example, it excludes the reduced visibility caused by fog. Two broadly different approaches have traditionally been used to define and quantify the value of good VAQ. One approach assesses the monetary value associated with visibility changes; the other assesses the psychological value of visual air quality. With respect to the latter, reduced VAQ is considered an environmental stressor (Campbell, 1983, [190172](#)) that is associated with heightened amounts of anxiety, tension, anger, fatigue, depression, and feelings of helplessness (Evans et al., 1987, [190347](#); Zeidner and Shechter, 1988, [191973](#)). Though the relationship between impaired VAQ and mental health is poorly understood, there are greater emergency calls associated with psychiatric disturbances during periods with reduced VAQ (Rotton and Frey, 1982, [190477](#)). Studies have shown that reduced VAQ affects people's behavior, including reductions in outdoor activities, and increased hostility and aggressive behavior (Evans et al., 1982, [190521](#); Cunningham, 1979, [191974](#); Jones and Bogat, 1978, [190396](#); Rotton et al., 1979, [190478](#)).

The value of VAQ (both monetary and non-monetary) has been investigated in two broadly different settings, non-recreational or urban settings and recreational settings, such as the national parks and wilderness areas where visibility is protected by the RHR (Trijonis et al., 1990, [157058](#)). In urban settings, public surveys have shown that greater than 80% of the participants are aware of poor VAQ conditions (Cohen et al., 1986, [190182](#)), though attitudes towards poor VAQ have been shown to vary by socio-economic status, health, and length of residence in the urban setting (Barker, 1976, [072137](#)). The economic importance of urban visibility has been examined by a number of studies designed to quantify the benefits (or willingness to pay) associated with potential improvements in urban visibility. Urban visibility valuation research prior to 1997 was summarized in Chestnut and Dennis (1997, [014525](#)), and was also described in the 2004 Air Quality for PM (EPA, 2004, [056905](#)) and the 2005 OAQPS PM NAAQS Staff Paper (U.S. EPA, 2005, [090209](#)). These reviews summarize 34 estimates (based on different cities or model specifications) from six different studies. Since the mid 1990s, however, only one new valuation study of urban visibility has been published (Beron et al., 2001, [156270](#)) which is summarized below (Section 9.1.4.6).

In recreational settings, experience based demand models have been developed using on-site and mail-in surveys to judge the relative importance to national park visitors of

various park attributes including good VAQ, to assess visitor awareness of VAQ conditions, and to explore possible relationships between VAQ and visitor satisfaction (Ross et al., 1987, [037420](#); Ross et al., 1985, [044287](#)). At the three western and two eastern national parks where this survey was conducted, visitors rated the attribute identified as “clean, clear air” among the most important features of the parks. A random sample of 1800 visitors at one of the parks (Grand Canyon) showed that visitor awareness of VAQ impacts increased as measured visibility conditions decreased, and that overall park enjoyment and satisfaction decreased with reduced VAQ. Grand Canyon visitors when asked to indicate how they would budget their time (e.g., between visiting an archaeological site or a view lookout point) indicated that they would be willing to significantly alter their behavior to experience views under improved VAQ (Malm et al., 1984, [044292](#)).

9.2.3. Monitoring and Assessment

Monitoring and the assessment of monitoring data serve a number of goals with regard to the visibility effects of PM, including improving the understanding of the physio/chemical/optical properties of the aerosol, characterizing spatial and temporal air quality patterns, and assessing the causes (i.e., pollution sources and atmospheric processes) that are responsible for visibility impairment. Information generated by special studies employing sophisticated instrumentation are typically needed to advance the understanding of aerosol properties, while characterizing trends is the product of analyzing routine monitoring data, whereas assessing the causes of haze usually involves a weight-of-evidence approach applied to special study and/or routine monitoring data sets plus the use of air quality simulation modeling. This section summarizes recently available information that is based on monitoring data.

9.2.3.1. Aerosol Properties

Particle size is the most influential physical property of aerosols with respect to their dry light extinction efficiency. Chemical composition by size is used to ascertain density (needed to convert aerodynamic to physical size and to determine particle mass as a function of size) and to identify the water growth characteristics of the aerosol (needed to calculate the particle size, density and index of refraction at ambient RH). To characterize aerosol properties of interest for visibility effects, field monitoring programs typically include particle size distribution monitoring, high size resolution particle sampling with

subsequent compositional analysis, and optical monitoring. These generate data that permit optical closure assessments where the light scattering and/or light extinction estimates from the aerosol data are compared to corresponding optical data. Since component contributions to visibility are generally assessed by applying the IMPROVE or some similar algorithm to measured or modeled aerosol concentration data, this section will include recent investigations that evaluate or address various assumptions inherent in the use of these simple algorithms.

One component of the Big Bend Regional Aerosol and Visibility Observational (BRAVO) Study, conducted at Big Bend NP, TX in the summer and fall of 1999, entailed use of detailed measurements of aerosol chemical composition, size distribution, water growth, and optical properties to characterize the aerosol and assess the relationship between aerosol physical, chemical and optical properties (Malm et al., 2003, [190434](#); Schichtel et al., 2004, [179902](#)). Fine ammoniated sulfate during the BRAVO Study was about half the fine particle mass concentration and was shown to be responsible for about 35% of the light extinction. Rayleigh scattering was the second largest contributor at about 25%, followed by coarse particle (about 18%), and organic compounds (about 13%). There was little fine particle nitrate (less than 5% of the mass concentration) and most of it is apparently in the form of sodium nitrate and two thirds of it was found in the coarse mode where it comprises about 8% of the coarse particle mass concentration. Both the composition of the nitrate and the fact of much of it being in the coarse size mode ($2.5 \mu\text{m} > D > 10 \mu\text{m}$) are inconsistent with the implied assumptions of the IMPROVE algorithm.

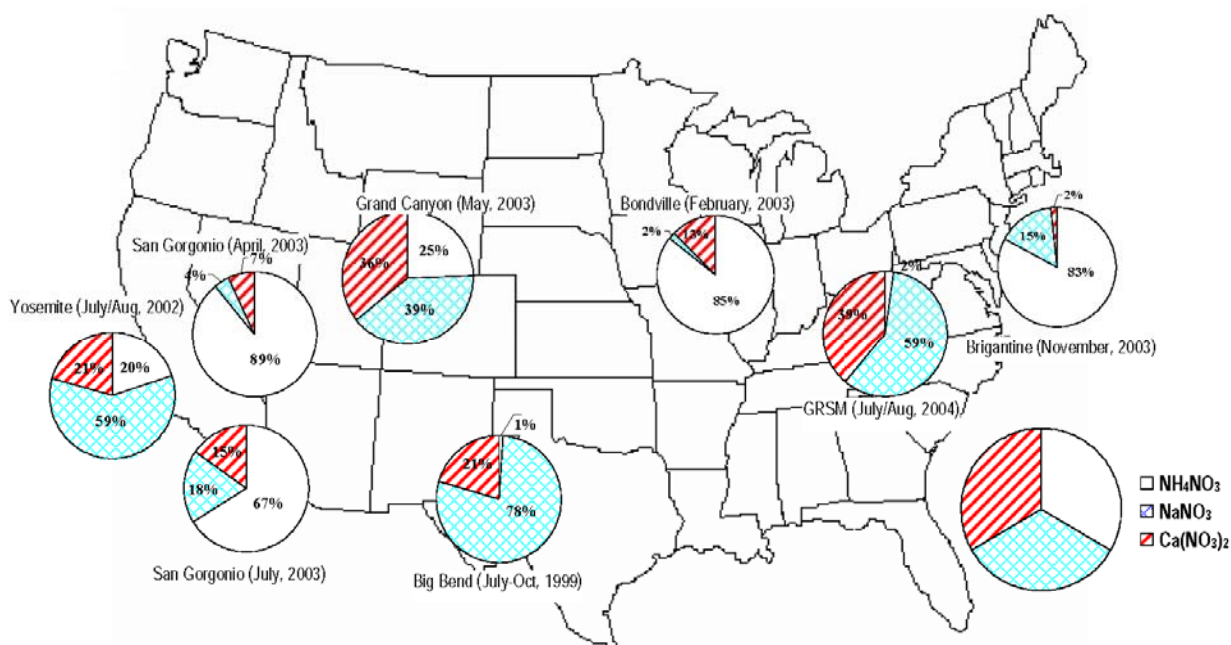
A year-long special study of coarse particle speciation was conducted at nine IMPROVE remote area monitoring sites during 2003 to 2004 to provide additional information about the geographic and seasonal variations in coarse particle composition (Malm et al., 2007, [156730](#)). The same sampling and analytical methodologies procedures were used for the PM_{10} samples as are routinely used on the IMPROVE $\text{PM}_{2.5}$ samples. The IMPROVE coarse particle speciation study did not include ammonium analysis, so SO_4^{2-} and nitrate ions were assumed to be ammonium sulfate and ammonium nitrate. As expected crustal minerals were the largest contributors to coarse mass overall (about 60%), though at Mt. Rainier the fraction of coarse PM that was organic exceeded the crustal mineral by nearly two to one (i.e., 59.2% compared to 33.5%) On average across sites the organic particulate contributed significantly at about one quarter of the coarse mass, while ammonium nitrate was the third largest contributor to coarse mass (about 8%). Seas salt

was negligible overall, but high at the one coastal site (i.e., 12% at Brigantine, NJ). The two California sites, San Geronio and Sequoia, had the highest coarse nitrate concentrations, 0.74 $\mu\text{g}/\text{m}^3$ and 0.69 $\mu\text{g}/\text{m}^3$, and high fine nitrates concentrations on average, 2.66 $\mu\text{g}/\text{m}^3$ and 2.14 $\mu\text{g}/\text{m}^3$, respectively. Brigantine, a coastal site in New Jersey, had the highest fraction of total nitrate in the coarse size range (36%). The authors speculate that Brigantine's particulate nitrate is likely sodium nitrate, the result of nitric acid reactions with sodium chloride. The nine-site average fraction of total nitrate in the coarse size range is 26%. By contrast, coarse SO_4^{2-} concentrations are small with only about ~1% of the total SO_4^{2-} in the coarse fraction.

Routine IMPROVE monitoring data include the mass concentration, but not the composition of the coarse PM fraction, so the algorithm used to estimate light extinction does not include any provision for varied coarse PM composition as shown in this study. This study shows that about 10% of the coarse mass across the nine monitoring sites is composed of hygroscopic materials (i.e., ammonium sulfate, ammonium nitrate and sea salt), which during high humidity conditions will scatter more light than estimated by the current algorithm (e.g., ~20% bias at ~90% relative humidity). However, at coastal sites such as the Brigantine, NJ, IMPROVE site where the combined concentration of the inorganic salts (i.e., sea salt, nitrate and SO_4^{2-}) constitute a significant fraction (~24% on average) of the coarse mass concentration, the IMPROVE algorithm underestimation of light extinction by coarse PM can be significant for high relative humidity conditions (~60% at ~90% relative humidity). The resulting underestimation of total light extinction is typically much smaller since fine particle light extinction generally exceeds that contributed by coarse particles. Another issue with regard to estimating light extinction from coarse PM concentration when the composition is not crustal minerals, as has been assumed, has to do with the lower average density of the coarse mode particles that results in greater particle numbers and/or larger particles and therefore a greater light extinction efficiency (Malm and Hand, 2007, [155962](#)).

Special studies with more complete, higher time resolution and size resolved particulate inorganic ion species chemistry and precursor gases were conducted at seven of the nine sites with IMPROVE coarse particle speciation monitoring (Lee et al., 2008, [156686](#)). This work confirmed the presence of sodium and calcium nitrate (referred to as mineral nitrate) primarily in the coarse particle size range in addition to fine particle ammonium nitrate where low temperatures, high humidity and excess ammonium (beyond

that required to neutralize the particulate SO_4^{2-}) favored particle phase equilibrium. Figure 9-4 is a map showing the locations and sample times and estimated composition of the total particulate nitrate for the seven locations for this special study. Sites with a high fraction of ammonium nitrate (e.g., San Gorgonio, Bondville, and Brigantine) have the highest nitrate contributions to total mass concentration and haze, whereas sites with high mineral nitrates tend to have low total nitrate contributions. This work shows that the common assumption that particulate nitrate is in the fine particle size range and consists principally of ammonium nitrate is not necessarily true.



Source: Lee et al. (2008, [156686](#))

Figure 9-4. Estimated fractions of total particulate nitrate during each field campaign comprised of ammonium nitrate, reacted sea salt nitrate (shown as NaNO_3), and reacted soil dust nitrate (shown as $\text{Ca}(\text{NO}_3)_2$).

Extinction efficiencies for individual particle species can be theoretically calculated from sized-resolved aerosol measurements and can be inferred using multiple linear regression applied to aerosol composition and light extinction measurement data. In a recent publication, Hand and Malm (2007, [155825](#)) reviewed the literature since 1990 in which aerosol mass scattering efficiency values were calculated or inferred. From these they have compiled normalized dry scattering efficiency values for the individual species.

Based on 93 separate determinations including marine, remote continental and urban areas data sets, the average dry mass scattering efficiency for ammonium sulfate is $2.5 \pm 0.6 \text{ m}^2/\text{g}$. Average values tended to be somewhat lower for the marine aerosol ($\sim 2 \text{ m}^2/\text{g}$) than for remote continental ($\sim 2.7 \text{ m}^2/\text{g}$) and urban ($2.6 \text{ m}^2/\text{g}$) areas, and values also tended to be lower for fairly clean arid locations compared with more humid polluted areas.

Based on 48 separate determinations including remote area and urban area data sets, the average dry mass scattering efficiency for ammonium nitrate is $2.7 \pm 0.5 \text{ m}^2/\text{g}$ (Hand and Malm, 2007, [155825](#)). Average values were higher in remote locations ($2.8 \pm 0.5 \text{ m}^2/\text{g}$) compared to urban locations ($2.2 \pm 0.5 \text{ m}^2/\text{g}$) though this might be accounted for by the predominate use of multiple linear regression for the remote areas, which can be biased high, compared to the use of theoretical calculations for the urban data sets.

Organic fine PM extinction efficiency of $3.9 \pm 1.5 \text{ m}^2/\text{g}$ is based on 58 separate determinations, though much higher values ($\sim 6 \text{ m}^2/\text{g}$) resulted for locations influenced by industrial and biomass combustion sources (Hand and Malm, 2007, [155825](#)). These organic fine PM extinction efficiency values were adjusted to use a consistent ratio of organic mass to OC (OC) of 1.8 for each determination of the mass concentration. This value is generally associated with aged organic PM, while for more freshly emitted PM, such as in an urban environment, a smaller ratio (e.g., 1.4) would be more appropriate. This could explain the discrepancy between two approaches used to estimate the organic PM light extinction efficiency for Phoenix (Hand and Malm, 2006, [156517](#)), which resulted in a significantly lower value where a site specific regression method was used compared to the value obtained from a method optimized for remote-area monitoring ($2.47 \text{ m}^2/\text{g}$ compared to $3.71 \text{ m}^2/\text{g}$). However in Fresno both the mass balance and light scattering balance was improved by using a ratio of 1.8 instead of 1.4 to estimate the organic compound mass (Watson and Chow, 2007, [157127](#)). Another possible or partial factor with respect to urban light extinction efficiency for organic PM may be that the size distribution of freshly emitted organic PM in urban areas extends significantly into the ultra-fine particle size range (Demerjian and Mohnen, 2008, [156392](#)) that is less efficient per mass concentration at light scattering than the generally larger-sized aged organic PM such as from a distant forest fire as was measured at the Baltimore Supersite.

Hand and Malm (2007, [155825](#)) also reviewed and made recommendation for extinction efficiencies for the other PM components including for mixed coarse mode ($1.0 \pm 0.9 \text{ m}^2/\text{g}$ based on 51 determinations) and fine mode dust or soil ($3.3 \pm 0.6 \text{ m}^2/\text{g}$ based

on 23 determinations, but recommending 1.0 m²/g for use with data from realistic collection efficiency samplers) and fine sea salt (4.5 ± 0.9 m²/g based on 25 determinations, but recommending 1.0 m²/g to 1.3 m²/g for use with data from realistic collection efficiency samplers). This work did not address light absorption efficiency of EC, CB, or crustal PM.

The Hand and Malm (2007, [155825](#)) average dry mass light scattering efficiency values are generally consistent with the values for the IMPROVE algorithm (as shown in equation 9-1). However the adoption of the IMPROVE algorithm by EPA for calculating the haze metric used to track trends and assess the nominal pace of progress for the RHR (EPA, 2001, [157068](#)) resulted in much greater scrutiny of its performance in estimating extinction (Lowenthal and Kumar, 2003, [156712](#); Malm, 1999, [025037](#); Malm and Hand, 2007, [155962](#); Ryan et al., 2005, [156934](#)). Among the issues raised is that the algorithm tended to underestimate the light extinction for the haziest conditions that occur principally during the summer in the southeastern U.S. and overestimate for near pristine conditions that tend to occur most often in the arid western U.S. Furthermore they showed the lack of mass or light scattering closure at coastal sites due to sea salt that was not accounted for by the IMPROVE algorithm. These assessments used mass concentration and light extinction closure and regression analysis methods to infer that the dry extinction efficiency for the major fine particle components would need to vary in order to avoid the biased estimates of light extinction at the extremes. Theoretical calculations of SO₄²⁻ dry extinction efficiencies for 41 days of size-resolved chemical composition data for Big Bend, Texas, as part of the BRAVO Study produced a range of results from ~2.4 m²/g to ~4.1 m²/g, with the larger dry extinction efficiency values tending to be associated with higher ammonium sulfate mass concentration and narrower size distributions (Schichtel et al., 2004, [179902](#)).

In response to the technical concerns raised about the performance of the IMPROVE algorithm, a revised algorithm was developed (Pitchford et al., 2007, [098066](#)). The revised version of the algorithm differs from the original algorithm by including a fine sea salt term related to the measured chloride ion concentration, increases by about 30% the mass concentration of the organic aerosol component by changing the ratio of organic compound mass to OC mass from 1.4 to 1.8, uses site elevation dependent Rayleigh scattering in place of 10 Mm⁻¹ that had been used at every site, added a NO₂ light absorption term and employs a split component model for the secondary particulate components (i.e., SO₄²⁻, nitrate and organic species) with new water growth terms to better estimate their

extinction at the high and low extremes of the range. The revised algorithm is displayed below in Equation 9-2.

$$\begin{aligned}
 b_{ext} \approx & 2.2 \times f_s(RH) \times [Small\ Sulfate] + 4.8 \times f_L(RH) \times [Large\ Sulfate] \\
 & + 2.4 \times f_s(RH) \times [Small\ Nitrate] + 5.1 \times f_L(RH) \times [Large\ Nitrate] \\
 & + 2.8 \times [Small\ Organic\ Mass] + 6.1 \times [Large\ Organic\ Mass] \\
 & + 10 \times [Elemental\ Carbon] \\
 & + 1 \times [Fine\ Soil] \\
 & + 1.7 \times f_{ss}(RH) \times [Sea\ Salt] \\
 & + 0.6 \times [Coarse\ Mass] \\
 & + Rayleigh\ Scattering\ (Site\ Specific) \\
 & + 0.33 \times [NO_2\ (ppb)]
 \end{aligned}$$

Equation 9-2

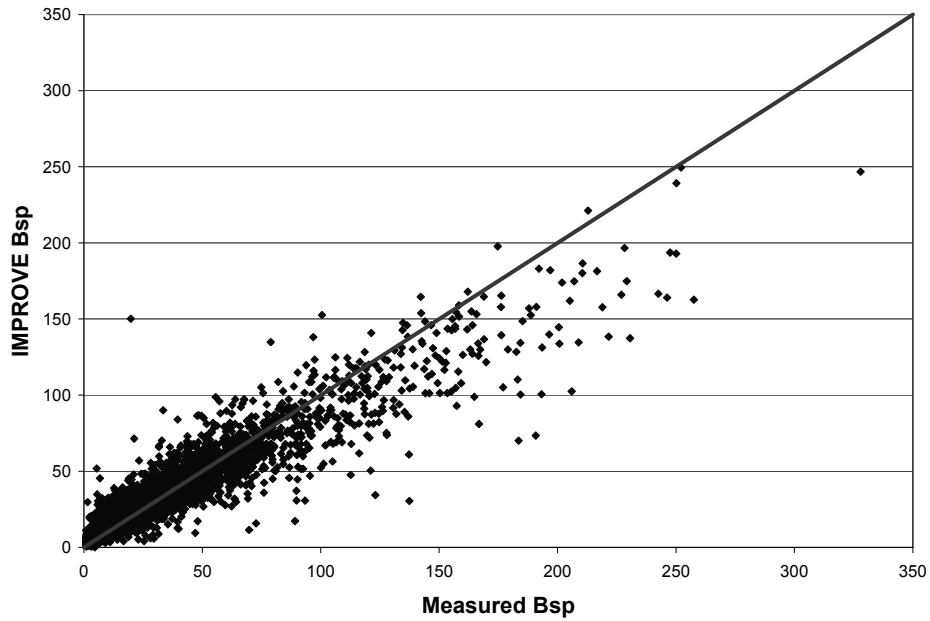
Small and large SO₄²⁻, nitrate and organic mass are used to refer to the splitting of the concentrations of each of those three species into two size distributions. This approach accounts for increased light extinction efficiency with mass by using a simple mixing model that assume that each of these three components are comprised of an external mixture of small and large particle size modes. Conceptually, the large mode particles represent aged or cloud-processed aerosol, while the small mode particles represent relatively newly generated particles from the gas phase precursors. The former are more likely to be associated with high concentrations while the latter are likely to be at relatively low concentration.

The geometric mean diameter and standard deviations assumed for these two size modes are 0.5 μm and 1.5 for the large mode particles and 0.2 μm and 2.2 for the small mode particles. Mie theory applied to these size distributions for the three species results in dry extinction efficiencies for the small and large mode ammonium sulfate (2.2 m²/g and 4.8 m²/g), ammonium nitrate (2.4 m²/g and 5.1 m²/g) and organic mass (2.8 m²/g and 6.1 m²/g). Water growth terms specifically derived for the small and large size distribution using the upper branch of the hygroscopic growth curves for ammonium sulfate are applied to both the SO₄²⁻ and nitrate PM. No water growth is assumed for organic PM.

A simple empirically developed apportionment approach that was evaluated by testing the new algorithms estimated light scattering at the 21 IMPROVE sites that have nephelometer-measured light scattering data. For each sample, the fraction of the fine particle component (SO₄²⁻, nitrate, or organic mass) that is assigned to the large mode is calculated by dividing the total concentration of the component by 20 μg/m³ (e.g., if the total

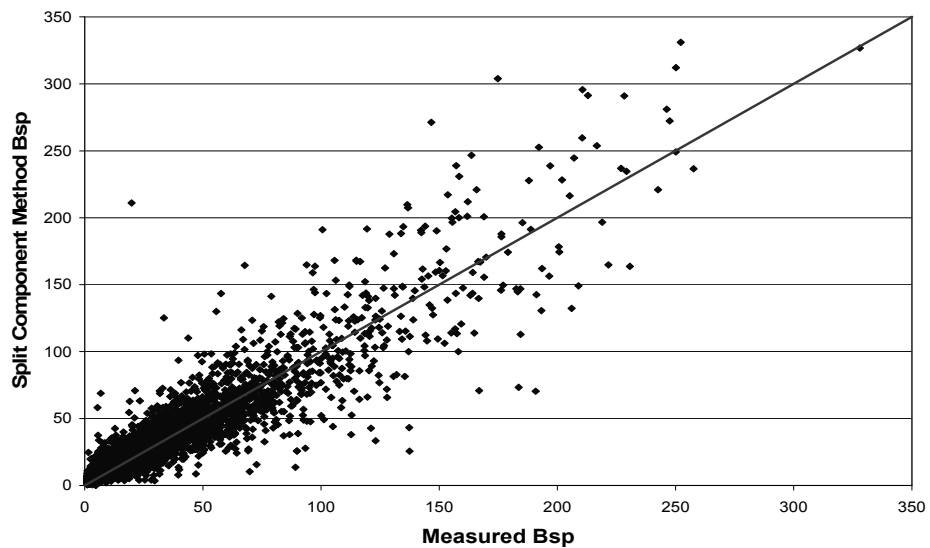
fine particle nitrate concentration is $4 \mu\text{g}/\text{m}^3$, the large mode concentration is $1/5$ of $4 \mu\text{g}/\text{m}^3$ or $0.8 \mu\text{g}/\text{m}^3$, leaving $3.2 \mu\text{g}/\text{m}^3$ in the small mode). If the total concentration of a component exceeds $20 \mu\text{g}/\text{m}^3$, all of it is assumed to be in the large mode.

The performance of the original and revised IMPROVE algorithms was evaluated using the data for 21 IMPROVE remote-area monitoring sites that also have nephelometer monitoring of particle light scattering. Figures 9-5 and 9-6 are scatterplots of the estimated versus measured light scattering for the two algorithms. The revised algorithm has noticeably reduced bias at the upper and lower extremes. However, the new algorithm estimates have somewhat reduced precision (i.e., the points are more broadly scattered). States have adopted the new algorithm for the technical assessments that support their RHR State Implementation Plans, but the revised algorithm was too recently developed to be incorporated into any of the peer-reviewed technical literature reported on below. In general the differences resulting from use of the original versus the revised IMPROVE algorithm in identifying best and worst haze conditions and the apportionment of the various PM components are small with exception of coastal locations where sea salt may be a significant contributor.



Source: Pitchford, et al. (2007, [098066](#))

Figure 9-5. A scatter plot of the original IMPROVE algorithm estimated particle light scattering versus measured particle light scattering.



Source: Pitchford, et al. (2007, [098066](#))

Figure 9-6. Scatter plot of the revised algorithm estimates of light scattering versus measured light scattering.

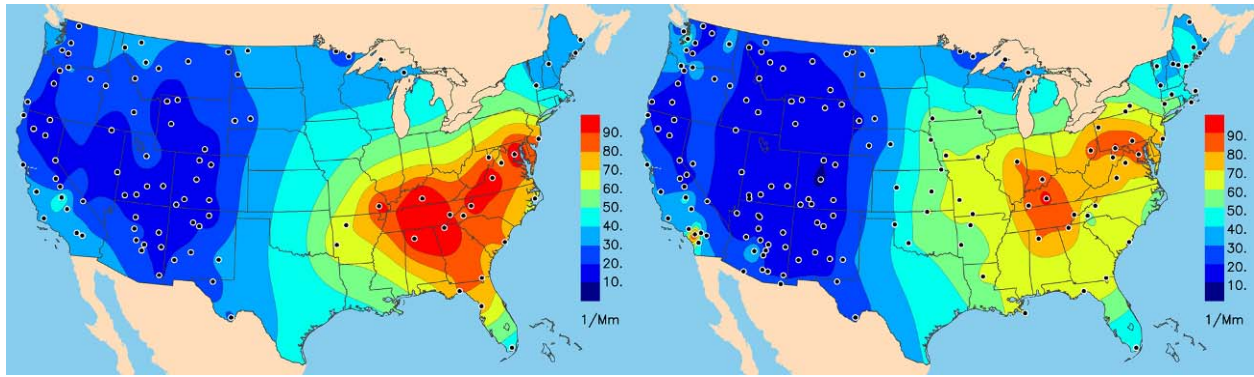
9.2.3.2. Spatial Patterns

The IMPROVE network is the basis for much of what is known about particulate species spatial and temporal patterns for remote areas of the U.S. Though IMPROVE includes some urban monitoring sites, most of what is known about urban particle speciation trends is based on the EPA Speciation Trend Network (STN) and other similarly operated state particle speciation sites jointly referred to as the Chemical Speciation Network (CSN) (Jayanty, 2003, [156605](#)). The number of IMPROVE network sites has increased considerably beginning in 2000, first to increase its ability to generate data representative of the 156 visibility-protected national parks and wilderness areas, then later as the states in the central U.S. requested additional remote-area monitoring to better understand their contributions to regional haze. The expansion of the network into the central U.S. significantly improved the understanding of spatial trends in a region of the country that had little speciation monitoring. Except as otherwise noted most of the information in this section was from the IMPROVE Report IV (DeBell, 2006, [156388](#)) and displays of data that are readily generated using the Visibility Information Exchange Web Site (VIEWS). VIEWS, the ambient monitoring data system, is one of several websites (as described in Table 9-1) sponsored by the Regional Planning Organizations (RPO) that documents substantial, though often otherwise unpublished, technical information generated to support implementation of the RHR.

Figure 9-7 shows maps of remote area light extinction estimates from PM speciation data for two yr selected to demonstrate the additional information available due to the expansion of the IMPROVE network into the central U.S. The locations of monitoring sites supplying the data shown as color contours are shown as dot on the maps. Users of such contour maps are usually cautioned that the contours are only there to guide the eye to sites with similar measurements and that nothing should be implied about spatial patterns where there are no monitoring sites. Certainly these plots give proof to the wisdom of such warnings. Prior to 2001 there were no IMPROVE or any other remote-area aerosol speciation monitoring sites in the central states between northern Minnesota and Michigan to the north and Arkansas and Kentucky to the south. The lack of monitoring over such a large region in the center of the country hid the presence of high average regional haze over the Midwestern U.S. Smaller scale differences are seen in the rest of the country and some of those are due to interannual variations as well as to better spatial resolution made possible by a more dense monitoring network.

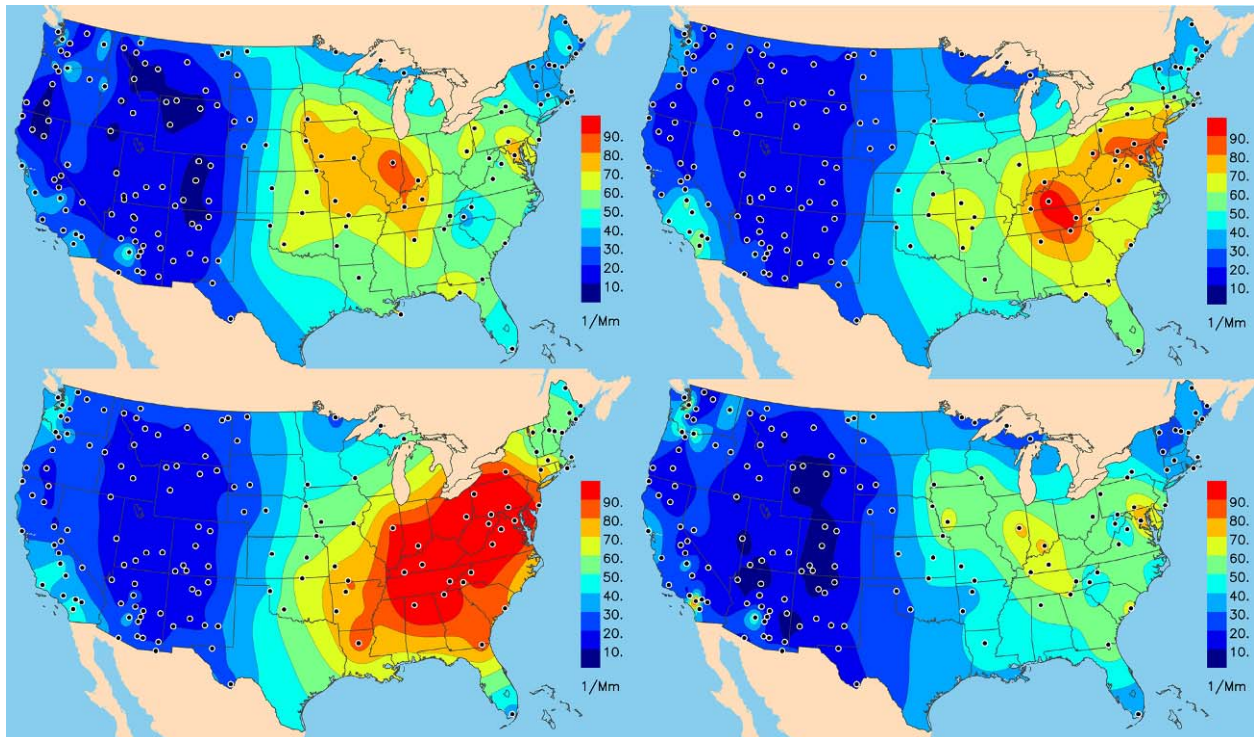
Table 9-1. Regional Planning Organization websites with visibility characterization and source attribution assessment information.

Type of Information	Name and Web Address	RPO	Information Content and Comments
RPO Home Pages	Western Regional Air Partnership http://www.wrapair.org/	WRAP	Organizational structure, plans, projects, reports and links to other sites with additional information. MANE-VU works in close cooperation with Northeast States for Coordinated Air Use Management (NESCAUM) and Mid-Atlantic Regional Air Management Association (MARAMA) to develop the technical information for RHR in the Northeast. All three web sites contain unique technical support information.
	Central Regional Air Planning Association http://www.cenrap.org/	CENRAP	
	Midwest Regional Planning Organization http://64.27.125.175/mrpo.html	MRPO	
	Visibility Improvement State and Tribal Association of the Southeast http://www.vistas-sesarm.org/	VISTAS	
	Mid-Atlantic/Northeast Visibility Union http://www.manevu.org/	MANE-VU	
	http://www.nescaum.org/topics/regional-haze http://www.marama.org/visibility/	NESCAUM MARAMA	
Visibility - Air Quality Monitoring Data	Visibility Information Exchange Web Site http://vista.cira.colostate.edu/views/	All RPOs	All IMPROVE and most other PM speciation data, RHR compatible derived parameters, and user-friendly tools to summarize and display data.
Emission Inventory Data	Emissions Data Management System http://www.wrappedms.org/default_login.asp	WRAP	WRAP emission inventory data warehouse and tools that provides a consistent approach to regional emissions tracking
Monitoring Data Assessment	Causes of Haze Assessment http://www.coha.dri.edu/	WRAP CENRAP	Monitoring site-specific descriptive characterizations and maps, seasonal and trends analysis, air flow analysis, & receptor modeling.
Visibility Modeling	U. of California-Riverside Modeling Center http://pah.cert.ucr.edu/aqm/308/ http://pah.cert.ucr.edu/aqm/cenrap/index.shtml http://pah.cert.ucr.edu/vistas/	WRAP CENRAP VISTAS	Descriptions of input data, performance, and results of regional scale modeling (CMAQ & CAMx) & source attribution for base and future yr regional haze.
Integrated Information to Support RHR SIP Preparations	Technical Support System http://matar.cira.colostate.edu/tss/	WRAP	Provides access and common formats to display and summarize emissions inventory information, monitoring data/ assessment and regional haze modeling result to aid state and tribal analyst prepare RHR implementation plans.



Source: VIEWS (<http://vista.cira.colostate.edu/views/>)

Figure 9-7. IMPROVE network PM species estimated light extinction for 2000 (left) and for 2004 (right).



Source: VIEWS (<http://vista.cira.colostate.edu/views/>)

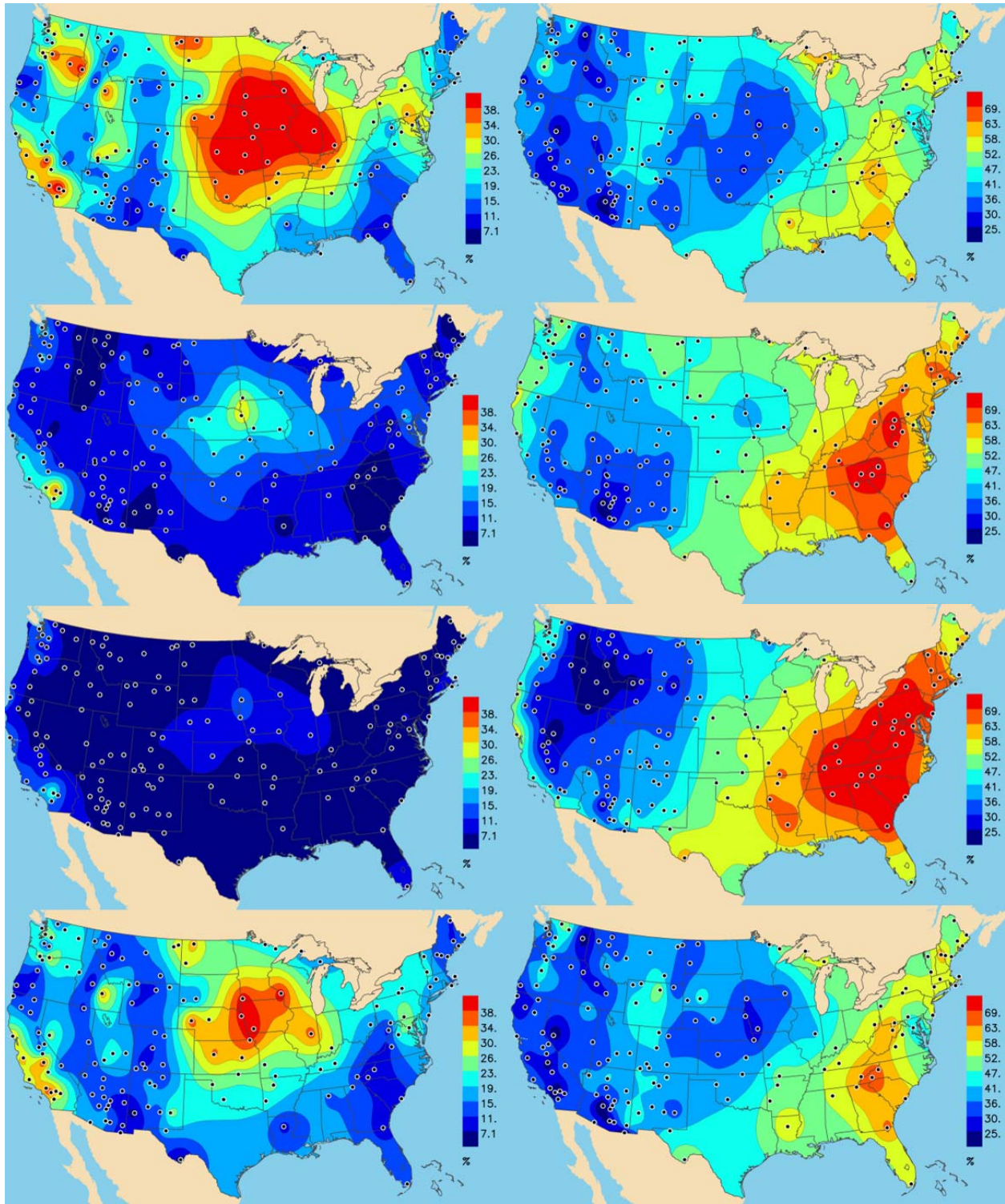
Figure 9-8. Mean estimated light extinction from PM speciation measurements for the first (top left), second (top right), third (bottom left), and fourth (bottom right) calendar quarters of 2004.

Figure 9-8 shows the seasonal pattern of PM species estimated light extinction using maps of mean values for each of the calendar quarter for 2004. The first quarter has the highest region of haze centered in the Midwestern U.S.; the warmer second and third quarters have the region of highest haze over the Ohio River Valley; and the fourth quarter is a composite with high haze in both the Midwest and Ohio River Valley. Smaller regions of haze show up in the Columbia River Valley (border between Washington and Oregon) in the colder first and fourth quarters and in Southern California in the warmer second and third quarters.

The IMPROVE algorithm permits each PM component contribution to light extinction to be separately estimated. Figures 9-9, 9-10 and 9-11 display the seasonal variation of the percent contribution to aerosol light extinction by the various component estimates. Figure 9-9 shows the contributions by SO_4^{2-} and nitrate particulate including the haze enhancement caused by the absorbed water in humid conditions. As shown in Figures 9-9, a large regional pattern of high contribution to haze by nitrate PM is centered in the Midwest, and during the cooler months the nitrate PM is the dominant cause of haze in the region responsible for a third to a half of the particulate light extinction. Midwestern particulate nitrate is responsible for the regional pattern of the highest haze conditions shifting from the Ohio River Valley during summer to the Midwest in the winter as shown in Figure 9-8. Particulate nitrate is also a significant contributor to particulate light extinction year-around in parts of California, where it generally contributes 20%-40%. The Pacific Northwest, parts of Idaho and Utah experience large contributions to particulate light extinction by nitrates during the colder seasons, with contributions of 20%-30%. Figure 9-9 also shows that particulate SO_4^{2-} is the predominate contributor in the eastern U.S., where it contributes 40% or more on average and during the summer months up to three quarters of the particulate light extinction over much of the East. In the western U.S. particulate SO_4^{2-} generally contribute 20-50% of the particle light extinction. Regions of the lowest fractional contributions by particulate SO_4^{2-} and nitrate for any calendar quarter are generally in the western U.S., and as are shown in the subsequent two figures have significant contributions by crustal PM components (i.e., coarse mass and fine soil) and by carbonaceous PM (i.e., organic mass and EC).

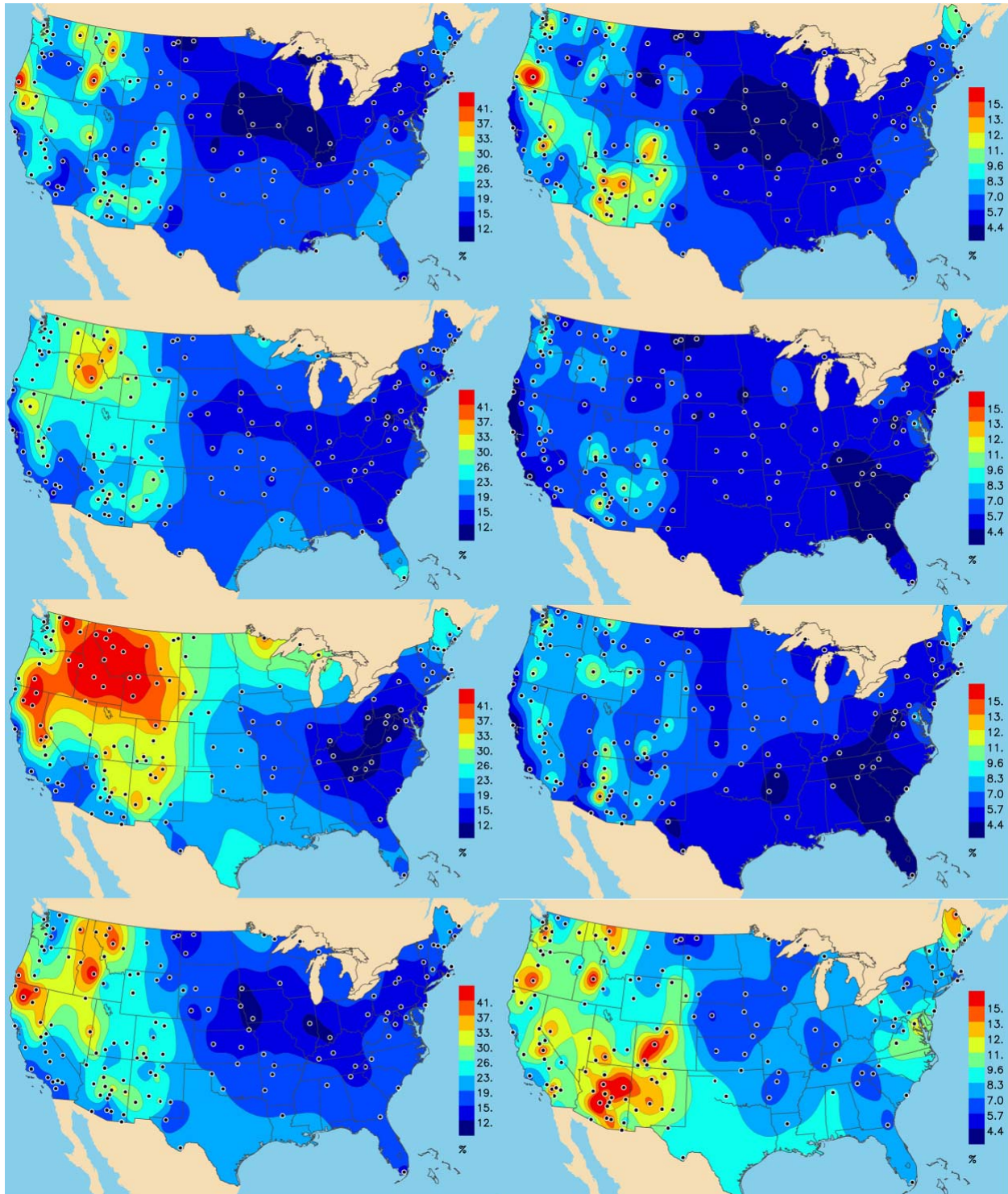
Figure 9-10 shows the contributions to haze by the carbonaceous PM components (i.e., organic mass and EC). They show broadly similar patterns with the greatest contributions in the western U.S. especially during the warmer months of the year. For the most part this

spatial pattern results from the dominant contributions to haze by SO_4^{2-} and nitrate PM in the eastern half of the U.S., leaving relatively little for other component contributions. The fractional contribution to haze by organic PM is generally two to five times that of EC. In absolute terms, both carbonaceous components tend to have two to three times higher concentrations in the eastern U.S. than in the non-coastal western states.



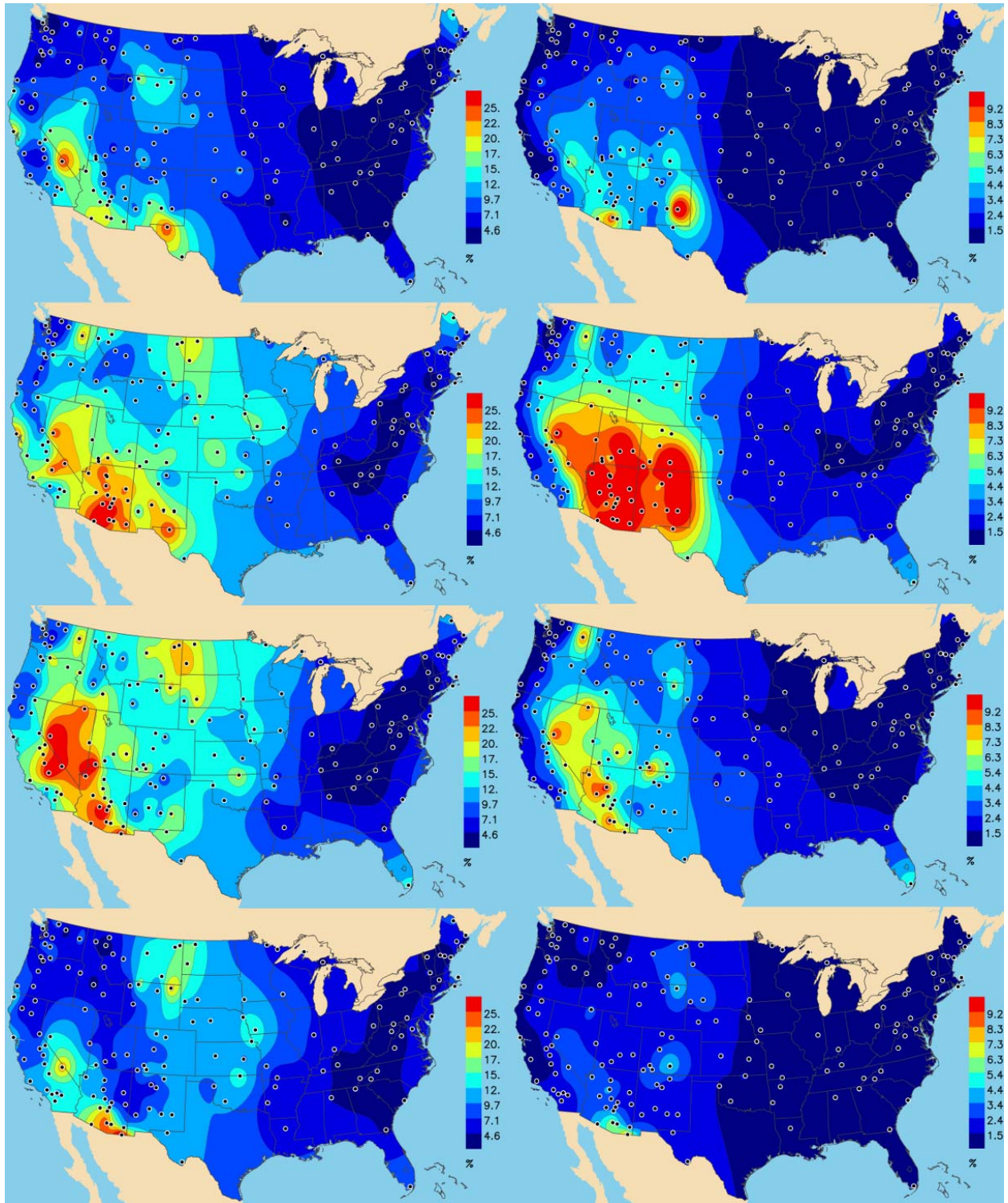
Source: VIEWS (<http://vista.cira.colostate.edu/views/>)

Figure 9-9. Percent contributions of ammonium nitrate (left column) and ammonium sulfate (right column) to particulate light extinction for each calendar quarter of 2004 (first through fourth quarter arranged from top to bottom). Note that the contour intervals are not the same for the two species contributions.



Source: VIEWS (<http://vista.cira.colostate.edu/views/>)

Figure 9-10. Percent contributions of organic mass (left column) and EC (right column) to particulate light extinction for each calendar quarter of 2004 (first through fourth quarter arranged from top to bottom). Note that the contour intervals are not the same for the two species contributions.



Source: VIEWS (<http://vista.cira.colostate.edu/views/>)

Figure 9-11. Percent contributions of coarse mass (left column) and fine soil (right column) to particulate light extinction for each calendar quarter of 2004 (first through fourth quarter arranged from top to bottom). Note that the contour intervals are not the same for the two species contributions.

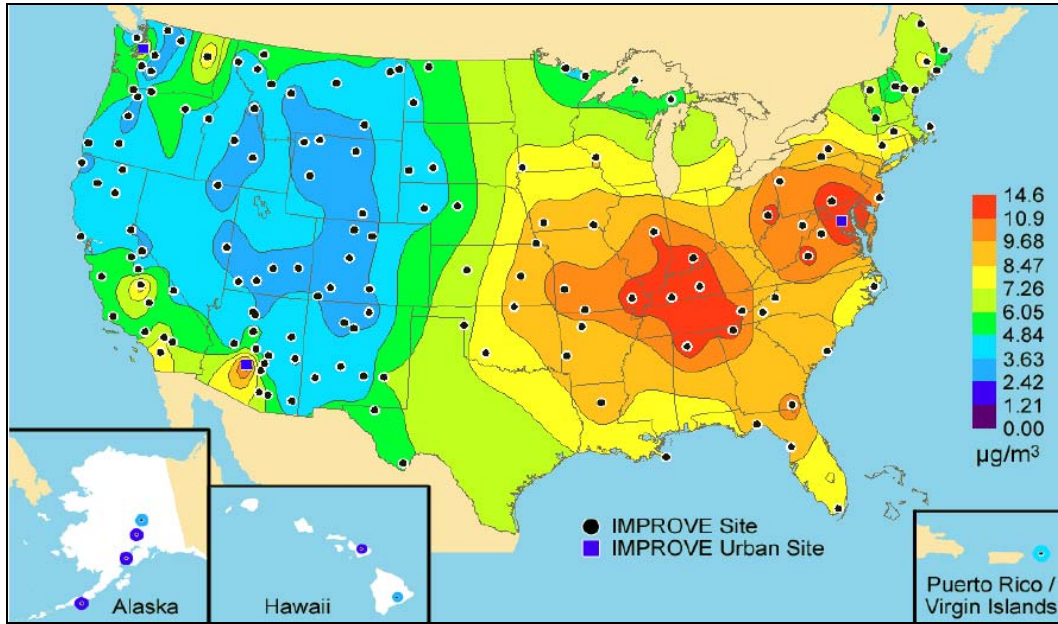
Figure 9-11 shows the contributions to haze by coarse mass and fine soil components. As with the carbonaceous components, these crustal dominated components have a similar spatial pattern with regions of highest contribution to haze in the western U.S., and just as for the carbonaceous PM, the explanation for low contributions in the eastern U.S. is the dominant contributions to haze by SO_4^{2-} and nitrate PM leaving relatively little for other components. The crustal components contribute more to haze in the arid regions of the west including the southwestern deserts. In absolute terms, coarse mass concentrations are as high in the rural areas of the center of the country (including Oklahoma, Arkansas, Kansas, Missouri, and Iowa) as they are in the Desert Southwest. Typically coarse mass contributions to haze exceed those of fine mass by a factor of 2-4.

9.2.3.3. Urban and Regional Patterns

Using a combination of IMPROVE and CSN data, it is possible to compare urban $\text{PM}_{2.5}$ concentrations and composition to corresponding remote-area regional values. These are shown as paired color contours maps for IMPROVE and IMPROVE plus CSN (see Figures 9-12 to 9-23). The degree of comparability of the data from these two networks was assessed by an analysis of two yr of co-located IMPROVE and CSN data from six urban areas. The CSN organic mass data were adjusted for a positive sampling artifact prior to inclusion in this assessment, in a fashion similar to that used for the IMPROVE data set (pages 29-30, DeBell, 2006, [156388](#)). Note that the contour scales are different between the two maps for each component pair of maps so that each contains as much information as possible using ten concentration contours. To assess the degree to which urban areas have higher PM component concentrations compared to regional background note how many contour intervals surround the urban monitoring sites. The U.S. EPA (2004, [190219](#)) used the pairing of IMPROVE and CSN monitoring sites at 13 selected urban areas to separate local and regional contributions of three major $\text{PM}_{2.5}$ components as shown in Figure 9-24.

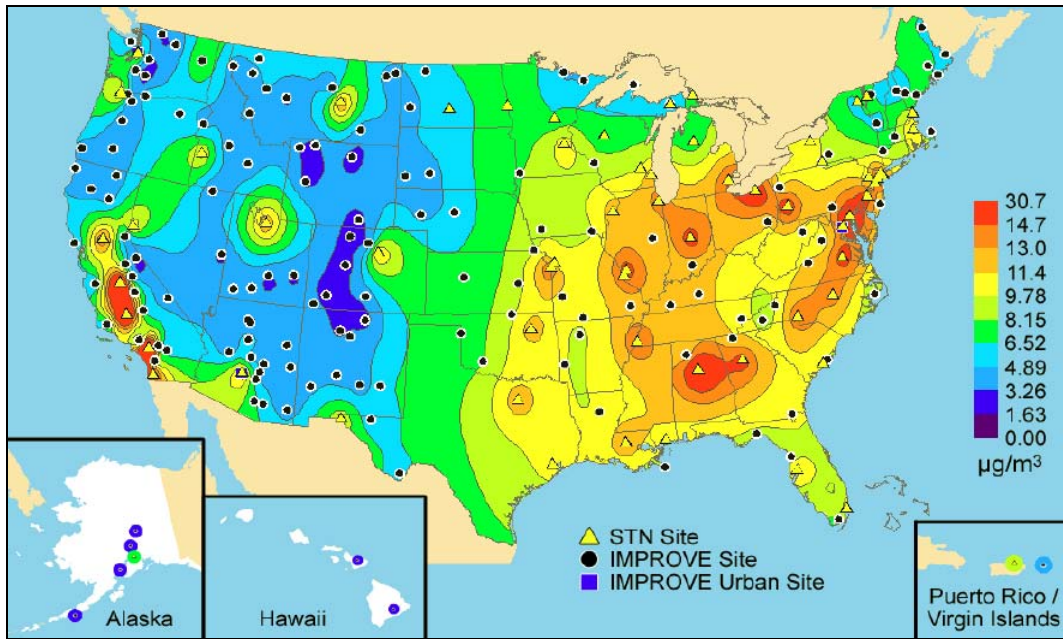
In Figures 9-12 and 9-13, urban $\text{PM}_{2.5}$ concentrations are systematically higher than those in the surrounding non-urban regions. The urban excess is generally much higher in the western U.S. than in the East (e.g., there are five contour intervals separating Salt Lake City from its remote regional area compared to only two for Indianapolis). This

implies that eastern and western urban $PM_{2.5}$ concentrations and resulting visibility are less different than the eastern and western regional concentrations and visibility.



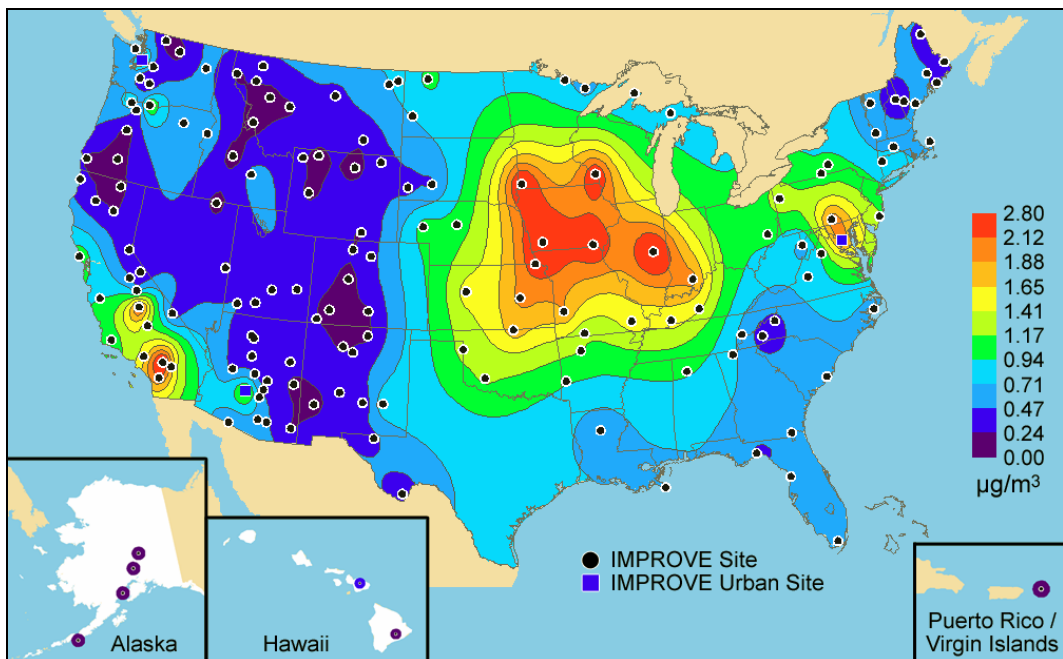
Source: Debell (2006, [156388](#)).

Figure 9-12. IMPROVE Mean $PM_{2.5}$ mass concentration determined by summing the major components for the 2000-2004.



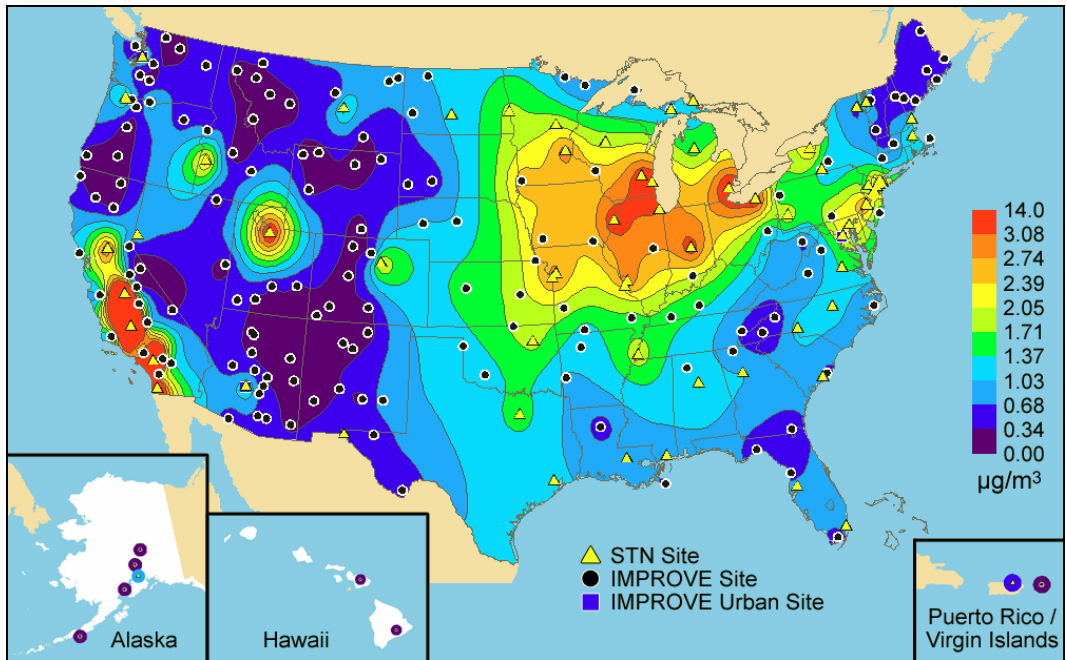
Source: Debell (2006, [156388](#)).

Figure 9-13. IMPROVE and CSN (STN) mean PM_{2.5} mass concentration determined by summing the major components for 2000-2004



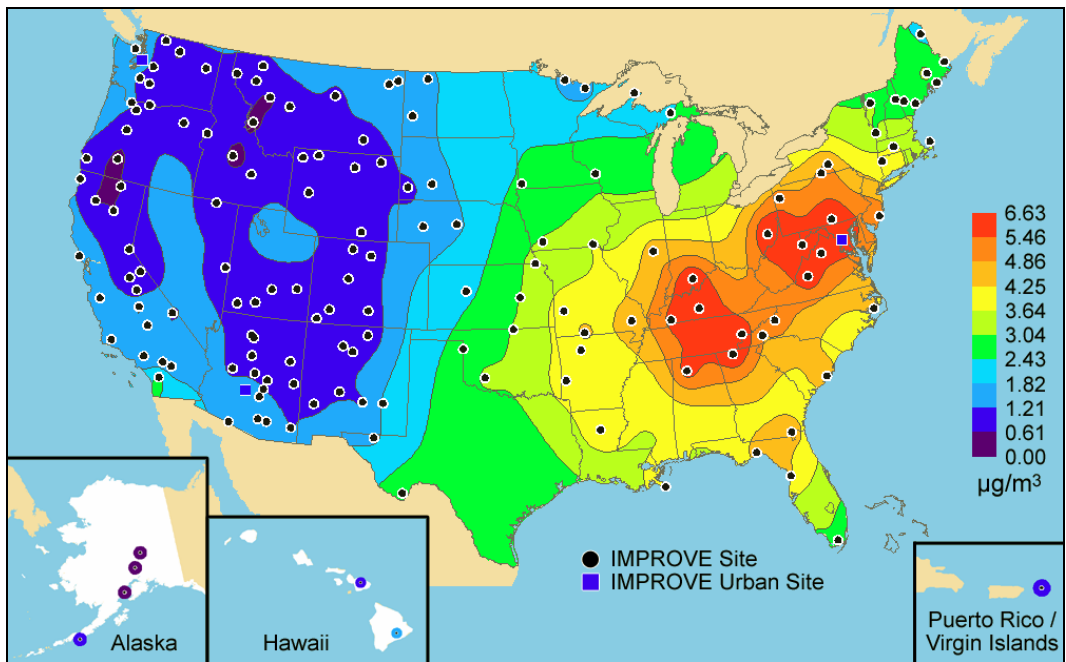
Source: Debell (2006, [156388](#)).

Figure 9-14. IMPROVE mean ammonium nitrate concentrations for 2000-2004.



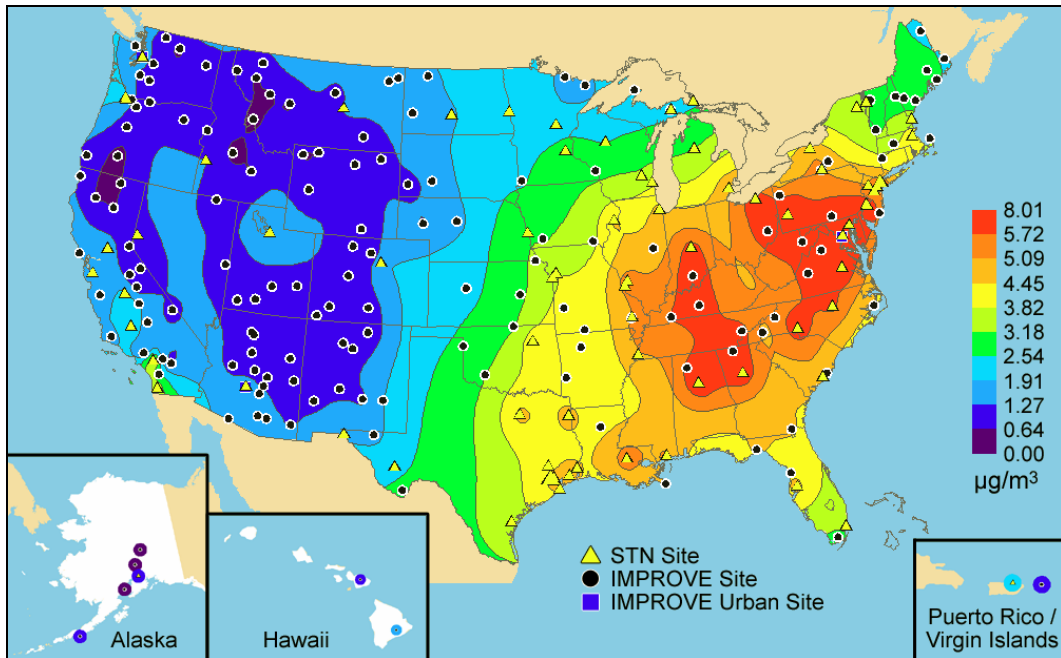
Source: Debell (2006, [156388](#)).

Figure 9-15. IMPROVE and CSN (STN) mean ammonium nitrate concentrations for 2000-2004.



Source: Debell (2006, [156388](#)).

Figure 9-16. IMPROVE mean ammonium sulfate concentrations for 2000-2004.



Source: Debell (2006, [156388](#)).

Figure 9-17. IMPROVE and CSN (STN) mean ammonium sulfate concentrations for 2000-2004.

Figures 9-14, 9-15, and 9-24 show the $PM_{2.5}$ nitrate in remote and urban areas. Here the western states have urban particulate nitrate concentrations that far exceed twice the remote area regional concentrations. For the Central Valley of California and Los Angeles areas, the urban excess of ammonium nitrate exceeds regional concentrations by $2 \mu\text{g}/\text{m}^3$ to $12 \mu\text{g}/\text{m}^3$. In the region of the Midwest nitrate bulge, the urban concentrations were less than twice the regional concentrations for an annual urban excess of about $1 \mu\text{g}/\text{m}^3$. Northeast and southeast of the Midwest nitrate bulge, annual urban particulate nitrate concentrations are several tenths to about one $\mu\text{g}/\text{m}^3$ above the remote area regional concentrations, with warmer southern locations tending to have the smaller concentrations of both regional and urban excess particulate nitrate.

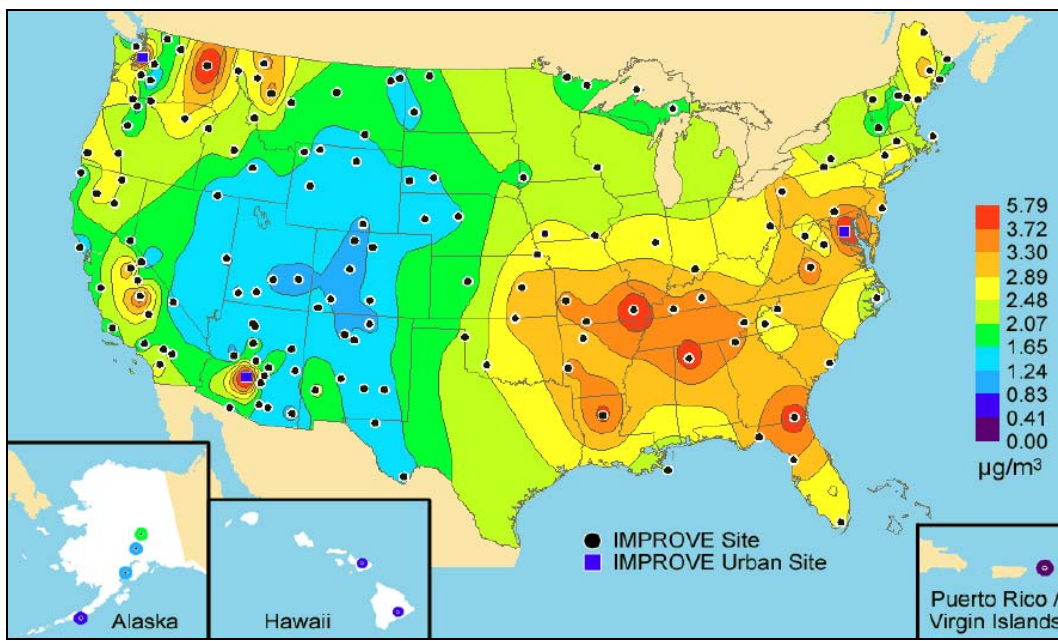
As shown in Figures 9-16, 9-17, and 9-24, annual-averaged urban particulate SO_4^{2-} concentrations are generally not much higher than the regional values, with urban excess generally of less than about a half $\mu\text{g}/\text{m}^3$. The exceptions apparent by comparing Figures 9-16 and 9-17 are in Texas and Louisiana where urban excess particulate SO_4^{2-} are greater than $1 \mu\text{g}/\text{m}^3$, perhaps caused by local emissions (e.g., from oil refineries). Urban contributions are a larger fraction of the total particulate SO_4^{2-} concentrations in the western U.S. because the regional concentrations are much lower than in the East. The modest additional particulate SO_4^{2-} concentrations associated with urban areas suggests

that most particulate SO_4^{2-} is regionally distributed, and that IMPROVE and CSN monitoring sites can be used together to enhance the ability to delineate particulate SO_4^{2-} spatial distributions. For example, note that the additional data from urban sites shown in Figure 9-17 extends north and south distribution of the high particulate SO_4^{2-} loading shown in Figure 9-16 over Tennessee and Kentucky, as well as the high loadings over southern Pennsylvania, eastern West Virginia and northern Virginia. (The color-contour suggested dip in concentrations between the two eastern particulate SO_4^{2-} high concentrations regions may not exist in the atmosphere, but this cannot be verified without speciation monitoring sites in southern Ohio, the boarder of Kentucky and West Virginia and western Virginia.)

Urban and remote area carbonaceous $\text{PM}_{2.5}$ are displayed in Figures 9-18 and 9-19 (organic mass), 9-20 and 9-21 (EC), and 9-24 (total carbon = organic + EC concentration). Just as with particulate nitrate both organic mass and EC concentrations are more than twice the remote-area background concentrations for western urban monitoring locations. One of the more interesting pairing of sites is for the Virgin Islands compared to the urban site at San Juan Puerto Rico (see the map cutout Figures 9-18 through 9-21). The San Juan urban excess OC is moderate, while the EC value is among the most extreme inferred in this manner. For eastern urban areas, approximately half the total carbon is local while the other half is regional. In eastern urban areas, carbonaceous and SO_4^{2-} particulate are the two major components of $\text{PM}_{2.5}$, with roughly equal contributions, and account for over 80% of the mass concentration. Edgerton et al. (2004, [156413](#)) showed that carbonaceous $\text{PM}_{2.5}$ is responsible for most of the urban excess above regional concentrations at four urban/rural paired Southeastern Aerosol Research and Characterization (SEARCH) monitoring sites in the southeastern U.S. However, the higher overall light extinction efficiency for SO_4^{2-} resulting from its hydrophilicity gives it ~ 2:1 dominance in responsibility for eastern urban light extinction.

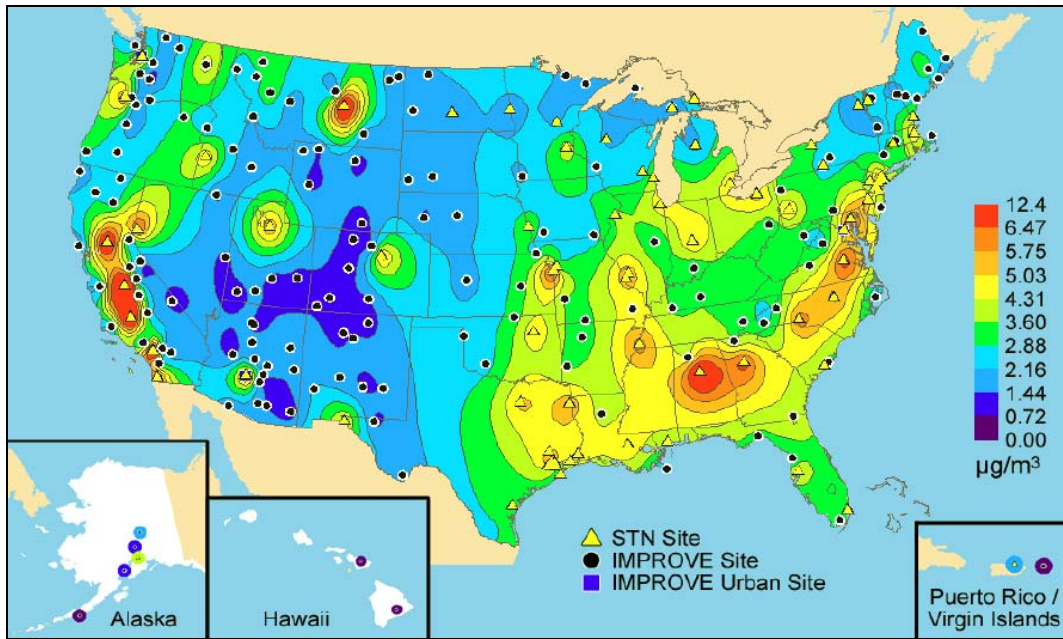
Urban and remote area fine soil $\text{PM}_{2.5}$ concentrations are displayed in Figures 9-22 and 9-23. Urban fine soil concentrations are at most a few tenths of a $\mu\text{g}/\text{m}^3$ higher than the regional background concentrations and in some regions they are much less. Just as with carbonaceous $\text{PM}_{2.5}$, the Virgin Island, San Juan, Puerto Rico pair are interesting for fine soil. In this case the interesting feature is that both of these island monitoring sites have high concentrations of fine soil, which is caused by their being in the trans-Atlantic transport path of dust from Africa (Prospero, 1996, [156889](#)).

No urban-remote pair of coarse mass concentration maps is available because CSN does not monitor coarse mass. In Malm et al. (2004, [156728](#)) a map of annual mean coarse mass concentration is shown for 2003 which includes the values for IMPROVE urban sites, including two in the western U.S. with much more coarse mass than the nearby remote areas monitoring sites (i.e., $\sim 24 \mu\text{g}/\text{m}^3$ compared to $\sim 9 \mu\text{g}/\text{m}^3$ for Phoenix, AZ, and $\sim 6 \mu\text{g}/\text{m}^3$ compared to $\sim 2 \mu\text{g}/\text{m}^3$ for Puget Sound, WA) and one eastern IMPROVE site at Washington, DC with less coarse mass than the surrounding remote area values ($\sim 2 \mu\text{g}/\text{m}^3$ compared to $\sim 4 \mu\text{g}/\text{m}^3$).



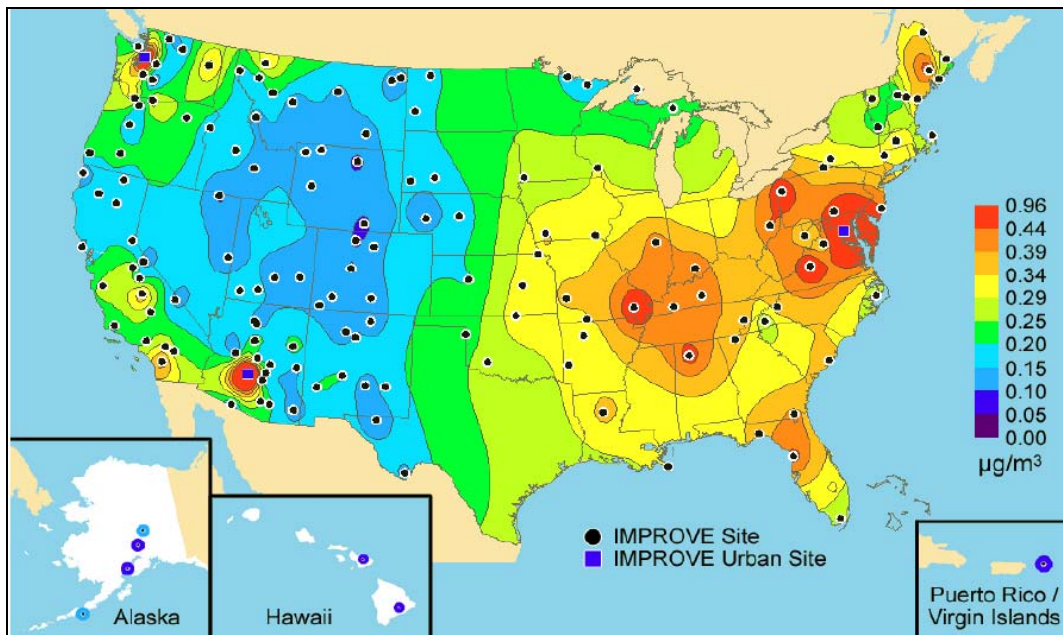
Source: Debell (2006, [156388](#)).

Figure 9-18. IMPROVE monitored mean organic mass concentrations for 2000-2004.



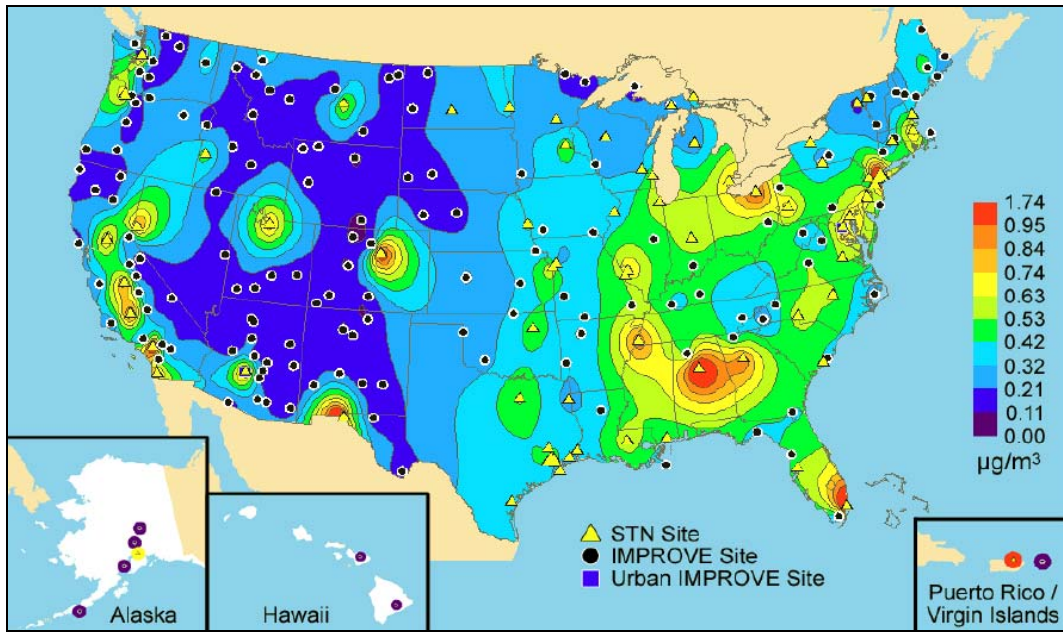
Source: Debell (2006, [156388](#)).

Figure 9-19. IMPROVE and CSN (STN) mean organic mass concentrations for 2000-2004.



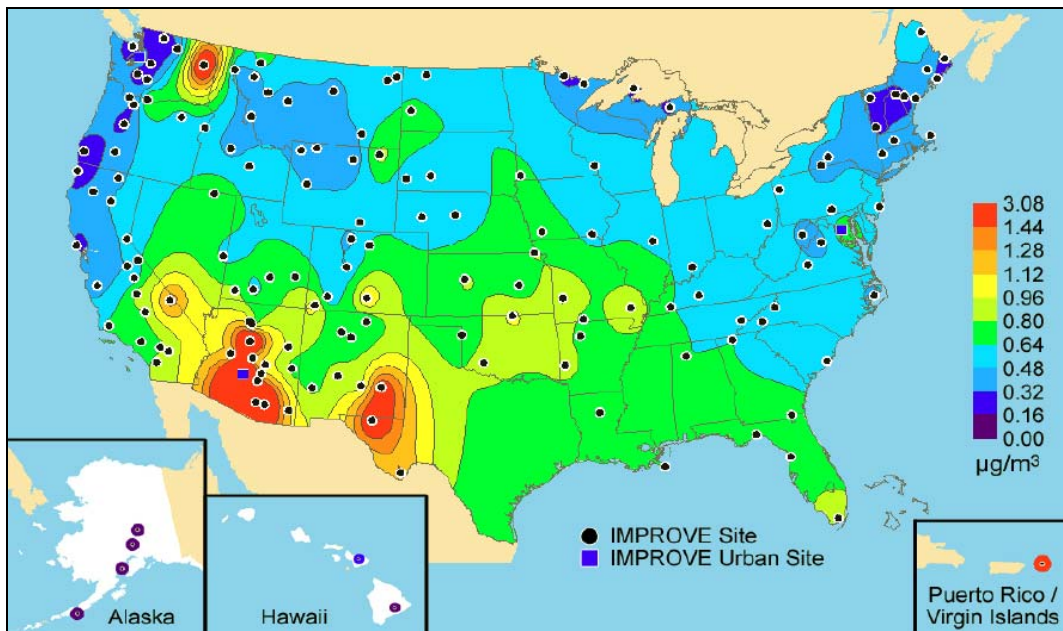
Source: Debell (2006, [156388](#)).

Figure 9-20. IMPROVE mean EC concentrations for 2000-2004.



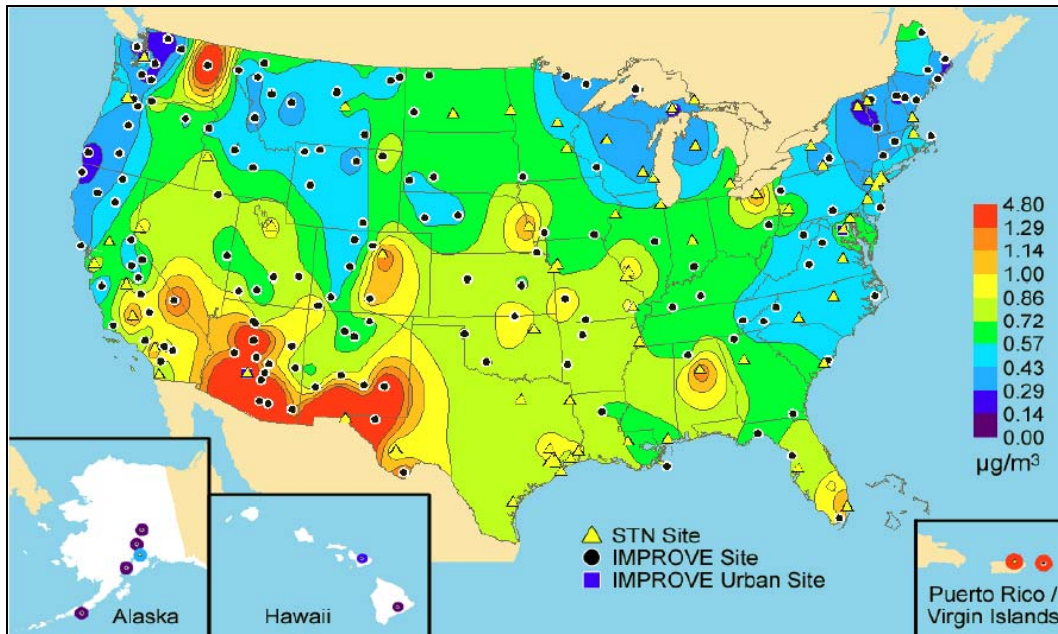
Source: Debell (2006, [156388](#)).

Figure 9-21. IMPROVE and CSN (STN) mean EC concentrations for 2000-2004.



Source: Debell (2006, [156388](#)).

Figure 9-22. IMPROVE mean fine soil concentrations for 2000-2004.



Source: Debell (2006, [156388](#)).

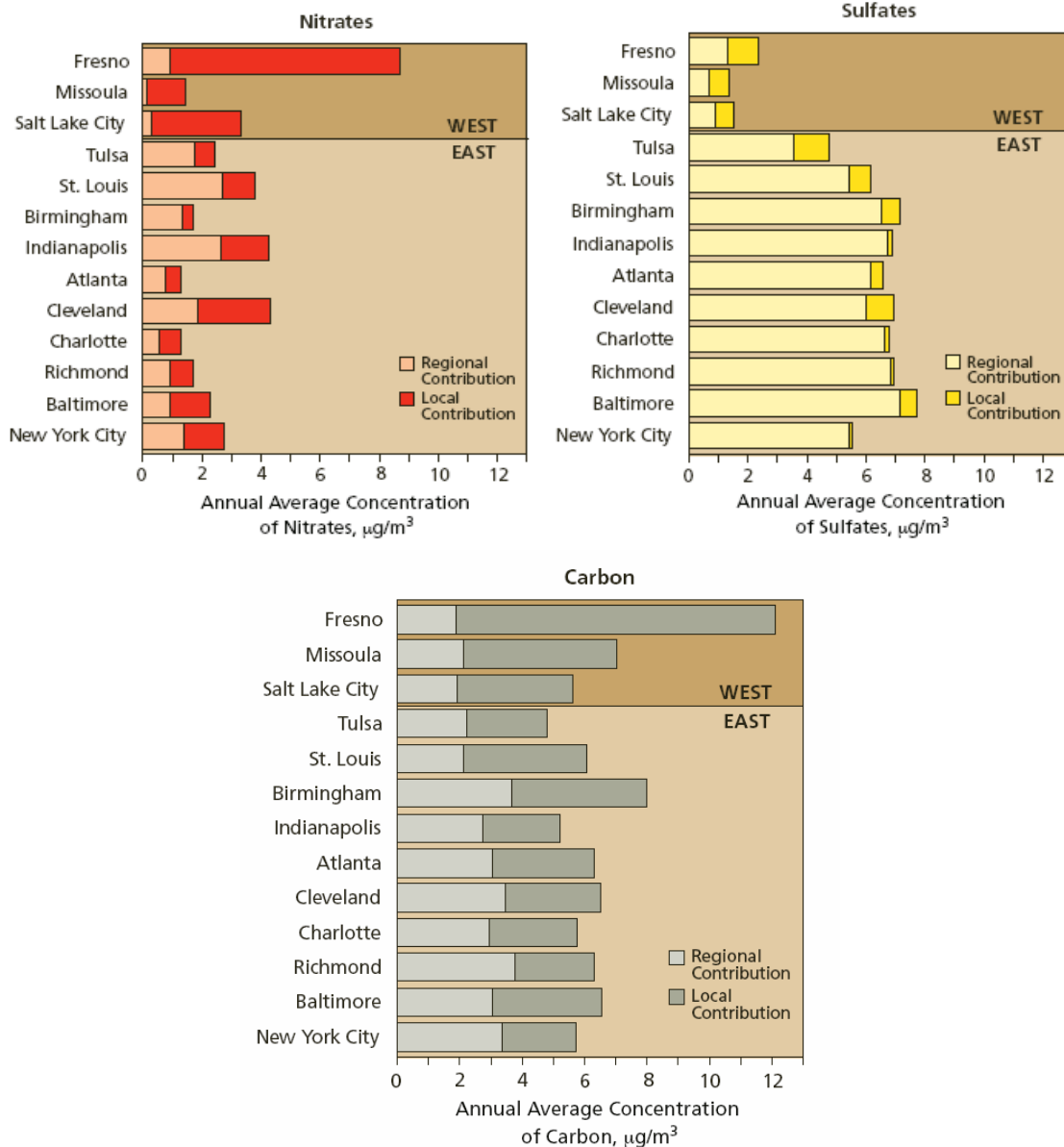
Figure 9-23. IMPROVE and CSN (STN) fine soil concentrations, 2000-2004.

Figure 9-25 shows the remote area coarse mass concentrations as measured by the IMPROVE network. The pattern of high coarse mass concentrations from Oklahoma to Iowa is comparable to the high concentrations in the desert southwest, though as shown in Figure 9-11 it contributes a smaller relative share of the light extinction because of the higher contributions to haze by particulate nitrate and sulfate in this agricultural region of the country. Comparing Figures 9-22 and 9-25 shows that the coarse mass and fine soil concentration patterns are similar for the desert southwest but there is a much lower fine soil to coarse mass concentration ratio for the agricultural center of the country, suggesting a regional difference in the size distribution of the coarse mass, perhaps due to differences in suspendable soil materials.

9.2.3.4. Temporal Trends

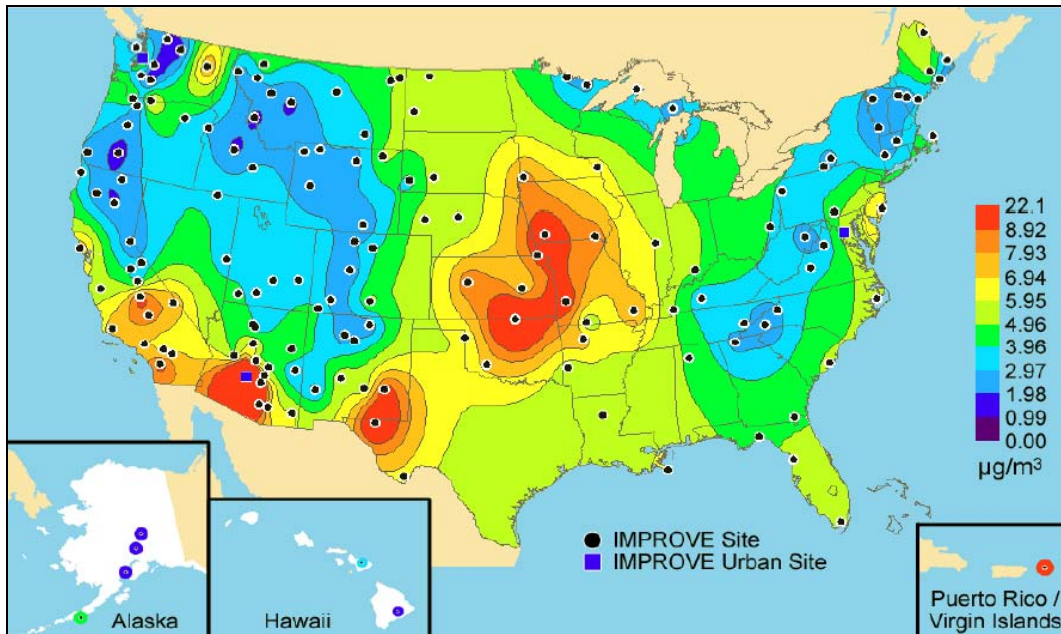
Visibility trend analysis requires relatively long data records to avoid having meteorologically driven interannual variability obscure more meaningful emissions-driven air quality trends. A requirement for long-term data limits the number of monitoring sites useful for trend analysis. Maps that show haze trends for IMPROVE sites for the 10-yr period from 1995 through 2004 for the mean of the 20% best and the 20% worst haze days where sites are required to have a minimum of 6 complete yr of data during the 10-yr

period are shown in Figures 9-26 and 9-27, respectively. The best haze days have improving haze at most sites (32 of 47), no trend at several sites (10 of 47) and degrading visibility at just one site (Great Sand Dunes, CO). The worst haze days have improving haze conditions at several sites (13 of 47), no trend at most sites (30 of 47) and degrading visibility at a few western sites (4 of 47).



Source: U.S. EPA (2004, [190219](#))

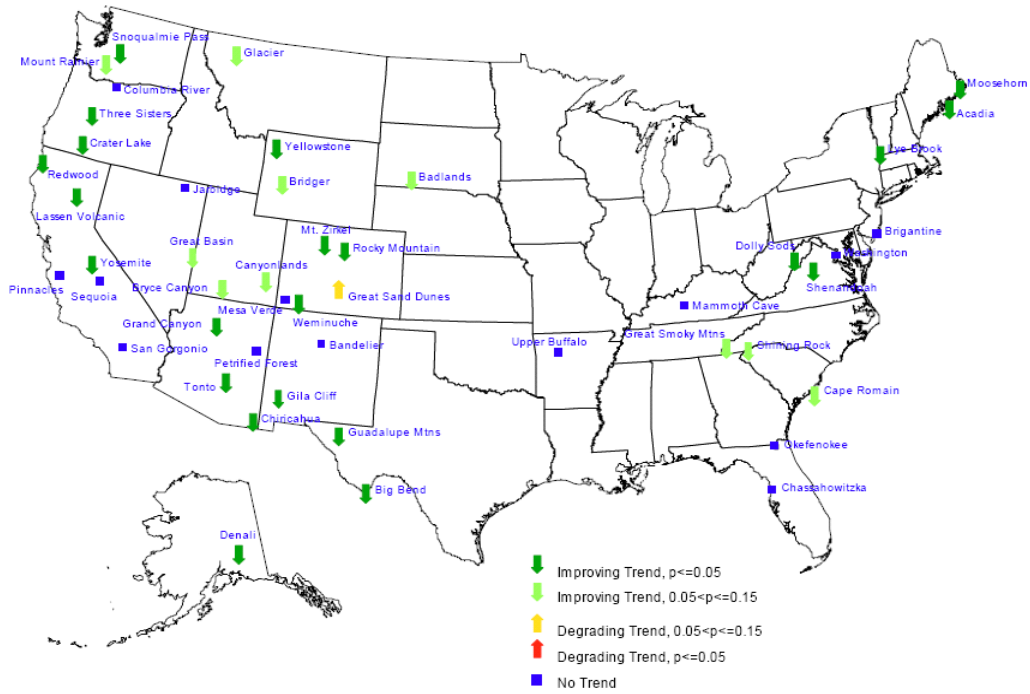
Figure 9-24. Regional and local contributions to annual average PM_{2.5} by particulate SO₄²⁻, nitrate and total carbon (i.e., organic plus EC) for select urban areas based on paired IMPROVE and CSN monitoring sites.



Source: Debell (2006, [156388](#)).

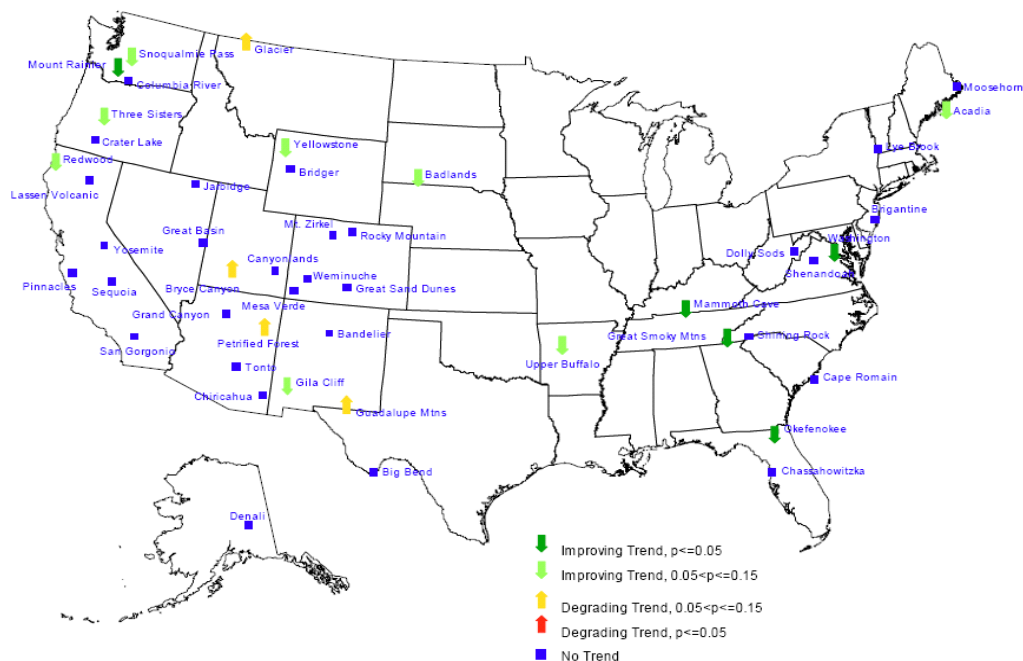
Figure 9-25. IMPROVE mean coarse mass concentrations for 2000-2004.

Eight-, ten-, and sixteen-yr trends analysis conducted for the Western Regional Air Partnership (WRAP) as part of the Causes of Haze Assessment (<http://www.wrapair.or>) show that improving trends for the 20% best haze days for the sites in the western U.S. generally correspond to improving trends for all of the major components with the exception of particulate nitrate. Trends assessment for the worst haze days at western sites show consistent reductions in particulate SO_4^{2-} , but otherwise have mixed increasing and decreasing haze component trends, many of which are not statistically significant. Substantial interannual and shorter term spatial and temporal wildfire activity variations have been shown to have a significant impact on the variability of haze in the Western U.S. (Park et al., 2006, [190469](#); Spracklen et al., 2007, [190485](#)). Edgerton et al. (2004, [156413](#)) showed a decreasing trend in $\text{PM}_{2.5}$ of about 18% (corresponding to $1 \mu\text{g}/\text{m}^3$ to $2 \mu\text{g}/\text{m}^3$) for four urban-rural paired SEARCH sites in the Southeastern U.S. corresponding to similar reductions in SO_4^{2-} and carbonaceous particulate.



Source: Debell (2006, [156388](#))

Figure 9-26. Ten-yr (1995-2004) haze trends for the mean of the 20% best annual haze conditions.



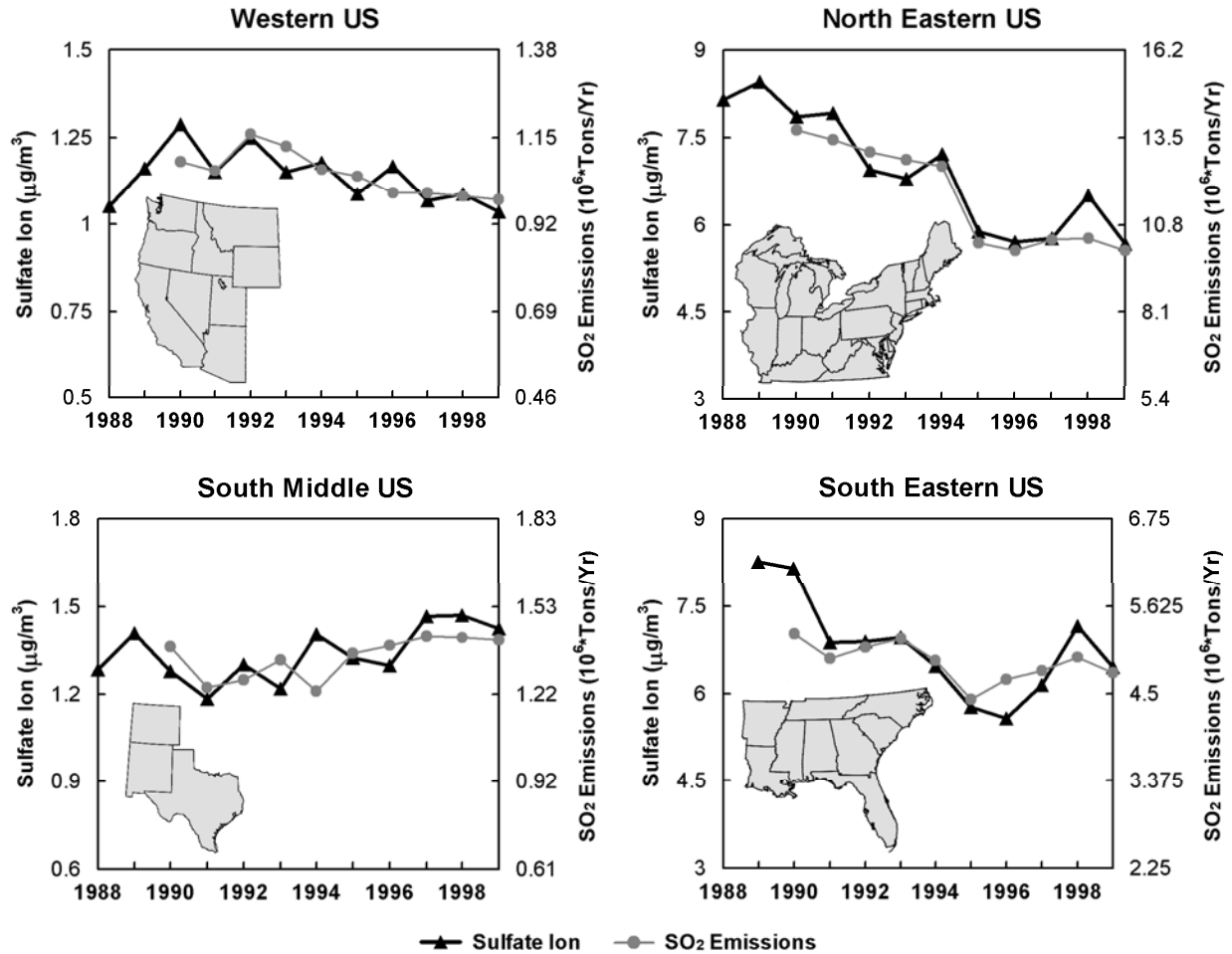
Source: Debell (2006, [156388](#))

Figure 9-27. Ten-yr (1995-2004) haze trends for the mean of the 20% worst annual haze conditions.

Malm et al. (2002, [156727](#)) conducted 10-yr (1988-1998) trends analyses on the combination of IMPROVE and CASTNET (Clean Air Status and Trends Network) (Baumgardner et al., 1999, [011308](#)) particulate SO_4^{2-} concentration datasets, which were shown to produce comparable SO_4^{2-} concentrations at 23 co-located monitoring sites. Figure 9-28 shows time plots of 80th percentile particulate SO_4^{2-} concentrations and annual average SO_2 emissions from the National Emissions Trends (EPA, 2000, [012211](#)) database for four regions of the U.S. Note that the concentration and emissions scales on the plots are each a factor of three, so that an equal percentage change in particulate SO_4^{2-} and SO_2 emissions slope in any plot will have the same trend line slope. Each plot shows a strong correspondence between 80th percentile particulate SO_4^{2-} and SO_2 emissions trends. The western U.S. had steadily declining trends in both, for an overall decrease of about 15%. The northeastern U.S. had a decrease of about 27% over the 10-yr period with the largest 1-yr decrease of about 20% between 1994 and 1995 as a result of the Phase I implementation of the Acid Rain Program. The southwestern U.S. (Texas, New Mexico and Colorado) had about a 15% increase in particulate SO_4^{2-} and SO_2 emissions over the ten-yr period. The southeastern U.S. had a declining trend for the early 1990s followed by an increasing trend for the later half of the decade, with a net decrease over the decade of less

than 10%. Others have shown similar decreasing particulate SO_4^{2-} concentration trends and a correspondence in trends between SO_2 emissions and particulate SO_4^{2-} concentration by region (EPA, 2004, [056905](#); Holland et al., 1999, [092051](#)).

Holland et al. (1999, [092051](#)) developed and compared NO_x emissions trends from 1989 to 1995 to corresponding trends in total nitrogen concentration (defined as particulate nitrate plus gaseous nitric acid) for the eastern U.S. (states between Louisiana to Minnesota and further east) based on data from 34 rural CASTNet dry deposition monitoring sites. They found a decrease in nitrogen median values of about 8% associated with a decrease of 5.4% in non-biogenic NO_x emissions. Trends in haze associated with particulate SO_4^{2-} and nitrate concentrations should correspond fairly well with trends in their concentration due to the simple relationship between concentration and light extinction at any relative humidity. However, nitrogen as defined in the Holland et al. (1999, [092051](#)) trend analysis includes the nitrogen from particulate nitrate and gaseous nitric acid, but nitric acid does not contribute to light extinction. For situations with limited atmospheric ammonia or elevated temperatures, trends in nitrogen may be principally in nitric acid with no net change in nitrate light extinction. Alternately with abundant ammonia and low temperatures the trend in nitrogen may be principally in particulate nitrate and the nitrate component of haze.



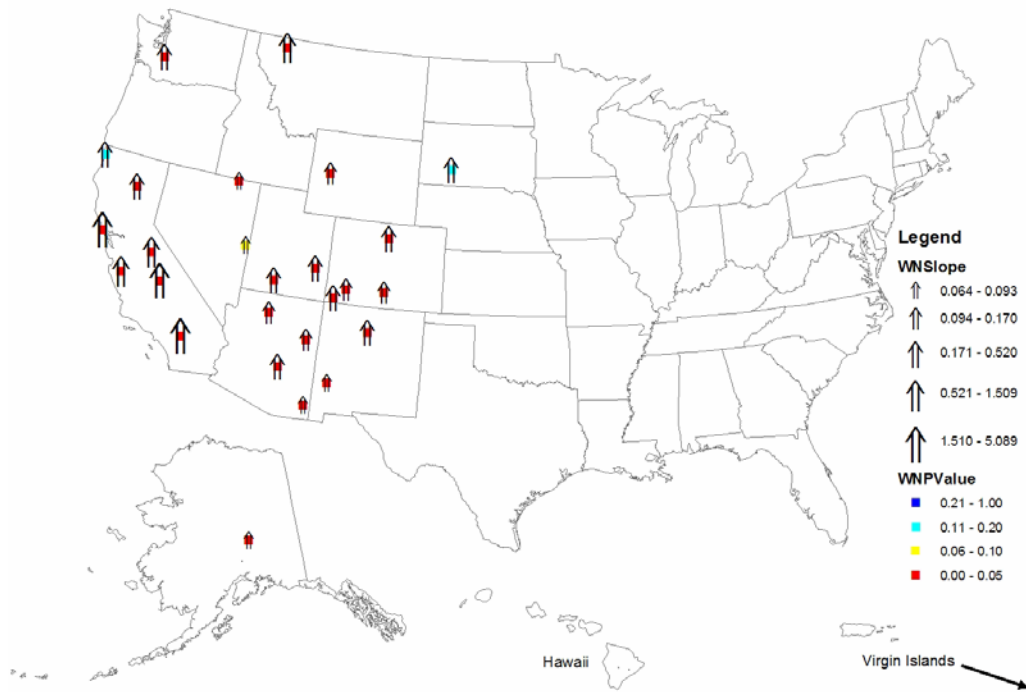
Source: Malm et al. (2002, [156727](#)).

Figure 9-28. Ten-yr trends in the 80th percentile particulate SO_4^{2-} concentration based on IMPROVE and CASTNet monitoring and net SO_2 emissions from the National Emissions Trends (NET) data base by region of the U.S.

Ten-yr trends (1994-2003) of particulate nitrate contribution to light extinction during the 20% worst haze conditions conducted as part of the Causes of Haze Assessment (see the link in Table 9-1) are shown in Figure 9-29. This indicates that haze from particulate nitrates is increasing across the western U.S. at a rate of several Mm^{-1} per year in parts of California and at a rate of several tenths of an Mm^{-1} across the Four-Corners states. A similar particulate nitrate trends map (not shown here) for the 20% best haze conditions that is available at the same web site shows decreasing particulate nitrate contribution to light extinction at nearly all of the western monitoring sites. While statistically significant, these trends for both the 20% worst and 20% best haze periods are influenced by an unexplained nationwide period of depressed nitrate concentrations measured by the

IMPROVE network during a 4-yr period from the winter of 1996-97 through the winter of 2000-01. Extensive examinations of plausible monitoring methodological explanations have failed to offer any evidence that the data are invalid (McDade, 2006, [192075](#)), but no satisfactory atmospheric or emissions-related explanation has been offered to account for this four-yr depression of nitrate. Similar analyses of particulate nitrate haze trends are not available for the rest of the country.

Maps of remote-area 8-, 10-, and 16-yr trends for carbonaceous and crustal PM species based on IMPROVE monitoring are available for the western U.S. conducted as part of the Causes of Haze Assessment. Generally these show a broad range of results (i.e., a mixture of statistically significant upward or downward trends and insignificant trends often with neighboring sites having opposing trends) that vary considerably depending on the number of years selected (i.e., 8, 10, or 16) and whether trends are for the best, worst, or middle of the haze distribution data. The scatter in these results is undoubtedly due to the high interannual variability and varying locations of wildfire and wind-suspended dust emissions that dominate the remote-area concentrations of the carbonaceous and crustal PM species in the western U.S.



Source: <http://www.coha.dri.edu/>

Figure 9-29. Map of 10-yr trends (1994-2003) in haze by particulate nitrate contribution to haze for the worst 20% annual haze periods. The orientation, size and color of the arrows indicate the direction, magnitude and statistical level of significance of the trends. These consistent upward trends may be a misleading result due to an unexplained sampling issue (see text for additional information).

9.2.3.5. Causes of Haze

In order to attribute haze to emissions from individual sources, source types, or source regions, scientists generally apply any of a number of receptor and air quality simulation modeling approaches and when using multiple approaches they reconcile the results of each using a weight-of-evidence methodology. Commonly this methodology has been applied to the extensive datasets generated by special studies designed to estimate source-receptor relationships for a few receptor locations or for individual emission sources (Pitchford et al., 1999, [156873](#); Pitchford et al., 2005, [156874](#); Schichtel et al., 2005, [156957](#)). More recently the Regional Planning Organizations (RPOs) have sponsored extensive regional haze source attribution assessments using weight-of-evidence methodologies to reconcile attribution results for virtually all of the remote-area IMPROVE sites to support the development of State Implementation Plans for the RHR. Additionally, a number of recent urban special

studies, including those sponsored by EPA PM Supersites program (Solomon and Hopke, 2008, [156997](#)), have addressed the causes of and sources contributing to urban excess PM concentrations above region concentrations. Attribution results uncertainties are generally larger than those of the measurements upon which they are based because they also include model uncertainties and assumptions, as well as issues of representativeness (e.g., How well does the data used in the analysis represent the typical emissions, air quality and meteorological conditions of interest?). As such it is advisable to treat the attribution results reported below as semi-quantitative.

The relative importance of the PM species that contribute to haze varies by region of the U.S. and time of year as seen in Figures 9-9, 9-10 and 9-11, above. Generally haze in the western half of the U.S. is not dominated by any one or two PM species. In the eastern half of the U.S., SO_4^{2-} , especially during summer and nitrate during the winter in the Midwest are the dominant haze species. As described above, urban haze can be viewed as a composite of the regional and local contributions where local contributions seem to be dominated by carbonaceous and to a lesser extent nitrate and crustal PM components. There have been far fewer urban investigations that explicitly consider visibility impacts, though there are numerous studies of urban PM source attribution. The order of discussion below on the cause of haze is by region beginning in the western U.S. and proceeding to the east, analogous to dominant air flow patterns across the lower 48 states and will include information from urban studies along side those of remote-area haze investigations.

Based on modeling of an episode (September 23-25, 1996) in the California South Coast Air Basin (SCAB) and another episode (January 4-6, 1996) in the San Joaquin Valley (SJV) by Ying and Kleeman (2006, [098359](#)), about 80% of the particulate SO_4^{2-} for both regions are from upwind sources (i.e., thought to be principally from offshore sources including marine shipping, long-range transport and natural marine sources), with most of the remaining associated with diesel and high-sulfur fuel combustion. Kleeman et al. (1999, [011286](#)), using a combination of measurements and modeling, showed that the upwind particulate SO_4^{2-} source region for the SCAB was over the Pacific Ocean (confirmed by measurements on Santa Catalina Island) and that these particles subsequently grew with accumulation of additional secondary aerosol material, principally ammonium nitrate as they traversed the SCAB. The majority of the nitric acid that forms particulate nitrate in the SCAB is from diesel and gasoline combustion (~63%), while much of the ammonia is from agricultural sources (~40%), catalyst equipped gasoline combustion (~16%), and

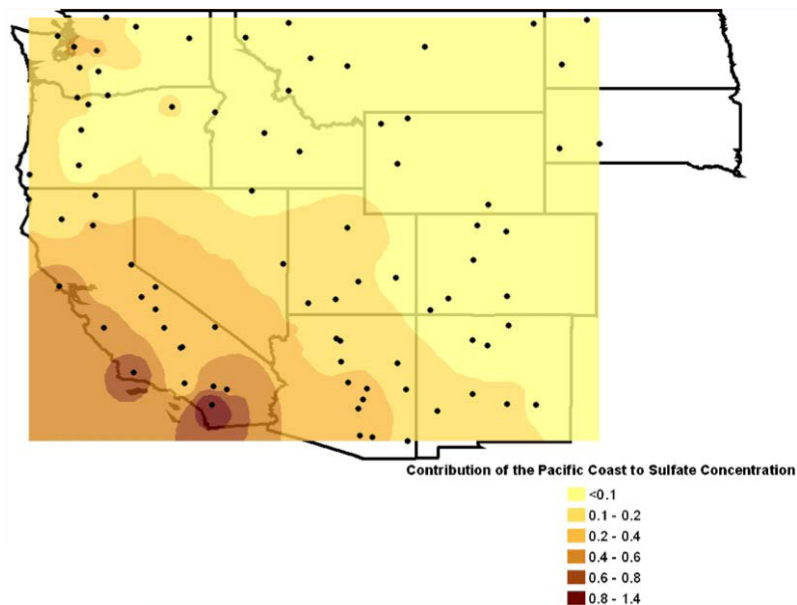
upwind sources (~18%). The majority of the OC found in SCAB was attributed in this study to primary emissions by transportation-related sources including diesel (~13%) and gasoline (~44%) engines and paved road dust (~12%). At the Fullerton site in the middle of the SCAB the concentration of locally generated organics is roughly double that of the locally generated nitrates (~5.6 $\mu\text{g}/\text{m}^3$ compared to ~2.4 $\mu\text{g}/\text{m}^3$), while at Riverside on the east edge of the SCAB and near the large agricultural sources of ammonia emissions, the particulate nitrate concentrations are nearly double that of organic PM (~17 $\mu\text{g}/\text{m}^3$ compared to ~10 $\mu\text{g}/\text{m}^3$).

Ying and Kleeman (2006, [098359](#)) showed that during the winter 1996 episode in the SJV most of the nitric acid that forms particulate nitrate is from upwind sources (~57%) with diesel and gasoline combustion contributing most of the rest (30%), while much of the ammonia is from upwind sources (~39%) and a combination of area, soil and fertilizer sources (~52%). In an assessment of PM particle size and composition in the SJV during the winter of 2000-2001, Herner et al. (2006, [135981](#)) showed that fresh emissions of carbonaceous PM from combustion sources in urban locations (Sacramento, Modesto, and Bakersfield, CA) move quickly from ultrafine particle size (i.e., diameter ~0.1 μm) to accumulation mode by condensation with accumulation mode (i.e., diameter ~0.5 μm) particles, and that secondary nitrate particle formation occurs preferentially on the surface of hydrated ammonium sulfate particles during the afternoon when gas-phase nitric acid is at peak photo-chemical production from NO_x . Given the abundance of ammonia emissions and low ambient temperatures, particulate nitrate production in this way is only limited by the availability of nitric acid. Due to the cool winter conditions there was little secondary organic aerosol production during this study. Sea salt was shown to dominate the larger coarse particle mode during on-shore wind at the background coastal monitoring site at Bodega Bay, north of San Francisco, CA.

Using a regression analysis to find the dependence of particulate SO_4^{2-} concentration measured over a 3-yr period (2000-2002) at 84 western IMPROVE monitoring sites on the modeled transport trajectories to the sites for each sample period, Xu et al. (2006, [102706](#)) were able to infer the source regions that supplied particulate SO_4^{2-} in the western U.S. Among the source regions included in this analysis was the near coastal Pacific Ocean (i.e., a 300 km zone off the coast of California, Oregon, and Washington). Up to half of the particulate SO_4^{2-} measured at Southern California monitoring sites was associated with this source region. As shown in Figure 9-30 the zone of impact from this source region

included large regions of California, Arizona, and Nevada. The authors made the case that high sulfur content fuel used in marine shipping and port emissions may be largely responsible. As a result, the WRAP RPO emissions inventory was modified to include marine shipping and a Pacific Offshore source region was added to source attribution by air quality simulation modeling.

The SO_4^{2-} attribution results of the WRAP air quality modeling (results available on the Technical Support System (TSS) website, see Table 9-1 for the web-link) credit the Pacific offshore source region with somewhat smaller contributions than those from the trajectory regression work by Xu et al. (2006, [102706](#)) with concentrations at the peak impact site in California that are about 45% compared to 50% by regressions and even greater differences for more distant monitoring sites. Based on the modeling attribution the Pacific offshore source region was responsible for 10%-20% of the nitrate measured in Southern California.



Source: Xu et al. (2006, [102706](#)).

Figure 9-30. Contributions of the Pacific Coast area to the ammonium sulfate ($\mu\text{g}/\text{m}^3$) at 84 remote-area monitoring sites in western U.S. based on trajectory regression for all sample periods from 2000-2002 (dots denote locations of the IMPROVE aerosol monitoring sites).

A coordinated effort by federal, state, and county air quality organizations to determine the causes of haze in the Columbia River Gorge (a deep and narrow gap in the

Cascade Mountains on the Washington/Oregon border) through extensive multiyear measurements and high spatial resolution air quality modeling of typical episodes demonstrated the multitude of emission sources that contribute to its impairment (Pitchford et al., 2008, [180159](#)). During the summer, gorge winds are generally from the west and relatively dry. More than half of the haze during a typical summer episode is from a combination of international and other distant sources (~22% at the western end of the gorge) plus regional natural sources including wildfire and secondary organic PM from biogenic emissions (~39% at the eastern end of the gorge). The Portland/Vancouver metropolitan area was responsible for a significant amount of the haze during the summer (~20% on in the western end of the gorge), while sources within the gorge were responsible for a moderate amount of haze (~6% and ~9% at the western and eastern ends of the gorge). The wind is much more often from the east during the winter. The highest haze conditions in the gorge are during the winter and are associated with fog conditions that rapidly convert precursor gaseous emissions of NO_x and SO₂ from local and regional combustion sources and NH₄ from local and regional agricultural activities to secondary nitrate and SO₄²⁻ PM that persist as a post-fog intense haze. Contributions by these sources east of the gorge contribute ~57% of the haze on the eastern end of the gorge, with half of the nitrate and SO₄²⁻ particulate from electric utility emissions and most of the rest from transportation sources. Other sources contributing during the winter haze at the eastern end of the gorge are from sources outside the modeling domain (i.e., most of Washington and Oregon) and within the gorge (~23% and ~10%, respectively).

An assessment of concurrent measurements at the nearby Mt. Hood IMPROVE monitoring site (45 km south of the Columbia River at 1531m ASL) shows that Columbia River Gorge haze conditions and especially the wintertime high nitrate/SO₄²⁻ contributions to haze are not typical of the generally higher elevation remote areas of the region (Pitchford et al., 2008, [180159](#)). However Gorge-like high wintertime nitrate and SO₄²⁻ are found at the Hells Canyon IMPROVE site, which is similarly situated in a narrow canyon of the Snake River almost 400 km east of the Gorge (from the VIEWS web site, see Table 9-1), implying that there may be a substantial vertical concentration gradient during winter in this complex terrain.

Several example monitoring locations distributed across the northern and southern portions of the western U.S. have been selected to illustrate the attribution results from the WRAP-sponsored attribution analysis tools that estimate the relative responsibility for

haze of the various PM species by source region and source type. The selected sites include Olympic NP (NP), WA; Yellowstone NP, WY; and Badlands NP, SD across the north, and San Gorgonio Wilderness (W), CA; Grand Canyon NP, AZ and Salt Creek W, NM across the south as shown in Figure 9-31.

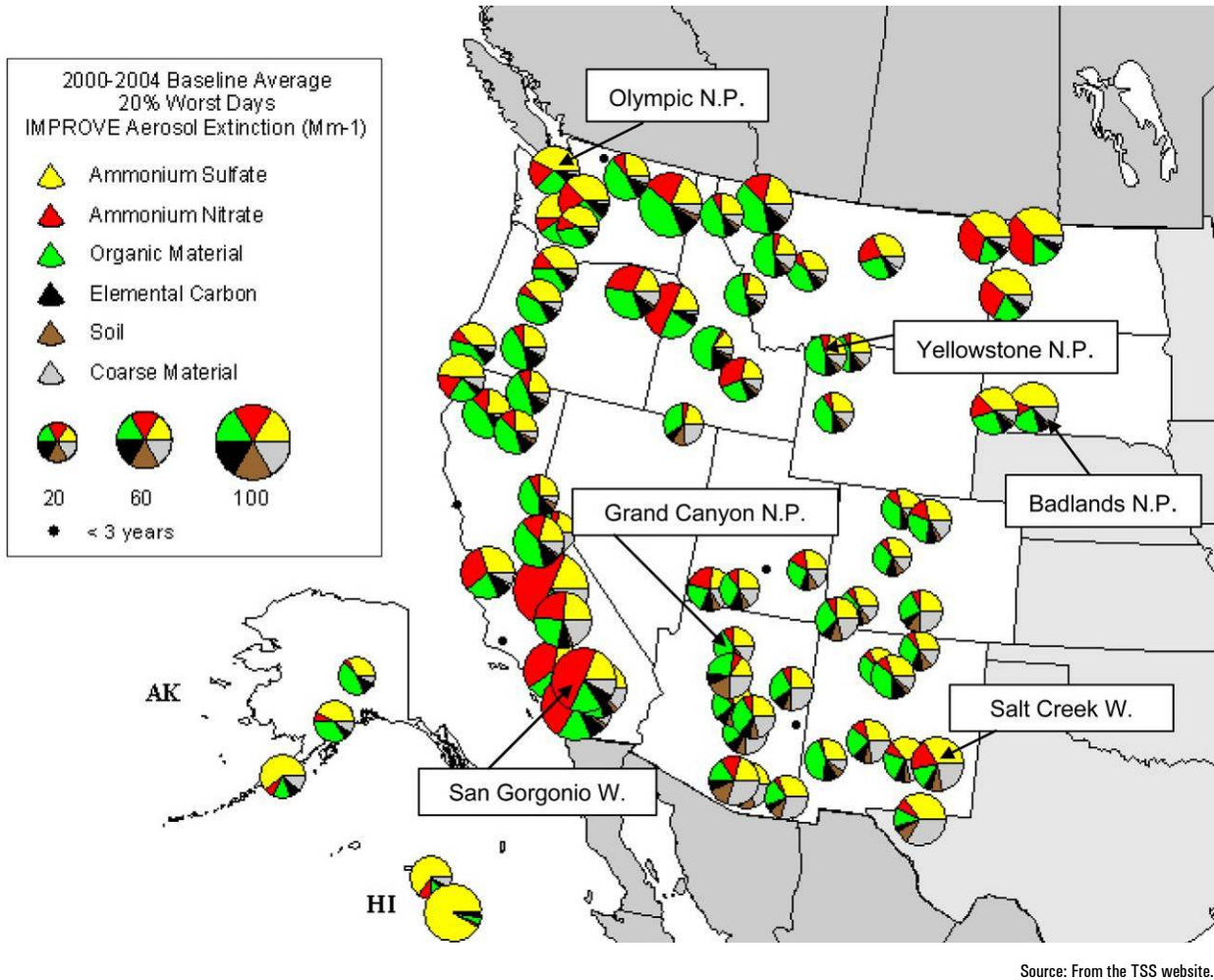


Figure 9-31. Shows the IMPROVE monitoring sites in the WRAP region with at least three yr of valid data and identifies the six sites selected to demonstrate the apportionment tools. Pie diagrams show the composition for the mean of the 20% worst haze conditions and the mean light extinction (Mm^{-1}) by the size of the circle (see figure key).

WRAP-sponsored CMAQ modeling for 2002 used virtual tracers of SO_2 and NO_x emissions that tracked the source region and category through the transport and transformation processes to particulate SO_4^{2-} and nitrate. This was used to produce pie diagrams of particulate SO_4^{2-} and nitrate attribution results by source region for each of

these sites as shown in Figure 9-32 (produced using the TSS, see Table 9-1). Based on these sites, over half of the particulate SO_4^{2-} in remote areas of the Pacific coastal states is from outside of the U.S. (Pacific offshore and outside of the domain). The outside of the domain values were derived by simulating the fate of the boundary condition concentrations, which for the WRAP air quality modeling were obtained using output from the GEOS-CHEM global air quality model (Fiore et al., 2003, [047805](#)). The SO_4^{2-} fraction from the region labeled outside of domain was approximately uniform throughout the western U.S. with site-to-site variation in the fraction caused mostly by variations in total SO_4^{2-} concentration. The more northerly sites have impacts from Canadian emissions, while the southern sites have impacts from Mexican emissions. Half of the Salt Creek, New Mexico SO_4^{2-} is from the domestic source emissions further to the east, which also contribute about 20% to Badlands particulate SO_4^{2-} concentrations. A breakout of the emission sources from within the WRAP region by source type (not shown) has most of the emissions from point sources, with the combination of motor vehicle, area and wildfire emissions contributing from a few percent at the furthest eastern sites to about half at San Geronio.

By comparison, the particulate nitrate is much more from domestic regional emission sources, with ~60%-80% being from emissions within the WRAP region. For the west coast sites about 25% of the nitrate is from a combination of Pacific offshore emissions (i.e., marine shipping) and outside domain regions. Canadian emissions are responsible for about 10%-30% of the particulate nitrate for the three northern sites, but Mexican emissions do not contribute appreciably to particulate nitrate for the three southern sites. Motor vehicles are the largest contributing NO_x source category responsible for particulate nitrate for these six WRAP sites, with a combination of point, area and wildfire source categories also contributing from about 10%-50% of the WRAP regional emissions.

WRAP only used the virtual tracer approach to investigate source locations and categories for SO_2 and NO_x emissions. A different type of virtual tracer modeling tool was used to track the various OC compounds and sort them into three groups for 2002. The first group labeled primary organics includes all of the organics that are emitted directly as PM from any source type and location. The second group labeled anthropogenic secondary organics is PM produced in the atmosphere by aromatic VOCs. The third category labeled biogenic secondary organics is PM produced in the atmosphere by biogenic VOCs. Organic PM in the biogenic secondary category includes those that would functionally be considered man-made emissions (e.g., those from agricultural crops and urban landscapes), though in

most remote areas of the west these man-made VOC emissions are small compared to those of the natural biogenic sources. Figures 9-33, 9-34 and 9-35 show the monthly averaged apportionment of organic PM for the six selected monitoring locations.

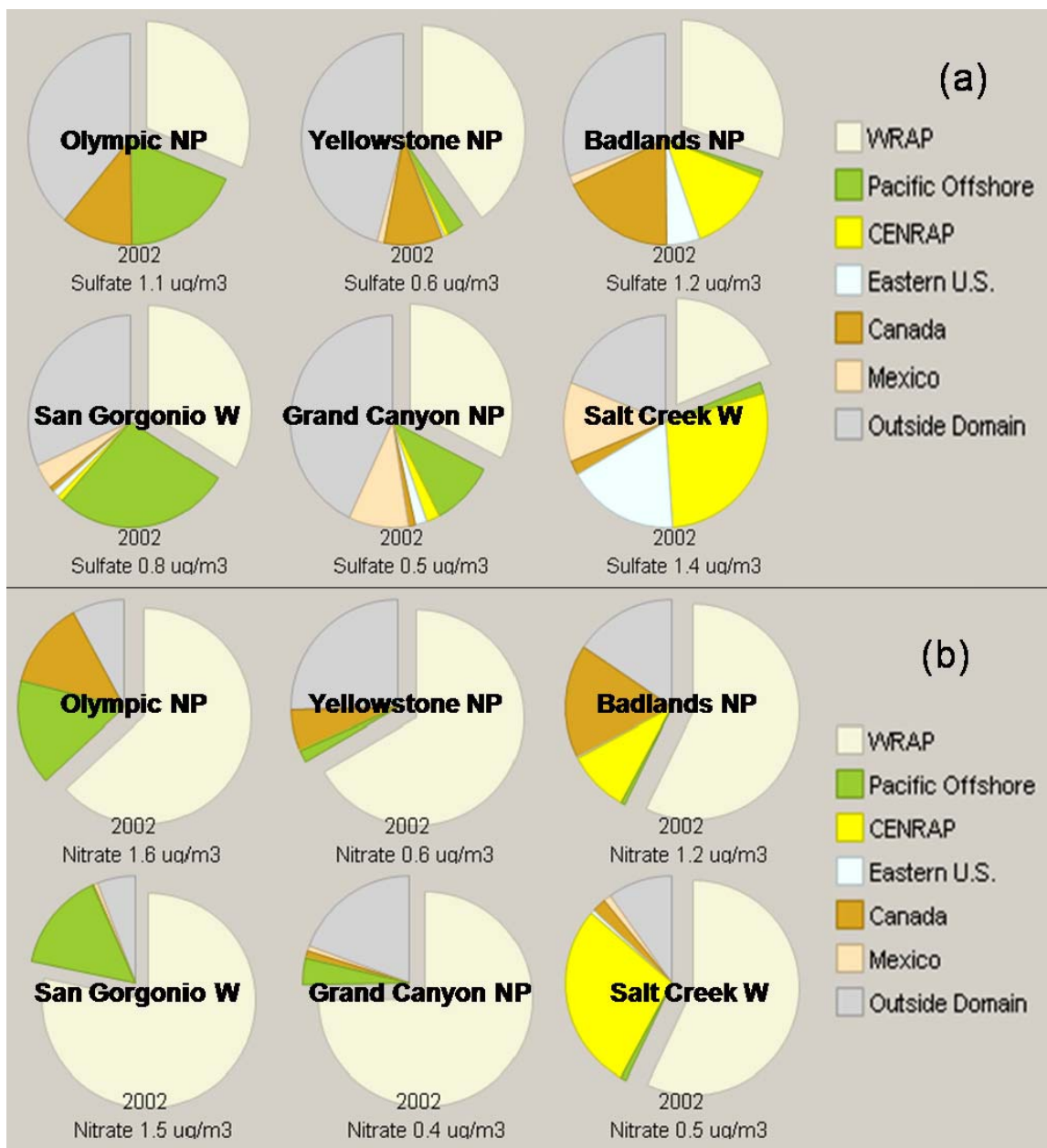
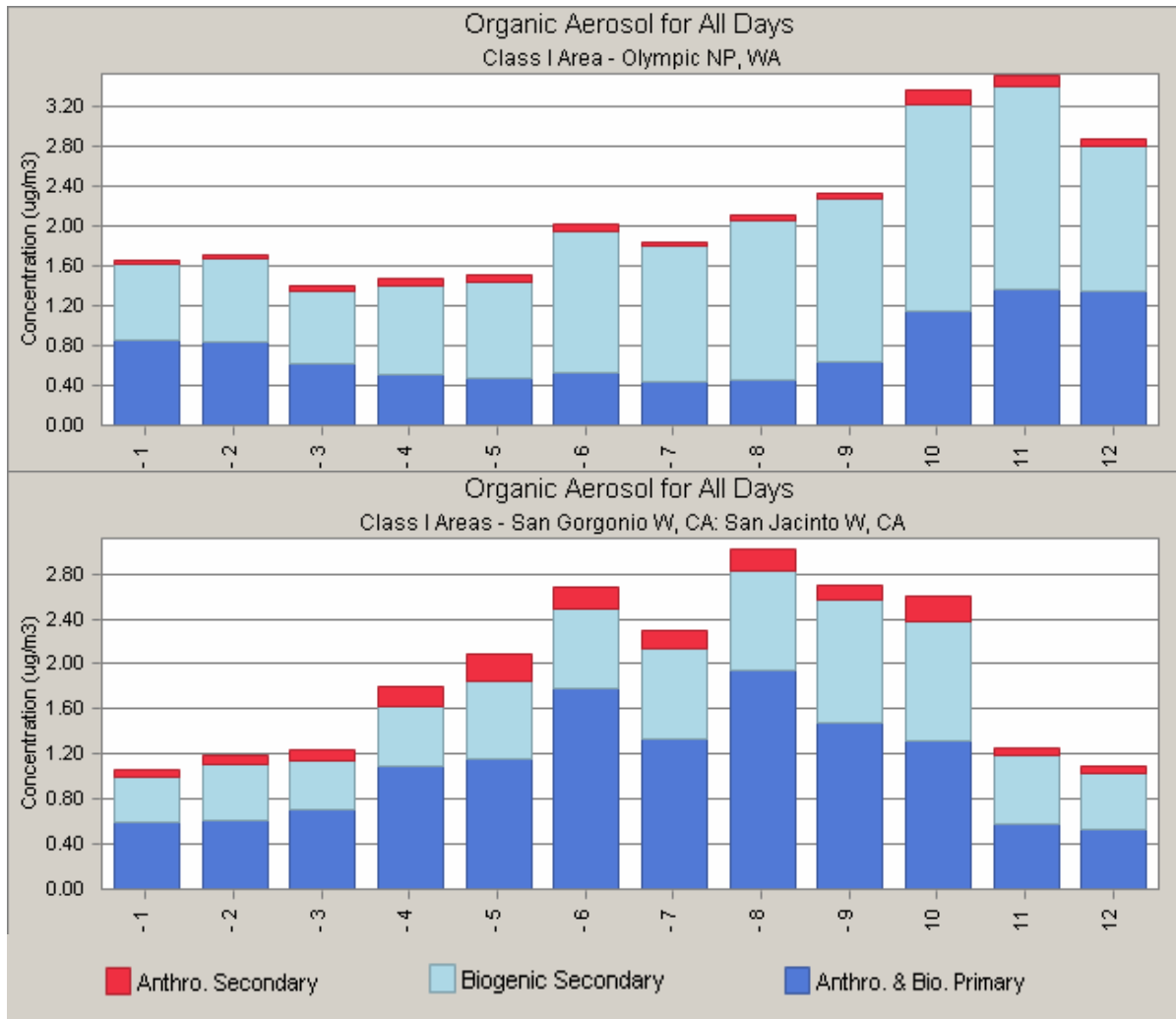


Figure 9-32. Particulate SO_4^{2-} (a) and nitrate (b) source attribution by region using CAMx modeling for six western remote area monitoring sites: top left to right Olympic NP, WA; Yellowstone NP, WY; Badlands NP, SD; bottom left to right San Gorgonio W, CA; Grand Canyon NP, AZ; and Salt Creek W, NM. WRAP includes ND, SD, WY, CO, NM and all states further west. CENRAP includes all states east of WRAP and west of the Mississippi River including MN. Eastern U.S. includes all states east of CENRAP. The Pacific Offshore extends 300km to the west of CA, OR, and WA. Outside Domain refers to the modeling domain, which extend hundreds of kilometers into the Pacific and Atlantic Oceans and from Hudson Bay Canada to just north of Mexico City. This figure was assembled from site-specific diagrams produced on the TSS web site (see Table 9-1) for 2002.

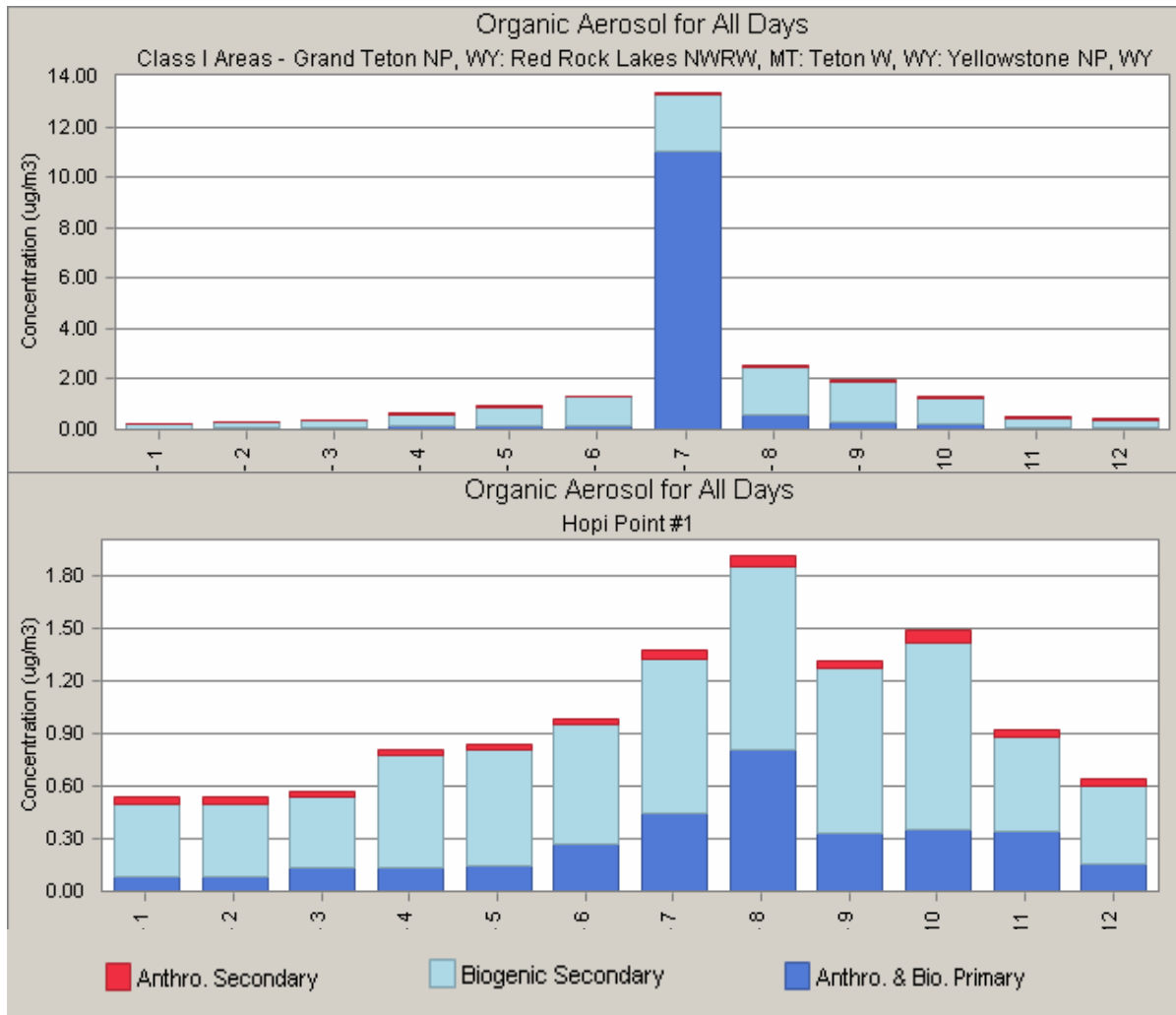


Source: From the TSS website, see Table 9-1.

Figure 9-33. Monthly averaged model predicted organic mass concentration apportioned into primary and anthropogenic and biogenic secondary PM categories for the Olympic NP (top) and San Geronio Wilderness (bottom) monitoring sites.

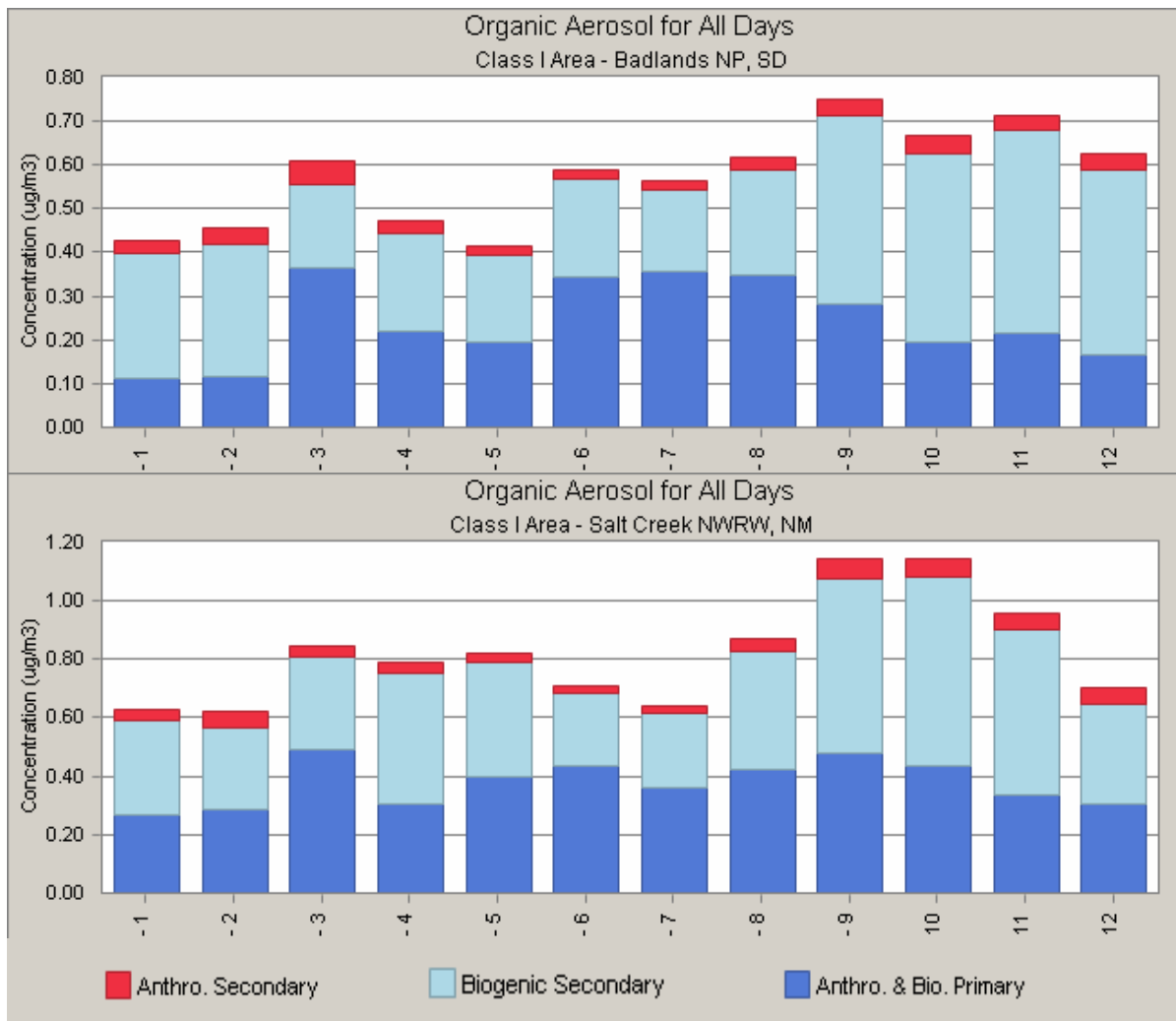
Based on the modeling results for these six sites and confirmed by measurements (see, e.g., Figure 9-10), a west to east decreasing gradient of organic mass exists with annual concentrations from $\sim 2 \mu\text{g}/\text{m}^3$ for the coastal state sites to $\sim 1 \mu\text{g}/\text{m}^3$ for the intermountain west sites to less than $1 \mu\text{g}/\text{m}^3$ for the sites just east of the Rocky Mountains, discounting the large fire impacts for July at Yellowstone NP which raised its annual mean to $\sim 2 \mu\text{g}/\text{m}^3$. At all of these remote-area sites anthropogenic secondary PM is estimated to be a small fraction of the organic mass, with the largest fractional contribution at the San Geronio monitoring site immediately downwind of the major Southern California urban areas, yet having less than 10% of the monthly mean organic mass from anthropogenic

secondary PM. Of the six selected monitoring sites, San Geronio has the highest fraction of the organic PM from primary emissions (~57%), followed by Yellowstone (~55%), then the two eastern-most sites (Badlands ~42% and Salt Creek 41%), and with Grand Canyon and Olympic national parks the lowest fraction by primary emissions (~37%). Yellowstone NP would have had the lowest fraction of organic PM by primary emissions had it not been for the month of July (the 11 month mean is 29%) when wild fire smoke contributed. Results from recent chamber and field studies, and modeling would seem to call into question apportionment of primary and secondary carbon done by traditional air quality model simulations of OC, as described above, due to the combined effects of extensive evaporation of semivolatile primary emissions when diluted and to photochemical reactions of low volatility gas phase species that substantially increases the amount of secondary organic PM (Robinson et al., 2007, [191975](#)).



Source: From the TSS website, see Table 9-1.

Figure 9-34. Monthly averaged model predicted organic mass concentration apportioned into primary and anthropogenic and biogenic secondary PM categories for the Yellowstone NP (top) and Grand Canyon (Hopi Point) (bottom) monitoring sites.



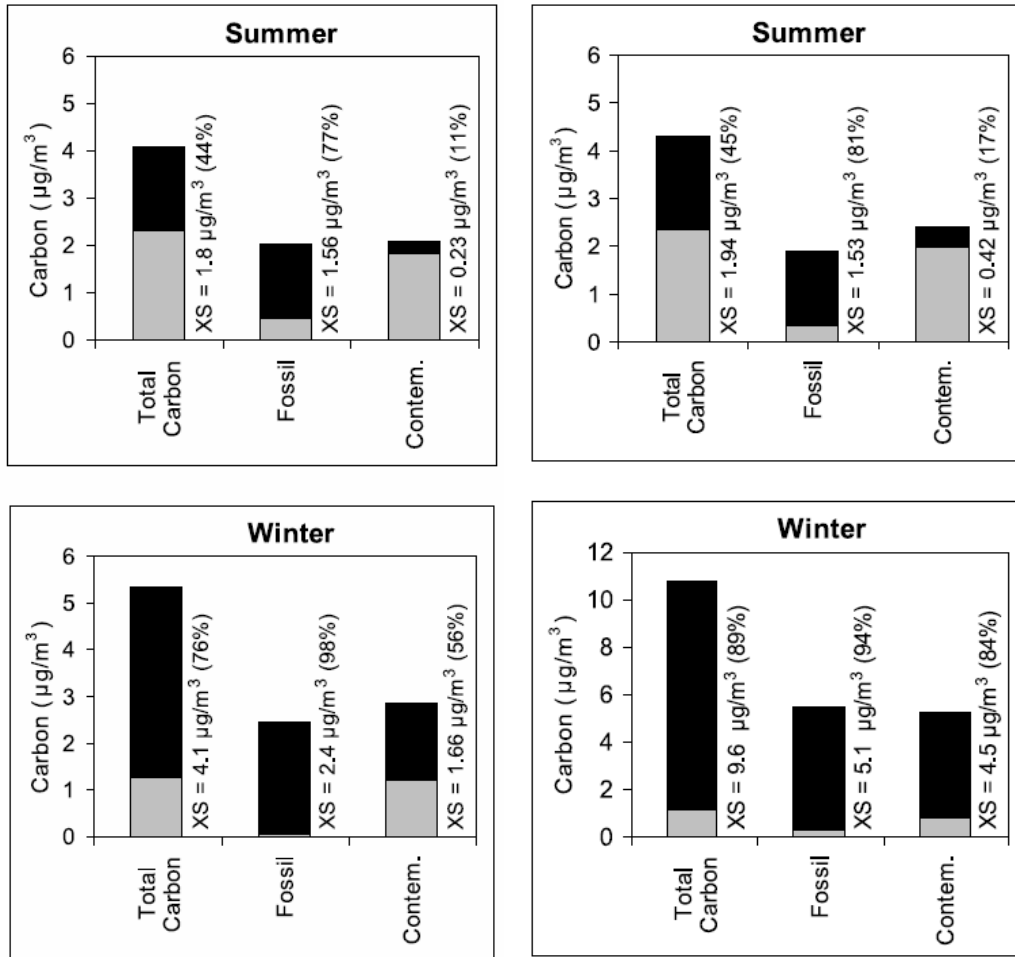
Source: From the TSS website, see Table 9-1.

Figure 9-35. Monthly averaged model predicted organic mass concentration apportioned into primary and anthropogenic and biogenic secondary PM categories for the Badland NP (top) and Salt Creek Wilderness (bottom) monitoring sites.

Radiocarbon (^{14}C) dating techniques were used to group ambient PM carbon into fossil and contemporary source categories at 12 IMPROVE monitoring sites across the U.S., 8 of which are in the WRAP region (Schichtel et al., 2008, [156958](#)). Results of this work showed that contemporary carbon accounts for about half the carbon in urban areas, 70%-97% in near-urban areas (i.e., San Geronio) and 82%-100% in remote areas. Comparing these radiocarbon dating results with the WRAP virtual tracer modeling results for organic aerosol (above), and presuming that the modeled anthropogenic secondary organic is fossil carbon and the biogenic secondary is contemporary carbon, suggests that a large fraction of

the model-determined regional primary organic PM is from contemporary carbon sources (e.g., smoke from wildfires).

Schichtel et al. (2008, [156958](#)) compared radiocarbon measurements at two sets of urban/rural paired sites in the west (Mount Rainer/Seattle, and Tonto/Phoenix). Figure 9-36 shows that most of total carbon urban excess (i.e., urban site concentration minus the regional site concentration) in the summer is from fossil carbon sources (87% and 79%, respectively), while in the winter there is a surprisingly high fraction of the urban excess at both sites that is from contemporary carbon sources (41% and 47%, respectively). This implies that urban, and therefore anthropogenic, activities generate almost as much PM_{2.5} carbon from contemporary sources (e.g., residential wood combustion) as from the fossil sources during the winter for these two western urban areas.



Source: Schichtel et al. (2008, [156958](#)).

Figure 9-36. Comparison of carbon concentrations between Seattle (Puget Sound site) and Mt. Rainer (left) and between Phoenix and Tonto (right) showing the background site concentration (gray) and the urban excess concentration (black) for total, fossil and contemporary carbon during the summer and winter studies.

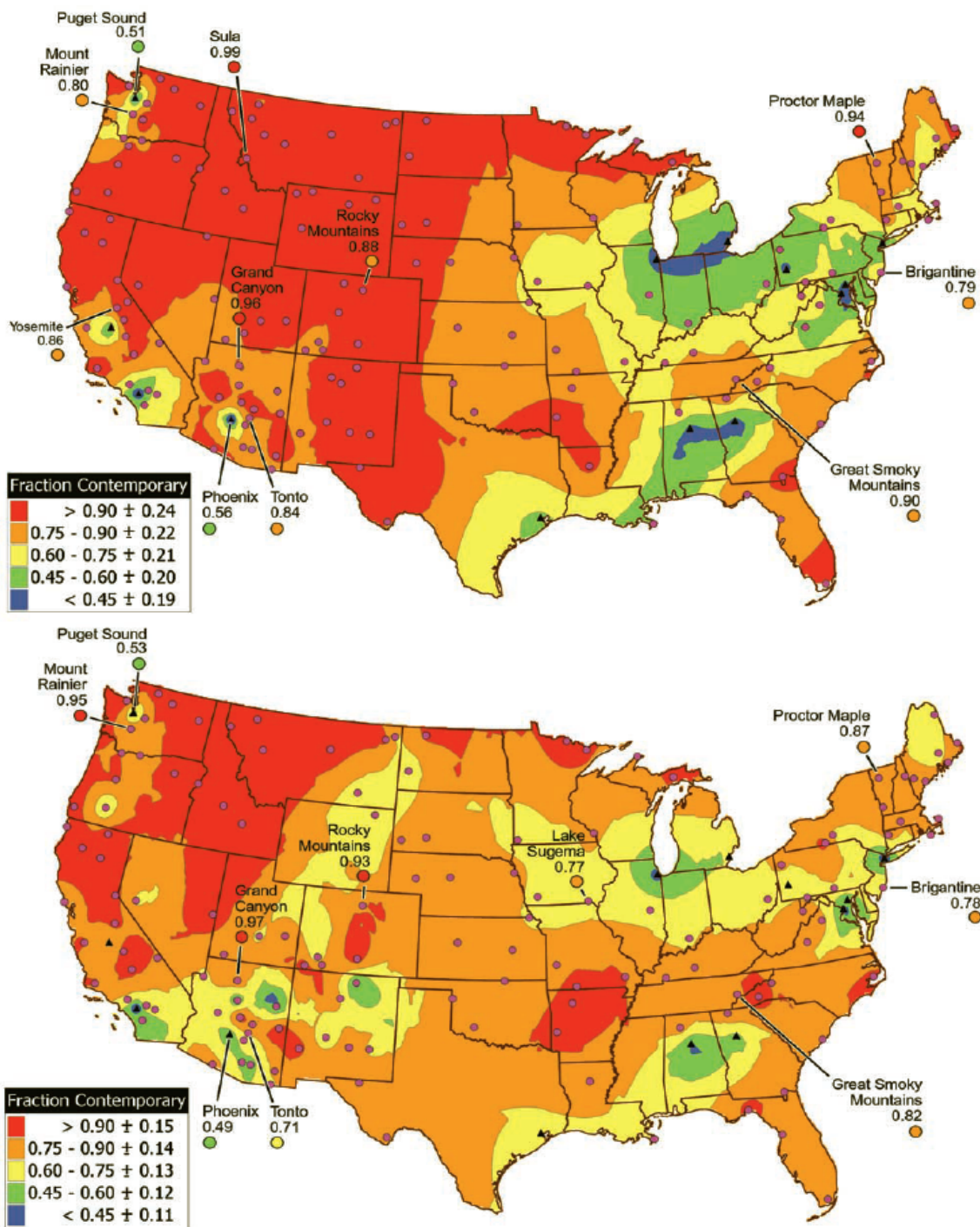


Figure 9-37. Average contemporary fraction of PM_{2.5} carbon for the summer (top) and winter (bottom), estimated from IMPROVE monitoring data (6/04 to 2/06) based on EC/TC ratios. The contemporary values from radiocarbon dating for the 12 monitoring sites are indicated in by colored circles with the site names. Color contours are shown to aid in showing sites with similar values. Site locations are indicated by circles for remote area sites and triangles for urban sites.

Contemporary carbon estimates for all of the IMPROVE network monitoring sites for data from two summer seasons (June, July and August, 2004/2005) and two winter seasons (December, 2004/2005, January and February, 2005/2006) were calculated from the measured EC to total carbon (EC/TC) ratios using the 12-site empirical relationship between radiocarbon determined contemporary carbon fraction and IMPROVE measured EC/TC ratio (Schichtel et al., 2008, [156958](#)). The results are displayed in color contour maps in Figure 9-37, which also shows the radiocarbon determined contemporary carbon for the 12 sites. The lowest contemporary carbon estimates (<60%) in both seasons are for urban areas. In the rural West, most of the sites have over 90% of their PM carbon from contemporary carbon sources during the summer and from 60%-over 90% during the winter. In the rural East, most of the sites have 45%-90% of their PM carbon from contemporary carbon sources during the summer and from 60%-over 90% in the winter.

Schichtel et al. (2008, [156958](#)) showed a strong relationship between the site-averaged EC/TC ratios and the site-averaged fraction of fossil carbon separately for the summer and winter data sets (i.e., R^2 of 0.71 and 0.87, respectively). Using regression analysis they estimated that the summer and winter EC/TC ratios associated with purely fossil carbon were 0.35 ± 0.039 and 0.46 ± 0.028 , respectively, and for purely contemporary carbon the EC/TC ratios were 0.12 ± 0.011 and 0.19 ± 0.0095 . These ratios are shown to be consistent with corresponding ratios from the literature for source testing primary fossil and contemporary combustion sources respectively. They are also shown to be consistent with the 90 percentile value of the EC/TC ratio from the urban IMPROVE monitoring sites (0.41 and 0.44 for summer and winter) and the 10th percentile values of the EC/TC ratio for remote areas IMPROVE monitoring sites (0.07 and 0.16 for summer and winter), which they argue are dominated by fossil and contemporary carbon, respectively.

The largest sources of contemporary carbon are primary emissions from biomass burning and secondary organic aerosol from biogenic precursor gases (e.g., terpenes from conifer forests). Schichtel et al. (2008, [156958](#)) estimated the 12-site overall contribution by secondary organic PM to the summer contemporary carbon fraction as $36 \pm 6.4\%$ by assuming the EC/TC ratio for contemporary carbon during the winter represented the ratio of primary emissions only (i.e., no secondary organic PM formation in the winter) and that the EC/TC ratio for primary emissions is independent of seasons. This approach should provide a lower bound estimate of the secondary OC species. The same method applied to the fossil carbon fraction yielded an estimate of $23 \pm 10\%$ of the fossil carbon PM from

secondary organic formation in the atmosphere during the summer. These estimates correspond to over 40% of the contemporary and over 35% of the fossil OC being from secondary PM formation.

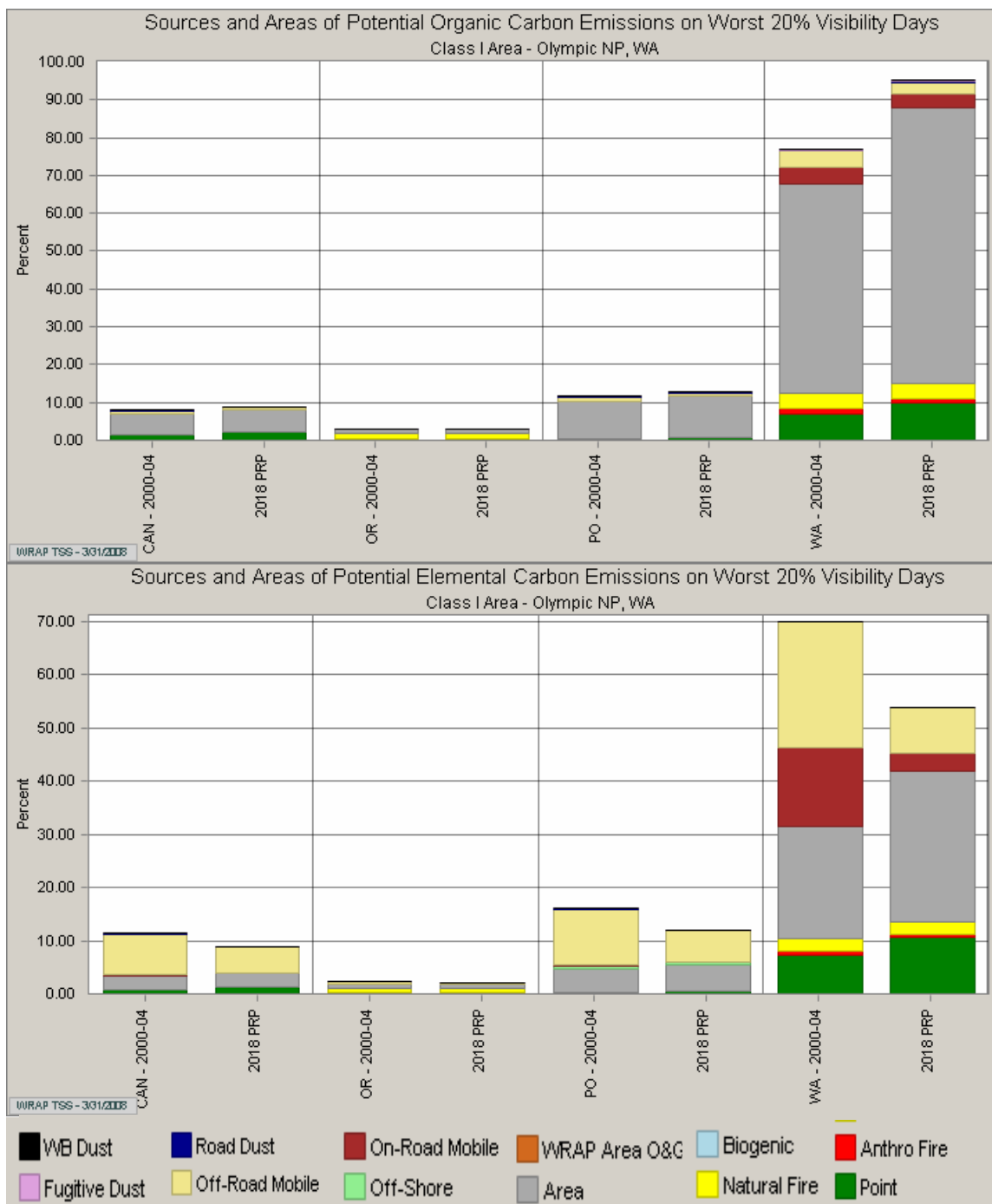
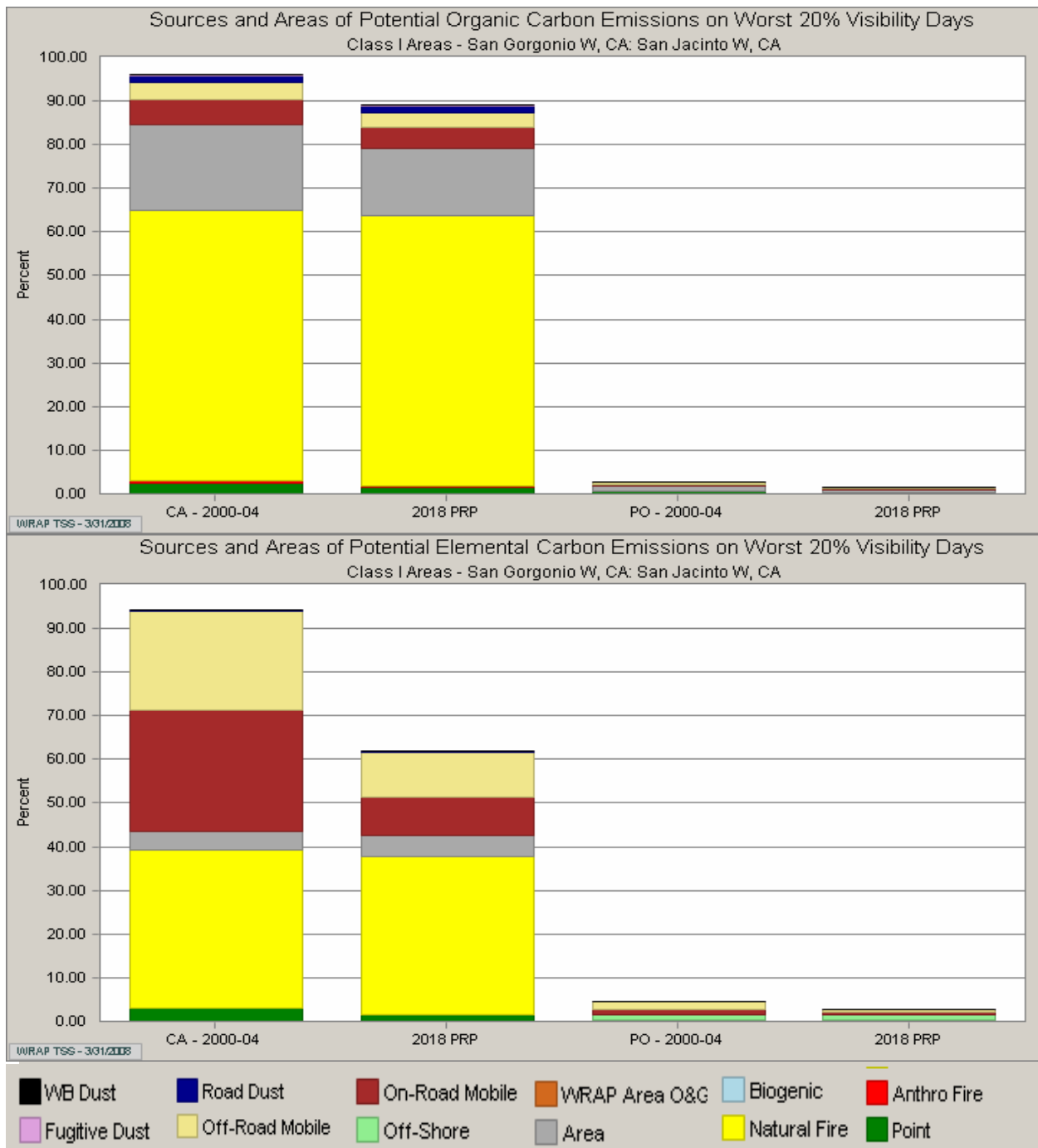


Figure 9-38. Results of the weighted emissions potential tool applied to primary OC emissions (top) and EC emissions (bottom) for the baseline and projected 2018 emissions inventories for Olympic NP. Only source regions (WRAP states and other regions) with the largest estimated contributions are shown (i.e., Canada, Oregon, Pacific Off-Shore, and Washington from left to right). The scale is normalized (i.e., unitless) one over distance weighted emissions multiplied by trajectory residence time.



Source: From the TSS website (see Table 9-1).

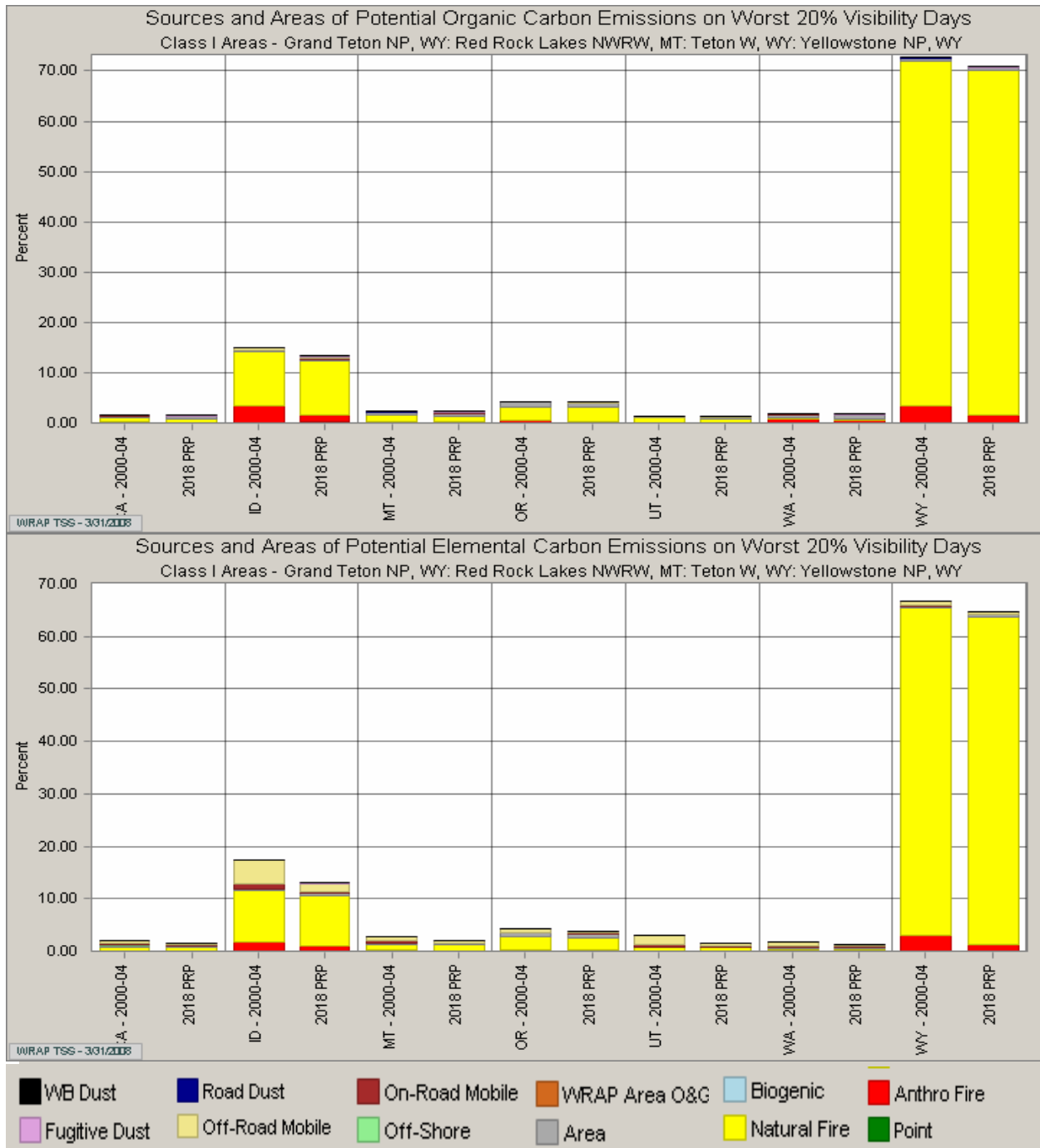
Figure 9-39. Results of the weighted emissions potential tool applied to primary OC emissions (top) and EC emissions (bottom) for the baseline and projected 2018 emissions inventories for San Geronio W. Only source regions (WRAP states and other regions) with the largest estimated contributions are shown (i.e., California and Pacific Off-Shore from left to right). The scale is normalized (i.e., unitless) one over distance weighted emissions multiplied by trajectory residence time.

WRAP applied a weighted emissions potential analysis tool that combined gridded emissions data with back-trajectory analysis that simulated the transport pathway to the various monitoring sites to infer likely source region and emission categories for the 20% best and 20% worst haze conditions for each of the IMPROVE PM speciation monitoring locations in the West. Unlike the virtual tracer approach that uses a full regional air quality simulation model, this method does not explicitly account for chemistry or removal processes and it does not incorporate the sophisticated dispersion estimates (i.e., it uses one over distance weighting for dispersion), so it should be considered a screening tool that has been found to be helpful in identifying the likely sources contributing to haze. More information on this approach is available elsewhere (see the link to the TSS in Table 9-1). Primary organic and EC PM species results from the weighted emissions potential tool for the worst 20% haze days using the 2000-2004 base years' emissions and trajectories, and the same trajectories with 2018-projected emissions for each of the six selected western monitoring locations are shown in Figures 9-38 through 9-43.

For Olympic NP (Figure 9-38), most of the primary organic as well as most of the EC PM is likely to be from the state of Washington during the worst haze days. This is because the multi-day trajectories that transport emissions on its worst days tend to be short (within 200 km based on maps available on TSS, see Table 9-1). Area sources, which include emissions from residential wood heating, watercraft, non-mobile urban and other sources too small to be labeled as point sources, are the big contributors to primary organic, while on- and off-road mobile emissions plus area sources are large contributors to the EC at Olympic NP. The 2018 projected growth in area sources and decrease in emissions of mobile source emissions is anticipated to increase the haze by primary organic while reducing the haze by EC at Olympic NP. The same analysis applied to San Geronio (Figure 9-39), is similar in that the majority of the emissions with the potential to contribute to primary organic and EC PM is from the home state, California in this case. However, the likely importance of natural fire emissions for carbonaceous PM species sites is substantially greater at San Geronio W. than it was for Olympic NP.

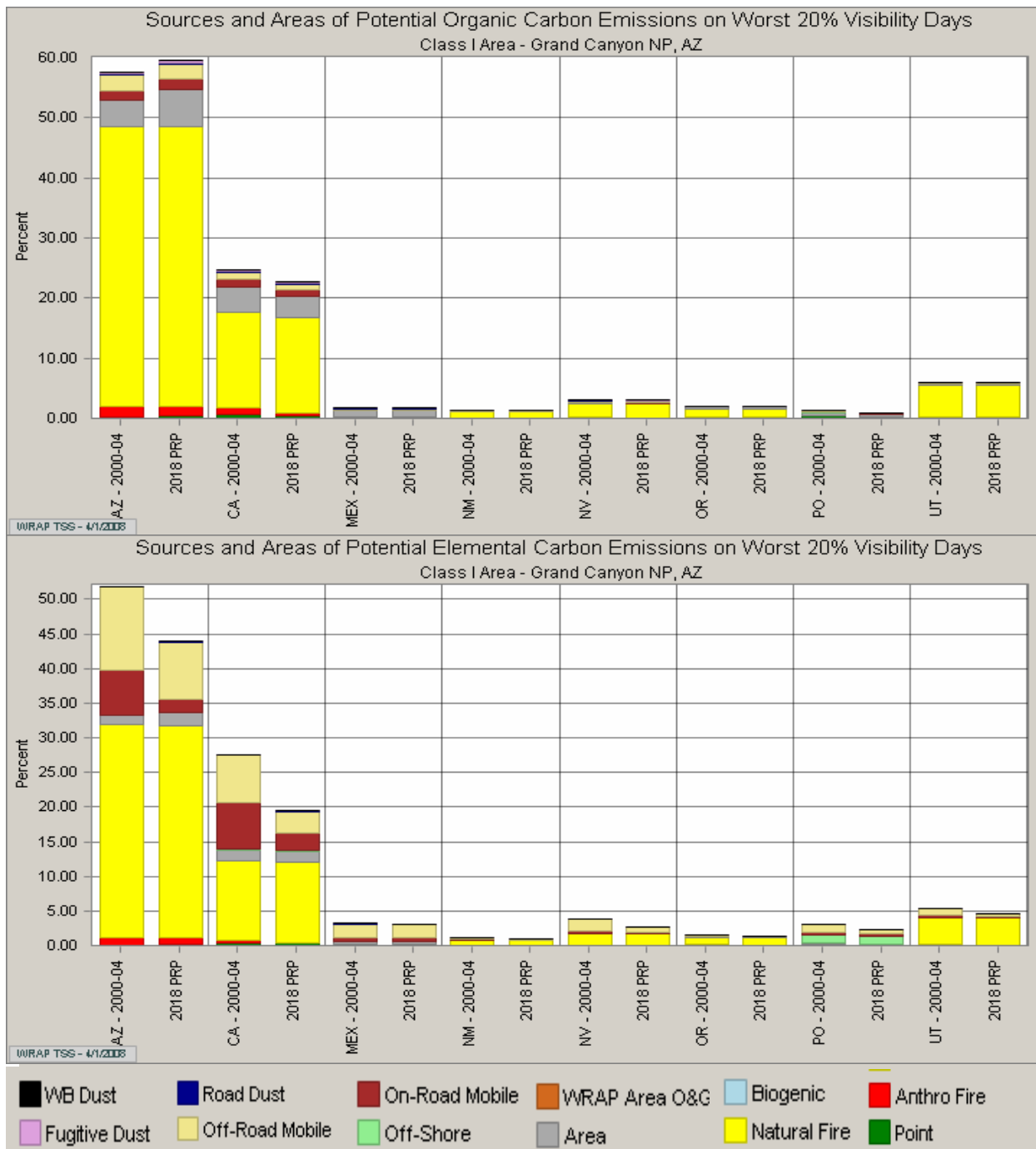
The weighted emissions potential results applied to Yellowstone NP and Grand Canyon NP (Figures 9-40 and 9-41) show the likely dominance of natural fire emissions in the intermountain western U.S. to primary organic and EC PM during worst haze conditions for these two locations. Numerous states have emissions that have the potential to contribute noticeably to these carbonaceous species, due to relatively long multi-day

trajectories (500 km to 1000 km) on worst haze days, though for both sites the home state has the greatest potential based on this inverse distance weighting approach. On- and off-road mobile sources in Arizona and California have significant potential to contribute to Grand Canyon carbonaceous particles, especially EC concentrations, probably due to some of the trajectories being over the populated areas of these two states to the south and southwest of Grand Canyon.



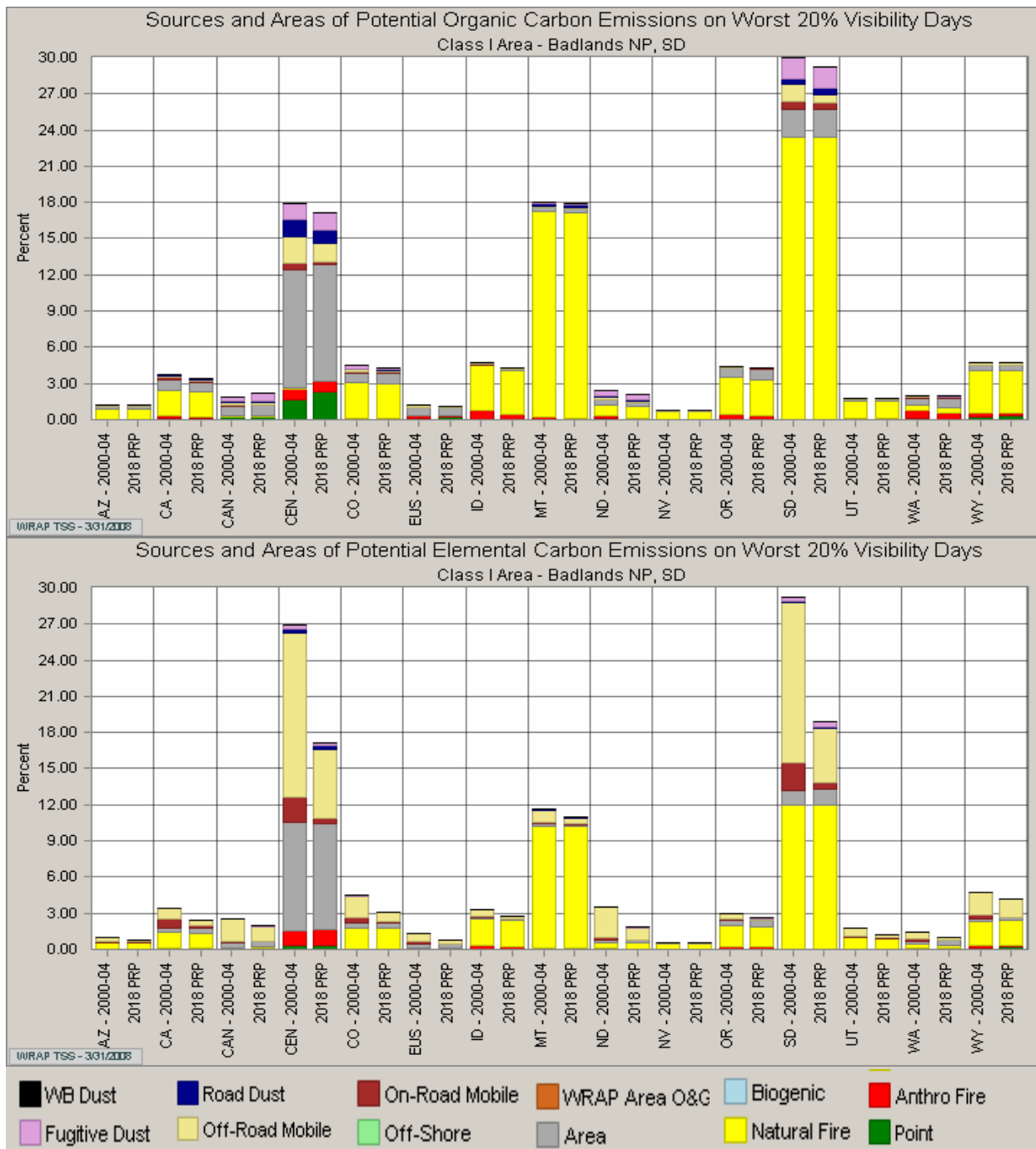
Source: From the TSS website (see Table 9-1).

Figure 9-40. Results of the weighted emissions potential tool applied to primary OC emissions (top) and EC emissions (bottom) for the baseline and projected 2018 emissions inventories for Yellowstone NP. Only source regions (WRAP states and other regions) with the largest estimated contributions are shown (i.e., California, Idaho, Montana, Oregon, Utah, Washington, and Wyoming from left to right). The scale is normalized (i.e., unitless) one over distance weighted emissions multiplied by trajectory residence time.



Source: From the TSS website (see Table 9-1).

Figure 9-41. Results of the weighted emissions potential tool applied to primary OC emissions (top) and EC emissions (bottom) for the baseline and projected 2018 emissions inventories for Grand Canyon NP. Only source regions (WRAP states and other regions) with the largest estimated contributions are shown (i.e., Arizona, California, Mexico, New Mexico, Nevada, Oregon, Pacific Off-shore and Utah from left to right). The scale is normalized (i.e., unitless) one over distance weighted emissions multiplied by trajectory residence time.



Source: From the TSS website (see Table 9-1).

Figure 9-42. Results of the weighted emissions potential tool applied to primary OC emissions (top) and EC emissions (bottom) for the baseline and projected 2018 emissions inventories for Badlands NP. Only source regions (WRAP states and other regions) with the largest estimated contributions are shown (i.e., Arizona, California, Canada, CenRAP, Colorado, eastern U.S., Idaho, Montana, North Dakota, Nevada, Oregon, South Dakota, Utah, Washington, and Wyoming from left to right). The scale is normalized (i.e., unitless) one over distance weighted emissions multiplied by trajectory residence time.

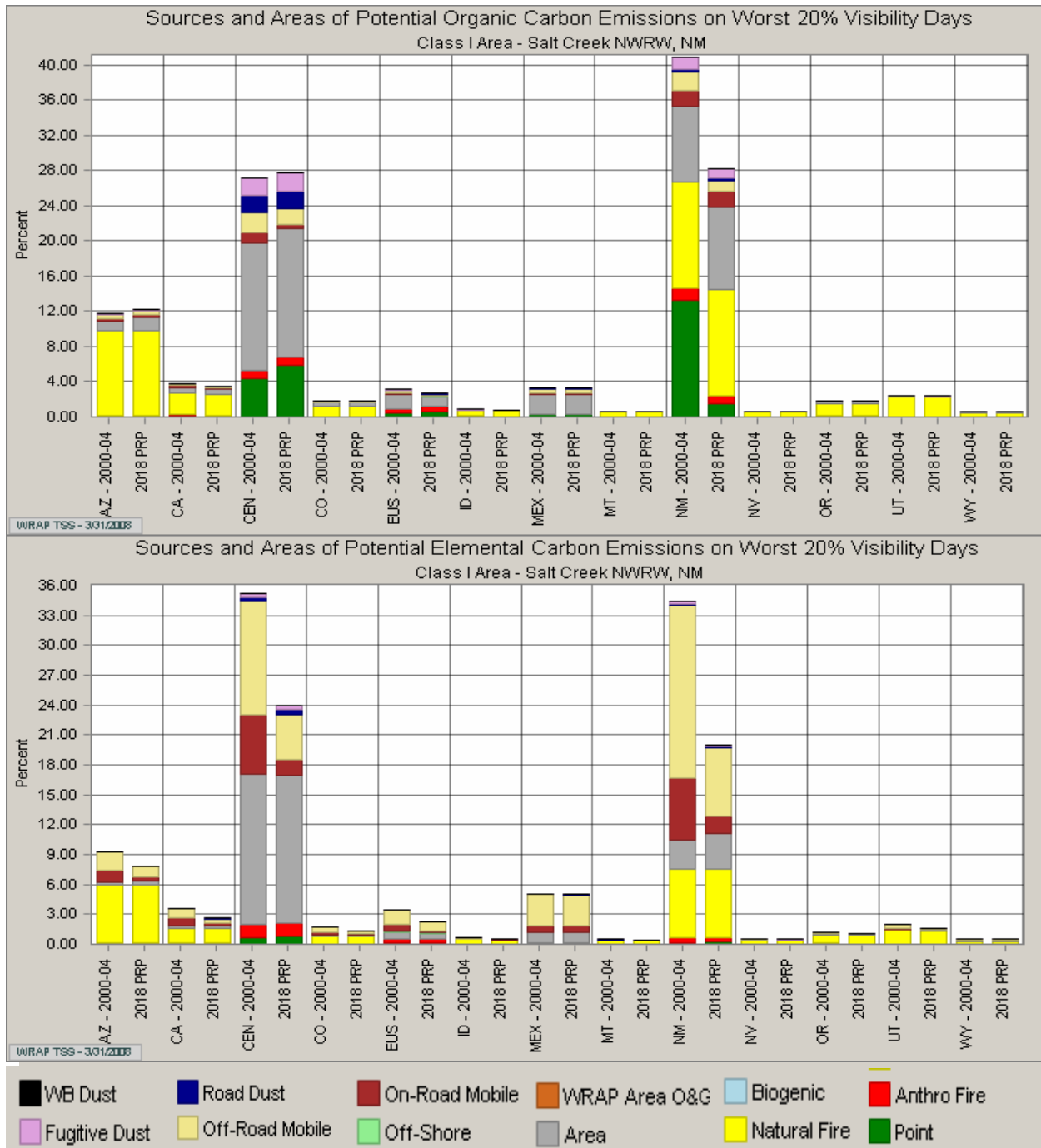


Figure 9-43. Results of the weighted emissions potential tool applied to primary OC emissions (top) and EC emissions (bottom) for the baseline and projected 2018 emissions inventories for Salt Creek W. Only source regions (WRAP states and other regions) with the largest estimated contributions are shown (i.e., Arizona, California, CenRAP, Colorado, eastern U.S., Idaho, Mexico, Montana, New Mexico, Nevada, Oregon, Utah, and Wyoming from left to right). The scale is normalized (i.e., unitless) one over distance weighted emissions multiplied by trajectory residence time.

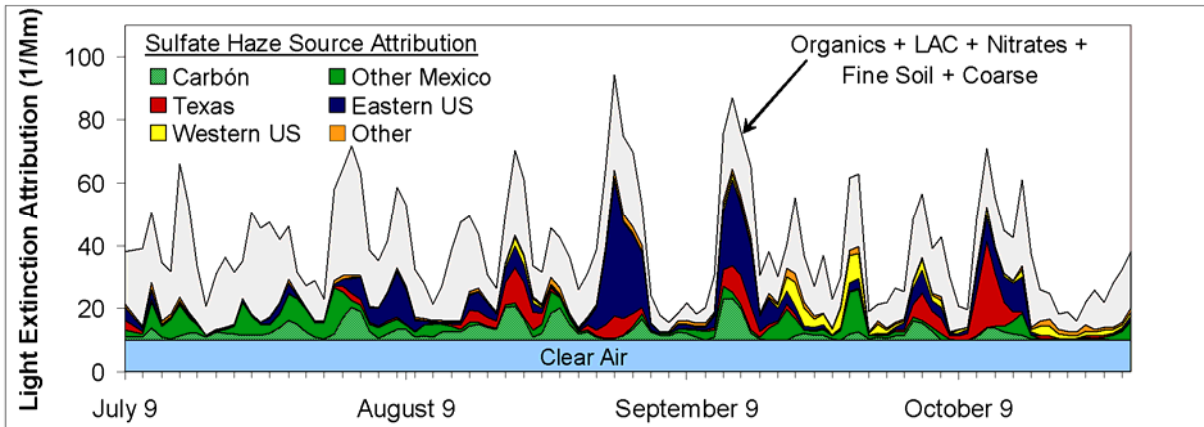
For the most easterly of the selected WRAP sites, Badlands NP and Salt Creek, the weighted emissions potential results for primary organic and EC (Figures 9-42 and 9-43) show potential contributions from a greater number of states and multi-state regions than for selected sites further to the west. This may be due in part to trajectories associated with worst haze conditions for these two sites being moderately long (~500 km) and in multiple directions. Natural fire emissions have the greatest potential to contribute to organic species PM at Badlands NP, but are less likely to be dominant at Salt Creek or at either site in its contribution to EC PM concentrations. The contributions by emissions from area and mobile sources from the home states and states to the east (Central States Regional Air Partnership states are labeled “CEN” in the figures) are potentially greater than by natural fire; this is especially true for contributions to EC PM.

WRAP applied the weighted emissions potential tool to assess likely source types and regions contributing to coarse mass concentrations. The results for the six selected monitoring sites (not shown) are as follows. Most dust at Olympic NP is likely to be from fugitive dust sources in Washington state, while at San Geronio it is likely more from road dust with smaller amounts from fugitive dust sources. The amount from wind-blown dust is small for both of these far westerly sites. Wind-blown dust is likely the largest source contributing to coarse mass at Grand Canyon NP, Badlands NP and Salt Creek Wilderness with most of it originating in the home-state for those sites. The weighted emissions potential results for coarse mass at Yellowstone are different from those of the other five selected sites in that Idaho and Montana each have a higher potential to contribute to coarse mass on the worst haze days than the home state (Wyoming), and that wind-blown and road dust both contribute substantially as does fugitive dust and natural fire.

In another WRAP-sponsored effort to better understand the causes of remote area haze in the western U.S., each of the worst haze days for all western IMPROVE monitoring sites where dust (defined as the sum of coarse mass and fine soil PM) was the largest

contributor to light extinction was separately assessed to categorize the most likely dust source (Kavouras et al., 2007, [156630](#); Kavouras et al., 2009, [191976](#)) and the Causes of Haze Website – see Table 9-1). Elemental composition was used to assess the likelihood that the dust was associated with long-range transport from Asia. A regression analysis at each site between dust concentrations and coincident local wind speed was used to generate site-specific estimates of local windblown dust for each sample period. Finally, back trajectory analysis combined with maps constructed of wind erosion potential (i.e., developed by combining soil types and land cover classifications) are used in a manner similar to the weighted emissions potential analysis to identify the likelihood of regionally transported wind-blown dust as the source. These assessments were conducted on each of the 610 so-called “worst dust haze days” at 70 monitoring sites for data from 2001-2003 to classify each day by its likely contributions from Asian dust, local windblown dust, upwind transport and undetermined. The undetermined category includes those sample periods that failed to be classified into one of the other three source categories suggesting that mechanically suspended dust activities (e.g., unpaved road dust, agricultural, construction and mining activities) may be responsible.

Of the 610 “worst dust haze days” at the 70 WRAP monitoring sites, 55 sample periods are classified as Asian dust influenced, almost exclusively in the spring; 201 sample period are classified as local windblown dust, mostly in the spring but some in all seasons; 240 sample periods are classified as upwind transported dust, with a broader seasonal distribution centered on summer and few instances during winter; and 114 are in the undetermined category with most in summer and least in winter. Most dust days occurred in the deserts of Arizona, New Mexico, Colorado, western Texas and southern California, and these were dominated by local and regionally transported wind-blown dust (e.g., 84% for Salt Creek W). Asian dust caused only a few of the worst dust days during the 3-yr assessment period, though it is an important source (i.e., 10-40% of the worst dust days) for sites in the more northern regions of the West with greater vegetative land-cover where local and regionally transported wind-blown dust was infrequent. The frequency of worst dust events classified as undetermined was greatest for sites in the vicinity of large urban and agricultural areas such as those in California and southern Arizona.



Source: Pitchford et al. (2005, [156874](#))

Figure 9-44. BRAVO study haze contributions for Big Bend NP, TX during a 4-mo period in 1999. Shown are impacts by various particulate SO_4^{2-} sources, as well as the total light extinction (black line) and Rayleigh or clear air light scattering.

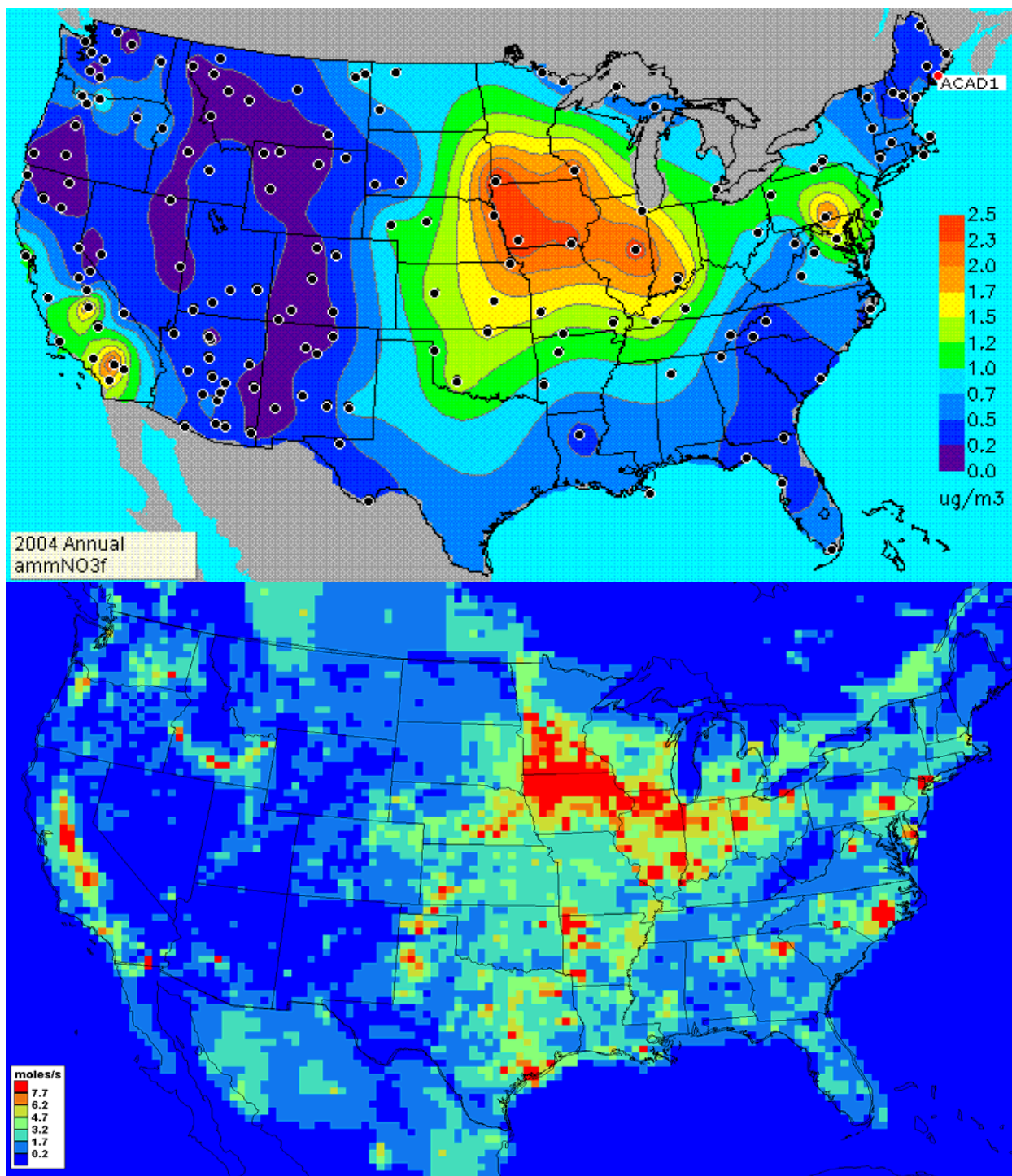


Figure 9-45. Maps of spatial patterns for average annual particulate nitrate measurements (top), and for ammonia emissions for April 2002 from the WRAP emissions inventory (bottom).

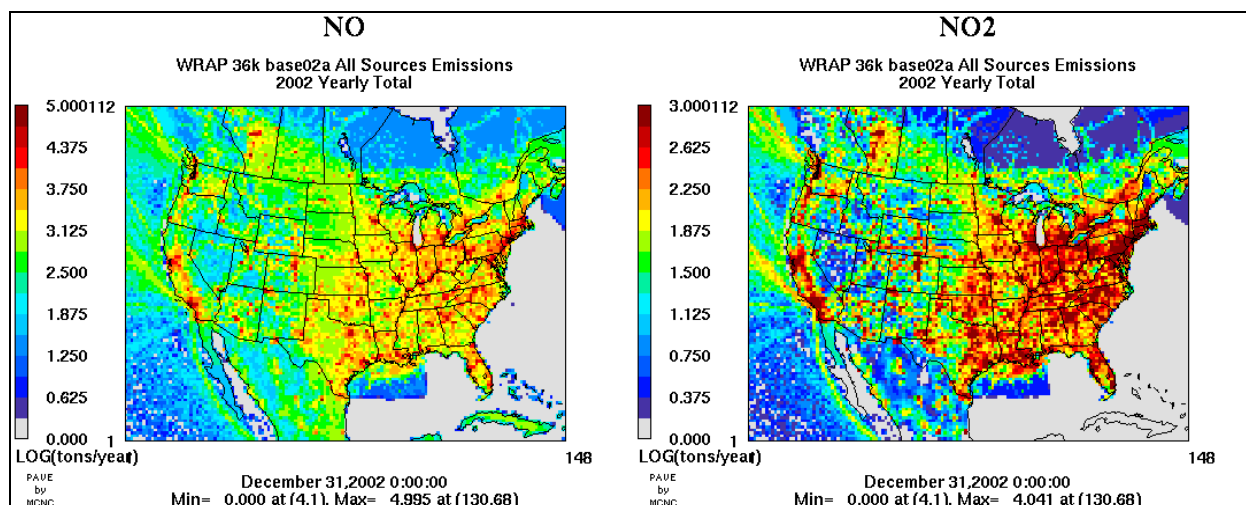


Figure 9-46. Maps of spatial patterns of annual NO (left) and NO₂ (right) emissions for 2002 from the WRAP emissions inventory.

Source attribution of the particulate SO₄²⁻ contribution to haze at Big Bend NP, TX was a primary motivation for the BRAVO study. Schichtel et al. (2005, [156957](#)) showed that during the four-month field monitoring study (July-October, 1999) SO₂ emissions sources in the U.S. and Mexico were responsible for ~55% and ~38% of the particulate SO₄²⁻, respectively. Among U.S. source regions, Texas was responsible for ~16%, eastern U.S. ~30%, and the western U.S. ~9%. A large coal fired power plant, the Carbón facility in Mexico, just south of Eagle Pass, TX, was responsible for about ~19%, making it the largest single contributor. Pitchford et al. (2005, [156874](#)) put these results into the context of other component contributions to regional haze, plus seasonal and longer-term variations in haze by particulate components. Figure 9-44 shows the temporal variation of the contributions by the various SO₂ emissions source regions plus the Carbón facility during the BRAVO study period. The largest particulate SO₄²⁻ peak haze periods are dominated by infrequent large contribution by emission sources in TX and eastern U.S., while Mexican sources including the Carbón facility are more frequent contributors to haze, but at generally lower light extinction values. Particulate nitrate contributions to haze at Big Bend NP are among the lowest measured in the U.S. (~3% of light extinction on average and for worst haze episodes).

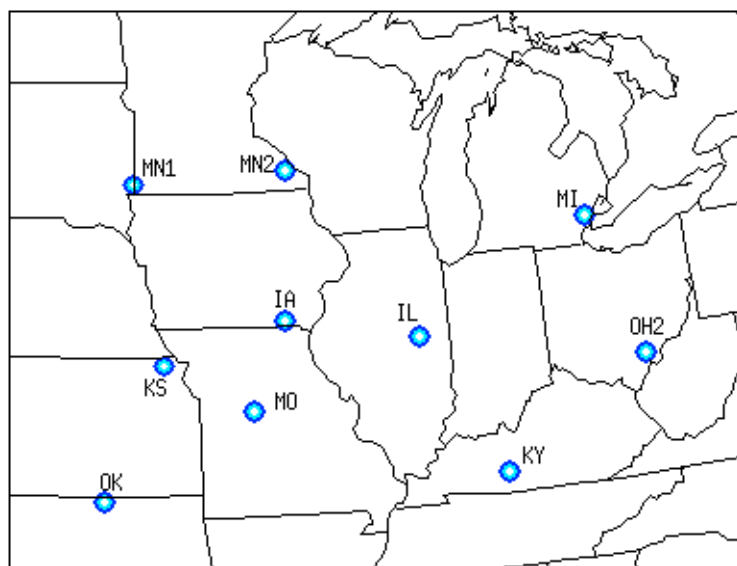
Nitrate concentrations are a significant contributor to light extinction further to the north of Texas in the center of the country. While SO₄²⁻ can be in particulate form though not fully neutralized by ammonia, nitric acid from NO_x emissions requires neutralization

by ammonium to become particulate ammonium nitrate. One way to explore the causes of the Midwest nitrate bulge is to compare its spatial distribution with the spatial distributions of NO_x and ammonia emissions. Figure 9-45 shows a map of the annual average particulate nitrate concentrations (top) with a map of ammonia emissions directly below it. Animal agriculture is responsible for most of the ammonia emissions in the Midwest. The striking similarity between the ambient particulate nitrate concentration and the ammonia emissions spatial patterns with regional maximum centered on Iowa is in contrast to the NO_x (i.e., $\text{NO} + \text{NO}_2$) emissions spatial patterns, shown in Figure 9-46. NO_x emissions are high over a broad region of the country associated with the larger population densities and greater numbers of fossil fuel electric generation plant generally to the east of the Midwest nitrate bulge. While both ammonia and nitric acid are needed to form particulate ammonium nitrate, the maps suggest the Midwest nitrate bulge is due primarily to the abundance of free ammonia (i.e., the amount beyond what is required to neutralize the acidic particulate SO_4^{2-}). By contrast the region to the east of the Midwest nitrate bulge should have plenty of nitric acid given the higher emissions of NO_x , but apparently has a deficiency of free ammonia. The few eastern monitoring sites with locally high particulate nitrate (near southeastern PA) are located within a small region of high density animal agricultural that shows up as a high ammonia emissions region in Figure 9-45. Note that California's South Coast and Central Valley have both high ammonia and high NO_x emissions, explaining the high particulate nitrate contribution to haze there.

To better understand the role of ammonia in the formation of the Midwest nitrate bulge, the Midwest RPO and Central States Regional Air Partnership deployed a measurement program from late 2003 through early 2005 at 10 locations (9 rural and 1 urban) in the region (see Figure 9-47) to monitor particulate SO_4^{2-} , nitrate, and ammonium ions, plus the precursor gases sulfur dioxide, nitric acid, and ammonia (Kenski et al., 2004, [192078](#); Sweet et al., 2005, [180038](#)). These data have been used as input for thermodynamic equilibrium modeling to assess the changes in PM concentrations that would result from changes to precursor concentrations (Blanchard and Tanenbaum, 2006, [192181](#); Blanchard et al., 2007, [098659](#)). Blanchard and Tanenbaum (2006, [192181](#)) and Blanchard et al. (2007, [098659](#)) conclude that the current conditions at nine of the ten sites are near the point of transition between the precursor species (nitric acid and ammonia) that limits the formation of particulate nitrate. If excess ammonia increases, either by greater ammonia

emissions or by anticipated decreases in SO₂ emissions, then nitric acid concentration would need to be reduced (via lower NO_x emissions) in order to reduce the particulate nitrate concentration.

Given the comparability of particulate SO₄²⁻ and nitrate with regard to their light extinction efficiencies, their visibility impacts are proportional to the sum of their mass concentrations. A reduction in SO₄²⁻ caused by SO₂ emission reductions would reduce the particulate SO₄²⁻ concentration, though according to the thermodynamic equilibrium modeling for these sites the particulate nitrate concentration will be increased somewhat. However the total particulate SO₄²⁻ plus nitrate concentration would be reduced so visibility impacts would be decreased. At current ammonium concentrations the predicted response of changes to SO₄²⁻ and nitric acid concentrations (i.e., SO₂ and NO_x emissions changes) are similar in respect to the resulting magnitude of changes to the total particulate SO₄²⁻ plus nitrate concentrations. At all but two sites the total particulate SO₄²⁻ plus nitrate concentrations would decrease if either ammonia or nitric acid were reduced.



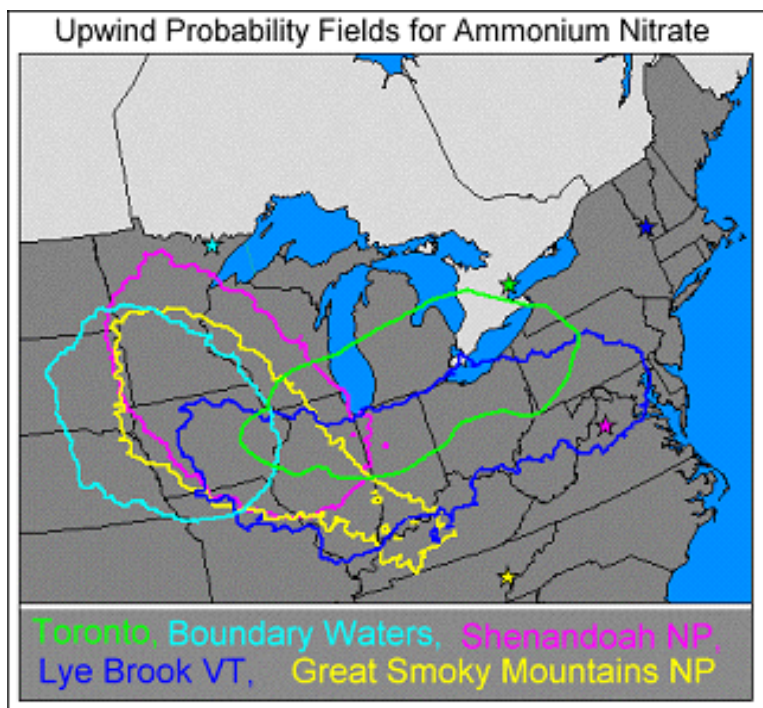
Source: Kenski et al. (2004, [192078](#))

Figure 9-47. Midwest ammonia monitoring network.

A further degree of complications in understanding the response of particulate nitrate to changes in precursor concentrations results from the temperature and humidity dependence of the partition between particulate ammonium nitrate and the disassociated

gaseous nitric acid and ammonia. This dependence causes seasonal and even diurnal differences in the expected responses of particulate nitrate concentrations to changes in precursor concentrations. As expected during the colder times of the year the total particulate concentrations are more sensitive to changes in ammonia and nitric acid concentrations than during the warmer seasons when SO_4^{2-} concentrations are greater.

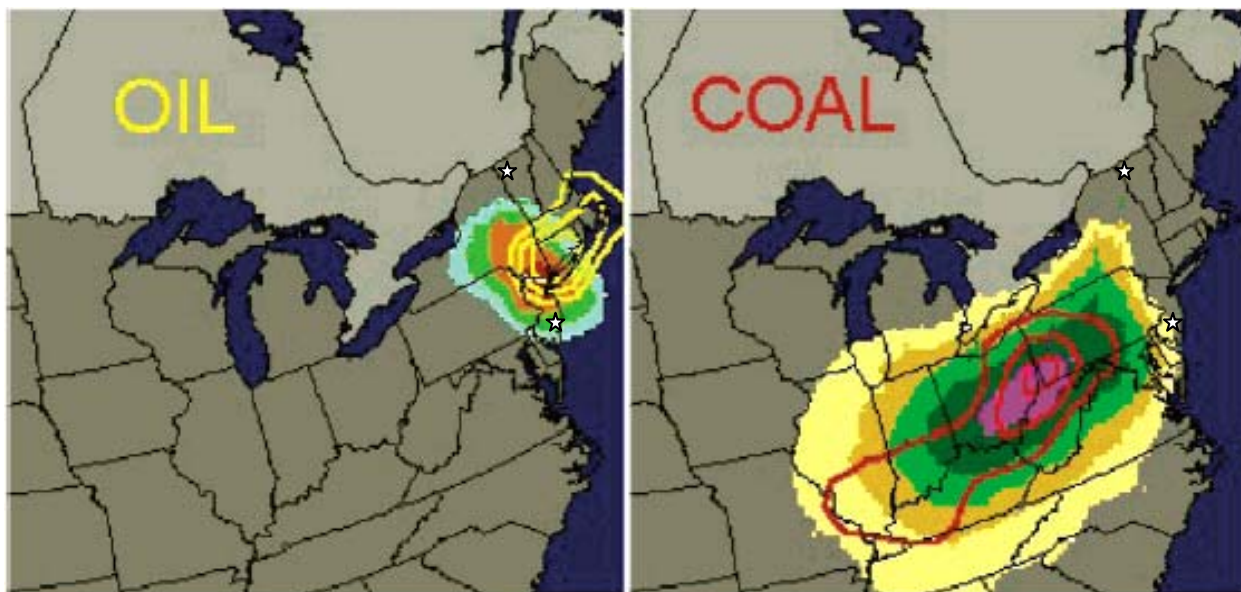
As shown in Figure 9-48, results of an air transport assessment to identify emission source areas associated with high particulate nitrate at five monitoring locations in the East (four remote-area sites and Toronto, Canada) implicate the high ammonia emissions region of the Midwest as a common source region (Canada-US Air Quality Committee, Subcommittee 2: Scientific, 2004, [190519](#)). This assessment does not preclude local sources of the precursor gases responsible for particulate ammonium nitrate, but does suggest that long-range transport of particulate nitrate or ammonia from the high emissions region of the Midwest is also contributing to eastern nitrate episodes.



Source: Canada-U.S. Air Committee (2004, [190519](#)).

Figure 9-48. Upwind transport probability fields associated with high particulate nitrate concentrations measured at Toronto, Canada; Boundary Water Canoe Area, MN; Shenandoah NP, VA; Lye Brook, VT; and Great Smoky Mountains NP, TN.

In a similar air transport assessment for measurements at Underhill, VT and at Brigantine, NJ, Hopke et al. (2005, [156567](#)) identified separate regions associated with particulate SO_4^{2-} accompanied by trace particulate components associated with coal burning (e.g., selenium) and accompanied by trace particulate components associated with oil burning (e.g., vanadium). As shown in Figure 9-49, the coal-burning related particulate SO_4^{2-} for these two monitoring sites is associated with long-range transport from the Ohio River Valley, while oil-burning related particulate SO_4^{2-} is from more nearby emissions in the high population region of coastal New York, New Jersey, Massachusetts, and Connecticut.

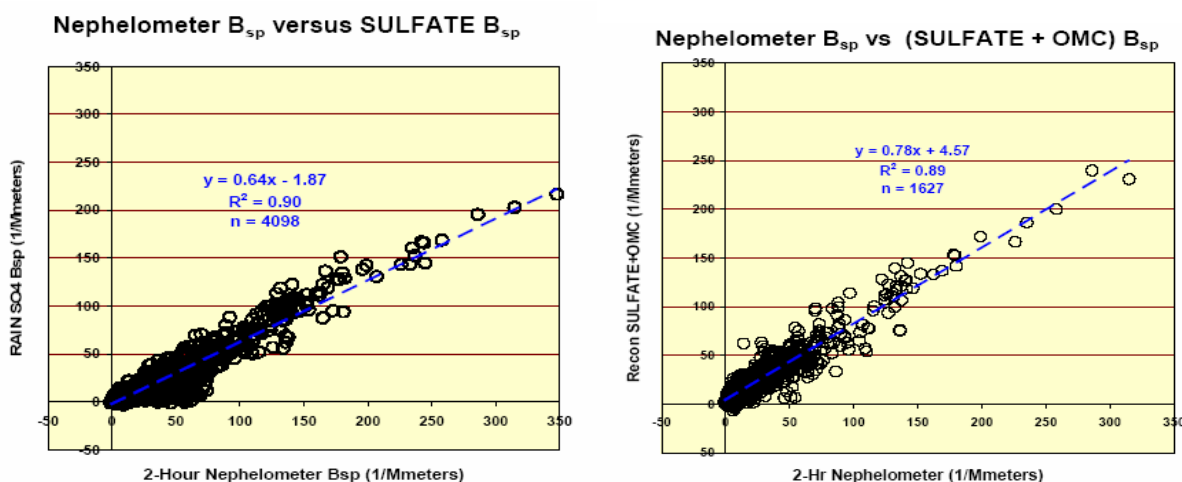


Hopke, et al. (2005, [156567](#)).

Figure 9-49. Trajectory probability fields for periods with high particulate SO_4^{2-} measured at Underhill, VT and Brigantine, NJ (shown as white stars) associated with oil-burning trace components (left) and with coal-burning trace components (right). Shown for comparison are the interpolated SO_2 emissions areal density contours for oil combustion sources (emissions times 10) and coal combustion sources, displayed as yellow and red contour lines, respectively.

The Regional Aerosol Intensive Network (RAIN) was established by MANE-VU to generate enhanced continuous visibility, plus fine particle mass and composition monitoring data at a string of three monitoring locations along the transport path from the Ohio River Valley to coastal Maine (NESCAUM, , [156802](#)). The dominant role of particulate SO_4^{2-} in the northeast is well demonstrated by a scatter plot of RAIN data that shows the

relationship between particulate SO_4^{2-} extinction, calculated using the IMPROVE algorithm plotted against directly measured particle light scattering for hourly data over a eight month period beginning in July 2004 at the Acadia NP, ME monitoring site (see Figure 9-50). Particulate SO_4^{2-} explains 90% of the variance in particulate light scattering even though it is responsible for only about 64% of the total light extinction (annual averaged value from the VIEWS web site). Adding the contribution by the second-largest regional contributor to light extinction, particulate OC with about 14%, does not improve the variance explained, but does increase the slope to 0.78. The noticeable difference between these two plots is that the particulate SO_4^{2-} alone underestimates light scattering during low haze periods (points on the plot are below the regression line for light scattering $<70\text{Mm}^{-1}$), while the agreement is improved with the addition of particulate OC contributions to haze (regression slope is nearer to one and reduced bias for low haze periods). This implies that particulate SO_4^{2-} and any other co-varying PM species are largely responsible for the highly impacted periods, while OC and other co-varying PM species contribute more during the less extreme haze periods. Particulate nitrate contribution to light extinction at Acadia is about 10% on average.



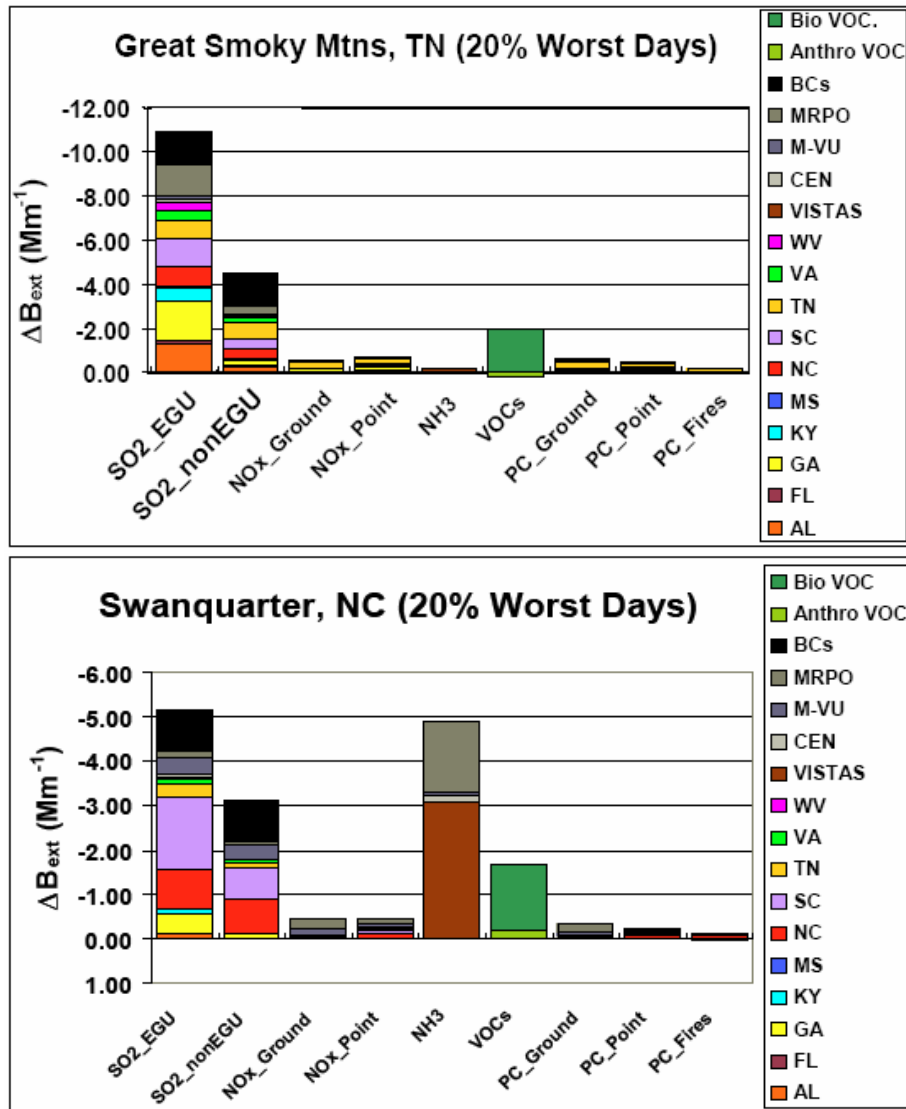
Source: RAIN Preliminary Data Analysis Report (NESCAUM, [156802](#))

Figure 9-50. Scatter plots of particulate SO_4^{2-} (left) and particulate nitrate and organic mass (right) versus nephelometer measured particle light scattering for Acadia NP, ME.

Particulate nitrate concentrations are considerably lower in the SO_4^{2-} -dominated warmer southeastern U.S. than in the Northeast and upper Midwest. Blanchard et al. (2007, [098659](#)) conducted thermodynamic equilibrium modeling on data from the eight

SEARCH monitoring sites and found that total particulate nitrate plus SO_4^{2-} is much more responsive to changes in SO_2 concentrations than to changes in nitric acid concentrations, which in turn is more responsive than changes in ammonia concentrations.

The VISTAS RPO commissioned an emissions sensitivity study using CMAQ modeling on winter and summer 2009 emissions projected from the 2002 emissions inventory (NCDENR, 2007, [156798](#)). Figure 9-51 contains bar plots for two North Carolina Class I areas that indicate projected changes in light extinction for the worst haze day due to 30% emissions reductions by particulate species, source types and location across the Southeastern states modeling domain (i.e., as far west as Texas, as far north as Pennsylvania, as far south as the Florida Keys, and as far east as ~300 km from the North Carolina coast). Great Smoky Mountains in the southern Appalachian Mountains has the greatest sensitivity to changes by SO_2 emissions from electrical generation units (EGU) and to a lesser extent other SO_2 emission sources in the region. Reductions of NO_x emissions from ground or point sources are not nearly as effective as SO_2 reductions in reducing the light extinction at Great Smoky Mountains. This is due principally to the worst days at Great Smoky Mountains occurring during the summer, when temperatures are too high to support high particulate nitrate concentrations. For the same reason, ammonia emission reductions are also ineffective. Swanquarter Wilderness, NC is a coastal location where some of the worst haze days are during the winter and include contributions from particulate ammonium nitrate. Both SO_2 and ammonia emissions reductions would be effective at reducing worst haze days at the Swanquarter Wilderness, though NO_x emissions are not as effective presumably because the atmosphere is ammonia-limited for particulate nitrate production.



Source: NCDENR (2007, [156798](#)).

Figure 9-51. CMAQ air quality modeling projections of visibility responses on the 20% worst haze days at Great Smoky Mountains NP, NC (top) and Swanquarter Wilderness, NC (bottom) to 30% reductions from a projected 2009 emission inventory of visibility-reducing pollutants by source category and geographic areas.

9.2.4. Urban Visibility Valuation and Preference

The Clean Air Act §302(h) defines public welfare to include the effects of air pollution on “...visibility, ... and personal comfort and wellbeing.” Though good visibility conditions in Class I (e.g., NPs) and wilderness areas have long been recognized as important to the public welfare (see discussions in EPA (2004, [056905](#); 2005, [090209](#)) and Chestnut and

Dennis (1997, [014525](#)), visibility conditions in urban areas also contribute to the public welfare. Although visibility impairment may be caused by either natural or manmade conditions (or both), it is only impairment that occurs as a result of air pollution (either alone or in combination with water vapor or other atmospheric conditions) that can be mitigated by regulations such as the RHR (40 CFR 51.300 through 309) or the Secondary National Ambient Air Quality Standards (NAAQS). The term visual air quality (VAQ) is used here to refer to the visibility effects caused solely by air quality conditions, so for example it excludes the reduced visibility caused by fog. Visibly poor air quality causes people to be concerned about substantive health risks, but degraded VAQ adversely affects people in additional ways. These include the aesthetic and wellbeing benefits of better visibility, improved road and air safety, and enhanced recreation in activities like hiking and bicycling. Because the human health impacts of air pollution are assessed under the Primary NAAQS, it is necessary to separate out these non-health components associated with the visibility condition produced by a given amount of air pollution when assessing the need for additional regulation to protect the public welfare effect of visibility under the Secondary NAAQS. The degree to which previous human preference and valuation studies for VAQ have adequately made this distinction and separation is an important issue in applying results from available studies in a Secondary NAAQS (or benefits estimation for any policy effecting VAQ) context. The remainder of this discussion is focused on those aesthetic and wellbeing qualities associated with a given VAQ in urban areas.

The term “urban visibility” is used to refer to VAQ throughout a city or metropolitan area. Urban visibility includes the VAQ conditions in all locations that people experience in their daily lives, including scenes such as residential streets and neighborhood parks, commercial and industrial areas, highway and commuting corridors, central downtown areas, and views from elevated locations providing a broad overlook of the metropolitan area. Thus urban visibility includes VAQ conditions in major cities and smaller towns and encompasses all the VAQ an individual resident sees on a regular basis. Visibility conditions in urban and suburban locations are therefore distinct from visibility in rural or wilderness settings such as the Class 1 areas defined by the Clean Air Act, which include NPs and similar natural settings.

Visibility has direct significance to people’s enjoyment of daily activities and their overall wellbeing. Visibility conditions can be described both as an aesthetic quality as well as a scientifically measurable set of atmospheric conditions. Due to the subjective nature of

aesthetics, people's preferences with respect to visibility are difficult to express or quantify, but people have expressed in many different ways that they enjoy and value a clear view. A number of social science disciplines have undertaken to link perceived urban visibility to an array of effects reflecting the overall desire for good VAQ, and the benefits of improving currently degraded VAQ. This wide range of diverse studies have identified types of benefits of good VAQ in addition to those directly connected with air-pollution related health effects such as respiratory diseases and premature mortality.

For example, psychological research has demonstrated that people are emotionally affected by low VAQ such that their overall sense of wellbeing is diminished (e.g., Bickerstaff and Walker, 2001, [156271](#)). Researchers have also shown that perception of pollution is correlated with stress, annoyance, and symptoms of depression (Evans and Jacobs, 1982, [179899](#); Jacobs et al., 1984, [156596](#); Mace et al., 2004, [180255](#)). Sociological research has demonstrated that VAQ is deeply intertwined with a "sense of place," effecting people's sense of the desirability of a neighborhood quite apart from the actual physical conditions of the area (e.g., ABT, 2002, [156186](#); Day, 2007, [156386](#); Elliot et al., 1999, [010716](#); Gilliland et al., 2004, [156471](#)). Public policy research finds that people think it is important to protect visibility, and accept the concept of setting standards to protect visibility (e.g., ABT, 2001, [156185](#); BBC Research & Consulting, 2002, [156258](#); Ely et al., 1991, [156417](#); Pryor, 1996, [056598](#)). Finally, economic valuation research has measured the amount of money that people are willing to pay to protect or improve both urban visibility (e.g., summary review in Beron et al., 2001, [156270](#); Chestnut and Dennis, 1997, [014525](#)) and natural locations such as NPs and other locations defined by the Clean Air Act as Class I visibility area (e.g., summary review in Chestnut and Dennis, 1997, [014525](#)).

Urban visibility has been examined in two types of studies directly relevant to the NAAQS review process: urban visibility preference studies and urban visibility valuation studies. The purpose of the remainder of this section is to review four urban preference studies, as well as one new urban visibility valuation study not previously discussed in previous EPA Criteria Documents or OAQPS Staff Papers.

Both types of studies are designed to evaluate individuals' desire (or demand) for good VAQ where they live, using different metrics to evaluate demand. Urban visibility preference studies examine individuals' demand by investigating what amount of visibility degradation is unacceptable while economic studies examine demand by investigating how much one would be willing to pay to improve visibility.

9.2.4.1. Urban Visibility Preference Studies

One group of urban visibility research projects focused on identifying preferences for urban VAQ without necessarily estimating the economic value of improving visibility. This group of preference studies used a common focus group method to estimate the visibility impairment conditions that respondents described as “acceptable.” The specific definition of acceptable was largely left to each individual respondent, allowing each to identify their own preferences.

There are three completed studies that used this method, and one additional pilot study (designed as a survey instrument development project) that provided additional information (Table 9-2). The completed studies were conducted in Denver, Colorado (Ely et al., 1991, [156417](#)), two cities in British Columbia, Canada (Pryor, 1996, [056598](#)), and Phoenix, Arizona (BBC Research & Consulting, 2002, [156258](#)). The pilot study was conducted in Washington, DC (ABT, 2001, [156185](#)).

Each study collected information in a focus group setting, presenting slides depicting various visibility conditions. All four studies used photographs of a single scene from the study’s city; each photo included images of the broad downtown area and spreading out to the hills or mountains composing the scene’s backdrop. The maximum sight distance under good conditions varied by city, ranging from 8 kilometers in Washington, DC to mountains hundreds of kilometers away in Denver. Multiple photos of the same scene were used to present approximately 20 different visibility impairment conditions. The Denver and British Columbia studies used actual photographs taken in the same location to depict various visibility conditions. The Phoenix and Washington, DC pilot study used photographs prepared using the WinHaze software from Air Resource Specialists (ARS). WinHaze is a computer-imaging software program that simulates visual air quality differences of various scenes, allowing the user to “degrade” an original near-pristine visibility condition photograph to create a photograph of each desired VAQ condition.

A common characteristic of the three visibility preference studies was that each were conducted in the West where distant mountains were shown in the photograph used to elicit local participant responses about visibility. Among other issues, the Washington D.C. pilot study was the first step in a process to expand the results to other regions where typical scenes may have different sensitivity to perceived visibility changes in PM air quality and where participants may have different acceptable visibility preference values.

One notable finding of the three visibility preference studies and the one pilot study is the general degree of consistency in the median preferences for an acceptable amount of visibility degradation. The range of median acceptable preference values from the four studies is 19-25 dv, the preferred measure of visibility impairment. Measured in terms of visual range (VR), these median acceptable values are between 59 and 32 km.

Table 9-2. Summary of urban visibility preference studies.

	Denver, CO	Phoenix, AZ	2 British Columbia cities	Washington, DC (pilot)
Report Date	1991	2003	1996	2001
Duration of session		45 min	50 mins	2 h
Compensation	None (civic groups)	\$50	None (class room exercise)	\$50
# focus group sessions	17	27 total at 6 locations, Including 3 in Spanish	4	1
# participants	214	385	180	9
Age range	adults	18-65+	University students	27-58
Annual or seasonal	Wintertime	Annual	Summertime	Annual
# total scenes presented	Single scene of downtown with mountains in background	Single scene of downtown and mountains, 42 km maximum distance	Single scene from each city	Single scene of DC Mall and downtown, 8 km maximum sight
# of total visibility conditions presented	20 conditions (+ 5 duplicates)	21 conditions (+ 4 duplicates)	20 conditions (10 each from each city)	20 conditions (+ 5 duplicates)
Source of slides	Actual photos taken between 9am and 3pm	WinHaze	Actual photos taken at 1pm or 4pm	WinHaze
Medium of presentation	Slide projection	Slide projection	Slide projection	Slide projection
Ranking scale used	7 point scale	7 point scale	7 point scale	7 point scale
Visibility range presented	11 to 40 dv	15 to 35 dv	13 to 25 dv (Chilliwack) 13.5 to 31.5 dv (Abbotsford)	9 to 38 dv
Health issue directions	Ignore potential health impacts; visibility only	Judge solely on visibility, do not consider health	Judge solely on visibility, do not consider health	Health never mentioned, "Focus only on visibility"
Key Questions asked	a) Rank VAQ (1-7 scale) b) Is each slide "acceptable" c) "How much haze is too much?"	a) Rank VAQ (1-7 scale) b) Is each slide "acceptable" c) How many days a yr would this picture be "acceptable"	a) Rank VAQ (1-7 scale) b) Is each slide "acceptable"	a) Rank VAQ (1-7 scale) b) Is each slide "acceptable" c) if this hazy, how many hs would it be acceptable (3 slides only) d) valuation question
Mean dv found "acceptable"	20.3 dv	23 to 25 dv	~ 23 dv(Chilliwack), ~ 19 dv(Abbotsford)	~ 20 dv (range 20-25)

9.2.4.2. Denver, Colorado Urban Visibility Preference Study

The Denver urban visibility preference study (Ely et al., 1991, [156417](#)) was conducted on behalf of the Colorado Department of Public Health and Environment (CDPHE). The study conducted a series of focus group sessions with 17 civic and community groups in which a total of 214 individuals were asked to rate slides. The slides depicted varying values of VAQ for a well-known Denver vista, including a broad view of downtown Denver with the mountains to the west composing the scene's background. The participants were instructed to base their judgments on three factors:

1. The standard was for an urban area, not a pristine national park area where the standards might be more strict;
2. The value of an urban visibility standard violation should be set at a VAQ value considered to be unreasonable, objectionable, and unacceptable visually; and
3. Judgments of standards violations should be based on visibility only, not on health effects.

Participants were shown 25 randomly ordered slides of actual photographs. The visibility conditions presented in the slides ranged from 11 to 40 dv, approximating the 10th to 90th percentile of wintertime visibility conditions in Denver. The participants rated the 25 slides based on a scale of 1 (poor) to 7 (excellent), with 5 duplicates included. They were then asked to judge whether the slide would violate what they would consider to be an appropriate urban visibility standard (i.e., whether the amount of impairment was “acceptable” or “unacceptable”). The individual's judgment of a slide's VAQ and whether the slide violated a visibility standard were highly correlated (Pearson correlation coefficient >80%), as were the VAQ ratings and the yes/no “acceptable” response. The participant's median response was that a visibility condition of 20.3 dv (extinction coefficient $b_{\text{ext}} = 76\text{Mm}^{-1}$, or VR ~51 km) was judged as “acceptable.” The CDPHE subsequently established a Denver visibility standard at this value (defined as $b_{\text{ext}} = 76\text{Mm}^{-1}$), based on the median 50% acceptability findings from the study.

9.2.4.3. Phoenix, Arizona Urban Visibility Preference Study

The Phoenix urban visibility preference study (BBC Research & Consulting, 2002, [156258](#)) was conducted on behalf of the Arizona Department of Environmental Quality. The Phoenix study patterned its focus group survey process after the Denver study. The study

included 385 participants in 27 separate focus group sessions. Participants were recruited using random digit dialing to obtain a sample group designed to be demographically representative of the larger Phoenix population. Focus group sessions were held at six neighborhood locations throughout the metropolitan area to improve the participation rate. Three sessions were held in Spanish in one region of the city with a large Hispanic population (25%), although the final overall participation of native Spanish speakers (18%) in the study was modestly below the targeted value. Participants received \$50 as an inducement to participate.

Participants were shown a series of 25 images of the same vista of downtown Phoenix, with South Mountain in the background at a distance of about 40 km. Photographic slides of the images were developed using WinHaze. The visibility impairment conditions ranged from 15-35 dv (the extinction coefficient, b_{ext} , range was approximately 45 Mm^{-1} to 330 Mm^{-1} , or a visual range of 87-12 km). Participants first individually rated the randomly shown slides on a VAQ scale of 1 (unacceptable) to 7 (excellent). Participants were instructed to rate the photographs solely on visibility, and to not base their decisions on either health concerns or what it would cost to have better visibility. Next, the participants individually rated the randomly ordered slides as “acceptable” or “unacceptable,” defined as whether the visibility in the slide is unreasonable or objectionable. Better visibility conditions (15 dv and 20 dv) were judged “acceptable” by 90% of all participants. At 24 dv nearly half of all participants thought the VAQ was “unacceptable,” with almost three-quarters judging 26 dv as unacceptable.

The Phoenix urban visibility study formed the basis of the decision of the Phoenix Visibility Index Oversight Committee for a visibility index for the Phoenix Metropolitan Area (Arizona Department of Environmental, 2000, [019164](#)). The Phoenix Visibility Index establishes an indexed system with 5 categories of visibility conditions, ranging from “Excellent” (14 dv or less) to “Very Poor” (29 dv or greater). The “Good” range is 15-20 dv. The environmental goal of the Phoenix urban visibility program is to achieve continued progress through 2018 by moving the number of days in lower quality categories into better quality categories.

9.2.4.4. British Columbia, Canada Urban Visibility Preference Study

The British Columbia urban visibility preference study (Pryor, 1996, [056598](#)) was conducted on behalf of the Ministry of Environment. The study conducted focus group

sessions that were also developed following the methods used in the Denver study. Participants were students at the University of British Columbia, who participated in one of four focus group sessions with between 7 and 95 participants. A total of 180 respondents completed surveys (29 did not complete the survey).

Participants in the study were shown slides of two suburban locations in British Columbia: Chilliwack and Abbotsford. Using the same general protocol as the Denver study, Pryor found that responses from this study found the acceptable level of visibility was 23 dv in Chilliwack and 19 dv in Abbotsford. Pryor (1996, [056598](#)) discusses some possible reasons for the variation in standard visibility judgments between the two locations. Factors discussed include the relative complexity of the scenes, potential bias of the sample population (only University students participated), and the different amounts of development at each location. Abbotsford (population 130,000) is an ethnically diverse suburb adjacent to the Vancouver Metro area, while Chilliwack (population 70,000) is an agricultural community 100 km east Vancouver in the Frazier Valley.

The British Columbia urban visibility preference study is being considered by the B.C. Ministry of the Environment as a part of establishing urban and wilderness visibility goals in British Columbia.

9.2.4.5. Washington, DC Urban Visibility Pilot Preference Study

The Washington, DC urban visibility pilot study (ABT, 2001, [156185](#)) was conducted on behalf of the EPA, and was designed to be a pilot focus group study, an initial developmental trial run of a larger study. The intent of the pilot study was to study both focus group method design and potential survey questions. Due to funding limitations, only a single focus group session was held, consisting of one extended session with 9 participants. No further urban visibility focus group sessions were held in Washington, DC.

Due to the small number of participants, it is not possible to make statistical inferences about the opinions of the general population. The study does, however, provide additional useful information about urban visibility studies, potentially helping to both better understand previous studies as well as design future studies.

The study also adopted the general Denver study method, modifying it as appropriate to be applicable in an eastern urban setting which has substantially different visibility conditions than any of the three western locations of the other preference studies. Washington's (and the entire East) visibility is typically substantially worse than western

cities, and has different characteristics. Washington's visibility impairment is primarily a uniform whitish haze dominated by sulfates, relative humidity values are higher, the low lying terrain provides substantially shorter maximum sight distances, and many residents are not well informed that anthropogenic emissions impair visibility on hazy days.

The Washington focus group session included questions on valuation, as well as on preferences. The focus group was asked to state its preferences measured in an increase in the general cost of living for certain increments of improvement in visibility on a typical summer day. A general cost of living approach is one payment vehicle approach that can be used in willingness to pay studies, especially for environmental issues arising from multiple diverse emission sources (e.g., transportation, electricity generation, industry, etc.) making a specific price increase potentially misleading.

The first part of the focus group session was designed to be an hour long, and was comparable to the focus group sessions in the Denver and Phoenix studies. A single scene was used; a panoramic shot of the Potomac River, Washington mall and downtown Washington, DC. In the first part of the session people were asked to rate the VAQ of 25 photographs (prepared using WinHaze, and projected on a large screen), judge the acceptability of visibility condition in each slide, and answer the valuation questions. The second half of the session, however, was a moderated discussion session about the format and content of the first phase of the session. In this moderated discussion, participants were asked about their understanding of each question asked in the first half of the session. Particular issues in designing a focus group session were also explored. Important participant comments included:

1. Participants had been asked how they reacted to the initial direction to base their answers only on visibility, but health was never explicitly mentioned by the focus group moderator. Participants strongly agreed with the decision to not mention that health effects are associated with visibility impairment. They understood the directions as meaning they should ignore health issues, and said their answers would have been different if they included health as well as visibility in their judgments.
2. Differentiating between haze and weather conditions was difficult. Weather was not discussed in the focus group session, and the photographs were WinHaze altered photos with identical weather conditions. Participants mentioned they were still confused about the role of weather and humidity in the different visibility conditions presented in the photos.

3. Questions about how many hours an impairment level would be acceptable were confusing. Most participants were normally indoors during most of the day, so questions about duration of outdoor conditions were difficult to answer.
4. Participants strongly agreed that not mentioning the purpose of the study, or the sponsor, until the very end (after all the questions were answered) was viewed as very important. Most felt this information would have influenced their answers.

9.2.4.6. Urban Visibility Valuation Studies

The one recent urban visibility benefit assessment not included in earlier reviews is “The Benefits of Visibility Improvement: New Evidence from the Los Angeles Metropolitan Area” (Beron et al., 2001, [156270](#)). Rather than a contingent valuation method (CVM) technique used in the majority of other urban visibility valuation studies, Beron et al. (2001, [156270](#)) used a housing market hedonic technique. The housing hedonic methods were used in previous urban visibility studies by Murdoch and Thayer (1988, [156788](#)) and Trijonis et al. (1985, [078468](#)). A housing market hedonic study views a housing unit as composed of a bundle of attributes, and uses housing sale price data from a large number of units in a metropolitan area to estimate the value of each component. Hedonic pricing has been used to estimate economic values for environmental effects that have a direct effect on housing market values. It relies on the measurement of differentials in property values under various environmental quality conditions including air pollution, visibility and other environmental amenities such as access to nearby beaches and parks, as well as by physical attributes of the house and attributes of the neighborhood.

Beron et al. (2001, [156270](#)) obtained data on approximately 840,000 owner-occupied, single family housing sales between 1980 and 1995 from the California South Coast Air Basin (composed of Los Angeles and Orange Counties, and the portions of Riverside and San Bernardino Counties in the greater metropolitan area). The real estate data included information on the sale price of the house, 13 housing attributes (square footage, number of bathrooms, etc.), 9 neighborhood attributes (percent poverty, school quality, FBI crime index, etc.), and three air pollution variables: ozone, particulates (measured by total suspended particulates, or TSP), and visibility. Visibility was measured as the annual average of visual range, measured in miles, and was obtained from seven airports within the study region. The visibility range was from 12.4 miles (Los Angeles International

Airport, 1991) to 31.9 miles (Palm Springs Airport, 1995). Ozone data (39 monitors) and TSP data (40 monitors) were obtained from the South Coast Air Quality Management District. Annual mean values for each year were calculated for ozone and TSP.

Beron et al. (2001, [156270](#)) presented results for a hypothetical basin-wide 20% visibility improvement, or an increase from 15.3 to 18.4 miles, which is equivalent to approximately 27.6 dv to 25.8 dv. The initial results reflect the change in the purchase price of a house associated with this difference in VAQ, which can be interpreted as a present value of a stream of annual values over the lifetime of the house. The authors therefore selected a time horizon (30 yr) and an interest rate (8%) to calculate an annual per household benefit per dv ranging from \$484 to \$1,756. The Beron results are higher than the CVM-based values summarized in Chestnut and Dennis (1997, [014525](#)), which ranged from \$12 to \$132 per dv. It should be noted that the \$132 CVM values cited by Chestnut and Dennis (1997, [014525](#)) is from a study in the Los Angeles area (Brookshire, 1979, [156298](#)). The Beron et al. (2001, [156270](#)) results are also higher than the Trijonis et al. (1990, [157058](#)) hedonic study in the Los Angeles area, which had a range of \$134 to \$360 per dv per year. All values reported here are in terms of 1994 prices.

A critical question for all urban visibility valuation studies is the extent to which the estimated values strictly reflect preferences for visibility, and do not include a component of preferences for reducing health risk from air pollution. The ability to isolate the value of visibility from within the collection of intertwined benefits from visual air quality, which is inherently multi-attributed, is a challenge for all visibility valuation studies. Each study attempts to isolate visibility from other effect categories, but different studies take different approaches.

Beron et al. (2001, [156270](#)) include two measures of air pollution directly related to health effects in their housing market hedonic study, ozone and particulates (using TSP as the metric for particulates), as well as visibility. They argue that the presence of the two health-related pollution conditions results in an estimated hedonic demand function for visibility that successfully separates the health component of demand for overall air quality from the visibility component. An alternative interpretation is that the estimated visibility function still includes a component of health risk because the housing market data does not support completely isolating the demand for visibility (due to correlated variables, omitted variables, measurement error, model specification error, etc.) from demand for health risk reductions measured by the two health related air quality metrics.

A key issue in interpreting the Beron et al. (2001, [156270](#)) results is whether the objective measures of air quality characteristics (e.g., visibility, PM concentrations, etc.) capture people's perceptions of the different aspects of air quality in a given location. To the extent the people simultaneously use what they see regarding VAQ as an indicator of the overall air quality including potential health risks, then including all the measures in the equation is not necessarily sufficient to isolate one effect from the other.

9.2.5. Summary of Effects on Visibility

Visibility impairment is caused by light scattering and absorption by suspended particles and gases. NO₂ is the only commonly occurring atmospheric pollutant gas that absorbs visible spectrum radiation, though in most situations the amount of light absorption by NO₂ is overwhelmed by the higher amounts of particulate light extinction (i.e., the combination of scattering and absorption) usually accompanying high NO₂ concentrations. Light scattering by gases in a pollutant-free atmosphere provides a limit to visibility in pristine conditions and is the largest contributor to the total light extinction during the least visibility-impaired periods in remote regions of the western U.S. There is strong and consistent evidence that PM is the overwhelming source of visibility impairment in both urban and remote areas. Elemental carbon (EC) and some crustal minerals are the only commonly occurring airborne particle components that absorb light. All particles scatter light, and generally light scattering by particles is the largest of the four light extinction components. Although a larger particle scatters more light than similarly shaped smaller particle of the same composition, the light scattered per unit of mass is greatest for particles with diameters from approximately 0.3-1.0 μm.

For studies where detailed data on particle composition by size data are available, accurate calculations of light extinction can be made. However, routinely available PM speciation data can be used to make reasonable estimates of light extinction using relatively simple algorithms that multiply the concentrations of each of the major PM species by its dry extinction efficiency and by a water growth term that accounts for particle size change as a function of relative humidity for hygroscopic species (e.g., SO₄²⁻, nitrate, and sea salt). This permits the visibility impairment associated with each of the major PM components to be separately approximated from PM speciation monitoring data. There are six major PM components: PM_{2.5} SO₄²⁻ usually assumed to be ammonium sulfate, PM_{2.5}

nitrate usually assumed to be ammonium nitrate, PM_{2.5} OC compound, PM_{2.5} EC, PM_{2.5} crustal material (referred to as fine soil), and PM_{10-2.5} or coarse mass.

Direct optical measurement of light extinction measured by transmissometer, or by combining the PM light scattering measured by integrating nephelometers with the PM light absorption measured by an aethalometer offer a number of advantages compared to algorithm estimates of light extinction based on PM composition and relative humidity data. The direct measurements are not subject to the uncertainties associated with assumed scattering and absorption efficiencies used in the PM algorithm approach. The direct measurements have higher time resolution (i.e., minutes to hours), which is more commensurate with the visibility effects compared with calculated light extinction using routinely available PM speciation data (i.e., 24-h duration).

Particulate SO₄²⁻ and nitrate are produced in the atmosphere from gaseous precursors, making them secondary PM species. They both have comparable light extinction efficiencies (haze impacts per unit mass concentration) at any relative humidity value, their light scattering per unit mass concentration increases with increasing relative humidity, and at sufficiently high humidity values (RH>85%) they are the most efficient particulate species contributing to haze. Particulate SO₄²⁻ is the dominant source of regional haze in the eastern U.S. (>50% of the particulate light extinction) and an important contributor to haze elsewhere in the country (>20% of particulate light extinction).

Particulate nitrate is a minor component of remote-area regional haze in the non-California western and eastern U.S., but an important contributor in much of California and in the upper Midwestern U.S. especially during winter when it is the dominant contributor to particulate light extinction. While both nitric acid (a reaction product of NO_x emissions) and ammonia are needed to form ammonium nitrate, the apparent reason for the Midwest nitrate bulge (i.e., region of high winter PM nitrate) is an abundance of atmospheric ammonia in this region principally from agricultural emissions. There is evidence that transport from the Midwest nitrate bulge region is responsible for some of the ammonium nitrate episodes experienced in downwind regions far to the east. Urban particulate nitrate concentrations are significantly elevated above surrounding remote-area background concentrations with the largest urban contributions in the western U.S. Particulate ammonium nitrate concentrations in California and the Midwestern nitrate bulge region are an order of magnitude greater than estimated natural ammonium

nitrate concentrations. Thermodynamic and air quality simulation modeling show that particulate nitrate concentrations are sensitive to changes in either NO_x emissions (from a combination of mobile and point sources) or ammonia emissions (principally from agricultural sources), with the responsiveness of particulate nitrate to emissions changes depending on the relative abundance of ammonia and nitric acid in the atmosphere.

EC and OC have the highest dry extinction efficiencies of the major PM species and are responsible for a large fraction of the haze especially in the Northwestern U.S., though absolute concentrations are as high in the eastern U.S. Both are a product of incomplete combustion of fuels, including those used in internal combustion processes (gasoline and diesel emissions) and open biomass burning (smoke from wild and prescribed fire). Organic compound PM species are also produced by atmospheric transformation of precursor gaseous emissions. Smoke plume impacts from large wildfires dominate many of the worst haze periods in the western U.S. Carbonaceous PM is generally the largest component of urban excess PM_{2.5} (i.e., the difference between urban and regional background concentration). Western urban areas have more than twice the average concentrations of carbonaceous PM than remote areas sites in the same region. In eastern urban areas PM_{2.5} is dominated by about equal concentrations of carbonaceous and SO₄²⁻ components, though the usually high relative humidity in the East causes the hydrated SO₄²⁻ particles to be responsible for about twice as much of the urban haze as that caused by the carbonaceous PM.

Radiocarbon dating of carbonaceous PM from twelve sites (eight in the West, two of which are urban) showed that about half of the urban area carbonaceous PM is from contemporary as opposed to fossil sources, while in remote areas the fraction that is contemporary ranges from 82%-100%. Summer urban excess carbonaceous PM is dominated by fossil carbon for the two western urban areas (Phoenix, AZ and Seattle, WA), but nearly half of the winter urban excess for these two urban areas are from contemporary carbon sources (e.g., residential wood combustion). An empirical relationship between the radiocarbon analysis results and the more widely measured elemental and OC data set was used to estimate the fraction of contemporary carbon at about 150 monitoring locations nationwide. The highest fraction of contemporary carbon is for the western remote areas sites during the summer (>90% contemporary) and the least was for eastern urban areas during the summer (<45% contemporary). Winter tended to have less extreme fractions of contemporary carbon for both remote and urban areas. A lower bound estimate of 40% of

the contemporary and 35% of the fossil carbon is from secondary conversion of gaseous precursor during the summer at the twelve radiocarbon monitoring sites, suggesting that primary carbonaceous PM whether from fossil or contemporary sources represent less than two thirds of the total carbonaceous PM.

PM_{2.5} crustal material (referred to as fine soil) and coarse mass (i.e., PM₁₀ minus PM_{2.5}) are significant contributors to haze for remote areas sites in the arid Southwestern U.S. where they contribute a quarter to a third of the haze, with coarse mass usually contributing twice that of fine soil. Coarse mass concentrations are as high in the Central Great Plains as in the Southwestern deserts though there are no corresponding high concentrations of fine soil as in the Southwest. Also, the relative contribution to haze by the high coarse mass in the Great Plains is much smaller because of the generally higher haze values caused by the high concentrations of SO₄²⁻ and nitrate PM in that region.

A comprehensive assessment of the 610 worst haze sample periods over a 3-yr period in the western U.S. where dust is the major contributor categorized each site/sampler period into four causal groups: Asian dust, local windblown dust, transported regional windblown dust, and undetermined dust (i.e., not in one of the three other groups). Most dust days occurred at sites in Arizona, New Mexico, Colorado, western Texas, and southern California, and these were dominated by local and regionally transported wind-blown dust. Asian dust caused only a few of the worst dust days during the 3-yr assessment period, though it is an important source of dust for the more northerly regions of the West (responsible for 10%-40% of their worst dust periods) where there is rarely any windblown dust probably due to the greater ground cover. The frequency of worst dust events classified as undetermined was greatest for sites in the vicinity of large urban and agricultural areas such as those in California and Southern Arizona.

Visibility has direct significance to people's enjoyment of daily activities and their overall sense of wellbeing. A number of social science disciplines have undertaken to link perceived urban visibility to an array of effects reflecting the overall desire for good VAQ, and the benefits of improving currently degraded VAQ. For example, psychological research has demonstrated that people are emotionally affected by poor VAQ such that their overall sense of wellbeing is diminished. Urban visibility has been examined in two types of studies directly relevant to the NAAQS review process: urban visibility preference studies and urban visibility valuation studies. Both types of studies are designed to evaluate individuals' desire for good VAQ where they live, using different metrics. Urban visibility

preference studies examine individuals' preferences by investigating the amount of visibility degradation considered unacceptable, while economic studies examine the value an individual places on improving VAQ by eliciting how much the individual would be willing to pay for different amounts of VAQ improvement.

There are three urban visibility preference studies and one additional pilot study (designed as a survey instrument development project) that have been conducted to date that provide useful information on individuals' preferences for good VAQ in the urban setting. The completed studies were conducted in Denver, Colorado (Ely et al., 1991, [156417](#)), two cities in British Columbia, Canada (Pryor, 1996, [056598](#)) and Phoenix, Arizona (BBC Research & Consulting, 2002, [156258](#)). The pilot study was conducted in Washington, DC (ABT, 2002, [156186](#)). One notable finding of the three visibility preference studies and the one pilot study is the general degree of consistency in the median preferences for an acceptable amount of visibility degradation. The range of median acceptable visibility preference values from the four studies is 19-25 dv. Measured in terms of visual range (VR), these median acceptable values are between 59 km and 32 km.

The economic importance of urban visibility has been examined by a number of studies designed to quantify the benefits (or willingness to pay) associated with potential improvements in urban visibility. Urban visibility valuation research prior to 1997 was summarized in Chestnut and Dennis (1997, [014525](#)), and was also described in the 2004 PM AQCD (EPA, 2004, [056905](#)) and the 2005 OAQPS PM NAAQS Staff Paper (U.S. EPA, 2005, [090209](#)). Since the mid-1990s, little new information has become available regarding urban visibility valuation.

Collectively, the evidence is sufficient to conclude **that a causal relationship exists between PM and visibility impairment.**

9.3. Effects on Climate

While most of this ISA is restricted to consideration of the emissions, transport and transformation, resulting concentrations, and effects from PM in the U.S., because the effects endpoint here is climate, a larger spatial domain is needed. However, this assessment is not intended to be comprehensive even as a survey of the enormous range and volume of science related to climate effects from PM; rather, particular attention has been paid to data relevant to the U.S.

The two principal sources for material in this section are Chapter 2, “Changes in Atmospheric Constituents and in Radiative Forcing,” (Forster et al., 2007, [092936](#)) in the comprehensive Working Group I report in the Fourth Assessment Report (AR4) from the Intergovernmental Panel on Climate Change (IPCC), *Climate Change 2007: The Physical Science Basis* (Intergovernmental Panel on Climate Change, 2007, [092765](#)), hereafter IPCC AR4; and the U.S. Climate Change Science Program Synthesis and Assessment Product 2.3, “Atmospheric Aerosol Properties and Climate Impacts,” by Chin et al. (2009, [192130](#)), hereafter CCSP SAP2.3. The EPA is a constituent agency member of the U.S. federated CCSP along with NOAA and NASA, which led production of CCSP SAP2.3 incorporating significant sections from EPA data and reports related particularly to U.S. emissions and measurements. Sections from each of these recent comprehensive reports are included here in their entirety or as emended as noted where they represent the most thorough summary of the climate effects of aerosols. (In the sections included from IPCC AR4 and CCSP SAP2.3, ‘aerosols’ is more frequently used than “PM” and that word is retained.)

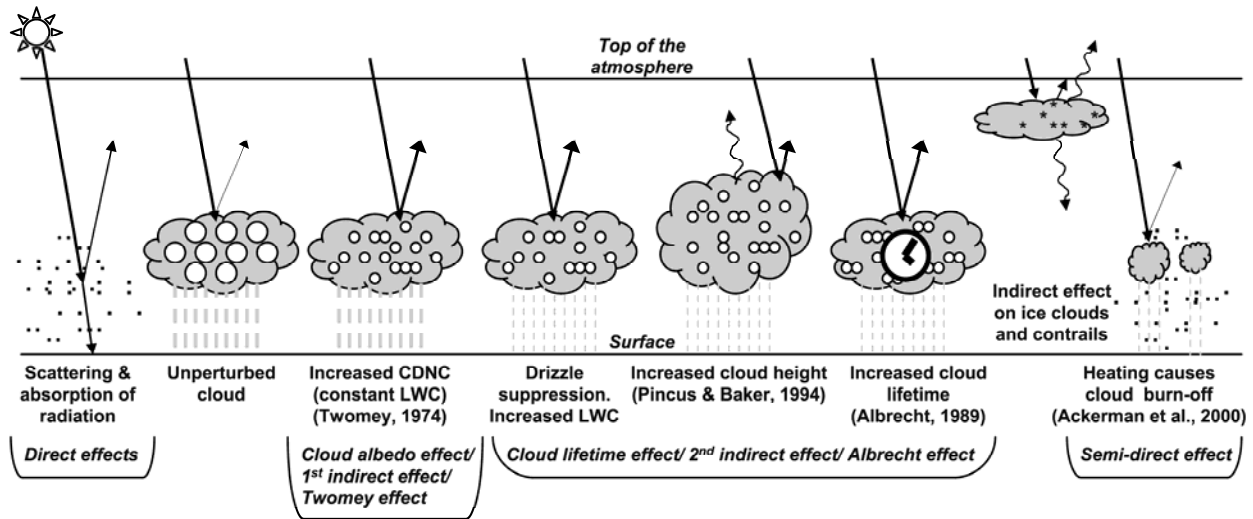
9.3.1. The Climate Effects of Aerosols

Section 9.3.1 comes directly from CCSP SAP2.3 Chapter 1 Section 1.2, with section, table, and figure numbers changed to be internally consistent with this ISA.

Aerosols exert a variety of impacts on the environment. Aerosols (sometimes referred to particulate matter or “PM,” especially in air quality applications), when concentrated near the surface, have long been recognized as affecting pulmonary function and other aspects of human health. Sulfate and nitrate aerosols play a role in acidifying the surface downwind of gaseous sulfur and odd nitrogen sources. Particles deposited far downwind might fertilize iron-poor waters in remote oceans, and Saharan dust reaching the Amazon Basin is thought to contribute nutrients to the rainforest soil.

Aerosols also interact strongly with solar and terrestrial radiation in several ways. Figure 9-52 offers a schematic overview. First, they scatter and absorb sunlight (McCormick and Ludwig, 1967, [190528](#); Mitchell, 1971, [190546](#); Charlson and Pilat, 1969, [190025](#)); these are described as “direct effects” on shortwave (solar) radiation. Second, aerosols act as sites at which water vapor can accumulate during cloud droplet formation, serving as cloud condensation nuclei or CCN. Any change in number concentration or hygroscopic properties of such particles has the potential to modify the physical and radiative properties of clouds, altering cloud brightness (Twomey, 1977, [190533](#)) and the likelihood and intensity with which a cloud will precipitate (Liou and Ou, 1989, [190407](#); Albrecht, 1989, [045783](#); e.g., Gunn and Phillips, 1957, [190595](#)). Collectively changes in cloud processes due to anthropogenic aerosols are referred to as *aerosol indirect effects*. Finally, absorption of solar radiation by particles is thought to contribute to a reduction in cloudiness, a phenomenon referred to as the *semi-direct effect*. This occurs because absorbing aerosol warms the atmosphere, which changes the atmospheric stability, and reduces surface flux.

The primary direct effect of aerosols is a brightening of the planet when viewed from space, as much of Earth's surface is dark ocean, and most aerosols scatter more than 90% of the visible light reaching them. The primary indirect effects of aerosols on clouds include an increase in cloud brightness, change in precipitation and possibly an increase in lifetime; thus the overall net impact of aerosols is an enhancement of Earth's reflectance (shortwave albedo). This reduces the sunlight reaching Earth's surface, producing a net climatic cooling, as well as a redistribution of the radiant and latent heat energy deposited in the atmosphere. These effects can alter atmospheric circulation and the water cycle, including precipitation patterns, on a variety of length and time scales (e.g., Ramanathan et al., 2001, [042681](#); Zhang et al., 2006, [190933](#)).



Source: IPCC (2007, [190988](#)) modified from Haywood and Boucher (2000, [156531](#)).

Figure 9-52. Aerosol radiative forcing. Airborne particles can affect the heat balance of the atmosphere, directly, by scattering and absorbing sunlight, and indirectly, by altering cloud brightness and possibly lifetime. Here small black dots represent aerosols, circles represent cloud droplets, and straight lines represent short-wave radiation, and wavy lines, long-wave radiation. LWC is liquid water content, and CDNC is cloud droplet number concentration. Confidence in the magnitudes of these effects varies considerably (see Chapter 3). Although the overall effect of aerosols is a net cooling at the surface, the heterogeneity of particle spatial distribution, emission history, and properties, as well as differences in surface reflectance, mean that the magnitude and even the sign of aerosol effects vary immensely with location, season and sometimes inter-annually. The human-induced component of these effects is sometimes called “climate forcing.”

Several variables are used to quantify the impact aerosols have on Earth's energy balance; these are helpful in describing current understanding, and in assessing possible future steps.

For the purposes of this report, *aerosol radiative forcing* (RF) is defined as the net energy flux (downwelling minus upwelling) difference between an initial and a perturbed aerosol loading state, at a specified level in the atmosphere. (Other quantities, such as solar radiation, are assumed to be the same for both states.) This difference is defined such that a negative aerosol forcing implies that the change in

aerosols relative to the initial state exerts a cooling influence, whereas a positive forcing would mean the change in aerosols exerts a warming influence.

There are a number of subtleties associated with this definition:

(1) The initial state against which aerosol forcing is assessed must be specified. For direct aerosol radiative forcing, it is sometimes taken as the complete absence of aerosols. IPCC AR4 (2001, [156587](#)) uses as the initial state their estimate of aerosol loading in 1750. That year is taken as the approximate beginning of the era when humans exerted accelerated influence on the environment.

(2) A distinction must be made between aerosol RF and the *anthropogenic contribution* to aerosol RF. Much effort has been made to distinguishing these contributions by modeling and with the help of space-based, airborne, and surface-based remote sensing, as well as in situ measurements. These efforts are described in subsequent chapters (of the CCSP SAP2.3).

(3) In general, aerosol RF and anthropogenic aerosol RF include energy associated with both the shortwave (solar) and the long-wave (primarily planetary thermal infrared) components of Earth's radiation budget. However, the solar component typically dominates, so in this document, these terms are used to refer to the solar component only, unless specified otherwise. The wavelength separation between the short- and long-wave components is usually set at around three or four micrometers.

(4) The IPCC AR4 (2007, [190988](#)) defines radiative forcing as the net downward minus upward irradiance at the tropopause due to an external driver of climate change. This definition excludes stratospheric contributions to the overall forcing. Under typical conditions, most aerosols are located within the troposphere, so aerosol forcing at TOA and at the tropopause are expected to be very similar. Major volcanic eruptions or conflagrations can alter this picture regionally, and even globally.

(5) Aerosol radiative forcing can be evaluated at the surface, within the atmosphere, or at top-of-atmosphere (TOA). In this document, unless specified otherwise, aerosol radiative forcing is assessed at TOA.

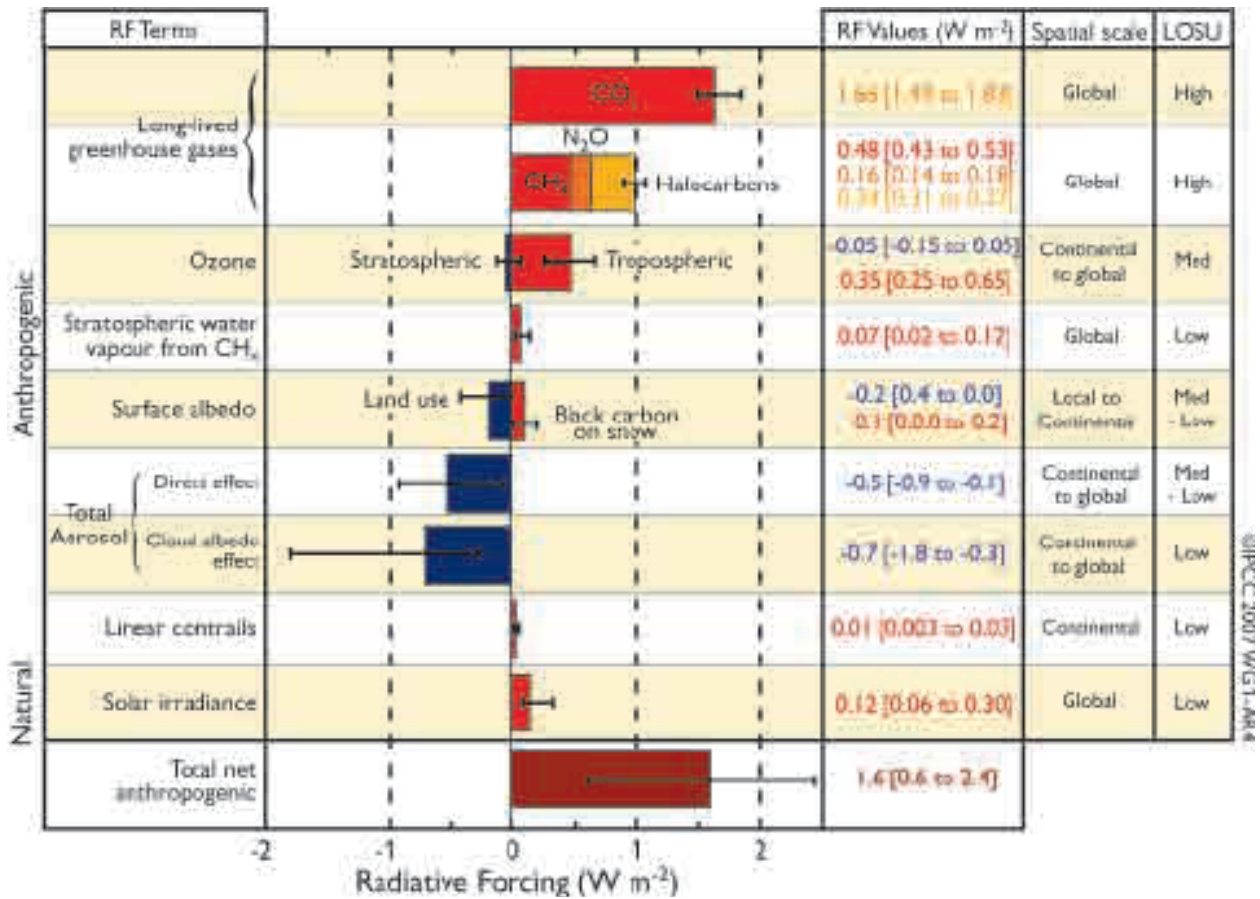
(6) As discussed subsequently, aerosol radiative forcing can be greater at the surface than at TOA if the aerosols absorb solar radiation. TOA forcing affects the radiation budget of the planet. Differences between TOA forcing and surface forcing represent heating within the atmosphere that can affect vertical stability, circulation on many scales, cloud formation, and precipitation, all of which are climate effects of aerosols. In this document, unless specified otherwise, these additional climate effects are not included in aerosol radiative forcing.)

(7) Aerosol direct radiative forcing can be evaluated under cloud-free conditions or under natural conditions, sometimes termed "all-sky" conditions, which include clouds. Cloud-free direct aerosol forcing is more easily and more accurately calculated; it is generally greater than all-sky forcing because clouds can mask the aerosol contribution to the scattered light. Indirect forcing, of course, must be evaluated for cloudy or all-sky conditions. In this document, unless specified otherwise, aerosol radiative forcing is assessed for all-sky conditions.

(8) Aerosol radiative forcing can be evaluated instantaneously, daily (24 h) averaged, or assessed over some other time period. Many measurements, such as those from polar-orbiting satellites, provide instantaneous values, whereas models usually consider aerosol RF as a daily average quantity. In this document, unless specified otherwise, daily averaged aerosol radiative forcing is reported.

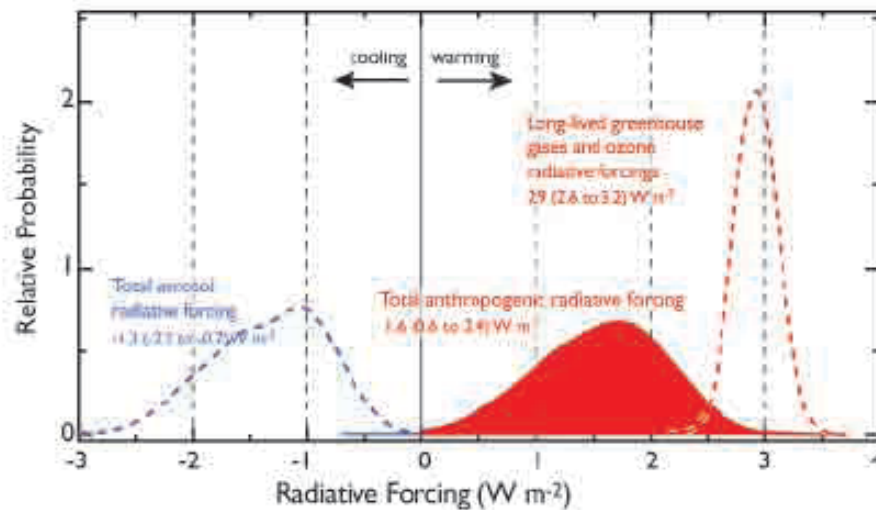
(9) Another subtlety is the distinction between a "forcing" and a "feedback." As different parts of the climate system interact, it is often unclear which elements are "causes" of climate change (forcings among them), which are responses to these causes, and which might be some of each. So, for example, the concept of aerosol effects on clouds is complicated by the impact clouds have on aerosols; the aggregate is often called aerosol-cloud interactions. This distinction sometimes matters, as it is

more natural to attribute responsibility for causes than for responses. However, practical environmental considerations usually depend on the net result of all influences. In this report, “feedbacks” are taken as the consequences of changes in surface or atmospheric temperature, with the understanding that for some applications, the accounting may be done differently.



Source: IPCC (2007, 190988).

Figure 9-53. Global average radiative forcing (RF) estimates and uncertainty ranges in 2005, relative to the pre-industrial climate. Anthropogenic CO₂, methane (CH₄), nitrous oxide (N₂O), ozone, and aerosols as well as the natural solar irradiance variations are included. Typical geographical extent of the forcing (spatial scale) and the assessed level of scientific understanding (LOSU) are also given. Forcing is expressed in units of watts per square meter (W/m^2). The total anthropogenic radiative forcing and its associated uncertainty are also given.



Source: Adapted from IPCC (2007, [190988](#)).

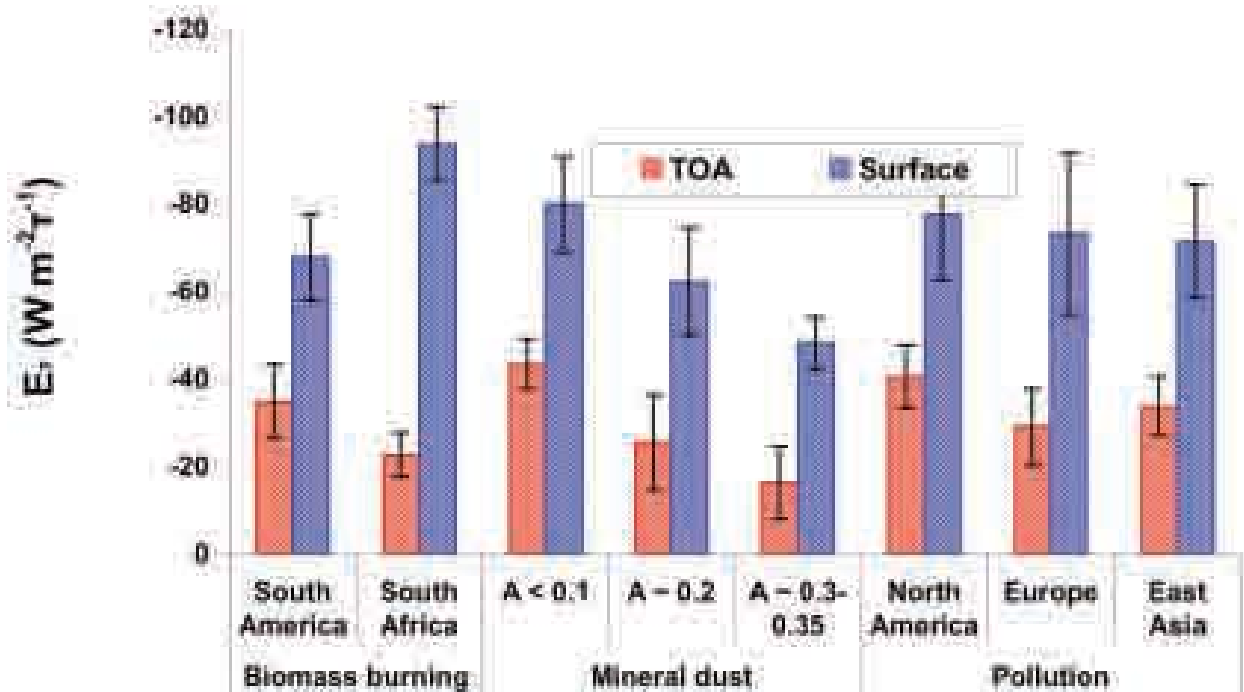
Figure 9-54. Probability distribution functions (PDFs) for anthropogenic aerosol and GHG RFs. Dashed red curve: RF of long-lived greenhouse gases plus ozone; dashed blue curve: RF of aerosols (direct and cloud albedo RF); red filled curve: combined anthropogenic RF. The RF range is at the 90% confidence interval.

In summary, aerosol radiative forcing, the fundamental quantity about which this report is written, must be qualified by specifying the initial and perturbed aerosol states for which the radiative flux difference is calculated, the altitude at which the quantity is assessed, the wavelength regime considered, the temporal averaging, the cloud conditions, and whether total or only human-induced contributions are considered. The definition given here, qualified as needed, is used throughout the report.

Although the possibility that aerosols affect climate was recognized more than 40 yr ago, the measurements needed to establish the magnitude of such effects, or even whether specific aerosol types warm or cool the surface, were lacking. Satellite instruments capable of at least crudely monitoring aerosol amount globally were first deployed in the late 1970s. But scientific focus on this subject grew substantially in the 1990s (e.g., Charlson and Wigley, 1994, [192011](#); 1991, [045793](#); 1992, [045794](#); Penner et al., 1992, [045825](#)), in part because it was recognized that reproducing the observed temperature trends over the industrial period with climate models requires including net global cooling by aerosols in the calculation (IPCC, 1995, [190991](#); 1996, [190990](#)), along with the warming influence of enhanced atmospheric greenhouse gas (GHG) concentrations – mainly carbon dioxide, methane, nitrous oxide, chlorofluorocarbons, and ozone.

Improved satellite instruments, ground- and ship-based surface monitoring, more sophisticated chemical transport and climate models, and field campaigns that brought all these elements together with aircraft remote sensing and in situ sampling for focused, coordinated study, began to fill in some of the knowledge gaps. By the Fourth IPCC Assessment Report, the scientific community consensus held that in global average, the sum of direct and indirect top-of-atmosphere (TOA) forcing by anthropogenic aerosols is negative (cooling) of about -1.3 W/m^2 (-2.2 to -0.5 W/m^2). This is significant compared to the positive forcing by anthropogenic GHGs (including ozone), about $2.9 \pm 0.3 \text{ W/m}^2$ (IPCC (Intergovernmental Panel on Climate, 2007, [190988](#)). However, the spatial distribution of the gases and aerosols are very different, and they do not simply exert compensating influences on climate.

The IPCC aerosol forcing assessments are based largely on model calculations, constrained as much as possible by observations. At present, aerosol influences are not yet quantified adequately, according to Figure 9-53, as scientific understanding is designated as “Medium-Low” and “Low” for the direct and indirect climate forcing, respectively. The IPCC AR4 (2007, [190988](#)) concluded that uncertainties associated with changes in Earth’s radiation budget due to anthropogenic aerosols make the largest contribution to the overall uncertainty in radiative forcing of climate change among the factors assessed over the industrial period (Figure 9-54).



Source: Adapted from Zhou et al. (2005, [156183](#)).

Figure 9-55. The clear-sky forcing efficiency E_{τ} , defined as the diurnally averaged aerosol direct radiative effect (W/m^2) per unit AOD at 550 nm, calculated at both TOA and the surface, for typical aerosol types over different geographical regions. The vertical black lines represent \pm one standard deviation of E_{τ} for individual aerosol regimes and A is surface broadband albedo.

Although AOD, aerosol properties, aerosol vertical distribution, and surface reflectivity all contribute to aerosol radiative forcing, AOD usually varies on regional scales more than the other aerosol quantities involved. *Forcing efficiency* (E_{τ}), defined as a ratio of direct aerosol radiative forcing to AOD at 550 nm, reports the sensitivity of aerosol radiative forcing to AOD, and is useful for isolating the influences of particle properties and other factors from that of AOD. E_{τ} is expected to exhibit a range of values globally, because it is governed mainly by aerosol size distribution and chemical composition (which determine aerosol single-scattering albedo and phase function), surface reflectivity, and solar irradiance, each of which exhibits pronounced spatial and temporal variations. To assess aerosol RF, E_{τ} is multiplied by the ambient AOD.

Figure 9-55 shows a range of E_{τ} , derived from AERONET surface sun photometer network measurements of aerosol loading and particle properties, representing

different aerosol and surface types, and geographic locations. It demonstrates how aerosol direct solar radiative forcing (with initial state taken as the absence of aerosol) is determined by a combination of aerosol and surface properties. For example, E_r due to southern African biomass burning smoke is greater at the surface and smaller at TOA than South American smoke because the southern African smoke absorbs sunlight more strongly, and the magnitude of E_r for mineral dust for several locations varies depending on the underlying surface reflectance. Figure 9-55 illustrates one further point, that the radiative forcing by aerosols on surface energy balance can be much greater than that at TOA. This is especially true when the particles have SSA substantially less than 1, which can create differences between surface and TOA forcing as large as a factor of five (e.g., Zhou, 2005, [156183](#)).

Table 9-3. Top-of-atmosphere, cloud-free, instantaneous direct aerosol radiative forcing dependence on aerosol and surface properties. Here TWP, SGP, and NSA are the Tropical West Pacific island, Southern Great Plains, and North Slope Alaska observation stations maintained by the DOE ARM program, respectively. Instantaneous values are given at specific solar zenith angle. Upper and middle parts are from McComiskey et al. (2008, [190523](#)). Representative, parameter-specific measurement uncertainty upper bounds for producing 1 W/m² instantaneous TOA forcing accuracy are given in the lower part, based on sensitivities at three sites from the middle part of the table.

Parameters	TWP	SGP	NSA
<i>AEROSOL PROPERTIES (AOD, SSA, G), SOLAR ZENITH ANGLE (SZA), SURFACE ALBEDO (A), AND AEROSOL DIRECT RF AT TOA (F)</i>			
AOD	0.05	0.1	0.05
SSA	0.97	0.95	0.95
g	0.8	0.6	0.7
A	0.05	0.1	0.9
SZA	30	45	70
F (W/m ²)	-2.2	-6.3	2.6
<i>SENSITIVITY OF CLOUD-FREE, INSTANTANEOUS, TOA DIRECT AEROSOL RADIATIVE FORCING TO AEROSOL AND SURFACE PROPERTIES, W/M² PER UNIT CHANGE IN PROPERTY</i>			
$dF/d(AOD)$	-45	-64	51
$dF/d(SSA)$	-11	-50	-60
dF/dg	13	23	2
dF/dA	8	24	6
<i>REPRESENTATIVE MEASUREMENT UNCERTAINTY UPPER BOUNDS FOR PRODUCING 1 W/M² ACCURACY OF AEROSOL RF</i>			
AOD	0.022	0.016	0.020
SSA	0.091	0.020	0.017
g	0.077	0.043	
A	0.125	0.042	0.167

Table 9-3 presents estimates of cloud-free, instantaneous, aerosol direct RF dependence on AOD, and on aerosol and surface properties, calculated for three sites maintained by the U.S. Department of Energy's Atmospheric Radiation Measurement (ARM) program, where surface and atmospheric conditions span a significant range of

natural environments (McComiskey et al., 2008, [190523](#)). Here aerosol RF is evaluated relative to an initial state that is the complete absence of aerosols. Note that aerosol direct RF dependence on individual parameters varies considerably, depending on the values of the other parameters, and in particular, that aerosol RF dependence on AOD actually changes sign, from net cooling to net warming, when aerosols reside over an exceedingly bright surface. Sensitivity values are given for snapshots at fixed solar zenith angles, relevant to measurements made, for example, by polar-orbiting satellites.

The lower portion of Table 9-3 presents upper bounds on instantaneous measurement uncertainty, assessed individually for each of AOD, SSA, g , and A , to produce a 1 W/m^2 top-of-atmosphere, cloud-free aerosol RF accuracy. The values are derived from the upper portion of the table, and reflect the diversity of conditions captured by the three ARM sites. Aerosol RF sensitivity of 1 W/m^2 is used as an example; uncertainty upper bounds are obtained from the partial derivative for each parameter by neglecting the uncertainties for all other parameters. These estimates produce an instantaneous AOD measurement uncertainty upper bound between about 0.01 and 0.02, and SSA constrained to about 0.02 over surfaces as bright as or brighter than the ARM Southern Great Plains site, typical of mid-latitude, vegetated land. Other researchers, using independent data sets, have derived ranges of E_r and aerosol RF sensitivity similar to those presented here, for a variety of conditions (Zhou, 2005, [156183](#); Yu, 2006, [156173](#); Christopher and Jones, 2008, [189985](#)).

These uncertainty bounds provide a baseline against which current and expected near-future instantaneous measurement capabilities are assessed in Chapter 2 (of the CCSP SAP2.3). Model sensitivity is usually evaluated for larger-scale (even global) and longer-term averages. When instantaneous measured values from a randomly sampled population are averaged, the uncertainty component associated with random error diminishes as something like the inverse square root of the number of samples. As a result, the accuracy limits used for assessing more broadly averaged model results corresponding to those used for assessing instantaneous measurements would have to be tighter, as discussed in Chapter 4 (of the CCSP SAP2.3).

In summary, much of the challenge in quantifying aerosol influences arises from large spatial and temporal heterogeneity, caused by the wide variety of aerosol sources, sizes and compositions, the spatial non-uniformity and intermittency of these sources, the short atmospheric lifetime of most aerosols, and the spatially and temporally non-uniform chemical and microphysical processing that occurs in the atmosphere. In regions having high concentrations of anthropogenic aerosol, for example, aerosol forcing is much stronger than the global average, and can exceed the magnitude of GHG warming, locally reversing the sign of the net forcing. It is also important to recognize that the global-scale aerosol TOA forcing alone is not an adequate metric for climate change (National Research, 2005, [057409](#)). Due to aerosol absorption, mainly by soot, smoke, and some desert dust particles, the aerosol direct radiative forcing at the surface can be much greater than the TOA forcing, and in addition, the radiative heating of the atmosphere by absorbing particles can change the atmospheric temperature structure, evolution, and possibly large-scale dynamical systems such as the monsoons (Kim et al., 2006, [190917](#); Lau et al., 2008, [190229](#)). By realizing aerosol's climate significance and the challenge of characterizing highly variable aerosol amount and properties, the U.S. Climate Change Research Initiative (CCRI) identified research on atmospheric concentrations and effects of aerosols specifically as a top priority (National Research, 2001, [053303](#)).

9.3.2. Overview of Aerosol Measurement Capabilities

9.3.2.1. Satellite Remote Sensing

Section 9.3.2 with the exception of the final paragraph, comes directly from CCSP SAP2.3 Chapter 2, Section 2.2 with section, table, and figure numbers changed to be internally consistent with this ISA.

A measurement-based characterization of aerosols on a global scale can be realized only through satellite remote sensing, which is the only means of characterizing the large spatial and temporal heterogeneities of aerosol distributions. Monitoring aerosols from space has been performed for over two decades and is planned for the coming decade with enhanced capabilities (King et al., 1999, [190635](#); Forster et al., 2007, [092936](#); Lee et al., 2006, [190358](#); Mischenko et al., 2007, [190543](#)). Table 9-4 summarizes major satellite measurements currently available for the tropospheric aerosol characterization and radiative forcing research.

Early aerosol monitoring from space relied on sensors that were designed for other purposes. The Advanced Very High Resolution Radiometer (AVHRR), intended as a cloud and surface monitoring instrument, provides radiance observations in the visible and near infrared wavelengths that are sensitive to aerosol properties over the ocean (Husar et al., 1997, [045900](#); Mischenko et al., 1999, [190541](#)). Originally intended for ozone monitoring, the ultraviolet (UV) channels used for the Total Ozone Mapping Spectrometer (TOMS) are sensitive to aerosol UV absorption with little surface interferences, even over land (Torres et al., 1998, [190503](#)). This UV-technique makes TOMS suitable for monitoring biomass burning smoke and dust, though with limited sensitivity near the surface (Herman et al., 1997, [048393](#)) and for retrieving aerosol single-scattering albedo from space (Torres et al., 2005, [190507](#)). (A new sensor, the Ozone Monitoring Instrument (OMI) aboard Aura, has improved on such UV-technique advantages, providing higher spatial resolution and more spectral channels; see (Veihelmann et al., 2007, [190627](#)). Such historical sensors have provided multi-decadal climatology of aerosol optical depth that has significantly advanced the understanding of aerosol distributions and long-term variability (e.g., Geogdzhayev et al., 2002, [190574](#); Massie et al., 2004, [190492](#); Mischenko and Geogdzhayev, 2007, [190545](#); Mischenko et al., 2007, [190542](#); Torres et al., 2002, [190505](#); Zhao et al., 2008, [190935](#)).

Over the past decade, satellite aerosol retrievals have become increasingly sophisticated. Now, satellites measure the angular dependence of radiance and polarization at multiple wavelengths from UV through the infrared (IR) at fine spatial resolution. From these observations, retrieved aerosol products include not only optical depth at one wavelength, but also spectral optical depth and some information about particle size over both ocean and land, as well as more direct measurements of polarization and phase function. In addition, cloud screening is much more robust than before and onboard calibration is now widely available. Examples of such new and enhanced sensors include the MODerate resolution Imaging Spectroradiometer (MODIS, see Box 2.1 of CCSP SAP2.3), the Multi-angle Imaging SpectroRadiometer (MISR, see Box 2.2 of CCSP SAP2.3), Polarization and Directionality of the Earth's Reflectance (POLDER, see Box 2.3 of CCSP SAP2.3), and OMI, among others. The accuracy for AOD measurement from these sensors is about 0.05 or 20% of AOD (Kahn RA Gaitley et al., 2005, [190966](#); Remer et al., 2005, [190221](#)) and somewhat better over dark water, but that for aerosol microphysical properties, which is useful for distinguishing aerosol air mass types, is generally low. The Clouds and the Earth's Radiant Energy System (CERES, see Box 2.4 of CCSP SAP2.3) measures broadband solar and terrestrial radiances. The CERES radiation measurements in combination

with satellite retrievals of aerosol optical depth can be used to determine aerosol direct radiative forcing.

Table 9-4. Summary of major satellite measurements currently available for the tropospheric aerosol characterization and radiative forcing research.

Category	Properties	Sensor/platform	Parameters	Spatial coverage	Temporal coverage
Column-integrated	Loading	AVHRR/NOAA-series	Optical depth	~ daily coverage of global ocean	1981-present
		TOMS/Nimbus, ADEOSI, EP		~ daily coverage of global land and ocean	1979-2001
		POLDER-1,2, PARASOL			1997-present
		MODIS/Terra, Aqua			2000-present (Terra) 2002-present (Aqua)
		MISR/Terra		~ weekly coverage of global land and ocean, including bright desert and nadir sun-glint	2000-present
		OMI/Aura		~ daily coverage of global land and ocean	2005-present
	Size, shape	AVHRR/NOAA-series	Ångström exponent	Global ocean	1981-present
		POLDER-1,2, PARASOL	Fine-mode fraction, Ångström exponent, non-spherical fraction	Global land and ocean	1997-present
		MODIS/Terra, Aqua	Fine-mode fraction	Global land and ocean (better quality over ocean)	2000-present (Terra)
			Ångström exponent		2002-present (Aqua)
			Effective radius	Global ocean	
		MISR/Terra	Ångström exponent, small, medium large fractions, non-spherical fractions	Global land and ocean	2000-present
	Absorption	TOMS/Nimbus, ADEOSI, EP	Absorbing aerosol index, single-scattering albedo, absorbing optical depth	Global land and ocean	1979-2001
		OMI/Aura			2005-present
		MISR/Terra	Single-scattering albedo (2-4 bins)		2000-present
Vertical-resolved	Loading, size, and shape	GLAS/ICESat	Extinction/backscatter	Global land and ocean, 16-day repeating cycle, single-nadir measurement	2003-present (~ 3 months/yr)
		CALIOP/CALIPSO	Extinction/backscatter, color ratio, depolarization ratio		2006-present

Complementary to these passive sensors, active remote sensing from space is also now possible and ongoing (see Box 2.5 of CCSP SAP2.3). Both the Geoscience Laser Altimeter System (GLAS) and the Cloud and Aerosol Lidar with Orthogonal Polarization (CALIOP) are collecting essential information about aerosol vertical distributions. Furthermore, the constellation of six afternoon-overpass spacecrafts (as illustrated in Figure 9-60), the so-called A-Train (Stephens and et, 2002, [190412](#)) makes it possible for the first time to conduct near simultaneous (within 15 minutes)

measurements of aerosols, clouds, and radiative fluxes in multiple dimensions with sensors in complementary capabilities.

The improved accuracy of aerosol products (mainly AOD) from these new-generation sensors, together with improvements in characterizing the earth's surface and clouds, can help reduce the uncertainties associated with estimating the aerosol direct radiative forcing (Yu H, et, 2006, [156173](#)); and references therein). The retrieved aerosol microphysical properties, such as size, absorption, and non-spherical fraction can help distinguish anthropogenic aerosols from natural aerosols and hence help assess the anthropogenic component of aerosol direct radiative forcing (Bellouin et al., 2005, [155684](#); Christopher et al., 2006, [155729](#); Kaufman et al., 2005, [155891](#); Yu H, et, 2006, [156173](#)). However, to infer aerosol number concentrations and examine indirect aerosol radiative effects from space, significant efforts are needed to measure aerosol size distribution with much improved accuracy, characterize aerosol type, account for impacts of water uptake on aerosol optical depth, and determine the fraction of aerosols that is at the level of the clouds (Kapustin et al., 2006, [190961](#); Rosenfeld, 2006, [190233](#)). In addition, satellite remote sensing is not sensitive to particles much smaller than 0.1 micrometer in diameter, which comprise of a significant fraction of those that serve as cloud condensation nuclei.

Finally, algorithms are being developed to retrieve aerosol absorption or SSA from satellite observations (e.g., Kaufman et al., 2002, [190955](#); Torres et al., 2005, [190507](#)). The NASA Glory mission, scheduled to launch in 2009 and to be added to the A-Train, will deploy a multi-angle, multispectral polarimeter to determine the global distribution of aerosol and clouds. It will also be able to infer microphysical property information, from which aerosol type (e.g., marine, dust, pollution, etc.) can be inferred for improving quantification of the aerosol direct and indirect forcing on climate (Mischenko et al., 2007, [190543](#)).

In summary, major advances have been made in both passive and active aerosol remote sensing from space in the past decade, providing better coverage, spatial resolution, retrieved AOD accuracy, and particle property information. However, AOD accuracy is still much poorer than that from surface-based sun photometers (0.01-0.02), even over vegetated land and dark water where retrievals are most reliable. Although there is some hope of approaching this level of uncertainty with a new generation of satellite instruments, the satellite retrievals entail additional sensitivities to aerosol and surface scattering properties. It seems unlikely that satellite remote sensing could exceed the sun photometer accuracy without introducing some as-yet-unspecified new technology. Spacebased lidars are for the first time providing global constraints on aerosol vertical distribution, and multi-angle imaging is supplementing this with maps of plume injection height in aerosol source regions. Major advances have also been made during the past decade in distinguishing aerosol types from space, and the data are now useful for validating aerosol transport model simulations of aerosol air mass type distributions and transports, particularly over dark water. But particle size, shape, and especially SSA information has large uncertainty; improvements will be needed to better distinguish anthropogenic from natural aerosols using space-based retrievals. The particle microphysical property detail required to assess aerosol radiative forcing will come largely from targeted in situ and surface remote sensing measurements, at least for the near-future, although estimates of measurement-based aerosol RF can be made from judicious use of the satellite data with relaxed requirements for characterizing aerosol microphysical properties.

MODerate resolution Imaging Spectroradiometer. MODIS performs near global daily observations of atmospheric aerosols. Seven of 36 channels (between 0.47 and 2.13 μm) are used to retrieve aerosol properties over cloud and surface-screened areas (Martins et al., 2002, [190470](#); Li et al., 2004, [190386](#)). Over vegetated land, MODIS retrieves aerosol optical depth at three visible channels with high accuracy of $\pm 0.05 \pm 0.2\tau$ (Kaufman and Fraser, 1997, [190958](#); Chu et al., 2002, [190001](#); Remer et al., 2005, [190221](#); Levy et al., 2007, [190379](#)). Most recently a deep blue algorithm (Hsu

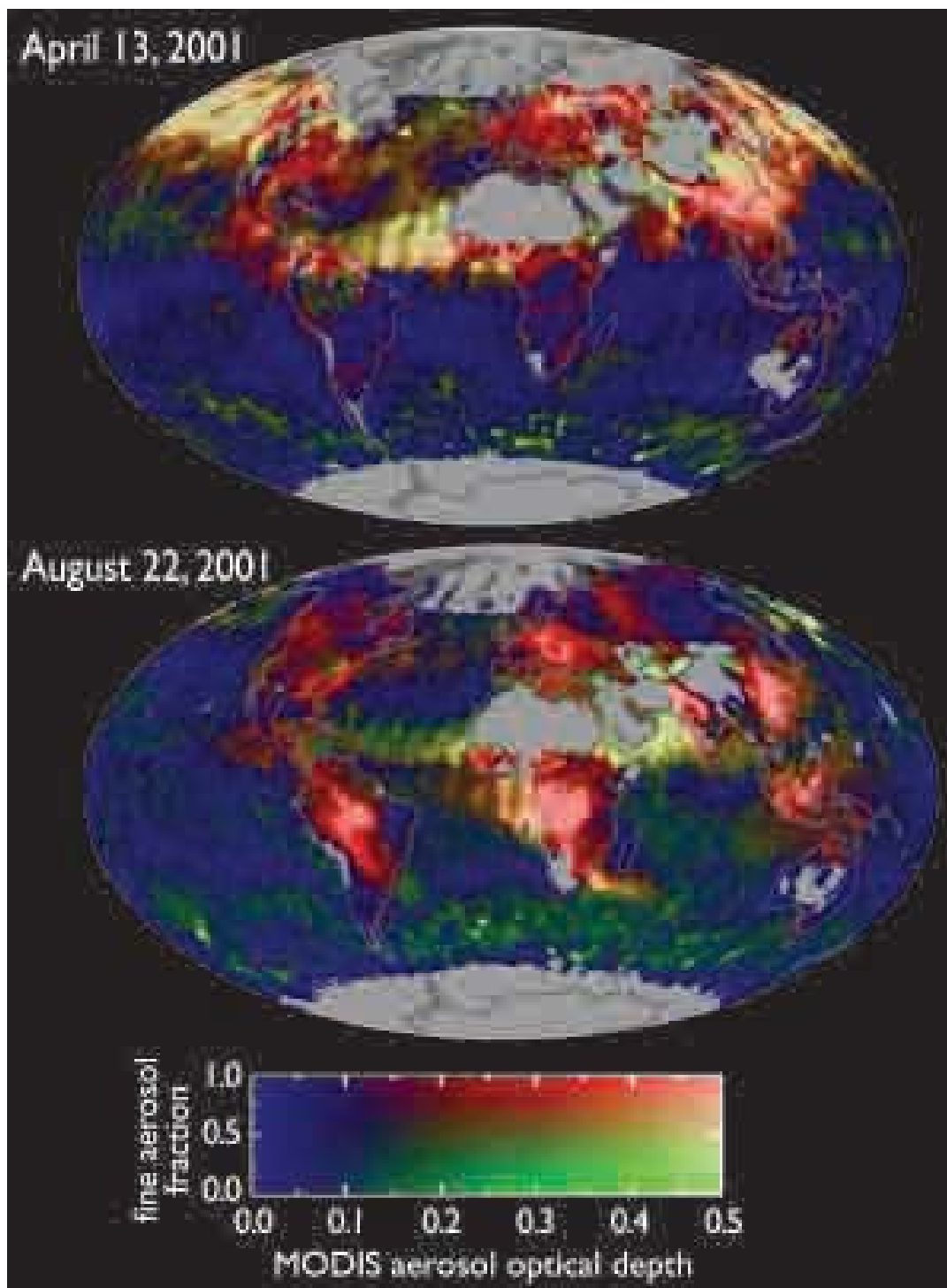
et al., 2004, [190622](#)) has been implemented to retrieve aerosols over bright deserts on an operational basis, with an estimated accuracy of 20-30%. Because of the greater simplicity of the ocean surface, MODIS has the unique capability of retrieving not only aerosol optical depth with greater accuracy, i.e., $\pm 0.03 \pm 0.05\tau$ (Tanré et al., 1997, [190452](#); Remer et al., 2002, [190218](#); 2005, [190221](#); Remer and et, 2008, [190224](#)), but also quantitative aerosol size parameters (e.g., effective radius, fine-mode fraction of AOD) (Kaufman et al., 2002, [190956](#); Remer et al., 2005, [190221](#); Kleidman et al., 2005, [190175](#)). The fine-mode fraction has been used as a tool for separating anthropogenic aerosol from natural ones and estimating the anthropogenic aerosol direct climate forcing (Kaufman et al., 2005, [155891](#)). Figure 9-56 shows composites of MODIS AOD and fine-mode fraction that illustrate seasonal and geographical variations of aerosol types. Clearly seen from the figure is heavy pollution over East Asia in both months, biomass burning smoke over South Africa, South America, and Southeast Asia in August, heavy dust storms over North Atlantic in both months and over Arabian Sea in August, and a mixture of dust and pollution plume swept across North Pacific in April.

Multi-Angle Imaging SpectroRadiometer. MISR, aboard the sun-synchronous, polar orbiting satellite Terra, measures upwelling solar radiance in four visible-near-IR spectral bands and at nine view angles spread out in the forward and aft directions along the flight path (Diner et al., 2002, [189967](#)). It acquires global coverage about once per week. A wide range of along-track view angles makes it feasible to more accurately evaluate the surface contribution to the TOA radiances and hence retrieve aerosols over both ocean and land surfaces, including bright desert and sunglint regions (Diner et al., 1998, [189962](#); Kahn RA Gaitley et al., 2005, [190966](#); Martonchik et al., 1998, [190472](#); 2002, [190490](#)). MISR AODs are within 20% or ± 0.05 of coincident AERONET measurements (Abdou et al., 2005, [190028](#); Kahn et al., 2005, [189961](#)). The MISR multi-angle data also sample scattering angles ranging from about 60° to 160° in midlatitudes, yielding information about particle size (Chen et al., 2008, [189984](#); Kahn et al., 1998, [190970](#); 2001, [190969](#); 2005, [190966](#)) and shape (Kalashnikova and Kahn, 2006, [190962](#)). The aggregate of aerosol microphysical properties can be used to assess aerosol air mass type, a more robust characterization of MISR-retrieved particle property information than individual attributes. MISR also retrieves plume height in the vicinity of wildfire, volcano, and mineral dust aerosol sources, where the plumes have discernable spatial contrast in the multi-angle imagery (Kahn et al., 2007, [190964](#)). Figure 9-57 is an example that illustrates MISR's ability to characterize the load, optical properties, and stereo height of near-source fire plumes.

POLarization and Directionality of the Earth's Reflectance. POLDER is a unique aerosol sensor that consists of wide field-of-view imaging spectro-radiometer capable of measuring multi-spectral, multi-directional, and polarized radiances (Deuzé et al., 2001, [192013](#)). The observed radiances can be exploited to better separate the atmospheric contribution from the surface contribution over both land and ocean. POLDER -1 and -2 flew onboard the ADEOS (Advanced Earth Observing Satellite) from November 1996 to June 1997 and April to October of 2003, respectively. A similar POLDER instrument flies on the PARASOL satellite that was launched in December 2004.

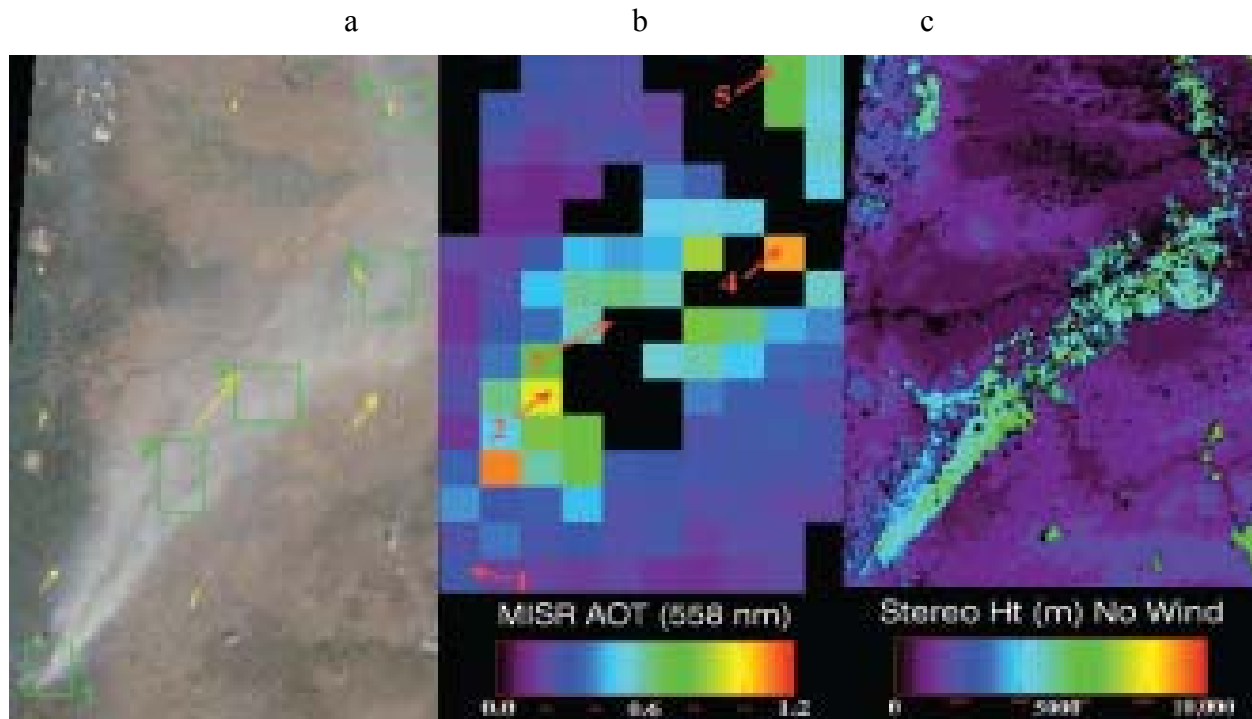
Figure 9-58 shows global horizontal patterns of AOD and Ångström exponent over the oceans derived from the POLDER instrument for June 1997. The oceanic AOD map (Figure 9-58.a) reveals near-coastal plumes of high AOD, which decrease with distance from the coast. This pattern arises from aerosol emissions from the continents, followed by atmospheric dispersion, transformation, and removal in the downwind direction. In large-scale flow fields, such as the trade winds, these continental plumes persist over several thousand kilometers. The Ångström exponent shown in Figure 9-58 exhibits a very different pattern from that of the aerosol optical depth; specifically, it exhibits high values downwind of industrialized regions and regions of biomass burning, indicative of small particles arising from direct emissions

from combustion sources and/or gas-to-particle conversion, and low values associated with large particles in plumes of soil dust from deserts and in sea salt aerosols.



Source: Adapted from (Chin et al., 2007, [190062](#)); original figure from Yoram Kaufman and Reto Stöckli.

Figure 9-56. A composite of MODIS/Terra observed aerosol optical depth (at 550 nm, green light near the peak of human vision) and fine-mode fraction that shows spatial and seasonal variations of aerosol types. Industrial pollution and biomass burning aerosols are predominately small particles (shown as red), whereas mineral dust and sea salt consist primarily of large particles (shown as green). Bright red and bright green indicate heavy pollution and dust plumes, respectively.



Source: taken from Kahn et al. (2007, [190964](#)).

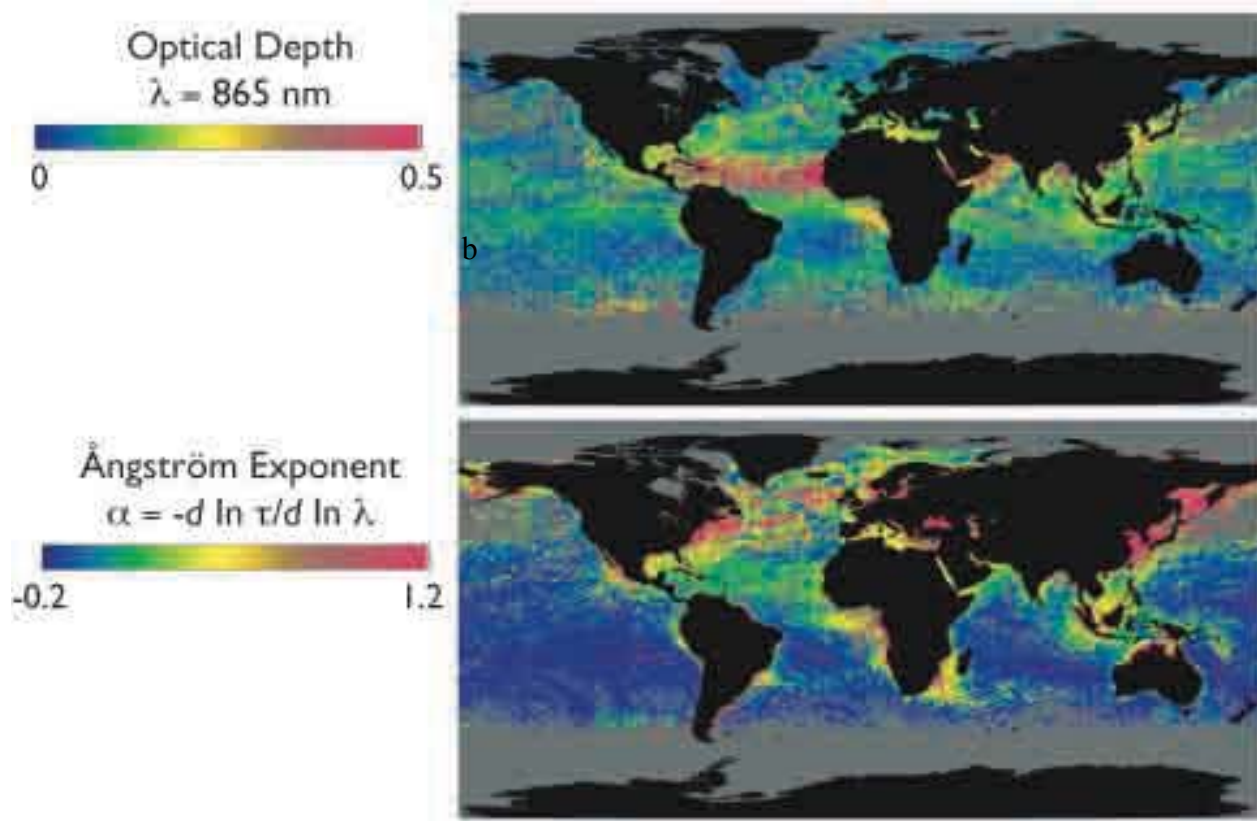
Figure 9-57. Oregon fire on September 4, 2003 as observed by MISR: (a) MISR nadir view of the fire plume, with five patch locations numbered and wind-vectors superposed in yellow; (b) MISR aerosol optical depth at 558 nm; and (c) MISR stereo height without wind correction for the same region.

9.3.2.2. Focused Field Campaigns

Over the past two decades, numerous focused field campaigns have examined the physical, chemical, and optical properties and radiative forcing of aerosols in a variety of aerosol regimes around the world, as listed in Table 9-5. These campaigns, which have been designed with aerosol characterization as the main goal or as one of the major themes in more interdisciplinary studies, were conducted mainly over or downwind of known continental aerosol source regions, but in some instances in low-aerosol regimes, for contrast. During each of these comprehensive campaigns, aerosols were studied in great detail, using combinations of in situ and remote sensing observations of physical and chemical properties from various platforms (e.g., aircraft, ships, satellites, and ground-based stations) and numerical modeling. In spite of their relatively short duration, these field studies have acquired comprehensive data sets of

regional aerosol properties that have been used to understand the properties and evolution of aerosols within the atmosphere and to improve the climatology of aerosol microphysical properties used in satellite retrieval algorithms and CTMs.

a



Reproduced with permission of Laboratoire d'Optique Atmosphérique (LOA), Lille, FR; Laboratoire des Sciences du Climat et de l'Environnement (LSCE), Gif sur Yvette, FR; Centre National d'études Spatiales (CNES), Toulouse, FR; and National Space Development Agency (NASDA), Japan.

Figure 9-58. Global maps at 18 km resolution showing monthly average (a) AOD at 865 nm and (b) Ångström exponent of AOD over water surfaces only for June, 1997, derived from radiance measurements by the POLDER.

9.3.2.3. Ground-Based In Situ Measurement Networks

Major U.S.-operated surface in situ and remote sensing networks for tropospheric aerosol characterization and climate forcing research are listed in Table 9-6. These surface in situ stations provide information about long-term changes and trends in aerosol concentrations and properties, the influence of regional sources on aerosol properties, climatologies of aerosol radiative properties, and data for testing models and satellite aerosol retrievals. The NOAA Earth System Research Laboratory (ESRL) aerosol monitoring network consists of baseline, regional, and mobile stations. These near-surface measurements include submicrometer and sub-10 micrometer scattering and absorption coefficients from which the extinction coefficient and single-scattering albedo can be derived. Additional measurements include particle concentration and, at selected sites, CCN concentration, the hygroscopic growth factor, and chemical composition.

Several of the stations, which are located across North America and world-wide, are in regions where recent focused field campaigns have been conducted. The measurement protocols at the stations are similar to those used during the field campaigns. Hence, the station data are directly comparable to the field campaign data so that they provide a longer-term measure of mean aerosol properties and their variability, as well as a context for the shorter-duration measurements of the field campaigns.

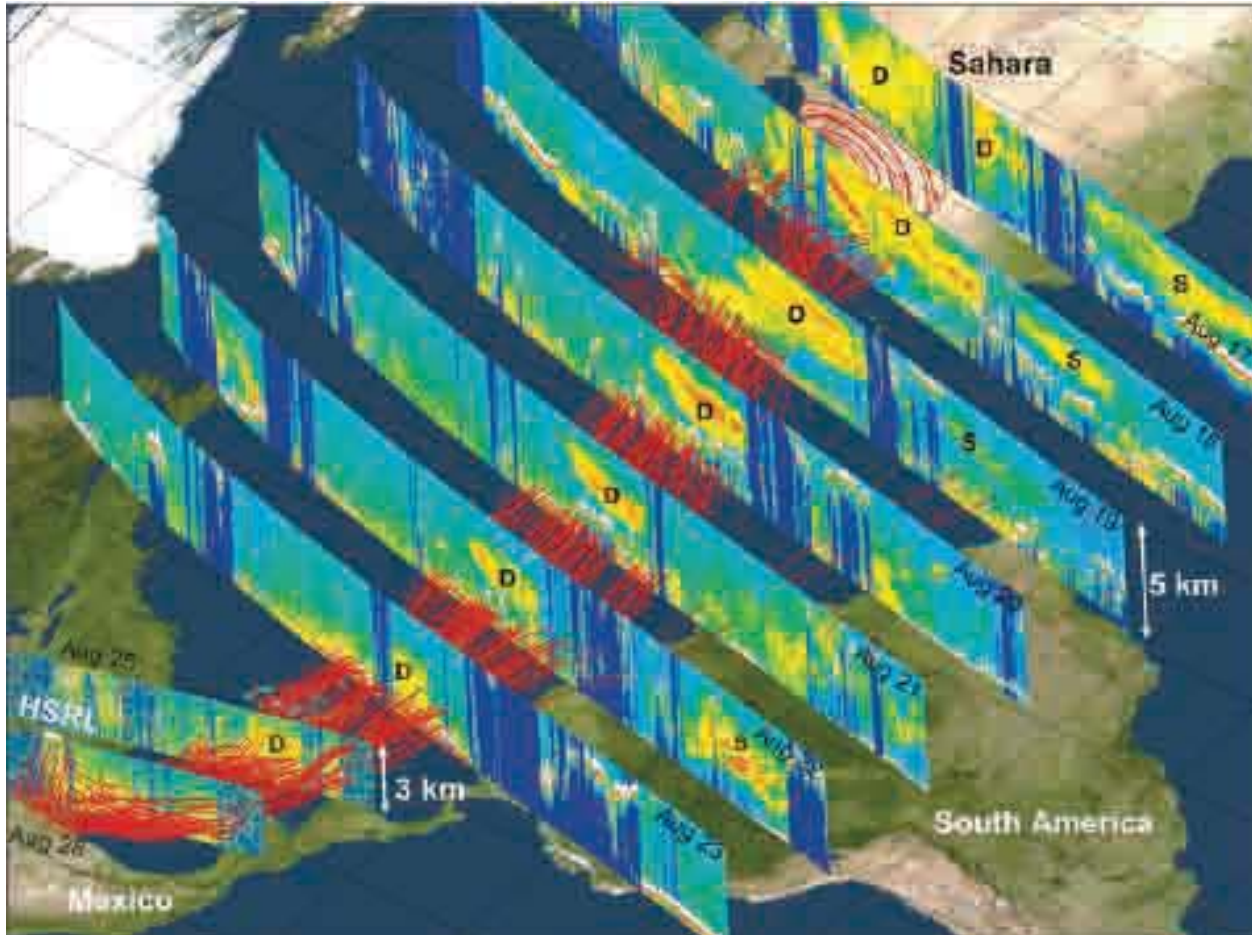
The Interagency Monitoring of Protected Visual Environment (IMPROVE), which is operated by the NP Service Air Resources Division, has stations across the U.S. located within national parks (Malm et al., 1994, [044920](#)). Although the primary focus of the network is air pollution, the measurements are also relevant to climate forcing research. Measurements include fine and coarse mode (PM_{2.5} and PM₁₀) aerosol mass concentration; concentrations of elements, sulfate, nitrate, organic carbon, and elemental carbon; and scattering coefficients.

In addition, to these U.S.-operated networks, there are other national and international surface networks that provide measurements of aerosol properties including, but not limited to, the World Meteorological Organization (WMO) Global Atmospheric Watch (GAW) network (<http://www.wmo.int/pages/prog/arep/gaw/monitoring.html>), the European Monitoring and Evaluation Programme (EMEP) (<http://www.emep.int/>), the Canadian Air and Precipitation Monitoring Network (CAPMoN) (http://www.msc-smc.ec.gc.ca/capmon/index_e.cfm), and the Acid Deposition Monitoring Network in East Asia (EANET) (<http://www.eanet.cc/eanet.html>).

Clouds and the Earth's Radiant Energy System. CERES measures broadband solar and terrestrial radiances at three channels with a large footprint (e.g., 20 km for CERES/Terra) (Wielicki et al., 1996, [190637](#)). It is co-located with MODIS and MISR aboard Terra and with MODIS on Aqua. The observed radiances are converted to TOA irradiances or fluxes using the Angular Distribution Models (ADMs) that are functions of viewing angle, sun angle, and scene type (Loeb and Kato, 2002, [190432](#); Loeb et al., 2005, [190436](#); Zhang et al., 2005, [190929](#)). Such estimates of TOA solar flux in clear-sky conditions can be compared to the expected flux for an aerosol-free atmosphere, in conjunction with measurements of aerosol optical depth from other sensors (e.g., MODIS and MISR) to derive the aerosol direct radiative forcing (Christopher et al., 2006, [155729](#); Loeb and Manalo-Smith, 2005, [190433](#); Patadia et al., 2008, [190558](#); Zhang and Christopher, 2003, [190928](#); Zhang et al., 2005, [190930](#)). The derived instantaneous value is then scaled to obtain a daily average. A direct use of the coarse spatial resolution CERES measurements would exclude aerosol distributions in partly cloudy CERES scenes. Several approaches that incorporate coincident, high spatial and spectral resolution measurements (e.g., MODIS) have been employed to overcome this limitation (Loeb and Manalo-Smith, 2005, [190433](#); Zhang et al., 2005, [190930](#)).

Active Remote Sensing of Aerosols. Following the success of a demonstration of lidar system aboard the U.S. Space Shuttle mission in 1994, i.e., Lidar In-space Technology Experiment (LITE) (Winker et al., 1996, [190914](#)), the Geoscience Laser Altimeter System (GLAS) was launched in early 2003 to become the first polar orbiting satellite lidar. It provides global aerosol and cloud profiling for a one-month period out of every three-to-six months. It has been demonstrated that GLAS is capable of detecting and discriminating multiple layer clouds, atmospheric boundary layer aerosols, and elevated aerosol layers (e.g., Spinhirne et al., 2005, [190410](#)). The Cloud-Aerosol Lidar and Infrared Pathfinder Satellite Observations (CALIPSO), launched on April 28, 2006, is carrying a lidar instrument (Cloud and Aerosol Lidar with Orthogonal Polarization - CALIOP) that has been collecting profiles of the attenuated backscatter at visible and near-infrared wavelengths along with polarized backscatter in the visible channel (Winker et al., 2003, [192017](#)). CALIOP measurements have been used to derive the above-cloud fraction of aerosol extinction optical depth (Chand et al., 2008, [189974](#)), one of the important factors

determining aerosol direct radiative forcing in cloudy conditions. Figure 9-59 shows an event of trans-Atlantic transport of Saharan dust captured by CALIPSO. Flying in formation with the Aqua, AURA, POLDER, and CloudSat satellites, the vertically resolved information is expected to greatly improve passive aerosol and cloud retrievals as well as allow the retrieval of vertical distributions of aerosol extinction, fine- and coarse-mode separately (Huneeus and O Boucher, 2007, [190624](#); Kaufman et al., 2003, [190954](#); Léon et al., 2003, [190366](#)).



Source: Liu et al. (2008, [156709](#)).

Figure 9-59. A dust event that originated in the Sahara desert on 17 August 2007 and was transported to the Gulf of Mexico. Red lines represent back trajectories indicating the transport track of the dust event. Vertical images are 532 nm attenuated backscatter coefficients measured by CALIOP when passing over the dust transport track. The letter "D" designates the dust layer, and "S" represents smoke layers from biomass burning in Africa (17-19 August) and South America (22 August). The track of the high-spectral-resolution-lidar (HSRL) measurement is indicated by the white line superimposed on the 28 August CALIPSO image. The HSRL track is coincident with the track of the 28 August CALIPSO measurement off the coast of Texas between 28.75°N and 29.08°N.

9.3.2.4. In Situ Aerosol Profiling Programs

In addition to long-term ground based measurements, regular long-term aircraft in situ measurements recently have been implemented at several locations. These programs provide a statistically significant data set of the vertical distribution of aerosol properties to determine spatial and temporal variability through the vertical column and the influence of regional sources on that variability. In addition, the measurements provide data for satellite and model validation. As part of its long-term ground measurements, NOAA has conducted regular flights over Bondville, Illinois since 2006. Measurements include light scattering and absorption coefficients, the relative humidity dependence of light scattering, aerosol number concentration and size distribution, and chemical composition. The same measurements with the exception of number concentration, size distribution, and chemical composition were made by NOAA during regular overflights of DOE ARM's Southern Great Plains (SGP) site from 2000-2007 (IOM et al., 2004, [190058](#)) (<http://www.esrl.noaa.gov/gmd/aero/net/index.html>).

In summary of Sections 9.3.2.2, 9.3.2.3, and 9.3.2.4, in situ measurements of aerosol properties have greatly expanded over the past two decades as evidenced by the number of focused field campaigns in or downwind of aerosol source regions all over the globe, the continuation of existing and implementation of new sampling networks worldwide, and the implementation of regular aerosol profiling measurements from fixed locations. In addition, in situ measurement capabilities have undergone major advancements during this same time period. These advancements include the ability to measure aerosol chemical composition as a function of size at a time resolution of seconds to minutes (e.g., Jayne et al., 2000, [190978](#)), the development of instruments able to measure aerosol absorption and extinction coefficients at high sensitivity and time resolution and as a function of relative humidity (e.g., Baynard et al., 2007, [151669](#); Lack et al., 2006, [190203](#)), and the deployment of these instruments across the globe on ships, at ground-based sites, and on aircraft. However, further advances are needed to make this newly developed instrumentation more affordable and turn-key so that it can be deployed more widely to characterize aerosol properties at a variety of sites worldwide.

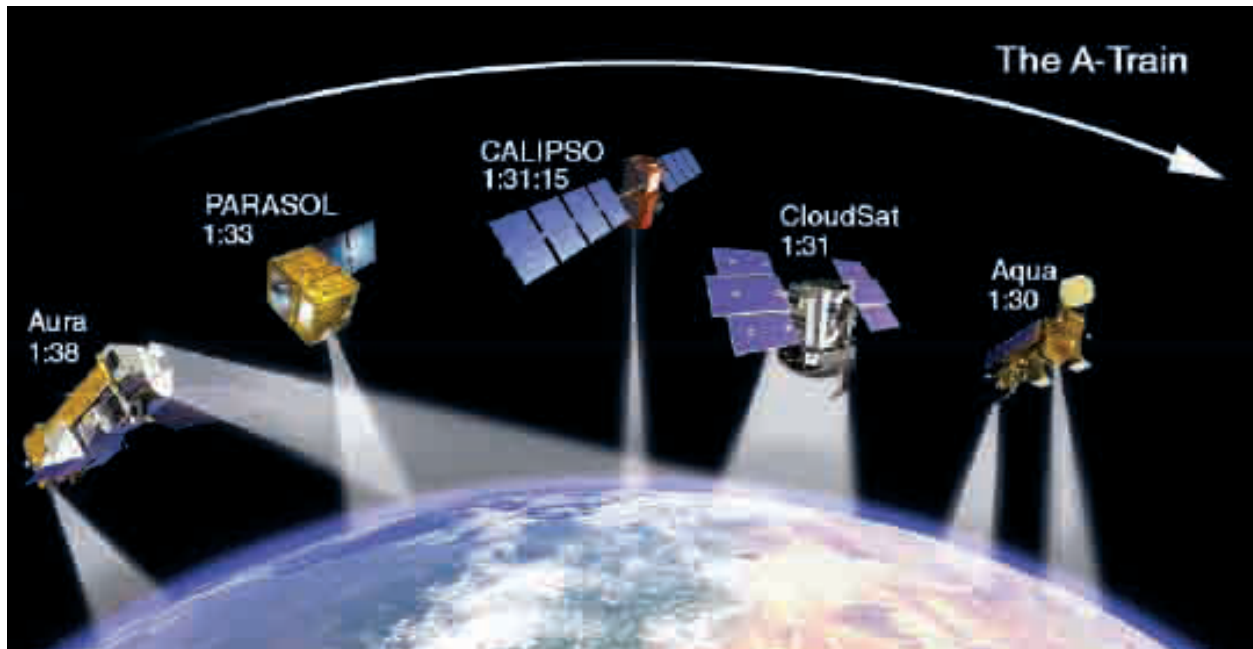


Figure 9-60. A constellation of five spacecraft that overfly the Equator at about 1:30 PM, the so-called A-Train, carries sensors having complementary capabilities, offering unprecedented opportunities to study aerosols from space in multiple dimensions.

Table 9-5. List of major intensive field experiments that are relevant to aerosol research in a variety of aerosol regimes around the globe conducted in the past two decades.

Aerosol Regimes	Intensive Field Experiments			Major References
	Name	Location	Time Period	
Anthropogenic aerosol and boreal forest from North America and West Europe	TARFOX	North Atlantic	July 1996	Russell et al. (1999, 190363)
	NEAQS	North Atlantic	July-August 2002	Quinn and Bates (2003, 049189)
	SCAR-A	North America	1993	Remer et al. (1997, 190216)
	CLAMS	East Coast of U.S.	July-August 2001	Smith et al. (2005, 190401)
	INTEX-NA, ICARTT	North America	Summer 2004	Fehsenfeld et al. (2006, 190531)
	DOE AIOF	Northern Oklahoma	May 2003	Ferrare et al. (2006, 190561)
	MILAGRO	Mexico City, Mexico	March 2006	Molina et al. (2008, 192019)
	TexAQS/GoMACCS	Texas and Gulf of Mexico	August-September 2006	Jiang et al. (2008, 156609); Lu et al. (2008, 190455)
	ARCTS	North-central Alaska to Greenland (Arctic haze)	March-April 2008	http://www.espo.nasa.gov/arctas/
	ARCTAS	Northern Canada (smoke)	June-July 2008	
	MINOS	Mediterranean region	July-August 2001	Lelieveld et al. (2002, 190361)
	LACE98	Lindberg, Germany	July-August 1998	Ansmann et al. (2002)

Intensive Field Experiments				
	Aerosols99	Atlantic	January-February 1999	Bates et al. (2001, 043385)
Brown haze in South Asia	INDOEX	Indian subcontinent and Indian Ocean	January-April 1998 & 1999	Ramanathan et al. (2001, 190196)
	ABC	South and East Asia	Ongoing	Ramanathan and Crutzen (2003, 190198)
Anthropogenic aerosol and desert dust mixture from East Asia	EAST-AIRE	China	March-April 2005	Li et al. (2007, 190392)
	INTEX-B	Northeastern Pacific	April 2006	Singh et al. (2008, 190394)
	ACE-Asia	East Asian and Northwest Pacific	April 2001	Huebert et al. (2003, 190623); Seinfeld et al. (2004, 190388)
	TRACE-P		March-April 2001	Jacob et al. (2003, 190987)
	PEM-West A & B	Western Pacific off East Asia	September-October 1991 February-March 1994	Hoell et al. (1996, 190607 ; 1997, 057373)
Biomass burning smoke in the tropics	BASE-A	Brazil	1989	Kaufman et al. (1992, 044557)
	SCAR-B	Brazil	August-September 1995	Kaufman et al. (1998, 089989)
	LBA-SMOCC	Amazon basin	September-November 2002	Andreae et al. (2004, 155658)
	SAFARI2000	South Africa and South Atlantic	August-September 2000	King et al. (2003, 094395)
	SAFARI92		September-October 1992	Lindesay et al. (1996, 190403)
	TRACE-ADABEX	South Atlantic	September-October 1992	Fishman et al. (1996, 190566)
	DABEX	West Africa	January-February 2006	Haywood et al. (2008, 190602)
Mineral dusts from North Africa and Arabian Peninsula	SAMUM	Southern Morocco	May-June 2006	Heintzenberg et al. (2008, 190605)
	SHADE	West coast of North Africa	September 2000	Tanrè et al. (2003, 190454)
	PRIDE	Puerto Rico	June-July 2000	Reid et al. (2003, 190213)
	UAE ²	Arabian Peninsula	August-September 2004	Reid et al. (2008, 190214)
Remote oceanic aerosol	ACE-1	Southern Oceans	December 1995	Bates et al. (1998, 190063); Quinn and Coffman (1998, 190918)

Source: (Yu, 2006, [156173](#)) (Updated)

Table 9-6. Summary of major U.S. surface in situ and remote sensing networks for the tropospheric aerosol characterization and radiative forcing research. All the reported quantities are column-integrated or column-effective, except as indicated.

Surface Network		Measured/Derived Parameters				Spatial Coverage	Temporal Coverage
		Loading	Size, Shape	Absorption	Chemistry		
In situ	NOAA ESRL aerosol monitoring (http://www.esrl.noaa.gov/gmd/aero/)	Near-surface extinction coefficient, optical depth, CN/CNN number concentrations	Ångström exponent, hemispheric backscatter fraction, asymmetry factor, hygroscopic growth	Single-scattering albedo, absorption coefficient	Chemical composition in selected sites and periods	5 baseline stations, several regional stations, aircraft and mobile platforms	1976 onward

		Measured/Derived Parameters					
	NPS/EPA IMPROVE (http://vista.cira.colostate.edu/improve/)	Near-surface mass concentrations and derived extinction coefficients by species	Fine and coarse separately	Single-scattering albedo, absorption coefficient	Ions, ammonium SO ₄ ²⁻ , ammonium nitrate organics, EC, fine soil	156 national parks and wilderness areas in the U.S.	1988 onward
Remote Sensing	NASA AERONET (http://aeronet.gsfc.nasa.gov)	Optical depth	Fine-mode fraction, Ångström exponents, asymmetry factor, phase function, non-spherical fraction	Single-scattering albedo, absorption optical depth, refractive indices	N/A	~ 200 sites over global land and islands	1993 onward
	DOE ARM (http://www.arm.gov)					6 sites and 1 mobile facility in N. America, Europe, and Asia	1989 onward
	NOAA SURFRAD (http://www.srb.noaa.gov/surfrad/)	N/A	N/A	N/A	7 sites in the U.S.	1995 onward	
	AERONET-MAN (http://aeronet.gsfc.nasa.gov/maritime_aerosol_network.html)				Global Ocean	2004-present periodically	
	NASA MPLNET (http://mplnet.gsfc.nasa.gov/)	Vertical profiles of backscatter/extinction coefficient	N/A	N/A	N/A	~ 30 sites in major continents, usually co-located with AERONET and ARM sites	2000 onward



Figure 9-61. Geographical coverage of active AERONET sites in 2006.

9.3.2.5. Ground-Based Remote Sensing Measurement Networks

The Aerosol Robotic Network (AERONET) program is a federated ground-based remote sensing network of well-calibrated sun photometers and radiometers (<http://aeronet.gsfc.nasa.gov>).

AERONET includes about 200 sites around the world, covering all major tropospheric aerosol regimes (Holben et al., 1998, [155848](#); 2001, [190618](#)), as illustrated in Figure 9-61. Spectral measurements of sun and sky radiance are calibrated and screened for cloud-free conditions (Smirnov et al., 2000, [190397](#)). AERONET stations provide direct, calibrated measurements of spectral AOD (normally at wavelengths of 440, 670, 870, and 1020 nm) with an accuracy of ± 0.015 (Eck et al., 1999, [190390](#)). In addition, inversion-based retrievals of a variety of effective, column-mean properties have been developed, including aerosol single-scattering albedo, size distributions, fine-mode fraction, degree of non-sphericity, phase function, and asymmetry factor (Dubovik and King, 2000, [190197](#); Dubovik et al., 2000, [190177](#); Dubovik et al., 2002, [190202](#); O'Neill et al., 2003, [180187](#)). The SSA can be retrieved with an accuracy of ± 0.03 , but only for AOD >0.4 (Dubovik et al., 2002, [190202](#)), which precludes much of the planet. These retrieved parameters have been validated or are undergoing validation by comparison to in situ measurements (e.g., Haywood et al., 2003, [190599](#); Leahy et al., 2007, [190232](#); Magi et al., 2005, [190468](#)).

Recent developments associated with AERONET algorithms and data products include:

- simultaneous retrieval of aerosol and surface properties using combined AERONET and satellite measurements (Sinyuk and et, 2007, [190395](#)) with surface reflectance taken into account (which significantly improves AERONET SSA retrieval accuracy) (Eck et al., 2008, [190409](#));
- the addition of ocean color and high frequency solar flux measurements; and
- the establishment of the Maritime Aerosol Network (MAN) component to monitor aerosols over the World oceans from ships of opportunity (Smirnov et al., 2006, [190400](#)).

Because of consistent calibration, cloud-screening, and retrieval methods, uniformly acquired and processed data are available from all stations, some of which have operated for over 10 years. These data constitute a high-quality, ground-based aerosol climatology and, as such, have been widely used for aerosol process studies as well as for evaluation and validation of model simulation and satellite remote sensing applications (e.g., Chin et al., 2002, [189996](#); Kahn RA Gaitley et al., 2005, [190966](#); Remer et al., 2005, [190221](#); Yu et al., 2003, [156171](#); 2006, [156173](#)). In addition, AERONET retrievals of aerosol size distribution and refractive indices have been used in algorithm development for satellite sensors (Levy et al., 2007, [190377](#); Remer et al., 2005, [190221](#)). A set of aerosol optical properties provided by AERONET has been used to calculate the aerosol direct radiative forcing (Procopio et al., 2004, [190571](#); Zhou M, et, 2005, [156183](#)), which can be used to evaluate both satellite remote sensing measurements and model simulations.

AERONET measurements are complemented by other ground-based aerosol networks having less geographical or temporal coverage, such as the Atmospheric Radiation Measurement (ARM) network (Ackerman and Stokes, 2003, [192080](#)), NOAA's national surface radiation budget network (SURFRAD) (Augustine et al., 2008, [189913](#)) and other networks with multifilter rotating shadowband radiometer (MFRSR) (Harrison et al., 1994, [045805](#); Michalsky et al., 2001, [190537](#)), and several lidar networks including:

- NASA Micro Pulse Lidar Network (MPLNET) (Welton et al., 2001, [157133](#)) (2002, [190631](#));
- Regional East Atmospheric Lidar Mesonet (REALM) in North America (Hoff and McCann, 2002, [190612](#); 2004, [190617](#));
- European Aerosol Research Lidar Network (EARLINET) (Matthias, 2004, [155971](#)); and
- Asian Dust Network (AD-Net) (e.g., Murayama T, et, 2001, [155992](#)).

Obtaining accurate aerosol extinction profile observations is pivotal to improving aerosol radiative forcing and atmospheric response calculations. The values derived from these lidar networks with state-of-the-art techniques (Schmid et al., 2006, [190372](#)) are helping to fill this need.

9.3.2.6. Synergy of Measurements and Model Simulations

Individual approaches discussed above have their own strengths and limitations, and are usually complementary. None of these approaches alone is adequate to characterize large spatial and temporal variations of aerosol physical and chemical properties and to address complex aerosol-climate interactions. The best strategy for characterizing aerosols and estimating their radiative forcing is to integrate measurements from different satellite sensors with complementary capabilities from in situ and surface based measurements. Similarly, while models are essential tools for estimating regional and global distributions and radiative forcing of aerosols at present as well as in the past and the future, observations are required to provide following, several synergistic approaches to studying aerosols and their radiative forcing are discussed.

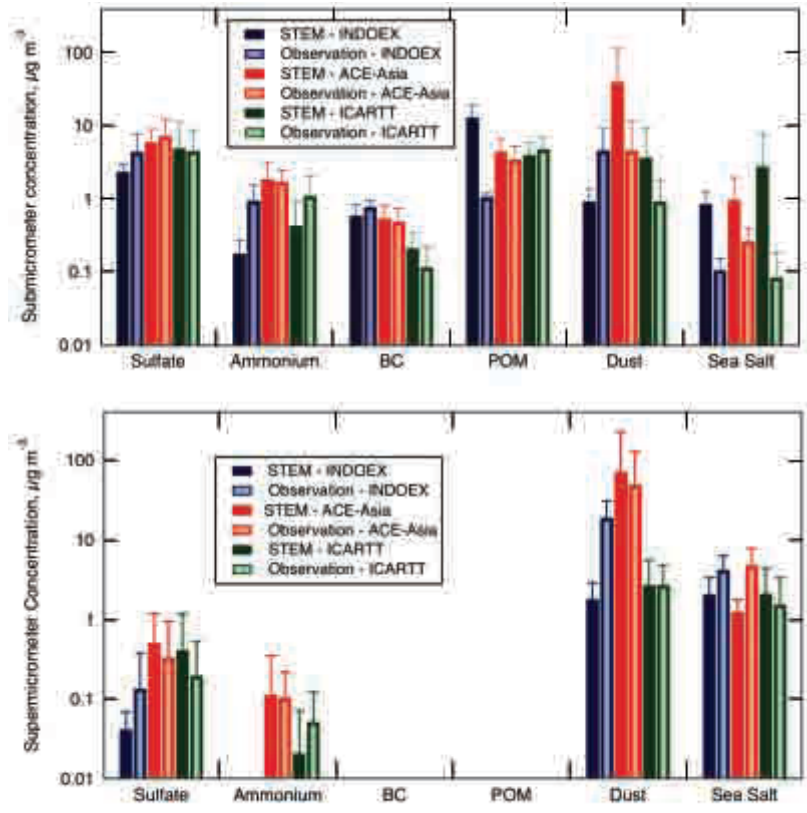
Closure Experiments. During intensive field studies, multiple platforms and instruments are deployed to sample regional aerosol properties through a well-coordinated experimental design. Often, several independent methods are used to measure or derive a single aerosol property or radiative forcing. This combination of methods can be used to identify inconsistencies in the methods and to quantify uncertainties in measured, derived, and calculated aerosol properties and radiative forcings. This approach, often referred to as a closure experiment, has been widely employed on both individual measurement platforms (local closure) and in studies involving vertical measurements through the atmospheric column by one or more platforms (column closure) (Quinn et al., 1996, [192021](#); Russell et al., 1997, [190359](#)).

Past closure studies have revealed that the best agreement between methods occurs for submicrometer, spherical particles such that different measures of aerosol optical properties and optical depth agree within 10-15% and often better (e.g., Clarke et al., 1996, [190003](#); Collins et al., 2000, [190059](#); Schmid and et, 2000, [190369](#); Quinn et al., 2004, [190937](#)). Larger particle sizes (e.g., sea salt and dust) present inlet collection efficiency issues and non-spherical particles (e.g., dust) lead to differences in instrumental responses. In these cases, differences between methods for determining aerosol optical depth can be as great as 35% (Doherty et al., 2005, [190027](#); Wang et al., 2003, [157106](#)). Closure studies on aerosol clear-sky DRF reveal uncertainties of about 25% for sulfate/carbonaceous aerosol and 60% for dust-containing aerosol (Bates et al., 2006, [189912](#)). Future closure studies could integrate surface- and satellite-based radiometric measurements of AOD with in situ optical, microphysical, and aircraft radiometric measurements for a wide range of situations. There is also a need to maintain consistency in comparing results and expressing uncertainties (Bates et al., 2006, [189912](#)).

Constraining Models with In Situ Measurements. In situ measurements of aerosol chemical, microphysical, and optical properties with known accuracy, based in part on closure studies, can be used to constrain regional CTM simulations of aerosol direct forcing, as described by Bates et al. (2006, [189912](#)). A key step in the approach is assigning empirically derived optical properties to the individual chemical components generated by the CTM for use in a Radiative Transfer Model (RTM). Specifically, regional data from focused, short-duration field programs can be segregated according to aerosol type (sea salt, dust, or sulfate/carbonaceous) based on measured chemical composition and particle size. Corresponding measured optical properties can be carried along in the sorting process so that they, too, are segregated by aerosol type. The empirically derived aerosol properties for individual aerosol types, including mass scattering efficiency, single-scattering albedo, and asymmetry factor, and their dependences on relative humidity, can be used in place of assumed values in CTMs. Short-term, focused measurements of aerosol properties (e.g., aerosol concentration and AOD) also can be used to evaluate CTM parameterizations on a regional basis, to suggest improvements to such uncertain model parameters, such as emission factors and scavenging coefficients (e.g., Koch et al., 2007, [190185](#)). Improvements in these parameterizations using observations yield increasing

confidence in simulations covering regions and periods where and when measurements are not available. To evaluate the aerosol properties generated by CTMs on broader scales in space and time, satellite observations and long-term in situ measurements are required.

Improved Model Simulations with Satellite Measurements. Global measurements of aerosols from satellites (mainly AOD) with well-defined accuracies offer an opportunity to evaluate model simulations at large spatial and temporal scales. The satellite measurements can also be used to constrain aerosol model simulations and hence the assessment of aerosol DRF through data assimilation or objective analysis process (e.g., Collins et al., , [189987](#); Yu et al., 2003, [156171](#); 2004, [190926](#); 2006, [156173](#); Liu et al., 2005, [190414](#); Zhang et al., 2008, [190932](#)). Both satellite retrievals and model simulations have uncertainties. The goal of data integration is to minimize the discrepancies between them, and to form an optimal estimate of aerosol distributions by combining them, typically with weights inversely proportional to the square of the errors of individual descriptions. Such integration can fill gaps in satellite retrievals and generate global distributions of aerosols that are consistent with ground-based measurements (Collins et al., , [189987](#); Yu et al., 2003, [156171](#); 2006, [156173](#); Liu et al., 2005, [190414](#)). Recent efforts have also focused on retrieving global sources of aerosol from satellite observations using inverse modeling, which may be valuable for reducing large aerosol simulation uncertainties (Dubovik et al., 2007, [190211](#)). Model refinements guided by model evaluation and integration practices with satellite retrievals can then be used to improve aerosol simulations of the pre- and post-satellite eras. Current measurement-based understanding of aerosol characterization and radiative forcing is assessed in Section 9.3.3 through intercomparisons of a variety of measurement-based estimates and model simulations published in literature. This is followed by a detailed discussion of major outstanding issues in Section 9.3.4.



Source: Bates et al. (2006, [189912](#)).

Figure 9-62. Comparison of the mean concentration ($\mu\text{g}/\text{m}^3$) and standard deviation of the modeled (STEM) aerosol chemical components with shipboard measurements during INDOEX, ACE-Asia, and ICARTT.

Further complexity is added when attempting to relate surface $\text{PM}_{2.5}$ to aerosol optical depths. The main approach to derive surface $\text{PM}_{2.5}$ from satellite optical depths from MISR is based on the use of model derived profiles to determine ratios of aerosol optical depth to surface $\text{PM}_{2.5}$ (Liu and Koutrakis, 2007, [187007](#); 2007, [192180](#); Van Donkelaar et al., 2006, [192108](#)). Van Donkelaar et al. (2006, [192108](#)) derived $r = 0.69$ (MODIS) and 0.58 (MISR) with annual average ground based $\text{PM}_{2.5}$ across the U.S. and Canada. For comparison, r between AERONET total AOD and surface measurements was 0.71 . On average, MODIS tended to overestimate surface $\text{PM}_{2.5}$ by about $5 \mu\text{g}/\text{m}^3$, while MISR estimates were biased high by about $3 \mu\text{g}/\text{m}^3$. Liu et al. (2007, [187007](#); 2007, [192180](#)) used MISR derived fractional AODs in their analysis and found improvement in the retrievals when fractional AODs were used instead of total AOD, allowing for better fits to the radiance data. They found that fractional AODs can explain 13-62% of the variability in $\text{PM}_{2.5}$ and its components in the eastern U.S. and 28-56% of the variability in the western U.S. The models tended to

underpredict $PM_{2.5}$ by ~7-8% in both the East and West. The relative errors in surface $PM_{2.5}$ were estimated to be 30% in the East and 34% in the West. For AODs >0.15 (nominal continental background values), dust particles could be distinguished from other particles with an estimated error of 4%. Performance improves substantially over polluted urban areas because they have much larger AOD. For example, Gupta et al. (2006, [137694](#)) derived a Pearson r between MODIS AOD and surface $PM_{2.5}$ of 0.96 for several urban areas around the world.

9.3.3. Assessments of Aerosol Characterization and Climate Forcing

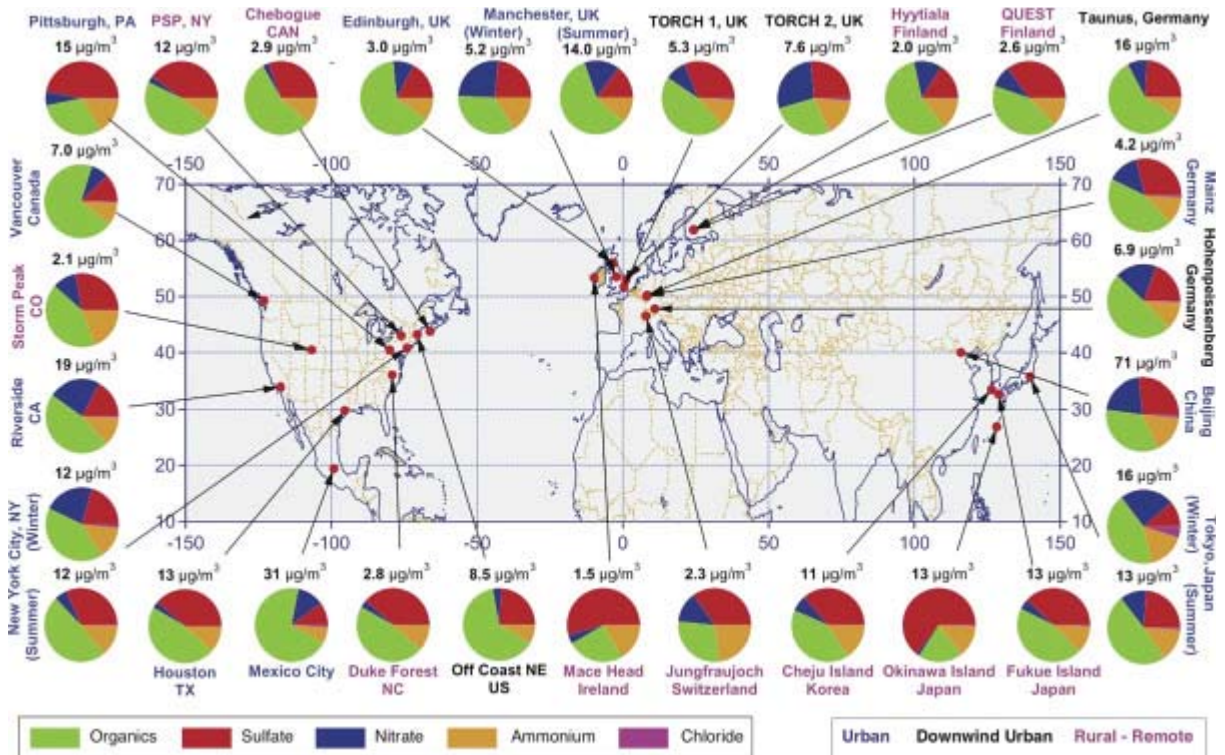
Sections 9.3.3 through 9.3.6 come directly from CCSP SAP2.3 Chapters 2, Section 2.3 through Chapter 3, Section 3.8, with section, table, and figure numbers changed to be internally consistent with this ISA.

This section focuses on the assessment of measurement-based aerosol characterization and its use in improving estimates of the direct radiative forcing on regional and global scales. In situ measurements provide highly accurate aerosol chemical, microphysical, and optical properties on a regional basis and for the particular time period of a given field campaign. Remote sensing from satellites and ground-based networks provide spatial and temporal coverage that intensive field campaigns lack. Both in situ measurements and remote sensing have been used to determine key parameters for estimating aerosol direct radiative forcing including aerosol single scattering albedo, asymmetry factor, optical depth. Remote sensing has also been providing simultaneous measurements of aerosol optical depth and radiative fluxes that can be combined to derive aerosol direct radiative forcing at the TOA with relaxed requirement for characterizing aerosol properties. Progress in using both satellite and surface-based measurements to study aerosol-cloud interactions and aerosol indirect forcing is also discussed.

9.3.3.1. The Use of Measured Aerosol Properties to Improve Models

The wide variety of aerosol data sets from intensive field campaigns provides a rigorous “testbed” for model simulations of aerosol properties and distributions and estimates of DRF. As described in Section 9.3.2.6, in situ measurements can be used to constrain regional CTM simulations of aerosol properties, DRF, anthropogenic component of DRF, and to evaluate CTM parameterizations. In addition, in situ measurements can be used to develop simplifying parameterizations for use by CTMs.

Several factors contribute to the uncertainty of CTM calculations of size-distributed aerosol composition including emissions, aerosol removal by wet deposition, processes involved in the formation of secondary aerosols and the chemical and microphysical evolution of aerosols, vertical transport, and meteorological fields including the timing and amount of precipitation, formation of clouds, and relative humidity. In situ measurements made during focused field campaigns provide a point of comparison for the CTM-generated aerosol distributions at the surface and at discrete points above the surface. Such comparisons are essential for identifying areas where the models need improvement.

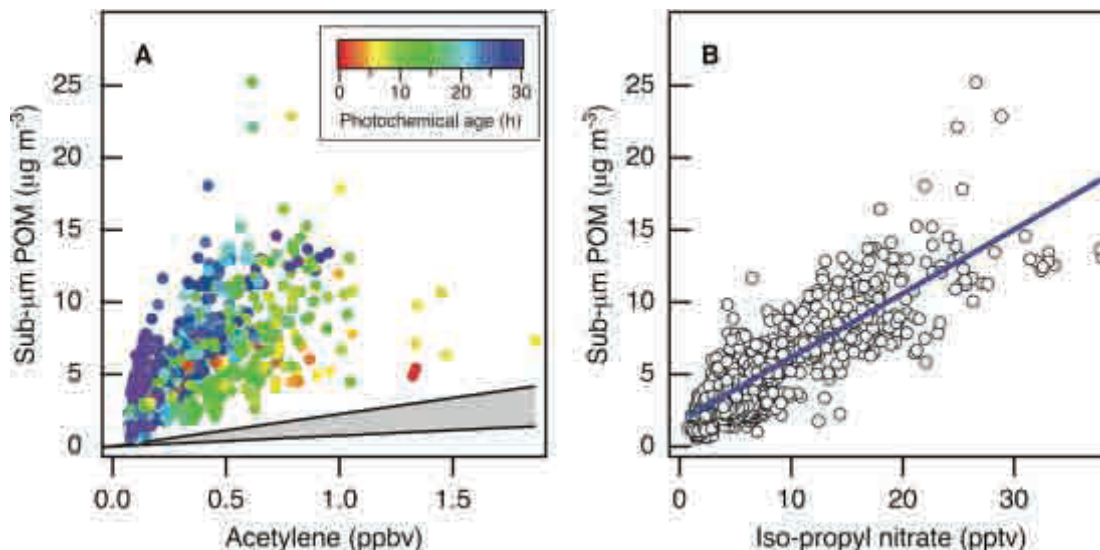


Source: Adapted from Zhang et al. (2007, 189998).

Figure 9-63. Location of aerosol chemical composition measurements with aerosol mass spectrometers. Colors for the labels indicate the type of sampling location: urban areas (blue), < 100 miles downwind of major cities (black), and rural/remote areas > 100 miles downwind (pink). Pie charts show the average mass concentration and chemical composition: organics (green), SO₄²⁻ (red), nitrate (blue), ammonium (orange), and chloride (purple), of non-refractory PM₁.

Figure 9-62 shows a comparison of submicrometer and supermicrometer aerosol chemical components measured during INDOEX, ACEAsia, and ICARTT onboard a ship and the same values calculated with the STEM Model (e.g., Bates et al., 2004, 189958; Carmichael et al., 2002, 148319; Carmichael et al., 2003, 190042; Streets et al., 2006, 157019; Tang and et, 2003, 190441; Tang and et, 2004, 190445). To permit direct comparison of the measured and modeled values, the model was driven by analyzed meteorological data and sampled at the times and locations of the shipboard measurements every 30 min along the cruise track. The best agreement was found for submicrometer sulfate and BC. The agreement was best for sulfate; this is attributed to greater accuracy in emissions, chemical conversion, and removal for this component. Underestimation of dust and sea salt is most likely due to errors in model-calculated emissions. Large discrepancies between the modeled and measured values occurred for submicrometer particulate organic matter (POM) (INDOEX), and for particles in the supermicrometer size range such as dust (ACE-Asia), and sea salt (all regions). The model underestimated the total mass of the supermicrometer aerosol by about a factor of 3. POM makes up a large and variable fraction of aerosol mass throughout the anthropogenically influenced northern hemisphere, and yet models have severe problems in properly representing this type of aerosol. Much of this discrepancy follows from the models inability to represent the formation of secondary organic aerosols (SOA) from the precursor volatile organic compounds (VOC). Figure 9-63 shows a summary of the results from aerosol mass spectrometer measurements

at 30 sites over North America, Europe, and Asia. Based on aircraft measurements of urban-influenced air over New England, de Gouw et al. (2005, [190020](#)) found that POM was highly correlated with secondary anthropogenic gas phase species suggesting that the POM was derived from secondary anthropogenic sources and that the formation took one day or more.



Source: Adapted from de Guow et al. (2005, [190020](#)).

Figure 9-64. Scatterplots of the submicrometer POM measured during NEAQS versus A) acetylene and B) iso-propyl nitrate. The colors of the data points in A) denote the photochemical age as determined by the ratios of compounds of known OH reactivity. The gray area in A) shows the range of ratios between submicrometer POM and acetylene observed by Kirchstetter et al. (1999, [010642](#)) in tunnel studies.

Figure 9-64 shows scatterplots of submicrometer POM versus acetylene (a gas phase primary emitted VOC species) and isopropyl nitrate (a secondary gas phase organic species formed by atmospheric reactions). The increase in submicrometer POM with increasing photochemical age could not be explained by the removal of VOC alone, which are its traditionally recognized precursors. This result suggests that other species must have contributed and/or that the mechanism for POM formation is more efficient than assumed by models. Similar results were obtained from the 2006 MILAGRO field campaign conducted in Mexico City (Kleinman et al., 2008, [190074](#)), and comparisons of GCM results with several long-term monitoring stations also showed that the model underestimated organic aerosol concentrations (Koch et al., 2007, [190185](#)). Recent laboratory work suggests that isoprene may be a major SOA source missing from previous atmospheric models (Kroll et al., 2006, [190195](#); Henze and Seinfeld, 2006, [190606](#)), but underestimating sources from certain economic sectors may also play a role (Koch et al., 2007, [190185](#)). Models also have difficulty in representing the vertical distribution of organic aerosols, underpredicting their occurrence in the free troposphere (FT) (Heald et al., 2005, [190603](#)). While organic aerosol presents models with some of their greatest challenges, even the distribution of well-characterized sulfate aerosol is not always estimated correctly in models (Shindell et al., 2008, [190391](#)).

Comparisons of DRF and its anthropogenic component calculated with assumed optical properties and values constrained by in situ measurements can help identify

areas of uncertainty in model parameterizations. In a study described by Bates et al. (2006, [189912](#)), two different CTMs (MOZART and STEM) were used to calculate dry mass concentrations of the dominant aerosol species (sulfate, organic carbon, BC, sea salt, and dust).

In situ measurements were used to calculate the corresponding optical properties for each aerosol type for use in a radiative transfer model. Aerosol DRF and its anthropogenic component estimated using the empirically derived and *a priori* optical properties were then compared. The DRF and its anthropogenic component were calculated as the net downward solar flux difference between the model state with aerosol and of the model state with no aerosol. It was found that the constrained optical properties derived from measurements increased the calculated AOD ($34 \pm 8\%$), TOA DRF ($32 \pm 12\%$), and anthropogenic component of TOA DRF ($37 \pm 7\%$) relative to runs using the *a priori* values. These increases were due to larger values of the constrained mass extinction efficiencies relative to the *a priori* values. In addition, differences in AOD due to using the aerosol loadings from MOZART versus those from STEM were much greater than differences resulting from the *a priori* vs. constrained RTM runs. In situ observations also can be used to generate simplified parameterizations for CTMs and RTMs thereby lending an empirical foundation to uncertain parameters currently in use by models. CTMs generate concentration fields of individual aerosol chemical components that are then used as input to radiative transfer models (RTMs) for the calculation of DRF. Currently, these calculations are performed with a variety of simplifying assumptions concerning the RH dependence of light scattering by the aerosol. Chemical components often are treated as externally mixed each with a unique RH dependence of light scattering. However, both model and measurement studies reveal that POM, internally mixed with water-soluble salts, can reduce the hygroscopic response of the aerosol, which decreases its water content and ability to scatter light at elevated relative humidity (e.g., Saxena et al., 1995, [077273](#); Carrico et al., 2005, [190052](#)). The complexity of the POM composition and its impact on aerosol optical properties requires the development of simplifying parameterizations that allow for the incorporation of information derived from field measurements into calculations of DRF (Quinn et al., 2005, [156033](#)). Measurements made during INDOEX, ACE-Asia, and ICARTT revealed a substantial decrease in $f_{\text{sp}}(RH)$ with increasing mass fraction of POM in the accumulation mode. Based on these data, a parameterization was developed that quantitatively describes the relationship between POM mass fraction and $f_{\text{sp}}(RH)$ for accumulation mode sulfate-POM mixtures (Quinn et al., 2005, [156033](#)). This simplified parameterization may be used as input to RTMs to derive values of $f_{\text{sp}}(RH)$ based on CTM estimates of the POM mass fraction. Alternatively, the relationship may be used to assess values of $f_{\text{sp}}(RH)$ currently being used in RTMs.

9.3.3.2. Intercomparisons of Satellite Measurements and Model Simulation of Aerosol Optical Depth

As aerosol DRF is highly dependent on the amount of aerosol present, it is of first-order importance to improve the spatial characterization of AOD on a global scale. This requires an evaluation of the various remote sensing AOD data sets and comparison with model-based AOD estimates. The latter comparison is particularly important if models are to be used in projections of future climate states that would result from assumed future emissions. Both remote sensing and model simulation have uncertainties and satellite-model integration is needed to obtain an optimum description of aerosol distribution.

Figure 9-65 shows an intercomparison of annual average AOD at 550 nm from two recent satellite aerosol sensors (MODIS and MISR), five model simulations (GOCART, GISS, SPRINTARS, LMDZ-LOA, LMDZ-INCA) and three satellite-model integrations (MO_GO, MI_GO, MO_MI_GO). These model-satellite integrations are conducted by using an optimum interpolation approach (Yu et al., 2003, [156171](#)) to

constrain GOCART simulated AOD with that from MODIS, MISR, or MODIS over ocean and MISR over land, denoted as MO_GO, MI_GO, and MO_MI_GO, respectively. MODIS values of AOD are from Terra Collection 4 retrievals and MISR AOD is based on early post launch retrievals. MODIS and MISR retrievals give a comparable average AOD on the global scale, with MISR greater than MODIS by 0.01~0.02 depending on the season. However, differences between MODIS and MISR are much larger when land and ocean are examined separately: AOD from MODIS is 0.02-0.07 higher over land but 0.03-0.04 lower over ocean than the AOD from MISR. Several major causes for the systematic MODIS-MISR differences have been identified, including instrument calibration and sampling differences, different assumptions about ocean surface boundary conditions made in the individual retrieval algorithms, missing particle property or mixture options in the look-up tables, and cloud screening (Kahn et al., 2007, [190963](#)). The MODIS-MISR AOD differences are being reduced by continuous efforts on improving satellite retrieval algorithms and radiance calibration. The new MODIS aerosol retrieval algorithms in Collection 5 have resulted in a reduction of 0.07 for global land mean AOD (Levy et al., 2007, [190379](#)), and improved radiance calibration for MISR removed ~40% of AOD bias over dark water scenes (Kahn et al., 2005, [190965](#)).

The annual and global average AOD from the five models is 0.19 ± 0.02 (mean \pm standard deviation) over land and 0.13 ± 0.05 over ocean, respectively. Clearly, the model-based mean AOD is smaller than both MODIS- and MISR-derived values (except the GISS model). A similar conclusion has been drawn from more extensive comparisons involving more models and satellites (Kinne et al., 2006, [155903](#)). On regional scales, satellite-model differences are much larger. These differences could be attributed in part to cloud contamination (Kaufman et al., 2005, [155891](#); Zhang et al., 2005, [190931](#)) and 3D cloud effects in satellite retrievals (Kaufman et al., 2005, [155891](#); Wen et al., 2006, [179964](#)) or to models missing important aerosol sources/sinks or physical processes (Koren et al., 2007, [190192](#)). Integrated satellite-model products are generally in-between the satellite retrievals and the model simulations, and agree better with AERONET measurements (e.g., Yu et al., 2003, [156171](#)). As in comparisons between models and in situ measurements (Bates et al., 2006, [189912](#)), there appears to be a relationship between uncertainties in the representation of dust in models and the uncertainty in AOD, and its global distribution.

For example, the GISS model generates more dust than the other models (Figure 9-66), resulting in a closer agreement with MODIS and MISR in the global mean (Figure 9-65). However, the distribution of AOD between land and ocean is quite different from MODIS- and MISR-derived values.

Figure 9-66 shows larger model differences in the simulated percentage contributions of individual components to the total aerosol optical depth on a global scale, and hence in the simulated aerosol single-scattering properties (e.g., single-scattering albedo, and phase function), as documented in Kinne et al. (2006, [155903](#)). This, combined with the differences in aerosol loading (as characterized by AOD) determines the model diversity in simulated aerosol direct radiative forcing, as discussed later. However, current satellite remote sensing capability is not sufficient to constrain model simulations of aerosol components.

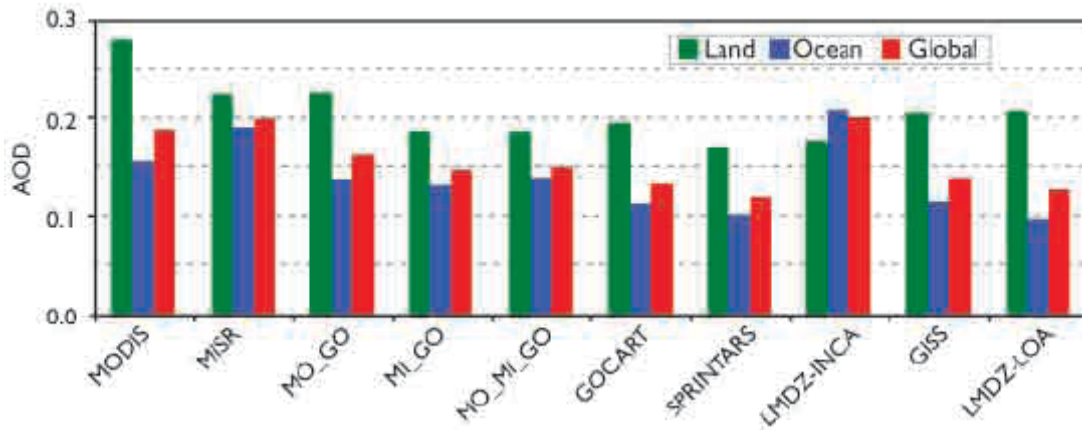


Figure 9-65. Comparison of annual mean aerosol optical depth (AOD)

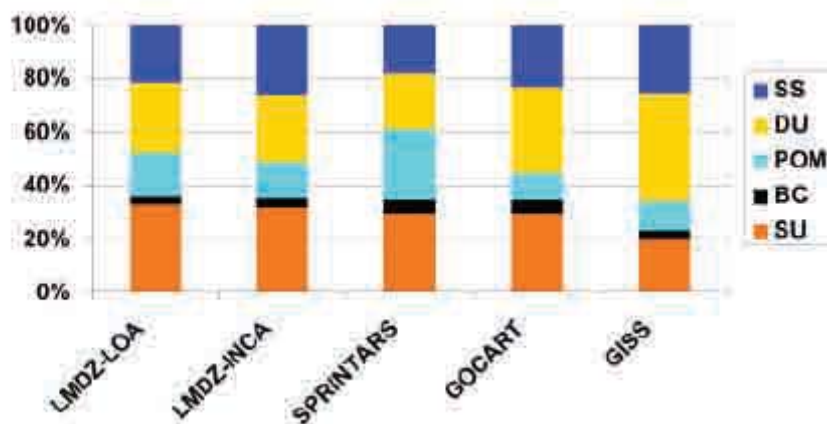


Figure 9-66. Percentage contributions of individual aerosol components (SU – sulfate, BC – BC, POM – particulate organic matter, DU – dust, SS – sea salt) to the total aerosol optical depth (at 550 nm) on a global scale simulated by the five models. Data taken from Kinne et al. (2006, [155903](#)).

9.3.3.3. Satellite-Based Estimates of Aerosol Direct Radiative Forcing

Table 9-7 summarizes approaches to estimating the aerosol direct radiative forcing, including a brief description of methods, identifies major sources of uncertainty, and provides references. These estimates fall into three broad categories, namely (A) satellite-based, (B) satellite-model integrated, and (C) model-based. As satellite aerosol measurements are generally limited to cloud-free conditions, the discussion here focuses on assessments of clear-sky aerosol direct radiative forcing, a net (downwelling minus upwelling) solar flux difference between with aerosol (natural + anthropogenic) and in the absence of aerosol.

Global Distributions. Figure 9-67 shows global distributions of aerosol optical depth at 550 nm (left panel) and diurnally averaged clear-sky TOA DRF (right panel) for March-April-May (MAM) based on the different approaches. The DRF at the surface follows the same pattern as that at the TOA but is significantly larger in magnitude because of aerosol absorption. It appears that different approaches agree on large-scale patterns of aerosol optical depth and the direct radiative forcing. In this season, the aerosol impacts in the Northern Hemisphere are much larger than those in the Southern Hemisphere. Dust outbreaks and biomass burning elevate the optical depth to more than 0.3 over large parts of North Africa and the tropical Atlantic. In the tropical Atlantic, TOA cooling as large as -10 W/m^2 extends westward to Central America. In eastern China, the optical depth is as high as 0.6-0.8, resulting from the combined effects of industrial activities and biomass burning in the south, and dust outbreaks in the north. The Asian impacts also extend to the North Pacific, producing a TOA cooling of more than -10 W/m^2 . Other areas having large aerosol impacts include Western Europe, midlatitude North Atlantic, and much of South Asia and the Indian Ocean. Over the “roaring forties” in the Southern Hemisphere, high winds generate a large amount of sea salt. Elevated optical depth, along with high solar zenith angle and hence large backscattering to space, results in a band of TOA cooling of more than -4 W/m^2 . However, there is also some question as to whether thin cirrus (e.g., Zhang et al., 2005, [190931](#)) and unaccounted-for whitecaps contribute to the apparent enhancement in AOD retrieved by satellite. Some differences exist between different approaches. For example, the early post-launch MISR retrieved optical depths over the southern hemisphere oceans are higher than MODIS retrievals and GOCART simulations. Over the “roaring forties,” the MODIS derived TOA solar flux perturbations are larger than the estimates from other approaches.

Table 9-7. Summary of approaches to estimating the aerosol direct radiative forcing in three categories: (A) satellite retrievals; (B) satellite-model integrations; and (C) model simulations.

Category	Product	Brief Description	Identified Sources of Uncertainty	Major References
A Satellite retrievals	MODIS	Using MODIS retrievals of a linked set of AOD, ω_0 , and phase function consistently in conjunction with a radiative transfer model (RTM) to calculate TOA fluxes that best match the observed radiances.	Radiance calibration, cloudaerosol discrimination, instantaneous-to-diurnal scaling, RTM parameterizations	Remer and Kaufman (2006, 190222)
	MODIS_A	Splitting MODIS AOD over ocean into mineral dust, sea salt, and biomass-burning and pollution; using AERONET measurements to derive the size distribution and single-scattering albedo for individual components.	Satellite AOD and FMF retrievals, overestimate due to summing up the compositional direct forcing, use of a single AERONET site to characterize a large region	Bellouin et al. (2005, 155684)
	CERES_A	Using CERES fluxes in combination with standard MODIS aerosol.	Calibration of CERES radiances, large CERES footprint, satellite AOD retrieval, radiance-to-flux conversion (ADM), instantaneous-to-diurnal scaling, narrow-to-broadband conversion	Loeb and Manalo-Smith (2005, 190433); Loeb and Kato (2002, 190432)
	CERES_B	Using CERES fluxes in combination with NOAA NESDIS aerosol from MODIS radiances.		
	CERES_C	Using CERES fluxes in combination with MODIS (ocean) and MISR (non-desert land) aerosol with new angular models for aerosols.		Zhang et al. (2005, 086743 ; 2005, 157185); Zhang and Christopher (2003, 190928); Christopher et al. (2006, 155729); Patadia et al. (2008, 190558)

Category	Product	Brief Description	Identified Sources of Uncertainty	Major References	
	POLDER	Using POLDER AOD in combination with prescribed aerosol models (similar to MODIS).	Similar to MODIS	Boucher and Tarré (2000, 190041); Bellouin et al. (2003, 189911)	
B. Satellite-model integrations	MODIS_G	Using GOCART simulations to fill AOD gaps in satellite retrievals.	Propagation of uncertainties associated with both satellite retrievals and model simulations (but the model-satellite integration approach does result in improved AOD quality for MO_GO, and O_MI_GO)	*Aerosol single-scattering albedo and asymmetry factor are taken from GOCART simulations *Yu et al. (2003, 156171 ; 2004, 190926 ; 2006, 156173)	
	MISR_G				
	MO_GO	Integration of MODIS and GOCART AOD.			
	MO_MI_GO	Integration of GOCART AOD with retrievals from MODIS (Ocean) and MISR (Land).			
	SeaWiFS	Using SeaWiFS AOD and assumed aerosol models.	Similar to MODIS_G and MISR_G, too weak aerosol absorption	Chou et al. (2002, 190008)	
C. Model simulations	GOCART	Offline RT calculations using monthly avg aerosols with a time step of 30 min (without the presence of clouds).	Emissions, parameterizations of a variety of sub-grid aerosol processes (e.g., wet and dry deposition, cloud convection, aqueous-phase oxidation), assumptions on aerosol size, absorption, mixture, and humidification of particles, Meteorology fields, not fully evaluated surface albedo schemes, RT parameterizations	Chin et al. (2002, 189996); Yu et al. (2004, 190926)	
	SPRINTARS	Online RT calculations every 3 hrs (cloud fraction = 0).			Takemura et al. (2002, 190438 ; 2005, 190439)
	GISS	Online model simulations and weighted by clear-sky fraction.			Koch and Hansen (2005, 190183); Koch et al. (2006, 190184)
	LMDZ-INCA	Online RT calculations every 2 hrs (cloud fraction = 0).			Balkanski et al. (2007, 189979); Schulz et al. (2006, 190381); Kinne et al. (2006, 155903)
	LMDZ-LOA	Online RT calculations every 2 hrs (cloud fraction = 0).			Reddy et al. (2005, 190207 ; 2005, 190208)

Source: Adapted from Yu et al. (2006, [156173](#)).

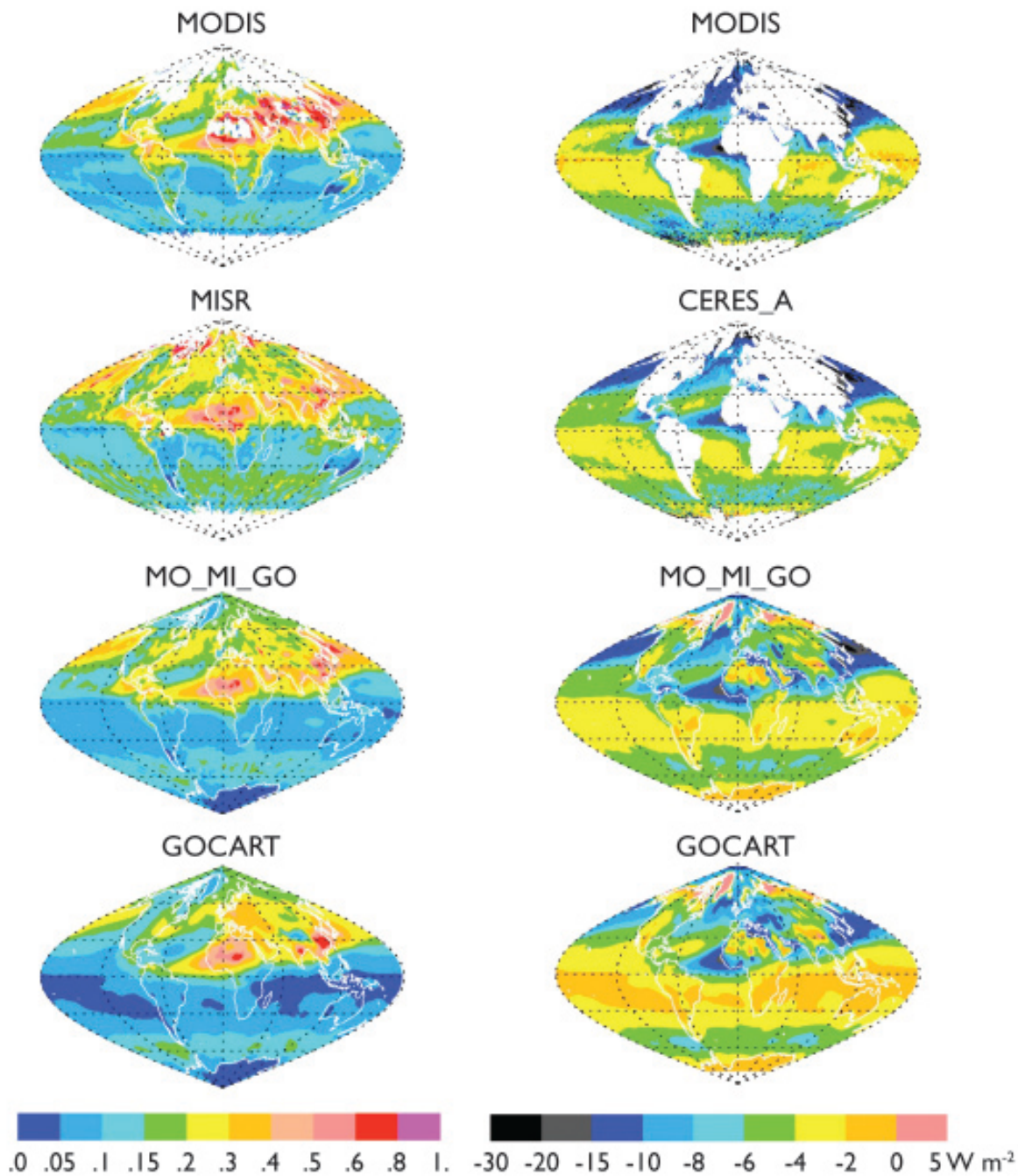


Figure 9-67. Geographical patterns of seasonally (MAM) averaged aerosol optical depth at 550 nm (left panel) and the diurnally averaged clear-sky aerosol direct radiative (solar spectrum) forcing (W/m^2) at the TOA (right panel) derived from satellite (Terra) retrievals. MODIS (Remer et al., 2005, [190221](#); Remer and Kaufman, 2006, [190222](#)); MISR (Kahn RA Gaitley et al., 2005, [190966](#)); and CERES_A (Loeb and Manalo-Smith, 2005, [190433](#)); GOCART simulations (Chin et al., 2002, [189996](#); Yu et al., 2004, [190926](#)); and GOCART-MODIS-MISR integrations (MO_MI_GO) (Yu H, et, 2006, [156173](#)).

Global Mean. Figure 9-68 summarizes the measurement- and model-based estimates of clear-sky annual-averaged DRF at both the TOA and surface from 60°S to 60°N. Seasonal DRF values for individual estimates are summarized in Table 9-8 and Table 9-9 for ocean and land, respectively. Mean, median and standard error ϵ ($\epsilon = \sigma / (n-1)^{1/2}$, where σ is standard deviation and n is the number of methods) are calculated for measurement- and model-based estimates separately. Note that although the standard deviation or standard error reported here is not a fully rigorous measure of a true experimental uncertainty, it is indicative of the uncertainty because independent approaches with independent sources of errors are used (see Table 9-7; in the modeling community, this is called the “diversity;” see Section 9.3.6).

Ocean: For the TOA DRF, a majority of measurement-based and satellite-model integration-based estimates agree with each other within about 10%. On annual average, the measurement-based estimates give the DRF of $-5.5 \pm 0.2 \text{ W/m}^2$ (mean $\pm \epsilon$) at the TOA and $-8.7 \pm 0.7 \text{ W/m}^2$ at the surface. This suggests that the ocean surface cooling is about 60% larger than the cooling at the TOA. Model simulations give wide ranges of DRF estimates at both the TOA and surface. The ensemble of five models gives the annual average DRF (mean $\pm \epsilon$) of $-3.2 \pm 0.6 \text{ W/m}^2$ and $-4.9 \pm 0.8 \text{ W/m}^2$ at the TOA and surface, respectively. On average, the surface cooling is about 37% larger than the TOA cooling, smaller than the measurement-based estimate of surface and TOA difference of 60%. However, the ‘measurement-based’ estimate of *surface* DRF is actually a calculated value, using poorly constrained particle properties.

Land: It remains challenging to use satellite measurements alone for characterizing complex aerosol properties over land surfaces with high accuracy. As such, DRF estimates over land have to rely largely on model simulations and satellite-model integrations. On a global and annual average, the satellite-model integrated approaches derive a mean DRF of -4.9 W/m^2 at the TOA and -11.9 W/m^2 at the surface respectively. The surface cooling is more than a factor of 2 larger than the TOA cooling because of aerosol absorption. Note that the TOA DRF of -4.9 W/m^2 agrees quite well with the most recent satellite-based estimate of $-5.1 \pm 1.1 \text{ W/m}^2$ over non-desert land based on coincident measurements of MISR AOD and CERES solar flux (Patadia et al., 2008, [190558](#)). For comparisons, an ensemble of five model simulations derives a DRF (mean $\pm \epsilon$) over land of $-3.0 \pm 0.6 \text{ W/m}^2$ at the TOA and $-7.6 \pm 0.9 \text{ W/m}^2$ at the surface, respectively. Seasonal variations of DRF over land, as derived from both measurements and models, are larger than those over ocean.

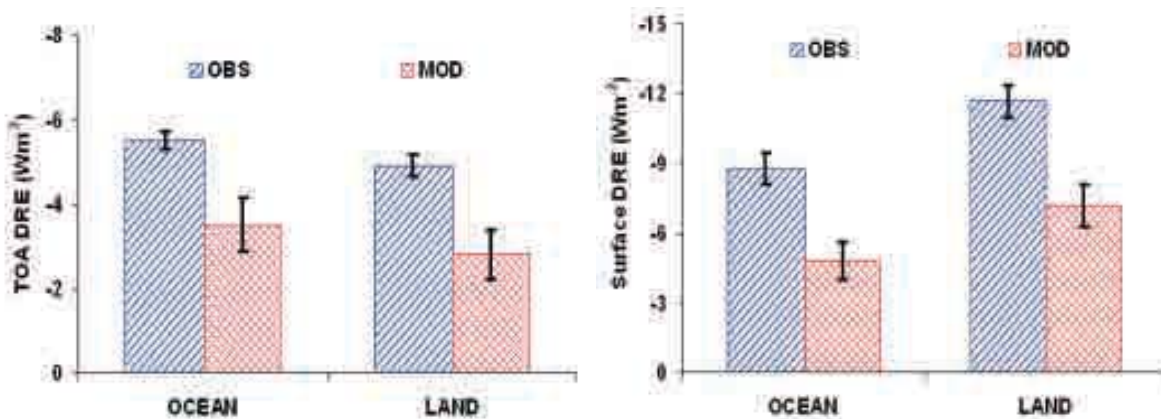


Figure 9-68. Summary of observation- and model-based (denoted as OBS and MOD, respectively) estimates of clear-sky, annual average DRF at the TOA and at the surface. The box and vertical bar represent median and standard error, respectively (taken from Yu H, et, 2006, [156173](#)).

Table 9-8. Summary of seasonal and annual average clear-sky DRF (W/m^2) at the TOA and the surface (SFC) over global OCEAN derived with different methods and data.

Products	DJF		MAM		JJA		SON		ANN	
	TOA	SFC	TOA	SFC	TOA	SFC	TOA	SFC	TOA	SFC
MODIS	-5.9		-5.8		-6.0		-5.8		-5.9	
MODIX_A*	-6.0	-8.2	-6.4	-8.9	-6.5	-9.3	-6.4	-8.9	-6.4	-8.9
CERES_A	-5.3		-6.1		-5.4		-5.1		-5.5	
CERES_B	-3.8		-4.3		-3.5		-3.6		-3.8	
CERES_C	-5.3		-5.4		-5.2				-5.3	
MODIS_G	-5.5	-9.1	-5.7	-10.4	-6.0	-10.6	-5.5	-9.8	-5.7	-10.0
MISR_G**	-6.4	-10.3	-6.5	-11.4	-7.0	-11.9	-6.3	-10.9	-6.5	-11.1
MO_GO	-4.9	-7.8	-5.1	-9.3	-5.4	-9.4	-5.0	-8.7	-5.1	-8.8
MO_MI_GO	-4.9	-7.9	-5.1	-9.2	-5.5	-9.5	-5.0	-8.6	-5.1	-8.7
POLDER	-5.7		-5.7		-5.8		-5.6		-5.7	
									-5.2***	-7.7***
SeaWiFS	-6.0	-6.6	-5.2	-5.8	-4.9	-5.6	-5.3	-5.7	-5.4	-5.9
Obs. Mean	-5.4	-8.3	-5.6	-9.2	-5.6	-9.4	-5.4	-8.8	-5.5	-8.7
Obs. Median	-5.5	-8.1	-5.7	-9.3	-5.5	-9.5	-5.4	-8.8	-5.5	-8.8
Obs. σ	0.72	1.26	0.64	1.89	0.91	2.10	0.79	1.74	0.70	1.65
Obs. μ	0.23	0.56	0.20	0.85	0.29	0.94	0.26	0.78	0.21	0.67
GOCART	-3.6	-5.7	-4.0	-7.2	-4.7	-8.0	-4.0	-6.8	-4.1	-6.9
SPRINTARS	-1.5	-2.5	-1.5	-2.5	-1.9	-3.3	-1.5	-2.5	-1.6	-2.7
GISS	-3.3	-4.1	-3.5	-4.6	-3.5	-4.9	-3.8	-5.4	-3.5	-4.8
LMDZ-INCA	-4.6	-5.6	-4.7	-5.9	-5.0	-6.3	-4.8	-5.5	-4.7	-5.8
LMDZ-LOA	-2.2	-4.1	-2.2	-3.7	-2.5	-4.4	-2.2	-4.1	-2.3	-4.1
Mod. Mean	-3.0	-4.4	-3.2	-4.8	-3.5	-5.4	-3.3	-4.9	-3.2	-4.9
Mod Median	-3.3	-4.1	-3.5	-4.6	-3.5	-4.9	-3.8	-5.4	-3.5	-4.8
Mod. σ	1.21	1.32	1.31	1.84	1.35	1.82	1.36	1.63	1.28	1.60
Mod. ϵ	0.61	0.66	0.66	0.92	0.67	0.91	0.68	0.81	0.64	0.80
Mod./Obs.	.60	.51	.61	.50	.64	.52	.70	.61	.64	.55

	DJF	MAM	JJA	SON	ANN
--	-----	-----	-----	-----	-----

* High bias may result from adding the DRF of individual components to derive the total DRF (Bellouin et al., 2005, [155684](#)).

** High bias most likely results from an overall overestimate of 20% in early post-launch MISR optical depth retrievals (Kahn RA Gaitley et al., 2005, [190966](#)).

*** Bellouin et al. (2003, [189911](#)) use AERONET retrieval of aerosol absorption as a constraint to the method in Boucher and Tanré (2000, [190041](#)), deriving aerosol direct radiative forcing both at the TOA and the surface.

Sources of data: MODIS (Remer & Kaufman, 2006), MODIS_A (Bellouin et al., 2005, [155684](#)), POLDER (Boucher and Tanré, 2000, [190041](#); Bellouin et al., 2003, [189911](#)), CERES_A and CERES_B (Loeb and Manalo-Smith, 2005, [190433](#)), CERES_C (Zhang et al., 2005, [190930](#)), MODIS_G, MISR_G, MO_GO, MO_MI_GO (Yu et al., 2004, [190926](#); 2006, [156173](#)), SeaWiFS (Chou et al., 2002, [190008](#)), GOCART (Chin et al., 2002, [189996](#); Yu et al., 2004, [190926](#)), SPRINTARS (Takemura et al., 2002, [190438](#)), GISS (Koch and Hansen, 2005, [190183](#); Koch et al., 2006, [190184](#)), LMDZ-INCA (Kinne et al., 2006, [155903](#); Schulz et al., 2006, [190381](#)), LMDZ-LOA (Reddy et al., 2005, [190207](#); Reddy et al., 2005, [190208](#)). Mean, median, standard deviation (σ), and standard error (ϵ) are calculated for observations (Obs) and model simulations (Mod) separately. The last row is the ratio of model median to observational median (taken from Yu H, et, 2006, [156173](#)).

Table 9-9. Summary of seasonal and annual average clear-sky DRF (W/m^2) at the TOA and the surface (SFC) over global LAND derived with different methods and data.

Products	DJF		MAM		JJA		SON		ANN	
	TOA	SFC	TOA	SFC	TOA	SFC	TOA	SFC	TOA	SFC
MODIS_G	-4.1	-9.1	-5.8	-14.9	-6.6	-17.4	-5.4	-12.8	-5.5	-13.5
MISR_G	-3.9	-8.7	-5.1	-13.0	-5.8	-14.6	-4.6	-10.7	-4.9	-11.8
MO_GO	-3.5	-7.5	-5.1	-12.9	-5.8	-14.9	-4.8	-10.9	-4.8	-11.6
MO_MI_GO	-3.4	-7.4	-4.7	-11.8	-5.3	-13.5	-4.3	-9.7	-4.4	-10.6
Obs. Mean	-3.7	-8.2	-5.2	-13.2	-5.9	-15.1	-4.8	-11.0	-4.9	-11.9
Obs. Median	-3.7	-8.1	-5.1	-13.0	-5.8	-14.8	-4.7	-10.8	-4.9	-11.7
Obs. σ	0.33	0.85	0.46	1.29	0.54	1.65	0.46	1.29	0.45	1.20
Obs. ϵ	0.17	0.49	0.26	0.74	0.31	0.85	0.27	0.75	0.26	0.70
GOCART	02.9	-6.1	-4.4	-10.9	-4.8	-12.3	-4.3	-9.3	-4.1	-9.7
SPRINTARS	-1.4	-4.0	-1.5	-4.6	-2.0	-6.7	-1.7	-5.2	-1.7	-5.1
GISS	-1.6	-3.9	-3.2	-7.9	-3.6	-9.3	-2.5	-6.6	-2.8	-7.2
LMDZ-INCA	-3.0	-5.8	-4.0	-9.2	-6.0	-13.5	-4.3	-8.2	-4.3	-9.2
LMDZ-LOA	-1.3	-5.4	-1.8	-6.4	-2.7	-8.9	-2.1	-6.7	-2.0	-6.9
Mod. Mean	-2.0	-5.0	-3.0	-7.8	-3.8	-10.1	-3.0	-7.2	-3.0	-7.6
Mod Median	-1.6	-5.4	-3.2	-7.9	-3.6	-9.3	-2.5	-6.7	-2.8	-7.2
Mod. σ	0.84	1.03	1.29	2.44	1.61	2.74	1.24	1.58	1.19	1.86
Mod. ϵ	0.42	0.51	0.65	1.22	0.80	1.37	0.62	0.79	0.59	0.93
Mod./Obs.	0.43	0.67	0.63	0.61	0.62	0.62	0.53	0.62	0.58	0.62

Sources of data: MODIS_G, MISR_G, MO_GO, MO_MI_GO (Yu et al., 2004, [190926](#); 2006, [156173](#)), GOCART (Chin et al., 2002, [189996](#); Yu et al., 2004, [190926](#)), SPRINTARS (Takemura et al., 2002, [190438](#)), GISS (Koch and Hansen, 2005, [190183](#); Koch et al., 2006, [190184](#)), LMDZ-INCA (Balkanski et al., 2007, [189979](#); Kinne et al., 2006, [155903](#); Schulz et al., 2006, [190381](#)), LMDZ-LOA (Reddy et al., 2005, [190207](#); Reddy et al., 2005, [190208](#)). Mean, median, standard deviation (σ), and standard error (ϵ) are calculated for observations (Obs) and model simulations (Mod) separately. The last row is the ratio of model median to observational median. (Taken from Yu H, et, 2006, [156173](#)).

The above analyses show that, on a global average, the measurement-based estimates of DRF are 55-80% greater than the model-based estimates. The differences are even larger on regional scales. Such measurement-model differences are a combination of differences in aerosol amount (optical depth), single-scattering properties, surface albedo, and radiative transfer schemes (Yu H, et, 2006, [156173](#)). As discussed earlier, MODIS retrieved optical depths tend to be overestimated by about 10-15% due to the contamination of thin cirrus and clouds in general (Kaufman et al., 2005, [155891](#)). Such overestimation of optical depth would result in a comparable overestimate of the aerosol direct radiative forcing. Other satellite AOD data may have similar contamination, which however has not yet been quantified. On the other hand, the observations may be measuring enhanced AOD and DRF due to processes not well represented in the models including humidification and enhancement of aerosols in the vicinity of clouds (Koren et al., 2007, [190192](#)).

From the perspective of model simulations, uncertainties associated with parameterizations of various aerosol processes and meteorological fields, as documented under the AEROCOM and Global Modeling Initiative (GMI) frameworks (Kinne et al., 2006, [155903](#); Textor et al., 2006, [190456](#); Liu et al., 2007, [190427](#)), contribute to the large measurement-model and model-model discrepancies. Factors determining the AOD should be major reasons for the DRF discrepancy and the constraint of model AOD with well evaluated and bias reduced satellite AOD through a data assimilation approach can reduce the DRF discrepancy significantly. Other factors (such as model parameterization of surface reflectance, and model-satellite differences in single-scattering albedo and asymmetry factor due to satellite sampling bias toward cloud-free conditions) should also contribute, as evidenced by the existence of a large discrepancy in the radiative efficiency (Yu H, et, 2006, [156173](#)). Significant effort will be needed in the future to conduct comprehensive assessments.

9.3.3.4. Satellite-Based Estimates of Anthropogenic Component of Aerosol Direct Radiative Forcing

Satellite instruments do not measure the aerosol chemical composition needed to discriminate anthropogenic from natural aerosol components. Because anthropogenic aerosols are predominantly sub-micron, the fine-mode fraction derived from POLDER, MODIS, or MISR might be used as a tool for deriving anthropogenic aerosol optical depth. This could provide a feasible way to conduct measurement-based estimates of anthropogenic component of aerosol direct radiative forcing (Kaufman et al., 2002, [190956](#)). Such method derives anthropogenic AOD from satellite measurements by empirically correcting contributions of natural sources (dust and maritime aerosol) to the sub-micron AOD (Kaufman et al., 2005, [155891](#)). The MODISbased estimate of anthropogenic AOD is about 0.033 over oceans, consistent with model assessments of 0.030~0.036 even though the total AOD from MODIS is 25-40% higher than the models (Kaufman et al., 2005, [155891](#)). This accounts for $21 \pm 7\%$ of the MODIS-observed total aerosol optical depth, compared with about 33% of anthropogenic contributions estimated by the models. The anthropogenic fraction of AOD should be much larger over land (i.e., $47 \pm 9\%$ from a composite of several models) (Bellouin et al., 2005, [155684](#)), comparable to the 40% estimated by Yu et al. (2006, [156173](#)). Similarly, the non-spherical fraction from MISR or POLDER can be used to separate dust from spherical aerosol (Kahn et al., 2001, [190969](#); Kalashnikova and Kahn, 2006, [190962](#)), providing another constraint for distinguishing anthropogenic from natural aerosols.

There have been several estimates of anthropogenic component of DRF in recent years. Table 9-10 lists such estimates of anthropogenic component of TOA DRF that are from model simulations (Schulz et al., 2006, [190381](#)) and constrained to some degree by satellite observations (Kaufman et al., 2005, [155891](#); Bellouin et al., 2005, [155684](#); Bellouin et al., 2008, [189999](#); Chung et al., 2005, [155733](#); Christopher et al., 2006, [155729](#); Matsui et al., 2006, [190495](#); Yu H, et, 2006, [156173](#); Quaas et al., 2008,

[190916](#); Zhao et al., 2008, [190936](#)). The satellite-based clear-sky DRF by anthropogenic aerosols is estimated to be -1.1 ± 0.37 W/m² over ocean, about a factor of 2 stronger than model simulated -0.6 W/m². Similar DRF estimates are rare over land, but a few studies do suggest that the anthropogenic DRF over land is much more negative than that over ocean (Yu H, et, 2006, [156173](#); Bellouin et al., 2005, [155684](#); Bellouin et al., 2008, [189999](#)). On global average, the measurement-based estimate of anthropogenic DRF ranges from -0.9 to -1.9 W/m², again stronger than the model-based estimate of -0.8 W/m². Similar to DRF estimates for total aerosols, satellite-based estimates of anthropogenic component of DRF are rare over land.

On global average, anthropogenic aerosols are generally more absorptive than natural aerosols. As such the anthropogenic component of DRF is much more negative at the surface than at TOA. Several observation-constrained studies estimate that the global average, clear-sky, anthropogenic component of DRF at the surface ranges from -4.2 to -5.1 W/m² (Yu et al., 2004, [190926](#); Bellouin et al., 2005, [155684](#); Chung et al., 2005, [155733](#); Matsui et al., 2006, [190495](#)), which is about a factor of 2 larger in magnitude than the model estimates (e.g., Reddy et al., 2005, [190208](#)).

Uncertainties in estimates of the anthropogenic component of aerosol DRF are greater than for the total aerosol, particularly over land. An uncertainty analysis (Yu H, et, 2006, [156173](#)) partitions the uncertainty for the global average anthropogenic DRF between land and ocean more or less evenly. Five parameters, namely fine-mode fraction (f) and anthropogenic fraction of fine-mode fraction (f_{ant}) over both land and ocean, and τ over ocean, contribute nearly 80% of the overall uncertainty in the anthropogenic DRF estimate, with individual shares ranging from 13-20% (Yu H, et, 2006, [156173](#)). These uncertainties presumably represent a lower bound because the sources of error are assumed to be independent. Uncertainties associated with several parameters are also not well defined. Nevertheless, such uncertainty analysis is useful for guiding future research and documenting advances in understanding.

Table 9-10. Estimates of anthropogenic components of aerosol optical depth (T_{ant}) and clear-sky DRF at the TOA from model simulations

Data Sources	Ocean		Land		Global		Estimated uncertainty or model diversity for DRF
	T_{ant}	DRF (W/m ²)	T_{ant}	DRF (W/m ²)	T_{ant}	DRF (W/m ²)	
Kaufman et al. (2005, 155891)	0.033	-1.4					30%
Bellouin et al. (2005, 155684)	0.028	-0.8	0.13		0.062	-1.9	15%
Chung et al. (2005, 155733)						-1.1	
Yu et al. (2006, 156173)	0.031	-1.1	-0.88	-1.8	0.048	-1.3	47% (ocean), 84% (land), and 62% (global)
Christopher et al. (2006, 155729)		-1.4					65%
Matsui and Pielke (2006, 190495)		-1.6					30°S-30°N oceans
Quaas et al. (2008, 190916)		-0.7		-1.8		-0.9	45%
Bellouin et al. (2008, 189999)	0.021	-0.6	0.107	-3.3	0.043	-1.3	Update to Bellouin et al. (2005) with MODIS Collection 5 data
Zhao et al. (2008, 190936)		-1.25					35%
Schulz et al. (2006, 190381)	0.022	-0.59	0.065	-1.14	0.036	-0.77	30-40%; same emissions prescribed for all models

Sources: Schulz et al., (2006, [190381](#)) approaches constrained by satellite observations, Kaufman et al. (2005, [155891](#)); Bellouin et al. (2005, [155684](#)) 2008; Chung et al. (2005, [155733](#)); Yu et al. (2006, [156173](#)); Christopher et al. (2006, [155729](#)); Matsui and Pielke (2006, [190495](#)); Quaas et al. (2008, [190916](#)); Zhao et al. (2008, [190936](#)).

9.3.3.5. Aerosol-Cloud Interactions and Indirect Forcing

Satellite views of the Earth show a planet whose albedo is dominated by dark oceans and vegetated surfaces, white clouds, and bright deserts. The bright white clouds overlying darker oceans or vegetated surface demonstrate the significant effect that clouds have on the Earth's radiative balance. Low clouds reflect incoming sunlight back to space, acting to cool the planet, whereas high clouds can trap outgoing terrestrial radiation and act to warm the planet. In the Arctic, low clouds have also been shown to warm the surface (Garrett and Zhao, 2006, [190570](#)). Changes in cloud cover, in cloud vertical development, and cloud optical properties will have strong radiative and therefore, climatic impacts. Furthermore, factors that change cloud development will also change precipitation processes. These changes may alter amounts, locations and intensities of local and regional rain and snowfall, creating droughts, floods and severe weather.

Cloud droplets form on a subset of aerosol particles called cloud condensation nuclei (CCN). In general, an increase in aerosol leads to an increase in CCN and an increase in drop concentration. Thus, for the same amount of liquid water in a cloud, more available CCN will result in a greater number but smaller size of droplets (Twomey, 1977, [190533](#)). A cloud with smaller but more numerous droplets will be brighter and reflect more sunlight to space, thus exerting a cooling effect. This is the first aerosol indirect radiative effect, or "albedo effect". The effectiveness of a particle as a CCN depends on its size and composition so that the degree to which clouds become brighter for a given aerosol perturbation, and therefore the extent of cooling, depends on the aerosol size distribution and its size-dependent composition. In addition, aerosol perturbations to cloud microphysics may involve feedbacks: for example, smaller drops are less likely to collide and coalesce; this will inhibit growth, suppressing precipitation, and possibly increasing cloud lifetime (Albrecht, 1989, [045783](#)). In this case clouds may exert an even stronger cooling effect.

A distinctly different aerosol effect on clouds exists in thin Arctic clouds (LWP <25 g m⁻²) having low emissivity. Aerosol has been shown to increase the longwave emissivity in these clouds, thereby *warming* the surface (Lubin and Vogelmann, 2006, [190466](#); Garrett and Zhao, 2006, [190570](#)).

Some aerosol particles, particularly black carbon and dust, also act as ice nuclei (IN) and in so doing, modify the microphysical properties of mixed-phase and ice clouds. An increase in IN will generate more ice crystals, which grow at the expense of water droplets due to the difference in vapor pressure over ice and water surfaces. The efficient growth of ice particles may increase the precipitation efficiency. In deep convective, polluted clouds there is a delay in the onset of freezing because droplets are smaller. These clouds may eventually precipitate, but only after higher altitudes are reached that result in taller cloud tops, more lightning and greater chance of severe weather (Rosenfeld and Lansky, 1998, [190230](#); Andreae et al., 2004, [155658](#)). The present state of knowledge of the nature and abundance of IN, and ice formation in clouds is extremely poor. There is some observational evidence of aerosol influences on ice processes, but a clear link between aerosol, IN concentrations, ice crystal concentrations and growth to precipitation has not been established. This report therefore only peripherally addresses ice processes. More information can be found in a review by the WMO/IUGG International Aerosol-Precipitation Scientific Assessment (Levin and Cotton, 2008, [190375](#)).

In addition to their roles as CCN and IN, aerosols also absorb and scatter light, and therefore they can change atmospheric conditions (temperature, stability, and surface fluxes) that influence cloud development and properties (Ackerman et al., 2000, [002987](#); Hansen et al., 1997, [043104](#)). Thus, aerosols affect clouds through changing cloud droplet size distributions, cloud particle phase, and by changing the atmospheric environment of the cloud.

9.3.3.6. Remote Sensing of Aerosol-Cloud Interactions and Indirect Forcing

The AVHRR satellite instruments have observed relationships between columnar aerosol loading, retrieved cloud microphysics, and cloud brightness over the Amazon Basin that are consistent with the theories explained above (Feingold et al., 2001, [190544](#); Kaufman and Fraser, 1997, [190958](#); Kaufman and Nakajima, 1993, [190959](#)), but do not necessarily prove a causal relationship. Other studies have linked cloud and aerosol microphysical parameters or cloud albedo and droplet size using satellite data applied over the entire global oceans (Han et al., 1998, [190594](#); Nakajima et al., 2001, [190552](#); Wetzel and Stowe, 1999, [190636](#)). Using these correlations with estimates of aerosol increase from the pre-industrial era, estimates of anthropogenic aerosol indirect radiative forcing fall into the range of -0.7 to -1.7 W/m² (Nakajima et al., 2001, [190552](#)).

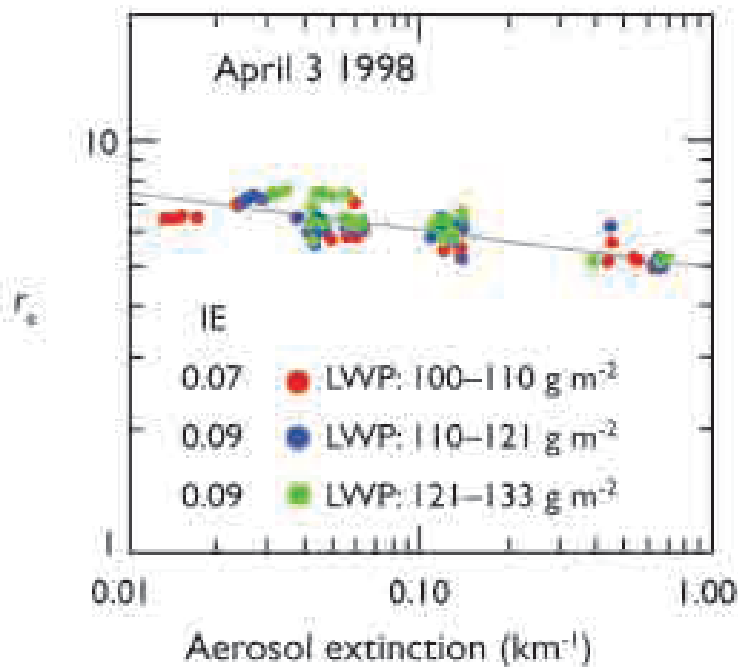
Introduction of the more modern instruments (POLDER and MODIS) has allowed more detailed observations of relationships between aerosol and cloud parameters. Cloud cover can both decrease and increase with increasing aerosol loading (Kaufman et al., 2005, [155891](#); Koren et al., 2004, [190187](#); Koren et al., 2005, [190188](#); Matheson et al., 2005, [190494](#); Sekiguchi et al., 2003, [190385](#); Yu and et, 2007, [093173](#)). The same is true of LWP (Han et al., 2002, [049181](#); Matsui et al., 2006, [190498](#)). Aerosol absorption appears to be an important factor in determining how cloud cover will respond to increased aerosol loading (Jiang and Feingold, 2006, [190976](#); Kaufman and Koren, 2006, [190951](#); Koren et al., 2008, [190193](#)). Different responses of cloud cover to increased aerosol could also be correlated with atmospheric thermodynamic and moisture structure (Yu and et, 2007, [093173](#)). Observations in the MODIS data show that aerosol loading correlates with enhanced convection and greater production of ice anvils in the summer Atlantic Ocean (Koren et al., 2005, [190188](#)), which conflicts with previous results that used AVHRR and could not isolate convective systems from shallow clouds (Sekiguchi et al., 2003, [190385](#)).

In recent years, surface-based remote sensing has also been applied to address aerosol effects on cloud microphysics. This method offers some interesting insights, and is complementary to the global satellite view. Surface remote sensing can only be applied at a limited number of locations, and therefore lacks the global satellite view. However, these surface stations yield high temporal resolution data and because they sample aerosol below, rather than adjacent to clouds they do not suffer from “cloud contamination”. With the appropriate instrumentation (lidar) they can measure the local aerosol entering the clouds, rather than a column-integrated aerosol optical depth. Under well-mixed conditions, surface in situ aerosol measurements can be used. Surface remote-sensing studies are discussed in more detail below, although the main science issues are common to satellite remote sensing.

Feingold et al. (2001, [190544](#)) used data collected at the ARM Southern Great Plains (SGP) site to allow simultaneous retrieval of aerosol and cloud properties. A combination of a Doppler cloud radar and a microwave radiometer was used to retrieve cloud drop effective radius r_e profiles in non-precipitating (radar reflectivity $Z < 17$ dBZ), ice-free clouds. Simultaneously, sub-cloud aerosol extinction profiles were measured with a lidar to quantify the response of drop sizes to changes in aerosol properties. Cloud data were binned according to liquid water path (LWP) as measured with a microwave radiometer, consistent with Twomey’s (1977, [190533](#)) conceptual view of the aerosol impact on cloud microphysics. With high temporal/spatial resolution data (on the order of 20s or 100s of meters), realizations of aerosol-cloud

interactions at the large eddy scale were obtained, and quantified in terms of the relative decrease in r_e in response to a relative increase in aerosol extinction ($d \ln r_e / d \ln \text{extinction}$), as shown in Figure 9-69. Examining the dependence in this way reduces reliance on absolute measures of cloud and aerosol parameters and minimizes sensitivity to measurement error, provided errors are unbiased. This formulation permitted these responses to be related to cloud microphysical theory. Restricting the examination to updrafts only (as determined from the radar Doppler signal) permitted examination of the role of updraft in determining the response of r_e to changes in aerosol (via changes in drop number concentration N_d). Analysis of data from 7 days showed that turbulence intensifies the aerosol impact on cloud microphysics.

In addition to radar/microwave radiometer retrievals of aerosol and cloud properties, measurements of cloud optical depth by surface based radiometers such as the MFRSR (Michalsky et al., 2001, [190537](#)) have been used in combination with measurements of cloud LWP by microwave radiometer to measure an average value of r_e during daylight when the solar elevation angle is sufficiently high (Min and Harrison, 1996, [190538](#)). Using this retrieval, Kim et al. (2003, [155899](#)) performed analyses of the r_e response to changes in aerosol at the same continental site, using a surface measurement of the aerosol light scattering coefficient instead of using extinction near cloud base as a proxy for CCN. Variance in LWP was shown to explain most of the variance in cloud optical depth, exacerbating detection of an aerosol effect. Although a decrease in r_e was observed with increasing scattering coefficient, the relation was not strong, indicative of other influences on r_e and/or decoupling between the surface and cloud layer. A similar study was conducted by Garrett et al. (2004, [190568](#)) at a location in the Arctic.



Source: Adapted from Feingold et al. (2003, [190551](#)).

Figure 9-69. Scatter plots showing mean cloud drop effective radius (r_e) vs. aerosol extinction coefficient (unit: km^{-1}) for various liquid water path (LWP) bands on April 3, 1998 at ARM SGP site.

They suggested that summertime Arctic clouds are more sensitive to aerosol perturbations than clouds at lower latitudes. The advantage of the MFRSR/microwave radiometer combination is that it derives τ from cloud optical depth and LWP and it is not as sensitive to large drops as the radar is. A limitation is that it can be applied only to clouds with extensive horizontal cover during daylight hours.

More recent data analyses by Feingold et al. (2003, [190551](#)), Kim et al. (2008, [130785](#)) and McComiskey et al. (2008, [190525](#)) at a variety of locations, and modeling work (Feingold, 2003, [190547](#)) have investigated (i) the use of different proxies for cloud condensation nuclei, such as the light scattering coefficient and aerosol index; (ii) sensitivity of cloud microphysical/optical properties to controlling factors such as aerosol size distribution, entrainment, LWP, and updraft velocity; (iii) the effect of optical- as opposed to radar-retrievals of drop size; and (iv) spatial heterogeneity. These studies have reinforced the importance of LWP and vertical velocity as controlling parameters. They have also begun to reconcile the reasons for the large discrepancies between various approaches, and platforms (satellite, aircraft *in situ*, and surface-based remote sensing). These investigations are important because satellite measurements that use a similar approach are being employed in GCMs to represent the albedo indirect effect (Quaas and Boucher, 2005, [190573](#)). In fact, the weakest albedo indirect effect in IPCC (2007, [189430](#)) derives from satellite measurements that have very weak responses of τ to changes in aerosol. The relationship between these aerosol-cloud microphysical responses and cloud radiative forcing has been examined by McComiskey and Feingold (2008, [190517](#)). They showed that for plane-parallel clouds, a typical uncertainty in the logarithmic gradient of a τ -aerosol relationship of 0.05 results in a local forcing error of -3 to -10 W/m², depending on the aerosol perturbation. This sensitivity reinforces the importance of adequate quantification of aerosol effects on cloud microphysics to assessment of the radiative forcing, i.e., the indirect effect. Quantification of these effects from remote sensors is exacerbated by measurement errors. For example, LWP is measured to an accuracy of 25 g m⁻² at best, and since it is the thinnest clouds (i.e., low LWP) that are most susceptible (from a radiative forcing perspective) to changes in aerosol, this measurement uncertainty represents a significant uncertainty in whether the observed response is related to aerosol, or to differences in LWP. The accuracy and spatial resolution of satellite-based LWP measurements is much poorer and this represents a significant challenge. In some cases important measurements are simply absent, e.g., updraft is not measured from satellite-based remote sensors.

Finally, cloud radar data from CloudSat, along with the A-train aerosol data, is providing great opportunity for inferring aerosol effects on precipitation (e.g., Stephens and Haynes, 2007, [190413](#)). The aerosol effect on precipitation is far more complex than the albedo effect because the instantaneous view provided by satellites makes it difficult to establish causal relationships.

9.3.3.7. In Situ Studies of Aerosol-Cloud Interactions

In situ observations of aerosol effects on cloud microphysics date back to the 1950s and 1960s (Gunn and Phillips, 1957, [190595](#); Squires, 1958, [045608](#); Warner, 1968, [157114](#); Warner and Twomey, 1967, [045616](#); Radke et al., 1989, [156034](#); Leitch et al., 1992, [045270](#); Brenguier et al., 2000, [189966](#); to name a few). These studies showed that high concentrations of CCN from anthropogenic sources, such as industrial pollution or the burning of sugarcane can increase cloud droplet number concentration N_d , thus increasing cloud microphysical stability and potentially reducing precipitation efficiency. As in the case of remote sensing studies, the causal link between aerosol perturbations and cloud microphysical responses (e.g., τ or N_d) is much better established than the relationship between aerosol and changes in cloud fraction, LWC, and precipitation (see also Levin and Cotton, 2008, [190375](#)).

In situ cloud measurements are usually regarded as “ground truth” for satellite retrievals but in fact there is considerable uncertainty in measured parameters such

liquid water content (LWC), and size distribution, which forms the basis of other calculations such as drop concentration, r_e and extinction. It is not uncommon to see discrepancies in LWC on the order of 50% between different instruments, and cloud drop size distributions are difficult to measure, particularly for droplets $<10 \mu\text{m}$ where Mie scattering oscillations generate ambiguities in drop size. Measurement uncertainty in r_e from in situ probes is assessed, for horizontally homogeneous clouds, to be on the order of 15- 20%, compared to 10% for MODIS and 15-20% for other spectral measurements (Feingold et al., 2003, [190551](#)). As with remote measurements it is prudent to consider relative (as opposed to absolute) changes in cloud microphysics related to relative changes in aerosol. An added consideration is that in situ measurements typically represent a very small sample of the atmosphere akin to a thin pencil line through a large volume. For an aircraft flying at 100 m/s and sampling at 1 Hz, the sample volume is on the order of 10 cm^3 . The larger spatial sampling of remote sensing has the advantage of being more representative but it removes small-scale (i.e., sub sampling volume) variability, and therefore, may obscure important cloud processes.

Measurements at a wide variety of locations around the world have shown that increases in aerosol concentration lead to increases in \dot{N}_a . However the rate of this increase is highly variable and always sub-linear, as exemplified by the compilation of data in Ramanathan et al. (2001, [042681](#)). This is because, as discussed previously, \dot{N}_a is a function of numerous parameters in addition to aerosol number concentration, including size distribution, updraft velocity (Leitch et al., 1996, [190354](#)), and composition. In stratocumulus clouds, characterized by relatively low vertical velocity (and low supersaturation) only a small fraction of particles can be activated whereas in vigorous cumulus clouds that have high updraft velocities, a much larger fraction of aerosol particles is activated. Thus the ratio of \dot{N}_a to aerosol particle number concentration is highly variable.

In recent years there has been a concerted effort to reconcile measured \dot{N}_a concentrations with those calculated based on observed aerosol size and composition, as well as updraft velocity. These so-called “closure experiments” have demonstrated that on average, agreement in \dot{N}_a between these approaches is on the order of 20% (Conant et al., 2004, [190010](#)). This provides confidence in theoretical understanding of droplet activation, however, measurement accuracy is not high enough to constrain the aerosol composition effects that have magnitudes $<20\%$.

One exception to the rule that more aerosol particles result in larger \dot{N}_a is the case of giant CCN (sizes on the order of a few microns), which, in concentrations on the order of 1 cm^{-3} (i.e., $\sim 1\%$ of the total concentration) can lead to significant suppression in cloud supersaturation and reductions in \dot{N}_a (O'Dowd et al., 1999, [090414](#)). The measurement of these large particles is difficult and hence the importance of this effect is hard to assess. These same giant CCN, at concentrations as low as 1/liter, can significantly affect the initiation of precipitation in moderately polluted clouds (Johnson, 1982, [190973](#)) and in so doing alter cloud albedo (Feingold et al., 1999, [190540](#)).

The most direct link between the remote sensing of aerosol-cloud interactions discussed in Section 9.3.3.6 and in situ observations is via observations of relationships between drop concentration \dot{N}_a and CCN concentration. Theory shows that if r_e -CCN relationships are calculated at constant LWP or LWC, their logarithmic slope is $-1/3$ that of the \dot{N}_a -CCN logarithmic slope (i.e., $d \ln r_e / d \ln \text{CCN} = -1/3 d \ln \dot{N}_a / d \ln \text{CCN}$). In general, \dot{N}_a -CCN slopes measured in situ tend to be stronger than equivalent slopes obtained from remote sensing – particularly in the case of satellite remote sensing (McComiskey and Feingold, 2008, [190517](#)). There are a number of reasons for this: (i) in situ measurements focus on smaller spatial scales and are more likely to observe the droplet activation process as opposed to remote sensing that incorporates larger spatial scales and includes other processes such as drop coalescence that reduce \dot{N}_a , and therefore the slope of the \dot{N}_a - CCN relationship (McComiskey et al., 2008, [190525](#)). (ii) Satellite remote sensing studies typically do

not sort their data by LWP, and this has been shown to reduce the magnitude of the κ -CCN response (Feingold, 2003, [190547](#)).

In conclusion, observational estimates of aerosol indirect radiative forcings are still in their infancy. Effects on cloud microphysics that result in cloud brightening have to be considered along with effects on cloud lifetime, cover, vertical development and ice production. For in situ measurements, aerosol effects on cloud microphysics are reasonably consistent (within $\sim 20\%$) with theory but measurement uncertainties in remote sensing of aerosol effects on clouds, as well as complexity associated with three-dimensional radiative transfer, result in considerable uncertainty in radiative forcing. The higher order indirect effects are poorly understood and even the sign of the microphysical response and forcing may not always be the same. Aerosol type and specifically the absorption properties of the aerosol may cause different cloud responses. Early estimates of observationally based aerosol indirect forcing range from -0.7 to -1.7 W/m^2 (Nakajima et al., 2001, [190552](#)) and -0.6 to -1.2 W/m^2 (Sekiguchi et al., 2003, [190385](#)), depending on the estimate for aerosol increase from pre-industrial times and whether aerosol effects on cloud fraction are also included in the estimate.

9.3.4. Outstanding Issues

Despite substantial progress, as summarized in Sections 9.3.2 and 9.3.3, most measurement-based studies so far have concentrated on influences produced by the sum of natural and anthropogenic aerosols on solar radiation under clear sky conditions. Important issues remain:

- Because accurate measurements of aerosol absorption are lacking and land surface reflection values are uncertain, DRF estimates over land and at the ocean surface are less well constrained than the estimate of TOA DRF over ocean.
- Current estimates of the anthropogenic component of aerosol direct radiative forcing have large uncertainties, especially over land.
- Because there are very few measurements of aerosol absorption vertical distribution, mainly from aircraft during field campaigns, estimates of direct radiative forcing of above-cloud aerosols and profiles of atmospheric radiative heating induced by aerosol absorption are poorly constrained.
- There is a need to quantify aerosol impacts on thermal infrared radiation, especially for dust.
- The diurnal cycle of aerosol direct radiative forcing cannot be adequately characterized with currently available, sun-synchronous, polar orbiting satellite measurements.
- Measuring aerosol, cloud, and ambient meteorology contributions to indirect radiative forcing remains a major challenge.
- Long-term aerosol trends and their relationship to observed surface solar radiation changes are not well understood.

The current status and prospects for these areas are briefly discussed below.

Measuring Aerosol Absorption and Single-Scattering Albedo: Currently, the accuracy of both in situ and remote sensing aerosol SSA measurements is generally ± 0.03 at best, which implies that the inferred accuracy of clear sky aerosol DRF would be larger than 1 W/m^2 (see Chapter 1 of the CSSP SAP2.3). Recently developed photoacoustic (Arnott et al., 1999, [020650](#)) and cavity ring down extinction cell (Strawa et al., 2002, [190421](#)) techniques for measuring aerosol absorption produce SSA with improved accuracy over previous methods. However, these methods are still experimental, and must be deployed on aircraft. Aerosol absorption retrievals from satellites using the UV-technique have large uncertainties associated with its sensitivity to the height of the aerosol layer(s) (Torres et al., 2005, [190507](#)), and it is unclear how the UV results can be extended to visible wavelengths. Views in and out of sunglint can be used to retrieve total aerosol extinction and scattering, respectively, thus constraining aerosol absorption over oceans (Kaufman et al., 2002, [190955](#)).

However, this technique requires retrievals of aerosol scattering properties, including the real part of the refractive index, well beyond what has so far been demonstrated from space. In summary, there is a need to pursue a better understanding of the uncertainty in SSA from both in situ measurements and remote sensing retrievals and, with this knowledge, to synthesize different data sets to yield a characterization of aerosol absorption with well-defined uncertainty (Leahy et al., 2007, [190232](#)). Laboratory studies of aerosol absorption of specific known composition are also needed to interpret in situ measurements and remote sensing retrievals and to provide updated database of particle absorbing properties for models.

Estimating the Aerosol Direct Radiative Forcing over Land: Land surface reflection is large, heterogeneous, and anisotropic, which complicates aerosol retrievals and DRF determination from satellites. Currently, the aerosol retrievals over land have relatively lower accuracy than those over ocean (Section 9.3.2.5) and satellite data are rarely used alone for estimating DRF over land (Section 9.3.3). Several issues need to be addressed, such as developing appropriate angular models for aerosols over land (Patadia et al., 2008, [190558](#)) and improving land surface reflectance characterization. MODIS and MISR measure land surface reflection wavelength dependence and angular distribution at high resolution (Moody et al., 2005, [190548](#); Martonchik et al., 1998, [190484](#); Martonchik et al., 2002, [190490](#)). This offers a promising opportunity for inferring the aerosol direct radiative forcing over land from satellite measurements of radiative fluxes (e.g., CERES) and from critical reflectance techniques (Fraser and Kaufman, 1985, [190567](#); Kaufman, 1987, [190960](#)). The aerosol direct radiative forcing over land depends strongly on aerosol absorption and improved measurements of aerosol absorption are required.

Distinguishing Anthropogenic from Natural Aerosols: Current estimates of anthropogenic components of AOD and direct radiative forcing have larger uncertainties than total aerosol optical depth and direct radiative forcing, particularly over land (see Section 9.3.3.4), because of relatively large uncertainties in the retrieved aerosol microphysical properties (see Section 9.3.2). Future measurements should focus on improved retrievals of such aerosol properties as size distribution, particle shape, and absorption, along with algorithm refinement for better aerosol optical depth retrievals. Coordinated in situ measurements offer a promising avenue for validating and refining satellite identification of anthropogenic aerosols (Anderson et al., 2005, [189993](#); 2005, [189991](#)). For satellite-based aerosol type characterization, it is sometimes assumed that all biomass-burning aerosol is anthropogenic and all dust aerosol is natural (Kaufman et al., 2005, [155891](#)). The better determination of anthropogenic aerosols requires a quantification of biomass burning ignited by lightning (natural origin) and mineral dust due to human induced changes of land cover/land use and climate (anthropogenic origin). Improved emissions inventories and better integration of satellite observations with models seem likely to reduce the uncertainties in aerosol source attribution.

Profiling the Vertical Distributions of Aerosols: Current aerosol profile data are far from adequate for quantifying the aerosol radiative forcing and atmospheric response to the forcing. The data have limited spatial and temporal coverage, even for current spaceborne lidar measurements. Retrieving aerosol extinction profile from lidar measured attenuated backscatter is subject to large uncertainties resulting from aerosol type characterization. Current space-borne Lidar measurements are also not sensitive to aerosol absorption. Because of lack of aerosol vertical distribution observations, the estimates of DRF in cloudy conditions and dust DRF in the thermal infrared remain highly uncertain (Schulz et al., 2006, [190381](#); Sokolik et al., 2001, [190404](#); Lubin et al., 2002, [190463](#)). It also remains challenging to constrain the aerosol-induced atmospheric heating rate increment that is essential for assessing atmospheric responses to the aerosol radiative forcing (e.g., Yu et al., 2002, [190923](#); Feingold et al., 2005, [190550](#); Lau et al., 2006, [190223](#)). Progress in the foreseeable future is likely to come from (1) better use of existing, global, space-based backscatter lidar data to constrain model simulations, and (2) deployment of new instruments, such as high-spectral-resolution lidar (HSRL), capable of retrieving both

extinction and backscatter from space. The HSRL lidar system will be deployed on the EarthCARE satellite mission tentatively scheduled for 2013 (http://asimov/esrin.esi.it/esaLP/ASESMYNW9SC_Lpearthcare_1.html).

Characterizing the Diurnal Cycle of Aerosol Direct Radiative Forcing:

The diurnal variability of aerosol can be large, depending on location and aerosol type (Smirnov et al., 2002, [190398](#)), especially in wildfire situations, and in places where boundary layer aerosols hydrate or otherwise change significantly during the day. This cannot be captured by currently available, sun-synchronous, polar orbiting satellites. Geostationary satellites provide adequate time resolution (TSI et al., 2002, [190031](#); Wang et al., 2003, [157106](#)), but lack the information required to characterize aerosol types. Aerosol type information from low earth orbit satellites can help improve accuracy of geostationary satellite aerosol retrievals (Costa et al., 2004, [190006](#); 2004, [192022](#)). For estimating the diurnal cycle of aerosol DRF, additional efforts are needed to adequately characterize the anisotropy of surface reflection (Yu et al., 2004, [190926](#)) and daytime variation of clouds.

Studying Aerosol-Cloud Interactions and Indirect Radiative Forcing:

Remote sensing estimates of aerosol indirect forcing are still rare and uncertain. Improvements are needed for both aerosol characterization and measurements of cloud properties, precipitation, water vapor, and temperature profiles. Basic processes still need to be understood on regional and global scales. Remote sensing observations of aerosol-cloud interactions and aerosol indirect forcing are for the most part based on simple correlations among variables, from which cause-and-effects cannot be deduced. One difficulty in inferring aerosol effects on clouds from the observed relationships is separating aerosol from meteorological effects, as aerosol loading itself is often correlated with the meteorology. In addition, there are systematic errors and biases in satellite aerosol retrievals for partly cloud-filled scenes. Stratifying aerosol and cloud data by liquid water content, a key step in quantifying the albedo (or first) indirect effect, is usually missing. Future work will need to combine satellite observations with in situ validation and modeling interpretation. A methodology for integrating observations (in situ and remote) and models at the range of relevant temporal/spatial scales is crucial to improve understanding of aerosol indirect effects and aerosol-cloud interactions.

Quantifying Long-Term Trends of Aerosols at Regional Scales: Because secular changes are subtle and are superposed on seasonal and other natural variability, this requires the construction of consistent, multi-decadal records of climate-quality data. To be meaningful, aerosol trend analysis must be performed on a regional basis. Long-term trends of aerosol optical depth have been studied using measurements from surface remote sensing stations (e.g., Hoyt and Frohlich, 1983, [190621](#); Augustine et al., 2008, [189913](#); Luo et al., 2001, [190467](#)) and historic satellite sensors (Massie et al., 2004, [190492](#); Mishchenko et al., 2007, [190542](#); Mishchenko and Geogdzhayev, 2007, [190545](#); Zhao et al., 2008, [190935](#)). An emerging multiyear climatology of high quality AOD data from modern satellite sensors (e.g., Remer and et, 2008, [190224](#); Kahn RA Gaitley et al., 2005, [190966](#)) has been used to examine the interannual variations of aerosol (e.g., Koren et al., 2007, [190189](#); Mishchenko and Geogdzhayev, 2007, [190545](#)) and contribute significantly to the study of aerosol trends. Current observational capability needs to be continued to avoid any data gaps. A synergy of aerosol products from historical, modern and future sensors is needed to construct as long a record as possible. Such a data synergy can build upon understanding and reconciliation of AOD differences among different sensors or platforms (Jeong et al., 2005, [190977](#)). This requires overlapping data records for multiple sensors. A close examination of relevant issues associated with individual sensors is urgently needed, including sensor calibration, algorithm assumptions, cloud screening, data sampling and aggregation, among others.

Linking Aerosol Long-Term Trends with Changes of Surface Solar Radiation:

Analysis of the long-term surface solar radiation record suggests significant trends during past decades (e.g., Stanhill and Cohen, 2001, [042121](#); Wild et

al., 2005, [156156](#); Pinker et al., 2005, [190569](#); Alpert et al., 2005, [190047](#)). Although a significant and widespread decline in surface total solar radiation (the sum of direct and diffuse irradiance) occurred up to 1990 (so-called solar dimming), a sustained increase has been observed during the subsequent decade. Speculation suggests that such trends result from decadal changes of aerosols and the interplay of aerosol direct and indirect radiative forcing (Stanhill and Cohen, 2001, [042121](#); Wild et al., 2005, [156156](#); Streets et al., 2006, [190425](#); Norris and Wild, 2007, [190555](#); Ruckstuhl and et, 2008, [190356](#)). However, reliable observations of aerosol trends are required test these ideas. In addition to aerosol optical depth, changes in aerosol composition must also be quantified, to account for changing industrial practices, environmental regulations, and biomass burning emissions (Novakov et al., 2003, [048398](#); Streets et al., 2004, [190423](#); Streets and Aunan, 2005, [156106](#)). Such compositional changes will affect the aerosol SSA and size distribution, which in turn will affect the surface solar radiation (e.g., Qian et al., 2007, [190572](#)). However such data are currently rare and subject to large uncertainties. Finally, a better understanding of aerosol-radiation-cloud interactions and trends in cloudiness, cloud albedo, and surface albedo is badly needed to attribute the observed radiation changes to aerosol changes with less ambiguity.

9.3.5. Concluding Remarks

Since the concept of aerosol-radiation-climate interactions was first proposed around 1970, substantial progress has been made in determining the mechanisms and magnitudes of these interactions, particularly in the last 10 yr. Such progress has greatly benefited from significant improvements in aerosol measurements and increasing sophistication of model simulations. As a result, knowledge of aerosol properties and their interaction with solar radiation on regional and global scales is much improved. Such progress plays a unique role in the definitive assessment of the global anthropogenic radiative forcing, as “*virtually certainly positive*” in IPCC AR4 (Haywood and Schulz, 2007, [190600](#)).

In Situ Measurements of Aerosols: New in situ instruments such as aerosol mass spectrometers, photoacoustic techniques, and cavity ring down cells provide high accuracy and fast time resolution measurements of aerosol chemical and optical properties. Numerous focused field campaigns and the emerging ground-based aerosol networks are improving regional aerosol chemical, microphysical, and radiative property characterization. Aerosol closure studies of different measurements indicate that measurements of submicrometer, spherical sulfate and carbonaceous particles have a much better accuracy than that for dust-dominated aerosol. The accumulated comprehensive data sets of regional aerosol properties provide a rigorous “test bed” and strong constraint for satellite retrievals and model simulations of aerosols and their direct radiative forcing.

Remote Sensing Measurements of Aerosols: Surface networks, covering various aerosol regimes around the globe, have been measuring aerosol optical depth with an accuracy of 0.01~0.02, which is adequate for achieving the accuracy of 1 W/m² for cloud-free TOA DRF. On the other hand, aerosol microphysical properties retrieved from these networks, especially SSA, have relatively large uncertainties and are only available in very limited conditions. Current satellite sensors can measure AOD with an accuracy of about 0.05 or 15-20% in most cases. The implementation of multi-wavelength, multi-angle, and polarization measuring capabilities has also made it possible to measure particle properties (size, shape, and absorption) that are essential for characterizing aerosol type and estimating anthropogenic component of aerosols. However, these microphysical measurements are more uncertain than AOD measurements.

Observational Estimates of Clear-Sky Aerosol Direct Radiative Forcing: Closure studies based on focused field experiments reveal DRF uncertainties of about 25% for sulfate/carbonaceous aerosol and 60% for dust at

regional scales. The high-accuracy of MODIS, MISR and POLDER aerosol products and broadband flux measurements from CERES make it feasible to obtain observational constraints for aerosol TOA DRF at a global scale, with relaxed requirements for measuring particle microphysical properties. Major conclusions from the assessment are:

- A number of satellite-based approaches consistently estimate the clear-sky diurnally averaged TOA DRF (on solar radiation) to be about $-5.5 \pm 0.2 \text{ W/m}^2$ (mean \pm standard error from various methods) over global ocean. At the ocean surface, the diurnally averaged DRF is estimated to be $-8.7 \pm 0.7 \text{ W/m}^2$. These values are calculated for the difference between today's measured total aerosol (natural plus anthropogenic) and the absence of all aerosol.
- Overall, in comparison to that over ocean, the DRF estimates over land are more poorly constrained by observations and have larger uncertainties. A few satellite retrieval and satellite-model integration yield the overland clear-sky diurnally averaged DRF of $-4.9 \pm 0.7 \text{ W/m}^2$ and $-11.8 \pm 1.9 \text{ W/m}^2$ at the TOA and surface, respectively. These values over land are calculated for the difference between total aerosol and the complete absence of all aerosol.
- Use of satellite measurements of aerosol microphysical properties yields that on a global ocean average, about 20% of AOD is contributed by human activities and the clear-sky TOA DRF by anthropogenic aerosols is $-1.1 \pm 0.4 \text{ W/m}^2$. Similar DRF estimates are rare over land, but a few measurement-model integrated studies do suggest much more negative DRF over land than over ocean.
- These satellite-based DRF estimates are much greater than the model-based estimates, with differences much larger at regional scales than at a global scale.

Measurements of Aerosol-Cloud Interactions and Indirect Radiative Forcing: In situ measurement of cloud properties and aerosol effects on cloud microphysics suggest that theoretical understanding of the activation process for water cloud is reasonably well-understood. Remote sensing of aerosol effects on droplet size associated with the albedo effect tends to underestimate the magnitude of the response compared to in situ measurements. Recent efforts trace this to a combination of lack of stratification of data by cloud water, the relatively large spatial scale over which measurements are averaged (which includes variability in cloud fields, and processes that obscure the aerosol-cloud processes), as well as measurement uncertainties (particularly in broken cloud fields). It remains a major challenge to infer aerosol number concentrations from satellite measurements. The present state of knowledge of the nature and abundance of IN, and ice formation in clouds is extremely poor.

Despite the substantial progress in recent decades, several important issues remain, such as measurements of aerosol size distribution, particle shape, absorption, and vertical profiles, and the detection of aerosol long-term trend and establishment of its connection with the observed trends of solar radiation reaching the surface, as discussed in Section 9.3.4. Furthering the understanding of aerosol impacts on climate requires a coordinated research strategy to improve the measurement accuracy and use the measurements to validate and effectively constrain model simulations. Concepts of future research in measurements are discussed in Chapter 4 “Way Forward” (of the CCSP SAP2.3).

9.3.6. Modeling the Effect of Aerosols on Climate

9.3.6.1. Introduction

The IPCC Fourth Assessment Report (AR4) (Intergovernmental Panel on Climate, 2007, [190988](#)) concludes that man's influence on the warming climate is in the category of “very likely”. This conclusion is based on, among other things, the

ability of models to simulate the global and, to some extent, regional variations of temperature over the past 50-100 yr. When anthropogenic effects are included, the simulations can reproduce the observed warming (primarily for the past 50 yr); when they are not, the models do not get very much warming at all. In fact, all of the models runs for the IPCC AR4 assessment (more than 20) produce this distinctive result, driven by the greenhouse gas increases that have been observed to occur.

These results were produced in models whose average global warming associated with a doubled CO₂ forcing of 4 W/m² was about 3°C. This translates into a climate sensitivity (surface temperature change per forcing) of about 0.75°C/(W/m²). The determination of climate sensitivity is crucial to projecting the future impact of increased greenhouse gases, and the credibility of this projected value relies on the ability of these models to simulate the observed temperature changes over the past century. However, in producing the observed temperature trend in the past, the models made use of very uncertain aerosol forcing. The greenhouse gas change by itself produces warming in models that exceeds that observed by some 40% on average (IPCC et al., 2007, [189430](#); IPCC (Intergovernmental Panel on Climate, 2007, [190988](#)). Cooling associated with aerosols reduces this warming to the observed level. Different climate models use differing aerosol forcings, both direct (aerosol scattering and absorption of short and longwave radiation) and indirect (aerosol effect on cloud cover reflectivity and lifetime), whose magnitudes vary markedly from one model to the next. Kiehl (2007, [190949](#)) using nine of the IPCC (2007, [189430](#); 2007, [190988](#)) AR4 climate models found that they had a factor of three forcing differences in the aerosol contribution for the 20th century. The differing aerosol forcing is the prime reason why models whose climate sensitivity varies by almost a factor of three can produce the observed trend. It was thus concluded that the uncertainty in IPCC (2007, [190988](#)) anthropogenic climate simulations for the past century should really be much greater than stated (Schwartz et al., 2007, [188938](#); Kerr, 2007, [190950](#)), since, in general, models with low/high sensitivity to greenhouse warming used weaker/stronger aerosol cooling to obtain the same temperature response (Kiehl, 2007, [190949](#)). Had the situation been reversed and the low/high sensitivity models used strong/ weak aerosol forcing, there would have been a greater divergence in model simulations of the past century.



Figure 9-70. Sampling the Arctic Haze. Pollution and smoke aerosols can travel long distances, from mid-latitudes to the Arctic, causing "Arctic Haze." Photo taken from the NASA DC-8 aircraft during the ARCTAS field experiment over Alaska in April 2008. Credit: Mian Chin, NASA.

Therefore, the fact that a model has accurately reproduced the global temperature change in the past does not imply that its future forecast is accurate. This state of affairs will remain until a firmer estimate of radiative forcing (RF) by aerosols, in addition to that by greenhouse gases, is available.

Two different approaches are used to assess the aerosol effect on climate. "Forward modeling" studies incorporate different aerosol types and attempt to explicitly calculate the aerosol RF. From this approach, IPCC (2007, [190988](#)) concluded that the best estimate of the global aerosol direct RF (compared with preindustrial times) is -0.5 (-0.9 to -0.1) W/m^2 . The RF due to the cloud albedo or brightness effect (also referred to as first indirect or Twomey effect) is estimated to be -0.7 (-1.8 to -0.3) W/m^2 . No estimate was specified for the effect associated with cloud lifetime. The total negative RF due to aerosols according to IPCC (2007, [190988](#)) estimates is then -1.3 (-2.2 to -0.5) W/m^2 . In comparison, the positive radiative forcing (RF) from greenhouse gases (including tropospheric ozone) is estimated to be $+2.9 \pm 0.3$ W/m^2 ; hence tropospheric aerosols reduce the influence from greenhouse gases by about 45% (15-85%). This approach however inherits large uncertainties in aerosol amount, composition, and physical and optical properties in modeling of atmospheric aerosols. The consequences of these uncertainties are discussed in the next section.

The other method of calculating aerosol forcing is called the “inverse approach” – it is assumed that the observed climate change is primarily the result of the known climate forcing contributions. If one further assumes a particular climate sensitivity (or a range of sensitivities), one can determine what the total forcing had to be to produce the observed temperature change. The aerosol forcing is then deduced as a residual after subtraction of the greenhouse gas forcing along with other known forcings from the total value. Studies of this nature come up with aerosol forcing ranges of -0.6 to -1.7 W/m² (Knutti et al., 2002, [190178](#); Knutti et al., 2003, [190180](#)); IPCC AR4 Chap.9); -0.4 to -1.6 W/m² (Gregory et al., 2002, [190593](#)); and -0.4 to -1.4 W/m² (Stott, 2006, [190419](#)). This approach however provides a bracket of the possible range of aerosol forcing without the assessment of current knowledge of the complexity of atmospheric aerosols.

This chapter of the CCSP SAP2.3 reviews the current state of aerosol RF in the global models and assesses the uncertainties in these calculations. First representation of aerosols in the forward global chemistry and transport models and the diversity of the model simulated aerosol fields are discussed; then calculation of the aerosol direct and indirect effects in the climate models is reviewed; finally the impacts of aerosols on climate model simulations and their implications are assessed.

9.3.6.2. Modeling of Atmospheric Aerosols

The global aerosol modeling capability has developed rapidly in the past decade. In the late 1990s, there were only a few global models that were able to simulate one or two aerosol components, but now there are a few dozen global models that simulate a comprehensive suite of aerosols in the atmosphere. As introduced in Chapter 1 (of the CCSP SAP2.3), aerosols consist of a variety of species including dust, sea salt, sulfate, nitrate, and carbonaceous aerosols (black and organic carbon) produced from natural and man-made sources with a wide range of physical and optical properties. Because of the complexity of the processes and composition, and highly inhomogeneous distribution of aerosols, accurately modeling atmospheric aerosols and their effects remains a challenge. Models have to take into account not only the aerosol and precursor emissions, but also the chemical transformation, transport, and removal processes (e.g., dry and wet depositions) to simulate the aerosol mass concentrations. Furthermore, aerosol particle size can grow in the atmosphere because the ambient water vapor can condense on the aerosol particles. This “swelling” process, called hygroscopic growth, is most commonly parameterized in the models as a function of relative humidity.

Estimates of Emissions. Aerosols have various sources from both natural and anthropogenic processes. Natural emissions include wind-blown mineral dust, aerosol and precursor gases from volcanic eruptions, natural wild fires, vegetation, and oceans. Anthropogenic sources include emissions from fossil fuel and biofuel combustion, industrial processes, agriculture practices, and human-induced biomass burning.

Following earlier attempts to quantify manmade primary emissions of aerosols (Turco et al., 1983, [190529](#); Penner et al., 1993, [045457](#)) systematic work was undertaken in the late 1990s to calculate emissions of black carbon (BC) and organic carbon (OC), using fuel-use data and measured emission factors (Lioussé et al., 1996, [078158](#); Cooke and Wilson, , [190046](#); Cooke et al., 1999, [156365](#)). The work was extended in greater detail and with improved attention to source-specific emission factors in Bond et al. (2004, [056389](#)), which provides global inventories of BC and OC for the year 1996, with regional and source-category discrimination that includes contributions from industrial, transportation, residential solid-fuel combustion, vegetation and open biomass burning (forest fires, agricultural waste burning, etc.), and diesel vehicles.

Emissions from natural sources—which include wind-blown mineral dust, wildfires, sea salt, and volcanic eruptions—are less well quantified, mainly because of the difficulties of measuring emission rates in the field and the unpredictable nature of the events. Often, emissions must be inferred from ambient observations at some distance from the actual source. As an example, it was concluded (Lewis and Schwartz, 2004, [192023](#)) that available information on size-dependent sea salt production rates could only provide order-of-magnitude estimates. The natural emissions in general can vary dramatically over space and time.

Aerosols can be produced from trace gases in the atmosphere via chemical reactions, and those aerosols are called *secondary* aerosols, as distinct from *primary* aerosols that are directly emitted to the atmosphere as aerosol particles. For example, most sulfate and nitrate aerosols are secondary aerosols that are formed from their precursor gases, sulfur dioxide (SO₂) and nitrogen oxides (NO and NO₂, collectively called NO_x), respectively. Those sources have been studied for many years and are relatively well known. By contrast, the sources of secondary organic aerosols (SOA) are poorly understood, including emissions of their precursor gases (called volatile organic compounds, VOC) from both natural and anthropogenic sources and the atmospheric production processes.

Globally, sea salt and mineral dust dominate the total aerosol mass emissions because of the large source areas and/or large particle sizes. However, sea salt and dust also have shorter atmospheric lifetimes because of their large particle size, and are radiatively less active than aerosols with small particle size, such as sulfate, nitrate, BC, and particulate organic matter (POM, which includes both carbon and non-carbon mass in the organic aerosol), most of which are anthropogenic in origin.

Because the anthropogenic aerosol RF is usually evaluated (e.g., by the IPCC) as the anthropogenic perturbation since the pre-industrial period, it is necessary to estimate the historical emission trends, especially the emissions in the pre-industrial era. Compared to estimates of present-day emissions, estimates of historical emission have much larger uncertainties. Information for past years on the source types and strengths and even locations are difficult to obtain, so historical inventories from preindustrial times to the present have to be based on limited knowledge and data. Several studies on historical emission inventories of BC and OC (e.g., Novakov et al., 2003, [048398](#); Ito and Penne, 2005, [190626](#); Bond et al., 2007, [190050](#); Fernandes et al., 2007, [190554](#); Junker and Liouise, 2008, [190971](#)), SO₂ (Stern, 2005, [190416](#)), and various species (Van Aardenne et al., 2001, [055564](#); Dentener et al., 2006, [088434](#)) are available in the literature; there are some similarities and some differences among them, but the emission estimates for early times do not have the rigor of the studies for present-day emissions. One major conclusion from all these studies is that the growth of primary aerosol emissions in the 20th century was not nearly as rapid as the growth in CO₂ emissions. This is because in the late 19th and early 20th centuries, particle emissions such as BC and POM were relatively high due to the heavy use of biofuels and the lack of particulate controls on coal-burning facilities; however, as economic development continued, traditional biofuel use remained fairly constant and particulate emissions from coal burning were reduced by the application of technological controls (Bond et al., 2007, [190050](#)). Thus, particle emissions in the 20th century did not grow as fast as CO₂ emissions, as the latter are roughly proportional to total fuel use—oil and gas included. Another challenge is estimating historical biomass burning emissions. A recent study suggested about a 40% increase in carbon emissions from biomass burning from the beginning to the end of last century (Mouillot et al., 2006, [190549](#)), but it is difficult to verify.

Table 9-11. Anthropogenic emissions of aerosols and precursors for 2000 and 1750.

Source	Species*	Emission# 2000 (Tg/yr)	Emission 1750 (Tg/yr)
Biomass burning	BC	3.1	1.03
	POM	34.7	12.8
	S	4.1	1.46
Biofuel	BC	9.1	0.39
	POM	9.6	1.56
	S		0.12
Fossil fuel	BC	3.0	
	POM	3.2	
	S	98.9	

Data source for 2000 emission: biomass burning – Global Fire Emission Dataset (GFED); biofuel BC and POM – Speciated Pollutant Emission Wizard (SPEW); biofuel sulfur – International Institute for Applied System Analysis (IIASA); fossil fuel BC and POM – SPEW; fossil fuel sulfur – Emission Database for Global Atmospheric Research (EDGAR) and IIASA. Fossil fuel emission of sulfur (S) is the sum of emission from industry, power plants, and transportation listed in Dentener et al. (2006, 088434).

* S=sulfur, including SO₂ and particulate SO₄²⁻. Most emitted as SO₂, and 2.5% emitted as SO₄²⁻.

Source: Adapted from Dentener et al. (2006, 088434).

As an example, Table 9-11 shows estimated anthropogenic emissions of sulfur, BC and POM in the present day (year 2000) and pre-industrial time (1750) compiled by Dentener et al. (2006, 088434). These estimates have been used in the Aerosol Comparisons between Observations and Models (AeroCom) project (Experiment B, which uses the year 2000 emission; and Experiment PRE, which uses pre-industrial emissions), for simulating atmospheric aerosols and anthropogenic aerosol RF. The AeroCom results are discussed below and in Section 9.3.6.3.

Aerosol Mass Loading and Optical Depth. In the global models, aerosols are usually simulated in the successive steps of sources (emission and chemical formation), transport (from source location to other area), and removal processes (dry deposition, in which particles fall onto the surface, and wet deposition by rain) that control the aerosol lifetime. Collectively, emission, transport, and removal determine the amount (mass) of aerosols in the atmosphere. Aerosol optical depth (AOD), which is a measure of solar or thermal radiation being attenuated by aerosol particles via scattering or absorption, can be related to the atmospheric aerosol mass loading as follows:

$$\text{AOD} = \text{MEE} \bullet \text{M}$$

Equation 9-3

where M is the aerosol mass loading per unit area (g m⁻²), MEE is the mass extinction efficiency or specific extinction in unit of m²/g, which is

$$\text{MEE} = \frac{3Q_{\text{ext}}}{4\pi\rho r_{\text{eff}}} \bullet \int$$

Equation 9-4

where Q_{ext} is the extinction coefficient (a function of particle size distribution and refractive index), r_{eff} is the aerosol particle effective radius, ρ is the aerosol particle density, and f is the ratio of ambient aerosol mass (wet) to dry aerosol mass M . Here, M is the result from model-simulated atmospheric processes and MEE embodies the aerosol physical (including microphysical) and optical properties. Since Q_{ext} varies

with radiation wavelength, so do MEE and AOD. AOD is the quantity that is most commonly obtained from remote sensing measurements and is frequently used for model evaluation (see Chapter 2 of the CCSP SAP2.3). AOD is also a key parameter determining aerosol radiative effects.

Here the results from the recent multiple global-model studies by the AeroCom project are summarized, as they represent the current assessment of model-simulated atmospheric aerosol loading, optical properties, and RF for the present-day. AeroCom aims to document differences in global aerosol models and compare the model output to observations. Sixteen global models participated in the AeroCom Experiment A (AeroCom-A), for which every model used their own configuration, including their own choice of estimating emissions (Kinne et al., 2006, [155903](#); Textor et al., 2006, [190456](#)). Five major aerosol types: sulfate, BC, POM, dust, and sea salt, were included in the experiments, although some models had additional aerosol species. Of those major aerosol types, dust and sea-salt are predominantly natural in origin, whereas sulfate, BC, and POM have major anthropogenic sources.

Table 9-12 summarizes the model results from the AeroCom-A for several key parameters: Sources (emission and chemical transformation), mass loading, lifetime, removal rates, and MEE and AOD at a commonly used, mid-visible, wavelength of 550 nanometer (nm). These are the globally averaged values for the year 2000. Major features and conclusions are:

- Globally, aerosol source (in mass) is dominated by sea salt, followed by dust, sulfate, POM, and BC. Over the non-desert land area, human activity is the major source of sulfate, black carbon, and organic aerosols.
- Aerosols are removed from the atmosphere by wet and dry deposition. Although sea salt dominates the emissions, it is quickly removed from the atmosphere because of its large particle size and near-surface distributions, thus having the shortest lifetime. The median lifetime of sea salt from the AeroCom-A models is less than half a day, whereas dust and sulfate have similar lifetimes of 4 days and BC and POM 6-7 days.
- Globally, small-particle-sized sulfate, BC, and POM make up a little over 10% of total aerosol mass in the atmosphere. However, they are mainly from anthropogenic activity, so the highest concentrations are in the most populated regions, where their effects on climate and air quality are major concerns.
- Sulfate and BC have their highest MEE at mid-visible wavelengths, whereas dust is lowest among the aerosol types modeled. That means for the same amount of aerosol mass, sulfate and BC are more effective at attenuating (scattering or absorbing) solar radiation than dust. This is why the sulfate AOD is about the same as dust AOD even though the atmospheric amount of sulfate mass is 10 times less than that of the dust.
- There are large differences, or diversities, among the models for all the parameters listed in Table 9-12. The largest model diversity, shown as the % standard deviation from the all-model-mean and the range (minimum and maximum values) in Table 9-12, is in sea salt emission and removal; this is mainly associated with the differences in particle size range and source parameterizations in each model. The diversity of sea salt atmospheric loading however is much smaller than that of sources or sinks, because the largest particles have the shortest lifetimes even though they comprise the largest fraction of emitted and deposited mass.

Table 9-12. Summary of statistics of AeroCom Experiment A results from 16 global models.

Quantity	Mean	Median	Range	Stddev/mean*
SOURCES (TG/YR)				
SO ₄ ²⁻	179	186	98-232	22%
BC	11.9	11.3	7.8-19.4	23%
Organic matter	96.6	96.0	53-138	26%
Dust	1840	1640	672-4040	49%

Quantity	Mean	Median	Range	Stddev/mean*
Sea salt	16600	6280	2180-121000	199%
REMOVAL RATE (DAY)				
SO ₄ ²⁻	0.25	0.24	0.19-0.39	18%
BC	0.15	0.15	0.066-0.19	21%
Organic matter	0.16	0.16	0.09-0.23	24%
Dust	0.31	0.25	0.14-0.79	62%
Sea salt	5.07	2.50	0.95-35.0	188%
LIFETIME (DAY)				
SO ₄ ²⁻	4.12	4.13	2.6-5.4	18%
BC	7.12	6.54	5.3-15	33%
Organic matter	6.54	6.16	4.3-11	27%
Dust	4.14	4.04	1.3-7.0	43%
Sea salt	0.48	0.41	0.03-1.1	58%
MASS LOADING (TG)				
SO ₄ ²⁻	1.99	1.98	0.92-2.70	25%
BC	0.24	0.21	0.046-0.51	42%
Organic matter	1.70	1.76	0.46-2.56	27%
Dust	19.2	20.5	4.5-29.5	40%
Sea salt	7.52	6.37	2.5-13.2	54%
MEE AT 550 NM (M²G⁻¹)				
SO ₄ ²⁻	11.3	9.5	4.2-28.3	56%
BC	9.4	9.2	5.3-18.9	36%
Organic matter	5.7	5.7	3.7-9.1	26%
Dust	0.99	0.95	0.46-2.05	45%
Sea salt	3.0	3.1	0.97-7.5	55%
AOD AT 550 NM				
SO ₄ ²⁻	0.035	0.034	0.015-0.051	33%
BC	0.004	0.004	0.002-0.009	46%
Organic matter	0.018	0.019	0.006-0.030	36%
Dust	0.032	0.033	0.012-0.054	44%
Sea salt	0.033	0.030	0.02-0.067	42%
TOTAL AOT AT 550 NM	0.124	0.127	0.056-0.151	18%

* Stddev/mean was used as the term "diversity" in Textor et al. (2006, 190456).

Source: Textor et al. (2006, 190456) and Kinne et al. (2006, 155903), and AeroCom website <http://nansen.ipsl.jussieu.fr/AEROCOM/data.html>

- Among the key parameters compared in Table 9-12, the models agree best for simulated total AOD – the % of standard deviation from the model mean is 18%, with the extreme values just a factor of 2 apart. The median value of the multi-model simulated global annual mean total AOD, 0.127, is also in agreement with the global mean values from recent satellite measurements. However, despite the general agreement in total AOD, there are significant diversities at the individual component level for aerosol optical thickness, mass loading, and mass extinction efficiency. This indicates that uncertainties in assessing aerosol climate forcing are still large, and they depend not only on total AOD but also on aerosol absorption and scattering direction (called asymmetry factor), both of which are determined by aerosol physical and optical

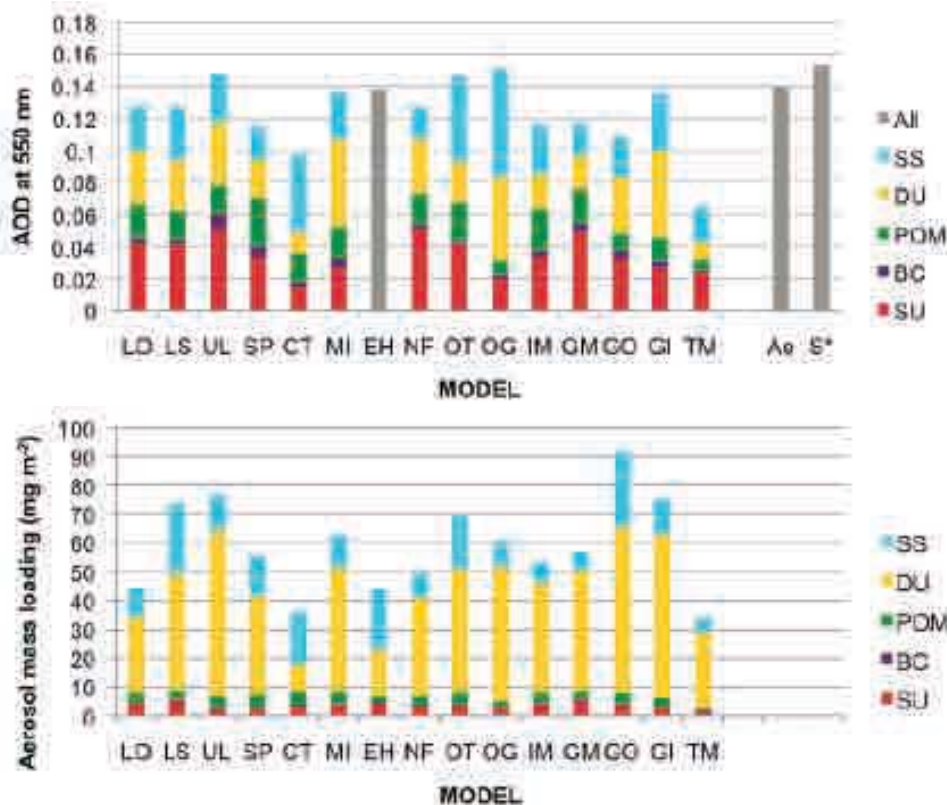
properties. In addition, even with large differences in mass loading and MEE among different models, these terms could compensate for each other (Equation 9-1) to produce similar AOD. This is illustrated in Figure 9-71. For example, model LO and LS have quite different mass loading (44 and 74 mg m⁻², respectively), especially for dust and sea salt amount, but they produce nearly identical total AOD (0.127 and 0.128, respectively).

- Because of the large spatial and temporal variations of aerosol distributions, regional and seasonal diversities are even larger than the diversity for global annual means.

To further isolate the impact of the differences in emissions on the diversity of simulated aerosol mass loading, identical emissions for aerosols and their precursor were used in the AeroCom Experiment B exercise in which 12 of the 16 AeroCom-A models participated (Textor et al., 2007, [190458](#)). The comparison of the results and diversity between AeroCom-A and -B for the same models showed that using harmonized emissions does not significantly reduce model diversity for the simulated global mass and AOD fields, indicating that the differences in atmospheric processes, such as transport, removal, chemistry, and aerosol microphysics, play more important roles than emission in creating diversity among the models. This outcome is somewhat different from another recent study, in which the differences in calculated clear-sky aerosol RF between two models (a regional model STEM and a global model MOZART) were attributed mostly to the differences in emissions (Bates et al., 2006, [189912](#)), although the conclusion was based on only two model simulations for a few focused regions. It is highly recommended from the outcome of AeroCom-A and -B that, although more detailed evaluation for each individual process is needed, multi-model ensemble results, e.g., median values of multi-model output variables, should be used to estimate aerosol RF, due to their greater robustness, relative to individual models, when compared to observations (Textor et al., 2006, [190456](#); Textor et al., 2007, [190458](#); Schulz et al., 2006, [190381](#)).

9.3.6.3. Calculating Aerosol Direct Radiative Forcing

The three parameters that define the aerosol direct RF are the AOD, the single scattering albedo (SSA), and the asymmetry factor (g), all of which are wavelength dependent. AOD is indicative of how much aerosol exists in the column, SSA is the fraction of radiation being scattered versus the total attenuation (scattered and absorbed), and the g relates to the direction of scattering that is related to the size of the particles (see Chapter 1 of the CCSP SAP2.3). An indication of the particle size is provided by another parameter, the Ångström exponent (\mathring{A}), which is a measure of differences of AOD at different wavelengths. For typical tropospheric aerosols, \mathring{A} tends to be inversely dependent on particle size; larger values of \mathring{A} are generally associated with smaller aerosols particles. These parameters are further related; for example, for a given composition, the ability of a particle to scatter radiation decreases more rapidly with decreasing size than does its ability to absorb, so at a given wavelength varying \mathring{A} can change SSA. Note that AOD, SSA, g , \mathring{A} , and all the other parameters in Equations 9.1 and 9.2 vary with space and time due to variations of both aerosol composition and relative humidity, which influence these characteristics.



Source: Kinne et al. (2006, [155903](#))

Figure 9-71. Global annual averaged AOD (upper panel) and aerosol mass loading (lower panel) with their components simulated by 15 models in AeroCom- A (excluding one model which only reported mass). SU=SO₄²⁻, BC=black carbon, POM=particulate OC, DU=dust, SS=sea salt. Model abbreviations: LO=LOA (Lille, Fra), LS=LSCE (Paris, Fra), UL=ULAQ (L’Aquila, Ita), SP=SPRINTARS (Kyushu, Jap), CT=ARQM (Toronto, Can), MI=MIRAGE (Richland, USA), EH=ECHAM5 (MPI-Hamburg, Ger), NF=CCM-Match (NCAR Boulder, USA), OT=Oslo-CTM (Oslo, Nor), OG=OLSO-GCM (Oslo, Nor) [prescribed background for DU and SS], IM=IMPACT (Michigan, USA), GM=GFDLMozart (Princeton, NJ, USA), GO=GOCART (NASA-GSFC, Washington DC, USA), GI=GISS (NASA-GISS, New York, USA), TM=TM5 (Utrecht, Net). Also shown in the upper panel are the averaged observation data from AERONET (Ae) and the satellite composite (S*).

In the recent AeroCom project, aerosol direct RF for the solar spectral wavelengths (or shortwave) was assessed based on the 9 models that participated in both Experiment B and PRE in which identical, prescribed emissions for present (year 2000) and pre-industrial time (year 1750) listed in Table 9-11 were used across the models (Schulz et al., 2006, [190381](#)). The anthropogenic direct RF was obtained by subtracting AeroCom-PRE from AeroCom-B simulated results. Because dust and sea salt are predominantly from natural sources, they were not included in the anthropogenic RF assessment although the land use practice can contribute to dust emissions as “anthropogenic”. Other aerosols that were not considered in the AeroCom forcing assessment were natural sulfate (e.g., from volcanoes or ocean) and POM (e.g., from biogenic hydrocarbon oxidation), as well as nitrate. The aerosol direct forcing in

the AeroCom assessment thus comprises three major anthropogenic aerosol components sulfate, BC, and POM.

Table 9-13. SO₄²⁻ mass loading, MEE and AOD at 550 nm, shortwave radiative forcing at the top of the atmosphere, and normalized forcing with respect to AOD and mass. All values refer to anthropogenic perturbation.

Model	Mass load (mg m ⁻²)	MEE (m ² g ⁻¹)	AOD att 550 nm	TOA Forcing (W/m ²)	Forcing/AOD (W/m ²)	Forcing/Mass (W g ⁻¹)
<i>PUBLISHED SINCE IPCC 2001</i>						
A CCM3	2.23			-0.56		-251
B GEOSCHEM	1.53	11.8	0.018	-0.33	-18	-216
C GISS	3.30	6.7	0.022	-0.65	-30	-197
D GISS	3.27			-0.96		-294
E GISS*	2.12			-0.57		-269
F SPRINTARS	1.55	9.7	0.015	-0.21		-135
G LMD	2.76			-0.42		-152
H LOA	3.03	9.9	0.03	-0.41	-14	-135
I GATORG	3.06			-0.32		-105
J PNNL	5.50	7.6	0.042	-0.44	-10	-80
K UIO-CTM	1.79	10.6	0.019	-0.37	-19	-207
L UIO-GCM	2.28			-0.29		-127
<i>AEROCOM: IDENTICAL EMISSIONS USED FOR YR 2000 AND 1750</i>						
M UMI	2.64	7.6	0.02	-0.58	-29	-220
N UIO-CTM	1.70	11.2	0.019	-0.36	-19	-212
O LOA	3.64	9.6	0.035	-0.49	-14	-135
P LSCE	3.01	7.6	0.023	-0.42	-18	-140
Q ECHAMS-HAM	2.47	6.5	0.016	-0.46	-29	-186
R GISS**	1.34	4.5	0.006	-0.19	-32	-142
S UIO-GCM	1.72	7.0	0.012	-0.25	-21	-145
T SPRINTARS	1.19	10.9	0.013	-0.16	-12	-134
U ULAQ	1.62	12.3	0.02	-0.22	-11	-136
Average A-L	2.70	9.4	0.024	-0.46	-18	-181
Average M-U	2.15	8.6	0.018	-0.35	-21	-161
Minimum A-U	1.19	4.5	0.006	-0.96	-32	-294
Maximum A-U	5.50	12.3	0.042	-0.16	-10	-80
Std dev A-L	1.09	1.9	0.010	0.202	7	68
Std dev M-U	0.83	2.6	0.008	0.149	8	35
%Stddev/avg A-L	40%	20%	41%	44%	38%	385
%Stddev/avg M-U	39%	30%	45%	43%	37%	22%

Model	Mass load (mg m ⁻²)	MEE (m ² g ⁻¹)	AOD att 550 nm	TOA Forcing (W/m ²)	Forcing/AOD (W/m ²)	Forcing/Mass (W g ⁻¹)
-------	------------------------------------	--	-------------------	------------------------------------	------------------------------------	--------------------------------------

Model abbreviations: CCM3 = Community Climate Model; GEOSCHEM = Goddard Earth Observing System-Chemistry; GISS = Goddard Institute for Space Studies; SPRINTARS = Spectral Radiation-Transport Model for Aerosol Species; LMD = Laboratoire de Meteorologie Dynamique; LOA = Laboratoire d'Optique Atmospherique; GATORG = Gas, Aerosol Transport and General circulation model; PNNL = Pacific Northwest National Laboratory; UIO-CTM = University of Oslo CTM; UIO-GCM = University of Oslo GCM; UMI = University of Michigan; LSCE = Laboratoire des Sciences du Climat et de l'Environnement; ECHAMS5-HAM = European Centre Hamburg with Hamburg Aerosol Module; ULAQ = University of IL'Aquila.
Source: Adapted from IPCC AR4 (Intergovernmental Panel on Climate, 2007, [190988](#)) and Schulz et al. (2006, [190381](#))

Table 9-14. Particulate organic matter (POM) and BC mass loading, AOD at 550 nm, shortwave radiative forcing at the top of the atmosphere, and normalized forcing with respect to AOD and mass.

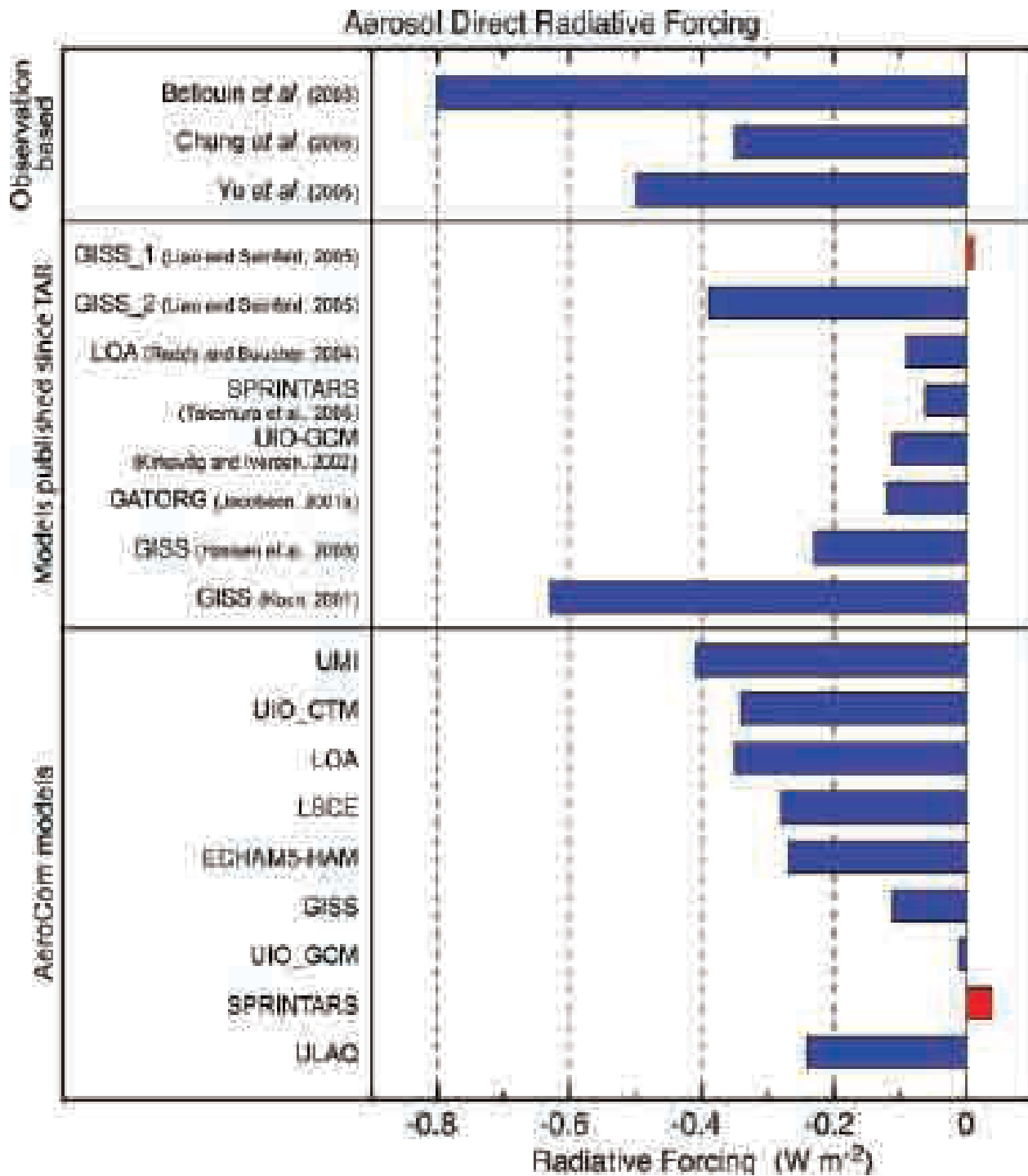
Model	Mass load (mg m ⁻²)	MEE (m ² g ⁻¹)	AOD at 550 nm	TOA Forcing (W/m ²)	Forcing/ AOD (W/m ²)	Forcing/ Mass (W g ⁻¹)	Mass load (mg m ⁻²)	MEE (m ² g ⁻¹)	AOD at 550 nm	TOA Forcing (W/m ²)	Forcing/ AOD (W/m ²)	Forcing/ Mass (W g ⁻¹)
<i>PUBLISHED SINCE IPCC 2001</i>												
A SPRINTARS				-0.24		-107				0.36		
B LOA	2.33	6.9	0.016	-0.25	-16	-140	0.37			0.55		
C GISS	1.86	9.1	0.017	-0.26	-15	-161	0.29			0.61		
D GISS	1.86	8.1	0.015	-0.30	-20	-75	0.29			0.35		
E GISS*	2.39			-0.18		-92	0.39			0.50		
F GISS	2.49			-0.23		-101	0.43			0.53		
G SPRINTARS	2.67	10.9	0.029	-0.27	-9	-23	0.53			0.42		
H GATORG	2.56			-0.06		-112	0.39			0.55		
I MOZGN	3.03	5.9	0.018	-0.34	-19							
J CCM							0.33			0.34		
K UIO-CTM							0.30			0.19		
<i>AEROCOM: IDENTICAL EMISSIONS FOR YR 2000 & 1750</i>												
L UMI	1.16	5.2	0.0060	-0.23	-38	-198	0.19	6.8	1.29	0.25	194	1316
M UIO-CTM	1.12	5.2	0.0058	-0.16	-28	-143	0.19	7.1	1.34	0.22	164	1158
N LOA	1.41	6.0	0.0085	-0.16	-19	-113	0.25	7.9	1.98	0.32	162	1280
OLSCE	1.50	5.3	0.0079	-0.17	-22	-113	0.25	4.4	1.11	0.30	270	1200
P ECHAMS-HAM	1.00	7.7	0.0077	-0.10	-13	-100	0.16	7.7	1.23	0.20	163	1250
Q GISS**	1.22	4.9	0.0060	-0.14	-23	-115	0.24	7.6	1.83	0.22	120	917
R UIO-GCM	0.88	5.2	0.0046	-0.06	-13	-68	0.19	10.3	1.95	0.36	185	1895
S SPRINTARS	1.84	10.9	0.0200	-0.10	-5	-54	0.37	9.5	3.50	0.32	91	865
T ULAQ	1.71	4.4	0.0075	-0.09	-12	-53	0.38	7.6	2.90	0.08	28	211
Average A-K	2.40	8.2	0.019	-0.24	-16	-102	0.37			0.44		1242
Average L-T	1.32	6.1	0.008	-0.13	-19	-106	0.25	7.7	1.90	0.25	153	1121
Minimum A-T	0.88	4.4	0.005	-0.34	-38	-198	0.16	4.4	1.11	0.08	28	211
Maximum A-T	3.03	10.9	0.029	-0.06	-5	-23	0.53	10.3	3.50	0.61	270	2103
Std dev A-K	0.39	1.7	0.006	0.09	4	41	0.08			0.06		384
Std dev L-T	0.32	2.0	0.005	0.05	10	46	0.08	1.6	0.82	0.09	68	450
%Stddev/avg A-K	16%	21%	30%	36%	26%	41%	22%			23%		31%

Model	Mass load (mg m ⁻²)	MEE (m ² g ⁻¹)	AOD at 550 nm	TOA Forcing (W/m ²)	Forcing/AOD (W/m ²)	Forcing/Mass (W g ⁻¹)	Mass load (mg m ⁻²)	MEE (m ² g ⁻¹)	AOD at 550 nm	TOA Forcing (W/m ²)	Forcing/AOD (W/m ²)	Forcing/Mass (W g ⁻¹)
%Stddev/avg L-T	25%	33%	56%	39%	52%	43%	32%	21%	43%	34%	45%	40%

Source: Based on IPCC AR4 (2007, [190988](#)) and Schulz et al. (2006, [190381](#)).

The IPCC AR4 (Intergovernmental Panel on Climate, 2007, [190988](#)) assessed anthropogenic aerosol RF based on the model results published after the IPCC TAR in 2001, including those from the AeroCom study discussed above. These results (adopted from IPCC AR4) are shown in Table 9-13 for sulfate and Table 9-14 for carbonaceous aerosols (BC and POM), respectively. All values listed in Table 9-13 and 9.14 refer to anthropogenic perturbation, i.e., excluding the natural fraction of these aerosols. In addition to the mass burden, MEE, and AOD, Table 9-13 and 9.14 also list the “normalized forcing”, also known as “forcing efficiency”, one for the forcing per unit AOD, and the other the forcing per gram of aerosol mass (dry). For some models, aerosols are externally mixed, that is, each aerosol particle contains only one aerosol type such as sulfate, whereas other models allow aerosols to mix internally to different degrees, that is, each aerosol particle can have more than one component, such as black carbon coated with sulfate. For models with internal mixing of aerosols, the component values for AOD, MEE, and forcing were extracted (Schulz et al., 2006, [190381](#)).

Considerable variation exists among these models for all quantities in Table 9-13 and 9.14. The RF for all the components varies by a factor of 6 or more: Sulfate from 0.16 to 0.96 W/m², POM from -0.06 to -0.34 W/m², and BC from +0.08 to +0.61 W/m², with the standard deviation in the range of 30 to 40% of the ensemble mean. It should be noted that although BC has the lowest mass loading and AOD, it is the only aerosol species that absorbs strongly, causing positive forcing to warm the atmosphere, in contrast to other aerosols that impose negative forcing to cool the atmosphere. As a result, the net anthropogenic aerosol forcing as a whole becomes less negative when BC is included. The global average anthropogenic aerosol direct RF at the top of the atmosphere (TOA) from the models, together with observation-based estimates (see Chapter 2 of the CCSP SAP2.3), is presented in Figure 9-72. Note the wide range for forcing in Figure 9-72. The comparison with observation-based estimates shows that the model estimated forcing is in general lower, partially because the forcing value from the model is the difference between present-day and pre-industrial time, whereas the observation-derived quantity is the difference between an atmosphere with and without anthropogenic aerosols, so the “background” value that is subtracted from the total forcing is higher in the models. The discussion so far has dealt with global average values. The geographic distributions of multi-model aerosol direct RF has been evaluated among the AeroCom models, which are shown in Figure 9-73 for total and anthropogenic AOD at 550 nm and anthropogenic aerosol RF at TOA, within the atmospheric column, and at the surface. Globally, anthropogenic AOD is about 25% of total AOD (Figure 9-73a and b) but is more concentrated over polluted regions in Asia, Europe, and North America and biomass burning regions in tropical southern Africa and South America. At TOA, anthropogenic aerosol causes negative forcing over mid-latitude continents and oceans with the most negative values (-1 to -2 W/m²) over polluted regions (Figure 9-73C). Although anthropogenic aerosol has a cooling effect at the surface with surface forcing values down to -10 W/m² over China, India, and tropical Africa (Figure 9-73E), it warms the atmospheric column with the largest effects again over the polluted and biomass burning regions. This heating effect will change the atmospheric circulation and can affect the weather and precipitation (e.g., Kim et al., 2006, [190917](#)).



Source: IPCC (2007, 190988).

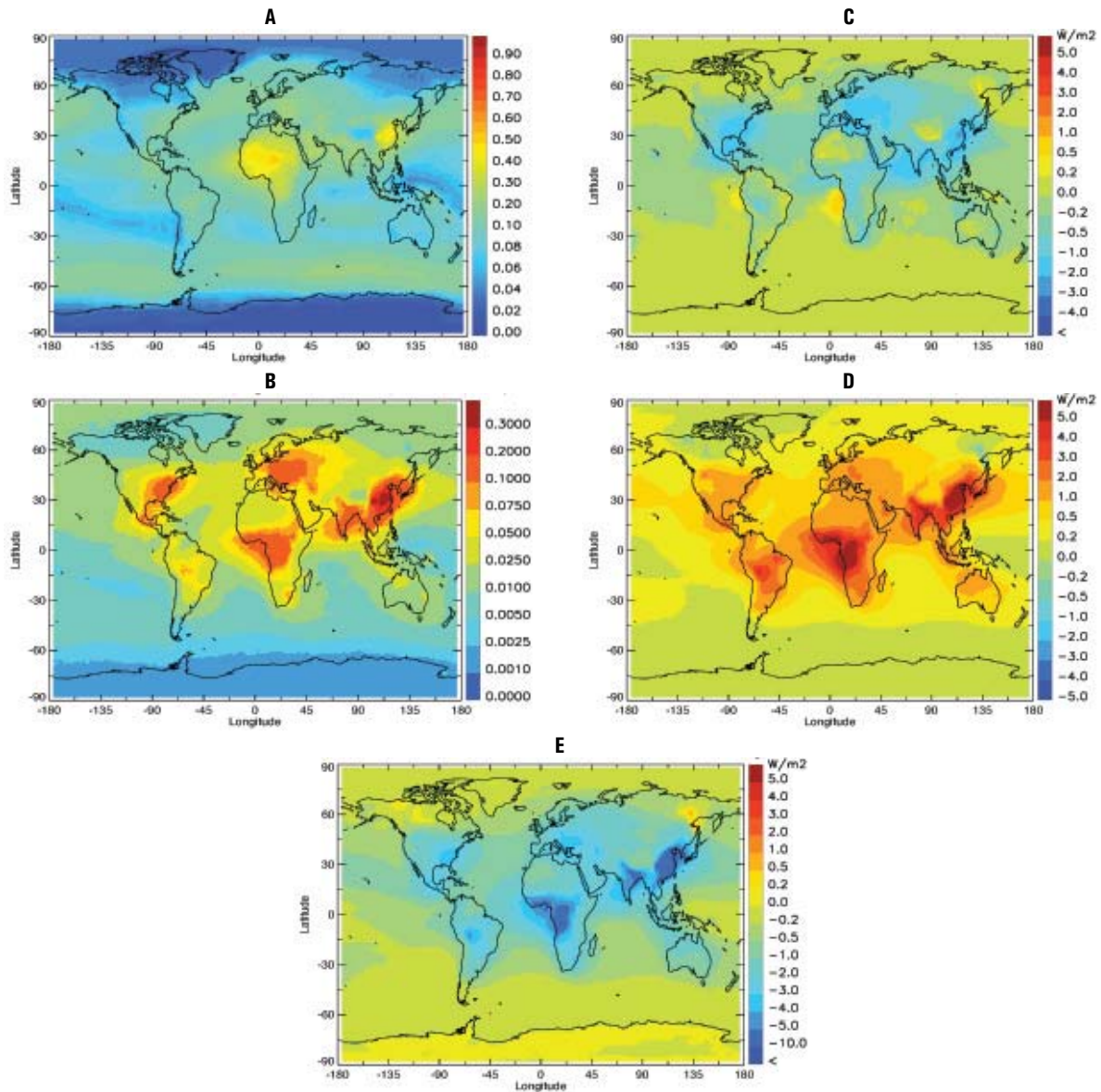
Figure 9-72. Aerosol direct radiative forcing in various climate and aerosol models. Observed values are shown in the top section.

Basic conclusions from forward modeling of aerosol direct RF are:

- The most recent estimate of all-sky shortwave aerosol direct RF at TOA from anthropogenic sulfate, BC, and POM (mostly from fossil fuel/biofuel combustion and

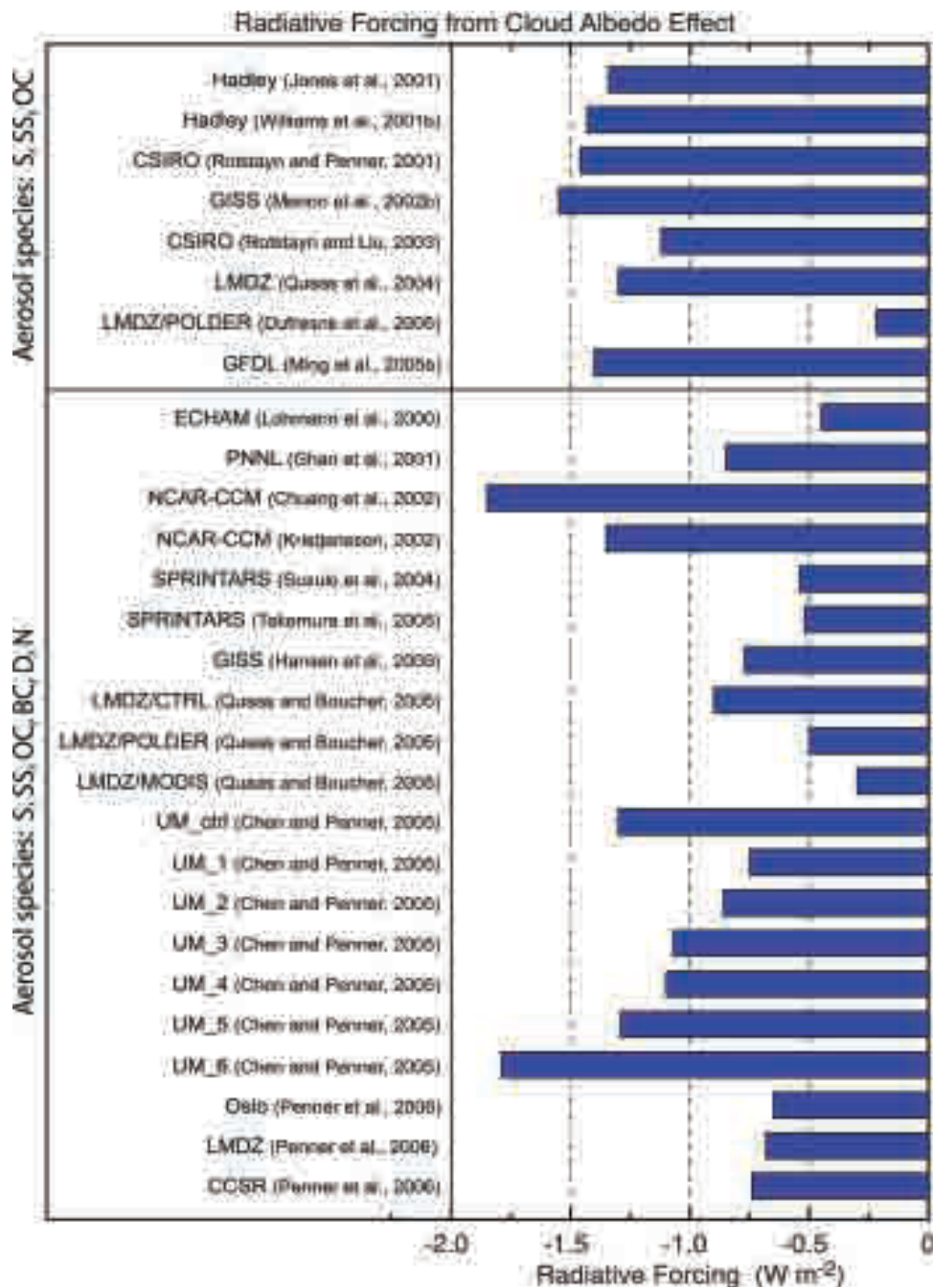
biomass burning) is -0.22 ± 0.18 W/m² averaged globally, exerting a net cooling effect. This value would represent the low-end of the forcing magnitude, since some potentially significant anthropogenic aerosols, such as nitrate and dust from human activities are not included because of their highly uncertain sources and processes. IPCC AR4 had adjusted the total anthropogenic aerosol direct RF to -0.5 ± 0.4 W/m² by adding estimated anthropogenic nitrate and dust forcing values based on limited modeling studies and by considering the observation-based estimates (see Chapter 2 of the CCSP SAP2.3).

- Both sulfate and POM negative forcing whereas BC causes positive forcing because of its highly absorbing nature. Although BC comprises only a small fraction of anthropogenic aerosol mass load and AOD, its forcing efficiency (with respect to either AOD or mass) is an order of magnitude stronger than sulfate and POM, so its positive shortwave forcing largely offsets the negative forcing from sulfate and POM. This points out the importance of improving the model ability to simulate each individual aerosol components more accurately, especially black carbon. Separately, it is estimated from recent model studies that anthropogenic sulfate, POM, and BC forcings at TOA are -0.4 , -0.18 , $+0.35$ W/m², respectively. The anthropogenic nitrate and dust forcings are estimated at -0.1 W/m² for each, with uncertainties exceeds 100% (Intergovernmental Panel on Climate, 2007, [190988](#)).
- In contrast to long-lived greenhouse gases, anthropogenic aerosol RF exhibits significant regional and seasonal variations. The forcing magnitude is the largest over the industrial and biomass burning source regions, where the magnitude of the negative aerosol forcing can be of the same magnitude or even stronger than that of positive greenhouse gas forcing.
- There is a large spread of model-calculated aerosol RF even in the global annual averaged values. The AeroCom study shows that the model diversity at some locations (mostly East Asia and African biomass burning regions) can reach ± 3 W/m², which is an order of magnitude above the global averaged forcing value of -0.22 W/m². The large diversity reflects the low level of current understanding of aerosol radiative forcing, which is compounded by uncertainties in emissions, transport, transformation, removal, particle size, and optical and microphysical (including hygroscopic) properties.
- In spite of the relatively small value of forcing at TOA, the magnitudes of anthropogenic forcing at the surface and within the atmospheric column are considerably larger: -1 to -2 W/m² at the surface and $+0.8$ to $+2$ W/m² in the atmosphere. Anthropogenic aerosols thus cool the surface but heat the atmosphere, on average. Regionally, the atmospheric heating can reach annually averaged values exceeding 5 W/m² (Figure 9-73D). These regional effects and the negative surface forcing are expected to exert an important effect on climate through alteration of the hydrological cycle.



Source: Schulz et al. (2006, [190381](#)) and AeroCom image catalog (<http://nansen.ipl.jussieu.fr/AEROCOM/data.html>).

Figure 9-73. Aerosol optical thickness and anthropogenic shortwave all-sky radiative forcing from the AeroCom study. Shown in the figure: total AOD (A) and anthropogenic AOD (B) at 550 nm, and radiative forcing at TOA (C), atmospheric column (D), and surface (E).



Source: IPCC (2007, 190988).

Figure 9-74. Radiative forcing from the cloud albedo effect (1st aerosol indirect effect) in the global climate models used from IPCC (2007, 190988), Chapter 2, Figure 2.14, of the IPCC AR4. Species included in the lower panel are SO_4^{2-} , sea salt, organic and BC, dust and nitrates; in the top panel, only SO_4^{2-} , sea salt and OC are included.

9.3.6.4. Calculating Aerosol Indirect Forcing

Aerosol Effects on Clouds. A subset of the aerosol particles can act as cloud condensation nuclei (CCN) and/or ice nuclei (IN). Increases in aerosol particle concentrations, therefore, may increase the ambient concentrations of CCN and IN, affecting cloud properties. For a fixed cloud liquid water content, a CCN increase will lead to more cloud droplets so that the cloud droplet size will decrease. That effect leads to brighter clouds, the enhanced albedo then being referred to as the “cloud albedo effect” (Twomey, 1977, [190533](#)), also known as the first indirect effect. If the droplet size is smaller, it may take longer to rainout, leading to an increase in cloud lifetime, hence the “cloud lifetime” effect (Albrecht, 1989, [045783](#)), also called the second indirect effect. Approximately one-third of the models used for the IPCC 20th century climate change simulations incorporated an aerosol indirect effect, generally (though not exclusively) considered only with sulfates.

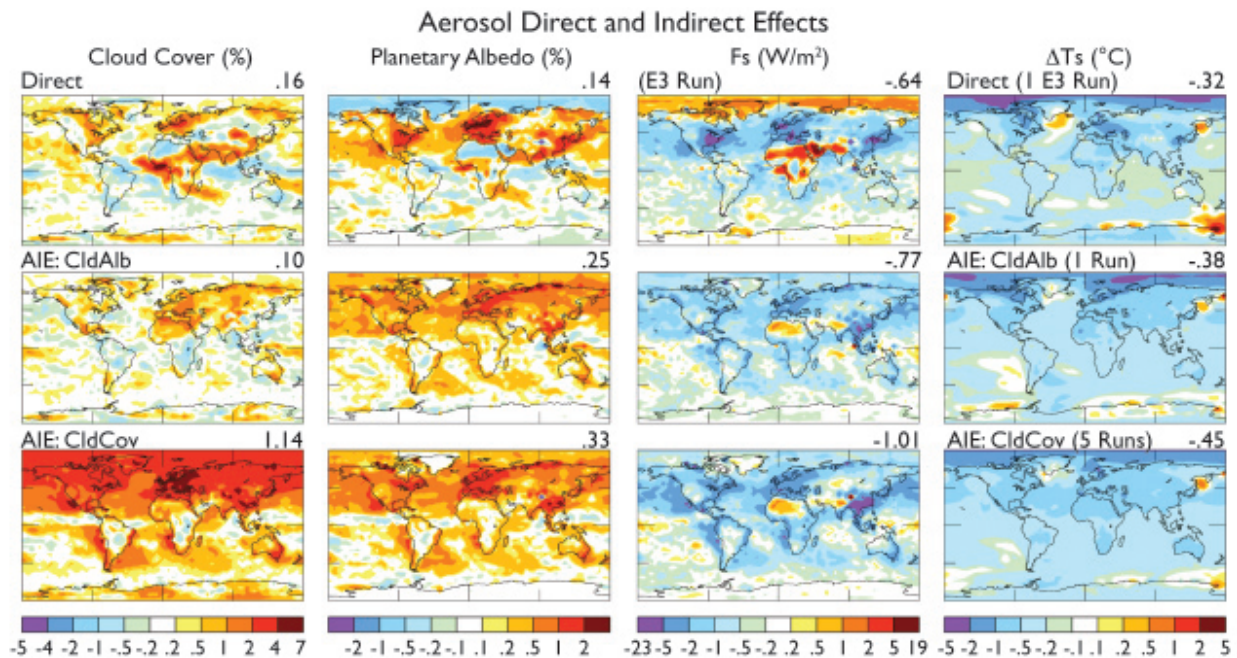
Shown in Figure 9-74 are results from published model studies indicating the different RF values from the cloud albedo effect. The cloud albedo effect ranges from -0.22 to -1.85 W/m²; the lowest estimates are from simulations that constrained representation of aerosol effects on clouds with satellite measurements of drop size vs. aerosol index. In view of the difficulty of quantifying this effect remotely (discussed later), it is not clear whether this constraint provides an improved estimate. The estimate in the IPCC AR4 ranges from +0.4 to -1.1 W/m², with a “best-guess” estimate of 0.7 W/m².

The representation of cloud effects in GCMs is considered below. However, it is becoming increasingly clear from studies based on high resolution simulations of aerosol-cloud interactions that there is a great deal of complexity that is unresolved in climate models. This point is examined below (*High Resolution Modeling*).

Most models did not incorporate the “cloud lifetime effect.” Hansen et al. (2005, [059087](#)) compared this latter influence (in the form of time-averaged cloud area or cloud cover increase) with the cloud albedo effect. In contrast to the discussion in IPCC (2007, [189430](#)), they argue that the cloud cover effect is more likely to be the dominant one, as suggested both by cloud-resolving model studies (Ackerman et al., 2004, [190056](#)) and satellite observations (Kaufman et al., 2005, [155891](#)). The cloud albedo effect may be partly offset by reduced cloud thickness accompanying aerosol pollutants, producing a meteorological (cloud) rather than aerosol effect (see the discussion in Lohman and Feichter, 2005, [155942](#)). The distinction between meteorological feedback and aerosol forcing can become quite opaque: as noted earlier, the term feedback is restricted here to those processes that are responding to a change in temperature. Nevertheless, both aerosol indirect effects were utilized in Hansen et al. (2005, [059087](#)), with the second indirect effect calculated by relating cloud cover to the aerosol number concentration, which in turn is a function of sulfate, nitrate, black carbon and organic carbon concentration. Only the low altitude cloud influence was modeled, principally because there are greater aerosol concentrations at low levels, and because low clouds currently exert greater cloud RF. The aerosol influence on high altitude clouds, associated with IN changes, is a relatively unexplored area for models and as well for process-level understanding.

Hansen et al. (2005, [059087](#)) used coefficients to normalize the cooling from aerosol indirect effects to between -0.75 and -1 W/m², based on comparisons of modeled and observed changes in the diurnal temperature range as well as some satellite observations. The response of the GISS model to the direct and two indirect effects is shown in Figure 9-75. As parameterized, the cloud lifetime effect produced somewhat greater negative RF (cooling), but this was the result of the coefficients chosen. Geographically, it appears that the “cloud cover” effect produced slightly more cooling in the Southern Hemisphere than did the “cloud albedo” response, with the reverse being true in the Northern Hemisphere (differences on the order of a few tenths °C).

Model Experiments. There are many different factors that can explain the large divergence of aerosol indirect effects in models (Figure 9-744). To explore this in more depth, Penner et al. (2006, [190564](#)) used three general circulation models to analyze the differences between models for the first indirect effect, as well as a combined first plus second indirect effect. The models all had different cloud and/or convection parameterizations. In the first experiment, the monthly average aerosol mass and size distribution of, effectively, sulfate aerosol were prescribed, and all models followed the same prescription for parameterizing the cloud droplet number concentration (CDNC) as a function of aerosol concentration. In that sense, the only difference among the models was their separate cloud formation and radiation schemes. The different models all produced similar droplet effective radii, and therefore shortwave cloud forcing, and change in net outgoing whole sky radiation between pre-industrial times and the present. Hence the first indirect effect was not a strong function of the cloud or radiation scheme. The results for this and the following experiments are presented in Figure 9-76, where the experimental results are shown sequentially from left to right for the whole sky effect and in Table 9-15 for the clear-sky and cloud forcing response as well.



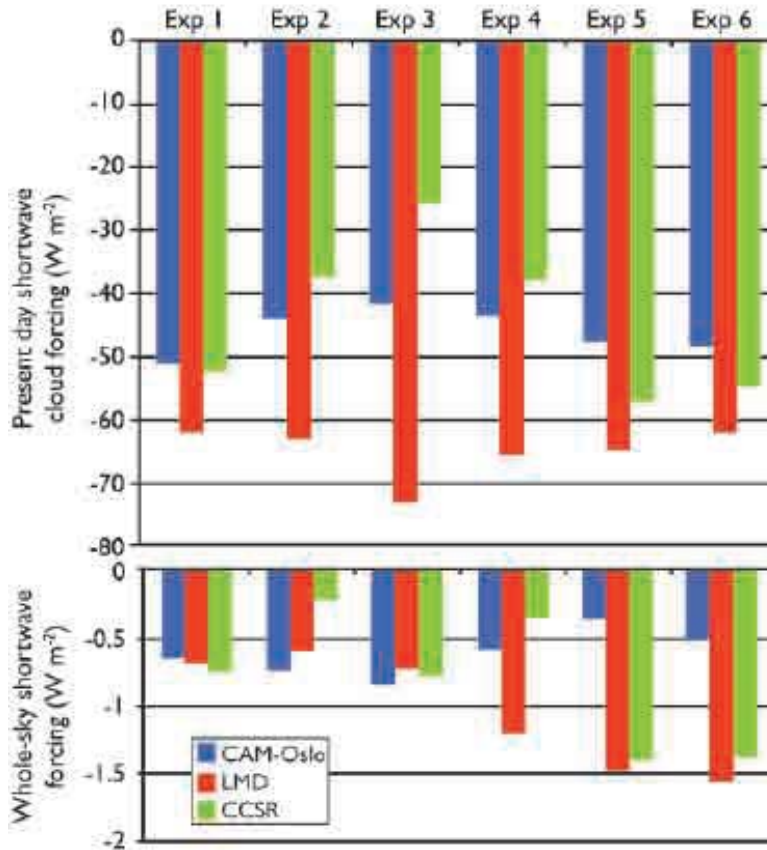
Source: Hansen et al. (2005, [059087](#)).

Figure 9-75. Anthropogenic impact on cloud cover, planetary albedo, radiative flux at the surface (while holding sea surface temperatures and sea ice fixed) and surface air temperature change from the direct aerosol forcing (top row), the first indirect effect (second row) and the second indirect effect (third row). The temperature change is calculated from years 81-120 of a coupled atmosphere simulation with the GISS model.

The change in cloud forcing is the difference between whole sky and clear sky outgoing radiation in the present day minus pre-industrial simulation. The large differences seen between experiments 5 and 6 are due to the inclusion of the clear sky component of aerosol scattering and absorption (the direct effect) in experiment 6.

In the second experiment, the aerosol mass and size distribution were again prescribed, but now each model used its own formulation for relating aerosols to droplets. In this case one of the models produced larger effective radii and therefore a much smaller first indirect aerosol effect (Figure 9.76, Table 9-15). However, even in the two models where the effective radius change and net global forcing were similar, the spatial patterns of cloud forcing differ, especially over the biomass burning regions of Africa and South America.

The third experiment allowed the models to relate the change in droplet size to change in precipitation efficiency (i.e., they were now also allowing the second indirect effect – smaller droplets being less efficient rain producers – as well as the first). The models utilized the same relationship for autoconversion of cloud droplets to precipitation. Changing the precipitation efficiency results in all models producing an increase in cloud liquid water path, although the effect on cloud fraction was smaller than in the previous experiments. The net result was to increase the negative radiative forcing in all three models, albeit with different magnitudes: for two of the models the net impact on outgoing shortwave radiative increased by about 20%, whereas in the third model (which had the much smaller first indirect effect), it was magnified by a factor of three.



Source: Adapted from Penner et al. (2006, [190564](#)).

Figure 9-76. Global average present-day short wave cloud forcing at TOA (top) and change in whole sky net outgoing shortwave radiation (bottom) between the present-day and pre-industrial simulations for each model in each experiment.

Table 9-15. Differences in present day and pre-industrial outgoing solar radiation (W/m^2) in the different experiments.

Model	EXP 1	EXP 2	EXP 3	EXP 4	EXP 5	EXP 6
WHOLE-SKY						
CAM-Oslo	-0.648	-0.726	-0.833	-0.580	-0.365	-0.518
LMD-Z	-0.682	-0.597	-0.722	-1.194	-1.479	-1.553
CCSR	-0.739	-0.218	-0.733	-0.350	-1.386	-1.386
CLEAR-SKY						
CAM-Oslo	-0.063	-0.066	-0.026	0.014	-0.054	-0.575
LMD-Z	-0.054	0.019	0.030	-0.066	-0.126	-1.034
CCSR	0.018	-0.007	-0.045	-0.008	0.018	-1.160
CLOUD-FORCING						
CAM-Oslo	-0.548	-0.660	-0.807	-0.595	-0.311	0.056
LMD-Z	-0.628	-0.616	-0.752	-1.128	-1.353	-0.518
CCSR	-0.757	-0.212	-0.728	-0.345	-1.404	-0.200

EXP1: tests cloud formation and radiation schemes

EXP2: tests formulation for relating aerosols to droplets

EXP3: tests inclusion of droplet size influence on precipitation efficiency

EXP4: tests formulation of droplet size influence on precipitation efficiency

EXP5: tests model aerosol formulation from common sources

EXP6: added the direct aerosol effect

Source: Adapted from Penner et al. (2006, [190564](#)).

In the fourth experiment, the models were now each allowed to use their own formulation to relate aerosols to precipitation efficiency. This introduced some additional changes in the whole sky shortwave forcing (Figure 9-76).

In the fifth experiment, models were allowed to produce their own aerosol concentrations, but were given common sources. This produced the largest changes in the RF in several of the models. Within any one model, therefore, the change in aerosol concentration has the largest effect on droplet concentrations and effective radii. This experiment too resulted in large changes in RF.

In the last experiment, the aerosol direct effect was included, based on the full range of aerosols used in each model. While the impact on the whole-sky forcing was not large, the addition of aerosol scattering and absorption primarily affected the change in clear sky radiation (Table 9-15).

The results of this study emphasize that in addition to questions concerning cloud physics, the differences in aerosol concentrations among the models play a strong role in inducing differences in the indirect effect(s), as well as the direct one.

Observational constraints on climate model simulations of the indirect effect with satellite data (e.g., MODIS) have been performed previously in a number of studies (e.g., Storlevmo et al., 2006, [190418](#); Lohmann et al., 2006, [190451](#); Quaas et al., 2006, [190915](#); Menon et al., 2008, [190534](#)). These have been somewhat limited since the satellite retrieved data used do not have the vertical profiles needed to resolve aerosol and cloud fields (e.g., cloud droplet number and liquid water content); the temporal resolution of simultaneous aerosol and cloud product retrievals are usually not available at a frequency of more than one a day; and higher level clouds often obscure low clouds and aerosols. Thus, the indirect effect, especially the second indirect effect, remains, to a large extent, unconstrained by satellite observations. However, improved measurements of aerosol vertical distribution from the newer generation of

sensors on the A-train platform may provide a better understanding of changes to cloud properties from aerosols. Simulating the top-of-atmosphere reflectance for comparison to satellite measured values could be another way to compare model with observations, which would eliminate the inconsistent assumptions of aerosol optical properties and surface reflectance encountered when compared the model calculated and satellite retrieved AOD values.

Additional Aerosol Influences. Various observations have empirically related aerosols injected from biomass burning or industrial processes to reductions in rainfall (e.g., Warner, 1968, [157114](#); Egan et al., 1974, [190231](#); Andreae et al., 2004, [155658](#); Rosenfeld, 2000, [002234](#)). There are several potential mechanisms associated with this response.

In addition to the two indirect aerosol effects noted above, a process denoted as the “semidirect” effect involves the absorption of solar radiation by aerosols such as black carbon and dust. The absorption increases the temperature, thus lowering the relative humidity and producing evaporation, hence a reduction in cloud liquid water. The impact of this process depends strongly on what the effective aerosol absorption actually is; the more absorbing the aerosol, the larger the potential positive forcing on climate (by reducing low level clouds and allowing more solar radiation to reach the surface). This effect is responsible for shifting the critical value of SSA (separating aerosol cooling from aerosol warming) from 0.86 with fixed clouds to 0.91 with varying clouds (Hansen et al., 1997, [043104](#)). Reduction in cloud cover and liquid water is one way aerosols could reduce rainfall.

More generally, aerosols can alter the location of solar radiation absorption within the system, and this aspect alone can alter climate and precipitation even without producing any change in net radiation at the top of the atmosphere (the usual metric for climate impact). By decreasing solar absorption at the surface, aerosols (from both the direct and indirect effects) reduce the energy available for evapotranspiration, potentially resulting in a decrease in precipitation. This effect has been suggested as the reason for the decrease in pan evaporation over the last 50 yr (Roderick and Farquhar, 2002, [042788](#)). The decline in solar radiation at the surface appears to have ended in the 1990s (Wild et al., 2005, [156156](#)), perhaps because of reduced aerosol emissions in industrial areas (Kruger and Grasl, 2002, [190200](#)), although this issue is still not settled.

Energy absorption by aerosols above the boundary layer can also inhibit precipitation by warming the air at altitude relative to the surface, i.e., increasing atmospheric stability. The increased stability can then inhibit convection, affecting both rainfall and atmospheric circulation (Ramanathan et al., 2001, [042681](#); Chung and Zhang, 2004, [190054](#)). To the extent that aerosols decrease droplet size and reduce precipitation efficiency, this effect by itself could result in lowered rainfall values locally.

In their latest simulations, Hansen et al. (2007, [190597](#)) did find that the indirect aerosol effect reduced tropical precipitation; however, the effect is similar regardless of which of the two indirect effects is used, and also similar to the direct effect. So it is likely that the reduction of tropical precipitation is because of aerosol induced cooling at the surface and the consequent reduced evapotranspiration. Similar conclusions were reached by Yu et al. (2002, [190923](#)) and Feingold et al. (2005, [190550](#)). In this case, the effect is a feedback and not a forcing.

The local precipitation change, through its impacts on dynamics and soil moisture, can have large positive feedbacks. Harvey (2004, [190598](#)) concluded from assessing the response to aerosols in eight coupled models that the aerosol impact on precipitation was larger than on temperature. He also found that the precipitation impact differed substantially among the models, with little correlation among them.

Recent GCM simulations have further examined the aerosol effects on hydrological cycle. Ramanathan et al. (2005, [190199](#)) showed from fully coupled ocean-atmosphere GCM experiments that the “solar dimming” effect at the surface,

i.e., the reduction of solar radiation reaching the surface, due to the inclusion of absorbing aerosol forcing causes a reduction in surface evaporation, a decrease in meridional sea surface temperature (SST) gradient and an increase in atmospheric stability, and a reduction in rainfall over South Asia. Lau and Kim (2006, [190226](#)) examined the direct effects of aerosol on the monsoon water cycle variability from GCM simulations with prescribed realistic global aerosol forcing and proposed the “elevated heat pump” effect, suggesting that atmospheric heating by absorbing aerosols (dust and black carbon), through water cycle feedback, may lead to a strengthening of the South Asia monsoon. These model results are not necessarily at odds with each other, but rather illustrate the complexity of the aerosol-monsoon interactions that are associated with different mechanisms, whose relative importance in affecting the monsoon may be strongly dependent on spatial and temporal scales and the timing of the monsoon. These results may be model dependent and should be further examined.

High Resolution Modeling. Largely by its nature, the representation of the interaction between aerosol and clouds in GCMs is poorly resolved. This stems in large part from the fact that GCMs do not resolve convection on their large grids (order of several hundred km), that their treatment of cloud microphysics is rather crude, and that as discussed previously, their representation of aerosol needs improvement. Superparametrization efforts (where standard cloud parameterizations in the GCM are replaced by resolving clouds in each grid column of the GCM via a cloud resolving model) (e.g., Grabowski, 2004, [190590](#)) could lead the way for the development of more realistic cloud fields and thus improved treatments of aerosol cloud interactions in large-scale models. However, these are just being incorporated in models that resolve both cloud and aerosols. Detailed cloud parcel models have been developed to focus on the droplet activation problem (that asks under what conditions droplets actually start forming) and questions associated with the first indirect effect. The coupling of aerosol and cloud modules to dynamical models that resolve the large turbulent eddies associated with vertical motion and clouds [large eddy simulations (LES) models, with grid sizes of ~100 m and domains ~10 km] has proven to be a powerful tool for representing the details of aerosol-cloud interactions together with feedbacks (e.g., Feingold et al., 1994, [190535](#); Kogan et al., 1994, [190186](#); Stevens et al., 1996, [190417](#); Feingold et al., 1999, [190540](#); Ackerman et al., 2004, [190056](#)). This section explores some of the complexity in the aerosol indirect effects revealed by such studies to illustrate how difficult parameterizing these effects properly in GCMs could really be.

The First Indirect Effect. The relationship between aerosol and drop concentrations (or drop sizes) is a key piece of the first indirect effect puzzle. (It should not, however, be equated to the first indirect effect which concerns itself with the resultant RF). A huge body of measurement and modeling work points to the fact that drop concentrations increase with increasing aerosol. The main unresolved questions relate to the degree of this effect, and the relative importance of aerosol size distribution, composition and updraft velocity in determining drop concentrations (for a review, see McFiggans et al., 2006, [190532](#)). Studies indicate that the aerosol number concentration and size distribution are the most important aerosol factors. Updraft velocity (unresolved by GCMs) is particularly important under conditions of high aerosol particle number concentration.

Although it is likely that composition has some effect on drop number concentrations, composition is generally regarded as relatively unimportant compared to the other parameters (Fitzgerald, 1975, [095417](#); Feingold et al., 2003, [190551](#); Ervens et al., 2005, [190527](#); Dusek et al., 2006, [155756](#)). Therefore, it has been stated that the significant complexity in aerosol composition can be modeled, for the most part, using fairly simple parameterizations that reflect the soluble and insoluble fractions (e.g., Rissler et al., 2004, [190225](#)). However, composition cannot be simply dismissed. Furthermore, chemical interactions also cannot be overlooked. A large uncertainty remains concerning the impact of organic species on cloud droplet growth kinetics, thus cloud droplet formation. Cloud drop size is affected by wet scavenging,

which depends on aerosol composition especially for freshly emitted aerosol. And future changes in composition will presumably arise due to biofuels/biomass burning and a reduction in sulfate emissions, which emphasizes the need to include composition changes in models when assessing the first indirect effect. The simple soluble/insoluble fraction model may become less applicable than is currently the case.

The updraft velocity, and its change as climate warms, may be the most difficult aspect to simulate in GCMs because of the small scales involved. In GCMs it is calculated in the dynamics as a grid box average, and parameterized on the small scale indirectly because it is a key part of convection and the spatial distribution of condensate, as well as droplet activation. Numerous solutions to this problem have been sought, including estimation of vertical velocity based on predicted turbulent kinetic energy from boundary layer models (Lohmann et al., 1999, [190443](#); Larson et al., 2001, [190212](#)) and PDF representations of subgrid quantities, such as vertical velocity and the vertically-integrated cloud liquid water ('liquid water path,' or LWP) (Pincus and Klein, 2000, [190565](#); Golaz et al., 2002, [190587](#); 2002, [190589](#); Larson et al., 2005, [190220](#)). Embedding cloud-resolving models within GCMs is also being actively pursued (Grabowski et al., 1999, [190592](#); Randall et al., 2003, [190201](#)). Numerous other details come into play; for example, the treatment of cloud droplet activation in GCM frameworks is often based on the assumption of adiabatic conditions, which may overestimate the sensitivity of cloud to changes in CCN (Sotiropoulou et al., 2007, [190405](#); Sotiropoulou et al., 2006, [190406](#)). This points to the need for improved theoretical understanding followed by new parameterizations.

Other Indirect Effects. The second indirect effect is often referred to as the "cloud lifetime effect", based on the premise that non-precipitating clouds will live longer. In GCMs the "lifetime effect" is equivalent to changing the representation of precipitation production and can be parameterized as an increase in cloud area or cloud cover (e.g., Hansen et al., 2005, [059087](#)). The second indirect effect hypothesis states that the more numerous and smaller drops associated with aerosol perturbations, suppress collision-induced rain, and result in a longer cloud lifetime. Observational evidence for the suppression of rain in warm clouds exists in the form of isolated studies (e.g., Warner, 1968, [157114](#)) but to date there is no statistically robust proof of surface rain suppression (Levin and Cotton, 2008, [190375](#)). Results from ship-track studies show that cloud water may increase or decrease in the tracks (Coakley and Walsh, 2002, [192025](#)) and satellite studies suggest similar results for warm boundary layer clouds (Han et al., 2002, [049181](#)). Ackerman et al. (2004, [190056](#)) used LES to show that in stratocumulus, cloud water may increase or decrease in response to increasing aerosol depending on the relative humidity of the air overlaying the cloud. Wang et al. (2003, [157106](#)) showed that all else being equal, polluted stratocumulus clouds tend to have lower water contents than clean clouds because the small droplets associated with polluted clouds evaporate more readily and induce an evaporation-entrainment feedback that dilutes the cloud. This result was confirmed by Xue and Feingold (2006, [190920](#)) and Jiang and Feingold (2006, [190976](#)) for shallow cumulus, where pollution particles were shown to decrease cloud fraction. Furthermore, Xue et al. (2008, [190921](#)) suggested that there may exist two regimes: the first, a precipitating regime at low aerosol concentrations where an increase in aerosol will suppress precipitation and increase cloud cover (Albrecht, 1989, [045783](#)); and a second, non-precipitating regime where the enhanced evaporation associated with smaller drops will decrease cloud water and cloud fraction.

The possibility of bistable aerosol states was proposed earlier by Baker and Charlson (1990, [190016](#)) based on consideration of aerosol sources and sinks. They used a simple numerical model to suggest that the marine boundary layer prefers two aerosol states: a clean, oceanic regime characterized by a weak aerosol source and less reflective clouds; and a polluted, continental regime characterized by more reflective clouds. On the other hand, study by Ackerman et al. (1994, [189975](#)) did not support such a bistable system using a somewhat more sophisticated model. Further observations are needed to clarify the nature of cloud/aerosol interactions under a variety of conditions.

Finally, the question of possible effects of aerosol on cloud lifetime was examined by Jiang et al. (2006, [133165](#)), who tracked hundreds of cumulus clouds generated by LES from their formative stages until they dissipated. They showed that in the model there was no effect of aerosol on cloud lifetime, and that cloud lifetime was dominated by dynamical variability.

It could be argued that the representation of these complex feedbacks in GCMs is not warranted until a better understanding of the processes is at hand. Moreover, until GCMs are able to represent cloud scales, it is questionable what can be obtained by adding microphysical complexity to poorly resolved clouds. A better representation of aerosol-cloud interactions in GCMs therefore depends on the ability to improve representation of aerosols and clouds, as well as their interaction, in the hydrologic cycle. This issue is discussed further in the next chapter.

9.3.6.5. Aerosol in the Climate Models

Aerosol in the IPCC AR4 Climate Model Simulations. To assess the atmospheric and climate response to aerosol forcing, e.g., changes in surface temperature, precipitation, or atmospheric circulation, aerosols, together with greenhouse gases should be an integrated part of climate model simulation under the past, present, and future conditions. Table 9-16 lists the forcing species that were included in 25 climate modeling groups used in the IPCC AR4 (2007, [190988](#)) assessment. All the models included long-lived greenhouse gases, most models included sulfate direct forcing, but only a fraction of those climate models considered other aerosol types. In other words, aerosol RF was not adequately accounted for in the climate simulations for the IPCC AR4. Put still differently, the current aerosol modeling capability has not been fully incorporated into the climate model simulations. As pointed out in Section 9.3.6.4, fewer than one-third of the models incorporated an aerosol indirect effect, and most considered only sulfates.

The following discussion compares two of the IPCC AR4 climate models that include all major forcing agencies in their climate simulation: the model from the NASA Goddard Institute for Space Studies (GISS) and from the NOAA Geophysical Fluid Dynamics Laboratory (GFDL). The purpose in presenting these comparisons is to help elucidate how modelers go about assessing their aerosol components, and the difficulties that entail. A particular concern is how aerosol forcings were obtained in the climate model experiments for IPCC AR4. Comparisons with observations have already led to some improvements that can be implemented in climate models for subsequent climate change experiments (e.g., Koch et al., 2006, [190184](#), for GISS model). This aspect is discussed further in Chapter 4 of the CCSP SAP2.3.

Table 9-16. Forcings used in IPCC AR4 simulations of 20th century climate change. This table is adapted from SAP 1.1 Table 5.2 (compiled using information provided by the participating modeling centers, see http://www.pcmdi.llnl.gov/ipcc/model-documentation/ipcc_model_documentation.php) plus additional information from that website. Eleven different forcings are listed: well-mixed greenhouse gases (G), tropospheric and stratospheric ozone (O), SO₄²⁻ aerosol direct (SD) and indirect effects (SI), black carbon (BC) and organic carbon aerosols (OC), mineral dust (MD), sea salt (SS), land use/land cover (LU), solar irradiance (SO), and volcanic aerosols (V). Check mark denotes inclusion of a specific forcing. As used here, "inclusion" means specification of a time-varying forcing, with changes on interannual and longer timescales.

	Model	Country	G	O	SD	SI	BC	OC	MD	SS	LU	SO	V
1	BCC-CMI	China	√	√	√								
2	BCCR-BCM2.0	Norway	√		√				√	√			
3	CCSM3	USA	√	√	√		√	√				√	√
4	CGCM3.1(T47)	Canada	√		√								
5	CGCM3.1(T63)	Canada	√		√								
6	CNRM-CM3	France	√	√	√		√						
7	CSIRO-Mk3.0	Australia	√		√								
8	CSIRO-Mk3.5	Australia	√		√								
9	ECHAMS/MPI-OM	Germany	√	√	√	√							
10	ECHO-G	Germany/ Korea	□	□	□	□						□	□
11	FGOALS-g1.0	China	□		□								
12	GFDL-CM2.0	USA	□	□	□		□				□	□	□
13	GFDL-CM2.1	USA	□	□	□		□				□	□	□
14	GISS-AOM	USA	□		□					□			
15	GISS-EH	USA	□	□	□	□	□	□	□	□	□	□	□
16	GISS-ER	USA	□	□	□	□	□	□	□	□	□	□	□
17	INGV-SXG	Italy	□	□	□								
18	INM-CM3.0	Russia	□		□							□	
19	IPSL-CM4	France	□		□	□							
20	MICROC3.2(hires)	Japan	□	□	□		□	□	□	□	□	□	□
21	MICROC3.2(medres)	Japan	□	□	□		□	□	□	□	□	□	□
22	MRI-CGCM2.3.2	Japan	□		□							□	□
23	PCM	USA	√	√	√							√	√
24	UKMO-HasCM3	U.K.	√	√	√	√							
25	UKMO-HadGEM1	U.K.	√	√	√	√	√	√				√	√

The GISS Model. There have been many different configurations of aerosol simulations in the GISS model over the years, with different emissions, physics

packages, etc., as is apparent from the multiple GISS entries in the preceding figures and tables. There were also three different GISS GCM submissions to IPCC AR4, which varied in their model physics and ocean formulation. (Note that the aerosols in these three GISS versions are different from those in the AeroCom simulations described in Sections 9.3.6.2 and 9.3.6.3.) The GCM results discussed below all relate to the simulations known as GISS model ER (Schmidt and et, 2006, [190373](#)) (see Table 9-16). Although the detailed description and model evaluation have been presented in Liu et al. (2006, [190422](#)), below are the general characteristics of aerosols in the GISS ER:

Aerosol fields: The aerosol fields used in the GISS ER is a prescribed “climatology” which is obtained from chemistry transport model simulations with monthly averaged mass concentrations representing conditions up to 1990. Aerosol species included are sulfate, nitrate, BC, POM, dust, and sea salt. Dry size effective radii are specified for each of the aerosol types, and laboratory-measured phase functions are employed for all solar and thermal wavelengths. For hygroscopic aerosols (sulfate, nitrate, POM, and sea salt), formulas are used for the particle growth of each aerosol as a function of relative humidity, including the change in density and optical parameters. With these specifications, the AOD, single scattering albedo, and phase function of the various aerosols are calculated. While the aerosol distribution is prescribed as monthly mean values, the relative humidity component of the extinction is updated each hour. The global averaged AOD at 550 nm is about 0.15.

Global distribution: When comparing with AOD from observations by multiple satellite sensors of MODIS, MISR, POLDER, and AVHRR and surface based sunphotometer network AERONET (see Chapter 2 of the CCSP SAP2.3 for detailed information about data), qualitative agreement is apparent, with generally higher burdens in Northern Hemisphere summer, and seasonal variations of smoke over southern Africa and South America, as well as wind blown dust over northern African and the Persian Gulf. Aerosol optical depth in both model and observations is smaller away from land. There are, however, considerable discrepancies between the model and observations. Overall, the GISS GCM has reduced aerosol optical depths compared with the satellite data (a global, clear-sky average of about 80% compared with MODIS and MISR data), although it is in better agreement with AERONET ground-based measurements in some locations (note that the input aerosol values were calibrated with AERONET data). The model values over the Sahel in Northern Hemisphere winter and the Amazon in Southern Hemisphere winter are excessive, indicative of errors in the biomass burning distributions, at least partially associated with an older biomass burning source used (the source used here was from (Liousse et al., 1996, [078158](#))).

Seasonal variation: A comparison of the seasonal distribution of the global AOD between the GISS model and satellite data indicates that the model seasonal variation is in qualitative agreement with observations for many of the locations that represent major aerosol regimes, although there are noticeable differences. For example, in some locations the seasonal variations are different from or even opposite to the observations.

Particle size parameter: The Ångström exponent (Å), which is determined by the contrast between the AOD at two or more different wavelengths and is related to aerosol particle size (discussed in Section 9.3.6.3). This parameter is important because the particle size distribution affects the efficiency of scattering of both short and long wave radiation, as discussed earlier. Å from the GISS model is biased low compared with AERONET, MODIS, and POLDER data, although there are technical differences in determining the Å . This low bias suggests that the aerosol particle size in the GISS model is probably too large. The average effective radius in the GISS model appears to be 0.3-0.4 μm , whereas the observational data indicates a value more in the range of 0.2-0.3 μm (Liu et al., 2006, [190422](#)).

Single scattering albedo: The model-calculated SSA (at 550 nm) appears to be generally higher than the AERONET data at worldwide locations (not enough absorption), but lower than AERONET data in Northern Africa, the Persian Gulf, and the Amazon (too much absorption). This discrepancy reflects the difficulties in modeling BC, which is the dominant absorbing aerosol, and aerosol sizes. Global averaged SSA at 550 nm from the GISS model is at about 0.95.

Aerosol direct RF: The GISS model calculated anthropogenic aerosol direct shortwave RF is -0.56 W/m^2 at TOA and -2.87 W/m^2 at the surface. The TOA forcing (upper left, Figure 9-77) indicates that, as expected, the model has larger negative values in polluted regions and positive forcing at the highest latitudes. At the surface (lower left, Figure 9-77) GISS model values exceed -4 W/m^2 over large regions. Note there is also a longwave RF of aerosols (right column), although they are much weaker than the shortwave RF.

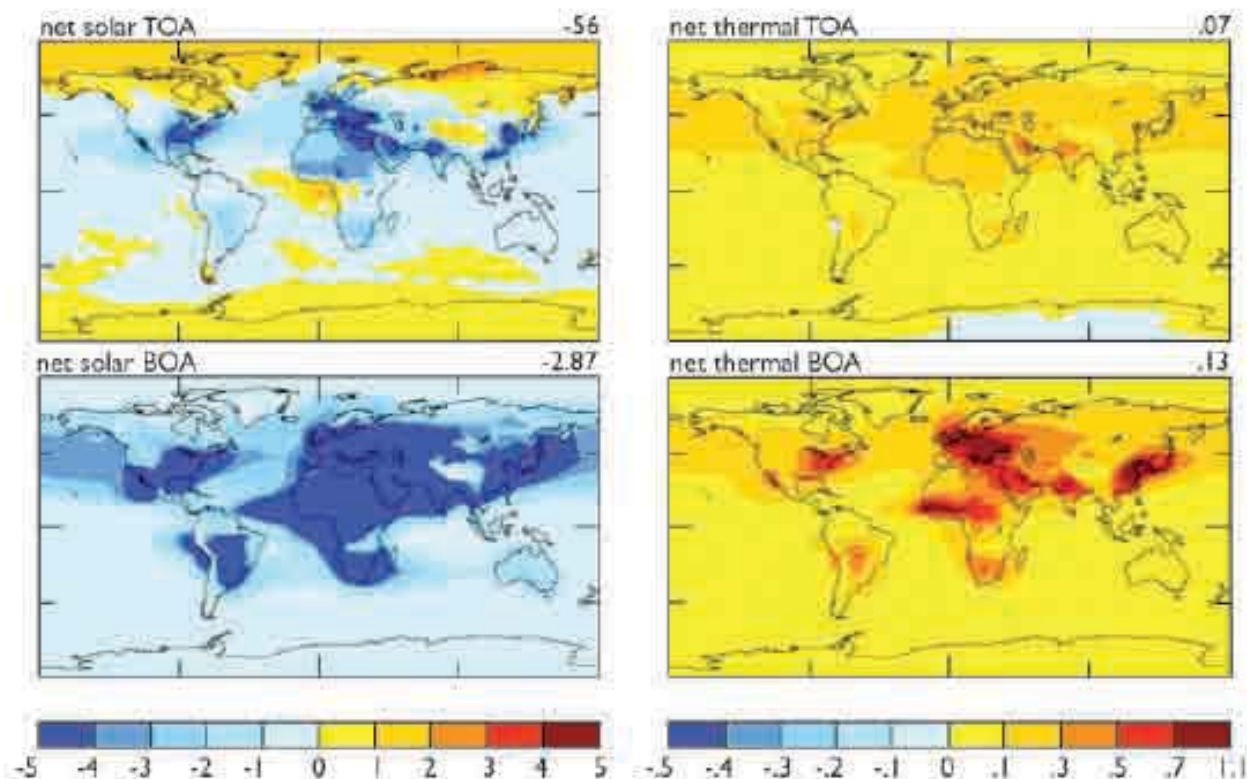
There are several concerns for climate change simulations related to the aerosol trend in the GISS model. One is that the aerosol fields in the GISS AR4 climate simulation (version ER) are kept fixed after 1990. In fact, the observed trend shows a reduction in tropospheric aerosol optical thickness from 1990 through the present, at least over the oceans (Mishchenko and Geogdzhayev, 2007, [190545](#)). Hansen et al. (2007, [190597](#)) suggested that the deficient warming in the GISS model over Eurasia post-1990 was due to the lack of this trend. Indeed, a possible conclusion from the Penner et al. (2002, [190562](#)) study was that the GISS model overestimated the AOD (presumably associated with anthropogenic aerosols) poleward of 30°N . However, when an alternate experiment reduced the aerosol optical depths, the polar warming became excessive (Hansen et al., 2007, [190597](#)). The other concern is that the GISS model may underestimate the organic and sea salt AOD, and overestimate the influence of black carbon aerosols in the biomass burning regions (deduced from Penner et al., 2002, [190562](#); Liu et al., 2006, [190422](#)). To the extent that is true, it would indicate the GISS model underestimates the aerosol direct cooling effect in a substantial portion of the tropics, outside of biomass burning areas. Clarifying those issues requires numerous modeling experiments and various types of observations.

The GFDL Model. A comprehensive description and evaluation of the GFDL aerosol simulation are given in Ginoux et al. (2006, [190582](#)). Below are the general characteristics:

Aerosol fields: The aerosols used in the GFDL climate experiments are obtained from simulations performed with the MOZART 2 model (Model for Ozone and Related chemical Tracers) (Horowitz et al., 2003, [057770](#); Horowitz, 2006, [190620](#)). The exceptions were dust, which was generated with a separate simulation of MOZART 2, using sources from Ginoux et al. (2001, [190579](#)) and wind fields from NCEP/NCAR reanalysis data; and sea salt, whose monthly mean concentrations were obtained from a previous study by Haywood et al. (1999, [040453](#)). It includes most of the same aerosol species as in the GISS model (although it does not include nitrates), and, as in the GISS model, relates the dry aerosol to wet aerosol optical depth via the model's relative humidity for sulfate (but not for organic carbon); for sea salt, a constant relative humidity of 80% was used. Although the parameterizations come from different sources, both models maintain a very large growth in sulfate particle size when the relative humidity exceeds 90%.

Global distributions: Overall, the GFDL global mean aerosol mass loading is within 30% of that of other studies (Chin et al., 2002, [189996](#); Tie and et, 2005, [190459](#); Reddy et al., 2005, [190207](#)), except for sea salt, which is 2 to 5 times smaller. However, the sulfate AOD (0.1) is 2.5 times that of other studies, whereas the organic carbon value is considerably smaller (on the order of 1/2). Both of these differences are influenced by the relationship with relative humidity. In the GFDL model, sulfate is allowed to grow up to 100% relative humidity, but organic carbon does not increase in size as relative humidity increases. Comparison of AOD with AVHRR and MODIS data for the time period 1996-2000 shows that the global mean value over the ocean (0.15) agrees with AVHRR data (0.14) but there are significant differences regionally,

with the model overestimating the value in the northern mid latitude oceans and underestimating it in the southern ocean. Comparison with MODIS also shows good agreement globally (0.15), but in this case indicates large disagreements over land, with the model producing excessive AOD over industrialized countries and underestimating the effect over biomass burning regions. Overall, the global averaged AOD at 550 nm is 0.17, which is higher than the maximum values in the AeroCom-A experiments (Table 9-12) and exceeds the observed value too (Ae and S* in Figure 9-71).



Source: Figure provided by A. Lacis, GISS.

Figure 9-77. Direct radiative forcing by anthropogenic aerosols in the GISS model (including sulfates, BC, OC and nitrates). Short wave forcing at TOA and surface are shown in the top left and bottom left panels. The corresponding thermal forcing is indicated in the right hand panels.

Composition: Comparison of GFDL modeled species with in situ data over North America, Europe, and over oceans has revealed that the sulfate is overestimated in spring and summer and underestimated in winter in many regions, including Europe and North America. Organic and black carbon aerosols are also overestimated in polluted regions by a factor of two, whereas organic carbon aerosols are elsewhere underestimated by factors of 2 to 3. Dust concentrations at the surface agree with observations to within a factor of 2 in most places where significant dust exists, although over the southwest U.S. it is a factor of 10 too large. Surface concentrations of sea salt are underestimated by more than a factor of 2. Over the oceans, the excessive sulfate AOD compensates for the low sea salt values except in the southern oceans. *Size and single-scattering albedo:* No specific comparison was given for

particle size or single-scattering albedo, but the excessive sulfate would likely produce too high a value of reflectivity relative to absorption except in some polluted regions where black carbon (an absorbing aerosol) is also overestimated.

As in the case of the GISS model, there are several concerns with the GFDL model. The good global-average agreement masks an excessive aerosol loading over the Northern Hemisphere (in particular, over the northeast U.S. and Europe) and an underestimate over biomass burning regions and the southern oceans. Several model improvements are needed, including better parameterization of hygroscopic growth at high relative humidity for sulfate and organic carbon; better sea salt simulations; correcting an error in extinction coefficients; and improved biomass burning emissions inventory (Ginoux et al., 2006, [190582](#)).

Comparisons between GISS and GFDL Model. Both GISS and GFDL models were used in the IPCC AR4 climate simulations for climate sensitivity that included aerosol forcing. It would be constructive, therefore, to compare the similarities and differences of aerosols in these two models and to understand what their impacts are in climate change simulations. Figure 9-78 shows the percentage AOD from different aerosol components in the two models.

Sulfate: The sulfate AOD from the GISS model is within the range of that from all other models (Table 9-13), but that from the GFDL model exceeds the maximum value by a factor of 2.5. An assessment in SAP 3.2 (CCSP, 2008, [192028](#); Shindell et al., 2008, [190393](#)) also concludes that GFDL had excessive sulfate AOD compared with other models. The sulfate AOD from GFDL is nearly a factor of 4 larger than that from GISS, although the sulfate burden differs only by about 50% between the two models. Clearly, this implies a large difference in sulfate MEE between the two models.

BC and POM: Compared to observations, the GISS model appears to overestimate the influence of BC and POM in the biomass burning regions and underestimate it elsewhere, whereas the GFDL model is somewhat the reverse: it overestimates it in polluted regions, and underestimates it in biomass burning areas. The global comparison shown in Table 9-14 indicates the GISS model has values similar to those from other models, which might be the result of such compensating errors. The GISS and GFDL models have relatively similar global-average black carbon contributions, and the same appears true for POM.

Sea salt: The GISS model has a much larger sea salt contribution than does GFDL (or indeed other models).

Global and regional distributions: Overall, the global averaged AOD is 0.15 from the GISS model and 0.17 from GFDL. However, as shown in Figure 9-78, the contribution to this AOD from different aerosol components shows greater disparity. For example, over the Southern Ocean where the primary influence is due to sea salt in the GISS model, but in the GFDL it is sulfate. The lack of satellite observations of the component contributions and the limited available in situ measurements make the model improvements at aerosol composition level difficult.

Climate simulations: With such large differences in aerosol composition and distribution between the GISS and GFDL models, one might expect that the model simulated surface temperature might be quite different. Indeed, the GFDL model was able to reproduce the observed temperature change during the 20th century without the use of an indirect aerosol effect, whereas the GISS model required a substantial indirect aerosol contribution (more than half of the total aerosol forcing; (Hansen et al., 2007, [190597](#)). It is likely that the reason for this difference was the excessive direct effect in the GFDL model caused by its overestimation of the sulfate optical depth. The GISS model direct aerosol effect (see Section 9.3.6.6) is close to that derived from observations (Chapter 2 of the CCSP SAP2.3); this suggests that for models with climate sensitivity close to $0.75^{\circ}\text{C}/(\text{W}/\text{m}^2)$ (as in the GISS and GFDL models), an indirect effect is needed.

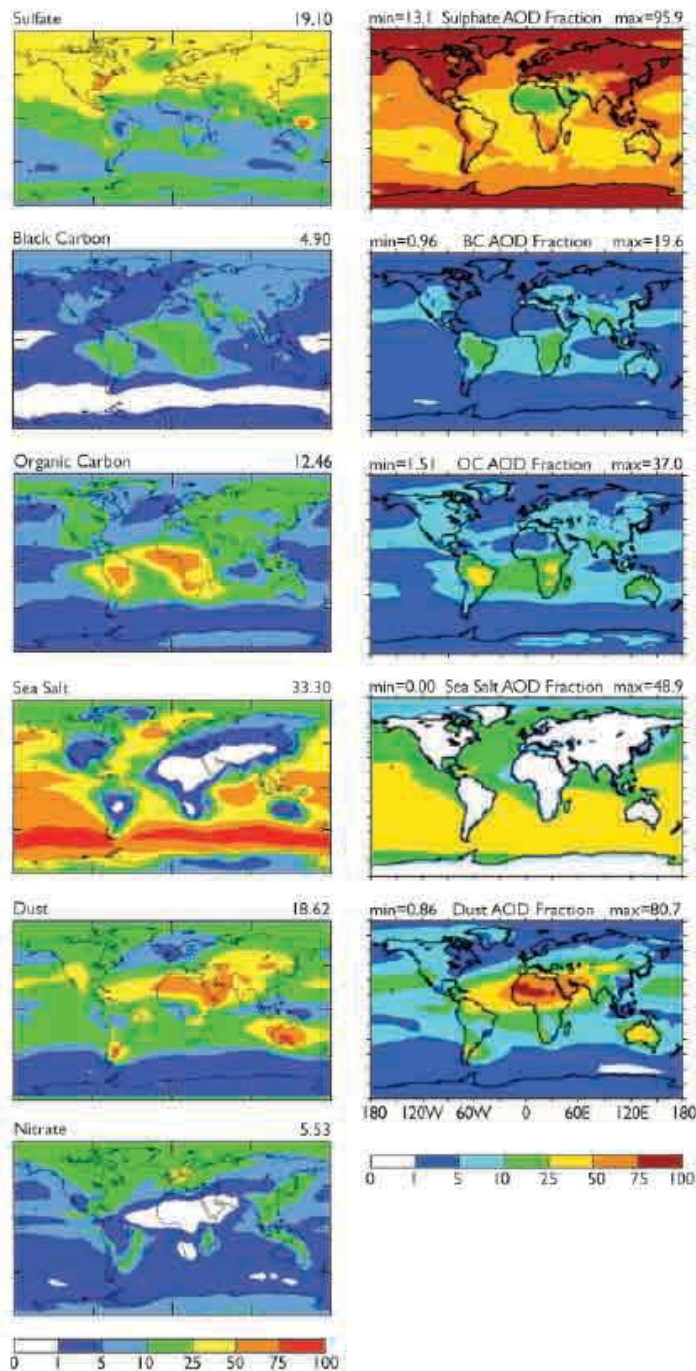


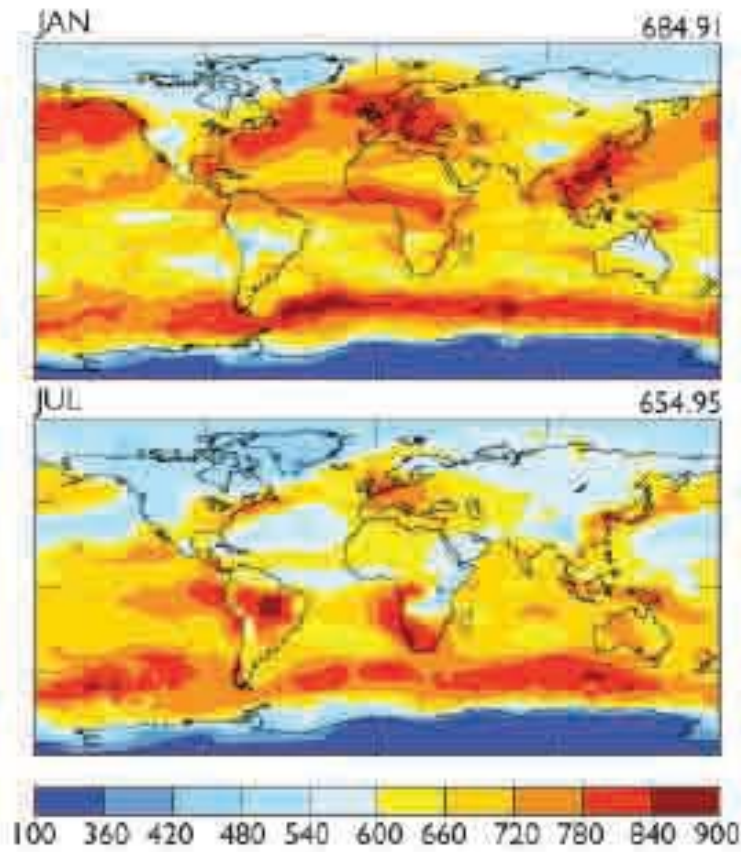
Figure 9-78. Percentage of aerosol optical depth in the GISS, left, based on Liu et al. (2006, [190422](#)), provided by A. Lacis, GISS, and GFDL, right, from Ginoux et al. (2006, [190582](#)). Models associated with the different components: SO_4^{2-} (1st row), BC (2nd row), OC (3rd row), sea-salt (4th row), dust (5th row), and nitrate (last row). Nitrate not available in GFDL model). Numbers on the GISS panels are global average, but on the GFDL panels are maximum and minimum.

Additional Considerations. *Long wave aerosol forcing:* So far only the aerosol RF in the shortwave (solar) spectrum has been discussed. Figure 9-77 (right column) shows that compared to the shortwave forcing, the values of anthropogenic aerosol long wave (thermal) forcing in the GISS model are on the order of 10%. Like the shortwave forcing, these values will also be affected by the particular aerosol characteristics used in the simulation.

Aerosol vertical distribution: Vertical distribution is particularly important for absorbing aerosols, such as BC and dust in calculating the RF, particularly when longwave forcing is considered (e.g., Figure 9-77) because the energy they reradiate depends on the temperature (and hence altitude), which affects the calculated forcing values. Several model inter-comparison studies have shown that the largest difference among model simulated aerosol distributions is the vertical profile (e.g., Lohmann et al., 2001, [190448](#); Penner et al., 2002, [190562](#); Textor et al., 2006, [190456](#)), due to the significant diversities in atmospheric processes in the models (e.g., Table 9-12). In addition, the vertical distribution also varies with space and time, as illustrated in Figure 9-79 from the GISS ER simulations for January and July showing the most probable altitude of aerosol vertical locations. In general, aerosols in the northern hemisphere are located at lower altitudes in January than in July, and vice versa for the southern hemisphere.

Mixing state: Most climate model simulations incorporating different aerosol types have been made using external mixtures, i.e., the evaluation of the aerosols and their radiative properties are calculated separately for each aerosol type (assuming no mixing between different components within individual particles). Observations indicate that aerosols commonly consist of internally mixed particles, and these “internal mixtures” can have very different radiative impacts. For example, the GISS-1 (internal mixture) and GISS-2 (external mixture) model results shows very different magnitude and sign of aerosol forcing from slightly positive (implying slight warming) to strong negative (implying significant cooling) TOA forcing (Figure 9-72), due to changes in both radiative properties of the mixtures, and in aerosol amount. The more sophisticated aerosol mixtures from detailed microphysics calculations now being used/developed by different modeling groups may well end up producing very different direct (and indirect) forcing values.

Cloudy sky vs. clear sky: The satellite or AERONET observations are all for clear sky only because aerosol cannot be measured in the remote sensing technique when clouds are present. However, almost all the model results are for all-sky because of difficulty in extracting cloud-free scenes from the GCMs. So the AOD comparisons discussed earlier are not completely consistent. Because AOD can be significantly amplified when relative humidity is high, such as near or inside clouds, all-sky AOD values are expected to be higher than clear sky AOD values. On the other hand, the aerosol RF at TOA is significantly lower for all-sky than for clear sky conditions; the IPCC AR4 and AeroCom RF study (Schulz et al., 2006, [190381](#)) have shown that on average the aerosol RF value for all-sky is about 1/3 of that for clear sky although with large diversity (63%). These aspects illustrate the complexity of the system and the difficulty of representing aerosol radiative influences in climate models whose cloud and aerosol distributions are somewhat problematic. And of course aerosols in cloudy regions can affect the clouds themselves, as discussed in Section 9.3.6.4.



Source: A. Lacis, GISS.

Figure 9-79. Most probable aerosol altitude (in pressure, hPa) from the GISS model in January (top) and July (bottom).

9.3.6.6. Impacts of Aerosols on Climate Model Simulations

Surface Temperature Change. It was noted in the introduction that aerosol cooling is essential in order for models to produce the observed global temperature rise over the last century, at least models with climate sensitivities in the range of 3°C for doubled CO_2 (or $\sim 0.75^{\circ}\text{C}/(\text{W}/\text{m}^2)$). The implications of this are discussed here in somewhat more detail. Hansen et al. (2007, [190597](#)) show that in the GISS model, well-mixed greenhouse gases produce a warming of close to 1°C between 1880 and the present (Table 9-17). The direct effect of tropospheric aerosols as calculated in that model produces cooling of close to -0.3°C between those same years, while the indirect effect (represented in that study as cloud cover change) produces an additional cooling of similar magnitude (note that the general model result quoted in IPCC AR4 is that the indirect RF is twice that of the direct effect).

Table 9-17. Climate forcings (1880-2003) used to drive GISS climate simulations, along with the surface air temperature changes obtained for several periods.

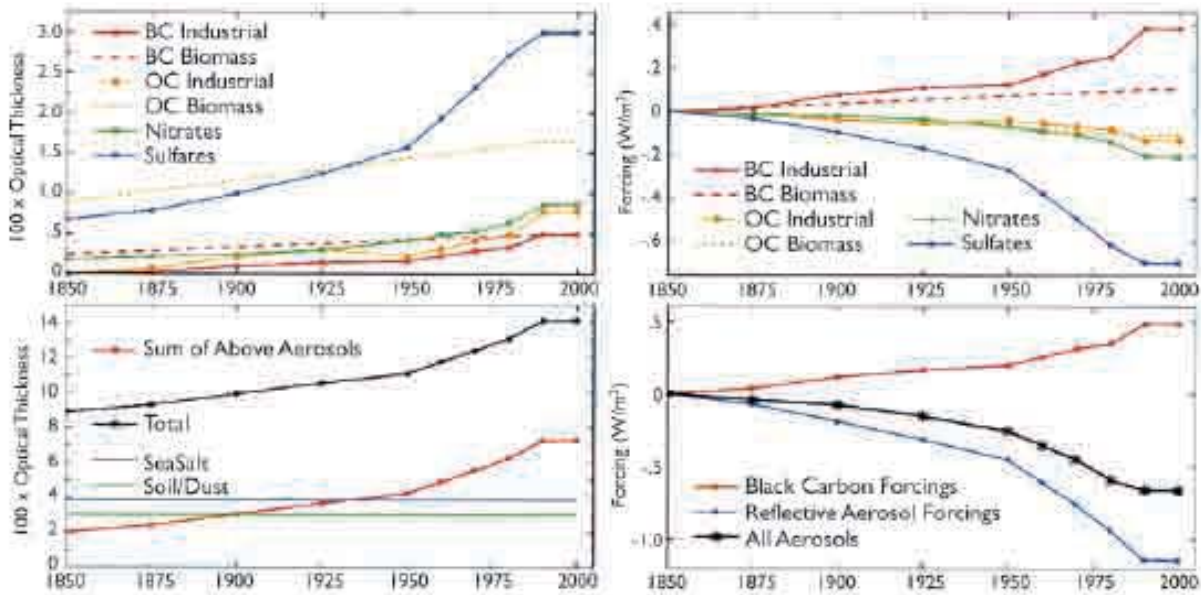
Forcing Agent	Forcing w M-2 (1880-2003)				ΔT Surface °C (yr to 2003)			
	Fi	Fa	Fs	Fe	1880	1900	1950	1979
Well-mixed GHGs	2.62	2.50	2.65	2.72	0.96	0.93	0.74	0.43
Stratospheric H ₂ O			0.06	0.05	0.03	0.01	0.05	0.00
O ₃	0.44	0.28	0.26	0.23	0.08	0.05	0.00	-0.01
Land use			-0.09	-0.09	-0.05	-0.07	-0.04	-0.02
Snow albedo	0.05	0.05	0.14	0.14	0.03	0.00	0.02	-0.01
Solar irradiance	0.23	0.24	0.23	0.22	0.07	0.07	0.01	0.02
Stratospheric aerosols	0.00	0.00	0.00	0.00	-0.08	-0.03	-0.06	0.04
Trop. aerosol direct forcing	-0.41	-0.38	-0.52	-0.60	-0.28	-0.23	-0.18	-0.10
Trop. aerosol indirect forcing			-0.87	-0.77	-0.27	-0.29	-0.14	-0.05
Sum of above			1.86	1.90	0.49	0.44	0.40	0.30
All forcings at once			1.77	1.75	0.53	0.61	0.44	0.29

Source: Hansen et al. (2007, [190597](#)). Instantaneous (Fi), adjusted (Fa), fixed SST (Fs) and effective (Fe) forcings are defined in Hansen et al. (2005, [059087](#)).

The time dependence of the total aerosol forcing used as well as the individual species components is shown in Figure 9-80. The resultant warming, $0.53 (\pm 0.04) ^\circ\text{C}$ including these and other forcings (Table 9-17), is less than the observed value of $0.6\text{-}0.7^\circ\text{C}$ from 1880-2003. Hansen et al. (2007, [190597](#)) further show that a reduction in sulfate optical thickness and the direct aerosol effect by 50%, which also reduced the aerosol indirect effect by 18%, produces a negative aerosol forcing from 1880-2003 of -0.91 W/m^2 (down from -1.37 W/m^2 with this revised forcing). The model now warms 0.75°C over that time. Hansen et al. (2007, [190597](#)) defend this change by noting that sulfate aerosol removal over North America and western Europe during the 1990s led to a cleaner atmosphere. Note that the comparisons shown in the previous section suggest that the GISS model already underestimates aerosol optical depths; it is thus trends that are the issue here.

The magnitude of the indirect effect used by Hansen et al. (2005, [190596](#)) is roughly calibrated to reproduce the observed change in diurnal temperature cycle and is consistent with some satellite observations. However, as Anderson et al. (2003, [054820](#)) note, the forward calculation of aerosol negative forcing covers a much larger range than is normally used in GCMs; the values chosen, as in this case, are consistent with the inverse reasoning estimates of what is needed to produce the observed warming, and hence generally consistent with current model climate sensitivities. The authors justify this approach by claiming that paleoclimate data indicate a climate sensitivity of close to $0.75 (\pm 0.25) ^\circ\text{C}/(\text{W/m}^2)$, and therefore something close to this magnitude of negative forcing is reasonable. Even this stated range leaves significant uncertainty in climate sensitivity and the magnitude of the aerosol negative forcing. Furthermore, IPCC (2007, [189430](#)) concluded that paleoclimate data are not capable of narrowing the range of climate sensitivity, nominally $0.375\text{-}1.13 ^\circ\text{C}/(\text{W/m}^2)$, because of uncertainties in paleoclimate forcing and response; so from this perspective the total aerosol forcing is even less constrained than the GISS estimate. Hansen et al. (2007, [190597](#)) acknowledge that “an equally good match to observations probably could be obtained from a model with larger

sensitivity and smaller net forcing, or a model with smaller sensitivity and larger forcing”.



Source: Hansen et al. (2007, [190597](#)).

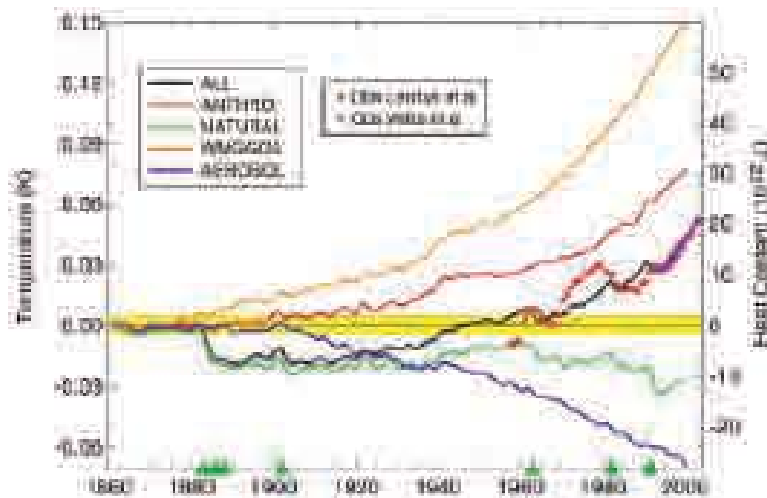
Figure 9-80. Time dependence of aerosol optical thickness (left) and climate forcing (right). Note that as specified, the aerosol trends are all “flat” from 1990-2000.

The GFDL model results for global mean ocean temperature change (down to 3 km depth) for the time period 1860-2000 is shown in Figure 9-81, along with the different contributing factors (Delworth et al., 2005, [190055](#)). This is the same GFDL model whose aerosol distribution was discussed previously. The aerosol forcing produces a cooling on the order of 50% that of greenhouse warming (generally similar to that calculated by the GISS model, Table 9-17). Note that this was achieved without any aerosol indirect effect.

The general model response noted by IPCC, as discussed in the introduction, was that the total aerosol forcing of -1.3 W/m^2 reduced the greenhouse forcing of near 3 W/m^2 by about 45%, in the neighborhood of the GFDL and GISS forcings. Since the average model sensitivity was close to $0.75 \text{ }^\circ\text{C}/(\text{W/m}^2)$, similar to the sensitivities of these models, the necessary negative forcing is therefore similar. The agreement cannot therefore be used to validate the actual aerosol effect until climate sensitivity itself is better known.

Is there some way to distinguish between greenhouse gas and aerosol forcing that would allow the observational record to indicate how much of each was really occurring? This question of attribution has been the subject of numerous papers, and the full scope of the discussion is beyond the range of this (CCSP SAP2.3) report. It might be briefly noted that Zhang et al. (2006, [157722](#)) using results from several climate models and including both spatial and temporal patterns, found that the climate responses to greenhouse gases and sulfate aerosols are correlated, and separation is possible only occasionally, especially at global scales. This conclusion appears to be both model and method-dependent: using time-space distinctions as opposed to trend detection may work differently in different models (Gillett et al.,

2002, [190576](#)). Using multiple models helps primarily by providing larger-ensemble sizes for statistics (Gillett et al., 2002, [190578](#)). However, even separating between the effects of different aerosol types is difficult. Jones et al. (2005, [155885](#)) concluded that currently the pattern of temperature change due to black carbon is indistinguishable from the sulfate aerosol pattern. In contrast, Hansen et al. (2005, [059087](#)) found that absorbing aerosols produce a different global response than other forcings, and so may be distinguishable. Overall, the similarity in response to all these very different forcings is undoubtedly due to the importance of climate feedbacks in amplifying the forcing, whatever its nature.



Source: Delworth et al. (2005, [190055](#)).

Figure 9-81. Change in global mean ocean temperature (left axis) and ocean heat content (right axis) for the top 3000 m due to different forcings in the GFDL model. WMGG includes all greenhouse gases and ozone; NATURAL includes solar and volcanic aerosols (events shown as green triangles on the bottom axis). Observed ocean heat content changes are shown as well.

Distinctions in the climate response do appear to arise in the vertical, where absorbing aerosols produce warming that is exhibited throughout the troposphere and into the stratosphere, whereas reflective aerosols cool the troposphere but warm the stratosphere (Hansen et al., 2005, [059087](#); IPCC (Intergovernmental Panel on Climate, 2007, [190988](#)). Delworth et al. (2005, [190055](#)) noted that in the ocean, the cooling effect of aerosols extended to greater depths, due to the thermal instability associated with cooling the ocean surface. Hence the temperature response at levels both above and below the surface may provide an additional constraint on the magnitudes of each of these forcings, as may the difference between Northern and Southern Hemisphere changes (IPCC et al., 2007, [189430](#), Chapter 9). The profile of atmospheric temperature response will be useful to the extent that the vertical profile of aerosol absorption, an important parameter to measure, is known.

Implications for Climate Model Simulations. The comparisons in Sections 9.3.6.2 and 9.3.6.3 suggest that there are large differences in model calculated aerosol distributions, mainly because of the large uncertainties in modeling the aerosol atmospheric processes in addition to the uncertainties in emissions. The fact that the total optical depth is in better agreement between models than the individual components means that even with similar optical depths, the aerosol direct forcing effect can be quite different, as shown in the AeroCom studies. Because the diversity

among models and discrepancy between models and observations are much larger at the regional level than in global average, the assessment of climate response (e.g., surface temperature change) to aerosol forcing would be more accurate for global average than for regional or hemispheric differentiation. However, since aerosol forcing is much more pronounced on regional than on global scales because of the highly variable aerosol distributions, it is insufficient or even misleading to just get the global average right. The indirect effect is strongly influenced by the aerosol concentrations, size, type, mixing state, microphysical processes, and vertical profile. As shown in previous sections, very large differences exist in those quantities even among the models having similar AOD. Moreover, modeling aerosol indirect forcing presents more challenges than direct forcing because there is so far no rigorous observational data, especially on a global scale, that one can use to test the model simulations. As seen in the comparisons of the GISS and GFDL model climate simulations for IPCC AR4, aerosol indirect forcing was so poorly constrained that it was completely ignored by one model (GFDL) but used by another (GISS) at a magnitude that is more than half of the direct forcing, in order to reproduce the observed surface temperature trends. A majority of the climate models used in IPCC AR4 do not consider indirect effects; the ones that did were mostly limited to highly simplified sulfate indirect effects (Table 9-16). Improvements must be made to at least the degree that the aerosol indirect forcing can no longer be used to mask the deficiencies in estimating the climate response to greenhouse gas and aerosol direct RF.

9.3.6.7. Outstanding Issues

Clearly there are still large gaps in assessing the aerosol impacts on climate through modeling. Major outstanding issues and prospects of improving model simulations are discussed below.

Aerosol composition. Many global models are now able to simulate major aerosol types such as sulfate, black carbon, and POM, dust, and sea salt, but only a small fraction of these models simulate nitrate aerosols or consider anthropogenic secondary organic aerosols. And it is difficult to quantify the dust emission from human activities. As a result, the IPCC AR4 estimation of the nitrate and anthropogenic dust TOA forcing was left with very large uncertainty. The next generation of global models should therefore have a more comprehensive suite of aerosol compositions with better-constrained anthropogenic sources.

Aerosol absorption. One of the most critical parameters in aerosol direct RF and aerosol impact on hydrological cycles is the aerosol absorption. Most of the absorption is from BC despite its small contribution to total aerosol short and long-wave spectral ranges, whereas POM absorbs in the near UV. The aerosol absorption or SSA, will have to be much better represented in the models through improving the estimates of carbonaceous and dust aerosol sources, their atmospheric distributions, and optical properties.

Aerosol indirect effects. The activation of aerosol particles into CCN depends not only on particle size but chemical composition, with the relative importance of size and composition unclear. In current aerosol-climate modeling, aerosol size distribution is generally prescribed and simulations of aerosol composition have large uncertainties. Therefore the model estimated “albedo effect” has large uncertainties. How aerosol would influence cloud lifetime/ cover is still in debate. The influence of aerosols on other aspects of the climate system, such as precipitation, is even more uncertain, as are the physical processes involved. Processes that determine aerosol size distributions, hygroscopic growth, mixing state, as well as CCN concentrations, however, are inadequately represented in most of the global models. It will also be difficult to improve the estimate of indirect effects until the models can produce more realistic cloud characteristics.

Aerosol impacts on surface radiation and atmospheric heating.

Although these effects are well acknowledged to play roles in modulating atmospheric circulation and water cycle, few coherent or comprehensive modeling studies have focused on them, as compared to the efforts that have gone to assessing aerosol RF at TOA. They have not yet been addressed in the previous IPCC reports. Here, of particular importance is to improve the accuracy of aerosol absorption.

Long-term trends of aerosol. To assess the aerosol effects on climate change the long-term variations of aerosol amount and composition and how they are related to the emission trends in different regions have to be specified. Simulations of historical aerosol trends can be problematic since historical emissions of aerosols have shown large uncertainties—as information is difficult to obtain on past source types, strengths, and even locations. The IPCC AR4 simulations used several alternative aerosol emission histories, especially for BC and POM aerosols.

Climate modeling. Current aerosol simulation capabilities from CTMs have not been fully implemented in most models used in IPCC AR4 climate simulations. Instead, a majority employed simplified approaches to account for aerosol effects, to the extent that aerosol representations in the GCMs, and the resulting forcing estimates, are inadequate. The oversimplification occurs in part because the modeling complexity and computing resource would be significantly increased if the full suite of aerosols were fully coupled in the climate models.

Observational constraints. Model improvement has been hindered by a lack of comprehensive datasets that could provide multiple constraints for the key parameters simulated in the model. The extensive AOD coverage from satellite observations and AERONET measurements has helped a great deal in validating model-simulated AOD over the past decade, but further progress has been slow. Large model diversities in aerosol composition, size, vertical distribution, and mixing state are difficult to constrain, because of lack of reliable measurements with adequate spatial and temporal coverage (see Chapter 2 of the CCSP SAP2.3).

Aerosol radiative forcing. Because of the large spatial and temporal differences in aerosol sources, types, emission trends, compositions, and atmospheric concentrations, anthropogenic aerosol RF has profound regional and seasonal variations. So it is an insufficient measure of aerosol RF scientific understanding, however useful, for models (or observation-derived products) to converge only on globally and annually averaged TOA RF values and accuracy. More emphasis should be placed on regional and seasonal comparisons, and on climate effects in addition to direct RF at TOA.

9.3.6.8. Conclusions

From forward modeling studies, as discussed in the IPCC (2007, [190988](#)), the direct effect of aerosols since pre-industrial times has resulted in a negative RF of about -0.5 ± 0.4 W/m². The RF due to cloud albedo or brightness effect is estimated to be -0.7 (-1.8 to -0.3) W/m². Forcing of similar magnitude has been used in some modeling studies for the effect associated with cloud lifetime, in lieu of the cloud brightness influence. The total negative RF due to aerosols according to IPCC (2007, [190988](#)) estimates is therefore -1.3 (-2.2 to -0.5) W/m². With the inverse approach, in which aerosols provide forcing necessary to produce the observed temperature change, values range from -1.7 to -0.4 W/m² (Intergovernmental Panel on Climate, 2007, [190988](#)). These results represent a substantial advance over previous assessments (e.g., IPCC TAR), as the forward model estimated and inverse approach required aerosol TOA forcing values are converging. However, large uncertainty ranges preclude using the forcing and temperature records to more accurately determine climate sensitivity.

There are now a few dozen models that simulate a comprehensive suite of aerosols. This is done primarily in the CTMs. Model inter-comparison studies have

shown that models have merged at matching the global annual averaged AOD observed by satellite instruments, but they differ greatly in the relative amount of individual components, in vertical distributions, and in optical properties. Because of the great spatial and temporal variations of aerosol distributions, regional and seasonal diversities are much larger than that of the global annual mean. Different emissions and differences in atmospheric processes, such as transport, removal, chemistry, and aerosol microphysics, are chiefly responsible for the spread among the models. The varying component contributions then lead to differences in aerosol direct RF, as aerosol scattering and absorption properties depend on aerosol size and type. They also impact the calculated indirect RF, whose variations are further amplified by the wide range of cloud and convective parameterizations in models. Currently, the largest aerosol RF uncertainties are associated with the aerosol indirect effect. Most climate models used for the IPCC AR4 simulations employed simplified approaches, with aerosols specified from stand-alone CTM simulations. Despite the uncertainties in aerosol RF and widely varying model climate sensitivity, the IPCC AR4 models were generally able to reproduce the observed temperature record for the past century. This is because models with lower/higher climate sensitivity generally used less/more negative aerosol forcing to offset the greenhouse gas warming. An equally good match to observed surface temperature change in the past could be obtained from a model with larger climate sensitivity and smaller net forcing, or a model with smaller sensitivity and larger forcing (Hansen et al., 2007, [190597](#)). Obviously, both greenhouse gases and aerosol effects have to be much better quantified in future assessments.

Progress in better quantifying aerosol impacts on climate will only be made when the capabilities of both aerosol observations and representation of aerosol processes in models are improved. The primary concerns and issues discussed in this chapter of the CCSP SAP2.3 include:

- Better representation of aerosol composition and absorption in the global models
- Improved theoretical understanding of subgrid-scale processes crucial to aerosol-cloud interactions and lifetime
- Improved aerosol microphysics and cloud parameterizations
- Better understanding of aerosol effects on surface radiation and hydrological cycles
- More focused analysis on regional and seasonal variations of aerosols
- More reliable simulations of aerosol historic long-term trends
- More sophisticated climate model simulations with coupled aerosol and cloud processes
- Enhanced satellite observations of aerosol type, SSA, vertical distributions, and aerosol radiative effect at TOA; more coordinated field experiments to provide constraints on aerosol chemical, physical, and optical properties. Progress in better quantifying aerosol impacts on climate will only be made when the capabilities of both aerosol observations and representation of aerosol processes in models are improved.

9.3.7. Fire as a Special Source of PM Welfare Effects

Much interest has developed in defining more precisely the role of pyrogenic C in the boreal C cycle. This is due to: (1) the resistance of pyrogenic C to decomposition; (2) its influence on soil processes; and (3) the absorption of solar radiation by soot aerosols (Preston and Schmidt, 2006, [156030](#)).

Preston and Schmidt (2006, [156030](#)) reviewed the current state of knowledge regarding atmospheric emissions of pyrogenic C in the boreal zone. They considered chemical structures, analytical methods, formation, characteristics in soil, loss mechanisms, and longevity. Biomass is largely converted to gaseous forms during burning,

but up to several percent is converted to pyrogenic C, and this includes charcoal and BC. Charcoal is defined visually; BC is defined chemically by its resistance to oxidation in the laboratory.

Andreae and Gelencsér (2006, [156215](#)) reviewed a different category of light-absorbing carbon, referred to as brown carbon. Operational methods used to measure all light-absorbing carbon are estimated to have a factor of 2 at present.

Within the boreal zone, fire is a critical driver of ecosystem process and nutrient cycling (Hicke et al., 2003, [156545](#)). For example, Bachelet et al. (2005, [156241](#)) estimated that 61% of the C gained in Alaska by primary production of boreal forests between 1922 and 1996 was lost to fire.

An updated modeling effort to evaluate the radiative effects of aerosols was presented by Stier et al. (2007, [157012](#)). Inclusion of refractive indices recommended by (2005, [155696](#)) significantly increased aerosol RF and resulted in better agreement with sun-photometer estimates. Although this stage of climate modeling improved the representation of aerosols, large uncertainties remain regarding the effects of aerosol mixing and aerosol-cloud interactions. Furthermore, Stier et al. (2007, [157012](#)) emphasized that these types of modeling efforts are dependent upon emission estimates that are likely to vary by a factor of 2 or more.

One important reason for the acknowledged uncertainty in estimating global emissions of carbonaceous aerosols is the influence of intermittent fires that can occur at scales large enough to affect hemispheric aerosol concentrations. To better quantify the effects of large-scale fire, Generoso et al. (2007, [155786](#)) used satellite observations of boreal fires in Russia in 2003 to evaluate the performance of a global chemistry and transport model in simulating aerosol optical thickness, transport, and deposition. Emissions estimates of BC and OC were adjusted in the model to better match satellite observations of pollutant transport over the North Pacific. This resulted in an increase in optical thickness and BC deposition by a factor of 2. The adjusted model estimated that the fires contributed 16-33% of the optical thickness and 40-56% of BC deposition north of 75° N in the spring and summer of 2003.

Large fires also occurred over the Iberian Peninsula and Mediterranean coast during 2003. A meso-scale atmospheric transport model was used with ground-based measurements and satellite optical measurements to characterize the dispersion of emitted smoke particles and quantify radiative effects across Europe (Hodzic et al., 2007, [156553](#)).

The modeled wildfire emissions resulted in increases in PM_{2.5} concentrations from 20 to 200%. The increased aerosol concentration was estimated to increase radiative forcing by 10-35 W/m² during the period of strong fire influence. Absorption of radiation by BC was also estimated to decrease rates of photolysis by 30%. In this simulation, all particles were assumed to be internally mixed, and secondary aerosol formation was not considered. Meteorological conditions in Europe during the exceptionally hot summer of 2003 were linked to enhanced photochemically derived pollutants, increased wild fires, and elevated aerosol concentrations in an analysis by (Vautard et al., 2007, [106012](#)).

In addition to incidental fires, routine biomass burning, usually associated with agriculture in eastern Europe, also has been shown to contribute to hemispheric concentrations of carbonaceous aerosols. In the spring of 2006, the most severe air pollution levels in the Arctic to date were recorded (Stohl et al., 2006, [156100](#)). Atmospheric transport modeling coupled with satellite fire detection data identified biomass burning for agriculture as the primary cause of the high pollution levels. Concentrations of PM_{2.5} peaked during the pollution episode at values of an order of magnitude greater than those recorded prior to the episode. The increased transport of pollution into the Arctic during 2006 was attributed to weather conditions that delayed preparations for crop planting into May. Weather patterns favorable for pollutant transport into the Arctic were related to unusually warm weather in late April and May, when the majority of agricultural biomass burning took place that year.

In the summer of 2004, 2.7 million ha were burned by wildfire in Alaska and 3.1 million ha were burned in Canada. Effects on atmospheric air quality were measured throughout the Arctic, although the concentrations of particulates varied considerably. Aerosol optical depths were also increased at all measurement stations, which indicated that the fires were likely to have had a significant effect on the atmospheric radiation budget for the Arctic (Stohl et al., 2006, [156100](#)). At one site, a pronounced drop in albedo was observed due presumably to high deposition of light absorbing particulates on the snow surface by the North American fires in 2004.

Investigations of the effects of large fires on climate forcing have typically focused on the absorptive effects of BC. However, these fires also release large amounts of CO₂ and CH₄, as well as light scattering compounds such as OC, and can enhance cloud formation. These fires also increase radiative surface absorption through BC deposition on snow and ice, and alter surface albedo and ecosystem energy budgets within the burn perimeter.

Randerson et al. (2006, [156038](#)) estimated the net climate forcing of greenhouse gases, aerosols, BC deposition on snow and ice and changes in albedo for the year subsequent to a fire and for 80 yr in the future in interior Alaska. The net effect of the fire in the first year was an increase in radiative forcing, but over the 80-yr recovery period, average net annual radiative forcing was decreased by the fire.

9.3.8. Radiative Effects of Volcanic Aerosols

Section 9.3.8.1. comes directly from IPCC AR4 Chapter 2, Section 2.7.2, with section, table, and figure numbers changed to be internally consistent with this ISA.

9.3.8.1. Explosive Volcanic Activity

Radiative Effects of Volcanic Aerosols. Volcanic sulfate aerosols are formed as a result of oxidation of the sulfur gases emitted by explosive volcanic eruptions into the stratosphere. The process of gas-to-particle conversion has an e-folding time of roughly 35 days (Bluth et al., 1992, [192029](#); Read et al., 1993, [192031](#)). The e-folding time (by mass) for sedimentation of sulfate aerosols is typically about 12 to 14 months (Baran and Foot, 1994, [192032](#); Barnes and Hofmann, 1997, [192044](#); Bluth et al., 1997, [192045](#); Lambert et al., 1993, [192231](#)). Also emitted directly during an eruption are volcanic ash particulates (siliceous material). These are particles usually larger than 2 μm that sediment out of the stratosphere fairly rapidly due to gravity (within three months or so), but could also play a role in the radiative perturbations in the immediate aftermath of an eruption. Stratospheric aerosol data incorporated for climate change simulations tends to be mostly that of the sulfates (Ammann et al., 2003, [192057](#); Hansen et al., 2002, [049177](#); Ramachandran et al., 2000, [192050](#); Sato et al., 1993, [192046](#); Stenchikov et al., 1998, [192049](#); Tett et al., 2002, [192053](#)). As noted in the Second Assessment Report (SAR) and the TAR, explosive volcanic events are episodic, but the stratospheric aerosols resulting from them yield substantial transitory perturbations to the radiative energy balance of the planet, with both shortwave and longwave effects sensitive to the microphysical characteristics of the aerosols (e.g., size distribution).

Long-term ground-based and balloon-borne instrumental observations have resulted in an understanding of the optical effects and microphysical evolution of volcanic aerosols (Deshler et al., 2003, [192058](#); Hofmann et al., 2003, [192062](#)). Important groundbased observations of aerosol characteristics from pre-satellite era spectral extinction measurements have been analysed by Stothers (2001, [192233](#); 2001, [192232](#)), but they do not provide global coverage. Global observations of stratospheric aerosol over the last 25 years have been possible owing to a number of satellite platforms, for example, TOMS and TOVS have been used to estimate SO_2 loadings from volcanic eruptions (Krueger et al., 2000, [192234](#); Prata et al., 2003, [192235](#)). The Stratospheric Aerosol and Gas Experiment (SAGE) and Stratospheric Aerosol Measurement (SAM) projects (e.g., McCormick and Trepte, 1987, [192328](#)) have provided vertically resolved stratospheric aerosol spectral extinction data for over 20 years, the longest such record. This data set has significant gaps in coverage at the time of the El Chichón eruption in 1982 (the second most important in the 20th century after Mt. Pinatubo in 1991) and when the aerosol cloud is dense; these gaps have been partially filled by lidar measurements and field campaigns (e.g., Antuña et al., 2003, [192251](#); Thomason and Peter, 2006, [192248](#)).

Volcanic aerosols transported in the atmosphere to polar regions are preserved in the ice sheets, thus recording the history of the Earth's volcanism for thousands of years (Kruysse, 1971, [192236](#); Mosley-Thompson et al., 2003, [192255](#); Palmer et al., 2002, [192319](#)). However, the atmospheric loadings obtained from ice records suffer from uncertainties due to imprecise knowledge of the latitudinal distribution of the aerosols, depositional noise that can affect the signal for an individual eruption in a single ice core, and poor constraints on aerosol microphysical properties. The best-documented explosive volcanic event to date, by way of reliable and accurate observations, is the 1991 eruption of Mt. Pinatubo. The growth and decay of aerosols resulting from this eruption have provided a basis for modeling the RF due to explosive volcanoes. There have been no explosive and climatically significant volcanic events since Mt. Pinatubo. As pointed out in Ramaswamy et al. (2001, [156899](#)), stratospheric aerosol concentrations are now at the lowest concentrations since the satellite era and global coverage began in about 1980. Altitude dependent stratospheric optical observations at a few wavelengths, together with columnar optical and physical measurements, have been used to construct the time-dependent global field of stratospheric aerosol size distribution formed in the aftermath of volcanic events. The wavelength-dependent stratospheric aerosol single-scattering characteristics calculated for the solar and longwave spectrum are deployed in climate models to account for the resulting radiative (shortwave plus longwave) perturbations.

Using available satellite- and ground-based observations, Hansen et al. (2002, [049177](#)) constructed a volcanic aerosols data set for the 1850-1999 period (Sato et al., 1993, [192046](#)). This has yielded zonal mean vertically resolved aerosol optical depths for visible wavelengths and column average effective radii. Stenchikov et al. (2006, [192260](#)) introduced a slight variation to this data set, employing UARS observations to modify the effective radii relative to Hansen et al. (2002, [049177](#)), thus accounting for variations with altitude. Ammann et al. (2003, [192057](#)) developed a data set of total aerosol optical depth for the period since 1890 that does not include the Krakatau eruption. The data set is based on empirical estimates of atmospheric loadings, which are then globally distributed using a simplified parameterization of atmospheric transport, and employs a fixed aerosol effective radius (0.42 μm) for calculating optical properties. The above data sets have essentially provided the bases for the volcanic aerosols implemented in virtually all of the models that have performed the 20th-century climate integrations (Stenchikov et al., 2006, [192260](#)). Relative to Sato et al. (1993, [192046](#)), the Ammann et al. (2003, [192057](#)) estimate yields a larger value of the optical depth, by 20 to 30% in the second part of the 20th century, and by 50% for eruptions at the end of 19th and beginning of 20th century, for example, the 1902 Santa Maria eruption (Figure 9-82).

The global mean RF calculated using the Sato et al. (1993, [192046](#)) data yields a peak in radiative perturbation of about -3 W/m^2 for the strong (rated in terms of emitted SO_2) 1860 and 1991 eruptions of Krakatau and Mt. Pinatubo, respectively. The value is reduced to about -2 W/m^2 for the relatively less intense El Chichón and Agung eruptions (Hansen et al., 2002, [049177](#)). As expected from the arguments above, Ammann's RF is roughly 20 to 30% larger than Sato's RF.

Not all features of the aerosols are well quantified, and extending and improving the data sets remains an important area of research. This includes improved estimates of the aerosol size parameters (Bingen et al., 2004, [192262](#)), a new approach for calculating aerosol optical characteristics using SAGE and UARS data (Bauman et al., 2003, [192265](#)), and intercomparison of data from different satellites and combining them to fill gaps (Randall et al., 2001, [192268](#)). While the aerosol characteristics are better constrained for the Mt. Pinatubo eruption, and to some extent for the El Chichón and Agung eruptions, the reliability degrades for aerosols from explosive volcanic events further back in time as there are few, if any, observational constraints on their optical depth and size evolution.

The radiative effects due to volcanic aerosols from major eruptions are manifest in the global mean anomaly of reflected solar radiation; this variable affords a good

estimate of radiative effects that can actually be tested against observations. However, unlike RF, this variable contains effects due to feedbacks (e.g., changes in cloud distributions) so that it is actually more a signature of the climate response. In the case of the Mt. Pinatubo eruption, with a peak global visible optical depth of about 0.15, simulations yield a large negative perturbation as noted above of about -3 W/m^2 (Hansen et al., 2002, [049177](#); Ramachandran et al., 2000, [192050](#)) (see also Section 9.2 of the IPCC AR4). This modeled estimate of reflected solar radiation compares reasonably with ERBS observations (Minnis et al., 1993, [190539](#)). However, the ERBS observations were for a relatively short duration, and the model-observation comparisons are likely affected by differing cloud effects in simulations and measurements. It is interesting to note (Stenchikov et al., 2006, [192260](#)) that, in the Mt. Pinatubo case, the Goddard Institute for Space Studies (GISS) models that use the Sato et al. (1993, [192046](#)) data yield an even greater solar reflection than the National Center for Atmospheric Research (NCAR) model that uses the larger (Ammann et al., 2003, [192057](#)) optical depth estimate.

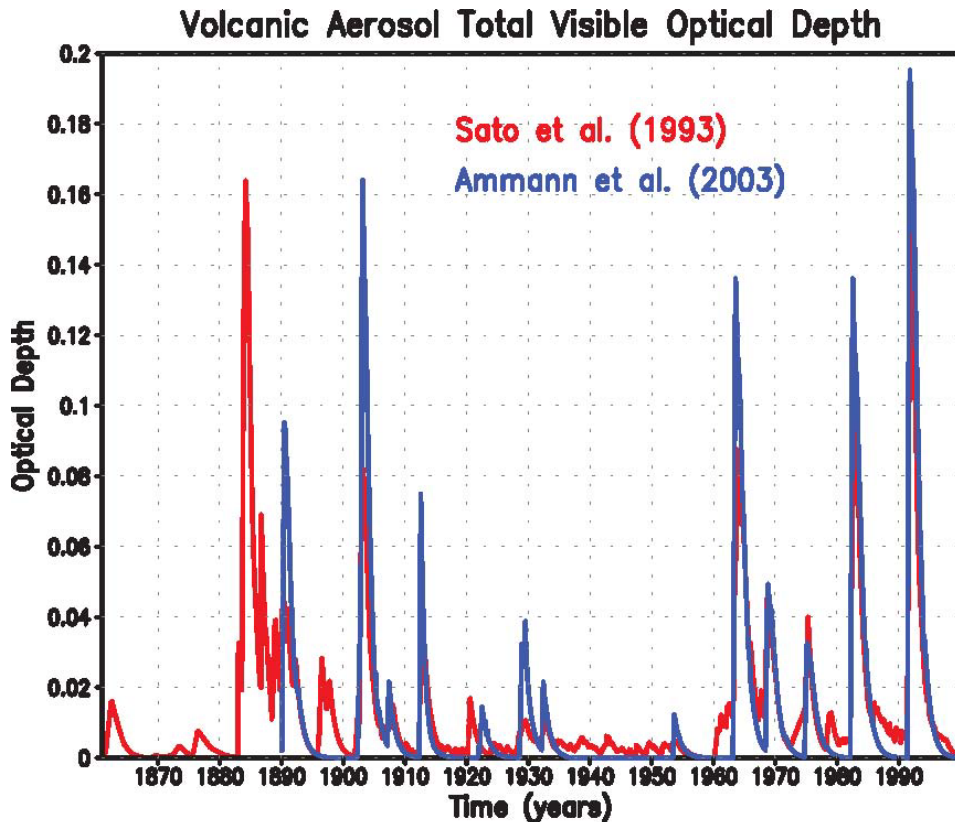


Figure 9-82. Visible (wavelength $0.55 \mu\text{m}$) optical depth estimates of stratospheric SO_4^{2-} aerosols formed in the aftermath of explosive volcanic eruptions that occurred between 1860 and 2000. Results are shown from two different data sets that have been used in recent climate model integrations. Note that the Ammann et al. (2003, [192057](#)) data begins in 1890.

Thermal, Dynamical and Chemistry Perturbations Forced by Volcanic Aerosols. Four distinct mechanisms have been invoked with regards to the climate response to volcanic aerosol RF. First, these forcings can directly affect the Earth's radiative balance and thus alter surface temperature. Second, they introduce horizontal and vertical heating gradients; these can alter the stratospheric circulation, in turn affecting the troposphere. Third, the forcings can interact with internal climate system variability (e.g., El Niño-Southern Oscillation, North Atlantic Oscillation, Quasi-Biennial Oscillation) and dynamical noise, thereby triggering, amplifying or shifting these modes (see Section 9.2 of the IPCC AR4) (Yang and Schlesinger, 2001, [192270](#); Stenchikov et al., 2004, [192274](#)). Fourth, volcanic aerosols provide surfaces for heterogeneous chemistry affecting global stratospheric ozone distributions (Chipperfield et al., 2003, [192275](#)) and perturbing other trace gases for a considerable period following an eruption. Each of the above mechanisms has its own spatial and temporal response pattern. In addition, the mechanisms could depend on the background state of the climate system, and thus on other forcings (e.g., due to well-mixed gases) (Meehl et al., 2004, [192279](#)), or interact with each other.

The complexity of radiative-dynamical response forced by volcanic impacts suggests that it is important to calculate aerosol radiative effects interactively within the model rather than prescribe them (Andronova et al., 1999, [192286](#); Broccoli et al., 2003, [192283](#)). Despite differences in volcanic aerosol parameters employed, models computing the aerosol radiative effects interactively yield tropical and global mean lower-stratospheric warmings that are fairly consistent with each other and with observations (Ramachandran et al., 2000, [192050](#); Hansen et al., 2002, [049177](#); Yang and Schlesinger, 2001, [192270](#); Stenchikov et al., 2004, [192274](#); Ramaswamy et al., 2006, [192284](#)); however, there is a considerable range in the responses in the polar stratosphere and troposphere. The global mean warming of the lower stratosphere is due mainly to aerosol effects in the longwave spectrum, in contrast to the flux changes at the TOA that are essentially due to aerosol effects in the solar spectrum. The net radiative effects of volcanic aerosols on the thermal and hydrologic balance (e.g., surface temperature and moisture) have been highlighted by recent studies (Free and Angell, 2002, [192281](#); Jones et al., 2003, [192278](#)) (see Chapter 6 of the IPCC AR4). See Chapter 9 (of the IPCC AR4) for significance of the simulated responses and model-observation comparisons for 20th-century eruptions. A mechanism closely linked to the optical depth perturbation and ensuing warming of the tropical lower stratosphere is the potential change in the cross-tropopause water vapour flux (Joshi and Shine, 2003, [192327](#)) (see Section 2.3.7 of the IPCC AR4).

Anomalies in the volcanic-aerosol induced global radiative heating distribution can force significant changes in atmospheric circulation, for example, perturbing the equator-to-pole heating gradient (Ramaswamy et al., 2006, [192273](#); Stenchikov et al., 2002, [192277](#)) (see Section 9.2 of the IPCC AR4) and forcing a positive phase of the Arctic Oscillation that in turn causes a counterintuitive boreal winter warming at middle and high latitudes over Eurasia and North America (Miller et al., 2005, [192258](#); Perlwitz and Graf, 2001, [192271](#); Perlwitz and Harnik, 2003, [192264](#); Rind et al., 2005, [192261](#); Shindell et al., 2003, [192069](#); Shindell et al., 2004, [192267](#); Stenchikov et al., 2002, [192277](#); Stenchikov et al., 2004, [192274](#); Stenchikov et al., 2006, [192260](#)).

Stratospheric aerosols affect the chemistry and transport processes in the stratosphere, resulting in the depletion of ozone (Brasseur and Granier, 1992, [192256](#); Chipperfield et al., 2003, [192275](#); Solomon et al., 1996, [192252](#); Tie et al., 1994, [192253](#)). Stenchikov et al. (2002, [192277](#)) demonstrated a link between ozone depletion and Arctic Oscillation response; this is essentially a secondary radiative mechanism induced by volcanic aerosols through stratospheric chemistry. Stratospheric cooling in the polar region associated with a stronger polar vortex initiated by volcanic effects can increase the probability of formation of polar stratospheric clouds and therefore enhance the rate of heterogeneous chemical destruction of stratospheric ozone, especially in the NH (Tabazadeh et al., 2002,

[192250](#)). The above studies indicate effects on the stratospheric ozone layer in the wake of a volcanic eruption and under conditions of enhanced anthropogenic halogen loading. Interactive microphysics-chemistry-climate models (Dameris et al., 2005, [192238](#); Rozanov et al., 2002, [192247](#); Rozanov et al., 2004, [192245](#); Shindell et al., 2003, [192069](#); Timmreck et al., 2003, [192254](#)) indicate that aerosol-induced stratospheric heating affects the dispersion of the volcanic aerosol cloud, thus affecting the spatial RF. However the models' simplified treatment of aerosol microphysics introduces biases; further, they usually overestimate the mixing at the tropopause level and intensity of meridional transport in the stratosphere (Douglass et al., 2003, [057260](#); Schoeberl et al., 2003, [057262](#)). For present climate studies, it is practical to utilize simpler approaches that are reliably constrained by aerosol observations.

Because of its episodic and transitory nature, it is difficult to give a best estimate for the volcanic RF, unlike the other agents. Neither a best estimate nor a level of scientific understanding was given in the TAR. For the well-documented case of the explosive 1991 Mt. Pinatubo eruption, there is a good scientific understanding. However, the limited knowledge of the RF associated with prior episodic, explosive events indicates a low level of scientific understanding.

9.3.9. Other Special Sources and Effects

International shipping has been identified as an additional source of carbonaceous aerosols. Simulations with a climate model that included aerosol effects and 3 different emissions inventories showed that shipping contributed 2.3-3.6% of the total SO₄²⁻ atmospheric aerosol content and 0.4-1.4% of the total BC atmospheric aerosol content, based on global means in 2000. This modeling also showed that aerosol optical thickness over the Indian Ocean, the Gulf of Mexico, and the northeastern Pacific Ocean varied by 8 to 10%. The corresponding all-sky (that includes both cloudy and clear skies) direct radiative forcings ranged from -0.011 W/m² to -0.013 W/m². The greatest effect of aerosols emitted from global shipping is likely to be an increase in cloud formation and the resulting change in reflectivity of shortwave radiation. Aerosols from shipping were estimated to contribute 17-39% of the total anthropogenic aerosol radiation forcing effect.

When BC is deposited to the surface of ice or snow, solar absorption and heating occur at the surface. This can melt additional snow or ice at the surface and the reflectivity of the surface can change. Both factors affect aspects of climate. Jacobson (2003, [155866](#); 2004, [155870](#)) and Jacobson et al. (2004, [180362](#)) estimated the warming due to fossil fuel BC and organic matter using the Gas, Aerosol, Transport, Radiation, General Circulation, Mesoscale and Ocean Model (GATOR-GCMOM). The modeling effort included consideration of the BC cycle, accounting for emissions, transport, aerosol coagulation, aerosol growth, cloud activation, aerosol-cloud coagulation, cloud-cloud coagulation, rainout, washout, dry deposition, and processes of precipitated and dry-deposited BC in snow and sea ice. Results

suggested that BC absorption in snow and sea ice increased near-surface temperatures over a 10-yr simulation by about 0.06°K (Jacobson, 2003, [189421](#)).

BC soot is a potentially important agent of climate warming in the Arctic, and northern boreal wildfires may contribute substantially to this effect. Soot is approximately twice as effective as CO₂ in altering surface air temperature, and can reduce sea ice formation and snow albedo (Hansen and Nazarenko, 2004, [156521](#)).

Kim et al. (2005, [155900](#)) investigated the relationships between northern boreal wildfires and reductions in Arctic sea ice and glacial coverage. They modeled the FROSTFIRE boreal forest control burn (Hinzman et al., 2003, [155845](#)) with respect to BC aerosol transport, dispersion, and deposition. Model results suggested that boreal wildfires could be a major source of BC soot to sea ice and glaciers in Alaska. This may exacerbate summer melting of sea ice and reduce recruitment of first-year ice into multiyear ice, thereby leading to an overall reduction in sea ice. Similarly, increased BC soot on glaciers would be expected to increase summer melting and lead to an overall reduction in glacial coverage (Kim et al., 2005, [155900](#)).

Jacobson (2002, [155865](#)) proposed, based on model simulations with 12 identifiable effects of aerosol particles on climate, emission reductions of fossil fuel particulate BC and associated organic matter could potentially slow warming for a specific period more than reduction of CO₂ or CH₄ for a specific period. Jacobson's (2006, [156599](#)) calculations suggested that fossil fuel BC plus organic matter emissions reductions could eliminate 8 to 18% of total anthropogenic warming, and 20 to 45% of net warming after accounting for aerosol cooling, within a period of 3-5 yr (Chock et al., 2003, [155727](#)). See also conflicting discussions (Feichter et al., 2003, [155772](#); Penner, 2003, [156851](#)); and further responses (Jacobson, 2003, [155867](#); Jacobson, 2003, [155868](#); Jacobson, 2003, [155869](#); Penner, 2003, [156851](#)).

Bond and Sun (2005, [156282](#)) reviewed published data regarding the warming potential of BC, compared with CO₂ and other GHG. Climatic effects of GHG are generally compared on the basis of top-of-the-atmosphere, globally averaged changes in radiative balance. On that basis, BC is one of the largest individual warming agents, after CO₂ and perhaps CH₄ (Bond and Sun, 2005, [156282](#); Jacobson, 2000, [056378](#); Sato et al., 2003, [156947](#)).

Reddy and Boucher (2007, [156042](#)) conducted an analysis that provided regional estimates of BC emissions from fossil fuels and biofuels. These estimates indicated that

East and Southeast Asia contributed over 50% of the global BC burden and its associated direct radiative forcing. Europe was found to be the largest BC contributor in the northern latitudes. The indirect effect of BC deposition on snow was also estimated to be highest for Europe.

To improve understanding of the role of aerosols in climate forcing, Chung and Seinfeld (2002, [155732](#)) estimated the global distribution of BC, primary organic particles (those directly emitted from combustion), secondary organic particles (primary organic compounds partially oxidized in the atmosphere), and SO_4^{2-} aerosols to model the overall radiative forcing of these groups of compounds. The model was run with the assumption that the BC particles do not combine with OC or SO_4^{2-} particles (termed an external mixture), and with the assumption that the particles are represented by a core of BC surrounded by a shell of light scattering aerosols. Modeling results suggested an overall radiative cooling effect from aerosols ranging from -0.39 to -0.78 W/m^2 .

Roberts and Jones (2004, [156052](#)) used a climate modeling approach to compare possible effects of BC on climate warming to those attributable to emissions from greenhouse gases. Results suggested that the warming effect from atmospheric BC aerosols may not be large relative to that from greenhouse gases. A different modeling approach by Roeckner et al. (2006, [156920](#)) evaluated the effects of BC and primary OC on climate under two scenarios of carbonaceous aerosol emissions. In the first scenario, BC and primary OC emissions decreased over Europe and China, but increased at lower latitudes. In the second scenario, emissions were frozen at 2000 levels. The effects of both scenarios on mean global temperature were found to be small, but higher aerosol emissions at low latitudes did result in atmospheric heating and corresponding land surface cooling that led to increased precipitation and runoff in this simulation.

Study of BC effects in tropical climates was undertaken by Wang (2007, [156147](#)). Substantial effects of direct radiative forcing by BC on the tropical Pacific were shown in model results that were similar to the El Niño Southern Oscillation activities both in the nature and scale of effects with enhancement of the Indian monsoon circulation. The model suggested that atmospheric heating by radiation absorption by BC can form temperature and pressure anomalies that favor propagation of convection from western to central and eastern Pacific. More work will be needed to distinguish between the aerosol signal and natural factors in controlling tropical precipitation in this region.

Table 9-18. Overview of the different aerosol indirect effects and their sign of the net radiative flux change at the top of the atmosphere (TOA).

Effect	Cloud Types Affected	Process	Sign of Change in TOA Radiation	Potential Magnitude	Scientific Understanding
Cloud albedo effect	All clouds	For the same cloud water or ice content more but smaller cloud particles reflect more solar radiation	Negative	Medium	Low
Cloud lifetime effect	All clouds	Smaller cloud particles decrease the precipitation efficiency thereby presumably prolonging cloud lifetime	Negative	Medium	Very low
Semi-direct effect	All clouds	Absorption of solar radiation by absorbing aerosols affects static stability and the surface energy budget, and may lead to an evaporation of cloud particles	Positive or Negative	Small	Very low
Glaciation indirect effect	Mixed-phase clouds	An increase in IN increases the precipitation efficiency	Positive	Medium	Very low
Thermodynamic effect	Mixed-phase clouds	Smaller cloud droplets delay freezing causing super-cooled clouds to extend to colder temperatures	Positive or Negative	Medium	Very low

Source: Denman (2007, [156394](#))

Table 9-19. Overview of the different aerosol indirect effects and their implications for the global mean net shortwave radiation of the surface F_{sc} (columns 2-4) and for precipitation (columns 5-7).

Effect	Sign of Change in F_{sc}	Potential Magnitude	Scientific Understanding	Sign of Change in Precipitation	Potential Magnitude	Scientific Understanding
Cloud albedo effect	Negative	Medium	Low	n.a.	n.a.	n.a.
Cloud lifetime effect	Negative	Medium	Very low	Negative	Small	Very low
Semi-direct effect	Negative	Large	Very low	Negative	Large	Very low
Glaciation indirect effect	Positive	Medium	Very low	Positive	Medium	Very low
Thermodynamic effect	Positive or Negative	Medium	Very low	Positive or Negative	Medium	Very low

Source: Denman (2007, [156394](#))

There are several other kinds of climate effects from aerosol PM. None is well understood or well quantified. The semi-direct effect, which involves absorption of solar radiation by soot particles followed by re-emission as thermal radiation, is expected to heat the air mass and increase its static stability relative to the surface. The semi-direct effect can also cause evaporation of cloud droplets, thereby partially offsetting the cloud albedo indirect effect. The glaciation effect involves an increase in IN, which is expected to cause rapid glaciation of a super-cooled liquid water cloud due to the differences in vapor pressure over ice and water. Unlike cloud droplets, these ice crystals can quickly reach precipitation size, with the potential to turn a non-precipitating cloud into a precipitating cloud. The thermodynamic effect involves a delay in freezing by the smaller cloud droplets, which can

cause super cooled clouds to occur under colder temperatures. The possible consequences to radiative flux of all of the processes are outlined in Table 9-18 (top of the atmosphere effects) and Table 9-19 (surface radiative and precipitation effects) (Denman et al., 2007, [156394](#)), though significant uncertainties remain. Nevertheless, the individual processes cannot be considered in isolation because of the numerous feedbacks, and because atmospheric aerosol concentrations and climate are intimately coupled (Denman et al., 2007, [156394](#); Dentener et al., 2006, [088434](#)).

9.3.9.1. Glaciers and Snowpack

Organic compounds are incorporated into snow by wet and dry deposition processes (Lei and Wania, 2004, [127880](#); Roth et al., 2004, [056431](#)). Atmospherically deposited organics appear to be ubiquitous in snowpacks at appreciable concentrations (Grannas et al., 2007, [156492](#)). Examples include PAHs, phthalates, alkanes, phenols, low molecular weight carbonyls, POPs, and low molecular weight organic acids (Halsall, 2004, [155822](#); Nakamura et al., 2000, [156792](#); Villa et al., 2003, [156139](#)). Humic-like substances found in the snowpack may release VOCs into the atmosphere via photo-oxidation (Grannas et al., 2004, [155803](#); Grannas et al., 2007, [156492](#)). Several thousand organic species were identified by Grannas et al. (2006, [155804](#)), based on molecular weight, from a single ice core collected in Russia. Little information is available, however, regarding the chemical properties of these chemical constituents. In addition to the diversity of chemicals that are deposited into the snowpack, there are also biological organisms, including bacteria and algae. Their role in influencing snow chemistry and volatilization processes is not understood (Grannas et al., 2007, [156492](#)).

Recent research has explored connections between the atmosphere and the cryosphere (land or sea covered by snow or ice). A seasonal maximum of 40% of the Earth's land surface is covered by snow or ice, as well as several percent of the oceans. Particulate deposition to snow and ice surfaces can affect melting rates. Deposition of PM to glacial ice surfaces can affect the subsequent rate of melting. A thin cover of debris contributes to accelerated melting. A thicker cover of debris, such as may result from a volcanic eruption, retards melting. The difference is due to the changing balance between enhanced absorption of shortwave radiation by PM and conductive heat flow (insulation) through a buildup of material having low heat conduction (Kirkbride and Dugmore, 2003, [156645](#)). This issue is particularly important for deposition of large quantities of volcanic material. To a lesser

extent, however, the same principles apply to PM deposition derived from air pollution. Under a thin layer of debris, ablation rates are higher than for clean ice. However, as the thickness of the debris layer increases, ablation rates systematically decline (Nicholson and Benn, 2006, [156806](#)). The threshold debris thickness that separates ablation increase from decrease is site specific and depends on local climate and the nature of the debris particles. Nicholson and Benn (2006, [156806](#)) presented a surface energy balance model to calculate ice melt beneath a surface debris layer, based on meteorological data and basic debris characteristics. Modeled melting rates matched observed rates, suggesting that the model produced useful results.

Long-range atmospheric transport of PM delivers a large fraction of the total input of POPs to the Arctic region (Halsall, 2004, [155822](#)). These contaminants can accumulate in Arctic food webs and have become the focus of international research and concern. Nevertheless, fate and transport of POPs within terrestrial and marine Arctic ecosystems are not well understood and are strongly affected by the presence of snow and ice. Sea ice provides a barrier to air-water exchange, and this hinders volatilization and re-emission of previously deposited contaminants (Halsall, 2004, [155822](#)). Thus, the effects of greenhouse gasses and PM on climate in the Arctic region have feedbacks to POP fate, transport, and toxicity. The transfer of POPs among the major abiotic environmental compartments in the Arctic are summarized in Figure 9-83 from Halsall (2004, [155822](#)). Recent studies detailing rate and transport of POPs are summarized in Table 9-20.

Table 9-20. Recent studies highlighting POP occurrence and fate in the major arctic compartments.

<i>ATMOSPHERE</i>		
1	Annual time-series of OC and PCB concentrations in the Norwegian Arctic	Oehme et al. (1996, 156001)
2	Long-term analysis of the chlordanes and their input to the Arctic with changing sources	Bidleman et al. (2002, 155691)
3	PAH occurrence at monitoring sites across the Arctic, seasonality and gas/particle partitioning	Halsall et al. (1997, 155821)
4	PCB occurrence at monitoring sites across the Arctic, spatial differences and seasonality	Stern et al. (1997, 156096)
5	Long-term analysis of PCB and OC trends in the Canadian Arctic and seasonal patterns	Hung et al. (2001, 155856 ; 2002, 155857)
6	Trans-Pacific LRAT and impact of Asian sources on the western Canadian Arctic	Bailey et al. (2000, 155670)
<i>FRESHWATER</i>		
7	Annual avg water concentrations in major Russian rivers for selected OC pesticides	Alexeeva et al. (2001, 155651)
8	Long-term (decades) PCB deposition profile in Arctic lake sediments	Muir et al. (1996, 155991)
9	Mass balance of selected OCs in Canadian Arctic lake conducted with data collected over 3 yrs	Helm et al. (2002, 155835)
10	Examining the biodegradation of HCHs in Canadian Arctic watersheds	Helm et al. (2000, 155834)

ATMOSPHERE

MARINE

11	Transport and entry of β -HCH into western Arctic Ocean via Pacific surface waters	Li et al. (2002, 156691)
12	Occurrence of current use pesticides in air, fog and surface seawater in the western Arctic Ocean	Chermyak et al. (1996, 155726)
13	Resolving petrogenic and anthropogenic PAH input to marine sediments in coastal Arctic seas	Yunker et al. (1996, 156175)
14	Quantifying abiotic and biotic degradation of HCHs in the Arctic Ocean water column	Harner et al. (2000, 156829)
15	PCBs and OCs in surface ocean water—Bering and Chukchi seas	Strachan et al. (2001, 156103)
16	Spatial patterns of HCHs and toxaphene in Arctic Ocean surface water	Jantunen and Bidleman (1998, 155877)

SNOW/AIR-FRESHWATER

17	PAHs (and inorganics) in surface snow layers (snowpit) at Summit, Greenland	Masclat et al. (2000, 155966)
18	PAHs measured in snow and ice layers on Agassiz ice-cap, Ellesmere Island, Canada	Peters et al. (1995, 156856)
19	Modeling OC behaviour and fate in the surface seasonal snow pack at Amituk Lake, Canada	Wania et al. (1998, 156148)
20	OCs, PCBs and PAHs in snow and ice of the Ob-Yenisey watershed of the Russian Arctic	Melnikov et al. (2003, 156753)

OCEAN/AIR

21	Transfer of α -HCH across the air/water interface in the western Arctic ocean	Jantunen and Bidleman (1996, 155876)
22	Calculated seasonality of OC air/water fluxes in the Canadian high Arctic	Hargrave et al. (1997, 155827)

OCEAN/ICE

23	Transport potential of contaminants across the Arctic ocean via sea-ice drift	Pfirman et al. (1997, 156864)
24	The importance of eastern Arctic sea-ice drift as a source of contaminants to the Norwegian sea	Korsnes et al. (2002, 156657)

Source: Halsall (2004, [155822](#))

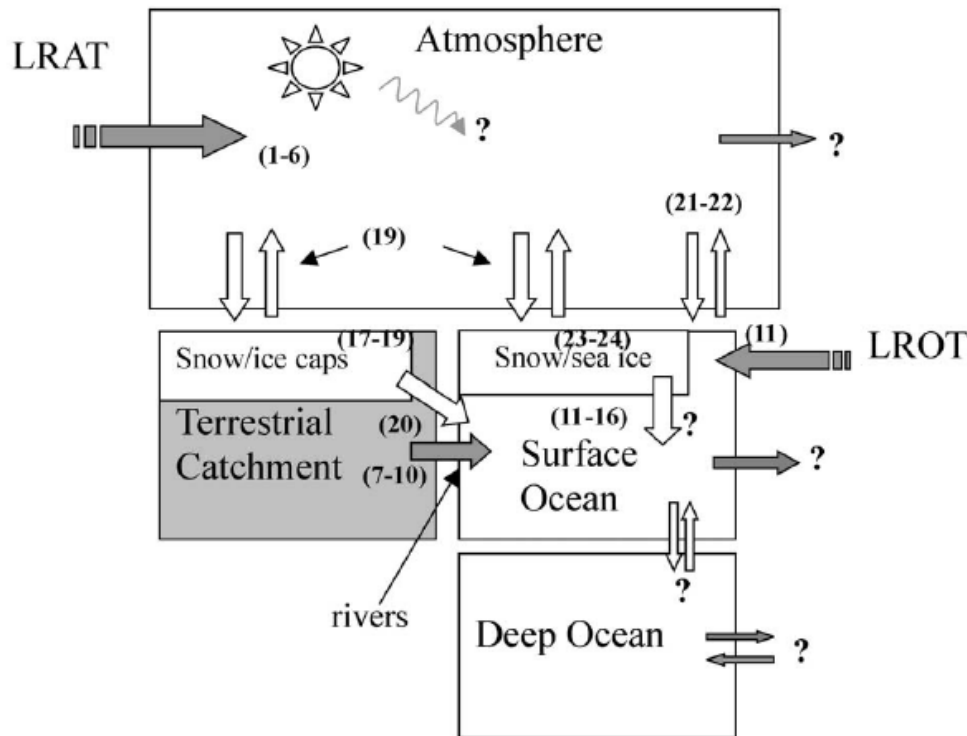


Figure 9-83. The transfer of POPs between the major abiotic compartments of the Arctic. Shaded arrows represent inputs/outputs of POPs to the Arctic. The numbers refer to selected studies detailing the occurrence and behavior of POPs, and are listed in Table 9-20. Question marks represent those areas that are least well understood. LRAT-long range atmospheric transport; LROT – long range oceanic transport.

9.3.9.2. Radiative Forcing by Anthropogenic Surface Albedo Change: BC in Snow and Ice

Section 9.3.9.2. comes directly from IPCC AR4 Chapter 2, Section 2.5.4, with section, table, and figure numbers changed to be internally consistent with this ISA.

The presence of soot particles in snow could cause a decrease in the albedo of snow and affect snowmelt. Initial estimates by Hansen et al. (2000, [042683](#)) suggested that BC could thereby exert a positive RF of +0.2 W/m². This estimate was refined by Hansen and Nazarenko (2004, [156521](#)), who used measured BC concentrations within snow and ice at a wide range of geographic locations to deduce the perturbation to the surface and planetary albedo, deriving an RF of +0.15 W/m². The uncertainty in this estimate is substantial due to uncertainties in whether BC and snow particles are internally or externally mixed, in BC and snow particle shapes and sizes, in voids within BC particles, and in the BC imaginary refractive index. Jacobson (2004, [155870](#)) developed a global model that allows the BC aerosol to enter snow via precipitation and dry deposition, thereby modifying the snow albedo and emissivity. They found modeled concentrations of BC within snow that were in reasonable agreement with those from many observations. The model study found that BC on snow and sea ice caused a decrease in the surface albedo of 0.4% globally and 1% in

the NH, although RFs were not reported. Hansen et al. (2005, [059087](#)) allowed the albedo change to be proportional to local BC deposition according to Koch (2001, [192054](#)) and presented a further revised estimate of 0.08 W/m². They also suggested that this RF mechanism produces a greater temperature response by a factor of 1.7 than an equivalent CO₂ RF, that is, the ‘efficacy’ may be higher for this RF mechanism (see Section 2.8.5.7 of the IPCC AR4). This report adopts a best estimate for the BC on snow RF of +0.10 ± 0.10 W/m², with a low level of scientific understanding (Section 2.9, Table 2.11, of the IPCC AR4).

9.3.9.3. Effects on Local and Regional Climate

Most effects of PM on climate, as assessed by IPCC (Stohl et al., 2007, [157015](#)) and summarized in this assessment, focus on global-scale processes and responses. In addition, it is also possible that PM emissions contribute to local and regional climate changes. These might include short-term cycles in rainfall or temperature and rainfall suppression, especially near cities and for orographic precipitation. Rainfall suppression, in particular, is believed to exacerbate water supply problems which are substantial in many regions, especially in the western U.S.

Aerosol particles, directly and through cloud enhancement, may reduce near-surface wind speeds locally. Slower winds, in turn, reduce evaporation. The overall impact can be a reduction in local precipitation. Jacobson and Kaufman (2006, [090942](#)) investigated the effects of PM on spatially-distributed wind speeds and resulting feedbacks to precipitation using the GATOR-GCMOM (Jacobson, 2001, [155864](#)) and supporting evidence from satellite data. The study focused on the South Coast Air Basin (SCAB) in California during February and August, 2002-2004. The modeled precipitation decrease over land in California was 2% of the baseline 1.5 mm/day due to emissions of anthropogenic aerosol particle and precursor gasses in the SCAB domain. However, the reduction over much of the Sierra Nevada, where most precipitation falls, was up to 0.5 mm/day, or 4 to 5% of the baseline 10 to 13 mm/day in that mountainous region (Jacobson, 2006, [156599](#)). The probable mechanism was described as follows. Aerosol particles and aerosol-enhanced clouds reduce wind speeds below them by stabilizing the air, reducing the vertical transport of horizontal momentum. In turn, the reduced wind speeds, and associated reduced evaporation and increased cloud lifetime, contributes to reduced local and regional precipitation (Jacobson, 2006, [156599](#)).

Effects of air pollution on regional precipitation were quantified by Givati and Rosenfeld (2004, [156475](#)). They found a 15-25% reduction in the orographic component of precipitation downwind of major coastal urban areas during the 20th century. Their study focused on orographically-forced clouds because these short-lived, shallow clouds are

expected to exhibit the largest effect of air pollution on precipitation. Substantially larger precipitation suppression due to aerosol particulate pollution was found between Fresno and Sacramento in California by Givati and Rosenfeld (2004, [156475](#)). Precipitation losses over topographical barriers in the Sierra Nevada amounted to 15%-25% of the annual precipitation at elevations less than 2,000 m. This precipitation suppression occurred mainly in the relatively shallow orographic clouds within the cold air mass of cyclones. The suppression that occurred on the upslope side of the mountains was coupled with similar percentage (but lower absolute volume) enhancement on the drier downslope eastern side (Givati and Rosenfeld, 2004, [156475](#)). Similar results were found in studies by Griffith et al. (2005, [156497](#)), Jirak and Cotton (2006, [156612](#)), Rosenfeld and Givati (2006, [156924](#)), and Rosenfeld et al. (2007, [156057](#)). At all of these study locations (California, Israel, Utah, Colorado, China), orographic precipitation decreased by 15-30% downwind of pollution sources, likely due to creation of more and smaller cloud droplets and resulting suppression of precipitation.

The study of Givati and Rosenfeld (2004, [156475](#)) was the first to quantify the microphysical effect of mesoscale precipitation. Following the findings of Givati and Rosenfeld (2004, [156475](#)), the effects of aerosol air pollution on precipitation at high elevation sites in the Front Range of Colorado adjacent to urban areas were investigated by Jirak and Cotton (2006, [156612](#)). Examination of precipitation trends showed that the ratio of upslope precipitation during easterly flows at high elevation west of Denver and Colorado Springs to the upwind urban sites decreased by about 30% over the past half century. These results provide further support for the hypothesis that aerosol pollution suppresses orographic precipitation downwind of pollution source areas.

Griffith et al. (2005, [156497](#)) found similar reductions in mountainous precipitation in Utah, downwind of Salt Lake City and Provo. The ratio of precipitation at mountain stations located in rural settings in Utah and Nevada remained stable, supporting the hypothesis that air pollution decreases R_o (the ratio of precipitation at the downwind site to precipitation at the upwind pollution source) over the mountains to the east of Salt Lake City.

Rosenfeld and Givati (2006, [156924](#)) extended the investigation of the suppression of precipitation by aerosol pollutants to a larger scale by examining the ratio between precipitation amounts over the hills to precipitation over upwind lowland areas throughout the western U.S. from the Pacific Coast to the Rocky Mountains. They found in these paired

analyses a pattern of decreasing precipitation by as much as 24% from the Mexican border to central California, with no decrease in northern California and Oregon and smaller decrease of 14% in Washington east of Seattle and Puget Sound. Similar decreases were found over Arizona and New Mexico (Rosenfeld, 2006, [190233](#)), Utah (Griffith et al., 2005, [156497](#)), and the east slope of the Colorado Rockies (Jirak and Cotton, 2006, [156612](#)).

Suppression of winter orographic precipitation appears to occur up to hundreds of kilometers inland of coastal urban areas (Rosenfeld, 2006, [190233](#)). Decreases in this precipitation ratio occurred during winter orographic precipitation, but not during convective summer precipitation over the same mountain ranges. This finding agrees with the expectation that aerosol-induced changes in the rate of precipitation formation would cause a decrease in precipitation from shallow and short-lived orographic clouds, but not necessarily from deeper and longer-lived thermally-driven convective clouds.

Results of these studies of aerosol effects on orographic precipitation suggest that human-caused air pollution, and fine particles in particular, have had a large effect on precipitation well beyond the local scales of the pollution sources (Rosenfeld, 2006, [190233](#)).

9.3.10. Summary of Effects on Climate

Aerosols affect climate through direct and indirect effects. The direct effect is primarily realized as planet brightening when seen from space because most aerosols scatter most of the visible spectrum light that reaches them. The IPCC AR4 reported that the radiative forcing from this direct effect was $-0.5 (\pm 0.4)$ W/m² and identified the level of scientific understanding of this effect as 'Medium-low'. The global mean direct radiative forcing from individual aerosol components varies from strongly negative for SO₄²⁻ to positive for BC with weaker positive or negative effects for other components, all of which can vary strongly over space and time and with aerosol size. The indirect effects are primarily realized as an increase in cloud brightness (termed the “first indirect” or “Twomey” effect), changes in precipitation, and possible changes in cloud lifetime. The IPCC AR4 reported that the radiative forcing from the Twomey effect was -0.7 (range: -1.1 to $+4$) and identified the level of scientific understanding of this effect as “Low”. The other indirect effects from aerosols were not considered to be radiative-forcing.

Taken together, direct and indirect effects from aerosols increase Earth's shortwave albedo or reflectance, thereby reducing the radiative flux reaching Earth's surface from the Sun. This produces net climate cooling from aerosols. The current scientific consensus

reported by IPCC AR4 is that the direct and indirect radiative forcing from anthropogenic aerosols computed at the top of the atmosphere, on a global average, is about -1.3 (range: -2.2 to -0.5) W/m^2 . Although the magnitude of this negative radiative forcing appears large in comparison to the analogous IPCC AR4 estimate of positive radiative forcing from anthropogenic GHG of about $2.9 (\pm 0.3)$ W/m^2 , the spatial and temporal distributions of these two very different radiative forcing agents are dissimilar; therefore, they do not simply cancel and regional differences can be large. These differences result from the much shorter atmospheric lifetime of aerosols than for the radiatively important trace gases, implying that the radiative effects of aerosols respond much more quickly to changes in emissions than do the effects from the gas-phase forcing agents. Moreover, the effect of present-day aerosols is to cool Earth's surface but, on average, to heat the atmosphere itself: within the atmospheric column, the radiative forcing effect from aerosols is estimated to range from $+0.8$ to $+2$ W/m^2 .

Considerable progress has been made with in situ and remotely-sensed aerosols concentrations including the MODIS, MISR, POLDER, and OMI satellite instruments; see the discussion in Section 3.4.1.6. The accuracy for aerosol optical depth (AOD) measured with these global-coverage remote sensing instruments is on the order of 0.05 or 20% of the AOD, but is still much lower than for the limited-area surface-based sun photometers which have accuracy in the range of 0.01-0.02. The differences remaining between surface and remotely sensed AOD and between estimates computed from measurements and from numerical model predictions are important because AOD is a significant element in determining radiative forcing. Hence, uncertainty and error in AOD measurements and modeling propagate into the range of estimates for total radiative forcing reported here.

Numerical modeling of aerosol effects on climate has also sustained remarkable progress since the 2004 PM AQCD (EPA, 2004, [056905](#)), though model solutions still display large heterogeneity in their estimation of the direct radiative forcing effect from anthropogenic aerosols. Differences among models are due in large measure to differences in: emissions of PM and precursors to secondary PM formation; in the representation of aerosol microphysical and optical processes; in regional- and global-scale transport and transformation; as well as in the effects of aerosol radiative forcing. The clear-sky direct radiative forcing over ocean due to anthropogenic aerosols is estimated from satellite instruments to be on the order of $-1.1 (\pm 0.37)$ W/m^2 while model estimates are -0.6 W/m^2 . The models' low bias over ocean is carried through for the global average: global average

direct radiative forcing from anthropogenic aerosols is estimated from measurements to range from -0.9 to -1.9 W/m², larger than the estimate of -0.8 W/m² from the models. Spatial heterogeneity in radiative forcing is expected to exert significant effects on regional climate, but because the effects of climate warming and cooling are not strictly co-located spatially or temporally with radiative forcing or with emissions in particular for precursors for secondary PM formation, assessments of effects for sub-global domains are even more uncertain than the global averages reported here.

Overall, the evidence is sufficient to conclude **that a causal relationship exists between PM and effects on climate, including both direct effects on radiative forcing and indirect effects that involve cloud feedbacks that influence precipitation formation and cloud lifetimes.**

9.4. Ecological Effects of PM

9.4.1. Introduction

PM is heterogeneous with respect to chemical composition and size, therefore it can cause a variety of ecological effects, which have been previously described by the U.S. EPA (2004, [056905](#)) and by Grantz et al. (2003, [155805](#)). Atmospheric PM has been defined, for regulatory purposes, mainly by size fractions and less clearly so in terms of chemical nature, structure, or source. Both fine and coarse-mode particles may affect plants and other organisms, however PM size classes do not necessarily relate to ecological effects (U.S. EPA, 1996, [079380](#)). More often the chemical constituents drive the ecosystem response to PM (Grantz et al., 2003, [155805](#)).

The previous PM assessment (U.S. EPA, 2004, [056905](#)) included the acidifying effects of particulate N and S. The 2008 NO_xSO_x ISA (U.S. EPA, 2008, [157074](#)) assessed the effects of particle- and gas-phase N and S pollution on acidification, N enrichment, and Hg methylation. Acidification of ecosystems is driven primarily by deposition resulting from SO_x, NO_x, and NH_x pollution. Acidification from the deposition resulting from current emission levels causes a cascade of effects that harm susceptible aquatic and terrestrial ecosystems, including slower growth and injury to forests and localized extinction of fishes and other aquatic species. In addition to acidification, atmospheric deposition of reactive N resulting from current NO_x and NH_x emissions along with other non-atmospheric sources (e.g., fertilizers and wastewater), causes a suite of ecological changes within sensitive

ecosystems. These include increased primary productivity in most N-limited ecosystems, biodiversity losses, changes in C cycling, and eutrophication and harmful algal blooms in freshwater, estuarine, and ocean ecosystems. In some watersheds, additional SO_4^{2-} from atmospheric deposition increases Hg methylation rates by increasing both the number and activity of S-reducing bacteria. Methylmercury is a powerful toxin that can bioaccumulate to toxic amounts in food webs at higher trophic levels. Effects of particulate metals and organics on ecosystems and ecosystem receptors are the focus in this PM ISA.

This assessment of PM effects on ecosystems considers both direct and indirect exposure pathways. Atmospheric PM may affect ecological receptors directly following deposition on surfaces or indirectly by changing the soil chemistry or by changing the amount of radiation reaching the Earth's surface. Indirect effects acting through the soil are often thought to be most significant because they can alter nutrient cycling and inhibit nutrient uptake (EPA, 2004, [056905](#)). The U.S. EPA (2004, [056905](#)) reported that the effects of PM can be both chemical and physical. Physical effects of particle deposition on vegetation may include abrasion and radiative heating. Chemical effects may be more significant (U.S. EPA, 2008, [157074](#)).

In general, anthropogenic stressors can result in damaged ecosystems that do not recover readily (Odum, 1993, [076742](#); Rapport and Whitford, 1999, [004595](#)). Ecosystems sometimes lack the capacity to adapt to an anthropogenic stress and are unable to maintain their normal structure and functions unless the stressor is removed (Rapport and Whitford, 1999, [004595](#)). These stresses result in a process of ecosystem degradation marked by a decrease in biodiversity, reduced primary and secondary production, and a lower capacity to recover and return to the original ecosystem state. In addition, there can be an increased prevalence of disease, reduced nutrient cycling, increased dominance of exotic species, and increased dominance by smaller, short-lived opportunistic species (Odum, 1985, [039482](#); Rapport and Whitford, 1999, [004595](#)).

Ecosystems are often subjected to multiple stressors, of which atmospheric PM deposition is only one. Additional stressors are also important, including O_3 exposure, climatic variation, natural and human disturbance, the occurrence of invasive non-native plants, native and non-native insect pests, disease, acidification, and eutrophication among others. PM deposition interacts with these other stressors to affect ecosystem patterns and processes.

The possible effects of particulate (and other) air pollutants on ecosystems have been categorized by Guderian (1977, [004150](#)) as follows:

- accumulation of pollutants in plants and other ecosystem components (such as soil and surface- and groundwater),
- damage to consumers as a result of pollutant accumulation,
- changes in species diversity because of shifts in competition,
- disruption of biogeochemical cycles,
- disruption of stability and reduction in the ability to self-regulate,
- breakdown of stands and associations, and
- expansion of denuded zones.

The general conclusion of the last PM assessment (U.S. EPA, 2004, [056905](#)) was that ecosystem response to PM can be difficult to determine because the changes are often subtle. For example, changes in the soil may not be observed until pollutant deposition has occurred for many decades, except in the most severely polluted areas around heavily industrialized point sources. The presence of co-occurring pollutants generally makes it difficult to attribute ecological effects to PM alone or to one constituent in the deposited PM. In other words, the potential for alteration of ecosystem function and structure exists but can be difficult to quantify except in cases of extreme amounts of deposition, especially when there are other pollutants present in the ambient air that may produce additive or synergistic responses.

New information on the ecological effects of coarse and fine particle PM is presented in the following discussion in the context of effects that were known from the last PM AQCD (EPA, 2004, [056905](#)). The general effects of the chemical constituents of PM are discussed; however, a rigorous assessment of each chemical constituent (e.g., Hg, Cd, Pb, etc.) is not given. Both direct and indirect effects will be discussed and the strength of the scientific evidence will be evaluated using the causality framework.

9.4.1.1. Ecosystem Scale, Function, and Structure

Information presented in this section was collected at multiple scales, ranging from the physiology of a given species to population, community, and ecosystem-level investigations. For this assessment, “ecosystem” is defined as a functional entity consisting of interacting groups of living organisms and their abiotic (chemical and physical) environment. Ecosystems cover a hierarchy of spatial scales and can comprise the entire globe, biomes at the continental scale, or small, well-circumscribed systems such as a small pond.

Ecosystems have both structure and function. Structure may refer to a variety of measurements including the species richness, abundance, community composition and biodiversity as well as landscape attributes. Competition among and within species and their tolerance to environmental stresses are key elements of survivorship. When environmental conditions are shifted, for example, by the presence of anthropogenic air pollution, these competitive relationships may change and tolerance to stress may be exceeded. “Function” refers to the suite of processes and interactions among the ecosystem components and their environment that involve nutrient and energy flow as well as other attributes including water dynamics and the flux of trace gases. Plant processes including photosynthesis, nutrient uptake, respiration, and C allocation, are directly related to functions of energy flow and nutrient cycling. The energy accumulated and stored by vegetation (via photosynthetic C capture) is available to other organisms. Energy moves from one organism to another through food webs, until it is ultimately released as heat. Nutrients and water can be recycled. Air pollution alters the function of ecosystems when elemental cycles or the energy flow are altered. This alteration can also be manifested in changes in the biotic composition of ecosystems.

There are at least three levels of ecosystem response to pollutant deposition: (1) the individual organism and its environment; (2) the population and its environment; and (3) the biological community composed of many species and their environment (Billings, 1978, [034165](#)). Individual organisms within a population vary in their ability to withstand the stress of environmental change. The response of individual organisms within a population is based on their genetic constitution, stage of growth at time of exposure to stress, and the microhabitat in which they are growing (Levine and Pinto, 1998, [029599](#)). The range within which organisms can exist and function determines the ability of the population to survive. Those able to cope with the stresses survive and reproduce. Competition among different

species results in succession (community change over time) and, ultimately, produces ecosystems composed of populations of species that have the capability to tolerate the stresses (Guderian R, 1985, [019325](#); Rapport and Whitford, 1999, [004595](#)). Available information on individual, population and community response to PM will be discussed.

9.4.1.2. Ecosystem Services

Ecosystem structure and function may be translated into ecosystem services. Ecosystem services identify the varied and numerous ways that ecosystems are important to human welfare. Ecosystems provide many goods and services that are of vital importance for the functioning of the biosphere and provide the basis for the delivery of tangible benefits to human society. Hassan et al. (2005, [092759](#)) define these to include supporting, provisioning, regulating, and cultural services:

- Supporting services are necessary for the production of all other ecosystem services. Some examples include biomass production, production of atmospheric O₂, soil formation and retention, nutrient cycling, water cycling, and provisioning of habitat. Biodiversity is a supporting service that is increasingly recognized to sustain many of the goods and services that humans enjoy from ecosystems. These provide a basis for three higher-level categories of services.
- Provisioning services, such as products (Gitay et al., 2001, [092761](#)), i.e., food (including game, roots, seeds, nuts and other fruit, spices, fodder), fiber (including wood, textiles), and medicinal and cosmetic products (including aromatic plants, pigments).
- Regulating services that are of paramount importance for human society such as (a) C sequestration, (b) climate and water regulation, (c) protection from natural hazards such as floods, avalanches, or rock-fall, (d) water and air purification, and (e) disease and pest regulation.
- Cultural services that satisfy human spiritual and aesthetic appreciation of ecosystems and their components.

9.4.2. Deposition of PM

Deposition of PM is discussed in Chapter 3.3.3. Additional material specifically related to ecosystems is discussed in this section.

9.4.2.1. Forms of Deposition

Research summarized by the previous NAAQS PM assessment illustrated the complexity of deposition processes. Airborne particles, their gas-phase precursors, and their transformation products are removed from the atmosphere by wet and dry deposition processes. These deposition processes transfer PM pollutants to other environmental media where they can alter the structure, function, diversity, and sustainability of complex ecosystems. Dry deposition of PM is most effective for coarse particles. These include primary geologic materials and elements such as iron and manganese. By contrast, wet deposition is more effective for fine particles of secondary atmospheric origin and elements such as cadmium, chromium, lead, nickel, and vanadium (Reisinger, 1990, [046737](#); Smith, 1990, [084015](#); U.S. EPA, 2004, [056905](#)). The relative magnitudes of the different deposition modes vary with ecosystem type, location, elevation, and chemical burden of the atmosphere (U.S. EPA, 2004, [056905](#)). There are differences in the deposition behavior of fine and coarse particles. Coarse particles generally settle nearer their site of formation than do fine particles. In addition, the chemical constitution of individual particles is correlated with size. For example, much of the base cation and heavy metal burden is present on coarse particles.

Fine PM is often a secondary pollutant that forms within the atmosphere, rather than being directly emitted from a pollution source. It derives from atmospheric gas-to-particle conversion reactions involving nucleation, condensation, and coagulation, and from evaporation of water from contaminated fog and cloud droplets. Fine PM may also contain condensates of VOCs, volatilized metals, and products of incomplete combustion, including polycyclic aromatic hydrocarbons (PAH) and BC (soot) (EPA, 2004, [056905](#)).

Fine PM may act as a carrier for materials such as herbicides that are phytotoxic. Fine PM provides much of the surface area of particles suspended in the atmosphere, whereas coarse PM provides much of the mass of airborne particles. Surface area can influence ecological effects associated with the oxidizing capacity of fine particles, their interactions with other pollutants, and their adsorption of organic compounds. Fine and

coarse particles also respond to changes in atmospheric humidity, precipitation, and wind, and these can alter their deposition characteristics.

Coarse PM is mainly a primary pollutant, having been emitted from pollution sources as fully formed particles derived from abrasion and crushing processes, soil disturbances, desiccation of marine aerosol emitted from bursting bubbles, hygroscopic fine PM expanding with humidity to coarse mode, and/or gas condensation directly onto preexisting coarse particles. Suspended primary coarse PM may contain iron, silica, aluminum, and base cations from soil, plant and insect fragments, pollen, fungal spores, bacteria, and viruses, as well as fly ash, brake lining particles, and automobile tire fragments. Coarse mode particles can be altered by chemical reactions and/or physical interactions with gaseous or liquid contaminants.

Exposure to a given mass concentration of PM may lead to widely differing phytotoxic and other environmental outcomes depending upon the particular mix of PM constituents involved. Especially important in this regard are S and N components of PM, which are addressed in the 2008 NO_xSO_x ISA, and effects of particulate heavy metals and organic contaminants. This variability has not been characterized adequately. Though effects of specific chemical fractions of PM have been described to some extent, there has been relatively little research aimed at defining the effects of unspiciated PM on plants or ecosystems.

9.4.2.2. Components of PM Deposition

Trace Metals

Atmospheric deposition can be the primary source of some metals to some watersheds. Metal inputs can include the primary crustal elements (Al, Ca, K, Fe, Mg, Si, Ti) and the primary anthropogenic elements (Cu, Zn, Cd, Cr, Mn, Pb, V, Hg). The crustal elements are derived largely from weathering and erosion, whereas the anthropogenic elements are derived from combustion, industrial sources, and other man-made sources (Goforth and Christoforou, 2006, [088353](#)).

Heavy metal deposition to ecosystems depends on their location as well as upwind emissions source strength. The deposition velocity tends to be dependent on particle size and chemical species. Larger particles deposit more efficiently than smaller particles. Heavy metals preferentially associate with fine particles. Fine particles also have the

longest atmospheric residence times. Depending on climate and topography, fine particles may remain airborne for days to months and may be transported thousands of kilometers from their source.

Ecosystems immediately downwind of major heavy metal emissions sources may receive locally heavy dry deposition. Trace element investigations conducted in roadside, industrial, and urban environments have also shown that substantial amounts of particulate heavy metals can accumulate on surfaces.

A significant trace metal component of PM is mercury (Hg). Mercury is toxic and can move readily through environmental compartments. Atmospheric and depositional inputs of Hg include both natural and anthropogenic sources. Natural geologic contributions to Hg in the environment include geothermal and volcanic activity, geologic metal deposits, and organic-rich sedimentary rocks. These natural emissions combine with anthropogenic emissions from such sources as power plants, landfills, sewage sludge, mine waste, and incineration (Gustin, 2003, [155816](#); Schroeder and Munthe, 1998, [014559](#)). Emissions from natural sources are controlled by geologic features, including substrate Hg content, rock type, the degree of hydrothermal activity, and the presence of heat sources (Gustin, 2003, [155816](#)). The significance of natural Hg sources relative to anthropogenic sources varies geographically. For example, Nevada occurs within a global mercuriferous belt, with area emissions about three times higher than the value assumed for global modeling (Gustin, 2003, [155816](#)). In Nevada, natural and anthropogenic Hg emissions are approximately equal (Gustin, 2003, [155816](#)).

The U.S. EPA (1997, [157066](#)) compiled an assessment of the sources and environmental effects of Hg in the U.S. A variety of factors were found to influence Hg deposition, fate and transport (Table 1). Such factors relate in particular to speciation of the Hg that is emitted, the forms in which it is deposited from the atmosphere, and transformations that occur within the atmosphere and within the aquatic, transitional, and terrestrial compartments of the receiving watershed. There have been studies that have reconstructed, from lake sediment records, the atmospheric depositional history of trace metals and PAHs in lakes adjacent to coal-fired power plants. For example, Donahue et al. (2006, [155751](#)) analyzed sediment from Wababun Lake, which is located in Alberta, Canada in proximity (within 35 km) to 4 power plants built since 1950. Trace metal concentrations of Hg, Cu, Pb, As, and Se in lake sediment increased by 1.2- to 4-fold. The total PAH flux to surface sediments was 730 to 1100 $\mu\text{g}/\text{m}^2/\text{yr}$, which was two to five times higher than in 2

lakes situated 20 km to the north and 70 km to the south. Further discussion of Hg effects on ecosystems can be found in Section 9.4.5.

Table 9-21. Factors potentially important in estimating mercury exposure.

Factor	Importance and Possible Effect on Mercury Exposure
Type of anthropogenic source of mercury	Different combustion and industrial process sources are anticipated to have different local scale impacts due to physical source characteristics (e.g., stack height), the method of waste generation (e.g., incineration or mass burn) or mercury control devices and their effectiveness.
Mercury emission rates from stack	Increased emissions will result in a greater chance of adverse impacts on environment.
Mercury species emitted from stack	More soluble species will tend to deposit closer to the source.
Form of mercury emitted from stack	Transport properties can be highly dependent on form.
Deposition differences between vapor and particulate-bound mercury	Vapor-phase forms may deposit significantly faster than particulate-bound forms.
Transformations of mercury after emission from source	Relatively nontoxic forms emitted from source may be transformed into more toxic compounds.
Transformation of mercury in watershed soil	Reduction and revolatilization of mercury in soil limits the buildup of concentration.
Transport of mercury from watershed soils to water body	Mercury in watershed soils can be a significant source to water bodies and subsequently to fish.
Transformation of mercury in water body	Reduction, methylation, and demethylation of mercury in water bodies affect the overall concentration and the MHg fraction, which is bioaccumulated in fish.
Facility locations	Effects of meteorology and terrain may be significant.
Location relative to local mercury source	Receptors located downwind are more likely to have higher exposures. Influence of distance depends on source type.
Contribution from non-local sources of mercury	Important to keep predicted impacts of local sources in perspective.
Uncertainty	Reduces confidence in ability to estimate exposure accurately.

Source: Modified from U.S. EPA (1997, [157066](#))

Organics

Organic compounds that may be associated with deposited PM include persistent organic pollutants (POPs), pesticides, SOCs, polyaromatic hydrocarbons (PAHs) and flame retardants among others. Organic compounds partition between gas and particle phases, and organic particulate deposition depends largely on the particle sizes available for adsorption (EPA, 2004, [056905](#)). Dry deposition of organic materials is often dominated by the coarse fraction. Gas-particle phase interconversions are important in determining the amount of dry deposition.

Most persistent organic pollutants (POPs) enter the biosphere via human activities, including synthetic pesticide application, output of polychlorinated dibenzo dioxins (PCDD) from incinerators, and accidental release of PCBs from transformers (Lee, 2006, [088968](#)). Once they are introduced into the environment, their accumulation and magnification in biological systems are determined by physiochemical properties and environmental

conditions (Section 9.4.5.7). Uptake by plants can occur at the soil/plant interface and at the air/plant interface. For lipophilic POPs, such as PCDDs and PCBs, the air/plant response route generally dominates (Lee, 2006, [088968](#); Thomas et al., 1998, [156118](#)), but uptake through above-ground plant tissue also occurs. In a study of zucchini (*Cucurbita pepo*), Lee et al. (2006, [088968](#)) found chlordane pesticide components in all vegetation tissues examined: root, stem, leaves, fruits.

Many pesticides and SOCs are carcinogenic or estrogenic and pose potential threats to aquatic and terrestrial biota. Although deposition of SOCs was previously reported for the Sierra Nevada Mountains in California and the Rocky Mountains in Colorado, little was previously known about the occurrence, distribution, or sources of SOCs in alpine, sub-Arctic, and Arctic ecosystems in the western U.S. The snowpack is efficient at scavenging of both particulate and gas phase pesticides from the atmosphere (Halsall, 2004, [155822](#); Lei and Wania, 2004, [127880](#)). Analysis of pesticides in snowpack samples from seven national parks in the western U.S. by Hageman et al. (2006, [156509](#)) illustrated the deposition and fate of 47 pesticides and their degradation products. Correlation analysis with latitude, temperature, elevation, PM, and two indicators of regional pesticide use suggested that regional patterns in historic and current agricultural practices are largely responsible for the distribution of pesticides in the national parks. Pesticide deposition to parks in Alaska was attributed to long-range atmospheric transport.

PAHs include hundreds of different compounds that are characterized by possessing two or more fused benzene rings. They are widespread contaminants in the environment, and are formed by incomplete combustion of fossil fuels and other organic materials. Eight PAHs are considered carcinogenic and 16 are classified by EPA as priority pollutants. They are common air pollutants in metropolitan areas, derived from vehicular traffic and other urban sources. Especially high concentrations have been found near Söderberg aluminum production industries and areas where wood heating during winter is common. Other sources, in addition to gasoline and diesel engines, include forest fires and various forms of fossil fuel combustion (Sanderson and Farant, 2004, [156942](#)).

The behavior of PAHs is strongly determined by their chemical characteristics, especially their nonpolarity and hydrophobicity. They readily adsorb to particulates in the air and to sediments in water. Srogi (2007, [180049](#)) provided a thorough review of PAH concentrations in various environmental compartments and their use for assessing environmental risks and possible effects on ecosystems and human health.

Deposition and fate of PAH has been an important area of research. Because they are carcinogenic, PAHs are important environmental contaminants. Root-soil behavior of PAHs is an area of active study. Soil-bound PAHs are associated with soil organic matter and are therefore generally not easily available for root uptake. PAHs are readily adsorbed to root surfaces but there seems to be little movement to the interior of the root or movement up to the shoots (Gao and Zhu, 2004, [155782](#)). Paddy rice is the main food crop planted in China. As an aquatic plant having aerial roots, the movement of PAHs into rice roots may be different than their movement into more widely studied land-grown food crops. PAH concentrations in the rice roots were more correlated with the water and air compartments than with the soil (Jiao et al., 2007, [155879](#)).

The total PAH concentration in grasses adjacent to a highway have been measured to be about eight times higher than in grasses from reference sites not close to a highway (Crépineau et al., 2003, [155741](#)). Howe et al. (2004, [155854](#)) found that concentrations of PAHs and hexachlorobenzene (HCB) in spruce (*Picea* spp.) needles at 36 sites in eastern Alaska varied by an order of magnitude. Samples collected near the city of Fairbanks generally had higher concentrations than samples collected from rural areas. The relative importance of combustion sources versus petrogenic sources was highest in the near-coastal areas, as reflected in variation in the concentration of ratios of isomeric PAHs.

Use of flame retardants has increased in recent years in response to fire product safety regulations. However, some flame retardant chemicals are toxic and are readily transported atmospherically. Use of some has been banned in Europe and some of the United States because of their persistence and tendency to bioaccumulate (Hoh et al., 2006, [190378](#)).

Base Cations

With respect to ecosystem effects from PM deposition, the inclusion of base cations (especially Ca, Mg, and K) in atmospheric deposition is generally considered to be a positive effect. Base cations are important plant nutrients that are in some locations present in short supply and that are further depleted by the acidic components of deposition. Increased base cation deposition can help to ameliorate adverse effects of acidification of soils and surface waters and reduce the toxicity of inorganic Al to plant roots and aquatic biota. These topics are covered in detail in the recent 2000 NO_xSO_x ISA (U.S. EPA, 2008, [157074](#)). Calcium supply is also well known to be important for breeding success in

passerine bird species. Eggshell thickness, egg size, clutch size, and hatchability of pied flycatcher (*Ficedula hypoleuca*) were found to be depressed near the Cu smelter at Harjavalta, SW Finland (Eeva and Lehtikoinen, 2004, [155762](#)). Availability of Ca-rich food to the birds was estimated by counting snail shells in the nests postfledging. The number of snail shells correlated positively with the Ca concentration of nestling feces and adult breeding success. In addition, the negative impact of Cu on the number of fledglings was stronger at locations where Ca concentration was low (Eeva and Lehtikoinen, 2004, [155762](#)).

Although the effects of base cation deposition inputs to terrestrial ecosystems are most commonly considered to be positive, under very high base cation deposition, plant health can be adversely affected. Dust that is high in base cations can settle on leaves and other plant structures and remain for extended periods of time. This is especially likely in arid environments because rainfall can serve to wash dry deposited materials off the foliage. Extended dust coverage can result in a variety of adverse impacts on plant physiology (Grantz et al., 2003, [155805](#)). For example, van Heerden et al. (2007, [156131](#)) documented decreased chlorophyll content, inhibition of CO₂ assimilation, and uncoupling of the oxygen-evolving complex in desert shrubs exposed to high limestone dust deposition near a limestone quarry in Namibia.

Based on the Integrated Forest Study (IFS) data, the U.S. EPA (2004, [056905](#)) concluded that particulate deposition has a greater effect on base cation inputs to soils than on base cation losses associated with the inputs of sulfur, nitrogen, and H⁺. These atmospheric inputs of base cations have considerable significance, not only to the base cation status of these ecosystems, but also to the potential of incoming precipitation to acidify or alkalize the soils in these ecosystems. This topic is discussed in detail in the recent NO_xSO_x ISA (U.S. EPA, 2008, [157074](#)).

9.4.2.3. Magnitude of Dry Deposition

Using Vegetation for Estimating Atmospheric Deposition

Whereas direct real-time measurement of deposition or air concentrations of atmospheric contaminants is desirable, it is not always practical (Howe et al., 2004, [155854](#)). Instead, passive time-integrative methods are frequently used. These can involve analysis of vegetative tissues as a record of pollutant exposure, or analysis of lake sediment cores or ice cores to determine changes in pollutant input over time. There is a general

assumption that the concentration of an analyte in vegetation reflects the time-integrated concentration of that analyte in the air. The development of deposition layers in sediment or ice cores allows the possibility of determining the effects of changes in the atmospheric concentration over periods of years, decades, or longer.

Biomonitoring methods are important in air pollution assessment and provide a complement for more typical instrumental analyses. It is well known that mosses can accumulate large amounts of heavy metals in response to atmospheric deposition. Mosses accumulate dissolved materials and PM deposited from the atmosphere and have been used extensively in Europe as surrogate collectors for estimating bulk (wet plus dry) deposition of metals. The ease and low cost of this method has enabled regional assessments to be conducted throughout Europe.

Despite its wide use, however, several papers have pointed out complications in the use of mosses to quantify metal deposition rates. Zechmeister (1998, [156178](#)) found that the uptake efficiency for 12 heavy metals in 3 species of moss was similar, but that uptake efficiency in a fourth species was uncorrelated with the other species for about half the metals considered. Zechmeister (1998, [156178](#)) also showed that productivity of an individual species can vary greatly among sites. To calculate atmospheric deposition of metals from accumulation in mosses, both the metal concentration and the rate of biomass production is needed. Further complication was shown in the study of Shakya et al. (2008, [156081](#)), which revealed that accumulation of Cu, Zn and Pb decreased chlorophyll content. Sites with greater deposition amounts may therefore have lower rates of productivity than cleaner sites.

Differences in uptake efficiencies among species and productivity among sites has led to the use of a single moss species placed in mesh bags that can be distributed to areas where that species of moss does not grow naturally. Studies to standardize this passive deposition monitoring approach have been limited. Adamo et al. (2007, [155644](#)) evaluated the effects of washing with water, oven drying, and acid washing as pretreatments and found little difference in uptake efficiencies, although the ratio of the collecting surface area to mass was found to be a key factor in uptake efficiency.

Couto et al. (2004, [155739](#)) investigated dry versus bulk deposition of metals using transplanted moss bags. This study showed that at some sites dry deposition exceeded bulk deposition, a likely outcome of wash-off of dry deposited particles. This study also documented intercationic displacement and leaching as a result of acidic precipitation. The

authors concluded that the accumulated metal concentration represented an unstable equilibrium between inputs and outputs of elements that were a function of the local environment and weather during the exposure period. They also concluded that it was not possible to extrapolate calibrations between metal accumulation in moss and atmospheric deposition of metals to areas with different weather conditions, precipitation pH, and air contaminant concentrations. Zechmeister et al. (2003, [157175](#)) also presented results demonstrating the problems with dry deposited particles that can be washed off by rain. These studies indicate that moss is not a completely effective collector of total particle deposition. Deposition estimates from moss accumulation probably represent values that fall between wet deposition and total deposition.

A European moss biomonitoring network has been in place since 1990 (Harmens et al., 2007, [155828](#)). Sampling surveys are repeated every 5 yr. The survey conducted in 2005/2006 occurred in 32 countries at over 7000 sites. The network reports metal concentrations associated with live moss tissue. Trends analysis of these data showed statistically significant decreases over time in moss concentrations for As, Cu, V, and Zn. Trends were not observed for Cr, Fe, or Ni. Results for individual countries participating in the survey have also been published. In Hungary, major pollution sources were readily detected by moss sampling (Ötvös, 2003). Somewhat higher metal concentrations in mosses in 1997 than in other European countries were attributed to the use of a different moss species in the Hungarian survey (Ötvös, 2003). Similar sampling in Romania showed regions with contamination that were among the highest in Europe. These results were consistent with known air quality problems in Romania (Lucaciu et al., 2004, [155947](#)). Because particulate deposition is not well characterized using this method, spatial patterns and temporal trends for particulate metal deposition in Europe only provide crude estimates of relative deposition patterns.

The use of moss to assess heavy metal deposition has received much less attention in the U.S. than in Europe. A study conducted in the Blue Ridge Mountains, VA, found that metal concentrations in moss were related to elevation and canopy species at some sites (Schilling and Lehman, 2002, [113075](#)). However, metal concentrations in moss were not related to concentrations in the O horizon of the soil. Other measurement methods for trace metal deposition were not available to compare with moss concentrations.

Epiphytic lichens have also been used to evaluate heavy metal accumulation. Helena et al. (2004, [155833](#)) found substantially increased concentrations of metals in lichens

transplanted from a relatively clean region to an area in proximity to a metal smelter. The presence of specific species of bryophyte or lichen can serve as an effective bioindicator of metal contamination (Cuny et al., 2004, [155742](#)). In some studies, tree bark has been used as a biomonitor for atmospheric deposition of heavy metals (Baptista et al., 2008, [155673](#); Pacheco and Freitas, 2004, [156011](#); Rusu et al., 2006, [156062](#)).

Biomonitoring using mosses, lichens, or other types of vegetation has been well established as a means of identifying spatial patterns in atmospheric deposition of heavy metals in relation to power plants, industry, and other point and regional emissions sources. More recently, a number of studies (López Alonso et al., 2002, [155943](#); 2003, [155944](#); 2003, [155945](#)) have used cattle that have been reared predominantly on local forage as a means of monitoring atmospheric inputs of Cu, Ar, Zn, and Hg. For example, Hg emissions from coal fired power plants in Spain had a substantial effect on Hg accumulation by calves (López Alonso et al., 2003, [155944](#)). Accumulation of Hg by cattle extended to ~140-200 km downwind from the source.

Yang and Zhu (2007, [156168](#)) investigated the effectiveness of pine needles as passive air samplers for SOCs, such as PAHs, that are partially or completely particle-associated in the atmosphere. PAH distribution patterns are complicated by their properties, which span a broad range of octanol-air partition coefficients. This allows them to be present in both vapor and particle phases. In addition, the air-plant partitioning of PAHs is affected by air temperature and atmospheric stability (Yang and Chen, 2007, [092847](#)). DeNicola et al. (2005, [155747](#)) documented the suitability of a Mediterranean evergreen oak (*Quercus ilex*) to serve as a passive biomonitor for atmospheric contamination with PAH in Italy.

Deposition to Canopies

Tree canopies have been shown to increase dry deposition from the atmosphere, including deposition of PM. Dry deposition rates in the canopy are commonly estimated by the difference between throughfall deposition and deposition measured by an open collector, although the use of this approach to specifically quantify particulate deposition is complicated by gaseous deposition to leaf surfaces and, for some elements, leaching and uptake. Avila and Rodrigo (2004, [155664](#)) found that trace metal deposition in throughfall in a Spanish oak forest were higher than bulk deposition for Cu, Pb, Mn, V, and Ni, but not for Cd and Zn. This study also found that dry deposition of Cu, Pb, Zn, Cd and V occurred, but that canopy uptake of Zn and Cd also occurred. Leaching of Mn and Ni from the foliage

was observed as well. Leaching of Ni, Cu, Mn, Rb, and Sr from a red spruce-balsam fir canopy by acidic cloud water was also measured in a study by Lawson et al. (2003, [089371](#)). These studies suggest that leaching of trace metals from forest canopies varies with tree species and the acidity of precipitation. Throughfall therefore cannot be assumed to represent total deposition of heavy metals without evaluating uptake and leaching at the specific study site.

Physical models have provided an alternative to estimating dry deposition to canopies with throughfall measurements. Recently, Pryor and Binkowski (2004, [116805](#)) identified an additional complication in that models typically hold particle size constant. Nevertheless, there may be significant modification of particle size distributions during the deposition process. Condensation processes in the vicinity of the canopy can increase particle size and may explain discrepancies between observations and modeled dry deposition that is based on air sampling of particulates above the canopy.

The use of pine and oak canopies as bioindicators of atmospheric trace metal pollution was investigated by Aboal et al. (2004, [155642](#)). Metal concentrations in leaves were found to be one to three orders of magnitude lower than in mosses collected in this study. As an ecosystem pool, metals in leaves were likely to be much more important than those in mosses. The authors concluded, however, that these tree species were not effective bioindicators of atmospheric deposition of heavy metals.

The effectiveness of tree canopies in capturing particulates was investigated as a method for improving air quality by Freer-Smith et al. (2004, [156451](#)). This study showed that with consideration of planting design, location of pollution source, and tree species, planting of trees can be effective at reducing particulate air pollution. However, this approach does not address the possible effects of the captured pollution on trees, soils and surface waters.

High-elevation forests generally receive larger particulate deposition loadings than equivalent low elevation sites. Higher wind speeds at high elevation enhance the rate of aerosol impaction. Orographic effects enhance rainfall intensity and composition and increase the duration of occult deposition. High-elevation forests are often dominated by coniferous species with needle-shaped leaves that enhance impaction and retention of PM delivered by all three deposition modes.

Deposition to Soil

As with mosses, accumulation of heavy metals in surface soils provides a general reflection of the spatial distribution of industrial pollution. The distribution of toxic elements in urban soils has been an important area of study (Madrid et al., 2002, [155956](#); Markiewicz Patkowska et al., 2005, [155963](#)). Generally, Cu, Pb, Zn, and Ni have accumulated in urban soils compared with their rural counterparts (Yuangen et al., 2006, [156174](#)). In the study of Romić and Romić (2003, [156055](#)), relationships were found between urban activities and concentrations of metals in soils in developed areas surrounding Zagreb, Croatia. Goodarzi et al. (2002, [155801](#)) compared deposition estimated by moss bags to concentrations of metals in A-horizon soils in the vicinity of a large smelter. Statistically significant correlations were observed between the moss bag deposition estimates and the soil metal concentrations for Cd, Pb, Zn, and in some cases also Cu. These correlations suggested that atmospheric deposition of metals caused elevated metal concentrations in the upper mineral horizon of these soils. No correlations were found for Hg or As in this study.

Studies have also looked at metal accumulation in peat because of the tendency of most metals to be immobilized through binding with organic matter. Steinnes et al. (2005, [156095](#)) presented geographical patterns of metal concentrations in surface peat throughout Norway that corresponded to pollution sources, although the peat samples were collected in 1979. Zaccone et al. (2007, [179930](#)) found that variations of metal concentrations with depth in a single Swiss peat core corresponded with the depositional history that would be expected from the industrial revolution, although Cs¹³⁷ activity exhibited a distribution in the profile that was not fully consistent with the Chernobyl nuclear reactor accident. A detailed study of Finish peat showed that relationships between depth profiles of metal concentrations and deposition history can match well for some metals at some sites, but not well for the same metals at other sites (Roberts et al., 2003, [156051](#)). They also found that Zn and Cd accumulation rates were independent of deposition history at each of three study sites.

Metal deposition to soil is also a significant concern adjacent to roadways. Urban stormwater can be rich in heavy metals and other contaminants derived from atmospheric deposition, and can be a major source of pollutant inputs to water bodies in urban settings. Urban stormwater runoff can also be toxic to aquatic biota, partly due to trace metal concentrations (Greenstein et al., 2004, [155808](#); Sabin et al., 2005, [088300](#); Schiff et al.,

2002, [156959](#)). These processes are largely a function of the impervious nature of much of the ground surface in urban areas (i.e., buildings, roads, sidewalks, parking lots, construction sites). Dry-deposited pollutants can build up, especially in arid and semi-arid environments, and then be washed into surface waters with the first precipitation event. The concentrations of Cd, Ca, Cu, Pb, and Zn in road runoff were found to be significantly higher during winter in Sweden. This seasonal pattern was attributed to the intense wearing of the pavement that occurred during winter due to the use of studded tires in combination with chemical effects of deicing salts (Bäckström et al., 2003, [156242](#)).

9.4.3. Direct Effects of PM on Vegetation

Exposure to airborne PM can lead to a range of phytotoxic responses, depending on the particular mix of deposited particles. This was well known at the time of the previous PM criteria assessment, as summarized below. Most direct phytotoxic effects occur in severely polluted areas surrounding industrial point sources, such as limestone quarries and other mining activities, cement kilns, and metal smelting facilities (U.S. EPA, 2006, [090110](#)). Experimental application of PM constituents to foliage typically elicits little response at the more common ambient concentrations. The diverse chemistry and size characteristics of ambient PM and the lack of clear distinction between effects attributed to phytotoxic particles and to other air pollutants further confound understanding of the direct effects on foliar surfaces.

Deposition of PM can cause the accumulation of heavy metals on vegetative surfaces. Low solubility limits foliar uptake and direct heavy metal toxicity because trace metals must be brought into solution before they can enter into the leaves or bark of vascular plants. In those instances when trace metals are absorbed, they are frequently bound in leaf tissue and are lost when the leaf drops off (Hughes, 1981, [156578](#)).

Depending on the size of the particles, the PM deposited on the leaf surface can affect the plant's metabolism and photosynthesis by blocking light, obstructing stomatal apertures, increasing leaf temperature and altering pigment and mineral content (Naidoo and Chirkoot, 2004, [190449](#)) (see Section 9.4.3.1.). Fine PM has been shown to enter the leaf through the stomata and penetrate into the mesophyll layers where it alters leaf chemistry (Da Silva et al., 2006, [190190](#)). Kuki et al. (2008, [155346](#)) also showed increased leaf permeability and increased activity of enzymes in response to fine PM lead (see discussion in Section 9.4.5.).

Studies of the direct toxic effects of particles on vegetation have not yet advanced to the stage of reproducible exposure experiments. In general, phytotoxic gases are deposited more readily, assimilated more rapidly, and lead to greater direct injury of vegetation as compared with most common particulate materials. The dose-response functions obtained in early experiments following the exposure of plants to phytotoxic gases generally have not been observed following the application of particles (EPA, 2004, [056905](#)).

9.4.3.1. Effects of Coarse-mode Particles

The current state of scientific knowledge regarding the direct effects of coarse PM on plants has not changed since publication of the previous PM criteria assessment (EPA, 2004, [056905](#)). The summary provided here is taken from that report. In many rural areas and some urban areas, the majority of the mass in the coarse particle mode derives from the elements silicon, aluminum, calcium, and iron, suggesting a crustal origin as fugitive dust from disturbed land, roadways, agriculture tillage, or construction activities. Large particles tend to deposit near their source (Grantz et al., 2003, [155805](#)) and rapid sedimentation of coarse particles tends to restrict their direct effects on vegetation largely to roadsides and forest edges, which often receive the greatest deposition (EPA, 2004, [056905](#))

Dust

Dust can cause both physical and chemical effects. Consequences are often mediated via impacts on leaf cuticles and waxes. Deposition of inert PM on above-ground plant organs sufficient to coat them with a layer of dust may result in changes in radiation received, a rise in leaf temperature, and the blockage of stomata. Crust formation can reduce photosynthesis and the formation of carbohydrates needed for normal growth, induce premature leaf-fall, damage leaf tissues, inhibit growth of new tissue, and reduce starch storage. Dust may decrease photosynthesis, respiration, and transpiration; and it may result in the condensation and reactivity of gaseous pollutants with PM, thereby causing visible injury symptoms and decreased productivity (EPA, 2004, [056905](#)). Leaves with trichomes may be more prone to the accumulation of dust on leaf surfaces (Kuki et al., 2008, [155346](#)).

The chemical composition of PM is usually the key phytotoxic factor leading to plant injury. For example, cement-kiln dust liberates calcium hydroxide on hydration. It can then

penetrate the epidermis and enter the mesophyll, causing an increase in leaf surface pH. In turn, surface pH can be important for surface microbial colonization and wax formation and degradation.

Salt

Sea-salt particles can serve as nuclei for the absorption and subsequent reaction of other gaseous and particulate air pollutants. Direct effects on vegetation reflect these inputs and salt injury caused by the sodium and chloride that constitute the bulk of these particles. The source of most salt spray is aerosolized ocean water. Sea salt can cause damage to plants; however, it is not covered in this assessment because it is not of anthropogenic origin. However particulate salt may be input to an ecosystem from deicing salt.

Injury to vegetation from the application of deicing salt is caused by salt spray blown or drifting from the highways (Viskari and Karenlampi, 2000, [019101](#)). The most severe injury is often observed nearest the highway. Conifers planted near roadway margins in the eastern U.S. often exhibit foliar injury due to toxic amounts of saline aerosols deposited from deicing solutions (EPA, 2004, [056905](#)).

Exposure of vegetation to atmospheric PM deposition can lead to varying levels of effects, depending on PM deposition amounts and the chemical make-up of the deposited materials. Nevertheless, most of the well-documented examples of direct PM effects have been caused largely by coarse particles deposited in close proximity to industrial point sources, such as limestone quarries, cement kilns, and metal smelting facilities (Grantz et al., 2003, [155805](#)). Fine particles tend to have wider atmospheric distribution, and their direct effects have not been as clearly demonstrated.

9.4.4. PM and Diffuse Light Effects

Atmospheric PM can affect ambient radiation, which can be considered in both its direct and diffuse components. Foliar interception by canopy elements occurs for both up- and down-welling radiation. Therefore, the effect of atmospheric PM on atmospheric turbidity influences canopy processes both by radiation attenuation and by changing the efficiency of radiation interception in the canopy through conversion of direct to diffuse radiation (Hoyt, 1978, [046638](#)). Diffuse radiation is more uniformly distributed throughout the canopy and increases canopy photosynthetic productivity by distributing radiation to

lower leaves. The enrichment in photosynthetically active radiation (PAR) present in diffuse radiation appears to offset a portion of the effect of an increased atmospheric albedo due to atmospheric particles.

The effects of regional haze on the yield of crops because of reduction in solar radiation were examined by Chameides et al. (1999, [011184](#)) in China, where regional haze is especially severe. They estimated that approximately 70% of crops were being depressed by at least 3 to 5% by regional scale air pollution and its associated haze (Chameides et al., 1999, [011184](#); EPA, 2004, [056905](#)).

The net effect of PM on photosynthesis depends on the balance between the reduction in total PAR (which decreases photosynthesis) and the increase in the diffuse fraction of PAR (which tends to increase photosynthesis). The ‘global dimming’ period occurred between 1950 and 1980 and was characterized by reduced PAR and increased diffuse light caused by anthropogenic aerosols. Mercado et al. (2009, [190444](#)) estimate the effects of variations in diffuse light on the terrestrial carbon sink during the last century using a global model. The results indicate that the terrestrial carbon sink increased by approximately 25% during the “global dimming” period, likely driven by increased diffuse light despite decreased PAR. However under a future scenario in which SO_4^{2-} and BC aerosols decline, the diffuse-radiation and the associated terrestrial C sink also decline.

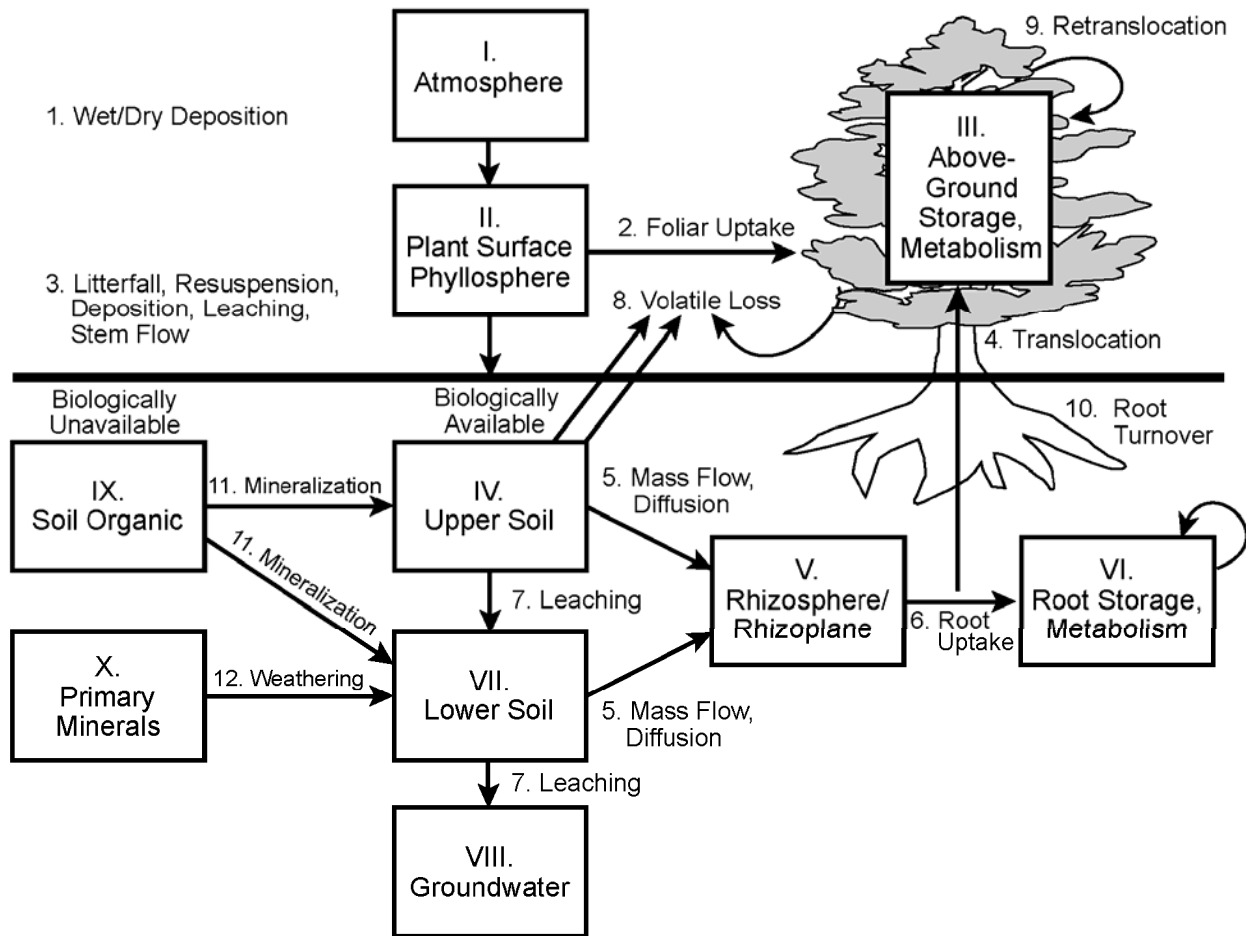
9.4.5. Effects of Trace Metals on Ecosystems

Trace metals may enter the ecosystems as both fine and coarse particles. All but 10 of the 90 elements that comprise the inorganic fraction of the soil occur at concentrations of <0.1% (1000 $\mu\text{g/g}$) and are termed “trace” elements or trace metals. Trace metals with a density greater than 6 g/cm^3 , referred to as “heavy metals” (e.g., Cd, Cu, Pb, Cr, Hg, Ni, Zn), are of particular interest because of their potential toxicity to plants and animals. Although some trace metals are essential for vegetative growth or animal health, they are all toxic in large quantities. Most trace elements exist in the atmosphere in particulate form as metal oxides (Ormrod, 1984, [046892](#)). Aerosols containing trace elements derive predominantly from industrial activities. Generally, only the heavy metals Cd, Cr, Ni, and Hg are released from stacks in the vapor phase (McGowan et al., 1993, [046731](#)). Atmospherically deposited PM can interact with a variety of biogeochemical processes. The potential pathways of accumulation of trace metals in terrestrial ecosystems, as well as the possible consequences of trace metal deposition on ecosystem functions, are summarized in Figure 9-84 (U.S. EPA,

2004, [056905](#)). A number of mass balance approaches (Macleod et al., 2005, [155954](#); Toose and Mackay, 2004, [156123](#)), and metal speciation and transport models (Bhavsar et al., 2004, [155689](#); Bhavsar et al., 2004, [155690](#); Gandhi et al., 2007, [155781](#)) have been developed in recent years.

Atmospheric Pb is a component of PM in some regions. The effects of Pb on ecosystems were discussed in the 2006 Pb AQCD (U.S. EPA, 2006, [090110](#)), which concluded that, due to the deposition of Pb from past human practices (e.g., leaded gasoline, ore smelting) and the long residence time of Pb in many aquatic and terrestrial ecosystems, a legacy of environmental Pb burden exists, over which is superimposed much lower contemporary atmospheric Pb loadings. The potential for ecological effects of the combined legacy and contemporary Pb burden to occur is a function of the bioavailability or bioaccessibility of the Pb. This, in turn, is highly dependent upon numerous site factors (e.g., soil OC content, pH, water hardness). Although the more localized ecosystem impacts observed around smelters are often striking, effects generally cannot be attributed solely to Pb, because of the presence of many other stressors (e.g., other heavy metals, oxides of sulfur and nitrogen) that can also act singly or in concert with Pb to cause readily observable environmental impacts (U.S. EPA, 2008, [157074](#); EPA, 2004, [056905](#)).

Effects of fine particle trace elements were described by the U.S. EPA (2004, [056905](#)), and some additional more recent research has also been conducted, especially on the topic of vegetative uptake of trace elements from the soil. The state of scientific understanding as presented by the U.S. EPA (2004, [056905](#)) as well as a discussion of more recent research findings are presented below.



Source: U.S. EPA (2004, [056905](#))

Figure 9-84. Relationship of plant nutrients and trace metals with vegetation. Compartments (roman numerals) represent potential storage sites; whereas arrows (Arabic numerals) represent potential transfer routes.

9.4.5.1. Direct Effects of Metals

Direct effects of trace elements on vegetation can result from their deposition and residence on foliar surfaces. Direct metal phytotoxicity can occur only if the metal can move from the surface into the leaf or directly from the soil into the root. Low solubility limits entry into plant tissue. Trace metals absorbed into leaf tissue are eventually transferred to the soil litter layer where they can affect litter decomposition, an important source of soil nutrients. Fungi and microorganisms living on leaves aid in leaf decomposition after leaves are dropped to the forest floor. Changes in litter decomposition processes in response to

metal toxicity can influence nutrient cycling in the soil and limit the supply of essential nutrients.

Foliar Effects

Da Silva et al. (2006, [190190](#)) have shown that PM had anatomical and physiological effects on plants growing near an iron pelletization factory in Brazil. The effects of PM occurred due to foliar uptake. Structural characteristics such as peltate trichomes, probably formed a barrier lessening the penetration of metallic iron into the mesophyll in some species. Iron was shown to penetrate the trichomes, epidermic cells (adaxial and abaxial surfaces), stomata, xylem cells, collenchyma, endodermis and mesophyll tissues. Once entering the stomata, the PM penetrates within the mesophyll, it may modify the chemical balance of the mesophyll (Da Silva et al., 2006, [190190](#)).

A greenhouse study evaluated the combined effects of iron dust on restinga vegetation (coastal vegetation of Brazil) that commonly grows near iron ore industries simulated field conditions. Kuki et al. (2008, [155346](#)) found that iron dust had differing effects on gas exchange, chlorophyll content, iron content and antioxidant enzyme activity on two plant species common to the restinga. *Schinus terebinthifolius* (an invasive exotic in the U.S.) was not affected by the iron dust. However, *Sophora tomentosa* showed increased iron content and membrane permeability to the leaves, increased activity of antioxidant enzymes. These results showed that the plants used different strategies to cope with PM pollution, *S. terebinthifolius* avoided stress, while *S. tomentosa* used antioxidant enzyme systems to partially neutralize oxidative stress.

Toxicity to Mosses and Lichens

At the time of the most recent air quality criteria report for PM (EPA, 2004, [056905](#)), trace metal toxicity to lichens had been demonstrated in relatively few cases. Nash (1975, [016763](#)) documented Zn toxicity in the vicinity of a Zn smelter near Palmerton, PA. Experimental data had suggested that lichen tolerance to Zn and Cd generally ranges between 200 and 600 ppm (Nash TH, 1975, [016763](#)).

The effects of deposited metals on the mosses have not been well studied. Tremper et al. (2004, [156126](#)) exposed mosses of two species to roadside conditions and sampled them over a period of three months. Under field conditions, chlorophyll concentrations in moss tissue were not affected by metal contamination and accumulation

Mosses and lichens readily take up metals from atmospheric deposition. Otnyukova (2007, [156009](#)) demonstrated vertical gradients within a coniferous forest canopy in the fruticose lichen genus *Usnea* with respect to lichen thallus morphology and heavy metal concentration. Abnormal thalli at the tree-top level contained higher concentrations of Al, Fe, Zn, F, Sr, and Pb. This vertical pattern within the tree canopy is in general accordance with known deposition of PM to plants (Otnyukova, 2007, [156009](#)).

There is an extensive literature on the use of mosses and lichens for estimating deposition (biomonitors) and indicating metal exposure in ecosystems (bioindicators) (see Section 9.4.2.3.).

9.4.5.2. Effects on Soil Chemistry

Trace metals are naturally found in small amounts in soils, ground water, and vegetation. Many are essential micronutrients required for growth by plants and animals. Naturally occurring mineralization can produce metal concentrations in soils and vegetation that are high compared to atmospheric sources. Many metals are bound by chemical processes in the soil, reducing their availability to biota. However, epiphytic or parasitic root colonizing microorganisms can solubilize and transport metals for root uptake (Lingua et al., 2008, [155935](#)). It can be difficult to assess the extent to which observed heavy metal concentrations in soil are of anthropogenic origin. This is because soil parent material, pedogenesis, and anthropogenic inputs all influence the amounts and distribution of trace elements in soil. Trace element concentrations in some natural soils that are remote from air pollution can be higher than soils derived from other parent materials that receive anthropogenic inputs (Burt et al., 2003, [155709](#)). The general effects of metals from atmospheric deposition are presented in the following discussion.

There is not a standard method available for quantifying the bioavailability of heavy metals in soil. A variety of models, isotopic studies, and sequential extraction methods have been used (Shan et al., 2003, [156972](#); Collins et al., 2003, [155737](#); Feng et al., 2005, [155774](#)). Total metal concentration in soil does not give a good indication of potential biological effects because soils vary in their ability to bind metals in forms that are not bioavailable. There are various methods available for assessing bioavailability of metals, but soils are heterogeneous and there is no ideal method for evaluating what conditions the soil biota experience. Almås et al. (2004, [155654](#)) argued that the actual measurement of biological effects is the best criterion for determining bioavailability. In particular, the

replacement of metal-sensitive microorganisms by metal-tolerant organisms within each functional group may be one of the most sensitive indicators of metal exposure. An increase in microbial trace metal tolerance per se would not be problematic if it was not for the fact that this increase in tolerance is generally accompanied by a decrease in microbial diversity (Lakzian et al., 2002, [156671](#); Almås ÅR et al., 2004, [155654](#)).

Heavy metals deposited from the atmosphere to forests accumulate either in the organic forest floor or in the upper mineral soil layers and metal concentration tends to decrease with soil depth. The accumulation of heavy metals in soil is influenced by a variety of soil characteristics, including pH, Fe and Al oxide content, amount of clay and organic material, and cation exchange capacity (CEC) (Hernandez et al., 2003, [155841](#)). Thus, the pattern of distribution of heavy metals in soils depends on both the soil characteristics and the metal characteristics.

Burt et al. (2003, [155709](#)) investigated the concentrations and chemical forms of trace metals in smelter-contaminated soils collected in the Anaconda and Deer Lodge Valley area of Montana, one of the major mining districts of the world for over a century (1864-1983). The relative distributions of trace metals within the more soluble soil extraction forms were similar to their respective total concentrations. This suggested a relationship between the concentrations of total trace elements and concentrations of soluble mobile fractions. Sequential extractions do not provide direct characterization of trace metal speciation, but rather an indication of chemical reactivity (Burt et al., 2003, [155709](#); Ramos et al., 1994, [046736](#)). Soluble and exchangeable forms are considered readily mobile and bioavailable. Those bound to clay minerals or organic matter are considered generally unavailable.

There is concern that Pb contamination of forest soil could move into groundwater. This would be important in view of the large quantity of Pb deposited from the atmosphere in the 1960s and 1970s in response to combustion of leaded gasoline. This issue was investigated by Watmough et al. (2004, [077809](#)) who applied a stable isotope (^{207}Pb) to the forest floors of white pine (*Pinus strobus*) and sugar maple (*Acer saccharum*) stands. Added Pb was rapidly lost from the forest floor, likely due to high litter turnover in these forest types. However, Pb concentrations in the upper 30 cm of mineral soil were strongly correlated with soil OM, suggesting that Pb does not readily move down the soil profile to the ground water, but rather is associated with the organic content of the upper soil layers (Watmough et al., 2004, [077809](#)).

The upper soil layers are typically an active site of litter decomposition and plant root uptake, both processes may be affected by metal components of PM. Surface litter decomposition is reduced in soils having high metal concentrations. This is likely due to the sensitivity to metals of microbial decomposers and reduced palatability of plant litter having high metal concentration (Johnson and Hale, 2008, [155881](#)). Root decomposition is a key component of nutrient cycling. Johnson and Hale (2008, [155881](#)) measured in situ fine root decomposition at Sudbury, Ontario and Rouyn-Noranda, Quebec. Elevated soil metal concentrations (Cu, Ni, Pb, Zn) did not necessarily reduce fine root decomposition. Only at sites having high concentrations of metals did decomposing roots show increased metal concentrations over time.

9.4.5.3. Effects on Soil Microbes and Plant Uptake via Soil

Upon entering the soil environment, PM pollutants can alter ecological processes of energy flow and nutrient cycling, inhibit nutrient uptake, change ecosystem structure, and affect ecosystem biodiversity. Many of the most important effects occur in the soil. The soil environment is one of the most dynamic sites of biological interaction in nature. It is inhabited by microbial communities of bacteria, fungi, and actinomycetes. These organisms are essential participants in the nutrient cycles that make elements available for plant uptake. Changes in the soil environment that influence the role of the bacteria and fungi in nutrient cycling determine plant and ultimately ecosystem response.

Many of the major indirect plant responses to PM deposition are chiefly soil-mediated and depend on the chemical composition of the individual components of deposited PM. Effects may result in changes in biota and in soil conditions that affect ecological processes, such as nutrient cycling and uptake by plants.

The soil environment is rich in biota. Bacteria and fungi are usually most abundant in the rhizosphere, the soil around plant roots that all mineral nutrients must pass through. Bacteria and fungi benefit from the nutrients that are present in root exudates and make mineral nutrients available for plant uptake. The soil-mediated ecosystem impacts of PM are largely determined by effects on the growth of bacteria and mycorrhizal fungi that are involved in nutrient cycling and plant nutrient uptake.

Soil Nutrient Cycling

Accumulation of heavy metals in litter can interfere with nutrient cycling.

Microorganisms are responsible for decomposition of organic matter, which contributes to soil fertility. Toxic effects on the microflora can be caused by Zn, Cd, and Cu. The U.S. EPA (2004, [056905](#)) judged that addition of only a few mg of Zn per kg of soil can inhibit sensitive microbial processes. Enzymes involved in the cycling of N, P, and S (especially arylsulfatase and phosphatase) seem to be most affected (Kandeler et al., 1996, [094392](#)).

Soil organic matter cycling is known to be sensitive to disturbance due to heavy metal pollution. This can cause increased litter accumulation at sites close to metal emissions point sources. The relative importance of the various processes that might be responsible for this observation is poorly known. Boucher et al. (2005, [155699](#)) conducted CO₂ evolution studies in microcosms having metal-rich and metal-poor plant materials. Their results suggested that there was a pool of less readily decomposable C that appeared to be preferentially preserved in the presence of high metal (Zn, Pb, Cd) concentrations in the leaves of the metallophyte *Arabidopsis halleri*. An additional possibility is that increased lignification of the cell walls increased the amount of insoluble C (Mayo et al., 1992, [155974](#)).

Yuangen et al. (2006, [156174](#)) found that urban soil basal respiration rates were positively correlated with soil acetic acid-extractable Cd, Cu, Ni, and Zn. The soil microbial biomass was negatively correlated with the concentrations of Pb fractions, but not with other metals. Overall microbial biomass was lower for urban soils as compared with rural soils (Yuangen et al., 2006, [156174](#)).

Metal Toxicity to Microbial Communities

It is believed that increased accumulation of litter in metal-contaminated areas is due to the effects of metal toxicity on microorganisms. Smith (1991, [042566](#)) reported the effects of Cd, Cu, Ni, and Zn on the symbiotic activity of fungi, bacteria, and actinomycetes. In particular, the formation of mycorrhizae has been shown to be reduced when Zn, Cu, Ni, and Cd were added to the soil.

Most studies of the effects of heavy metals on soils have been conducted under laboratory conditions. However, Oliveira and Pampulha (2006, [156827](#)) performed a field study to evaluate long-term changes in soil microbiological characteristics in response to heavy metal contamination. Dehydrogenase activity, soil ATP content, and enumeration of

major soil microbial groups illustrated the effects of contamination. There was a marked decrease in total numbers of the different microbial groups. In particular, asymbiotic nitrogen-fixers and heterotrophic bacteria were found to be sensitive. Dehydrogenase activity was confirmed to be a good assay for determining the effect of heavy metals on physiologically active soil microbial biomass.

The toxic effects of heavy metals on soil microorganisms are well known. However, less is known about the relative sensitivity of different types of soil microorganisms (Rajapaksha et al., 2004, [156035](#)). Vaisvalavicius et al. (2006, [157080](#)) assessed the toxicity of high concentrations of Pb (839 mg/kg), Zn (844 mg/kg), and Cu (773 mg/kg) in the upper 0 to 0.1 m soil layer. Microbial abundance of all groups was reduced and enzymatic activity was lower than for uncontaminated soil. In particular, actinomycetes, oligonitrophobic and mineral N assimilating bacteria were most affected.

Effects of heavy metals in soil on microbes depends on soil pH, organic content, and the type of heavy metal exposure (Kucharski and Wyszowska, 2004, [156662](#)). Some studies have shown that heavy metals inhibit microbial activity in soil (Smejkalova et al., 2003, [156987](#); Vasundhara et al., 2004, [156133](#)). However, Wyszowska et al. (2007, [179948](#)) showed that heavy metals can either inhibit or stimulate the growth of soil microbes. Populations of *Azotobacter* spp. decreased, but populations of oligotrophic and copiotrophic bacteria, actinomyces, and fungi increased in response to heavy metal exposure. Acute metal stress causes a decrease in microbial biomass as metal-sensitive microbes are inhibited (Joynt et al., 2006, [155887](#)).

Studies of the impacts of metal stress on the microbial community composition in soil have generally been based on microbial culturing techniques that can select only a subset of the natural soil population of microbes. More recent culture-independent studies have been conducted using phospholipids or nucleic acid biomarkers to reveal information regarding changes in microbial community structure (Joynt et al., 2006, [155887](#)). Using this approach, Joynt et al. (2006, [155887](#)) demonstrated that soils contaminated with both metals (Pb, Cr) and organic solvent compounds over a period of several decades had undergone changes in community composition, but still contained a phylogenetically diverse group of bacteria. This may reflect adaptation to the potentially toxic conditions through such processes as natural selection, gene exchange, and immigration. Comparison between a severely contaminated soil with a similar soil that had much lower amounts of contamination showed considerably lower microbial diversity in the contaminated soil, particularly for

asymbiotic nitrogen fixers and heterotrophic bacteria (Oliveira and Pampulha, 2006, [156827](#)).

As pollution increases, it is expected that the more sensitive species will be lost and the more tolerant species remain. This gives rise to the concept of pollution-induced community tolerance (PICT), which has been demonstrated for populations of bacteria and fungi (Davis et al., 2004, [155744](#)). These researchers assessed the effects of long-term Zn exposure on the metabolic diversity and tolerance to Zn of a soil microbial community across a gradient of Zn pollution. PICT was found to correlate better with total soil Zn than with the concentration of Zn in soil pore water.

Soil Microbe Interactions with Plant Uptake of Metals

Atmospherically-deposited metals accumulate in upper soil horizons where fine roots are most developed. The availability for plant uptake of metals in soil depends on metal speciation and soil pH. In addition, metal binding to dissolved organic matter (DOM) reduces bioavailability (Sauvé, 2001, [156948](#)). Because organic matter typically decreases with soil depth, the affinity of metals for organic matter can influence metal bioavailability at different soil depths. Fine roots (<2 mm diameter) provide the major site of uptake and transport to the above-ground plant and generally contain a large proportion of the total metals found in plants (Gordon and Jackson, 2000, [155802](#)).

Fine roots are often colonized by mycorrhiza and interact with other soil microbes. Recent published evidence supports that mycorrhiza and bacteria influence plant uptake and tolerance of metals. Mycorrhiza are fungi that colonize plant roots to form a symbiosis. Mycorrhiza uptake nutrients from the soil and transfer them to the plant in exchange for carbon from the plant. Like plants, some species and strains of mycorrhiza are more tolerant of metals in the soil (Ray et al., 2005, [190473](#)), so that unpolluted and polluted sites may host different species and strains of mycorrhiza (Vogel-Mikus et al., 2005, [190501](#)).

Mycorrhiza have been observed to cause a range of effects on plants. In some cases, plants colonized with mycorrhiza showed improved nutrient uptake and decreased metal uptake (Berthelsen et al., 1995, [078058](#); Vogel-Mikus et al., 2006, [190502](#); Nogueira et al., 2004, [190460](#)). Mycorrhiza have been shown to accumulate metals and act as a sink (Berthelsen et al., 1995, [078058](#); Carvalho et al., 2006, [155715](#)) often preventing the metals in the roots from allocation to shoots (Kaldorf et al., 1999, [190399](#); Zhang et al., 2005,

[192083](#); Soares and Siqueira, 2008, [190482](#)). For example, estuarine salt marshes are often located close to urban and industrial areas and receive elevated amounts of trace metal contaminants from point and nonpoint (including atmospheric deposition) sources. Vegetation is important in the retention and accumulation of heavy metals in salt marshes. Carvalho et al. (2006, [155715](#)) conducted experiments on the effects of arbuscular mycorrhizal fungi (AMF) on the uptake of Cd and Cu by *Aster tripolium*, a common plant species in polluted salt marshes and a host of AMF. Carvalho et al. (2006, [155715](#)) found that AMF colonization increased metal accumulation in the root system of *Aster tripolium* without enhancing translocation to the shoot. By trapping toxic metals in the roots, this plant species may reduce the extent of vegetative stress caused by metal exposure and act as an effective sink for these metals. In a review paper Christie et al. (2004, [190174](#)) concluded that mycorrhiza may directly improve plant tolerance to metals by binding and immobilizing metals and indirectly improve plant tolerance by improving uptake of nutrients that increase plant growth.

There is recent evidence that bacteria and mycorrhiza act together to improve plant tolerance to metals. Like mycorrhiza some bacteria are more tolerant to metals than others (Vivas et al., 2003, [190499](#)). Combined inoculation of *Trifolium sp.* by the arbuscular mycorrhiza *Glomus mosseae* and the bacterium *Brevivacillus sp.* conferred tolerance to Cd by increasing nutrient status and rooting development and by increasing Cd uptake by the plant (Vivas et al., 2003, [190499](#)). A similar results was observed for Zn uptake (Vivas et al., 2006, [190500](#)).

In some cases mycorrhizae will not prevent metal uptake (Weissenhorn et al., 1995, [073826](#)). In fact mycorrhiza may facilitate the accumulation of metals in plants and mycorrhiza will enhance the translocation of metals from the root to the shoot (Vogel-Mikus et al., 2005, [190501](#); Citterio et al., 2005, [190176](#); Zimmer et al., 2009, [192085](#)). There is evidence of variable responses depending on the combination of mycorrhiza and bacteria species. Zimmer et al. (2009, [192085](#)) recently showed that the willow tree *Salix sp.* colonized with the ectomycorrhizal fungus *Hebeloma crustuliniforme* and the bacteria *Micrococcus luteus* increased total Cd and Zn accumulation due to enhanced mycorrhizal formation. In these cases where soil microbes cause increased metal accumulation, there is a potential to use the system for phytoremediation.

Plants also vary in the extent to which they take up heavy metals from the soil. Variability has been shown to occur in response to different plant species and different

metals. For example, Szabó and Fodor (2006, [156109](#)) exposed winter wheat (*Triticum aestivum*), maize (*Zea mays*) and sunflower (*Helianthus annuus*) to a variety of micro-pollutants. Cadmium accumulation was significant in both vegetative and reproductive plant parts. Vegetative winter wheat accumulated substantial amounts of Hg, but the other species did not. Lead, Cu, and Zn showed only moderate enrichment in crops (Szabó and Fodor, 2006, [156109](#)).

There is some evidence to support that shallow-rooted plant species are most likely to take up metals from the soil (Martin and Coughtry, 1981, [047727](#)). However, there is little evidence confirming this observation. It may be more likely that shallow roots of species are likely to take up metals because the metal often accumulates in shallow soil layers. Even though atmospheric PM will usually deposit on soils before being taken up by plants, it could also be deposited to aquatic systems with subsequent transfer to terrestrial plants. Contamination of stream sediments by heavy metals can impact adjacent terrestrial ecosystems when high flows cause resuspension and subsequent streamside deposition of sediment particles. For example, Ozdilek et al. (2007, [156010](#)) showed that metal concentrations in vegetation along the Blackstone River in Massachusetts and Rhode Island were generally inversely related to the distance from the riverbank, with higher metal concentrations in plant tissues located near the river. The ability of plants to take up metals from soil is an important part of metal cycling in the environment. This uptake process allows the metals to enter the food web, where they might exert mutagenic, carcinogenic, and teratogenic effects (Hunaiti et al., 2007, [156579](#)).

9.4.5.4. Plant Response to Metals

Some metals, including Cu, Co, Ni, and Zn, are essential micronutrients needed for plant growth. Others, including Hg, Cd, and Pb are not essential for plants. Though all heavy metals can be directly toxic at sufficiently high concentrations, only Cu, Ni, and Zn have been documented as being frequently toxic to plants (EPA, 2004, [056905](#)), while toxicity due to Cd, Co, and Pb has been observed less frequently (Smith, 1990, [046896](#)). Toxic doses depend on the type of ion, ion concentration, plant species and the stage of plant growth (Memon and Schroder, 2009, [190442](#)). Toxicity response is also dependent on the nutritional status of the plant and the development of mycorrhizae (Strandberg et al., 2006, [156105](#)). Plants respond to high concentrations of metals in soil through a variety of mechanisms and there are substantial differences among plant species

in their response to heavy metal exposure. Mechanisms of metal tolerance included exclusion or excretion rates, genetics (Patra et al., 2004, [081976](#); Yang et al., 2005, [192104](#)), mycorrhizal interactions (Gohre and Paszkowski, 2006, [190355](#)), storage capability and accumulation (Clemens, 2006, [190179](#)), and various cellular detoxification mechanisms (Hall, 2002, [190365](#); Gratao et al., 2005, [190364](#)).

One of the most important mechanisms that increases plant tolerance to metals is chelation with phytochelatins, such as metallothioneins and peptide ligands that are synthesized within the plant from glutathione (Memon and Schroder, 2009, [190442](#)). Phytochelatins are intracellular metal-binding peptides that act as specific indicators of metal stress. Because they are produced by plants as a response to sublethal concentrations of heavy metals, they can indicate that heavy metals play a role in forest decline (Gawel et al., 1996, [012278](#)). Phytochelatin concentrations have previously been measured in coniferous trees in the northeastern U.S. The U.S. EPA (2004, [056905](#)) and Grantz et al. (2003, [155805](#)) summarized studies indicating that both the number of dead red spruce trees and phytochelatin concentrations increased sharply with elevation in the northeastern U.S. Red spruce stands showing varying degrees of decline indicated a systematic and significant increase in phytochelatin concentrations associated with the extent of tree injury. These data suggest that metal stress might contribute to tree injury and forest decline in the northeastern U.S. The extent to which low to moderate amounts of heavy metal deposition, which might occur at locations that are not in close proximity to a large point source, contribute to adverse impacts on forest vegetation is not known. Although the phytochelatin data suggest a linkage, more direct experimental data would be needed to confirm such a finding.

In general plant growth is negatively correlated with trace metal and heavy metal concentration in soils and plant tissue (Audet and Charest, 2007, [190169](#)). Trace metals, particularly heavy metals can influence forest growth. Growth suppression of foliar microflora has been shown to result from Fe, Al, and Zn. These three metals can also inhibit fungal spore formation, as can Cd, Cr, Mg, and Ni (see Smith, 1990, [046896](#)). Metals cause stress and decreased photosynthesis (Kucera et al., 2008, [190408](#)) and disrupt numerous enzymes and metabolic pathways (Strydom et al., 2006, [190486](#)). Excessive concentrations of metals result in phytotoxicity through: (i) changes in the permeability of the cell membrane; (ii) reactions of sulfhydryl (-SH) groups with cations; (iii) affinity for reacting

with phosphate groups and active groups of ADP or ATP; and (iv) replacement of essential ions (Patra et al., 2004, [081976](#)).

In addition to disrupting photosynthesis and other metabolic pathways, metals have been shown to alter frost hardiness and impair nutrition. A recent review by Taulavuori (2005, [190489](#)) suggests that metal-induced stress reduces frost hardiness of plants, a particular concern at high elevation sites. Kim et al. (2003, [155899](#)) found decreased concentration of K in needles and Ca in stems of *Pinus sylvestris* seedlings exposed to Cd addition. This response suggests a disturbance of nutrition in response to Cd. Pollutant-caused needle loss can reduce the interception of pollutants from the atmosphere, and therefore reduce their concentrations in stemflow. This may be responsible for the observation that species diversity of lichens is sometimes higher on trees affected by die-back (Hauck, 2003, [155830](#)).

Plant foliage can accumulate elemental Hg over time in response to air exposure and concentrations in soil (Frescholtz et al., 2003, [190352](#); Ericksen et al., 2003, [155769](#)). A mesocosm experiment was conducted by Ericksen et al. (2003, [155769](#)) where aspen trees were grown in gas-exchange chambers in Hg-enriched soil ($12.3 \pm 1.3 \mu\text{g/g}$) and the Hg content in the foliage was analyzed. Foliar Hg increased with leaf age for two to three months and then stabilized at leaf concentrations near 150 ng/g . About 80% of the Hg found in above-ground biomass was present in the leaves. The concentration of Hg in trees grown in the same mesocosms in containers of low Hg soil ($0.03 \pm 0.01 \mu\text{g/g}$) exhibited foliar Hg concentrations that were similar to those of trees grown in Hg-enriched soil. Almost all of the foliar Hg originated from the atmosphere. Clearly, plant foliage can be a major sink for airborne Hg, which can subsequently enter the soil after litterfall (Ericksen et al., 2003, [155769](#)). However, this study did not determine the extent to which atmospheric Hg was dry-deposited on the foliage, as opposed to gaseous uptake through the stomata. Foliar/air Hg exchange has been shown to be dynamic and bi-directional (Millhollen et al., 2006, [190447](#)). These investigators compared foliar Hg accumulation over time in three tree species with fluxes measured using a plant gas-exchange system subsequent to soil amendment with HgCl_2 . Root tissue Hg concentrations were strongly correlated with soil Hg concentrations, suggesting that below-ground accumulation of Hg by roots may be an important process in the biogeochemical cycling of Hg in soil systems. Nevertheless, measured foliar Hg fluxes indicated that deposition of atmospheric Hg constituted the dominant flux of Hg to the leaf surface (Millhollen et al., 2006, [190447](#)). Grigal (2003,

[155811](#)) also found that Hg in vegetation is derived almost exclusively from the atmosphere. Mercury uptake from soil is limited, partly because roots adsorb Hg but transport it to foliage very poorly (Grigal, 2002, [156498](#)). Grigal (2003, [155811](#)) provided a thorough review of the sequestration of Hg in forest and peatland ecosystems. A fundamental aspect of Hg cycling is its strong relationship to organic matter. For that reason, peatlands sequester much larger quantities of Hg than would be expected on the basis of their land area. Thus, if global climate change affects C storage, it may indirectly affect Hg storage because of the strong relationship between Hg and organic matter (Grigal, 2003, [155811](#)).

Arbuscular mycorrhizal (AM) fungi can play important roles in mitigating toxicity of heavy metals in plants. For example, AM symbiosis is known to be involved in plant adaptation to As-contaminated soils. Higher plants that are adapted to As contaminated soils are generally associated with mycorrhizal fungi (Gonzalez-Chavez et al., 2002, [155800](#)). It has also been shown that AM symbioses can influence plant coexistence and community diversity (O'Connor, 2002). Some plants associated with AM fungi can successfully colonize sites that are heavily contaminated by heavy metals (Pennisi, 2004, [156018](#)).

Dong et al. (2008, [192106](#)) cultivated white clover (*Trifolium repens*) and ryegrass (*Lolium perenne*) in As-contaminated soil (water extractable As 82.7 mg/kg). The growth and P nutrition of both species largely depended on AM symbiosis. The AM-inoculated plants showed selective uptake and transfer of P over As.

PM pollution has the potential to alter species composition over long time scales. Kuki et al. (2009, [190411](#)) showed that early establishment stages of *Sophora tomentosa* species were negatively affected by the combination of iron ore and acidifying particles. The deleterious effects of the PM included deficient germination and toxic concentrations in roots. In contrast, *S. terebinthifolius* was not affected by the PM revealing species resistance to the pollution. The difference among species response suggests that over a long time period the imbalance will likely change the species composition (Kuki et al., 2009, [190411](#)).

The process of removing toxins from soil or water using photoautotrophs is referred to as phytoremediation. Some plant species have good ability to extract heavy metals from soil, thereby offering potential for phytoremediation (Clemens, 2006, [190179](#); Hooda, 2007, [190382](#); Padmavathiamma and Li, 2007, [190465](#)). For example, several species of willow (*Salix* spp.) accumulate high concentrations of Zn and Cd in aboveground biomass

(Lunácková et al., 2003, [155948](#); Meers et al., 2007, [155977](#); Rosselli et al., 2003, [156058](#)). A first estimation of the order of magnitude of potential metal removal by willow was 2 to 27 kg/ha/yr of Zn and 0.25 to 0.65 kg/ha/yr for Cd (Meers et al., 2007, [155977](#)). Build-up of high concentrations of trace metals in soil is difficult to remediate because of the long residence times of metals in the environment. Plants that survive on heavy metal-contaminated soils have been studied to elucidate the mechanisms that allow them to tolerate such conditions and interactions between soil contamination and vegetation composition (Becker and Brändel, 2007, [156260](#); Hall, 2002, [190365](#)). There are numerous other plants that have been investigated for application to phytoremediation. Plants that hyperaccumulate metals have special potential for remediation of metal-contaminated sites. About 400 species have been reported. Brassicaceae has the largest numbers of taxa, with 11 genera and 87 species known to hyperaccumulate one or more metal contaminants (Prasad and De Oliveira Freitas, 2003, [156885](#)).

Plant uptake is often the first step for a metal to enter higher levels of the food web. Consumers of vegetation may often receive heavy loading of metals from their diets. Metals may also bioaccumulate in some species and tissue concentrations are magnified at the higher trophic levels, so-called biomagnifications (see Section 9.4.5.7. on Biomagnification).

9.4.5.5. Effects on Aquatic Ecosystems

The atmospheric deposition of PM into the ocean has important implications for primary productivity and carbon sequestration. This is because metals in PM deposition limit phytoplankton growth in parts of the ocean (Crawford et al., 2003, [156370](#)). In particular, Fe and Zn can influence the productivity of algae that are involved in CaCO₃ production. The production of both particulate organic C and CaCO₃ drive the ocean's biological carbon pump (Shulz et al., 2004, [156087](#)). Thus, in oceanic areas of trace metal limitation, changes in trace metal atmospheric deposition can affect biogenic calcification, with potential consequences for CO₂ partitioning between the ocean and atmosphere.

A study by Sheesley et al. (2004, [156084](#)) illustrated the value of bioassay procedures to provide an initial screening of ambient PM toxicity. They used two species of green algae and two extraction methods to compare the toxicities of atmospheric PM collected at two urban/industrial sites and one rural site near the southern shore of Lake Michigan. Toxicities varied by site, by extraction solvent, and by bioassay. Results suggested that toxicity was not related to the total mass of PM in the extract, but to the chemical

components of the PM. It is noteworthy that the concentrations of contaminants in PM in this type of short-term and acute toxicity testing are much higher than would be found in the natural environment. Thus, the purpose of this type of testing is to provide an initial screening-level comparison of relative toxicities of atmospheric PM from different source areas. It does not provide the data that would be needed to assess risk (Sheesley et al., 2004, [156084](#)).

9.4.5.6. Effects on Animals

There has been little work focusing on animal indicators of PM effects in the field. However, there have been several recent studies on snails, amphibians, earthworms, and bivalves that are discussed below.

Bioindicator organisms can be especially useful for monitoring PM effects over geographical and temporal scales. Terrestrial invertebrates have been used to monitor contaminants in both air and soil. Snails (*Helix* spp.) accumulate trace metals and agrochemicals, and can be used as effective biomonitors for urban air pollution (Beeby and Richmond, 2002, [155680](#))(Viard et al., 2004, [055675](#))(Regoli et al., 2006, [156046](#)). Demonstrated biological effects include growth inhibition, impairment of reproduction, and induction of metallothioneins that are involved in metal detoxification (Gomot-de Vaufleury and Kerhoas, 2000, [155798](#))(Regoli et al., 2006, [156046](#)). The use of sentinel species to detect the effects of complex mixtures of air pollutants is of particular value because the chemical constituents are difficult to characterize, exhibit varying bioavailability, and are subject to various synergistic effects.

Regoli et al. (2006, [156046](#)) caged land snails (*Helix aspersa*) at five locations in the urban areas of Ancona, Italy. After four weeks of exposure to ambient air pollution, the snails were analyzed for trace metals and PAHs. Biomarkers were measured that correlated with contaminant accumulation, including concentrations of metallothioneins, activity of biotransformation enzymes, and peroxisomal proliferation. In addition, indicators of oxidative stress were measured, such as oxyradical scavenging capacity, onset of cellular damage, and loss of DNA integrity. Results documented substantial accumulation of metals and PAHs in snail digestive tissues in urban areas having high traffic congestion. Cellular reactivity was also found, suggesting that this species is an effective bioindicator for multipollutant air quality and PM monitoring.

Some amphibian ecotoxicological research has focused on heavy metal exposure. Contaminant uptake can occur by oral, pulmonary, and dermal exposure (Lambert, 1997, [155916](#))(Johnson et al., 1999, [155880](#))(James et al., 2004, [155874](#)). This is potentially important because of documented declines in amphibian populations in the U.S. and elsewhere in recent decades (Houlahan et al., 2000, [155853](#)). Toads were shown to be fairly tolerant of Cd exposure (James et al., 2004, [155874](#)). It is not clear whether current amounts of terrestrial metal contamination pose an increased risk to amphibians in general.

Estuarine and marine bivalves provide potential bioindicators for Hg bioaccumulation. For example, Coelho et al. (2006, [190181](#)) investigated Hg concentrations in *Scrobicularia plana*, a long-lived, deposit-feeding bivalve in southern Europe. Annual bioaccumulation rates were shown to be strongly correlated with Hg concentrations in suspended particulate matter (SPM), a response to their deposit-feeding tactics (Verdelhos et al., 2005, [190497](#)). The ability to predict annual accumulation rates for indicator species, such as this bivalve, may facilitate management actions to avoid deleterious effects on humans through consumption of bivalves above a certain age/size class.

Earthworms often constitute a large percentage of soil animal biomass and they are considered to be relatively sensitive indicators of soil metal contamination. They are continuously exposed to the soil via dermal contact in the soil solution or ingestion of large quantities of soil pore water, polluted food and/or soil particles (Lanno et al., 2004, [190415](#)). Hobbelen et al. (2006, [190371](#)) determined the important metal pools for bioaccumulation by earthworms *Lumbricus rubellus*, which live in the upper 5cm of soil and *Aporrectodea caliginosa*, which live in the upper 25 cm of soil. Soil concentration explained much of earthworm concentrations, however Cd concentration in *A. caliginosa* was best explained by pore water concentrations and no variable tested explained Zn tissue concentrations. Massicotte et al. (2003, [155968](#)) compared the cell viability and phagocytic potential of three earthworm species (*Lumbricus terrestris*, *Eisenia andrei*, and *Aporrectodea tuberculata*) in response to atmospheric emissions of metals from a cement factory in Quebec, Canada. Cell viability actually increased in proximity (0.5 km) to the cement factory for *A. tuberculata*, and this might have been due to beneficial effects of increased Ca deposition. There were no significant differences observed for the other two species (Massicotte et al., 2003, [155968](#)).

Biogeochemical cycling of Hg in the Arctic has been investigated, in part because observed Hg concentrations in marine animals may pose health risks for local human populations. The lifetime of gaseous elemental Hg (GEM) in the atmosphere, which constitutes about 95% of atmospheric Hg, is generally about 1-yr (Lin and Pehkonen, 1999, [190426](#)). However, during spring (typically March through June), the lifetime of GEM in the Arctic is much shorter, and atmospheric GEM can be depleted in less than one day during atmospheric Hg depletion episodes (MADE) (Lindberg et al., 2002, [190429](#)) (Skov et al., 2004, [190481](#)). During the AMDE, GEM is rapidly oxidized to reactive gaseous Hg that can be deposited to the ground surface (Skov et al., 2004, [190481](#)). Because of the increased solar flux to the Arctic during spring and seasonal melting of sea ice, there may be an increased efficiency of Hg bioaccumulation in Arctic food webs than would be expected based on data collected at mid-latitudes. Skov et al. (2004, [190481](#)) developed a simple parameterization for AMDE and included it in the Danish Eulerian Hemispheric Model (DEHM). The model was shown to reproduce the general structure of AMDE, suggesting that the limiting factor for AMDE may be the surface temperature of sea ice.

9.4.5.7. Biomagnification across trophic levels

Biomagnification is the progressive accumulation of chemicals with increasing trophic level (LeBlanc, 1995, [155921](#)). Organic Hg is the most likely metal to biomagnify, in part because organisms can efficiently assimilate methylmercury and it is slowly eliminated (Croteau et al., 2005, [156373](#); Reinfelder et al., 1998, [156047](#)). Of the trace metals, there is also evidence that Cd, Pb, Zn, Cu and Se biomagnify.

The study of trophic transfer and biomagnification is limited by the difficulty in discriminating food webs and the uncertainty associated with assignment of trophic position to individual species (Croteau et al., 2005, [156373](#)). Use of stable isotopes can help to establish linkages. However, it is difficult to determine the extent to which biomagnification occurs in a given ecosystem without thoroughly investigating physiological biodynamics, habitat, food web structure, and trophic position of relevant species. Thus, development of an understanding of ecosystem complexity is necessary to determine what species might be at greatest risk from toxic metal exposure (Croteau et al., 2005, [156373](#)).

Terrestrial

Bioaccumulation of heavy metals can occur through the plant-herbivore and litter-detrivore food webs. The U.S. EPA (2004, [056905](#)) concluded that Cd and Zn can bioaccumulate in earthworms. Other invertebrates inhabiting soil litter may also accumulate metals. Although food web accumulation of a metal may not result in mortality, it might reduce breeding potential or result in other non-lethal effects that adversely affect organism responses to environmental cues.

Metal accumulation in litter can be found mainly around brass works and Pb and Zn smelters. Organisms that feed on earthworms living in soils with elevated metal concentrations may also accumulate Pb and Zn. Increased concentrations of heavy metals have been found in a variety of mammals living in areas with elevated heavy metal concentrations in the soils.

The transfer of metals from plants to terrestrial snails is an interesting system for biomagnifications because snails accumulate metals in their soft tissue and can contribute significantly to the transfer of pollutants to primary consumers and terrestrial predators (Dallinger et al., 2001, [192109](#)). Notten et al. (2005, [190461](#)) studied the transfer of Cu, Zn, Cd and Pb in terrestrial soil-plant-snail food chains in metal-polluted soils of the Netherlands. The food chain included perennial plant species *Urtica dioica* and the herbivorous snail *Cepaea nemoralis*. The transfer of metal from the soil to the plant compartment was low (coefficient of determination $R^2 = 0.20$). Total concentration of metals in soils was a poor predictor of leaf concentration. Low metal concentration in the leaves was thought to be due to low pore water metal concentrations and was also thought to be partly caused by low translocation from roots within the plant. The Cu, Zn and Cd concentrations in the snails were always higher than concentrations in the leaves indicating bioaccumulation. The metal transfer from the leaf to snail was highest among all routes tested, suggesting that transfer from diet is important. Similar results were found by Beeby and Richmond (2002, [155680](#)) with the snail *Helix aspersa* and the plant *Taraxacum sp.* for Zn, Pb, Cd, but not for Cu.

Many types of predators including shrews, thrushes and beetle larvae include snails as part of their diet (Gomot-De Vaufleury and Pihan, 2002, [190357](#); Seifert et al., 1999, [190480](#)). Seifert et al. (1999, [190480](#)) found the shrews eating snails with elevated Cd had critical levels of Cd in their kidneys. Scheifler et al. (2007, [190379](#)) found that Cd in snails lead to toxic levels in beetle larvae that caused increased amounts of mortality.

Aquatic

In general, it has been assumed that metal biomagnification in aquatic ecosystems is an exception rather than the rule (Gray, 2002, [155806](#)). More recent research has demonstrated aquatic biomagnification of certain metals. For example, Stewart et al. (2004, [156097](#)) used stable isotopes of C and N to show biomagnification of Se in San Francisco Bay food webs. Croteau et al. (2005, [156373](#)) identified trophic position of estuarine organisms and food web structure in the delta of San Francisco Bay to document Cd biomagnification in invertebrates that live on macrophytes and also in fish. Concentrations of Cd were biomagnified 15 times within two trophic links in each food web. In contrast, no tendency towards biomagnification was observed for Cu.

In aquatic ecosystems, biomagnification of trace metals does not necessarily occur. Nguyen et al. (2005, [155997](#)) found biodiminution for most metals in Lake Balaton, Hungary, with the exception of slight enrichment of Zn from PM to zooplankton and of Cd from sediment to mussel.

Once transported to aquatic ecosystems, trace metals often preferentially bind to sediment particles. Some of these sediment-bound metals may be unavailable to biota; in contrast, metals bound to sediment organic matter may exhibit varying degrees of bioavailability (Di Toro et al., 2005, [155750](#)). Piol et al. (2006, [156028](#)) studied the bioavailability of sediment-bound Cd to the freshwater oligochaete *Lumbriculus variegatus*. They found that Cd uptake depended on the amount of free dissolved Cd(II), and the Cd contribution from sedimentary particles to biological uptake was negligible.

Marine bivalve mollusks bioaccumulate trace metals and other contaminants (LaBrecque et al., 2004, [155913](#)) and therefore may be used as bioindicators of contamination. In addition, they constitute an important link to human health by virtue of their importance as a food source (Cheggour et al., 2005, [155723](#); Li et al., 2002, [156691](#)).

9.4.5.8. Effects near Smelters and Roadsides

The high PM concentrations in proximity to mining, smelting, roadsides and other industrial sources result in heavy metal loadings that may be particularly damaging to nearby ecosystems.

Smelters

The Harjavalta region is one of the most intensively studied heavy metal polluted areas in the world. Kiikkilä et al. (2003, [156637](#)) reviewed available data on heavy metal deposition and environmental effects in this area. Emissions from the smelter were as high as 1100 t/yr of dust, 140 t/yr Cu, 96 t/yr Ni, 162 t/yr Zn, and 94 t/yr Pb in 1987. Deposition amounts decreased substantially after 1990, to only a few percent of the amounts that occurred during the 1980s.

Kiikkilä (2003, [156637](#)) investigated the effects of heavy metal pollution in proximity to a Cu-Ni smelter at Harjavalta, Finland. The deposition of heavy metals increased within 30 km of the smelter. Only slight changes in the understory vegetation were observed at distances greater than 8 km from the smelter. At 4 km distance, species composition of vegetation, insects, birds, and soil microbiota changed and tree growth was reduced. Within about 1 km, only the most resistant organisms were surviving.

The number of soil organisms clearly decreased and their community structure was altered close to the Harjavalta smelter (Kiikkilä, 2003, [156637](#)). However, this effect was only pronounced within about 2 km of the smelter. This suggests that the soil microfauna are relatively resistant to metal pollution effects.

Soil microbial activity decreased close to the Harjavalta smelter (Kiikkilä, 2003, [156637](#)), as reflected by microbial respiration, distribution of species within physiological groups, and microbial and fungal biomass. The fungi appeared to be more sensitive to metal contamination than the bacteria (Pennanen et al., 1996, [156016](#)). The rate of litter decomposition decreased, causing an accumulation of needle litter on top of the forest floor near the smelter (Fritze et al., 1989, [079635](#)).

Inhibition of nutrient cycling and displacement by Cu and Ni of base cations from cation exchange sites on the soil resulted in a decrease in base cation concentrations in the organic soil layer (Derome and Lindroos, 1998, [155749](#); Kiikkilä, 2003, [156637](#)) close to the Harjavalta smelter. In addition, Mg, Ca, and Mn concentrations in Scots pine needles were low, and this was attributed by Kiikkilä (2003, [156637](#)) to the toxic effects of Cu and Ni to plant fine roots and also to ectomycorrhizal root tips (Helmisaari et al., 1999, [155836](#)). Nutrient translocation during fall was also affected close to the smelter; as a consequence needle concentrations of K were relatively high (Nieminen et al., 1999, [155998](#)).

Tree growth (Scots pine) has been poor (Mälkönen et al., 1999, [155961](#)) and most vegetation was absent within 0.5 km of the smelter. Effects on plant species occurrence

close to the smelter were almost entirely negative. In contrast, some animal species responded positively, including a leaf miner, three species of aphid, and some ants, beetles, and spiders.

Salemaa et al. (2004, [156069](#)) investigated heavy metal concentrations in understory plant species growing at varying distances from the Harjavalta Cu-Ni smelter. Heavy metal concentrations (except Mn) were highest in bryophytes, followed by lichens, and were lowest in vascular plants. Vascular plants are generally able to restrict the uptake of toxic elements, and therefore were able to grow closer to the smelter than lichens. A pioneer moss (*Pohlia nutans*) was unusual in that it survived close to the smelter despite its accumulation of high amounts of Cu and Ni.

Changes in breeding success of cavity-nesting passerine birds close to the Harjavalta smelter were attributed by Kiikkilä (2003, [156637](#)) to habitat changes in response to metal toxicity. In particular, there was an apparent decrease in the proportion of green insect larvae in the diet of nestlings. In addition, pollution stress was inferred from increased heavy metals and decreased Ca in the diet of the pied fly catcher (*Ficedula hypoleuca*) (Eeva et al., 2000, [155761](#)).

Documentation of effects on individual species, such as was reported above, does not reveal what the impacts might be on ecosystem function. Nevertheless, the mere fact that multiple species, operating at different trophic levels, have been shown to be affected by the ambient deposition in proximity to the smelter suggests that effects on ecosystem function may indeed have occurred. More research is needed, however, to fully evaluate effects on function as opposed to abundance of individual species.

Roadsides

Heavy metal particles are important constituents of road dust. These particles accumulate on the road surface from brake linings, road paint, tire debris, DE, road construction materials, and catalyst materials. Road dust can be suspended in the atmosphere and contribute metals to soil, air, and urban runoff (Adachi and Tainosho, 2004, [081380](#); Davis et al., 2001, [024933](#); Smolders and Degryse, 2002, [156091](#)). In particular, Zn oxide comprises 0.4 to 4.3% of tire tread (Smolders and Degryse, 2002, [156091](#)) and tire wear is a substantial source of environmental Zn pollution. Adachi and Tainosho (2004, [081380](#)) used a field emission screening electron microscope equipped with an energy dispersive x-ray spectrometer to characterize heavy metal particles embedded in tire dust.

Samples were classified into four likely source categories, based on cluster analysis. Based on morphology and chemical composition, the samples were identified as having derived from yellow paint (CrPbO₄ particles), brake dust (particulate Ti, Fe, Cu, Sb, Zr, Ba and heavy minerals [Y, Zr, La, Ce]), and tire tread (Zn oxide).

Since publication of EPA's 2004 PM criteria assessment, some additional research has been conducted on the effects of windblown PM. Effects on physical, chemical, and biological attributes of both plants and animals have been documented (Englert, 2004, [087939](#); Gleason et al., 2007, [155794](#); Kappos et al., 2004, [087922](#)). Experiments by Gleason et al. (Gleason et al., 2007, [155794](#)) suggest that most direct effects on plants of windblown PM originating from on-road surfaces occur within 40 m of the source. Windblown PM from roads or agriculture can cover plant photosynthetic structures (Sharifi et al., 1999, [156082](#)), cause impact damage (Armbrust and Retta, 2002, [156225](#)), or interfere with physiological mechanisms (Burkhardt et al., 2002, [155708](#)). As previously discussed in Section 9.4.4.6 land snails in urban areas have been shown to be a good indicator of traffic pollution.

9.4.6. Organic Compounds

VOCs in the atmosphere are partitioned between the gas and particle phases. As described by the U.S. EPA (2004, [056905](#)), the partitioning depends on vapor pressure, temperature, surface area of the particles, and the nature of the particles and of the chemical being adsorbed. A wide variety of organic contaminants are deposited from the atmosphere. These include chemicals such as DDT, PCBs, and PAHs.

Important organic atmospheric contaminants are generally those that are transported long distances in the atmosphere, subsequently deposited into remote locations, and bioaccumulated to sufficient concentrations that they can affect humans, wildlife, or other biota (Swackhamer et al., 2004, [190488](#)). Certain physical and chemical properties facilitate the movement of these contaminants from land and water surfaces into the atmosphere, provide stability, and enhance accumulation in lipids. Some, including the relatively small (up to 4 rings) PAHs degrade relatively rapidly in the atmosphere or at the surface subsequent to atmospheric deposition. Below is a summary of the findings of the U.S. EPA (2004, [056905](#)), followed by discussion of more recent research findings.

Plants may be used as passive monitors to compare the deposition of organic compounds between sites. Vegetation can be used semi-quantitatively to indicate organic pollutant amounts if the mechanism of accumulation is considered. Organic compounds can

enter the plant via the roots or be deposited as particles on the leaves and be taken up through the cuticle or stomata. The pathways depend on the chemical and its physical properties. These include, for example, lipophilicity, water solubility, vapor pressure, and Henry's law constant. Environmental conditions can also be important, including temperature and organic content of soil, plant species, and the foliar surface area and lipid content.

Organic particulates in the atmosphere are diverse in their makeup and sources. Vegetation itself is an important source of hydrocarbon aerosols. Terpenes, particularly α -pinene, β -pinene, and limonene, released from tree foliage may react in the atmosphere to form submicron particles. These naturally generated organic particles contribute significantly to the blue haze aerosols formed naturally over forested areas (Geron et al., 2000, [019095](#); U.S. EPA, 2004, [056905](#)).

The low water solubility and high lipo-affinity of many organic xenobiotics control their interaction with the vegetative components of natural ecosystems. Foliar surfaces are covered with a waxy cuticle layer that helps reduce moisture loss and short-wave radiation stress. This epicuticular wax consists largely of long-chain esters, polyesters, and paraffins, which accumulate lipophilic compounds. Organic air contaminants in the particulate or vapor phase can be adsorbed to, and accumulate in, the epicuticular wax of leaf surfaces. Direct uptake of organic contaminants through the cuticle and vapor-phase uptake through the stomata are not well characterized for most trace organics.

Topographic and vegetative characteristics exert different influence on deposition modes. In general, dry deposition is most affected by plant morphology (Grantz et al., 2003, [155805](#)). The potential effects of PM on vegetation include the full range of biological organization, with exposures occurring through the soil and through vegetative surfaces. In general, soil-mediated exposure is thought to be more significant (Grantz et al., 2003, [155805](#)). Soil acts as an important storage compartment for POPs, including PCBs and PAHs. There is a continuous process of partitioning between the soil pool and the atmosphere, and this controls the regional and global transport of these compounds (Backe et al., 2004, [155668](#); Wania and Mackay, 1993, [157110](#)). Over time, POPs move towards equilibrium between the environmental compartments, and this process can be described using the fugacity concept (Backe et al., 2004, [155668](#); Mackay, 1991, [042941](#)). Fugacity reflects the tendency of a chemical constituent to escape one environmental compartment and move to another. When an equilibrium distribution is achieved, the fugacity quotient

values in each compartment will be equal. Soil/air partitioning is controlled by a variety of factors. These include soil properties, such as organic matter content, moisture, porosity, texture, and structure, as well as the physiochemical properties of the pollutant, including vapor pressure and water solubility.

The accumulation of PAHs in vegetation, due to their lipophilic nature, could contribute to human and other animal exposure via food consumption. As a result, plant uptake of PAHs has been an important area of research (Gao and Zhu, 2004, [155782](#)). Most bioaccumulation of PAHs by plants occurs by leaf uptake (Tao et al., 2006, [156112](#)). Root uptake also occurs. It appears that roots preferentially accumulate the lower molecular weight PAHs due to their greater water solubility (Wild and Jones, 1992, [156155](#)).

Various models have been developed to simulate plant uptake of organic contaminants. The simple partition-limited model of Chiou et al. (2001, [156342](#)) has been further expanded to increase complexity and to include root uptake pathways (e.g., Fryer and Collins, 2003, [156454](#); Yang et al., 2005, [192104](#); Zhu et al., 2004, [156184](#)).

In evaluating receptor choice for studies of contaminant exposure to plants, and also remediation potential, it is important to consider differences among species. For example, Parrish et al. (2006, [156014](#)) assessed the bioavailability of PAHs in soil. During the first growing season, zucchini (*Cucurbita pepo* ssp. *pepo*) accumulated significantly more PAHs than did other related plant species, including up to three orders of magnitude greater concentrations of the six-ring PAHs. Parrish et al. (2006, [156014](#)) also noted differences in PAH uptake by two different species of earthworm.

The leaves of *Quercus ilex* have been shown to readily accumulate PAHs in situ. Young leaves accumulated PAHs within three weeks of bud break. Mature leaves showed seasonality, with higher PAH concentrations during winter (Alfani et al., 2005, [154319](#)).

It is difficult to discriminate between PAHs that are adsorbed to plant root surfaces as opposed to those that are actually taken up by the roots. In general, soil bound PAHs are associated with soil organic matter and are therefore not readily available for root uptake (Fismes et al., 2002, [141156](#); Jiao et al., 2007, [155879](#)). Wild et al. (2005, [156156](#)) used two-photon excitation microscopy to visualize the uptake and transport of two PAHs (anthracene and phenanthrene) from a contaminated soil into living wheat and maize roots. Jiao et al. (2007, [155879](#)) developed a sequential extraction method to discriminate between PAH adsorption in rice roots.

Maize roots and tops of plants have been shown to directly accumulate PAHs from aqueous solution and from air in proportion to exposure amounts. Root concentration factors are log-linear functions of log-based octanol-water partition coefficients ($\log K_{ow}$); similarly, leaf concentration factors are log-linear functions of log-based octanol-air partition coefficients ($\log K_{oa}$) (Lin et al., 2007, [155933](#)). Although the bulk concentrations of PAHs in various plant tissues can differ greatly, the observed differences disappear after they are normalized to lipid content (Lin et al., 2007, [155933](#)). This suggests that the lipid content of different plant tissues may influence PAH distribution within the plant.

Previously, there was relatively little information available regarding incorporation of atmospherically deposited PAHs into aquatic food webs. It is known that PAHs can be transferred to higher trophic levels, including fish, and that this transfer can be mediated by aquatic invertebrates, which generally comprise an important part of fish diets. High mountain lakes offer an effective receptor for quantification of biomagnification in aquatic ecosystems from atmospheric PM deposition. There are typically no sources of organic contaminants in their watersheds, and atmospheric inputs dominate as sources of contamination. In addition, such lakes tend to have relatively simple food webs. Vives et al. (2005, [157099](#)) investigated PAH content of brown trout (*Salmo trutta*) and their food items. Total PAH concentrations tended to be highest in organisms that occupy littoral habitats, and lowest in pelagic organisms. This may reflect more efficient transfer of PAHs to underlying sediments in shallower water and associated degradation within the water column.

Some atmospheric organic contaminants have been shown to accumulate in biota at remote locations. For example, polybrominated diphenyl ethers (PBDEs), which are man-made chemicals used as flame retardants in materials manufacturing, have been found to accumulate in lichens and mosses collected at King George Island, maritime Antarctica (Yogui and Sericano, 2008, [189971](#)). Because contaminant concentrations were not statistically different at sites close to and distant from human facilities in Antarctica, the authors concluded that long-range atmospheric transport was the likely primary source of PBDEs to King George Island. Law et al. (2003, [190420](#)) reviewed available data for accumulation of PBDEs and other brominated flame retardants in wildlife. These compounds have become widely distributed in the environment, including in the deep-water, oceanic food webs.

Ohyama et al. (2004, [190462](#)) chose salmonid fish, mainly rainbow trout (*Oncorhynchus mykiss*), as an indicator species to evaluate the transport and bioaccumulation of organochloride compounds in the northern and central Sierra Nevada. They found that elevation was an important factor affecting residual concentrations of polychlorinated biphenyls (PCBs) in fish muscle tissue. On this basis, Ohyama et al. (2004, [190462](#)) concluded that PCB residue in rainbow trout, a widely distributed salmonid species, provided a good monitoring tool for studying the effects of mountainous topography on the long-range transport and distribution of persistent organic pollutants.

Semivolatile compounds can undergo repeated volatilization on surfaces, such as plant foliage, in response to diel changes in temperature. As a consequence, such compounds can be deposited, re-emitted, and re-deposited multiple times. This behavior can cause these compounds to move large distances in a leap-frog fashion. It is believed that POPs can be atmospherically transported throughout the world because of their volatility and response to changes in temperature. This “global distillation theory” (Holmqvist et al., 2006, [190380](#); Wania and Mackay, 1993, [157110](#)) predicts that POPs in the northern hemisphere are generally transported towards the Arctic, and in the southern hemisphere they are transported toward the Antarctic. In general, POP concentrations measured in the Arctic are higher than in the Antarctic. They have been detected in all levels of the Arctic food web (Oehme et al., 1995, [011267](#)). Bioconcentration of organochlorines has been shown in the Arctic food web, including fish, seals, and polar bears (Oehme et al., 1995, [011267](#)). Concentrations measured in Arctic polar bears are especially high (Arctic Monitoring and Assessment Programme, 2004, [190168](#)).

Holmqvist et al. (2006, [190380](#)) measured levels of PCBs in longfin eels (*Anguilla dieffenbachii*) in 17 streams on the west coast of South Island, New Zealand. The PCBs were at low levels, and were believed to originate from atmospheric transport from industrial areas in Asia. Characteristics of the longfin eel that make it susceptible to bioaccumulation of lipophilic persistent pollutants include high lipid content (up to 40%), long lifespan (up to 90 yr), and position near the top of the food chain (Holmqvist et al., 2006, [190380](#)).

Long-range transport of atmospherically deposited contaminants can be augmented by biotransport. A good example of this phenomenon was documented by Ewald et al. (1998, [190348](#)), who showed that biotransport by migrating sockeye salmon (*Oncorhynchus nerka*) in the Copper River watershed, Alaska, had a greater influence than atmospheric transport

on bioaccumulation of PCBs and DDT in lake food webs. Organic pollutants accumulated by salmon during their ocean residence were effectively transferred 410 km inland to their spawning lake. Arctic grayling (*Thymallus arcticus*) in the salmon spawning lake were found to contain organic pollutants more than twice as high as arctic grayling in a near-by salmon-free lake. The pollutant composition of the grayling in the salmon spawning lake was similar to that of the migrating salmon (Ewald et al., 1998, [190348](#)), suggesting that salmon migration contributed to bioaccumulation of organic contaminants in the lake used for spawning by the salmon.

An assessment of the ecological effects of airborne metals and SOCs was conducted for eight NPs by the Western Airborne Contaminants Assessment Project (WACAP) (Landers et al., 2008, [191181](#)). From 2002-2007, WACAP researchers conducted analysis of the biological effects of airborne contaminants in seven ecosystem compartments: air, snow, water, sediments, lichens, conifer needles and fish. The goals were to identify where the pollutants were accumulating, identify ecological indicators for those pollutants causing ecological harm, and to determine the source of the air masses most likely to have transported the contaminants to the parks.

The results from WACAP were summarized by Landers et al. (2008, [191181](#)), which concluded that bioaccumulation of SOCs were observed throughout park ecosystems. Vegetation tended to accumulate PAHs, CUPs, and HCHs. Conifer needles were a good indicator of pesticides, however the ecological consequences of this accumulation are unexamined. SOCs in vegetation and air showed different patterns, possibly because each medium absorbs different types of SOCs with varying efficiencies. Mean ammonium nitrate concentration in ambient fine particulates <2.5 µm diameter was a good predictor of dacthal, endosulfan, chloradane, trifluralin, DDT and PAH concentrations in vegetation.

Concentrations of SOCs were five to seven orders of magnitude higher in fish tissue than in sediments. Fish accumulated more PCBs, chlordanes, DDT and dieldrin than vegetation. Fish lipid and age were the most reliable predictors of SOC concentrations. Most fish appeared normal during field necropsies; however, individuals with both male and female reproductive organs were collected at two sites. The incidence of this condition has increased since the pre-organic pollutant era. Additionally, elevated concentrations of vitellogenin, a female protein involved in egg production, were found in male fish from three sites, and directly related to the concentration of several organochlorines at one site.

The lake sediment records showed steadily increasing mercury deposition over time at lakes in two parks, Mt. Ranier NP and Rocky Mountain NP. Apportionment of the mercury to its atmospheric sources is not quantified at this time; however, the pattern in the sediment suggests a local source rather than a global source. Mercury concentrations in fish exceeded contaminant health thresholds for some piscivorous fish, mammals and birds in most parks. The average mercury concentration in fish from one site and individual fish from three additional sites exceeded the U.S. EPA contaminant health thresholds for humans.

Although this assessment focuses on chemical species that are components of PM it does not specifically assess the effects of particulate vs. gas-phase forms, therefore in most cases it is difficult to apply the results to this assessment based on particulate concentration and size fraction.

9.4.7. Summary of Ecological Effects of PM

Ecological effects of PM include direct effects to metabolic processes of plant foliage; contribution to total metal loading resulting in alteration of soil biogeochemistry, plant and animal growth and reproduction; and contribution to total organics loading resulting in bioaccumulation and biomagnification across trophic levels. These effects were well-characterized in the 2004 PM AQCD (U.S. EPA, 2004, [056905](#)). Thus, the summary below builds upon the conclusions provided in that review.

PM deposition comprises a heterogeneous mixture of particles differing in origin, size, and chemical composition. Exposure to a given concentration of PM may, depending on the mix of deposited particles, lead to a variety of phytotoxic responses and ecosystem effects. Moreover, many of the ecological effects of PM are due to the chemical constituents (e.g., metals and organics) and their contribution to total loading within an ecosystem.

Investigations of the direct effects of PM deposition on foliage have suggested little or no effects on foliar processes, unless deposition levels were higher than is typically found in the ambient environment. However, consistent and coherent evidence of direct effects of PM has been found in heavily polluted areas adjacent to industrial point sources such as limestone quarries, cement kilns, and metal smelters (Sections 9.4.3. and 9.4.5.8.). Where toxic responses have been documented, they generally have been associated with the acidity, trace metal content, surfactant properties, or salinity of the deposited materials.

An important characteristic of fine particles is their ability to affect the flux of solar radiation passing through the atmosphere directly, by scattering and absorbing solar radiation, and, indirectly, by acting as cloud condensation nuclei (CCN) that, in turn, influence the optical properties of clouds. Regional haze has been estimated to diminish surface solar visible radiation. Crop yields can be sensitive to the amount of sunlight received, and crop losses have been attributed to increased airborne particle concentrations in some areas of the world. PM has been observed to cause a decrease in photosynthetically active radiation (PAR) via thick haze occurring in China that decreases plant growth in the diffuse light portion of PAR. However, a global model showed that PM can increase the diffuse light fraction of PAR. On a global scale, the diffuse light fraction of PAR has been shown to increase growth. Consequently, it was shown that when PM is decreased, plant growth and C storage are also decreased. Further research is needed to determine net effects of PM alteration of light conditions on the growth of vegetation in the U.S.

The deposition of PM onto vegetation and soil, depending on its chemical composition, can produce responses within an ecosystem. The ecosystem response to pollutant deposition is a direct function of the level of sensitivity of the ecosystem and its ability to ameliorate resulting change. Many of the most important ecosystem effects of PM deposition occur in the soil. Upon entering the soil environment, PM pollutants can alter ecological processes of energy flow and nutrient cycling, inhibit nutrient uptake, change ecosystem structure, and affect ecosystem biodiversity. The soil environment is one of the most dynamic sites of biological interaction in nature. It is inhabited by microbial communities of bacteria, fungi, and actinomycetes, in addition to plant roots and soil macro-fauna. These organisms are essential participants in the nutrient cycles that make elements available for plant uptake. Changes in the soil environment can be important in determining plant and ultimately ecosystem response to PM inputs.

There is strong and consistent evidence from field and laboratory experiments that metal components of PM alter numerous aspects of ecosystem structure and function. Changes in the soil chemistry, microbial communities and nutrient cycling, can result from the deposition of trace metals. Exposures to trace metals are highly variable, depending on whether deposition is by wet or dry processes. Although metals can cause phytotoxicity at high concentrations, few heavy metals (e.g., Cu, Ni, Zn) have been documented to cause direct phytotoxicity under field conditions. Exposure to coarse particles and elements such as Fe and Mg are more likely to occur via dry deposition, while fine particles are more likely

to contain elements such as Ca, Cr, Pb, Ni, and V. Ecosystems immediately downwind of major emissions sources can receive locally heavy deposition inputs. Phytochelatins produced by plants as a response to sublethal concentrations of heavy metals are indicators of metal stress to plants. Increased concentrations of phytochelatins across regions and at greater elevation have been associated with increased amounts of forest injury in the northeastern U.S.

Overall, the ecological evidence is sufficient to conclude **that a causal relationship is likely to exist between deposition of PM and a variety of effects on individual organisms and ecosystems, based on information from the previous review and limited new findings in this review.** However, in many cases, it is difficult to characterize the nature and magnitude of effects and to quantify relationships between ambient concentrations of PM and ecosystem response due to significant data gaps and uncertainties as well as considerable variability that exists in the components of PM and their various ecological effects.

9.5. Effects on Materials

Effects of air pollution on materials are related to both aesthetic appeal and physical damage. Deposited particles, primarily carbonaceous compounds, cause soiling of building materials and culturally important items, such as statues and works of art. Physical damage from dry deposition of PM also can accelerate natural weathering processes. The major deterioration phenomenon affecting building materials in response to atmospheric deposition is probably sulfation, leading to secondary salt crystallization which forms gypsum (Marinoni et al., 2003, [092520](#)).

This section (a) summarizes information on exposure-related effects on materials associated with particulate pollutants as addressed in the 2004 PM AQCD (U.S. EPA, 2004, [056905](#)) and (b) presents relevant information derived from very limited research conducted and published since completion of that document. Most recent work on this topic has been conducted outside the U.S.

There is a variety of factors that contribute to the deterioration of monuments and buildings of cultural significance. They include: (1) biodeterioration processes; (2) weathering of materials exposed to the air; and (3) air pollution from both anthropogenic and natural sources (Herrera and Videla, 2004, [155843](#)). Because of the diversity in climate,

proximity to marine aerosol sources, and pollution of various types, the magnitude and relative importance of these causal agents vary by location.

Much existing literature on damage to structural materials of cultural heritage has not seriously considered the importance of biodeterioration processes and the relationship that often exists between environmental characteristics and the microbial communities that colonize monuments and buildings. In general, high humidity, high temperature, and air pollution often enhance the biodeterioration hazard. Herrera and Videla (2004, [155843](#)) concluded that heterotrophic bacteria, fungi, and cyanobacteria were the main microbial colonizers of buildings that they investigated in Latin America. Their analyses suggested that the major deterioration mechanism of limestone at the Mayan site of Uxmal in a non-polluted rural environment was biosolubilization induced by metabolic acids produced by bacteria and fungi. The rock decay at Tulum, near the seashore, was mainly attributed to the marine influence. At Medellin, it appeared that biodeterioration effects from microbes synergistically enhanced the effects of atmospheric factors on material decay. Deterioration of structural material in the Cathedral of La Plata, located in a mixed urban/industrial environment, was attributed mainly to atmospheric pollutants (Herrera and Videla, 2004, [155843](#)).

Ambient particles can cause soiling of man-made surfaces. Soiling generally is considered an optical effect. Soiling changes the reflectance from opaque materials and reduces the transmission of light through transparent materials. Soiling can represent a significant detrimental effect, requiring increased frequency of cleaning of glass windows and concrete structures, washing and repainting of structures, and, in some cases, reduces the useful life of the object. Particles, especially carbon, may also help catalyze chemical reactions that result in the deterioration of materials (U.S. EPA, 2004, [056905](#)).

Soiling is dependent on atmospheric particle concentration, particle size distribution, deposition rate, and the horizontal or vertical orientation and texture of the exposed surface (Haynie, 1986, [157198](#)). The chemical composition and morphology of the particles and the optical properties of the surface being soiled will determine the time at which soiling is perceived by human observers (Nazaroff and Cass, 1991, [044577](#)).

Ferm et al. (2006, [155135](#)) reported development of a simple passive particle collector for estimating dry deposition to objects of cultural heritage. The observed mass of deposited particles mainly belonged to the coarse particulate mode. The sampler collects particles

from all directions. It replicates at least some of the complexity of particle deposition to actual objects, and is easier to analyze than a precious object (Ferm et al., 2006, [155135](#)).

Soiling of urban buildings constitutes a visual nuisance that leads to the loss of architectural value. Soiling can include reversible darkening of the building surfaces and also irreversible damage. Water runoff patterns on the building surfaces are influenced by the type of surface material, architectural elements, and climate. Therefore, soiling does not occur uniformly across the building. Public perception of soiling entails complex interactions between the extent of soiling, architecture, and aesthetics (Grossi and Brimblecombe, 2004, [155813](#)).

One of the most significant air pollution damage features affecting urban buildings and monuments is the formation of black crusts. Quantification of different forms of carbon in black crusts is difficult. There is often a carbonate component which is derived from the building material, plus OC and EC, derived from air pollution. EC is considered to be a tracer for combustion sources, whereas OC may derive from multiple sources, including atmospheric deposition of primary and secondary pollutants, and the decay of protective organic treatments (Bonazza et al., 2005, [155695](#)). Bonazza et al. (2005, [155695](#)) quantified OC and EC in damage layers on European cultural heritage structures. OC predominated over EC at almost all locations investigated. Traffic appeared to be the major source of fine carbonaceous particles, with organic matter as the main component (Putaud et al., 2004, [055545](#)). Viles and Gorbushina (2003, [156138](#)) found that soiling in Oxford, U.K. showed a relationship with traffic and NO₂ concentrations.

In addition to the soiling effects of EC, much soiling appears to be largely of microbiological origin (Viles and Gorbushina, 2003, [156138](#)). Microbial biofilms, composed mainly of fungi, can stain exposed rock surfaces with yellow, orange, brown, gray, or black colors. Microorganisms may be able to trap PM more efficiently than the stone surface itself. In addition, microbial growth may be stimulated by organic or nutrient constituents in PM deposition.

Viles et al. (2002, [156137](#)) investigated the nature of soiling on limestone tablets in relation to ambient air pollution and climate at 3 contrasting sites in Great Britain over periods of 1-8 yr. Spectrophotometer and microscope observations suggested that there were not consistent trends in soiling over time at the study sites. Each site behaved differently in terms of the temporal development of soiling and the differences between sheltered and

exposed limestone tablets. In addition, organisms played important roles in the soiling response, even at the highly polluted site.

Some work has been conducted on public perception regarding the lightness of historic buildings and the aesthetic need for cleaning subsequent to soiling by air pollution. Brimblecombe and Grossi (2005, [155703](#)) found a strong relationship between the perceived lightness of a building and the opinion that it was dirty. This relationship was used to establish levels of blackening that might be publicly acceptable.

Recently, the importance of organic contaminant deposition to the overall air pollution damage to building materials has been recognized. Low molecular weight organic anions such as formate, acetate, and oxalate are ubiquitous in black crusts in damage layers on stones and mortars sampled from monuments and buildings throughout Europe (Sabbioni et al., 2003, [049282](#)). This has been observed at urban, suburban, and rural sites.

9.5.1. Effects on Paint

Studies have evaluated the soiling effects of particles on painted surfaces (U.S. EPA, 2004, [056905](#)). Particles composed of EC, acids, and various other constituents are responsible for the soiling of structural painted surfaces. Coarse-mode particles ($>2.5 \mu\text{m}$) initially contribute more soiling of horizontal and vertical painted surfaces than do fine-mode particles ($<2.5 \mu\text{m}$), but are more easily removed by rain (Haynie and Lemmons, 1990, [044579](#)). Rain interacts with coarse particles, dissolving the particle and leaving stains on the painted surface (Creighton et al., 1990, [044578](#); Haynie and Lemmons, 1990, [044579](#)). Particle deposition contributes to increased frequency of cleaning of painted surfaces and physical damage to the painted surface. Air pollution affects the durability of paint finishes by promoting discoloration, chalking, loss of gloss, erosion, blistering, and peeling (U.S. EPA, 2004, [056905](#)). There have been no new developments in this field subsequent to the review of the U.S. EPA (2004, [056905](#)).

9.5.2. Effects on Metal Surfaces

Metals undergo natural weathering processes. The effects of air pollutants on natural weathering processes depend on the nature of the pollutant(s), the deposition rate, and the presence of moisture (U.S. EPA, 2004, [056905](#)). Pollutant effects on metal surfaces are governed by such factors as the presence of protective corrosion films and surface

electrolytes, the orientation of the metal surface, and surface moisture. Surface moisture facilitates particulate deposition and promotes corrosive reactions. Formation of hygroscopic salts increases the duration of surface wetness and enhances corrosion.

A corrosion film, such as for example the rust layer on a metal surface, provides some protection against further corrosion. Its effectiveness in retarding the corrosion process is affected by the solubility of the corrosion layer and the pollutant exposure. Other than the effects of acidifying compounds, there has not been additional research conducted in recent years on the effects of PM deposition on metal corrosion.

9.5.3. Effects on Stone

Air pollutants can enhance the natural weathering processes on building stone. The development of crusts on stone monuments has been attributed to the interaction of the stone's surface with pollutants, wet or dry deposition of atmospheric particles, and dry deposition of gypsum particles. Because of a greater porosity and specific surface, mortars have a high potential for reacting with environmental pollutants (Zappia et al., 1998, [012037](#)).

Most research evaluating the effects of air pollutants on stone structures has concentrated on gaseous pollutants (U.S. EPA, 2004, [056905](#)). The dark color of gypsum is attributed to soiling by carbonaceous particles. A lighter gray colored crust is attributed to soil dust and metal deposits (Ausset et al., 1998, [040480](#); Camuffo, 1995, [076278](#); Lorusso et al., 1997, [084534](#); Moropoulou et al., 1998, [040485](#)). Lorusso et al. (1997, [084534](#)) attributed the need for frequent cleaning and restoration of historic monuments in Rome to exposure to total suspended particulates.

Grossi et al. (2003, [155812](#)) investigated the black soiling rates of building granite, marble, and limestone in two urban environments with different climates. Horizontal specimens were exposed, both sheltered and unsheltered from rainfall. Limestone showed soiling proportional to the square root of the time of exposure, but granite and marble did not.

Black soiling is caused mainly by particulate EC (PEC). For that reason, it is most prevalent in urban environments due to the formation of carbonaceous fine particles from the incomplete combustion of fossil fuels. Traffic emissions, especially from diesel engines, and wood burning are important sources of PEC (Grossi et al., 2003, [155812](#)).

Kamh (2005, [155888](#)) studied the effects of weathering on Conway Castle, an historical structure in Great Britain built about 1289 AC. The weathering was identified as honeycomb, blackcrust, exfoliation, and discoloration, with white salt efflorescence at some parts. These features are diagnostic for salt weathering (Goudie et al., 2002, [156486](#)), and this was confirmed by laboratory analyses, including scanning electron microscopy and x-ray diffraction. The authors concluded that the salt was derived from three sources: sea spray, chemical alteration of the carbonate in mortar into SO_4^{2-} salts by acidic deposition, and wet deposition of air pollutants on the stone surface. The salt content on the rock surface fills the rock pores and then exerts high pressure on the rock texture due to hydration of the salt in the cold humid environment. In particular, CaSO_4 and Na_2SO_4 exert enough pressure on hydration as to deteriorate construction rock at both the micro- and macroscale (Moses and Smith, 1994, [156785](#)).

9.5.4. Summary of Effects on Materials

Building materials (metals, stones, cements, and paints) undergo natural weathering processes from exposure to environmental elements (wind, moisture, temperature fluctuations, sunlight, etc.). Metals form a protective film of oxidized metal (e.g., rust) that slows environmentally induced corrosion. However, the natural process of metal corrosion is enhanced by exposure to anthropogenic pollutants. For example, formation of hygroscopic salts increases the duration of surface wetness and enhances corrosion.

A significant detrimental effect of particle pollution is the soiling of painted surfaces and other building materials. Soiling changes the reflectance of opaque materials and reduces the transmission of light through transparent materials. Soiling is a degradation process that requires remediation by cleaning or washing, and, depending on the soiled surface, repainting. Particulate deposition can result in increased cleaning frequency of the exposed surface and may reduce the usefulness of the soiled material. Attempts have been made to quantify the pollutant exposure at which materials damage and soiling have been perceived. However, to date, insufficient data are available to advance the knowledge regarding perception thresholds with respect to pollutant concentration, particle size, and chemical composition. Nevertheless, the evidence is sufficient to conclude that **a causal relationship exists between PM and effects on materials.**

Chapter 9 References

- Abdou W; Diner D; Martonchik J; Bruegge C; Kahn R; Gaitley B; Crean K; Remer L; Holben B. (2005). Comparison of coincident Multiangle Imaging Spectroradiometer and Moderate Resolution Imaging Spectroradiometer aerosol optical depths over land and ocean scenes containing Aerosol Robotic Network sites. , 110. [190028](#)
- Aboal JR; Fernández JA; Carballeira A. (2004). Oak leaves and pine needles as biomonitors of airborne trace elements pollution. *Environ Exp Bot*, 51: 215-225. [155642](#)
- ABT. (2001). Assessing Public Opinions on Visibility Impairment Due to Air Pollution: Summary Report. [156185](#)
- ABT. (2002). Sense of Place and Stewardship: Final Focus Group Report. [156186](#)
- Ackerman A; Kirkpatrick M; Stevens D; Toon O. (2004). The impact of humidity above stratiform clouds on indirect aerosol climate forcing. *Nature*, 432: 1014-1017. [190056](#)
- Ackerman AS; Toon OB; Stevens DE; Heymsfield AJ; Ramanathan V; Welton EJ. (2000). Reduction of tropical cloudiness by soot. , 288: 1042-1047. [002987](#)
- Ackerman T; Stokes G. (2003). The atmospheric radiation measurement program. , 56: 38-44. [192080](#)
- Adachi K; Tainosho Y. (2004). Characterization of heavy metal particles embedded in tire dust. *Environ Int*, 30: 1009-1017. [081380](#)
- Adamo P; Crisafulli P; Giordano S; Minganti V; Modenesi P; Monaci F; Pittao E; Tretiach M; Bargagli R. (2007). Lichen and moss bags as monitoring devices in urban areas. Part II: Trace element content in living and dead biomonitors and comparison with synthetic materials. , 146: 392-399. [155644](#)
- Albrecht B. (1989). Aerosols, cloud microphysics, and fractional cloudiness. , 245: 1227-1230. [045783](#)
- Alexeeva LB; Strachan WMJ; Shlychkova VV; Nazarova AA; Nikanorov AM; Korotova LG. (2001). Organochlorine pesticides and trace metal monitoring of Russian rivers flowing to the Arctic Ocean. *Mar Pollut Bull*, 43: 71-85. [155651](#)
- Alfani A; De Nicola F; Maisto G; Prati MV. (2005). Long-term PAH accumulation after bud break in *Quercus ilex* L leaves in a polluted environment. *Atmos Environ*, 39: 307-314. [154319](#)
- Allen GA; Lawrence J; Koutrakis P. (1999). Field validation of a semi-continuous method for aerosol black carbon (aethalometer) and temporal patterns of summertime hourly black carbon measurements in southwestern PA. *Atmos Environ*, 33: 817-823. [048923](#)
- Almås ÅR; Bakken LR; Mulder J. (2004). Changes in tolerance of soil microbial communities in Zn and Cd contaminated soils. *Soil Biol Biochem*, 36: 805-813. [155654](#)
- Alpert P; Kishcha P; Kaufman Y; Schwarzbard R. (2005). Global dimming or local dimming?: Effect of urbanization on sunlight availability. , 32: 17. [190047](#)
- Ammann CM; Meehl GA; Washington WM; Zender CS. (2003). A monthly and latitudinally varying volcanic forcing dataset in simulations of 20th century climate. *Geophys Res Lett*, 30: 1657. [192057](#)
- Anderson HR; Atkinson RW; Bremner SA; Marston L. (2003). Particulate air pollution and hospital admissions for cardiorespiratory diseases: are the elderly at greater risk?. *Eur Respir J*, 40: 39s-46s. [054820](#)
- Anderson T; Charlson R; Bellouin N; Boucher O; Chin M; Christopher S; Haywood J; Kaufman Y; Kinne S; Ogren J. (2005). An “A-Train” strategy for quantifying direct climate forcing by anthropogenic aerosols. , 86: 1795-1809. [189993](#)
- Anderson T; Wu Y; Chu D; Schmid B; Redemann J; Dubovik O. (2005). Testing the MODIS satellite retrieval of aerosol fine-mode fraction. , 110: D18204. [189991](#)
- Andreae MO; Gelencsér A. (2006). Black carbon or brown carbon? The nature of light-absorbing carbonaceous aerosols. , 6: 3131-3148. [156215](#)
- Andreae MO; Rosenfeld D; Artaxo P; Costa AA; Frank GP; Longo KM; Silva-Dias MAF. (2004). Atmospheric science: smoking rain clouds over the Amazon. , 303: 1337-1341. [155658](#)
- Andronova NG; Rozanov EV; Yang F; Schlesinger ME; Stenchikov GL. (1999). Radiative forcing by volcanic aerosols from 1850 to 1994. *J Geophys Res*, 104: 16807-16826. [192286](#)
- Antuña JC; Robock A; Stenchikov G; Zhou J; David C; Barnes J; Thomason L. (2003). Spatial and temporal variability of the stratospheric aerosol cloud produced by the 1991 Mount Pinatubo eruption. *J Geophys Res*, 108: 4624. [192251](#)

Note: Hyperlinks to the reference citations throughout this document will take you to the NCEA HERO database (Health and Environmental Research Online) at <http://epa.gov/hero>. HERO is a database of scientific literature used by U.S. EPA in the process of developing science assessments such as the Integrated Science Assessments (ISA) and the Integrated Risk Information System (IRIS).

- Arctic Monitoring and Assessment Programme (AMAP). (2004). AMAP Assessment 2002: Persistent Organic Pollutants in the Arctic. AMAP. Oslo, Norway. [190168](#)
- Arizona Department of Environmental Quality. (2000). Phoenix metropolitan area visibility briefing paper. [019164](#)
- Armbrust DV; Retta A. (2002). Wind and sandblast damage to growing vegetation. , 39: 273-284. [156225](#)
- Arnott WP; Moosmuller H; Rogers CF; Jin T; Bruch R. (1999). Photoacoustic spectrometer for measuring light absorption by aerosol; instrument description. Atmos Environ, 33: 2845-2852. [020650](#)
- Audet P; Charest C. (2007). Heavy metal phytoremediation from a meta-analytical perspective. , 147: 231-237. [190169](#)
- Augustine J; Hodges G; Dutton E; Michalsky J; Cornwall C. (2008). An aerosol optical depth climatology for NOAA's national surface radiation budget network (SURFRAD). , 113: D11204. [189913](#)
- Ausset P; Bannery F; Del Monte M; Lefevre RA. (1998). Recording of pre-industrial atmospheric environment by ancient crusts on stone monuments. Atmos Environ, 32: 2859-2863. [040480](#)
- Avila A; Rodrigo A. (2004). Trace metal fluxes in bulk deposition, throughfall and stemflow at two evergreen oakstands in NE Spain subject to different exposure to the industrial environment. Atmos Environ, 38: 171-180. [155664](#)
- Babich P; Wang PY; Allen G; Sioutas C; Koutrakis P. (2000). Development and Evaluation of a Continuous Ambient PM_{2.5} Mass Monitor. Aerosol Sci Technol, 32: 309-324. [156239](#)
- Bachelet D; Lenihan J; Neilson R; Drapek R; Kittel T. (2005). Simulating the response of natural ecosystems and their fire regimes to climatic variability in Alaska. Can J For Res, 35: 2244-2257. [156241](#)
- Backe C; Cousins IT; Larsson P. (2004). PCB in soils and estimated soil-air exchange fluxes of selected PCB congeners in the south of Sweden. Environ Pollut, 128: 59-72. [155668](#)
- Bailey R; Barrie LA; Halsall CJ; Fellin P; Muir DCG. (2000). Atmospheric organochlorine pesticides in the western Canadian Arctic: evidence of trans-Pacific transport. J Geophys Res, 105: 11805-11811. [155670](#)
- Baker M; Charlson R. (1990). Bistability of CCN concentrations and thermodynamics in the cloud-topped boundary layer. [190016](#)
- Balkanski Y; Schulz M; Claquin T; Guibert S. (2007). Reevaluation of mineral aerosol radiative forcings suggests a better agreement with satellite and AERONET data. , 7: 95. [189979](#)
- Baptista MS; Vasconcelos MTSD; Cabral JP; Freitas MC; Pacheco AMG. (2008). Copper, nickel and lead in lichen and tree bark transplants over different periods of time. Environ Pollut, 151: 408-413. [155673](#)
- Baran AJ; Foot JS. (1994). New application of the operational sounder HIRS in determining a climatology of sulphuric acid aerosol from the Pinatubo eruption. J Geophys Res, 99: 25673-25679. [192032](#)
- Barker ML. (1976). Planning for environmental indices: observer appraisals of air quality. In K Craig; E Zube (Ed.), Perceiving Environmental Quality (pp. 175-203). New York: Plenum Press. [072137](#)
- Barnes JE; Hofmann DJ. (1997). Lidar measurements of stratospheric aerosol over Mauna Loa Observatory. Geophys Res Lett, 24: 1923-1926. [192044](#)
- Bates T; Anderson T; Baynard T; Bond T; Boucher O; Carmichael G; Clarke A; Erlick C; Guo H; Horowitz L. (2006). Aerosol direct radiative effects over the northwest Atlantic, northwest Pacific, and North Indian Oceans: estimates based on in-situ chemical and optical measurements and chemical transport modeling. , 6: 175-362. [189912](#)
- Bates T; Huebert B; Gras J; Griffiths B; Durkee P. (1998). The International Global Atmospheric Chemistry (IGAC) Project's First Aerosol Characterization Experiment (ACE 1)-Overview. , 103: 16297-16318. [190063](#)
- Bates T; Quinn P; Coffman D; Covert D; Miller T; Johnson J; Carmichael G; Uno I; Guazzotti S; Sodeman D. (2004). Marine boundary layer dust and pollutant transport associated with the passage of a frontal system over eastern Asia. , 109. [189958](#)
- Bates TS; Quinn PK; Coffman DJ; Johnson JE; Miller TL; Covert DS; Wiedensohler A; Leinert S; Nowak A; Neususs C. (2001). Regional physical and chemical properties of the marine boundary layer aerosol across the Atlantic during Aerosols99: an overview. J Geophys Res, 106: 20,767-20,782. [043385](#)
- Bauman JJ; Russell PB; Geller MA; Hamill P. (2003). A stratospheric aerosol climatology from SAGE II and CLAES measurements: 2. Results and comparisons. J Geophys Res, 108: 4383. [192265](#)
- Baumgardner RE Jr; Isil SS; Bowser JJ; Fitzgerald KM. (1999). Measurements of rural sulfur dioxide and particle sulfate: analysis of CASTNet data, 1987 through 1996. J Air Waste Manag Assoc, 49: 1266-1279. [011308](#)
- Baynard T; Lovejoy ER; Pettersson A; Brown SS; Lack D; Osthoff H; Massoli P; Ciciora S; Dube WP; Ravishankara AR. (2007). Design and application of a pulsed cavity ring-down aerosol extinction spectrometer for field measurements. Aerosol Sci Technol, 41: 447-462. [151669](#)

- BBC Research & Consulting. (2002). Phoenix Area Visibility Survey. Draft Report. Available at http://www.azdeq.gov/viron/air/download/vis_021903f.pdf. [156258](#)
- Becker T; Brändel M. (2007). Vegetation-environment relationships in a heavy metal-dry grassland complex. , 42: 11-28. [156260](#)
- Beeby A; Richmond L. (2002). Evaluating *Helix aspersa* as a sentinel for mapping metal pollution. , 1: 261-270. [155680](#)
- Bellouin N; Boucher O; Haywood J; Reddy MS. (2005). Global emissions of aerosol direct radiative forcing from satellite measurements. , 438: 1138-1141. [155684](#)
- Bellouin N; Boucher O; Tanré D; Dubovik O. (2003). Aerosol absorption over the clear-sky oceans deduced from POLDER-1 and AERONET observations. , 30: 1748. [189911](#)
- Bellouin N; Jones A; Haywood J; Christopher S. (2008). Updated estimate of aerosol direct radiative forcing from satellite observations and comparison against the Hadley Centre climate model. , 113. [189999](#)
- Beron K; Murdoch J; Thayer M. (2001). The Benefits of Visibility Improvement: New Evidence from the Los Angeles Metropolitan Area. , 22: 319-337. [156270](#)
- Berthelsen BO; Olsen RA; Steinnes E. (1995). Ectomycorrhizal heavy metal accumulation as a contributing factor to heavy metal levels in organic surface soils. *Sci Total Environ*, 170: 141-149. [078058](#)
- Bhavsar SP; Diamond ML; Evans LJ; Gandhi N; Nilsen J; Antunes P. (2004). Development of a coupled metal speciation–fate model for surface aquatic systems. *Environ Toxicol Chem*, 23: 1376– 1385. [155689](#)
- Bhavsar SP; Diamond ML; Gandhi N; Nilsen J. (2004). Dynamic coupled metal transport–speciation model: application to assess a zinc-contaminated lake. *Environ Toxicol Chem*, 23: 2410–2420. [155690](#)
- Bickerstaff K; Walker G. (2001). Public understandings of air pollution: the ‘localisation’of environmental risk. *Global Environ Change*, 11: 133-145. [156271](#)
- Bidleman TF; Jantunen LMM; Helm PA; Bronstrom-Lunden E; Juntto S. (2002). Chlordane isomers and enantiomers suggest changing sources in Arctic air. *Environ Sci Technol*, 36: 539-544. [155691](#)
- Billings WD. (1978). *Plants and the ecosystem*. Belmont, CA: Wadsworth Publishing Company, Inc. [034165](#)
- Bingen C; Fussen D; Vanhellefont F. (2004). A global climatology of stratospheric aerosol size distribution parameters derived from SAGE II data over the period 1984?2000: 2. Reference data . *J Geophys Res*, 102: D06202. [192262](#)
- Blanchard CL; Tanenbaum S. (2006). Weekday/Weekend differences in ambient air pollutant concentrations in atlanta and the southeastern United States. , 56: 271-284. [192181](#)
- Blanchard CL; Tanenbaum S; Hidy GM. (2007). Effects of sulfur dioxide and oxides of nitrogen emission reductions on fine particulate matter mass concentrations: regional comparisons. *J Air Waste Manag Assoc*, 57: 1337-50. [098659](#)
- Bluth GJS; Doiron SD; Schnetzler CC; Krueger AJ; Walter LS. (1992). Global tracking of the SO₂ clouds from the June, 1991 Mount Pinatubo eruptions . *Geophys Res Lett*, 19: 151-154. [192029](#)
- Bluth GJS; Rose WI; Sprod IE. (1997). Stratospheric loading of sulfur from explosive volcanic eruptions. , 105: 671-683. [192045](#)
- Bonazza A; Sabbioni C; Ghedini N. (2005). Quantitative data on carbon fractions in interpretation of black crusts and soiling on European built heritage. *Atmos Environ*, 39: 2607-2618. [155695](#)
- Bond T; Bhardwaj E; Dong R; Jogani R; Jung S; Roden C; Streets D; Trautmann N. (2007). Historical emissions of black and organic carbon aerosol from energy-related combustion, 1850-2000. *Global Biogeochem Cycles*, 21. [190050](#)
- Bond TC; Anderson TL; Campbell D. (1999). Calibration and Intercomparison of Filter-Based Measurements of Visible Light Absorption by Aerosols. *Aerosol Sci Technol*, 30: 582-600. [156281](#)
- Bond TC; Bergstrom RW. (2005). Light absorption by carbonaceous particles: an investigative review. *Aerosol Sci Technol*, 39: 1-41. [155696](#)
- Bond TC; Streets DG; Yarber KF; Nelson SM; Woo J-H; Klimont Z. (2004). A technology-based global inventory of black and organic carbon emissions from combustion. *J Geophys Res*, 109: D14203. [056389](#)
- Bond TC; Sun H. (2005). Can reducing black carbon emissions counteract global warming?. *Environ Sci Technol*, 39: 5921-5926. [156282](#)
- Boucher O; Tanré D. (2000). Estimation of the aerosol perturbation to the Earth's radiative budget over oceans using POLDER satellite aerosol retrievals. *Geophys Res Lett*, 27: 1103-1106. [190041](#)
- Boucher U; Balabane M; Lamy I; Cambier P. (2005). Decomposition in soil microcosms of leaves of the metallophyte *Arabidopsis halleri*: Effect of leaf-associated heavy metals on biodegradation. , 135: 187-194. [155699](#)
- Brasseur G; Granier C. (1992). Mount Pinatubo aerosols, chlorofluorocarbons, and ozone depletion. , 257: 1239-1242. [192256](#)

- Brenguier J; Chuang P; Fouquart Y; Johnson D; Parol F; Pawlowska H; Pelon J; Schuller L; Schroder F; Snider J. (2000). An overview of the ACE-2 CLOUDYCOLUMN closure experiment. , 52: 815-827. [189966](#)
- Brimblecombe P; Grossi CM. (2005). Aesthetic thresholds and blackening of stone buildings. *Sci Total Environ*, 349: 175-189. [155703](#)
- Broccoli AJ; Dixon KW; Delworth TL; Knutson TR; Stouffer RJ; Zeng F. (2003). Twentieth-century temperature and precipitation trends in ensemble climate simulations including natural and anthropogenic forcing. *J Geophys Res*, 108: 4798. [192283](#)
- Brookshire D. (1979). Methods Development for Assessing Air Pollution Control Benefits. Volume 2: Experiments in Valuing Nonmarket Goods. A Case Study of Alternative Benefit Measures of Air Pollution in the South Coast Air Basin of Southern California. . . . [156298](#)
- Burkhardt J; Kaiser H; Kappen L; Goldbach HE. (2002). The possible role of aerosols on stomatal conductivity for water vapour. , 2: 351-364. [155708](#)
- Burt R; Wilson MA; Mays MD; Lee CW. (2003). Major and trace elements of selected pedons in the USA. *J Environ Qual*, 32: 2109-2121. [155709](#)
- Bäckström M; Nilsson U; Håkansson K; Allard B; Karlsson S. (2003). Speciation of heavy metals in road runoff and roadside total deposition. *Water Air Soil Pollut*, 147: 343-366. [156242](#)
- Campbell D; Copeland S; Cahill T. (1995). Measurement of Aerosol Absorption Coefficient from Teflon Filters using Integrating Plate and Integrating Sphere Techniques. *Aerosol Sci Technol*, 22: 287-292. [190171](#)
- Campbell FW. (1983). Ambient Stressors. , 15: 355-380. [190172](#)
- Camuffo D. (1995). Physical weathering of stones. Presented at In: Saiz-Jimenez, C., ed. The deterioration of monuments: proceedings of the 2nd international symposium on biodeterioration and biodegradation; January 1994; Sevilla, Spain. *Sci. Total Environ*. 167: 1-14. [076278](#)
- Canada-US Air Quality Committee, Subcommittee 2: Scientific Cooperation. (2004). Canada-United States transboundary particulate matter science assessment. Meteorological Service of Canada. Toronto, Ontario, Canada. En56-203/2004E. http://www.msc-smc.ec.gc.ca/saib/smog/transboundary/toc_e.html. [190519](#)
- Carmichael G; Tang Y; Kurata G; Uno I; Streets D; Thongboonchoo N; Woo J; Guttikunda S; White A; Wang T. (2003). Evaluating regional emission estimates using the TRACE-P observations. , 108: 10.1029. [190042](#)
- Carmichael GR; Calori G; Hayami H; Uno I; Cho SY; Engardt M; Kim SB; Ichikawa Y; Ikeda Y; Woo JH; Ueda H; Amann M. (2002). The MICS-Asia study: model intercomparison of long-range transport and sulfur deposition in East Asia. *Atmos Environ*, 36: 175-199. [148319](#)
- Carrico C; Kreidenweis S; Malm W; Day D; Lee T; Carrillo J; McMeeking G; Collett J. (2005). Hygroscopic growth behavior of a carbon-dominated aerosol in Yosemite National Park. *Atmos Environ*, 39: 1393-1404. [190052](#)
- Carvalho LM; Caçador I; Martins-Loução MA. (2006). Arbuscular mycorrhizal fungi enhance root cadmium and copper accumulation in the roots of the salt marsh plant *Aster tripolium* L. *Plant Soil*, 285: 161-169. [155715](#)
- CCSP. (2008). Climate Projections Based on Emissions Scenarios for Long-lived and Short-lived Radiatively Active Gases and Aerosols. A Report by the U.S. Climate Change Science, Program and the Subcommittee on Global Change Research. Department of Commerce. Washington, DC. [192028](#)
- Chameides WL; Yu H; Liu SC; Bergin M; Zhou X; Mearns L; Wang G; Kiang CS; Saylor RD; Luo C; Huang Y; Steiner A; Giorgi F. (1999). Case study of the effects of atmospheric aerosols and regional haze on agriculture: an opportunity to enhance crop yields in China through emission controls?. *Proc Natl Acad Sci U S A*, 96: 13626-13633. [011184](#)
- Chand D; Anderson T; Wood R; Charlson R; Hu Y; Liu Z; Vaughan M. (2008). Quantifying above-cloud aerosol using spaceborne lidar for improved understanding of cloudy-sky direct climate forcing. *J Geophys Res*, 113: D13206. [189974](#)
- Charlson R; Pilat M. (1969). Climate: the influence of aerosols. , 8: 1001-1002. [190025](#)
- Charlson R; Wigley T. (1994). Sulfate aerosol and climatic change. *Sci Am*, 270: 28-35. [192011](#)
- Charlson RJ; Ahlquist NC; Horvath H. (1968). On the generality of correlation of atmospheric aerosol mass concentration and light scatter. *Atmos Environ*, 2: 455-464. [095355](#)
- Charlson RJ; Langner J; Rodhe H; Leovy CB; Warren SG. (1991). Perturbation of the northern hemisphere radiative balance by backscattering from anthropogenic sulfate aerosols. , 43AB: 152-163. [045793](#)
- Charlson RJ; Schwartz SE; Hales JM; Cess RD; Coakley JA Jr; Hansen JE; Hofmann DJ. (1992). Climate forcing by anthropogenic aerosols. , 255: 423-430. [045794](#)
- Cheggour M; Chafik A; Fisher NS; Benbrahim S. (2005). Metal concentrations in sediments and clams in four Moroccan estuaries. *Mar Environ Res*, 59: 119-137. [155723](#)

- Chen W; Kahn R; Nelson D; Yau K; Seinfeld J. (2008). Sensitivity of multiangle imaging to the optical and microphysical properties of biomass burning aerosols. , 113. [189984](#)
- Chernyak SM; Rice CP; McConnell LL. (1996). Evidence of currently used pesticides in air, ice, fog, seawater and surface microlayer in the Bering and Chukchi Seas. *Mar Pollut Bull*, 32: 410-419. [155726](#)
- Chestnut LG; Dennis RL. (1997). Economic benefits of improvements in visibility: acid rain Provisions of the 1990 Clean Air Act Amendments. *J Air Waste Manag Assoc*, 47: 395-402. [014525](#)
- Chin M; Diehl T; Ginoux P; Malm W. (2007). Intercontinental transport of pollution and dust aerosols: implications for regional air quality. , 7: 5501-5517. [190062](#)
- Chin M; Ginoux P; Kinne S; Torres O; Holben B; Duncan B; Martin R; Logan J; Higurashi A; Nakajima T. (2002). Tropospheric aerosol optical thickness from the GOCART model and comparisons with satellite and Sun photometer measurements. *J Trace Elem Med Biol*, 59: 461-483. [189996](#)
- Chin M; Kahn RA; Remer LA; Yu H; Rind D; Feingold G; Quinn PK; Schwartz SE; Streets DG; DeCola P; Halthorne R. (2009). Atmospheric aerosol properties and climate impacts. Synthesis and assesment product 2.3. A report by the U.S. Climate Change Science Program and the Subcommittee on Global Change Research. National Aeronautics and Space Administration. Washington, DC. [192130](#)
- Chiou CT; Sheng G; Manes M. (2001). A partition-limited model for the plant uptake of organic contaminants from soil and water. *Environ Sci Technol*, 35: 1437-1444. [156342](#)
- Chipperfield MP; Randel WJ; Bodeker GE; Johnston P. (2003). Global ozone: past and future. In *Scientific Assessment of Ozone Depletion: 2002* (pp. 4.1-4.90). Geneva: World Meteorological Organization. [192275](#)
- Chock DP; Song Q; Hass H; Schell B; Ackermann I. (2003). Comment on "Control of fossil-fuel particulate black carbon and organic matter, possibly the most effective method of slowing global warming" by Jacobson, M. Z. *J Geophys Res*, 108: ACH12.1-ACH13.4. [155727](#)
- Chou M; Chan P; Wang M. (2002). Aerosol radiative forcing derived from SeaWiFS-retrieved aerosol optical properties. *J Trace Elem Med Biol*, 59: 748-757. [190008](#)
- Chow JC; Watson JG; Edgerton SA; Vega E. (2002). Chemical composition of PM10 and PM25 in Mexico City during winter 1997. *Sci Total Environ*, 287: 177-201. [036166](#)
- Chow JC; Watson JG; Lowenthal DH; Richards LW. (2002). Comparability between PM25 and particle light scattering measurements. *Environ Monit Assess*, 79: 29-45. [037784](#)
- Christie P; Li XL; Chen BD. (2004). Arbuscular mycorrhiza can depress translocation of zinc to shoots of host plants in soils moderately polluted with zinc. *Plant Soil*, 261: 209-217. [190174](#)
- Christopher S; Jones T. (2008). Short-wave aerosol radiative efficiency over the global oceans derived from satellite data. , 60: 636-640. [189985](#)
- Christopher SA; Zhang J; Kaufman YJ; Remer L. (2006). Satellite-based assessment of the top of the atmosphere anthropogenic aerosol radiative forcing over cloud-free oceans. *Geophys Res Lett*, 111: L15816. [155729](#)
- Chu D; Kaufman Y; Ichoku C; Remer L; Tanré D; Holben B. (2002). Validation of MODIS aerosol optical depth retrieval over land. , 29: 8007. [190001](#)
- Chung C; Zhang G. (2004). Impact of absorbing aerosol on precipitation: Dynamic aspects in association with convective available potential energy and convective parameterization closure and dependence on aerosol heating profile. , 109. [190054](#)
- Chung CE; Ramanathan V; Kim D; Podgorny IA. (2005). Global anthropogenic aerosol direct forcing derived from satellite and ground-based observations. *J Geophys Res*, 110: D24207. [155733](#)
- Chung SH; Seinfeld JH. (2002). Global distribution and climate forcing of carbonaceous aerosols. *J Geophys Res*, 107: 4407. [155732](#)
- Citterio S; Prato N; Fumagalli P; Aina R; Massa N; Santagostino A; Sgorbati S; Berta G. (2005). The arbuscular mycorrhizal fungus *Glomus mosseae* induces growth and metal accumulation changes in *Cannabis sativa* L. *Chemosphere*, 59: 21-29. [190176](#)
- Clarke A; Porter J; Valero F; Pilewskie P. (1996). Vertical profiles, aerosol microphysics, and optical closure during the Atlantic Stratocumulus Transition Experiment: Measured and modeled column optical properties. , 101: 4443-4453. [190003](#)
- Clemens S. (2006). Toxic metal accumulation, responses to exposure and mechanisms of tolerance in plants. *Biochimie*, 88: 1707-1719. [190179](#)
- Coakley JA; Walsh CD. (2002). Limits to the aerosol indirect radiative effect derived from observations of ship tracks. *J Trace Elem Med Biol*, 59: 668-680. [192025](#)
- Coelho JP; Rosa M; Pereira E; Duarte A; Pardal MA. (2006). Pattern and annual rates of *Scrobicularia plana* mercury bioaccumulation in a human induced mercury gradient (Ria de Aveiro, Portugal). , 69: 629-635. [190181](#)

- Cohen S; Evans GW; Stokols D; Krantz DS. (1986). Behavior, Health, and Environmental Stress. New York: Plenum Press. [190182](#)
- Collins D; Johnsson H; Seinfeld J; Flagan R; Gasso S; Hegg D; Russell P; Schmid B; Livingston J; Ostrom E. (2000). In situ aerosol-size distributions and clear-column radiative closure during ACE-2. , 52: 498-525. [190059](#)
- Collins RN; Merrington G; McLaughlin MJ; Morel JL. (2003). Organic ligand and pH effects on isotopically exchangeable cadmium in polluted soils. Soil Sci Soc Am J, 67: 112-121. [155737](#)
- Collins W; Rasch P; Eaton B; Khattatov B; Lamarque J; Zender C. O. Simulating aerosols using a chemical transport model with assimilation of satellite aerosol retrievals: Methodology for INDOEX. , 106. [189987](#)
- Conant W; VanReken T; Rissman T; Varutbangkul V; Jonsson H; Nenes A; Jimenez J; Delia A; Bahreini R; Roberts G. (2004). Aerosol-cloud drop concentration closure in warm cumulus. , 109. [190010](#)
- Cooke W; Wilson J. O. A global black carbon aerosol model. , 101. [190046](#)
- Cooke WF; Lioussé C; Cachier H; Feichter J. (1999). Construction of a 1° x 1° fossil fuel emission data set for carbonaceous aerosol and implementation and radiative impact in the ECHAM 4 model. J Geophys Res, 104: 22137-22162. [156365](#)
- Costa M; Silva A; Levizzani V. (2004). Aerosol characterization and direct radiative forcing assessment over the ocean. Part I: Methodology and sensitivity analysis. , 43: 1799-1817. [190006](#)
- Costa MJ; Levizzani V; Silva AM. (2004). Aerosol characterization and direct radiative forcing assessment over the ocean. Part II: Application to test cases and validation. , 43: 1818-1833. [192022](#)
- Couto JA; Fernández JA; Aboal JR; Carballeira A. (2004). Active biomonitoring of element uptake with terrestrial mosses: a comparison of bulk and dry deposition. Sci Total Environ, 324: 211-222. [155739](#)
- Covert DS; Charlson RJ; Ahlquist NC. (1972). A study of the relationship of chemical composition and humidity to light scattering by aerosols. , 11: 968-976. [072055](#)
- Crawford DW; Lipsen MS; Purdie DA; Lohan MC; Statham PJ; Whitney FA; Putland JN; Johnson WK; Sutherland N; Peterson TD; Harrison PJ; Wong CS. (2003). Influence of zinc and iron enrichments on phytoplankton growth in the northeastern subarctic Pacific. Limnol Oceanogr, 48: 1583-1600. [156370](#)
- Creighton PJ; Liou PJ; Haynie FH; Lemmons TJ; Miller JL; Gerhart J. (1990). Soiling by atmospheric aerosols in an urban industrial area. J Air Waste Manag Assoc, 40: 1285-1289. [044578](#)
- Croteau MN; Luoma SN; Stewart AR. (2005). Trophic transfer of metals along freshwater food webs: Evidence of cadmium biomagnification in nature. Limnol Oceanogr, 50: 1511-1519. [156373](#)
- Crépineau C; Rychen G; Feidt C; Le Roux Y; Lichtfouse E; Laurent F. (2003). Contamination of pastures by polycyclic aromatic hydrocarbons (PAHs) in the vicinity of a highway. J Agric Food Chem, 51: 4841-4845. [155741](#)
- Cunningham M. (1979). Weather, mood, and helping behavior: Quasi experiments with the sunshine Samaritan. , 37: 1947-1956. [191974](#)
- Cuny D; Denayer FO; De Foucault B; Schumacker R; Colein P; Van Haluwyn C. (2004). Patterns of metal soil contamination and changes in terrestrial cryptogamic communities. Environ Pollut, 129: 289-297. [155742](#)
- Da Silva LC; Oliva MA; Azevedo AA; De Araujo JM. (2006). Responses of restinga plant species to pollution from an iron pelletization factory. , 175: 241-256. [190190](#)
- Dallinger R; Wang Y; Berger B; Mackay EA; Kägi JH. (2001). Spectroscopic characterization of metallothionein from the terrestrial snail, *Helix pomatia*. , 268: 4126-4133. [192109](#)
- Dameris M; Grewe V; Ponater M; Deckert R; Eyring V; Mager F; Matthes S; Schnadt C; Stenke A; Steil B; Brühl C; Giorgetta MA. (2005). Long-term changes and variability in a transient simulation with a chemistry-climate model employing realistic forcing. , 5: 2121-2145. [192238](#)
- Davis AP; Shokouhian M; Ni S. (2001). Loading estimates of lead, copper, cadmium, and zinc in urban runoff from specific sources. Chemosphere, 44: 997-1009. [024933](#)
- Davis MRH; Zhao FJ; McGrath SP. (2004). Pollution-induced community tolerance of soil microbes in response to a zinc gradient. Environ Toxicol Chem, 23: 2665-2672. [155744](#)
- Day R. (2007). Place and the experience of air quality. Health Place, 13: 249-260. [156386](#)
- De Gouw J; Middlebrook A; Warneke C; Goldan P; Kuster W; Roberts J; Fehsenfeld F; Worsnop D; Canagaratna M; Pszenny A. (2005). Budget of organic carbon in a polluted atmosphere: Results from the New England Air Quality Study in 2002. , 110. [190020](#)
- De Nicola F; Maisto G; Prati MV; Alfani A. (2005). Temporal variations in PAH concentrations in *Quercus ilex* L. (holm oak) leaves in an urban area. Chemosphere, 61: 432-440. [155747](#)
- DeBell L. (2006). Spatial and seasonal patterns and temporal variability of haze and its constituents in the United States: Report IV. 1Cooperative Institute for Research in the Atmosphere. Colorado State University Fort Collins, CO. [156388](#)

- Delworth T; Ramaswamy V; Stenchikov G. (2005). The impact of aerosols on simulated ocean temperature and heat content in the 20th century. , 32. [190055](#)
- Demerjian KL; Mohnen VA. (2008). Synopsis of the temporal variation of particulate matter composition and size. *J Air Waste Manag Assoc*, 58: 216-233. [156392](#)
- Denman KL; Brasseur G; Chidthaisong A; Ciais P; Cox PM; Dickinson RE; Hauglustaine D; Heinze C; Holland E; Jacob D; Lohmann U; Ramachandran S; da Silva Dias PL; Wofsy SC; Zhang X. (2007). Couplings Between Changes in the Climate System and Biogeochemistry. . : [156394](#)
- Dentener F; Stevenson D; Ellingsen K; Van Noije T; Schultz M; Amann M; Atherton C; Bell N; Bergmann D; Bey I; Bouwman L; Butler T; Cofala J; Collins B; Drevet J; Doherty R; Eickhout B; Eskes H; Fiore A; Gauss M; Hauglustaine D; Horowitz L; Isaksen ISA; Josse B; Lawrence M; Krol M; Lamarque JF; Montanaro V; Muller JF; Peuch VH; Pitari G; Pyle J; Rast S; Rodriguez J; Sanderson M; Savage NH; Shindell D; Strahan S; et al. (2006). The global atmospheric environment for the next generation. *Environ Sci Technol*, 40: 3586-3594. [088434](#)
- Derome J; Lindroos A-J. (1998). Effects of heavy metal contamination on macronutrient availability and acidification parameters in forest soil in the vicinity of the Harjavalta Cu-Ni smelter, SW Finland. *Environ Pollut*, 99: 225-232. [155749](#)
- Deshler T; Hervig ME; Hofmann DJ; Rosen JM; Liley JB. (2003). Thirty years of in situ stratospheric aerosol size distribution measurements from Laramie, Wyoming (41°N), using balloon-borne instruments . *J Geophys Res*, 108: 4167. [192058](#)
- Deuzé J; Bréon F; Devaux C; Goloub P; Herman M; Lafrance B; Maignan F; Marchand A; Nadal F; Perry G. (2001). Remote sensing of aerosols over land surfaces from POLDER-ADEOS-1 polarized measurements. , 106: x. [192013](#)
- Di Toro DM; McGrath JH; Berry WJ; Paquin PR; Mathew R; Wu KB; Santore RC. (2005). Predicting sediment metal toxicity using a sediment biotic ligand model: Methodology and initial application. *Environ Toxicol Chem*, 24: 2410-2427. [155750](#)
- Diner D; Beckert J; Bothwell G; Rodriguez J. (2002). Performance of the MISR instrument during its first 20 months in Earth orbit. *IEEE Trans Geosci Remote Sens*, 40: 1449-1466. [189967](#)
- Diner D; Beckert J; Reilly T; Bruegge C; Conel J; Kahn R; Martonchik J; Ackerman T; Davies R; Gerstl S. (1998). Multi-angle Imaging SpectroRadiometer(MISR) instrument description and experiment overview. *IEEE Trans Geosci Remote Sens*, 36: 1072-1087. [189962](#)
- Doherty S; Quinn P; Jefferson A; Carrico C; Anderson T; Hegg D. (2005). A comparison and summary of aerosol optical properties as observed in situ from aircraft, ship, and land during ACE-Asia. , 110. [190027](#)
- Donahue WF; Allen EW; Schindler DW. (2006). Impacts of coal-fired power plants on trace metals and polycyclic aromatic hydrocarbons (PAHs) in lake sediments in central Alberta, Canada. *J Paleolimnol*, 35: 111-128. [155751](#)
- Dong Y; Zhu YG; Smith FA; Wang Y; Chen B. (2008). Arbuscular mycorrhiza enhanced arsenic resistance of both white clover (*Trifolium repens* Linn.) and ryegrass (*Lolium perenne* L.) plants in an arsenic-contaminated soil. *Environ Pollut*, 155: 174-181. [192106](#)
- Douglass AR; Schoeberl MR; Rood RB; Pawson S. (2003). Evaluation of transport in the lower tropical stratosphere in a global chemistry and transport model. *J Geophys Res*, 108D9. [057260](#)
- Dubovik O; Holben B; Eck TF; Smirnov A; Kaufman YJ; King MD; Tanre D; Slutsker I. (2002). Variability of absorption and optical properties of key aerosol types observed in worldwide locations . *J Trace Elem Med Biol*, 59: 590-608. [190202](#)
- Dubovik O; King MD. (2000). A flexible inversion algorithm for retrieval of aerosol optical properties from sun and sky radiance measurements. *J Geophys Res*, 105: 20673-20696. [190197](#)
- Dubovik O; Lapyonok T; Kaufman Y; Chin M; Ginoux P; Sinyuk A. (2007). Retrieving global sources of aerosols from MODIS observations by inverting GOCART model. , 7: 3629-3718. [190211](#)
- Dubovik O; Smirnov A; Holben BN; King MD; Kaufman YJ; Eck TF; Slutsker I. (2000). Accuracy assessments of aerosol optical properties retrieved from AERONET sun and sky radiance measurements. *J Geophys Res*, 105: 9791-9806. [190177](#)
- Duriscoe DM; Luginbuhl CB; Moore CA. (2007). Measuring Night-Sky Brightness with a Wide-Field CCD Camera. , 119: 192-213. [156411](#)
- Dusek R; Frank GP; Hildebrandt L; Curtius J; Schneider J; Walter S; Chand D; Drewnick F; Hings S; Jung D; Borrmann S; Andreae MO. (2006). Size matters more than chemistry for cloud-nucleating ability of aerosol particles. 1375-1378. [155756](#)
- Eagan RC; Hobbs PV; Radke LF. (1974). Measurements of cloud condensation nuclei and cloud droplet size distributions in the vicinity of forest fires. , 13: 553-557. [190231](#)

- Eck TF; Holben BN; Reid JS; Dubovik O; Smirnov A; O'Neill NT; Slutsker I; Kinne S. (1999). Wavelength dependence of the optical depth of biomass burning, urban, and desert dust aerosols . *J Geophys Res*, 104: 31333-31350. [190390](#)
- Eck TF; Holben BN; Reid JS; Sinyuk A; Dubovik O; Smirnov A; Giles D; O'Neill NT; Tsay SC; Ji Q; Mandoos AAI; Khan MR; Reid EA; Schafer JS; Sorokine M; Newcomb W; Slutsker I. (2008). Spatial and temporal variability of column- integrated aerosol optical properties in the southern Arabian Gulf and United Arab Emirates in summer. *J Geophys Res*, 113: in press. [190409](#)
- Edgerton ES; Hartsell BE; Jansen JJ; Hansen DA; Waid CJ; Kandasamy K. (2004). 5-Year Trend Analysis of PM2.5 Data from the SEARCH Network. Presented at , . [156413](#)
- Eeva T; Lehikoinen E. (2004). Rich calcium availability diminishes heavy metal toxicity in Pied Flycatcher. *Funct Ecol*, 18: 548-553. [155762](#)
- Eeva T; Tanhuanpää S; Råbergh C; Airaksinen S; Nikinmaa M; Lehikoinen E. (2000). Biomarkers and fluctuating asymmetry as indicators of pollution- induced stress in two hole-nesting passerines. *Funct Ecol*, 14: 235-243. [155761](#)
- Elliot SJ; Cole DC; Krueger P; Voorberg N; Wakefield S. (1999). The power of perception: health risk attributed to air pollution in an urban industrial neighborhood. *Risk Anal*, 19: 621-634. [010716](#)
- Ely DW; Leary JT; Stewart TR; Ross DM. (1991). The Establishment of the Denver Visibility Standard. Presented at . [156417](#)
- Englert N. (2004). Fine particles and human health - a review of epidemiological studies. *Toxicol Lett*, 149: 235-242. [087939](#)
- EPA. (2000). National air pollutant emission trends, 1900-1998. U.S. Environmental Protection Agency. Washington, D.C.. . . [012211](#)
- EPA. (2001). Draft Guidance for tracking progress under the regional haze rule. U.S. Environmental Protection Agency. Washington, D.C.. . . [157068](#)
- Ericksen JA; Gustin MS; Schorran DE; Johnson DW; Lindberg SE; Coleman JS. (2003). Accumulation of atmospheric mercury in forest foliage. *Atmos Environ*, 37: 1613-1622. [155769](#)
- Ervens B; Feingold G; and SMKreidenweis SM. (2005). The influence of water-soluble organic carbon on cloud drop number concentration. *J Geophys Res*, 110: D18211.1-D18211.14. [190527](#)
- Evans GW; Jacobs SV. (1982). Air Pollution and Human Behavior. In Evans, GW (Ed.), *Environmental Stress* (pp. 105-132). New York, NY: Cambridge University Press. [179899](#)
- Evans GW; Jacobs SV; Dooley D; Catalano R. (1987). The Interaction of Stressful Life Events and Chronic Strains on Community Mental Health. , 15: 23-24. [190347](#)
- Evans GW; Jacobs SV; Frager NB. (1982). Behavioral responses to air pollution. In A Baum; J Singer (Ed.), *Advances in Environmental Psychology* (pp. 237-269). Hillsdale, NJ: Erlbaum. [190521](#)
- Ewald G; Larsson P; Linge H; Okla L; Szarzi M. (1998). Biotransport of organic pollutants to an inland Alaska lake by migrating sockeye salmon (*Oncorhynchus nerka*). , 51: 40-47. [190348](#)
- Fehsenfeld FC | Ancellet G | Bates TS | Goldstein AH | Hardesty RM | Honrath R | Law KS; Lewis AC; Leaitch R; McKeen S; Meagher J; Parrish DD; Pszenny AAP; Russell PB; Schlager H; Seinfeld J; Talbot R; Zbinden R. (2006). International consortium for atmospheric research on transport and transformation (ICARTT): North America to Europe -overview of the 2004 summer field study . *J Geophys Res*, 111: D23S01.1-D23S01.36. [190531](#)
- Feichter J; Sausen R; Graßl H; Fiebig M. (2003). Comment on "Control of fossil-fuel particulate black carbon and organic matter, possibly the most effective method of slowing global warming" by M. Z. Jacobson. *J Geophys Res*, 108 (D24), 4767, doi:10.1029/2002JD003223. [155772](#)
- Feingold G. (2003). Modeling of the first indirect effect: Analysis of measurement requirements. *Geophys Res Lett*, 30: ASC7.1-ASC7.4. [190547](#)
- Feingold G; Furrer R; Pilewskie P; Remer LA; Min Q; Jonsson; Hafliidi. (2003). Aerosol indirect effect studies at southern great plains during the May 2003 intensive operations period . *J Geophys Res*, 111: D5. [190551](#)
- Feingold G; Jiang H; Harrington J. (2005). On smoke suppression of clouds in Amazonia. *Geophys Res Lett*, 32: L02804.1-L02804.4. [190550](#)
- Feingold G; Remer LA; Ramaprasad J; Kaufman YJ. (2001). Analysis of smoke impact on clouds in Brazilian biomass burning regions: An extension of Twomey's approach. *J Geophys Res*, 106: 22907-22922. [190544](#)
- Feingold G; Stevens B; Cotton WR; Walko RL. (1994). An explicit microphysics/LES model designed to simulate the Twomey Effect. , 33: 207-233. [190535](#)
- Feingold GW; Cotton WR; Kreidenweis SM; Davis JT. (1999). The impact of giant cloud condensation nuclei on drizzle formation in stratocumulus: Implications for cloud radiative properties. *J Trace Elem Med Biol*, 56: 4100-4117. [190540](#)

- Feng MH; Shan XQ; Zhang SZ; Wen B. (2005). Comparison of a rhizosphere-based method with other one-step extraction methods for assessing the bioavailability of soil metals to wheat. *Chemosphere*, 59: 939-949. [155774](#)
- Ferm M; Watt J; O'Hanlon S; De Santis F; Varotsos C. (2006). Deposition measurement of particulate matter in connection with corrosion studies. *Anal Bioanal Chem*, 384: 1320-30. [155135](#)
- Fernandes SD; Trautmann NM; Streets DG; Roden CA; Bond TC. (2007). Global biofuel use, 1850-2000. *Global Biogeochem Cycles*, 21: GB2019.1-GB2019.15. [190554](#)
- Ferrare R; Feingold G; Ghan S; Ogren J Schmid B; Schwartz SE; Sheridan P. (2006). Preface to special section: Atmospheric radiation measurement program May 2003 intensive operations period examining aerosol properties and radiative influences. *J Geophys Res*, 111: D05S01. [190561](#)
- Fiore AM; Jacob DJ; Mathur R; Martin RV. (2003). Application of empirical orthogonal functions to evaluate ozone simulations with regional and global models. *J Geophys Res*, 108D14: . [047805](#)
- Fishman J; Hoell JM; Bendura RD; McNeal RJ; Kirchoff V. (1996). NASA GTE TRACE A experiment (September- October 2002): Overview. *J Geophys Res*, 101: 23865-23880. [190566](#)
- Fismes J; Perrin-Ganier C; Empereur-Bissonnet P; Morel JL. (2002). Soil-to-root transfer and translocation of polycyclic aromatic hydrocarbons by vegetables grown on industrial contaminated soils. , 31: 1649-1656. [141156](#)
- Fitzgerald JW. (1975). Approximation formulas for the equilibrium size of an aerosol particle as a function of its dry size and composition and the ambient relative humidity. , 14: 1044-1049. [095417](#)
- Forster P; Ramaswamy V; Artaxo P; Betts R; Fahey DW; Haywood J; Lean J; Lowe DC; Myhre G; Nganga J; Prinn R; Raga G; Schultz M; Van Dorland R. (2007). Changes in atmospheric constituents and in radiative forcing. In Solomon, S.; Qin, D.; Manning, M.; Chen, Z.; Marquis, M.; Averyt, K. B.; Tignor, M.; Miller, H. L. (Ed.), *Climate Change 2007: the physical science basis. Contribution of Working Group I to the fourth assessment report of the intergovernmental panel on:* . [092936](#)
- Fraser R; Kaufman Y. (1985). The relative importance of aerosol scattering and absorption in remote sensing. *IEEE Trans Geosci Remote Sens*, GE-23: 625-633. [190567](#)
- Free M; Angell JK. (2002). Effect of volcanoes on the vertical temperature profile in radiosonde data. *J Geophys Res*, 107: 4101. [192281](#)
- Freer-Smith PH; El-khatib A; Taylor G. (2004). Capture of particulate pollution by trees: a comparison of species typical of semi-arid areas (*Ficus nitida* and *Eucalyptus globulus*) with European and North American species. *Water Air Soil Pollut*, 155: 173-187. [156451](#)
- Frescholtz TF; Gustin MS; Schorran DE; Fernandez GCJ. (2003). Assessing the source of mercury in the foliar tissue of quaking aspen. *Environ Toxicol Chem*, 22: 2114-2119. [190352](#)
- Fritze H; Niini S; Mikkola K; Makinen A. (1989). Soil microbial effects of a Cu-Ni smelter in southwestern Finland. , 8: 87-94. [079635](#)
- Fryer ME; Collins CD. (2003). Model intercomparison for the uptake of organic chemicals by plants. *Environ Sci Technol*, 37: 1617-1624. [156454](#)
- Gandhi N; Bhavsar SP; Diamond ML; Kuwabara JS; Marvin-DiPasquale M; Krabbenhoft DP. (2007). Development of a mercury speciation, fate, and biotic uptake (BIOTRANSPEC) model: Application to Lahontan Reservoir (Nevada, USA). *Environ Toxicol Chem*, 26: 2260-2273. [155781](#)
- Gao YZ; Zhu LZ. (2004). Plant uptake, accumulation and translocation of phenanthrene and pyrene in soils. *Chemosphere*, 55: 1169-1178. [155782](#)
- Garrett T; Zhao C; Dong X; Mace G; Hobbs P. (2004). Effects of varying aerosol regimes on low-level Arctic stratus. *Geophys Res Lett*, 31: L17105.1-L17105.4. [190568](#)
- Garrett TJ; Zhao C. (2006). Increased Arctic cloud longwave emissivity associated with pollution from mid-latitudes. *Nature*, 440: 787-789. [190570](#)
- Gawel JE; Ahner BA; Friedland AJ; Morel FMM. (1996). Role for heavy metals in forest decline indicated by phytochelatin measurements. , 381: 64-65. [012278](#)
- Generoso S; Bey I; Attié J-L; Bréon F-M. (2007). A satellite- and model-based assessment of the 2003 Russian fires: impact on the arctic region. *J Geophys Res*, 112: 5302. [155786](#)
- Geogdzhayev I; Mishchenko M; Rossow W; Cairns B; Lacis AA. (2002). Global two-channel AVHRR retrievals of aerosol properties over the ocean for the period of NOAA-9 observations and preliminary retrievals using NOAA-7 and NOAA-11 data. *J Trace Elem Med Biol*, 59: 262-278. [190574](#)
- Geron C; Rasmussen R; Arnts RR; Guenther A. (2000). A review and synthesis of monoterpene speciation from forests in the United States. *Atmos Environ*, 34: 1761-1781. [019095](#)
- Gillett NP; Hegerl GC; Allen MR; Stott PA; Schnur R. (2002). Reconciling two approaches to the detection of anthropogenic influence on climate. *J Clim*, 15: 326-329. [190576](#)

- Gillett NP; Zwiers FW; Weaver AJ; Hegerl GC; Allen MR; Stott PA. (2002). Detecting anthropogenic influence with a multi-model ensemble. *J Geophys Res*, 29: 31.1-31.4. [190578](#)
- Gilliland FD; Li YF; Saxon A; Diaz-Sanchez D. (2004). Effect of glutathione-S-transferase M1 and P1 genotypes on xenobiotic enhancement of allergic responses: randomised, placebo-controlled crossover study. *Lancet*, 363: 119-125. [156471](#)
- Ginoux P; Chin M; Holben B; Lin SJ; Tegen I; Prospero JM; Dubovik O. (2001). Sources and distributions of dust aerosols simulated with the GOCART model. *J Geophys Res*, 20: 20255-20273. [190579](#)
- Ginoux P; Horowitz LW; Ramaswamy V; Geogdzhayev IV; Holben BN; Stenchikov G; Tie X. (2006). Evaluation of aerosol distribution and optical depth in the geophysical fluid dynamics laboratory coupled model CM2.1 for present climate. *J Geophys Res*, 111: D22210. [190582](#)
- Gitay H; Brown S; Easterling W; Jallow B. (2001). Ecosystems and their goods and services. In *Climate change 2001: impacts, adaptation and vulnerability. Contribution of working group II to the third assessment report of the Intergovernmental Panel on Climate Change* (pp. 237-342). Cambridge, United Kingdom: Cambridge University Press. [092761](#)
- Givati A; Rosenfeld D. (2004). Quantifying precipitation suppression due to air pollution. , 43: 1038-1056. [156475](#)
- Gleason SM; Faucette DT; Toyofuku MM; Torres CA; Bagley CF. (2007). Assessing and mitigating the effects of windblown soil on rare and common vegetation. *Environ Manage*, 40: 1016-1024. [155794](#)
- Goforth MR; Christoforou CS. (2006). Particle size distribution and atmospheric metals measurements in a rural area in the South Eastern USA. *Sci Total Environ*, 356: 217-227. [088353](#)
- Gohre V; Paszkowski U. (2006). Contribution of the arbuscular mycorrhizal symbiosis to heavy metal phytoremediation. *Planta*, 223: 1115-1122. [190355](#)
- Golaz JC; Larson VE; Cotton WR. (2002). A PDF based model for boundary layer clouds. Part I: Method and model description. *J Trace Elem Med Biol*, 59: 3540-3551. [190587](#)
- Golaz JC; Larson VE; Cotton WR. (2002). A PDF-Based Model for Boundary Layer Clouds. Part II: Model Results. *J Trace Elem Med Biol*, 59: 3552-3571. [190589](#)
- Gomot-de Vaufleury A; Kerhoas I. (2000). Effects of cadmium on the reproductive system of the land snail *Helix aspersa*. , 64: 434-442. [155798](#)
- Gomot-De Vaufleury A; Pihan F. (2002). Methods for toxicity assessment of contaminated soil by oral or dermal uptake in land snails: Metal bioavailability and bioaccumulation. *Environ Toxicol Chem*, 21: 820-827. [190357](#)
- Gonzalez-Chavez C; Harris PJ; Dodd J; Meharg AA. (2002). Arbuscular mycorrhizal fungi confer enhanced arsenate resistance on *Holcus lanatus*. *New Phytol*, 155: 163-171. [155800](#)
- Goodarzi F; Sanei H; Garrett RG; Duncan WF. (2002). Accumulation of trace elements on the surface soil around the Trail smelter, British Columbia, Canada. , 43: 29-38. [155801](#)
- Gordon W; Jackson R. (2000). Nutrient concentrations in fine roots. *Ecology*, 81: 275-280. [155802](#)
- Goudie AS; Elaine W; Viles HA. (2002). The roles of salt and fog in weathering: a laboratory simulation of conditions the northern Atacama Desert, Chile. *Catena*, 48: 255-266. [156486](#)
- Grabowski WW. (2004). An improved framework for superparameterization. [embedding of cloud-resolving model in each column of large-scale model for small-scale and mesoscale processes representation] . *J Trace Elem Med Biol*, 61: 1940-1952. [190590](#)
- Grabowski WW; Wu X; Moncrieff MW. (1999). Cloud resolving modeling of tropical cloud systems during phase III of GATE. Part III: Effects of cloud microphysics . *J Trace Elem Med Biol*, 56: 2384-2402. [190592](#)
- Grannas AM; Hockaday WC; Hatcher PG; Thompson LG; Mosley-Thompson E. (2006). New revelations on the nature of organic matter in ice cores. *J Geophys Res*, 111, D04304, doi:10.1029/2005JD006251. [155804](#)
- Grannas AM; Jones AE; Dibb J; Ammann M; Anastasio C; Beine HJ; Bergin M; Bottenheim J; Boxe CS; Carver G; Chen G; Crawford JH; Dominé F; Frey MM; Guzmán MI; Heard DE; Helmig D; Hoffmann MR; Honrath RE; Huey LG; Hutterli M; Jacobi HW; Klán P; Lefer B; McCo. (2007). An overview of snow photochemistry: evidence, mechanisms and impacts. , 7: 4329-4373. [156492](#)
- Grannas AM; Shepson PB; Filley TR. (2004). Photochemistry and nature of organic matter in Arctic and Antarctic snow. *Global Biogeochem Cycles*, 18(1), GB1006, doi:10.1029/2003GB002133. [155803](#)
- Grantz DA; Garner JHB; Johnson DW. (2003). Ecological effects of particulate matter. *Environ Int*, 29: 213-239. [155805](#)
- Gratao PL; Polle A; Lea PJ; Azevedo RA. (2005). Making the life of heavy metal-stressed plants a little easier. *Funct Plant Biol*, 32: 481-494. [190364](#)
- Gray JS. (2002). Biomagnification in marine systems: The perspective of an ecologist. *Mar Pollut Bull*, 45: 46-52. [155806](#)

- Greenstein D; Tiefenthaler L; Bay S. (2004). Toxicity of parking lot runoff after application of simulated rainfall. *Arch Environ Contam Toxicol*, 47: 199-206. [155808](#)
- Gregory JM; Stouffer RJ; Raper SCB; Stott PA; Rayner NA. (2002). An observationally based estimate of the climate sensitivity. *J Clim*, 15: 3117-3121. [190593](#)
- Griffith DA; Solak ME; Yorty DP. (2005). Is air pollution impacting winter orographic precipitation in Utah? Weather modification association. *J Weather Modif*, 37: 14-20. [156497](#)
- Grigal DF. (2002). Inputs and outputs of mercury from terrestrial watersheds: a review. , 10: 1-39. [156498](#)
- Grigal DF. (2003). Mercury sequestration in forests and peatlands: A review. *J Environ Qual*, 32: 393-405. [155811](#)
- Grossi CM; Brimblecombe P. (2004). Aesthetics of simulated soiling patterns on architecture. *Environ Sci Technol*, 38: 3971-3976. [155813](#)
- Grossi CM; Esbert RM; Díaz-Pache F; Alonso FJ. (2003). Soiling of building stones in urban environments. , 38: 147-159. [155812](#)
- Guderian R ed. (1985). Air pollution by photochemical oxidants: formation, transport, control, and effects on plants. New York: Springer-Verlag. [019325](#)
- Guderian R. (1977). Accumulation of pollutants in plant organs. In *Air pollution: phytotoxicity of acidic gases and its significance in air pollution control* Berlin, Germany: Springer-Verlag. [004150](#)
- Gunn R; Phillips BB. (1957). An experimental investigation of the effect of air pollution on the initiation of rain. *J Trace Elem Med Biol*, 14: 272-280. [190595](#)
- Gupta P; Christopher SA; Wang J; Gehrig R; Lee Y; Kumar N. (2006). Satellite remote sensing of particulate matter and air quality assessment over global cities. *Atmos Environ*, 40: 5880-5892. [137694](#)
- Gustin MS. (2003). Are mercury emissions from geologic sources significant? A status report. *Sci Total Environ*, 304: 153-167. [155816](#)
- Hageman KJ; Simonich SL; Campbell DH; Wilson GR; Landers DH. (2006). Atmospheric deposition of current-use and historic-use pesticides in snow at national parks in the western United States. *Environ Sci Technol*, 40: 3174-3180. [156509](#)
- Hall JL. (2002). Cellular mechanisms for heavy metal detoxification and tolerance. *J Exp Bot*, 53: 1-11. [190365](#)
- Halsall CJ. (2004). Investigating the occurrence of persistent organic pollutants (POPs) in the Arctic: their atmospheric behaviour and interaction with the seasonal snow pack. *Environ Pollut*, 128: 163-175. [155822](#)
- Halsall CJ; Barrie LA; Fellin P; Muir DCG; Rovinski FY; Kononov EY. (1997). Spatial and temporal variation of polycyclic aromatic hydrocarbons in the arctic atmosphere. *Environ Sci Technol*, 31: 3593-3599. [155821](#)
- Han Q; Rossow WB; Chou J; Welch RM. (1998). Global survey of the relationship of cloud albedo and liquid water path with droplet size using ISCCP. *J Clim*, 11: 1516-1528. [190594](#)
- Han Q; Rossow WB; Zeng J. (2002). Three different behaviors on liquid water path of clouds in aerosol-cloud interactions. *J Trace Elem Med Biol*, 59: 726-735. [049181](#)
- Hand JL; Kreidenweis SM; Sherman DE; Collett JL Jr; Hering SV; Day DE; Malm WC. (2002). Aerosol size distributions and visibility estimates during the big bend regional aerosol visibility and observational study (BRAVO). *Atmos Environ*, 36: 5043-5055. [190367](#)
- Hand JL; Malm WC. (2006). Review of the IMPROVE Equation for Estimating Ambient Light Extinction Coefficients-Final Report. . . . [156517](#)
- Hand JL; Malm WC. (2007). Review of aerosol mass scattering efficiencies from ground-based measurements since 1990. *J Geophys Res*, 112: . [155825](#)
- Hansen AC; Zhang Q; Lyne PWL. (2005). Ethanol-diesel fuel blends--a review. *Bioresour Technol*, 96: 277-285. [059087](#)
- Hansen AD; Rosen AH; Novakov T. (1982). Real-Time Measurement of the Absorption Coefficient of Aerosol Particles. *Appl Opt*, 21: 3060-3062. [190368](#)
- Hansen ADA; Rosen H; Novakov T. (1984). The aethalometer - an instrument for the real-time measurement of optical absorption by aerosol particles. *Sci Total Environ*, 36: 191-196. [002396](#)
- Hansen J; Nazarenko L. (2004). Soot climate forcing via snow and ice albedos. Presented at , . [156521](#)
- Hansen J; Sato M; Mazarenko L; Ruedy R; Lacis A; Koch D; Tegen I; Hall T; Shindell D; Santer B; Stone P; Novakov T; Thomason L; Wang R; Wang Y; Jacob D; Hollandsworth S; Bishop L; Logan J; Thompson A; Stolarski R; Lean J; Willson R; Levitus S; Antonov J; Rayner N; Parker D; Christy J. (2002). Climate forcings in Goddard Institute for Space Studies S12000 simulations. *J Geophys Res*, 107. [049177](#)

- Hansen J; Sato M; Ruedy R; Kharecha P; Lacis A; Miller R; Nazarenko L; Lo K; Schmidt GA; Russell G; Aleinov I; Bauer S; Baum E; Cairns B; Canuto V; Chandler M; Cheng Y; Cohen A; Del Genio A; Faluvegi G; Fleming E; Friend A; Hall T; Jackman C; Jonas J; Kelley M; Kiang NY; Koch D; Labow G; Lerner J; Menon S; Novakov T; Oinas V; Perlwitz JA; Perlwitz Ju; Rind D; Romanou A; Schmunk R; Shindell D; Stone P; Sun S; Streets D; Tausnev N; Thresher D; Unger N; Yao M; Zhang S. (2007). Climate simulations for 1880-2003 with GISS modelE. , 29: 661-696. [190597](#)
- Hansen J; Sato M; Ruedy R; Lacis A; Oinas V. (2000). Global warming in the twenty-first century: an alternative scenario. Proc Natl Acad Sci U S A, 97: 9875-9880. [042683](#)
- Hansen J; Sato M; Ruedy R; Nazarenko L; Lacis A; Schmidt GA; Russell G; Aleinov I; Bauer M; Bauer S; Bell N; Cairns B; Canuto V; Chandler M; Cheng Y; Del Genio A; Faluvegi G; Fleming E; Friend A; Hall T; Jackman C; Kelley M; Kiang N; Koch D; Lean J; Lerner J; Lo K; Menon S; Miller R; Minnis P; Novakov T; Oinas V; Perlwitz JA; Perlwitz Ju; Rind D; Romanou A; Shindell D; Stone P; Sun S; Tausnev N; Thresher D; Wielicki B; Wong T; Yao M; Zhang S. (2005). Efficacy of climate forcings. J Geophys Res, 110: D18104. [190596](#)
- Hansen JE; Sato M; Ruedy R. (1997). Radiative forcing and climate response. J Geophys Res, 102: 6831-6864. [043104](#)
- Hargrave BT; Barrie LA; Bidleman TF; Welch HE. (1997). Seasonality in exchange of organochlorines between arctic air and seawater. Environ Sci Technol, 31: 3258-3266. [155827](#)
- Harmens H; Norris DA; Koerber GR; Buse A; Steinnes E; Rühling A. (2007). Temporal trends in the concentration of arsenic, chromium, copper, iron, nickel, vanadium and zinc in mosses across Europe between 1990 and 2000. Atmos Environ, 41: 6673-6687. [155828](#)
- Harner T; Jantunen LMM; Bidleman TF; Barrie LA; Kylin H; Strachan WMJ; Macdonald RW. (2000). Microbial degradation is a key elimination pathway of hexachlorocyclohexanes from the Arctic Ocean. Geophys Res Lett, 27: 1155-1158. [155829](#)
- Harrison L; Michalsky J; Berndt J. (1994). Automated multifilter rotating shadow-band radiometer: an instrument for optical depth and radiation measurements. Appl Opt, 33: 5118-5125. [045805](#)
- Harvey LDD. (2004). Characterizing the annual-mean climatic effect of anthropogenic CO₂ and aerosol emissions in eight coupled atmosphere-ocean GCMs. , 23: 569-599. [190598](#)
- Hassan R; Scholes R; Ash N. (2005). Ecosystems and human well-being: current state and trends, volume 1. [092759](#)
- Hauck M. (2003). Epiphytic lichen diversity and forest dieback: The role of chemical site factors. Bryologist, 106: 257-269. [155830](#)
- Haynie FH. (1986). Environmental factors affecting corrosion of weathering steel. Presented at Materials degradation caused by acid rain: developed from the 20th state-of-the-art symposium of the American Chemical Society; June 1985; Arlington, VA., Washington, DC. [157198](#)
- Haynie FH; Lemmons TJ. (1990). Particulate matter soiling of exterior paints at a rural site. Aerosol Sci Technol, 13: 356-367. [044579](#)
- Haywood J; Boucher O. (2000). Estimates of the direct and indirect radiative forcing due to tropospheric aerosols: A review. Rev Geophys, 38: 513-543. [156531](#)
- Haywood J; Francis P; Osborne S; Glew M; Loeb N; Highwood E; Tanré D; Myhre G; Formenti P; Hirst E. (2003). Radiative properties and direct radiative effect of Saharan dust measured by the C-130 aircraft during SHADE: 1. Solar spectrum : The Saharan Dust Experiment (SHADE). , 108: SAH 4-1. [190599](#)
- Haywood J; Schulz M. (2007). Causes of the reduction in uncertainty in the anthropogenic radiative forcing of climate between IPCC (2001) and IPCC (2007). Geophys Res Lett, 34: L20701. [190600](#)
- Haywood JM; Pelon J; Formenti P; Bharmal N; Brooks M; Capes G; Chazette P; Chou C; Christopher S; Coe H; Cuesta J; Derimian Y; Desboeufs K; Greed G; Harrison M; Heese B; Highwood EJ; Johnson B; Mallet M; Marticorena B; Marsham J; Milton S; Myhre G; Osborne SR; Parker DJ; Rajot JL; Schulz M; Slingo A; Tanré D; Tulet P. (2008). Overview of the dust and biomass burning experiment and African monsoon multidisciplinary analysis special observing Period-0. J Geophys Res, 113: D00C17. [190602](#)
- Haywood JM; Ramaswamy V; Soden BJ. (1999). Tropospheric aerosol climate forcing in clear-sky satellite observations over the oceans. , 283: 1299-1303. [040453](#)
- Heald CL; Jacob DJ; Park RJ; Russell LM; Huebert BJ; Seinfeld JH; Liao H; Weber RJ. (2005). A large organic aerosol source in the free troposphere missing from current models. Geophys Res Lett, 32: L18809.1-L18809.4. [190603](#)
- HEI; Ackerman A; Toon O; Hobbs P. (1994). Reassessing the dependence of cloud condensation nucleus concentration on formation rate. Nature. [189975](#)
- Heintzenberg J. (2008). The SAMUM-1 experiment over Southern Morocco: overview and introduction. , 61: 2-11. [190605](#)

- Helena P; Franc B; Cvetka RL. (2004). Monitoring of short-term heavy metal deposition by accumulation in epiphytic lichens (*Hypogymnia Physodes* (L.) Nyl.). , 49: 223-230. [155833](#)
- Helm PA; Diamond ML; Semkin R; Bidleman TF. (2000). Degradation as a loss mechanism in the fate of α -hexachlorocyclohexane in Arctic watersheds. *Environ Sci Technol*, 34: 812-818. [155834](#)
- Helm PA; Diamond ML; Semkin R; Strachan WMJ; Teixeira C; Gregor D. (2002). A mass balance model describing multi-year fate of organochlorine compounds in a high arctic lake. *Environ Sci Technol*, 36: 996-1003. [155835](#)
- Helmisaari H-S; Makkonen K; Olsson M; Viksna A; Mälkönen E. (1999). Fine-root growth, mortality and heavy metal concentrations in limed and fertilized *Pinus silvestris* (L.) stands in the vicinity of a Cu-Ni smelter in SW Finland. *Plant Soil*, 209: 193-200. [155836](#)
- Henze DK; Seinfeld JH. (2006). Global secondary organic aerosol from isoprene oxidation. *Geophys Res Lett*, 33: L09812.1-L09812.4. [190606](#)
- Herman JR; Bhartia PK; Torres O; Hsu C; Seftor C; Celarier E. (1997). Global distribution of UV-absorbing aerosols from Nimbus 7/TOMS data. *J Geophys Res*, 102: 16911-16922. [048393](#)
- Hernandez L; Probst A; Probst JL; Ulrich E. (2003). Heavy metal distribution in some French forest soils: Evidence for atmospheric contamination. *Sci Total Environ*, 312: 195-219. [155841](#)
- Herner JD; Ying Q; Aw J; Gao O; Chang DPY; Kleeman MJ. (2006). Dominant Mechanisms that Shape the Airborne Particle Size and Composition Distribution in Central California. *Aerosol Sci Technol*, 40: 827-844. [135981](#)
- Herrera LK; Videla HA. (2004). The importance of atmospheric effects on biodeterioration of cultural heritage constructional materials. *Int Biodeterior Biodegradation*, 54: 125-134. [155843](#)
- Hicke JA; Asner GP; Kasischke ES; French NHF; Randerson JT; Collatz GJ; Stocks BJ; Tucker CJ; Los SO; Field CB. (2003). Postfire response of North American boreal forest net primary productivity analysed with satellite observations. , 9: 1145-1157. [156545](#)
- Hinzman LD; Fukuda M; Sandberg DV; Chapin III FS; Dash D. (2003). FROSTFIRE: an experimental approach to predicting the climate feedbacks from the changing boreal fire regime. *J Geophys Res*, 108 (D1), 8153, doi:10.1029/2001JD000415. . [155845](#)
- Hobbelen PHF; Koolhaas JE; van Gestel CAM. (2006). Bioaccumulation of heavy metals in the earthworms *Lumbricus rubellus* and *Aporrectodea caliginosa* in relation to total and available metal concentrations in field soils. , 144: 639-646. [190371](#)
- Hodzic A; Madronich S; Bohn B; Massie S; Menut L; Wiedinmyer C. (2007). Wildfire particulate matter in Europe during summer 2003: meso-scale modeling of smoke emissions, transport and radiative effects. , 7: 4043-4064. [156553](#)
- Hoell JM; Davis DD; Liu SC; Newell R; Shipham M; Akimoto H; McNeal RJ; Bemdura RJ; Drewry JW. (1996). Pacific exploratory mission-west A (PEM-WEST A): September- October, 1991. *J Geophys Res*, 101: 1641-1653. [190607](#)
- Hoell JM; Davis DD; Liu SC; Newell RE; Akimoto H; McNeal RJ; Bendura RJ. (1997). The Pacific exploratory mission-west phase B: February-March, 1994. *J Geophys Res*, 102: 28223-28239. [057373](#)
- Hoff R; Engel-Cox J; Krotkov N; Palm S; Rogers R; McCann K; Sparling L; Jordan N; Torres O; Spinhirne J. (2004). Long-range transport observations of two large forest fire plumes to the northeastern U.S. In *Proceedings of the 22nd International Laser Radar Conference* (pp. 683-686). Paris: European Space Agency. [190617](#)
- Hoff RM; McCann KJ. (2002). Regional East Atmospheric Lidar Mesonet: REALM. In L. Bissonette; G Roy; G Vallée (Ed.), *Lidar Remote Sensing in Atmospheric and Earth Sciences* (pp. 281-284). Val-Bélair, Quebec: Def. R&D Can. Valcartier. [190612](#)
- Hofmann D; Barnes J; Dutton E; Deshler T; Jäger H; Keen R; Osborn M. (2003). Surface-based observations of volcanic emissions to stratosphere. In *Volcanism and the Earth's Atmosphere* (pp. 57-73). Washington, DC: American Geophysical Union. [192062](#)
- Hoh E; Zhu L; Hites RA. (2006). Dechlorane plus, a chlorinated flame retardant, in the Great Lakes. *Environ Sci Technol*, 40: 1184-1189. [190378](#)
- Holben BN; Eck TF; Slutsker I; Tanré D; Buis JP; Setzer A; Vermote E; Reagan JA; Kaufman YJ; Nakajima T; Lavenu F; Jankowiak I; Smirnov A. (1998). AERONET: A federated instrument network and data archive for aerosol characterization. , 66: 1-16. [155848](#)
- Holben BN; Smirnov A; Eck TF; Slutsker I; Abuhassan N; Newcomb WW; Schafer JS; Tanre D; Chatenet B; Lavenu F. (2001). An emerging groundbased aerosol climatology: aerosol optical depth from AERONET. *J Geophys Res*, 106: 12067-12098. [190618](#)
- Holland EA; Dentener FJ; Braswell BH; Sulzman JM. (1999). Contemporary and pre-industrial global reactive nitrogen budgets. , 46: 7-43. [092051](#)

- Holmqvist M; Stenroth P; Berglund O; Nystrom P; Olsson K; Jellyman D; McIntosh AR; Larsson P. (2006). Low levels of persistent organic pollutants (POPs) in New Zealand eels reflect isolation from atmospheric sources. *Environ Pollut*, 141: 532-538. [190380](#)
- Hooda V. (2007). Phytoremediation of toxic metals from soil and waste water. *J Environ Biol*, 28: 367-376. [190382](#)
- Hopke PK; Zhou L; Poirot RL. (2005). Reconciling Trajectory Ensemble Receptor Model Results with Emissions. *Environ Sci Technol*, 39: 7980-7983. [156567](#)
- Horowitz L. (2006). Past, present, and future concentrations of tropospheric ozone and aerosols: Methodology, ozone evaluation, and sensitivity to aerosol wet removal. *J Geophys Res*, 111: D22211.1-D22211.16. [190620](#)
- Horowitz LW; Walters S; Mauzerall DL; Emmons LK; Rasch PJ; Granier C; Tie X; Lamarque J-F; Schultz MG; Tyndall GS; Orlando JJ; Brasseur GP. (2003). A global simulation of tropospheric ozone and related tracers: description and evaluation of MOZART, version 2. *J Geophys Res*, 108: in press. [057770](#)
- Houlahan JE; Findlay CS; Schmidt BR; Meyer AH; Kuzmin SL. (2000). Quantitative evidence for global amphibian population declines. *J Geophys Res*, 105: 752-755. [155853](#)
- Howe TS; Billings S; Stolzberg RJ. (2004). Sources of polycyclic aromatic hydrocarbons and hexachlorobenzene in spruce needles of eastern Alaska. *Environ Sci Technol*, 38: 3294-3298. [155854](#)
- Hoyt D; Frohlich C. (1983). Atmospheric transmission at Davos, Switzerland 1909-1979. *Clim Change*, 5: 61-71. [190621](#)
- Hoyt DV. (1978). A model for the calculation of solar global insolation. *J Geophys Res*, 83: 27-35. [046638](#)
- Hsu NC; Tsay SC; King MD; Herman JR. (2004). Aerosol properties over bright-reflecting source regions. *IEEE Trans Geosci Remote Sens*, 42: 557-569. [190622](#)
- Huebert BJ; Bates T; Russell PB; Shi G; Kim YJ; Kawamura K; Carmichael G; Nakajima T. (2003). An overview of ACE-Asia: Strategies for quantifying the relationships between Asian aerosols and their climatic impacts. *J Geophys Res*, 108: 8633. [190623](#)
- Hughes MK. (1981). Cycling of trace metals in ecosystems. *Environ Sci Technol*, 15: 1565-1578. [156578](#)
- Hunaiti AA; Al-Oqlah A; Shannag NM; Abukhalaf IK; Silvestrov NA; Von Deutsch DA; Bayorh MA. (2007). Toward understanding the influence of soil metals and sulfate content on plant thiols. *J Toxicol Environ Health A*, 70: 559-567. [156579](#)
- Huneus N; O Boucher O. (2007). One-dimensional variational retrieval of aerosol extinction coefficient from synthetic LIDAR and radiometric measurements. *J Geophys Res*, 112: D14303.1-D14303.14. [190624](#)
- Hung HH; Halsall CJ; Blanchard P. (2001). Are PCBs in the Canadian Arctic atmosphere declining? Evidence from 5 years of monitoring. *Environ Sci Technol*, 35: 1303-1311. [155856](#)
- Hung HH; Halsall CJ; Blanchard P; Li HH; Fellin P; Stern G; Rosenberg B. (2002). Temporal trends of organochlorine pesticides in the Canadian Arctic atmosphere. *Environ Sci Technol*, 36: 862-868. [155857](#)
- Husar RB; Prospero JM; Stowe LL. (1997). Characterization of tropospheric aerosols over the oceans with the NOAA advanced very high resolution radiometer optical thickness operational product. *J Geophys Res*, 102: 16,889-16,909. [045900](#)
- Intergovernmental Panel on Climate Change (IPCC). (2007). Climate change 2007: the physical science basis Contribution of Working Group I to the fourth assessment report of the Intergovernmental Panel on Climate Change. [092765](#)
- IOM; Andrews E; Sheridan P; Ogren J; Ferrare R. (2004). In situ aerosol profiles over the Southern Great Plains cloud and radiation test bed site: 1. Aerosol optical properties. *J Geophys Res*, 109: D06208. [190058](#)
- IPCC (Intergovernmental Panel on Climate Change). (1996). Radiative forcing of climate change. In *Climate Change 1995* (pp. np). New York: Cambridge University Press. [190990](#)
- IPCC (Intergovernmental Panel on Climate Change). (2007). Changes in Atmospheric Constituents and in Radiative forcing. In *Climate Change 2007* (pp. np). New York: Cambridge University Press. [190988](#)
- IPCC. (1995). Radiative forcing of climate change and an evaluation of the IPCC IS92 emission scenarios. In *Climate Change 1994* (pp. np). New York: Cambridge University Press. [190991](#)
- IPCC. (2001). *Climate Change 2001: The Scientific Basis*. Cambridge University Press. Cambridge. [156587](#)
- IPCC; IOM; Inoue K-i; Takano H; Yanagisawa R; Sakurai M; Ueki N; Yoshikawa T. (2007). Effects of diesel exhaust particles on cytokine production by splenocytes stimulated with lipopolysaccharide. *J Appl Toxicol*, 27: 95-100. [189430](#)
- Ito A; Penne JE. (2005). Historical emissions of carbonaceous aerosols from biomass and fossil fuel burning for the period 1870-2000. *Global Biogeochem Cycles*, 19: GB2028.1-GB2028.14. [190626](#)
- Jacob DJ; Crawford JH; Kleb MM; Connors VS; Bendura RJ; Raper JL; Sachse GW; Gille JC; Emmons L; Heald CL. (2003). The Transport and Chemical Evolution over the Pacific (TRACE-P) aircraft mission: design, execution, and first results. *J Geophys Res*, 108: 9000. [190987](#)

- Jacobs SV; Evans GW; Catalano R; Dooley D. (1984). Air pollution and depressive symptomatology: Exploratory analyses of intervening psychosocial factors. , 7: 260-272. [156596](#)
- Jacobson MZ. (2000). A physically-based treatment of elemental carbon optics: implications for global direct forcing of aerosols. *Geophys Res Lett*, 27: 217-220. [056378](#)
- Jacobson MZ. (2001). GATOR-GCMM: a global through urban scale air pollution and weather forecast model: 1. Model design and treatment of subgrid soil, vegetation, roads, rooftops, water, sea ice, and snow. *J Geophys Res*, 106: 5385-5402. [155864](#)
- Jacobson MZ. (2002). Control of fossil-fuel particulate black carbon and organic matter, possibly the most effective method of slowing global warming. *J Geophys Res*, 107: 4410. [155865](#)
- Jacobson MZ. (2003). Development of mixed-phase clouds from multiple aerosol size distributions and the effect of the clouds on aerosol removal. *J Geophys Res*, 108 D8, 4245, doi:10.1029/2002JD002691. [155866](#)
- Jacobson MZ. (2003). Reply to comment by D. P. Chock et al. on "Control of fossil-fuel particulate black carbon and organic matter, possibly the most effective method of slowing global warming". *J Geophys Res*, 108 D24, 4770, doi:10.1029/2003JD003707. [155867](#)
- Jacobson MZ. (2003). Reply to comment by J. E. Penner on "Control of fossil-fuel particulate black carbon and organic matter, possibly the most effective method of slowing global warming". *J Geophys Res*, 108 (D24), 4772, doi:10.1029/2003JD003403. [155868](#)
- Jacobson MZ. (2003). Reply to comment by J. E. Penner on "Control of fossil-fuel particulate black carbon and organic matter, possibly the most effective method of slowing global warming. *J Geophys Res*, 108 (D24), 4772, doi:10.1029/2003JD003403. [189421](#)
- Jacobson MZ. (2003). Reply to comment by J. Feichter et al. on "Control of fossil-fuel particulate black carbon and organic matter, possibly the most effective method of slowing global warming". *J Geophys Res*, 108 D24, 4768, doi:10.1029/2002JD003299,. [155869](#)
- Jacobson MZ. (2004). Climate response of fossil fuel and biofuel soot, accounting for soot's feedback to snow and sea ice albedo and emissivity. *J Geophys Res*, 109, D21201, doi:10.1029/2004JD004945. [155870](#)
- Jacobson MZ. (2006). Effects of externally-through-internally-mixed soot inclusions within clouds and precipitation on global climate. *J Phys Chem B*, 110: 6860-6873. [156599](#)
- Jacobson MZ; Kaufman YJ. (2006). Wind reduction by aerosol particles. *Geophys Res Lett*, 33. [090942](#)
- Jacobson MZ; Seinfeld JH; Carmichael GR; Streets DG. (2004). The effect on photochemical smog of converting the U.S. fleet of gasoline vehicles to modern diesel vehicles. *Geophys Res Lett*, 31: L02116. [180362](#)
- James SM; Little EE; Semlitsch RD. (2004). Effects of multiple routes of cadmium exposure on the hibernation success of the American toad (*Bufo americanus*). *Arch Environ Contam Toxicol*, 46: 518-527. [155874](#)
- Jantunen LMM; Bidleman TF. (1996). Air-water gas exchange of hexachlorocyclohexanes (HCHs) and the enantiomers of α -HCH in Arctic regions. *J Geophys Res*, 101: 28837-28846. [155876](#)
- Jantunen LMM; Bidleman TF. (1998). Organochlorine pesticides and enantiomers of chiral pesticides in Arctic Ocean water. *Arch Environ Contam Toxicol*, 35. [155877](#)
- Jayanty R. (2003). Overview of PM_{2.5} chemical speciation network program. Presented at . [156605](#)
- Jayne JT; Leard DC; Zhang X; Davidovits P; Smith KA; Kolb CE; Worsnop DR. (2000). Development of an aerosol mass spectrometer for size and composition analysis of submicron particles. *Aerosol Sci Technol*, 33: 49-70. [190978](#)
- Jeong MJ; Li Z; Chu DA; Tsay SC. (2005). Quality and Compatibility Analyses of Global Aerosol Products Derived from the Advanced Very High Resolution Radiometer and Moderate Resolution Imaging Spectroradiometer. *J Geophys Res*, 110: np. [190977](#)
- Jiang H; Feingold G. (2006). Effect of aerosol on warm convective clouds: Aerosol-cloud-surface flux feedbacks in a new coupled large eddy model. *J Geophys Res*, 111: D01202. [190976](#)
- Jiang J; Oberdrster G; Elder A; Gelein R; Mercer P; Biswas P. (2008). Does nanoparticle activity depend upon size and crystal phase?. , 2: 33-42. [156609](#)
- Jiang W; Smyth S; Giroux E; Roth H; Yin D. (2006). Differences between CMAQ fine mode particle and PM 25 concentrations and their impact on model performance evaluation in the lower Fraser valley. *Atmos Environ*, 40: 4973-4985. [133165](#)
- Jiao XC; Xu FL; Dawson R; Chen SH; Tao S. (2007). Adsorption and absorption of polycyclic aromatic hydrocarbons to rice roots. , 148: 230-235. [155879](#)
- Jirak IL; Cotton WR. (2006). Effect of air pollution on precipitation along the Front Range of the Rocky Mountains. , 45: 236-245. [156612](#)
- Johnson D; Hale B. (2008). Fine root decomposition and cycling of Cu, Ni, Pb, and Zn at forest sites near smelters in Sudbury, ON, and Rouyn-Noranda, QU, Canada. , 14: 41-53. [155881](#)
- Johnson DB. (1982). The role of giant and ultragiant aerosol particles in warm rain initiation. , 39: 448-460. [190973](#)

- Johnson MS; Franke LS; Lee RB; Holladay SD. (1999). Bioaccumulation of 2,4,6-trinitrotoluene and polychlorinated biphenyls through two routes of exposure in a terrestrial amphibian: Is the dermal route significant?. *Environ Toxicol Chem*, 18: 873–878. [155880](#)
- Jones GS; Jones A; Roberts DL; Stott PA; Williams KD. (2005). Sensitivity of global-scale climate change attribution results to inclusion of fossil fuel black carbon aerosol. *Geophys Res Lett*, 32, L14701, doi:10.1029/2005GL023370. [155885](#)
- Jones JW; Bogat GA. (1978). Air pollution and human aggression. *Psychol Rep*, 43: 721-722. [190396](#)
- Jones PD; Moberg A; Osborn TJ; Briffa KR. (2003). Surface climate responses to explosive volcanic eruptions seen in long European temperature records and mid-to-high latitude tree-ring density around the Northern Hemisphere. In Robock A; Oppenheimer C (Ed.), *Volcanism and the earth's atmosphere* (pp. 239–254). Washington, DC: American Geophysical Union. [192278](#)
- Joshi M; Shine K. (2003). A GCM study of volcanic eruptions as a cause of increased stratospheric water vapor. *J Clim*, 16: 3525-3534. [192327](#)
- Joynt J; Bischoff M; Turco R; Konopka A; Nakatsu CH. (2006). Microbial community analysis of soils contaminated with lead, chromium and petroleum hydrocarbons. *Microb Ecol*, 51: 209-219. [155887](#)
- Junker C; Lioussé C. (2008). A global emission inventory of carbonaceous aerosol from historic records of fossil fuel and biofuel consumption for the period 1860-1997. , 8: 1195-1207. [190971](#)
- Kahn R; Banerjee P; McDonald D. (2001). The sensitivity of multiangle imaging to natural mixtures of aerosols over ocean. *J Geophys Res*, 106: 18219-18238. [190969](#)
- Kahn R; Banerjee P; McDonald D; Diner D. (1998). Sensitivity of multiangle imaging to aerosol optical depth, and to pure-particle size distribution and composition over ocean. *J Geophys Res*, 103: 32195-32213. [190970](#)
- Kahn R; Gaitley B; Martonchik J; Diner D; Crean K; Holben B. (2005). Multiangle Imaging Spectroradiometer (MISR) global aerosol optical depth validation based on 2 years of coincident Aerosol Robotic Network (AERONET) observations. *J Geophys Res*, 110: D10S04. [189961](#)
- Kahn R; Li W; Martonchik J; Bruegge C; Diner D; Gaitley B; Abdou W; Dubovik O; Holben B; Smirnov A; Jin Z; Clark D. (2005). MISR low-light-level calibration, and implications for aerosol retrieval over dark water. , 62: 1032-1052. [190965](#)
- Kahn R; Li W; Moroney C; Diner D; Martonchik J; Fishbein E. (2007). Aerosol source plume physical characteristics from space-based multiangle imaging. *J Geophys Res*, 112: D11205. [190964](#)
- Kahn RA Gaitley BJ; Martonchik JV; Diner DJ Crean KA; Holben B. (2005). MISR global aerosol optical depth validation based on two years of coincident AERONET observations. *J Geophys Res*, 110: D10S04. [190966](#)
- Kahn RA Garay MJ; Nelson DL; Yau KK; Bull M; Gaitley BJ; Martonchik JV; Levy R. (2007). Satellite-derived aerosol optical depth over dark water from MISR and MODIS: Comparisons with AERONET and implications for climatological studies. *J Geophys Res*, 112: D18205. [190963](#)
- Kalashnikova O; Kahn R. (2006). Ability of multiangle remote sensing observations to identify and distinguish mineral dust types: Part 2 Sensitivity over dark water. *J Geophys Res*, 111: D11207. [190962](#)
- Kaldorf M; Kuhn AJ; Schroder WH; Hildebrandt U; Bothe H. (1999). Selective element deposits in maize colonized by a heavy metal tolerance conferring arbuscular mycorrhizal fungus. *J Plant Physiol*, 154: 718-728. [190399](#)
- Kamh GME. (2005). The impact of landslides and salt weathering on Roman structures at high latitudes - Conway Castle, Great Britain: A case study. , 48: 238-254. [155888](#)
- Kandeler E; Kampichler C; Horak O. (1996). Influence of heavy metals on the functional diversity of soil microbial communities. , 23: 299-306. [094392](#)
- Kappos AD; Bruckmann P; Eikmann T; Englert N; Heinrich U; Hoppe P; Koch E; Krause GH; Kreyling WG; Rauchfuss K; Rombout P; Schulz-Klemp V; Thiel WR; Wichmann HE. (2004). Health effects of particles in ambient air. *Int J Hyg Environ Health*, 207: 399-407. [087922](#)
- Kapustin VN; Clarke AD; Shinozuka Y; Howell S; V Brekhovskikh V; Nakajima T; Higurashi A. (2006). On the determination of a cloud condensation nuclei from satellite: Challenges and possibilities. *J Geophys Res*, 111: D04202. [190961](#)
- Kaufman Y. (1987). Satellite sensing of aerosol absorption. *J Geophys Res*, 92: 4307-4317. [190960](#)
- Kaufman Y; Boucher O; Tanré D; Chin M; Remer L; Takemura T. (2005). Aerosol anthropogenic component estimated from satellite data. *Geophys Res Lett*, 32: L17804. [155891](#)
- Kaufman Y; Fraser R. (1997). The effect of smoke particles on clouds and climate forcing. , 277: 1636-1639. [190958](#)
- Kaufman Y; Haywood J; Hobbs P; Hart W; Kleidman R; Schmid B. (2003). Remote sensing of vertical distributions of smoke aerosol off the coast of Africa. *Geophys Res Lett*, 30: 1831. [190954](#)

- Kaufman YD; Tanré D; Boucher O. (2002). A satellite view of aerosols in the climate system. *Nature*, 419: 215-223. [190956](#)
- Kaufman YJ; Hobbs PV; Kirchoff VWJH; Artaxo P; Remer LA; Holben BN; King MD; Ward DE; Prins EM; Longo KM; Mattos LF; Nobre CA; Spinhirne JD; Ji Q; Thompson AM; Gleason JF; Christopher SA; Tsay S-C. (1998). Smoke, clouds, and radiation--Brazil (SCAR-B) experiment. *J Geophys Res*, 103: 31783-31808. [089989](#)
- Kaufman YJ; Koren I. (2006). Smoke and pollution aerosol effect on cloud cover. , 313: 655-658. [190951](#)
- Kaufman YJ; Martins JV; Remer LA; Schoeberl MR; Yamasoe MA. (2002). Satellite retrieval of aerosol absorption over the oceans using sunglint. *Geophys Res Lett*, 29: 34.1-34.4. [190955](#)
- Kaufman YJ; Nakajima T. (1993). Effect of Amazon smoke on cloud microphysics and albedo—Analysis from satellite imagery. , 32: 729-744. [190959](#)
- Kaufman YJ; Setzer A; Ward D; Tanre D; Holben BN; Menzel P; Pereira MC; Rasmussen R. (1992). Biomass Burning Airborne and Spaceborne Experiment in the Amazonas (BASE-A). *J Geophys Res*, 97: 14581-14599. [044557](#)
- Kavouras IG; Etyemezian V; DuBois DW; Xu J; Pitchford M. (2009). Source reconciliation of atmospheric dust causing visibility impairment in Class I areas of the western United States. , 114: x. [191976](#)
- Kavouras IG; Etyemezian V; Xu J; DuBois DW; Green M; Pitchford M. (2007). Assessment of the local windblown component of dust in the western United States. *J Geophys Res*, 112: . [156630](#)
- Kenski DM; Gay D; Fitzsimmons S. (2004). Ammonia and its role in midwestern haze. Presented at Regional and Global Perspectives on Haze: Causes, Consequences and Controversies Visibility Specialty Conference, Asheville, NC. [192078](#)
- Kerr R. (2007). Another global warming icon comes under attack. , 317: 28-29. [190950](#)
- Kiehl JT. (2007). Twentieth century climate model response and climate sensitivity. *Geophys Res Lett*, 34: np. [190949](#)
- Kiikkilä O. (2003). Heavy-metal pollution and remediation of forest soil around the Harjavalta Cu-Ni smelter, in SW Finland. , 37: 399-415. [156637](#)
- Kim CG; Bell JNB; Power SA. (2003). Effects of soil cadmium on *Pinus sylvestris* L. seedlings. *Plant Soil*, 257: 443-449. [155899](#)
- Kim MK; Lau KM; Chin M; Kim KM; Sud Y; Walker GK. (2006). Atmospheric teleconnection over Eurasia induced by aerosol radiative forcing during boreal spring. *Proc Natl Acad Sci U S A*, 19: 4700-4718. [190917](#)
- Kim SW; Yoon SC; Kim J. (2008). Columnar Asian dust particle properties observed by sun/sky radiometers from 2000 to 2006 in Korea. *Atmos Environ*, 42: 492-504. [130785](#)
- Kim Y; Hatsushika H; Muskett RR; Yamazaki K. (2005). Possible effect of boreal wildfire soot on Arctic sea ice and Alaska glaciers. *Atmos Environ*, 39: 3513-3520. [155900](#)
- King M; Kaufman Y; Tanré D; Nakajima T. (1999). Remote sensing of tropospheric aerosols from space: Past, present, and future. , 80: 2229-2259. [190635](#)
- King MD; Platnick S; Moeller CC; Revercomb HE; Chu DA. (2003). Remote sensing of smoke, land, and clouds from the NASA ER-2 during SAFARI 2000. *J Geophys Res*, 108: SAF38.1-SAF38.12. [094395](#)
- Kinne S; Schulz M; Textor C; Guibert S; Balkanski Y; Bauer SE; Berntsen T; Berglen TF; Boucher O; Chin M; Collins W; Dentener F; Diehl T; Easter R; Feichter J; Fillmore D; Ghan S; Ginoux P; Gong S; Grini A; Hendricks J; Herzog M; Horowitz L; Isaksen I; Iversen T; Kirkevåg A; Kloster S; Koch D; Kristjansson JE; Krol M; Lauer A; Lamarque JF; Lesins G; Liu X; Lohmann U; Montanaro V; Myhre G; Penner J; Pitari G; Reddy S; Seland O; Stier P; Takemura T; Tie X. (2006). An AeroCom initial assessment—optical properties in aerosol component modules of global models. , 6: 1815-1834. [155903](#)
- Kirchstetter TW; Harley RA; Kreisberg NM; Stolzenberg MR; Hering SV. (1999). On-road measurement of fine particle and nitrogen oxide emissions from light- and heavy-duty motor vehicles. *Atmos Environ*, 33: 2955-2968. [010642](#)
- Kirkbride MP; Dugmore JA. (2003). Glaciological response to distal tephra fallout from the 1947 eruption of Hekla, south Iceland. , 49: 420-428. [156645](#)
- Kleeman MJ; Hughes LS; Allen JO; Cass GR. (1999). Source contributions to the size and composition distribution of atmospheric particles: southern California in September 1996. *Environ Sci Technol*, 33: 4331-4341. [011286](#)
- Kleidman R; O'Neill N; Remer L; Kaufman Y; Eck T; Tanré D; Dubovik O; Holben B. (2005). Comparison of Moderate Resolution Imaging Spectroradiometer (MODIS) and Aerosol Robotic Network (AERONET) remote-sensing retrievals of aerosol fine mode fraction over ocean. *J Geophys Res*, 110: 1-16. [190175](#)

- Kleinman MT; Araujo JA; Nel A; Sioutas C; Campbell A; Cong PQ; Li H; Bondy SC. (2008). Inhaled ultrafine particulate matter affects CNS inflammatory processes and may act via MAP kinase signaling pathways. *Toxicol Lett*, 178: 127-130. [190074](#)
- Knutti R; Stocker TF; Joos F; Plattner GK. (2002). Constraints on radiative forcing and future climate change from observations and climate model ensembles. *Nature*, 416: 719-723. [190178](#)
- Knutti R; Stocker TF; Joos F; Plattner GK. (2003). Probabilistic climate change projections using neural networks. , 21: 257-272. [190180](#)
- Koch D. (2001). Transport and direct radiative forcing of carbonaceous and sulfate aerosols in the GISS GCM. *J Geophys Res*, 106: 20311–20332. [192054](#)
- Koch D; Bond TC; Streets D; Unger N; van der Werf GR. (2007). Global impact of aerosols from particular source regions and sectors. *J Geophys Res*, 112: D02205. [190185](#)
- Koch D; Hansen J. (2005). Distant origins of Arctic black carbon: A Goddard Institute for Space Studies ModelE experiment. *J Geophys Res*, 110: D04204. [190183](#)
- Koch D; Schmidt G; Field C. (2006). Sulfur, sea salt, and radionuclide aerosols in GISS ModelE. *J Geophys Res*, 111: D06206. [190184](#)
- Kogan YL; Lilly DK; Kogan ZN; Filyushkin V. (1994). The effect of CCN regeneration on the evolution of stratocumulus cloud layers. , 33: 137-150. [190186](#)
- Koren I; Kaufman YJ; Remer LA; Martins JV. (2004). Measurement of the effect of Amazon smoke on inhibition of cloud formation. *Science*, 303: 1342-1345. [190187](#)
- Koren I; Kaufman YJ; Rosenfeld D; Remer LA; Rudich Y. (2005). Aerosol invigoration and restructuring of Atlantic convective clouds. *Geophys Res Lett*, 32: L14828. [190188](#)
- Koren I; Martins JV; Remer LA; Afargan H. (2008). Smoke invigoration versus inhibition of clouds over the Amazon. , 321: 946-949. [190193](#)
- Koren I; Remer KA; Kaufman YJ; Rudich Y; Martins JV. (2007). On the twilight zone between clouds and aerosols. *Geophys Res Lett*, 34: L08805. [190192](#)
- Koren I; Remer LA; Longo K. (2007). Reversal of trend of biomass burning in the Amazon. *Geophys Res Lett*, 34: L20404. [190189](#)
- Korsnes R; Pavlova O; Godtlielsen F. (2002). Assessment of potential transport of pollutants into the Barents Sea via sea ice--an observational approach. *Mar Pollut Bull*, 44: 861-869. [156657](#)
- Kroll JH; Ng NL; Murphy SM; Flagan RC; Seinfeld JH. (2006). Secondary organic aerosol formation from isoprene photooxidation. *Environ Sci Technol*, 40: 1869-1877. [190195](#)
- Krueger AJ; Schaefer SJ; Krotkov N; Bluth G; Barker S. (2000). Ultraviolet remote sensing of volcanic emissions. In *Remote Sensing of Active Volcanism* (pp. 25-43). Washington, DC: American Geophysical Union. [192234](#)
- Kruger O; Grasl H. (2002). The indirect aerosol effect over Europe. *Geophys Res Lett*, 29: 1925. [190200](#)
- Kruysse A. (1971). Acute inhalation toxicity of acrolein in hamsters. *Central Institute for Nutrition and Food Research. The Netherlands. R 3516*. [192236](#)
- Kucera T; Horakova H; Sonska A. (2008). Toxic metal ions in photoautotrophic organisms. , 46: 481-489. [190408](#)
- Kucharski J; Wyszowska J. (2004). Inter-relationship between number of microorganisms and spring barley yield and degree of soil contamination with copper. , 50: 243–249. [156662](#)
- Kuki KN; Oliva MA; Costa AC. (2009). The simulated effects of iron dust and acidity during the early stages of establishment of two coastal plant species. , 196: 287-295. [190411](#)
- Kuki KN; Oliva MA; Pereira EG; Costa AC; Cambraia J. (2008). Effects of simulated deposition of acid mist and iron ore particulate matter on photosynthesis and the generation of oxidative stress in *Schinus terebinthifolius* Raddi and *Sophora tomentosa* L. , 403(1-3): 207-214. [155346](#)
- LaBrecque JJ; Benzo Z; Alfonso JA; Cordoves Manuelita Quintal PR; Gomez CV; Marcano E. (2004). The concentrations of selected trace elements in clams, *Trivela mactroidea* along the Venezuelan coast in the state of Miranda. *Mar Pollut Bull*, 49: 659-667. [155913](#)
- Lack D; Lovejoy E; Baynard T; Pettersson A; Ravishankara A. (2006). Aerosol absorption measurements using photoacoustic spectroscopy: sensitivity, calibration, and uncertainty developments. *Aerosol Sci Technol*, 40: 697-708. [190203](#)
- Lakzian A; Murphy P; Turner A; Beynon JL; Giller KE. (2002). *Rhizobium leguminosarum* bv. *viciae* populations in soils with increasing heavy metal contamination: abundance, plasmid profiles, diversity and metal tolerance. *Soil Biol Biochem*, 34: 519-529. [156671](#)
- Lambert A; Grainger RG; Remedios JJ; Rodgers CD; Corney M; Taylor FW. (1993). Measurements of the evolution of the Mt. Pinatubo aerosol cloud by ISAMS. *Geophys Res Lett*, 20: 1287–1290. [192231](#)

- Lambert MRK. (1997). Environmental effects of heavy spillage from a destroyed pesticide store near Hargeisa (Somaliland) assessed during the dry season, using reptiles and amphibians as bioindicators. *Arch Environ Contam Toxicol*, 32: 80–93. [155916](#)
- Landers DH; Simonich SL; Jaffe DA; Geiser LH; Campbell DH; Schwindt AR; Schreck CB; Kent ML; Hafner WD; Taylor HE; Hageman KJ; Usenko S; Ackerman LK; Schrlau JE; Rose NL; Blett TF; Erway MM. (2008). The Fate, Transport and Ecological Impacts of Airborne Contaminants in Western National Parks (USA). U.S. Environmental Protection Agency, Office of Research and Development, NHEERL, Western Ecology Division. Corvallis, Oregon. [191181](#)
- Lanno R; Wells J; Conder J; Bradham K; Basta N. (2004). The bioavailability of chemicals in soil for earthworms. *Ecotoxicol Environ Saf*, 57: 39-47. [190415](#)
- Larson VE; Golaz J-C; Jiang H; Cotton WR. (2005). Supplying local microphysics parameterizations with information about subgrid variability: Latin hypercube sampling. *J Trace Elem Med Biol*, 62: 4010-4026. [190220](#)
- Larson VE; Wood R; Field PR; Golaz J-C. (2001). Small-scale and mesoscale variability of scalars in cloudy boundary layers: One-dimensional probability density functions. *J Trace Elem Med Biol*, 58: 1978-1996. [190212](#)
- Latimer DA; Ireson RG. (1980). Workbook for estimating visibility impairment. U.S. Environmental Protection Agency. Research Triangle Park, NC. EPA-450/4-80-031. [035723](#)
- Lau K-M; Kim K-M. (2006). Observational relationships between aerosol and Asian monsoon rainfall, and circulation. *Geophys Res Lett*, 33: L21810. [190226](#)
- Lau K-M; Kim K-M; Walker G; Sud G. (2008). A GCM study of the possible impacts of Saharan dust heating on the water cycle and climate of the tropical Atlantic and Caribbean regions. *Proc Natl Acad Sci U S A*, in press: in press. [190229](#)
- Lau K; Kim M; Kim K. (2006). Asian summer monsoon anomalies induced by aerosol direct forcing—the role of the Tibetan Plateau. , 36: 855-864. [190223](#)
- Law RJ; Alae M; Allchin CR; Boon JP; Lebeuf M; Lepom P; Ster GA. (2003). Levels and trends of polybrominated diphenylethers and other brominated flame retardants in wildlife. *Environ Int*, 29: 757-770. [190420](#)
- Lawson ST; Scherbatskoy TD; Malcolm EG; Keeler GJ. (2003). Cloud water and throughfall deposition of mercury and trace elements in a high elevation spruce-fir forest at Mt Mansfield, Vermont. *J Environ Monit*, 5: 578-583. [089371](#)
- Leahy L; Anderson T; Eck T; Bergstrom R. (2007). A synthesis of single scattering albedo of biomass burning aerosol over southern Africa during SAFARI 2000. *Geophys Res Lett*, 34: L12814. [190232](#)
- Leaitch WR; Banic CM; Isaac GA; Couture MD; Liu PSK; Gultepe I; et al. (1996). Physical and chemical observations in marine stratus during the 1993 North Atlantic Regional Experiment: Factors controlling cloud droplet number concentrations. *J Geophys Res*, 101: 29123-29135. [190354](#)
- Leaitch WR; Isaac GA; Strapp JW; Banic CM; Wiebe HA. (1992). The relationship between cloud droplet number concentrations and anthropogenic pollution: observations and climatic implications. *J Geophys Res*, 97: 2463-2474. [045270](#)
- LeBlanc GA. (1995). Trophic-level differences in the bioconcentration of chemicals: Implications in assessing environmental biomagnification. *Environ Sci Technol*, 29: 154-160. [155921](#)
- Lee JK. (2006). Toxicity and tissue distribution of magnetic nanoparticles in mice [erratum]. *Toxicol Sci*, 90: 267. [088968](#)
- Lee T; Yu XY; Ayres B; Kreidenweis SM; Malm WC; Collett JL. (2008). Observations of fine and coarse particle nitrate at several rural locations in the United States. *Atmos Environ*, 42: 2720-2732. [156686](#)
- Lee TE; Miller SD; Turk FJ; Schueler C; Julian R; Deyo S; et al. (2006). The NPOESS VIIRS day/night visible sensor. , 87: 191-199. [190358](#)
- Lei YD; Wania F. (2004). Is rain or snow a more efficient scavenger of organic chemicals?. *Atmos Environ*, 38: 3557-3571. [127880](#)
- Lelieveld J; Berresheim H; Borrmann S; Crutzen PJ; Dentener FJ; Fischer H; et al. (2002). Global air pollution crossroads over the Mediterranean. , 298: 794-799. [190361](#)
- Levin Z; Cotton WR. (2008). Report from the WMO/ IUGG International Aerosol Precipitation Science, Assessment Group (IAPSAG). In *Aerosol pollution impact on precipitation: A scientific review* (pp. 482). Geneva, Switzerland: World Meteorological Organization. [190375](#)
- Levine JS; Pinto JP. (1998). The production of CO by biomass burning. Presented at . [029599](#)
- Levy R; Remer L; Dubovik O. (2007). Global aerosol optical properties and application to MODIS aerosol retrieval over land. *J Geophys Res*, 112: D13210. [190377](#)

- Levy R; Remer L; Mattoo S; Vermote E; Kaufman Y. (2007). Second-generation algorithm for retrieving aerosol properties over land from MODIS spectral reflectance. *J Geophys Res*, 112: D13211. [190379](#)
- Lewis ER; Schwartz SE. (2004). Sea salt aerosol production: Mechanisms, methods, measurements and models: A critical review. Washington, DC: American Geophysical Union. [192023](#)
- Li R-R; Kaufman YJ; Hao WM; Salmon JM; Gao B-C . (2004). A technique for detecting burn scars using MODIS data. *IEEE Trans Geosci Remote Sens*, 42: 1300-1308. [190386](#)
- Li Y-F; MacDonald RW; Jantunen LMM; Harner T; Bidleman TF; Stachen WMJ. (2002). The transport of β -hexachlorocyclohexane to the western Arctic Ocean: a contrast to α HCH. *Sci Total Environ*, 291: 229-246. [156691](#)
- Li Z; Chen H; Cribb M; Dickerson R; Holben B; Li C; et al. (2007). Preface to special section on East Asian studies of tropospheric aerosols: An international regional experiment (EAST-AIRE). *J Geophys Res*, 112: D22S00. [190392](#)
- Lin CJ; Pehkonen SO. (1999). The chemistry of atmospheric mercury: a review. *Atmos Environ*, 33: 2067-2070. [190426](#)
- Lin H; Tao S; Zuo Q; Coveney RM. (2007). Uptake of polycyclic aromatic hydrocarbons by maize plants. *Environ Pollut*, 148: 614-619. [155933](#)
- Lindberg SE; Brooks S; Linn CJ; Scott KJ; Landis MS; Stevens RK; Goodsite M; Richter A. (2002). Dynamic oxidation of gaseous mercury in the Arctic troposphere at polar sunrise. *Environ Sci Technol*, 36: 1245-1256. [190429](#)
- Lindesay JA; Andreae MO; Goldammer JG; Harris G; Annegarn HJ; Garstang M; et al. (1996). International Geosphere Biosphere Programme/International Global Atmospheric Chemistry SAFARI-92 field experiment: Background and overview. *J Geophys Res*, 23521-23530: 101. [190403](#)
- Lingua G; Franchin C; Todeschini V; Castiglione S; SBiondi; Burlando B; Parravicini V; PTorrigiani; GBerta. (2008). Arbuscular mycorrhizal fungi differentially affect the response to high zinc concentrations of two registered poplar clones. , 153: 137-147. [155935](#)
- Liou KN; Ou S-C. (1989). The role of cloud microphysical processes in climate: an assessment from a one-dimensional perspective. *J Geophys Res*, 94: 8599-8607. [190407](#)
- Liousse C; Penner JE; Chuang C; Walton JJ; Eddleman H; Cachier H. (1996). A global three-dimensional model study of carbonaceous aerosols. *J Geophys Res*, 101: 19,411-19,432. [078158](#)
- Liu H; Pinker R; Holben B. (2005). A global view of aerosols from merged transport models, satellite, and ground observations. *J Geophys Res*, 110: D10S15. [190414](#)
- Liu J; Ballaney M; Al-Alem U; Quan C; Jin X; Perera F; Chen LC; Miller RL. (2008). Combined Inhaled Diesel Exhaust Particles and Allergen Exposure Alter Methylation of T Helper Genes and IgE Production In Vivo. *Toxicol Sci*, 102: 76-81. [156709](#)
- Liu L; Lacis AA; Carlson BE; Mishchenko MI; Cairns B. (2006). Assessing Goddard Institute for Space Studies ModelE aerosol climatology using satellite and ground-based measurements. *J Geophys Res*, 111: D20212. [190422](#)
- Liu X; Penner J; Das B; Bergmann D; Rodriguez J; Strahan S; et al. (2007). Uncertainties in global aerosol simulations: Assessment using three meteorological data sets. *J Geophys Res*, 112: D11212. [190427](#)
- Liu Y; Koutrakis P. (2007). Estimating Fine Particulate Matter Component Concentrations and Size Distributions Using Satellite- Retrieved Fractional Aerosol Optical Depth: Part 1—Method Development. *J Air Waste Manag Assoc*, 57: 1351-1359. [187007](#)
- Liu, Y; Franklin, M; Kahn, R; Koutrakis, P. (2007). Using aerosol optical thickness to predict ground-level PM sub(2) sub(.) sub(5) concentrations in the St. Louis area: A comparison between MISR and MODIS . , 107: 33-44. [192180](#)
- Loeb N; Kato S. (2002). Top-of-atmosphere direct radiative effect of aerosols over the tropical oceans from the Clouds and the Earth's Radiant Energy System (CERES) satellite instrument. *Proc Natl Acad Sci U S A*, 15: 1474-1484. [190432](#)
- Loeb N; Manalo-Smith N. (2005). Top-of-Atmosphere direct radiative effect of aerosols over global oceans from merged CERES and MODIS observations. *J Clim*, 18: 3506-3526. [190433](#)
- Loeb NG; Kato S; Loukachine K; Smith NM. (2005). Angular distribution models for top-of-atmosphere radiative flux estimation from the Clouds and the Earth's Radiant Energy System instrument on the Terra Satellite. part I: Methodology. , 22: 338-351. [190436](#)
- Lohman U; Feichter J. (2005). Global indirect aerosol effects: a review. , 5: 715-737. [155942](#)
- Lohmann U; Feichter J; Chuang CC; Penner JE. (1999). Prediction of the number of cloud droplets in the ECHAM GCM. *J Geophys Res*, 104: 9169-9198. [190443](#)
- Lohmann U; Koren I; Kaufman YJ. (2006). Disentangling the role of microphysical and dynamical effects in determining cloud properties over the Atlantic. *Geophys Res Lett*, 33: L09802. [190451](#)

- Lohmann U; Leaitch WR; Barrie L; Law K; Yi Y; Bergmann D; et al. (2001). Vertical distributions of sulfur species simulated by large scale atmospheric models in COSAM: Comparison with observations. , 53: 646 - 672. [190448](#)
- Lorusso S; Marabelli M; Troili M. (1997). Air pollution and the deterioration of historic monuments. *J Environ Pathol Toxicol Oncol*, 16: 171-173. [084534](#)
- Lowenthal DH; Kumar N. (2003). PM_{2.5} mass and light extinction reconstruction in IMPROVE. *J Air Waste Manag Assoc*, 53: 1109-1120. [156712](#)
- Lowenthal DH; Rogers CF; Saxena P; Watson JG; Chow JC. (1995). Sensitivity of estimated light extinction coefficients to model assumptions and measurement errors. *Atmos Environ*, 29: 751-766. [045134](#)
- Lu M-L; Feingold G; Jonsson H; Chuang P; Gates H; Flagan RC; Seinfeld JH. (2008). Aerosol-cloud relationships in continental shallow cumulus. *J Geophys Res*, 113: D15201. [190455](#)
- Lubin D; Vogelmann AM. (2006). A climatologically significant aerosol longwave indirect effect in the Arctic. *Nature*, 439: 453-456. [190466](#)
- Lubin DS; Satheesh S; McFarquar G; Heymsfield A. (2002). Longwave radiative forcing of Indian Ocean tropospheric aerosol. *J Geophys Res*, 107: 8004. [190463](#)
- Lucaciu A; Timofte L; Culicov O; Frontasyeva MV; Oprea C; Cucu-Man S; Mocanu R; Steinnes E. (2004). Atmospheric deposition of trace elements in Romania studied by the moss biomonitoring technique. , 49: 533-548. [155947](#)
- Lunácková L; Masarovicová E; Králová K; Stresko V. (2003). Response of fast growing woody plants from family Salicaceae to cadmium treatment. , 70: 576-585. [155948](#)
- Luo Y; Lu D; Zhou X; Li W; He Q. (2001). Characteristics of the spatial distribution and yearly variation of aerosol optical depth over China in last 30 years. *J Geophys Res*, 106: 14501. [190467](#)
- Léon J; Tanré D; Pelon J; Kaufman Y; Haywood J; Chatenet B. (2003). Profiling of a Saharan dust outbreak based on a synergy between active and passive remote sensing. *J Geophys Res*, 108: 8575. [190366](#)
- López Alonso M; Benedito JL; Miranda M; Castillo C; Hernández J; Shore RF. (2002). Cattle as biomonitors of environmental semi-metal and trace metal concentrations in Galicia (NW Spain). *Arch Environ Contam Toxicol*, 43: 103-108. [155943](#)
- López Alonso M; Benedito JL; Miranda M; Castillo C; Hernández J; Shore RF. (2003). Mercury concentrations in cattle from NW Spain. *Sci Total Environ*, 302: 93-100 . [155945](#)
- López Alonso M; Benedito JL; Miranda M; Fernández JA; Castillo C; Hernández J; Shore RF. (2003). Large-scale spatial variation in mercury concentrations in cattle in NW Spain. *Environ Pollut*, 125: 173-181. [155944](#)
- Mace BL; Bell PA; Loomis RJ. (2004). Visibility and Natural Quiet in National Parks and Wilderness Areas: Psychological Considerations. , 36: 5-31. [180255](#)
- Mackay D. (1991). Multimedia environmental models: the fugacity approach. Chelsea, MI: Lewis Publishers. [042941](#)
- Macleod M; McKone TE; Mackay D. (2005). Mass balance for mercury in the San Francisco Bay area. *Environ Sci Technol*, 39: 6721-6729. [155954](#)
- Madrid L; Diaz-Barrientos E; Madrid F. (2002). Distribution of heavy metal contents of urban soils in parks of Seville. *Chemosphere*, 49: 1301-1309. [155956](#)
- Magi B; Hobbs P; Kirchstetter T; Novakov T; Hegg D; Gao S; et al. (2005). Aerosol properties and chemical apportionment of aerosol optical depth at locations off the United States East Coast in July and August 2001. *J Trace Elem Med Biol*, 62: 919-933. [190468](#)
- Malm W; Bell P; McGlothin GE. (1984). Field testing a methodology for assessing the importance of good visual air quality. Presented at . [044292](#)
- Malm WC. (1999). Introduction to visibility. [025037](#)
- Malm WC; Day DE. (2001). Estimates of aerosol species scattering characteristics as a function of relative humidity. *Atmos Environ*, 35: 2845-2860. [190431](#)
- Malm WC; Day DE; Kreidenweis SM; Collett JL; Lee T. (2003). Humidity dependent optical properties of fine particle during the Big Bend Regional Aerosol and Visibility Observational Study (BRAVO). , 108: 4279. [190434](#)
- Malm WC; Hand JL. (2007). An examination of the physical and optical properties of aerosols collected in the IMPROVE program. *Atmos Environ*, 41: 3407-3427. [155962](#)
- Malm WC; Pitchford ML. (1997). Comparison of calculated sulfate scattering efficiencies as estimated from size-resolved particle measurements at three national locations. *Atmos Environ*, 31: 1315-1325. [002519](#)
- Malm WC; Pitchford ML; McDade C; Ashbaugh LL. (2007). Coarse particle speciation at selected locations in the rural continental United States. *Atmos Environ*, 41: 2225-2239. [156730](#)

- Malm WC; Schichtel BA; Ames RB; Gebhart KA. (2002). A ten-Year spatial and temporal trend of sulfate across the United States. *J Geophys Res*, . [156727](#)
- Malm WC; Schichtel BA; Pitchford ML; Ashbaugh LL; Eldred RA. (2004). Spatial and monthly trends in speciated fine particle concentration in the United States. *J Geophys Res*, 109: 3306. [156728](#)
- Malm WC; Trijonis J; Sisler J; Pitchford M; Dennis RL. (1994). Assessing the effect of SO₂ emission changes on visibility. *Atmos Environ*, 28: 1023-1034. [044920](#)
- Marinoni N; Birelli MP; Rostagno C; Pavese A. (2003). The effects of atmospheric multipollutants on modern concrete. *Atmos Environ*, 37: 4701-4712. [092520](#)
- Markiewicz Patkowska J; Hursthouse A; Przybyla-Kij H. (2005). The interaction of heavy metals with urban soils: sorption behaviour of Cd, Cu, Cr, Pb and Zn with a typical mixed brownfield deposit. *Environ Int*, 31: 513-521. [155963](#)
- Martin MH; Coughtrey PJ. (1981). Impact of metals on ecosystem function and productivity. In Lepp, N. W. (Ed.), *Effect of heavy metal pollution on plants: volume 2, metals in the environment* (pp. 119-158). Barking, United Kingdom: Applied Science Publishers. [047727](#)
- Martins J; Tanré D; Remer L; Kaufman Y; Mattoo S; Levy R; et al. (2002). MODIS cloud screening for remote sensing of aerosol over oceans using spatial variability. *Geophys Res Lett*, 29: MOD4. [190470](#)
- Martonchik J; Diner D; Crean K; Bull M. (2002). Regional aerosol retrieval results from MISR. *IEEE Trans Geosci Remote Sens*, 40: 1520-1531. [190490](#)
- Martonchik J; Diner D; Pinty B; Verstraete M; Myneni R; Knjazikhin Y; Gordon H. (1998). Determination of land and ocean reflective, radiative, and biophysical properties using multiangle imaging. *IEEE Trans Geosci Remote Sens*, 36: 1266-1281. [190484](#)
- Martonchik JD; Diner D; Kahn R; Verstraete M; Pinty B; Gordon H; Ackerman T. (1998). Techniques for the Retrieval of aerosol properties over land and ocean using multiangle data. *IEEE Trans Geosci Remote Sens*, 36: 1212-1227. [190472](#)
- Masclat PP; Hoyau V; Jaffrezo JL; Cachier H. (2000). Polycyclic aromatic hydrocarbons deposition on the ice sheet of Greenland. Part I. Superficial snow. *Atmos Environ*, 34: 3195-3207. [155966](#)
- Massicotte R; Robidoux PY; Sauve S; Flipo D; Fournier M; Trottier B. (2003). Immune response of earthworms (*Lumbricus terrestris*, *Eisenia andrei* and *Aporrectodea tuberculata*) following in situ soil exposure to atmospheric deposition from a cement factory. *J Environ Monit*, 5: 774-779. [155968](#)
- Massie S; Torres O; Smith S. (2004). Total ozone mapping spectrometer (TOMS) observations of increases in Asian aerosol in winter from 1979 to 2000. *J Geophys Res*, 109: D18211. [190492](#)
- Matheson MA; Coakley JA; Tahnk WR. (2005). Aerosol and cloud property relationships for summertime stratiform clouds in the northeastern Atlantic from Advanced Very High Resolution Radiometer observations. *J Geophys Res*, 110: D24204. [190494](#)
- Matsui T; Masunaga H; Kreidenweis SM; Pielke RA; Tao W-K; Chin M; et al. (2006). Satellite-based assessment of marine low cloud variability associated with aerosol, atmospheric stability, and the diurnal cycle. *J Geophys Res*, 111: D17204. [190498](#)
- Matsui T; Pielke R. (2006). Measurement-based estimation of the spatial gradient of aerosol radiative forcing. *Geophys Res Lett*, 33: L11813. [190495](#)
- Matthias I, et al.. (2004). Multiyear aerosol observations with dual wavelength Raman lidar in the framework of EARLINET. *J Geophys Res*, 109, D13203, doi:10.1029/2004JD004600: . [155971](#)
- Mayo JM; Legge AH; Yeung EC; Krupa SV; Bogner JC. (1992). The effects of sulphur gas and elemental sulphur dust deposition on *Pinus contorta* x *Pinus banksiana*: Cell walls and water relations. , 76: 43-50. [155974](#)
- McComiskey A; Feingold G. (2008). Quantifying error in the radiative forcing of the first aerosol indirect effect. *Geophys Res Lett*, 35: L20810. [190517](#)
- McComiskey A; Feingold G; Frisch AS; Turner D; Miller M; Chiu JC; et al. (2008). An assessment of aerosol-cloud interactions in marine stratus clouds based on surface remote sensing. *J Geophys Res*, 114: D09203. [190525](#)
- McComiskey A; Schwartz SE; Schmid B; Guan H; Lewis ER; Ricchiazzi P; et al. (2008). Direct aerosol forcing: Calculation from observables and sensitivity to inputs. *J Geophys Res*, 113: D09202. [190523](#)
- McCormick M; Trepte C. (1987). Polar stratospheric optical depth observed between 1978 and 1985. *J Geophys Res*, 92: 4297-4306. [192328](#)
- McCormick R; Ludwig J. (1967). Climate modification by atmospheric aerosols. , 9: 1358 - 1359. [190528](#)
- McDade C. (2006). Summary of IMPROVE Nitrate Measurements. Retrieved 29-JUL-09, from http://vista.cira.colostate.edu/improve/publications/GrayLit/gray_literature.htm. [192075](#)
- Mcfiggans G; Artaxo P; Baltensperger U; Coe H; Facchini MC; Feingold G; et al. (2006). The effect of physical and chemical aerosol properties on warm cloud droplet activation. , 6: 2593-2649. [190532](#)
- McGowan TF; Lipinski GE; Santoleri JJ. (1993). New rules affect the handling of waste fuels. 122-128. [046731](#)

- McMurry PH. (2000). A review of atmospheric aerosol measurements. *Atmos Environ*, 34: 1959-1999. [081517](#)
- Meehl GA; Washington WM; Ammann CM; Arblaster JM; Wigley TML; Tebaldi C. (2004). Combinations of natural and anthropogenic forcings in twentieth-century climate. *J Clim*, 17: 3721–3727. [192279](#)
- Meers E; Vangronsveld J; Tack FMG; Vandecasteele B; Ruttens A. (2007). Potential of five willow species (*Salix* spp.) for phytoextraction of heavy metals. *Environ Exp Bot*, 60: 57-68. [155977](#)
- Melnikov S; Carroll J; Gorshkov A; Vlasov S; Dahle S. (2003). Snow and ice concentrations of selected persistent organic pollutants in the Ob-Yenisey River watershed. *Sci Total Environ*, 306: 27-37. [156753](#)
- Memon AR; Schroder P. (2009). Implications of metal accumulation mechanisms to phytoremediation. *Environ Sci Pollut Res Int*, 16: 162-175. [190442](#)
- Menon S; Del Genio AD; Kaufman Y; Bennartz R; Koch D; Loeb N; Orlikowski D. (2008). Analyzing signatures of aerosol cloud interactions from satellite retrievals and the GISS GCM to constrain the aerosol indirect effect. *J Geophys Res*, 113: D14S22. [190534](#)
- Mercado LM; Bellouin N; Sitch S; Boucher O; Huntingford C; Wild M; Cox PM. (2009). Impact of changes in diffuse radiation on the global land carbon sink. *Nature*, 458: 1014-U1087. [190444](#)
- Michalsky J; Schlemmer J; Berkheiser W;. (2001). Multiyear measurements of aerosol optical depth in the Atmospheric Radiation Measurement and Quantitative Links program. *J Geophys Res*, 106: 12099-12108. [190537](#)
- Middleton WEK. (1952). *Vision through the atmosphere*. Toronto, ON, Canada: University of Toronto Press. [016324](#)
- Mie G. (1908). Beiträge zur Optik trüber Medien, speziell kolloidaler Metallösungen. , 330: 377-445. [155983](#)
- Miller RL; Schmidt GA; Shindell DT. (2005). Forced annular variations in the 20th century Intergovernmental Panel on Climate Change Fourth Assessment Report models. *J Geophys Res*, 111: D18101. [192258](#)
- Millhollen AG; Gustin MS; Obrist D. (2006). Foliar mercury accumulation and exchange for three tree species. *Environ Sci Technol*, 40: 6001-6006. [190447](#)
- Min Q; Harrison LC. (1996). Cloud properties derived from surface MFRSR measurements and comparison with GEOS results at the ARM SGP site. *Geophys Res Lett*, 23: 1641- 1644. [190538](#)
- Minnis P; Harrison EF; Stowe LL; Gibson GG; Denn FM; Doelling DR; Smith WL Jr. (1993). Radiative Climate Forcing by the Mount Pinatubo Eruption. , 259: 1411-1415. [190539](#)
- Mischenko M; Cairns B; Kopp G; Schueler CF; Fafaul BA; Hansen JE; et al. (2007). Accurate monitoring of terrestrial aerosols and total solar irradiance. , 88: 677-691. [190543](#)
- Mishchenko MI; Geogdzhayev IV. (2007). Satellite remote sensing reveals regional tropospheric aerosol trends. , 15: 7423-7438. [190545](#)
- Mishchenko MI; Geogdzhayev IV; Cairns B; Rossow WB; Lacis AA. (1999). Aerosol retrievals over the ocean by use of channels 1 and 2 AVHRR data: sensitivity analysis and preliminary results. *Appl Opt*, 38: 7325-7341. [190541](#)
- Mishchenko MI; Geogdzhayev IV; Rossow WB; Cairns B; Carlson BE; Lacis AA; Liu L; Travis LD. (2007). Long-term satellite record reveals likely recent aerosol trend. , 315: 1543. [190542](#)
- Mitchell JM Jr. (1971). The effect of atmospheric aerosols on climate with special reference to temperature near the Earth's surface. , 10: 703-714. [190546](#)
- Molina LT; Madronich S; Gaffney JS; Singh HB. (2008). Overview of MILAGRO/INTEX-B Campaign. International Global Atmospheric Chemistry (Newsletter). Seattle, WA. http://www.igac.noaa.gov/newsletter/igac38/Apr_2008_IGAC_38.pdf. [192019](#)
- Moody E; King M; Platnick S; Schaaf C; Gao F. (2005). Spatially complete global spectral surface albedos: value-added datasets derived from Terra MODIS land products. *IEEE Trans Geosci Remote Sens*, 43: 144-158. [190548](#)
- Moosmüller H; Arnott WP; Rogers CF; Chow JC; Frazier CA; Sherman LE; Dietrich DL. (1998). Photoacoustic and filter measurements related to aerosol light-absorption during the northern front range air quality study (Colorado 1996/1997). *J Geophys Res*, 103: 28149-28157. [192073](#)
- Moropoulou A; Bisbikou K; Torfs K; Van Grieken R; Zezza F; Macri F. (1998). Origin and growth of weathering crusts on ancient marbles in industrial atmosphere. *Atmos Environ*, 32: 967-982. [040485](#)
- Moses CA; Smith BJ. (1994). Limestone weathering in the supratidal zone: an example from Mallorca. : . [156785](#)
- Mosley-Thompson E; Mashiotta TA; Thompson LG. (2003). High resolution ice core records of Late Holocene volcanism: Current and future contributions from the Greenland PARCA cores. In *Volcanism and the Earth's Atmosphere* (pp. 153–164). Washington, DC: American Geophysical Union. [192255](#)
- Mouillot F; Narasimha A; Balkanski Y; Lamarque J-F. (2006). Global carbon emissions from biomass burning in the 20th century. *Geophys Res Lett*, 33: L01801. [190549](#)

- Muir DCG; Omelchenko A; Grift NP; Savoie DA; Lockhart WL; Wilkinson P; Brunskill GJ. (1996). Spatial trends and historical deposition of polychlorinated biphenyls in Canadian midlatitude and arctic lake sediments. *Environ Sci Technol*, 30: 3609-3617. [155991](#)
- Murayama T, et al. (2001). Ground-based network observation of Asian dust events of April 1998 in East Asia. *J Geophys Res*, 106: 18345-18360. [155992](#)
- Murdoch JC; Thayer MA. (1988). Hedonic price estimation of variable urban air quality. *J Environ Econ Manage*, 15: 143-146. [156788](#)
- Mälkönen E; Derome J; Fritze H; Helmisaari H-S; Kukkola M; Kytö M; Saarsalmi A; Salemaa M. (1999). Compensatory fertilization of Scots pine stands polluted by heavy metals. , 55: 239–268. [155961](#)
- Naidoo G; Chirkoot D. (2004). The effects of coal dust on photosynthetic performance of the mangrove, *Avicennia marina* in Richards Bay, South Africa. , 127: 359-366. [190449](#)
- Nakajima T; Higurashi A; Kawamoto K; Penner JE. (2001). A possible correlation between satellite-derived cloud and aerosol microphysical parameters. *Geophys Res Lett*, 28: 1171-1174. [190552](#)
- Nakamura K; Nakawo M; Ageta Y; Goto-Azuma K; Kamiyam K. (2000). Post-depositional loss of nitrate in surface snow layers of the Antarctic ice sheet. , 17: 11-16. [156792](#)
- Nash TH III. (1975). Influence of effluents from a zinc factory on lichens. *Ecol Monogr*, 45: 183-198. [016763](#)
- National Research Council. (2001). Climate change science: an analysis of some key questions. [053303](#)
- National Research Council. (2005). Radiative forcing of climate change: expanding the concept and addressing uncertainties. [057409](#)
- Nazaroff WW; Cass GR. (1991). Protecting museum collections from soiling due to the deposition of airborne particles. *Atmos Environ*, 25: 841-852. [044577](#)
- NCDENR. (2007). Technical Analyses Supporting Regional Haze State Implementation Plan. . . . [156798](#)
- NESCAUM. (0). Regional Aerosol Intensive Network (RAIN) Preliminary Data Analysis. . . . [156802](#)
- Nguyen HL; Leermakers M; Elskens M; De Ridder F; Doan TH; Baeyens W. (2005). Correlations, partitioning and bioaccumulation of heavy metals between different compartments of Lake Balaton. *Sci Total Environ*, 341: 211-226. [155997](#)
- Nicholson L; Benn DI. (2006). Calculating ice melt beneath a debris layer using meteorological data. , 52: 463-470. [156806](#)
- Nieminen T; Derome J; Helmisaari H-S. (1999). Interactions between precipitation and Scots pine canopies along a heavy-metal pollution gradient. *Environ Pollut*, 106: 129–137. [155998](#)
- Nogueira MA; Magalhaes GC; Cardoso EJB. (2004). Manganese toxicity in mycorrhizal and phosphorus-fertilized soybean plants. , 27: 141-156. [190460](#)
- Norris J; Wild M. (2007). Trends in aerosol radiative effects over Europe inferred from observed cloud cover, solar “dimming”, and solar “brightening”. *J Geophys Res*, 112: D08214. [190555](#)
- Notten MJM; Oosthoek AJP; Rozema J; Aerts R. (2005). Heavy metal concentrations in a soil-plant-snail food chain along a terrestrial soil pollution gradient. *Environ Pollut*, 138: 178-190. [190461](#)
- Novakov T; Ramanathan V; Hansen JE; Kirchstetter TW; Sato M; Sinton JE; Sathaye JA. (2003). Large historical changes of fossil-fuel black carbon aerosols. *Geophys Res Lett*, 30. [048398](#)
- O'Dowd C; McFiggans G; Creasey DJ; Pirjola L; Hoell C; Smith MH; Allan BJ; Plane JMC; Heard DE; Lee JD; Pilling MJ; Kulmala M. (1999). On the photochemical production of new particles in the coastal boundary layer. *Geophys Res Lett*, 26: 1707-1710. [090414](#)
- O'Neill NT; Eck TF; Smirnov A; Holben BN; Thulasiraman S. (2003). Spectral discrimination of coarse and fine mode optical depth. *J Geophys Res*, 108: 4559. [180187](#)
- Odum EP. (1985). Trends expected in stressed ecosystems. , 35: 419-422. [039482](#)
- Odum EP. (1993). Major ecosystem types of the world. In Odum, E. P. (Ed.), *Ecology and our endangered life-support systems* Sunderland, MA: Sinauer Associates, Inc. [076742](#)
- Oehme M; Biseth A; Schlabach M; Wiig O. (1995). Concentrations of polychlorinated dibenzo-p-dioxins, dibenzofurans and non-ortho substituted biphenyls in polar bear milk from Svalbard (Norway). *Environ Pollut*, 90: 401-407. [011267](#)
- Oehme M; Haugen J-E; Schlabach M. (1996). Seasonal changes and relation between levels of organochlorines in Arctic ambient air: First results from an all-round-year monitoring program at Ny-Ålesund, Norway. *Environ Sci Technol*, 30: 2294-2304. [156001](#)
- Ohyama K; Angermann J; Dunlap DY; Matsumura F. (2004). Distribution of polychlorinated biphenyls and chlorinated pesticide residues in trout in the Sierra Nevada. *J Environ Qual*, 33: 1752-1764. [190462](#)
- Oliveira A; Pampulha ME. (2006). Effects of long-term heavy metal contamination on soil microbial characteristics. , 102: 157-161. [156827](#)
- Ormrod DP. (1984). Impact of trace element pollution on plants. In Treshow, M. (Ed.), *Air pollution and plant life* Chichester, United Kingdom: John Wiley & Sons Ltd. [046892](#)

- Otnyukova T. (2007). Epiphytic lichen growth abnormalities and element concentrations as early indicators of forest decline. , 146: 359-365. [156009](#)
- Ouimette JR; Flagan RC. (1982). The extinction coefficient of multicomponent aerosols. *Atmos Environ*, 16: 2405-2420. [025047](#)
- Ozdilek HG; Mathisen PP; Pellegrino D. (2007). Distribution of heavy metals in vegetation surrounding the Blackstone River, USA: Considerations regarding sediment contamination and long term metals transport in freshwater riverine ecosystems. *J Environ Biol*, 28: 493-502. [156010](#)
- Pacheco AMG; Freitas MC. (2004). Are lower epiphytes really that better than higher plants for indicating airborne contaminants? An insight into the elemental contents of lichen thalli and tree bark by INAA. *Journal of Radioanal Chem*, 259: 27-33. [156011](#)
- Padmavathamma PK; Li LY. (2007). Phytoremediation technology: Hyper-accumulation metals in plants. , 184: 105-126. [190465](#)
- Palmer AS; Morgan VI; Curran MAJ; van Ommen TD; Mayewski PA. (2002). Antarctic volcanic flux ratios from Law Dome ice cores. *Ann Glaciol*, 35: 329-332. [192319](#)
- Park RJ; Jacob DJ; Kumar N; Yantosca RM. (2006). Regional visibility statistics in the United States: Natural and transboundary pollution influences, and implications for the regional haze rule. *Atmos Environ*, 40: 5405-5423. [190469](#)
- Parrish ZD; White JC; Isleyen M; Gent MPN; Iannucci-Berger W; Eitzer BD; Kelsey JW; Mattina MI. (2006). Accumulation of weathered polycyclic aromatic hydrocarbons (PAHs) by plant and earthworm species. *Chemosphere*, 64: 609-618. [156014](#)
- Patadia F; Gupta P; Christopher SA. (2008). First observational estimates of global clear-sky shortwave aerosol direct radiative effect over land. *J Geophys Res*, 35: L04810. [190558](#)
- Patra M; Bhowmik N; Bandopadhyay B; Sharma A. (2004). Comparison of mercury, lead and arsenic with respect to genotoxic effects on plant systems and the development of genetic tolerance. *Environ Exp Bot*, 52: 199-223. [081976](#)
- Pennanen T; Frostegård Å; Fritze H; Bååth E. (1996). Phospholipid fatty acid composition and heavy metal tolerance of soil microbial communities along two heavy metal-polluted gradients in coniferous forests. *Appl Environ Microbiol*, 62: 420-428. [156016](#)
- Penner J; Quaas J; Storelvmo T; Takemura T; Boucher O; Guo H; et al. (2006). Model intercomparison of indirect aerosol effects. , 6: 3391-3405. [190564](#)
- Penner JE. (2003). Comment on "Control of fossil-fuel particulate black carbon and organic matter, possibly the most effective method of slowing global warming. *J Geophys Res*, 108: 4771. [156851](#)
- Penner JE; Dickinson RE; O'Neill CA. (1992). Effects of aerosol from biomass burning on the global radiation budget. , 256: 1432-1433. [045825](#)
- Penner JE; Eddleman H; Novakov T. (1993). Towards the development of a global inventory for black carbon emissions. *Atmos Environ*, 27: 1277-1295. [045457](#)
- Penner JE; Zhang SY; Chin M; Chuang CC; Feichter J; Geogdzhayev IV; et al. (2002). A comparison of model- and satellite derived aerosol optical depth and reflectivity. *J Trace Elem Med Biol*, 59: 441-460. [190562](#)
- Pennisi E. (2004). The secret life of fungi. , 304: 1620-1622. [156018](#)
- Perlwitz J; Graf HF. (2001). Troposphere-stratosphere dynamic coupling under strong and weak polar vortex conditions. *J Geophys Res Lett*, 28: 271-274. [192271](#)
- Perlwitz J; Harnik N. (2003). Observational evidence of a stratospheric influence on the troposphere by planetary wave reflection. *J Clim*, 16: 3011-3026. [192264](#)
- Peters AJ; Gregor DJ; Teixeira CF; Jones NP; Spencer C. (1995). The recent depositional trend of polycyclic aromatic hydrocarbons and elemental carbon to the Agassiz Ice cap, Ellesmere Island, Canada. *Sci Total Environ*, 160/161: 167-179. [156856](#)
- Pfirman SL; Kögeler JW; Rigor I. (1997). Potential for rapid transport of contaminants from the Kara Sea. *Sci Total Environ*, 202: 111-122. [156864](#)
- Pincus R; Klein SA. (2000). Unresolved spatial variability and microphysical process rates in large-scale models. *J Geophys Res*, 105: 27059-27065. [190565](#)
- Pinker R; Zhang B; Dutton E. (2005). Do satellites detect trends in surface solar radiation?. , 308: 850-854. [190569](#)
- Piol MN; López AG; Miño LA; Dos Santos Afonso M; Verrengia Guerrero NR. (2006). The impact of particle-bound cadmium on bioavailability and bioaccumulation: A pragmatic approach. *Environ Sci Technol*, 40: 6341-6347. [156028](#)
- Pitchford M; Green M; Kuhns H; Tombach I; Malm W; Scruggs M; Farber R; Mirabella V; White WH; McDade C. (1999). Project MOHAVE Final Report. [156873](#)

- Pitchford M; Maim W; Schichtel B; Kumar N; Lowenthal D; Hand J. (2007). Revised algorithm for estimating light extinction from IMPROVE particle speciation data. *J Air Waste Manag Assoc*, 57: 1326-36. [098066](#)
- Pitchford ML; Green MC; Morris R; Emery C; Sakata R; Swab C; Mairose PT. (2008). Columbia River Gorge Air Quality Study: Science Summary Report. Southwest Clean Air Agency. Vancouver, WA. [180159](#)
- Pitchford ML; Malm WC. (1994). Development and applications of a standard visual index. *Atmos Environ*, 28: 1049-1054. [044922](#)
- Pitchford ML; Polkowsky BV; McGown MR; Malm WC; Molenaar JV; Mauch L. (1990). Percent change in extinction coefficient: A proposed approach for federal visibility protection strategy. : . [156871](#)
- Pitchford ML; Schichtel BA; Gebhart KA; Barna MG; Malm WC; Tombach IH; Knipping EM. (2005). Reconciliation and Interpretation of the Big Bend National Park Light Extinction Source Apportionment: Results from the Big Bend Regional Aerosol and Visibility Observational Study- Part II. *J Air Waste Manag Assoc*, 55: 1726-1732. [156874](#)
- Prasad MNV; De Oliveira Freitas HM. (2003). Metal hyperaccumulation in plants - Biodiversity prospecting for. *Electron J Biotechnol*, 6: 110-146. [156885](#)
- Prata A; Rose W; Self S; O'Brien D. (2003). Global, long-term sulphur dioxide measurements from TOVS data: a new tool for studying explosive volcanism and climate. In *Volcanism and the Earth's Atmosphere* (pp. 75-92). Washington, DC: American Geophysical Union. [192235](#)
- Preston CM; Schmidt MWI. (2006). Black (pyrogenic) carbon: a synthesis of current knowledge and uncertainties with special consideration of boreal regions. , 3: 397-420. [156030](#)
- Procopio AS; Artaxo P; Kaufman YJ; Remer LA; Schafer JA; Holben BN. (2004). Multiyear analysis of Amazonian biomass burning smoke radiative forcing of climate. *J Geophys Res*, 31: L03108. [190571](#)
- Prospero JM. (1996). Saharan dust transport over the North Atlantic Ocean and Mediterranean: an overview. In Guerzoni S; Chester R (Ed.), *The Impact of Desert Dust Across the Mediterranean* (pp. 133-152). The Netherlands: Kluwer Academic Publishers. [156889](#)
- Pryor SC. (1996). Assessing public perception of visibility for standard setting exercises. *Atmos Environ*, 30: 2705-2716. [056598](#)
- Pryor SC; Binkowski FS. (2004). An analysis of the time scales associated with aerosol processes during dry deposition. *Aerosol Sci Technol*, 38: 1091-1098. [116805](#)
- Putaud J-P; Raes F; Van Dingenen R; Brüggemann E; Facchini M-C; Decesari S; Fuzzi S; Gehrig R; Hüglin C; Laj P; Lorbeer G; Maenhaut W; Mihalopoulos N; Müller K; Querol X; Rodriguez S; Schneider J; Spindler G; ten Brink H; Tørseth K; Wiedensohler A. (2004). A European aerosol phenomenology-2: chemical characteristics of particulate matter at kerbside, urban, rural and background sites in Europe. *Atmos Environ*, 38: 2579-2595. [055545](#)
- Qian Y; Wang W; Leung L; Kaiser D. (2007). Variability of solar radiation under cloud-free skies in China: The role of aerosols. *Geophys Res Lett*, 34: L12804. [190572](#)
- Quaas J; Boucher O. (2005). Constraining the first aerosol indirect radiative forcing in the LMDZ GCM using POLDER and MODIS satellite data. *Geophys Res Lett*, 32: L17814. [190573](#)
- Quaas J; Boucher O; Bellouin N; Kinne S. (2008). Satellite-based estimate of the direct and indirect aerosol climate forcing. *J Geophys Res*, 113: D05204. [190916](#)
- Quaas J; Boucher O; Lohmann U. (2006). Constraining the total aerosol indirect effect in the LMDZ GCM and ECHAM4 GCMs using MODIS satellite data. , 5: 9669-9690. [190915](#)
- Quinn PK; Anderson T; Bates T; Dlugi R; Heintzenberg J; Von Hoyningen-Huene W; Kumula M; Russel P; Swietlicki E. (1996). Closure in tropospheric aerosol-climate research : A review and future needs for addressing aerosol direct shortwave radiative forcing. , 69: 547-577. [192021](#)
- Quinn PK; Bates TS. (2003). North American, Asian, and Indian haze: similar regional impacts on climate?. *Geophys Res Lett*, 30. [049189](#)
- Quinn PK; Bates TS; Baynard T; Clarke AD; Onasch TB; Wang W; Rood MJ; Andrews E; Allan J; Carrico CM; Coffman D; Worsnop D. (2005). Impact of particulate organic matter on the relative humidity dependence of light scattering: A simplified parameterization. *Geophys Res Lett*, 32: 1-4. [156033](#)
- Quinn PK; Coffman D; Kapustin V; Bates TS; Covert DS. (1998). Aerosol optical properties in the marine boundary layer during ACE 1 and the underlying chemical and physical aerosol properties. *J Geophys Res*, 103: 16547-16563. [190918](#)
- Quinn PK; Coffman DJ; Bates TS; Welton EJ; Covert DS; Miller TL; et al. (2004). Aerosol optical properties measured aboard the Ronald H. Brown during ACE-Asia as a function of aerosol chemical composition and source region. *J Geophys Res*, 109: 109. [190937](#)
- Radke LF; Coakley JA; King MD. (1989). Direct and remote sensing observations of the effects of ships on clouds. , 246: 1146-1149. [156034](#)

- Rajapaksha R; MT-K; Bååth E. (2004). Metal toxicity affects fungal and bacterial activities in soil differently. *Appl Environ Microbiol*, 5: 2966 – 2973. [156035](#)
- Ramachandran S; Ramaswamy V; Stenchikov GL; Robock A. (2000). Radiative impact of the Mount Pinatubo volcanic eruption: Lower stratospheric response. *J Geophys Res*, 105: 24409-24429. [192050](#)
- Ramanathan V; Crutzen P. (2003). Atmospheric Brown “Clouds”. *Atmos Environ*, 37: 4033-4035. [190198](#)
- Ramanathan V; Crutzen P; Lelieveld J; et al. (2001). Indian Ocean Experiment: An integrated analysis of the climate forcing and effects of the great Indo-Asian haze. *J Geophys Res*, 106: 28371-38398. [190196](#)
- Ramanathan V; Crutzen PJ; Kiehl JT; Rosenfeld D. (2001). Aerosols, climate and the hydrological cycle. , 294: 2119-2124. [042681](#)
- Ramanathan V; et al. (2005). Atmospheric brown clouds: Impact on South Asian climate and hydrologic cycle. , 102: 5326-5333. [190199](#)
- Ramaswamy V; Boucher O; Haigh J; Hauglustaine D; Haywood J; Myhre G; Nakajima T; Shi G; Solomon S; Betts RE. (2001). Radiative Forcing of Climate Change: PNNL-SA-39648. New York: Cambridge University Press. [156899](#)
- Ramaswamy V; Ramachandran S; Stenchikov G; Robock A. (2006). A model study of the effect of Pinatubo volcanic aerosols on the stratospheric temperatures+. In Kiehl JT; Ramanathan V (Ed.), *Frontiers of climate modeling* (pp. 152–178). Cambridge, UK: Cambridge University Press. [192273](#)
- Ramaswamy V; Schwarzkopf MD; Randel WJ; Santer BD; Soden BJ; Stenchikov GL. (2006). Anthropogenic and natural influences in the evolution of lower stratospheric cooling. , 311: 1138-1141. [192284](#)
- Ramos L; Hernandez LM; Gonzalez MJ. (1994). Sequential fractionation of copper, lead, cadmium and zinc in soils from or near Donana National Park. *J Environ Qual*, 23: 50-57. [046736](#)
- Ramsey JM. (1966). Concentrations of carbon monoxide at traffic intersections in Dayton, Ohio. *Arch Environ Occup Health*, 13: 44-46. [013946](#)
- Randall CE; Bevilacqua RM; Lumpe JD; Hoppel KW. (2001). Validation of POAM III aerosols: Comparison to SAGE II and HALOE. *J Geophys Res*, 106: 27525–27536. [192268](#)
- Randall D; Khairoutdinov M; Arakawa A; Grabowski W. (2003). Breaking the cloud parameterization deadlock. , 84: 1547-1564. [190201](#)
- Randerson JT; Liu H; Flanner MG; Chambers SD; Jin Y; Hess PG; Pfister G; Mack MC; Treseder KK; Welp LR; Chapin FS; Harden JW; Goulden ML; Lyons E; Neff JC; Schuur EAG; Zender CS. (2006). The impact of boreal forest fire on climate warming. , 314: 1130-1132. [156038](#)
- Rapport DJ; Whitford WG. (1999). How ecosystems respond to stress: common properties of arid and aquatic systems. , 49: 193-203. [004595](#)
- Ray P; Reddy UG; Lapeyrie F; Adholeya A. (2005). Effect of coal ash on growth and metal uptake by some selected ectomycorrhizal fungi in vitro. , 7: 199-216. [190473](#)
- Read WG; Froidevaux L; Waters JW. (1993). Microwave limb sounder measurement of stratospheric SO₂ from the Mt. Pinatubo Volcano. *Geophys Res Lett*, 20: 1299–1302. [192031](#)
- Reddy M; Boucher O; Balkanski Y; Schulz M. (2005). Aerosol optical depths and direct radiative perturbations by species and source type. *Geophys Res Lett*, 32: L12803. [190208](#)
- Reddy M; Boucher O; Bellouin N; Schulz M; Balkanski Y; Dufresne J; Pham M. (2005). Estimates of multi-component aerosol optical depth and direct radiative perturbation in the LMDZT general circulation model. *J Geophys Res*, 110: D10S16. [190207](#)
- Reddy MS; Boucher O. (2007). Climate impact of black carbon emitted from energy consumption in the world's regions. *Geophys Res Lett*, 34: 1802. [156042](#)
- Regoli F; Gorbi S; Fattorini D; Tedesco S; Notti A; Machella N; Bocchetti R; Benedetti M; Piva F. (2006). Use of the land snail *Helix aspersa* sentinel organism for monitoring ecotoxicologic effects of urban pollution: An integrated approach. , 114: 63-69. [156046](#)
- Reid J. (2008). An overview of UAE2 flight operations: Observations of summertime atmospheric thermodynamic and aerosol profiles of the southern Arabian Gulf. *J Geophys Res*, 113: D14213. [190214](#)
- Reid J; Kinney J; Wesphal D; et al. (2003). Analysis of measurements of Saharan dust by airborne and ground-based remote sensing methods during the Puerto Rico Dust Experiment (PRIDE). *J Geophys Res*, 108: 8586. [190213](#)
- Reinfelder JR; Fisher NS; Luoma SN; Nichols JW; Wang W-X. (1998). Trace element trophic transfer in aquatic organisms: A critique of the kinetic model approach. *Sci Total Environ*, 219: 117-135. [156047](#)
- Reisinger LM. (1990). Analysis of airborne particles sampled in the southern Appalachian Mountains. *Water Air Soil Pollut*, 50: 149-162. [046737](#)
- Remer L; et al. (2008). An emerging aerosol climatology from the MODIS satellite sensors. *J Geophys Res*, 113: D14S01. [190224](#)

- Remer L; Gassó; Hegg D; Kaufman Y; Holben B. (1997). Urban/industrial aerosol: ground based sun/sky radiometer and airborne in situ measurements. *J Geophys Res*, 102: 16849-16859. [190216](#)
- Remer L; Kaufman Y. (2006). Aerosol direct radiative effect at the top of the atmosphere over cloud free ocean derived from four years of MODIS data. , 6: 237-253. [190222](#)
- Remer L; Kaufman Y; Tanré D; Mattoo S; Chu D; Martins J; Li R; Ichoku C; Levy R; Kleidman R; Eck T; Vermote E; Holben B. (2005). The MODIS aerosol algorithm, products and validation. *J Trace Elem Med Biol*, 62: 947-973. [190221](#)
- Remer L; Tanré D; Kaufman Y; Ichoku C; Mattoo S; Levy R; Chu D; Holben B; Dubovik O; Smirnov A; Martins J; Li R; Ahman Z. (2002). Validation of MODIS aerosol retrieval over ocean. *Geophys Res Lett*, 29: 8008. [190218](#)
- Richards LW; Dye TS; Arthur M; Byars MS. (1996). Analysis of ASOS Data for Visibility Purposes, Final Report . Systems Applications International, Inc., San Rafael, CA. STI-996231-1610-FR. [190476](#)
- Rind D; Perlwitz J; Lonergan P. (2005). AO/NAO response to climate change: 1. Respective influences of stratospheric and tropospheric climate changes. *J Geophys Res*, 110: D12107. [192261](#)
- Rissler J; Swietlicki E; Zhou J; Roberts G; Andreae MO; Gatti LV; Artaxo P. (2004). Physical properties of the sub-micrometer aerosol over the Amazon rain forest during the wet-todry season transition—comparison of modeled and measured CCN concentrations. , 4: 2119-2143. [190225](#)
- Roberts DL; Jones A. (2004). Climate sensitivity to black carbon aerosol from fossil fuel combustion. *J Geophys Res*, 109: 6202. [156052](#)
- Roberts ES; Richards JH; Jaskot R; Dreher KL. (2003). Oxidative stress mediates air pollution particle-induced acute lung injury and molecular pathology. *Inhal Toxicol*, 15: 1327-1346. [156051](#)
- Robinson A; Donahue N; Shrivastava M; Weitkamp E; Sage A; Grieshop A; Lane T; Pierce J; Pandis S. (2007). Rethinking organic aerosols: Semivolatile emissions and photochemical aging. , 315: 1259. [191975](#)
- Roderick ML; Farquhar GD. (2002). The cause of decreased pan evaporation over the past 50 years. , 298: 1410-1411. [042788](#)
- Roeckner E; Stier P; Feichter J; Kloster S; Esch M; Fischer-Bruns L. (2006). Impact of carbonaceous aerosol emissions on regional climate change. , 27: 553-571. [156920](#)
- Romic M; Romic D. (2003). Heavy metals distribution in agricultural topsoils in urban area. , 43: 795-805. [156055](#)
- Rood MJ; Covert DS; Larson TV. (1987). Hygroscopic properties of atmospheric aerosol in Riverside, California. *Tellus B Chem Phys Meteorol*, 39B: 383-397. [046397](#)
- Rosenfeld D. (2000). Suppression of rain and snow by urban and industrial air pollution. , 287: 1793-1796. [002234](#)
- Rosenfeld D. (2006). Aerosols, clouds, and climate. , 312: 1. [190233](#)
- Rosenfeld D; Dai J; Yu X; Yao Z; Xu X; Yang X; Du C. (2007). Inverse relations between amounts of air pollution and orographic precipitation. , 315: 1396-1398. [156057](#)
- Rosenfeld D; Givati A. (2006). Evidence of orographic precipitation suppression by air pollution-induced aerosols in the western United States. , 45: 893-911. [156924](#)
- Rosenfeld D; Lansky I. (1998). Satellite-based insights into precipitation formation processes in continental and maritime convective clouds. , 79: 2457-2476. [190230](#)
- Ross DM; Malm WC; Loomis RJ. (1985). The psychological valuation of good visual air quality by national park visitors. Presented at Presented at: 78th annual meeting of the Air Pollution Control Association; June; Detroit, MI. Pittsburgh, PA: Air Pollution Control Association; paper no. 85-10.4. [044287](#)
- Ross DM; Malm WC; Loomis RJ. (1987). An examination of the relative importance of park attributes at several national parks. In Bhardwaja, P. S. (Ed.), *Visibility protection: research and policy aspects*, an APCA international specialty conference Grand Teton National Park, WY; Pittsburgh, PA: Air Pollution Control Association. [037420](#)
- Rosselli W; Keller C; Boschi K. (2003). Phytoextraction capacity of trees growing on a metal contaminated soil. *Plant Soil*, 256: 265-272. [156058](#)
- Roth CM; Goss K-U; Schwarzenbach RP. (2004). Sorption of diverse organic vapors to snow. *Environ Sci Technol*, 38: 4078-4084. [056431](#)
- Rotton J; Barry T; Milligan M; Fitzpatrick M. (1979). The air pollution experience and interpersonal aggression. , 9: 397-412. [190478](#)
- Rotton J; Frey J. (1982). Atmospheric conditions, seasonal trends, and psychiatric emergencies. In *Replications and Extensions* (pp. Unknown). Washington, DC: American Psychological Association. [190477](#)
- Rozanov EV; Schlesinger ME; Andronova NG; Yang F; Malyshev SL; Zubov VA; Egorova TA; Li B. (2002). Climate/chemistry effects of the Pinatubo volcanic eruption simulated by the UIUC stratosphere/troposphere GCM with interactive photochemistry. *J Geophys Res*, 107: 4594. [192247](#)

- Rozanov EV; Schlesinger ME; Egorova TA; Li B; Andronova N; Zubov VA. (2004). Atmospheric response to the observed increase of solar UV radiation from solar minimum to solar maximum simulated by the University of Illinois at Urbana-Champaign climate-chemistry model. *J Geophys Res*, 109: D01110. [192245](#)
- Ruckstuhl C; et al. (2008). Aerosol and cloud effects on solar brightening and recent rapid warming. *Geophys Res Lett*, 35: L12708. [190356](#)
- Russell P; Kinne S; Bergstrom R. (1997). Aerosol climate effects: local radiative forcing and column closure experiments. *J Geophys Res*, 102: 9397-9407. [190359](#)
- Russell P; Livingston J; Hignett P; Kinne S; Wong J; Chien A; Bergstrom R; Durkee P; Hobbs P. (1999). Aerosol-induced radiative flux changes off the United States mid-Atlantic coast: comparison of values calculated from sun photometer and in situ data with those measured by airborne pyranometer. *J Geophys Res*, 104: 2289-2307. [190363](#)
- Rusu A-M; Jones GC; Chimonides PDJ; Purvis OW. (2006). Biomonitoring using the lichen *Hypogymnia physodes* and bark samples near Zlatna, Romania immediately following closure of a copper ore-processing plant. *Environ Pollut*, 143: 81-88. [156062](#)
- Ryan PA; Lowenthal D; Kumar N. (2005). Improved light extinction reconstruction in interagency monitoring of protected visual environments. *J Air Waste Manag Assoc*, 55: 1751-1759. [156934](#)
- Sabbioni C; Ghedini N; Bonazza A. (2003). Organic anions in damage layers on monuments and buildings. *Atmos Environ*, 37: 1261-1269. [049282](#)
- Sabin LD; Lim JH; Stolzenbach KD; Schiff KC. (2005). Contribution of trace metals from atmospheric deposition to stormwater runoff in a small impervious urban catchment. *Water Res*, 39: 3929-3937. [088300](#)
- Salemaa M; Derome J; Helmisaari HS; Nieminen T; Vanha-Majamaa I. (2004). Element accumulation in boreal bryophytes, lichens and vascular plants exposed to heavy metal and sulfur deposition in Finland. *Sci Total Environ*, 324: 141-160. [156069](#)
- Samuels HJ; Twiss S; Wong EW. (1973). Visibility, light scattering and mass concentration of particulate matter: report of the California Tri-City Aerosol Sampling Project. [070601](#)
- Sanderson EG; Farant JP. (2004). Indoor and outdoor polycyclic aromatic hydrocarbons in residences surrounding a Soderberg aluminum smelter in Canada. *Environ Sci Technol*, 38: 5350-5356. [156942](#)
- Sato M; Hansen J; Koch D; Lucis A; Ruedy R; Dubovik O; Holben B; Chin M; Novakov T. (2003). Global atmospheric black carbon inferred from AAEONET. Presented at Proceedings of the National Academy of Science. [156947](#)
- Sato M; Hansen JE; McCormick MP; Pollack JB. (1993). Stratospheric aerosol optical depths, 1850-1990. *J Geophys Res*, 98: 22987-22994. [192046](#)
- Sauvé S. (2001). Speciation of metals in soils. Presented at , Pensacola, FL. [156948](#)
- Saxena P; Hildemann LM; McMurry PH; Seinfeld JH. (1995). Organics alter hygroscopic behavior of atmospheric particles. *J Geophys Res*, 100: 18,755-18,770. [077273](#)
- Schichtel BA; Gebhart K; Barna MG; Malm WC; Green MC. (2004). Big Bend Regional Aerosol and Visibility Observational (BRAVO) Study Results: Air Quality Data and Source Attribution Analyses Results from the National Park Service. . . . [179902](#)
- Schichtel BA; Gebhart KA; Malm WC; Barna MG; Pitchford ML; Knipping EM; Tombach IH. (2005). Reconciliation and interpretation of big bend national park particulate sulfur source apportionment: Results from the big bend regional aerosol and visibility observational study-part I. *J Air Waste Manag Assoc*, 55: 1709-1725. [156957](#)
- Schichtel BA; Malm WC; Bench G; Fallon S; McDade CE; Chow JC; Watson JG. (2008). Fossil and contemporary fine particulate carbon fractions at 12 rural and urban sites in the United States. *J Geophys Res*, 113: . [156958](#)
- Schiff K; Bay S; Stransky C. (2002). Characterization of stormwater toxicants from an urban watershed to freshwater and marine organisms. , 4: 215-227. [156959](#)
- Schilling JS; Lehman ME. (2002). Bioindication of atmospheric heavy metal deposition in the Southeastern US using the moss *Thuidium delicatulum*. *Atmos Environ*, 36: 1611-1618. [113075](#)
- Schmid B; et al. (2000). Clearsky closure studies of lower tropospheric aerosol and water vapor during ACE-2 using airborne sunphotometer, airborne in situ, space-borne, and ground-based measurements. , 52: 568-593. [190369](#)
- Schmid B; Ferrare R; Flynn C; et al. (2006). How well do state-of-the-art techniques measuring the vertical profile of tropospheric aerosol extinction compare?. *J Geophys Res*, 111: 0. [190372](#)
- Schmidt GA; et al. (2006). Present-day atmospheric simulations using GISS Model E: Comparison to in situ, satellite and reanalysis data. *J Clim*, 19: 153-192. [190373](#)

- Schoeberl MR; Douglass AR; Zhu Z; Pawson S. (2003). A comparison of the lower stratospheric age spectra derived from a general circulation model and two data assimilation systems. *J Geophys Res*, 108D3. [057262](#)
- Schroeder WH; Munthe J. (1998). Atmospheric mercury -- an overview. *Atmos Environ*, 32: 809-822. [014559](#)
- Schulz M; Textor C; Kinne S; et al. (2006). Radiative forcing by aerosols as derived from the AeroCom present-day and preindustrial simulations. , 6: 5225-5246. [190381](#)
- Schwartz J; Zanobetti A; Bateson TF; Schwartz J; Sarnat JA; Coull BA; Wilson WE. (2007). Effects of exposure measurement error on particle matter epidemiology: a simulation using data from a panel study in Baltimore, MD. , 17: S2. [188938](#)
- Seifert M; Anke S; Holzinger S; Jaritz M; Arnhold W; Anke M. (1999). Cadmium and strontium content of mice, shrews. and some invertebrates. , 17: 357-365. [190480](#)
- Seigneur C; Johnson CD; Latimer DA; Bergstrom RW; Hogo H. (1984). Users manual for the Plume Visibility Model (PLUVUE II). Final report 23 Feb-29 Aug 83. . . . [156965](#)
- Seinfeld JH; Carmichael GR; Arimoto R; et al. (2004). ACEAsia: Regional climatic and atmospheric chemical effects of Asian dust and pollution. , 85: 367-380. [190388](#)
- Sekiguchi M; Nakajima T; Suzuki K; et al. (2003). A study of the direct and indirect effects of aerosols using global satellite data sets of aerosol and cloud parameters. *J Geophys Res*, 108 D22: 4699. [190385](#)
- Shakya K; Chettri MK; Sawidis T. (2008). Impact of heavy metals (copper, zinc, and lead) on the chlorophyll content of some mosses. *Arch Environ Contam Toxicol*, 54: 412-421. [156081](#)
- Shan XQ; Wang ZW; Wang WS; Zhang SZ; Wen B. (2003). Labile rhizosphere soil solution fraction for prediction of bioavailability of heavy metals and rare earth elements to plants. *Anal Bioanal Chem*, 375: 400-407. [156972](#)
- Sharifi MR; Gibson AC; Rundel PW. (1999). Phenological and physiological responses of heavily dusted creosote bush (*Larrea tridentata*) to summer irrigation in the Mojave Desert. , 14: 369-378. [156082](#)
- Sheesley RJ; Schauer JJ; Hemming JD; Barman MA; Geis SW; Tortorelli JJ. (2004). Toxicity of ambient atmospheric particulate matter from the Lake Michigan (USA) airshed to aquatic organisms. *Environ Toxicol Chem*, 23: 133-140. [156084](#)
- Shindell DT; Chin M; Dentener F; et al. (2008). A multi-model assessment of pollution transport to the Arctic. , 8: 5353-5372. [190391](#)
- Shindell DT; Levy H; Schwarzkopf II MD; Horowitz LW; Lamarque JF; Faluvegi G. (2008). Multimodel projections of climate change from short-lived emissions due to human activities. *J Geophys Res*, 113: D11109. [190393](#)
- Shindell DT; Schmidt GA; Mann ME; Faluvegi G. (2004). Dynamic winter climate response to large tropical volcanic eruptions since 1600. *J Geophys Res*, 109: D05104. [192267](#)
- Shindell DT; Schmidt GA; Miller RL; Mann M. (2003). Volcanic and solar forcing of climate change during the preindustrial era. *J Clim*, 16: 4094-4107. [192069](#)
- Shulz KG; Zondervan I; Gerringa LJA; Timmermans KR; Veldhuls MJW; Riebesell U. (2004). Effect of trace metal availability on coccolithophorid calcification. , 430: 673-676. [156087](#)
- Singh HB; Brune WH; Crawford JH; Flocke F; Jacob DJ. (2008). Chemistry and Transport of Pollution over the Gulf of Mexico and the Pacific: Spring 2006 INTEX-B Campaign Overview and First Results. , 0: 0. [190394](#)
- Sinyuk A; et al. (2007). Simultaneous retrieval of aerosol and surface properties from a combination of AERONET and satellite data. , 107: 90-108. [190395](#)
- Skov H; Christensen JH; Goodsite ME; Heidam NZ; Jensen B; Wahlin P; Geernaert G. (2004). Fate of elemental mercury in the Arctic during atmospheric mercury depletion episodes and the load of atmospheric mercury to the Arctic. *Environ Sci Technol*, 38: 2373-2382. [190481](#)
- Sloane CS. (1983). Optical properties of aerosols--comparison of measurements with model calculations. *Atmos Environ*, 17: 409-416. [025039](#)
- Sloane CS. (1984). Optical properties of aerosols of mixed composition. *Atmos Environ*, 18: 871-878. [025040](#)
- Sloane CS. (1986). Effect of composition on aerosol light scattering efficiencies. *Atmos Environ*, 20: 1025-1037. [045954](#)
- Sloane CS; Wolff GT. (1985). Prediction of ambient light scattering using a physical model responsive to relative humidity: validation with measurements from Detroit. *Atmos Environ*, 19: 669-680. [045953](#)
- Smejkalova M; Mikanova O; Boruvka L. (2003). Effects of heavy metal concentrations on biological activity of soil microorganisms. , 49: 321-326. [156987](#)
- Smirnov A; Holben B; Eck T; Dubovik O; Slutsker I. (2000). Cloud screening and quality control algorithms for the AERONET database. , 73: 337-349. [190397](#)

- Smirnov A; Holben B; Eck T; Slutsker I; Chatenet B; Pinker R. (2002). Diurnal variability of aerosol optical depth observed at AERONET (Aerosol Robotic Network) sites. *Geophys Res Lett*, 29: 2115. [190398](#)
- Smirnov A; Holben B; Sakerin S; et al. (2006). Shipbased aerosol optical depth measurements in the Atlantic Ocean, comparison with satellite retrievals and GOCART model. *Geophys Res Lett*, 33: L14817. [190400](#)
- Smith Jr WL; et al. (2005). EOS Terra aerosol and radiative flux validation: An overview of the Chesapeake Lighthouse and aircraft measurements from satellites (CLAMS) experiment. *J Trace Elem Med Biol*, 62: 903-918. [190401](#)
- Smith WH. (1990). Forest nutrient cycling: toxic ions. In *Air pollution and forests: interactions between air contaminants and forest ecosystems* New York, NY: Springer-Verlag. [046896](#)
- Smith WH. (1990). Forests as sinks for air contaminants: vegetative compartment. In *Air pollution and forests: interactions between air contaminants and forest ecosystems* (pp. 147-180). New York, NY: Springer-Verlag. [084015](#)
- Smith WH. (1991). Air pollution and forest damage. *Chem Eng News*, 6945: 30-43. [042566](#)
- Smolders E; Degryse F. (2002). Fate and effect of zinc from tire debris in soil. *Environ Sci Technol*, 36: 3706-3710. [156091](#)
- Soares CRFS; Siqueira JO. (2008). Mycorrhiza and phosphate protection of tropical grass species against heavy metal toxicity in multi-contaminated soil. , 44: 833-841. [190482](#)
- Sokolik I; Winker D; Bergametti G; et al. (2001). Introduction to special section: outstanding problems in quantifying the radiative impacts of mineral dust. *J Geophys Res*, 106: 18015-18027. [190404](#)
- Solomon PA; Hopke PK. (2008). A Special Issue of JA&WMA Supporting Key Scientific and Policy-and Health-Relevant Findings from EPA's Particulate Matter Supersites Program and Related Studies: An Integration and Synthesis of Results. *J Air Waste Manag Assoc*, 58: 137. [156997](#)
- Solomon S; Portmann RW; Garcia RR; Thomason LW; Poole LR; McCormick MP. (1996). The role of aerosol variations in anthropogenic ozone depletion at northern midlatitudes. *J Geophys Res*, 101: 6713-6727. [192252](#)
- Sotiropoulou REP; Medina J; Nenes A. (2006). CCN predictions: is theory sufficient for assessments of the indirect effect?. *Geophys Res Lett*, 33: L05816. [190406](#)
- Sotiropoulou REP; Nenes A; Adams PJ; Seinfeld JH. (2007). Cloud condensation nuclei prediction error from application of Kohler theory: Importance for the aerosol indirect effect. *J Geophys Res*, 112: D12202. [190405](#)
- Spinhirne J; Palm S; Hart W; Hlavka D; Welton E. (2005). Cloud and Aerosol Measurements from the GLAS Space Borne Lidar: initial results. *Geophys Res Lett*, 32: L22S03. [190410](#)
- Spracklen DV; Logan JA; Mickley LJ; Park RJ; Yevich R; Westerling AL; Jaffe DA. (2007). Wildfires drive interannual variability of organic carbon aerosol in the western U.S. in summer. *Geophys Res Lett*, 34: L16816. [190485](#)
- Squires P. (1958). The microstructure and colloidal stability of warm clouds: Part I - the relation between structure and stability. , 10: 256-261. [045608](#)
- Srogi. (2007). Monitoring of environmental exposure to polycyclic aromatic hydrocarbons: a review. , 5: 169-195. [180049](#)
- Stanhill G; Cohen S. (2001). Global dimming: a review of the evidence for a widespread and significant reduction in global radiation with discussion of its probable causes and possible agricultural consequences. , 107: 255-278. [042121](#)
- Steinnes E; Hvatum OØ; Bølviken B; Varskog P. (2005). Atmospheric supply of trace elements studied by peat samples from ombrotrophic bogs. *J Environ Qual*, 34: 192-197. [156095](#)
- Stenchikov G; Hamilton K; Robock A; Ramaswamy V; Schwarzkopf MD. (2004). Arctic Oscillation response to the 1991 Pinatubo eruption in the SKYHI GCM with a realistic quasi-biennial oscillation. *J Geophys Res*, 109: D03112. [192274](#)
- Stenchikov G; Hamilton K; Stouffer RJ; Robock A; Ramaswamy V; Santer B; Graf H-F. (2006). Arctic Oscillation response to volcanic eruptions in the IPCC AR4 climate models. *J Geophys Res*, 111: D07107. [192260](#)
- Stenchikov G; Robock A; Ramaswamy V; Schwarzkopf MD; Hamilton K; Ramachandran S. (2002). Arctic Oscillation response to the 1991 Mount Pinatubo eruption: Effects of volcanic aerosols and ozone depletion. *J Geophys Res*, 107: D24. [192277](#)
- Stenchikov GL; Kirchner I; Robock A; Graf H-F; Antuña JC; Grainger RG; Lambert A; Thomason L. (1998). Radiative forcing from the 1991 Mount Pinatubo volcanic eruption. *J Geophys Res*, 103: 13837-13857. [192049](#)
- Stephens G; et al. (2002). The CloudSat mission and the A-Train. , 83: 1771-1790. [190412](#)
- Stephens GL; Haynes JM. (2007). Near global observations of the warm rain coalescence process. *Geophys Res Lett*, 34: L20805. [190413](#)

- Stern DI. (2005). Global sulfur emissions from 1850 to 2000. *Chemosphere*, 58: 163-175. [190416](#)
- Stern GA; Halsall CJ; Barrie LA; Muir DCG; Fellin P; Rosenberg B. (1997). Polychlorinated biphenyls in arctic air. 1. Temporal and spatial trends: 1992-1994. *Environ Sci Technol*, 31: 3619-3628. [156096](#)
- Stevens B; Feingold G; Walko RL; Cotton WR. (1996). On elements of the microphysical structure of numerically simulated non-precipitating stratocumulus. *J Trace Elem Med Biol*, 53: 980-1006. [190417](#)
- Stewart AR; Luoma SN; Schlekot CE; Doblin MA; Hieb KA. (2004). Food web pathway determines how selenium affects aquatic ecosystems. *Environ Sci Technol*, 38: 4519-4526. [156097](#)
- Stier P; Seinfeld JH; Kinne S; Boucher O. (2007). Aerosol absorption and radiative forcing. , 7: 5237-5261. [157012](#)
- Stohl A; Andrews E; Burkhardt JF; Forster C; Herber A; Hoch SW; Kowal D; Lunder C; Mefford T; Ogren JA; Sharma S; Spichtinger N; Stebel K; Stone R; Ström J; Tørseth K; Wehrli C; Yttri KE. (2006). Pan-Arctic enhancements of light absorbing aerosol concentrations due to North American boreal forest fires during summer 2004. *J Geophys Res*, 111, D22214, doi:10.1029/2006JD007216: . [156100](#)
- Stohl A; Berg T; Burkhardt JF; Fjæraa AM; Forster C; Herber A; Hov Ø; Lunder C; McMillan WW; Oltmans S; Shiobara M; Dimpson D; Solberg S; Stebel K; Ström J; Tørseth K; Treffeisen R; Virkkunen K; Yttri KE. (2007). Arctic smoke - record high air pollution levels in the European Arctic due to agricultural fires in Eastern Europe in spring 2006. , 7: 511-534. [157015](#)
- Storlevmo T; Kristjansson JE; Myhre G; Johnsdud M; Stordal F. (2006). Combined observational and modeling based study of the aerosol indirect effect. , 6: 3583-3601. [190418](#)
- Stothers RB. (2001). A chronology of annual mean effective radii of stratospheric aerosols from volcanic eruptions during the twentieth century as derived from ground-based spectral extinction measurements. *J Geophys Res*, 106: 32043-32049. [192233](#)
- Stothers RB. (2001). Major optical depth perturbations to the stratosphere from volcanic eruptions: Stellar extinction period, 1961-1978. *J Geophys Res*, 106: 2993-3003. [192232](#)
- Stott PA. (2006). Observational constraints on past attributable warming and predictions of future global warming. *J Clim*, 19: 3055-3069. [190419](#)
- Strachan WMJ; Burniston DA; Williamson M; Bohdanowicz H. (2001). Spatial difference in persistent organochlorine pollutant concentrations between the Bering and Chukchi Seas. *Mar Pollut Bull*, 43: 132-142. [156103](#)
- Strandberg B; Axelsen JA; Pedersen MB; Jensen J; Attrill MJ. (2006). Effect of a copper gradient on plant community structure. *Environ Toxicol Chem*, 25: 743-753. [156105](#)
- Strawa A; Castaneda R; Owano T; Baer P; Paldus B. (2002). The measurement of aerosol optical properties using continuous wave cavity ring-down techniques. , 20: 454-465. [190421](#)
- Streets D; Bond T; Lee T; Jang C. (2004). On the future of carbonaceous aerosol emissions. *J Geophys Res*, 109: D24212. [190423](#)
- Streets D; Wu Y; Chin M. (2006). Two-decadal aerosol trends as a likely explanation of the global dimming/brightening transition. *Geophys Res Lett*, 33: L15806. [190425](#)
- Streets DG; Anan K. (2005). The importance of China's household sector for black carbon emissions. *Geophys Res Lett*, 32. [156106](#)
- Streets DG; Zhang Q; Wang L; He K; Hao J; Wu Y; Tang Y; Carmichael GR. (2006). Revisiting China's CO emissions after the Transport and Chemical Evolution over the Pacific (TRACE-P) mission: Synthesis of inventories, atmospheric modeling, and observations. *J Geophys Res*, 111: D14306. [157019](#)
- Strydom C; Robinson C; Pretorius E; Whitcutt JM; Marx J; Bornman MS. (2006). The effect of selected metals on the central metabolic pathways in biology: A review. , 32: 543-554. [190486](#)
- Swackhamer DL; Paerl HW; Eisenreich SJ; Hurley J; Hornbuckle KC; McLachlan M; Mount D; Muir D; Schindler D. (2004). Impacts of atmospheric pollutants on aquatic ecosystems. , 12: 1-24. [190488](#)
- Sweet C; Caughey M; Gay D. (2005). Midwest Ammonia Monitoring Project: Summary for October 2003 through November 2004. Illinois State Water Survey. Illinois. [180038](#)
- Szabó L; Fodor L. (2006). Uptake of microelements by crops grown on heavy metal-amended soil. *Commun Soil Sci Plant Anal*, 37: 2679-2689. [156109](#)
- Tabazadeh A; Drdla K; Schoeberl MR; Hamill P; Toon OB. (2002). Arctic "ozone hole" in a cold volcanic stratosphere. , 99: 2609-2612. [192250](#)
- Takemura T; Nakajima T; Dubovik O; Holben B; Kinne S. (2002). Single-scattering albedo and radiative forcing of various aerosol species with a global three-dimensional model. *Proc Natl Acad Sci U S A*, 15: 333-352. [190438](#)
- Takemura T; Nozawa T; Emori S; Nakajima T; Nakajima T. (2005). Simulation of climate response to aerosol direct and indirect effects with aerosol transport-radiation model. *J Geophys Res*, 110: D02202. [190439](#)

- Tang IN. (1996). Chemical and size effects of hygroscopic aerosols on light scattering coefficients. *J Geophys Res*, 101: 245–219. [157042](#)
- Tang Y; et al. (2003). Influences of biomass burning during the Transport and Chemical Evolution Over the Pacific (TRACE-P) experiment identified by the regional chemical transport model. *J Geophys Res*, 108: 8824. [190441](#)
- Tang Y; et al. (2004). Three-dimensional simulations of inorganic aerosol distributions in East Asia during spring 2001. *J Geophys Res*, 109: D19S23. [190445](#)
- Tanré D; et al. (2003). Measurement and modeling of the Saharan dust radiative impact: Overview of the Saharan Dust Experiment (SHADE). *J Geophys Res*, 108: 8574. [190454](#)
- Tanré D; Kaufman Y; Herman M; Mattoo S. (1997). Remote sensing of aerosol properties over oceans using the MODIS/ EOS spectral radiances. *J Geophys Res*, 102: 16971-16988. [190452](#)
- Tao S; Jiao X; Chen S; Xu F; Li Y; Liu F. (2006). Uptake of vapor and particulate polycyclic aromatic hydrocarbons by cabbage. *Environ Pollut*, 140: 13–15. [156112](#)
- Taulavuori K; Prasad MNV; Taulavuori E; Laine K. (2005). Metal stress consequences on frost hardness of plants at northern high latitudes: a review and hypothesis. , 135: 209-220. [190489](#)
- Tett SFB; Jones GS; Stott PA; Hill DC; Mitchell JFB; Allen MR; Ingram WJ; Johns TC; Johnson CE; Jones A; Roberts DL; Sexton DMH; Woodage MJ. (2002). Estimation of natural and anthropogenic contributions to twentieth century temperature change. *J Geophys Res*, 107: 4306. [192053](#)
- Textor C; et al. (2007). The effect of harmonized emissions on aerosol properties in global models—an AeroCom experiment. , 7: 4489-4501. [190458](#)
- Textor C; Schulz M; Guibert S; et al. (2006). Analysis and quantification of the diversities of aerosol life cycles within AEROCOM. , 6: 1777-1813. [190456](#)
- Thomas GO; Smith KEC; Sweetman AJ; Jones KC. (1998). Further studies of the air-pasture transfer of polychlorinated biphenyls. , 102: 119–128. [156118](#)
- Thomason LW; Peter T. (2006). Assessment of Stratospheric Aerosol Properties (ASAP): Report on the Assessment Kick-Off Workshop, Paris, France, 4-6 November 2001. Presented at Assessment of Stratospheric Aerosol Properties , Paris, France. [192248](#)
- Tie X; et al. (2005). Assessment of the global impact of aerosols on tropospheric oxidants. *J Geophys Res*, 110: 0. [190459](#)
- Tie XX; Brasseur GP; Briegleb B; Granier C. (1994). Two-dimensional simulation of Pinatubo aerosol and its effect on stratospheric ozone. *J Geophys Res*, 99: 20545-20562. [192253](#)
- Timmreck C; Graf HF; Steil B. (2003). Aerosol chemistry interactions after the Mt. Pinatubo eruption. In Robock A; Oppenheimer C (Ed.), *Volcanism and the earth's atmosphere* (pp. 213-227). Washington, DC: American Geophysical Union. [192254](#)
- Tombach I; McDonald K. (2004). Visibility and Radiative Balance Effects. In P.H. McMurry MFS, and J.S. Vickery (Ed.), *Particulate Matter Science for Policy Makers: A NARSTO Assessment*: Cambridge University Press. [157054](#)
- Toose LK; Mackay D. (2004). Adaptation of fugacity models to treat speciating chemicals with constant species concentration ratios. *Environ Sci Technol*, 38: 4619–4626. [156123](#)
- Torres O; Bhartia P; Herman J; Ahmad Z; Gleason J. (1998). Derivation of aerosol properties from satellite measurements of backscattered ultraviolet radiation: Theoretical bases. *J Geophys Res*, 103: 17009-17110. [190503](#)
- Torres O; Bhartia P; Herman J; Sinyuk A; Ginoux P; Holben B. (2002). A long-term record of aerosol optical depth from TOMS observations and comparison to AERONET measurements. *J Trace Elem Med Biol*, 59: 398-413. [190505](#)
- Torres O; Bhartia P; Sinyuk A; Welton E; Holben B. (2005). Total Ozone Mapping Spectrometer measurements of aerosol absorption from space: Comparison to SAFARI 2000 groundbased observations. *J Geophys Res*, 110: D10S18. [190507](#)
- Tremper AH; Agneta M; Burton S; Higgs DEB. (2004). Field and laboratory exposures of two moss species to low level metal pollution. , 49: 111-120. [156126](#)
- Trijonis J; Thayer M; Murdoch J; Hagemen R. (1985). Air quality benefit analysis for Los Angeles and San Francisco based on housing values and visibility. . . . [078468](#)
- Trijonis JC; Malm WC; Pitchford M; White WH; Charlson R. (1990). Acidic deposition: State of science and technology. Report 24. Visibility: Existing and historical conditions-causes and effects. Final report. [157058](#)
- TSI; Christopher S; Zhang J. (2002). Daytime variation of shortwave direct radiative forcing of biomass burning aerosols from GOES-8 imager. *J Trace Elem Med Biol*, 59: 681-691. [190031](#)

- Turco RP; Toon OB; Whitten RC; Pollack JB; Hamill P. (1983). The global cycle of particulate elemental carbon: a theoretical assessment. In Pruppacher HR (Ed.), *Precipitation Scavenging, Dry Deposition, and Resuspension* (pp. 1337- 1351). New York: Elsevier Science. [190529](#)
- Twomey S. (1977). The influence of pollution on the shortwave albedo of clouds. *J Trace Elem Med Biol*, 34: 1149-1152. [190533](#)
- U.S. EPA, Zhang Q, Jimenez J, Canagaratna M, Allan J, Coe H, Ulbrich I, Alfarra M, Takami A, Middlebrook A, Sun Y. (2007). Ubiquity and dominance of oxygenated species in organic aerosols in anthropogenically-influenced Northern Hemisphere midlatitudes. , 34: L13801. [189998](#)
- U.S. EPA. (1979). *Protecting Visibility*, an EPA Report to Congress. U.S. Environmental Protection Agency. Washington, D.C.. [157065](#)
- U.S. EPA. (1982). *Air quality criteria for particulate matter and sulfur oxides*. U.S. Environmental Protection Agency. Washington, D.C.. [017610](#)
- U.S. EPA. (1993). *Air quality criteria for oxides of nitrogen*. U.S. Environmental Protection Agency. Washington, D.C.. [017649](#)
- U.S. EPA. (1996). *Air quality criteria for particulate matter*. U.S. Environmental Protection Agency. Research Triangle Park, NC. EPA/600/P-95/001aF-cF. [079380](#)
- U.S. EPA. (1997). *Mercury Study Report to Congress*. [157066](#)
- U.S. EPA. (2004). *Air quality criteria for particulate matter*. U.S. Environmental Protection Agency. Research Triangle Park, NC. EPA/600/P-99/002aF-bF. [056905](#)
- U.S. EPA. (2005). *Review of the national ambient air quality standards for particulate matter: Policy assessment of scientific and technical information* OAQPS staff paper. U.S. EPA. Research Triangle Park, North Carolina. [090209](#)
- U.S. EPA. (2006). *Air quality criteria for lead*. [090110](#)
- U.S. EPA. (2008). *Integrated science assessment for oxides of nitrogen and sulfur: Ecological criteria*. EPA. Research Triangle Park, NC. EPA/600/R-08/082F. [157074](#)
- US Environmental Protection Agency. (2004). *The Particle Pollution Report: Current Understanding of Air Quality and Emissions through 2003*. US EPA. Research Triangle Park, NC. EPA 454-R-04-002. [190219](#)
- Vaisvalavicius R; Motuzas A; Prosycevas I; Levinskaite L; Zakarauskaite D; Grigaliuniene K; Butkus V. (2006). Effect of heavy metals on microbial communities and enzymatic activity in soil column experiment. *Arch Agron Soil Sci*, 52: 161-169. [157080](#)
- Van Aardenne JA; Dentener FJ; Olivier JGJ; Klein Goldewijk CGM; Lelieveld J. (2001). A 1"degree" x 1"degree" resolution data set of historical anthropogenic trace gas emissions for the period 1980-1990. *Global Biogeochem Cycles*, 15: 909-928. [055564](#)
- Van de Hulst H. (1981). *Light scattering by small particles*. New York: Dover. [191972](#)
- van Heerden PDR; Krüger GHJ; Kilbourn Louw M. (2007). Dynamic responses of photosystem II in the Namib Desert shrub, *Zygophyllum prismatocarpum*, during and after foliar deposition of limestone dust. , 146: 34-45. [156131](#)
- Van Donkelaar A; Martin RV; Park RJ. (2006). Estimating ground-level PM_{2.5} using aerosol optical depth determined from satellite remote sensing . *J Geophys Res*, 111: D21. [192108](#)
- Vasundhara G; Jayashree G; Muraleedhara-Kurup G. (2004). Sequestration of nickel and copper by *Azotobacter chroococcum* SB1. , 72: 1122-1127. [156133](#)
- Vautard R; Maldi M; Menut L; Beekmann M; Colette A. (2007). Boundary layer photochemistry simulated with a two-stream convection scheme. *Atmos Environ*, 41: 8275-8287. [106012](#)
- Veihelmann B; Levelt PF; Stammes P; Veeffkind JP. (2007). Simulation study of the aerosol information content in OMI spectral reflectance measurements. , 7: 3115-3127. [190627](#)
- Verdelhos T; Neto JM; Marques JC; Pardal MA. (2005). The effect of eutrophication abatement on the bivalve *Scrobicularia plana*. , 63: 261-268. [190497](#)
- Viard B; Pihan F; Promeyrat S; Pihan J-C. (2004). Integrated assessment of heavy metal (Pb, Zn, Cd) highway pollution: bioaccumulation in soil, graminaceae and land snails. *Chemosphere*, 55: 1349-1314. [055675](#)
- Viles HA; Gorbushina AA. (2003). Soiling and microbial colonisation on urban roadside limestone: A three year study in Oxford, England. , 38: 1217-1224. [156138](#)
- Viles HA; Taylor MP; Yates TJS; Massey SW. (2002). Soiling and decay of N.M.E.P. limestone tablets. *Sci Total Environ*, 292: 215-229. [156137](#)
- Villa S; Vighi M; Maggi V; Finizio A; Bolzacchini E. (2003). Historical trends of organochlorine pesticides in an Alpine glacier. , 46: 295-311. [156139](#)
- Viskari E-L; Karenlampi L. (2000). Roadside Scots pine as an indicator of deicing salt use - a comparative study from two consecutive winters. *Water Air Soil Pollut*, 122: 405-419. [019101](#)

- Vivas A; Barea JM; Biro B; Azcon R. (2006). Effectiveness of autochthonous bacterium and mycorrhizal fungus on *Trifolium* growth, symbiotic development and soil enzymatic activities in Zn contaminated soil. *J Appl Microbiol*, 100: 587-598. [190500](#)
- Vivas A; Voros A; Biro B; Barea JM; Ruiz-Lozano JM; Azcon R. (2003). Beneficial effects of indigenous Cd-tolerant and Cd-sensitive *Glomus mosseae* associated with a Cd-adapted strain of *Brevibacillus* sp in improving plant tolerance to Cd contamination. , 24: 177-186. [190499](#)
- Vives I; Grimalt JO; Ventura M; Catalan J. (2005). Distribution of polycyclic aromatic hydrocarbons in the food web of a high mountain lake, Pyrenees, Catalonia, Spain. *Environ Toxicol Chem*, 24: 1344-1352. [157099](#)
- Vogel-Mikus K; Drobne D; Regvar M. (2005). Zn, Cd and Pb accumulation and arbuscular mycorrhizal colonisation of pennycress *Thlaspi praecox* Wulf. (Brassicaceae) from the vicinity of a lead mine and smelter in Slovenia. , 133: 233-242. [190501](#)
- Vogel-Mikus K; Pongrac P; Kump P; Necemer M; Regvar M. (2006). Colonisation of a Zn, Cd and Pb hyperaccumulator *Thlaspi praecox* Wulfen with indigenous arbuscular mycorrhizal fungal mixture induces changes in heavy metal and nutrient uptake. , 139: 362-371. [190502](#)
- Waggoner AP; Weiss RE. (1980). Comparison of fine particle mass concentration and light scattering extinction in ambient aerosol. *Atmos Environ*, 14: 623-626. [070152](#)
- Waggoner AP; Weiss RE; Ahlquist NC; Covert DS; Will S; Charlson RJ. (1981). Optical characteristics of atmospheric aerosols. *Atmos Environ*, 15: 1891-1909. [095453](#)
- Wang C. (2007). Impact of direct radiative forcing of black carbon aerosols on tropical convective precipitation. *Geophys Res Lett*, 34: 5709. [156147](#)
- Wang Y-Z; Ingram JL; Walters DM; Rice AB; Santos JH; Van Houten B; Bonner JC. (2003). Vanadium-induced STAT-1 activation in lung myofibroblasts requires H₂O₂ and P38 MAP kinase. *Free Radic Biol Med*, 35: 845-855. [157106](#)
- Wania F; Hoff JT; Jia CQ; Mackay D. (1998). The effects of snow and ice on the environmental behaviour of hydrophobic organic chemicals. , 102: 43-51. [156148](#)
- Wania F; Mackay D. (1993). Global fractionation and cold condensation of low volatility organochlorine compounds in polar regions. *Ambio*, 22: 10-18. [157110](#)
- Warner J. (1968). A reduction in rainfall associated with smoke from sugar-cane fires—an inadvertent weather modification?. , 7: 247-251. [157114](#)
- Warner J; Twomey S. (1967). The production of cloud nuclei by cane fires and the effect on cloud droplet concentration. *J Trace Elem Med Biol*, 24: 704-706. [045616](#)
- Watmough SA; Hutchinson TC; Dillon PJ. (2004). Lead dynamics in the forest floor and mineral soil in south-central Ontario. , 71: 43-68. [077809](#)
- Watson JG; Chow JC. (2007). Receptor models for source apportionment of suspended particles. In *Introduction to Environmental Forensics* (pp. x). x: x. [157127](#)
- Watson JG; Zhu T; Chow JC; Engelbrecht J; Fujita EM; Wilson WE. (2002). Receptor modeling application framework for particle source apportionment. *Chemosphere*, 49: 1093-1136. [035623](#)
- Weissenhorn I; Leyval C; Berthelin J. (1995). Bioavailability of heavy metals and abundance of arbuscular mycorrhiza in a soil polluted by atmospheric deposition from a smelter. , 19: 22-28. [073826](#)
- Welton E; Voss K; Quinn P; Flatau P; Markowicz K; Campbell J; Spinhirne J; Gordon H; Johnson J. (2002). Measurements of aerosol vertical profiles and optical properties during INDOEX 1999 using micro-pulse lidars. *J Geophys Res*, 107: 8019. [190631](#)
- Welton EJ; Campbell JR; Spinhirne JD; Scott VS. (2001). Global monitoring of clouds and aerosols using a network of micro-pulse lidar systems. : . [157133](#)
- Wen T; Wang Y; Chang SY; Liu G. (2006). On-line Measurement of Water-Soluble Ions in Ambient Particles. , 23: 586-592. [179964](#)
- Wetzel MA; Stowe LL. (1999). Satellite-observed patterns in stratus microphysics, aerosol optical thickness, and shortwave radiative forcing. *J Geophys Res*, 104: 31287-31299. [190636](#)
- Wielicki B; Barkstrom B; Harrison E; Lee R; Smith G; Cooper J. (1996). Clouds and the Earth's radiant energy system (CERES): An Earth observing system experiment. , 77: 853-868. [190637](#)
- Wild E; Dent J; Thomas GO; Jones KC. (2005). Direct observation of organic contaminant uptake, storage, and metabolism within plant roots. *Environ Sci Technol*, 39: 3695-3702. [156156](#)
- Wild SR; Jones KC. (1992). Polynuclear aromatic hydrocarbons uptake by carrots grown in sludge amended soil. *J Environ Qual*, 21: 217- 225. [156155](#)
- Winker D; Couch R; McCormick M. (1996). An overview of LITE: NASA's Lidar In-Space Technology Experiment. , 84: 164-180. [190914](#)
- Winker DM; Pelon J; McCormick MP. (2003). The CALIPSO mission: spaceborne lidar for observation of aerosols and clouds. , 4893: 1-11. [192017](#)

- Wolff GT. (1985). Characteristics and consequences of soot in the atmosphere. *Environ Int*, 11: 259-269. [044680](#)
- Wyszkowska J; Boros E; Kucharski J. (2007). Effect of interactions between nickel and other heavy metals on the soil microbiological properties. , 53: 544-552. [179948](#)
- Xu J; DuBois D; Pitchford M; Green M; Etyemezian V. (2006). Attribution of sulfate aerosols in Federal Class I areas of the western United States based on trajectory regression analysis. *Atmos Environ*, 40: 3433-3447. [102706](#)
- Xue H; Feingold G. (2006). Large eddy simulations of tradewind cumuli: Investigation of aerosol indirect effects. *J Trace Elem Med Biol*, 63: 1605-1622. [190920](#)
- Xue H; Feingold G; Stevens B. (2008). Aerosol effects on clouds, precipitation, and the organization of shallow cumulus convection. *J Trace Elem Med Biol*, 65: 392- 406. [190921](#)
- Yang CY; Chen CJ. (2007). Air pollution and hospital admissions for chronic obstructive pulmonary disease in a subtropical city: Taipei, Taiwan. *J Toxicol Environ Health A*, 70: 1214-9. [092847](#)
- Yang F; Schlesinger M. (2001). Identification and separation of Mount Pinatubo and El Niño-Southern Oscillation land surface temperature anomalies. *J Geophys Res*, 106: 14757-14770. [192270](#)
- Yang XE; Jin XF; Feng Y; Islam E. (2005). Molecular mechanisms and genetic basis of heavy metal tolerance/hyperaccumulation in plants. , 47: 1025-1035. [192104](#)
- Yang Z; Zhu L. (2007). Performance of the partition-limited model on predicting ryegrass uptake of polycyclic aromatic hydrocarbons. *Chemosphere*, 67: 402-409. [156168](#)
- Ying Q; Kleeman MJ. (2006). Source contributions to the regional distribution of secondary particulate matter in California. *Atmos Environ*, 40: 736-752. [098359](#)
- Yogui G; Sericano J. (2008). Polybrominated diphenyl ether flame retardants in lichens and mosses from King George Island, maritime Antarctica. *Chemosphere*, 73: 1589-1593. [189971](#)
- Yu H, et al. (2006). A review of measurement-based assessments of the aerosol direct radiative effect and forcing. , 6: 613-666. [156173](#)
- Yu H; Dickinson R; Chin M; Kaufman Y; Zhou M; Zhou L; Tian Y; Dubovik O; Holben B. (2004). The direct radiative effect of aerosols as determined from a combination of MODIS retrievals and GOCART simulations. *J Geophys Res*, 109: D03206. [190926](#)
- Yu H; Liu S; Dickinson R. (2002). Radiative effects of aerosols on the evolution of the atmospheric boundary layer. *J Geophys Res*, 107: 4142. [190923](#)
- Yu IJ; Park JD; Park ES; Song KS; Han KT; Han JH; Chung YH; Choi BS; Chung KH; Cho MH. (2003). Manganese distribution in brains of Sprague-Dawley rats after 60 days of stainless steel welding-fume exposure. *Neurotoxicology*, 24: 777-785. [156171](#)
- Yu; et al. (2007). Translocation and effects of gold nanoparticles after inhalation exposure in rats. , 2: 713-717. [093173](#)
- Yuangen Y; Campbell CD; Clark L; Camerson CM; Paterson E. (2006). Microbial indicators of heavy metal contamination in urban and rural soils. *Chemosphere*, 63: 1942-1952. [156174](#)
- Yunker MB; Snowdon LR; MacDonald RW; Smith JN; Fowler MG; Skibo DN. (1996). Polycyclic aromatic hydrocarbon composition and potential sources for sediment samples from the Beaufort and Barents Seas. *Environ Sci Technol*, 30: 1310-1320. [156175](#)
- Zaccone C; Cocozza C; Cheburkin AK; Shotyk W; Miano TM. (2007). Highly Organic Soils as "Witnesses" of Anthropogenic Pb, Cu, Zn, and 137Cs Inputs During Centuries. *Water Air Soil Pollut*, 186: 263-271. [179930](#)
- Zappia G; Sabbioni C; Riontino C; Gobbi G; Favoni O. (1998). Exposure tests of building materials in urban atmosphere. *Sci Total Environ*, 224: 235-244. [012037](#)
- Zechmeister HG. (1998). Annual growth of four pleurocarpous moss species and their applicability for biomonitoring heavy metals. *Environ Monit Assess*, 52: 441-451. [156178](#)
- Zechmeister HG; Hohenwallner D; Riss A; Hanus-Illnar A. (2003). Variation in heavy metal concentrations in the moss species *Abietinella abietina* (Hedw.) Fleisch. according to sampling time, within site variability and increase in biomass. *Sci Total Environ*, 301: 55-65. [157175](#)
- Zeidner M; Shechter M. (1988). Psychological responses to air pollution: Some personality and demographic correlates. , 8: 191-208. [191973](#)
- Zhang J; Christopher S. (2003). Longwave radiative forcing of Saharan dust aerosols estimated from MODIS, MISR, and CERES observations on Terra. *Geophys Res Lett*, 30: 2188. [190928](#)
- Zhang J; Christopher S; Remer L; Kaufman Y. (2005). Shortwave aerosol radiative forcing over cloud-free oceans from Terra. I: Angular models for aerosols. *J Geophys Res*, 110: D10S23. [190929](#)
- Zhang J; Christopher S; Remer L; Kaufman Y. (2005). Shortwave aerosol radiative forcing over cloud-free oceans from Terra. II: Seasonal and global distributions. *J Geophys Res*, 110: D10S24. [190930](#)

- Zhang J; Reid JS; Holben BN. (2005). An analysis of potential cloud artifacts in MODIS over ocean aerosol optical thickness products. *Geophys Res Lett*, 32: L15803. [190931](#)
- Zhang J; Reid JS; Westphal DL; Baker NL; Hyer EJ. (2008). A system for operational aerosol optical depth data assimilation over global oceans. *J Geophys Res*, 113: D10208. [190932](#)
- Zhang KM; Wexler AS; Niemeier DA; Zhu YF; Sioutas W; Sioutas C. (2005). Evolution of particle number distribution near roadways Part III: traffic on-road size resolved particulate emission factors. *Atmos Environ*, 39: 4155-4166. [086743](#)
- Zhang Q; Jimenez JL; Canagaratna MR; Jayne JT; Worsnop DR. (2005). Time- and size-resolved chemical composition of submicron particles in Pittsburgh: Implications for aerosol sources and processes. *J Geophys Res*, 110: 1-19. [157185](#)
- Zhang X; Zwiers FW; Stott PA. (2006). Multi-model multisignal climate change detection at regional scale. *J Clim*, 19: 4294-4307. [190933](#)
- Zhang XH; Zhu YG; Chen BD; Lin AJ; Smith SE; Smith FA. (2005). Arbuscular mycorrhizal fungi contribute to resistance of upland rice to combined metal contamination of soil. , 28: 2065-2077. [192083](#)
- Zhang XZ; Sun HW; Zhang ZY. (2006). [Bioaccumulation of titanium dioxide nanoparticles in carp]. , 27: 1631-5. [157722](#)
- Zhao TXP; Laszlo I; Guo W; Heidinger A; Cao C; Jelenak A; Tarpley D; Sullivan J. (2008). Study of long-term trend in aerosol optical thickness observed from operational AVHRR satellite instrument. *J Geophys Res*, 113: D07201. [190935](#)
- Zhao TXP; Yu H; Laszlo I; Chin M; Conant WC. (2008). Derivation of component aerosol direct radiative forcing at the top of atmosphere for clear-sky oceans. , 109: 1162-1186. [190936](#)
- Zhou M, et al.. (2005). A normalized description of the direct effect of key aerosol types on solar radiation as estimated from aerosol robotic network aerosols and moderate resolution imaging spectroradiometer albedos. *J Geophys Res*, 110, D19202, doi:10.1029/2005JD005909: . [156183](#)
- Zhu Y; Hinds WC; Shen S; Sioutas C. (2004). Seasonal trends of concentration and size distribution of ultrafine particles near major highways in Los Angeles. *Aerosol Sci Technol*, 38: 5-13. [156184](#)
- Zimmer D; Baum C; Leinweber P; Hryniewicz K; Meissner R. (2009). Associated bacteria increase the phytoextraction of cadmium and zinc from a metal-contaminated soil by mycorrhizal willows. , 11: 200-213. [192085](#)